FOURTH

ICA

1962

I

Preface

The Organization Committee of The Fourth International Congress on Acoustics has found that the value of the Congress will be increased to a considerable extent if the manuscripts for the papers of the delegates are available already at the opening of the Congress. Thus, it will be far easier to the individual congress members to select the papers of which they want to attend the reading than in the case they are guided by a short summary only. Furthermore - and this is maybe the most important thing - the members of the Congress will be able to study the manuscripts during and immediately after the Congress instead of having to wait for one year before these are available to the public.

The authors have been very obliging to the Organization, and by a thorough rationalization of the production technique it has been possible to postpone the delivery of the manuscripts to June 15th, i.e. approximately two months before the opening of the Congress. Unfortunately, it has, for technical reasons, been completely impossible to accept manuscripts received after the expiry of the time limit.

This publication, Congress Report I, contains all the papers of the members, whereas the invited papers will be printed and published after the Congress in the form of Congress Report II.

Congress Report I is devided into the following ten sections:
1) Speech analysis and synthesis (section G), 2) Physiological and psychological acoustics (section H), 3) Molecular acoustics (section J), 4) Ultrasonics and underwater sound (section K), 5) Noise and noise control (section L), 6) Room acoustics (section M), 7) Electroacoustics (section N), 8) Physical acoustics (section O), 9) Mechanical vibrations (section P), 10) Musical acoustics (section P 5).

This division corresponds to the one to be used during the Congress, and the sequence within each section corresponds to the one planned for the papers.

The Organization Committee extends its best thanks to the United Nations Educational Scientific and Cultural Organization as well as to the Danish Government Fund for Scientific and Industrial Research for the financial support rendered at the publishing of Congress Report I.

Copenhagen, June 15th, 1962. A.Kjerbye Nielsen.

Vorwort

Das Organisationskomitee für The Fourth International Congress on Acoustics ist der Ansicth gewesen, dass der Kongress erheblich an Wert gewinnen würde, falls die Manuskripte über die Vorträge der Delegierten bereits bei der Eröffnung des Kongresses vorliegen könnten. Dadurch wird es dem einzelnen Kongressteilnehmer viel leichter, diejenigen Vorträge zu wählen, denen er beiwohnen möchte, als wenn nur kurze Zusammenfassungen vorliegen würden. Ferner - und das ist vielleicht das Bedeutendste - werden die Teilnehmer die Manuskripte während des Kongresses und umittelbar nach seinem Abschluss studieren können und nicht etwa ein Jahr warten müssen, bis sie öffenlich erhältlich sind.

Der Organisation ist von Seiten der Verfasser ein sehr grosses Entgegenkommen gezeigt worden, und mit Hilfe einer durchgreifenden Rationalisierung auf dem Gebiet der Reproduktionstechnik ist es gelungen, den Zeitpunkt für die Einlieferung der Manuskripte auf den 15. Juni zu verschieben, d.h. etwa 2 Monate vor Eröffnung des Kongresses. Bedauerlicherweise ist es aus technischen Gründen nicht möglich gewesen, Manuskripte, die nach Ablauf dieser Frist eingegangen sind, zu akzeptieren.

Die gegenwärtige Publikation, Kongress-Bericht I, enthalt alle Teilnehmervorträge, während die Plenarvorträge als Kongress-Bericht II nach Abschluss des Kongresses gedruckt und herausgegeben werden.

Kongress-Bericht I ist in folgende 10 Abteilungen aufgeteilt: 1) Sprache, Analyse und Synthese (Sektion G), 2) Physiologische und psychologische Akustik (Sektion H), 3) Molekularakustik (Sektion J), 4) Ultraschall und Wasserschall (Sektion K), 5) Lärm und Lärmabwehr (Sektion L), 6) Raumakustik (Sektion M), 7) Elektroakustik (Sektion N), 8) Physikalische Akustik (Sektion O), 9) Körperschall (Sektion P), 10) Musikalische Akustik (Sektion P 5). Diese Aufteilung entspricht derjenigen, die während des Kongresses zur Anwendung kommt, und die Reihenfolge innerhalb jeder Abteilung entspricht der geplanten Reihenfolge der Vorträge.

Das Organisationskomitee bringt The United Nations Educational Scientific and Cultural Organization sowie dem dänischen technisch-wissenschaftlichen Staatsfonds für die ökonomische Unterstützung bei der Herausgabe des Kongress-Berichtes I seinen besten Dank zum Ausdruck.

Kopenhagen, den 15. Juni 1962 A. Kjerbye Nielsen

Avant-Propos

Le comité organisateur du Quatrième Congrès International de l'Acoustique a trouvé que la valeur du congrès augmenterait considérablement, si les manuscrits pour les conférences des délégués étaient disponibles déjà lors de l'ouverture du congrès. De cette facon il sera beaucoup plus facile pour chaque congressiste de choisir les conférences, auxquelles il veut assister, que s'il n'y a à disposition que des résumés très sommaires. D'autre part - et en voici peut-être le point le plus important - les participants auront la possibilité pour étudier les manuscrits durant le congrès et immédiatement après la clôture de celui-ci au lieu d'avoir à attendre environ une année la publication officielle.

Le comité organisateur a trouvé beaucoup de bienveillance de la part des auteurs, et grâce à une rationalisation rigoureuse de la technique de reproduction on a réussi à proroger le délai de la remise des manuscrits jusqu'au 15 juin, à peu pres 2 mois avant l'ouverture du congrès. C'est à déplorer que, pour des raisons techniques, il a été tout à fait impossible d'accepter des manuscrits parvenus après l'expiration du délai.

Cette publication, Rapport du congrès I, contient l'ensemble des conférences particulières, alors que les conférences générales seront tirées et éditées à titre de Rapport du congrès II après la clôture du congrès.

Le rapport du congrès I est divisé dans les 10 sections suivantes: 1) Langage, analyse et synthèse (section G), 2) Acoustique physiologique et psychologique (section H), 3) Acoustique moléculaire (section J), 4) Ultrasons et acoustique des fluides (section K), 5) Bruit et lutte contre le bruit (section L), 6) Acoustique des salles (section M), 7) Electroacoustique (section N), 8) Acoustique physicale (section O), 9) Vibrations méchaniques (section P), 10) Acoustique musicale (section P 5).

Cette division est conforme à celle venant être appliquée pendant le congrès, et l'ordre de chaque section correspond à l'ordre prévu des conférences.

Le comité organisateur présent ses meilleurs remerciements à l'Organisation des Nations Unies pour l'Education, la Science et la Culture et à Le fonds d'Etat de la Recherche Scientifique et Technique de Danemark du concours économique au tirage du Rapport du congrès I.

CONGRESS REPORT I

of the

FOURTH INTERNATIONAL CONGRESS ON ACOUSTICS

COPENHAGEN, 1962

CONTRIBUTED PAPERS

Dr. A. Kjerbye Nielsen
Editor

Reproduction of the contents of the separate articles must take place only after permission in writing from the authors of the articles in question.

Published by the Organization Committee of the FOURTH INTERNATIONAL CONGRESS ON ACOUSTICS, Copenhagen, 1962. Address: The Acoustical Laboratory, 10 Øster Voldgade, Copenhagen, K.

Printers: Harlang & Toksvig, Advertising Agency Ltd.
Copenhagen

L. C. 58-30838

FOURTH INTERNATIONAL CONGRESS ON ACOUSTICS
COPENHAGEN 21.-28. AUGUST 1962

ALPHABETICAL INDEX OF AUTHORS

Adam, M. M31
Alim, T. Abdel H11 H25
Allen, W. B. K13
Angelini, T. O16
Angeluscheff, Z. D. H12
Anthony, J. G43
Arnaud, J. F. G31
Arnold, J. B. G22
Arni, P. M11
Arns, U. P34
Atal, B. S. H31 M21

Badilian, B. K44
Bang, B. E. N12
Baron, P. L13
Bateman, T. B. K26
Bauer, H.-J. J44
Backer, C. H. K34
Becker, G. W. K42
Bell, J. F. W. J52
Benson, R. W. K35
Bertolotti, M. J26
Betzhold, C. L14
Birch, W. B. K45
Bird, C. M21
Birecki, W. H33
Bismuth, W. P35
Blackstock, D. T. O15
Blake, D. G. N13
Blazier, W. E. L23 L24
Bljakhman, E. A. O17
Bobber, R. J. K33
Bobbert, G. L15
Bodner, S. R. P36
de Boer, E. H13
Boerger, G. N15
Bömmel, H. E. K36
Bonsignour, D. P35
Booker, J. J45
Bordoni, P. G. J12 J53
Borenius, J. M11 M12
Bos, C. E. H13
Boucher, R. M. G. K41
Boutros-Attia, R. M42
Boyd, J. H32
Bradfield, G. J54 K17
Brandt, O. L57 M35
Brekhovskikh, L. B. K21
Brittain, F. H. N21
Broch, J. T. N17
Bruckmayer, F. L16
Brugger, K. J42
Bücklein, R. M41

Burgeat, M. H14
Burger, J. F. M13
van der Burgt, C. M. K22 N18
Burgtorf, W. M14
Burris-Meyer, H. H15

Canac, F. O16
Candau, S. J13 J14
Carbonell, J. R. H17
Cardinell, R. L. H15
Cardozo, B. Lopes H16
Carmel, P. H49
Carome, E. F. K23
Carterette, E. C. G54
Cerf, R. J13 J14
Chalupová, V. H47
Chen, Y. N. L17
Chernov, L. A. O17
Chiba, S. G21
Chistovich, L. A. H18
Chocholle, R. H19
Chromov, V. O18
Chubachi, N. L36
Clark, W. E. L28
Cohen, A. G51
Colbert, H. M. K52
Cole, J. N. L18
Coles, R. R. A. H21
Colton, E. H22
Cook, B. D. O21
Cook, R. K. O43
Corliss, E. L. R. N22
Corsain, G. O16
Corso, J. F. H23
Crawford, A. E. N23
Cremer, L. N15
Dalsgaard, S. C. N24
Dämmig, P. M23
Danielmeyer, H. G. J55
David, E. E. H24 H27 N25
Davies, P. O. A. L. L19 L27
Davis, C. M. J56
Degrois, M. K44
Delany, M. E. N26
Delsasso, L. P. M16 M45
Dietz, F. L. K45
Dion, D. J. N27
Doelle, L. L. M22
Dorland, W. D. L25
Dubout, P. M46
Dwyer, M. J. L19
Dyer, I. O44

Eichler, E. L26
Eisenmenger, W. K46
Eknadiosyants, O. K. O11
Elco, R. A. K54
Essama, E. H11 H25

Fanti, F. J33
Fiala, W. T. N36
Filipczyński, L. P44
Fischer, R. N31
Fisher, M. J. L27
Flanagan, J. L. H26 H27
Fletcher, J. L. H28
Fleury, P. A. K23
Forgie, C. D. G11
Forgie, J. W. G11
Fowweather, F. N32
Franssen, N. V. G12
Freeman, F. E. K51
Fridman, W. M. N33 N58
Fujii, Y. K24
Funakoshi, Y. M51

Galloway, W. J. L28
Gavini, H. H29
Geluk, J. J. M52
Giełdanowski, J. H33
v. Gierke, H. E. L18
Gill, J. S. G33
Giua, P. J12
Gold, B. G34
Goldberg, G. A. M53
Goldberg, Z. A. O45
Gomperts, M. C. M54
Goodman, R. R. K53
Greenspan, M. P12
Gregory, P. L31
Greguss, P. O13
Grumazescu, M. M55
Guillermin, J. N34

Hanson, R. L. H24
Harris, C. M. G47 O54
t' Hart, J. G51
Harwood, H. D. N35
Häusler, E. P11
Havinga, E. E. N18
Heckl, M. F. O55
Heinz, J. M. G46
Henderson, M. C. J25
Heydemann, P. J15
Hida, N. M56
Hiedemann, E. A. J41
Hieken, M. H. L33
Hiki, S. G26
Hille, H. K. L18
Hilliard, J. K. N36
Hiraicho, F. M56
Hiramatsu, K. G32
Hirschfeld, J.-P. N39
Hirschwehr, E. M33
Holmes, J. N. G13
Holmes, R. J31
House, A. S. G22 G23
van Houten, J. J. N36
Hovorka, F. J45
Hub, D. R. J51
Hübner, G. L34
Hughes, W. F. K54
Hunt, F. V. N37
Hunter, J. L. J21
Huszty, D. O51

Illenyi, A. N38
Ingard, U. O33
Inomata, S. G15
Issakovich, M. A. K55

Jacquemot, M. L13
Jamroz, A. H32
Jankowski, W. H33
Járfás, T. G16
Jassem, W. G17
Jensen, J. A. L35
Johnson, F. R. M15
Jones, C. K. K36
Jörgen, G. O. M24

Kacprowski, J. G55
Kagawa, Y. P17
Kahn, J. S. K45
Kapustin, A. P. J23
Karsai, M. M25
Kaszynski, G. O19
Kato, Y. G21
Kelly, J. L. G42
Khokhlov, R. V. O34
Kido, K. L36 P17
Kikuchi, Y. N56
Kirschner, F. L37
Kneser, H. O. J55
Knight, J. J. H34
Knopoff, L. P14
Knudsen, V. O. M27
Kobrynski, M. L22
Kolmer, F. H35
Kolsky, H. P41
Koppelmann, J. K56
Kraut, E. A. O35
Krauth, E. M41
Krom, M. N. O17
Kuhl, W. M28
Kurtze, G. L41
Kurz, K. L42
Kuttruff, H. H31 J24
Kuzmin, Y. I. G35

Lampio, E. N42
Lang, J. M29
Lang, W. W. M32

Lange, T. H36
Larsen, H. L35
Lauber, A. L43
Lawrence, W. G43
Lázár, D. L44
Legouix, J.-P. H37
Lehmann, R. H14 H38
Leipp, E. P51
Leman, H. S. G36
Leonard, R. W. M45
Levelt, W. J. M. P55
Lewis, T. B. J21
Lewis, W. J. L45
Liaghati, G. A. N43
Liebermann, P. G37
Lienard, P. N14
Lierke, G. P42
Lindh, G. 037
Lindsay, R. B. K24
Lippert, W. K. R. M46
Liska, E. J44
Litovitz, T. A. J56
Lloyd, E. A. K51
Lochbaum, C. C. G42
Lochner, J. P. A. M13
Loeb, M. H28
Logan, B. F. G41
Lord, N. W. K25
Lord, P. P31
Louden, M. 038
Lowenstein, C. D. 041
Lyamshev, L. M. 036

Magyar, P. E. L46
Malecki, I. 042
Maling, G. C. 033
Manley, D. M. J. P. H39
Martin, D. W. P52
Martin, T. B. G25
Mártony, J. G45
Mason, W. P. J42 K26
Mathews, M. V. N25
Matsuda, R. N52
Matsui, M. L47
May, J. E. K31
Mayer, W. G. P13
McSkimin, H. J. K26
Mechel, F. 024
Meecham, W. C. 046
Meister, F. J. L48
Meitzler, A. H. N44
Menkes, J. 047
Merle, M. 048
Messinð, D. J34
Meyer, J. P53
Middleton, D. L21
Mikhailov, I. G. J43
Mikhaltzev, I. E. K21
Møller, A. R. G54 H41
Morfey, C. L. L51
Müller, E. H. K. P15

Nägerl, H. J15
Nagata, K. G21
Nakamura, K. L47
Naugolnich, K. A. 045
Nederveen, C. J. P16
Neely, K. K. H42
Nemec, J. L52
Newman, R. B. M47
Nickson, A. F. B. L53
Niese, H. N19
de Niet, E. N11
Nimura, T. L36 P17
Nomoto, O. J11
Nordby, K. S. M32
Nowitzky, B. G. N33 N58
Nuovo, M. J33 J53
Nutsch, J. M44

Oberst, H. M57
Oestreicher, H. 052
Ohman, S. E. G. G53
Olson, H. F. G14
Onoe. M. N44
Ostergaard, P. B. M58
Otani, T. K43
Oyer, H. J. G52

Pajewski, W. 042
Parfitt, G. G. P21
Paul, A. P. G22 G23
Pauthier-Camier, S. K32
Pedersen, S. Boel N45
Peetz, E. P15
Petersen, P. E. Møller N41
Pfafflin, S. M. N25
Pickett, J. M. G24
Piercy, J. E. H46
Pikler, A. G. P54
Pimonow, L. H43
Pithey, E. R. P31
Plomp, R. P55
Pohlman, R. P42
Pollack, I. H44
Polyakova, A. L. 053
Port, E. H45
Powell, A. 022
Powell, R. G. L18
Prestigiacomo, A. J. G41
Putzrath, F. L. G25

Rademacher, H.-J. K42
Radionova, E. A. H55
Raes, A. M43
Rasmussen, G. N51
Richards, E. J. L12 L21
Rimski-Korsakov, A. V. H57
Ritsma, R. J. H51 H58
Roth, W. N13

ALPHABETICAL INDEX OF AUTHORS

Rother, P. M44
Rudmose, W. H52
Rudnick, I. J22 M45
Rybak, S. A. P43

Sacerdote, C. Bordone N16
Sachs, T. D. O23
Saito, I. K43
Saito, S. N52
Saulnier, C. H19
Scharf, B. H53
Schilz, W. O24
Scholl, H. H56
Schreiber, L. N53
Schroeder, M. R. G41 H31 M21 O25
Seed, A. N54
Sekey, A. R. H59
Sessler, G. M. N55 O25
Sette, D. J26 J34
Shapiro, K. A. J22
Sharland, I. J. L12
Shaw, E. A. G. H46
Shibayama, K. N56 P17
Siegert, H. K11
Sirotyuk, M. G. K55 O26
Slavík, J. B. H47
Smith, E. L. H48
Smith, F. A. J31
Snowdon, J. C. P22
Soluyan, S. I. O27
Starr, A. H49
Stewart, E. S. K12
Stewart, J. L. K12 K13
Stevens, K. N. G22 G23
Strasberg, N. O28
Straszewicz, W. M26
Struve, W. M28
Stuijts, A. L. K22
Subbarao, K. L56
Sugimoto, T. G26
Sykes, A. O. L54
Széchey, B. L55

Talavage, J. J. G25
Tarnóczy, T. G27 M25
Tartakowskii, B. D. P43
Tedrick, R. N. O12
Teer, K. N11
Tempest, W. J31
Terkildsen, K. H54
Thiessen, G. J. L56
Thorne, E. A. P23
Tiutekin, V. V. P24 P45
Tjaden, D. L. A. N11
Tolstoy, I. K14
Trott, W. J. K33
Tschiegg, C. P12

Urabe, Y. K43
Urushihara, K. K24

Vagi, O. G. M22
Venzke, G. M34
Verdini, L. J12 J53
Victorov, I. A. P33
Vigneaux, G. A, O31
Viktorova, R. N. P45
Voce, J. D. L31
Vovk, E. A. P45

Wagner, W. J. K23
Wahlström, S. L57
Wahrman, C. G. N57
Walkling, R. A. P32
Walther, L. N46
Wanderlingh, F. J34
Ward, F. L. L11
Waterhouse, R. V. O32
Wathen-Dunn, W. G44
Watson, B. J. H27
Wehr, J. S. K15 P35
Weiss, M. R. G47
Weissler, A. J32
Wells, R. J. L23 L24
Werner, H. L58
West, J. E. N55
Westerberg, G. M35
Westphal, W. M36
White, D. L. K16
White, J. E. O14
Winckel, F. M37
Winkler, U. L58

Yeager, E. J45

Zana, R. J13 J14
Zankel, K. L. K52
Zosel, A. J15

INDEX OF PAPERS

Section G: Speech Analysis and Synthesis

G11 A Computer Program for Recognizing the English Fricative Consonants |f| and |θ|.
(James W. Forgie & Carma D. Forgie).

G12 The Mechanism of the Human Voice and Wind Instruments.
(N. V. Franssen).

G13 An Investigation of the Volume Velocity Waveform at the Larynx during Speech by Means of an Inverse Filter.
(J. N. Holmes).

G14 Speech Machine Considerations.
(Harry F. Olson).

G15 Program for Active Segmentation and Reduction of Phonetic Parameters.
(Syuiji Inomata).

G16 Investigations of the directivity pattern of speech-sounds.
(Thomas Járfás).

G17 Noise spectra of Swedish, English and Polish fricatives.
(Wiktor Jassem).

G21 Spoken digit recognizer for Japanese language.
(Kuniichi Nagata, Yasuo Kato & Seibi Chiba).

G22 Acoustical Description of Syllabic Nuclei: Data Derived by Automatic Analysis Procedures.
(A. S. House, A. P. Paul, K. N. Stevens & Jane B. Arnold).

G23 Acoustical Description of Syllabic Nuclei: An Interpretation in Terms of a Dynamic Model of Articulation.
(A. S. House, K. N. Stevens & A. P. Paul).

G24 Tactual Vocoder as an Aid for the Deaf.
(J. M. Pickett).

G25 Electronic Model of the Human Auditory System.
(T. B. Martin, J. J. Talavage & F. L. Putzrath).

G26 On the Fxtraction of the Pitch Signal Using the Body Wall Vibration at the Throat of the Talker.
(Toshitaka Sugimoto & Shizuo Hiki).

G27 Sprachliche Verschiedenheiten erhalten durch Sprechchormethode.
(Thomas Tarnóczy).

G31 L'écoute stéréophonique chez l'auditeur.
(J. F. Arnaud).

G32 Speech parameters extracted by processing of S.S.B.-clipping.
(Keiji Hiramatsu).

G33 Estimation of larynx-pulse timing during speech.
(J. S. Gill).

G34 Description of a Computer Program for Pitch Detection.
(Bernard Gold).

G35 Mobile Palatography as a Tool for Acoustic Study of Speech Sounds.
(Y. I. Kuzmin).

G36 Shape of Human Mouth based on Speech Pressure Distribution close to the Mouth.
(H. S. Leman).

G37 Pitch Perturbations of Normal and Pathologic Larynxes.
(Philip Lieberman).

G41 New Methods for Speech Analysis-Synthesis and Bandwidth Compression.
(M. R. Schroeder, B. F. Logan & A. J. Prestigiacomo).

G42 Speech Synthesis.
(John L. Kelly & Carol C. Lochbaum).

G43 A Resonance Analogue Speech Synthesiser.
(J. Anthony & W. Lawrence)

G44 On Peak Factors and Assymetries of Acoustical Speech Signals.
(Weiant Wathen-Dunn).

G45 On Perceptual Cues for Swedish Fricatives.
(János Mártony).

G46 An Analysis of Speech Spectra in Terms of a Model of Articulation.
(J. M. Heinz).

G47 Concerning the Effect of Word Length on Rates of Change of Formant Frequencies.
(Mark R. Weiss & Cyril M. Harris).

G51 Segmentation of the Speech Continuum, (A. Cohen & J. 't Hart).

G52 Manipulation of the Acoustical Component of Language By A Specially Structured Ortographic System. (Herbert J. Oyer).

G53 Perception of gated Swedish consonants in VC and CV syllables. (S. E. G. Öhman).

G54 The Perception of Real and Synthetic Vowels After Very Sharp Filtering. (Edward C. Carterette & A. Møller).

G55 Preliminary Synthesis of Polish Vowels by Means of the "Terminal-Analog" Speech Synthesizer. (Janusz Kacprowski).

Section H: Physiological and Psychological Acoustics (apart from speech analysis and synthesis)

H11 Proper Evaluation of Audiometric Results. (T. Abdel Alim & E. Essama).

H12 On Biochemistry of Hearing. (Z. D. Angeluscheff).

H13 On the concept of the critical band. (E. de Boer & C. E. Bos).

H14 Etude experimentale de la propagation des ondes acoustiques dans les liquides cochleaires. (M. Burgeat & R. Lehmann).

H15 Applied Psychoacoustics. (Harold Burris-Meyer & Richmond L. Cardinell).

H16 Frequency Discrimination of the Human Ear. (B. Lopes Cardozo).

H17 A Tentative Model on Binaural Hearing. (Jaime R. Carbonell).

H18 Temporal Course of Speech Sound Perception. (Experiments with shadowing and letter writing reaction to consonants). (L. A. Chistovich).

H19 L'effet d'un bruit blanc contralateral tant sur le seuil absolu que sur le seuil differentiel. (René Chocholle & Christiane Saulnier).

H21 Some Considerations Concerning the Effects on Hearing of the Noise of Small-Arms. (R. R. A. Coles).

H22 On the Contribution of Synchronization Patterns to Semantic Meaning. (Ernest Colton).

H23 Age and Sex Differences in Pure-Tone Thresholds from 18 to 65 Years. (John F. Corso).

H24 Binaural Hearing and Free Field Effects. (E. E. David, Jr. & R. L. Hanson).

H25 The Effect of Noise on Hearing in the Egyptian Industrial Schools. (E. Essamma & T. Abdel Alim).

H26 Computer Simulation of Basilar Membrane Displacement. (James L. Flanagan).

H27 Physiological Correlates of Binaural Lateralization. (J. L. Flanagan, E. E. David, Jr. & B. J. Watson).

H28 Free Field Threshold Shift and Temporary Threshold Shift Reduction as Measures of Efficiency of Ear Protective Devices. (John L. Fletcher).

H29 Le perception du son d'interruption dans la stimulation acoustique intermittente. (Hélène Gavini).

H31 Perception of Coloration in Filtered Gaussian Noise - Short-Time Spectral Analysis by the Ear. (B. S. Atal, M. R. Schroeder & K. H. Kuttruff).

H32 Preliminary Report on Comparison of Binaural and Monaural Group Hearing Aids. (John Boyd & Anthony Jamroz).

H33 Die Bedeutung des vegetativen Nervensystems für die Entstehung des Reizfolgestroms. (Wiktor Jankowski, Jerzy Giełdanowski & Władysław Birecki).

H34 Effect of Jet-Aircraft Noise on Hearing. (J. J. Knight).

H35 Der Einfluss des Geräusches auf die Lokalisierung und Verständlichkeit bei der dreikanaligen Stereophonie. (Felix Kolmer).

H36 Ein Zusammenhang zwischen Schwerpunktsfrequenz, Tiergrösse und akustischer Reichweite. (Th. Lange).

H37 Etude du potentiel microphonique cochleaire dans diverses conditions modifiant les proprietés mecaniques de l'oreille interne. (J.-P. Legouix).

H38 Contribution à l'étude du masquage de la parole. (R. Lehmann).

H39 Some Experiments on the Assessment of Subject Judgement to the Quality and Signal to Noise Ratio of Programme. (D. M. J. P. Manley).

H41 On the Transmission Characteristic of the Middle Ear. (Aage R. Møller).

H42 The Implementation of a Hearing Conservation Program. (Keith K. Neely).

H43 Réponse de l'oreille aux phénomènes transitoires. (Léonid Pimonow).

H44 Methods for Obtaining Unbiased Rating Scales. (Irwin Pollack).

H45 Zur Lautstärke einzelner Rauschimpulse. (E. Port).

H46 Audiometry and Physiological Noise. (E. A. G. Shaw & J. E. Piercy).

H47 Über die Kurven gleicher Sprachverständlichkeit. (Vera Chalupová & Josef B. Slavík).

H48 Relative Power Transmission Characteristics of the Ear and the Skull from Hearing Threshold Data. (Ernest L. Smith).

H49 Middle Ear Muscle Effect on Round Window Responses During Prolonged Sound. (Peter W. Carmel & Arnold Starr).

H51 The Domain of Existence of the Tonal Residue. (R. J. Ritsma).

H52 Pressure vs Free Field Thresholds at Low Frequencies. (Wayne Rudmose).

H53 Loudness Summation in Conductive Deafness. (Bertram Scharf).

H54 Clinical determination of the acoustic impedance of the eardrum. (K. Terkildsen).

H55 On the Short Acoustical Signal Intensity Measurement at the First Neuron Level of the Auditory System. (E. A. Radionova).

H56 Verdeckung von Tönen durch pulsierende Geräusche. (H. Scholl).

H57 Correlation of Binaural Noise Signals and Sound Image Localization. (A. V. Rimski-Korsakov).

H58 A Model of Human Pitch-Extraction Based on Additive Correlation. (R. J. Ritsma).

H59 Auditory Adaption in Pitch Shift Detection. (Andrew Sekey).

Section J: Molecular Acoustics

Investigations of molecular properties by acoustic means

J11 Sound Velocity in Liquids and Solutions in Relation to the Cell Model Theory of Liquids. (Otohiko Nomoto).

J12 A New Dissipation Process in Copper, Silver and Gold. (Piero Giorgio Bordoni, Paolo E. Giua & Livio Verdini).

J13 Sur les anomalies des spectres d'absorption ultrasonore dans les solutions de hauts polymères: Essai d'interpretation. (R. Cerf, S. Candau & R. Zana).

J14 Mesures d'absorption ultrasonore par des solutions de polymerès. (S. Candau, R. Zana & R. Cerf).

J15 Vergleich der dynamischen Schub-, Elastizitäts- und Kompressionsmoduln von plastifizierten Polyvinylchloriden im Temperaturbereich -80 bis +100° C bei 1 kHz.
(P. Heydemann, A. Zosel & H. Nägerl.

J21 Ultrasonic Relaxation in Fractionated Polysiloxanes.
(J. L. Hunter & T. B. Lewis).

J22 Experimental Determination of the Sound Velocity in Liquid Helium at and below the Lambda Point.
(Kenneth A. Shapiro & Isadore Rudnick).

J23 Die Kinetik des Wachstums und der Auflösung von Monokristallen im Ultraschallfeld.
(A. P. Kapustin).

J24 Sonolumineszenz in Quecksilber.
(H. Kuttruff).

J25 Thermal Relaxation in N_2, O_2, and CO with Admixtures.
(Malcolm C. Henderson).

J26 On Nucleation Processes in Ultrasonic Cavitation and Bubble Chambers.
(M. Bertolotti & D. Sette).

J31 Vibrational Relaxation in Oxygen-Argon, Oxygen-Helium and Oxygen-Hydrogen Mixtures.
(R. Holmes, F. A. Smith & W. Tempest).

J32 Ultrasonic Cavitation Measurements by Chemical Methods.
(Alfred Weissler).

J33 Bordoni Peak in Aluminum.
(Fausta Fanti & Mario Nuovo).

J34 On the Nucleation Process in Ultrasonic Cavitation.
(Diana Messinò, Daniele Sette & Francesco Wanderlingh).

J41 A Characteristic Number for the Interaction Between a Sound Field and a Colloid.
(Egon A. Hiedemann).

J42 Effect of Interstitials Due to Water on the Attenuation and Velocity of Ultrasonic Waves, and on the Thermal Resistance of Sodium Chloride Crystals.
(Warren P. Mason & Konrad Brugger).

J43 New data on sound velocity in aquaeous solutions.
(I. G. Mikhailov).

J44 Schwingungsrelaxation von CO_2 in Mischungen mit Helium.
(H.-J. Bauer & E. Liska).

J45 Ultrasonic Vibration Potentials in Polyelectrolytes.
(Jonathan Booker, Ernest Yeager & Frank Hovorka).

J51 Measurements of Velocity and Attenuation of Sound in Iron up to the Melting Point.
(D. R. Hub).

J52 Some Acoustic Effects at Phase Changes.
(J. F. W. Bell).

J53 Dislocation Relaxation in Some B.C.C. Metals.
(Piero Giorgio Bordoni, Mario Nuovo & Livio Verdini).

J54 The Influence of Texture and Plastic Deformation on the Elasticity of Polycrystalline Metals.
(G. Bradfield).

J55 Schwingungsrelaxation in flüssigem und festem Brom.
(H. G. Danielmeyer & H. O. Kneser).

J56 The Origin of Sound Absorption in Water.
(C. M. Davis, Jr. & T. A. Litovitz).

Section K: Ultrasonics and Underwater Sound
Ultrasonic techniques in general

K11 Ultraschallabsorptionsuntersuchungen an höher konzentrierten, wässrigen Kobaltsulfatlösungen.
(H. Siegert).

K12 Hypersonic Resonance of Quartz from 3ooo to 1o ooo Megacycles.
(Ellen S. Stewart & James L. Stewart).

K13 Pseudonoise-Correlation Techniques in Underwater Acoustic Studies.
(J. L. Stewart & W. B. Allen).

K14 Trapping of Sound by Density Gradients.
(Ivan Tolstoy).

K15 Classification and Discussion of Interference Methods for Measuring the Propagation Velocity of Ultrasonic Waves.
(J. S. Wehr).

K16 The Ultrasonic Travelling Wave Amplifier.
(D. L. White).

K17 Measurement at High Pressures of the Dynamic Complex Elasticity of Solids and Liquids including Polymers and of Dynamic Viscosity.
(G. Bradfield).

K21 Acoustics and Oceanology.
(L. B. Brekhovskikh & I. E. Mikhaltzev).

K22 Low-Porosity Ferrites for High-Intensity Ultrasonic Radiators.
(C. M. van der Burgt & A. L. Stuijts).

K23 Theoretical and Experimental Studies of the Propagation of Acoustic Impulses in Relaxing Liquids.
(E. F. Carome, P. A. Fleury & W. J. Wagner).

K24 Ultrasonic Absorption and Relaxation Times in Nitrogen, Oxygen, and Water Vapor.
(Yahei Fujii, Robert Bruce Lindsay & Kiyoshi Urushihara).

K25 Fluctuating Acoustic Refraction in Deep Ocean Water.
(Norman W. Lord).

K26 Attenuation of High Frequency Longitudinal and Transverse Waves in Germanium, Silicon and Z-cut Quartz and Their Relation to Thermally Determined Parameters.
(Warren P. Mason, H. J. McSkimin & T. B. Bateman).

K31 New Trends in Ultrasonic Device Technology.
(John E. May, Jr.)

K32 Mise en évidence au moyen d'ondes ultrasonores transversales, des variations des constantes élastiques de solides soumis à des contraintes statiques. Application à la détection de faibles anisotropies initiales.
(Suzanne Pauthier-Camier).

K33 Transducer Calibration from Near-Field Data.
(W. James Trott & Robert J. Bobber).

K34 Quantum Electronics of Optical Phonons.
(C. H. Becker).

K35 Hysteresis and Residual Stress in Solids.
(Robert W. Benson).

K36 Hypersonic Attenuation in Fused Quartz at Low Temperatures.
(H. E. Bömmel & C. K. Jones).

K41 Influence of Large Amplitude Sound Waves upon Aerosol Scrubbing.
(R. M. G. Boucher).

K42 Mechanisches Verhalten von Polymeren bei sinusförmigen Deformationen grosser Amplitude.
(G. W. Becker & H.-J. Rademacher).

K43 On the Directivity Control of the Underwater Sound Receiving System.
(Isao Saito, Yasumasa Urabe & Takahiko Otani).

K44 Relation dans certains liquides ultrasonnés entre la luminescence et la relaxation des cavitations de gaz et de vapeur.
(M. Degrois & B. Badilian).

K45 The Relationship between Wind Speed and Shallow Water Ambient Noise.
(Frank T. Dietz, J. Steven Kahn & William B. Birch).

K46 Bestimmung der Stossfrontdicke in Flüssigkeiten aus dem akustischen Spektrum.
(W. Eisenmenger).

K51 The Measurement of Liquid Borne Ultrasonic Power.
(F. E. Freeman & E. A. Lloyd).

K52 Time Dependent Optical Methods for the Study of Ultrasonic Waves.
(K. L. Zankel & H. M. Colbert).

K53 A New Variational Method for Ray Path Calculations.
(Ralph R. Goodman).

K54 Acoustic Waveguide Mode Interference and Damping in Viscous Fluids.
(Richard A. Elco & William F. Hughes).

K55 A Solid Resonant Device for Ultrasound Focusing.
(M. A. Issakovich & M. G. Sirotyuk).

K56 Mechanische und dielektrische Relaxationserscheinungen in Hochpolymeren bei Ultraschallfrequenzen.
(Jan Koppelmann).

Section L: Noise Control
Noise problems in general, insulation in connection with specific noise and vibration problems

L11 The Accelerometer Pick-Up as a Diagnostic Tool in Noise Studies in Buildings.
(F. L. Ward).

L12 Sources of Noise in Axial Flow Fans.
(E. J. Richards & I. J. Sharland).

L13 Le bruit des moteurs électriques.
(P. Baron & M. Jacquemot).

L14 Der Einfluss der Luftschalldämmung auf das Innengeräusch von Strassenfahrzeugen.
(Christian Betzhold).

L15 Wie laut ist es in meinem Auto?
(G. Bobbert).

L16 Beurteilung von Lärmbelästigungen durch Bezug auf den Störpegel.
(Friedrich Bruckmayer).

L17 Effekt der Halslänge und der Kanalwandschallabsorption auf nichtlineare ungedämpfte Resonatoren.
(Y. N. Chen).

L18 Noise Produced During Launchings of Rocket Powered Vehicles and Some Human Factor Siting Considerations.
(John N. Cole, Harald K. Hille, Robert G. Powell & Henning E. von Gierke).

L19 Theoretical and Experimental Studies of Steep Fronted Waves in Pipes.
(P. O. A. L. Davies & M. J. Dwyer).

L21 Discrete Frequency Noise from Ejector Nozzles.
(D. Middleton & E. J. Richards).

L22 Technique de mesure du bruit des fusées.
(M. Kobrynski).

L23 A Procedure for Noise Evaluation of Sound Power Data.
(W. E. Blazier, Jr. & R. J. Wells).

L24 A Procedure for Computing the Subjective Reaction to Complex Noise.
(R. J. Wells & W. E. Blazier).

L25 Characteristics of the Saturn Space Booster as a Noise Source.
(Wade D. Dorland).

L26 Akustische Schaltungen unter Gleichströmung.
(Ewald Eichler).

L27 Experimental Studies of Jet Turbulence and Their Relation to Jet Noise.
(P. O. A. L. Davies & M. J. Fisher).

L28 Prediction of Noise from Motor Vehicles in Freely Flowing Traffic.
(W. J. Galloway & W. E. Clark).

L31 Noise Characteristics of Coaxial Nozzles.
(P. Gregory & J. D. Voce).

L33 Methods for Generation of High Intensity Sound.
(M. H. Hieken).

L34 Vorausberechnung der aerodynamischen Geräusche elektrischer Maschinen.
(G. Hübner).

L35 Quality Control by Noise Analysis.
(J. August Jensen & Holger Larsen).

L36 On the Relation between the Exhaust Noise and the Mechanical Output Power of Some Combustion Engines.
(Ken'iti Kido, Noriyoshi Chubachi & Tadamoto Nimura).

L37 Vibration and Noise Control by High Efficiency Viscoelastic Damping Materials.
(Francis Kirschner).

L41 Anwendung von Sandwichblechen zur Lärmbekämpfung.
(Günther Kurtze).

L42 Zur Deutung einiger typischer Frequenzanalysen von Fahrzeuginnengeräuschen.
(Karl Kurz).

L43 Die Anwendung elektronischer Rechenmaschinen bei Lärmbekämpfungsarbeiten.
(Anselm Lauber).

L44 Die zulässigen Störpegel in den Studios.
(Dezsó Lázár).

L45 The Correlation of Jet Noise Frequency Spectra.
(W. J. Lewis).

L46 Etude sur Maquette de la Réduction du Bruit par l'interposition d'une Barrière.
(P. E. Magyar).

L47 A Proposed Sound-Absorbing Device in the High Velocity Duct Systems.
(Masayuki Matsui & Kinya Nakamura).

L48 FAA-Richtlinien der Flughafenrand-bebauung und akustische Belastung. (F. J. Meister).

L51 Transmission of Sound in Ducts. (C. L. Morfey).

L52 The Blading of Fans in Its Influence on Noise. (Jaroslav Nemec).

L53 Quietening a Cyclone Extractor to Reduce Community Annoyance. (A. F. B. Nickson).

L54 Multi-Mount Isolation Systems. (Alan O. Sykes).

L55 Geräuschmessungen an den normalen und geschweissten Schienen. (Béla Széchey).

L56 Effect of Reverberation on Reaction to Impact Noise. (G. J. Thiessen & K. Subbarao).

L57 Experimental buildings for sound insulation studies. (O. Brandt & S. Wahlström).

L58 Geräuschkontrolle und Lärmbekämpfungs-massnahmen an Heizkesseln. (Herbert Werner & Ulrich Winkler).

Section M: Room Acoustics

Sound absorption and insulation in general - Acoustic properties of rooms

M11 On the Correlation of the Results of Air Borne Sound Insulation Measurements Recommended by ISO and a New Method Based on the Research of van den Eijk. (Paavo Arni & Juhani Borenius).

M12 Testing small talks-studios with a simple method intended for diffusion measurements. (Juhani Borenius).

M13 Pulse Tests in Acoustic Models. (J. P. A. Lochner & J. F. Burger).

M14 Ein Verfahren zur Nachbildung von Schallfeldern in Räumen und zur Untersuchung ihrer subjektiven Wirkungen. (W. Burgtorf).

M15 Acoustical Design of La Grande Salle, A 3,000-Seat Multi-use Auditorium, Montreal, Canada. (Frederick Russell Johnson).

M16 The Dependence of Reverberation Time upon Seat Spacing. (L. P. Delsasso).

M21 Digital Computers in Room Acoustics. (M. R. Schroeder, B. S. Atal & Carol Bird).

M22 Acoustical Design of the Quebec Academy Auditorium, Quebec, Canada. (Leslie L. Doelle & Oscar G. Vagi).

M23 Zur Schalldämmung gelochter Blech-platten. (Peter Dämmig).

M24 Sound Insulation Requirements in Building Practice. (Gunnar O. Jörgen).

M25 Absorptionsmessungen für Eichung eines kleinen Hallraumes. (Marta Karsai & Thomas Tarnóczy).

M26 Une méthode d'analyse acoustique spatiale. (Witold Straszewicz).

M27 Acoustics of Music Rooms. (Vern O. Knudsen).

M28 Die Kopplung von Doppelwänden am Fundament als Grenze ihrer Schalldämmung. (W. Kuhl & W. Struve).

M29 Schalldämmung von Fenstern und Türen mit Fugen verschiedener Luftdurchlässigkeit. (Judith Lang).

M31 Ein Betonbunker wird Kongresshalle. (Max Adam).

M32 Reverberation Chamber Power Level Measurements on Sound Sources. (W. W. Lang & K. S. Nordby).

M33 Breitbandabsorber mit hohen Absorptionsgraden. (E. Hirschwehr).

M34 Die Schallabsorption von gelochten und ungelochten Platten bei grossen Wandabständen. (Günter Venzke).

M35 Studies on flanking transmission in an experimental building. (O. Brandt & G. Westerberg).

M36 Beeinflussung der Schalldämmung von Wänden durch Resonatoren. (Wolfgang Westphal).

M37 Über den Einfluss der Deckenhöhe auf die Klangqualität in Konzertsälen. (Fritz Winckel).

M41 Modellversuche zur Ermittlung des Einflusses von Schallspiegeln auf die Hörsamkeit.
(Ekkehart Krauth & Roland Bücklein).

M42 Instantaneous Subjective Pre-Determination of Room Acoustics.
(Radamis Boutros-Attia).

M43 Transient Sound Transmission Losses.
(Auguste C. Raes).

M44 Prinzip und Anwendung einer neuartigen Wandverkleidung für reflexionsarme Räume.
(Peter Rother & Joachim Nutsch).

M45 The New Acoustic Facilities at UCLA.
(R. W. Leonard, I. Rudnick & L. P. Delsasso).

M46 Demonstration Box for Sound Insulation.
(W. K. R. Lippert & P. Dubout).

M47 Influence of Acoustics on Design and Construction of Buildings in America Today.
(Robert B. Newman).

M51 Acoustical Effects of Movable Sound Reflectors in Auditoriums.
(Yoshifusa Funakoshi).

M52 Measuring Methods for Distinctness in time and Distinctness in frequency in Studio Acoustics.
(J. J. Geluk).

M53 A Method for the Investigation of Sound Diffusiveness in Rooms.
(G. A. Goldberg).

M54 The "Sound Insulation" of Circular and Slit-shaped Apertures.
(M. C. Gomperts).

M55 Considerations sur l'efficacité du traitement acoustique pour l'insonorisation des salles bruyantes.
(M. Grumazescu).

M56 Graphic Solution for Acoustical Designing in Auditorium.
(Naoto Hida).

M57 Geschlossenzelliger Weich-PVC-Schaumstoff als Luftschallabsorptionsmittel.
(Hermann Oberst).

M58 The Use of Lead in Improving Sound Transmission Loss.
(Paul B. Ostergaard).

Section N: Electroacoustics
Transducers, measuring methods in general

N11 Magnetic Recording of Audio Signals at Low Tape Speed.
(E. de Niet, K. Teer & D. L. A. Tjaden).

N12 A.F. Nonlinear Distortion Measurement by Wide Band Noise.
(Bjarne E. Bang).

N13 Acoustic Probe for Intraocular Pressure Measurement.
(Wilfred Roth & Dale G. Blake).

N14 Analyse et dépouillement automatique des réponses transitoires.
(P. Lienard).

N15 Ein mechanischer Kettenleiter für Verzögerungszwecke.
(Georg Boerger & Lothar Cremer).

N16 Power Handling Capacity of Loudspeakers.
(Cesarina Bordone Sacerdote).

N17 On the Use of Warble Tone and Random Noise for Acoustic Measurement Purposes.
(Jens T. Broch).

N18 Finite-Strain Response of the Piezoelectric Transducer Ceramics Pb-Ba and Pb-Sr Zirconate-Titanate.
(C. M. van der Burgt & E. E. Havinga).

N19 Die Nachbildung der Hörrichtwirkung bei Lautstärkemessmikrofonen.
(H. Niese).

N21 A Push-Pull Stereophonic Loudspeaker based on New Concepts in 2-channel Stereophony.
(F. H. Brittain).

N22 Indication Limit.
(Edith L. R. Corliss).

N23 High Power Ultrasonic Transducers Using Piezoelectric Ceramics.
(Alan E. Crawford).

N24 On the Sensitivity of Condenser Microphones to a Non-Uniform Pressure Distribution on the Diaphragm.
(S. C. Dalsgaard).

N25 An Energy Detection Model for Monaural Auditory Detection.
(E. E. David, Jr., M. V. Mathews & Sheila M. Pfafflin).

N26 A New Determination of the Acoustical Impedance of Human Ears.
(M. E. Delany).

N27 Contrôle des Lecteurs Stéréophoniques par Disques de Fréquence Glissante.
(D. J. Dion).

N31 Gerät zur Anzeige des "subjektiven Spektrums" und der Lautheit von Dauergeräuschen.
(R. Fischer).

N32 Attenuation Measurements on a Mobile Audiometric Unit.
(Frank Fowweather).

N33 Die Erregung von Schwingungen mit einer grossen Schallintensität in Gasen mittels eines magnetostriktiven Schallgebers.
(B. G. Nowitzky & W. M. Friedmann).

N34 Essais de mesures objectives de la fidélité de transmission d'un quadripole acoustique par corrélation.
(Jean Guillermin).

N35 The Effect on Stereophonic Reproduction of Frequency-Dependent Crosstalk Between Left and Right Channels.
(H. D. Harwood).

N36 The Air Modulated Loudspeaker and Its Application to Acoustic Environmental Testing.
(John K. Hilliard, Walter T. Fiala & John J. Van Houten).

N37 The Rational Design of Phonograph Pickups.
(F. V. Hunt).

N38 Analyse des stereofonen Schallfeldes.
(András Illényi).

N39 Die obere Frequenzgrenze bei der Kalibrierung piezoelektrischer Beschleunigungsaufnehmer mit elektrodynamischen Schwingtischen.
(Jan-Peter Hirschfeld).

N41 Problems in Feedback Control of Narrow Band Random Noise.
(P. E. Møller Petersen).

N42 Development of a Spheric Artificial Head for Acoustical Measurements of Telephone Instruments.
(Eero Lampio).

N43 Akustisches Goniometer.
(G. A. Liaghati).

N44 Effects of High Electromechanical Coupling on Characteristics of Piezoelectric Ceramic Transducers.
(Morio Onoe & Allen H. Meitzler).

N45 Some Results on Using a Signal with a Continuous Spectrum for Distortion Measurements.
(S. Boel Pedersen).

N46 Eine Methode zur Bestimmung des Querkontraktionskoeffizienten piezoelektrischer Keramiken.
(Ludwig Walther).

N51 Miniature Pressure Microphones.
(Gunnar Rasmussen).

N52 Qualitive Study of Transmission Frequency Response.
(Shuzo Saito & Ryoichi Matsuda).

N53 Eine Apparatur zur ohrgemässen Tonhöhenanzeige.
(Ludwig Schreiber).

N54 Non-Linear Effects in Quartz Resonators.
(A. Seed).

N55 High-Quality Push-Pull Condenser Transmitters.
(G. M. Sessler & J. E. West).

N56 Electromechanical Constants of Thick Barium Titanate Disks.
(Kimio Shibayama & Yoshimitsu Kikuchi).

N57 Methods of Checking the RMS Properties of RMS Instruments.
(Carl Gustav Wahrman).

N58 Production of High-Intensity Acoustic Vibrations by Means of Hydrodynamic Transducers.
(V. M. Fridman & B. G. Novitsky).

Section O: Physical Acoustics

General theoretical acoustics, radiation problems, non-linear acoustics etc.

O11 On Interaction of Aerosol Particles in an Acoustic Field.
(O. K. Eknadiosyants).

O12 Determination of Zones Subject to Meteorological Focusing.
(Richard N. Tedrick).

O13 Beiträge zu dem Mechanismus des aktiven akustischen Feldes.
(P. Greguss).

O14 Inhomogeneous Elastic Media with Constant Velocity.
(J. E. White).

015 Dissipative Propagation of Finite-Amplitude Waves in a Tube.
(David T. Blackstock).

016 Production de bruits blancs par des claquettes.
(F. Canac, G. Corsain & Th. Angelini).

017 The Focal System Influence over Statistical Characteristics of Wave Propagated through the Medium with Random Inhomogeneties.
(E. A. Bljakhman, L. A. Chernov & M. N. Krom).

018 Generalization of Kirchoff's Theorem for an Arbitrarily Moving Surface.
(V. Chromov).

019 Die Störung des Schallfeldes durch Hindernisse verschiedener Form.
(G. Kaszynski).

021 Calculations of Finite-Amplitude Distortion.
(Bill D. Cook).

022 Nature of the Feedback Mechanism in Some Fluid Flows Producing Sound.
(Alan Powell).

023 Mutual Interaction of High Energy Pulsed Sound Beams at Varying Relative Angles.
(Thomas D. Sachs).

024 Akustische Beeinflussung der Strömungsgrenzschicht in Luft.
(F. Mechel & W. Schilz).

025 Interaction of Sound Waves with a Gas Discharge.
(G. M. Sessler & M. R. Schroeder).

026 A Double Temperature Jump Associated with the Onset of Cavitation.
(M. G. Sirotyuk).

027 Non-Linear Theory of Spherical and Cylindrical Acoustic Waves in Viscous Heat-Conducting Medium.
(S. I. Soluyan).

028 Sound Radiation from Slender Bodies in Axisymmetric Vibration.
(M. Strasberg).

031 Experiments on the Propagation of Sound in Foams.
(G. A. Vignaux).

032 Diffraction Effects in a Random Sound Field.
(Richard V. Waterhouse).

033 Amplitude Fluctuations of Sound in Atmospheric Turbulence.
(Uno Ingard & George C. Maling).

034 An Approach in Non-Linear Acoustics.
(R. V. Khokhlov).

035 Anisotropic Elastic Wave Propagation.
(Edgar A. Kraut).

036 Diffraction Theory of Noise Generated by Turbulent Flows and Boundary Layers.
(L. M. Lyamshev).

037 The Transmission of a Spherical Transient Wave Through a Liquid Layer.
(Gunnar Lindh).

038 A New Method for Determining the End Correction of Pipes by Means of a Pulse.
(Mohy Louden).

041 Synthesis of Directive Arrays - II.
(C. D. Lowenstein).

042 Radiation Impedance of Systems with Arbitrary Shape.
(Ignacy Malecki & Wincenty Pajewski).

043 Radiation of Sound by Ocean Waves.
(Richard K. Cook).

044 Acoustic Instability of Burning Gases.
(Ira Dyer).

045 On the Radiation Pressure of Standing Waves.
(Z. A. Goldberg & K. A. Naugolnich).

046 On Sound Propagation in a Randomly Inhomogeneous Medium.
(William C. Meecham).

047 Blast Waves in a Heterogeneous Atmosphere.
(J. Menkes).

048 Rôle d'un baffle sur l'émission sonore d'un jet d'air sonique.
(Marie Merle).

051 Neuere Beiträge zur Theorie der Schallstrahlung.
(Dénes Huszty).

052 On Acoustic Wave Propagation in Horns.
(Hans L. Oestreicher).

053 Finite Perturbations in Relaxing Media.
(A. L. Polyakova).

054 Absorption of Sound in Air in the Audio Frequency Range.
(Cyril M. Harris).

055 Einfluss der Randbedingungen auf die Schallabstrahlung von Platten.
(Manfred Heckl).

Section P: Mechanical Vibrations

P11 Ein optisches Verfahren zur Untersuchung geführter elastischer Wellen. (E. Häusler).

P12 Audio-Frequency Compliances of Prestressed Quartz, Fused Silica, and Aluminum. (Martin Greenspan & Carl Tschiegg).

P13 On the Conversion of Longitudinal to Surface Waves in Solids. (Walter G. Mayer).

P14 Dispersion of Elastic Surface Waves in a Tapering Layered Medium. (L. Knopoff).

P15 Über die Aufspaltung von Biegeschwingungen bei fehlerhaften Platten. (Erich H. K. Müller & Eugen Peetz).

P16 Measurements of E and G Moduli and Poisson's Ratio of Polymethylmethacrylate over a Large Frequency Range. (C. J. Nederveen).

P17 Analysis of Inextensional Vibration of a Curved Cone. (Yukio Kagawa, Kimio Shibayama, Ken'iti Kido & Tadamoto Nimura).

P21 The Effect of Cuts in Damping Tapes. (G. G. Parfitt).

P22 Utilization of High-Damping Rubbers in Vibration Control. (J. C. Snowdon).

P23 The Measurement of High Temperatures by the Determination of the Velocity of Sound Waves in Materials. (E. A. Thorne).

P24 Propagation of Flexural Waves in Unhomogeneous Plates with Slowly Changing Parameters. (V. V. Tiutekin).

P31 Mechanical Internal Energy Losses at Audio Frequencies in High Polymer Solids Related to Cross Link Density. (P. Lord & E. R. Pithey).

P32 A Seismic Displacement Pickup. (R. A. Walkling).

P33 Flexural Waves of Finite Amplitude in a Plate. (I. A. Victorov).

P34 Die Messung der absoluten Schwingungsauslenkung bei tiefen Frequenzen ohne festen Bezugspunkt. (Ulrich Arns).

P35 Propagation des ondes de torsion dans le plexiglas. (W. Bismuth, D. Bonsignour & J. Wehr).

P36 On Anomalous Resonances in Stressed Crystalline Solids. (Sol R. Bodner).

P41 The Propagation of Acoustic Pulses in Linear Viscoelastic Solids. (H. Kolsky).

P42 Umwandlung mechanischer Rotationsenergie in mechanische Schwingungsenergie. (R. Pohlman & E. G. Lierke).

P43 On Vibration of Layered Plate with Losses. (B. D. Tartakowskii & S. A. Rybak).

P44 Propagation of Ultrasonic Waves in Spirals. (Leszek Filipczyński).

P45 Method of Measurements of Acoustic Material Visco-Elastic Parameters. (E. A. Vovk, R. N. Viktorova & V. V. Tiutekin).

Section P5: Musical Acoustics

P51 La cavité buccale, paramètre sensible des spectres rayonnés par les instruments à vent. (Emile Leipp).

P52 Musical Implications of Standardized Tuning Frequency. (Daniel W. Martin).

P53 Unharmonische Komponenten im "Klang der Orgelpfeifen". (Jürgen Meyer).

P54 Musical Transfer Functions. (Andrew G. Pikler).

P55 Musical Consonance and Critical Bandwidth. (R. Plomp & W J. M. Levelt).

ERRATA

J13 M. R. Cerf, R. Zana et S. Candau. - Page 1, cinquième ligne avant la fin: au lieu de "dilatation" lire "déformation".

J54 G. Bradfield. - P. 2, 6 l. up: alter "Δ_{ii}" to "$\overset{VR}{\Delta}_{ii}$"; 4 l. up: alter "i=i" to "i=1".

K17 G. Bradfield. - P. 1, 9 l. up: alter "o.25" to ".o25"; Fig. 9: alter lower R. H. arrow to central block.

L14 Christian Betzhold. - Auf Seite 1 unten muss die Gleichung 3 lauten wie folgt:

$$\frac{p_1^2}{p_2^2} = \frac{1}{W^2}\left(1 - \frac{p_K^2}{p_2^2}\right)$$

und auf Seite 2 unten muss die Formel 6 lauten:

$$\Delta R = 10 \log \left(\frac{p_{21}^2 - p_K^2}{p_{22}^2 - p_K^2}\right) \frac{p_{22}^2}{p_{21}^2}$$

L28 W. J. Galloway. - The Equation for Passenger Car Noise Levels at the bottom of P. 2 which now reads: PNdb = 35 + 30 $\log_{10}V$ should read: PNdb = 28 + 30 $\log_{10}V$. Similarly the 3 curves for Passenger Cars in Fig. 3 should have 7 db subtracted for all values.

M32 W. W. Lang and K. S. Nordby. - P. 3, Appendix equation (2) should read: $PWL_S = \overline{SPL}_S + 20 \log_{10} r + 7.5$. P. 4, Fig. 1: Curve A should be designated "SEMI ANECHOIC CHAMBER".

028 M. Strasberg. - The points plotted in Fig. 1 contain a numerical error. A corrected reprint can be obtained from the author.

P32 R. A. Walkling. - Page 3, fifth line from the bottom: for ".495 and 1.o6 for ".495 and 1.o6 volts/micron" read "4.95 and 1o.6 millivolts/micron". Page 1, foot note: read: This study was supported in part by funds made available under a contract with the (U. S.) Office of Naval Research.

G11

FOURTH INTERNATIONAL CONGRESS ON ACOUSTICS
COPENHAGEN 21.-28. AUGUST 1962

A Computer Program for Recognizing the English Fricative Consonants |f| and |θ|

James W. Forgie and Carma D. Forgie
Lincoln Laboratory* - M. I. T.

The English labio-dental fricative |f| and the lingua-dental fricative |θ| pose problems for both mechanical and human speech recognizers. The spectra of the fricative portion of these sounds are not dramatically different, and their effects on adjacent vowels differ only slightly. Our studies have not shown any single measurement of any aspect of these consonants which could alone achieve much better than chance separation of the two. We have, however, observed a number of different cues, each of which can be relied upon for separation of some small fraction of the cases. Potentially useful cues appear in the spectral shape of the frictional energy itself, in the brief, nearly silent interval between fricative and vowel, and in the movement of the vowel formants. The program to be described here is an attempt to utilize enough such cues to achieve recognition scores approaching those of human listeners.

Fricative Spectrum Cues

Examination of averaged spectra for the fricative portions of |f| and |θ| for a large sample of different speakers and contexts reveals little of help in separating them. Differences which appear in the averages are less than the observed deviations. If spectra are averaged as a function of individual speakers, some differences become apparent. |f| has relatively more energy in some part of the region from about 750 to 3500 cps. |θ| has more energy between 3500 and 10000 cps. The spectra may cross each other several times in these regions. The frequency location of the maximum difference varies greatly from speaker to speaker as does the amplitude of the difference. These differences are more pronounced for fricatives in final position in a syllable. If spectra are averaged as a function of adjacent-phoneme context, one observes that |θ| is more nearly independent of context, while |f| shows a tendency to have more energy in the region of the second formant of a following vowel. The effect of a preceding vowel is not pronounced. The influence of a following vowel or sonorant on |f| can be expected because the tongue can be in position for the following sound while the fricative energy is still being produced by the lip-teeth constriction. A result of this influence is a tendency to bias |f|'s followed by |i| or |I| toward |θ| in recognition experiments. Both human listeners and the computer program exhibit this bias.

Transient Cues

Examination of either waveform or spectral data indicates that, when |f| or |θ| is followed by a vowel or sonorant, there is a distinct difference in the persistence of the fricative energy into the beginning of the voiced sound. For a period of a few milliseconds, as the fricative energy dies away and the voiced sound is building up, there is a more high-frequency energy present in |θ| than in |f|. This effect is quite clear when word pairs such as "first-thirst" by the same speaker are compared. The problem in utilizing this cue lies in finding appropriate normalizing schemes, because the energy at this time also varies greatly from speaker to speaker and from one context to another. A further problem lies in determining the appropriate time at which to measure this phenomemon. The optimum time in most cases corresponds to the point of minimum overall sound intensity between the fricative and the following

---

* Operated with support from the U. S. Army, Navy, and Air Force.

voiced sound. In some cases, usually where the fricative energy is relatively weak, the overall sound intensity rises almost continuously, making it difficult to pick the proper time for measurement. The persistence of |θ| into a following voiced sound may have its counterpart in the case where |θ| is preceded by a voiced sound, but in that case any reverberation of the lower-frequency energy of the voiced sound would tend to obscure the boundary. The speech samples used for this study were all recorded under moderately reverberant conditions, and no attempt was made to utilize this transient cue except when the fricative was followed by a voiced sound.

Formant Cues

Since the places of articulation of |f| and |θ| are not far apart, the influence of these fricatives on adjacent vowels is quite similar. Schultz[1] has measured the average formant movements associated with these sounds. His results show that with a few exceptions the movements are in the same direction and of similar magnitude. The differences in many cases are quite small. No numbers are given concerning the variability of the data. Our data also show small average formant motions but high variability. The filter bank connected to our computer has limited resolution in the upper part of the second formant and third formant ranges where the bandwidths are several hundred cycles wide. The formant movements for both |f| and |θ| are thus often less than one filter width in magnitude. A different filter bank with more resolution might show some separation, but the great variability present with |f| and |θ| indicates that formant cues, like the others, can be expected to help in only a fraction of the cases. As yet, our formant-movement programs, which show promise for recognizing voiced stops, have contributed little of value for |f| - |θ| separation and are not used in the recognition experiments described here.

Nature of Computer Input

Speech samples used in this study were all English words beginning or ending with |f| or |θ|. All were recorded using an Electro-Voice Model 666 cardioid microphone. Some recordings were made in a room about 20 feet square with a hard floor and acoustic tile on upper walls and ceiling. Others were made in an audiometric testing booth. A speaker-to-microphone distance of about 30 inches was used in the large room. A closer spacing of about 15 inches was required in the booth. Since the program accumulates statistics about the sounds fed to it, the frequency response of the microphone and the characteristics of the room reverberation become important parameters in the system. In this case the two different acoustical situations produced no significant differences in performance, but some experiments with a different microphone with poorer high-frequency response showed a large effect. The poorer microphone would presumably have been adequate it it had been used to gather the statistics as well as test the results.

For input to the computer, the recorded speech is first passed through a compressor which reduces its dynamic range by an average of about 10 db. A filter bank then splits the frequency range of 100-10000 cps into 35 bands with a bandwidth of 50 cps at the low-frequency end. The filter bandwidths begin expanding logarithmically above 500 cps and reach 1 KC at the high-frequency end. The filter outputs are envelope-detected with a simple RC smoothing circuit having a time constant of 50 ms. The envelope-detector outputs are scanned by an electronic commutator at a rate which gives 180 full scans per second. The commutator output is converted to digital form and fed directly into the Lincoln Laboratory TX-2 computer. All further processing is done by the computer program. The signal-to-noise ratio of the speech input system is limited in practice by an 8-bit quantization used in the analog-to-digital conversion process.

Organization of the Computer Program

The computer program first makes a primitive segmentation of the speech into phoneme classes (e.g., --vowel, fricative, nasal). The fricative segments, which concern us here, are classified into four groups, |s|, |ʃ|, |h|, and |f-θ|, on the basis of the properties of the frictional energy. For this purpose the spectral samples corresponding to the fricative segment are averaged into a single spectral

pattern. The length of the segment before averaging, its amplitude in relation to the more intense vowel on either side of it, and four measurements of its spectral shape are used by the fricative classification program. If the output of this program is the |f-θ| class, then further operations are performed which attempt to use the cues described above to decide between |f| and |θ|. In the following discussion it is assumed that the preliminary processes of segmentation and fricative separation to the |f-θ| class have taken place without error, but in practice about 10% of |f|'s and |θ|'s are too weak to appear as fricative segments without special gain adjustments, and perhaps another 8% are mis-classified, |f| usually being confused with |h|, and |θ| with |s|.

Space limitations prohibit a detailed description of the measurements actually used to extract the information from the cues used by the program. The measurements which apply to the fricative spectra all involve computing the ratio of energy ir one part of the spectrum to that in another. If the values obtained from a particular measurement are tallied over a number of utterances, the resulting distributions show large overlap, seldom less than 75 or 80%. The decision process must then rely on the tails of the distributions, and enough independent measurements must be used to insure than an unknown has a reasonably high probability of falling into the tail of the distribution of at least one measurement. As an example, one of the measurements which gives relatively good separation of |f| and |θ| in final position in a word is

$$M_F = \frac{A}{A+2B}$$

where A = Sum of 6 filter channels from 890 to 1700
and B = Sum of 5 filter channels from 4700 to 8100.

The program computes a total of eight different measurements of the fricative spectrum.

When an |f| or |θ| is followed by a vowel or sonorant, a further five measurements are made in attempt to utilize the information contained in the transient cues discussed above. One measurement is of the form

$$M_{T_1} = \frac{A - B}{A + B}$$

where A = Sum of 8 filter channels from 4000 to 10,000 cps measured at a time 5.5 ms. before the point of minimum intensity between the fricative and the following sound.
and B = Sum of same channels at a time 11.0 ms. after the minimum-intensity point.
Another measurement is of the form

$$M_{T_2} = \frac{C}{D}$$

where C = Sum of filter channels from 3 channels above F2 (as picked by the program) to 10,000 cps., measured at a time 11.0 ms. after the beginning of the following vocalic segment,
and D = Sum of filter channels from 2 channels below F2 to 10,000 cps., measured at the same time as C.
The other measurements are essentially variations on these two, with the principal variation being in the rule for picking the measuring times.

The final recognition process involves a voting operation. On the basis of a preceding statistical tally, each possible measurement value is assigned a vote for |f|, |θ|, or neither. The voting is done in two stages, the first being a conservative vote which has a low probability of error but a higher probability of making no decision at all. In the case that the first vote produces no decision, a second, less conservative one is taken, which makes use of measurement values falling farther into the overlapped regions of the distribution. This second vote is both more likely to produce a decision and more likely to err. This process could be continued indefinitely, but in this case two stages leave only about 5% of the cases undecided, and these can be settled by guessing randomly with little loss in overall performance.

Listening Test Comparisons

The performance of the program has been tested against a jury of human listeners. For the test, a word list containing 19 English word pairs differing only in |f| and |θ|

in initial and final position was recorded by 5 male and 5 female talkers. The tapes were filtered to the 10 KC band used by the computer. The signal-to-noise ratio was determined by the room conditions and recording equipment and was not artificially reduced. The recordings were randomized both with respect to |f| and |θ| and with respect to speaker. For testing, the tapes were played through Beyer DT48 headphones at a comfortable level. Two groups of listeners were used for the tests. The first group contained some of the talkers used in the test and others who were familiar with the talkers' voices, while the second group was made up of people who had little if any familiarity with the talkers' voices. The results showed no significant differences in the average scores; so the results were pooled.

The results of both the listening tests and the computer program are summarized in Table I. While the average scores of the listeners look good, there is evidence of considerable guessing. Retesting of several listeners revealed that while they obtained very nearly the same total scores, only about 2/3 of their correct responses came on the same words. This finding, taken with the number of words missed by more than 1/5 but less than 1/2 of the listeners,would seem to indicate that the listeners are guessing approximately 1/3 of the time in |f|-|θ| discrimination. The worst initial-fricative words for both listeners and computer were "fief" and "fie", both of which had strong biases toward "thief" and "thigh". The best pairs for listeners were "frill-thrill","free-three", and "first-thirst." For the computer "first-thirst" was the best pair with the other two following. The worst and best final fricative words for the listeners display the bias toward |θ|. The best words were "Ruth" and "myth"; the worst word was "miff" with "rafe" and "deaf" following. A number of words including "Ruth", "miff","deaf", and "rafe" were never missed by the computer. None of the words was missed significantly more than any other by the computer.

The scores for the listeners and the computer compare favorably in the case of the final fricatives. People have a strong bias toward |θ| which the computer does not exhibit.

With beginning fricatives, people do considerably better than the computer, Also the computer has a bias toward |f|. The difference may be due to use by the listeners and not by the computer of one or more of the following cues: a)formant transition cues discussed above, in some if not all cases; b) more use of vowel information in setting criteria for the beginning fricatives which do vary with the vowel; c) use of pitch or other speaker cues which could help indicate the amount of high frequency energy to expect from the speaker. Any or all of these might be incorporated into the recognition system; however, we question whether such added complexity is warranted for these phonemes.

TABLE I

Summary of Results

		Scores in Per Cent				
		Initial		Final		
		f	θ	f	θ	
Computer Program		70	70	72	75	
Listening Tests	Average	80	82	66	85	
	Best Listener	92		91		
	Worst Listener	73		54		
	"Good" words	57		46		Missed by less than 1/5 of listeners
	"Questionable words	31		39		Missed by more than 1/5 less than 1/2
	"Bad" words	12		15		Missed by more than 1/2

(1) Schultz, Martin C. A Preliminary Investigation of the Acoustical Characteristics of Inter-Phonemic Transitions, Ph. D. Thesis, State University of Iowa, June 1955.

H11

FOURTH INTERNATIONAL CONGRESS ON ACOUSTICS
COPENHAGEN 21.-28. AUGUST 1962

Proper Evaluation of Audiometric Results

by

T. Abd El Alim & E. Essama

Hearing is a sensation experienced by the individual, when there is an energy leading to movement of the air particles in a frequency situated in the audible scale, and having an intensity wi-whin the hearing ability of the individual. An audiogram is actually a registration of the stimulus which evokes the sensation of hearing and not the hearing itself.

Making an audiogram is the most exact and academic method in our hands, to know the degree of the hearing defect and its nature.

We observed thet the results obtained by different audiologists are variable due to several factors and difference in technique. The aim of this work is to suggest a standard technique minimising the variability in the results. The responsible factors in play can be grouped under three main headings.

1) Factors related to the audiometer
2) Acoustic factors
3) Non-acoustic factors.

Factors related to the audiometers:

1) Nature of the sound used. In children and even in adults, we get better results with the pulse noise, probably because it is more attractive. A continuous non-audible noise, may be heared once it is interrupted. The pulse noise, again, is of value in adults to differentiate the masking from the signal noise.

2) We should agree about the intensity to be registered, whether it is the minimal audible, or the maximal inaudible, as there is a difference of 5 d.b., between the two readings.

3) It is preferred to start from audibility to non-audibility giving the individual a chance to recognise the noise he is going to hear, thus avoiding the probability of the lowest audible intensity to pass unnoticed especially in children.

4) The audiometer must at all times be in calibration, so that both air and bone curve averag e "0" for a group of normal hearing adults.

5) The effect of the vehicles and undergrounds, in the vicinity should be abolished by doing the test in a specially designed

studio suspended by shock-absorbers. If this not available, we advise a carpet floor, acoustic tile on walls, and oeiling the testing room with a double door.

II.- Acoustic Factors:-

1) Physical elements due to the anatomical construction of the ear. Anatomical variations in the middle and inner ear are negligeable to affect our audiometric results. As regards the external ear external meatus and concha variability in size may be big enough to effect our results.

This has been proved experimentally to amount up to 3 c.c. in a group of adults of different body sizes.

On dividing the audible range into high, middle and low tones, each band is found to possess a specific factor which enhances its audibility. Low frequencies are rich in sound power. The natural resonance of the ear favours the middle range frequencies. High patched tones are heard further by the normally hearing individual as a function of frequency.

In the normal audiogram, the threshold curve is practically a straight line, as the factors favouring specific segments, balance each other.

In addition to the above mentioned factors, we have still other factors in play, mainly, the resistance of the air column in the concha and external auditory meatus, and the damping effect of the meatal wall.

A pathologic process, may constitute an davance influence on our factor only. In perceptive deafness for example, the advantage of the greater high frequency acuity is lost clearly. Stenosis of the external auditory meatus will lead to a shift of the frequencies to which the air column normally resonates.

Most of the above mentioned factors are due to the presence of an air column, between the ear-phone and the drum. Using an ear-mould specially designed, is a good idea to displace this air column, thus reducing the air in the external meatus to the minimum and so abolishing the effect of resonance, resistance and damping.

Also an ear mould will guarantee the proper fittness and correct direction of the ear phone on the outer opening of the external auditory meatus.

2) Discriminative power of the cochlea: An audiogram may give us a false idea about the hearing acuity. If we make a tone audiometric test and a speech test in the same individual we usually get a higher level in the tone test than in the speech test, because in

the latter, we are actually doing a tone test and at the same time testing the discriminative power of the ear.

In practice we are not going to hear simple tones, but a combination of tones which we must be capable to discriminate between them, in order that they will be intelligible to us as speech. The musical affinity being variable in the different individuals, means that in spite of the more or less, normal audiogram, the individual may get a variable degree of word deafness. Speech tests of a standard intensity, should be recorded and the number of word score is registered by the individual through speech audiometry.

Tone audiometry, still has got its academic value. We can know, the nature of the deafness whether conductive or perceptive. Also we can detect cases of high tone deafness, even if the hearing acuity as regards speech may be not affected.

So, we advise when taking an audiogram to ask the person, when we change the tone used, whether he can notice this or not, and data acheived should be registered. Normal comprehension of speech, depends on two things. The first is normal tone hearing acuity, and the second is normal musical affinity. So we can easily understand now, that a normal audiogram level in itself, does not essentially mean normal speech hearing.

In tone audiometry, the highest frequency used is 8000 c.p.s. We advise doing an additional test, which consists of a well designed peice of music in which most of the high audible frequencies are represented. The person is allowed to hear this music in bits and is asked to repeat what he hears. This can substitute the high frequency audiometer as it is not always handy and is expensive.

III.- Non-Acoustic Factors/

1) Psychological State: The audiologist should try to make his clinic as attractive to the patient as possible. We have to gain the friendship of the patient by offering toys to the child and a touching speech for the adults. If the reflexes towards the sound impulse are not synchronous, this means that the individual is either frightened or intentionally lier, or mentally backward.

2) Capacity of concentration. in children sometimes they are unable to concentrate on the test. This may happen even in adults So we advise a rest between the examination of the two ears. By using the pulse noise and making the test carefully, but reasonably quickly we lessen the errors due to fatigue, adaptation or tone decay.

3) Intelligence. Before doing an audiometric test in children, we must explain it clearly first.It is the custom that we must find out the intelligence quotion in every case of hardness of hearing before being condemned of having any grade of deafness. In some cases, the deafness is apparent and is actually due to the backwardness in the mentality of the child and finding out the I.Q. will prove that.

Actually it is very difficult to examine a child who has got a combined handicap, of being partially deaf and mentally backward. Such a child should always be allowed to join the deaf children of the same grade, and if he does not prove that he is of

the same mental standard, he should shift to join the mentally backward.

Watching the child during the test is very important as his manouvre, may give us a good idea about his intelligence.

C o n c l u s i o n .

From the above data we can understand that there are several factors, which may change our audiometric results. Most of these factors are amenable of being controlled.

1) Physical factors could be reduced to minimum by using special ear moulds.

2) An authorised standard technique should be followed by all audiometrists, thus giving a reasonable chance for audiograms by different specialists, being compared.

3) Non acoustic factors could only be overcomed by the experience and patience of the examiner.

4) The help of a psychatrist is of great value in children.

Dr. Talaat Abel Alim
In charge of the Audiology Unit
School Health Service
4, Abo Tamman Street
Koubba Gardens
Cairo - Egypt.

J11

FOURTH INTERNATIONAL CONGRESS ON ACOUSTICS
COPENHAGEN 21.-28. AUGUST 1962

SOUND VELOCITY IN LIQUIDS AND SOLUTIONS

IN RELATION TO THE CELL MODEL THEORY OF LIQUIDS

OTOHIKO NOMOTO Tokyo Univ. of Agriculture & Technol. and
Kobayasi Institute of Physical Research, Tokyo, Japan

Sound velocity in liquids being closely related to the intermolecular force, a close examination permits one to obtain the intermolecular potential energy on the one hand, and to explain the behaviour of the sound velocity on the other hand. Various methods of approach are to be considered. Here, however, a thermodynamical treatment is performed based on the cell-model theory and postulating the Lennard-Jones' 12:6 potential. Although the work is rather preliminary, because of some simplifying assumptions and approximations involved, some interesting results are obtained.

The sound velocity c being related to the pressure p and the molar volume v by

$$c^2 = - \frac{v^2}{M}\left(\frac{\partial p}{\partial v}\right)_s , \qquad (1)$$

and the pressure being related to the internal energy (per mole) E by

$$- p = \left(\frac{\partial E}{\partial v}\right)_s = \left(\frac{\partial E}{\partial v}\right)_T + \left(\frac{\partial E}{\partial T}\right)_v \left(\frac{\partial T}{\partial v}\right)_s . \qquad (2a, 2b)$$

we have by substitution of (2a) in (1) the relation:

$$\left(\frac{\partial^2 E}{\partial v^2}\right)_s = \frac{M}{v^2} c^2 \qquad (3)$$

In these equations, M means the molecular weight and s the entropy. We have for non-structural liquids

$$E = E_p + E_k + E_r + E_s \qquad (4)$$

where E_p means the potential energy of the intermolecular force ($E_p < 0$), and E_k, E_r and E_s the translational, rotational and vibrational energies of the molecules, respectively. When equipartition is established for the translational and the rotational energies, we have $E_k + E_r = nRT$, where R denotes the universal gas constant and T the absolute temperature. n is 3 for ordinary organic liquids, 5/2 for straight line molecules, and 3/2 for monatomic liquids.

Assuming the Lennard-Jones' 12:6 potential, we have by taking into account the interaction between the nearest neighbours, but omitting the interaction between the second and third neighbours, the relation:

$$E_p = E_m\left[\left(\frac{v_m}{v}\right)^4 - 2\left(\frac{v_m}{v}\right)^2\right] \qquad (5)$$

Here the Boltzmann distribution in the potential well of the cell is also omitted. v_m means the molar volume corresponding to the potential energy minimum, and E_m the depth of the minimum ($E_m > 0$). The equation of state is obtained from (2b) as

$$- p = \left(\frac{\partial E_p}{\partial v}\right)_T + C_v\left(\frac{\partial T}{\partial v}\right)_s , \qquad (6)$$

when it is assumed that

$$\left[\partial(E_k + E_r + E_s)/\partial v\right]_T = 0. \qquad (7)$$

Here C_v means the molar heat capacity at constant volume. We intend to express E_m in terms of the sound velocity and other thermodynamical quantities. In the zero approximation case corresponding to (5) we have

$$(\partial E_p/\partial T)_v = 0 \qquad (8)$$

and

$$\left(\frac{\partial^2 E_p}{\partial v^2}\right)_s = -\frac{8}{v^2} E_p - \frac{7}{v}\left(\frac{\partial E_p}{\partial v}\right)_s . \tag{9}$$

This becomes, by (6), as

$$\left(\frac{\partial^2 E_p}{\partial v^2}\right)_s = -\frac{8}{v^2} E_p + \frac{7}{v}\left[p + C_v\left(\frac{\partial T}{\partial v}\right)_s\right]. \tag{10}$$

Now it is easy to show that

$$\left(\frac{\partial T}{\partial v}\right)_s = -\frac{T\alpha}{C_v \beta_T} = -\frac{T\alpha}{C_p \beta_s} = -\frac{T\alpha Mc^2}{v C_p} = -\frac{C_p - C_v}{C_v}\frac{1}{v\alpha} \tag{11}$$

where β_T and β_s mean the isothermal and the adiabatic compressibility respectively, α the expansion coefficient and C_p the molar heat capacity at constant pressure. Now that

$$\left(\frac{\partial^2 E}{\partial v^2}\right)_s = \left(\frac{\partial^2 E_p}{\partial v^2}\right)_s + \left(\frac{\partial^2 (E_k + E_r + E_s)}{\partial v^2}\right)_s \tag{12}$$

we have to compute the second term on the right hand side of this equation. First we have

$$\left(\frac{\partial (E_k + E_r + E_s)}{\partial v}\right)_s = \left(\frac{\partial (E_k + E_r + E_s)}{\partial v}\right)_T + \left(\frac{\partial (E_k + E_r + E_s)}{\partial T}\right)_v \left(\frac{\partial T}{\partial v}\right)_s ,$$

This becomes by (7) and (8) as

$$\left(\frac{\partial (E_k + E_r + E_s)}{\partial v}\right)_s = C_v\left(\frac{\partial T}{\partial v}\right)_s = -\frac{T}{C_v}\left(\frac{\partial p}{\partial T}\right)_v = -\frac{T\alpha Mc^2}{v\gamma} , \tag{13}$$

where γ means the ratio of the specific heats. Then we have after a short computation

$$\left(\frac{\partial^2 (E_k+E_r+E_s)}{\partial v^2}\right)_s = -T\frac{\partial^2 p}{\partial v \partial T} - \left[T\left(\frac{\partial^2 p}{\partial T^2}\right)_v + \left(\frac{\partial p}{\partial T}\right)_v\right]\left(\frac{\partial T}{\partial v}\right)_s = -T\frac{\partial^2 p}{\partial v \partial T} - \left(\frac{\partial C_v}{\partial v}\right)_T \left(\frac{\partial T}{\partial v}\right)_s + \frac{C_v}{T}\left(\frac{\partial T}{\partial v}\right)_s^2$$

This becomes, as $(\partial C_v/\partial v)_T = 0$ by (4), (7) and (8),

$$\left(\frac{\partial^2 (E_k + E_r + E_s)}{\partial v^2}\right)_s = T\frac{\alpha Mc^2}{v^2\gamma} - \frac{T}{v}\left[\frac{\partial}{\partial v}\left(\frac{\alpha Mc^2}{\gamma}\right)\right]_T + \left(\frac{\alpha Mc^2}{v}\right)^2 \frac{T}{\gamma C_p}. \tag{14}$$

In the following calculations, we omitted the term containing the derivative of $(\alpha Mc^2/\gamma)$ in this equation. Substituting this result together with (3) and (10) into (12), we have

$$-E_p = \frac{1}{8}\left[Mc^2\left(1 + 6\frac{T\alpha}{\gamma} - \frac{T\alpha^2}{\gamma C_p} Mc^2\right) - 7pv\right] . \tag{15}$$

The last term containing pv is so small at ordinary pressures, that it is to be omitted. Thus we have

$$-E_p = \frac{1}{8} Mc^2 \Phi \; ; \; \Phi = 1 + \frac{1}{\gamma}\left(6 T\alpha - \frac{T\alpha^2}{C_p} Mc^2\right). \tag{16a, b}$$

Here γ is to be computed from α, C_p and c by the known relation:

$$\gamma = 1 + \frac{T\alpha^2 Mc^2}{C_p}. \tag{17}$$

Now we can calculate E_m as follows. We have at $v = v_m + \Delta v$,

$$E_p = (E_p)_o + (E_p')_o \Delta v + \frac{1}{2}(E_p'')_o (\Delta v)^2 = -E_m + 4\frac{E_m}{v^2}(\Delta v)^2, \tag{18}$$

Here the primes indicates the derivatives with respect to v and at constant temperature, and the suffix 0 indicates the values at $v = v_m$. The second half of (18) follows because we have $E_p = -E_m$ and $E_p' = (\partial E_p/\partial v)_T = 0$ at v_m, while $E_p'' = (\partial^2 E_p/\partial v^2)_T = 8 E_m/v^2$ from (5). On the other hand we have also the relation:

$$E_p' = (E_p')_o + (E_p'')_o \Delta v = \frac{8 E_m}{v^2}\Delta v. \tag{19}$$

If v corresponds to the actual volume, then it must satisfy the equation of state (6), or

$$\left(\frac{\partial E_p}{\partial v}\right)_T = -p + \frac{T\alpha Mc^2}{\gamma v} \fallingdotseq \frac{T\alpha Mc^2}{\gamma v} \tag{20}$$

So we have from (19) and (20)

$$\Delta v = \frac{1}{8}\,\frac{v}{E_m}\,\frac{T\alpha Mc^2}{\gamma}\,. \tag{21}$$

Then we have from (18) and (21)

$$E_p = -E_m\left[1 - \left(\frac{T\alpha Mc^2}{4\,E_m\,\gamma}\right)^2\right]. \tag{22}$$

As the second term in the brackets is a small correction, we have approximately from this

$$E_m = -\left[1 + \left(\frac{T\alpha Mc^2}{4\,E_p\gamma}\right)^2\right]E_p = \frac{1}{8}\,Mc^2\left[\Phi + \left(\frac{2T\alpha}{\gamma}\right)^2\,\frac{1}{\Phi}\right], \tag{23}$$

in which Φ is given by (16b).

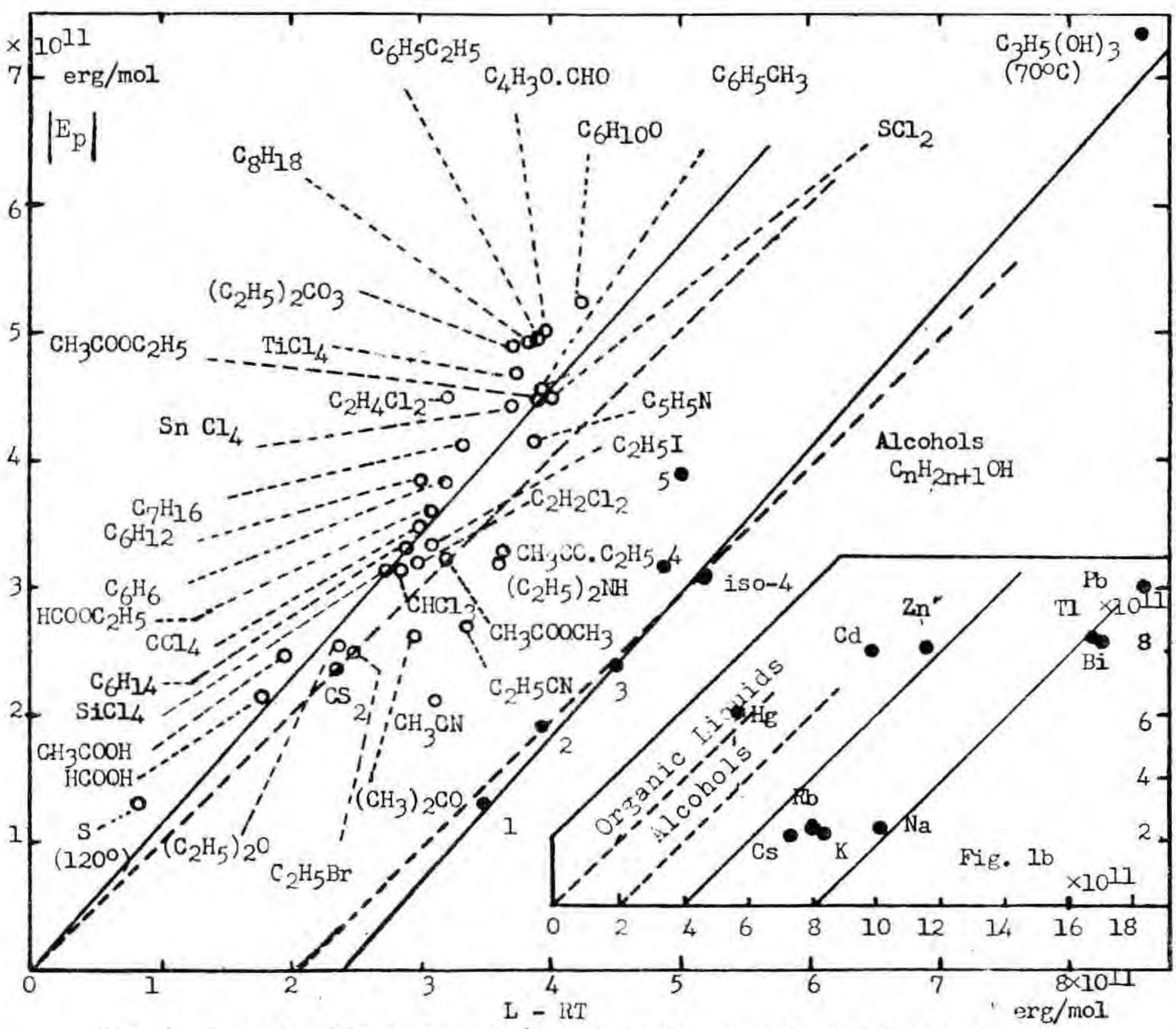

Fig. 1. Relationship between $|E_p|$ and L–RT for organic and inorganic liquids at ordinary temperatures

Fig. 1b. Relationship between $|E_p|$ and L–RT for molten metals

Table 1 shows the values of $(1/8)Mc^2$, Φ , $-E_p$, E_m, L-RT, $-E_p/(L-RT)$, T_b and kT_b/ε_m $(= 6RT_b/E_m)$ for some liquids. Here L means the heat of vaporization (per mole) at the same temperature with the measurements of c, α and C_p, RT is the work of expansion by the vaporization, T_b the boiling point, and k the Boltzmann constant. ε_m is the energy constant of the Lennard-Jones' 12:6 potential and we have $\varepsilon_m = E_m/6N$ in case of the close-packed arrangement of molecules with 12 nearest neighbours, where N means the Avogadro number. The values of c are taken from the existing ultrasonic data, and α, C_p and L from "International Critical Tables" and Landolt-Börnsteins' tables. α means the true expansion coefficient at the temperature considered, and are computed from tabular values. Theoretically it is to be expected that $|E_p| = L - RT$. The result shows that the ratio $-E_p/(L-RT)$ is nearly 1 except for alcohols.

Fig. 1 shows the relationship between E_p and L-RT for many liquids. The dotted line represents the theoretical curve $-E_p = L-RT$, while the solid line represents the mean observed value (except alcohols), the slope of this line being 1.172. Alcohols deviate clearly from this line, the lower members of aliphatic alcohols corresponding to

$$L-RT = |E_p| + 2 \times 10^{11} \text{ erg/mol} = |E_p| + 5 \text{ kcal/mol} \qquad (24)$$

If it is assumed that the relaxational compressibility due to the breaking of hydrogen bonds is comparatively small in alcohols, so that the observed sound velocity is not so lowered by this effect, we may conclude that the value of E_p obtained from sound velocity data corresponds to the Van der Waals force, while the difference of 5 kcal/mol corresponds to the energy of the hydrogen bonds. The energy of hydrogen bond in alcohols is known to be of the order of 5 kcal/mol. So we may conclude that almost all the molecules of alcohols are hydrogen-bonded with 1 bond per molecule. Alcohols of longer molecules seems to have the tendency of decreasing hydrogen bonds with molecular length. Glycerine with three OH-groups seems to have only one hydrogen bond at 70°C. It is to be noticed that the formic acid and the acetic acid show no deviation from the normal $E_p/(L-RT)$ ratio. This means, presumably, that these carbonic acids are associated also in the vapour phase(1), so that the value of L is also decreased.

Also the molten metals show a marked decrease of $|E_p|$ as compared to L-RT, the difference attaining 10~20 kcal/mol in cases, though Hg seems to exhibit normal behaviour.

A drawback intrinsic to this approximate treatment is, that the value of E_m is temperature-dependent, as is to be noticed in Table 1. To get rid of this, it may be necessary to use a better approximation for the potential expression (5), including the effect of the Boltzmann distribution in the potential valley, and to conserve various derivatives in the calculations. Effet of the second and third neigbours must be also taken into account. This reduces, roughly speaking, the value of E_m by about 20 %, while the value of E_p remains the same.

Table 1

Liquids	T(°C)	$(1/8)Mc^2$ $\times 10^{11}$	Φ	$-E_p$ $\times 10^{11}$	E_m $\times 10^{11}$	L-RT $\times 10^{11}$	$-E_p/(L-RT)$	T_b(°K)	kT_b/ε_m
S_2Cl_2	26	2.323	1.927	4.476	4.672	4.003	1.118	411	0.439
$SiCl_4$	20	1.247	2.522	3.145	3.332	2.736	1.149	332	0.497
$TiCl_4$	30	2.266	2.078	4.709	4.931	3,754	1.254	409.5	0.414
$SnCl_4$	30	1.993	2,223	4.430	4.662	3.716	1.192	387	0.414
CCl_4	0	1.954	2.000	3.908	4.096	3.125	1.251	350	0.426
	30	1.571	2.235	3.511	3.697	2.972	1.181		0.472
CS_2	0	1.350	1.859	2.509	2.629	2.470	1.042	319.4	0.606
	40	1.078	2.133	2.299	2.423	2.307	0.9965		0.658
CH_3OH	0	0.5641	2.372	1.338	1.401	3.585	0.3732	337.7	1.203
	40	0.4464	2.758	1.231	1.291	3.391	0.3630		1.305
C_6H_6	10	1.845	2.070	3.819	4.009	3.207	1.191	353.2	0.440
	80	1.078	2.831	3.052	3.239	2.783	1.097		0.544
mean (96 liquids)			2.189				1.172*		0.466**

* 31 liquids excluding alcohols ** 85 liquids

(1) George C. Pimentel and Aubrey L. McClellan, "The Hydrogen Bond", Freeman & Co. (1960)

K11

FOURTH INTERNATIONAL CONGRESS ON ACOUSTICS
COPENHAGEN 21.-28. AUGUST 1962

Ultraschallabsorptionsuntersuchungen an höher konzentrierten, wäßrigen Kobaltsulfatlösungen

Dr. H. Siegert, Institut f.Angew.Physik, Heidelberg

1. Einleitendes zur Ultraschallabsorption von 2-2-wertigen Elektrolytlösungen

Kobaltsulfat gehört zu der Gruppe von 2-2-wertigen Elektrolyten, die sich vor anderen, sogenannten "starken" 1-1- und 1-2-wertigen Elektrolyten dadurch auszeichnen, daß die Ultraschallabsorption je Wellenlänge im Frequenzbereich von einigen kHz bis ca. 200 MHz zwei ausgeprägte Maxima durchläuft, die Relaxationsvorgängen in der Elektrolytlösung zugeordnet werden müssen. Die nähere Untersuchung, ob es sich hierbei um die Relaxation der Wechselwirkung der Ionen mit den Wassermolekülen oder der Ionen untereinander handelt, führte schließlich nach EIGEN und TAMM [1] dazu, als Erklärung für die beobachteten Relaxationsvorgänge eine stufenweise Dissoziationsreaktion in der Elektrolytlösung anzunehmen. Gestützt wird diese Vorstellung durch den experimentellen Befund, daß die starke Ultraschallabsorption nur bei gleichzeitiger Anwesenheit vom 2-2-wertigen Anion und Kation beobachtet wird, d.h. Kobaltchlorid- und Schwefelsäure-Lösungen besitzen eine wesentlich geringere Absorption als eine Kobaltsulfatlösung gleicher Konzentration. Ein weiterer Befund ist die starke Variation der Frequenzlage des bei tieferen Frequenzen beobachteten Absorptionsmaximum mit der Natur des 2-wertigen Kations, im Gegensatz zu einer geringen Variation der Frequenzlage des bei höheren Frequenzen auftretenden Maximum.

Beide Tatsachen werden verständlich, wenn man annimmt, daß in der Elektrolytlösung nicht nur freie Ionen und undissoziierte Molekeln vorhanden sind, sondern auch Übergangszustände (Ionenpaare genannt), bei denen das 2-wertige Kation über ein oder mehrere Wassermoleküle an das Anion gebunden ist. Jeder dieser Zustände von Anion und Kation (freie Ionen, Ionenpaare, Molekeln) besitzt infolge der verschiedenen Wechselwirkung mit den umgebenden Wasserdipolen ein verschiedenes effektives Volumen. Dieser Volumunterschied ist mit die Ursache dafür, daß sich die relative Besetzungswahrscheinlichkeit der Zustände (ihre Konzentration) bei einer Änderung der äußeren Bedingungen mit dem Wechseldruck einer Schallwelle verschiebt. Die Zeitkonstante der Wiedereinstellung des gestörten Gleichgewichtes gibt die reziproke Ultraschallkreisfrequenz an, bei der eine maximale Absorption auftritt.

Das einfachste Schema einer solchen mehrstufigen Dissoziationsreaktion lautet:

$$\underset{\overset{1}{[\delta c]}}{(Me^{++})_{aq}} + \underset{}{(SO_4^{--})_{aq}} \underset{k_{21}}{\overset{k_{12}}{\rightleftharpoons}} \underset{\overset{2}{[\alpha(1-\delta)c]}}{(Me^{++}OH_2SO_4^{--})_{aq}} \underset{k_{32}}{\overset{k_{23}}{\rightleftharpoons}} \underset{\overset{3}{[(1-\alpha)(1-\delta)c]}}{(MeSO_4)_{aq}}$$

Hierin bedeutet δ den Gesamtdissoziationsgrad des diffusionsbestimmten Schrittes 1-2, α den Umwandlungsgrad des durch die Aktivierungs-

energie der Umwandlung bestimmten Schrittes 2-3 und c die gesamte Salzkonzentration. Dieses Schema bietet in einfacher Weise eine Erklärung für das Auftreten zweier gekoppelter Relaxationsvorgänge in 2-2-wertigen Elektrolytlösungen. Da die beobachteten Relaxationszeiten um etwa zwei Größenordnungen differieren, stellt sich das bei Kobaltsulfat schnellere Diffusionsgleichgewicht annähernd so ein, als ob das Umwandlungsgleichgewicht garnicht vorhanden wäre. Umgekehrt befindet sich während der Einstellung des rechten Gleichgewichtes das linke immer annähernd im Gleichgewicht. Diese relativ einfachen Verhältnisse gestatten es, die theoretischen Aussagen über ein solches zweistufiges Dissoziationsgleichgewicht quantitativ mit den Meßergebnissen zu vergleichen. Aus der Lage der Relaxationsfrequenzen gewinnt man Aussagen über die Kinetik der Dissoziationsreaktion und aus der Höhe der Ultraschallabsorption Angaben über Konzentration und Volumen der verschiedenen Zustände.

Die maximale Ultraschallabsorption je Wellenlänge, bezogen auf die Zahl der absorbierenden Teilchen in der Volumeinheit, wird häufig "maximales Absorptionsvolumen" genannt und ergibt sich nach EIGEN und TAMM zu:

$$\left(\frac{2\alpha\lambda}{n}\right)_{I,II} = (Q\lambda)_{max\ I,II} = \frac{\pi}{N_L RT\ \beta_\infty}\left[G^+ \cdot (\Delta V)^2\right]_{I,II} .$$

Hierin bedeutet G^+ eine Funktion, die von dem Dissoziations- und Umwandlungsgrad abhängt, ΔV eine Linearkombination der Volumdifferenzen, die beim Übergang eines Teilchens aus dem Zustand 1 in Zustand 2 bzw. vom Zustand 2 in Zustand 3 auftreten, N_L die Loschmidtzahl, R die Gaskonstante, T die absolute Temperatur und β_∞ die Kompressibilität der Lösung bei Frequenzen weit oberhalb der Relaxationsfrequenz.

Für die Relaxationszeiten des "oberen" und "unteren" Maximum ergibt sich

$$\tau_I = \gamma_I / k_{21} \quad \text{und} \quad \tau_{II} = \gamma_{II} / k_{32} .$$

Hierin sind k_{21} bzw. k_{32} die Geschwindigkeitskonstanten der Zerfallsreaktionen der Zustände 2 und 3 und γ_I und γ_{II} wieder Funktionen, die nur den Dissoziations- bzw. Umwandlungsgrad enthalten. Der spezielle Wert, den eine Untersuchung der Konzentrationsabhängigkeit der Ultraschallabsorption besitzt, wird an Hand dieser Formeln für die Relaxationszeiten besonders deutlich, wenn man bemerkt, daß die Funktionen γ_I und γ_{II} für stark verdünnte Lösungen dem Grenzwert eins zustreben. Das heißt, aus akustischen Absorptionsmessungen können unmittelbar einzelne Geschwindigkeitskonstanten abgelesen werden.

2. Meßmethode und Apparatur

Es gibt verschiedene Meßmethoden, die jeweils in verschiedenen Frequenzbereichen die Ultraschallabsorption vorteilhaft zu bestimmen gestatten. Hier interessierte der Frequenzbereich 0,2...2 MHz, in dem weder das bekannte Resonatorverfahren noch das übliche Ausbreitungsverfahren angewandt werden konnte. Wegen der geringen Größe der zu messenden Absorptionskoeffizienten wurde ein neueres Substitutionsverfahren von CARSTENSEN [2] ausgewählt, das die Ultraschall-

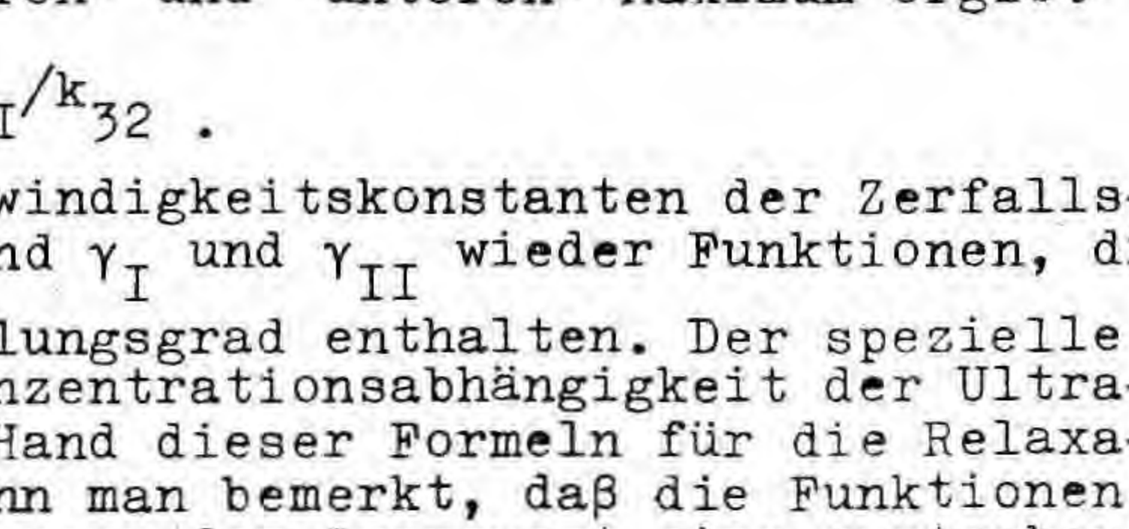

Abb. 1 Schematische Versuchsanordnung

absorption in ebenen fortschreitenden Wellen mißt.(Siehe Abb.1) Sender und Empfänger tauchen bei diesem Verfahren in je eine von zwei Kammern, die durch eine schalldurchlässige Membran voneinander getrennt sind, und können, starr miteinander verbunden, relativ zur Trennwand verschoben werden. In der einen Kammer befindet sich die Meßflüssigkeit, in der anderen eine Vergleichsflüssigkeit gleicher Schallgeschwindigkeit und bekannter, sehr kleiner Dämpfung(NaCl). Da der Abstand Sender-Empfänger während einer Messung konstant bleibt, hat hier eine Schallbündeldivergenz keinen Einfluß auf die Absorptionsmessung. Bei der verwendeten Apparatur wird ein Ultraschall-Schwingungsimpuls von 30...100 µsec-Dauer pro 50 Hz-Periode in die Lösung abgestrahlt, nach Durchlaufen der Meßstrecke wieder empfangen, gleichgerichtet und der Wert der entstehenden Differenz-Gleichspannung(nach weitgehender Vorkompensation zu Beginn einer Messung)einem Pegelschreiber zugeführt. Durch Ausschaltung kleiner akustischer und elektrischer Störungen war es möglich, noch Absorptionskoeffizienten von 0,01 dB/cm in der Elektrolytlösung sicher zu bestimmen.

3. Meßergebnisse

Die Ergebnisse der Ultraschallabsorptionsmessungen an Kobaltsulfatlösungen gehen aus den folgenden Abbildungen hervor. Abb.2 zeigt das Absorptionsvolumen von Kobaltsulfat in Einheiten von $10^{-30} m^3$ über der Frequenz in doppelt logarithmischem Maßstab. Die Meßkurven für Konzentrationen von 0,02...0,1 Mol pro Liter durchlaufen im Frequenzbereich von 0,2...2 MHz ein Maximum und fallen praktisch zusammen. Abb.3 zeigt eine starke Abnahme des Absorptionsvolumen mit zunehmender Konzentration. Die Konzentrationsabhängigkeiten der Relaxationsfrequenz und des Maximum der beobachteten Absorption, welche für die Auswertung der Meßergebnisse von Bedeutung sind, zeigen die Abb. 4 und Abb. 5. Aus dem unteren Grenzwert der Relaxationsfrequenz bei kleinen Konzentrationen läßt sich eine Geschwindigkeitskonstante des Umwandlungsschrittes 3-2 von

$$k_{32} \approx 2{,}8 \cdot 10^{-6}/\text{sec}$$

ablesen. Aus dem Verhältnis vom oberen zum unteren Grenzwert ergibt sich ein Umwandlungsgrad $\alpha \approx 0{,}75$. Dem entspricht ein Verhältnis der Konzentrationen der Zustände 2 und 3 von etwa drei zu eins, bzw. eine Geschwindigkeitskonstante für den Umwandlungsschritt 2-3 von

$$k_{23} = 0{,}92 \cdot 10^{-6}/\text{sec}.$$

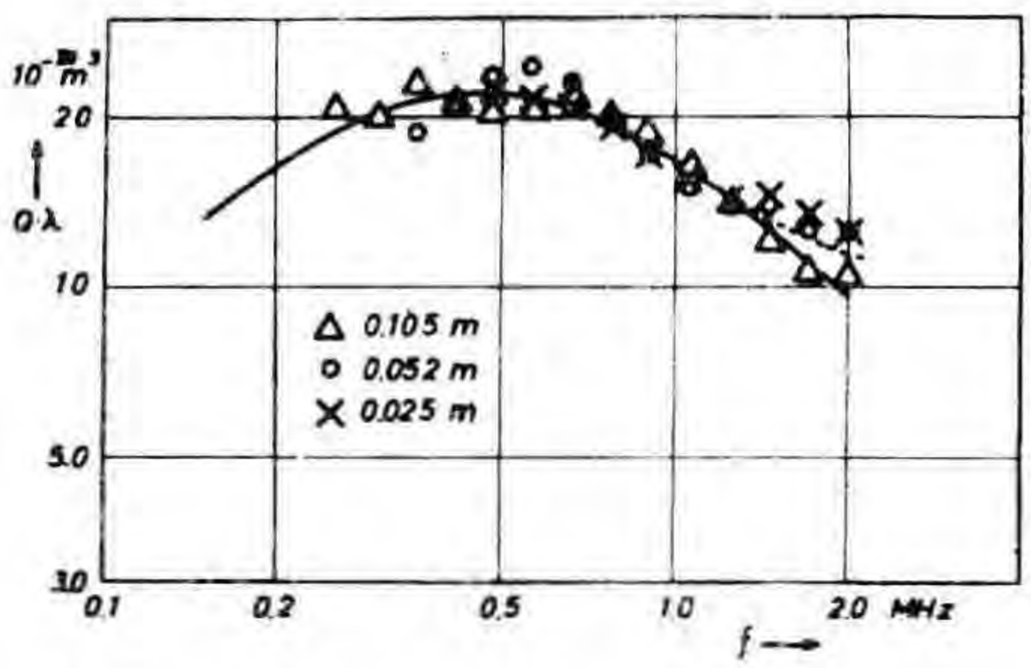

Abb. 2 Absorptionsvolumen von $CoSO_4$-Lösungen in Abhängigkeit von der Frequenz für Konzentrationen von 0.105 bis 0.025 Mol/l

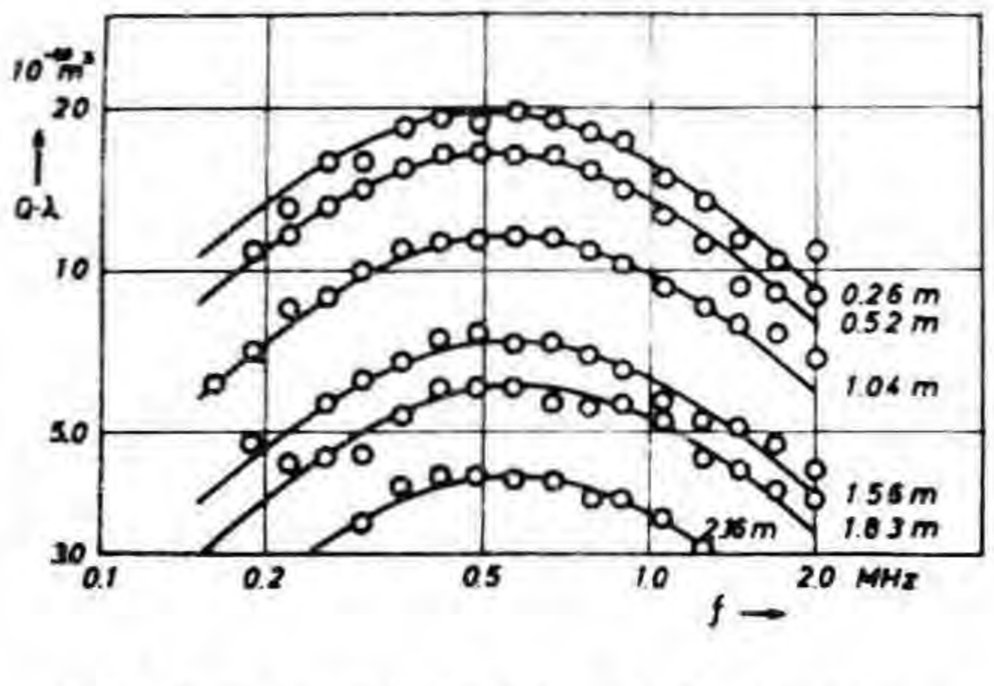

Abb. 3 Absorptionsvolumen 0·λ von $CoSO_4$-Lösungen in Abhängigkeit von der Frequenz für Konzentrationen von 0.26 bis 2.16 Mol/l

Abb.5 zeigt eine Auftragung der Wurzel des maximalen Absorptionsvolumens von Kobaltsulfat linear über der Konzentration, die (etwas überraschend) zu einer sehr einfachen Gesetzmäßigkeit führt, welche im

gesamten untersuchten Konzentrationsbereich bis zur Löslichkeitsgrenze erfüllt ist. Es gilt bei 20°C:

$(Q\lambda)_{max\ II} = 22{,}5 \cdot (1-0{,}27 \cdot c)^2$,

wenn $Q\lambda$ in $10^{-30} m^3$ und c in Mol pro Liter gemessen werden.

Eine gesicherte quantitative Auswertung aller Parameter der vorliegenden stufenweisen Dissoziationsreaktion läßt sich bisher noch nicht durchführen, da die Konzentrationsabhängigkeit des oberen, bei ca.120 MHz auftretenden Relaxationsmaximum bisher nicht genügend genau bekannt ist. Folgende abschließende Bemerkungen mögen darum nur zeigen, auf welche Weise eine quantitative Deutung der Ultraschallabsorptionsmessungen mit Hilfe der angenommenen zweistufigen Dissoziationsreaktion möglich ist.

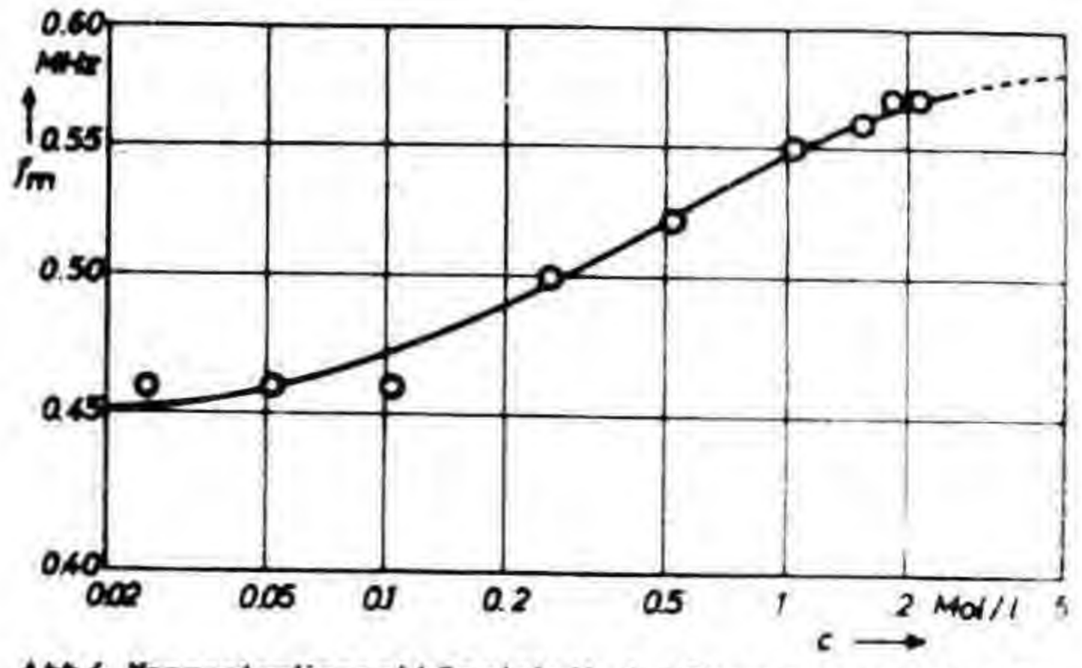

Abb.4 Konzentrationsabhängigkeit der Frequenz maximalen Absorptionsvolumens von $CoSO_4$ im Bereich 0.2...2MHz

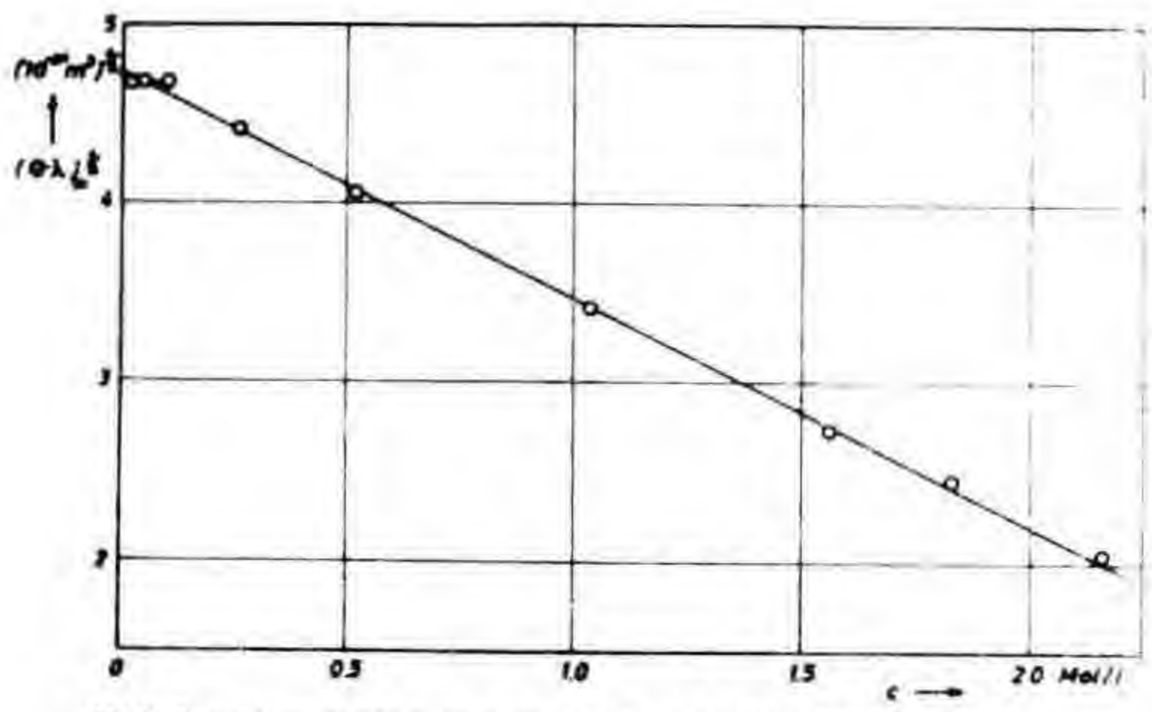

Abb.5 Konzentrationsabhängigkeit des maximalen Absorptionsvolumens $(Q\lambda)_m$ von $CoSO_4$ im Frequenzbereich 0.2...2 MHz

Aus der Konzentrationsabhängigkeit der Relaxationsfrequenz des unteren Absorptionsmaximum ergibt sich, wie bereits gezeigt, der Umwandlungsgrad α. Aus der Konzentrationsabhängigkeit der Relaxationsfrequenz des oberen Maximum läßt sich mit dem Umwandlungsgrad -unter Zuhilfenahme gewisser Annahmen über den Konzentrationsverlauf der Aktivitätskoeffizienten- der jeweilige Gesamtdissoziationsgrad δ bestimmen. Alsdann folgt aus dem Verhältnis der maximalen Absorptionsvolumina bei der unteren und oberen Relaxationsfrequenz das Verhältnis der Übergangsvolumdifferenzen zwischen den Zuständen 1-2 und 2-3. Schließlich liefert eine genaue Dichtemessung der Elektrolytlösungen in Abhängigkeit von der Konzentration die 5. notwendige Meßgröße, um die Absolutwerte der effektiven Volumina der Zustande 1,2 und 3 bei der jeweiligen Konzentration festlegen zu können. Somit sind(abgesehen von den aus elektrischen Messungen gewonnenen und bei hohen Salzkonzentrationen etwas fragwürdig erscheinenden Daten über die Aktivitätskoeffizienten)alle Parameter der stufenweisen Dissoziationsreaktion leicht auswertbar und man darf hoffen,daß aus den akustischen Absorptionsmessungen noch einiges über Elektrolytlösungen hoher Konzentration zu erfahren ist.

Literatur

[1] M.EIGEN, K.TAMM: Zeitschr.f.Elektrochem.66(1962) 93
K.TAMM: Handbuch d.Physik Bd.XI,1 (1961) 202

[2] E.L.CARSTENSEN: J.Acoust.Soc.Amer. 26 (1954) 858, 862

L11

FOURTH INTERNATIONAL CONGRESS ON ACOUSTICS
COPENHAGEN 21.-28. AUGUST 1962

THE ACCELEROMETER PICK-UP AS A DIAGNOSTIC TOOL IN NOISE STUDIES IN BUILDINGS

F.L. WARD, B.Sc., A.Inst.P., A.M.I.E.E.
RESEARCH DEPARTMENT, BRITISH BROADCASTING CORPORATION.

INTRODUCTION: One of the functions carried out by the B.B.C. Engineering Research Department is to investigate problems of noise in sound and television studios and to suggest solutions for them.

There are special difficulties with measurements in the field, notably:- (1) Time is usually very limited, (2) Apparatus needs to be easily transportable, (3) Working conditions may be very noisy. Consequently, measurement techniques which produce quickly an indication of the nature of the problem and an order of magnitude are often more useful than those which, while being rigorous, involve much labour and time.

In the case of broadcasting studios especially, where transmission through air paths is reduced to a minimum, the sound level in the room due to an external noise source is often entirely the result of vibration of the room surfaces. Common exceptions to this arise with transmission along ventilation trunking, and through inadequate door-seals.

The methods of analysis which involve measuring directly the amplitude of vibration or of velocity, require a stable mounting unaffected by sound fields and vibration elsewhere in the enclosure. Measurements of acceleration by means of a piezo-electric element (in conjunction with a small mass) do not have this disadvantage. The type found to be most useful is a standard commercial product using barium titanate as the piezo-electric material, and weighing about 20 gms.

The advantages of such a transducer are (a) it will operate immediately on any surface without adjustment, (b) it produces negligible effect due to mass or restraint on most surfaces encountered in buildings, (c) for a constant velocity amplitude the output rises with increasing frequency at a rate of 6 dB per octave; this is an advantage from the point of view of signal-to-noise ratio, as most noises encountered in studios tend to have lower energies at high frequencies, (d) a well-designed accelerometer is very insensitive to direct sound fields, (e) it is normally very robust.

A disadvantage is that such transducers have rather low sensitivities and high noise levels compared with a moving-coil device.

MOUNTING: The accelerometer is designed to be secured to a stud or tapped hole. Where this is not possible, it has been found entirely satisfactory to mount the accelerometer with a pellet of modelling clay; the clay has negligible effect on the sensitivity of the transducer. An extension of this principle employing a special mounting device has been used where the latter method is not suitable. This consists of a thin circular duralumin plate, of thickness 3 mm, and diameter 50 mm, into which the accelerometer is screwed. The front surface of the plate is normally covered with a 2 mm layer of modelling clay which is itself covered with a thin plastic sheet. This assembly is attached to a back-plate by three resilient mounts. In operation the back-plate is held in the hand, or with a sprung lever device, and the plastic covered surface of the clay is thereby pressed lightly against the surface to be examined. With thin panels care has to be taken that the light pressure required does not unduly affect the action of the surface. With constructional walls and most light partitions however it forms a reliable and convenient method of transferring the movement of a surface to the accelerometer, and the point of measurement can be changed at intervals of a few seconds if required. The co-axial cable is treated with a silicone fluid which prevents the electrostatic noise caused by movement of the cable. (Ref. R.D. Hole Electronic Engineering, Dec. 1960).

AMPLIFICATION AND MEASUREMENT: A cathode-follower amplifying stage with an input impedance of 40 megohms is used to link the transducer to a conventional high gain amplifier. It incorporates a simple integrating circuit for use when direct measurements of velocity amplitude are required. In a large number of cases the output of the amplifier is recorded for subsequent analysis, usually with a second track carrying the signal from a microphone or a second accelerometer. When it is necessary to examine signals at frequencies below the working frequency of the recording machine a suppressed-carrier modulation system may be employed, the carrier being recorded on the second channel.

The type of final indicator or detector used will depend on the nature of the signal, and may be an R.M.S. meter, level-recorder, oscilloscope or a Peak Programme Meter (P.P.M.) similar to that used for programme control in the B.B.C. Band-pass filters may be incorporated in the analysis chain when broad-band noises are being studied, a bandwidth of one octave being generally used as a suitable compromise.

A barium titanate accelerometer is sufficiently stable to be able to rely on a laboratory calibration over long periods of time. If desired a microphone calibrator of the type employing falling balls provides a useful comparative check of sensitivity.

VIBRATION SOURCES: An interfering noise source may be a continuous or quasicontinuous vibration, or some form of impact noise. For experimental work three types of test signal are commonly used:- (1) A continuous tone with or without frequency modulation, particularly in connection with sound insulation measurement, (2) Narrow band or broad-band "white" noise, again employed as a source for sound insulation measurements, (3) Impact source, for a variety of tests in connection with tracing transmission paths. A standard "footsteps" machine employing five hammers is often used. Where a peak programme meter, as opposed to an R.M.S. indicator, is used for measurement a single hammer-blow repeated at intervals of a few seconds may be suitable. An ordinary hammer held in the hand is entirely satisfactory for some investigations; although appearing to be crude, it does in fact provide a substantially stable source of convenient level.

It is desirable, if possible, to mount a second accelerometer close to the striking point of the hammer to provide a control signal. This is especially necessary where there is a risk that the successive blows will modify the surface and consequently change the character of the signal transmitted to the structure.

TYPES OF PROBLEM: In practice the investigation of a particular problem may involve measurements of more than one type:- (1) Identification of noise sources. An accelerometer may be of value in two ways in cases where there is a complex noise with a variety of possible sources: (a) A comparison of levels at different parts of the structure may indicate the position of the source of noise. (b) Where the character of the noise radiated from a source differs markedly from that transmitted into the structure, the source may be identifiable by an aural or instrumental comparison of the character of the received noise with the signal detected at a point in the structure near the assumed source. (2) Tracing the transmission route. Measurements of the relative levels in a structure due to a known source make it possible to assign a relative importance to the various radiating surfaces in an enclosure and to the different routes by which energy reaches these surfaces. This in turn leads to the efficient use of remedial measures. (3) Efficiency of isolation measures. Measurements are usually directed to providing information regarding the efficiency of specific isolation measures in existing installations, or determining whether a specified isolation has been achieved and what further measures are likely to be worthwhile. The problems studied include antivibration mountings for various machines, resilience of floor coverings, and isolation measures in the building structure. Comparison measurements may be made: (a) on both sides of an isolating system. (b) before and after the modification to an existing system. (c) on similar equipment with and without isolating systems. (4) Estimation of expected sound pressure level (SPL). The need for estimating the SPL to be expected from the vibration level in existing surfaces arises where alterations to the existing internal treatment of a room are to be made.

A large number of points of observation on the surface are required for accuracy due to the large variation of vibration level with position commonly encountered. (5) Establishment of vibration level criteria. Occasions arise where it is necessary to specify maximum permissible vibration levels generated by equipment to be used in particular conditions. In other cases the specification refers to the maximum level

to which a particular piece of apparatus, for example, a high stability oscillator, may be subjected. Criteria are established by measuring levels in existing installations where the "nuisance value" of the interference is known. (6) Sound insulation of Partitions. Estimates of the transmission loss of certain structures may be made in a limited number of cases, particularly where the surface is not highly absorbent and is homogeneous. An accelerometer technique is especially useful where measurements must be carried out in the presence of heavy flanking transmission and where a correlation technique, which might otherwise be used, would be too slow and complex.

The transmission loss is derived from the comparison of the SPL on the source side of the partition and the accelerometer level on the far side. The measurements of the accelerometer levels on the source side also provides information about the characteristics of the partition when it is complex, and may be the only measurement required for transmission loss when the partition is a simple homogeneous structure.

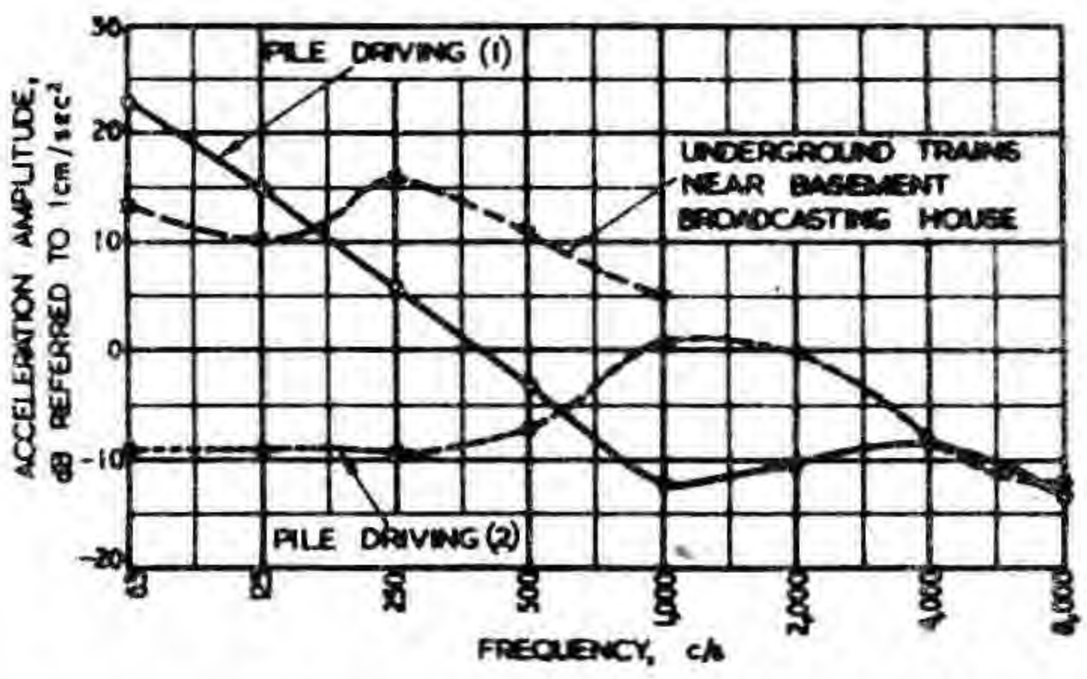

Fig. 1 - Comparison of vibration levels due to two methods of pile-driving and underground trains

EXAMPLES OF ACCELEROMETER MEASUREMENTS:

(A) Vibration levels due to pile-driving

It was required to determine whether the driving of piles for a new building close to an existing studio centre would interfere with the operation of the studios. Fig. 1 shows levels obtained during pile-driving operations on two building sites, where different methods of driving were being employed these being the loudest methods investigated. The levels are compared with those obtained in the lower basement of Broadcasting House, London, from underground trains. It is known from special experiments carried out in Broadcasting House basement that isolation measures giving at least 20 dB attenuation of train noise are required for satisfactory operation of studios there.

The results obtained support the aural impression of a heavy low-frequency "thump" in (1) and a medium-frequency "clang" in the case of (2). As a result of these measurements, together with airborne analysis, it was decided that both methods should be avoided for the proposed building operation.

(B) Comparison of wall structures. Fig. 2a shows the octave band analysis of the output of an accelerometer placed at four representative points on the structure of a studio suite. The analysis was made with a peak programme meter from recordings, the source being a hand-held hammer dropping on to the street pavement from which serious interference, due to footsteps, had been experienced. Fig. 2b shows the equivalent measurements for a similar studio in the same building, considered entirely satisfactory. The existence of an additional partition of building board and plasterboard was not discovered until the accelerometer measurements revealed the rapid decrease in vibration level at high frequencies. A small hole was then cut in the partition to allow measurements to be made on the structural wall.

Comparing the two sets of curves there are clear indications of a difference in construction between the two cases. In case (1) most of the attenuation takes place across the outer wall of the studio, indicating that this is a complex wall with at least one cavity, while in case (2) there is heavy attenuation between the pavement and the studio wall and none at all across the wall itself which is clearly a solid, single-leaf construction.

(C) Vibration levels in a ceiling. During the course of modifications in the studio suite described above, the vibration levels shown in Fig. 3 were obtained, from a hammer-blow source on the pavement. The measurements were obtained on newly-constructed inner partitions in the studio and ceiling void, and on the structural and studio ceilings.

It was concluded from these measurements, together with measurements of SPL in the studio and void, that:- (1) The studio ceiling rather than the studio partition was the major contributor to the unwanted sound energy in the studio. (2) At low frequencies, the vibration energy in the studio ceiling was due to the high airborne level in the void, which itself originated mainly in the void partition, rather than direct transmission from the structural ceiling through the ceiling ties.

THE ACCELEROMETER PICK-UP AS A DIAGNOSTIC TOOL IN NOISE STUDIES IN BUILDINGS

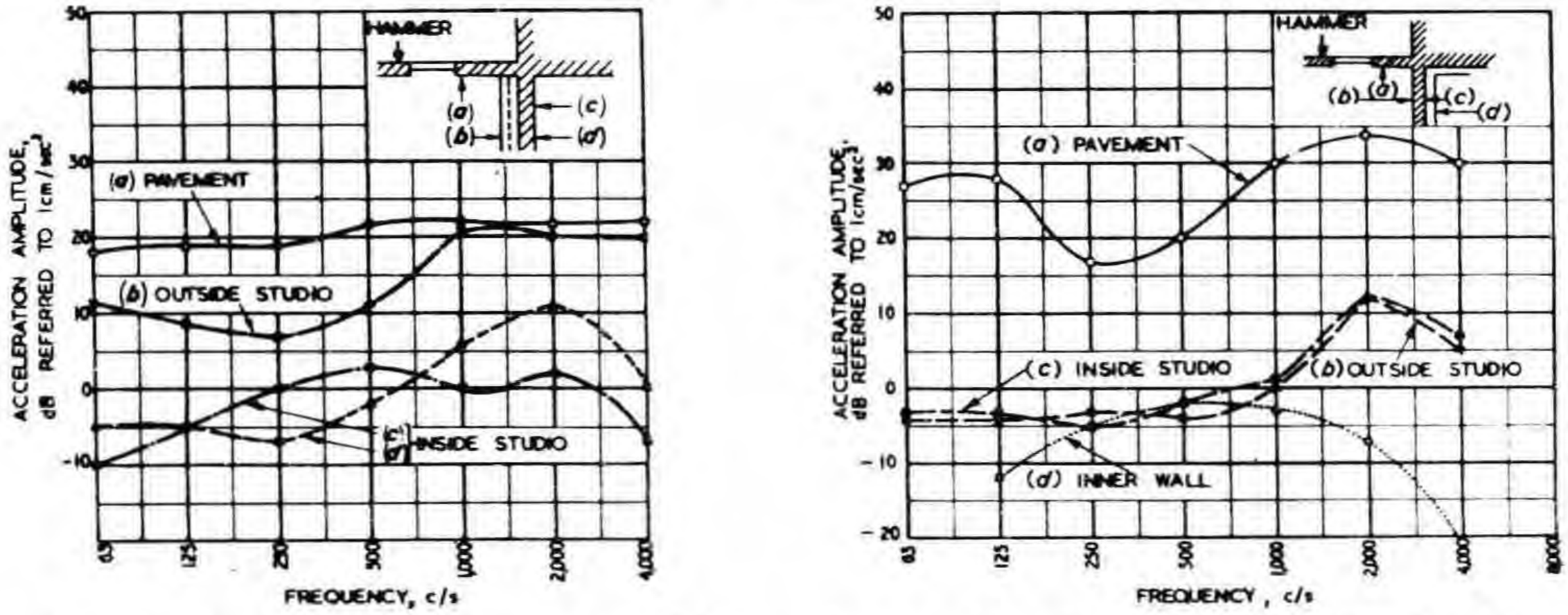

Fig. 2 - vibration levels due to standard hammer blows on street pavement. Comparison of wall structures in two studios

Fig. 3 - Vibration levels in studio due to standard hammer-blows on street pavement

(a) Partition in ceiling void
(b) Structural ceiling
(c) Studio ceiling
(d) Partition in studio

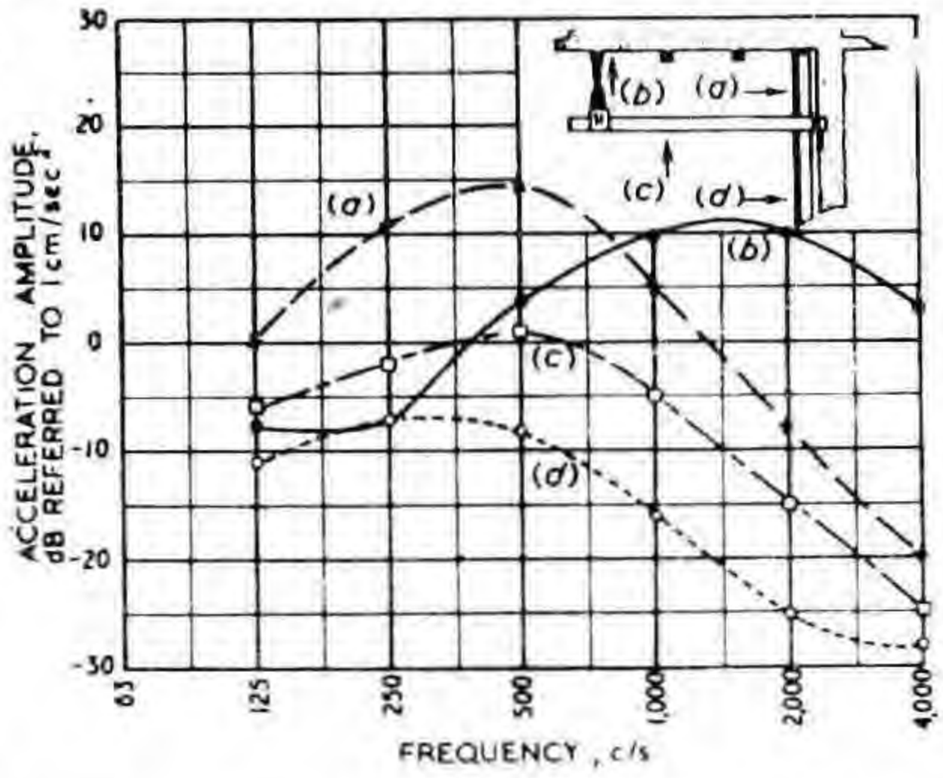

Fig. 4 - Comparison of micropnone and accelerometer. Measurements of transmission loss of steel door

(3) At high frequencies, the structural ceiling was the principal source. (4) The attenuation due to the ceiling ties was at least 25 dB at frequencies of 2 kc/s and above.

It was concluded that no further isolating measures would be economically worthwhile.

(D) Transmission loss. Fig. 4 shows the Transmission loss of a steel door, (a) computed by comparison of SPL measured with an omni-directional microphone and (b) by comparison of SPL in the source room and accelerometer measurements. The same frequency-modulated tone signal was used in the source room for both measurements. After necessary corrections for reverberation time and sample area, the values of transmission loss obtained with a microphone near the surface of the door and in the reverberation sound field were identical within experimental error.

It will be seen that for frequencies about 300 c/s the transmission loss by accelerometer is much higher than the microphone measurement when the door was fitted with its original sealing system. It rises at a rate of about 9 dB/octave compared with the substantially constant microphone measurement.

This clear indication of the presence of flanking transmission was supported by an examination of the sealing system, which appeared unsatisfactory. Special additional measures were then taken to seal the door temporarily and under these conditions the microphone measurement gave values approaching the accelerometer values.

ACKNOWLEDGEMENTS: This paper is published by permission of the Director of Engineering of the British Broadcasting Corporation. The author wishes to acknowledge the assistance of his Colleagues in the B.B.C. Research Department, in particular that of Mr. A.N. Burd.

M11

FOURTH INTERNATIONAL CONGRESS ON ACOUSTICS
COPENHAGEN 21.-28. AUGUST 1962

On the Correlation of the Results of Air Borne Sound Insulation Measurements Recommended by ISO and a new Method Based on the Research of van den Eijk.

Paavo Arni, Chief Engineer, the Finnish Broadcasting Co., Helsinki
Juhani Borenius, Senior Studio Engineer, " "

In practice there are many cases in which the exact and due sound insulation measurement according to the ISO Recommendation R 140 takes too much time and is too expensive. When for instance all the walls between the accommodation units of a hotel as well as the walls bordering to the corridors in a newly completed building have to be inspected, this would mean that only for measuring one wall, the pressure level has to be measured in both rooms in several points at all the 16 measuring frequencies. In addition to that the reverberation time of the receiving room has to be measured at the same frequencies. This takes at least one hour. For calculating and examining the results double that time is needed.

The measurement has to be carried out when the building is completely quiet, i.e. practically always only at night. However, when the building is completed, it is taken to use immediately, which means that there are only a few nights for carrying out the measurements. As in one night only 8 walls can be measured and two work days are needed for calculating the results, insulation can mostly be inspected only at random, and even then it is unreasonably expensive. Therefore it would be important to create a quick measuring method which with required exactness gives the quality of insulation.

Van den Eijk[1)] has put forth in the ICA Congress in 1959 that in most cases the octave band 400...800 c/s determines the quality of insulation and put a question whether it is worth while to put requirements and carry out measurements at frequency bands below 400 c/s and above 800 c/s. The research of van den Eijk concerns mostly disturbances caused by neighbor's radio, but as radio programs in general consist of sounds of normal life, the study obviously reveals even a more general value.

The requirements for the air borne sound insulation in many countries are based on standard curves, under which the insulation values measured in laboratories or buildings under practical conditions must not lie. In fig. 1 are two examples of this kind of standard curves. If it must be verified whether the insulation between two rooms meets the requirements, the measured insulation curve is compared with the standard curve, which in Finland is done by

forming the so called "Protection Value" (Schutzmass) about as in the DIN-norm n:o 4109. The Protection Value is determined by transferring the standard curve in vertical direction in the coordination until the measured curve passes the standard curve to the allowable extent (together not more than 16 dB) The Protection Value (dB) is the perpendicular difference between the transferred curve and the standard curve at its original position.

In the Finnish Proposals to requirements of sound insulation are given the highest allowed noise levels, dB(A), in disturbed rooms, supposing that the noise load causing the above mentioned air borne sound, is in some other dwelling 85 dB(B).

Controlling the normalized sound level difference with a noise load, with frequency band 400...800 c/s, is a very easy and simple task, taking only the time of about 5 min. On the sound source side no big amplifiers and heavy loudspeakers are needed. Standardized sound level meters are used for measuring sound levels. The correction caused by reverberation can normally be estimated exactly enough. The reverberation time in an unfurnished room in general is 1...2 seconds.

To find out the correlation between the noise value caused by the above mentioned noise load, which in this text is called the Y-figure and the Protection Value of the insulation, we have carried out numerous measurements in different buildings. On the loudspeaker side we used an octave filter of Siemens and two Sinus loudspeaker-p'.lars PB 87. The spectrum of the noise 400...800 c/s, which we used, measured in an anechoic chamber, is shown in fig. 2. It considerably differs from the ideal, but the calculations showed that the Y-figure did not very much depend on the form of the spectrum.

The Protection Value has been determined by comparing the insulation curves with the Standard curve proposed in Finland, fig. 1. Since the requirements at the band 400...800 c/s are relatively high, the curve being upward convex, it is to be expected that the correlation between the Protection Value and the Y-figure is in general very obvious. However, sometimes, for instance because of resonances, insulation at the frequency band 1600...3150 c/s might be relatively poor. In this case it is to be expected that the Y-figure gives too good a picture of the insulation of the wall.

The results of 24 insulation measurements have been marked in coordination fig. 3, the ordinate representing the Protection Value and the abscissa the Y-figure. In some cases the Y-figure has been measured twice with different meters. The measured values have been marked either with black circles or black squares. Those cases, in which the Protection Value is, because of the special "abnormal" form of the insulation curve, determined by other frequencies than 400...800 c/s, have been marked with black squares. The "normal"

cases have been marked with black circles. The calculated values corresponding to the ideal octave band noise have been marked with respective white marks. The straight line representing the mutual dependence between the Protection Value and the Y-figure as well as the greatest spreading limits have been marked in the graph. It can be noted that almost all the "abnormal" cases are below the mean line and give too good a picture of the insulation. The "normal" cases marked with circles are for the most part above the mean line, the more the Protection Value depends on the insulation at the frequency band 400...800 c/s.

Even though the measuring points are considerably spread on both sides of the mean line, the Y-figure has some practical importance. When for instance a new dwelling house has been completed, the different types of walls and floors in the building are measured using both methods mentioned above, and the measuring is continued by determining the Y-figure for all walls, in order to find out the constructional defects. When in a big house there are hundreds of walls and floors, the total number of different constructions is limited to tens. The possibility to save time is obvious.

1) J. van den Eijk: My Neighbour's Radio,
Proceedings of the Third International Congress on Accoustics, Stuttgart, 1959.

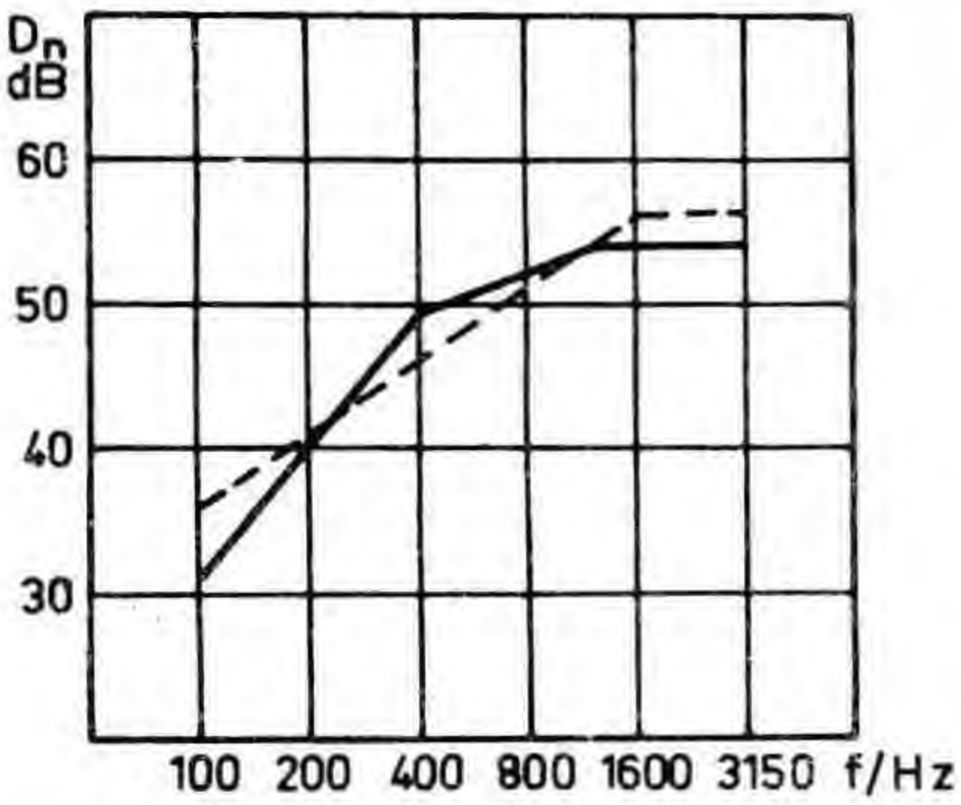

Fig. 1. Standard curves for insulation of air borne sound
— proposed Finnish Standard Class II
– – -Building Research Station, England.

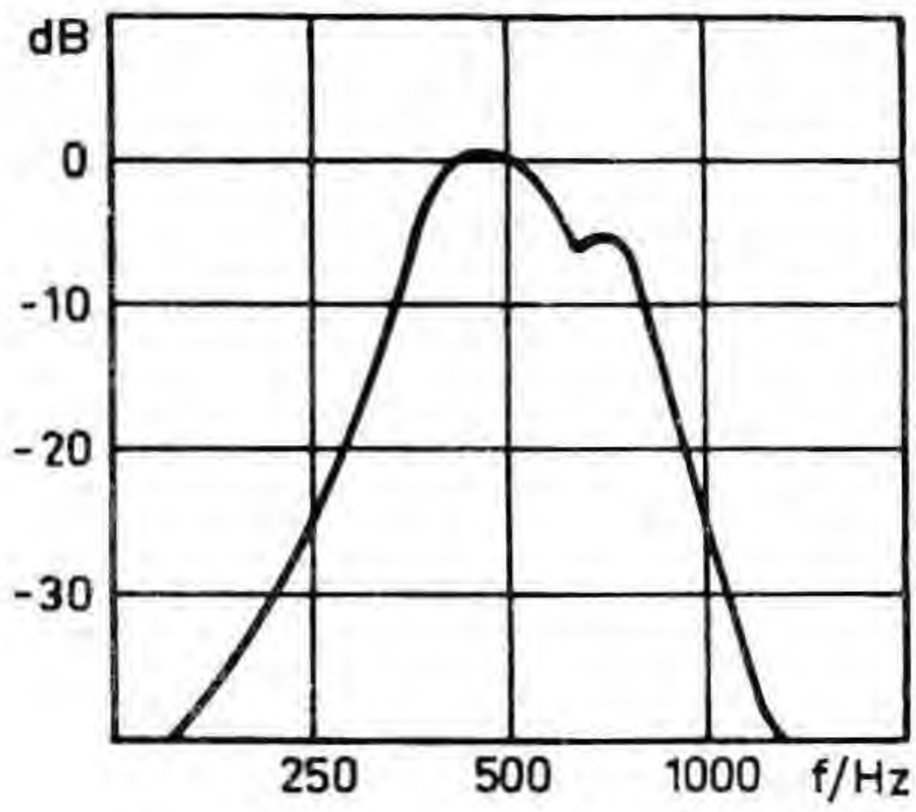

Fig. 2. The spectrum of the noise 400···800 Hz used in the sound insulation measurements.

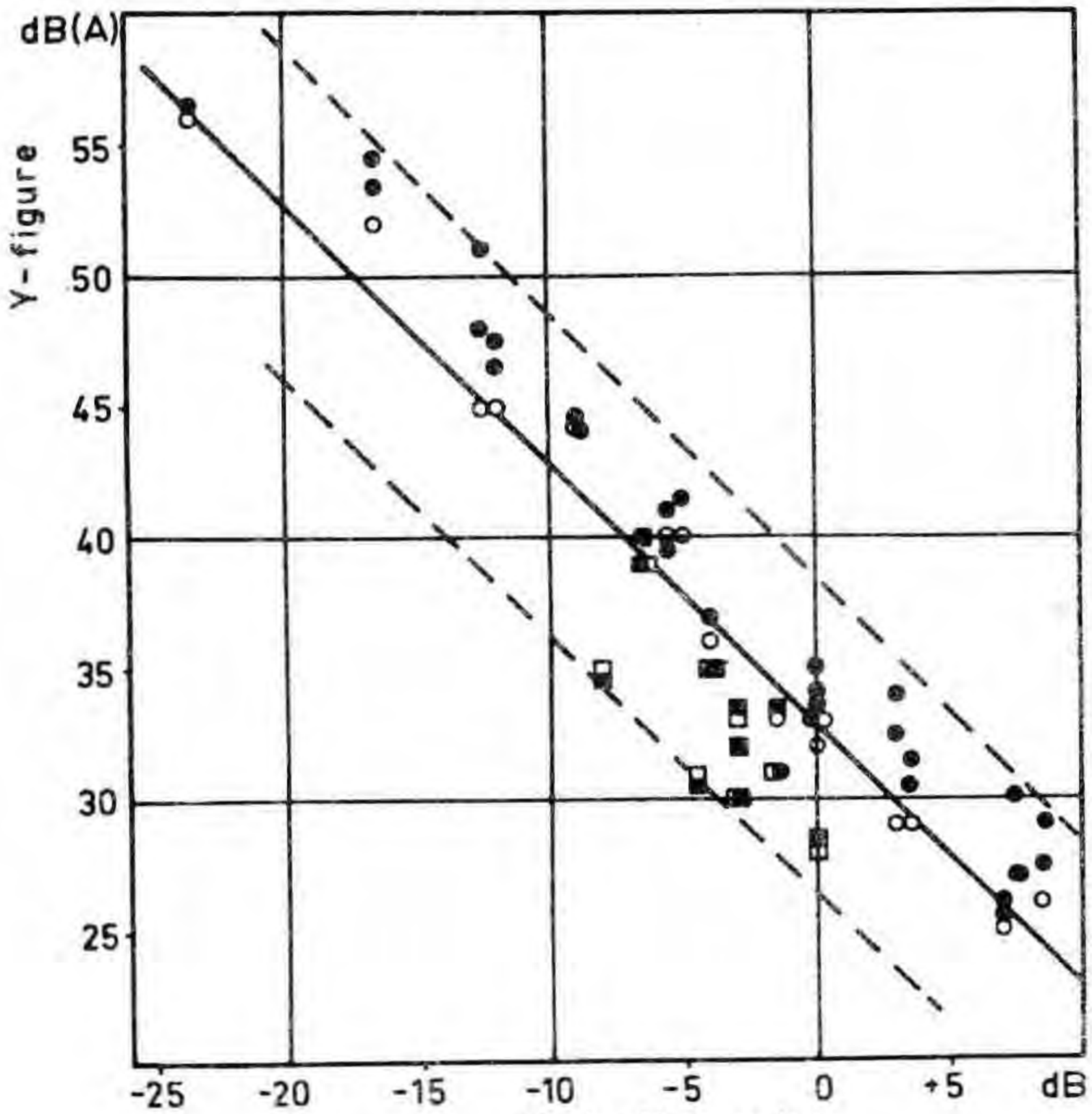

Fig. 3. The correlation between the protection value and the Y-figure

N11

FOURTH INTERNATIONAL CONGRESS ON ACOUSTICS
COPENHAGEN 21.-28. AUGUST 1962

MAGNETIC RECORDING OF AUDIO SIGNALS AT LOW TAPE SPEEDS.

E. de Niet, K. Teer, D.L.A. Tjaden

In recent years the problem of high quality sound recording at low tape speeds got quite a lot of attention in several laboratories. This effort was highly stimulated by the publications and demonstrations of the C.B.S. laboratory in 1959 and later, the endeavour being to solve the problem of developing a simple cartridge recorder for pre-recorded tapes, easy to handle and with such a tape consumption and musical quality that a competitive position with respect to the disc would be possible[1]. We do not, of course, wish to pay much attention here to the commercial and design problems in this field: rather do we wish to give an impression of the investigations and results which have been obtained in our laboratories in the study of refined recording methods for the purpose mentioned
When tape speed is brought to a lower value the minimum wavelength naturally becomes smaller. This means an increase of the influence in the writing and reading process of such quantities as separation, gap length and rate of extinction of the recording field.
As is generally known, recording of small wavelengths demands a rapid decrease of the h.f. bias field in the region of the critical field strength(s). In the normal head configuration this can be obtained by a narrow recording gap and a relatively low bias level, leading to a small recording depth. On the other hand, this small recording depth can be accepted in play back because due to the rapid decrease in resolving power of play-back head with separation for small wavelengths, only a very thin surface layer (λ/π, say) can contribute to the output.
This situation however, is not too compatible with that for long wavelengths, where a large recording depth is useful in order to overcome poor signal to noise condition. Hence, for low tape speeds, there is a very large variation throughout the whole wavelength range in optimum recording parameters, and the choice of the several parameters such as gap length and H.F. bias level can only be a compromise between favourable conditions for long wavelengths and those for short wavelengths. With this situation in mind, the attempt was made to modify the recording process in such a way that more parameters are involved, so making possible a better approximation towards optimum conditions throughout the whole wavelength range*). This was especially carried out for a tape speed of 1 7/8" p.s.. The solution was found in a dual gap recording in which recording of long and short wavelengths takes place on separate locations under separate circumstances but in the same track.

---

*) The first idea goes as far back as 1953 (D.Kleis Patent specification 775.090) but the work on practical realization did not start before 1959. Good results were obtained fairly rapidly and a first demonstration outside our company followed in the middle of 1960. Since then, a number of papers on magnetic recording from other laboratories have been published these considering principles identical to those applied by ourselves: hence, the basic idea seems to have been found in other places independently.

J.F.Woodward: Audio Engineering Society Convention Oct. '61
D.F.Eldridge and E.D.Daniel: Convention IRE March 1962

In this method a low frequency part of the signal is first recorded with suitable gap length and bias level and then the high frequency part with a second gap and a second bias field. The first recording will, of course, be partly erased by the second but this is only effective in a very thin layer, the low frequency output thus being only slightly affected. On the other hand, however, the absence of low frequencies in that part of the tape where the high frequencies are recorded is an advantageous feature from the point of view of intermodulation distortion.
It will be clear that without special precautions a time delay between highs and lows will occur in playback. This difficulty can be overcome in several ways. In the first place the recorded signal could be read out with two gaps, but this was not considered a very valuable proposition. In the second place time equalization can be applied by using a delay line for the high frequency part before recording. In the third place one may try to bring both gaps very close together so that the time difference is not perceptible. After some experiments with time equalization the third solution was chosen. The distance between the gaps is 1 mm this giving a time difference of 20 m sec, which can be said to be imperceptible.
The cross-over frequency is about 2000 c/s. At this frequency, both gaps are equivalent in recording ability, the value being determined by the bias setting and tape characteristics. The first bias field is adjusted for optimum results at 500 c/s, whereas for the second gap the value is 10000 c/s.
In fig. 1 the recording capability of the system is illustrated for B.A.S.F. tape L.G.S. 26 and a track width of 1.5 mm. In this figure the maximum loading of the tape for a prescribed amount of distortion is given in curve A as the playback output with an unequalized amplifier and negligible gap loss.
In order to judge the quality, two reference curves are drawn. In the first place reference can be made to curve B, which is the recording result obtained with one gap and optimum H.F. biasing at each frequency. In the second place curve A can be referred to the noise output.

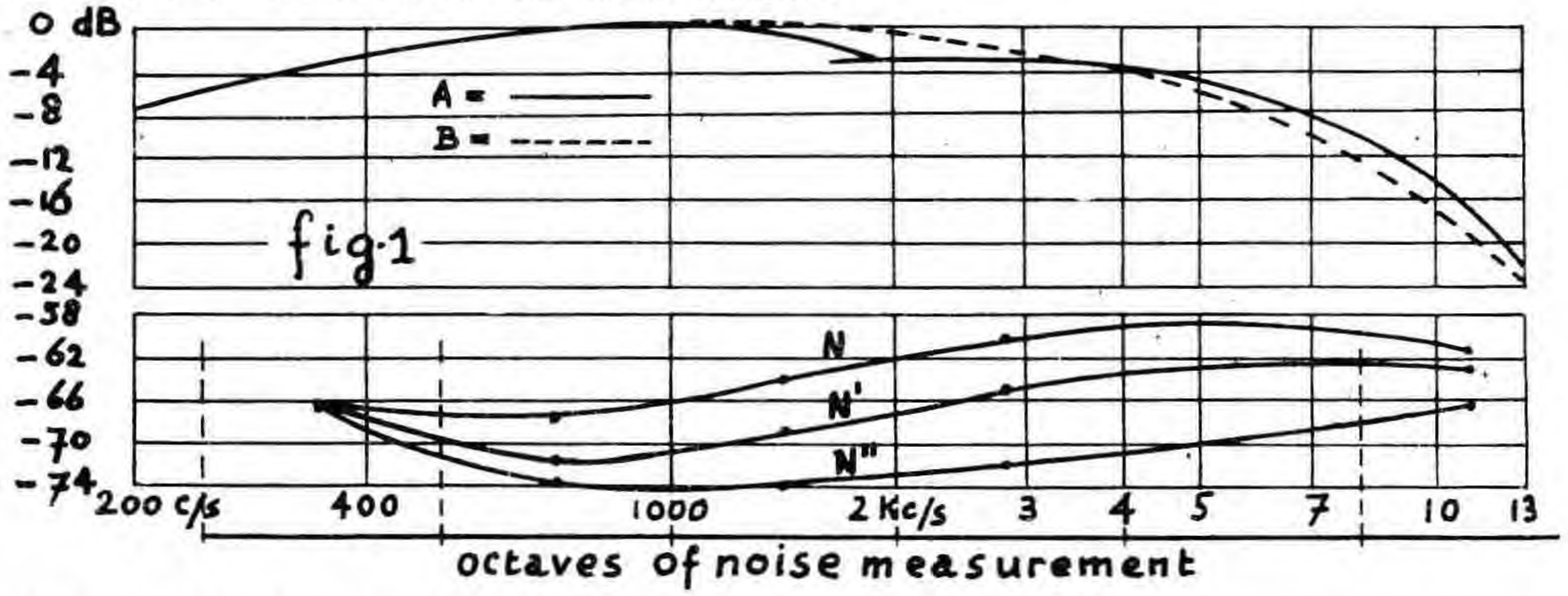

fig-1

It can be seen that A is very near to B and that at high frequencies curve A even exceeds curve B. This might seem impossible but we have to bear in mind that in our system two gaps are applied. The second gap is better matched to high frequency recording than the gap applied in measuring curve B, which has to be suitable for the whole frequency range.
The recording ability of the second gap was studied extensively. Four major points had to be considered.
a) The maximum output (with prescribed distortion) for 10000 c/s.
b) The rate of decrease in output with bias field below or in excess of the optimum value.
c) The erasure effect on the preceding recording.

d) The influence of drop outs and irregularities in tape travel.
In the table below the results are given for three different gap lengths, these being 1.5/u, 4/u and 10/u.

Gap length	recording at 10000 c/s	3 dB decrease bias field in % of opt.value		erasure effect for 2000 c/s
1.5/u	0 dB	55%	170%	3 dB
4/u	-2 dB	77%	140%	4 dB
10/u	-5 dB	82%	120%	4,5 dB

It will be clear that the smallest gap is preferable with respect to recording and erasure effect. The drop out sensitivity, however, is larger. As the latter drawback can be overcome by careful mechanical design, it will be obvious why a narrow gap has been chosen. Such is even necessary when this gap is also used as playback gap, which is advisable not only for reasons of simplicity but also from the point of view of tape guide.
When the signal to noise characteristics of the system are considered on the basis of fig. 1, it has first to be clearly stated what distortion limit is used. For the investigation of recording ability it is suitable to use the compression in the output-input relation as a distortion criterion. This means that the output amplitude is plotted as a function of input amplitude for a given frequency and that the deviation from linearity is measured. With respect to the harmonic distortion measurement this method is advantageous because it is independent of overall frequency characteristic and applicable in the full frequency range. With respect to intermodulation distortion it avoids difficulties due to wow, flutter and noise. Thirty percent compression corresponds to 10% intermodulation. Curves A and B are based on a compression of 30%!
The noise in the output can be split up in two contributions: the equipment noise (playback head and playback amplifier) and the tape noise. The latter is understood here as being the noise in absence of a recorded signal, the modulation noise being left out of account. It is well known that the tape noise is far less for a bulk erased tape than for a bias erased tape. Unfortunately, we have to work with bias in action; hence with a noise level which is considerably higher than originates from a well degaussed tape. In fig. 1 this effect is illustrated by the difference between curve N (noise output for bias erased tape) and curve N' (bulk erased tape). It is not yet well understood what the mechanism of the bias noise might be, so that nothing can be said about measures for improvement. Apart from this effect the tape noise is, of course, completely determined by tape technology.
The equipment noise, given by curve N'' in fig. 1, can be kept at a low level by applying a head with a high efficiency in its magnetic circuit and a high Q in its electronic circuit, well matched to a low noise amplifier. In this respect the figures for ferrite heads are superior to those for mu metal heads. Although at the moment the ratio between tape noise and equipment noise is such that optimum figures for head quality are not wholly necessary, use of mu metal heads thus being possible, future development of tape may lead to lower tape noise levels and higher demands on head quality, these being met by ferrite heads. From a design point of view, too, the use of ferrite as head material is better suited to narrow gap and dual gap design than is mu metal [2]. In principle the signal to noise properties of the system are determined by curves A and N. To obtain actual values the pre-emphasis and equalization characteristics have to be known. These curves are such of course that in combination with the tape characteristic a flat frequency characteristic is obtained. In our system this holds up to 13000 c/s (3 dB point). This tape characteristic is given in fig. 2A measured at a level which is about 20 dB below maximum loading.

Ideally, the pre-emphasis characteristic has to be chosen in such a way that for all frequencies in the musical signal the tape is optimally loaded. It will be clear that this depends on the programme material and that only a mean curve can be found, derived from a lot of practical tests.

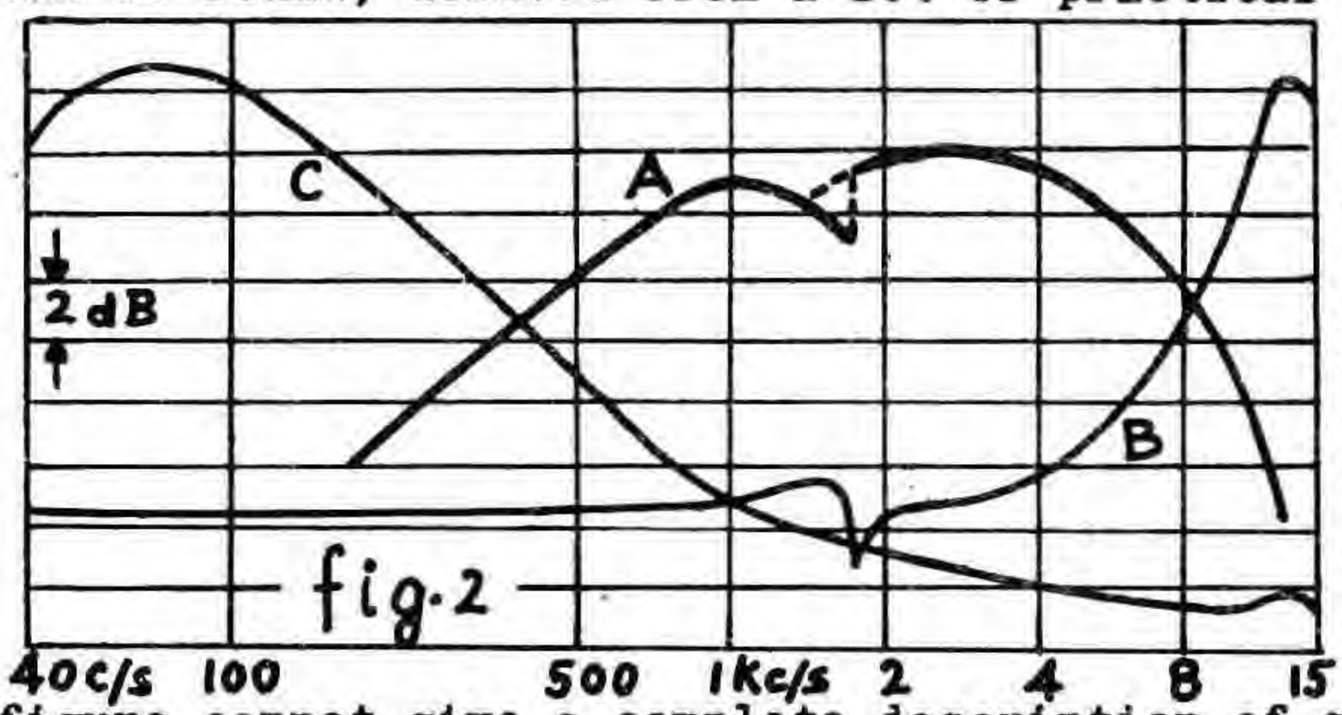

fig.2

The pre-emphasis characteristic is given in fig. 2B and the playback equalization in fig. 2C. Small corrections in the latter in the upper frequency end may be necessary in order to overcome variations in tape and head. With A, B and C 3 dB points are at 50 c/s and 13000 c/s.
It is common practice to give the signal to noise behaviour of a system in one single figure. It has to be borne in mind that this figure cannot give a complete description of quality and that a good evaluation is only possible when a listening test is included. A single figure for the signal to noise ratio has reference here to a maximum tape load for 30% compression at 1000 c/s and to the intigrated noise power in the band from 250 c/s up to 16 kc/s. For the data given in fig. 1 this value is 55 dB. With experimental tape and a somewhat improved playback amplifier circuit a value of 58 dB could be reached.
As stated above, a good evaluation can only be based on listening tests. This paper is therefore followed by a short demonstration of the musical quality. Now the demand for a listening test does not mean that this is a simple, unambiguous criterion. As the reader will know, it is rather easy to bring an audience in a listening test to a favourable conclusion by a suitable choice of programme material, reference quality (if present), loudspeaker arrangement and the acoustics of the listening room.
In our demontration we try to make the test as severe and instructive as possible. For this purpose it is first of all necessary that the music has a considerable amount of highs in the upper end of the frequency characteristic. The second condition is a larger dynamic range because one of the typical shortcomings in slow speed recording is the limited dynamic range, which makes the result very critical for the right setting of the recording level. If this level is too low there will be too much annoyance from the noise in the silent parts, whilst if set to high, there will be over-modulation in the fortissimos. Due to the large amount of pre-emphasis for the high frequencies this over-modulation does not directly lead to what in audio reproduction is normally understood as distortion but rather to a decrease in high notes, this giving a lack of transparency.
Another point of weakness which may occur in a system where the frequency spectrum is split up into two parts which are handled differently is the transient behaviour, especially in the middle range. With respect to this point too the music must enable the listener to test critically.
Finally, the increased sensitivity of low-speed small-track recordings to drop outs must be tested, and also the general shortcomings of magnetic recording: wow, flutter, and modulation noise (for which piano music is very suitable).
In the demonstration all of these points are catered for. A comparison is made with professional quality at 15'' p.s. In order to make the arrangement not too complicated, a copy is made of the slow speed recording at professional speed, in such a way that professional and slow speed quality can be reproduced sequentially.

LW

Eindhoven, 29-4-1962

References

1. P.C.Goldmark, C.D.Mee, J.D.Goodell and W.P.Guckenburg, Convention Record I.R.E. part 7, 116-126, March 1960.
2. S.Duinker, Philips Res. Rep. 16, 307-322, 1961.

O11

FOURTH INTERNATIONAL CONGRESS ON ACOUSTICS
COPENHAGEN 21.-28. AUGUST 1962.

On Interaction of Aerosol Particles in an Acoustic Field.

O.K.Ekmadiosyants

There are some hypotheses about mechanism of acoustic aerosol coagulation, but hardly some of them are justified experimentally. For the purpose of studying the indicated processe in greater detail we ran some high-speed macro-and microfilm tests of polydisperse aerosol particles in an acoustic field of vertical coagulation chamber. The speed of filming varied in the limits from 300 to 5000 frames/sec. Twin horn electrodynamic laudspeakers of nominal output of 50w each, situated in the upper part of steel chamber, radiated sound between 300 and 3000c. The coagulation chamber consisted of several sections and one of them placed opposite the camera was narrowed and glazed. The internal dimensions of the sections were 60 x 40, in the narrow part 60 x 10. The main experimental part of the work was conducted in sound standing waves with the travelling wave ratio within 0,15 and 0,35 and the pressure level (in narrowing) in the loops from 140 to 150 db. Sound pressure distribution was checked with the aid of ceramic sound pressure pickup probe, smoothly transfered along the chamber axes. The signal was sinusoidal above 700c, the third and strongly expressed the second harmonics were present in more low frequencies. Aerosol particles were illuminated with a lamp perpendicular to the filming. The vibrational partical traces on the film had the form given in the fig.1. When the speed of filming was less (numerically) than that of frequency of radiation the trace length was correspondent to double particle amplitude displacement. The sizes of all particles (suspended aluminium powder)

fall within limits from 3 to 30μ. The sizes of the most frequently occurring particles were within the limits from 5 to 10μ. The behaviour of bronze powder particles was quite analogous.

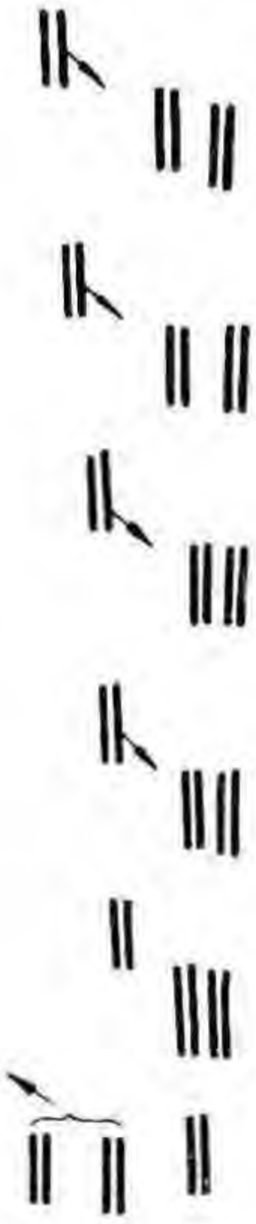
fig.1

The phenomenon of aggregation of polydisperse aerosol particles was the most important result of the experiment. According to high-speed filming the vibrating particles form in a sound field stable spatial aggregates, consist of 2("pairs"), 3("threes"), 4("fours") and rather greate number of vibrating particles, which are some distance d_o apart from each cther. This distance d_o decreased with the growth of frequency. The aggregates could travel as a whole along and aeross the field. It was revealed the stable systems resembling flakes consist of 8,10 and more number of vibrating particles. The number of component particles in aggregates is determined, however, by aerosol concentration, frequency and sound pressure level. Similar aggregation occured always in a given frequency (300-3000c) within the dynamic range of 135db and much higher. The same could be observed with sinusoidal and distorted forms of the signal. The most intensive aggregate formation occured in pressure node region, that is in loop velocity. In some experiments the sound was suddenly switched on, which lead to strong circular streaming formation, and the aggregation began immediately before the streamings set up. It is obvious, that necessary condition for such aggregate formation should be the presence as of repulsive forces, as well as attractive ones simultaneausly, which were dependent somehow upon the distance between the vibrating particles. According to high-speed filming no electrical forces in aggregate formation exist. Otherwise the particle attraction and repulsion could be revealed immediately

after the removal of radiating. But it was not the case. Soon after the field was switched out the more heavy aggregate particles began to move down and surpass other more light ones, but the distance between them in horizontal direction remains constant. It is evident that the interaction of particles and aggregates is hydrodynamical. No direct contact was revealed experimentally, the same was with the orthokinetic interaction. Aggregate formation and their recombination are illustrated by filmdiagrams, one of which could be seen in the fig.1. A "pair" (see from upper to down), interacting with a "four", takes half of the vibrating particles, forms a new "four" and removes backwards. Fig.2 shows the relation of d_o and the double viscous layer 2δ in μ (broken line) upon the frequency f in kc.

Two upper experimental points of the curve are that of Staszewski /1/ who studied the interaction of the sphere with the diameters of 0,33 and 0,39mm, situated on an inclined plane with their central line perpendicular to the field. Beginning with 300c the curve falls down then turn up in the region of 1100c and goes almost parallely to the axis till 3000c at least. The last experimental point shown in the fig.2 corresponds to 2070c. It is interesting to note that in given conditions there is no direct contact between the particle and according to the curves the distance d_o is of the order of 2δ.

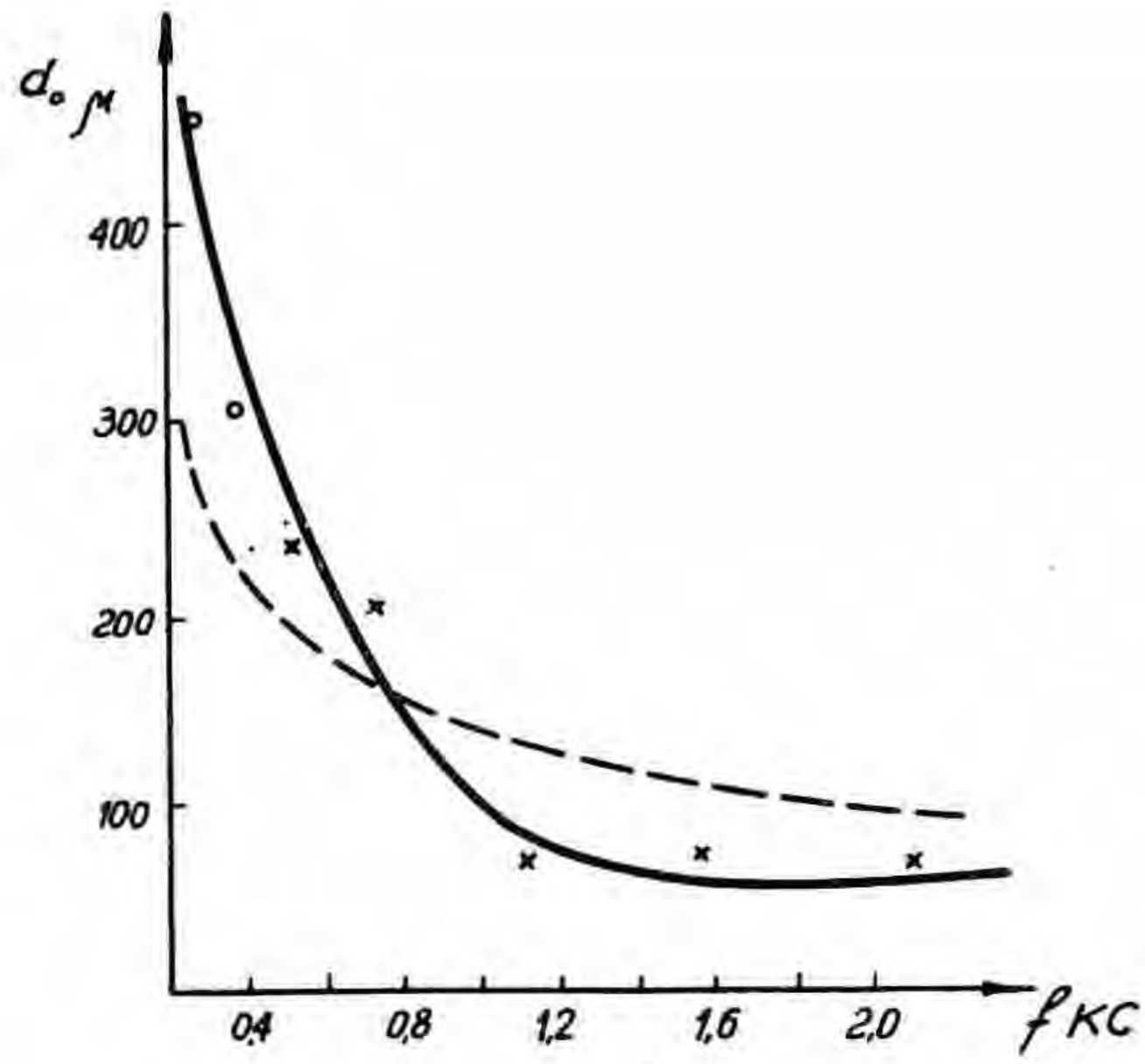

fig.2

References

/1/. Staszewski W. On the mutual influence of spheres in vibrating air. Acta Physica Polonica, 1958. 13. 3. 209-224.

P11

FOURTH INTERNATIONAL CONGRESS ON ACOUSTICS
COPENHAGEN 21.-28. AUGUST 1962

Ein optisches Verfahren zur Untersuchung geführter elastischer Wellen.

E.Häusler

Während in unbegrenzt ausgedehnten schubspannungsfreien Medien nur elastische Wellen mit einheitlicher Geschwindigkeit (Schallgeschwindigkeit) vorkommen, ist ihre Ausbreitung in Medien begrenzter Dimensionen von diesen abhängig. In einer schubspannungsfreien Platte breiten sich sogenannte Plattenwellen aus. Ihre Geschwindigkeit hängt von Frequenz und Plattendicke ab. Ähnliche Dispersionseigenschaften zeigt auch ein aus einer schubspannungsfreien Schicht über einem schubspannungsfreien Halbraum zusammengesetztes System. In beiden Fällen spricht man von „geführten" elastischen Wellen. Solche Wellen spielen eine große Rolle in der Geophysik, wo man aus ihrer Ausbreitungsgeschwindigkeit auf die Zusammensetzung des Erdmantels schließt (1). In Modellversuchen mit derartigen, meist aus festen Medien aufgebauten Systemen kann man die Gruppengeschwindigkeit geführter Wellen mit dem Ultraschall-Impuls-Verfahren ermitteln. Auch zur zerstörungsfreien Materialprüfung können derartige Wellen benutzt werden (2). Solche Messungen ergeben jedoch nur eine sehr grobe Vorstellung über den Mechanismus der Wellenausbreitung. Im folgenden soll daher eine Apparatur beschrieben werden, mit der es gelingt, Aufbau, Ausbreitung und Abbau geführter elastischer Wellen sichtbar zu machen.

Wir beschränken uns dabei auf ein schubspannungsfreies, gemäß Abb. 1 aufgebautes System. Die geführten Wellen muß man sich als zickzackförmig in der Schicht hin- und herlaufende Schallwellen vorstellen, die an der oberen, schallharten Grenzfläche mit dem Phasensprung 0, an der unteren Grenzfläche mit einem vom Einfallswinkel α abhängigen Phasensprung reflektiert werden, da an dieser Grenzfläche Totalreflexion auftritt. Durch Anwendung des Prinzips der konstruktiven Interferenz kann man die Einfallswinkel ermitteln, bei denen für eine bestimmte Frequenz und Schichtdicke eine ungedämpfte Ausbreitung der Wellen möglich ist. Dieser Einfallswinkel bestimmt auch die Spur- oder Phasengeschwindigkeit der geführten Wellen: $c = c_1/\sin\alpha$. Wegen der Totalreflexion an der Grenzfläche Schicht-Halbraum bleibt die Welle nicht auf die Schicht beschränkt, sondern setzt sich als quergedämpfte, inhomogene Welle in den Halbraum fort. Ihre Eindringtiefe hängt von der Spurgeschwindigkeit ab:

$z/\lambda_1 = {}^{c_2}/_{2\pi c_1}\sqrt{c_2^2/c^2-1}$ wobei $\lambda_1 = f/c_1$ (f = Frequenz). Für den Grenzwinkel der Totalreflexion ist sie also ∞ , für streifenden Einfall in unserem Fall: $z = 0{,}37\ \lambda_1$. Die Ermittlung der Abhängigkeit der Spurgeschwindigkeit von Schichtdicke und Frequenz (Geschwindigkeitsgleichung) erfolgt einfacher durch Annahme zweier parallel zur Grenzfläche laufender Wellen, die durch die Randbedingungen (Verschwinden der Normalkomponente der Verschiebungen an der oberen schallharten Begrenzung, Übereinstimmung von Schalldruck und Verschiebungen an der Grenzfläche Schicht-Unterlage) miteinander gekoppelt sind. Das dadurch erhaltene homogene Gleichungssystem hat nur dann eine Lösung, wenn die Determinante der Koeffizienten verschwindet. Die Auflösung dieser Gleichung liefert die transzendente Geschwindigkeitsgleichung:

$$tg\left[2\pi d\frac{f}{c}\sqrt{\frac{c^2}{c_1^2}-1}\right]=\frac{\varrho_1\sqrt{1-\frac{c^2}{c_2^2}}}{\varrho_2\sqrt{\frac{c^2}{c_1^2}-1}}$$

In Abb. 2 ist der Zusammenhang graphisch dargestellt. Die Schichtdicke ist auf λ_1 normiert. Für sehr kleine Schichtdicken nähert sich die Phasengeschwindigkeit c der Wasserschallgeschwindigkeit c_2 . Mit wachsender Schichtdicke nimmt sie ab und erreicht - nur die 1. Mode betrachtet - asymptotisch c_1 . Bei $d \approx 1{,}1\ \lambda_1$ beginnt die 2. Mode mit $c = c_2$. Mit wachsender Schichtdicke nähert sich c ebenfalls, aber langsamer als bei der 1. Mode, asymptotisch c_1. Bei $d \approx 2{,}05\ \lambda_1$ beginnt die 3. Mode. Ihre Geschwindigkeit nähert sich noch langsamer der Geschwindigkeit c_1. Die verschiedenen Moden können durch freie Wellen im Benzol, die die entsprechende Spurgeschwindigkeit haben, angeregt werden.

Das beschriebene System wurde realisiert durch ein Aquarium mit planparallelen durchsichtigen Seitenflächen gemäß Abb.3. Die Anregung der geführten Wellen erfolgt durch einen Keramikschwinger, der Ultraschall-Impulse (Frequenz 300 kHz, Impulsdauer 100 µs) mit einer der Phasengeschwindigkeit der geführten Wellen entsprechenden Spurgeschwindigkeit in das Benzol abstrahlt. Das Aquarium befindet sich innerhalb einer normalen Schlierenapparatur mit 2 Hohlspiegeln (vgl. Abb.4). Die Lichtquelle ist eine periodische angeregte gesteuerte Funkenstrecke. Während der Ultraschall-Impuls durch den 1.Impuls eines Doppelimpulsgenerators gesteuert wird, erfolgt die Auslösung der Funkenstrecke durch dessen 2.Impuls. Dieser kann gegenüber dem 1.Impuls verzögert werden und gestattet eine Beobachtung des Ultraschall-Impulses zu einem beliebigen Zeitpunkt nach seiner Anregung.

Abb. 5 zeigt damit erhaltene Schlierenbilder bei einer normierten Schichtdicke zwischen 0,23 und 0,68 (f = 300 kHz, d = 1-3 mm). Es ist also nur die 1.Mode angeregt. Mit zunehmender Schichtdicke nehmen Wellenlänge und Eindringtiefe ab. Die Kopplung der in der Schicht laufenden Welle mit der zugehörigen inhomogenen Welle im Wasser ist deutlich zu erkennen, da sie ihre Fortsetzung im Wasser darstellt. Die außerdem im Wasser sichtbaren freien Wellen haben eine größere Wellenlänge.

Abb. 6 zeigt geführte Wellen bei größeren Schichtdicken (d/λ_1 = 1,13-1,36), wo also auch die 2.Mode angeregt ist. Gegenüber Abb. 5b und c ist die Eindringtiefe wieder größer, doch stark räumlich moduliert. Abb. 6e und f unterscheiden sich nur durch die mittlere Spurgeschwindigkeit der anregenden freien Wellen (1350 bezw. 1465 m/s). Die Druckverteilung in Schicht und Unterlage hängt also auch vom Einstrahlwinkel ab. Da der Schwinger keine ebenen Wellen abstrahlt, werden in jedem Fall beide Moden angeregt. Je nach der Intensität der Anregung der einzelnen Moden ergibt sich eine unterschiedliche Druckverteilung in der Schicht. Die Modulation der Eindringtiefe der inhomogenen Welle ist ebenfalls durch Interferenz der beiden mit unterschiedlicher Phasengeschwindigkeit laufenden Moden zu erklären.

Wenn die Spurgeschwiodigkeit der anregenden freien Welle im Benzol stark von der zu der Schichtdicke gehörenden Phasengeschwindigkeit abweicht, beobachtet man eine Druckverteilung, wie sie Abb.7 zeigt. (Spurgeschwindigkeit der anregenden Wellen 1465 m/s, aus der Schichtdicke resultierende Phasengeschwindigkeit 1340 m/s, normierte Schichtdicke ≈ 1, 2.Mode also noch nicht angeregt). Bei einzelnen Phasenflächen in der Schicht fehlt hier die zugehörige, der inhomogenen Welle entsprechende Fortsetzung ins Wasser. Bei anderen ist deren Intensität und Eindringtiefe dagegen besonders groß. Es handelt sich um einen Abstrahlungsvorgang, bei dem die Energie der in der Schicht laufenden Welle an das Wasser abgegeben wird. Diese Wellen sind also in der Fortpflanzungsrichtung stark gedämpft. Sie sind ein akustisches Analogon zu der bei elektromagnetischen Wellen auftretenden Hohlleiterdämpfung, wobei in letzterem Fall allerdings die Energie nicht in ein 2.Medium abgestrahlt, sondern reflektiert wird.

Den Abbau einer geführten Welle zeigt Abb.8. Am Ende der als schallharte Begrenzung dienenden Stahlplatte wird die geführte Welle in eine freie, unter dem ihrer Phasengeschwindigkeit entsprechenden Winkel im Benzol laufenden Welle umgewandelt. Ein anderer Teil läuft im Wasser weiter und wird erst später in das Benzol abgestrahlt. In der Nähe der Kante besteht noch eine Kopplung mit der im Benzol laufenden Welle. Es handelt sich um ein Analogon zur Seitenversetzung einer totalreflektierten Welle.

Das beschriebene Verfahren zur Sichtbarmachung geführter Wellen gestattet eine sehr genaue Analyse des, schon bei den untersuchten relativ einfachen Systemen, recht komplizierten Mechanismus bei Anregung, Ausbreitung und Umwandlung solcher geführter Wellen. Für weitere Untersuchungen wäre an kompliziertere Systeme z.B. Medien mit komplexen elastischen Eigenschaften, stetige Schichtungen u.s.w. zu denken. Für komplizierte Beugungsprobleme bei der Ausbreitung elektromagnetischer Wellen, die sich mathematisch schwer erfassen lassen, bietet dieses optische Verfahren eine Möglichkeit, an Hand von Modellversuchen mit elastischen Wellen Anhaltspunkte für die theoretische Behandlung solcher Probleme zu finden.

Literatur: (1) Ewing, Jardetzky, Press: "Elastic Waves in Layered Media", New York 1957

(2) Häusler,E. : Materialprüfung 2, 51, 1960

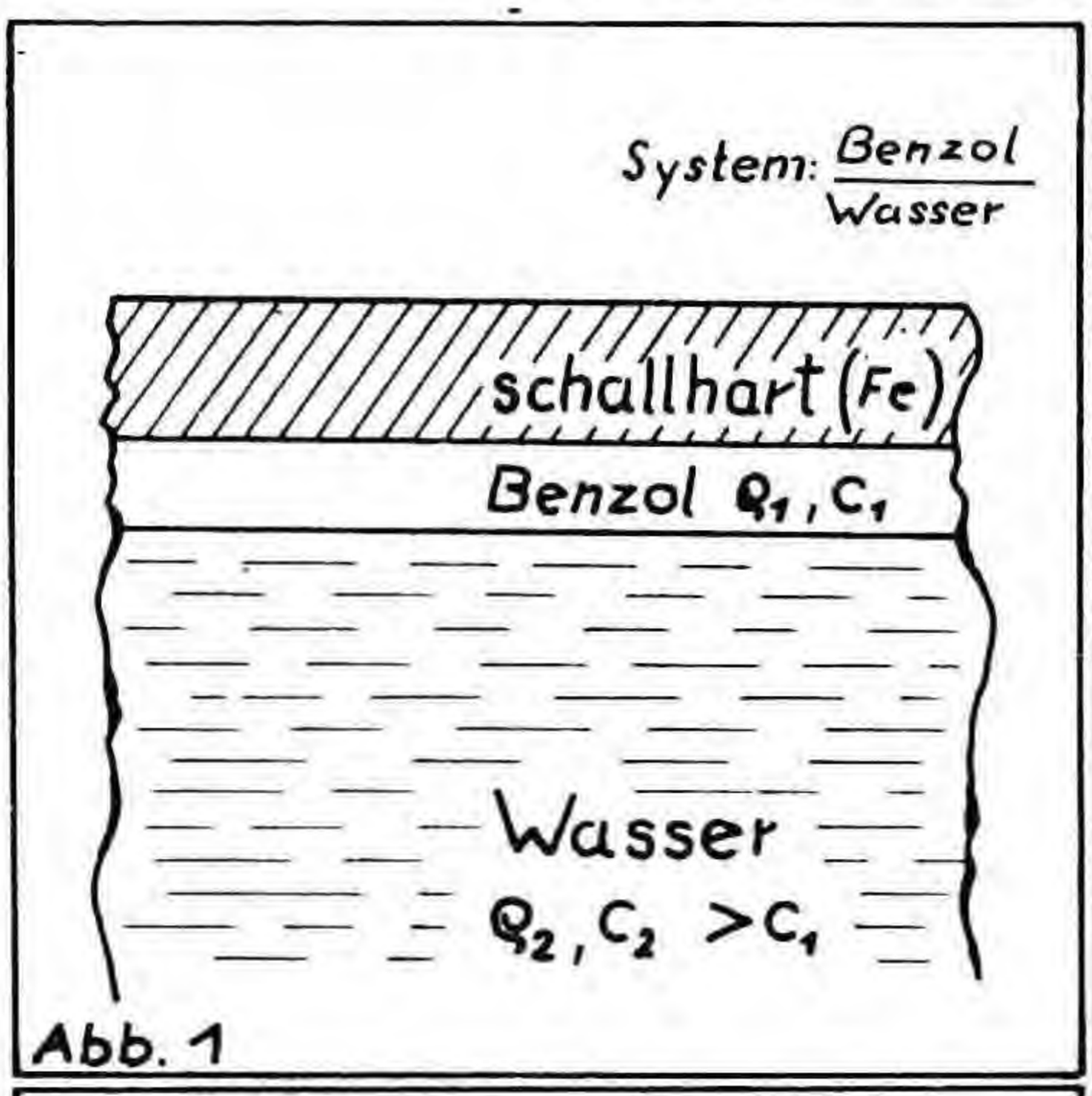

Abb. 1

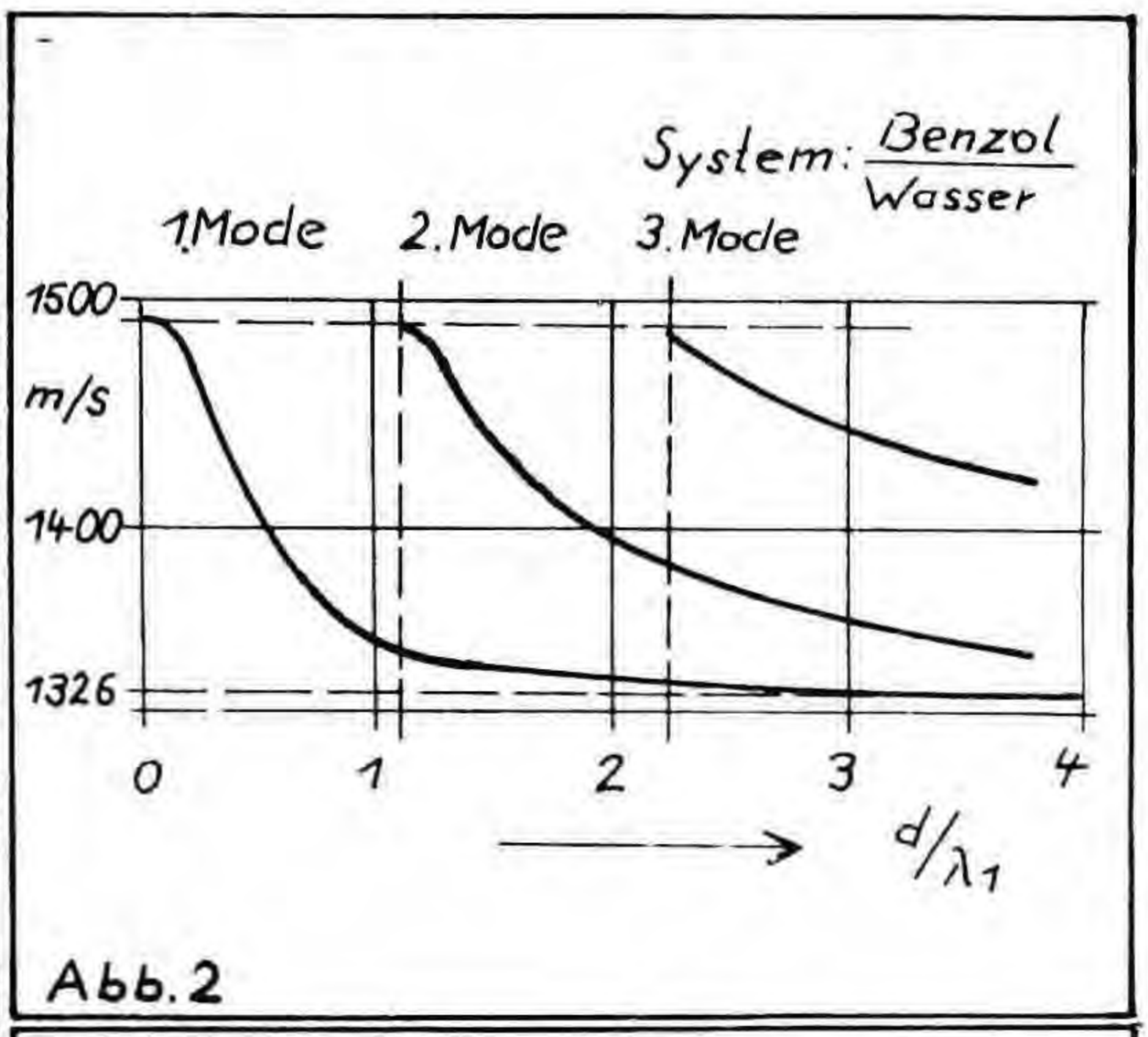

Abb. 2

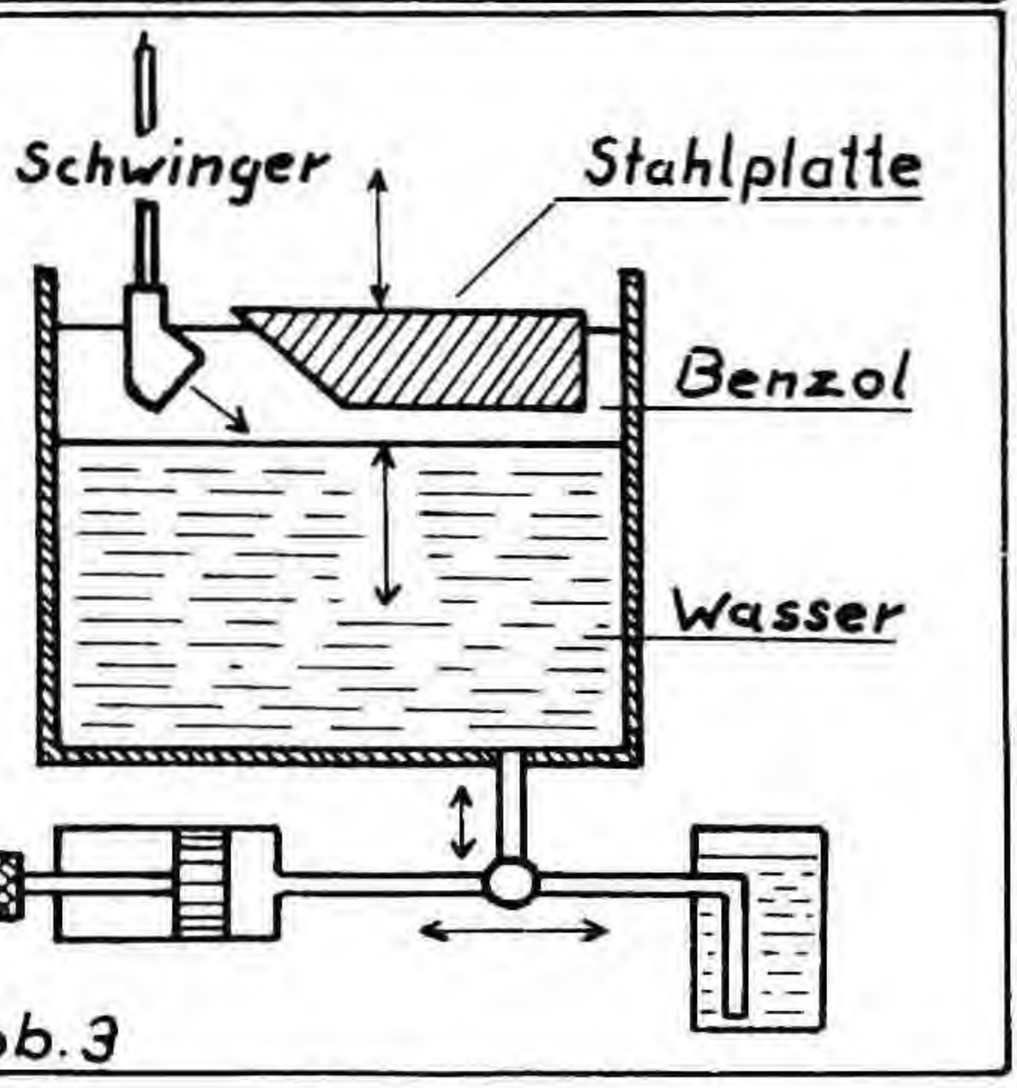

Abb. 3

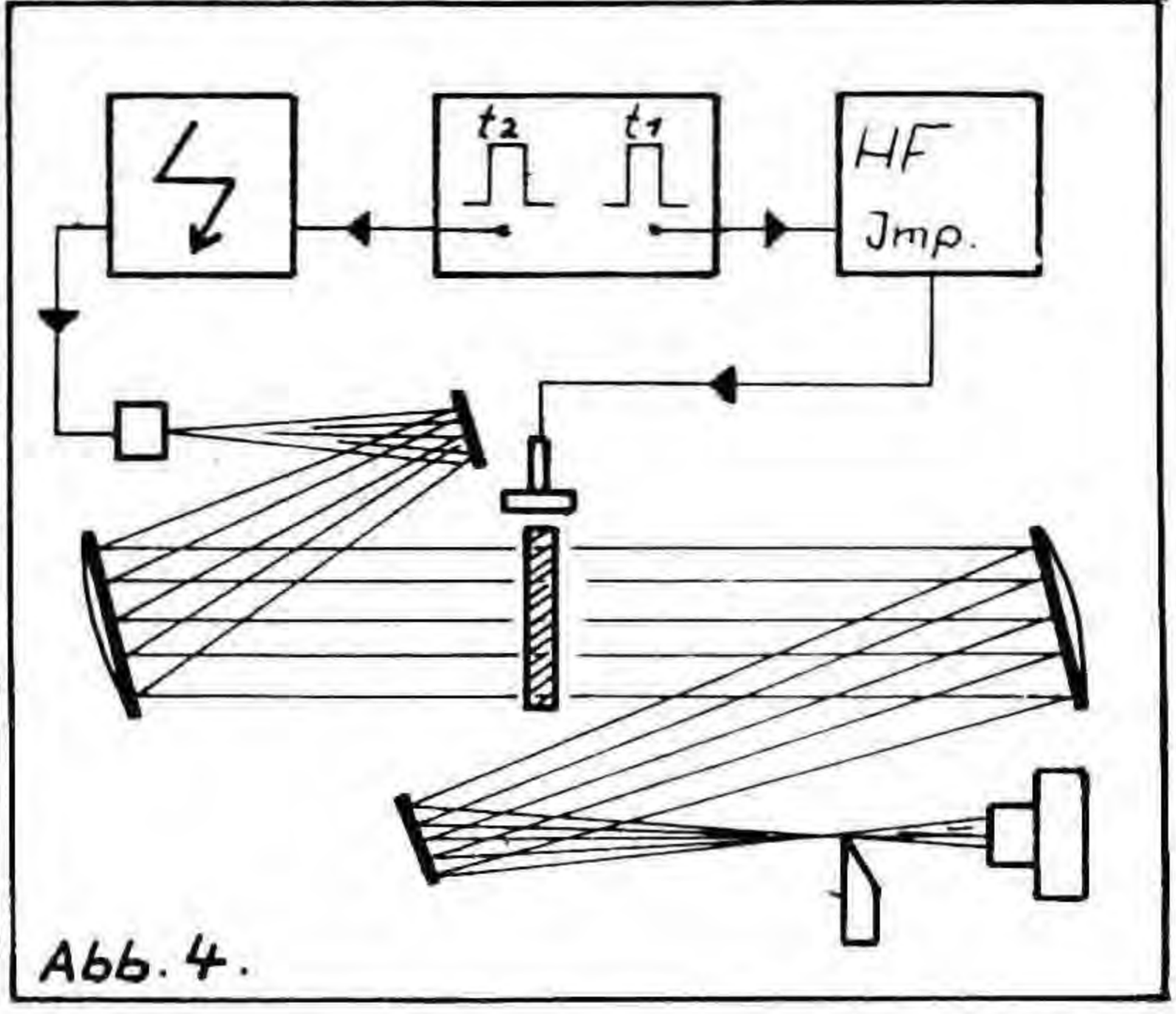

Abb. 4.

G12

FOURTH INTERNATIONAL CONGRESS ON ACOUSTICS
COPENHAGEN 21.-28. AUGUST 1962

THE MECHANISM OF THE HUMAN VOICE AND WIND INSTRUMENTS

N.V. Franssen

PHILIPS RESEARCH LABORATORIES

Musical instruments may be divided into three main catagories. Percussion instruments, the piano, the harpsichord and so on belong to one group. For those instruments a pulse of energy is applied to a more or less complicated passive filter with a certain number of resonances. In the second group, comprising string instruments such as the violin, the instrument can be considered as a relaxation oscillator, whose frequency is determined and fixed by the resonant element the string. Wind instruments and the human voice belong to the third category. Here a continuous stream of air is supplied to the instrument and its D.C. energy is converted into air vibrations. The stream of air can evidently be compared with the D.C. supply of an electrical generator and the instrument with the electrical generator itself. An electrical generator contains a tuning element and an amplifier. Comparison of musical instruments with electrical generators implies that both elements, tuning and amplification, must be present in the wind instruments. For the tuning element this gives no difficulties; the pipe for a flute, the reeds for the reedstops of an organ, the vocal cords for the human voice, all determine the pitch of the sound emitted. The concept amplification is more difficult. Amplification means that a small effect causes a larger similar effect in phase or antiphase. It can be shown that this effect really occurs in the wind instrument. In the lip-pipes of an organ a thin stream of air is divided into two parts by the lip (fig. 1). A small difference between the pressure in the pipe and the pressure outside causes a deviation of the whole stream to the low-pressure side and therefore a much larger difference in pressure. In the human-voice mechanism the air pressure in the chamber below the vocal cords is diminished by the displacement of the vocal cords. But when this displacement is large enough a gap between the two vocal cords arises and the air can escape through this gap, causing a much larger diminution of air pressure. It can be shown that this mechanism has a great resemblance with a normal colpitts oscillator (fig. 2).

The displacement of the vocal cords can be represented by the voltage on the condenser S and this voltage opens the tube. The stream of air through the gap, however, will be regulated not only by the dimensions of this gap but equally by the difference before and behind the vocal cords, so that the airstream depends on the product of gap and difference in pressure. This can be represented by a voltage on a second multiplicative grid.

The cavities of mouth, throat and nose form a second tuning circuit and generally the whole mechanism can be represented as in the diagram in fig. 3: an amplifier A and two tuning circuits, the vocal cords and mouth cavities. Reed instruments like the clarinet and lip instruments like the trumpet can be represented in a similar way. The pitch of the sound emitted is determined mainly by the resonance of one tuning system, the other system determines the formant. In the voice mechanism the pitch belongs to the resonance of the vocal cords; the cavities of mouth and nose have little influence on the pitch. In wind instruments, however, the pitch is determined by the length of the tube, which can be tuned with the aid of side holes; the formants are given there by the resonances of the reeds and lips. But the pitch frequency as well as the formant frequencies are generated: the formant filters do not filter the signal in a passive way but are incorporated in a generating system. In general we may say that one tuning circuit generates the pitch frequency and that the distortion products of this signal in the amplifier help the formantcircuits to generate. This behaviour is rather complicated, especially at the onset of a tone, and is therefore responsible for the complicated transients of musical tones. Conversely the transient can be responsible for the ultimate pitch of the generated tone: the start of blowing the instrument determines whether the instrument will be overblown: the well-known difficulty in playing horn.

Although the lip-pipes of organs contain only one tuning element, i.e. the tube itself, most of them possess a formant region. The tuning circuit has a certain number of eigentones. These eigentones are not completely harmonic. The overtones of the fundamental formed by distortion in the amplifier are harmonic. It will then be more difficult to generate certain overtones in an active way the more remote are those overtones from the eigentones (fig. 4). However a second effect influences the generation of overtones: the noise in the stream of air helps the generation of formants in a similar way as distortion products. This means that the generated overtones are not completely defined by the distortion products of the fundamental but have some degree of freedom.

Each pipe itself has some chorus effect.

These considerations have some consequences for the construction of electronic musical instruments. Firstly it seems to be insufficient to produce formants with the aid of passive filters: the generation of transients needs an active generation of formants. Secondly since overtones must have some degree of freedom, relaxation oscillators are not very suitable for the formation of notes. Furthermore it is clear that frequency dividers must be avoided, unless a chorus effect can be introduced afterwards.

LH

Eindhoven, May 29th 1962

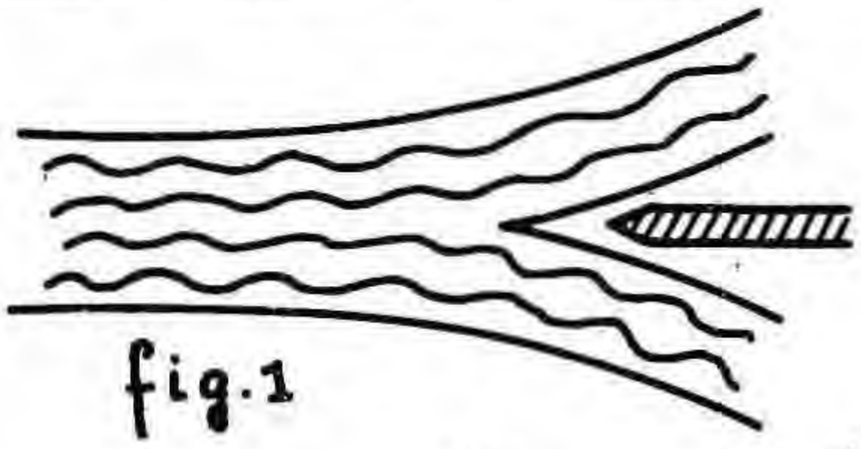

fig.1

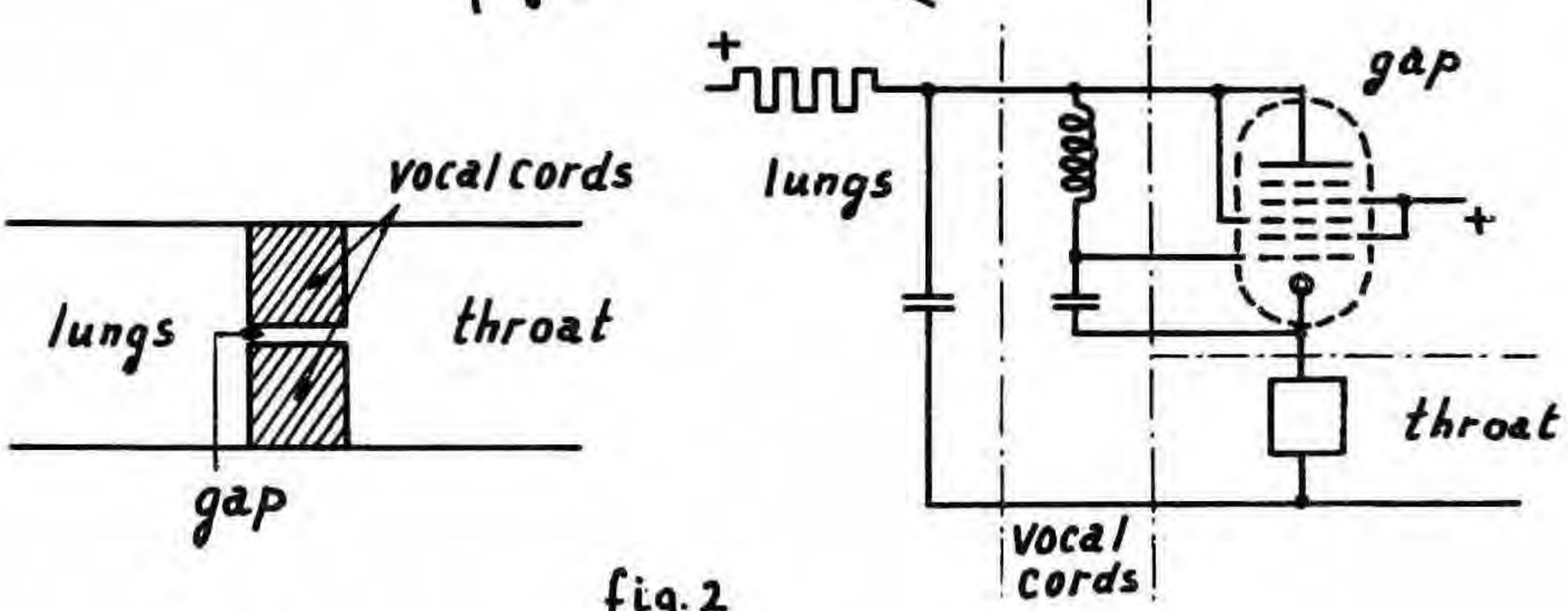

fig.2

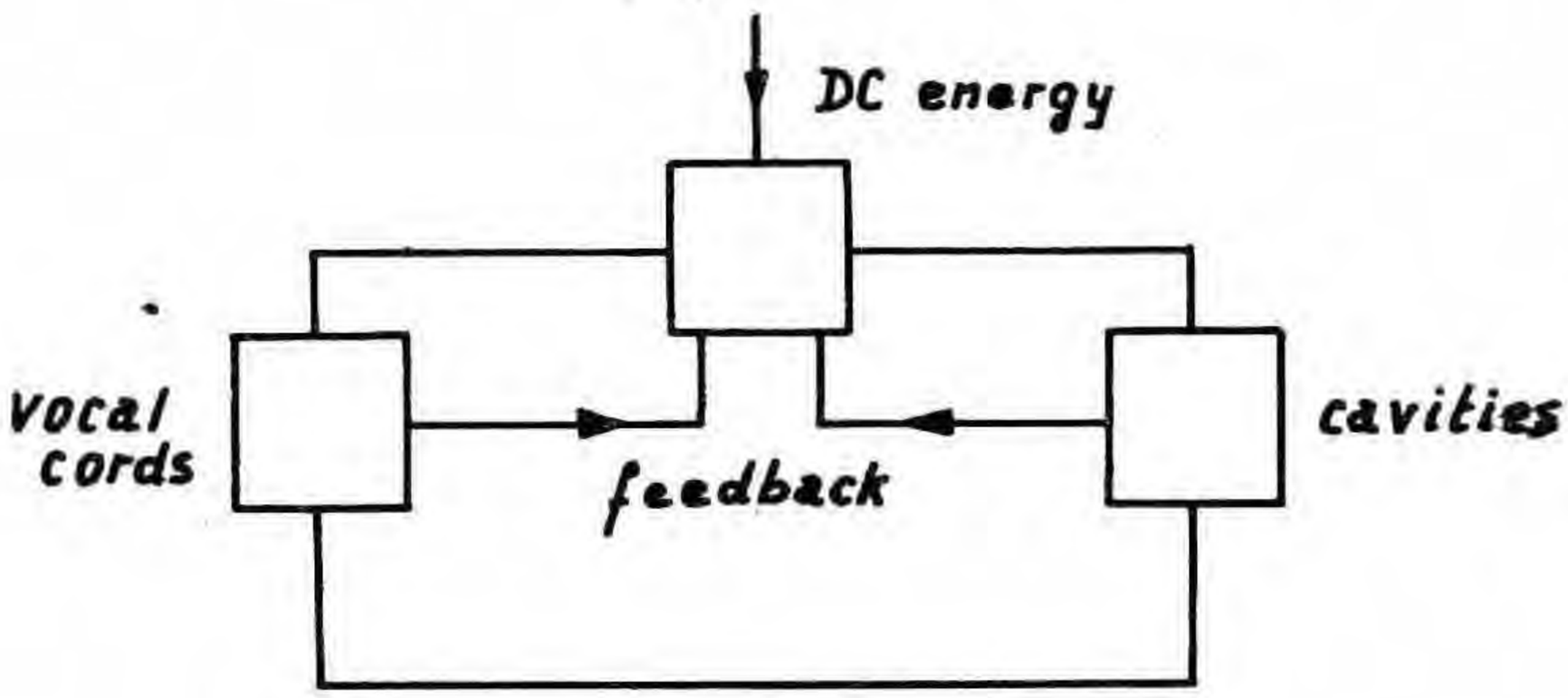

fig.3

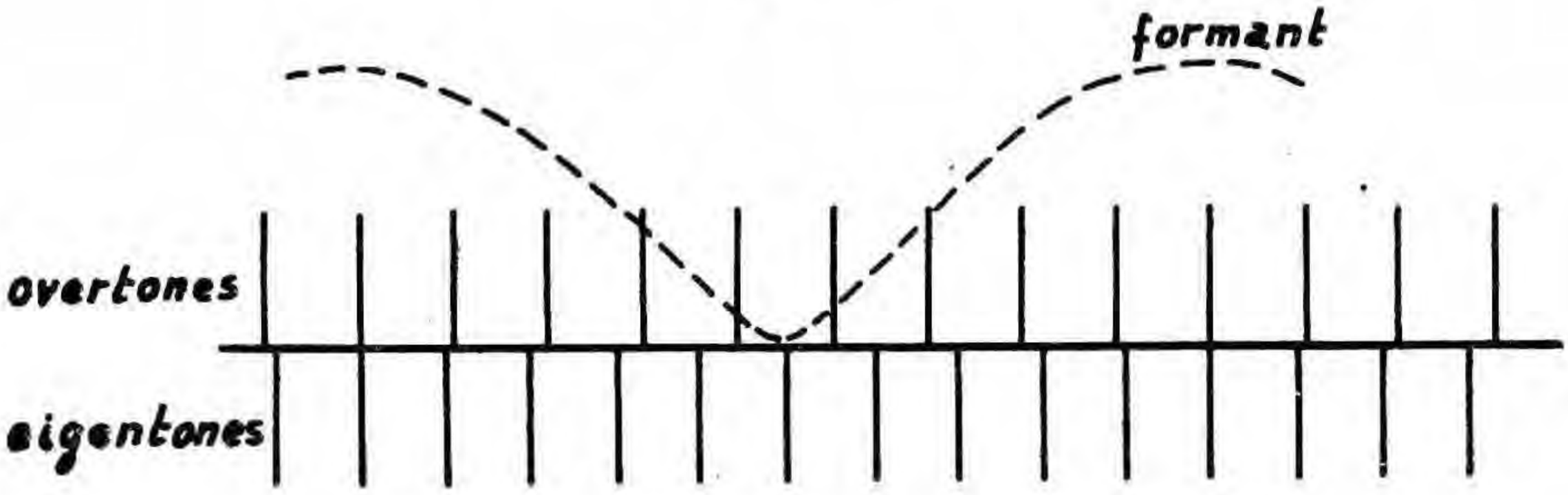

fig. 4

H12

FOURTH INTERNATIONAL CONGRESS ON ACOUSTICS
COPENHAGEN 21.-28. AUGUST 1962

ON BIOCHEMISTRY OF HEARING

Z. D. ANGELUSCHEFF, M.D.

Vibratory energy is converted by sensory cells into electro-chemical energy. Any frequency calls forth a cyto-chemical reaction and produces the subjective sensation of hearing.

The chemoreceptors of the nerve cells are an integral part of the transducing system of the mitochondrium. The main biochemical function of the mitochondrial system is to harness electrons and induce oxydation and phosphorylation. The mitochondrium thereby furthers the synthesis of amino-acids and fatty acids into higher polymers.

Submolecular movement of electrons in the living cell is a manifestation of life. Organic matter consists of units of chemically bound atoms. These adherent atoms are easily broken down by vibratory energy.

"When the mitochondrium exposed to sonic vibrations is disintegrated its enzymes become detached from the Electron Transport System and the capacity for citric and fatty acids oxydation cycles is lost." (Linnane)

This degeneration of mitochondrial components under the impact of vibratory energy has recently been demonstrated by the electron microscope.

The disruption of the molecules of the nerve cells can deprive them of their primordial functions. When a submolecular motion is generated in the cell by adequate frequencies, resonance results. Under such a condition the nerve cell attains its maximum depletion of enzymes, electrolites and amino acids. These cell components being freed of their chemical ties are liberated. They leave the cell and the specific band of the amino-acids is no longer obtainable in the spectroscope. Succindehydrase, cytochrome oxydase taking part in oxydation are thus lost. Glycolysis taking place in the hair-cells of organ of Corti and spiral ganglion is stopped. The plasma itself undergoes degeneration. (Vinnikov) The failure of the synthesis of high polymers incapacitates the nerve cells so that they can not fullfil their specific biological function.

The Electron Transport System (ETS) accounts for more than 50% of the total protein. The protein under impact of vibratory energy drops. The degeneration of the high proteins (RNA, DNA) leads to deficiency of the cellular function and failure of the hearing. In experiments with rats exposed to sublethal vibratory stimulation, the Purkinje cells in the brain tissue has been found in higher percentage. These cells are "densified," filled with granules, with low physiological function and are progressively decaying. The chemical substance of the granules has been identified by staining and ultraviolet spectrum to be Ribonucleic acid (RNA). This RNA proved to be denaturated and denuded of its primordial physiological function.

The proof for the denaturation of RNA has been established.

Decaying granules of RNA (in histological sections) have been reactivated by treatment with enzymes (ribonuclease). (Dunaevski)

The new knowledge of disruption and fragmentation of the minute mitochondrium by vibratory energy is of paramount importance for the medical and for the acoustical sciences. Any stress of the mitochondrial cell system, by vibratory energy or any noise, is capable of disrupting its synthetic system and undermining the highest biological activity of the cell. The biological system which converts the vibratory sonic energy into electro-chemical energy then disappears.

One should keep in mind that a population not exposed to noise thus preserves its normal hearing capacity, usually till very advanced age. The population in industrial areas, on the contrary, loses its hearing very rapidly and becomes hard of hearing during middle age.

Recent investigations have confirmed the previous advanced assertion, that the primary etiological factor in progressive deafness is vibratory energy; sonic and ultrasonic.

"The solution of the problem of progressive deafness, its cause, prevention and cure is to be found through the study of biological effects of soundwaves on the human ear." (Angeluscheff)

Vibratory energy can be perceived as noise or as silent, ultrasonics.

The pathologic affects upon the biological structures in both cases are essentially identical.

A dental drill of 40 kc/sec. arrests the growing process of the teeth in 95% of the experimental animals. The late effect of the vibratory energy is necrosis of mandibula, maxilla and degeneration of the nerve. (Kennedy J.)

"Frequencies which are not perceptible by the ear, ultrasonics, can be damaging. The effect of sonic and ultrasonic frequencies are especially dangerous for the ganglionic cells and those of the central nervous system of the spinal cord and brain . . . An irreversible paralysis and under circumstances death of the cells can result." (Lehmann G.)

Japanese investigators have recently scrutinized all aspects of biochemistry of acoustic trauma. They came to the following conclusion:

"Actually the ear of animal as affected by exposure to shock waves is the effect of vibration alone." (Yasushi Koide)

Our society accepts vibratory energy as a full fledged member, under the generic name - noise. But this evildoer is now under scrutiny. The French popular movement for healthy living has proclaimed that "noise is public enemy No. 1."

Fifty years ago Robert Koch, the discoverer of tubercule bacillus said:

"The day will come when man will have to fight mercilessly noise as the worst enemy of his health, as he did long ago with cholera and the plague."

This day is now upon us. The tremendous impact of vibratory energy is exerting its destructive effect. The victims of such bombardment present themselves to physicians everywhere. Unfortunately we must confess that we are helpless. We do not have the remedy or the answer. Being here where my colleagues are concerned with acoustical problems, allows me a special appeal. As physicians and acousticians we are concerned with the vital responsibility of Man, his health, his happiness and his functional serviceability.

"The concern of man and his destiny must always be the chief interest of all technical efforts. Never forget it among your diagrams and equations."

These prophetic words of Einstein must be the slogan of all interdisciplinary sciences devoted to the ultimate health & hearing destiny of man!

J12

FOURTH INTERNATIONAL CONGRESS ON ACOUSTICS
COPENHAGEN 21.-28. AUGUST 1962

A NEW DISSIPATION PROCESS IN COPPER, SILVER AND GOLD.

Piero Giorgio BORDONI - Università di Roma
Istituto Nazionale di Ultracustica "O. M. Corbino"
Paolo E. GIUA - Istituto Nazionale di Ultracustica "O. M. Corbino" Roma.
Livio VERDINI - Istituto Nazionale di Ultracustica "O. M. Corbino" Roma.

The first dissipation process observed at low temperatures in fcc metals and associated with the geometrical imperfections of the lattice was the relaxation effect due to the dislocations (1). A typical feature of this effect is that the temperature of the dissipation peak is considerably below the room temperature for vibration frequencies in the kilocycle range. Owing to the sharpness of the peak, the dissipation coefficient Q^{-1} at room temperature is then about one tenth of the value corresponding to the peak, or is even smaller. (Fig. 1, curve A).

A second dissipation process, having an entirely different character, has been recently found in polycrystalline fcc metals. It has been observed that if these metals are ground at room temperature with some abrasive material, such as carborundum paper, the dissipation at room temperature becomes very large, of the same order as that measured at the top of the dislocation peak at low temperature. If the material has undergone a permanent strain before grinding, the dislocation peak is still observed in the experimental curve, but it is superposed to a strong " background" dissipation (Fig. 1, curve B).

To isolate the second dissipation process from other causes of energy dissipation, the material must be annealed at high temperature in high vacuum, in order to cancel the dissipation peak, and to obtain a very small value of the dissipation (Fig. 2, curve A). The material is then ground at room temperature, and a low temperature run is made immediately after grinding. The experimental technique is the same which has been used in previous investigations upon the dislocation peak in fcc and bcc metals (2). The measurements have been made on 99.88 % gold at about 13 kc s^{-1}, on 99.80 silver between 7 and 31 kc s^{-1}, and on 99.78 copper between 8 and 30 kc s^{-1}. The experimental curves (Fig. 2, curve B) show that the dissipation coefficient due to grinding is almost linearly dependent upon temperature between 60 and 300 °K, and that no appreciable dislocation peak is introduced by grinding.

For a given temperature the value of Q^{-1} increases with grinding until a saturation is reached. The highest values which have been measured at room temperature after a very long grinding treatment are:

$$\text{for} \begin{cases} \text{gold} & Q^{-1} = 140 \cdot 10^{-5} \\ \text{silver} & Q^{-1} = 150 \cdot 10^{-5} \\ \text{copper} & Q^{-1} = 70 \cdot 10^{-5} \end{cases}$$

Of course the above values, like those of Fig. 2, correspond to the stress range in which the behaviour of the solid is linear, and are therefore independent of the amplitude of stress or strain. This condition imposes a rather sever limitations upon the maximum vibration amplitude, as the upper limit of linear elasticity is generally very low after an high temperature anneal, even when this treatment is followed by grinding.

It may be interesting to note that the straight line which may be drawn through the experimental values of the dissipation measured after grinding crosses the temperature axis at about 20 °K for gold (Fig. 2). The same happens with the corresponding line, for copper, whilst for silver the intersection is somewhat nearer to the absolute zero. This seems to indicate that the second dissipation process is related to the thermal energy associated with a frequency somewhat lower than the average Debye's value for the material.

The geometrical imperfections introduced in the metal lattice by grinding seem to diffuse easily at room temperature, even across the grain boundaries. There is also some evidence that the introduction of this second dissipation process is favoured by grains of large size.

The dissipation due to grinding is not entirely stable at room temperature, but anneals out in a time of several days, as it is shown for gold the curves of Fig. 3. A large number of measurements has been made for gold and silver to investigate the dependence of the rate of annealing upon temperature. The experiments have been made in the temperature interval 273 - 312 °K, measuring the value of the dissipation coefficient after grinding as a function of time at fixed temperatures. The curves obtained in this way have the same aspect as the usual recovery curves as it is shown by Fig. 3. It may be added that the resonant frequency of the specimens increases with time while the energy dissipation decreases and approaches asymptotically an lower limit.

The analysis of the experimental data concerning the recovery of the defects introduced by grinding shows that the experimental curves cannot be represented satisfactorily by a single exponential function, but rather by a sum of exponentials, each corresponding to a different characteristic time. However in the initial part of the experimental curves the fastest recovery effect predominates, and it is possible to compute the smallest characteristic time associated with the recovery, from the initial slope of the experimental curves. Assuming that the characteristic time is related to the temperature of recovery by the usual Arrhenius equation, the activation energy for the recovery seems to be near 0.6 eV for gold and to 0.2 eV for silver.

CONCLUSIONS

The geometrical imperfections introduced in fcc metal lattices by grinding give rise to a process of energy dissipation which is basically different from the well-known relaxation effects. In this second process the dissipation coefficient is roughly proportional to the absolute temperature, or to say better,

to the difference between T and a threshold value near to 20 °K.

No appreciable dependence of the dissipation coefficient upon frequency has been detected. However this result must not bee, considered as final, owing to the narrowness of the frequency range, and to the well-known difficulties which are found when this dependence is investigated.

The imperfections responsible for the second process anneal out at room temperature with a characteristic time of some days. This time decreases with increasing temperature; the corresponding activation energy for gold is of the same order as that associated with the diffusion of point defects.

REFERENCES

(1) A considerable amount of experimental evidence on the dislocation relaxation is collected in the paper by P. G. BORDONI, Resonance and Relaxation in Metals (American Soc. for Metals, Chicago 1962) VI, Dislocation Relaxation at High Frequencies, or by the same A.: Nuovo Cimento Suppl. 17, 43 (1960).

(2) A review of the experimental methods has been recently given by M. NUOVO, Ricerca Scientifica, 31, (II-A), 212 (1961).

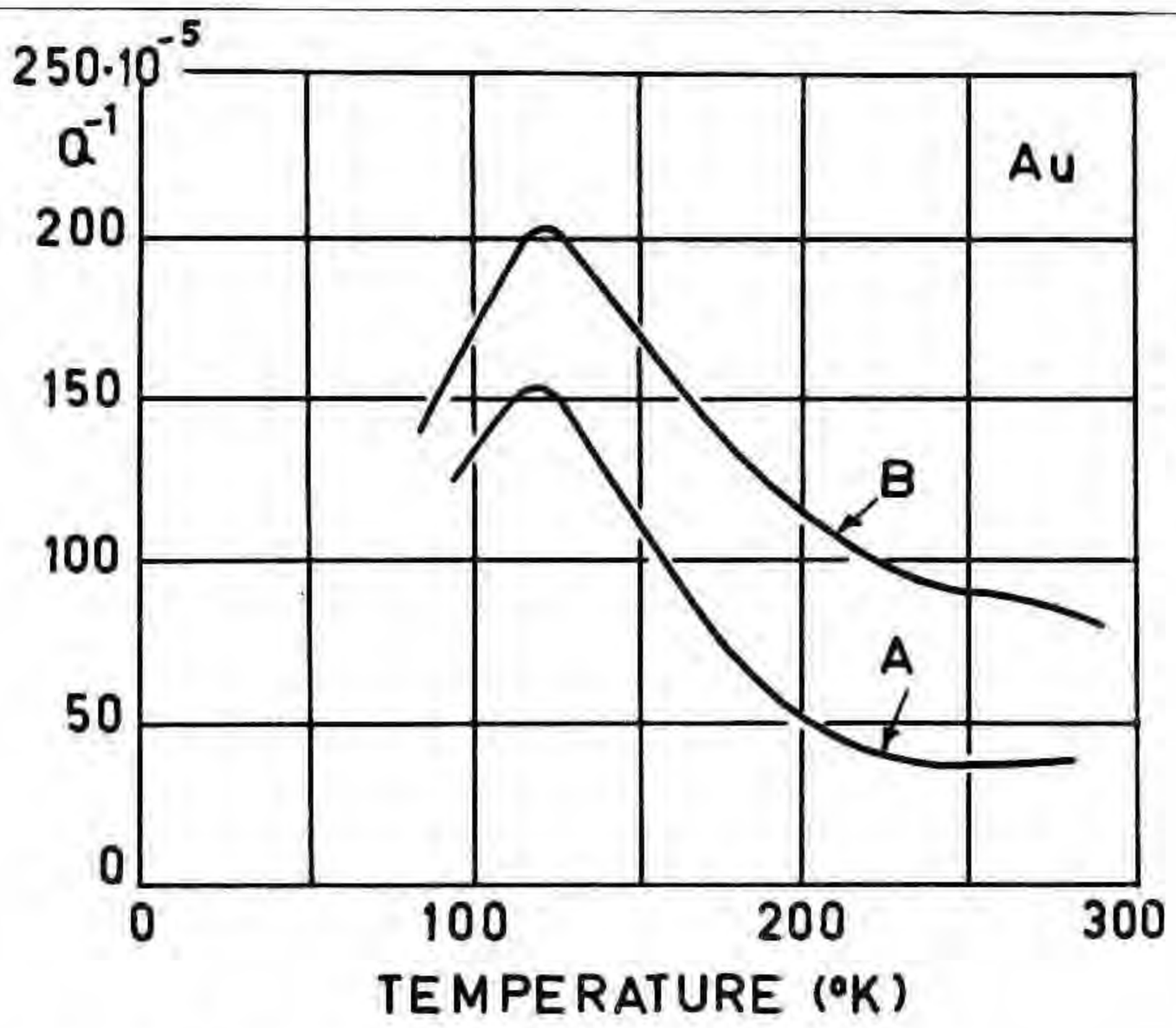

Fig. 1 - Curve A, relaxation peak due to the dislocations; Curve B, relaxation peak superposed to the second dissipation process due to grinding.

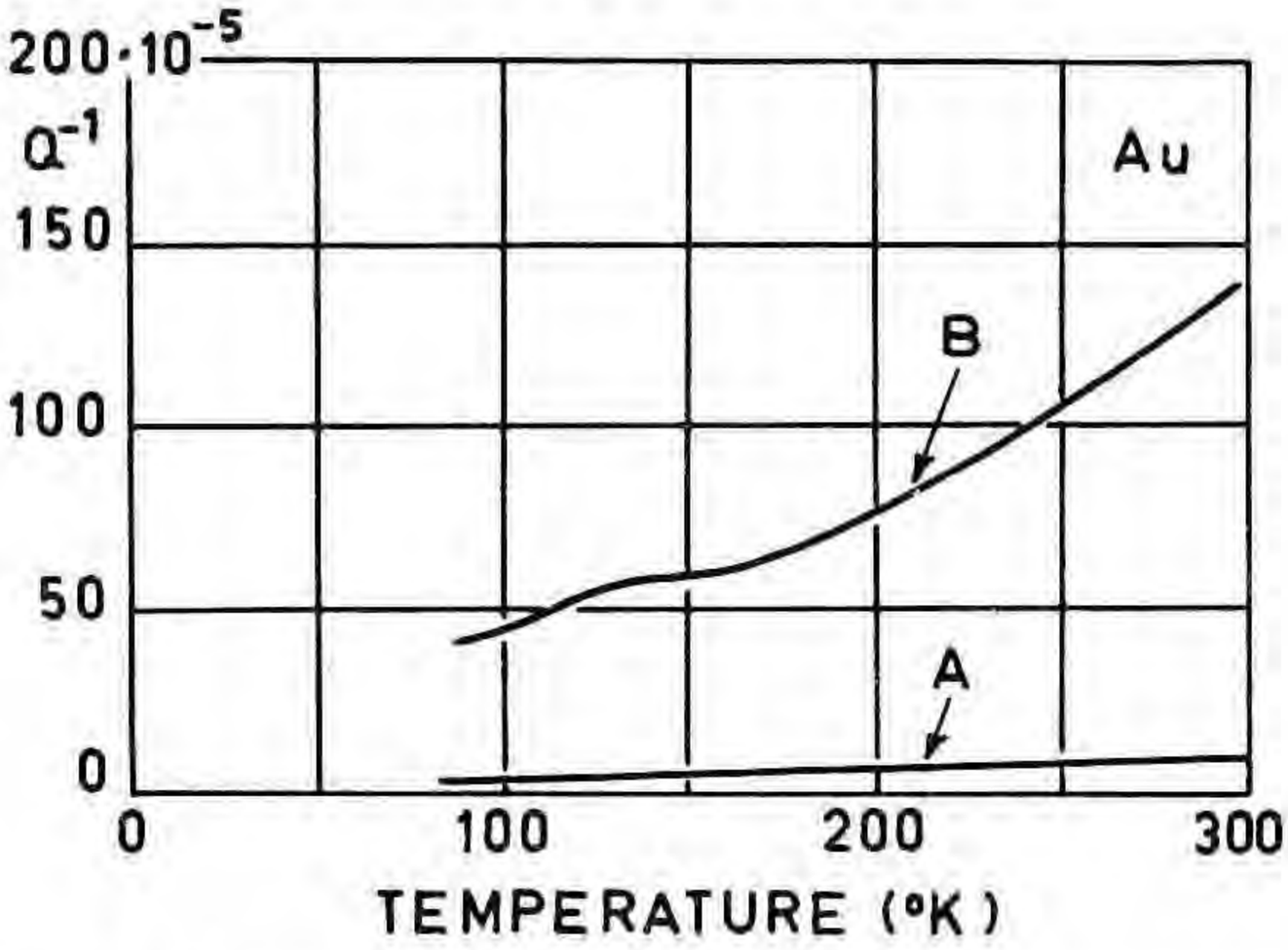

Fig. 2 - Curve A after an high temperature anneal; Curve B, immediately after grinding.

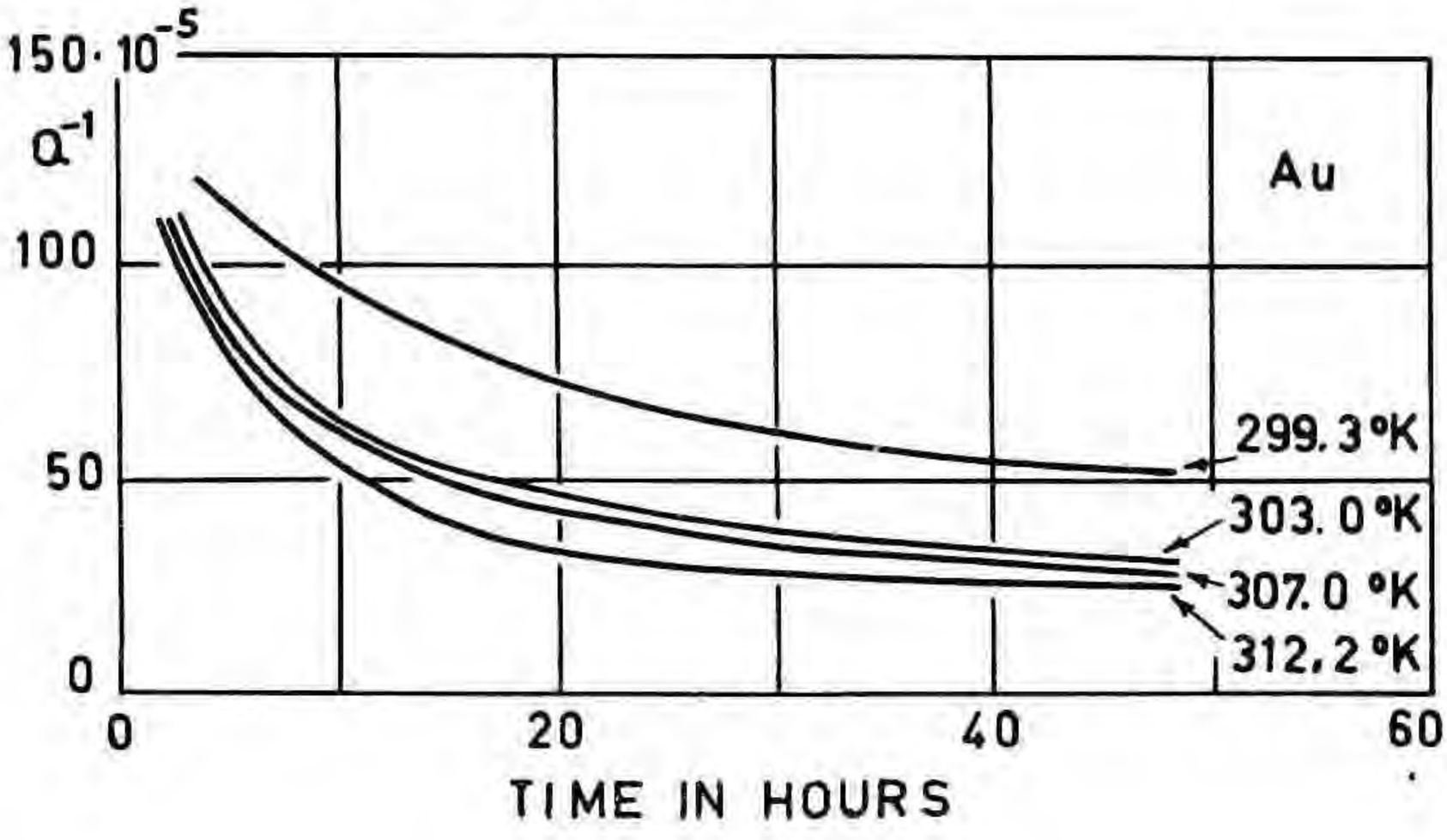

Fig. 3 - Recovery curves.

FOURTH INTERNATIONAL CONGRESS ON ACOUSTICS
COPENHAGEN 21.-28. AUGUST 1962

Hypersonic Resonance of Quartz from 3000 to 10 000 Megacycles

Ellen S. Stewart and James L. Stewart, U. S. Navy Electronics Laboratory, San Diego 52, California, USA

The excitation and propagation of hypersonic waves in quartz have been studied by Baranskii[1] using optical detection of continuous waves and by Bömmel and Dransfeld[2] and by Jacobsen[3] using electrical detection of pulses. We proposed[4] applying the ultrasonic resonator and interferometer methods to the hypersonic region in order to extend such measurements to highly attenuating solids and liquids in which the pulse methods are impractical due to the high losses in the thick samples required for pulse resolution. This required the development of a quartz resonator capable of operation at room temperature as the source. Last year we resonated[5] quartz crystals at 3000 Mc; now we have also resonated quartz at 10 000 Mc and have radiated sound into water and aluminum.

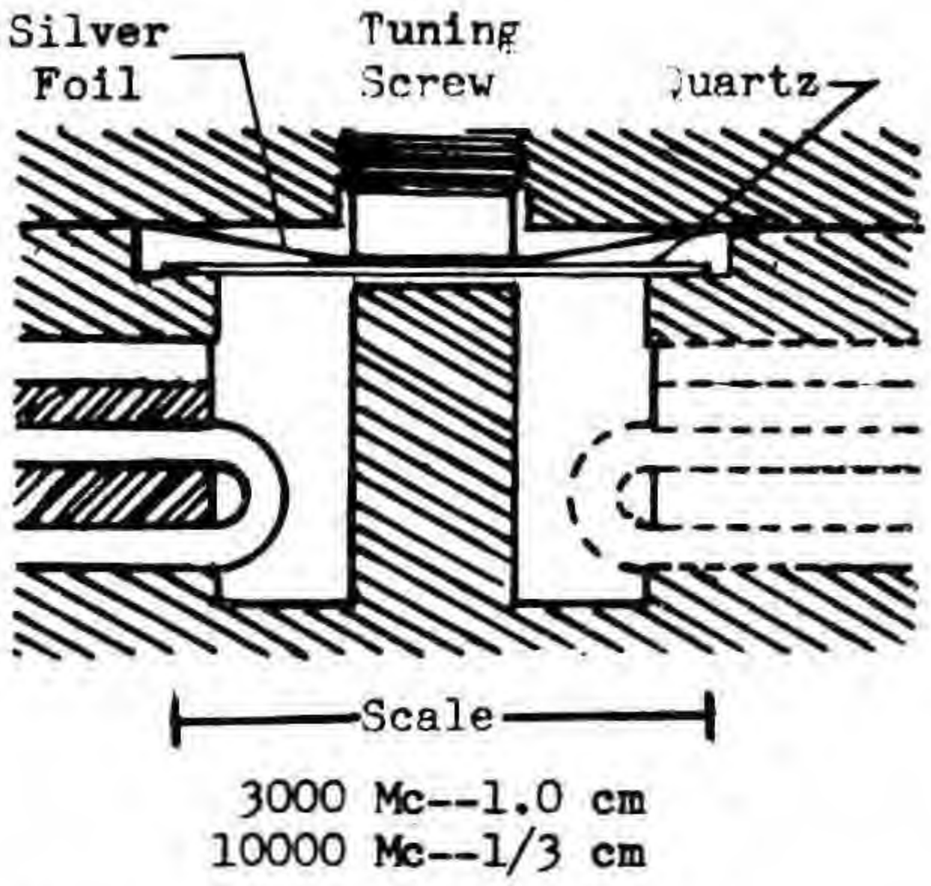

Figure 1. A microwave quartz-cavity resonator.

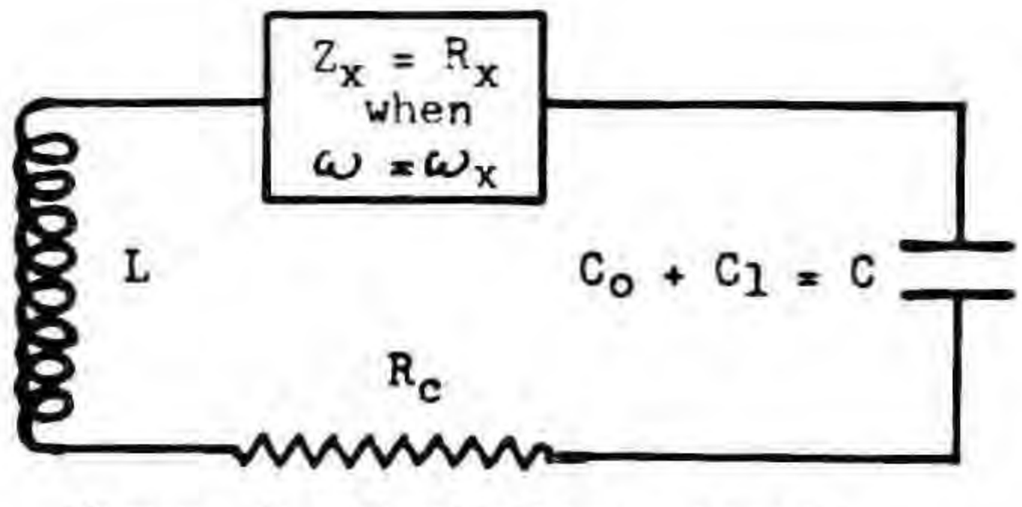

Figure 2. Equivalent circuit of reentrant cavity with piezo-electric crystal in gap.

An X cut quartz crystal is located in the gap of a reentrant cylindrical cavity, Fig. 1, as suggested by Slater.[6] The cavity, which is made of brass and gold-plated, is closed at the top by silver foil that is tightly clamped to the brass. The tuning screw is used to vary the air gap between the foil and the upper surface of the quartz, and thereby the cavity is tuned to the odd harmonics of the crystal which are in the range of our S-band oscillator (2950 - 3600 Mc) or our X-band oscillator (8600 - 10 000 Mc). Two cavities are used. The 3000 Mc cavity was designed according to Fujisawa[7]; the 10 000 Mc cavity was scaled down exactly one-third from the 3000 Mc one.

The crystal is supported only on its outer edge which is out of the electric field. There are air gaps a few microns thick between the center post and the bottom of the crystal and between the silver foil and the top of the crystal. Because the electric field excites mechanical vibrations only at the middle of the crystal, any radial vibrations which may be excited are damped out before they reach the edge of the crystal and the resonance is probably a pure thickness resonance of longitudinal waves.

For resonance to be observable the crystals must be thin since the attenuation is high and must be very plane-parallel since the wavelengths are short. In the 3000 Mc cavity the crystals are 100 microns (0.01 cm) thick and 1.0 cm in diameter. Since the acoustic wavelength is just under two microns or four wavelengths of green light, these crystals were made plane-parallel to one-quarter wavelength of green light. At 10 000 Mc where the acoustic wavelength is the same as that of light we used crystals, provided by the U. S. Army Signal Research and Development Laboratory, which are 30 microns thick, 0.50 cm in diameter, and plane-parallel to one-tenth wavelength of green light. These 30-micron crystals were also resonated at 3000 Mc by using an adaptor ring to hold them in the cavity.

The microwave input from the oscillator and the output to the crystal detector are made through coupling loops. The coupling is kept small to avoid damping the cavity and to decrease the reaction back on the source. The microwave oscillators can be used in either single frequency or swept frequency operation. Usually the reaction of the mechanical resonance of the piezoelectric quartz on the electrical resonance of the cavity has been observed by sweeping the frequency of the microwave oscillator. Oscillograph traces such as those reproduced in Fig. 3 show the sharper inverted resonance or "crevasse" of the quartz superimposed on the broader resonance of the cavity tuned to the same frequency. The microwave power into the cavity is estimated to be less than one-tenth milliwatt. It is kept low to avoid heating the specimens. All of the measurements were made at room temperature because of our interest in studying hypersonic properties of normal liquids.

In order to analyze the observations, the usual parallel equivalent circuit of a vibrating piezoelectric crystal has been transformed into a series equivalent circuit and combined with that of the cavity to give the circuit of Fig. 2. The cavity is represented by the resonant circuit L, R_c, and $C = C_o + C_1$ where C_o is the capacitance of the quartz and air in the gap and C_1 is the leakage capacitance[7] due to the field outside the gap. Z_x is the series electrical impedance due to the piezoelectric coupling of the mechanical vibration of the quartz.

$$Z_x = \left[\frac{2DC_o}{\omega C}\right]^2 \frac{1}{Z_m} = R_x + jX_x \qquad (1)$$

where D is the piezoelectric constant and Z_m, the mechanical impedance of the quartz, is

$$Z_m = W + j(\omega M - \frac{1}{\omega C_m}). \qquad (2)$$

The mechanical resistance W is the sum of all the losses including the attenuation in the crystal, the radiation loss into the second medium, the mounting loss, radial radiation generated in directions other than thickness, and radiation lost due to incoherent reflection. M is half the mass of that portion of the crystal which is in the gap, and C_m is its compliance.

The frequency response of this circuit is illustrated in Fig. 3 for the case where the resonant frequency of the cavity and that of an odd harmonic of the crystal are the same and the mechanical Q of the quartz is large compared with the electrical Q of the cavity. Near the resonant frequency the cavity response rises toward the usual maximum, but it is depressed in the region of the crystal's resonance. This dip is the inverted resonance curve of the crystal and is called a "crevasse". Crevasses occur at all odd harmonics of the fundamental thickness mode of vibration of the crystal.

At a crevasse minimum $Z_x = R_x$, $Z_m = W$, and $R_x = (2DC_o/\omega C)^2 W^{-1}$. If i_c and i_x are respectively the currents at the resonant frequency with the crystal static and vibrating,

$$\frac{i_c}{i_x} = \frac{R_c + R_x}{R_c} \text{ and } \frac{i_x}{i_c - i_x} = \frac{R_c}{R_x} = R_c\left[\frac{\omega C}{2DC_o}\right]^2 W \qquad (3)$$

whence it is possible to determine W. W can also be independently determined from the bandwidth of the crevasse and the vibrating mass of the crystal.

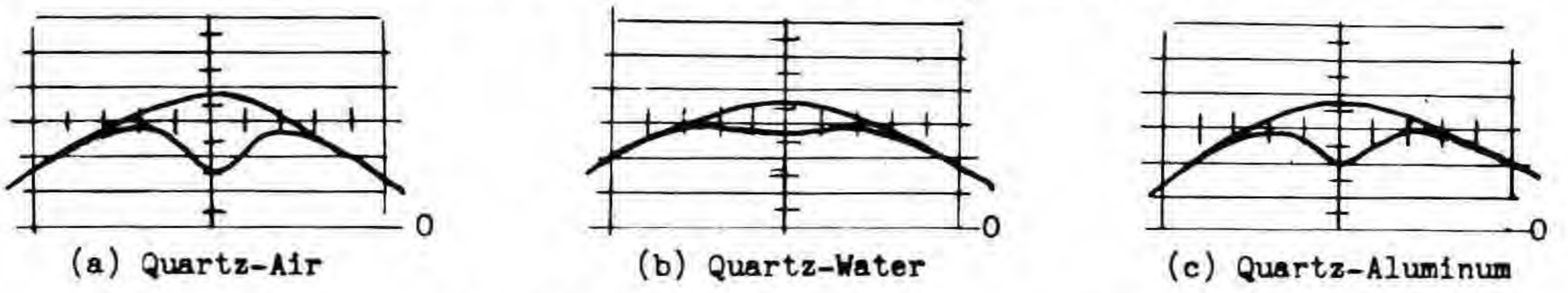

(a) Quartz-Air (b) Quartz-Water (c) Quartz-Aluminum

d = 100 microns; f = 3200 Mc; n = 113

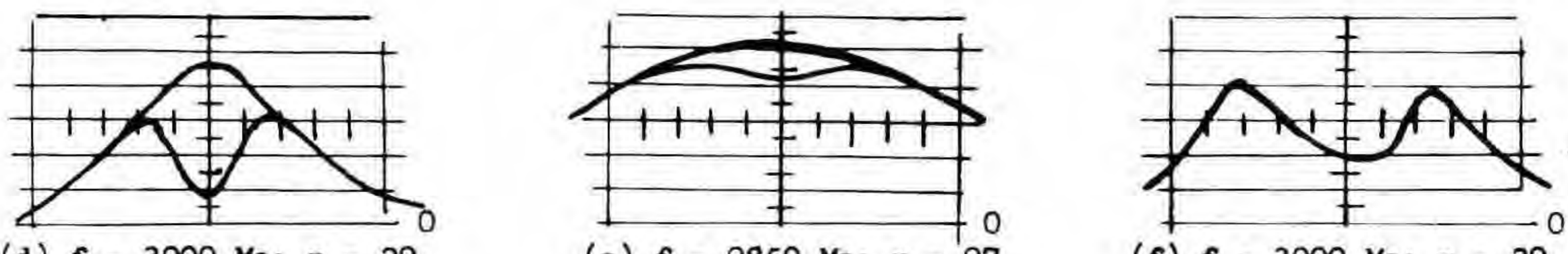

(d) f = 3000 Mc; n = 29 (e) f = 9850 Mc; n = 97 (f) f = 3000 Mc; n = 29

d = 30 microns; Quartz-Air

Figure 3. Frequency response of quartz-cavity resonators.

Oscilloscope traces of six quartz-cavity resonators are reproduced in Fig. 3. The frequency scale is approximately 1 Mc/division except in 3(e) where it is about 2 Mc/division. In the legend, d is the thickness of the quartz crystal, f is the frequency, and n is the order of the harmonic. In Figs. 3(a) and 3(d) the depths of the crevasse at the same frequency for different thicknesses of quartz are contrasted. Since the mechanical resistance due to internal absorption is smaller for the thinner crystal, the crevasse is deeper. Fig. 3(e) at 9850 Mc shows the effect on the crevasse depth of the f^2 increase of attenuation which causes Q to vary inversely with frequency.

The frequencies of the odd harmonics in the range of the oscillators were measured and the fundamental computed; the precision is ±0.004%. The frequency of the fundamental was also measured directly. Any dispersion between the fundamental and 3000 Mc and between 3000 and 10 000 Mc is less than 0.03% which is within the accuracy of the present calibrations. The observed velocity of sound in quartz is $5.74 \times 10^5 \pm 1\%$. The one percent error comes from difficulty in measuring the thickness of the quartz.

The Q of the quartz determined from the crevasse bandwidth at the half-power points is 4400 ± 400 at 3200 Mc and 1600 ± 300 at 9600 Mc. These correspond to attenuations of 4 and 33 nepers/cm. The values of Q predicted from the quartz absorption extrapolated from the data of Bömmel and Dransfeld[2] at 1000 Mc using a frequency square dependence are 3900 and 1300 respectively. The agreement is gratifying since Bömmel and Dransfeld observed a frequency dependence of absorption slightly less than quadratic. Consequently, other losses such as those due to insufficient plane-parallelism or generation of radial radiation are small indicating that we have approximately a pure thickness mode of vibration. A crystal which was plane-parallel to only one wavelength gave a Q of 2700 ± 200 at 3200 Mc. This extra loss is ascribed to insufficient plane-parallelism. Some 30-micron crystals plane-parallel to only two wavelengths did not resonate observably at either 10 000 Mc or 3000 Mc, probably for the same reason.

While symmetric crevasses such as that in Fig. 3(d) were observed for one-third of the crystals 30 microns thick and 5 mm in diameter when they were supported by an adaptor

ring in the larger 3000 Mc cavity, asymmetric crevasses such as that in Fig. 3(f) were more typical. This is in contrast with the symmetric crevasses of Figs. 3(a) and 3(e) which were observed in every case when the crystal diameter was greater than the cavity diameter. In more detail the pattern of Fig. 3(f) appears to be a group of partially resolved multiple resonances which are characteristic of the individual crystals. Possible explanations for these unwanted resonances are radial resonances of longitudinal waves in the crystal, shear wave resonances in thickness, and longitudinal wave resonances in thickness where some parts of the surface are out of phase with other parts. We favor the first explanation because only excitation of radial radiation depends upon whether the edges of the crystal are in or out of the electric field.

Since our primary interest is in the study of liquids, we wanted to know if sound could be radiated into liquids at these high frequencies. If a thin layer of liquid such as water is placed on the crystal the crevasse depth is decreased by an amount depending on the radiation of sound by the quartz into the liquid. In Fig. 3(b) is shown the effect of water on the crevasse of Fig. 3(a). From this effect the specific acoustic impedance of water can be calculated. The average of a number of measurements is $\rho c = (1.5 \pm 0.6) \times 10^5$ g cm^{-2} sec^{-1} at 3200 Mc. We also observed damping due to radiation into water at 9800 Mc but the effect, although of the correct order of magnitude, was too small for a quantitative determination.

The overall efficiency of conversion of electromagnetic energy in the cavity to sound radiated into water in our present 3000 Mc cavity is about 10%. This can be improved by a more optimal design of the cavity dimensions. The radiation into water was 1.5 times the radiation absorbed in the quartz for the 100-micron crystals and would be proportionately greater for the 30-micron crystals.

Aluminum coatings of different thicknesses between one and four microns, which are greater than the electromagnetic skin depth at 3000 Mc, were evaporated on three of the 100 -micron crystals. The resonance of one of these is illustrated in Fig. 3(c). The crystal vibration was damped only slightly, indicating that the thin film of aluminum is not too attenuating to hypersound. When a layer of water was placed on the aluminized surface, the crystal vibration was significantly damped; therefore, sound had been radiated through the aluminum into the water. This demonstrates the feasibility of aluminum windows which will transmit hypersound outside the cavity while serving as its top electrical conductor. Aluminum was chosen because it has the same ρc as quartz. An acoustical-optical interferometer employing the aluminized crystal as source and a transparent optical flat as reflector is being assembled to study the acoustic properties of liquids at hypersonic frequencies.

REFERENCES

1. K. N. Baranskii, Doklady Akad. Nauk S.S.S.R. 114, 517 (1957); translation: Soviet Phys.--Doklady 2, 237 (1958).
2. H. Bömmel and K. Dransfeld, Phys. Rev. Letters 1, 234 (1958); 2, 298 (1959); Phys. Rev. 117, 1245 (1960).
3. E. H. Jacobsen, Phys. Rev. Letters 2, 249 (1959).
4. J. L. Stewart, J. Acoust. Soc. Am. 31, 836 (1959).
5. J. L. Stewart and E. S. Stewart, J. Acoust. Soc. Am. 33, 538 (1961); 33, 1147 (1961).
6. J. C. Slater, U. S. Patent 2,773,996 (1956); J. Acoust. Soc. Am. 29, 758 (1957).
7. K. Fujisawa, IRE Trans. on Microwave Theory and Techniques 6, 344 (1958).

L12

FOURTH INTERNATIONAL CONGRESS ON ACOUSTICS
COPENHAGEN 21.-28. AUGUST 1962

Sources of Noise in Axial Flow Fans

E.J. Richards and I.J. Sharland

Introduction

In recent years the need has arisen for detailed knowledge of the origin and behaviour of noise generated in axial flow fans. To this end, many investigations are now under way, ranging from multistage aircraft engine compressors to single stage ventilating fans. At the University of Southampton measurements are being made on a three stage model compressor having a tip diameter of 6 inches, a hub tip ratio of $\frac{2}{3}$ and a maximum speed of 15000 rpm. Each stage consists of 16 rotor blades and 15 stator blades and there is a row of 15 inlet guide vanes. The geometry of the fan is variable in respect of number of stages, number of blades, blade incidence and blade spacing, and by measuring the noise radiated from different configurations it is hoped to establish which are the most important mechanisms of generation.

Measurements of fan noise show that the frequency spectra are characteristic in shape. There is generally a broad spectrum centred around one kilocycle on which is superimposed a number of sharp peaks. These peaks are found to occur at the fundamental blade passing frequency and its harmonics. It is convenient to study fan noise under two headings - broad band noise associated with random disturbances on the blades, and discrete frequency noise associated with blade rotation.

Broad Band Noise

Broad band noise is generated by random force fluctuations on the blades, and these forces can appear in the following forms.

(i) pressure fluctuations produced by turbulent boundary layers over the blades
(ii) lift fluctuations due to trailing edge vortex shedding in the boundary layers
(iii) local lift fluctuations on the blades due to turbulence in the incident airstream

In an attempt to establish the relative importance of these sources a simple experiment was carried out in which a small flat plate was held at zero incidence in the turbulent mixing region of an air jet. The noise was measured at right angles to the plate for a number of jet velocities and the test was repeated with the aerofoil in the laminar core of the jet. The order of magnitude of the noise was then estimated for each of the three sources mentioned above, and compared with the measured results.

The basis for calculating the noise produced by a solid body immersed in a compressible flow has been established by Curle (1955) in an extension of Lighthill's theory of aerodynamic noise which includes the influence of solid boundaries.

It can be shown that

$$W = \frac{1}{6\pi\rho a^3}\overline{\left[\int_S \frac{\partial p_i}{\partial t}\cdot dS\right]^2} \qquad \ldots(1)$$

where W is the acoustic power, p_i is the pressure on the surface, and the integral is over the surface S of the body.

Case (i): For boundary layer pressure fluctuations the integral in equation (1) can be expressed in terms of the RMS surface pressure fluctuations $\sqrt{\overline{p_i^2}}$, a correlation area S_c, and the curvature at the origin of the autocorrelation coefficient R, so that

$$W = \frac{1}{6\pi\rho a^3}\cdot S\cdot S_c\cdot\overline{p_i^2}\left[\frac{\partial^2 R}{\partial\tau^2}\right]_{\tau=0} \qquad \ldots(2)$$

Since the angular distribution of intensity is that for a dipole (this was confirmed during the tests), the sound pressure at 90° to the plate can be expressed in terms of the total acoustic power. Evaluating the constants, and using experimental results for S_c, $\overline{P_i^2}$, and R, yields for the sound pressure level at 90°,

$$SPL = 60 \log U - 98.5 \text{ db} \quad \ldots(3)$$

where U is the free stream velocity. (All sound pressure levels are expressed in db re. 2×10^{-4} dynes/cm^2).

Case (ii): For this case the relevant parameters can be obtained dimensionally. The acoustic intensity is proportional to the mean square of the acoustic pressure fluctuation $\overline{p^2}$ i.e.

$$I \propto \frac{\overline{p^2}}{\rho a} \quad \ldots(4)$$

The acoustic pressure can be expressed in terms of (ρU^2) with the constant of proportionality generally a function of Reynolds Number, Mach Number, some characteristic dimension of the body, b, and the polar co-ordinate of the observer r, θ, ϕ.

Then $$I \propto f(R_e, M, \frac{b}{r}, \theta, \phi). \frac{\rho U^4}{a} \quad \ldots(5)$$

From energy conservation considerations the intensity would be expected to vary like $1/r^2$. The Mach Number must appear as a multiplier since the intensity must become zero for an incompressible fluid ($a \to \infty$). The general form of M is a power series and it can be shown that the term giving dipole radiation is M^2. The final form is then, assuming axial symmetry and inserting the form of θ for a dipole,

$$I = c.f(R_e) \frac{S \rho U^6}{r^2 a^3} \cdot \cos^2\theta \quad \ldots(6)$$

where the surface area S has been written for b^2.

A similar expression has been derived by Lilley (1961) and it is suggested that the constant, c, is of the order of 10^{-4} and $f(R_e)$ is $(R_e)^{-0.4}$. The expression for sound pressure level is then

$$SPL = 56 \log U - 63.4 \text{ db} \quad \ldots(7)$$

Case (iii): If the incident airstream is turbulent, fluctuations of velocity normal to the aerofoil produce fluctuations in incidence and hence in lift. The pressure in equation (1) may be identified with lift/unit area over the aerofoil and, if the scale of turbulence is larger than or comparable to the chord, this is given by

$$P_i = \tfrac{1}{2} \rho U^2 . a_0 \left(\frac{v'}{U}\right) \quad \ldots(8)$$

where a_0 is the lift curve slope and v' is the perturbation velocity normal to the aerofoil. For small incidences and to a first order approximation it can be shown from equation (8) that

$$\frac{\partial P_i}{\partial t} = \tfrac{1}{2} \rho U . a_0 \left(\frac{\partial v'}{\partial t}\right) \quad \ldots(9)$$

Substituting into equation (1) gives

$$W = \frac{\rho a_0^2}{24\pi d^2} \overline{\left[\int_S U^2 \left(\frac{\partial v'}{\partial t}\right) dS\right]^2} \quad \ldots(10)$$

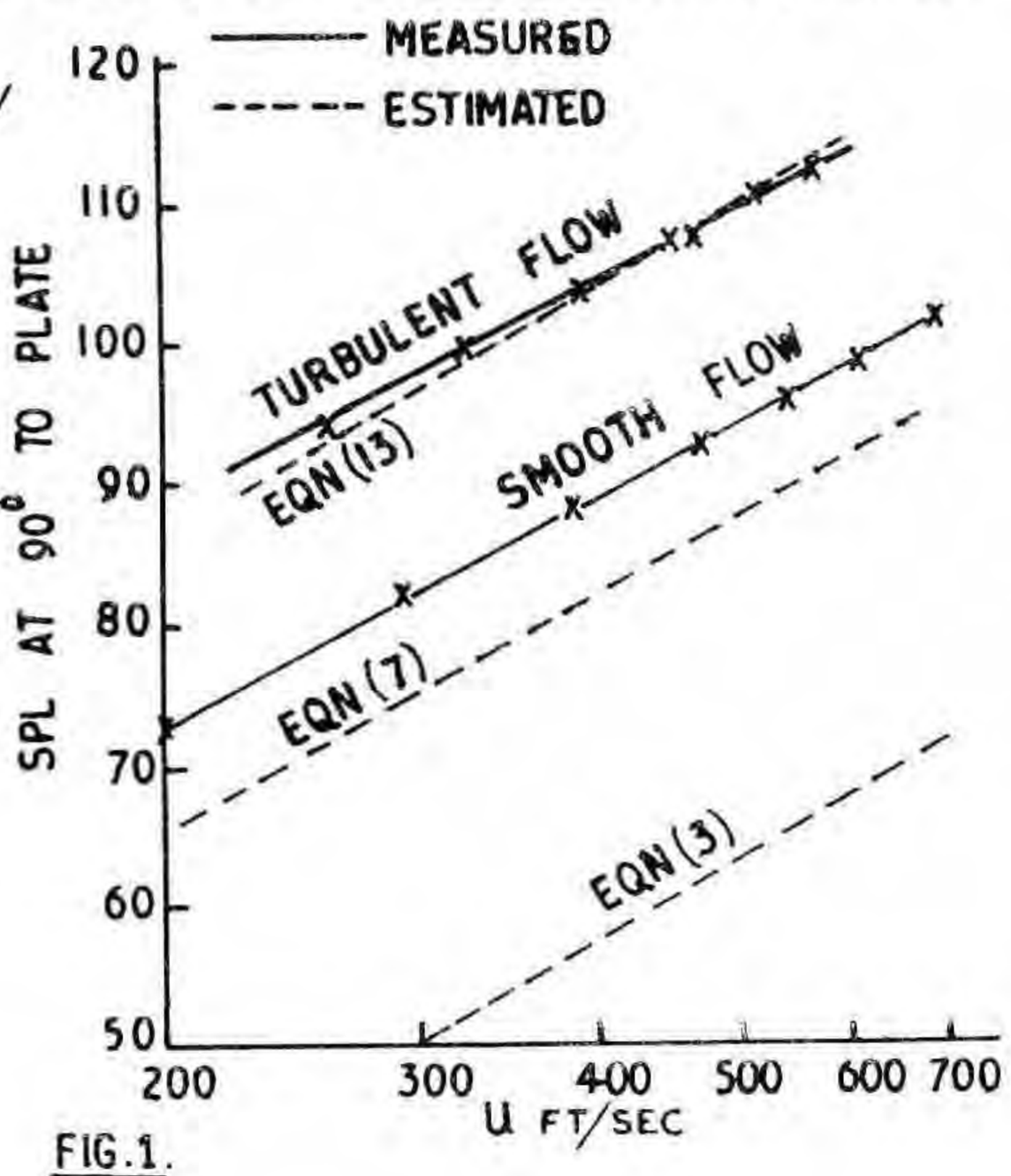

FIG.1.

and this can be written

$$W = \frac{\rho a_0^2}{24\pi a^3} \int_S U^2 \overline{v'^2} S_c \omega^2 dS \quad \ldots(11)$$

The characteristic frequency ω, is of order $U/2\pi l$ where l is some typical turbulence scale, and the correlation area S_c should be of order πl^2. Then

$$W = \frac{\rho a_0^2}{96\pi^2 a^3} \int_S U^6 \left(\frac{\overline{v'^2}}{U^2}\right)^2 dS \quad \ldots(12)$$

The integral in equation (12) was evaluated using typical velocity and turbulence intensity distributions for a circular jet and the sound pressure level is then

$$SPL = 60 \log U - 52.2 \text{ db} \quad \ldots(13)$$

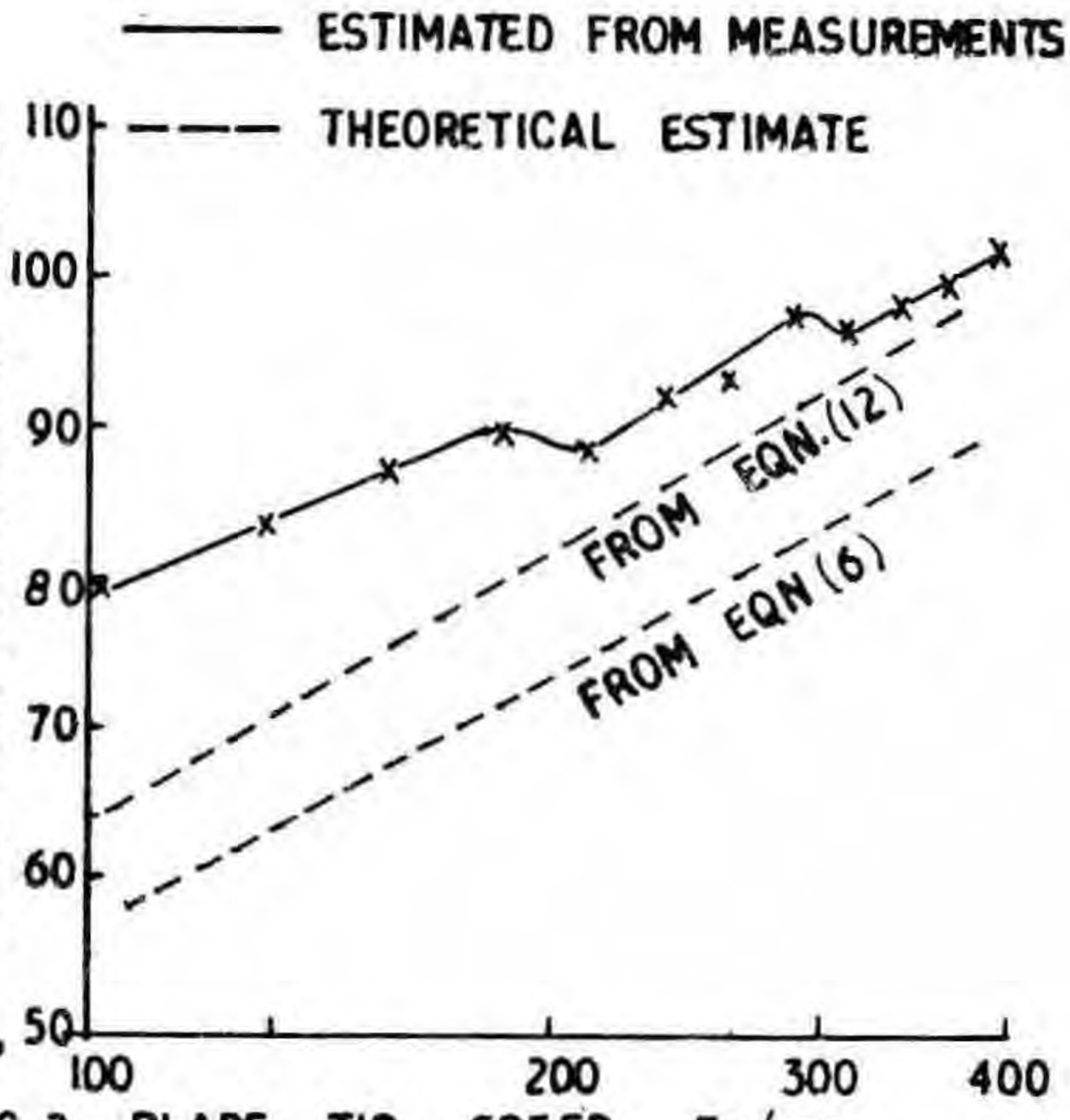

FIG.2.

Noise from single aerofoil: The empirical expressions derived above have been compared with the measured noise from a flat plate in both turbulent and smooth jet flows, and are shown in Fig. 1. The results indicate that for an aerofoil in a smooth flow field the noise radiated is of the same order as that expected from lift fluctuations due to boundary layer effects at the trailing edge. If, however, the flow field is turbulent the noise arising from lift fluctuations set up by the turbulence will dominate. Noise generated by wall pressure fluctuations in a turbulent boundary layer does not appear to be significant. If was confirmed during the tests that the noise of the jet itself was well below the aerofoil noise.

Broad band fan noise: General agreement with the conclusions drawn from the single aerofoil tests was obtained from measurements on the compressor operating with one rotor row and one stator row. The broad band acoustic power was obtained by subtracting the power in the first three harmonics of the discrete noise from the overall power. The variation with fan speed is shown in Fig. 2.

Under ideal conditions the flow would be smooth over all the blade area, but in fact the tips of the blades operate in a turbulent boundary layer on the wall of the fan casing. Using estimated values of the thickness and turbulence intensity in this boundary layer the acoustic power was calculated from equation (12). This result and the power calculated using equation (6) is compared with the measured noise in Fig. 2. If these estimates are of the right order then it appears that even a small area of the blade over which the flow is turbulent can radiate a significant amount of acoustic energy.

Another indication of the effects of airstream turbulence was observed during tests on the fan operating with one rotor row only. When the cascade stalled the overall acoustic power increased by some 10 db, (see Fig. 4) and the spectrum of the noise showed that it was almost entirely broad band noise. This same effect, but to a smaller degree, was observed by Williams and Sharland (1961) when a flat plate was stalled in the smooth flow region of a jet. It seems that the noise increase is a result of increased

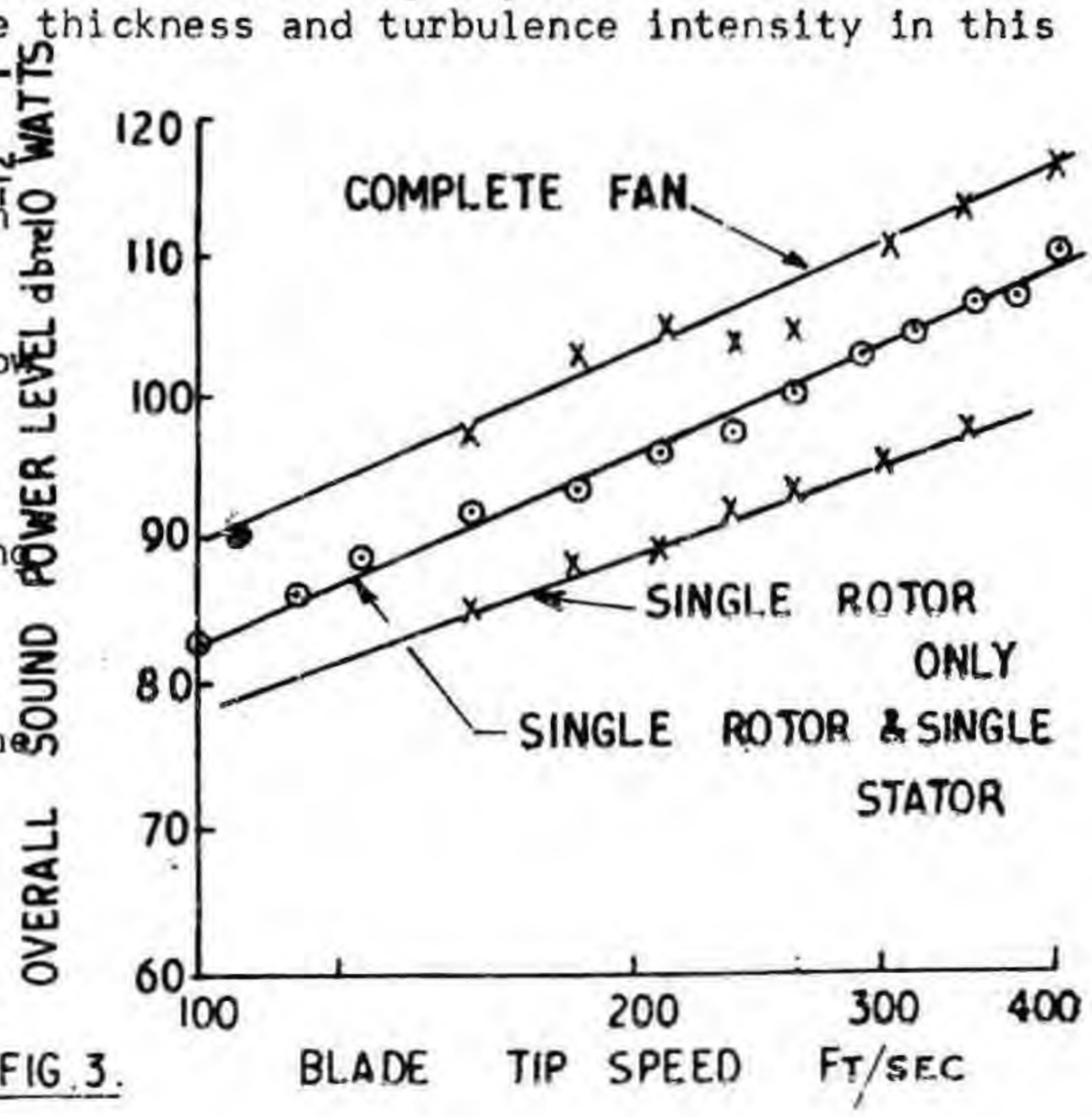

FIG.3.

turbulence over the blade which sets up fluctuating pressures on the blade itself and in the case of the fan rotor, possibly on adjacent blades.

Discrete Frequency Noise

Consider first a single row rotor operating well away from any solid obstacle. In this case discrete frequency noise originates from force fluctuations at a fixed point in the rotor plane which are cuased by the passage of successive blades. This type of noise has been considered in some detail for open running propellers and it has been shown that the fluctuating forces can be replaced by a distribution of dipoles whose strength can be expressed in terms of the torque and thrust on the blades.

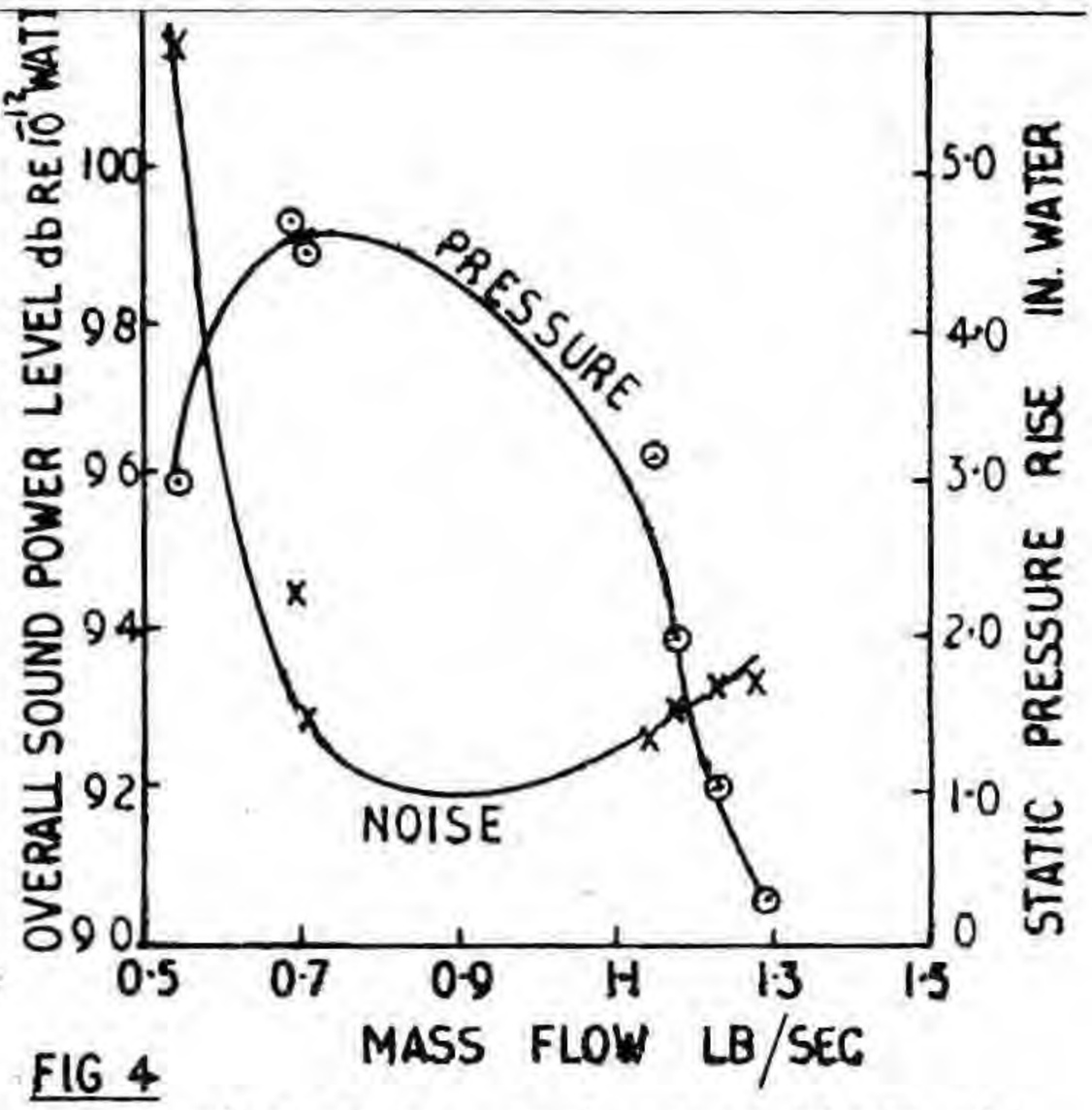

FIG 4

If now a solid obstacle is placed near the rotor the velocity field through which the rotor blades pass will no longer be uniform . In the case of a rotor operating near a row of stators, each rotor blade wil experience a periodic velocity and hence force fluctuation as it passes successive stator blades. Moreover by a similar mechanism the force on each stator blade will vary periodically. These interaction effects may well be a significant source of discrete noise. The frequencies which are radiated have been discussed by Tyler & Sofrin (1961), but the magnitude is much more difficult to analyse.

To obtain some idea of the order of interaction noise, overall sound power levels were measured for the fan with first a single rotor row only and then with one rotor row and a following stator row. The results are shown in Fig. 3, together with a curve for the complete three-stage fan. Taking the lower curve as representative of the propeller noise generated by the single rotor row, the interaction noise due to the addition of a stator row is about 6 db.

The addition of two more stages to the fan produces an increase in noise which is of the order expected on the basis of this result for one stage. These results indicate that interaction noise can make an important contribution to discrete noise, but how this is affected by such parameters as axial blade spacing and blade numbers has yet to be determined.

Returning to the single row rotor, a typical noise and static pressure curve is shown in Fig. 4. The noise decreases slowly with increasing pressure to reach a minimum at some point near the maximum pressure rise and then increases sharply as the blades stall. This minimum noise point has been observed by other authors and generally corresponds to the blade design point.

Summary

From the results obtained so far from experimental investigation into fan noise it is possible to draw the following general conclusions.

Any turbulence over the blade will give a significant increase in broad band noise. Stator blades placed near a rotor will produce an additional component of discrete noise which can be of a higher order than the noise produced by the rotor alone. At a given speed minimum noise is observed near maximum blade efficiency but at mass flows low enough to case the blades to stall a large increase in broad band noise will result.

In the above discussion the emphasis has been on the strength of the various noise sources. The aim of the present research programme which is continuing is to identify these sources with the flow conditions in the fan. When this has been achieved one can look for methods of reducing fan noise at its source.

References: Curle, N.,Proc. Roy. Soc. A231: Lilley, G.M., Private Communication: Tyler, J.M. & Sofrin, T.G., S.A.E. Aero. Meeting: Williams, D.J.M. & Sharland, I.J. Southampton University Aero. Note.

M12

FOURTH INTERNATIONAL CONGRESS ON ACOUSTICS
COPENHAGEN 21.-28. AUGUST 1962

Testing small talks-studios with a simple method intended for diffusion measurements

Juhani Borenius
Finnish Broadcasting Company, Helsinki

The sound field prevailing in a room can roughly be divided into two components, i.e. the free wave from the sound source and the reverberant sound field caused by reflections. The free wave is damped 6 dB for every doubling of the distance from the sound source whereas the reverberant field remains constant independently of place, the better the more diffuse the field is. The qualities of the sound source, only, effect the free wave, whereas the reverberant field is dependent on the qualities of the room, too. Close to the sound source the free wave is prevailing, but farther away from it its role is negligible in comparison to the reverberant field. At the distance of the so called reverbertion radius these components are equally strong. The length of the reverberation radius is proportional to the square root of the total absorption.

In talk recordings the most important criterium of the quality is the clearness and the intelligibility of reproduction. Especially when lectures and discussions are broadcasted, there is a wish to eliminate the acoustical effects of the place of performance, so that the listener gets the impression that the performance takes place in his own home. This is attained by damping the talks-studios heavily and by using a short microphone distance, in other words by placing the microphone inside the reverberation radius. However, it is not desirable to make the studios completely dead since this is unpleasant to the performers. As a suitable reverberation time for talks-studios smaller than 100 m^3 might be regarded 0,3...0,4 sec.

For economical reasons the talks-studios are often made smaller than recommendable acoustically. The result is that normal modes are too few on the fundamental frequencies of speech (100...250 c/s). Few, unevenly spread and weakly damped resonancies cause a hollow tone in the reproduction, which disturbance is increased by the fact that damping does not take place on the fundamental frequency but on the normal frequencies of the room. This phenomenon is called coloration /1/. The loudspeaker resonance of ordinary radio sets often falls on the above mentioned frequency range thus making the situation worse.

For eliminating the unwanted effects of normal modes it is recommended that the reverberation time curve somewhat sinks at lower frequencies. Inspite of this bad

resonancies often are observed in small talks-studios. The average reverberation time thus obviously does not well enough revealall the acoustical defects. Moreover, the measurement of the reverberation time in small rooms at low frequencies is a very problematic task. The reverberation phenomenon as observed with a level recorder is very vague and the spreading of results great.

Measuring methods would have to be invented, with which it would be possible to find out and examine the acoustical defects of talks-studios and other especially heavily damped rooms and their effects on normal microphone distances in different places and directions, and thus to obtain additional information in comparison to ordinary reverberation time measurement. In the following I will comment on a simple measuring method used by the Finnish Broadcasting Co, the idea of which has been received from the diffusion research of the International Broadcasting and Television Organization (OIRT).

The conception diffusion and its measuring have during the last few years aroused vivid interest. Well known are for instance the directional diffusion measurements of Thiele with sharply directed microphones. The method however takes much time and its use is limited to larger halls and medium and high frequencies.

Furduyev has proposed the use of normal microphones having cardioid or "eight" characteristic for diffusion measurements. The principle of this method is shown in fig. 1. The microphone is turned at the measuring point as in a directivity pattern measurement. The received polar pattern is compared with the directivity pattern measured in an anechoic chamber (i. e. in a completely nondiffuse field) and with the pattern received in a completely diffuse field, which, despite of the microphone characteristic, is a circle. Furduyev has also shown an expression based on the areas of the patterns for calculating the degree of diffusion.

When we test heavily damped rooms at short microphone distances using the above mentioned microphone technique, the received polar patterns differ comparatively little from those measured in an anechoic chamber. The greatest level differences can be noted in those directions where the microphone is the least sensitive. Because of this we have done so (fig. 2) that we have measured the output voltage when the microphone is firstly directed towards the sound source (direction x) and secondly turned away from it (directions y-, z and 180°). The corresponding angular deviation losses have been marked with D_y, D_z (eight characteristic) and D_{180^o} (cardioid characteristic). The free wave from the sound source may be regarded in this case as a signal which we try to eliminate with the directional effect of the microphone, so that the interferences caused by the room can be measured.

As the sound source we have used Danavox spherical earphone. Its response range starts from about 100 c/s and its directional effect below 1000 c/s is negligible.

As microphone we have used Neumann KM 56 condenser microphone which has three directivity patterns namely circle, cardioid and figure eight. As measuring sound we have used the 1/3 octave band noise. Because of the nature of the sound the measuring instrument is damped in order to get the angular deviation losses measured within measuring tolerances of $\pm$ 1 dB. The most suitable microphone distance proved to be 0,75... 1 m.

Fig. 3 shows typical measuring results received with microphone having "eight" characteristic at one meter's distance from the sound source. Curve 1 has been measured in the anechoic chamber of the Technical University, curves 2 in a relatively large dramastudio, which is considered acoustically satisfactory (210 m^3, T≈0,6 sec), and curves 3 in a relatively small laboratory room (35 m^3, T≈0,6 sec). The higher D_z value at higher frequencies is most likely caused by the reflection from the floor and the table. In general the angular deviation loss was, measured with the eight characteristic at the distance mentioned above, in satisfactory or good talks studios $\gtrsim$ 10 dB. If the loss was much smaller than 10 dB, the effect of the room is considered too great. The angular deviation loss of the cardioid microphone proved to be too small (about 8 dB) for this purpose at low frequencies.

The number of measurements carried out using this method has been so limited that nothing definitive can so far be said about the importance of angular deviation losses as a criterium of the quality of talks-studios. It is obvious that there is a correlation between angular deviation losses and the reverberation time of the room (especially the quantity $\sqrt{V/T}$). Most likely this method can best be applied in almost dead rooms (anechoic studios), which are not so ideally planned as the anechoic measuring rooms, but the reverberation time of which cannot easily be measured because of its shortness. This measuring method might also be used for studying the bad effects of room resonancies in small rooms at low frequencies. However, this method might hardly be of help in obtaining additional information in comparison to the reverberation time measurements in larger and more reverberant rooms.

Literature: 1. Gilford: The Acoustic Design of Talks-Studios and Listening Rooms, Proc. IEE Vol 106 B p. 245

2. Furduyev and Tchen-Tun: Methods of Measuring Diffusion of Sound Field in Broadcasting and Sound Recording Studios, OIRT Doc TK-II-23/57.

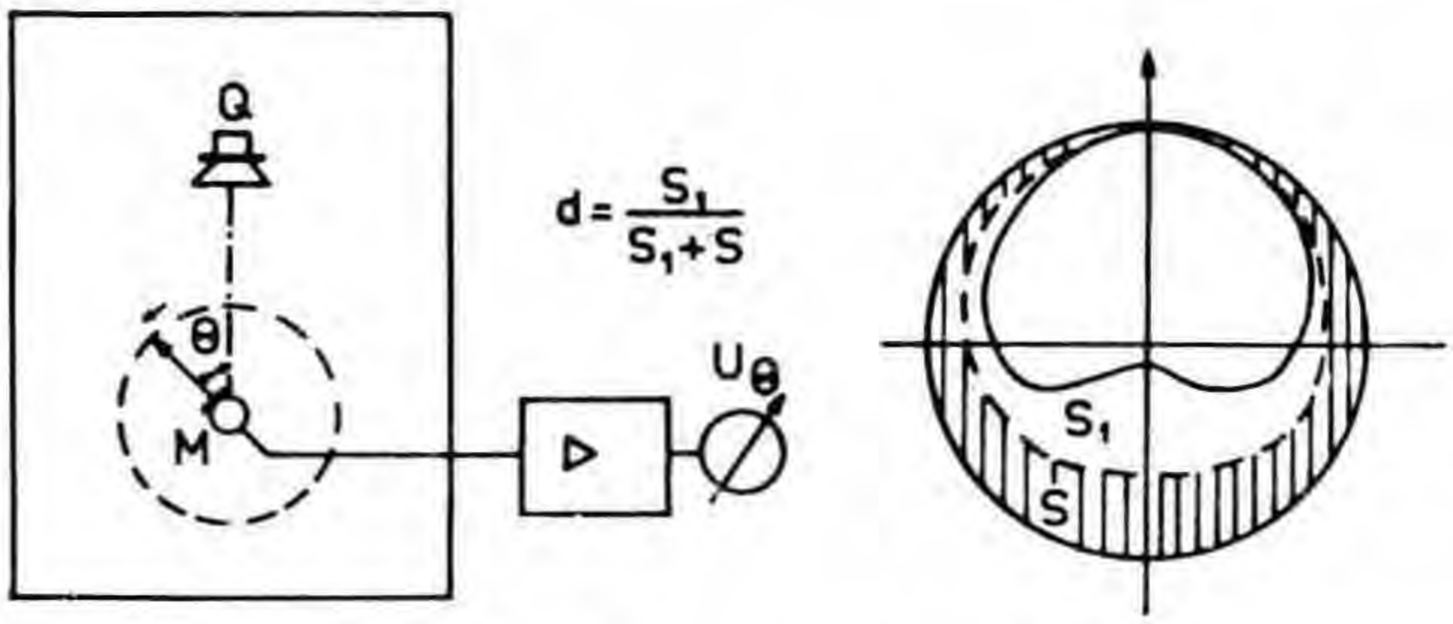

Fig. 1. The method for measuring diffusion proposed by Furduyev

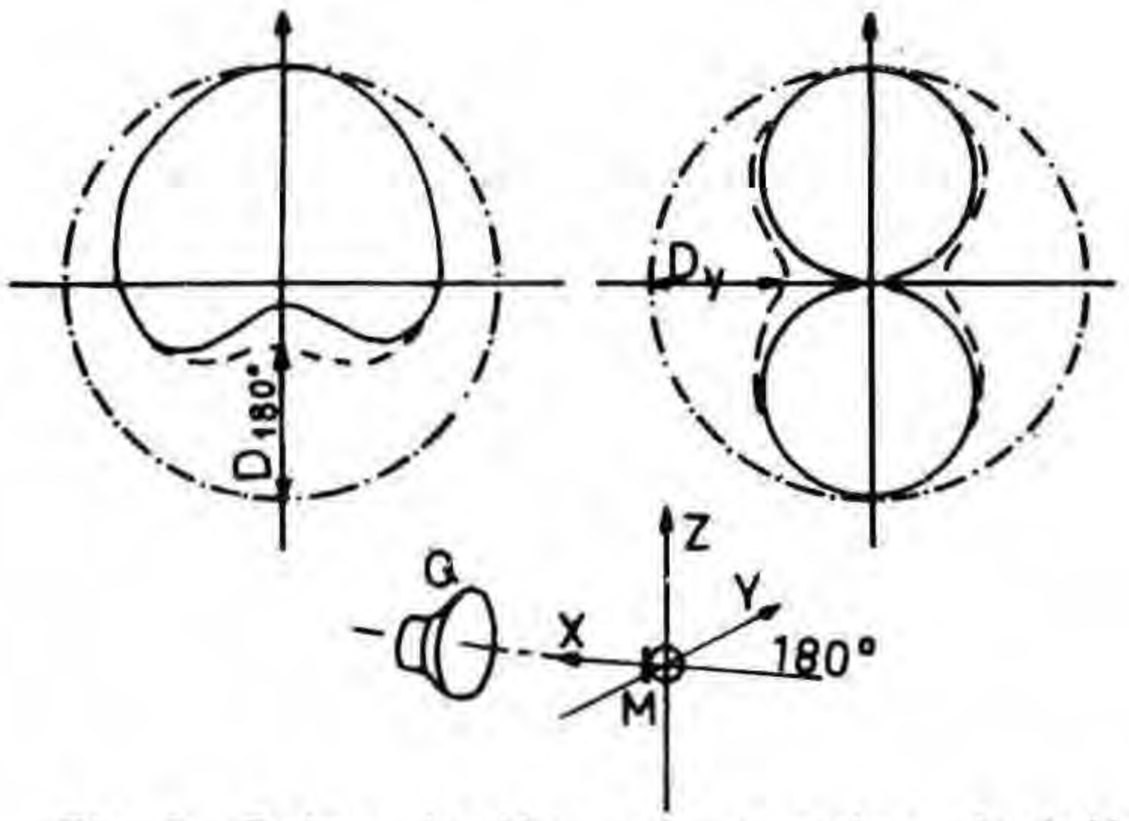

Fig. 2. Determination of angular deviation losses.

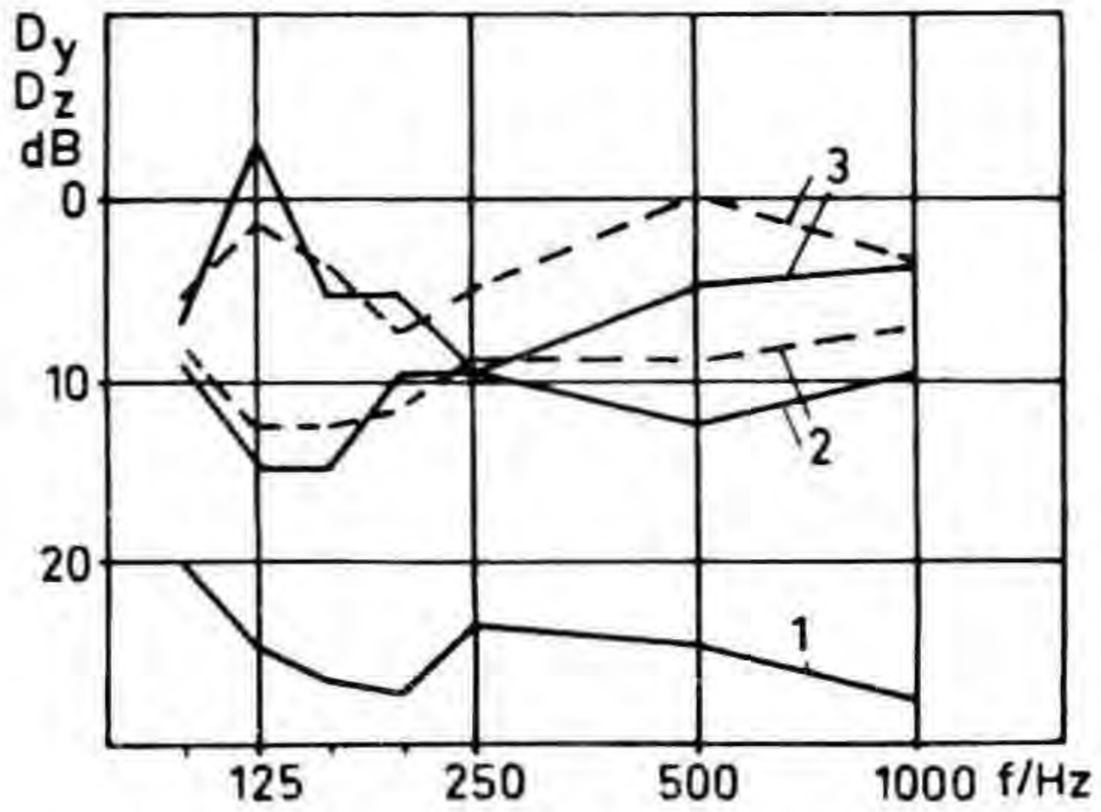

Fig. 3. Augular deviation losses measured in an anechoic chamber (1), in a talks studio (2) and a usual laboratory room (3). D_z is marked with dotted lines.

N12

FOURTH INTERNATIONAL CONGRESS ON ACOUSTICS
COPENHAGEN 21.-28. AUGUST 1962

A.F. Nonlinear Distortion Measurement by Wide Band Noise

Bjarne E. Bang, Electrical Engineer, A/S Brüel & Kjær

In electro-acoustic systems various forms of distortion are present. The nonlinear distortion, which will be discussed in the following, arises from nonlinear characteristics in the transmission system. If a pure sine-wave is applied to the input of the system, the nonlinearity produces harmonics and, additionally, when two or more sine-waves are applied, intermodulation between the signals will result. Usually, the nonlinear distortion is measured using pure sine-wave signals. By this method, however, the sound system is operated under very special circumstances. Therefore it may be more realistic to use a test signal which has a character similar to speech and music. A nonlinear distortion measuring method utilizing a signal of this type is described in the CCITT Livre Rouge Tome IV, page 189. In this paper it is suggested that a statistical signal (white noise) be used as test signal. A white noise signal can be considered as a signal containing an infinite number of sine-waves within its band, the magnitudes of which are statistically distributed. A white noise signal often used in measurements to simulate among other things speech and music, has a Gaussian (normal) magnitude distribution.

Applying a white noise signal U_n to a system containing nonlinearities, a new noise signal U_{n2} can arise on the output of the system in combination with the transmitted signal U'_n. Fig. 1. It is produced from the harmonics as well as from the combination signals (mixing products). The level and spectrum density will depend on the degree and character of the system nonlinearities. This effect can be utilized in nonlinear distortion measurements. To be able to measure the signal U_{n2} produced by the nonlinearities it is necessary to introduce a band-stop Δf in the input noise signal. Fig.2. The signal level U_{n2} produced within this band-stop can then be measured at the output of the system under test by a selective indicator having a band-pass with center frequency f_o and width Δf equal to that of the band-stop.

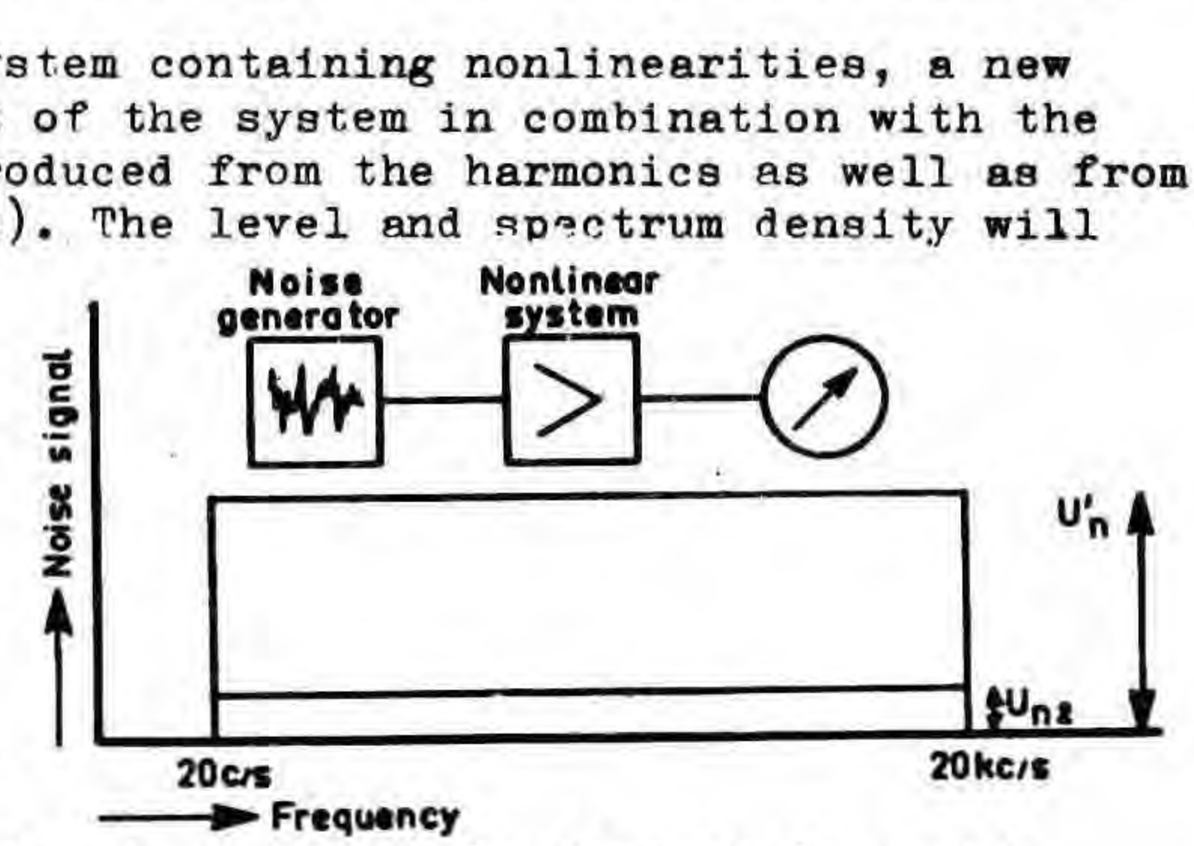

Fig.1. The signals derived from wide band noise U_n transmitted through a system containing nonlinearities.

The principle, using ideal filters, is illustrated in fig.2. In practice, the band-stop and band-pass filters will have a more or less steep slope and will not show zero an infinite attenuation outside the stop band and the pass band respectively. These properties determine the limit of the noise measuring method.

The effective bandwidth Δf of the band-stop filter should be narrow compared to the effective bandwidth F of the system under investigation. The attenuation required at the "stop-bandwidth" depends on the degree of distortion which has to be measured. By "stop-bandwidth" is here meant the bandwidth Δf of the band-stop filter where it equals the effective bandwidth Δf of the following band-pass filter. In the measurements discussed later the attenuation at the stop-band limits was 13 dB approximately.
The bandwidth Δf of the band-pass filter should as mentioned be as narrow as the width of the stop-band Δf of the band-stop filter. A filter which is even narrower, i.e. only a part of Δf can also be used. The attenuation at all frequencies

well away from the pass-band should be high. It should in any case be higher than the difference in wide band noise level U'_n (F) to narrow band noise level U'_n (Δf). In practical measurements there is also a limit to how narrow the band-pass can be. For a filter only a few cycles wide the integration time of the associated indicating meter has to be inconveniently long. For a filter more than

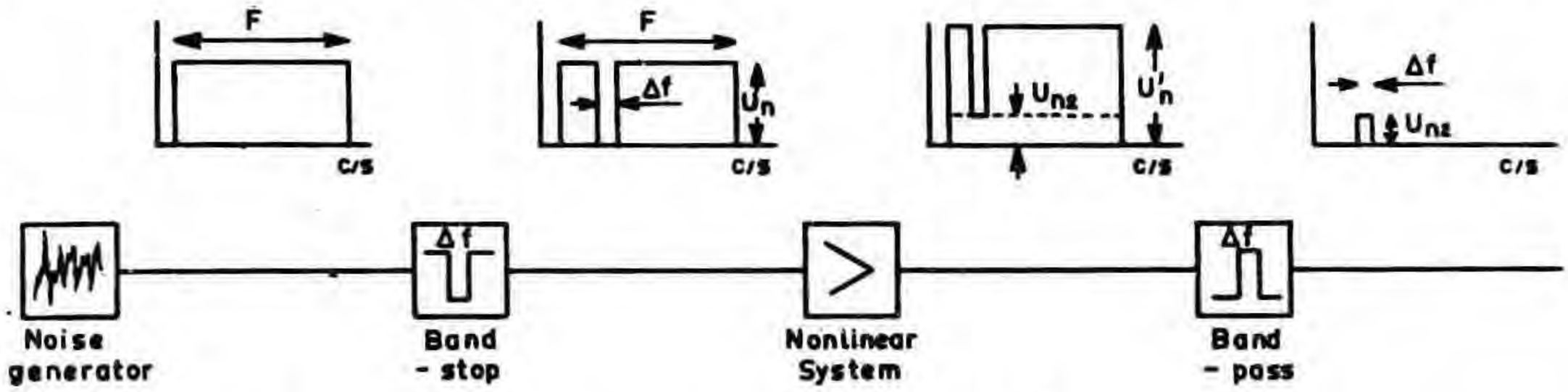

Fig.2. Principle of measuring nonlinear distortion by wide band noise.

10 c/s wide the integration time, suggested for Precision Sound Level Meters (I.E.C. Helsinki 1961), will in many cases suffice.
The measurements can be carried out using a few pairs of filters with fixed center frequency, or better, the two filters can be continuously variable. A refinement would be if the band-stop and band-pass filters could be scanned in synchronism with each other through the complete frequency range. In combination with a level recorder the measurements could in this manner be carried out automatically. Two filter types can be considered, viz. filters showing constant absolute bandwidth (heterodyne filters) or filters with constant percentage bandwidth. In both instances the signal U_{n2} produced by the system nonlinearities have to be measured in relation to the complete signal $U'_n + U_{n2}$ which has passed the system, thus containing both the original U'_n and the produced signal U_{n2}. Using a filter with constant absolute bandwidth the complete signal $U'_n + U_{n2}$ can be measured either by a wide band indicator or by a narrow band indicator. With this measuring arrangement no "frequency compensation" is necessary in either case. For filters showing constant percentage bandwidth the ratio will depend on frequency when the signal $U'_n + U_{n2}$ is measured by a wide band indicator, as the signal level of the produced signal U_{n2} will increase by 3 dB/octave increasing frequency when measured by such a filter. If, on the other hand, $U'_n + U_{n2}$ is also measured by the narrow band indicator with center-frequency f_o equal to that of the band-stop filter, this signal level will additionally increase by 3 dB/octave, making the measured ratio independent of frequency. Utilizing the latter method, the band-stop filter has to be taken out of circuit during the selective measurement of the signal $U'_n + U_{n2}$.

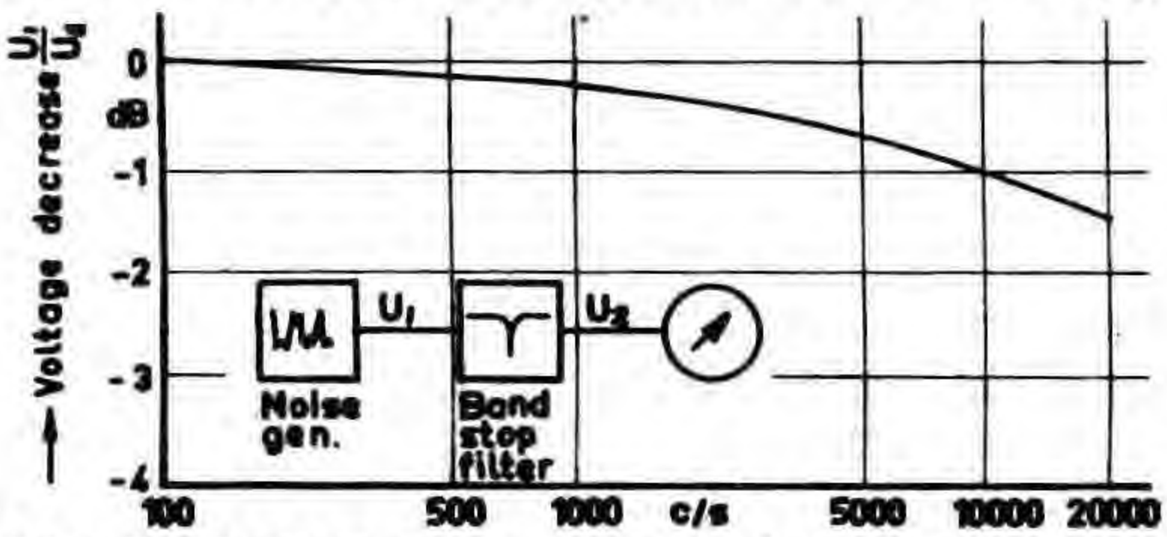

Fig.3. Decrease in r.m.s. level of wide band noise caused by inserting a band-stop filter.

Practical Measurements

Since, to the author's knowledge, no special equipment is available commercially, an equipment was devised using standard electro-acoustic measuring instruments, i.e.

Random noise generator, giving uniform spectrum density (white noise) with Gaussian distribution in the frequency range 20 c/s - 20 kc/s.
Band-stop (rejection) filter. 20 c/s - 20 kc/s continuously variable, having constant percentage bandwidth.

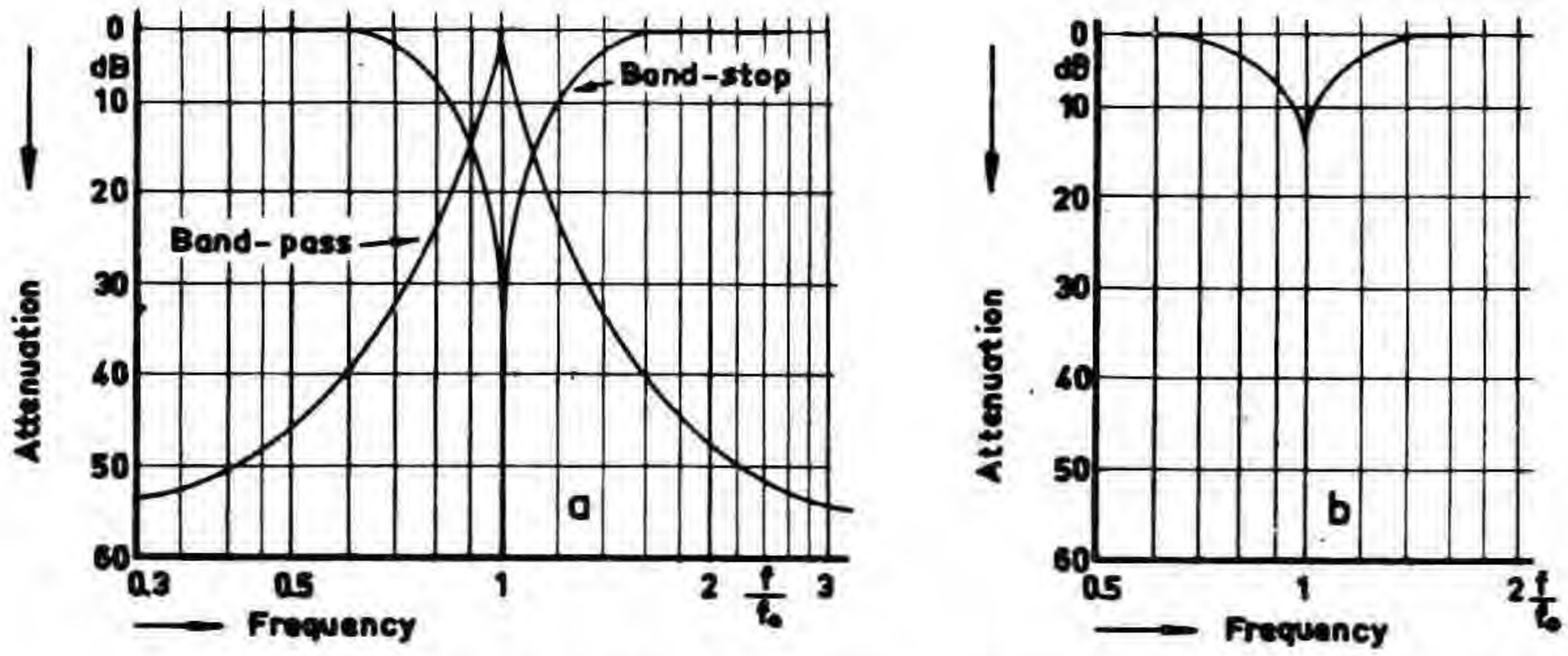

Fig.4. a. Amplitude versus frequency characteristics of band-stop and band-pass filters as measured by sine wave.
b. Band-stop filter's frequency characteristic measured via the band-pass filter and using a white noise signal.

Band-pass filter, 20 c/s - 20 kc/s continuously variable, having a 3 dB constant percentage bandwidth of 6%.
Indicating meter, 2 c/s - 40 kc/s measuring r.m.s.

Firstly, the capability of the instrumentation was checked. A filter had to be chosen which would not extract too much energy from the effective white noise signal. After investigating various band-stop filters, sometimes using two units in cascade, it was decided to employ a single filter having an effect as shown in fig.3. The filter was later found to give a ratio $U'_n + U_{n2}$ to U_{n2} of about 13 dB. Fig.4b. Its frequency characteristic compared with the band-stop filter was as illustrated in fig. 4a.

Some distortion measurements were carried out on a hearing aid. The measuring arrangement used can be seen in fig.5. The noise generator supplies a white noise signal to the band-stop filter and further to a loudspeaker via an amplifier. Therefore, it was placed in a special hearing aid test box ensuring reflexion-free transmission from loudspeaker to hearing aid microphone. The ear piece was placed in an artificial ear, the output of which was fed to the band-pass filter via an amplifier. Finally, the various levels were measured by an r.m.s. indicating meter.
For the sake of comparison, the distortion as a function of frequency was measured first by sine-wave for input sound pressure levels of both 60 and 70 dB at the hearing aid microphone. Fig.6. Note the increase in distortion at 1500 c/s. For the measurements using noise the sound pressure level was adjusted to a wide band

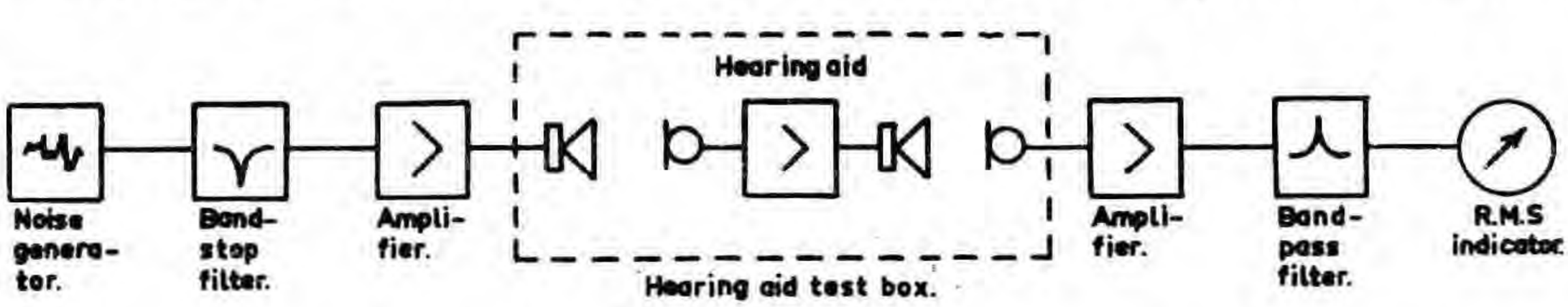

Fig.5. Arrangement for nonlinear distortion measurement on a hearing aid by using a wide band noise signal.

input level U_n of 60 dB and 70 dB respectively. As constant percentage bandwidth filters are used, the complete signal $U'_n + U_{n2}$ was measured selectively by the band-pass filter and with the band-stop filter out of circuit. The ratio, complete signal $U'_n + U_{n2}$ to produced signal U_{n2} is expressed in dB, derived from

the expression

$$2o \log \frac{\sqrt{U'_n{}^2 + U_{n2}{}^2}}{U_{n2}} \text{ dB}$$

From the curve in fig.6 it can be seen that at 6o dB sound pressure level and high frequencies the ratio tends towards 13 dB, which was found earlier to be the highest ratio measurable by the equipment used. At 7o dB level and towards the lower frequencies the ratio reaches 0 dB. As 0 dB is the lowest ratio measurable by this principle ($U'_n + U_{n2}$ measured selectively by the band-pass filter) a limit of maximum distortion measured by this equipment is attained. A great difference in the results obtained by the sine-wave measuring method and the noise method is noted at high frequencies for both sound pressure levels. The sine-wave method shows a large increase in distortion at 15oo c/s whereas the noise method tends to decrease. The reason for this difference may be that the noise peaks which are able to excite the possible resonance at 15oo c/s, have a much lower energy level than does the distinct sine-wave used during the sine-wave measurement. If the bandwidth of the noise is assumed to be in the order of say ± loo c/s, the r.m.s. level within this narrow band compared to the r.m.s. level U'_n of the effective bandwidth F of the hearing aid, will be:

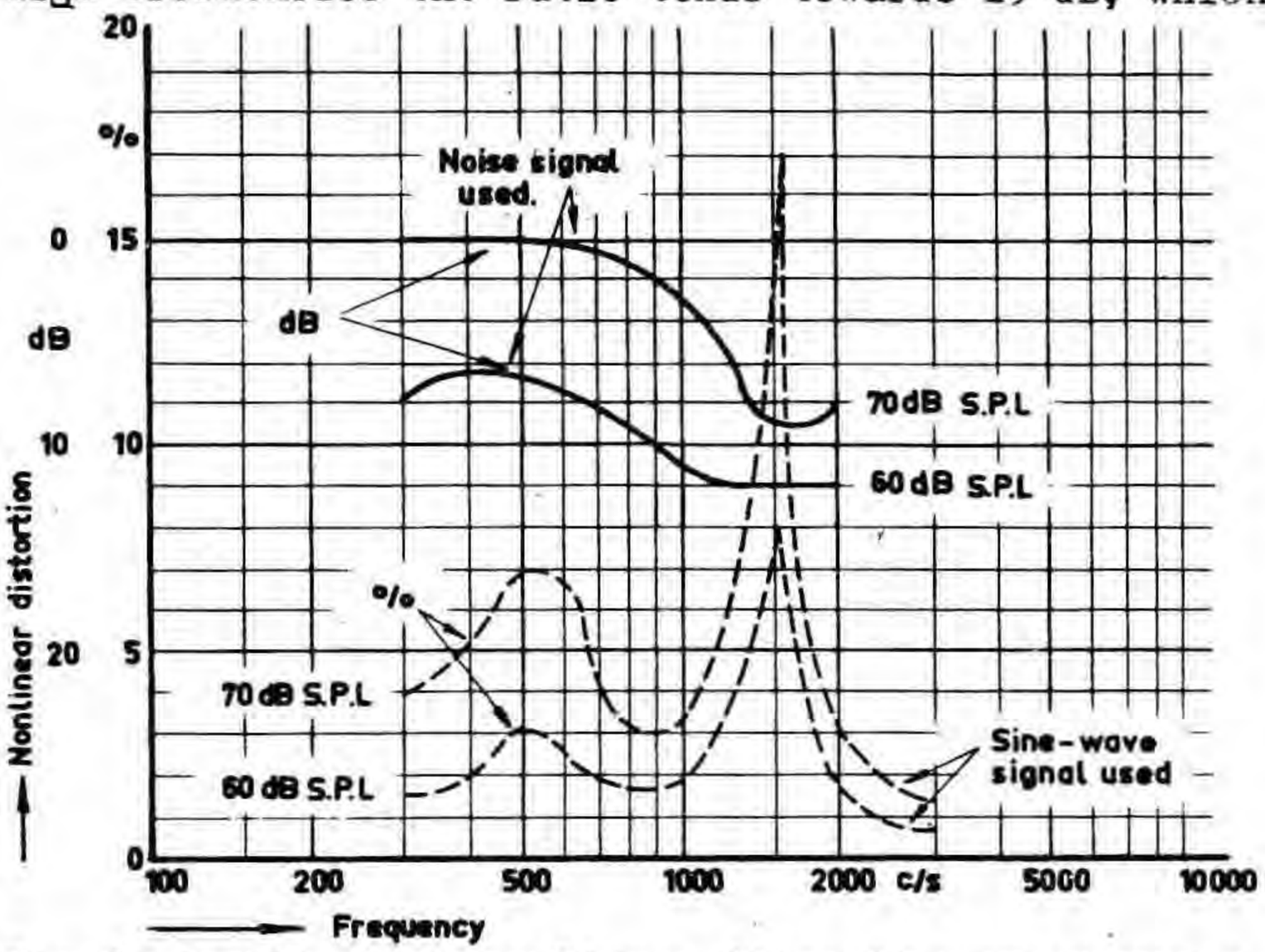

Fig.6. Results from nonlinear distortion measurement on a hearing aid. Test signals: noise (full lines), sine wave (dashed lines).

$$\sqrt{\frac{F}{\Delta f}} = \sqrt{\frac{3ooo}{2oo}} = 4 \text{ times} \sim 12 \text{ dB lower}$$

F = 3ooo c/s approx.

Accordingly, the produced signal U_{n2} will also be of a low value, thus making the ratio $\frac{\sqrt{U'_n{}^2 + U'_{n2}{}^2}}{U_{n2}}$ high. Note that both $U'_n + U_{n2}$ and U_{n2} are measured via the band-pass filter (Δf).

The measurements show that by using wide band random noise together with the discussed instrumentation it is possible to obtain data illustrating the nonlinear distortion in sound systems, though within certain limits. In the first instance the obtained data have to be interpreted from subjective investigations as the system, for which the described measuring method is intended, is used for sound transmission. With experience it can be established if a system showing a particular amount of distortion expressed in per cent. or, as in the examples, in dB, exhibits low or high subjective nonlinear distortion. The distortion measuring method discussed here is in some countries used on multi channel telecommunication equipment. The reason why the method is not widely used for more simple electro acoustic systems may be that commercial filters with adequate data have not been available.

Bibliography:
Comité Consultatif International Télégraphique et Téléphonique (C.C.I.T.T.)
Livre Rouge Tome IV.
Lennart Brandqvist: Ny metod för mätning av förvrängning vid ljudåtergivning.
RADIO OCH TELEVISION - Nr. 8 - 1958.
W. Reichardt: Grundlagen der Elektroakustik

O12

FOURTH INTERNATIONAL CONGRESS ON ACOUSTICS
COPENHAGEN 21.-28. AUGUST 1962

DETERMINATION OF ZONES SUBJECT TO METEOROLOGICAL FOCUSING

Richard N. Tedrick

Several authors[1,2,3] have shown that acoustic energy propagating away from the earth's surface through the atmosphere can, under specified circumstances, be refracted (bent) back toward the ground. In the past, this effect has rarely been of interest because of the limited signal strengths which it was possible to sustain over appreciable periods. However, since the development of the large rocket engine, this refractive effect has assumed greater importance, especially in the civilian areas surrounding the test sites for such large rocket engines.[4]

The acoustical focusing problem posed by the static test firing of the Saturn booster is greater because of the proximity of the city of Huntsville, Alabama. The city is on the north and east boundaries of Redstone Arsenal about 5 to 12 miles from the Saturn Test Tower.

Meteorologically, the MSFC-Huntsville area is dominated by a general westerly-southwesterly prevailing wind pattern. During the winter months, this pattern intensifies and is quite often accompanied by a strong surface temperature inversion. This causes the acoustic velocity profile along the azimuth toward the city to assume proportions similar to FIGURE 1. Such profiles do not occur every day, nor do they often last more than a few hours. Nevertheless, examination of the past meteorological data shows that such focusing conditions may exist for varying lengths of time during any season or month.

In order to consider the path of propagation of acoustic energy, it is convenient to utilize the concept of the "ray", i.e., an infinitely small segment of the acoustical wave front which, because of its incremental dimensions, can be mathematically treated in the same way as the light ray in optics. Not only does this device enable the acoustician to simplify his computational procedures, but by relating the convergence or divergence of the rays to the normally-assumed sperical radiation, he can approximate the gain or loss in signal strength due to such refraction.

Snell's Law, when applied to acoustical energy traveling through a horizontally-stratified atmosphere where each layer of such an atmosphere contains a constant velocity gradient, takes the form:

$$\cos\theta = \frac{C}{C_{max}}; \quad C_{max} = \frac{C}{\cos\theta} \qquad (1)$$

θ is the angle which the ray makes with the horizontal at the altitude where the velocity of sound along the path of propagation is C. C_{max} is the acoustic velocity at the altitude where the ray path is horizontal.

Equation 1 states that if the attitude (angle from the horizontal) and the velocity of sound at some given altitude is known, the attitude of the ray may be calculated from every height where the velocity of sounds is known. Thus, all that

is needed to trace the path of a sound ray as it moves through the atmosphere is the acoustic velocity profile and one measured or defined angle. If one is interested in certain well-defined boundary conditions where (by definition) the attitude is known, then it is possible to determine the ray paths defined by those conditions. The intersection of these ray paths with the earth surface will define the boundaries of the intersection of the entire acoustic wave front with the ground.

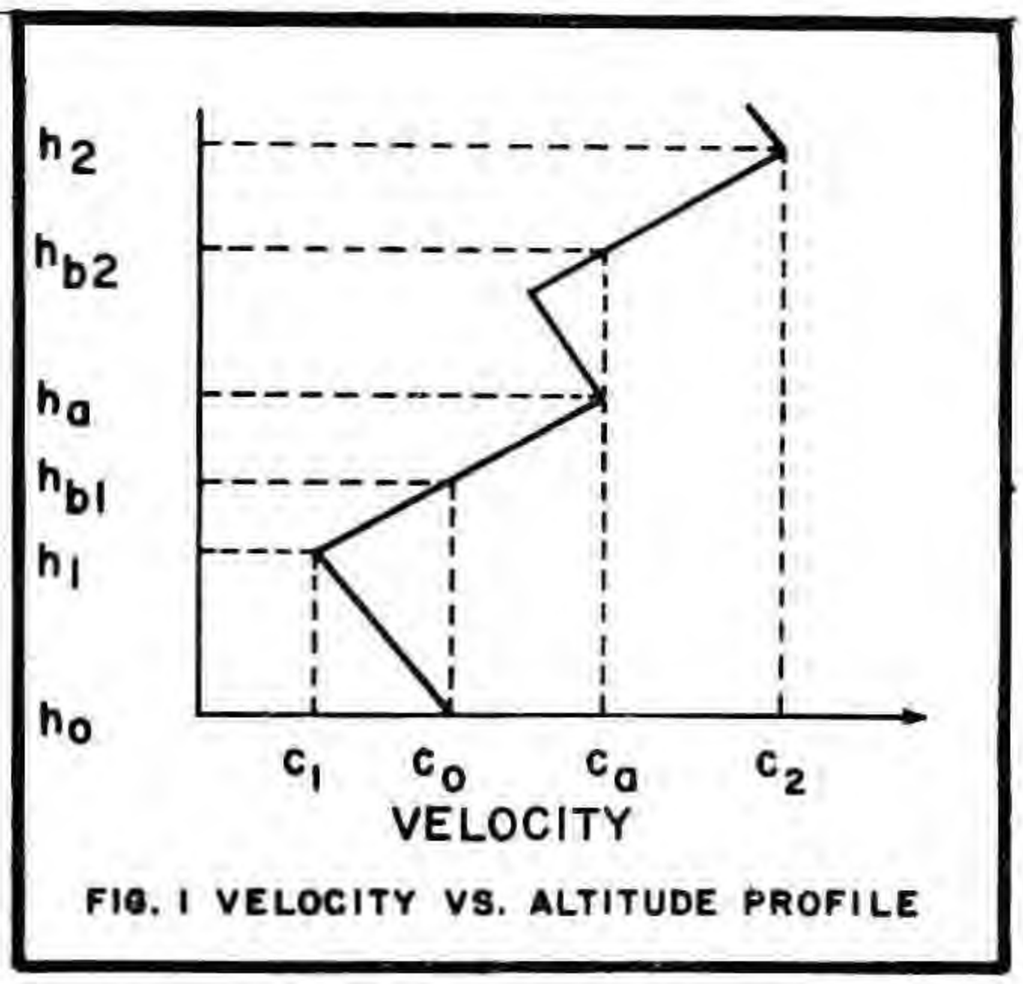

FIG. 1 VELOCITY VS. ALTITUDE PROFILE

The aforementioned problem here is one of locating the boundaries of one or more zones which may be subjected to focusing the acoustic energy. These boundary conditions may be defined within the accuracy limits placed upon the problem by the meteorological data acquisition techniques. The boundaries may be considered to be determined by two angles; the minimum and the maximum angles with which energy can originate at the source and be refracted back to earth in a single continuous wave. If there are several waves (or more precisely, several portions of the same acoustic front) which return to earth, a corresponding rise occurs in the number of boundaries to be calculated.

The velocity profile may be assumed to follow the general pattern shown in FIGURE 1 in those cases in which focusing is important. Of course, this pattern may vary or may be composed of a number of smaller layers which follow the general trend of FIGURE 1. In some cases the altitude, h_1, may be zero.

Assuming an acoustic source at the surface, the lowest possible angle of transmission is zero degrees. Because an acoustic front bends toward the lower velocity end of any gradient when C_1 is less than C_o, this grazing ray will curve upward. At height h_1, the velocity of sound is C_1 and the attitude of the ray may be expressed:

$$\cos \theta = C_1/C_{max} \qquad (2)$$

However, for this ray, C_{max} is equal to C_o since the sound travels horizontally at the surface. Equation 2 then becomes:

$$\cos \theta = C_1/C_o \qquad (3)$$

It may be seen that at height, h_b, where C is equal to C_o, cos θ equals unity, therefore, the boundary ray has been bent to the horizontal. Since any increment of positive gradient above the level, h_b, would cause the cosine to be greater than one, h_{b1} may be considered as the zenith altitude of one of the boundary rays.

In a layer of thickness, h, bounded by velocities C_n and C_{n+1} and containing a constant velocity gradient, the ray path follows an arc of a circle e which is subtended by the angles θ_n and θ_{n+1} as shown in FIGURE 2. The horizontal distance X, traversed by the sound in the layer is given by the equation:

$$X = \frac{h}{\tan \frac{\theta_n + \theta_{n+1}}{2}} \qquad (4)$$

Since, assuming a horizontally-stratified atmosphere, the acoustic ray passes twice through each layer, the horizontal distance, R, from the source to the reincident point is equal to twice the summation of X.

$$R = 2 \sum_{c=0}^{C=C_{max}} X \qquad (5)$$

Another boundary of the reincident energy zone may be found by considering the maximum angle of transmission which can result in energy being refracted back to earth. This will occur to the ray which is horizontal to the maximum velocity. Equation 1, for the condition in FIGURE 1, then becomes:

$$\cos \theta_o = \frac{C_o}{C_2}$$

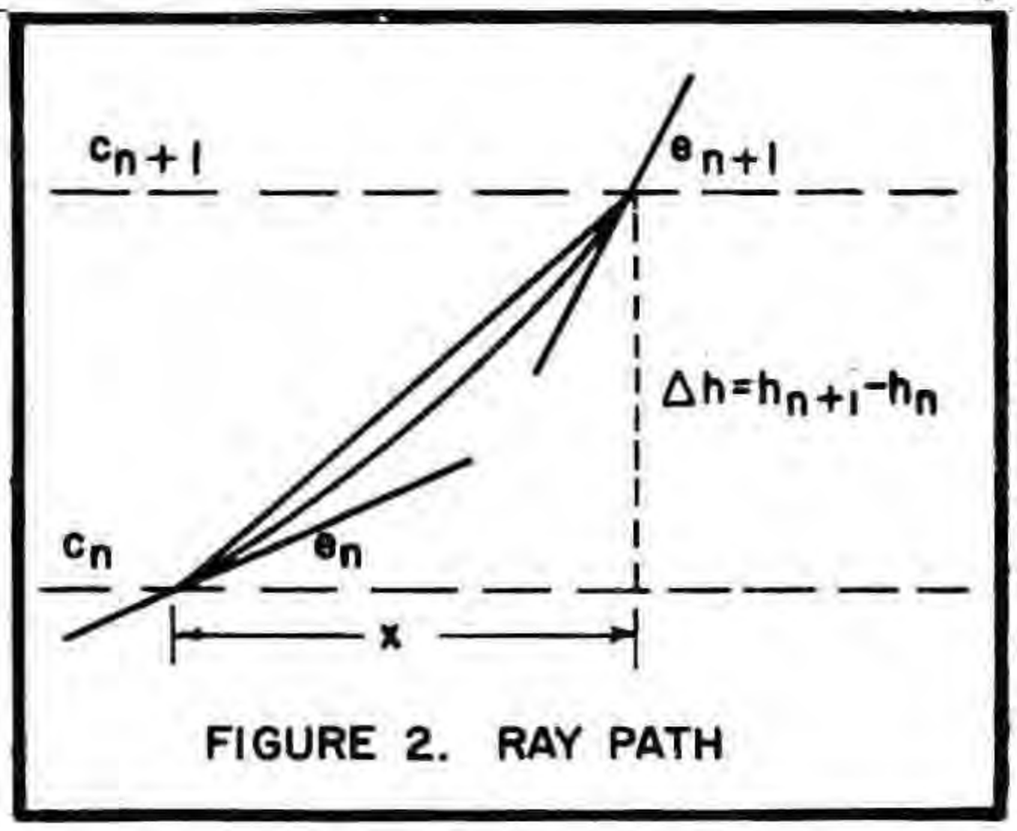

FIGURE 2. RAY PATH

Using this new value of θ_o in Equations 4 and 5, R is calculated in the same way as above.

The atmosphere sometimes becomes fairly complex and the resulting acoustic velocity profiles then may contain several local maxima and minima below the over-all maximum. By definition, a maximum point on the sound velocity profile is one where, above and below it in altitude, the velocity is less than at that point, or put another way, any level which has a positive gradient beneath and a negative gradient above. Since the negative gradient will bend the sound upward while the positive gradient bends it down, there will result a dead zone from that altitude to some point on the ground.

Significant levels are those altitudes at which occur the above-mentioned maxima and minima. With the exception of the over-all maximum, for each local maximum there is some altitude above it at which the velocity equals that local maximum. This is a boundary level. There is a radius, R, to be calculated for each maximum and each boundary level. Thus, in FIGURE 1, there would be two reincident focal zones; one bounded by the values of R, calculated for heights h_{b1} and h_a, the other by values of R for heights h_{b2} and h_2.

Up to this point, it has been assumed that the velocity profile is known. Usually the only informational input is from radiosonde data. This gives, in tabular form, the temperature, T, and the wind speed, V, and direction, oc, as functions of altitude, H, above mean sea level.

Since the wind is a vectorial quantity, the effect of the wind upon the velocity of sound propagation is affected by the wind direction α, and the azimuth, β, along which the various R's will be calculated. If γ is defined as the angle between α and β then:

$$C = 1052 + 1.106T + 1.467V \cos \gamma ,$$

where V is in miles per hour, T in degrees Fahrenheit, and C in feet per second.

If γ is less than 90 degrees, then the sign of V cos is negative.

Thus, because the wind changes direction with altitude, the acoustic velocity profiles vary with azimuth and the values of R must be recalculated for each azimuth of interest.

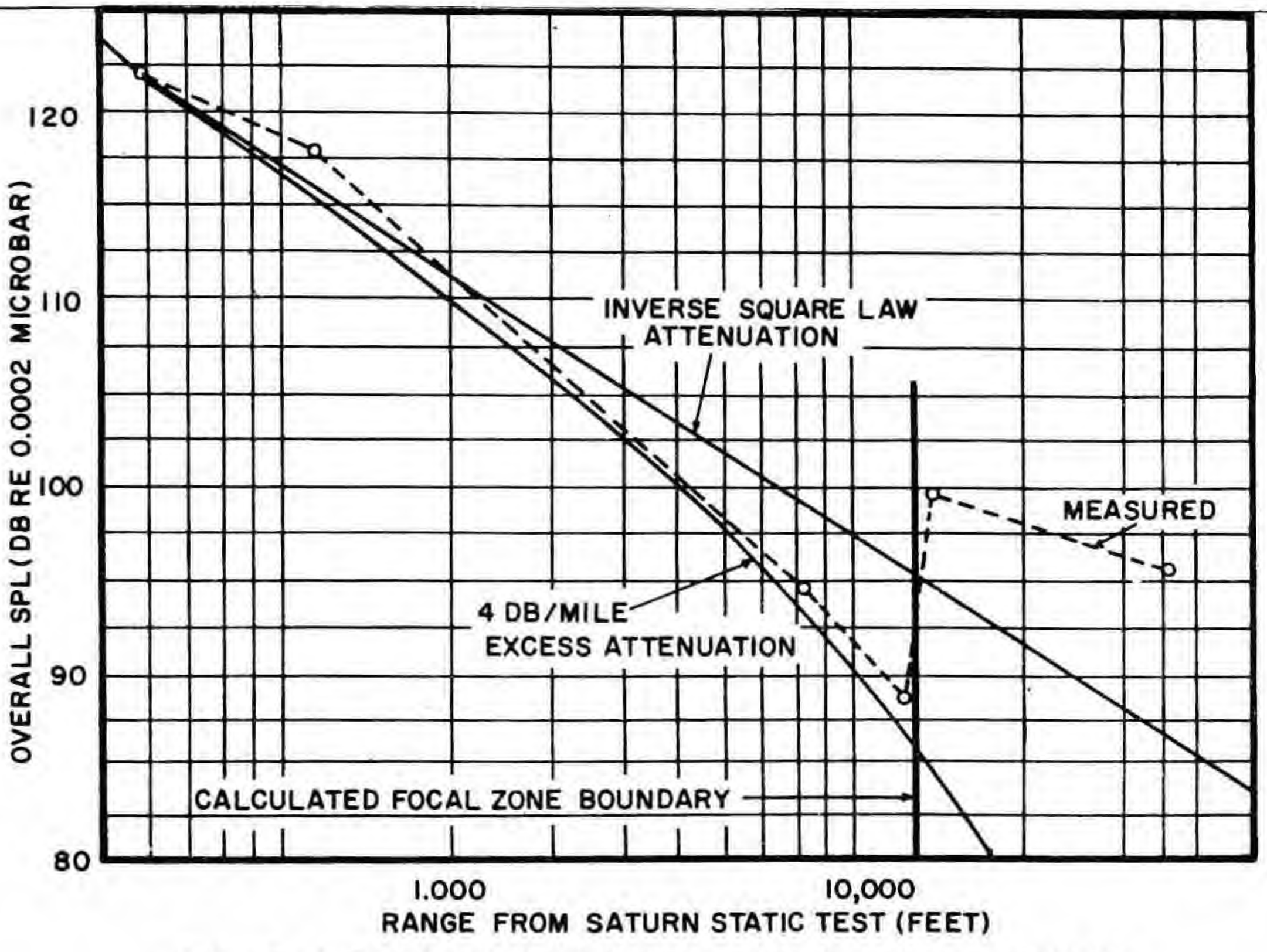

FIG. 3 VARIATION OF SOUND LEVELS UPON ENTRY TO FOCAL AREA, HUNTSVILLE, ALA., DEC. 10, 1960

To better judge the effects of meteorological focusing, MSFC personnel were assigned to monitor various locations with sound-level measuring equipment during test periods.[5] The results of one of these measurements are shown in FIGURE 3. As can be seen from the example, the measurements generally agreed with the predicted focal area and resulted in rises of between 20 and 30 decibels over those normally expected

REFERENCES

1. Perkins, Beauregard Jr., et al, "Forecasting the Focus of Air Blasts Due to Meteorological Conditions in the Lower Atmosphere", BRL Report 1118, Aberdeen Proving Ground, October 1960.

2. Cox, Everett F., et al, "Meteorology Directs Where Blast Will Strike", Bull of American Meteorology Society, Vol. 35, pp 95 - 103, 1954.

3. Barnes, Thomas G., "Velocity Gradient Method of Ray Tracing in the Atmosphere", Schellenger Research Foundation, August 1956.

4. Tedrick, Richard N. and Dorland, Wade D., "Anticipated RMS Sound Levels Around Static Tests of Large Vehicles", NASA-Marshall, MTP-61-20, November, 1961.

5. Tedrick, Richard N., "Acoustic Focal Zones Around Saturn Static Tests", NASA-Marshall, MTP-61-21, December 1961.

P12

FOURTH INTERNATIONAL CONGRESS ON ACOUSTICS
COPENHAGEN 21.-28. AUGUST 1962

Audio-Frequency Compliances of Prestressed Quartz, Fused Silica, and Aluminum

Martin Greenspan and Carl Tschiegg
National Bureau of Standards, Washington, D. C.

I. Introduction

According to E.R. Fitzgerald,[1] the dynamic shear compliances of many crystalline materials exhibit resonance dispersion in the range 100 to 5000 cps. The resonances are observed in the presence of static stress, either residual, or resulting from an external load.

The measured compliances conform to a simple equivalent circuit. Corresponding to each resonance peak, i, of which there may be a dozen or more, there is in parallel with the ordinary (static or ultrasonic) compliance s_o, a simple series m_i, s_i, R_i-chain. Thus if we examine the total compliance s beginning at high frequencies ($s = s_o$), then each time we pass through a resonance, the compliance increases by the corresponding s_i. In Fitzgerald's experiments on fused silica[2], for instance, the total shear compliance in the 100 to 1000 cps region is in the range 20 to 40 (in one case, about 85) times the ordinary compliance, s_o. The origin of the excess compliances s_i, the effective masses per unit length m_i, and the losses R_i, is supposed to be connected with the existence of slip planes induced by the static stress; the details are given by Fitzgerald[1]. The dynamic compliance in question is that on a pair of axes of which one is normal to the slip plane and the other is in the slip plane along the direction of slip.

Fitzgerald's method of measurement employs two disk-like specimens each about 6mm in diameter and some 2 to 5mm thick, pressed against a large mass. This pressure, which is necessary to hold the specimens in place, is also the source of the static stress responsible for the effects in question. The specimens are very stiff, so that it is possible that they resonate parts of the massive apparatus at audio frequencies. To circumvent this difficulty, if it be one, we undertook the measurements to be described.

II. Experimental method

The specimen consists of a clamped-free beam (reed) with dimensions such that the first three modes of vibration are in the range of frequencies desired. It consists of a duplex +5° LR X-cut quartz bender with a sheet of the test material cemented to each broad face. The static stresses are thermal in origin and can be varied by change of temperature; piezoelectric stressing can also be used.

The compliances of the material are calculated from the resonant frequencies of the reed. Measurements are made in a bridge assembled from a special transformer[3], the specimen, and an air condenser of the same static capacity as the specimen. The properties of the transformer are such that if the bridge is balanced at a frequency off resonance of the specimen, it will remain accurately balanced over the entire frequency range of interest unless the impedance of the specimen changes. As the generator frequency is varied, the bridge output therefore remains at zero until a resonance of the specimen is reached, resulting in a sharp peak. The frequency is then measured with a counter.

---

[1] E.R. Fitzgerald, J Acoust Soc Am 32, 1270 (1960). This is a summary paper and gives references to several of Fitzgerald's other papers on the subject.

[2] E.R. Fitzgerald, Phys Rev 112, 765 (1958).

[3] Replacement transformer for General Radio Co. Impedance Comparator 1605-A. See General Radio Experimenter 30, April 1956.

The specimen is clamped by cementing to a pair of blocks of mass about 315 g. The total flexural effective compliance of the specimen in the first mode (0.971 times the static value) resonates the effective mass of the specimen (1/4 the actual mass of about 0.5 g) at the lowest frequency of interest; any possible resonance with the mass of the clamp is then far lower. The lowest frequency at which the axial compliance of the specimen would resonate with the clamp is much higher than the highest frequency of interest.

Clearly, the proposed method is not suited to the accurate determination of elastic constants. The resonant frequency is affected by coupling to other modes; the conditions at the fixed end are ill defined; and the elementary theory requires corrections which are known only approximately. The degree of agreement between the elementary theory and experiment was therefore assessed by measurements on a +5° LR X-cut duplex quartz bender 0.508 mm thick, and 4.8 mm wide, cemented into the clamp so that the free length, ℓ, was 55.5 mm. The resonant frequencies, f_1, f_2, f_3, corresponding to the first three modes were determined and the frequency constants $f_1\ell^2$ were calculated. The specimen was then shortened by sawing a bit from the free end and the measurements repeated. In all, 13 lengths were used, the shortest being 32.3 mm.

According to the elementary theory, the frequency constant can be gotten from

$$f_i = \frac{m_i^2}{2\pi} \frac{(B/\rho)^{1/2}}{\ell^2} , \qquad (1)$$

in which B is the flexural rigidity per unit width and ρ is the mass per unit length per unit width, and

$$m_1 = 1.875,\ m_2 = 4.694,\ m_3 = 7.855. \qquad (2)$$

The theoretical frequency constants $(FC)_i$ were calculated from eq (1) using published values of the properties of quartz and the measured dimensions, and found to be

$FC_1 = 4429,\ FC_2 = 27,760,\ FC_3 = 77,720\ cm^2\ sec^{-1}$.

The ratios $f_i\ell^2/(FC)_i$ (measured/calculated) for all 39 cases were in the range 0.97 to 1.00, the variation with ℓ and i(=1,2,3) being erratic. The various corrections to the elementary theory (rotatory inertia, dynamical asymmetry, shear, twisting due to anisotropy), which altogether amount to much less than 1%, were therefore not applied. If the present method can be relied upon to within, say, 2% for f_1, then the compliance can be determined within about 4%. As we are in search of changes in compliance of some thousands of percent, the method is probably adequate.

III. The specimens

A typical specimen is shown schematically in fig. 1. The inner core is a soldered duplex +5° X-cut LR bender. x_1 is the crystallographic x-axis, x_3 is the Z-axis, and x_2, which is along the length, is in the yz-plane at +5° from y. The sample materials (all isotropic) are affixed with a very thin layer of epoxy cement. The adequacy of such an epoxy joint was tested on several duplex quartz elements so cemented. These were stressed piezoelectrically and the deflection at the ends measured with a micrometer microscope. The measured and calculated deflections agreed within the experimental error.

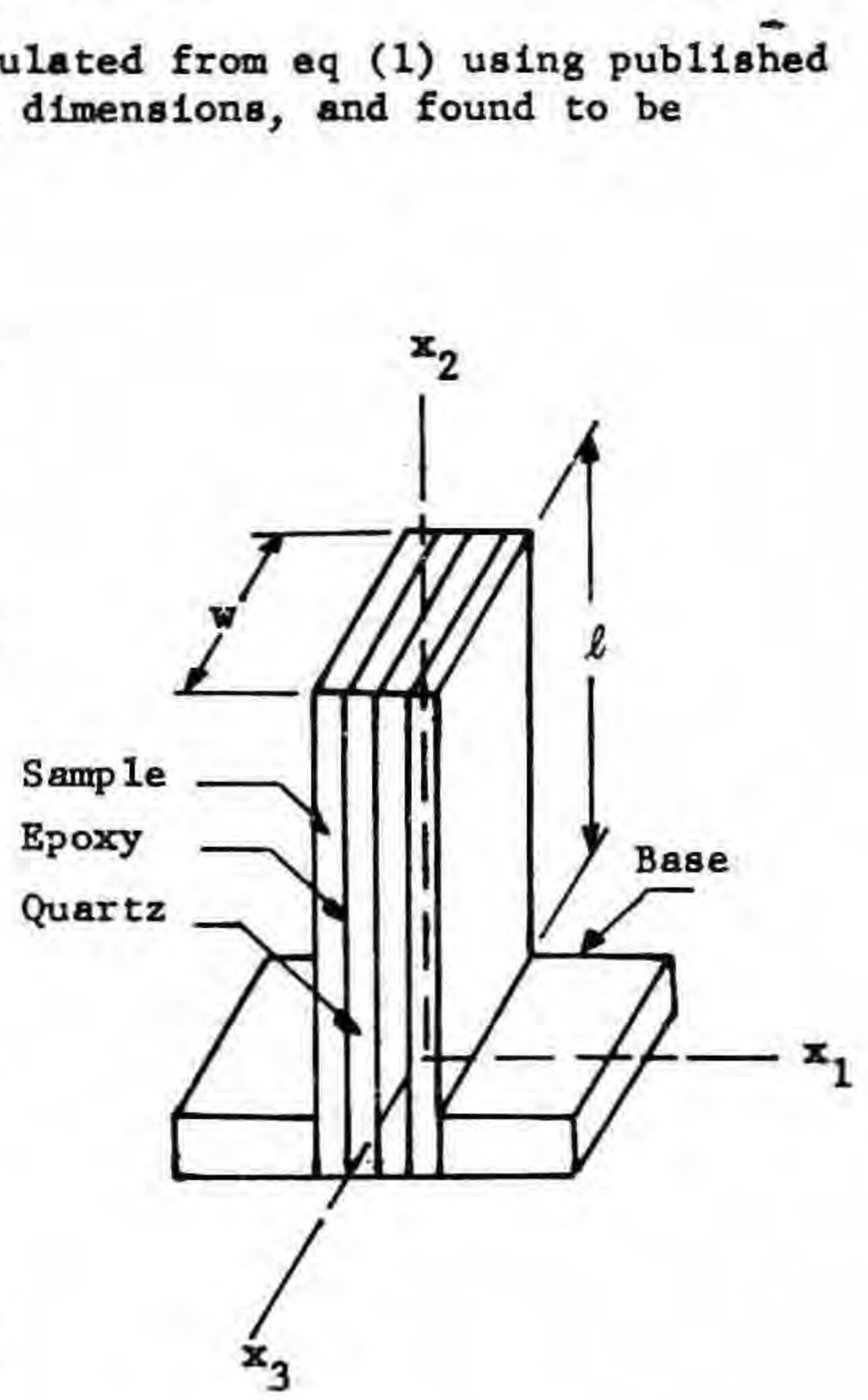

Fig. 1

The samples were cut from (a) an optically clear fused silica rod, (b) a "high purity" continuous-cast aluminum rod, and (c) a 99.992% pure aluminum sheet. In all cases the total thickness was about 1 mm of which about half was the quartz core. The widths were in the range 2-5 mm and the lengths 4 to 5 cm.

IV. The static stress and its effect on the compliances

The thermal stresses corresponding to a difference θ between the temperature at which the resin is cured and that of test can be calculated by the ordinary theory, extended somewhat to allow for anisotropy. The maximum shearing stress occurs on a pair of axes x_1', x_2', which together with an x_3' make up a set of axes having direction cosines α_{ij} relative to the frame x_1, x_2, x_3. As θ is increased, the slip postulated by Fitzgerald will occur first on the x_1', x_2' axes, the material being isotropic. On the original axes, the compliances are

$$s_{mnop} = \alpha_{mi}\, \alpha_{nj}\, \alpha_{ok}\, \alpha_{pl}\, s'_{ijkl}. \tag{3}$$

For an isotropic material, $s_{mnop} = s'_{ijkl}$, but on account of the postulated slip on the x_1', x_2' axes, $s'_{66}(=4s'_{1212})$ is according to the Fitzgerald mechanism, increased by a factor F to $4Fs'_{1212}$; the other compliances are unchanged. In our reed experiment the decisive compliance is $s_{2222} = s_{22}$, which according to eq (3) is now

$$s_{22} = s'_{22} + (F-1)\, \alpha_{21}^2\, \alpha_{22}^2\, s'_{66}/4. \tag{4}$$

If k is the fraction of the total flexural rigidity in the absence of prestress contributed by the sample (in the present instances, $k \approx 7/8$), then it is easily shown that

$$F = 1 + \frac{4}{\alpha_{21}^2\, \alpha_{22}^2}\, \frac{s'_{22}}{s'_{66}}\, \frac{1-(f/f_o)^2}{k-1+(f/f_o)^2}, \tag{5}$$

in which f_o and f are corresponding resonant frequencies of the reed without and with prestress, respectively.

The fused silica specimens were cemented at 57°C and tested at various temperatures down to 25°C, corresponding to a maximum static shearing stress of 105×10^6 dyne cm^{-2}. Fitzgerald[2] estimates his value at 5×10^6 dyne cm^{-2}. For the sheet aluminum specimens the corresponding values were 57°C, 22°C, and 108×10^6 dyne cm^{-2}, and for the cast aluminum specimens they were 49°C, 26°C, and 77×10^6 dyne cm^{-2}. It is difficult to say what value of static stress was used by Fitzgerald[4]. He compressed his samples 1.9% and found no permanent set after removal from the apparatus. An elastic recovery of even 0.1% for his material would be impressively large.[5]

---

[4] E.R. Fitzgerald, Phys Rev 108, 690 (1957).

[5] Metals Handbook, 8 Ed, Vol I. Am Soc Metals (1961).

V. Results

The first three resonant frequencies under zero static stress are given in the following table.

Sample material	Length cm	Width mm	$f_{1,o}$ c/s	$f_{2,o}$ c/s	$f_{3,o}$ c/s
fused silica	5.12	4.9	333.4	2091	5834
fused silica	4.81	4.9	372.7	2332	6501
fused silica	5.07	2.6	336.5	2114	5899
fused silica	4.19	2.6	487.7	3066	8539
sheet Al	5.00	4.9	306.9	1950	5500
sheet Al	4.47	4.9	377.5	2377	6674
sheet Al	4.90	2.3	309.7	1946	5450
sheet Al	4.44	2.3	375.5	2367	6649
cast Al	5.26	3.1	264.7	1675	4687
cast Al	4.79	3.1	316.1	2001	5606

In all cases the values in the table are within a few percent of those calculated from eqs (1) and (2) and the published values of s_{22}. As the static stress was increased by lowering the temperature, no significant change in the resonant frequencies occurred. In the case of aluminum, the resonant frequency gradually increased, by an amount in every case less than 2% over the entire temperature range, as would be expected from the temperature dependence of the elastic compliances. In the case of fused silica, the thermal effects in the silica and in the quartz core tend to cancel; the observed change in resonant frequency was in every case less than 0.1%.

In eq (5) the α's and s's are such that the factor $(4/\alpha_{21}^2\ \alpha_{22}^2)\ (s'_{22}/s'_{66})$ is about 8.8 for the silica and 7.0 for the aluminum, specimens. With k about 0.9, we find that even if we admitted a 1% decrease in f, owing to Fitzgerald's postulated mechanism, then F, the factor by which the shear compliance is increased, is about 1.2 for both the silica and the aluminum. Fitzgerald's values of F, in the range 100 to 1000 c/s for four pairs of samples of silica (all cut from the same rod but of different dimensions), are about 30, 85, 40, and 20, and for his pair of aluminum samples,[6] F is about 20. From eq (5) f/f_o is about 1/3 for F = 20. Similar comparisons can be made at the higher frequencies.

Many tests were performed on asymmetrical specimens made by cementing a layer of the sample material (fused silica or aluminum) to a layer of -18.5° X-cut quartz using thermal stressing. The results were negative.

Fitzgerald's[2] results for α-quartz are similar to those for fused silica. Therefore, we made our first tests on +5° LR X-cut benders using high-voltage piezoelectric stressing. The results were negative.

We conclude that the slip mechanism proposed by Fitzgerald is not adequate for the explanation of his results.

[6] Fitzgerald measures his compliance in directions at 45° to those of the maximum static shearing stress, so that the actual values of F are higher than those quoted by a factor which could approach 4.

G13

FOURTH INTERNATIONAL CONGRESS ON ACOUSTICS
COPENHAGEN 21.-28. AUGUST 1962

An Investigation of the Volume Velocity Waveform at the Larynx during Speech by Means of an Inverse Filter

J.N. Holmes (Joint Speech Research Unit of the British Post Office, Eastcote)

Introduction

In recent years there has been much interest in the nature of the vibration of the vocal chords. This interest has arisen from various applications in the fields of medicine, phonetics, and communications engineering.

There are various methods of study available, of which high speed cine-photography has been the most widely used.[1,2,3] This method is expensive if a lot of data is required, but it gives very detailed information about the form of the larynx vibration It has the disadvantage that ordinary speaking conditions cannot be studied because of the necessity for a laryngoscope mirror in the mouth.

In the field of communications, where one is primarily interested in the acoustic output from the larynx, the inverse filtering method[4,5] is preferable because the results are cheaply and easily obtainable during normal speech and are obtained directly in the form of volume velocity waveforms.

In addition certain features of the vocal chord wave, such as the time instants when the main pulsings of the vocal cavities occur, are very clearly shown by this method. It has been stated by Miller[4] that in general the main instant of excitation of the second formant is at the closure of the glottis, but it will be shown here that in many cases there are also well defined instants of excitation of the second and higher formants at other points in the larynx wave.

Experimental Method

It has been shown by Fant[6] that for non-nasalized vowels the transfer function of the vocal tract can be closely approximated in the range up to 5000 c/s by a function having four or five suitably chosen conjugate pole pairs, a correction for higher poles and a zero at zero frequency to represent the effect of radiation from the mouth. Similarly an inverse network can be made with a few suitably placed zeros, a higher zero correction, and a pole at zero frequency. In practice it will suffice if the transfer function has the correct amplitude and phase characteristic in the range 50 c/s to 5000 c/s, and so the pole need not be at the origin, provided the effect of its displacement from the origin is compensated in the frequency range required.

The inverse filter used in the experiments described here consists of five cascaded similar networks whose transfer functions each have one complex conjugate zero pair adjustable in frequency and bandwidth, together with a higher pole pair which is well above the frequency range of interest. The correction for higher zeros is included in the inter-network couplings. The low frequency pole which corrects for the radiation at the mouth is included in the formant-one zero circuit, and may be switched out if the differentiated larynx wave is required. Each adjustable zero network is arranged to give a low frequency transmission which is independent of the frequency of the zero, and to have facilities for disconnecting the zero circuit without affecting the low frequency gain. This latter facility is useful for showing the effect of inverse filtering all except one of the formants, so that the excitation pattern of each formant can be seen separately.

The sounds are magnetically recorded and replayed repeatedly from a tape loop into the inverse filter. An oscilloscope, whose time-base is synchronized to the loop, is used for studying the filter output. The frequencies and bandwidths of the zeros are then adjusted to produce minimum formant-frequency ripple in the output waveform. During vowels this condition is usually well defined, and provides, incidentally, an accurate measure of the formant frequencies. The waveform with all the formant ripple removed represents the volume velocity at the larynx.

Precautions to minimize errors

The required inverse filter settings are normally well defined, but the correct larynx waveforms will not be obtained unless all the conditions assumed in the theoretical model are met. The serious danger here is that if these conditions are not quite met there may be a setting of the inverse filter controls which will give a waveform which is at least credible as a larynx wave, but which will have a shape very different from that of the volume velocity wave at the larynx.

It is thus essential to take many precautions to prevent errors. As non-nasalized vowels are assumed it was necessary to avoid those near to nasal consonants. A good anechoic chamber was used to achieve free field radiation, and a condenser microphone to reproduce the sound pressure waveform accurately.

It was impossible to avoid the presence of very low frequency noise in the microphone output due to slight variations in room air pressure, and air movements caused by breathing and slight body movements. This noise made it essential to limit the low frequency response of the system by means of A.C. couplings in the amplifiers, but even so some remaining noise, mainly in the region of 10 c/s, caused slight variations of the base line on the measured larynx waves.

In the electrical equipment the combined effect of phase distortion in all amplifier A.C. couplings was corrected, and extreme precautions were taken to avoid distortion and noise in the magnetic recorder.

Fortunately it was possible to test the overall performance of the complete electrical system. A test waveform was generated consisting of a 50 c/s square wave feeding an all-pole network similar to that needed to synthesize a neutral vowel. This waveform was fed into the microphone amplifier through a capacitor equal in value to the microphone capacitance. The zeros of the inverse filter were adjusted to the frequencies of the poles of the test network, and the waveform was displayed without the low frequency pole of the inverse filter in operation. The quality of the square wave so obtained is shown in fig. 1. As can be seen it is not a perfect square wave, but the errors are not sufficient to make an appreciable difference to the measured larynx waveforms.



Fig. 1. Test waveform

Results

Study of several different examples of larynx waves show results similar to those already published[3,4,5,7,8,] but with quite large differences in waveshape and in length of the closed period for different talkers, different degrees of stress, and different frequency of vibration. Two typical such waveforms are shown in figs. 2 and 3. Further study of the sample in fig. 3 was made to see how the formants are excited. This was done by differentiating the larynx wave to emphasize the higher frequencies, and removing the zero from the inverse filter for one formant at a time. The results for the first three formants are shown in figs. 4, 5 and 6. It can be seen from these figures that the first formant is excited once per cycle at the closure of the larynx. The second formant has two main excitation points of nearly equal intensity, one at the closure and another at the re-opening of the larynx. The third formant has the same two excitation points, but in this case the opening pulse is of much less intensity than the closure. This sort of variation between formants is typical of a large number of samples examined, and the more complicated patterns of excitation are noticed most in the higher formants. It will be seen from these figures, and it has been found to be generally true for most speakers, that successive larynx wave cycles are almost identical, even in fine detail. It is well known, however, that considerable variations between successive cycles occur frequently for some talkers, and on some occasions for almost all talkers. The vibrations of a habitually irregular larynx have not yet been studied, but several cases have been investigated in which the behaviour of a normal larynx is changing. Fig. 7 shows a vowel starting from a glottal stop, and it can be seen that the three cycles shown are of very different form. The The step on the opening phase of the third cycle persisted for the remainder of the

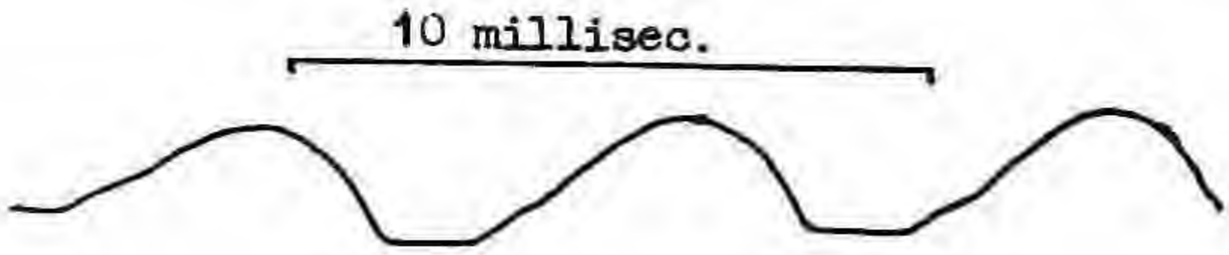

Fig. 2. Talker L.V.C.
Typical larynx wave



Fig. 3. Talker A.H.T.
Typical larynx wave

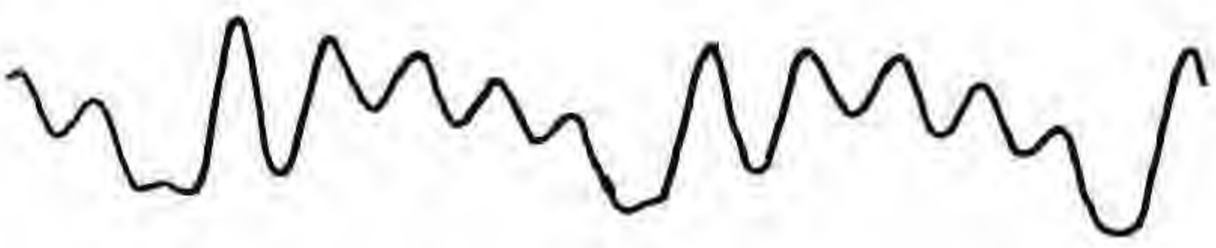

Fig. 4. Differentiated larynx wave with the inverse filter for formant 1 removed. Same speech sample as Fig. 3.



Fig. 5. Differentiated larynx wave with inverse filter for formant 2 removed. Same speech sample as Fig. 3.



Fig. 6. Differentiated larynx wave with the inverse filter for formant 3 removed. Same speech sample as Fig. 3.

vowel, and was found to be a frequently seen characteristic of that speaker. Several other cases of initiation and cessation of voicing have been examined, both with a glottal stop and with an open glottis condition adjoining. After an initial glottal stop about three cycles of vibration are generally needed to achieve full amplitude, and sometimes a few more to establish a repetitive pattern. Voicing starting from an open glottis has been observed to take about twice as many cycles to build up.

Examination of one sample of an /h/ sound between two vowels shows voicing with a volume velocity wave whose peak-to-peak amplitude is not significantly different from in the vowels but which does cease to have a completely closed period. Successive cycles of the vibration to differ appreciably during the /h/. Examination of the excitation of the formants shows that the first and second formants derived their excitation mainly from the larynx vibration, whereas the higher formants were mainly excited by friction, which appeared to be continuously present through each larynx cycle. It is assumed that the mean volume velocity during the /h/ is much higher than in the vowels, but this would not be shown because the apparatus response is not maintained below 50 c/s.

Several other examples of larynx vibration have been studied by this method but space limitation prevents any more being shown here.

Conclusions

The main facts brought out by this investigation are:-

(i) The fine detail of the larynx wave is normally very complicated, in particular in its effect in exciting the higher formants. The lack of this complexity in the excitation normally used in speech synthesis leads one to suspect that this may be a partial cause of unnaturalness in synthetic speech.

(ii) For most speakers the period, form, and even fine detail, of vibration do not often change suddenly except in regions near intentional changes in larynx behaviour.

References

1. FARNSWORTH, D.W., "High-speed motion pictures of the human vocal chords". Bell Laboratories Record, 18, 203-208 (1940).
2. MOORE, P. and LEDEN, von H., "Dynamic variations of the vibratory pattern in the normal larynx". Folia Phoniatrica, 10, 205-238 (1958).
3. GILL, J.S., "Estimation of vocal excitation during speech with particular reference to the requirements of analysis-synthesis telephony". Ph.D. Thesis, University of London (1961).
4. MILLER, R.L., "Nature of the Vocal Chord Wave". J. Acoust. Soc. Amer. 31, 667-677, (1959).
5. SPEECH TRANSMISSION LABORATORY QUARTERLY PROGRESS AND STATUS REPORT, Royal Institute of Technology, Stockholm, (July-September 1960).
6. FANT, C.G.M., "Acoustic Theory of Speech Production". Mouton & Co. (1960).
7. FLANAGAN, J.L., "Some properties of the glottal sound source". J. Speech and Hearing Research, 1, 99-116 (1958).
8. SONESSON, B., "On the anatomy and vibratory pattern of the human vocal folds", Acta-Oto-Laryngologica, Supplementum 156, (1960).



Fig. 7. Talker J.N.H. Larynx wave after a glottal stop.

Fig. 8. Talker L.V.C. Differentiated larynx wave with the inverse filter for formant 4 removed



(a) during a voiced /h/ sound, showing mainly fricative excitation.



(b) during the preceding vowel, showing excitation mainly from the larynx closure.

10 millisec.

H13

FOURTH INTERNATIONAL CONGRESS ON ACOUSTICS
COPENHAGEN 21.-28. AUGUST 1962

On the concept of the critical band.

E. de Boer and C.E.Bos.
Physical Laboratory, Ear-nose-throat clinic
Wilhelmina Hospital, Amsterdam, Netherlands.

When a tone is perceived against a background of wide-band noise, only a part of the noise spectrum contributes to the masking. The ear appears to integrate only noise components over a band of frequencies situated around the tone's frequency. In the "classical" experiment (Fletcher) this band - called the critical band - is found to be rather narrow: being less than 60 c/s wide at frequencies below 500 c/s, and amounting to about 7 % of the frequency at higher frequencies.
Numerous other, more recent, experiments (Feldtkeller and Zwicker) on signal resolution and frequency integration have led to a critical bandwidth that is from 2,5 to 4 times larger than the classical value. For low frequencies the critical band is found to be around 100 c/s, increasing to become approximately 18 % of the frequency at higher frequencies. The discrepancy between the two sets of values calls for an explanation. It will be suggested that the modern (large) values of the critical bandwidth are to be preferred. One argument is contained in a criticism of the classical type of experiment: audible noise fluctuations will affect measurements of masking to a large extent. As a second argument an experiment will be described that aims at refining the critical-band concept without involving disturbances due to noise fluctuations.
The influence of noise fluctuations on masking data can be studied with reference to the intensity difference limen for noise bands of various widths. Consequently, experiments have been performed on the intensity discrimination of band-limited noise as well as experiments on the masking of a pure tone by the same bands of noise. Frequency regions of 125 - 4000 c/s are explored; the test tone always remains at the centre of the noise band. The results of both types of experiment indeed coincide over a large range of bandwidths. This shows that the intensity discrimination is the major determinant of pure-tone masking. As Zwicker has shown, intensity discrimination of noise bands is worse for smaller band widths; the difference limen depends only on the bandwidth and does not depend upon the frequency. We must conclude that the critical bandwidth cannot be determined from

masking experiments of this type.
In our further measurements the influence of fluctuations is decreased by using exclusively wide-band noise as masking signal. A gap is produced in the noise spectrum by a sharp band-rejection filter. The width of the rejected band can be changed in steps. Fig. 1 shows frequency response curves of the filter. The masking of a pure tone, situated at the (geometrical) centre of the gap will then reflect the critical-band action: masking will be less the wider is the gap in the spectrum. Expermentally the masking does not decrease as fast as it could in view of the extreme steepness of the filter response. We cannot escape the conclusion that the filtering action of the ear is not as perfect as the conventional model of the critical band implies.
With a few simplifying assumptions we can describe this by analogy with a (realistic) filter. Assume that the perception of a tone (e.g. of 1000 c/s) is mediated by a " receptor" that is maximally sensitive to the tone's frequency, but that has a lower sensitivity at other frequencies. Assume further that the masking is equivalent to the intensity passed by a filter having the same response curve as the receptor under consideration. From the response curves of the noise filter and the experimental data, the equivalent receptor response curve can be determined. Fig. 2 shows this function for the region of 1000 c/s, as based on measurements averaged over five listening subjects. As a filter response it approximates a band-pass filter of the third degree (e.g. a full Zobel section). The effective width of this response function can be taken as a datum for the critical band. As Fig 3 shows, the values found are considerably larger than the "classical" values. In effect they are slightly larger than Zwicker's values, but they follow the same course as a function of frequency.
In further expermenting a few interesting features were found, especially in asymmetrical masking situations. The perception sometimes appears not to be mediated by the receptor that is maximally sensitive to the tone's frequency. Instead one may assume that it is mediated by the receptor that has the most favourable signal - to - noise ratio. This hypothesis also explains the masking patterns of single pure tones, which are decidedly narrower than the critical band. The extended critical-band model also served to explain the pure-tone difference limen for frequency, a well-known stumbling-block of auditory theory (See the slope of the function of Fig 2).
It is to be concluded that in the concept of the critical band one should not emphasize the integration aspect too much. Indeed, perception of narrow-band signals is determined by their temporal course, not by their integrated frequency spectrum. One should instead put the emphasis on the separability

of signals (as exemplified by the receptor response function).

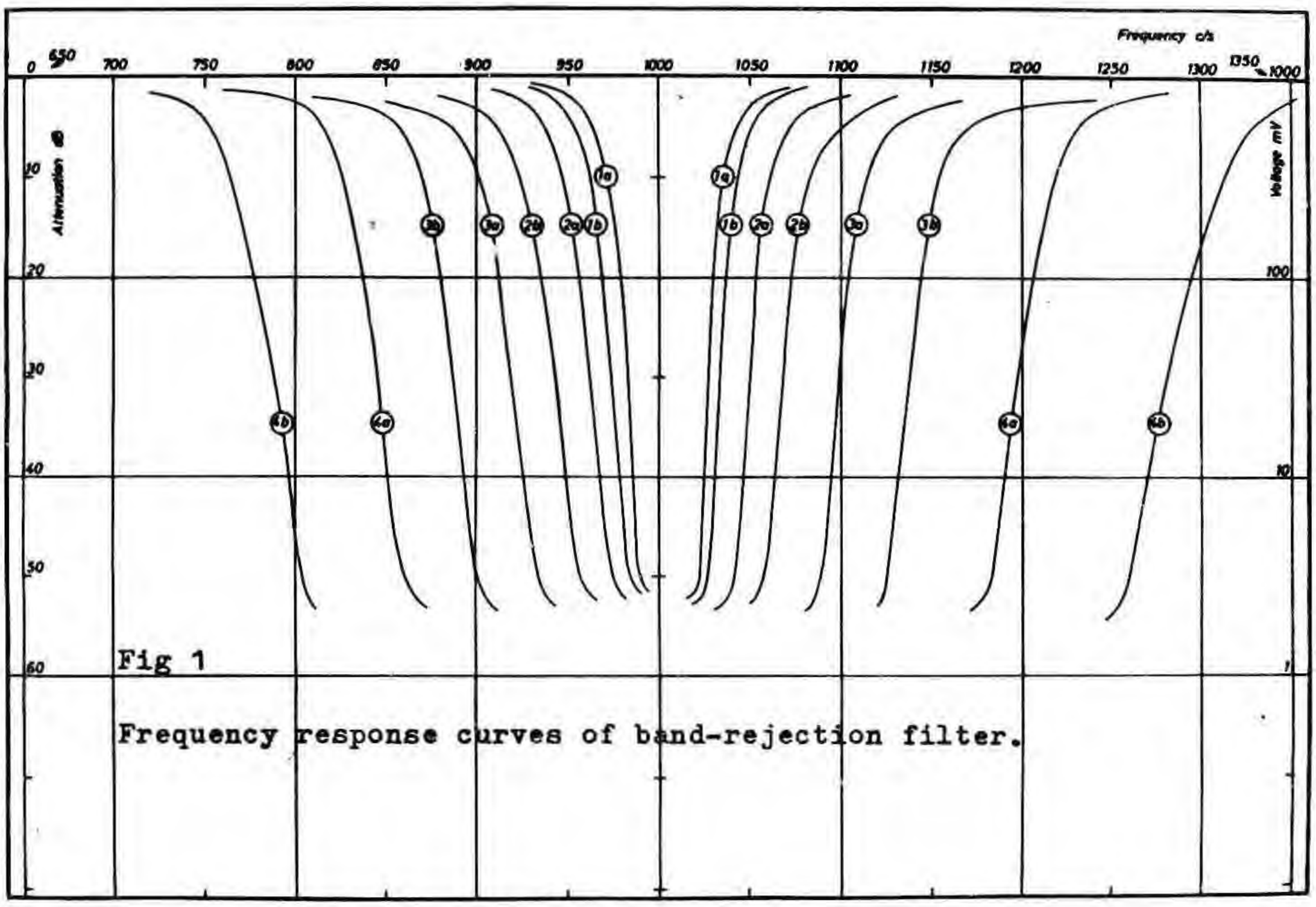

Fig 1

Frequency response curves of band-rejection filter.

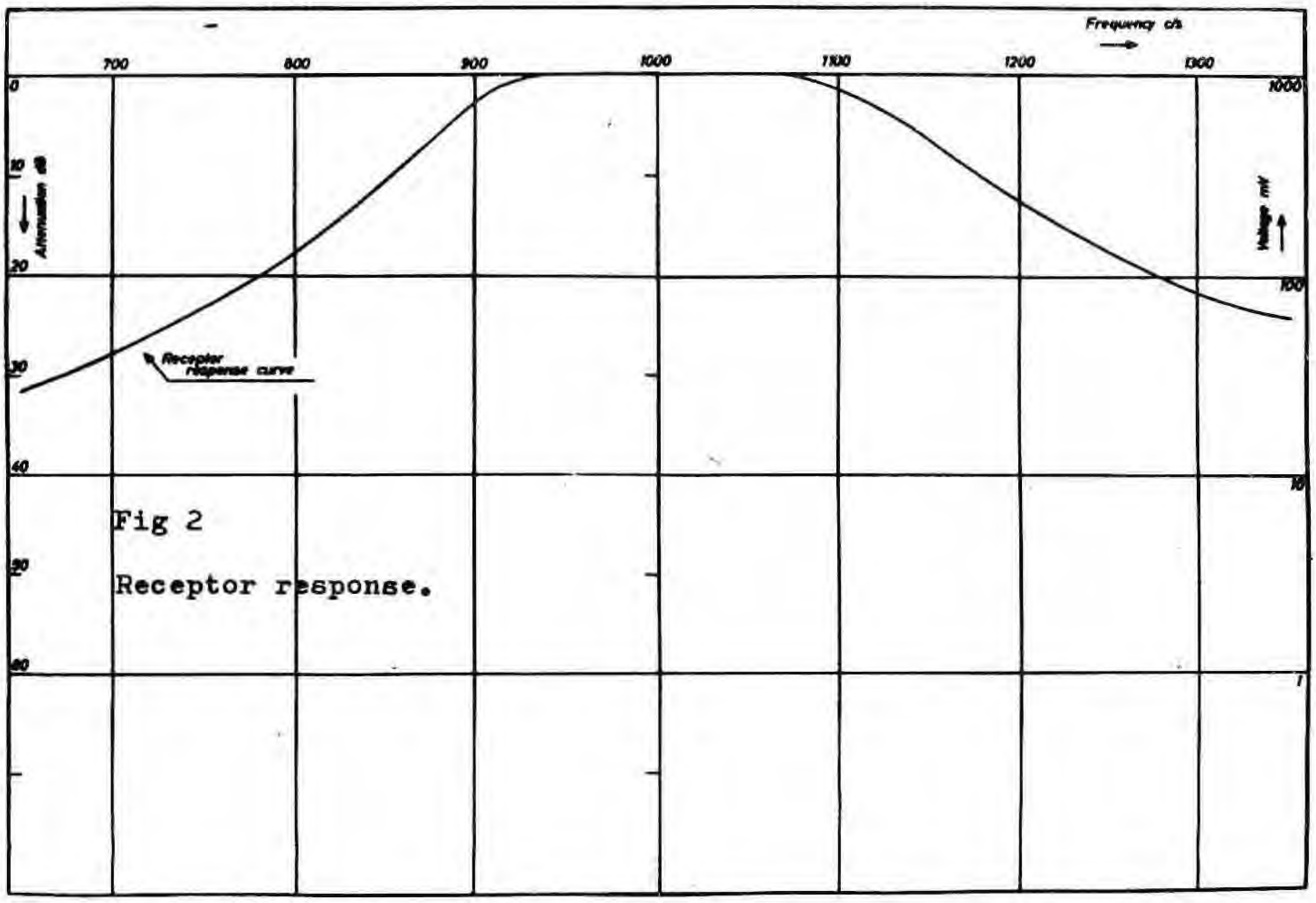

Fig 2

Receptor response.

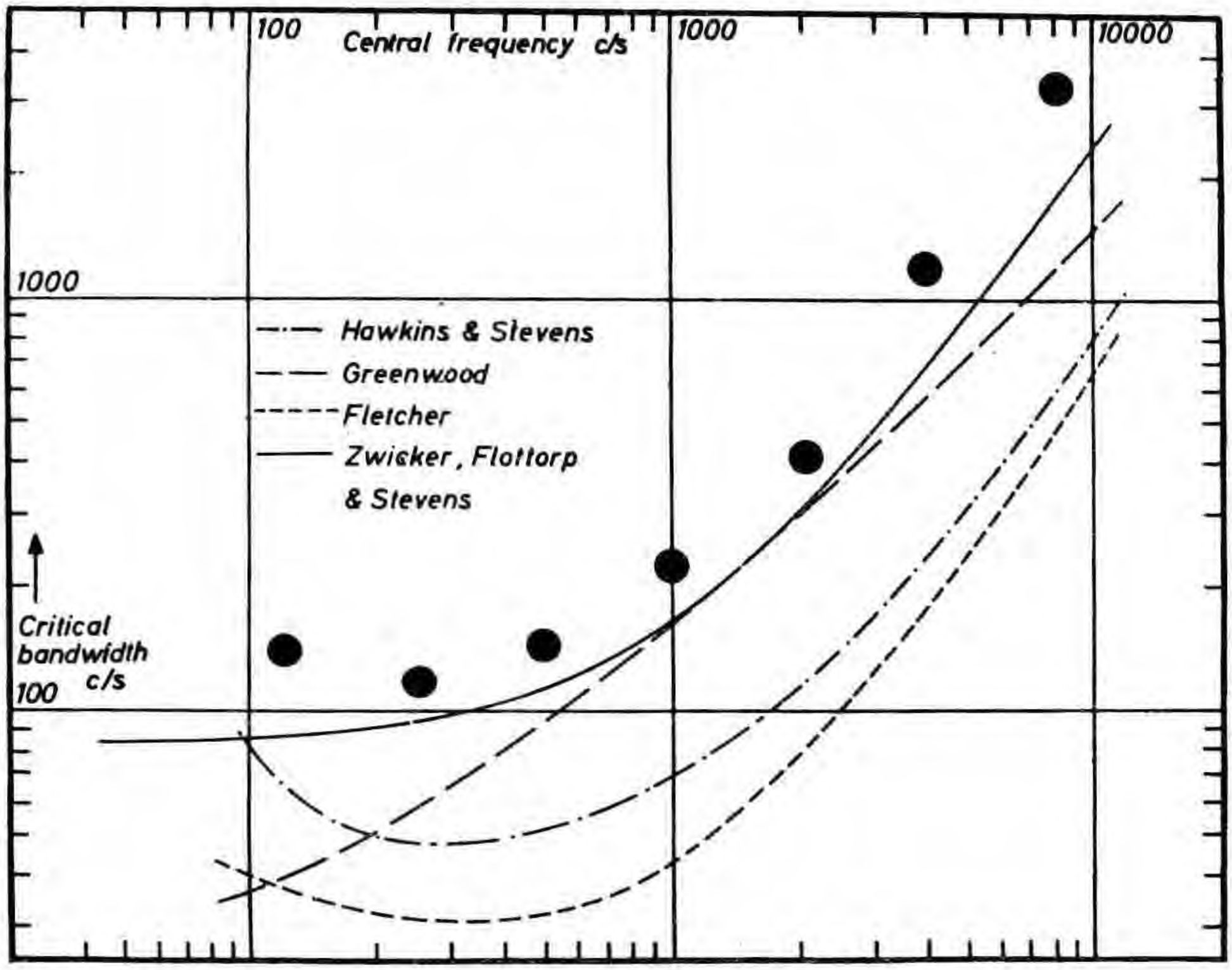

Fig 3.

Comparison of critical-band values effective width of receptor response curve.

J13

FOURTH INTERNATIONAL CONGRESS ON ACOUSTICS
COPENHAGEN 21.-28. AUGUST 1962

SUR LES ANOMALIES DES SPECTRES D'ABSORPTION ULTRASONORE DANS LES SOLUTIONS DE HAUTS POLYMERES : ESSAI D'INTERPRETATION.

R. CERF, S. CANDAU et R. ZANA
Centre de Recherches sur les Macromolécules, Strasbourg, France.

Nous avons étudié, au cours des deux années écoulées, l'absorption ultrasonore de solutions macromoléculaires à l'aide d'un dispositif qui nous permet d'effectuer les mesures en variant la fréquence de manière continue dans certains intervalles du domaine 0,8 Mc/s-27 Mc/s (1). Cette spectroscopie ultrasonore à fréquence continûment variable a révélé, tout d'abord pour une solution de polystyrène dans le benzène, l'existence d'une anomalie consistant en une brusque chute du coefficient d'absorption α se produisant à une fréquence bien définie (1). La courbe α/N^2 en fonction de la fréquence N affecte pratiquement la forme d'une marche d'escalier.

Ce phénomène a été observé ensuite pour d'autres couples polymère-solvant ; la chute de α/N^2 en fonction de N est généralement plus étalée que pour le polystyrène dans le benzène, mais reste néanmoins trop rapide pour ressembler aux décroissances que l'on enregistre lors d'un phénomène de relaxation. Des études systématiques ont permis de préciser l'influence de la concentration, de la masse moléculaire et de la structure du polymère dissous, ainsi que l'influence de la nature du solvant (2,3). Il est à noter, en particulier, que la fréquence caractéristique augmente ici avec la masse moléculaire M, alors qu'elle devrait diminuer lorsque M augmente, s'il s'agissait d'un processus de relaxation.

Tous les renseignements recueillis indiquent que le phénomène observé est d'origine intramoléculaire et qu'il affecte des portions limitées des macromolécules. Nous pensons qu'il est possible de l'expliquer par un changement local de configuration des molécules de type coopératif. Nous allons préciser les hypothèses que nous avons faites pour obtenir une variation brusque de α/N^2 en fonction de N. On verra qu'elles ne paraissent pas artificielles à la lumière des considérations les plus récentes sur la statistique des chaînes. De plus, ces mêmes hypothèses font prévoir que la spectroscopie ultrasonore doit pouvoir être appliquée à un problème actuel de la physico-chimie macromoléculaire : l'analyse de la stéréorégularité. Des résultats de mesures effectuées sur trois échantillons de polyméthacrylate de méthyle, respectivement atactique, syndiotactique et isotactique illustreront cette possibilité.

Nous supposons que les molécules en solution sont toutes identiques entre elles. Nous envisageons ici des chaînes à squelette carboné de type aliphatique (exemple le polystyrène $[-CH_2-CH(C_6H_6)-]_p$). On sait que chaque chaînon $C_j - C_{j+1}$ est astreint à se trouver sur un cône d'axe $C_{j-1} \rightarrow C_j$ dont le demi-angle au sommet est le supplément de l'angle de valence (cône de valence). Les différentes configurations obtenues par rotation de chaque chaînon sur son cône de valence ne sont toutefois pas également probables, du fait d'interactions attractives et répulsives entre les substituants.

De plus, des changements de configuration se produisent nécessairement du fait de l'agitation thermique, et, le cas échéant, sous l'effet d'un champ de forces, par exemple le champ acoustique. Nous admettrons que dans les longues molécules flexibles, les changements de configuration les plus fréquents sont tels que la déformation de la chaîne reste aussi localisée que possible. Ainsi, en l'absence d'un champ de forces, l'agitation thermique produirait des réorganisations locales respectant les positions relatives des portions non déformées de la molécule. De même, lors d'une faible dilatation de la molécule, comme il s'en produit dans champ ultrasonore, quelques segments comprenant chacun un petit nombre de chaînons subiraient une réorganisation aboutissant à un allongement dans la direction de dilatation, tandis que les morceaux de molécule intermédiaires ne subiraient que des translations les uns par rapport aux autres.

Nous schématiserons ici en admettant :

1) Que les segments subissant des changements de configuration ont une longueur bien définie. Nous entendons par là que la fréquence des changements de configuration présente, en fonction du nombre n de monomères prenant part à la réorganisation locale, un maximum aigu autour d'une certaine valeur n_e de n.

2) Que ces segments présentent (au moins) trois états particulièrement stables : deux états appelés 1' et 1" entre lesquels la transition est facile (barrières de potentiel de l'ordre de RT/mole de segments), et un état appelé 2 séparé de 1' et de 1" par une barrière de potentiel très supérieure à RT/mole de segments. L'apport d'énergie libre produisant la transformation respectivement de 1' en 2 et de 1" en 2 en l'absence de champ est supposé être sensiblement le même, et sera appelé ΔF.

Dans un champ acoustique, des vibrations (à la fréquence N du champ) ont lieu localement dans des segments comprenant $n \sim n_e$ monomères, avec passage de l'état 1' à l'état 1" et réciproquement. On appellera ν le nombre de segments en vibration dans chaque molécule ; l'amplitude de la dilatation des macromolécules doit être proportionnelle à l'amplitude de la déformation locale du milieu ; on voit immédiatement que ν doit par suite être également proportionnel à cette dernière amplitude. Les segments en vibration sont susceptibles d'occuper, au cours du temps, des positions variables le long de la chaîne, mais ce fait ne sera pas pris en considération ici. On notera que chacun des ν segments contient une énergie vibratoire E(N) indépendante de l'amplitude du champ ultrasonore, puisque la vibration se fait par passages $1' \rightleftarrows 1"$ d'amplitude bien définie, indépendante de celle du champ.

Nous nous demanderons maintenant quelle est la proportion de segments en vibration qui subissent un changement de configuration les faisant passer à l'état 2. Lors d'une telle transition le segment peut être considéré comme étant dans un état unique 1 dont le passage à l'état 2 exige un apport d'énergie libre réduit à $\Delta F - E(N)$.

Dans ces conditions, on voit immédiatement que la fraction f des segments demeurés à l'état 1 est :

$$(1) \qquad f = (1 + \exp -[\Delta F - E(N)]/RT)^{-1} = (1/2)\,(1 + \mathrm{Th}[\Delta F - E(N)]/2RT)$$

Lorsque N croît de zéro à l'infini, f décroît de un à zéro. La décroissance de f se produit dans un domaine de fréquence d'autant plus étroit que ΔF est plus grand, et la transition se fait à la fréquence N* qui annule $\Delta F - E(N)$; pour $N = N^*$, $f = 0{,}5$. A la limite, si ΔF était infiniment grand devant RT/mole de segments (la fréquence de transition restant finie), la décroissance de f prendrait l'aspect d'une marche d'escalier (*).

Le modèle que nous avons proposé montre ainsi la possibilité d'un changement réversible de configuration des molécules produit par l'ultrason à une fréquence caractéristique. Comme dans la théorie de la relaxation, on considère un déplacement d'équilibre entre deux formes moléculaires. Mais ce déplacement d'équilibre, au lieu de varier sinusoïdalement au cours du temps avec la fréquence de l'onde (théorie de la relaxation), est ici indépendant du temps pour une valeur donnée de la fréquence.

(*) Une fonction de la forme (1) ci-dessus, mais sans terme vibratoire, apparaît dans la théorie de la dénaturation des protéines. Une forme simplifiée (4) de cette théorie fournit en effet, l'expression suivante de la fraction φ des molécules demeurées sous forme ordonnée (non dénaturée) :

$$(2) \qquad \varphi = (1 + \exp -\Delta F/RT)^{-1}$$

où ΔF représente l'apport d'énergie libre nécessaire pour convertir une molécule de la forme ordonnée à la forme désordonnée. La transition peut être obtenue par variation de la température, et la température de transition est celle qui annule $\Delta F = \Delta H - T\Delta S$. A la limite, si ΔF était infiniment grand devant RT/mole (molécule infiniment grande), la variation de φ en fonction de la température prendrait la forme d'une marche d'escalier.

Les fonctions f et φ sont de la même forme générale que la fonction de Fermi-Dirac, laquelle prend, comme on sait, la forme d'une marche d'escalier au zéro absolu.

Il importe de noter que pour des valeurs de ΔF relativement peu élevées, par exemple ΔF de l'ordre de 10 RT/mole de segments, c'est-à-dire de l'ordre de 6 Kcal/mole de segments, la chute de f est encore très rapide ici, comparativement à celle que fournirait la théorie de la relaxation pour la quantité correspondante.

Effectivement, pour la valeur indiquée de ΔF, f tombe de 0,95 à 0,05 dans un intervalle de fréquence $\Delta N \sim 0,3\ N^*$. Au contraire, dans la théorie de la relaxation, la fonction $\psi = (1+4\pi^2N^2\tau^2)$ (où τ désigne le temps de relaxation), montre la même variation dans un intervalle de fréquence $\Delta N \sim 4N_*$; N^* et N_* désignent respectivement les valeurs de N pour lesquelles les fonctions f et ψ sont l'une et l'autre tombées à 0,5.

Le caractère rapide de la variation de f étant constaté, il faut connaître la variation concomitante de l'absorption. Ce problème ne sera pas envisagé ici, mais il n'est pas douteux que le coefficient d'absorption varie de manière rapide à la fréquence N^*. D'autre part, on peut voir immédiatement qu'en dehors du domaine de fréquence, où se produit la transition, le terme d'absorption α_d dû à la déformation périodique des molécules est tel que α_d/N^2 soit constant. Ainsi le modèle proposé conduit-il bien à une variation rapide de α/N^2 à une fréquence caractéristique.

Il est à noter que rien ne s'oppose à ce que des niveaux énergétiques supplémentaires conduisent à l'existence de plusieurs transitions du type envisagé, chacune se produisant à sa fréquence caractéristique. Signalons à cet égard que dans le polyméthacrylate de méthyle nous avons observé non pas une mais deux chutes d'absorption ; les deux fréquences caractéristiques augmentent d'ailleurs avec la masse moléculaire, de sorte que les deux chutes doivent traduire des phénomènes de même nature ([2]).

On peut objecter que notre modèle moléculaire présente un certain caractère "ad hoc", et qu'il suppose un nombre de configurations stables beaucoup plus réduit que ne le voudrait la statistique des chaînes sous sa forme classique. Mais, par ailleurs, il a déjà été suggéré que les molécules en chaînes pourraient comporter des séquences de monomères régulièrement ordonnés, chacune constituant un segment hélicoïdal ([5]). Il convient alors de noter que des calculs récents ([6]) concernant des structures hélicoïdales montrent que le potentiel intramoléculaire présente un petit nombre de minima, dont la disposition relative justifierait souvent notre hypothèse n° 2 ci-dessus. Les résultats de ces calculs permettent de voir également que si les segments considérés ici comportent un nombre de monomères de l'ordre de la dizaine, la quantité ΔF atteint déjà des valeurs de l'ordre de 6 Kcal/mole de segments, donc suffisantes, d'après ce que l'on a vu, pour assurer la rapide décroissance de f ([+]).

Sans vouloir lier nécessairement le phénomène au caractère hélicoïdal des segments, les considérations qui précèdent conduisent à prévoir que les spectres d'absorption ultrasonore doivent être différents selon le type et selon le taux de stéréorégularité d'un polymère ([++]).

La figure représente les spectres ultrasonores pour un polyméthacrylate de méthyle (PMM) atactique de masse moléculaire moyenne en poids M_w = 80.000, un PMM syndiotactique de masse M_w = 100.000, donc sensiblement égale à la précédente, et un PMM isotactique de masse M_w = 400.000 ([3]), tous trois en solution dans le benzène (concentration c, en polymère, respectivement égale à $5,78.10^{-2}$; $4,82.10^{-2}$; $3,68.10^{-2}$ gr/cm^3). On a porté en

---

([+]) Dans une molécule hélicoïdale ΔF est une fonction linéaire du nombre de monomères.

([++]) Un polymère est dit stéréorégulier lorsque la structure spatiale des molécules qui le composent représente une régularité bien définie. Ainsi, dans un polymère isotactique les carbones asymétriques ont la même disposition dans l'espace ; dans un polymère syndiotactique les carbones asymétriques ont alternativement une disposition dans l'espace et sa symétrique par rapport à un plan. A ces deux types de polymères stéréoréguliers s'oppose le polymère atactique dans lequel la disposition des carbones asymétriques le long de la chaîne est désordonnée.

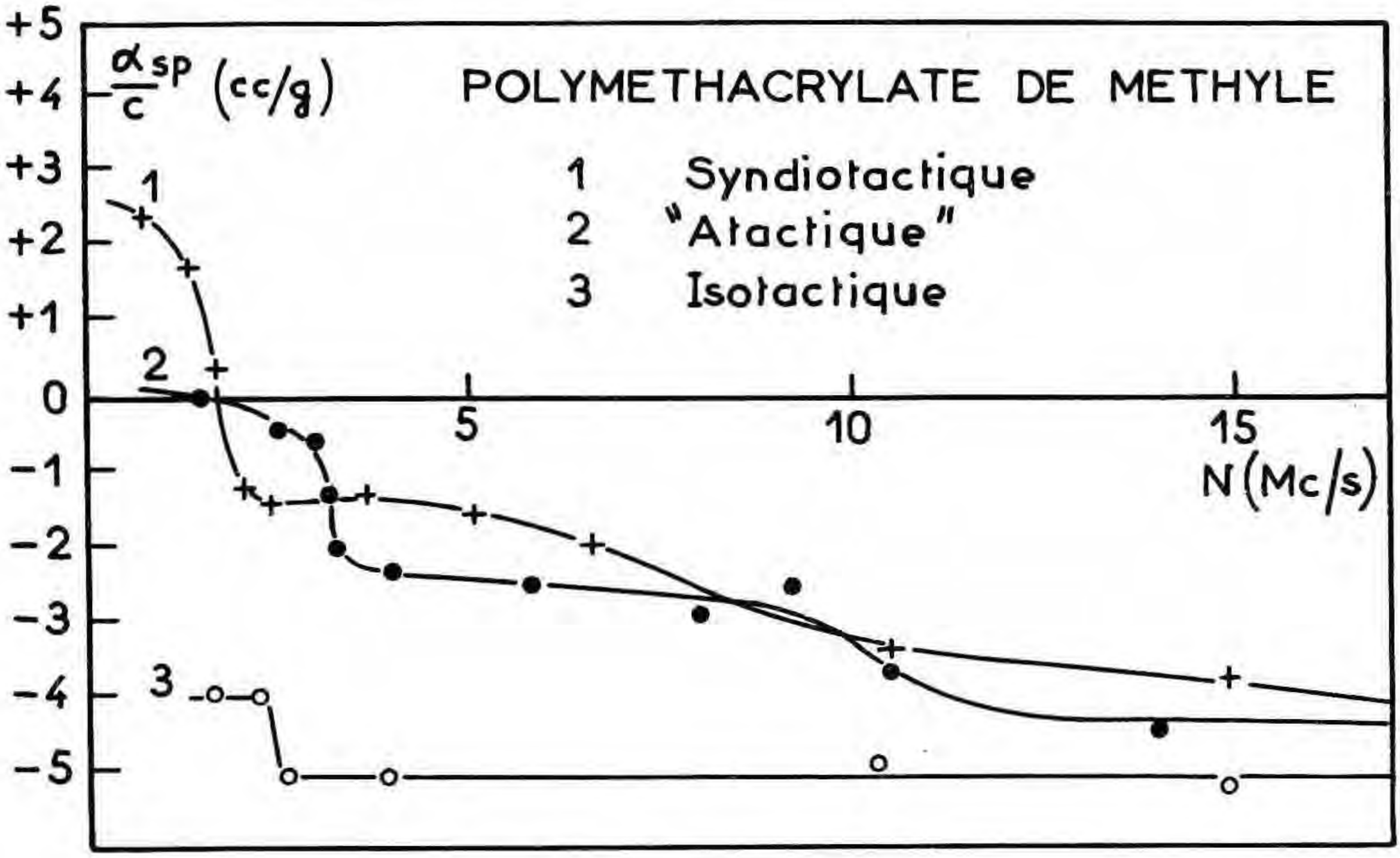

ordonnée la quantité $\alpha_{sp}/c = (\alpha - \alpha_0)/\alpha_0 c$ (α_0: absorption du solvant); pour la clarté du dessin on a renoncé à reporter les points expérimentaux obtenus à des fréquences supérieures à 15 Mc/sec.

On voit notamment qu'à masse moléculaire égale les fréquences caractéristiques sont environ deux fois plus petites pour l'échantillon syndiotactique que pour l'échantillon atactique, et que, dans le domaine de fréquence exploré, la variation de l'absorption spécifique de l'échantillon isotactique est considérablement réduite comparativement aux variations enregistrées pour les deux autres échantillons.

Ces résultats font apparaître de nouvelles perspectives pour l'analyse de la stéréorégularité, et la question sera reprise plus en détail dans la communication suivante.

Références

(1) R. CERF, R. ZANA et S. CANDAU, C.R. Acad. Sci., Paris, 252, 1961, 681 ; Zeits. Elektrochemie, 65, 1961, 687.
(2) S. CANDAU, R. ZANA et R. CERF, C.R. Acad. Sci., Paris, 252, 1961, 2229.
(3) R. ZANA, S. CANDAU et R. CERF, C.R. Acad. Sci., Paris, 254, 1962, 1061.
(4) J. SCHELLMAN, C.R. Lab. Carlsberg, 29, 1955, 223.
(5) M. VOLKENSTEIN, J. Polymer Sci., 29, 1958, 441.
(6) P. de SANTIS, E. GIGLIO, A. LIQUORI, et A. RIPAMONTI, manuscrit obligeamment communiqué par les auteurs, à paraître au J. Polymer Sci.
(7) Les échantillons syndiotactique et isotactique sont dus à l'obligeance respectivement de la Cie ROHM et HAAS, et de Melle M. SAVINO.

K13

FOURTH INTERNATIONAL CONGRESS ON ACOUSTICS
COPENHAGEN 21.-28. AUGUST 1962

Pseudonoise-Correlation Techniques in Underwater Acoustic Studies

J. L. Stewart and W. B. Allen
U.S. Navy Electronics Laboratory, San Diego 52, California

It is the purpose of this paper to present the method of pseudorandom signal (pseudonoise) correlation measurements and to demonstrate theoretically and experimentally that the results are different from and unpredictable from those obtained by employing the usual filtering and detection of impulsive (explosive) or single frequency signals. Since the crosscorrelation of the received underwater acoustic signal with that transmitted is a measure of the feasibility of signal processing techniques employing coherent time averaging, these measurements are of practical importance. A study of such correlation coefficients as a function of the averaging time, frequency, and bandwidth of the signal and of the locations and motions of the source and receiver will lead finally to a determination of those properties of the medium and its boundaries which perturb underwater acoustic propagation.

Two earlier experiments of a similar nature should be mentioned. In air acoustics, Goff[1] crosscorrelated the signals received at one point in a machine shop with the signal recorded next to a particular machine to identify the component due to that particular machine at the distant point. In radar, Lincoln Laboratory's Venus echo ranging experiment[2] employed a series of single frequency pulses 'interval modulated' by a pseudorandom sequence generator and correlated the envelopes of the transmitted and returned pulse trains to suppress the range ambiguity.

Since the system being presented determines the input-output crosscorrelation of the ocean with a broadband pseudorandom signal as input, one might expect by the theorem of Weiner, Lee and Wiesner[3] that the result would be identical with the impulsive response of the ocean obtained by firing explosives and analyzing the received impulses in the same bandwidth. This would be correct if everything were stationary but when reflections from a moving surface or motions of the source or receiver in a nonhomogeneous medium are involved the results may be quite different. That is, the shot measures one sample of the changing impulsive response while the correlation measures its time average. Since the time averaged impulsive response is the Fourier transform of the single frequency response of the medium, one might also expect that the result of the pseudorandom signal correlation might be predictable from propagation studies made with long pulses of different single frequencies. This would be correct even if the situation of medium, boundaries, and terminals were nonstationary; if all the different frequencies in the band could be observed simultaneously; and if the phase spectra of the different frequencies were measured as well as their amplitude spectra. Since in practice only the power response at a few frequencies are measured and these at different times, the single frequency results cannot predict the correlation responses or coefficients for the broadband signals.

Woodward's signal ambiguity function[4] is the squared magnitude of the autocorrelation function with respect to both time and frequency displacement. From a study of the ambiguity functions of available waveforms[5], it is easily seen that the pseudorandom (PR) signals of large time-bandwidth product are much superior to all other waveforms for our purposes. They alone permit simultaneous high resolution of the received signals both in range and in Doppler. The PR waveforms, which are generated by shift reg. encoders,[6] are even superior to sample signals from a real noise generator because all possible sequences of the shift register length occur once and only once before the whole sequence repeats. The PR signals can be completely reproduced with any desired

time delay and time compression by a similar shift register encoder.

The correlator employed must be capable of continuous search over the region of uncertainty in both range and Doppler of the source. Two possibilities presently exist, a matched filter or a time compression correlator. The delay line time compressor (Deltic[7,8]) correlator system we employ uses infinite peak clipping. Clipping has been found to have many practical advantages such as eliminating dynamic range problems, permitting digital storage and shift register time delay techniques. The differences between polarity correlation and complete amplitude correlation are well known[9]. The variations in correlation output due to clipping, sampling, and lack of precise Doppler matching have been observed in the laboratory to be much less than the variations observed in the field which are thus presumably due to the motion of the source or of the medium.

The experiments are conducted by employing an experimental broadband transducer mounted on a submarine operating at sufficient depth to be out of surface wave action and running slowly at right angles to the sound path to produce a low and very constant range rate. The receiving hydrophone is mounted on the continental slope close to the depth of the deep sound channel axis, as in Sofar. The PR signals transmitted are accurately clock driven and repeat every 41 seconds which is much longer than the duration of the sequence of significant arrivals observed. The received and reference signals, which have been heterodyned down to be close to zero frequency, are sampled at twice the signal bandwidth. The 'receive' Deltic compresses and stores the latest 5000 samples of the received signal and correlates it continuously with a similarly compressed fixed set of 5000 samples of the reference signal in the 'reference' Deltic. Since the two signals are heterodyned down with frequencies differing by 10 cps, the output of the correlator is an AC signal which is analyzed in a bank of eleven Doppler filters. The system thus searches continuously in range and Doppler with a time delay resolution which is the reciprocal of the signal bandwidth and a Doppler frequency shift resolution which is the reciprocal of the integration time, i.e. 0.01 seconds for the 100 cps bandwidth and 1/25 cps for the 25 second integration time we have employed. The reference PR signal generator is run faster or slower to match the Doppler of the received signal to center the display.

Figure 1 illustrates our records. It was made with a 760 cps carrier at a range of about 60 nautical miles in the middle of a storm with confused seas. Time is running from right to left. On the right are four unprocessed tenth-second pings which preceded the PR transmissions on the left. On the left are two adjacent Doppler output channels (#5 and #6) with the signal mostly in the upper channel (#6) for the duration of the run. The records have been retraced to place the correlation peaks, which repeat every 41 seconds, adjacent to each other by omitting the blank parts of the record as indicated by the breaks in the base line. Thus the record represents about 15 minutes of PR transmissions. The linewidth resolution on the paper is about equal to the duration of one-tenth second pings but does not resolve the correlation functions with their 1/100th second resolution.

Since the Doppler channels are separated by 1/6th knot at 760 cps, the record indicates that the range rate of the source submarine was constant within 1/12 knot for 15 minutes which makes it an ideal platform for correlation studies. Of course, the surface, bottom, and thermal structure involved in the transmission path did change slowly during the experiment as the source submarine changed slowly in bearing and drifted slightly in range, and to this must be attributed the observed variations.

We do not as yet know the calibrations or linearity of our system to any precision so we can not obtain absolute values but the relative values are of interest. When all of the power is in a single arrival, as happens occasionally in Figure 1, we obtain the highest correlation. The correlation of these main arrivals dropped slowly from the higher values to lower values in long periods of the order of several minutes. Most of this variation is to be associated with the build up of one or two other arrivals and is simply a clipper normalization effect. The curve of dots in Figure 1 is

the sum of amplitudes of the two highest peaks of the observed multiple arrivals in the output of the correlator. The relative stability of the sum indicates that about half of the time the total correlation is constant. Some of the residual variation is due to splitting between Doppler channels, but most of the variation must be due to perturbations of the medium or boundaries such as reflection off the surface or bottom.

The precursor, marked p about 1.2 seconds ahead of the main arrival, is believed to have traveled by an almost purely refracted path with one less top to bottom skip than the main arrival, as is crudely suggested by the ray marked P in the diagram at the top of Figure 1. It will be noted toward the end of the run that, while the main arrival appears frequently in the lower Doppler channel the precursor does so only once, although they both have comparable amplitudes in the upper channel. This is evidence of a very small Doppler difference of the order of 1/12th knot between these two arrivals.

It will be noted that some tails marked t appear about 1.3 seconds after the main arrival in the pings. They presumably take one more top to bottom skip than the main arrival. While they appear with amplitudes comparable with the precursors in the ping records on the right; they do not appear in the correlator output on the left. Such uncorrelated tails can of course also explain why the sum of the correlator peaks is not conserved at all times.

An obvious explanation of the missing tails is that they are more perturbed than the main arrival due to more reflections off the violently moving surface and at higher angles with the surface. Numerically the tails might have angles with the surface of 15° while the main arrivals have angles of 7°. Then the surface perturbation per reflection would be twice as much for a tail arrival as for the main arrival and could be greater than a half wavelength while the perturbation of the main arrival could be less than a half wavelength. Since the dominant period of ocean waves is known to be in the 5 to 10 second region[10] (continuous amplitude modulations of this period were observed on single frequency transmissions) and our integration time is 25 seconds, the tail correlations were wiped out. On this basis, we would expect the tails to hold their correlation for integration times less than 5 seconds.

In our future plans, we hope to obtain the absolute calibration of the searching polarity correlator herein described. We also hope to employ it to synchronize the local PR generator with one of the arrivals. Then we can employ a nonsearching but completely analogue DC correlator to obtain absolute correlation coefficients as a function of averaging time. With these improvements, the pseudorandom signal (pseudonoise) correlation technique is expected to be a valuable tool for the study of the propagation of signals including those of underwater acoustics.

References

[1] K. W. Goff, J. Acoust. Soc. Am. 27, p. 223-246 (1955).
[2] R. Price, Science 129, p. 751-753 (1959).
[3] Y. W. Lee, Statistical Theory of Communication (John Wiley & Sons, 1960) p. 341-348.
[4] P. M. Woodward, Probability and Information Theory with Applications to Radar (McGraw-Hill, 1953) p. 115-125.
[5] J. L. Stewart and E. C. Westerfield, Proc. IRE 47, p. 872-881 (1959).
[6] S. W. Golomb, L. R. Welch, and R. M. Goldstein, Jet Propulsion Lab Progress Report 20-389 (1959), "Cycles from Nonlinear Shift Registers".
[7] V. C. Anderson, Harvard Acoustics Research Laboratory TM-37 (Jan 5, 1956).
[8] W. W. Scanlon and G. Lieberman, Proc. IRE 47, p. 910-920 (May 1959).
[9] J. J. Faran and R. H. Hills, Harvard Acoustics Research Laboratory TM-27 (Sept 15, 1952).
[10] H. O. Publication No. 603, "Practical Methods for Observing and Forecasting Ocean Waves," p. 48 (1955).

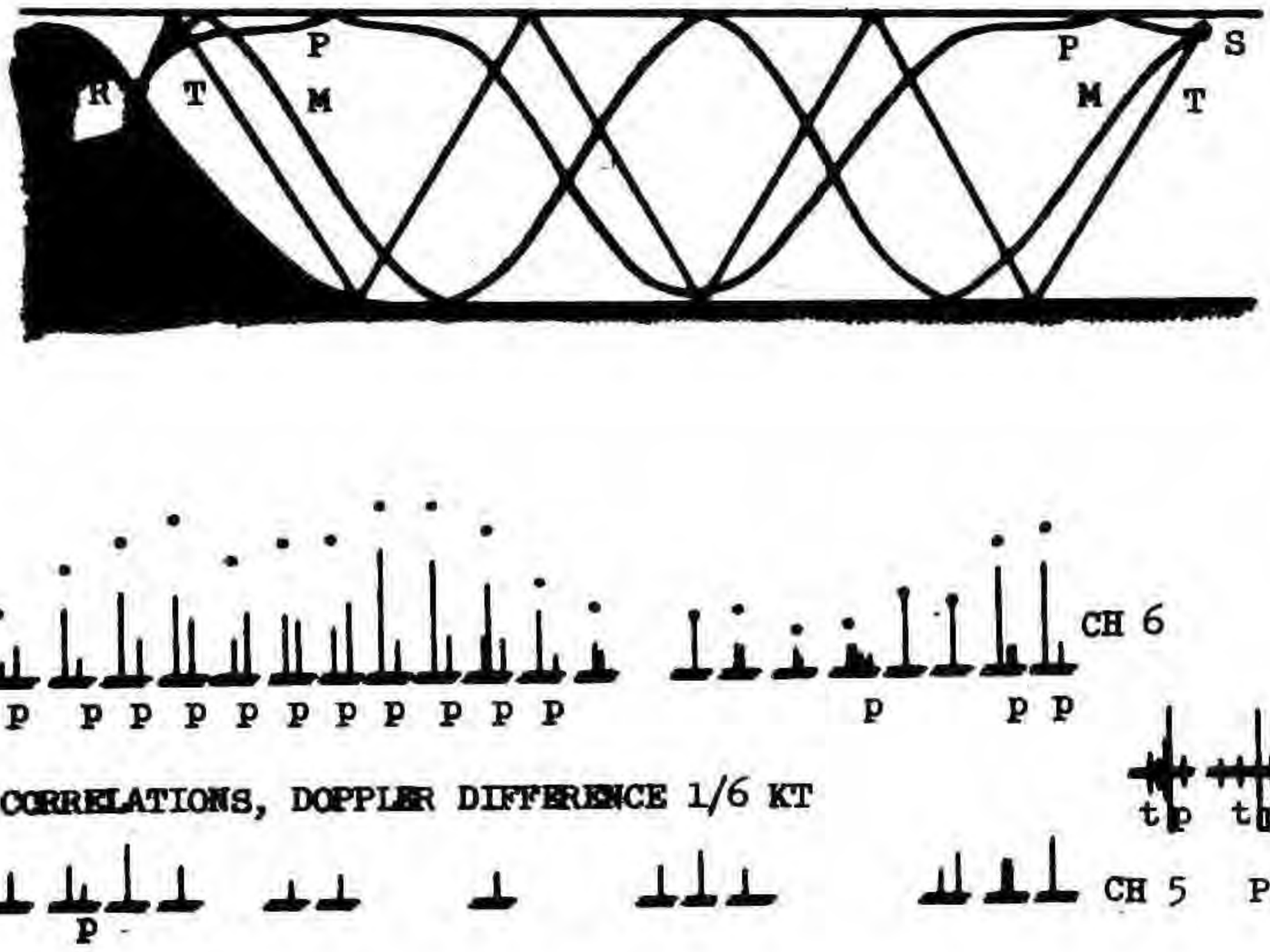

FIGURE 1.

Figure 1. Crosscorrelations of received PR signals with the reference PR signal at about 60 n. mi. range and 760 cps center frequency all shown on the left below. Time runs from right to left. The correlations occurring every 41 seconds (the repetition time of the PR signal generator) are shown in sequence with the blank parts of the record omitted. They occur in two Doppler channels 6 and 5, 1/6th knot apart. The tenth second, 760 cps, calibration pings appear on the right. The main arrivals (unlabeled) are accompanied by precursors p and tails t at separation of 1.2 and 1.3 seconds respectively. Their possible ray paths labeled P and T respectively along with that of the main arrival labeled M from source S to receiver R are suggested in the diagram above.

L13

FOURTH INTERNATIONAL CONGRESS ON ACOUSTICS
COPENHAGEN 21.-28. AUGUST 1962

LE BRUIT DES MOTEURS ELECTRIQUES

Messieurs BARON et JACQUEMOT

Les moteurs électriques auxquels nous nous sommes intéressés sont les moteurs asynchrones utilisés dans les centrales thermiques ; leur puissance s'échelonne entre une centaine et quelque milliers de kW.

Code d'essais

Etant donné la diversité de forme, d'encombrement et de rayonnement acoustique des moteurs, on ne peut les comparer correctement entre eux qu'en déterminant, sinon la puissance acoustique exacte, du moins une quantité qui n'en diffère sensiblement que par une constante.

Dans ce but, le moteur est placé dans un local tel, qu'à l'endroit de la mesure, l'influence des réflexions sonores soit négligeable - inférieure à 1 dB -. On trace autour de lui un contour cylindrique sur lequel on répartit régulièrement 10 - ou 20 - points de mesure et calcule le niveau sonore correspondant à la moyenne quadratique des pressions. Le rayon du cylindre est normalement de 1,50 m et la génératrice de 3,50 m. Pour les gros moteurs, ces dimensions peuvent être multipliées par $\sqrt{2}$ ou par 2 mais on ajoute alors aux résultats la quantité 20 log $\sqrt{2}$ ou 20 log 2.

L'expérience a montré que ce code d'essais permet de définir le bruit d'un moteur à 1 - ou 2 - dB près, étant entendu qu'on utilise un sonomètre de précision.

L'essai se fait à vide, ce qui est suffisant quand le bruit est d'origine aérodynamique. Quand il est d'origine magnétique, on peut être amené à faire également un essai en charge, au besoin en centrale, les conditions de précision étant alors généralement moins bonnes.

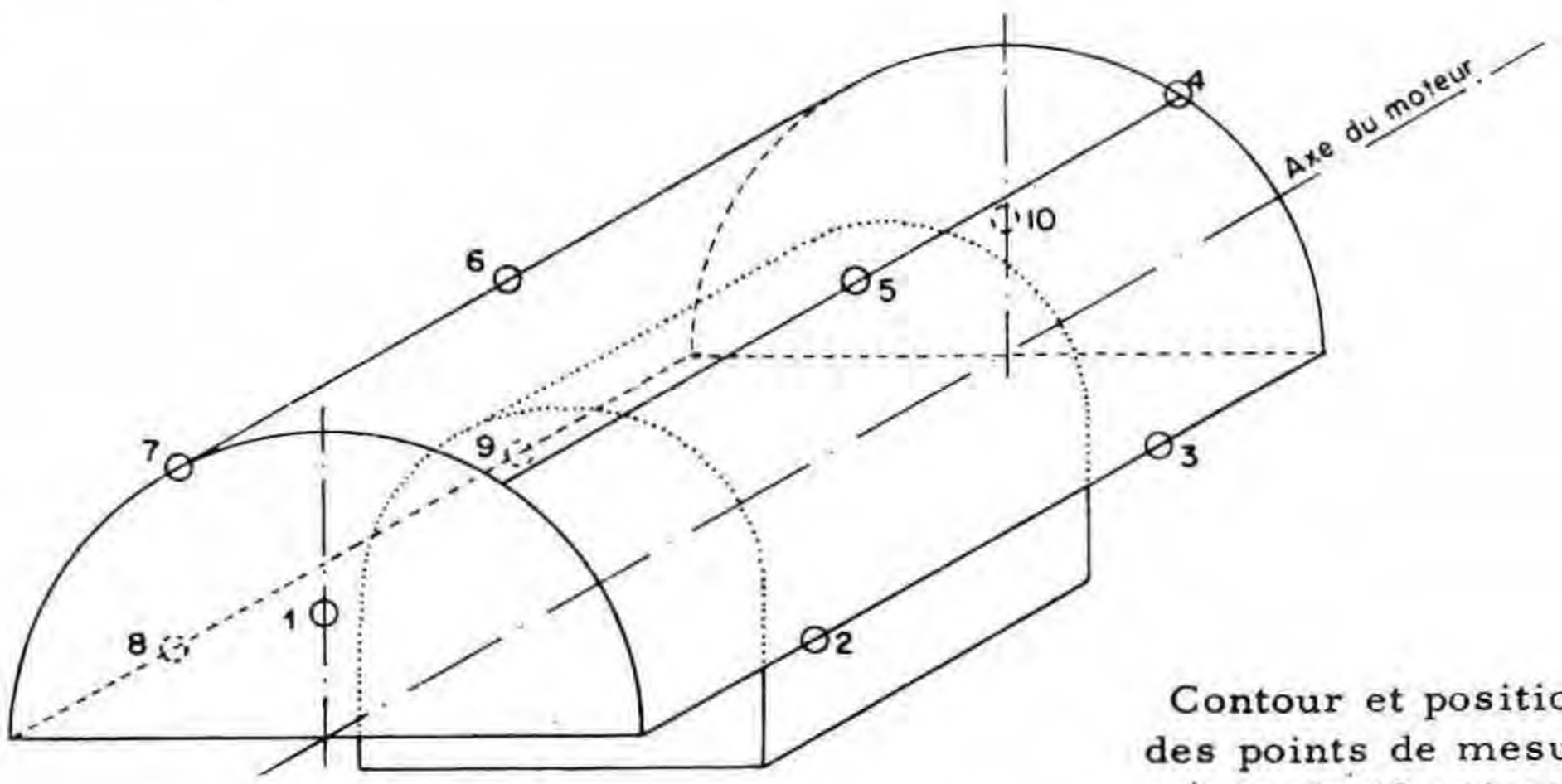

Contour et position des points de mesure (cas de 10 points)

Réglementation

Pour obtenir des conditions d'ambiance convenables, Electricité de France a été amenée à imposer les valeurs maximales suivantes :
. 85 dB pour la valeur globale A ;
. 80 dB par tiers d'octave, les niveaux relevés étant affectés de l'affaiblissement défini par la courbe A.

Tout dépassement est sanctionné par des pénalités, voire par le rebut.
La réglementation par tiers d'octave a pour but de pénaliser les sons purs. Elle entraine une augmentation importante de la durée de l'essai, aussi ne fait-on l'analyse que lorsqu'un son pur se manifeste à moins, évidemment, que la mesure ait un caractère de recherche.

Origines du bruit

Le bruit peut être d'origine magnétique, aérodynamique ou mécanique (roulements). Jusqu'à présent, on s'est surtout occupé du bruit magnétique, lequel a été étudié depuis bien longtemps et, accessoirement, du bruit des roulements. Et pourtant, dans le cas des moteurs refroidis par air et suffisamment rapides - à partir de 1 000 tr/mn le bruit aérodynamique domine généralement. C'est ainsi que le démontage du ventilateur d'un moteur 3 000 tr/mn peut faire baisser le niveau sonore d'une trentaine de dB (A). Pour cette raison, notre attention a surtout été portée sur le bruit aérodynamique et c'est seulement de lui qu'il sera question dans ce qui va suivre.

Caractéristiques du bruit aérodynamique

Le bruit aérodynamique peut se décomposer en :
- un bruit de sirène (spectre de raies),
- un bruit de turbulence (spectre continu).

Le bruit de sirène est assez facile à combattre par éloignement des parties fixes et des parties tournantes du ventilateur et par décalage des canaux de ventilation des tôles rotor et stator.

Quant au bruit de turbulence, pour un type de ventilateur et un circuit de ventilation donnés, il est parfaitement défini et obéit à la loi :

$$10 \log \frac{P_a}{P_o} = 70 \log D + 50 \log N + Cte \qquad (1)$$

$10 \log \frac{P_a}{P_o}$: niveau de la puissance acoustique

D : diamètre du ventilateur

N : vitesse du ventilateur

Il s'agit là de la puissance physique, c'est-à-dire correspondant à l'utilisation d'une courbe de réponse du sonomètre indépendante de la fréquence. Quand on utilise la courbe A, l'influence de la vitesse augmente et le coefficient 50 devient plutôt 55.

Quand la construction est homogène et que les dimensions du ventilateur correspondent exactement à ce qui est nécessaire pour obtenir un échauffement constant, le niveau de la puissance acoustique varie linéairement avec le niveau de la puissance mécanique, les droites obtenues aux différentes vitesses étant sensiblement parallèles. On obtient alors une relation de la forme :

$$10 \log \frac{P_a}{P_o} = 18 \log Pm + 50 \log N + Cte \qquad (2)$$

Pm : puissance mécanique du moteur

Il arrive assez souvent, principalement dans le cas des grosses unités, que la construction ne soit pas homogène, en sorte que la dispersion des résultats est plus élevée en considérant la formule (2) que la formule (1).

D'un constructeur à l'autre et pour le même type de moteur, le bruit aérodynamique varie couramment de 5 à 10 dB.

Possibilités de réduire le bruit aérodynamique.

Dès qu'on arrive à des puissances de quelques centaines de kW à 3 000 tr/mn, la limite de 85 dB (A) imposée est normalement dépassée.

Nous allons indiquer comment le problème a été résolu dans un certain cas, les résultats de cette expérience pouvant être étendus à tous les types de moteurs. Il s'agissait d'un moteur à tubes de 1 470 kW tournant à 1 500 tr/mn (croquis 1). Son niveau de bruit était de 104 dB (C) et de 101,5 dB (A), valeurs qui peuvent être considérées comme normales. Le spectre sonore (courbe 1) est sensiblement continu, avec toutefois une légère pointe dans le tiers d'octave centré sur 640 Hz, qui renferme le son fondamental du ventilateur (24 ailettes, soit 600 Hz).

On a commencé par munir de flasques les ouvertures d'aspiration et de refoulement, flasques qu'on a coiffés de silencieux (croquis 2). Le niveau sonore est tombé à 93 dB (C) et 84 dB (A), l'efficacité des silencieux étant plus faible aux basses fréquences (courbe 2). Par ailleurs, le champ acoustique était plus régulier et la valeur maximale du niveau sonore réduite de 20,5 dB (A). En fait, le bruit de ventilation n'était maintenant guère supérieur au bruit des roulements (courbe 5).

La garantie était ainsi tenue mais ces silencieux sont onéreux, encombrants, lourds et, par ailleurs, ils gênent l'exploitation.

On a alors repris le moteur original mais remplacé le ventilateur par un autre, comportant 12 ailettes en profil d'aile d'avion, fortement inclinées vers l'arrière et précédé d'un pavillon ayant pour but de guider les filets d'air et d'en éviter le décollement. Le spectre sonore (courbe 3) présente un maximum dans le tiers d'octave centré sur 320 Hz renfermant le son fondamental du ventilateur mais son niveau est néanmoins d'une dizaine de dB inférieur à la valeur initiale et, ailleurs, la réduction est nettement plus forte encore. Pour le bruit global, elle est de 15 dB (A), en sorte que le niveau de bruit est passé à 86,5 dB (A). Il convient de noter que cette réduction de bruit s'est accompagnée d'une augmentation du débit d'air de 35%.

Finalement, on a placé, à l'aspiration et au refoulement, endroits où le niveau sonore était le plus élevé, des écrans absorbants. Le niveau sonore est tombé à 88,5 dB (C) et 81 dB (A) (courbe 4), ces valeurs étant d'ailleurs nettement influencées par le bruit des roulements (il s'agissait de roulements à rouleaux).

En résumé, en utilisant un ventilateur convenablement profilé, précédé d'un pavillon, et en munissant les entrées et sorties d'air d'écrans, on est arrivé à gagner 20 dB (A) sur la valeur moyenne du bruit et 22 dB (A) sur sa valeur maximale, tout en augmentant notablement le débit d'air.

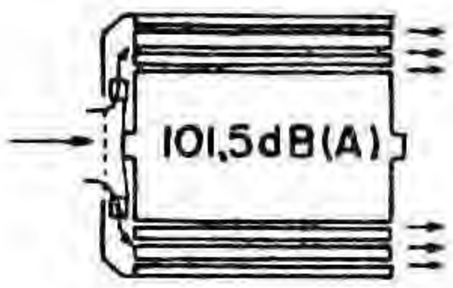

1_ Moteur original

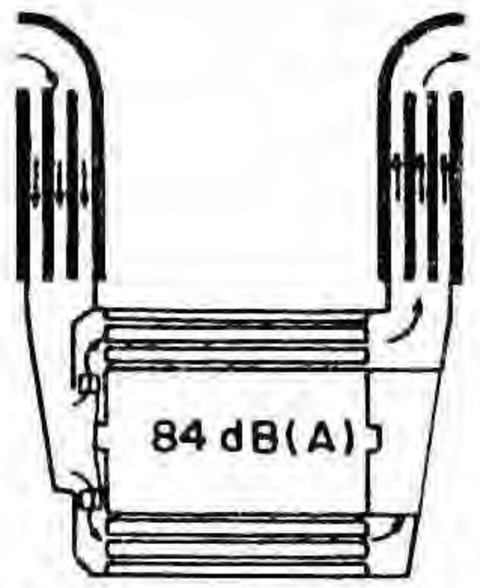

2_ Mêmes dispositions que 1 mais avec silencieux

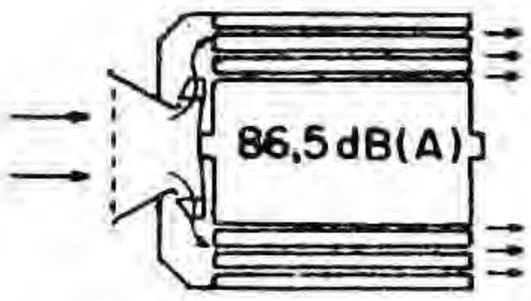

3_ Moteur équipé d'un ventilateur aérodynamique précédé d'un pavillon

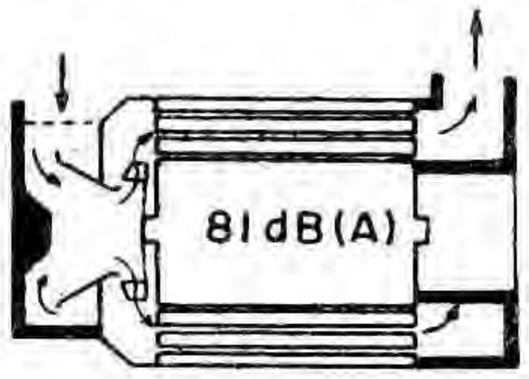

4_ Mêmes dispositions que 3 mais avec écrans absorbants

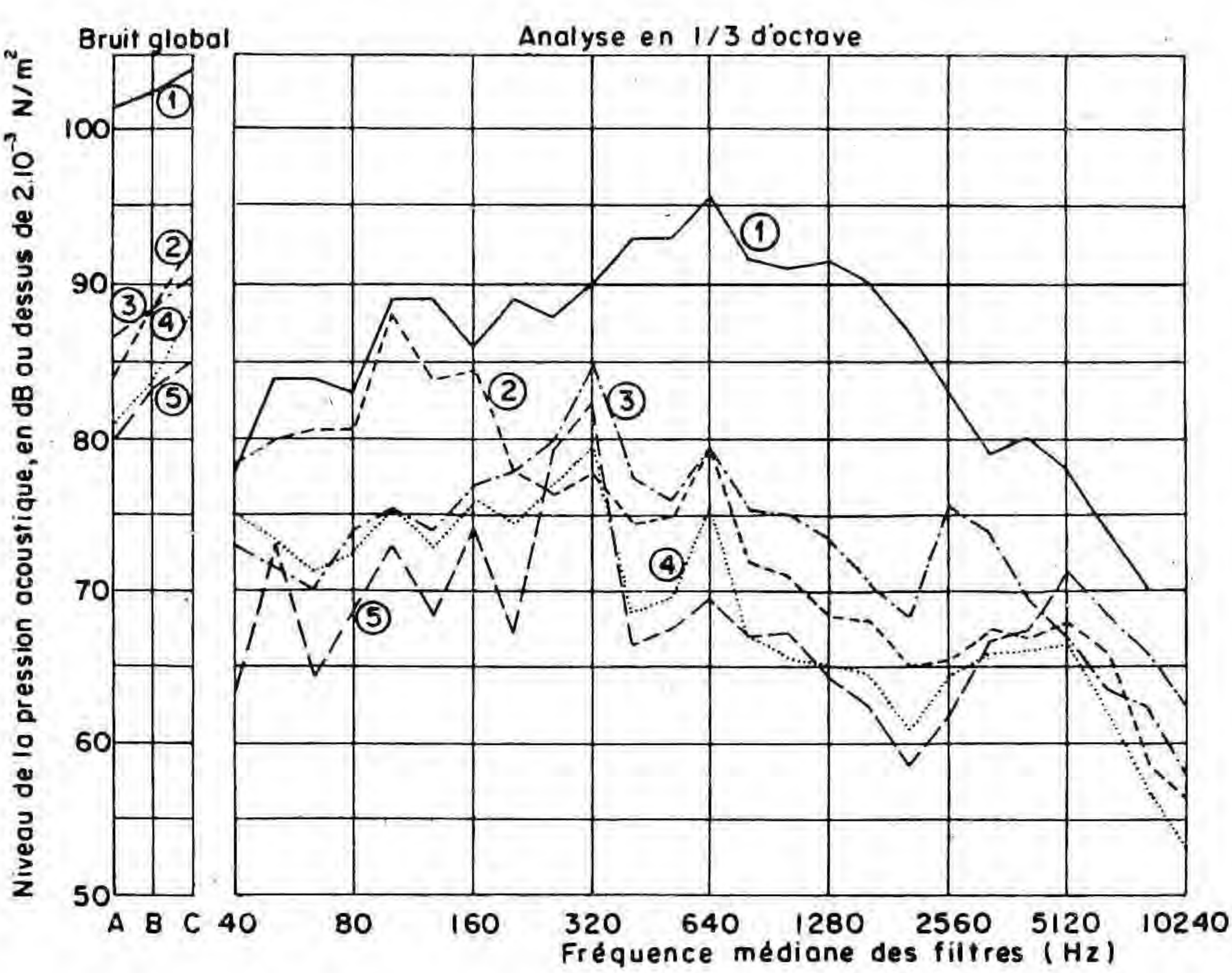

NOTA_ La courbe 5 correspond au croquis 1, ventilateur démonté

M13

FOURTH INTERNATIONAL CONGRESS ON ACOUSTICS
COPENHAGEN 21.-28. AUGUST 1962

PULSE TESTS IN ACOUSTIC MODELS.

J.P.A. LOCHNER and J.F. BURGER.

National Physical Research Laboratory, Pretoria, South Africa.

SUMMARY.

A description is given of tests that were carried out in acoustic models of two widely differing rooms. The results, which were used to compute the percentage articulation to be expected, are compared with measurements and articulation tests carried out in the actual rooms. The agreement is satisfactory.

INTRODUCTION.

A method has been described[1] whereby the results of pulse tests in rooms can be used to compute speech intelligibility. This method has now been applied to two acoustic models built to a scale of 1:16. The results are sufficiently encouraging to warrant further development of the method, in particular the instrumentation. In its present state of development it is already adequate for preliminary tests on proposed rooms, and should be very useful in assessing the relative merits of different designs.

EXPERIMENTAL TECHNIQUE.

In the full-scale tests, use is made of a 10 ms burst of a 1 KHz sine wave. For the 1:16 scale models, 10 cycles of a 16 KHz sine wave were used. An electrostatic loudspeaker, terminated in a thin tube to render it omnidirectional, was used as a sound source, and a Neumann MM5 condenser microphone was used to pick up the sound in the model. Recordings were made on magnetic tape running at 30 i.p.s. and played back at 1/16th of this speed to obtain a normal time scale.

To compute the expected speech intelligibility, it is necessary to know the relative energy and time of arrival of the reflections reaching the listener. This was done by selecting 10 ms intervals (taking the arrival of the direct sound as t=0), squaring the electrical signal and integrating it.

The first 100 ms contribute toward the effective signal level, and sound arriving later than 100 ms after the direct sound acts as masking noise. A detailed investigation, in 10 ms intervals, was therefore only made of the first 100 ms, and in addition a measurement of the total energy reaching the observer was made. This last measurement was performed by integrating over 0-1500 ms, after which time all reflections have died out.

In analyzing the results obtained with the model, the difference in air absorption at 1 KHz and 16 KHz must be taken into account. From published results[2] an attenuation of 0.0025 dB/m at 1 KHz and 0.4 dB/m at 16 KHz were assumed. Since the effect is continuous, the correction factor in dB is a linear function of time and comes to 7.8 dB/s. To obtain a correction factor for the sound energy arriving after 100 ms, where no detailed analysis was carried out, it was simply assumed that the sound decayed exponentially. The reverberation time of the model, measured from the slowed down tape, was approximately 1s. The sound intensity can therefore be written as $P = P_o \epsilon^{-13.8\ t}$; the correction of

7.8 dB/s that must be applied is nearly $\epsilon^{1.8t}$. Consequently

$$\frac{E_{corr}}{E_{meas}} = \frac{\int_{0.1}^{1.5} \epsilon^{-12t}\,dt}{\int_{0.1}^{1.5} \epsilon^{-13.8t}\,dt} \quad \text{which comes to 1.4 dB} \qquad (1)$$

The following table is given as an example:

Time ms	Energy	Correction dB	E_{corr}	αE_{corr}
0-10	367	0.039	370	370
10-20	55	0.117	57	57
20-30	343	0.195	359	359
.	.	.	.	.
.	.	.	.	.
90-100	109	0.74	129	
0-1500	2610		3055	
0-100	1918		2099	1366
100-1500	692	1.4	956	

The factor α in the last column is due to the integration characteristics of the ear, and is a function of the intensity and the delay time of an echo.

In addition to the pulse tests, measurements were made of the relative intensities at the various measuring points in the model, when a constant 1/3 octave band of random noise centered about 16 KHz was radiated by the loudspeaker. If this is I_j at measuring point j, we can say that

$$I_j \propto \sum_{0}^{1500} E_{corr} \qquad (2)$$

and the effective signal at point j is then

$$S_j = \frac{\sum_{0}^{100} \alpha . E_{corr}}{\sum_{0}^{1500} E_{corr}} \cdot I_j \qquad (3)$$

$$\text{The effective noise is } N_j = \frac{\sum_{100}^{1500} E_{corr}}{\sum_{0}^{1500}} \cdot I_j \qquad (4)$$

To the noise given by eq 4, any constant background noise that may be present is added on a power basis. Knowing the effective signal and the total noise at a measuring point, the percentage articulation can be found from curves previously published[1].

RESULTS OBTAINED.

Tests were made in models of the Aula - an auditorium seating 1000 people - of the University of Pretoria, and of our reverberation room (which has a volume of 430 m^3 and a reverberation time of 9 s at 1 KHz). In addition, pulse and articulation tests were carried out in the actual rooms.

Fig. 1 shows the word intelligibility for the Aula calculated from model tests (solid lines) and from full scale tests (dotted lines); results of articulation tests are shown as dots. A constant background noise, giving 40 dB at position 4, was artificially added.

Fig. 2 shows the floor plan of the Aula, with the measuring points indicated by the numbered circles.

Fig. 3 shows results of model tests (solid line) full scale tests (dotted line) and articulation tests (dots) for the reverberation room, with results calculated and obtained under anechoic conditions added as reference. A constant background noise of 50 dB was used during the articulation tests.

DISCUSSION.

In general, the results of the model tests are in good agreement with the experimental results obtained in the actual rooms. It must be pointed out, however, that these rooms had surfaces that were either wholly reflective or absorptive. If models are made of rooms that have surfaces that are partially absorptive, it may become difficult to duplicate these characteristics at the scaled up frequency.

Difficulty due to the directional sensitivity of the transducers used in the models may also arise. In our case, the microphone was not perfectly omnidirectional, and its orientation in the models could affect the results obtained. In actual fact, it was used pointing vertically upwards in the model of the Aula because, since the floor was absorptive, no reflections would reach the microphone from its least sensitive direction. For the model of the reverberation room, four measurements were carried out with the microphone pointing in different directions. The mean value of these measurements was used for the calculations.

It is thought that such deviations as exist between the model tests and the actual tests are to a large extent due to the directionality of the microphone. In spite of this, however, the method seems to be highly promising, and the authors have little doubt that acoustical models can be of great value in the design of auditoria.

REFERENCES.

1. Lochner, J.P.A. and Burger, J.F. "The intelligibility of speech under reverberant conditions" Acustica Vol. 11 No. 4, 1961.

2. Harris, C.M., Handbook of noise control, McGraw-Hill 1957.

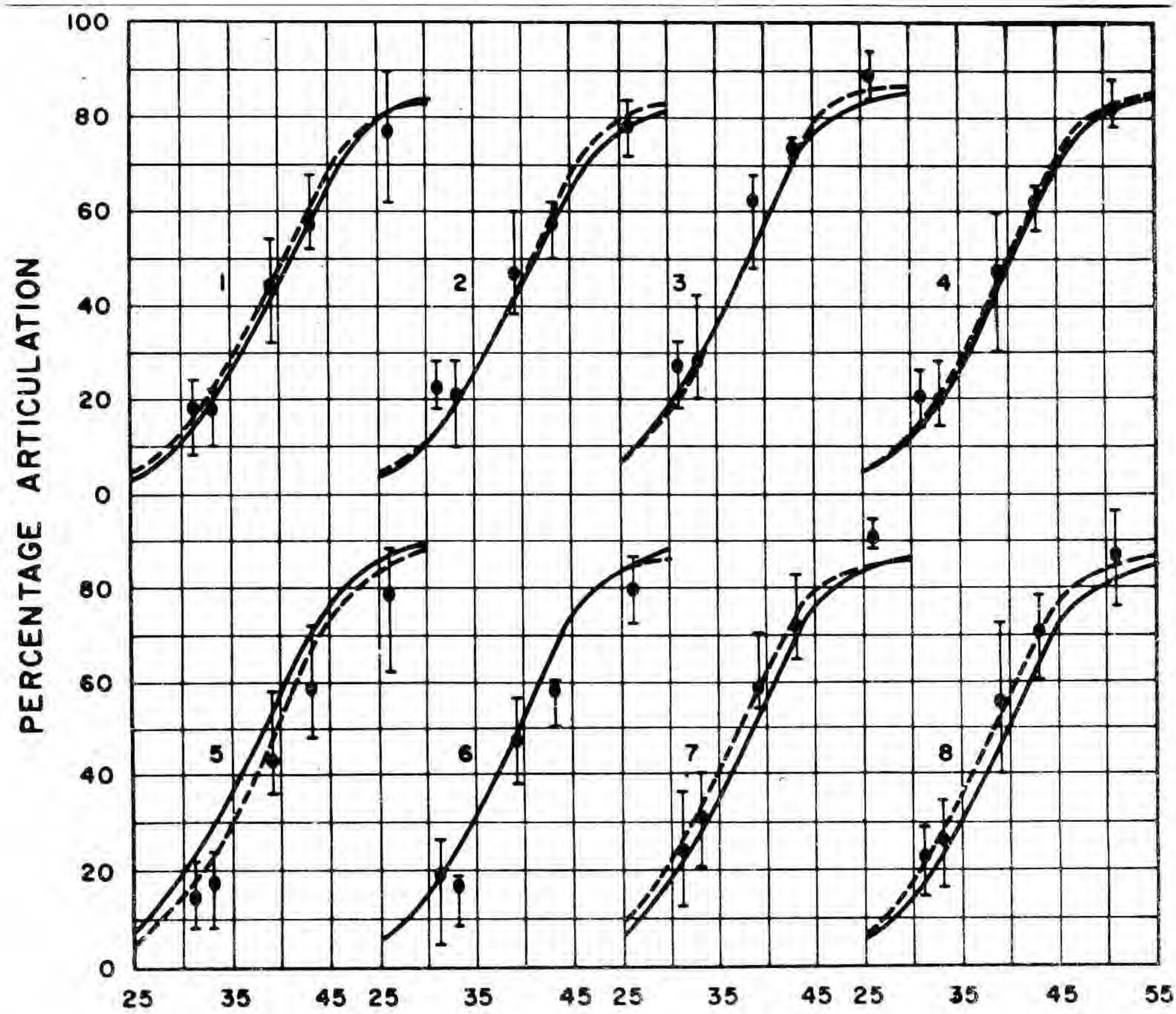

FIG. 1.

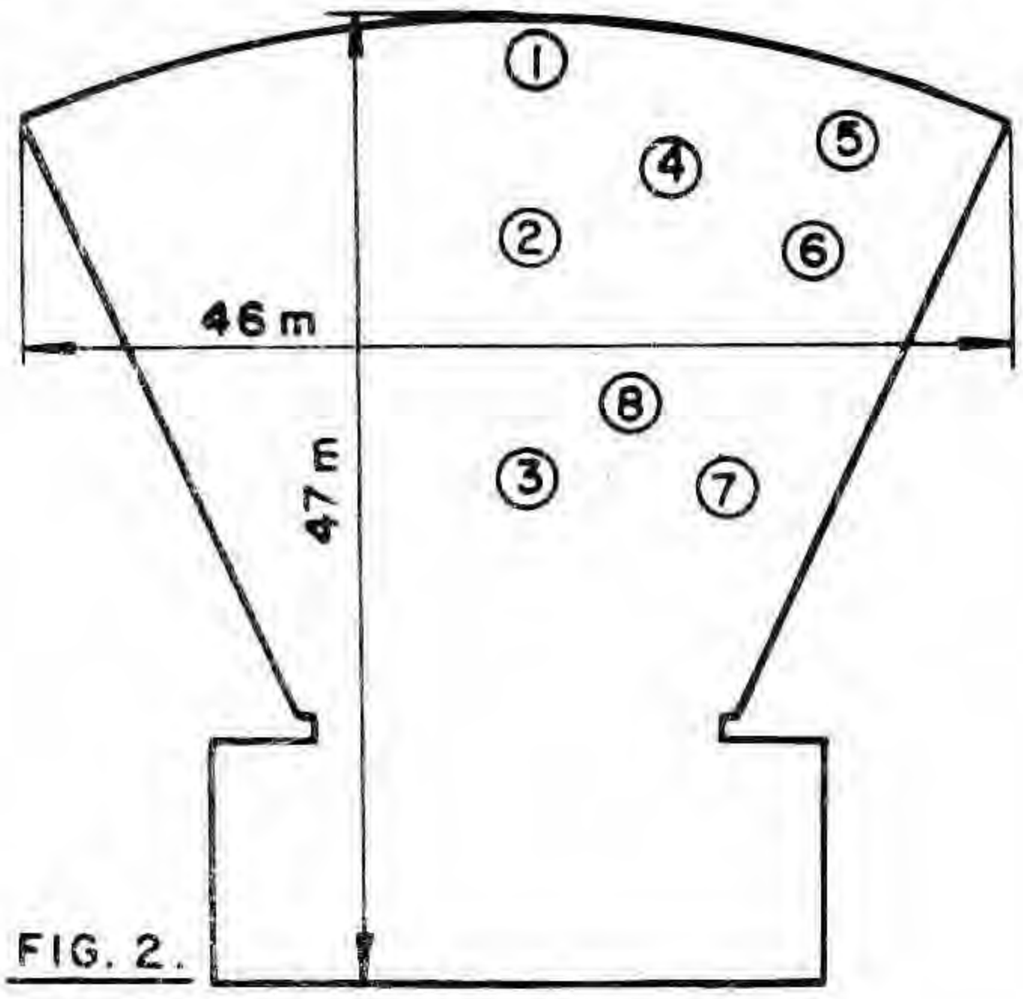

FIG. 2.

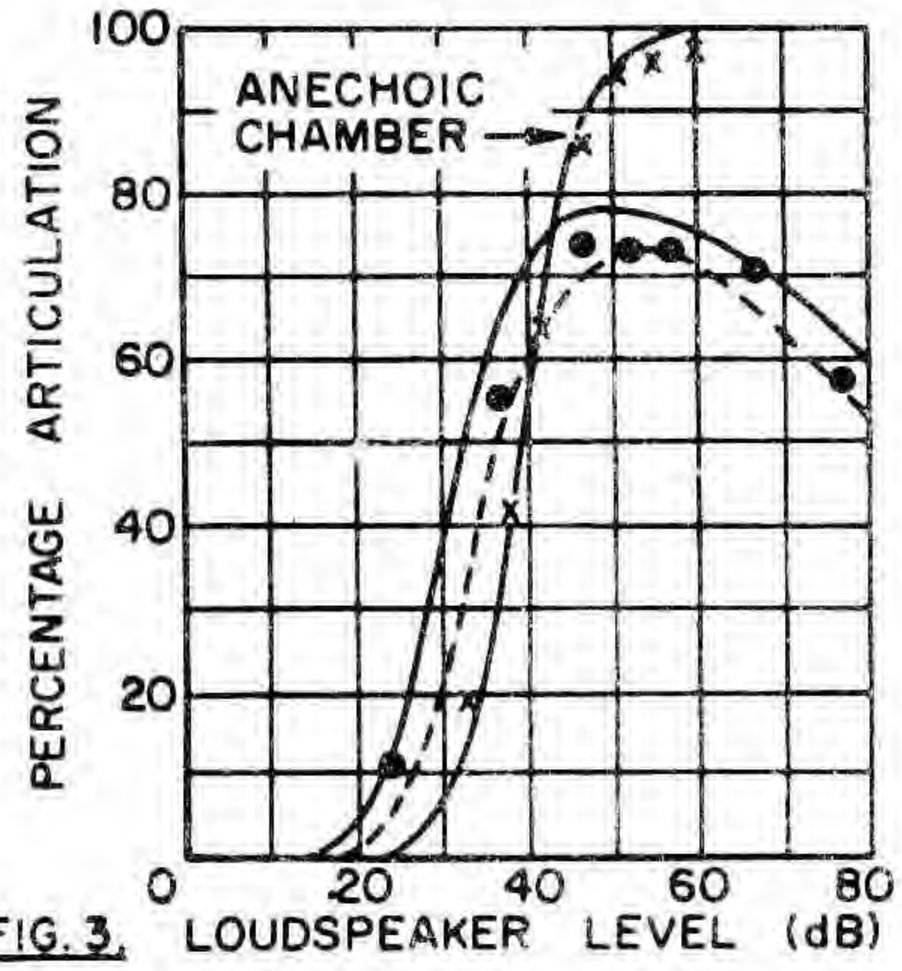

FIG. 3.

N13

FOURTH INTERNATIONAL CONGRESS ON ACOUSTICS
COPENHAGEN 21.-28. AUGUST 1962

ACOUSTIC PROBE FOR INTRAOCULAR PRESSURE MEASUREMENT

Wilfred Roth, Ph. D. and Dale G. Blake

I. Introduction:

The tissues of the eye are normally flexible and elastic. Structural stability is provided by fluid under pressure within the globe. This pressure, termed the intraocular pressure or IOP, is usually maintained reasonably constant over extended periods of time by a balanced flow of fluid into and out of the eye. In the normal eye, the IOP is in the range of 15 to 25 mm Hg. When the balance of the fluid flow is upset by either anatomical or functional defects, the IOP can change radically. A pressure rise of 3 or 4 times normal is not uncommon. Prolonged high pressure, such as occurs in glaucoma, results in the destruction of the optic nerve and retina, causing blindness. Because the symptoms of glaucoma are often mild and transitory, early detection depends on the measurement of IOP by devices called tonometers. If diagnosis is made before substantial damage occurs, continued degeneration and subsequent blindness can be prevented by controlling the intraocular pressure with drugs or surgery.

As early as 1860[1], it was recognized that glaucoma was characterized by increased IOP but it took more than 40 years to devise a useful instrument for pressure measurement. The early workers generally either pushed a plunger against the cornea and attempted to determine the indentation or measured the area of aplanation when a plane surface was pressed against the eye.

In 1905, Hjalmar Schiøtz published[2] a calibration scale for the instrument which he invented and now bears his name. The Schiøtz tonometer introduced a new concept by allowing a curved footplate to rest on the surface of the cornea and a plunger, operating through the footplate, to indent the cornea. Through the action of simple levers, the depth of indentation is indicated on a scale. The Schiøtz tonometer gained rapid acceptance and is the most widelv used instrument today. The instruments of Gradle, McLean and Bailliart[3] are mechanical variations of the Schiøtz which introduce no new concepts. Electronic variations of these instruments have been devised but have resulted in no vast improvements. The Schiøtz tonometer has limited accuracy by virtue of defects in both the instrument and the measuring technique. The force of the basic 16. 5 gm mass of the Schiøtz against the cornea causes gross deformation which increases the IOP significantly, often by a factor of two or more. Thus, the measurement is made with the eye in other than its normal condition. Variations in corneal thickness, radius of curvature and resistance to deformation introduce significant, sometimes gross errors. The error in reading the scale alone amounts to ± 10%

II. Theory of the Vibration Tonometer:

Intraocular pressure is closely associated with an effective spring constant of the eye. The Schiøtz and other tonometers measure this statically, but gross deformation of the cornea is required. Our studies revealed that this spring constant could be measured dynamically without increasing the IOP significantly if displacements were kept small. Figure 1 is a simplified lumped constant equivalent mechanical circuit of a vibrating mass in contact with the eye. Since the spring constant and viscous losses of the vi-

This investigation was supported in part by a PHS Research Grant (B-1007) from the National Institute of Neurological Diseases and Blindness.

bration probe which has been developed are negligible they are not considered here. For a small vibration amplitude, the dynamic mass of the eye is small compared to the mass of the probe.

If an oscillating force $F(\omega)$ is applied across the network terminals, the velocity, $V(\omega)$, is a measure of the system response. By varying the frequency of the force generator and by measuring the response, the values of the circuit elements can be obtained. Since the network is a simple resonant system, conventional velocity and phase response vs. frequency plots are applicable. Since M is known if the effective dynamic mass of eye is small compared to that of the probe, an accurate evaluation of K_d can be made by measuring the resonant frequency of the system. Knowledge of the effective spring constant, K_d, leads, in turn, to the measurement of IOP.

III. Dynamic Spring Constant of the Eye:

Goldmann and Schmidt[4] derived and experimentally verified equations for a static aplanation Tonometer in which a small area of the cornea is flattened by a plane surface. A simple derivation, neglecting surface tension forces due to tears and cornea bending forces follows. By inspection of Fig. 2, we find that $R^2 = (R - x)^2 + (d/2)^2$, $F = AP = \pi P (d/2)^2 = \pi P [R^2 - (R - x)^2]$. For measurement on a dynamic basis, the slope of the force - displacement curve is of interest. If we define $K_d = dF/dx$ = dynamic spring constant, from above, $K_d = 2\pi P (R - x)$. For a measuring technique using small displacements $x \ll R$ so $K_d \cong 2\pi PR$. The resonant frequency of a vibration tonometer is given by $\omega_0^2 = K_d/M = 2\pi PR/M$.

A significant variation in resonant frequency can be obtained as a function of IOP but there is also a similar dependence on the radius of curvature of the cornea. In the general population, the variation in corneal radius is quite small so only small errors will be introduced. In those cases where the corneal radius of curvature is markedly different from normal, the radius can be determined by other means and the reading corrected. In any case, we find that the dependence of the vibration tonometer on corneal curvature is considerably less for most radii and pressures than the Schiøtz. For the vibration tonometer, the correction for R is independent of IOP while, with the Schiøtz, the correction for R is a complicated function of IOP.

The neglected surface tension and bending forces have been evaluated by Goldmann and Schmidt[5]. These factors increase the complexity of the final equation but do not grossly affect the results given above on the basis of the simplified derivation.

IV. Description of the Vibration Tonometer:

The following criteria were selected as research goals for the vibration tonometer: high degree of safety, accurate, portable, convenient to use and rugged. Only small forces were to be generated in order that change of IOP and corneal deformation would be negligible. The vibration tonometer which has been developed meets these requirements. The instrument, Fig. 3, comprises a probe and a small electronic unit. The probe, designed to be hand held, contains an electromagnetic force generator and a velocity pick-up transducer. A hollow steel shaft with a flat tip on one end and transducer elements attached along its length, is mounted axially within the probe case. This shaft, supported by ruby bearings, is free to move axially within the limits of mechanical stops with very low friction. The driving and pick-up transducers are designed to provide constant force and sensitivity, respectively, over a wide range of axial position of the probe shaft assembly.

Measurements are made by resting the plastic tip (1/4" diameter disc) at the end of the shaft on the cornea. The velocity pick-up develops a voltage proportional to the velocity of the cornea. This signal is amplified by a high gain transistor amplifier and applied to the driver as regenerative feedback. The system oscillates at the resonant frequency determined primarily by the mass of the probe armature and dynamic spring

constant of the eye. Frequency measuring circuits display the reading on a micro-ammeter.

The force transducer generates a d. c. force with a superimposed a. c. force at the oscillation frequency. The d. c. force component insures that the aplanating tip remains in contact with the cornea. The average force of 1. 5 grams raises the IOP less than 0. 5 mm Hg. Over the extremes of IOP, the resonant frequency varies from 30 to 160 cps. Since the driver is a constant velocity generator, the amplitude of vibration is an inverse function of frequency for a particular Q of the eye. At 100 cps the peak-to-peak displacement is approximately 0. 08 mm. on a whole pork eye.

V. Experimental Results:

In early 1961, after a preliminary evaluation at the Roth Laboratory, a first generation instrument was sent to the Howe Laboratory of Ophthalmology at the Massachusetts Eye and Ear Infirmary in Boston, Massachusetts. Readings as a function of IOP were obtained on whole rabbit and human eyes and anterior hemispheres of human eyes in a Friedenwald Frame. The curve in Fig. 4 was obtained by the Howe Laboratory while evaluating the vibration tonometer on an enucleated whole human eye.

Several different types of tips were under evaluation at that time. This particular curve was obtained with a small nonaplanating tip. This tip later proved too difficult to position and led to scatter in the data.

The Howe Laboratory conducted experiments to determine the effects of ocular rigidity and the degree of precision necessary in placing the tip on the cornea to get reproducible results. Their results regarding ocular rigidity indicated that rigidity effects were small. The probe did prove to be difficult to position. In this prototype instrument, the longitudinal dynamic range of operation of the probe was small.

In the spring of 1961, an improved probe and circuits were constructed and used at Roth Laboratory. During the following months a large number of pressure runs were made on pig and bovine eyes and simulated eye models. The data in Fig. 5, using an organic membrane to simulate the eye, is typical. Further improvements were made in both the probe and the circuits as a result of these experiments. The aplanating tip was found to be easy to position and gave the most reproducible results.

Analysis of data indicated that the resonant frequency of the eye-probe mechanical system was proportional to $(\text{Pressure} + \text{Constant})^{1/2}$. The constant is due to the effects of a small internal spring constant within the probe and surface tension[6].

The vibration tonometer has been used on 182 en vivo human eyes to date. Satisfactory operation was achieved on 180 eyes. For reasons as yet unknown, the instrument failed to perform properly on one subject. The instrument has been convenient to use and the data has been reproducible within a few percent.

Positive correlation with the Schiøtz tonometer was obtained. However, when the readings are plotted against each other, there is considerable scatter. This is not surprising because the Schiøtz, alone, exhibits large scatter when its readings are plotted against known pressures in the eye.

Further and more exacting experiments are now in progress on five vibration tonometers. These include comparison with the Goldmann aplanation tonometer and Schiøtz tonometer. Experiments will also be performed on excised eyes. When the general utility of the vibration tonometer has been firmly established, experiments will be made to determine the feasibility of clinical measurement of IOP with the probe tip operating on the sclera or on the cornea with the eyelid interposed. Preliminary results indicate the possibility of success in this direction. Further effort is also being directed toward use of vibration principles and a modified probe tip to measure corneal and scleral rigidity.

VI. Conclusions:

The vibration tonometer shows promise as a more accurate instrument to measure intra-

ocular pressure. The forces applied to the eye by the probe are so small that negligible change in pressure occurs during measurement. It is simple to use and has proved to be reproducible. Clinical correlation studies are in progress to determine its ultimate usefulness as a general medical instrument.

Fig. 1 Equivalent Mechanical Circuit

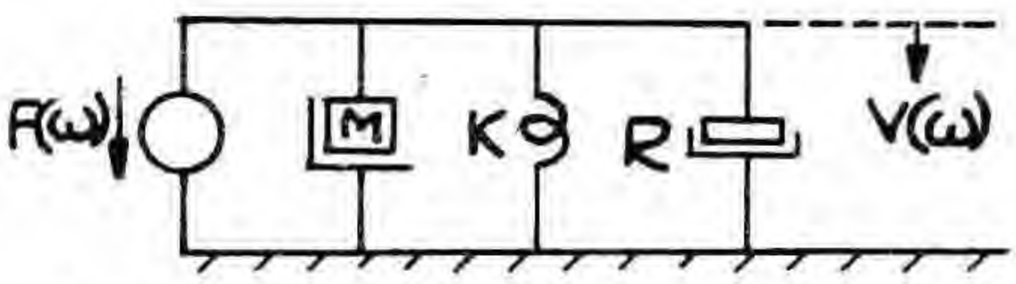

where:
M = mass of the vibration probe assembly & dynamic mass of the eye
K = effective spring constant of the eye
R = viscous dissipation in the eye
V(ω) = velocity of the system
F(ω) = force generator

Fig. 2

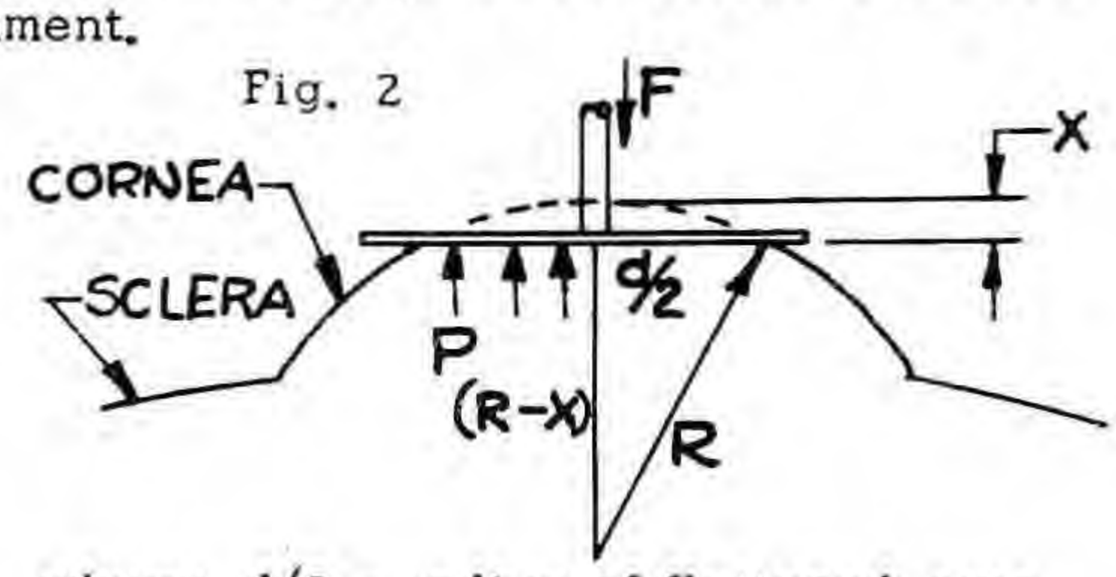

where: d/2 = radius of flattened area
R = radius of curvature of cornea
x = displacement of cornea
F = force necessary for flattening
A = area of contact = $\pi(d/2)^2$

Fig. 3 Probe & Block Diagram

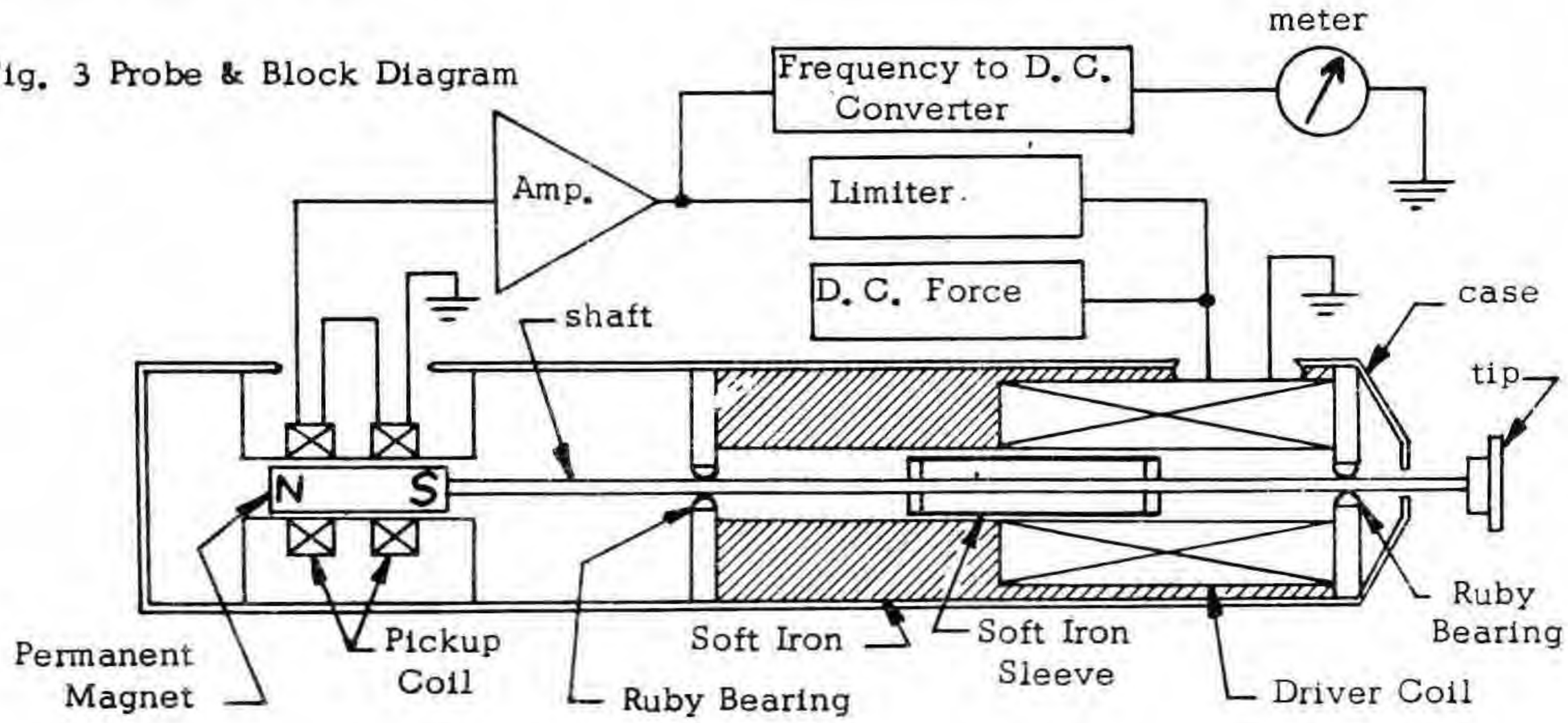

Fig. 4 Human Eye

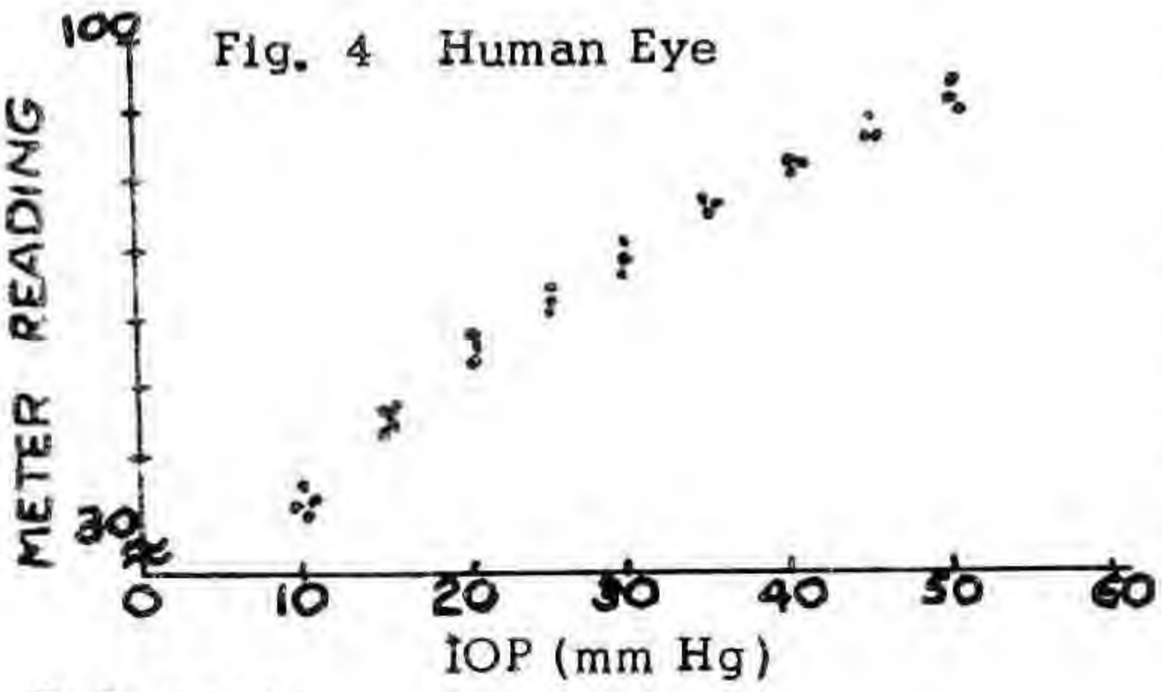

Fig. 5 Organic Membrane

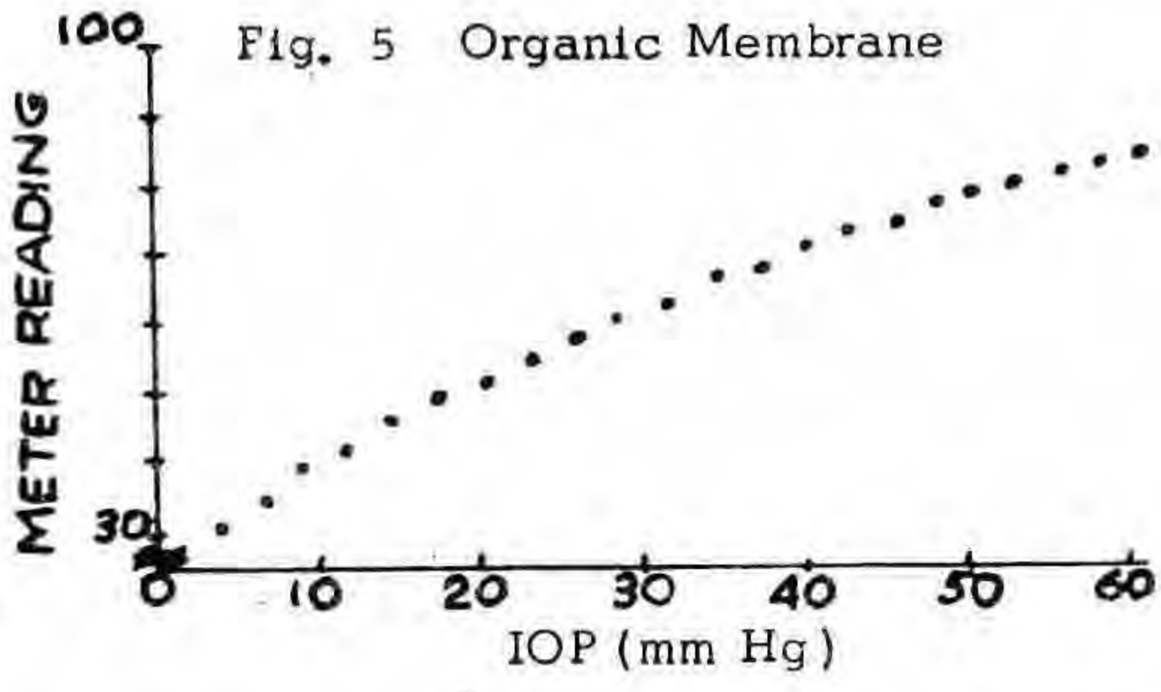

References:
[1]Jonas S. Friedenwald, M. D., Standardization of Tonometers, Decennial Report 1954, Calibration of Tonometers, p. 94. [2]Ibid., p. 97. [3]Ibid., p. 96.
[4]Goldmann and Schmidt, Ophthalmologica, 134, 221 (1957). [5]Ibid. [6]Ibid.

O13

FOURTH INTERNATIONAL CONGRESS ON ACOUSTICS
COPENHAGEN 21.-28. AUGUST 1962

Beiträge zu dem Mechanismus des aktiven akustischen Feldes

P. GREGUSS

Ultraschall-Laboratorium, Wissenschaftliches Forschungsinstitut für Eisenbahnwesen, Budapest

Der akustischen Energie - oft als Ultraschall bezeichnet - und den durch seine Anwendung ergebenen Möglichkeiten wird auf den verschiedensten theoretischen Gebieten immer annehmender Interesse entgegengebracht. Dieser erhöhte Interesse am Ultraschall ist durch die Sonderheiten bedingt, die ihn von anderen Energiesorten unterscheiden. Die intensive akustische Energie hat häufig beträchtliche Veränderungen des ihn fortleitenden Mediums zur Folge, so dass es gerecht scheint in diesen Fällen - im Gegensatz zu den Methoden, wo der Ultraschall zur zerstörüngsfreie Erforschung der physikálisch-chemischen Eigenschaften verschiedenster Systeme angewandt wird - über aktiven akustische Energie zu sprechen.

Für die obenerwähnten beträchtlichen physikalisch-chemischen Veränderungen in dem aktiven akustischen Felde steht in manchen Fällen eine eindeutige Erklärung noch aus. Im allgemeinen führt man diese, oft verblüffende Vorgänge auf die in einer Schallwelle herrschenden intensiven Schallstrahlungsdrucke, Wechseldrucke, - die am meisten fast gleichzeitig von sekundären Wirkungen, wie Kavitation, thermische Effekten usw. begleitet sind, - zurück. Wenig Aufmerksamkeit wurde aber bis zur Zeit auf jene enormen Werte der Amplituden der Teilchenbeschleunigung gewidmet, die im Ultraschallgebiet bis zur zehnfachen Wert der Erdbeschleunigung ohne besondere Massnahmen - wie z. B. Fokus-

sierung des Strahlenbündels - zu erreichen sind.

Das aktive akustische Feld kann ohne weiteres als von Mikrogravitationsfeldern aufgebautes disperses System betrachtet werden. Ein System ist nämlich in dispersem Zustand, - wie es nach einer, von W. Ostwald stammenden Definition bekannt ist, - wenn irgendeine seiner Eigenschaften räumliche Periodizität aufweist. Dieses trifft auch dann zu, wenn das disperse System nur stationär existiert, also immer und immer aufgebaut und wieder vernichtet wird. Darum sind in diesem Sinne auch Schall- und Ultraschallwellen als stationär-disperse Systeme zu betrachten, wie es Auerbach /1/ in einer seiner Veröffentlichungen auch tat.

Sowohl bei stehenden, wie bei fortschreitenden Wellen, bei einzelnen Wellen, wie bei interferierenden Wellenpaketen besteht nicht nur eine räumliche Periodizität der Dichte, der Brechungsexponenten, sondern auch eine räumliche Periodizität der Beschleunigungsamplitude.

Während ein einzelnes Wellenfeld, hinsichtlich der Dichte, Brechungsexponenten usw., partielldisperse und zwar im allgemeinen lamellar orientierte Systeme ergibt, handelt es bei der Beschleunigungsamplitude um im Raume total-disperse Systeme, da das Gravitationsfeld der Erde mit den Beschleunigungsamplituden der Schallwelle interferiert. Nachdem die beiden Beschleunigungswerte im allgemeinen nicht gleich sind, handelt es sich fast immer um eine räumlich anisotrope Disperside, deren Längsausdehnung in Richtung der grösseren Werte verläuft. Dass jene Beschleunigungskräfte bei den Effekten im akustischen Felde eine Rolle spielen können, kommt - unter anderen - aus den Versuchen hervor, die bestätigten, dass bei Veränderung der Richtung der Wellenfronts eine quantitative, und manchmal sogar eine qualitative Anderung der Vorgänge zu beobachten sind, ohne dass andere Parameter sich ge-

ändert hätten.

Die erste Erscheinung, die unsere Aufmerksamkeit auf den gerade dargestellten Gedanken lenkte, hing mit unseren ausführlichen Untersuchungen über den Einfluss von Ultraschall auf den Vorgang der Präzipitation von Kreide zusammen. Wir fanden nämlich, dass bestimmte Kristallformen häufiger gebildet wurden, wenn die Richtung des aktiven akustischen Feldes 90° mit der Richtung der Erdbeschleunigung einschloss, als wenn sie damit parallel war.

Als wir die Untersuchungen von Kapustin /2/ über das Verhalten von Plexiglas im intensiven Ultraschallfeld wiederholten, konnten wir nicht nur seine veröffentlichte Ergebnisse bestätigen, sondern fanden noch, dass die Intensität und Form der von den Ultraschallwellen hervorgerufenen Spannungen, bei gleichbleibenden Schallfeldparametern, von der Beschallungsrichtung abhängt.

Diese beiden Beispiele lassen keinen Zweifel, dass man bei der Erklärung des Wirkungsmechanismus des aktiven akustischen Feldes mit der Beschleunigungsamplitude zu rechnen ist. Wie aber die Beschleunigungswerte zu den Veränderungen im intensiven akustischen Felde beitragen, ist noch heute in meisten Fällen eine offene Frage.

Bei der Auslegung der Ergebnisse über den Einfluss der intensiven akustischen energie auf den Vorgang

$$Ca/OH/_2 + CO_2 = CaCO_3 + H_2O$$

gingen wir von der Tatsache aus, dass die Kristallform des Produktes stark temperaturabhängig ist. Wir benutzten nur reine Ausgangsstoffe, arbeiteten bei Zimmertemperatur und so erwarteten wir als Präzipitatum nur feine Kalcitkristalle, da von reinen Lösungen - wie bekannt - unter $30^{o}C$ nur Kalcit ausscheidet. Das war auch der Fall, wenn kein intensives akustisches Feld vorhanden war, aber man erhielt auch Arago-

nitkristalle, als man intensive Ultraschallwellen von 800 kHz anlegte. Der Anteil der Aragonitkristalle hing aber nicht nur von der Intensität der Ultraschallwellen, sondern auch von der Beschallungsrichtung. War diese horizontal, so war der Aragonitanteil grösser, als bei senkrechter Bescahllung. Alle Parameter blieben unverändert, so konnte man nur auf den Schallstrahlungsdruok oder auf die Beschleunigungsamplitude als Grund für die Entstehung von Aragonit denken. Da aber bei Beschallung von oben nach unten der Aragonitanteil keinen wesentlichen Unterschied aufwies, kam nur die Beschleunigungsamplitude in Frage.

Um die Erscheinung zu erklären, gingen wir zur vielbestrittenen Theorie von Erdélyi /3/ zurück, die behauptet, wo Beschleunigungsunterschiede vorhanden sind, auch Temperaturgradienten auftreten. Nach dieser Konzeption ist das Aragonitanteilerhöhen bei horizontaler Beschallung verständlich, da in diesem Falle bei unveränderlichen US-Intensitäten mit einer grösseren Beschleunigungsamplitude zu rechnen ist, als bei vertikaler Bestrahlung. Dieser Temperaturgradient kann bei 6g - 10g mehrere $10^{o}C$ erreichen, was bedeutet, dass in dem durch US erzeugten stationär-dispersen System solche Temperaturerhöhungen vorhanden sein können. Geht der beschriebene Vorgang in einer der erwähnten Punkte vor, so bildet sich ein Kristall gemäss der lokalen Temperatur.

Selbstverständlich sind diese Ergebnisse noch keine eindeutige Beweise weder für die Theorie von Erdélyi, noch für die heterodisperse Auffassung des aktiven akustischen Feldes, jedoch weisen sie auf die Wichtigkeit der Frage der Beschleunigungsamlpitude. Weitere Versuche sind im Gange.

Literatur: R. Auerbach: Kolloid Z. 119 /1950/ 166
A. P. Kapustin: Prim. Ultraakust. Issledow. Vesh. 6/1958/139.
I. Erdélyi: Acta Technica Ac.Sci.Hung.XXVII./1959/ 128.

P13

FOURTH INTERNATIONAL CONGRESS ON ACOUSTICS
COPENHAGEN 21.-28. AUGUST 1962

ON THE CONVERSION OF LONGITUDINAL TO SURFACE WAVES IN SOLIDS

Walter G. Mayer
Physics Department, Michigan State University,
East Lansing, Michigan, U.S.A.

Various experimental techniques for the production of surface waves on a free surface of a solid have been described in the past (1). Quite frequently one uses the method of converting a longitudinal wave in a solid to a surface wave on another solid in contact with the first. The present paper is concerned with this type of mode conversion because the energy transfer from a longitudinal to a surface wave seems to offer possibilities for decreasing the intensity of the reflection of the longitudinal wave in the solid through which it is propagated. Some experimental results for a specific case are given here.

The production of a surface wave is usually accomplished by the familiar wedge method shown in Figure 1. The amplitude of the surface wave reaches a maximum (2) when the angle of incidence α is chosen that the ratio $V_L/V_S = \sin\alpha$, where V_L is the velocity of the longitudinal wave in solid I, and V_S is the velocity of the surface wave on solid II. An arrangement of this type has the disadvantage that one cannot easily determine how much energy contained in the longitudinal wave is transferred to the surface wave. A slightly different wedge was therefore used, shown in Figure 2. An ultrasonic pulse is emitted by transducer E. If the bottom surface of the wedge is in contact with air the pulse will be totally reflected and will be picked up by the receiving transducer R. The amplitude of the received pulse is taken as reference for the subsequent experiment in which the wedge is placed on the smooth surface of solid II. In the experiments described here solid II is aluminum while solid I is Plexiglas. The velocities V_L and V_S were determined experimentally by a conventional pulse method. Placing the Plexiglas wedge on the aluminum surface allows the mode conversion from a longitudinal wave in the wedge to a surface wave on the aluminum. The wedge is cut in such a way that the angle of incidence α satisfies the above condition for optimum surface wave production. With the wedge on solid II there is no more total reflection of the incident pulse, and the amplitude of the signal received by transducer R should decrease by an amount determined by the energy converted to the surface wave. However, it is found that using the Plexiglas wedge the amplitude of the received pulse increases when the wedge is placed on the aluminum. This may be explained by considering the loss mechanisms. If the wedge is not in contact with solid II every part of the sound signal emitted by transducer E travels the same distance in the wedge before it reaches transducer R. The absorption in the Plexiglas is quite high. If the wedge is then placed on the aluminum a surface wave is generated between the two solids. As this wave propagates along the surfaces it may radiate energy back into the wedge. If the absorption of this wave should be less than the absorption of the longitudinal wave in the wedge a signal of higher amplitude would be received at R than if the signal had traveled entirely in the Plexiglas.

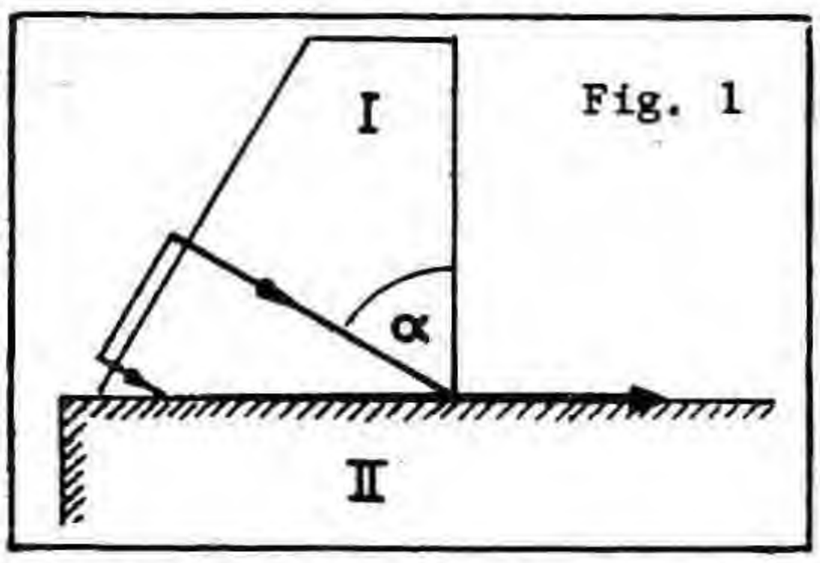

Fig. 1

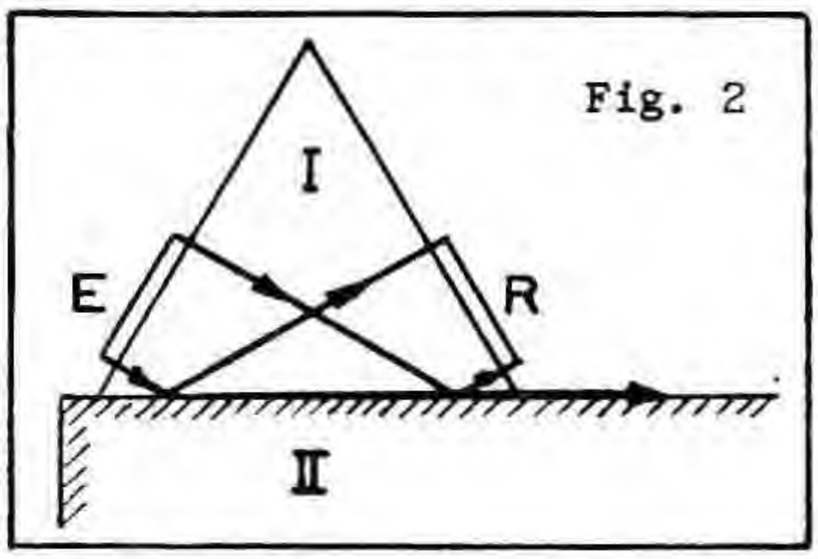

Fig. 2

One would, therefore, like to minimize this radiation back into solid I. Ideally, one would like to separate the surface wave from the bottom of the wedge as soon as it is generated. But this wave is generated over a finite area of contact between the two solids, and the size of this area is determined by the size of the emitting transducer and the angle of incidence; one therefore encounters certain experimental limitations in separating the surface wave from the bottom of the wedge. Since the central portion of the ultrasonic signal emitted from transducer E contains more energy than the outside of the beam one might remove the corresponding most intense portion of the surface wave by rounding off one edge of solid II and placing it in relation to the wedge as indicated in Figure 3. The radius of curvature of the rounded edge is big enough so that the surface wave will travel around it (3). Adjusting the relative positions of the wedge and solid II in this manner one transfers the most intense part of the longitudinal wave in the wedge to a surface wave which is then conducted away from the wedge, thus reducing radiation back toward the receiving transducer.

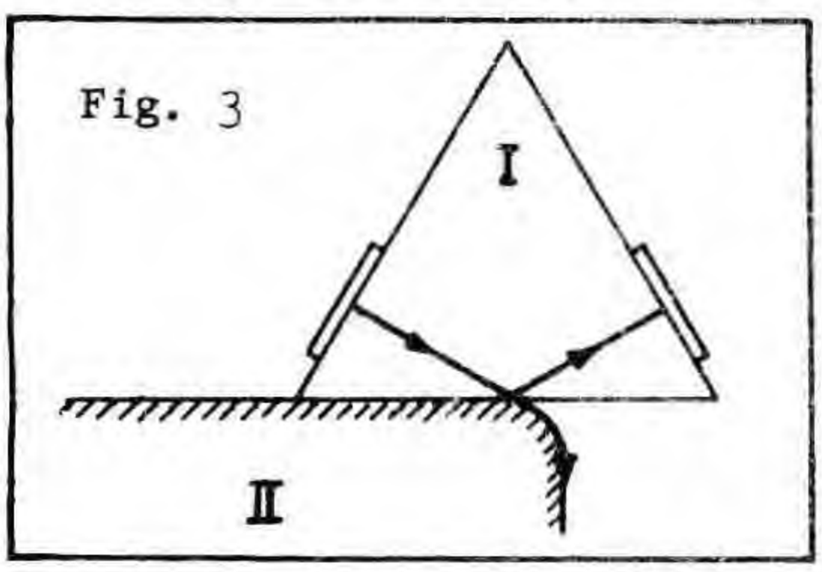

Fig. 3

In order to decrease further the area of contact in which surface waves are generated one can decrease the dimensions of the emitting transducer. Doing this one narrows the width of the longitudinal wave impinging on solid II and one can reduce the received signal by replacing the aluminum block by a solid aluminum cylinder as shown in Figure 4. This reduces the area of contact between the two solids and assures a more efficient separation of the surface wave from the bottom of the wedge. Changing the size of the aluminum cylinder changes the effective area of contact and thus the amplitude of the received pulse. The angle of incidence α is not affected by the size of the cylinder.

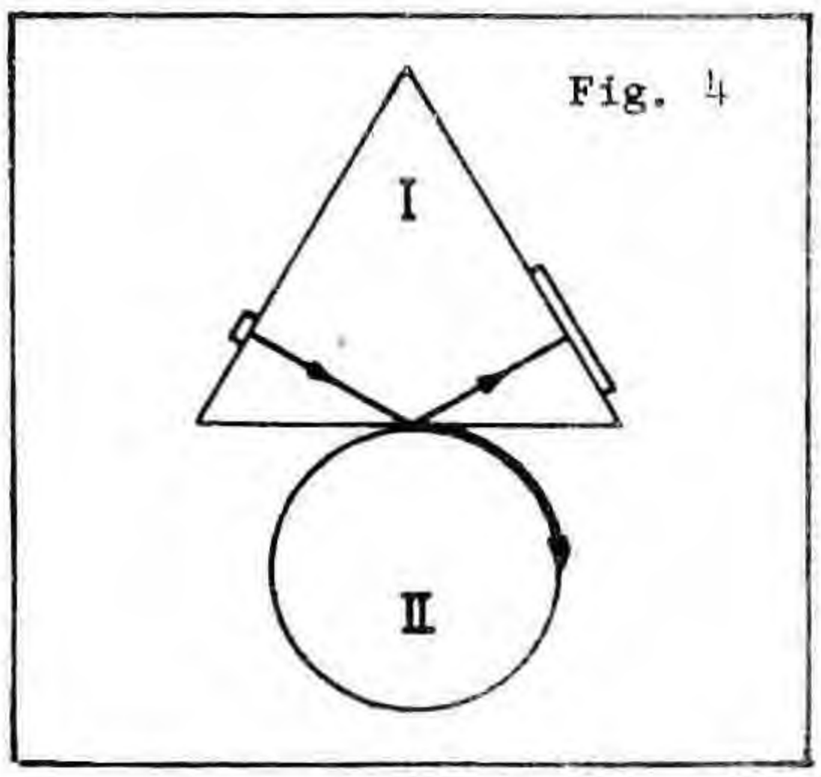

Fig. 4

The surface wave traveling around the cylinder is absorbed by placing some suitable liquid on the cylinder; if this is not done, the wave completes the circle and reaches the wedge again where it is converted back into a longitudinal wave which travels toward R. In this case one has a short delay line.

The efficiency of mode conversion from longitudinal to surface wave for the various arrangements described can be seen from the results of experiments using Plexiglas and aluminum. Using a 5 Mc pulse from a 1.2 x 2.5 cm transducer and placing the entire wedge on the aluminum one receives a signal whose amplitude is shown in Figure 5b. The reference amplitude (wedge in air) is shown in Figure 5a. The amplitude of the signal has increased by about 50 percent; thus, placing the entire wedge on the aluminum block does not reduce the reflections back into the wedge. Figure 5c shows the received amplitude of the reflected longitudinal wave recorded with the arrangement indicated in Figure 3. In this case the amplitude has decreased somewhat. A more effective energy transfer is attainable if the wedge is placed on a solid aluminum cylinder. The received amplitude is indicated in Figure 6b, compared with the reference amplitude in Figure 6a (wedge in air). The diameter of the cylinder was 1.85 cm. The effective area of contact between the two solids was increased slightly by using a solid aluminum cylinder with a diameter of 0.34 cm. In this case the received signal had an amplitude shown in Figure 6c. The results shown in Figure 6 were ob-

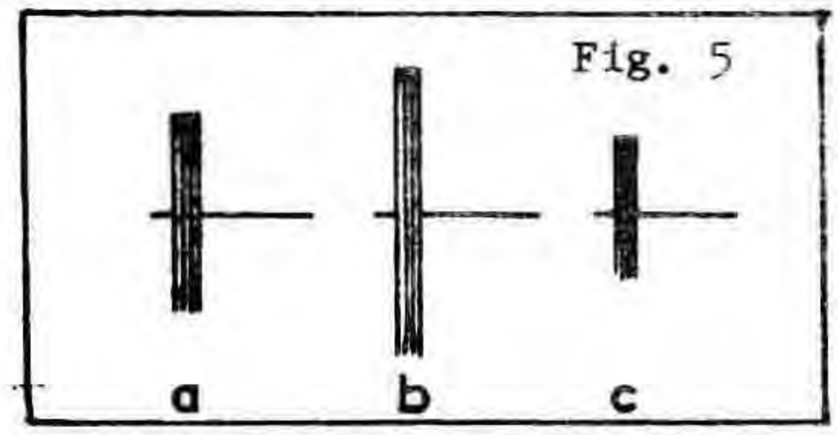

Fig. 5

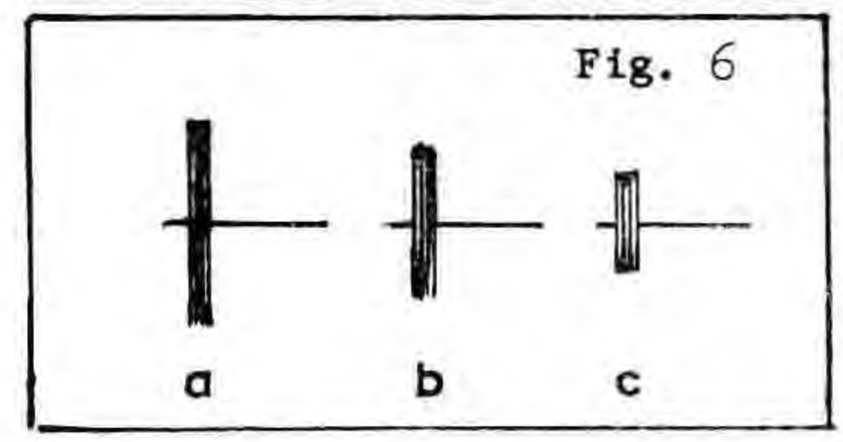

Fig. 6

tained by using an emitting transducer with dimensions 0.25 x 2.5 cm which minimized further the effective area of surface wave production. It is seen that the reflected longitudinal wave decreases to about half its amplitude in the last case shown in Figure 6.

This reduction in amplitude of the reflected longitudinal wave indicates that an appreciable part of the energy in the longitudinal wave can be taken out of solid I by mode conversion to a surface wave on solid II, especially if one considers that the greatest part of the cross-section of the sound beam is impinging on the Plexiglas-air interface and only a small part on the Plexiglas-aluminum interface. The resulting surface wave can be absorbed very easily so that it will not be reflected back into solid I. That fraction of the longitudinal wave in solid I which was not converted to a surface wave at the boundary can be reduced further by repeating the process as indicated in Figure 7. In principle, it should be possible to use this technique for the surpression of reflections of an ultrasonic wave in a solid. Since the absorption of the resulting surface wave presents no problem one should be able to approach the production of progressive ultrasonic waves in solids using the method outlined here, provided the velocity of the longitudinal wave in the solid in question is smaller than the velocity of the surface wave on solid II. (This work was supported by the Office of Naval Research, U.S. Navy.)

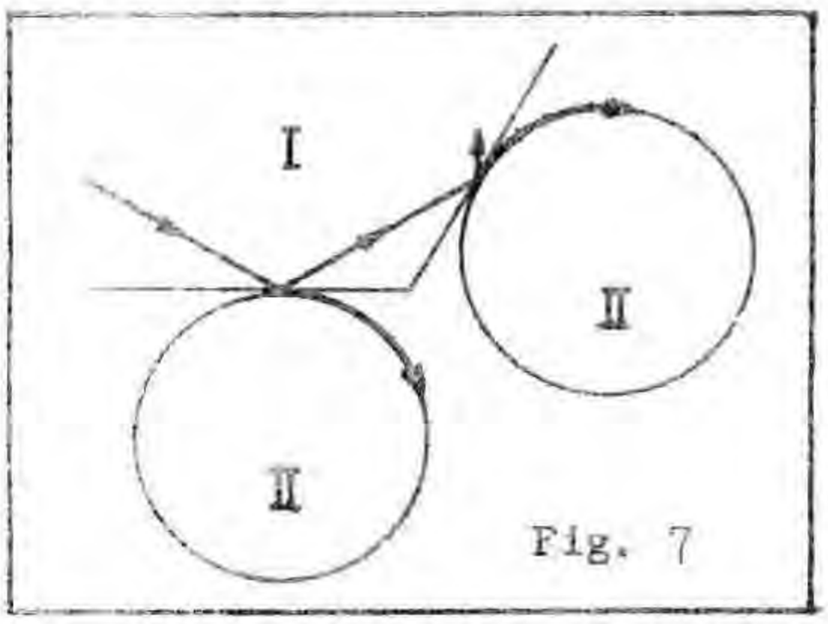

Fig. 7

Bibliography

(1) I. A. Viktorov, Soviet Phys.- Acoustics 7, 236 (1962).
(2) E. G. Cook and H. E. Van Valkenburg, ASTM Bull. No. 198, 81 (1954).
(3) I. A. Viktorov, Soviet Phys.- Acoustics 7, 70 (1961).

G14

FOURTH INTERNATIONAL CONGRESS ON ACOUSTICS
COPENHAGEN 21.-28. AUGUSTI 1962

SPEECH MACHINE CONSIDERATIONS

Harry F. Olson

RCA Laboratories, Princeton, New Jersey, U. S. A.

I. Introduction

The general subject of the analysis and synthesis of speech leads to products which may be useful for many applications in the speech processing field. These may range from a system that responds to a few simple commands which will actuate certain functions in a machine to the ultimate machine speech writer in which the voice produces the perfect typed copy. The purpose of this paper is to classify speech recognition machines and describe some of the speech characteristics and the methods of analysis.

II. Types of Speech Recognition Systems and Machines

In addition to other classifications, it is possible to categorize speech systems and machines in terms of their service in connection of "what" was said, "how" it was said, by "whom" it was said and "where" it was said. A number of services that could be put into categories based on "what", "how", "who", and "where" are shown in Table I. Some of the characteristics of speech which may be used to implement the various services will be outlined in the sections which follow.

III. Speech Characteristics

There are many properties of speech which may be employed to determine the "who", "what", "how" and "where" of speech. The characteristics may be determined by various types of analyzers. The selections which follow will describe some of the characteristics of speech and the means for obtaining these characteristics.

A. Spectrum vs Time Analysis

The most basic analysis of speech involves some form of spectrum analysis as a function of the time. There are many variations and ramifications of this type of speech analysis. In one form of the analyzing system the analysis is in the form of eight frequency bands, one step of amplitude and five steps of time.

B. Fine Structure Analysis

The eight frequency channels of the system described in the preceding section will not provide adequate analysis and a finer division is necessary. However, with only eight channels, successive phonations by even the same person are not always depicted the same, indicating that eight channels are too many when variations in speaking are considered. This becomes more pronounced when different speakers are considered. The difficulty can be overcome by employing as few channels as possible to analyze the speech entities required with the least variations. The main analyzer is followed by a fine structure analyzer the output of which is not to be fed to the spectral memory but to a category sorter providing a number that could be handled by a reasonable size memory.

C. Normalizers for Spectrum vs Time Analyzers

Tests have shown that an individual even when speaking in a normal voice cannot control the amplitude or speed of talking. Variations in these quantities will change the analysis as provided by the spectrum vs time system. Therefore, normalizers are required to compensate for the loudness and speed of talking.

1. Loudness Normalizer

The amplitude can be normalized by the use of a conventional amplitude compressor. A more sophisticated system may be employed consisting of an anticipation and delay system.

In addition to the compressor, an amplitude comparison system may be employed in the analyzer. In this system, instead of quantizing amplitude in predetermined steps against a fixed or variable threshold the output of each channel is compared to the adjacent ones. This is similar to obtaining the second derivature by finite differences and identifying the points of inflection that are concave downward. The advantage of this system is that it is less sensitive to absolute levels and that secondary peaks, removed from the larger ones in frequency, are indicated more clearly, than if reference is made to a common threshold.

2. Time Compensated Memories

The speed of talking may be compensated in the spectrum vs time system by employing a time compensation in which the time steps of analysis are not advanced until a charge occurs in the spectrum.

D. Speech Envelope Analysis

The envelope of a speech wave provides information on the characteristics of speech. This could be included in the spectrum vs time analysis but the envelope analysis is more convenient.

1. Growth and Decay Analysis

The envelope analysis provides information on the growth and decay of speech. Investigations have shown that the starting characteristics of speech are more dependent upon the person talking than on the specific word which is spoken. Analysis has shown that a stop consonant tends to have a faster decay than one that ends in a vowel.

2. Unbalance of Peak Amplitudes of the Bilateral Envelopes of Speech

Measurements on the output of the vowel sounds show that the wave is of the sawtooth shape with the negative portion flattened to some extent. The flattening on one side gives rise to an unbalance in the two directions. The unbalance characteristics are maintained in speech at the output of the mouth. An inspection of the bilateral envelopes of speech shows that the unsymmetrical nature of speech provides additional information on the analysis of speech.

E. Frequency Deviation Analysis

Early work on the synthesis of music and speech showed the importance of the deviations from the mean to achieve artistic rendition of music and the natural quality of speech. Deviations in pitch or frequency are a case in point. There are important deviations during growth and decay. There is a fine structure of deviations over and above the more obvious deviations in pitch such as vibrato and other forms of frequency modulation. This fine structure is always present in the case of sound generators like the human voice which starts with relaxation oscillations.

Speech transduced into electrical energy and transmitted over a single channel can be represented as a function of amplitude and time. A trace of such a function contains all the information which is transmitted. An investigation of the frequency deviation may be facilitated by reducing the trace to a lower frequency. The frequency reduction can be obtained by rerecording a modulatèd carrier. In one form of the system the speech was reduced 64 to 1 in frequency and recorded by means of a pen recorder. An inspection of the trace indicated deviations in the frequency.

F. Inflection Analysis

Inflection in speech for the most part involves a change in frequency and amplitude. The systems for analysis of amplitude and frequency provide information on the inflection of speech.

G. Location Analysis

The location of the origin of speech sound involves the determination of two parameters namely, direction and distance. The direction of a sound source with respect to the observation point may be determined by means of a directional microphone. The use of two spaced directional microphones provides the location of a sound source.

IV. Summary

A review of the characteristics of speech and the means for obtaining these characteristics indicates that useful products represented by the services depicted in Table I can indeed be created by the application of additional research and development because the work has progressed beyond the questionable stage.

TABLE I

Services Based on Recognizing the "What", the "How", the, by "Whom", and the "Where" of Speech

	WHAT	HOW	WHO	WHERE
High fidelity reproduction of speech	x	x	x	
Stereo reproduction of speech	x	x	x	x
Phonetic Typewriter	x			
Speech locator and recognizer	x			x
Voice signature and command recognizer	x		x	
Voice locator and signature and command recognizer	x		x	x
Voice recognizer			x	
Voice locator and recognizer			x	x
Speech locator				x
Speech and inflection recognizer	x	x		
Speech recognizer, locator and inflection recognizer	x	x		x
Speech inflection recognizer		x		
Speech locator and inflection recognizer		x		x
Voice and inflection recognizer		x	x	
Voice locator and inflection recognizer		x	x	x

H14

FOURTH INTERNATIONAL CONGRESS ON ACOUSTICS
COPENHAGEN 21.-28. AUGUST 1962

ETUDE EXPERIMENTALE DE LA PROPAGATION DES ONDES ACOUSTIQUES DANS LES LIQUIDES COCHLEAIRES.

M.BURGEAT & R.LEHMANN - Paris (France).
Faculté de Médecine & Centre National d'Etudes des Télécommunications.

I/ TECHNIQUE

Plusieurs animaux (14 Cobayes et 7 Mériones) ont été anesthésiés au Dial, puis fixés sur une table de stéréotaxie de Horsley-Clark.
Les tiges à oreille, creuses, ont été reliées à un haut-parleur du type à chambre de compression, par l'intermédiaire d'un tube plastique de 10 mm de diamètre. Deux sondes acoustiques identiques de 4/10 mm de diamètre peuvent être mises en place,, à l'aide d'un micromanipulateur, dans les rampes vestibulaire et tympanique de la cochlée. L'enregistrement des sons qui se propagent dans les liquides cochléaires a été réalisé à l'aide d'un microphone électrostatique étalon relié à un oscilloscope bicourbe dont l'image peut être photographiée. Les diverses mesures ont été effectuées à des fréquences de 400 Hz.

2/ ETUDE COMPARATIVE DE LA PROPAGATION DANS LES RAMPES VESTIBULAIRE ET TYMPANIQUE.

2.1. Chaine des osselets intacte.

a) la pression acoustique présente la même fréquence dans les deux rampes,
b) la pression acoustique dans la rampe vestibulaire est une fonction linéaire de la pression acoustique produite dans le conduit auditif, dans les limites correspondant à une dynamique de 30 dB dans un domaine de niveaux inférieurs à 100 dB au dessus de 2.10^{-5} Pascal.
c) la pression acoustique dans la rampe tympanique est de 25 à 30 dB inférieure à celle dans la rampe vestibulaire, les deux pressions ne semblent pas être en phase.

2.2. Interruption de la chaine ossiculaire.

La cochlée étant exposée de telle sorte que soit visible et facilement accessible l'articulation enclume-étrier, des mesures furent effectuées dans les rampes vestibulaire et tympanique du premier tour de spire, avant et après rupture de l'articulation. Après rupture, il y a disparition immédiate du signal dans les deux rampes. L'amplitude de cette chute a toujours été d'au moins 55 à 60 dB, valeur correspondant à la limite mesurable, du fait du passage direct du son dans les sondes.

2.3. Evidement de la bulle tympanique.

Après avoir constaté la disparition de l'onde acoustique qui se propage dans les deux rampes à la suite de la rupture de l'articulation enclume-étrier, un évidement complet de la bulle a été pratiqué.
On enlève d'abord soigneusement le tympan et le marteau, puis l'enclume, l'étrier restant en place. Dans ces conditions il a été possible d'assister dans certains cas à un retour de la propagation intra-cochléaire. Dans l'ensemble, il a semblé, dans les cas où un retour de la propagation acoustique était constaté, que la pression acoustique dans la rampe tympanique était, soit plus grande, soit égale à celle dans la rampe vestibulaire. Il semble donc que l'onde acoustique puisse, dans certaines conditions, pénétrer dans la cochlée par la fenêtre ronde. D'ailleurs son amplitude s'est avérée être d'environ 40 à 50 dB inférieure à l'amplitude normale enregistrée dans la rampe vestibulaire. Cette valeur représente environ 1% de la pression initiale, c'est à dire ce que l'on doit s'attendre à trouver, lorsqu'on passe du milieu aérien à faible impédance au milieu liquide à impédance élevée, en l'absence de toute adaptation.

2.4. Influence de la variation de la pression statique dans la bulle tympanique.
Les sondes acoustiques étant mises en place dans les orifices des rampes vestibulaire et tympanique, la bulle tympanique est refermée au ciment après mise en place d'un tube en Y. Ce dernier est relié par deux tuyaux en plastique, d'une part à une seringue de 30 cm^3 permettant de faire varier la pression statique, d'autre part à un manomètre à eau fixé devant l'écran de l'oscilloscope. Il est ainsi possible de photographier les variations du niveau du manomètre avec l'image oscilloscopique des variations de pression sonore dans les rampes vestibulaire et tympanique.
Dans ces conditions, nous avons constaté, au cours d'une dépression progressive: a) une diminution de la pression sonore dans la rampe vestibulaire, b) une légère chute ou le maintient à un niveau constant, suivi d'une nette augmentation, de la pression sonore dans la rampe tympanique.

3/ VERIFICATIONS EXPERIMENTALES COMPLEMENTAIRES.
3.1. Preuve de l'origine cochléaire des sons enregistrés.
a) Le retrait de la sonde de l'orifice cochléaire, au cours de l'émission sonore, annule complètement le signal, même lorsque l'extrémité de la sonde est maintenue à l'intérieur de la bulle,
b) la rupture de la chaine ossiculaire annule de la même façon la propagation sonore dans la cochlée. Dans ce cas, une augmentation de l'intensité sonore permet d'enregistrer un signal dont l'amplitude ne change pas lors du retrait de la sonde. Ce n'est donc qu'à des intensités supérieures à 80 dB au niveau du tympan que la transmission commence à se faire directement à travers les parois de la sonde.
3.2. Preuve de la propagation liquidienne intra-cochléaire.
La sonde acoustique étant en place au niveau de la rampe vestibulaire du 3^{è} tour, l'aspiration du liquide périlymphatique au niveau du 2e tour annule complètement la réponse. Celle-ci réapparait avec une amplitude égale lorsqu'on injecte du sérum par l'orifice d'aspiration.
3.3. Propagation acoustique dans les différents tours de la cochlée.
Les caractéristiques des enregistrements effectués au niveau des rampes vestibulaire et tympanique du premier tour sont applicables aux autres tours de spire de la cochlée. En effet trois orifices étant pratiqués au niveau de la rampe vestibulaire des 1er,2^{è}, et 3^{è} tour de spire, les valeurs des pressions sonores aux fréquences 400-800 et 1600 Hz, dans chaque tour. sont sensiblement identiques. Il n'a été constaté qu'une variation maximale de 6 dB, due principalement aux difficultés de mise en place correcte de la sonde. Aucune variation de phase n'a été enregistrée.

4/ DISCUSSION.
4.1. La pression sonore existant dans la rampe tympanique doit très vraisemblablement provenir de la rampe vestibulaire, comme le prouve sa disparition lorsqu'on supprime toute pression sonore dans cette rampe après rupture de la chaine ossiculaire.Le passage doit se faire à travers la rampe médiane (canal cochléaire) avec une perte de 25 à 30 décibels et un décalage de phase dû vraisemblablement au fait que l'onde sonore doit traverser un milieu présentant une impédance acoustique différente.
4.2. Le rôle de la chaine des osselets est donc bien de transmettre l'onde acoustique en provenance du tympan au liquide périlymphatique de la rampe vestibulaire. sans déperdition d'énergie, grâce à son rôle d'adaptateur d'impédance entre les milieux aérien et liquide . Par contre, il n'a pas été possible, chez le Cobaye et la Mérione, de constater un déphasage entre l'onde acoustique frappant le tympan et celle transmise à la cochlée.
4.3. Le rôle de la fenêtre ronde.
a) Normalement , il semble que la fenêtre ronde puisse avoir pour rôle principal d'assurer une compensation suffisante, au cours des mouvements de grande amplitude et de basse fréquence de la chaine des osselets, tels que ceux que l'on constate au cours des contractions musculaires ou ceux qui sont dus aux mouvements d'air dans

l'oreille moyenne, à travers la trompe d'Eustache.
En ce qui concerne son rôle proprement auditif, on peut estimer avec LINK (1) qu'il doit se limiter, à l'aide d'un très faible volume d'air déplacé, comme WEVER l'a montré, à assurer la transmission ossiculaire normale des sons graves surtout. Enfin, nous pensons qu'elle doit aussi assurer la compensation des pressions statiques élevées dans la rampe vestibulaire, survenant pour des sons intenses.
b) En cas d'évidement de la bulle tympanique, il semble que la fenêtre ronde puisse, lorsqué l'obsatcle que sont pour elle le tympan et les deux premiers osselets est supprimé, assurer une certaine transmission sonore, mais avec une forte déperdition d'énergie.
4.4. La mobilisation de la membrane basilaire.
a) Normalement. Le mouvement résultant de la membrane basilaire, qui a seul une signification physiologique, puisque ce sont les ondes qui se propagent le long de cette membrane (BEKESY-2-) qui stimulent les cellules ciliées de l'organe de Corti, est provoqué par l'onde acoustique qui se déplace dans la rampe vestibulaire.
En effet, la pression sonore recueillie dans la rampe tympanique et provenant de la rampe vestibulaire, par passage à travers la rampe médiane, ne peut avoir qu'un effet limité sur la membrane basilaire. En admettant, par exemple, que la pression sonore dans la rampe tympanique soit de 30 dB inférieure et qu'elle ait un retard de phase de 90° par rapport à la pression sonore dans la rampe vestibulaire, la construction d'un diagramme de Fresnel montre que le vecteur résultant a pratiquement le même sens et la même grandeur que celui représentant la pression sonore dans la rampe vestibulaire.
b) Anormalement. Dans certains cas, cependant, la mobilisation de la membrane basilaire peut être provoquée par la pression sonore qui se propage dans la rampe tympanique. Dans ces cas, l'amplitude du déplacement de la membrane basilaire est beaucoup plus faible que lorsque l'effet de la rampe vestibulaire est prédominant et on peut observer un déphasage total du déplacement.
Ceci, comme nous l'avons vu, peut survenir après évidement de la bulle tympanique. C'est vraisemblablement aussi le cas lors des varaitions de pression statique dans la bulle tympanique. Au cours d'une dépression progressive dans la bulle, la pression sonore dans la rampe vestibulaire s'abaisse progressivement, tandis que dans la rampe tympanique, après avoir amorcé une chute, elle montre une augmentation très nette, au moins jusqu'à -6 ou -7 cm d'eau.
Ces faits sont à rapprocher d'un travail que l'un de nous a précédemment effectué (3) et qui avait montré une diminution progressive du potentiel microphonique cochléaire (380 Hz) au cours d'une variation négative de la pression statique dans la bulle s'annulant pour -6 cm d'eau, et réapparaissant pour une dépression plus accentuée, avec un déphasage de 180°. Il est vraisemblable, comme semblent l'indiquer les enregistrements de la pression sonore dans les rampes vestibulaire et tympanique que les modifications du mouvement de la membrane basilaire au cours des variations de pression statique peuvent se décomposer en trois étapes: a) diminution de la pression sonore dans les rampes vestibulaire et tympanique engendrant une diminution de l'amplitude des mouvements de la membrane basilaire, donc des potentiels microphoniques cochléaires, b) augmentation de la pression sonore dans la rampe tympanique par passage direct à travers la fenêtre ronde puis, lorsqu'elle a la même action que la pression sonore dans la rampe vestibulaire, mais une phase opposée, annulation des mouvements de la membrane basilaire, donc des potentiels microphoniques cochléaires,
c) enfin, lorsque le rapport entre les pressions sonores mesurées dans la rampe vestibulaire et dans la rampe tympanique atteint une certaine valeur, les potentiels microphoniques cochléaires réapparaissent, mais sont de phase opposée, les mouvements de la membrane basilaire étant alors provoqués par la rampe tympanique.
L'expérience prouve, d'ailleurs, que l'annulation des potentiels microphoniques cochléaires ne survient que pour une valeur très critique de la dépression dans la bulle. Il est évident qu'étant donné les difficultés de mesure, ces conclusions ne sont que schématiques. Il serait intéressant, en effet, de connaitre en particulier la valeur de la "pression actuelle" qu'il serait nécessaire d'appliquer dans

chacune des rampes, pour obtenir un déplacement de la membrane basilaire d'amplitude identique et de phase opposée.
Des résultats de portée semblable ont été relatées par LEGOUIX (4) au cours de l'étude de la variation des potentiels microphoniques cochléaires en fonction des pressions acoustiques appliquées directement dans les rampes tympanique et vestibulaire.

5/ CONCLUSIONS.

5.1. La transmission des ondes acoustiques à travers la chaine ossiculaire semble se faire sans modification significative de la phase.
5.2. Normalement, la propagation acoustique se fait uniquement dans la rampe vestibulaire avec, cependant, la transmission d'une faible pression sonore dans la rampe tympanique, à travers la rampe médiane.
5.3. Cette propagation se fait strictement à travers le liquide périlymphatique sans aucune déperdition d'énergie ni aucun changement de phase, dans les trois premiers tours de spire.
5.4. A l'état normal, le rôle essentiel de la fenêtre ronde semble être d'assurer une certaine compensation mécanique dans les mouvements de grande amplitude et de basse fréquence de la chaine des osselets (contractions musculaires, aération de la caisse). Il semble qu'elle permette ainsi une bonne transmission ossiculaire, surtout pour les fréquences graves, ainsi qu'une compensation pour les pressions statiques développées dans la rampe vestibulaire pour des sons intenses.
Anormalement , après évidement ou au cours d'une variation négative de la pression statique dans la bulle, il semble que la fenêtre ronde puisse, dans certains cas, assurer le passage d'une très faible pression acoustique. Mais, en ce qui concerne la membrane de la fenêtre ronde, il nous semble nécessaire de distinguer:
1) la "pression acoustique incidente"dépendant des obstacles interposés (tympan, osselets), -2) et la "pression acoustique transmise"au liquide de la rampe tympanique, qui dépend des caractéristiques physiques de la membrane au moment considéré.
5.5. Les mouvements de la membrane basilaire sont normalement provoqués par l'onde acoustique qui se propage dans la rampe vestibulaire.
Dans les cas où la propagation dans la rampe tympanique est plus active que dans la rampe vestibulaire, le mouvement résultant de la membrane basilaire est de faible amplitude, et se fait avec un décalage de phase de 180°. Il semble nécessaire d'envisager, dans chacune des deux rampes, et pour une fréquence donnée, la notion d'une "pression acoustique actuelle"engendrant des déplacements d'amplitude semblable de la membrane basilaire.

BIBLIOGRAPHIE

-1- LINK,R. -"Zur Funktion der Membran des runden Fensters under des Schalleitungs apparatus" - Der Hals-Nasen-U.Ohrenartz. 33,I,421-467, 1943.

-2- BEKESY,G,v. -"Zur Theorie des Hörens. Die Schwingungsform der basilar Membran". - Physik.Zschr.29,793-810, 1928.

-3- AUBRY,M.- PIALOUX,P.- BURGEAT,M.- "Amplitude et phase des microphoniques cochléaires en fonction des variations de pression à l'intérieur de la bulle tympanique chez la Mérione et le Cobaye". -Annales O.R.L. 1962 (à paraitre)

-4- LEGOUIX,J.P. -"Etude du fonctionnement des fenêtres ronde et ovale, au moyen de stimulations endocochléaires".-Journ. de Physiologie, Juin 1958.

J14

FOURTH INTERNATIONAL CONGRESS ON ACOUSTICS
COPENHAGEN 21.-28. AUGUST 1962

MESURES D'ABSORPTION ULTRASONORE PAR DES SOLUTIONS DE POLYMERES.

S. CANDAU, R. ZANA et R. CERF
Centre de Recherches sur les Macromolécules, Strasbourg, France.

Nous poursuivons ici l'étude expérimentale de l'absorption ultrasonore par les solutions de polymères. Les premiers résultats avaient montré l'existence de brusques chutes du coefficient d'absorption à des fréquences caractéristiques ([1]), et, dès les premières mesures systématiques, le caractère intramoléculaire du phénomène responsable de ces chutes s'était manifesté ([2,3]). Il est apparu également que le phénomène moléculaire doit affecter des segments limités des chaînes polymériques ([3]), et finalement, dans la communication précédente (qui sera désignée par les lettres CP), un mécanisme moléculaire susceptible d'expliquer les observations a été proposé.

On aborde ici l'étude du comportement des copolymères (c'est-à-dire des polymères comprenant différentes espèces monomères), et l'on poursuit l'étude des polymères stéréoréguliers amorcée dans la CP. Toutes les mesures ont été effectuées à 25°C.

I. COPOLYMERES. Le fait que le phénomène moléculaire responsable de l'effet observé affecte des segments limités, évalués à une dizaine de chaînons (CP), comporte les conséquences suivantes. Si pour chacun des constituants d'un copolymère les séquences de monomères de même espèce comprennent un grand nombre d'unités, l'absorption ultrasonore du copolymère ne devrait pas différer notablement de celle des homopolymères qui le composent. Au contraire, si les séquences sont courtes, l'absorption ultrasonore du copolymère devrait différer de celle du mélange des homopolymères, et montrer un comportement caractéristique du mode d'enchaînement des espèces monomères. Les résultats qui suivent sont en accord avec ces deux conclusions ; ils confirment par conséquent les opinions précédemment exprimées, et dans le cas des copolymères à courtes séquences, conduisent à prévoir des applications à l'étude de la structure locale.

a) Copolymères à longues séquences. Nous avons étudié un copolymère composé de deux séquences polyoxyéthylèneglycol (POEG) de masse moléculaire en poids M_w= 2500 séparées par une séquence polystyrène (PST) M_w= 5000. Sur la figure 1 on a porté, pour une solution benzénique de ce polymère, la quantité $\alpha_{sp}/c = (\alpha - \alpha_s)/\alpha_s c$ (α: absorption de la solution, α_s: absorption du solvant, c : concentration en grammes par centimètre cube) en fonction de la fréquence N. La concentration en polymère était $c = 4{,}6.10^{-2}$. Sur la même figure, on a porté la quantité α_{sp}/c pour un mélange d'un POEG de masse M_w= 3000 et d'un PST de masse M_w= 5000. La concentration totale en polymère et la proportion en monomères de chaque espèce étaient les mêmes pour les deux solutions. On voit que les deux courbes sont pratiquement confondues. La chute d'absorption est due à la molécule de PST, celle de POEG ne donnant aucune chute d'absorption dans le domaine de fréquence envisagé ([2]).

Des résultats analogues ont été obtenus pour des copolymères à longues séquences polystyrène-polyméthacrylate de méthyle.

b) Copolymères à courtes séquences. La figure 2 représente les variations de α_{sp}/c en fonction de la fréquence N pour deux solutions benzéniques à concentration $c = 3.10^{-2}$ de copolymères butadiène-styrène non fractionnés aimablement fournis par la Sté Hüls ; les proportions relatives en poids des deux monomères sont respectivement égales à 77/23 et 60/40 ; les viscosités intrinsèques des polymères dans le toluène sont respectivement égales à 220 et 270. On a représenté en pointillé les courbes qui correspondraient aux deux mélanges d'homopolymères de masses moléculaires élevées avec respectivement les proportions en poids ci-dessus. Les mélanges d'homopolymères fournissent ici des courbes qui diffèrent de celles obtenues pour les copolymères correspondants.

Des mesures effectuées sur des solutions de copolymères alternés styrène-méthacrylate de méthyle ont également fourni des résultats s'écartant de ceux que l'on obtiendrait pour un mélange d'homopolymères.

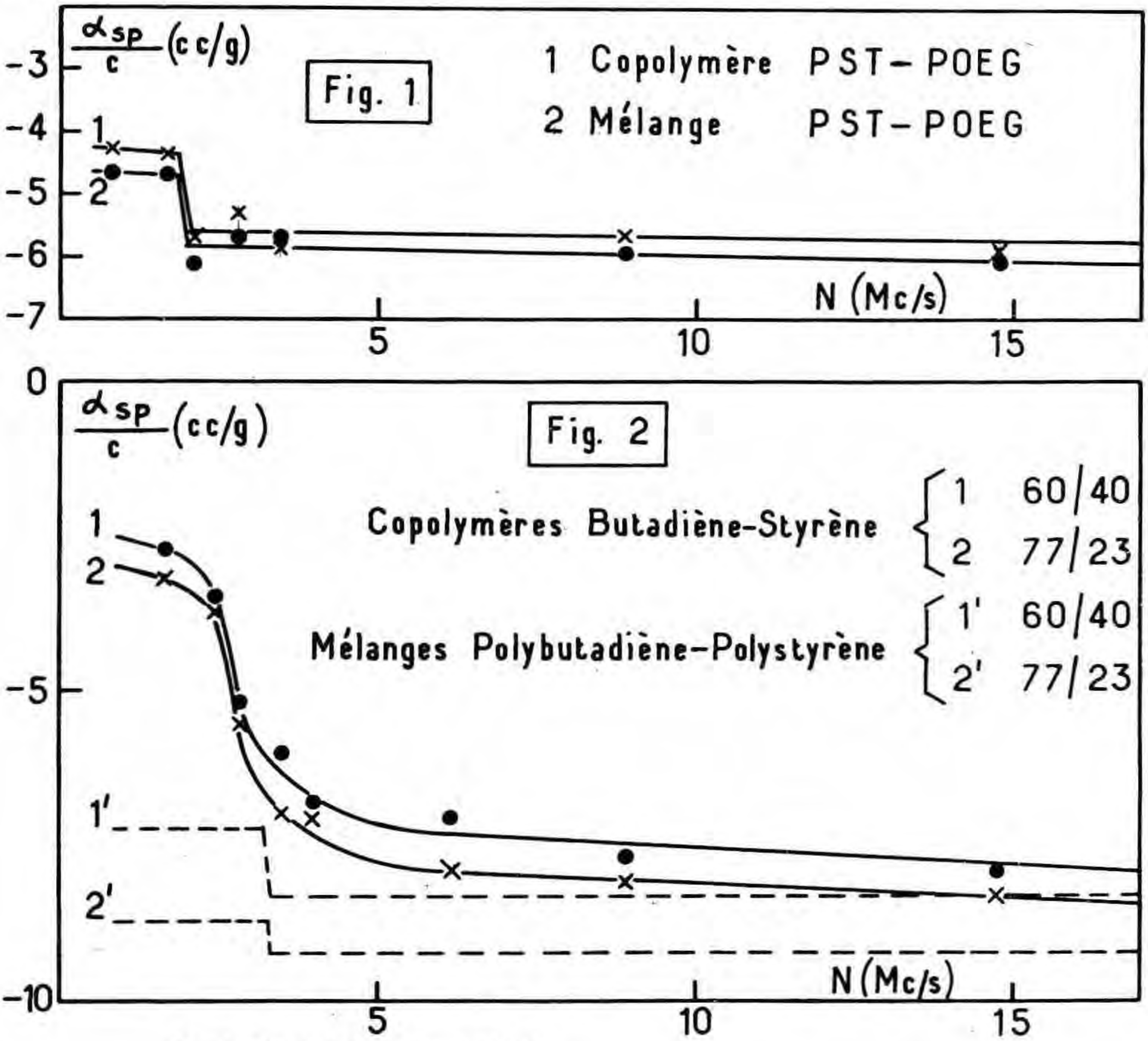

Fig. 1

1 Copolymère PST-POEG

2 Mélange PST-POEG

Fig. 2

Copolymères Butadiène-Styrène { 1 60/40 ; 2 77/23

Mélanges Polybutadiène-Polystyrène { 1' 60/40 ; 2' 77/23

II. <u>POLYMERES STEREOREGULIERS</u>.

a) <u>Polystyrène</u>. La figure 3 représente la courbe α_{sp}/c en fonction de N pour une solution dans le bromoforme à la concentration c = 2.10^{-2} d'un polystyrène isotactique qui nous a été aimablement fourni par la Sté Montecatini. Ce produit a un taux d'isotacticité de 97 %, sa viscosité intrinsèque dans le tétrahydronaphtalène à 130°C est égale à 385. Sur la même figure on a porté la courbe relative à un polystyrène atactique de masse moléculaire M_w = 465000. La comparaison des deux courbes met en évidence la sensibilité de l'absorption ultrasonore à la stéréorégularité.

Il convient de noter que dans le bromoforme la chute d'absorption fournie par le polystyrène atactique est très étalée, contrairement à ce que nous avions observé dans d'autres solvants.

b) <u>Polyvinylisobutylether,(PVIBE)</u>. La figure 4 représente les courbes α_{sp}/c en fonction de N pour des solutions benzéniques à la concentration c = 4.10^{-2} de deux fractions de PVIBE, l'une atactique, l'autre isotactique. Ces deux fractions étaient chacune

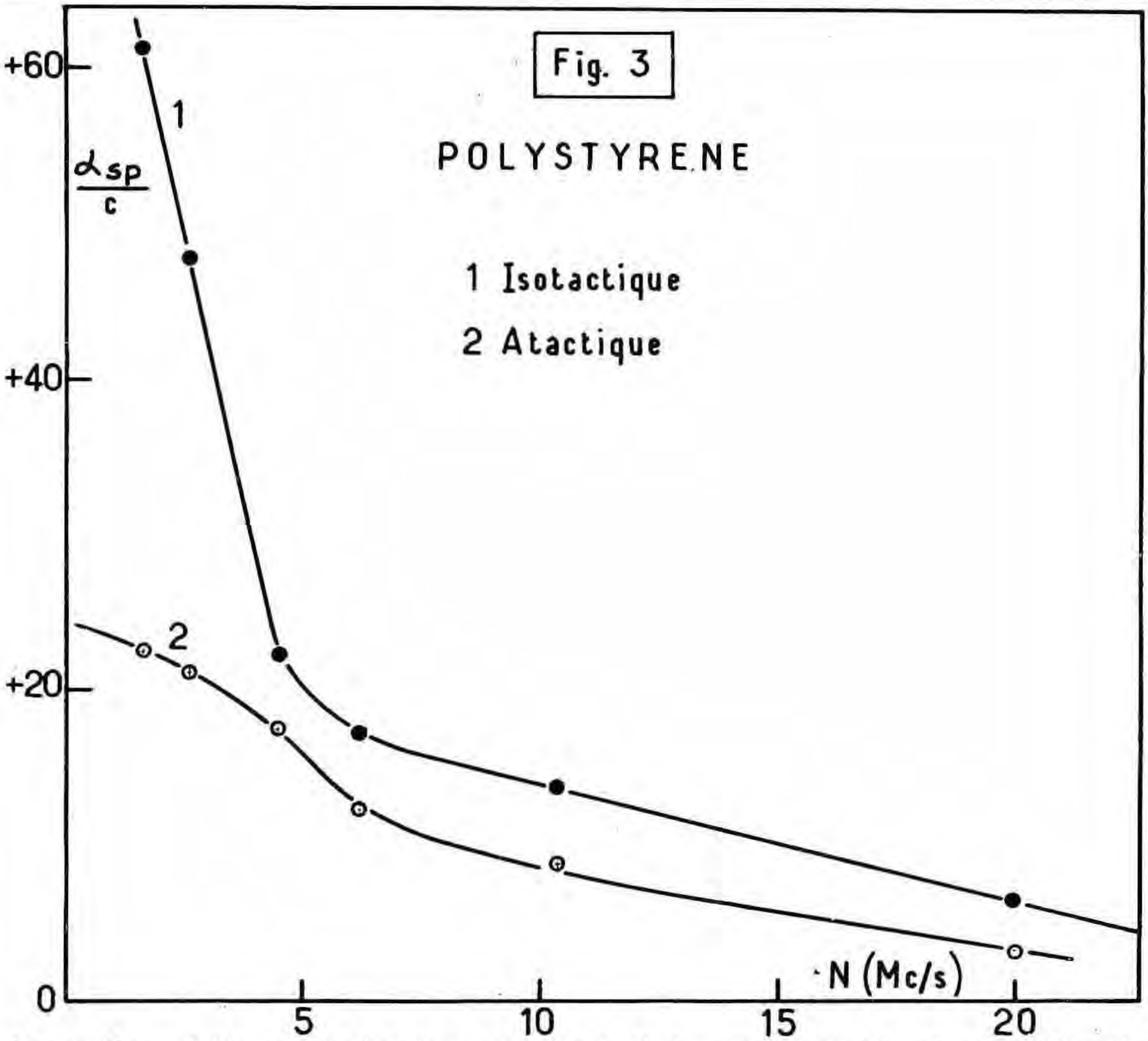

la première soluble dans le benzène, respectivement des parties amorphe et cristalline obtenues par dissolutions dans la méthyléthylcétone d'un échantillon brut de PVIBE. Une différence, quoique moins marquée que précédemment, apparaît dans les deux courbes de la figure 4.

c) Polyméthacrylate de méthyle.(PMM). Ce polymère a déjà été envisagé dans la CP, où l'on a donné les spectres ultrasonores pour deux échantillons stéréoréguliers, l'un isotactique, l'autre syndiotactique, ainsi que pour un échantillon dit "atactique". Il faut noter qu'il est encore difficile à l'heure actuelle de préciser le taux de syndiotacticité d'un PMM, et qu'un échantillon "atactique" (tel celui de la CP) peut fort bien contenir des séquences syndiotactiques. Ces résultats de la CP, et ceux qui suivent, font précisément espérer que la spectroscopie ultrasonore apportera des informations à cet égard.

Nous nous sommes surtout proposé, pour le moment, de multiplier les mesures sur des échantillons qualifiés respectivement isotactique et syndiotactique, d'origines différentes, de manière à vérifier la généralité des caractéristiques dégagées précédemment(CP).

Nous disposions d'un échantillon isotactique de masse moléculaire M_w= 970000 aimablement fourni par la Cie Rohm et Haas, et deux échantillons syndiotactiques, de masses moléculaires M_w = 190000 et M_w= 500000 dus à l'obligeance respectivement de MM. Sigwalt et Leng.

1) Les spectres, que nous ne donnons pas ici, confirment que la variation de l'absorption spécifique en fonction de la fréquence est atténuée par l'isotacticité et amplifiée par la syndiotacticité.

2) Sur la figure 5 on a porté la fréquence de la première chute d'absorption en fonction de $\log M_w$ pour les deux échantillons stéréoréguliers de la CP et les trois échantillons envisagés. On a également reporté sur la même figure les points relatifs à une série d'échantillons préparés par la méthode de Swarc dans le tétrahydrofuranne à -78°C. Ces échantillons sont dus à l'obligeance de M. Rempp et possèdent un taux de stéréorégularité moindre. L'échantillon qualifié "atactique" dans la CP appartient à cette série.

Malgré la disposition irrégulière des points relatifs aux échantillons stéréoréguliers, il se confirme que la stéréorégularité abaisse les fréquences auxquelles se produisent les chutes d'absorption.

Références.

(1) R. CERF, R. ZANA et S. CANDAU, C.R. Acad. Sci., Paris, 252, 1961, 681.
(2) S. CANDAU, R. ZANA et R. CERF, C.R. Acad. Sci., Paris, 252, 1961, 2229.
(3) R. ZANA, S. CANDAU et R. CERF, C.R. Acad. Sci., Paris, 254, 1962, 10061.

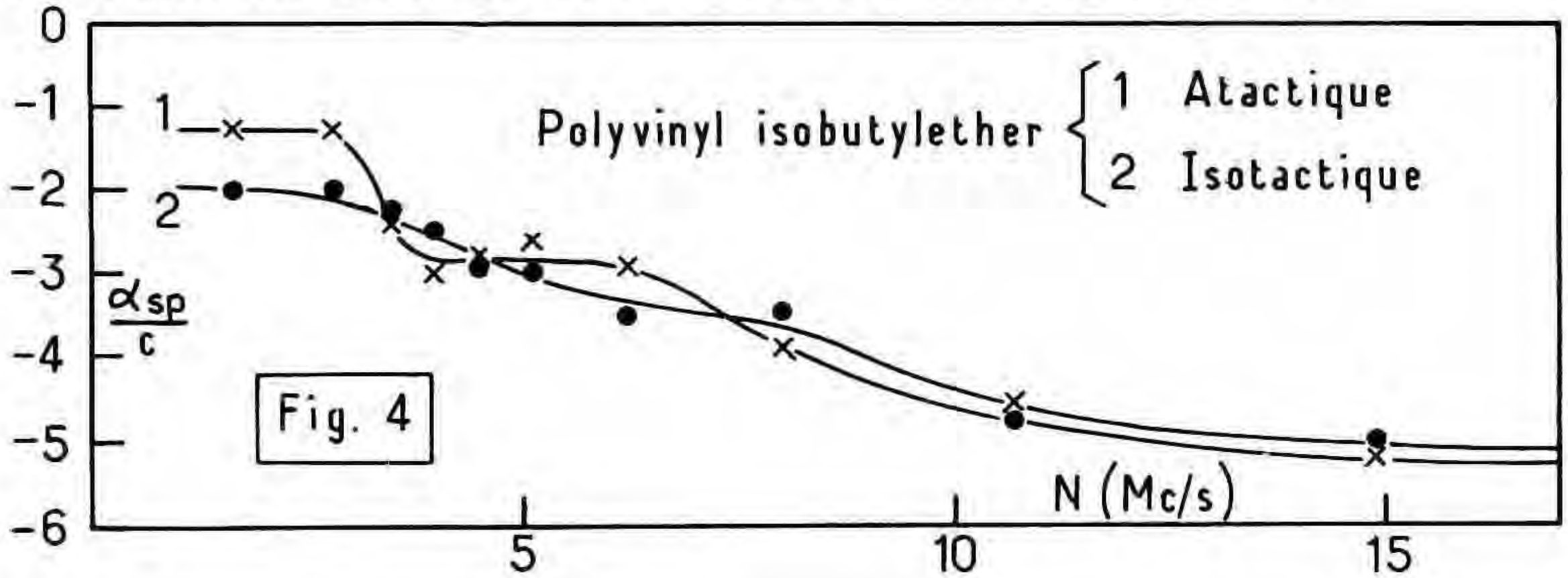

Fig. 4

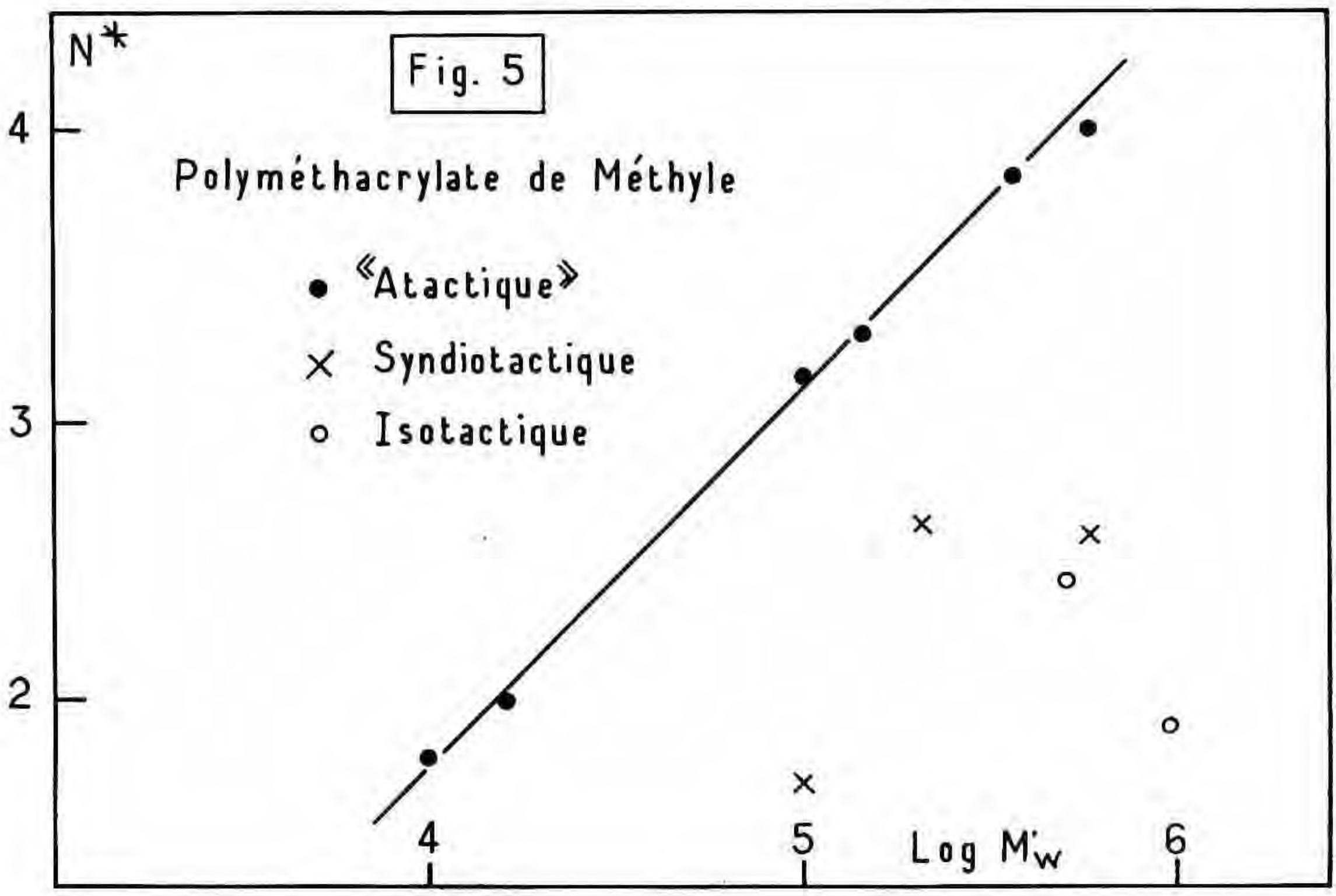

Fig. 5

K14

FOURTH INTERNATIONAL CONGRESS ON ACOUSTICS
COPENHAGEN 21.-28. AUGUST 1962

TRAPPING OF SOUND BY DENSITY GRADIENTS

Ivan Tolstoy

1. Total reflection by density gradients

Consider a fluid at rest, of density ρ and sound velocity c. Let ρ, c depend on the z coordinate only (stratified fluid). The equations of small motion are well known and may be put in various forms.[1-3] For present purposes we neglect gravity and assume that the displacements from equilibrium ξ, ζ are limited to two dimensions x, z. If we further restrict ourselves to harmonic waves of the form $f(z)e^{i(\alpha x - \omega t)}$, then ζ, ξ and the pressure perturbation p obey the equations:

$$\frac{d^2\zeta}{dz^2} + \frac{d\zeta}{dz} \cdot \frac{d}{dz} \log\left(\frac{\rho}{\beta^2}\right) + \zeta\beta^2 = 0 \qquad (1.1)$$

$$\xi = -i\alpha\beta^{-2} \frac{d\zeta}{dz} \qquad (1.2)$$

$$p = -\rho\omega^2\beta^{-2} \frac{d\zeta}{dz} \qquad (1.3)$$

where $\rho(z)$ is the unperturbed equilibrium density, and

$$\beta^2 = \omega^2 c^{-2} - \alpha^2 \qquad (1.4)$$

The transformation $$\zeta = \beta\rho^{-\frac{1}{2}} h \qquad (1.5)$$

gives: $$\frac{d^2h}{dz^2} + \gamma^2 h = 0 \qquad (1.6)$$

$$\gamma^2 = \beta^2 - \tfrac{1}{4}\left(\frac{d}{dz}\log\frac{\rho}{\beta^2}\right)^2 - \tfrac{1}{2}\frac{d^2}{dz^2}\log\frac{\rho}{\beta^2} \qquad (1.7)$$

Hence there is for given z, a frequency ω_o such that for $\omega < \omega_o$, $\gamma^2 < 0$, i.e., the waves are damped. A simple model is c = constant and

$$\rho = \rho_o e^{-2\nu z} \qquad (1.8)$$

Then $$\gamma^2 = \beta^2 - \nu^2 \qquad (1.9)$$

is constant, and $$\omega_o = \nu c \qquad (1.10)$$

is the low-frequency cutoff for sound waves in an exponentially density-stratified fluid. It is the resonant frequency for vertical oscillations of a fluid column. The

* This work was supported by the Office of Naval Research. It is Columbia University, Hudson Laboratories Contribution No. 146.

[1] Biot, M. A., J. Appl. Phys. 11, 522-530 (1940).
[2] Bergman, P., J. Acoust. Soc. Am. 17, 329-333 (1946).
[3] Eckart, C., Hydrodynamics of Oceans and Atmospheres (Pergamon Press, New York, 1960).

fluid is opaque to frequencies $\omega<\omega_o$

Now, γ,a are the z,x components of the wave number k, and

$$\omega^2 = k^2 c^2 + \omega_o^2 \quad . \tag{1.11}$$

Thus, frequencies $\omega>\omega_o$ are dispersed. The characteristic curve in the ω, k plane is a hyperbola (Fig. 1). If we consider two half spaces characterized by ν_1, ν_2 [Eq. (1.8)] such that $\omega_{o1}<\omega_{o2}$, a plane wave of frequency $\omega_{o1}<\omega<\omega_{o2}$ in medium (1) will be totally reflected after incidence upon the boundary of medium (2), irrespective of angle of incidence or of the numerical value of c_2/c_1. The criteria and effects of total reflection can be defined more sharply by considering the reflection coefficient (for displacements):

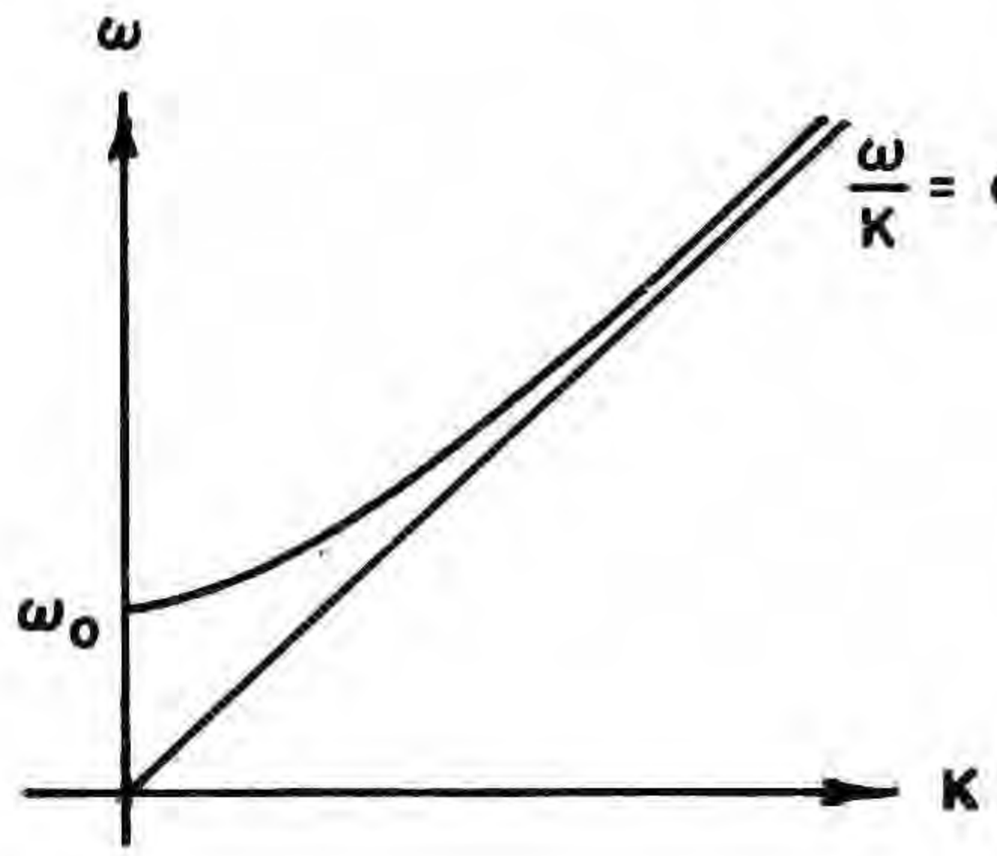

Fig. 1

$$R = \frac{i\gamma_1 - \nu_1 + (\nu_2 - i\gamma_2)\,\beta_1^2/\beta_2^2}{i\gamma_1 + \nu_1 - (\nu_2 - i\gamma_2)\,\beta_1^2/\beta_2^2} \tag{1.12}$$

which may be derived by standard procedures. In (1.12) it is assumed that ρ is continuous at the plane boundary between the media. The condition of total reflection is that γ_2 be imaginary: the shaded areas in Fig. 2 correspond to total reflection.

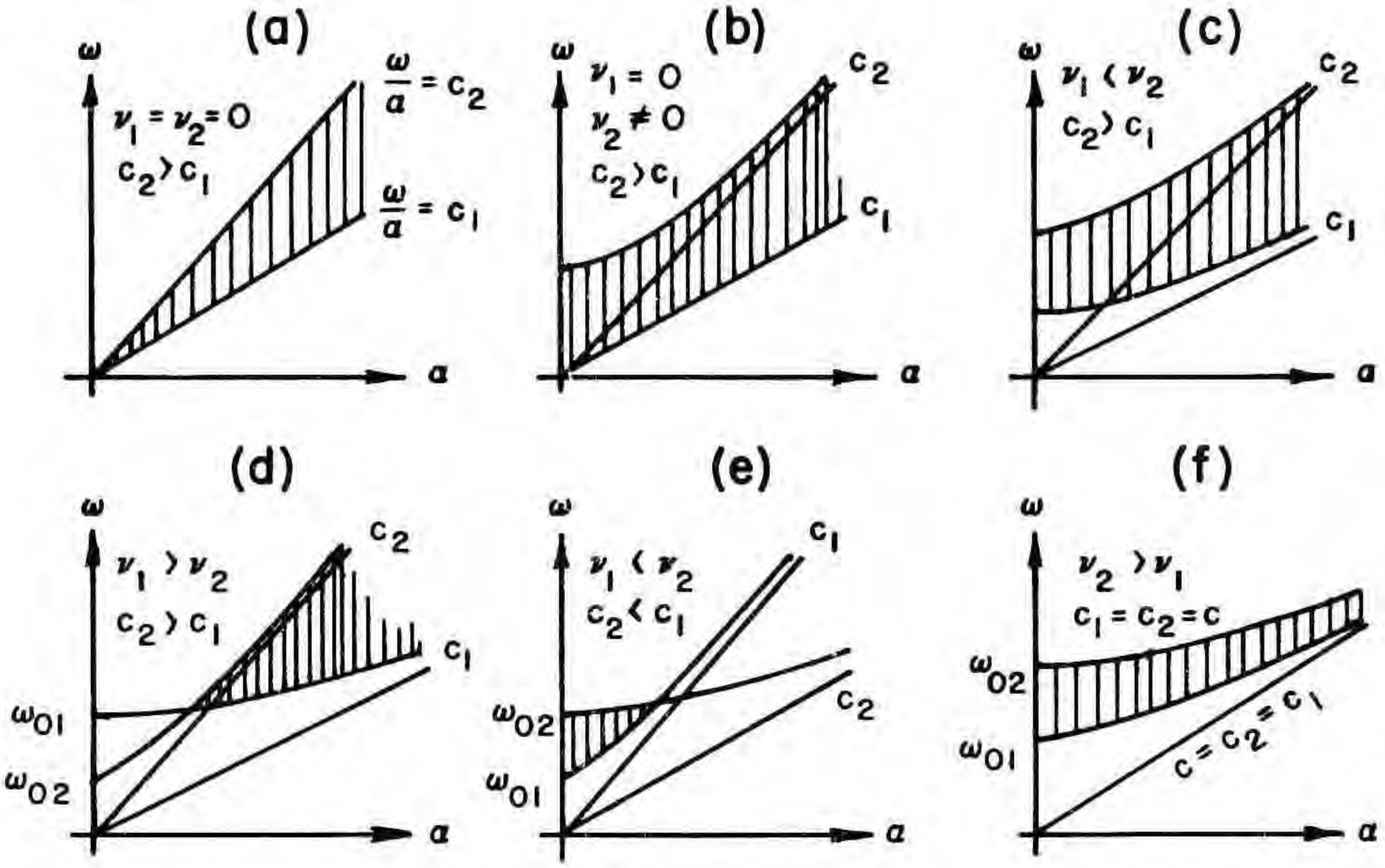

Fig. 2

Writing $$\gamma_2 = i\gamma_2' \qquad (1.13)$$

one has $$R = e^{2iX} \quad ; \qquad (1.14)$$

$$\chi = -\operatorname{Arctan} \frac{1}{\gamma_1} \left[-\nu_1 + \nu_2 \frac{\beta_1^2}{\beta_2^2} + \gamma_2' \frac{\beta_1^2}{\beta_2^2} \right] \qquad (1.15)$$

2. Waveguides

It is now obvious that if we consider a layer of medium (1) imbedded in an infinite medium (2), one may have waves totally reflected at both boundaries: even when $c_1 \geq c_2$, the layer can act as a waveguide. The characteristic equation is easily obtained from the interference condition between up- and downgoing plane waves in the layer.[4,5]

We confine ourselves here to a simple problem having the merit of exhibiting properties similar to those of the Earth's upper atmosphere. Recent data,[6] based upon rocket and satellite measurements, imply that $\omega_o(z)$ and $c(z)$ vary in the manner shown in Fig. 3. Therefore, the simplified model of Fig. 4 may give us a qualitative description of acoustic waves in the thermosphere. For the sake of mathematical simplicity it is assumed that

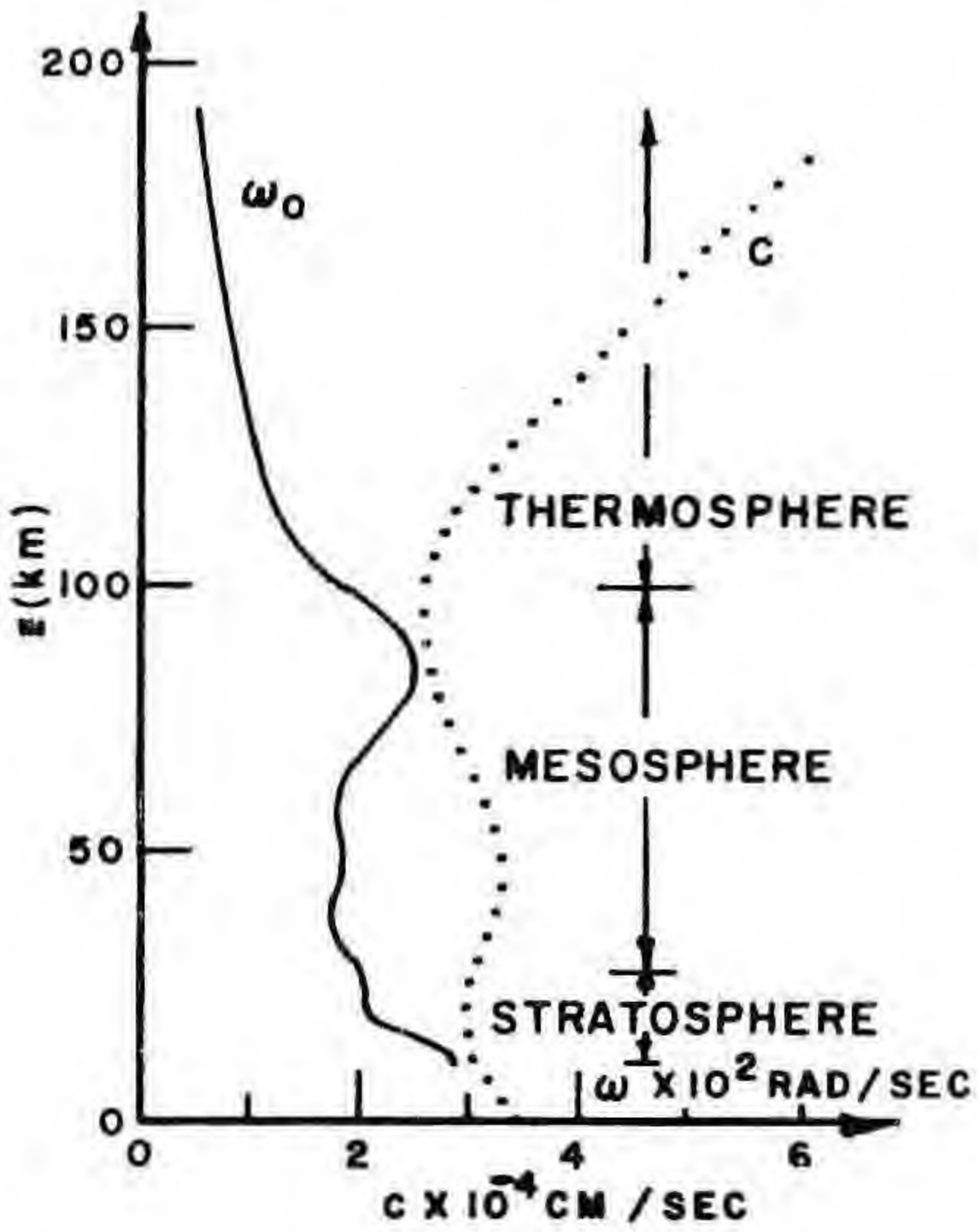

Fig. 3

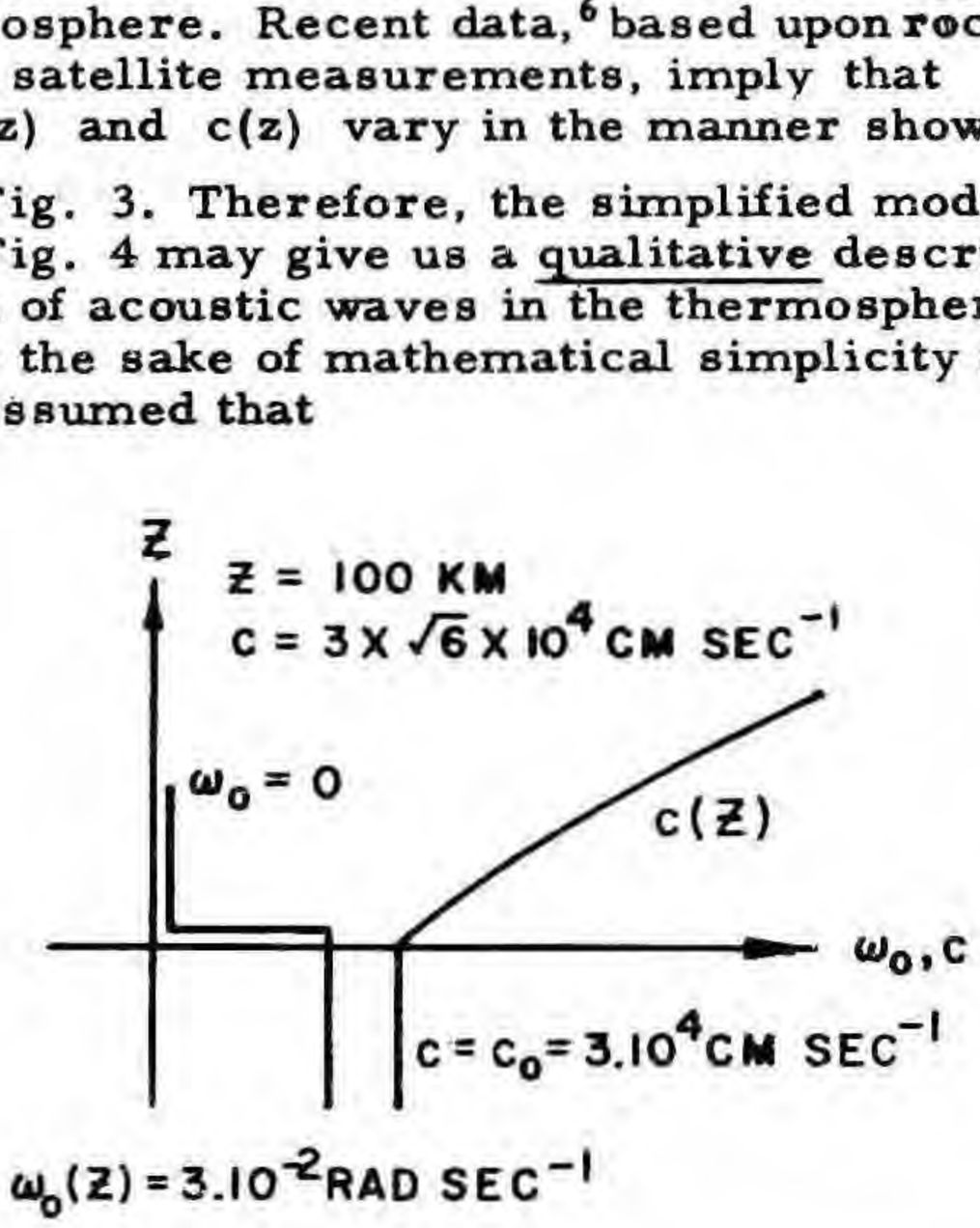

Fig. 4

$$z > 0 \quad \begin{cases} c(z) = (p\,z + q)^{-\frac{1}{2}} \\ \omega_o = 0 \quad ; \end{cases} \qquad (2.1)$$

$$z < 0 \quad \begin{cases} c(z) = c_o = \text{const} \\ \omega_o = \text{const} = 3.10^{-2} \end{cases} \qquad (2.2)$$

where p,q are chosen to give the desired values of c at z = 0 and z = 100 km (corresponding respectively to altitudes at 100 and 200 km). Waves in the thermosphere ($z > 0$) corresponding to ω, a values falling below the characteristic curve $\gamma_2 = \gamma_2' = 0$

[4] Tolstoy, I., J. Acoust. Soc. Am. 27, 274-277 (1955).
[5] Brekhovskikh, L.M., Waves in Layered Media (Academic Press, New York, 1960).
[6] U.S.A.F. Geophysics Res. Directorate: Handbook of Geophysics (Macmillan, New York, 1960).

will be totally reflected back into the thermosphere, with a change of phase:

$$\chi = - \text{Arctan} \frac{\gamma_2' + \nu_2}{\beta_o} \quad ; \tag{2.3}$$

$$\gamma_2' \doteq (\nu_2^2 - \beta_o^2)^{\frac{1}{2}} \quad . \tag{2.4}$$

In the region $z > 0$, the energy travels along curved ray paths which turn at $z = z_T$ $[\beta(z_T) = 0]$. When using the W.K.B. method it is necessary to approximate the effect of the turning point by a change in phase $\frac{\pi}{2}$.[5] The phase change due to the rest of the curved path is

$$2S = 2\int_{z=0}^{z_T} \beta \, dz = - \frac{4}{3\omega^2 p} \beta_o^3 \tag{2.5}$$

The interference condition[4,5] for guided modes is then simply the Bohr-Sommerfeld eigenvalue equation, modified to include the change in phase at the lower boundary:

$$S + \frac{\pi}{4} + \chi = m\pi \tag{2.6}$$

This equation has real roots defining the three dispersive modes of propagation in Fig. 5. These have low-frequency cutoffs at $a = 0$, corresponding to normal incidence, and high cutoffs where $\omega(a)$ intersects $\gamma_2' = 0$. The periods of these modes cover a range of about 1 to 10 min. An interesting feature is that, although for $z < 0$, $\zeta \to 0$ as $z \to -\infty$ like $e^{(\nu_2 + \gamma_2')z}$, the pressure $p \to +\infty$ like $e^{(\gamma_2' - \nu_2)z}$ $[\nu > \gamma_2'$ by Eq. (2.4)]. The energy density, however, vanishes like $\rho\zeta^2$, i.e., like $e^{2\gamma_2' z}$. Thus, although the energy is strongly concentrated, the observed pressure perturbations at depth (e.g., near the Earth's surface) may be large.

If a similar model with a rigid wall at $z = -100$ km is used, total reflection obtains also in the ω, a region above the hyperbola $\gamma_2' = 0$ in Fig. 4. In this case the dispersion curves will not be cut off as shown. The segments indicated in this figure remain almost unchanged, but they intersect the $\gamma_2' = 0$ curve and merge, for higher ω values, into the $\omega(a)$ curves one would obtain by a theory of a velocity stratified atmosphere of constant density. The curves in Fig. 5 would then be approximations to the low-frequency behavior of the lowest two or three modes.

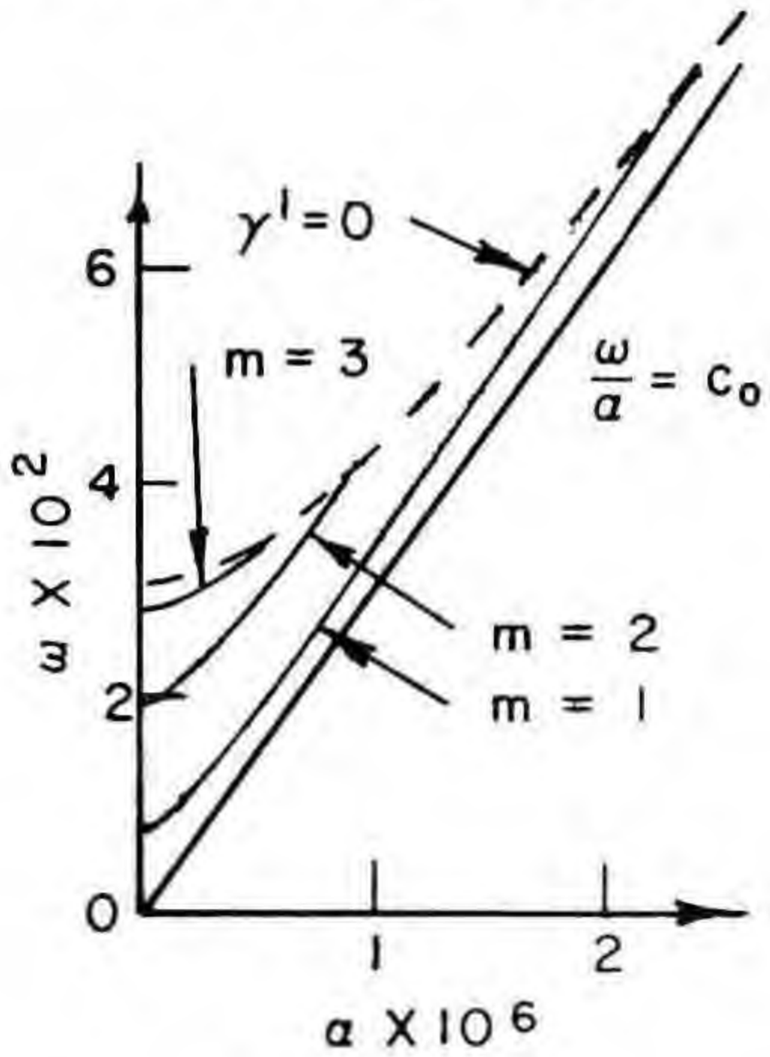

Fig. 5

A more exact treatment would have to be based not only upon a more elaborate and realistic model, but should also include the effect of gravity upon these very low-frequency acoustic waves. This, however, would not change things qualitatively.

Of course, these effects will be observable only if the equations of motion used are valid for the very long mean free paths L of the molecules at these altitudes $(10^2 \text{ m} \geq L \geq 1 \text{ m})$. However, we see that $aL \ll 1$, and it would seem that, as long as $\zeta \gg L$, our equations should apply.

Insofar as the oceans are concerned, these phenomena will also exist in principle, but the energy concentrations will be too weak to be perceptible. This is the explanation for certain types of solution noted by Eckart.[3]

L14

FOURTH INTERNATIONAL CONGRESS ON ACOUSTICS
COPENHAGEN 21.-28. AUGUST 1962

Der Einfluss der Luftschalldämmung auf das Innengeräusch von Strassenfahrzeugen

Christian Betzhold

Die Schwierigkeiten, die sich bisher bei der Lärmbekämpfung an Fahrzeugen ergaben, sind fast ausschliesslich auf die wenig übersichtliche Zusammensetzung des Fahrzeuggeräusches aus zahlreichen Komponenten zurückzuführen. Um jedoch der immer stärker werdenden Forderung nach leiseren Fahrzeuginnengeräuschen gerecht zu werden, ist eine Minderung aller Geräuschkomponenten notwendig, hierfür ist ihre genaue Kenntnis und die systematische Trennung der einzelnen Energieanteile Voraussetzung. Über die Messmethode und die Problemstellung berichteten früher Kurz und Oberst (4).

Für die Trennung der Körperschall- und Luftschallanteile des Motorgeräusches im Fahrzeuginnenraum wird im folgenden eine neue Methode beschrieben. Sie geht von der Feststellung aus, dass in fast allen Fällen Einzelmassnahmen bei der Lärmbekämpfung in Fahrzeugen, z.B. die Anwendung von Dämmatten, nicht die Wirkung erreichen, die nach Kenntnis ihrer Materialeigenschaften zu erwarten gewesen war. Dieser Unterschied hat seine Ursache zu einem sehr wesentlichen Teil in den Geräuschkomponenten, die häufig von den getroffenen Einzelmassnahmen nicht beeinflusst wurden, den sogenannten Nebenweganteilen.

1.) Schalldämmung von Trennwänden in Fahrzeugen

Es wird zunächst angenommen, dass das Geräusch im Innenraum des Fahrzeuges bei gegebenem Geräuschpegel im Motorraum und gegebenem Absorptionsvermögen des Innenraumes nur von der Schalldämmung der Trennwand abhängt und der Lärmpegel im Motorraum und das Absorptionsvermögen des Innenraumes nicht verändert werden. Durch den vom Motor erregten Körperschall wird jedoch der Geräuschpegel im Fahrzeuginnenraum über den durch die Trennwanddämmung gegebenen Betrag erhöht, so dass der Schalldruck p_2 im Innenraum aus beiden Schalldruckanteilen zusammengesetzt ist, der direkt über die Trennwand (p_D) und der auf dem Körperschallnebenwege (p_k) übertragen wird.

$$p_2^2 = p_D^2 + p_k^2 \qquad (1)$$

Von diesen Anteilen ist der direkt über die Trennwand zwischen Motor- und Fahrgastraum übertragene Anteil p_D gegeben durch

$$p_D = p_1 \cdot W \qquad (2)$$

mit p_1 dem Schalldruck im Motorraum und W dem Verhältnis der Trennwandimpedanz zur Impedanz des anschliessenden Fahrzeuginnenraumes.

Zur Vereinfachung wird Gleichung 1 nach p_1 aufgelöst und durch p_2 dividiert.

$$\frac{p_1}{p_2} = \frac{1}{W^2}\left(1 - \frac{p_k^2}{p_2^2}\right) \qquad (3)$$

Durch Logarithmieren ergibt sich

$$10 \log \frac{p_1^2}{p_2^2} - 10 \log \frac{1}{W^2} + 10 \log \left(1 - \frac{p_K^2}{p_2^2}\right) \qquad (4)$$

bzw. nach Einführung von $R_K = 10 \log \frac{p_1^2}{p_2^2}$ und $R = 10 \log \frac{1}{W^2}$

$$R_K = R + 10 \log \left(1 - \frac{p_K^2}{p_2^2}\right) \qquad (5)$$

Da gemäss Gleichung 1 p_k kleiner als p_2 ist, wird der Ausdruck für den auf dem Körperschallwege übertragenen Geräuschanteil $10 \log \left(1 - \frac{p_K^2}{p_2^2}\right)$ negativ, wofür also $-R_n$ gesetzt werden kann.

$$R_K = R - R_N \qquad (5a)$$

Bei eingebauten Fahrzeugtrennwänden ist die vor und hinter der Trennwand gemessene Pegeldifferenz R_K gleich der Schalldämmung der Trennwand R (Schalldämmzahl nach DIN 52210) vermindert um den auf dem Körperschallwege übertragenen Geräuschanteil R_N, wegen der bei Fahrzeugen unvermeidbaren Nebenwege.

2.) Berechnung des Körperschallanteils durch Änderung der Schalldämmung

Solange die Schalldämmzahl einer Fahrzeugtrennwand nicht bekannt ist, können für die Bestimmung des Nebenweganteiles die Gleichungen 5 und 5b noch nicht verwendet werden, sie bieten jedoch die Voraussetzung dafür, dass durch Änderung der Schalldämmung um einen bekannten Betrag der Nebenweganteil abzuschätzen ist. Dies kann im Versuch beispielsweise durch den Einbau einer Dämmatte geschehen, deren Wirkung von Labormessungen her bekannt ist.

Es wird hierbei vorausgesetzt, dass diese Dämmatte den Nebenweg nicht beeinflusst, und dass die z.B. im bauakustischen Prüfstand nach DIN 52210 festgestellte Dämmverbesserung im Fahrzeug die gleiche ist. Die erste dieser beiden Annahmen lässt sich experimentell bestätigen, die zweite Voraussetzung hat sich innerhalb der bisher bei Fahrzeuggeräuschmessungen üblichen Messgenauigkeit als annehmbar erwiesen.

Vor dem Einkleben der Matte besteht gemäss Gleichung 5 die Beziehung

$$R_{K1} = R_1 + 10 \log \left(1 - \frac{p_K^2}{p_{21}^2}\right) \qquad (5b)$$

und nach dem Einkleben der Matte die Beziehung

$$R_{K2} = R_1 + 10 \log \left(1 - \frac{p_K^2}{p_{22}^2}\right) \qquad (5c)$$

Aus der Differenz ergibt sich schliesslich der gesuchte Körperschallanteil p_K

$$\Delta R = 10 \log \left(\frac{p_{21}^2 - p_K^2}{p_{22}^2 - p_K^2}\right) \qquad (6)$$

Mit Hilfe der Gleichung 6 und unter Verwendung geeigneter Messunterlagen kann nunmehr der über den Nebenweg übertragene Körperschallanteil abgeschätzt werden. Auch gestattet diese Formel die Berechnung der zu erwartenden Geräuschminderung bei Änderung der Schalldämmung. Schliesslich kann mit Hilfe des nunmehr bekannten Körperschallanteiles die Wirkung weiterer Massnahmen am Fahrzeug vorausgesagt werden, soweit die Kenndaten der verwendeten Materialien von Prüfstand- bzw. Labormessungen her bekannt sind.

3.) Vergleich mit anderen Verfahren zur Abschätzung der Körperschall-übertragung in Fahrzeugen

Nach dem von Zboralski (5) beschriebenen Verfahren zur Abschätzung der Körperschallanteile des Fahrzeuginnengeräusches von Eisenbahnfahrzeugen werden zunächst die Aussen- und Innenpegel von Schienenfahrzeugen gemessen. Sodann wird mit einem Lautsprecher im Fahrzeuginneren ein Geräuschpegel erzeugt, durch den ausserhalb des Fahrzeuges ein Pegel entsteht, der im Nahfeld der Fahrzeugwand gemessen wird. Durch Versuche gelangt Zboralski zu einer Endformel, welche obiger Gleichung 5 entspricht.

Zur Erfassung der über Körperschallwege in das Fahrzeuginnere von Schienenfahrzeugen eingeleiteten Geräuschanteile hat der Verfasser in einer früheren Arbeit (1) empfohlen, den Luftschall innerhalb als auch ausserhalb des Wagens sowohl auf riffelfreien als auch auf riffelbehafteten Schienen zu messen, sinngemäss wird bei den Körperschallmessungen verfahren. Bei der Berechnung wird sowohl von der obigen Gleichung (1) ausgegangen, als auch von der Überlegung, dass die Differenz zwischen dem gemessenen Aussenluftschall und dem reinen Luftschallanteil des Innengeräusches gleich der Schalldämmung der Waggonwand, also unabhängig von den Eigenschaften des Oberbaues ist.

Die nach den vorgenannten Verfahren ermittelten Werte stimmen innerhalb der Messgenauigkeit überein.

Bobbert (2, 3) empfiehlt, das Fahrzeuginnengeräusch in zwei Versuchen zu bestimmen. Beim ersten Versuch wird das Innengeräusch am normalen, fahrbereiten Fahrzeug gemessen. Beim zweiten Versuch wird der Motor in seinen Aufhängungen bzw. auf dem Rollenprüfstand die Karosserie vom Fahrgestell gelöst. Dieses Verfahren gestattet die direkte Bestimmung des Körperschallanteiles.

4.) Zusammenfassung

Bei systematischen Versuchen zur Geräuschsenkung in Fahrzeugen wurden die vier geschilderten Verfahren zur Trennung der Luft- und Körperschallanteile des Innengeräusches angewendet. Der Vergleich der Mess- und Rechenergebnisse ergab Übereinstimmung innerhalb der Messgenauigkeit, so dass sowohl theoretisch als auch in der Praxis die erwünschte Gleichwertigkeit besteht. Welches Verfahren jeweils anzuwenden ist, richtet sich allein nach den praktischen Gegebenheiten. Das neue Verfahren bedingt Änderungen der im Fahrzeug eingebauten Isolation. Das ältere Verfahren benötigt verhältnismässig viel Rechenaufwand und erfordert im allgemeiner. zwei bis drei Körperschallmess-Stellen. Dem gegenüber benötigt das Zboralskische Verfahren einen hohen apparativen Aufwand, diesstösst bei Messungen an schnellfahrenden und verhältnismässig kleinen Strassenfahrzeugen auf praktische Schwierigkeiten. Das von Bobbert vorgeschlagene Verfahren fordert das Lösen der Karosserie vom Fahrgestell und setzt einen Rollenprüfstand voraus. Schliesslich ist das Lösen des Motors von seinen Aufhängungen aus konstruktiven Gründen meist mit Schwierigkeiten verbunden und erfordert daher mehr Zeit als die zuerst genannten Verfahren. Diesen Nachteilen der einzelnen Verfahren stehen andererseits eine Reihe von Vorteilen, insbesondere die erwünschte Kenntnis über die Zusammensetzung der Schallenergien gegenüber, so dass die Anwendung wenigstens eines der genannten Verfahren bei fahrzeugakustischen Untersuchungen zu empfehlen ist.

Der Überblick über die Messergebnisse bestätigt ausserdem, dass sich die Geräusche im Innenraum von Fahrzeugen nur durch geeignete Kombination verschiedener Massnahmen wesentlich vermindern lassen. Insbesondere ist es möglich, den Einfluss einzelner Massnahmen theoretisch abzuschätzen, und so bestimmte Massnahmen zielstrebig durchzuführen.

Für dieses Ziel lohnt sich die Anwendung eines oder möglichst mehrerer der miteinander verglichenen Verfahren zur Abtrennung der Nebenweganteile des Innengeräusches von Fahrzeugen.

Literatur:

(1) Ch. Betzhold, "Beitrag zur Fahrzeugakustik"
Glasers Annalen 83, (1959) S. 352

(2) G. Bobbert, "Geräusche im Innenraum von Personenwagen"
VDI-Zeitschrift, Bd. 101 (1959) Nr. 26 - 1217/24

(3) G. Bobbert, "Lärmbekämpfung bei Personenwagen und ihre Beurteilung"
ATZ 61, (1959) S. 42

(4) K. Kurz und W. Oberst, "Zum Problem der Lautstärkeverminderung von Kraftfahrzeugen"
ATZ 60, (1958) S. 133

(5) D. Zboralski, "Körperschall- und Nebenweganteile im Fahrzeuggeräusch, ein Beitrag zur Vervollkommnung der Geräuschisolierung"
Glasers Annalen 81, (1957) S. 246

M14

FOURTH INTERNATIONAL CONGRESS ON ACOUSTICS
COPENHAGEN 21.-28. AUGUST 1962

Ein Verfahren zur Nachbildung von Schallfeldern in Räumen und zur Untersuchung ihrer subjektiven Wirkungen

W. Burgtorf

III. Physikalisches Institut der Universität Göttingen

Bei der Neuplanung eines Raumes steht der Akustiker vor der Aufgabe, die vom Architekten gelieferte Grundkonzeption so zu erweitern, daß der fertige Raum den gewünschten akustischen Anforderungen gerecht wird. Seine Kunst besteht darin, die einzelnen raumakustischen Elemente wie Nachhallzeit, Diffusität, Schallstärkeverteilung, starke Einzelrückwürfe usw. so zu bemessen, daß das aus ihrem Zusammenwirken sich ergebende Schallfeld in seiner Hörsamkeit in der fertigen Ausführung des projektierten Raumes der gewünschten Vorstellung entspricht.

Mit der hier beschriebenen Anlage sollen mit elektroakustischen Mitteln Schallfelder wirklicher Räume in einem reflexionsfreien Raum durch Zusammensetzen aus ihren zeitlichen und räumlichen Komponenten (Direktschall, Rückwürfe, Nachhall) nachgebildet und von einer Versuchsperson hinsichtlich ihrer Hörsamkeit beurteilt werden. Für Vergleichsmöglichkeiten und quantitative Aussagen müssen die Einzelelemente des Schallfeldes, also Zeitlage, Einfallsrichtung, Pegel und Klangfarbe der Rückwürfe sowie der Nachhall innerhalb gewisser Grenzen unabhängig voneinander variierbar sein.

Der Direktschall wird nachhallfrei oder zumindest sehr nachhallarm monophon oder auch stereophon von einem Magnetophon M_1 geliefert. Die Verwendung endloser Bandschleifen ist möglich und zum Teil zweckmäßig. Für die Erzeugung der Rückwürfe stehen fünf Verzögerungseinrichtungen $M_2 \ldots M_6$ zur Verfügung (Magnetophone mit gegeneinander versetzten Wiedergabeköpfen). Insgesamt sind 17 verzögerte Wiedergaben des Direktsignals möglich, die zwischen 0 und 1 s praktisch beliebig einstellbar sind.

Der Verstärkerteil der Anlage besteht aus 12 voneinander unabhängigen 15 W-Verstärkerkanälen mit jeweils einem davorgeschalteten geeichten Flachbahnregler zur Einstellung einer definierten Vordämpfung. Zur Abstrahlung der einzelnen Schallsignale werden im reflexionsfreien Raum konzentrisch zu dem Platz der Versuchsperson in der jeweils benötigten Richtung bis zu 30 hochwertige elektrodynamische

Lautsprecher aufgestellt. - Den einzelnen Darbietungen kann Nachhall in der gewünschten Stärke zugesetzt werden. Dies geschieht entweder mit der Hallplatte nach Kuhl, die derart erweitert wurde, daß sich ein räumlich wirkender Nachhall erzeugen läßt, oder mit Hilfe eines Hallraumes, der zuvor durch geeignete Auskleidung mit Absorptionsmaterialien auf die gewünschte Nachhallzeit eingestellt wurde, bzw. mit Hilfe eines anderen Raumes (z.B. Hörsaal).

Die Verbindung der Verzögerungsgeräte mit den Verstärkerkanälen und mit den Lautsprechern geschieht entweder direkt über Steckverbindungen oder über vom reflexionsfreien Raum aus fernbedienbare Auswahlschalter, um in bestimmten Verstärkerkanälen Verzögerungszeit, Dämpfung und Einfallsrichtung variieren zu können. Hierdurch wird ermöglicht, daß verschiedene Schallfeldkonfigurationen in schnell wechselnder Folge zur Beurteilung dargeboten werden können. Für quantitative Messungen und zur Kontrolle der Anlage sind eine Reihe von Hilfseinrichtungen vorhanden. Sie erlauben z.B., daß der Versuchsleiter seine eigene Versuchsperson sein kann. - Auf Einzelheiten und Besonderheiten der Anlage und auf eigentliche Nachbildungsexperimente soll im Rahmen dieser Ausführungen nicht eingegangen werden.

Wirkliche Schallfelder bestehen aus einer Vielzahl verschiedenartigster Rückwürfe. Objektiv exakte Nachbildungen scheitern von vornherein an dem zu betreibenden technischen Aufwand. Sie sind auch nicht notwendig, da das Auflösungsvermögen des Gehörs nach Zeit und Richtung begrenzt ist. Umfangreiche Untersuchungen über die subjektiven Wirkungen von Rückwurffolgen - über einige wird berichtet werden - zeigen, daß es einen sinnvollen Kompromiß gibt zwischen einem noch "vernünftigen" apparativen Aufwand und der zu fordernden "Natürlichkeit" des nachgebildeten Schallfeldes. Es wurden hierbei die Rückwürfe ermittelt, die in einfachen oder zusammengesetzten Rückwurffolgen nicht zur Wahrnehmung gelangen, also bei Nachbildungen fortgelassen werden dürfen. Die Untersuchungen führen vielfach auf spezielle Fragen der psychologischen Akustik.

Die Durchführung der Versuche geschah im einfachsten Fall in der Weise, daß auf ein Schallsignal S_o, dessen Ankunft bei der Versuchsperson den Zeit-Nullpunkt festlegte, eine verzögerte Wiederholung dieses Ereignisses ($S_{\Delta t}$) als Testschall folgte. Dessen Pegel war von der Versuchsperson so einzustellen, daß bei Successivvergleich der Darbietungen mit bzw. ohne Testschall kein Unterschied festzustellen war. Die so gemessene Schwelle für die Erkennbarkeit des Testschalles wurde "Absolute Wahrnehmbarkeitsschwelle" genannt

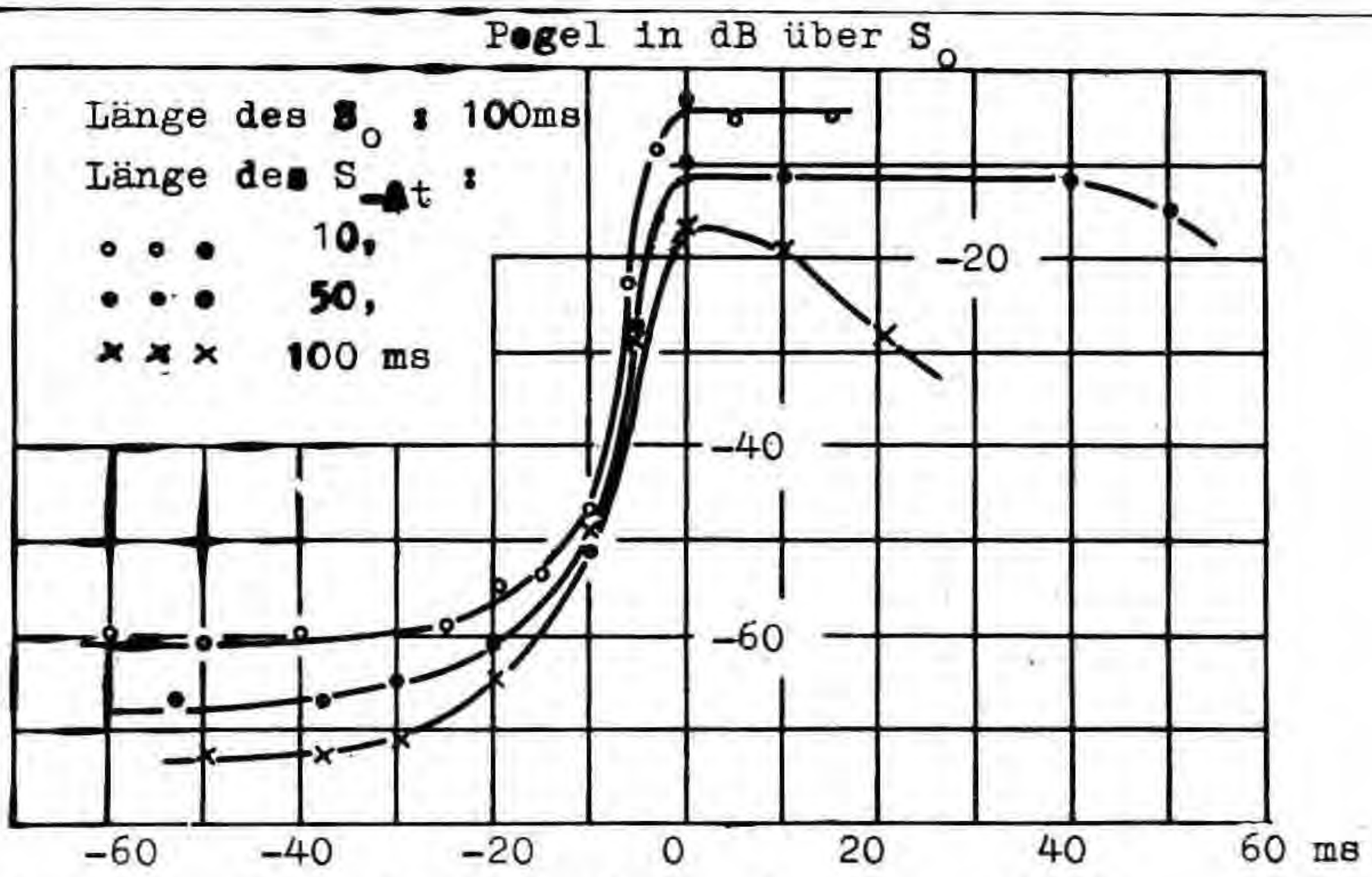

Bild 1 : Verdeckung durch "backward masking".

und in Abhängigkeit von der Zeitverzögerung des Testschalles und für zahlreiche Kombinationen der Einfallsrichtungen der beteiligten Schallsignale gemessen. Der zugrundeliegende Effekt ist die bekannte Vorwärtsverdeckung (forward masking).

Hier soll nun über einige Untersuchungen berichtet werden, bei denen einem zur Zeit Null ankommendem Hauptsignal S_o ein diesem gleichartiges mit einer quasi "negativen" Verzögerung als Testschall vorauseilte ($S_{-\Delta t}$). Der Schwellenverlauf wurde als Funktion der Voreilung und der Einfallsrichtung gemessen. Dieses zunächst befremdlich erscheinende Phänomen der Rückwärtsverdeckung (backward masking) ist z.B. auch von Raab und von Pickett untersucht worden, allerdings unter ganz anderen Versuchsbedingungen und von anderen Fragestellungen ausgehend.

Als Motiv dienten mit weißem Rauschen aufgefüllte Rechteckimpulse. Bei Richtungsgleichheit (Schalleinfall von vorn) und mit der Länge des verdeckten Impulses als Parameter erhält man die Schwellenverläufe nach Bild 1. Der verdeckende Impuls war 100 ms lang. Für große Voreilungen gehen die Schwellen über in die Hörschwellen des einzeln dargebotenen Testimpulses. Diese sind - ebenso wie die Maxima der Kurven - entsprechend dem Anstieg der Lautstärke mit der Impulslänge in Ordinatenrichtung verschoben. Die Rückwärtsverdeckung erstreckt sich nur über einen relativ kleinen Zeitbereich (in diesem Fall etwa 30 ms) im Gegensatz zur Vorwärtsverdeckung (siehe Kurvenverlauf in Bild 1 über der positiven Zeitachse).

Bild 2 zeigt für zwei Richtungskombinationen (Einfall des Haupt-

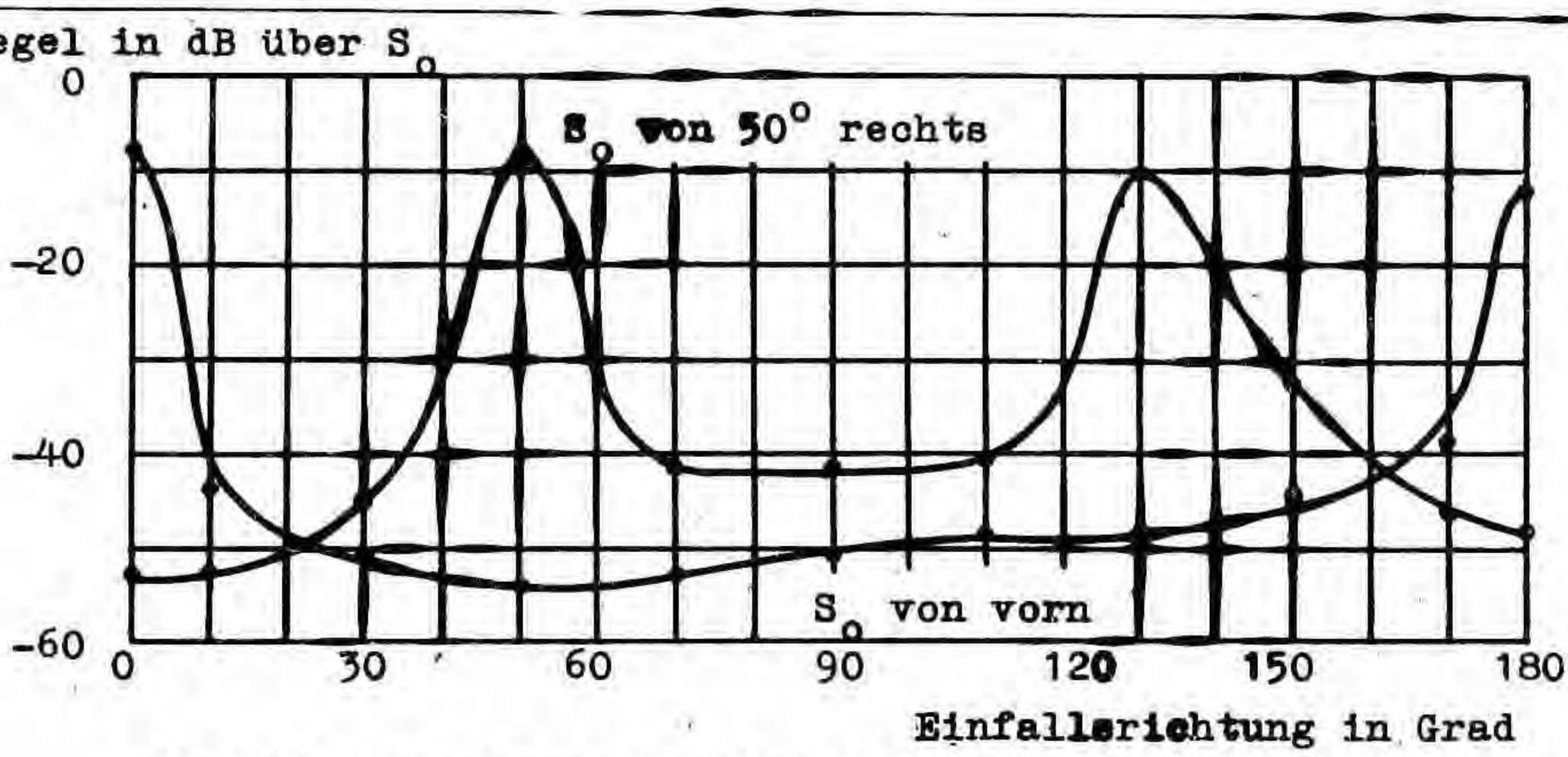

Bild 2 : Richtungsabhängigkeit des "backward masking".

signales von vorn und von 50° rechts) den Schwellenverlauf in Abhängigkeit von der Einfallsrichtung des verdeckten Signales (verdeckender Impuls loo ms lang, um 5 ms voreilender verdeckter Impuls lo ms lang). Die Kurven zeigen zwei sehr ausgeprägte Maxima. Das eine tritt auf bei Richtungsgleichheit von verdeckendem und verdecktem Schall, das andere liegt symmetrisch zu der gemeinsamen Einfallsrichtung. Symmetrieachse ist die Senkrechte auf der Blickrichtung. Dies und die Stärke der Maxima deuten darauf hin, daß die Rückwärtsverdeckung und speziell ihre Richtungsabhängigkeit sehr amplituden- und phasenabhängig ist. Die gängige Erklärung der Rückwärtsverdeckung mit Hilfe einer von der Reizstärke abhängigen Fortpflanzungsgeschwindigkeit der Erregung im Nervensystem scheint für sich allein nicht ausreichend zu sein.

Wie dieses Beispiel zeigt, eignet sich die beschriebene Anlage nicht nur zur Untersuchung raumakustischer Fragen mit Hilfe von Schallfeldnachbildungen, sondern sie läßt sich auch mit Erfolg einsetzen für Versuche auf dem Gebiet der psychologischen Akustik, die unter Freifeldbedingungen durchgeführt werden können.

Literatur:

(1) W. Burgtorf — Acustica, 11 (1961), 97; Acustica, 12 (1962)
(2) H.P.Seraphim — Acustica, 11 (1961), 80; Acustica, 12 (1962)
(3) David H.Raab — J.Acoust.Soc.Amer., 33(1961), 137
(4) J.M.Pickett — J.Acoust.Soc.Amer., 31(1959), 1613

N14

FOURTH INTERNATIONAL CONGRESS ON ACOUSTICS
COPENHAGEN 21.-28. AUGUST 1962

Analyse et dépouillement automatique des réponses transitoires

P. LIENARD (O.N.E.R.A. - France)

L'analyse classique des phénomènes acoustiques par filtres suppose que la pression sonore mesurée est, soit une fonction périodique du temps, soit une fonction aléatoire stationnaire, soit une somme des deux. Or, nous rencontrons souvent des phénomènes transitoires non directement analysables par les filtres usuels, tels que le bruit dû au passage rapide d'un avion, même subsonique; l'onde de choc d'un mobile supersonique, certaines fluctuations en soufflerie, etc... Leur analyse doit être faite par le calcul à partir du relevé des ordonnées de la fonction correspondante, à des intervalles rapprochés.

L'étalonnage de microphones très peu sensibles, pour bruits allant jusqu'à 180 dB, a nécessité l'analyse de la réponse de ces microphones à une impulsion ou un échelon de pression, car il n'est pas possible de produire économiquement des pressions sinusoïdales permanentes de forte intensité, et bien connues.

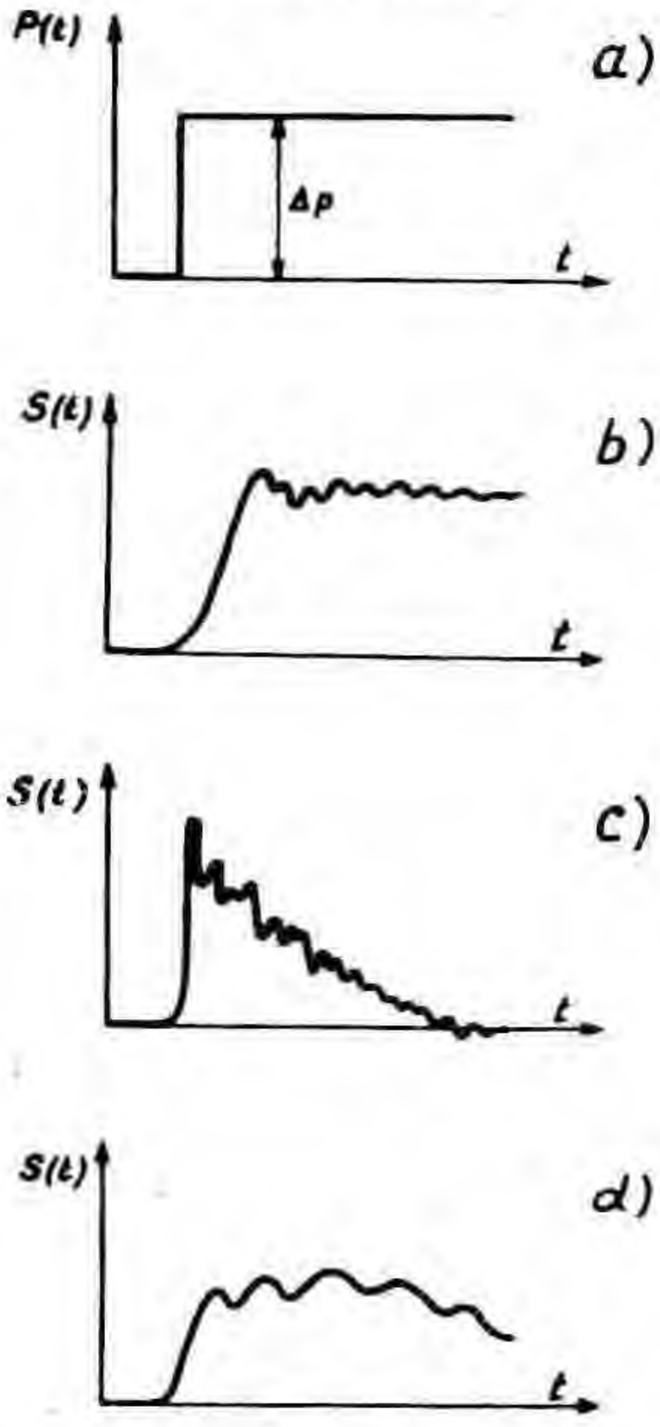

fig. 1

Par contre, il est possible au moyen d'un tube à choc, de produire un échelon unité de pression de hauteur bien connue, et d'une durée suffisante pour que les fréquences basses de son spectre soient physiquement définies [1].

Le capteur de pression en étude étant fixé à l'extrémité fermée de la chambre de détente du tube, avec les précautions convenables d'isolement des vibrations de parois et d'étanchéité, il reçoit une pression représentée par la figure 1a, et le signal qu'il transmet, qui

serait identique à 1a si le capteur était parfait, est de l'une des formes 1b, c, d mettant en évidence son temps de réponse, ses fréquences propres, etc...

La fonction de transfert du capteur est le rapport complexe des transformées de LAPLACE, de la fonction de sortie s(t) et de la fonction d'entrée p(t).

Mais l'échelon de pression p(t) étant de durée limitée (60 ms par exemple, avec un tube de 25 m de long), le calcul des intégrales correspondantes n'est possible que si la fonction de sortie est arrivée au bout de ce temps, à une valeur stable (fig.1b et 1c). Le cas de la figure 1d n'est pas analysable, car la réponse complète du capteur n'est pas connue.

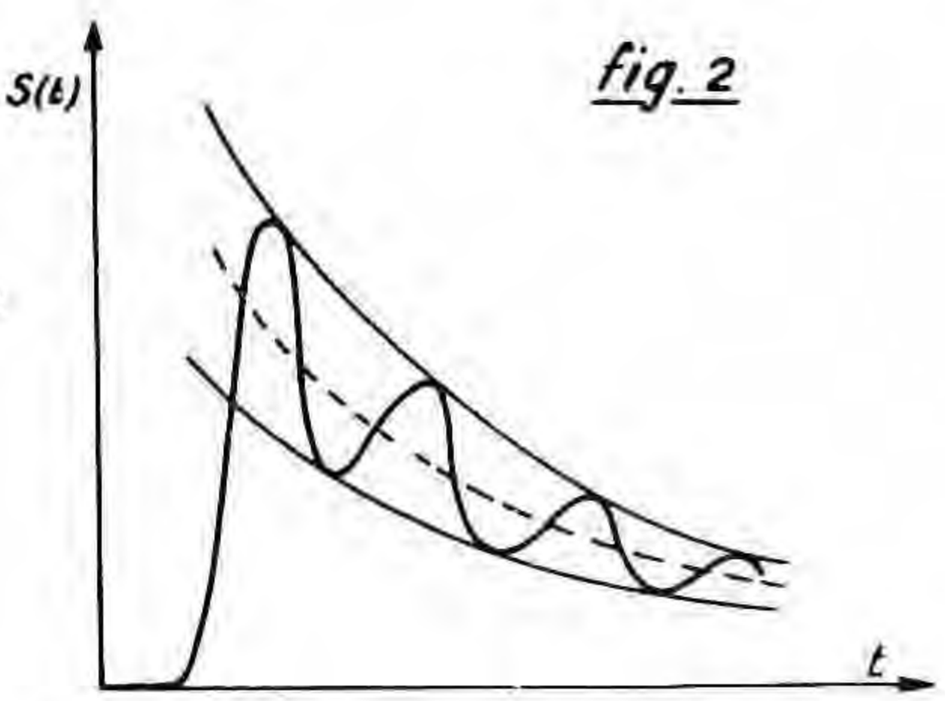

fig. 2

Toutefois, une étude est en cours afin d'analyser les réponses transitoires presque stabilisées (fig.2), dans le cas où la valeur moyenne de la réponse transitoire est proche d'une exponentielle décroissante, autour de laquelle la fluctuation d'amplitude est elle-même décroissante.

Le calcul de la fonction de transfert est possible, dans les cas tels que 1b et 1c, en supposant que la figure tracée est la moitié d'une période de pression à variation rectangulaire : c'est à dire qu'une fonction d'entrée telle que a (fig.3) conduirait à une réponse telle que b ou c.

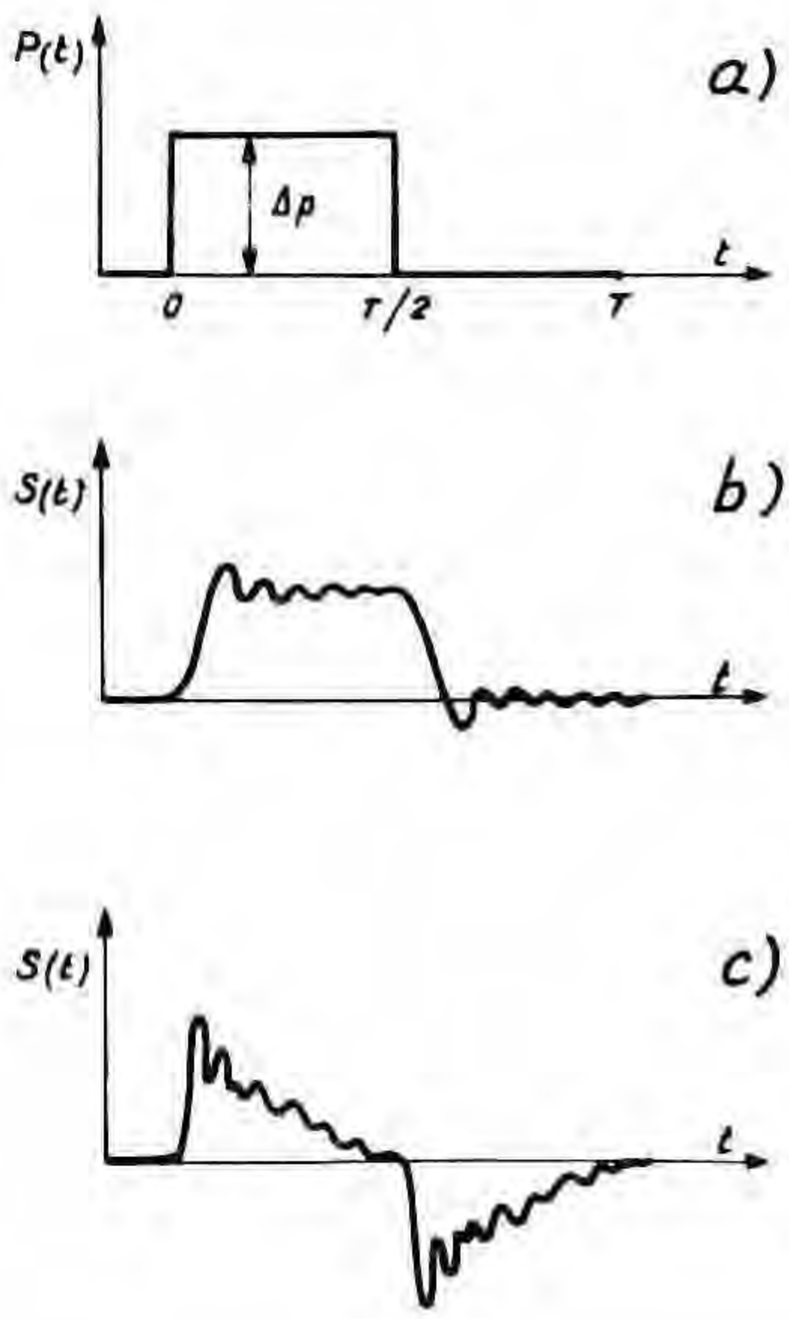

fig. 3

Les aires des 2 fonctions sont alors bien déterminées et calculables par exemple par méthode des trapèzes ainsi que les produits $s(t)\cos\omega t$ pour toute valeur donnée de ω.

Le calcul pratique nécessite donc le relevé des ordonnées s(t) de la courbe de réponse expérimentale, pour des valeurs de t aussi rapprochées que possible, afin de pouvoir définir le spectre de cette fonction pour des fréquences élevées.

Pour cela, l'enregistrement oscillographique de la réponse est agrandi, retracé, afin d'avoir un trait suffisamment fin, et cette courbe (fig. 4 a) est enroulée sur un tambour de lecture de " fac-similé " BELIN. Un spot lumineux est à chaque tour, interrompu successivement par l'axe des x (arbitraire) et la courbe ; une cellule photo-électrique envoie à ces deux moments un "top" qui commande la marche et l'arrêt d'un compteur. Le chiffre du compteur est mis en mémoire, pour perforation d'un ruban codé, puis le compteur mis à zéro pour recevoir le nombre suivant, qui représentera l'ordonnée s (t+Δt), etc...

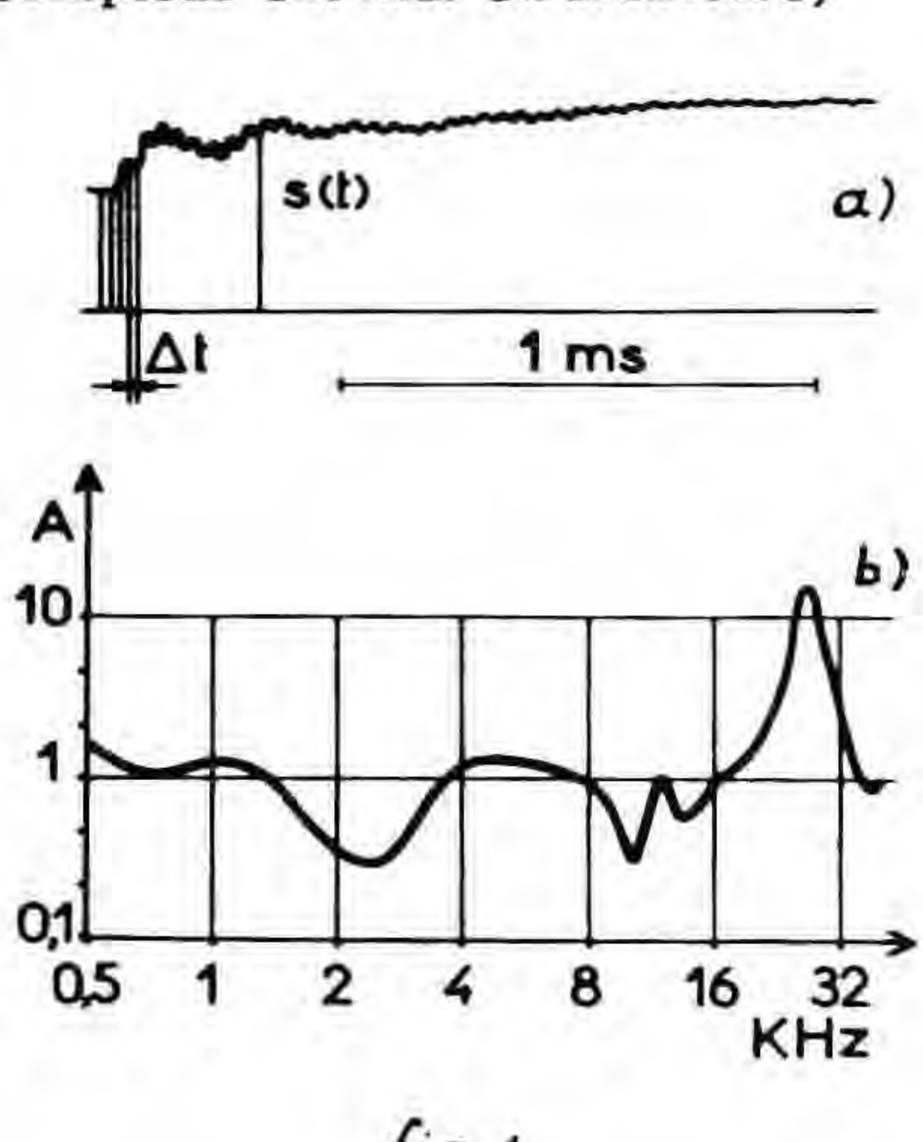

fig. 4

Le ruban perforé est ensuite utilisé pour la perforation de cartes, et un programme de calcul assez classique [2] détermine, pour les différentes valeurs de la fréquence données d'avance, les termes réel et imaginaire, le module et la phase, de la fonction de transfert du capteur de pression étudié (fig. 4 b).

La figure 5 donne la réponse transitoire expérimentale b (capteur de pression ONERA type 20 H44) à une onde balistique a (balle de fusil) [3] et la courbe correspondante calculée de réponse des amplitudes en fonction de la fréquence (c).

La même méthode permet d'analyser un infra-son enregistré photographiquement, dont on prend un échantillon pendant un temps suffisant.

La forme de pression due à une onde de détonation d'avion supersonique est analysable aussi de cette façon.

L'appareillage d'analyse automatique a été réalisé par l'O.N.E.R.A., en utilisant en partie un tambour BELIN et du

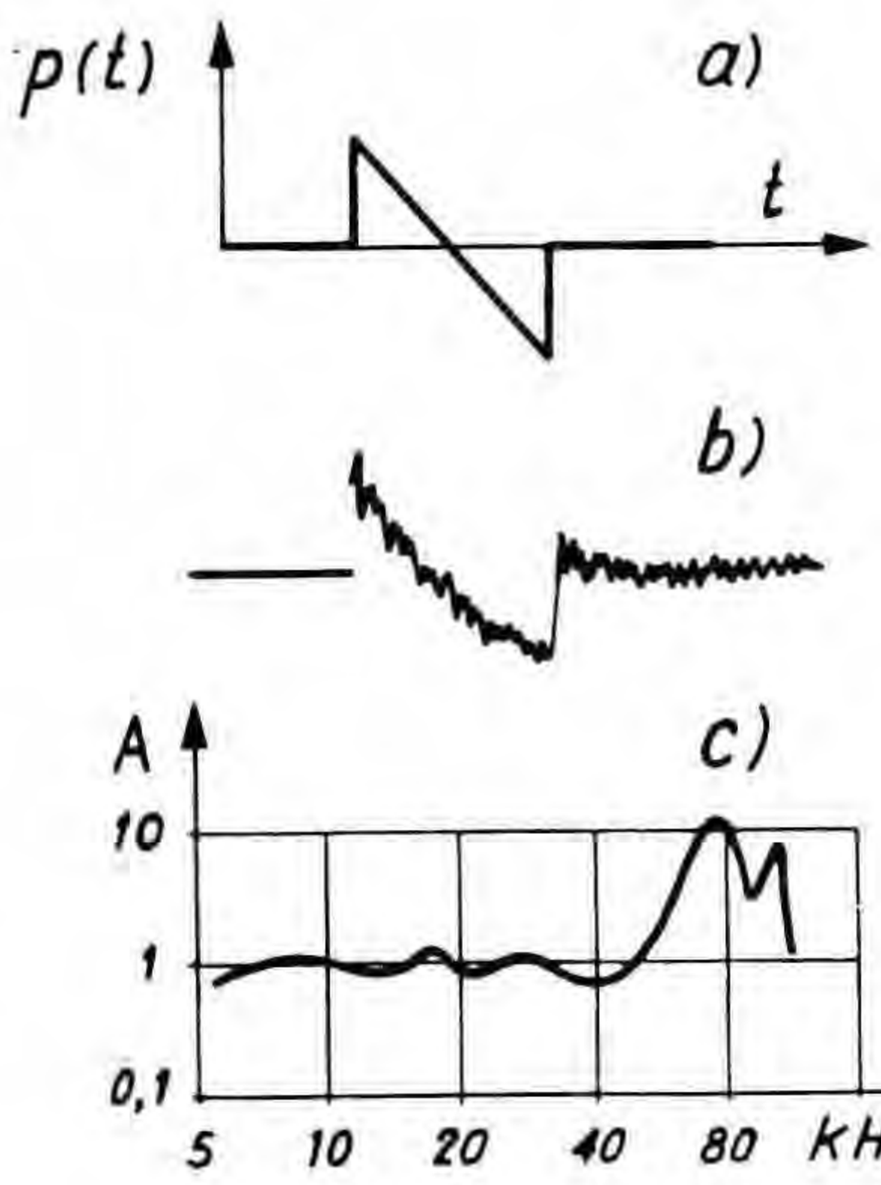

fig. 5

matériel mécanographique BULL.

Ces résultats sont l'aboutissement d'un travail d'équipe entre les Divisions d'Acoustique et d'Electronique, et le Centre de Calcul de la Direction de Physique de l'O.N.E.R.A. MM. MIQUEL et CHOLAT ont établi les principes de base et effectué les premières expériences. M. PLANCHAIS a réalisé l'appareillage définitif de dépouillement et en assure l'exploitation, et Madame GAUDFERNAU a établi les programmes de calcul.

Références :

(1) - J. CHOLAT-NAMY - Etude de méthodes d'étalonnage dynamique de capteurs de pressions.
La Recherche Aéronautique n°80 - Janvier/Février 1961 - p.37 .

(2) - R. LAFON - Transformée de FOURIER directe et inverse.
Note Technique O.N.E.R.A. 4-2265 P - Septembre 1958.

(3) - J. MATTEI - Les mesures d'ondes de choc.
La Recherche Aéronautique n°50 - Mars/Avril 1956 - p.39.

O14

FOURTH INTERNATIONAL CONGRESS ON ACOUSTICS
COPENHAGEN 21.-28. AUGUST 1962

INHOMOGENEOUS ELASTIC MEDIA WITH CONSTANT VELOCITY

J. E. White

The Ohio Oil Company, Denver Research Center, Littleton, Colorado

INTRODUCTION

In order to obtain a realistic description of the propagation of sound over long distances in the atmosphere or in the ocean, or to compute the paths deep in the earth followed by earthquake waves, one must take into account the continuous variations in properties of the atmosphere, the ocean, or the earth. With these and other applications in mind, authors have published dozens of articles on wave propagation in inhomogeneous media, and a chapter is devoted to this subject in each of two recent books. [1, 2]. Attention has been focused exclusively on situations where velocity varies from point to point, and techniques for computing curved ray paths have been developed quite fully. It is the purpose of this paper to examine the case where density and elastic constants vary in direct proportion, so that the propagation velocity is constant throughout the medium. An interest in the propagation of elastic waves in a thin wedge led to this study, and the relation between a thin wedge and a linearly inhomogeneous medium is discussed.

INHOMOGENEOUS LIQUIDS

ARBITRARY FUNCTION OF POSITION

Any small elementary volume of the liquid is characterized by density and bulk modulus, and we assume that these two quantities vary together from point to point, according to some arbitrary function $f(x, y, z)$. Let us denote density $\rho = rf$ and bulk modulus $B = bf$. Pressure at any point is proportional to dilatation Δ:

$$-p = bf\Delta \qquad (1)$$

In this equation, $\Delta = \frac{\partial u}{\partial x} + \frac{\partial v}{\partial y} + \frac{\partial w}{\partial z}$, where u, v, and w are components particle displacement along the x-, y-, and z- axes. The acceleration of an elementary volume by the pressure gradient is expressed thus:

$$rf \frac{\partial^2 u}{\partial t^2} = - \frac{\partial p}{\partial x}$$

$$rf \frac{\partial^2 v}{\partial t^2} = - \frac{\partial p}{\partial y} \qquad (2)$$

$$rf \frac{\partial^2 w}{\partial t^2} = - \frac{\partial p}{\partial z}$$

Elimination of pressure between Equations (1) and (2) and further manipulation leads to an equation involving dilatation only:

$$\frac{1}{\alpha^2}\frac{\partial^2\Delta}{\partial t^2} = \nabla^2\Delta + \frac{1}{f}\left(\frac{\partial f}{\partial x}\frac{\partial\Delta}{\partial x} + \frac{\partial f}{\partial y}\frac{\partial\Delta}{\partial y} + \frac{\partial f}{\partial z}\frac{\partial\Delta}{\partial z}\right)$$
$$+ \frac{1}{f}\nabla^2 f\,\Delta - \frac{1}{f^2}\left[\left(\frac{\partial f}{\partial x}\right)^2 + \left(\frac{\partial f}{\partial y}\right)^2 + \left(\frac{\partial f}{\partial z}\right)^2\right]\Delta \qquad (3)$$

In this equation, α is the speed of compressional waves, equal to $\sqrt{b/r}$.

We shall confine our attention to instances where f depends on one coordinate only, which we shall take to be x. For plane waves of sinusoidal time dependence, the dilatation can be expressed as

$$\Delta = F(x)\, e^{i\ell z}\, e^{-i\omega t} \qquad (4)$$

With these conditions, Equation (3) yields:

$$\frac{d^2F}{dx^2} + \left(\frac{df}{dx}/f\right)\frac{dF}{dx} + \left[\frac{d^2f}{dx^2}/f - \left(\frac{df}{dx}/f\right)^2 + \frac{\omega^2}{\alpha^2} - \ell^2\right]F = 0 \qquad (5)$$

Various functions specifying the variation of elastic constants will be substituted into this equation, from which the dependence of dilatation on the x- coordinate can then be seen.

LINEAR DEPENDENCE ON POSITION

We assume that density and bulk modulus are proportional to distance, rx and bx, respectively. Then $f(x) = x$, $\frac{df}{dx}/x = \frac{1}{x}$, and $\frac{d^2f}{dx^2} = 0$. Equation (5) then becomes

$$\frac{d^2F}{dx^2} + \frac{1}{x}\frac{dF}{dx} + \left(\frac{\omega^2}{\alpha^2} - \ell^2 - \frac{1}{x^2}\right)F = 0 \qquad (6)$$

Solutions for F are $H_1^{(1)}(mx)$ or $H_1^{(2)}(mx)$, where $m^2 = (\omega^2/\alpha^2 - \ell^2)$. As a representative solution, we take $H_1^{(1)}(mx)$, describing a wave traveling in the positive x-direction.

$$\Delta = A\, H_1^{(1)}(mx)\, e^{i\ell z}\, e^{-i\omega t} \qquad (7)$$

$$p = -Abx\, H_1^{(1)}(mx)\, e^{i\ell z}\, e^{-i\omega t} \qquad (8)$$

$$u = (m A \alpha^2/\omega^2)\, H_0^{(1)}(mx)\, e^{i\ell z}\, e^{-i\omega t} \qquad (9)$$

$$w = (i\ell A \alpha^2/\omega^2)\, H_1^{(1)}(mx)\, e^{i\ell z}\, e^{-i\omega t}$$

DEPENDENCE ON SECOND POWER

With density given as rx^2 and bulk modulus as bx^2, substitution into Equation (5) gives

$$\frac{d^2F}{dx^2} + \frac{2}{x}\frac{dF}{dx} + \left(\frac{\omega^2}{\alpha^2} - \ell^2 - \frac{2}{x^2}\right)F = 0 \qquad (10)$$

Solutions to this involve spherical Bessel functions:

$$\Delta = A\, h_1^{(1)}(mx)\, e^{i\ell z}\, e^{-i\omega t} \tag{11}$$

$$p = -Ab\, x^2\, h_1^{(1)}(mx)\, e^{i\ell z}\, e^{-i\omega t} \tag{12}$$

$$u = (mA\,\alpha^2/\omega^2)\, h_0^{(1)}(mx)\, e^{i\ell z}\, e^{-i\omega t} \tag{13}$$

$$w = (i\,\ell\, A\,\alpha^2/\omega^2)\, h_1^{(1)}(mx)\, e^{i\ell z}\, e^{-i\omega t}$$

SINUSOIDAL DEPENDENCE

If we take $\rho = r \sin ax$ and $B = b \sin ax$, then Equation (5) leads to the result:

$$\frac{1}{a^2}\frac{d^2F}{dx^2} + \cot ax\, \frac{1}{a}\frac{dF}{dx} + \left[\frac{1}{a^2}\left(\frac{\omega^2}{\alpha^2} - \ell^2\right) - \frac{1}{\sin^2 ax}\right] F = 0 \tag{14}$$

Solutions to this are the Associated Legendre Functions, $P_n^1(\cos ax)$ and $Q_n^1(\cos ax)$, where $n(n+1) = (\omega^2/\alpha^2 - \ell^2)/a^2$. Defining $R_n^m(\cos ax)$ as $[P_n^m(\cos ax) + \frac{2i}{\pi} Q_n^m(\cos ax)]$, solutions are:

$$\Delta = A\, R_n^1(\cos ax)\, e^{i\ell z}\, e^{-i\omega t} \tag{15}$$

$$p = -Ab \sin ax\, R_n^1(\cos ax)\, e^{i\ell z}\, e^{-i\omega t} \tag{16}$$

$$u = \left[(1 - \ell^2\alpha^2/\omega^2)/a\right] A\, R_n^0(\cos ax)\, e^{i\ell z}\, e^{-i\omega t}$$

$$w = (\alpha^2/\omega^2)\,(i\ell + a \cot ax)\, A\, R_n^1(\cos ax)\, e^{i\ell z}\, e^{-i\omega t} \tag{17}$$

SOLID WITH LINEAR DEPENDENCE

Following steps comparable to those given above for a liquid, Ewing, Jardetzky and Press [1] give the equations of motion for an inhomogeneous solid. For the special case of linear dependence on one coordinate (ρx, λx, and μx), and with the requirements that the y-component of displacement be zero and that all quantities be independent of y, a simple pair of equations results:

$$\rho\frac{\partial^2 u}{\partial t^2} = (\lambda + 2\mu)\left(\frac{\partial\Delta}{\partial x} + \frac{\Delta}{x}\right) + \mu\left(\frac{\partial^2 u}{\partial z^2} - \frac{\partial^2 w}{\partial x \partial z} - \frac{2}{x}\frac{\partial w}{\partial z}\right)$$

$$\rho\frac{\partial^2 w}{\partial t^2} = (\lambda + 2\mu)\frac{\partial\Delta}{\partial z} + \mu\left(\frac{\partial^2 w}{\partial x^2} - \frac{\partial^2 u}{\partial x \partial z} + \frac{1}{x}\frac{\partial w}{\partial x} + \frac{1}{x}\frac{\partial u}{\partial z}\right) \tag{18}$$

THIN WEDGE

By analogy with Love's treatment of wave propagation in a thin plate [3], it was assumed that propagation in a very thin wedge would take place with the normal stress $p_{\theta\theta} = 0$ throughout. Furthermore, displacements and stresses were averaged through the thickness of the wedge. In terms of average displacements, the equations of motion are the same as Equation (18), with λ' replacing λ, where $\lambda' = (2\lambda\mu)/(\lambda + 2\mu)$.

Waves travelling in the direction of thickening of the wedge, namely, the radius of cylindrical coordinates, are described by particularly simple expressions. For z-component of displacement zero and the radial component independent of z, the counterpart of Equation (18) reduces to:

$$\rho \frac{\partial^2 u_r}{\partial t^2} = (\lambda' + 2\mu) \left(\frac{\partial^2 u_r}{\partial r^2} + \frac{1}{r} \frac{\partial u_r}{\partial r} \right) \tag{19}$$

The solution for displacement is:

$$u_r = A H_0^{(1)} (kr) e^{-i\omega t} \tag{20}$$

where $k^2 = \rho\omega^2/(\lambda' + 2\mu)$. This is seen to be a longitudinal wave travelling at "plate speed", $\sqrt{(\lambda' + 2\mu/\rho}$.

For zero radial displacement, a transverse wave results, with displacement

$$u_z = A H_0^{(1)} (qr) e^{-i\omega t} \tag{21}$$

where $q^2 = \omega^2\mu/\rho$.

CONCLUSION

Inhomogeneous media in which elastic wave velocities are constant throughout exhibit some interesting properties. For instance, displacements may involve cylindrical Bessel functions or spherical Bessel functions, even though the coordinates are rectangular. An inhomogeneous medium with constants proportional to one coordinate is shown to be equivalent to a thin wedge of homogeneous material. Wave propagation in a wedge is not fully described and merits further attention.

REFERENCES

1. Ewing, Jardetzky, and Press. Elastic Waves in Layered Media. McGraw-Hill, 1957.

2. Brekhovskikh, Leonid M. Waves in Layered Media. English Translation. Academic Press, 1960.

3. Love, A. E. H. A Treatise on the Mathematical Theory of Elasticity. Dover, 1944.

P14

FOURTH INTERNATIONAL CONGRESS ON ACOUSTICS
COPENHAGEN 21.-28. AUGUST 1962

Dispersion of Elastic Surface Waves in a Tapering Layered Medium.

L. Knopoff

A geophysical problem of considerable interest is the nature of elastic wave propagation in an elastic wedge-shaped region bounded at one surface by a dissimilar semi-infinite elastic region; the other surface is stress-free. This is an improved model approximating the cross-sectional geometry of the earth in certain regions. The usual model considered is that of a semi-infinite half-space with one layer overlying it where both boundaries are parallel to each other. At the continental margins and perhaps at the flanks of mountain ranges, the bottom of the earth's crust is not parallel to the surface of the earth. In sufficiently small regions, this may be approximated by a wedge-shaped region overlying a half-space; the vertex of the wedge is considered remote from the region of interest. Much work has been done on acoustic wave propagation in wedges with walls having infinite impedance, where the walls are either stress-free or perfectly rigid. The mathematical difficulties that arise are associated with the singularity of the geometry at the vertex and the need to express the corresponding singularity in the mathematical solution at the vertex. There have been no solutions presented for the wedge with the mixed boundary conditions considered here, although some work has been done on wedges with impedance boundary conditions. One difficulty with the use of impedance boundary conditions or perfectly reflecting boundaries is that surface waves do not arise in the solutions or are difficult to introduce.

In this paper we consider only the surface waves that exist in the problem of the tapering layer with mixed boundary conditions at one surface. This problem is made simpler if the vertex of the wedge, the source of the preceding mathematical difficulties, is removed from the problem. This is the case if the wedge is of small angle and the points of observation are located at great distance from the vertex.

The solution to the problem may be set up in two ways. As in the case of the

plane-layered medium, we may write down a ray solution as well as a mode solution. In the case of the mode solution, we extend the procedure due to Homma. In the wedge, we write down solutions appropriate to the geometry of the wedge. For Love waves we write as the solution in the wedge for outgoing waves,

$$u_1 = A(r)\, H_p^{(1)}\left(\frac{\omega r}{\beta_1}\right) \cos p(\theta-\theta_0)\, e^{-i\omega t}$$

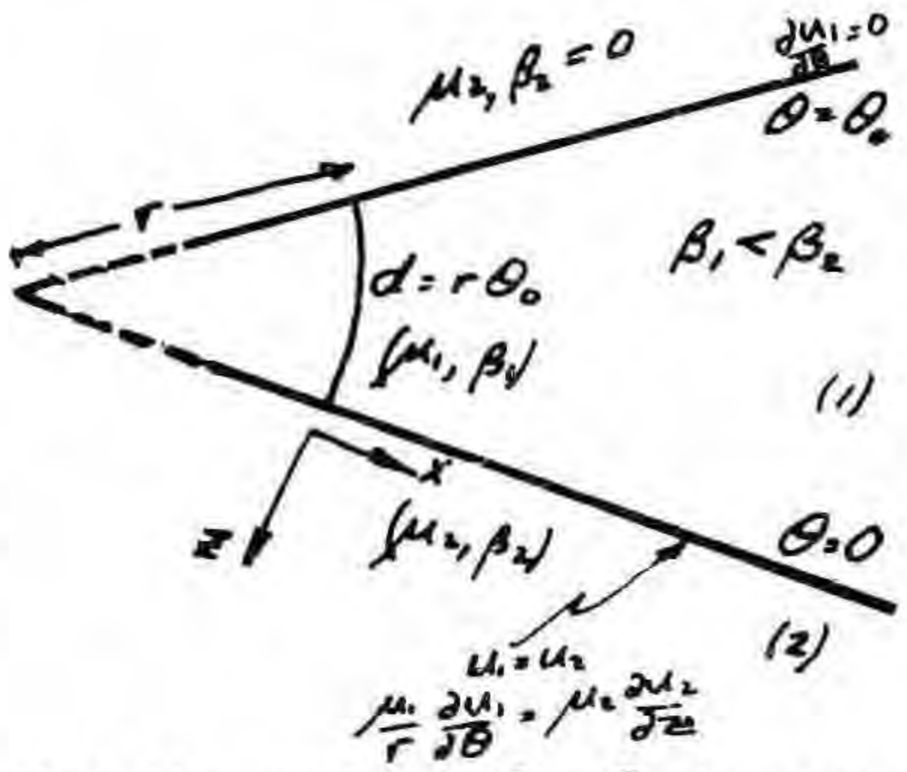

at a point with cylindrical coordinates (r,θ) where $H_p^{(1)}$ is the ordinary Hankel function and (β_1, μ_1) are the shear wave velocity and shear modulus, ω is the angular frequency and A is at best a function of p only and does not depend upon r. This solution has been selected so that the surface $\theta = \theta_0$ is stress-free. In the half space we write

$$u_2 = B(p)\, e^{i(kx + \eta_2 z - t)\omega + i\phi(p)}$$

where we now use a solution to the wave equation in cartesian coordinates for this region for outgoing waves only and where B and ϕ are functions of p only and $\eta_2^2 = k^2 - 1/\beta_2^2$. Our problem is to compute $k(\omega)$ as the eigenvalues of the system, subject to the boundary conditions

$$\mu_2 \frac{\partial u_2}{\partial z} = \frac{\mu_1}{r}\frac{\partial u_1}{\partial \theta}, \quad u_1 = u_2 \quad ; \text{at } \theta = 0.$$

Applying these boundary conditions, we see that the eigenvalue equation for outgoing surface waves is

$$\tan \omega d \xi_1 = \frac{\mu_2 \eta_2}{\mu_1 \xi_1} \tag{1}$$

where we set the distance $d = r\theta_0$, the arc length across the wedge at the distance r and where $\xi_1 = \frac{p}{\omega r}$. Since this eigenvalue equation is a function of r, we see that we obtain a different set of eigenvalues at different distances from the vertex.

The eigenvalue equation has been represented in a form analogous to the solution for the plane-parallel case, $\theta_0 \longrightarrow 0$, $r \longrightarrow \infty$ where d is now the thickness of the layer: $\tan \omega d \eta_1 = \frac{\mu_2 \eta_2}{\mu_1 \eta_1}$, $\eta_1^2 = \frac{1}{\beta_1^2} - k^2$.

Hence we should be able to obtain the dispersion equation in the limit as $\theta_0 \longrightarrow 0$. This is done by representing the Hankel function by its asymptotic expansion for large values of argument and order:

$$H_p^{(1)}(y) = \left(\frac{2}{\pi}\right)^{1/2} (y^2 - p^2)^{-\frac{1}{4}} \exp\left[i(y^2-p^2)^{1/2} - ip\cos^{-1}\frac{p}{y} + \cdots\right] e^{-\frac{i\pi}{4}}, \quad y > p \gg 1$$

We further expand this solution to describe waves moving past a particular point r_o. We let $r = r_o + r_1$, $r_1 \ll r_o$ and compare the phases in the waves by equating the coefficients of r_1 and x in the exponents. We thus obtain the additional equation

$$k\beta_1 = \frac{(y_o^2 - p^2)^{\frac{1}{2}}}{y} + \frac{i}{2}\frac{y_o}{y_o^2 - p^2} + \frac{y_o(y_o^2 + 4p^2)}{8(y_o^2 - p^2)^{\frac{5}{2}}} + \cdots \qquad (2)$$

where $y_o = p/\beta_1\xi_1$

Equations (1) and (2) may be solved simultaneously to obtain the wave number $k(\omega)$. These equations have been solved numerically. The number of terms in the asymptotic expansion $H_p(y)$ determines the number of terms in the expansion for $k(\omega)$ written as a function of Q_β.

The numerical results, taken to three terms in the power series expansion show, as the lowest approximation, a solution identical with that for the plane-parallel case of a slab of thickness d. In the next order, the principal effect is an attenuation for outward going waves and an amplification for inward traveling waves; the attenuation factor is frequency dependent and has a maximum close to (but not identical with) the period of the minimum group velocity. For the values $\frac{\alpha_1}{\beta_1} = 1.8$, $\beta_2/\beta_1 = (.6)^{\frac{1}{2}}$, the maximum value of the attenuation factor is about $\frac{1}{4}Q_\beta\omega/\beta_1$

In the second order approximation, the phase velocity of surface waves is shifted from the value in the plane-parallel case. For waves propagating outward from the wedge, high frequencies show a decrease in phase velocity over and above the velocities obtained in the plane-parallel solution, while the low frequencies show an increase in phase velocity. The signs are reversed for waves propagating toward the vertex. The crossover in the shift in velocity due to the inclination of the two surfaces can be explanied on geometrical grounds: The ray is rotated by $2\theta_o$ upon each reflection at the surface. This corresponds to the lengthening of the ray path for outward going waves and hence to a decrease in phase velocity. For constructive interference we must take into account not only the phase shifts due to the change in path length but also the phase shifts upon reflection from the half-space; these magnitudes are dependent upon the angle of incidence in a manner opposite to the effect of the change of path length. For the parameters above, the

shift in phase velocity at short periods is negligible due to either effect. At long periods however, the phase velocity shift becomes appreciable and has a maximum at about $\frac{0.3\theta_0^2 c^2}{\beta_1}$ where c is the unperturbed phase velocity. The crossover occurs at roughly the frequency corresponding to the minimum group velocity.

The phase velocity can also be computed by a ray construction. The sum of all the multiply reflected rays, with strengths that depend upon the angle-dependent reflection coefficient, can be written down. Here, the strengths are written as a series; it has been possible to sum the series, in the limit of small wedge angle, only for the case of perfectly reflecting walls. By the application of Watson's transformation, it is possible to convert the series into an integral, which may then be evaluated by the method of steepest descents. If several higher order terms in the solution by steepest descents are obtained, the features observed in the construction by modes, considered earlier, are reproduced.

The case of the mode solution for Rayleigh waves is somewhat more complex algebraically but the solution is formally similar, although some caution must be taken in the asymptotic expansion of the two Hankel functions with different arguments corresponding to the compression and shear modes. The algebra is more complex as it is necessary to solve two simultaneous transcendental equations, as before, but here the equations are themselves sixth order determinants, corresponding to the six boundary conditions. Numerical solutions, however, show results similar to those obtained in the case of Love waves.

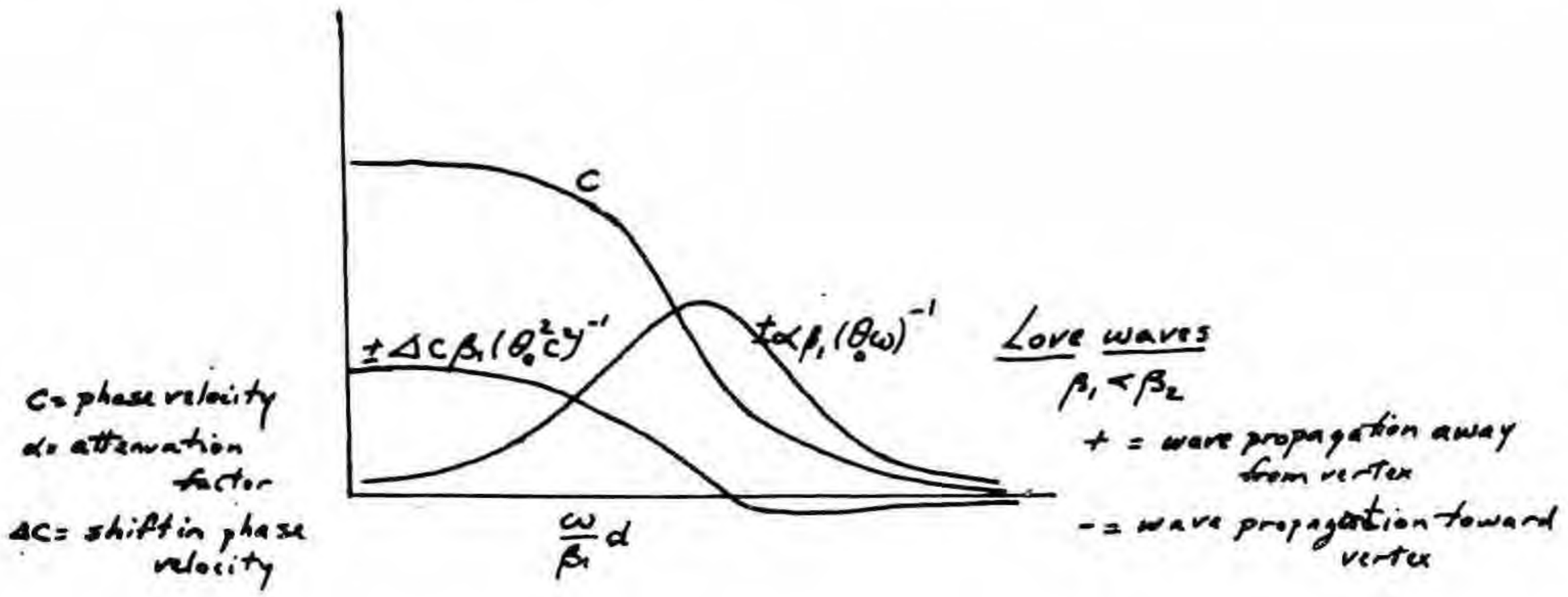

G15

FOURTH INTERNATIONAL CONGRESS ON ACOUSTICS
COPENHAGEN 21.-28. AUGUST 1962

PROGRAM FOR ACTIVE SEGMENTATION AND REDUCTION OF PHONETIC PARAMETERS*

Syuji Inomata, Research Laboratory of Electronics, Massachusetts Institute of Technology, Cambridge, Mass., U.S.A. and Electrotechnical Laboratory, Tokyo, Japan

1. Introduction

The so-called "active"[1] or "analysis-by-synthesis"[2] method of speech data processing has, up to the present time, been applied experimentally at the acoustical level and has been used primarily for extracting formant frequencies. The method is also being used currently to obtain approximations to the time-varying articulatory configurations used in speech production.[3] This paper describes an experiment that attempts to extend the method to the extraction of quasi-discrete parameters at the physiologico-anatomical level.

The analysis scheme is based on a source-transfer function concept of the speech production process at the physiological and anatomical levels. The continuous articulatory motions that occur in speech are described by a set of so-called phonetic parameters, which are considered to be the result of a set of neuro-muscular instructions or excitations that operate on the mechanical system consisting of the lips, tongue, velum, etc. It is hypothesized that for a given speech sound these excitations assume a set of steady values, but jump discontinuously from one set of values to another as a sequence of speech sounds is generated. It is assumed that a unique set of such excitations is associate with each speech sound. The relations between the excitations and the resulting articulatory motions are undoubtedly not linear, but it is convenient to characterize the mechanical properties of the articulatory structures in an approximate manner by a set of system functions.

The present paper examines the problem of determining a set of quasi-discrete or ideal phonetic parameters when a set of continuous phonetic parameters is given. The scheme used for accomplishing the analysis is shown in block diagram form in Fig. 1. The input to the analyzer consists of a set of continuous phonetic parameters that describe certain continuous articulatory motions. In the present experiments the input phonetic parameters are derived from measurements on cineradiographic films. (If the analysis scheme were to be incorporated in an automatic speech recognition system, then these parameters would, of course, have to be derived from the acoustic speech signal.) The output of the analyzer consists of a set of ideal quasi-discrete phonetic parameters. The internal generative model simulates the above-mentioned articulatory processes--it accepts ideal phonetic parameters at its input and operates on these to yield continuous phonetic parameters at its output. Comparison is made between the input parameters and the internally-generated parameters, and new inputs to the internal model are tried until a best match is obtained in the comparator. Preliminary analysis and segmentation are carried out in order to obtain approximate first guesses for the ideal parameters.

In the preliminary studies described here, four parameters $f_i(t)$, $i = 1 \sim 4$, were selected tentatively as input signals. These are shown in the mid-sagittal section of Fig. 2. They are (A) the distance between

the lips on the midline, (C) and (D) the x- and y-coordinates of the highest point of the tongue relative to a fixed set of axes, and (B) the vertical dimension between tongue and hard palate at the position shown in the figure. Frame-by-frame measurements from cineradiographic films[4] were used to obtain these four input parameters for the final (stressed) syllable of several utterances of the form /hə'C_1VC_2/, where the initial and final consonants C_1 and C_2 are identical. Time functions that depict the four parameters for a typical utterance (the word /hə pɪp/) are shown by the dotted curves in Fig. 3. The output data consist of the values of four ideal phonetic parameters corresponding to each of three time intervals, and the values of two switching times for each parameter, one corresponding approximately to the boundary between C_1 and V and the other corresponding to the boundary between V and C_2. The experimental studies also permit estimates to be made of time constants that characterize the approximate system functions corresponding to each of the four parameters.

2. Description of Program

The analysis scheme shown in Fig. 1 has been programmed on a digital computer. The analysis consists of two main parts: a preliminary analysis and an active analysis.

Preliminary analysis. Preliminary analysis is accomplished by locating inflection points in each parameter and then by performing a set of associated logical operations. The inflection points are obtained by first double differentiating each curve $f_i(t)$, yielding $f_i''(t)$, and then finding the minimum of $|f_i''(t)|$. Two such minima are in general found in each parameter during a symmetrical consonant-vowel-consonant syllable. The time locations of these minima, t_{1i} and t_{2i} ($i = 1 \sim 4$), represent first guesses of the segmentation point. It should be noted that no constraint is imposed to require that the values of t_{1i} and t_{2i} be the same for different values of i, i.e., for different parameters. The next step in the program is to determine whether $f_i''(t)$ is positive or negative in the interval (t_{1i}, t_{2i}). If $f_i''(t)$ is positive in this interval, then the minimum value of $f_i(t)$ is determined in the interval, and the maximum values of $f_i(t)$ are determined in the two intervals $t < t_{1i}$ and $t > t_{2i}$. These three maximum or minimum values are considered to be first guesses of the ideal phonetic parameters. The opposite procedure is used when $f_i''(t)$ is negative in the interval (t_{1i}, t_{2i}).

As a result of the preliminary analysis, tentative values for 20 parameters are obtained. These consist of the eight time segmentation points (two for each parameter) and the values of 12 ideal phonetic parameters. While not sufficiently accurate to be considered as final outputs, these tentative values help to reduce the search area of the active analysis stage to be described in the following section.

Active analysis. As Fig. 1 shows, the development of an active analysis scheme requires that an internal model of the generative process be simulated. Data on the dynamic characteristics of the articulatory mechanism are, unfortunately, not available in detail, and hence it is necessary to make assumptions concerning the nature of the model. As noted above, a linear model is assumed in the present study. The model adopted in the present work is of the Gaussian type, such that the impulse response for a given parameter i ($i = 1 \sim 4$) is given by

$$h_i(t, G_i) \begin{cases} = \dfrac{1}{\sqrt{2\pi}G_i} \exp[-(t-t_o)^2/2G_i^2] & t \geq 0 \\ = 0 & t < 0 \end{cases} \qquad (1)$$

where G_i is a constant that is a measure of the duration or time constant of the response. The input to the model is a set of four ideal phonetic parameters, each of which can be written as follows

$$g_i(t,t_{1i},t_{2i},f_{1i},f_{2i},f_{3i}) \begin{cases} = f_{1i}\,, & t < t_{1i} \\ = f_{2i}\,, & t_{1i} \le t \le t_{2i} \\ = f_{3i}\,, & t_{2i} < t \end{cases} \qquad (2)$$

The output of the model for each i is thus given by

$$F_i(t;G_i t_{1i},t_{2i},f_{1i},f_{2i},f_{3i}) = \int_o^\infty h_i(\tau,G_i)g_i(t-\tau;t_{1i},t_{2i},f_{1i},f_{2i},f_{3i})d\,\tau \qquad (3)$$

In the analysis procedure of Fig. 1, a measure is obtained in the comparator of the degree to which each internally generated parameter $F_i(t)$ matches the input parameter $f_i(t)$. The distance function that is used to provide this measure is

$$D[\mathbb{G},\mathbb{T}_1,\mathbb{T}_2,\mathbb{F}_1,\mathbb{F}_2,\mathbb{F}_3]$$

$$\sum_{i=1}^{4} a_i \int_{T_1}^{T_2} \left| F_i(t;G_i,t_{1i},t_{2i},f_{1i},f_{2i},f_{3i}) - f_i(t)\right|^2 dt \qquad (4)$$

where T_1 and T_2 are the beginning and the end of an utterance, and $\mathbb{G} \equiv (G_1,G_2,G_3,G_4)$, $\mathbb{T}_1 \equiv (t_{11},t_{12},t_{13},t_{14})$, $\mathbb{T}_2 \equiv (t_{21},t_{22},t_{23},t_{24})$, $\mathbb{F}_1 = (f_{11},f_{12},f_{13},f_{14})$, $\mathbb{F}_2 = (f_{21},f_{22},f_{23},f_{24})$, and $\mathbb{F}_3 = (f_{31},f_{32},f_{33},f_{34})$ are all vectors. The constants, $a_1 \sim a_4$, are weighting quantities which are selected to provide an efficient search. In effect, therefore, the active analysis has reduced to a hole-searching problem involving a distance function of 22 dimensions.

The searching technique employed in this program is the Golf method[5] developed by the author. In that method, the motion of a mass point on the surface of a hyper surface $D[\mathbb{G},\ldots,\mathbb{F}_3]$ in 23-dimensional space is simulated to obtain the global minimum. The method could be regarded as a sophisticated version of the method of steepest descent or ascent. The initial values of $\mathbb{F}_1$, $\mathbb{F}_2$ and $\mathbb{F}_3$ are determined directly by the output of the preliminary analysis. The initial $\mathbb{T}_1$ and $\mathbb{T}_2$ are adjusted so that the delay effect of the impulse response may be taken into account, and the initial values of $\mathbb{G}$ are selected randomly, say, in the interval (0,1).

3. Experimental Results

Programs that accomplish the preliminary analysis and the active analysis described above have been written for the IBM 7090 computer at the M.I.T. Computation Center, using the Fortran system. Data have been obtained for the final syllable of several utterances of the form /hə'CVC/ in which the initial and final consonants are bilabial stop consonants. Results of the preliminary analysis stage for the word /hə'pIp/ are shown by the solid rectangular-shaped wave in Fig. 3. These results indicate for each of the four phonetic parameters the times at which preliminary segmentation is made and the preliminary values of each parameter during the three intervals within the syllables. At the time of preparing this paper, data from the active analysis procedure have not been analyzed in detail. It is expected, however, that results of this part of the analysis will be presented at the meeting.

4. Acknowledgments

Many thanks are due to Prof. K. N. Stevens for his useful suggestions, discussions, and aid in preparing this paper, and to the staff of the M.I.T. Computation Center for their help during this work. Discussions with Prof. O. Fujimura of the University of Electro-Communications, Tokyo, are also acknowledged.

Footnotes and References

* This work was supported in part by the U. S. Army Signal Corps, the Air Force Office of Scientific Research, and the Office of Naval Research; in part by the National Science Foundation under Grant G-10800; and in part by the U. S. Air Force Cambridge Research Laboratories under Contract No. AF 19(604)-6102.

1. S. Inomata, Paper 3-2-5, Meeting Record, Acoustical Society of Japan (May 1960), and Bull. Electrotech. Lab. 24, 8 (August 1960), Tokyo.

2. K. N. Stevens, J. Acoust. Soc. Am. 32, 1 (January 1960).

3. J. M. Heinz, paper published in these proceedings.

4. These films were obtained with the cooperation of Dr. James Bosma and his associates at the National Institute of Dental Research, National Institutes of Health, Bethesda, Md., U.S.A.

5. S. Inomata, Bull, Electrotech. Lab. 25, 2(February 1961), Tokyo.

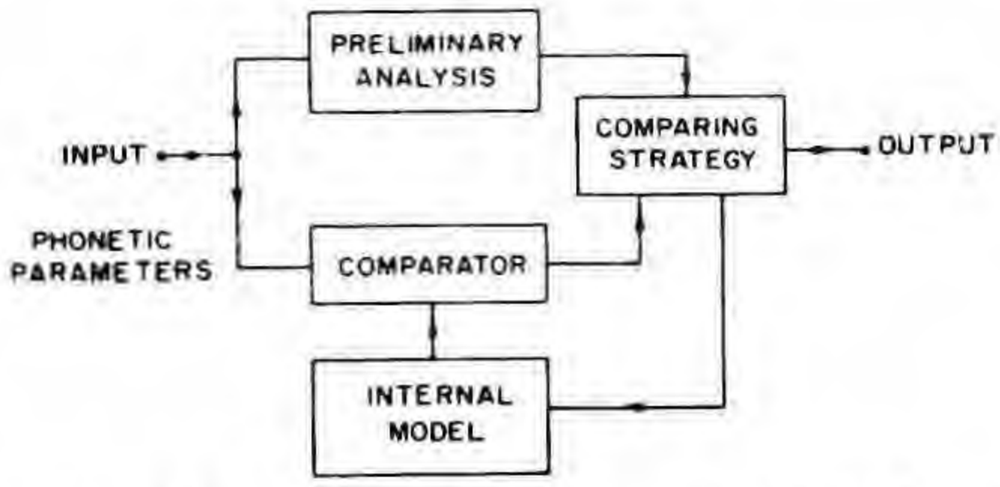

Fig. 1. Analysis by synthesis extended to physiologico-anatomical level.

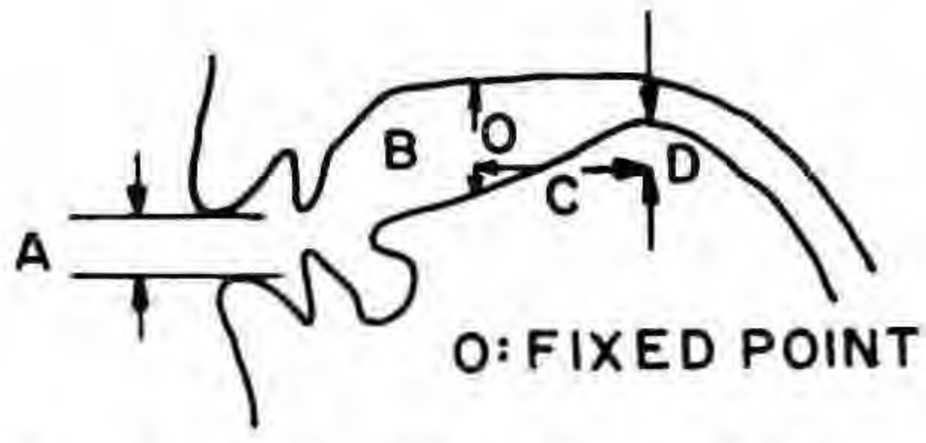

Fig. 2. Mid-sagittal representation of phonetic parameters.

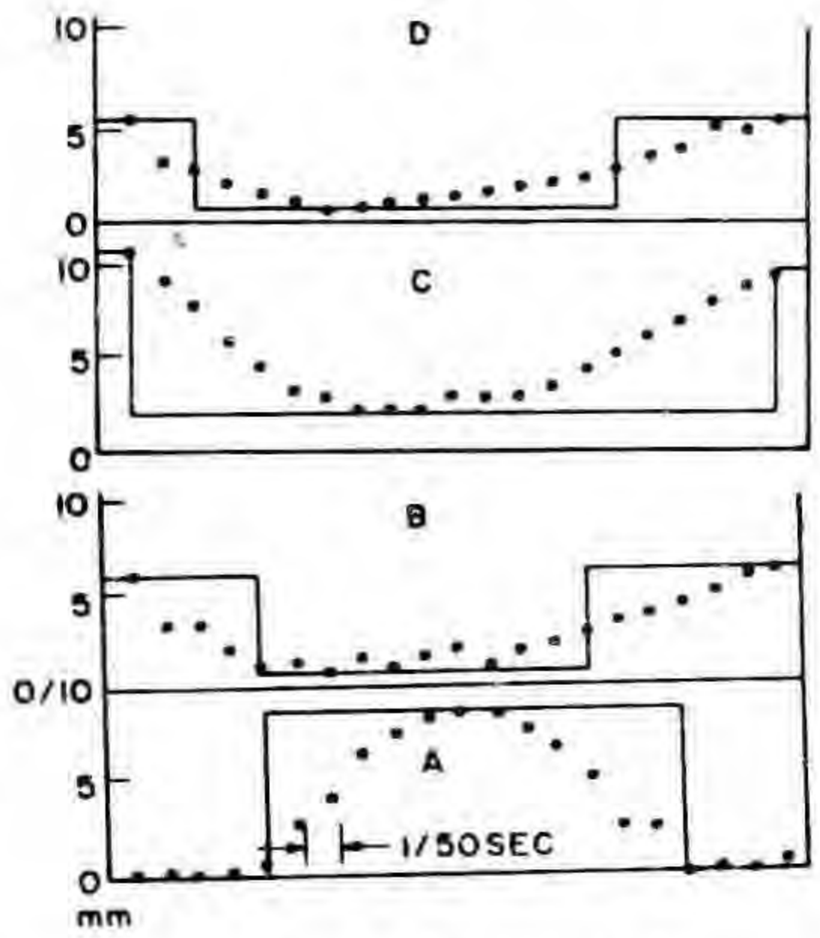

Fig. 3. Input(dotted) and output (solid) of the preliminary analyzer.

H15

FOURTH INTERNATIONAL CONGRESS ON ACOUSTICS
COPENHAGEN 21.-28. AUGUST 1962

APPLIED PSYCHOACOUSTICS

HAROLD BURRIS-MEYER and RICHMOND L. CARDINELL

The Glossary of Terms Frequently used in Acoustics, (1) published by the American Institute of Physics lists psychoacoustics on the cover, but prudently omits any definition of this intriguing expression. Undeterred by the slight, the term gets around, and has, since first pronounced by Dr. Theodore Forbes in 1942 gathered beneath its encompassing cloak a large motley array of ancient observations of the behavior of men when they heard a noise, of more recently observed audio-psycho-physical phenomena, of energetically exploited consumer services and quite a lot of nonsense.

Psychoacoustics as a subject of research has spawned a literature of some magnitude and passing scientific respectability. Not so applied psychoacoustics. For scientifically valid search for links between the sound and the psyche has turned up precious little that is used for anything, and the application of auditory stimuli to the presumed needs of men rests principally upon a foundation of hunch, faith, commercial expediency, and the desire to see one's name in the paper.

The two largest current enterprises which undertake to do something to people via acoustical phenomena use music. They are, functional music employed in industry, offices, restaurants, and music played for people who are ill, in connection with occupational therapy or recreational programs, but often called by those who employ it Music Therapy.

Functional music is for the most part a proprietary commodity. It is sold by wire music services and imitated on independent plant and hospital sound systems and by radio stations broadcasting what is called "work music" or "music for dining!

At its best, it provides a background of melody which some people like in restaurants, where it has displaced the orchestra. It may serve as a stimulus, or relief from tension as the occasion may demand, for the industrial worker. It creates a not unpleasant amient sound level partially to mask the clatter of dishes or machinery.

During the decade 1937 to 1947, a number of serious attempts were made to find out what music would really do to people at work and how to devise and present a program which could produce a predictable result in terms of performance or some other measurable index. They met with some success and are well documented (2) in acoustical literature.

But the fundamental problem of classifying music according to its effect upon man was not solved. Variations in conditions of performance were never adequately related to observed effect. There is still no scale of affective intensity. And when a little reasonably valid experimental data seemed to support the theory that functional music was a valuable commodity, all work on how to make it good stopped.

---

(1) H. M. Trent and B. Anderson, GLOSSARY OF TERMS FREQUENTLY USED IN ACOUSTICS, Am. Inst. Physics, New York (undated)

(2) H. Burris-Meyer, Mech. Eng. 65, 31 (1943) R. L. Cardinell and H. Burris-Meyer, J. Aeous. Soc. Am., 19, 547-549 (1947)

The music services have researched consumer preference (previously shown to be independent of functional effectiveness) (3) and continued to build programs on hunch, consumer preference, guess and subjective evaluation by the programmer. The so called "emotional content" scale on which the programmer rates the music has no basis in the measurement of any physiological index of emotional state change or rate of change.

During the brief time that making music functional was studied it was learned that at least three kinds of industrial programs were needed to apply to different kinds of work. Similarly two office programs were a minimum if the music were not to be as bad in some places as it was good in others. The fact that different kinds of restaurants require different types of music seemed obvious, and was indeed proved experimentally to be the case.

Also, it takes a minimum of 20 minutes to build a mood with music unless it is so presented as to command attention, and therefore interferes with what is going on. This is not the purpose.

No music service offers more than one each of industrial, office and restaurant programs. The best known, sells a single program for public spaces, of which certain segments are advertised as being specifically programmed for offices and for industry and can be separated out for such customers. Traditionally the playing periods last thirteen minutes-- about two thirds of what is minimum for functional effectiveness if everything else is good.

The use of music to promote the recovery of people ill in mind or body, called by its promoters, "Music Therapy" has more historical authority than modern scientific basis. AESCULEPIUS observed that "for sorrowful thought, concerts of music, cymbals and noise are useful. Yet the patients must be oftener humored than contradicted and the mind must be led by slow degrees". (4) David "played on a harp" and alleviated King Saul's distress, (5) and "the chanting of mystic lays" is credited as an element in the cure of Ulysseys' knee, injured in a boar hunt on Pasnassus. (6)

Experiments first reported in 1943 (2) in the use of music to improve the performance of people at work in factories, stimulated a renewed interest in the possibility of curing the ill with music. Music was already being used as entertainment in hospitals. It became the darling of a host of eager promoters, whose wild claims gave the evil flavor of charlatanism to what might well be an important aid to healing. The so-called theraputic uses of music outran the understanding of what the music actually did. In fact nobody knows yet.

The so-called research in this field has been woefully disappointing. Reports indicate that patients have been "observed" not measured. The stated systems of music classification are scientifically meaningless to those who hoped for something one could count on. Several attempts have been made to establish comparative values of music and phrenotrapic drugs. These have generally shown that music can reduce the need for sedatives. But that apple cart was once rudely upset when so-called "slumber music" made disturbed patients aggressive. (7) Music has been tried as an adjunct to psychiatric diagnosis with encouraging results. (8) Such clinical experiences, however have little theoretical and less experimental authority behind them.

---

(3) R. L. Cardinell and H. Burris-Meyer, J. Acous. Soc. Am, 19, 547-549 (1947)

(4) EPIDAURAN Temple/Record, Inscriptiones Graecae IV^2, i, 121-124 - see also R. Herzog "Die Wunderheilungen Von Epidaurus", Philol. Supl. III 3.

(5) 1 Samuel, 16:23

(6) Homer, ODYSSEY, Book 19

(7) E.C. Dax, EXPERIMENTAL STUDIES IN PSYCHIATRIC ART, Lippencott, Phila. (1953)

When music is selected for otherwise undefined "emotional content" and classified by similarly vague "diagnostic function" or "social meaning", it is manifestly improbable that any two independent researchers can get comparable results. So most hospitals using music, use it as a recreational activity and in occupational therapy. In a moment of realistic modesty the journal Music Therapy published an article containing the statement: "It is not the music which is the real theraputic agent, but the music therapist." (9)

Less well publicized psychoacoustic applications have appeared to have a more solid scientific foundation, although their effects have not been quantitively measurable. In 1944 Project BATTLE NOISE (10) developed a program and technique for rough screening of naval recruits, and it did identify young men who under subsequent psychiatric examination showed themselves unqualified for the stress of battle. The project languished during an internecine struggle among the psychologists who had an interest in it. Finally the marines hauled the equipment away and used it for training. The project has never been revived.

Dr. Harry Cherry has used music as an aid to anaesthesia for oral surgery, with spectacular results. But although it has been approved after several years of critical evaluation and has been adequately reported, (11) the Cherry method appears to have made little headway.

Long ago Drs. Kubie and Margolin found that the sounds of slow rythmic breathing helped to induce sleep. (12) Now someone has made a machine called a "respiratory regulator." A loudspeaker under the pillow projects the sound, and if the conditions are right the subject goes to sleep (13) The loudspeaker under the pillow repeating a lesson all night has also been tried as a teaching device.

Dr. Liklider found that a buzz in the ear minimizes a pain in the jaw. (14) His commercial device for auditory analgesia also plays music, in case you get tired of the buzz.

And man's old enemy, noise (originally defined and still sentimentally regarded as unwanted sound) has been rehabilitated by the psychoacousticians. We first deplored, then tolerated noise. We are now assured that its embrace is comforting to the soul and soothing to the spirit--although bad for the ear. We make a steady noise to minimize the annoyance of an intermittent noise. A whole Madison Avenue-like folklore has grown up about this phenomenon. The definitions of common words are even adjusted to the theory. One well known acoustician has been quoted as saying "Silence is the lack of noise" and "quiet is the lack of distraction". (15) To follow this orwellian unthink just a tiny step farther we can easily conclude that noise is quiet. And, by extrapolation: we want what we don't want.

---

(8) Ibid

(9) MUSIC THERAPY 1952, Nat. Assn for Music Therapy, Inc., Lawrence, Kans., (1953)

(10) H. Burris-Meyer and V. Mallory, J. Acous. Soc. Am, 32, 1568-1574 (1960)

(11) H. Cherry and I. M. Pallin, Anesthesiology 8 (1947)

(12) Lawrence S. Kubie and Sidney Margolin AN ACOUSTIC RESPIROGRAPH: A method for the study of respiration through the graphic recording of breath sounds Journal of Clinical Investigation March 1943 V 22 No 2 pp 221-224

(13) N. Y. Times, Apr 11, 1962

(14) a. W. J. Gardner and J. C. Licklider, J. Acous. Soc. Am. 31, 117A (1959)
b. W. J. Gardner and J. C. R. Licklider, J. Acous. Soc. Am. 31, 850-851A (1959)

(15) TIME, March 2, 1962, p. 53

(16) H. Burris-Meyer and V. Mallory, SOUND IN THE THEATRE, Radio Magazines, Inc., Mineola, N. Y., (1959)

(17) K. D. Kryter and K. S. Pearsons, JUDGMENT TESTS OF THE SOUND FROM PISTO TURBOJET AND TURBOFAN AIRCRAFT, Sound, Vol 1, No. 2, March-April 1962

This is a bleak picture. Yet those of us, who have moved many people to pity and terror with auditory stimuli, (16) employing little more than classic showman's techniques, believe that consistent relationships between auditory stimuli and the emotional responses of the subject can be identified and measured, and that such knowledge can be applied to the control of the emotional determinants of action.

Sound, in any form, is susceptible of analysis, recording, reproduction, measurement and mathematical study. The physiological concomitants of emotional state, change and rate of change are also measurable--objectively without the subject being aware that he is a subject. Such measurements may be expressed in mathematical form. Yet a perusal of the literature reveals no instance of employing the techniques here indicated to establish a reliable, repeatable, scientifically valid relationship between the stimulus and the emotion and thereby give to psychoacoustics a sound basis for application.

Not only is the basis for the most significant application of psychoacoustics neglected, but it seems to us that there is a singular inversion of interest, and current effort in the investigations which should support applications of psychoacoustics. We find noise studies directed toward finding how much the human carcass or psyche can take, how adaptable we are to unpleasant environment. There is little comfort in the knowledge that a jet aircraft sounds noiser than it is. (17)

We submit that it is high time we honestly set about finding out what sound does to people. We suggest a few approaches:

1. Revival of the Rockland State project which was planned in 1947 to try to improve the discharge rate of manic, regressed, and depressive patients. One hundred matched pairs of patients (one subject one control) in each category were to be studied for a year. The program provided for the patients was to be music taken from the most nearly applicable program pattern already experimentally validated in industry and non-musical stimuli taken from wartime investigations. This project, abandoned for want of the last twenty percent of the required funds, could give us a gross, empirically derived starting point for more precise studies. At least the conditions were ideally controllable and if the discharge rate were improved, the project would pay for itself.

2. Revival and extension of the studies of music in industry in which program design and presentation are controllable for experimental purposes, and the performance index remains a reliable measure of the emotional involvement of the subject.

3. Laboratory studies in which (a) the sound is designed in all its details: spectrum, direction, reverberant characteristics, level. (b) The presentation is controlled so that the design pattern does not vary in any respect. This rules out live performance of music for research purposes. (c) The response of the subjects is measured without their knowing that they are subjects. Instrumentation for this purpose developed ten years ago has never been used.

4. Field validation studies in theatres, churches, night clubs, political meetings, using principles derived in 3 (above) and measurement of the audiences without their knowledge.

5. A project to find out, on the basis of objective measurement of the subjects, what the most pleasant and healthful acoustical climate is, so that we could have a design objective for things which make or control noise.

We submit that only when these or comparable studies are pursued and the results applied in the conduct of the church service, the opera, the commencement oration, will psychoacoustics achieve the respectability of other branches of acoustics, and be applicable as a reputable science for the benefit of those it touches.

J15

FOURTH INTERNATIONAL CONGRESS ON ACOUSTICS
COPENHAGEN 21.-28. AUGUST 1962

Vergleich der dynamischen Schub-, Elastizitäts- und Kompressionsmoduln von plastifizierten Polyvinylchloriden im Temperaturbereich -80 bis +100° C bei 1 kHz

P. Heydemann, A. Zosel, H. Nägerl
III.Physikalisches Institut der Universität Göttingen

Ältere Messungen von Koppelmann [1] an Plexiglas zeigen, daß die Querkontraktionszahl μ im Nebendispersionsgebiet ein Minimum durchläuft. Außerdem stimmt der aus Koppelmanns Werten für den Schub- und den Elastizitätsmodul nach der Gleichung $\frac{1}{K} = \frac{9}{E} - \frac{3}{G}$ berechnete Kompressionsmodul K nicht mit eigenen experimentellen Werten überein [2].

Daher wurden Messungen der drei Moduln in Abhängigkeit von Frequenz und Temperatur an Polyvinylchlorid mit 0, 10, 20 und 30 % Weichmachergehalt im Hauptdispersionsgebiet durchgeführt. Der Kompressionsmodul wurde nach einer von Marvin und McKinney vorgeschlagenen Methode gemessen [3]. Schub- und Elastizitätsmodul wurden aus Eigenschwingungen von Stäben und aus der Ausbreitung fortschreitender Wellen auf Stäben bestimmt [4]. Dazu werden ca. 30 cm lange, schlanke Stäbe mit rechteckigem Querschnitt am oberen Ende fest eingespannt. Am unteren Ende werden durch eine aufgesetzte Spule, die sich im Feld eines Permanentmagneten befindet, längs des Stabes fortschreitende Torsions- oder Biegewellen angeregt. Die Abtastung der Schwingungen erfolgt mit einer optischen Methode. Das optische Abtastsystem wird längs des Stabes bewegt und die der jeweiligen Torsions- oder Biegeamplitude proportionale Ausgangsspannung auf einen Pegelschreiber registriert. Die Wellenlänge wird gleichzeitig durch Phasenvergleich bestimmt. Bei tieferen Temperaturen und kleineren Verlustfaktoren wurden die komplexen Moduln aus den Eigenschwingungen von einfachen oder lamellierten Stäben ermittelt. Die nach den verschiedenen Verfahren gemessenen Kurven schließen sehr gut aneinander an.

Die Streuung der Meßwerte ist bei den Resonanzmethoden kleiner als 2 % und bei den fortschreitenden Wellen kleiner als 5 %. Alle Proben wurden vor der Messung sorgfältig getempert. Sämtliche Stäbe einer Meßreihe wurden aus der gleichen Platte geschnitten. Auf Grund eingehender Untersuchungen konnte der Einfluß der Luftreibung, Abstrahlung, Einspannung und dergleichen eliminiert werden. Kontrollmessungen mit Plexiglasstäben ergaben gute Übereinstimmung mit den Ergebnissen anderer Autoren. Variation der Anregungsspannung in einem weiten Bereich ergab

keine systematische Änderung der Ergebnisse.

Als Funktion der Temperatur bei konstanter Frequenz aufgetragen zeigen die Kurven für den Schubmodul G und den Elastizitätsmodul E die bekannte Dispersion begleitet von Maxima der Verlustfaktoren. Mit steigendem Weichmachergehalt wird das Dispersionsgebiet breiter und das Maximum der Verlustfaktoren verschiebt sich zu tieferen Temperaturen. In allen Fällen sind die Verlustfaktoren etwa gleich groß, jedoch sind die Maxima von η_G gegenüber η_E zu tieferen Temperaturen verschoben. Die Temperaturdifferenz steigt mit dem Weichmachergehalt. Weiterhin zeigen die reduzierten Kurven bzw. die Relaxationszeitenspektren (Abb.1), daß auch die Verteilungsfunktionen und damit die Form der Kurven für E und G verschieden sind. Und zwar nimmt bei der Schubbeanspruchung die

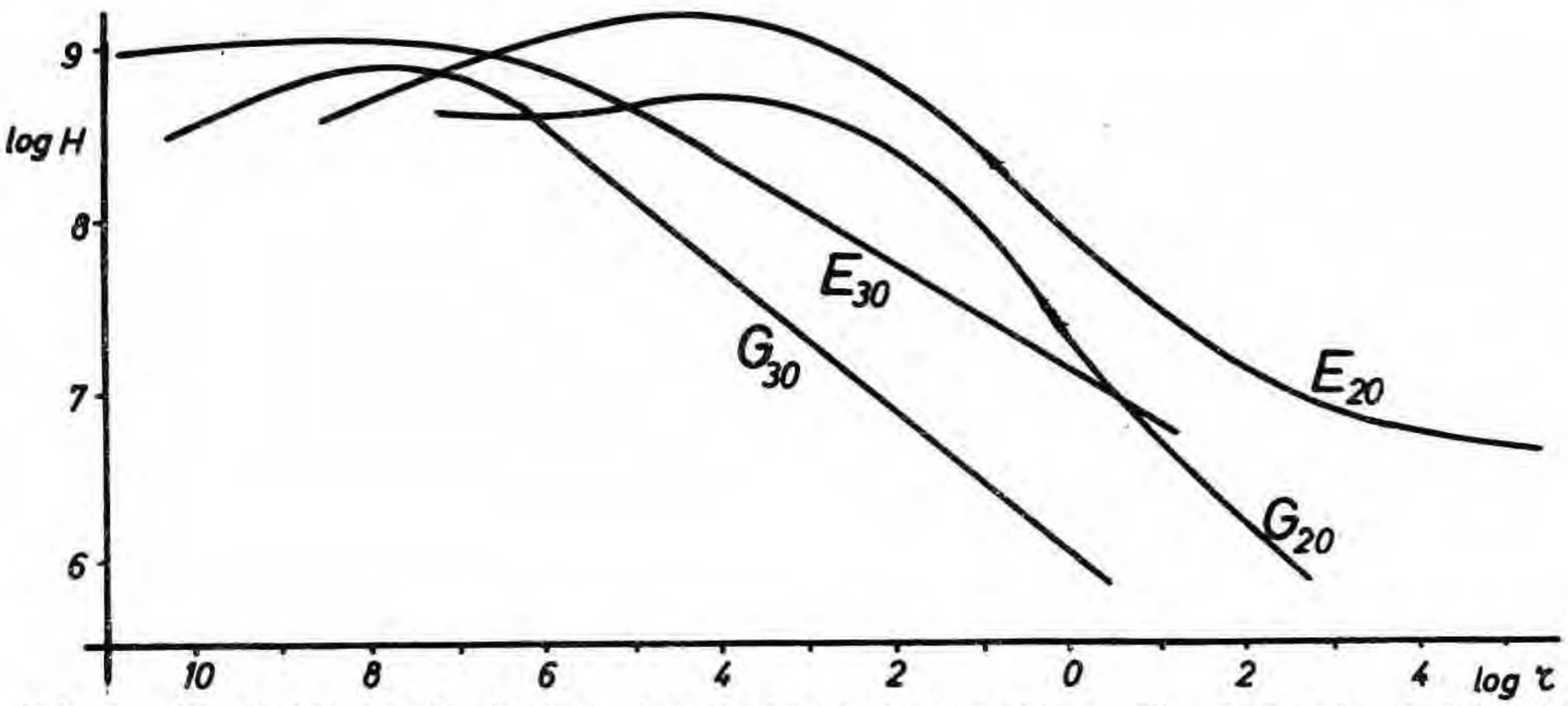

Abb.1 Verteilungsfunktion der Relaxationszeiten für Polyvinylchlorid mit 20 und 30 % Weichmachergehalt.

Verteilungsfunktion nach langen Zeiten hin stärker ab als bei Biegebeanspruchung.

Für den Kompressionsmodul K konnte eine Dispersion bisher nicht nachgewiesen werden. Unterhalb der Einfriertemperatur T_g ändert sich der Modul nur wenig mit der Temperatur. Oberhalb T_g nimmt er entsprechend dem größeren Ausdehnungskoeffizienten stärker ab.

Die Berechnung der Querkontraktionszahl μ aus E und G nach (1) als Funktion der Temperatur führt in allen Fällen zu Kurven mit einem ausgeprägten Minimum. Als Beispiel sind die hier besprochenen Kurven für Polyvinylchlorid mit 30 % Weichmachergehalt (Dioctylphtalat) in Abb.2 eingetragen. Bei tiefen Temperaturen ist $\mu = 0.37 \ldots 0.38$; oberhalb der Dispersionsstufe wird $\mu = 0{,}5$ angenähert. Die Berechnung von μ aus G und K bzw. aus E und K nach (2) ergibt einen allmählichen, dispersions

artigen Übergang von 0,38 auf 0,5.

$$\mu' + j\mu'' = \frac{1}{2}\,\frac{E'(1+j\eta_E)}{G'(1+j\eta_G)} \quad ; \quad \mu' + j\mu'' = \frac{3K^x - 2G^x}{6K^x + 2G^x} \qquad (1),\ (2)$$

Das Minimum kann offensichtlich nicht durch Meßfehler erkärt werden. Die Variationsbreite für μ_{EG} bei einem Fehler von $\pm$ 5 % bei E und G ist in Abb.2 angedeutet. Erst bei einem Meßfehler von $\pm$ 20 bis $\pm$ 40 % für beide Moduln würde das Minimum der Querkontraktionszahl als Meßfehler angesehen werden können. Außerdem sprechen der Wert von μ = 0,38 bei tiefen und μ = 0,5 bei hohen Temperaturen für die Genauigkeit der Messung. Die berechnete Querkontraktionszahl hat in allen Fällen unterhalb des Minimums einen negativen und oberhalb einen positiven Imaginärteil, der bei höheren und tieferen Temperaturen gegen Null geht. Die Streuung der berechneten Kurvenpunkte von Real- und Imaginärteil der Querkontraktionszahl ist erstaunlich klein. Fehler bei der Bestimmung der Meßtemperatur scheiden ebenfalls aus, da diese mindestens 4 bis 6° C betragen müßten.

Mit einfachen Modellrechnungen kann das gefundene Minimum der berechneten Querkontraktionszahl auf zwei Arten nachgebildet werden: Erstens durch die Annahme je einer Relaxationszeit für die Schub- und

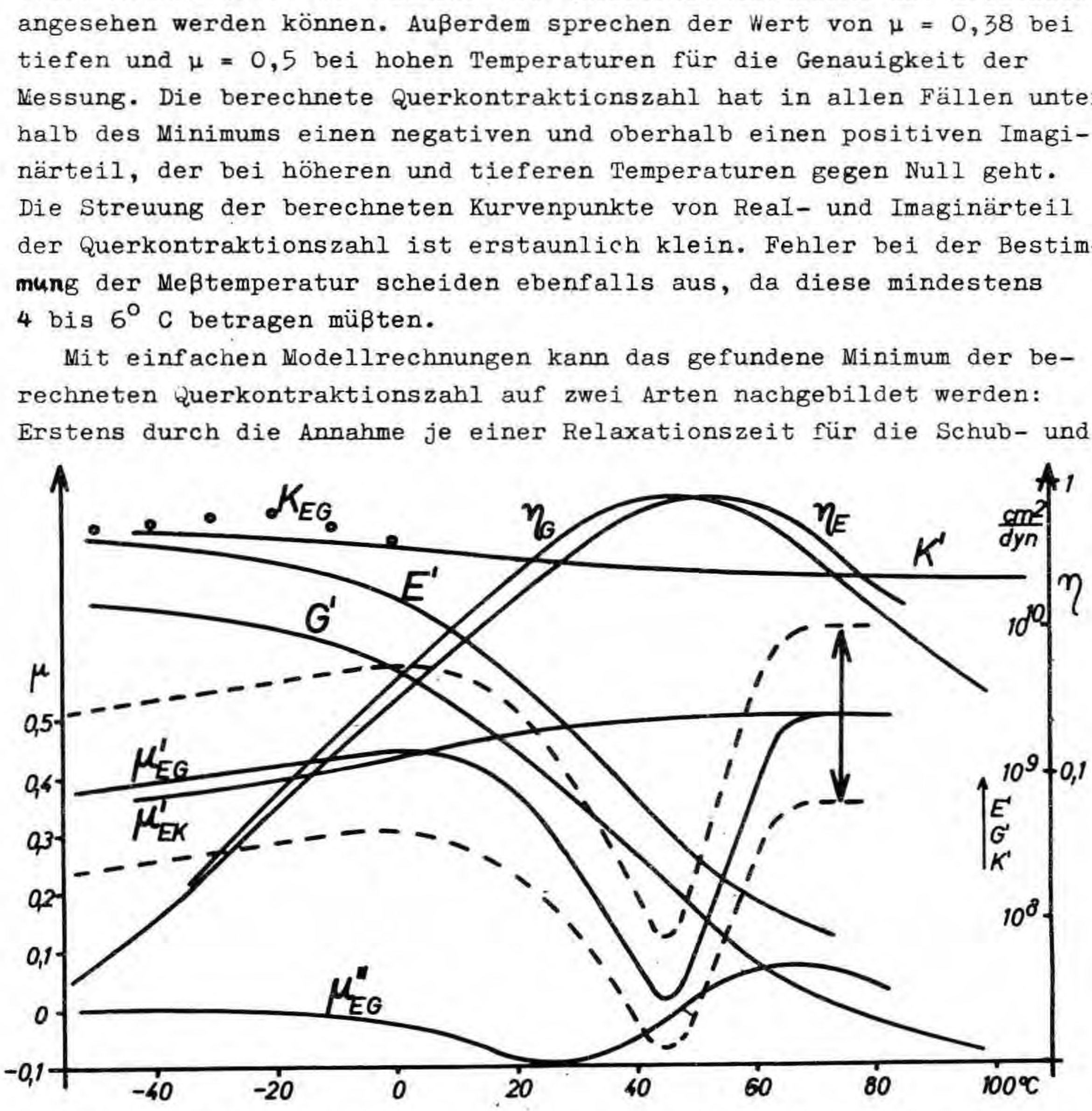

Abb.2 Meßwerte für Schubmodul G, Elastizitätsmodul E, Kompressionsmodul K und die Verlustfaktoren von E und G. Berechnete Werte der Querkontraktionszahl μ_{EG}(aus E und G), μ_{KG} und μ_{KE}(aus K und G bzw.K und E) und des Kompressionsmoduls K_{EG}(aus E und G). Polyvinylchlorid mit 30 % Weichmacher. f_m = 1 kHz.

die Biegebeanspruchung, wobei $\tau_E < \tau_G$ sein muß, oder durch die Annahr einer Relaxationszeit τ_G für die Schubbeanspruchung und zweier Zeiten τ_{E1} und τ_{E2} für die Biegebeanspruchung mit $\tau_{E1} < \tau_G < \tau_{E2}$. Die Relaxationsstärken können dabei gleich oder verschieden sein. Abb.3 enthält ein Beispiel für die Dispersionskurven und die Querkontraktion, die sich mit einer solchen Verteilung ergibt. In keinem Fall wird der Imaginärteil der Querkontraktionszahl richtig wiedergegeben.

Die Berechnung des Kompressionsmoduls K von Plexiglas aus Schub- und Elastizitätsmodul im Nebenrelaxationsgebiet führte in einer früheren Untersuchung [2] im Gegensatz zu den damaligen Messungen zu einem Minimum von K im Dispersionsgebiet. Es ist nicht möglich, die gleiche Berechnung auch im Hauptdispersionsgebiet durchzuführen, da hierfür die Meßgenauigkeit von E und G nicht ausreicht. Eine Abschätzung von K aus G und den ausgeglichenen Werten von μ_{EG} deutet jedoch auch hier ein tiefes Minimum an der gleichen Stelle wie μ_{EG} an, was auch wieder dem sehr gehauen Meßwerten widerspricht. Bei tiefen Temperaturen stimmen sowohl K_{GE} als auch $K_{G\mu}$ recht gut mit den gemessenen Werten überein.

Literatur

[1] J.Koppelmann Rheologica Acta 1958, Nr.1, 20
[2] P.Heydemann Acustica 9 (1959), 446
[3] J.E.McKinney,S.Edelmann,R.S. Marvin J.Appl.Phys. 27 (1956), 425
[4] P.Heydemann, A.Zosel Acustica 12 (1962)

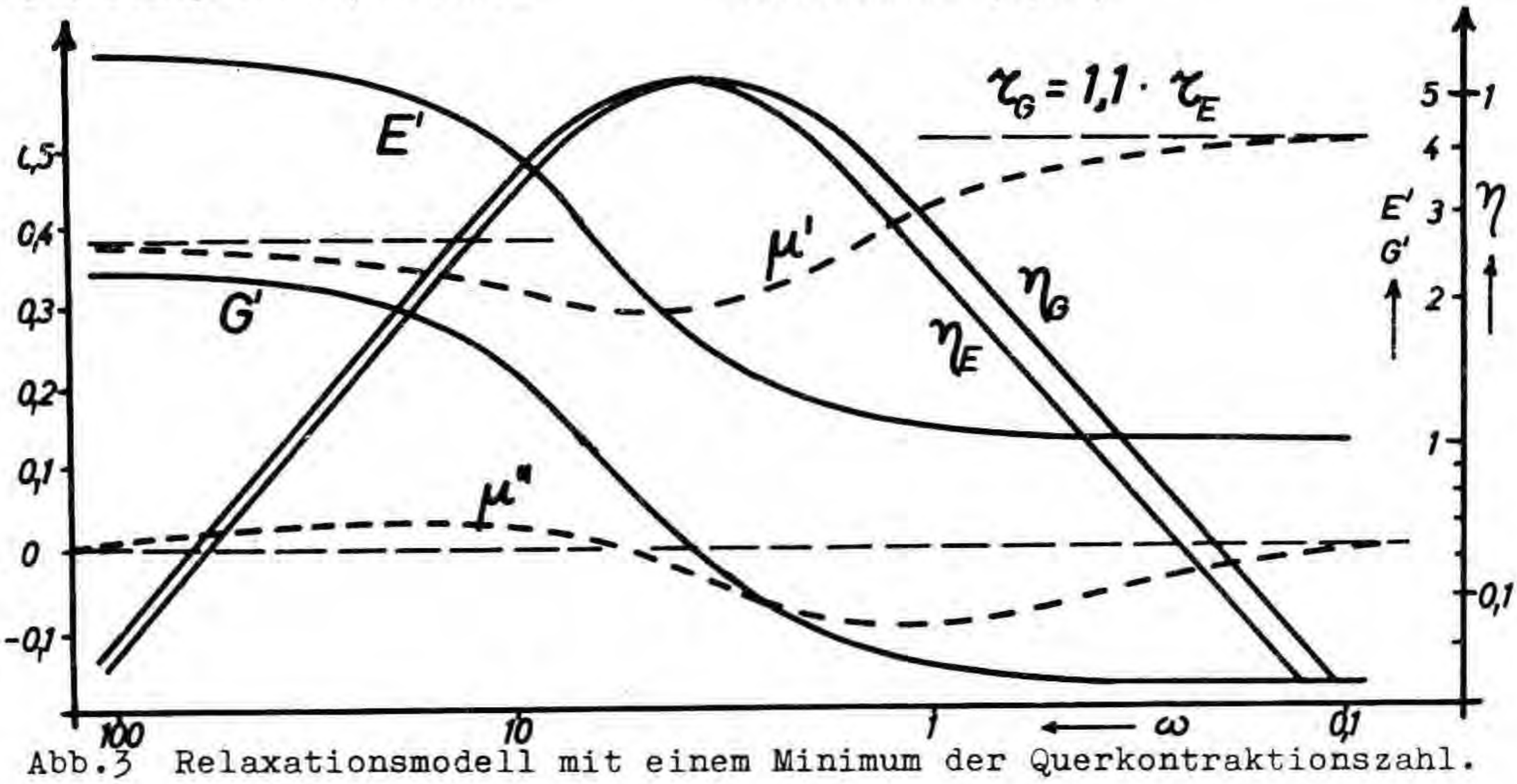

Abb.3 Relaxationsmodell mit einem Minimum der Querkontraktionszahl.

K15

FOURTH INTERNATIONAL CONGRESS ON ACOUSTICS
COPENHAGEN 21.-28. AUGUST 1962

CLASSIFICATION AND DISCUSSION OF INTERFERENCE METHODS FOR MEASURING THE PROPAGATION VELOCITY OF ULTRASONIC WAVES

J.S. WEHR, D.S., WARSAW, POLAND, POLISH ACADEMY OF SCIENCES

The aim of the present, rather arbitrary classification is to draw the reader's attention to the variety, simplicity and precision of interference methods which have been so far underestimated in ultrasonic measurements. The interference methods, the principle of which has been known for long, have been somewhat put aside by the development of advanced pulse techniques. In fact the proper combining of both pulse and interference techniques permits us to obtain the utmost advantages and to solve many important practical problems, e.g.: interferometric velocity measurements in liquids with high attenuation and at high temperatures, thickness measurements in attenuating layers and on uneven surfaces, accurate measurements of longitudinal and transversal wave velocities in rods and plates, required for determination of elastic constants etc.

The characteristic feature of the interference method has been assumed to be the superposition of two or more wave trains, the resulting amplitude of which depends on the phase shifts between individual components /the most evident example being the resonance of plane waves in a rod or in a column of fluid/. The considerations have been limited to the case of a single electric source of vibrations /the interferences of independent sound and light waves being thus excluded/.

The classification pattern is formed by relating two groups of parameters:

I. Type of interference and the conditions of ultrasonic wave propagation in the material;

II. Main features of the measuring equipment and the measuring techniques.

In the first group we shall distinguish <u>2 types of interference</u>:

1.-./ -the "ultrasonic" interference resulting from the phase difference of two or more ultrasonic wave trains /which can be additionally produced in the standard material, if necessary/.

2.-./ -the "electric" interference produced by a purely electric superposition of the oscillator voltage upon the electric signal converted from ultrasonic vibrations.

Further subdivision of group I. is based on <u>3 patterns of ultrasonic wave propagation</u>:

-.1./ -ultrasonic signal available with one delay only, the influence of multiple reflections being negligible;

-.2./ -propagation of ultrasonic waves along two geometrically different paths;

-.3./ -multiple reflections of ultrasonic waves within one given path.

The kinds of interference described in group I. can be produced and observed under various conditions of the measuring equipment. From this point of view 3 parameters are proposed with the following subdivision.

<u>Type of modulation</u>: /1.-.-. -continuous wave,
/2.-.-. -pulse modulation.

<u>Use of transducers</u>: /-.1.-. -the same transducer for transmission and recept.
/-.2.-. -separate transducers for transmission and "

<u>Adjusting system:</u> /-.-.1. -mechanical adjusting /change of distance or of angle
/-.-.2. -electrical adjusting/e.g.frequency tuning/

Even such an off - hand classification yields 48 methods /see page 2./;about 30 of those seem to be applicable and 20 have been so far examined by the author. The equipment, constructed as complete measuring apparatus by the author and his co-workers, is additionally marked in the classification table with the type symbols.

CLASSIFICATION AND DISCUSSION OF INTERFERENCE METHODS FOR MEASURING THE PROPAGATION VELOCITY OF ULTRASONIC WAVES

interfer. type			1.-./ ultrasonic interference			2.-./ electric interference		
equipment features			-.1./ one ultr.path	-.2./two diff. paths	-.3./ mult. reflections	-.1./ one ultr. path	-.2./ two diff. paths	-.3./ mult. reflections
continuous wave	/-.1.-. one T-R transducer	/-.-.1.mech.	1.1./1.1.1.	1.2./1.1.1.	1.3./1.1.1. liquids; resonance interferom. IUR-3	2.1./1.1.1. Note: the applications have been chosen arbitrarily	2.2./1.1.1.	2.3./1.1.1.
		/-.-.2. el.	1.1./1.1.2.	1.2./1.1.2.	1.3./1.1.2. layers; resonance thick.meter GUR-3	2.1./1.1.2.	2.2./1.1.2.	2.3./1.1.2.
	/-.2.-. separate transd.	/-.-.1.mech.	1.1./1.2.1.	1.2./1.2.1. plates-C_T	1.3./1.2.1. liquids gases	2.1./1.2.1. liquids rods /l.f./ /high att./	2.2./1.2.1.	2.3./1.2.1. liquids rods/l.f./
				ordinary electronic	resonance interferom.	amplitude and phase		
		/-.-.2. el.	1.1./1.2.2.	1.2./1.2.2. plates-C_T	1.3./1.2.2. resonant plates-C_L	2.1./1.2.2. plates-C_L /high att./	2.2./1.2.2.	2.3./1.2.2. plates-C_L
				generators and amplif. + nonrefl. probe-heads		indicator UF - 1		
pulse modulation	/-.1.-. one T-R transducer	/-.-.1.mech.	1.1./2.1.1. liquids rods-C_L	1.2./2.1.1. rods-C_T	1.3./2.1.1. liquids gases /flow,	2.1./2.1.1. liquids gases tanks/	2.2./2.1.1.	2.3./2.1.1.
			elastometer		pulse gauge-interferom.			
		/-.-.2.el.	1.1./2.1.2. rods-C_L	1.2./2.1.2. rods-C_T	1.3./2.1.2. plates /uneven surf./	2.1./2.1.2. plates /high att./	2.2./2.1.2. rods-C_L,C_T	2.3./2.1.2. rods-C_L,C_T
					pulse thick.meter GUR-4			
			elastometer based on the pulse - echo system					
	/-.2.-. separate transd.	/-.-.1.mech.	1.1./2.2.1. liquids plates,rods -C_L,C_T	1.2./2.2.1. plates-C_T	1.3./2.2.1. liquids gases /high temp./	2.1./2.2.1. liquids gases /high att./	2.2./2.2.1.	2.3./2.2.1.
			elastometer UE - 1		pulse interferom. UI-6			
		/-.-.2.elect.	1.1./2.2.2. plates-C_L rods-C_L /scattering/	1.2./2.2.2. rods-C_T	1.3./2.2.2. plates-C_L rods-C_L,C_T	2.1./2.2.2. plates-C_L rods-C_L,C_T /high att./	2.2./2.2.2. rods-C_L,C_T	2.3./2.2.2. rods-C_L,C_T
			universal ultrasonic elastometer UE - 1					

Being limited in space the author can present a few examples only.

1.1./2.2.1. -the method of phase coincidence of 2 pulses, introduced by Merkulov, consists in superposing 2 h.f. pulses transmitted between 2 pairs of ultrasonic probe-heads. One of those pairs is a calibrated and adjustable liquid delay-line. The delay in sample is thus compared with that in the delay line/Fig. 1a/. The coincidence of two pulses is determined very exactly, as the signals are added or canceled in phase. The measured velocity is

$$C_x = C_o \left/ l_{o2} - l_{o1} \right.^{-1} \qquad /1/$$

where C_o - velocity in standard liquid

l_{o1}, l_{o2} - paths in liquid with the probe-heads pressed to each other and with the sample between them, respectively.

The above method, which is very accurate but uncovenient for media with high dispersion, can be then replaced by the author's method of zero-point interference /1.1./2.2.2./. The method requires frequency adjusting when 2 pulses are superposed: one being sent through the sample and the other one through a standard with the known delay t_s. If the envelopes of the pulse fronts intersect, one obtains, every Δf, in the intersection point zero of the resulting amplitude at phase opposition /Fig.1b/. Then the velocity

$$C_x = 1/t_s \pm 1/\Delta f \left.^{-1}\right. \qquad /2/$$

/$\pm$ for $t_s \lesseqgtr t_x$/.

The advantages of the pulse-interference methods become apperent in thickness measurements of attenuating layers /method 2.1./2.1.2./ and in thickness measurements in the case of rough or curved layer surface /method 1.3./2.1.2./.

The problems of very accurate interferometric measurements in liquids at high temperatures as well as in liquids with very high attenuation may be successfully solved by the methods /1.3./2.2.1./ and /2.1./2.2.1./. The pulse modulation permits us to apply the separating the transducers and the liquid. The pulse length, on the other hand, is kept long enough to permit the interference of multiple reflections in the liquid between the ends of the rods /method 1.3./2.2.1./. If there are no multiple reflections, the signal transmitted through the liquid interferes with the electric signal introduced on the electric way from the oscillator to the amplifier /method 2.1./2.2.1./. Changing the distance between the rods we obtain the extreme values of the resulting amplitude every Δl. Hence, for the frequency f=const

$$c = 2 f \Delta l \quad \text{/method 1.3./2.2.1./}$$
$$c = f \Delta l \quad \text{/method 2.1./2.2.1./} \qquad /3/$$

The oscilloscopic comparison of the electric signal of the oscillator with the c.w. signal received after multiple reflections in the material permits us to determine easily the phase shift between them in the function of distance or frequency /methods 2.3./1.2.1. and 2.3./1.2.2./. From the plot: phase shift versus $2\pi l/\lambda$ conclusions may be drawn as to velocity as well as attenuation of ultrasonic waves [1].

Different geometrical paths of ultrasonic waves, as, for instance, in the case of side-reflections in rods with subsequent transformation of longitudinal waves into transversal ones, may require the pulse modulation and the superposition of a long-pulse electric component over the short pulses passing through the sample /method 2.3./2.2.2./. Changing the frequency and measuring its differences between adjacent maxima or minima of particular pulses, as shown in Fig. 3., we obtain

$$C_L = 2l/\Delta f_{L2}^{-1} - \Delta f_L^{-1} \left.^{-1}\right. \qquad /4/$$

$$C_T = 2l\left[/\Delta f_{L2}^{-1} - \Delta f_L^{-1}/^2 + 4l^2 d^{-2}/\Delta f_T^{-1} - \Delta f_L^{-1}/^2\right]^{-1/2} \qquad /5/$$

The error analysis of the function /5/ shows that the method 2.3./2.2.2. may be used for not too thin rods /$l/d \lesssim 5$/, while for thinner ones the method 1.2./2.2.2. is to be preferred.

References

[1] J. Wehr: "Application of nonreflecting transducers in ultrasonic measurements", Proc. of Vibrations Problems, 4/1960 /Warsaw/.

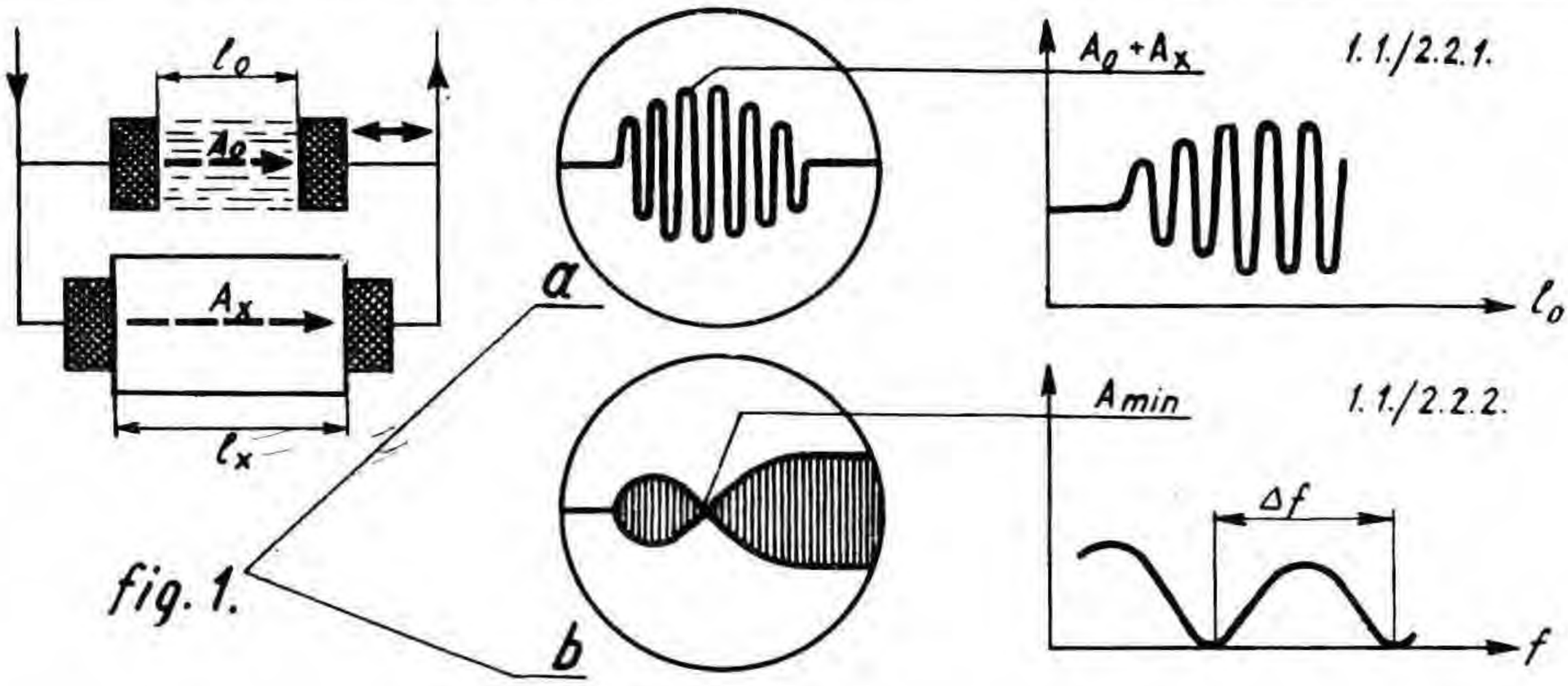

fig. 1.

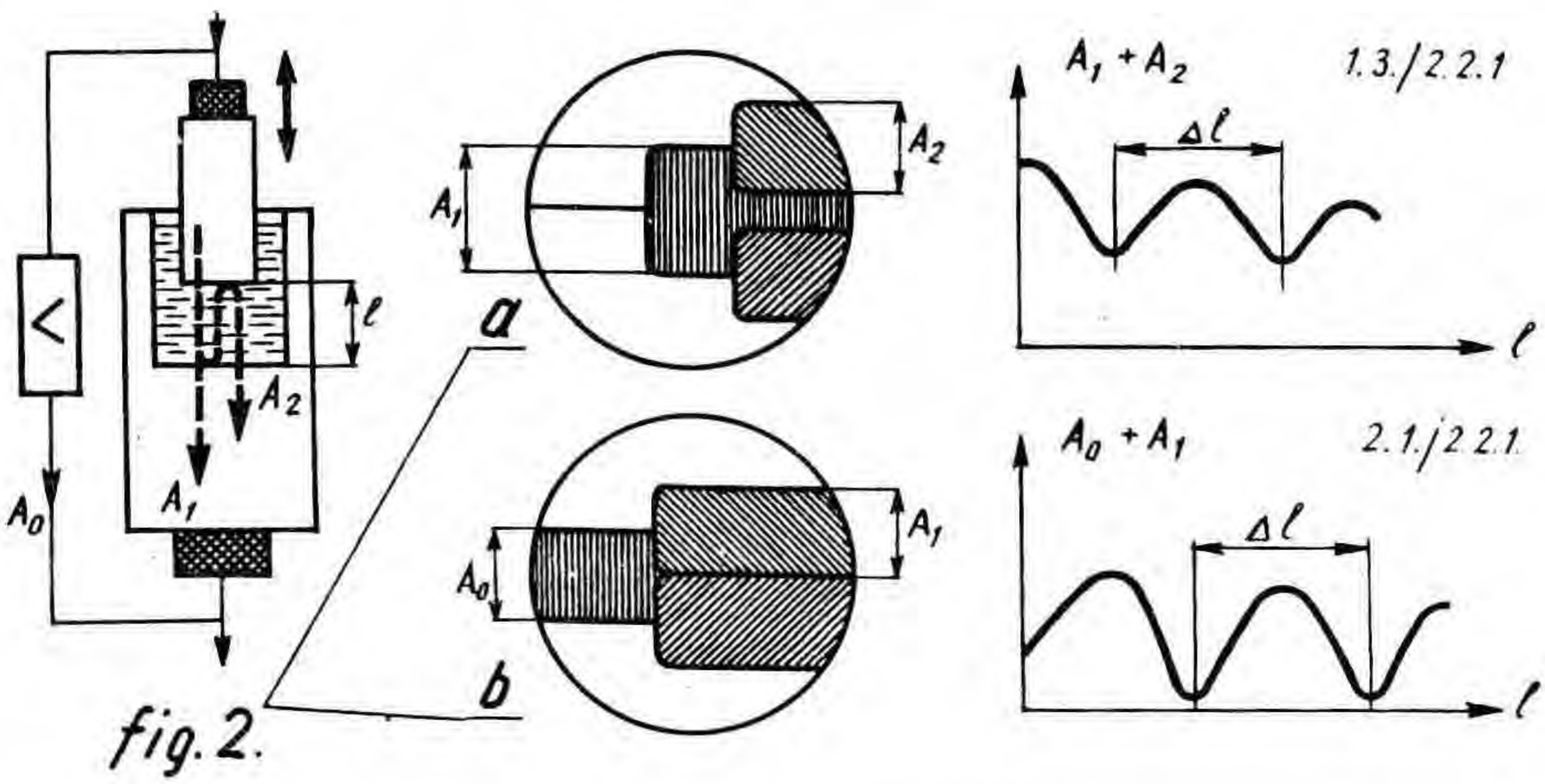

fig. 2.

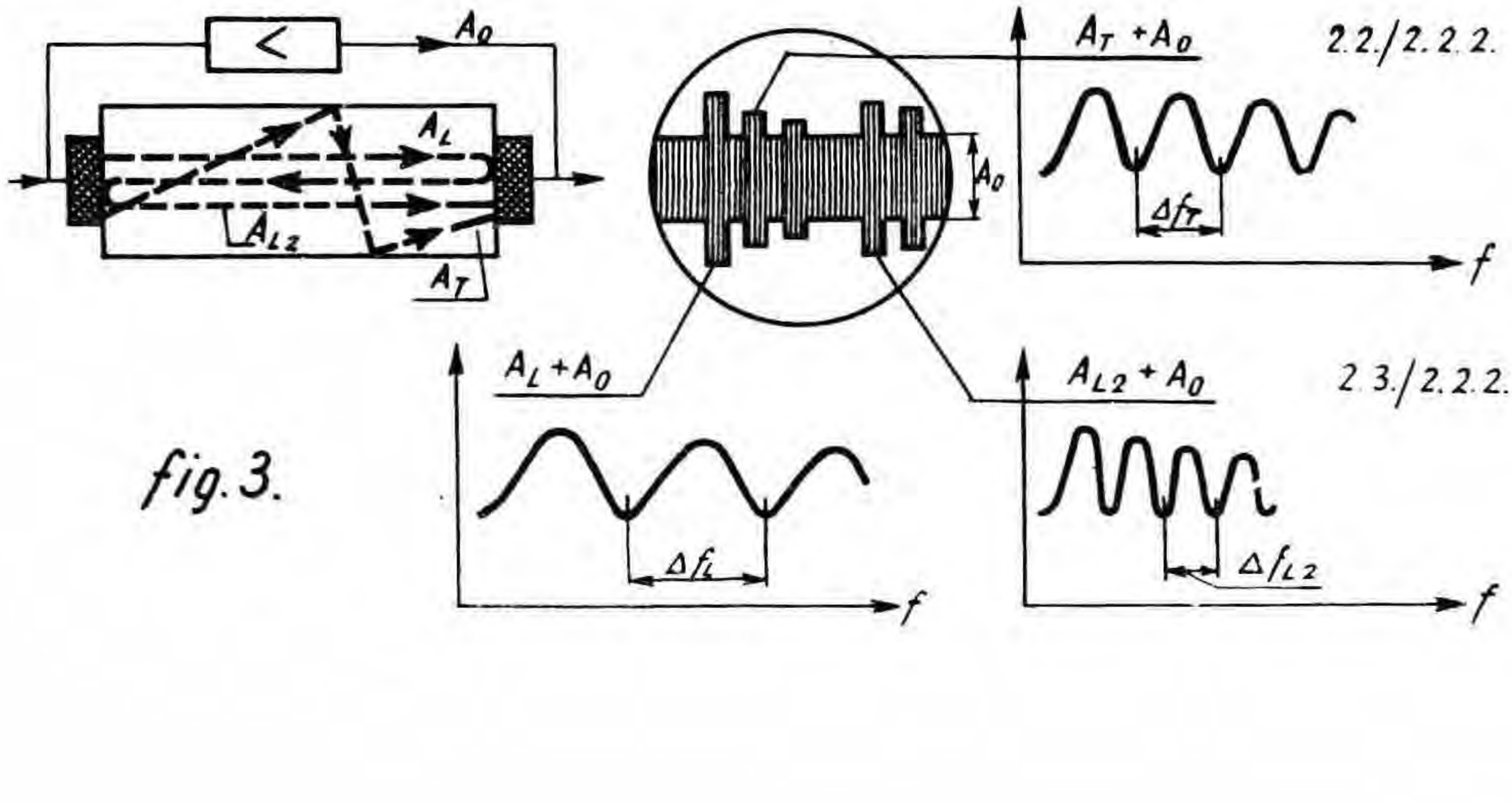

fig. 3.

L15

FOURTH INTERNATIONAL CONGRESS ON ACOUSTICS
COPENHAGEN 21.-28. AUGUST 1962

Wie laut ist es in meinem Auto?

G. Bobbert, Neckarsulm, Deutschland

Die Lautstärke ist als das Ergebnis einer bestimmten Meßmethode definiert, die auf einen subjektiven Hörvergleich mit einem Normalton oder einem Normalgeräusch hinausläuft. Da dieses Verfahren in der Praxis nur schwierig oder gar nicht durchführbar ist, wurde eine Reihe von Methoden erdacht und erprobt, mit deren Hilfe das richtige Ergebnis mit objektiven Messungen angenähert werden kann.

Am Beispiel des Geräusches im Innenraum von Kraftwagen soll über die mit verschiedenen dieser Methoden ermittelten Ergebnisse berichtet werden. Die definierte Methode selbst, der subjektive Hörvergleich wurde dabei nicht eingeschlossen. Es schien schwierig, die akustischen Verhältnisse im Innenraum eines Kraftwagens so nachzuahmen, daß für eine Hörergruppe aus mehreren Personen die wirklichen Verhältnisse des fahrenden Kraftwagens bestanden. Dazu sei daran erinnert, daß die Schallverteilung im Wageninnern örtlich sehr verschieden ist [1,2,3], ja, daß der Höreindruck sich wesentlich ändern kann, wenn der Hörer - etwa durch Drehen oder Vorbeugen des Kopfes - seine Position wechselt. Auch ist die verzerrungsfreie Wiedergabe der im Kraftwagen vorherrschenden tiefen und tiefsten Frequenzen mittels Lautsprecher in der Originalstärke von z.B. 90 dB bei 20 Hz nicht möglich (sh. Bild 1).

In mehreren Wagen verschiedener Hersteller, die sich nach Größe und Motorleistung unterschieden, wurde, teils bei mehreren Geschwindigkeiten, teils bei verschiedenen Getriebegängen, teils an verschiedenen Stellen im Wageninnern selbst, der Schallpegel mittels eines Terzfilters analysiert. Aus den erhaltenen Meßdaten wurden rechnerisch die Werte für den Gesamtpegel in dB(F)[1], dB(B)[2], dB(A), dB(CCIR)[3], sowie der NR-Wert nach den international vorgeschlagenen Grenzkurven (Noise Rating Numbers) [5] ermittelt und die Lautstärken nach Stevens [5] und Zwicker [5] berechnet.

---

1) (F) = flat. Mit dB(F) soll ausgedrückt werden, daß im Gegensatz zu dB(C) auch bei sehr tiefen Frequenzen keine Bewertung erfolgte.

2) dB (B) = DIN-phon.

3) CCIR bedeutet Bewertung nach der Psophometerkurve des CCIR [4].

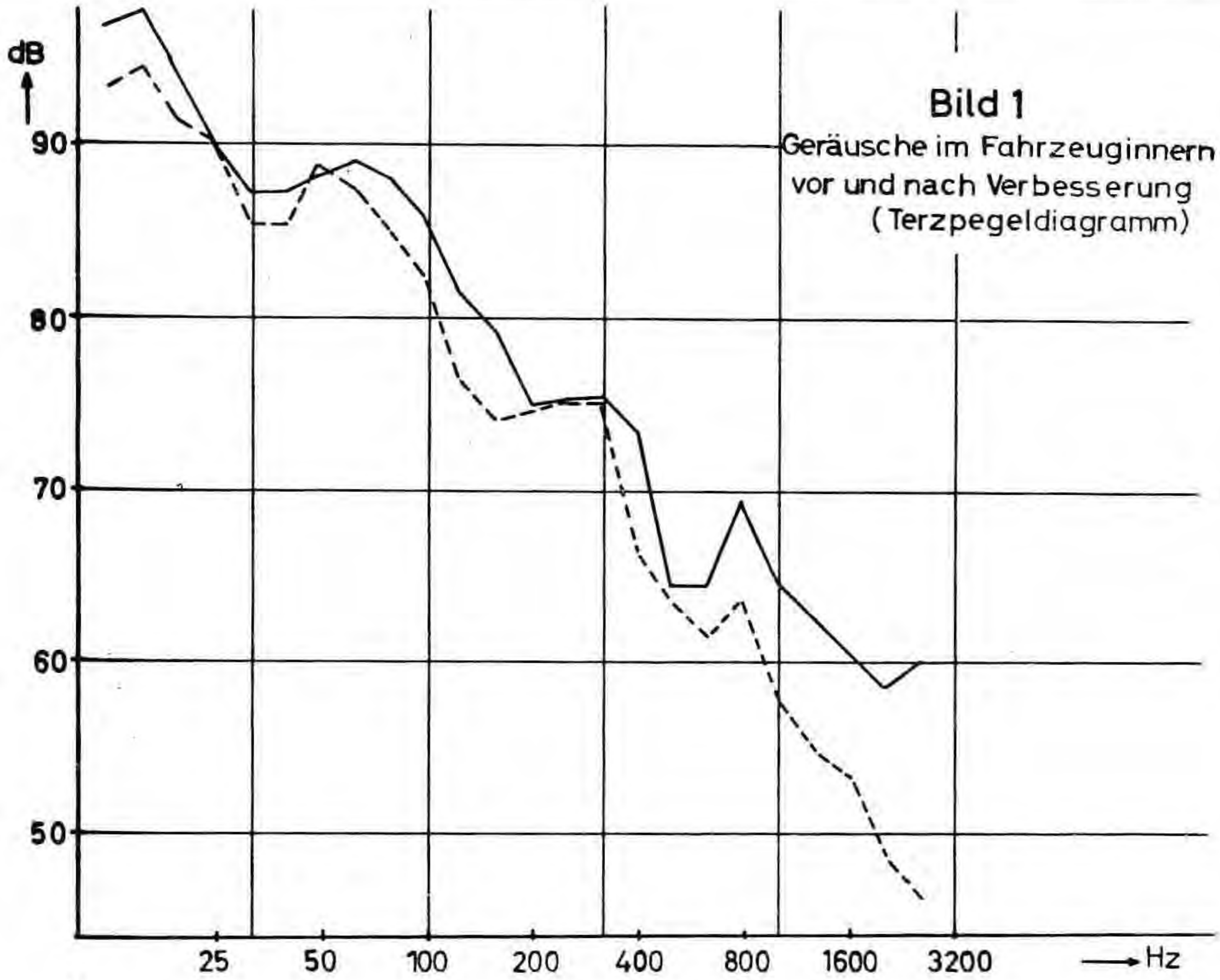

Bild 1
Geräusche im Fahrzeuginnern
vor und nach Verbesserung
(Terzpegeldiagramm)

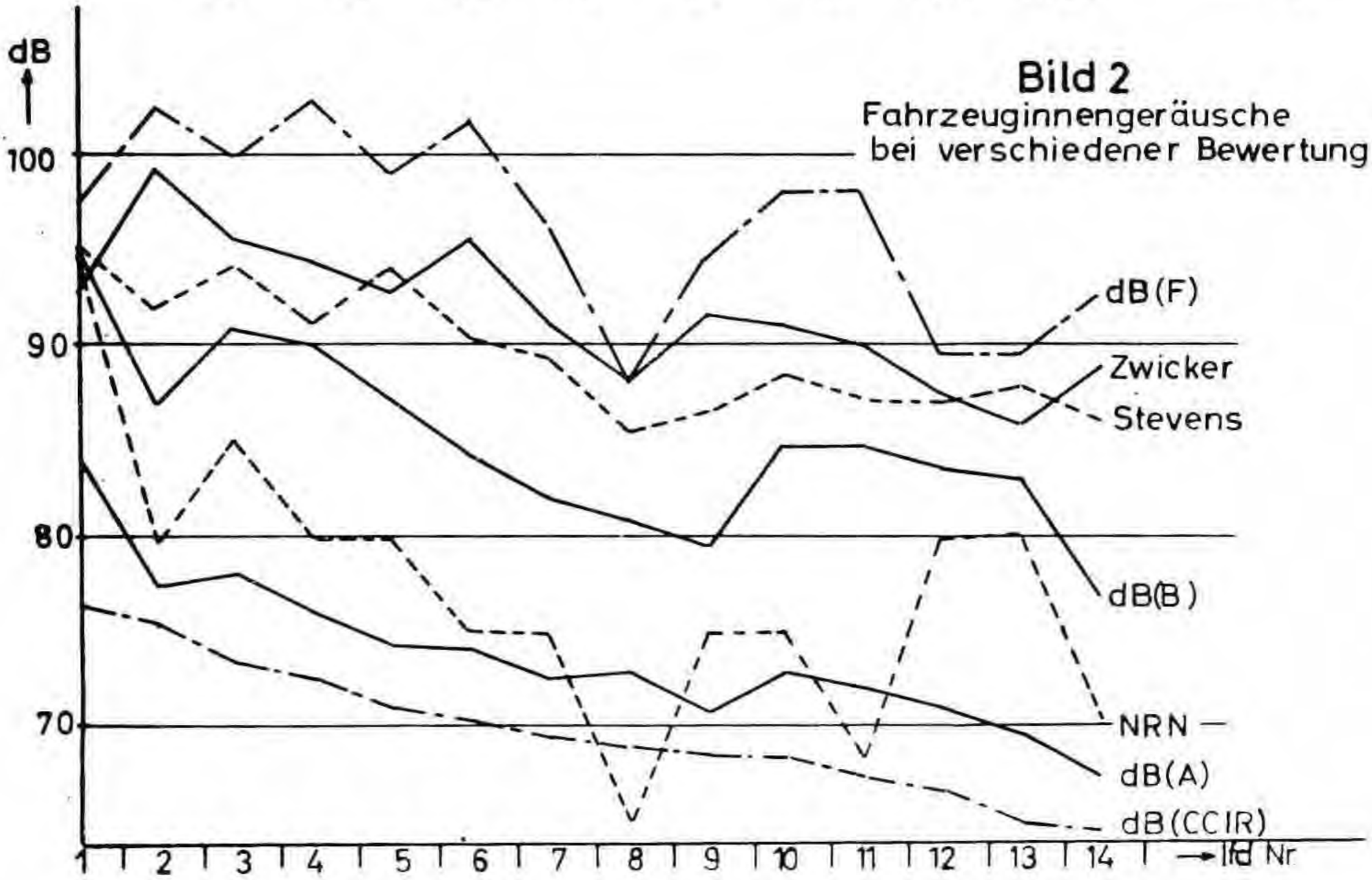

Bild 2
Fahrzeuginnengeräusche
bei verschiedener Bewertung

Die Bewertung nach den international empfohlenen Kurven A und B [6] sowie die nach der für die Geräuschspannungsmessung auf Rundfunkleitungen festgelegten Psophometerkurve [4] bedeuten dabei keine Schwierigkeit. Zur Bestimmung der Grenzkurven (NR-Wert) wurden je 3 Terzen zu einer Oktave zusammengefaßt und dann diejenige Grenzkurve gesucht, die von dem Oktavpegeldiagramm gerade nicht mehr erreicht wurde. Definitionsgemäß sind die Grenzkurven dabei von 5 zu 5 dB abgestuft.

Die Lautstärkeberechnung nach Stevens ist an einige Voraussetzungen geknüpft, die bei den Geräuschen im Wageninnern teilweise nicht voll zutreffen. So soll das Schallfeld diffus sein, was aber für die vorherrschenden tief- und sehr tieffrequenten Komponenten nicht der Fall ist. Auch soll das Spektrum breitbandig sein und keine herausragenden Einzeltöne aufweisen. Im Bild 1 ist das Spektrum zweier der untersuchten Geräusche (Nr. 2 und 6) dargestellt. Man erkennt daraus, daß die an das Stevensverfahren geknüpften Bedingungen auch in diesem Punkte nicht ganz zutreffen, da an mindestens zwei Stellen Eigentöne herausragen[4]. Trotzdem wurden die Werte nach Stevens ermittelt und in die Zusammenstellung mit aufgenommen.

Bei der Berechnung nach Zwicker sind keine derartigen Voraussetzungen zu beachten. Man hat auch die Wahl, die Berechnung für ein freies oder diffuses Schallfeld anzuwenden. Wenngleich die Berechnung für das freie Feld eine gewisse Berechtigung hätte, wurde hier doch ein diffuses Feld zugrunde gelegt, um den Anschluß an die Stevens-Berechnung zu haben, die nur für diffuse Felder möglich ist.

Im Bild 2 sind die erhaltenen Werte für 14 verschiedene Geräusche, geordnet nach fallenden Werten für dB(CCIR), zusammengestellt. Die zugrunde liegenden Spektren sind alle vom Typus des im Bild 1 gezeigten. Wenn auch der Pegel der Komponenten bei mittleren und höheren Frequenzen stark differiert, haben doch alle ihren Höchstwert unter, meist weit unter 100 Hz. Der Pegel dieser Maxima liegt jeweils zwischen 90 und 100 dB. Nur Geräusch Nr. 1 hat sein Maximum (97 dB) bei 160 Hz. Wenn man von den absoluten Zahlenwerten (in dB), die bei jeder der 7 Berechnungsarten stark abweichen (sh. Bild 2), absieht, so wäre auch die Rangordnung der 14 Geräusche in Bild 2 nach jeder Berechnungsart eine andere. Welche der möglichen Rangfolgen dem wirklichen Ohreindruck am besten entspräche, müßte durch einen subjektiven Hörvergleich mit Normaltönen oder -geräuschen bestimmt werden [7] . Da dies - wie oben dargelegt - nicht möglich war, mußte man sich auf das Urteil der Fahrer verlassen, die teils unmittelbar hintereinander, teils nach längeren Zeitabständen in den einzelnen Wagen gefahren waren. Diesem Urteil entsprach am besten die Rangfolge bei der Bewertung nach der CCIR-Kurve. Am Beispiel der im Bild 1 gezeigten Geräuschspektren Nr. 2 und 6 ist dies deutlich. Die Geräuschminderung im Wagen, die von der durchgezogenen Kurve zu der gestrichelt aufgetragenen führte, und die bei allen Beobachtern eine subjektiv empfundene merkliche Besserung bedeutete, hatte nur in der Bewertung nach CCIR einen Unterschied von 5 dB zur Folge. (Ebenso in der NRN-Bewertung, was aber zufällig durch die grobe Stufung von 5 zu 5 dB der Grenzkurve bedingt ist.) Bei den anderen Bewertungen lag die Minderung zwischen nur 0,5 und 3 dB.

---

4) Die Einzeltöne, die im Terzpegeldiagramm nur undeutlich zu erkennen sind, wurden durch eine genauere Analyse nachgewiesen.

Zwar reichen die Erfahrungen heute noch nicht aus, für die Geräusche im Kraftwagen eine bestimmte Bewertung, z.B. die nach CCIR, ausschließlich zu empfehlen, doch scheint die vorliegende Untersuchung zu zeigen, daß die üblichen Berechnungsmethoden offenbar auf die Besonderheiten der Kraftfahrzeuginnengeräusche nicht zugeschnitten sind. Alle Methoden, mit Ausnahme der CCIR-Bewertung, und in etwa auch der A-Bewertung, heben anscheinend die tiefen und sehr tiefen Frequenzen zu sehr hervor, während alle subjektiven Beobachtungen dafür sprechen, daß es mehr auf die Komponenten im mittleren Frequenzbereich ankommt. Schließlich könnte auch der von verschiedenen Autoren [8, 9] gesuchte aber nicht nachzuweisende Unterschied zwischen Lautheitseindruck und sog. Lästigkeit oder Störwirkung möglicherweise bei diesem Typus von Spektren eine Bedeutung haben.

Schrifttum

1. G. Bobbert: Verkehrsgeräusche, ihre Messung und ihre Beurteilung. Deutsch. Kraftfahrtforschung Nr. 91, VDI-Verlag 1956

2. G.W. Becker, H. Oberst: Grenzen der Geräuschminderung durch Körperschalldämpfung im Kraftfahrzeug. Acustica 8 (1958) S. 11/18

3. H. Nakamura, S. Sato, J. Sakagami: On Cavity Resonance of a Car Room and its Abatement. SAE Transactions, Jan. 1961

4. CCIF-Grünbuch 1956, Bd. 4, S. 129/31

5. ISO Draft Recommendation 1961 (unveröffentlicht)

6. IEC-Publication 123

7. ISO-Recommendation R 131

8. G. Quietzsch: Objektive und subjektive Lautstärkemessungen; Acustica 5 (1955) S. 49/66.

9. H.J. Rademacher: Die Lautstärke von Kraftfahrzeuggeräuschen; Acustica 9 (1959) S. 93/108.

M15

FOURTH INTERNATIONAL CONGRESS ON ACOUSTICS
COPENHAGEN 21.-28. AUGUST 1962

Acoustical Design of La Grande Salle,

A 3,000-Seat Multi-use Auditorium, Montreal, Canada

Frederick Russell Johnson

50 Moulton Street, Cambridge, Massachusetts, U.S.A.

In Europe large multi-use auditoriums seating 2000 to 3400 people can be found, but most of the opera house-concert halls in Europe seat 1000 to 2000. In North America, most multi-use halls in use or under construction seat about 2400 to 3200. It is probably fair to say that the acoustical-architectural design problem of the large multi-use civic auditorium is native to North America.

All aspects of good acoustics are served best by relatively small halls. Clarity, fullness of tone, intelligibility, sufficient loudness and reverberation, balance between a singer on stage and an accompanying orchestra in the pit, the quality of musical sound, balance between various sections of an orchestra, freedom from various types of echo--all of these desired characteristics and others are easily achieved in 1400 to 1800 seat halls. Conversely, increasing the seating capacity to 2200 to 2800 requires, in order to achieve satisfactory acoustics, that all of the basic architectural aspects of the room be molded in conformity with acoustical needs.

The major architectural parameters affecting the acoustical quality of a hall include the area used for audience seating (L.L.Beranek, JASA, p.661, 1960), the cubage, the cubage per unit area of sound absorption (primarily audience), shaping, height and width of hall. The area used for audience seating and aisles should not exceed 10,000 to 14,000 sq ft for best results. The cubage of the hall, including the concert enclosure, should not exceed 500,000 to 600,000 cu ft. The cubage should, at the same time, be about 40 to 45 cu ft per sq ft of sound absorption. Overhead there should be large areas--roughly horizontal--providing sound reflection, located not more than 24 ft to 28 ft above stage level. At the sides at the front of the hall there should be sound-reflecting surfaces, roughly parallel, no more than 30 to 35 ft from the centerline of the hall. The Musikvereinssaal in Vienna is an example of a hall that meets these requirements.



FIG 1 MUSIKVEREINSSAAL, VIENNA - 1680 SEATS

In North America where there is an apparently inexorable demand for halls seating more than 2000 to 2200 these specifications usually cannot be fulfilled, and therefore our group has been studying, during the past eight years, ways to optimize the acoustical qualities of large multi-use halls. During the first half of this century, most multi-use halls in North America were not only too large, but most of them did not have sufficient ceiling height for adequate reverberation. They also had fan plans which reflected the sound away from the seating areas where it was most needed. Most of these auditoriums were very wide and very deep. Aside from the negative effects of these stretched dimensions, the resulting surfaces led to the use of large areas of sound-absorbing treatment, thus further reducing the sound produced by singers and orchestras. The large dimensions of these halls were due partly to large seating capacities, partly to the trend towards luxurious "leg room," and partly to the style trend of incorporating only one or two balconies at the rear of the hall. Multi-tiered halls with "horseshoe shaped" shallow balconies have been essentially nonexistent in North America since the end of the last century.

In 1954, our group designed a new "perforated" ceiling canopy for the Tanglewood Music Shed (JASA, p.475, 1961). This canopy, about 22 ft above the concert platform and about 20 ft below the ceiling, consists of 50% void and 50% large sound-reflecting panels. It provides the desired short-time-delay sound reflections and at the same time enables the cubage over the canopy to supply the reverberation needed for music performance. The success of this canopy supplied one of the keys to the frustrating

acoustical problems facing auditorium architects in North America. Beginning in 1956, 1958 and 1959, our group incorporated, in a series of hall designs, suspended sound-reflecting canopies, half open and half closed, following the Tanglewood canopy con-



FIG 2 LA GRANDE SALLE PLACE DES ARTS, MONTREAL

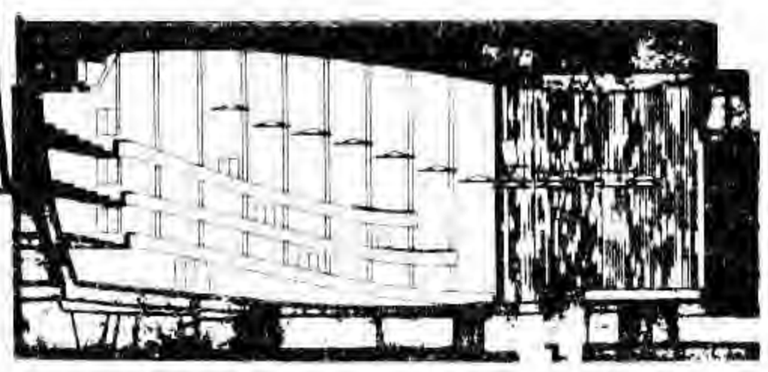

FIG 3 PHILHARMONIC HALL LINCOLN CENTER, NEW YORK CITY

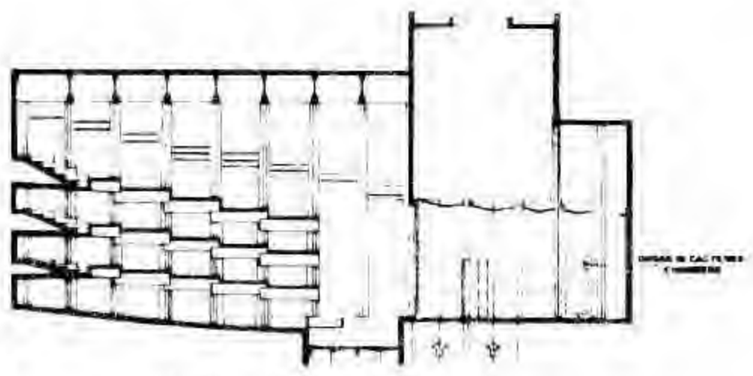

FIG 4 CLOWES HALL INDIANAPOLIS, INDIANA

cept. Three of these halls not only incorporate this layer of suspended sound reflectors, but are also alike in their basic seating arrangement--three "horseshoe shaped" tiers of seating above the parquet. Two of these halls, La Grande Salle in Montreal and Clowes Hall in Indianapolis, are multi-use halls, and the other, Philharmonic Hall in Lincoln Center, is a concert hall. The suspended panels in the Indianapolis and Lincoln Center projects are independent units. In the case of the Montreal hall, the suspended panels are interconnected with plaster "arms" and "bridges," weaving an overall ceiling pattern that effectively conceals the space above, used to develop reverberation.

Although these three halls have basic similarities, only one of them is a concert hall. Concert halls (auditoriums with concert platforms--no stagehouse) are only infrequently constructed. In the last fifty years only one concert hall has been constructed in North America--Buffalo's Kleinhans Hall--and even now the owner is considering converting Kleinhans into an opera house type by adding a theatre stagehouse. There are only four major halls in North America that have no provision for theatrical production--Massey Hall, Toronto; Orchestra Hall, Chicago; Symphony Hall, Boston, and Kleinhans Hall. The Lincoln Center concert hall will be inaugurated in September 1962, and the only other concert hall currently planned in North America is one in Pittsburgh.

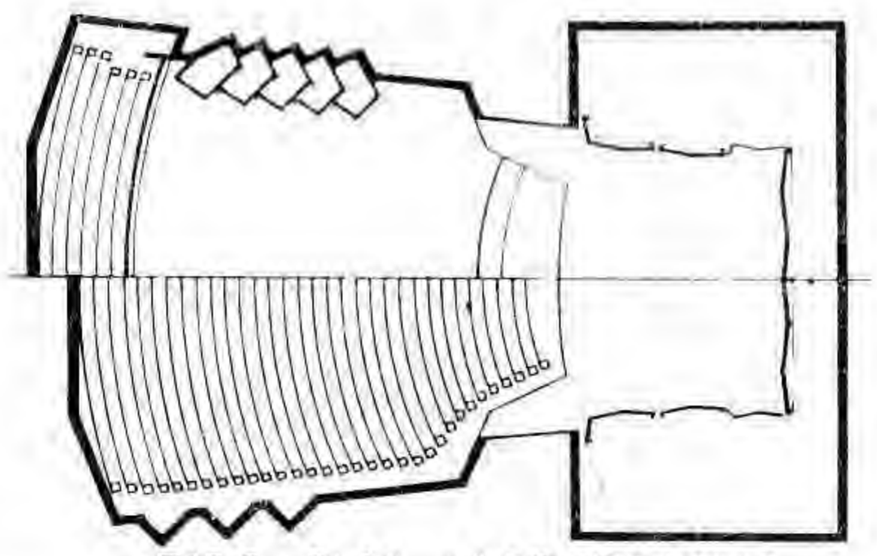

FIG 5 PLAN, LA GRANDE SALLE

The 3,000-seat hall now being constructed in Montreal was referred to as a concert hall during the early planning stages four to six years ago. However the activities which will take place in this hall when it is finished require a full theatrical stagehouse. One of the project's brochures stated that the Great Hall will be twice the size of the other two auditoriums currently in use in Montreal and that "it will bring to Montreal symphony, opera, ballet, operetta, musical comedy, major dramatic productions and concert artists." A report prepared for the building owner by a market research firm stated that the hall should have complete facilities for stage productions and be suitable for opera, concert and ballet. This report also states that the hall should be a compromise between a concert hall and a large opera house and that it should be designed primarily for major concerts and ballet performances with full provision for opera, large scale operetta and musical comedy. Thomas Archer (Montreal Gazette, 14 June 1958) supported the need for a multi-use hall in Montreal by pointing out that it is possible for a symphony orchestra to perform in an opera house, but opera cannot be staged in a concert hall.

Peter Collins, an architectural commentator, reported in the 2 May 1959 Montreal Star, that "for various practical reasons it was considered advisable to plan the building as an opera house." He also wrote that the acoustical requirements "were very lax in that every kind of performance from orchestra to musical comedy had to be provided for."

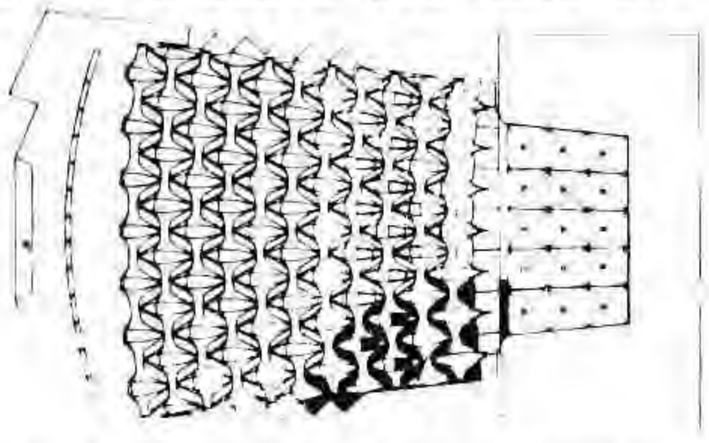

FIG 6 PLAN OF SUSPENDED SOUND REFLECTING PANELS, LA GRANDE SALLE

Eric McLean, music critic of the Montreal Star, expressed the hope in one of his columns that the new hall would lead to the formation of a permanent opera company in Montreal. In another column he wrote, "For the European the term 'concert hall' has a very definite meaning and the term 'opera house' is something else again. In our case, however, the two will have to be equated somehow, since the building will have to house orchestral concerts, opera, and theatre and ballet as well. As far as I could learn from the people in the business in France, Italy, and Germany, such a building does not exist in Europe. Their concert halls, both old and new, have no other function. They consist of an auditorium with a platform for the performers--nothing else. There is no stagehouse. Their opera houses, on the other hand, are unsuitable for concerts. Most Montrealers know perfectly well that their new building will be an opera house, or that opera will be one of its functions at least. By calling it a concert hall, we give it a much more sober air and the term suggests a sensible approach to finances. But our concert hall will necessarily differ from the best European opera houses in much more than name. Consider the capacity, for instance. Europeans in the business feel that 1600 to 1800 is about the maximum for good acoustics and good visibility. But because our hall must serve for theatre, concerts, opera and ballet, and because it must pay its way as much as possible, the figure under discussion is something around 2500. The architects of our concert hall-opera house-theatre will not be able to side-step this peculiar problem, and should they find a satisfactory solution they may well set a pattern for future theatres in other cities of this continent."

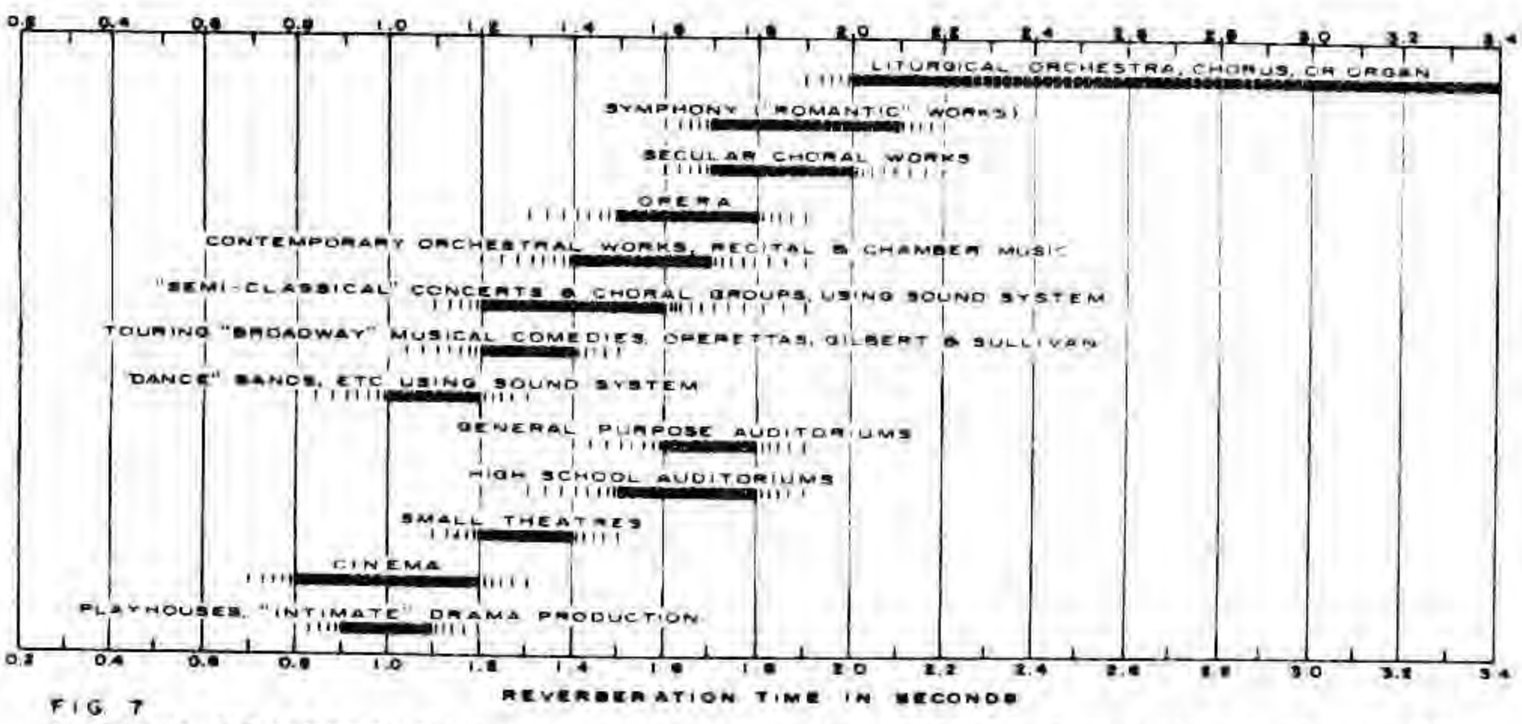

FIG 7
OPTIMUM REVERBERATION (500/1000 CPS) FOR AUDITORIUMS AND SIMILAR FACILITIES

Expressed in terms of source of income, the use of the hall was projected in a report (September 1958) to the owner as: ballet, 20%; recitals, 20%; symphony orchestra, 20%; touring symphony, 15%; musical comedy, light opera and revue, 10%; choral concert with and without orchestra, 5%; grand opera, 5%; motion picture, conventions and spectacles, 3%; drama, 2%. The market research firm employed by the owner, after studying the potential sources of rental income, reported that approximately 3,100 seats would be required to pay operating costs at acceptable box-office prices.

It can be seen that this hall presented the acoustical designer with the problem typically encountered in North America--a large, multi-use hall. The three balconies wrap around the side walls in "horseshoe shape." The re-entrant balconies are quite deep at the rear of the hall, and this will have an effect on the acoustic conditions in the rear of these "pockets." The audience seating area is 22,100 sq ft. The cubage including the demountable concert enclosure is 936,800 cu ft. This indicates a maximum reverberation time (with a full symphony on stage and a full audience, including audience in the orchestra pit) of 1.7 to 1.75 seconds (500/1000 cps). The reverberation time of the completed hall will depend in part on the finish materials used in the aisles. We recommended the use of a sound-reflecting materials in the aisles. This recommendation was mandatory due to the high ratio of aisle area to seating area in a hall which has audience seating on four levels. The acoustical design incorporates no permanent sound-absorbing material other than the seats and

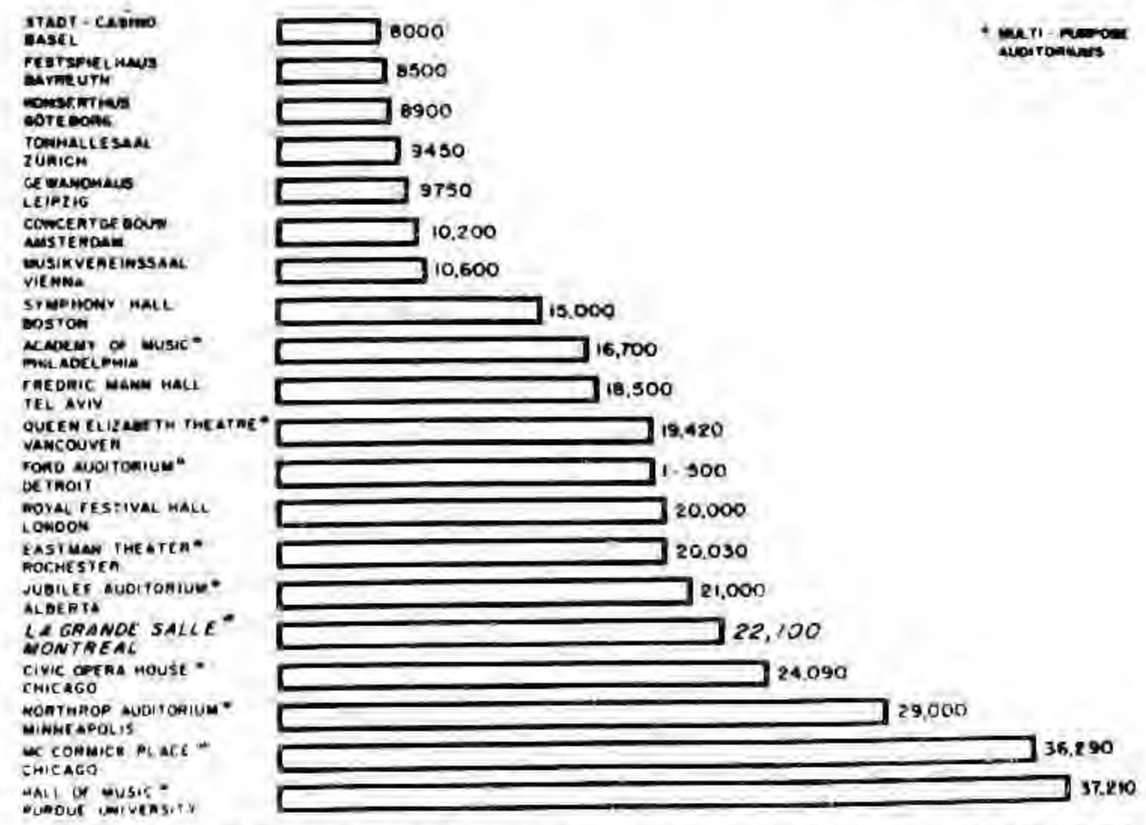

FIG 8 AUDIENCE AREA (INCLUDING AISLES UP TO 3.5 FT.)

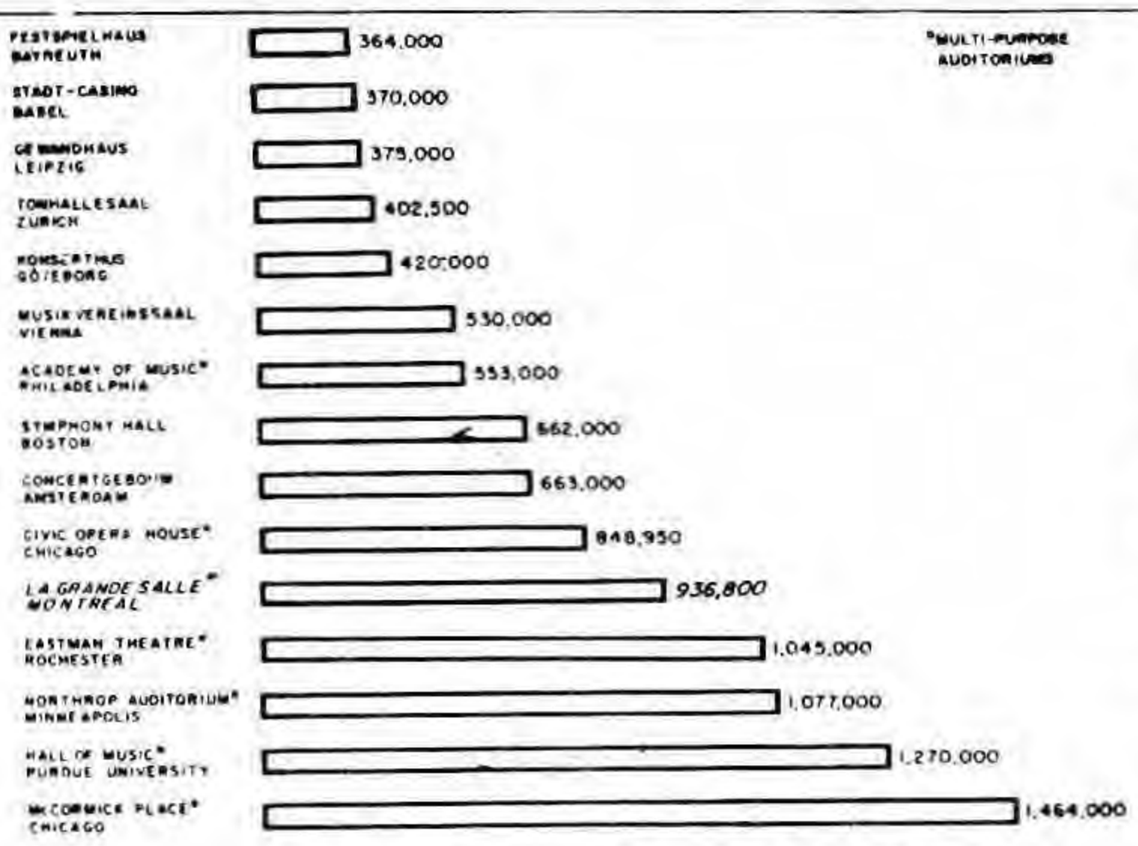

FIG 9 VOLUME (CUBAGE)

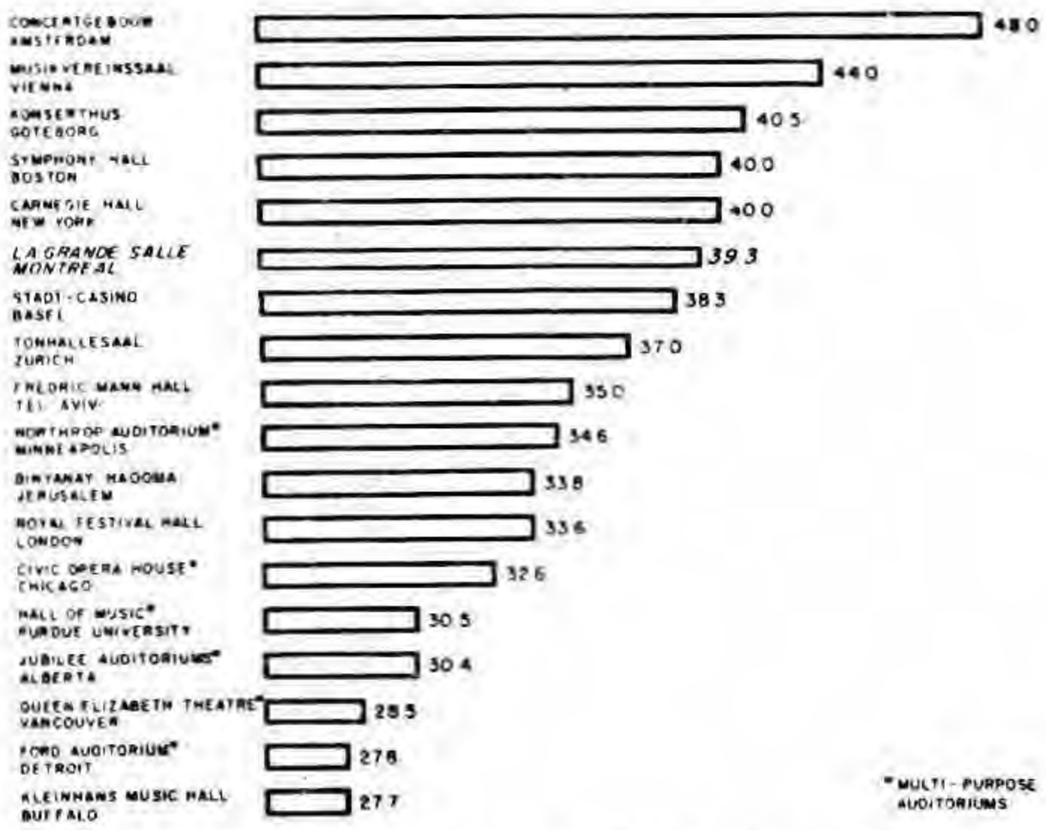

FIG.10 VOLUME PER UNIT AREA OF SOUND ABSORPTION (PRIMARILY AUDIENCE)

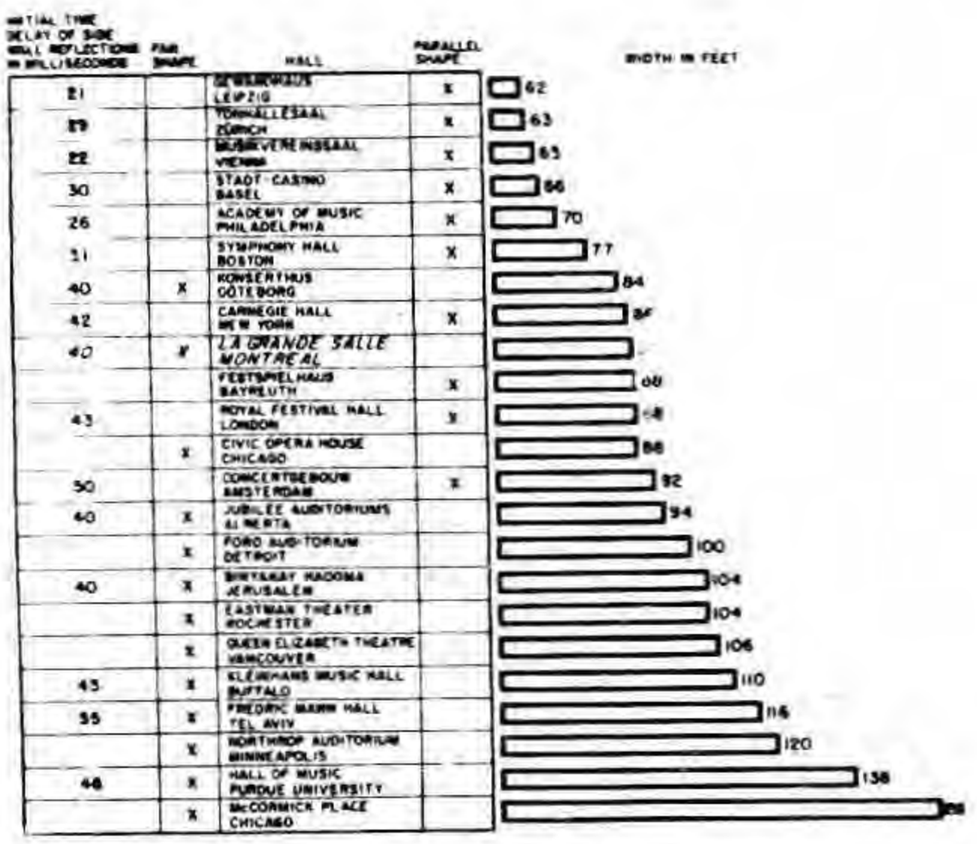

FIG.11 WIDTH AND SHAPING

carpet beneath the seats. The carpet beneath the seats was recommended as reverberation compensation for less than capacity audiences. The upper ceiling is constructed of $1\frac{1}{2}$" thick plaster, also to help augment the low frequency reverberation. Similarly, the suspended sound-reflecting panels are $1\frac{1}{2}$" thick plaster, and the plaster is troweled on the top side to minimize high frequency absorption by dust. All of the walls of the hall are constructed of 4" (or heavier) masonry units, with a directly-applied plaster finish. This is to augment the low frequency reverberation, as required in halls of more than 300,000 to 500,000 cu ft.

By studying the optimum reverberation time for various uses (Fig. 7) in conjunction with the projected uses of this hall, it can be seen that the predicted reverberation time of this hall will lie between the optimum for symphony performance and the optimum for unamplified speech and opera. Even though the 1.9 second mid-frequency reverberation desired for symphony performance will not be achieved, the predicted 1.7 seconds will be too high for certain conditions of use. For this reason, our design incorporates 6000 sq ft of sound-absorbing curtain on tracks in the space above the suspended panels.

For symphony concerts, all of this sound-absorbing material will be retracted, by remote motorized control, into housings constructed of heavy plaster. For the infrequent performances of Shakespeare and opera these curtains will be exposed, lowering the reverberation, with full audience, about 0.3 second.

The average width of the hall in the front half is 87 ft. In the center third of the auditorium the walls are spaced about 104 ft apart. The requirement for a width of 60 to 70 ft is not met, but the need to seat approximately 3,000 people in this hall made it necessary to seek compromises. Figs. 8, 9, 10 and 11 compare some of the basic architectural parameters of the Montreal hall with other existing halls.

The firms collaborating on the architectural-acoustical design of the hall include Ben Schlanger and Donald Oenslanger, auditorium and stage consultants, Affleck, Desbarats, Dimakopoulos, Lebensold and Sise, architects, and Bolt Beranek and Newman Inc., acoustical consultants. The hall will be completed by the fall of 1963.

N15

FOURTH INTERNATIONAL CONGRESS ON ACOUSTICS
COPENHAGEN 21.-28. AUGUST 1962

Ein mechanischer Kettenleiter für Verzögerungszwecke

Georg Boerger und Lothar Cremer
Heinrich-Hertz-Institut für Schwingungsforschung,
Berlin-Charlottenburg

Im Zusammenhang mit verschiedenen Problemen der Signalübertragungstechnik entsteht die Aufgabe, ein Signal zu verzögern. Es sei z.B. an die Unterstützung eines Redners durch eine Lautsprecheranlage erinnert, wobei angestrebt ist, das Originalsignal als erste Wellenfront an einem Hörerplatz zu empfangen, da nur dann erreichbar ist, daß der Hörer als Schallquelle den Redner ortet und nicht etwa einen ihm viel näher gelegenen Lautsprecher. Als zweites Beispiel sei an die Erzeugung künstlichen Nachhalls gedacht. Ferner werden Verzögerungseinrichtungen für jede Korrelationsanalyse benötigt.

Zur Erzeugung von Laufzeiten kann man entweder von der Anwendung des Magnettonverfahrens Gebrauch machen, wobei die Laufzeit des Tonträgers vom Aufnahmekopf zum Wiedergabekopf ausgenutzt wird, oder man kann elektrische oder mechanische Leitungsgebilde mit ihrer natürlichen Laufzeit anwenden.

Eine dispersionsfreie Wellenausbreitung besitzen bekanntlich nur die Longitudinal- und die Torsionswelle. In einem kreisrunden Stab beträgt die Phasengeschwindigkeit

$$\text{für die Longitudinalwelle } c_L = \sqrt{\frac{E}{\varrho}} \qquad (1)$$

$$\text{und für die Torsionswelle } c_T = \sqrt{\frac{G}{\varrho}}\ , \qquad (2)$$

wobei E der Elastizitätsmodul, G der Schubmodul und ϱ die Dichte ist. Elastizitäts- und Schubmodul sind für isotrope Stoffe durch die Poissonsche Querkontraktionszahl μ miteinander verknüpft:

$$E = 2(1 + \mu)G \qquad (3)$$

Für die meisten hier interessierenden Werkstoffe kann man die Näherung schreiben

$$G \approx 0{,}4\ E, \qquad (4)$$

so daß der Torsionswelle der Vorzug zu geben ist, wenn eine geringe Phasengeschwindigkeit angestrebt wird. Betrachtet man selbst ein so schweres und dabei nachgiebiges Material wie Blei, so ergibt sich, daß dessen Phasengeschwindigkeit

$$c_{T\,Pb} \approx 800 \text{ m/sec} \qquad (5)$$

um ein Vielfaches größer ist, als die Schallgeschwindigkeit in Luft. Die Torsionswellenausbreitung in einem Stab würde daher keinen konstruktiven Vorteil gegenüber der Luftschallausbreitung etwa in einem Rohr bringen.

Niedrige Ausbreitungsgeschwindigkeiten sind - auch bei Anwendung der Torsion - offenbar nur mit einem Kettenleiter erreichbar. Mit einem solchen Übergang zu einem diskontinuierlichen Wellenleiter ist allerdings eine Einschränkung des übertragbaren Frequenzbandes verbunden.

Es soll von einer in Berlin entwickelten Anordnung berichtet werden, die, wie wir nachträglich feststellten, bereits von anderen Autoren, insbesondere von W.P. Mason /1/ vorgeschlagen und untersucht wurde, und deren Prinzip in Abbildung 1 gezeigt ist:

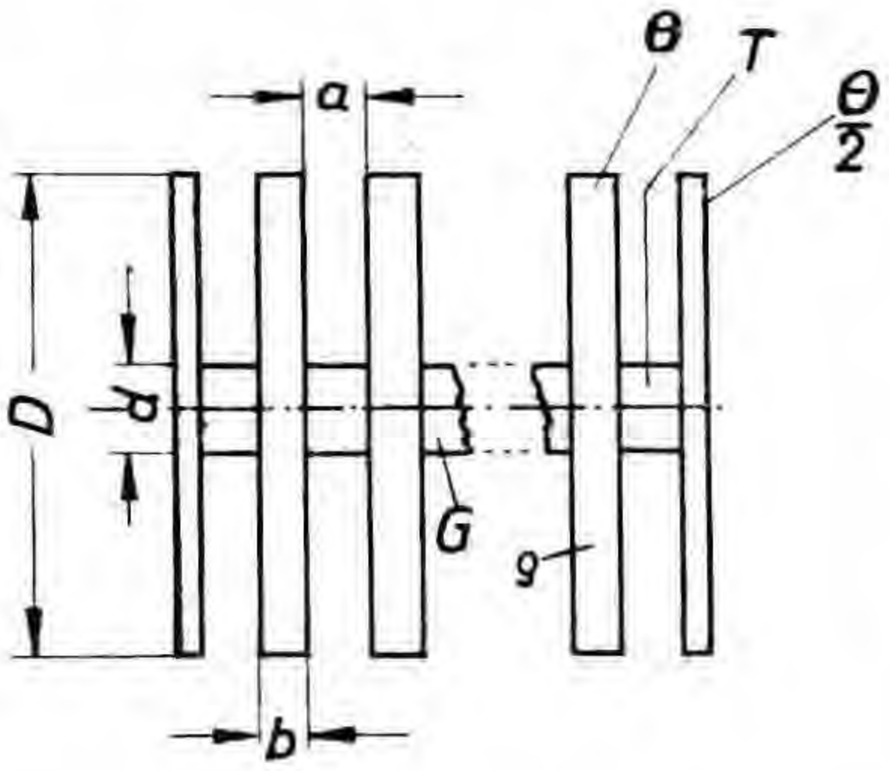

Abb. 1

Setzt man voraus, daß die großen Scheiben mit dem Trägheitsmoment Θ sich als starre Körper verhalten, und die dazwischen liegenden Elemente eine Torsionssteife T, aber eine vernachlässigbare Trägheitswirkung haben, so hat diese Anordnung einen Tiefpaßcharakter. Das Phasenmaß und die Gruppenlaufzeit innerhalb des Durchlaßbereiches ergeben sich zu /2,3/:

$$b = 2\arcsin\frac{\omega}{\omega_g} \qquad (6)$$

$$\tau_{gr} = \frac{2n}{\omega_g}\sqrt{\frac{1}{1-(\omega/\omega_g)^2}}\,, \qquad (7)$$

wobei n die Zahl der Glieder und

$$\omega_g = \sqrt{\frac{T}{\Theta}} = \frac{2}{\sqrt{ab}}\left(\frac{d}{D}\right)^2\sqrt{\frac{G}{\varrho}} \qquad (8)$$

die Grenzfrequenz des Kettenleiters ist. Die Gruppengeschwindigkeit beträgt dann

$$c_{Tgr} = \frac{n(a+b)}{\omega_{gr}} \qquad (9)$$

In einem Bereich konstanter Gruppenlaufzeit, d.h. für Frequenzen weit unterhalb der Grenzfrequenz ergeben sich folgende Beziehungen:

$$b_o = 2n\,\frac{\omega}{\omega_g} = n\omega\sqrt{ab}\,\left(\frac{D}{d}\right)^2\sqrt{\frac{\varrho}{G}} \qquad (10)$$

$$\tau_o = \frac{2n}{\omega_g} = n\sqrt{ab}\,\left(\frac{D}{d}\right)^2\sqrt{\frac{\varrho}{G}} \qquad (11)$$

$$\tau_o\omega_g = 2n \qquad (12)$$

$$c_{To} = \frac{a+b}{2}\,\omega_g = \frac{a+b}{\sqrt{ab}}\,\left(\frac{d}{D}\right)^2\sqrt{\frac{G}{\varrho}} \qquad (13)$$

$$c_{To}/\omega_g = \frac{a+b}{2}\,. \qquad (14)$$

Für eine sinnvolle Dimensionierung des Kettenleiters wird man sich also bemühen, die Längen a und b der Elemente möglichst gering zu machen, um eine geringe Phasengeschwindigkeit zu erhalten. Bei vorgegebener Grenzfrequenz ergibt sich dabei auch ein kleiner Wert für das Verhältnis d/D der beiden Durchmesser. Eine Grenze in dieser Richtung ist durch die Tatsache gegeben, daß die Trägheitselemente nicht mehr als starre Körper anzusehen sind, wenn die Betriebsfrequenz in die Nähe der ersten Eigenfrequenz der am Umfang der Federungselemente eingespannten großen Scheiben kommt. Diese erste Eigenfrequenz ist näherungsweise durch

$$\omega_o \approx \frac{4d}{D^2} \sqrt{\frac{2G}{\varrho}} \qquad (15)$$

gegeben. Man muß also einen gewissen Mindestwert des Durchmessers der Federungselemente in Kauf nehmen, wenn ω_o oberhalb des Übertragungsbereiches liegen soll. Um trotz dieser Grenze die Federungselemente nachgiebiger zu machen, wurde die einfache Scheibenform verlassen und tellerförmige Elemente entwickelt, wie sie in Abbildung 2 angedeutet sind. In dieser Anordnung sind die doppeltschraffiert gezeichneten Bereiche als die elastisch deformierbaren anzusehen. Durch geeignete Dimensionierung dieser Bereiche sind beliebige Torsionssteifen zu erzielen. Eine solche Konstruktion ist allerdings erst möglich, wenn man dazu übergeht, den Kettenleiter aus einzelnen Elementen zusammenzubauen. Die mechanische Verbindung der Elemente geschah, indem diese auf eine dünne Stahlsaite aufgereiht und dann durch eine axiale Verspannung in mechanischen Kontakt gebracht wurden.

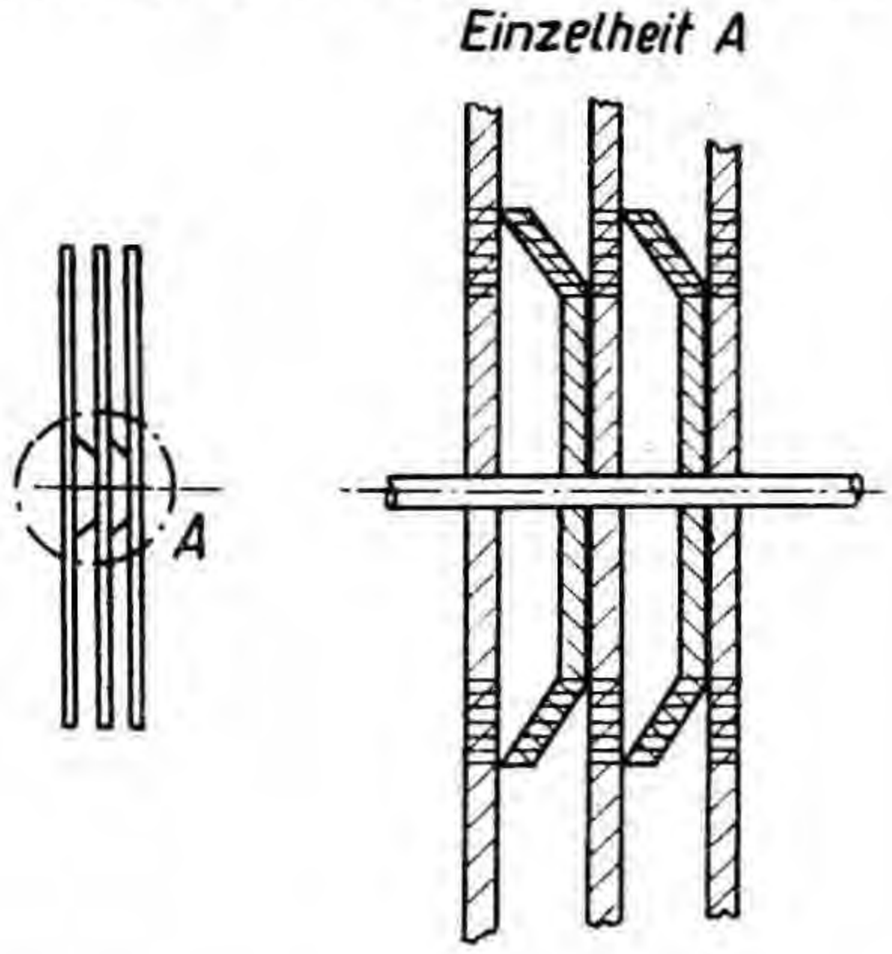

Abb. 2

Die Wellenanregung erfolgt an einem Ende des Kettenleiters durch einen elektromagnetischen Wandler. Die Abtastung der Wellenbewegung kann entsprechend der gewünschten Laufzeit an irgendeiner Stelle des Kettenleiters an der Peripherie eines Trägheitselementes erfolgen. Verwendet wurde dazu ein elektrodynamischer Wandler mit sehr geringem mechanischen Eingangswiderstand. Der dadurch entstehende Reflexionsfaktor war vernachlässigbar.

Zur Vermeidung von Reflexionen am Ende des Kettenleiters wurden dort eine Reihe verlustbehafteter Kunststoffelemente angebaut, die die Energie der eindringenden Welle verzehren.

Die Abbildung 3 zeigt den Pegel- und Laufzeitfrequenzgang eines entsprechenden Kettenleiters, der für ein Frequenzband von 0...4,5 kHz und einer Laufzeit von 50 $\pm$ 3 ms ausgelegt worden ist. Der Abfall im Pegelfrequenzgang oberhalb 3 kHz ist durch die Grenzfrequenz des sendeseitigen Wandlers bedingt und nicht durch die Grenzfrequenz des Kettenleiters, die bei 11 kHz liegt. Die Ausbreitungsgeschwindigkeit beträgt 20 m/sec. Die Ausbreitungsgleichung dieser Ausführung ist in Abbildung 4 dargestellt.

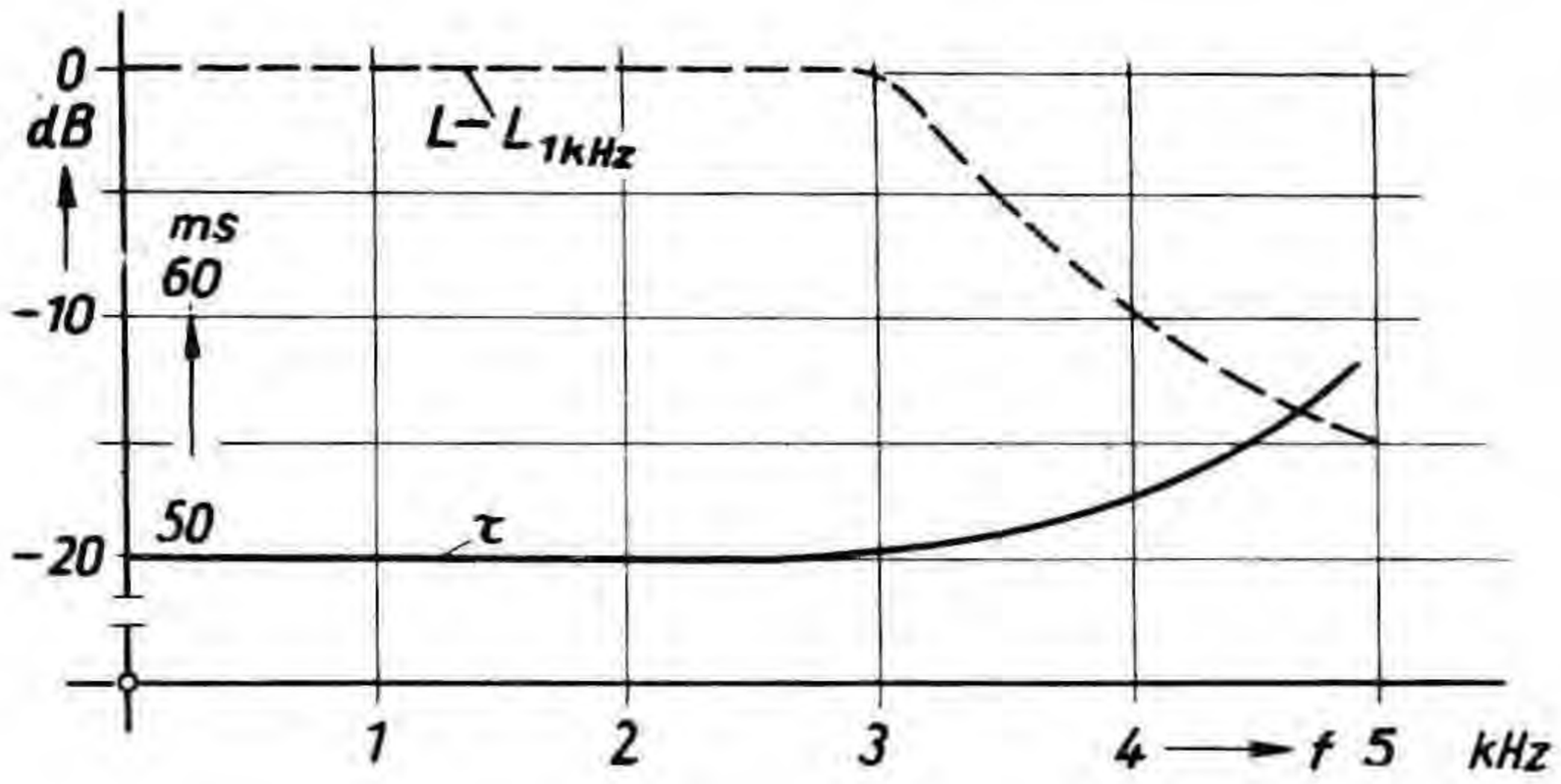

Abb. 3

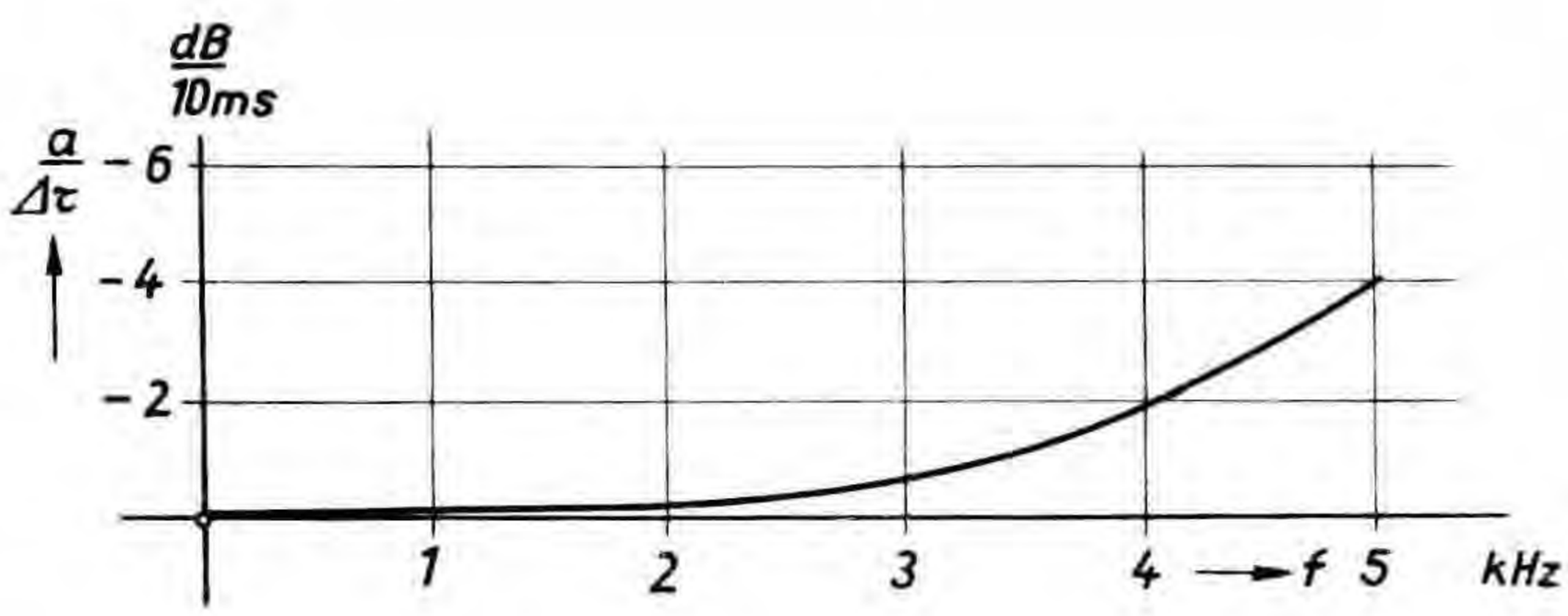

Abb. 4

Literatur

/1/ USA Patent 2 906 971

/2/ L. Cremer, The Propagation of Structure-borne Sound. Department of Scientific and Industrial Research, Sponsored Research (Germany) Report No. 1. (Series B).

/3/ Meinke/Gundlach, Taschenbuch der HF-Technik.

O15

FOURTH INTERNATIONAL CONGRESS ON ACOUSTICS
COPENHAGEN 21.-28. AUGUST 1962

DISSIPATIVE PROPAGATION OF FINITE-AMPLITUDE WAVES IN A TUBE*

David T. Blackstock

General Dynamics/Electronics, Rochester 1, New York (U.S.A.)

A long standing problem in the field of finite-amplitude sound has been the "missing 3 db of Thuras, Jenkins, and O'Neil". Consider a plane sound wave produced by pure sinusoidal excitation at a plane in space. Because of nonlinear propagation effects, the wave suffers distortion as it progresses. A very simple theoretical treatment of the applicable hydrodynamics equations shows that the second-harmonic component of the distortion grows linearly with distance from the source. In an experiment in which the waves were contained by a tube Thuras, Jenkins, and O'Neil[1] (1935) confirmed the linear growth of the second harmonic with distance but found a discrepancy as to magnitude. The experimental points lay about 3 db below the theoretical curve. Thuras, et al took tube-wall losses into account by analyzing a phenomenological model of the experiment. For the range of the experimental measurements the losses were very small and in any case not enough to account for the 3-db deviation. Geertsen[2] (1951) repeated the experiment and found no 3-db deviation; his measurements agreed quite well with the theoretical prediction. The work that is described in this paper was undertaken (1) to give a rigorous theoretical analysis of the role played by tube-wall losses, and (2) to add new experimental data so as to try to settle the question of the "missing 3-db".

The goal in the theoretical treatment is to solve the equations of hydrodynamics for plane-wave motion in a viscous, thermally conducting perfect gas contained in a rigid, semi-infinite tube. The boundary conditions are (1) that the variational pressure $p-p_0$ vary as $B \sin \omega t$ at $x = 0$, (2) that there be no source of waves at $x = \infty$, (3) that the tangential component u and the normal component v of particle velocity vanish at the wall $r = a$, and (4) that the variational temperature vanish at $r = a$.

In order to make the problem tractable, it is necessary to introduce some approximations. First we assume that the frequency range and tube radius are such that (1) the tube wall losses, though small, are much more important than the viscosity and heat conduction losses within the main body of the gas, and (2) the tube radius is much larger than the acoustic boundary-layer thickness. Mathematically these assumptions amount to

$$\frac{1}{\sqrt{\delta}} \gg ka \gg \sqrt{\delta} \quad ; \qquad \delta \ll 1$$

where $k = \omega/c_0$, $\delta = k\nu/c_0$, ν is the kinematic viscosity, and c_0 is the small-signal speed of sound under lossless conditions. When the above inequalities hold, the influence of the curvature of the circular tube on the thin boundary layer is so small that the tube may, for mathematical purposes, be approximated by a pair of infinite parallel plates of separation distance a. Finally, we employ a modified version of the approximation procedure outlined by Lighthill in his treatment of plane waves of infinite extent in a viscous, thermally conducting gas[3] and obtain

---

Supported in part by the USAF Office of Scientific Research.

$$P_r^{-1}\delta\nabla^4\phi - \nabla^2\phi_\tau + \phi_{\tau\tau\tau} = -\tfrac{1}{2}(\gamma+1)[\phi_\tau^2]_{\tau\tau} \qquad (1a)$$

$$\delta\nabla^2\psi - \psi_\tau = 0 \qquad (1b)$$

as the equations that must be solved. Here $z = kx$, $\eta = ky$ (y is the coordinate normal to the parallel plates), Pr is the Prandtl number, $\tau = \omega t$, γ = ratio of specific heats, and ϕ and ψ are potentials such that $u = c_0(\phi_z + \psi_\eta)$, $v = c_0(\phi_\eta - \psi_z)$, and $p-p_0 = -\gamma p_0 \phi_\tau$. These equations, despite the seemingly large number of approximations used to derive them, are broad enough to govern a wide range of problems.

Equations (1) are solved by a perturbation method in which $\varepsilon = B/\gamma p_0$ is the small parameter for the series expansions, for example,

$$p-p_0 = \gamma p_0 \left[\varepsilon p^{(1)} + \varepsilon^2 p^{(2)} + \ldots \right] . \qquad (2)$$

It turns out that although the particle velocity varies greatly through the boundary layer, the pressure is very nearly constant over the entire cross-section of the channel. In particular at the wall, where the measurements reported below were taken, the first two pressure components are given by

$$p^{(1)} = e^{-\alpha z}\sin[\tau-(1+\alpha)z] \qquad (3a)$$

$$p^{(2)} = \frac{(\gamma+1)(\sqrt{2}+1)}{8\alpha}\left\{e^{-\sqrt{2}\alpha z}\sin 2\left[\tau-\left(1+\frac{\alpha}{\sqrt{2}}\right)z-\frac{\pi}{8}\right] - e^{-2\alpha z}\sin 2\left[\tau-(1+\alpha)z-\frac{\pi}{8}\right]\right\}, \qquad (3b)$$

where $\alpha = (ka)^{-1}(\delta/2)^{1/2}[1+(\gamma-1)Pr^{-1/2}]$ and only leading terms in δ have been retained. Thus the second harmonic signal is composed of two waves, each with its own damping and dispersion. In the phenomenological approach used by Thuras, et al[1] the effect of dispersion was missing.

Next consider the ratio of the root-mean-square value of the second harmonic to that of the fundamental:

$$\frac{P_2}{P_1} = \frac{(\gamma+1)\varepsilon}{4(2-\sqrt{2})\alpha} e^{-\frac{\alpha z}{\sqrt{2}}}\left[\cosh(2-\sqrt{2})\alpha z - \cos(2-\sqrt{2})\alpha z\right]^{\frac{1}{2}}. \qquad (4)$$

The solid curve in the figure represents Eq. (4) for the case $\alpha = 2.97 \times 10^{-3}$ and $\varepsilon = 3.16 \times 10^{-3}$, which values correspond to the experimental conditions described below. The abscissa is given in units of $\bar{x} = [\tfrac{1}{2}(\gamma+1)k\varepsilon]^{-1}$, which is the distance at which a shock would form if there were no losses; for the value of ε given, $\bar{x} \doteq 94.7$ ft. For small values of $\sigma = x/\bar{x}$ dissipation is almost negligible. The curve approaches the prediction of lossless theory, namely $P_2/P_1 = \tfrac{1}{2}\sigma$. As σ increases, dissipation limits the growth of the second harmonic. Eventually a maximum is reached at $\sigma \doteq 1.6$, at which point the second harmonic is about 9.5 db below the fundamental. If α is maintained constant and ε lowered, σ_{max} and $(P_2/P_1)_{max}$ decrease; if ε is raised, σ_{max} and $(P_2/P_1)_{max}$ increase. In actual practice for the case illustrated higher-order nonlinear effects would cause σ_{max} and $(P_2/P_1)_{max}$ to be less than the values shown.

Some preliminary experimental data are also shown in the figure along with a sketch of the experimental arrangement. The SPL at the first measurement hole was

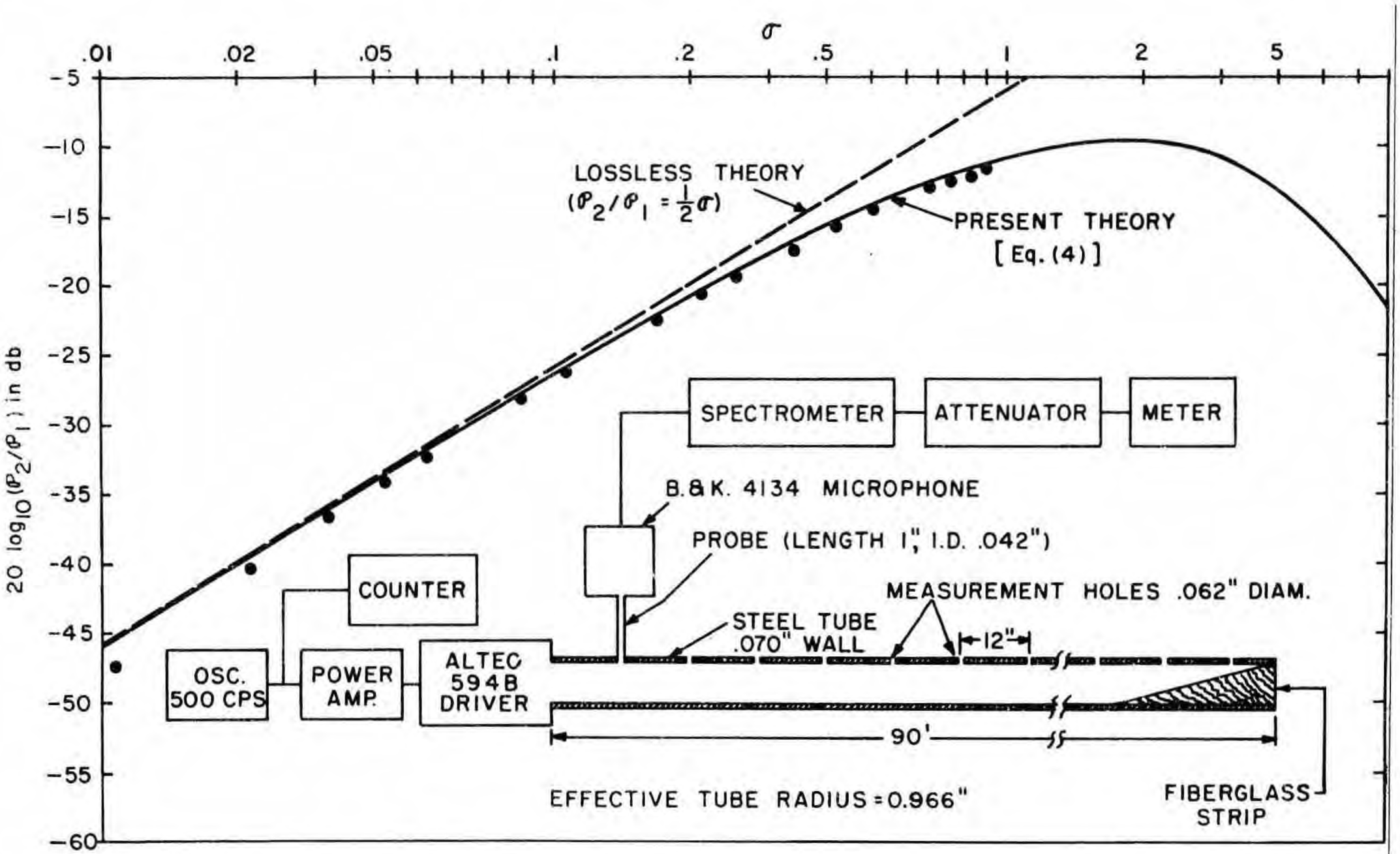
σ
.01
.02
.05
.1
.2
.5
1
2
5
-5
-10
-15
-20
-25
-30
-35
-40
-45
-50
-55
-60
20 log10 (P2/P1) in db
LOSSLESS THEORY
(P2/P1 = 1/2 σ)
PRESENT THEORY
[Eq. (4)]
SPECTROMETER
ATTENUATOR
METER
B.&K. 4134 MICROPHONE
PROBE (LENGTH 1", I.D. .042")
COUNTER
MEASUREMENT HOLES .062" DIAM.
STEEL TUBE
.070" WALL
12"
OSC.
500 CPS
POWER
AMP.
ALTEC
594B
DRIVER
90'
EFFECTIVE TUBE RADIUS = 0.966"
FIBERGLASS
STRIP

143.9 db. Measurement holes not in use were closed with plastic tape. The fibre-glass strip reduced reflections to the point that no standing-wave phenomena were observed for frequencies about 150 c/s. The microphone-probe unit was calibrated against a B. and K. Type 4131 microphone that had previously been calibrated by a coupler reciprocity method.

For the region measured, $\sigma \lesssim 0.9$, the data confirm theoretical predictions and hence agree with the data of Geertsen instead of that of Thuras, et al. Neither of the latter reported measurements for $\sigma >$ 0.43. It is evident that more measurements for high values of σ need to be made.

REFERENCES

1. A. L. Thuras, R. T. Jenkins, and H. T. O'Neil, J. Acoust. Soc. Am. 6, 173 (1935).

2. O. N. Geertsen, Tech. Rep. No. 3, Dept. of Physics, University of California at Los Angeles, May 1951.

3. M. J. Lighthill, Surveys in Mechanics, edited by G. K. Batchelor and R. M. Davies (Cambridge Univ. Press, England, 1956), pp 264-267.

P15

FOURTH INTERNATIONAL CONGRESS ON ACOUSTICS
COPENHAGEN 21.-28. AUGUST 1962

Über die Aufspaltung von Biegeschwingungen bei fehlerhaften Platten

Erich H. K. Müller und Eugen Peetz

Die bekannten Chladnischen Klangfiguren von elastischen Platten, die in Resonanz-Biegeschwingungen versetzt werden, reagieren auf Unregelmäßigkeiten des Plattenmaterials in bezug auf Massenverteilung, Elastizität und Plattengeometrie durch Änderung der Lage und Gestalt der Knotenlinien. Gleichzeitig ändert sich die Eigenfrequenz der Schwingung. Je nach ihrem durch das Knotenlinienbild charakterisierten Typ reagieren die Schwingungen unterschiedlich auf vorhandene Unregelmäßigkeiten. Es ist auch bekannt, daß diese eine Aufspaltung von Resonanzschwingungen zur Folge haben. Theoretisch untersucht sind solche Aufspaltungen bei gleichmäßig gespannten Membranen mit kreisförmiger oder geradliniger Begrenzung unter der Wirkung einer punktförmigen Zusatzmasse[1]. In diesen Fällen spalten die Eigenschwingungen im allgemeinen in je zwei Schwingungen auf, deren Knotenlinienbilder so beschaffen sind, daß die eine Frequenz ein Maximum, die andere ein Minimum wird. Ähnlich verhalten sich schwingende Platten, doch ist in der Literatur wenig von der Aufspaltung, sondern bevorzugt von der Deformation der Knotenlinien und der Änderung von Frequenz und Amplitude die Rede[2-5].

Es wurden Versuche an Platten durchgeführt, um die Aufspaltung der Biegeschwingungen unter dem Einfluß von Materialunregelmäßigkeiten zu untersuchen. Rechteckige Plattengeometrie, einander parallele und rechtwinklige Seiten und konstante Plattendicke sorgten dafür, daß die Messungen nicht durch geometrische Unregelmäßigkeiten verfälscht

---

1) Lord Rayleigh, Theory of Sound, Vol. I (1926), 2nd edit., § 208.
2) A. Kalähne, Handbuch d. Physik, Bd. VIII (1927), Kap. 5.
3) J. Zenneck, Ann. d. Phys., Bd. 67 (1899), S. 165.
4) H.C. Hayes, J.A.S.A., Vol. 8 (1937), S. 220.
5) R.E. Roberson, J. appl. Mech. 1951, S. 280 und S. 349.

wurden. Im Hintergrund stand die Frage, ob man umgekehrt aus der Aufspaltung der Biegeschwingungen auf das Vorhandensein unbekannter Materialfehler schließen und damit eine Methode zur zerstörungsfreien Prüfung solcher Platten gewinnen kann.

Untersucht worden sind Stahlplatten verschiedener Größe bis zu großen Schiffsblechen. Sie wurden an wenigen Stellen symmetrisch zu beiden Hauptachsen gelagert oder eingespannt, kleinere Platten beispielsweise im Schnittpunkt der Hauptachsen zwischen zwei Stempel, größere an den vier Schnittpunkten der Hauptachsen mit den Plattenseiten. Zur Messung wurden einwandfreie, ultraschallgeprüfte Platten und solche mit natürlichen und künstlichen Materialfehlern verwendet. Die Schwingungen wurden mit Tauchspulschwingern, bei kleineren und dünneren Platten auch berührungsfrei mit elektromagnetischen Gebern erzeugt.

Die Untersuchungen bestätigten, daß die Neigung der einzelnen Schwingungstypen zur Aufspaltung bei Materialfehlern sehr unterschiedlich ist. Das Ergebnis vieler Messungen lautet: Die gewünschte Aufspaltung erfolgt regelmäßig nur bei einem bestimmten Schwingungstyp, der Knotenlinien besitzt, die alle parallel zur großen Hauptachse in Längsrichtung der Platte verlaufen. Diese Knotenlinien dürfen von keinen anderen querverlaufenden gekreuzt werden mit einer Ausnahme, nämlich genau am Ort der kleinen Hauptachse. Bild 1 zeigt schematisch einen solchen Schwingungstyp mit drei Knotenlinien in Längsrichtung eines fehlerfreien Bleches. Anstelle von drei kann die Anzahl der Knotenlinien auch zwei, vier, fünf und mehr betragen.

Betrachtet sei eine Platte mit Materialunregelmäßigkeiten, die nicht genau symmetrisch zur kleinen Hauptachse verteilt sind, was für die in der Praxis vorkommenden Fehler in der Regel zutrifft. Eine Schwingung nach Bild 1 läßt sich bei dieser Platte nicht erzeugen. Statt dessen beobachtet man, daß das gesuchte Knotenlinienbild an der kleinen Hauptachse geteilt ist und jeder Teil bei einer anderen Frequenz nur auf der einen oder nur auf der anderen Plattenseite auftritt. Beispielsweise sieht man die gesuchten Knotenlinien bei einer bestimmten Frequenz f_1 nur auf der Plattenseite links von der kleinen Hauptachse gemäß Bild 2a. Sie erstrecken sich dort von der Schmalseite bis etwa zur Plattenmitte, während das Blech auf der anderen Seite gar nicht oder mit andersartigen oder zumindest stark verzerrten Knotenlinien schwingt. Bei einer anderen, von f_1 unterschiedlichen Fre-

quenz f_2 tritt das Knotenlinienbild der gesuchten Schwingung seitenverkehrt auf der gegenüberliegenden Plattenseite und nur dort gemäß Bild 2b auf.

Bei Vorhandensein von Materialfehlern ist somit der ausgewählte Schwingungstyp mit Knotenlinien in Längsrichtung der Platte in zwei Teilschwingungen aufgespalten. Die eine tritt nur auf der einen Plattenseite, die andere bei einer abweichenden Frequenz nur auf der anderen auf.

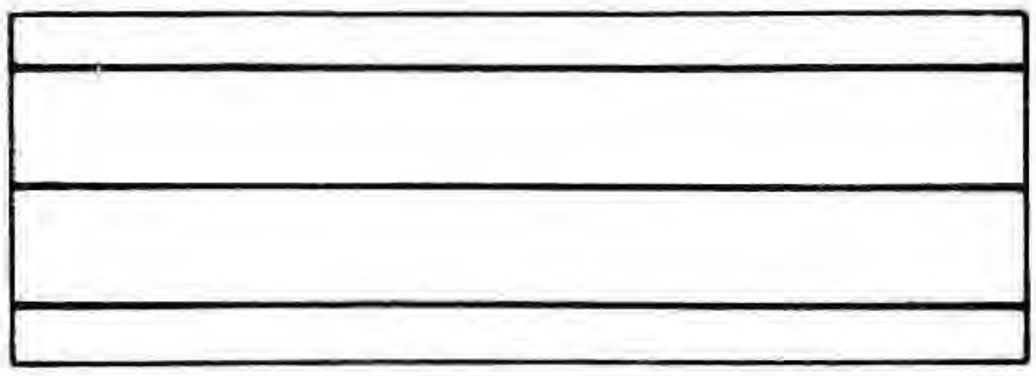

Frequenz f_o

Bild 1. Knotenlinien bei einer fehlerfreien rechteckigen Platte.

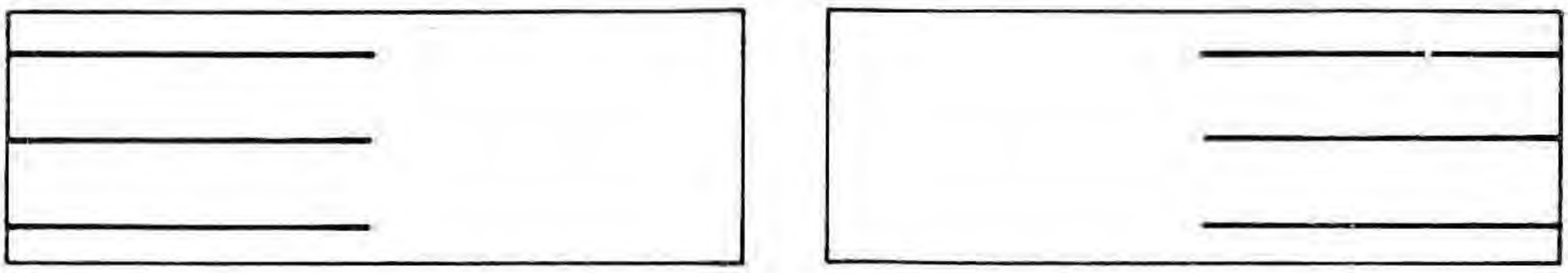

a) Frequenz f_1 b) Frequenz f_2

Bild 2. Aufspaltung der Knotenlinien in zwei Anteile verschiedener Frequenz bei vorhandenen Materialfehlern.

Die relative Frequenzdifferenz ist gering und liegt bei natürlichen Blechfehlern meist zwischen 0,5 und 3 %. Sie hängt außer von der Stärke und Ausdehnung der Unregelmäßigkeiten auch von deren Lage und Verteilung zur kleinen Hauptachse und zu den Knotenlinien ab. Künstliche Bohrungen bei verschiedenen Platten mit von Messung zu Messung wachsendem Durchmesser haben gezeigt, daß die Frequenzdifferenz im allgemeinen mit der Bohrlochgröße zunimmt.

Die halbe Wellenlänge der Schwingung, d.h. der Abstand der Knotenlinien voneinander, darf nicht zu groß oder zu klein im Verhältnis zur Ausdehnung einer Fehlstelle sein, die man durch Aufspaltung der Schwingung nachweisen möchte. Bei großem Knotenlinienabstand werden vorwiegend großflächige Fehler gemessen. Durch richtige Wahl des Knotenlinienabstandes läßt sich somit erreichen, daß sehr kleine Fehlstellen, an deren Nachweis man in der Praxis nicht interessiert ist, keine Aufspaltung bewirken und daher nicht angezeigt werden.

Unsymmetrisch verteilte Materialunregelmäßigkeiten von größenordnungsmäßig bekannter Ausdehnung lassen sich demnach mit Hilfe des genannten Schwingungstyps auf folgende Weisen ausfindig machen: Einmal durch Sichtbarmachung der Knotenlinien und Beobachtung, ob sie nur auf einer Plattenseite gemäß Bild 2a oder Bild 2b auftreten oder nicht, zum anderen in bevorzugter Weise durch Messung der Frequenzdifferenz der ausgewählten Schwingung an beiden Plattenseiten. Dazu ist eine Sichtbarmachung der Knotenlinien nicht unbedingt erforderlich, sofern durch geeignete Schwingeranordnung gewährleistet ist, daß die Schwingung der Platte vom gewünschten Typ ist.

Weiter ist es nach den bisherigen Kenntnissen möglich, die Schwingungen unterschiedlicher Frequenz an beiden Plattenseiten nicht nur zeitlich nacheinander, sondern auch gleichzeitig zu erzeugen. Hingegen lassen sich Fehlstellen nicht lokalisieren.

Weitere Untersuchungen werden gegenwärtig zur Vertiefung der Erkenntnisse und Überprüfung praktischer Anwendungsmöglichkeiten ausgeführt.

G16

FOURTH INTERNATIONAL CONGRESS ON ACOUSTICS
COPENHAGEN 21.-28. AUGUST 1962

Investigations of the directivity pattern of speech-sounds.

Thomas Járfás,
Acoustical Research Group, Budapest, Hungary.

Though the physical aspects and the problem of directivity pattern of human-speech has been investigated by a number of researchers, the studying of directivity patterns of speech-sounds remained a neglected question. Yet the experiments of Trendelenburg (1) and those of Flanagan (2) with the life-size mannequin and transducer are of account. The results of Flanagan refer to sine waves and therefore are hard to applicate for speech-sounds, while Trendelenburg defines only three speech-sounds.

This time we wanted to give an account of our investigations made for repeating and completing those of Trendelenburg, accomplished more than 30 years ago. Our experiments are made with more subjects (test-individuals) and speech-sounds by help of modern instruments, and besides the features of speech-sounds the influence of individual timbre and pronounciation has been studied as well.

The measurements have been carried out according to the definition of directivity pattern. Measuring in the horizontal plain, set across the mouth, the relation was investigated between the absolute value of sound pressure level measured in direction φ (SPL_φ), and the SPL_o, obtained in the axis against the subject ($\varphi = 0$). The two microphons, measuring SPL_φ and SPL_o were set along the arc (line) of a circle of a radius of 100, 75 and 50 cm in course of the experiments. The figures are given for 75 cm distance, this seemed to be most characteristic. We measured generally in 15° steps,but in some cases in $7{,}5^o$ steps too. The directivity patterns were presumed symmetrical, like by Trendelenburg and are given between 0° and 180°.

No exact value of intensity of uttered speech-sounds can be given because of fluctuations in amplitude, but it was about the intensity of normal colloquial speech. Care was taken that the SPL_φ belonging always to the same SPL_o (0 dB) should be read during the measurement of a directivity pattern. The measurements took place in the anechoic room of the Technical University, Budapest, using a pair of microphons, microphon-amplifiers, and vacuum-tube voltmeters.

(Types of Brüel and Kjaer, Radiometer, Orion-EMG). This time only the ready-state period of the radiation characteristics was investigated.

The insufficient absorption for lower frequencies of the anechoic chamber and the fact, that there was no possibility for automatizing the measuring, caused some difficulties.

Some of our characteristic results should be presented, as follows. Fig.1. is an example for the dispersion of measuring. On the horizontal axis the angles from 0° to 180° may be read, on the vertical one the sound pressure in dB. This way of demonstration seemed to be easier to survey than that of a polar diagram. The two curves show the directivity pattern of a man blowing an "a"-pipe (440 Hz) measured and read two times. This method was used instead of making the subject utter a speech-sound for eliminating the effect of subjective articulations. The reason of the differences is in the little deviation of the synchronity of reading the instruments. The average difference is less than 0,5 dB.



Fig.1. Exemple for dispersion of the measuring. Directivity patterns of a male person, blowing an "a"-pipe. (440 Hz). Distance 75 cm.

Fig.2. shows the uttering dispersion of a subject. The directivity pattern of an "ü" is to be seen three times repeated by the same person. It is a typical example for the average dispersion.

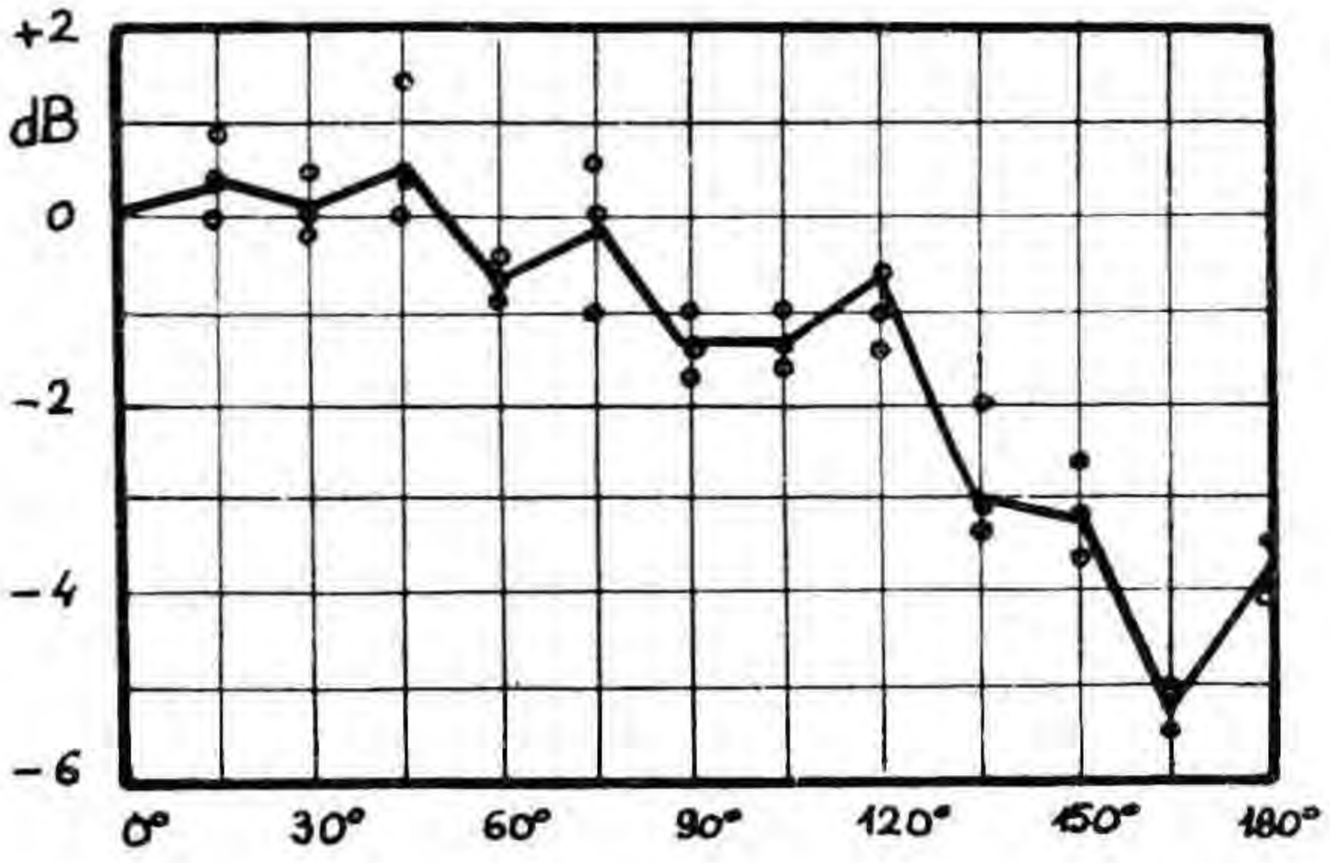

Fig.2. Directivity pattern and dispersion of a speech-sound "ü" uttered by a male person. Distance 75 cm.

It can be explained by the fact, that the way of uttering can't be kept perfectly unchanged during the whole measurement. Using 15° step-adjustments, the subjects have to pronounce every speech-sound for each characteristic 13-times. On account of the decreasing of attentiveness and self control various differences are produced in each direction. The maximal ones are about 1,3 dB.

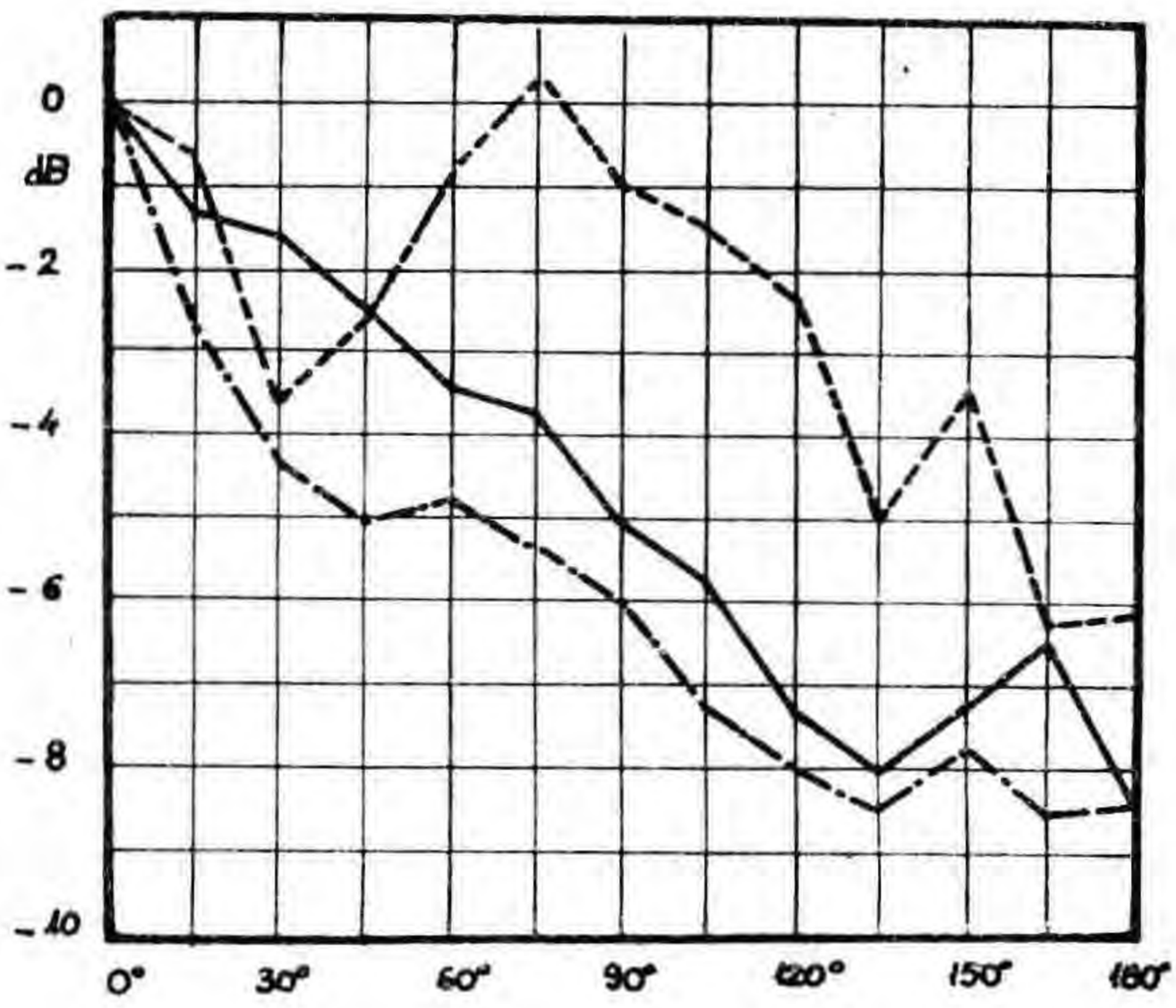

Fig.3. Example for individual influance on the directivity pattern. Curves of three different persons uttering an "ā" (I. female, II. and III. male). Distance 75 cm.

Fig.3. demonstrates the individual influence of the subjects on the directivity pattern. Each curve is averaged from several measuring series. The individual character is formed on one hand by the sound formation (larynx, mouth, cavities, etc.) and on the other hand by the diffraction and absorption of the head and body (geometric form, density of hair, clothes, stc.).

A relation between the directivity pattern of speech-sounds and their first formants is presented in Fig.4. Having made a series (3, 4) of the investigated speech-sounds according to their first formants (n, $\bar{u}$, $\bar{u}$, m; i, $\bar{o}$; $\bar{e}$, $\bar{o}$, å; ε, ā; $\int$, s) we may obtain patterns more and more directed. The human head and body as a complex radiating source has a sharper directivity at higher frequencies. The higher formants have also an effect, but in this case they are not to be taken into consideration, because higher formants radiate only a small part of their energy in the 90°-180° part of directivity pattern. Chief differences are to be found, however, just in this part. The characteristics correspond to the respective results of Dunn and Farnsworth and Flanagan.

The directivity pattern of a speech-sound, as it was shown, is determined by the uttering person and by the speech-sound. The theoretical treatment of the problem would be very interesting, but also most difficult. Researchers couldn't find a right model for represent-

ing the spatial distribution of sound pressure around the head till now (1, 2). The head and body must be considered as a complex radiator, because larynx and chest are radiating as well as mouth and nose. For being able to calculate the radiation velocity distribution should be known. The irregularities of the characteristics, e.g. some maxima greater than 0 dB (Fig.2. and 4.) can be explained also by this way of radiation. Further irregularities like interfering effects can also be seen between 165° and 180°. For giving more precise explanations of above described phenomena, we are going to continue the experiments.

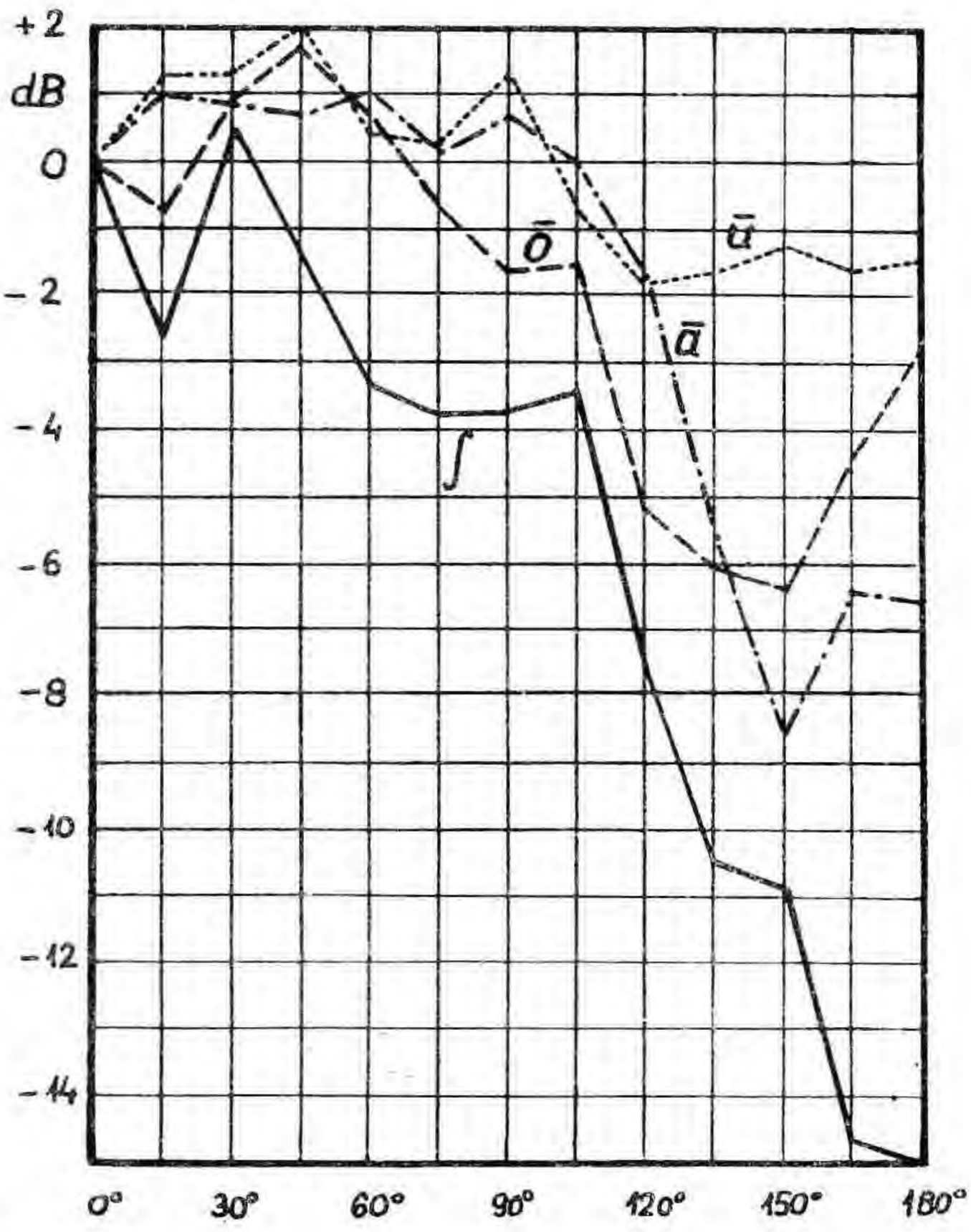

Fig.4. Directivity patterns of speech-sounds "ū", "ō", "ā", "ʃ" of a female person. First formants about 280-380 Hz, 600-800 Hz and 3000-4000 Hz. Distance 75 cm.

Bibliography.

1. F. Trendelenburg: Z. Techn. Physik 1o, 558 (1929).
2. J.L. Flanagan: J. Acoust. Soc. Am. 32, 1613 (1960).
3. T. Tarnóczy: Akust.Z. 8, 22 (1943).
4. T. Tarnóczy: Word 4, 71 (1948).

H16

FOURTH INTERNATIONAL CONGRESS ON ACOUSTICS
COPENHAGEN 21.-28. AUGUST 1962

FREQUENCY DISCRIMINATION OF THE HUMAN EAR

B.LOPES CARDOZO

INSTITUUT VOOR PERCEPTIE ONDERZOEK

- EINDHOVEN - NETHERLANDS -

INTRODUCTION

E.Mach (Lotos, 1873) reported that a 128 cps tone has to last at least some 35 msec in order to bring about a pitch sensation. The effect of the duration Δt of a sinusoid on pitch quality has been explored more extensively in this century, notably by Doughty and Garner (J.Exp.Psych., 1947) who found that sinusoid pulses of only a few milliseconds lack 'tone pitch', but can still be attributed to 'click pitch'. Von Békésy (Physik. Zeits., 1929) made more quantitative measurements. He found the j.n.d. Δf for frequency in pulsed sinusoids (at f = 800 cps) to be nearly constant at $\Delta f = 0.003f$ for $\Delta t > 0.25$ sec and an increase of Δf for $\Delta t < 0.25$ sec. These measurements have later been extended by other investigators, e.g. by Oetinger (Acustica, 1959) and by Liang Chih-an and Chistovitch (Sov.Physics, Acoustics, 1960). Similar measurements have also been made at the Institute for Perception Research, Eindhoven.

THE J.N.D. FOR FREQUENCY IN TONE PULSES WITHOUT NOISE.

Working mainly with two trained subjects it was found, that smaller Δf values can be obtained by gating the sinusoid in the axis crossings, rather than in a random phase. An acceptable acoustic representation of the signal can be obtained in this way, as illustrated in fig. 1.

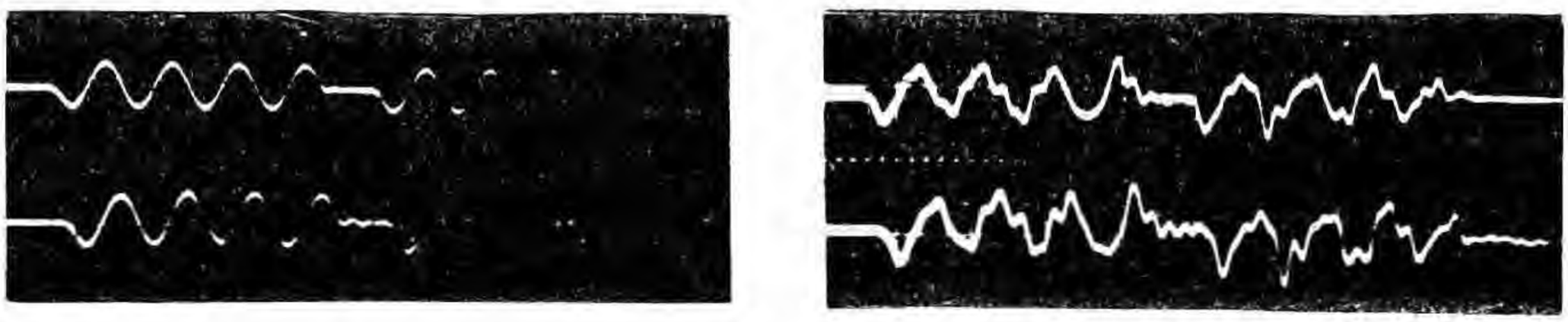

Fig.1. Two pairs of sinusoid pulses, right with noise (d = 12) left without noise ($d = \infty$). The upper traces show the voltage, the lower ones the acoustic reproduction of the electric signal as measured by inserting a condensor microphone into the P.D.R.-10 headphone cushion. The sinusoids have frequencies of 1000 cps and a duration of about 4 msec. For longer tone pulses, the acoustic signal is a slightly better replica of the electric one. In shorter tone pulses, however, the acoustic signal tends to continue longer than the electric one. The interval between two pulses of a pair (normally 0.1 sec) was taken slightly less than 1 msec for the sake of this illustration. The frequency difference between two members of a pair was 'just noticable'.

The subject was presented binaurally at 30-50 dB sensation level with two tone pulses of equal amplitude and of equal number 2^n ($n = 0,1,....,10$) of periods, differing by an amount of Δf cps in frequency (controlled to the nearest 0.1 cps). The interval between these two pulses was 0.1 sec. The interval between two pairs of pulses was long. A ready way of measuring the j.n.d. in this situation would be to apply the method of adjustment, in which the subject himself tries to set $\Delta f = 0$. The residual error is then taken to be a measure of the j.n.d. After considerable effort with this and kindred methods, it had to be discarded, partly because the results showed contamination due to the subject's anticipation, partly because in this method the amount of information which the subject has at his disposal is ill-defined.

Results to be reported in this paper have all been obtained with the more laborious AX-method, which is free from anticipation and has the important feature that every single response is based on just one stimulus presentation. It proved to be possible to reduce the number of trials to about 200 per j.n.d. by sampling sequentially and by choosing the trial values of Δf according to the up-and-down method. The Δf values obtained in this way correspond to the 0.70 correct response level, chance successes (amounting to 0.50) included. In this scale the standard deviation due to the fluctuations both in the sampling method and in the subject is about 0.10, which, by rule of thumb is equivalent to a factor 1.5 to 2 in Δf. Results are shown in fig.2. The full line represents the average of two subjects.

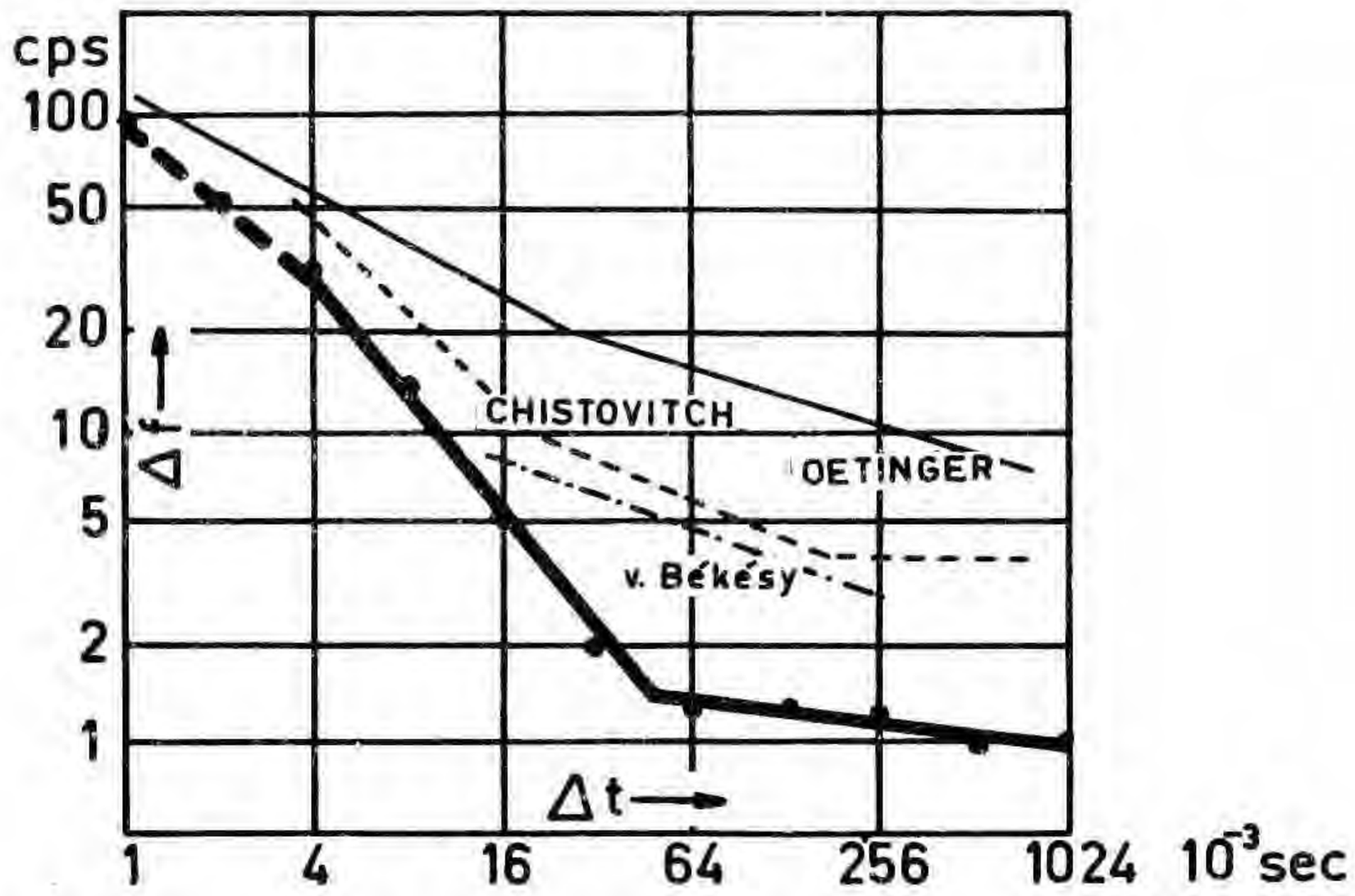

Fig. 2. The j.n.d. for frequency Δf as a function of the duration of a tone pulse on a double logarithmic scale. Broken lines show the results obtained by investigators making use of relay-gated sinusoids. The upper line represents results obtained with sinusoid pulses having a Gaussian envelope. The heavy full line shows the j.n.d. averaged over two subjects.

Results of other investigators are also given for comparison. These results indicate that the j.n.d. for $f = 1000$ cps and $\Delta t > 0.05$ sec is nearly constant at $\Delta f = 0.001\ f$. For $\Delta t < 0.05$ sec, the j.n.d. can approximately be described by

$$\Delta f . \Delta t = c \qquad (1)$$

For $f = 1000$ cps the value of the constant c is of the order of 0.05, differing by a factor 2 between subjects.

It is convenient to introduce the 'uncertainty product' $\psi \equiv \Delta f . \Delta t$
A value of the uncertainty product as small as $\psi = 0.05$ seems to call for comment. Suppose one had to build a physical instrument of equal accuracy and of equally quick response. One type of instrument would consist of a bank of low-Q filters with an additional discriminating network localizing the maximal response. Not counting the possibility of interpolation, these filters would have to show a 1 cps spacing near f = 1000 cps. As the sinusoids become shorter, their spectrum widens and gets flatter. The discriminating network could be described by the requirement that a difference ΔI in energy between two adjacent filters must be estimated correctly (in (0.70 - 0.50).2 = 0.40 of the cases) provided $\Delta I \geq 0.01$ I, I being the energy absorbed in either filter. This instrument would then behave as indicated by the full line in fig. 2.

An alternative instrumentation would be to measure the time interval between successive tops or zeros of the sinusoid, or, for better accuracy, the average over the number of periods contained in 0.05 sec. With a 50 μ sec. clock pulse the instrument would than again behave similarly.

FREQUENCY DISCRIMINATION IN TONE PULS S WITH NOISE

By adding Gaussian white noise to the sinusoids, a situation is created in which ψ is no longer determined solely by the technical implementation of an instrument. In this case the signal-to-noise ratio sets an ultimate lower bound to the frequency discrimination. In the rest of this paper an attempt will be made to express the frequency discrimination of the human ear in terms of this absolute lower bound, borrowing from statistical decision theory.
An ideal frequency discriminator (I.F.D.) is introduced being a conceptual instrument which is supposed to make the best possible use of all the information present both apriori and in the noise corrupted signal, thus attaining the absolute lower bound to ψ .

C.W.Helstrom (Proc.I.R.E.,1955) has computed along this line the behaviour of the I.F.D. in a situation where two, mutually exclusive, sinusoid pulses of known frequencies f and f+Δf may start with equal apriori probability at a known epoch in a known phase. The pulses are thought to be embedded in white Gaussian noise of spectral power density N, the bandwidth of which is large compared to $1/\Delta t$. The pulses have equal energies E and their cross-correlation is

$$\lambda = (2/\Delta t)\int_0^{\Delta t} \sin 2\pi f u . \sin 2\pi (f+\Delta f)u . du \qquad (2)$$

The probability P of a correct decision by the I.F.D. is then given by

$$P = 0.5 + 0.5\ \mathrm{erf}\left[(d\sqrt{1-\lambda})/2\right] \qquad (3)$$

with $d = \sqrt{2E/N}$, the signal-to-noise figure.

Standardizing P at 0.70 as in the experiment, we obtain

$$d\sqrt{1-\lambda} = 0.74 \qquad (4)$$

In the experiment a noise band 0 - 4000 cps was used which is fairly large compared to $1/\Delta t$. In the experiment the sinusoid energies E would differ slightly, being inversely proportional to 1/f. A check was made, however, that this difference, which was 6 percent or 1/2 dB at most, provided no clue to the observer. The epoch of the sinusoid was, in the experimental situation, clearly and unequivocally marked to the subject by gating the sinusoid and the noise simultaneously.

It therefore appears admissable to compare the human performance with that of the I.F.D. as given by (4). The cross-correlation may be approximated by

$$\lambda = (\sin 2\pi\psi)/2\pi\psi \qquad \text{since } \Delta f \ll f \qquad (5)$$

Putting, with small error for $2\pi\psi < 1$,

$$\sqrt{1-\lambda} = 2\pi\psi \qquad (6)$$

we find the lower bound to be

$$\psi = 0.12/d \qquad \text{for} \qquad 2\pi\psi < 1 \qquad (7)$$

Thus the j.n.d. Δf of the I.F.D. is found to be inversely proportional to the product of duration of the sinusoid and the signal-to-noise figure. It may be remarked that for $\psi \gg 2\pi$, the cross-correlation is virtually zero and the I.F.D. acts as a signal detector rather than as a discriminator. The probability of a correct decision by the I.F.D. will then no longer depend on Δf, but on d only. In fig. 3 the dotted lines show the absolute lower bound to Δf as a function of Δt with the signal-to-noise figure d as a parameter. Full lines represent Δf values obtained by one human observer under comparable conditions. Fig. 4 contains the results of another subject in a similar representation. Although a full discussion is preserved for the congress meeting, it may be remarked that the human frequency discrimination power falls behind that of the I.F.D. by about 1 order of magnitude in the most favourable conditions.

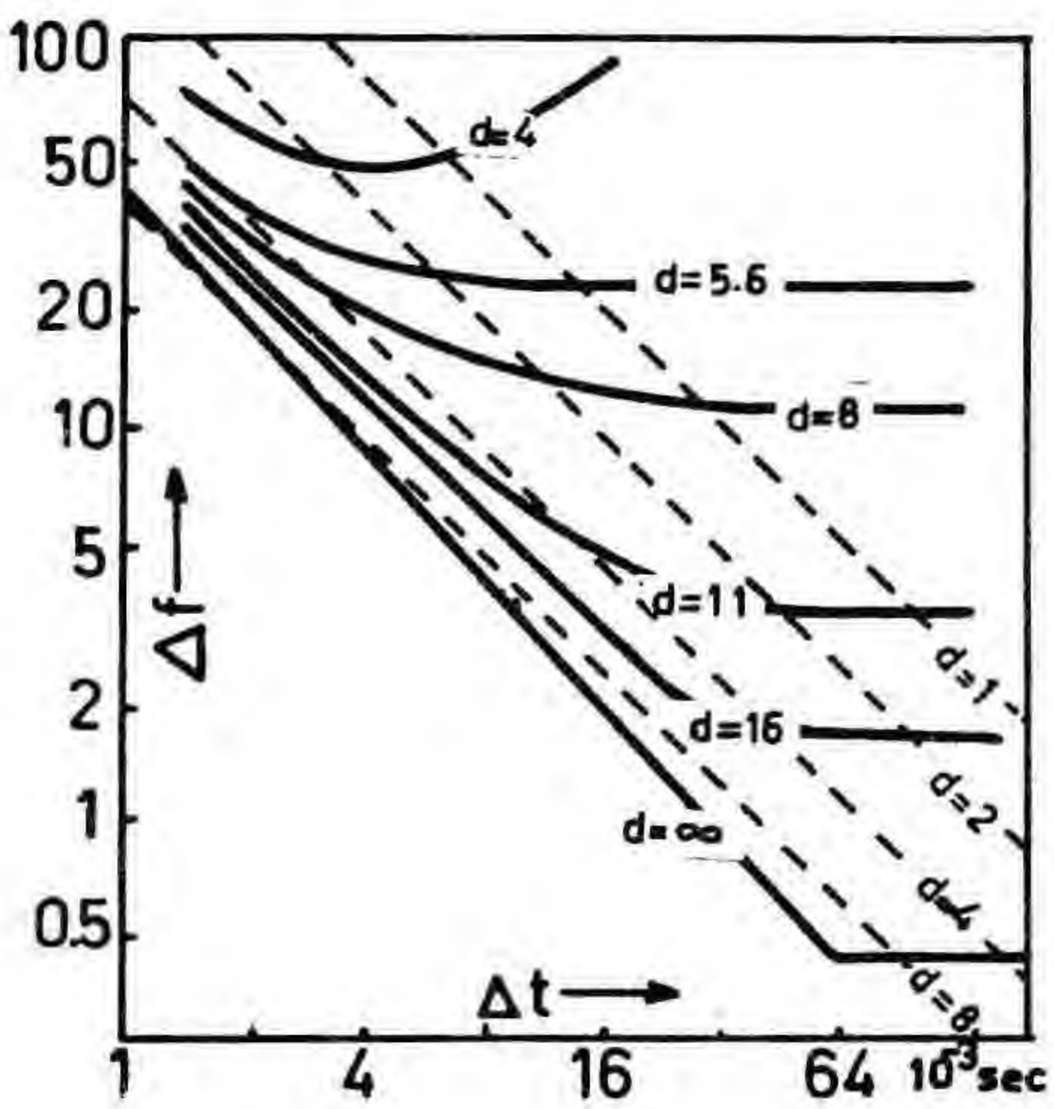

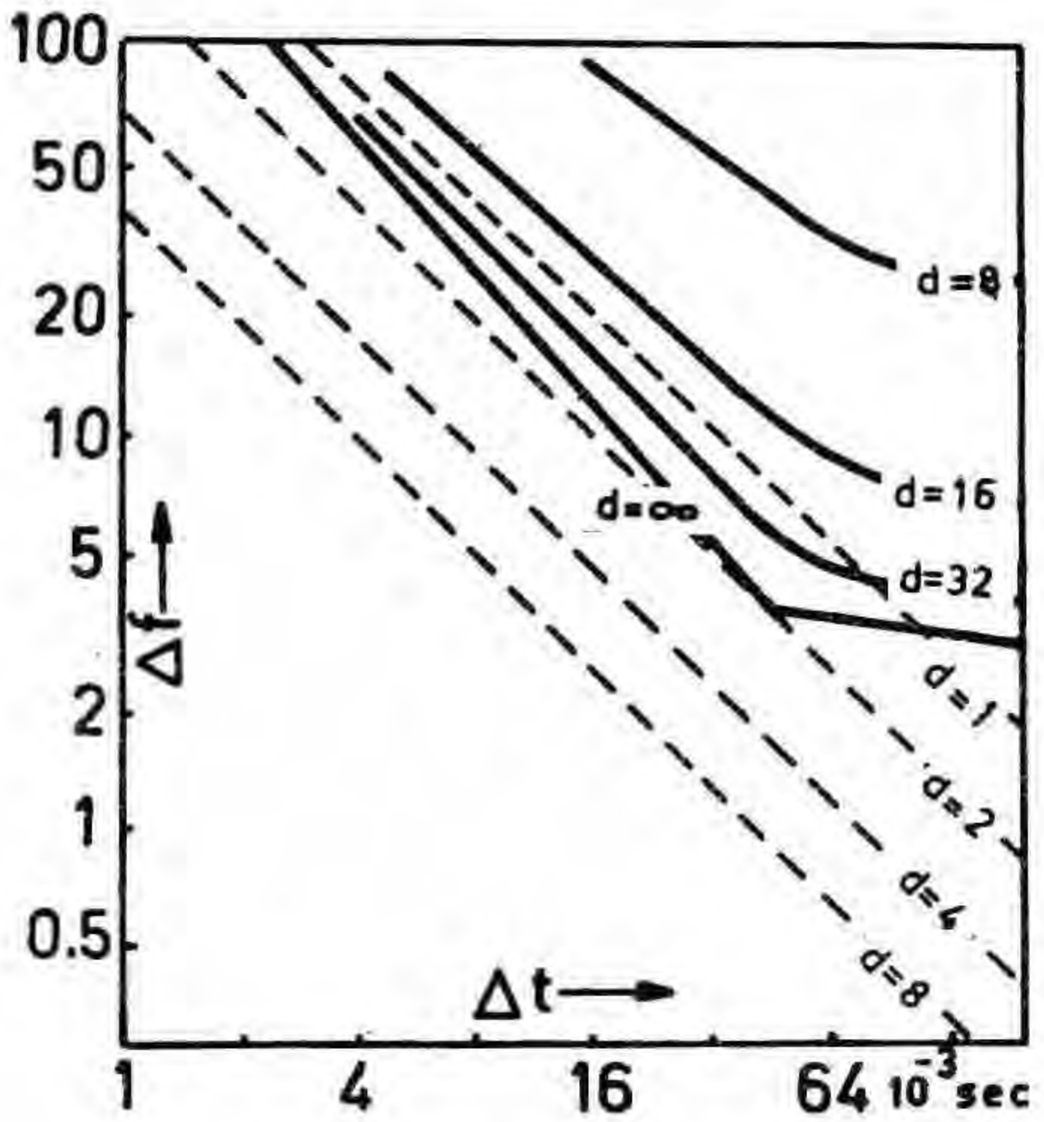

Figs. 3 and 4 showing the j.n.d. f as a function of the duration t with the signal-to-noise figure d as a parameter for two subjects respectively. Broken lines represent the behaviour of the ideal frequency discriminator in the same way.

K16

FOURTH INTERNATIONAL CONGRESS ON ACOUSTICS
COPENHAGEN 21.-28. AUGUST 1962

THE ULTRASONIC TRAVELLING WAVE AMPLIFIER

D. L. White, Bell Telephone Laboratories, Incorporated
Whippany, New Jersey

Theory of Ultrasonic Amplification--An ultrasonic wave travelling in certain directions in a piezoelectric semiconducting crystal is accompanied by an alternating electric field and current. Since the current produces joule heating, the ultrasonic wave is attenuated[1]. When a direct current flows through the crystal and the electron drift velocity exceeds the velocity of sound, it is possible to invert the loss mechanism and make the ultrasonic wave grow in amplitude[2].

To calculate the propagation constants for an ultrasonic wave in an n-type semiconductor we start with the piezoelectric equations of state for the stress, T, and the electric displacement, D. They are $T=cS - eE$ and $D=eS + E$, where c is the elastic constant, e the piezoelectric constant, ε the electric permittivity and E the electric field. For plane waves the strain, S, may be written as $\partial u/\partial x$ where u is the mechanical displacement of the medium. Of particular interest are crystals with a wurtzite structure (such as CdS, CdSe and ZnO) and those with a zinc blende structure (such as GaAs). If we consider only waves shown in the chart below, all the important quantities in the equations are scalar.

Structure	Wave	Propagation Direction	Particle Motion	Elastic Constant	Piezoelectric Constant
Wurtzite	Longitudinal	c-axis	c-axis	c_{33}	e_{33}
Wurtzite	Shear	$\perp$ c-axis	c-axis	c_{44}	e_{15}
Zinc Blende	Longitudinal	{111}	{111}	$(c_{11}+2c_{12}+4c_{44})/3$	$2e_{14}/\sqrt{3}$
Zinc Blende	Shear	{110}	{001}	c_{44}	e_{14}

The elastic wave equation and Gauss's equation in a piezoelectric medium are

$\frac{\partial T}{\partial x} = \rho \frac{\partial^2 u}{\partial t^2} = c \frac{\partial^2 u}{\partial x^2} - \frac{\partial E}{\partial x}$ and $\frac{\partial D}{\partial x} = e \frac{\partial^2 u}{\partial x^2} + \frac{\partial E}{\partial x} = -qn_1$ where $-q$ is the electron charge and $-qn_1$ is the space charge and ρ is the mass density. The current density is $J = q\mu nE - q\mathcal{D}\,\partial n/\partial x$ where the electron density is $n = n_o + n_1 e^{j(kx-\omega t)}$, n_o being the equilibrium electron density and n_1 the electron bunching due to the presence of the ultrasonic wave, and $E = E_{dc} + E_1 e^{j(kx-\omega t)}$, E_{dc} being the applied field and E_1 the internal a.c. field. The electron mobility is μ and the diffusion constant is. . The propagation constant is $k = j\alpha + \omega/v$ where α is the attenuation and v the phase velocity. With the help of the continuity equation, $\partial J/\partial x - q\partial n/\partial t = 0$, we have enough equations to calculate the attenuation and the velocity. Assuming $\alpha \ll \omega/v$ we have

$$\alpha = \frac{e^2}{2\varepsilon c}\,\frac{\omega_c}{v_s}\,\frac{\gamma}{\gamma^2 + \left(\frac{\omega_c}{\omega} + \frac{\omega}{\omega_D}\right)^2} \qquad v = v_s\left[1 + \frac{e^2}{2\varepsilon c}\,\frac{\gamma^2 + \frac{\omega_c}{\omega_D} + \frac{\omega^2}{\omega_c\omega_D}}{\gamma^2 + \left(\frac{\omega_c}{\omega} + \frac{\omega}{\omega_D}\right)^2}\right]$$

where $v_s = \sqrt{c/\rho}$ is the velocity of sound when there is no piezoelectricity, $\gamma = 1+\mu E_{dc}/v_s$, $\omega_c = \frac{\sigma}{\varepsilon}$, $\sigma = n_o q\mu$ is the conductivity, and $\omega_D = v_s^2/\mathcal{D}$ is called the diffusion frequency. If the electron bunching is calculated from the Boltzmann transport equation instead of from the J used above it can be shown that the diffusion frequency is one third as high as the value shown. Otherwise both derivations give the same formulae. If the electron drift velocity, $-\mu E_{dc}$, exceeds the velocity of sound, the attenuation is negative, i.e. the wave grows in amplitude as it travels through the crystal. The gain can be very large. For instance if $e^2/\varepsilon c = 0.03$, the amplitude of the ultrasonic wave may gain four percent or about 0.35 db per wave length. Calculated curves of α and velocity are shown in figures 1 and 2 as a function of the ratio of electron drift velocity, v_d, to the velocity of sound, v_s. The concentration, mobility and diffusion constant of the electrons and the piezoelectric coupling of the medium can be calculated by expimentally fitting the curves. If both electrons and holes are present, these same quantities can be calculated for both carriers. Figure 3 shows gain and attenuation for a case where both electrons and holes are present.

Experiments--The most quantitative experiments have been performed in the frequency range of 10 to 50 mc with CdS and CdSe. Since these crystals are photoconductive, the conductivity was controlled by illumination. In the experiments a d.c. pulse, which could be as much as several thousand volts, was applied across the crystal. A pulse was used to prevent spontaneous oscillation and undue heating. During the time the voltage was applied a short burst of ultrasonic energy was transmitted through the crystal. Figures 4, 5 and 6 show loss and gain as a function of electric field in CdS and CdSe in the 15 mc range. In general the maximum gain was not as great as the maximum loss. The most gain observed was 57 db for 45 mc shear waves in a 1.2 cm bar of CdSe. The piezoelectric coupling, as determined from the magnitude of the loss, and the mobility, as determined by the field required for zero loss, are in fair agreement with values obtained by other means.

Effects of Inhomogenities--If the resistivity varies throughout the bulk of the crystal, experimental observations gives an average α, not the true α of the material. Figure 7 shows calculated loss and gain α for crystals having the same resistance but different resistivity distributions along the length. Other reasonable resistivity gradients give similar results. The experimental curves more closely fit the calculated curves of figure 7 than those of figure 1. Therefore before modifying the theory to obtain a better fit with experimental data, it seems prudent to first study the material used. To check for resistivity inhomogenities, the voltage was measured over the surface by a probe. The electric field in samples which were believed to be high quality was often found to vary by a factor of two. As a further check a very short d.c. pulse, a quarter or half of a microsecond, was applied across the crystal while an ultrasonic wave was passing through. The ultrasonic wave in various parts of the crystal were then amplified or attenuated by an amount characteristic of the resistivity and field at that particular point in the crystal. An oscilloscope trace of a typical output pulse is shown in figure 8. Only the middle part of the long pulse, from two to eight microseconds, has been amplified. The leading edge of the amplified portion corresponding to the end of the crystal near the output transducer underwent more gain than the trailing edge. As a further refinement the output transducer has been split into several smaller transducers. Thus the rays passing through various parts of the crystal could be observed separately. By studying the amplitude of the output as a function of the driving current, it is possible, in principle, to determine the resistivity and mobility point by point throughout the bulk of the crystal.

Non Linear Effects--In the theory presented above only terms involving the driving frequency were considered. If higher order terms are included, the harmonic power, the direct current from phonon drag, and the saturation in the gain of the fundamental frequency can all be calculated. The small signal theory assumes the electron bunching is small compared to the average electron concentration in the conduction band, i.e. $n_1 \ll n_0$. This is true if $\mu^2 e^2 S^2 \ll \gamma^2 + (\omega_c/\omega + \omega/\omega_D)^2$. For CdS the strain should usually be much less than 3×10^{-5}. In amplifiers with large gain care must be taken to keep the output strain below this value or else the gain will saturate. If a resistor, R, is placed across the ends of the crystal, the d.c. voltage developed is $V = \frac{Rc\mu}{\sigma} (e^{-2\alpha L} - 1)(R + R_C)^{-1} S^2$ where R_C is the resistance of the crystal and L is its length. As an example at 15 mc an ultrasonic wave with a strain of 10^{-6} can produce several volts across a two millimeter thick piece of 10,000 ohm cm material. With quiet amplifiers it should be possible to detect strains thousands of times smaller. The d.c. output of ultrasonic waves has been detected up to frequencies of 900 mc. The theory indicates an ultrasonic wave will produce direct current at any frequency where $\alpha \neq 0$. Hence this detection method should work at microwave frequencies. Since this is a bulk property of the material, the faces of the sample do not need to be parallel to the incoming wave front. At high frequencies, where conventional transducers must be extremely parallel, this is a great experimental convenience. If the ultrasonic wave is amplified as it passes through the semiconductor, the d.c. output is also amplified. Thus an ultrasonic amplifier can both amplify and detect weak ultrasonic signals. Since this is a square law detector amplitude modulation on the ultrasonic wave is distorted, but digital information can be easily handled.

Applications--The ultrasonic amplifier should find applications in a number of varied fields. In semiconductor physics it can be used to examine the electrical properties of the material. As a tool in ultrasonics, especially at very high frequencies, intense ultrasonic waves can be produced and weak waves detected. Device applications, particularly under 1000 mc where it should be capable of operating continuously without destructive heating, include low loss wide band ultrasonic delay lines and possibly amplification of electrical signals.

REFERENCES

1. J. J. Kyame, J. Acoust, Soc. Am., 26, p. 990 (1954).
A. R. Hutson and D. L. White, J. App. Phys., 33, p. 40 (1962).

2. A. R. Hutson, J. H. McFee, D. L. White, Phys. Rev. Letters, 7, p. 237 (1961).
D. L. White, to be published J. App. Phys., 33, July, 1962.

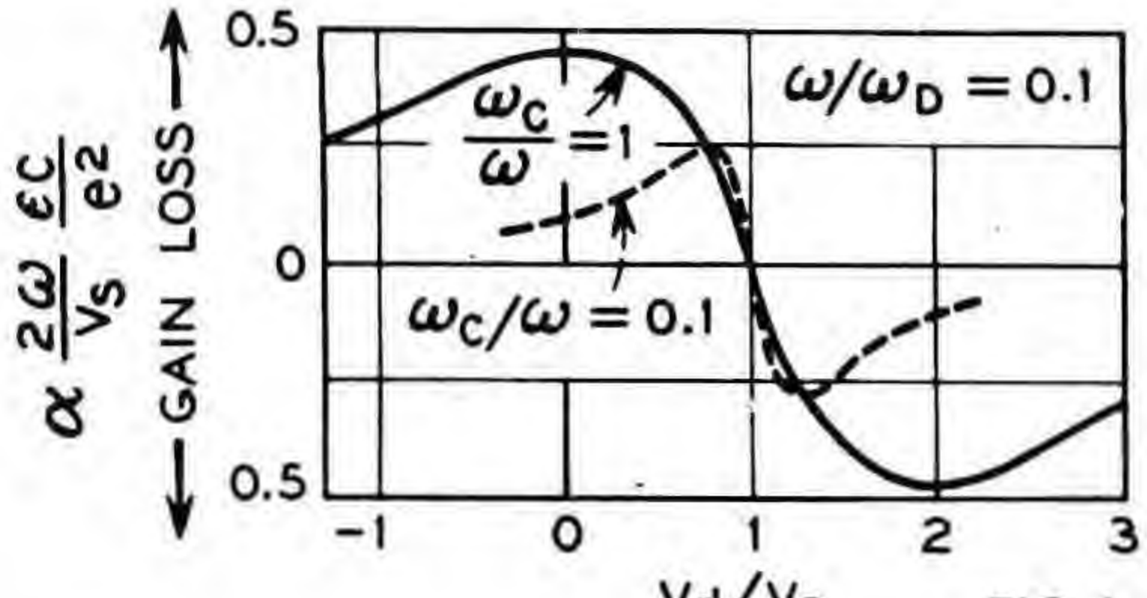

FIG. 1

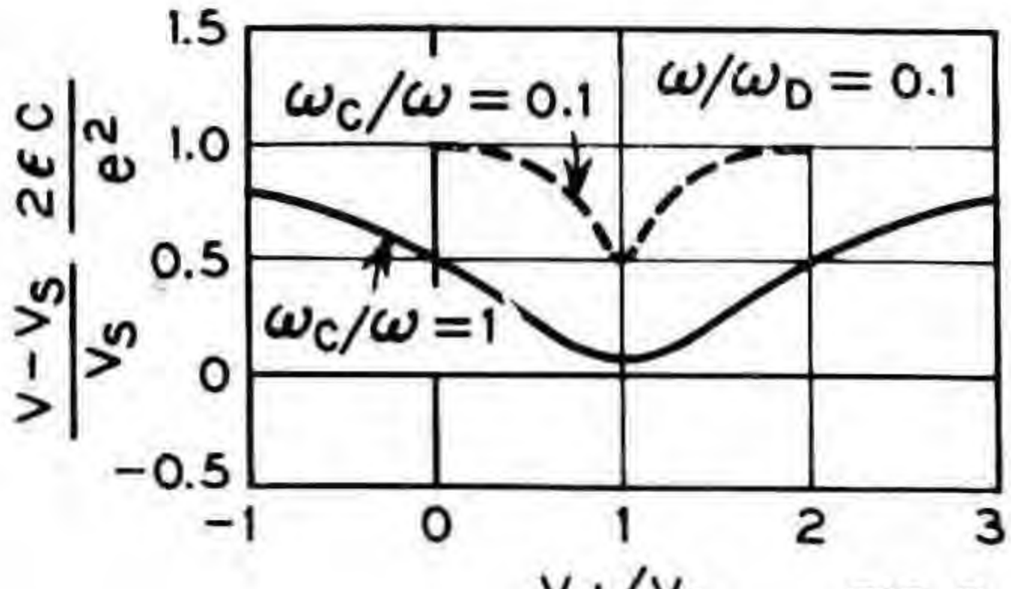

FIG. 2

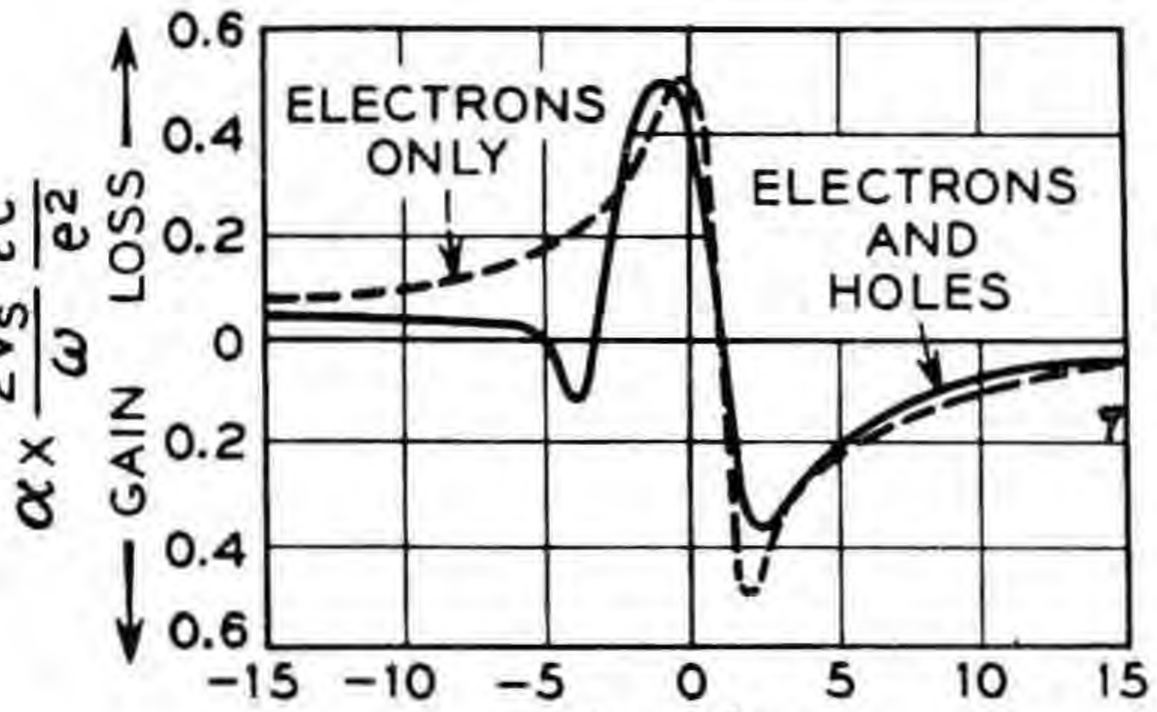

FIG. 3

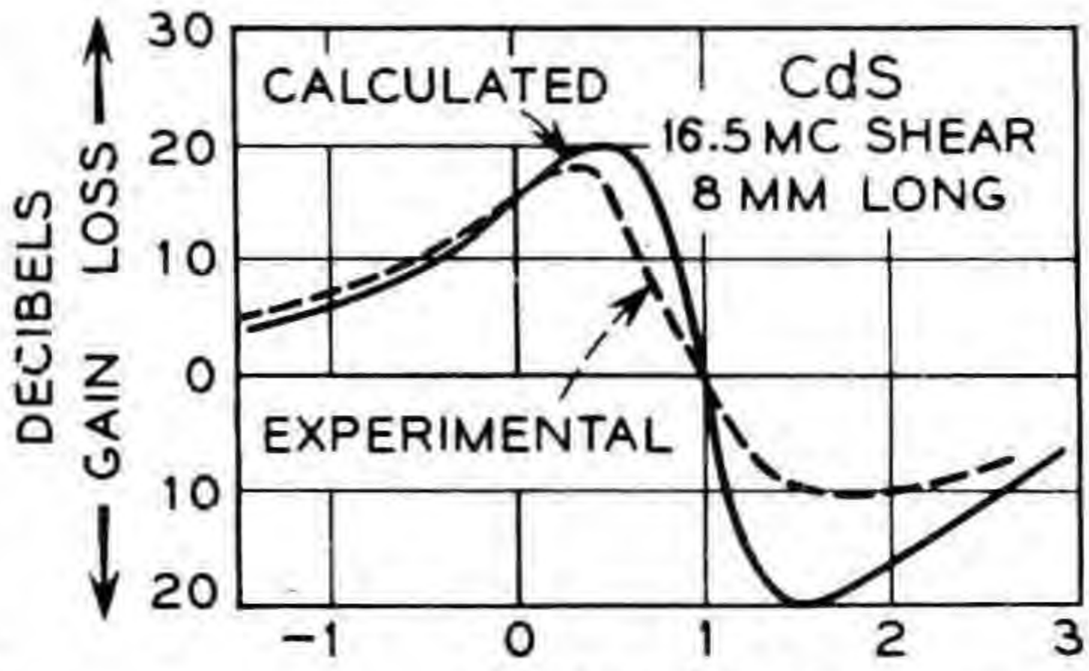

FIG. 4

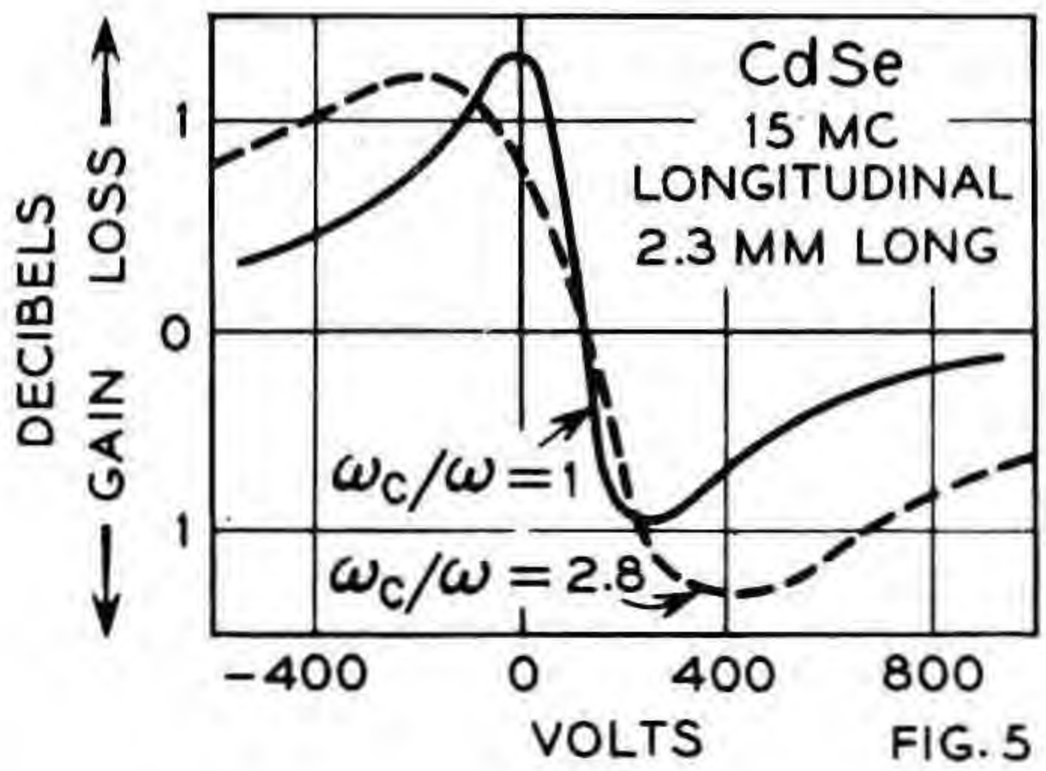

FIG. 5

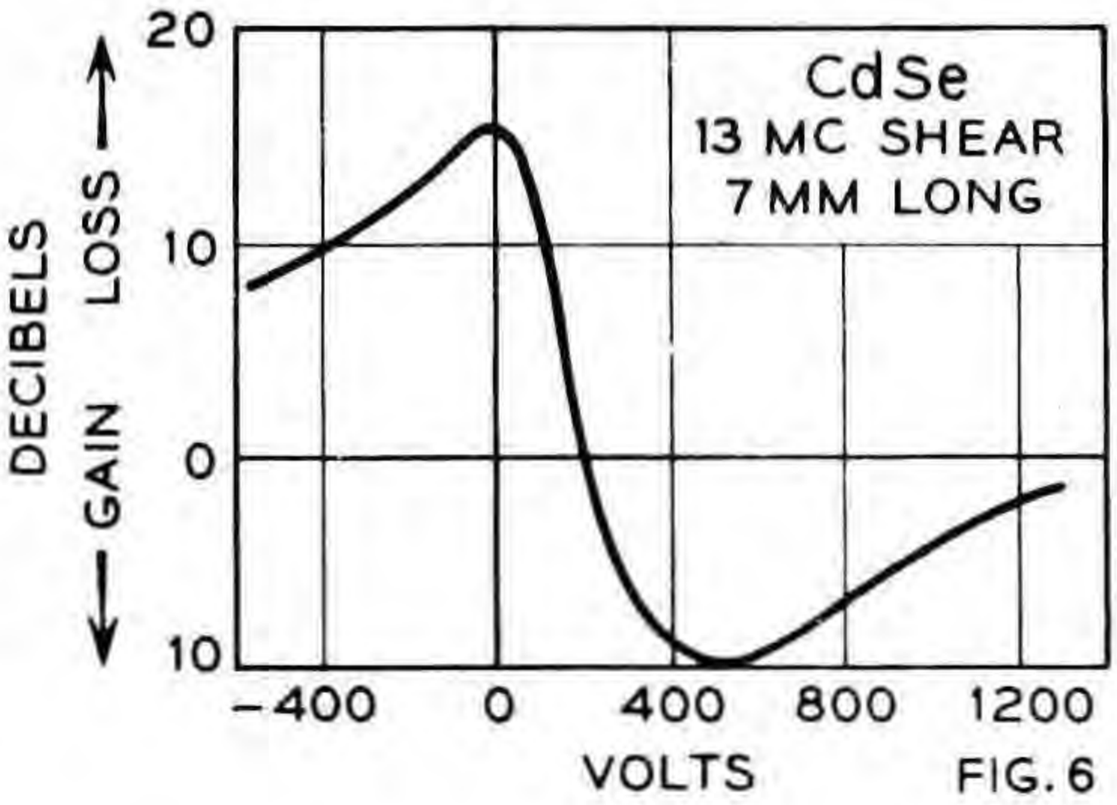

FIG. 6

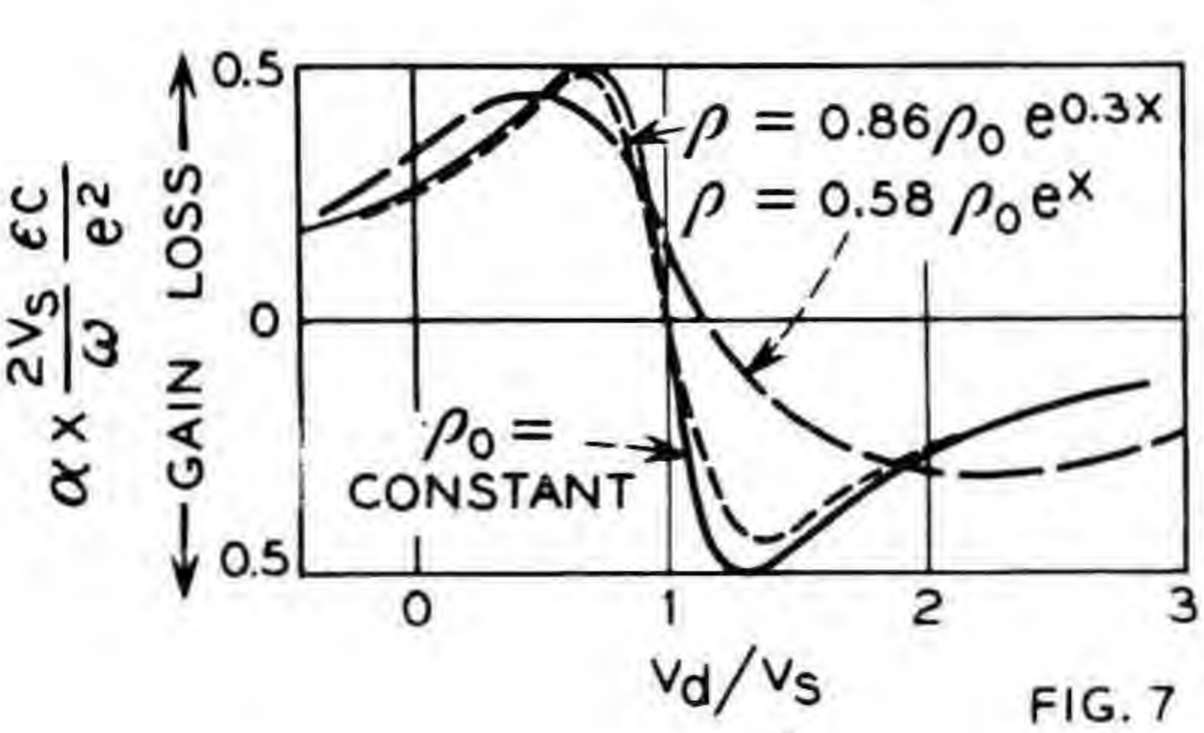

FIG. 7

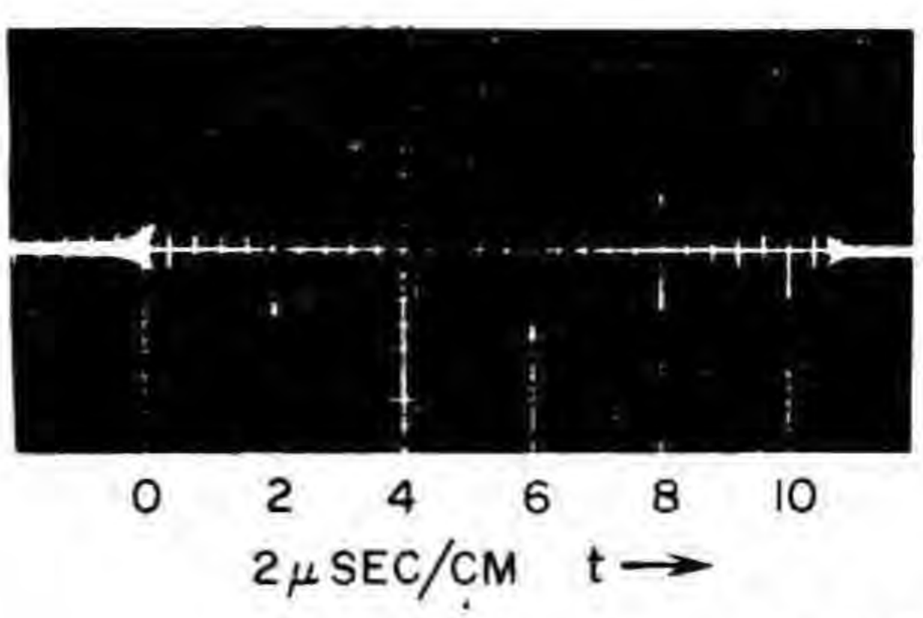

FIG. 8

L16

FOURTH INTERNATIONAL CONGRESS ON ACOUSTICS
COPENHAGEN 21.-28. AUGUST 1962

Beurteilung von Lärmbelästigungen durch Bezug auf den Störpegel.

Prof. Dr.Ing. Friedrich Bruckmayer, Leiter der Staatlichen Versuchsanstalt für Wärme- und Schalltechnik in Wien.

1. Störung und Grenze der zumutbaren Störung

Zur Beurteilung von Lärmbelästigungen vor oder in Wohnhäusern hat sich der Bezug des gemessenen Lärmpegels auf den gleichzeitig gemessenen Störpegel (background noise level) bewährt (1).

Ist der Lärm vom Störpegel verdeckt, so ist er unhörbar (2). Erhebt er sich stärker über den Störpegel, so wird er störend; die "Grenze der zumutbaren Störung" liegt bei einer Erhebung um 10 dB. Diese Festlegung ist in ÖNORM B 8115 und für spezielle Fälle auch in einem ISO Draft Secretariat Proposal enthalten.

Der Störpegel ist der geringste an einem Ort zu einer bestimmten Zeit gemessene Schallpegel, der durch entfernte Geräusche, wie Verkehr, verursacht ist und bei dessen Empfinden Ruhe zu herrschen scheint.

Bild 1a zeigt, aus einer Schallpegelregistrierung in einer städtischen Hauptverkehrsstraße, den Störpegel um 1 Uhr nachts mit 46 dB(A), die Lärmspitzen sind von vorbeifahrenden Kraftfahrzeugen verursacht.

2. Erfassung des Ort- und Zeiteinflusses auf die Störung

Die Störpegelmessung ergibt einfach diese Einflüsse, sei es z.B. die trotz gleichem Lärmpegel ganz verschiedene Störung in einem straßen- bzw. hofseitigen Zimmer derselben Wohnung, sei es die auch ganz verschiedene Störung bei Tag bzw. bei Nacht. Es erscheint unmöglich, den Ort- und Zeiteinfluß etwa durch feste Korrekturen zu einer Beurteilungsmethode mit festen Grenzkurven genügend genau zu erfassen.

Der Lärm und der Störpegel (bei abgestellter Lärmquelle) sind jedenfalls bei offenen Fenstern zu messen, wenn der zu beurteilende Lärm als Luftschall von außen kommt, bzw. jedenfalls bei geschlossenen Fenstern, wenn er als Körperschall durch die festen Bauteile eindringt.

Beim Schließen von Doppelfenstern nimmt der Störpegel im groben Durchschnitt um 15 dB ab.

Richtwerte für die Störpegelhöhe nach Lage und Tageszeit sind folgende (die Richtwerte für die "Grenze der zumutbaren Störung" liegen um 10 dB höher):

in ruhiger Lage (Wohngebiet, Dorf), im Raum:[1]		tags 25,	nachts 15 dB(A)
	" Freien:	" 40, "	30 "
in verkehrsreicher Lage (Stadtgebiet)[2], im Raum:[1]		" 35, "	25 "
	" Freien:	" 50, "	40 "

1) Bei geschlossenen Doppelfenstern
2) Bei Lage in geschlossenem Hof gelten die vorhergehenden Angaben

3. Zergliederung des Störpegelaufbaues

Sowohl in ruhiger Lage, d.i. im Dorf oder im Wohngebiet einer Stadt, als auch in verkehrsreicher Lage, d.i. im Stadtkern, ist der Störpegel überwiegend vom Verkehrslärm bestimmt.

In Bild 1a - c ist nun an Ausschnitten einer 24-stündigen Registrierung des Schallpegels in einer verkehrsreichen Lage im Stadtkern gezeigt, daß der Störpegel gemäß der Auswertung in Tafel 1 etwa mit dem zehnfachen Logarithmus der Zahl der vorbeifahrenden Fahrzeuge zunimmt.

Tafel 1

Störpegelaufbau

Bild 1	Störpegel dB(A)	Zeit	Fahrzeugvorbeifahrten in 15 Minuten	Störpegelzunahme dB gemessen	gerechnet [1]
a	46	0.45-1	20	Bezugswert	
b	50	22.45-23	50	4	4
c	54	19.30-19.45	90	8	7

[1] $\Delta L = 10 \log n$ (n ... Vervielfachung der Fahrzeugvorbeifahrten)

Die Unterschiede in den obenstehenden Richtwerten würden sonach bedeuten, daß an einem Ort tags durchschnittlich die zehnfache Zahl an Fahrzeugen gegenüber nachts verkehrt, bzw. in verkehrsreicher Lage die zehnfache Zahl gegenüber der in ruhiger Lage.

Damit sind nun Verfeinerungen des zu erwartenden Störpegels mittels abgeschätzter Verkehrsdichte möglich. Im Wohngebiet wird letztere tags und nachts nicht sehr unterschiedlich sein und der Störpegelunterschied daher z.B. nur 5-10 dB ausmachen. Im Stadtzentrum kann hingegen zwischen Tag und Nacht ein Unterschied bis 15-20 dB auftreten.

4. <u>Störpegelverlauf für die verkehrsreiche Lage</u>

Für den Stadtkern Wiens wurden für kennzeichnende Stellen 24-stündige Schallpegelregistrierungen (außerhalb von Wohnungsfenstern) durchgeführt, von denen in Bild 2a - e eine Auswahl dargestellt ist. In Abhängigkeit von der Tageszeit ist die Zeitdauer in % angegeben, in welcher ein bestimmter Schallpegel überschritten ist, der Störpegel ergibt sich demnach für 100% Zeitdauer.

In Tafel 2 ist abgerundet Höhe und zeitlicher Verlauf des Störpegels für einige Verkehrslagen dargestellt, wobei durch die ausgewiesene Pegelabnahme für die Abend- und Morgenstunden bzw. die Nachtstunden die obenstehenden Ausführungen bestätigt erscheinen.

Tafel 2

Störpegelverlauf

Bild 2	L a g e	Störpegel tags dB(A)	Zeit	Nachtzeiten mit einer Abnahme des Störpegels um 5 dB	10 dB	15 dB	20 dB
a	Kreuzung von Hauptverkehrsadern (IV)	65	6-21	21-24	-	0-1 5-6	1-5
b	Hauptverkehrsader (IX)	60	6-20	20-23	5-6	23-5	-
c	Garten 200 m entfernt von der Hauptverkehrsader (IX)	55	6-21	21-23	23-1 5-6	1-5	-
d	Hauptstraße (II)	55	7-19	19-20 6-7	20-6	-	-
e	Nebenstraße parallel zu Hauptstraße (IX)	55	7-10	10-21 6-7	21-6	-	-

Der Zusammenhalt der Störpegelwerte und der Zeitdauer der verkehrsbedingten hohen Lautstärken zeigt, daß eine längere Nachtruhe nur in der Hauptstraße (2d) und in der Nebenstraße zu einer Hauptstraße (2e) eintritt.

5. Oktavbandanalyse des Störpegels und ihre Reihung

Zweckmäßig erfolgt eine Schallanalyse für den Lärm und den Störpegel. Übersteigt das Lärmspektrum das um 10 dB nach oben verschobene Störpegelspektrum, so ist die "zumutbare Grenze der Störung" überschritten.

Die Schar der bekannten Schallpegelreihungskurven nach ISO dient einer Einstufung von Lärm (noise rating) und es liegt nahe, sie auch zu einer Einstufung des Störpegels heranzuziehen. Allerdings bedingt der häufig viel flachere Verlauf des Störpegelspektrums dabei eine ungenaue Beurteilung.

Vom Verfasser wurde für ISO vor längerem vorgeschlagen, die Schar der A-Bewertungskurven für die Einstufung von Lärm zu benützen. Es wurde daher jetzt für 20 kennzeichnende Störpegelspektren ein Vergleich durch Einstufung nach den ISO- und nach den A-Kurvenscharen vorgenommen.

Im Ergebnis wurde für keine der 20 Kurven ein Unterschied festgestellt, so daß diesbezüglich die Kurvenscharen gleichwertig erscheinen.

Es ist noch zu erwähnen, daß die Einstufung von Lärm mittels Schallpegelreihungskurven, ergänzt durch vorgegebene feste Korrekturen, für viele Zwecke wie Gebietswidmungen, Feststellung der akustischen Eignung von Räumen und dgl. vorteilhaft ist, daß jedoch nach Ansicht des Verfassers in speziellen Fällen die genauere Beurteilung der Lärmstörung durch Bezug auf den Störpegel erforderlich ist.

(1) Ausführliche Darstellung siehe F. Bruckmayer: Handbuch der Schalltechnik im Hochbau, Verlag F. Deuticke, Wien 1962

(2) Masking noise by noise, siehe W.A. Munson in C.M. Harris: Handbook of Noise Control, Mc Graw-Hill Book Comp. Inc., New York 1957

Bild 1 Zunahme des Störpegels mit der Verkehrsdichte

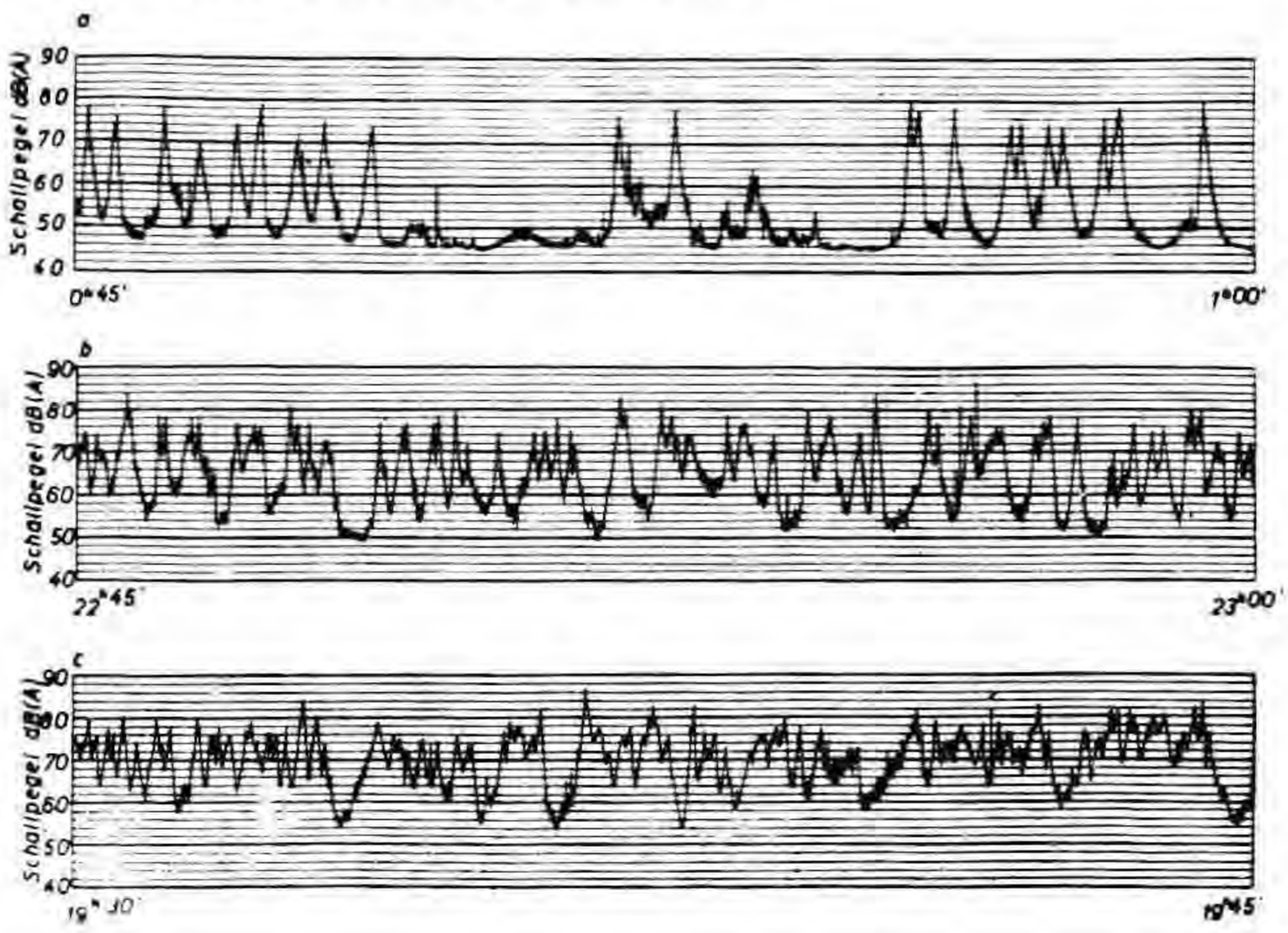

Bild 2 : Störpegelverlauf mit der Tageszeit

a. Kreuzung von Hauptverkehrsadern (IV)

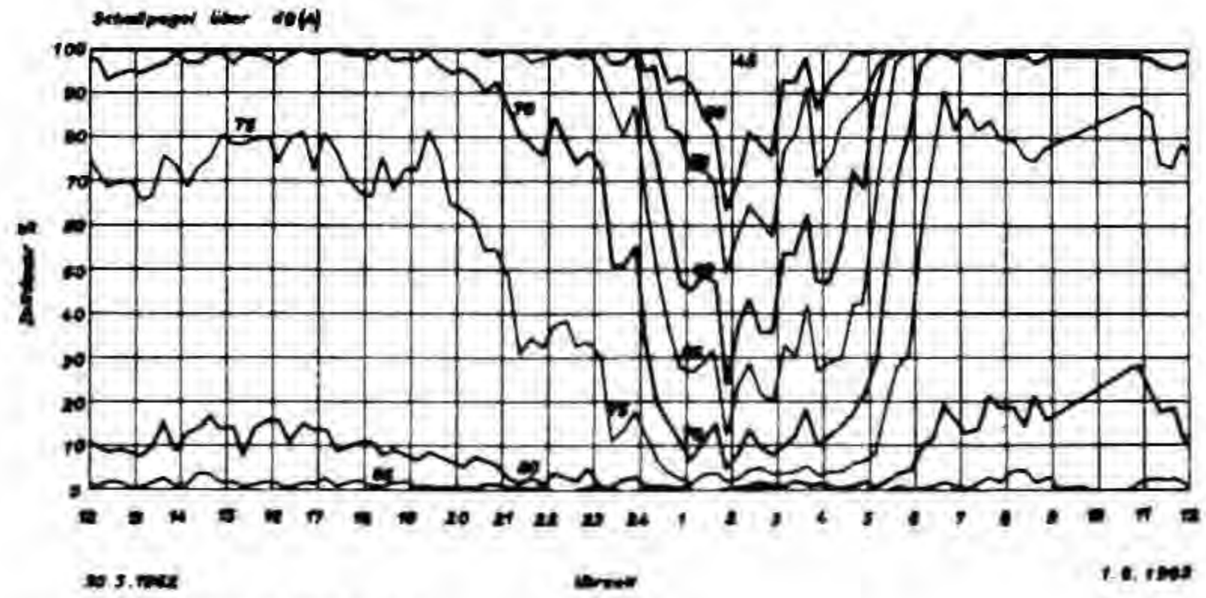

b. Hauptverkehrsader (IX)

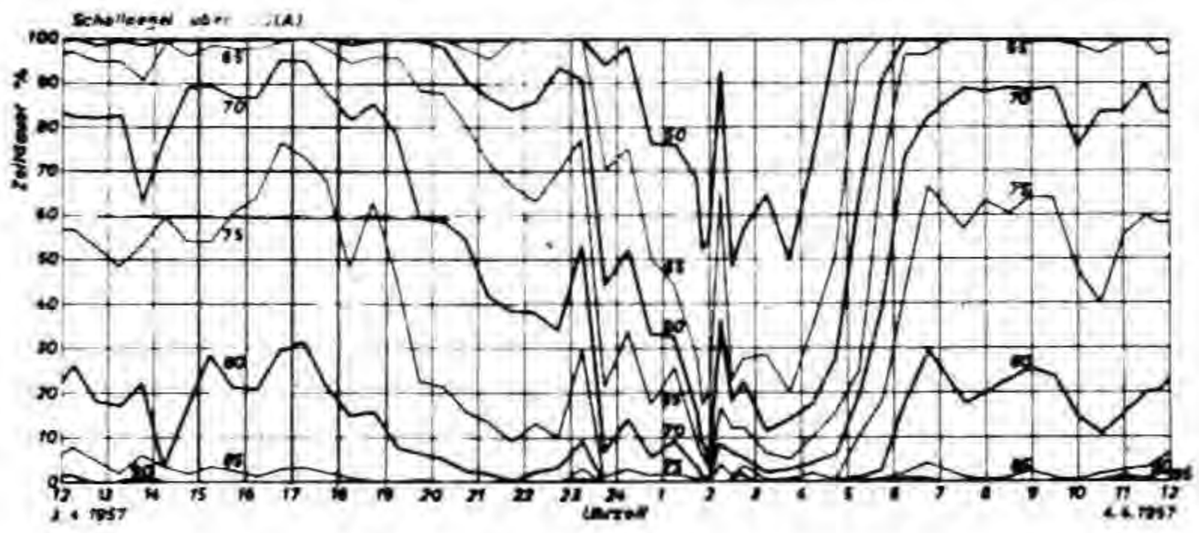

c. 200m entfernt von der Hauptverkehrsader (IX)

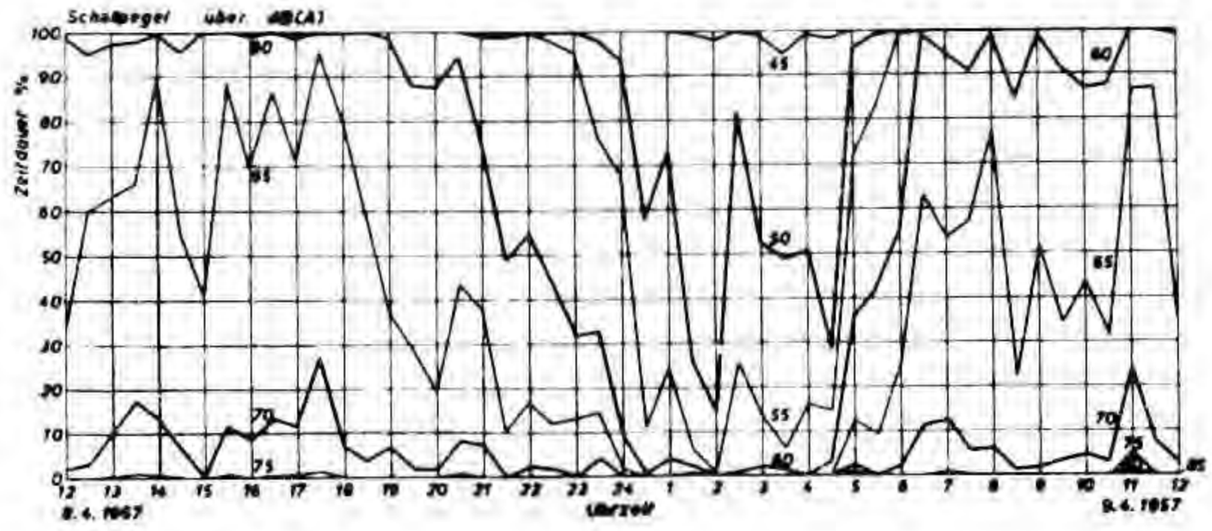

d. Hauptstraße (X)

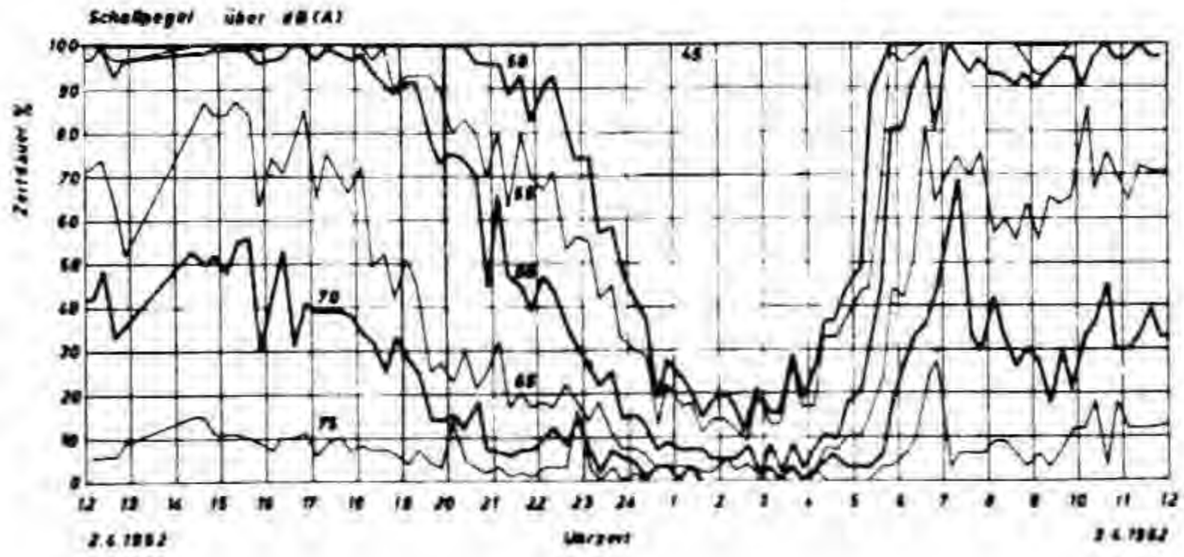

e. Nebenstraße parallel zu Hauptstraße (IX)

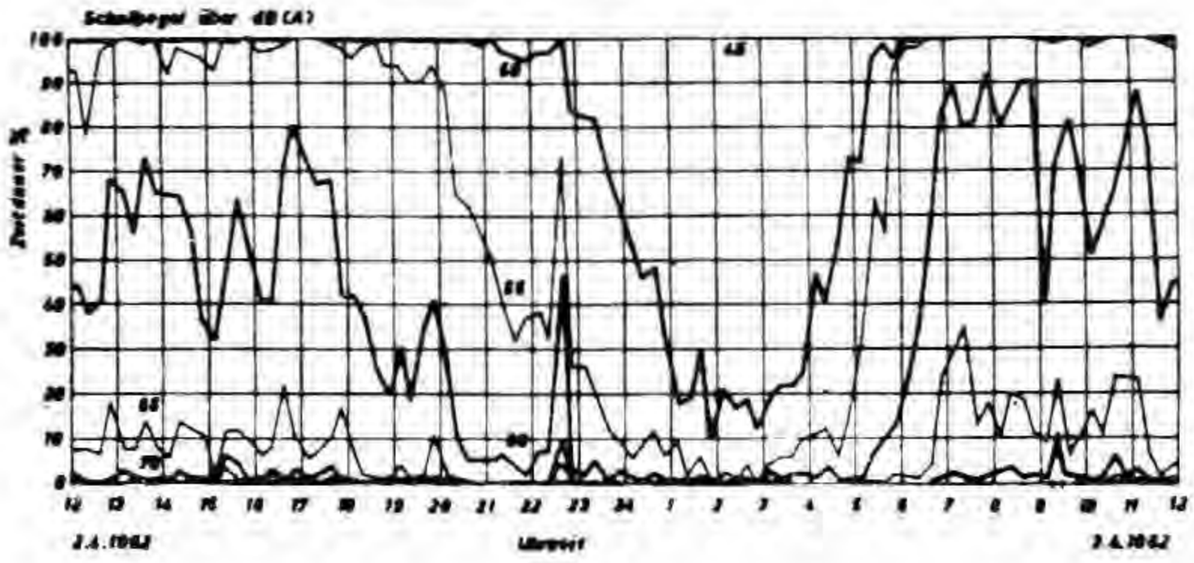

M16

FOURTH INTERNATIONAL CONGRESS ON ACOUSTICS
COPENHAGEN 21.-28. AUGUST 1962

THE DEPENDENCE OF REVERBERATION TIME UPON SEAT SPACING

L. P. Delsasso, Department of Physics
University of California, Los Angeles

In this paper I wish to present the experimental results of changing the seat spacing in three enclosures, a reverberation room, an all purpose auditorium of 600,000 cu. ft. seating 2560 and a new teaching theater of 120,000 cu. ft. seating 600.

The reverberation room at U.C.L.A. has a volume of 6080 cu. ft. and a reverberation characteristic at 38% Relative Humidity as shown on the first slide. Eight upholstered theater chairs were placed in two rows of four chairs each and the reverberation times for ½ octave bands of white noise measured on a B & K logarithmic recorder. Measurements were obtained for spacings between rows of 15", 32" and 120" for the empty chairs and for frequencies from 125 c.p.s. to 8000 c.p.s. These results are shown on the next slide. You will note that the computed absorption per chair varies irregularly at the low frequencies for the three spacings, reaches the same value of 3.4 for the three at 500 c.p.s. and then keeps between 3 and 4 up to 4000 c.p.s The absorption for the different spacings is again identical at 8000 c.p.s. reaching a value of 5.3. No clear cut conclusion can be drawn from these measurements on empty chairs to indicate a common trend as they are separated.

For the two spacings used with people in the chairs there is an increase at all frequencies from 125 c.p.s. to 4000 c.p.s. of at least 1 unit for the 120" spacing over the 32" spacing. The curves cross at 5700 c.p.s. and differ in the reverse direction by 3.4 units at 8000 c.p.s.

The first building tested was the Multipurpose Municipal Auditorium in Santa Monica, California. This building has a large central floor area which can be tilted from horizontal to 7°. On this 1610 folding chairs with both seats and backs padded and covered with "nogahide" can be placed. A balcony which "matches" with the movable floor, when it is tilted, has 952 fixed upholstered theater seats.

The reverberation characteristics of this auditorium with all 2560 seats but without audience is shown in the next slide. These observations and similar ones, with every other row of the portable chairs removed and with all of the portable chairs removed, were made. The results are given in the next slide. Here the absorption per seat has been determined for 1610 seats with rows spaced 2.5 ft. apart and with 828 seats spaced 5.0 ft. apart. You will note that above 1000 c.p.s. the absorption per seat is essentially the same but that below 1000 c.p.s. there is a rather pronounced peak in each curve. This occurs at 250 c.p.s. for the 2.5 ft. spacing and at 500 c.p.s. at the 500 ft. spacing. Although the accuracy with which such determinations can be made in a room of this size with around 16000 S of fixed absorption at 500 c.p.s is not great both of these effects appear to be real.

The third auditorium investigated was the Teaching Theater at U.C.L.A. This has a volume of 120,000 cu. ft. and a capacity of 600. For purposes of instruction it is provided with a standard large stage of 488,000 cu. ft. Here again reverberation measurements were made after the auditorium was completed but before the seats were installed, when every other row was in place and finally with all seats in place. The results are shown in the following slides.

These experiments suggest that the absorption provided by audience areas is a complex problem of spacing construction and audience clothing and that more detailed studies in theaters, music halls and in large reverberant rooms are required.

N16

FOURTH INTERNATIONAL CONGRESS ON ACOUSTICS
COPENHAGEN 21.-28. AUGUST 1962

POWER HANDLING CAPACITY OF LOUDSPEAKERS

Cesarina Bordone Sacerdote - Istituto Elettrotecnico Nazionale " Galileo Ferraris "
- Corso Massimo d'Azeglio, 42 - Torino

A recent document issued by the I.E.C., 29 (Secretariat) 45, recommends that the rated power handling capacity that a manufacturer assigns for his loudspeaker should be controlled applying a special noise signal, for 100 continuous hours at that specified power, and verifying that after this test the loud speaker survives without significant deterioration.

Some tests of this kind have been carried out in the laboratory of the I.E.N., during which measurements have been made, to put into evidence any eventual change of behaviour of the loudspeaker during the test.

The frequency response and the resonance frequency of the tested loudspeaker were measured from time to time during the life test: the figures report some results. It has been noticed that the resonance frequency of the loudspeaker decreases during the test: fig. 1 reports the resonance frequency of three loudspeakers of mean quality and dimensions (25 - 20 cm of diameter) as a function of the time during which the test is carried on.

To another loudspeaker, 15 cm of diameter, low quality, only 1/8 of its power handling capacity was applied: the resonance frequency did not decrease so much during this test (fig. 2). Then the loudspeaker remained quiet 16 hours: after this rest the resonance frequency had increased a little. To the loudspeaker then 3/8, and 3/4 of its power handling

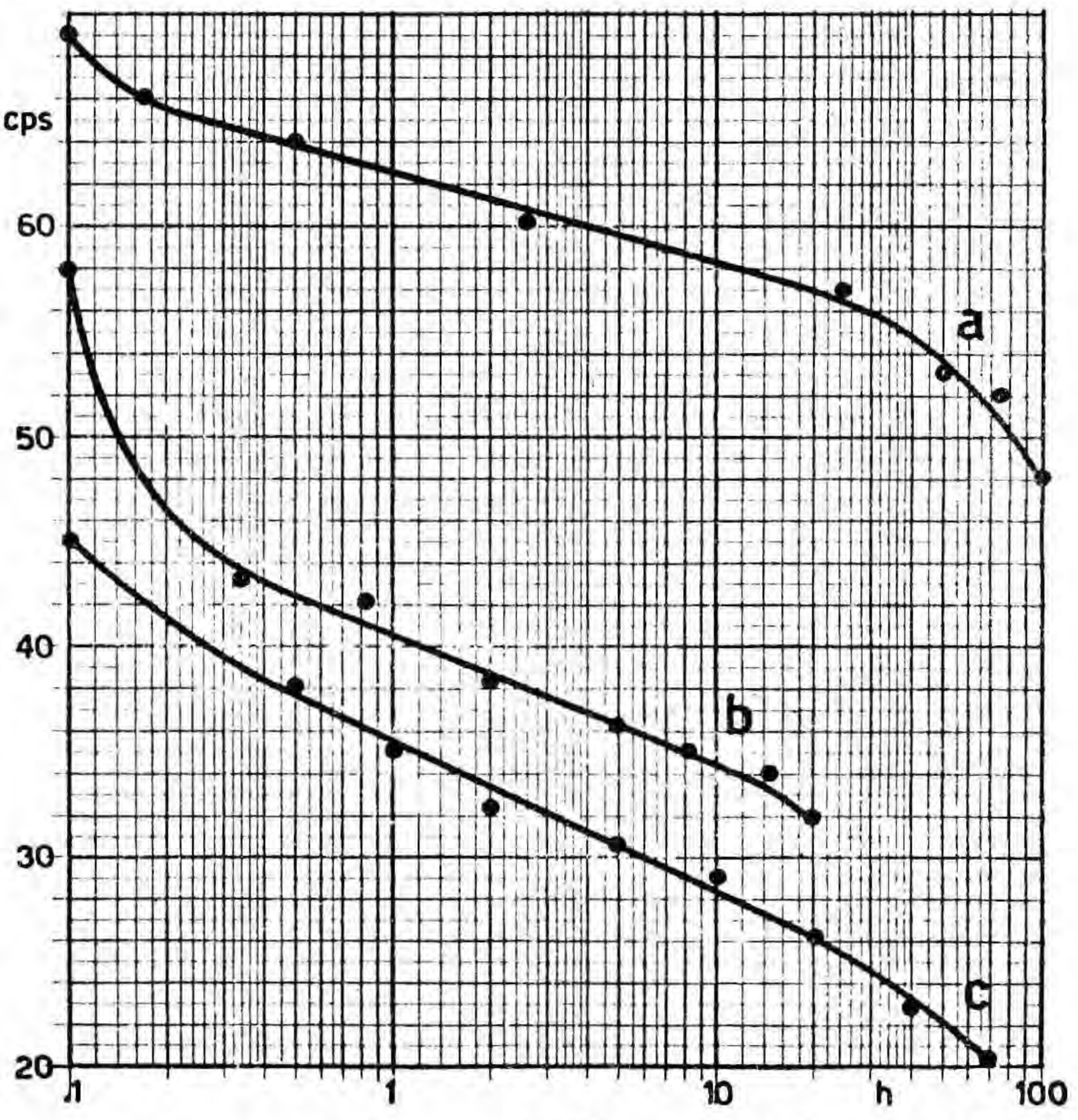

Fig. 1 - Resonance frequency of different loudspeakers as a function of the time during a life test.

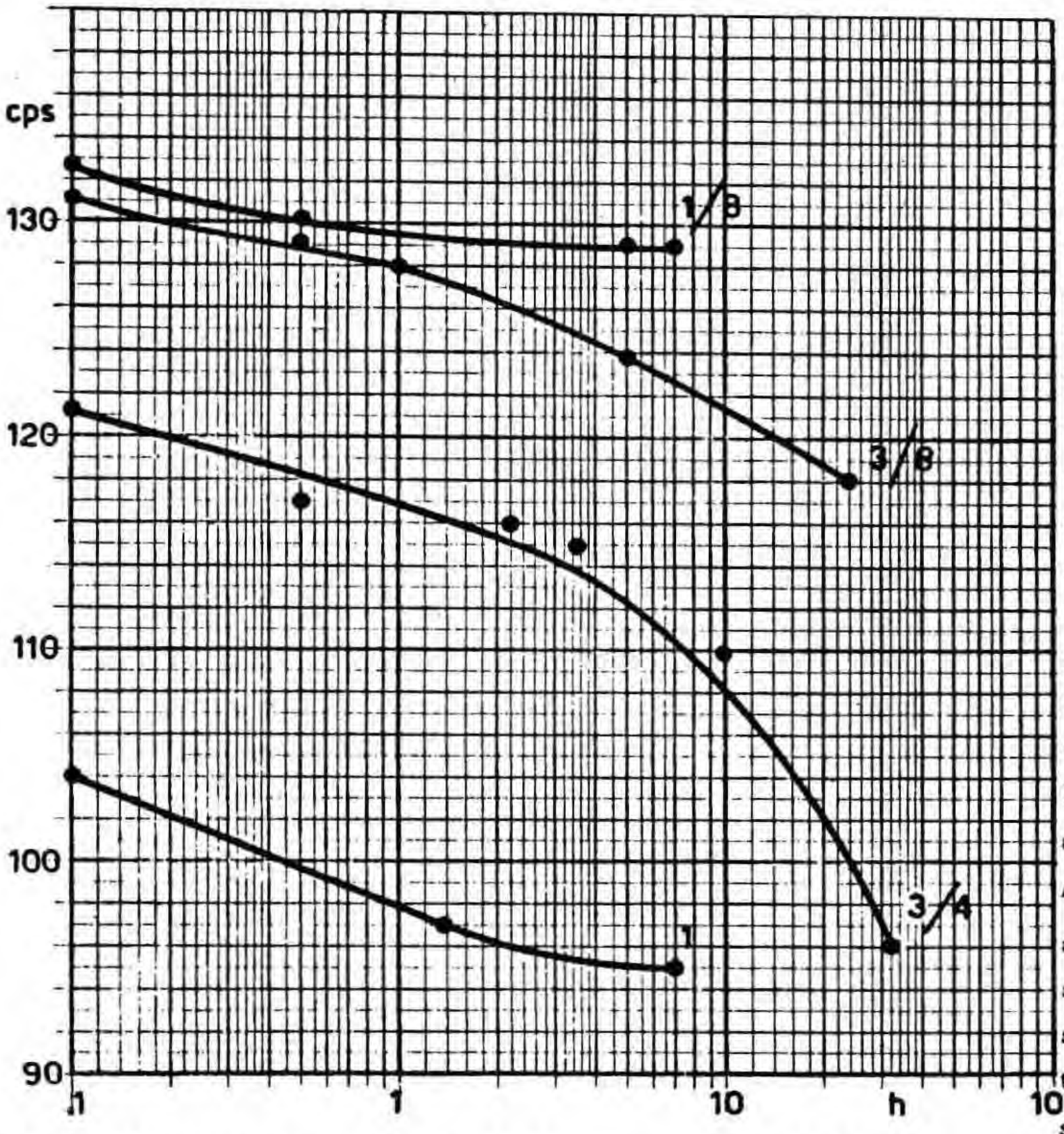

Fig. 2 - Resonance frequency of a loudspeaker to which different powers have been applied (1/8; 3/8; 3/4; 1; referred to its power handling capacity) for some hours (at the abscissa), inserting a period of rest between the different tests.

capacity were applied: the resonance frequency decreased more rapidly, but there was still an increase after every rest. When the whole power was applied, the loudspeaker was damaged after 7 hours.

The response of loudspeakers, measured at 400 cps, as a function of the time during the life test, results practically unvaried for some loudspeaker, increases up to 6 dB for others, due to the softening of the movement of the membrane and of the voice coil assembly.

As for the frequency response also for loudspeakers that survive the test there is some change: fig. 4 reports two examples. For one loudspeaker (mean quality, 25 cm of diameter) a peak, around 1000 cps, flattens as a function of the time, and its frequency goes down to 850 cps; in correspondence of a through, around 1250 cps, a new peak arises (fig. 3a). In the frequency range from 400 to 1000 cps the distortion, which was lower than 3% for the new loudspeaker, increases to 8% after the life test.

For another loudspeaker (good quality, 20 cm of diameter) the continuous slope at low frequencies gives place to an intermediate flat response, around 500 cps, and the response increases at high frequencies (fig. 3b).

In some cases the loudspeaker did not survive the test because its membrane was broken around its corrugated part near the edge: in every case this part of the loudspeaker resulted deteriorated. We thought then that the decrease of the resonance frequency was due to the change of the elastic properties of the paper in the corrugated zone.

Two new equal loudspeakers were chosen (mean quality, 25 cm of diameter) with the same frequency response and resonance frequency. One of them supported the life test, the other was kept unemployed. After the test, that the loudspeaker survived, measurements were made on the elastic properties of the corrugated part of the membrane. Small samples were cut radially from the membrane, 2.4 cm large and 3.0 cm long. The sample was clamped at one end in a rigid support, at the other in a weight of 45 g,

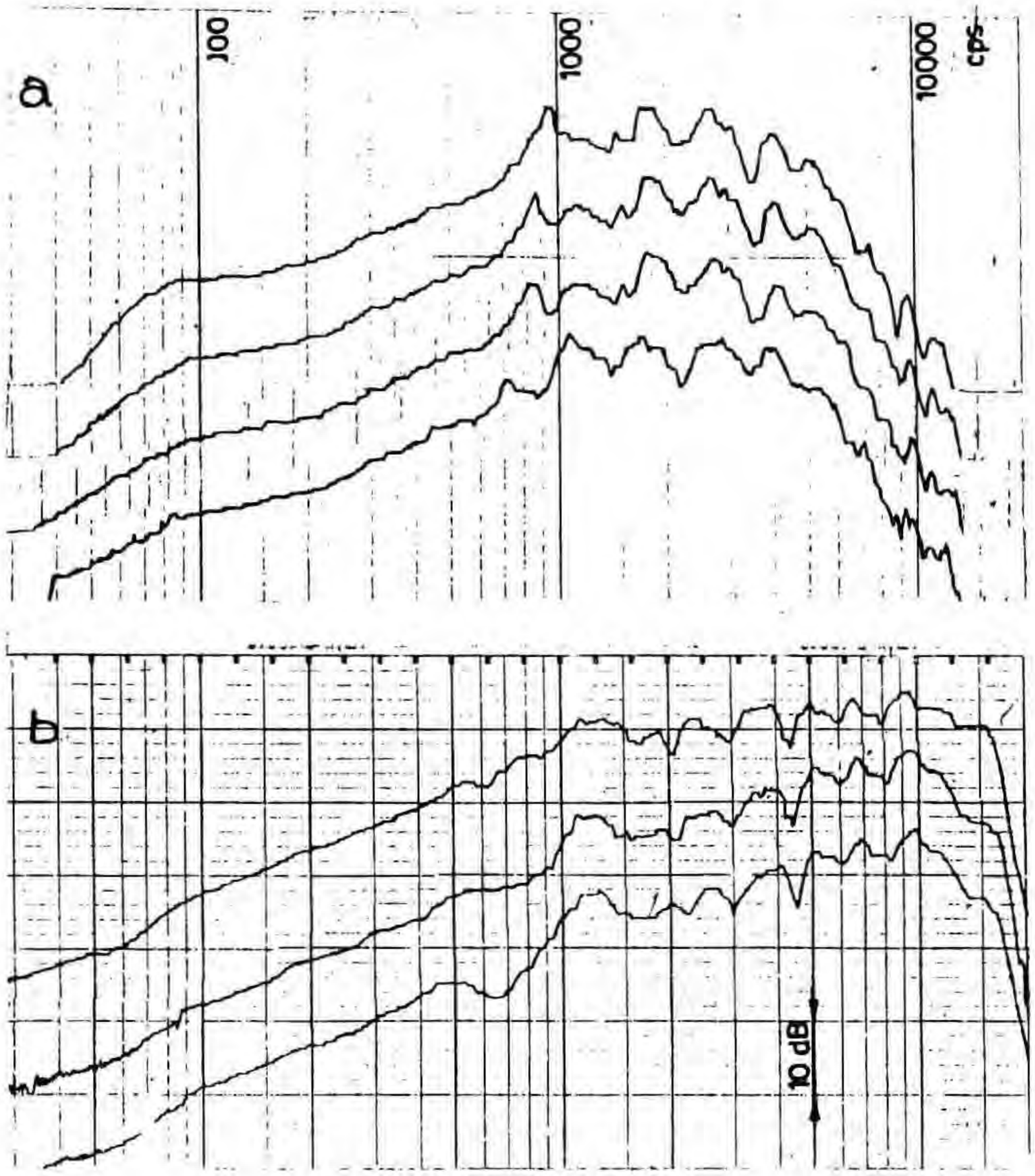

Fig. 3 - a) Frequency response of a loudspeaker during the life test after 0; 7; 30 and 96 hours (from the top).
b) Frequency response of a loudspeaker during the life test after 0; 1.30 and 6 hours of test (from the top).

which kept it vertical. Under the weight an electromagnet excited the sample to vibrate: a piezoelectric device into the support detected its reaction to these vibrations. The resonance frequency of the samples is reported in fig. 4 as a function of the angle of the cone: it results to have a behaviour due to the manufacturing process.

A remarkable difference of resonance frequency was found measuring the impedance of the loudspeaker without membrane (that is the impedance of the voice coil assembly): the tested loudspeaker has a lower resonance frequency (fig. 5b). We can suppose then that for this kind of loudspeakers the decrease of resonance frequency is partly due to the voice coil assembly.

Different behaviours may be found for different loudspeakers: some had the moving coil interrupted during the life test, another had the wires coming out of the membrane broken.

Life tests were also made employing music from broadcasting instead of the noise signal: to evaluate the power applied to the loudspeaker the music signal was superposed random 8 times on a magnetic record (following a method employed by Tarnozcky).

The test with noise signal results to be more severe: its spectrum contains more low frequency components than the spectrum of music, according to some analysis carried out in our laboratory and by different authors.

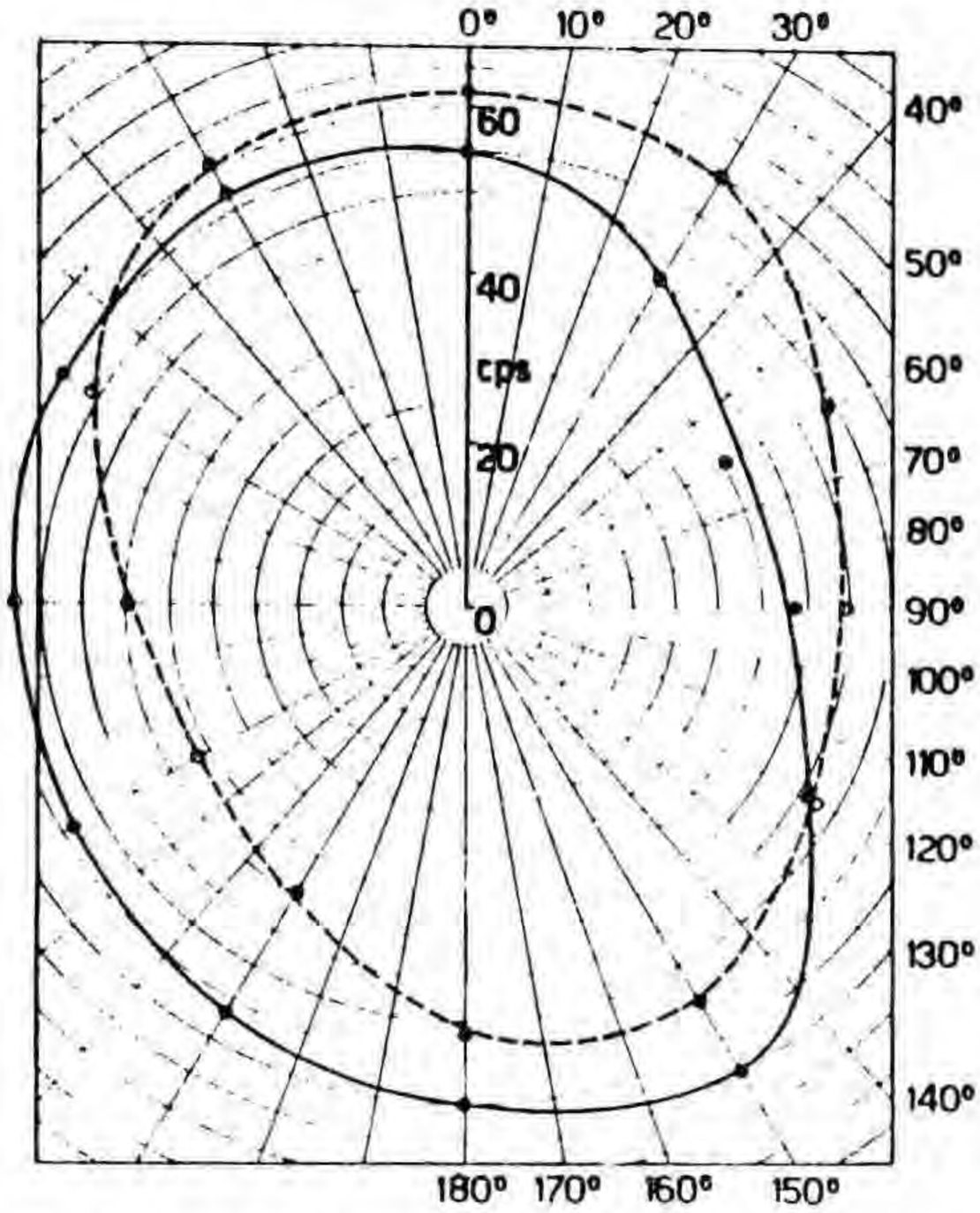

Fig. 4 - Resonance frequency of samples cut from the corrugated part of the membrane of two loudspeakers as a function of the angle of the cone: the continuous curve concerns a tested loudspeaker, the dotted a new one.

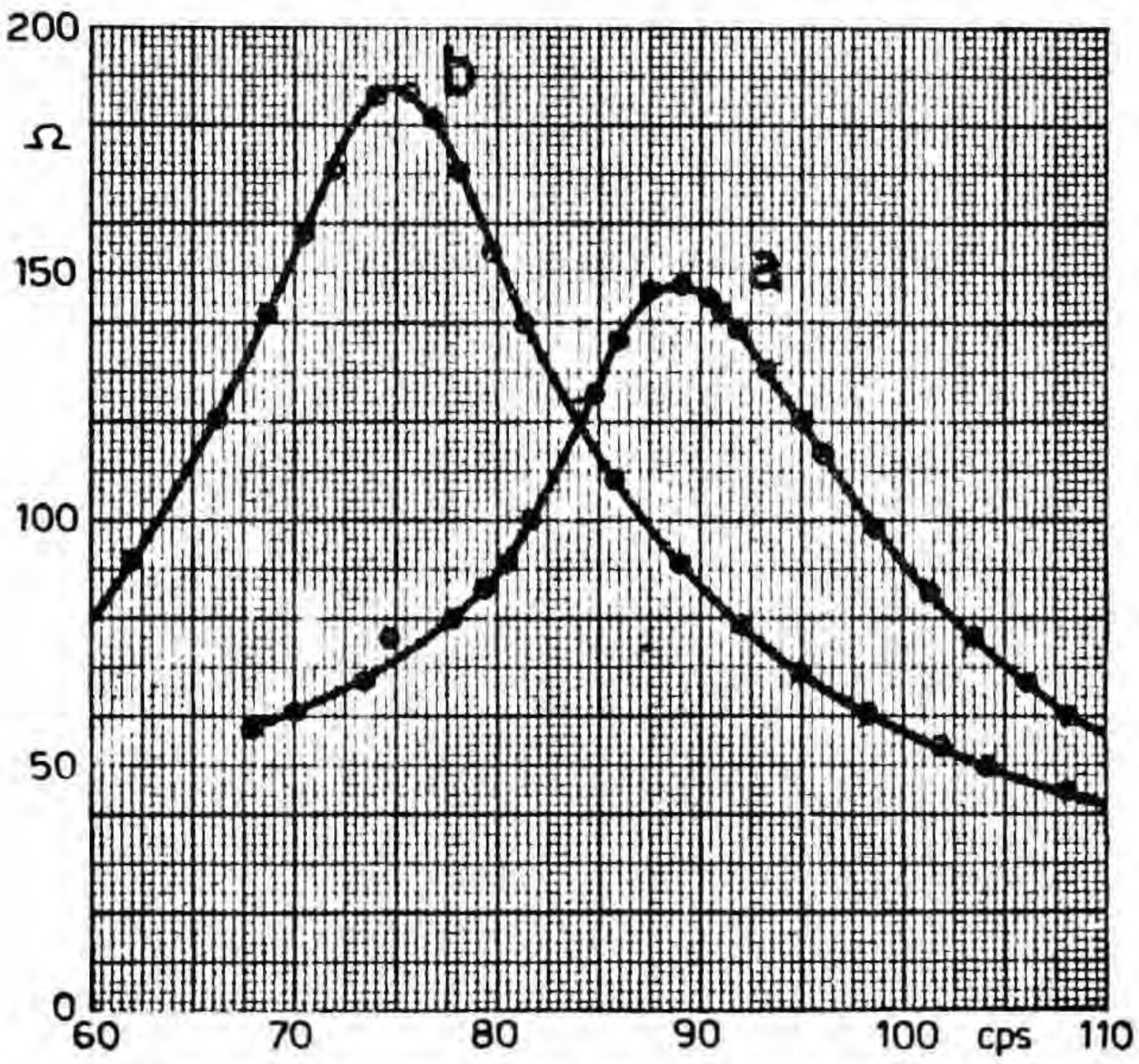

Fig. 5 - Impedance of the voice coil assembly of a loudspeaker before (a) and after (b) the life test.

O16

FOURTH INTERNATIONAL CONGRESS ON ACOUSTICS
COPENHAGEN 21.-28. AUGUST 1962

Production de bruits blancs par des claquettes

F. CANAC, G.CORSAIN & Th.ANGELINI (Centre de Recherches Scientifiques et Industrielles de Marseille)

Certaines mesures d'acoustique nécessitent l'emploi de "tops" et, en particulier, de tops constitués par des "bruits blancs" . Lorsque ces mesures se font sur le chantier ou dans certains édifices, il est souvent assez difficile de disposer d'appareils électriques. Nous avons cherché à pallier ces difficultés en utilisant des "claquettes" . En particulier, s'il s'agit de connaître les réactions d'un local au point de vue de la compréhension du langage parlé, il ne faut pas oublier que la durée d'émission d'une syllabe est comprise entre 1/10 et 2/10 de seconde. C'est précisément la durée d'émission des claquettes que nous avons réalisées. On se trouve ainsi dans les conditions optima pour étudier l'influence de la réverbération. Enfin, le bruit blanc permet de s'affranchir des ondes stationnaires.

Dans leur réalisation la plus simple, les claquettes sont constituées par deux rectangles de métal ou de bois réunis par une charnière. (On peut d'ailleurs dans certains cas donner aux deux éléments une forme particulière : trapèze, triangle, etc ...). En première réalisation, la claquette est manoeuvrée à la main. L'expérience montre qu'avec de l'habitude l'émission est constante à 1 ou 2 décibels près.

Dans un deuxième type d'appareil, la claquette est constituée par une boite peu profonde avec son couvercle. On peut aussi réaliser deux éléments creux identiques réunis toujours par une charnière, de façon à ce que les deux éléments puissent bien s'appliquer l'un sur l'autre. On dispose alors de trois paramètres correspondant aux trois dimensions de la boite.

Dans une première réalisation, nous avons utilisé des claquettes formées de deux rectangles de bois épais, contreplaqué ou non (ce qui modifie l'amortissement), ou encore des rectangles de fer ou de duralumin.

On analyse directement le bruit de choc reçu par un microphone électrostatique dans un analyseur de fréquence, après filtration par 1/3 d'octave. On peut aussi enregistrer sur magnétophone et reprendre les résultats avec l'analyseur.

Les bruits provenant de la claquette sont de trois origines :

1°) Mise en vibration du volume d'air compris entre les deux éléments mobiles. Dans le cas d'une claquette du type "boite" les fréquences sont données par la formule

$$f = \frac{V}{2}\left(\frac{p^2}{a^2} + \frac{q^2}{b^2} + \frac{r^2}{c^2}\right)^{1/2}$$

V vitesse du son dans l'air
a, b, c dimensions de la boite
p, q, r nombres entiers : 0, 1, 2, ...

Dans le cas d'une claquette formée simplement de deux plateaux, on considèrera la lame d'air comprise entre eux au moment de la fermeture et l'on applique, comme nous l'avons vérifié, la formule précédente en faisant $r = 0$.

2°) Mise en vibration des plateaux ou des parois de la boite. Elle dépend de la nature et des dimensions des parois.

3°) Vibration de la lame d'air expulsée par la compression. Formation possible de tourbillons. Ceci rappelle ce qui se passe lors du bruit d'un jet d'air comprimé : en gros, fréquences discrètes, décroissantes quand la pression croît.

Les fréquences précédentes se retrouvent dans la décomposition en série de Fourier du top initial, et constituent des irrégularités dans le spectre. On peut facilement les repérer.

Par exemple :

- claquette en fer rectangulaire (20 x 12 cm), fréquence calculée 1700, maximum observé autour de 1600;
- claquette en bois, rectangle de 5 x 6,5 cm, fréquence calculée 3200, maximum observé vers 3500;
- claquette en bois, rectangle de 20 x 9 cm, fréquence calculée 1890, maximum observé vers 2000;
- claquette en bois rectangulaire (6 x 20 cm), fréquence calculée 3200, maximum observé 3500.

Ce dernier résultat est assez intéressant. En effet, jusqu'à 1000 la courbe spectrale est à peu près horizontale. Puis, elle remonte graduellement jusqu'à 3500. On a ainsi une émission cantonnée dans les hautes fréquences de la voix.

Beaucoup de maxima ainsi observés correspondent à une demi-longueur d'onde (ou une longueur d'onde) égale à la grande dimension de la claquette, comme si la lame d'air considérée vibrait ainsi qu'un tube ouvert aux deux bouts.

On obtient des résultats bien meilleurs en utilisant des claquettes du type "boite" , c'est à dire en faisant intervenir une troisième dimension. Ainsi, des claquettes formées de deux demi boites en bois (300 x 100 x 100 mm) donnent un bruit blanc de 50 à 5000 constant avec seulement deux écarts de ± 2,5 dB. Une autre (350 x 145 x 32 mm) donne un spectre sonore décroissant assez régulièrement de 6 dB entre 125 et 8000. On peut arriver à retoucher une claquette de façon à étendre la constante du spectre dans les graves (autour de 100) et dans les aigus (jusqu'à 10.000), soit en amortissant les parois par des pièces métalliques pour faciliter certaines résonances au dépens d'autres, soit en s'inspirant de la technique des luthiers en facilitant l'ébranlement du fond de la boite par une "âme" sur laquelle vient frapper le couvercle. C'est ainsi qu'a été réalisé la dernière claquette signalée ci-dessus.

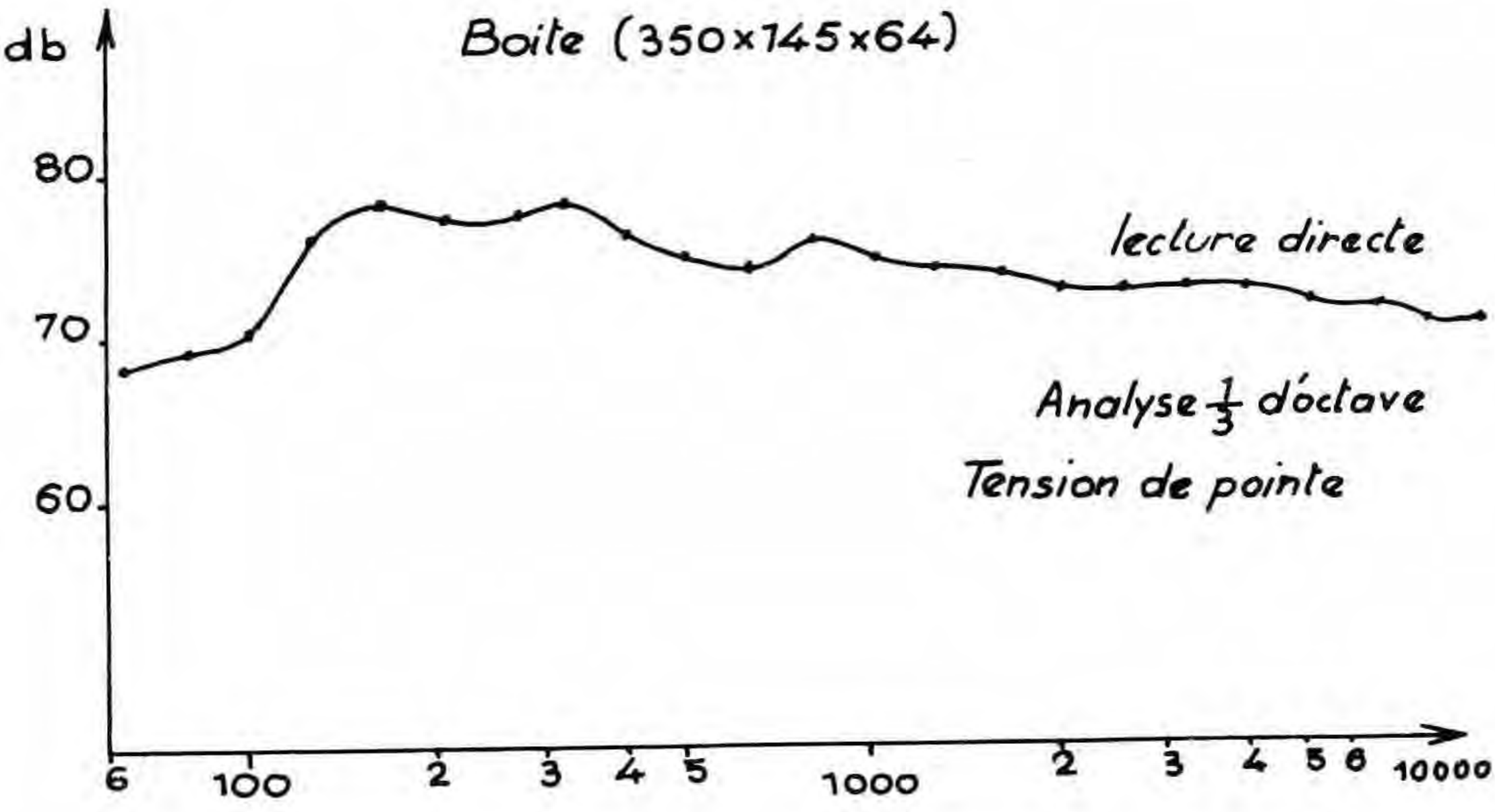

P16

FOURTH INTERNATIONAL CONGRESS ON ACOUSTICS
COPENHAGEN 21.-28. AUGUST 1962

"Measurement of E and G moduli and Poisson's ratio of polymethylmethacrylate over a large frequency range"

Ir. C.J. Nederveen.

Central Laboratory T.N.O. - DELFT, The Netherlands.

SUMMARY.

With creep and with vibrational experiments E and G of polymethylmethacrylate were measured at room temperature in the frequency-range between 10^{-5} and 10^{4} Hz. Poisson's ratio was calculated. Contrary to earlier observations, no minimum has been found.

INTRODUCTION.

In studies of the mechanical behaviour of high polymers[1] the moduli of elasticity and Poisson's ratio are important and useful quantities, especially in the region where stress and strain are linearly dependent upon each other. A modulus of elasticity is defined as the quotient of the stress and the strain at this stress. As high polymers show so-called visco-elastic behaviour, the mechanical energy applied to the specimen is dissipated partly and the modulus appears to be dependent on time and temperature. Accordingly, with cyclic deformations, the strain will lag behind the stress, so that the modulus should be considered as a complex quantity. When the absolute value of the dynamic modulus measured at a frequency ν is compared with the static modulus measured at a time

$$t = (2\pi\nu)^{-1} \qquad (1)$$

after the start of the experiment, the numerical values of both quantities theoretically agree with each other to a good approximation.
The most commonly used moduli are G (shear-) E (Young's) and K (bulkmodulus). Apart from the moduli, Poisson's ratio, μ, is an important quantity. The direct measurement of Poisson's ratio is difficult and mostly it is calculated by means of one of the following formulae :

$$\mu = \frac{E}{2G} - 1 = \tfrac{1}{2}\left(1 - \frac{3G}{G+3K}\right) = \tfrac{1}{2}\left(1 - \frac{E}{3K}\right) \qquad (2).$$

Experimentally it is observed and theoretically it can be proved, that G, E and K decrease with time. The slope of the curves against log time (approximately equal to minus the damping tan δ) is always negative and shows maxima and minima. The course of μ is still a point of discussion. A monotonous course seems most probable, but theoretically this has not been proved so far. Experiment should yield the ultimate decision here.

One of the aims of the investigation was the time dependence of Poisson's ratio. The results, as a function of time at constant temperature showed a monotonous course, contrary to corresponding measurements of Koppelmann[2] on the same material, which showed a minimum. Another aim was to improve the interrelationship of results obtained by various techniques (see Fig. 1) in our laboratory. This difficulty of achieving a satisfactory relationship seems to be a more generally appearing problem[3]. Besides, these inaccuracies of measurement could be responsible for the observed minima and maxima in Poisson's ratio; so both aims of the investigation cannot be sharply distinguished.

Because the damping gave no difficulties regarding the interrelationship, this quantity was not investigated further.

EXPERIMENTAL PROCEDURE.

The quantities we chose to measure were G and E and they were measured respectively in torsion and in bending. Poisson's ratio, as calculated from these two moduli, is not very accurate, which is an implicit property of Eq. (2).

It is generally accepted that a time- or frequencydependence of the modules can be interpreted as a temperature dependence, and vice versa. Although the realization of a wide temperature range is easiest, we nevertheless preferred measuring of the frequency dependence directly. This implied the construction of several apparatuses, one for each frequency region.

The measurements were carried out on specimens with rectangular cross section 3.5 x 7 mm^2 and lengths of 20, 57 and 120 cm, all manufactured from the same sheet polymethylmethacrylate (perspex of I.C.I.). All measurements were carried out on the specimen of 20 cm length, except those on the standing bending vibrations of very low frequencies.

Static as well as dynamic experiments were carried out. The boundary of ease of handling between both kinds of measurements lies at about 1 second. In Fig. 1 a survey of the techniques used is given. For the static experiments creep tests were chosen in which the strain is measured at a constant stress. In the dynamical experiments the specimen with or without an additional mass is set into resonance vibration. For torsional vibrations the specimen is fixed at one end and at the other provided with a cross-bar with additional masses. For bending vibrations the specimen is provided with two equal masses at each end. By varying the magnitude of the masses the frequency can be varied between a very low value and about 5000 Hz. At this upper frequency the additional masses are practically zero, i.e. in the specimen standing vibrations are generated.

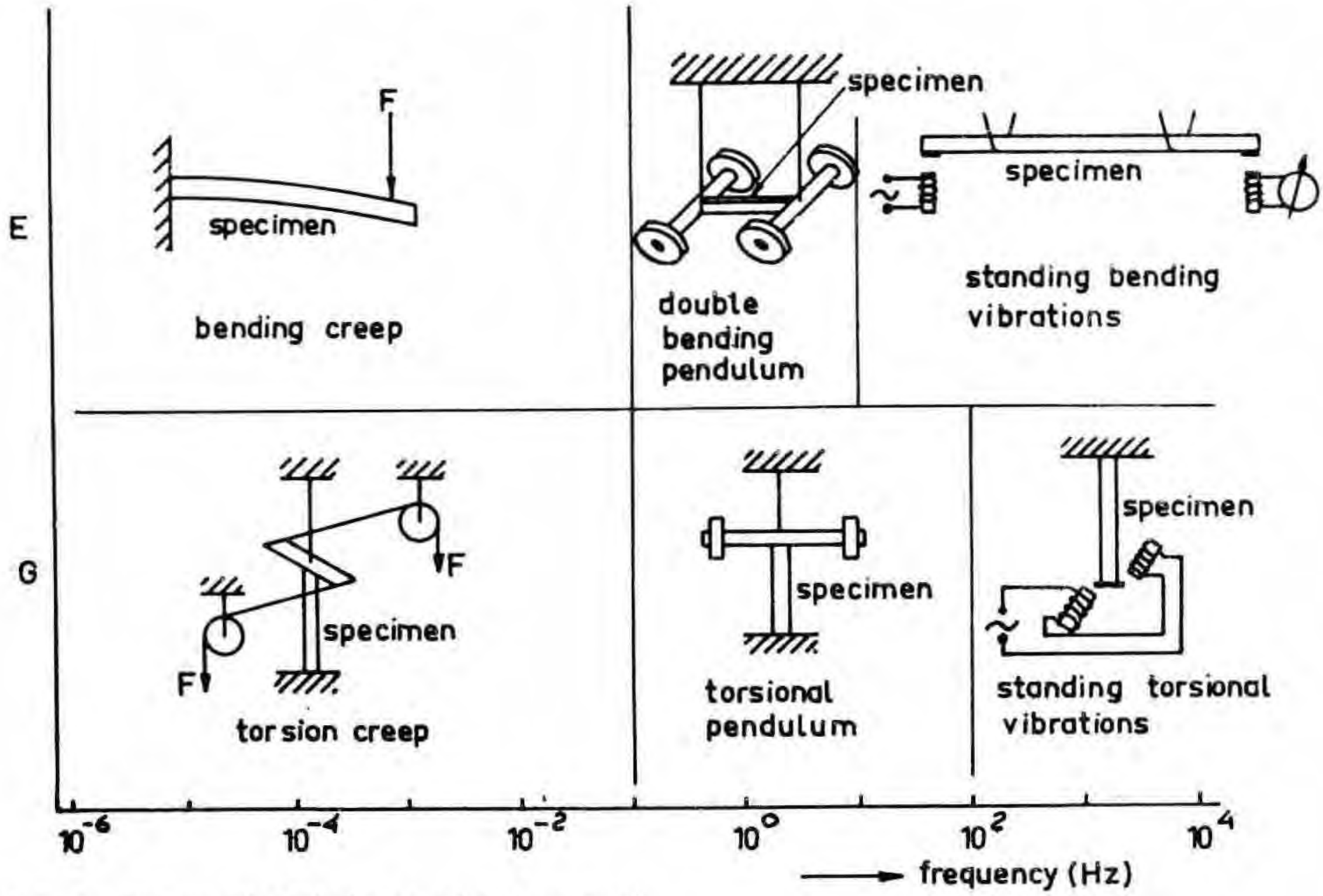

Fig. 1. Survey of techniques of measurement.

In order to reach this upper frequency with bending vibrations use must be made of higher vibrational modes.

Special care should be taken that nothing else is measured than what had been theoretically intended. Especially for torsion experiments everything must be in one line and placed vertically. The clamp should preferably possess one screw and enclose the end of the specimen completely. The clamps should be sufficiently stiff with respect to the specimen and must not possess resonance frequencies in the region of the measurement.

The measurement of the resonance frequency boils down to reading an audio frequency oscillator, which feeds an electromagnet mounted in the neighbourhood of the masses. The vibration is detected electromagnetically or with a system consisting of lamp, little mirror and photocell. At the lowest frequencies (1 Hz) a measurement in free damped vibration was preferred which was registered by an electrical spark-over of one of the arms of the cross-bar to a rotating drum.

FORMULAS.

For the torsional pendulum is generally valid

$$kl \tan kl = j_G/J \tag{3}$$

where J is the rotational moment of inertia of the additional mass,

$$k = \omega\sqrt{\frac{j_G}{G\ T\ 1}} \tag{4}$$

and 1, j_G and G T respectively represent the length, the moment of inertia about the length axis and the torsion stiffness per unit of length of the specimen. $\omega = 2\pi$ times the frequency of the vibration. When j_G/J is smaller than 0,7 the modulus is given with an accuracy of 1 % by :

$$G = \frac{\omega^2\ 1\ J}{T}\left(1 + \frac{j_G}{3J}\right) \tag{5}$$

For the double bending pendulum which is used in the region around 1 Hz, the modulus is given with an accuracy of 1 % by

$$E = \frac{6\ \omega^2\ 1\ J}{bh^3} \quad \text{if} \quad \frac{\rho S\ 1^3}{12\ J} < 0.01 \tag{6}$$

where ρ, b and h denote density, breadth and thickness of the specimen.

For standing vibrations in bending, where the additional masses are negligible with respect to the mass of the specimen, the modulus can be calculated from

$$E = \frac{78\ \nu^2\ 1^4\ \rho}{(2S+1)^4\ h^2} \tag{7}$$

where S is the number of the vibrational mode.

RESULTS.

The results are given in Fig. 2, where the shear and Young's moduli and the Poisson's ratio's calculated from these are plotted as a function of frequency *).

---

*) $10^9\ N/m^2 = 10^{10}\ dyn/cm^2 \simeq 10^4\ kgf/cm^2$.

The spread and uncertainty of both moduli is not smaller than 2 %, so that in Poisson's ratio uncertainties of 12 % and more appear. Making allowance for these uncertainties, our results show a monotonous course of μ, with a most probable value between 0.28 and 0.35. We did not observe a minimum of 0.12 at 10 Hz, as was found by Koppelmann[2].

LITERATURE.

1) STUART, H.A., Die Physik der Hochpolymeren IV.
2) KOPPELMANN, J., Rheologica Acta 1 (1958) 20.
3) YIN, T.P. and J.D. FERRY, J. Colloid Sci. 6 (1961) 166.

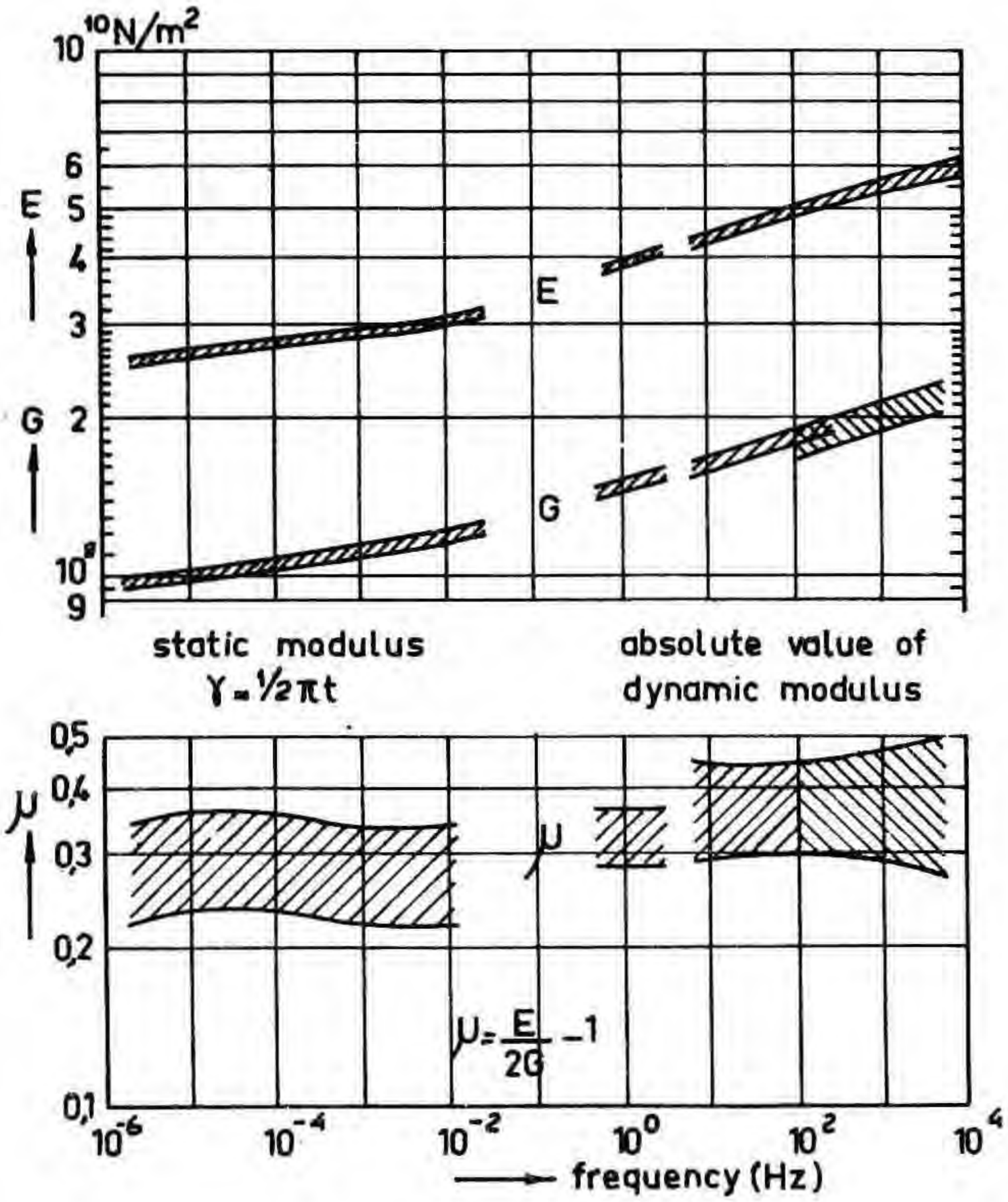

Fig. 2. E, G and Poisson's ratio as a function of the frequency at 20 °C of polymethylmethacrylate.

G17

FOURTH INTERNATIONAL CONGRESS ON ACOUSTICS
COPENHAGEN 21.-28. AUGUST 1962

Noise spectra of Swedish, English and Polish fricatives

Wiktor Jassem, Dr. Doc.
Speech Transmission Laboratory, Royal Institute of Technology,
Stockholm 70, Sweden

Some vocoder systems designed to achieve a maximum reduction of the information flow in the transmission channel and most devices attempting mechanical speech recognition depend on the automatic identification of phonetic units, preferably at the phoneme level. The main difficulty in the theoretical and technical solution of recognition devices lies in the fact that stretches of the speech-wave which are to be identified as representing one particular phoneme are often very different from each other in many respects such as spectral energy distribution, intensity or duration. In most cases the identification of phonetic units depend mainly on the distribution of energy with frequency. The differences in the spectra of acoustic signals representing a particular phoneme are mainly due to (a) differences among individual speakers, (b) effects of "coarticulation" (contextual variation), and (c) non-identity of the articulation on repeated performances. A study of these variations is also one of the basic requirements for establishing common ground for acoustic phonetics and linguistics.

Selecting one class of speech sounds, the fricatives, this investigation attempts to obtain estimates as to the extent of the variation in their spectra due to factors (a) and (c). The material consists of short syllables of the consonant-vowel-consonant or consonant-vowel type. The analysis was performed by a spectrum analyzer constructed at the Speech Transmission Laboratory, Royal Institute of Technology in Stockholm. When this analyzer - called RASSLAN - is used, the spectrum of an acoustic signal shows the distribution of energy in 180 channels, with center frequencies spaced 50 cps apart for a range of 0 - 9 kcps or 100 cps for a range of 0-18 kcps. Several band-widths and several integration time values are available. On the basis of preliminary measurements involving the use of various combinations of the various possibilities it was decided to employ mainly a filter bandwidth of 250 cps and a 5 cps cut-off low-pass smoothing filter (integration time constant = 80 msec). This reduced the randomness in the spectral amplitude to a mean value of 0.8 dB. The maximum of the memory curve occurred in the middle or in the second half of the fricative segment.

The first part of the materials includes syllables consisting of a voiceless consonant followed by each of the three vowels /i a u/ pronounced by three male and three female Swedish voices. The females will here receive the labels I, II and III, and the males IV, V and VI. This part of the investigation is mainly directed towards establishing the extent of differences

among individual speakers of one language. The speakers read quasi-words consisting of combinations of letters which would correspond to the expected combinations of sounds. Two male and two female speakers used the consonants [f] (labio-dental), [s] (post-dental), [ɕ] (palatal) and [ʃ] (alveolar), one female speaker used [ɧ] (labio-velar) instead of [ʃ] and one male speaker used both [ʃ] and [ɧ], all according to their normal speech habits. Thus, there were differences at the phonetic level. To estimate differences in the spectra of phonetically equivalent fricatives the frequencies of the formants and regularly occurring higher-frequency peaks were measured. In each spectrum points along the frequency axis were also taken at which the level of the spectral envelope was -10, -20 and -30 dB relative to the highest level in the envelope.

(1) The most consistent difference among the individual speakers has been observed in a rather high frequency region, viz. between 5 and 13 kcps. For each phoneme a particular speaker either has no regular formant-like energy concentration here, or has one, two or three at very definite frequencies. The following table gives, in kcps these spectral peaks:

	voice	f	s	ʃ	ɕ	ɧ
female	I	7.3 8.5	8.4 10.6 12.2	8.3	7.5	not used
	II	5.3	7.9 8.6 9.7	5.3	13.6	not used
	III	6.8 8.5	8.5 12.3	not used	—	5.0 5.5
male	IV	6.5	7.9	-----	—	not used
	V	5.3 6.4	9.1 10.6 12.3	5.6 6.2 9.7	—	--------
	VI	———	———	-----	—	not used

Other higher-frequency peaks are irregular.

(2) The speakers also differ fairly consistently in the distinctness of the F-pattern in the particular phonemes. Whilst in /f/ all show distinct formants, F_2 F_3 and F_4 of /s/ can be traced in voice IV and V but F_3 is suppressed completely in voice II and III, and rather difficult to discern in voice I. In /ɕ/ F_2 F_3 and F_4 are fairly distinct in voices I, II and IV, voice III shows no trace of F_2 in the spectrum and F_4 is indistinct in voice V and VI. Such features occurred regularly in all the three variants of each phoneme.

(3) When the frequency region is measured within which the spectral level is not more than 10 dB below the highest peak in the spectrum, and the center point of this frequency region is taken, a crude indication of the main spectral energy concentration is obtained. In the three variants of /s/ this point - call it Max - regularly occurred higher in the female voices than in the male voices (around 8.5 for females and 7.0 for males). This female-male distinction is somewhat less regular in /ɕ/ and /ʃ/. With one exception Max was lowest in all variants of all the phonemes in voice IV. The /f/ variants show very irregular Max.

(4) The F-patterns of the individual variants of /f/ and /ç/ were compared among the 6 speakers. Relating all individual F values to the corresponding ones in voice IV, the differences averaged in the F-patterns of the /f/ phoneme were: +16 % for I, +43 % for II, +17 % for III and +14 % for V and VI. The F-pattern was, on an average, 15 % higher in /f/ for the female voices than for the male voices. Similar figures were obtained for /ç/, where the female F-pattern was, on an average, 11 % higher in frequency.

The other part of our materials consists of series of consonant-vowel or consonant-vowel-consonant combinations including all fricatives occurring in Swedish, Polish and English. One speaker was selected for each of the three languages, and at time intervals of approx. 1 month recordings were made of the series. There were three series for each speaker. Each consonant occurred in each series in combination with three different vowels of the [i a u] types. The main purpose of this part of the investigation was to see how much the variations in the spectra of fricative phonemes may be due to non-identity of articulation in an individual speaker on repetition of phonetically equivalent utterances.

For each formant frequency in each of the six variants of /f/ an average from three (or two) specimens was taken and the spread expressed in per cent. For one of the three speakers the deviations ranged from 0 (within measurement accuracy) to 5 % with an average for all the F-patterns of 1 1/2 %. Similar calculations gave a spread of 2 % for the second speaker (with a range of 0 - 5 %) in his /f/ phoneme. The estimation of variations in the spectrum on repeated speech samples is still in progress, but it is believed that the figures just given are reasonably representative.

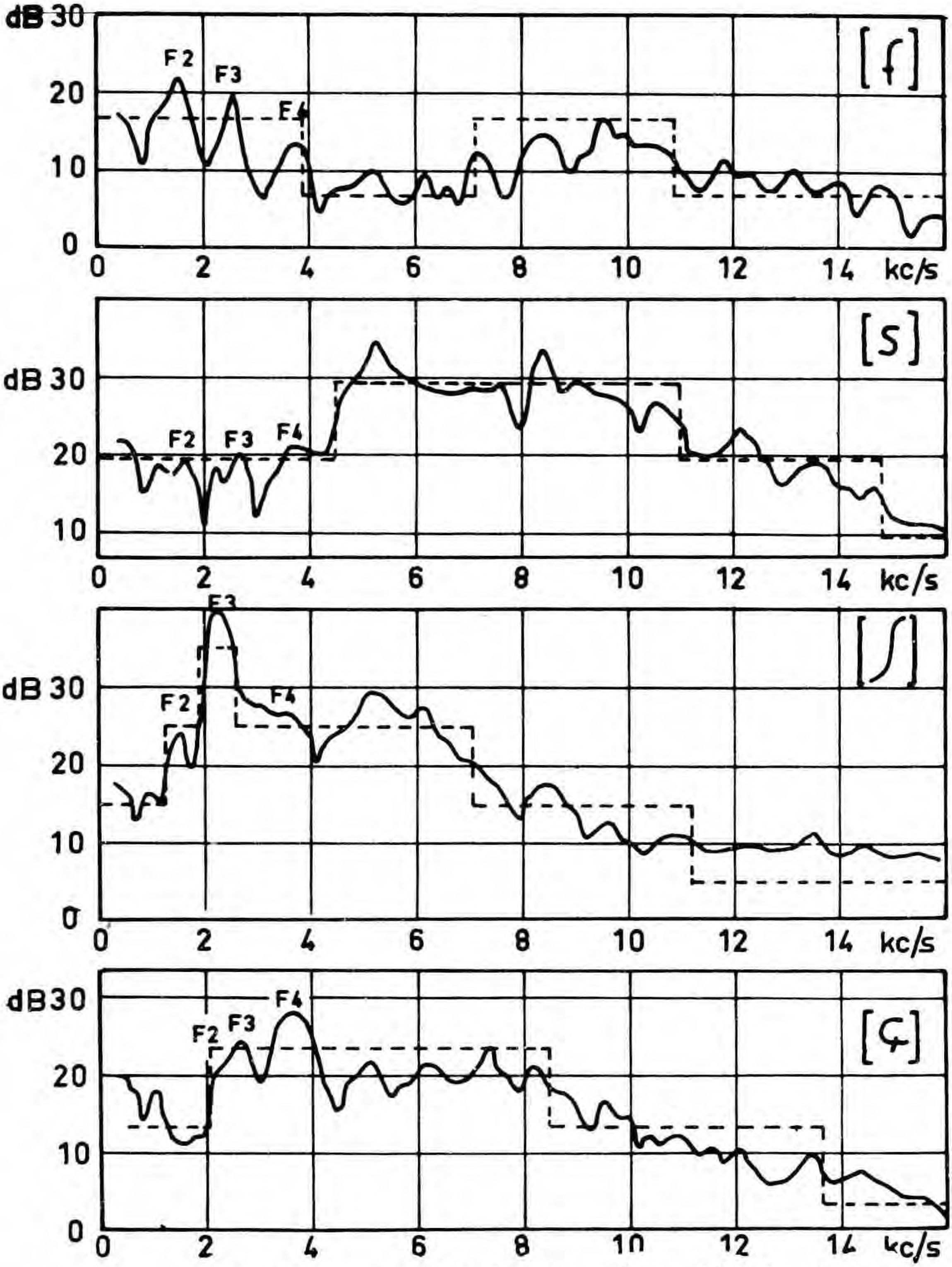

Spectra of the Swedish fricatives /f s ç ʃ/ before [a:] with 10 dB quantization levels. Spectrum level in 250 c/s bands at 1 m distance, 80 ms integration time.

H17

FOURTH INTERNATIONAL CONGRES ON ACOUSTICS
COPENHAGEN 21.-28. AUGUST 1962

A TENTATIVE MODEL ON BINAURAL HEARING.

by

Jaime R. Carbonell.
University of Uruguay, Montevideo, Uruguay.(+)

The present study proposes a model that attempts to explain certain aspects of binaural hearing such as binaural fusion, sound localization, and the binaural threshold shift (BTS). The BTS is the improvement in the masked threshold of signals through binaural listening when the signal and the noise come from sources with different spatial configurations, and has been loosely called "cocktail-party effect" in the past[1]. The theoretical performance of the model is not in contradiction with the results of the classical as well as the most recent psychoacoustic experiments; furthermore, the model attempts to take into account the present status of knowledge about the ear and the nervous system at its different levels. The model postulates that binaural signals are processed by active mechanisms which tend to optimize the output to higher levels, and consist of adjustable transfer functions and switching devices, voluntarily though unconsciously controlled by means of feedback loops[2]. It is also assumed that sound localization is at a higher stage than the BTS and that localization judgments would be made through a "measure of the effort" required to optimize the output to higher levels.

I. Description of the model.

A general scheme of the model is presented in Fig.1. The input signal to each ear passes through a device with an adjustable transfer function (T_L or T_R); the type of the function is the same for both channels, though the instantaneous values may be different,

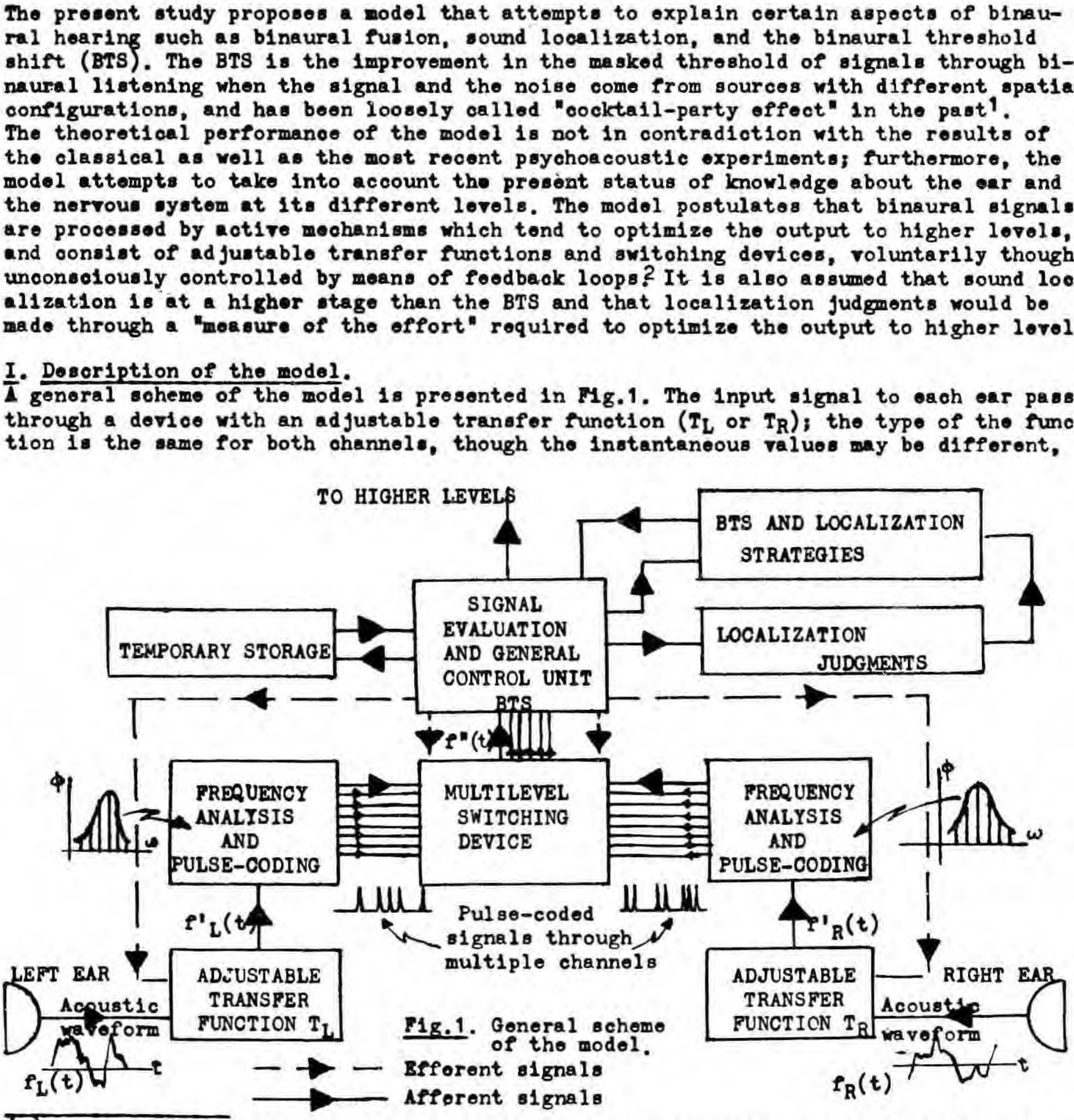

Fig.1. General scheme of the model.

(+) This work was performed while on leave at the Massachusetts Institute of Technology, as a fellow of the International Cooperation Administration.

in order to modify in a different way the two signals transmitted to the central system; this may be either a change in the overall amplitude, or a relative time-delay, or a change in their spectra, or, in general, a combination of these effects. Also, the operations defined by T_L and T_R may be linear or non-linear. Though the processes taking place in the actual mechanisms would undoubtedly be more complicated, it seems a reasonable assumption to consider the transfer functions as linear devices, capable of introducing only a relative time delay between the two signals. The instantaneous value of T_L and T_R is in the model controlled through a feedback loop which operates with the tendency to optimize the final output, as will be explained below. The problems of what the transfer functions may actually be and where they may be located (before, after, or partially before and partially after the next step in the model) will not be considered here.[2]

The next black boxes roughly correspond to the inner ears. It is known that the inner ear (namely the basilar membrane) performs a broad-band frequency analysis on the signals received, and that the signals transmitted from the inner ear to higher levels consist of impulses which, like all neural volleys, are of the all-or-nothing type. In agreement with the mixed place-time theories for frequency discrimination, the model postulates, from the inner ear on: a) transmission of pulses through many parallel channels (at velocities which increase as the intensity of the stimulus increases); b)firing of neurons in relation with the onset of sounds, with the individual cycles for low frequencies, and with the "envelope" for complex sounds with high frequency components.[3] Of course, due to the differences in both the refractory periods and thresholds of individual neurons, the firing of neurons can only be treated in a statistical way.

In the model, each left fiber or group of fibers meets the corresponding right fiber or group of fibers in a logical switching device; there are many such switching devices operating in parallel. Though there are many different ways in which suitable switching devices may be built, only one of them is presented in Fig.2. As will be seen below, the components included in it are all logical components known to exist in the nervous system and the brain. One and-gate, three not-gates, and one exclusive-or-gate (which in turn may be derived from two not-gates and one or-gate)[4] give several possible operating modes. The control is performed by descending fibers from a higher stage. If no path is blocked by a control signal, the result is an inclusive-or logical device. When control pulses block the exclusive-or-gate, only impulses arriving (statistically) in phase from the two ears will go through the and-gate. Other possible operating modes, that account for different psychoacoustical experiments, are also possible (see below).

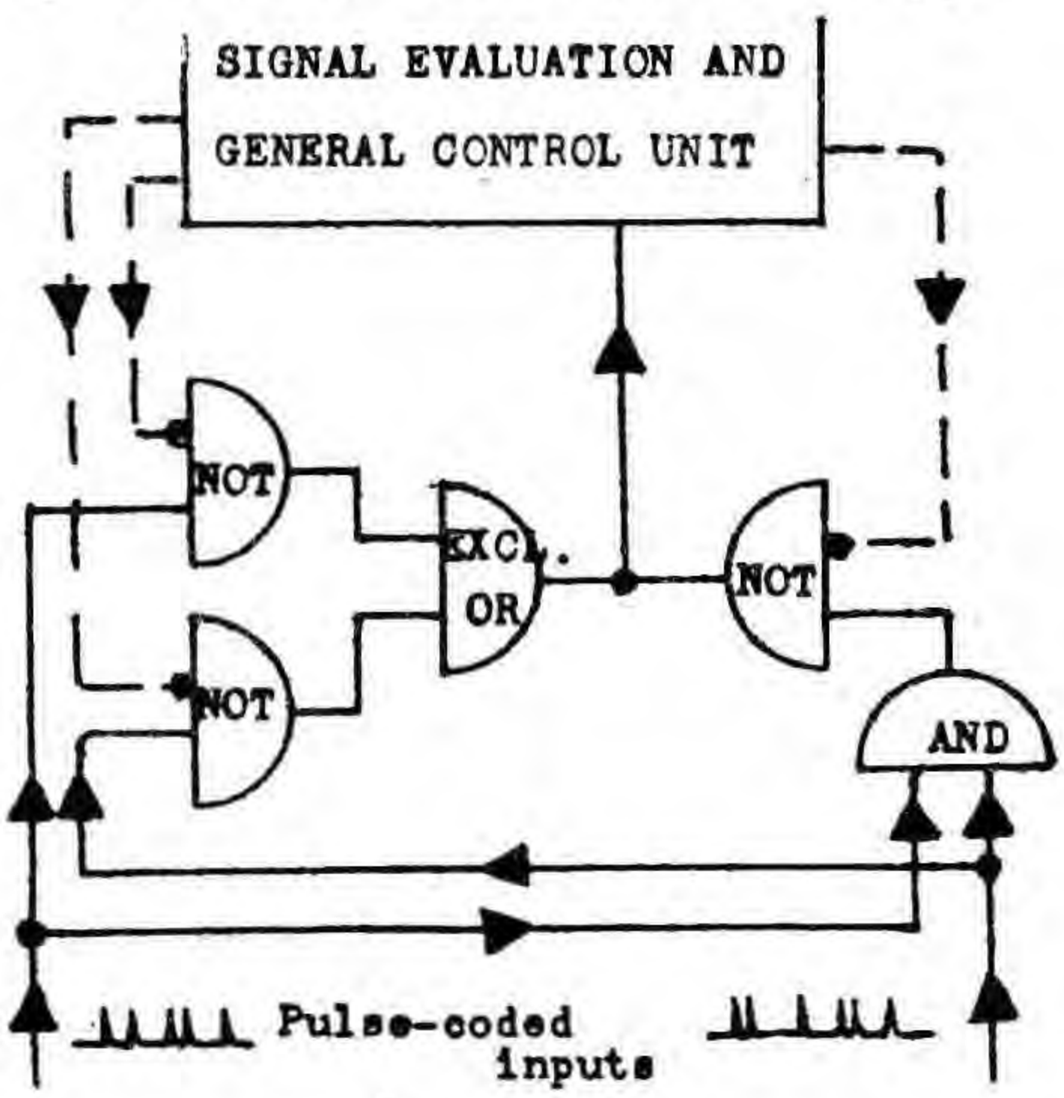

Fig.2. One of the possible schemes for each switching device.
Afferent signals
Efferent signals

The output of the multilevel switching device goes to the black box labeled "Signal Evaluation and General Control Unit", which is responsible for the BTS by controlling the adjustable transfer functions and the multilevel switching device by means of feedback loops.

A temporary storage mechanism is also included at the higher levels of the model, as well as a general strategy unit (see Fig.1). Connected to the signal evaluator and control unit, a localization unit is responsible for the judgments about the position of the sound source, by estimating the "effort" required to optimise the desired signal. Finally, it has been necessary to include in the model a general output to higher levels. This output carries the general information content of the signal, which will be processed, stored, and generally used in any way by the brain.

II. How the model behaves.

We will assume that complex audio waveforms $f_L(t)$ and $f_R(t)$, each one composed of a desired signal plus noise, reach the two inputs (the ears). Therefore:

$$f_L(t) = s_L(t) + n_L(t)$$
$$f_R(t) = s_R(t) + n_R(t)$$

The two signals and the two noises will in general differ in a different way if the corresponding sources occupy different positions in space; the differences will be in time of arrival, in spectral distribution and in overall intensity. The model is concerned with time and intensity differences, the latter being converted into time differences according to what both binaural time-intensity trade experiments and physiological data about the velocity of nervous signals indicate. There are several different cases:

A) In unattentive listening no control signal would be acting, and therefore both signals $f_L(t)$ and $f_R(t)$, after suffering only a broad-band frequency analysis and pulse coding, would go through to higher levels.

B) In normal attentive listening, the first assumption of the model is that the binaural hearing mechanism tends to transform each one of the two desired signals into a common signal s(t) by adjusting the transfer functions to proper values; however, the noises will still be different. At their outputs $f_L(t)$ and $f_R(t)$ are transformed into:

$$f'_L(t) = s(t) + n'_L(t)$$
$$f'_R(t) = s(t) + n'_R(t)$$

The simplest and most efficient way to do this is to turn the head and face the signal source, but the model also postulates an alternative way to do so (at a more or less peripheral level) by introducing an adjustable time-delay in each one of the two auditory pathways. In Fig.1 it has been located before the cochlea where the frequency analysis and pulse-coding of the signals are performed, but physiologically it might be located further on. Pulses corresponding to s(t) arrive in statistical coincidence at the multilevel switching device, while pulses corresponding to the noises arrive uncorrelated. Control pulses block the inputs to the exclusive-or-gate and only coincident signal pulses go through the and-gate.There will also be a few noise pulses, due to their statistical nature; they constitute the weakened background noise. Therefore, the output will be:

$$f''(t) = s(t) + E(t)$$

, where E(t) is the error in the filtering process achieved through the switching devices.

We will now refer to several special cases encountered in different binaural experiments related to the BTS[5,6]. Case (C) corresponds to experiments where a signal is delivered to the left ear and noise to the right one (or viceversa). The obvious solution is to block both the output of the and-gate and the right-hand input to the exclusive-or-gate. The output will have the same form as in case (B), but the error is much smaller since there is no possibility of coincidence of noise pulses (in agreement with experiments with earphones that show practically no cross-masking between the ears). D) For a signal in both ears and noise in one, switching according either to cases (B) or (C) is suitable. E) For a signal in one ear and correlated noises in both, the noises would be made to coincide and would be eliminated by blocking the and-gate and leaving the exclusive-or-gate opened. This also explains one case of antiphasic presentation[6], while the other corresponds to switching mode (B). The advantage of the antiphasic presentation over the heterophasic one[6], is also easily explained in terms of the model.

In all cases, the signal evaluation and control unit estimates how well the desired signal is perceived, and, according to a pre-established strategy, it issues the general control orders to improve and finally optimize (through what might be called a scanning process) the perception of the signal. The temporary storage mechanism supplies information to the evaluator from adjustments made just previously. These previous data can be used to expedite both the next adjustments and the final optimization of the result. In turn, the strategy unit reflects all the past experience of the listener as such; it is the consequence of many past trials. It should be then capable of more or less slow modification in order to explain learning processes for handling new cases, such as unnatural experiments through earphones. The strategy unit would also be responsible for the use of visual and other cues as aids for binaural hearing.

Connected to the signal evaluator and control unit, and after the BTS is obtained, the localization unit judges the position of the sound source by estimating the "effort" required to have the optimum possible output; and it seems logical for that effort to be evaluated in terms of the estimated equivalent movement of the head that produces the

same optimized result. We would, in a way, "synthesize" that muscular effort without actually doing it.
The model then postulates that the BTS occurs at a lower level in the binaural hearing mechanism than sound localization. It is an every day experience that we "pay attention" to the sources we want to localize; we "concentrate"on them, and only then we are able to localize them. Of course, for simple lateralization judgments, there should be some kind of weighting mechanism, probably located within the localization unit, capable of giving a left or right indication. Besides, that mechanism would help to make a first rough guess (a starting point for further adjustments) before the other devices start to operate.

III. Relation of the model with physiological and psychoacoustical data.
The plan of the model and the components included in it are generally considered among the group of possible patterns and possible components to be encountered in the auditory system, as well as in the nervous system and the brain. The idea of feedback control loops in man and in animals, to account for many functions, was first proposed by Norbert Wiener[7] and extensively used by others such as McCulloch[8] who stated that "...the principal function of the central nervous system is that of a computer for an enormously complex, multiple closed-loop servo system." Evidence of the existence of feedback loops in the auditory system has existed for some time[9]. On the other hand, there is also experimental evidence of the existence of and-, not-, and or-gates in the nervous system and the brain[4,8]. Furthermore, the model takes into account other physiological facts such as the frequency analysis and pulse-coding of the auditory signals.
Classical binaural experiments by Hirsh[5], by Licklider[6], by Pollack[1], and by many others are satisfactorily explained in terms of the model. More recent data by David and his associates[3] have also been taken into account. Klumpp and Eady[10], and Tobias and Zerlin[11] have found in independent experiments that the longer the stimulus, the better the interaural time difference threshold; this should be expected from a scanning process. The 6 microsecond limit in accuracy[11]might be probably due to the error or "internal noise" of the system. Finally Tobias and Schubert[12] measured the counterbalance of the transient disparity with the ongoing disparity and found that "...the larger the reported ongoing disparity value, the smaller the per-unit effectiveness of the ongoing cue". In terms of the model, the easier the task to be performed (larger ongoing disparity), the less time required to perform the scanning task, and the less improvement if longer time is allowed.

IV. Main features of the present model.
The present model, built according to physiological and psychoacoustical data, accounts for such binaural phenomena as binaural fusion, sound localization and the BTS. By postulating that sound localization is at a higher stage than the BTS, both phenomena are presented as the result of active mechanisms which tend to optimize the output to higher levels; these mechanisms consist of adjustable transfer functions and switching devices, voluntarily though unconsciously controlled by means of feedback loops.

Acknowledgements. The author is very grateful to Prof. Kenneth N. Stevens for his invaluable suggestions and encouragement throughout this research work.

References. 1.- Pollack, I., and J.Pickett, J.A.S.A., 30, No.2, p.131.
2.- Carbonell, J., Unpublished Thesis, M.I.T., Dept.of E.E., 1960.
3.- David, E.E. and others, several papers, J.A.S.A. and Bell Syst.Techn.J.
4.- Goode, H., and R. Machol, System Engineering, McGraw-Hill, 1957.
5.- Hirsh, I., J.A.S.A., 20, p.536, and 22, No.3, p.196.
6.- Licklider, J., J.A.S.A., 20, No.2, p.150.
7.- Wiener, N., Cybernetics, The Technology Press, 1947.
8.- McCulloch, W., I.R.E.Trans.on Electr.Comp., EC-6, No.3, p.190.
9.- Galambos, R., Physiol.Review, 34, No.3, p.497.
10.- Klumpp, R., and H. Eady, J.A.S.A., 28, No.5, p.859.
11.- Tobias, J., and S. Zerlin, J.A.S.A., 31, No.12, p.1591.
12.- Tobias, J., and E. Schubert, J.A.S.A., 31, No.12, p.1595.

K17

FOURTH INTERNATIONAL CONGRESS ON ACOUSTICS
COPENHAGEN 21.-28. AUGUST 1962

Measurement at High Pressures of the Dynamic Complex Elasticity of Solids and Liquids including Polymers and of Dynamic Viscosity.

G. Bradfield
National Physical Laboratory, Teddington, England.

Introduction

In the study of metals it has been found that the elastic behaviour of alloys is very much dependent on the lattice strain produced by the solute and the extent of this dependence is closely related to the change of elastic constants when the pure solvent is compressed. The equipment described yields the necessary information.

Solids such as rocks may have very different elasticity if porosity is present; for example, a sandstone with a normalised density of 0.78 compared with that of α-quartz may have its elasticity reduced to a normalised value of 0.1 due to this cause. When compressed, the pores of rocks close up and then behaviour is much closer to that of a rock constituting the path of e.g. waves encountered in geophysical survey or earthquakes. The equipment can test rock specimens under pressure to provide this valuable information.

Solids such as polymers behave like porous rocks in some respects and their elastic moduli increase markedly under pressure as the "free volume" is reduced. At a critical value of this free volume many polymers may change from "rubbery" behaviour to "glass-like" behaviour. This change may also occur as the polymer is cooled, even for polymers possessing a high degree of crystallinity. The study of the pressure-temperature relations for constant free-volume seems profitable to separate this parameter from the effects of increased thermal agitation.

The fabrication of polymers involves rates of application of stress which may be quite slow, say a stress cycle in several minutes. In such circumstances creep and recovery take place and the stress/strain relation depends very much on the duration of stressing. Methods are described for the evaluation of this relationship at slow rates of change of stress over wide variations of temperature and pressure and for the measurement of hysteresis also.

The "free-volume" effect on compressibility exists also in polymeric liquids, but in addition this effect governs the viscosity behaviour to a marked extent. Associated liquids frequently also possess a dynamic compliance or springiness, which becomes increasingly important compared with viscous resistance at high shearing rates. The study of these effects can be normalised in terms of pressure and temperature using the "static" value of the viscosity and a nearly constant value for the compliance. In liquids under constant volume conditions, viscosity change against pressure change is related to viscosity/temperature change by a series of coefficients which bear some relation to the composition. (Bradfield, I.E.E. Monograph 521M).

When relaxation effects occur, in polymeric solids at least, there seems to be a relation between the shift caused by temperature change and the shift caused by pressure change; this approximates to 0.25°C per bar in such different solids as rubber vulcanizate, polyisobutylene and polyvinyl acetate. (McKinney et al.Priv.Comm.)

Unified Design and Scope of Measurements for which Equipment is intended

The equipment to be described comprises broadly two parts, the first of which (Fig. 1) is the combination of a pump, a gauge and a pressure vessel operating up to 3,000 atmospheres, with a temperature control system operating from -30° to +130°C. The second part of the equipment comprises a number of interchangeable units which enable measurements of elastic constants to be made in solids and liquids over a range from 15 Mc/s down to, at present, 20 c/s with a further extension under construction

for very slow cycling of about half hour duration. These slow speed equipments provide information on internal friction also and this can be measured at 10, 36, 108, 250 and (possibly) 700 Kc/s. Viscosity measurements can be made on liquids at 10, 36, 108, 205 and (possibly) 700 Kc/s.

Brief Description of Individual Units

Figure 2 shows the use of a piezoelectric crystal outside the pressure vessel transmitting waves through a hard steel bolt, into the specimen inside the vessel. Either irrotational or rotational waves can be used. Figure 2a shows the adaptation of this device to the measurement of velocity in liquids. Figure 3 shows a lower frequency method of test using two piezoelectric crystals, one acting as receiver and one acting as transmitter, spaced at distances of 1 cm and 2 cms apart in successive experiments; the crystals are changed to operate at either $\frac{1}{2}$, 1 or $2\frac{1}{2}$ Mc/s to evaluate the frequency dependence of the constants. By the use of range/amplitude corrections evaluated by Seki et al (J.Acoust. Soc. Am., 28, 230), and the phase change effects evaluated by Bradfield and Goodwin (Phil.Mag., 6, 1065), it is possible, in combination with waveguide corrections adapted from Carome et al (J.Acoust. Soc. Am., 33, 1417), to evaluate both attenuation and velocity in the materials under test to a fair degree of accuracy.

Figure 3a shows a modification of Fig. 3 equipment for the measurement of liquids. Again similar corrections to amplitude and phase are necessary.

Figure 4 illustrates a torsionally vibrating specimen about 3 cms long and $5\frac{1}{2}$ cms diameter set in motion by a pair of piezomagnetic transducers as described by the writer (Brit. J.Appl. Phys., 11, 478) in 1950 (and in more detail in 1959, 1962), the motion being picked up by another similar pair of transducers. At present this equipment has only been operated on metals and there the frequencies involved are about 100 Kc/s with harmonic operation at about 200 and about 300 Kc/s.

Figure 5 shows an ultrasonic torsionally vibrating transducer which is used in the equipment for measuring viscosity at various frequencies; described by the writer (Monograph 521M) in 1961, this has a cobalt-iron-vanadium piezomagnetic element peripherially magnetised and excited with an axial field.

Figure 6 shows the adaptation of the torsionally vibrating viscometer to the measurement of solid polymers in the form of fairly short thick-walled tubes which are attached to a shortened vibrator and form a composite resonator assembly; from the impedence of this at various frequencies near resonance the modulus of rigidity and the internal friction of a polymer specimen can be evaluated. The devices shown in Figs. 5 and 6 can resonate as low as 10 Kc/s and up to 250 Kc/s with a possible extension to 700 Kc/s. Separate transducers are used for 10 Kc/s and 36 Kc/s and 130 Kc/s and harmonic operation of each of these is possible. The device has the advantage that the coil can remain in position undisturbed while the transducers are quickly inter-changed for the various frequencies of operation. In Fig. 7, for operation at much lower frequencies, ($\approx$ 20 c/s), we can no longer rely on the sinusoidal oscillations of uniform rods: it is necessary to use lumped mechanical reactances, the equipment constituting a torsional pendulum. To avoid limitation to a vertical axis, the inertia cylinder is mounted on a shaft in ballbearings driven by a torsional motor of the moving "iron" type. Decay and period of oscillations is monitored with the winding of the motor in a 10 Kc/s bridge circuit using change of inductance to indicate amplitude and period of the decay. Calibration is by means of metal specimens of known modulus of rigidity.

In the modification of the above shown in Fig. 8, very much slower stress cycling is employed, varying from $\frac{1}{2}$ hr to one second per cycle. A more powerful torsional motor is used in two parts. The pole-to-armature air gaps are smaller in order to reduce the wattage in the coils and avoid heating. The angular strain is measured (see Fig. 8a) somewhat as in Fig. 7 but using inductance change on a 120 tooth armature system, so providing measurement to a small fraction of a degree. Calibration is as before. For these measurements the liquids used inside the sealed vessels are either di (2 ethyl hexyl) sebacate or methyl cyclohexane. Possibly iso-pentane may be used later to facilitate very low temperature operation.

Additional Facilities

The pressure vessel illustrated in Fig. 1 is specially designed with a small bore of 1.8 cms to be capable of operation up to 12500 atm., but, at present, the pump, gauge and adaptor system is only suitable for operation up to about 3,500 atms. By a relatively simple modification, however, a pressure intensifier can be introduced between the outlet of the present gauge adaptor and pressure vessel in order to reach 12500 atm. Nevertheless, although such a high pressure is very valuable for precision in the evaluation of the elastic constants of metals under high pressures, the testing of polymers merely up to 1000 atm. provides a great deal of very valuable information.

The present system of testing lacks one important link in the provision of complete information concerning polymers. This is the evaluation of compressibility at relatively low frequencies. Here the method described by McKinney, Belcher and Marvin (Trans. Soc. Rheo. IV, 347) can fill the gap. A preliminary design has been worked out to adapt the interchangeable unit system to a long thin strong chamber to house the piezoelectric "crystals and specimen involved in this system of testing. It is then hoped to be able to operate over the range from 20 cycles up to 2,000 cycles per second in order to compare relaxation and elastic behaviour at these frequencies with the information obtained from the measurements of the modulus of rigidity as already described.

We are interested in the measurement of elasticity of e.g. metals and semiconductors and of elements undergoing transformations (such as to bismuth) at pressures up to 100,000 atms., and we are proposing to modify the 4-ram tetrahedron compression system, devised by Tracey Hall (Scientific American, 201, 61), as in Fig. 9 which resembles Fig. 2 of this account. A pressure pad below one of the tungsten carbide anvils is drilled to 8 mm diameter and on the tungsten carbide anvil itself a common transmit-receive crystal is cemented to send a wave to the end of the specimen under test. By suitable design of strengthening members in the pyrophillite around the specimen it is hoped that the distortion arising from the high pressure flow can be reduced so as to yield a reflection from the end of the specimen and thus provide information on its elasticity by a travel time measurement.

Acknowledgment

The work forms part of the research programme of the National Physical Laboratory and is published by permission of the Director.

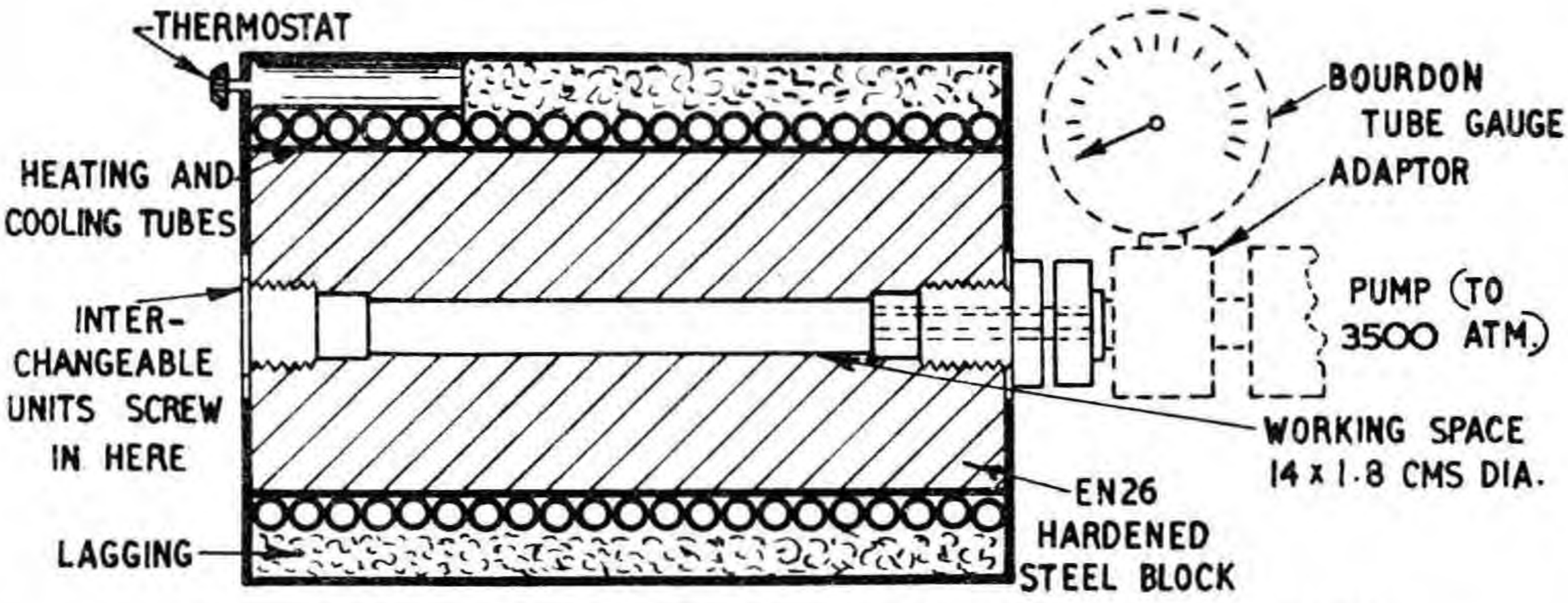

FIG. 1. ASSEMBLY OF PUMP, GAUGE, ADAPTOR AND PRESSURE VESSEL

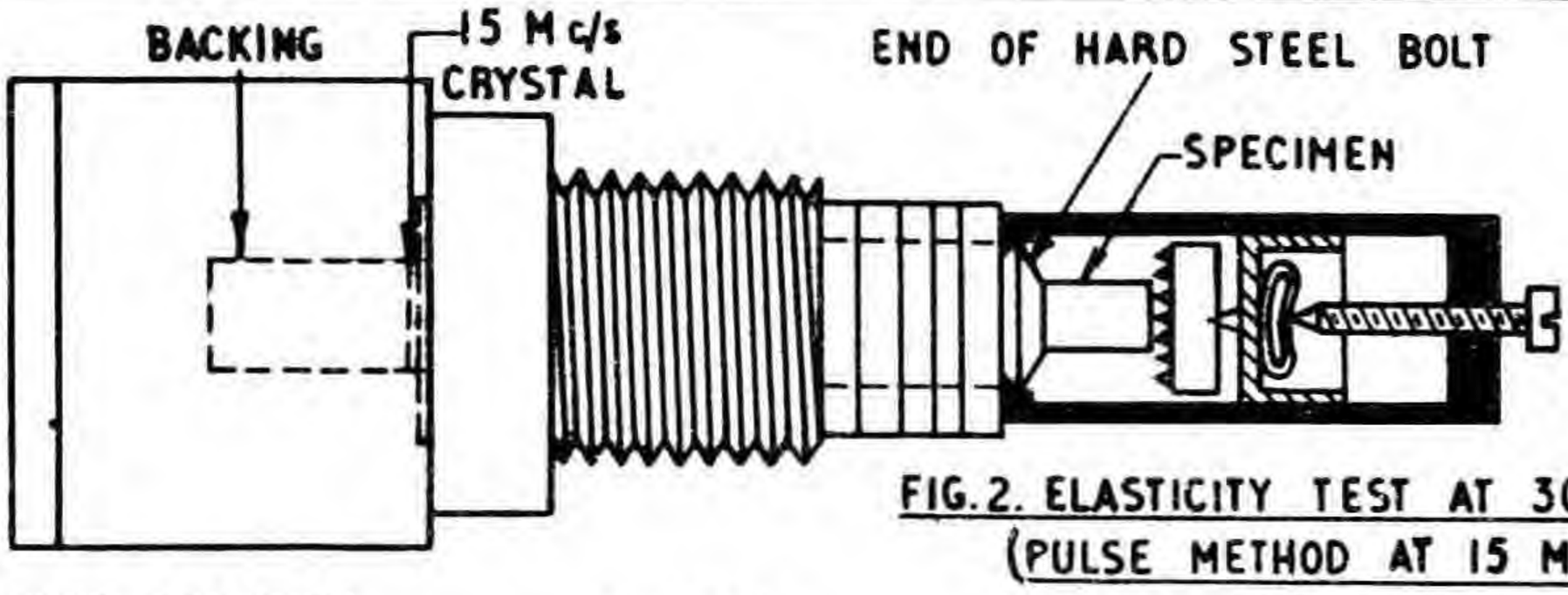

FIG. 2. ELASTICITY TEST AT 3000 ATM (PULSE METHOD AT 15 Mc/s)

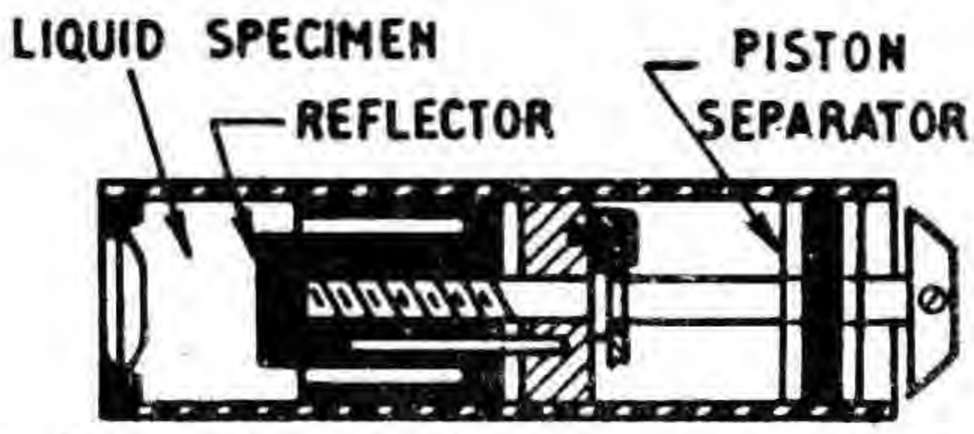

FIG. 2A. COMPRESSIBILITY AT 15 Mc/s

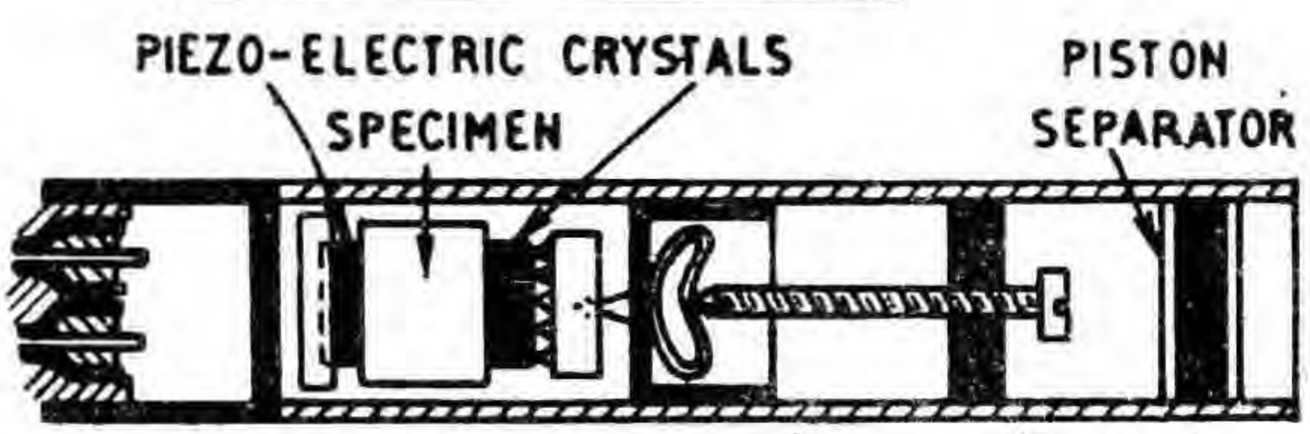

FIG. 3. ELASTICITY TEST AT ½, 1, 2½ Mc/s

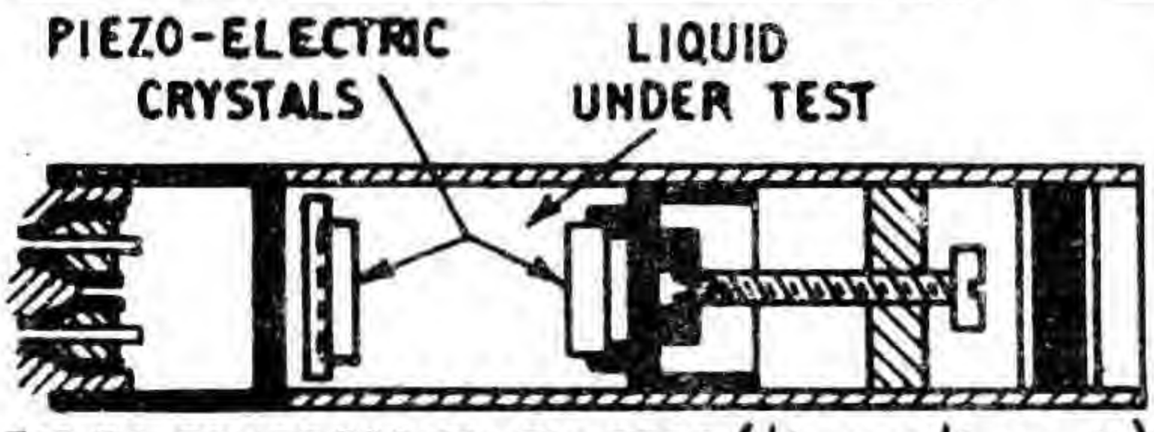

FIG. 3A. COMPRESSIBILITY TEST (½, 1, 2½ Mc/s)

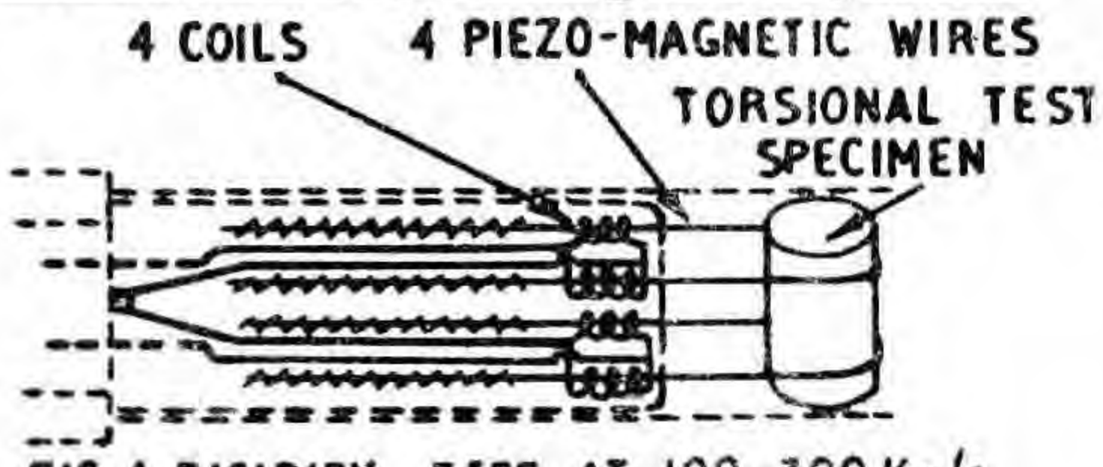

FIG. 4. RIGIDITY TEST AT 100-300 Kc/s

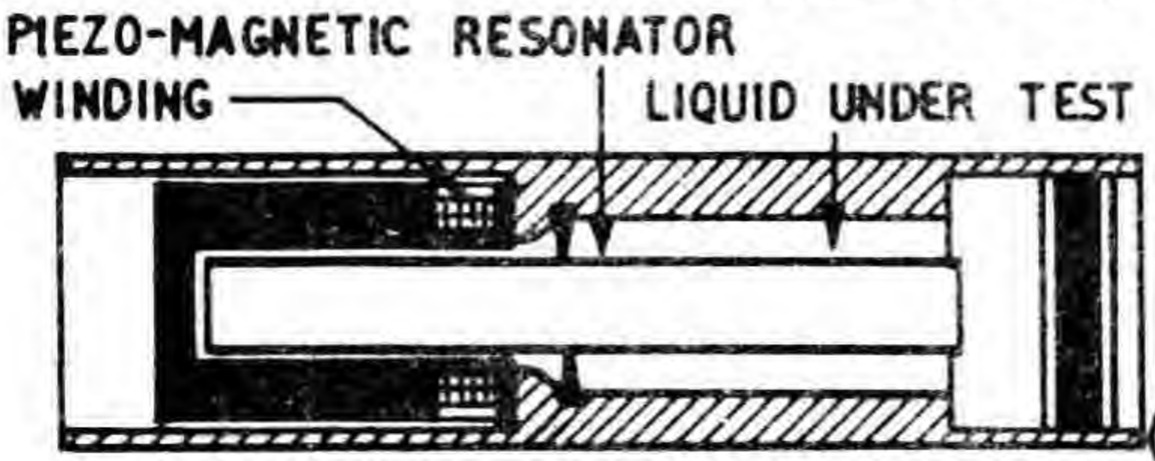

FIG. 5. VISCOSITY TEST AT 36-250 Kc/s

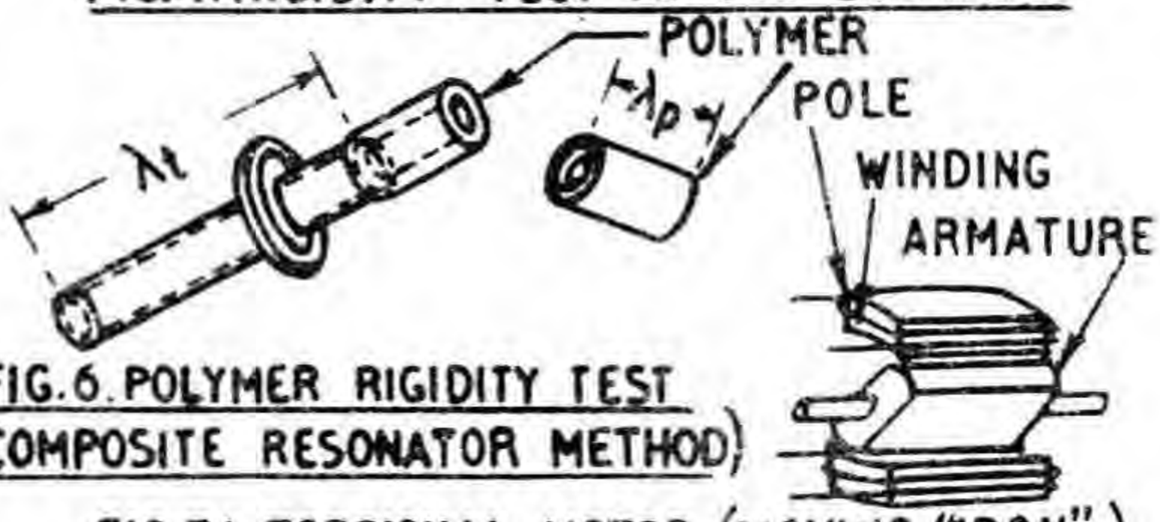

FIG. 6. POLYMER RIGIDITY TEST (COMPOSITE RESONATOR METHOD)

FIG. 7A. TORSIONAL MOTOR (MOVING "IRON")

FIG. 7. POLYMER 20 c/s RIGIDITY TEST

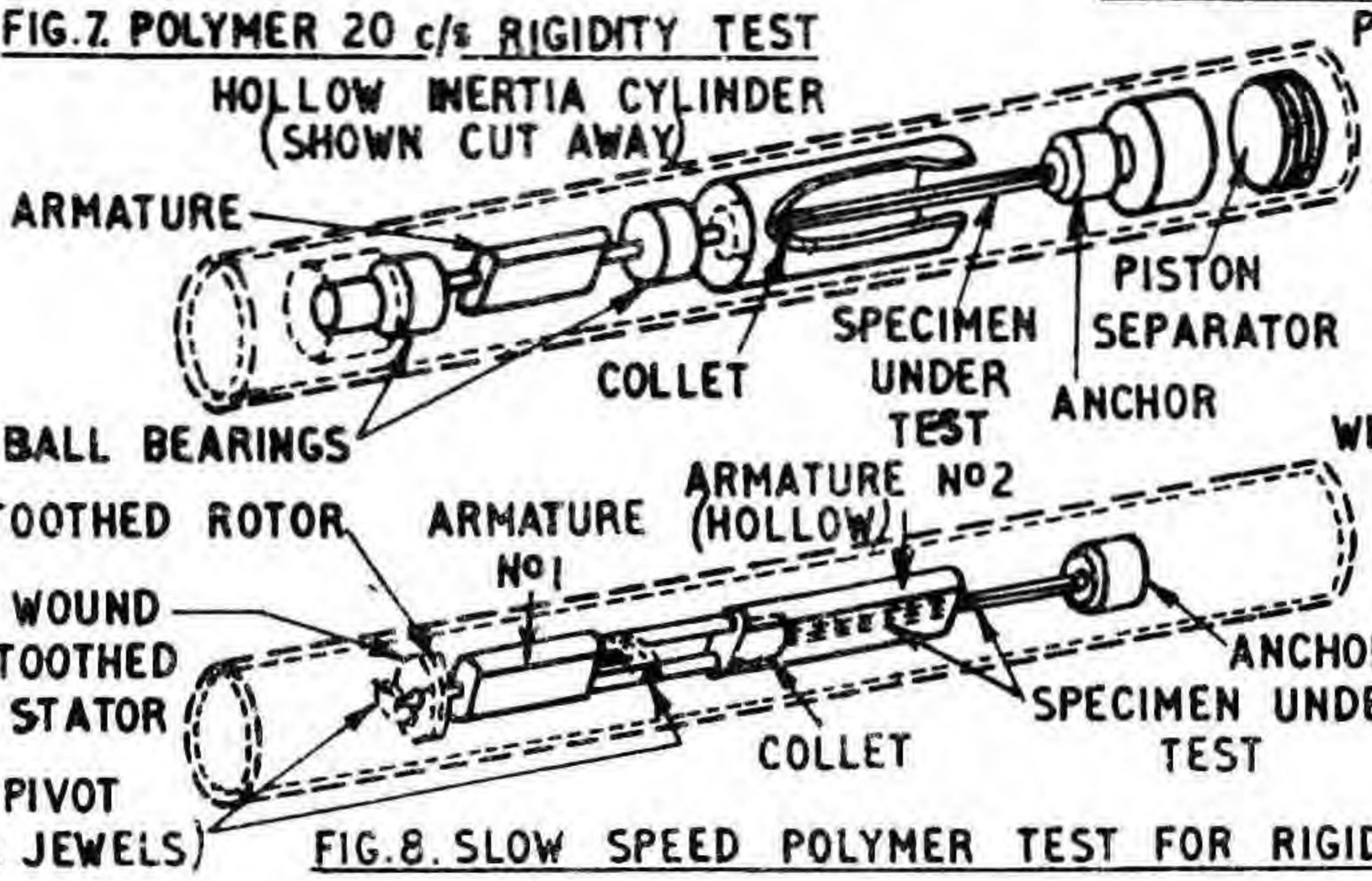

FIG. 8. SLOW SPEED POLYMER TEST FOR RIGIDITY.

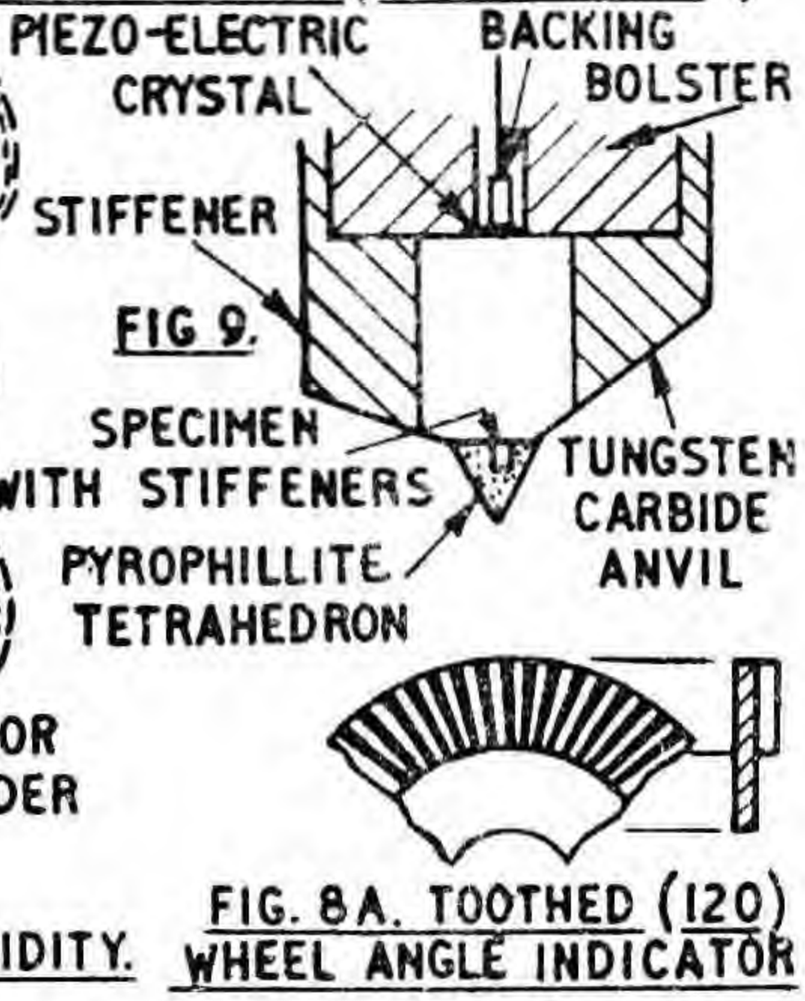

FIG. 8A. TOOTHED (120) WHEEL ANGLE INDICATOR

L17

FOURTH INTERNATIONAL CONGRESS ON ACOUSTICS
COPENHAGEN 21.-28. AUGUST 1962

Effekt der Halslänge und der Kanalwandschallabsorption auf nichtlineare, ungedämpfte Resonatoren

Dr. Y.N. Chen
Forschungslaboratorium für Schwingungen und Lärmbekämpfung,
Gebr. Sulzer A.G., Winterthur, Schweiz

1. Einleitung

Wegen ihres geringen Gegendruckes werden Resonatoren häufig als Auspuffschalldämpfer von Dieselmotoren angewandt. Durch die grosse Lärmintensität und die hohe Strömungsgeschwindigkeit treten aber ungünstig wirkende Nichtlinearitäten auf. Der starke Auspufflärm erregt die Gasmasse im Hals, welcher die Resonatorkammer mit der Auspuffleitung verbindet, zu starken Schwingungen. Die aus dem Hals austretenden Gase bilden infolge der grossen Schwingschnelle einen Strahl[1], welcher sich mit der Auspuffströmung kreuzt und zu Wirbelbildungen führt.

Solche Wirbel erzeugen in der Leitung einem zusätzlichen Lärm durch Querresonanz, Pfeiftöne und Pseudoschall[2)3)4)] und beeinträchtigen dadurch die Wirkung des Resonators.

Diese Störungen können jedoch an der Quelle bekämpft werden, indem man z.B. den obenerwähnten Strahl durch ein Drahtgewebe an der strömungsseitigen Halsmündung dämpft und damit aufteilt, um die Wirbelbildung zu verhindern. Eine solche Massnahme ist leider für sehr heisse Strömungsmedien, wie es bei den Auspuffgasen von grösseren Dieselmotoren mit einer Temperatur bis 550°C der Fall ist, wegen Verzunderung nicht geeignet.

Bei Grossdieselmotor-Auspuffschalldämpfern kann deshalb die Entstehung der Wirbel kaum verhindert werden. Es muss vielmehr danach getrachtet werden, die Energie der Wirbel dauernd zu entziehen. Wie die Untersuchungen zeigen, ist die Auskleidung der die Halsmündungen umgebenden Kanalwände mit schallabsorbierendem Material sehr geeignet, die Wirbel bereits in deren Nähe zu dämpfen. Eine Verlängerung der Hälse kann ebenfalls in beschränktem Masse der Nichtlinearität der Resonatoren entgegenwirken.

2. Nichtlinearität und Pseudoschall

Fig. 1a zeigt einen Resonator für kleine Schallintensität. Wegen der kleinen Schwingschnelle kann sich der Gasstrom aus der Halsmündung an die Umgebungskontur schmiegen. Die ausserhalb der Mündung befindliche Gasmasse, welche durch den Gasstrom mit in Bewegung gesetzt wird (Holmholtzsche Korrektur), lässt sich angenähert berechnen, da der Einfluss der Wände des die Mündung umgebenden Raumes nur schwer erfassbar ist[5)6)].

Bei grosser Schallintensität bildet sich ein Strahl nach der Mündung aus (Fig. 1b). Wenn die Strömung in der Leitung eine hohe Geschwindigkeit V hat, kann sie beim Kreuzen des Strahls aus dem Hals zur Wirbelbildung führen. Eine starke Steigerung der Turbulenz der Gasströmung nahe der Resonatoröffnung wurde bereits von Schilz[4)] gefunden (vgl. Bild 18 in seiner Arbeit). Wenn eine Resonatorkammer durch mehrere gleichmässig verteilte Hälse mit der Leitung verbunden ist (s. Fig. 2), dann wird die Wirbelbildung regelmässig auftreten. Ein Pseudoschall mit der Frequenz

$$\nu = \frac{V}{s}$$

wird mit der Strömungsgeschwindigkeit stromabwärts wandern[4)].

Der Pseudoschall kann nach obiger Darstellung in Zusammenhang mit dem Strahl aus dem Hals gebracht werden. Die Halsmündungen selbst dürften wegen dem Vorhandensein der Grenzschicht

nur eine kleine Störung auf die Strömung verursachen. Diese Annahme lässt sich aus einem Versuch von Meyer u.a.[2], wo der Pseudoschall durch Abdeckung der Halsmündung auf der Kammerseite mit einem dichten seidenen Gewebe unterdrückt werden konnte, bestätigen. Hätte die Halsmündungsöffnung an der Leitungswand hierbei die Hauptrolle gespielt, so müsste der Pseudoschall nach wie vor auftreten. Das seidene Gewebe dämpfte jedoch die Schwingung so stark, dass am Austritt sich kein starker Strahl mehr ausbilden konnte.

Ein weiterer Versuch derselben Autoren zeigte, dass eine Abdeckung der strömungsseitigen Halsmündung durch ein weitmaschiges Gewebe den Pseudoschall ebenfalls unterdrückte. Hieraus ergibt sich die Annahme, dass der aus dem Hals austretende Strahl durch das grobe Gewebe in lauter kleine Strahlen aufgeteilt wurde (Fig. 3). Dies nunmehr kurze Strahlenbündel störte die Strömung in der Leitung nur wenig, wodurch keine nennenswerte Wirbelbildung auftrat und somit kein Pseudoschall erzeugt wurde.

Diese Methoden sind leider bei Grossdieselmotoren nicht verwendbar, da das Gewebe schnell durch das Rauchgas verbrannt würde.

3. Dämpfung von Pfeiftönen, Pseudoschall und Querresonanz durch Auskleidung der Leitungswände mit Absorptionsmaterial

Ein Auspuffschalldämpfer aus zwei Resonatoren nach dem Prinzip von Fig. 4a wurde an einem 4-Takt-6-Zyl.-Dieselmotor (850 PS) untersucht. Der Resonator I war für Vollast (n = 850 U/min) und der zweite für Leerlauf (n = 430 U/min) abgestimmt. Die mittlere Strömungsgeschwindigkeit in der Auspuffleitung betrug für Vollast ca. 74 m/s und für Leerlauf 12 m/s. Der Lärm wurde bei Vollast im Abstand von 1 m seitlich der Auspuffleitungsmündung ohne und mit Schalldämpfer gemessen. Fig. 5 zeigt die Messresultate, und zwar Kurve 1 für Messungen ohne und Kurve 2 für Messungen mit Schalldämpfer. Wenn man die beiden Kurven vergleicht, entdeckt man zwei Hauptgebiete der Schalldurchbrüche: das erste bei 200 bis 400 Hz und das zweite bei 1600 bis 2000 Hz.

Der Abstand zweier benachbarter Hälse betrug 40 mm. Es sollte einen Pseudoschall von einer Frequenz von

$$\nu = \frac{74}{0{,}04} = 1800 \text{ Hz}$$

auftreten.
Die Quereigenfrequenz der Auspuffleitung wird nach folgender Formel berechnet:

$$f_q = 0{,}586 \frac{a}{d}$$

wobei a = Schallgeschwindigkeit des Rauchgases
d = Durchmesser der Auspuffleitung
sind. Mit $a = 540$ m/s und $a = 0{,}21$ wird

$$f_q = 0{,}586 \frac{540}{0{,}21} = 1500 \text{ Hz}$$

Das zweite Schalldurchbruchgebiet kann hiermit auf den Pseudoschall und die Quereigenfrequenz zurückzuführen sein. Das erste Gebiet dürfte durch Pfeiftöne, welche an den Halsmündungen erregt werden, hervorgerufen werden.

Bei Leerlauf-Drehzahl des Dieselmotors zeigt die Dämpfung des Schalldämpfers einen ähnlichen Verlauf wie bei Vollast-Drehzahl.

Als einen weiteren Schritt der Untersuchung wurden die die Hälse umgebenden Rohrwände mit Schallabsorptionsmaterial ausgekleidet (Fig. 4b). Die Ausführung der Auskleidung ist aus Bild 4c ersichtlich. Der Abstand der Hälse im Resonator I (für Vollast) war auf 60 mm vergrössert. Mit diesem neuen Dämpfer ausgerüstet, wurde der Lärm des Dieselmotors nochmals gemessen. Kurve 3 in Fig. 5 zeigt das Messresultat. Das erste Schalldurchbruchgebiet des alten Dämpfers wurde mit Erfolg unterdrückt. Das zweite Schalldurchbruchgebiet konnte ebenfalls abgeschwächt werden. Er war nach den tieferen Frequenzen verschoben, da die Frequenz des Pseudoschalls des neuen Dämpfers folgendem Wert

$$\nu = \frac{74}{0{,}06} = 1230 \text{ Hz}$$

entsprach.

Die Wirkung des Absorptionsmantels um die Hälse ist spezifisch für die an den Halsmündungen auftretenden Wirbel, deren Turbulenzenergie sofort am Entstehungsort stark absorbiert wird und eine Fortpflanzung unterbindet. Wenn sich ein äquivalenter Absorptionsmantel statt im Resonator in der Auspuffleitung befände, ist sein Effekt unwesentlich klein. Die Wirkung dieses Schallabsorptionsmantels kann nicht auf blosse Absorption des Schalls zurückgeführt werden. Eine kurze Berechnung kann dies bestätigen:

Nach King u.a.[7)8)] würde die Absorption

	3 db	bei 300 Hz
und	11 db	bei 1000 Hz

für einen rein akustischen Fall ohne Strömung betragen. Wenn man die Erhöhung der Impedanz des Absorptionsmaterials und der Vergrösserung der Wellenlänge durch die hohe Strömungsgeschwindigkeit von 74 m/s berücksichtigt, dann würde nach Gerber[9)] bei 250 Hz keine Dämpfung, bei 1000 Hz nur ca. 1 db Dämpfung auftreten. Somit ist klar, dass der Mantel nicht als direkter Absorptionsdämpfer des Schalls angesehen werden darf.

Um die obige Behauptung experimentell zu überprüfen, wurde ein zum Resonatordämpfer führendes Bogenstück von etwa 500 mm Länge mit Schallabsorptionsmaterial ausgekleidet. Es wurde hierdurch, wie erwartet, keine nennenswerte, zusätzliche Dämpfung erzielt.

4. Erhöhung der Dämpfung des Resonators durch Verlängerung der Hälse

Nach Versuchen von Meyer[2)] wird die Dämpfungskurve des Resonators mit höher werdender Strömungsgeschwindigkeit in der Leitung immer flacher (Fig. 6). Dies kann einerseits auf die Aenderung der Impedanz des Resonators und andererseits auf die Nichtlinearität desselben zurückgeführt werden. Nach Schilz[4)] wird die aus dem Hals austretende Schwingschnelle durch die Strömung mitgerissen. Eine Richtungsänderung der Schwingschnelle von 40° wurde bei demselben Verfasser für einen speziellen Fall aufgefunden. Da diese Schwingschnelle nichtlinear ist, kann durch die Ueberlagerung der Strömungsgeschwindigkeit die Abstimmung des Resonators beeinträchtigt werden. Je länger der Hals ist, um so schwächer wird sich diese nichtlineare Störung auf die Gasmasse im Hals auswirken. Somit wird die Dämpfung des Resonators verbessert.

Um dies zu überprüfen, wurden zwei Resonatoren mit gleicher Resonanzfrequenz, aber mit verschiedenen Halslängen an einem 12 Zyl.-4Takt-Dieselmotor (2500 PS) ausgemessen. Die Halslänge des ersten Resonators betrug nur 3 mm (gleich Blechdicke), mit 18 mm Durchmesser, und diejenige des zweiten 42 mm mit 15 mm Innendurchmesser. Wie in Fig. 7 dargestellt ist, besass der Resonator mit den längeren Hälsen eine Dämpfungsverbesserung von 1 bis 1,5 db, gegenüber der gesamten Resonatordämpfung von 8 bis 11 db.

5. Zusammenfassung

Hohe Strömungsgeschwindigkeiten verursachen in ungedämpften Resonatoren (z.B. Auspuffschalldämpfer für Dieselmotoren) tieffrequente Pfeiftöne und hochfrequente Pseudoschallwellen. Die schwingende Gasmasse der Resonatorhälse wird zudem in die Strömungsrichtung mitgerissen. Diese Störungen lassen sich wirksam bekämpfen, wenn man unter Verzicht auf schwer durchführbare Dämpfungsmassnahmen in den Resonatorhälsen diese lediglich verlängert und nur in der Nähe ihrer Oeffnungen die Kanalwände mit schallabsorbierendem Material auskleidet.

Literatur

1) Barthel, Frequenz 12 (1958), 72. 2) Meyer, Mechel und Kurtze, J. Acoust. Soc. Amer. 30 (1958), 165. 3) Mechel, Acustica 10 (1960), 133. 4) Schilz, Acustica 11 (1961) 137. 5) Bolt, Labate und Ingard, J. Acoust. Soc. Amer. 21 (1949), 94. 6) Schröder, Acustica 3 (1953), 54. 7) King, "Technical Aspect of Sound", 1953, Bd. 1, 178. 8) King, Engineering 165 (1948), 97, 145. 9) Gerber, VDI-Berichte Bd. 24, Schwingungsabwehr, 1957, 139.

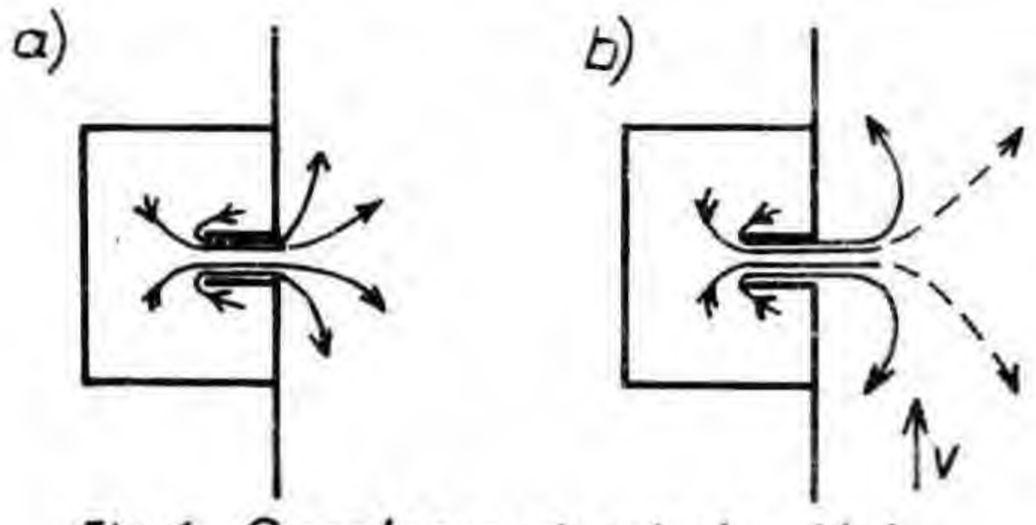

Fig 1. Gasstrom durch den Hals
a) akustisch (linear)
b) hydrodynamisch (nichtlinear)

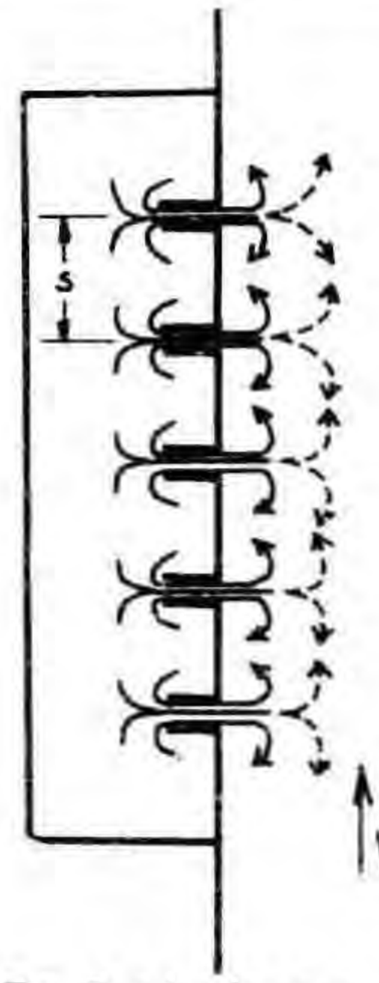

Fig. 2 Hintereinander geschaltete Hülse

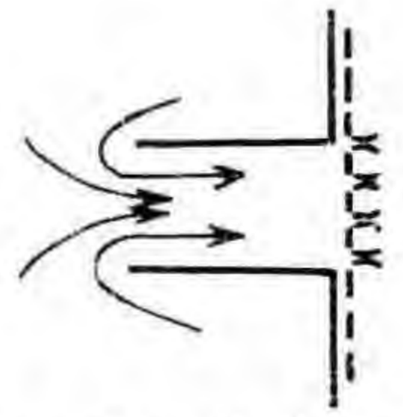

Fig. 3 Aufteilung des Strahls

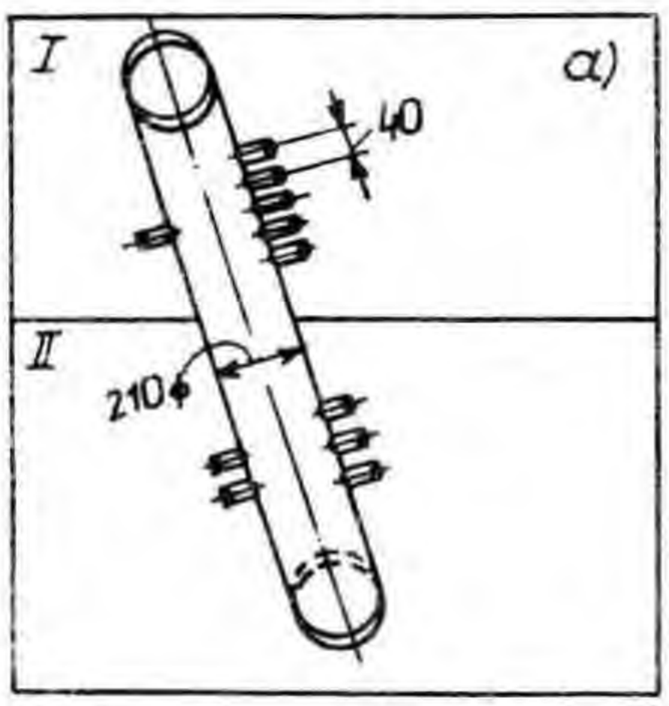

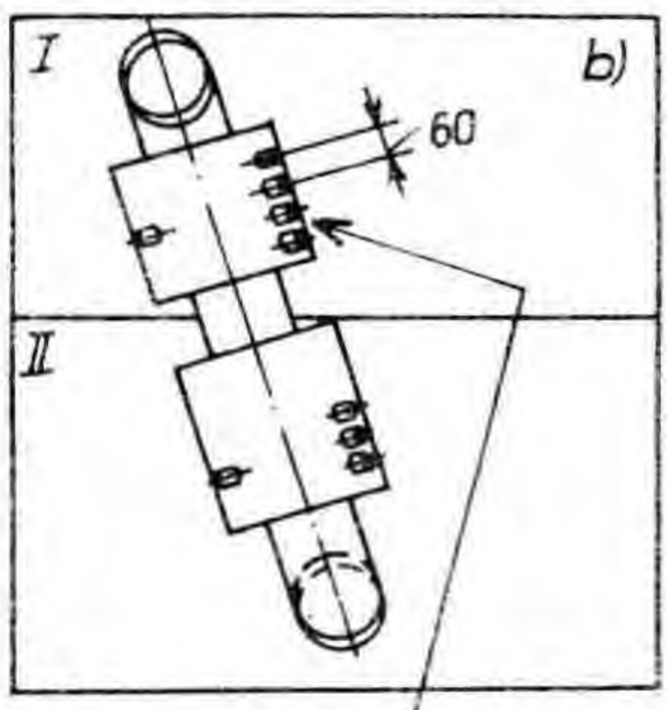

Fig. 4 Resonator-Schalldämpfer
a) ohne Absorptionsmantel
b) mit Absorptionsmantel
c) Absorptionsmantel

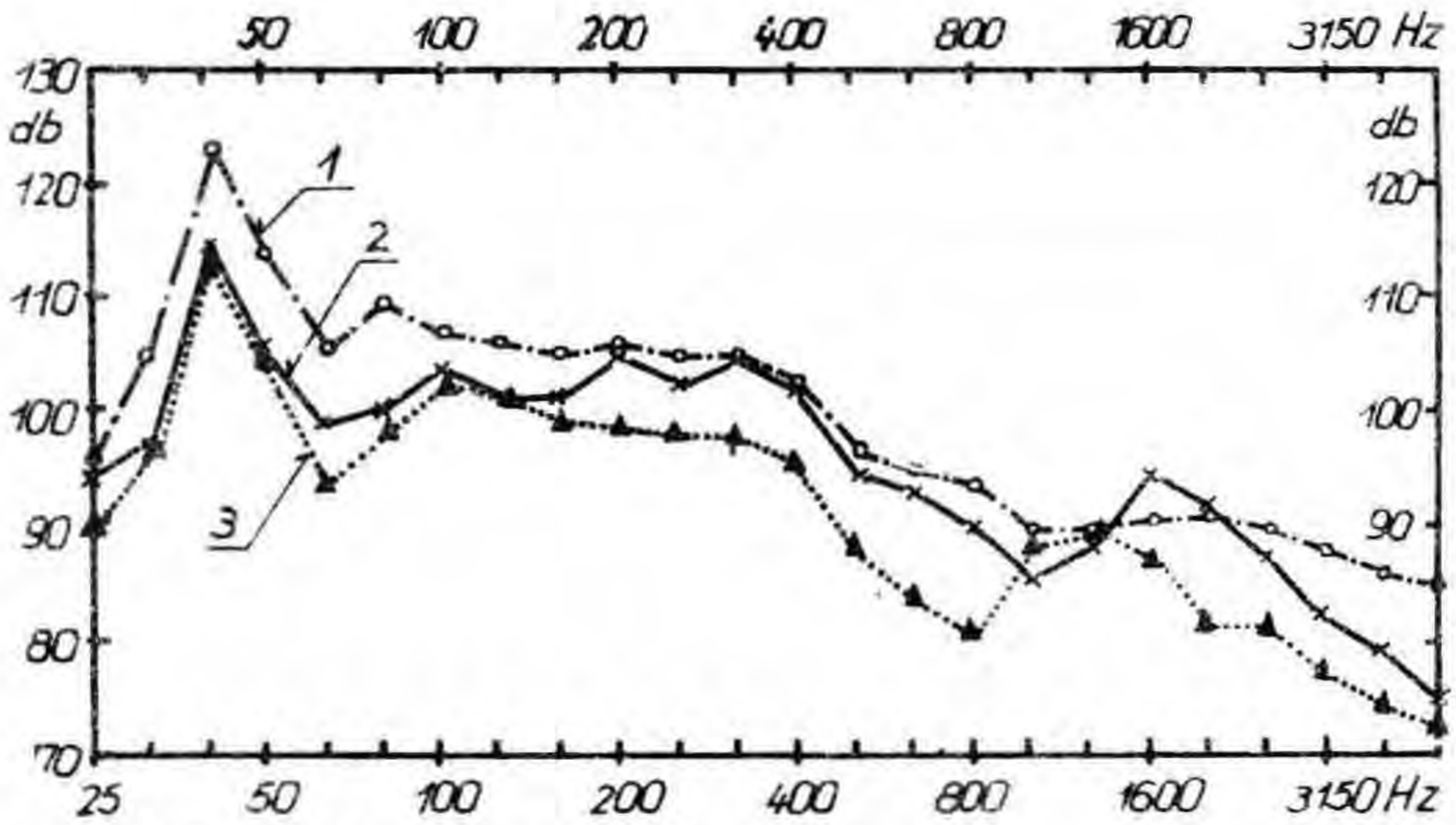

Fig. 5 Schallspektren in Terz
Kurve 1: ohne Schalldämpfer
Kurve 2: mit Schalldämpfer ohne Absorptionsmantel
Kurve 3: mit Schalldämpfer mit Absorptionsmantel

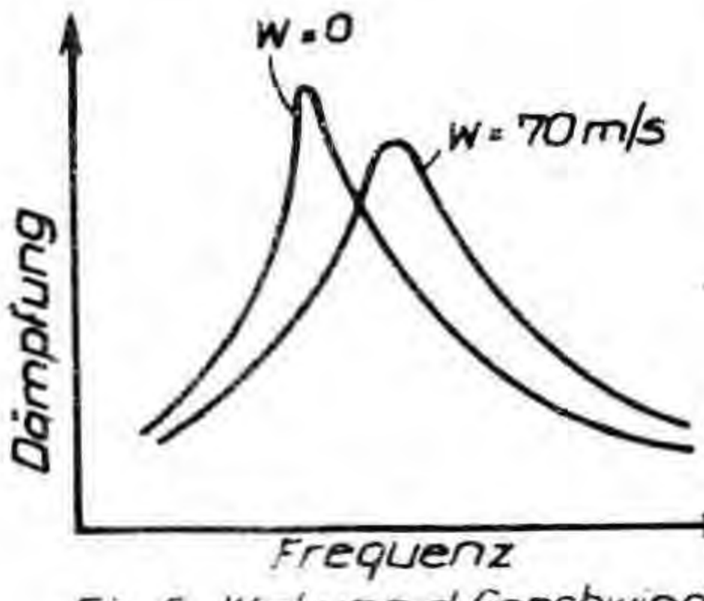

Fig. 6 Wirkung d. Geschwindigkeit

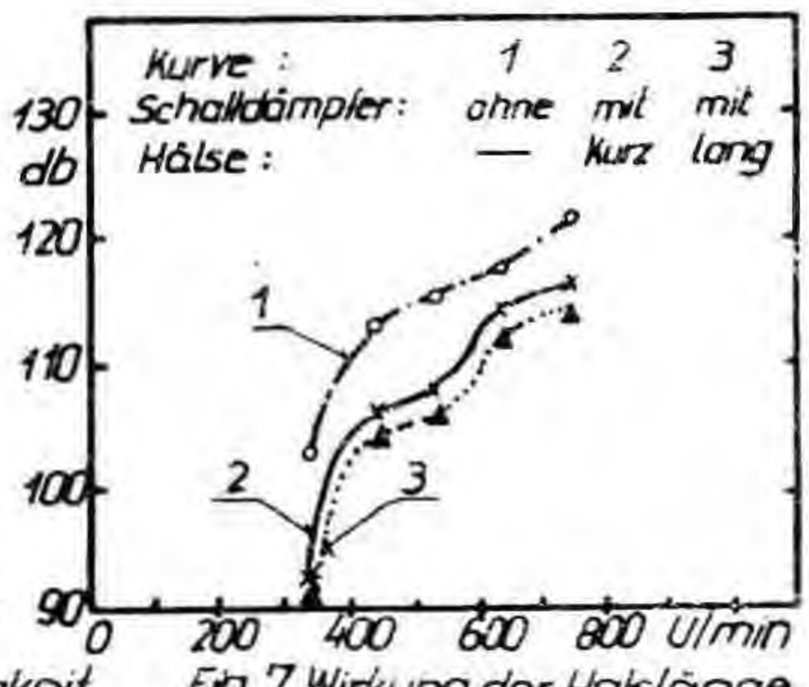

Fig. 7 Wirkung der Halslänge

N17

FOURTH INTERNATIONAL CONGRESS ON ACOUSTICS
COPENHAGEN 21.-28. AUGUST 1962

On the Use of Warble Tone and Random Noise for Acoustic Measurement Purposes.

Jens T.Broch, Dipl.Ing. E.T.H.
A/S Brüel & Kjær

The study of the various branches of acoustics require a somewhat different measurement technique, and the requirements to the signal source will therefore also vary.

As long as the exact behaviour of, for example, electro-mechanical-acoustical transducers is investigated, the most convenient signal to use is the simple, pure sinewave. However, most phenomena related to room- and psycho-acoustics, and noise control, such as speech, music and noise are complex and transient in nature. Also, in room acoustics the physical dimensions of the boundaries within which the sound waves travel are of the same order of magnitude as the wavelength of the sound. Such conditions require, for more realistic and convenient measurements, some sort of a complex test signal, instead of pure sine-waves, as well as a relatively simple method of time and space averaging.

Two main types of test signals have, in the course of time, been suggested and found wide-spread use for these types of measurements, namely "warbled tones" and controlled, electrically produced, bands of random noise.

Now, what are the significant difference between the two types of signals and which type of signal should be chosen for a particular measurement problem.

Let it be stated at once that warbled tones are easier to produce and "control" than random noise, and measuring equipment used in conjunction with warbled tones will thus, in most cases, be the least expensive. However, in certain cases where "beats" and non-linearities are involved, the use of a random noise test signal may be the only way to produce realistic measuring results. In all circumstances it seems that random noise can substitute the warbled tone, - while the converse is not true.

The significant differences between the two types of signal can be understood when the physical characteristics of the signals are known. Starting with the warbled tone this is a "simple" frequency modulated signal.

The frequency spectrum of such a signal will, when the modulating signal consist of a periodic wave, consist of discrete lines spaced at multiples of the fundamental modulation frequency around the carrier, see Fig.1a.

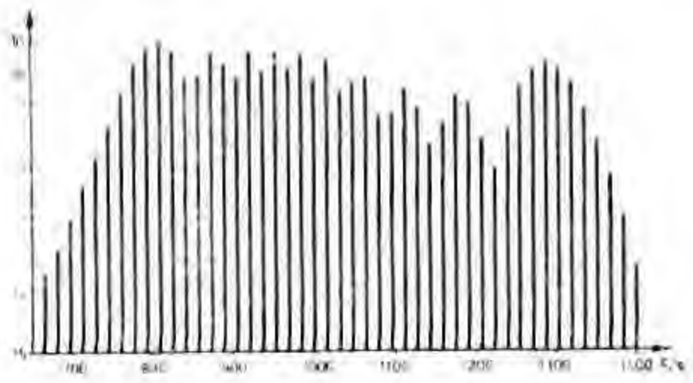

Fig. 1a

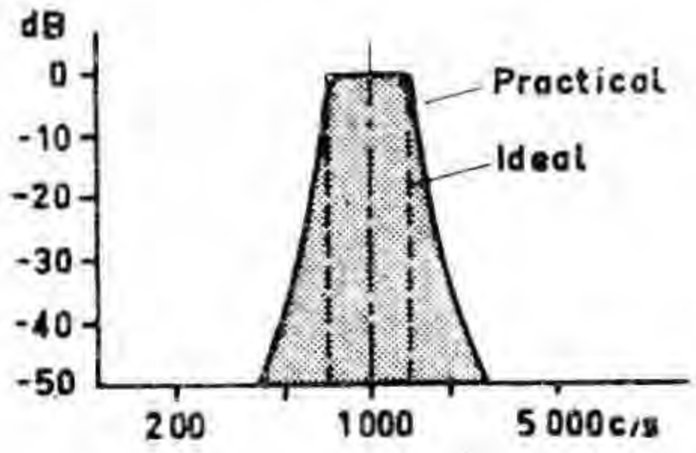

Fig. 1b

If, on the other hand, bands of random noise are used as test signal, no discrete lines are obtained, the spectrum in this case being completely continuous within the band considered, Fig. 1b.

However, also another, significant difference exist between the two types of signal, namely the amplitude vs. time relationship. Fig.2a shows a time record of a warbled signal and Fig. 2b the same for a band of random noise photographed off the screen of a cathode ray oscilloscope. It can be seen from the figure that while the maximum amplitude remains fairly constant for the warbled signal, it varies considerably with time for the noise band.

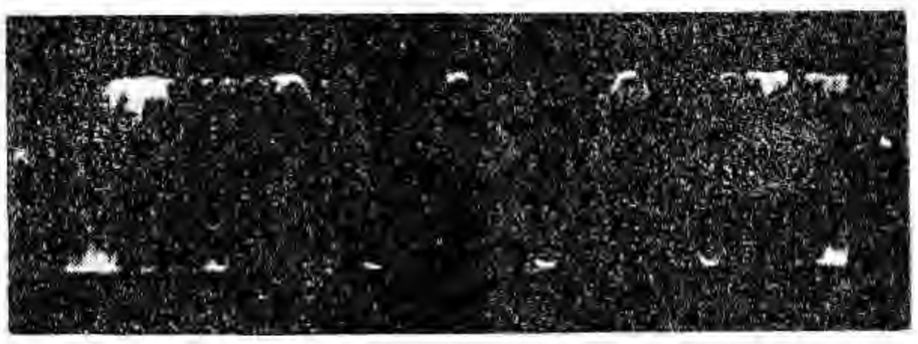

Fig. 2a.

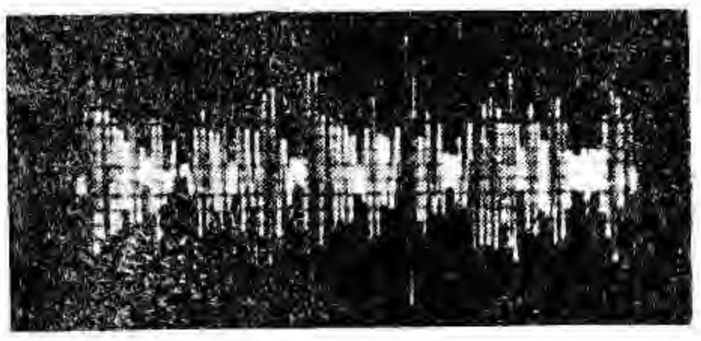

Fig. 2b.

Regarding the use of the two types of signal it must be viewed in relation to the actual measurement problems. In most room acoustic measurements one of the main problems is to obtain a realistic space averaging. As is well known to acoustical engineers the room resonances form a rather complicated scheme of sound distribution vs. space coordinates at medium and higher frequencies. Investigate the usefulness of warbled signals, relative to bands of noise M.I.Karnovski (U.S.S.R.) has studied the auto-correlative function for the two types of signal in the presence of reflecting surfaces and assumed that if the correlation coefficient $R(\tau) < 0{,}1$ a practically diffuse sound field existed. He found the following expressions for the auto-correlation:

For "ideal" bands of random noise:

$$R_n(\tau) = \frac{\sin\left(\frac{\Delta\omega\tau}{2}\right)}{\frac{\Delta\omega\tau}{2}} \cdot \cos\omega_0\tau$$

For an "ideal" warbled signal:

$$R_w(\tau) = \frac{\sin\left(\frac{\Delta\omega\tau}{2}\right)}{n \sin\left(\frac{\Delta\omega\tau}{2n}\right)} \cdot \cos\omega_0\tau$$

where $\omega_0 = 2\pi f_0$ = angular center frequency of the band considered, $\Delta\omega$ = bandwidth, τ = time difference between the direct and reflected signal at the point of measurement and $n = 2m$ (m = modulation index of the warbled signal). It can be seen from (2) and (3) that if $n \to \infty$ then $R_n = R_w$, which means that for high modulation indices (m) of the warbled signal the influence picture for a band of random noise and a warbled signal of the same bandwidth and center frequency will be the same.

The factor $E_{(n)} = \frac{\sin\left(\frac{\Delta\omega\tau}{2}\right)}{n \cdot \sin\left(\frac{\Delta\omega\tau}{2n}\right)}$ is plotted in Fig.3 for various values of n.

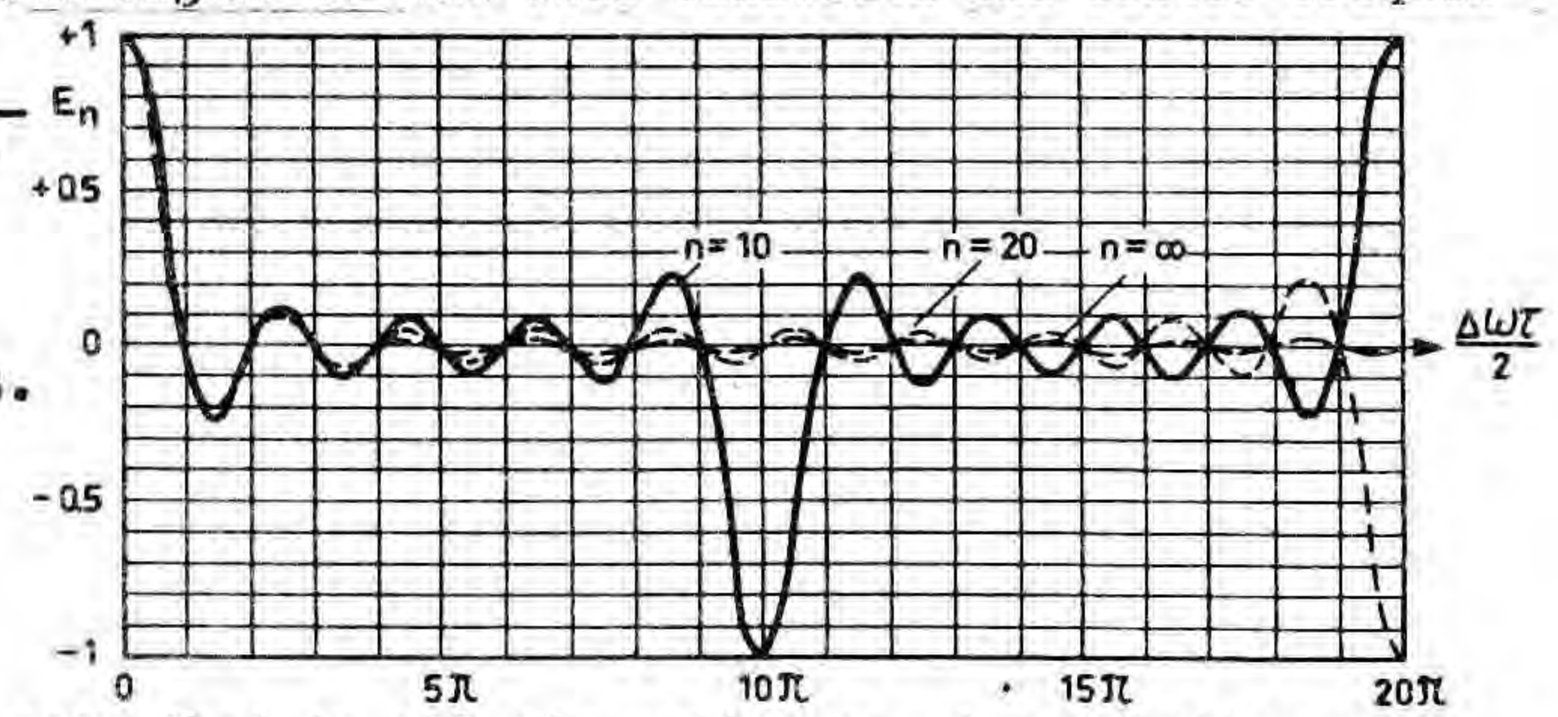

Fig. 3.
(From M.I.Karnovski)

From the figure it can be seen that in all circumstances, i.e. whether a warbled tone or a noise band is used as test signal, a distinct interfe-

rence picture will be obtained near the reflecting surface. However, in the case of warbled tones also a second, third, etc. strong interference range is obtained with a maximum determined by the relation $\frac{\Delta\omega\tau}{2}=n\pi$. If τ is set equal to $2\frac{l}{c}$ where l is the distance from the surface and c is the velocity of sound the second interference maximum will occur at

$$l = \frac{n \cdot c}{2\Delta f} = \frac{m \cdot c}{\Delta f}$$

where m is the modulation index of the warbled signal. For a modulation index of 10 (n=20, see also Fig.3) and a bandwidth Δf =350 c/s, this second interference maximum will thus occur at a distance of around 10 m from the reflecting surface. For higher modulation indices the distance will be still greater and it may thus be assumed that when modulation indices of 10 or higher are used, very little difference will exist in practice between the interference picture of a warbled tone and the equivalent noise-band, even if a bandwidth as high as 350 c/s is employed.

Also the effect of the bandwidth can be seen from Fig.8. The relation $R(\tau)<0,1$ is obtained for the first interference range when $\frac{\Delta\omega\tau}{2} \approx 3\pi$.
Again solving this for l gives $l = \frac{3c}{2\Delta f}$
This means that the greater the bandwidth is, the narrower will the disturbing interference range be. In practice bandwidths greater than around 350 c/s are not very feasible for controlled warble tone or narrow band noise generators, which means that the first strong interference range will be present up to distances around 1,5 m from the reflecting surface.

The above theory assumes perfectly reflecting surfaces. If the surface contains sound absorbing material, this will affect the interference picture as to reduce the calculated maxima.

Now, what is the significance of the difference in amplitude vs. time characteristics of the two types of signal with regard to room-acoustical measurements? This question may be answered by considering the linearity of acoustic absorbers commonly used for the acoustic treatment of rooms, as well as the amplitude vs. time characteristics of "natural sounds". Most acoustic materials show an almost exact linearity over the range of sound levels encountered in normal music and speech rooms. However, a certain type of Helmholtz resonators with relatively small "necks" show a distinct non-linearity with sound pressure level. This subject has been treated by L.J.Sivian, K.Uno Ingard and S.Labate (USA) and also by F.Barthel(Germany). Ingard and Labate suggested that non-linearity should start already at a sound pressure level of around 65 db. However, although non-linearity seems to be measurable at sound pressure levels around 80 db, serious non-linear effects of the absorbers when applied to the acoustic treatment of rooms are not likely to start at sound pressure levels lower than 110-120 db.

Measurements on a single resonator at Brüel & Kjær, carried out by means of the standing wave method, also showed a distinct non-linearity with sound pressure level, although at considerably higher levels than those mentioned in the literature.

As long as linear relationship hold true, and a fairly high modulation index is used for the warbled signal, no significant measurement difference will exist in practice, whether a warbled tone or the equivalent band of random noise is used as test signal. This will, in most cases, be valid in room-acoustic measurements. However, as soon as non-linearity enters the picture, the use of random noise becomes important. As an example of this cathegory of problems some investigations have been made at Brüel & Kjær on the attenuation characteristics of an automobile muffler.

The muffler was first mounted on a car and a $\frac{1}{2}$" microphone Type 4134 installed at the muffler input. Tape recordings were then made on a high quality type recorder (lin.freq.response 2-2000 c/s) and the overall sound pressure levels

monitored on a true R.M.S.-measuring amplifier, both with idling engine and with the engine running at around full speed. The R.M.S. sound pressure levels were found to be in the region of 130-140 db re.2 x 10^{-4} µbar and an analysis of the instantaneous amplitude distribution showed amplitude density curves of the type given in Fig.4. Pictures were also taken off the screen of a cathode ray oscilloscope of the variation in waveform of the sound. One of the photos is reproduced in Fig.5 and shows a fairly distinct periodicity in the sound waves, but a considerable variation in maximum amplitude with time. These characteristics are almost exactly those of narrow band noise.

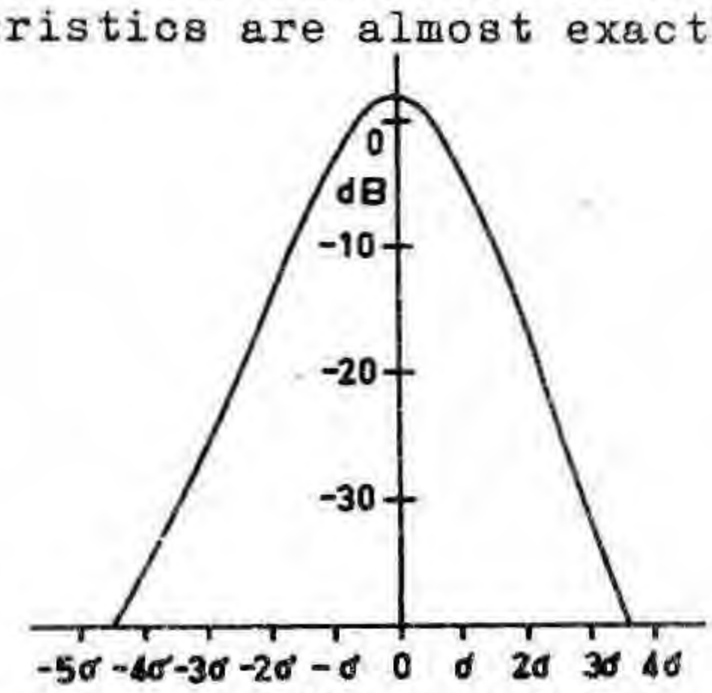

Fig.4.

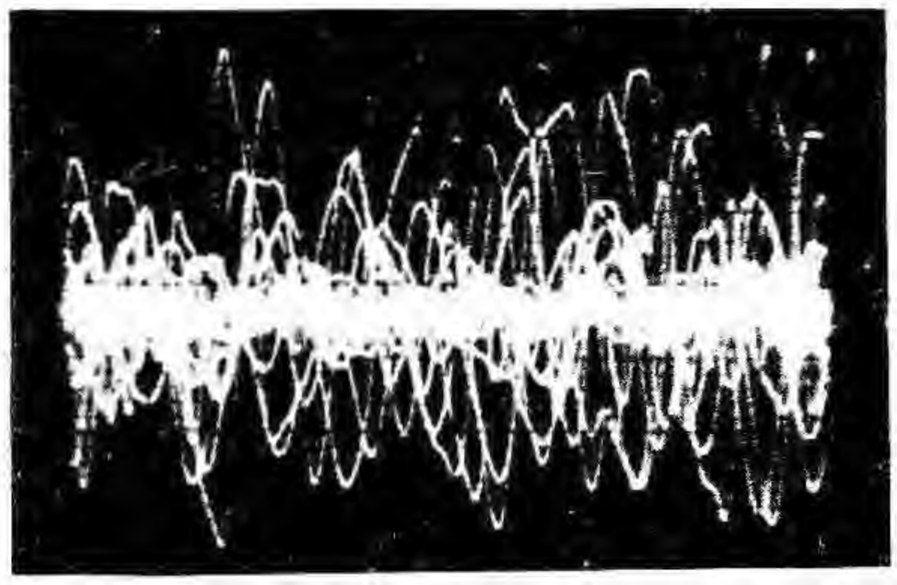

Fig.5.

To determine possible non-linearities in the muffler this was dismounted from the car and mounted on the Brüel & Kjær Constant Sound Pressure Source Type 4211 which is very well suited for measurements at low frequencies and with high sound pressure levels.

By feeding the muffler first with sinusoidal sound waves of constant R.M.S. levels (113 db and 126 db) and then with narrow bands of noise (Δf-10 c/s) at the same R.M.S. input sound pressure levels the curves shown in Fig.6 were recorded at the muffler output. The difference between the curves are clearly noticed and are due partly to the difference in "bandwidths" of the sweeping signals and partly to some slight nonlinearities in the muffler.

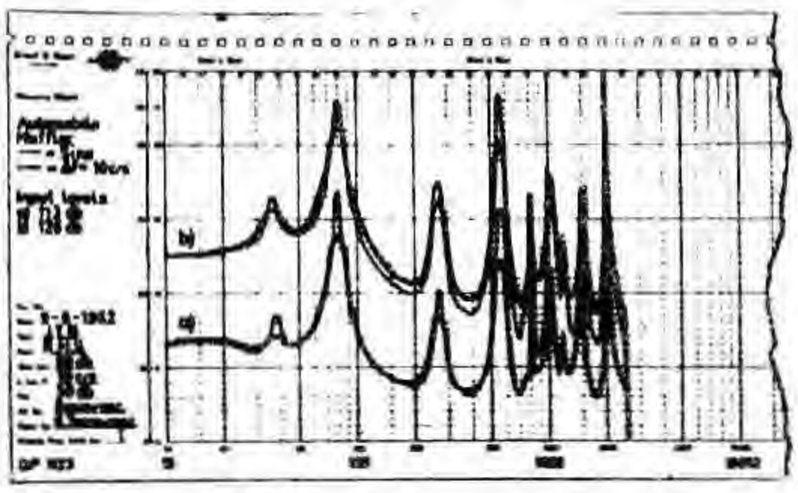

Fig.6.

From the foregoing discussion the following conclusions may be drawn on the use of warbled tone and bands of random noise for acoustic measurement purposes:

1) Wherever acoustic measurements are to be made in spaces or on equipment designed for operation in complex sound fields and where non-linearities are present, bands of random noise should be used as test signals.
2) If measurements are to be made in spaces or on equipment which behave strictly linear with sound pressure level, warbled tones may be used as test signal instead of random noise, even if the sound field in actual operation is random in nature.

The discussion in this paper has been mainly concerned with the measurement problems in room acoustics and noise control. However, also in electro- and psycho-acoustics sometimes the use of complex test signals are convenient, such as in the testing of loud-speakers and experiments on the masking effect of the ear. Also in these cases the above conclusion hold true with regard to the choice of test signal type, and it may be generally stated that when a complex test signal is wanted bands of random noise will be the most desirable type of signal to use, while economical considerations may sometimes result in the substitution of this type of signal with warbled tones.

O17

FOURTH INTERNATIONAL CONGRESS ON ACOUSTICS
COPENHAGEN 21.-28. AUGUST 1962

The Focal System Influence over Statistical Characteristics of Wave Propagated through the Medium with Random Inhomogeneties.

E.A.Bljakhman, L.A.Chernov, M.N.Krom.

It is well known from acoustic and astronomic observations, that when a wave has passed through a real medium (atmosphere, ocean) the diffraction image produced by a focusing system fluctuates.

This phenomenon could be explained by the fact that the random inhomogeneties of the refractive index in the medium produces fluctuations of the wave coming to the lens. The object of the theory consists in explanation of the dependence of averaged diffraction pattern a spatial distribution and spectral composition of field fluctuations near the focus upon the fluctuation values in the incident wave and upon focusing system dimensions.

For the first time these problems were considered in [I] , where general formulae for calculation of average intensity and field fluctuations in the vicinity of the focus in the dependence on the autocorrelation functions of the fluctuations of the level and phase of the signal on a paraxial lens were obtained. For some particular cases general formulas were investigated with the aid of autocorrelation function calculated according to the assumption of Gaussian correlation of refractive index fluctuations.

Present authors have carried out a more complete study of this problem. It is shown, that the average intensity in the focus decreases with the increase of the incident wave fluctuations and the effect is more marked for greater dimensions of the lens.

By focusing of unperturbed wave the curve of intensity distribution represents a system of decreasing maxima. With perturbations the averaged diffraction pattern and blurring occurs with decrease of

maximums and rise of miniums.

The larger is the lens, the more essential is this deformation. For large fluctuations in the incident wave average intensity decreases monotonously. Blurring of the averaged diffraction pattern leads to decrease of the resolving power of the lens. The same resultes are obtained with the homogeneous and isotropic turbulence.

Theoretical conclusions co-ordinate well with experimental curves of averaged distributions which were obtained by observations of scintillations of star images through the telescope in a number of observatories.

The spatial distribution of field fluctuations near the focus has been also studied. If lens dimensions are small in comparison with the correlation radius of the refractive index fluctuation the distribution in the focal plane has an oscillatory form, similar to the form of average intensity distribution. For lenses of the dimensions much larger than correlation radius fluctuations decrease monotonously from its maximal value in the focus.

In the focus of any lens the ration of fluctuation to the average intensity increases continiously from the zero to unity with fluctuation increase in the incident wave. Relative fluctuation distribution in the focal plane has an oscillatory form its minima coinciding with maxima of the average intensity and vice versa. Increased pulsations in the incident wave result in the straithening of the distribution curve; relative fluctuation approaches then unity everywhere.

The spectral density of the fluctuations was calculated on the assumption, that local changes of the retractive index were caused only by the motion of the inhomogeneities. Two cases were considered:constant speed motion (drift) and chaotic movements.

In the case of a drift spectral density represents the product of spectral density in front of the lens and of a diffraction factor identi-

cal with respect to its structure with the distribution of the intensity in the Fraungofer diffraction pattern from the diaphragm. This factor determines the filter effect of the lens, consising in emphasising of characteristic frequencies.

In the case of a chaotic movement the spectral density was calculated in the limiting cases of large and small fluctuations in the incident wave and only for lenses much larger or much smaller in comparison with the scale of the inhomogeneities. For a large lens the spectral density is changed from Rayleigu spectra in the incident wave in the focal Gaussion plane. The spectral density is not changed by a small lens. The dependence of the average square frequency of the field fluctuation has been also found in dependence from the size of the lens a good agreement was found with the experimental data of scintillation observations with the aid of variable aperture telescopes.

We should like to note in the conclusion, that the problem studied was the first where the influence of regular (lens) and random inhomogeneities on the passing wave was taken into account. The solution had proved that the effects created by these two types of inhomogeneities, generally are not additive.

Literature Cited

[1] Chernov L.A. Wave Propagation in a Random Medium. McGraw-Hill. 1960.

[2] Татарский В.И. Теория флюктуационных явлений при распространении волн в турбулентной атмосфере. Изд.АН СССР. 1959. (Translated English).

P17

FOURTH INTERNATIONAL CONGRESS ON ACOUSTICS
COPENHAGEN 21.-28. AUGUST 1962

ANALYSIS OF INEXTENSIONAL VIBRATION OF A CURVED CONE

Yukio Kagawa, Kimio Shibayama, Ken'iti Kido and Tadamoto Nimura
Tohoku University, Japan

Introduction

McLachlan* gives two kinds of salient types of vibration of a conical shell. They are (a) radial modes, which are associated with bending and (b) symmetrical modes, which depend on bending and extension.

Though the first type of vibration does not influence the volume displacement of a cone-type loudspeaker, this is important concerning a non-linear distortion, for its amplitude happens to be very large because of the littleness of the bending energy.

In this paper, we treat the first case about a curved cone. The base of this analysis depends on the "Inextensional Theory", in which the same treatment is made as Love** analized the vibration of a cylindrical shell in his book. This type of vibration of a conical shell, Dr. Shibayama*** analized as "Inextensional Vibration".

Coordinate

The coordinate used in this analysis is similar to a polar coordinate. Fig. 1 indicates the coordinate and the median surface of a curved cone.

The cone is curved along its meridional line, whose angle from the axis is $\theta = \alpha + mr$, which is proportional to the distance from o point. The proportional constant m is the parameter of the curve of the shell. α is the angle at $r = 0$.

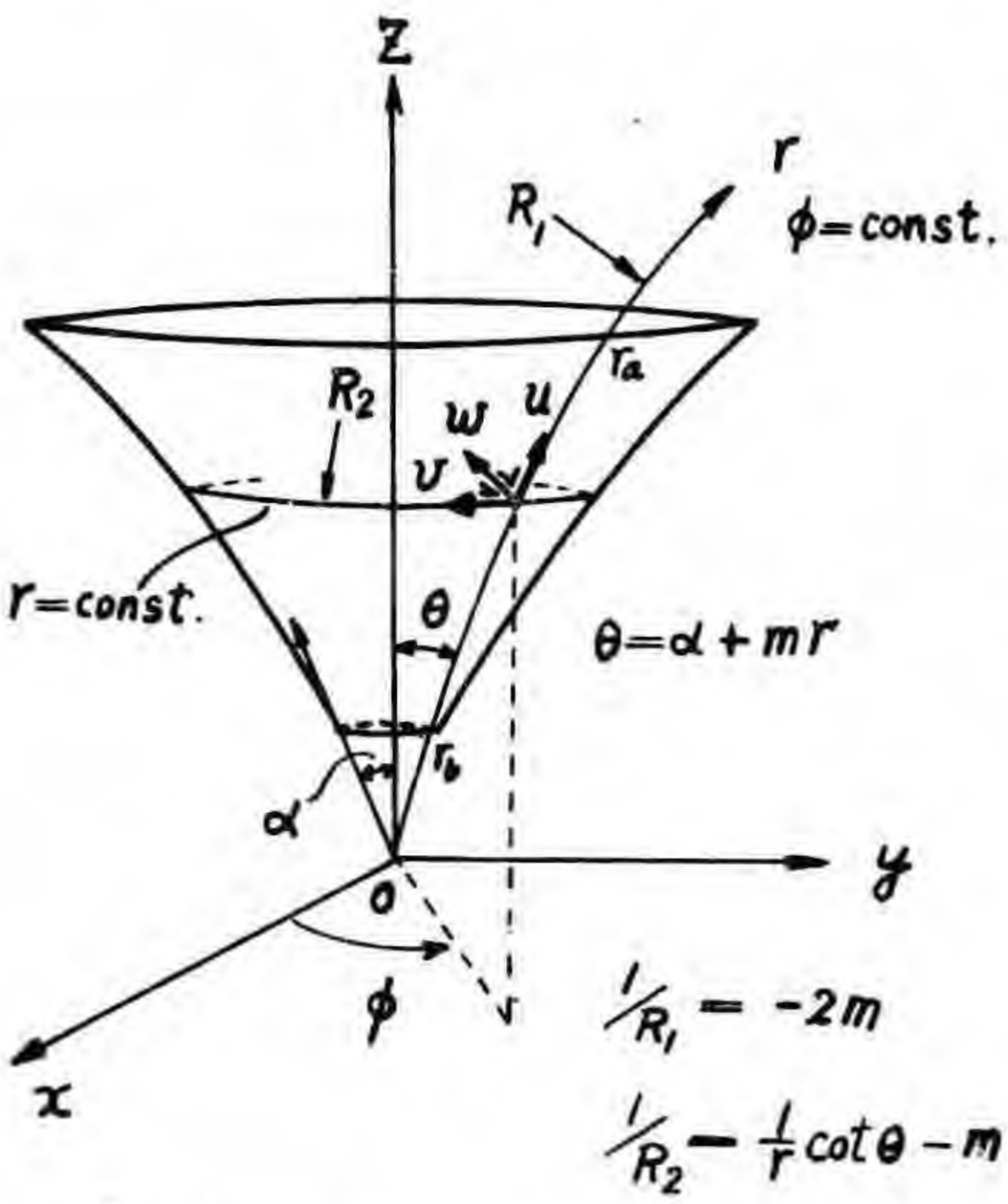

Fig. 1. Curved cone and its coordinate

The basical conditions

(1) Vibrations are associated with bending and only the nodal radii (radial modes) appear.

(2) Inextensional theory does not allow that there are extension to each directions and a change of angle between the two directions on the median surface after deformation.

(3) As mr is so small as to satisfy the following condition

$$(mr)^2 \ll 1 \quad ,$$

a solution is accurate in the first order approximation about m.

Equations

From the condition (2), we obtain three differential equations concerning the displacements to each directions u, v and w,

$$\frac{du}{dr} + 2mw = 0 \qquad (1)$$

$$\frac{1}{r\cdot\sin\theta}\frac{dv}{d\phi}+\frac{u}{r}-\frac{w}{r}\cot\theta+m\cot\theta\cdot u+mw=0 \qquad (2)$$

$$\frac{dv}{dr}+\frac{1}{r\cdot\sin\theta}\frac{du}{d\phi}-\frac{u}{r}-m\cot\theta\cdot v=0 \qquad (3)$$

Boundary conditions

The outer radius of a speaker cone is suspend-ed loosely with a surrounding divice, whose condition we consider to be "free" as an ideal case. The inner radius is connected with a voice coil bobbin, whose condition we consider to be "figid". This condition which restrains displacements in the inner radius means $u=v=w=0$ at $r=r_b$.

Analysis and Calculation

Equations (1), (2) and (3) can be analitically solved with the method of a series expansion. As displacements u, v and w are symmetrical around the axis of the cone, equations can be given under the separation of variables.
Suppose $v=v_0(r)\cos n\phi$, where n is an integer, we obtain the following equation about v_0 from equations (1), (2) and (3).

$$r\cdot\sin\theta(-\cos\theta+mr\cdot\sin\theta)\frac{d^2v_0}{dr^2}-2mr\cdot\sin^2\theta\frac{dv_0}{dr}+2m(1-n^2)v_0=0 \qquad (4)$$

The same treatment as shown above can be done about displacements u and w.
The solution of equation (4) given by the method of a series expansion has a sufficient accuracy in the first order approximation about the parameter of curvature m, because mr is very small and $(mr)^2$ can be neglected.
Solution of equation (4) is given as the following,

$$v_n=\left\{A_n r\left(1-\frac{n^2-\cos^2\alpha}{\sin\alpha\cdot\cos\alpha}mr\right)+B_n\left(1-\frac{1}{\sin\alpha\cdot\cos\alpha}mr\right.\right.$$
$$\left.\left.\times\left[2(n^2-1)\log r+5\sin^2\alpha-2n^2+1\right]\right)\right\}\cdot\cos n\phi \qquad (5)$$

, where A_n and B_n are arbitrary constants decided under the boundary conditions. Solutions about u and w is also given after the same calculation.

The eigen frequencies are given under the principle of an energy conservation, that is, potential energy V_n plus kinetic energy T_n in this system equals to zero.

$$V_n+T_n=0 \qquad (6)$$

$$V_n=\frac{D}{2}\int_{r_b}^{r_a}r\cdot dr\int_0^{2\pi}d\phi\cdot\sin\theta\left\{(\kappa_1+\kappa_2)^2-2(1-\sigma)(\kappa_1\kappa_2-\tau^2)\right\} \qquad (7)$$

$$T_n=-\omega_n^2 h_1\rho\int_{r_b}^{r_a}r\cdot dr\int_0^{2\pi}d\phi\cdot\sin\theta\left\{u_n^2+v_n^2+w_n^2\right\} \qquad (8)$$

, where D is a flexural rigidity and equals to $2Eh_1^3/3(1-\sigma^2)$, $2h_1$ and ρ are the thickness and the density of a shell, E is Young's modulus, σ is Poisson's ratio and ω_n is an eigen angular frequency. κ_1, κ_2 and τ are changes of curvature and the twist component of the coordinate.

It is the problem to calculate these energy.

Now, we introduce a new idea for a parameter to indicate the effect of a curve, which means the increment coefficient of an eigen frequency by a curve. This coefficient equals to differentiating an eigen frequency by m.
The increment coefficient of an eigen frequency by a curve G_n is shown as the following ;

$$G_n=\frac{1}{\omega_n}\frac{d\omega_n}{dm}$$
$$=\frac{1}{2}\left[\frac{\frac{d}{dm}\int r\cdot dr\int d\phi\cdot\sin\theta\left\{(\kappa_1+\kappa_2)^2-2(1-\sigma)(\kappa_1\kappa_2-\tau^2)\right\}}{\int r\cdot dr\int d\phi\left\{(\kappa_1+\kappa_2)^2-2(1-\sigma)(\kappa_1\kappa_2-\tau^2)\right\}}\right.$$

$$- \frac{\frac{d}{dm}\int r\cdot dr \int d\phi \cdot \sin\theta \left\{ u_n^2 + v_n^2 + w_n^2 \right\}}{\int r\cdot dr \int d\phi \left\{ u_n^2 + v_n^2 + w_n^2 \right\}} \Bigg] \qquad (9)$$

Equation (9) is differentiated by m, its solution is sufficiently accurate in the zero-th order approximation about m and does not contain m.

After we calculate the integration of equation (9), we can obtain the eigen frequency f_n of a curved cone with a parameter m.

$$f_n = e^{mG_n} \cdot f_c \qquad (10)$$

, where f_c is the eigen frequency of a conical shell in the case of $m = 0$, which is given by Dr. Shibayama.

Conclusion and Discussion

For example, we calculate when the following constants are given;

$\rho = 0.858/cm^3$
$E = 5.48\times10^{10}\ dyne/cm^2$
$\sqrt{E/\rho} = 2.54\times10^5\ cm/sec.$
$h_1 = 0.013\ cm$
$\sigma = 0$
$\alpha = 60^\circ = 1.047\ rad.$
$r_a = 10\ cm$
$r_b = 0.98\ cm$
$m = 0.005 \sim 0.05$

The calculated values of the eigen frequencies of a curved cone and a straight cone and an increment coefficient to the numbers of the nodal radii are shown in Fig. 2.

The eigen frequencies greatly increase even by a slight bend.

The increment coefficient increases according to the increase of the numbers of the nodal radii.

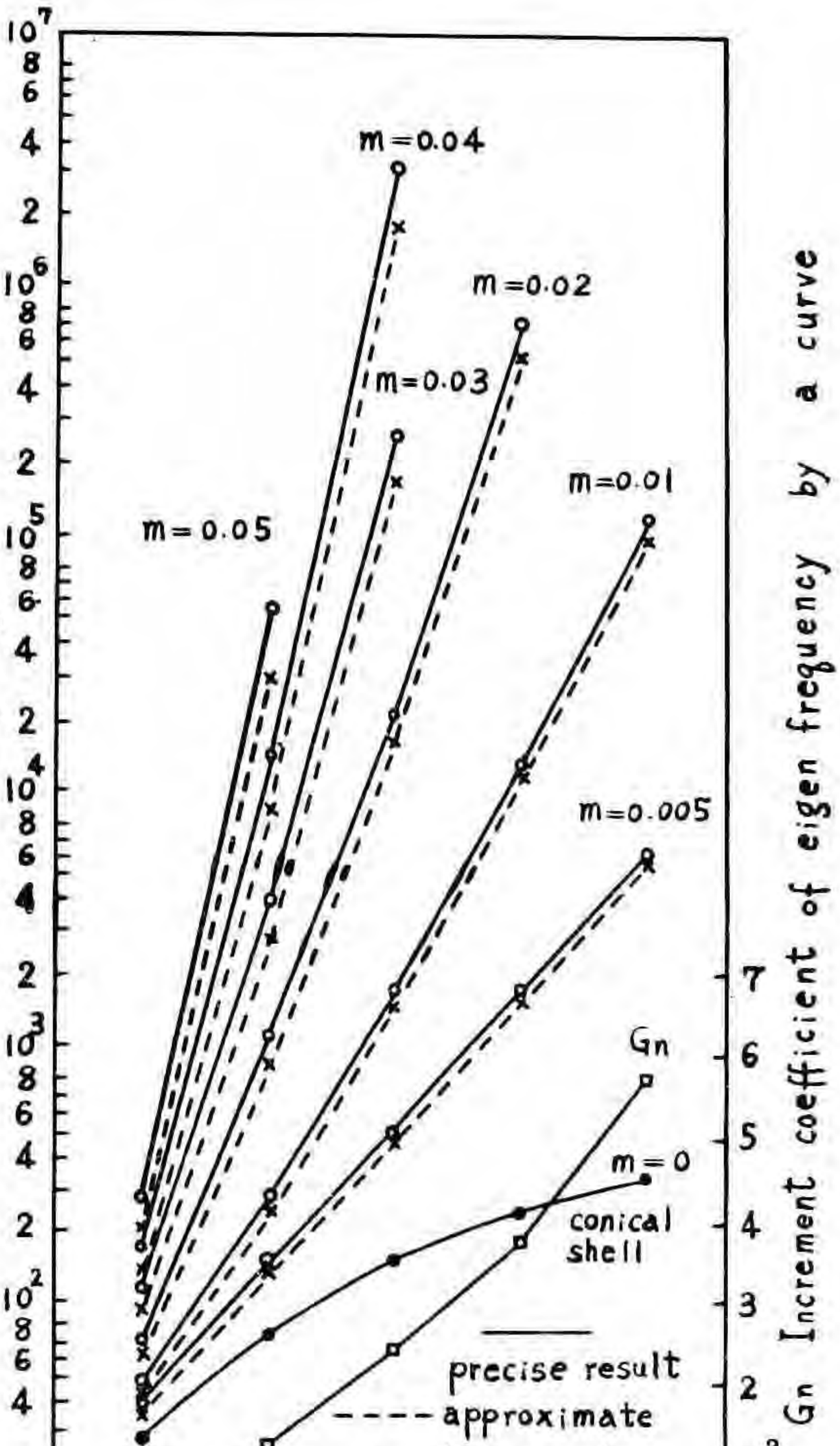

Fig. 2

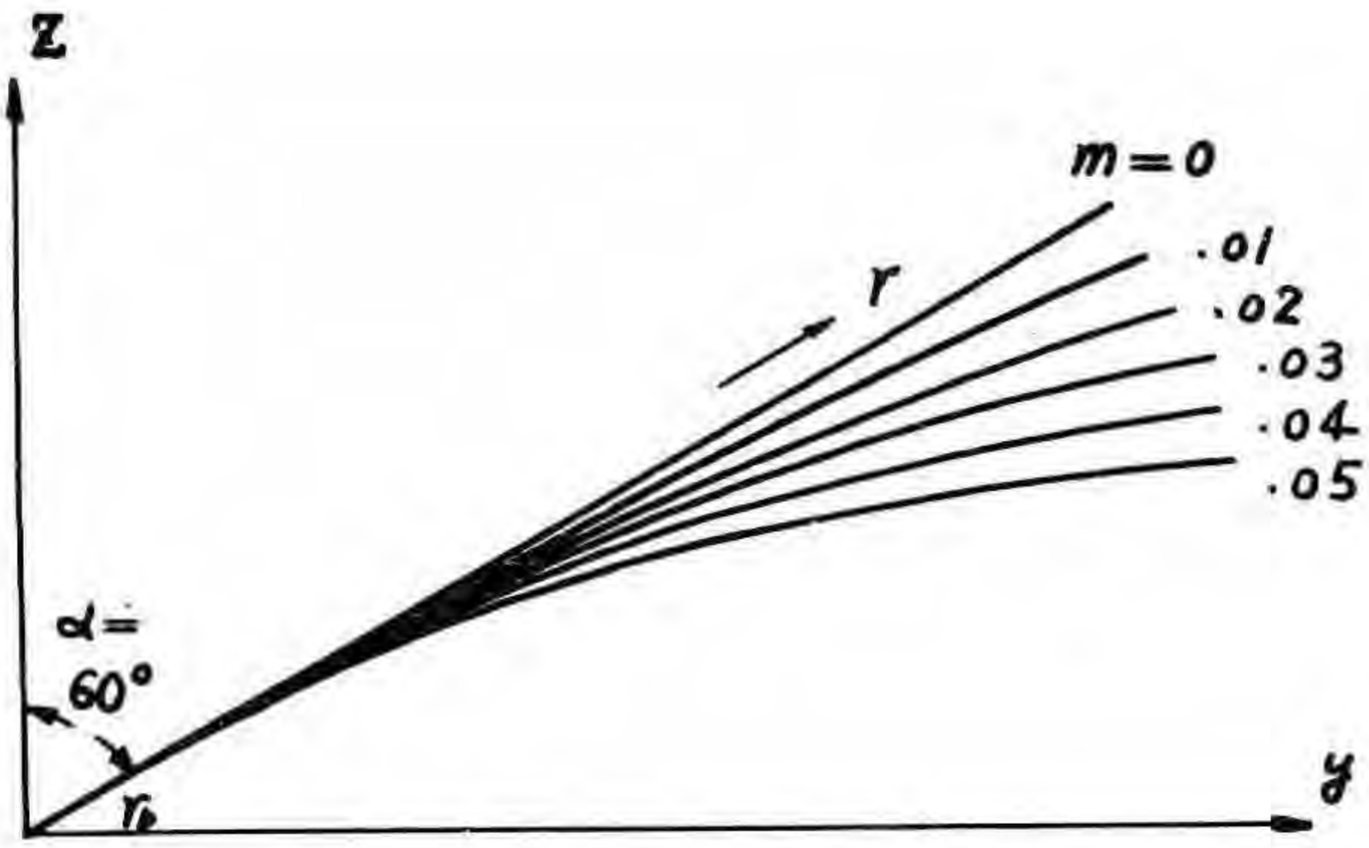

Fig. 3 Curvature of a shell

This means that the increase of the bending energy in the system is equivalent to the increase of the effective thickness of the shell. To curve a conical shell along its meridional line is useful to reduce the non-linear distortion in a cone-type loud speaker.
Fig. 3 shows the curvature of a shell to the parameter m in the case of $\alpha = 60°$.

Reference
* McLachlan: Loud Speaker Oxford 1934
** Love: The Mathematical Theory of Elasticity Cambridge 1934
*** Kimura and Shibayama: Studies on the Cone Type Loud Speakers II On the Inextensional Vibration of a Conical Shell
S C I. REP. R I T E., B-(Elect. Comm.)
Vol. 3, No. 2, March 1952

H18

FOURTH INTERNATIONAL CONGRESS ON ACOUSTICS
COPENHAGEN 21.-28. AUGUST 1962

TEMPORAL COURSE OF SPEECH SOUND PERCEPTION
(Experiments with shadowing and letter writing reaction to consonants).

L.A. CHISTOVICH
Pavlov Institute of Physiology, Leningrad.

It is well known, that the human subject makes use of numerous acoustic cues for the identification of speech signals. Almost nothing is known about the human strategy in processing and accumulating this useful information: does hg immediately make some preliminary decisions and then correct them,or does he at first store the long portions of data without interpreting them; what are his decisions about - do they concern the distinctive features, or phonemes, or syllables, or words ?

We tried to study this problem by investigating first the patterns of articulation produced by the subject in the course of rapid shadowing of syllables and secondly the latencies of letter writing reactions to consonants.

The set of devices for simultaneous continuous ink recording of the parameters of consonant articulation,constructed by Kozhevnikov, Shuplakov and Kuzmin,was used. The recorded parameters were: the contact of the lips, the contacts of the tongue with various areas of the artificial palate, the voicing, the oral and nasal air flow.

In the shadowing experiments the simultaneous recording of the speaker's and the subject's articulation was made. The subject heard the speaker's speech through head earphones. Two subjects were occupied in two experimental sessions.In the first session vowel-consonant- vowel syllables (vowel: a and conso - nants: p,b,m,f,v,t,d,n,s,z)were used.In the second session consonant-vowel syllables (vowels:u,o,a and consonants: t,t',d,d' n,n',l,l',s,s',z,z') were used. I000 consonant shadowing patterns have been obtained for the analysis.

The results indicate short latencies of consonant shadowing (Ioo-I20 msec in vowel-consonant-vowel conditions and I50-200 msec in consonant-vowel conditions).In vowel-consonant-vowel conditions the subject starts to shadow the consonant before

the speaker has released the closure i.e. before all the useful information about the speaker's consonant can appear and be heard. The subject reacts very rapidly, but not very correctly. It is interesting, that in many cases he produces two closures (dental and labial) at once.

As a rule, the initially incorrect pattern of the articulation improves to the end of the consonant shadowing articulation, Fig. I demonstrates this effect. The heights of the white columns indicate the number of cases, when the initial pattern of the subject's consonant does not coincide with the speaker's consonant in the distinctive feature labelled below (I-dental vs labial, 2- voiced vs voiceless, 3- stop vs fricative, 4-nasal vs oral). The heights of the black columns indicate the number of cases when the final pattern of the subject's consonant does not correspond to the speaker's consonant.

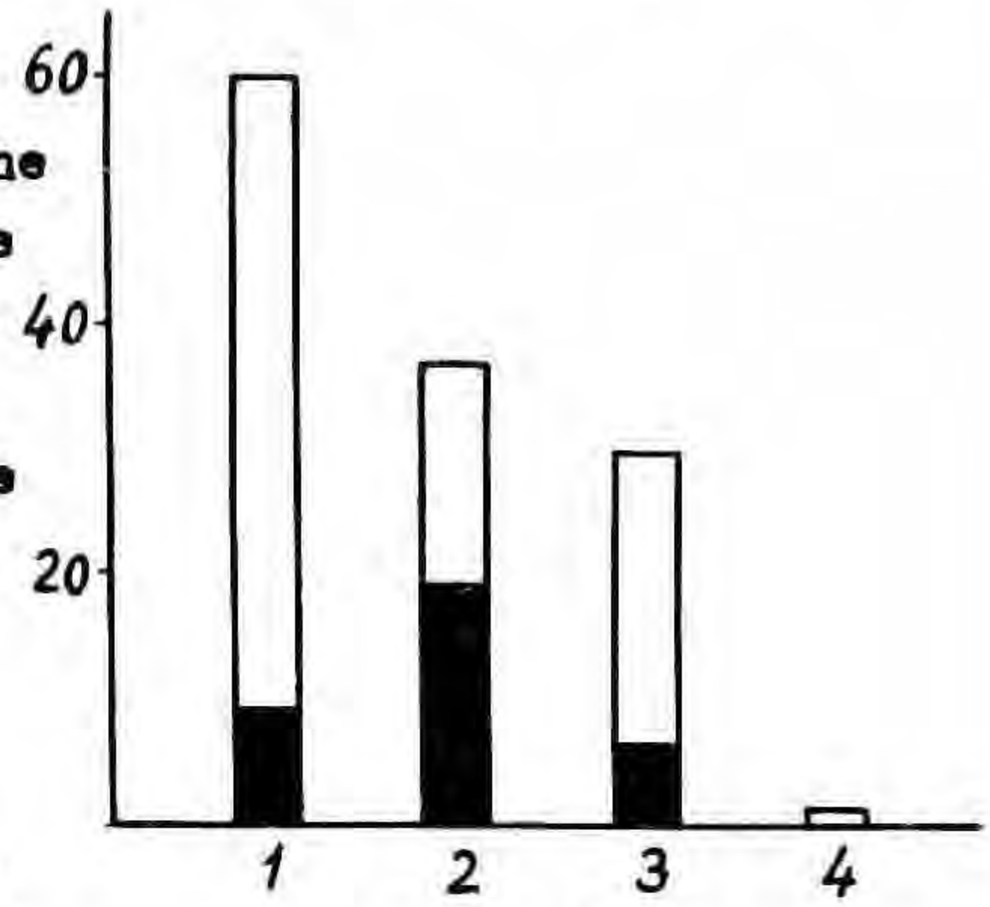

Fig. 1

It can be seen, that the effect of running correction on the shadowing articulation is drastic.

The results obtained can not be treated from the point of view of the primary choice of phoneme. The subject reacts before he perceives the whole consonant, he makes reactions which are not possible in his language (two closures at once).

A better explanation is that the subject makes a number of simple decisions about the articulatory origin of the heard acoustic events (e.g. he hears something dental, something voiceless, something nasal), corrects them, and at last accumulates the whole set of features which forms the phoneme. In other words we may suppose, that the shadowing movements are the visible signs of phoneme creation (synthesis) from the more simple decisions about its articulatory parameters.

According to this hypothesis the choice of phonemic symbol has to be the final result of the phoneme creation and naturally it has to be related not to the onset of the consonant shadowing

but to the end of it. In order to test this hypothesis we studied the latencies of latter writing reactions to consonants.

Four subjects were to write the heard consonant on a metallic plate. The intervals between the end of the speaker's consonant (release of the contacts) and the touch of the pencil to the plate were measured. Consonant-vowel syllables (vowels: u, o,a, and consonants: t,t', d,d', n.n', l,l', s,s', z,z') were used. Each subject has written 720 consonant.

The solid line in Fig.2 indicates the average latencies of letter-writing reaction for different consonants labelled below. The dashed line indicates the latencies of the end of consonant shadowing (the intervals between the speaker's and the subject's release of the contacts). Agreement between two sets of data seems to be rather good. Thus the consonant writing really appears to be related to the end of the consonant shadowing.

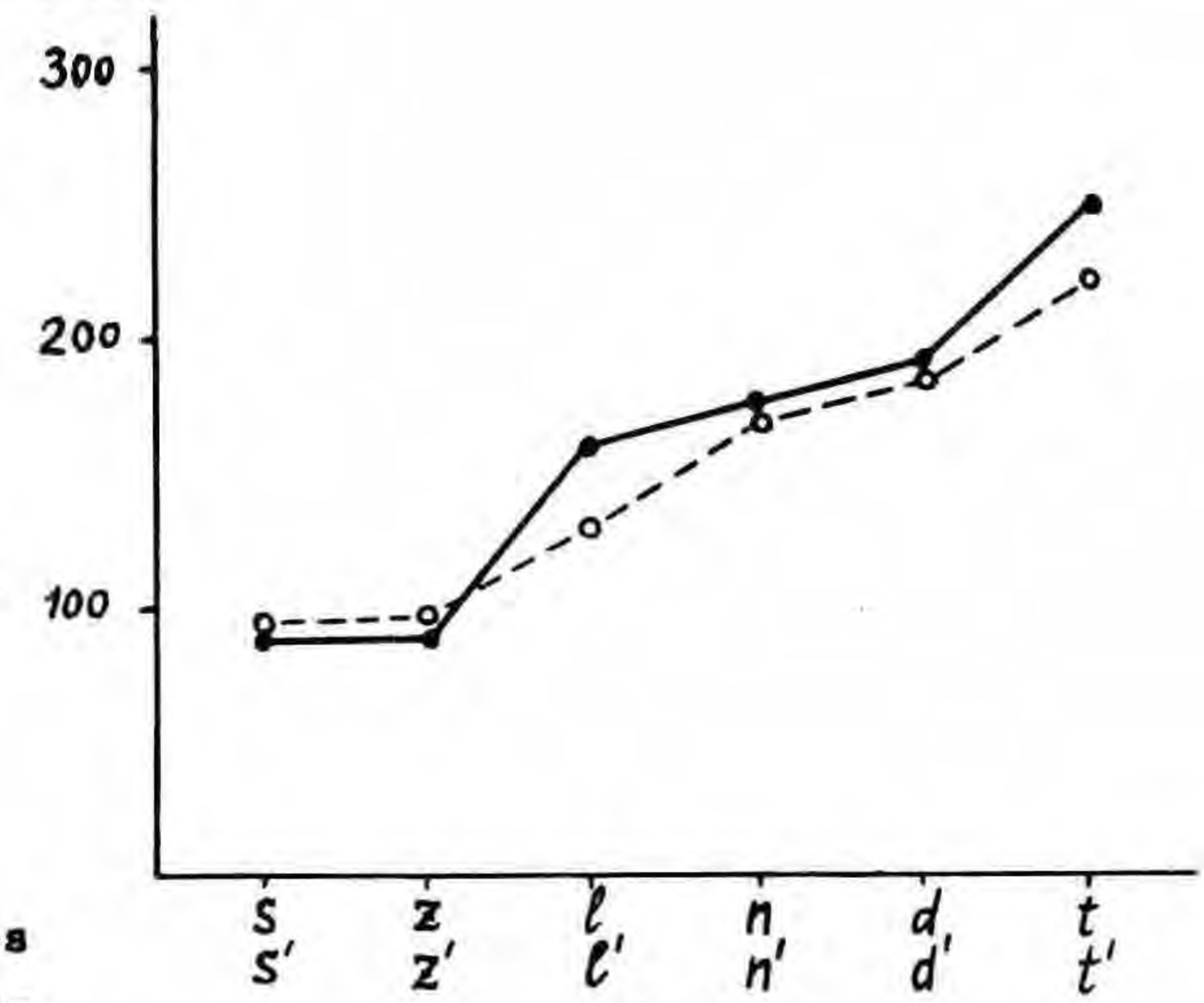

Fig.2

It is worth noting, that the rather odd dependence of the latencies upon the consonant quality, (Fig.2) can be simply explained by some of the rules of shadowing articulation. It was found, that the end of consonant shadowing was allowed only after all the preceding components of the consonant articulation had been performed. When the latencies of the end of consonant shadowing had been measured from the last of two events (the end of the speaker's consonant and the subject's preceding articulatory movement), the latencies for different consonants appeared to be equal.

L18

FOURTH INTERNATIONAL CONGRESS ON ACOUSTICS
COPENHAGEN 21.-28. AUGUST 1962

Noise Produced During Launchings of Rocket Powered Vehicles and Some Human Factor Siting Considerations

John N. Cole, Harald K. Hille, Robert G. Powell, and Henning E. von Gierke; 6570th Aerospace Medical Research Laboratories, Wright-Patterson AFB, Ohio, U.S.A.

INTRODUCTION. Mankind's continuing efforts to explore space will require increasingly larger propulsion units to lift these vehicles from the earth's surface. The potential hazards associated with the launchings of such vehicles include blast, fireball, fragmentation, noise and toxicity. All of these factors must be considered in the selection of launching sites so as to insure the safety of operational personnel and the surrounding community populace.

The subject of this paper concerns acoustic noise as an environmental factor. Future large space vehicle boosters such as NOVA will produce, according to present estimates, as much as 500 megawatts of acoustic energy which will radiate outward into the surrounding areas creating unprecedented, high noise levels. Sufficient separation distances between communities and the launch site must be provided for in the planning of future facilities so that the noise levels reaching these communities are neither hazardous nor intolerable. This paper reports a research study designed to provide a better understanding and improved prediction methods for estimating the levels and durations of these adverse environments. This five month noise study was recently conducted at Cape Canaveral, Florida, U.S.A. (Atlantic Missile Range) by the 6570th Aerospace Medical Research Laboratories, Wright-Patterson AFB, Ohio.

Included in this paper to illustrate the usefulness of these data are a few estimated noise environments of a future large space vehicle booster. Also considered are some of the human factors regarding community acceptability or reaction to these future environments.

CAPE CANAVERAL NOISE SURVEY. The purpose of this study was to measure the sound levels produced during present-day launch operations at Cape Canaveral in order to document present noise environments and more importantly to obtain basic information which would be useful in better estimating the noise environment of future systems.

To this end a systematic collection of environmental data was undertaken to measure the sound pressure level-time (SPL-time) histories at as many as 10 locations surrounding the launch site during each of 23 launchings made during the period of 13 July 1961 to 17 November 1961. These tests are briefly summarized in Table I and include systems ranging in thrust size from the solid propellent powered Pershing

TABLE I. LAUNCHES MEASURED AND SYSTEM DESCRIPTION

SYSTEM	NUMBER OF LAUNCHES MEASURED	THRUST IN POUNDS	NUMBER OF BOOSTER ENGINES	PROPELLANT
PERSHING	2	28,000	1	SOLID
POLARIS	1	82,600	1	SOLID
BLUESCOUT	1	102,000	1	SOLID
JUPITER	1	150,000	1	LIQUID
THOR	1	150,000	1	LIQUID
MINUTEMAN	1	178,000	1	SOLID
TITAN	8	305,000	2	LIQUID
ATLAS D	2	368,000	3	LIQUID
ATLAS E AND F	5	389,000	3	LIQUID
SATURN	1	1,310,000	8	LIQUID

to the Saturn which is boosted by a cluster of eight liquid fuel engines.

The general geographic characteristics of Cape Canaveral and surrounding area are shown on Figure 1. Also shown are the 13 microphone measuring locations established on the Cape and the six locations established in the surrounding communities. These microphone locations were 150 to 96,000 feet from the active launching sites. Several different instrumentation systems were used to acquire data. Most of these microphone locations constituted a fixed network of transducers transmitting data via direct wire, or in one case via microwave link, to a centralized recording facility. These microphone locations were selected on the basis of availability of power, communication, and signal transmission lines and, of course, on geographic location from the viewpoint of obtaining the desired array of sensors. Some of these transducers were installed at tracking, guidance and telemetry installations so as to provide environmental data on the acoustic levels generated at these critical instrumentation facilities. A simplified schematic, Figure 2, illustrates the basic instrumentation employed in this program. Several of the measurement locations shown in Figure 1 were monitored with independent, vehicle-mounted instrumentation. All microphones were mounted in a cylindrical, nylon-covered windscreen and placed 6 - 10 feet above the ground (or roof) and clear of other reflecting surfaces. All systems were fully calibrated from microphone to graphic level recorder inclusively using both electrical and acoustical calibration procedures.

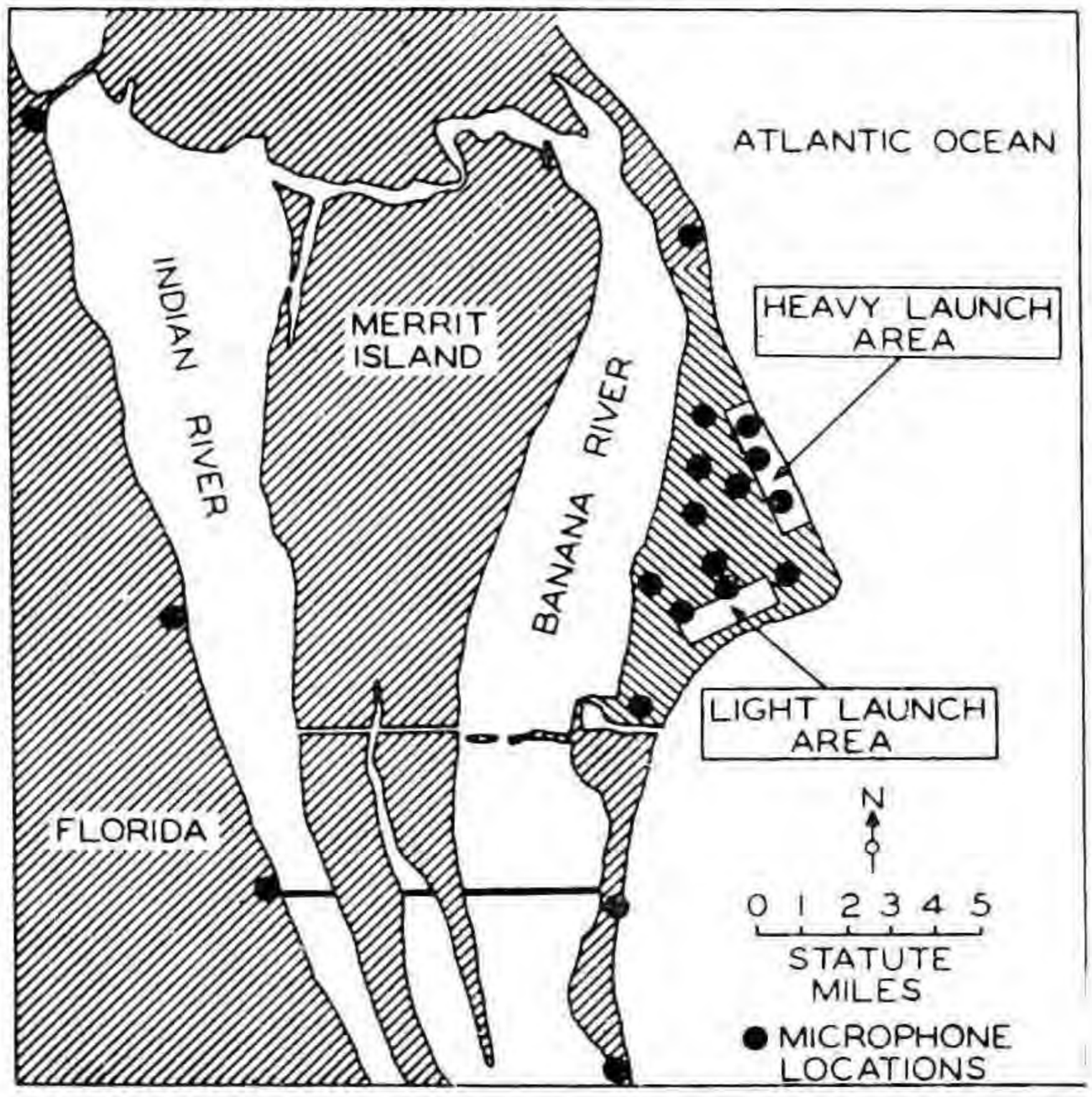

FIGURE 1. CAPE CANAVERAL MISSILE TEST FACILITY

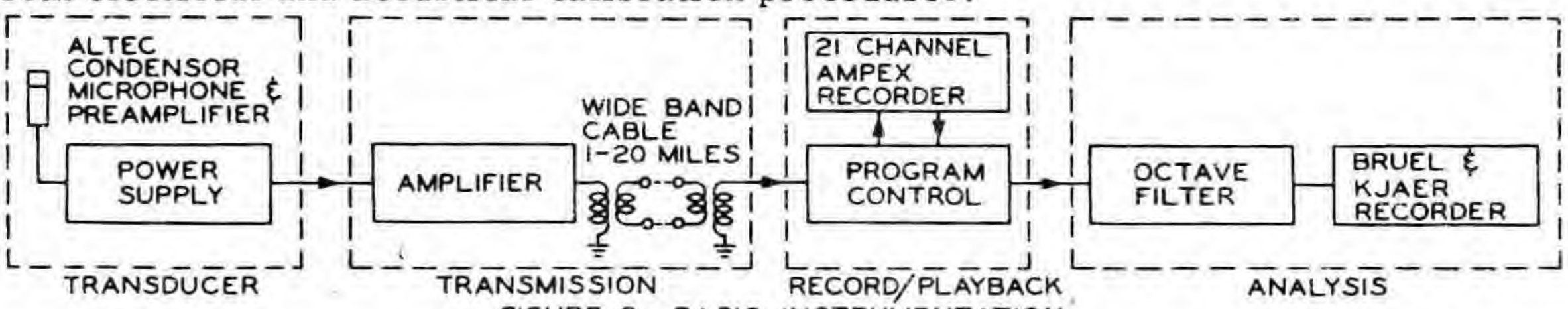

FIGURE 2. BASIC INSTRUMENTATION

The recorded data from each microphone location for each test (a total of 174 records) were reduced into octave band SPL-time functions. Eleven standard octave bands were utilized ranging from the 4.7-9.4 cps band to the 4800-9600 cps band. For most data an effective averaging time of approximately 3 seconds was electronically applied to smooth the filtered signal after amplification for purposes of graphic presentation.

A few typical measured overall SPL-time histories, Figure 3, are given as a function of distance from the launch sites for Pershing, Atlas and Saturn launchings. The zero reference in time is the first whole second before first motion of the vehicle.

The initial peak in some of these data can be directly related to the gas flow emitted by the rocket engine(s) interacting with the launch stand or ground during the initial lift off phase of flight.

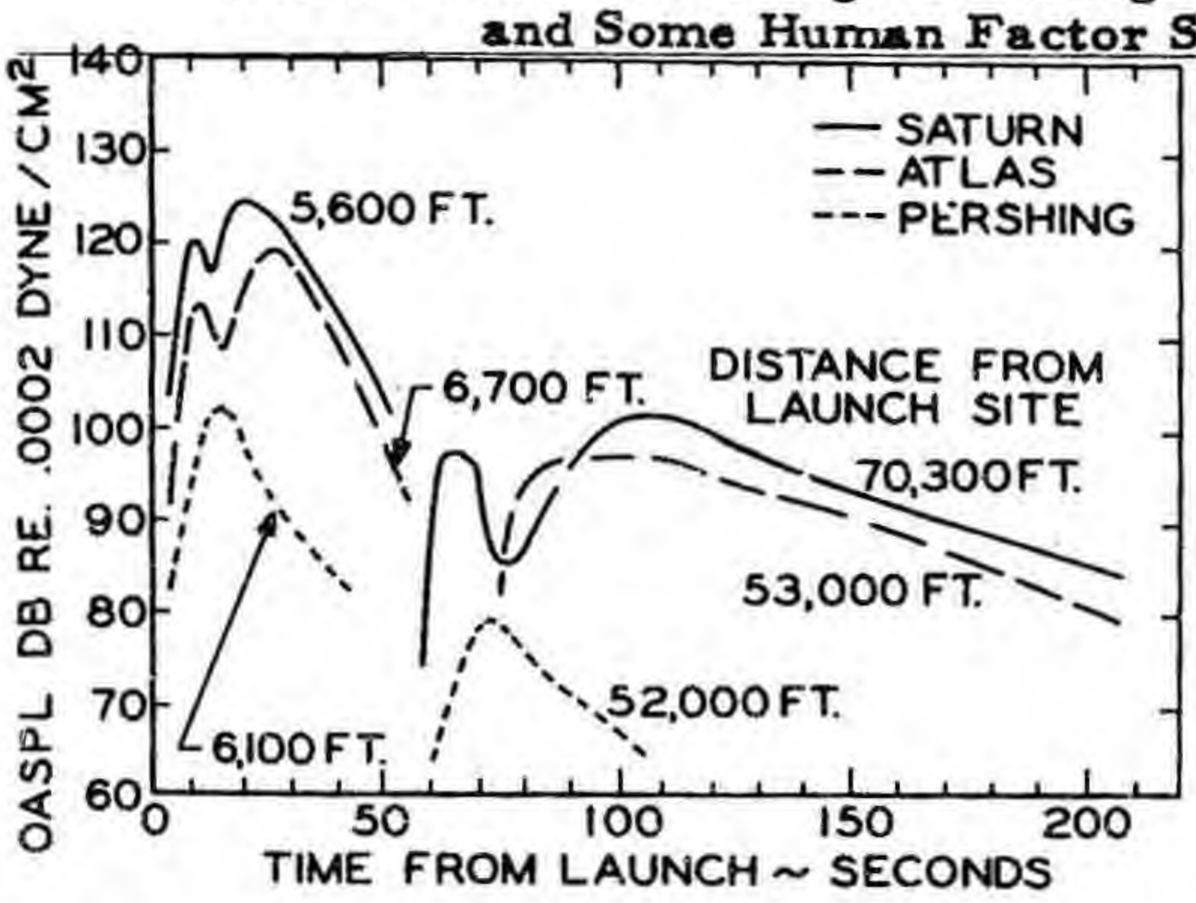

FIG. 3 TYPICAL OASPL ENVIRONMENTS

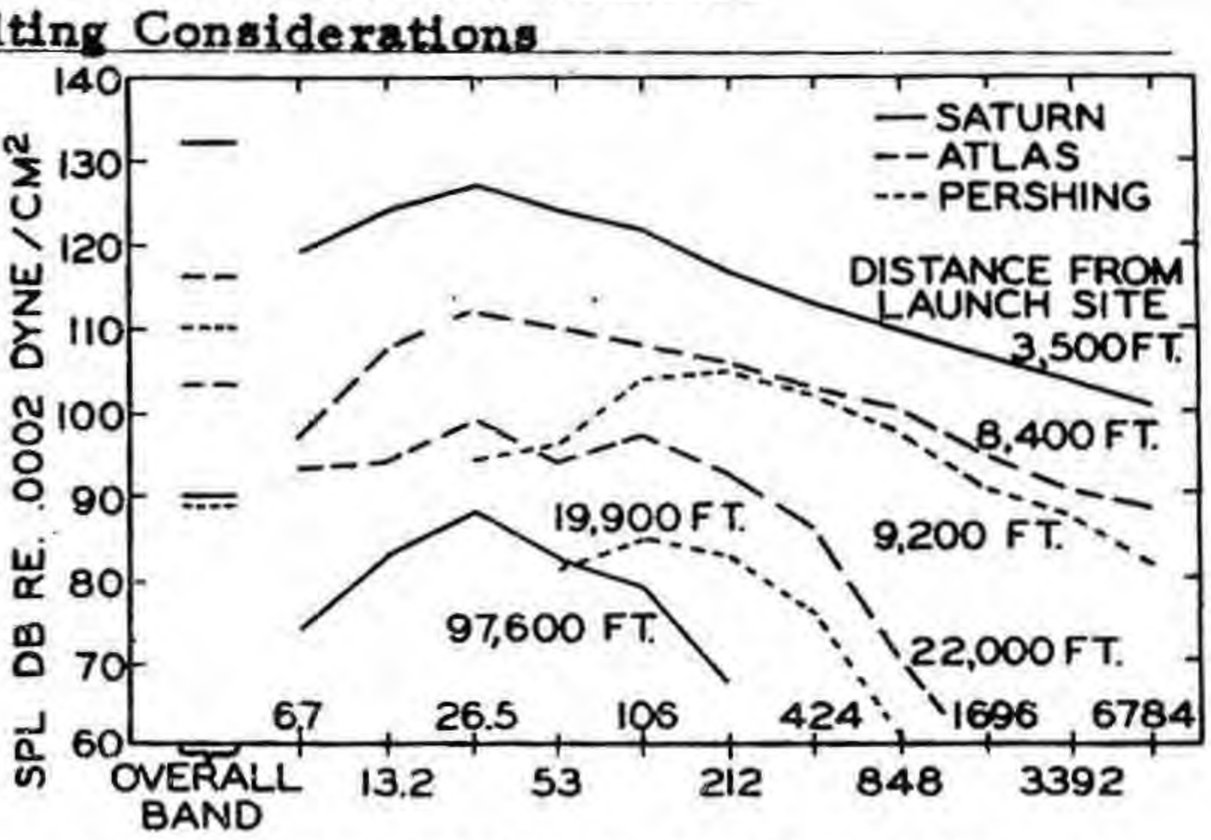

FIG. 4 TYPICAL MEASURED SPL SPECTRA

Representative spectral distributions, Figure 4, indicate the dependency of the peak pressure frequency on vehicle size and distance from launch site. This peak frequency is directly proportional to the effective flow diameter of the source and inversely proportional to the distance from the launch site.

This shift of energy to progressively lower frequencies as the vehicle size increases and as the distance to the point of interest increases (which it does when more powerful noise sources are involved) becomes very significant when considering the potential noise environments of future large booster vehicles.

All data obtained during this study is also contained in digital form and analytical methods utilizing computer techniques are currently being performed to determine regression and correlation coefficients relating the dependency of the environment on selected variables. (1)

NOISE OF FUTURE LARGE SPACE VEHICLES AND SOME HUMAN FACTOR CONSIDERATIONS. Although detailed discussions of the analytical results of the Cape study and the more general methods of predicting noise environments are beyond the scope of this paper, a few estimates are presented on Figure 5 of the maximum overall and octave band SPL's expected to be produced at distances of 1, 5 and 20 miles from the launch site of a 22 x 10^6 pound thrust vehicle. Conventional fuel-oxidizer mixtures and a nominally vertical launching trajectory have been assumed. Substantial energy is estimated below 20 cps. These estimates were based on an extrapolation of generalized, empirical data.

One facet of the acoustic problem associated with launch operations concerns the exposure of surrounding civilian communities to the noise produced during those operations. Some of these human factor considerations will be briefly discussed herein to illustrate the application and need for not only basic environmental data such as obtained during the Cape survey, but also the need for improved and broadened criteria relating community response to noise exposure.

Assume that the noise spectra estimated in Figure 5 reasonably well represent future typical noise levels at distances out to 20 miles from the launch site. Exposure of the community to such noise is usually interpreted in terms of certain criteria relating to hazardous exposure, interference with communication or annoyance. Present day criteria, however, have been based on research in the audio frequency range (20-12,000 cps) since no practical requirements for detailed studies in the sub-audio range (2-20cps) have heretofore existed. Although no criteria exist for exposure to sub-audio noise, it is known that the ear is relatively insensitive in this lower frequency range and, consequently, is not expected to be the body organ which limits tolerance. Whereas the pain threshold is between 135 and 140 db from 10 to 1,000 cps,

the pain threshold is approximately 151 db for 7 cps, 157 db for 5 cps, 162 db for 3 cps and 175 db for slow static pressure changes. (2) From these limited data it can be concluded that the sub-audio frequency energy will be no problem with respect to pain or damage to the ear or hearing loss; nor is it expected to contribute anything to the "loudness" of the noise perceived by the ear.

On the other hand, it must be expected and it is known from qualitative observations that these sub-audio frequencies and the lower frequencies of the audio range excite vibration of various parts of the body such as head, eyes, nasal and pharyngeal cavities, chest, abdomen, etc. (3) All these vibrations result in a stimulation of various receptor organs in the skin and elsewhere. The vibrations are definitely "felt" and would constitute a new experience to people never before exposed to these environments. Psychological factors such as startle and fear will strongly influence voluntary tolerance.

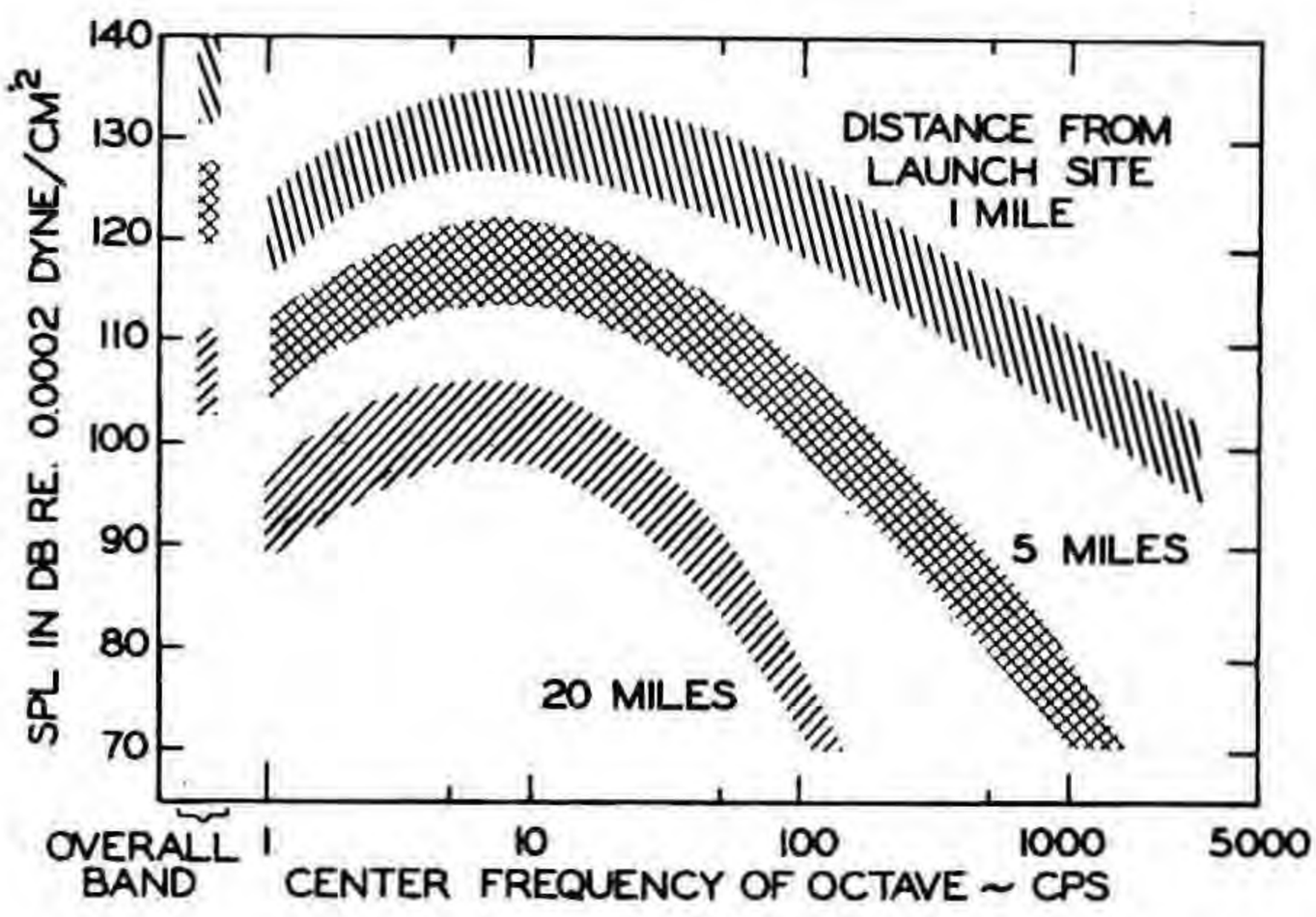

FIGURE 5

A tentative criterion of 115 db overall SPL for the type of spectra under consideration is currently used as a tentative upper limit to which a community should be exposed assuming 2 to 3 launches per month and assuming that the community population has been well educated to expect the noise, recognize it and not worry.

The type of data obtained by the Cape Canaveral noise survey and the resulting estimates made of both the environment and the response of the community to these environments represent the best estimates presently available and have been used by planners to assist in locating launch site facilities for vehicles to be used in the lunar landing program. But to overcome remaining deficiencies in the state-of-the-art and to keep ahead of technical information requirements, more work needs to be done in both the physical and bioacoustic aspects of this unique and challenging problem.

REFERENCES

1. J.N. Cole, R.G. Powell and H.K. Hille, "Acoustic Measurements at Cape Canaveral Missile Test Annex, Atlantic Missile Range," Aeronautical Systems Division Technical Report 61-608, June 1962.

2. Benox Report "An Exploratory Study of the Biological Effects of Noise," (Contract No. ORI-020, Task Order 44, ONR Project NR 144079, between ONR and University of Chicago), 1 December 1953.

3. D.E. Goldman and C.E. Crede, "Handbook of Shock and Vibration" (C.M. Harris, editor), "Shock and Vibration; Limits of Comfort and Safety." McGraw Hill Book Co., New York, N.Y., 1961.

N18

FOURTH INTERNATIONAL CONGRESS ON ACOUSTICS
COPENHAGEN 21.-28. AUGUST 1962

FINITE-STRAIN RESPONSE OF THE PIEZOELECTRIC TRANSDUCER CERAMICS Pb-Ba AND Pb-Sr ZIRCONATE-TITANATE

C.M. van der Burgt and E.E. Havinga
Philips Research Laboratories, Kastanjelaan, EINDHOVEN, Netherlands

1. Previously Published Large-Signal Data on Charge Release of Piezo-Ceramics

Just before the 3rd ICA Congress L.W.Doremus published the first large-signal data on the "Charge Release of Several Ceramic Ferroelectrics Under Various Temperature and Stress Conditions", Proc.Inst.Radio Engrs. 47, 921-924, May 1959. Since quite a number of papers afforded a broad information on the large-signal behaviour of modified types of barium titanate and lead zirconate-titanate. In particular H.H.A.Krueger and D.Berlincourt demonstrated the "Effects of High Static Stress on the Piezoelectric Properties of Transducer Materials", J.Acoust. Soc.Amer. 33, 1339-1344, Oct.1961, whilst Bogdanov, Vul, and Razbash described "The Piezoelectric Properties of Polycrystalline Barium Titanate at High Pressures", Soviet Physics-Cryst. 6, 58-61, July-August 1961, and 211-213, Sept.-Oct. 1961. Bogdanov found that the charge generated by the initial pressure application is greater than the charge generated by the subsequent pressure release, and is also greater for the first cycle of measurement than for the second. In other words, Bogdanov was the first to publish graphical data on the pressure-induced depolarization of a previously poled sample with positive longitudinal electrostriction. Unfortunately Bogdanov used the same sample at various levels of increasing pressure, whereas it would be more interesting to know the charge release of fresh specimens for each value of the pressure in order to eliminate any effects dependent upon past history. Moreover Bogdanov and his colleagues confined themselves to barium titanate. Therefore the effect of large-signal pressure cycling on fresh samples of lead zirconate-titanates was investigated.

2. Lead Zirconate-Titanates Used in the Present Large-Signal Experiments

At the 3rd ICA Congress, Sept.1959 (Proc.pp.1226-1228) A.E. Crawford stated that lead zirconate-titanates can be profitably used in ignition systems for internal combustion engines and explosive missiles. Ignition of photoflash lamps could have been mentioned too (W.F. Albrecht, US Patent 2, 868, 003, publ. Jan. 13, 1959). Partly in view of such applications it was decided to measure the open-circuit output voltage rather than the short-circuit charge release. Although the available electrostatic voltmeters had a sufficiently high leakage resistance ($>10^{14}\Omega$) their inertia enabled reliable measurements only if the decay time or RC-time of the piezoceramic in question was much longer than 5 seconds (>100 s, say) even at the upper limit of the temperature region -50 to 80°C to be covered. In view of the high permittivity of the piezoceramics resistivities better than $10^{10}\Omega$m were required at 80°C. Such high values can be easily obtained by adding small amounts of 3-valent or 5-valent cations like La, Nd, or Ta, Nb, respectively, as shown by F. Kulcsar, J.Amer.Cer.Soc. 42, 343-349, July 1959. Kulcsar also pointed out that each of these additives is still effective if part of the lead is replaced by strontium in order to improve the small-signal piezoelectric and dielectric properties. However, in the period preceding the present investigation it had already been found that La is somewhat more effective than the other additives if barium supersedes part of the lead. Consequently it was decided to carry out the static high-pressure measurements on large batches of Pb-Sr and Pb-Ba zirconate-titanates with La additive. The chemical compositions were chosen so as to result in nearly equal Curie temperatures. In addition, a Pb-Ba composition with a much lower Curie temperature was investigated. Moreover another large batch of the Pb-Sr composition

showing different porosity, different coercive force, etc., was duly paid attention to. Pertinent chemical and physical data for the four batches are compiled in table I.

Table I Average values of physical properties of ceramics having the approx. chemical composition $Pb_{1-x-y}Sr_xBa_y(Zr_{0.54}Ti_{0.46})O_3$ + 100z wt.% La_2O_3

Batch Nr.	Chemical composition 100x --	100y --	100z --	Curie temp. a) °C	Specific mass (±0.1) X-ray g/cm^3	Appar g/cm^3	Coercive field kV/mm	Permittivity Rise by poling %	Value after poling --	Planar coupling factor (±0.015) --	Resistivity at 20°C $10^{10}\Omega m$	Resistivity at 70°C $10^{10}\Omega m$	(RC-) decay time at 70°C seconds
Sr5A	5	0	1.5	263	7.82	7.69	1.5	20.6	1620	0.500	25	8	1450
Sr5B	5	0	1.5	258	7.82	7.64	1.3	13.4	1650	0.500	22	7	1250
Ba10	0	10	1.2	270	7.80	7.59	1.0	13.4	1540	0.495	20	6	1100
Ba16 b)	0	16	1.0	220	7.71	7.46	0.8	6.5	1960	0.505	10	3	750

a) The Curie temperature is roughly 390 - 1050x - 650y - 5500z.
b) Batch with Zr/Ti ratio 55/45 instead of 54/46.

3. Experimental Set-Up

Methods of "Static" Pressure Cycling

Ceramic disks, 16 mm diam., 1 mm thick, were provided with sprayed-on burnt-on silver electrodes, so that a flatness better than ±5 μ was obtained. After poling only disks having a planar coupling coefficient within ±0.015 around the average value were used for experiments. Pairs of samples were inserted into the pressure device sketched in fig. 1. Fresh pairs of samples were used for each pressure cycling experiment at each predetermined pressure amplitude (σ_3 = -1, -2, -3, -4, -5, -7½, -10x10^7 N/m^2) and at each chosen temperature (T=-48, 23, 80°C). For each (σ_3, T) three fresh pairs of disks were given a series of "static" pressure cycles. Fig. 2 sketches such an experiment yielding the value of the pos. field generated by the pressure application E_{appl} and (after transient short-circuiting; SC in fig.2) the neg.field generated by the pressure release E_{rel}. Usually six successive pressure cycles were applied to a pair of fresh disks. They were subsequently stored at room temperature during 24 h, whereupon the new value of the planar coupling coefficient was measured (k_{pI}). In a few other experiments with other fresh pairs of disks the samples were removed from the pressure device after each of the

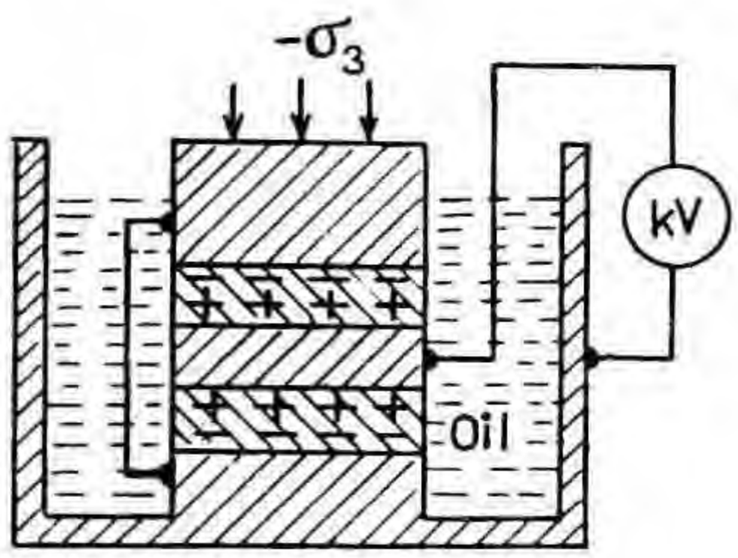

FIG.1

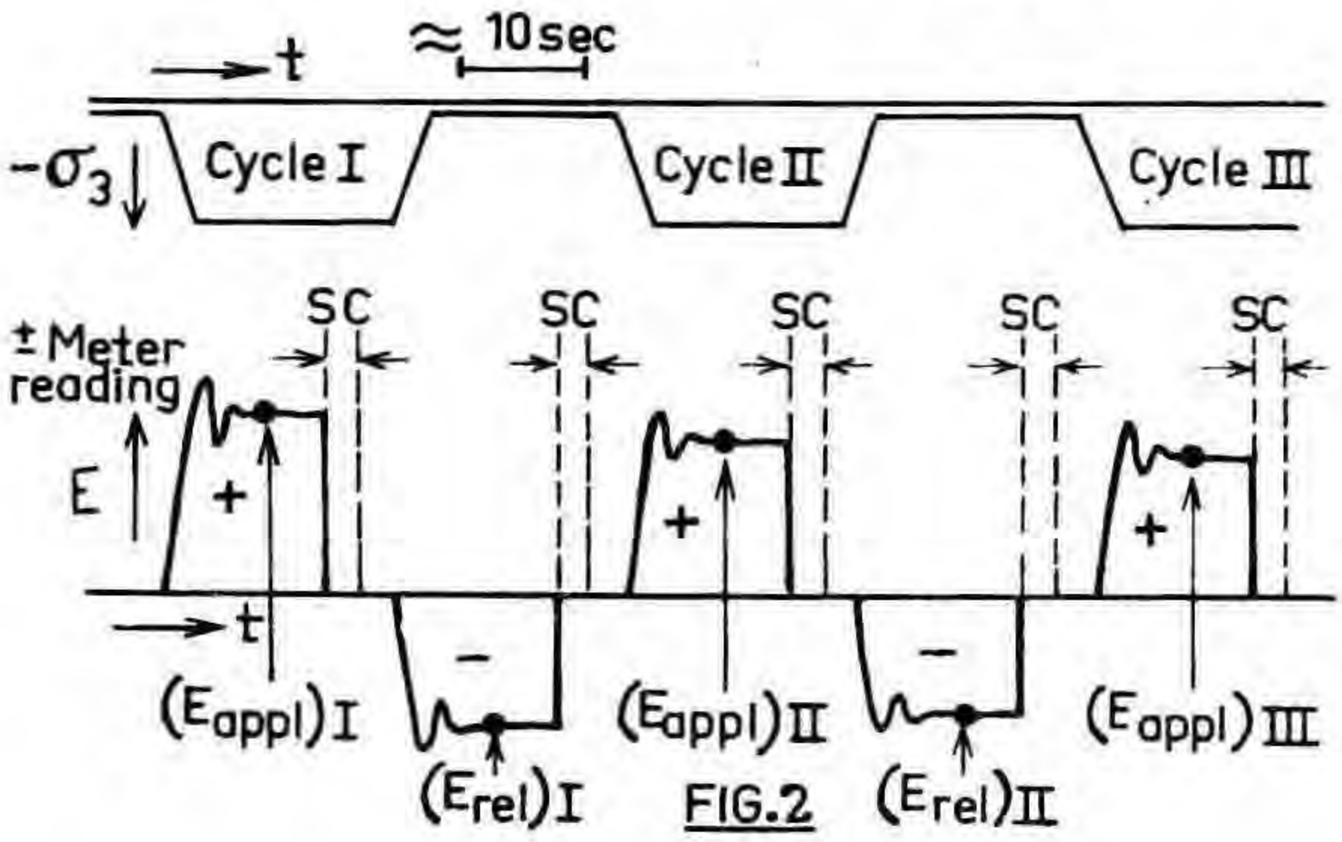

FIG.2

cycles I, II,.... VI and were stored at room temperature for 24 h, whereupon the intermediate values of the coupling k_I, k_{II}, ... k_{VI} were determined. Immediately afterwards the next pressure cycle at the temperature in question was started. Due to the inertia of the electrostatic voltmeter any reading within 5 sec. after reaching full pressure or zero pressure is unreliable, as sketched in fig.2. Consequently E_{appl} and E_{rel} were read at about t=5 sec. Moreover for a limited number of samples the curve E_{rel}-versus-time was recorded up to t=300. Fig. 3 contains typical log E_{rel}-versus-t curves for pairs of disks from each batch at 70°C. Obviously ageing phenomena (domain reorientation after pressure variation) exert a distinct influence for the first hundred seconds in each batch. If readings had been done at t=100 instead of at t=5 sec., a small change of the general outlook might have been found for the graphical data on pressure-induced fields shown below.

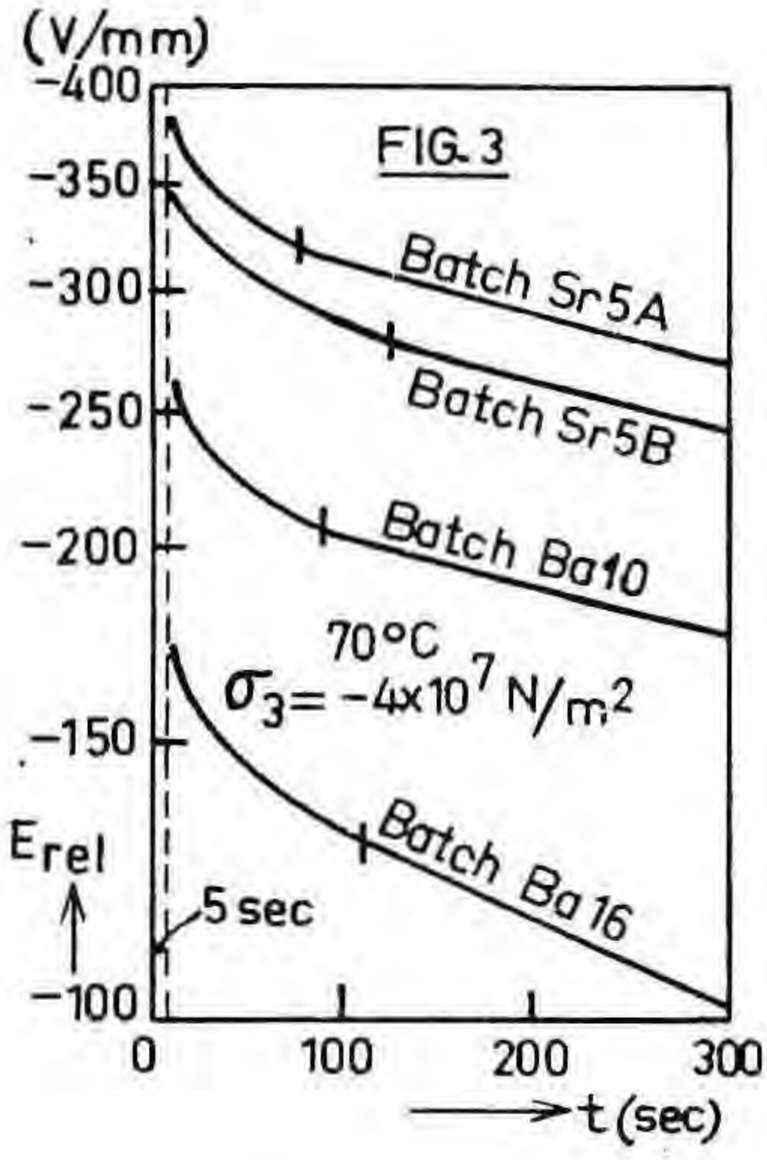

4. Induced Field Intensity and Irreversible Depolarisation in Successive Pressure Cycles at Various Pressure Amplitudes and Various Temperatures

Figs 4-11 display part of the data found on a few hundred samples of each of the batches. From these graphs and table I several conclusions can readily be drawn: 1) During pressure cycling the induced field E_{appl} falls off more rapidly and the ratio $-E_{rel}/E_{appl}$ for the first cycle is the lower the more the coercivity is lower; 2) During pressure

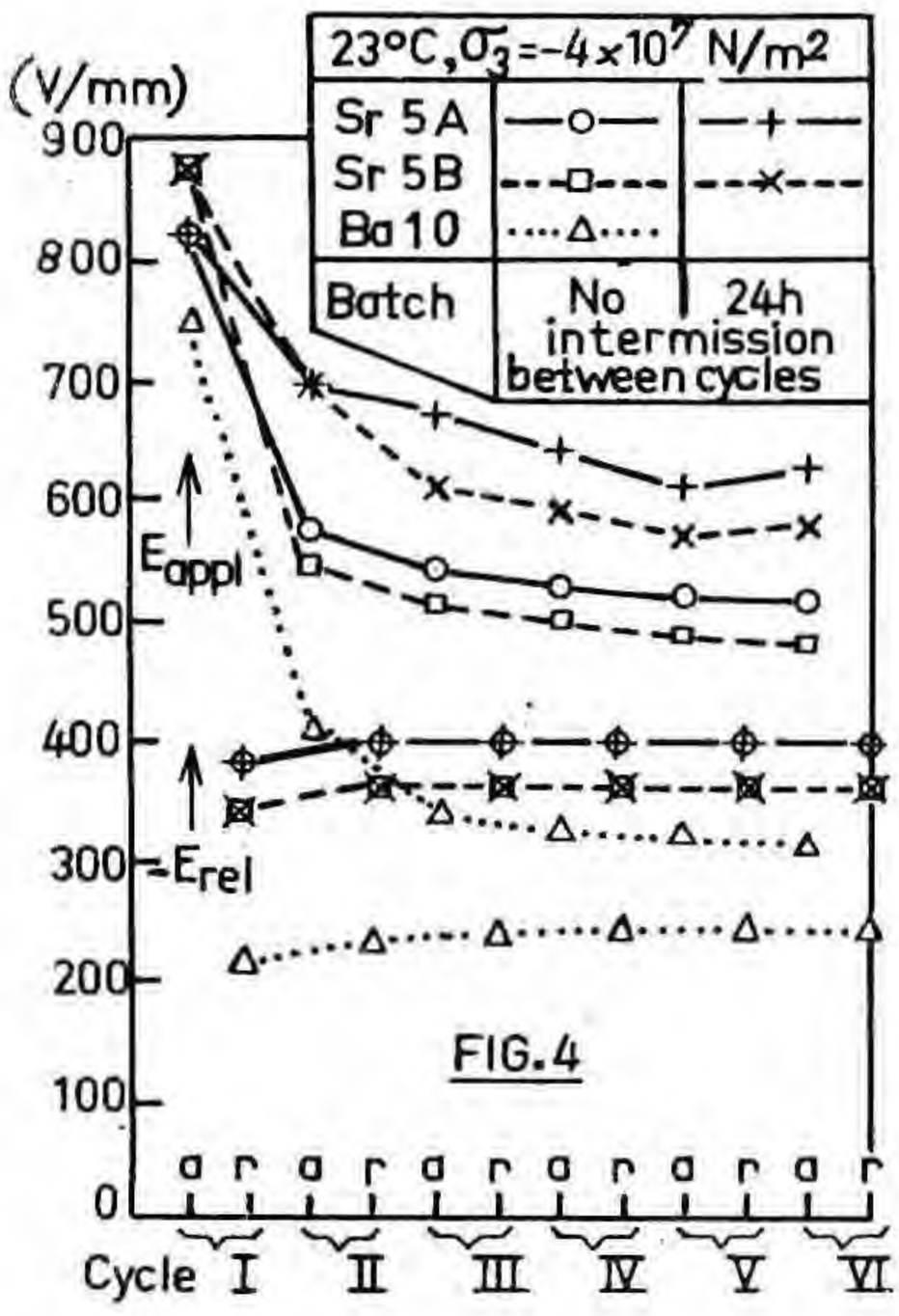

FIG.4

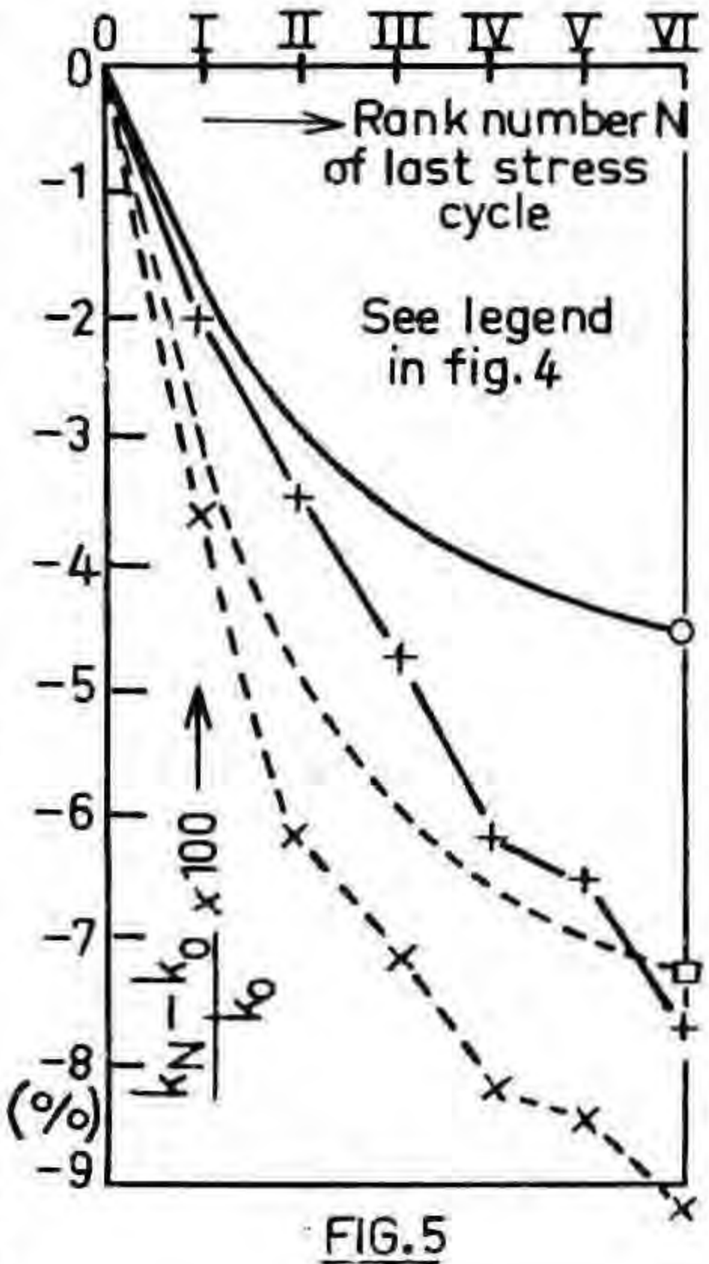

FIG.5

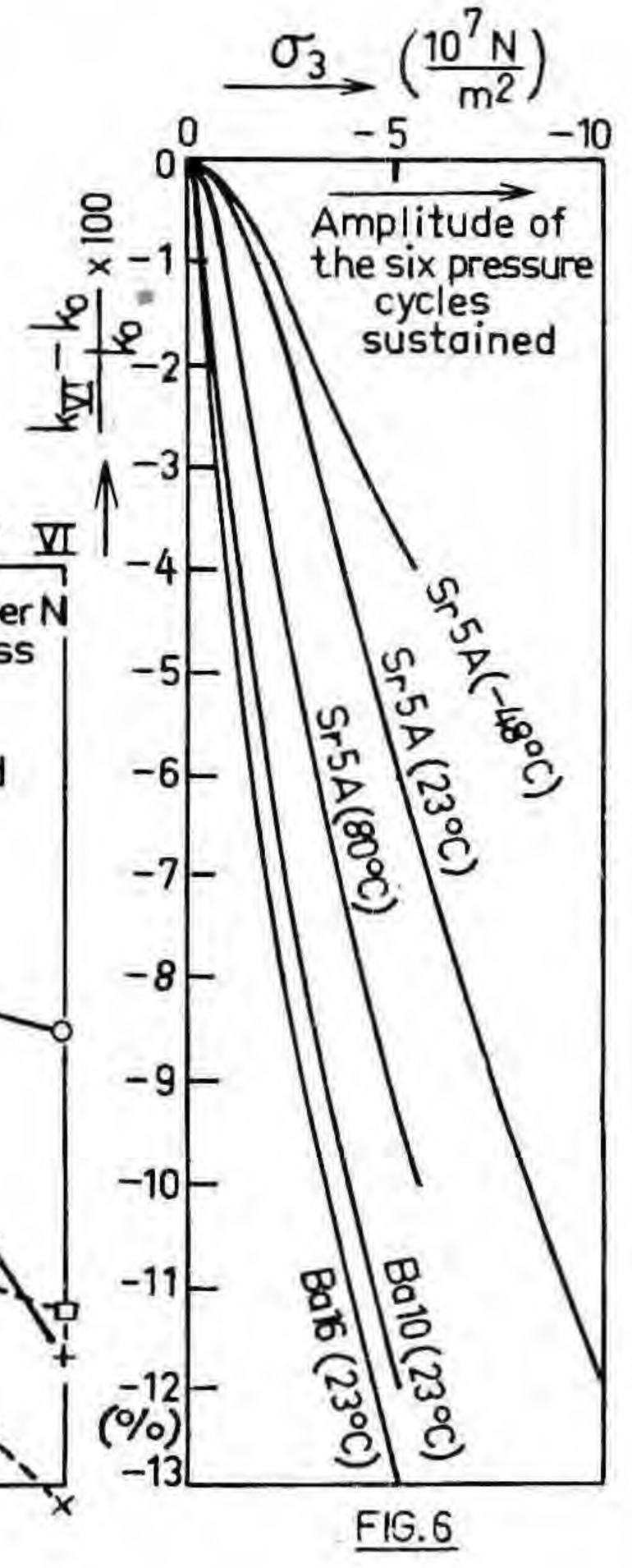

FIG.6

cycling the induced field E_{rel} is nearly constant; a 24 hours intermission between successive cycles has no effect; 3) The decrease of the planar coupling coefficient k evidences that the poled samples suffer more rapidly irriversible depolarization the more the coercivity is lower; 4) At higher temperature this depolarization is larger, whereas the induced fields are weaker; 5)The large-signal response of Sr5A is much better than that of Ba10,which has nearly the same Curie temperature but a lower coercivity; on the other hand the small-signal response (pickups, hydrophones!) is slightly lower for Sr5A than for Ba10. Since the La-content is not the same, the effect of La needs further investigation. Various Zr/Ti ratios should also be studied.

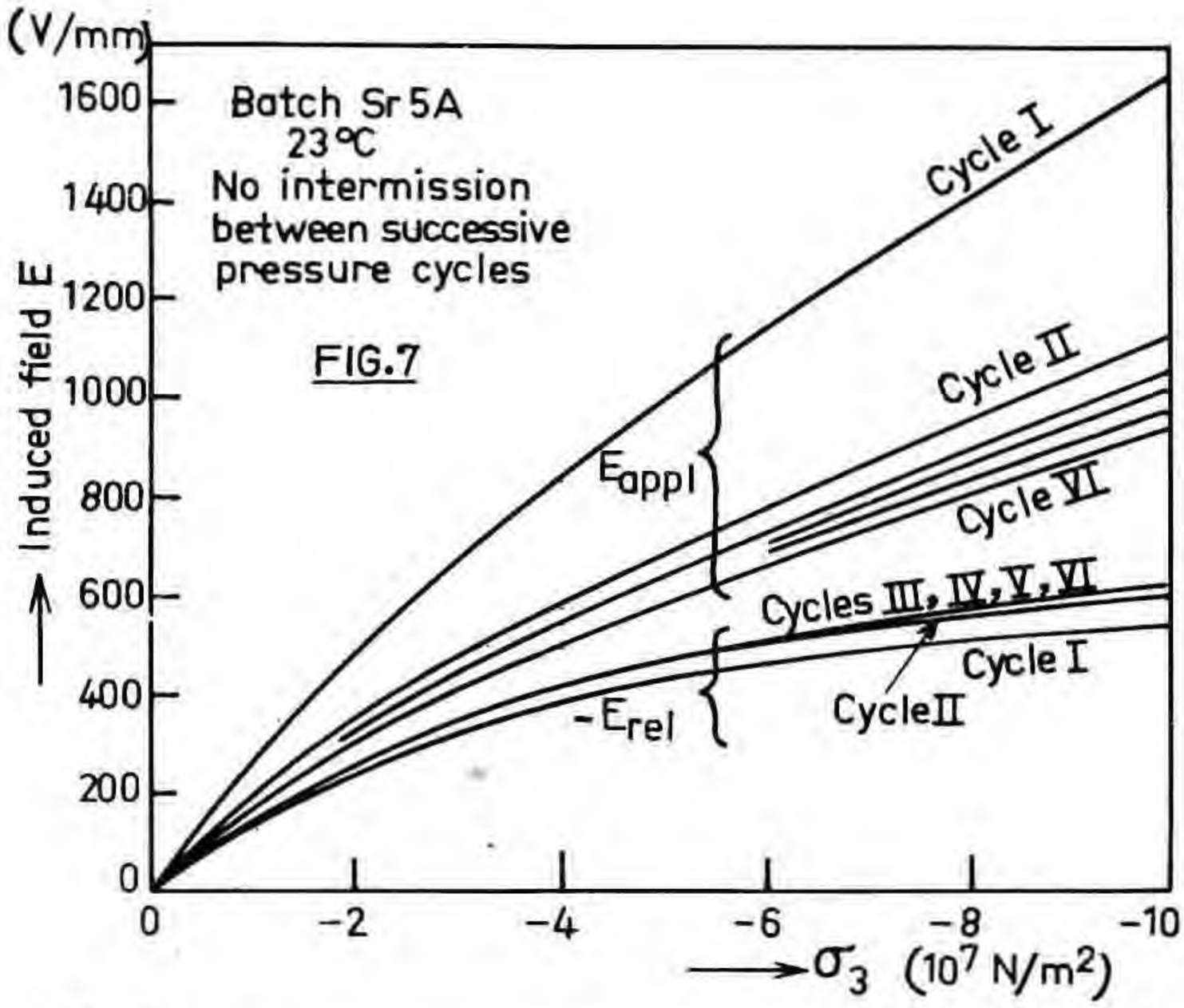

FIG.7

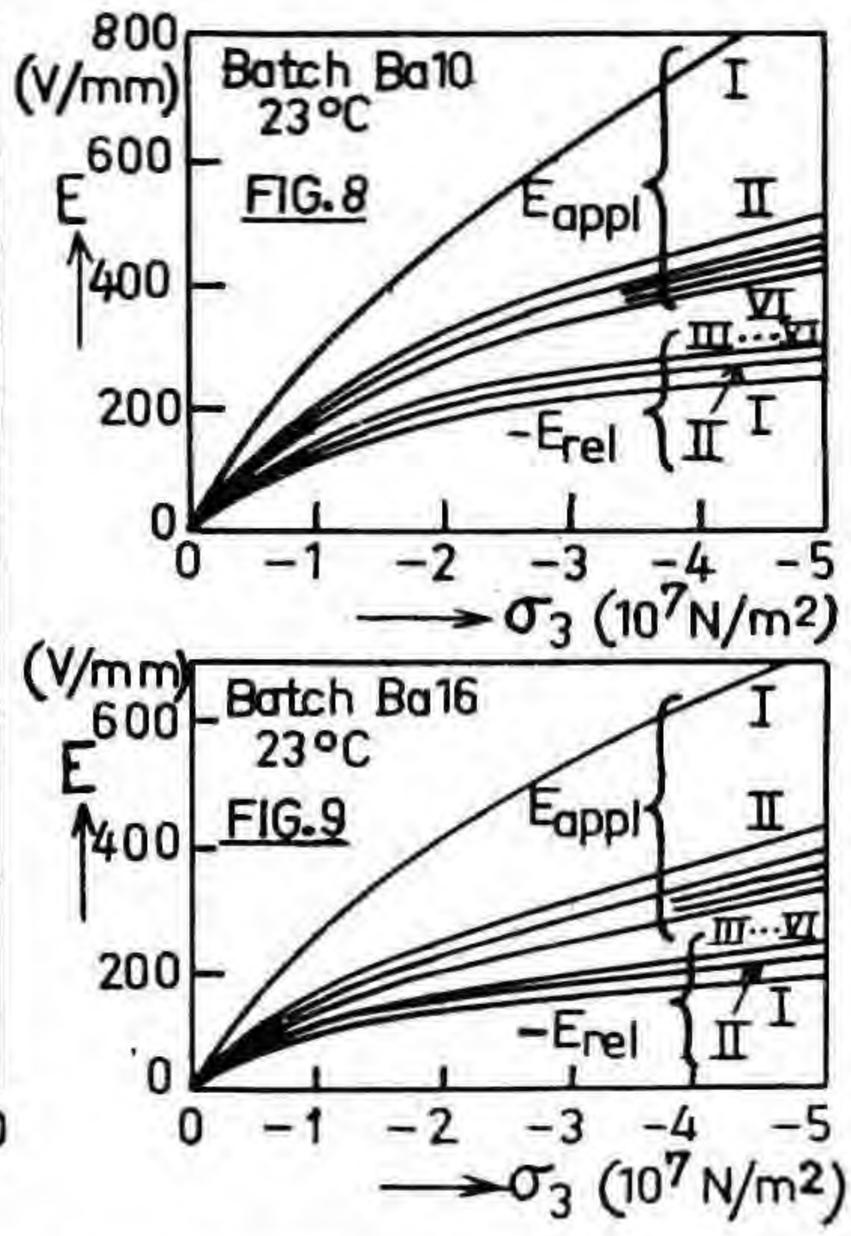

FIG.8

FIG.9

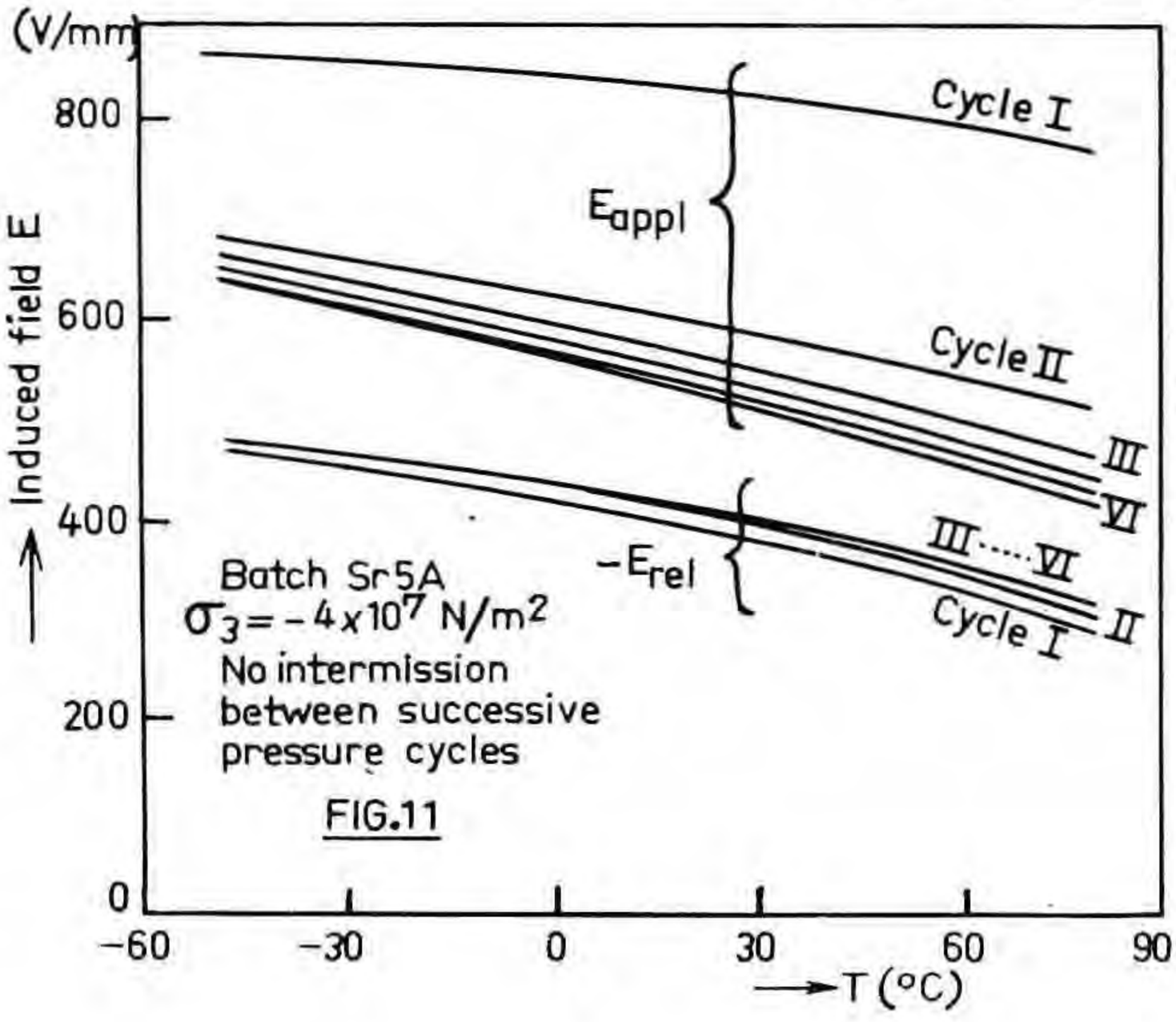

FIG.11

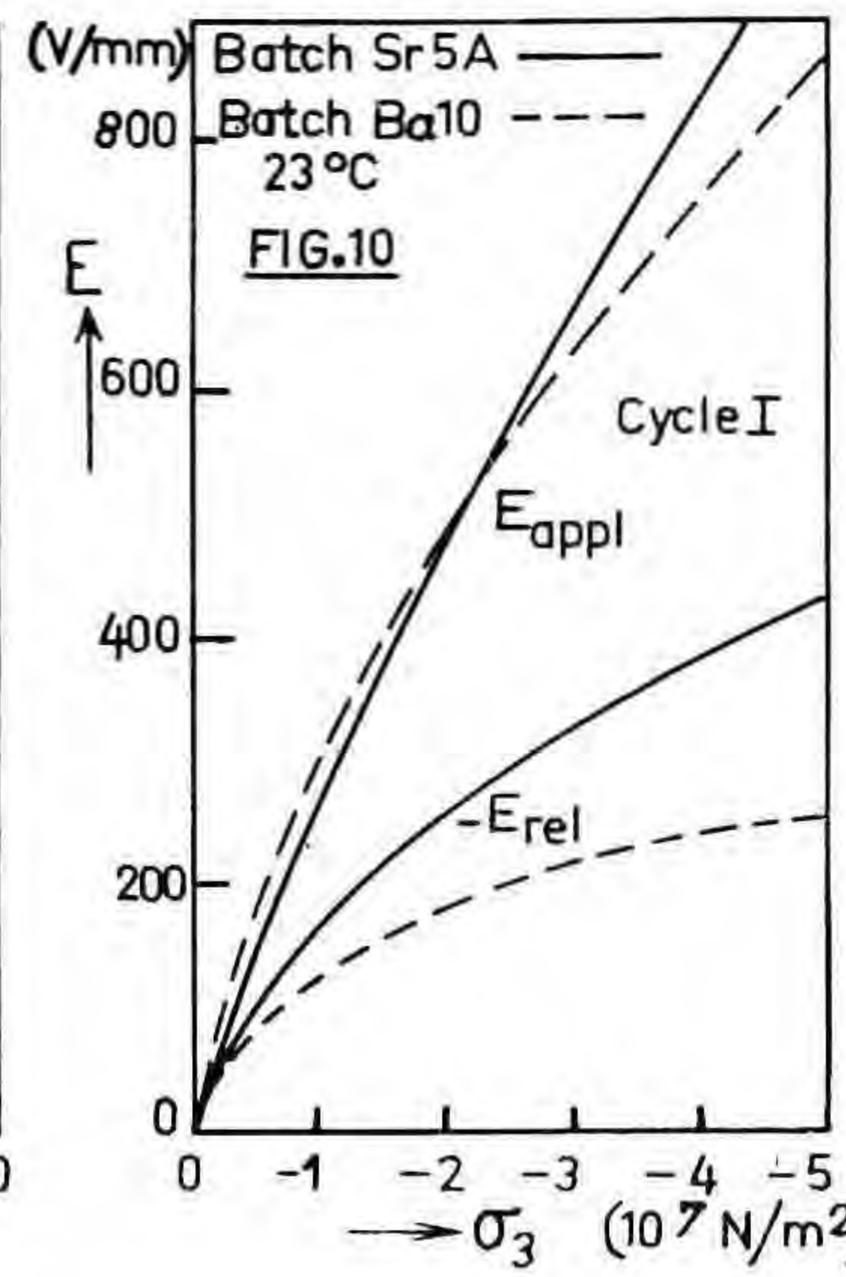

FIG.10

O18

FOURTH INTERNATIONAL CONGRESS ON ACOUSTICS
COPENHAGEN 21.-28. AUGUST 1962

Generalization of Kirchoff's Theorem for an Arbitrarily Moving Surface.

V.Chromov

A generalization Kirchoff's formula is proposed for the case of the integration surface moving in the space.

If

$$\Delta\varphi - \frac{1}{c^2}\frac{\partial^2\varphi}{\partial t^2} = 0 \qquad /1/$$

is written in the form

$$\Box\varphi = 0 \qquad /3/$$

where $\Box = \sum_{i=1}^{4}\frac{\partial^2}{\partial x_i^2}$ and

$$x_1 = x\ ,\ x_2 = y,\ x_3 = z\ ,\ x_4 = ict \qquad /2/$$

Than the dynamical problem is reduced to the soltuion of a statical equation /3/ in the fourdimensional space.

Equation /3/ can be considered as an analogue of the usuall Laplace equation.

It is possible to obtain Green's formula for the fourdimensional space in the same manner as for threedimensional space:

$$\int_V (W\Box\varphi - \varphi\Box W)dV = \int_S (W\frac{\partial\varphi}{\partial N} - \varphi\frac{\partial W}{\partial N})dS \qquad /4/$$

V - fourdimensional region bounded by threedimensional surface S, φ and W are function of four variable continuous with their first and second derivatives in the region V and on the surface S

N -unit vector in the direction of the external normal to S .

Let x_i' denote the coordinates of the observation point lying inside S, and x_i coordinates of the variable point on S .

The distance between these points is

$$R = \sqrt{\sum_{i=1}^{4} (x_i' - x_i)^2} \qquad /5/$$

It is easy to show directly that equation /3/ is satisfied by

$$W = \frac{1}{R^2} \qquad /6/$$

everywhere except point R=0.

Let us draw a hypersphere of radius R' around this point. Substituting /6/ into /4/ and assuming $R' \to 0$ it is possible to obtain.

$$\varphi(x_1', x_2', x_3', x_4') = \frac{1}{4\pi^2} \int_S \left[\frac{1}{R^2} \frac{\partial \varphi}{\partial N} - \varphi \frac{\partial}{\partial N} \left(\frac{1}{R^2} \right) \right] dS \qquad /7/$$

the solution of one is expressed in the form of integral taken along the hypersurface S .

If

$$F(x_1, x_2, x_3, x_4) = 0 \qquad /8/$$

is the equation of this hypersurface it is possible to consider it as the equation of a usual surface moving in threedimensional space.

The nondimensional normal velocity $\beta_n^2 = \frac{\frac{\partial F}{\partial t}}{\sum_{i=1}^{3} \left(\frac{\partial F}{\partial t} \right)^2}$ of the surface[x)] can be found

$$\beta_n^2 = \frac{\frac{\partial F}{\partial t}}{\sum_{i=1}^{3} \left(\frac{\partial F}{\partial t} \right)^2} \qquad /9/$$

Direction cosines of the fourdimensional normal $N[\cos(x_i, N)]$ can be expressed in terms of normal surface velocity β_n and direction cosines of the normal n in the threedimensional space:

$$\cos(x_4, N) = \frac{\beta_n}{i\sqrt{1-\beta_n^2}} , \cos(x_i, N) = \frac{\cos(x_i, n)}{\sqrt{1-\beta_n^2}} \qquad i = 1,2,3 \qquad /10/$$

It is possible to show that for hypersurface element dS holds the relation

$$dS = dS \sqrt{1-\beta_n^2}\, dx_4 ,$$

x) It is assumed that $1 - \beta_n^2 > 0$

Where dS -twodimensional surface element.

/7/ can be rewritten in the form

$$\varphi(x_1', x_2', x_3', x_4) = \frac{1}{4\pi^2} \int_S dS \int_{x_4} \frac{1}{R^2} \frac{\partial \varphi}{\partial N} - \varphi \frac{\partial}{\partial N}\left(\frac{1}{R^2}\right) \Big\} \sqrt{1-\beta_n^2}\, dx_4 \qquad /11/$$

After integration between the limits $x_4 = a_1 \to -\infty \quad x_4 = a_2 \to +\infty$

and using the relation $\frac{\partial(\ldots)}{\partial N} = \sum_{i=1}^{4} \frac{\partial(\ldots)}{\partial x_i} \cos(x_i, N)$

and/10/ it is possible to express $\frac{\partial \varphi}{\partial N}$ and $\frac{\partial}{\partial N}\left(\frac{1}{R^2}\right)$ in terms of

and of derivatives in respect

It is easy to show that all integrals in /11/ can be reduced to the

form $\int_{-\infty}^{\infty} \frac{1}{R^2}(\ldots)\, dx_4$

The integrands have poles in points

$$|x_4' - x_4| = -i\tau \qquad x_4' - x_4 = i\tau,$$

Where τ -distance in the threedimensional space. The integration in the plane of complex variable x_4 gives φ

$$\varphi(x', y', z', t') = \frac{1}{4\pi} \int_S \Big\{ \frac{1}{r(1-\beta_{nr})} \frac{\partial \varphi}{\partial n} - \frac{\partial}{\partial n}\Big[\frac{1}{r(1-\beta_{nr})}\Big] \varphi +$$

$$+ \frac{\frac{\partial r}{\partial n}}{c\, r(1-\beta_{nr})} \frac{\partial \varphi}{\partial t} - \frac{2\beta_n}{c\, r(1-\beta_{nr})} \frac{\partial \varphi}{\partial t} - \frac{\frac{\partial \beta_n}{\partial t}}{c\, r(1-\beta_{nr})} \varphi \Big\} dS \qquad /12/$$

The values in integrand are taken for the moment $t = t' - \frac{r}{c}$

where r -distance in the moment t'. For $\beta_n = 0$ /12/ is reduced to the usual Kirchoff's formula.

In this manner the value of $\varphi(x', y', z', t')$ is determined by values of φ, $\frac{\partial \varphi}{\partial n}$, $\frac{\partial \varphi}{\partial t}$ on the moving surface.

For harmonical fields $\varphi = \psi e^{i\omega t}$ /12/ gives

$$\varphi(x', y', z', t) = \frac{e^{i\omega t}}{4\pi} \int_S \Big\{ \frac{e^{-ikr}}{r(1-\beta_{nr})} \frac{\partial \psi}{\partial n} - \qquad /13/$$

$$- 2ik\beta_n \frac{e^{-ikr}}{r(1-\beta_{nr})} \psi - \frac{\partial \beta_n}{\partial r} \frac{e^{-ikr}}{r(1-\beta_{nr})} \psi \Big\} dS$$

H19

FOURTH INTERNATIONAL CONGRESS ON ACOUSTICS
COPENHAGEN 21.-28. AUGUST 1962

L'EFFET D'UN BRUIT BLANC CONTRALATERAL TANT SUR LE SEUIL ABSOLU QUE SUR LE SEUIL DIFFERENTIEL

René CHOCHOLLE et Christiane SAULNIER (PARIS)

Des expériences antérieures nous avaient montré l'effet de sons purs sur une oreille tant sur le seuil absolu que sur le seuil différentiel de fréquence ou d'intensité mesuré sur l'autre oreille .

Nous avons jugé utile de reprendre ces expériences en remplaçant le son pur sur l'oreille opposée par un bruit blanc . Le bruit blanc utilisé n'était pas filtré et s'étendait sur une bande de fréquences certainement plus large que la bande des fréquences audibles, même compte tenu de la courbe de réponse de l'écouteur électrodynamique utilisé ; son niveau était de 40 dB au-dessus du seuil . Les expériences furent faites toujours sur un son de 1000 Hz sur l'autre oreille .

Les mesures furent conduites, toujours en chambre sourde, par la méthode des stimuli constants améliorée (CHOCHOLLE,1) de façon à faire collaborer activement les sujets aux expériences et à les mettre dans le meilleur état d'attention possible ; en particulier ceux-ci faisaient apparaître eux-mêmes les stimuli ou leurs variations : après un faible signal lumineux qui les invitait à se préparer, ils appuyaient sur une clé (ou sur deux clés à la suite l'une de l'autre s'il s'agissait de mesurer un seuil différentiel) et ceci trois fois de suite à chaque valeur testée, avec un court intervalle de temps entre chaque essai ; les clés étaient suffisamment silencieuses pour ne pas détourner l'attention des sujets ; ceux-ci devaient indiquer au moyen d'une clé de réponse et selon un code convenu, le nombre de fois qu'ils pensaient avoir perçu le stimulus ou sa variation ; 50 essais furent effectués à chaque valeur testée . Les seuils ont été déterminés aux 50% de réponses positives sur les courbes de réponse (courbes donnant les variations du nombre de réponses positives en fonction de l'intensité aux niveaux juxtaliminaires), et également calculés par la méthode des moindres carrés, de même que les écarts-types et les erreurs-types sur la moyenne .

Les mesures furent faites en suites croissantes et décroissantes alternées de stimuli (ou de variations de stimuli, celles-ci étant toujours prises dans le sens positif, c'est-à-dire dans le sens des accroissements de stimulus), et les résultats additionnés quel que soit le sens des suites, afin de compenser les sous-évaluations et les surévaluations provenant de celui-ci ; par ailleurs, des suites avec bruit blanc sur l'oreille opposée et des suites en absence de bruit étaient alternées au cours de chaque série, afin de pouvoir tenir compte dans la mesure du possible des variations de sensibilité d'une période de temps à une autre . Chaque série de mesures était toujours précédée de la mesure du seuil absolu de chaque oreille au stimulus utilisé, et les intensités fixées par rapport à ce seuil .

4 sujets furent testés .

Dans une première série d'expériences, nous avons étudié les seuils absolus en présence d'un bruit blanc sur l'oreille contralatérale . L'appareillage utilisé ne posait aucun problème particulier ; il comprenait un oscillateur et un générateur de bruit blanc, ainsi que deux atténuateurs et deux écouteurs électrodynamiques ; les impédances étaient correctement adaptées dans les deux sens . Tous les sujets montrent une augmentation du seuil absolu du son de 1000 Hz due à la présence du bruit blanc ; cette augmentation allait d'un à plus 5 dB selon les sujets, mais n'était vraiment très significative que pour 3 sujets sur 4 . Ces résultats rappellent ceux obtenus dans des expériences précédentes (CHOCHOLLE, 4) en présence de sons purs de fréquence voisine de celle à laquelle sont faites les mesures sur l'autre oreille, puisque dans les deux cas le seuil absolu est augmenté ; toutefois, l'augmentation est moins importante pour un bruit blanc que pour un son pur de fréquence voisine de celle sur laquelle on fait les mesures à même niveau d'audition (intensité en décibels au-dessus du seuil) .

Dans une deuxième série d'expériences, nous avons recherché l'effet de la présence d'un bruit blanc invariable sur une oreille sur le seuil différentiel d'intensité mesuré sur l'autre oreille .

Les variations d'intensité étaient obtenues en court-circuitant brusquement à l'entrée comme à la sortie l'un des deux atténuateurs placés à la suite l'un de l'autre, après compensation préalable de l'atténuation sur l'autre atténuateur de façon que le niveau initial d'intensité soit toujours le même à chaque essai quelle que soit la différence introduite . Le sujet disposait de deux clés ; il faisait apparaître simultanément le son sur une oreille et le bruit sur l'autre oreille en appuyant sur la première clé, puis la variation d'intensité sur la première oreille tout en laissant constant le bruit sur la deuxième en appuyant sur la deuxième clé, au bout d'un temps suffisant mais pas trop long ; enfin, il revenait au silence sur les deux oreilles en relâchant les clés au bout du temps nécessaire à une comparaison correcte du stimulus entendu avant et après avoir appuyé sur la deuxième clé ; il devait prendre bien garde de ne pas se laisser guider par l'apparition possible de clics au moment de la variation . L'intensité du son de 1000 Hz sur lequel étaient faites les mesures a toujours été de 10 dB au-dessus du seuil . Le seuil différentiel d'intensité paraît plus grand en présence d'un bruit blanc qu'en absence de tout bruit sur l'oreille opposée (quelques dixièmes de décibels), au moins pour 3 sujets sur 4 ; toutefois, la différence n'est nettement significative que pour un seul des sujets ; ainsi, il y aurait seulement tendance à une certaine augmentation du seuil différentiel d'intensité en présence d'un bruit blanc sur l'oreille contralatérale . Le seuil différentiel d'intensité tend donc à être plus grand en présence d'un bruit blanc comme en présence d'un son pur de même fréquence ou de fréquence voisine sur l'oreille opposée (CHOCHOLLE,2) ; mais, comme pour le seuil absolu envisagé précédemment, l'augmentation est beaucoup moins nette qu'en présence d'un son pur de même fréquence ou de fréquence voisine .

Dans une troisième série d'experiences, nous avons étudié l'effet de la présence d'un bruit blanc sur une oreille sur le seuil différentiel de fréquence mesuré sur l'autre oreille . Les variations de fréquence étaient obtenues en introduisant brusquement des capacités dans un des circuits oscillants d'un générateur à battements au moyen d'un relais commandé par une clé silencieuse mise à la disposition du sujet . Comme dans les expériences sur le seuil différentiel d'intensité, celui-ci faisait apparaître d'abord simultanément le son sur une oreille et le bruit sur l'autre oreille en appuyant sur une première clé, puis la variation sur l'une des deux oreilles seulement en appuyant sur une deuxième clé, sans relâcher la première ; enfin, il reve-

nait au silence en relâchant les deux clés . Les variations de fréquence furent mesurées avec une grande précision en fractions de hertz au moyen d'un compteur électronique et vérifiées sur un oscillographe cathodique bicourbe à grand écran en utilisant les figures de LISSAJOUS, ainsi que par comparaison avec le balayage . Le niveau du son de 1000 Hz sur lequel ont été faites les mesures a toujours été de 10 dB au-dessus du seuil . Dans ce cas encore, pour tous les sujets, le seuil différentiel est toujours très significativement augmenté en présence d'un bruit blanc sur l'oreille opposée (augmentation de quelques hertz), mais nettement moins toutefois qu'en présence d'un son pur de même fréquence ou de fréquence voisine (CHOCHOLLE et SAULNIER,5) .

Ainsi, l'effet de la présence d'un bruit blanc sur une oreille, que ce soit sur le seuil absolu ou sur le seuil différentiel de fréquence ou d'intensité mesuré sur l'autre oreille, est analogue à celui de la présence d'un son de même fréquence ou de fréquence voisine de celle sur laquelle on fait les mesures, puisqu'il y a une augmentation nette du seuil absolu et plus encore du seuil différentiel de fréquence, et tendance également à une augmentation du seuil différentiel d'intensité . Comme ceci a été montré à propos de l'effet de la présence des sons purs sur l'oreille opposée tant sur les seuils absolus que sur les seuils différentiels de fréquence ou d'intensité, cette augmentation est due dans tous les cas à des interférences à des niveaux supérieurs des voies nerveuses auditives droite et gauche, et qui plus est probablement au niveau cortical, tant physiologique que psychique .

Mais cette augmentation est dans tous les cas nettement inférieure à celle que l'on obtiendrait en présence d'un son pur contralatéral de même fréquence ou de fréquence voisine de celle utilisée dans les mesures, à un même niveau d'intensité évalué par rapport au seuil . Comment expliquer qu'un bruit blanc puisse avoir un effet moindre qu'un son pur de même fréquence ou de fréquence voisine ? Les auteurs ont tendance à admettre que l'oreille est capable d'analyser tout son complexe, et un bruit blanc par conséquent, en ses composantes, et d'autre part qu'il existerait des bandes critiques au-delà desquelles certains effets ne se produiraient plus ou pourraient être différents : ainsi, dans l'effet de masque homolatéral d'un bruit blanc sur un son pur par exemple, seule n'interviendrait qu'une bande assez étroite de fréquences située de part et d'autre de la fréquence masquée, à l'exclusion des autres composantes du bruit blanc ; mais s'il en était ainsi, l'effet d'un bruit blanc ne devrait pas être inférieur à celui d'un son de même fréquence ou de fréquence voisine ; peut-être même il pourrait être un peu plus grand, puisqu'un bruit blanc n'est pas limité à une seule fréquence, mais comprend en principe une série infinie de fréquences . En réalité, l'oreille doit être un mauvais analyseur, si tant est qu'elle puisse faire une certaine analyse en présence d'un son aussi complexe qu'un bruit blanc dont le spectre est continu et continuellement variable, et les interactions qui se produisent à divers niveaux des voies nerveuses auditives doivent encore modifier les messages transmis le long de ces voies à partir de la cochlée ; d'autre part, il n'est pas certain que seules n'aient d'effet que les fréquences situées à l'intérieur d'une certaine bande .

En réalité, la comparaison avec les expériences faites sur des sons purs montre que les bandes éloignées interviennent dans l'effet d'un bruit blanc sur l'oreille contralatérale tant sur le seuil absolu que sur le seuil différentiel de fréquence ou d'intensité mesuré sur l'autre oreille ; en effet, comme les expériences antérieures l'ont montré (CHOCHOLLE, 2,4 ; CHOCHOLLE et SAULNIER,5), seuls les sons de même fréquence ou de fréquence voisine sur une oreille ont pour effet une augmentation du seuil absolu comme du seuil différentiel de fréquence ou d'intensité mesuré sur l'autre oreille ; les fréquences éloignées par contre semblent sans effet significatif net sur les seuils absolus (CHOCHOLLE,2), amènent une réduction nette du seuil différentiel d'intensité (CHOCHOLLE,4), et tendent à amener parfois également une

réduction plus ou moins nette selon les sujets du seuil différentiel de fréquence (CHOCHOLLE et SAULNIER, 5) ; tout semble donc se passer comme si l'effet d'un bruit blanc sur l'oreille opposée dépendait à la fois des fréquences voisines et des fréquences éloignées de la fréquence de mesure, ces dernières tendant à contrebalancer plus ou moins selon les cas l'effet des premières ; ceci met en cause l'idée de bande critique ; et même, si on voulait maintenir la notion de bande critique malgré les objections précédentes, leur largeur ne pourrait pas être la même selon les types d'expériences envisagées (seuils absolus, seuils différentiels de fréquence ou seuils différentiels d'intensité) . On pourrait évidemment s'étonner de constater que les fréquences éloignées ne contrebalancent pas plus encore l'effet des fréquences voisines de celle sur laquelle ont été faites les mesures ; mais il faut se rappeler que le niveau d'audition (intensité en décibels au-dessus du seuil), comme le niveau isosonique de chacune des composantes possibles d'un bruit blanc, doivent différer largement selon les composantes aux intensités moyennes utilisées, en raison même des variations de la sensibilité de l'oreille dans tout le spectre acoustique audible; et la fréquence de 1000 Hz à laquelle ont été faites les mesures sur l'autre oreille se trouve par hasard dans la zone de meilleure sensibilité, de l'oreille .

BIBLIOGRAPHIE

1) CHOCHOLLE R.- Le déclenchement des stimuli par le sujet en Physiologie sensorielle .-J. Psychol., 1949, 42,p. 339-344 .

2) CHOCHOLLE R.- La sensibilité auditive différentielle d'intensité en présence d'un son contralatéral de même fréquence .- Acustica, 1957, 7, p. 75-83 .

3) CHOCHOLLE R.- Le seuil différentiel d'intensité en présence d'un son contralatéral de fréquence différente .- Acustica, 1959, 9, p.309-315 .

4) CHOCHOLLE R.- Le seuil auditif monaural en présence d'un son de fréquence différente sur l'oreille opposée .- J. Physiol., 1960, 52, p.51-52 .

5) CHOCHOLLE R., SAULNIER C.- Le seuil différentiel de fréquence .: l'effet de la présence simultanée d'un son ou d'un bruit blanc sur l'oreille opposée .- J. Physiol., 1962 (sous presse) .

L19

FOURTH INTERNATIONAL CONGRESS ON ACOUSTICS
COPENHAGEN 21.-28. AUGUST 1962

THEORETICAL AND EXPERIMENTAL STUDIES OF STEEP FRONTED WAVES IN PIPES

P.O.A.L. Davies and M.J. Dwyer

Introduction

The general approach to Internal Combustion engine silencing has been to consider the engine exhaust as a noise source consisting of a train of acoustic pulses. The resulting sound waves are attenuated by acoustic filters and absorbers. Although this has given some insight into silencer performance, practical results have often been disappointing.

A better approach is to consider the pulses as being independent disturbances, as they are effectively widely separated within the system. This can be illustrated by a practical example. A four stroke four cylinder engine running at 3000 rpm produces 100 impulses per second. These however, travel at around 1800 fps, which means that the primary exhaust pulses traverse the exhaust pipe separated by 18 ft. At 6000 rpm, these pulses will still be 9 ft. apart.

A major objection to acoustic theory is that the pressure changes are not infinitesimal, but of the order of half an atmosphere. Small perturbation theory is not applicable either, as it does not take account of the large changes of density that accompany the unsteady flow. Shock tube theory, on the other hand, meets these objections and has been well developed.

It remains however, to show that exhaust pulses will give rise to the same type of disturbances as the bursting of the diaphragm in a shock tube. In the example quoted above, if the exhaust valve takes 10 crank angle degrees to open, the time taken will be of the order of 600 microsecs. This is of the same order as the time taken to burst the diaphragm in a conventional shock tube, therefore, the performance of the two systems should be similar.

The unsteady flow in the exhaust system can be examined using the results of shock tube theory. The exhaust pipe outlet can now be considered as a source of sound produced by unsteady gas flow in the exhaust system. If the pressure and gas velocity variations here can be predicted, the sound radiation can be calculated by piston theory. It is clear that if these pressure variations are minimised, the sound radiated will be a minimum. The aim of silencer design will therefore be to reduce the amplitude of the pressure changes due to the unsteady flow from the engine, without impeding that flow.

The unsteady flow in representative parts of a silencer system has been examined both theoretically and experimentally using single disturbances. An outline of the relevant theory is given together with a summary of the experimental results obtained in a special shock tube. These illustrate principles which can be employed to predict silencer performance.

An Outline of Shock Tube Theory

A shock tube consists of a pipe separated in two by a diaphragm. The two chambers thus formed are charged with air or other gas at different pressures. When the diaphragm between them is burst, the high pressure gas expands into the low pressure chamber producing an unsteady flow. A short time after the flow starts, the situation will be as sketched in Fig. 1. The shock wave 1-2 is advancing into the low pressure gas 1. which remains at rest. The shock itself is very thin, of the order of 10^{-4}mm under present conditions, and the original gas is accelerated through it and also compressed to a steady value which exists throughout region 2. The contact surface separating region 2 from region 3 represents the division between what

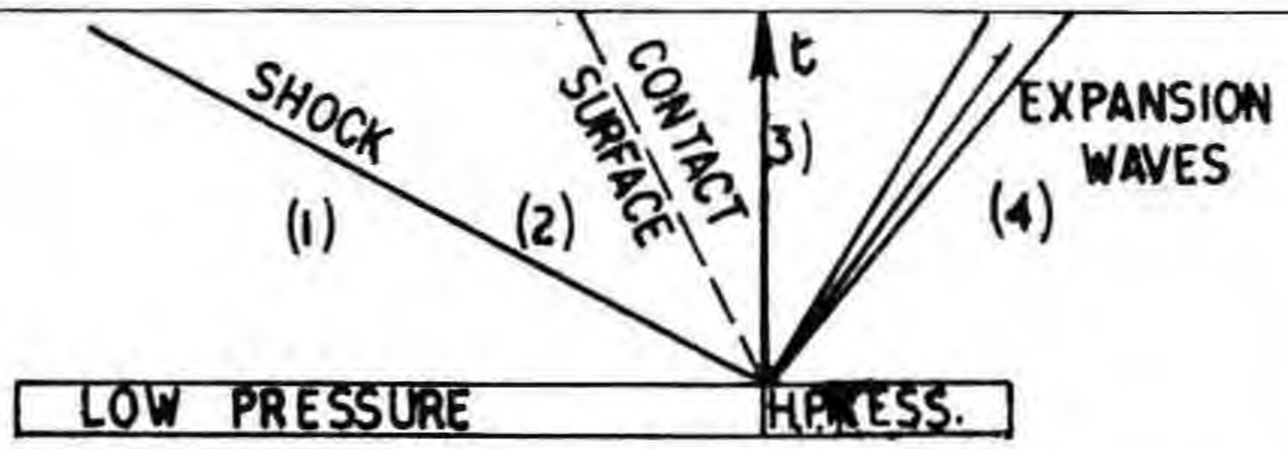

FIG.1.

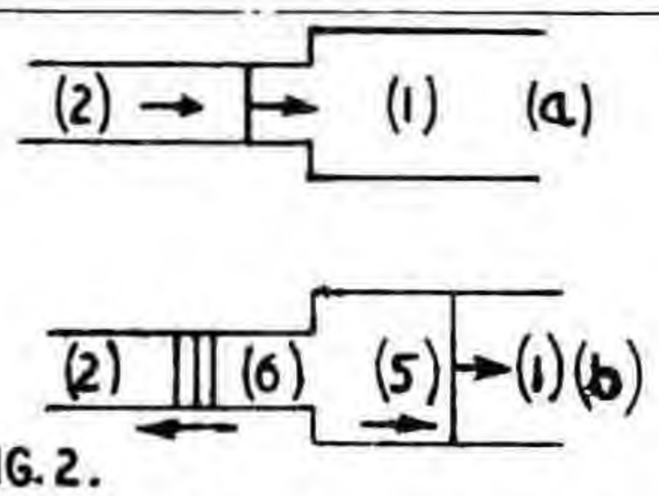

FIG.2.

was originally high and low pressure gas. The pressure and velocity in region 3 are the same as those for 2, but the temperature will, in general, be different. At 4 the gas remains in its original high pressure state and expands isentropically through a series of expansion waves to region 3, each wave moving at the local gas acoustic velocity. The gas conditions at 3 are thus the result of an isentropic expansion from 4, while those at 2 are produced by a shock compression from 1. This gives rise to the change in gas temperature across the contact surface.

Representing the pressure ratio across the shock as p_{21}, the gas velocity behind the shock in region 2 is given by (Ref. 1).

$$\frac{U_2}{a_1} = (p_{21}-1)\left[\frac{2/\gamma_1}{(\gamma_1+1)p_{21}+(\gamma_1-1)}\right]^{1/2} \qquad \ldots(1)$$

where a1 is the acoustic velocity in region 1, and γ_i is the ratio of specific heats for the gas. The velocity after the isentropic expansion is given by

$$\frac{U_3}{a_4} = \frac{2}{\gamma_4+1}\left[1-(p_{34})^{\frac{\gamma_4-1}{2\gamma_4}}\right] \qquad \ldots(2)$$

Using $U_2 = U_3$, provided the conditions at 1 and 4 are known, the shock pressure step p_{21} can be calculated in terms of the original pressure ratio p_{41}.

The flow through an expansion with area ratio A, is illustrated in Fig. 2. The conditions just before and just after the passage of the shock are illustrated. Equations 1 and 2 now apply to the processes 1 - 5 and 2 - 6 respectively. Between 6 and 5 a steady flow will exist which must obey the continuity relation:

$$\rho_5 U_5 = A \rho_6 U_6 \qquad \ldots(3)$$

The solution of the problem requires some other assumptions about the flow between 6 and 5, and a first approximation is to assume it is isentropic and one dimensional. For the exhaust system, it is also reasonable to assume that the local flow Mach number at 6 is always less than unity, although it might just reach this value. The solution for this part of the flow can then be performed using the tables of isentropic flow functions (Ref. 2).

The flow through a contraction can be treated in an analogous manner, but here the wave 2 - 6 will be a reflected shock and not an expansion wave. Bends in the pipe will produce some secondary refraction effects and can be ignored, while branches can be treated as expansion of the pipe. The flow through an orifice can be treated as a contraction followed by an expansion. This is possible because the shock wave is so very thin compared with the length of the hole in the plate.

Finally, conical expansions and contractions will behave very similarly to the sharp ones. But the wave reflected from a cone will be spread out. In the case of a compression wave, the separate reflected shocks will coalesce and form a simple shock front some distance along the pipe, while an expansion wave will remain spread out.

Experiments

The analysis above omits certain characteristics of the flow which are of practical interest, and assumes all the processes are ideal ones. Furthermore, the majority of the literature on shock tubes is concerned with strong shocks and relatively simple configurations. Experiments were performed to confirm the validity of the assumption of ideal processes, and to check other approximations made in the analysis. In addition the theoretical predictions for the more complicated flow processes required confirmation.

Two basic measurements are of interest here: (i) the amplitude of the largest pressure step reaching the exhaust outlet, which sets the maximum sound level, and (ii) the mean pressure behind the primary shock system, which determines the effective exhaust back pressure. Four basic shapes have been investigated, namely, an orifice, an expansion chamber, a cone, and a side branch. The first two of these have been studied in some detail.

The shock tube was approximately 2 in diameter and 7 ft or so long divided into four sections. The high pressure chamber was followed by 3 ft of plain tube, then the test section which was of variable length and finally a plain tube 2 ft long. Pressure measurements were made in the plain tubes before and after the test section using piezo-electric pressure gauges. The frequency response of these was in the neighbourhood of 200 kilocycles.

Results

The observed pressure steps were compared with the predicted performance for each of the basic test rigs. Calibration runs with a plain 1 ft long tube for a test section were made first. For an initial high pressure of 25 psi giving a diaphragm pressure ratio of 2.7, the ideal shock pressure ratio is 1.615 giving a pressure step of 9.0 psi. The observed pressure step at the upstream measuring station was 8.2 psi average while that at the further station was 7.4 psi. This represents a decay of 0.3 psi per foot along the tube. The losses would be smaller in a larger tube, and have therefore been ignored in calculating the ideal performance of expansion chambers, except that the incident step was taken as 8.0 psi for the ideal performance calculations.

The measurements for the orifice plate and the expansion chamber are plotted on Fig. 3, with an ideal curve for comparison. The agreement is very good except at the small area ratios, where the effects of friction loss are most important. If the ideal curve is adjusted for this effect the agreement is almost complete.

Since the performance should depend only on area ratio, orifice plates with one, four and sixteen holes having the same total area were also tested. These gave exactly the same results for the same total area contraction ratio. Similarly, the length of the expansion chamber should have no effect on the results. This was found to be true for length diameter ratios of 1, 2, 3 and 6, as far as the transmitted step was concerned. The reflected wave system, however, was modified slightly with the shortest expansion chamber. This will alter the back pressure on the engine. Otherwise the behaviour is exactly what is predicted by the ideal theory.

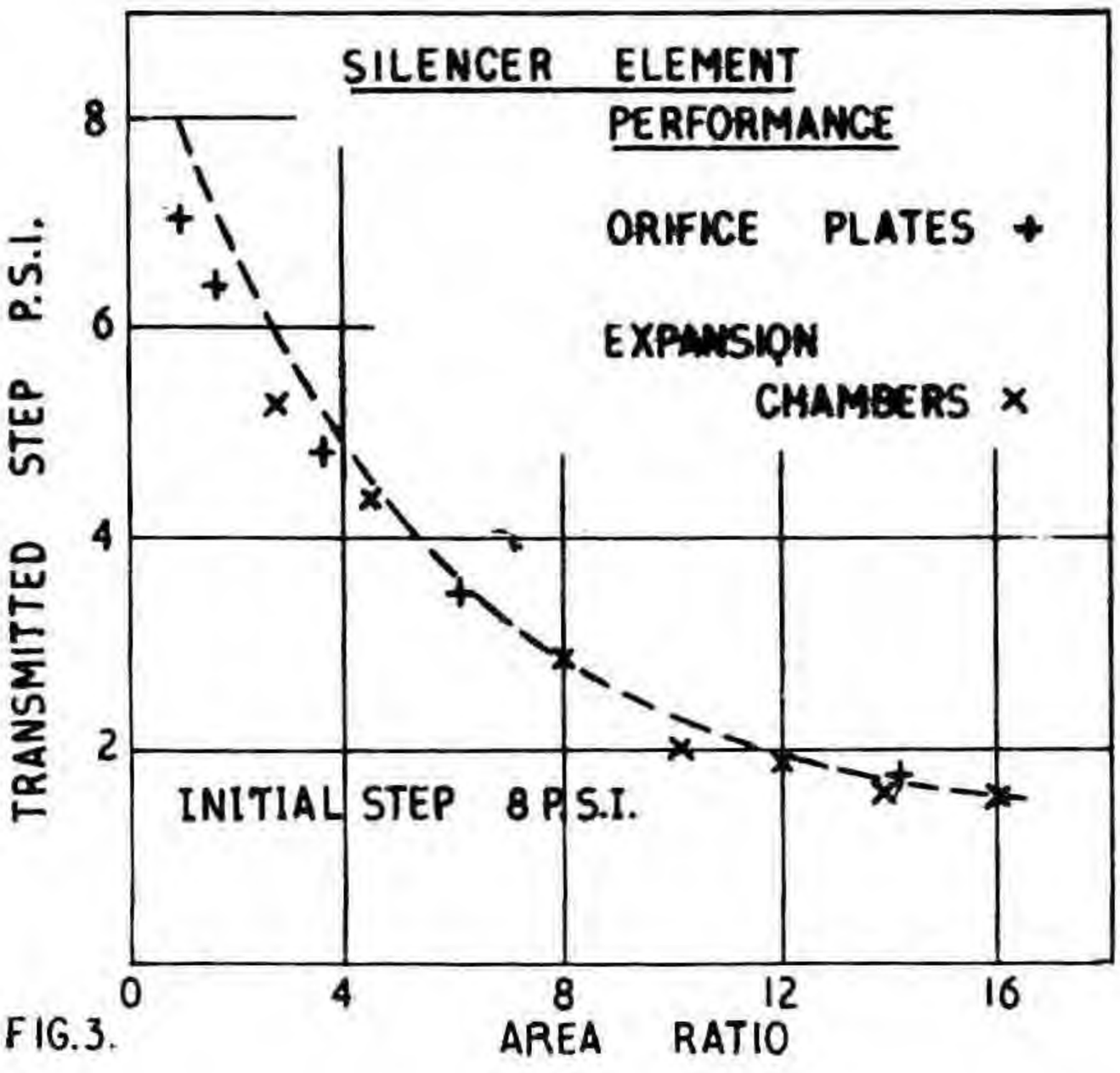

FIG. 3.

A	ΔPz		ΔPs	
	IDEAL	ACTUAL	IDEAL	ACTUAL
1	5·7	5·5	5·7	4·9
0·28	6·4	5·9	2·8	2·8
0·16	6·8	7·1	1·7	1·7
0·07	7·4	7·3	0·9	0·8

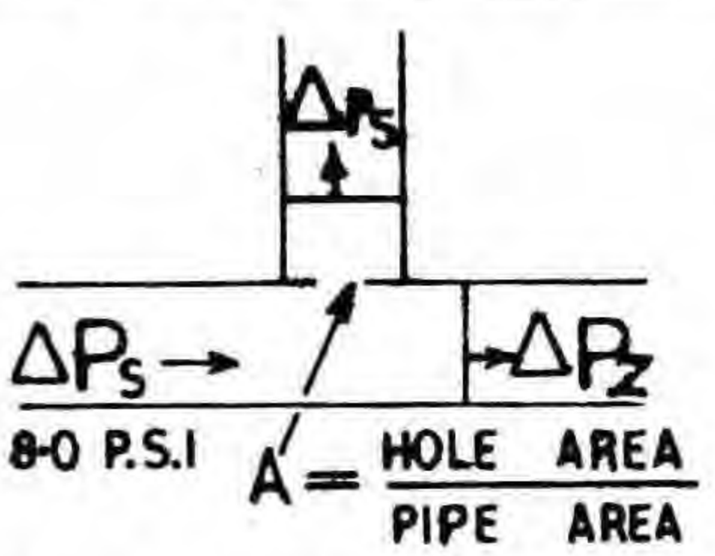

SIDE BRANCH PERFORMANCE

FIG. 4.

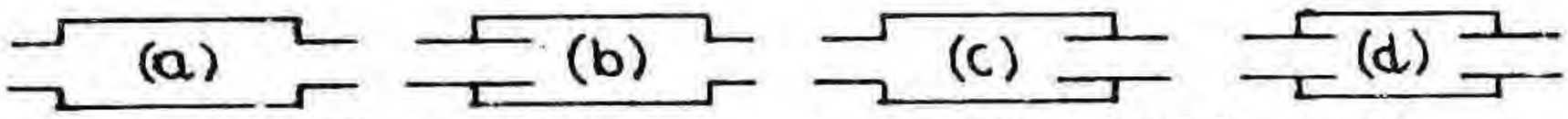

FIG 5 MODIFIED EXPANSION CHAMBERS

	IDEAL	ACTUAL
a	4·6	4·4
b	2·6	3·5
c	3·1	3·1
d	1·6	2·2

Side branches were also investigated to determine their performance. The ideal analysis was again based on one dimensional flow with area changes. Strictly however the turning of the wave front becomes a three dimensional process and, although theory exists for this situation, the labour of the calculations is hardly justified. The area of the orifice leading to the side branch was varied to investigate the performance of pierced tube. As can be seen in Fig. 4, the results again agree with the predicted performance except for the largest area ratio, where it was anticipated the theory would break down.

Similar results were obtained with a modified expansion chamber. These, with the modifications, are illustrated in Fig. 5. Since the wave can expand in both directions the modification 5b will increase the effective expansion ratio without increasing the expansion chamber diameter. Ideally on a one dimensional basis, the area ratio is increased from 4.5 to 8 giving two weaker pressure waves travelling in opposite directions. The measured performance does not agree with this, due to three dimensional effects which are even more serious than for the side branch case.

Modification 5c on the other hand prevents the recompression of the shock flow at the end of the expansion chamber, and is a very effective way of reducing the transmitted pulse amplitude. The reflected pulse is stronger in this instance. The predicted behaviour of 5d also falls short of the ideal due to the reasons already discussed above.

Finally, experiments with conical expansions and contractions gave very good agreement between ideal and measured performance.

Conclusions

The results of the experiments show that is possible to predict the behaviour of silencer system elements on the basis of one dimensional shock tube theory. The experiments point to a design such as is shown in Fig. 5d as being a very effective silencer, and practical experience on a test engine have proved this to be the case.

Acknowledgements

The authors would like to thank Professor E.J. Richards and their colleagues for their interest and advice. Thanks are also due to Mr. A. Hawkins who built the equipment.

References

(1) H.W. Liepmann & A. Roshko, 'Elements of Gas Dynamics' Chapter 3. John Wiley, 1956.

(2) Keenan & Kaye, 'Gas Tables, Table 30' John Wiley 1948.

N19

FOURTH INTERNATIONAL CONGRESS ON ACOUSTICS
COPENHAGEN 21.-28. AUGUST 1962

Die Nachbildung der Hörrichtwirkung bei Lautstärkemeßmikrofonen

H. Niese, Dresden

Es läßt sich zeigen, daß die Richtcharakteristik des Aufnahmemikrofons bei Lautstärkemessungen den Meßwert stark beeinflußt. Übliche Mikrofone besitzen eine Richtcharakteristik, die bei tiefen Frequenzen kugelförmig ist und mit steigender Frequenz mehr und mehr eine Keulenform annimmt. Der Übergang von der Kugel-zur Keulenform erfolgt bei umso niedrigeren Frequenzen je größer die geometrischen Abmessungen des Mikrofons sind.

Einerseits ergeben sich Meßwertunterschiede, die vom verwendeten Mikrofontyp abhängen. Andererseits entstehen sie bei Geräten gleichen Fabrikats durch die Ausrichtung des Mikrofons im Schallfeld, die dem Benutzer überlassen ist. Üblicherweise werden Lautstärkemesser so benutzt, daß das Mikrofon in Richtung der Schallquelle zeigt. Diese vermeintliche richtige Benutzung kann dann nicht konsequent eingehalten werden, wenn gleichzeitig mehrere Schallquellen aus verschiedenen Richtungen wirken. Das ist der Fall: bei Verkehrsgeräuschen, in Maschinensälen, in Räumen mit Büromaschinen oder auf den Führungsständen von Großmaschinen und Fahrzeugen. In solchen Fällen ist der Benutzer geneigt, das Mikrofon so auszurichten, daß es mit der Blickrichtung der Person am Arbeitsplatz übereinstimmt. Er glaubt dann, denjenigen Meßwert zu ermitteln, den die Person empfindet. Es entstehen jedoch Meßfehler, die sowohl von der Richtcharakteristik des Meßmikrofons als auch von seiner Kalibrierung abhängen.

Keine Meßfehler entstehen dann, wenn immer nur in einem solchen Schallfeld gemessen wird, in dem das Meßgerät gemäß der Lautstärkeempfindung kalibriert wurde. Speziell führt man die Kalibrierung entweder im ebenen oder diffusen Schallfeld durch. Wurde die Kalibrierung in der ebenen Welle vorgenommen, wobei das Mikrofon zur Schallquelle zeigt, so ergibt sich der größte Meßfehler, wenn bei Messungen höherfrequente Schallanteile von der Seite her einfallen. Genügt hierbei das Mikrofon den IEC-Empfehlungen für den Präzisions-Schallpegelmesser, die im Frequenzgebiet um 8 kHz bis zu 10 dB Empfindlichkeitsabfall bei

seitlichem gegenüber frontalem Schalleinfall zulassen, so steht die Mikrofonrichtcharakteristik im Widerspruch zur Ohrrichtempfindlichkeit. Die Ohrempfindlichkeit ist im gleichen Frequenzgebiet um 7 dB größer, wenn der Schallvon der Seite her einfällt gegenüber frontalem Einfall. Insgesamt ergibt sich ein Meßfehler von 17 phon, der bei der betrachteten Beschallung und Mikrofonkalibrierung entsteht. Selbst wenn unter Verzicht auf absolute Empfindlichkeit ein sehr kleines Mikrofon benutzt würde, das bei diesen Frequenzen noch Kugelrichtempfindlichkeit besitzt, so verbleibt dennoch ein Meßfehler von 7 phon.

Kalibriert man andererseits das Mikrofon in senkrechter Stellung in der ebenen Welle, so ist die azimutale Empfindlichkeit richtungsunabhängig, jedoch verbleiben auch hier bei seitlichem Schalleinfall die 7 phon Meßfehler durch die Ohrrichtwirkung. Fällt ein höherfrequentes Schallereignis von oben ein, so ist gemäß der genannten IEC-Empfehlung die Mikrofonempfindlichkeit bis zu 10 dB größer, die Hörempfindlichkeit ist aber gegenüber frontalem Schalleinfall nur 5 dB größer, so daß ein Meßfehler von 5 phon zu erwarten ist.

Ebenso entstehen Meßfehler, wenn das Mikrofon im diffusen Schallfeld kalibriert wird und bei der Messung gerichtete Schallstrahlen einfallen.

Diese Meßfehler lassen sich ganz vermeiden, wenn ein Mikrofon benützt wird, das die Richtcharakteristik des beidohrigen Hörens besitzt. Es ist beliebig kalibrierbar und mißt in jedem Schallfeld fehlerfrei, wenn es in Blickrichtung des Beobachters benutzt wird. Auch für die Aufnahme von Geräuschspektren zur Anwendung von Lautstärkeberechnungsmethoden ergeben sich Vorteile. Einerseits muß nicht mehr zwischen ebenem und diffusem Schallfeld entschieden werden und andererseits lassen sich auch hier die Meßfehler vermeiden, die wie vorstehend erläutert entstehen, wenn keines der Normalschallfelder vorliegt.

Die Richtcharakteristik des zweiohrigen Hörens wurde in verschiedenen Instituten in Abhängigkeit von der Frequenz für eine Kugelfläche ermittelt. Je nach Autor schwanken diese Ergebnisse etwas. Sie lassen sich durch Mittelung allgemeingültig darstellen.

Mit Hilfe einer größeren Anzahl Abschattungsstudien wurde der Versuch unternommen, durch einen auf das Mikrofon aufsteckbaren Abschattungskörper die Richtempfindlichkeit des Gehörs nachzubilden. Als günstig-

ste Annäherung wurde ein Blechdoppelwinkel mit den Abmessungen 80 mm x 55 mm x 55 mm entwickelt, der mit Hilfe zweier Federn an das Mikrofongehäuse geklemmt werden kann. Verwendet wurde ein Kondensatormikrofon von 40 mm Gehäusedurchmesser. Der Blechwinkel ist von der Gestalt, daß die Mikrofonmembran bei höheren Frequenzen von vorn und von unten abgeschattet wird, wodurch die keulenförmige Richtcharakteristik des Mikrofons in zwei seitwärts gerichtete Keulen aufgespaltet und die Empfindlichkeit bei Schalleinfall von unten gegenüber eines solchen von oben herabgedrückt wird. Entsprechend der Abmessungen des Abschattungswinkels beginnt dessen Wirkung oberhalb der Frequenz von etwa 2 kHz. Bis zu dieser Frequenz wird auch die Absolutempfindlichkeit des Mikrofons bei senkrechtem Schalleinfall nicht beeinflußt. Oberhalb von 2 kHz wird gleichzeitig durch die frontale Abschattungswirkung eine Linearisierung des Frequenzganges erreicht. Der Frequenzgang steigt gewöhnlich bei Mikrofonen ohne Abschattungskörper mit der Frequenz an, so daß mit Abschattungskörper geringere Mikrofonentzerrungsmittel benötigt werden.

Die beigefügten Diagramme zeigen den Vergleich der Richtcharakteristiken zwischen den subjektiven Sollkurven und den objektiven Istkurven bei den Terzbandmittenfrequenzen von 2,25 kHz; 4,5 kHz und 8 kHz, für den Azimut-und Erhebungswinkel, sowohl für das Mikrofon allein als auch für das Mikrofon mit aufgesteckten Abschattungskörper. Der Abschattungskörper wurde so entwickelt, daß die in den Diagrammen schraffiert dargestellten Fehlerflächen ein Minimum werden und daß sich die positiven Fehler mit den negativen möglichst kompensieren. Man erkennt, daß die Nachbildung mit einer Genauigkeit von $\pm$ 4 dB gelungen ist.

Mit der nachgebildeten Hörrichtwirkung entnimmt das Mikrofon dem Schallfeld die Meßgröße immer in angenähert subjektiver Übereinstimmung. Es kann somit in jedem beliebigen Schallfeld gemessen werden, ohne daß Schallfeld-Entzerrungsschalter für diffuses und ebenes Feld am Meßgerät bedient werden müssen. Günstig ist es auch, Spektralanalysen mit einem solchen richtungsentzerrten Mikrofon durchzuführen und die Lautstärkeberechnungsmethoden darauf abzustimmen, so daß diese Methoden unabhängig von der Schallfeldform benutzt werden können und nicht auf spezielle Normschallfelder beschränkt bleiben müssen. Die Abmessungen des Mikrofons sind hierbei ohne Bedeutung, so daß auch größere Mikrofone mit größeren Absolutempfindlichkeiten benutzt werden können und somit auch kleinere Lautstärken meßbar werden.

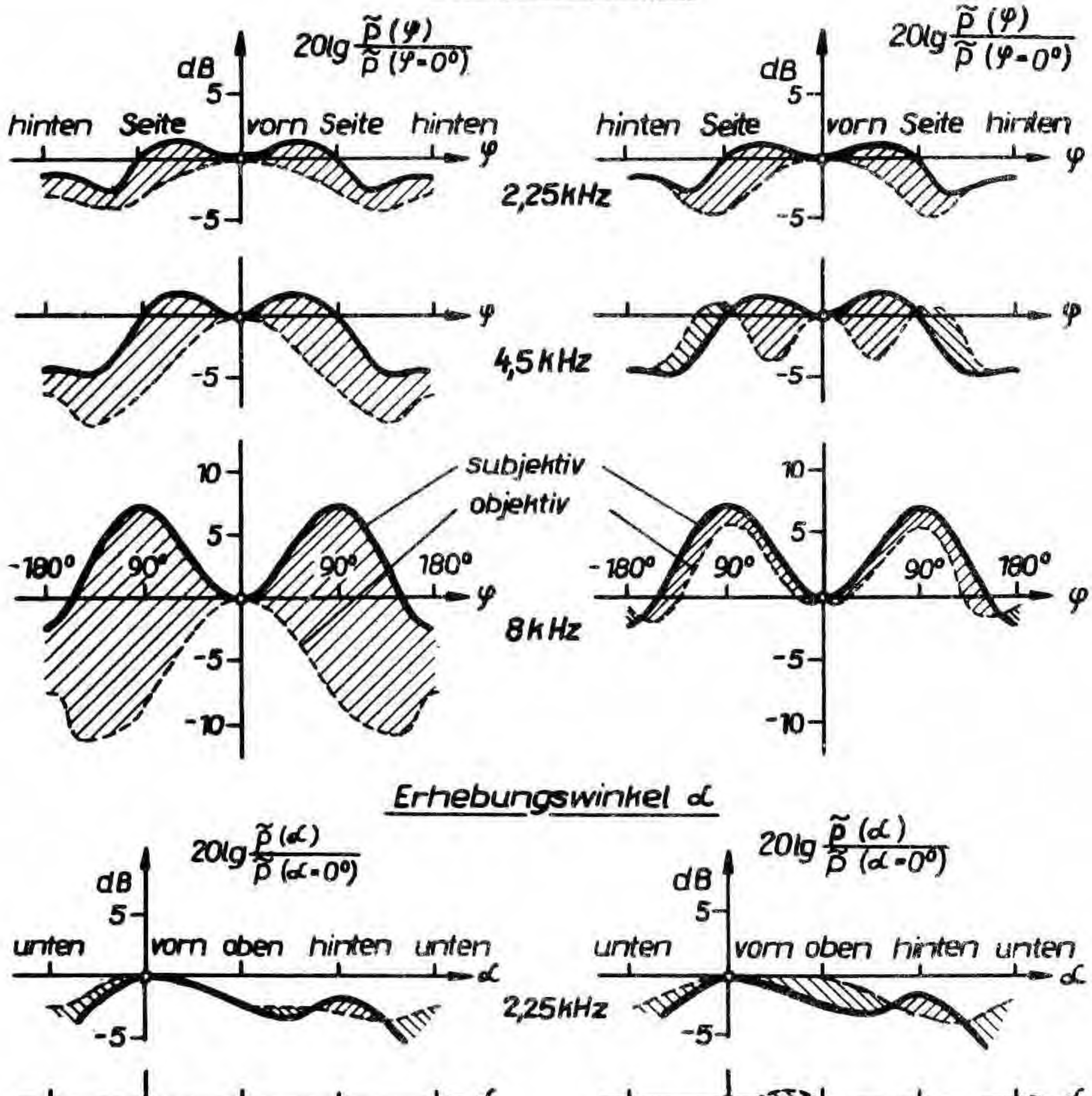
Azimutwinkel φ
20lg P̃(φ) / P̃(φ=0°)
dB
5
-5
hinten Seite vorn Seite hinten
φ
2,25kHz
4,5kHz
8kHz
10
-10
-180°
90°
180°
subjektiv
objektiv
Erhebungswinkel α
20lg P̃(α) / P̃(α=0°)
unten vorn oben hinten unten
α
-90°
270°
ohne — Abschattungskörper — mit

O19

FOURTH INTERNATIONAL CONGRESS ON ACOUSTICS
COPENHAGEN 21.-28. AUGUST 1962

Die Störung des Schallfeldes durch Hindernisse verschiedener Form

G.Kaszynski, Heinrich-Hertz-Institut für Schwingungsforschung d.Deutschen Akademie d.Wissenschaften z.Berlin,Bln.-Adlershof

1. Allgemeines

Jeder starre Körper, der in ein Schallfeld gebracht wird, verursacht eine Störung dieses Feldes. Die Größe der Störung ist von den Abmessungen und der geometrischen Gestalt des Körpers sowie von der Wellenlänge und der Art des Schallfeldes abhängig. Anfangs war diese Erscheinung nur von akademischem Interesse, während heute die Kenntnis der Schallfeldstörung in der akustischen Meßtechnik sowie bei der Entwicklung von Gradientenmikrofonen von großem Nutzen ist.

Von Rayleigh, Sivian und O'Neil, Stenzel, Morse, Schwarz, Primakoff, Klein, Keller, Carstensen, Brosze u.a. ist das Schallfeld in der Umgebung von Körpern verschiedener Form untersucht worden. Ergänzend zu diesen Arbeiten soll im folgenden die Störung des Schallfeldes durch eine Scheibe, Zylinder, abgeflachte Kugeln und Vollkugeln sowie an zwei hintereinander angeordneten Scheiben experimentell untersucht werden, da eine Berechnung sehr aufwendig ist.

2. Versuchsanordnung

Um Störungen des Schallfeldes durch die Meßeinrichtung zu vermeiden, wurden die Untersuchungen an Holzmodellen von 38 cm Ø im Frequenzbereich von 140 Hz bis 2850 Hz durchgeführt, dem entspricht ein Wert von kR = 0,5 bis 10, wenn k die Kreiswellenzahl und R der Radius sind.

Die Messungen wurden in einem reflexionsfreien Raum durchgeführt. Als Schallquelle wurde ein Lautsprecher in einer Schallbox verwendet. Der Abstand zwischen Schallquelle und Modell betrug nahezu 3 m, so daß sich das Modell angenähert in einer ebenen fortschreitenden Schallwelle befand.

Zur Messung des Schalldruckes wurde ein Kondensatormikrofon mit einer Sonde von 5 mm Durchmesser verwendet. Zur Ermittlung der Schallfeldverteilung in einer Ebene war das Sondenmikrofon an einem bewegbaren

Arm von 1,35 m Länge angeordnet, der sich mit einer Geschwindigkeit von 0,6 m/s und einem Hub von 1,35 m auf einem Teil eines Kreisbogens auf- und abwärts bewegte. Gleichzeitig bewegt sich diese Anordnung mit einer Geschwindigkeit von 2,5 mm/s in Längsrichtung. Neben dem Sondenmikrofon war, wie bei Harvey und Kock, eine Glimmlampe angeordnet, der die verstärkte Mikrofonspannung zugeführt wurde, so daß die Schalldruckschwankungen in Helligkeitsschwankungen umgewandelt und dann fotografisch registriert werden. Um Aussagen über die Größe der auftretenden Schalldruckpegelschwankungen machen zu können, wurde außerdem der Graukeil aufgenommen. Zwischen weiß und schwarz lassen sich mit Hilfe des menschlichen Auges maximal 10 Helligkeitsabstufungen erkennen, die in diesem Fall jeweils einer Schalldruckpegeländerung von 1 dB entsprechen.

3. Versuchsergebnisse

Abbildung 1 zeigt die Störung des Schallfeldes durch eine starre Kugel vor und hinter der Kugel in Schallausbreitungsrichtung für kR = 2 und 8. Auf der Abszisse wurde als Maß für die Störung des Schallfeldes $S = 20 \lg \frac{p_{\text{mit Körper}}}{p_{\text{freies Feld}}}$ und auf der Ordinate der auf den Kugelradius R normierte Abstand d, gemessen von der Oberfläche der Kugel, aufgetragen. Zum Vergleich wurden die von Brosze errechneten Werte mit eingetragen.

Wird von der Kugel ein Kugelabschnitt mit einer Höhe h von 3 cm abgeschnitten, d.h. $\frac{h}{R} = 0{,}16$, so erkennt man aus der Abb. 2, daß die Amplitude der Schallfeldstörung und auch die Anzahl der Schwankungen bei kR = 8 gegenüber der Störung bei der Vollkugel größer geworden sind, während bei kR = 2 die Veränderungen gegenüber der Vollkugel nur geringfügig sind. Betrachtet man dagegen die Störung des Schallfeldes durch eine Halbkugel, siehe Abb. 3, so zeigt sich, daß die Amplitude der Schallfeldstörung und auch die Anzahl der Schwankungen bei kR = 2 und kR = 8 sich erheblich vergrößert haben. Die Störung des Schallfeldes vor der Halbkugel ist nahezu die gleiche wie vor einer Scheibe gleichen Durchmessers, während das Schallfeld hinter der Halbkugel beträchtlich von dem einer gleich großen Scheibe oder eines Zylinders abweicht.

Außerdem wurde die Störung des Schallfeldes quer zur Schallausbreitungsrichtung längs einer Achse untersucht, die durch das Zentrum auf der Vorder- bzw. Rückseite der Hindernisse geht. Die gewonnenen Ergebnisse an Scheibe, Zylinder, abgeflachter und Vollkugel und an zwei in verschiedenem Abstand voneinander angeordneten Scheiben werden mitgeteilt.

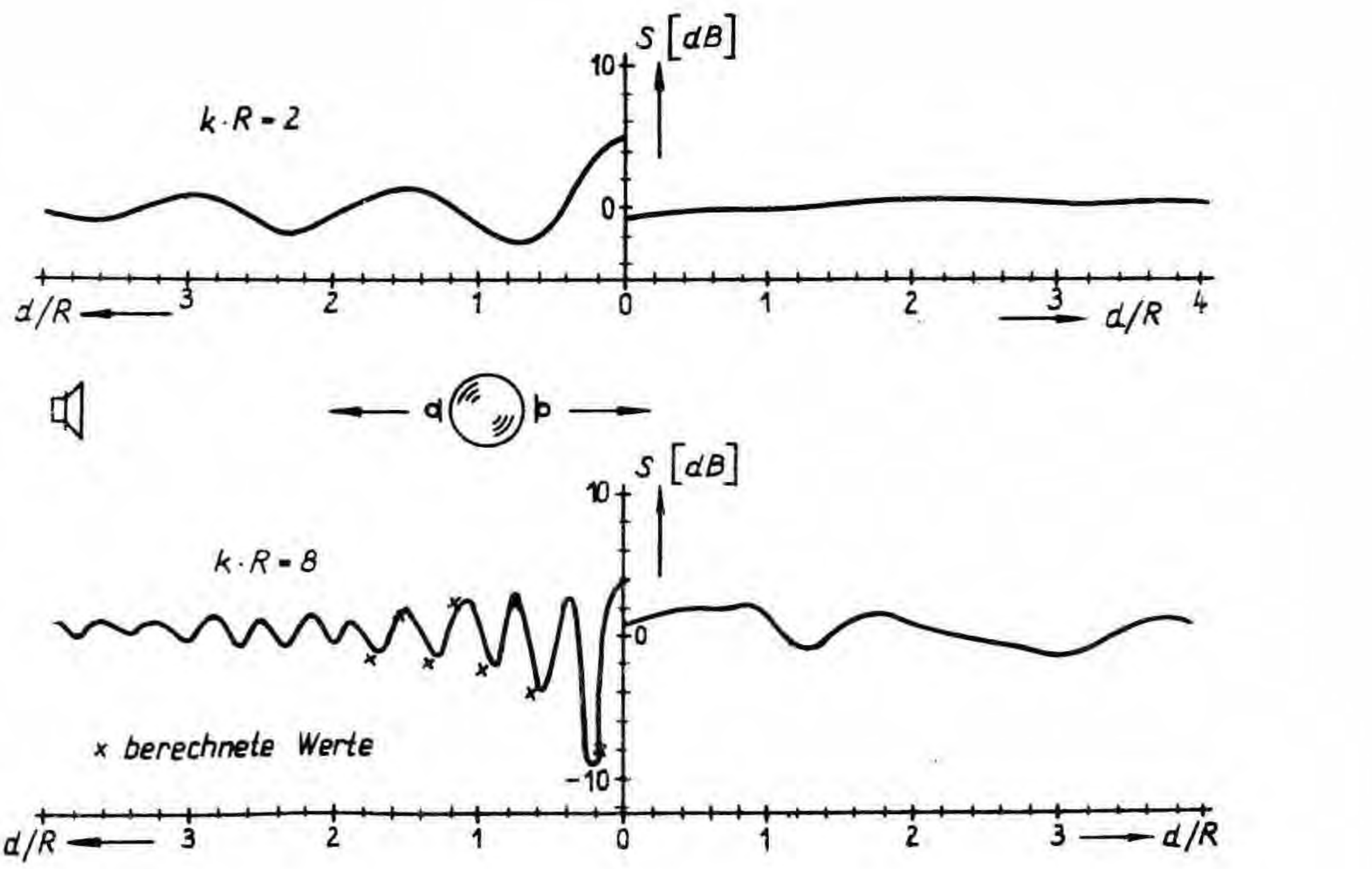

Abb.1 Störung des Schallfeldes vor und hinter einer starren Kugel

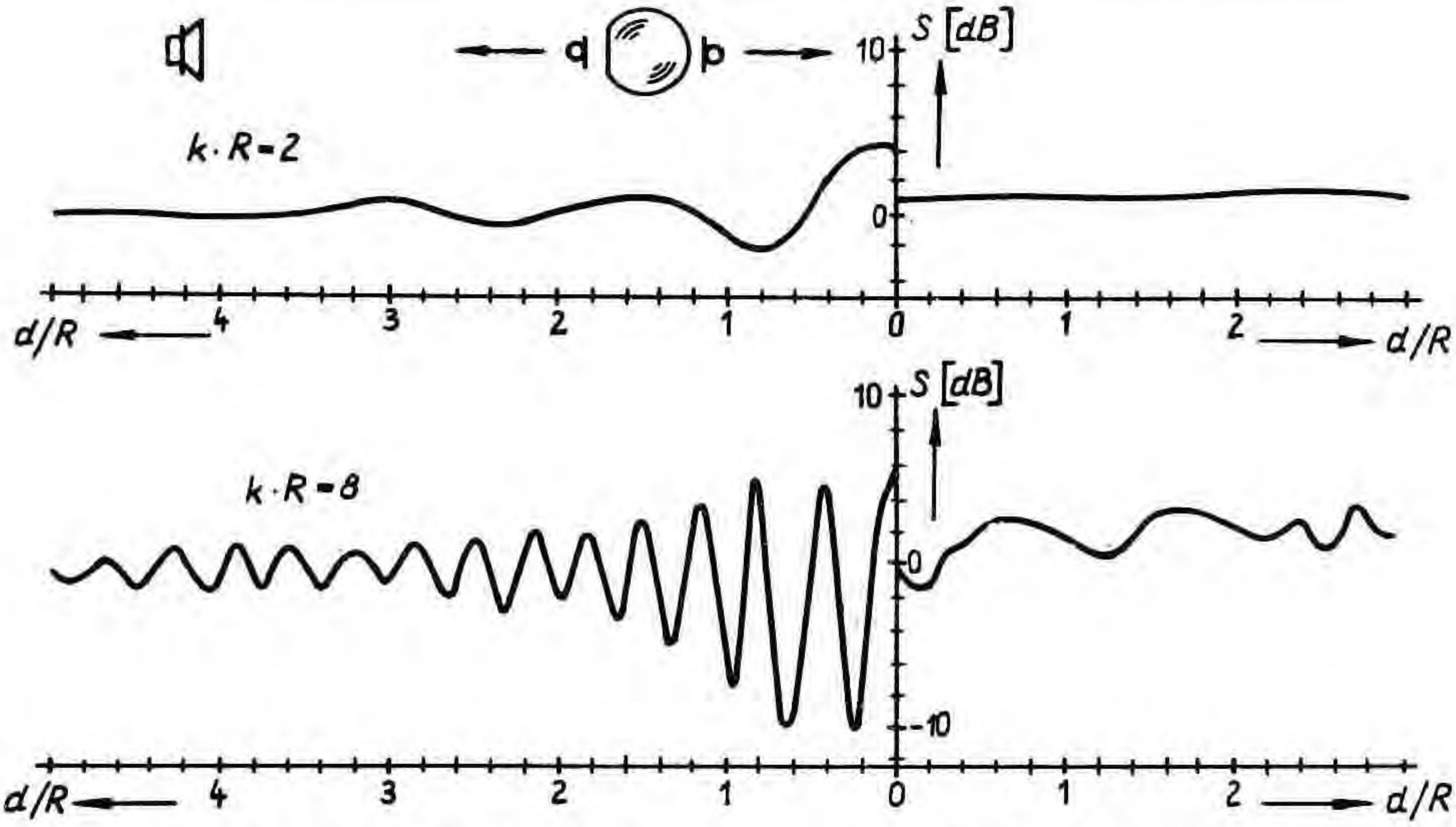

Abb.2 Störung des Schallfeldes vor und hinter einer abgeflachten starren Kugel $\frac{h}{R} = 0.16$

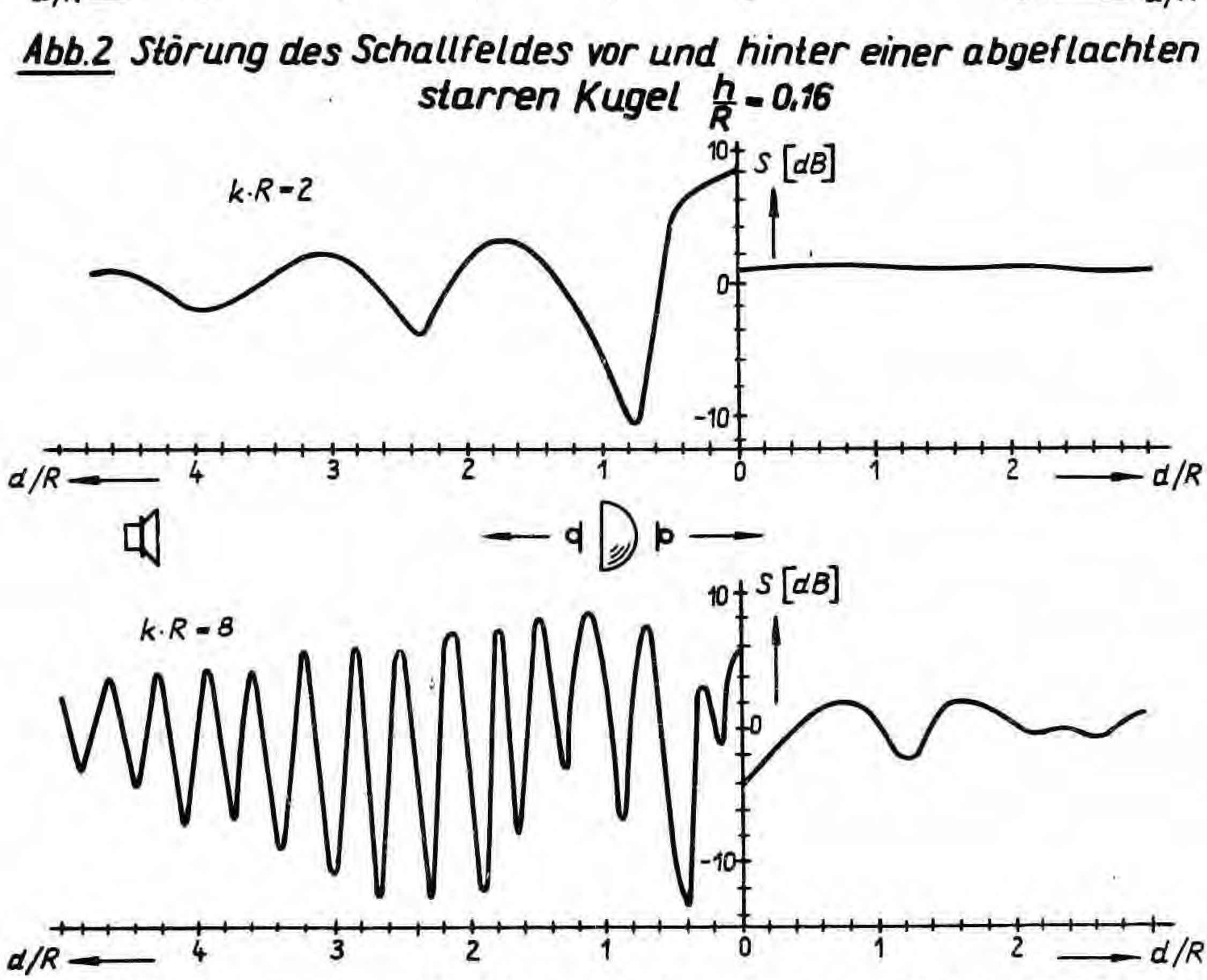

Abb.3 Störung des Schallfeldes vor und hinter einer starren Halbkugel

G21

FOURTH INTERNATIONAL CONGRESS ON ACOUSTICS
COPENHAGEN 21.-28. AUGUST 1962

Spoken digit recognizer for Japanese language

Kuniichi Nagata, Yasuo Kato and Seibi Chiba
Nippon Electric Co., Ltd. Tokyo, Japan.

Introduction

A spoken digit recognizer for Japanese has been designed and constructed. An outline of the scheme is described.

In designing this scheme, we assumed that one of the ten words representing the ten Japanese digits, from zero to nine, was to be uttered in isolation. The features which seem to characterize the individual spoken digits most efficiently have been looked for by examining sonagrams of typical utterances, and the eight features as described in the following section were derived.

Transistor circuits have been designed for extracting the features and also for decision-making. The determination of the digit was made by computing the *a posteriori* probabilities for all digits from the occurrence patterns of the features and then selecting the digit having the largest *a posteriori* probability.

Particular care has been exercised in the design of this scheme in order that utterances by both male and female speakers can be accepted by the machine without any additional informations about the talker.

Japanese spoken digits

Japanese spoken digits (0 to 9) are transcribed phonemically as:

0	1	2	3	4	5	6	7	8	9
/rei/ /zero/	/itʃi/	/ni/	/saN/	/joN/ /si/	/go/	/roku/	/nana/ /hitʃi/ /sitʃi/	/hatʃi/	/kju/ /ku/

There are several ways in reading the digits 0, 4, 7 and 9. In our experiment, the talker is required to pronounce the digits only in the way given in the first row of the table above.

For these phonemic sequences, furthermore, there can be some variations of utterances phonetically. For example, the last vowels of 1, 6 and 8 are often (but not alwasy) devoiced. These variabilities are taken into consideration in the present system.

Extracted features

The effect of superposed random noise, such as that introduced in the telephone line, must be minimized in order to secure a satisfactory performance of the recognizer in

practical applications. Taking this into consideration, a weight was put on the voiced portions of the speech signal when the features to be used in the decision process were selected. Since the number of words to be recognized is limited, the features that are useful particularly for the discrimination within the word set have been defined and utilized. Eight features thus selected are:

(1) the number of voiced intervals within the utterance,

(2) the location of the first and second formants in the F_1-F_2 diagram at the onset of the first voiced interval,

(3) the location in the F_1-F_2 diagram at the time moment 100 msec after the onset of the first voiced interval,

(4) the slope of the F_2 transition at the onset of the first voiced interval,

(5) the location in the F_1-F_2 diagram at the end of the first voiced interval

(6) F_2 in the second voiced interval or in the corresponding devoiced portion,

(7) the presence or absence of a marked unvoiced consonantal portion at the onset of the utterance,

(8) the movement of F_1 during the first voiced interval.

(F_1: the frequency of the first formant, F_2: the frequency of the second formant)

It is desirable to select the features so that each of them is perfectly independent of the others. In the practical system designs in accordance with the requirement that the scheme be realizable by use of comparatively simple circuits, a compromise in this respect has to be made. The eight features given above are to some extent correlated among each other. The fourth feature, for example, represents the slope of the F_2 transition at the onset of the first voiced interval, and in practice it is extracted as the difference between the F_2 near the voice onset and that at the time moment 100 msec later. The fourth feature thus extracted is evidently not independent of the second or the third feature. In this scheme, however, the F_1-F_2 plane is divided into eleven sections in order to avoid an excessive complication of the system. Accordingly, the F_2 values which determine the second and third features are given in terms of a gross categorization. The fourth feature is extracted before the categorization, and therefore it is not necessarily correlated with the second or the third feature, and is worth extracting as an independent feature.

Possible states for the eight features are shown as follows:

Feature 1: three possible states — one voiced interval (for 0, 2, 3, 4, 5, 7, 9), two voiced intervals (for 1, 6, 8) or a di-syllable with a devoiced final vowel (for 1, 6, 8).

Feature 2: twelve possible states — one of eleven sections of the F_1-F_2 diagram, or outside any of them.

Feature 3: thirteen possible states — one of the eleven sections of F_1-F_2 diagram, outside any of them, or cessation of the voiced portion before sampled time.

Feature 4: four possible states — negative slope (two levels), zero slope, or positive slope.

Feature 5: same as Feature 2.

Feature 6: four possible states — three frequency bands or outside any of them.

Feature 7: two possible states — presence or absence.

Feature 8: six possible states — patterns of the F_1 movement across predetermined three frequency values.

Possible states for each feature are mutually exclusive and only one state can correspond to one input signal. Consequently, the number of occurence patterns of the features is 1,078,272, at most.

Decision procedure

We can consider a set of occurence patterns of the eight features by a probabilistic model. An unknown spoken digit, therefore, is determined on a statistical basis by examining the occurence pattern of the features.

In the present scheme, the recognition is performed in the following steps. The *a posteriori* probabilities are computed for all digits from the observed occurence pattern of the features, and the digit having the largest *a posteriori* probability is determined. A"dead-zone" of decision is provided when the largest *a posteriori* probability falls below a predetermined threshold.

If we assume that the eight features are mutually independent, then the following relation holds:

$$P\{i|A\cdot B\cdot \cdots \cdot H\} = P\{i|A\} \cdot P\{i|B\} \cdot \cdots \cdot P\{i|H\}$$

where A, B, ..., H represent the states of the eight features; $P\{i|A\cdot B\cdot \cdots \cdot H\}$ represents the probability that the unknown spoken digit is i when the eight features are known as A, B, ..., H; and $P\{i|A\}$ represents the probability that the unknown spoken digit is i when the first feature is known as A. The most probable spoken digit is easily found by a circuit shown in Fig. 1.

Circuits

A simplified block diagram of the circuit employed is shown in Fig. 2. The "Interval-and-pitch extractor" extracts the information as to the time portion of a voiced interval, the time portion of a voiced interval without a buzz bar (very low frequency component), whether the fundamental frequency is higher than a predetermined value or lower, and some others. The controller generates control signals which trigger or reset the formant extractor, the feature extractor, and the decision circuit according to the informations supplied by the interval-and-pitch extractor. At the same time, in the formant extractor, the two formant frequencies F_1 and F_2 are estimated by digitally counting the zero-crossings of the output waveforms from the pertinent filters. For F_2, two parallel circuits

are provided in connection with two different filters that are suitable for male and female utterances. The choice among the two parallel circuits is made according to the information concerning the fundamental frequency. The selection is triggered by the control signal sent from the controller.

The eight features are then extracted, and each feature extractor generates a D.C. output signal that indicates the state of the feature. Finally, the most probable digit is chosen and the result is indicated at the output terminal.

The result of the experiment using utterances of a number of speakers will be reported in some detail at the conference.

Acknowledgments

The authors are indebted to Dr. O. Harashima and Dr. T. Suzuki for their instructive suggestions and constant encouragement and to Dr. T. Kurokawa and Mr. K. Tsuzaki for their assistance in building the equipment.

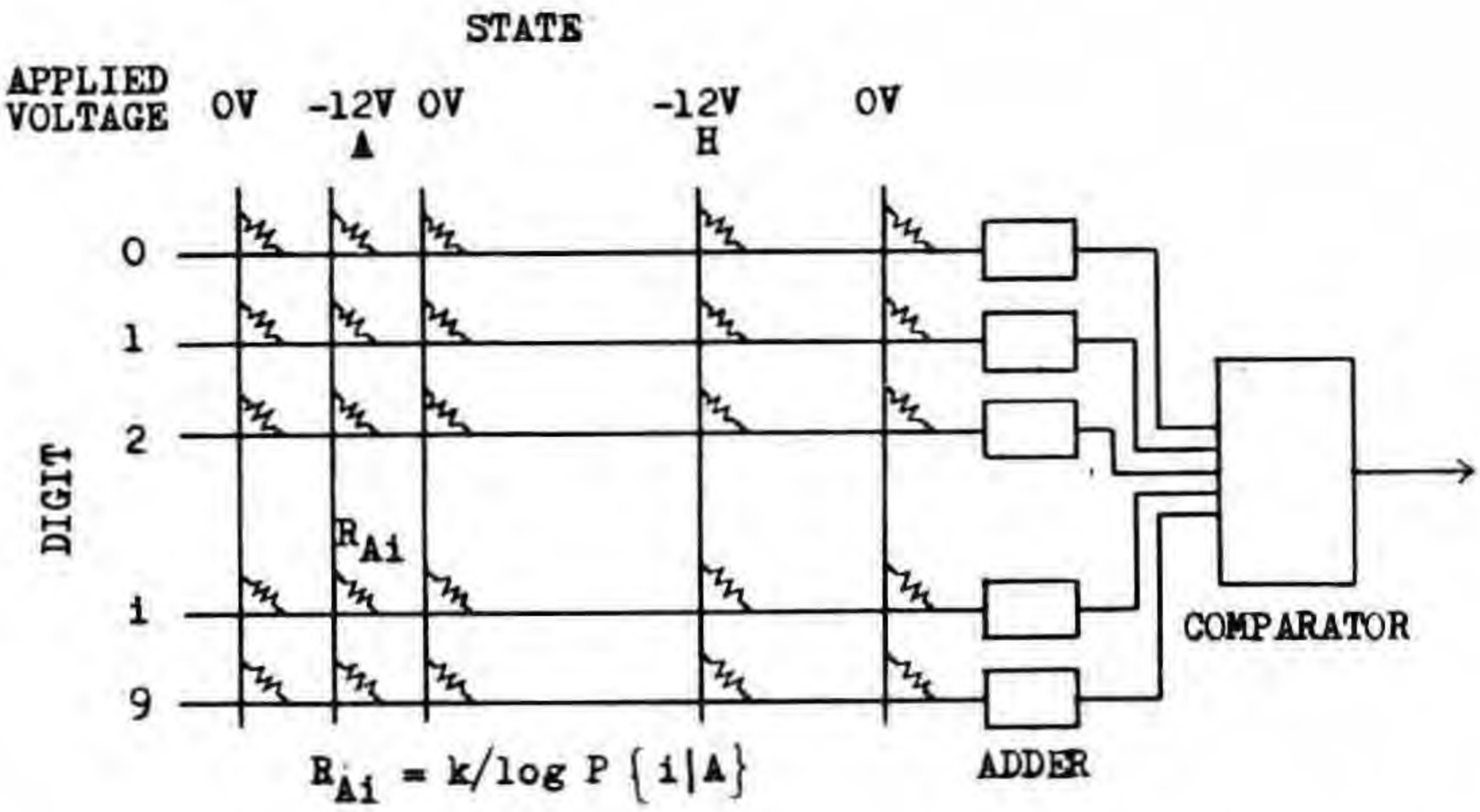

FIG.1. Decision circuit to choose the most probable digit.

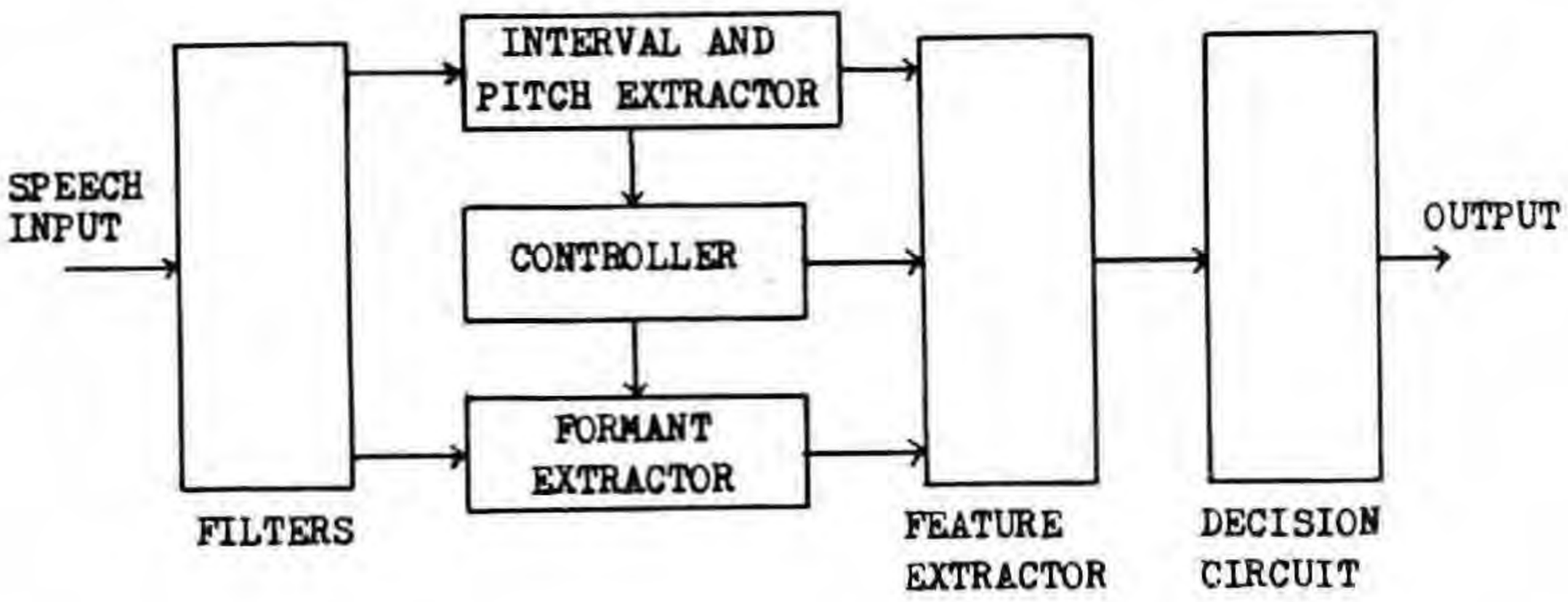

FIG.2. Simplified block diagram of the equipment.

H21

FOURTH INTERNATIONAL CONGRESS ON ACOUSTICS
COPENHAGEN 21.-28. AUGUST 1962

SOME CONSIDERATIONS CONCERNING THE EFFECTS ON HEARING OF THE NOISE OF SMALL-ARMS.

Surgeon Lieutenant Commander R. R. A. Coles, R.N.

(Royal Naval Medical School, Alverstoke, England)

In the British Armed Services the recent advent of a new rifle reputedly noisier than its predecessor, already a recognised hazard e.g. Knight and Coles (1959), provided a good opportunity for the introduction of much stricter hearing conservation measures than hitherto. In order to lend force to arguments at all levels as to the necessity for this, two pieces of information were needed; firstly, to know how much the new rifle is noisier than the old one, and secondly to ascertain what would be the effects of the noise on men's hearing if they continued to disregard the need for ear-protection.

This paper deals, in brief, with the main results of the investigations designed to answer these questions. Also described, in more detail, are two of the more interesting side issues; namely, some measurements of temporary hearing losses following repeated noise exposures, and a study of the relationship between acoustic reflex threshold and noise-induced hearing loss.

Whilst the whole study formed part of the research programme of the R.N. Personnel Research Committee (Medical Research Council), the opinions and interpretations given here are at present those of the author alone. The noise measurements were made by the Admiralty Research Laboratory, Teddington, but the rest of the work was carried out in collaboration with J.J. Knight, of the scientific staff of the M.R.C. Wernher Research Unit on Deafness.

THE PHYSICAL NATURE OF THE STIMULUS

The weapon in question was the self-loading rifle (S.L.R.), a British modification of the Belgian F.N. 7.62 mm. rifle. A standard method of measuring impulsive noise was employed, the overall bandwidth of the apparatus being approximately 20 - 10,000 c/s.

The sound field was found to be symmetrical and, with rifle and microphone 2 feet above grass, the peak positive pressures measured (relative to an r.m.s. sound pressure of 0.0002 dynes/cm^2) were as follows:-

2 ins. from either ear of marksman	168 dB
At approximate position of instructor's ears	174 dB
At approximate position of next marksman in line (6 ft. away)	170 dB

The initial positive pressure wave lasted about 0.2 m.sec.

With the old (No. 4) rifle, the .303 in. Lee-Enfield, the field was also symmetrical but the peak pressures were on the average some 7 dB lower than with the S.L.R.

HEARING LOSSES

A total of 202 recruits to the Royal Marines were audiometrically surveyed at intervals to provide information on hearing states at entry, half way through training and on its completion. The principle noise hazard during their training was the S.L.R., and V. 51-R ear plugs were provided for protection against it.

A typical case is illustrated in Figure 1(A), whilst the hearing state of one of his weapon-training instructors is shown in Figure 1(B).

Approximately a third of one squad which used little ear protection during their training had sustained hearing losses of at least 25 dB at 3, 4 or 6 Kc/s, or of 30 dB

at 8 Kc/s, in one or both ears when retested some three weeks after their last noise exposure.

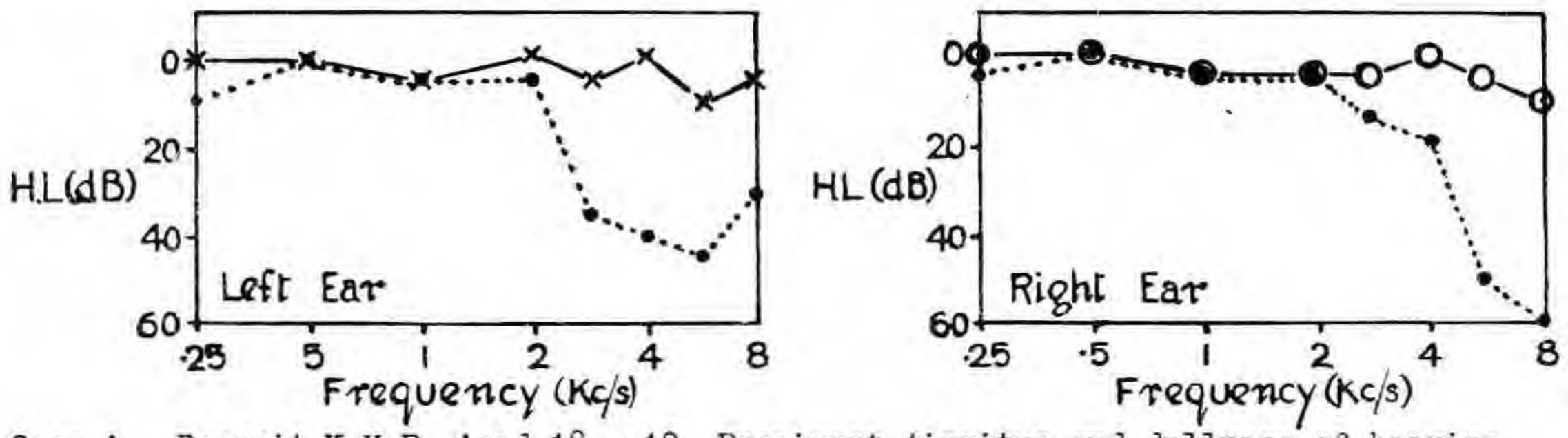

Case A. Recruit K.H.P. Aged 18 - 19. Prominent tinnitus and dullness of hearing immediately after shooting if he wore no ear protection. Protected his ears on 4 out of every 5 occasions of firing.

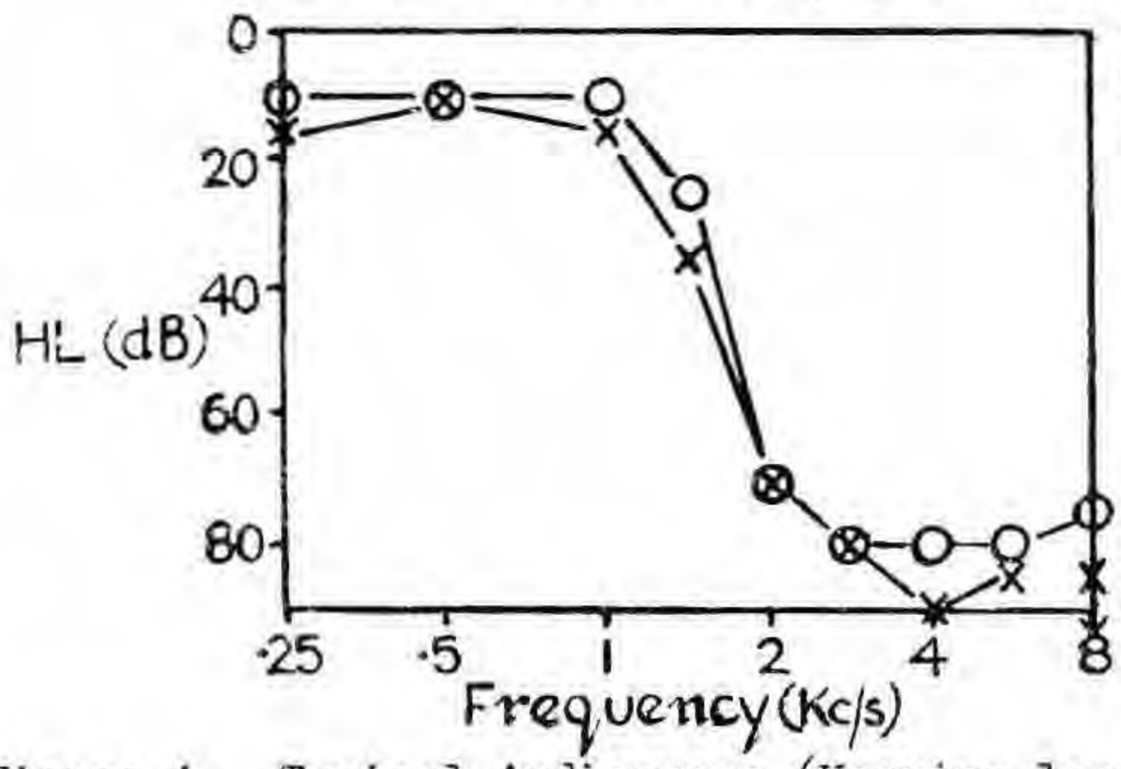

× —— × = hearing before training (L.ear)
○ —— ○ = hearing before training (R.ear)
• ····· • = hearing after training.

Case B. Corporal W.N.N. Aged 23. Weapon-training instructor 3 years. Minimal temporary symptoms after shooting. Thinks he is slightly hard-of-hearing now.

× —— × = Left Ear.
○ —— ○ = Right Ear.

Figure 1. Typical Audiograms (Hearing loss, H.L., is shown relative to British Standard (2497) Normal Threshold for Hearing of Pure-tones).

T.T.S. FOLLOWING REPEATED NOISE EXPOSURES

Two men exposed their ears without protection to 20 roundsof S.L.R. noise (in a position corresponding to peak pressure of 177 dB) once a week under constant conditions. Audiometric checks confirmed that no measurable permanent hearing loss had occurred at any stage of the experiment.

The noise was mildly painful and resulted in visible reddening and occasional small haemorrhages on their ear-drums. Measurements on seven occasions confirmed the finding of Reid (1946), and others, that considerable day-to-day variations in T.T.S., superimposed on a progressive reduction, result from such exposures. Reid suggested that this might have been caused by learning to contract voluntarily the intra-aural muscles in anticipation of the blast, or to a "toughening" of the basilar membrane.

Averaged over 3, 4 and 6 Kc/s, the maximum T.T.S. was 32.5 dB (on the first occasion) and in the same ear this fell to a minimum of zero after the fifth exposure.

Recovery rates were also studied and for full recovery at all test frequencies this fell in the more sensitive subject from needing 4 days after the first exposure, to between 20 and 70 minutes on the second occasion, and to less than 20 minutes on the fifth.

During all the first seven exposures firings were at regular intervals and immediately preceded by a warning; on two subsequent occasions the rate was irregular and without warning. Subjectively, this was reported as being more unpleasant, and in fact it resulted in the T.T.S. returning almost to the initial level.

The conclusion to be drawn from these experiments is that T.T.S. falls with consecutive exposures to impulsive noise. Further, it is suggested that the effect described may be due partly to an increase in recovery rate and partly to the acoustic reflex becoming conditioned to come into action before each expected noise exposure, and perhaps to operate more efficiently also. It is interesting however to note that, in common with other workers, the author has found no such process to result from continuous pure-tone noise exposures.

MEASUREMENTS OF THRESHOLD OF ACOUSTIC REFLEX

Stapedius and tensor tympani are the names given to two small muscles present in each ear. They can be caused to contract, usually involuntarily, by exposure of either ear to a sufficiently loud sound. Their action is believed to impede conduction of sound to the receptor organ in the inner ear and thereby act as a physiological protective mechanism against noise; this is known as the acoustic reflex.

At the time of the final retest of the last two squads of marine recruits a Madsen Acoustic Impedance Meter, Model ZO.61, became available. Time permitted measurements of the threshold of acoustic reflex at 1 and 4 Kc/s in 40 of the men.

The principle of the technique and the essentials of the apparatus have recently been described by Terkildsen and Scott Nielsen (1960). As their account could be applied exactly to the instrument used in the present work, no further description of it will be given here.

Our first finding of interest was that the ascending threshold was frequently up to 10 dB higher than the descending one. This suggests that recent experience of supra-threshold noise itself lowers that threshold, a change somewhat akin to the conditioning process suggested in the section above.

In treatment of the main data of this section, the 40 noise exposed men were divided into three subgroups according to the state of their high-tone hearing. The median reflex thresholds of the subgroups at 1 and 4 Kc/s were then calculated and are illustrated in Figure 2.

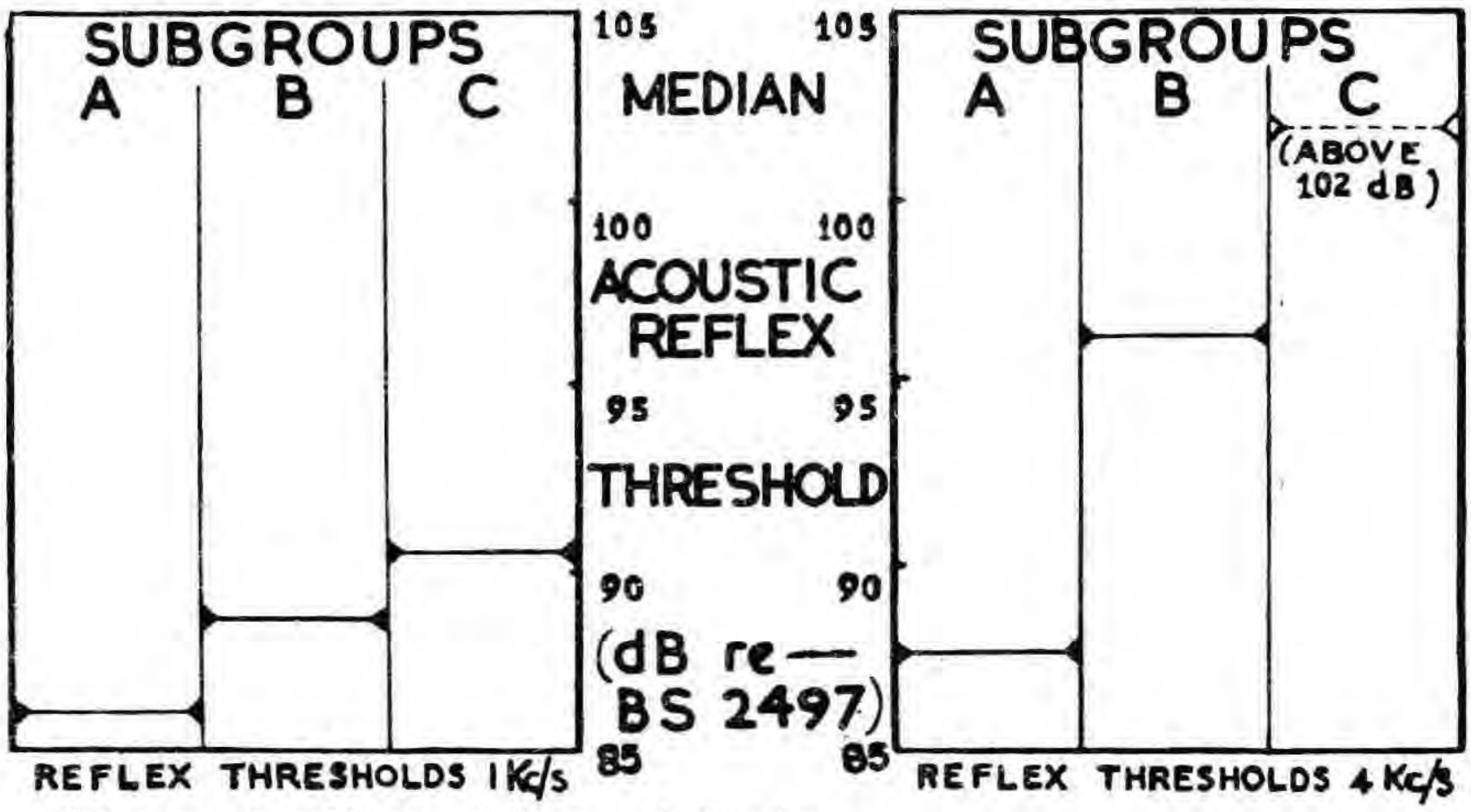

Subgroup A = 20 men with normal hearing.
Subgroup B = 10 men with slight high-tone hearing loss.
Subgroup C = 10 men with marked high-tone hearing loss.

Figure 2. Median Acoustic Reflex Thresholds at 1 and 4 Kc/s, Subdivided by Three Grades of Hearing Acuity.

It is once apparent that there is a relationship between noise-induced hearing loss and the threshold of acoustic reflex both at 1 Kc/s and at 4 Kc/s. The observed differences in reflex threshold can hardly be related to the original hearing state of the men in the three subgroups, because even after training their median hearing losses at 1 Kc/s were almost identical. Moreover, the distribution of hearing and reflex thresholds in the three subgroups at 1 Kc/s was equivalent to that measured in a control group of 23 new-entry recruits.

Further evidence is gained from 16 men whose actual change of hearing after noise exposure had been measured. Those who developed more than average high-tone loss also had the higher average reflex threshold at 1 Kc/s.

With 4 Kc/s tones Jepsen (1951) failed to elicit an acoustic reflex in only one out of 98 ears and Metz (1952) made no mention of any such cases. On the contrary, in our control series no reaction could be obtained in 11 out of 46 ears (24%), the maximum stimulus intensity being 100 dB and with atmospheric pressure in the external auditory meatus. No reaction was found more frequently still (31%) in the noise exposed men, but this probably resulted from a degree of special attention given in this group to those with high-tone hearing losses. At 1 Kc/s however, acoustic reflexes were obtainable (maximum S.P.L.=110 dB) in all but 2 of the 126 ears tested.

Metz, Thomsen (1955) and others have described the use of measurement of acoustic reflex threshold in testing for recruitment. Thomsen in particular has stated that a positive test result, i.e. a normal reflex threshold, confirms recruitment and that a negative one, whilst not completely excluding a recruiting perceptive lesion, is often explained by a conductive element in the hearing loss. In the present work on the other hand, a positive result at 4 Kc/s was often absent in cases of 4 Kc/s hearing loss which were of perceptive type attributable to acoustic trauma. Time at our disposal did not allow other tests of recruitment, but it is usually accepted that it is present in cases of noise-induced hearing loss, e.g. Glorig and Davis (1961). If this is so, then the men probably had poor acoustic reflexes before they developed their hearing losses and a causal relationship between the two is indicated.

It should be noted in passing that with individuals, as distinct from the average, wide variations were found between hearing loss and acoustic reflex threshold. There are in addition some less acceptable explanations of the above relationship: noise may damage the mechanism of the reflex threshold either independently of hearing loss or by means of hearing loss without recruitment. A prospective study including other tests of recruitment is needed to elucidate these points.

CONCLUSIONS

The measurements of the noise of the S.L.R. and of its effects on hearing are convincing as to the necessity of protecting the ears of men using this weapon. Protection would appear to be particularly important early in training because, even in absence of noise induced hearing loss, sensitivity to noise appears to lessen with increasing noise experience. It must be worn by <u>all</u> exposed personnel, until a really reliable and easy test of individual sensitivity to noise becomes available; towards this goal, measurements of the acoustic reflex seem to offer the possibility of an interesting new approach.

REFERENCES

GLORIG, A. and DAVIS, H. (1961) Ann. Otol. 70, 556.
JEPSEN, O. (1951). Acta Otolaryng., 39, 406.
KNIGHT, J.J. and COLES, R.R.A. (1960) J. Acoust. Soc. Am., 32, 800.
METZ, O. (1952) Arch. Otolaryng., 55, 536.
REID, G. (1946) J. Laryng. and Otol., 61, 609.
TERKILDSEN, K. and NIELSEN, S. SCOTT (1960). Arch. Otolaryng., 72, 339.
THOMSEN, K.A. (1955). Acta Otolaryng., 54, 544.

Acknowledgements: The author wishes to express his thanks to the Medical Director General of the Navy for sponsoring this contributed paper, and to the Superintendent of Admiralty Research Laboratory, Teddington, for permission to publish some details of the noise measurements.

J21

FOURTH INTERNATIONAL CONGRESS ON ACOUSTICS
COPENHAGEN 21.-28. AUGUST 1962

ULTRASONIC RELAXATION IN FRACTIONATED POLYSILOXANES

J. L. Hunter and T. B. Lewis, John Carroll University, Cleveland, Ohio, USA

Ultrasonic absorption and velocity measurements have been obtained in nine fractionated polysiloxanes. These polymers were selected because they represent a series of linear chain molecules of gradually varying length whose chemical structure is well known. Preliminary measurements were conducted on the polysiloxanes of lowest molecular weight (from two to ten siloxane radicals per molecule). After this preliminary investigation, the 6- and 10-atom liquids were selected for detailed investigation over a frequency range of 30 to 270 Mc, and a temperature range of -50 to +30 ^{o}C.

A two-crystal invar absorption cell was designed for the longitudinal measurements. The very low temperature-coefficient of expansion of invar was vital for the maintenance of parallelism at the upper frequency of 270 Mc, over the eighty degree temperature change. A standard pulse technique was used, similar to that of Litovitz[1], including a comparison signal from a Hewlett-Packard signal generator. The frequencies were 30, 50, 70, 90, 110, 130, 170, and 270 Mc (nominal). The samples of fractionated polysiloxanes (dimethyl siloxane polymers) obtained from the Dow Corning Corporation were specified as 99.9% pure.

It was ascertained by preliminary measurements that the velocity dispersion was negligible, and therefore, velocities were measured at the single frequency, 49.85 Mc, for the main purpose of computing the Stokes value of the absorption coefficient. For velocity, a continuous wave measurement was made, utilizing the signal generator and an r-f amplifier. In this way the frequency was precisely known.

Curves showing the absorption values are given in Figs. 1 and 2. At 50, 70, 90, 110, and 130 Mc, the reproducibility is 1%; at 30 and 270 Mc, about 3%: the signal-to-noise ratio is beginning to fall at 270 Mc, and the low value of absorption and probably the presence of diffraction effects limit the accuracy at 30 Mc.

An attempt was made to fit the curves of Figs. 1 and 2 with the aid of a computer to the single-relaxation time equation:

$$\frac{\alpha}{f^2} = \frac{A}{1 + (f/f_o)^2} + B$$

The parameters of the equation were obtained by use of the following program: A value of B was chosen, and resulting values of A and f_o were provided by the computer, along with the rms deviations. This process was continued until minimum deviations were obtained. The corresponding values of A, B, and f_o may be taken tentatively as a most probable triplet of values. Another choice of B will give a different triplet of values. It was found that the curves may be fitted within the experimental error for a range of values of each of the three parameters. For the higher temperature curves where only a slight curvature occurs between 30 and 270 Mc, the ranges are so broad as to be almost meaningless. However, for temperatures below -30 ^{o}C, the ranges of all three parameters are small enough to be significant. The parameters obtained from this program are listed in Table 1, along with the corresponding Stokes value of absorption. Where a comparatively small change in α/f^2 occurs, the inflection point will be rather ill-defined, and this lack of precision will be borne out in the greater range of f_o values.

The most immediately interesting observation that can be made is that the most probable values of the "B" parameter are less than the Stokes value of the absorption

coefficient. In some cases the difference is small, but in others, it is well beyond the degree of accuracy of the experiment. It is difficult to interpret this fact from the point of view of a theory of single relaxation. If our curves had fitted a single relaxation equation with a fall-off asymptotic to the Stokes value, the logical explanation would be a relaxation of compressional viscosity, with the residual absorption due to the shear viscosity. The f_o would then correspond to t_c, the relaxation time of compressional viscosity, the A would be proportional to the unrelaxed compressional viscosity, and the B to the unrelaxed shear viscosity.

TABLE 1

SINGLE RELAXATION PARAMETERS

Temp (°C)	A ($cm^{-1} \times 10^{-17}$)	B ($cm^{-1} \times 10^{-17}$)	f_o (Mc)	α/f^2 Stokes ($cm^{-1} \times 10^{-17}$)
10-atom Polysiloxanes				
-45	220 - 255	257 - 260	74 - 87	320
-40	199 - 217	231 - 234	88 - 99	286
-30	153 - 162	204 - 210	112 - 131	256
-20	125 - 129	180 - 196	148 - 187	229
6-atom Polysiloxanes				
-50	127 - 128	165 - 180	135 - 170	184
-45	104 - 126	130 - 160	170 - 250	169
-40	88 - 123	110 - 152	180 - 300	157

But, if A is associated with compressional viscosity, the presence of B less than Stokes' value can only be interpreted as relaxation of the shear viscosity. Let us, therefore, consider an alternate possibility of single relaxation --- that the shear viscosity alone is relaxing, while the compressional viscosity remains constant. Here there is merely an exchange of the significance of the A and B parameters, A now representing unrelaxed shear viscosity and B unrelaxed compressional viscosity. The value of A should now equal the Stokes value. We find, however, that the A values are in general much smaller than the Stokes values (They are in fact always less than the B values).

We are thus forced to the conclusion that both viscosities are present in the fre-

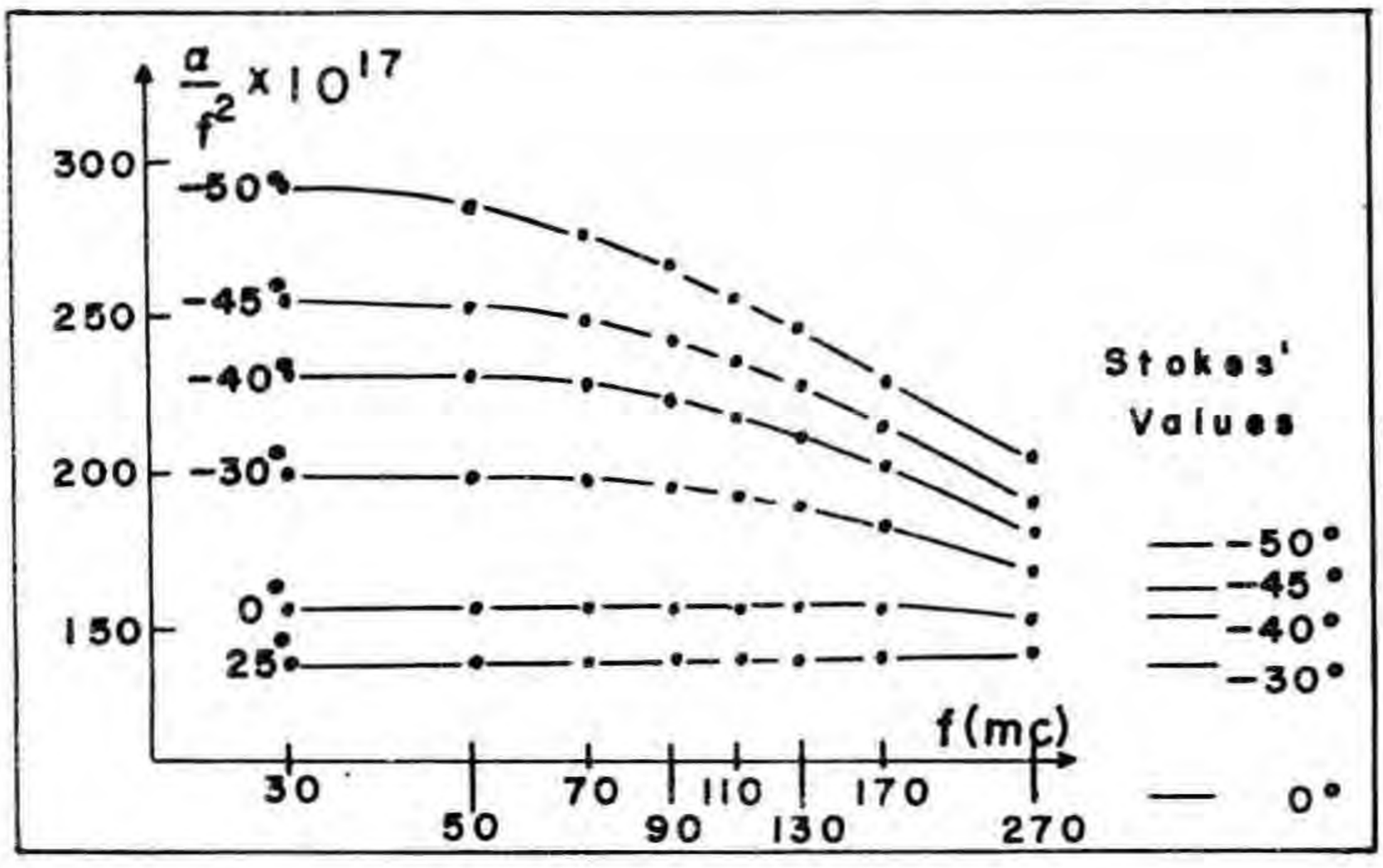

Fig. 1. Absorption of longitudinal ultrasonic waves in the dimethyl siloxane polymer containing 6 silicon atoms per molecule.

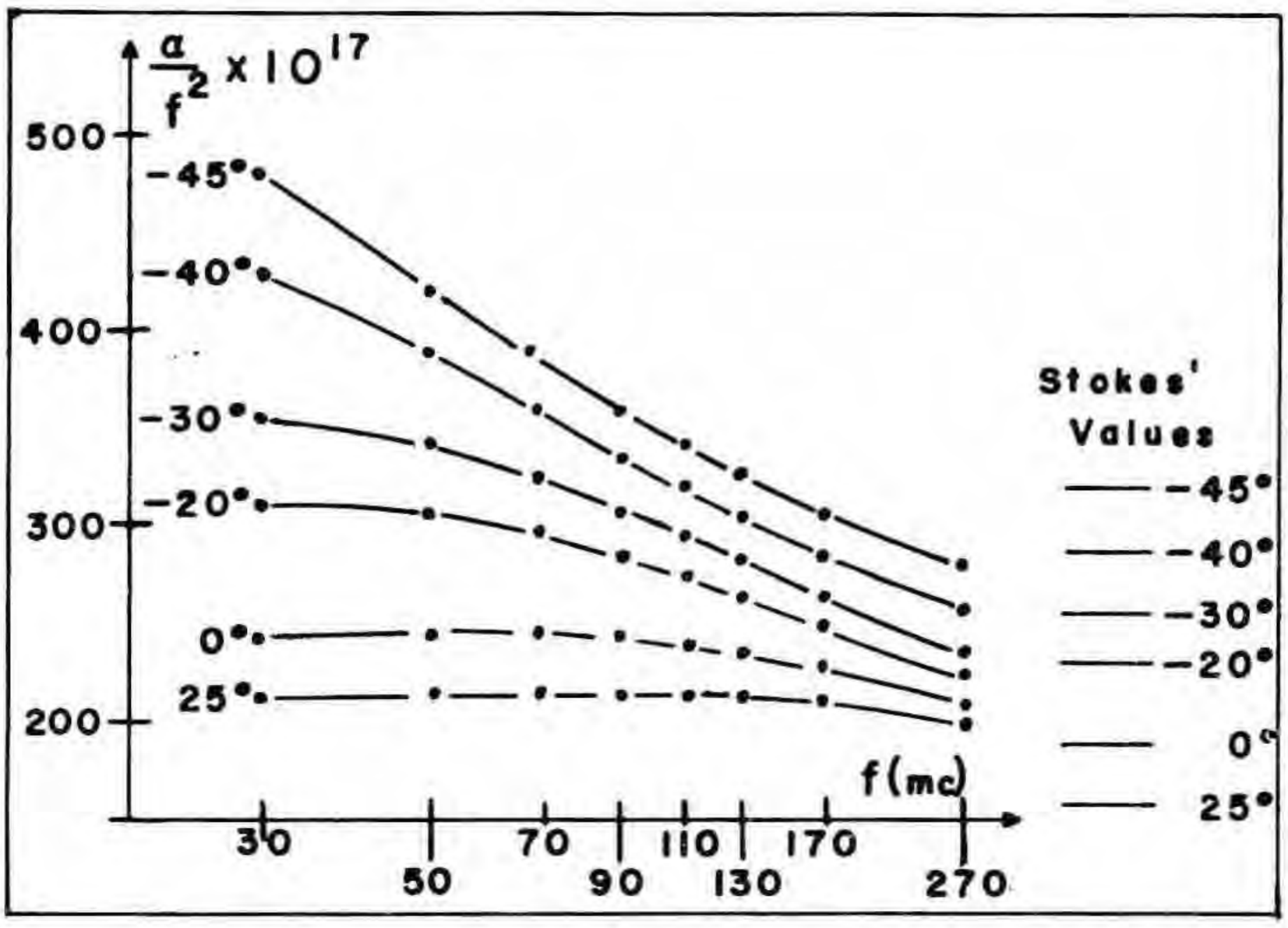

Fig. 2. Absorption of longitudinal ultrasonic waves in the dimethyl siloxane polymer containing 10 silicon atoms per molecule.

quency region of measurement and that both are relaxing. We are further of the opinion that, as in the case of water, the two viscosities represent a total explanation of absorption in the silicones. This opinion is reinforced by the temperature dependence of the absorption and the relatively small ratios of experimental-to-classical absorption at the low-frequency limit. With both viscosities relaxing in the same region, the relaxation equation would be of the form:

$$\frac{\alpha}{f^2} = \frac{A}{1 + (f/f_c)^2} + \frac{B}{1 + (f/f_s)^2} ,$$

where f_c is the relaxation frequency for compressional viscosity and f_s the relaxation frequency for shear viscosity. It should be possible to set up a program in which a value of B and a value of f_c/f_s would be assumed, and the values of A and f_c computed. This however, has not yet been done, and it is difficult to estimate the degree of success with which two relaxation times could be found, considering the relatively small fall-off in most of the curves.

The relaxation of the shear viscosity in nonfractionated silicone fluids (Dow Corning 200-series) has been recognized in shear impedance measurements by McSkimin[2], and in longitudinal absorption measurements by Carome, Hunter, and Pasquesi[3]. McSkimin's measurements show a linear increase of impedance vs. flow viscosity to 10 centistokes, but a marked tapering-off between 10 and 100 centistokes (flow viscosity) and practically constant dynamic shear impedance beyond 100 centistokes (flow viscosity). His computed dynamic shear viscosity has the same general characteristic, which yields a very low shear modulus as well as relaxation frequencies low by comparison with most other liquids. The longitudinal absorption measurements have the same type of variation, i.e. the absorption follows the same tapering-off between 10 and 100 centistokes (flow viscosity), and is practically constant beyond 100 centistokes (flow viscosity).

The more interesting results may be summarized as follows:

1. The relaxation process in 6-atom and 10-atom dimethyl polysiloxanes becomes apparent below 0°C, although lower temperatures are required for the fall-off to become a significant fraction of the total absorption.

2. Low-frequency absorption values exceed those computed from the Stokes low-frequency equation. This is in contrast to values obtained in Dow Corning 200-series silicones of high flow viscosity.

3. Absorption values at 270 Mc in the 10-atom polysiloxane are less than the

Stokes value. The experimental values at 270 Mc in the 6-atom polysiloxane are slightly above the Stokes values, but the extrapolated limiting values are below the Stokes values.

4. There is evidence of relaxation of both compressional and shear viscosity within the frequency region 30 to 270 Mc.

REFERENCES

1. T. Litovitz, T. Lyon, and L. Peselnick, J. Acoust. Soc. Am., 26, 566 (1954).
2. H. J. McSkimin, Bell Telephone Technical Memorandum, 59-121-21, July 10, 1959.
3. E. F. Carome, J. L. Hunter, and R. J. Pasquesi, J. Acoust. Soc. Am., 32, 1510 (1960).

K21

FOURTH INTERNATIONAL CONGRESS ON ACOUSTICS
COPENHAGEN 21.-28. AUGUST 1962

Acoustics and Oceanology.

L.B.Brekhovskikh, I.E.Mikhaltzev.

Sound is the only form of energy being able to propagate in the ocean thousands of miles. Light is scattered in sea water practically after the first ten meters of propagation; electromagnetic waves extinguish on distance of the order of hundred meters. This is the principal reason for acoustics to become of great importance in ocean investigation.

Three lines of contact of acoustics and oceanology may be distinguished. First-it is the investigation of sound propagation, absorption and scattering; many characteristics of ocean surface, water masses and bottom might be gotten. Secondly-studying of noise and sounds of the ocean could give valuable information on sea life and meteorological conditions above the ocean surface. The utilization of sound waves and acoustical methods in ocean investigation could represent the third line of contact of the two sciences.

The investigation of sound propagation in the ocean gives us the possibility to get information about water masses inhomogeneity. The presence of the upper isotermic layer in the ocean forms conditions known as a surface acoustic channel; a structure of ocean water masses and main termocline form a SOFAR - channal. Investigation of sound propagation of a signal given by some calibrated source (e.g.a charge of TNT of a certain weight) on a distance of hundreds and thousands of miles permits to characterise the depth of constant temperature layer as well as mean structure of temperature distribution in deep layers. Changes in acoustical signal characteristics received after crossing big scale temperature inhomogeneities (e.g.streems and current convergences could be used as a measure of such inhomogeneities. The change in intensity of sound after crossing the layer of large temperature gradients gives data of gradient magnitude.

Investigation of sound absorption in sea water (connected with electrolytic processes) permints to obtain information of integral salinity; the possibility of more exact chemical analysis of sea water based on the role of Mg - ions in dissipation of sonic waves is also very im-

portant. The dependence of sound energy absorption in water in the presence of gas or solid inclusions allows to measure the quantity of free gas and solid particals in the subsurface layers.
The scattering of sound by gas bubbles, sea flora and fauna permints to obtain average characteristics of quantity of their presence in a given part of the ocean.
Temperature fluctuations make sound propagation, even on a short distance, a statistical process.
Measuring phase and amplitude fluctuations of a sound wave gives much information on the temperature microstructure of the water along the sound path. Thus the degree of turbulence of various oceanic layers could be found out.

Concerning the second line of contact between acoustics and oceanology some aspects of studying of "acoustical life" of the ocean should be pointed out.
Ocean meteorology can obtain valuable information about conditions over vast ocean area receiving infrasound produced by stormes and coming to the point of reception from the distance of hundreds of miles It is quite possible to find out the course of typhoon motion by acoustical direction finding of its center in the infralow frequency band.
The biological acoustics of ocean becomes an important field of research. The life of a great many of sea animals is connected with transmission of sound. Scientific and practical interest and namely the identefication and investigation of behaviour of oceanliving animals "in situ" make this new branch of science of great importance. It may be said that analogous possibilities were disclosed some years ago for astronomy by radiophysics and radiotechnic; radiotransmission of unvisible stars and nebulae made possible to discover and study new cosmic bodies. Undoubtedly, studying acoustical life of ocean animals will give new valuable data to biology.
Dynamical processes on the bottom of oceans generate sound; recording of these sounds we can obtain geological information which would be impossible to get in any other ways. Such phenomenon as "tsunamy" can be predicted by acoustical observations.

Utilization of sound waves and acoustical methods and instruments permits to speed progress practically in all branches of oceanological research work.
Most widely, and already for many years, acoustical methods are used

in geology of ocean. Echo sounding became a routine method of bathimetric work in the ocean. Seismoacoustics is practically the only possible method to get information of structure of layers many kilometers beneath the ocean bottom. Thickness, mechanical and elastic properties of distant layers can be calculated with the help of data of waves refracted and reflected from the body of the ocean. Identification of the type of ground (sand, rock etc.) is possible by observations of deformation of reflected pulse; more precise data can be obtained by measuring the amplitude and phase of the reflected wave.
Using acoustical methods of investigation in marine biology began by utilization of standard echo sounders for fishing purposes.
Modern multifrequency fish locators permit to distingwish between various species of marine animals. Wideband acoustical pulse source (e.g.a little TNT charge) makes possible to get the quantitative information and stratification data and, some times, identification of species of animals on the depthes of hundreds of meters. Investigation upon reception of sound by marine animals enables to point out the perspectiveness of practical or commercial use of acoustical "bait"; this method might be thousands times more effective then widespread method of fishing with a light source.
Acoustical methods in hydrological investigations can give valuable information on dynamics of large scale heterogeneities in water masses (e.g.on the fronts of currents convergences). The change of temperature or/and density of water creates phase and amplitude changes in transmitted acoustical signal; variation measurements of phase and amplitude of acoustical signal in two (or more) points along the transmission path (e.g.from two ships or anchored buoys) can give the picture of dynamics of hydrology on the sound trace. The investigation of "microstructure" of heterogeneity of sea water on various depth horizons can be effectively performed by acoustical measurements of streaming and local sound velocity variations. Statistical characteristics of surface waves can be obtained by measuring surface reverberation.
If a surface acoustic channel is present, the mean statistical data of sea surface state can be obtained by observations of pulsed sound transmission in this channel.
In addition the possibilities of hydrochemical investigations in the ocean with the help of acoustical methods can be mentioned. The measurement of quantity of free gas and the dimensions of gas bubbles may be performed investigating the reverberation in a distinct volume;

utilizing frequencies of the order of hundreds of kc the concentration of bubbles with dimensions of about hundredth of mm can be measured, which is practically impossible by photooptical method.
In conclusion, the outstanding importance of various oceanological devices and instruments using the acoustical channel of communication and transmission of information and command must be stated. It is impossible in this short report to review all the directions and the coming advantages of the contact of acoustics and oceanology. We hope that the new geophysical aspect of acoustics would draw attention of a vast group of scientists and bring outstanding results.
Thank you.

L21

FOURTH INTERNATIONAL CONGRESS ON ACOUSTICS
COPENHAGEN 21.-28. AUGUST 1962

Discrete Frequency Noise from Ejector Nozzles

D. Middleton and E.J. Richards

The Nature of the Problem

The noise from the engines of jet-powered airliners tends to be so severe that methods of reduction must be considered even in the preliminary project stage of the aircraft. For this reason work has been undertaken by the Department of Aeronautics and Astronautics in the University of Southampton to investigate how ejectors might reduce the exhaust noise of the supersonic transport aircraft.

The idea is to surround the primary nozzle of a jet engine with a tube as Figure 1 illustrates. The mixing of the primary stream A with the induced annular secondary airflow B results in a final efflux C consisting of a greater quantity of gas than the primary jet and moving at a lower velocity. Exhaust velocity being the dominating parameter on which the noise of a jet usually depends, a reduction in sound output is anticipated.

The resulting attenuation must depend on the geometry and the aerodynamic characteristics of the installation at the design operating pressure ratio, and a range of cylindrical ejectors has been under study, with lengths between 3 and 32 times the diameter of the primary nozzle, and of cross-sectional area between 2 and 4 times that of the primary nozzle.

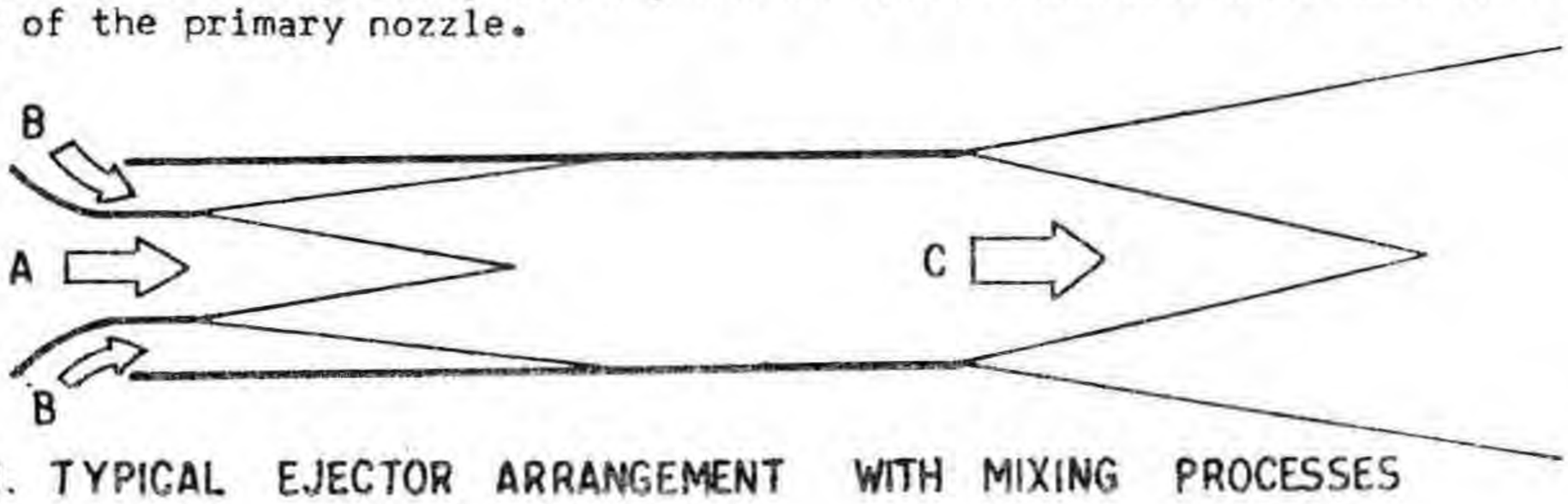

FIG.1. TYPICAL EJECTOR ARRANGEMENT WITH MIXING PROCESSES

Noise tests carried out in the Acoustics Laboratory of the University showed that several of the ejectors gave significant noise reductions, but it also became apparent, especially with the shorter shrouds, that discrete noises were present, and often in sufficient strength to more than offset the reduction achieved in the broad band noise which characterises the usual jet discharge. This is illustrated by Figure 2 which shows plotted against pressure ratio the overall noise levels recorded at the same position, of the primary nozzle alone and of a typical short ejector. The steady increase in noise level for the simple jet follows the usual relationship of being proportional to approximately the eighth power of the jet velocity, until at a pressure ratio somewhere above choking a rapid increase in noise level of some 10 db is registered. On the other hand, mainly in the region below a pressure ratio of about 1.5, the curve for the ejector shows some ranges where the measured levels are somewhat higher than anticipated. Further along the curve an increase in noise is again registered at a condition above choking. Narrow band analysis has shown that these excesses are due entirely to the presence of discrete frequencies in the noise output.

Discrete Frequencies at Pressure Ratios Above Choking

A decade ago Reference 1 reported work on the discrete frequencies which may exist for a simple axi-symmetric jet operating under choked conditions. The present work has shown that the phenomenon is also able to occur when the flow is contained within a duct, and a typical spectrum analysis with ejector in position is shown in Figure 3. Harmonics of the fundamental are detectable up to the limit of the narrow band analysis.

The frequency of the fundamental is plotted against pressure ratio in Figure 4 for the primary nozzle both unshrouded and with a typical ejector. The main characteristics are the same. These are that the fundamental frequency generally falls gradually with increase in pressure ratio but at certain conditions discontinuities in this frequency occur, and some hysteresis in going from one domain to another may

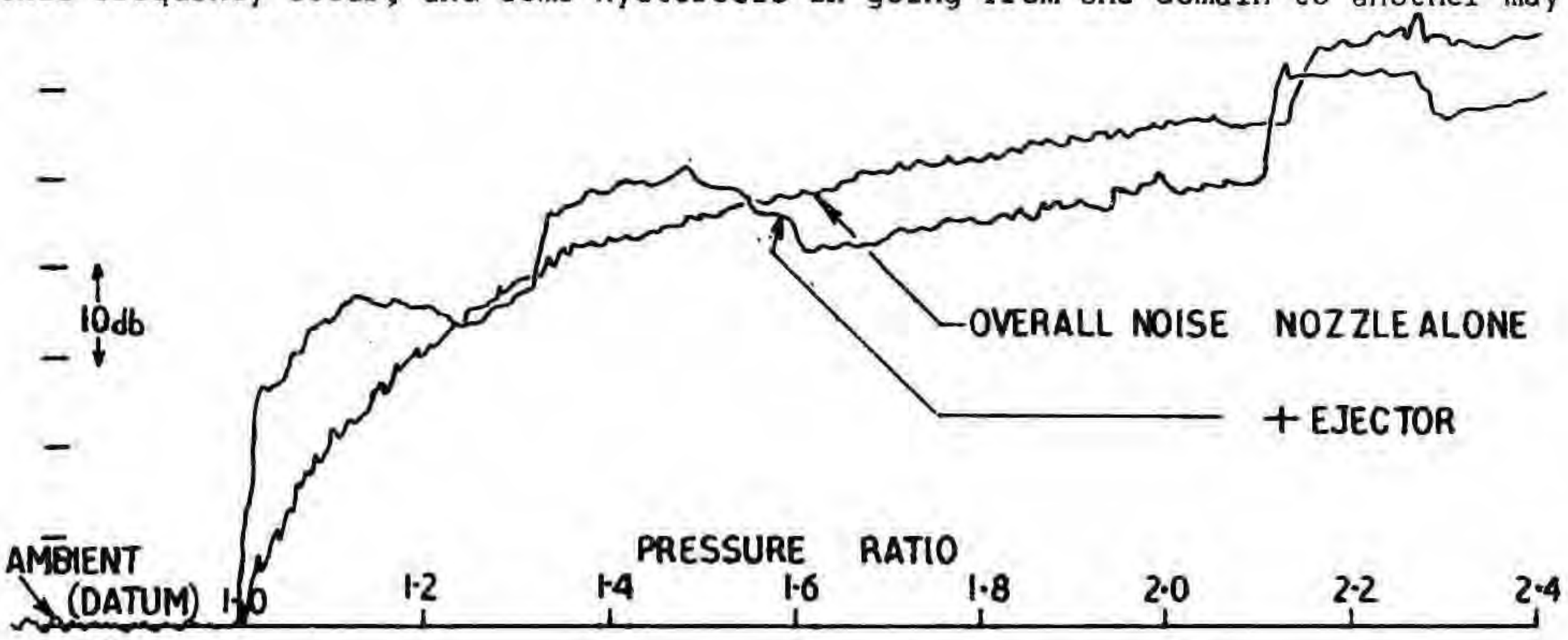

FIG.2.

be apparent. However over part of the pressure range the frequencies of the present primary nozzle do not agree with those quoted by other workers, suggesting that the manifestation depends crucially on initial conditions.

These discrete frequencies have been detected when the final efflux, (C), is subsonic, though the primary flow (A) is necessarily sonic at the nozzle. This means that they are associated with the primary discharge and therefore the generation mechanism must take place within the ejector itself as the primary flow expands through its shock pattern to subsonic flow. The hypothesis has been made for unshrouded flow that a 'disturbance' initiated at the mouth of the nozzle causes an acoustic wave to be emitted as it passes through a cell end in the shock pattern which

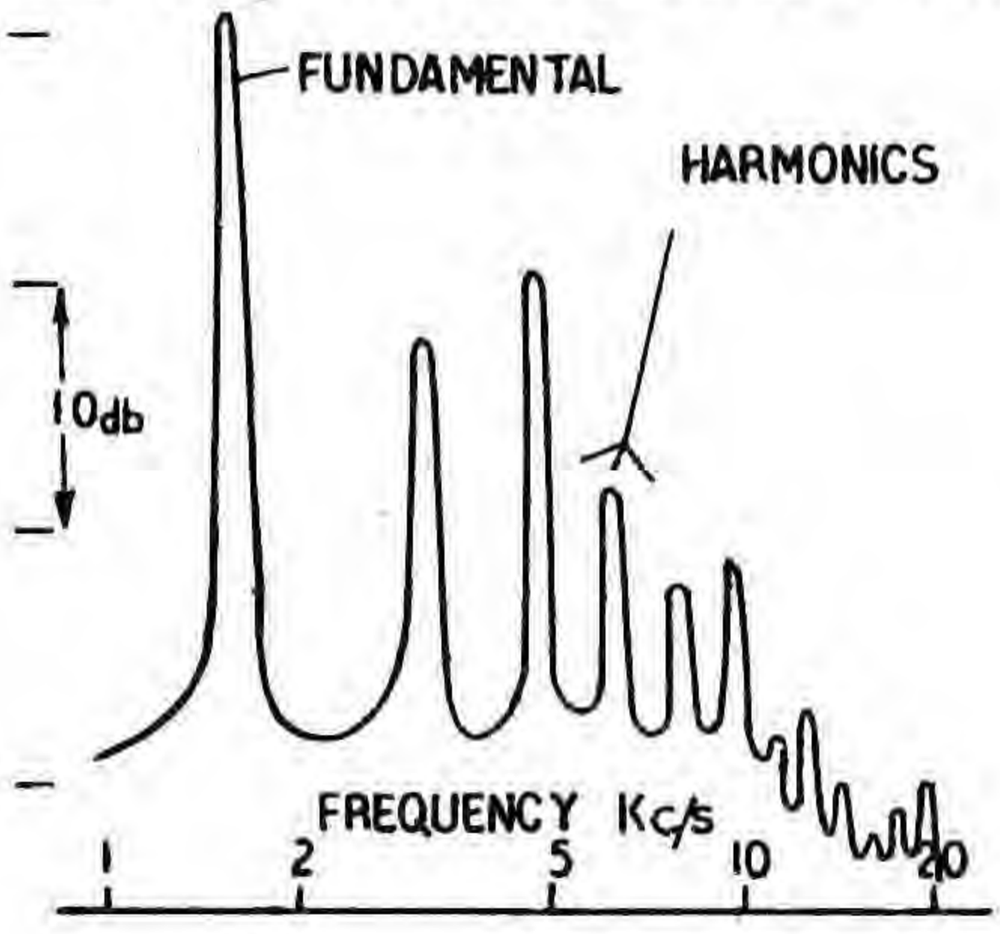

FIG.3.

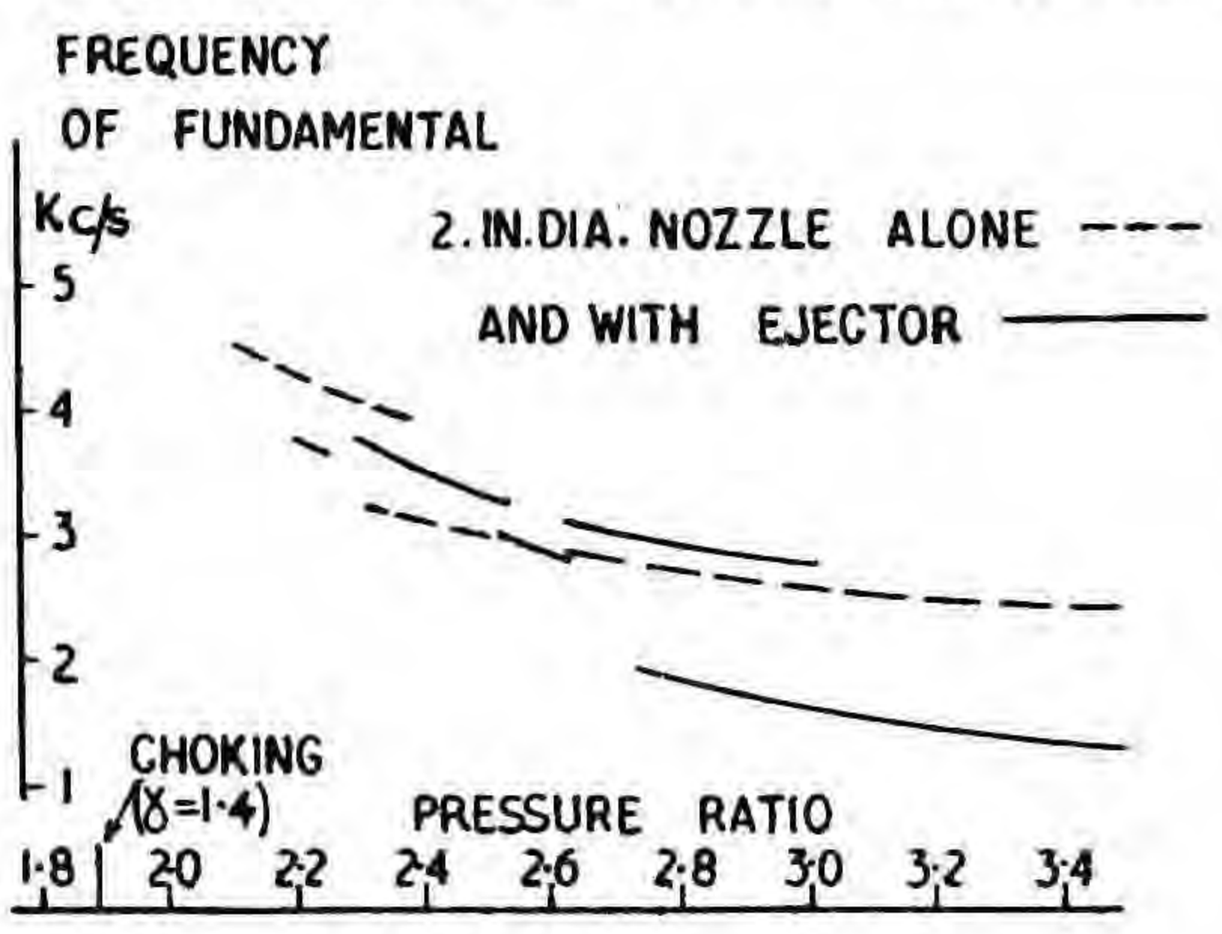

FIG.4.

exists downstream. On striking the nozzle lip this acoustic waves generates a second pulse which is convected downstream, and so the loop cycle is formed. The general similarity of the ejector results to the unshrouded case suggests that the mechanism is essentially the same, with the acoustic wave travelling upstream against the subsonic secondary flow. Clearly the pattern is somewhat more complicated than in the unshrouded jet case, as exemplified by there being more frequency ranges, and work is therefore continuing to elucidate the facts.

Discrete Frequencies at Pressure Ratios Below Choking

Figure 5 shows a typical spectrum obtained from an ejector when no part of the flow was sonic. The discrete frequencies which are present appear to be related by the formula $(1.5)^p qn$ where p and q are integers, $p \geq 0$, $q \geq 1$, and n is the lowest detectable discrete frequency. Thus successive values of q give the simple harmonics of the note $(1.5)^p n$. In contrast with the case already considered, these frequencies increase as the pressure ratio rises. Since there is a change of frequency with operating condition we are not dealing with simple organ-piping.

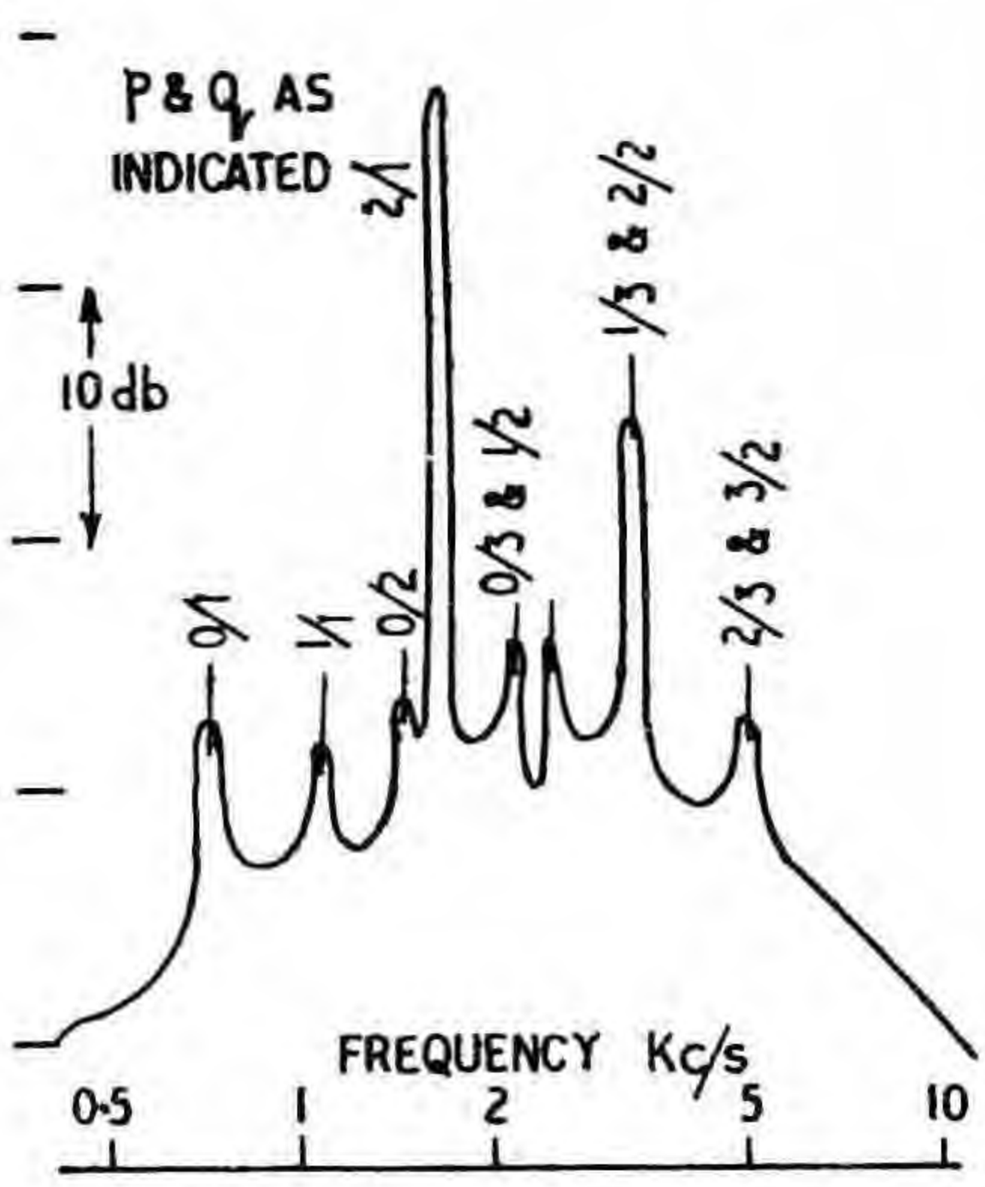

FIG 5

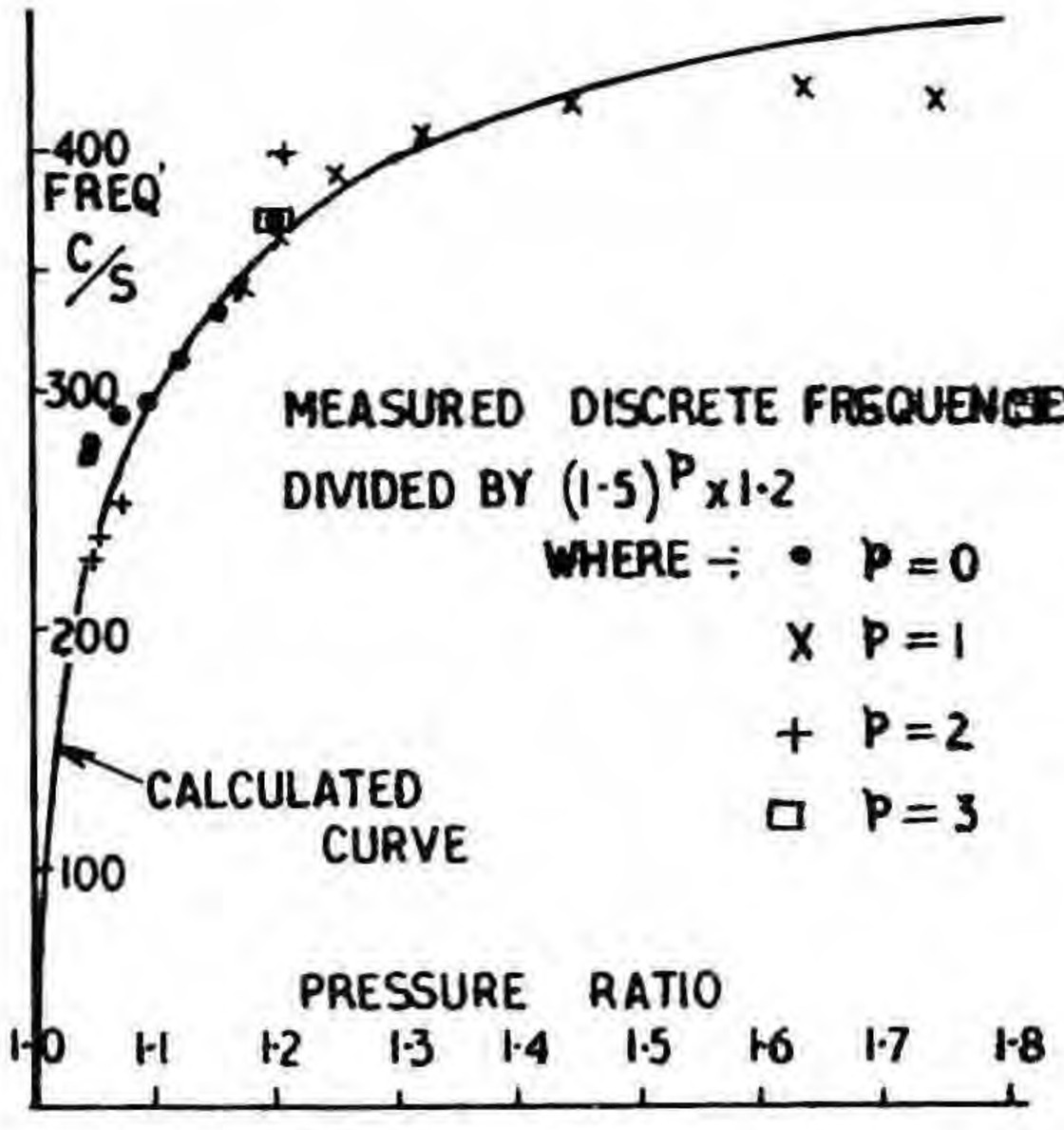

FIG.6

Neither the addition of a thick layer of damping material nor of a large quantity of mass made any difference to the intensities of these frequencies or their values showing that the particular problem here is not one of mechanical vibration. It therefore appears that the phenomenon is once more acoustic and an initial attempt has been made at calculation, based again on a feedback system, as follows:-

In a short ejector it is known that the primary and secondary streams pass through virtually unmixed. Consider then a flow irregularity propagated down the tube from the nozzle with a velocity equal to the speed of the primary jet. If on reaching the end of the ejector this generates an acoustic wave, this latter will reach the nozzle most quickly by travelling upstream against the lower speed of the secondary airflow. The initiation of another 'eddy' from the mouth of the primary nozzle by this wave completes the cycle. In the longer ejectors mixing is much more advanced, so that such an idealized situation does not occur. This may explain why in these cases the discrete frequencies are much weaker or even not detectable.

Figure 6 plots against pressure ratio the frequency calculated in this way for a particular ejector. Also shown are the measured frequencies divided by a

factor $(1.5)^p q$ x 1.2, with values of p as appropriate. The additional factor of 1.2 gives best agreement between the recorded points and the curve, and may be a result of end effects, that is, the ejector having an effective length slightly different from its physical length.

Methods of Reduction of Discrete Frequencies

As in certain cases discrete frequencies have been measured whose spectrum levels are up to 40 db more than those of the surrounding broad band noise, with octave levels increased by over 30 db and overall noise by perhaps as much as 20 db, this double problem of these two forms of discrete frequencies cannot be overlooked when consideration is given to a full scale ejector design. Investigation of the phenomenon rather than methods of reduction or elimination has been the principal concern so far, but nevertheless two partially successful methods of reducing the discrete notes have been discovered. In a supercritical case, roughening the inside of the primary nozzle was found to reduce the overall noise by some 5 db to a level only 2 db above the broad band noise level. In the sub-critical case, roughening the inside of the ejector brought about a reduction. The octave in which the principal discrete frequency was located, was lowered by 15 db, and the overall noise by 12 db to bring it to within 4 db of the 'pure jet noise'. In no case did this roughening appear to change the broad band noise in any way.

Acknowledgement

The assistance of Raymond J. Hale in the preparation of the paper is acknowledged.

References

(1) Alan Powell — On the Mechanism of Choked Jet Noise
Proceedings of the Physical Society, Vol.66B, p.1039, 1953.

M21

FOURTH INTERNATIONAL CONGRESS ON ACOUSTICS
COPENHAGEN 21.-28. AUGUST 1962

DIGITAL COMPUTERS IN ROOM ACOUSTICS

M. R. Schroeder, B. S. Atal and Carol Bird, Bell Telephone Laboratories, Incorporated, Murray Hill, New Jersey

This paper describes a method for evaluating the acoustics of concert halls, prior to construction, by simulating the sound transmission in the hall on a digital computer. Frequency and space responses of rooms can also be simulated on a digital computer by a Monte Carlo method and evaluated to determine characteristics of these responses which cannot be computed analytically.

Summary of Computer Simulation of Concert Hall Acoustics

A reverberation-free sound signal is sampled, quantized and fed into the computer. The computer adds echoes and reverberation to this signal and produces two output signals. These signals, when radiated from two loudspeakers in an anechoic chamber, combine at the ears of a centrally seated listener to form echo responses similar to those in the real hall. In the simulation, we distinguish between "discrete echoes" which influence the acoustical quality individually and "continuous reverberation" in which individual echoes are not distinguishable but act collectively. The computer program allows the specification of the individual discrete echoes in amplitude, delay and direction of incidence. The continuous reverberation is simulated with adjustable frequency-dependent reverberation time, shape of decay curve, diffusion, echo density and frequency response irregularity.

Simulation of Discrete Echoes

The hall to be simulated is considered from the point of view of "geometrical acoustics," i.e., the sound is assumed to travel along straight paths (rays). The reflectionsat the boundaries obey the laws of geometrical optics. This approach, although approximate, has been found useful in studying the acoustics of large halls.[1,2]

Seraphim[3] has established a criterion to determine which of the discrete echoes in a room individually influence its acoustical quality. The delays, amplitudes and directions of these echoes are determined from plan drawings of the hall. In principle, these echoes can be reproduced from many loudspeakers located in appropriate directions in an anechoic chamber. However, we have taken a different approach. By taking into account the sound diffraction around the listener's head, we simulate echoes arriving from arbitrary front directions by radiating from only two fixed loudspeakers. The signals from the two loudspeakers combine at each ear to form pressure waves corresponding to echoes from different directions. The operations to obtain the required loudspeaker signals are also performed in the computer. If desired, strong reflections from the back of the hall and the ceiling can be reproduced by using one or two additional loudspeakers.

Figure 1 illustrates the signals $x_1(t)$ and $x_2(t)$ required at the two loudspeakers to produce pressure waves at the two ears that will simulate a single echo arriving from an imaginary source S. The impulses at the ears from the near loudspeaker are shown by full lines, those from the far loudspeaker are shown as dashed lines. As can be seen, all but the first impulses at each ear cancel each other. The remaining two

---

[1] E.Meyer and W.Burgtorf, "Ueber die Zeitabhaengigkeit der Schallrichtungsverteilung in Raeumen bei Impulsartiger Anregung," Akustische Beihefte, Heft 1, 313 (1957).

[2] L.Cremer, "Welcher Aufwand an Information ist erforderlich, um einen Raum akustisch zu chacterisieren," Proceedings of the Third International Congress on Acoustics, (Elsevier Publishing Company, Amsterdam, 1961), p.831.

[3] H.P.Seraphim, "Ueber die Wahrnehmbarkeit mehrerer Rueckwuerfe von Sprachschall," Acustica 11, 80 (1961).

impulses have amplitudes and relative delays corresponding to an echo from source S. A method of obtaining the appropriate loudspeaker signals for various source directions is described in the Appendix. For simplicity, we have assumed that the interaural time and amplitude differences depend only on angle of incidence and not on frequency. Experiments in an anechoic chamber with speech signals have confirmed the validity of this approximation. With loudspeakers located at ±22.5°, external virtual sound images have been created at 0°, ±12°, ±37°, ±48°, ±66°, and ±90°. The images are stationary for head movements up to ±10°.

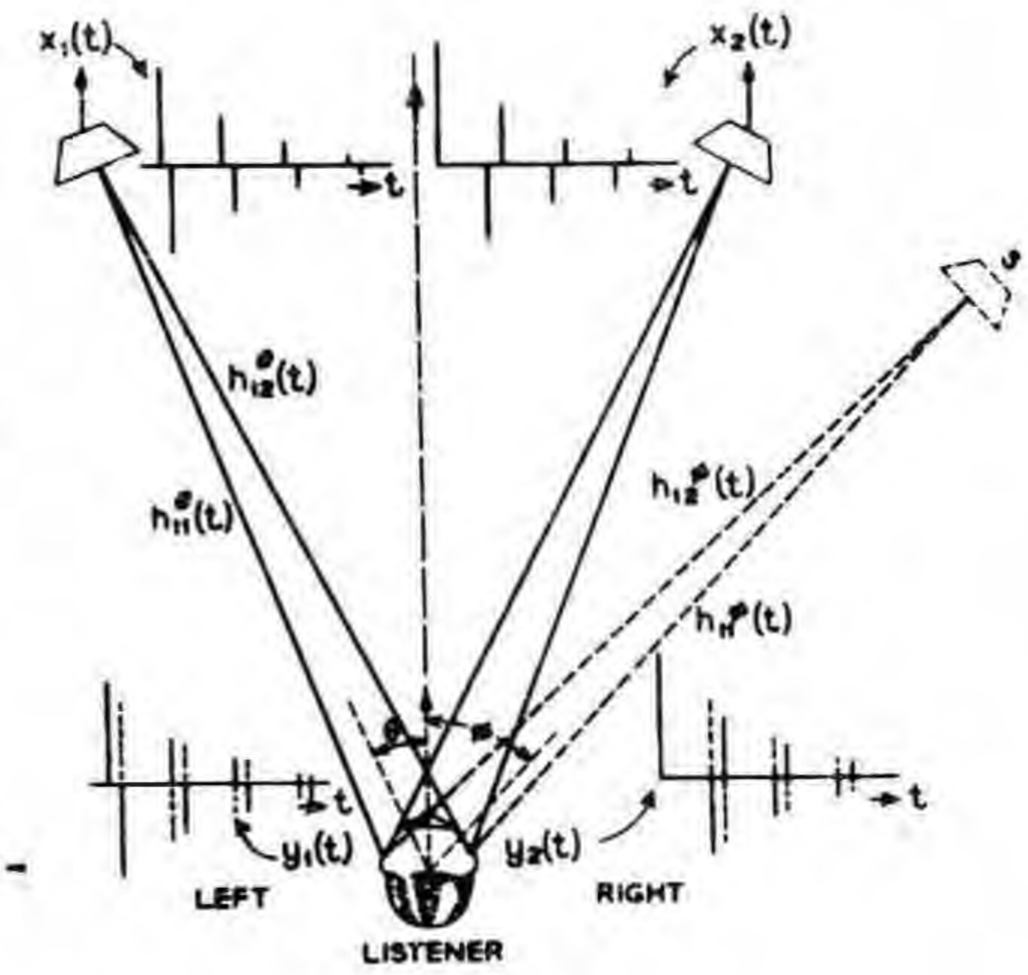

Figure 1

Simulation of Continuous Reverberation

Continuous reverberation with any desired characteristics (reverberation time, including its variation with frequency, shape of the decay curve, echo density, state of diffusion, and frequency response irregularity) can be produced on a digital computer. A block diagram of a (monophonic) reverberator is shown in Fig. 2. The reverberator consists of several "comb-filters" (delay line in a feedback loop) connected in parallel and two all-pass filters[4] in series. The comb-filters determine the reverberation time, the all-pass filters the echo density. A minimum of 4 comb-filters in parallel is required to produce a frequency response statistically similar to that of a room. However, the number of comb-filters may be altered to produce any desired frequency response irregularity. For exponential sound decays, the gains g_1 through g_4 are adjusted according to the formula $T = \frac{3\tau_n}{(-\log |g_n|)}$, where T is the desired reverberation time. Nonexponential decays can be realized by choosing comb-filters with different decay rates according to the desired distribution of reverberation times. For a frequency-dependent reverberation time, gains g_1 through g_4 are made dependent on frequency.

The echo density[5] produced by the reverberator at a time t is given by $(\tau_5 \tau_6/2 \sum_{i=1}^{4} 1/\tau_i)t^2$. The variation of echo density with time is the same as in a room ($\frac{4\pi c^3}{V} t^2$, where V is the volume of the room). Thus, the desired echo density can be obtained by suitable choice of the delays τ. The gains g_5 and g_6 are most conveniently made equal to 0.7.

To make the continuous reverberation spatially diffuse, several differently reverberated signals radiated from a number of loudspeakers located around the listener could be used. Instead, we use only two artificial reverberators, one with positive gains (g_1 through g_6) and the other with negative gains. Two such reverberators have almost uncorrelated impulse responses and produce a diffuse reverberation similar to that found in real halls. The outputs of the two artificial reverberators are reproduced at the listener's ears by radiating from the two loudspeakers with proper compensation for the sound diffraction around the listener's head.

Programming the Digital Computer

A "block diagram compiler"[6] is used to translate the acoustical data into a language understood by the IBM 7090 digital computer. First a block diagram is prepared which

[4] M.R.Schroeder, "Improved quasi-stereophony and 'colorless' artificial reverberation," J.Acous. Soc. Am., 33, 1061 (1961).
[5] H.Kuttruff, "Kuenstlicher Nachhall," Frequenz, 16, 91 (1961).
[6] J.L.Kelly, Jr., Carol C.Lochbaum, and V.A.Vyssotsky, "A block diagram compiler," Bell Syst. Tech. J., 40, 669 (1961).

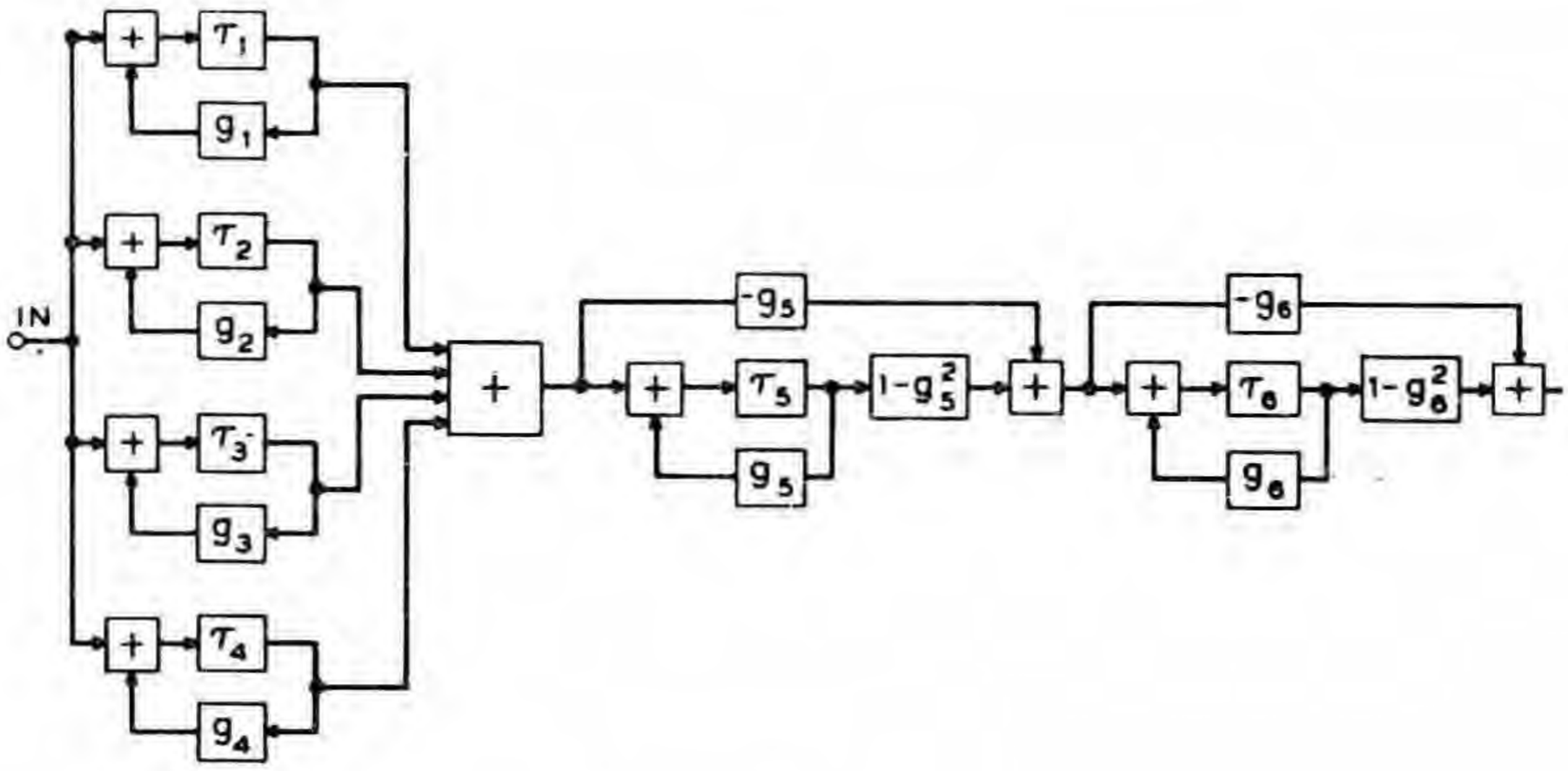

Figure 2

will produce two output signals with the desired discrete echoes and continuous reverberation. This reverberator includes a network to compensate for the sound diffraction around the listener's head. The block diagram information is punched on IBM-cards which are fed into the computer. The output of the computer is a program which will simulate the specified reverberator. Samples of reverberation-free speech or music are then recorded on a digital tape. This tape is read and processed by the compiled program. The two output tapes from the computer are converted into a stereo tape which is played back over two loudspeakers in an anechoic chamber. Based on the listener's evaluations, the architectural plan of the hall can be modified to obtain the desired acoustics.

Monte Carlo Compuations in Room Acoustics

Sound transmission in rooms is a complex phenomenon. In virtually all cases, treatment as a boundary value problem is impractical. Therefore, it is not possible to compute the exact sound pressure distribution. Fortunately, this is not necessary. All that is required is knowledge of certain average quantitites, for example, the average initial slope of a sound decay curve. These average quantities can be obtained by statistical methods. This has long been recognized and a statistical theory of room acoustics based on the ray approximation of sound transmission has been developed.[7] In 1954, the statistical approach[8] was extended to sound waves (as opposed to rays).

With the tools of "statistical wave acoustics," many properties of frequency and space responses in rooms can be computed. An example is the average frequency spacing between adjacent maxima of the frequency response.[9] However, some problems are not amenable to analytical treatment. In these cases, a Monte Carlo method, executed on a large digital computer, has proved useful. For large rooms, the Monte Carlo method is based on the fact that real and imaginary parts of the sound transmission function between two points in a reverberant sound field are Gaussian processes[8] - either as functions of frequency or space. The "macroscopic" properties of the room (reverberation time, diffusion, etc.) determine the "spectrum" of the Gaussian process. Accordingly, the first step in the Monte Carlo computation is the generation of a sequence of independent Gaussian-distributed numbers. This discrete Gaussian process is then

---

[7] L.Cremer, Statistische Raumakustik (published by S.Hirzel Verlag,Stuttgart, 1961).

[8] M.R.Schroeder, "Die statistischen Parameter der Frequenzkurven von grossen Raeumen," Acustica 4, 594 (1954).

[9] M.R.Schroeder and K.H.Kuttruff, "On frequency response curves in rooms," J. Acoust. Soc. Am. 34, 76 (1962).

"filtered" to give it the proper spectrum. By further transformations, a random function is derived which has the same statistical properties as the room acoustical function under study. This function is then evaluated in the computer much like an experimentalist evaluates his measurements on an actual room. Further details about digital Monte Carlo computation can be found in reference 9. Here we shall limit ourselves to the illustration of two results obtained by this method.

Figure 3 shows the "frequency irregularity" (the average level difference in decibels between maxima and minima of the frequency response) as a function of the ratio of direct sound intensity to total sound intensity. This ratio is a function of the distance between sound source and receiver. The ratio of direct-to-reverberant sound intensity is important in telephony where it determines the "clarity" of the received signal. The function shown in Fig. 3 allows one to determine this ratio by measuring the frequency irregularity (for example, with a level recorder).

Figure 4 shows the frequency autocorrelation function of the frequency response (in terms of pressure squared) of a room with uniform reverberation time T_{60}. In this case, the result can also be obtained by analytical means. The Monte Carlo computation was undertaken to check the accuracy of this method. As can be seen, the agreement between analytical theory (full curve) and Monte Carlo results (small circles) is quite close.

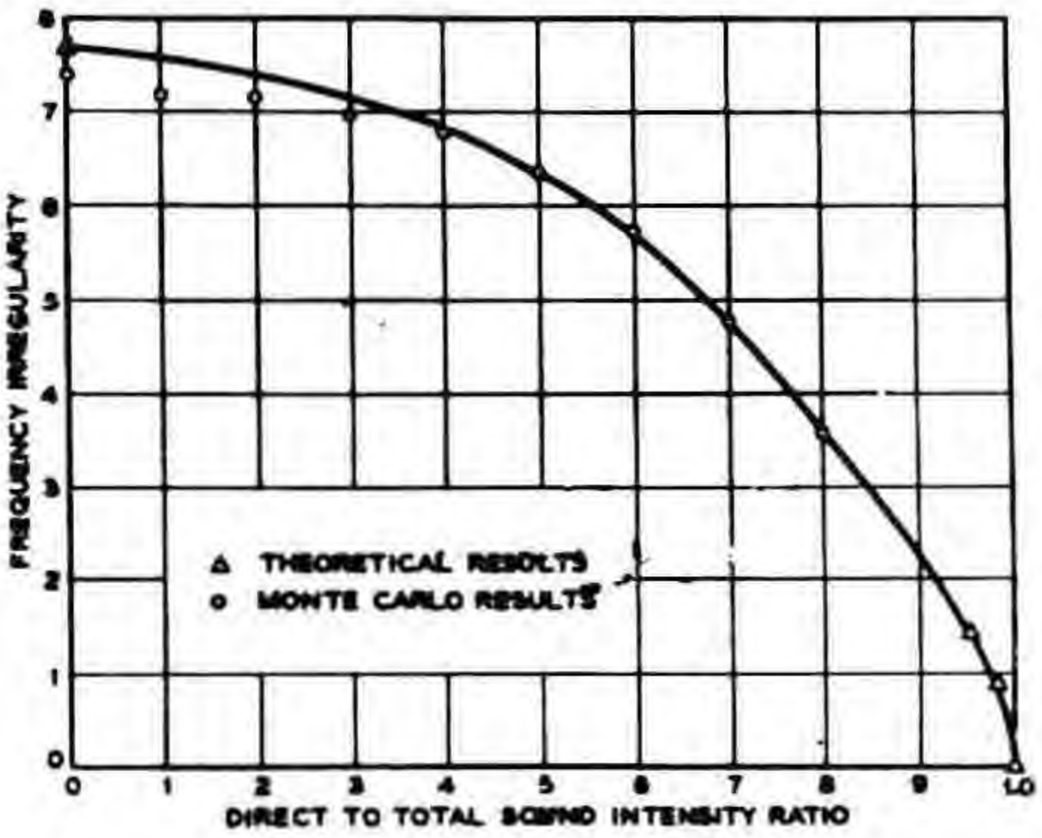

Figure 3

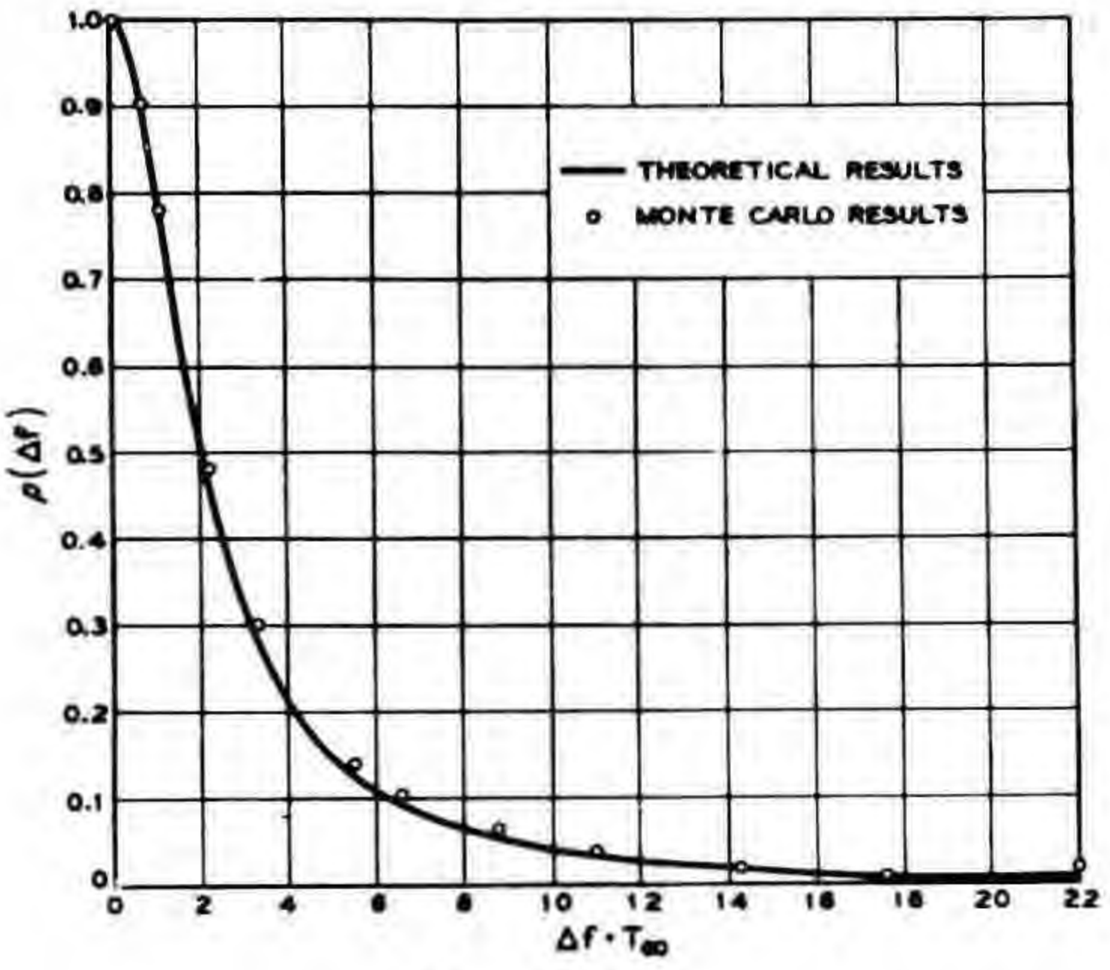

Figure 4

Appendix

Consider two loudspeakers at angles $\pm\theta$ in front of a listener seated in an anechoic chamber (Fig. 1). Let $h_{11}^{\theta}(t)$ and $h_{12}^{\theta}(t)$ be the pressure responses at the listener's left and right ear, respectively, when a short voltage pulse is fed to the left loudspeaker. Let $h_{11}^{\varphi}(t)$ and $h_{12}^{\varphi}(t)$ be the pressure responses at the two ears from a source in any given direction φ. Then (assuming a symmetrical head) the required loudspeaker signals $x_1(t)$ and $x_2(t)$ to simulate an echo from direction φ are given by the following equations:

$$h_{12}^{\varphi}(t) = x_1(t) * h_{11}^{\theta}(t) + x_2(t) * h_{12}^{\theta}(t) , \qquad (1)$$

$$h_{11}^{\varphi}(t) = x_1(t) * h_{12}^{\theta}(t) + x_2(t) * h_{11}^{\theta}(t) , \qquad (2)$$

where the asterisks signify convolution. $x_1(t)$ and $x_2(t)$ are obtained from Eqs. (1) and (2) by taking the Fourier transforms on both sides, solving for x_1 and x_2, and then taking inverse Fourier transforms. This yields

$$x_1(t) = [\, h_{11}^{\theta}(t) * h_{12}^{\varphi}(t) - h_{12}^{\theta}(t) * h_{11}^{\varphi}(t)] * a(t) ,$$

$$x_2(t) = [\, h_{11}^{\theta}(t) * h_{11}^{\varphi}(t) - h_{12}^{\theta}(t) * h_{12}^{\varphi}(t)] * a(t) ,$$

where $a(t)$ is the inverse Fourier transform of $1/[H_{11}^2(\omega) - H_{12}^2(\omega)]$, and $H_{11}(\omega)$ and $H_{12}(\omega)$ are the Fourier transforms of $h_{11}^{\theta}(t)$ and $h_{12}^{\theta}(t)$, respectively.

N21

FOURTH INTERNATIONAL CONGRESS ON ACOUSTICS
COPENHAGEN 21.-28. AUGUST 1962

A Push-Pull Stereophonic Loudspeaker

based on New Concepts in 2-channel Stereophony

F.H. Brittain

Part I Binaural Audition.

Part II The design of a push-pull loudspeaker.

Part I Binaural Audition

Ideal Stereophony. The aim of stereophony should be: (i) "that the listener should not be able to differentiate between the original and the reproduced sound fields". (ii) "that the listener should perceive the sound field that the producer intended". (This sound field may not necessarily bear any relation to any natural sound field).

Practical Stereophony. A particular system will be described in order to study its requirements in detail. This system will have two loudspeakers situated on a base line not exceeding 6 m in length, the listener will be seated somewhere opposite the base line of the loudspeakers and not nearer than 2.5 m to either loudspeaker.

Specified Performance. The system must produce an easily combined or "fused" sound image. A sound image, intended to be at one end of the base line must not appear to come from a position which is displaced more than half-way towards the centre of the base line wherever the position of the listener may be.

Gestalt. The brain makes use of all available factors in determining the position of a sound, most weight being given to a comparison of the time of arrival of the "wanted" sound at the two ears. In order that the arrival time at the two ears may be compared, the brain has to decide what sounds are to be considered, and what are to be rejected; roughly, what to listen to. This can only be done by means of a brain image or "gestalt". Under normal conditions the sounds picked up by the ear will contain the direct and the reflected or reverberant sounds as well. For sound location and for the accurate hearing of sound detail, it is very necessary to be able to separate the direct from the reverberant sound.

Time-Parallax. A small movement of the head is used to alter the arrival times at the two ears; this head movement may be as little as 3 mm. since the brain can detect aural time differences of less than 10 μs. Head movement permits the "gestalt" to be made much sharper - only those sounds with the same time-behaviour will be grouped together to form the "gestalt". All other sounds having different or random time-behaviour will be rejected.

Running Auto-Correlation. It has been shown that inter aural time differences as short as 10 μs. can be used by the brain for sound location. It may seem surprising that detailed structure can be preserved through such mechanical systems as the middle ear, cochlea and neural responses. However, since the auto-correlation is continuous or running, it is only necessary for the information provided by the two ears to be sufficiently similar to be recognised by the brain and to provide a comparison for time-parallax. Thus the behaviour of the two ears does not have to be identical. All that is required is that the degree of mutilation by either ear does not prevent correlation. Partial deafness, or malformation of the ear does not influence the position of a sound unless the brain cannot recognise the "gestalt" formed by the deficient ear.

An Image. It has been shown by a number of experimenters that a sound image, differing in position from either of the two loudspeakers producing it, can

/ be

be produced in the mind of a listener situated equidistant from the two loudspeakers. The twin signals, one from each loudspeaker, arrive at one ear and can be fused together to form a single signal with an effective arrival time somewhere between that of the two components if the time interval does not exceed approximately 600 μs. Fusion is less certain with longer time intervals and varies greatly with the particular listener, it is virtually impossible beyond about 5,000 μs.

The Mind. Since auto-correlation between the two ears is done at brain level it may be supposed that it is controlled by the mind to some extent. Consider the case where the loudspeakers subtend an angle of 90° to the "on axis" listener. The pairs of signals at each ear will be separated by approximately 300 μs. The listener may take either the first arriving signals or the mean of each pair, in both cases the sound image will appear straight ahead in the centre. If now the "on axis" listener turns to face loudspeaker A its signal will reach both ears simultaneously. The signal from loudspeaker B will reach the nearer ear almost simultaneously with the sound from A, it will reach the remote ear approximately 600 μs. later. The listener can combine the signals from each ear due to loudspeaker A, and deduce that the image is at A, ignoring the late signal from B. Alternatively, the listener can fuse the double signal from loudspeaker B in the remote ear and apply auto-correlation to this "mean time". This will give a fused image with approximately 300 μs. time difference, that is, the image will be at 45° to the direction in which the listener is facing, at the centre mid way between the two loudspeakers.

Listening. It has been shown experimentally that if the sound from one loudspeaker is increased, and that from the other reduced, the effective arrival time of the pair of signals at one ear will shift towards the louder signal. A difference of 25 dB between the two loudspeakers is sufficient to "lock" an image firmly over to that loudspeaker which is loudest. Not all listeners demand an image somewhere on the base line, they are satisfied if some sounds appear to come from one end of the base line and different sounds from the other end. In this case which is effectively a "double monophonic" system, it is only necessary to provide a separation of 25 dB between the loudspeakers anywhere in the listening area.

As soon as the listener moves off the central axis where both loudspeakers are equidistant, the double sounds at one ear become separated by a much longer interval of time. This interval, of roughly 3,000 μs. per metre of path length difference is something not encountered in nature and some listeners are unable to fuse the double sounds into one.

Part II The design of a push-pull stereophonic loudspeaker

Special requirements. The first requirement is that the sounds from the two loudspeakers should be easily fused together to form a single "gestalt" which can then be located by normal auto-correlation procedure. It has been found that the more sharply defined is the arrival time from a loudspeaker, the more easily and accurately it can be fused with the other loudspeaker to give a mean arrival time. Also, very important, the sharp arrival time of the sound direct from the loudspeaker prevents it being confused with reflected sound, whose arrival time is always less clearly defined. This may be achieved in practice by making the loudspeaker small in the horizontal plane and extending it in a vertical plane if this is necessary to ensure adequate radiation of various frequencies.

Off axis listening. In order to produce a central image it is necessary for the two loudspeakers to appear to be equally loud when heard from any listening position. This means that the loudspeakers must be slightly directional in a horizontal plane so that the nearer loudspeaker radiates less sound and the remote loudspeaker more sound to the off-axis listener. It is important that the directionality of the loudspeakers is maintained at all frequencies above about 300 Hz. Below this frequency the sound waves are so distorted by the walls of the room that little directional information can be obtained from them.

The Cabinet. This consists of a Helmholtz resonator tuned to a very low frequency by means of an internal pipe. Two low frequency loudspeaker units are used

/ mounted

mounted in push-pull which greatly reduces harmonic distortion at low frequencies. The form of the cabinet is tall and narrow in the horizontal plane. At the bottom of the cabinet is the opening of the duct or port of the Helmholtz resonator. Just above it the forward facing low frequency loudspeaker unit is mounted on the front panel of the cabinet. Just behind it, sloping upwards at an angle of approximately 45° is the wall of the duct, and in this wall the second loudspeaker of the push-pull pair is, mounted, also at 45°. This arrangement gives the tightest possible coupling between the two loudspeakers and permits full advantage to be taken of the push-pull system. In this arrangement the front of the second low frequency unit radiates into the cabinet proper and the back of the unit radiates into the listening room via the port. In order to make the output from the second loudspeaker add to that of the first, the electrical signal to the second loudspeaker is reversed in phase.

Air Resonances. Since the bottom of the cabinet proper is arranged at an angle of 45° it very effectively reduces the main vertical mode of air resonance in the cabinet. The back to front mode of vibration of the air is effectively reduced by making the front of the cabinet not parallel with the back. The actual angle is chosen to give the polar distribution required for equal sound pressures along the listening line. Even when all precautions have been taken in the design of the cabinet, some trace of air resonance remains. This is best removed by a "membrane" adsorber which is much more efficient at low frequencies than the soft damping material usually employed.

Upper Frequencies. The low frequency units are used up to 1,500 Hz. Small pressure units are used for the range 1,500 to 12,000 Hz. From 12,000 to 25,000 Hz. a ribbon horn unit is used and gives a worth while improvement when a high quality programme is supplied to the loudspeaker.

Polar Response. It has been found possible to obtain a polar response which will give approximately equal sound pressures, in any 1/3 octave band above 500 Hz. from the two loudspeakers anywhere in the listening area. This polar response is maintained constant with frequency by progressively reducing the horizontal dimension of the radiator as the frequency is increased. For this purpose the electrical cross over circuits used are not sharp so that the effective width of the radiator is gradually reduced.

Transient Response. In order to produce a sharp arrival time and a clear "gestalt" it is very important to have particularly good transient response at all frequencies. This is achieved at low frequencies by the design of the cabinet and the use of membrane adsorbers. At 1,500 Hz. an electrical filter is used on the loudspeaker side of the cross over network to counteract the fundamental mode of resonance of the upper frequency pressure unit.

Frequency response. The range extends from 30 to 25,000 Hz. and is sensibly flat. The low frequency performance is governed by the acoustical impedance presented to the cabinet by the listening room; there is a slight fall off of low frequencies when the cabinet is radiating into a sphere as in an anechoic room. There is no bass fall off when the unit is radiating into a hemisphere, that is, when standing on a solid floor. The bass response rises if the cabinet is placed on a solid floor near a wall, that is, radiating into 1/4 of a sphere; it rises considerably if it is placed in a corner of a room, radiating into 1/8 sphere.

This cabinet was designed by F.H. Brittain and B.J. Webb.

PUSH - PULL STEREOPHONIC MONITOR LOUDSPEAKER

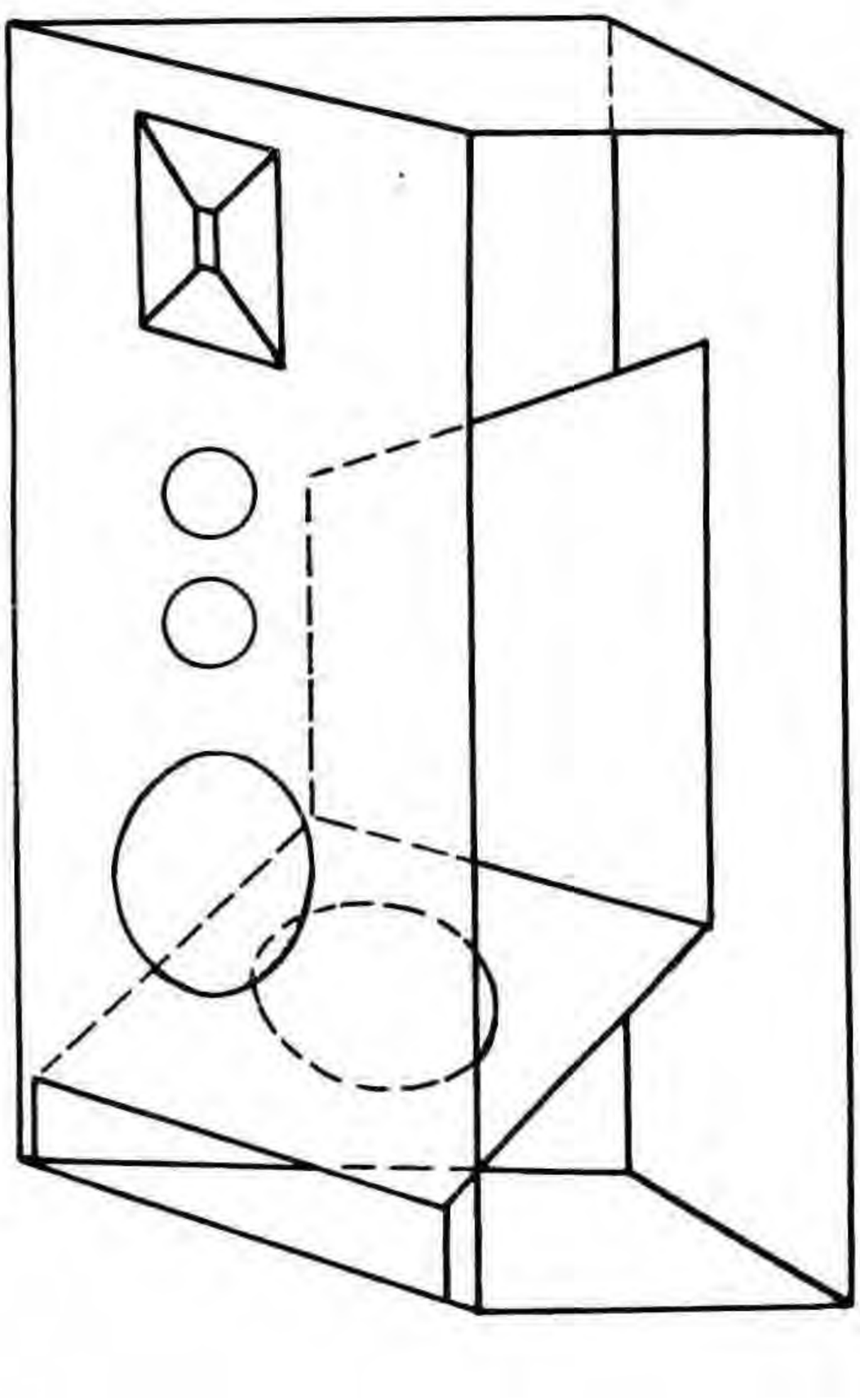

O21

FOURTH INTERNATIONAL CONGRESS ON ACOUSTICS
COPENHAGEN 21.-28. AUGUST 1962

Calculations of Finite-Amplitude Distortion.

Bill D. Cook, Research Assistant, Physics Department, Michigan State University, East Lansing, Michigan, U.S.A.

Abstract: The distortion of plane finite amplitude sound waves in a dissipative, non-dispersive medium can be calculated by an iterative process of allowing the wave to distort and then correcting for the absorption. Results of such calculations are presented.

In the last few years, there has been considerable interest in the problem of finite-amplitude sound waves in dissipative media, primarily, because of the excess absorption of these waves. Most theoretical attempts to calculate finite-amplitude distortion and, consequently, the absorption have not been entirely successful. The chief difficulty with these theoretical attempts, which are usually based on equations approximating the exact differential equations, is that the range of reliability usually extends only up to the neighborhood of the discontinuity distance as given by the dissipationless theory. However, from the phenomenological aspects of the problem, a simple model can be formulated from which solutions for greater distances can be calculated. In this paper, an outline of this model is given and some of the more interesting conclusions are noted.

This model basically consists of applying distortion and absorption mechanisms in an iterative manner. This model is based on two fundamental processes which describe the distortion and absorption mechanisms independently. The mechanism for the distortion is described by a change in phase velocity directly proportional to the particle velocity. This may be written as

$$c = c_o + [(B/2A) + 1]\, u \qquad (1)$$

where c_o is the velocity of sound waves of infinitesimal amplitude and u is the instantaneous particle velocity. The terms A and B, which are constants for a given medium and a given temperature, are defined by the equation of state relating the instantaneous pressure p and density ρ in the following equation:

$$p = p_o + A\left[\frac{\rho-\rho_o}{\rho_o}\right] + (B/2)\left[\frac{\rho-\rho_o}{\rho_o}\right]^2 \qquad (2)$$

where the zero subscripts refer to the undisturbed medium. For this model it is assumed that only this linear change in phase velocity causes the wave to distort. This distortion is produced as points on the wave having larger values of particle velocity tend to overtake points of lesser values. (see Fig. 1).

The absorption mechanism is described by assuming that the rate of absorption may be obtained by calculating the absorption of each harmonic independently according to the amount of the harmonic present and to the square of the frequency of the harmonic. This assumes that the absorption mechanisms are linear. With these two mechanisms, the procedure for the calculation of finite-amplitude distortion is the following: assume an initial waveform f(x) which may be described by a set of Fourier coefficients b_n; allow the wave to distort while propagating a small distance, producing the function $f_1(x)$ described by the coefficients $b_{n,1}$; correcting

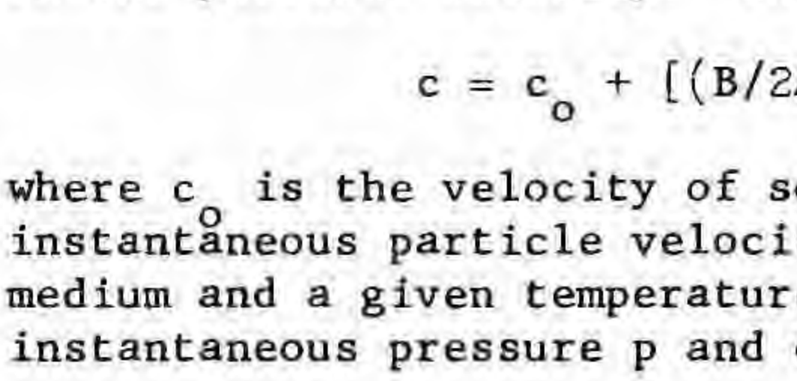

Figure 1.

coefficients for absorption; and then allowing these coefficients to describe the new waveform and continuing this process in an iterative manner. By assuming that the waveshape does not become multiple valued because of the absorption, one may calculate by this continuing process the shape of the wave at all distances. Although the generation and absorption of harmonics are treated independently in each interval, the end result contains the interaction between these mechanisms.

A model somewhat based on the same aspects outlined here was used by Fox and Wallace(1) in their attempt of calculating absorption coefficients for finite-amplitude waves. They graphically analysed the waveforms to obtain the Fourier coefficients. However, it is possible to use a parametric integration method for calculating the distortion process which allows the problem to be easily adapted to high speed computation. If the function $f(x)$ is known analytically, the function $f_1(\theta)$ may be obtained by introducing $x = \theta + k\, f(\theta)$ into $f(x)$. The term $kf(\theta)$ introduces the distortion mechanism required by Eq. 1. The quantity k represents the distance the wave has propagated in the interval in terms of the fractional distance to the discontinuity distance L for an initially sinusoidal wave. Introduction of the parameter θ allows the coefficients $b_{n,1}$ to be calculated from

$$b_{n,1} = \frac{2}{\pi} \int_o^{\pi} \left\{ f(\theta) \sin [n\theta + nk\, f(\theta)] \right\} [1 + k\, f'(\theta)]\, d\theta \qquad (3)$$

The discontinuity distance L represents the distance which initially sinusoidal waveform travels in a dissipationless medium before becoming multiple valued. At this distance, the wavefront has an infinite slope, however, the peak has moved only the distance of one radian with respect to the zero points of the wave. The distance L is given by

$$L = c_o^2 \left\{ 2[(B/2A) + 1]\, U_1(0)\, \pi f \right\}^{-1} \qquad (4)$$

where f is the frequency of the wave and $U_1(0)$ is the maximum particle velocity of the initial sinusoidal wave. For this model, this distance L is sufficient to describe the distortion mechanisms and, consequently, is an important parameter in describing the results.

The absorption coefficient α_o of a wave of infinitesimal amplitude with the frequency of the fundamental component completely describes the absorption mechanism; hence, it is another important parameter for this model. Each harmonic is absorbed essentially exponentially for each interval in each iteration. The property of heat-conducting, viscous media having an absorption coefficient dependent on the square of the frequency is also taken into account.

Using the model previously described, calculations were made using a high speed electronic computer. To accurately retain the shape of the waveform, as many as sixteen harmonics were computed. The value of k, the length of each iteration was taken to be 0.05, one twentieth of the discontinuity distance. The results are presented in terms of the dimensionless product $\alpha_o L$ which adequately describes both distortion and absorption mechanisms. This parameter $\alpha_o L$ is related to the inverse of the Reynolds number.

This model is not expected to be valid for extremely intense sound waves which may produce periodic shock fronts but rather for sound waves of moderate amplitudes travelling in a fairly absorbing medium. The results presented are within these limitations.

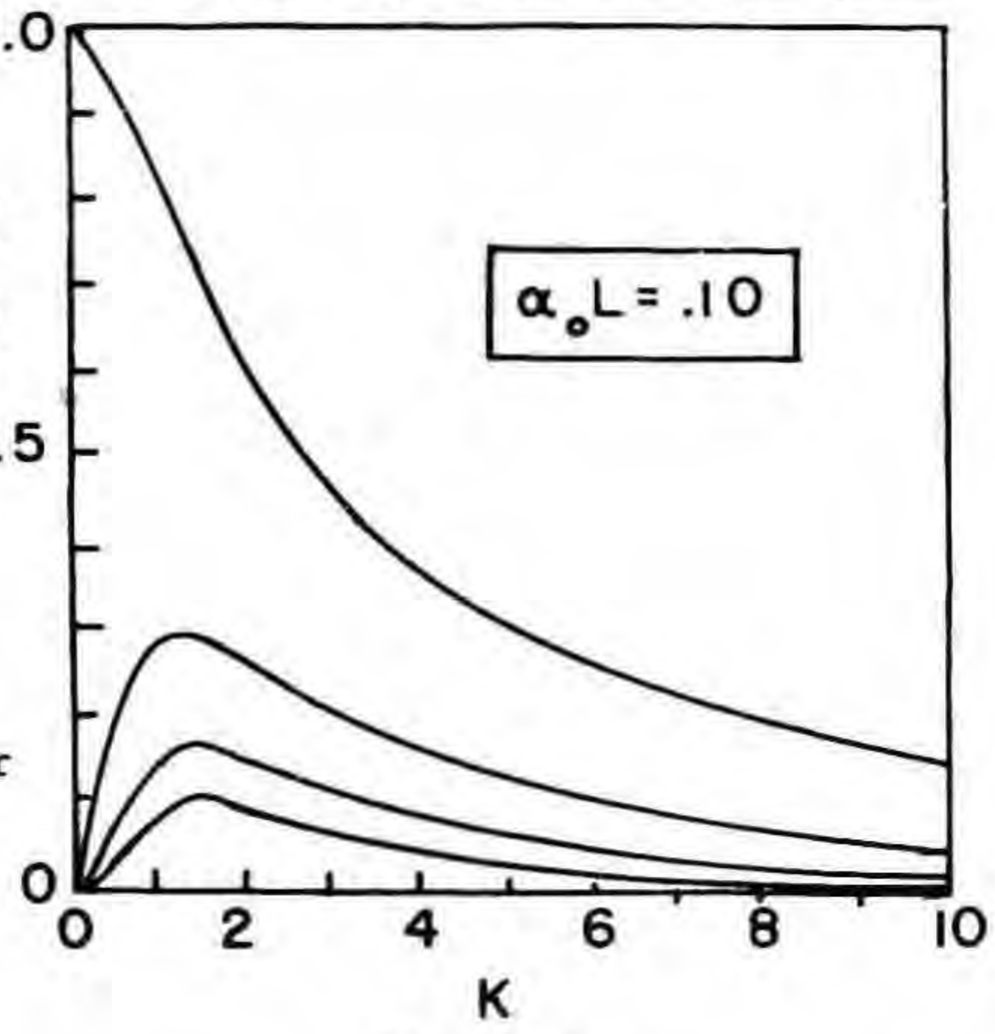

Figure 2.

Figure 3.

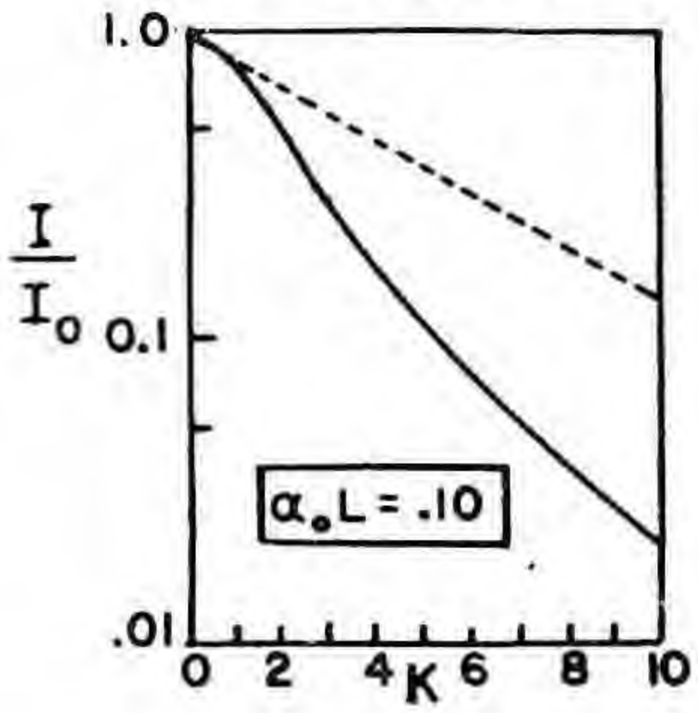

Figure 4.

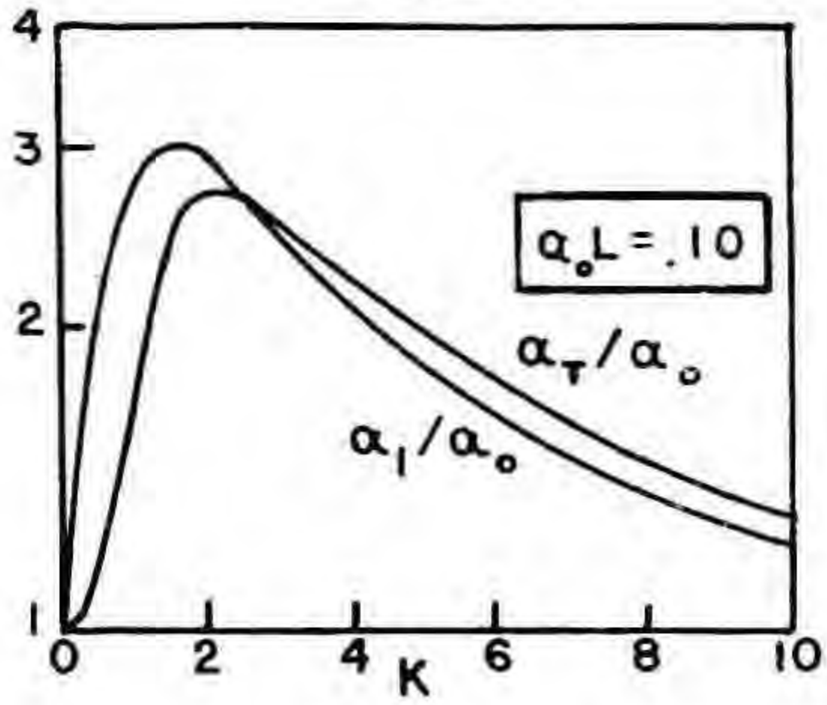

Figure 2 shows typical results from calculations made from this model. The amplitude of the particle velocity $U_n(K)$ of the harmonics are normalized to the amplitude $U_1(0)$ of the initial sinusoidal wave. The value of $\alpha_o L$ equals 0.10 for these curves. The abscissa, capital K, measures the distance the wave travels in units of the discontinuity distance. It is to be particularly noted that these calculations extend to 10 times the discontinuity distance. For these calculations, the amplitudes of the higher harmonics have their peak in the region where K is between 1 and 2.

Figure 3 shows the effect of the nonlinear propagation on the dissipation of the sound intensity calculated from the previous curves. As expected, there is a large difference between the exponential decay (dashed line) and the decay predicted by this model (solid line). The predicted greater absorption is, of course, caused by the higher rate of absorption of the generated harmonics. To describe this higher rate of absorption, one may define a finite amplitude absorption coefficient as

$$\alpha_T = -\frac{1}{2I}\frac{dI}{dx} \tag{5}$$

This coefficient describes the rate at which the energy of the total wave is being dissipated at any given distance. One may similarly define a coefficient α_1 for the energy carried by the fundamental component as

$$\alpha_1 = -\frac{d(U_1^2)}{2U_1^2\,dx} \tag{6}$$

The absorption coefficient α_1 measures the rate of loss of energy from the fundamental component alone while α_T measures that from the total wave.

Figure 4 shows these coefficients (normalized to α_o) for the parameter $\alpha_o L = 0.10$. It is important to note that the absorption coefficient α_1 for the fundamental frequency differs from the total absorption coefficient α_T for most values of K. It can be concluded that the total absorption coefficient can not be always obtained by measurements of the fundamental component only. The differences between α_1 and α_T can be very large at small distances where the energy carried by the fundamental is being lost by both distortion and absorption, while the energy of the total wave is being lost only by absorption.

As the results depend on the parameter $\alpha_o L$, it is interesting to investigate the dissipation of the intensity as a function of this parameter. Figure 5 shows a semi-logarithmic plot of the

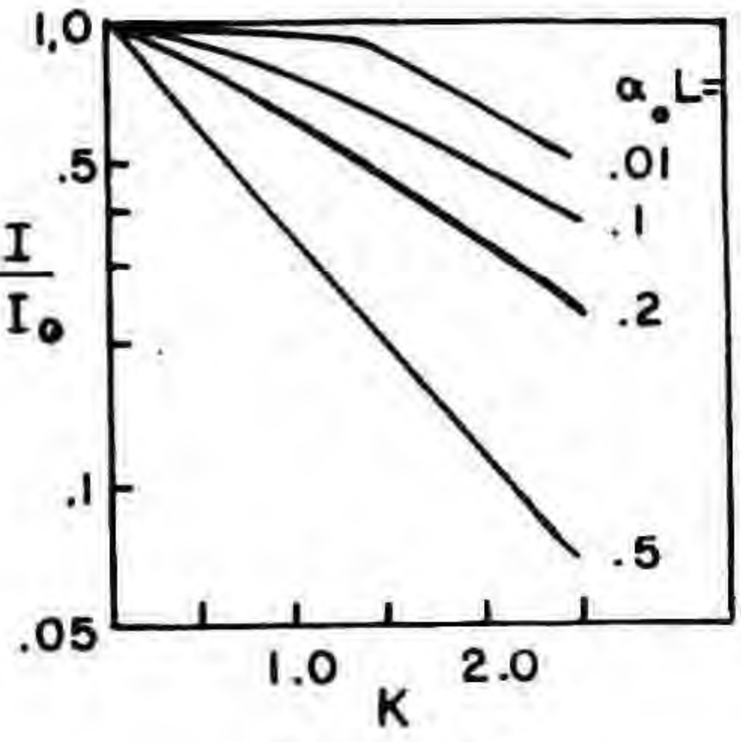

Figure 5.

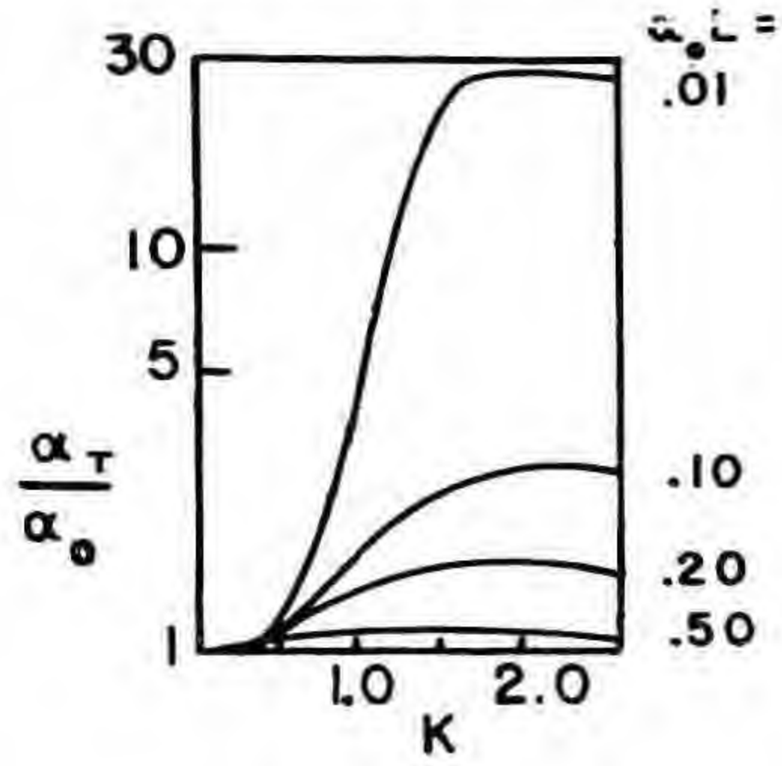

Figure 6.

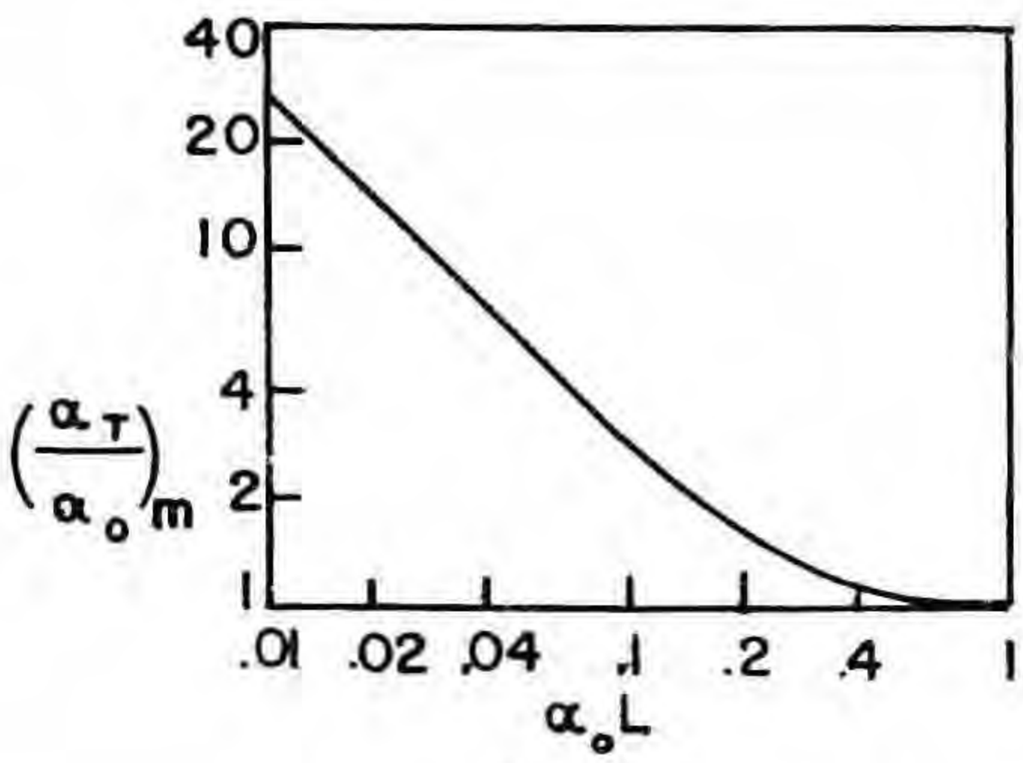

Figure 7.

intensity for different values of $\alpha_o L$. For large values of $\alpha_o L(>0.5)$, where the absorption is large or where the nonlinear effects are small, the decay is nearly exponential as the lower curve in Figure 5 is almost a straight line. In these cases, the wave is absorbed so fast that the nonlinear effects do not become appreciable. Hence, there is little or no excess absorption. For smaller values of $\alpha_o L$, the wave becomes appreciably distorted and the excess absorption becomes noticeable. The upper-most curve of Figure 5 shows that the excess absorption becomes prominent after the wave has propagated to the vicinity of the discontinuity distance.

The differential absorption coefficient α_T gives a more detailed view of the rate of absorption. Figure 6 shows the absorption coefficients corresponding to the curves in Figure 5. For the smaller values of $\alpha_o L$, the absorption coefficients have their maxima in the vicinity of K = 1.6 L. This corresponds to the situation that the peak of the initial wave move $\pi/2$ with respect to the zero points of the wave. Physically, the movement of this peak is limited to this range as the particles cannot move through each other.

In Figure 7 the maximum values obtained by the absorption coefficient are plotted as a function of $\alpha_o L$. For values of large $\alpha_o L(>1)$, the finite amplitude distortion is completely negligible. For small values of $\alpha_o L$, i.e., large nonlinear effects, the maximum absorption becomes inversely proportional to the parameter $\alpha_o L$. In other words, at large sound pressures, the maximum absorption coefficient is directly proportional to the initial sound pressure. The nature of the curve in Figure 7 agrees somewhat with the theoretical results as outlined in the review paper of Zarembo and Krasil'nikov (2).

Although this model approach is an over simplification of the problem of finite-amplitude distortion, the results obtained from it are beneficial in understanding some of the properties of finite-amplitude distortion. At present there is not a sufficient amount of experimental data to check the range of validity of the results obtained using this model. (This work was supported by the Office of Naval Research, U.S. Navy and the U.S. Army Research Office (Durham)).

References.

1. F. E. Fox and W. A. Wallace, J. Acoust. Soc. Am. 26, 994-1006 (1954).
2. E. K. Zarembo and V. A. Krasil'nikov, Soviet Physics- Uspekhi 2, 580-599 (1959).

P21

FOURTH INTERNATIONAL CONGRESS ON ACOUSTICS
COPENHAGEN 21.-28. AUGUST 1962

The Effect of Cuts in Damping Tapes

G.G. Parfitt, Physics Department, Imperial College,
London, S.W.7, England

Introduction:

For many years it has been a growing practice to apply layers of damping material to metal structures such as automobile and aircraft bodies to absorb vibrational energy. A more recent development is the use of damping tape, which consists of a metal tape or foil coated with a damped, adhesive compound by which it is attached to the metal panel. The first analysis of the behaviour of the three-layer sandwich so formed was made by Kerwin[1] and his co-workers in the U.S.A. He showed in particular that the damping introduced by the tape was substantial only in a limited frequency range determined by the relative dimensions and elastic constants of the three layers (see fig 2 for $L = \infty$). It was observed experimentally by D. Lambeth and the author[2] that in an actual tape the damping tended to be less frequency-dependent than was predicted, and this was found to be partially due to wrinkling of the foil or 'backing'. The effect was emphasised if the backing was not merely wrinkled but cut through at intervals. The current paper presents a theory of the effect of such cutting.

This theory is based on the analysis of Kerwin[1], and adopts the same assumptions, in particular that the thickness of the layers is small compared with all wavelengths concerned, and that the central layer is not too heavily damped and is relatively elastic compared with the other two. When the composite bar is bent with curvature $\partial\alpha/\partial x$ (fig 1), the central layer in general undergoes shear through an angle ψ as well as bending. Kerwin showed that α and ψ are connected by the relation

$$\frac{\partial^2\psi}{\partial x^2} - \left[\frac{G_2^*}{E_3 H_2 H_3}\right]\psi = \frac{H_{30}}{H_2}\frac{\partial^2\alpha}{\partial x^2} \qquad \text{.....(1)}$$

The notation is such that E_j, H_j and H_{jo} represent for the jth layer

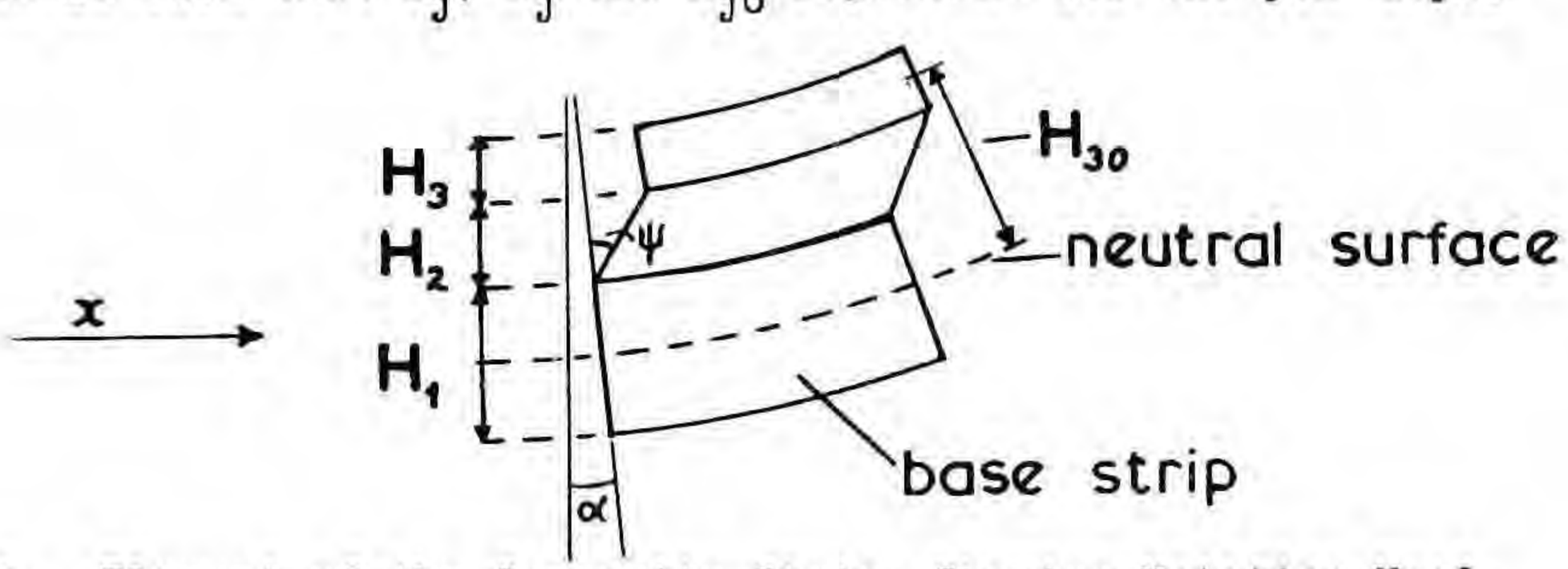

Fig. 1. Element of the Composite Strip, Showing Notation Used.

(j = 1 for the base strip) the Young's Modulus, the thickness and the distance of its central plane from the neutral surface of bending respectively. $G_2^* = G_2(1+i\beta)$ is the complex shear modulus of the damping layer. If the strip remains flat (α=0), but a tangential force is applied to the foil layer at its end, x=0, then equation (1) has the solution

$$\psi = \psi_{x=0} \exp(-x/D)$$

if the difference between G_2^* and its real part G_2 is neglected (i.e. the damping is small), where

$$D^2 = \frac{E_3 H_2 H_3}{G_2} \qquad \ldots\ldots\ldots\ldots(2)$$

D is thus a measure of the "diffusion length", i.e. the distance over which the shear introduced at x=0 penetrates or diffuses along the damping layer. D is independent of the properties of the base strip.

The Divided Tape

We consider now the solution of equation (1) for the case of progressive sinusoidal bending waves in the strip, assumed to be of infinite extent and to be covered with a damping tape cut across so as to divide it into sections of length L.

The aim of the present analysis is simply to bring out the physical mechanism involved, and so to minimise algebraic complication it will be assumed that the damping tape is sufficiently thin that the strain configuration of the base strip is essentially unchanged by its presence. Thus the motion of the panel can be represented as

$$\alpha = A \exp(i(\omega t - px)) \qquad \ldots\ldots\ldots\ldots(3)$$

where $2\pi/p$ is the wavelength λ of bending waves in the panel.

Equation (1) can now be solved by conventional methods, giving as the solution for the typical section of strip 0<x<L

$$\psi = \frac{AH_{30}p^2D^2\exp(i\omega t)}{H_2(1+p^2D^2)} \left[\exp(-ipx) + \frac{\{\exp(i(p-d)L)-1\}\exp(dx) + \{\exp(i(p+d)L)+1\}\exp(-dx)}{ipD\{\exp(i(p-d)L) - \exp(i(p+d)L)\}} \right] \ldots(4)$$

which produces zero tension in the backing layer at the positions x=0 and x=L of the cuts. Here d is written for 1/D for convenience.

The elastic energy stored per unit volume of the central layer is $\frac{1}{2}|G_2^*| \cdot |\psi|^2$ if certain terms involving extensions of the layer are neglected. These can be shown to be of secondary importance in the cases of interest provided that D is large compared with the thickness H_2. The energy dissipated per cycle per unit volume is then $\pi\beta G_2 |\psi|^2$. The total energy stored in the system, under the assumptions made, lies mainly in the base strip, and has a peak value of

$\frac{1}{24} E_1 H_1^2 \left|\frac{d\alpha}{dx}\right|^2$ per unit volume. If these two latter quantities are integrated over a length L of the composite strip the ratio of the results is 2π times the effective damping coefficient of the strip η_e. Calculation of this quantity from equations (3) and (4), assuming again that D^2 may be supposed purely real, leads to the expression

$$\eta_e = 12 \frac{\beta G_2}{E_1} \cdot \frac{D^2 H_{30}^2}{H_2 H_1^3} \cdot \frac{g}{(1+g)^2} [\theta] \qquad \ldots\ldots\ldots\ldots(5)$$

where $\theta = 1 + \frac{g(g-3)}{(g+1)} \left[\frac{\cosh L/D - \cos pL}{(L/D) \sinh L/D} \right] + g \left[\frac{1 - \cos pl \cosh L/D}{\sinh^2 L/D} \right]$ ...(6)

and $g = 1/p^2D^2 = (\lambda/2\pi D)^2$ .....(7)

g is the quantity called by Kerwin the "shear parameter": it is proportional to the square of the bending wavelength on the strip and hence inversely proportional to frequency.

Discussion

The effects of cutting the tape are contained in the function θ. When L is infinite, i.e. no cuts are made, θ becomes unity, and equation (5) reduces to the quantity outside the square bracket, which is the value given by Kerwin. Fig 2 shows the frequency-dependent part of equation (5), viz $g\theta/(1+g)^2$, plotted as a function of frequency (actually the parameter $1/g$ or $(2\pi D/\lambda)^2$.

For L infinite, the damping curve shows a symmetrical peak centred at the frequency where the bending wavelength is equal to $2\pi D$. With cuts at intervals L, the curve reaches a constant value for frequencies below that at which $L \sim \lambda$: the point $L = \lambda/4$ is marked by a vertical bar on each curve. The magnitude of this constant value is greatest for a particular value of L given by

$$L = 3.28D \qquad \ldots\ldots\ldots\ldots(8)$$

With this optimum value of L the tape gives a virtually constant damping at all frequencies up to a certain critical value, and this constant damping is similar in magnitude to that which is otherwise obtainable only in the immediate neighbourhood of this critical frequency. Thus a substantial practical advantage can be obtained at no extra cost in weight or materials. The optimum cut spacing 3.28D is a property of the damping tape only, and so can be specified by its manufacturer independently of its application. It provides a rational figure for the width of a tape, which could then be applied to a panel normal to the plane of bending.

The physical mechanism underlying this behaviour is readily understood. Analysis of the equations for an uncut tape shows that for $g \gg 1$ (low frequencies) the composite strip bends as a single unit, so that there is little shear in the central layer and hence little damping (there is of course a small damping due to extension of the layer and represented by energy terms neglected here). Conversely, for $g \ll 1$, there is substantial shear but only a small fraction of the total elastic energy is stored in the central layer where it can be dissipated. Solely in the transitional region $g \sim 1$ is the resultant damping substantial.

Now if a single cut is made in a tape working in the low-frequency or pure-bending range, the edges of the cut will open and close under vibration and intense shears in the damping layer may develop over a length of about D on either side of the cut. (This action was suggested independently by D.J. Mead of Southampton University). Shear energy is

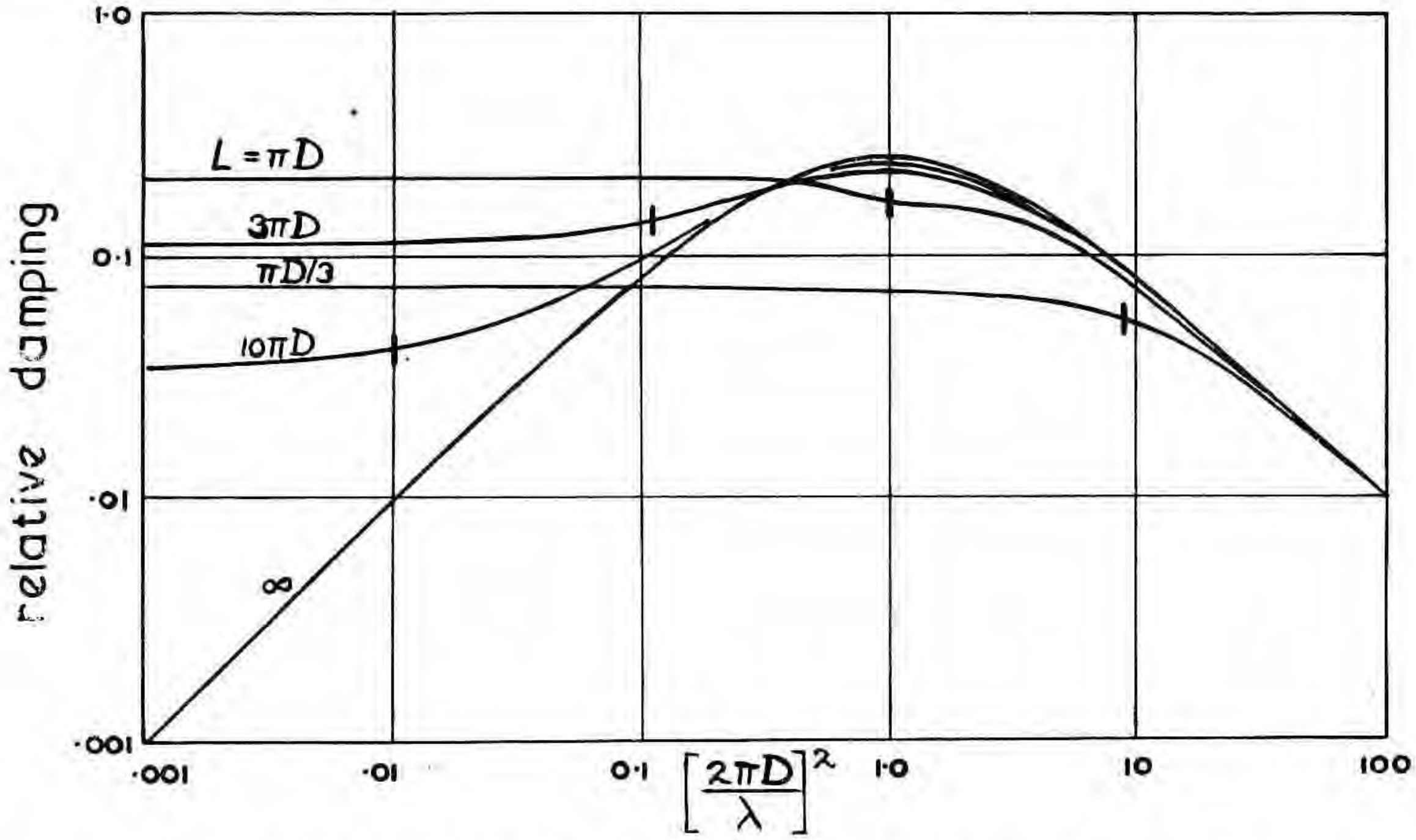

Fig. 2. Damping Produced by a Tape Cut Into Lengths L.

now dissipated here and the amount of it increases with the number of cuts until the diffusion lengths D from neighbouring cuts begin to overlap. When in fact $L \ll D$, the resulting short 'islands' of tape will simply ride to and fro on the base strip with little internal deformation. The existence of an optimum length is thus understandable.

When the tape is working at high frequencies, substantial shear is already present in the central layer, so that cutting tends to relieve it and reduce damping. However if $L > \lambda$ in either regime, any effect of cutting is confined to a small region of about $\lambda/4$ on either side of the cut and the damping does not then depart much in either direction from that of an uncut tape.

References

(1) Kerwin, E.M. J. Acoust. Soc. Amer., 31 952 1959.
(2) Parfitt, G.G. and Lambeth, D. Aeronautical Research Council Report ARC 22,250 (National Physical Laboratory, Teddington, Middlesex).

G22

FOURTH INTERNATIONAL CONGRESS ON ACOUSTICS
COPENHAGEN 21.-28. AUGUST 1962

ACOUSTICAL DESCRIPTION OF SYLLABIC NUCLEI:

DATA DERIVED BY AUTOMATIC ANALYSIS PROCEDURES*

A. S. House, A. P. Paul, K. N. Stevens and Jane B. Arnold,
Research Laboratory of Electronics, Massachusetts Institute of Technology, Cambridge, Mass., U. S. A.

One method for reducing the speech wave to a specification in terms of the time-varying vocal-tract resonances has made use of a procedure called analysis by synthesis.[1] In general, the method involves the comparison of sampled speech spectra with spectra that are synthesized within the analyzer according to rules based on an acoustical theory of speech production.[2] The analysis of each input spectrum results in a set of parameters that describe the synthesized spectrum providing the best match. In the procedure to be discussed here, these parameters specify the locations of the poles and zeros of the vocal-tract transfer function.

Figure 1 illustrates the general scheme and also indicates two different modes of operation that have been implemented. All operations are programmed on a digital computer. The input speech has previously been processed by a suitable set of analog filters with rectifiers and smoothing circuits, and stored in digital form in the computer. Time samples are taken every 8.3 msec, frequency is sampled at 36 points over a 7-kcps range, and amplitude is specified to within 1 db. The box in Fig. 1 labeled 'spectrum generator' accepts at its input the locations of one or more poles and/or zeros in the complex-frequency plane and computes a spectrum; the box labeled 'comparator' compares this internally computed spectrum with sampled input spectra taken from temporary storage. The general idea in the analysis process is to adjust the position and number of poles and/or zeros until a best match is obtained with the spectrum under analysis. In the case of vowel analysis, it is in general necessary to specify only poles, whose locations must be described in terms of frequency and bandwidth values. Such poles represent, of course, the vowel formants.

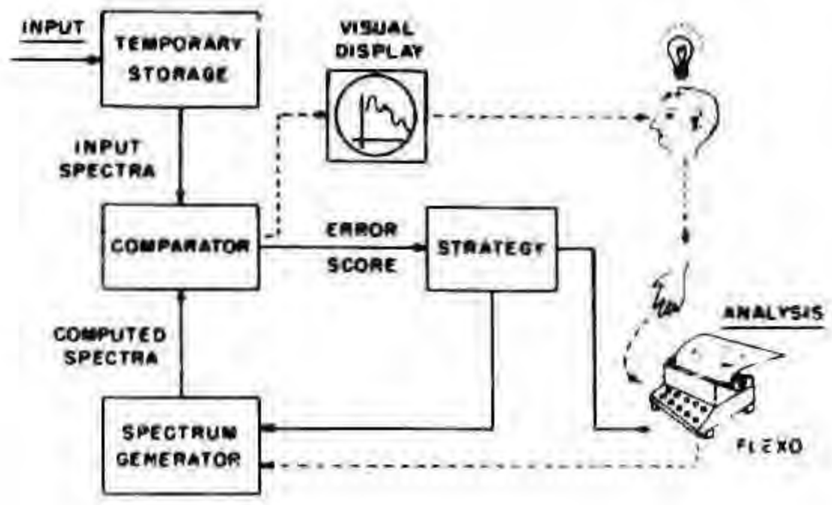

Fig. 1. Paradigm of the analysis-by-synthesis reduction scheme. The control strategy can be carried out automatically or by an experimenter, as shown.

As the figure indicates, convergence toward the best match can be achieved in either a manual mode--epitomized by the human head and hand in the loop--or automatically through an internally stored strategy. Of particular interest is the output provided by an automatic strategy designed to analyze vowel sounds in a manner similar to a sophisticated manual method. This paper will (1) outline the

main features of the automatic strategy, (2) demonstrate the validity of the output of this automatic strategy by comparing it to data obtained through manual procedures, and (3) introduce a scheme for describing and organizing vowel data obtained by the automatic procedure.

The speech materials that provide the vowels for analysis consist of bisyllabic nonsense utterances of three adult male speakers of American English. The first syllable of each word is an unstressed carrier; the second syllable is stressed and has the general form consonant-vowel-consonant with the consonants representing the same phoneme. These materials include eight common vowels of American English in 15 consonant contexts.

The automatic analysis scheme incorporates two different strategies. When the analyzer is confronted by the first spectral sample in a vowel, its strategy is to first find approximate values for the locations of the formant frequencies (within 200-300 cps). In this mode of operation the approximate locations of the formant frequencies are found by assembling comparison spectra from a small set of stored curves. When approximate values of the formant frequencies are available, or have been found, the strategy that controls the way in which the frequency and bandwidth of a particular pole is moved from one trial to the next makes use of the detailed shape of the error curve that describes the difference between the speech spectrum and the internally generated spectrum. When the second strategy is in effect, there are eight parameters which can be varied by the automatic program: the frequency and bandwidth of F1, F2 and F3, the frequency of F4, and the value of a real-axis zero, corresponding to a 'tilt' or glottal spectrum correction curve.

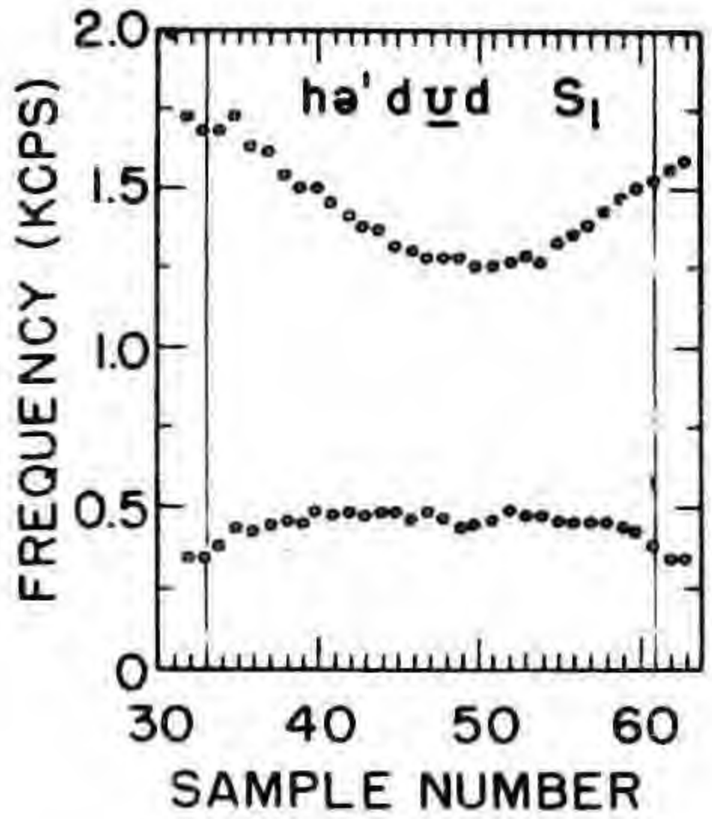

Fig. 2. Example of data on the frequencies of F1 and F2 obtained by the automatic analysis program. The light lines at samples 33 and 61 represent vowel boundaries obtained from visual examination of spectrograms.

In order to demonstrate the validity of the output of the automatic analysis program, three consecutive spectral samples located medially in the stressed vowel of each utterance were processed by both the automatic and the manual procedure. The manual procedure was used by two experimenters familiar with the constraints imposed on speech spectra by articulation processes. These experimenters based their strategy on a visual estimation of the over-all spectral match and on various numerical estimates of mismatch provided by the computer. When the average values of the three consecutive samples derived by the two methods of analysis were compared, 75% of the time the automatic program was found to provide values of F1 and F2 within $\pm$ 20 cps of those obtained manually; in 90% of the cases this difference was within $\pm$ 35 cps. Results such as these suggest strongly that the automatic procedure leads to valid data on formant locations.

Typical data obtained from the automatic matching procedure are shown in Fig. 2. The plotted points represent the frequencies of the first two formants as found by the automatic procedure for spectral samples at 8.3-msec intervals throughout the vowel. Instants of initiation and termination of voicing, as estimated from spectrograms of the utterances, are indicated by vertical lines.

The remainder of this paper and all of a companion paper[3] will be concerned with a discussion of procedures for describing data such as those of Fig. 2, and will consider the interpretations of such data. The curves depicting F_1 and F_2 as a function of time for the symmetrical consonant environments used in this study usually have a form similar to that shown in this figure. Each formant begins at some value that is presumably dependent upon the vocal-tract configuration for the initial consonant. The curve then proceeds toward a maximum or minimum value associated with some target configuration, and finally tends toward a value determined by the vocal-tract configuration for the final consonant.

Examination of data from a number of vowels has suggested that the plotted points for each formant of each vowel might be approximated by two parabolic segments, one for the initial portion of the vowel and the other for the final portion. The rationale for selecting parabolic curves to approximate formant motions is not based on quantitative theoretical considerations relating to the dynamics of articulation. The curves seem to provide reasonable fits to the data, however, and are of a form that facilitates interpretation of the data in articulatory terms. Each parabolic segment is of the form

$$F_i = a_i (t - T_i)^2 + F_{i0}$$

where F_i represents formant frequency, t is time, and a_i, T_i and F_{i0} are parameters that are selected to give a best fit; ($i = 1$ for the first formant and $i = 2$ for the second formant). The parameter F_{i0} represents the maximum or minimum value reached by the formant, and T_i indicates the point in time at which this maximum or minimum value occurs. The parameter a_i is a measure of the curvature of the formant, and can be positive or negative. Figure 3 shows the parabolic curves that give good fits to the data points plotted in Fig. 2. The parabolic curves used in Fig. 3 were selected from a set of curves similar to those shown in Fig. 4. The parameter values on these curves arbitrarily will be

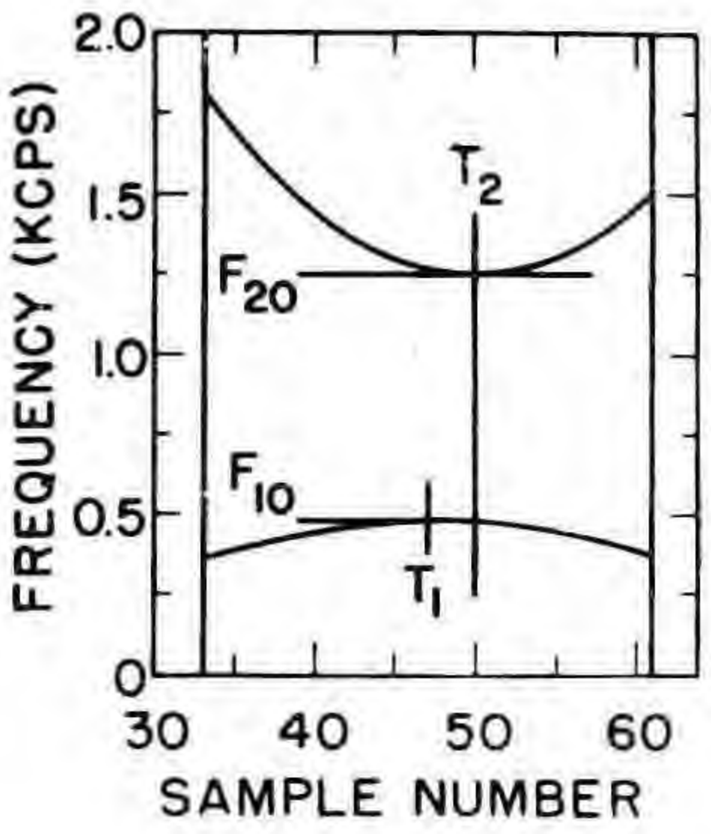

Fig. 3. Approximations to the data in Fig. 2 obtained by fitting parabolic curves to the plotted points within the vowel boundaries. The two curves are completely described by the parameters F_{10}, F_{20}, T_1, and T_2, together with the 'curvature values' for the parabolas.

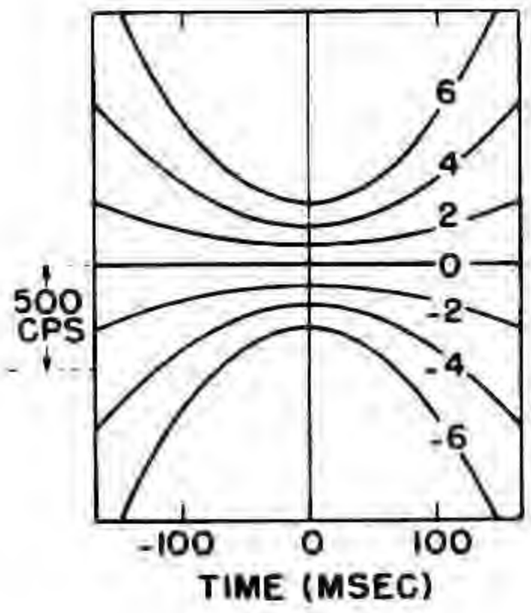

Fig. 4. Examples of parabolic curves used to specify vowel formant data. The parameter is the so-called 'curvature value.'

called 'curvature values.'

The automatic computational methods and the data reduction procedures outlined in this paper appear to provide simple yet accurate descriptions of time-varying articulatory events throughout the vocalic portions of speech. The procedures have been used to analyze an ensemble of speech materials; some of these results are reported in a companion paper.[3]

* This work was supported in part by the U. S. Army Signal Corps, the Air Force Office of Scientific Research, and the Office of Naval Research; in part by the National Science Foundation under Grant G-10800; and in part by the U. S. Air Force Cambridge Research Laboratories under Contract No. AF 19(604)-6102.

1. C. G. Bell, et. al., Reduction of speech spectra by analysis-by-synthesis techniques, J. Acoust. Soc. Am. 33, 1725-1736 (1961).

2. G. Fant, Acoustic Theory of Speech Production. Mouton: 's-Gravenhage, 1960.

3. A. S. House, K. N. Stevens and A. P. Paul, Acoustical description of syllabic nuclei: An interpretation in terms of a dynamic model of articulation. These Proceedings.

H22

FOURTH INTERNATIONAL CONGRESS ON ACOUSTICS
COPENHAGEN 21.-28. AUGUST 1962

ON THE CONTRIBUTION OF SYNCHRONIZATION PATTERNS TO SEMANTIC MEANING

Ernest Colton

Human languages are learned rather than innate characteristics. This implies that the receivers and speakers of such languages must be capable of learning them. Such learning occurs under an enormous heterogeneity of conditions and for a wide range in the intrinsic or innate characteristics of the various receivers and senders. Gestalt theory implies that the structure of a receiver must be such as to normally "perceive" (receive) something as being either "it" or "not it" -- e.g. either an apple or not. [1] Part of an initial attempt to develop a "Prinzipientheorie" of meaning dynamics from these postulates is here briefly outlined, followed by a brief, expository, crude "ad hoc" description and "justification" of one of its results and its implications.

The above postulates imply that there exists a property -- significance. Equality of significance is a necessary and sufficient condition for meaning equilibrium between two or more brain systems or subsystems in direct or indirect communicative contact. (E.g. if two communicating persons had reached fully identical "conclusions" about some topic further discussion between them about this topic would no longer alter the significance of the topic for them -- unless, of course, their meaning equilibrium would be disturbed by introducing additional factors related to the topic into the system.)

The mathematical definition of a property is that it must have a perfect differential. For convenience the differential of significance will here be referred to as "understanding". It is a function of other variables, e.g. perceptability, brain capacity, memory accessibility. All points in significance space are not necessarily accessible to every point; e.g. after studying a puzzle or an equation one might eventually "see" it in a new "light" and then can no longer return to how one "saw" it earlier; or one can "reach" its solution only along a certain path and not along another. In other words, understanding must be expressed in the form of a Pfaffian expression. By Carathéodory's theorem any change in significance must admit of an integrating denominator or multiplier in the expression for understanding. A particular multiplier (constant) "helps" to define a Gestalt -- a one parameter hypersurface whose differential is zero, i.e. a hypersurface of constant significance; all points on such a surface are accessible to each other. The family of all such hypersurfaces can be regarded as a function. Its differential will here be referred to as semantic meaning. Lexical meaning will here be defined as the product of an integrating denominator times the derivative of its associated Gestalt with respect to the total semantic meaning of the system. Total semantic meaning is thus an extensive property which corresponds to the intensive property lexical meaning. Lexical meaning and semantic meaning are conjugate properties. Since there are processes in meaning dynamics in which significance changes (increases) irreversibly it follows that usually understanding is equal to or greater than the conjugate product of lexical meaning times semantic meaning.

This formulation bears great similarity to that of thermodynamics -- except for the inequality direction. This is not so surprising. Thermodynamics is the one branch of classical physics which deals with some system properties which are not directly measurable. Although some of the mathematical apparatus developed in thermodynamics and quantum statistical mechanics (the "atomistic" approach) can be readily plagiarized this will not be done here. The only result which will be discussed here is that a concept or variable can often only be explained in terms of the product (antonym) rather than the sum (synonym) of other variables. This does not say that the summing of values is useless or that only algebraic manipulations occur. For example, taking the vectorial sum of the forces acting on a body is certainly a valid operation. What is emphasized here is that the concept of force is defined as the product of mass times acceleration and has no value without it. This does not imply that the integration of a force field along some curve has no value or that static or electromagnetic forces cannot exist.

Some readers may prefer to regard the above conclusions that any concept, observation, or word should be regarded as a complementary product of other variables as an assumption. Such a conclusion or assumption is at first rather surprising. The remainder of this article is a hermeneutical attempt to indicate some of its value in a primitive fashion.

The assumption that language is learned suggests that one can investigate how language is learned and how it develops. It implies that human language develops and is used directly and indirectly by groups of individuals or societies rather than by an individuum in isolation. It can be shown that a group of individuals linked through an efficient, flexible communication system will often have a survival advantage over individuals not linked in such a fashion. (Ashby's [2] mechanisms are as applicable to groups as to individuals.) Such a communication system "acts" primarily to synchronize the actions of the parts of the group with that of the whole. Thus one can formulate a model in which primitive language "acts to synchronize" the behavior of complex computers each of which is connected to its own perception and motion capabilities and arranged for asynchronous or parallel operation with the others.

It is clear that such a language must "provide" a means to "control" the behavior of such an abstracted primitive-group. The individual computer in such a group (a primitive hunting party for instance) can sense its own positions and actions relative to an environment which includes the other computers of the group. This implies environment linked feedbacks and controls. An individual computer can be instructed to observe or to "look for" something (which might involve an "automatic" response to do something). Multiple environment connected feedbacks are active. To keep the group "acting" as a unit it is necessary that each of its units "performs" properly relative to that of the others; e.g. if one unit slows down or speeds up relative to the others it must be "told" to "correct" this. This implies that most words must have antonyms or words of opposite meaning. Compare with the necessity of both positive and negative potentials for controlling servo-mechanisms (error signal detection as ratio of reference signal).

In such primitive computer ensembles the environmental feedbacks keep the servo-motor controls -- (social) words -- from running wild. For example, if one of the individuals is told to move "down" the "natural" environment would let him "know" if he had "overshot" his mark too much, even if the "social" environment did not. Such an "overshoot" results in an "up" command, and so forth till the "desired" group synchronization tolerance of an action is achieved. Thus, as a first step, one might regard a word and its antonym as a set of complementary quantities. Their product defines a third word or variable; e.g. "left" times "right" defines a "sideward" direction (and this product is recognized (or learned) before the conjugate antonym-synonym set is differentiated).

In the previous example an overshoot in either "down" or "up" is "correctable" by the other which is always implicitly available. This appears to have resulted in an adequate language for such groups. In actual societies the individual units and subunits (humans) are, of course, linked in complex, shifting series-parallel arrays. The environmental controls may not be "adequate" to "correct" overshoots and synchronization errors in such ensembles. Before this matter can be elucidated further this argument must be interrupted for two digressions.

The above crude "ad hoc" descriptions may indicated how language develops in a generalized, abstract society which is in turn defined by the language it develops. (Brevity requirements might have made the description somewhat "vitalistic". Analysis will indicate that this is not so; it implies realizable experiments.) A society "outlives" and replaces its component parts just as an individual its component cells and these their component atoms. The part "replacement" must "fit into" the society similar to the way a new cell "fits into" an organ. It is largely "shaped" by its society. It usually acquires the language developed by its subsociety. Thus it is instructive to inquire how such a language is acquired by a new unit.

The "mother method" is, of course, well known and some schemes [3] have been proposed to relate it to the structure of the infant brain. Here another facet needs to be emphasized. The parent usually "desires" the infant to "do" something -- be it merely to "look" at some object which is held in front of him or given him, to "say" or "repeat" something, to "pay attention" to something, or to "perform" some other (simple) act. This can be considered in terms of parent-child "computer" connections. The parent "desires" a certain amount of synchronization of the child's behavior with his own actions relative to the common environment. (Much, if not all, of the "listening" by the child is, of course, "accidental" and independent of any parental "desires"; however, the synchronization effect is almost the same as if it had been "purposeful". -- "accidental" goal or equilibrium seeking even if the equilibrium is not "willfully" disturbed by a parent.) Similarly, an infant's sounds tend to synchronize the parent's behavior with its own (physiological and psychological) requirements of the "moment".

In general, any semantically meaningful communication (oral, written, etc.) implies at least a certain amount of synchronization between two or more individuals. It is always "desired" that the receiver computer "observes" or "does" something which is synchronized relative to an environment which includes the "sender" at least implicitly -- not necessarily overtly through its available motor responses but at least internally through "associated equivalent mental patterns". (The author, like most persons in the field, has his own notions about the "workings of the brain". These agree substantially with those of Hebb [4] and Rosenblatt [5] but include the concept of "time clocks". The brain is considered as a collection of computer subunits which are in changeable, complex parallel and series connection with each other and which tend to be specialized in structural location aggregates which may have their own "master clocks". The dominant operation of the moment of such a subunit aggregate is defined as "awareness". Consciousness is defined as the dominant operation of the moment of the total unit -- involving at least partial series operation of the subunit aggregates which are connected with each other through some central "switchboard" intimately associated with biochemical "master" control clocks and gates. ("Emotional words" tend to "activate" these chemical controls.) A detailed knowledge of the receiver structure is not necessary for the present purposes. The receiver must be capable of associating a variety of symbols with their environmental patterns. Thus very general requirements such as those discussed by Ashby [2] are the only ones needed here.

These imply that any mental concept, picture, or symbol must be the product of perceivable patterns (possibilities) times associable patterns (possibilities; including past associations). The actually perceived patterns are complementarily determined by "learning" [2,4]. The environment is sufficiently constant so that individuals exposed only to very roughly similar social and physical environments tend to form such mental concepts, pictures, and symbols wich have enough similarity among individuals that for most conditions a more or less "agreed average" or lexical meaning can be assigned to their word labels. It is convenient to define "understanding" as the particular mental pattern associated with a word under a particular condition for a particular sender or receiver; semantic meaning can then be defined as that multiplier which will let lexical meaning equal understanding.

It is thus clear that effective communication requires that the sending and receiving brains must have been exposed to quite similar environments. It is not feasible to describe colors or sunsets to a congenitally blind person or to one reared in darkness. Similarly, one cannot describe music or noise to a congenitally deaf person. (It is, of course, possible to describe the properties of sound in terms of those of light and vice versa, but it is likely that

such descriptions would be of very limited value to a person who lacks the background to "interpret" them properly.) The more similar the environments of the communicators have been the more predictable their message understanding will be and the fewer the symbols necessary to convey the message. Hence, it is obvious that effective communication must imply at least a minimum amount of synchronization of the communicators's mental patterns. But since these patterns can usually only be similar to the extent they have been shaped by the same environmental conditions (environmental to the "brains", not the bodies) it is self-evident that one can regard semantic meaning as defined above as a measure of the synchronizability of the lexical meaning passing between the brains of particular listener-talker systems at a particular time under particular conditions.

Any (effective) communication must thus always involve some synchronization. Any talk to which one at least partially listens "forces" one's brain through some synchronization with the talker's. The more synchronized the communicating brains are, the more (mutual) understanding they can convey during any fixed time interval (at a constant rate of lexical meaning). (At the extreme case of complete synchronization no "useful" lexical meaning could be conveyed; this would correspond to infinite semantic meaning times zero lexical meaning -- no communication would be necessary or could result in a change in significance, i.e. it would be "meaningless".) Conversely, the less synchronized the communicating brains are, the more lexical meaning must be communicated to achieve a certain amount of (mutual) understanding. (Again, at the extreme case of no possibility of any "useful" synchronization no communication could result in a change in (meaningful) significance -- this would correspond to infinite lexical meaning times zero semantic meaning.) This implies also that messages rich in semantic meaning, e.g. poems, songs, clichés, have relatively little specific lexical meaning -- their significance involves broad, generalized, large-group-aggregate synchronizations which cannot have very specific lexical meaning. It also implies that a particular brain will have great difficulty in attempting to comprehend material of very little semantic meaning (as defined above) to it, e.g. technical or legal descriptions or directions to the layman (if written for the layman these would tend to become very lengthy as the author tries to be "explicit" and "exact" -- but unless he can build up necessary synchronization (which is seldom attempted) the result will be quite unreadable). Communication in these cases implies very specific synchronization and this synchronization is not yet established. (A good example of the effort required to introduce new lexical concepts into a "society" which was not synchronized for it has been given by Abbott [6]; communication involving the six-dimensional physical universe [7] is still not generally feasible.) These are the reasons why what an instructor regards as a good textbook may not be regarded as such by a student -- till he has "digested" it. Unfortunately, it also implies that this article will require considerable effort on part of the reader if it is to be understood by him.

Since understanding and lexical and semantic meanings as defined herein may import on a "first look" basis a certain amount of vagueness, a few remarks about "exact" scientific knowledge may be helpful at this point. Perhaps the most familiar quantitative scientific law is that "force equals mass times acceleration". (At least one "feels" that this is a very precise "law" which one thoroughly "understands" -- probably because one learned it at an early age, before one's thymus gland degenerated.) This law was, of course, originally stated in terms of the derivative of momentum with respect to time. (When the great Newton introduced his laws of motion he had to introduce dynamic concepts such as force, momentum, mass and define them in terms of the then familiar kinematic (geometric "plus" "time") concepts. He defined momentum as the product of the mass of a body times its velocity -- his first law of motion states that this product is constant in the absence of acting forces. He defined the mass of a body (or a gas) as the product of its volume times its density. Density was "familiar" in his time because of the work of the alchemists. Today density could be defined by the general (ideal or universal) gas law as pressure divided by temperature times a constant, where the constant is necessary because the units have been chosen inappropriately [7]. But pressure, an intensive property, is the canonical conjugate of volume, an extensive property, just as temperature, an intensive property, is the canonical conjugate of entropy, an extensive property. Thus even in modern elementary physics -- with which one is familiar as a clear and precise science -- one finds that at an introductory level one can thus far only define many "derived" (or abstract) concepts only in terms of complementary products.) But the interest here is not in how this law was introduced nor in its limitations but in how it is presently taught in most (American) schools. One notes that the units defined by this equation must be such that no constant is needed. To measure force in a mechanical system one must measure a mass and its acceleration (the principle of inertial frame of reference equivalence is here implicitly assumed). But to measure a mass one must measure its acceleration under the influence of a known force, and acceleration can only be observed if one has a mass (body) to indicate it. The concept of product quantities is quite basic to elementary quantitative science. One can use it with at least some amount of confidence to describe many phenomena with considerable accuracy.

Discovering the appropriate complementary product quantities can be difficult. It was not "a priori" obvious that the complement of distance is time [7]. The human brain must have a separate semantic meaning for each word. But the complementarity of word concepts is a function of the environment. Although human knowledge and adjustment to the physical environment is inadequate, this environment is relatively more constant than man's modern social environment. Thus his adjustment to the physical world is at present more adequate than his adaptation to the modern social world. The latter changes relative to him. This implies that the synchronization must change. This means that words change their semantic meaning, new words come into use -- and over a few generations the lexical meaning of some words changes also. Ashby's [2] mechanisms indicate that over a time period of many generations the structure (grammar, orthography, etc.) of a language would tend to become simpler after its original development.

Subgroups have to develop some specific synchronization before they can function as identifiable units. Thus each family has a few particular words and symbols (gestures) which it uses in a special way or synchronization sense. Age subgroups in modern society develop or adapt some words to express their "synchronization with" or "belonging to" their particular groups. This is especially noticeable among modern teenagers and their subgroups. These synchronization symbols are used extensively on very many occasions as the individuals go through the learning

process of adapting to stay properly synchronized with their various groups and learn to identify who belongs to what group under what circumstances, i.e. what synchronization symbol corresponds to what and when. Human society has, of course, very many subgroups. Under some circumstances a particular subgroup will "choose" to have minimum communicational contacts with outside groups, at other times the same subgroup may "choose" to have so many communication links with one or more other groups that it becomes so synchronized with these that it can no longer be directly identifiable as a unit. Ashby's [2] description of the advantages and disadvantages of richly and poorly joined systems is fully applicable to human society in this group sense.

Much of the specialized technical jargon (and ritual) "acts" mainly as a "generalized synchronization symbol" to block outside "non-belonging" check signals. This is particularly clear in the institutionalized forms of the spiritual, military, and legal "functions". (The great Veblen [8] and Sumner [9] have described these processes and how institutions "shape" (synchronize) their members -- although from different perspectives.) Modern society "has found" special schools and special training particularly effective for imparting sufficient synchronization or indoctrination. However, modern mass media of communication "interfere" to some extent with the group isolation adjustments. Some groups thus tend to compete for their basic substance and food, i.e. members. Such competition takes on, in part, the form of a battle of "equivocation" in synchronization symbols. Words symbolizing a person's identification (synchronization) with one group are "craftily" extended and adapted and controverted to other "purposes" [10].

Unfortunately, an adult human has difficulty in relearning or changing the semantic significance of such symbols. Thus, like Hoffer's True Believer [11], he fails to compensate for changes in the meaning of the generalized "belonging" symbols. The group to which he "belongs" reinforces this process by "appropriate means" [12]. The group fails to develop adequate synchronization symbols for "moving" in the "opposite" direction -- this is similar to a group developing only a symbol for "left" and not for "right", except that these generalized belonging symbols have a far richer semantic impact. The resulting synchronization overshoots become eventually corrected by the group's environment, but this process may "exact" a high price from the group, including its possible destruction and that of its component members. Wiener's [13] truism that "what is used as an element of a machine, is in fact an element in the machine" is particularly applicable in the battles for the minds of mobs.

The large group aggregates have "reached" the (evolutionary) state where they "find" "semantic warfare" adaptive, but this practice has been overdone and the environmental controls will undoubtedly make themselves felt eventually. Language "had barely adapted" to the unavoidable natural meaning equivocation before the "artificial" mass media noise was added. Modern advertising (including its political use) and its results indicate that much work needs to be done in meaning dynamics. Particularly such conjugate variables as "war" and "peace" should be quantitatively investigated and their implications explored. But this is perhaps less urgent as the development of techniques to "save" an individual from his group training, discipline, and conditioned learning. Otherwise a society might well develop which is a cross between those visualized by Orwell (particularly in "1984") and by Huxley (especially in "Brave New World") -- combining the worst features of each.

An implication of this approach is that language research should usually be carried out on groups rather than individuals. Conferences are very convenient groups for some such studies. The haggling, "schooling", inherent slowness, degeneration, etc. of some such groups are very illuminating from a synchronization perspective [14]. Some soldier and some industrial and some commercial groups are also very convenient for synchronization studies [12].

In isolated individuum studies one must be very careful. The theory discussed above indicates that one reaches a limit of accuracy with which an individuum study can be isolated from disturbing factors. Below this limit the effect of the observation or measurement on the individuum introduces unpredictable effects. Fortunately, the environment in which human brains exist is sufficiently uniform so that most presently observed data are not yet "invalidated" by this limit. Individuum studies are, of course, very necessary at present where a single brain is regarded as a "working group" of subunits -- a different limit applies to such experiments.

Finally, it should be noted that this theory should not be confused with Fichte's formulation of thesis, antithesis, and synthesis to which it might bear a superficial resemblance. Semantic implications are, of course, best expressed by a poet. The great word artist and writer Goethe came perhaps closest in anticipating some of the above results:
"... Denn eben wo Begriffe fehlen, Da stellt ein Wort zur rechten Zeit sich ein. Mit Worten lässt sich trefflich streiten, Mit Worten ein System bereiten, An Worte lässt sich trefflich glauben, Von einem Wort lässt sich kein Jota rauben. ... Gewöhnlich glaubt der Mensch, wenn er nur Worte hört, Es müsse sich dabei doch auch was denken lassen. ..."

References

1. F. Allport, *Theories of Perception and the Concept of Structure*, John Wiley, New York, 1955.
2. R. Ashby, *Design for a Brain*, John Wiley, New York, 2nd. ed., 1960.
3. W. Penfield and L. Roberts, *Speech and Brain-Mechanisms*, Princeton Univ. Press, Princeton, N.J., 1959.
4. D. Hebb, *The Organization of Behavior*, John Wiley, New York, 1949.
5. F. Rosenblatt, *The Perceptron*, CAL Report VG-1196-G-1 (1958), PB151247, OTS, U.S. Dept. of Commerce.
6. E. Abbott, *Flatland*, Dover, New York, 1952.
7. E. Colton, *Bull. Am. Phys. Soc.*, 6 (1961) 432 (uncorrected abstract).
8. M. Lerner, ed., *Veblen*, Viking, New York, 1948.
9. W. Sumner, *Folkways*, Dover, New York, 1959.
10. E. Walker and R. Heyns, *Anatomy for Conformity*, Prentice-Hall Englewood Cliffs, N.J., 1962.
11. E. Hoffer, *The True Believer*, Mentor, New York, 1958.
12. E. Colton, unpublished notes.
13. N. Wiener, *The human use of human beings*, Doubleday Anchor, Garden City, N.Y., 2nd. ed., 1954.
14. E. Colton, *J. Acoust. Soc. Am.*, 33 (1961) 1656 (abstract).

J22

FOURTH INTERNATIONAL CONGRESS ON ACOUSTICS
COPENHAGEN 21.-28. AUGUST 1962

EXPERIMENTAL DETERMINATION OF THE SOUND VELOCITY IN LIQUID HELIUM AT AND BELOW THE LAMBDA POINT

Kenneth A. Shapiro and Isadore Rudnick, Physics Department,
University of California, Los Angeles 24, California, U.S.A.

The lambda transition in liquid helium below which liquid helium exhibits superfluid properties, is thermodynamically characterized by the fact that the specific heat at constant pressure appears to approach infinity logarithmically on both sides of the transition temperature T_λ, according to the law (1)

$$C_p = 4.55 - 3.00 \log_{10} |T - T_\lambda| + 5.20\,\Delta \quad \text{joules/gm-deg}$$

where $\Delta = 1$ for $T < T_\lambda$ and $\Delta = 0$ for $T > T_\lambda$. The temperature dependence of the zero frequency adiabatic sound velocity can be shown to have a sharp cusp at the lambda point (1), (2). Previous measurements by Chase (3), made at one megacycle, show the existence of a relaxation phenomenon associated with the transition. The resultant attenuation and dispersion very near the lambda point (within approximately 1 millidegree) mask the above-mentioned velocity dependence. A much closer approach to the lambda point can be made at lower frequencies and the purpose of this paper is to describe apparatus and measurements made at 10 kc.

The rationale of the measurements consists of determining the velocity by measuring the frequency of a plane wave mode of a rigid-walled cylindrical resonator. Since ρc for helium is small (3220 cgs), the requirement for rigidity can be easily met. The resonator, complete with heat exchanger fins, was machined out of a single bar of very high purity silver. The high thermal conductivity of the silver ensured temperature homogeneity.

Two identical solid dielectric transducers, of the type shown in Figure 1, one being used as a source and the other as a receiver, terminated each end of the tube. The resultant cylindrical cavity had a diameter of 1.00 cm and a length of 3.57 cm. The stretched diaphragm, G (0.00065 cm thick), lies in the plane of the back plate and is separated from it only by the surface roughness of the back plate.

The source transducer is operated without bias so that the resultant sound field has twice the frequency of the driving voltage. The Q of the system was sufficient to allow changes of velocity of one part in 10,000 to be measured. Figure 2 shows the results of our measurements over a range of 20 millidegrees on either side of the lambda point. Because of the excellent thermal properties of HeII, data below the lambda point can be more reliably obtained than above the lambda point. Also, a closer approach to the lambda point is possible. The crosses are our measurements and the triangles are Chase's data (4). The line is the theoretical result (1), (2), using -100 atm/^{o}K for the slope of the lambda line which gives the best fit. The experimental data were made to fit the curve at 2 millidegrees above T_λ.

Of primary interest is the data close to T_λ, which is shown to good advantage in Figure 3. The theoretical curve is again made to fit the data at $T - T_\lambda =$ 2 millidegrees. It is impossible to fit the data for $T < T_\lambda$ with any reasonable choice for the value of the slope of the lambda line. The value of -100atm per ^{o}K, which produces the best fit for the data above T_λ, is to be compared with the value of -96 atm/^{o}K given by Chase (5). There is no way of fitting the data with Buckingham and Fairbank's value of -130 atm/^{o}K, (1).

It is possible that the discrepancy for $T < T_\lambda$ can be due to the unusual nature of sound propagation in liquid helium II. Compressional waves, or first sound, are non-isentropic waves and therefore will travel with a velocity which differs from the adiabatic velocity. This velocity was first calculated by Tisza (6) and is given by

$$U_I^2 = U_{ad}^2 + \epsilon \frac{U_I^2 \quad U_{II}^2}{U_I^2 - U_{II}^2}$$

where U_I is the first sound velocity, U_{II} is the second sound velocity, U_{ad} is the adiabatic sound velocity, ϵ is the temperature dependent coupling constant and is given by $1 - 1/\gamma$, where γ is the ratio of the specific heats. Calculations indicate this correction is orders of magnitude smaller than the discrepancy.

The diaphragm of the transducer may be selectively permeable to the superfluid component of liquid helium II. If this is true, the response of the transducer will not simply be determined by the pressure in the standing wave. The possibility that this is involved in the observed discrepancy has not been ruled out. Experiments investigating the mode of operation of the transducer are now in progress.

<u>References:</u>

1) M.J. Buckingham and W.M. Fairbank, Progress in Low Temperature Physics, Vol III (Edited by C.J. Gortor) Chap III, North-Holland Publishing Co., Amsterdam, 1961
2) C.E. Chase, Phys. Rev. Letters, 2, 197 (1959).
3) C.E. Chase, Physics of Fluids, 1, 193 (1958).
4) C.E. Chase, Proc. 5th Conf. Int. Low Temp. Phys., Madison, Wisconsin (1951) p. 73.
5) C.E. Chase, E. Maxwell and W.E. Millett, Physica, 27, 1129 (1961).
6) F. London, Superfluids, Vol II (John Wiley and Sons, New York) (1954) pp 83-85.

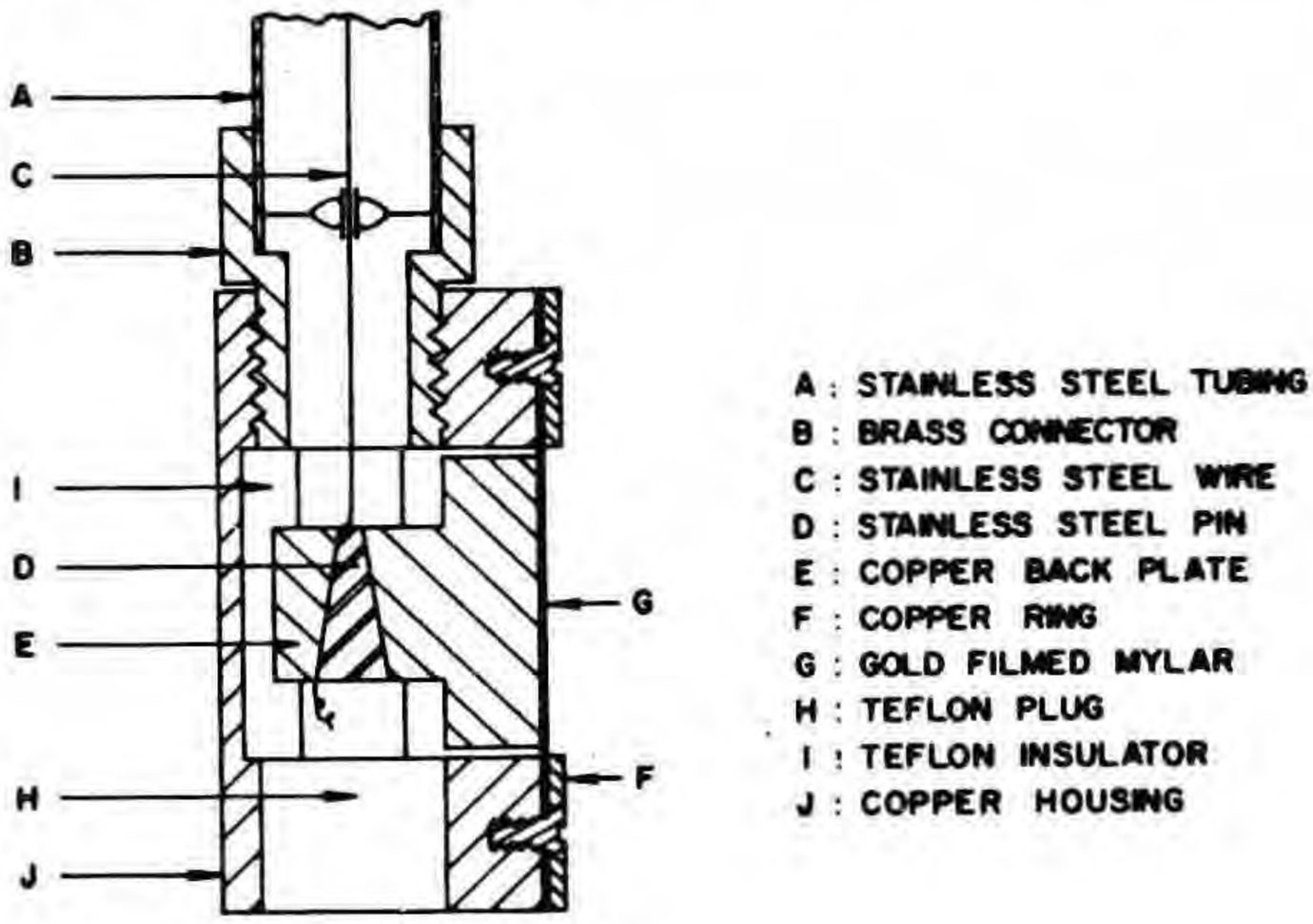

FIGURE 1. CROSS SECTION OF THE MICROPHONE

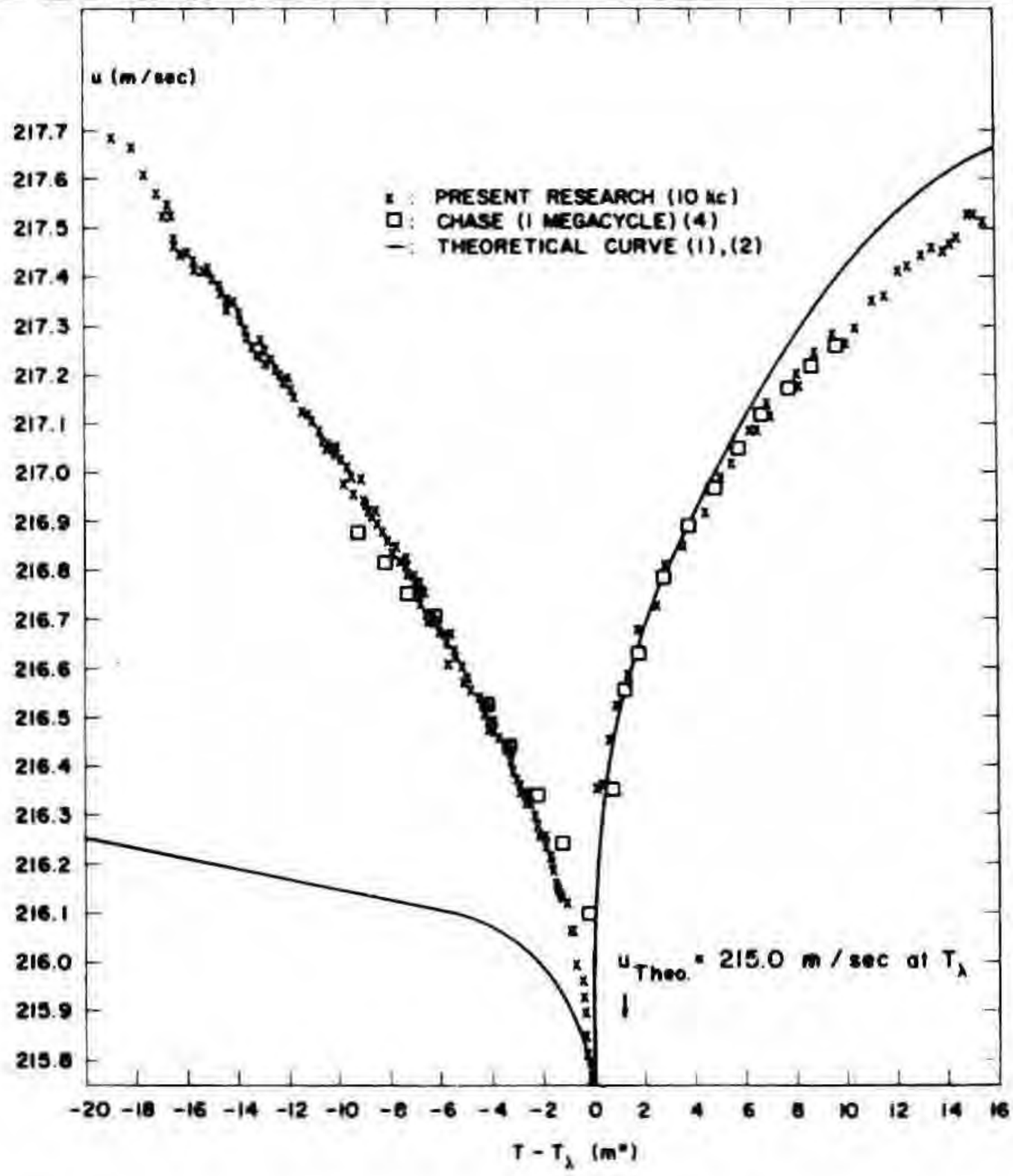

FIGURE 2. VELOCITY OF SOUND VERSUS $T-T_\lambda$.

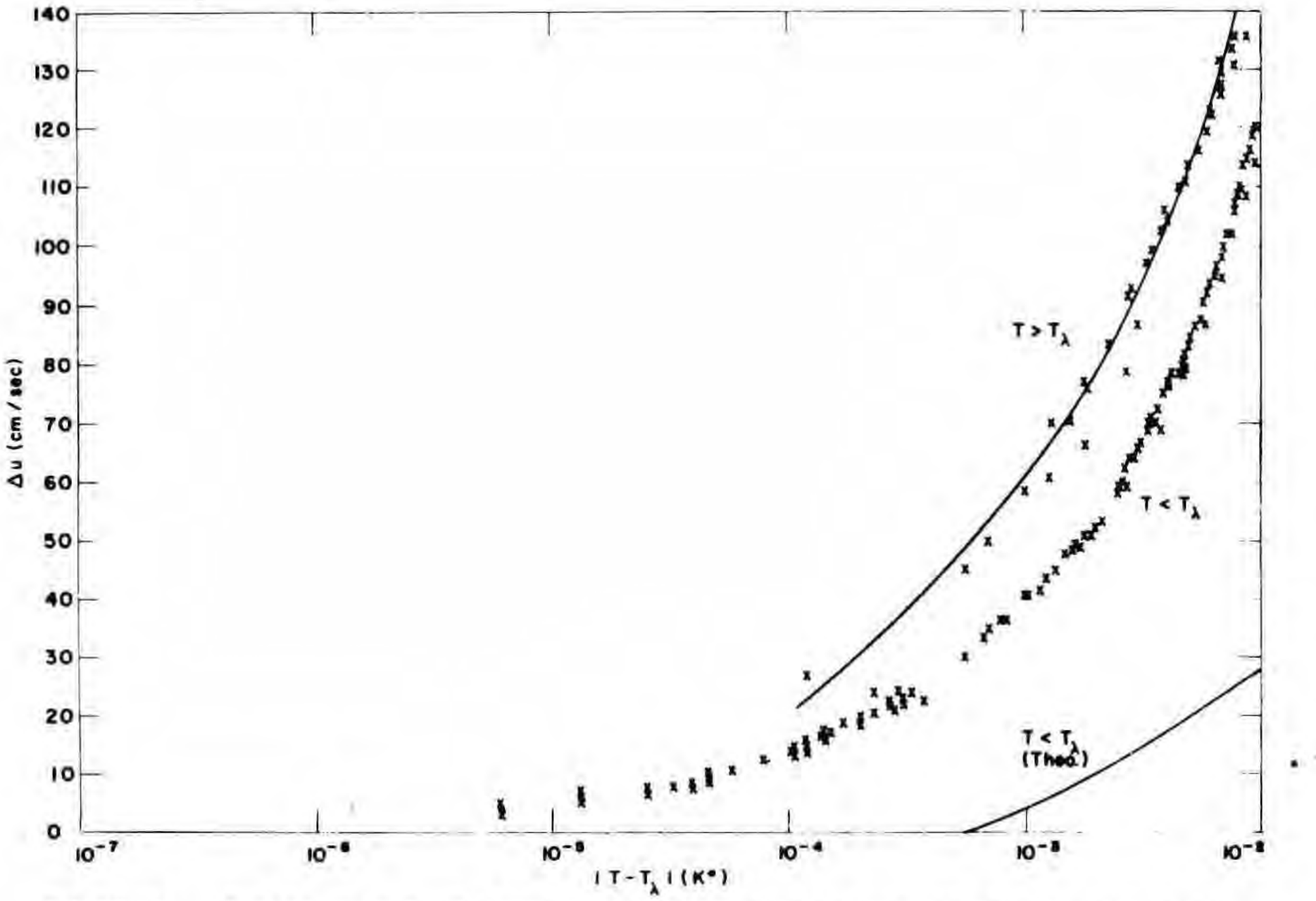

FIGURE 3. CHANGE IN THE VELOCITY OF SOUND FROM ITS VALUE AT THE LAMBDA POINT VERSUS $|T - T_\lambda|$ (AT 10kc)

K22

FOURTH INTERNATIONAL CONGRESS ON ACOUSTICS
COPENHAGEN 21.-28. AUGUST 1962

LOW-POROSITY FERRITES FOR HIGH-INTENSITY ULTRASONIC RADIATORS

C.M. van der Burgt and A.L. Stuijts
Philips Research Laboratories, Kastanjelaan, EINDHOVEN, Netherlands

1. High k_{opt} and low H_{opt} as criterions for high-intensity transducer materials

Piezomagnetic alloys and ceramics used for high-intensity ultrasonic transducer cores exhibit a reasonably high value of the effective piezomagnetic coupling coefficient k, and a reasonably low value of the transducer loss figure $\alpha \approx [\delta_{magn}\ \delta_{mech}]^{\frac{1}{2}}/k$. Here δ_{magn} is the magnetic loss angle as measured at the usual amplitude of the magnetic induction while keeping the core clamped, and δ_{mech} is the mechanical loss angle as measured at the usual amplitude of the mechanical excursion while keeping the coil short-circuited and the "radiating" face free from the usual acoustic load. Since the fractional bandwidth of an electrically tuned transducer equals $k/(1-k^2)^{\frac{1}{2}}$, a high k is desirable not only for acoustical and electrical communication elements, but also for resonant radiators (see below). However, increasing k does not necessarily mean lower α. Keeping δ_{magn} constant, α is even more or less independent of k. Writing $\delta_{mech} = \delta_i + \delta_e$ (i for internal friction, e for external mechanical losses) and neglecting electrical losses in the copper winding one may derive from theoretical and experimental data [1], that for well-sintered ceramic cores the loss angle δ_i very roughly equals $k^2\,\delta_{magn}$, so that:

Electroacoustic efficiency $\eta_{ea} \approx 1-2\alpha \approx 1-2\delta_{magn}\left[1+(\delta_e/\delta_i)_{mech}\right]^{\frac{1}{2}}$.

Since magnetic hysteresis losses decrease with increasing bias, the so-called "optimum" bias (H_{opt}, B_{opt}) yielding a maximum coupling (k_{opt}) is often profitably replaced by a bias somewhat closer to saturation. This requires rather strong fields $H_o \gg H_{opt}$, so that new materials with low values of the coercive and "optimum" fields would be welcomed. Moreover, the reduction of δ_{magn} and δ_{mech} by an $H_o \gg H_{opt}$ has another profitable consequence, viz. a better stability of the electrical and mechanical resonance frequencies f. These frequencies decrease with increasing δ's (increasing power level) roughly in accordance with Rayleigh's hysteresis relations. Denoting the "clamped" permeability by μ and the "short-circuit" modulus of Young by E, the Rayleigh relations are:

$$\frac{\Delta\mu}{\mu} = -2\frac{\Delta f_{elec}}{f_{elec}} = \frac{3\pi}{4}\Delta\delta_{magn}, \quad \cdots \frac{\Delta(1/E)}{1/E} = -2\frac{\Delta f_{mech}}{f_{mech}} = \frac{3\pi}{4}\Delta\delta_{mech}.$$

In the search for new ferrites or essentially improved ferrites having much higher k_{opt} and much lower H_{opt} (i.e., much lower δ_{magn} for the same H_o), the preliminary results are highly promising, as will be shown below.

2. The series of mixed ferrites prepared for the present investigation

Several authors have already described the piezomagnetic behaviour of ferrites that presumably had exactly or nearly the same chemical compositions as those chosen for the present investigation: $(Ni_{1-y-z}\ Cu_yZn_z)_{1-x}Co_xFe_a^{2+}Fe_{2-a}^{3+}O_4$, with $x \leqslant 0.03$. Since a low sintering temperature was used, the ferrous ferrite content a was small and will not be discussed here. Similarly a full account of the technological procedure lies outside the scope of this paper and will be published elsewhere by one of the authors (St). In the above series of mixed ferrites Kikuchi [2] reported a maximum coupling coefficient for roughly y=z=0.2, but Kikuchi applied the same sintering temperature and the same biasing field for all compositions, whereas the Ni-rich ferrites require a higher sintering temperature (to obtain samples with reasonably low porosity) and a stronger

biasing field (to reach optimum coupling). However, a porosity $< 3\%$ has never been reported for Ni-Co ferrites. Cu substitutions [3]) or Zn substitutions were necessary in order to reach a porosity of about 1%. It was decided to try to reduce the porosity to below 0.5% for all compositions. In such a low-porosity quaternary system of Ni-Co-Cu-Zn ferrites the maximum coupling is expected near Ni on the Ni-Co edge or close to that in the Ni-Co-Cu face, because the saturation magnetostriction ε_{sat} sharply decreases with increasing Zn content but is nearly constant for various Cu contents, and because ε_{sat} and k_{opt} satisfy the relation [4] [5]

$$\varepsilon_{sat}^2 \, E/k_{opt}^2 \approx \left[\begin{matrix}\text{Crystal}\\ \text{anisotropy}\end{matrix}\right] + \left[\begin{matrix}\text{Internal stress}\\ \text{anisotropy}\end{matrix}\right] + \left[\begin{matrix}\text{Internal shape anisotropy}\\ \text{of non-spherical pores}\end{matrix}\right].$$

Although the crystal anisotropy can be made to pass through zero at any desired temperature T_o by substituting an appropriate amount of Co, the crystal anisotropy will strongly vary with temperature around T_o. Consequently extremely sharp peaks are expected around T_o in the k_{opt}- vs-T curve, the μ-vs-T curve, etc.

3. Measuring techniques. The exact evaluation of coupling coefficients

Rings with an average diameter D_{av} = 24 mm, a radial width of 4 mm, and an axial height of 4 mm were machined from the solid disks available after the sintering process. Extensional and torsional vibrations were excited by passing an AC current of an appropriate frequency through a toroidal winding (n turns), which did not touch the ring. In the extensional experiment an additional DC current I_o through the toroidal winding supplied the average biasing field $H_o = nI_o/\pi D_{av}$ ...(A/m). In the torsional experiment the axis of the ring was made to coincide with the axis at the centre of an electromagnet. However, the demagnetising field of the ring was much stronger than the internal biasing field and was therefore nearly equal to the external field $H_{external}$ supplied by the magnet, so that the average biasing induction could be derived from: $B_o = H_{external} \times 8\pi \times 10^{-7}$... ($Wb/m^2$). Both the extensional coupling coefficient k_{33} and the torsional coupling coefficient k_{15} were evaluated from the relative distance $\Delta f/f_r = (f_a - f_r)/f_r$ between the so-called antiresonance frequency f_a (at minimum electrical impedance) and the resonance frequency f_r (at maximum electrical impedance). Exact expressions and curves were used, because the widely used approximate relations would yield much too high values of k (see table I and fig.1) and should only be used for evaluating small k's.

4. Preliminary results. Conclusion

Table II and figs. 2-8 display a choice of numerical and graphical data obtained in the preliminary stages of the present investigation. Since in the technological procedure not all of the important factors have been optimized for all of the samples, still higher values of k_{opt} and still lower values of H_{opt} may be obtained in the future. For instance, values of k_{33} between 0.50 and 0.60 are conceivable for low-porosity Ni-Co ferrites with or without a small Cu content. The transition temperature T_o can readily be shifted towards a desired value (sec.2) using the approx. relations $\Delta T_o \approx 5000 \Delta x$ for Ni-Co ferrites and $\Delta T_o \approx 7500 \Delta x$ for Ni-Cu-Co ferrites with Ni/Cu ratio 80/20.

References

1) C.M. van der Burgt, Philips Res.Rep. 8, 91-132, 1953 (Eq. 19 + Fig. 1a).
2) Y. Kikuchi, French Pat. 1, 214, 857, publ. April 12, 1960.
3) C.M. van der Burgt, J. Acoust. Soc. Amer. 28, 1020-1032, 1956, and Electronic Technol. 37, 330-341, 1960.
4) See Eq. 15 of ref. 1.
5) This approx.relation is valid for both extension and torsion.
6) C.M. van der Burgt, Matronics, Philips Techn.Inform.Bull. No.15,273-304, Sept. 1958.
7) Kearfott, Advance Tech.Data Sheet, effective April 15, 1958.

Table I The evaluation of coupling coefficients from the relative distance $\Delta f/f_r = (f_a-f_r)/f_r$ between the resonance and antiresonance frequencies (n = 1, 2, 3 = direction of AC flux; m = 1, 2,..6 = dir.of strain; 3=bias dir.)

	Uniform strain in the resonating sample	Sinusoidal spatial distribution of strain in the resonating sample ($\lambda/2$)
Exact relations ——— in fig. 1	$\frac{(k_{nm})_u^2}{1-(k_{nm})_u^2} = 2\frac{\Delta f}{f_r}\left(1+\frac{1}{2}\frac{\Delta f}{f_r}\right)$	$\frac{(k_{nm})_\sim^2}{1-(k_{nm})_\sim^2} = \frac{\pi}{2}\left(1+\frac{\Delta f}{f_r}\right)\tan\frac{\pi}{2}\frac{\Delta f}{f_r}$
Approx.relations --- in fig. 1	$(k_{nm})_u^2 \approx 2\frac{\Delta f}{f_r}$	$(k_{nm})_\sim^2 \approx \frac{\pi^2}{4}\frac{\Delta f}{f_r}$

Table II Properties of some low-porosity ferrites and commercially available transducer ferrites (Philips Ferroxcube 7A1 and Kearfott "N-51") having the approx.chemical composition $(Ni_{1-y-z}Cu_yZn_z)_{1-x}Co_xFe_a^{2+}Fe_{2-a}^{3+}O_4$.

Name	Approx. Chemical Composition After Sintering 100x %	100y %	100z %	100s %	Specific Mass ρ 10^3 kg/m^3	Fract. poros. 100p %	Satur. Magneto strict. $10^6\varepsilon_{sat}$ --	Curie Temp. T_c °C	Trans ition Temp. T_o °C	Values at T_o: Init. Perm. $/\mu_i$ --	Field Intensity H_c 10^2 A/m	H_{opt}	Max.33-Coupl. $100k_{opt}$ --
7A1 6)	≈2	≈20	0	3-4	5.15-5.30	1-4	-28	540	≈15	≈80	2-4	12-20	25-32
Cu20-Co1.8	1.8	20	0	≤1	5.36	≤0.2	-28	540	18	110	1.3	3.8	45.5
Zn5-Co2.8	2.8	0	5	≤2	5.325	≤0.5	-27	560	22½	130	1.1	2.3	44
N-51 7)	≈2.7	0	0	2-3	5.05-5.15	4-6	≈-29	590	≈25	≈90	1.2	6-7	37-39
Co2.8	2.8	0	0	0.7	5.325	≤0.6	≈-29	590	34½	125	1.8	3.5	49.5

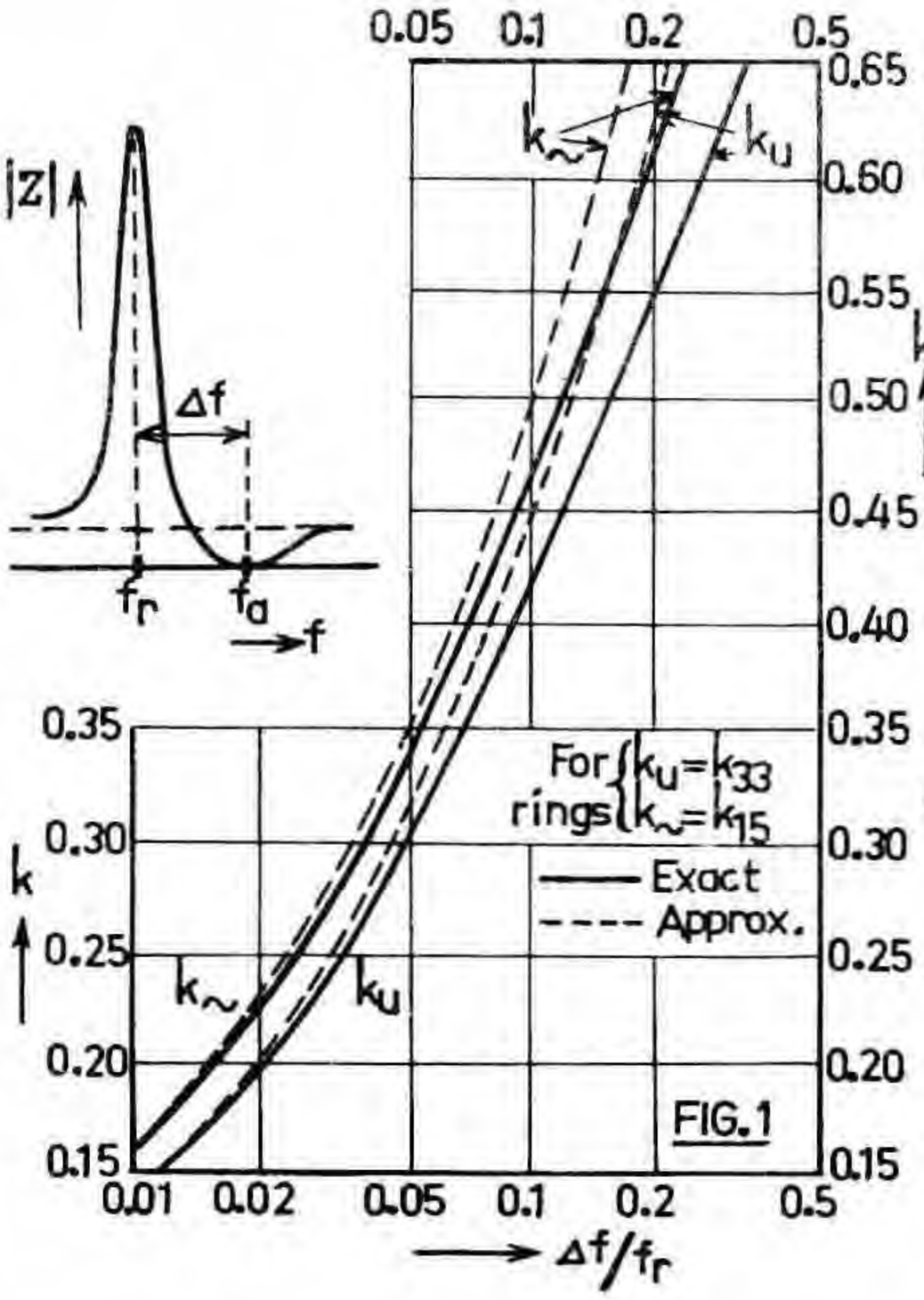

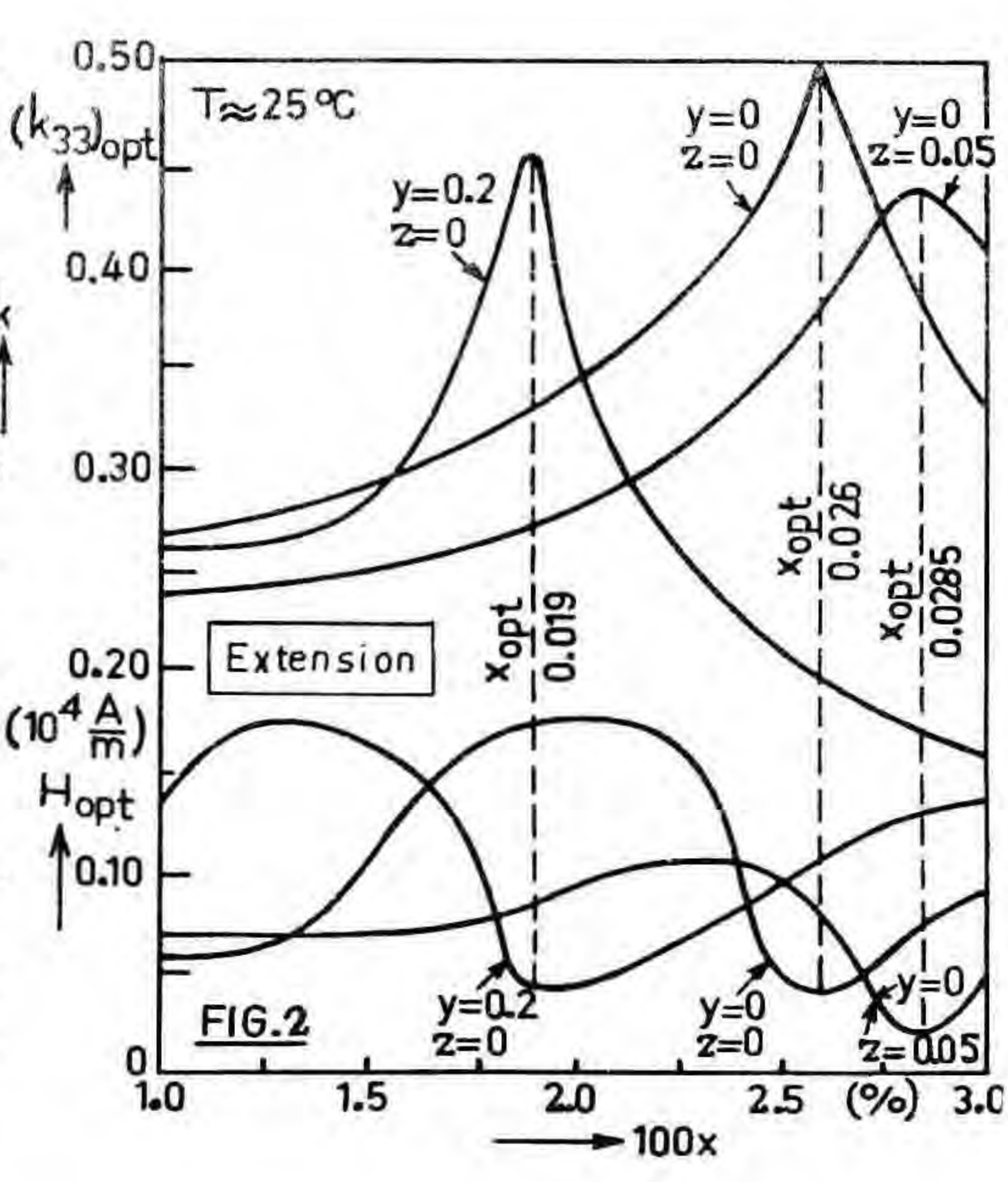

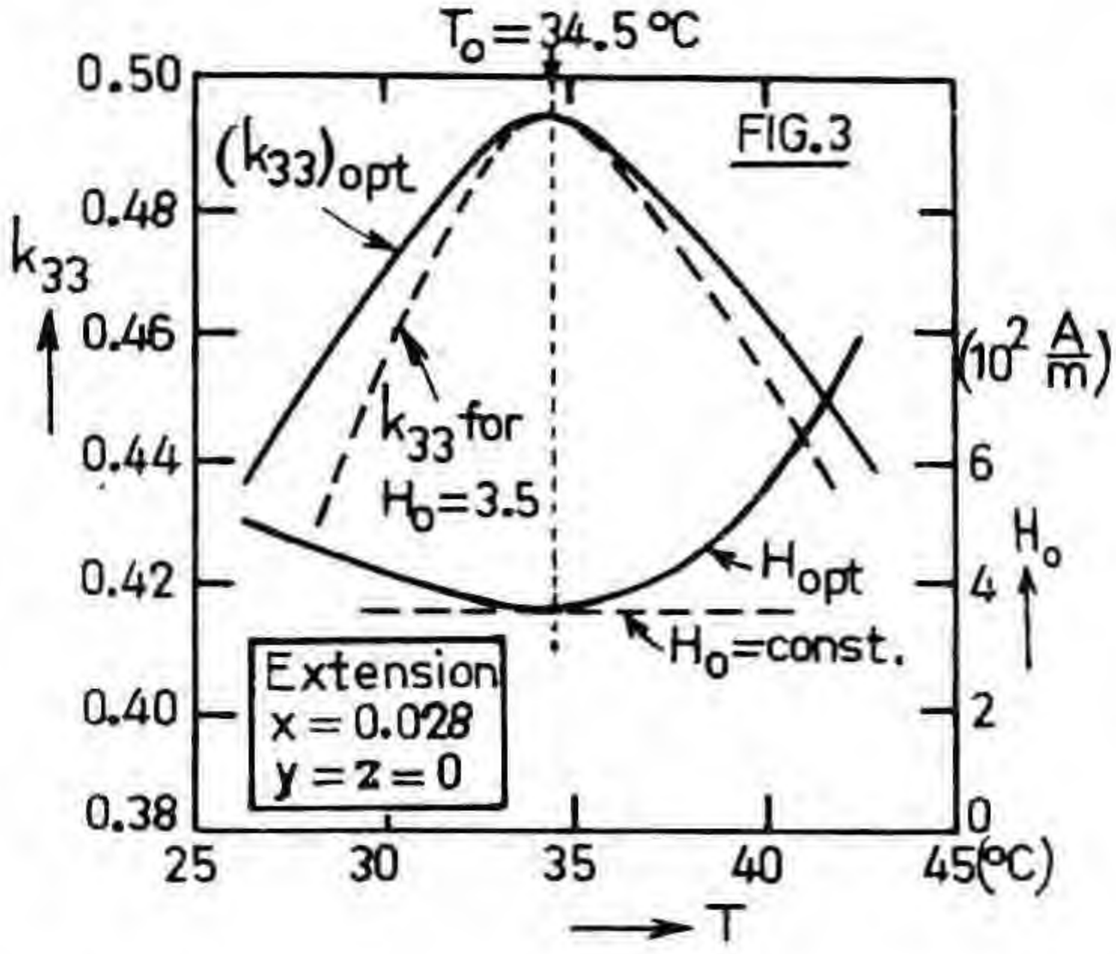

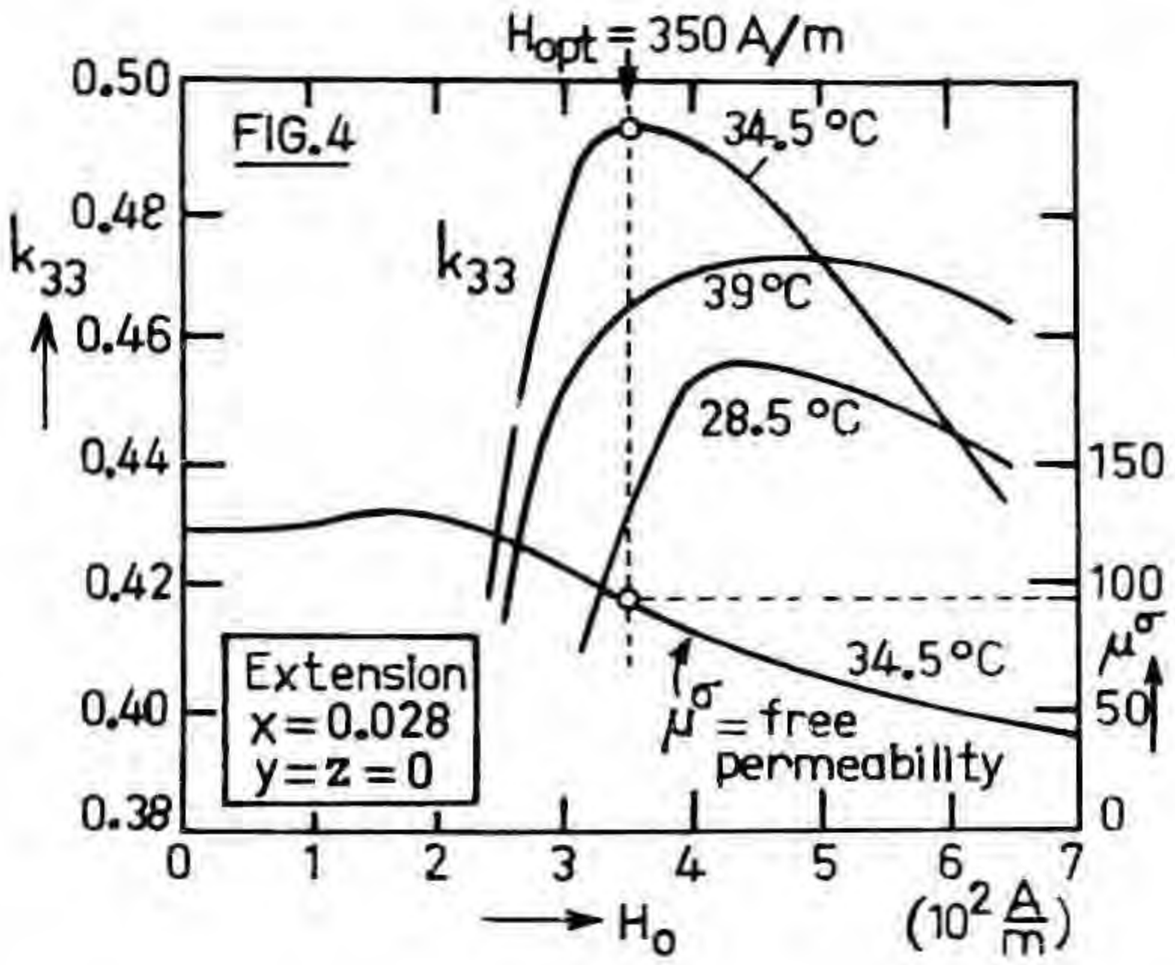

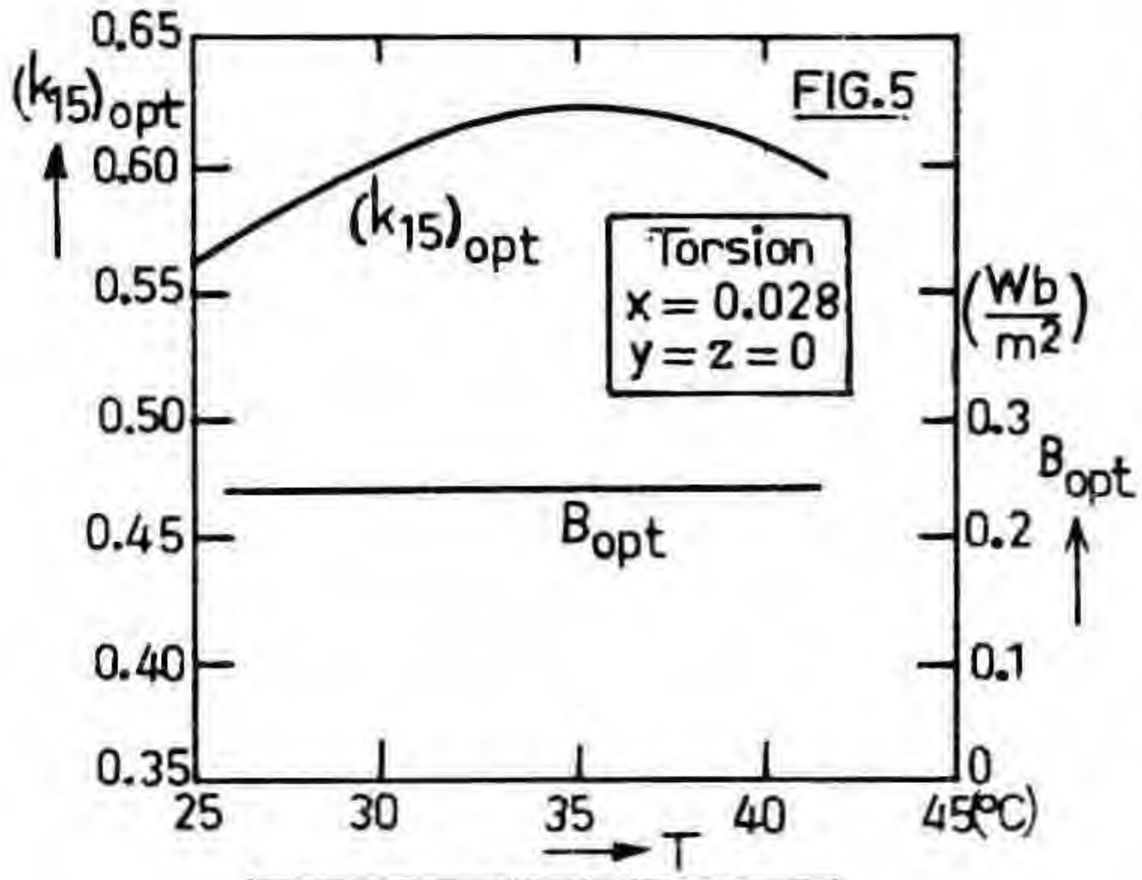

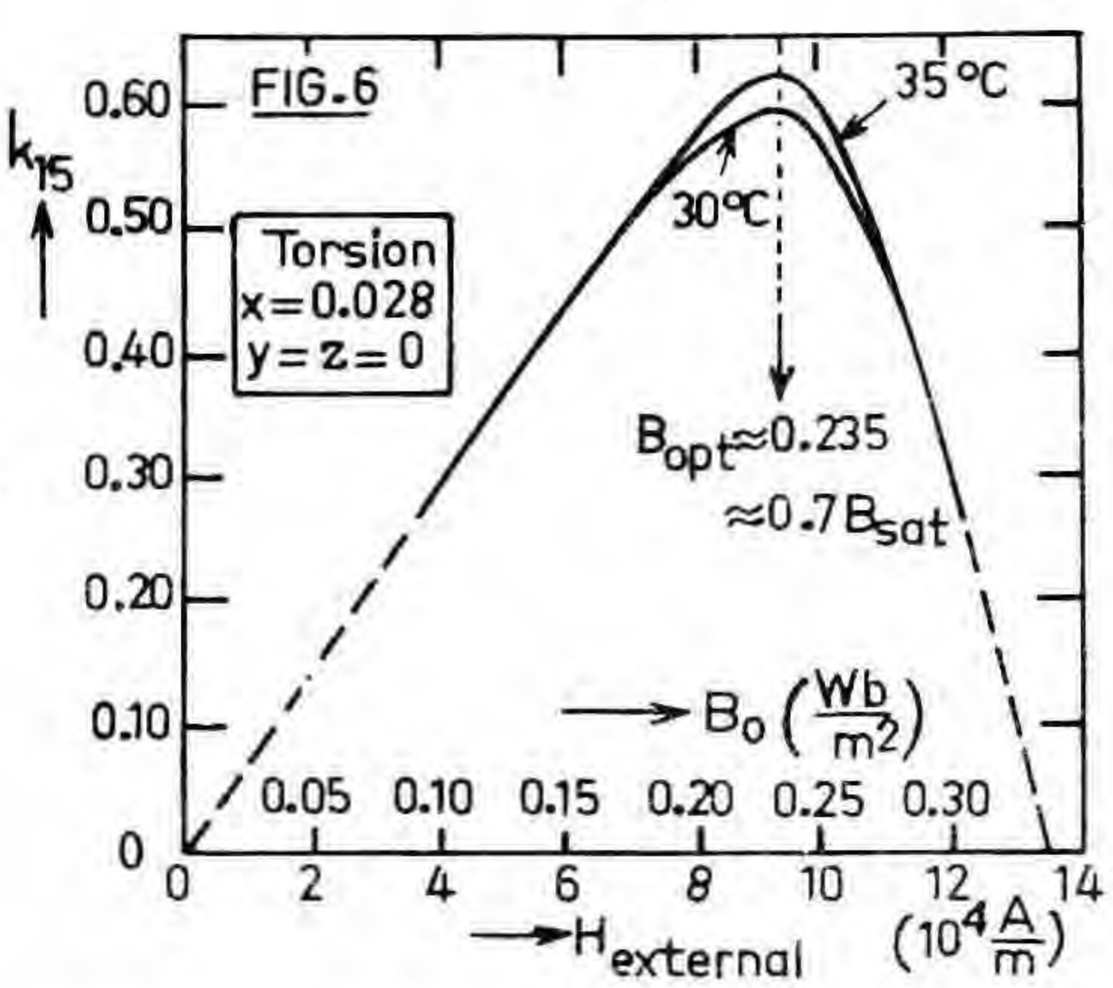

Curve →	1	2	3	4
100 x	1.8	2.2	2.8	2.8
100 y	20	20	0	0
100 z	0	0	5	0

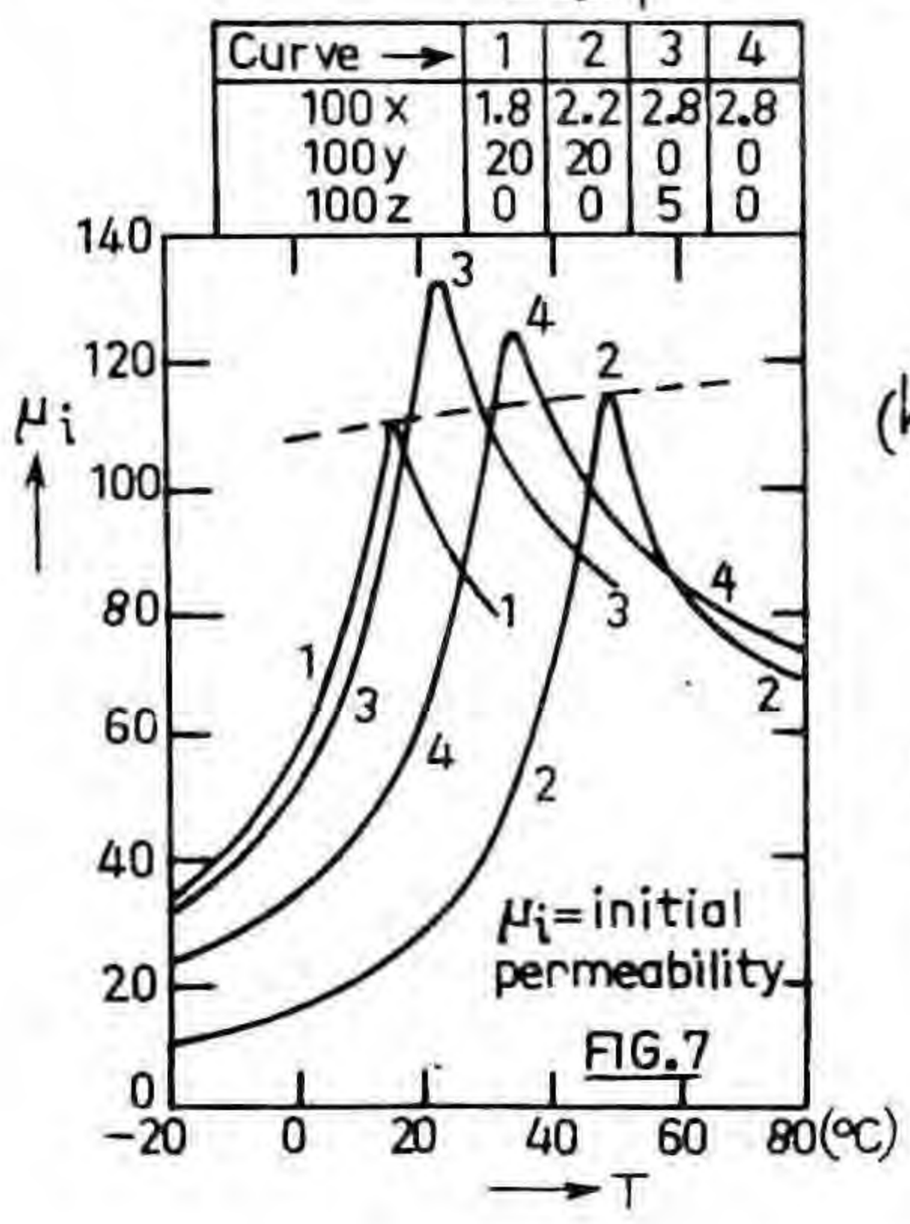

100y	0	0	20
100z	0	5	0
$100\, x_{opt}$	2.6	2.85	1.9

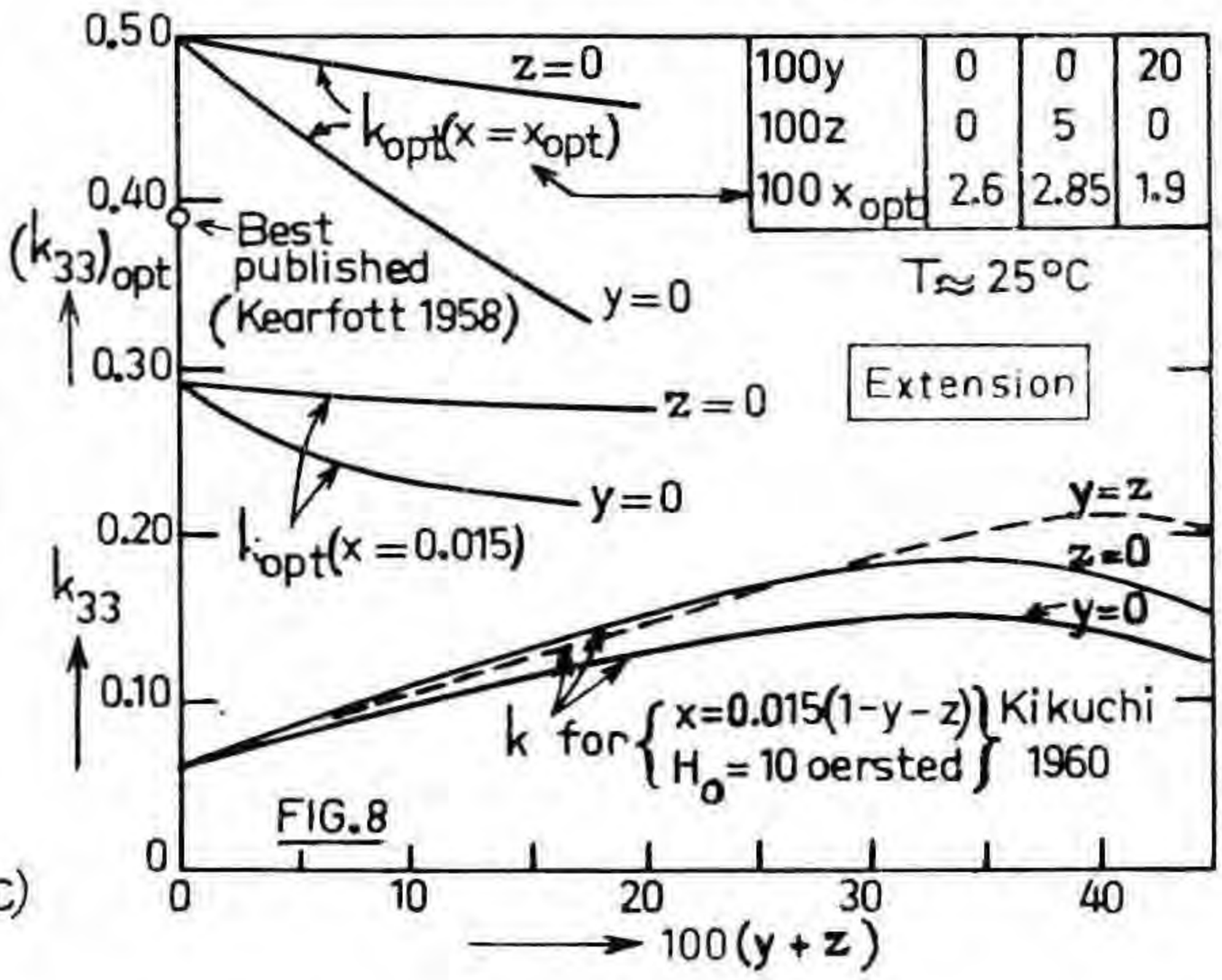

L22

FOURTH INTERNATIONAL CONGRESS ON ACOUSTICS
COPENHAGEN 21.-28. AUGUST 1962

TECHNIQUE DE MESURE DU BRUIT DES FUSEES

M. KOBRYNSKI (O.N.E.R.A. - FRANCE)

Les caractéristiques du bruit des jets et des régimes vibratoires instationnaires dûs à la combustion instable sont examinées sur 4 moteurs fusées à propergol solide de 8 à 20 tonnes de poussée.

Champ sonore du jet : Celui-ci est défini par la pression efficace dans le plan horizontal du jet, analysé par octaves de fréquence, par la puissance acoustique, sa densité spectrale, et par l'indice de directivité.

Méthode d'étude : Les propulseurs fonctionnent sur un banc horizontal à moins de 1 m du sol. L'aire de mesure, plate et dégagée, est jalonnée de repères, disposés suivant des rayons, ayant pour origine le centre de la tuyère. Le secteur étudié est compris entre les angles de 90° et 160°, comptés depuis l'avant du propulseur (fig. 1).

Le champ acoustique proche (jusqu'à 20 m) est exploré par des microphones mobiles sur rail et le champ lointain (jusqu'à 50 m) en des points discrets.

Les voies de mesure comprennent les microphones électrostatiques et adaptateurs de ligne étudiés par l'O.N.E.R.A. [1], peu sensibles aux vibrations mécaniques.

Leur courbe de réponse est rectiligne à ± 2 dB entre 0,02 et 20 KHz, le taux de distorsion à 2 KHz inférieur à 5% pour 174 dB et la sensibilité absolue est de 75 μ V/Pa. Les enregistreurs magnétiques utilisés sont à 7 et 14 pistes. Sur le terrain, toutes les voies

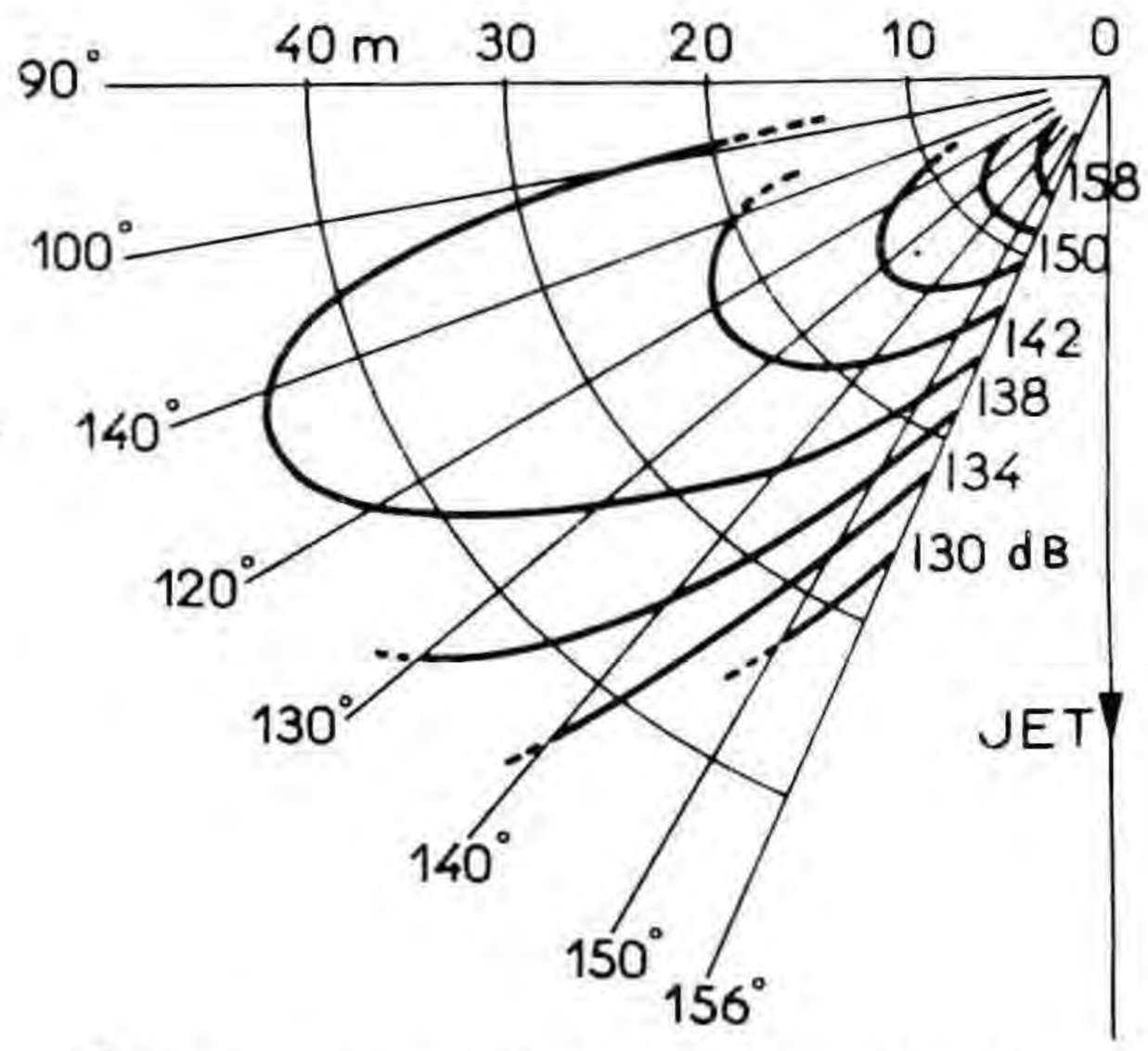

fig. 1 - Courbes d'égal niveau de bruit
Propulseur de 8000 Kg de poussée.

de mesure sont contrôlées avant les essais au moyen d'une source sonore portative.

Résultats : La répartition spatiale de pression sonore des fusées (voir fig. 1 et 2) [2] est semblable à celle obtenue pour les jets subsoniques. Comme pour ceux-ci, les réseaux d'isobares par octaves indiquent l'existence, sur le pourtour du jet d'"anneaux émissifs" correspondant aux diverses fréquences du spectre.

La puissance acoustique totale W_a (intégrée sur l'hémisphère) est, suivant les propulseurs, de 350 à 1100 Kw, d'où un facteur d'émission sonore de 0,5% environ.

Pour le champ lointain, l'indice de directivité calculé, indique un maximum à 110° pour les fréquences hautes et à 140° pour les basses fréquences.

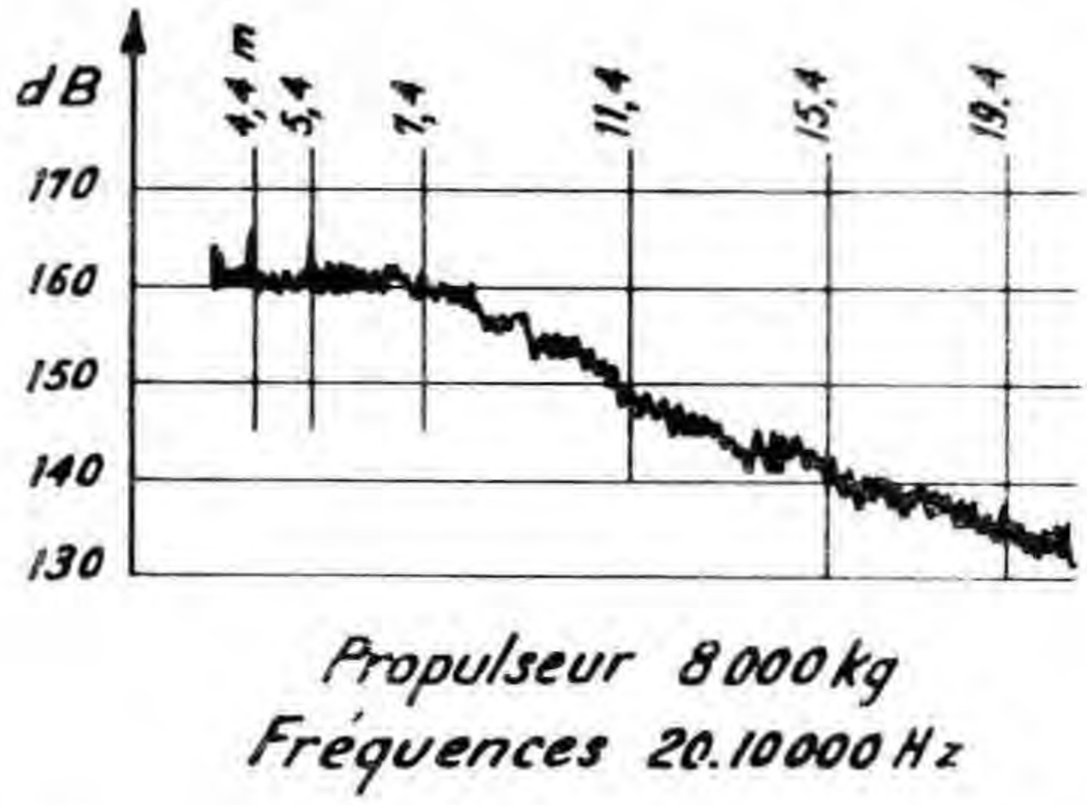

fig. 2 - Niveau de bruit le long d'un rayon à 24° de l'axe du jet.

Le spectre généralisé de puissance ψ (f) en fonction de la fréquence f, obtenue par la représentation de la grandeur sans dimension $10 \log \frac{V}{d} \cdot \frac{\psi(f)}{W_a}$ dB (V = vitesse des jets, d = diamètre des tuyères) en fonction du nombre de STROUHAL $\frac{f\,d}{V}$ présente une courbe de variation moyenne (fig. 3) en bon accord avec celle donnée par [3].

Analyse des instabilités de combustion : La combustion instable du propergol peut exciter les cavités du bloc de poudre suivant ses modes principaux de vibrations propres. La mesure des fréquences émises permet de connaître les modes prédominants.

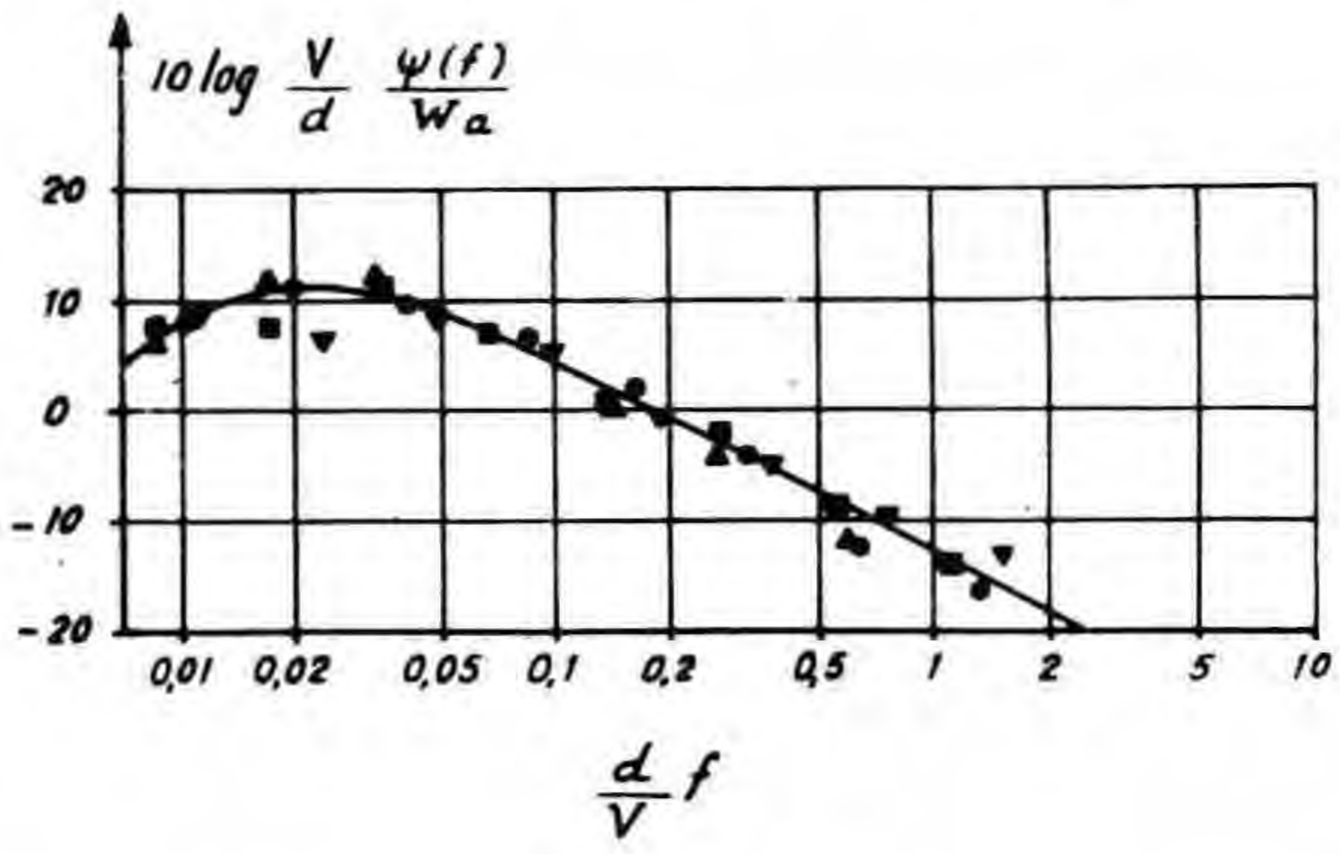

fig. 3 - Spectre de puissance généralisé.

Méthode d'analyse : Les signaux donnés par un microphone disposé près du fond avant du propulseur sont enregistrés sur ruban magnétique. En raison des variations rapides des fréquences à mesurer, la lecture de l'enregistrement est effectuée à une vitesse 10 fois plus faible que celle adoptée pour l'inscription du phénomène.

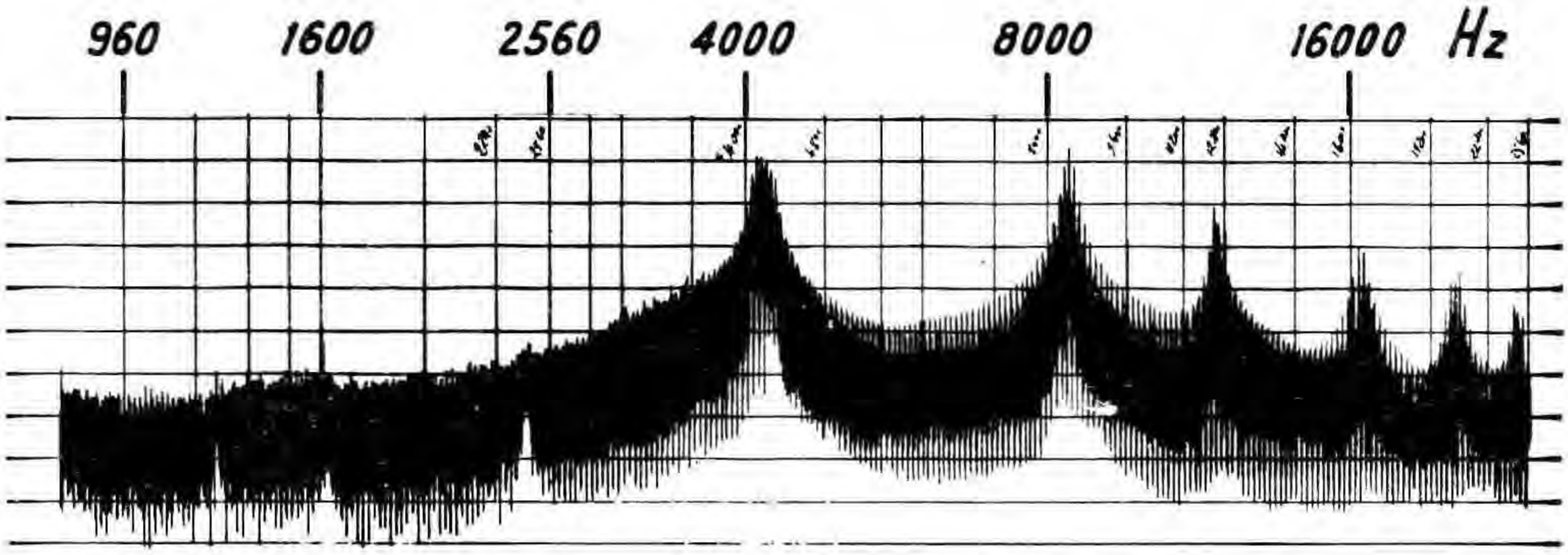

fig. 4 - Bruit de combustion - Spectre de raies.

Des tronçons correspondant à 0,2 s du temps réel sont extraits à des époques repérées avec précision. L'analyse fine de ces tronçons, mis en boucle, et sur laquelle les fréquences n'ont pas varié de manière appréciable, donne le spectre de raies correspondant aux époques choisies (fig. 4). Revenant à l'enregistrement complet, la courbe de variation de chaque harmonique, sur toute la durée de combustion, s'obtient par comparaison des fréquences instantanées avec des fréquences fixes f_0 en repérant le temps où chaque fréquence passe par la valeur f_0. Afin de séparer les diverses composantes, des filtres 1/3 d'octave sont insérés successivement dans le circuit de lecture (fig. 5), les fréquences de coupure du filtre choisi encadrant la fréquence recherchée.

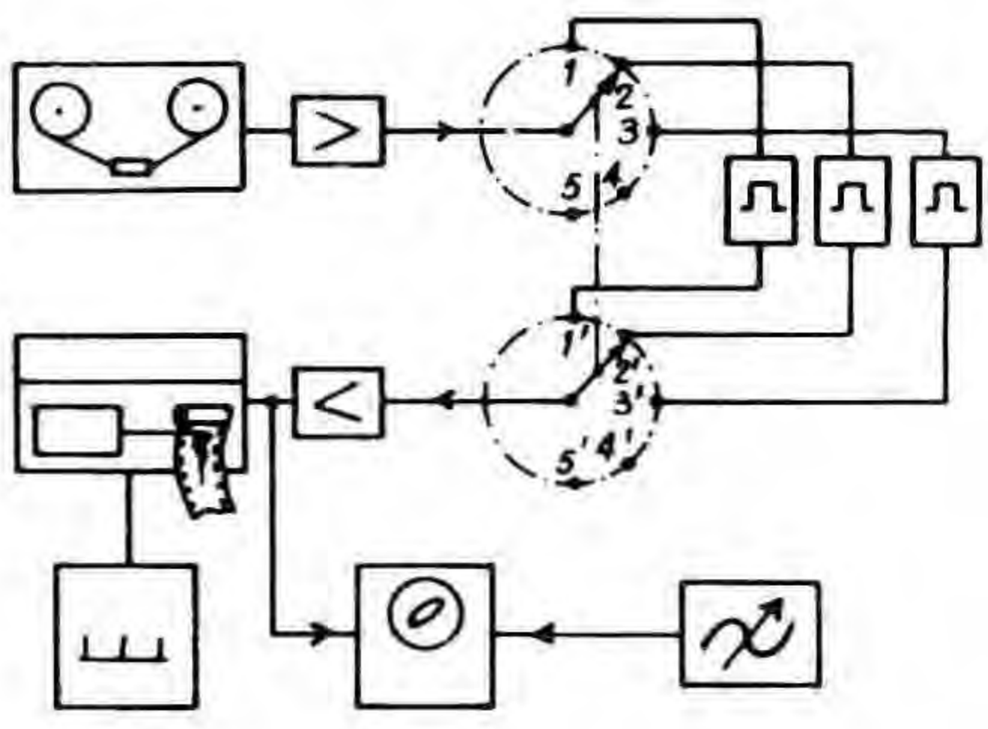

fig. 5 - Appareillage d'analyse.

Résultats : L'accord étroit entre les fréquences mesurées et calculées [4], pour les mêmes époques du tir (fig. 6) montre que dans certains pro-

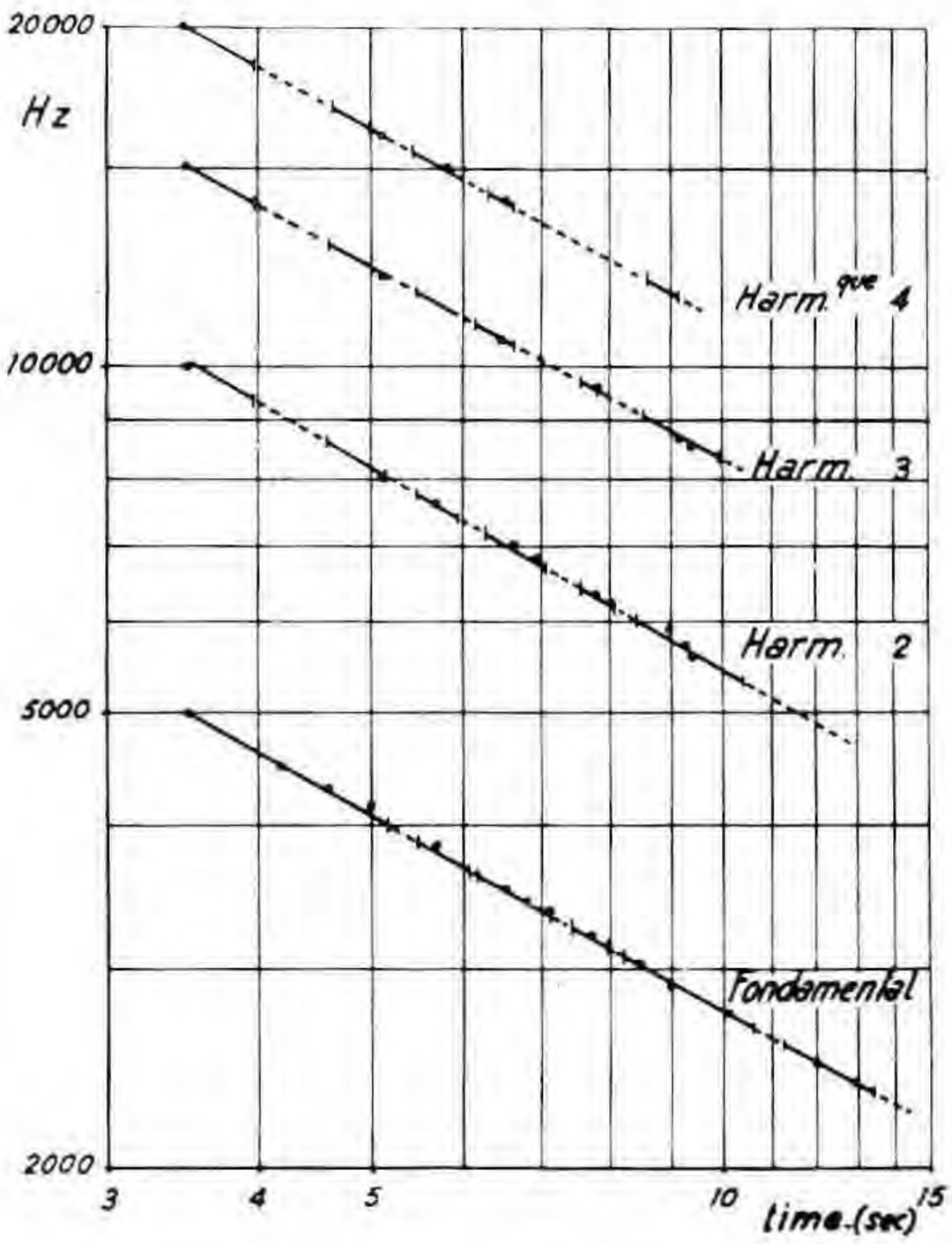

fig. 6 - Analyse du bruit de combustion en fonction du temps.
—— calculée
mesurée

propulseurs les instabilités de combustion engendrent des vibrations tangentielles des cavités du bloc. Les fréquences émises sont fonction de la vitesse de combustion de la poudre et du diamètre de la cavité.

---

(1) P. LIENARD - G. BOEGLIN - Chaînes de mesure de bruit des fusées.
(A paraître - Electronique Industrielle 1962).

(2) M. KOBRYNSKI - Sur la structure du champ sonore des turboréacteurs.
La Recherche Aéronautique n° 58 (1957), p. 29

(3) J.N. COLE etc. - Noise radiation from fourteen types of rockets in the 1000 to 130000 pounds thrust range.
TR 57-354, Aero Medical Lab. WADC, décembre 1957

(4) M. BARRERE - Les instabilités de combustion du type acoustique dans les fusées à propergol solide.
La Recherche Aéronautique n° 83, juillet/août 1961, p. 17.

M22

FOURTH INTERNATIONAL CONGRESS ON ACOUSTICS
COPENHAGEN 21.-28. AUGUST 1962

Acoustical Design of the Quebec Academy Auditorium, Quebec, Canada

Leslie L. Doelle, Acoustical Consultant and Oscar G. Vagi, Architectural Associate, Montreal, Canada

General Considerations, Room Shape

The 1000 seat Auditorium was designed primarily for lectures but the ever increasing interest of Quebec's population in all kinds of theatrical and musical performances necessitated the construction of a General Purpose Hall which is both aesthetically and acoustically suitable for speech, stage presentations, concerts and moving pictures alike.
For visual and acoustical reasons a fan shaped plan was preferred with a balcony which brings the audience as close as possible to the stage. (Fig. 1 and 2). The maximum balcony overhang is about 3.5 m (11 ft), so that all seats benefit from the short-time-delay ceiling reflections. A row of recessed boxes have been accommodated along both side walls. A coffered-serrated ceiling covers the entire audience area. A demountable orchestra shell separates the stage tower from the acting stage area, for concert purposes (Fig. 3).
The architect for the entire Academy project is Gaston Amyot and his staff, Quebec.

Important Architectural-Acoustical Data

Volume without stage tower	8500 m^3	(300000	ft^3)
Overall seating area, including aisles	725 m^2	(7800	ft^2)
Number of audience seats		1000	
Volume per audience seat	8.5 m^3	(300	ft^3)
Floor area per audience seat	0.72 m^2	(7.8	ft^3)
Max. distance between seat and proscenium opening	32 m	(105	ft)
Orchestra pit floor area	70 m^2	(755	ft^2)
Stage area	350 m^2	(3770	ft^2)
Max. stage floor area within orchestra shell	150 m^2	(1600	ft^2)
Mid-frequency reverberation time		1.4 sec	

Acoustical Design Objectives

The various functions in the Auditorium would require different reverberation times, varying from about 1.0 sec (for speech) to about 1.8 sec (for symphony music). Since the application of variable absorbers did not seem to be feasible, a medium reverberation time of 1.4 sec has been chosen which will create ideal acoustical conditions for theatrical presentations, but will be somewhat long for speech programs and short for romantic music. In order to secure the mid-frequency reverberation time of 1.4 sec, and to minimize the consequences of a compromised reverberation characteristic, the following measures have been taken in the overall architectural-acoustical design of the Auditorium:

1. The application of absorptive treatments has been limited to a minimum and confined to the rear wall portion of the room and to the gallery balustrade.
2. A large number of adequately sized, spherical plastic diffusers have been distributed along the two side walls. These contribute to the

appearance of the room and are used as lighting fixtures at the same time (Fig. 4).

3. A meticulously detailed, basically reflective, lath and plaster ceiling has been designed above the seating area and this blends into a directional canopy above the proscenium opening. This provides for short delayed reflections toward every part of the audience area and beneficial reflections for the sound waves originating from the orchestra pit. These periodic short-delay reflections • increase definition, reducing thereby the effect of the reverberation time which would be too long for speech. The ceiling is also a source of useful back reflections towards the stage area and it supplies efficient diffusion by properly proportioned surface irregularities. The ceiling also accommodates the required openings for downlighting and slots for spotlights, floodlights and ventilating grilles. Uniformly distributed and unobtrusive openings in the ceiling couple the air space above to the Auditorium space, which improves reverberation characteristics for musical presentations.

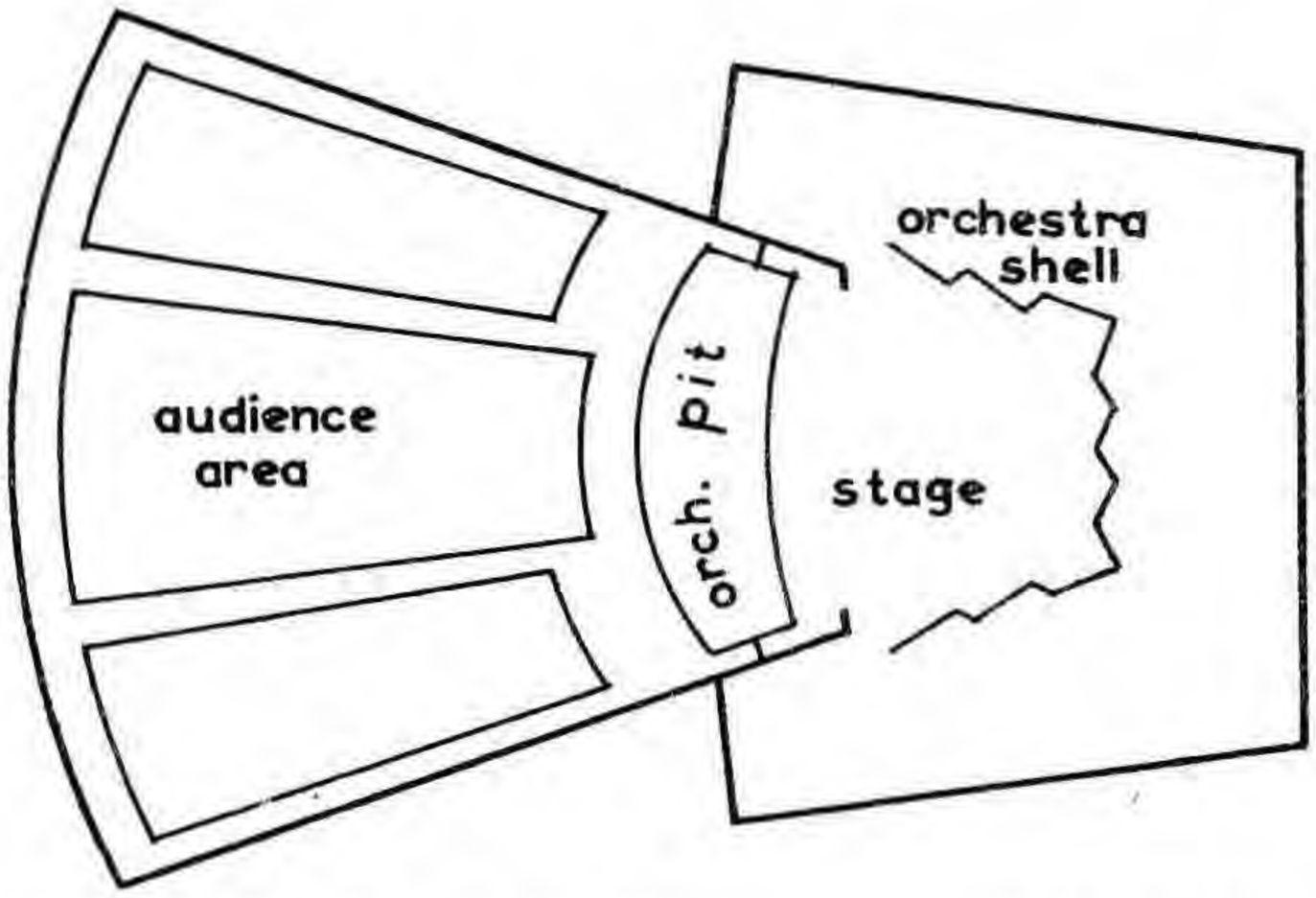

Fig.1. GROUND FLOOR PLAN

4. The demountable orchestra shell provides additional reflective and diffusive surfaces around the musicians and soloists. The capacity of this orchestra shell can be adjusted to accommodate any performing ensemble from full symphony orchestra to chamber quartet.

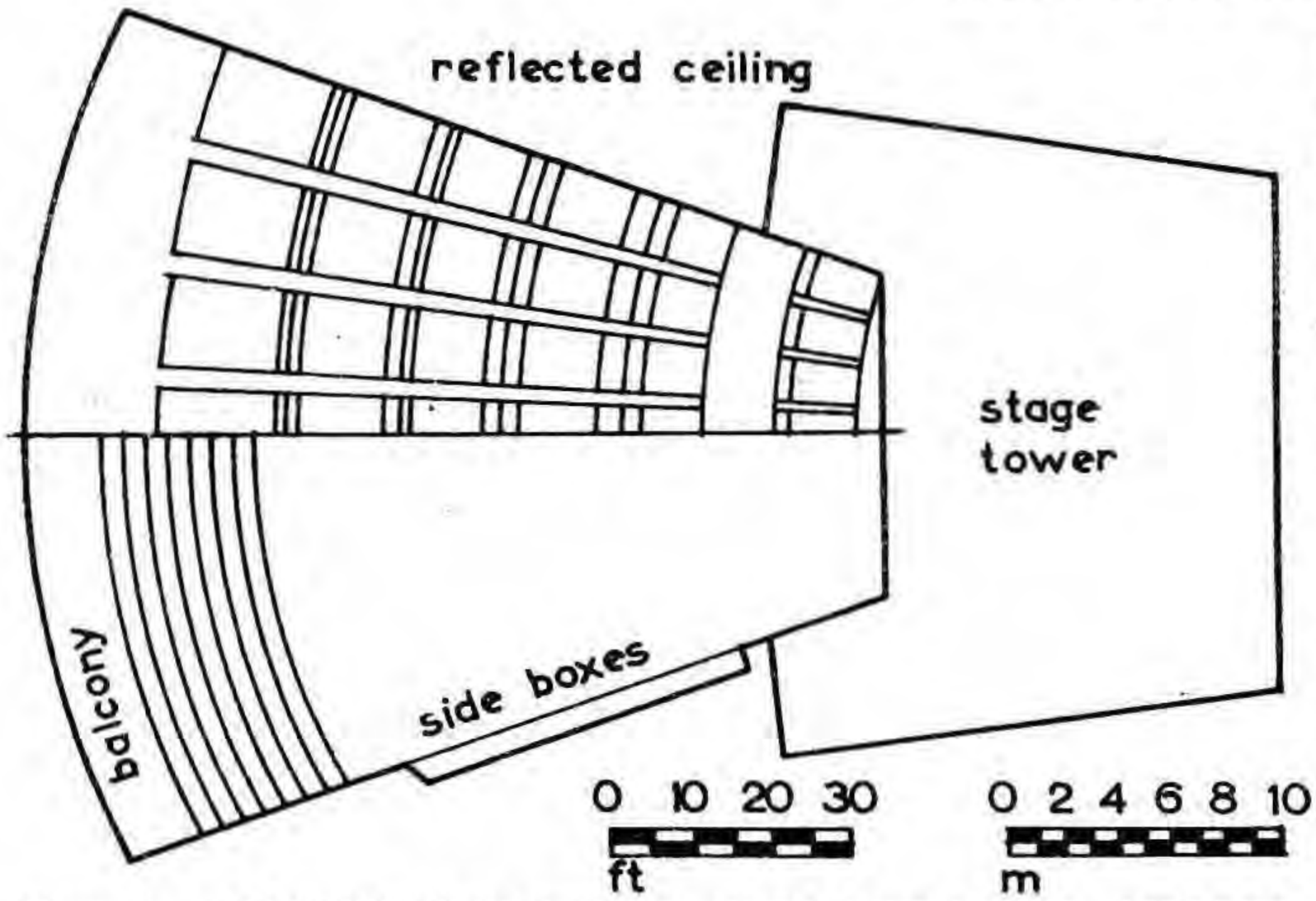

Fig.2. BALCONY FLOOR PLAN WITH REFLECTED CEILING

Finish of Materials

To secure proper balance between low, medium, and high frequency reverberation time, an absorptive wood-slat treatment, with protective alum-

inum bars at dado height, will be installed along the rear walls of the ground floor and gallery floor and also on the gallery balustrade facing the stage. This kind of treatment provides a reasonably uniform absorption over the entire audio-frequency range (Fig. 5).

Fig.3. LONGITUDINAL SECTION

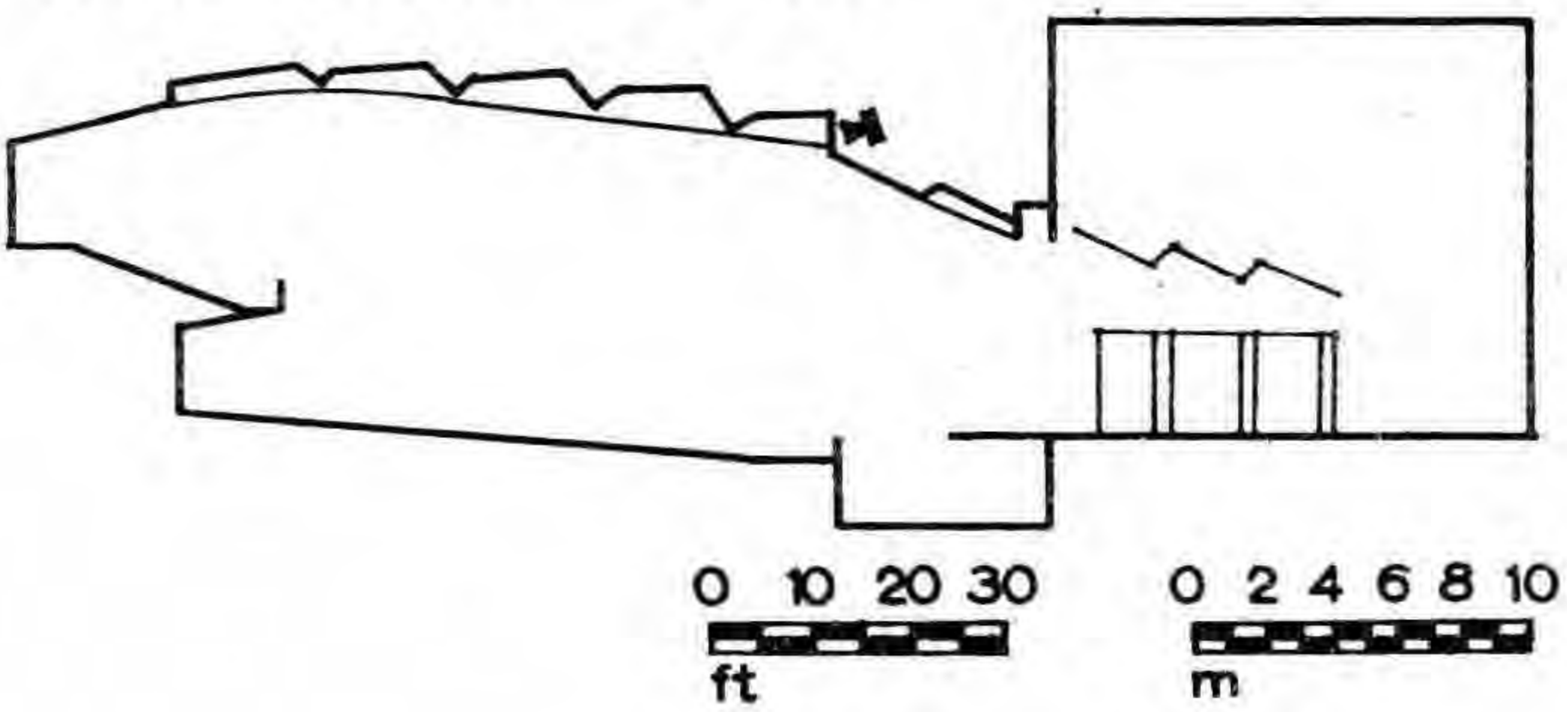

Longitudinal ribs divide the previously described lath and plaster ceiling above the entire audience area into seven bays. This ceiling and also the plywood orchestra shell constitute low frequency absorbers, counterbalancing the pronounced medium and high frequency absorption of the audience and seating.

The finish of the side walls consists mostly of a reflective, flexible wood panelling (Flexwood), glued to the plastered wall. Close to the stage the mosaic finished side wall with the adjacent plastered canopy forms an integrated proscenium opening assembly.

The audience area has a vinyl flooring which adequately eliminates footstep noises and facilitates cleaning. Aisles will be covered with carpets.

Fig.4. INTERIOR VIEW

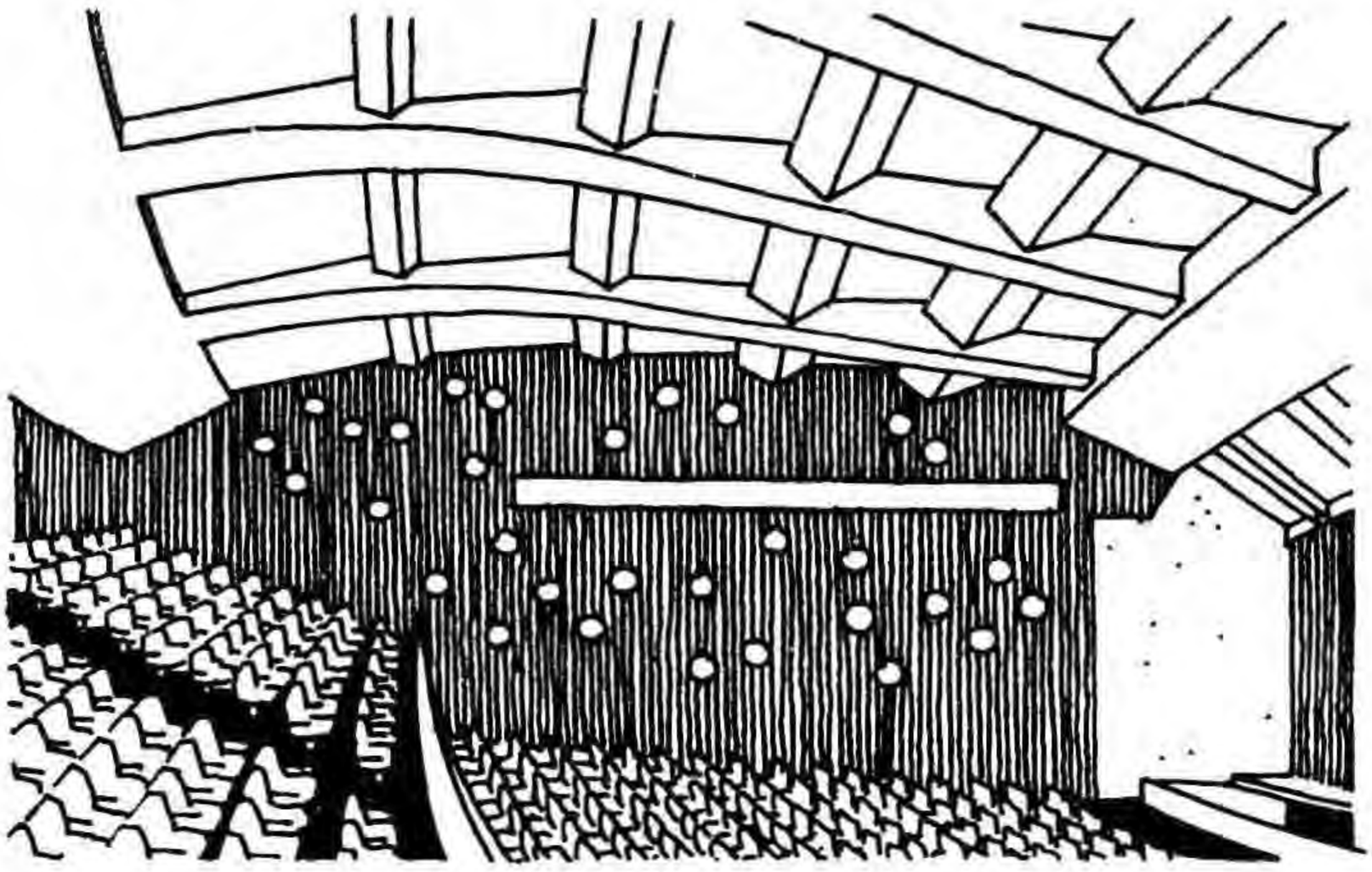

The orchestra pit has an elevated resonant wood floor and plywood covered side walls all around. The solid balustrade between audience and orchestra pit beneficially directs the sounds of the hidden orchestra onto the stage, promoting thereby balance and unison. The orchestra shell is constructed of 12 mm (½") thick plywood, on a randomly braced framing, divided into easily demountible folding sections. The roof portion of this shell can also be separated into sections and flown up into the stage tower.

Noise Control

Since the Academy is situated in a quiet suburb of Quebec, a not too distant aircraft route constituted the only exterior noise source which had to be considered. Particular attention was, therefore, given to the roof construction which consists of 10 cm (4") thick light weight pre-fabricated concrete slabs supported by steel trusses. A horizontal, uninterrupted suspended lath and plaster ceiling is attached to the bottom of the trusses, creating thereby a fairly deep air space between the roof slabs and the horizontal ceiling. A 5 cm (2") thick isolation blanket is placed on top of this ceiling. The serrated-coffered ceiling is suspended below this horizontal isolation ceiling.

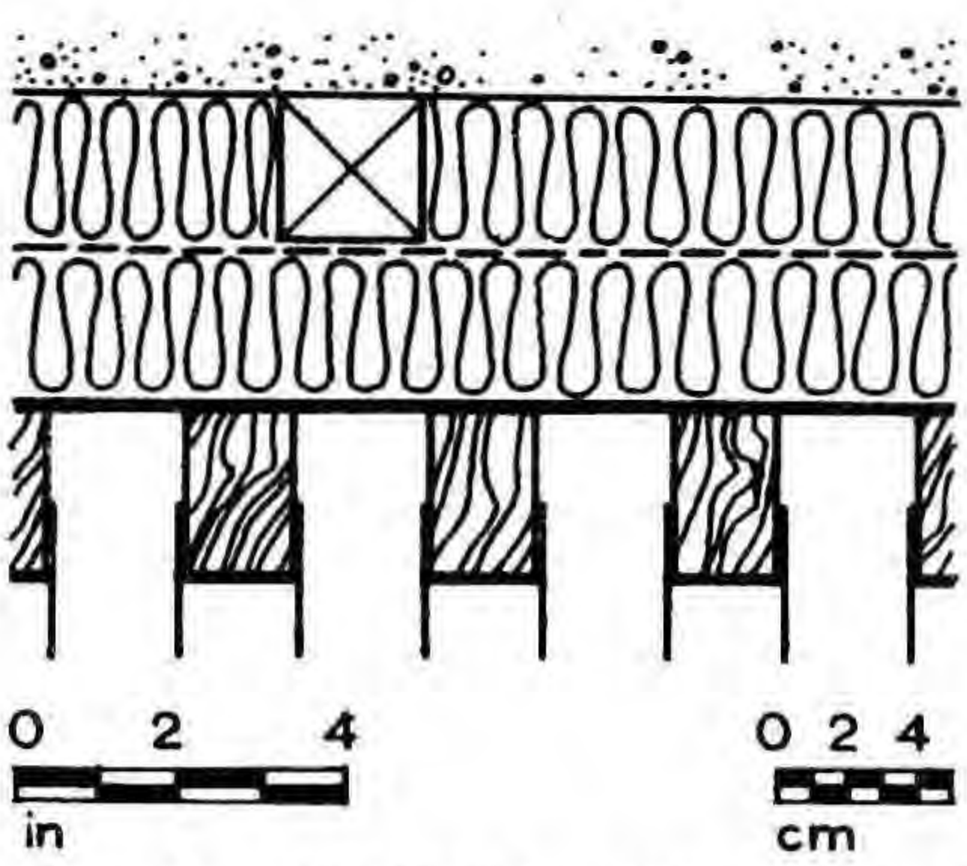

Fig.5. ACOUSTICAL TREATMENT AT REAR WALL

Entrance doors leading into the Auditorium are sound insulating to exclude unwanted building noise.

Interior noises and vibrations caused by mechanical equipment or the movie projectors are reduced to inaudibility in the Auditorium.

Sound Reinforcement System

In order to supply sufficient reflected-sound energy throughout the listening area, highly reflective surfaces have been provided around the proscenium opening, however, in view of the relatively large volume of the Auditorium, a sound amplification system will be installed for the reinforcement of speech sound or music when the sound source is particularly weak. A central loudspeaker cluster will be hidden behind a grille, in the vertical portion of the canopy above the stage, so that both natural and amplified sounds will arrive to the listeners from the same direction and almost simultaneously. The amplified sound will be radiated at a level adequate to assure a reasonable increase in speech intelligibility.

The music played in the orchestra pit will be assisted by two loudspeakers at the two sides of the same canopy plane where the central loudspeaker will be located. Thus the orchestra will be "raised" out of the pit to which it is tied for functional and visual reasons. The same loudspeaker system can be used for any "on-stage" musical presentation if this should be necessary.

An electro-acoustical equipment will be installed in a control room, providing various facilities for the audience, staff, and artists in the normal everyday routine of a multipurpose Auditorium.

N22

FOURTH INTERNATIONAL CONGRESS ON ACOUSTICS
COPENHAGEN 21.-28. AUGUST 1962

INDICATION LIMIT

Mrs. Edith L. R. Corliss
National Bureau of Standards, Washington 25, D. C.

The limits of resolution of an analyzing system may be represented graphically by an irreducible limit in a three-dimensional space, a region in which no information about a signal can be found. This region is shown in Figure 1, plotted in terms of relative differentials in energy, frequency, and time, corresponding to the limits of resolution of the analyzer for each of these respective variables. The resulting volume is here termed the indication limit. It is defined by the triple product

$U = \frac{\Delta E}{E_o}.\frac{\Delta f}{f_o}.\frac{\Delta t}{T_o}$. As this product is invariant for any given energy resolution limit $\frac{\Delta E}{E_o}$, it may be used to calculate the remaining resolution limit if any pair are known. Its derivation sheds light on the factors limiting the resolution of an analyzer, and it may be used to apportion the errors in measuring transient phenomena as advantageously as possible.

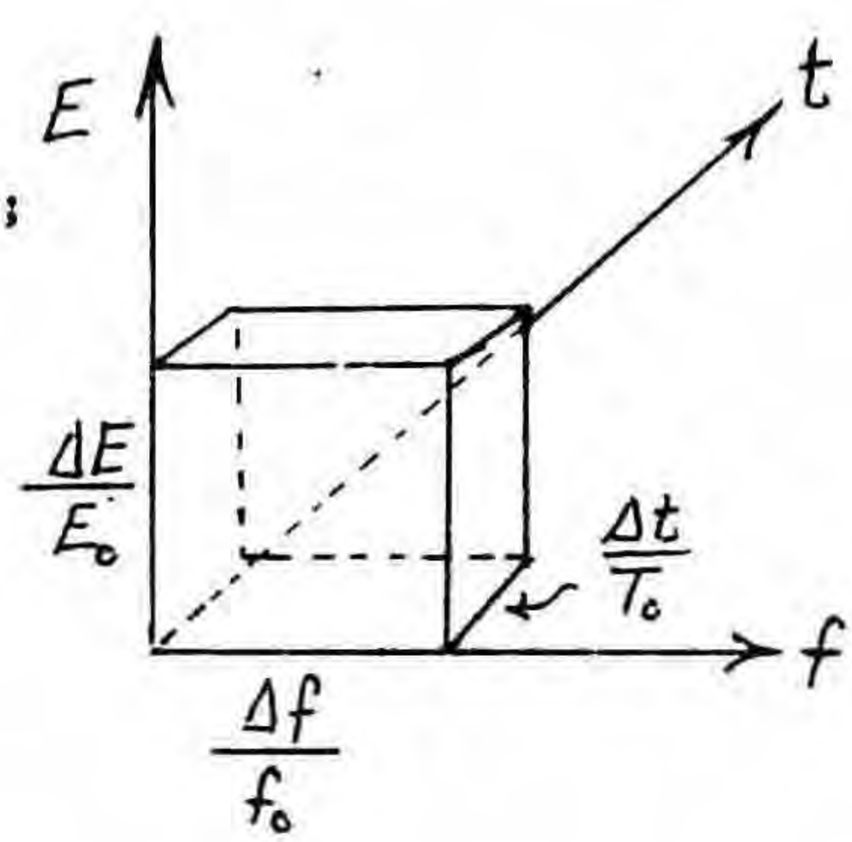

Figure 1. Resolution limits of an analyzer forming the indication limit, U. T_o is the period corresponding to f_o, the central frequency of the analyzer; E_o is the total energy stored in the reactive components at the beginning of the differential time interval, Δt.

This derivation is applied to an analyzer characterized by a second-order differential equation. The relative proportions between the resolution limits $\frac{\Delta f}{f_o}$ and $\frac{\Delta t}{T_o}$ are determined by Q_o, the "figure of merit" for the analyzer, i.e., the ratio of its energy-storage capacity to its mean rate of energy dissipation. Although the <u>shape</u> of the limiting region changes with Q_o, the volume, U, of the indication limit is fixed by the energy-resolving properties of the system. Because the volume of the indication limit is given by an energy <u>ratio</u>, many of the equations derived from it may be used interchangeably for power or energy.

The indication limit may be computed in terms of an exponential factor, α, defined as follows: The energy in the system must change to a fraction $e^{-\alpha}$ times its original value in order for the change in energy stored in the system to be indicated, i.e. $\Delta E = (1 - e^{-\alpha})\ E_o$ or, for power, $\Delta W = (1 - e^{-\alpha})\ W_o$.

Where the transient behavior of the analyzer is concerned, the decay of the signal stored in the system must exceed $e^{-\alpha}$ to be discernible. Thus the factor $e^{-\alpha}$ applies to the exponential envelope of the energy in the system. Therefore, from the relation $E_o e^{-\alpha} = E_o \exp(-2\pi\Delta t/Q_o T_o)$ the resolution limit along the time axis in terms of the natural period of the system is:

$$\frac{\Delta t}{T_o} = \frac{\alpha Q_o}{2\pi}$$

Along the frequency axis, the steady-state response of the analyzer must be reduced by a factor $e^{-\alpha}$ before any change is discernible; this determines the finest frequency resolution limit surrounding f_o, the natural frequency to which the analyzer is tuned. At frequencies other than its natural frequency, the response of the analyzer is a fraction, F, of its maximum response. Thus the limiting fraction may be stated as:

$$F = e^{-\alpha} \frac{1}{f^2/f_o^2 + Q_o^2\ (1 - f^2/f_o^2)^2}$$

The frequency resolution limit derived from this equation proves to be:

$$\frac{\Delta f}{f_o} = \frac{\sqrt{e^{\alpha} - 1}}{Q_o}$$

The resolution limits in frequency and time depend in a complementary fashion upon Q. Thus Q affects the relative size of the resolution limits, but it is eliminated from their product, which is the signal uncertainty equation:

$$\Delta f.\Delta t = \frac{\alpha}{2\pi} \sqrt{e^{\alpha} - 1}$$

From these relations one may compute the indication limit:

$$U = \alpha e^{-\alpha} \frac{(e^{\alpha} - 1)^{3/2}}{2\pi} = \frac{\Delta E}{E_o}.\frac{\Delta f}{f_o}.\frac{\Delta t}{T_o}$$

In many cases α is an intrinsic property of the analyzer, but if the limitation of energy resolution is caused by noise present with the signal, α becomes an extrinsic property. A common instance of this condition is encountered where one is dealing with the detection of a sinusoidal signal in noise. Although the derivations presented here are most simply expressed in terms of the exponent α, the basic variable in the E-f-t coordinates is of course, $\frac{\Delta E}{E_o}$ The results are also most easily interpreted in terms of $\frac{\Delta E}{E_o}$. The definition of α implies the relation $\alpha = \ln(1 - \frac{\Delta E}{E_o})$, from which the appropriate substitutions may be made.

Where one is dealing with the detection of a sinusoidal signal in noise, it is most convenient to use the signal-to-noise ratio as the basic variable. In that case:

$$\frac{\Delta E}{E_o} = \frac{N}{S + N} = \frac{1}{S/N + 1}$$

It is interesting to interpret the functional relation between U and the signal-to-noise ratio.

$$U = \frac{(S/N)^{-3/2}}{2\pi} \cdot \left[- \frac{S/N}{S/N + 1} \ln \frac{S/N}{S/N + 1} \right]$$

The right-hand factor is related directly to the function " - p ln p" that describes the flow of information in a noisy channel. One can see this from the fact that the quantity known as the "expectation" is the product of the probability that an event will occur and the intrinsic content of the event. It is just the "expectation" values of the signal and noise powers that are observed as the long-time average signal-to-noise ratio.

A particular instance, often important in practice, is the presence of a large amount of "white noise" accompanying the signal. The analyzer is selective in the energy it stores, and the noise energy stored may be found by integrating over the system response. For a white noise whose power distribution is n_f energy units per cycle, which forms the background for an input sinusoidal signal of power W_i, the maximum signal-to-noise ratio attainable with the analyzer is given by:

$$S/N = \frac{Q_o W_i}{\pi^2 n_f f_o}$$

The results of the foregoing discussion are summarized in the table accompanying this article. A detailed derivation and a bibliography of related papers are included in a forthcoming paper, "Resolution Limits of Analyzers and Oscillatory Systems", to be published in the Journal of Research of the National Bureau of Standards.

The first line of the table summarizes the results in terms of the basic variable $\frac{\Delta E}{E_o}$. The second line gives the general results again, expressed in terms of the exponential term, α, converted to the form equivalent to $\frac{\Delta E}{E_o}$. The third line summarizes the results for the condition where $\frac{\Delta E}{E_o}$ is limited by noise, i.e.

$$\frac{\Delta E}{E_o} = \frac{N}{S + N}$$

This work was sponsored by the Office of Naval Research.

TABLE I

RESOLUTION LIMITS OF ANALYZERS AND OSCILLATORY SYSTEMS

Basic Variables:			Resolution Limits:		Uncertainty Relation:	Indication Limit:
$\frac{\Delta E}{E_o}$	α	S/N	$\Delta f/f_o$	$\Delta t/T_o$	$\Delta f \Delta t$	U
$\frac{\Delta E}{E_o}$	$-\ln(1-\frac{\Delta E}{E_o})$	$\frac{1-\frac{\Delta E}{E_o}}{\frac{\Delta E}{E_o}}$	$\frac{1}{Q_o}\sqrt{\frac{\frac{\Delta E}{E_o}}{1-\frac{\Delta E}{E_o}}}$	$-\frac{Q_o}{2\pi}\ln(1-\frac{\Delta E}{E_o})$	$\frac{1}{\pi}\sqrt{\frac{\Delta E}{E_o}}\cdot\frac{1}{\sqrt{1-\frac{\Delta E}{E_o}}}\ln\frac{1}{1-\frac{\Delta E}{E_o}}$	$\frac{1}{2\pi}\left(\frac{\frac{\Delta E}{E_o}}{1-\frac{\Delta E}{E_o}}\right)^{3/2}\cdot\left[-\left(1-\frac{\Delta E}{E_o}\right)\ln\left(1-\frac{\Delta E}{E_o}\right)\right]$
$1-e^{-\alpha}$	α	$\frac{1}{e^{\alpha}-1}$	$\frac{\sqrt{e^{\alpha}-1}}{Q_o}$	$\frac{\alpha Q_o}{2\pi}$	$\frac{\alpha}{2\pi}\sqrt{e^{\alpha}-1}$	$\frac{\alpha e^{-\alpha}}{2\pi}\quad(e^{\alpha}-1)^{3/2}$
$\frac{1}{S/N+1}$	$\ln\frac{S/N+1}{S/N}$	S/N	$\frac{1}{Q_o\sqrt{S/N}}$	$\frac{Q_o}{2\pi}\ln\frac{S/N+1}{S/N}$	$\frac{1}{2\pi\sqrt{S/N}}\ln\frac{S/N+1}{S/N}$	$\frac{(S/N)^{-3/2}}{2\pi}\cdot-\frac{S/N}{S/N+1}\ln\frac{S/N}{S/N+1}$

O22

FOURTH INTERNATIONAL CONGRESS ON ACOUSTICS
COPENHAGEN 21.-28. AUGUST 1962

NATURE OF THE FEEDBACK MECHANISM IN SOME FLUID FLOWS PRODUCING SOUND

Alan Powell

There is a wide class of flows which undergo self-generated periodic disturbances, often accompanied by sound emission, whose mechanism is of feedback nature. The mechanism may often be analysed in terms of the feedback elements shown in Fig 1; in other cases such analysis is yet tentative since details have yet to be explored.

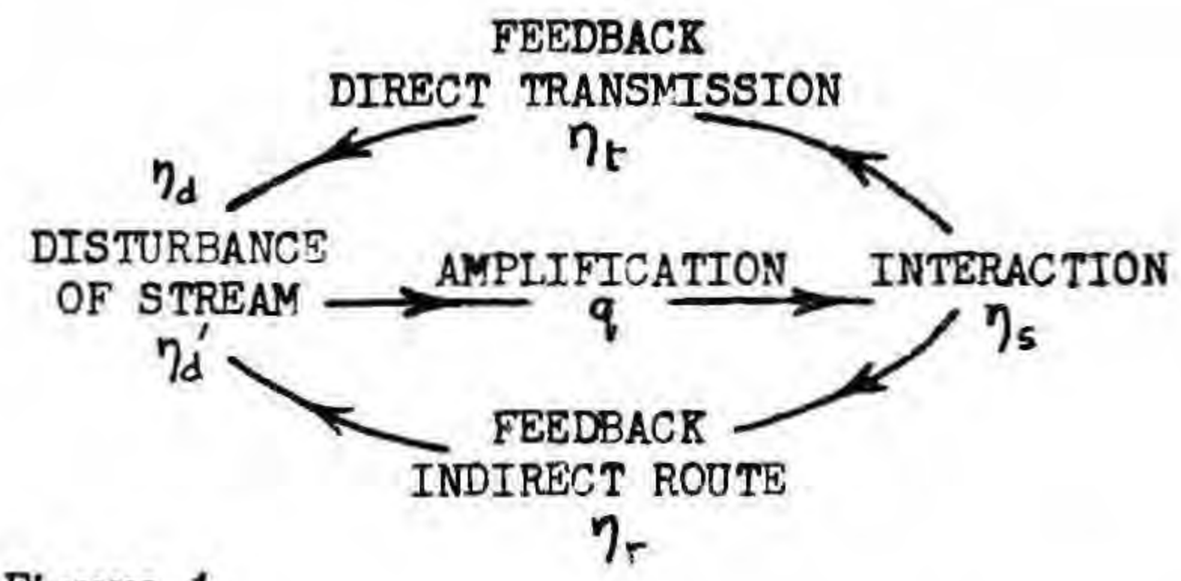

Figure 1

Edgetone at low speeds The edgetone is the best understood example at the present time; here the indirect feedback path shown in Fig 1 does not exist. The stream is a plane laminar jet and the sinuosities, or vortex formations, in it interact with the edge E, Fig 2. The fluid motion due to this interaction may be represented equally well by a dipole D associated with the lateral fluctuating force on the edge, 1)2), or by the vortex motion there, 3)4) The stream leaving the nozzle N is disturbed by this motion, and its sinuosities are amplified by a factor q by the stream instability as they are carried to the edge E. Thus the feedback loop is completed. For a sinusoidally varying oscillation of constant amplitude we must have

$$\eta_s \eta_t \eta_d q = 1 \qquad (1)$$

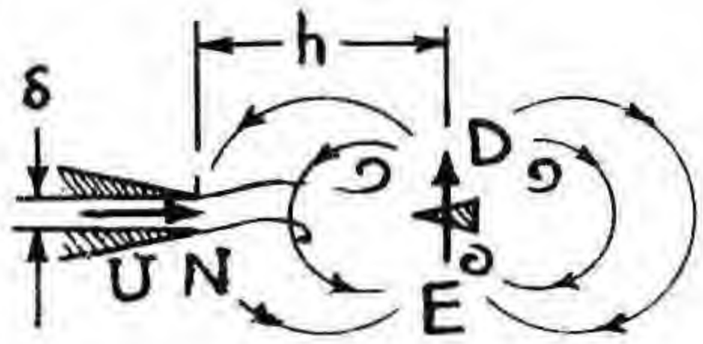

Figure 2

Each factor is a conveniently defined ratio, the same measure being used in the denominator of one factor as in the numerator of the one following, 1)2)4).

Actually the jet flow is sufficiently unstable for this criterion to be satisfied, so far as amplitudes are concerned, over a wide band of frequency, as shown shaded in Fig 3. Here the frequency f is represented by Strouhal number S, and the velocity by Reynolds number R. But in a feedback mechanism a consistency of phase is essential for periodicity. One may follow the action around the loop at the appropriate phase velocity and note the phase shifts as transfer is made between each segment of the loop: Upon returning to the starting point there will be some phase shift of p cycles. Let there be (N'+p') wavelengths of length λ' moving at the mean convection velocity u_{con} between nozzle N and edge E, and (N"+p") wavelengths λ'' moving at speed c in the acoustic path from edge E to nozzle N. Here we keep p', p" 1. Then we must have, in general

$$(p' + p'')/f = (h - N'\lambda')/u_{con} + (h - N''\lambda'')/c \qquad (2)$$

Putting N = N' + N" and since p = p' + p", we find that

$$f = (N + p)/(1 + M_{con}).u_{con}/h \qquad (3)$$

Here $M_{con} = u_{con}/c$, the Mach number. This is the generalised frequency formula, and consistent with it are these:

$$f = (N' + p')u_{con}/h \qquad (4)$$

$$f = (N'' + p'')c/h \qquad (5)$$

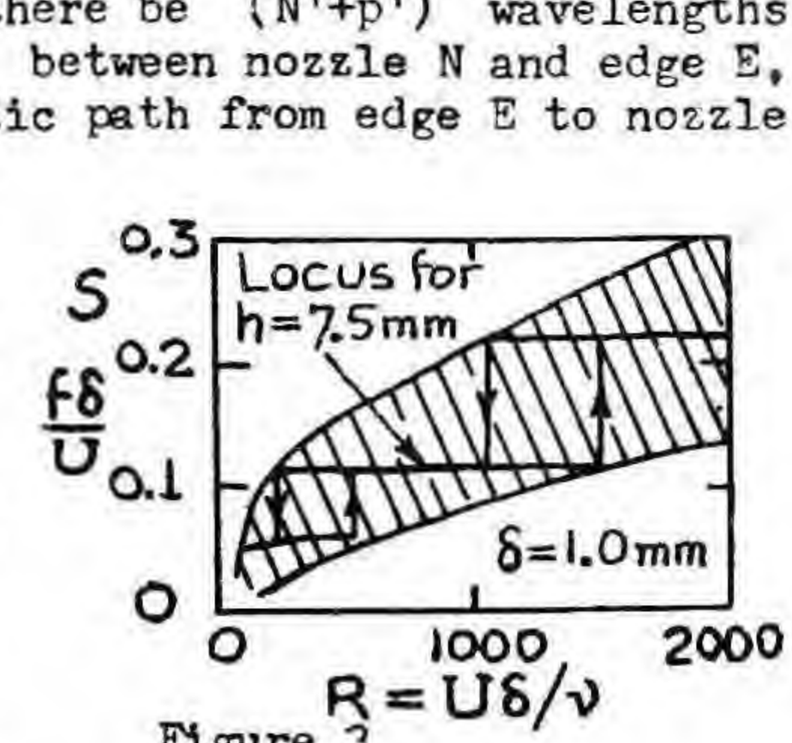

Figure 3

In general u_{con} is a function of h/δ and R, but often the

variation is small in a given mode (i.e. given N) so then S remains almost constant; the phase velocity near a source may differ somewhat from the sound speed. For the low speed edgetones $M_{con} \ll 1$ and $h \ll \lambda''$, and then (2) reduces to (3) and the value $p = 1/4$ is supported by experiment and theory,1)2)3). The frequencies in three stages, N = 1,2,3 are shown in Fig 3 for fixed h as the velocity is varied.

Edgetone at high speeds At high speeds the wavelength is short, $\lambda'' < h$, so the eigenvalues must be taken from (2). In this case the feedback is truly acoustic in nature. The sound field is now attributable to alternating periodic displacements of fluid on either side of the edge with separate monopole radiation on each side, instead of there being reduction to dipole form,1).

Ringtones The ringtone has been constructed as a symmetrical form of the edgetone for here alternate swellings and contractions of the jet interact with a circular ring of approximately the orifice diameter. The behavior is in many ways analogous to edgetones, but it is more complex, it being discovered that downwards as well as upwards jumps in frequency may occur with increasing speed. Since here the jet is symmetrically disturbed at the nozzle by pressure fluctuations, some coupling with the approach to the nozzle may be expected, even if the overt resonances are successfully eliminated. Another distinguishing feature is that due to the symmetry the dipole radiation from the ring must be oriented along the axis, associated with the fluctuating axial force on the ring; measurements have confirmed such a directionality,5).

Oscillations of choked jets Like the high speed edgetone, the feedback is acoustic in nature, but now the sound emanates from the end of each of the distinctive cells of such a supersonic jet. The jet is quite unstable over a continuous range of the frequency, and here again there is a set of eigenfrequencies,6)7). These are also given by (2) provided that effective values are chosen for h and p. However here the effectiveness of the feedback also depends on how much the waves from each source reinforce each other at the nozzle N, see Fig 4, so here η_t is highly frequency dependent. On taking the varying time delays into account, if a_n is the strength of the n'th source from the nozzle N, we find

$$\eta_t \sim \sum_n \frac{a_n}{ns} e^{-2\pi f(ns/c)(1 + 1/M_{con})} \quad (6)$$

Since $\eta_{t,max} = \sum a_n/ns$, a measure of the selectivity of the feedback transmission is $|\eta_t|/\eta_{t,max}$. The plausible values $a_1 = a_4 = 1$, and $a_2 = a_3 = 2$ give the result of Fig 4; the peak recurs at values 2,3,.

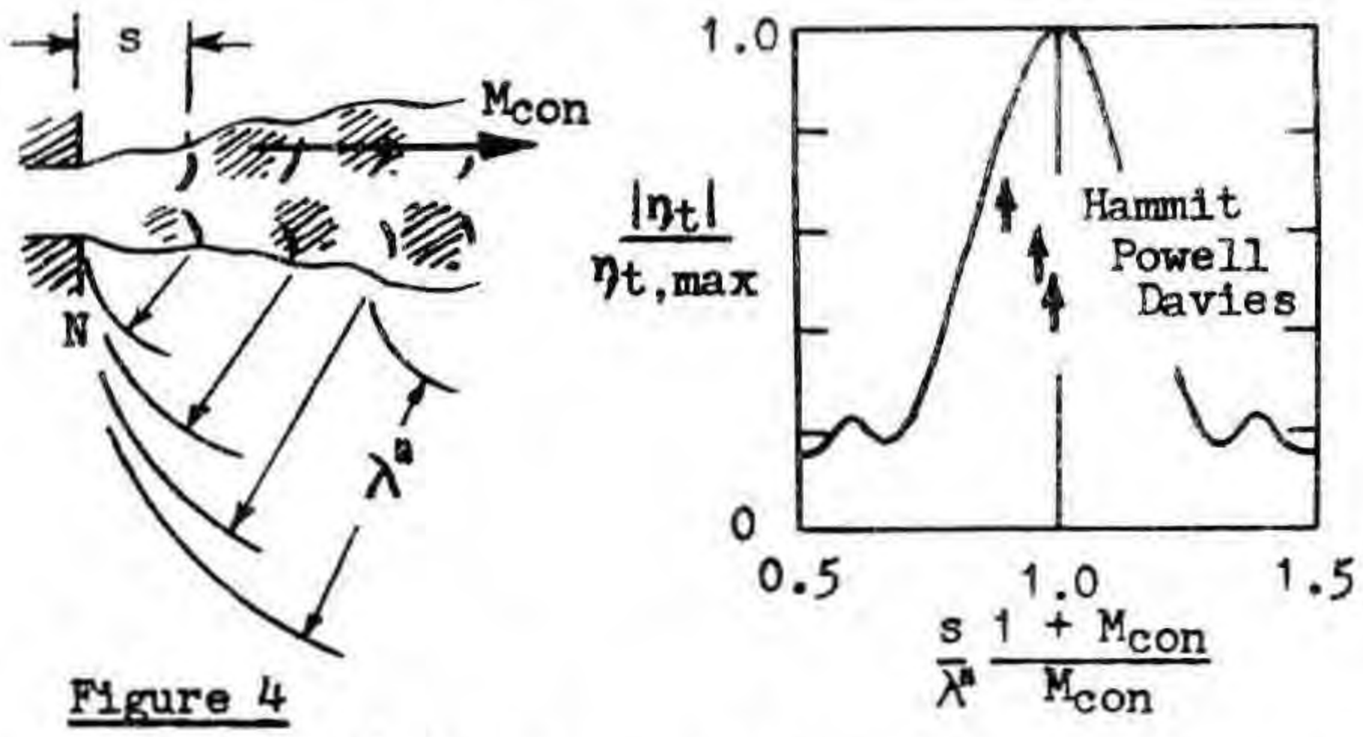

Figure 4

Thus the frequency of oscillation is to be expected to be that eigenfrequency nearest a peak of η_t provided that the jet instability there is adequate. This expectation is borne out by the results of three observers,6)8)9), as may be seen from the averaged results shown in Fig 4.

It is always uncertain as to what are the relative strengths of each of the sources Their effective position cannot be precisely predicted, since because of the greatly enhanced jet spread, convection causes the sound to emerge as from a little downstream of the cell ends. Therefore it is important to note that the overt peak for η_t is relatively insensitive to the actual strengths chosen for the a_n and to variation in the cell length s and the disturbance speed M_{con}.

Turning now from rectangular to circular jets, the frequency of the latter suffers marked jumps as the mode of oscillation suddenly changes,7); here λ''/s, mostly about 2.5, may become as low as 1.75. For proximity to the first maximum of η_t we find $M_{con} > 1$, which is impossible. But for the next maximum we find $M_{con} = 0.4$, which is very plausible. Thus we see how η_t plays an important role in the selection of the proper eigenfrequency for the oscillations of a choked jet.

Edgetone with a reflector

The susceptibility of the low speed edgetone to feedback of a purely acoustical nature is demonstrated by the effect of reflections from a plane, i.e. the direct feedback is supplemented by feedback via an indirect route, Figs 1 and 5. The criterion may now be written as

$$\eta_s(\eta_t + \eta_r)\eta_d q = 1 \qquad (7)$$

(neglecting any difference between η_d and η_d'). If the edge distance be increased so that the tone just vanishes, introduction of a plane reflector may augment the feedback adequately near each of its maxima for the criterion to be met. Thus in the author's apparatus an oscillation occurs for R = 1630 and h = 2.90 mm, with S = 0.135, while no oscillation occurs at h = 2.85 mm. For a plane reflector the calculated augmentation for h = 2.85 mm is as shown in Fig 5: Oscillation actually did occur for the approximate values H = 7,13 and 18 cm, even though the augmentation is extremely small.

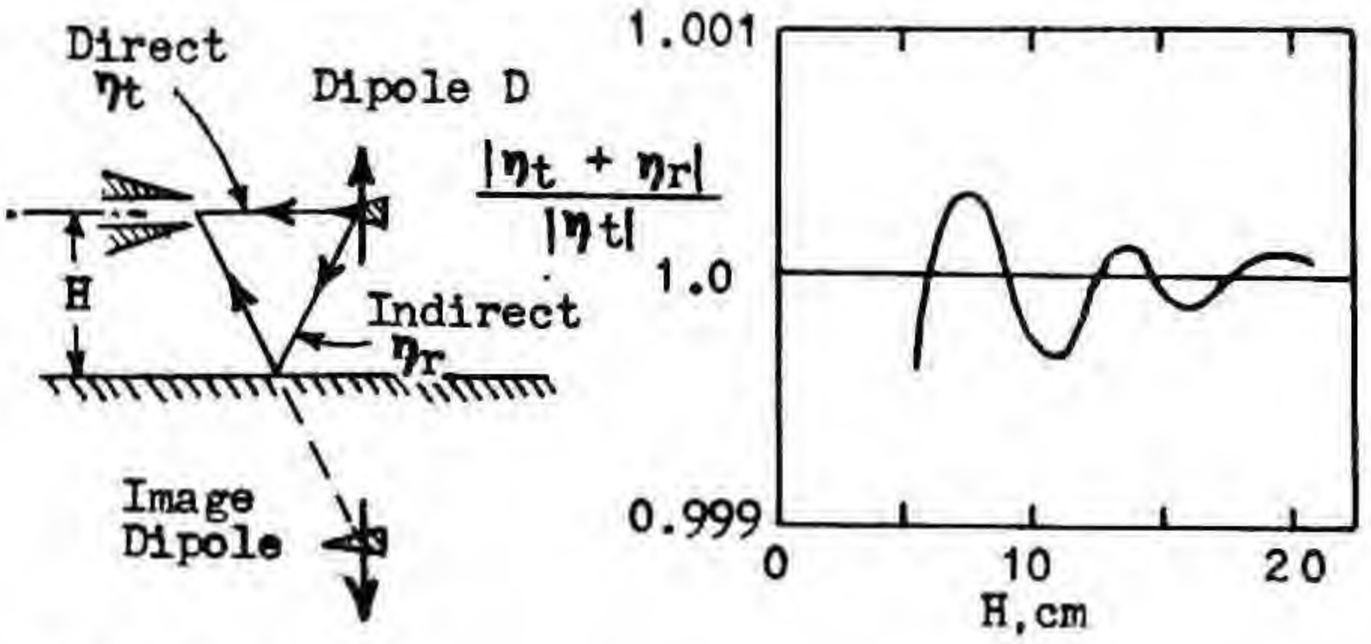

Figure 5

Birdcall The birdcall, briefly discussed by Rayleigh, 10), is similar to the ring tone except that the ring is replaced by a plate with a circular hole in it, and the jet emerges from an orifice in a plate parallel to the first one. Thus reflection occurs from the boundary of the plates. The frequency characteristics have much in common with edgetones, witness von Gierke's observations, 11), but recent work has shown that, as in ringtones to which it is closely related, there may also be frequency jumps of the opposite sense, dependent upon the diameter of the plates. For the larger plates the sound is to be expected to be associated with flow pulsations from the hole, and measurements do disclose a sound field much more uniform than that of a dipole,5).

Oscillations in flow past a wall cavity

The mechanism here is also thought to be of analogous feedback character, it occuring from the rear "edge" E of the cavity to the front edge N, the shear layer being the unstable element, Fig 6; it somewhat resembles a one-sided edgetone with a local reflecting surface, the frequencies being proportional to the velocity with a minimum h for the shear layer to provide adequate amplification to maintain the action, 12). At subsonic speeds the sound radiation is by the periodic interaction at rear edge E. At supersonic speeds the wavelength is shorter and the multiple heavily damped to-and-fro reflections in the cavity result in periodic pressure maxima, which generate additional sound waves extending out into the supersonic steady flow. These may have a crinked appearance because of the pressure maxima oscillating in position. Experiments show the crinkle wavelength λ_c to be consistent with the wavelength λ' of the disturbed shear layer and the cavity length h, 13).

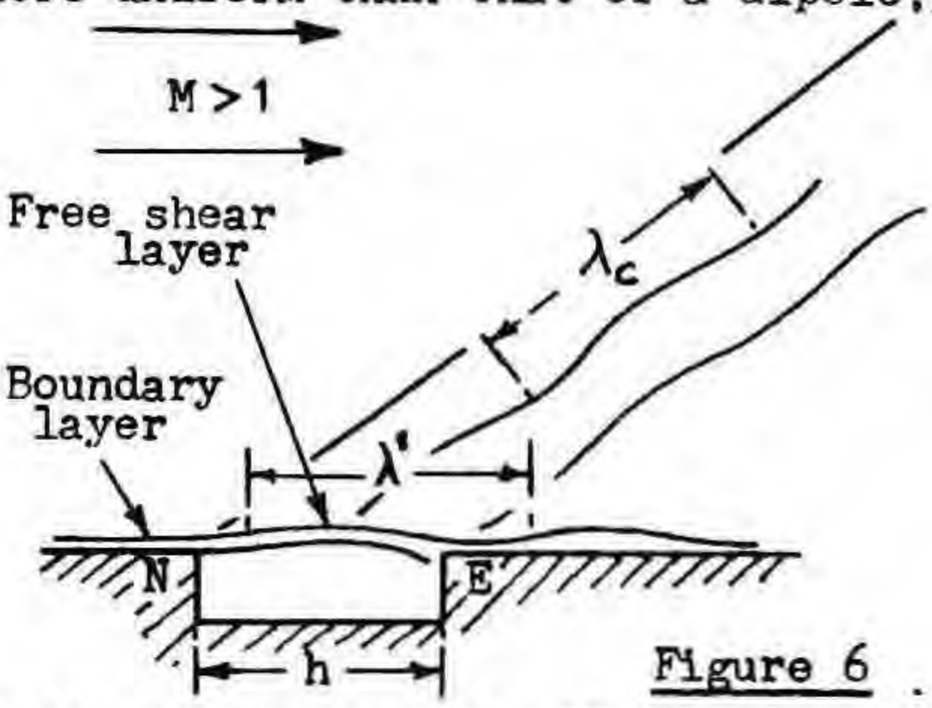

Figure 6

Hartmann Ocsillator Here a supersonic jet is directed straight into a cavity also of circular cross-section; the strogly resonant acoustical properties were reported in some detail by Hartmann of Copenhagen, 14). Recent schlieren photographs have shown that during part of the cycle the jet almost wholly enters the cavity; about half a cycle later the compressed fluid is expelled to form a powerful sound-producing vortex. The photographs also show that the sound so generated causes axisymmetric disturbances in the supersonic jet leaving the nozzle. Corresponding eddies, and the local narrowing of the jet stream, are also evident in the two-dimensional case, where a destabilising trip wire has to be inserted in front of the cavity. These new observations are highly suggestive that the basic character of the mechanism of operation is of the class under discussion here, 15).

Organ type tones Here a pipe introduces a powerful resonance into the indirect feedback path, so that η_{fr} has a sharp maximum at each of the resonant modes of the pipe: Here we have the condition

$$\eta_s(\eta_t\eta_d + \eta_r\eta_d')q = 1 \qquad (8)$$

A symmetrical open pipe was added to the edgetone system of Fig 3 so that the edgetone system lay across its center, the results being shown in Fig 7. The three bands of S for activity are apparently associated with the edgetone stages, although in the changed circumstances exactly similar action is not to be expected. At the lowest speed the action is ragged, dominated by three major unsteady components, not harmonically related, as shown by the shading; the lower two evidently correspond to two "edgetone" modes, while the highest one is centered on the fundamental pipe frequency. Resonant action first commences here then jumps to the next lower "edgetone" mode as the speed increases; later it jumps to the lowest mode. In all of these the pipe is resonating in its first, fundamental, mode at almost its natural frequency. But there is a very significant intermediate stage where this fundamental frequency is away from an edgetone region: Here the action jumps to the second mode of the pipe, which does coincide with such a region. Strong harmonics are present at the higher speeds; adjacent to the fifth harmonic shown in Fig 7 is a limited but clearly defined note of constant S, characteristic of the edgetone itself.

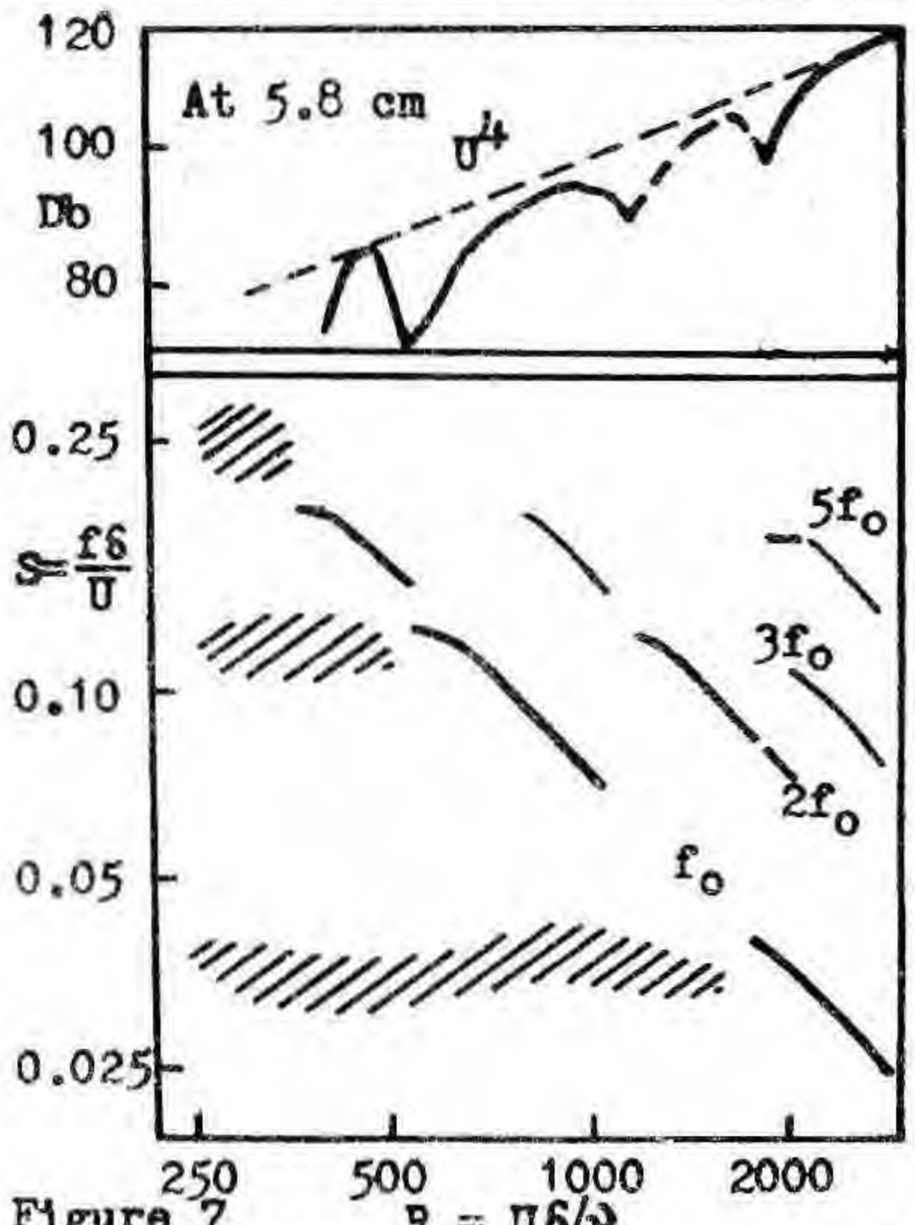

Figure 7

The characteristic variation of sound intensity as each stage is passed through is shown in Fig 7. The succesive maxima vary nearly as U^4, consistent with excitation at constant frequency by a dipole whose limiting force varies as U^2, 2).

At higher speeds than shown in Fig 7 a jump again occurs from the first pipe mode to the second; this restores the action to the lowest "edgetone" mode. At even higher speeds a similar jump occurs from the second to the third mode of pipe resonance, 16).

Essential character of the self-maintained oscillations A number of flow situations have been discussed with the emphasis on the nature of the feedback mechanisms involved. It is important to note that the oscillations of these jet-like flows are far from minor perturbations of any steady flow picture, but are an integral part of the overt flow characteristics, apart from any interesting consequent acoustic output.

In the choked jet the oscillations involve powerful alternate vortex formations which cause a radical increase in the angle of spread of the jet and in the rate of the energy dissipation. Similarly, in the edgetone the alternate vortices spread out very rapidly compared to the steady laminar flow along the sides of a thin edge at below the minimum h for oscillation. On the other hand, these vortices spread much less rapidly than when the steady laminar jet is completely bifurcated by a blunt (though possibly still small) edge, 17). This latter case is analogous to the Hartmann oscillator, for the non-oscillatory supersonic jet strikes the obstructing cavity and is deflected to spread as a turbulent fan jet of large angle; the angle of the flow is very markedly decreased when this conical jet is replaced by the series of powerful ring vortices which pass downstream past the cavity tube.

Thus the occurrence of these acoustical phenomena are indicative of very fundamental changes in the basic flow patterns due to the self-maintained oscillations.

1) A.Powell, Acoustica 3 163 1953; 2) A.Powell, JASA 33 395 1961; 3) N.Curle, Proc Roy Soc A216 412 1953; 4) A.Powell, JASA 34 163 1962; 5) A.Powell, R.C.Chanuad, unpublished work; 6) A.Powell, Aero Quart 4 103 1953; 7) A.Powell, Proc Phys Soc B 66 1039 1953; 8) M.G.Davies, Aero Research Council Report 19016, 1957; 9) A.G.Hammit, J Aerospace Sci 28 673 1961; 10) Lord Rayleigh, The Theory of Sound, vol 2; 11) H. von Gierke, Z Phys 3 97 1950; 12) K.Krishnamurty, NACA TN 3487 1955; 13) A.Powell,A.F.Charwat and G.G.Barnes, unpublished work; 14) J.Hartmann, Acad. Tech. Sci, Copenhagen, 4 1939; 15) A.Powell and T,J.B.Smith, unpublished work; 16) A.Powell, unpublished work; 17) A.Powell,R.C.Chanaud Dept Engineering, University of California,Report 62-8 1962.

P22

FOURTH INTERNATIONAL CONGRESS ON ACOUSTICS
COPENHAGEN 21.-28. AUGUST 1962

UTILIZATION OF HIGH-DAMPING RUBBERS IN VIBRATION CONTROL

J. C. SNOWDON, Ordnance Research Laboratory

The Pennsylvania State University, University Park, Pa.

The performance of anti-vibration mountings employing natural rubber and a high-damping rubber, in either a series or parallel configuration, has been evaluated for a two-stage mounting system supported by a non-rigid foundation. Knowledge of the mechanical properties of natural rubber and two high-damping rubbers has enabled realistic calculations to be made.

High-damping rubbers can be effectively utilized in vibration control, if the manner in which their mechanical properties depend on frequency is properly understood. It is the purpose of this paper to demonstrate theoretically the value of anti-vibration mountings composed of a high-damping rubber and natural rubber, either in a series or in a parallel configuration.

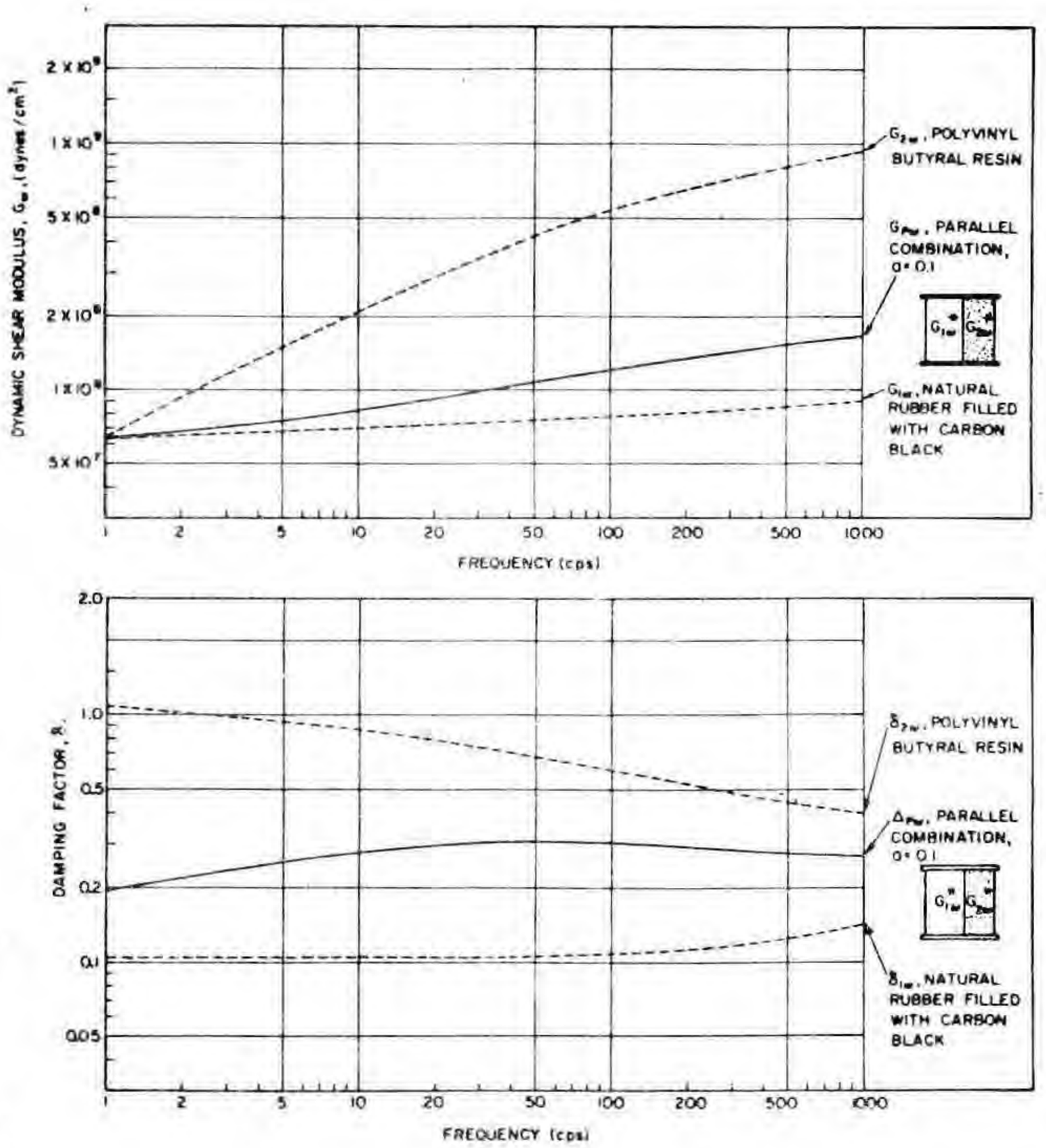

Fig. 1

High mount damping is generally recognized to be of value in reducing the vibration of a mounting system at its resonant frequencies, and in suppressing the lower modes of vibration of any non-rigid foundation that might support the mounting system.[1] Unfortunately, the dynamic stiffness of high-damping rubbers increases very rapidly with frequency - in contrast to the stiffness of natural rubber, which remains constant or increases only slowly with frequency. In consequence, at frequencies well above the natural frequency of a one-stage mounting, for example, the isolation afforded by a high-damping rubber does not increase in proportion to the square of frequency, as simple theory predicts for a spring, but at a slower rate. The amount

by which the isolation of the high-damping rubber differs from the level predicted by simple theory or from the isolation afforded by natural rubber, which closely follows this level, is usually appreciable.

It is helpful now to refer to Figs. 1 and 2, in which the dynamic shear modulus, G_ω, and damping factor, δ_ω, of two high-damping rubbers, natural rubber and natural rubber filled with fifty parts by weight of carbon black are presented as functions of frequency, ω (refer to broken lines). The parameters G_ω and δ_ω are related to the complex shear modulus G^* of the materials in the usual way, namely,

$$G^* = G_\omega(1+j\delta_\omega).$$

Value of G_ω and δ_ω for Thiokol RD and natural rubber have been deduced by the method of reduced variables from experimental data published by W. P. Fletcher and A. N. Gent.[2] The data for plasticized polyvinyl butyral resin, also obtained by the method of reduced variables, were made available in their present form by K. M. Sinnott and R. K. Eby.[3] The dynamic modulus possessed by polyvinyl butyral resin and Thiokol RD is seen to increase rapidly with frequency, although the modulus of natural rubber varies only slowly with frequency. The damping factor of polyvinyl butyral resin is of interest since it decreases as frequency increases, the transition frequency of the material falling below 1 cps at room temperature.*

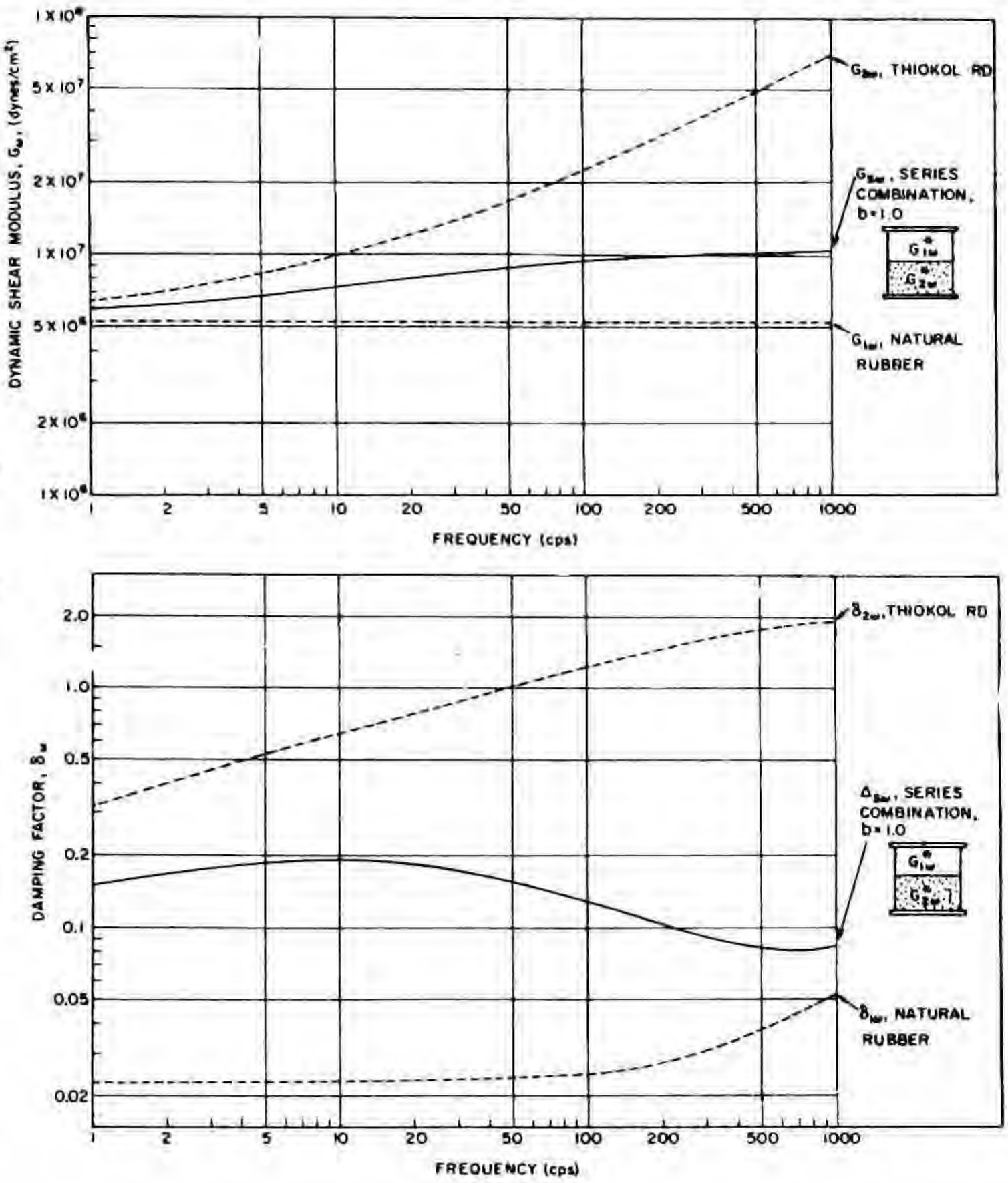

Fig 2

Since the poor performance of the high-damping rubbers at high frequencies will normally detract from their value as anti-vibration mount materials, it is necessary to inquire whether the rubbers could be utilized in other ways so that the benefit of their high damping is not lost, yet the limitation of their large high-frequency stiffness is avoided. Two such methods are now considered, whereby the high-damping

*It is important to realize that the mechanical properties of high-damping rubbers are temperature sensitive, and that the dynamic modulus and damping factor of the high-damping rubbers to which Figs. 1 and 2 refer will take appreciably different values at temperatures not closely neighboring room temperature.

material is mechanically combined in parallel with natural rubber of suitable cross-section, as in Fig. 1, or combined in series with natural rubber of suitable thickness, as in Fig. 2. The shear modulus and damping factor of the parallel and series combinations are shown as full lines in these figures, the constants "a" and "b" refer to the ratio of the cross-sectional areas, and to the ratio of the lengths of the high-damping rubber to the natural rubber, respectively.

The so-called parallel and series mountings are seen to possess a dynamic modulus that increases only slowly with frequency, yet their damping factor takes values - intermediate to those of the constituent low- and high-damping rubbers - which are of significant magnitude. The dynamic modulus and damping factor have been determined from relations that are readily derived in the following form:

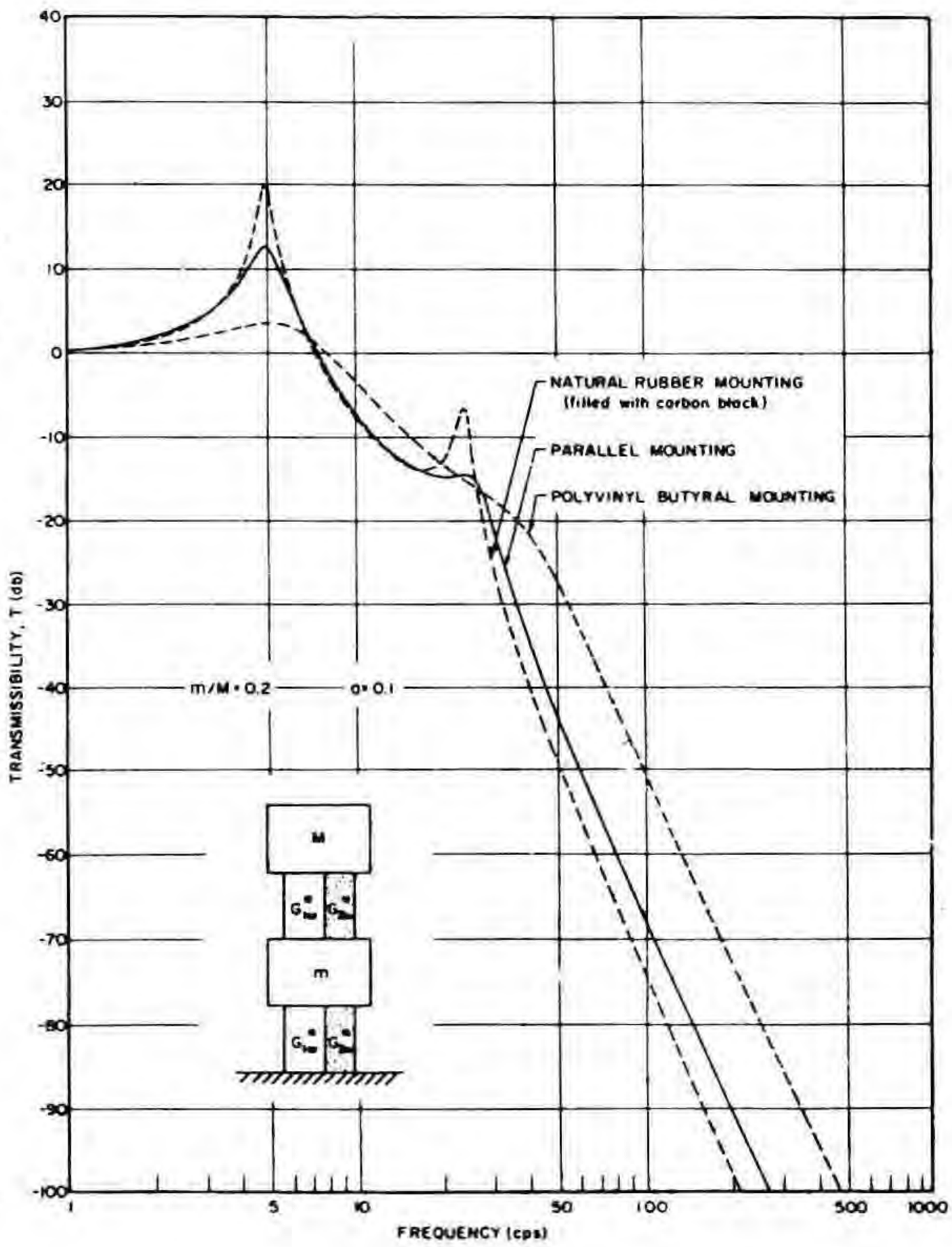

Fig. 3

1. Parallel Mounting

$$G_{p\omega} = \left[\frac{G_{1\omega} + aG_{2\omega}}{1 + a}\right]$$

$$\Delta_{p\omega} = \left[\frac{G_{1\omega}\,\delta_{1\omega} + aG_{2\omega}\,\delta_{2\omega}}{G_{1\omega} + aG_{2\omega}}\right]$$

2. Series Mounting

$$\boxed{G_{s\omega} = \frac{(1+b)G_{1\omega}G_{2\omega}}{(bG_{1\omega}+G_{2\omega})}\left[\frac{(1-\delta_{1\omega}\,\delta_{2\omega}) + (\delta_{1\omega} + \delta_{2\omega})\,\Gamma_{\omega}}{(1+\Gamma_{\omega}^{2})}\right]}$$

$$\Delta_{s\omega} = \left[\frac{(\delta_{1\omega}+\delta_{2\omega}) - (1-\delta_{1\omega}\,\delta_{2\omega})\,\Gamma_{\omega}}{(1-\delta_{1\omega}\delta_{2\omega})+(\delta_{1\omega}+\delta_{2\omega})\,\Gamma_{\omega}}\right]$$

where

$$\Gamma_{\omega} = \left[\frac{bG_{1\omega}\,\delta_{1\omega} + G_{2\omega}\,\delta_{2\omega}}{bG_{1\omega} + G_{2\omega}}\right]$$

To illustrate the effectiveness of the parallel and series mountings, their performance in a two-stage or compound system is now discussed. In one case, the mounting system is considered to be supported by an ideally rigid foundation (Fig. 3), and in the second, by a non-rigid foundation of finite mechanical impedance Z_ω (Fig. 4). The impedance of the non-rigid foundation has been simulated by the driving-point impedance of an internally damped beam. The characteristics of this impedance, and the properties of the mounting system are described in detail in Ref. 1, where an expression is given from which the transmissibility and response ratio* of the system may be calculated [Eq. (6.6)]. Figures 3 and 4 represent the results of one such calculation, which utilizes the values of G_ω and δ_ω presented graphically in Figs. 1 and 2. In this example, the non-rigid foundation is one-fiftieth as massive as the mounted item M, and possesses a constant damping factor $\delta_f = 0.01$. The mounting system employs an intermediate mass m = 0.2 M.

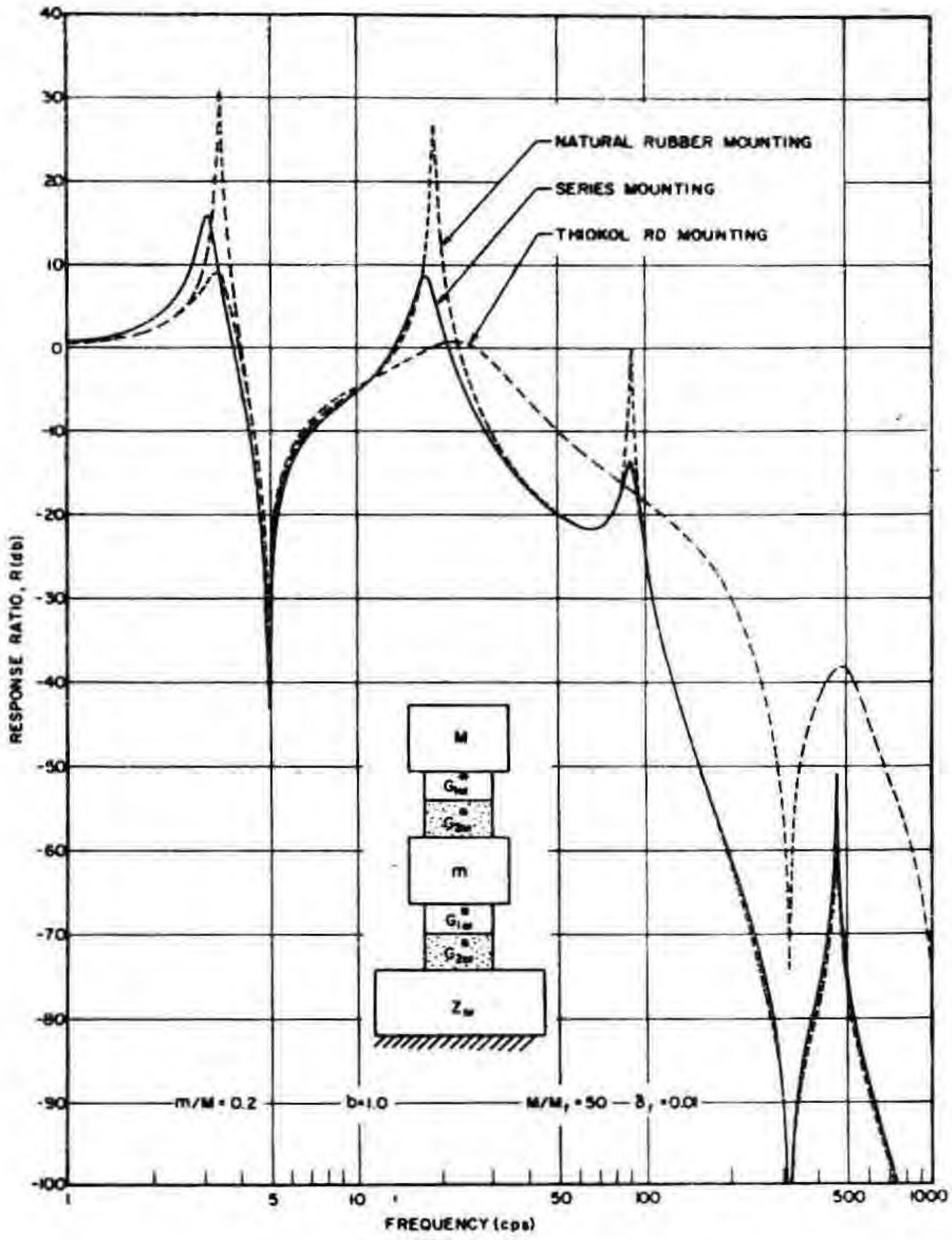

Fig. 4

As anticipated, Figs. 3 and 4 show that although the high-damping mounts heavily "suppress" the resonances of the mounting system and its foundation, they afford less isolation than natural rubber and the composite mountings at other frequencies. The difference in isolation becomes very large indeed at frequencies greater than about 30 cps. In contrast, it is apparent that the parallel and series mountings reduce the resonant motion of the compound system and its foundation appreciably, yet provide an isolation which closely resembles that of natural rubber at all other frequencies.

REFERENCES

1. J. C. Snowdon, J. Acoust. Soc. Am. 34, 54 (1962)
2. W. P. Fletcher and A. N. Gent, Brit. J. Appl. Phys. 8, 194 (1957)
3. K. M. Sinnott and R. K. Eby, private communication (to be published)

*Response ratio is defined as the magnitude of the ratio of the foundation velocity observed when the vibrating item M is resiliently mounted, as in Fig. 4, to the velocity observed when M is connected to the foundation directly.

G23

FOURTH INTERNATIONAL CONGRESS ON ACOUSTICS
COPENHAGEN 21.-28. AUGUST 1962

ACOUSTICAL DESCRIPTION OF SYLLABIC NUCLEI:

AN INTERPRETATION IN TERMS OF A DYNAMIC MODEL OF ARTICULATION*

A. S. House, K. N. Stevens and A. P. Paul, Research Laboratory of Electronics, Massachusetts Institute of Technology, Cambridge, Mass., U. S. A.

A companion paper[1] has described certain data reduction procedures that have been developed for the analysis of vowels, and has indicated that these procedures were used to obtain data for a number of utterances by three talkers. Specifically, the automatic analysis technique was used to obtain formant frequencies throughout the vowel portions of 360 syllables. The syllables were constructed from eight different stressed vowels occurring in 15 different symmetrical nonnasal consonant environments. The boundaries of the vocalic portions of these syllables were established from visual examination of spectrograms of the utterances, and the automatic analysis program was instructed to determine frequencies and bandwidths of the first three formants for spectral samples spaced 8.3 msec apart throughout these vocalic portions.

In the case of the first two formant frequencies, the output of this program took the form shown in Fig. 1. These data were then further reduced by fitting parabolic curves in the manner already described.[1] The results of this procedure led to a description of each vowel in terms of several parameters: the maximum or minimum values F_{10} and F_{20} of the frequencies of the first two formants; the times T_1 and T_2 at which these maximum or minimum frequencies occurred; 'curvature values' for the initial and final segments of the curves depicting F_1 and F_2 as a function of time; and the total vowel duration. In this paper we shall be concerned primarily with the formant frequency values F_{10} and F_{20} and with the curvature values.

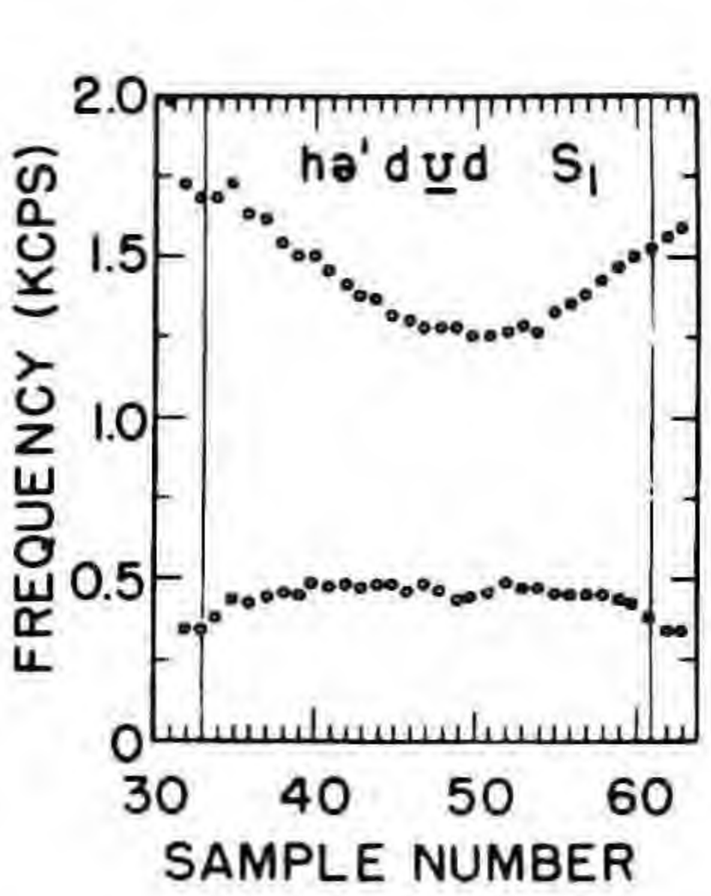

Fig. 1. Example of data on the frequencies of first two formants obtained by the automatic analysis program. Spectral samples occur 120 per sec. The light lines at samples 33 and 61 represent vowel boundaries obtained from visual examination of spectrograms.

In order to interpret these acoustic data it is appropriate to examine the nature of the articulatory activities producing these time-varying formant frequencies. As is well known, a rigorous relation exists between articulatory configurations and formant frequencies since the formant frequencies can be viewed as natural resonances of the vocal tract.[2] A syllable such as that represented in Fig. 1 starts with a constricted articulatory configuration appropriate to the production of the initial consonant. Acoustic manifestations of this configuration are a second-formant transition in the

vowel, originating from a so-called hub or locus,[3-5] and a first-formant transition originating from a frequency near zero. Following the initial consonant configuration, the vocal tract maneuvers toward a relatively unconstricted configuration appropriate to the vowel. During this maneuver the formant frequencies tend toward target values characteristic of the vowel in question. Finally, these continuous activities produce a configuration appropriate to the terminal consonant, and the formant frequencies approach corresponding consonant loci.

The curvature values for the parabolic curves that are matched to the time-varying formants such as those in Fig. 1 provide measures of the extent of the transitions of the formants between consonant loci and vowel targets. It is generally assumed that certain consonants are produced with configurations that are relatively independent of the vowel context; such consonants should be characterized by stable formant loci. Certain consonant phonemes, however, are influenced by vowel context, and thus cannot be characterized by a single set of formant loci.

In Fig. 2, a postdental consonant, which is known to have a relatively stable place of articulation, is examined in different vowel contexts. Each of the plotted symbols indicates the extremal formant frequency F_{20} and the curvature values, averaged over three talkers. There are systematic changes in curvature values from negative to positive as the frequency F_{20} decreases from high to low values, and this change differs slightly for the long and short vowels. The point of intersection of the two functions with the point of zero curvature value is about 1700 cps; when the frequency of F2 for a vowel is less than 1700 cps its curvature value is positive, and conversely when F_{20} is greater than 1700 cps the curvature is negative. In other words the value 1700 cps describes the articulatory context provided by the postdental stop consonant /d/, that is, the so-called F2 locus of /d/ is at about 1700 cps. When other postdental consonants such as /t s z/ are examined in this fashion, a similar consonant locus is obtained. Palatal and interdental consonant contexts produce graphic functions highly similar to those in Fig. 2, except that the respective loci are slightly higher and lower in frequency. When the consonantal context is bilabial, the vowel symbols arrange themselves in a less systematic fashion, and lie primarily to the left of the line representing zero curvature. As expected, the formant locus for this consonantal context is not well-defined, although the data suggest that it has a low frequency in the vicinity of 1000 cps. Contexts such as /k g/ seem always to produce positive curvature values, and again provide a poorly defined formant locus, probably at some high frequency above 2000 cps.

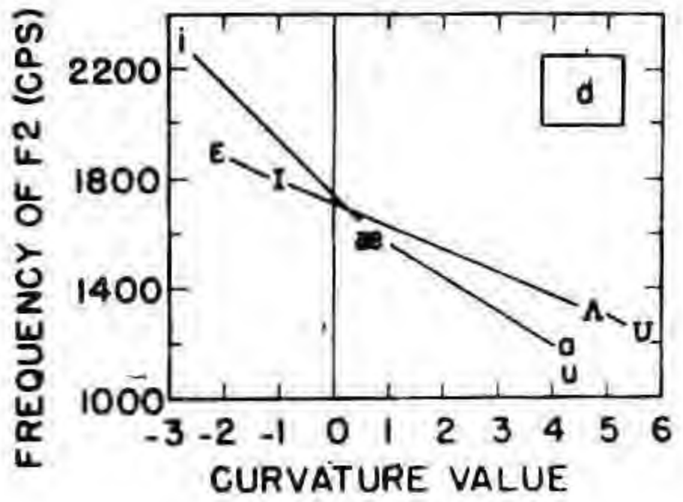

Fig. 2. Frequency F_{20} versus curvature value for various vowels preceded and followed by the consonant /d/. Each point represents average data for three talkers.

The extremal formant frequencies F_{10} and F_{20} can be thought of as estimates of target values appropriate to the vowel. The degree to

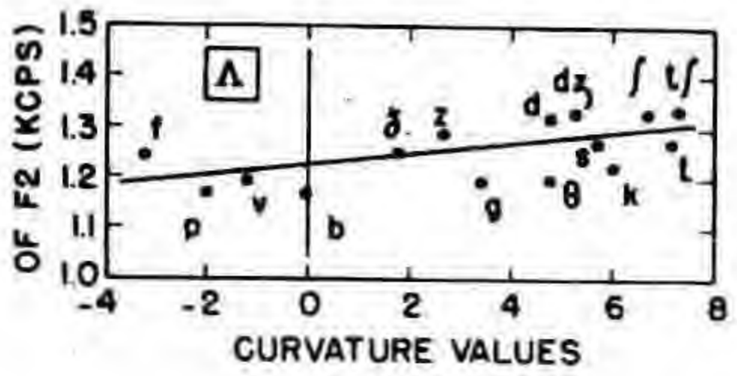

Fig. 3. Frequency F_{20} versus curvature values for a vowel in various symmetrical consonant contexts as indicated. Each point represents average data for three talkers. The straight line was fitted visually to the data.

which F_{20} is dependent upon consonantal context can be demonstrated by a graph of the type shown in Fig. 3. The data display a wide variation in curvature value, but there is a small but apparently systematic increase in F2 as the curvature values become more positive. If the straight line can be interpreted as representing a best fit to the plotted points, then the frequency 1220 cps corresponding to zero curvature value can be interpreted as the so-called F2 target value of this vowel, that is, the F2 value associated with an idealized vowel articulation. When the curvature value is negative, the maximum value of F_2 is less than the target value; for positive curvature values, the minimum value of F_2 is greater than the target value.

Plots of the type shown in Fig. 3 have been obtained for other vowels and indicate similar trends, although the magnitude of the effect differs from one vowel to another. Consonantal context appears to have the greatest influence on the value of F_{20} for rounded vowels. In all cases the effect is such that the extremal value of the second formant frequency is displaced from the ideal target value toward the frequency of the consonantal locus. In articulatory terms, this suggests that there is an effective inertia in the articulatory processes giving rise to undershoot in the system response during the production of syllabic nuclei.

Such an interpretation has implications in the formulation of theories of speech perception and in the design of machines for speech recognition. Both the listener and the machine must be prepared to account for variances in the acoustic signal contributed by dynamic constraints in the articulatory processes.

---

* This work was supported in part by the U. S. Army Signal Corps, the Air Force Office of Scientific Research, and the Office of Naval Research; in part by the National Science Foundation under Grant G-10800; and in part by the U. S. Air Force Cambridge Research Laboratories under Contract No. AF 19(604)-6102.

1. A. S. House, A. P. Paul, K. N. Stevens and Jane B. Arnold, Acoustical description of syllabic nuclei: Data derived by automatic analysis procedures. These Proceedings.

2. L. Hermann, Nachtrag zur Untersuchung der Vocalcurven. Pflueger's Arch. ges. Physiol. 58, 264-279 (1894).

3. R. K. Potter, G. A. Kopp and Harriet C. Green, Visible Speech. New York: Van Nostrand, 1947.

4. P. Delattre, A. M. Liberman and F. S. Cooper, Acoustic loci and transitional cues for consonants. J. Acoust. Soc. Am. 27, 769-773 (1955).

5. K. N. Stevens and A. S. House, Studies of formant transitions using a vocal-tract analog. J. Acoust. Soc. Am. 28, 578-585 (1956).

H23

FOURTH INTERNATIONAL CONGRESS ON ACOUSTICS
COPENHAGEN 21.-28. AUGUST 1962

Age and Sex Differences in Pure-Tone Thresholds from 18 to 65 Years

Dr. John F. Corso

INTRODUCTION

The current interest in the relationship between noise exposure and auditory functions has led to a growing concern about the validity of the American reference level for normal hearing. The reference level is fundamentally involved in the specification of the amount of permanent hearing impairment which may result from excessive noise exposure. This problem has become increasingly important in recent years due to (1) the development of jet aircraft, rocket engines, and other devices which can generate overall sound pressure levels of 130 db or more re 0.0002 dyne/sq. cm., and (2) the passing of certain state court rulings which hold that industrial deafness is an occupational disease, thus entitling the affected worker to a schedule award under the Workmen's Compensation Law.

Since it is now clearly established that prolonged exposure to noises having certain intensity and frequency characteristics can produce permanent shifts in man's auditory thresholds, two major issues remain to be resolved if the amount of damage attributable to noise exposure is to be evaluated properly: (1) the method for measuring and specifying the degree and type of hearing loss must be precisely described, and (2) the degree and type of auditory impairment must be related to its practical significance in a social setting. The present paper is restricted to a consideration of the first issue.

The measurement and specification of hearing loss involves a large number of related factors. These may be grouped into the following five classes: (1) the kind of material on which the individual is to be tested; (2) the psychophysical testing procedure to be used; (3) the environmental conditions under which the testing is to be done; (4) the psychological characteristics of the individual to be tested, and (5) the training and qualifications of the test administrator. Assuming that these and other factors which influence the accuracy of auditory threshold measurements can be reasonably well controlled in a laboratory situation, a crucial problem arises when the attempt is made to specify an individual's threshold of hearing in terms of hearing loss, i.e., relative to the values for a group of individuals with "normal" hearing. To properly evaluate the effects of noise exposure, the normative data serving as the baseline of comparison must be derived from individuals with little or no history of noise exposure and must reflect those changes in hearing which may be generally expected to accrue as a function of age.

STATEMENT OF THE PROBLEM

The primary objective of this study was to obtain pure-tone threshold data on a large sample of subjects stratified by age and by sex and drawn from a population exposed to minimal levels of industrial noise. The study was conducted in State College, Pennsylvania from 1952 to 1962, after a careful physical analysis of the ambient noise levels in the general area indicated the absence of excessively high noise levels such as those associated with industry or heavy traffic. It was anticipated that the data of the study would (1) provide a valid reference level for the assessment of hearing loss due to noise exposure, (2) yield an unbiased extimate of the effects of presbycusis, i.e., reduced hearing acuity with advancing age, and (3) serve as a basis for further consideration in the re-establishment of the American reference level for normal hearing.

METHODOLOGY

Subjects. The subjects tested (N = 912) were selected from six age categories: (1) 18 to 24 years; (2) 26 to 32 years; (3) 34 to 40 years; (4) 43 to 49 years; (5) 51 to 57 years; and (6) 59 to 65 years, inclusive. The subjects in the youngest age group were taken from the undergraduate student population at The Pennsylvania State University; the remaining subjects were selected at random

from the lists of registered voters for State College, Pennsylvania. This latter procedure was adopted to restrict the sample of subjects in the older age groups to more-or-less permanent residents.

All subjects in the study were required to complete a three-step experimental sequence. This included: (1) a comprehensive hearing survey questionnaire administered by a trained interviewer; (2) an otological examination performed by a qualified physician; and (3) an audiometric test given by an experienced student in psychology within 48 hrs. after the otological examination. When each subject had completed the three-step requirement, he was presented with the results of both his otological examination and audiometric test on standard forms. Not all subjects contacted by the interviewers agreed to participate in the study. The most common reason for refusal was the lack of time to fulfill the three-step requirement. In the five oldest age groups, 62% of the individuals sampled (862 in 1381) actually participated as subjects in the study and completed all requirements.

Apparatus. All subjects were tested on a Beltone audiometer, Model 10-A, which was appropriately modified with an impedance matching network to permit the use of Permoflux PDR-8 earphones mounted in MX-41/AR cushions. The resistive network also reduced the output voltage over the frequency range tested by approximately 15 to 30 db below the normal values of the U. S. Public Health Survey, as reduced to equivalent PDR-8 pressures by the National Bureau of Standards. For the two oldest age groups, an additional stage of amplification was added to the audiometer to provide a fixed gain of approximately 7 db above the maximal value at each frequency as provided by the manufacturer. The sound pressure output of the audiometer was calibrated periodically in a National Bureau of Standards coupler 9-A in accordance with recommended procedures. Periodic calibration checks were also made on the frequency of the generated signals and on the characteristics of the hearing-loss attenuator.

Testing Procedure. The testing procedure followed the method of limits with 2-db changes in intensity when the signal was near threshold strength. Three tone pulses were presented at each intensity setting near threshold and the criterion of hearing was set at two of three responses. The duration of each tone pulse was approximately 1.0 sec. and the interpulse intervals ranged from 0.6 sec. to several sec. depending on the particular age group being tested. Threshold measurements were made at nine frequencies in the following order: 1000, 500, 250, 1000, 1500, 2000, 3000, 4000, 6000, and 8000 cps. (The initial 1000 cps test was discarded as a practice trial in the analysis of data.) At each frequency, the threshold was crossed in a series of two ascending and two descending trials presented in alternation. The absolute threshold for a given ear for a given subject was taken as the mean audible intensity for these four trials. The sequence of testing right and left ears was alternated between subjects and a 5-min. rest period was provided between the tests for each ear. The total testing time per subject was approximately 50 min. All tests were individually administered in an anechoic chamber provided with a two-way voice communication system and a closed-loop television system.

RESULTS AND CONCLUSIONS

The basic data of this study consisted of individual threshold values for both right and left ears expressed in terms of sound pressure level (SPL), i.e., db re 0.0002 dyne/sq. cm, at each of nine test frequencies. From these data, derived measures of central tendency and variability were computed at each frequency for the six groups of subjects. The derived measures were analyzed at each frequency by age groups, by ears, and by sex in terms of three types of distributions: (1) original distributions which contained the data for all subjects selected in the study, (2) screened distributions which contained the data for only those subjects who passed rigid screening criteria related to otological disorders, military service, and the extent of environmental noise exposure, and (3) truncated distributions which contained only data ± 15 db from the mode of the screened distributions.

In order to compare the data of the present study with the data on presbycusis published by the American Standards Association, the threshold data for right and left ears were combined at each test frequency for both men and women in each of the six age groups. The combined mean thresholds for the 18 to 24 year old group next were used as a baseline and, by subtracting these values from the obtained mean thresholds at each frequency for each of the five remaining age groups, estimates of presbycusis were obtained for the men and for the women in the original sample. For the men, there was a general similarity in the two sets of curves but, except for 4000 cps, the data of the

present study indicate that the major "break" in the audibility curves occurs at about 32 years of age, with less than 2 db hearing loss for any frequency below this point. The 4000 cps threshold is depressed starting with the 26 to 32 year old group and the curve is consistently lower (poor hearing) than that of the American Standards Association up to approximately 54 years of age. In general, there is a trend for the magnitude of the discrepancies between the two sets of data to decrease as a function of increasing age. For the 59 to 65 year old group, the maximal discrepancy is approximately 2 db (at 4000 cps).

The data for the women in the original distribution seem to support the contention of the American Standards Association that the "break" in the audibility curves occurs at about 37 years of age. At ages younger than this, there is less than 5 db hearing loss; beyond this, there are differential frequency effects but not so marked as for men. The differences in thresholds between frequencies for women are also not so great as those for men. In general, except for 500 and 1000 cps in the 43 to 49 year old group, the data for the women in the original sample of the present study beyond 37 years of age differ from those of the American Standards Association in three ways: (1) the present data show greater hearing losses as a function of age; (2) the differences between frequencies are smaller than those shown by the curves of the American Standards Association; and (3) while all the curves of the American Standards Association appear to "level-off" beyond 60 years, the present curves for 2000, 3000, and 4000 cps have a marked negative slope in this age region.

While the data for the original sample tend to conform in some degree to the curves of the American Standards Association, the original samples were known to contain subjects with otologically abnormal ears, as well as subjects who had been exposed to high levels of noise. Consequently, the effects of these extraneous factors probably served to inflate the derived values of the present study. To obtain more valid estimates of presbycusis, rigid screening criteria were applied to the original sample of subjects to eliminate those subjects with a history of excessive noise exposure and/or otological abnormalities. Noise exposures were considered whether they were related to vocational training, living environment, military service, occupational setting, hobbies, or transportation. The information on noise exposure was obtained from the hearing survey questionnaire. The results of the screening procedure showed the following percentages of subjects eliminated in the six age groups: (1) 18 to 24, 22%; (2) 26 to 32, 41%; (3) 34 to 40, 36%; (4) 43 to 49, 34%; (5) 51 to 57, 26%; and (6) 59 to 65, 25%. In each age group, more men than women were eliminated. The large percentage of subjects eliminatedin each age group indicates that the screened samples were required to pass a relatively stringent set of criteria.

Since threshold data were collected for both right and left ears on all subjects, tests of significance were performed at each frequency for the differences in means and in variances for men and for women within each age group. Where significant differences did occur, the maximal difference between ears was approximately 9 db, with nearly all remaining differences being 5 db or less. Thus, it was concluded that for practical purposes, the threshold data of the screened distributions for right and left ears could be combined and that no appreciable biasing effect would be introduced by this procedure.

The mean threshold SPL's (combined ears) as a function of frequency, with age as the parameter, are shown in Figure 1 for the men and in Figure 2 for the women of the screened samples. The curves show that, in general, (1) hearing acuity diminishes (thresholds are higher) with advancing age, regardless of sex; (2) the effects of advancing age for both men and women are most pronounced for frequencies above 1000 cps, approximately, than below; (3) for a given age group, men have poorer hearing than women at and above 3000 cps, but the women in the two oldest age groups have poorer hearing at and below 1000 cps; and (4) regardless of age, threshold values for men and women do not differ by more than 6 db at and below 2000 cps. The standard deviations associated with these data points are, in general, smaller for women than for men, particularly above 3000 cps; exceptions occur in the two oldest age groups at certain low frequencies.

(The data for the truncated distributions are not presented in this report.)

SUMMARY

Audiometric measurements were made from 250 to 8000 cps on 912 subjects, ranging in age from 18 to 65 years and selected from a population exposed to minimal levels of industrial noise. The results for a screened sub-sample (N = 624 subjects) indicate that (1) hearing acuity diminishes with advancing age, (2) the effects of presbycusis depend upon frequency, with the greatest effects occurring above 1000 cps, (3) in general, men have poorer hearing than women, age held constant, and (4) the effects of presbycusis differ for men and women. These findings relate to the assessment of noise-induced hearing-loss and to the specification of future audiometric standards.

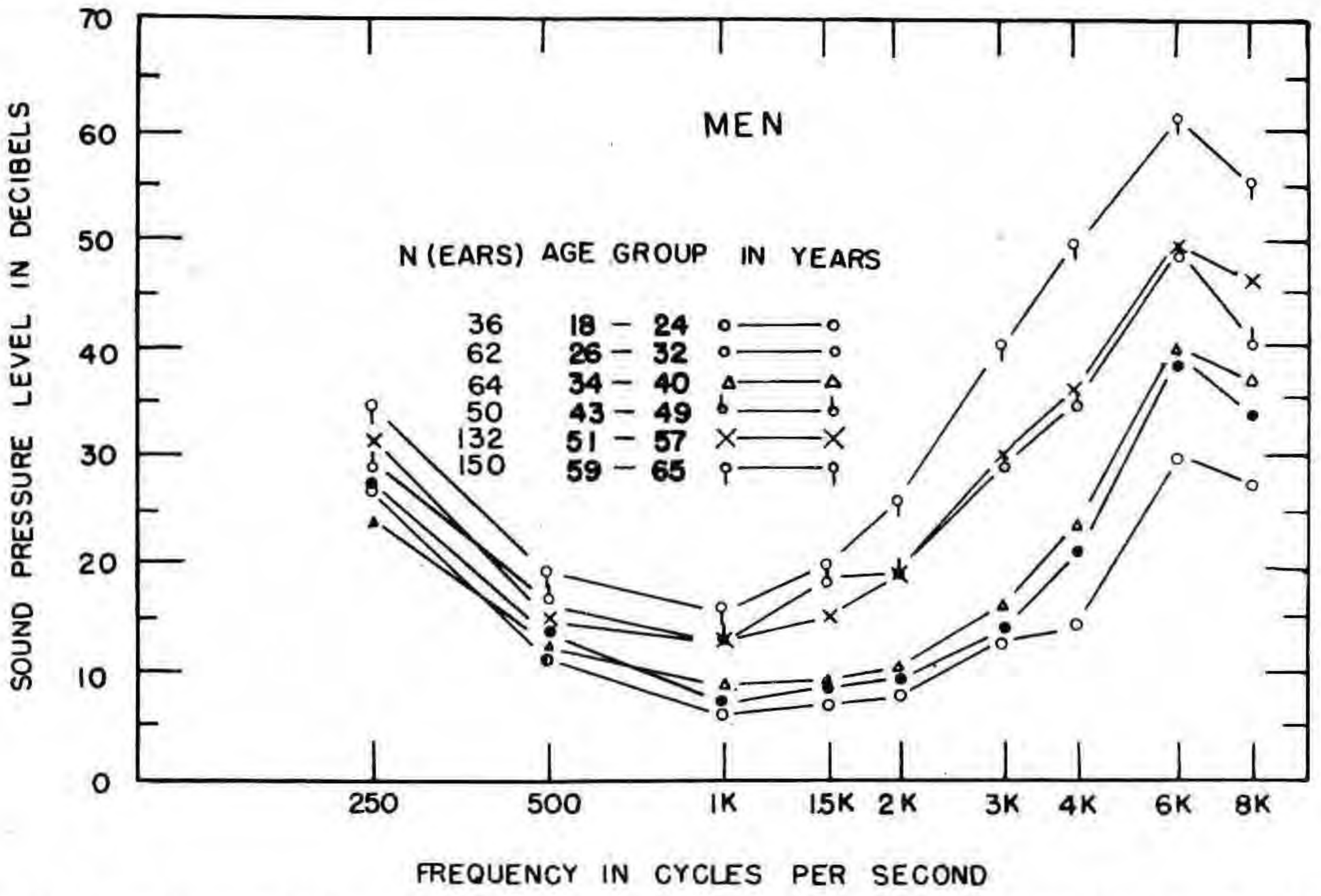

Fig. 1. Mean threshold sound pressure levels in db re 0.0002 dyne/sq.cm. for the combined right and left ears of the men in the screened sample of subjects.

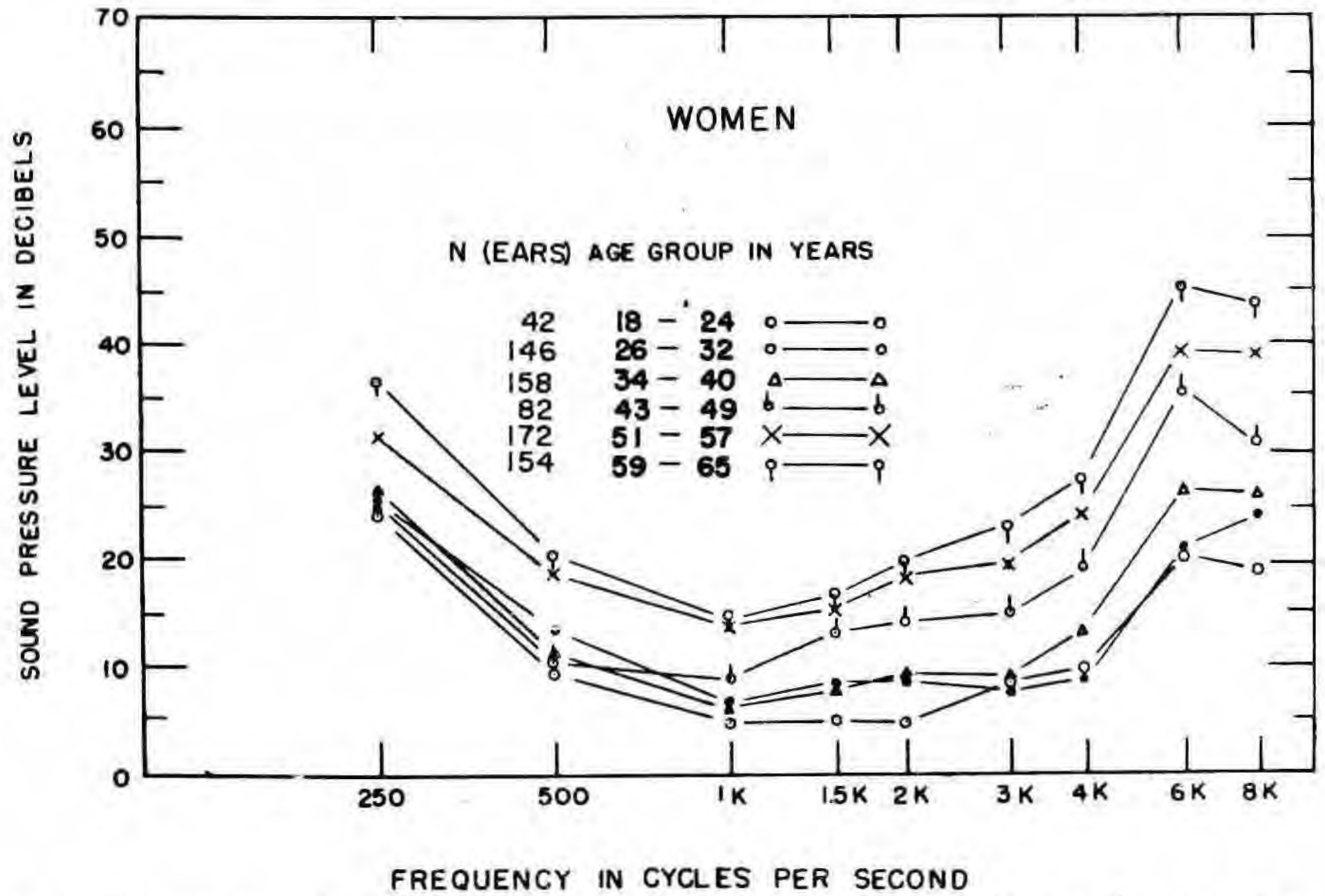

Fig. 2. Mean threshold sound pressure levels in db re 0.0002 dyne/sq.cm. for the combined right and left ears of the women in the screened sample of subjects.

J23

FOURTH INTERNATIONAL CONGRESS ON ACOUSTICS
COPENHAGEN 21.-28. AUGUST 1962

Die Kinetik des Wachstums und der.Auflösung von Monokristallen im Ultraschallfeld.

A.P.Kapustin

1. Einfluß Ultraschalls hoher Frequenz auf die Bildung und Auflösung von Monokristallen

Der Bildungsprozess Polykristalliner Struktur unter dem Einfluß von Ultraschall wurde bereits von vielen Forschern untersucht. Die Frage, ob der Ultraschall auf das.Wachstum eines Monokristalls Einfluß hat, bleibt aber noch ungeklärt. Während seines Wachstums erhält das Kristall nur von dem Medium Moleküle oder ihre Aggregate, das sich mit ihm in unmittelbarer Berührung befindet. Das geschieht dank dem Konzentrationsfluß und der Diffusion der stärker konzentrierten Lösung über die dem Kristall anliegende Schicht fast gesättigter Lösung. Es ist von Interesse, ob der Ultraschall auf den Prozess des Austauschs von Molekülen und im Einzelnen auf den Diffusionsprozess Einfluß haben kann. Die Klärung dieser Frage könnte viele, heute bekannte, Wirkungen des Ultraschalls erläutern.

Außerdem eröffnen die durch Ultraschall auf der Oberfläche eines festen Körpers hervorge rufenen Veränderungen Möglichkeiten zum Studium des Einflußes plastischer Formänderung auf den Charakter der Vergrößerung von Kristallflächen.

In diesem Zusammenhang wurde der Versuch gemacht, den Einfluß des Ultraschalls auf die lineare Kristallisationsgeschwindigkeit.einer Oktaederfläche des Monokristalls von Kalialaunen zu untersuchen. Dieser Einfluß sollte bestimmt werden durch Vergleich der Wachstumsgeschwindigkeit des Monokristalls im Ultraschallfeld mit seiner Wachstumsgeschwindigkeit bei sonst gleichen Bedingungen außerhalb eines Ultraschallfeldes. Als Ultraschallquelle diente eine Quarzplatte, angeregt durch einen Röhrengenerator mit einer Grundfrequenz von 2 MHz. Die maximale Intensität lag nicht über 0,2 W/cm^2.

Der Versuch wurde folgendermaßen durchgeführt. Die Lösung wurde mit einer Temperatur, die 7-8 C über der Sättigungstemperatur liegt, in mit Dampf behandelte Kristallisatoren abgefüllt. Diese wurden mit Deckeln verschlossen, in denen Öffnungen zur Einführung der Kristalle und eines Thermometers vorgesehen waren. Danach wurden die vorher abgewogenen Kristalle in die Kristallisatoren eingeführt, von denen einer mit Ul-

traschall behandelt wurde. Auf die entsprechenden Flächen beider Kristalle sind optische Rohre zur Beobachtung der Flächenwanderung während des Wachstumsprozesses eingerichtet worden. Die Werte der linearen. Flächenwanderung wurden 15-30 min Nach Versuchsbeginn festgehalten. Nach der Differenz des Anfangs- und Endgewichtes bildeten wir uns ein Urteil über die Zunahme der Masse der Kristalle. Unter bestimmten Bedingungen konnte man auch die Auflösung der Kristalle beobachten.
Die Versuchsergebnisse zeigen, daß bei einer Temperatur, die über der Sättigungstemperatur leigt, im Ultraschallfeld die Auflösung des eingeführten Kristalles intensiver verläuft. So übersteigt die mittlere lineare Geschwindigkeit der Flächenwanderung bei Ultraschalleinfluß die mittlere lineare Auflösungsgeschwindigkeit unter Normalbedingungen ungefähr um das doppelte.
Wenn die Lösung übersättigt wird, ist eine hohe Geschwindigkeit des Flächenzuwachses im Ultraschallfeld zu verzeichnen. In diesem Fall übersteigt die mittlere lineare Wandergeschwindigkeit senkrecht zur Fläche um 2-3 mal die mittlere lineare Wachstumsgeschwindigkeit des Kristalls ohne Ultraschllfeld. Es wurde ermittelt, daß der Ultraschall nicht nur das Wachstum der Strahlungsquelle zugewandten Fläche, sondern auch das der übrigen Flächen beschleunigt.
Um den Einfluß der Intensität des Ultraschalls auf das Wachstum der Monokristalle zu untersuchen, wurden Versuche mit Kristallen durchgeführt, deren Anfangsgewicht bei ca 23 mg lag. Die Sättigungstemperatur betrugt 25,5 C. Die bei der Durchführung des Versuches angewandte maximale Intensität des Ultraschalls betrugt 0,25 W/cm^2. In sämtlichen Fällen wurde die Lösung erst dann dem Ultraschall ausgesetzt, als der Auflösungsprozess der Kristalle beendet war. Bei einer Intensität J=0,006W/cm^2 und bei einer linearen Geschwindigkeit des Flächenzuwaehses unter gewöhnlichen Bedingungen von 0,027 mm/h hat der Ultraschall keinerlei Einfluß auf das Wachstum der Fläche. Eine weitere Intensitätserhöhung führt zur Verringerung der Wachstumsgeschwindigkeit der Fläche, gleichzeitig entstehen in der Lösung Kristalle und die Temperatur der Lösung steigt an.

2. Einfluß Ultraschalls niedriger Frequenz auf das Wachstum von Monokristallen der Kaliala'ne.

Bei den Versuchen wurden Intensitäten angewandt, bei denen keine Kavitationserscheinungen auftauchten (J=0,2W/cm^2). Die Kristalle wurden in den Bauch und in den Knoten einer stehenden Welle gebracht. Die Keimkristalle hatten eine Masse von 22mg und 22,3mg. Die Anfangsgeschwindigkeit des Flächenwachstums betrug 0,06 mm/n. Die Lösungstemperatur änderte sich von 23 bis 22,2 C. Die Sättigungstemperatur betrug 26 C.

Die Erfahrung zeigt, daß ein Kristall, welches bei Ultraschalleinfluß im Druckknoten aufgewachsen ist, senkrecht zur Ausbreitungsrichtung des Ultraschalls gegenüber einem Kristall, das in einer nichtbeschallten Lösung aufwuchs, etwas langgezogen erscheint. Ein Kristall,das bei Ultraschall im Druckbauch gezüchtet wurde, sieht gestreckt parallel zur Ultraschallstrahlrichtung aus. In den Druckknoten überwiegt der Tangentialzuwachs der Fläche, in den Schwingungsbäuchen-der Normalzuwachs.

3. Die Kristallisation von Kalialaunen in Lösungen unter Ultraschalleinfluß.

Die experimentelle Untersuchung des Ultraschalleinflußes (f=30kHz) auf die Kristallisationskinetik in Lösungen gestattet es, eine Reihe neuer interessanter Erscheinungen festzustellen.

In einer übersättigten Lösung (6-8 C unter der Sättigungstemperatur) entsteht bei Anwesenheit eines kleinen Kristalls bei genügender Intensität sofort nach dem Einschalten eine große Menge Kristallisationsherde, die bald das ganze Lösungsvolumen ausfüllen. Diese Erscheinung ist bei einer Frequenz ca 700 kHz zu beobachten. Nach Ausfällen der vom Niederschlag abgegossenen Lösung beträgt die Sättigungstemperatur den Wert der Zimmertemperatur oder um 1-2 C mehr. Die aus der Lösung ausgefällten Kristalle haben das Aussehen von Nadeln oder Plättchen. Ihre Entstehung und Entwicklung hängt von der Intensität des Ultraschalls, von der Lösungskonzentration und von der Lage des Keimkristalles im Kristallisator ab. Ein wesentlicher Faktor für die Bildung einer großen Menge Kristallisationherde in der Lösung ist ebenfalls das Vorhandensein einer stabilen stehenden Welle.

Man sollte noch auf folgende Erscheinungen hinweisen. Bei einer bestimmten Übersättigung der Lösung entsteht im Druckbauch der Welle ein "Klumpen" kleiner Kristalle. Zu ihm stoßen aus dem umgebenden Medium kleine Kristalle hinzu und gleichzeitig werden größere ausgestoßen. Wenn man in die Lösung einen großen Kristall hineinbringt und ihn senkrecht zur Wellenfront aufstellt, so bleibt ein Teil der kleinen Kristalle nach Erreichen der Fläche des großen Kristalls fest an ihr haften. Die Untersuchung dieser Präparate hat gezeigt, daß die größte Menge der anhaftenden Kristalle mit dem Hauptkristall parallele Verwachsungen bildet. Dieses Ergebnis trägt zum Verstehen des Wachstumsablaufs der Kristalle bei.

4. Herstellung von Ätzfiguren durch Ultraschalleinwirkung.

Es wurde festgestellt, daß Ultraschall auf das Anfangsstadium der Auflösung von Monokristallen, namentlich auf die Bildung von Ätzfiguren Einfluß hat. Heute ist im wesentlichen die Ursache der leichteren

Verletzbarkeit einzelner Stellen der Kristalloberfläche (Ätzfiguren) bekannt.

In der Regel besteht ein Zusammenhang zwischen den Figuren, die auf der Oberfläche des Monokristalls beim Ätzen entstehen, und den Dislokationsausgängen auf diese Oberfläche. In einem tatsächlichen Kristall stellen die Austrittspunkte der Dislokationen defekte Stellen dar, in denen sich elementare Vertiefungen bilden; ihre Etnwicklung führt zum Entstehen von Ätzfiguren.

Bei der von uns vorgeschlagenen Methode zur Erzeugung von Ätzfiguren wird Ultraschall angewandt. Das Kristall wird in eine gesättigte Mutterlösung gebracht und einer kurzzeitigen Bestrahlung im schwachen Ultraschallfeld im Druckbauch ausgesetzt. So erhielten wir Ätzfiguren auf der Oktaederfläche eines Al-K-Alaunkristalls, auf der Verbundfläche eines Benzophenonkristalles und eines Stückes Kaliumbichromat und and. Zur Ultraschallerzeugung wurde ein magnetischer Striktionsvibrator mit einer Schwingungsfrequenz 25 kHz verwendet. Die Intensität des Ultraschalls betrug ca 0,5 W/cm^2. Es hat sich herausgestellt, daß Ätzfiguren auf der Kristalloberfläche im Keim bei jedem Auflösungsstadium entstehen, was anscheinend durch die erhöhte Auflösungsgeschwindigkeit des Kristalls an den defekten Stellen erklärt werden muß.

Weitere Beobachtungen wurden mit Monokristallen von Lithiumfluorid durchgeführt. Unter gewöhnlichen Bedingungen entstehen auf der Oberfläche eines kurzzeitig ins Wasser gebrachten LiF-Monokristalls keine Ätzfiguren.

Die Vorbereitungstechnik der Kristalle zur Ultrabeschallung in Wasser und die Durchführung des Versuches selbst waren sehr einfach.Aus einem Monokristall Lithiumfluorid wird in der Verbundebene ein Stück von 1,05 x0,2cm ausgebrochen. Das Kristall wird an einem Stabende befestigt und in den Druckbauch einer stehenden Ultraschallwelle gebracht. Nach der Bestrahlung wurde die Fläche (100) des Kristalls mit Hilfe eines Polarisationsgerätes überprüft. Durch die Wirkung des Ultraschalls haben sich auf der Kristalloberfläche des Lithiumfluorid Vertiefungen mit einer richtigen Pyramidenform gebildet, die in Kettenform angebracht waren. Weitere Beobachtungen haben gezeigt, daß bei längerer Bestrahlung die Vertiefungen größer werden während ihre Anzahl relativ unverändert bleibt. Das berechtigt zu der Annahme, daß die Ätzfiguren sich auf den Dislokationen gebildet haben. Es ist nicht unwesentlich festzustellen, daß Ultraschall die Möglichkeit gibt, nich nur die Figuren herauszustellen, die den individuellen Dislokationen entsprechen, sondern es können auch andere Figuren ermittelt werden, die anscheinend durch andere Defekte des Kristallgitters bedingt sind.

Diese Arbeiten hoffen wir weiter fortzusetzen.

K23

FOURTH INTERNATIONAL CONGRESS ON ACOUSTICS
COPENHAGEN 21.-28. AUGUST 1962

Theoretical and Experimental Studies of the Propagation of Acoustic Impulses in Relaxing Liquids

E. F. Carome, P. A. Fleury, and W. J. Wagner
John Carroll University, Cleveland 18, Ohio, USA

Introduction

Experimental and theoretical studies are being made of the propagation of acoustic impulses in various highly absorbing liquids, some of which exhibit relaxation effects. Small amplitude unidirectional pressure pulses of widths between 0.1 and 1.0 microseconds have been used. The liquids studied experimentally include carbon tetrachloride, benzene, acetic and propionic acid, carbon disulphide, and castor oil. The results already obtained are quite promising. From a purely experimental aspect, these indicate that impulse propagation studies may yield certain types of acoustic information more readily than conventional pulse modulation or continuous wave ultrasonic techniques. There also appears to be good agreement between the experimental results and the theoretical predictions in a number of cases, though some differences are apparent.

It is to be noted immediately, however, that the theoretical predictions are based on the current theories of the propagation of ultrasound in absorbing and relaxing fluids. These theories, in turn, were developed to describe the propagation of sinusoidal disturbances. It appeared that they also should apply to small amplitude impulse disturbances because of the applicability of the superposition principle. However, in the development of a qualitative theory of the propagation of impulses in relaxing liquids several fundamental questions have arisen regarding the validity of using the current theories. These questions, which are discussed in a later section of this paper, are being investigated, and they indicate that impulse studies may yield new information regarding sound propagation in relaxing fluids.

Theory

Two different plane wave equations are available in the current acoustic theories, to describe the propagation of impulses in the various liquids mentioned in the introduction. The first applies to absorbing liquids, such as carbon tetrachloride, which do not exhibit relaxation effects within the frequency spectrum of the impulse; it is of the form

$$\frac{\rho}{\rho_0}\frac{\partial^3 \xi}{\partial x^2 \partial t} + c_0^2 \frac{\partial^2 \xi}{\partial x^2} - \frac{\partial^2 \xi}{\partial t^2} = 0 \qquad (1)$$

For liquids like acetic and propionic acid, which are known to relax within the frequency spectrum of the impulses studied here, the appropriate wave equation is

$$\frac{\partial^3 \xi}{\partial x^2 \partial t} - \frac{1}{c_\infty^2}\frac{\partial^3 \xi}{\partial t^3} + \omega_0 \frac{\partial^2 \xi}{\partial x^2} - \frac{\omega_0}{c_0^2}\frac{\partial^2 \xi}{\partial t^2} = 0 \qquad (2)$$

Here c_0 and c_∞ are the low and high frequency velocities, $\omega_0/2\pi$ is the relaxation frequency and ρ is the appropriate viscosity or loss coefficient.

Approximate Fourier integral solutions for Eq. (1) are available for impulse disturbances,[1] but attempts to find similar solutions for Eq. (2) have not been successful. Since these equations are linear, as mentioned in the introduction, the superposition principle applies, and Fourier analysis techniques may be used if repetitive disturbances are assumed. Numerical calculations have been made of the pulse shape as a function of path length assuming the input pressure pulse to be one oscillation (i.e., $0 \leq t \leq T_1$) of the function of $P_m \sin^2(\pi t/T_1)$. With the repetition rate $1/T$ set so that $T = 100\ T_1$ the first two hundred terms of the Fourier series, of fundamental frequency $f_0 = 1/T$, represents the impulse to a high degree of accuracy.

Calculations were carried out on a digital computer for carbon tetrachloride, acetic and propionic acids, using available absorption and velocity data.[2,3] In each case the impulse input width T_1 equaled 0.12 μsec, as compared to the measured relaxation times τ = 0.2 μsec and 0.08 μsec at 20°C for acetic and propionic acids, respectively. For such an impulse the amplitudes of the Fourier components are constant to about 5 Mc. Above this frequency they decay to zero in an oscillatory fashion, becoming negligible beyond 13 Mc.

The predicted variation of the shape of the impulse is strongly dependent on the characteristics of the medium. In the non-relaxing case for CCl_4, the impulse spreads continuously with increasing path length, but remains symmetrical about its peak. In agreement with the earlier approximate development,[1] the impulse shape becomes Gaussian at large distances. In the two relaxing cases, acetic and propionic acids, the rise and fall time of an initial peaked portion of the impulse remains roughly constant but an elongated tail developes on the lagging side. Finally, at large distances, only the tail is evident.

It is interesting to note that the leading edge of the impulse travels at the high frequency velocity c_∞ in acetic acid, while the peak propagates at the constant phase velocity c_o in non-relaxing cases.

Experimental Procedure

Consideration has been given in a number of recent papers to methods of generating and receiving acoustic impulses with piezoelectric tranducers.[4,5] For the present study cylindrical ceramic tranducers have been used as piston-like sources. The fundamental extensional mode of these elements was about 150 kc. It has been possible to generate a satisfactory pressure impulse approximating that discussed in the previous section by applying a square voltage pulse, 0.1 μsec in width and 50 volts in amplitude, across the ends of the cylinder. Thin X-cut quartz plates with fundamental frequencies in the range from 16 to 25 Mc have been used as receivers. Except at the shortest path lengths in the lowest absorbing liquids, where some ringing at the receiver frequency was evident, these served as satisfactory receivers for impulses of various shapes and widths. A high impedance cathode follower probe was used to monitor the voltage across the receiver. The output of the probe was amplified by a wide-band (3 cps to 17 Mc) amplifier and displayed on the delayed sweep of an oscilloscope. The overall gain and noise level of this system was such that the minimum useable output of the receiver was approximately .001 volt.

The repetition rate of the pulse generator used to excite the source was set at 3000 cps, though it could be varied widely without affecting the shape of the received impulse.

An effort was also made to determine if propagation phenomena, such as diffraction or beam spreading, affected the experimental results. Measurements were taken in water and the impulse shape remained the same for path lengths up to 10 cm, which was the maximum used in the experiments considered here.

Experimental Results and Comparison with Theory

Measurements have been made in all of the liquids mentioned in the introduction. Emphasis is placed here on the data obtained in CCl_4 and acetic acid, however, because more extensive calculations have been carried out for these two than for the others.

In CCl_4, as predicted, the impulse decays and spreads with increasing path length and remains quite symmetrical. However, at path lengths greater than 0.5 cm, the receiver voltage reverses polarity slightly on the trailing edge of the impulse. Currently we are investigating various possible sources for this reversal, including acoustic scattering effects.

In acetic acid, again as predicted, the rise time of the leading edge of the impulse remains relatively constant and a definite delayed tail developes. This general shape, i.e. a relatively rapid rise to the maximum followed by a much slower, almost exponential decay, is evident in all of the measurements made in relaxing liquids. It occurs even in carbon disulphide, for which the relaxation frequency is far above the maximum frequency passed by the amplifier, and for which theory predicts negligible departure from symmetry.

Quantitative comparison of theory and experiment can best be made from a tabulation of the impulse peak height versus path length, since this is the most definite characteristic of the data.
In Table I the theoretical and experimental relative maxima are tabulated; in each case the experimental values have been obtained from a curve of impulse height versus path length which has been normalized to unit height at zero path length. There is excellent agreement between theory and experimental for CCl_4, and fair agreement for acetic acid, where the measured decay is somewhat greater .

Table I. Comparison of theoretical and experimental impulse maxima as functions of path length in CCl_4, and acetic acid for an input impulse approximately 0.12 μsec wide.

Path Length in cm.	CCl_4		Acetic Acid	
	Theo.	Exp.	Theo.	Exp.
0.5	0.90	0.90	0.75	0.70
0.8	0.87	0.88	0.68	0.60
1.3	0.81	0.83	0.58	0.42
1.9	0.75	0.77	0.43	0.27
2.5	0.70	0.72	0.30	0.20
3.2	0.65	0.68	0.23	0.16
5.1	0.55	0.57	----	----

Discussion and Conclusion

The difference between impulse propagation in non-relaxing and relaxing liquids, qualitatively at least, may be explained quite simply. For example, from a frequency spectrum viewpoint, the delayed tail in the relaxing cases may be attributed to dispersion: the lower frequency Fourier components travel at lower velocities approaching c_o. Also the rise time of the leading edge of the impulse remains constant because the higher frequencies travel at velocities approaching c_∞ . On the other hand, from an impulse and relaxation aspect, the delayed tail may be attributed to a delay in the release of energy from internal or relaxing states.
It was this type of qualitative reasoning which led to the present study. From the outset, however, consideration was given to the problem of propagation of two closely spaced impulses. Suppose that, in a relaxing liquid, the time delay between the two impulses were short enough so that little of the energy fed into the internal states during the period of the first impulse could leak out before the arrival of the second. Under this condition one would expect that the second impulse would be absorbed less and possibly travel at higher velocity than the first.
These latter qualitative predictions differ from those derived from current acoustic theories. Referring to Eq. (2), since it is a linear differential equation, the superposition principle applies; its solution for two time delayed impulses is just the time delayed sum of their two separate solutions. Therefore, the use of Eq. (2) implies that the second pulse will be propagated in exactly the same manner as the first.

Thus the present study appears to have brought to light a fundamental problem. Current acoustic theories, developed for sinusoidal disturbances, imply the applicability of the superposition principle. On the other hand, relaxation theories indicate the possibility that saturation effects and time dependent specific heats and compressibilities should lead to previously unpredicted effects in impulse propagation. The results of preliminary experiments with double impulses have not led to definite conclusions regarding these effects. Measurements with single and double impulses are being continued. Consideration is being given to possible modifications of the theory to explain both the oberved single pulse effects and the anticipated double pulse effects.

REFERENCES

1. Landau and Lifshitz, Fluid Mechanics, p. 301, Pergammon Press, (1959).

2. Lamb and Pinkerton, Proc. Roy. Soc., A199, 114 (1949).

3. Lamb and Huddart, Trans. Faraday Soc., 46, 540 (1950).

4. E. G. Cook, IRE Convention Reports, 9, 6 (1956).

5. M. Redwood, J. Acoust. Soc. Am., 33, 527 (1961).

L23

FOURTH INTERNATIONAL CONGRESS ON ACOUSTICS
COPENHAGEN 21.-28. AUGUST 1962

A PROCEDURE FOR NOISE EVALUATION OF SOUND POWER DATA

W. E. Blazier, Jr.
York Division, Borg-Warner Corporation, York, Pennsylvania, U.S.A.
and
R. J. Wells
General Electric Company, Schenectady, New York, U.S.A.

There is considerable activity in the United States on subjects relating to the measurement of sound power and to the problem of obtaining a proper rating for the noise of various types of equipment. The air conditioning and refrigeration industry is particularly interested in this work--since many product applications are in noise-sensitive environments and thus vulnerable to complaints.

It has been generally recognized that data on equipment noise, expressed in terms of sound power rather than pressure, have several advantages. This is particularly true when measurements made in different source environments are to be correlated. Also, when the question of noise ratings is considered for these equipments, a quantity such as sound power is more convenient to handle since the level is not normally dependent on the characteristics of the source environment. Consequently, a trend has been established for expressing the noise output of air conditioning and refrigeration equipment on a sound power basis. The preferred bandwidth for sound analysis is a variable, dependent upon the characteristics of the spectrum and ultimate use for the data.

The transition in method of description, from relative sound pressure to power, has occurred more rapidly than suitable procedures have become available for rating or interpreting these data subjectively. Although the subjective reaction to noise is a function of the environment, the individual and the situation, there are procedures for evaluating these factors in specific cases. Most criteria, however, are on a sound pressure level basis and thus depend upon properties of the environment in their relationship to sound power. While it is possible to make use of these sound pressure level criteria in rating noise on a power basis, the scope of the rating procedure, for any particular class of equipment, must be limited to applications where the range of acceptable environmental criteria is relatively small. A number of people have used NC curves[1] as the basis for subjective noise criteria in various environmental situations. Typical examples are the criteria for offices, hotels, apartments, residences, hospitals, etc., in which a limit is placed on background noise corresponding to maximum levels defined by a particular NC curve. As a rule, these criteria range within the limits of NC 35 $\pm$ 10 db. This suggests that equipment for these categories of application might be rated on the basis of weighted sound power level contours assigned a shape similar to NC curves. For example, if the NC 35 curve were taken as a reference, the use of parallel power contours having this shape would introduce negligible error. A method based on this approach was introduced by Fehr and Wells in 1955.[2] A rating number was assigned the octave band power level spectrum of the noise source based on the highest reference contour tangent to the data. This is analogous to the present convention of assigning a sound pressure level spectrum an NC number based on its tangency to one of the NC curves.

A single number approach for sound rating has practical merit in estimating potential noise problems. From a purely technical viewpoint it is naturally desirable to have a more complete description of the spectrum. However, it is recognized that this involves too many numbers for most situations where sound ratings are applied. A simple, yet reliable, one number approach is needed which considers the subjective properties of the spectrum as well as the level in deriving a rating number. The tangent contour method is obviously a poor choice for rating noise subjectively since it ignores the effects of spectrum shape, pure tone content and other adverse spectral characteristics. This is a frequent criticism of the NC rating scheme--particularly when applied to components of an air conditioning system as a condition of acceptance. An example is shown in Figure 1 for three typical aerodynamic noise spectra which have been adjusted in level so that each has the same NC rating number. Spectrum A corresponds to the levels of an NC 40 curve. Spectra B and C are generalized curves with

shapes typical of the noise produced by terminal devices in an air distribution system. By convention, each spectrum would be assigned an NC 40 rating although the loudness levels (Stevens, Mark VI)[3] differ considerably. Spectrum C, for example, has a loudness less than one-half that of the NC 40 curve represented by Spectrum A. If C were to be realigned in level to a loudness the equivalent of A, the corresponding NC rating would rise about 10 db. Similarly, Spectrum B could be raised in level 5 db.

One might expect the subjective reaction to broadband noise to be more dependent upon relative loudness than NC number. However, if the spectral content of the noise includes pure tones, pulsed spectra or beats, the computed loudness also ceases to be a reliable index of relative acceptability. Spectrum D in Figure 1 is a modification of B in which a pure tone has been added to the one-third octave band centered at 200 cps. The presence of the tone in this spectrum alters neither the computed loudness(Mark VI) nor NC number--but in a given situation D might be judged more annoying than B.

A new procedure for evaluating sound power data is being studied. It includes a method for deriving single number ratings on the basis of relative annoyance. Although the details of this procedure and some experimental results will be discussed in a subsequent paper,[4] several aspects of the method are of special interest at this time. There is the question of an appropriate reference contour against which a noise spectrum can be evaluated and interpreted on the basis of relative annoyance. Assuming that the optimum shape of such a contour will not vary much with level within the application range of the rating system, a family of parallel contours expressed on a sound power level basis may be employed. The optimum shape for the contour is more uncertain. If the subjective reaction to noise is dependent on loudness, one choice might be an equal-loudness contour. Also, there are the equal-noisiness contours devised by Kryter[5] and, of course, the NC curves from which to choose.

Figure 2 provides a comparison among these parameters on a one-third octave band basis. The selected range of sound pressure levels is suitable for many applications. Notice the 1 noy curve lies above the 1 sone contour (Mark VI) over about two-thirds of the spectrum. This suggests the noisiness of a sound may be less than its loudness at the lower end of the spectrum and also in the range around 1000 cps. Intuitively, we would expect annoyance to be a function of both loudness and noisiness but varying with greater complexity than described by a simple curve. On the other hand, the NC 40 curve seems to be a compromise between these relative factors out to about 2000 cps. However, the 1 noy and 1 sone curves cross above 3000 cps indicating the relationship between noisiness and loudness apparently reverses. The level of the NC curve lies well above either of the others in this area of the spectrum. If subjective reaction is assumed to be primarily a function of loudness and noisiness, the shape of the NC curve is probably not a reliable criterion of acceptability in this region. The rapid drop-off in the noy curve at high frequencies also seems a little extreme, particularly for broadband noise. Measurements of jet engine noise figured heavily in the derivation of this contour. The strong subjective weighting of the high frequencies may reflect a source characteristic particularly one containing pure tones.

For complex noise which includes pure tones in an otherwise continuous spectrum, the new procedure proposes to treat these factors separately in deriving the subjective rating. The general shape of the reference curve is considered to approximate an equal-acceptance contour for bands of distributed noise. Initially, the shape of the NC 35 curve has been adopted for the contour up to 2000 cps. Above this frequency, the contour shape follows approximately the (Mark VI) 1 sone curve.

Another point frequently discussed, in connection with the reliability of subjective rating schemes, is the optimum bandwidth to use for noise measurements. The types of sounds experienced in practice fall into three general categories. The first type is one in which the spectrum is nominally continuous and termed broadband. Only a few noise sources actually meet this test. In the applicable cases, octave band data are generally adequate for use in subjective rating. A second type noise, however, is one with audible pure tone components in an otherwise broadband spectrum. This is a common form of mechanical equipment noise. In evaluating sources of this type, it is essential to determine frequency and amplitude of the pure tone, relative to masking noise present, if subjective reaction is to be predicted or correlated with any reliability. Naturally, a critical bandwidth analyzer would be an optimum instrument to select--although such an approach seems impractical at the present time. However, a system of measurement in one-third octave bands can be made to approximate this type of analysis.

In the companion paper presented by Mr. Wells,[4] a procedure is discussed for deriving an approximate correction for pure tones, relative to level in a critical band, on the basis of one-third octave data. Finally, typical mechanical equipment noise also includes pulsed sources such as reciprocating compressors. Very little quantitative data exist suitable for predicting subjective response to this type of noise spectrum. While measurements in one-third octave bands are unquestionably useful in evaluating sources of this nature, supplementary data are generally necessary--particularly regarding peak factors in the spectrum.

It is interesting to consider the application of single number noise ratings in estimating relative acceptance, tolerance, or, rejection for a particular background noise. It is assumed that such ratings include an adjustment for the subjective factors discussed previously and are expressed on a power level basis as "equivalent" to some reference contour for which the relative acceptance is known. The alignment chart shown in Figure 3 relates a sound pressure criterion, established for the environment, to a corresponding input sound power as a function of room volume and absorption. The chart is similar to the type introduced by Fehr and Wells[2] except for modifications to increase the flexibility of application. The extreme left hand scale is used to select an environmental noise criterion. This is expressed as the level of some reference contour for which a suitable subjective response is expected. NC curve numbers may be used in those situations where the criterion is known to be valid. This scale is used in conjunction with room volume to convert the selected pressure level criterion (re 0.0002 microbar), assumed to exist in the reverberant field, to an equivalent power level contour (re 10^{-13} watt). In aligning the volume scale, an average sound absorption characteristic of 0.2 has been assumed representative of normal rooms. For live rooms ($a=0.1$), the computed power level contours may be decreased by 3 db, or, for dead rooms ($a \geq 0.4$), increased 3 db. Next, the ICR scale (Indoor Contour Rating) is entered at the rating number assigned the sound power spectrum of the noise in question. This in turn is used in connection with the design power level contour derived previously in estimating the result on the noise acceptance scale. If the design power level contour is numerically matched by the rating number, the predicted response lies 5 db within the acceptable range. A 5 db mismatch places the estimated acceptance at the marginal boundary. This marginal region is 10 db wide and assumed proportional to frequency of complaints. A 15 db mismatch is considered unacceptable and corresponds to a high complaint rate.

The scales on the right hand side of the alignment chart are used to estimate subjective acceptance of sound sources located outdoors in noise-sensitive residential areas. The OCR scale (Outdoor Contour Rating) is analogous to the ICR scale mentioned earlier. Typical applications occur when the heat rejection equipment of an air conditioning system is to be located near the open windows of a bedroom in an adjacent residence. To reduce the possibility of a neighbor complaint, a minimum source to window distance can be established relative to the source power level and whatever subjective criteria fits the receiving environment.[6] In alignment of the distance scale, hemispherical spreading of the source power was assumed in calculating sound pressure levels just outside the open windows. Sound pressure levels inside the bedroom are assumed to drop another 10 db. This is consistent with average values reported by Hunter and Carome[7] based on a series of field measurements. The noise acceptance scale has been aligned such that the NC 35 curve, taken as a reference contour, lies 5 db within the acceptable range. On this same basis, the marginal region extends from NC 40 to NC 50.

The reliability of such alignment charts depends primarily on the method of deriving rating numbers to be inserted on the ICR and OCR scales. A rating based simply on tangency to a reference contour, disregarding spectrum shape and structure is the least dependable. A rating method believed to result in numbers significantly more reliable as inputs to these charts will be discussed in the following paper.[4]

1. L.L.Beranek, NOISE CONTROL 3,19 (Jan 57); 2. R.O.Fehr, R.J.Wells, NOISE CONTROL 1,30 (Jan 55); 3. S.S.Stevens, J. Acoust. Soc. Am. 33,1577 (1961); 4. R.J.Wells, W.E.Blazier,Jr., Proc. Fourth ICA (1962); 5. K.D.Kryter, NOISE CONTROL 6,12 (Sept - Oct 1960); 6. W.E.Blazier,Jr., NOISE CONTROL 5,48 (Jan 59); 7. J.L.Hunter, E.F.Carome, J. Acoust. Soc. Am. 32,1523 (1960).

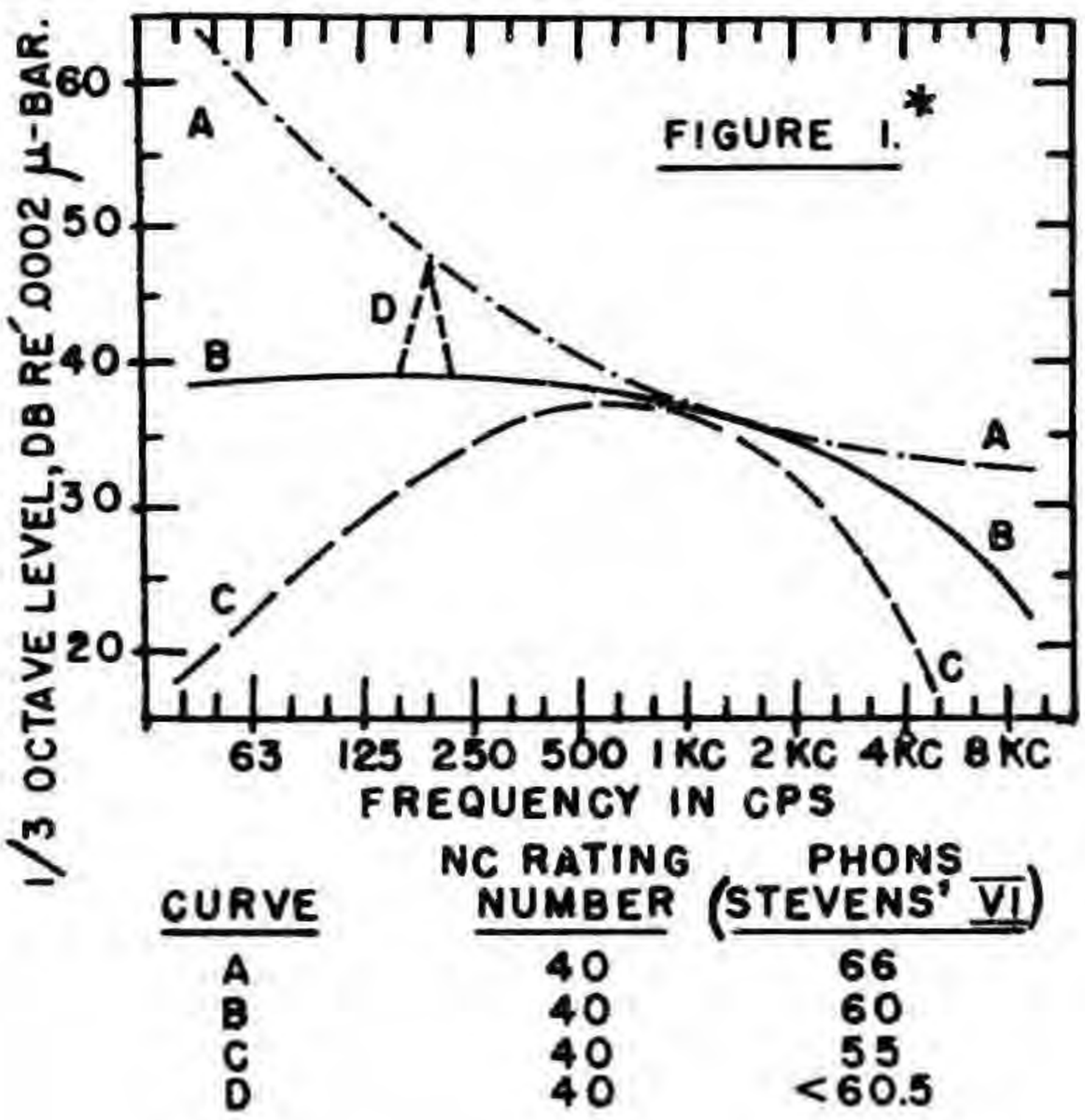

FIGURE 1.*

CURVE	NC RATING NUMBER	PHONS (STEVENS' VI)
A	40	66
B	40	60
C	40	55
D	40	<60.5

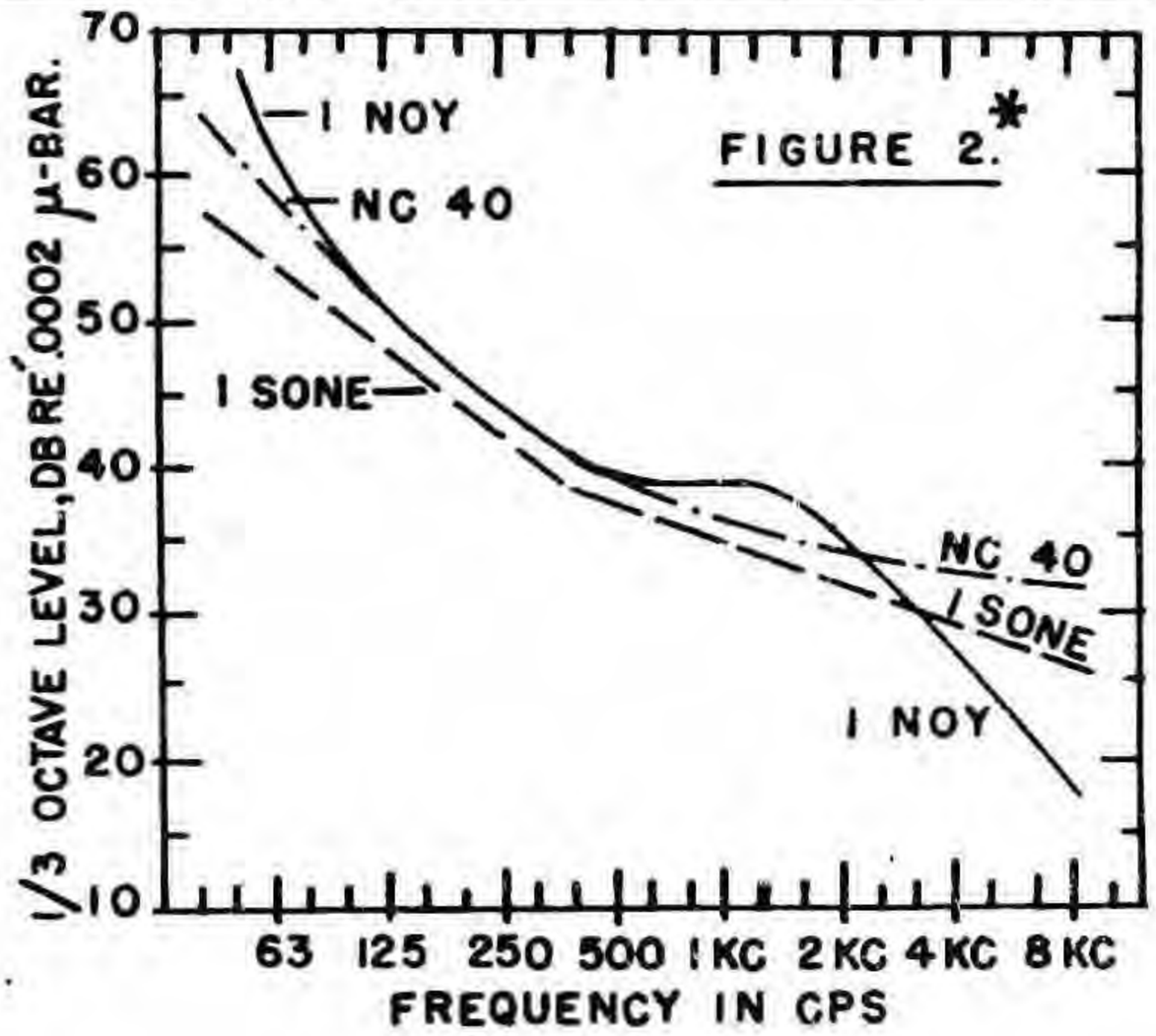

FIGURE 2.*

FIGURE 3.* NOISE EVALUATION CHART

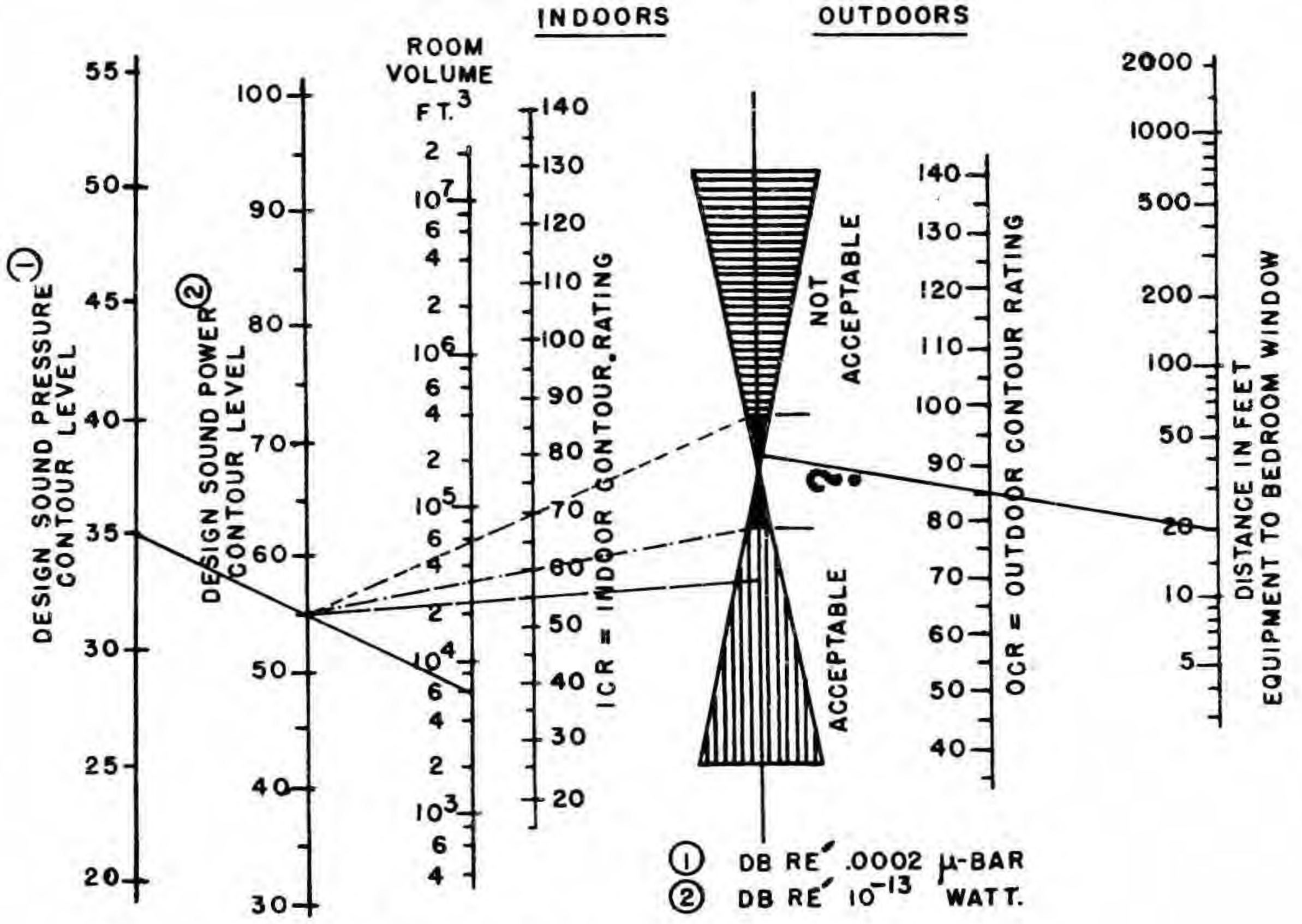

* FOR DISCUSSION OF FIGURES, SEE TEXT.

M23

FOURTH INTERNATIONAL CONGRESS ON ACOUSTICS
COPENHAGEN 21.-28. AUGUST 1962

Zur Schalldämmung gelochter Blechplatten.

Peter Dämmig, Braunschweig
Physikalisch-Technische Bundesanstalt

Einleitung.

Im Fahrzeug- und Schiffsbau erhebt sich gelegentlich die Frage nach der Luftschallübertragung durch Wände, die aus gelochten Blechplatten bestehen. Das Verhalten gelochter oder geschlitzter Konstruktionen im Schallfeld ist zwar schon oft theoretisch und durch Messung untersucht worden (zusammenfassende Darstellungen z.B. in [1...4]). Meist interessiert dabei der Schallabsorptionsgrad von Konstruktionen, die als Resonatoren wirken, nur geringe Bautiefe aufweisen und bei denen die Verluste wesentlich durch strömungsresistentes Material innerhalb der Absorber hervorgerufen werden. Mit der hier geschilderten Untersuchung sollte dagegen ermittelt werden, wie sich einschalige, gelochte Blechwände unter bestimmten Bedingungen bezüglich der Schalldämmung verhalten.

Die Messungen wurden an einer Stahlblechplatte von 1 mm Dicke (Flächengewicht M = 8 kg/m^2) ausgeführt. Sie war als 1 x 2 m^2 großes "Fenster" auf einer Rahmenkonstruktion mit Mittelrippe und schalldichtem Randschluß in eine 24 cm dicke, beiderseits verputzte Vollziegelwand (480 kg/m^2) von 11,4 m^2 Gesamtfläche zwischen den beiden Meßräumen des Wandprüfstands der Physikalisch-Technischen Bundesanstalt eingebaut. Zur Lochung der Blechwand wurden Bohrungen von 8 mm Durchmesser, entsprechend 0,5 cm^2 Fläche, in statistischer Anordnung angebracht. Gemessen wurde die Schalldämmung der ungelochten Blechwand, sowie bei Lochzahlen zwischen 6 und 192. Der größte Lochungsgrad betrug also $4{,}8.10^{-3}$. Grundlage der Messungen war DIN 52210. Insbesondere wurde also das Schalldämmaß gemäß

$$R = L_1 - L_2 + 10 \log S/A_2 \qquad (1)$$

ermittelt (L_1, L_2 = Schallpegel im Sende- bzw. Empfangsraum, S = Prüffläche, A_2 = äquivalente Absorptionsfläche im Empfangsraum). Als Meßgeräusch diente auf Terzbreite eingeschränktes weißes Rauschen. Der durch die 24 cm dicke Ziegelwand tretende Schallanteil wurde aus deren bekannter Schalldämmung bestimmt und an den Ergebnissen rechnerisch berücksichtigt.

Ergebnisse und Diskussion.

Die an der Blechwand gemessene Schalldämmung ist in Abhängigkeit von der Frequenz und mit der Lochzahl als Parameter in Abb.1a dargestellt. Läßt man die an der unteren Grenze des Frequenzbereichs sich andeutende Resonanzerscheinung außer acht, so entspricht der Kurvenverlauf für die ungelochte Wand angenähert den für das Wandgewicht auf Grund des Massengesetzes zu erwartenden Werten. Bei Lochung der Wand erniedrigt sich die Dämmung um Beträge, die bei geringen Lochzahlen fast frequenzunabhängig sind, bei steigender Lochzahl mit wachsender Frequenz dagegen etwas ansteigen.

Die hier geschilderte experimentelle Untersuchung bezieht sich zwar ausdrücklich auf statistische Lochverteilung, jedoch wird für die folgende theoretische Abschätzung näherungsweise eine regelmäßige Gitteranordnung der Löcher zugrunde gelegt. Ferner wird vereinfachend angenommen, daß die Wand unendlich dünn ist und daß sich die Wellen jenseits der Wand unabhängig von der Einfallsrichtung bevorzugt in Richtung der Wandnormalen ausbreiten. Man kann sich jedes Loch (Radius a) durch eine masselose Membran abgeschlossen denken, die der Schallbewegung trägheitslos folgt. Im Mittel ist jedes Loch von dem Teil $F_1 = F/n$ (n = Lochzahl auf der Gesamtfläche F) der Wandfläche umgeben. Man kann für die Schallimpedanz angenähert schreiben

$$W/\varrho c \approx 1 + j\,16\,k F_1/(3a\pi^2) = w + jq$$

(k = Wellenzahl). Für Schalleinfall unter dem Winkel ϑ gilt dann der Absorptionsgrad

$$\alpha(\vartheta) = 1 - \left|\frac{W/\varrho c \cdot \cos\vartheta - 1}{W/\varrho c \cdot \cos\vartheta + 1}\right|^2 .$$

Bei Umrechnung auf Schalleinfall auf die Wand aus allen Richtungen eines Halbraumes, also bei Berücksichtigung des diffusen Schallfelds im Senderaum, ergibt die Auswertung des Integrals $\alpha = \int_0^{\pi/2} \alpha(\vartheta)\sin 2\vartheta\, d\vartheta$

$$\alpha = \frac{8w}{w^2+q^2} + \frac{8w}{(w^2+q^2)^2}\left\{\frac{w^2-q^2}{q}\operatorname{arctg}\frac{q}{1+w} - w\ln\left[(1+w)^2+q^2\right]\right\} .$$

Der Verlauf dieses Schallabsorptionsgrads ist für die experimentellen Daten in Abhängigkeit vom Verhältnis Frequenz f / Lochzahl n in Abb.2 dargestellt. In einem großen Bereich läßt er sich annähern durch

$$\alpha \approx 0{,}32/(f/n)^2 . \qquad (2)$$

Erfolgt die Schallübertragung durch die gelochte Wand ohne Dissipationsverluste, so kann der Schallabsorptionsgrad näherungsweise gleich dem die Dämmung charakterisierenden Transmissionsgrad τ gesetzt werden, und man erhält für das Schalldämmaß

$$R \approx 10\log 1/\tau \approx 10\log 1/\alpha .$$

Es wird nun angenommen, daß die durch die ungelochte Wand allein und durch die Löcher allein aus dem Sende- in den Empfangsraum übertrage-

nen Energieanteile näherungsweise additiv zusammengesetzt werden können. Zu der Energiedichte E_2 im Empfangsraum, die sich für die ungelochte Wand nach (1) aus

$$10 \log E_2 = 10 \log E_1 - R + 10 \log S/A_2$$

ergibt, addiert sich dann der Anteil $E_2' = E_1 S \alpha / A_2$. Nach Durchführung der Rechnung erhält man schließlich eine Erniedrigung der Schalldämmung auf Grund der Lochung der Wand um

$$\Delta R = 10 \log (1 + \alpha 10^{R/10}), \qquad (3)$$

wobei R die Schalldämmung der ungelochten Wand bedeutet.
Die damit gewonnenen theoretischen Ergebnisse sind in Abb.1b den gemessenen Werten der Abb.1a gegenübergestellt. Für R wurden die theoretischen Dämmungswerte der Stahlblechwand eingesetzt. Die Kurven sind nur so weit gezeichnet, wie die bei der Rechnung gemachte Voraussetzung $\lambda \gg d$ (λ = Wellenlänge, d = mittlerer Lochabstand) erfüllt ist. Experimentell ergibt sich eine größere Dämmungsverminderung als nach der theoretischen Abschätzung.
Die mittlere Dämmungsverminderung für eine gewisse Lochzahl läßt sich angeben, wenn man in (3) den Verlauf der Schalldämmung R z.B. durch die übliche Näherung R = 20 log f + const. ausdrückt und dabei die Konstante aus der dem Wandgewicht entsprechenden mittleren Schalldämmung $R_m = 14 \log M + 14$ [3] berechnet. Es ergibt sich
$R = 20 \log (8{,}9 . 10^{-3} M^{0,7} f)$ und mit (2)

$$\Delta R = 10 \log (1 + 2{,}6 \cdot 10^{-5} M^{1,4} n^2). \qquad (4)$$

In dieser Näherung ist die Dämmungsverminderung also unabhängig von der Frequenz. Unter Berücksichtigung der experimentellen Daten gilt bei kleinen Lochzahlen $\Delta R \approx 2{,}1 . 10^{-3} n^2$, bei größeren dagegen
$\Delta R \approx 20 \log n - 33$.
Die durch (4) gegebene Kurve sowie die aus den Kurven der Abb.1a errechneten mittleren Dämmungsverminderungen sind in Abb.3 dargestellt. Auch hier zeigt sich, daß die gemessenen Dämmungsverminderungen etwas größer sind als die berechneten Werte.

Literatur.

[1] L.L.Beranek. Acoustics. McGraw-Hill Publ.Comp.Ltd. London, 1954.
[2] E.Skudrzyk. Die Grundlagen der Akustik. Springer-Verlag Wien, 1954.
[3] L.Cremer. Die wissenschaftlichen Grundlagen der Raumakustik, Bd. III. S.Hirzel Verlag Leipzig, 1950.
[4] Ph.M.Morse. Vibration and Sound. McGraw-Hill Publ.Comp.Ltd. London, 1948.

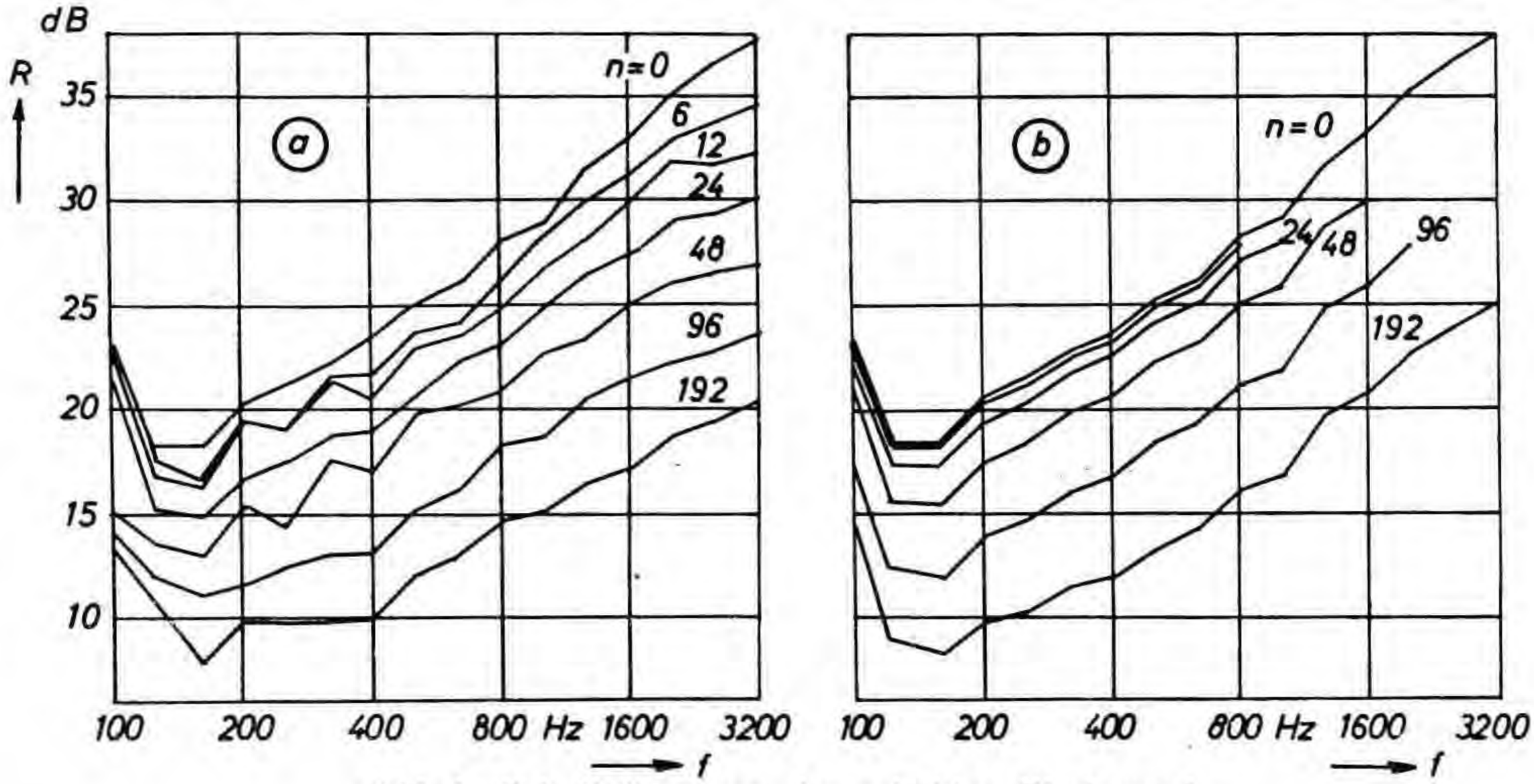

Abb. 1 Schalldämmung der gelochten Blechwand
Parameter: Lochzahl
a) gemessen b) berechnet

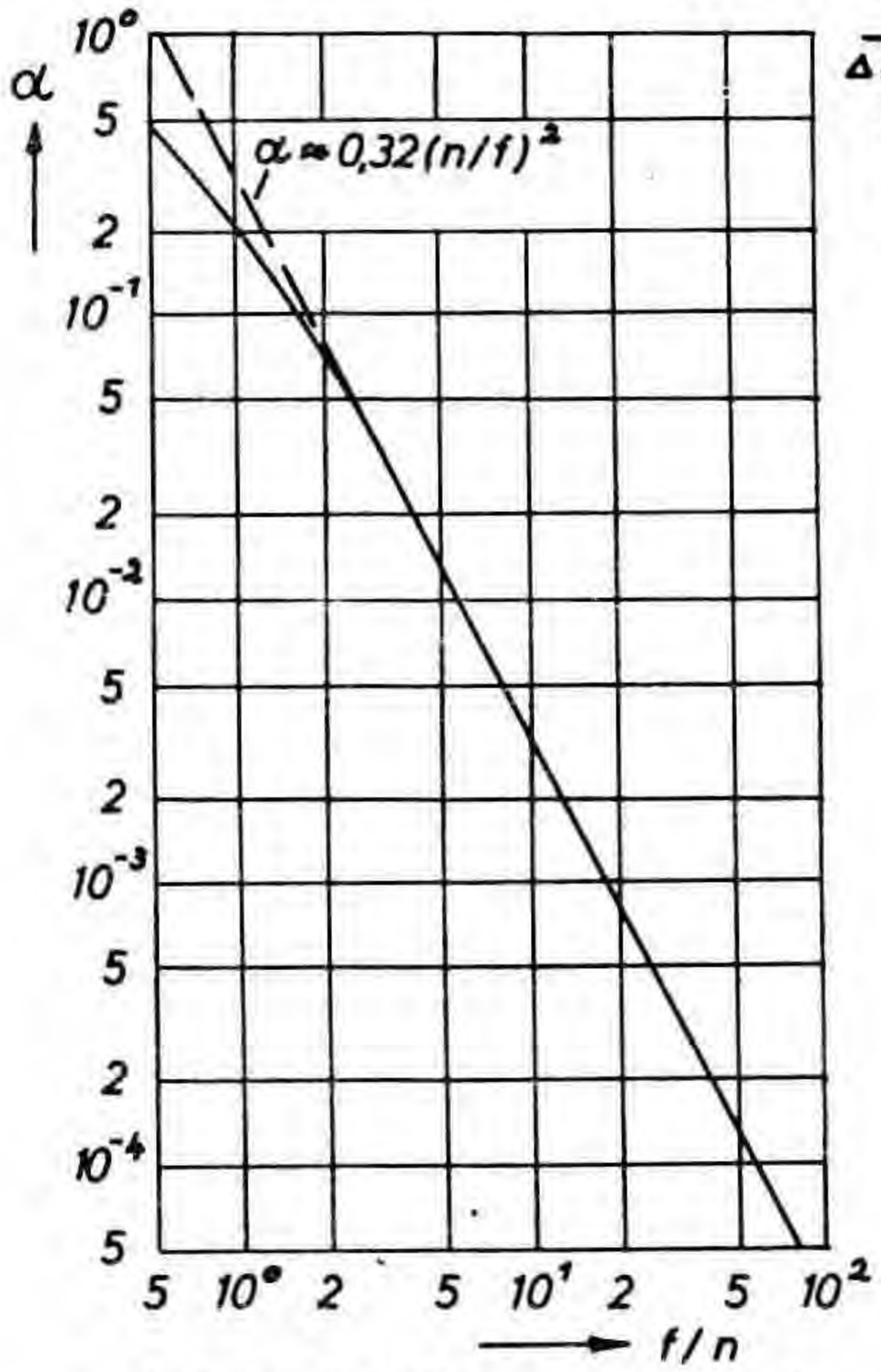

Abb. 2 Schallabsorptionsgrad
als Funktion von
Frequenz / Lochzahl

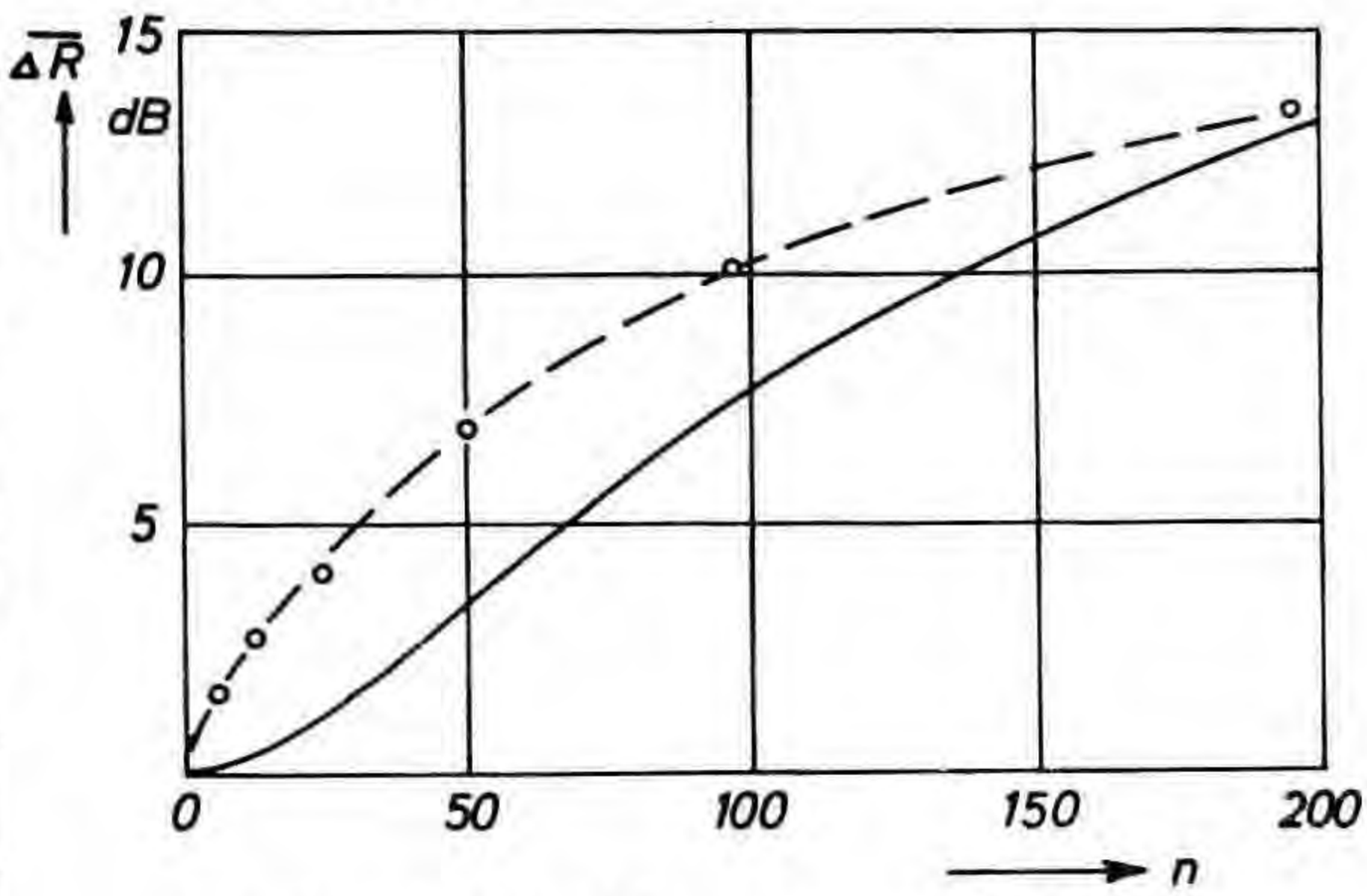

Abb. 3 Mittlere Dämmungsverminderung
als Funktion der Lochzahl
—— berechnet o gemessen

N23

FOURTH INTERNATIONAL CONGRESS ON ACOUSTICS
COPENHAGEN 21.-28. AUGUST 1962

HIGH POWER ULTRASONIC TRANSDUCERS USING PIEZOELECTRIC CERAMICS

ALAN E. CRAWFORD, SONICS DIVISION, ELLIOTT BROS (LONDON) LTD.

The increasing use of high power ultrasonic energy for industrial and military applications has stimulated both the development of new piezoelectric materials and advanced transducer design. The greatest advancement has been in the field of polycrystalline piezoelectric ceramics and few new single crystal piezoelectrics have been developed. The initial discovery of the ferroelectric properties in barium titanate was quickly followed by the development of lead zirconate-titanate (Ref. 1). These materials provide the transducer designer with easily fabricated high efficiency electro-acoustic converters but inherent disadvantages have so far limited their applications to relatively high frequency generation.

Many factors must be considered in the choice of high power transducer materials, but basically they should be efficient in electromechanical conversion and be capable of withstanding high mechanical stresses. Losses inevitably occur and these are mainly composed of dielectric and internal mechanical inefficiencies. It is almost impossible to rapidly dissipate the heat produced due to the poor thermal conductivity of the piezoelectric ceramic and there is a corresponding increase in losses due to the temperature rise within the material. In lead zirconate-titanate the dielectric loss alone increases by a factor of 10 over the range 25°C to 160°C and thus rapidly promotes an avalanche effect. This increasing temperature also produces other undesirable changes such as a variation in frequency constant and a large increase in the permittivity. Curves showing these changes in lead zirconate-titanate with a strontium additive are given in Fig. 1.

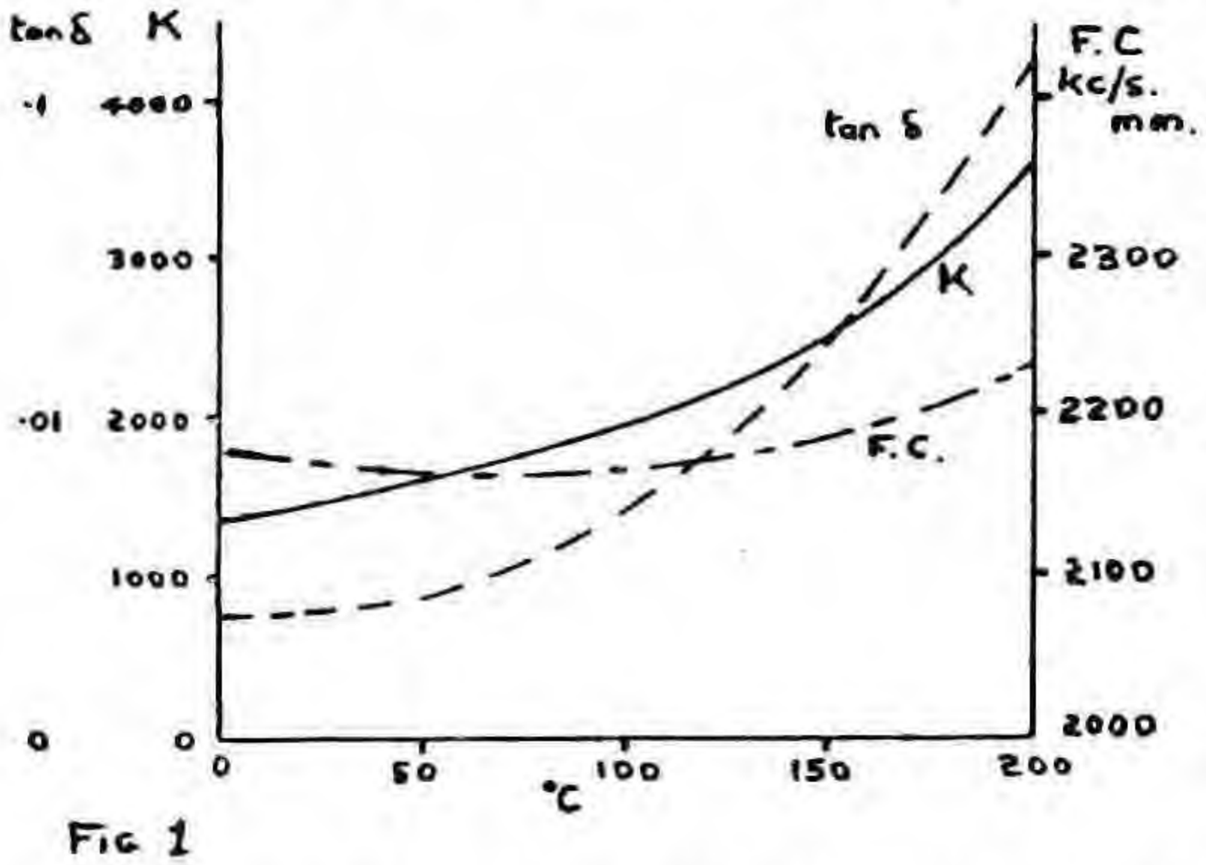

Fig 1

In the case of high power propagation in liquids it is often desirable to promote active cavitation and it has been shown that this effect becomes progressively greater as the frequency decreases (Ref. 2). Practical considerations dictate a limit at about 20 Kc/s but it is clearly impractical to produce a thickness resonant half-wave ceramic block for this frequency, the length being of the order of 8 cms in lead zirconate-titanate. There are obvious manufacturing difficulties due to the high voltage needed for polarisation and the problems encountered in forming homogeneous blocks of ceramic of this size.

There have been many attempts to produce low frequency piezoelectric transducers, perhaps the earliest being due to Langevin (Ref. 3). This was based on the mass loading of a relatively thin section of piezoelectric material and is generally known as the sandwich transducer. Two blocks of heavy material such as brass or steel are placed on each side of a number of thin quartz crystals. The system operates as a half wave resonator with the quartz crystals located at a nodal point. Since the Q of the system is basically the ratio between the acoustic impedance of the steel radiator and the acoustic impedance of the liquid in contact with the face it will be comparatively high. This will necessitate accurate tuning of the energising frequency and would limit its application for industrial use.

Similar principles are used in the 'Multipower' transducer (Ref. 4.), but the technique of operation is somewhat different. In this case the loading masses are of dissimilar metals, one being of considerably lower density than the other. Each mass will be approximately a quarter wavelength in length, while the fundamental thickness resonant frequency of the piezoelectric ceramic element is considerably higher than the lumped resonant frequency of the sandwich.

The particle velocity at the radiating surfaces of the two masses will be different to satisfy the law of conservation of momentum. This is obvious as the momentum must be equal for both blocks and the particle velocities will be in inverse ratio to the densities. Using aluminium and steel as the dissimilar masses a particle displacement ratio of about 3.33 to 1 will be obtained. The major displacement will occur at the face of the lighter metal and will thus radiate a greater proportion of the stored vibratory energy in the structure.

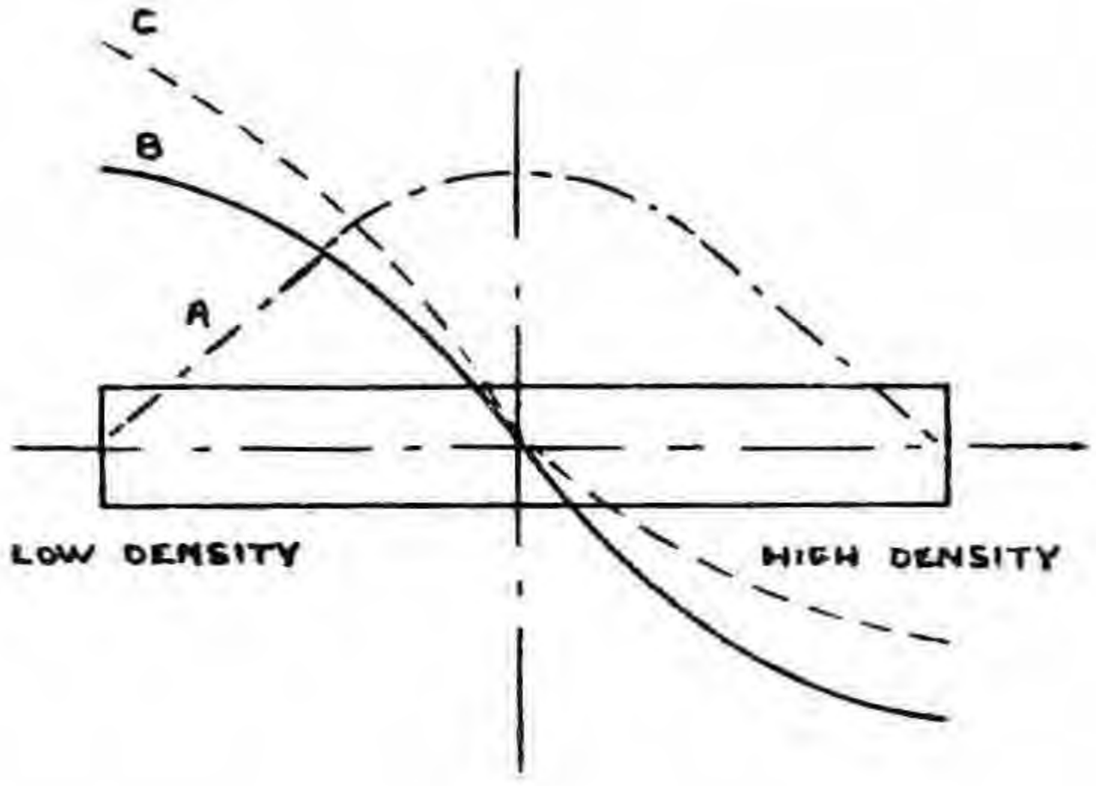

FIG. 2

Fig. 2. represents a half wave longitudinal vibrator. The stress or strain is given by Curve A and reaches a maximum at the nodal point. When the velocity of sound is the same in both sections this point will be at the geometric centre. With loading masses of similar densities the amplitude can be represented by Curve B, while with dissimilar densities the amplitude will follow Curve C. The maximum amplitude in this case occurs at the face of the lower density mass and is correspondingly greater with the same energy input.

The nodal point is the obvious position for exciting the structure into resonance, but as seen from Curve A the strain or stress will be at a maximum across the jointing faces between the piezoelectric element and the metal masses. Under high amplitude conditions a normal cemented joint will fail during the extension phase. This can be overcome by bolting the two halves together and adjusting the exerted compressive stress to be higher than the maximum negative stress experienced during operation. The choice of the tensioning device is critical as mechanical

hysteresis and creep effects must be kept to a minimum. A conical disk spring is used as it provides a compact assembly in the loading direction and is capable of supporting large compressive loads with little hysteresis. They are also characterised by a decrease in effective stiffness with an increase in loading, allowing less restraint as the amplitude increases (Ref. 5).

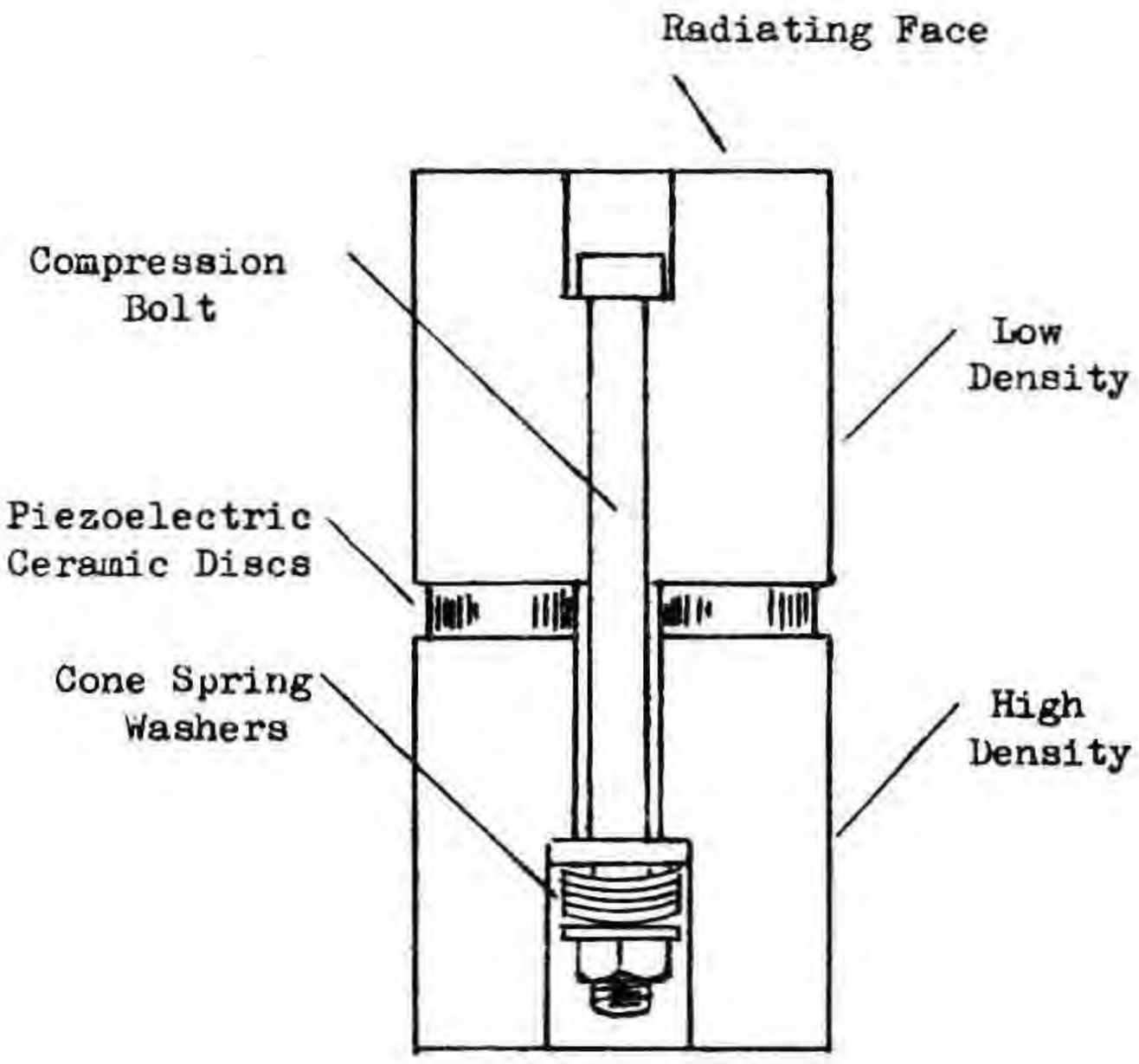

Fig. 3.

Fig. 3. shows the construction of a practical transducer employing these principles. The piezoelectric elements are four barium titanate or lead zirconate-titanate discs arranged symmetrically in a square section configuration. If contacting faces between the metal and ceramic are accurate in flatness, it is possible to disperse with cements, but normally a thin film of cement is used to obtain good acoustic energy transfer.

The advantages of this type of transducer are manifold. Since the radiated power is asymmetrically distributed between the two vibrating faces the unused acoustic energy produced at the rear face is considerably reduced with a corresponding gain at the operative surface. The radiating surface is metallic and can be secured to a transmission diaphragm by mechanical means, such as bolting or welding. Large pieces of ceramic are avoided and economic construction is possible. Heat is rapidly conducted away from the ceramic through the metal masses and the transducer operates at low temperatures and higher efficiency. Finally, the system provides a means of generating acoustic energy at frequencies normally associated with magnetostrictive elements.

Transducers based on these principles are now being widely used for many applications of high power ultrasonics. Cleaning baths and ultrasonic drills can be built showing higher efficiencies of operation than with conventional transducers and have proved to be very reliable over long operational periods. The inherent low Q and the relatively low input impedance enables fixed frequency transistorised power sources to be used (Ref. 6.). With full advantage being obtained from lead zirconate-titanate the economic production of low frequency ultrasonic power can be practically realised.

References

(1). Jaffe B., Roth R.S., and Marzullo S. (1954) J. Appl. Phys. 25. 809.

(2). Noltingk B.E., and Neppiras E.A. (1950) Proc. Phys. Soc. Lond. B63. 674.

(3). Langevin P. Brit. Pat. 145,691 (1921).

(4). Rich S. Brit. Pat. 868,784 (1957).

(5). Brickman A.D. (1962) J.A.S.A. 34. 305.

(6). Acoustica Associates Inc., Los Angeles, U.S.A.

O23

FOURTH INTERNATIONAL CONGRESS ON ACOUSTICS
COPENHAGEN 21.-28. AUGUST 1962

MUTUAL INTERACTION OF HIGH ENERGY PULSED SOUND BEAMS AT VARYING RELATIVE ANGLES

Thomas D. Sachs
University of Vermont, Burlington, Vermont, U.S.A.

Non-linearities of the hydrodynamic equations for large amplitude sound waves have led to the expectation that such waves should interact and produce sum and difference frequencies.[1-11] Interactions of two waves with like propagation vectors and phase, that is the interaction of a wave with itself, have received a great deal of attention;[1,11] the interactions of waves of different frequencies propagating parallel and superimposed have received somewhat less.[5,10] The study of waves of different frequencies propagating in different directions were first investigated theoretically by Ingard[3] using Lighthill's[4] perturbation method. Westervelt[12,13] later challenged both theory and experiment and his results showed that no second order interaction was to be expected for waves not parallel and superimposed. He also pointed out that interaction could be expected on any surface where both waves were incident at the same time, such as transmitting or receiving transducer surfaces.

Investigation of these conflicting theories was undertaken by means of a pulse technique which allowed the separation of the two initial beam pulses from the interaction pulse by means of timing and geometry.

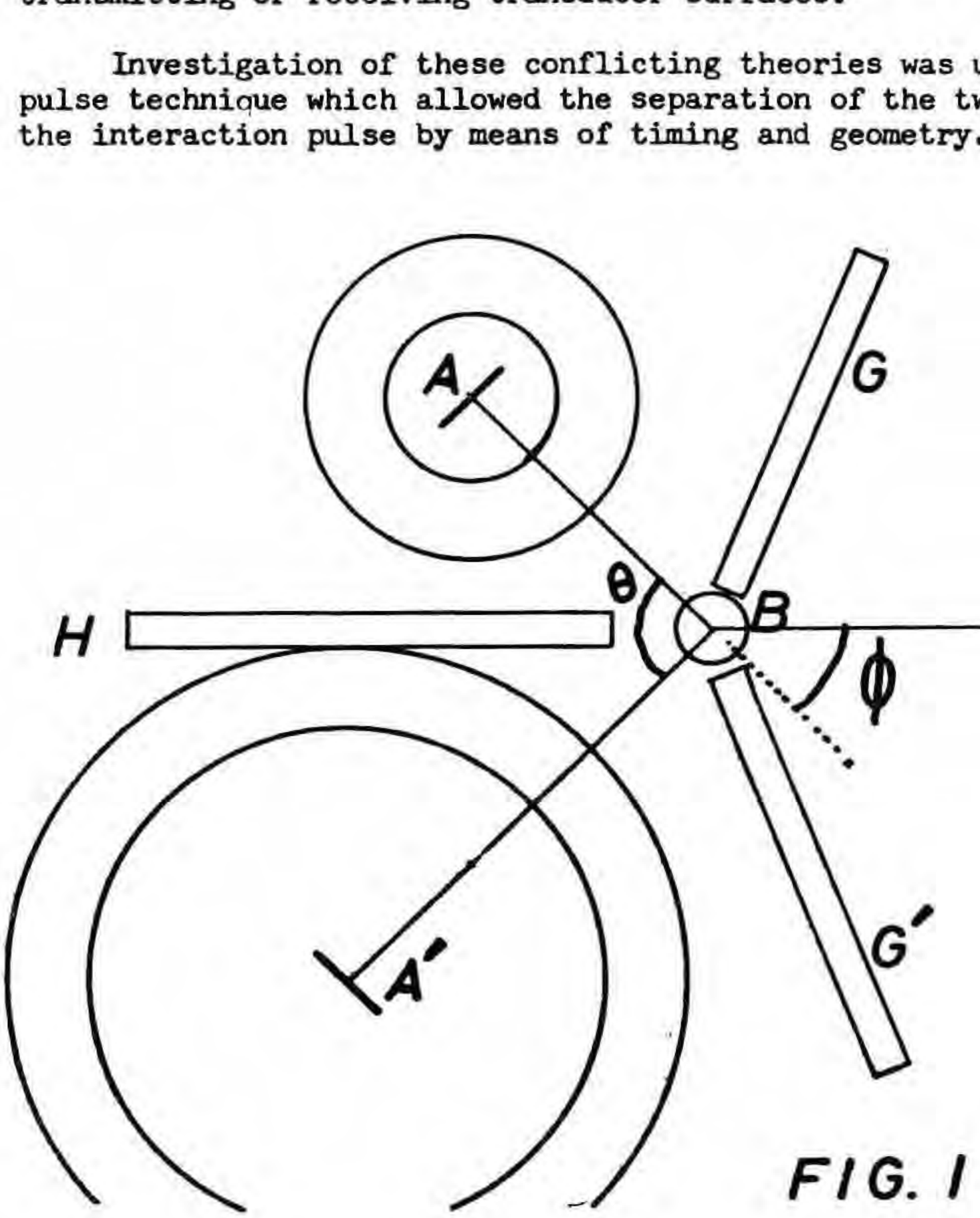

FIG. 1

In Fig. 1, A and A' are the transmitting transducers which are aimed at an arbitrary volume B. D is the receiving transducer which is tuned to the sum frequency and aimed at the volume B. A is closer to B than is A' by a distance at least as long as the physical length of the pulse in the water in which the experiment was carried out. The two pulses arrive at B concurrently and radiate an interaction pulse to D. This interaction pulse, however, arrives at D after the direct signals from A and A' would have arrived. Thus the two initial pulses do not arrive at D at the same time as the interaction pulse and thus we observe the signal from D only at the time during which the interaction pulse would be arriving, if it exists. The two concentric areas around A and A' indicate the physical positions of the two pulses after they have been emitted by the transmitters. Due to the chosen geometry, A pulses some time after A' and thus the two electrical circuits are not in operation at the same time and thus cannot interact with one another. Further separation of interaction pulse from initial pulses was obtained by tuning the transducer D to the sum frequency and making all transducers shown highly directional so that A and A' transmit little energy to D. In addition, D discriminates against this energy both as to frequency and direction. Absorbers are placed in the direct paths between A and D and between A' and D. The possible interactions which could occur on the surface of the transmitters were reduced in two ways: Neither transmitting transducer was in operation at the time that the pulse from the other transducer impinged on it except when the transmitters were very close together, and an absorber H was placed between them.

The requirements for the electronics were largely concerned with: 1. The sharpness of the cutoff of the transmitted pulse, as a "tail" on one pulse could occur at the receiver at the same time as the other pulse and thus cause interaction. 2. With the recovery time for the pre-amplifier for the receiver, since it would be saturated by a primary pulse just before measurement was to be made. 3. With the relative timing of the pulse transmitters and the observation time of the oscilloscope. To make sure that the two initial pulses actually coincided in the interaction volume, both in space and time, a small probe microphone was built and placed in a cylindrical coordinate system in the interaction volume. The cut off of the transmitters was accomplished by using a high impedance resonant circuit and clamping it at the end of the pulse. The low noise and rapid recovery time of the pre-amplifier were accomplished by using cascaded cascode circuits in the input and RC coupling throughout with short RC times.

Reflected signals from the sides of the tank interfered with the measurement at some configurations. To prevent such troubles, two coordinate systems were built, a polar one centered around the interaction volume and probe microphone, and a cartesian system on carts which carried the interaction volume to any desired part of the tank. The ability to move the interaction volume at will without disturbing the rest of the geometry, enabled us to cut the noise level considerably by avoiding reflected pulses.

The calibration of the system was carried out by an ultrasonic power meter which was constructed to have the same cross section as the non-resonant quartz microphone which was to be calibrated. The tuned transducers were then calibrated at the appropriate frequencies against this quartz standard.

The apparatus was set up by placing the probe microphone in the interaction volume and aiming both transmitting transducers at it. The relative timing of the transmitter pulses was adjusted for co-incidence by observing the output of the probe. The receiving transducer was then placed in the main beam from a transmitter and the delay of the oscilloscope sweep set so that it would trigger

just before the signal arrived, which total delay time is exactly that of the interaction pulse regardless of the relative positions of the transmitting and receiving transducers. The receiver was then swung to the measuring position.

So long as the probe microphone was left in the interaction volume, an interaction signal which had an amplitude modulation was recorded by the receiving transducer. As soon as this object was removed from the interaction volume, the level of the signals fell below noise level. This would indicate that interactions do take place at surfaces. Further experiments with other objects also produced like interactions.

To evaluate the data in relation to Westervelt's[12,13] and Ingard's[3] predictions, an "Excess Sensitivity" S_e was defined as the ratio between the signal predicted by Ingard and that which we could have measured with our apparatus where the limiting factor was the noise level. The excess sensitivity was measured as a function of two angles, θ and ϕ. θ was the angle between the two transmitting transducers, i.e. A'BA and ϕ was the angle between one incoming beam and the interaction signal going to the receiver, i.e. the supplement of the angle ABD. The noise level consisted not only of thermal noise in the input stages of the amplifier but also of stray energy from the transmitters, reflections, energy still present from previous pulses and so forth. This noise was geometry dependant and was taken into account in S_e. The value of S_e varied from 70-94 decibels. It should be noted that measurements could not be made closer than 45° from one or the other of the beams as insufficient time difference was available for smaller angles.

We found it possible to investigate the case of parallel superimposed beams, for energy radiated at an angle from these beams.

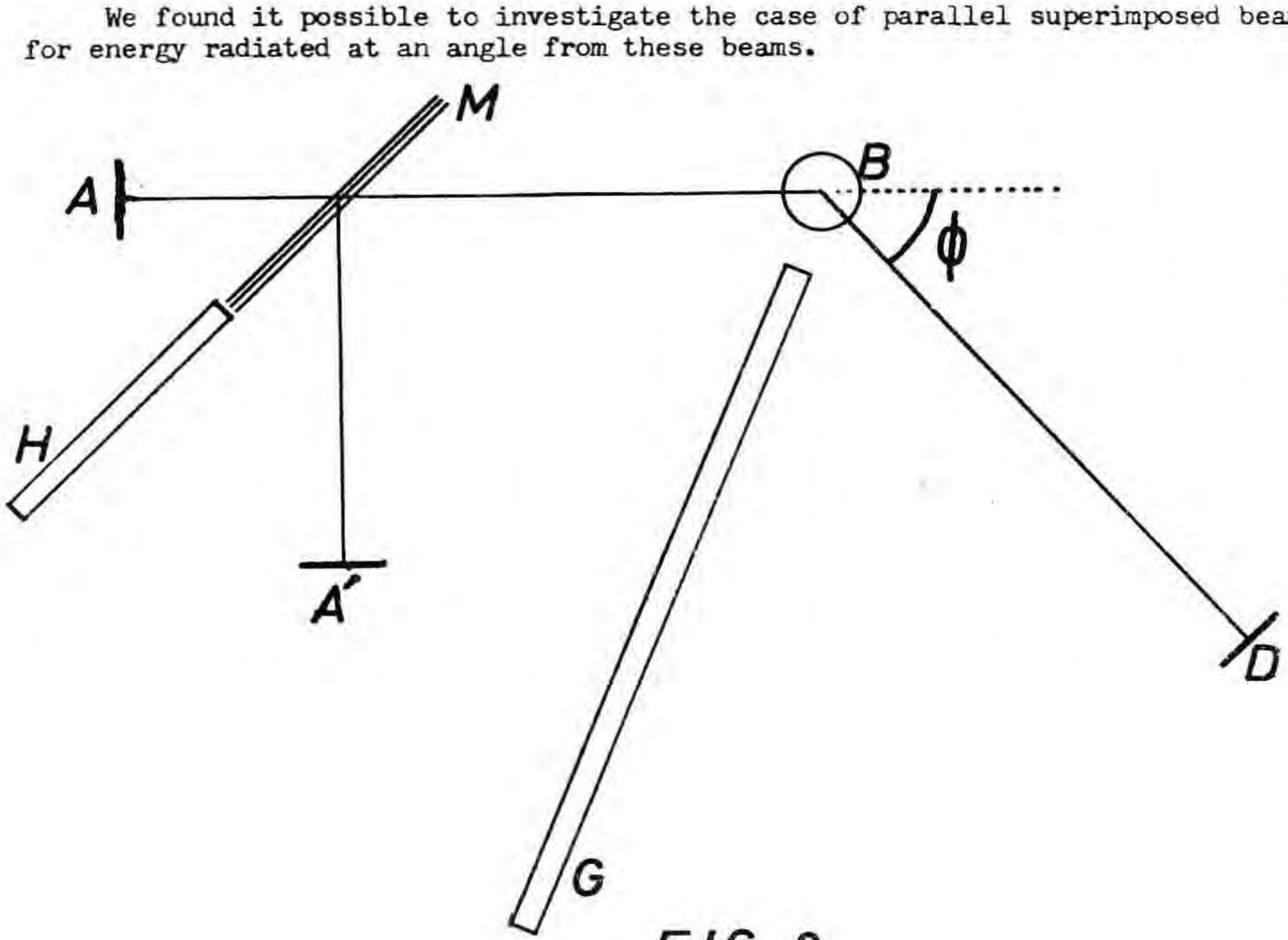

FIG. 2

The transducers A and A' were aimed at right angles to each other at a partially reflecting surface M as shown in Fig. 2. The beam from A is partially transmitted and that from A' partially reflected to form a set of parallel superimposed beams. The partially reflecting surface M was constructed of a thin sheet of polystyrene wrapped with aluminum foil until the desired reflectivity was achieved. The surface itself produced interactions, as expected, but after the beam had left this surface it propagated further down the tank and interactions at the down beam positions in the tank were used to make the investigation. The volume B was chosen as the volume to be examined and the timing of the oscilloscope sweep so chosen that the output of D would be observed only when the interaction signal was coming from the volume B. Since the direct signals from the transmitting transducers as well as the interaction signal from the semi-reflector were all arriving at D by more direct paths, a time separation could be achieved for this case also. The S_e measured in this case was 68 decibels. This is not to be taken to mean that parallel superimposed sound beams do not interact, but only that they do not radiate at an angle to the initial beam directions, which seems reasonable on the basis of momentum conservation.

The author wishes to thank Professors F. V. Hunt of Harvard and P. J. Westervelt of Brown for their assistance and encouragement on this problem and to express his particular thanks to Professor Joseph Kolb of the Physikalisches Institut der Universitaet Innsbruck, Innsbruck, Austria, where this work was carried out.

Bibliography

1. Fay, JASA 222 (1931)
2. Gorelik and Zverev Sov. Physics-Acoustics 1 353 (1955)
3. Ingard and Pridmore-Brown JASA 28 367 (1956)
4. Lighthill Proc. Roy. Soc. London A 211 567 (1952)
5. Mikhailov Doklady Akad. Nauk SSSR 4 663 (1953)
6. Mikhailov Doklady Akad. Nauk SSSR 109 603 (1956)
7. Mikhailov Sov. Physics - JETP 30 100 (1956)
8. Mikhailov Sov. Physics-Acoustics 2 409 (1956)
9. Rayleigh Theory of Sound Vol. 11 Dover (1945)
10. Thuras, Jenkins and O'Neil JASA 6 173 (1935)
11. Zarembo, Krasil'nikov, Shklovskaia-Kordi Doklady Akad. Nauk. SSSR 109 485 (1956)
12. Westervelt JASA 29 199 (1957)
13. Westervelt JASA 29 934 (1957)

P23

FOURTH INTERNATIONAL CONGRESS ON ACOUSTICS
COPENHAGEN 21.-28. AUGUST 1962

The Measurement of High Temperatures by the Determination of the Velocity of Sound Waves in Materials.

E. A. THORNE - Dragon Project
U.K.A.E.A. - Winfrith - UNITED KINGDOM

The measurement of temperature is an essential requirement in any nuclear reactor and its accompanying research and development programme. Up to the present thermocouples have been used but there are several disadvantages such as incompatibility with reactor construction materials which increases with rising temperature and alternative methods of measuring temperatures under these conditions need to be investigated.

The Dragon Project is concerned with the development of a high temperature gas cooled reactor with a fuel temperature of up to approximately 1500°C with helium as the coolant. The main construction material in the reactor core is graphite which at such high temperatures presents serious problems of compatibility and restricts the choice of materials that can be introduced into the reactor core for the purpose of temperature measurement.

A system originated by Professor J. F. W. Bell of the Royal Naval College, Greenwich, which was described in Philosophical Magazine Volume II, No. 21 of September 1957, offered a possible method of measuring temperatures and is being examined with this end in view. It is a sensitive method of showing structural and physical changes in materials by measuring the velocity of sound waves in thin rods and as such has a number of useful applications, but our interest is focused entirely on its employment as a means of temperature measurement.

The transducer is a polarised nickel tube around which is placed a transmitting coil and a receiving coil and electrical pulses fed to the former, cause sound waves to travel along the tube. The probe, a rod of 1 or 2 mm diameter has a notch or shoulder cut into it at a suitable point and it is joined to the nickel tube via an impedance matching piece. Sound waves passing along the tube therefore pass along the probe and are reflected back to the receiving coil and this signal is amplified and displayed on an oscilloscope screen. As there is mass discontinuity at the shoulder a portion of the sound wave will be reflected at this point, the remainder passing to the end of the probe and being reflected from there. A single pulse transmitted will be shown on the oscilloscope as a straight line with a strong signal originating from the echo at the shoulder and another caused by the echo from the end of the probe. There are several other echoes such as that from the joint of the matching piece and the probe etc., but these are small in comparison with the shoulder and end echoes. Now, if a pair of pulses are launched, correctly spaced, the first pulse of the pair will travel to the end of the probe and be echoed back, meeting the echo from the shoulder of the second pulse of the pair, combining with it and giving rise to a large combined signal. A high degree of sensitivity is achieved by transmitting alternate pairs of pulses with intervals slightly greater than and slightly less than the correct frequency. Both these combined signals are shown on the oscilloscope and when, by adjusting the frequency, the two amplitudes are equal the frequency is correct. Pulses are generated by a crystal calibrated oscillator and conventional electronic circuits select the pairs of pulses and arrange the small plus and minus frequency difference between pulses

.../of each pair.

of each pair. The pulse width is variable and this is important in achieving output signals with a good degree of symmetry. As the velocity of sound waves vary with the temperature of the medium there are obvious possibilities of using this system as a thermometer. It has the disadvantage that it is not possible to measure temperatures at a point; that which is measured is the mean temperature of the probe between the shoulder and the end, a distance of say 8 cms and upward.

The properties required in a probe which is to be used in a reactor are as follows:-

1. A high melting point.

2. Results must be reproducible with a curve showing no phase changes or hysteresis loop with heating and cooling cycling.

3. It must be compatible with its surrounding materials, e.g. the hot graphite of a high temperature reactor core.

4. It must possess a reasonably low neutron absorption cross section, if used in a reactor core.

The first choice of material was naturally graphite but the results were disappointing. There is a wide hysteresis loop for a heating and cooling cycle. Re-cycling merely diminishes the width of the loop slightly. There is also a negative dip with a minima at approximately 180°C. This disappears with successive heatings but returns after a rest period of several days. The attributes of this material, its high melting point and complete compatibility, are offset by these drawbacks and a search for a more suitable material has been made.

The properties of tungsten appeared to fit those listed above but it has proved, so far, to have an unfortunate tendency of exhibiting a slight change of slope for successive heatings. However, in view of its suitability otherwise, further investigations are being carried out with this material.

Alumina gave readings which were widely spread and which were not reproducible. There is a sharply defined change of condition at 1400°C and this may in some application be useful as a temperature calibration point, but as a probe it is unsuitable.

Niobium showed a similar change of condition at 460°C. A similar effect was found in tantalum by S. Ke who showed that it was due to relaxation phenomena, namely the diffusion of interstitual atoms of carbon nitrogen and oxygen between holes in the lattice.

Molybdenum produces very promising results. The curve is smooth and reproducible. Attenuation of the signal at 1500°C is small, indicating that it may be usable up to quite near its melting point. Readings were taken with molybdenum rods of 2 mm diameter. These were replaced by probes of 1 mm diameter wires and as a notch cut into it would weaken a wire of this dimension, the notch was replaced by a kink in the wire and proved to be satisfactory.

The ideal conditions for the apparatus in use are that the tube and coils be at room temperature with the probe inserted into the high temperature zone. Should the tube and coils be required to be at higher temperatures, difficulties arise. Coils wound with aluminium wire insulated by an anodised alumina coating are satisfactory but the curie point of nickel is 358°C above which temperature

.../polarisation

polarisation is lost. However, it appears that there are possible transducer materials with curie points far in excess of this temperature and these are being examined.

A minor but useful application of the system enables measurements of a number of temperatures to be read accurately. The probe has a number of pits drilled in it and these are filled with selected materials. Whilst the fillings are solid there is no echo, but upon their melting points being reached a large echo appears. An advantage of this method is that as only single pulses of no particular frequency are required the electronic requirements are simple.

G24

FOURTH INTERNATIONAL CONGRESS ON ACOUSTICS
COPENHAGEN 21.-28. AUGUST 1962

TACTUAL VOCODER AS AN AID FOR THE DEAF

J.M.Pickett, Ph.D. x)
Speech Transmission Laboratory, Royal Inst. of Technology, Stockholm

Communication through the skin offers interesting possibilities for adding to our ways of receiving information. Visual and auditory reception are sometimes fully occupied, or they may be limited in capacity by extreme vibration, noise, or sensory deficit. Then one looks for an alternative path for communication. One convenient way would be direct communication of speech by tactual stimuli and this has interested many investigators, especially as an aid for the deaf. The present paper describes some new tests of tactual speech transmission as a mode of presenting speech information to the deaf.

The most recent tests of speech aids for the deaf are those reported by Lövgren and Nykvist (1959); the results are summarized here. They explored, with brief training and tests on four deaf children, the transmission of speech by a 16-channel vocoder with a visual display and by the present tactual vocoder. Lövgren and Nykvist conclude that visual and tactual aids of this type have good potentialities for development as classroom devices in instruction of the deaf.

The tactual vocoder operated essentially as follows. The speech signal was first amplified and subjected to emphasis of the high frequencies (+4 dB/oct). The resulting signal was divided by overlapping filters into ten channels having center frequencies of 210, 400, 580, 830, 1050, 1800, 2250, 3320, 5800, and 7700 c/s. The response curves of the channel filters were triangular with sides having slopes that approached 12 dB/oct. The output signal from each channel was rectified and smoothed to yield a control voltage. Each of the ten control voltages modulated the amplitude of a 300-c/s sinusoidal signal. The varying 300-cycle signals were amplified and led to 10 bone-conduction transducers which served as vibrators for stimulating the ventral tips of the subject's fingers. Proceeding from left to right across the dorsal view of the two hands, the frequency channels were presented to the fingers in order beginning with the lowest channel and proceeding to the highest channel.

A tactual aid for the deaf would be of greatest value if it operated as a complement to lip-reading; in this role a tactual vocoder should provide indications of speech features that are difficult to identify by watching the talker. This mode of operation was explored in a series of tests at Manilla School for the Deaf, Stockholm. The main procedure was to compare the discrimination of speech sounds through the tactual vocoder with the discrimination of the same sounds by lip-reading.

Initially only two different Swedish syllables were used in a test. The tests were then increased in difficulty as the subjects (S's)

---

x) Author now at A.F. Cambridge Research Laboratories, Bedford, Mass. Research performed during tenure of a Research Fellowship from the National Institute of Mental Health, U.S. Public Health Service.

became more familiar with their tasks. Except where noted, the test utterances were isolated Swedish words. Each test was preceded by a practice period during which the talker spoke about ten examples of each word while an experimenter indicated on a card the word which was being spoken. For the subject receiving tactually, one of the experimenters indicated the tactual pattern of the utterance, using appropriate rhythmic gestures across the row of vibrators.

The procedure for testing was as follows. The talker spoke, one at a time, a list made up from equal numbers of each test utterance arranged in a random order. They were received simultaneously by two S's. One S received by lip-reading; the other S received only by feeling the output of the tactual vocoder on his fingers. After each utterance was received the S's spoke the utterance they believed the talker had spoken or pointed to the utterance on a card showing only the utterances of the test in progress. The experimenters then recorded the responses and informed the S's of the correct utterance. A visual ready signal was then given, the talker spoke the next test utterance, and the procedure was repeated to the end of the test. A test typically required 10 to 15 minutes, including training time. After one such test, S's exchanged positions and the test was repeated.

The lip-reading conditions were kept as constant as possible. The talker sat at a distance of 3 meters from S. The talker's face was illuminated from above and left by a 60 W incandescent lamp in a light cloth shade.

Lip-reading tests and tactual tests were undertaken with two classes of profoundly deaf children as subjects. All the deaf subjects were of normal or higher intelligence.

For discrimination tests where only two alternative words were used, the test scores were expressed in terms of percent discrimination relative to chance as zero. To obtain the percent discrimination, the original percent wrong response was subtracted from the percent correct response. For identification tests, where more than two words were used, the test scores were expressed as percent correct response. The statistical significance of a difference between test scores was tested by calculating the probability, p, of the obtained difference, assuming that the difference arose between two random samples from a single binomial population.

Test results are shown in Fig. 1 for tests with the Swedish words sy, ty, så, and tå, /sy, ty, so, to/. It will be noted that tactual discrimination of the two consonants, /s, t/, is better than by lip-reading while the opposite is true for the discrimination between the vowels /y, o/. The lip-position for the Swedish /y/ is protruded and very closely rounded relative to /o/.

Fig. 1. Comparison of results with two talkers (class 7) no"tala"

PERCENT DISCRIMINATION OR IDENTIFICATION

	Lip-Reading			Tactual Vocoder		
Test Words	sy, så	sy, ty	sy, ty, så, tå	sy, så	sy, ty	sy, ty, så, tå
FEMALE TALKER	85.0	46.7	75.8	63.3	60.0	51.4
MALE TALKER	91.6	46.7	78.3	57.5	78.3	57.?

There is a slight interaction between tactual discrimination of /s, t/ and the following vowel. The tactual discrimination of /s, t/ was 43.3 % before /y/ and 60.0 % before /o/, a difference significant at $p = .06$. This interaction may have its origin in the amount of apparent vibratory movement. A brief stimulus movement is felt between the /s/-vibration and the little movement is felt after /t/. A large movement is felt between /s/ and /o/ but only a small one between /s/ and /y/ or /i/. Thus, if the subject uses the movement as a cue for /s/, he receives a larger cue when the vowel is /o/.

A set of two tests were designed to combine discrimination of an initial consonant feature with discrimination of the number of syllables. In the first test, one-, two-, or three-syllable utterances with initial /j/ or /ç/ were combined to give a 6-word test. In a second test, /m/ and /b/ were chosen as the initial consonants in order to provide a consonant distinction that is difficult to lip-read. The results are shown by the matrices of Fig. 2. In the test with /j, ç/, tactual reception was better, overall, than lip-reading and the confusions indicate primarily a better transmission of the number of syllables. On the other hand, /j, ç/-discrimination was better when lip-reading. In the test with /m, b/, tactual reception is much better than lip-reading due to rather good discrimination between /m/ and /b/ as compared with lip-reading.

A final set of tests was performed to determine the combined performance using both lip-reading and tactual vocoder in comparison with lip-reading alone. The same procedure was followed as before but the subject at the tactual vocoder now faced the talker and received approximately the same visual information as the lip-reading subject. A graded series of three tests were carried out.

The results of the final test are shown in Fig. 3. Twelve words from previous tests were used. Lip-reading of labial words vs nonlabial words was perfect but the number of syllables, the /m, b/-distinction, and the /ç, j/-distinction were poorly resolved by lip-reading. The addition of tactual information improved these three discriminations greatly.

It is concluded from these experiments that a tactual vocoder can be of considerable aid in speech communication with the deaf, particularly in furnishing cues a. to time-intensity patterns and gross spectral information.

References

(1) Geldard, F.A.: "Cutaneous channels of communication", Chap. 4, pp. 73-87, Sensory Communication, W.A. Rosenblith (Ed.), Wiely and Sons, New York 1961.

(2) Rösler, G.: "Über die Vibrationsempfindung. Literaturdurchsicht und Untersuchungen im Tonfrequenzbereich", Z.Exp.Angew. Psychol., 4, pp. 549-602 (1957).

(3) Lövgren, Å. and Nykvist, O.: "Talöverföring och talträning med döva barn på visuell och taktil väg under utnyttjande av speciell apparatur" (Speech transmission and speech training for the deaf child by visual and tactual means using special devices), Nord.Tidskr.Dövundervis., pp. 122-143 (1959).

LIP-READING

RESPONSE

word spoken	järn	gärna	gärningen	känn	känna	kännande
järn	24	2		2		
gärna	6	16	1		4	1
gärningen	6	11	2	2	4	3
känn	4			23	1	
känna		2		3	18	5
kännande	1			4	4	19

TACTUAL VOCODER

RESPONSE

	järn	gärna	gärningen	känn	känna	kännande
	23			5		
		17		1	10	
		1	17		5	5
	8	1		18	1	
		9			18	1
			1			27

word spoken	men	mena	menade	ben	bena	benade
men	18			9	1	
mena		17			10	1
menade	1	3	13		4	7
ben	8	2		18		
bena		10			18	
benade		2	12		2	12

	men	mena	menade	ben	bena	benade
	27			1		
		25			3	
		1	25			2
	1			27		
		2			26	
			2		1	25

Fig. 2. Identification of Swedish words by lip-reading and by tactual vocoder. Seven deaf subjects. A male talker spoke four of each word to a pair of subjects, one receiving by lip-reading and the other through the tactual vocoder.

LIP-READING

RESPONSE

MALE TALKER WORD SPOKEN	men	mena	menade	ben	bena	benade	känn	känna	tjänade	järn	gärna	gärningen
men	14			6	1							
mena		9	1		9	2						
menade			8		1	12						
ben	9			12								
bena		7		1	13							
benade	2		8		1	10						
känn							19			2		
känna							3	14	2		1	1
tjänade							1	3	11	1	2	3
järn							2			19		
gärna								3	1		17	
gärningen								1	8	3	9	5

59.8 % correct

TACTUAL VOCODER AND LIP-READING

RESPONSE

	men	mena	menade	ben	bena	benade	känn	känna	tjänade	järn	gärna	gärningen
	15			6								
		15			6							
			18			3						
	2			19								
		2			19							
			3			18						
							19			2		
								20			1	
									16		2	3
							1			20		
								2			19	
									1	1	2	17

85.3 % correct

Fig. 3. Identification of Swedish words by lip-reading alone and by combined lip-reading and tactual vocoder. A male talker spoke three of each word to each of seven deaf subjects under each receiving condition.

H24

FOURTH INTERNATIONAL CONGRESS ON ACOUSTICS
COPENHAGEN 21.-28. AUGUST 1962

BINAURAL HEARING AND FREE FIELD EFFECTS

E. E. David, Jr. and R. L. Hanson, Bell Telephone Laboratories, Inc.
Murray Hill, New Jersey - U.S.A.

Binaural earphone experiments using well-controlled, simplified stimuli have provided major additions to auditory theory and to the understanding of auditory mechanisms. On the other hand, many of the most compelling binaural effects, such as "precedence" and "cocktail-party" phenomena are found in the free-field, and are difficult to relate to basic mechanisms. The few efforts along this line, though valuable, have been far from complete.[1] In this paper, we will present results which show that free-field effects involve factors not usually considered in earphone experiments.

The precedence effect,[2] sometimes called the Haas Effect,[3] involves multiple sources of the same sound. The nearest source, providing the first arrival at the listener's ears, controls the localization. Data demonstrating the effect can be obtained by placing two loudspeakers equidistant from a listener, as shown in Fig. 1. The same sound is projected by each except that interspeaker time and intensity differences can be introduced. With zero differences, the image appears midway between the speakers. When one sound is delayed by even as little as 0.1 ms, the image shifts toward the leading speaker. The image can be brought back to the center by increasing the intensity of the delayed sound. For long delays, two sources are apparent and the subject balances loudness. The relation between the interspeaker differences so measured shows a sharp rise for delays less than 2 or 3 milliseconds, reaches a peak and then begins to decrease. Actually, the detailed shape of the curve changes with the nature of the projected sounds, and is variable from listener to listener. Note that there are two arrivals at each ear, one from each speaker, as shown in Fig. 1. We label the left ear arrivals $L1_A$ and $L2_B$, and the right ear arrivals $R1_B$ and $R2_A$. (Subscripts refer to the source.) The second arrivals are of lower intensity due to head shadowing.

In explanation, David[4] has proposed that the initial rising portion of the curve reflects a time-intensity exchange with respect to the image formed by $R1_B$ and $L1_A$, the image from $R2_A$ and $L2_B$ being masked and not affecting localization.[2] The falling portion of the curve was attributed to monaural masking of the second arrival in each ear by the first. We now have results which indicate that some revision of these notions is in order.

Our experiments were done under essentially earphone conditions. Stimuli for each ear were provided by special loudspeakers very close to the listener's ears (see Fig. 2), thereby allowing the listener to recline comfortably on a headrest between the speakers. Head shadowing provided 40-db isolation from the opposite ear. Through the electrical arrangement shown in Fig. 2, the stimulus conditions corresponding to Fig. 1 can be recreated. When two pulses (high-passed to 400 cps to emphasize the isolation) are presented to each ear as shown, and the listener is required to balance a delay of source B (or A) by an intensity decrease of source A (or B), the solid curve of Fig. 2 is generated. This curve is the conventional precedence result. If now the second arrivals in each ear are eliminated, that is, only $R1_B$ and $L1_A$ are presented, and the same balancing undertaken, the dotted curve is obtained.

Clearly, the falling portions (beyond 8-10 milliseconds) of the curves are nearly identical. Since there can be no monaural masking in the latter case, the

implication is that the masking must be binaural in both cases. In other words, in the two-pulse case, the earlier pulse in one ear is masking the later in the other. This effect is equivalent to the masking of one binaural image by another, as consideration of the four-pulse case shows. Indeed, subjectively, observers feel they are equating the loudness of two percepts separated spatially. The degree of masking is indicated by the increased intensity as indicated by the falling tails of the precedence curve.

For delays less than about 5 ms, the data from our two experiments are definitely divergent. The presence of the second arrivals in each ear reduces the intensity difference necessary to balance a given delay. In this region, subjects tend to hear a single broad source, not two distinct images. When only $R1_B$ and $L1_A$ are used, the principal phenomenon seems to be a simple time-intensity exchange as has been previously reported.[5] The similar shape of the curve when $R2_A$ and $L2_B$ are added argues that this exchange is effective here also with an additional influence from the second arrivals. These, in effect, seem somehow to supplement the intensity of the lagging pulse, $R1_B$, or decrease that of the leading pulse, $L1_A$. A further experiment was done to clarify the matter.

The same experimental arrangement was used substituting three-pulse for four-pulse stimuli.[6] Results are shown in Fig. 3. Notice that the addition of the smaller second arrival, $R2_A$, has no effect. We find the same curve with and without it. The larger second arrival, $L2_B$, produces a marked effect. Looking at the stimulus pattern in this case, we see that $L2_B$ may be interacting in two ways; (1) it may be masking $L1_A$ retroactively, and (2) it may be forming a "secondary" image with $R1_B$ which affects the "primary" image from the fusion of $R1_A$ and $L1_B$. The latter seems the more likely, since the effect of $L2_B$ increases with interval between it and $L1_A$, the opposite from that expected in retroactive masking.

Let us examine the latter possibility more carefully. An image from $R1_A$ and $L1_B$ taken as a pair will be off-center toward the left since B/A is less than required. An image from $L2_B$ and $R1_B$ will be toward the right because of the direction of the time and intensity differences. Thus apparently the overall image position is a weighted compromise between those obtained from the individual pairs. This observation implies, and it has been confirmed by listening, that in the balance condition with $R1_B$, $L1_A$, and $L2_B$, removal of $L2_B$ from the left ear causes the image to move to the left, a paradox unless "position-averaging" is postulated. Note also that we are led to conclude that binaural interaction can occur simultaneously between a single event in one ear and each of two temporally separated events in the other.

Over what range of separation can such double interactions occur? From the data of Figs. 2 and 3, the range would seem to extend as far as 3-5 milliseconds with no minimum limit. Clearly some minimum must exist since monaural summation must take place at intervals where events can no longer be resolved temporally. This effect is easily shown by another experiment in which the "second arrival," $L2_B$ is varied in position while $R1_B$ and $L1_A$ are held fixed with no interaural time or intensity difference between them. Thus, alone they yield a centered image. As the position of $L2_B$ is varied, the observer judges the position of the resultant image. The results, Fig. 4, show that when $L2_B$ leads $L1_A$ by 0.2 ms or more, the image position is largely controlled by $R1_B$ and $L2_B$. The reader can confirm this fact by comparing in Fig. 4 the result for $R1_B$ and $L2_B$ alone with that when $L1_A$ is present. The slight right displacement in the latter case reflects the effect of $L1_A$ as previously discussed. When $L2_B$ lags $L1_A$ by 0.1 ms or more, the same effect shifts the $R1_B$-$L1_A$ image to the right. In between, the image is shifted to the left. Here $L1_A$ and $L2_B$ are reinforcing each other presumably by simply adding at the stimulus or basilar membrane level.

These results make it clear that the precedence effect involves a variety of phenomena. There is the conventional interaural time-intensity exchange, but in addition such unaccustomed factors as binaural masking, multiple binaural interactions, and image-position averaging apparently play a part. We should expect that comparable factors will be found in other free-field phenomenon such as the

cocktail-party effect. Here the listener is subjected to multiple sources of different sounds, presumably resulting in multiple images, one of which is selected and reinforced at the expense of others. The selection process undoubtedly partakes of a variety of factors. There is selectivity in space, frequency, pitch, and semantic and linguistic content, but there are less obvious factors, too.

One possibility is time gating. Speech is far from a continuous process. Rather it is off and on at the syllabic rate or faster. If two speech waveforms are added, much of the time their waveforms do not overlap. If the unwanted signal could be removed from the gaps in the wanted signal, it might be enhanced. Where and how could an appropriate gating signal be generated? Consider the following: if volleys from a particular basilar frequency channel provide the temporal cues for localization, then a straight-through perceptual chain seems unlikely. Speech perception probably calls for a stimulus representation different from that appropriate for localization. At the output of a localization center, low-frequency envelope information, such as that required for periodicity pitch, is likely available. If so, it can be used as a selective time gate to reinforce a particular signal. These operations are indicated in Fig. 5 and are arranged to reinforce an on-axis talker. Envelope data at the output of the coincidence detector is used to vary the effective gain in synchrony with the desired talker. Kaiser and David[8] have demonstrated that such gating can produce "cocktail party" type results. The advantage to be had decreases as the interference becomes more continuous temporally, a result in harmony with measurements by Hirsh,[8] and Pollak and Pickett.[9]

In conclusion, we see that earphone and free-field experiments have numerous points of contact. No one can doubt the value of controlled binaural experiments in trying to understand the complexities of the free-field. Yet we are only beginning to encompass the variety of factors which contribute to our binaural experiences.

REFERENCES

1. Notable work along this line has been recently reported by N. V. Franssen, "Some Considerations on the Mechanism of Directional Hearing," PhD Thesis, Univ. of Delft, 6 July 1960.
2. H. Wallach, E. B. Newman, and M. R. Rosenzweig, "The Precedence Effect," Am. J. Psychol., 62 (1949) 315.
3. H. Haas, "Uber den Einfluss Eines Einfachechos Auf Die Hörsamkeit von Sprache," Acustica, 1 (1951) 49; E. Meyer and G. R. Schodder, "Uber den Einfluss von Schallrückwürfen auf Richtungslokalisation und Lautstärke bei Sprache," Nachr. Akad. Wissensch, Göttingen, (1952) Nr 6, 31-42.
4. E. E. David, Jr., "Comment on the Precedence Effect," Proc. III Int. Cong. Acous., 1959, 144-146.
5. E. E. David, Jr., N. Guttman, W. A. van Bergeijk, "Binaural Interaction of High-Frequency Complex Stimuli," J. Acous. Soc. Am., 31, (1959) 774-782.
6. N. Guttman, W. A. van Bergeijk, and E. E. David, Jr., "Monaural Temporal Masking Investigated by Binaural Interaction," J. Acous. Soc. Am., 32, (1960) 1329-1336.
7. J. F. Kaiser and E. E. David, Jr., "Reproducing the Cocktail Party Effect," J. Acous. Soc. Am., 32, (1960) 918.
8. I. J. Hirsh, "The Relation between Localization and Intelligibility," J. Acous. Soc. Am., 22, (1950), 196-200.
9. I. Pollak and J. M. Pickett, "Sterephonic Listening and Speech Intelligibility against Voice Babble," J. Acous. Soc. Am., 30, (1958), 131-133.

FIGURE [illegible] - In the precedence effect, the source nearest the listener provides the first arrival and prompts localization of the virtual image.

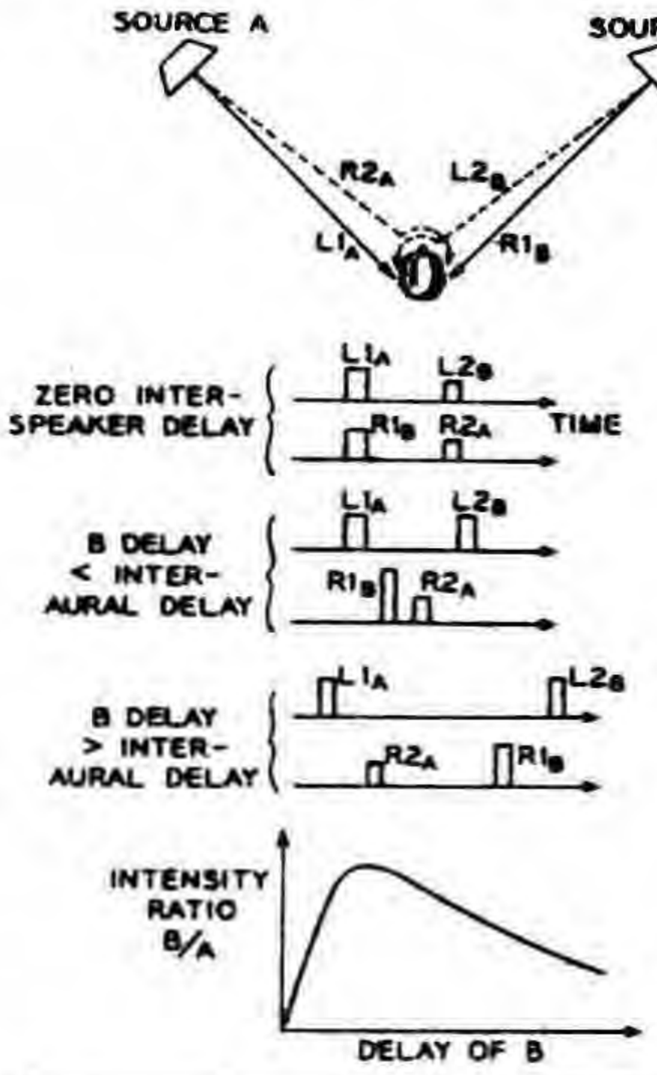

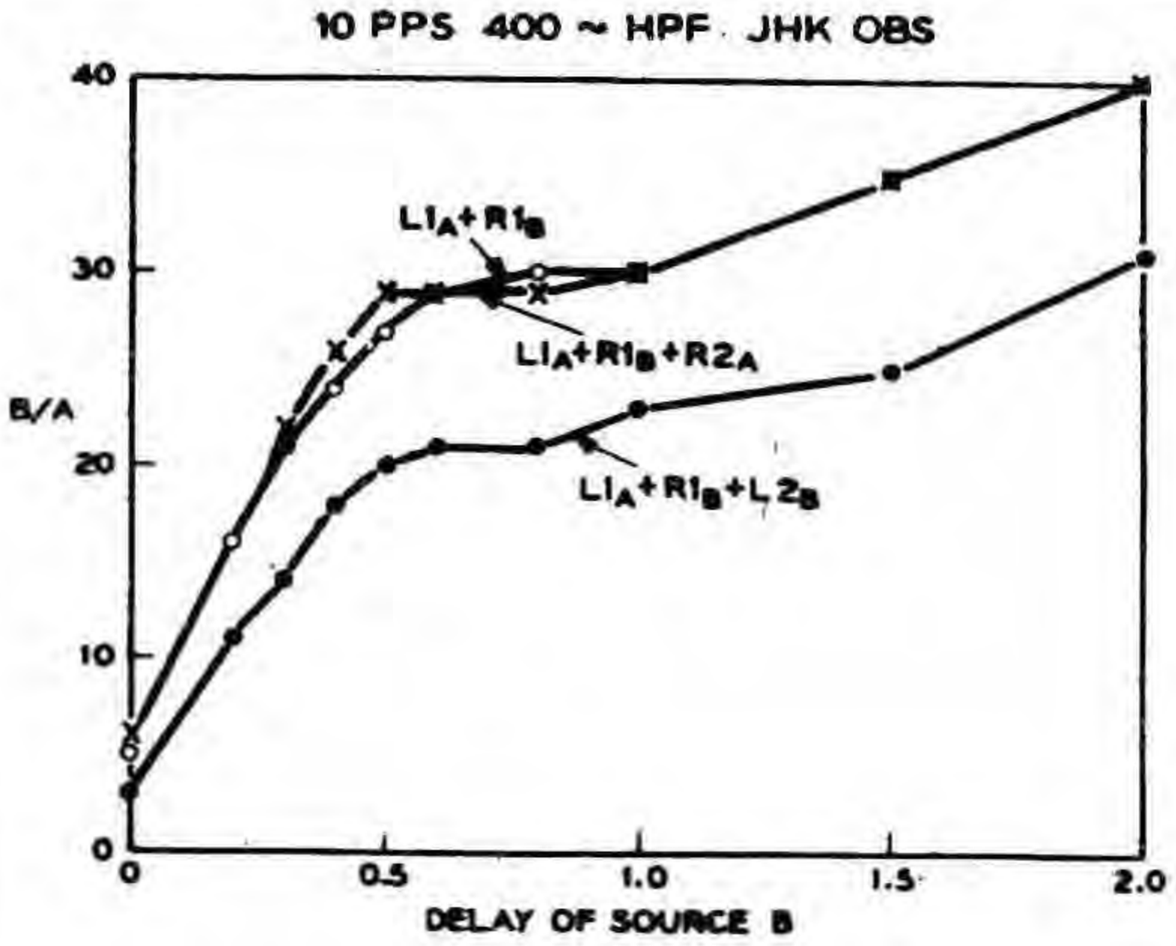

FIGURE 3 - Delay-intensity equivalence is affected more by the larger secondary arrival than by the smaller.

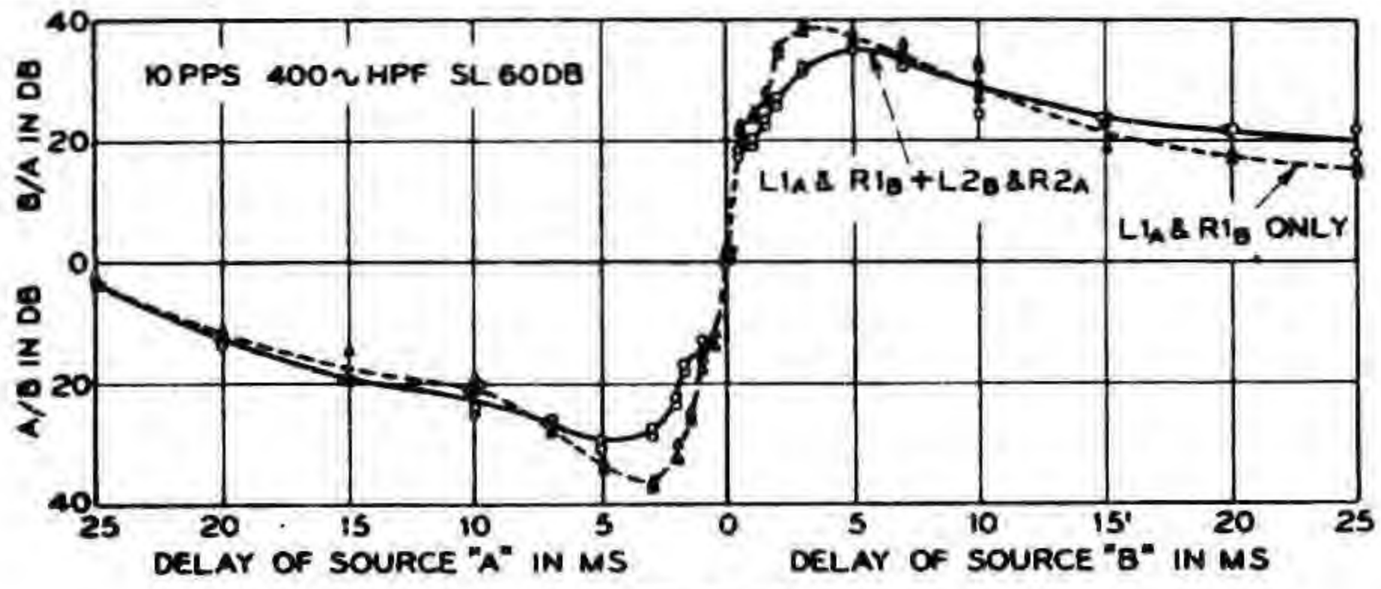

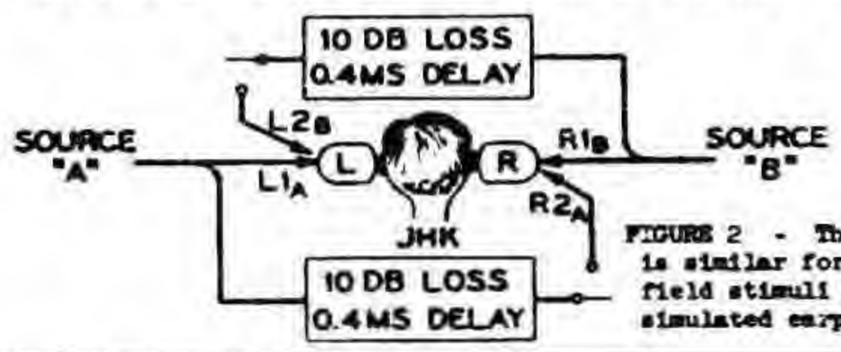

FIGURE 2 - The delay-intensity equivalence is similar for four-pulse, simulated free-field stimuli to that for the two-pulse, simulated earphone condition.

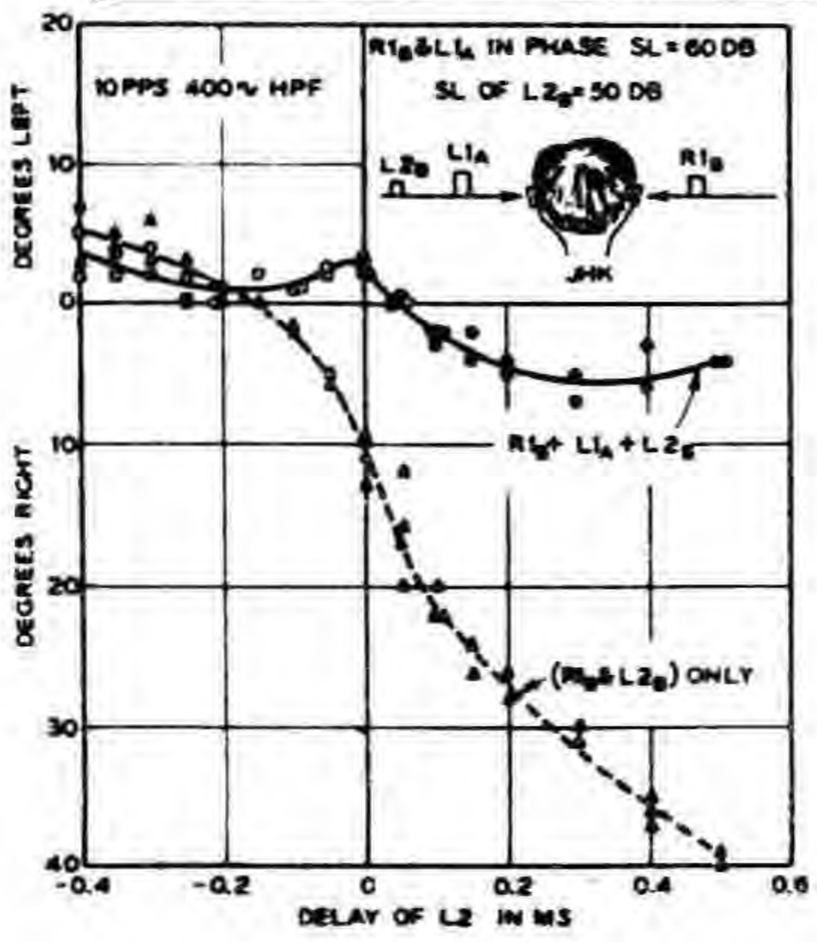

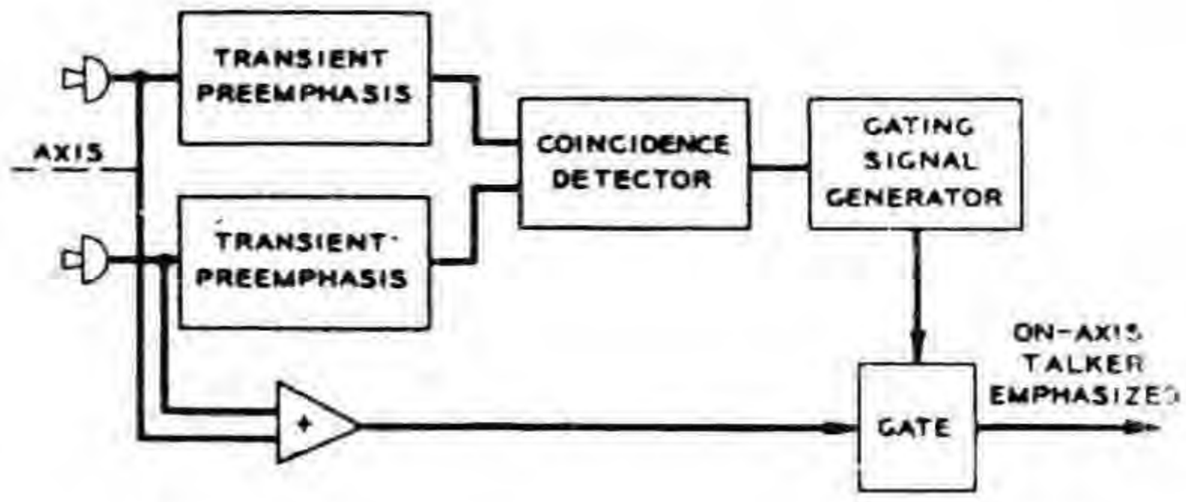

FIGURE [illegible] - Position of the virtual image depends [illegible] secondary. Both image-position asymmetry and [illegible] appear, but in different delay regions.

Sonolumineszenz in Quecksilber

H. Kuttruff
III. Physikalisches Institut, Universität Göttingen

Im Jahre 1959 hat JARMAN festgestellt, daß die Intensität der Sonolumineszenz proportional dem Quotienten aus dem Quadrat der Oberflächenspannung und dem Dampfdruck der beschallten Flüssigkeit ist. Falls diese Gesetzmäßigkeit allgemein gilt, sollte man bei Quecksilber besonders kräftige Lumineszenzerscheinungen erwarten, da hier der erwähnte Quotient etwa 75 000-mal größer ist als bei Wasser.

Leider hat die Undurchsichtigkeit des Quecksilbers große Beschränkungen in der Wahl der Beobachtungsmethode zur Folge. Zur Untersuchung einer etwaigen Sonolumineszenz in Quecksilber ist man daher gezwungen, die Kavitation, von der das Leuchten ausgeht, an einer durchsichtigen Grenzfläche zu erzeugen, durch die das entstehende Licht austreten kann.

Bei den hier zu beschreibenden Versuchen wurde ein Schwinger aus Glas verwendet, der durch ein Bariumtitanatrohr zu Longitudinalschwingungen erregt wurde (s. Abb. 1). Das Bariumtitanatrohr wird in der üblichen Weise in seiner ersten Längseigenschwingung erregt; die Frequenz beträgt 25 kHz. Der angekittete Glasstab, dessen Länge ebenfalls einer halben Dehnwellenlänge entspricht und dessen Querschnitt sich in der Mitte sprunghaft ändert, taucht mit seinem unteren Ende in das Quecksilber ein. Die Kavitationsblasen entstehen auf der unteren Endfläche des Stabes. Infolge der hohen Dichte des Quecksilbers und wegen der durch den Querschnittssprung bewirkten Schnelletransformation im Verhältnis 1 : 3,36 erhält man eine gute Anpassung des Schwingers an das Medium.

Das Leuchten kann entweder durch das Bariumtitanatrohr oder schräg von oben durch

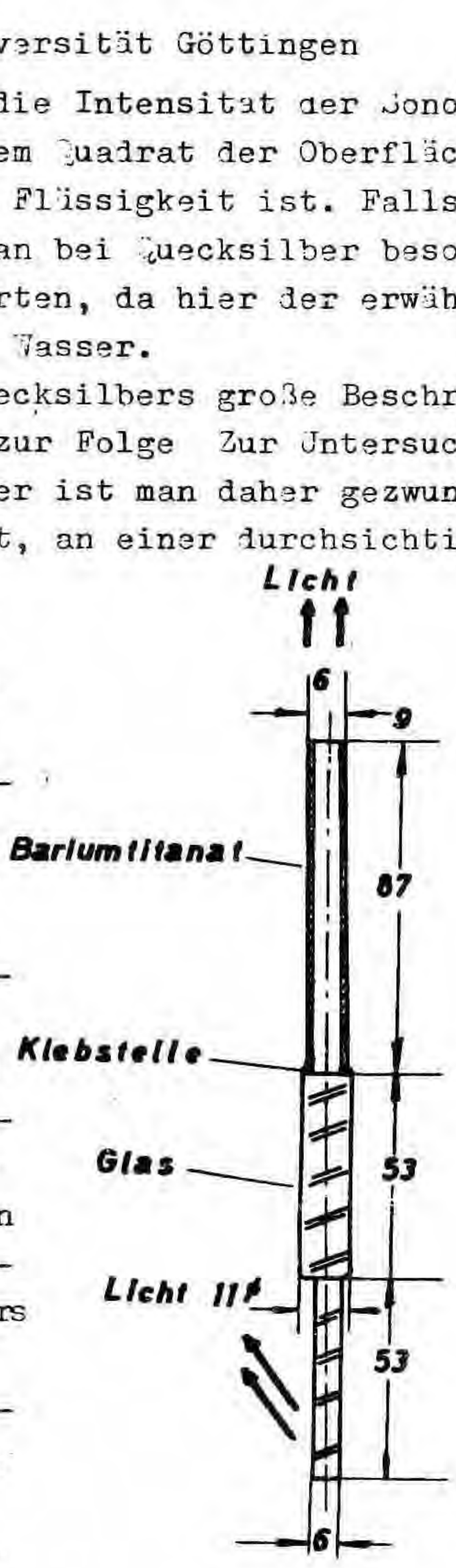

Bild 1

das untere Ende des Glasstabs beobachtet werden. Schon bei den ersten Versuchen konnten kräftige Leuchterscheinungen beobachtet werden, deren Intensität sehr viel höher ist als die der mit derselben Anordnung an Glyzerin oder Äthylglykol erhaltenen Sonolumineszenz. Das mag als Bestätigung der eingangs erwähnten Gesetzmäßigkeit angesehen werden. Es blieb allerdings noch nachzuweisen, daß dieses Leuchten identisch ist mit der von anderen Flüssigkeiten her bekannten Sonolumineszenz.

Hierzu wurde zunächst der zeitliche Ablauf des Leuchtens mit einem Photomultiplier registriert. Die so erhaltenen Oszillogramme weisen eine große Zahl von Spitzen auf, von denen jede einem emittierten Lichtblitz entspricht. Diese Lichtblitze treten während jeder Schallperiode in einem bestimmten Zeitintervall auf und sind statistisch über dieses verteilt. -

Zur zeitlichen Zuordnung der Lichtblitze zu dem Verhalten der Kavitationsblasen wurden die von den letzteren erzeugten Stosswellen herangezogen, und zwar erzeugt jede zusammenschlagende Blase im Endstadium der Implosion eine sich in die Flüssigkeit ausbreitende Stoßwelle. Zum Stoßwellennachweis diente ein eigens hierfür entwickeltes Sondenmikrophon (s. Abb. 2). Es besteht im wesentlichen aus einem Nickeldraht, dessen eines Ende sich in unmittelbarer Nähe des Schwingers befindet. Eine auf das Drahtende auftreffende Stoßwelle erzeugt im Draht einen Dehnenwellenstoß, welcher infolge der Magnetostriktion mit einer entsprechenden Magnetisierung verknüpft ist. Diese Magnetisierung pflanzt sich mit Dehnwellengeschwindigkeit im Draht fort. Bei der Reflexion der Dehnwelle am Drahtende ändert sich der magnetische Fluß, der einen kleinen dicht davor befindlichen Ferritzylinder durchsetzt und in der um das Ferritstück gewickelten Spule wird eine Leerlaufspannung induziert, die ein getreues Abbild des Dehnwellenstoßes darstellt. - Da die Dehnwellengeschwindigkeit im Nickeldraht als bekannt anzusehen ist, kann man aus dem Auftreten eines Spannungsstoßes an der Induktionsspule auf das erfolgte Zusammenschlagen einer Kavitationsblase schließen. Es stellte sich heraus, daß zumindest jeder stärkere Lichtblitz von einer deutlich feststellbaren Blasenimplosion begleitet wird und mit dieser zeitlich zusammenfällt. Dieser Sachverhalt ist aber ein charakteristisches Merkmal der Sonolumineszenz überhaupt.

Einen weiteren Anhaltspunkt liefert das Spektrum des Leuchtens. Es besteht aus einer verwaschenen Linie mit einer Wellenlänge von ungefähr 550 mu und einem sich über den ganzen sichtbaren Spektralbereich erstreckenden Kontinuum. Ein solches kontinuierliches Spektrum ist ebenfalls charakteristisch für die Sonolumineszenz. Die Natur des an be-

schalltem Quecksilber beobachteten Leuchtens ist damit klargestellt.

Die Tatsache, daß die Sonolumineszenz auch in Quecksilber auftritt und daß ihre Intensität hier sogar besonders hoch ist, gestattet nun weitreichende Schlüsse auf den Erzeugungsmechanismus des Leuchtens. Die Heranziehung elektrischer Effekte als Ursache der Sonolumineszenz scheidet von vornherein wegen der elektrischen Leitfähigkeit des Quecksilbers aus. Auch durch die Kavitation ausgelöste chemische Reaktionen kommen als Leuchtursache nicht in Betracht· dazu ist Quecksilber einfach zu verschieden von allen anderen bisher untersuchten Flüssigkeiten; eine Bildung von Wasserstoffperoxyd in Quecksilber z.B. ist nicht vorstellbar. Dagegen bestätigen die Versuche die zuerst von NOLTINGK und NEPPIRAS geäußerte Vermutung, wonach die Sonolumineszenz thermische Ursachen hat Hiernach wird das Gas, das in die Kavitationsblasen eindiffundiert, während der plötzlichen Implosion der Blasen adiabatisch komprimiert und hoch erhitzt. Die Implosion einer Kavitationsblase verläuft umso rascher und das in ihr befindliche Gas wird umso höher komprimiert, je weniger Gas in der Kavitationsblase vorhanden ist, d h auch je geringer die Löslichkeit des Gases in der Flüssigkeit ist. Das erklärt wenigstens teilweise die hohe Leuchtintensität bei Quecksilber, die übrigens mit einer sehr starken Materialerosion Hand in Hand geht. Die hohe Oberflächenspannung sorgt weiterhin dafür, daß eine implodierende Kavitationsblase relativ lange ihre Kugelform bewahrt, wodurch die Heftigkeit der Implosion ebenfalls gesteigert wird. Die Sonolumineszenz ist somit als thermisch angeregtes Gasleuchten aufzufassen, ein Resultat, für das auch zahlreiche frühere Versuchsergebnisse sprechen.

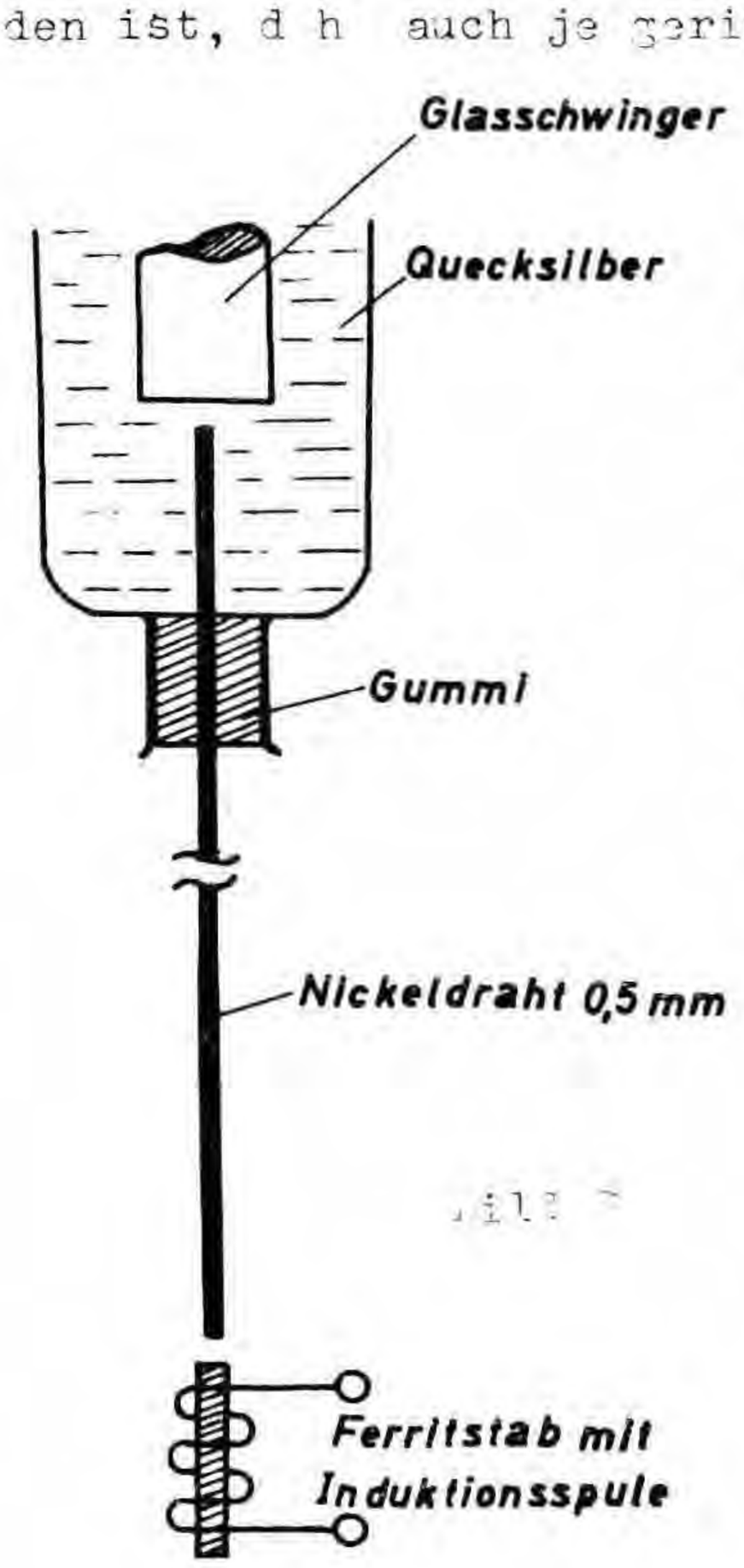

K24

FOURTH INTERNATIONAL CONGRESS ON ACOUSTICS
COPENHAGEN 21.-28. AUGUST 1962

Ultrasonic Absorption and Relaxation Times in Nitrogen, Oxygen, and Water Vapor

Yahei Fujii, Robert Bruce Lindsay, and Kiyoshi Urushihara

The sound absorption coefficient, α, in argon, nitrogen, oxygen, and water vapor is measured by a direct method using a pulse modulated signal of about 65 kc/s. A cylindrical vacuum-tight tank, which is 50 cm in diameter and 126 cm long, is used as a gas container and is placed in a heat bath whose temperature is regulated up to 190°C. A sound source and a receiver, both made of lead-zirconate-titanate ceramic tube and aluminum coupler, are placed on the center line of the tank, and the separation between them, r, is changeable by moving the source along the center line. Since the received acoustic excess pressure is proportional to $e^{-\alpha r}/r$ for sufficiently large r, α is obtained directly from the amplitude of the received signals which are given as a function of r. Precautions are taken to avoid the effect of echoes and other factors which may cause deviations from the relation that the received signal is proportional to $e^{-\alpha r}/r$. A block diagram of the apparatus is shown in Fig. 1.

The sound absorption coefficient in argon is measured to calibrate the apparatus. The results agree with the theoretical classical absorption coefficient, α_{cl}, within 1%.

It can be shown that the absorption coefficient is approximated by the sum, $\alpha_{cl} + \alpha_{rel}$, where

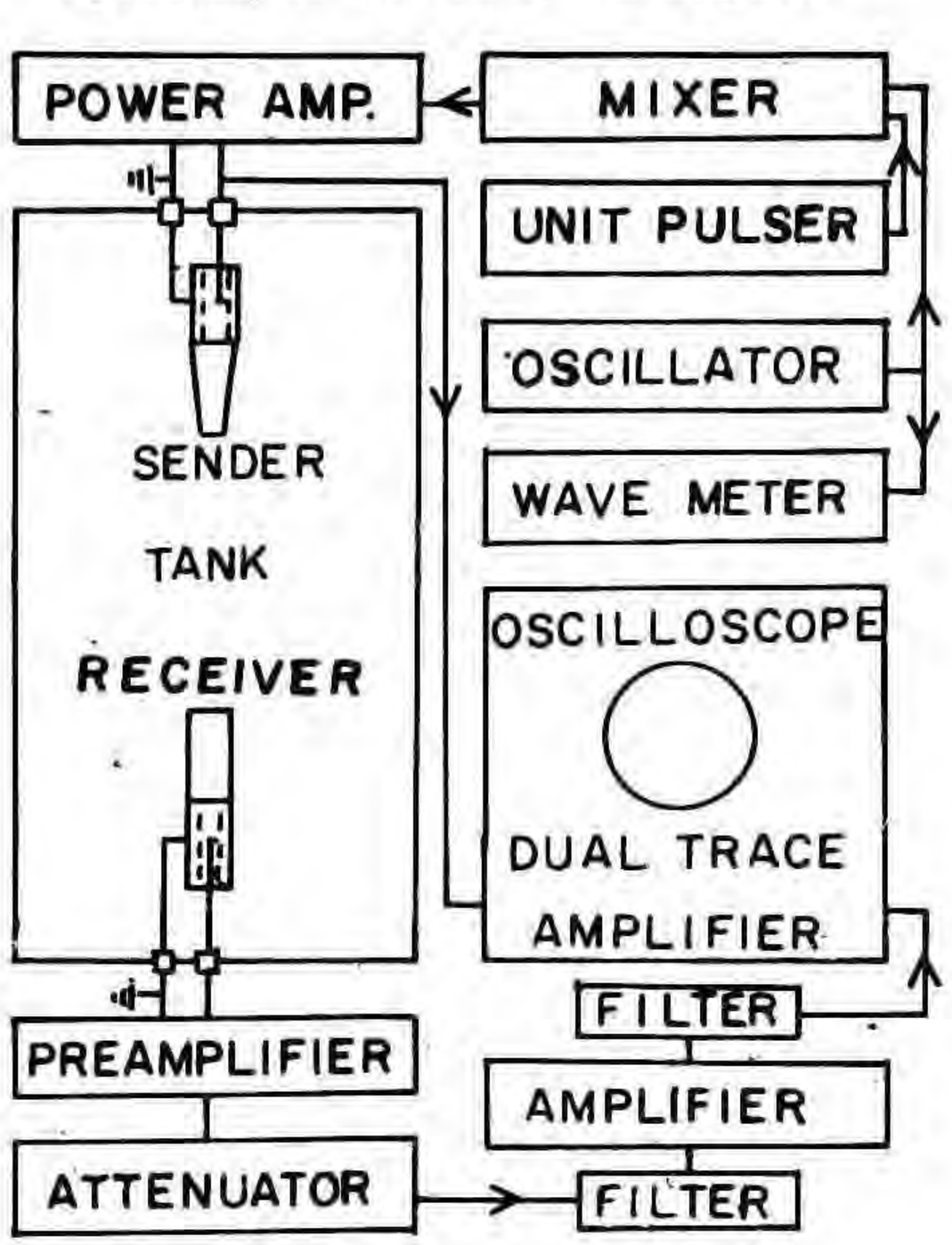

Fig. 1. Block Diagram of the Apparatus.

$$\alpha_{rel} = \frac{\omega V_p}{2c_o^2} \frac{RC_i}{C_v(C_p - C_i)} \frac{\omega \frac{(C_p - C_i)}{C_p} \tau}{1 + \omega^2 \frac{(C_p - C_i)^2}{C_p^2} \tau^2} \qquad (1)$$

where α_{rel}, τ, c_o, V_p, C_p, C_v, C_i, R, and ω are respectively the relaxational absorption coefficient, relaxation time, sound velocity at very low frequency, phase velocity, constant pressure specific heat, constant volume specific heat, specific heat of the internal degree of freedom, ideal gas constant for unit mass, and the angular frequency. The relaxational absorption coefficient per wave length, $\alpha_{rel}\lambda$, has its maximum when ω is equal to $C_p/(C_p - C_i)\tau$. Since τ is inversely proportional to the pressure, p, it is possible to obtain the relaxation time by the measurement of sound absorption over a sufficiently wide range of ω/p. If the complete information about the internal specific heat, C_i, is given, τ can be obtained from the equation,

$$\tau_{std} = (\alpha_{rel}p/f^2 P_{std})(2c_o C_v C_p/RC_i), \qquad (2)$$

obtained from Eq. (1) for $\omega \ll C_p/C_p - C_i)\tau$, where the subscript std indicates that the pressure is 1 atmosphere, and f is the frequency.

The sound absorption coefficients in nitrogen and oxygen are measured for 22°C and in the pressure range from 4 to 300 mmHg, i.e., in the range of ω/p from 1 to 80 Mc/atm. The product of α and p is approximately constant for fixed frequency and temperature; hence the relaxation time is much smaller than $1/\omega$, and Eq. (2) can be applied in these cases. Since the vibrational relaxation time in oxygen or nitrogen is reported to be very long, α_{rel} is considered to be due to rotational relaxation in this case. Hence we obtain, by insertion of the experimental $\alpha_{rel}p$, $C_i(= R)$, and other thermodynamical values into (2), for 22°C;

$$\tau_{rot,std} = (7.6 \pm 0.6) \times 10^{-10} \text{ sec in nitrogen,}$$

$$\tau_{rot,std} = (5.1 \pm 0.4) \times 10^{-10} \text{ sec in oxygen.}$$

These values agree with previously reported values[1,2,3] fairly well.

The absorption coefficient in water vapor is measured over the range of ω/p

from 1 to 50 Mc/atm. and the range of temperature from 42°C to 183°C. No relaxation peak is found in the experiments, and the product αp is approximately constant for each temperature. In Fig. 2, the experimental values of $\alpha p/f^2 p_{std}$ and theoretical values of $\alpha_{cl} p/f^2 p_{std}$ are plotted against the temperature. In the range of ω/p and temperature reported here, the relaxational absorption consists of vibrational and rotational absorption. The relaxational absorption is observed to increase rapidly with temperature. The theoretical specific heat of the vibrational degree of freedom with the lowest eigenfrequency, given as

$$C_i = \frac{R(\theta/T)^2 e^{\theta/T}}{(e^{\theta/T}-1)^2}, \quad (3)$$

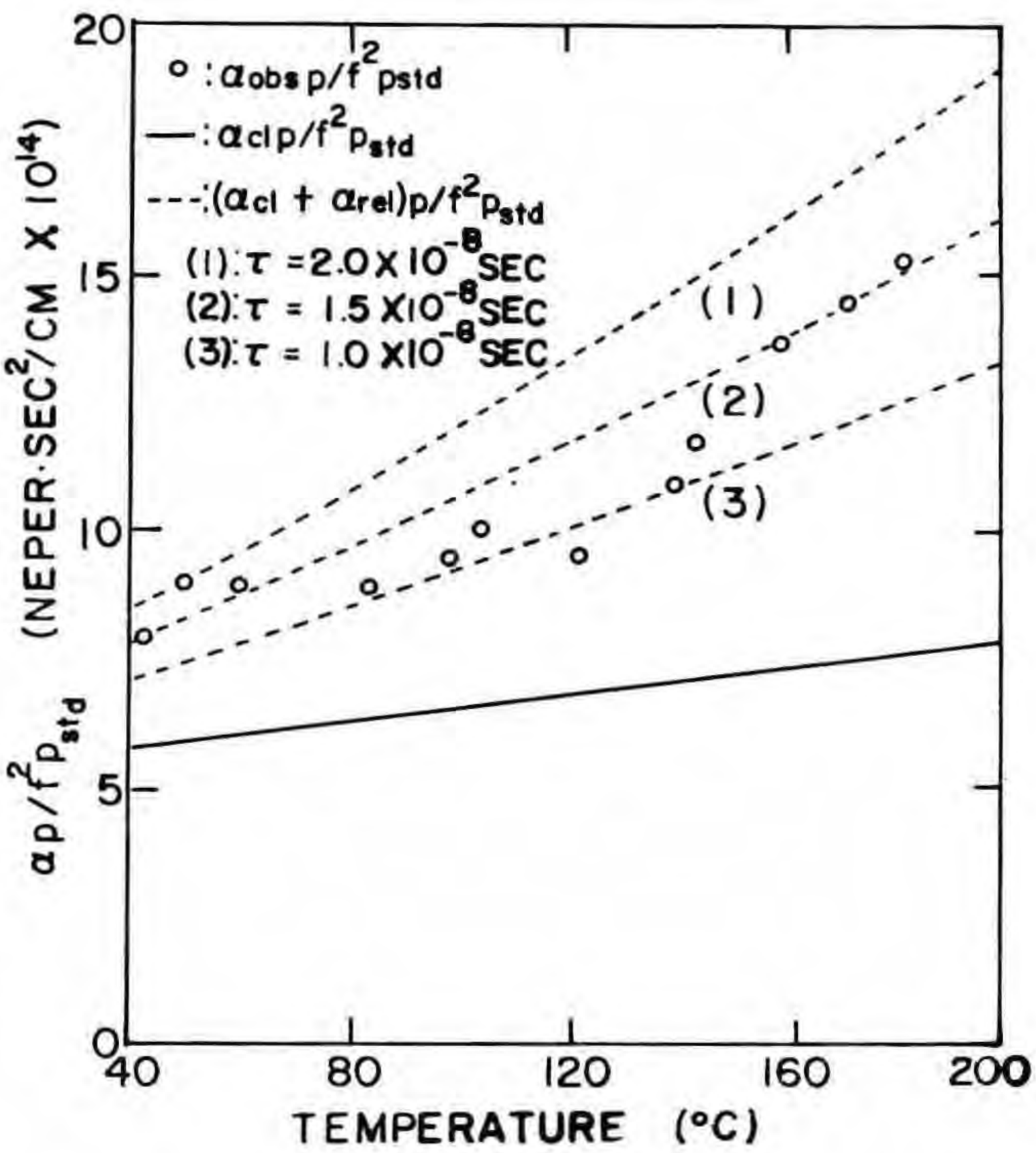

Fig. 2. Temperature Dependence of Absorption Coefficient in Water Vapor.

where θ is the characteristic temperature and is equal to 2294°K in this case, also increases nearly proportionally to α_{rel}, while the specific heat of rotational states remains practically constant since its characteristic temperature is very low. For this reason, α_{rel} is considered to be primarily due to vibrational relaxation. The use of the experimental α_{rel} and theoretical values of C_i, C_p, and C_v yields the vibrational relaxation time at 1 atmospheric pressure as ranging in values from 0.8 to 2.0 x 10^{-8} sec, as the temperature goes from 42°C to 183°C.

These values are of the same order of magnitude as values previously reported,

namely: 1) by Huber and Kantrowitz,[4] from 2 to 4 x 10^{-8} sec in the temperature range from 213°C to 433°C and 2) by Eden, Lindsay, and Zink,[5] about 4 x 10^{-8} sec in the temperature range from 235°C to 401°C.

References:

1. H. D. Parbrook and W. Tempest, Acustica, 6, 345 (1958)
2. G. Sessler, Acustica, 6, 395 (1958)
3. M. Greenspan, J. Acoust. Soc. Amer., 31, 155 (1959)
4. P. W. Huber and A. Kantrowitz, J. Chem. Phys., 15, 275 (1947)
5. D. D. Eden, R. B. Lindsay and H. Zink, Trans. ASME. J. Engineering for Power, 137 (1961)

L24

FOURTH INTERNATIONAL CONGRESS ON ACOUSTICS
COPENHAGEN 21.-28. AUGUST 1962

A Procedure for Computing the Subjective Reaction to Complex Noise.

R. J. Wells, General Electric Co., Schenectady, N. Y.
W. E. Blazier, Jr., York Division, Borg-Warner Corp., York, Penna.

In recent years, the use of parallel or approximately parallel contours of sound pressure level versus frequency has gained wide acceptance as a form of acoustic criteria. Such curves satisfy what seems to be a basic requirement for usable noise criteria -- they are expressible as a single number. As long as their use is confined to broadband spectra of similar shape, correlations between sound measurements and subjective reaction are good. It was originally intended that such contours should be so restricted. However, in actual practice, noises vary widely in spectral shape and pure tones often project well above the broadband noise in a given frequency range. During the last few years, there has been an increasing tendency to apply contours to all such spectra, simply by labeling the spectrum of interest with the number of the contour tangent to the spectrum, regardless of its shape or pure tone content. This procedure has created considerable chaos, since these factors are definitely not negligible. In addition, the picture has been further confused by the almost universal use of octave-band spectra; and at the higher frequencies octave bands are so wide that they may not reveal the presence of quite audible discrete tones.

In order to clarify the situation, let us suppose, for the moment at least, that we confine our attention to continuous noise spectra consisting of broadband noise plus not more than one strong pure tone. Suppose further that the broadband noise exhibits a single general peak at some frequency, f_B, while the tone occurs at a frequency, f_T. When we ask the question, "How do we assign a proper contour number to such a spectrum?", there are several characteristics of the noise spectrum which must be considered, regardless of whether we are concerned with loudness or the more elusive aspect of annoyance. These characteristics include:

1. The location of the broadband peak, f_B.
2. The shape, or width, of the broadband noise spectrum.
3. The frequency of the tone, f_T.
4. The level of the tone relative to the broadband noise at the same frequency.
5. The level of the tone relative to the peak of the broadband noise.
6. The bandwidth of the sound analyzer used in obtaining the data.

We shall begin by assuming that the contours described in the previous paper provide an adequate evaluation of the first factor. Let us turn our attention, then, to the second spectral characteristic; the shape of the broadband noise spectrum. In an attempt to evaluate this parameter, we considered four broadband noise spectra as indicated in Fig. 1 -- all tangent to the same contour at about 1000 cps, but with different shapes. One of these spectra approximated a contour itself, two others were broadband peaks of different widths, and the fourth was a single third-octave band of noise centered at 1000 cps. Free-field acoustic spectra of these shapes were produced by a loudspeaker in an anechoic room; and listeners were asked to rate their relative annoyance by adjusting the sound level until the particular spectrum of interest at the moment was judged to have the same annoyance as the contour-type spectrum at a given constant level. The results of this jury test are indicated in Fig. 2. In other words, the spectra shown here are now considered to have equal annoyance. From this we may conclude that the original spectra -- though all tangent to the same contour -- differed in subjective annoyance by nearly 15 decibels! Hence, the need of some contour level correction procedure is clearly indicated.

There may be some doubt as to what we mean by "annoyance". Actually most psychoacoustic experts tend to avoid this term as there are often non-acoustical factors which contribute to a feeling of annoyance when one hears a given sound. However, we believe that one can logically speak of "annoyance" if he limits himself to a some-

what narrow range of situations in which a continuous noise exists that is completely unrelated to his current occupation or desires. In our case, the jurors made the annoyance judgments under the assumption that they were relaxed and in the presence of a steady undesirable noise of long time duration.

Now, after obtaining these judgments, an attempt was made to correlate them with a number which could be easily determined from the shape of the spectrum. Since we are, in effect, trying to integrate the deviations from a contour shape, the idea of attempting correlation with the number of third-octave bands within 5 decibels of the tangent contour came to mind. (This is somewhat analogous to a Q-factor in a resonance curve). When this correlation was made, the top curve of Fig. 3 was obtained. (This curve was arbitrarily normalized to 0 for $n \approx 10$ in order to minimize adjustments to the tangent contour number for "typical" spectra.) The lower curve, shown dotted, results from correlations of the same parameter, n, against loudness computations by the latest method of Stevens.[1] For spectra with a sharp peak, it is apparent that our judgment of "annoyance" is more severe than would be expected from a judgment of "loudness". This we feel to be realistic. In fact, an intuitive feeling that this should be the case really led to this study.

These initial studies have been confined to broadband noise peaking at about 1000 cps. For similar cases with peaks at different frequencies, it is quite possible that a somewhat different contour correction curve may be obtained. Perhaps the abscissa scale of Fig. 4 should include a function of frequency.

Now let us consider noise spectra containing a strong pure tone. Here, the previously mentioned factors of frequency, relative levels, analyzer bandwidth, etc., are closely related. However, a logical approach to the problem may be made using the concept of critical bands of the ear.

For the moment, let us sidestep the arguments of the various authorities on this subject and assume that we really know what these critical bands are. Assume further that we have set up a series of contiguous critical bands, and constructed a sound analyzer employing these bands. With such an analyzer, our contour spectrum would be "distorted" about as indicated in Fig. 4. As we all know, however. a pure tone will be determined as having the same level regardless of analyzer bandwidth. But, when using our CB analyzer, the tone should appear in approximately its proper "perspective" as far as the ear is concerned. Hence, a logical procedure as a first step in evaluating the annoyance of the tone would seem to be the application of a correction which places the tone as many decibels above the third octave spectrum as the uncorrected tone exceeds the critical band spectrum. However, as the critical band is usually defined, a tone just at the threshold of audibility would increase the critical band level by 3 decibels. This would seem to be a slightly excessive "penalty" for an almost inaudible tone. Also, the threshold of annoyance - if such a thing can be defined - may not be identical with the threshold of audibility. For these reasons, it would seem desirable to mathematically depress the tone by N decibels before adding it to the broadband noise in the critical bandwidth, the value of N being determined as a function of frequency by jury tests. At this point it is of interest to note the mathematical form of the proposed correction. Denoting,

p = projection, in decibels, of tone above average level of broadband noise in the two adjacent analyzer bands

B = bandwidth, in decibels, of the analyzer at the tone frequency (10 x logarithm of bandwidth in cps)

CB = critical bandwidth, in decibels, of the ear at the tone frequency

N = decibel quantity, discussed above

it can be readily shown that the correction to be added to the analyzer reading for the band containing the one - i.e., the correction to the peak - is given by

$$10 \log_{10} \left\{ 1 + \text{antilog}_{10} \left(\log_{10} \left[\text{antilog}_{10} \left(\frac{p}{10} \right) - 1 \right] + \frac{B - (CB+N)}{10} \right) \right\} - p$$

Observe that the quantities CB and N appear only as the sum CB+N. Thus, in carrying out an experimental program we need not know CB explicity. Our tests really determine the quantity CB+N which might be considered as a modified or pseudo critical

bandwidth suitable for our purposes.

Jury tests to date correlate best with values of CB+N of 16 at 100 cps and 19 at 1000 cps. A comparison of these values with critical bandwidths suggested by various investigators in this field reveals that they fall about 3 db below the curve of Zwicker, Flottorp, and Stevens.[2] If we assume this as a trend, we can immediately draw correction charts applicable to analyzers of various bandwidths. Essentially this process has been followed in drawing tentative charts for octaves and third-octaves. The results for third-octaves are shown at the bottom of Fig. 5.

Although this matter obviously needs further study, it should be apparent that a correction of this general nature must be made to compensate for the difference in bandwidth between octave and third-octave data. If no correction is made, a little thought will show that the user of third-octave equipment is actually penalized about 5 db relative to the user of full octave equipment - since the measured level of the noise decreases with bandwidth while that of the tone does not.

During the studies reported here, pure tones of various levels at both 100 and 1000 cps were superimposed upon a single broadband spectrum. Fig. 5 shows the specific spectra thus obtained, and their numerical designations. Pure tone corrections are indicated.

In order to correlate jury tests with spectral characterisitcs, some computational method must be devised for effectively combining the annoyance of broadband and pure tone components of a noise spectrum. The method which we have tentatively adopted is summarized in Table I. For completeness, all spectra of Fig. 1 and Fig. 5 are included here. For purely broadband spectra, the correction to the tangent contour is determined solely from the number, n, of third-octave bands within 5 db of the contour and the correction curve of Fig. 3. For spectra containing a pure tone, a double computation is employed. First, the broadband portion is considered as above. Second, the contour tangent to the corrected tone level is obtained. Then 6 decibels is subtracted from this level (applying Fig. 3 for n=1) to obtain the corrected pure tone contour. Finally, the composite corrected contour is obtained by adding the corrected broadband and pure tone components as decibel levels.

How well this simple calculation agrees with subjective tests for this limited study is indicated in Table I. Preliminary results of a similar study in a normal room are comparable. Although the correlation appears rather good for a first attempt, it should be noted that we have not exhausted the capabilities of this general approach. So far, we have assumed that the quantity CB+N is simply a function of frequency. Actually, there is no reason why this quantity cannot vary with the projection p. If such variation is allowed, it becomes entirely practical to construct a set of correction curves so that computed contour level correlates exactly with subjective tests for all cases of broadband noise plus a single tone of any frequency and level.

Although only spectra with single strong tones have been studied to date, the extension of this approach to a reasonably small number of tones appears obvious. One would anticipate correlation simply by combining the computed contours for all the tones and the broadband noise. Also, it would seem logical to consider a double-peaked broadband noise as the superposition of two single peaks, etc. It has also been suggested that spectra consisting almost entirely of a large number of pure tones might be analyzed by a similar approach, perhaps by raising the entire spectrum about 6 db to compensate for the increased annoyance. In other words, a correction for n=1 might be applied throughout.

In conclusion, it should be noted that this procedure can be used with parallel sound power contours - such as those discussed in the preceding companion paper - to give a single decibel number evaluation of the potential annoyance of a given noise source. An alignment chart, also discussed in the previous paper, may then be used as an application guide.

The authors wish to acknowledge innumerable contributions from their co-members of ASHRAE and ARI committees. Particularly helpful were discussions with Mr. C. M. Ashley, Mr. P. Baade, and Mr. R. E. Parker.

References: 1) S. S. Stevens, "Procedure for Calculation Loudness, Mark VI, JASA, Vol. 33, No. 11, pp. 1577-1585, Nov. 1961.
2) E. Zwicker, G. Flottorp, S. S. Stevens, "Critical Bandwidth in Loudness Summations", JASA, Vol. 29, No. 5, p. 548, May 1957.

FIG. 1

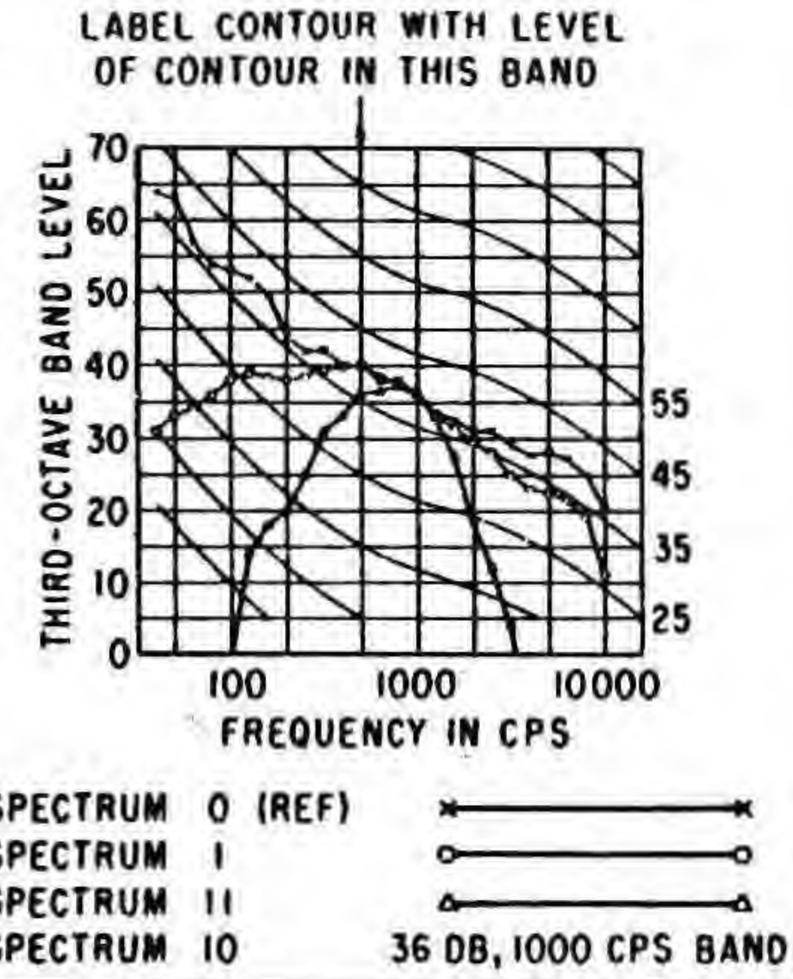

FIG. 2

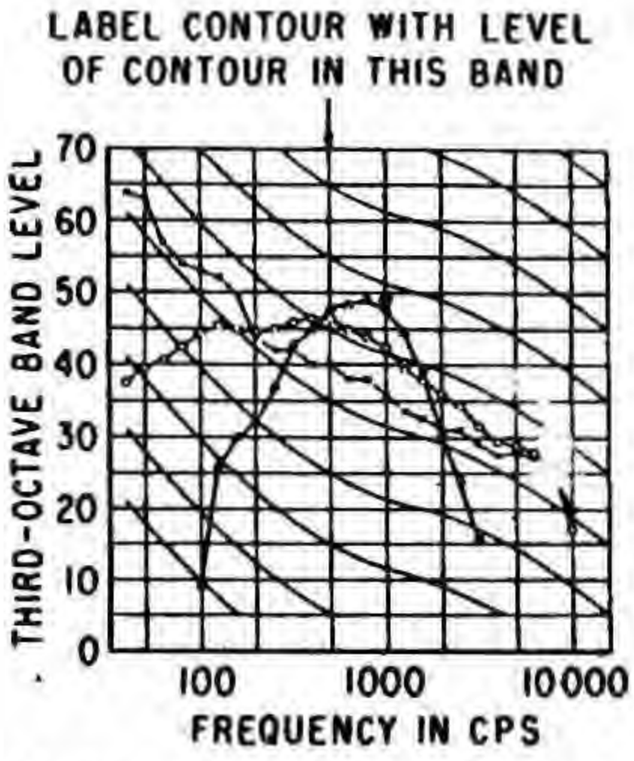

LEVEL OF SPECTRA ADJUSTED FOR JUDGEMENT OF EQUAL ANNOYANCE

FIG. 3

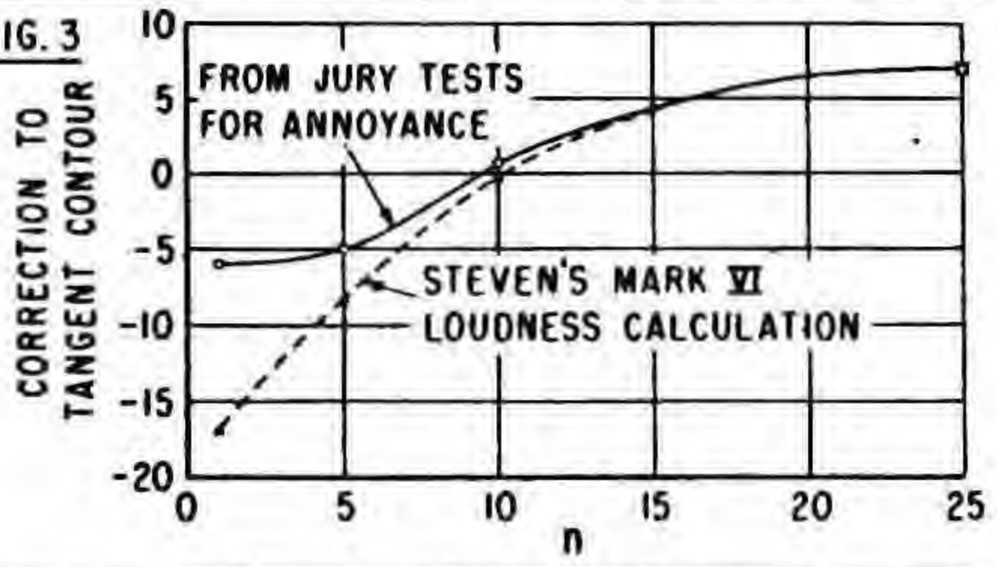

FIG. 4

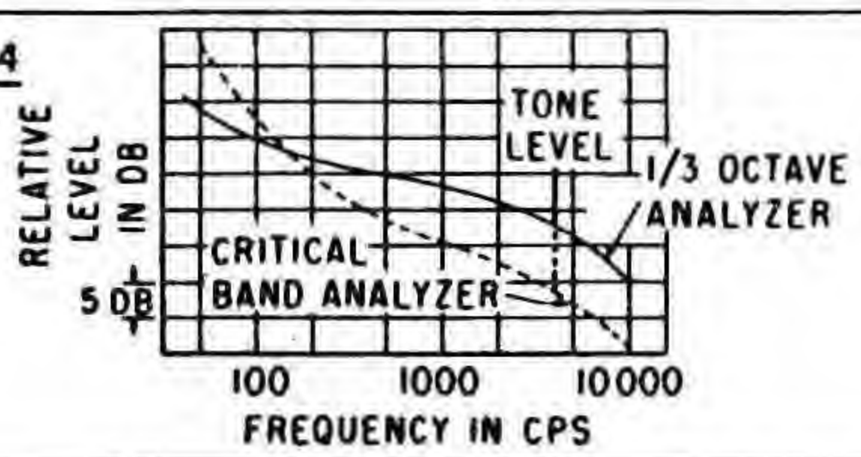

FIG. 5

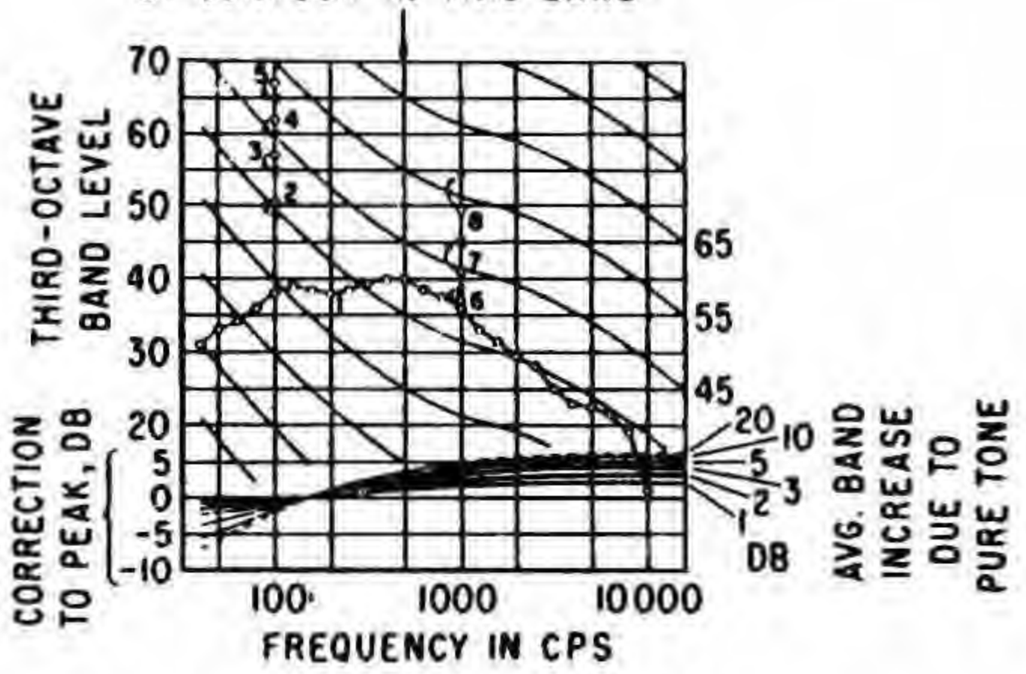

SPECTRUM DESIGNATIONS FOR TABLE I:
SPECTRUM 9 IS A 36 DB, 1000 CPS TONE
SPECTRUM 10 IS A 36 DB, 1000 CPS BAND

TABLE I

COMPUTED AND SUBJECTIVE CONTOUR LEVELS

Spectrum	0	1	2	3	4	5	6	7	8	9	10	11
BB Contour	40	40	40	40	40	40	40	40	40		40	40
	25	10	10	10	10	10	10	10	10		1	5
Correction	7	0.5	0.5	0.5	0.5	0.5	0.5	0.5	0.5		-6	-5
Corr. BB Contour	47	40.5	40.5	40.5	40.5	40.5	40.5	40.5	40.5		34	35
Tone Contour			34	40.5	45.5	50.5	42	48.5	58		44.5	
			1	1	1	1	1	1	1		1	
Correction			-6	-6	-6	-6	-6	-6	-6		-6	
Corr. Tone Contour			28	34.5	39.5	44.5	36	42.5	52		38.5	
Composite Corr. Contour Level	47	40.5	40.8	41.5	43.1	46	41.8	44.7	52.2		38.5	34	35
Subjective Contour Level	47	40.5	41.5	43.5	44.1	46	42.5	44.5	49.5		41.5	34	35

M24

FOURTH INTERNATIONAL CONGRESS ON ACOUSTICS
COPENHAGEN 21.-28. AUGUST 1962

SOUND INSULATION REQUIREMENTS in BUILDING PRACTICE

Gunnar Ö. Jörgen, Architect MNAL
Norwegian Building Research Institute

The physical basis of sound insulation requirements are:
Room insulation (sound pressure level difference between two rooms),
Sound reduction index (transmission loss, airborne sound insulation of the partition),
Impact sound level (sound pressure level caused by impacts).

The administrative basis of sound insulation requirements are standard curves, defining the room insulation wanted, or maximum permissible impact sound level.

To accomplish these standards, a simple method is required, allowing a reasonably accurate calculation of insulating properties of the constructive elements, satisfying the standards in the completed building.

Denmark, Norway and Sweden recently established common standards of sound insulation, differing in formulation only. The practical accomplishment of these standards is, however, different in the three countries. Danish standards are based on practical instructions, published by the Danish Building Research Institute. The Swedish standards are very comprehensive, including several practical instructions.

The Norwegian Building Research Institute has been working on sound insulating problems since 1955. We have felt the need of a basic system, which more easily would transmit the results from international acoustics research to practical applications in building practice. This paper describes a basic system, developed from communications between our institute and building constructors.

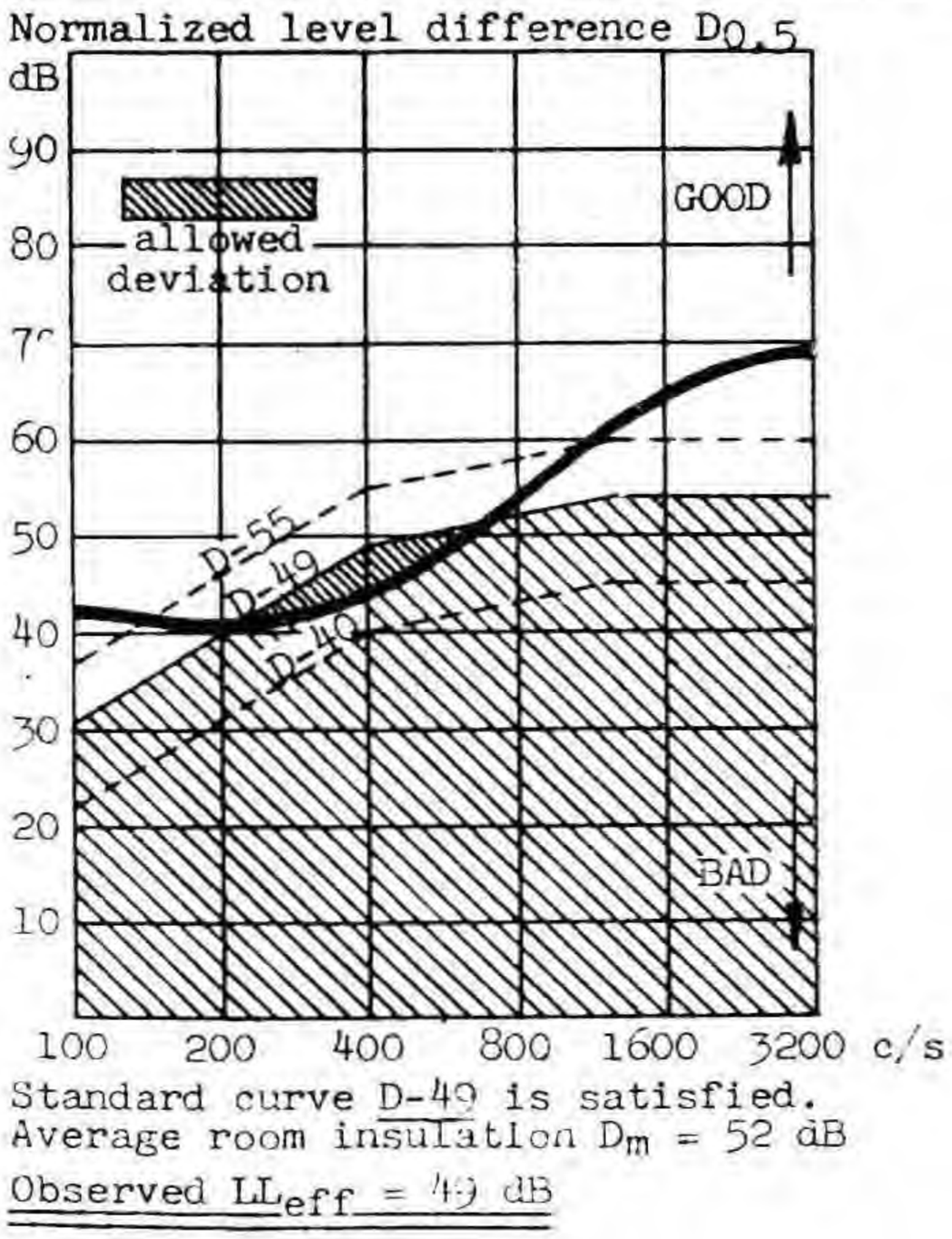

Standard curve D-49 is satisfied.
Average room insulation D_m = 52 dB
Observed LL_{eff} = 49 dB

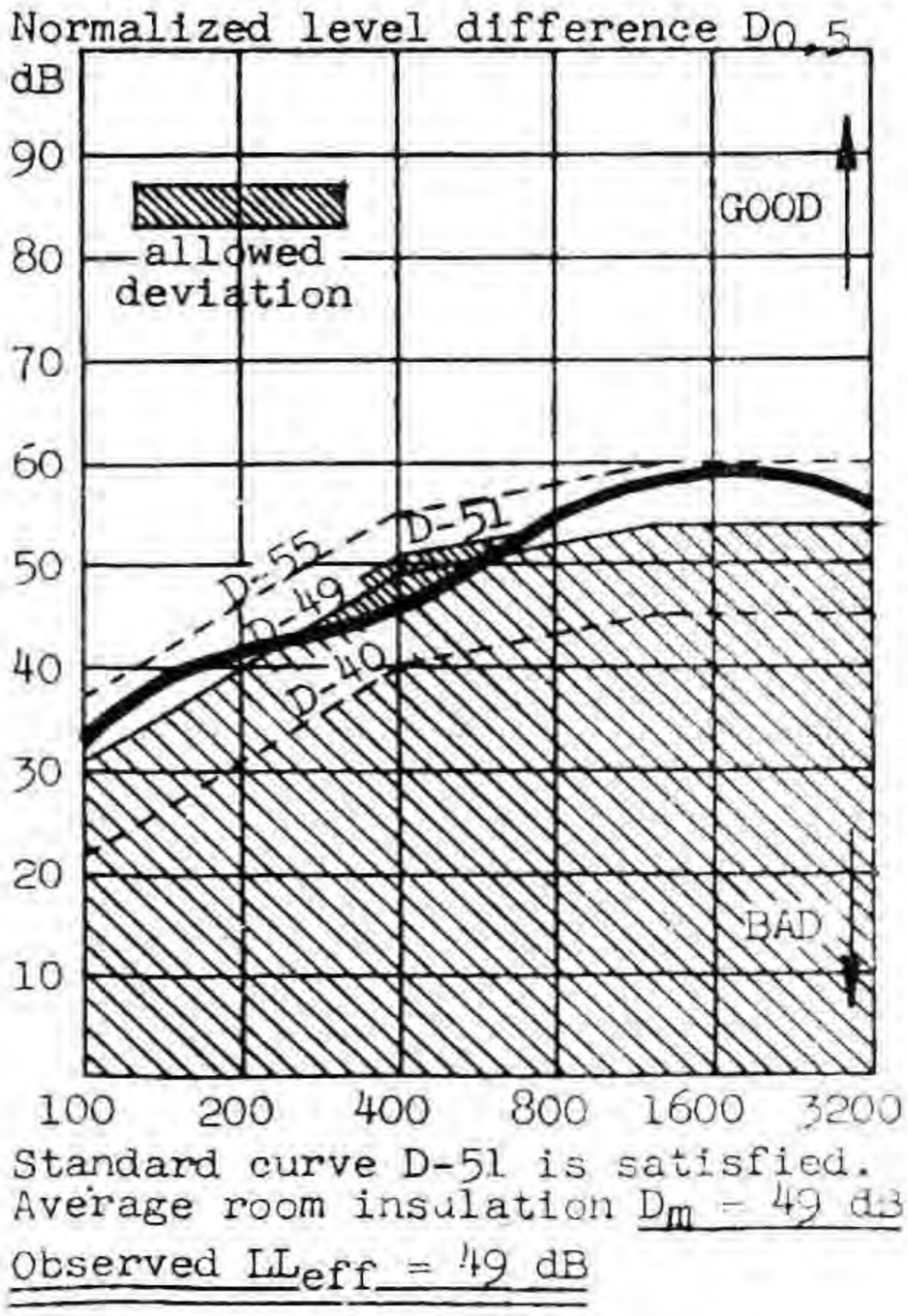

Standard curve D-51 is satisfied.
Average room insulation D_m = 49 dB
Observed LL_{eff} = 49 dB

AIRBORNE SOUND INSULATION

For practical reasons we have chosen the symbol D-49 for the standard curve between dwellings. The parallel curve 6 dB above is D-55, etc., as shown in the figures on the previous page.

Room insulation between dwellings must satisfy the standard curve D-49. Maximum allowed mean deviation is 1 dB under the standard curve. In addition, the average room insulation D_m shall be minimum 49 dB. One of these two requirements will be decisive in an actual case, as shown in the figures.

To characterize observations just satisfying these requirements, we will introduce the term effective airborne sound insulation with the symbol LL_{eff}. Accordingly, the minimum standard requirement between dwellings is indicated with $LL_{eff} = 49$ dB. A larger number means higher effective sound insulation.

In building practice it is also necessary to know the sound insulating properties of a partition, resulting in $LL_{eff} = 49$ dB in the completed building. Or, we might ask for the sound insulating properties of the partition, when we have observed an effective sound insulation $LL_{eff} = 49$ dB.

For this purpose we define the airborne sound number of the partition, symbol LL. When the sound transmitting partition has an area = 10 m2, the observation room has a volume = 50 m3 and a reverberation time = 0,5 s, and if the flanking effects are "normal", then $LL = LL_{eff}$.

With differing conditions, corrections are introduced, to be shown in this example:

Observed effective airborne sound insulation	LL_{eff} = 49 dB
Area of sound transmitting partition = 20 m2	+ 3 dB
Volume of observation room = 64 m3	+ 1 dB
Reverberation time of observation room = 0,5 s	+ 0 dB
"Great" flanking transmission	+ 1 dB
Calculated airborne sound number of the partition	LL = ca.52 dB

The calculation is exact, with the exeption of flanking effects, which must be estimated in each case. A larger number of LL means better insulation properties of the partition.

--o--

To avoid confusion, we notice that the effective airborne sound insulation LL_{eff} is not identical with the average room insulation D_m, and the airborne sound number LL is not identical with the sound reduction index R_m. It seems to be the following correlations between R_m and LL:		Laboratory measurements: Sound reduction index R_m	Building measurements: Airborne sound number LL
20 cm solid concrete wall	460 kgs/m2	58 dB	ca. 53 dB
15 cm solid concrete wall	350 kgs/m2	55 dB	ca. 50 dB
23 cm solid brick wall, plastered ...	450 kgs/m2	50 dB	ca. 50 dB
11 cm solid brick wall, plastered ...	230 kgs/m2	46 dB	ca. 45 dB
7 cm lightweight concrete slab	60 kgs/m2	38 dB	ca. 37 dB

IMPACT SOUND INSULATION

For practical reasons we have chosen the symbol T-50 for the standard curve between dwellings. The parallel curve 5 dB below is T-55, etc., as shown in the figure.

For impact sound insulation between dwellings, the impact sound level under a floor must satisfy the standard curve T-50. Maximum allowed mean deviation is 1 dB above the standard curve.

To characterize observations just satisfying this requirement, we will introduce the term effective impact sound insulation with the symbol TT_{eff}. Accordingly, minimum standard requirement between dwellings is indicated with TT_{eff} = 50 dB. A larger number means higher effective impact sound insulation (a lower impact sound level).

In building practice it is also necessary to know the impact sound insulation properties of a floor, resulting in TT_{eff} = 50 dB in the completed building. Or, we might ask for the impact sound insulating properties of the floor, if we have observed an effective impact sound insulation TT_{eff} = 50 dB.

For this purpose we define the impact sound number of the floor, symbol TT. When observation room under the floor has a volume = 50 m3 and a reverberation time = 0,5 s, and if the flanking effects are "normal", then TT = TT_{eff}.

With different conditions, corrections are introduced, to be shown in this example:

Observed effective impact sound insulation	TT_{eff} =	50 dB
Volume of observation room = 32 m3	+	2 dB
Reverberation time of observation room = 0,5 s	+	0 dB
"Small" flanking transmission	+	1 dB
Calculated impact sound number of the floor	TT = ca.	51 dB

The calculation is exact, with the exeption of flanking effects, which must be estimated in each case. The area of the floor is of less importance in this case, assuming a small part of the floor as the actual sound source. A larger number of TT means better impact sound insulation properties of the floor.

Correction factors for the calculation of LL or TT out of the observed LL_{eff} or TT_{eff}

transm. area	room volume	reverb. time	flanking effect	correction factor
20 m2	25 m3	1,o s	"extraord."	+ 3 dB
16 m2	32 m3	0,8 s	"very great"	+ 2 dB
13 m2	40 m3	0,6 s	"great"	+ 1 dB
10 m2	50 m3	0,5 s	"normal"	+ 0 dB
8 m2	64 m3	0,4 s	"small"	÷ 1 dB
6 m2	80 m3	0,3 s	"very small"	÷ 2 dB
5 m2	100 m3	0,25s	"none"	+ 3 dB

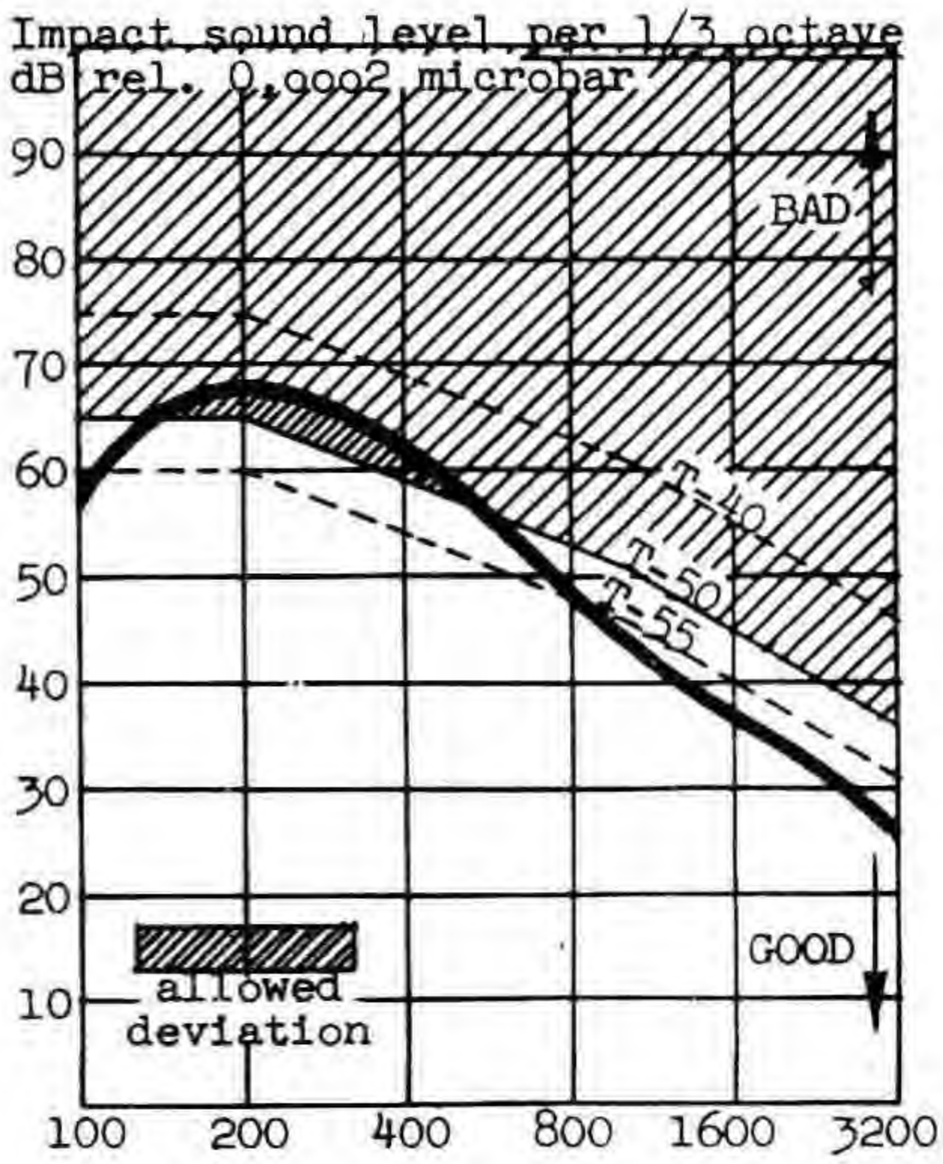

Standard curve T-50 is satisfied.
Observed TT_{eff} = 50 dB

USEFULNESS OF THE SYSTEM

Today it is impossible to predict the flanking transmission by calculation, and it is often difficult to measure. This will be the situation for several years to come. The problem should be solved by comparing numerous measurements in laboratory and in buildings.

Laboratory measurements can solve many problems of importance, but the results are frequently of less interest in building practice. Often we see unsatisfactory practical applications, based on laboratory measurements that were not fully understood.

We think one should not leave it to building practice, trying to estimate the flanking effect in every actual case. This can better be done in general by people with some experience in the acoustical behaviour of building constructions. In our opinion an estimated "normal" flanking transmission is a better starting point for practical calculations. The flanking transmission is considered "normal", when all connected building elements are fairly equivalent.

According to our experience, results from laboratory measurements should be reduced 2-3 dB or more when applied with "normal" flanking transmission. By disadvantageous combinations of building elements, the flanking transmission may increase 3-4 dB as compared with "normal" transmission, in exeptional cases even more.

On this basis we concluded our studies with the system described in this paper. The system works to our satisfaction, and has the advantage of being easily understood by building constructors. "Airborne sound number" and "Impact sound number" of various elements and structures can be tabulated, varying between ca. 58 dB and ca.22 dB or lower. The tables are very useful for building authorities, architects, contractors and producers of building materials. In this way excellent communications have been established between acoustical research and building practice in Norway.

We continue the experiments with our system, but, of course, we are ready to change to a future internationally accepted system, hoping this to be equally useful for practical purposes.

Example: Table of results
Floors and walls

Airborne sound number LL				Impact sound number TT
55	18 cm solid concrete;	T&G boards "floating" on mineral wool	450 kgs/m2	58
54	14 cm solid concrete;	T&G boards "floating" on mineral wool	360 kgs/m2	56
53	11 cm solid concrete;	T&G boards "floating" on mineral wool	290 kgs/m2	54
52	9 cm solid concrete;	T&G boards "floating" on mineral wool	240 kgs/m2	52
54	14 cm solid concrete;	concrete screed "floating" on mineral wool.	420 kgs/m2	50
52	18 cm solid concrete;	2,5 mm linoleum on 2 mm pure cork	430 kgs/m2	51
52	18 cm solid concrete;	2,5 mm linoleum on 2 mm felt	430 kgs/m2	48
50	14 cm solid concrete;	6,7 mm corklinoleum	340 kgs/m2	50
50	14 cm solid concrete;	2,5 mm linoleum	340 kgs/m2	30
52	joist floor;linoleum,fiberpl.,T&G b.;sand pugging on boards;plasterb.ceiling			52
53	20 cm solid concrete wall		460 kgs/m2	
50	15 cm solid concrete wall		350 kgs/m2	
46	10 cm solid concrete wall		230 kgs/m2	
50	23 cm solid brick wall, plastered on both sides		450 kgs/m2	
45	11 cm solid brick wall, plastered on both sides		230 kgs/m2	
43	25 cm lightweight concrete wall		150 kgs/m2	
37	7 cm lightweight concrete slab		60 kgs/m2	
51	10 mm plasterboard 18 cm apart on separate studs; 100 mm min.wool		28 kgs/m2	
50	= min. LL for walls betw. dwellings.			
52	= min. LL for floors betw. dwellings.	For floors betw.dwellings: min. TT =		50

N24

FOURTH INTERNATIONAL CONGRESS ON ACOUSTICS
COPENHAGEN 21.-28. AUGUST 1962

ON THE SENSITIVITY OF CONDENSER MICROPHONES TO A NON-UNIFORM PRESSURE DISTRIBUTION ON THE DIAPHRAGM.

S.C.Dalsgaard,
Acoustical Laboratory, Royal Technical University, Copenhagen

1. Introduction

In many measurements, e.g. coupler calibration of receivers and microphones, the measuring microphone will be exposed to a sound pressure, that is non-uniformly distributed on the diaphragm (1,2,4). This will also be the case in free field measurements due to diffractional effects at higher frequencies (3). The pressure distribution can in most cases be considered rotational symmetrical.

Due to the fact, that a microphone normally is calibrated for a uniform pressure on the diaphragm, a non-uniform sound pressure distribution will cause an error of measurement, because a microphone is normally most sensitive at the centre of the diaphragm, and will consequently not measure the mean sound pressure on the diaphragm.

This paper describes a method of estimating the error in the measured sound pressure.

2. Determination of the sensitivity function M(r)

Let $d = d(r)$ be the distance between the electrodes at a distance r from the centre, and $y = y(r)$ the deflection of the diaphragm at this point due to the sound pressure. Neglecting edge effects and assuming rotational symmetry we get the following expression for the electromotive force e

$$e = K \int_o^a \frac{y \, 2\pi r \, dr}{d^2} \qquad (2.1)$$

where K is a constant and a the radius of the diaphragm. If the static deflection caused by the polarizing voltage is very small we can consider d as a constant d_o. In this case the electromotive force e will be

$$e = \frac{K}{d_o^2} \int_o^a y \, 2\pi r \, dr \qquad (2.2)$$

The electromotive force is in this case proportional to the total volume displacement of the diaphragm.

We must now determine the total volume displacement for an arbitrary, axial symmetrical pressure distribution on the diaphragm. The method given by Morse (5) is to express the given pressure distribution by a series of characteristic functions for the diaphragm. The total volume displacement is then determined as the sum of the solutions for each of the terms in the series. This method however leads to rather laborious calculations.

The general differential equation determining the motion of the diaphragm is

$$L(y) = y'' + \frac{1}{r} y' + f(r)\, y = p/T \qquad (2.3)$$

where T is the tension of the diaphragm, f(r) a function of r, determined by the construction of the microphone and p = p(r) the pressure acting on the diaphragm.

The boundary conditions to be satisfied are y = 0 for r = a and y' = 0 for r = 0.

Let now $y_1 = y_1(r)$ and $y_2 = y_2(r)$ be the solutions to the equations $L(y_1) = p_1(r)/T$ and $L(y_2) = p_2(r)/T$ respectively. We then have

$$\int_o^a \frac{p_1}{T} y_2 \, 2r \, dr = \int_o^a y_2 \left[y_1'' + \frac{1}{r} y' + f(r) \, y \right] 2r \, dr \qquad (2.4)$$

The integral can be evaluated using integration by parts and we get with the given boundary conditions

$$\int_o^a p_1 \, y_2 \, 2r \, dr = \int_o^a p_2 \, y_1 \, 2r \, dr \qquad (2.5)$$

If $p_2 = p_o$, where p_o is a constant, independent of r, and y_o is the corresponding solution to equation 2.3, we get from 2.5

$$\int_o^a y_1 \, 2r \, dr = \frac{1}{p_o} \int_o^a p_1 \, y_o \, 2r \, dr \qquad (2.6)$$

i.e the total volume displacement for an arbitrary pressure distribution can be determined, provided that the solution to the differential equation 2.3 for a uniform sound pressure is known.

If the electrodes are assumed to be parallel, the electromotive force is proportional to the total volume displacement. If e_1 is the voltage produced by the pressure p_1, and e_m the voltage, that would be produced by a uniform pressure equal to the mean pressure p_m, we can express the error of measurement D as

$$D = e_1/e_m = \int_o^a \frac{p_1}{p_m} M(r) \, 2r \, dr \qquad (2.7)$$

The normalized sensitivity function M(r) is given by

$$M(r) = y_o / I \qquad (2.8)$$

where

$$I = \int_o^a y_o \, 2r \, dr \qquad (2.9)$$

If the static deflection of the diaphragm is significant, the sensitivity function will be modified. In this case y_o in 2.8 will be replaced by y_a determined by

$$L(y_a) = p_o / d^2 \, T \qquad (2.10)$$

3. The sensitivity function for a simple condenser microphone

We will consider a simple condenser microphone with a constant distance between the electrodes. We will further assume, that the reaction of the air on the diaphragm is determined by the average displacement of the diaphragm. The differential equation 2.3 is in this case

$$y'' + \frac{1}{r} y' + k^2 \, y = p/T \qquad (3.1)$$

The solution for a uniform sound pressure is well known, and we get

$$M(r) = \frac{J_o(kr) - J_o(ka)}{J_2(ka)} \qquad (3.2)$$

In the vicinity of the first resonance frequency, determined by $J_o(k_1 a) = 0$, the sensitivity function will be

$$M(r) = J_o(k_1 r)/J_2(k_1 a) \qquad (3.3)$$

and at low frequencies the sensitivity function will be

$$M(r) = \frac{2(a^2 - r^2)}{a^2} \qquad (3.4)$$

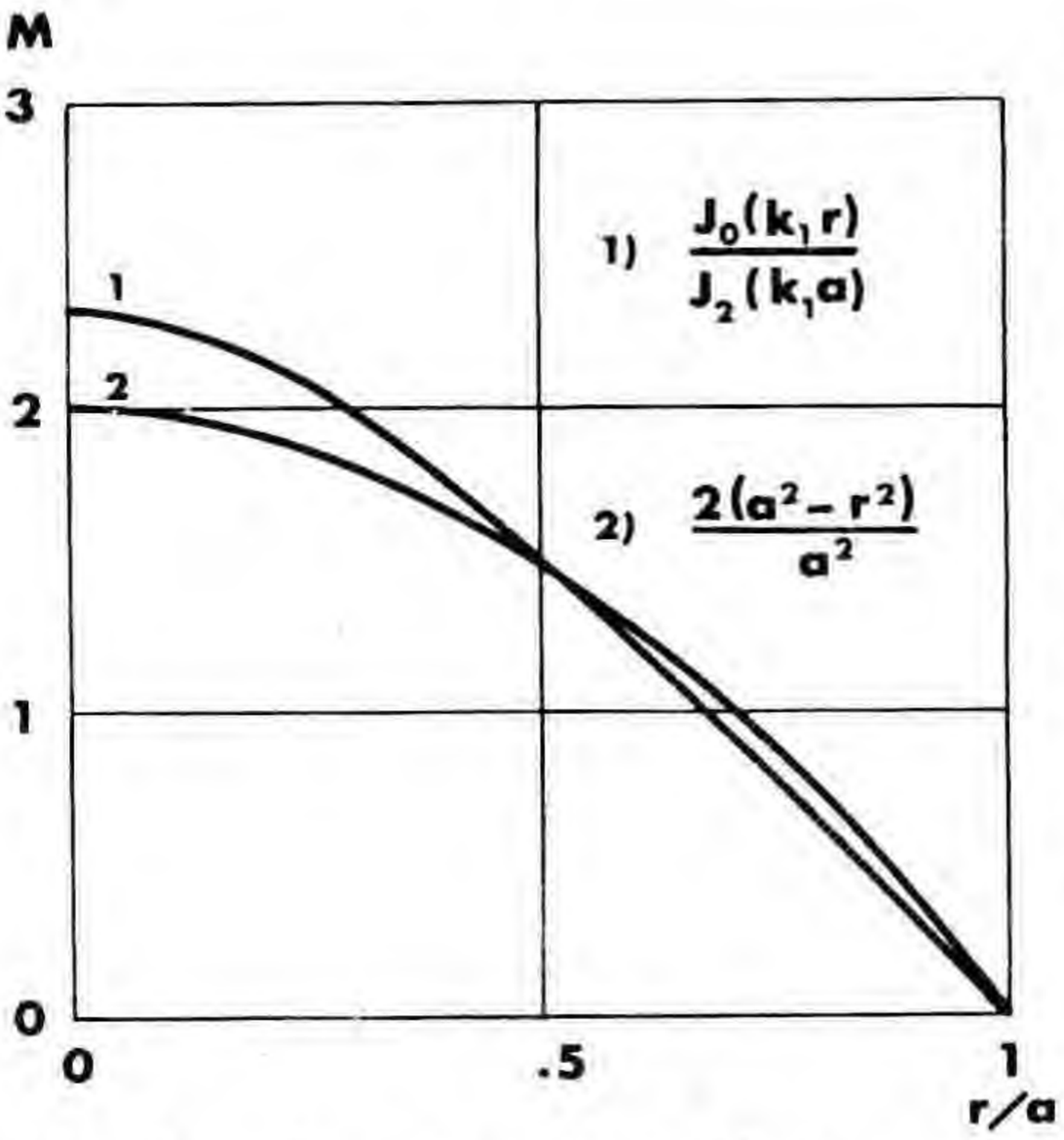

Fig.1. The function M(r).

The expressions 3.3 and 3.4 are illustrated on fig. 1.

Brüel and Rasmussen (3) have reported measurements of the sensitivity function for an actual microphone. There is good agreement between the measured values and the theoretical expressions given above for frequencies below the resonance frequency of the diaphragm.

At higher frequencies however, the motion of the diaphragm is more complicated than assumed here due to the influenc of the air damping, and the simple differential equation 3.1 is no longer valid.

The above mentioned method has been used to calculate the error of measurement on different 2 cm^3 couplers for hearing aid measurements, the couplers having internal diameters 1.5 , 2 , 2.5 and 3 cm, and the corresponding microphones having the same diameter as the couplers.

The calculation of the sound pressure distribution on the diaphragm has been described earlier (2), and shall not be mentioned here. An example of the calculated sound pressure distribution is shown on fig. 2 for a coupler with a diameter of 3 cm.

The calculations were carried out, using an approximate integration:

$$\int_o^a p(r)\, M(r)\, 2r\, dr \simeq \sum_o^N p(\tfrac{na}{N})\, M(\tfrac{na}{N})\, \tfrac{2na}{N}\, \tfrac{a}{N} \quad , N = 10.$$

The results of the calculations are shown on fig. 3. It should be noted, that allthough the mean sound pressure on the diaphragm is independent of the non-uniform pressure distribution, an error of measurement will occur due to the greater sensitivity at the centre of the microphone.

The expression 3.3 was used for the calculations shown on fig. 3. The difference between the results using expression 3.3 and 3.4 was in the investigated cases less than .3 db.

The method described in this paper has been found useful when estimating the influence of a non-uniform pressure distribution on a microphone, and by using approximate integration it can be employed even when a mathematical expression for the pressure distribution does not exist.

At frequencies below the resonance frequency the expressions 3.3 and 3.4 are reasonable approximations and can be used in most cases.

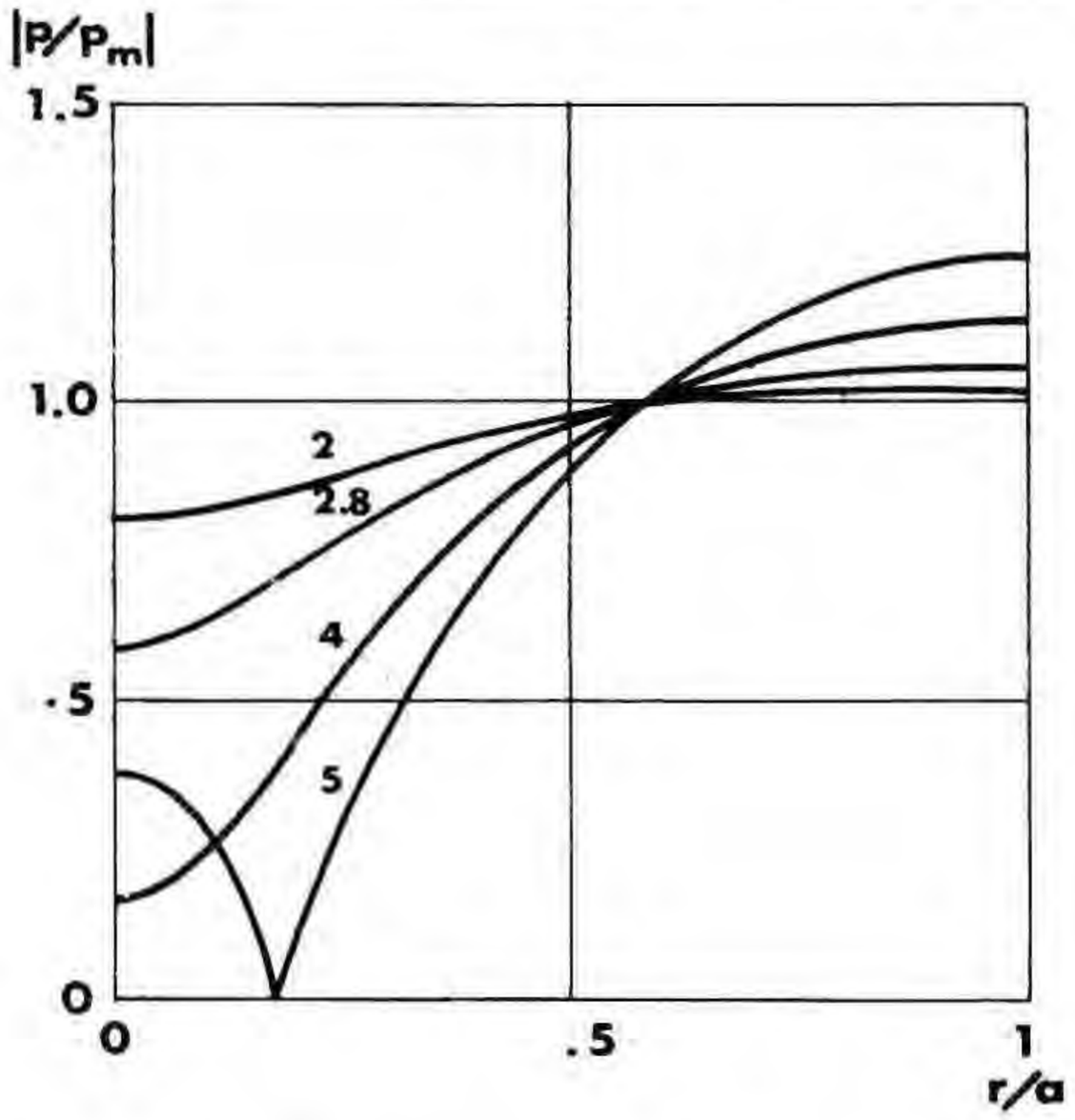

Fig.2. Sound pressure distribution in 2 cm³ coupler. Diameter 2a = 2 cm. Frequencies 2, 2.8, 4 and 5 kc/s

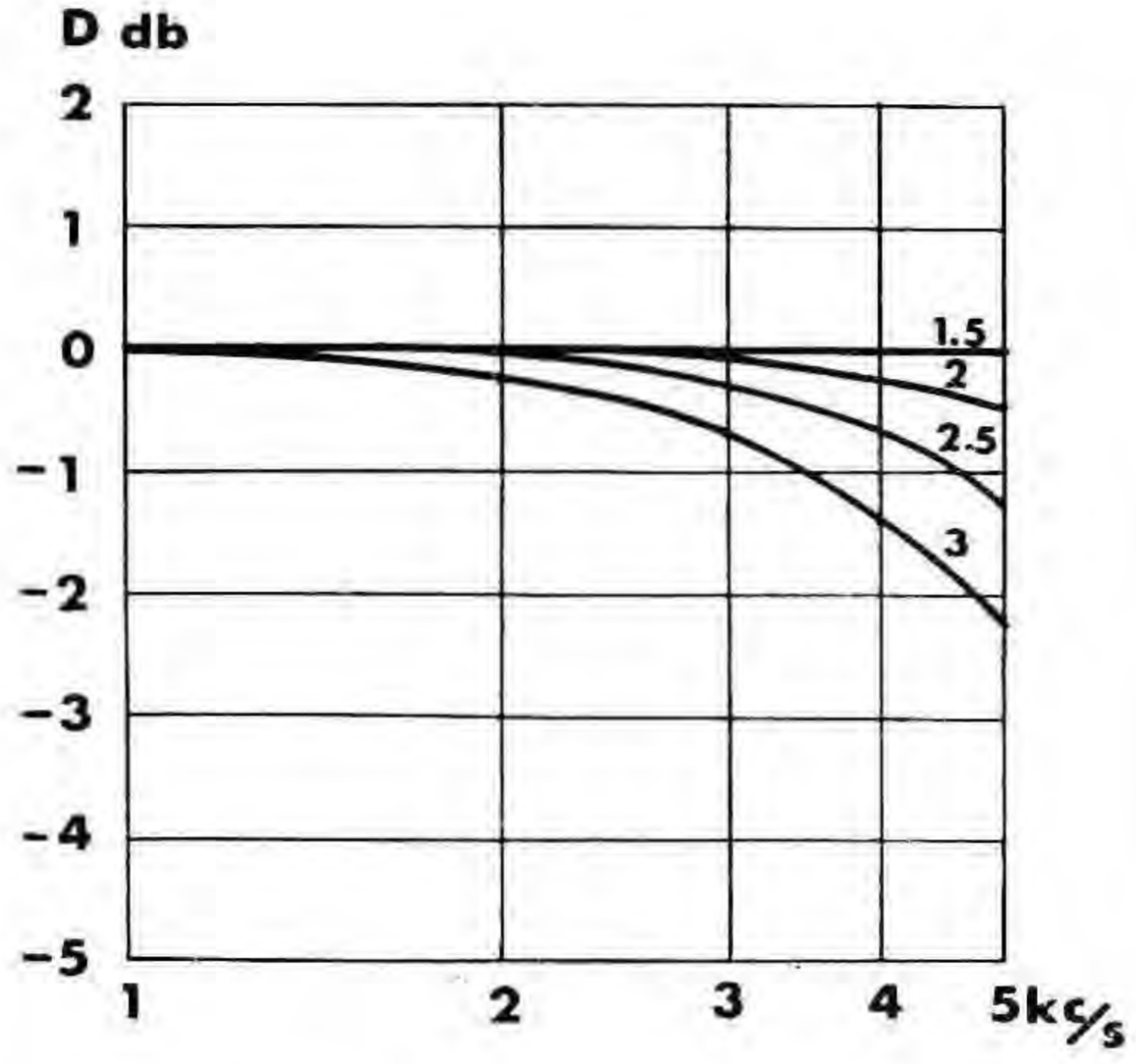

Fig.3. Deviation between measured sound pressure and mean sound pressure as a function of frequency for couplers with diameters 1.5 2, 2.5 and 3 cm. Diameter of microphone diaphragm equal to coupler diameter.

References:

1. J.L.Glaser, K.C.Morrical and K.W.Benson, J.A.S.A.,21 (1949), 190.

2. S.C.Dalsgaard, Proc.III.ICA Cong.,Elsevier,Amsterdam 1961,624.

3. P.V.Brüel and G.Rasmussen, B.& K.Tech.Rev. No 2 1959, 5.

4. A.K.Nielsen, Mikrofonmaalinger, diss.København 1949, 75-80.

5. P.M.Morse, Vibration and Sound 2.ed.,Mc Graw-Hill New York 1948,198

O24

FOURTH INTERNATIONAL CONGRESS ON ACOUSTICS
COPENHAGEN 21.-28. AUGUST 1962

Akustische Beeinflussung der Strömungsgrenzschicht in Luft.

F. Mechel und W. Schilz
III. Physikalisches Institut, Universität Göttingen

1. Messanordnung

In der Grenzschicht einer Luftströmung an einer ebenen Platte kann durch Schalleinstrahlung der Übergang von laminarer zu turbulenter Grenzschicht beeinflußt werden. Zur Untersuchung dieser Grenzschichtbeeinflussung wurde in einem Windkanal von 10x10 cm^2 Querschnitt eine ebene Platte mit scharfer Schneide eingesetzt, auf der sich die Grenzschicht entwickelt. Durch Veränderung der Absaugung unterhalb der Schneide kann der Störgrad der Grenzschicht eingestellt werden. In diese Platte ist eine kolbenförmig schwingende Membran so eingesetzt, daß sie im Ruhezustand die Strömung nicht stört. Sie wird von o,1 bis 3,5 kHz elektrodynamisch betrieben. In einer weiteren Messung wird die Membrane durch eine poröse Platte ersetzt. Diese besteht aus zusammengesinterten Bronzekugeln (o,3 mm Ø) und ist 10 cm lang. Durch die Platte wird eine ebene Schallwelle in die Grenzschicht eingestrahlt. Das System erlaubt Messungen im Bereich von o,1 bis 5 kHz.

Beim Übergang von der laminaren zu der turbulenten Grenzschicht treten zunächst schwache, fast periodische Geschwindigkeitsschwankungen auf, aus denen nach einem gewissen Laufweg Einzelwirbel mit wesentlich größerer Amplitude ausbrechen. Diese wachsen im weiteren Verlauf zu voll entwickelter Turbulenz zusammen. Der Einfluß der Schalleinstrahlung auf die Amplitude der periodischen Störung, die Häufigkeit der Einzelwirbel und die Lage des Umschlagpunktes auf der Platte werden gemessen.

2. Grenzschichtbeeinflussung mit der Kolbenmembran

2.1 Abhängigkeit von Frequenz und Reynoldszahl

Die Wirkung der Schalleinstrahlung auf die Grenzschicht zeigt eine starke Abhängigkeit von der Frequenz des Schallsignals. Mißt man die Häufigkeit der Einzelwirbel als Funktion der Signalfrequenz bei konstanter Schallschnelle und Windgeschwindigkeit, so unterscheidet man 3 Bereiche: 1) Bei niedrigen Frequenzen ist das Schallfeld ohne Einfluß auf die Grenzschicht. 2) In einem mittleren Frequenzbereich

tritt Anfachung der Störung auf. 3) Bei höheren Frequenzen wird die Störung unterdrückt.

Die Frequenzgrenzen des Anfachungsgebietes sind in einem Bereich von mehr als 30 dB unabhängig von der Stärke des Schallsignales und dem Grad der vorgegebenen Störung. Mit wachsender Reynoldszahl verbreitert sich das Anfachungsgebiet und verschiebt sich gleichzeitig zu höheren Frequenzen. Abb. 1 zeigt die Lage der 3 Bereiche. Abszisse ist die mit der Verdrängungsdicke gebildete Reynoldszahl; die Ordinate zeigt die Signalfrequenz. Den Reynoldszahlen entsprechen Windgeschwindigkeiten von 10 bis 30 m/s. Unterhalb der kritischen Reynoldszahl, Re_{kr} = 420, wurde keine Anfachung der Störung gefunden. Die zur Anfachung und Unterdrückung notwendigen Schallschnellen sind sehr klein, verglichen mit der mittleren Turbulenzschnelle. Schallschnellen von 10^{-2} bis 10^{-3} cm/s reichen aus, um den Umschlag laminar-turbulent bei einer ungestörten Strömung herbeizuführen, bzw. bei einer gestörten Strömung die Laminarhaltung zu erzwingen. Demgegenüber treten in den Einzelwirbeln Geschwindigkeiten bis zu 10 m/s auf.

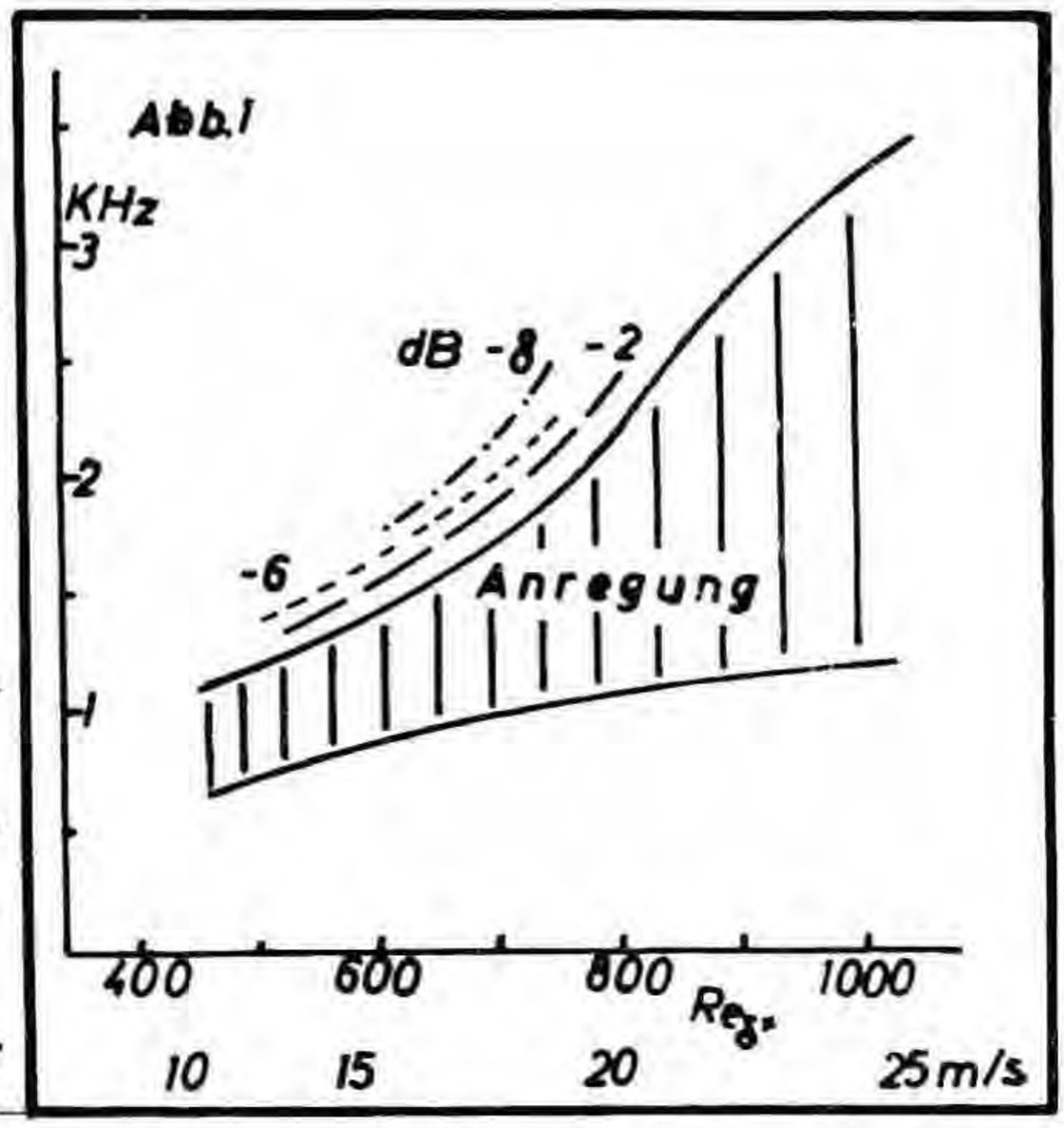

Ein Vergleich mit der Stabilitätstheorie der ebenen Plattenströmung zeigt, daß der hier gefundene Anfachungsbereich frequenzmäßig oberhalb des Instabilitätsbereiches der Tollmien-Schlichting-Wellen liegt. Daraus ist ersichtlich, daß die mit der schwingenden Platte induzierte Grenzschichtstörung von anderer Art als die natürliche Störung ist, da gerade die bei der natürlichen Störung kritischen Frequenzen ohne Einfluß auf die Grenzschicht sind. In Abb. 1 sind oberhalb des Anfachungsgebietes einige Kurven gleicher Störunterdrückung eingetragen. Die dB - Werte geben die Abnahme der vorgegebenen Störung (Wirbelhäufigkeit) bei konstanter Signalschnelle an.

2.2 Störanfachung

In Abb. 1 sind nur die obere und untere Grenze des Anfachungsgebietes eingetragen. Innerhalb dieses Gebietes ist die Stärke der Anregung von der Frequenz und der Signalschnelle abhängig. Mit wachsender

Reynoldszahl verschiebt sich der Beginn der Anfachung zu kleineren Signalschnellen. Dies erklärt sich aus dem Verhalten der periodischen Grenzschichtwellen, aus denen nach Erreichen einer Maximalamplitude die Einzelwirbel ausbrechen (Abb.2).Der Anfachungsexponent dieser Grenzschichtwellen nimmt nach der Theorie mit wachsender Reynoldszahl zu, d.h. die Strömung wird mehr und mehr störanfällig. Die akustische Beeinflußbarkeit der Grenzschichtstörungen hört praktisch auf, wenn die Einzelwirbel zu voller Turbulenz zusammengewachsen sind.

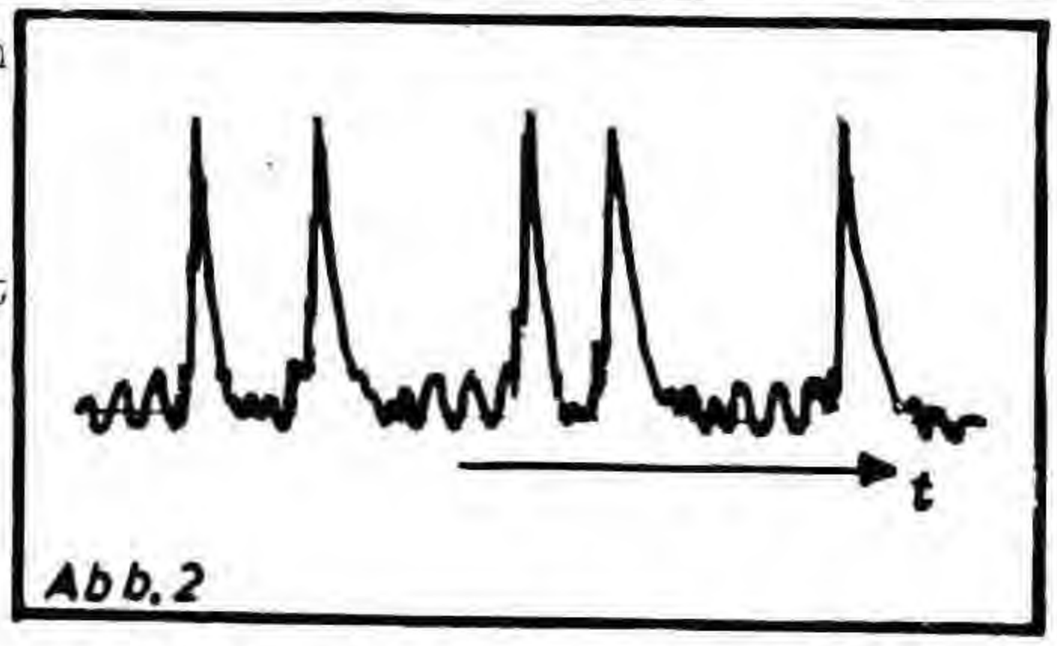

Abb.2

2.3 Störunterdrückung

Die genaueren Untersuchungen der Störunterdrückung wurden bei Windgeschwindigkeiten um 25 m/s und einer Frequenz von 12,4 kHz durchgeführt. Diese Frequenz liegt weit oberhalb des Anfachungsgebietes. Zur Schallerzeugung diente ein Aluminiumzylinder von 70 mm Ø, der in der ersten Längsresonanz betrieben wurde. Seine Oberfläche war mit einem Ringspalt von o,1 mm eben in die Platte eingesetzt.

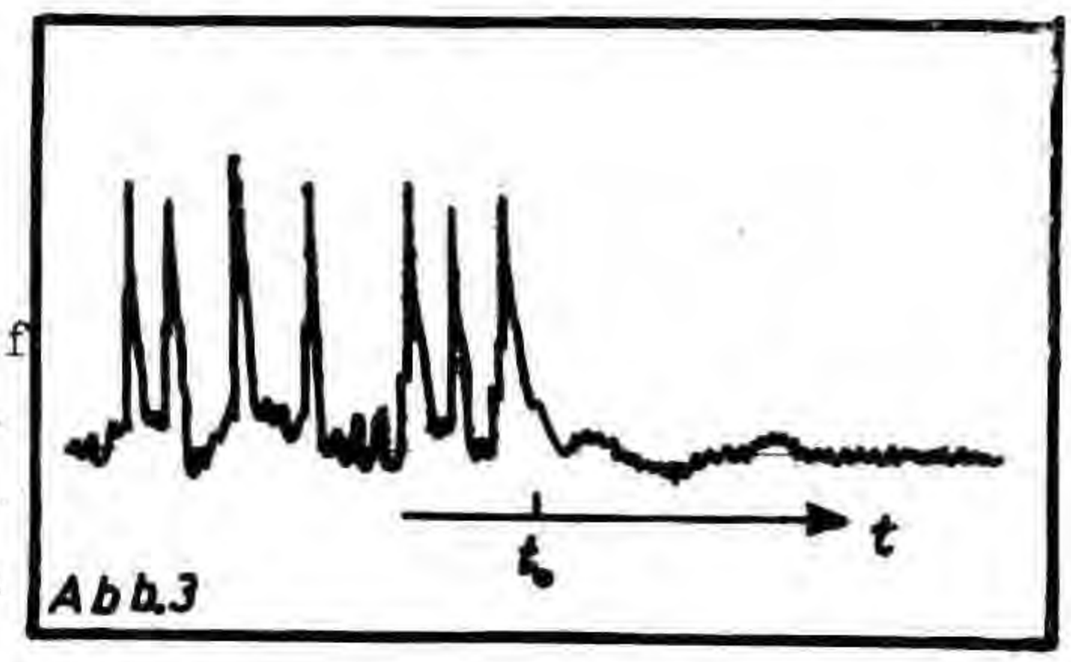

Abb.3

Die Untersuchung erstreckte sich auf die durch Schalleinstrahlung hervorgerufene Änderung des Amplitudenexponenten der natürlichen Grenzschichtwellen und der Wirbelhäufigkeit.Dieser wird mit wachsender Schallschnelle erniedrigt und negativ, so daß trotz instabiler Störung die Stabilität der Grenzschicht erzwungen wird. Bei Überschreiten einer bestimmten Schallschnelle hören die Einzelwirbelausbrüche im Schallfeld spontan auf (Abb.3). In dem Zeitpunkt t_o wurde das Schallsignal eingeschaltet. Die Schallschnelle beträgt o,o5 cm/s. Wenn die Wirbel so dicht aufeinander folgen, daß sie sich gegenseitig durchdringen, so liegen zwischen den Wirbeln keine Grenzschichtwellen mehr vor und die Beeinflussbarkeit durch das Schallfeld hört auf,ebenso wie bei der Anfachung der Störung.Voll ausgebildete Turbulenz läßt sich nicht unterdrücken.

3. Messungen an der porösen Platte

Im Gegensatz zu den obenstehenden Messungen wird an der porösen Platte keine Störunterdrückung durch das Schallfeld beobachtet. Im ganzen Frequenzbereich wird die Grenzschichtstörung angefacht, bzw. eine

vorgegebene Störung vergrößert. Gemessen wurde in Abhängigkeit von Frequenz und Signalamplitude bei verschiedenen Windgeschwindigkeiten die mittlere Turbulenzschnelle und der Ort des Umschlagpunktes zu turbulenter Strömung auf der Platte.

Mit wachsender Signalamplitude steigt die Häufigkeit der Einzelwirbel, wobei diese gleichzeitig breiter werden. Die Maximalschnelle der Wirbel bleibt nahezu konstant. Die Auftragung der Turbulenz als Funktion der Schallschnelle zeigt einen etwa gleichen Anstieg der Turbulenz bei allen Frequenzen, jedoch verschiebt sich der Einsatzpunkt der Störanfachung über einen Bereich von mehr als 4o dB. Hierin zeigt sich eine starke Frequenzabhängigkeit der Störanfachung, die bei jeder Windgeschwindigkeit ein ausgeprägtes Maximum aufweist. Das gleiche gilt für die Verschiebung der Lage des Umschlagpunktes, dessen Ort als Funktion der Frequenz für zwei Signalschnellen in Abb.4 wiedergegeben ist. (Windgeschwindigkeit 34 m/s). Mit wachsender Signalschnelle verschiebt sich der Umschlagpunkt monoton stromaufwärts, wobei die Lage des Maximums erhalten bleibt. Auch hierbei sind die Schallschnellen an der Platte klein gegen die Turbulenzschnelle.

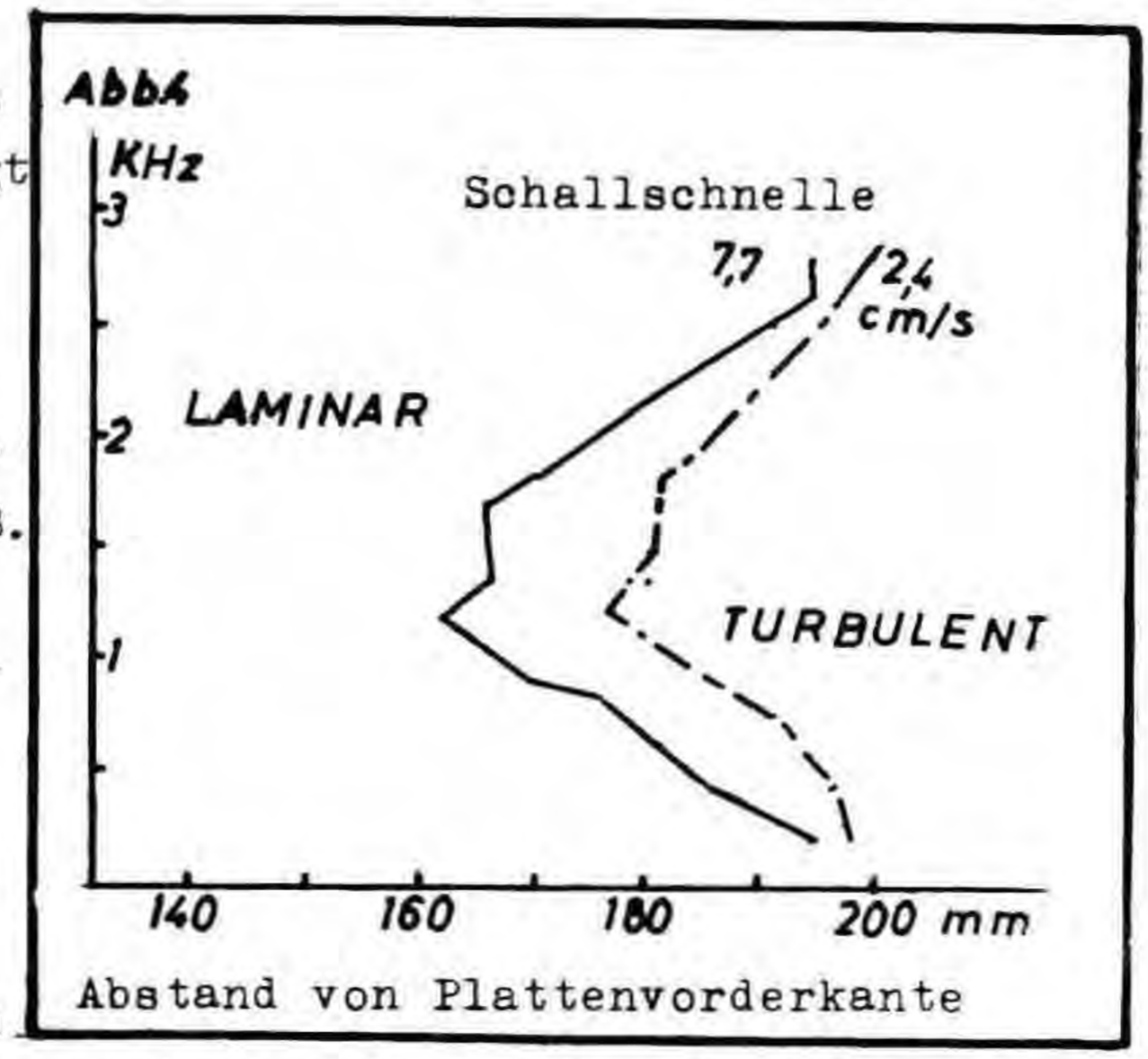

Die Schalleinstrahlung durch die poröse Platte kann als periodische Absaugung und Ausblasung der Grenzschicht beschrieben werden. Da in der Ausblasphase ruhende Luft der Grenzschicht zugeführt wird, ist dann eine besonders starke Störung der Grenzschicht zu erwarten. Bei tiefen Frequenzen ist die Zeitdauer eines Einzelwirbels klein gegen die Periodenlänge des Schallsignals, so daß man aus dem Oscillographenbild die Lage des Wirbelausbruches bestimmen kann. Man beobachtet stets einen Ausbruch im Maximum einer Halbwelle. Dieser Ausbruch erfolgt bei kleinen Schallschnellen nur, wenn schon eine Störung der Grenzschicht vorliegt, bei größeren Schallschnellen in jeder Periode. Bei höheren Frequenzen konnte die genaue Phasenlage zwischen Wirbelausbruch und Schallsignal noch nicht bestimmt werden.

P24 FOURTH INTERNATIONAL CONGRESS ON ACOUSTICS
COPENHAGEN 21.-28. AUGUST 1962

Propagation of Flexural Waves in Unhomogeneous Plates with Slowly Changing Parameters.

V.V.Tiutekin

The propagation of flexural waves in unhomogeneous plates and rods have some particularities compared with the propagation of sound in unhomogeneous liquid media.

Let us consider a plate cylindrical stiffness $D = Eh^3/12(1-\sigma^2)$ and density ρ of which are arbitrary continuous functions of one coordinate X in limit of $0<X<\ell$. Here h is the thickness of the plate, E and σ are Youngs modulus and Poisson ratio of the plate material. Considering for simplicity the flexural waves propagate along axis X only, we have a system determining the motion of the plate:

$$V = W' ; \quad M = -DV' ; \quad F = M' ; \quad -\kappa^4 DW = F' \qquad /1/$$

Here W is the displacement of a middle plane of the plate, V is the slope of this plane, M is the flexural moment, F is stress force, $\kappa^4 = \rho h \omega^2 / D$, where ω is the cycle frequency; a touch denotes differentiation with respect to coordinate X.

To obtain the solution of the system /1/ instead of values W, V, M and F we should introduce new functions P_1, P_2, P_3 and P_4, connected with above values by the following relations:

$$W = P_1 + P_2 + P_3 + P_4 ; \qquad V = \kappa(iP_1 - iP_2 + P_3 - P_4),$$

$$M = D\kappa^2(P_1 + P_2 - P_3 - P_4); \qquad F = D\kappa^3(iP_1 - iP_2 - P_3 + P_4) \qquad /2/$$

Substituting /2/ into /1/ we obtain a system of four linear differential equations of the first order:

$$P'_m = \sum_{n=1}^{4} \alpha_{mn} P_n \qquad m = 1,2,3,4 \qquad /3/$$

The coefficients α_{mn} are the functions of X and are expressed as follows:

$$\left.\begin{matrix}\alpha_{11}\\ \alpha_{22}\end{matrix}\right\} = \pm iK - \frac{\gamma+3\beta}{2} \quad ; \quad \left.\begin{matrix}\alpha_{33}\\ \alpha_{44}\end{matrix}\right\} = \pm K - \frac{\gamma+3\beta}{2} \quad ;$$

$$\alpha_{12} = \alpha_{21} = \alpha_{34} = \alpha_{43} = \frac{\beta}{2} \quad ;$$

$$\alpha_{13} = \alpha_{24} = \alpha_{32} = \alpha_{41} = (1+i)\frac{\gamma+2\beta}{4} \quad ;$$

$$\alpha_{14} = \alpha_{23} = \alpha_{31} = \alpha_{42} = (1-i)\frac{\gamma+2\beta}{4} \quad ,$$

where

$$\gamma = \frac{D'}{D} \quad \text{and} \quad \beta = \frac{K'}{K}$$

The solution can not be found for the general case, but for the case of small parameters variations on a wave length the approximate solution can be easily found.

For this purpose we assume:

$$P_m = p_m e^{\int_0^x \alpha_{mm} dx} \qquad /4/$$

Substituting /4/ into /3/ we shall obtain a new system, similar to /3/ but which does not held diagonal terms:

$$p'_m = \sum_{n=1}^{4} (1-\delta_{mn}) \alpha_{mn} p_n e^{\int_0^x (\alpha_{nn} - \alpha_{mm}) dx}$$

$$\delta_{mn} = \begin{cases} 1 & m = n \\ 0 & m \neq n \end{cases} \qquad /5/$$

For small variations of the plate parameters the system /5/ can be written in the form:

$$p'_m = \sum_{n=1}^{4} (1-\delta_{mn}) \varepsilon A_{mn} p_n \qquad /6/$$

where ε is a small parameter, and the values of are easily determined

from /5/.

We will seek a solution /6/ in the form of a power series:

$$p_m = \sum_{\kappa=0}^{\infty} \varepsilon^{\kappa} p_m^{(\kappa)} \qquad /7/$$

where $p_m^{(\kappa)}$ is κ-approximation of function p_m.

It is possible to show that the values $p_m^{(\kappa)}$ satisfy a following system of the equations:

$$p_m^{(\kappa)\prime} = \sum_{n=1}^{4} (1-\delta_{mn}) A_{mn} p_n^{(\kappa-1)} \qquad /8/$$

At the zero approximation, supposing $A_{mn}=0$, we obtain $p_m^{(0)\prime}=0$, or $p_m^{(0)} = C_m$, where values C_m are constant. Substituting the values $p_m^{(0)}$ and α_{mn} into /4/ the following expressions for functions $P_m^{(0)}$ could be obtain:

$$\left.\begin{matrix} P_1^{(0)} \\ P_2^{(0)} \end{matrix}\right\} = \frac{C_{1,2}}{\sqrt{D\kappa^3}} \ell^{\pm i\int_0^x \kappa dx} \quad ; \quad \left.\begin{matrix} P_3^{(0)} \\ P_4^{(0)} \end{matrix}\right\} = \frac{C_{3,4}}{\sqrt{D\kappa^3}} \ell^{\pm \int_0^x \kappa dx} \qquad /9/$$

The physical meaning of the functions $P_m^{(0)}$ is easily seen from these expressions. For κ =const and D =const functions $P_1^{(0)}$ and $P_2^{(0)}$ describe flexural sinusoidal waves, which propagate in positive and negative directions of X-axis, correspondingly; the functions $P_3^{(0)}$ and $P_4^{(0)}$ describe the waves of exponential type, increasing and decreasing along X-axis, respectively. It is evident that in the similar way functions $P_m^{(0)}$ could be interpreted in the unhomogeneous plate.

The solution /9/ of the system /5/ is an approximation of geometrical optics. This approximation describes the propagation of waves of any kind independent from each other and their mutual transformation is not taken into consideration. In order to take into account this transformation it is necessary to consider the following approximation. Substituting $p_m^{(0)} = C_m$ into /8/ we obtain at the first approximation:

$$p_1^{(1)} = \int_0^x \Big(\sum_{n=1}^{4} (1-\delta_{1n}) A_{1n} C_n \Big) dx \; ; \quad p_3^{(1)} = \int_\ell^x \Big(\sum_{n=1}^{4} (1-\delta_{3n}) A_{3n} C_n \Big) dx$$

$$p_2^{(1)} = \int_\ell^x \Big(\sum_{n=1}^{4} (1-\delta_{2n}) A_{2n} C_n \Big) dx \; ; \quad p_4^{(1)} = \int_0^x \Big(\sum_{n=1}^{4} (1-\delta_{31}) A_{4n} C_n \Big) dx \qquad /10/$$

The limits of integration in /10/ were chosen from the physical considerations: each wave receives "contribution" from other waves on a definite part of the unhomogeneous portion of the plate.

Substituting, further, /10/ into /8/ it is possible to find values p_m in subsequent approximations. It easily could be seen, that in any order of the approximation solution of the system /8/ would held four arbitrary constants C_m which have to be determined from boundary conditions at $x = 0, \ell$.

G25

FOURTH INTERNATIONAL CONGRESS ON ACOUSTICS
COPENHAGEN 21.-28. AUGUST 1962

ELECTRONIC MODEL OF THE HUMAN AUDITORY SYSTEM

T. B. Martin, J. J. Talavage and F. L. Putzrath
Radio Corporation of America, Camden, N. J., U. S. A.

I. INTRODUCTION

Many creatures have specialized organs and nerves for hearing. These systems have evolved to the particular degrees of sophistication required for the survival of each species. The auditory system of genus homo sapiens evolved similarly so that man, developing a spoken language, learned to form speech sounds to be compatible with a hearing system which had basically evolved to detect the sounds of approaching enemies, a mate, or food. Thus, human speech is formed to be processed by the human auditory system, a system which responds only selectively to the gross auditory environment. This selectivity, occurring naturally in man, must become an integral part of any machine whose object is to "understand" speech. To facilitate the study of the human auditory system responding to complex sounds, an electronic model is being built based upon the most recent findings in the fields of biology and psychology. It is the purpose of this paper to briefly review the anatomy of the ear, the neurophysiology of the auditory system, and the psychology of hearing. The main section of this paper covers the development of the electronic model, relating its performance capabilities to the naturally observed phenomena.

II. ANATOMY OF THE EAR

Acoustic energy impinging upon the tympanic membrane is transmitted by the ossicles to the base of the cochlea, the transmission efficiency decreasing at frequencies above 3000 cps. The transmitted energy produces mechanical waves in the basilar membrane. As the wave progresses towards the apex of the cochlea the amplitude of vibration builds up gradually to a broad maximum (Fig. 1A), but decreases rapidly beyond this point. These vibrations set up mechanical stresses within the basilar membrane which correspond to a spatial derivative of the amplitude function (Fig. 1B). The place of maximum stress moves from the apex of the cochlea toward the base as frequency of vibration is increased (Fig. 2). The relative amplitudes of these maxima increase about 5 db per octave but remain constant above 1000 cps[1]. Thus, the cochlea transforms mechanical frequency into linear space, permitting a large number of neurons to be stimulated by the acoustic signals.

The motion of the basilar membrane is sensed by two types of hair cells, the outer cells responding to the vibration of the membrane and the inner cells responding to the longitudinal stresses within the membrane[1]. The mechanical deformation of the cells releases electrical energy which indirectly excites neurons.

The controlled electrical energy, spatially distributed along the cochlea, influences a network of neurons which performs logical operations upon the input information. The electrical energy received by each neuron can be excitatory and/or inhibitory, the output pulse repetition rate of each neuron being determined by the difference between these quantities. After a temporal integration of the pulses, these pulses become the excitatory or inhibitory stimuli to other neurons.

The response of primary neurons to various audio input frequencies has been explored. With no external stimulation a neuron may be quiescent or have a low, spontaneous firing rate. Upon application of an excitatory stimulus, the pulse repetition rate may reach 800 pulses per second[2]. Many neurons respond to a range of audio frequencies rather than to a single frequency. The shape of the response area is closely correlated to the mechanical stresses in the basilar membrane (Fig. 3A). The distribution of the neurons along the length of the cochlea is not constant. Starting near the base, the ganglion density increases slightly but then drops significantly as the apex of the cochlea is reached.

The amount of knowledge about neural processes decreases rapidly as the auditory cortex is approached. It is known, however, that the response areas of the neurons become

increasingly sharpened (Fig. 3B). It is also significant that there is a decrease in the number of neurons that respond to steady-state tones, whereas there is an increasing number of neurons responding to the onset or the termination of a stimulus.

III. PSYCHOLOGY OF HEARING

The minimum acoustic energy required for the perception of a sustained tone determines the threshold of hearing. The hearing acuity of man is greatest at about 2000 cps, gradually decreasing above and below this frequency.

The threshold of hearing of a particular tone can be increased by the presence of a second tone. A low-level masking tone affects only signals near its frequency, whereas a high-level tone masks additional frequencies, particularly those in the higher frequency regions.

White noise can also mask any signal that falls within the noise spectrum. The bandwidth of this noise can be reduced without diminishing its masking effect, until a certain critical bandwidth is reached. Beyond this point the effectiveness of the masking is reduced. This observation and related psychoacoustic tests have shown that the critical bandwidth varies exponentially as the frequency increases. (Physically this bandwidth is equivalent to one millimeter along the length of the basilar membrane.)

IV. DEVELOPMENT OF THE MODEL

INTRODUCTION - In order that the electronic model be a reliable replica of the human listening system, all of the biological and psychological effects discussed above have to be considered. However, it must also be possible to build the model and to determine its effectiveness in the analysis of speech. Thus, a balance has to be maintained between the faithfulness of copying nature and the economic realities.

THE COCHLEA - In the model, the acoustic energy is initially transformed into electrical signals. The lowpass characteristics of the middle ear take the form of an R-C and an L-C filter (Fig. 4). The output of this filter drives an isolation amplifier which in turn supplies the electrical signals to the simulated cochlea. The electrical response of each cochlea section closely resembles the mechanical motion of the biological organ (Fig. 5). The effect of the graduated level of the maxima along the length of the structure is achieved by the insertion of fixed attenuators into the filter sections. Since it is not planned to make tests on binaural hearing, the model does not include the 5-ms transmission delay between the input and output sections. If desired, this effect could be included by the use of a multitapped delay line.

The concept of critical bandwidth is used as a guide in determining the filter spacing. Since the model will be used for speech analysis, the limited frequency range is accommodated by 19 filter sections whose center frequencies are listed in Table I.

SIMULATED NEURON - Each neuron is simulated by a four-transistor circuit (Fig. 7) and is capable of performing all the essential characteristics of the biological neurons; this means being responsive to excitation and inhibition and generating a variable pulse-repetition rate, which is based upon a refractory period occurring after each pulse. The only important (but logically inconsequential) deviation from the biological neuron is that the electronic model simultaneously generates positive and negative pulses used for excitation and inhibition, respectively. The natural neuron generates only positive pulses; inhibition probably is achieved by an inversion at the synapse.

NEURON RESPONSE AREAS - The primary row of artificial neurons is connected to the electrical cochlea to approximate the neural responses generated by the inner hair-cells. Each neuron is excited by the signal in one filter and inhibited by the signal in the next higher-frequency filter. Thus these neurons have response areas which are identical to the response areas of the primary biological neurons: the neuron is most readily stimulated by a particular frequency; its sensitivity decreases slowly for lower frequencies and quite rapidly for higher frequencies. The sounding of a single tone causes many neurons to fire, yet only the neuron exhibiting the highest firing rate can designate the frequency of a tone.

THRESHOLD OF HEARING - The threshold of hearing of the model is determined by the level of an input signal which just evokes the firing of a neuron. This level is not constant for all audio frequencies since the transfer function of the network is determined by 1) the lowpass network representing the middle ear, 2) the attenuators simulating the graded level of maximal stresses along the filter network and 3) the graded filter-neuron interconnections simulating the variations in ganglion density. Figure 8

shows the comparison between the model and the psychoacoustic phenomena.

MASKING EFFECTS - The networks mentioned in the previous paragraph also give the model the effect of masking. A low-amplitude 800-cps tone may be just sufficient to fire the neuron between filter sections 15 and 16. A 400-cps tone of moderate amplitude will also excite this neuron but will not be perceived as an 800-cps tone since at this station the neural activity is not at a maximum. To barely perceive an 800-cps tone in the presence of the 400-cps tone, that is, to form a local maximum of neural firing rate between filters 15 and 16, a large-amplitude 800-cps signal must be applied. Thus, the high-frequency signal has been masked by the presence of the low-frequency tone. Figure 6 shows a comparison between masking in the model and the psychoacoustic phenomena.

CAPABILITY OF SIMULATED NEURAL LOGIC - The exact circuitry of the model has not been determined beyond this point; yet neural logic has been developed that can simulate known or conjectured neural activity. Three basic functions are of particular interest: 1) contrast enhancement, 2) logical AND, and 3) ON and OFF response. The function of contrast enhancement has been found in living organisms and can be achieved by mutual inhibition of adjacent neurons (Fig. 9). If input A is only slightly larger than input B, output A' is enhanced while output B' is diminished.

The logical operation required to note the presence of two simultaneous features (AND) is difficult to achieve. The basic problem is caused by the fact that an output is desired when two small input signals are present, but no output must occur when only one large-amplitude input signal is present. A circuit consisting of three neurons can be used to achieve signal multiplication (Fig. 10). The inhibition connections from neurons 1 and 2 to neuron 3 are made lower in resistance than the direct excitatory inputs to neuron 3. Thus a single excitatory input cannot cause an output signal. However, the cross inhibition input connections are sufficient to cause an output if both input signals are present.

The neural responses to a change in input signals found in the cortical areas have been simulated. The OFF response is typified by a burst of pulses that occurs at the termination of the input signal, followed by a diminishing rate of firing which eventually ceases altogether (Fig. 11). Thus the firing rate tells how long ago a particular event ceased.

Simulated neurons can be used to isolate local maxima, minima, and slopes of energy within a network and to follow their changes in magnitude or location. The simultaneous occurrence or absence of these features can be recognized so that speech can be processed and analyzed in real time.

V. CONCLUSION

The model under development is not completed. The specific logic required to abstract the important features of speech remains to be determined. Yet the knowledge necessary to complete this work is rapidly being accumulated: the biologist is increasing his understanding of the living organism, the engineer is expanding the logic capability of simulated neural networks. The continuing exchange of information between these two disciplines should make the goals of both sciences more attainable.

The support of this work under U. S. Air Force Sponsorship (Contract AF 33(657)-7405) is acknowledged.

REFERENCES

1. G. Von Bekesy, Experiments in Hearing, McGraw-Hill Book Co., Inc. New York, 1960, pp. 440-449.
2. Katsuki, Y., et al., "Electric Responses of Auditory Neurons in Cat to Sound Stimulation," J. Neurophysiol., 1958, vol. 21, pp. 575, 576.
3. Greenwood, D. D., "Auditory Masking and the Critical Band," J. Acoust, Soc. Am., 1961, vol. 33, pp. 484-502.
4. J. Egan, H. Hake, "On the Masking Pattern of a Simple Auditory Stimulus," J. Acoust, Soc. Am., vol. 22, 1950, p. 622.
5. L. Sivian, S. White, "On Minimum Audible Sound Fields," J. Acoust. Soc. Amer., vol. 4, 1933, pp. 288-321.

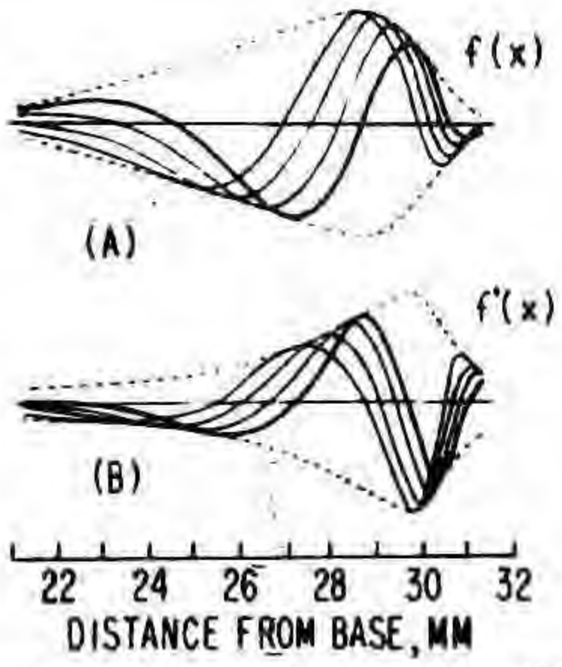

FIG. 1. TRAVELING WAVE AND STRESS ALONG BASILAR MEMBRANE (BEKESY[1]).

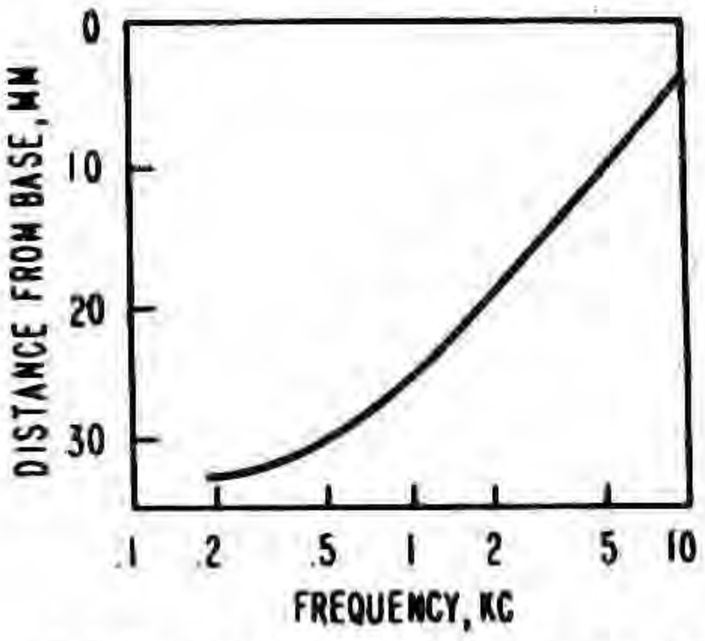

FIG. 2. PLACE OF MAXIMUM STIMULATION VS. FREQUENCY.

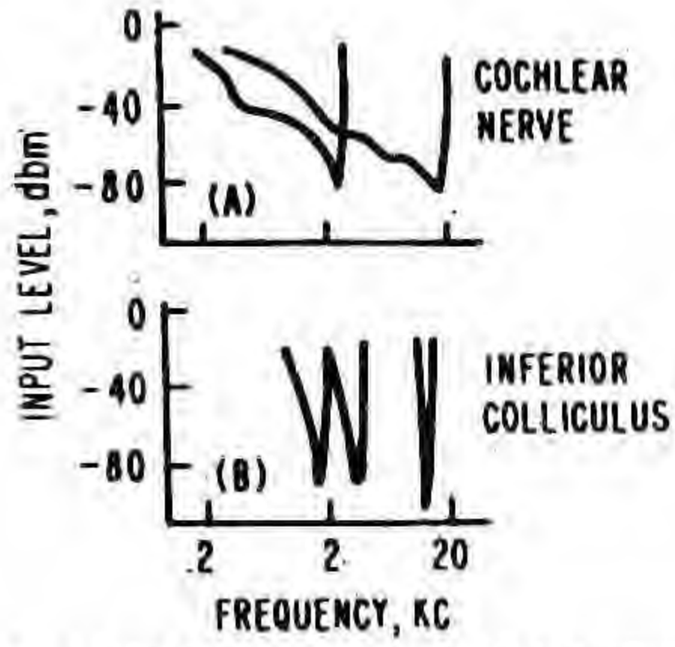

FIG. 3. RESPONSE AREAS OF SINGLE NEURONS (KATSUKI, ET AL.[2]).

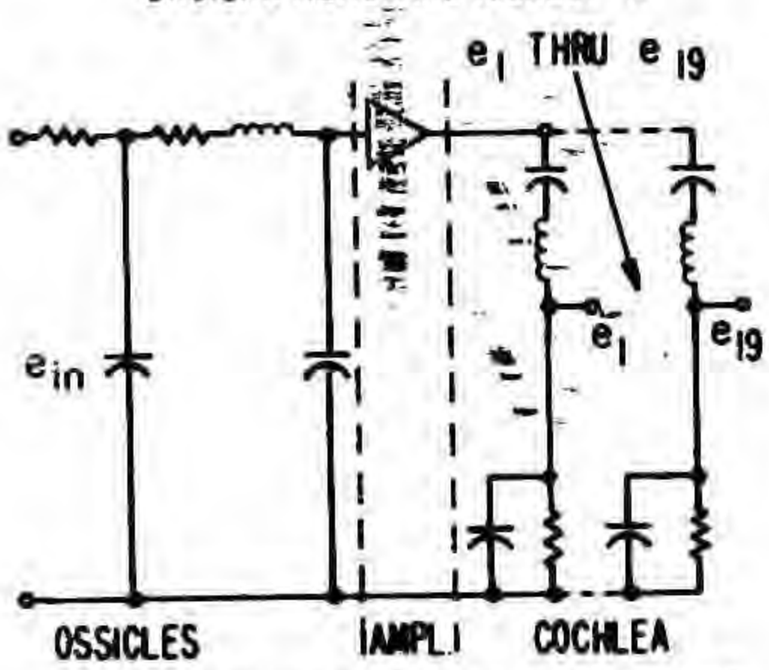

FIG. 4. ELECTRONIC MODEL OF OSSICLES AND COCHLEA.

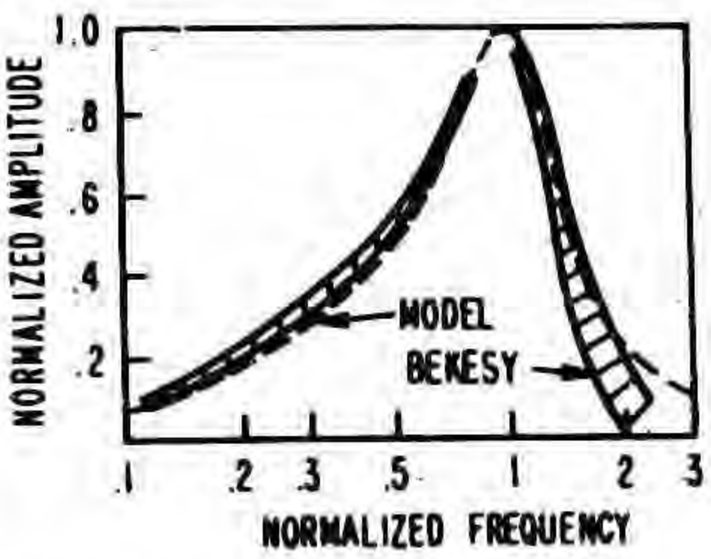

FIG. 5. MOTION OF BASILAR MEMBRANE (BEKESY[1]).

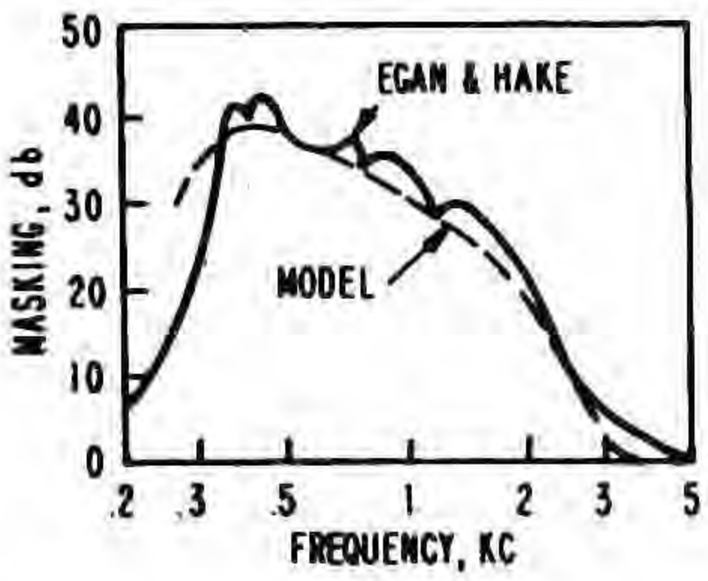

FIG. 6. MASKING CHARACTERISTICS (EGAN & HAKE[4]).

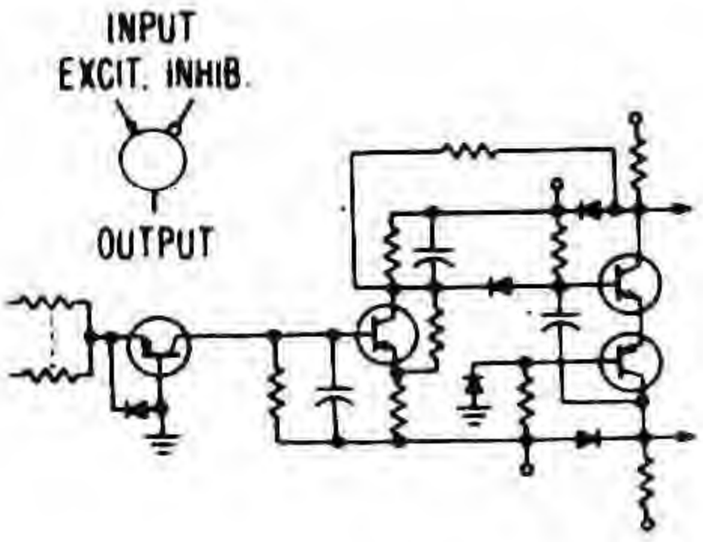

FIG. 7. SIMULATED NEURON: SCHEMATIC AND SYMBOL.

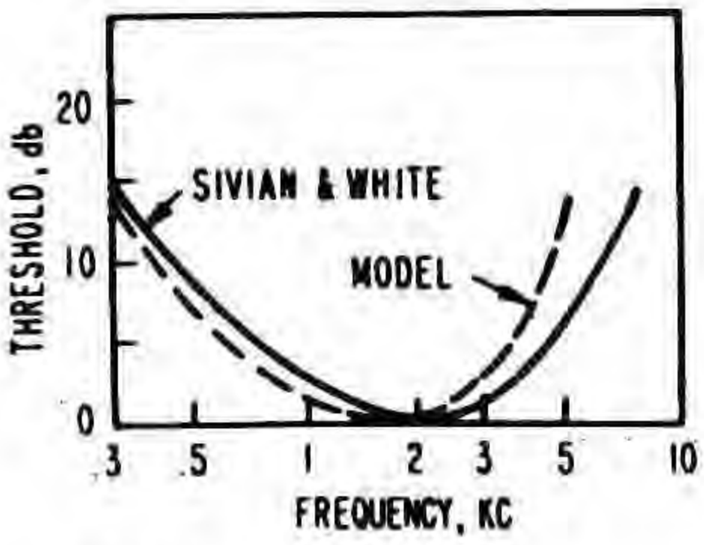

FIG. 8. THRESHOLD OF HEARING (SIVIAN & WHITE[5]).

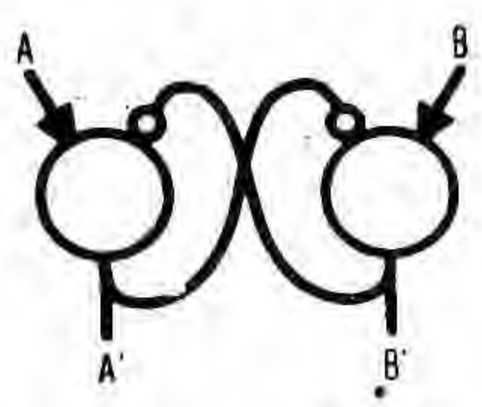

FIG. 9 CONTRAST ENHANCEMENT

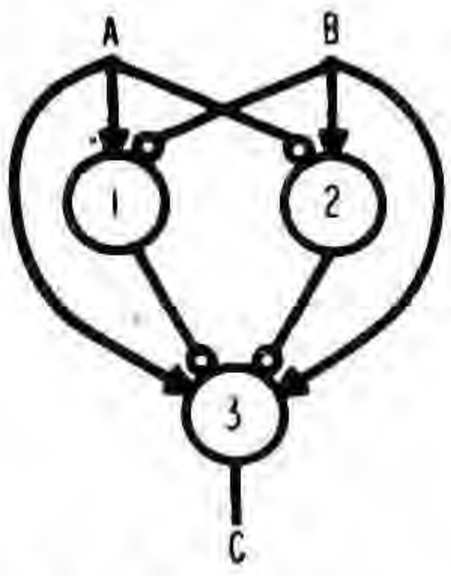

FIG. 10. "AND" FUNCTION.

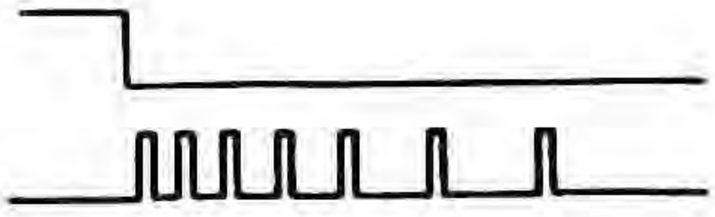

FIG. 11. "OFF" RESPONSE.

FILTER SECT. NO	RES. FREQ.	FILTER SECT. NO	RES FREQ
1	8710	11	1630
2	6570	12	1398
3	5275	13	1198
4	4570	14	1022
5	3960	15	868
6	3405	16	735
7	2960	17	572
8	2550	18	394
9	2200	19	259
10	1897		

RESONANT FREQUENCIES OF FILTER SECTIONS
TABLE I

H25

FOURTH INTERNATIONAL CONGRESS ON ACOUSTICS
COPENHAGEN 21.-28. AUGUST 1962

The Effect of Noise on Hearing in the Egyptian Industrial Schools.

By
E. ESSAMMA & T. ABDEL ALIM.

This survey was done on 1000 candidate. An audiometric design aiming at economy of time was followed, by doing group testing 1st., using an arabic speech test, to screen out the normal cases & then a tone test for the positive cases with impairment more than 20 db. Our standard in tone audiometry is that any case with impairment of 15 db or more in 2 frequencies in the field between 125 and 2000 c.p.s. or of 20 db or more in one frequency in the field between 4000 & 8000 c.p.s. is condemned to have some degree of deafness.

Clinical examination done to exclude out other causes of deafness not related to the profession. Students of the 1st. year were taken as our standard, about 7% showed some degree of deafness. Our results in the different sections are illustrated in table I.

Spectroscopic analysis of the various noises & their intensities are shown in table II. We attacked the problem by investigating the following points:

1. Duration & time distribution of noise during a typical work day. Our data agreed with the well known fact that the longer the time of exposure & the less the period of interruption of noise, the more the % of deafness. The intermittent exposure to noise appears to be less injurious than continuous exposure of the same total time even though the intermittent exposures are accompanied by considerably higher over all noise levels.

2. Intensity of noise: to find out the injurious level. This was found to be as low as 95 db.

3. Nature of noise whether steady or pulse. This could be practically ignored, as in the pulse noise e.g. smithing section, several units are working at the same time leading to continuity of noise.

4. Nature of the deafness: most cases are perceptive in origin. Deafness begins as a temporary loss due to nerve fatigue. After some time (may be as long as several years), permanent damage occurs. The unawareness of occupational deafness is actually due to the fact that in factories vocation is in a loud voice to overshadow the sounds generated by the engines. Added to this, the slow insiduous onset of deafness which may take years to manifest itself offering ample time for the person to be a good lip reader and explain the unawareness of the person of his handicap until too late.

The combined study of the spectograms & audiograms in the various sections makes one believe in the non-localisation theory of hearing.

Table I.

The Incidence of deafness in the different sections

Profession	Class	Total No.	Group Audiometry		Cases with Clinical Deafness	Tone Audiometry:		%
			Normal	Deaf?		Apparent Deafness	Prof. Deafness	
Fitting Section	2nd Y.	31	23	8	1	-	7	23%
	3rd Y.	65	46	19	-	4	15	20%
	Staff	8	-	-	-	-	3	37%
Metal Turning Section	2nd Y.	45	40	5	2	-	3	7%
	3rd Y.	80	68	12	-	-	12	15%
	Staff	10	-	-	-	-	5	50%
Smithing Section	2nd Y.	18	15	3	2	-	1	7%
	3rd Y.	16	13	3	-	-	3	19%
	Staff	4	-	-	-	-	3	75%
Electronic Section	2nd Y.	26	21	5	1	2	2	8%
	3rd Y.	28	25	3	-	-	3	11%
	Staff	6	-	-	1	1	1	33%
Electrical Section	2nd Y.	92	80	12	5	-	7	8%
	3rd Y.	53	48	4	-	-	4	7%
	Staff	11	-	-	-	-	1	10%
Motor-car Section	2nd Y.	70	65	5	-	-	5	7%
	3rd Y.	51	47	4	-	-	4	8%
	Staff	11	-	-	1	-	2	20%
Foundry Section	2nd Y.	27	23	4	1	-	3	12%
	3rd Y.	-	-	-	-	-	-	-
	Staff	7	-	-	1	-	2	33%
Pattern Welding Section	Staff	4	-	-	-	-	1	25%

Table II.

Readings of the Spectrograms.

Section	Intensity of Noise		Fundamental Tone	Combination Tone
Metal Turning Section	Position I	86 db	1000 cps	60 - 8000 cps
	II	83 db	4000 cps	60 - 8000 cps
	III	83 db	4000 cps	65 - 8000 cps
	IV	106 db	4000 cps	60 - 8000 cps
	V	105 db	4000 cps	60 - 8000 cps
Foundry Section	Position I	95 db	125 cps	60 - 8000 cps
	II	80 db	175 cps	60 - 8000 cps
Pattern Making Section	Position I	95 db	175 cps	
	II	85 db	175 cps	
Seldering Section	Outside the Soldering Cabin	95 db	60 cps	85 - 8000 cps
	Inside the Soldering Cabin	87 db	500 cps	60 - 8000 cps

It had been noticed that the noise inside the cabin is less than outside. This is due to the noise in the neighbouring room.

Smithing Section	Fans only	85 db	700 cps	60 - 8000 cps
	Fans and Hammers	112 db	2000 cps	60 - 8000 cps
Motor-car Section	Mean Value of two Positions	85 db	1000 cps	60 - 8000 cps
Fitting Section		79 db	700 cps	60 - 8000 cps

Beside the effect of the noise on the nerve, quite a good number of occupational deafness is conductive in origin. In smithing section, for example, the students work infront of the ovens, and suddenly going outside when the lesson finishes. This results in sore throats and sinusites with Eustachean catarrh and consequent middle ear troubles. Also, in weaving section; the inhalation of dust and cotton particles, may lead to irritation of nasal and tubal mucosa and even to secretory otitis media, if person is allergic.

Preventive measures :

1. Audiometric testing of the newly admitted students every 6 months to pick up cases as early as possible. If medical treatment (V.B1., V. B12., V. C., V. A), with intermittent exposure to noise fail, we advise changing the job to a less noisy one.

2. Ear plugs specially designed to be more sound proof by putting a layer or two of an isolating substance e.g. cork or glass wool. This should not prevent the student from hearing loud speech or warning signals.

3. Measures to suppress the noise, necessitating the help of architects and consulting engineers in their building projects.

4. Measures to minimize the number of conductive deafness:

a - Avoiding sudden changes of temperature by offering a rest room in the vicinity of the smithing section.

b - A mask should be worne in the weaving section plus measures to minimize the dust in the air.

c - The irritation of chemicals to the nasal and tubal mucosa in the soldering section, should be guarded against.

J25

FOURTH INTERNATIONAL CONGRESS ON ACOUSTICS
COPENHAGEN 21.-28. AUGUST 1962

Thermal Relaxation in N_2, O_2, and CO with Admixtures.

Malcolm C. Henderson

The Catholic University of America, Washington 17, D.C.

(Work supported by the Office of Naval Research.)

As reported in the Journal of the Acoustical Society of America, 34, 349 (1962), the author has developed an acoustical resonance tube capable of operating at pressures up to at least 150 atmospheres and temperatures of several hundred degrees C. A fuller account of the instrumentappears in the June issue of that journal (MCH & G.J.Donnelly, "Acoustic Resonance Tube for High Pressures and Low f/p.) The frequency range extends from 450 cps to above 10 Kc, and the corresponding frequency/pressure ratios run from 3 cps/atm to 20,000 cps/atm and more. This is a region that has not thus far been readily accessible to experiment, particularly the lower end thereof. J.G.Parker, J. Chem. Phys. 34, 1763 (1961) gives the theory of operation of such tubes concisely. It will not be repeated here, excpet to recall that the amplitude absorption coefficient, α, is given by $\pi\delta/v$, where δ is the width of the resonance peak in cycles per second at the half-power points, and v is the velocity under the experimental conditions. This α is the sum of the "tube absorption" and "relaxation absorption", "classical absorption" being negligible under these conditions.

In calibration runs with this tube, using gases for which C', the relaxing specific heat, is zero, it was established that the Helmholtz-Kirchhoff relation for tube absorption must be increased by about 11% if it is to agree with experiment. This moderate increase is a familiar phenomenon in resonance tubes, and is thus far without adequate explanation. However, its consistency with a number of non-relaxing gases was such as to permit the calculation of the tube absorption in a relaxing gas with confidence.

In the present work all gases were stored at 1000 psi or more over "Drierite" ($CaSO_4$) as a drying agent before being used. This material is in equilibrium with 0.005 mg/liter of water vapor at room temperature (J.H.Bower, Nat. Bu. Stan. J. Rsch. 12, 241 (1934) and ibid. 33, 199 (1944)), corresponding to a vapor pressure of 6.25×10^{-6} atm. and representing a correspondingly small mole-fraction. Adsorption and de-sorption from the walls of the metal tube and piping is probably an important source of vapor, in spite of repeated heating and evacuating.

In a gas having no measurable vibrational specific heat, i.e. C'=0, the tube absorption as a function of pressure and temperature appears as in Fig. 1, which shows the measured δ for nitrogen at room temperature, plotted on log-log scale. Here there is a steady fall in the absorption with successive increases in pressure, in successive curves of slope 1/2, crowding together as the gas begins to depart from ideality.

In oxygen, on the other hand, in Fig. 2 there is a divergence from the $(f/p)^{1/2}$ law even at as low a pressure as 1.2 atm. The straight lines in the lower part of the figure are the calculated tube absorptions, corrected, for the pressures as labelled. If they are now subtracted point by point, from the corresponding measured δ, the resulting differences may be converted to the absorption per wave length, $\alpha\lambda$, and plotted against log f/p as parameter. This procedure results in the data shown in Fig. 3. The position of the maximum gives the value of f_o/p_o, in this case 90 cps/atm. These three figures are typical of the data and results obtained.

If CO_2 be added to the oxygen in suitable amounts, the position of the peak is shifted to higher values of f/p. Table I gives the values of $(f/p)_{max}$ as a function of added mole-percent of CO_2. These data fit a straight line of equation $f_o = 66 + 440m$, f_o in cps/atm and m in mole-percent. (The 1% point omitted from calculation.) These figures are taken from Mr. E.J.Queen's Master's Dissertation.

Table I, Oxygen with CO_2 at room temperature.

m	0	0.233	0.507	0.970	1.920	mole-percent
f_o	69	168	282	520	905	cps/atm

The frequency of relaxation of pure oxygen at 23°C is thus about 66 cps/atm and the shift is about 440 cps/atm per mole-percent.

This figure of 66 cps is in approximate agreement with the Knötzels and others (H. & L.Knötzel, Ann. der Physik, 2, 393 (1948), but disagrees with Parker (loc. cit.) who gives 8.8±8.8. However, Parker assumed that oxygen at atmospheric pressure shows no relaxation absorption, and used the pure oxygen figures as a base line to subtract from the absorption in mixtures. This procedure should lead to a figure of zero for the pure oxygen relaxation frequency.

From this figure of 440 cps/atm per mole-percent it may be shown that the CO_2 molecule is about 630 times as effective in a collision with an O_2 molecule as is another O_2. This result may be compared with corresponding figures for N_2 and CO in O_2 (MCH loc. cit.): a shift of one cycle per percent of N_2 and 4 cycles per percent of CO. There is thus a slight difference between N_2 and CO in the direction reported long ago by Kneser and Knudsen (Ann. der Physik, 21, 682 (1934/35), but somewhat less than the factor of 13 they give.

For nitrogen to exhibit measurable relaxation absorption the temperature must be raised enough to make the vibrational specific heat appreciable. At 200°C N_2 has about the same C' as O_2 at room temperature, 0.046R, and the extra absorption becomes easily measurable. Data on the relaxation of nitrogen, pure and with hydrogen admixture, have already been published (MCH loc. cit.). Further data on the admixture with CO_2 have now been obtained, with the results shown in Table II.

Table II, Nitrogen with CO_2 at 203°C.

m	.25	.50	1.0	2.0	4.0	mole-percent
f_o	60	130	275	550	1100.	cps/atm

The line $f_o = (-6.6) + 277m$ fits these figures, giving a pure N_2 relaxation frequency less than zero. This means merely that there is sufficient error in the determinations to make the extrapolation meaningless. A figure of 1 cps/atm has been published (loc. cit.) but recent runs with the same apparatus show that even this low figure is too high and that the true figure is at least an order of magnitude lower. Recent work by R.C.Millikan (Phys. Rev. letters 8, 253 (1962) and private communication) shows that in carbon monoxide the fluorescence spectrum cannot be obtained unless the water vapor and CO_2 content are reduced below a part per million. His data lead to a vibrational relaxation time of 10 seconds. Since the nitrogen vibration levels are still higher, presumably the same considerations apply, and in consequence the relaxation time in the pure gas is so long that the effectiveness of the N_2-N_2 collision is essentially zero compared to other processes: e.g. walls, minute impurities, etc.

Preliminary work with CO (Matheson CP grade) showed, as expected, barely detectable absorption at room temperature (C' substantially zero) but at 100°C, C' = 0.017R and the effect is measurable. The relaxation frequency obtained, 73 cps/atm for the gas direct from the cylinder

(through drierite), is, in accordance with the preceding paragraph, far too high and more careful purification will be needed. However, runs with admixtures of H_2 and CO_2 produced the curious result that they are of equal effectiveness, molecule for molecule, each shifting the relaxation frequency by 225 cps/atm at 1.45% by volume.

A summary of some of the experimental results with various mixtures can be seen in the following table, covering a limited number of gases and contaminants. Since the amounts of the contaminants are very small (except for CO and N_2 in O_2), it is to be expected that even if the relaxation frequency for the pure gas is in error, the rate of change with per-cent of contaminant will not be affected. The data is expressed as $f_o = a_1 + a_2 m$, at one atmosphere, in cps and molepercent.

Table III

Base Gas	Added Gas	a_1	a_2	Notes	Reference.
CO_2	H_2O	30,000	700,000		F.A.Gutowski, J. Acoust. Soc. Am 28, 478 (1956)
O_2	H_2O	40	1,950	(13,200m^2)	H. & L. Knötzel, Ann. der Phys. 2, 393 (1948
N_2	H_2O	(.01)est	?		
CO	H_2O	(.03)est	(12,500)est		R.C. Millikan, priv. comun. MCH's est.
O_2	H_2	8.8	636		J.G.Parker, J. Chem. Phys. 34, 1763 (1961)
O_2	D_2	8.8	47		" "
O_2	He	8.8	47		" "
CO_2	H_2	32,000	110,000		MCH & J.Z.Klose, JASA 31, 29 (1959)
N_2	H_2	(0.0)	18	(203°C)	MCH, ibid. 34, 349 ('62)
CO	H_2	(73)	155	(100°C)	This paper
CO	CO_2	(73)	155	(100°C)	" "
O_2	CO_2	66	440		E.J.Queen, Dissertation. C.U.Am 1962
N_2	CO_2	(.01)	277	(203°C)	This paper
O_2	CO	90	4	(50°C)	MCH loc. cit.
O_2	NH_3	60	12,200		Knötzel & Knötzel, l.c.
O_2	N_2	90	1	(50°C)	MCH loc. cit.

This work is continuing, and it is hoped to present further data and an analysis of it at a later time.

Fig. 1

N_2 at 50.3°C.

$\int$ vs. N, the Harmonic Number

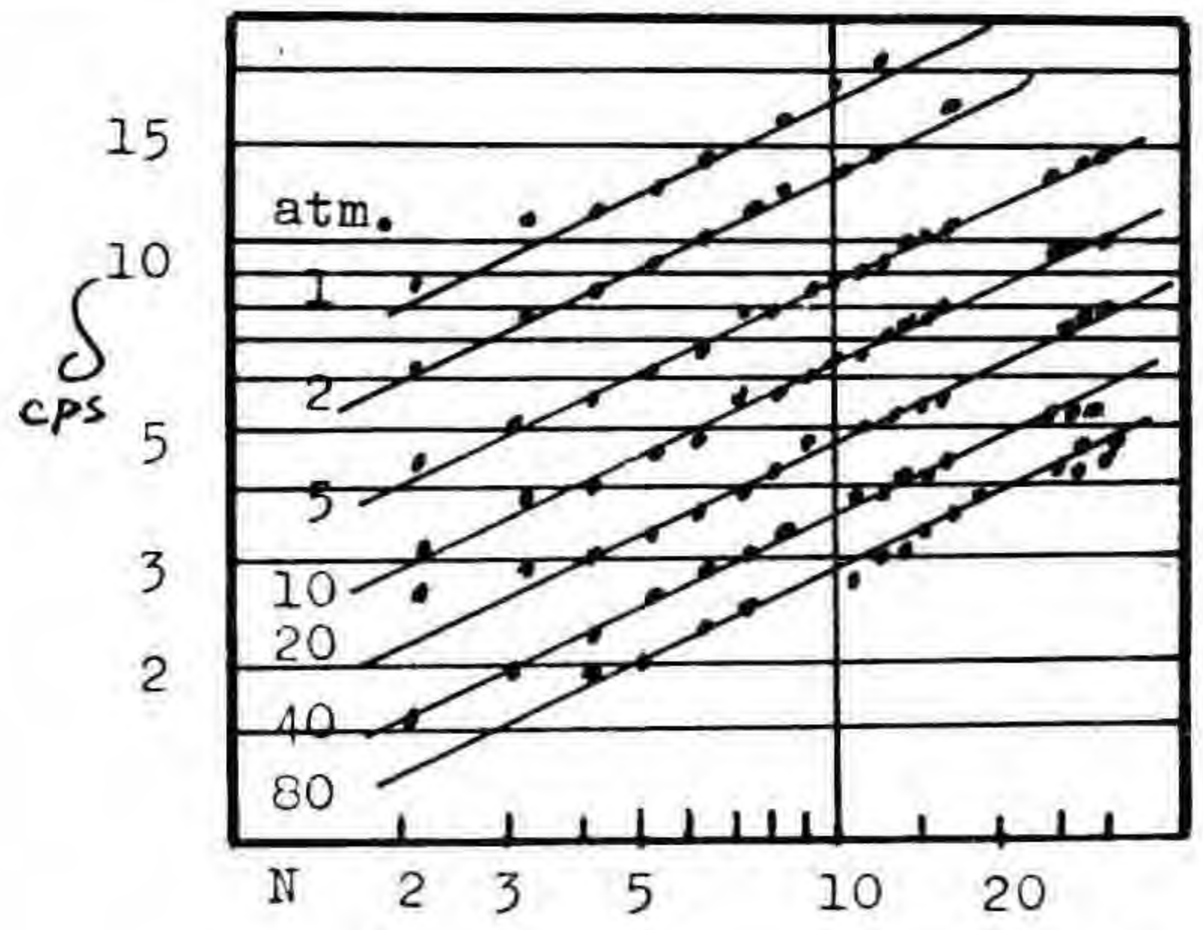

Fig. 2

O_2 at 50.6°C

$\int$ vs. N, the Harmonic Number

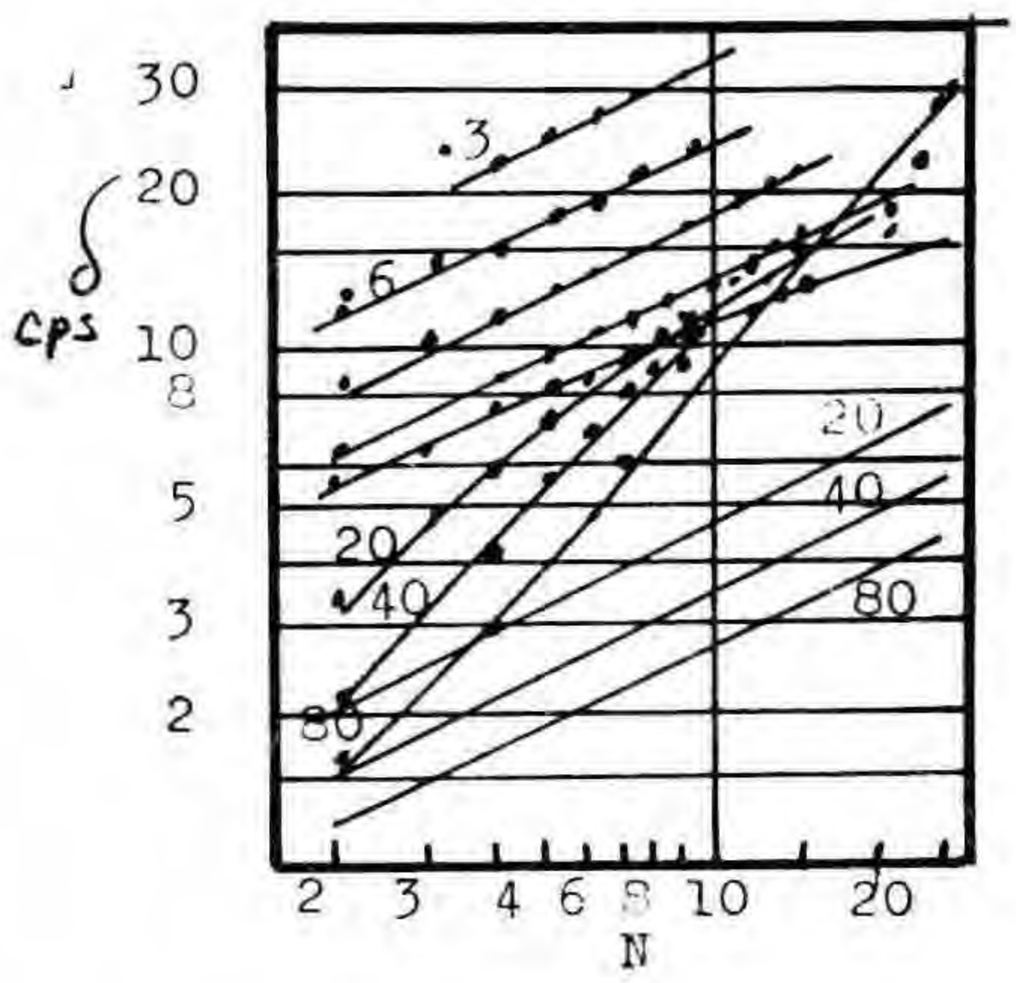

Fig. 3

O_2 at 50.6°C

$\alpha\lambda$ vs. f/p

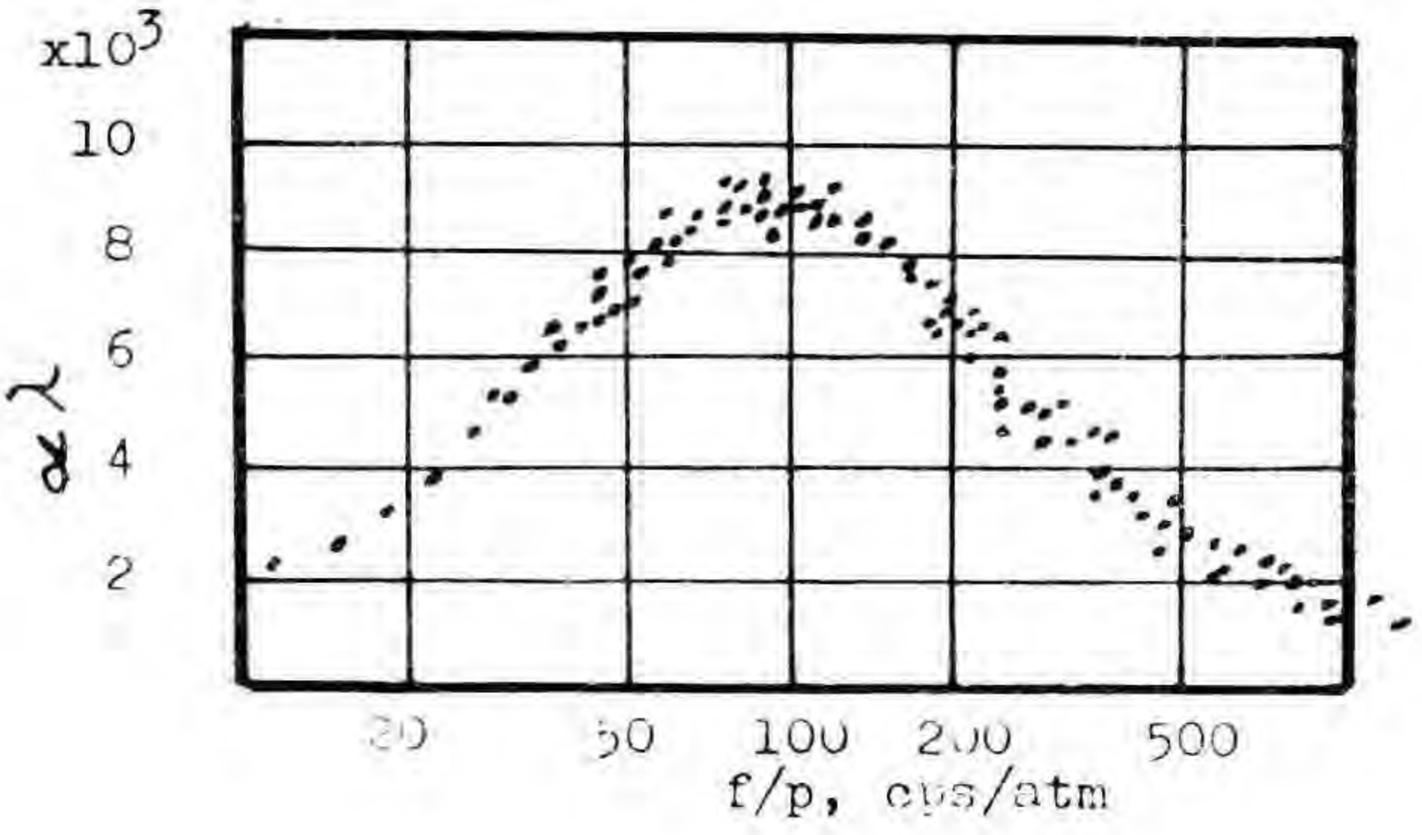

K25

FOURTH INTERNATIONAL CONGRESS ON ACOUSTICS
COPENHAGEN 21.-28. AUGUST 1962

FLUCTUATING ACOUSTIC REFRACTION IN DEEP OCEAN WATER*

Norman W. Lord

Columbia University, Hudson Laboratories

Long-distance transmission of acoustic energy which has been confined to the deep interior of an ocean medium is affected by spatial and temporal variation of the propagation velocity. I shall describe here a partially successful attempt at measuring those variations that occur with time at a point in the water medium hypothetically fixed with respect to the earth, i.e., the temporal variations. A meter[1] using short pulses of high frequency sound transmitted over a short folded path was used in situ over great depth ranges at three representative areas: In June, 1961 an oceanic station 1000 miles northeast of Barbados and another several miles southwest of Bermuda were each studied for several days using a single velocity meter at depths between 200 and 2500 m. In October, 1961 at a shallower place on the continental shelf 60 miles east of Boston in the Gulf of Maine two meters 61 m apart were used in a 12-hr test between 40 and 300 m.

At the oceanic stations, in the depth range 600-1700 m, where the velocity has a minimum around 1500/sec, the peak-to-peak amplitudes of velocity variations at various depth levels ranged up to 1 m/sec. The Gulf of Maine area had a total depth of 300 m and a flat velocity minimum of 1500 m/sec. Similar velocity variations occurred here.

At all stations, a 3000-ton vessel anchored to the ocean bottom, was the suspension point for the velocity meter on an armored cable (see Fig. 1). The meter regis-

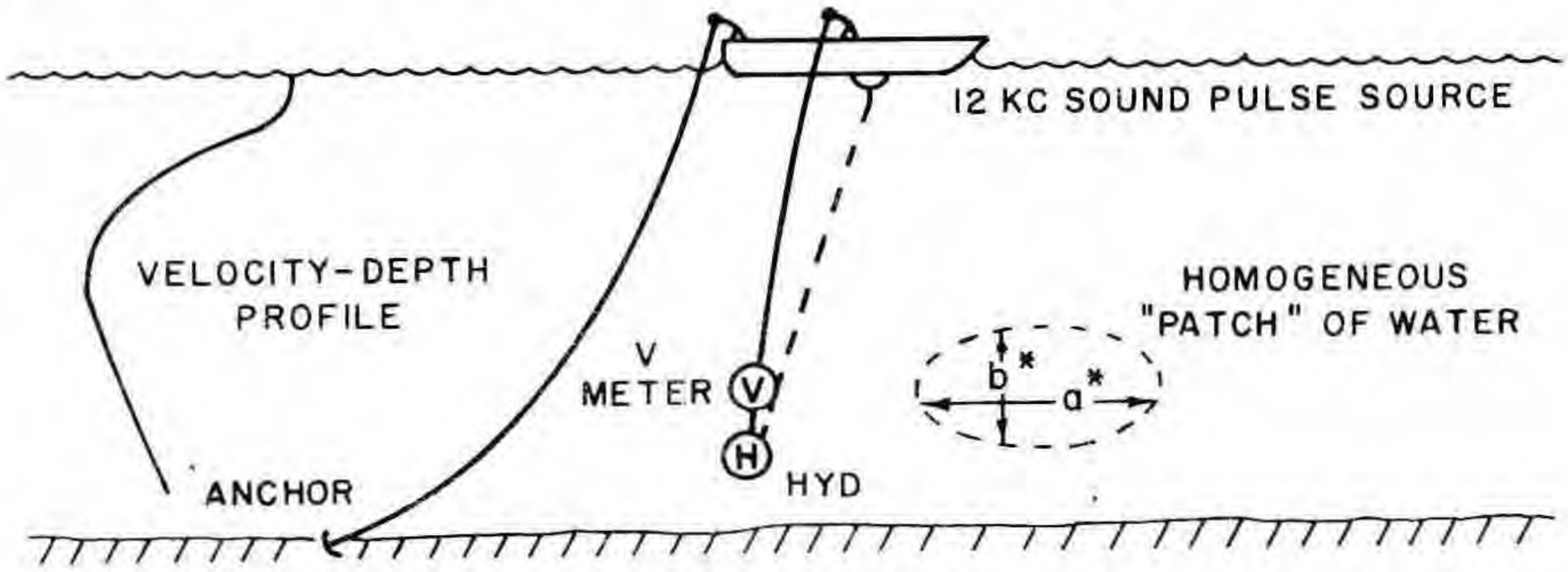

Fig. 1 Experimental arrangement; in Gulf of Maine a second velocimeter is added 61 m above the one shown and a pressure gauge replaces the hydrophone

tered sound velocity as a pulse repetition rate, or operating frequency. If they correspond to the definition advanced for temporal variation, the fluctuations in velocity registered on the meter occurred within a closely localized space and were due presumably to physical and chemical variation in the water flowing through it. However, other velocity changes, spurious to our definition, can be registered. They are considered in terms of their origins.

* This work was supported by the Office of Naval Research. It is Columbia University, Hudson Laboratories Informal Documentation No. 2.

[1] Carl E. Tschiegg and Earl E. Hays, "Transistorized velocimeter for measuring the speed of sound in the sea," J. Acoust. Soc. Am. 33, 1038-1039 (L) (1959).

I Meter movement: A depth change of 50 m can cause a 1 m/sec shift through pressure change alone. Also, movement in any direction where very rapid spatial variations of velocity exist can present an apparently temporal variation. However, these motions are severely limited in speed by the large drag forces on the cable. Any periodicities induced by movement would be much slower than the observed correlation time intervals (see below) indicated. At the two mid-oceanic positions direct sound pinging from the ship determined that the ship-to-velocimeter length was constant within 1 m. For depths greater than 300 m the cable drag limits meter falling speeds to 25 m/hr. In the Gulf of Maine the depth was monitored with a precision pressure gauge, and this indicated no changes greater than 2 m. Moreover amplitudes and periods of velocity variations here were large compared to the two oceanic sites. Swinging cable effects would be relatively much smaller.

II Unstable operating frequency of meter: The stable operation of the velocimeter itself was assured by testing and calibrating in pure isothermal water at temperatures of 5-50° C. The electronic pulse generation circuit was thermally isolated and separately controlled in temperature.[2] In a separate rigorous test using water stabilized at 75° C, the frequency was constant within the least count, 1:70,000, for several hours. At this temperature the sound velocity of distilled water is at a maximum. There would then be practically no spatial temperature gradients in the bath. Any velocity fluctuations registered by the meter would have had to come from its own operational instabilities.

III Frequency dependence of sound velocity: For long-distance transmission we are concerned with audio sound frequencies while the velocimeter uses 3 Mc as the fundamental of its pulse. It is possible for apparent fluctuations in 3 Mc sound velocity to be peculiar to high frequencies. As a partial check on the likelihood of this circumstance an experiment was performed by J. Shaffer[3] of this laboratory. He suspended at 131 m a 400-cycle resonant-pipe velocimeter[4] alongside the NBS meter. Temporal velocity variations were followed for $2\frac{1}{2}$ hr, and they appear in almost perfect concordance on the two meters. Still, at greater depths further comparisons are clearly needed.

From the above considerations it is fair to count at least 80 percent of the variation as real and pertinent to the physical problem.

At each location a similar procedure was followed. A velocimeter was lowered to different depth levels in steps and its frequency was measured every 20 sec. In the Gulf of Maine, however, two meters 61 m apart were lowered. The first station had 130 levels spread over a depth range of 0-2400 m; the second, 35 over 0-2200 m; and the third, 10 over 0-500 m. Over half the levels of the first two stations and all of the third were followed for periods of 15-40 min. It is this data which is considered here; the rest did not indicate any unsuspected divergences from the conclusions presented. To compile statistics that reflect the variations systematically the following analysis was carried out for each depth level.

Let $c(t)$ = Propagation velocity at time t and at a particular depth level
$\bar{c}(t)$ = Average of c for all data at one level
$\delta(t) = c - \bar{c}$ = Deviation in velocity from the average
$\mu = \langle \delta^2(t) \rangle^{\frac{1}{2}} / \bar{c}$ = Coefficient of variation of velocity $c(t)$

$$N(\tau) = \frac{\int_0^{T-\tau} \delta(t)\, \delta(t-\tau)\, dt}{\left[\int_0^{T-\tau} \delta^2(t)\, dt\right]^{\frac{1}{2}} \left[\int_0^{T-\tau} \delta^2(t-\tau)\, dt\right]^{\frac{1}{2}}} = \text{Approximately normalized correlation function of } \delta \text{ for interval, } \tau \text{ minutes}$$

---

[2] N. W. Lord, "Precise calibration of sea going velocimeters," J. Acoust. Soc. Am., (L), forthcoming.
[3] John D. Shaffer, Columbia University, Hudson Laboratories Technical Memorandum, forthcoming.
[4] John D. Shaffer, "Low frequency underwater sound velocity meter," Rev. Sci. Instr. 31, 1318-1320 (1960).

τ^* = First crossover time for $N(\tau)$ = correlation time interval.

The quantities μ and τ^* have been defined so as to provide together a rough, overall characterization of the fluctuation statistics for any set of data taken at one depth level. The usual set of data is not long enough for an adequate statistical treatment. The values of τ^* range from 1 to 10 min. Choosing the first crossover avoids using the $N(\tau)$ curve for larger τ. Close to $\tau = 0$ these curves were well behaved, and a comparison of the data at different depth levels and for different stations seems justified on the basis of μ and τ^* as defined. The values for each depth level are considered together with the data from other levels within a range of 400 m or so. It is apparent from the sequence of data at various levels that if μ, τ^* were redefined to pertain to a period of 30 min, there would be great temporal variation in their magnitudes. The two-velocimeter Gulf of Maine results show this clearly by considering the sequential probing of similar depth levels. Also very recent data taken by A. Berman of this laboratory show the same effects in records of several days' extent at one level for oceanic stations.

As expected, μ and τ^* have a wide range for each set of depth levels. The distribution of μ and τ^* values is shown in Fig. 2. As a check on the possibility

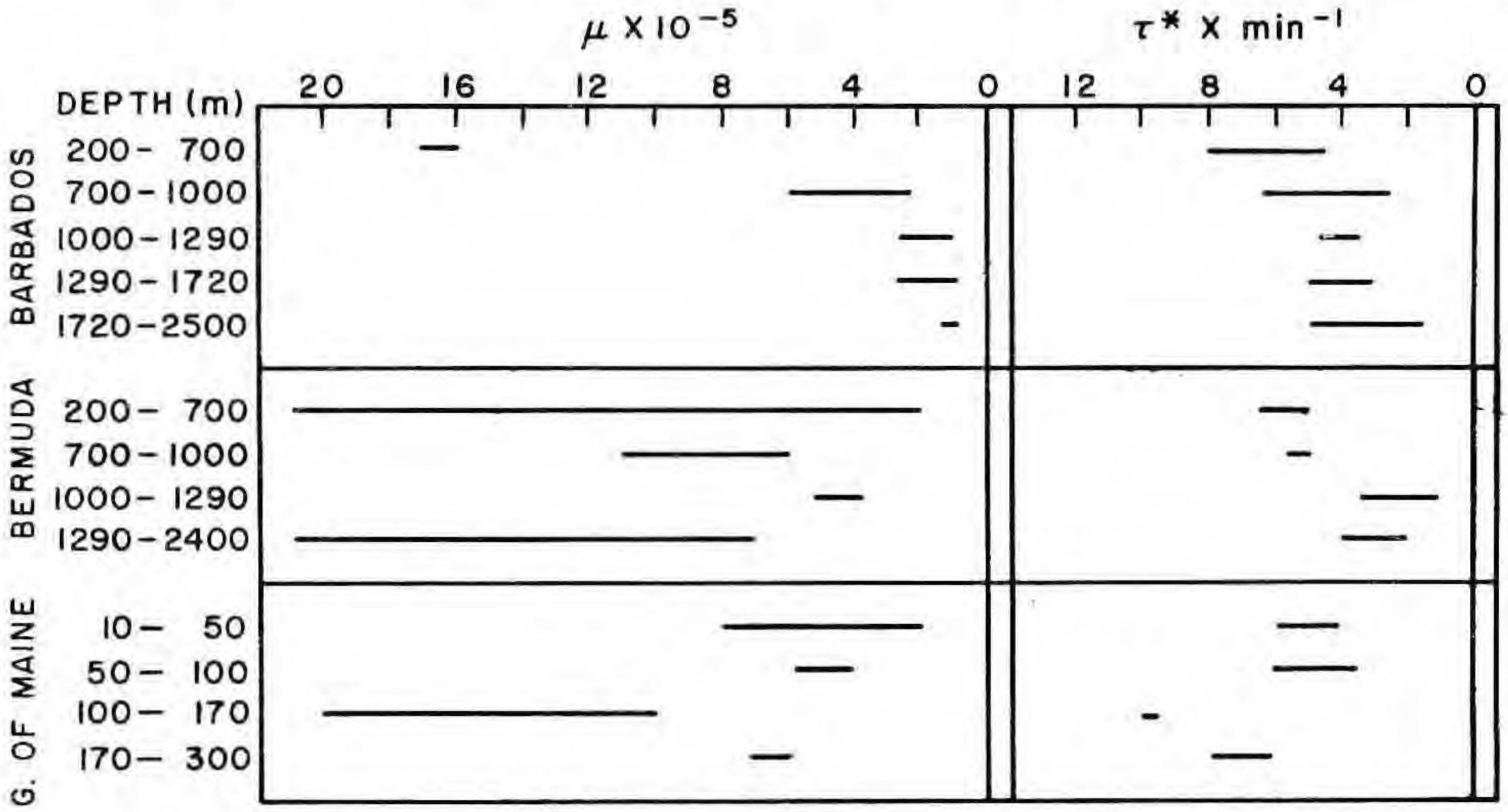

Fig. 2 Bars show ranges of μ and τ^* which contain approximately half of the values pertaining to the depth range

that varying run lengths would induce spurious trends in the data a parallel statistical analysis was carried out. Instead of the $\bar{c}(t)$ as defined above, a moving average calculated for a time interval [t-6 min, t + 6 min] was used in the formula for $\delta(t)$. Generally the values of μ were smaller while τ^* did not change. The overall trends, however, were maintained.

The sea environments at the three locations were somewhat different, and this is reflected in the data. Northeast of Barbados the bottom was 4600 m deep and fairly flat; winds were from the northeast and around 40 km/hr. Southwest of Bermuda the bottom was 2900 m deep and sloping upward sharply toward Bermuda; winds and surface currents were extremely variable. In the Gulf of Maine the bottom was flat and 300 m deep, winds were steady from the northwest, and the surface currents were variable and evidently different from strong deep currents.

At the Barbados station μ and τ^* values cluster toward very small μ and slightly smaller τ^* for the three depth regions below 1000 m. At Bermuda where the water currents are apparently more variable the μ, τ^* distribution of the shallow regions seems to persist to at least below 2000 m. The Gulf of Maine results

show an increase with depth in both μ and τ^*. The Barbados-Bermuda comparison points to water movement as the origin of the velocity fluctuations. Peak-to-peak variations in water properties of as little as 0.1°C or 0.2 °/oo S would make $3\mu \simeq 2.10^{-4}$. In the Gulf of Maine at the time of the experiment which was immediately after a storm, the very shallow water would be too thoroughly mixed to retain the variations in water temperature and salinity that may prevail at depths below 100 m. On the water current basis we can speculate a little more about the oceanic locations. Similarly to τ^* a horizontal correlation distance, a^*, can be defined in terms of the correlation of velocity variation along the direction x:

$$N(a) = \frac{\int_o^{L-a} \delta(x)\,\delta(x-a)\,dx}{\left(\int_o^{L-a} \delta^2(x)\,dx\right)^{\frac{1}{2}}\left(\int_o^{L-a} \delta^2(x-a)\,dx\right)^{\frac{1}{2}}}$$

If we consider the temporal variation of velocity to be generated by the movement of inhomogeneous water past a geodetically fixed point, we can estimate a^* from the values of τ^*. Present data on ocean currents including recent observations by A. Berman point to little variation in magnitude below 600 m from a value of 0.3 m/sec. For the smallest τ^*, about 1 min, a^* would be 20 m. We can also define a vertical correlation distance, b^*, and use the Gulf of Maine results to shed some light on it. A cross correlation of the two velocimeter readings was carried out for five pairs of depths 61 m apart, giving values for

$$N(12) = \frac{\int_o^{T} \delta 1(t)\,\delta 2(t)\,dt}{\left(\int_o^{T} \delta 1^2(t)\,dt\right)^{\frac{1}{2}}\left(\int_o^{T} \delta 2^2(t)\,dt\right)^{\frac{1}{2}}}$$

For the five pairs of depths $N(12)$ was both positive and negative and almost always below 0.3. Hence the value of b^* is almost certainly under 60 m. If we take the average τ^* for the Gulf of Maine as 4 min this gives $a^* = 80$ m. Intuitively one expects $b^* < a^*$ in a layered medium.

In addition to water currents it is also possible that the observed velocity variations are caused by internal waves. In the thermocline region, 200-1000 m, vertical movement of the water layers would present large temperature changes to our geodetically fixed point. At greater depths internal waves can vary only the pressure with amplitudes that are much too small to account for observed velocity variation. It seems especially tenuous to correlate the Gulf of Maine results with internal waves. Here the water is thoroughly mixed and the density almost constant from top to bottom. For the Bermuda and Barbados areas an internal wave origin reinforces the argument about a^*, since internal waves can be expected to have wavelengths over 50 m.[5] In any case a correlation distance, greater than 20 m, seems pertinent for deep water and should replace Liebermann's frequently used value of 0.6 m that had been obtained at a shallow depth. The character of acoustic transmission over very long ranges is greatly affected by such a change.

---

[5] C. W. Ufford, "Internal waves measured at three stations," Am. Geophys. Union. Trans., 28, 87 (1947).

L25

FOURTH INTERNATIONAL CONGRESS ON ACOUSTICS
COPENHAGEN 21.-28. AUGUST 1962

CHARACTERISTICS OF THE SATURN SPACE BOOSTER AS A NOISE SOURCE

WADE D. DORLAND

INTRODUCTION:

With the advent of large thrust rocket systems for space exploration, it became necessary to analyze the problems caused by noise from tests and launches of the vehicles. Accordingly, several theoretical studies of the environments were made, and measurement projects are currently under way. Because the SATURN booster is the first of the vehicles producing over 1,000,000 pounds of thrust, empiricle information on its noise fields were considered basic in the approaches to handling environmental problems anticipated with other vehicles, which may have thrusts up to 20,000,000 pounds.

The purpose of this report is to summarize the results and describe the characteristics of SATURN noise.

PROCEDURE AND EVALUATION OF MEASUREMENTS:

The sound was measured by placing microphones on the ground around the tower used for restrained tests of the vehicle (termed "static test") and the pad where the vehicle is launched. The microphone signals were recorded on instrumentation tape recorders, and then replayed through various analyzing systems, thus producing the distribution of the sound pressures with frequency. This data was further processed to show the characteristics of the noise in terms of the energy produced, the directivity of the energy propagation, and the frequency distribution of the energy.

Because these results were not obtained from experiments where acoustic evaluations are an important consideration, the results cannot be completely generalized. One limitation in the evaluation results from the method of restrained firing, where the rocket exhausts down onto a jet deflector which turns the flow through an angle of 120 degrees. Thus the exhaust jet is dissipated into the air at an angle of 30 degrees above the horizontal.

For many reasons including measurement limitations, propagation of the sound in a horizontal plane parallel to the ground is of greatest interest; therefore, the results are given in terms of the horizontal plane. However, these characteristics may be peculiar to the given rocket system and deflector used and should not be considered to be a free field description of the noise source. Despite this limitation, all other planned rocket vehicles in this thrust class will produce noise under similar conditions, so the results of this survey can be used in estimates of noise environments of test and launch facilities of other boosters.

The noise produced during static tests is very stable and can be evaluated very easily with averaging times up to 40 seconds, but noise from launching is more difficult to handle because the noise source is usually moving in space thus causing a further limitation on the results. Even so, the SATURN launch sequence has an initial restrained phase which may last up to 3 seconds. Noise measured during this phase, termed the "On Pad" conditions, may be compared to restrained test results if it is kept in mind that the deflector used on the launch pad is a wedge shaped device which splits the jet stream and turns the jets through 90° allowing the exhaust to flow parallel with the ground in opposite directions. The noise after the vehicle lifts off changes as the vehicle moves away, so very short averaging times are used to determine the sound pressure levels. These results, termed "flight" conditions, can be corrected for the changing ranges and angular relationships to give an approximation of noise from the undeflected jet stream as a sound source under the nearest approximation to free field conditions available.

Because the basic measurements were made at radius of 600 feet from the test tower or launch pad, and due to the wide frequency range of the data, some doubt may arise over the presumption that SATURN noise is attenuated in accordance with the inverse square law of radiation. However, the recorded data show a reasonable balance between too much attenuation for some frequencies and too little for others. Therefore, it is considered that such a presumption is valid, within feasibility, and in accordance with established practice for making far-field noise surveys.

TABLE 1 - COMPARISON OF SATURN NOISE SOURCE PARAMETERS

PARAMETER	STATIC TEST	ON PAD	LAUNCH[1]
OVERALL POWER LEVEL	205.5	203	205
MEASURED ACOUSTIC POWER IN MEGAWATTS	25 to 40	18 to 22	28 to 40
ACOUSTIC EFFICIENCY IN PERCENT	0.5	0.3	0.5
NOMINAL THRUST IN KILOPOUNDS	1300	1300	1300

NOTES:
1. Averaged over first 25 seconds of flight.
2. In decibels where db = 10 log (acoustic power/10^{-13} watts) and based on 9 to 11 pressure measurements at 600 foot radius.

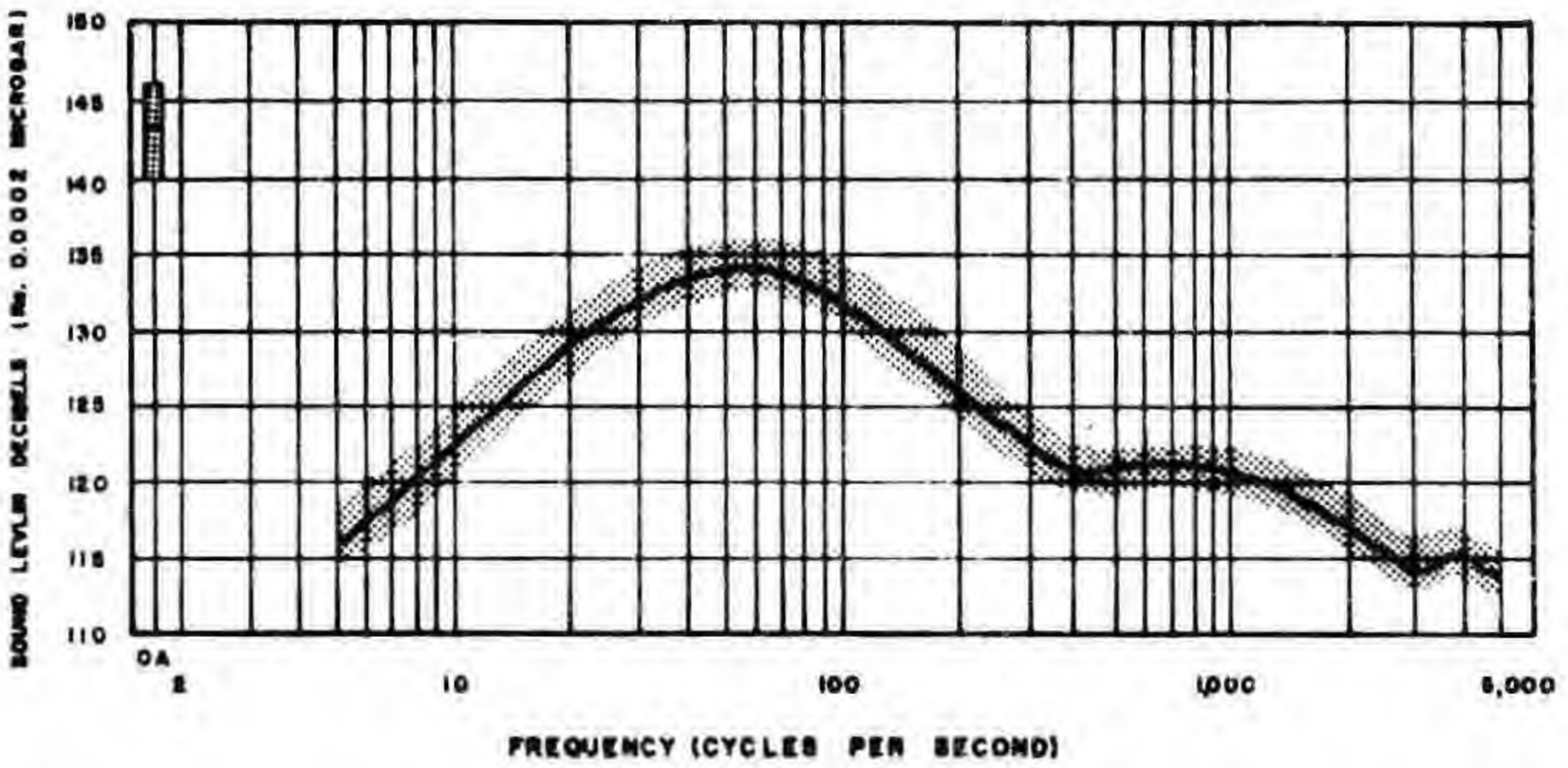

FIG. 1. AVERAGE AND RANGE OF DATA FROM TYPICAL MEASUREMENT LOCATION

DESCRIPTION OF SATURN NOISE:

Initially, the sound measurements were analyzed to show the frequency distribution of the root-mean-square sound pressure levels. A typical spectrum shape in terms of the range and average of data for several static tests is presented in FIGURE 1. Further processing of the data from measurements at different ranges and angular coordinates allow evaluation of the more general parameters such as spectrum levels, directivity patterns, and conversion efficiency of the kinetic jet stream energy of acoustic energy, i.e., acoustic efficiency. In TABLE 1 the overall noise characteristics are listed.

The overall directivity patterns, which depend primarily on the directivity of the radiation in frequencies below 100 cps, are presented in FIGURE 2, and the generalized spectrum level characteristics are presented in FIGURE 3.

It is of interest to note that the overall noise energy generated and the spectral distribution of this energy is quite similar for all three jet conditions, which are: (1) for static tests using a cooled unilateral deflector turning the jet through 120°;

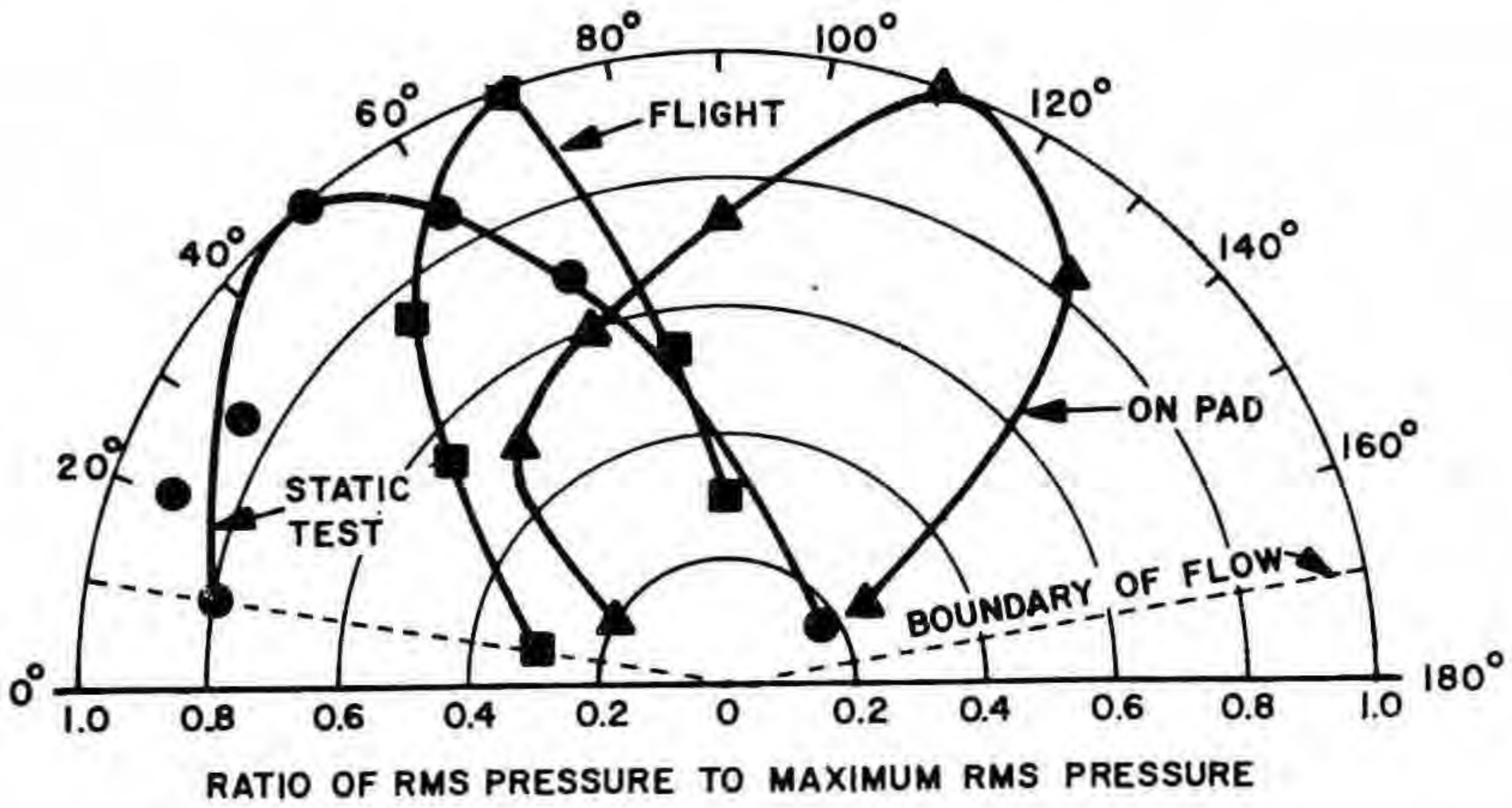

FIGURE 2. SATURN OVERALL DIRECTIVITY PATTERNS

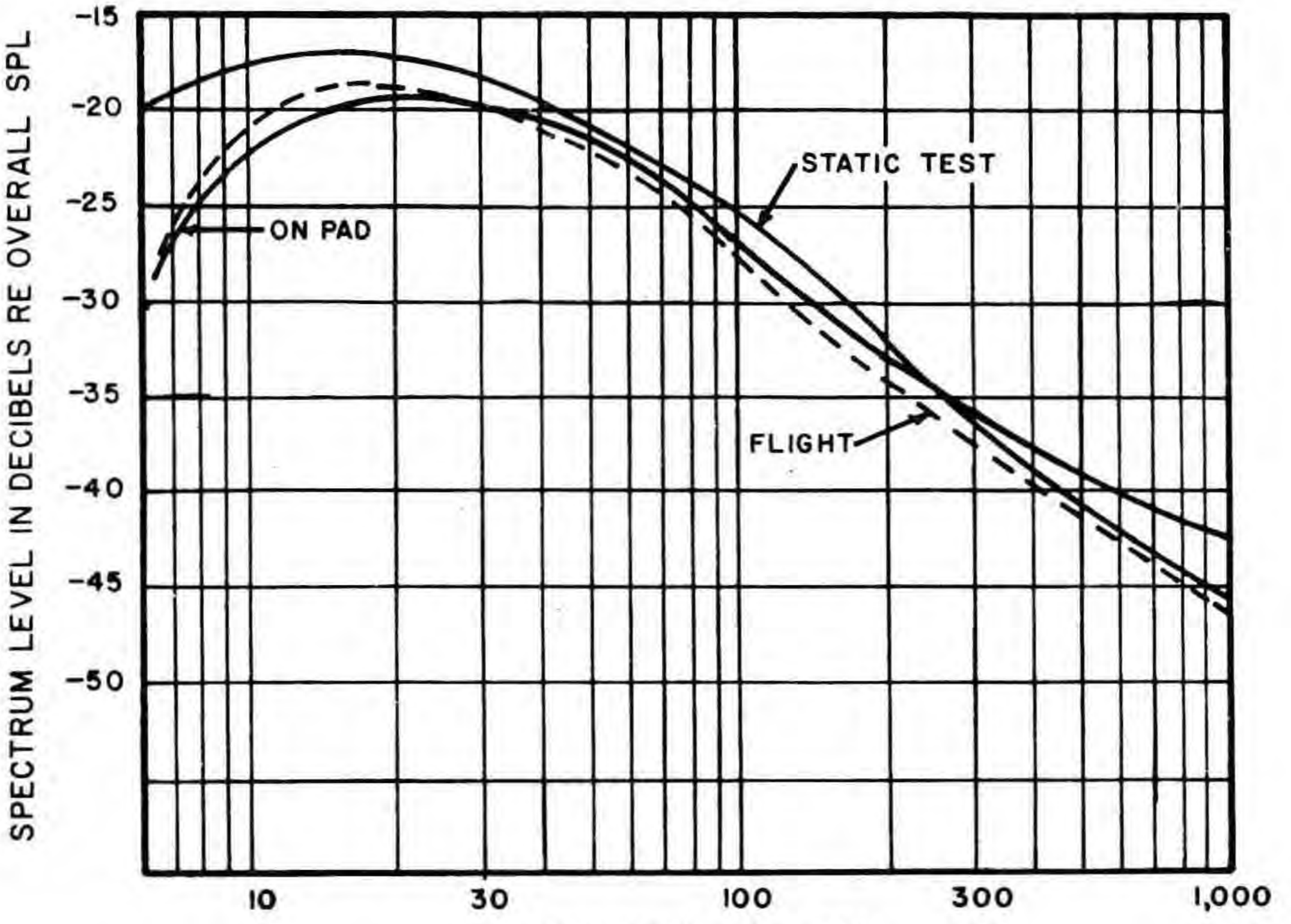

FIGURE 3. SATURN FREQUENCY SPECTRUM CHARACTERISTICS

(2) for the bilateral wedge deflector splitting the jet into two streams, each turned through 90° used on the launch pad; and (3) for the free flowing jet stream in flight. However, the directivity patterns for each of these measurement conditions are quite different and indicate that the radiation of the sound is directly dependent on the deflector configuration.

CONCLUSIONS:

The results of noise measurement during the SATURN vehicle development produced valuable data for reducing uncertainties in present estimation procedures for noise environments. Use of these procedures permits an estimate of power levels of large rocket engines and their spectra with an accuracy adequate for many engineering purposes. Only the effect of the deflector on directivity patterns produces a large uncertainty in estimates, and the range of uncertainty will probably be reduced as other deflector configurations are tested and evaluated while the large boosters are being developed.

M25

FOURTH INTERNATIONAL CONGRESS ON ACOUSTICS
COPENHAGEN 21.-28. AUGUST 1962

Absorptionsmessungen für Eichung eines kleinen Hallraumes.

Marta Karsai und Thomas Tarnóczy,
Akustische Forschungsgruppe, Budapest, Ungarn.

Der neue Normungsvorschlag von ISO hat den kleinsten, für Schluckmaterialienmessung nötigen Hallraum in 18o m^3 festgestellt (1). Wir möchten nun beweisen, dass es auch in einem geeignet aufgebauten kleinen Hallraum möglich ist zuverlässige Messungen durchzuführen.

Die Einzelheiten der Konstruktion des Hallraumes hat man bereits bekanntgegeben (2). Hier seien nur die wichtigsten Angaben wiederholt. Unsere Hallkammer wurde nach dem "Haus-im Haus" Methode mit einen Luftspalt von 4 cm errichtet. Alle Grenzflächen des inneren Hallraumes bestehen aus 2 mm starken Eisenplatten. Der Raum hat ein Volumen von 10 m^3 und eine innere Oberfläche von 3o,5 m^2.

Der Gegenstand der Messungen ist daher das Material Sillan SP 100, Dimension: 5o x 1oo x 5 cm. Aehnlich wie bei der internationalen Rundmessung, haben auch wir in verschiedenen Anordnungen gemessen. Die Messungen wurden in zwei Phasen durchgeführt. In der ersten Phase hatte man als Diffusoren vier massive, lackierte Holzkugeln, mit Durchmesser von 3o cm, in verschiedenen Höhen des Raumes aufgehängt. Die Anordnungen wurden auf Grund folgender drei Gesichtspunkte variiert:

1) Anordnung der Platten,
2) Oberflächengrösse der Platten,
3) Flächenverhältnis der freibleibenden Ränder.

Das Material wurde in drei Variationen angeordnet: auf dem Boden, auf einer einzigen Wand und auf drei Wänden. Laut Grösse der Oberflächen hat man mit einer "nominellen" Oberfläche von 1,5, 2,o, bzw. 3,o m^2 gearbeitet. Unter "nominellen" Oberfläche verstehen wir die obere Fläche der Platten. Bei der Auswertung der Messungsergebnisse wurde jedoch auch die Oberfläche der freibleibenden Ränder hinzugerechnet, man hat also mit der "effektiven" Oberfläche gerechnet. Um das Verhältnis der freien Ränder zu der Gesamtoberfläche zu variieren, wurden die Platten dicht neben einander und dann auch die einzelnen Platten voneinander entfernt gemessen.

Die Berechnungen wurden zuerst bezüglich der nominellen Oberfläche mit der durch die ISO Norm gegebene Formel durchgeführt und nach-

her mit Rücksicht auf die effektive Oberfläche korrigiert. Diese letztere Rechnungsmethode erwies sich als zuverlässiger, was ja auch zu erwarten war, wenn man berücksichtigt, dass bei einer F_o-Fläche von 3o,5 m^2 sehr wesentlich ist, ob man mit einer nominellen Oberfläche von 3 m^2, oder einer effektiven Oberfläche von 3,67 m^2 rechnet. Die Anordnung der Materialplatten beeinflusst ebenfalls wesentlich das Resultat. So z.B. ergaben sich nach Abb.1. ähnliche Kurven einerseits wenn die Platten mit einer nominellen Oberfläche von 1,5 oder 2 m^2 auf derselben Wandfläche von einander entfernt angeordnet waren, und andererseits mit Platten von einer nominellen Oberfläche von 3 m^2, falls diese auf drei Flächen zerstreut angebracht waren. Die Kurve gestaltet sich dagegen verschieden, falls man das 3 m^2 Material auf einer Fläche unterbringt. Ein auffallend niedriger Wert wurde nur in einem Falle gemessen, undzwar als 1,5 m^2 Oberfläche, also drei Platten, in einer Ecke des Hallraumes, auf drei Flächen und ganz nahe zueinander untergebracht war. Der Eckeneffekt ist also sehr stark.

An den Absorptionskurven findet man auch, dass bei 4000 Hz der Absorptionsgrad sehr niedrig ist. Davon konnte man die Folgerung ziehen, dass der Hallraum an höheren Frequenzen nicht genügend diffus war. Darum wurden in der zweiten Phase der Messungen kleinere Aenderungen durchgeführt.

Um den Randeffekt zu vermeiden, hatte man die Sillanplatten in Metallrahmen unterbracht. Die Ergebnisse haben die Erwartung erfüllt.

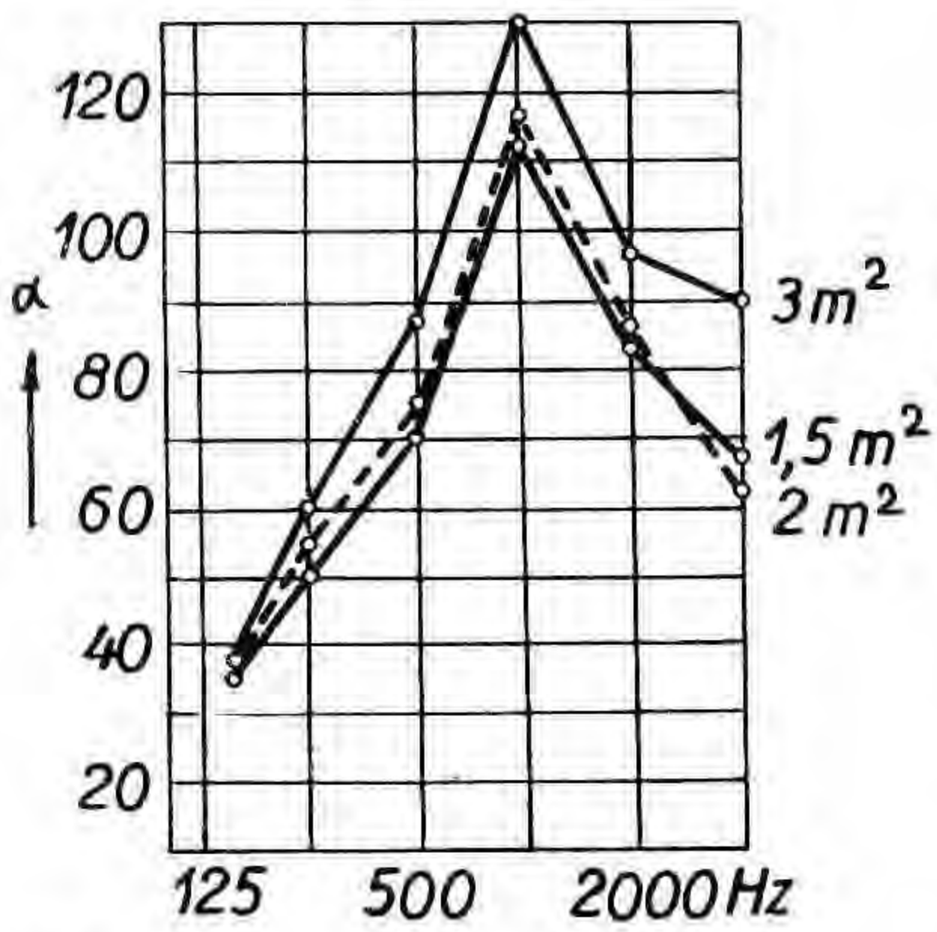

Abb.1. Absorptionswerte im halbdiffusem Raum von 10 m^3 gemessen, mit verschiedenen Materialoberflächen.

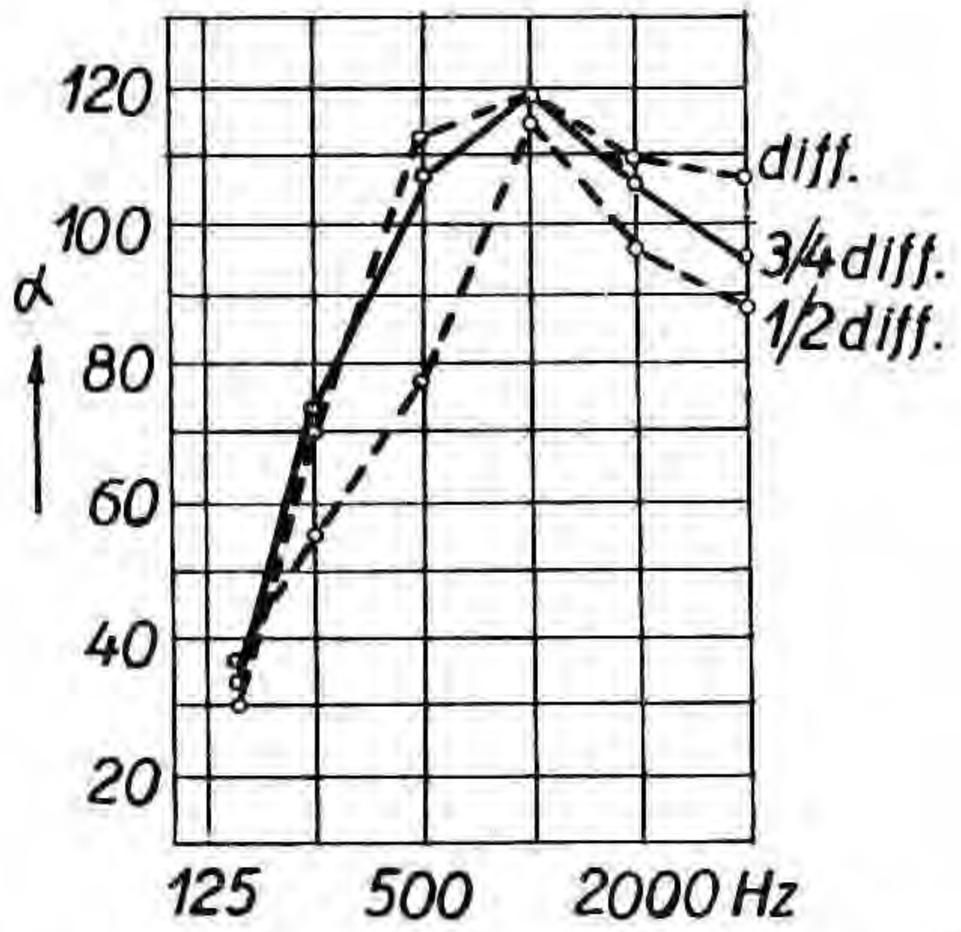

Abb.2. Absorptionswerte im 10 m^3 Raum, mit die Diffusität als Parameter.

Die Absorptionskurven der auf eine oder drei Flächen, nebeneinander oder zerstreut aufgelegten Platten zeigen viel kleinere Diskrepanz. Der Eckeneffekt blieb unverändert. Ebenfalls - wenn sich auch eine kleine Besserung zeigte - blieb das Problem der Diffusität bei 4000 Hz ungelöst. Deswegen haben wir weitere Diffusoren im Hallraum angebracht, u.zw. sieben Kegel, deren Durchmesser 20 cm und Höhe 16,5 cm ist. Von den Messergebnissen ist es ersichtlich, dass die Diffusität wesentlich grösser geworden ist (Abb.2.).

Nun wollen wir sehen, wie die Ergebnisse eigener Messungen zu denjenigen der in der Internationalen Kooperation seinerzeit beteiligten Laboratorien passen. Die Methode der Bestimmung des Absorptionskoeffizienten von akustischen Materialien durch stationären Wellen ist allgemein bekannt. Diese sehr einfache und reproduzierbare Messung hat jedoch den Nachteil, dass infolge der geringen Materialoberfläche nur die senkrechte Inzidenz betrachtet wird, weshalb die auf diese Weise gemessenen Absorptionskoeffizienten wesentlich kleiner sind, als die laut der Raummethode gemessenen Werte. Hier liegt teilweise auch der Grund dafür, dass ein Grossteil der Akustiker gegen die Anwendung von kleindimensionierten Hallräumen Stellung nimmt. Es unterliegt ja keinem Zweifel, dass ein diffuses Schallfeld mittels unregelmässig angeordneter Diffusoren in einem grossen Raum leichter herstellbar ist. Studiere man jedoch einige Beispiele von den Ergebnissen der grösseren Laboratorien. Im 251,5 m^3 grossen akustischen Laboratorium von Ottawa

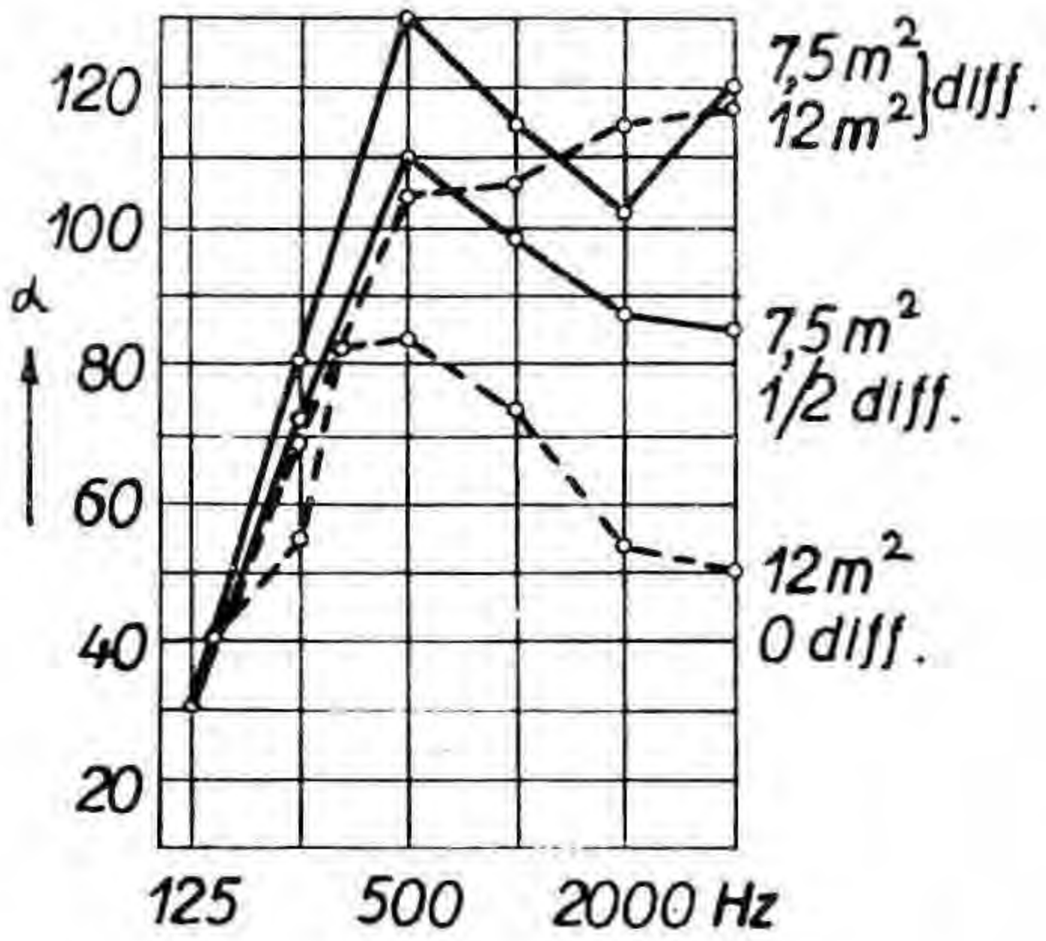

Abb.3. Absorptionswerte im Laboratorium von Ottawa, 251,5 m^3

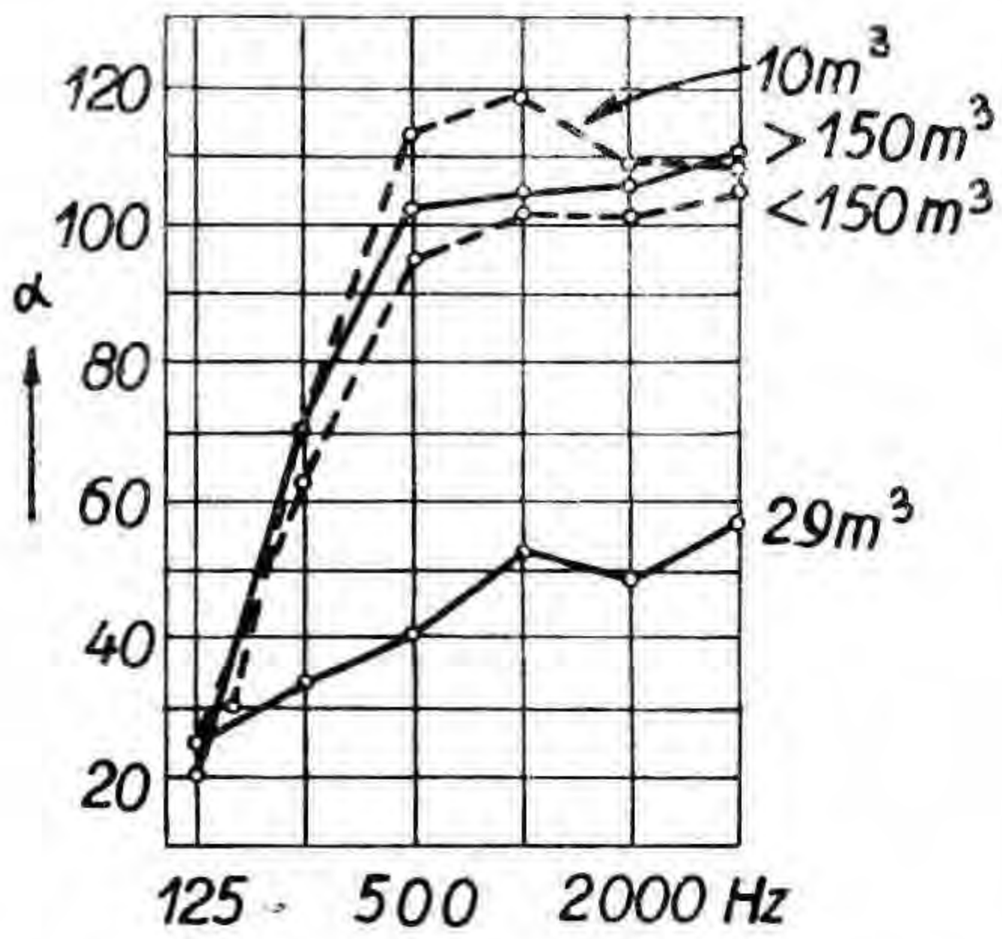

Abb.4. Vergleichungskurven von Mittelwerte, gemessen in Hallräumen mit verschiedenem Rauminhalt.

ergeben sich Abweichungen von mehr als 25 % zwischen den Ergebnissen der nach verschiedenen Anordnungen durchgeführten Messungen (Abb.3.). Man hat diesen Beispiel nur aufs Geratewohl hervorgehoben, da die Resultate der übrigen beteiligten Laboratorien auch dasselbe Bild zeigen.

Wenn nun unsere eigene Messergebnisse mit der von Resultaten der internationalen Messkooperation resultierenden Gesamtkurve verglichen werden (Abb.4.), ersieht man Folgendes: Die obere Kurve zeigt den Mittelwert der Messergebnisse von acht Laboratorien über 150 m^3, die zweite Kurve den Mittelwert der unsererseits ermittelten Messergebnisse. Wenn unsere Messergebnisse zwischen den Kurven sämtlicher Laboratorien aufgezeichnet werden, so würden sich diese unter deren Streuungen vollständig verlieren. Wir müssen noch bemerken, dass unsere Messwerte sich am stärksten eben von denen des 29 m^3 grossen Laboratoriums von Palaisseau abweichen, wo sich ausserordentlich kleine Absorptionswerte ergaben.

Zum Schluss möchte man hier noch auf folgende Beobachtung hinweisen: Laut der seitens des Fachausschusses ISO/TC 43 angegebenen Grenzfrequenz-Formel wäre in einem Hallraum von 10 m^3 $f_o^{\cdot}$ = 327,5 Hz die niedrigste Frequenz, bei welcher noch präzise Messungen durchgeführt werden können. In dem unsererseits entworfenen Hallraum konnte man dagegen, laut Beweis der Nachhallkurven, eine Oktave tiefer, also auch bei 160 Hz mit gut auswertbaren Nachhallkurven arbeiten.

Zusammenfassend kann man daher feststellen, dass in geeignet ausgebildeten, kleindimensionierten Hallräumen Messungen durchgeführt werden können, deren Ergebnisse mit den Schallabsorptionsmessungen der grossen Laboratorien vergleichbar sind. Die wirtschaftliche Bedeutung einer solchen Feststellung ist ebenfalls merkenswürdig, mit Rücksicht sowohl auf die Baukosten des Laboratoriums, als auch auf das Quantum des verbrauchten Materials.

Literatur.

1. Draft ISO recommendation No. 477, 1961.
2. T. Tarnóczy: Proc. III. ICA-Congress, Stuttgart 1959, Elsevier, Amsterdam 1961. 868.
3. C.W. Kosten: Acustica 10. 400. (1960).

N25

FOURTH INTERNATIONAL CONGRESS ON ACOUSTICS
COPENHAGEN 21.-28. AUGUST 1962

An Energy Detection Model for Monaural Auditory Detection

E. E. David, Jr., M. V. Mathews, and Sheila M. Pfafflin, Bell
Telephone Laboratories, Incorporated, Murray Hill, New Jersey

It has recently been reported by various experimenters that signal detection performance improves markedly when a "Pedestal" is added to the stimulus. In a typical experiment, the subject is presented with two sinusoids partially masked by noise and asked which is larger. The signal energy is defined as the energy of the difference signal, and the pedestal is the amplitude of the smaller sinusoid. With zero pedestal, the curve relating the proportion of correct responses to the ratio of the signal energy to the noise spectral density rises more steeply than a correlation detector would predict. By "correlation detector" we refer to a detector in which the test statistic is the integral of the product of the stimulus and the signal. It has been referred to by some as an "ideal observer," and is the type of detector which has been commonly assumed as a model in signal detection experiments. As the pedestal is increased, the probability of being correct increases and the curve approaches the slope predicted by the correlation detector.

We should like to show that a well-known detection process, which we shall call an energy detector, gives good agreement to this type of data, both as to the effects of the pedestal and the shape of the curves.

The energy detector consists of a band-pass filter centered about the signal frequency, a rectifier or square law device which measures the instantaneous energy from the filter, and an integrator which integrates this energy over some time interval to produce a statistic φ. For a two-interval experiment, the assumption is made that a value of Φ for each interval is obtained and the response corresponds to the largest Φ.

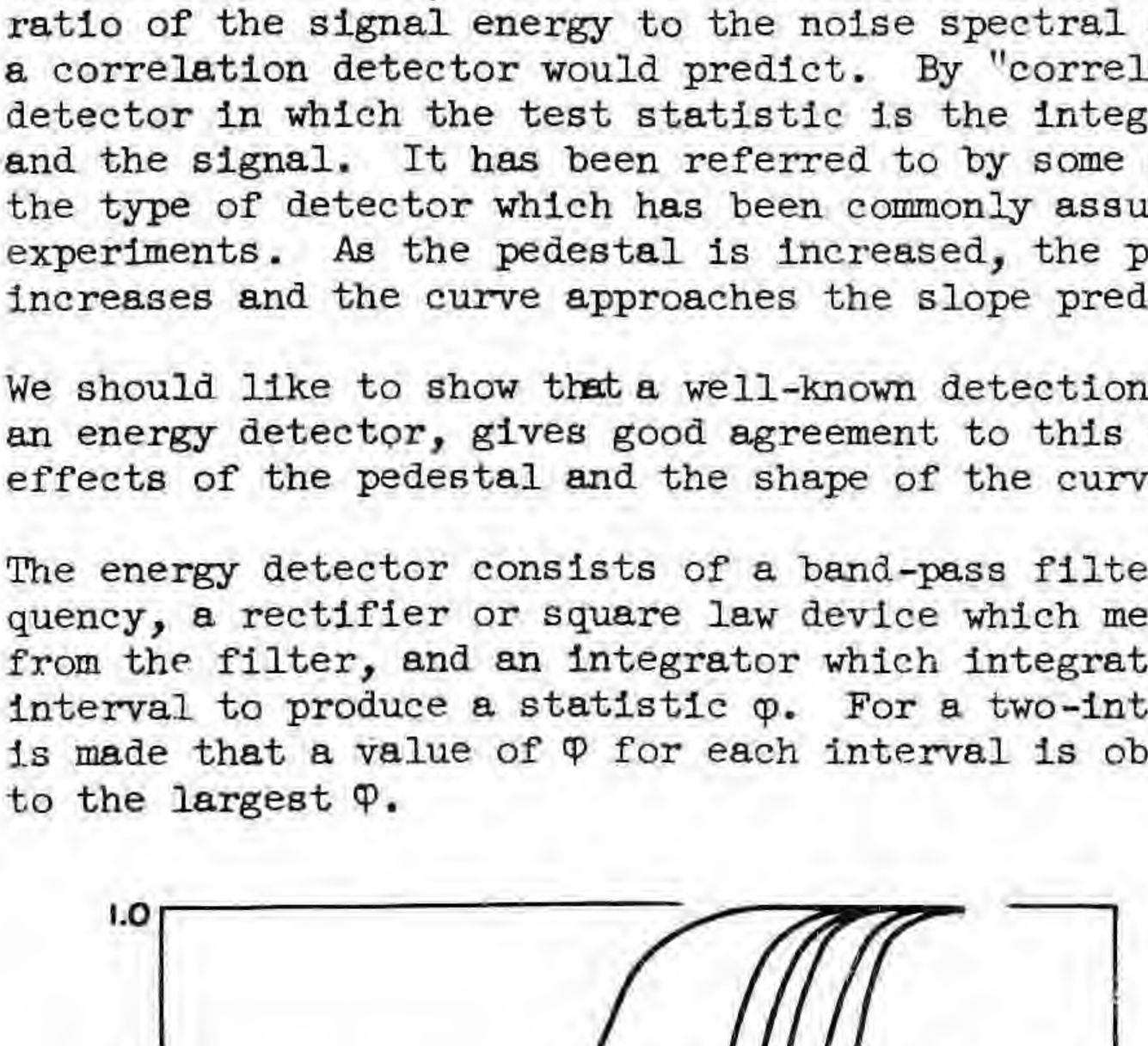

Fig. 1. Probability of correct response, P(c), for an energy detector as a function of E/No, the signal energy divided by the noise spectral density, for various bandwidths of the filter, in the absence of pedestal. Stimulus duration is 100 msec. Performance of a correlation detector is shown for comparison.

Detector performance has been calculated for a 1000 cps signal at various intensities of signal and pedestal for several bandwidths of the filter. Typical curves of the probability of a correct response as a function of signal-to-noise ratio for various bandwidths of the filter and zero pedestal are shown in Fig. 1. All the curves rise more steeply than that of the correlation detector. The main effect of increasing bandwidth is to move the curves to the right.

Its performance for two bandwidths, one narrow and one broad, is shown as a function of the signal-to-noise ratio, with pedestal as a parameter, in Fig. 2. The curves closely approach that of a correlation detector for large pedestals.

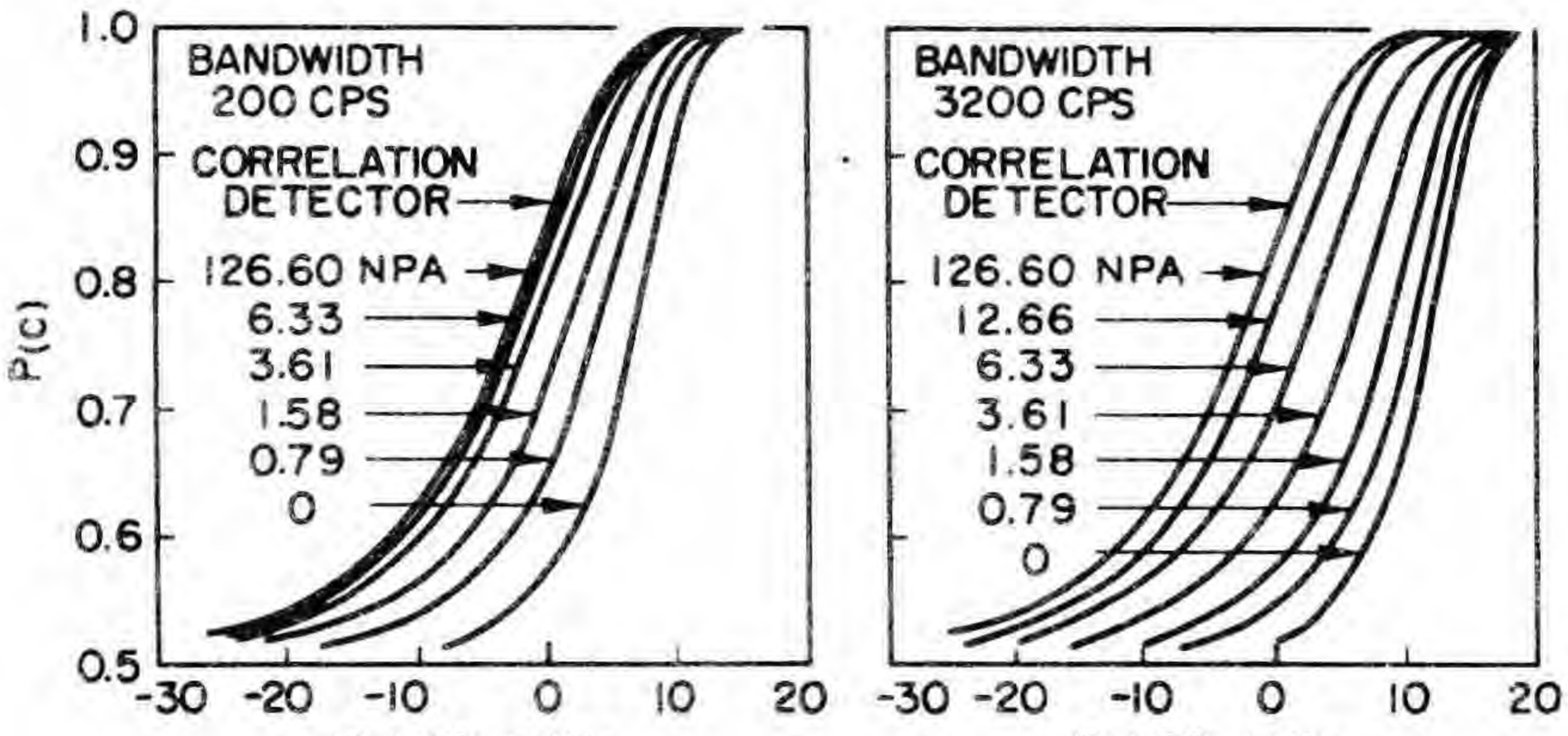

Fig. 2. Probability of correct response, P(c), for an energy detector as a function of normalized pedestal amplitude (NPA) for narrow and wide bandwidth. E/No is the signal energy divided by the noise spectral density.
Stimulus duration is 100 ms. Normalized pedestal amplitude equals pedestal amplitude/$(No/T)^{1/2}$. Performance of a correlation detector is shown for comparison.

One other effect is predicted by the energy detector model. If the pedestal is 90 degrees out of phase with the signal, then no improvement in performance should result from it. This prediction was tested in a two-interval forced choice signal detection experiment. The two stimulus intervals were 100 msec. long, contained random noise, the pedestal, and, in one, randomly selected, the signal. Both pedestal and signal were 1000 cps sinusoids. The subjects, four high school girls, listened binaurally with TDH 39 earphones and attempted to select the interval which had contained the signal. The background noise level was 76 db, and the ratio of the signal energy to the noise spectral density was 12 db.

The results of this experiment are shown in Fig. 3 where the proportion of responses correct is plotted as a function of pedestal intensity. When the pedestal is added in phase with the signal, the detectability of the signal is improved. When the pedestal is added 90 degrees out of phase with the signal, however, there is no improvement in signal detectability. The accuracy with which the model predicts the magnitude of the changes in detectability with changes in in-phase pedestal levels can be determined by comparing the solid curves, which indicate the performance of the model, with the data. Three of the subjects appear to fit well, the fourth, who had less training, shows poorer detectability than predicted. These curves were generated assuming a 200 cps bandwidth for the filter, and are shifted 10 db to the right to account for degradation in performance from other sources than the noise from the filter.

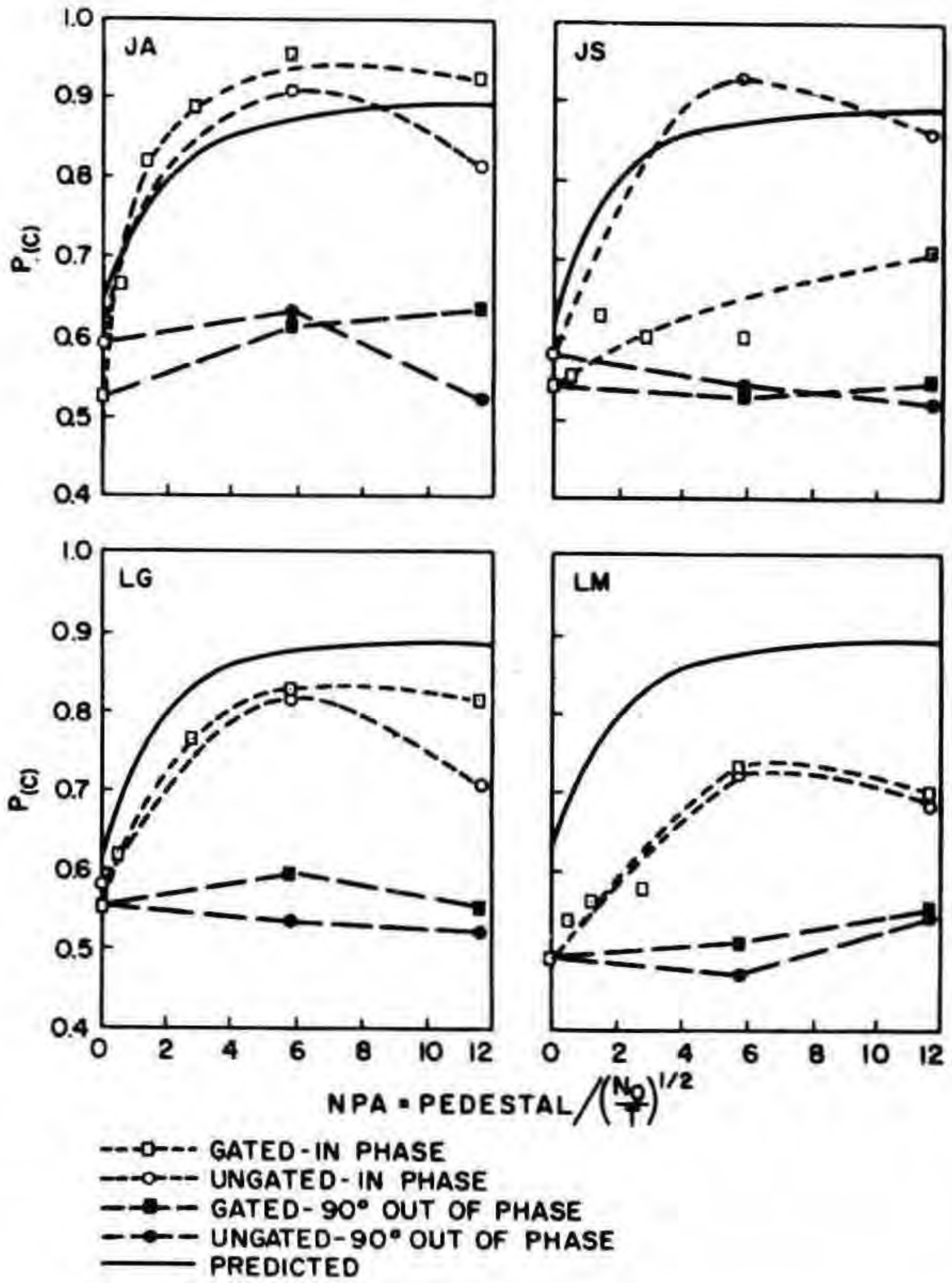

Fig. 3. Probability of correct response, P(c) as a function of normalized RMS pedestal amplitude (NPA) for four subjects for pedestal and signal in phase, pedestal and signal 90 degrees out of phase, stimulus gated, and stimulus ungated conditions. The solid curves give the energy detector performance with a 200 cps bandwidth and a 10 db abscissa shift. E/No, the signal energy divided by the noise spectral density is 12 db. The stimulus duration (T) is 100 ms. Gated refers to a procedure in which the noise and pedestal were on only during the stimulus intervals; ungated to one in which they were on continuously.

Further experiments were undertaken using the same general procedure and a range of signal-to-noise ratios with a wide range of pedestal amplitudes. The results, shown in Fig. 4, indicate that the model fits the data fairly well until high pedestal values are reached. There detectability begins to decrease while the model predicts constant detectability. This decrease may be attributed to noise in the subjects detection mechanism which is not included in the model.

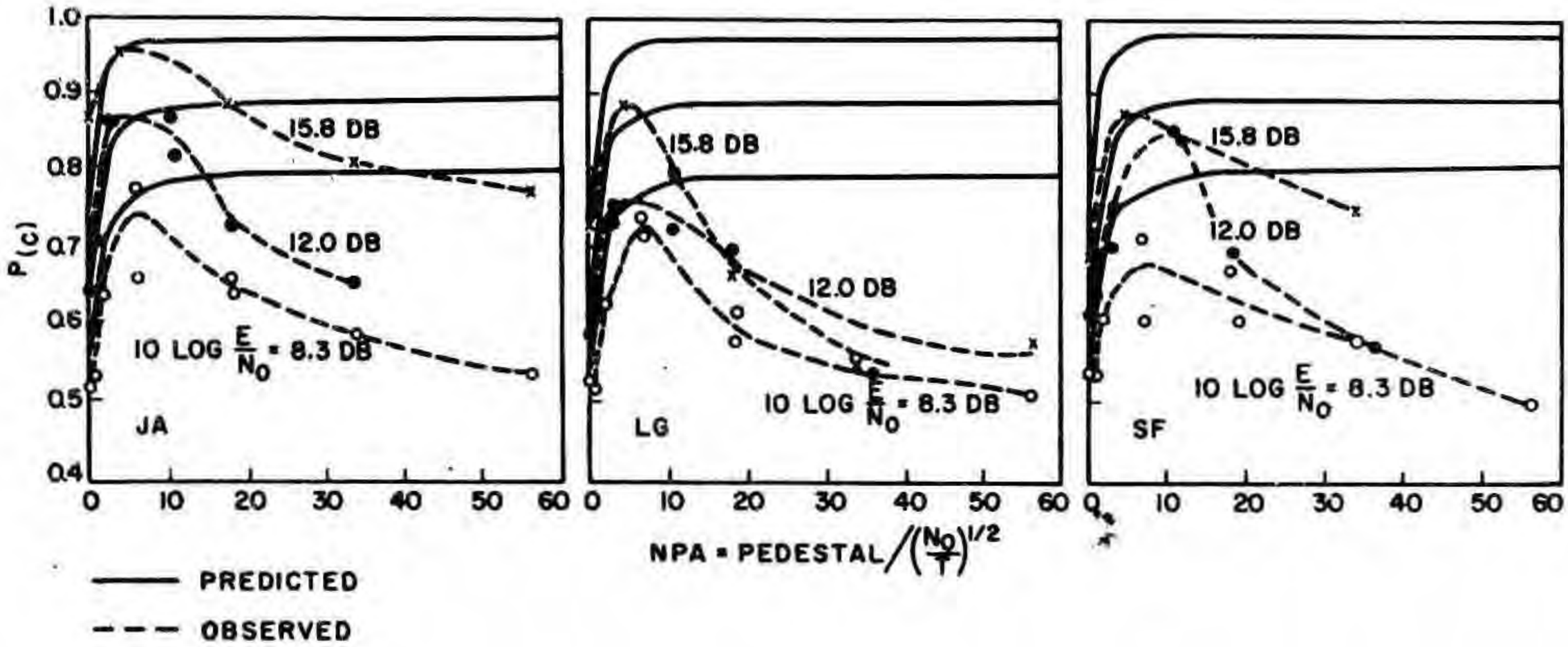

Fig. 4. Probability of correct response, P(c), as a function of normalized RMS pedestal amplitude (NPA) for three values of E/No, the signal energy divided by the noise spectral density. The solid curves give the energy detector performance with a 200 cps bandwidth and a 10 db abscissa shift. Stimulus duration (T) is 100 ms, and a gated method of presentation is used. All pedestals are in phase with the signal.

The explanation suggested here for the pedestal effect differs from those previously offered which assume that the presence of the pedestal eliminates the need for memory of the signal on the part of a subject using a correlation detection process. It is difficult to determine definitely which explanation is correct because the memory hypothesis is vague in its predictions about the quantitative effects of pedestals. The lack of effect of a 90 degree out-of-phase pedestal presents a difficulty for the memory hypothesis, since such a pedestal contains as much information about the frequency and phase of the signal as an in-phase pedestal, but even in this case, the predicted result depends upon which of several possible assumptions is made. While a clear decision is thus impossible, the very vagueness of the memory hypothesis argues against its usefulness. The energy detector predicts those phenomena associated with the presence of pedestals for which the memory explanation is adequate, and permits quantitative comparison. The energy detector, further, predicts the shape of the detection curve in the absence of pedestal. It is a simpler device than the correlation detector, to which the memory hypothesis is appropriate, and physiological evidence suggests that the energy detector would be a reasonable model to postulate for the ear. The energy detector thus appears to be a more fruitful model to employ in dealing with signal detection data than the optimum detectors previously employed.

O25

FOURTH INTERNATIONAL CONGRESS ON ACOUSTICS
COPENHAGEN 21.-28. AUGUST 1962

INTERACTION OF SOUND WAVES WITH A GAS DISCHARGE

G. M. Sessler and M. R. Schroeder, Bell Telephone Laboratories,
Incorporated, Murray Hill, New Jersey

Interaction of sound waves with noise generated by a dc-discharge in rarefied air (pressure of about 1 mm mercury and discharge currents of about 100 ma) has been observed acoustically and optically at frequencies between 10 and 20 kc. The measurements show that the discharge noise in some frequency bands is reduced or increased by sound waves penetrating the discharge, and having frequencies within or without these noise bands. The interaction can be explained by the strong dependence of the frequency of the discharge oscillations on the parameters of the discharge.

Introduction

The noise level of a dc-discharge in narrow frequency bands has been measured both acoustically (with a microphone) and optically (with a photocell). The influence of an applied acoustic wave on the noise level has been determined. The measurements have been taken in air at pressures between 1 and 3 mm mercury. The discharge is sustained by a current of between 50 and 100 ma, flowing either perpendicular or parallel to the direction of propagation of the applied sound wave. The measurements have been performed at frequencies between 10 and 20 kc.

Experimental Setup

The setup for the experiment is shown in Fig. 1. The bell jar, which is connected to a vacuum system, contains the acoustical system and the electrical (discharge) system. The optical system is outside of the bell jar and is not shown in the figure.

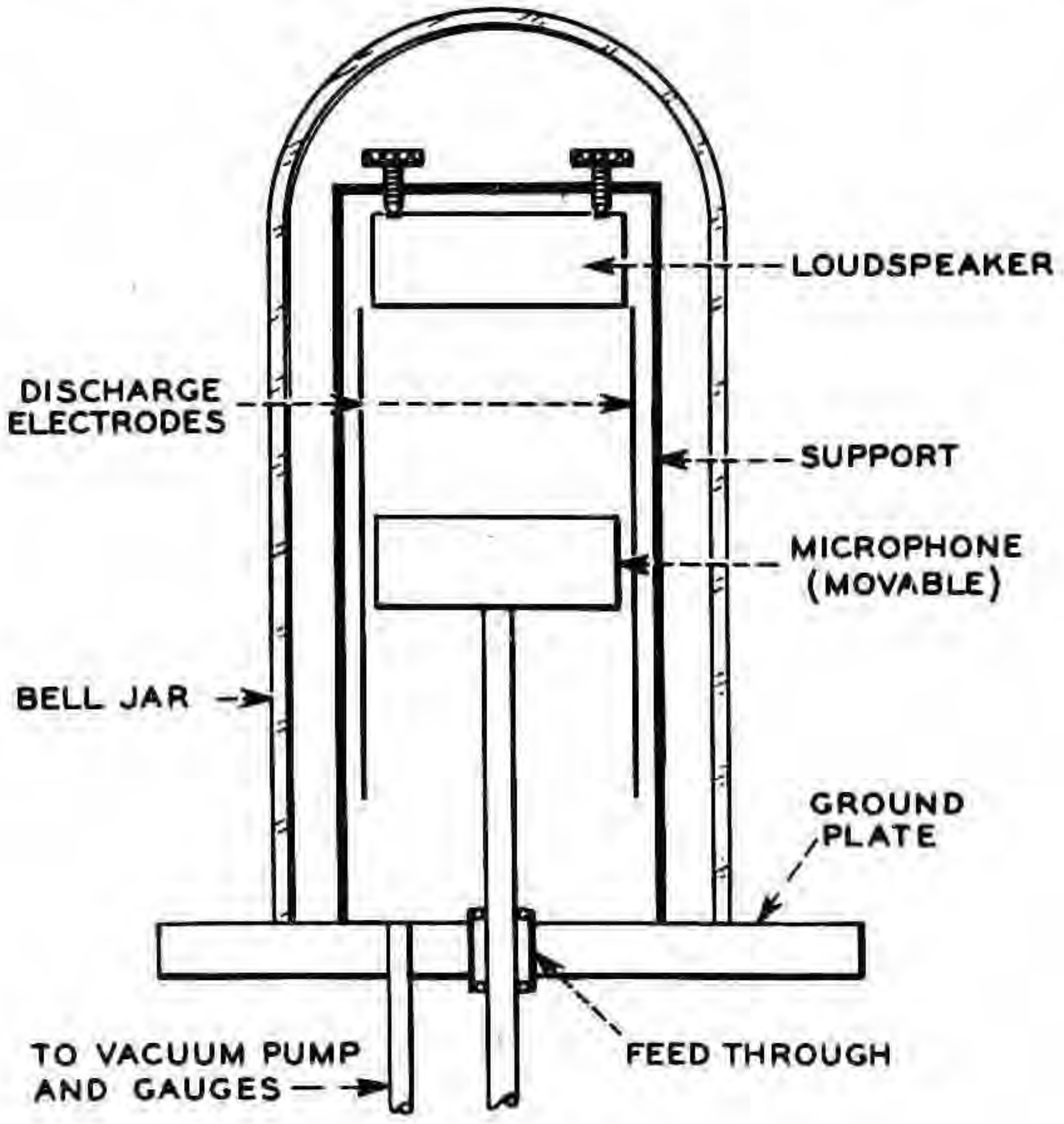

Figure 1

The acoustical system consists of an adjustable, but otherwise fixed, loudspeaker and a movable microphone. Loudspeaker and microphone are electrostatic transducers with solid dielectric. Their use in gases under reduced pressures has been described by Meyer and Sessler.[1] The distance between loudspeaker and microphone is between 6 and 8 cm. Under these conditions, the sound wave between loudspeaker and microphone contains only a small standing wave for the interesting frequencies. Without discharge the signal-to-noise ratio of the unfiltered microphone output exceeds 50 db.

Figure 1 also shows the electrodes for the discharge perpendicular to the direction of sound propagation. The electrodes are sheets of molybdenum whose dimensions are 4.5×9 cm^2. The distance between electrodes is 6 cm. A discharge current of 50 to 100 ma can be sustained by a voltage of about 500 to 600 v. Measurements with an electric probe show the resulting electron density in the center of the discharge to be in the order of 10^{10} electrons/cm^3. The density of the ions is higher by a factor of 2 or 3. The density of the neutral particles at 1 mm mercury is $3.6 \cdot 10^{16}$ cm^{-3}.

Two removable electrodes (not shown in Fig. 1) are used for operating the discharge parallel to the direction of sound propagation. They consist of a wire mesh (about 50% open) and thus permit propagation of a part of the sound wave to the microphone. These electrodes are placed parallel to and about 1 cm in front of the acoustic transducers.

The vacuum system consists of a rotary oil pump and several McLeod vacuum gauges. A small container of phosphorus pentoxide is placed in the bell jar to eliminate all water vapor in the gas.

Outside the bell jar a photocell is mounted for the optical measurements. An image of the cathode or anode is reproduced on the photocell by a f/2 lens. The voltages generated by the discharge noise at the output of the photocell are 10 db (anode) and 20 db (cathode) above other noise voltages.

Noise of a Gas Discharge

The noise spectrum of the discharge depends strongly on gas pressure, discharge current, geometrical dimensions of the discharge, and the condition of the electrodes. The "noise spectrum" can consist of a single frequency, of a fundamental frequency and some of its harmonics, or of wide-band noise. The strongest components of the spectrum are usually below 100 kc. However, in some cases frequencies as high as the plasma-frequency of the ions (which is in the order of 10 mc) and the plasma frequency of the electrons have been reported. The source of the low-frequency oscillations is still doubtful. They may be caused by ion waves, by oscillations of the cathode sheath, by potential-minimum oscillations, by striations, by anode spots, or by other sources. A review of this problem has been given recently by Crawford and Kino,[2] and some new results for gas pressures of about 1 mm mercury have been reported by Fite.[3]

At the relatively low frequencies considered here, ions are the primary source of oscillations. But the neutral particles, by collision with the ions, also take part in the oscillations. The longitudinal component of the ion oscillations represents a density oscillation of the charged particles. This causes an amplitude modulation of the emitted light which can be detected by the photocell. The longitudinal oscillations of the neutral particles can be observed with the microphone.

Method of Measurements

The noise level of the discharge in a certain fixed frequency band has been measured as a function of the frequency of the applied sound wave. For this purpose, the noise of the discharge (measured either with the microphone or with the photocell) has been band-pass filtered in a superheterodyne receiver with a constant bandwidth of about

---

[1] E.Meyer and G.Sessler; Z. Physik 149 (1957), p.15.
[2] F.W.Crawford and G.S.Kino; Proc. IRE 49 (1961), p.1767.
[3] W.L.Fite, University of Pennsylvania Report AD 47514, (1955).

200 cps. With the filter frequency fixed, the frequency of the loudspeaker is automatically driven across the band from about 10 to 20 kc. Simultaneously, the band-pass filtered noise, coming from the output of the receiver, has been recorded with a level recorder using a 50-db potentiometer. The level of the sound wave is usually about 30 db higher than the discharge noise in the above mentioned filter band. Most of the recordings show a constant noise level and a sharp peak when the filter frequency is equal to the frequency of the applied sound wave.

An example is given in Fig. 2 (Section A) which shows the noise level of the discharge at a filter frequency of 13.2 kc as a function of the applied sound wave frequency. The gas pressure is 3.9 mm mercury, the discharge current 77 ma. The discharge noise without applied sound wave is shown in the recording in Section B.

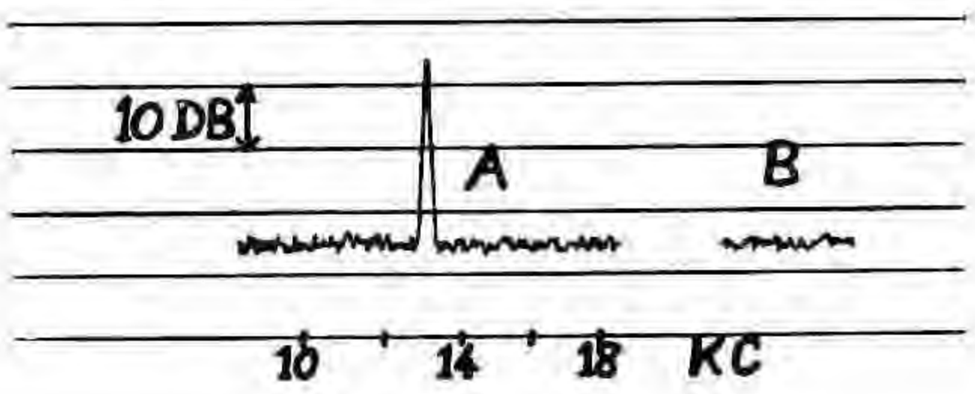

Figure 2

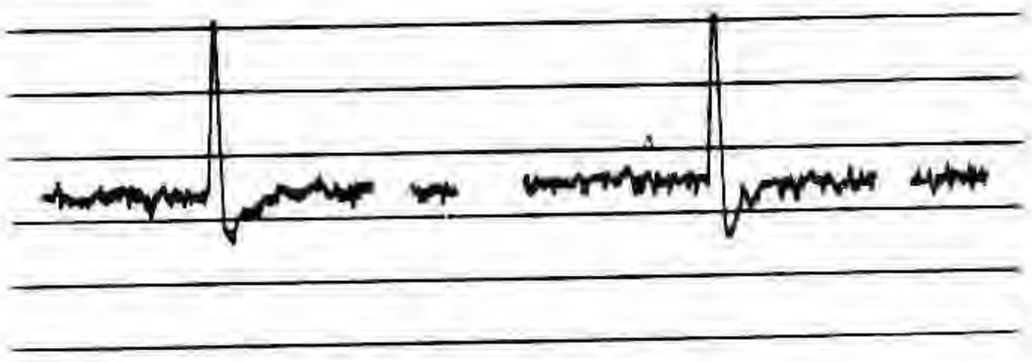

Figure 3

Many of the recordings show a more complicated behavior than the one in Fig. 2 and thus indicate an interaction between the sound wave and the discharge noise. Some of these recordings will be dealt with in the next paragraph.

Experimental Results

All results reported here have been taken with the discharge running perpendicular to the direction of sound propagation. Measurements taken with a parallel discharge indicate less interaction between sound wave and discharge noise.

Figure 3 shows two recordings taken with the microphone at a filter frequency of 13.95 kc, a discharge current of 82 ma and a pressure of 2.3 mm mercury. Figure 3 shows that the measurements are reproducible within short times in which the parameters of the discharge do not change substantially.

Figure 4 shows recordings taken with the microphone and the photocell at a filter frequency of 13.28 kc, a pressure of 2.6 mm mercury and a discharge current of 78 ma. The optical system is adjusted so that only light from the anode falls on the photocell. Figure 4a and b show the microphone recordings, Fig. 4c, d and e the photocell recordings. Figure 4f is a reference measurements taken with the photocell without discharge. It is recorded with the same amplification as Fig. 4c, d, and e. The strong signal at the filter frequency in Fig. 4f is electrical crosstalk. The agreement between the microphone and photocell measurements is noteworthy.

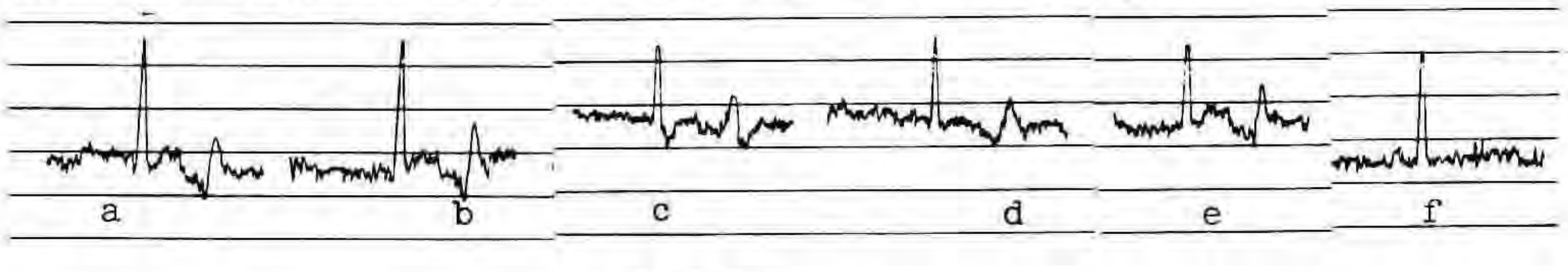

Figure 4

Explanation of the Interaction

For simplicity we shall assume that the interaction depends only upon one of the discharge parameters, called g, which consists of a static part g_o and a part $g_1 e^{i\omega t}$ which is caused by the applied sound wave:*

$$g = g_o + g_1 e^{i\omega t}, \qquad (1)$$

where ω is the radian frequency of the sound wave. In the simplest case, the internal noise of the discharge consists of pulses with a repitition rate ν. How are these pulses influenced by the applied sound wave?

It has been shown[3] that in some cases the frequencies of fluctuations in glow discharges change without noticeable variation in the discharge parameters. This indicates a very strong dependence of these frequencies upon the parameters. This can be expressed by an equation of the form

$$\nu = Ag - \nu_o \ , \qquad (2)$$

where A and ν_o are constants. It is assumed that Eq. 2, with slightly different values of A and ν_o, is valid also in the case where g is a periodic variable with a constant average value. Then Eq. 2 gives the dependence of ν on the momentary value of g at the time when the pulse is released. Substituting Eq. 1 into Eq. 2 yields

$$\nu = A(g_o + g_1 e^{i\omega t}) - \nu_o \ . \qquad (3)$$

Equation 3 indicates that ν depends upon the phase of the applied sound wave. If the initial value of ν is not too different from $f = \omega/2\pi$, ν will be shifted by the sound wave so that $\nu = f$. The frequency limits $\nu_{1,2}$ for this can be found from Eq. 3 by taking $e^{i\omega t} = \pm 1$ and $\nu = f$:

$$f = A(g_o \pm g_1) - \nu_o = \nu_{1,2} \pm Ag_1 \ , \qquad (4)$$

which yields

$$\nu_{1,2} = f \mp Ag_1 = f \mp Ag_o \cdot \frac{g_1}{g_o} \ . \qquad (5)$$

As an example, a relative sound pressure $p_1 = 10^{-3} p_o$ where p_o is the static gas pressure, has been used in the experiments. This results in an approximately equal relative amplitude of oscillation of g:

$$\frac{g_1}{g_o} \approx \frac{p_1}{p_o} = 10^{-3} \qquad (6)$$

Many of the recordings show (see Fig. 3) that discharge oscillations are influenced by a sound wave when the frequency of the oscillation is within 5 percent of the frequency of the sound wave. With these frequency limits substituted for ν_1 and ν_2, Eqs. 5 and 6 yield

$$Ag_o = 50 \ f$$

Using this value in Eq. 2 gives a relation between ν and g which has been confirmed experimentally in many cases.

The above calculations seem to offer a semi-quantitative explanation of the observed interaction between discharge oscillations and sound waves. A complete theory of these phenomena has to take account of possible phase differences between sound wave and discharge oscillations. These phase differences probably depend upon the geometry and the physical parameters of the discharge and determine whether the sound wave gains or looses energy from the interaction with the noise.

Conclusions

The formation of noise in a discharge is a phenomenon which, at present, is not completely understood. The fact that in some cases the discharge noise depends strongly upon the parameters of the discharge and therefore can be influenced by a penetrating sound wave may provide some clues as to the origin of the noise.

Another important point is that the sound wave itself might be influenced in amplitude and velocity by the discharge oscillations. This is suggested not only by the explanation which is given above but also by some experimental results. These seem to indicate that the sound wave undergoes an absorption or amplification at certain frequencies in addition to the classical absorption and th. normal absorption introduced by the discharge. However, more material has to be collected to further clarify this matter.

The authors are pleased to acknowledge the aid in mechanical design by C. F. Mattke and the assistance in the measurements by J. E. West.

---

*The quantity g can be any parameter of the discharge, such as pressure, temperature, discharge current, electron or ion density, etc.

G26

FOURTH INTERNATIONAL CONGRESS ON ACOUSTICS
COPENHAGEN 21.-28. AUGUST 1962

ON THE EXTRACTION OF THE PITCH SIGNAL USING THE BODY WALL VIBRATION AT THE THROAT OF THE TALKER

Toshitaka SUGIMOTO and Shizuo HIKI

(Electrical Communication Laboratory of N.T.T. Tokyo JAPAN)

INTRODUCTION

The reliable method of the extraction of the voice pitch has been an important problem in the fields of the analysis-synthesis scheme, the synthesis of speech and the fundamental research on the voice pitch. The wave form of the glottal vibration has estimated to be a simple triangularlike form and it may show a clearly definite period. The speech wave radiated from the mouth is, however, a very complicated one with the effects of the resonance character of the vocal tract and the transition of the phonemes. The normal pitch extracter will, therefore, sometimes fail in extracting the information of the correct pitch period.

It is well known that the body vibration caused by the pronunciation is picked up at various positions of the speaker. A large amplitude of the vibration is ,especially, found at the throat. If the body wall vibration originated from the vocal cord vibration is picked up without the influence of the vocal tract resonances, it is expected that it precisely carries the information of the pitch period. In this paper, the position of picking up the body wall vibration was examined for the purpose of the extraction of the pitch information and the most suitable position was determined to give a simple wave form originated from the glottal vibration which is scarcely influenced with the articulation of the speech. From this body wall vibration, the more reliable pitch information was delivered than that from the speech sounds. The low pass filtering action of the path from the glottis to the outer skin and the spectrum envelope of the glottal vibration were also discussed.

SUITABLE PICK-UP POSITION

Microphone

In order to decide the most suitable position forthe extraction of the pitch information experimentally, the body wall vibrations on the various points of the speaker's throat were picked up with a microphone and their wave forms were investigated in detail on various conditions of the pronunciation. MR-103 condenser microphone was used, which was about 25 mm. in diameter. The rubber ring was patched around the microphone to give the air gap between the diaphram and the skin and to avoid the noise of the circumference. The frequency response of the microphone was almost flat to 8000 cps.

In the case of the long time experiment, it is preferable to use a light microphone. For this purpose, the moving coil microphone weighing about 50 grams was developed as shown in Fig. 1. The frequency responce is equalized with a integrating network and in ±2dB from 100 cps to 2000 cps. With this microphone, the body wall vibration was picked up steadily and there was no obstruction in the pronunciation.

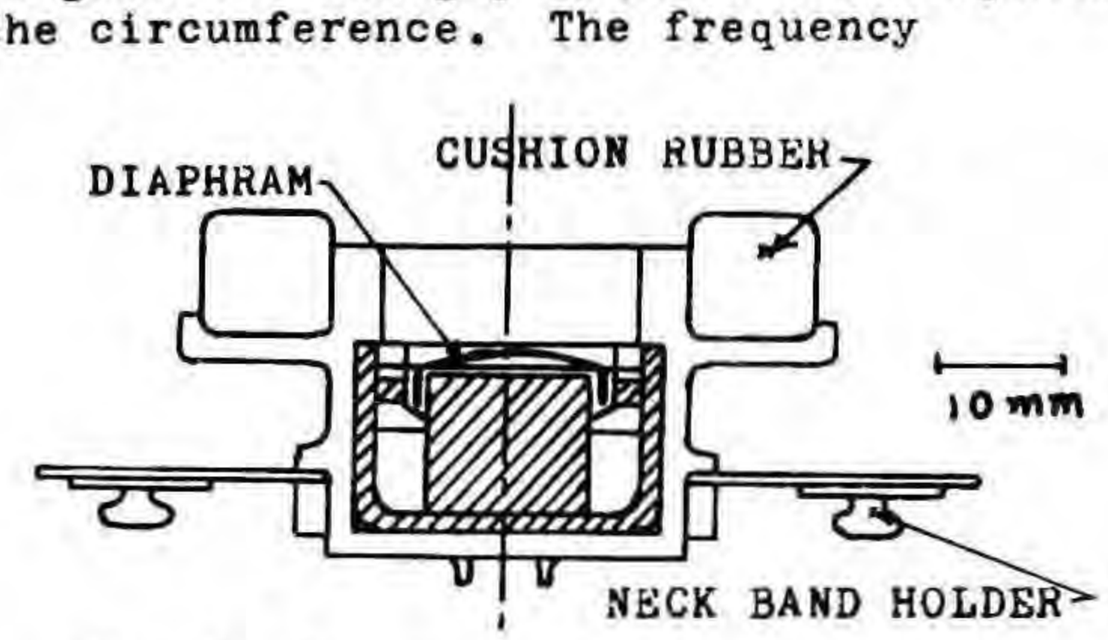

Fig.1. The moving coil microphone developed for picking-up the body vibration at the throat.

The Most Suitable Position

The body wall vibration were picked up at the various positions shown in Fig. 2 with regard to five Japanese vowels uttered by the adult male. (Pitch was about 120 cps.) The speech waves were simultaniously measured at the point of 10 cm. from the mouth with another condenser microphone which had nearly the same frequency response as that of the throat. Both wave forms were photographed. From the photographs, the wave forms of the body vibration were seen to be effected with the vocal resonances at the upper positions from the glotis but to be very simple and to be scarcely effected by the articulation at the lower positions .

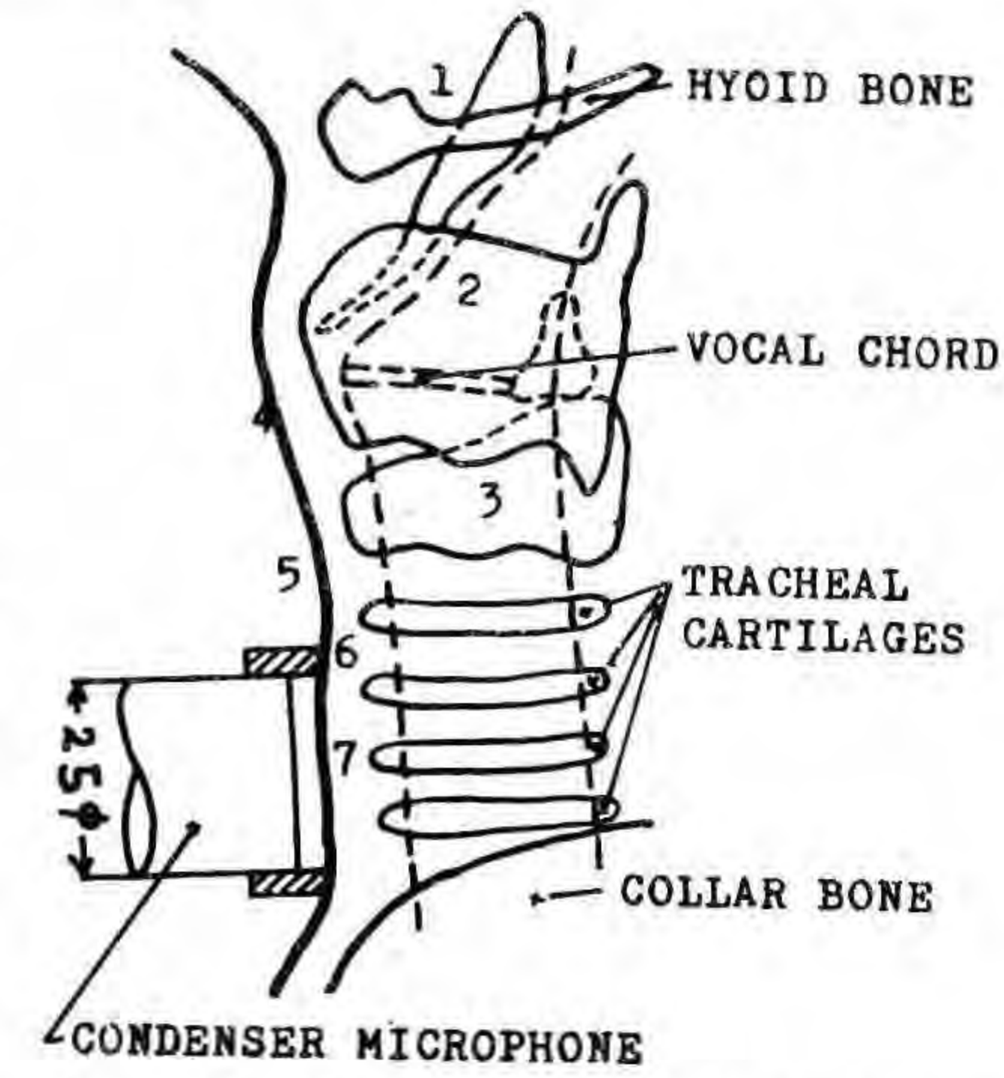

Fig. 2. Sketch of the larynx and the trachea, indicating the pick-up positions of the microphone.

For the selection of the suitable pick-up position, next items were taken into consideration; namely
(1) the clearness of the fundamental period,
(2) small difference among the articulation of vowels,
(3) the sufficient pressure level,
(4) little infulence to the pronunciation and (5) the stability.

The most suitable pick-up position was selected to be on the outer skin on the tracheal cartilages near the collar bone on anterior posterior line. This position is given in Fig.2 with the mark "7". The examples of the wave forms picked up at this position are shown in Fig. 3. (They are traced from the photographs of the oscilloscope.)

It is found that they are very similar to the glottal wave expected from the various experiments[1] and are clear in the fundamental period. The pitch information is ,therefore, expected to be easily extracted with the ordinary pitch extracter. Above all, the pressure level is about 20 dB higher than the speech level obtained from the oral output and this fact improves the signal-to-noise ratio of the signal used for the pitch extraction.

Same results were held to those obtained by five male and twe female talkers.

The body wall vibrations are clearly originated from the vocal cord vibration but they are much affected by the frequency response from the vocal cord to the skin. This response is supposed to be a kind of a low pass filter because the wall of the tracheal and the skin are both the soft materials. This response will be estimated by the spectrum analyses as explained below.

ADVANTAGE TO THE PITCH EXTRACTION

When the body wall vibration is utilized to the pitch extraction, there are many advantages compared with the extraction from the speech sounds.
(1) It has a clearly definite fundamental period which is not affected by the kind of phonemes. Namely, there is only single peak in one fundamental period.
(2) Above character is found to be the same among the speaker's sex and the individuality.



Fig. 3. Waveforms of the body vibration with a pronaunciation of various vowels picked up at the most suitable position. (Traced from the photograghs of scope.)

(3) Same character is also found in the change of the voice effort, pitch and the production of the nasals and blähhlaut sounds.
(4) The body vibration shows a very smoothed envelope.
(5) There are no disturbances at the start and end of the pronunciation.
(6) No effect is seen in the production of the voiceless sounds.

From above reasons, this method is much superior in the pitch extraction than that from the speech waves.

THE ESTIMATION OF THE FILTERING ACTION

The body wall vibration is distorted by the filtering action of the path from the glottis to the pick-up point. This character of filtering is not directly determined. It is ,therefore, estimated by the spectrum analyses of both the waves of the body vibration and speech. When the spectra of the body vibration and the speech are exprssed to be $/G'(\omega)/$ and $/F(\omega)/$ respectively, the following equations are given:

$$/G'(\omega)/=/L(\omega)/\times/G(\omega)/ \qquad (1)$$

$$/F(\omega)/=/P(\omega)/\times/G(\omega)/ \qquad (2)$$

where $F(\omega)$, $G'(\omega)$ and $G(\omega)$ are the spectra of the speech wave, the body vibration and the glottal vibration respectively, $P(\omega)$ is the response of the vocal tract containing the radiation characteristics and $L(\omega)$ is the filtering action of the path from the vocal cord to the skin. From above equations, $L(\omega)$ is given as follows.

$$/L(\omega)/=\frac{/G'(\omega)/\times/P(\omega)/}{/F(\omega)/} \qquad (3)$$

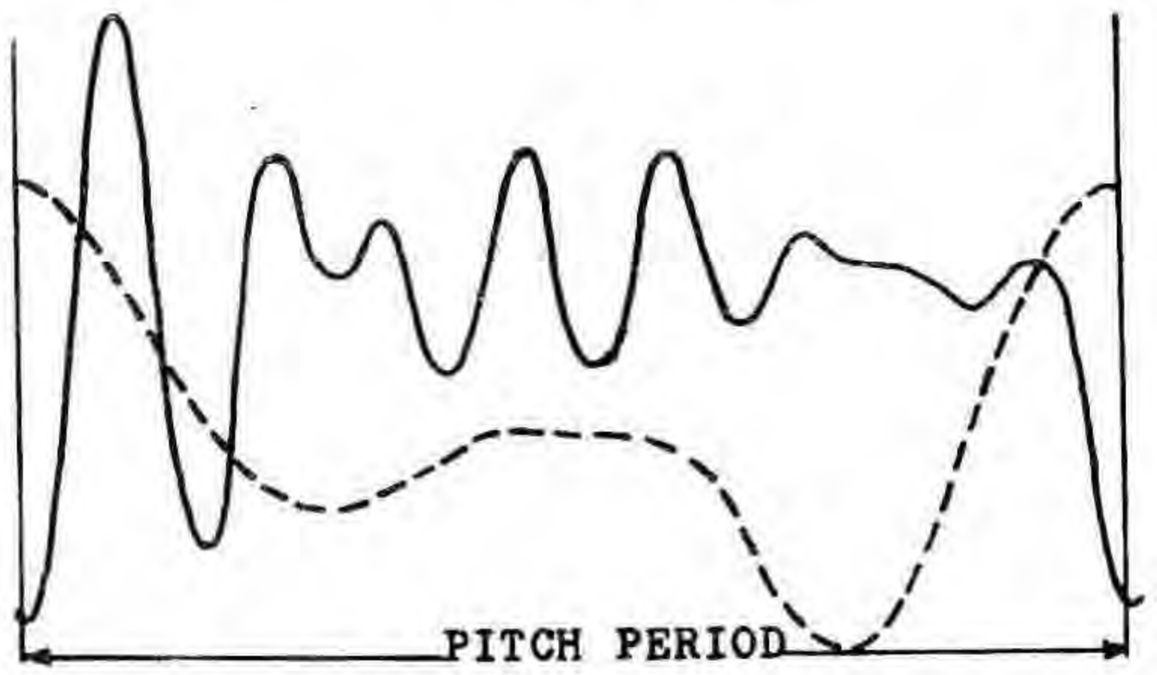

Fig. 4. Selected waveforms of a vowel /a/ and a corresponding body vibration plotted from digital data.

When $P(\omega)$ is given, $L(\omega)$ will be estimated from the spectrum data of the $G'(\omega)$ and $F(\omega)$. If the formant frequencies and their bandwidths are given, $P(\omega)$ will be computed by the theory of the speech production developed by G. Fant.[2] Namely $P(\omega)$ is given approximately as follows;

$$/P(\omega)/=/Z_r(\omega)/\times/K_{r3}(\omega)/\,\frac{\pi}{2}\,\frac{1}{\sqrt{\left(1-\frac{f^2}{F_n^2}\right)^2+\frac{f^2}{F_n^2Q_n^2}}} \qquad (4)$$

where $Z_r(\omega)$ is the radiation character and $K_{r3}(\omega)$ the correction factor introduced by neglecting the higher formants and F_n and Q_n are the n-th formant frequency and its bandwidth respectively. F_n was determined from the spectrum analysis and Q_n was assumed to be 100 cps.

The body wall vibrations and the speech waves of the isolated five Japanese vowels were simultaniously picked up and recorded by 2 channel tape recorder. The data were then sampled at the rate of 6400 samples/sec. and digitalized into 8 bits. The corresponding data in one pitch period were selected from a steady part of the signals. One example on /a/ is shown in Fig. 4. The spectra of $G'(\omega)$ and $F(\omega)$ were ,then, computed with a digital computer.

The results from the above calculation are given in Fig. 5. The average response of $L(\omega)$ is also shown. From this figure, it is seen that the $L(\omega)$ shows a low pass filter-like character having the cut-off frequency of 400 cps. The spectrum of the glottal wave ,$G(\omega)$, was also estimated and its spectrum envelope is found to have -12 dB/oct. slope.

These results are not free from the error in estimating the formant frequencies and their bandwidths. They show ,therefore, the comparatively complicated responses. It will be improved by using the data of more correct

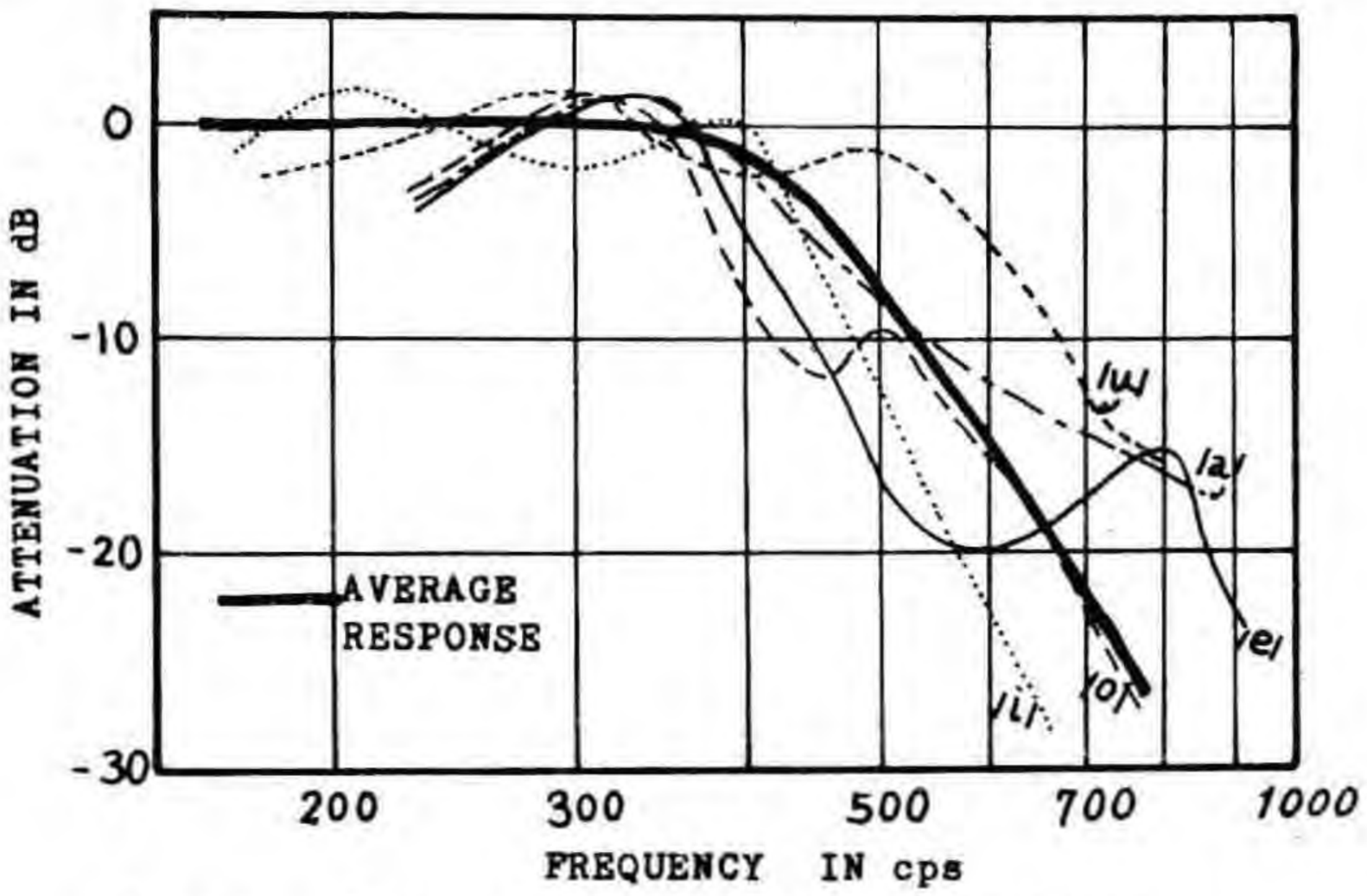

Fig. 5. Responses of the filtering action.

values determined by a analysis-by-synthesis method.

CONCLUSION

The body wall vibration at the region between the cricoid cartilage and the sternum of the talker is found to have a clearly definite period and not to be affected by the articulation of phonemes. The reliable pitch information is easily extracted by using this signal. The filtering action from the glottis to the pick-up point is measured to be a kind of a low pass filter. This character is also seen to have much advantage to the pitch-extraction.

When the pitch signal obtained by this method was applied to a vocoder, the quality of the remade speech was found to be much improved. This method will also give a standard signal for the improvement of the normal pitch extracter and an information dividing the voiced signal from the unvoiced one. The wave form of the body wall vibration will be utilized to the medical examination.

ACKNOWLEDGMENTS

The authors are grateful to Dr. T. Miura for his encouragement of this study and wish to thank Mr. S. Hashimoto and Mr. S. Takahira who made the digital computer calculation.

REFERENCES

(1) R.L. Miller: Nature of the vocal cord wave, J. Acoust. Soc. Am. 31 667 ('59)
(2) G. Fant: Acoustic analysis and synthesis of speech with applications to Swedish, Ericsson Techinics 15 3 ('59)

H26

FOURTH INTERNATIONAL CONGRESS ON ACOUSTICS
COPENHAGEN 21.-28. AUGUST 1962

Computer Simulation of Basilar Membrane Displacement

James L. Flanagan, Bell Telephone Laboratories, Inc.,
Murray Hill, New Jersey, U.S.A.

In earlier work[1] a computational model was derived for describing basilar membrane displacement in the human ear in response to an arbitrary sound pressure at the eardrum. The model consists of rational-function approximations to physiologically-measured transmissions between eardrum and stapes, and between stapes and membrane.[2] In addition to mathematical tractability, the rational function format has the advantage of being realizable in terms of lumped-constant electrical circuits. The model, in conjunction with ancillary schemes for processing membrane displacement information, has been found a useful tool for analyzing auditory signals and for relating perceptual and physiological behavior.[3] Some of the analyses, particularly those for speech signals, require rapid computation and the storage of substantial amounts of data. Large-scale digital computers are very adept at this. The ear model has therefore been simulated on an IBM 7090 digital computer.

The functions of the peripheral ear embraced by the model are shown schematically in Fig. 1. $p(t)$ is the time function of sound pressure at the eardrum; $x(t)$ is the equivalent linear displacement of the stapes; and $y_\ell(t)$ is the basilar membrane displacement at a distance ℓ from the stapes. The lower diagram indicates the functional relations between the quantities. The frequency-domain (Laplace) transforms $G(s)$ and $F_\ell(s)$ are respectively the middle-ear transmission and the transmission from stapes to point ℓ on the membrane. These quantities are approximated by rational functions. From the earlier work one such approximation is

$$G(s) = \frac{c_o}{(s+a)[(s+a)^2+b^2]}$$

$$F_\ell(s) = c_1\beta_\ell^4 \left(\frac{2000\pi\beta_\ell}{\beta_\ell+2000\pi}\right)^{0.8} \left(\frac{s}{s+\beta_\ell}\right) \left[\frac{1}{(s+a_\ell)^2+\beta_\ell^2}\right]^2 e^{-3\pi s/4\beta_\ell},$$

Where: s is the complex frequency $(\sigma+j\omega)$,
c_o, c_1 are positive real constants chosen to yield correct absolute values of displacements,
$b = 2a = 2\pi(1500)$ rad/sec
$\beta_\ell = 2a_\ell$ = radian frequency to which point ℓ responds maximally
$e^{-3\pi s/4\beta_\ell}$ is a delay factor of $3\pi/4\beta_\ell$ sec which brings the phase response of the model into line with the physiological measurements.

Because all other factors are constant, the model $G(s)F_\ell(s)$ is completely specified by the membrane place frequency β_ℓ. The middle-ear approximation, $G(s)$, exhibits simple, complex-conjugate poles at $s = (-a \pm jb) = 2\pi(1500)(-1/2 \pm j1)$, and a real-axis pole at $s = -a = -\pi(1500)$. The membrane function $F_\ell(s)$ has double complex-conjugate poles at $s = (-\alpha_\ell \pm j\beta_\ell) = \beta_\ell(-1/2 \pm j1)$, a zero at $s = 0$, and a real-axis pole at $s = -\beta_\ell$.

As one might do in realizing the analog electrical circuit, the digital representation of the model can easily be constructed from sampled-data equivalents of the individual complex pole-pairs and the individual real poles and zeros. The sampled-data equivalents approximate the continuous functions over the frequency band of interest. The present digital simulation was made within the format of a special compiler known as BLODI.[4] The computer operations used to simulate the necessary poles and zeros are shown in Fig. 2. All of the square boxes labelled D are delays equal to the time between successive digital samples. The input sampling frequency, 1/D, in the present simulation is 20 Kcps, and the input data is quantized to 11 bits. All of the triangular boxes are "amplifiers" which multiply their input samples by the gain factors shown in the boxes.

Each of the digital operations enclosed by dashed lines is treated as a component block in the program. The block shown in Fig. 2(a) is labelled CP for conjugate-pole. It has the transfer function

$$\frac{Y_a(s)}{X_a(s)} = \left[e^{-2\theta} e^{-2sD} - 2e^{-\theta}\cos\Phi\ e^{-sD} + 1 \right]^{-1}$$

which has poles at

$$e^{-(\theta+sD)} = \cos\Phi \pm j \sin\Phi ,$$

or

$$s = \frac{1}{D}\left[-\theta \pm j(\Phi + 2n\pi)\right],\ n = 0,1,2\ldots.,$$

so that

$$\theta_\ell = \alpha_\ell D \text{ and } \Phi_\ell = \beta_\ell D,$$

where α_ℓ and β_ℓ are the real and imaginary parts of the pole-pair to be simulated. The pole constellation of the sampled-data function repeats at $\pm j2n\pi/D$ (or at $\pm j2n\pi/5X10^{-5}$ for the 20 Kcps sampling frequency).

Single real-axis poles are approximated as shown by the P block in Fig. 2(b). The transfer function is

$$\frac{Y_b(s)}{X_b(s)} = \left[1 - e^{-(\theta+sD)}\right]^{-1}$$

and has poles at $s = \frac{1}{D}(-\theta \pm j2n\pi)$, $n = 0,1,2\ldots.$

The single zero is simulated by the Z block in Fig. 2(c). Its transfer function is the reciprocal of the P block and is

$$\frac{Y_c(s)}{X_c(s)} = 1 - e^{-(\theta+sD)}$$

with zeros at $s = \frac{1}{D}(-\theta \pm j2n\pi)$, $n = 0,1,2\ldots.$

In the present simulation the zero is placed at the origin, so that $\theta = 0$.

The computer operations diagrammed by these blocks were used to simulate the model $G(s)F_\ell(s)$ for 40 points along the basilar membrane. The points represent 0.5 mm increments of length and span the frequency range 75 to 4600 cps. The blocks are put together in the program as shown in Fig. 3. The amplifier boxes c_o and c_ℓ in Fig. 3 take into account not only the model amplitude constants c_0 and c_1 and the $(2000\pi\beta_\ell/\beta_\ell + 2000\pi)^{0.8}$ factor but also the amplitude responses of the digital component blocks. For example, it is convenient to make the zero-frequency gain of the CP boxes unity, so each c_ℓ amplifier effectively includes a $[e^{-2\theta}-2e^{-\theta}\cos\Phi + 1]^2$ term. The overall effect of the c_o and c_ℓ gain adjustments is to yield the amplitudes specified by $G(s)F_\ell(s)$. The delay to each membrane point, $3\pi/4\beta_\ell$, is simulated in terms of integral numbers of sample intervals. In the present simulation it is consequently represented to the nearest 50 μsec.

An illustrative output from the simulation, plotted automatically by the computer, is shown in Fig. 4. The displacement response of the membrane at 40 points is shown as a function of time. The characteristic frequencies of the membrane points are marked along the y-axis, starting with 4600 cps at the lower(basal) end and going to 75 cps at the upper (apical) end. Time is represented along the x-axis. The input signal p(t) is alternate positive and negative pulses of 100 μsec duration produced at a fundamental frequency of 100 cps. The time between alternate pulses is therefore 5 msec. At the apical (low frequency) end of the membrane, the frequency resolution is best, and the displacement builds up to the fundamental sinusoid. At the basal (high frequency) end the membrane resolves the individual pulses in time. The responses also reflect the transit delay along the membrane.

Various schemes for processing the membrane displacements for speech and other signals have also been simulated. All are computer operations performed upon the outputs $y_1(t)$ --- $y_{40}(t)$ shown in Fig. 3. Space precludes their description here. One such processing, however, has been the simulation of a pulse threshold function described earlier.[5] The displacement outputs are rectified, smoothed and raised to the 0.6 power. A basilar membrane "sound spectrogram" is thereby obtained in which features such as formants, voicing, friction, etc., can be discerned. This type of processing of membrane displacement information appears to offer some interesting possibilities for speech pattern matching, formant tracking and related analyses.

REFERENCES

1. J. L. Flanagan, Models for approximating basilar membrane displacement, Bell System Tech. J. 39, 1163-1191, (1960). Part II:Effects of middle-ear transmission and some relations between subjective and physiological behavior, Bell System Tech. J. 41, 959-1009,(1961).
2. G. v. Békésy, Experiments In Hearing, (McGraw-Hill, Inc., New York, (1960).
3. J. L. Flanagan, E. E. David, Jr., and B. J. Watson, Physiological correlates of binaural lateralization, Proceedings of IV International Congress on Acoustics, Copenhagen, 1962.
4. J. L. Kelly, Jr., V. A. Vyssotsky, and C. Lochbaum, A block diagram compiler, Bell System Tech. J. 40, 669-676, (1961).
5. J. L. Flanagan, Audibility of periodic pulses and a model for the threshold, J. Acoust. Soc. Am. 33, 1540-1549, (1961).

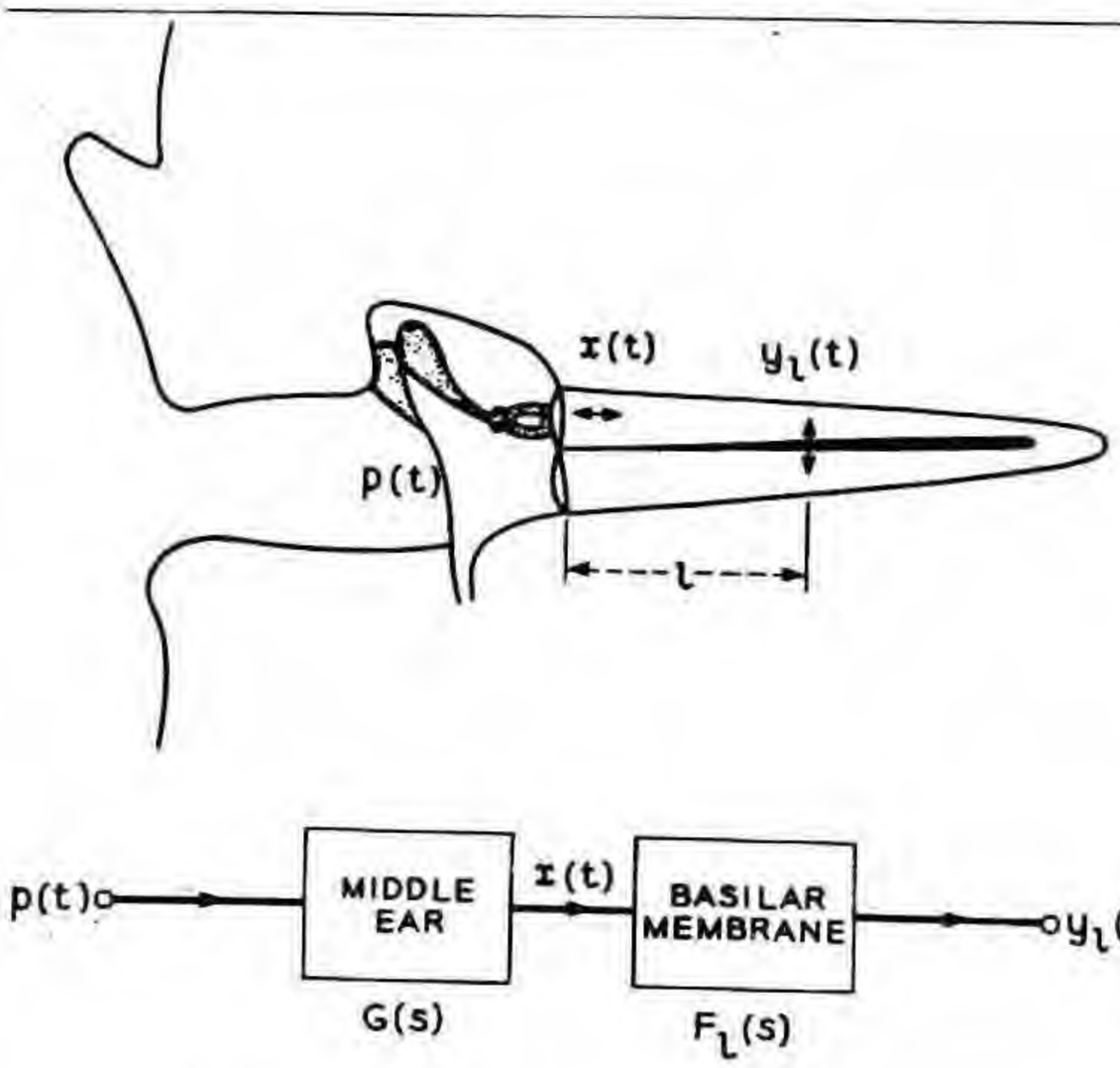

$$\frac{Y_l(s)}{P(s)} = \frac{X(s)}{P(s)} \cdot \frac{Y_l(s)}{X(s)} = G(s) \cdot F_l(s)$$

FIG. 1

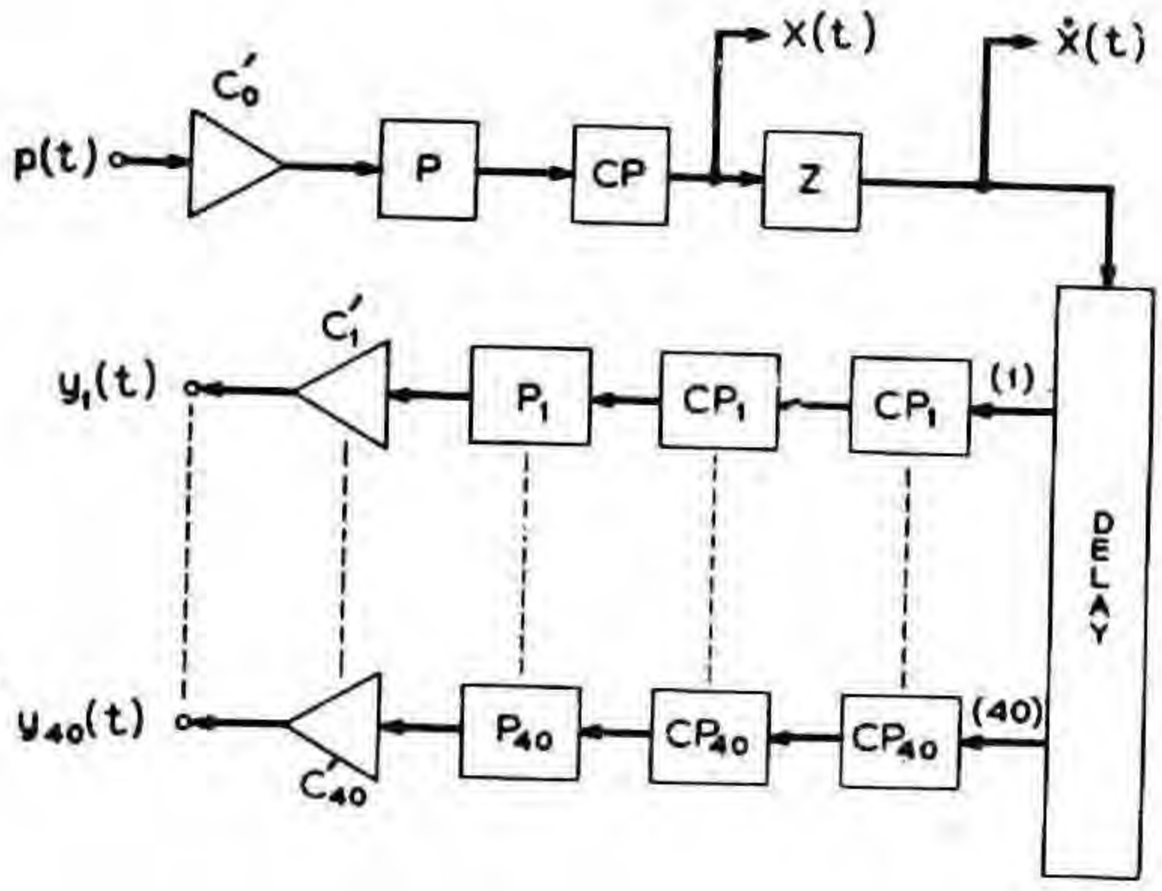

FIG. 3

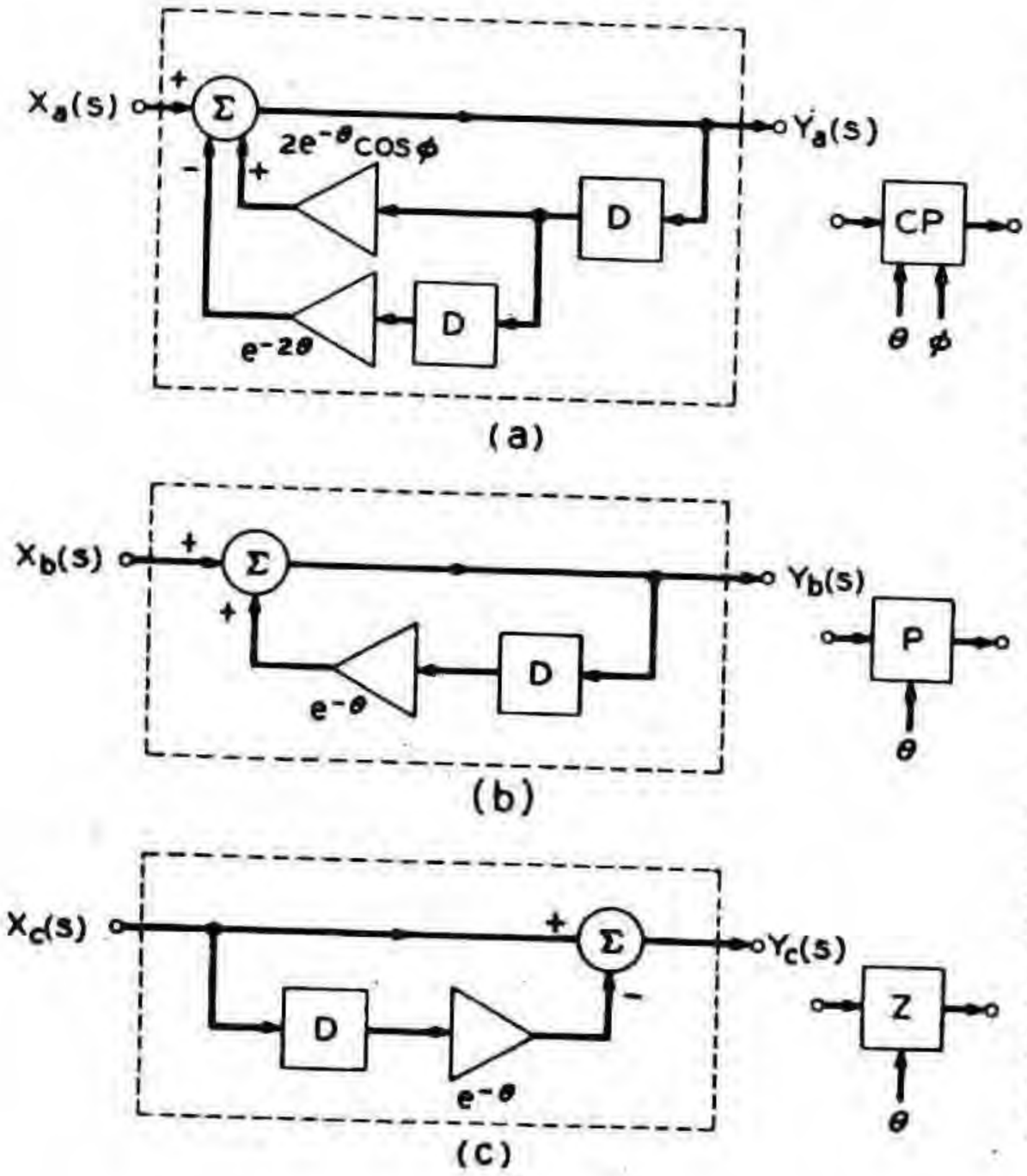

FIG. 2

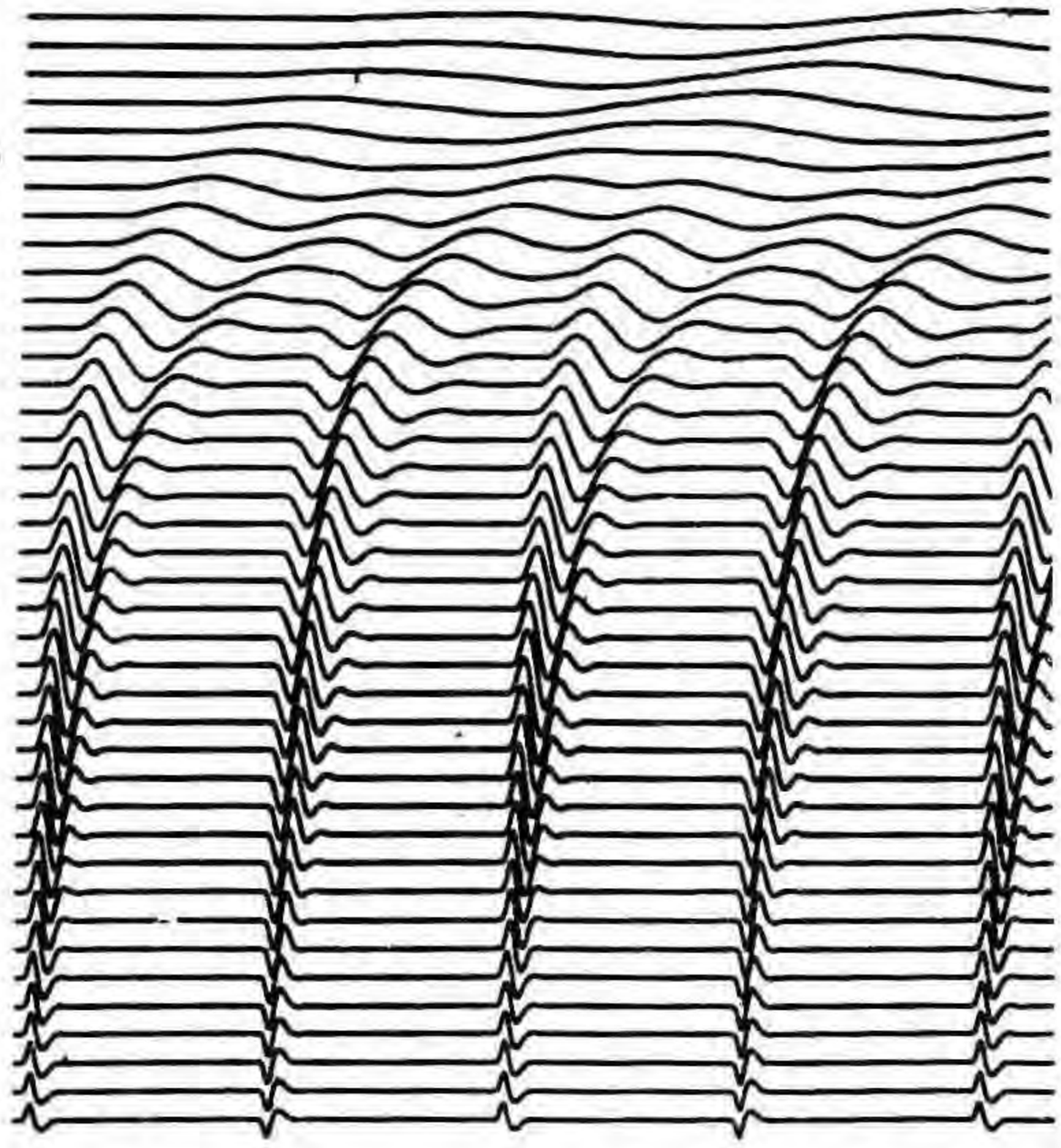

TIME →

FIG. 4

J26

FOURTH INTERNATIONAL CONGRESS ON ACOUSTICS
COPENHAGEN 21.-28. AUGUST 1962

ON NUCLEATION PROCESSES IN ULTRASONIC CAVITATION AND BUBBLE CHAMBERS

M.Bertolotti (Fondaz. U.Bordoni, Ist.Superiore P.T.,Roma)
D.Sette (Università di Roma,Istituto d'Ultracustica,Roma)

1-Introduction.

Experimental evidence has been found (1) that cosmic ray neutrons may be at the origin of ultrasonic cavitation in water through the creation of microbubbles: oxygen nuclei of water knocked-on by neutrons would act as nucleating agents.
Seitz (2) has proposed an explanation of nucleation in bubble chambers. This theory however does not give results in agreement with experiments in ultrasonic cavitation.We have therefore tried to modify the theory in order to explain both phenomena maintaining Seitz's suggestion that delta-rays are involved in the nucleation mechanism.This seems possible using a statistical treatment and taking into account radiolytic processes that, as it is well known, are produced in water at the passage of fast ionizing particles.

2-Bubble chamber theory.

Let us suppose that the delta-rays emitted along the path of the charged particle produce suitable conditions for creation of bubbles which subsequently may grow to visibility.The probability P that the bubble develops from the region interested by the delta-ray is simply calculated.The practical range of a delta-ray of energy W is an indicative quantity of its travel; delta-electrons suffer a great number of collisions and therefore their energy is absorbed by a great number of molecules in a relatively large region which can approximatively be taken as a sphere of diameter equal to the range.We assume

that the delta-ray energy distributes among all the molecules (N) in the region, producing a temperature raise of $\Delta T = W/kN$. The fluctuation theory applied to a great number of these regions allows the calculation of the number n of molecules that, as a consequence of the temperature raise, have a kinetic energy greater or equal to that corresponding to the critical temperature T_c. These molecules can no more be considered as a part of the liquid and by assembling in groups may originate gaseous microcavities. Let us call q the number of molecules contained in a bubble of the critical size at the temperature and pressure conditions of chamber operation. The probability that a region interested by a delta-ray originates a bubble is therefore given by the probability that at least q of the n molecules with energy larger than that at the critical temperature be close to each other. In the case that $q \ll N, n$ (as it usually is) one gets:

$$P(W) = Ne^{-Wq/kT}$$

The number n_b of bubbles created by a fast particle is:

$$n_b = \int_{W_{min}}^{W_{max}} n(W)P(W)dW$$

where n(W) is the number of delta-rays of energy W created by the fast particle. The integration is extended from the minimum energy W_{min} which a delta-ray must have to interest a volume equal to the bubble volume (it may be seen that otherways one may not have bubble formation) to the maximum energy W_{max} that it may receive from the colliding incident particle. One finds:

$$n_b = 1.56 \times 10^4 \frac{aZ^2 p^2 \rho}{\beta^2 \sigma^3 A} e^{-\frac{\sigma^3 A^2 T_c}{p^2 \rho^2 Z^3 T_{op}} 10^{-14} W_{min}^5 (eV)} \quad \text{bubbles/cm}$$

where:

a - number of electrons per molecule useful for delta-rays production (cm^{-3})

Z - atomic number of the liquid
A - atomic weight of the liquid
ρ - density (gr/cm^3)
σ - surface tension (dynes/cm^2)
p - operation pressure (atmos)
T_{op} - operation temperature (°K)
β - fast particle velocity ratio to light velocity

This formula when applied, for example, to the case of a propane chamber working in standard conditions (T_{op} - 328°K, p - 10atmos) gives $n_b \simeq 40/\beta^2$ against $n_b \simeq 10/\beta^2$ as it is experimentally found.

3-Theory of cavitation in water.

When a fast charged particle passes through water it produces three kinds of effects: molecule ionization with consequent thermal heating, radiolysis, delta-ray emission.A cylindrical region along the particle path exists in which heating and radiolytic effects are produced approximatively in a uniform way.In fact the incoming fast particle produces ionized molecules which lie near its path; if the ejected electrons have low energy, they can travel only a short distance before ionizing other molecules.The ionized molecules originate radiolytic processes which lead, through a number of chemical reactions, to formation of H_2,O_2,H_2O_2.It seems reasonable to assume that the ionized molecules and the reaction products move in a diffusive manner through some molecular distances extending the interested region to the aforementioned cylinder which therefore may be assumed to have a radius of the order of $1-2x10^{-7}$ cm.

Delta-rays emitted by the fast particle produce the same effects in a larger quantity.Therefore in the damage cylinder arround the fast particle there are regions where radiolysis and heating are gretly intensified by the passage of a delta-ray.We may calculate an upper energy limit E_o for the incoming particle so that the most of delta-rays travel in the damaged matrix of the liquid arround the particle path.Let us now consider the damaged cylinder along the particle

path between the points where its energy is E_o and nearly zero; it has a radius of $1-2x10^{-7}$ cm. The diffused damage produced by the first two processes is not sufficient to create large cavities; the damaged region may however be considered as a overheated and oversaturated liquid in which large fluctuations are present. It seems possible to assume that delta-rays traveling in such a matrix may produce cavities which grow to the dimentions of the damaged region ($r \cong 10^{-7}$ cm). If the delta-ray number in the cylinder is sufficiently large the microcavities created in this way come in contact and coalesce in a single bubble due to the surface energy gain. In a very short time the whole cylinder passes from the metastable state of a strongly disturbed liquid to the gaseous state and assumes a spherical form.

By appling these considerations to oxygen and hydrogen knocked-on nuclei in water one finds that after a proton has been slowed down to about 0.4MeV the most of the delta rays travel in the cylinder; the same happens for oxygen nuclei below 6MeV. One may then see that in the proton case the microbubbles created by delta-rays never succeed to coalesce whilst oxygen nuclei may gasify the whole volume arround their trajectory. The radius of the resulting bubble may be calculated as about $5x10^{-5}$ cm which is sufficient to explain cavitation experiences in water.

Bibliography.

(1) D.Sette and Wanderling,F.: Phys.Rev. 125, 409 (1962)

(2) F.Seitz: Phys. of Fluids 1 , 2 (1958)

K26

FOURTH INTERNATIONAL CONGRESS ON ACOUSTICS
COPENHAGEN 21.-28. AUGUST 1962

Attenuation of High Frequency Longitudinal and Transverse Waves in Germanium, Silicon and Z-cut Quartz and Their Relation to Thermally Determined Parameters

WARREN P. MASON, H. J. McSKIMIN and T. B. BATEMAN

Bell Telephone Laboratories, Incorporated, Murray Hill, New Jersey

The final cause for attenuation of sound waves in semiconducting and insulating crystals such as silicon, germanium and Z-cut quartz is the direct conversion of acoustic waves into heat, or phonon-phonon interactions. This follows since investigations[1] have shown that dislocations in silicon and germanium are few in number and moreover are completely immobilized by oxygen impurities while in Z-cut quartz[2] longitudinal stresses do not move dislocations.

Measurements have been made for shear and longitudinal waves in germanium and longitudinal waves in silicon and Z-cut quartz with the results shown by Fig. 1. The frequencies of all measurements were in the range 300 to 500 MC which is high enough to give measurable attention, but low enough to minimize trouble with the coupling seals which were silicone liquid and 4 methyl 1-pentene[3]. The results obtained for germanium are comparable with those measured by Dobbs, Chick and Truell,[4] but the seal losses and the probable errors are smaller.

Previous calculations,[2] and the new results discussed below indicate that the attenuation due to phonon-phonon interactions should be of the form

$$A(\text{nepers/cm}) = \frac{2\pi^2 f^2}{\rho V^3}\left[\frac{D\left[\frac{E_o}{C_v}\frac{K}{\bar{V}^2}\right]}{1+\omega^2\tau^2}\right] \quad ; \quad \tau_{THERMAL} = \frac{3K}{C_v\bar{V}^2} \qquad (1)$$

where f is the frequency, ρ the density, V the sound velocity, D a constant to be calculated, E_o is the thermal energy and C_v the specific heat per cubic cm, K is the thermal conductivity in erg cm/cm^{2}x°Kxsec, $\bar{V}$ is the Debye weighted average of the longitudinal and transverse wave velocities, $\omega = 2\pi$ times the frequency and τ the relaxation time for interchange of energy between the various phonon modes.

Since all the thermal quantities for these three materials are known, the attenuations of Fig. 1 can be used to check this relation. For silicon and germanium the velocities and densities are given by previous measurements.[5] For quartz $\rho = 2.65$, $V_\ell = 6.318\text{x}10^5$ cms/sec. Figure 2 shows the calculated values for longitudinal waves in germanium and silicon and shear waves in germanium using an adjustable constant D to obtain the best fit. In silicon a very low temperature relaxation occurs which is believed to be of the type observed[3] previously in sodium chloride. The most likely impurity causing the effect is oxygen. This relaxation will be investigated further.

For shear waves in germanium and longitudinal waves in Z-cut quartz, the entire curves are in agreement with a fall off in attenuation determined by the thermal time constant τ. For longitudinal waves in silicon and germanium a better fit is obtained with a time constant from 2 to 4 times the thermal constant. For shear waves the indicated constant D = 1 in agreement with previous calculations[2] and as verified by previous measurements. The attenuation in X-cut quartz[6], as shown by Fig. 3, has a different temperature relation from that found for Z-cut quartz and gives evidence of dislocation damping.

The constant D can be calculated when the third order elastic moduli are known. Such measurements have recently been made for germanium[7] and the following calculation shows that the measured and calculated D values are comparable. The model considered is the one first suggested by Akheizer[8] but these calculations are the first ones to relate the attenuation to the third order moduli. In this model, a sound wave passing through the crystal modulates the thermal phonons and produces a change in the distribution of the thermal energies so that they are not in the equilibrium Planck distribution. The re-establishment of equilibrium proceeds with a time constant τ and results in an increase in entropy and hence an absorption of sound. It is assumed that all phonon directions and all wave types are considered. The thermal energy for all modes of one polarization will be of the Debye form

$$E_1 = \frac{9Nh}{\nu_g^3}\int_0^{\nu_g} \frac{\nu^3 d\nu}{\left[e^{h\nu/kT} - 1\right]} \quad ; \quad \nu_g = GV/\ell \tag{2}$$

where G is a constant depending on the number of modes per unit volume, ℓ is the path length, V the velocity of the wave, N is the number of modes per mole of the type under consideration, h is Planck's constant, ν the frequency of the mode, ν_g the limiting frequency, k is Boltzmann's constant and T is the absolute temperature. The total internal energy U will be the sum of the elastic energy plus the thermal energy. For a strain S_1 along the X-axis, U can be written

$$U = c_{11}^{\theta} S_1^2/2 + \Sigma E_1 \tag{3}$$

where c_{11}^{θ} is the isothermal elastic constant. If we suddenly change the dimension in the X-direction by a strain S_{1_o}, the stress is given by

$$T_1 = \partial U/\partial S_{1_o} = c_{11}^{\theta} S_{1_o} + \sum \frac{\partial}{\partial S_{1_o}} \left(\frac{9Nh}{\nu_g^3}\int_0^{\nu_g} \frac{\nu^3 d\nu}{(e^{h\nu/kT}-1)}\right) \tag{4}$$

Since the integral is really the sum of all the modes times their thermal energies, and since the entropy will not be changed by a dimensional change, the integral will be invariant to the change and (4) becomes

$$T_1 = c_{11}^{\theta} S_{1_o} - 3\left(\frac{d\nu_g}{\partial S_{1_o}}/\nu_g\right)\left[\frac{9Nh}{\nu_g^3}\int_0^{\nu_g} \frac{\nu^3 d\nu}{(e^{h\nu/kT}-1)}\right] = c_{11}^{\theta} S_{1_o} - 3\sum E_1\left(\frac{\partial \nu_{g_1}}{\partial S_{1_o}}/\nu_{g_1}\right) \tag{5}$$

The variation of ν_g will from equation (2) depend on the variation of the velocity with S_{1_o} divided by the dimensional change $(1+S_{1_o}\cos\theta)$ where θ is the angle between X and the direction of phonon propagation. As shown by reference (7), this variation can be calculated for any direction when the third order moduli are known. For example, for a longitudinal wave along X, with a constant superposed strain S_{1_o},

$$\nu_g = \frac{GV}{1+S_{1_o}} = G\sqrt{\frac{c_{11}}{\rho}}\left[1 + \frac{S_{1_o}}{2}\left(3+6\,\frac{c_{111}}{c_{11}}\right)\right] = GV_o(1-\beta_1 S_{1_o}) \; ; \; \beta_1 = 1.34 \tag{6}$$

where C_{111} is one of the six third order moduli. For any other direction or any other mode, the change in v_g will have the form of (6), so that the effect of a suddenly applied strain S_{1_o} is to produce a stress

$$T_1 = c_{11}^{\theta} S_{1_o} + 3 \sum \frac{E_i \beta_i}{1 - \beta_i S_{1_o}} \doteq \left[c_{11}^{\theta} + 3 \sum E_i \beta_i^2 \right] S_{1_o} + 3 \sum E_i \beta_i \qquad (7)$$

The last term represents the stress required to keep the volume constant as the temperature varies, with no superposed strain S_{1_o}. The other term adds to the elastic modulus, which will therefore increase in the presence of the acoustic wave by the amount inside the bracket summed for all directions. This increase will relax down to the adiabatic modulus with the short relaxation time τ. This increase in modulus produces an attenuation given by

$$A+jB = \frac{j\omega}{\sqrt{c_{11}/\rho}} \doteq \frac{2\pi^2 f^2}{\rho V^3} \left[3 \sum E_i \beta_i^2 - \frac{\alpha^2 (c_{11}+2c_{12})^2 T}{C_v} \right] \left[\frac{\omega\tau}{1+\omega^2\tau^2} \right] + \frac{j}{\sqrt{c_{11}^{\sigma}/\rho}} \qquad (8)$$

Since we have neglected dispersion in this model, and hence can only hope to obtain an approximate value, it does not seem worth while to carry out the integral for all directions. The waves along [100], [110] and [111] directions are easily solved for from the data of reference (7), and these have been summed after assigning (1/39)th of the energy to each vibration. We find the sum to be $1.34E_o = 1.34 \times 3.5 \times 10^9$ ergs/cc at 300°K, giving a total increase of 3 times this or 14×10^9 d/cm^2 for the modulus increase. Subtracting the adiabatic modulus 2.66×10^9 d/cm^2, we find D to be 9.8 compared to a measured value of 11.1.

For a shear wave, similar calculations show that most of the change is due to dimensional factors - which give a constant $E_o/3$ - giving D = 1 in agreement with previous calculations[2] and measurements.[4]

References

1. Pearson, Read and Feldmann, Acta. Met. 5, 181 (1957). Lamb, Redwood and Steinshlifer, Phys. Rev. Letters, 3, 28, (1959).
2. W. P. Mason, J. Acous. Soc. Amer. 32, 458 (1960).
3. K. Brugger and W. P. Mason, Phys. Rev. Letters 7, 270 (1961).
4. Dobbs, Chick and Truell, Phys. Rev. Letters 3, 332 (1959); Dobbs, VII Int. Conf. on Low Temperature Physics 5-3, p. 15 (1960).
5. H. J. McSkimin, J. Appl. Phys. 24, 988 (1953).
6. H. E. Bömmel and K. Dransfeld, Phys. Rev. 117, 1245 (1960).
7. Bateman, Mason and McSkimin, J. Appl. Phys. 32, 928 (1961).
8. A. Akheizer, J. Phys. U.S.S.R. 1, 277 (1939).

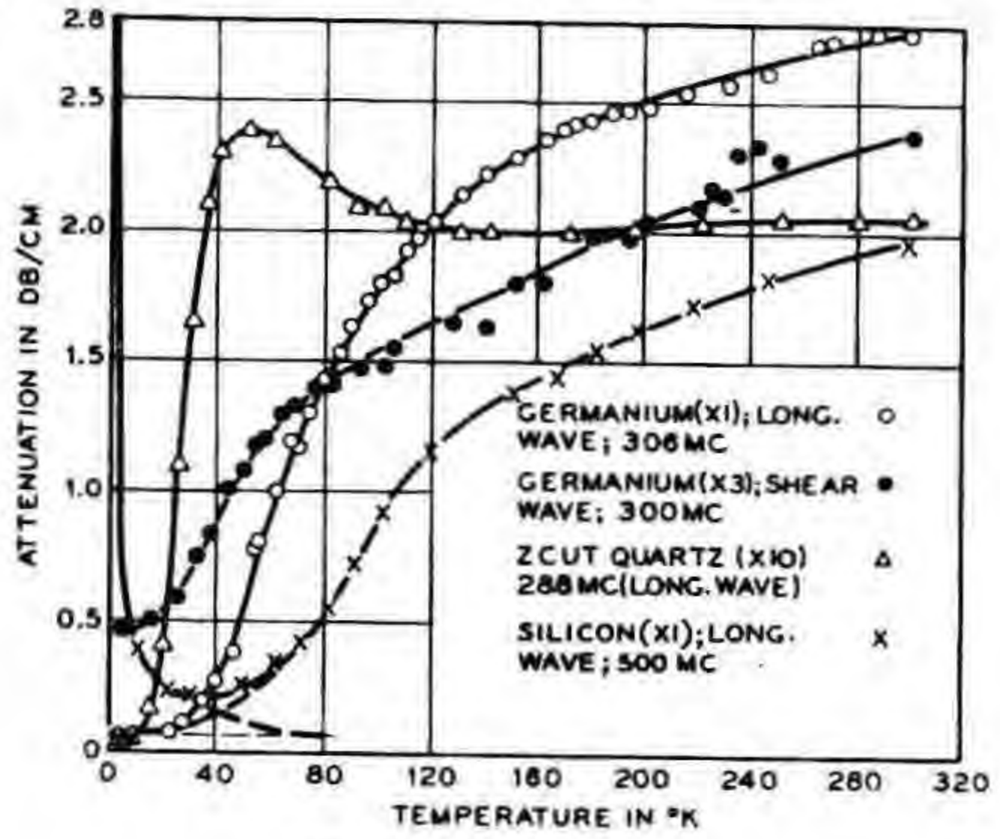

Figure 1

Measurements of the attenuations of longitudinal and shear waves in germanium, silicon and Z-cut quartz. In order to show all curves on the same figure the attenuation in Z-cut quartz is multiplied by 10 and shear attenuation in germanium by 3. Note relaxation effect in silicon at low temperatures.

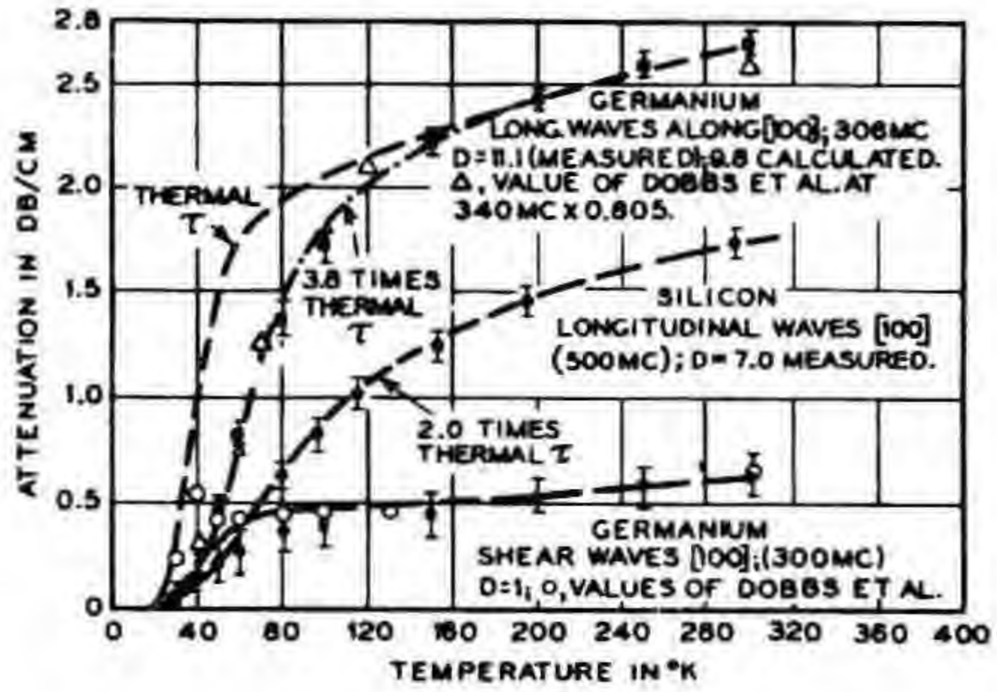

Figure 2

Comparison of measured and theoretical curves for germanium and silicon. Factor D is chosen to obtain the best fit.

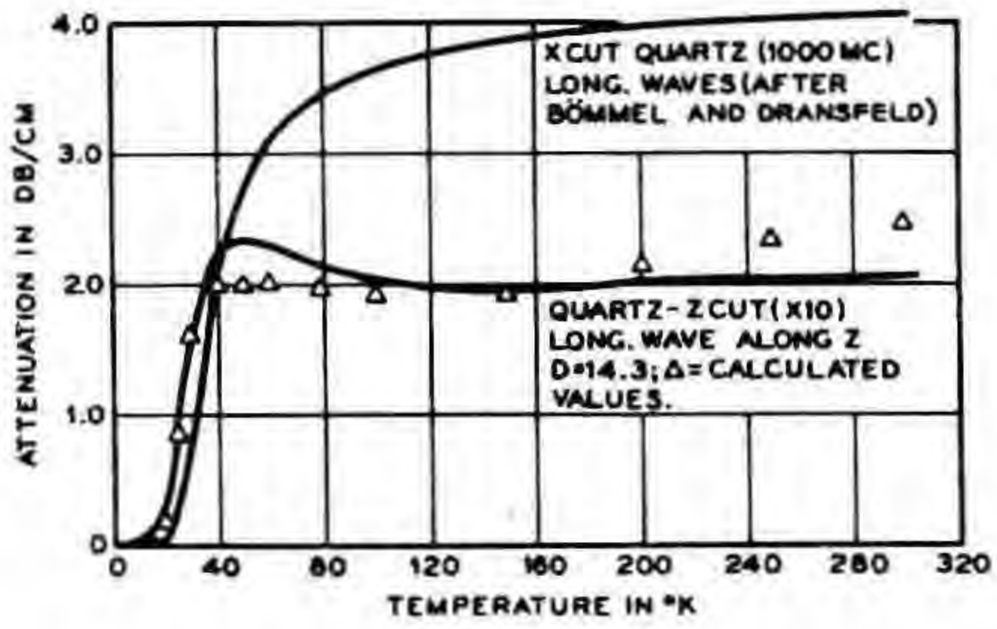

Figure 3

Comparison of measured and theoretical curves for Z-cut quartz with factor D chosen to obtain the best fit. The attenuation for X-cut quartz measured at 1000 MC is shown for comparison.

L26

FOURTH INTERNATIONAL CONGRESS ON ACOUSTICS
COPENHAGEN 21.-28. AUGUST 1962

AKUSTISCHE SCHALTUNGEN UNTER GLEICHSTRÖMUNG

Ewald Eichler
Bolt Beranek and Newman Inc, Cambridge, Massachusetts

ZUSAMMENFASSUNG. Beim Hinzutreten einer Gleichströmung ändern akustische Elemente ihre Schaltungseigenschaften, und neue akustische Widerstände treten auf. Diese Wirkungen werden in elementarer Weise berücksichtigt und ihre Vorteile werden gezeigt. Wir untersuchen einfache Schaltungen aus Volumina, Rohren und Öffnungen und beziehen ihre Schalldämpfung auf den Druckverlust.

EINLEITUNG. Bei der Untersuchung akustischer Schaltungen ist eine etwa überlagerte Gleichströmung oft außer acht gelassen worden. Sobald eine Gleichströmung zum Schall hinzutritt, ändern aber akustische und hydrodynamische Elemente wie Rohre, Blenden, Düsen und Widerstände ihre akustischen Eigenschaften. Unter Vernachlässigung der Viskosität errechnen sich die Veränderungen als Korrekturen von zweiter Ordnung in der Machzahl $M_o = v_o/c_o$ der Gleichströmung. Viskosität jedoch führt in praktischen Fällen zu Turbulenz und zu drastischeren Veränderungen. Turbulenz ist auch verantwortlich für zusätzliche akustische Verluste und Widerstände, die erst mit der Gleichströmung auftreten.

Wenn auch solche Wirkungen noch keineswegs hinreichend erforscht sind, so wollen wir im folgenden doch versuchen, sie in einer vorläufigen und elementaren Weise zu erfassen, und zu zeigen, daß die Eigenschaften akustischer Schaltungen wesentlich von ihnen abhängen. Wir beschränken uns dabei durchwegs auf kleine akustische Signale, die einer Unterschall-Gleichströmung überlagert sind.

VERÄNDERTE SCHALTUNGSEIGENSCHAFTEN. Es ist bekannt, daß Rohre akustisch länger werden, sowie sie eine Gleichströmung führen, und zwar ist die Wellenlänge $\lambda = \lambda_o(1-M_o^2)$ um den Faktor $1-M_o^2$ kleiner als im ruhenden Medium. Dieselbe Korrektur finden wir theoretisch für die Impedanz von Blenden und für die Strahlungsimpedanz offener Rohre, vorausgesetzt daß die Strömung laminar ist. Dieselbe Korrektur sollte auch für jenen Teil einer Öffnungsimpedanz gelten, der einer Querströmung ausgesetzt ist.

NEUE SCHALTUNGSEIGENSCHAFTEN. Bei hinreichend hoher Geschwindigkeit wird die Strömung turbulent, und die erstbesprochenen Veränderungen werden durch neue Erscheinungen verdeckt, wenn auch nicht aufgehoben. In einer turbulenten Gleichströmung treten Druckabfälle auf, welche empirisch als "Reibungsgesetze" erfaßt werden. Wenn wir annehmen, daß diese Gesetze momentan gültig sind, also auch für die Gleichströmung mit überlagerter Wechselströmung, so können wir die resultierenden akustischen Widerstände und Verluste berechnen. Experimentelle[1] und theoretische[2,3] Ergebnisse auf diesem Gebiet sind noch spärlich. Vor-

---

[1] C.E.McAuliffe: The influence of high-speed air flow on the behavior of acoustic elements. M.S.Thesis, M.I.T., 1950

[2] P.J.Westervelt: Acoustic impedance in terms of energy functions. J.A.S.A. 23, 347(1950)

läufig wollen wir annehmen, daß die momentane Betrachtungsweise gilt, solange das Element klein zur Wellenlänge und die Frequenz kleiner als die Strouhalfrequenz[3] ist, und wir beschränken uns auf diesen tieffrequenten Bereich.

Zur Berücksichtigung der turbulenten Verluste in einem Rohr fügen wir der Impulsgleichung das Glied RQv^2 hinzu. (In der Literatur findet man $R = 0{,}016/D$ für die Reibungszahl von Luft in technischen Stahlrohren vom Durchmesser D.) Für ein akustisches Signal $\sim \exp(i\omega t - ikx)$ ergeben sich die Fortpflanzungszahlen

$$k = \pm\left\{1 - i\gamma(1 \pm M_o^2/2) + \gamma^2\left[(2-M_o^2)^2 - M_o^2\right]/8(1 \mp M_o) + O(\gamma^3)\right\} k_o/(1 \pm M_o),$$

wo $\gamma = RM_o/k_o$ und $k_o = \omega/c_o$. Das obere Vorzeichen gehört der Welle die mit der Strömung läuft, das untere der rückläufigen. Die zugehörigen Wellenwiderstände sind $Z = \pm\rho_o c_o\left[1 - i\gamma(1 \pm 3M_o/2 + M_o^2/2) + O(\gamma^2)\right]$.

Das Reibungsgesetz für eine Blende oder die Öffnung eines Rohrs ist $p_1 - p_2 = R_e\rho_2 v_e^2/2$ (Abb.1). ρ_2 ist die Dichte auf der Leeseite und v_e ist die fiktive Strömungsgeschwindigkeit durch die Öffnungsfläche A_e, die mit ρ_2 den tatsächlichen Massefluß $f = A_e\rho_2 v_e$ ergibt. Wenn zur Rechten

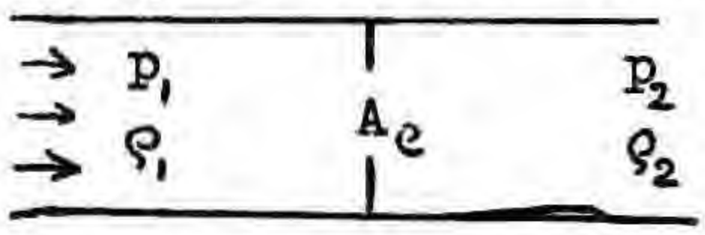

Abb.1. Blende in einem Rohr

ein akustischer Widerstand Z_r liegt (auf die Blendenöffnung bezogen), so ist der resultierende akustische Gesamtwiderstand

$Z = P/V = R_e v_e \rho_2 (1 + Z_r v_e/\rho_2 c_o^2) + Z_r$. v_e und ρ_2 sind hier Gleichwerte. (Für kleine Blenden in einem Rohr ist $R \doteq 2$, für die Endöffnung eines Rohrs von 2cm Durchmesser ergab sich $R = 0{,}4$.[4])

Turbulenz führt nicht nur zu Verlusten sondern auch zu einer drastischen Verminderung der Reaktanz einer Öffnung auf etwa 3/8 ihres Werts, und dieser Effekt tritt schon bei ziemlich kleinen Geschwindigkeiten auf.

Bei laminarer Strömung gelten Reibungsgesetze der Form $p_1 - p_2 = R_L v$. Bei mittleren Strömungsgeschwindigkeiten liegt ein Übergangsgebiet zwischen laminarer und turbulenter Strömung, in welchem die Reibungszahlen R_L, R, oder R_e nicht mehr konstant sind sondern sich mit der Reynoldszahl ändern. Wir können auf dieses interessante Gebiet hier leider nicht eingehen. Abschätzungen zeigen, daß in vielen praktischen Fällen der turbulente Widerstand die akustische Impedanz dominiert.

DRUCKVERLUST. Der Gleichdruckabfall oder kurz Druckverlust eines Elements oder einer Schaltung ergibt sich aus den Reibungsgesetzen. Er besteht aus zwei Teilen. Der erste Teil rührt von der Gleichströmung her und ist $DV = RL\rho_o v_o^2$ für ein (kurzes) Rohr der Länge L, $DV = R_e\rho_2 v_e^2/2$ für eine Blende oder ein Rohrende. Der zweite Teil des Druckverlusts rührt von der Wechselströmung her. Er ist durchwegs von zweiter Ordnung in der Wechselamplitude, also unter unseren gegenwärtigen Voraussetzungen zu vernachlässigen.

---

[3] H.G.Elrod: Pulsating flow through a nozzle. Unveröffentlichte Mitteilung, Mai 1962

[4] B.G.Watters, R.M.Hoover, and P.A.Franken: Designing a muffler for small engines. Noise Control 5, 98(1959)

SCHALLDÄMPFUNG. Unter den akustischen Schaltungen denen die Theorie gilt, sind vor allem Schalldämpfer von der Art wie wir sie bei Kolbenkraftmaschinen finden. Ihre akustische Wirkung wird durch die Schalldämpfung SD beschrieben, das Verhältnis der abgestrahlten Schalleistung mit und ohne Schalldämpfer. Wir können hier nur kurz die Ergebnisse für einige einfache Schaltungen hersetzen. Dabei wollen wir die Schalldämpfung auf den Druckverlust beziehen, denn das sind die beiden Größen die oft am meisten interessieren.

Die Schalldämpfung eines an eine Verschiebungsquelle angekoppelten Rohrstücks ist bekanntlich kleiner als eins, außer wenn die Rohrlänge ein vielfaches der halben Rohrwellenlänge ist. Dazwischen liegen Minima deren Tiefe durch die Verluste begrenzt wird. Für ein turbulentes Rohrstück ergibt sich $SD_{min} = [r+\gamma\varphi(1-M_o^2/2)]^2 - 3\gamma xM$ zu zweiter Ordnung in γ und $r+ix = Z/\rho_o c_o$, wo Z den akustischen Gesamtwiderstand am Rohrende (Öffnung oder Blende) und $\varphi = 2\pi L/\lambda$ bedeuten. Wenn wir die Strahlungsimpedanz Z_r am Ende vernachlässigen, bleibt

$$SD_{min} = \left[\frac{2DV}{\kappa p_o M_o} + \frac{1-M_o^2/2}{1-M_o^2}\cdot\frac{\Delta DV}{\kappa(p_o+DV)M_o}\right]^2$$

(DV Druckverlust im Rohr, ΔDV Druckverlust am Rohrende, p_o Atmosphärendruck, κ Verhältnis der spezifischen Wärmen). Für eine Massequelle ergibt sich in erster Näherung $SD_{min} = M_o^2 + 2\frac{\Delta DV+2DV(1-M_o^2)}{\kappa(p_o+DV)}$. Exaktere Formeln sind beträchtlich länger.

Für den durchströmten Resonator an einer Massequelle (Abb.2.) ergeben sich die in Abb.3 dargestellten Kurven der Schalldämpfung. Jede der

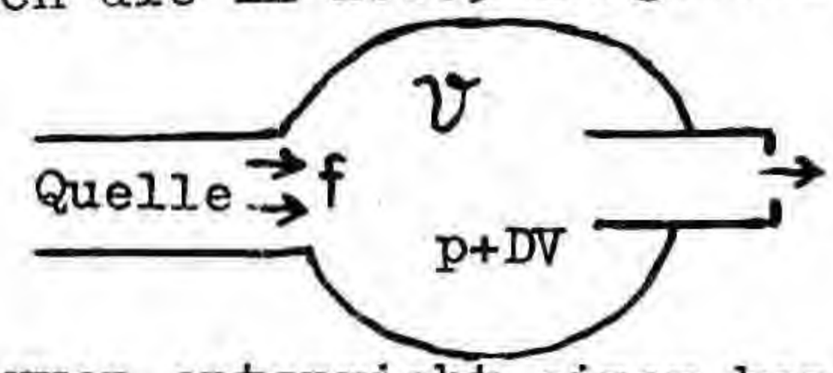

Abb.2. Durchströmter Resonator

Kurven entspricht einem konstanten Druckverlust, der implizit durch die Schalldämpfung SD_o bei der Resonanzfrequenz gegeben ist; die Beziehungen unterscheiden sich je nachdem der Strömungswiderstand des Resonators laminar oder turbulent ist (Abb.2. zeigt ein Rohrstück mit Blende). $\mathcal{V}$ ist das Volumen des Hohlraums, und f_o der mittlere Massefluß. Wir sehen, daß der turbulente Resonator bei gleichem Druckverlust dem laminaren bis zu 6db überlegen ist, besonders um die Resonanzfrequenz. Was geschieht, wenn die Quelle ihre Stärke proportional zur Frequenz (und der Drehzahl) ändert, zeigt Abb.4. Jede der dargestellten Kurven gibt die abgestrahlte Schalleistung eines Resonators, der durch seine Schalldämpfung bei der Resonanzfrequenz charakterisiert ist.

SCHLUSSBEMERKUNG. Die vorgebrachten elementaren Methoden sollten sich bei der Behandlung von akustischen Schaltungen unter Strömung als nützlich erweisen. Wir hoffen auch, daß sie dazu anregen werden, die Eigenschaften von Rohren, Blenden, Öffnungen, und anderen hydrodynamischen und akustischen Elementen genauer zu erforschen.

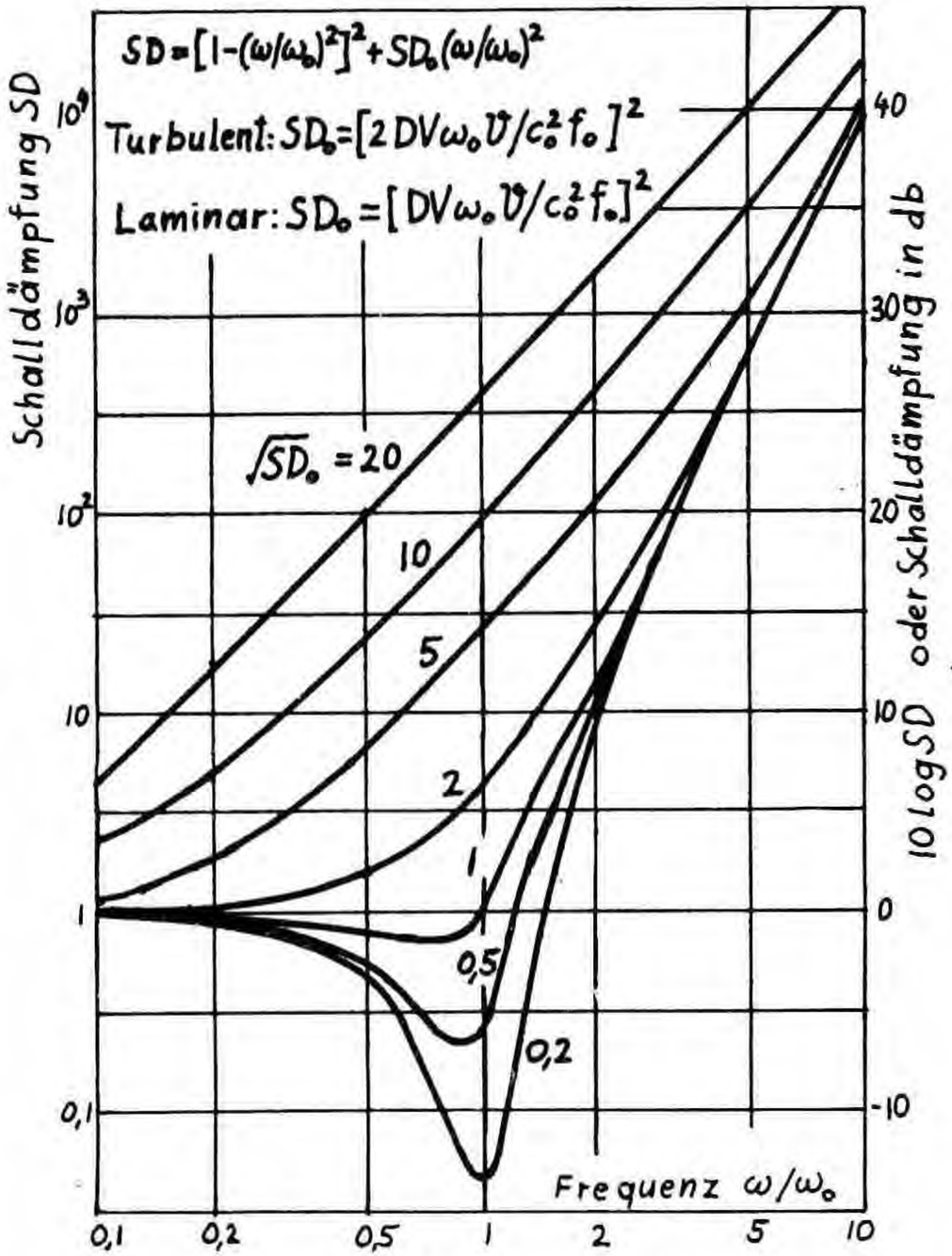

Abb.3. Schalldämpfung des durchströmten Resonators als Funktion vonFrequenz und Druckverlust

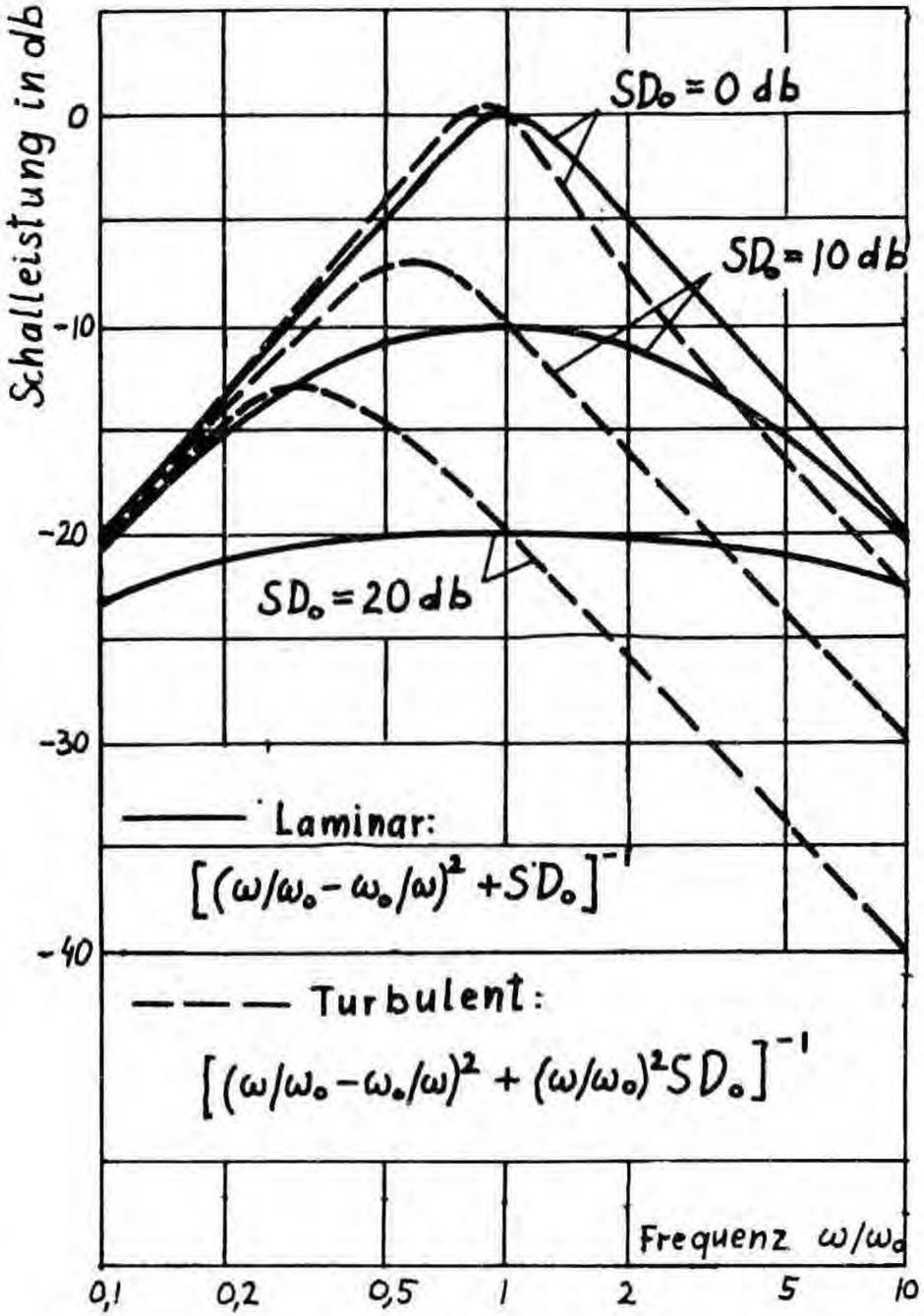

Abb.4. Abgestrahlte Schalleistung bezogen auf die Leistung bei $\omega=\omega_0$ onne Schalldämpfer

M26

FOURTH INTERNATIONAL CONGRESS ON ACOUSTICS
COPENHAGEN 21.-28. AUGUST 1962

Une méthode d'analyse acoustique spatiale

Witold Straszewicz

La méthode bien connue d'analyse graphique d'un interieur qu'on effectue dans le plan d'une section verticale oblongue n'est pas suffisante si la forme architectonique de cet interieur est trop compliquée, Cette methode cesse d'être applicable du tout dans le cas ,où les plans du plafond ne sont pas orthogonaux au plan de la section. Il est alors necessaire de recourir a une analyse spatiale. Dans ce qui suit on indique un procédé graphique et son analogue analytique qui peuvent servir à une telle analyse.

Il s'agit ici d'une construction représentée sur la fig.1 en projection axonometrique. La source du son se trouve ici au point S du plan sonorisé horizontal π .Un point R de la surface reflétante et le plan α tangent à cette surface en R étant donnés, on cherche sur le plan π la trace X du rayon reflété en R . On détermine dans ce but la normale RR_n au plan α ; ensuite on construit dans le plan de reflexion l'angle R_nRx égal à l'angle d'incidence $\varphi = \sphericalangle SRR_n$ On peut utiliser le fait que le rayon reflété passe par la source imaginaire S_i , c'est à dire par le point symétrique à la source S par rapport au plan α .

Les images axonometriques ont l'avantage de parler bien à l'imagination, mais leur construction comme celle /non indiquée/ qui a conduit à le fig.1, n'est pas assez simple. De plus,l'analyse acoustique doit se baser sur des dessins architectoniques exécutés de règle en projections orthogonales sur deux plans perpendiculaires.Notre construction doit donc être effectuée aussi par la methode de Monge.Ceci montre la fig.2 sur un exemple assez proche aux cas qu'on rencontre dans la pratique. La source S du son est donnée ici par ses projections /S',S"/ de Monge, le plan reflétant par les projections A'B'C' et A"B"C"d'un triangle ABC. Sur le plan horizontal de projection on a déterminé les traces A_o, B_o, C_o des rayons reflétés on A,B,C. Pour trouver les projections de ces rayons on peut rabattre les plans de reflexion sur le plan horizontal; sur la fig.2 le point C a été rabattu en C_k. On peut aussi utiliser dans ce but la source imaginaire S_i,ce qui donne un moyen de contrôler l'exactitude du dessin.

Dans certains cas, par exemple si l'inclinaison du plan reflétant au plan horizontal est insensible ou bien si les distances mutuelles des points A,B,C sont relativement petites, la construction peut devenir trop peu exacte. On peut alors traiter le problème par le calcul. Admettons que l'origine du système de coordonnées se trouve en S et que λ, μ, ν sont les cosinus directeur de la normale au plan contenant les points A,B,C,..Les coordonnées de la source imaginaire S_i s'expriment alors par les formules

$$x_i = 2\lambda k \,,\quad y_i = 2\mu k \,,\quad z_i = 2\nu k \quad \text{où} \quad k = \lambda x_A + \mu y_A + \nu z_A$$

et le rayon reflété, disons au point B, est déterminé par les équations

$$\frac{x - x_i}{x_B - x_i} = \frac{y - y_i}{y_B - y_i} = \frac{z - z_i}{z_B - z_i}$$

En y adpignant l'equation f/x,y,z/=o /p.ex. z = o/ de la surface sonorisée, on calcule de ce système d'equations les coordonnées /x,y,z/ de la trace cherchée B_o .

On a pu constater qu'il est souvent avantageux de combiner ces deux méthodes en determinant d'abord par le calcul la position du point S_i et en effectuant ensuite une construction géométrique pour trouver les traces A_o,B_o,C_o ...

En se servant d'un tel procédé pour analyser la sonorisation yenant d'une première reflexion dans le cas d'une salle de 10000 m³ au plafond couvert de 20 prismes, chacune à 2 faces reflétantes triangulaires, on a eu besoin de 6 heures du travail. La méthode semble donc acceptable dans la pratique.

Il se pose souvent devant l,acousticien projetant un problème inverse au précedent. On connait la surface qui doit recevoir une sonorisation supplementaire au moyen de l'energie émise par une source comme S et reflétée une premiere fois; on cherche la forme, l'étandue et l'inclinaison de la surface reflétante convenable.

On peut résoudre un tel problème en transposant la construction précédante. Une construction de ce genre montre la fig.3. On donne sur le plan horizontal un quadrangle A_o,B_o,C_o et la source S de l'energie et on choisit un point P /P',P''/, Il s,agit de trouver un quadrangle ABCD dont les diagonales se couperaient en P et tel que les rayons reflétés au points A,B,C,D du plan α = ABCD passeraient par A_o,B_o, C_oD_o respectivement . On determinée d'abord la normale au plan cherché en rabattant le plan SPP_o sur le plan horizontal, ensuite on trouve la source imaginaire S_i et enfin les points A,B,C,D. Il est recommandable d'exécuter cette dernière opération par le calcul.

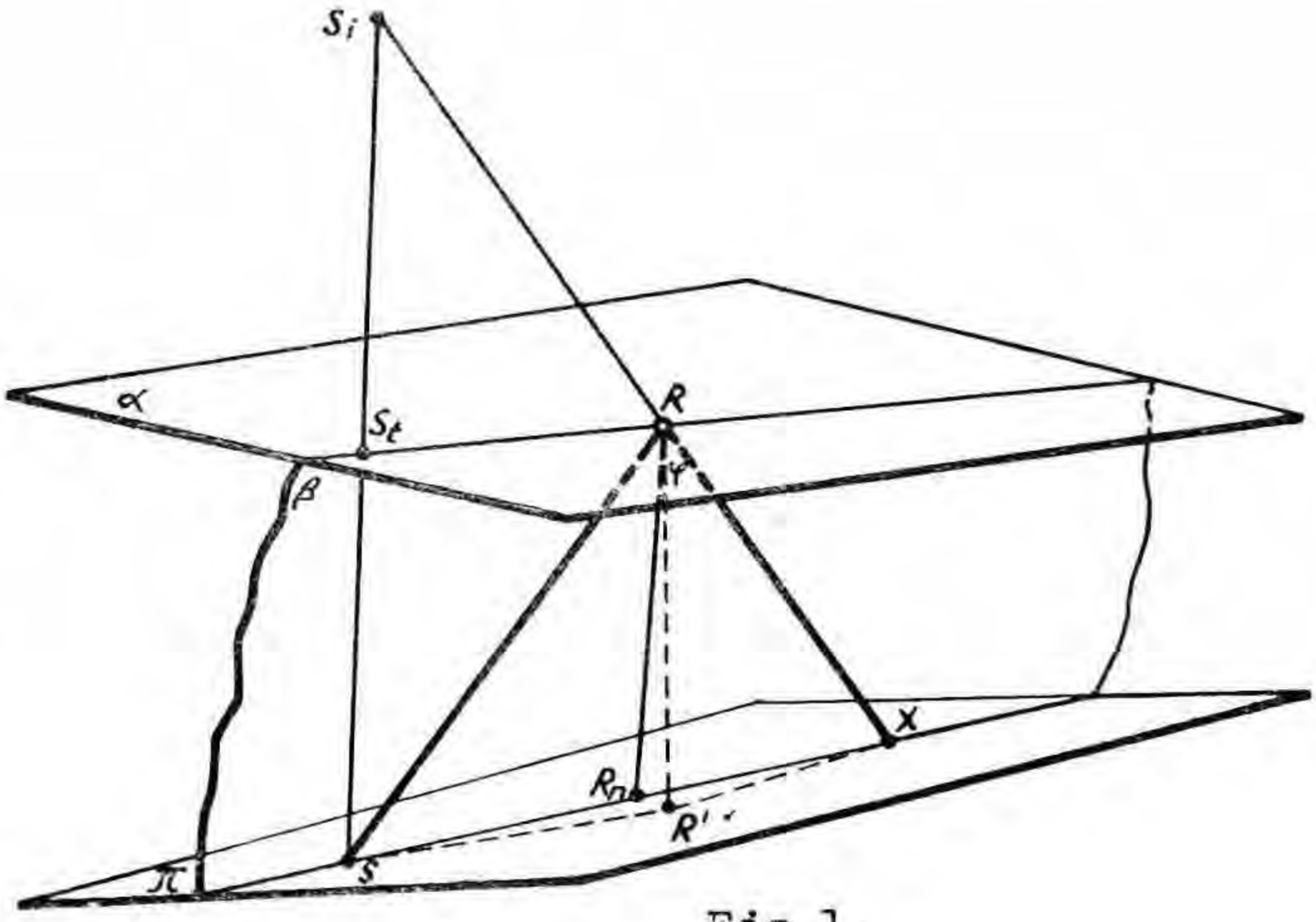

Fig.1.

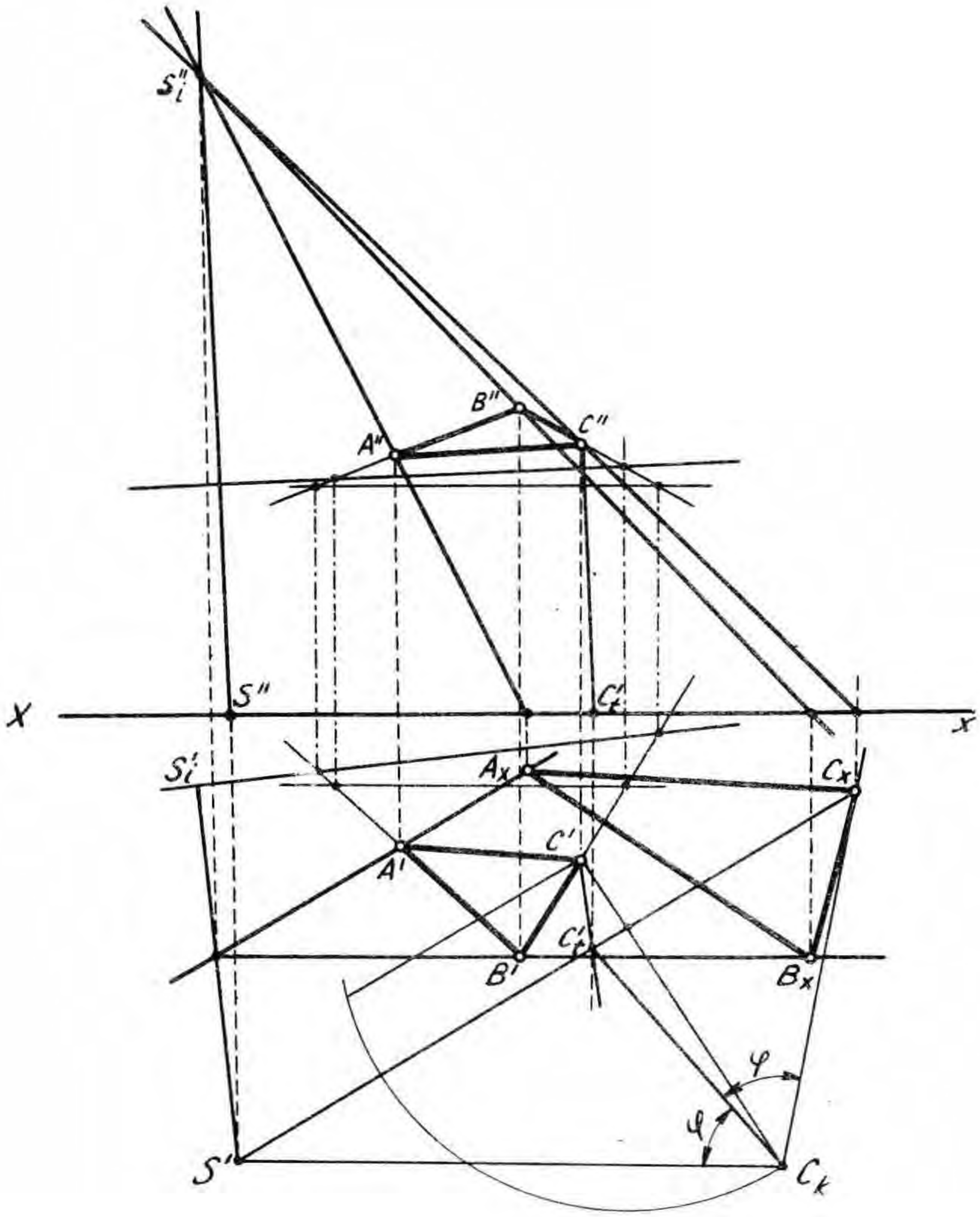

Fig.2.

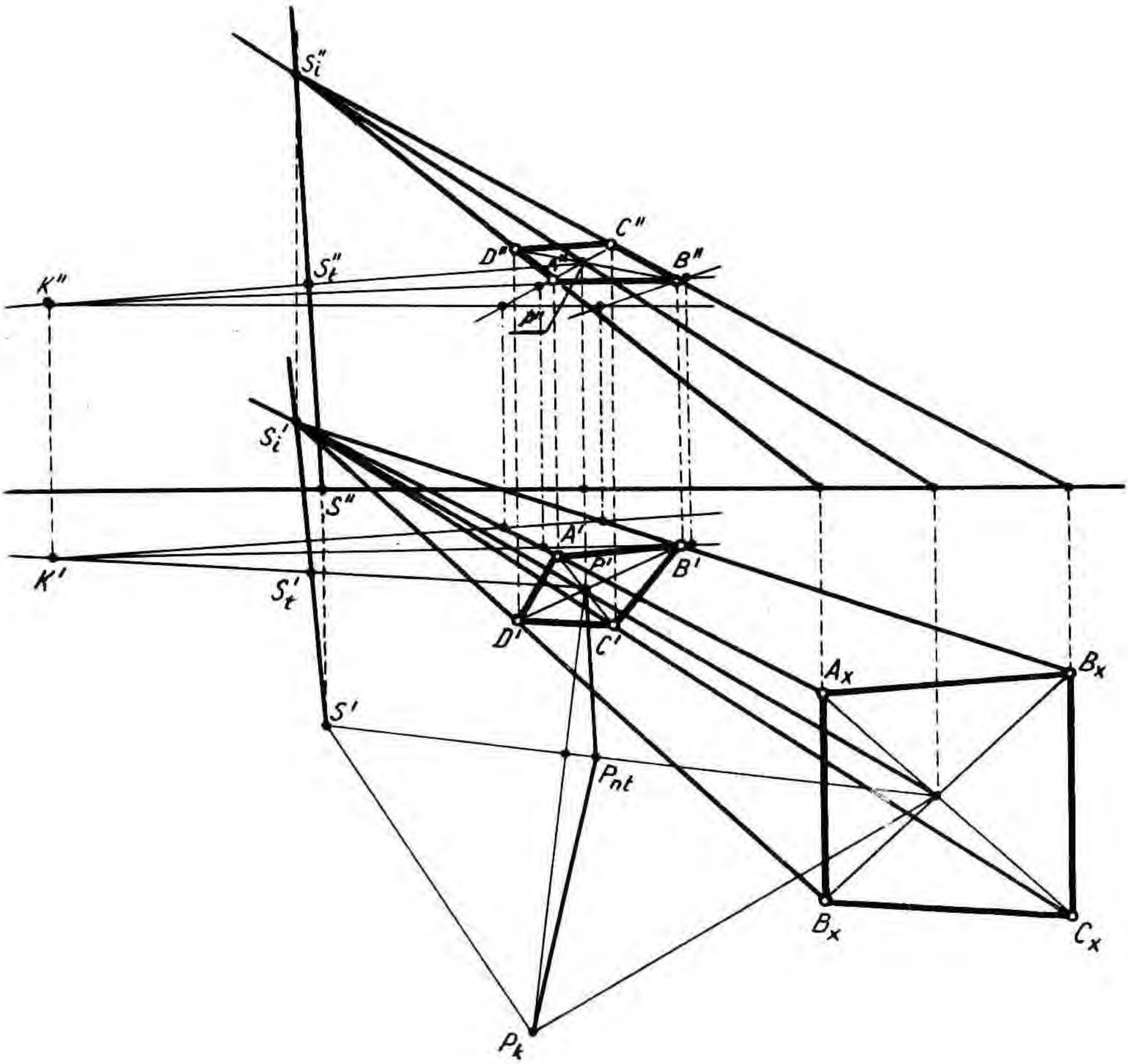

Fig.3.

N26

FOURTH INTERNATIONAL CONGRESS ON ACOUSTICS
COPENHAGEN 21.-28. AUGUST 1962

A NEW DETERMINATION OF THE ACOUSTICAL IMPEDANCE OF HUMAN EARS

Dr. M.E. Delany

National Physical Laboratory, Teddington, England.

1. Introduction

One factor limiting accuracy in the increasingly important field of pure-tone audiometry is the precision with which the sensitivity of the measuring earphone, when applied to the normal human ear, may be determined. Basically a comparison of the sensitivity of the earphone with a reference earphone may be effected subjectively, using a number of otologically normal people, but the process is time-consuming and costly. It has to be restricted to a small number of earphones maintained as standards of their respective patterns or to inter-laboratory comparisons such as those recently completed under the auspices of the International Organization for Standardization. For routine purposes an objective method is indispensable, and in its simplest form this is based on a rigid, hard-walled cavity of simple shape within which the sound pressure produced by a known electrical excitation of the earphone is measured. This is a convenient means of realizing the calibration of an audiometer, providing the latter is equipped with a type of earphone for which the corresponding normal threshold of hearing is known. However, there is no simple connection between the earphone response on a coupler and on a human ear due to lack of acoustical and geometrical similarity. Attempts to overcome this limitation with artificial ears based on the acoustical properties of the average real ear have been made and various forms have been adopted as national standards, but none appears to be adequate for accurately comparing the true sensitivities of earphones of different types.

The International Electrotechnical Commission has recently taken up the question of specifying an improved artificial ear, so that audiometer calibrations may be subject to less uncertainties and the exchange of information greatly facilitated, and the present work was undertaken with the work of IEC in view.

There is more than one approach to the design of an artificial ear, but a knowledge of the acoustical impedance presented to earphones by the typical human ear is regarded as fundamental. A number of investigations with this objective have been reported over the last 30 years, but interest has been mainly confined to the range of frequencies important in telephonometry. Moreover, results are so discordant as to preclude the possibility of deducing reliable impedance values, particularly at lower frequencies where variable leakage between earcap and ear affects results severely. In audiometry one endeavours to minimize this variability in the sound pressure generated for given earphone excitation, by specifying a certain headband pressure.

The means of taking leakage into account is a vexed question, but it seems to us logical in the first instance to specify the impedance of the human ear under "no leakage" conditions. In the ordinary use of telephones leakage is unavoidably present and for telephonometric purposes it may well be necessary to determine typical values of leakage and to introduce an additional simulating element into the artificial ear.

The investigation reported here furnishes new data on the acoustical impedance of human ears viewed from the aperture of various earcaps with particular reference to types fitted to earphones for audiometry, preliminary to the design of an improved artificial ear. The force of application of earcap to auricle has been controlled pneumatically and acoustical leakage effects minimized.

2. Measurement of acoustical impedance of ears

Since it is impracticable to measure directly at a point the simultaneous acoustical pressure and volume velocity, the complex ratio of which gives the acoustical impedance, recourse must be made to an indirect method. West (1) used a resonance-tube technique. Inglis, Gray and Jenkins (2), Loncheval (3), Zwicker (4) and various determinations by the Bell Telephone Manufacturing Co., Antwerp (5) have used a reaction-on-source technique, while Nábělek (6) and Pirlet (7) used a standing-wave method. However, in none of these determinations does there appear to have been any systematic means of controlling the force of application of earcap to ear, which affects the acoustical leakage.

For the present work the equipment consisted of a probe employing two high-impedance electrostatic transducers (B & K 4134), one generating a known volume velocity and the other providing a measure of the resulting sound pressure. A similar technique has been used by Mawardi (8) for measuring the acoustic impedance of absorbing materials, by Møller (9) for measurements of middle-ear impedance, and most recently by Brüel et al (10), who measured the modulus of the impedance of a number of ears as seen through the aperture of one particular earcap. The source transducer was coupled to the ear cavity via a very short, large-diameter tube and a similar tube coupled the receiving transducer to the ear volume, the two probe tubes being separated by only two or three millimetres. The electrical output of the receiving transducer was amplified and its relative magnitude and phase measured using systems having very narrow bandwidths. By maintaining the driving voltage constant the volume velocity generated increased directly with increasing frequency and for a purely capacitative acoustic load (a loss-free cavity of dimensions small compared with the wavelength) a pressure constant with respect to frequency would be produced. The impedance of the ear deviates from that of a simple capacitative load so that the amplitude of the sound pressure was not constant, but typically 0.1 Newton m^{-2} at 1 kc/s.

Theoretically it is possible to compute the applied acoustic load from observation of the input and output voltages of the respective transducers and their known complex transduction coefficients. In practice, however, it is expedient to calibrate and check the performance of the probe unit as a whole prior to use by applying known impedances using a rigid-walled impedance tube.

The impedance measuring unit is very small and light and can be fitted with any desired shape of earcap, the two probe holes being arranged to coincide with the normal aperture of the earcap, and the whole is applied to the ear with known force by a light-weight pneumatically-operated headband.

3. Results

Preliminary measurements on ears of six people showed that, in accordance with the findings of Metz (11), there is little difference between the impedance of the left and right ears of the same person. It was also established that under fixed test conditions the variance of repeated measurements on the same person was appreciably less than variance arising due to differences between subjects. For instance, at 1 kc/s the standard deviation in $|Z|$ for replication on a typical subject was about 10% of the mean, whereas that between the values for 23 subjects was 30%. To obtain a value for the impedance, as a function of frequency, characteristic of the average human ear, measurements have been made on one ear of each of 23 subjects, through the aperture of an MX41/AR cushion (rubber) and of a 4026A earcap, types fitted to earphones for audiometry, and through a small aperture in a plane disc. The measuring device was adjusted until the subject reported a good fit, and to aid adjustment a low-intensity 200 c/s tone was generated by the source. Median and quartile values for the impedance seen through the aperture of an MX41/AR cushion (as used with the Telephonics TDH39 earphone) for an applied force of 1 Kg. wt. are shown by way of example in the Figure. The arithmetic mean tends to a slightly larger value and the modal value to a

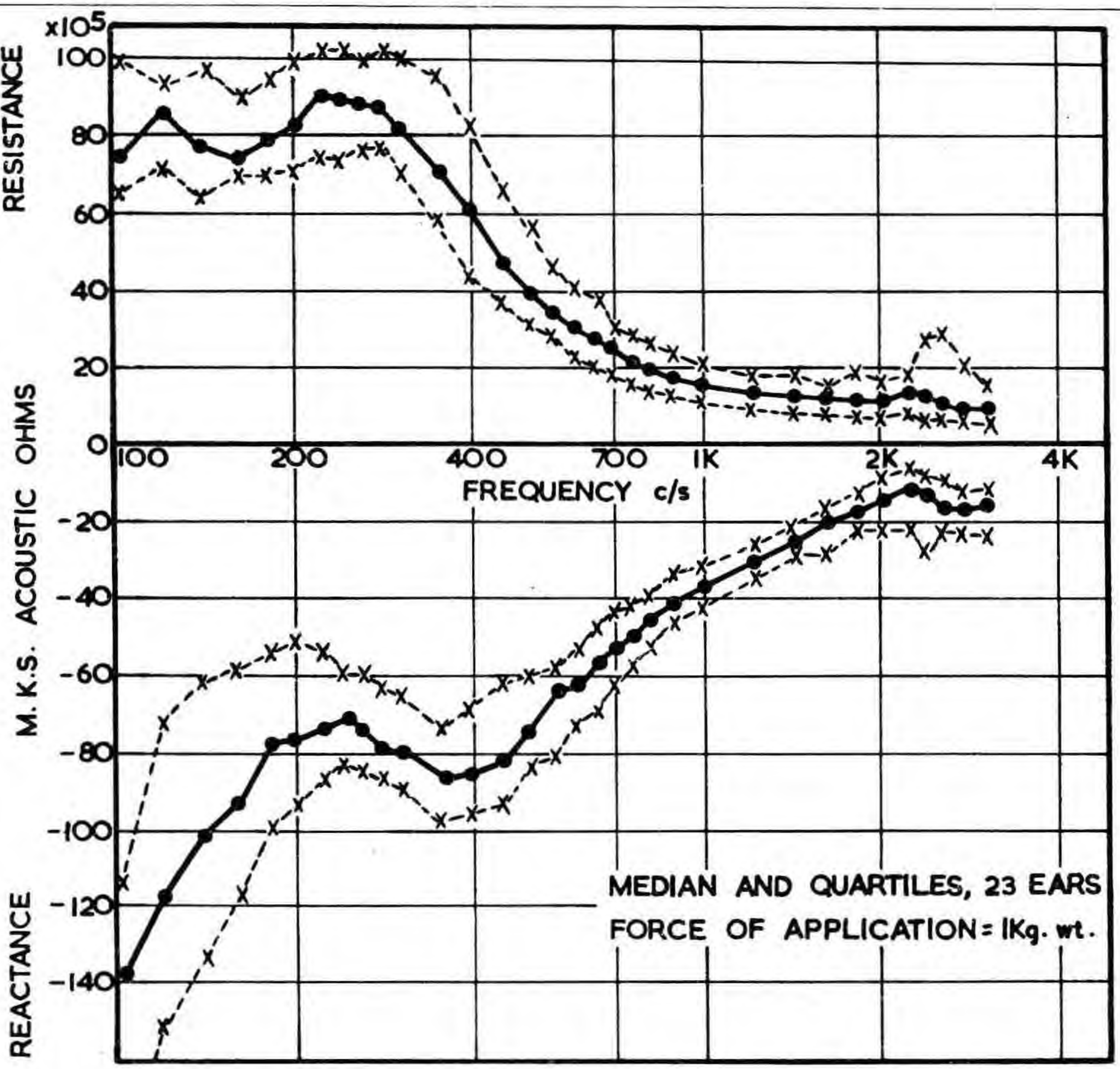

ACOUSTICAL IMPEDANCE OF THE HUMAN EAR
MEASURED THROUGH APERTURE OF MX 41/AR CUSHION

slightly lower value than the median shown. Complex-plane presentation of these median results (and of results for each individual person tested) shows two secondary resonances. One occurs at approximately 260 c/s, below which considerable increase in the effective volume of the ear occurs (from about 6.0 to 16.0 cm^3), an effect hitherto noticed only by Brüel (10). Experiments are being carried out to localize the source of this phenomenon. A second resonance occurring at approximately 2.2 kc/s probably originates at the tympanic membrane, for Békésy (12) has shown that the conical portion of the eardrum ceases to act as a stiff membrane above this frequency, when movements of the manubrium lag behind the vibrations of the adjoining portions of the tympanic membrane.

Above 500 c/s median values of impedance are in good agreement with those recently obtained by Zwicker (4), but below this frequency his results are affected by acoustic leakage. In the low-frequency range, however, the modulus of impedance approaches the values obtained by Brüel (10) with an earcap sealed to the ear with petroleum jelly. Work is proceeding to extend the range of measurement to other earcaps and to frequencies up to 10 kc/s.

Acknowledgements

The work described was carried out as part of the research programme of the National Physical Laboratory and the paper is published by permission of the Director.

References

(1) WEST, W. P.O.E.E.J. 21, 293, (1929)
(2) INGLIS, A.H., GRAY, C.H.G. and JENKINS, R.T. B.S.T.J. 11, 293, (1932)
(3) LONCHEVAL, A. Acustica 4, 161, (1958)
(4) ZWICKER, E. N.T.Z. 8, 397, (1961)
(5) BELL TEL. MFG. CO., ANTWERP. Reps. LTN 7106V (1952) and LTN 7069V (1960)
(6) NÁBĚLEK, I. Slaboproudy Obzor. 21, 210, (1960)
(7) PIRLET, R. Electroacoustique No. 6, July, 1962
(8) MAWARDI, O. J. Acoust. Soc. Amer. 21, 84, (1949)
(9) MØLLER, A. J. Acoust. Soc. Amer. 32, 250, (1960)
(10) BRÜEL, P.V., FREDERIKSEN, E. and RASMUSSEN, G. B & K Techn. Rev. No. 4 (1961)
(11) METZ, O. Acta oto-laryng. Supp. 63, (1946)
(12) BÉKÉSY, G. von. Akust. Zeits. 6, 1, (1941)

O26

FOURTH INTERNATIONAL CONGRESS ON ACOUSTICS
COPENHAGEN 21.-28. AUGUST 1962

A Double Temperature Jump Associated with the Onset of Cavitation.

M.G.Sirotyuk.

Several hypotheses have been put forward acounting for luminescence of liquids accompanying cavitation, the most plausible from these beeing: an electric discharge in the rarefied gas in the cavitation cavern [1] ; an adiabatic heating of the gas during the collapse of the bubbles [2] .

In this report an attempt to measure directly the heating of a liquid subjected to cavitation is given.

If the temperature of the gas filling collapsing bubbles, is increased a termocouple introduced into cavitation region would indicate the temperature change. The initial portions of dependence curves of luminescence brightness and averaged thermocouple temperature in the focal region of a concentrator from electrical tension (frequency 500 kc) feeding the concentrator [3] are given in the figure. The numbers to the right from vertical coordinate axis correspond to tension U_f from the amplifier increasing photocurrent of the photomultiplier ФЭУ-17 which was supported on the reactor cylinder of the consentrator and registrates integral luminescence in the focal sport.

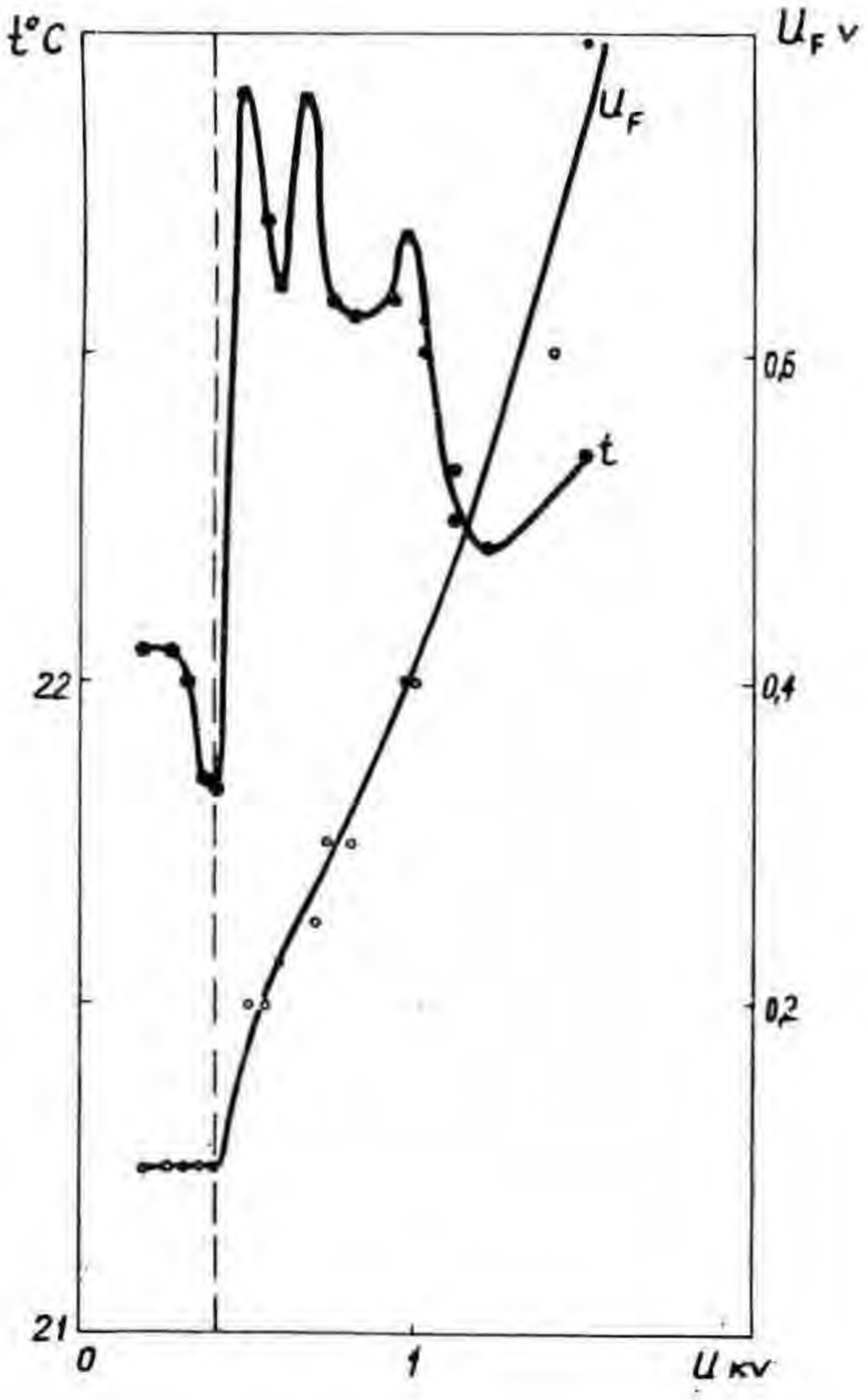

First of all it was ascertained that the luminescence of cavitation bubbles begins with the onset of cavitation itself. The exact moment of this onset was established with the aid of a hydrophone placed at a certain distance from the focal region. In the figure the tension corresponding to the cavitation onset is marked by a broken line. Simultanously with the registration of the cavitation the temperature in the focal region was measured with the aid of a thermocouple copper-constantane.

In order that the second end of the thermocouple should have constant temperature during measurement the thermocouple was soldered to thick copper leads placed at sufficient distance from the focus and the measurement itself was conducted during a short period of time - 15sec. (the period of measurement was slightly longer than the period of

heat inertion of the thermocouple). The measurements were carried up to the tension of 1,5 kv on the concentrator. With further increase of sound intensity the water in the reactive cylinder of the consentrator is heated which leads arroneous temperature readings. Experimental results are presented in the figure (curve t). It is seen that the cavitation onset is accompanied by a double temperature jump.

The decrease of temperature before the beginning of cavitation could be explained by several hypotheses (for example by sharp increase of average radius of bubbles at its approach to the resonant size which leads to cooling of the gas contained in bubbles).However, the lack of facts in favour of any hypotheses does not give possibility to explain this temperature decrease. The sharp increase of temperature during at the onset of cavitation can indicate that the gas in the bubbles becomes heated.

On the base of the present paper following conclusions can be drawn.

1) The beginning of luminescence of the bubbles corresponds exactly to the moment of cavitation onset.

2) The beginning of the cavitation is accompanied by double jump of temperature of the termocouple surrounded by cavitation bubbles.

It could be assumed that temperature jump upward, in the main, is called forth by adiabatic phenomena in bubbles.

The author thanks L.D.Rosenberg for valuable suggestions.

Literature Cited

1. I.Frenkel. Acta Phys.Chim. USSR, 1940, 12, 317.
2. B.E.Noltingk, E.A.Neppiras. Proc.Phys.Soc. 1950, 63B, 9, 674.
3. L.D.Rosenberg, M.G.Sirotyuk. Acoust.J. USSR, 1959, 5, 2, 206.

G27

FOURTH INTERNATIONAL CONGRESS ON ACOUSTICS
COPENHAGEN 21.-28. AUGUST 1962

Sprachliche Verschiedenheiten erhalten durch Sprechchormethode.

Thomas Tarnóczy

Akustische Forschungsgruppe, Budapest, Ungarn.

Die Sprechchormethode ermöglicht die Untersuchung der Feinstruktur des Sprechspektrums (1-3). Auf Grund unserer bisherigen Untersuchungen ist es uns wahrscheinlich gelungen, die physikalischen Aequivalente der Verschiedenheiten in Klangfarbe und Aussprache zu identifizieren (2). Die Bearbeitung der Methode wurde aber mit ungarischem Material durchgeführt. Wenn man auf eine andere Sprache übergehen will, können zwei wichtige Fragen auftauchen: 1) was für einen spektralen Unterschied zwei verschiedene Sprachen bedeuten und 2) wieweit die mit der ungarischen Sprache ausgewiesene Gesetzmässigkeiten auf anderen Sprachen nachweisbar sind.

Um das Problem besprechen zu können, haben wir mit Personen deutscher Muttersprache und mit deutschem Sprechmaterial Untersuchungen vorgenommen. Die Personen wurden aus den in Budapest studierenden 18-20 jährigen deutschen Studenten und Studentinnen ausgewählt. In den einzelnen Gruppen sprachen je 14 Personen, u.zw. entweder Jungen oder Mädchen, auf einmal. In Anbetracht des Dialektes hatte man keine Möglichkeit zu wählen, die Studenten stammten aus verschiedenen Gebieten von Sachsen, Thüringen, Brandenburg und Mecklenburg.

Die Aufnahme des Sprechgeräusches geschah mit der früher beschriebenen Methode (2-4), doch mit Einrichtung besserer Qualität und moderner Ausführung. In dem Aufnahmestudio von 2400 m^3 der Ungarischen Schallplattenfabrik wurden 7 Mikrofone mit achter Charakteristik aufgestellt. Die Distanz bzw. Lautstärke der an der gegenüberstehenden Seite des Mikrofons sprechenden Personen wurde vorhergehend so eingestellt, dass nebst gleicher Verstärkung der einzelnen Kanäle, im Aussteuerungsmesser je gleiche durchschnittliche Sprechstärke abzulesen war. Die Sprechenden haben dann gleichzeitig Zeitungstext vorgelesen, natürlich jede Person einen anderen Text. Um die Gleichmässigkeit des Sprechgeräusches steigern zu können, wurde die Sprechgeschwindigkeit auf etwa 6,5 Silben/sec erhöht.

Zur Aufnahme wurde das Magnettongerät Typ M 10 der Firma TELEFUNKEN verwendet. Als Magnettonband verbrauchte man AGFA FR 22. Zur

Auswertung wurde der neue Typ des Terzfilter-Analysators und des Pegelschreibers der Firma Brüel & Kjaer angewandt. Das Abspielen des endlosen Bandes geschah durch TELEFUNKEN Magnettongerät. Die elektroakustische Kette wurde vom Mikrofon bis zur Abspiel-Vorrichtung mit Messungen kontrolliert und die ausgewerteten Endergebnisse wurden mit den entsprechenden Korrektionen versehen.

Die als Ergebnisse erhaltenen Sprechspektren der deutschen Sprache für Männer- und Frauenstimmen sind im Spektrumpegel in Abb. 1. und 2. gezeichnet. Da aus weiblichen Stimmen zwei separate Gruppen zur Verfügung standen, so hatten wir die Möglichkeit, die von der Ungenauigkeit des Verfahrens und von der persönlichen Zusammenstellung des Sprechchors entstandene Streuung zu kontrollieren. Die Abweichungen zwischen den Spektren, welche sich aus der Terzfilter-Analyse der zwei Gruppen ergaben, waren nicht grösser als 1,5 dB.

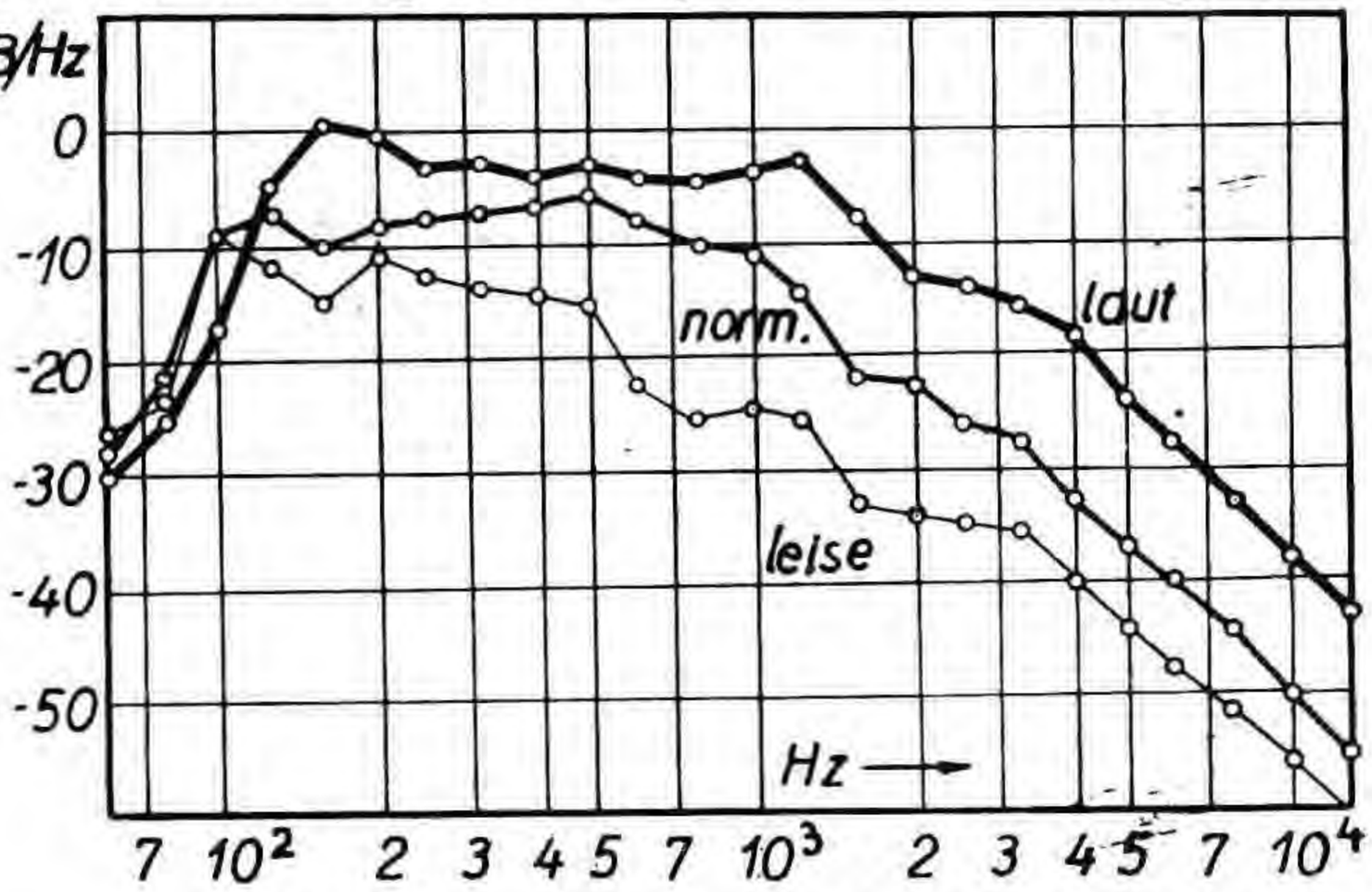

Abb.1. Spektren der deutschen Männerstimme auf leises, normales und lautes Sprechen.

Der Lauf der Spektren ist im grossen und ganzen ähnlich zu diesen, welche früher auf ungarische Sprache erhalten wurden. Einige ausdrücklich bemerkbaren Unterschiede werden nachstehend vorgeführt.

Abb.3. veranschaulicht den Vergleich der Spektren von normal-lauten Männerstimmen. Der Gesamtpegel des deutschen Sprechens normaler Lautstärke meldet sich etwa 3 dB höher, das "normale" deutsche Sprechen ist also etwas lauter, als das ungarische. Der wesentli-

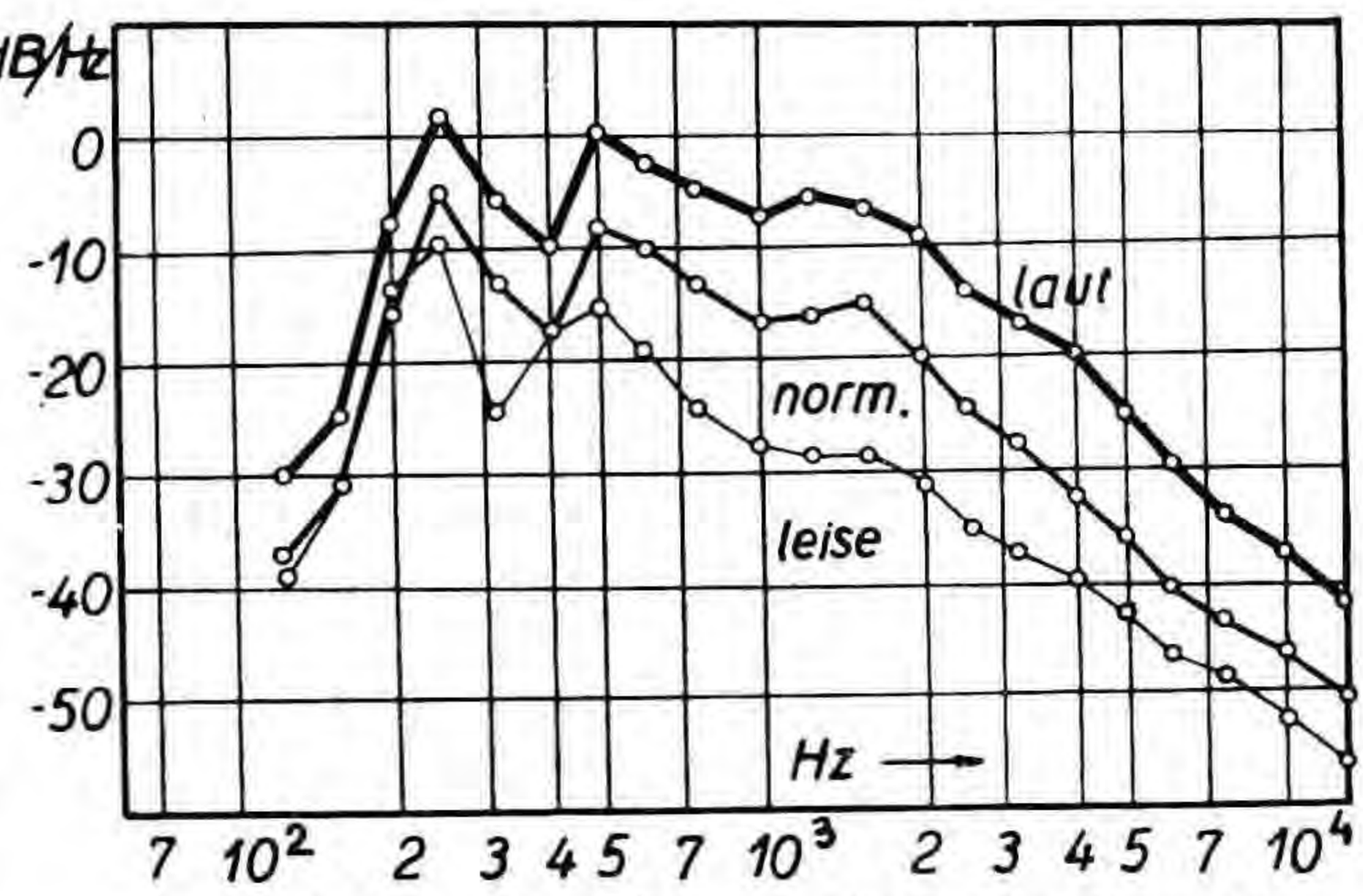

Abb.2. Wie Abb.1., aber für Frauenstimmen.

che Unterschied zwischen den zwei Spektren zeigt sich gegen 800 bis 1250 Hz, wobei das deutsche Spektrum im Pegel viel höher steigt, als das ungarische. Ansonsten laufen die zwei Spektren praktisch miteinander, nur bei niedrigen Frequenzen sieht man noch nicht sehr wesentliche Abweichungen.

Etwas anders steht die Sache bei Frauenstimmen. Die erhöhten Spektralanteile der deutschen Sprache melden sich diesmal etwas höher: zwischen 1000...2000 Hz (Abb.4.). Einen grossen Unterschied sieht man aber auch bei tiefen Tönen, der mit dem tieferen durchschnittlichen Grundton der ungarischen weiblichen Stimme in Zusammenhang stehen kann. Das erste Maximum und das erste Minimum liegen beide um einen Terz tiefer bei Ungarischen, als bei Deutschen. Es ist noch eine interessante Erscheinung zu bemerken, u.zw. dass man zwischen den ersten Maximum und Minimum beim deutschen Sprechen einen Pegelunterschied von 15 dB ablesen kann, wogegen beim Ungarischen dieser Unterschied den Wert von 5 dB nicht überschreitet. Dies gilt nicht nur auf "normales", sondern auch auf "leises" und "lautes" Sprechen.

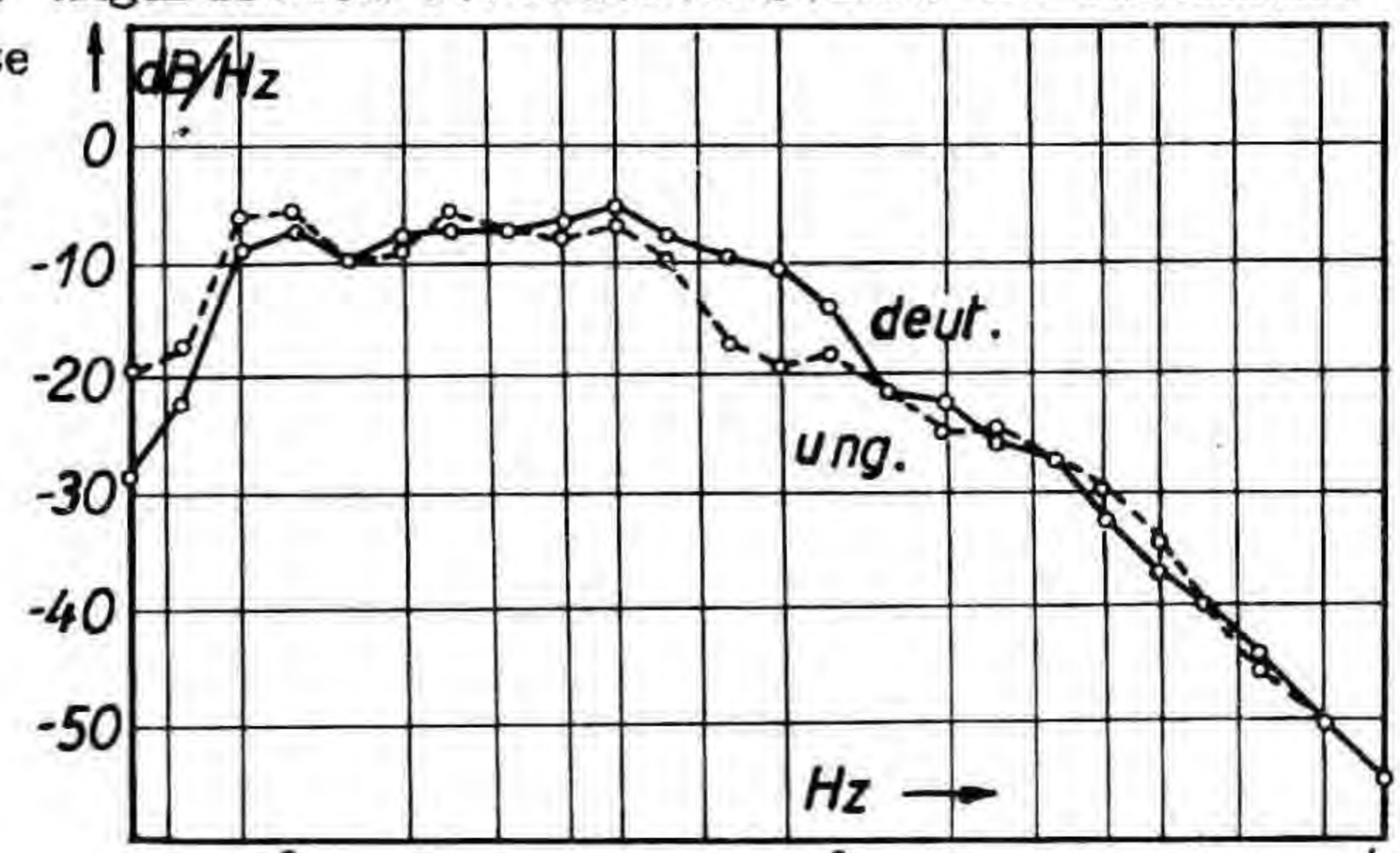

Abb.3: Spektren des normal-lauten deutschen und ungarischen männlichen Sprechens.

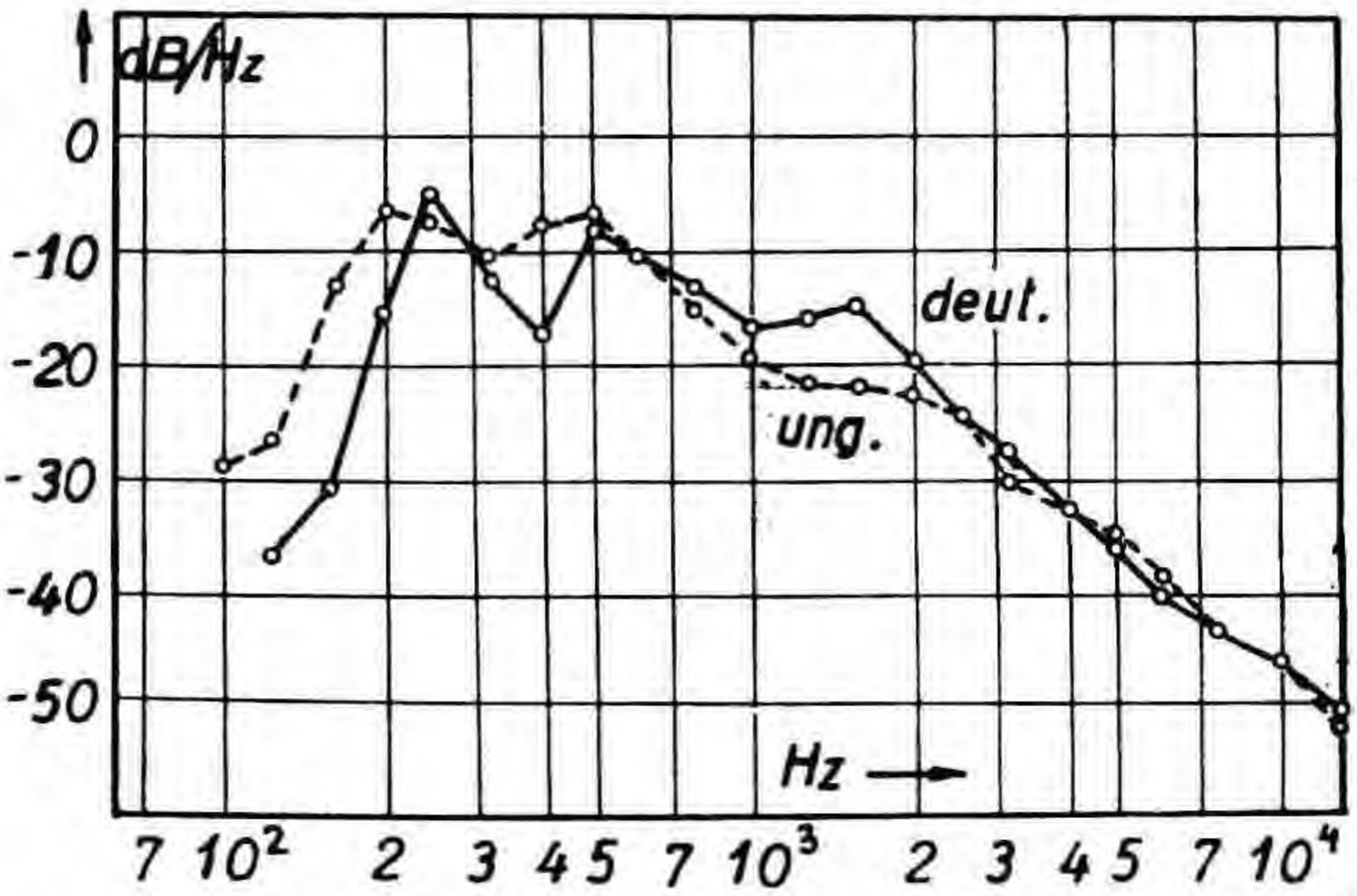

Abb.4. Wie Abb.3., aber für weibliches Sprechen.

Das zum Vergleich dienende ungarische Material war das Sprechgeräusch von 10 Männer und 10 Frauen (1, 3). Das Alter der Personen, die aus dem technischen Beamtenstand des Ungarischen Radios hierzu berufen wurden, war zwischen

26-30 Jahre. Diese Personen waren zweifellos mehr geübt und mehrere davon haben schon an früheren Versuchen teilgenommen. Das Aufnahmestudio und die angewandten Aufnahmevorrichtungen waren auch anderartig. Die in der Routine der Personen und in der Akustik des Aufnahmeraumes sich meldenden Unterschiede können die gewissermassen grössere Lautstärke der deutschen Experimente erklären. Die grössere Lautstärke und der Altersunterschied kann weiters eine Verschiebung im Grundton verursachen. Die weiteren Unterschiede sind aber mit sprachlichen Verschiedenheiten anknüpfbar. Diese Feststellung gilt besonders im Bereich gegen 1000 Hz, wo der Unterschied unbedingt signifikant ist. Es ist annehmbar, dass dieser Spektralunterschied mit einem Unterschied zwischen der Häufigkeit des Vorkommens von Vokalen, die in diesem Bereich Formanten haben, erklärt werden kann. Es ist aber auch möglich, - und hiezu besteht eine grössere Wahrscheinlichkeit, - dass man hier mit den allgemeinen Eigenschaften der deutschen Aussprache zu tun hat. Die zweierlei Sprechgeräusche nacheinander anhörend, ist die nach höheren Frequenzen verschobene Klangfarbe der Deutschen unbezweifelbar. Der Unterschied zwischen den zwei Spektren bei 400 Hz ist schwerer zu diskutieren, da dieser nur in weiblichen Stimmen nachweisbar war.

Die Wirkung der Lautstärke wurde auch untersucht. Die Verschiebung der niedrigen Spektralanteile nach höheren Frequenzen mit der sich steigernden Lautstärke ist so in Abb.1., wie in Abb.2. klar ersichtlich. Wenn alle Spektren sich auf denselben Gesamtpegel beziehen, so erhält man die relativen Unterschiede zwischen den Spektrumformen. Die Erfahrung zeigt, dass der relative Ablauf der Spektren bei niedrigen Frequenzen mit steigender Lautstärke sinkt, bei höheren Frequenzen dagegen sich erhöht. Wenn man die anderen Spektren mit den "normalen" vergleicht, so liegen die Pegel der "lauten" Spektralanteile unter 200 Hz niedriger, zwischen 500 und 5000 Hz aber höher, als bei "normalen", die Pegel der "leisen" Spektralanteile benehmen sich dagegen eben umgekehrt. Mit erhöhten Lautstärke wird also nicht nur eine Verschiebung nach höheren Frequenzen entstehen, sondern umkippt das Spektrum zu Gunsten der höheren Spektralkomponenten. Dieselbe Erscheinung wurde auch in ungarischen Sprechspektren beobachtet (3).

Literatur.

1. T. Tarnóczy: J.Acoust.Soc.Am. 28, 1270 (1956) - Acta Phys.Hung. 7, 87 (1957) - Acustica 8, 329 (1958).
2. T. Tarnóczy: Acta ORL Ibero-Amer. 11, 145 (1960) - IV. Int.Congr. Phon. Helsinki 1961.
3. T. Tarnóczy: II. Akust. Konf., Budapest 1961.

H27

FOURTH INTERNATIONAL CONGRESS ON ACOUSTICS
COPENHAGEN 21.-28. AUGUST 1962

Physiological Correlates of Binaural Lateralization

J. L. Flanagan, E. E. David, Jr., and B. J. Watson, Bell Telephone Laboratories, Inc., Murray Hill, New Jersey, U.S.A.

In earlier work[1] we have made efforts to relate subjective auditory behavior to the physiological operation of the ear. The correlations have been facilitated by a computational model which quantitatively describes the basilar membrane displacement for an arbitrary sound pressure at the eardrum. Details of the model have been given previously.[2] This general approach has appeared particularly promising in the areas of pitch perception, threshold discrimination, and binaural lateralization. The present experiment is an extension in the latter area.

Figure 1 illustrates features of the peripheral ear embraced by the model. The lower left shows a schematic diagram of the ear with the cochlea uncoiled. The horizontal partition in the cochlea represents the basilar membrane. $p(t)$ is the sound pressure at the eardrum; $x(t)$ is the equivalent linear displacement of the stapes; and $y_\ell(t)$ is the basilar membrane displacement at distance ℓ from the stapes.

If a pulse of pressure rarefaction is produced at the eardrum, the drum is initially drawn outward; the stapes also is initially drawn outward; and the membrane is initially drawn upward. The stapes and membrane displacements in response to a rarefaction pulse of 100 μsec duration are shown by the waveforms at the right of the figure. The pulse responses of three different membrane points are shown, namely the points maximally responsive to 2400 cps, 1200 cps and 600 cps. The stapes displacement is a slightly integrated version of the input. The membrane responses reflect the vibratory behavior of the particular points as well as the traveling-wave transit delay to the points.

According to the model, the greatest membrane displacements take place near the middle portion, roughly in the region maximally responsive to about 1500 cps. The amplitude of displacement is less both for points more toward the base and toward the apex. We hypothesize that the most significant neural activity is generated at the membrane point displacing with the greatest amplitude. Further, electro-physiological data suggest that neural firings occur at some threshold only on upward motions of the basilar membrane; that is, motions which drive it toward the tectorial membrane. The oscillatory behavior of the pulse response suggests, too, that multiple or secondary firings might be elicited for a single stimulus pulse.

If pulses are supplied to both ears, a centered sound image is heard provided the significant neural activity is elicited simultaneously. Suppose the input pulses are identical rarefaction pulses. The maximum membrane displacements occur near the middle. For simplicity imagine that the neural firings are triggered somewhere near the positive crests of the displacement waves. For this cophasic condition a centered image is heard if the input pulses are produced simultaneously, or if the interaural time is zero. Suppose now that the pulse to one of the ears is reversed in phase to a pressure condensation. The membrane responses for this ear also change sign and are the negatives of those shown in Fig. 1. Their first positive crests now occur later by

one-half cycle of the displacement. At the middle of the membrane this half-cycle amounts to between 300 and 400 μsec. To produce a centered image for this antiphasic condition, then, one would expect that the condensation pulse would have to be advanced in time by this amount.

The membrane point which displaces with the greatest coherent amplitude can be manipulated by adding masking noise of appropriate frequency content. That is, the place which normally responds with greatest amplitude can be obscured by noise, and the significant displacement can be caused to occur at a less sensitive place. For example, suppose that the basal end of the membrane in one ear is masked by high-pass noise, and the apical end of the membrane in the other ear is masked by low-pass noise. If the subject is required to adjust stimulus pulses to produce a centered image, the fusion must be made from apical-end information in one ear and basal-end in the other. The resulting interaural time would then reflect both the oscillatory characteristics of the specific membrane points and the traveling-wave delay between them.

We conducted an experiment to determine whether these time dependencies are actually manifest in subjective behavior. The experimental procedure is shown in Fig. 2. Identical pulse generators produce 100 μsec pulses at a rate of 10 per second. Pulse amplitude is set to produce a 40 db sensation level. The subject, seated in a sound-proof room, listens to the pulses over condenser earphones. (Good acoustic transduction of the pulses is important). He has a switch available to reverse the polarity of the pulses delivered to the right ear so that it can be made a condensation instead of the normal rarefaction. The subject also has a delay control which varies the relative times of occurence of the two pulses over a range of ±5 msec. Two uncorrelated noise generators supply additive masking noise via variable filters. A completely separate experiment was conducted to determine the filtered noise levels necessary to mask prescribed spectral sections of the pulse stimuli.

For a given masking and pulse polarity condition, the subject is required to adjust the delay to produce a sound image centered in his head. Multiple images are frequently heard, with the more subtle, secondary images apparently being elicited on secondary bounces of the membrane. In the present report we will discuss only the stronger, principal images. The masking conditions used in the present experiment were 600 HP and 2400 LP. The unmasked condition was included as a control. The results of the measurements are shown in Fig. 3(a) and 3(b).

Fig. 3(a) gives the results for the unmasked and the symmetrically-masked conditions. The data are for four subjects, and each point is the median of approximately 15 principal-image responses. Each two sets of points is bracketed along the abscissa. The set labelled C is the cophasic response. That labelled A is the antiphasic. Each bracket corresponds to the masking condition represented by the schematic cochleas drawn below the brackets. The labelling at the top of each cochlea gives the masking condition for that ear. For example, the UN means unmasked. The cross-hatching on the cochleas indicates the membrane regions obscured by masking noise. The double arrow between each pair of cochleas approximately indicates the membrane points of greatest unmasked displacement. The cophasic conditions are rarefaction pulses in both ears. The antiphasic conditions are rarefaction in the left ear and condensation in the right ear.

The single arrows in the vicinity of the plotted responses are estimates of the interaural times made from the model. The estimates are made by assuming the neural firings to be produced at the positive

crests of the displacement at the most significant place. The arrows therefore represent the time differences between the first positive crests at the places indicated in the cochlear diagrams. As such they include the transit time to the particular place, plus the initial quarter-cycle duration of the pulse response. The actual displacement threshold for neural firing is not known and very likely is dependent upon place. In the symmetrically-masked conditions a knowledge of the threshold is not so important since the threshold epoch, whether it is at the crest or down from the crest, should be about the same in the two ears. The interaural time for antiphasic lateralization should then be simply the half-cycle time. The measured responses for the symmetrically-masked cases do in fact agree relatively well with this estimate. All of the principal cophasic fusions are made for essentially zero time, and the antiphasic lateralizations reflect the half-cycle disparity of the appropriate places. The condensation pulse always leads.

The agreement is not as good for the asymmetrically-masked cases. These are shown in Fig. 3(b). Signal loudnesses are quite different in the two ears, and the neural thresholds probably vary with place. The times of the initial positive crests would not be expected to give very realistic estimates of the interaural times. It becomes much more important to have knowledge of the threshold levels and the relative amplitudes of the displacements. Even so, it is interesting to see to what extent the simple positive-crest estimates follow the data.

The relatively wider spread of the subject medians in the symmetrical cases, and in particular for the cases involving 2400 LP, shows that these lateralizations were considerably more difficult and more variable than the symmetrical cases. It is clear that the simple assumption of neural firing at the positive crests of the displacement is not completely adequate to specify all of the interaural times. The real threshold for firing is likely some other level. In fact, these data and the results from the model, offer the distinct possibility for working backwards to deduce information on the neural thresholds. Finally, the present results, as do our earlier ones, continue to support the notion that subjective response is closely related to the detailed motion of the basilar membrane.

REFERENCES

1. J. L. Flanagan, E. E. David, Jr., and B. J. Watson, Binaural lateralization of cophasic and antiphasic clicks, J. Acoust. Soc. Am., 33, 840(A), (1961).

   — Effects of masking upon the binaural lateralization of cophasic and antiphasic clicks. J. Acoust. Soc. Am., 33, 1670(A), (1961).

2. J. L. Flanagan, Models for approximating basilar membrane displacement, Bell System Tech. Jour., 39, 1163-1191, (1960).

   — Models for approximating basilar membrane displacement; Part II: Effects of middle ear transmission and some relations between subjective and physiological behavior, Bell System Tech. Jour., 41, 959-1009, (1962).

FIG. 1

FIG. 2

FIG. 3(a)

FIG. 3(b)

L27

FOURTH INTERNATIONAL CONGRESS ON ACOUSTICS
COPENHAGEN 21.-28. AUGUST 1962

Experimental Studies of Jet Turbulence and Their Relation to Jet Noise

P.O.A.L. Davies and M.J. Fisher

Introduction

The turbulence in the highly sheared mixing region of a jet has been related to the noise output by Lighthill (Ref. 1), who has derived the fundamental relations describing the aerodynamic generation of sound.

Comparing the exact equations of motion in a compressible medium with the equations of sound propagation in a medium at rest he showed that the exact equations may be written in the form

$$\frac{\partial^2 \rho}{\partial t^2} - a_o^2 \nabla^2 \rho = \frac{\partial^2}{\partial x_i \partial x_j} T_{ij} \qquad \ldots(1)$$

where $T_{ij} = \rho v_i v_j + p_{ij} - a_o^2 \rho \delta_{ij}$ and v_i is the velocity in the x_i direction, ρ the density, a_o the velocity of sound in the fluid at rest and p_{ij} the compressive stress tensor. In the absence of solid boundaries the dominant term in the stress tensor T_{ij} is the Reynolds stress $\rho v_i v_j$. Lighthill goes on to show that this forcing term gives rise to a distribution of acoustic quadrupoles. At high Mach numbers these are convected at a speed U_c (Ref.2). The radiation field relative to the position from which the sound is emitted by a moving quadrupole is expressed by

$$p - p_o = \frac{x_i x_j \partial^2 T_{ij}(t - r/a_o)}{4\pi r^3 (1 - M_c \cos\theta)^3} \qquad \ldots(2)$$

where $T_{ij}(t)$ is the strength at time t, r is the distance from the observer to the point of emission, θ the angle between this direction and the direction of motion and M_c the convection velocity divided by the speed of sound a_o.

Developing ideas put forward by Proudman, Lilley (Ref. 3) showed how turbulence measurements could be used to estimate the acoustic power output. He showed that the sound intensity per unit volume of turbulence is given approximately by

$$I(r) = \frac{0.02 \sin^2\theta \cos^2\theta}{\rho a_o^5 x^2 (1 - M_c \cos\theta)^5} L_{ij}^5 e_{12}^6 \bar{\rho}^2 \overline{v^2} \alpha \qquad \ldots(3)$$

where L_{ij} is the integral velocity scale of the turbulence, e_{12} the dominant rate of strain (corresponding to a velocity gradient $\partial U_1 / \partial x_2$) α an isotropy factor and the bars represent temporal mean values. It has not been possible to specify these characteristics of the turbulence theoretically and they must be determined experimentally.

The Characteristics of the Turbulent Motion

The quantities to be determined experimentally can be derived from velocity measurements which can be made with a hot wire anemometer. The details of the experimental techniques are reported in Ref. 4. The measurements required include the length scale L_{ij}, the velocity or mean shear $\partial U_1 / \partial x_2$, the convection velocity U_c and the mean square velocity fluctuations $\overline{v^2}$.

In a turbulent flow velocity measurements at nearby points are well correlated while those at points more remote from each other are almost uncorrelated. We can therefore use correlation techniques to define L_{ij}. For two points separated by a distance x we can define a space correlation coefficient as

$$R_{x_i} = \frac{1}{T} \int_o^T \frac{\overline{v_i(0)\, v_i(x)}}{\overline{v_i^2}} \, dt \qquad \ldots(4)$$

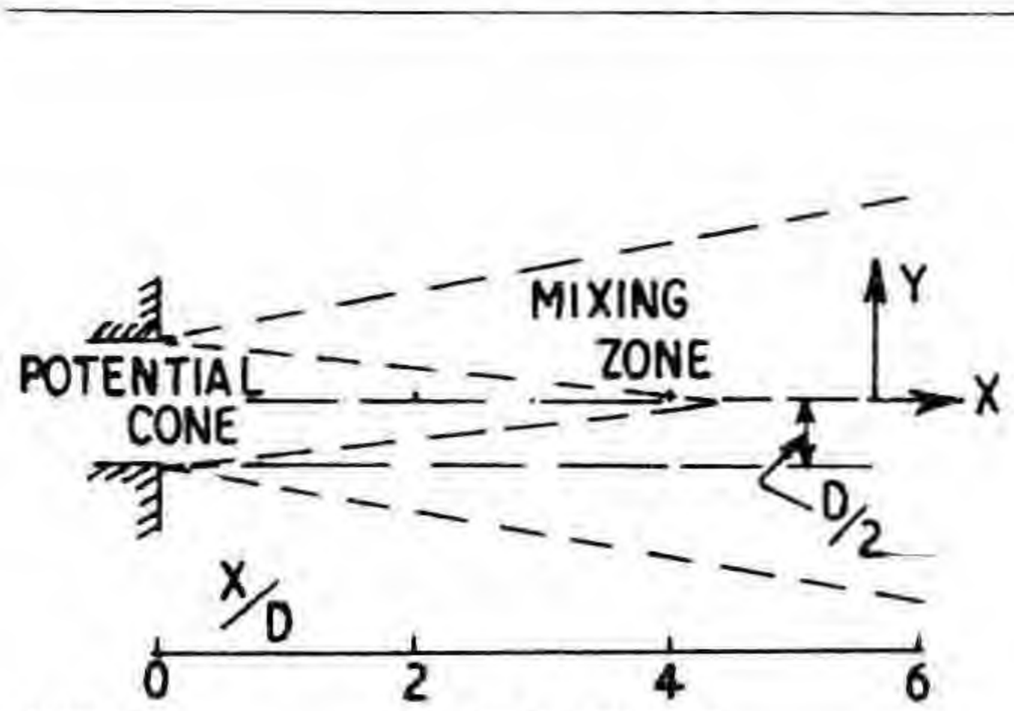

FIG.1. JET FLOW

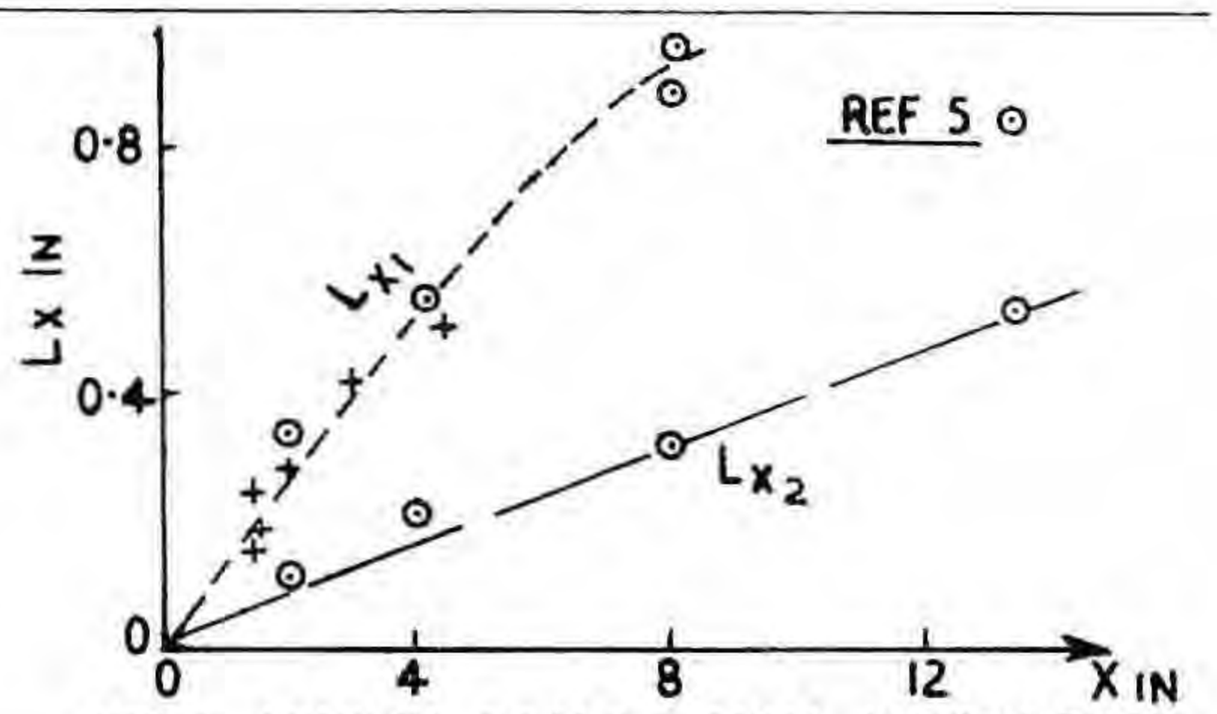

FIG.2. LENGTH SCALE – AXIAL FLUCTUATIONS

And the integral space scale can then be defined by

$$L_{x_i} = \int_0^\infty R_{x_i}\, dx \qquad \ldots(5)$$

To define the convection velocity we need to measure the correlation between points separated both in space and time. We can do this by delaying one of the signals above a time delay τ before correlating it with the other, to give the time separation. This is termed the cross correlation defined as

$$R_{x\tau} = \frac{1}{T}\int_0^T \left[\left(\overline{v_1(0,0)\, v_1(x,\tau)}\right)/\overline{v_1^2}\right] dt \qquad \ldots(6)$$

where v_1 is the axial component of the velocity fluctuation. If the values $R_{x\tau}$ are plotted against time delay for a series of increasing wire separations the whole family of curves define an optimum correlation envelope in time. A point on the envelope corresponds to a space separation and this with the appropriate time can be used to define the convection velocity U_c of the energy bearing eddies.

Experimental Results

The general structure of a circular jet is well known and when the density of the jet is the same as that of the surroundings is similar for all jets. As shown in Fig. 1, a mixing zone of intense turbulence surrounds a cone of potential flow which extends for about 4 diameters from the jet outlet. The mixing zone boundaries spread at a constant angle.

The integral length scales defined in (5) also exhibits this similarity, and for the first six or so jet diameters the axial scale of axial fluctuations L_{x_1} is well represented by

$$L_{x_1} = 0{\cdot}13X \quad ; \quad 0 < X < 6D \qquad \ldots(7)$$

This curve has been plotted on Fig. 2 for a one inch jet. Similar results from Ref.5 for D = 3.5 in are also plotted on Fig. 2 together with measurements of the radial scale of axial fluctuation L_{x_2}. These results imply the radial scale is about $\frac{1}{3}$ that

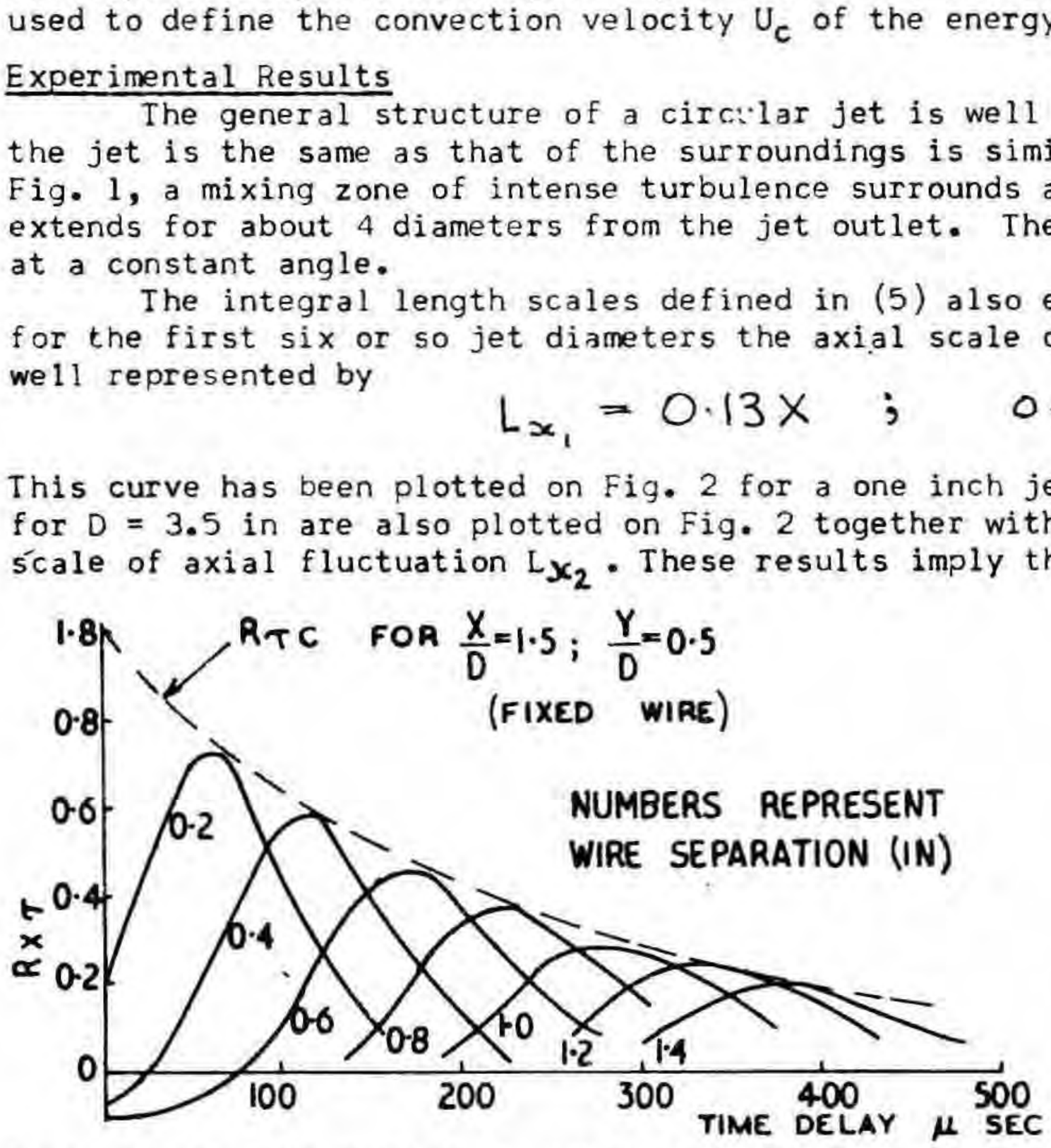

FIG.3. CROSS CORRELATION – AXIAL FLUCTUATIONS

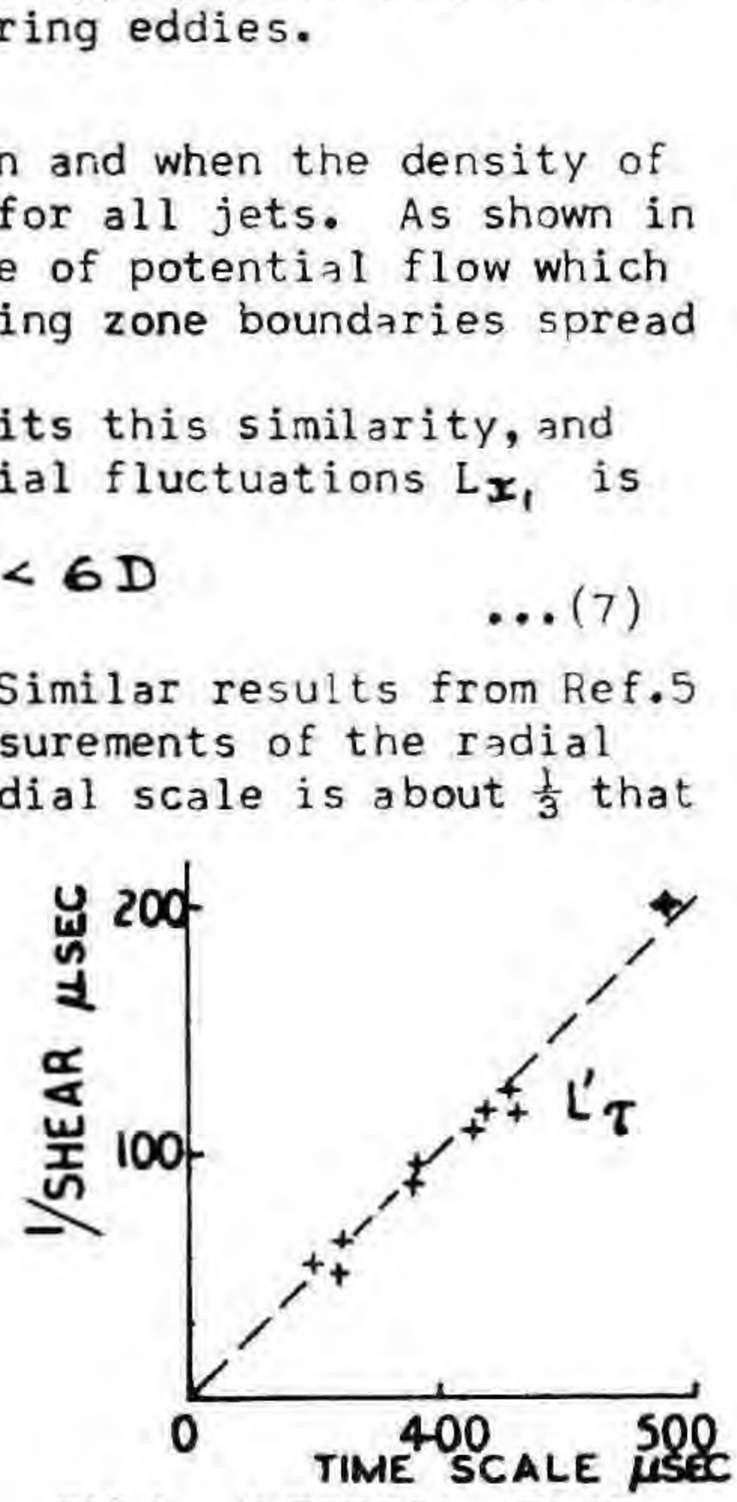

FIG.4. INTEGRAL TIME SCALE.

of the axial. There is good evidence that further downstream the rate of increase of L_{x1} decreases to about half the value indicated by equation (7). The results showed that the length scale was independent of jet velocity and varied slightly with radial position (Ref. 4).

A typical family of curves representing the cross correlation of the velocity signals is shown on Fig. 3. Here the time scale of the diagram is almost exactly inversely proportional to jet velocity indicating a strong Strouhal number dependence in the turbulent motion. The envelope of these curves represents the auto-correlation of the energy containing eddies in a frame moving with U_c. The integral of the envelope is the moving axis time scale of the turbulence, while its Fourier transform is the spectrum function of the velocity fluctuations in a moving frame.

This can be seen if one first considers the form Fig. 3 would take if the turbulence were a frozen pattern being swept past the stationary hot wire. Each curve representing a wire separation would rise to a peak value of unity, so the extent by which they fail to do this is a measure of the rate at which the velocity pattern changes. The time scale is therefore related to the rate at which the velocity pattern is distorted, that is to the rate of generation of new turbulence.

If one considers the turbulence in terms of vorticity components, one radial, one axial, and one tangential, the generation of new turbulence is directly related to the rate at which the vorticity filaments are stretched. The mean tangential filaments represent the mean shear, and the radial filaments will be the ones most strongly stretched by the shear. This implies a feed of energy into rotations about radial axes, therefore, one could expect the longitudinal and tangential fluctuations and scales to be larger than the radial ones, as has already been demonstrated. This also implies a relation between time scale and the mean shear which also proves to be the case as can be seen in Fig. 4.

Returning to Fig. 3, the time delay at which each separation curve touches the envelope will define the convection velocity U_c. To an observer moving with this velocity the rate of change of the turbulence structure will be a minimum. This convection velocity is plotted together with the mean velocity U_1 on Fig. 5. It can be seen that the convection velocity changes more slowly with radial displacement than does the mean velocity.

For mean velocity profiles such as that plotted on Fig. 5 the maximum shear was found to be almost proportional to the jet velocity. A good fit to the measurements for M_o 0.45 is given by the relation

$$\left(\partial U_1/\partial x_2\right)_{max} = \frac{6U_o}{X + ka_o}\ sec^{-1} \quad ; \quad M_o = 0.45 \qquad ...(8)$$

where ka_o will depend on the thickness of the boundary layer in the flow leaving the jet nozzle. For the 1 in diameter jet ka_o was found to be 0.4 in indicating an origin about 0.4 in upstream from the orifice. This shows that similarity breaks down close to the jet orifice and the turbulent flow structure takes a few inches to become established. The results for a 3.5 in jet from Ref. 5 also fit equation 8 at the same Mach Number.

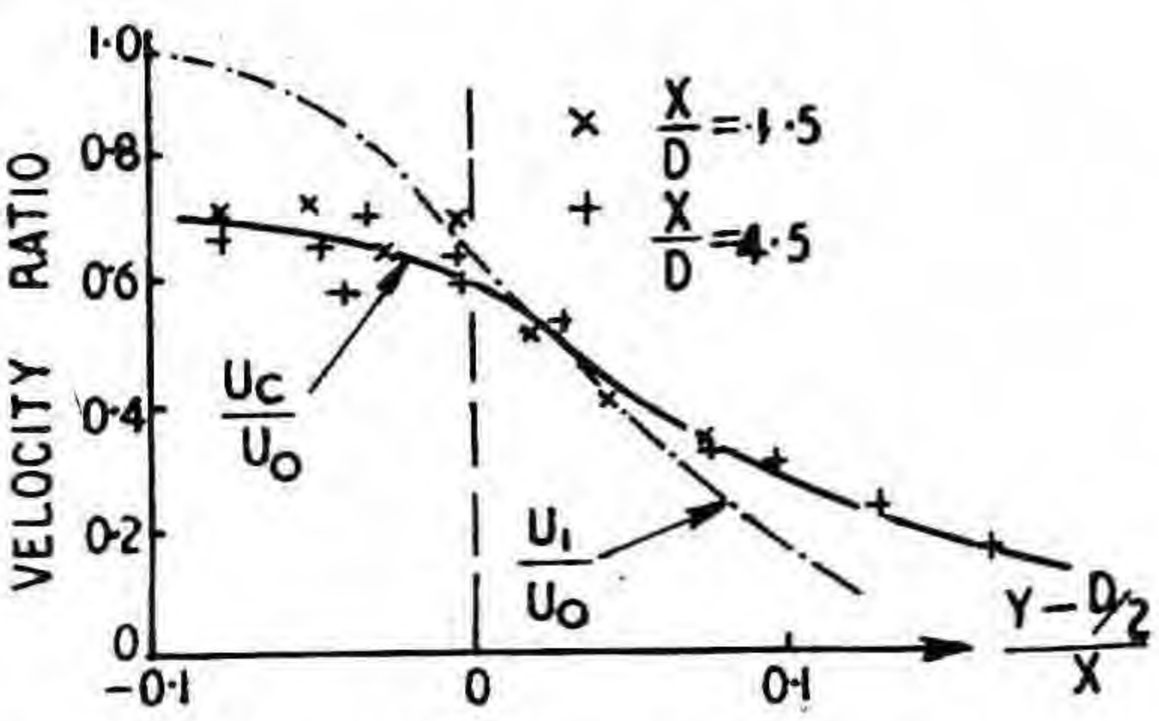

FIG. 5. CONVECTION VELOCITY

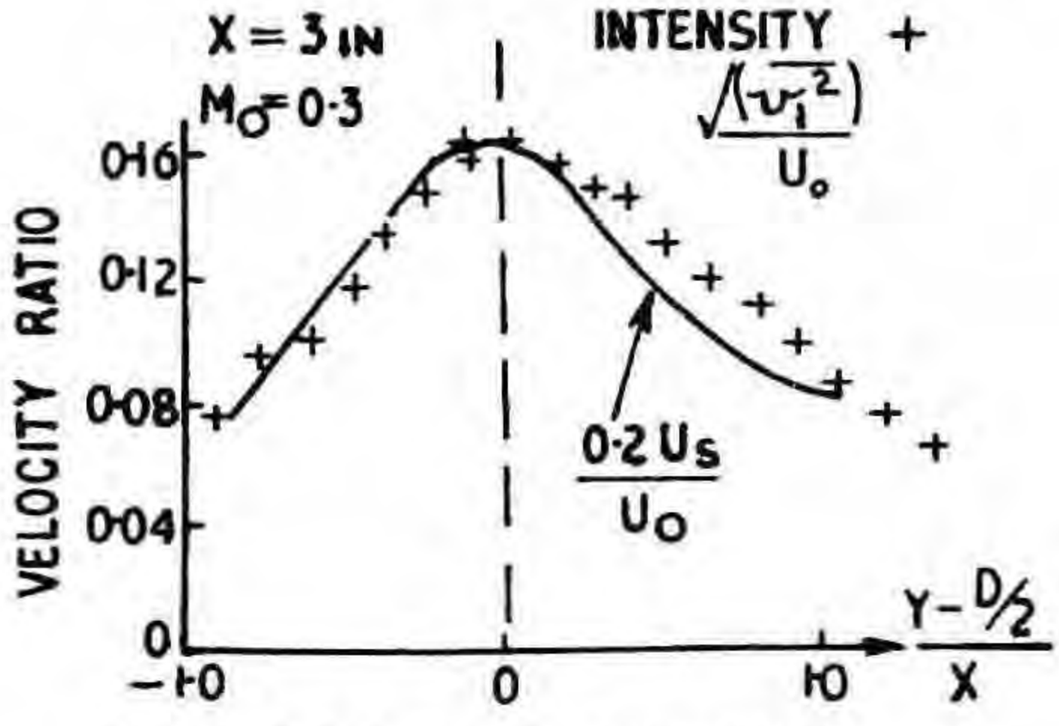

FIG 6. TURBULENT INTENSITY

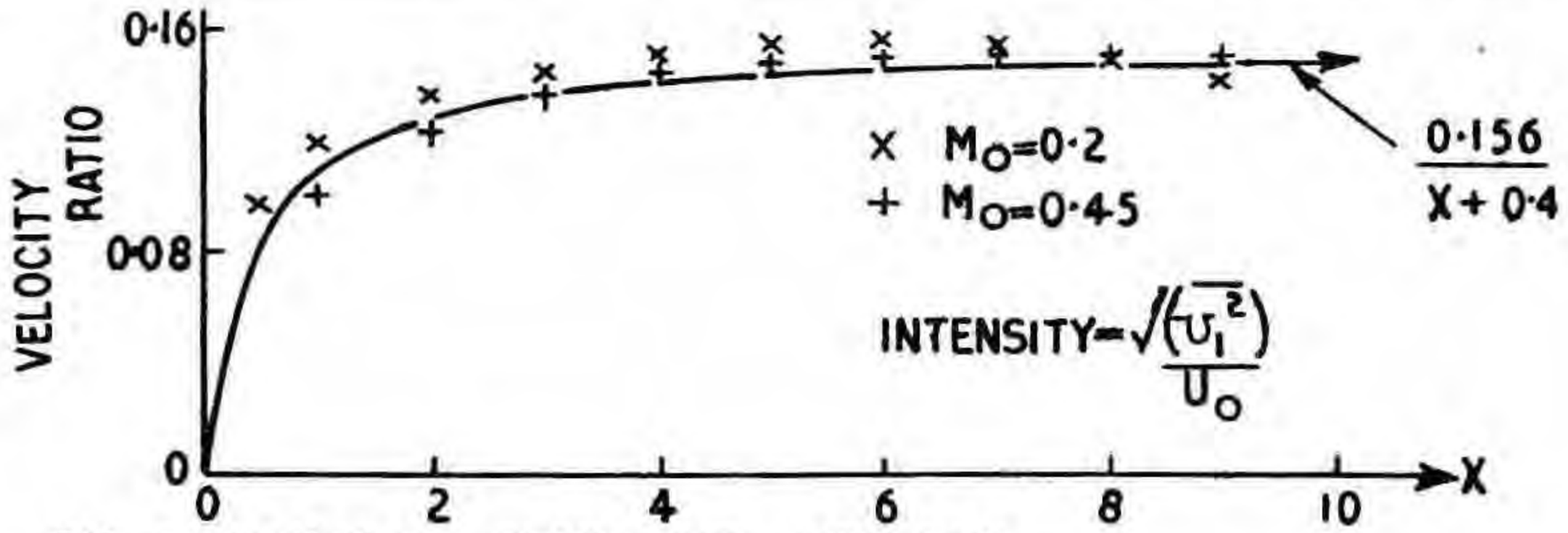

FIG 7 MAXIMUM TURBULENT INTENSITY

Turbulence intensity, defined as $\sqrt{\overline{v_1^2}}/U_o$ was measured throughout the mixing region for the first 10 diameters downstream from the orifice. A typical radial distribution of axial intensity is plotted in Fig. 6. The distributions were found to be similar if they were compared on the basis of the origin found for the mean shear.

If the mean shear is multiplied by the integral length scale L_{x1} the resulting product has the dimensions of a velocity, termed hereafter the shear velocity U_s. The quantity $0.2U_s/U_o$ is also plotted on Fig. 6 and it can be seen that it agrees closely with the intensity measurements. This indicates a simple relation exists between the shear and the turbulent intensity, which is not altogether surprising as a simple relation also exists between the integral time scale and the shear. This conclusion is supported by plotting the axial distribution of maximum intensity and comparing this with the shear velocity defined by (7) and (8), as can be seen in Fig. 7. This leads finally to

$$\sqrt{(v_1^2)} = 0.2 L_{x_1} \frac{\partial U_1}{\partial x_2} \qquad \ldots(9)$$

with some Mach Number dependence for the shear.

Conclusions

Returning now to the unknown terms in equation 3, it has been shown that the kinematic characteristics of the turbulence can be specified in terms of simple relationships involving the distance downstream as a length scale and the inverse of the shear as a time scale. The convection velocity differs from the mean velocity as is shown in Fig. 5, and is equal to about $0.6\ U_o$ in the region of maximum shear.

The turbulence measurements have shown that there are well defined similarity relationships for the first six or eight diameters of the jet flow. There is some evidence that the relations will alter somewhat further downstream but additional experiments are required to confirm this.

These can be used to define the statistical characteristics of the turbulence so that it is possible to estimate the acoustic output per unit volume of the turbulence in the mixing region.

The experiments indicate that the acoustic output per unit volume can be estimated by a relation which represents the turbulence by shear to the eighth power times distance from the orifice cubed. There is some evidence that e_{12} is not quite proportional to the jet Mach Number, but the exact relationship is not yet established.

Acknowledgements

The authors wish to thank Professor E.J. Richards and other members of the department for many helpful suggestions offered during the course of the work. Thanks are also due to D.S.I.R. for their support and interest in the investigation.

References

(1) Lighthill, M.J. Proc. Roy. Soc. A211, 1952, 564-587
(2) Lighthill, M.J. The Bakerian Lecture 1961. RAE Tech Memo No.DIR,8, 1961.
(3) Lilley, G.M. ARC.20,376 - N.40 - FM2724 1958.
(4) Davies, P.O.A.L., Barratt, M.J., Fisher, M.J., ARC.23,728 - N200 - FM3138,1962.
(5) Laurence, J. NACA Report No. 1292, 1956.

M27

FOURTH INTERNATIONAL CONGRESS ON ACOUSTICS
COPENHAGEN 21.-28. AUGUST 1962

ACOUSTICS OF MUSIC ROOMS

VERN O. KNUDSEN

1. Good and Bad Acoustics. Some distinguished musicians assert that they are not aware of the acoustics of a room unless it has conspicuous faults. In contrast, most critics, conductors, performing artists, and of course all ardent acousticians, aver that there are many gradations of acoustical quality, from dire perversity to perfect ideality.

The requirements for ideal acoustics, which we all strive to attain, are based on the needs and desires of both performers and listeners. These requirements should guide the design of all music rooms.

I shall not even list the numerous and important requirements, (see Knudsen, J.A.S.A., 2, 434-467 (1931)), but they underlie the three I discuss in this brief report, namely, (1) the shape of the total enclosure; (2) the design of the stage and music shell in the multi-purpose auditorium; and (3) the optimal reverberation for various types of music rooms.

2. Shape. The optimal shape of music rooms is a requirement of the highest priority. Many architects and others believe that faulty shapes can be corrected by covering the offending surfaces with highly absorptive materials, and by providing the optimal reverberation. Many innovations using concave concrete shells are acoustical perversions, which can be only partially ameliorated by the treatment of the offending surfaces with absorptive materials, and/or major surgery. A bad shape is a permanent liability.

The optical method devised by R. W. Leonard (J.A.S.A., 26, 937 (1954)) is useful for revealing defects in faulty shapes and for devising shapes, in plan and in section, that will give the most favorable distribution of geometrically reflected sound. Leonard, Delsasso and I used this technique for determining the optimal shape for Schoenberg Hall at the University of California, Los Angeles, (J.A.S.A., 29, 177 (1957)), which is highly acclaimed for its good acoustics. Leonard's optical technique has been used for the acoustical designing of several other music rooms, recently completed or now under construction.

The optical studies of two-dimensional models, and my own observations, do not reveal the advantages, claimed by some authorities, for a generally rectangular shape (with a preferred ratio of length, width and height) over shapes with moderately diverging side walls. But experience and ratings by competent listeners indicate that for generally rectangular rooms having volumes (V) between 500 and 4000 m^3, a favorable ratio of length to width is about four to three, and a satisfactory ceiling height is about $0.6V^{1/3}$ meters. Thus, for a chamber music room seating about 200, or a rehearsal room for a school band, orchestra or chorus, favorable dimensions would be about 16 x 12 x 6 meters (52 x 40 x 20 feet), but suitable means should be provided for preventing flutter echoes between pairs of parallel walls, such as slightly diverging side walls, stepped up (raked) seating, diffusive

panels, or other effective measures.

For music rooms having a volume of more than about 3000 m^3, the shape should be investigated by means of optical or even acoustical models. (See papers by Bücklein, by Spandöck, and by Krauth.) The recent work of Schroeder (Bell Laboratory Record, 39, 444 (1961)) has led to a promising method of simulating in an electronic digital computer the acoustics of existing or planned music rooms, which, after appropriate programming, is recorded on a multitrack tape, and then reproduced by the appropriate number of loudspeakers in an anechoic chamber, thus simulating the delayed reflections, reverberation, and directionality that would occur in the auditorium under study.

By means of the foregoing and other techniques it is possible to design shapes that will provide suitable time delays in the successive reflections reaching typical listener positions and also insure the optimal distribution of reflected sound. Thus, for rooms having volumes of about 5000 to 10,000 m^3, the first reflections should be delayed not more than about 30 to 40 milliseconds and these should be followed by a succession of reflections that will give a relatively smooth but slightly undulating (simulating a vibrato) reverberation of the optimal duration and frequency characteristic. For larger rooms than these, the first reflections should be delayed by somewhat longer times, but not more than about 45 to 50 milliseconds. This usually will require at the front of the room a lowering of the ceiling and/or a stepped up platform, and, for auditoriums with prosceniums and stage enclosures, a properly designed music shell.

3. Stage Design. The acoustical design of the stage enclosure of a multi-purpose music room or auditorium is as important as is that for the audience enclosure. In order to fulfill the requirements for both performers and listeners:

(1) The reverberation characteristic of the stage space, with its normal equipment and hangings - and its music shell in its storage position-, should differ only slightly from that of the audience space. For example, if the optimal time at middle frequencies is 1.8 seconds for the audience, the optimal time for the stage enclosure is about 2.0 seconds.

(2) There must be a properly designed music shell which simulates the acoustical conditions normally existing in the performers' end of a good concert hall. A good example is the new shell designed by George Izenour and Robert Newman for the Northrop Auditorium in Minneapolis. A shell patterned after the Minneapolis one has been designed for a multi-purpose 3000-seat auditorium for Arizona State University (W. W. Peters and Taliesin Associates, Architects). The walls of the shell are to be fabricated of 12 gauge steel conic sections (to provide diffuse reflections of sound), and the ceiling is of rolled cylindrical steel. The rear surfaces of the steel are heavily doped to prevent panel resonance. Several of the steel panels at the bottom of the rear and side walls are perforated and can be made reflective or absorptive, as required for the optimal "tuning" and balancing of the shell enclosure. A novel feature of this "Izenour" shell allows the side walls and ceiling to fold against the rear wall, thus requiring only a small space for storage.

Figure 1 is a photograph of a recently completed shell for the Seattle Opera House (Priteca and Chiarelli, Architects; Veneklasen and Knudsen, Consultants). This shell consists of slightly convex panels of plywood.

The walls are free standing, mounted on counter-weighted dollies for convenient moving and storage. The ceiling splays are suspended, and, for storage, can be drawn up into the fly gallery, as can also the rear wall. The two shells here described have stepped up platforms for orchestras and/or choruses. The shells and platforms simulate good concert hall acoustics; all instruments and performers can be seen and heard by all listeners, thus promoting good definition and balance, and also the acoustical "intimacy" advocated by Beranek (Sat. Rev., 44, 43 (1961)).

5. Optimal Reverberation. My experience indicates that the optimal reverberation times at 1000 c.p.s. for music rooms are: about 0.5 second for small practice rooms (volume ~ 15 m^3); 0.8 to 1.0 second for rehearsal rooms (200 to 400 m^3); 1.1 to 1.3 seconds for chamber music rooms (1000 to 2000 m^3); 1.4 to 1.6 seconds for multi-purpose school auditoriums (3000 to 10,000 m^3); 1.7 to 1.9 seconds for large concert halls (10,000 to 20,000 m^3); and about 2.0 to 2.2 seconds in larger halls used frequently for organ music and choral works. European habits and experience give preference to slightly longer times (about 10 percent longer) than these, but deviations of ± 0.1 second from the above values are readily acceptable if the rooms meet the other major requirements for good acoustics.

How should the reverberation time vary with frequency? What criteria should determine the optimal reverberation characteristic? Should it be the same for all frequencies? Or a composite based on the absorption characteristics of the audience, furnishings, air, and the walls and ceiling of typical music rooms? Should it be based on the frequency distribution of sound energy in the music, so that all components of music, on the average, will die away to inaudibility in the same length of time? Or should it be such that the rate of growth or decay of loudness level will be the same for all frequency components? Fortunately, the last three criteria lead to about the same characteristic for frequencies below 1000 c.p.s., namely, a gently rising one in which the reverberation time is about 50 percent longer at 62 c.p.s. than it is at 1000 c.p.s. The criterion that makes the rate of change of loudness level the same for all frequency components, first proposed by McNair, is probably the most reasonable one, and it has the advantage that it is easy to evaluate and is the same for different kinds of music. I have computed the characteristic from the mean of the equal loudness level contours of (1) Fletcher and Munson and (2) Robinson and Dadson, at the loudness levels between 50 and 80 db. The resulting optimal reverberation times are obtained by multiplying the 1000 c.p.s. optimal time by the following factors:

Frequency, c.p.s.	62	125	250	500	1000	2kc	4kc
Factor	1.5	1.3	1.15	1.1	1.0	1.1	1.15

This proposed reverberation characteristic differs only slightly from the one I recommended in Architectural Acoustics in 1932, and my experience of the past thirty years supports it as the optimal one for good music room acoustics.

N27

FOURTH INTERNATIONAL CONGRESS ON ACOUSTICS
COPENHAGEN 21.-28. AUGUST 1962

Contrôle des Lecteurs Stéréophoniques par Disques de Fréquence Glissante

D.J. DION
Ing. E.S.E., A/S Brüel & Kjær

Introduction

Les enregistrements stéréophoniques sur disques commerciaux sont susceptibles à l'heure actuelle de présenter des performances dépassant largement les possibilités des appareils de lecture de grande série et l'on peut affirmer en règle générale que la qualité de la reproduction sonore par disques est limitée par celle de la tête de lecture ("pick-up"). Ceci est particulièrement valable en ce qui concerne la reproduction stéréophonique où la tête de lecture est l'élément qui effectue la distinction entre les deux signaux 45°/45° dont la résultante est donnée par la modulation du sillon. Il est donc important d'étudier de près les caractéristiques des têtes de lecture, et en particulier la séparation entre canaux lorsqu'il s'agit d'équipement stéréophonique dont l'intérêt réside dans cette séparation même.

La séparation entre canaux est le pourcentage de modulation (b_o) du canal B par rapport à la modulation (a) du canal A, lorsque seul le canal A est modulé. Elle s'exprime généralement en décibels:

$$S(dB) = 20 \log_{10} \frac{a}{b_o}$$

et réciproquement

$$S'(dB) = 20 \log_{10} \frac{b}{a_o}$$

La séparation varie d'une manière très irrégulière avec la fréquence. On s'efforce de la maintenir maximum dans la partie centrale, la plus signifiante, de la gamme audible. Les mesures de séparation s'effectuent, en même temps que le tracé de la courbe de réponse, à l'aide d'un disque de fréquence glissante, c'est à dire un enregistrement étalonné d'un signal d'amplitude déterminée et de fréquence continûment variable d'une extrémité à l'autre de la gamme audible.

Disques de fréquence glissante stéréophoniques

Ces enregistrements étalons sont généralement réalisés avec un balayage de fréquence logarithmique en fonction du temps. La vitesse de rotation des platines d'entraînement pouvant sans difficulté être contrôlée avec une grande précision (celle de la fréquence du secteur) l'erreur de détermination de la fréquence est pratiquement celle du générateur BF employé à l'enregistrement. Avec un générateur à battement du commerce par exemple, on peut obtenir une échelle de fréquence logarithmique à $\pm$ 2% près de la valeur absolue sur trois décades.

La gamme de fréquence enregistrée doit recouvrir largement la gamme audible. De façon à inclure les fréquences musicales les plus basses (piano, orgue) la limite inférieure ne doit pas être supérieure à 2o Hz. D'autre part, il est nécessaire pour déterminer l'influence de la résonance du stylet de monter le plus haut possible en fréquence. En enregistrant jusqu'à 20 KHz, on pourra, d'après la pente finale de la courbe de réponse, estimer cette influence même dans le cas de lecteurs de hautes performances, bien que la précision absolue soit réduite à une fréquence aussi élevée.

A 20 KHz cependant l'amplitude de l'enregistrement est limitée en raison des distorsions et déformations qui s'accentuent dès que la courbure de la sinusoïde enregistrée atteint une valeur comparable à celle de l'extrémité de la pointe de lecture. La courbure de la sinusoïde enregistrée est par exemple d'environ 2o µ à 2o KHz pour une vitesse de sillon de 3o cm/s et un niveau de vitesse de 3 cm/s

efficace. C'est pourquoi les caractéristiques d'enregistrement adoptées ne comportent pas d'amplification des hautes au dessus de 1ooo Hz. Un exemple est montré en figure 1. - La partie basse fréquence correspond à la définition généralement adoptée:

$$V = V_o \sqrt{\frac{1 + \frac{1}{\omega^2 t_3^2}}{1 + \frac{1}{\omega^2 t_2^2}}}$$

avec t_3 = 10 t_2 = 3180 us. (Recommandations de la C.E.I., publication nº 98-1).

A la reproduction, un filtre restituant soit l'amplification des hautes fréquences pour obtenir une caractéristique normalisée, soit les basses fréquences de façon à avoir un niveau de référence à vitesse constante pour l'essai des lecteurs électrodynamiques, doit être intercalé dans la chaîne de mesure.
La réponse en fréquence d'un lecteur stéréophonique qui en principe est un transducteur bidimensionnel ne peut être représentée que par un réseau de courbe.
En pratique, l'étude se fait dans quatre directions différentes:

(1) horizontale, avec des modulations égales et en phase des deux canaux (a = b)
(2) verticale, correspondant à des modulations en opposition de phase (a = -b)
(3) 45° gauche, correspondant à la modulation d'un seul canal (soit a, avec b=o)
(4) 45° droite, correspondant à la modulation de l'autre canal seul (b, a = o).

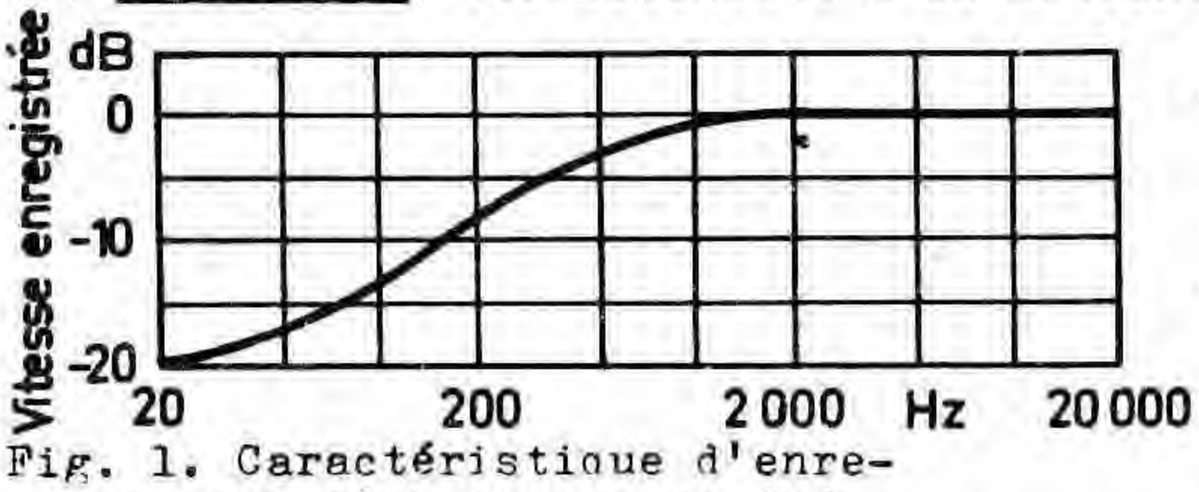

Fig. 1. Caractéristique d'enregistrement d'un disque de fréquence glissante montant jusqu'à 20 KHz.

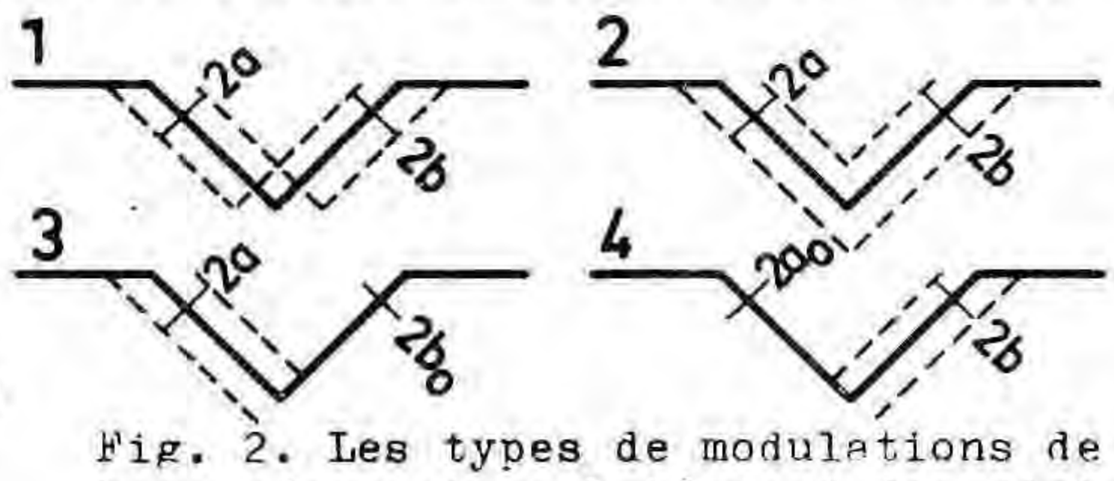

Fig. 2. Les types de modulations de base nécessaires à l'essai des pick-ups stéréophoniques.

L'ensemble, pour les deux canaux, demande donc le tracé de 8 courbes de réponse. Ces courbes présentant souvent de nombreuses irrégularités, un tracé détaillé est nécessaire et l'usage d'un enregistreur est pratiquement indispensable. De plus, aux fréquences élevées, les résultats sont fonction dans une certaine mesure de la vitesse de sillon et il est souhaitable de répéter les essais sur des enregistrements étalons de diamètres différents ou de vitesse de rotation différentes.

Mesures de séparation avec filtrage synchrone

Suivant la définition donnée en introduction, la séparation sera mesurée par le rapport des signaux de sortie du lecteur traçant les gammes de modulation unilatérale (3) et (4) ci-dessus. Cependant, la mesure du signal résiduel du canal non modulé n'est possible que si ce signal a une amplitude dépassant le niveau de bruit de fond. Dans les conditions discutées ci-dessus (niveau maximum de modulation égal à 3 cm/s efficace, et restitution soit des basses soit des hautes par filtre correcteur) le niveau de bruit de fond équivalent dans la gamme 2o Hz - 2o KHz est de l'ordre de 0,2 cm/s efficace. Ceci correspond, suivant les conditions de lecture, à un niveau situé de 2o à 26 dB sous le niveau de modulation, qui interdit donc les mesures de séparation dépassant 2o dB. En omettant le filtre correcteur, il est possible de pousser les mesures jusqu'à 32 dB dans la partie plate de la caractéristique d'enregistrement (au dessus de 1 KHz).
Cependant les lecteurs produits actuellement, même de grande série, présentent couramment une séparation supérieure dans une région plus ou moins étendue de la gamme audible. Les niveaux de bruit cités ci-dessus ont été mesurés sur des enregistrements réalisés par ORTOFON suivant les plus hauts standards actuels. Une réduction sensible de ces niveaux par amélioration du procédé d'enregistrement

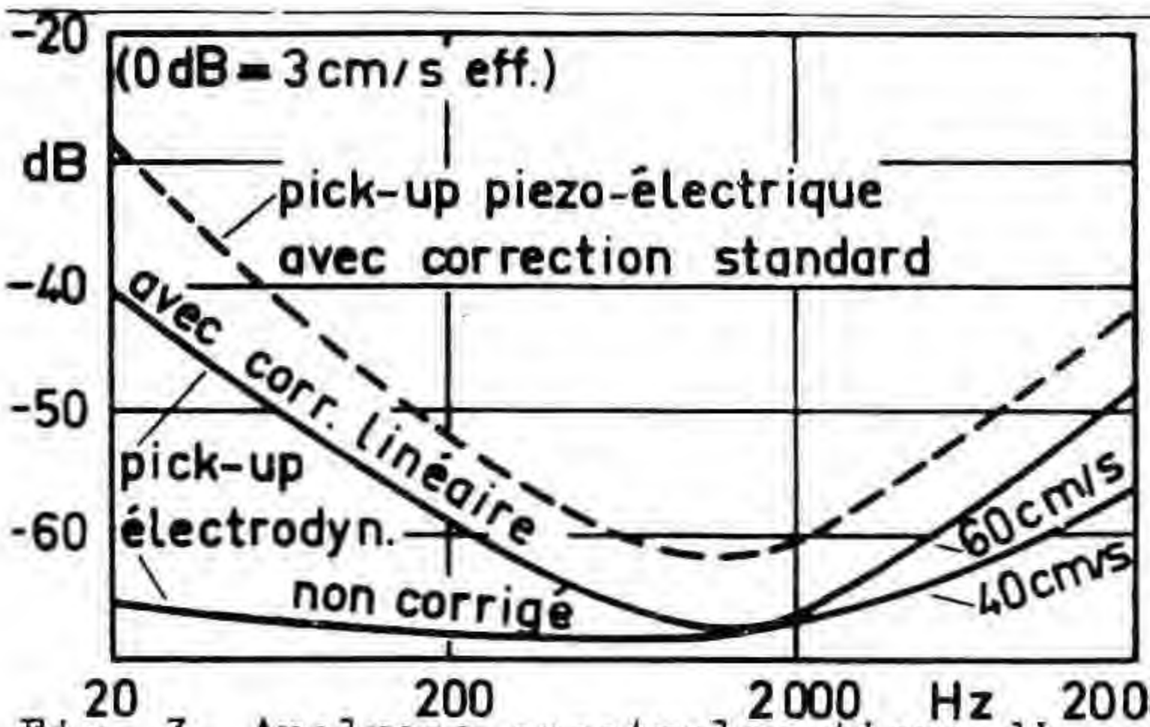

Fig. 3. Analyses spectrales tiers d'octave du bruit de fond dans quelques cas typiques.

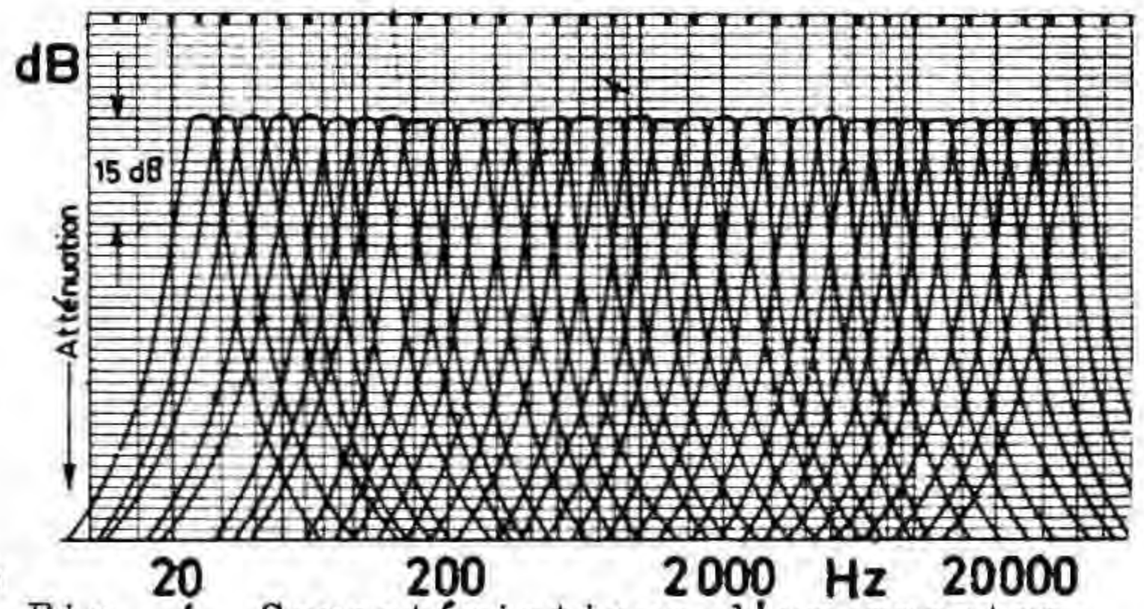

Fig. 4. Caractéristique d'un spectromètre de sonomètrie à filtres tiers d'octave.

est difficile à obtenir.
Par contre il est possible de réduire le bruit à la lecture par filtrage. Ceci a permis de mesurer avec un lecteur de bonne qualité des séparations d'environ 4o dB de 5oo Hz à 2ooo Hz. Evidemment il est difficile à ce niveau (1%) de distinguer le signal résiduel enregistré du signal résiduel dû à la lecture. Mais de nombreux fabricants d'équipement d'enregistrement déclarent atteindre des séparations dépassant largement 40 dB dans la partie la plus importante de la gamme audible, et il est hors de doute que ces performances d'enregistrement seront courantes dans l'avenir. La méthode de filtrage synchrone décrite ci-dessous, qui rejette le niveau de bruit à plus de 60 dB sous le signal à 1 KHz (Fig. 3) donne en tout cas un moyen de pousser les recherches dans cette voie. Des essais à vitesses différentes permettent de déterminer la séparation du disque lui-même.

Dispositif de mesure automatique de séparation en fréquence glissante.

Le filtrage doit atténuer à la fois les fréquences hautes contenant le bruit de surface et les fréquences basses provenant des imperfections mécaniques des platines d'entraînement. On doit donc disposer d'un filtrage passe-bande encadrant et suivant la fréquence de modulation sans troubler les mesures.

Parmis les divers procédés pouvant être utilisés, l'emploi d'un spectromètre de sonomètrie comportant une série de filtres tiers d'octave jointifs donne des résultats particulièrement sûrs. L'entraînement du sélecteur de filtre peut être effectué sans difficulté à la cadence appropriée. La synchronisation en fréquence n'est critique qu'aux points de commutation d'un filtre à l'autre. Avec le spectromètre dont la caractéristique est représentée en figure 4, on obtient des pics négatifs aux passages d'un filtre à l'autre, mais leur localisation étant déterminée à l'avance ils seront faciles à distinguer au cours des mesures. Leur amplitude permet de plus de contrôler la synchronisation: étant donnée la pente déjà importante des caractéristiques des filtres aux points de commutation, tout écart de fréquence entraîne une augmentation importante de l'amplitude des pics. L'écart inhérent à la précision en fréquence du disque étalon n'a qu'une influence réduite: une erreur en fréquence de 2% provoquera un pic de 5 dB au lieu de 3 dB normalement.
De façon à ne pas troubler l'entraînement du disque qui doit être exempt de toute vibration, la commande automatique du spectromètre doit de préférence être indépendante mécaniquement de la platine tourne-disque. Dans le dispositif ci-après, la synchronisation est réalisée d'une part à partir d'un signal de départ enregistré sur le disque, d'autre part à partir de la fréquence du secteur. Les vitesses de balayage respectives sont en effet règlées, soit stroboscopiquement, soit par moteur synchrone, sur la fréquence du secteur. La coïncidence en fréquence des deux plages logarithmiques est réalisée en faisant démarrer l'arbre d'entraînement du spectromètre à l'instant même où cesse le signal de départ de fréquence fixe 1 KHz enregistré immédiatement avant le balayage logarithmique (2o Hz - 2o KHz).
Le dispositif est schématisé en figure 5. Le signal de départ est amplifié par

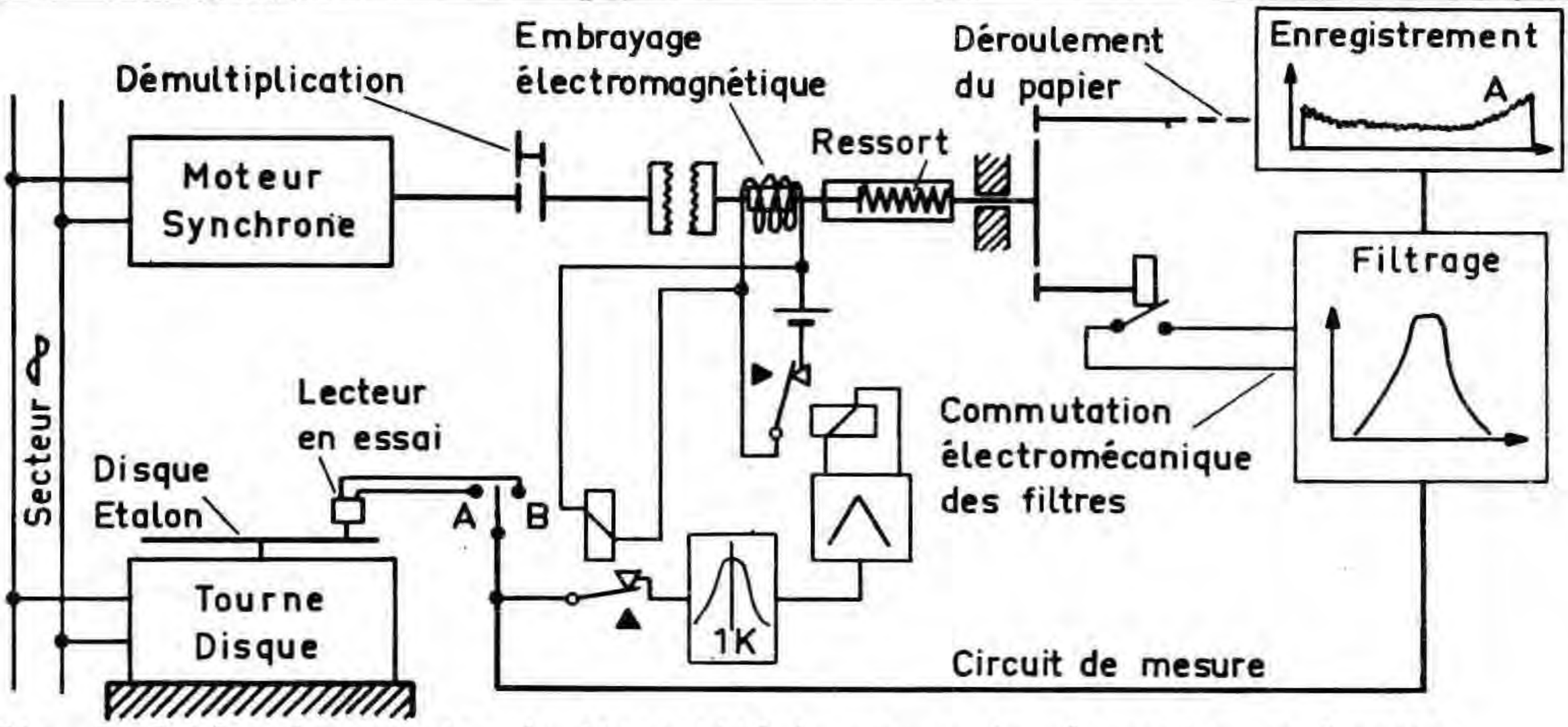

Fig. 5. Schéma de principe du dispositif de mesure de séparation en fonction continue de la fréquence avec filtrage synchrone.

un amplificateur sélectif qui n'est connecté au circuit de mesure que lorsque la transmission mécanique est débrayée. A la sortie de l'amplificateur, un système de relais coupe le circuit de débrayage à la fin de l'impulsion de départ. Le débrayage est donc relâché à cet instant, et si le moment d'inertie des pièces à démarrer est faible par rapport au moment d'inertie, rapporté à l'arbre d'embrayage, du rotor du moteur synchrone tournant en permanence, le démarrage est pratiquement instantané.
L'ensemble à démarrer comprend d'une part la came actionnant électromécaniquement le spectromètre et d'autre part le déroulement de papier d'un enregistreur à potentiomètre logarithmique. Une étendue dynamique de mesure de 5o dB est nécessaire pour permettre l'enregistrement sur le même papier des courbes de réponse du canal modulé et du canal non modulé. Un exemple de courbes données automatiquement par ce procédé est montré fig. 6. Dans l'interprétation des résultats obtenus au dessus de 15 KHz, il faut tenir compte éventuellement des pertes inhérentes dues à la compliance du disque qui ne sont négligeables que si la masse équivalente de la pointe de lecture et sa pression sur le disque sont suffisamment faibles.

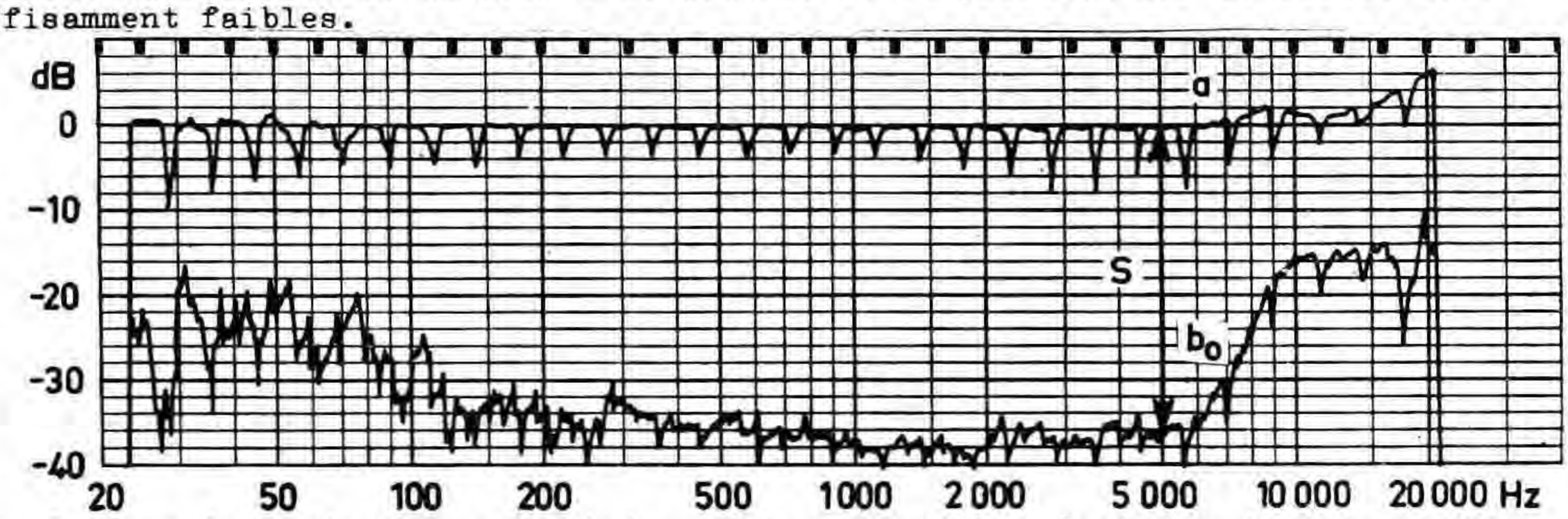

Fig. 6. Exemple typique de résultat expérimental obtenu à l'aide du dispositif de la fig. 5. La limite basse fréquence du premier filtre est 22 Hz.

En conclusion, j'adresse mes remerciements à Mr. O. Heilsberg, qui a mis au point une série de disques étalons ainsi qu'un dispositif de synchronisation entièrement automatique, et a bien voulu m'aider dans la présentation de cette technique.

O27

FOURTH INTERNATIONAL CONGRESS ON ACOUSTICS
COPENHAGEN 21.-28. AUGUST 1962

NON-LINEAR THEORY OF SPHERICAL AND CYLINDRICAL ACOUSTIC WAVES IN VISCOUS HEAT-CONDUCTING MEDIUM.

S. I. SOLUYAN

The spherical and cylindrical acoustic waves of finite amplitude cannot be considered on the basis of linear gasodynamic equations. On the other hand it is extremely difficult to find solution of non-linear equations even in absence of energy losses. There is no analogue of the Riemann's solution. The approximate study of spherical and cylindrical waves was undertaken only for mediums in which Reynolds-factor had an order of unity. ($Re \sim 1$)

In the present report the convergent and divergent spherical and cylindrical acoustic waves of finite amplitude in viscous heat-conducting medium are considered on the basis of the approximate method. This method is valid for small initial velocity v and density $\rho' = \rho - \rho_0$ disturbances, small energy losses and large radii of sphere or cylinder comparative to the wave-length. In first approximation the spherical and cylindrical waves have shape of plane waves (the zero-approximation), but this shape slowly varies with radius. If one passes to the "excorting" coordinate system $\tau = t - r/c_0$ and $r' = \mu r$ where c_0 is the sound-velocity, t - time and μ - the small parameter, the system of gasodynamic equations can be reduced in the first approximation to one partial non-linear equation of the second order.

This equation is

$$\frac{\partial v}{\partial r} + \frac{v}{\alpha r} - \beta v \frac{\partial v}{\partial \tau} = \delta \frac{\partial^2 v}{\partial \tau^2} \qquad (I)$$

where $\alpha = 1$ for spherical waves and $\alpha = 2$ for cylindrical waves,

$$\beta = (\gamma+1)/2c_0^2 \quad , \quad \delta = \left[\tfrac{4}{3}\eta + \zeta + \varkappa\left(\tfrac{1}{c_v} - \tfrac{1}{c_p}\right)\right] / 2\rho_0 c_0^3$$

ρ_0 - density of undisturbed medium, η and ζ viscosity coefficients respectively, $\varkappa$ - coefficient of heat-corductivily.

Assume the boundary condition on the oscillating sphere or cylinder is

$$v = v_0 \sin \omega t \qquad \text{when} \quad r = r_0 \qquad (2)$$

and find the steady-state with τ solution of equation (I), which describes the travelling convergent and divergent spherical and cylindrical waves.

The solution of equation (I) makes clear a series of interesting peculiarities for devergent accoustic waves. In the most interesting case $Re \gg 1$ the distances from the boundary can be divided up into three regions. In the first region the effects of energy losses can be neglected and the non-linear effects lead to the conversion of the sinusoidal wave to the sawtooth one. In the second region the losses play the essential role, so that the front of each shock wave diffuses and the wave become sinusoidal one again. Further the third region of the wave propagation begins. Due to dissipation and divergence losses in this last-region the wave amplitude becomes so small so that the standart linear treatment of divergent sound waves can be used.

The non-linear distortion of waves, the diffusion of shock fronts and the characteristic intervals of these motions are different for spherical and cylindrical waves.

The second region of propagation of divergent spherical and cylindrical waves is the most interesting one. In this region the non-linear and dissipative effects simultaneously play essential roles. The expression for the wave shape in this region can be written as

$$v = \frac{v_0 f(z)}{1+\alpha Z_0 |\psi(z)|}\left(-\omega\tau + \pi th\frac{\omega\tau}{\Delta}\right) \qquad (3)$$

where $Z_0 = \beta\omega v_0 z_0$, $f(z) = z_0/z$, $\psi(z) = \ln\frac{z}{z_0}$ - for spherical waves, and for cylindrical waves $f(z) = \sqrt{z_0/z}$ and $\psi(z) = 1 - \sqrt{z/z_0}$

The parameter Δ is dimentionless and express the front - width of waves and it is equal

$$\Delta = \frac{1+\alpha Z_0|\psi(z)|}{\alpha\pi Re} f(z) \qquad (4)$$

The solution (3) - (4) was obtained by means of the combination of the solution, describing sawtooth wave and the solution, describing quasi-stationary front structure. The features of the propagation of divergent waves is demonstrated in Fig.I , where the characteristic parameters of the forming quasi-discontinuite wave Z_1 and of the convertion of shock wave to the sinusoidal one Z_2 are pointed out:



Fig 1

When the wave is convergent, the dissipation losses and the convergence effect act in the different directions [relation (4)]. The growth of the frontwidth obliging to losses is being suppressed by the amplitude growth because of convergence.

Dissipative widening of the fronts of the convergent spherical and cylindrical waves displays in full measure in the long-focal systems, where initial radii are large. [Parameter Z_0] The case $Z_0 >> Re$ has a special interest, because the dimentionless front width can become equal (or even more) than π . However, for the distances, corresponding to $\Delta \geqslant \pi$ the wave amplitude, accordingly to (3) has the second order of magnitude and the wave behavior obeys the laws of the linear theory. In other words the linear theory is valid up to the begining of the second forming of shock waves, because of the convergent growth of the amplitude. The amplitude behavior for convergent spherical and cylindrical waves in this case is qualitative demonstrated on Fig.2, where the parameters Z^1 and Z^2 limit the region of validity of the linear theory. The dashed curve shows the amplitude accordingly to the linear theory. The second forming of shock waves begins from point Z^2 .

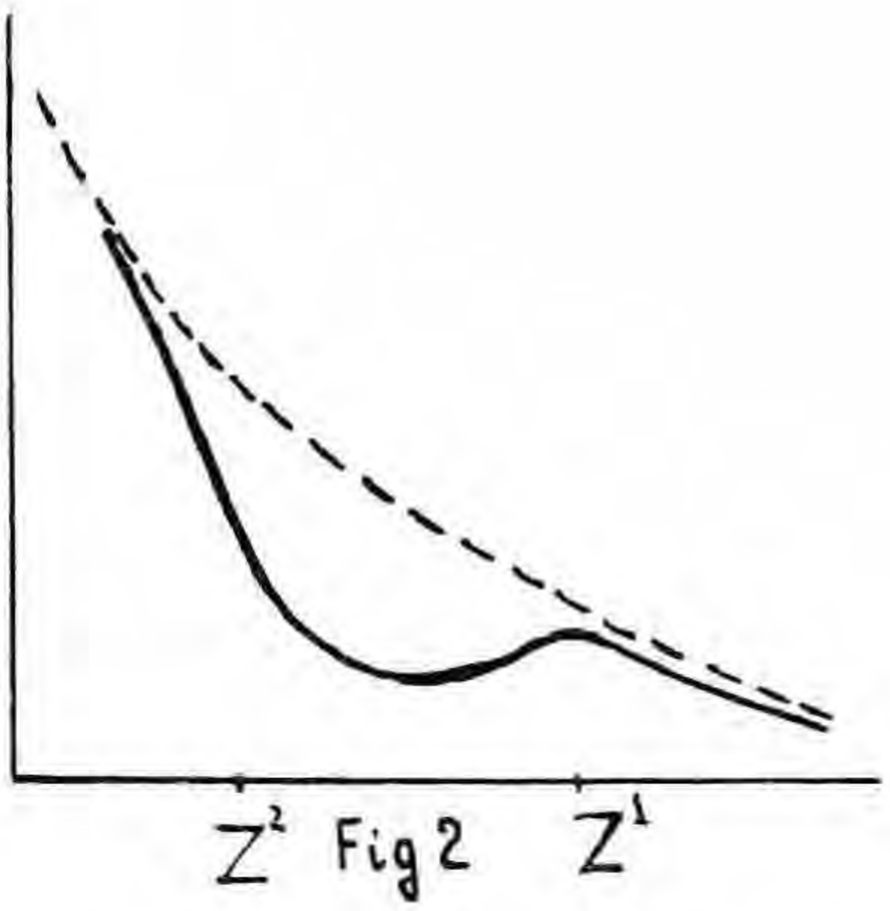

Fig 2

On the basis of the found analytical expressions, describing the wave in the non-linear dissipative medium it is easy to write the expression for sound wave energy. The dissipation energy is determined by the difference of the energy of the linear sound wave and the energy, which is brought by the sound wave, taking in to account the nonlinearity and the losses. The enrgy dissipation is proportional to the energy density of wave, but, this proportionality, in difference from the linear approximation, cannot be described by the absorbtion coefficient $\delta\omega^2 = \text{const}$. The relative energy of dissipation is maximum in the point $\Delta = \Delta_{max}$

It is interesting to note, that the convergent spherical wave always becomes the shock one, but the cylindrical wave can converge without noticeable distortion.

By the simple changing of variables equation (I) can be reduced to the equation, which describes the plane wave in the medium with ex-

pongntially increasing or decreasing viscosity for divergent or convergent spherical waves respectively or linear increasing or decreasing viscosity for divergent or covergent spherical waves.

H28

FOURTH INTERNATIONAL CONGRESS ON ACOUSTICS
COPENHAGEN 21.-28. AUGUST 1962

FREE FIELD THRESHOLD SHIFT AND TEMPORARY THRESHOLD SHIFT REDUCTION AS MEASURES OF EFFICIENCY OF EAR PROTECTIVE DEVICES

Capt John L. Fletcher, MSC (Ph.D.) and Michel Loeb, Ph.D.

I. Introduction

Basic to the problem of hearing conservation is the development of ear protective devices. Essential to such development are valid, reliable tests of the protection afforded the wearer by the device. The most widely accepted evaluation technique is the free field threshold shift (FFTS) method suggested by the American Standards Association[1]. This method requires a binaural determination of the shift of an individual's free-field threshold while wearing the particular device. Specific, discrete, frequencies are used and measurement of at least 10 persons with the procedure repeated at least three times for each individual is recommended. This method provides, essentially, a measure of the effective attenuation of the device for low intensity levels of pure tones. It is assumed that the attenuation at high intensity levels is comparable.

Another evaluation technique which provides a measure of protection for near injurious levels of noise is obtained by comparing the temporary threshold shift (TTS) induced in the hearing of an individual following exposure with and without ear protection. TTS is observed in the same person following exposure to a given noise environment with no ear protection and on another date to the same environment while wearing the protecting device. The reduction in TTS (TTSR) in the protected condition as compared to that observed in the unprotected state is taken as an index of the protection afforded by the device. This method was used by Zwislocki[2] in the evaluation of a new insert type protector. Cohen[3] utilized a similar method to evaluate the protective characteristics of a helmet.

Cohen's study which employed both continuous and impulse (gunfire) noise, suggests that the protection afforded by the helmet for impulse noise was less than that provided for continuous noise. He reported that the helmet provided significant protection against continuous noise but little or no protection against impulse noise of equal total energy. These results would seem to suggest that evaluation by the FFTS method with steady tones is inadequate for protective devices that will be used to shield the wearer from impulse exposure. The possibility exists that the use of a TTSR technique would make the evaluation of a protector more generalizable.

The purpose of the present study was to evaluate the protection (attenuation) of two inserts and one helmet type ear protector by means of the FFTS and TTSR techniques using both continuous and impulse noise exposure. A comparison of the results obtained was made to determine the limitations, advantages, and disadvantages of each method of evaluation.

II. Method, Apparatus, Procedure, and Subjects

The experimentation was conducted in three related but separate phases. The first phase entailed the exposure of 13 subjects, unprotected, to gunfire at a rate of 75 rounds per min. The average peak sound pressure level (SPL) of the blank rounds,

as measured by a General Radio sound level meter and impact noise analyzer was 155 db.

The subjects were initially exposed to a small number of rounds, and the exposure was gradually increased until a TTS of at least 12 but no more than 64 db was observed at some frequency. This procedure was instituted as a safety factor to assure that no permanent threshold shift would result.

After each subject met the minimum-maximum TTS requirement, he was exposed to the same number of rounds but protected by plug A, plug B, or the helmet. In all phases of the experiment order of wearing of the devices was counterbalanced. The plugs and helmet were individually fitted to the subjects prior to their participation in the experiment. At that time, they were instructed and supervised in the proper method of donning the device and in the wearing and care of the items. From that time on, whenever wearing of a protector was indicated, the subject himself put the device in place.

Phase I. In a typical experimental session of Phase I, the impulse noise, TTSR phase, the subject was given a pre-exposure sweep frequency audiogram from 1000-6000 cps and then seated on a stool just behind the machine gun. The number of rounds previously determined to be sufficient to induce a TTS of 12 db or more at some one of the sweep frequencies tested was then fired. Upon completion of the firing, the subject immediately entered the sound trailer and his post-exposure audiogram was determined. The post-exposure audiogram was begun within 15-25 sec. of the firing of the last round.

Phase II. After all subjects had completed the impulse noise phase of the experiment, the FFTS data were collected on the same 13 subjects. In general, the real ear method of evaluation proposed by the American Standards Association[1] was used. The method was modified to include the use of a recording attenuator and oscillator to determine by the Bekesy technique the discrete frequency thresholds for 125, 250, 500, 1000, 2000, 3000, 4000, 6000, and 8000 cps. The individual's threshold for each frequency was followed for 30 sec. with and without the protective device. Preliminary findings indicated that this method of threshold determination would decrease threshold variability by allowing the subject to accustom himself to the task.

In the experimental sessions the subjects were seated in an anechoic chamber with their chin in a chin rest, facing a speaker. The speaker output was controlled by a switch available to the subject. Utilizing this switch to control the output, the subjects determined their threshold with and without the protecting devices. Their discrete frequency threshold for 125 cps was determined by the above noted modified FFTS technique, and then, in ascending order of frequency, thresholds were determined for the remaining frequencies. The differences in hearing level (in db) at each frequency for the two conditions were presumably due to the attenuation of the device being investigated.

Phase III. In this phase the subjects were first exposed unprotected to a broad band noise source for increasing lengths of time until their measured TTS at 6000 cps matched that incurred previously from exposure to impulse noise. The criterion for a match was $\pm$ 6 db. No attempt was made to match the TTS at any other frequency. One subject from the original group used in the two previous phases was absent from the laboratory during the running of this phase. The overall SPL of the exposure noise at the ear of the listener was 109 db (re . 0002 dyne/cm^2), as measured by a

Brüel and Kjaer (BK) spectrum analyzer and BK Model 4131 microphone. The subject was seated with his chin in a chin rest equidistant from the three speakers, which were enclosed in a plywood reverberation room inside the anechoic chamber.

After determination of the duration of noise exposure necessary to induce sufficient TTS (unprotected) to match the impulse induced TTS, subjects were exposed to the noise on separate days while wearing the protective devices. The subjects were brought into the anechoic chamber, had their pre-exposure audiograms taken, were exposed to the noise, and then underwent post-exposure thresholds (determined usually within 10-15 sec. after termination of exposure). The TTSR characteristics of the items were determined by noting the differences in TTS between that observed following unprotected exposure and that noted following protected exposure. For all of the TTSR portions of the experiment, TTS was examined for the frequencies 1, 1.5, 2, 3, 4, 5, and 6 KC.

The raw data, then, are db of TTSR for each of the devices for the firing and noise phases of the experiment, and db of free field threshold shift attributable to the wearing of each protective item for the FFTS part of the study.

The subjects used in this experiment were all USAMRL staff members, ranging in age from 20-39 years. With one exception, all had normal hearing (here defined as not more than 15 db hearing loss at the octave frequencies 125-8000 cps). All were skilled in the Békésy technique.

IV. Discussion

It was demonstrated in this experiment that certain continuous and impulse noise exposures which would be hazardous if presented habitually would not be hazardous to observers wearing any of the three protective devices. While a determination of attenuation by the usual physical or threshold shift methods may be easier to perform than the TTSR technique, the TTSR method would appear to have certain advantages.

There are now generally accepted damage risk criteria for continuous noise exposure and we have no reason to doubt the validity and generality of the physical and FFTS attenuation figures as they apply to continuous noise. It is probably feasible then,if the level of a continuous noise exposure is know, to subtract these attenuation figures to determine the noise impinging on the ear. A fairly reliable estimate of the potential hazard can be made. For impulsive noise, however, the case is different. The attenuation figures obtained by the usual methods may not predict the attenuation of loud impulsive noise. Flottorp and Quist-Hanssen[8] have shown that attenuation of explosive noise by some devices exceeds that predictable from the usual pure-tone attenuation measurements. Moreover, criteria for safe exposure to impulsive noise do not currently exist. However, it is possible to accept tentatively Glorig's[6] et al standards for permissible TTS following exposure and to employ a TTSR method to determine whether a given device offers sufficient protection for a known exposure.

While the present data suggest negligible correlation between susceptibility to continuous and to impulse noise, the authors are loath to affirm such a conclusion on this basis alone. Other related experiments may be suggested. One such investigation might involve restriction of the range or ranges of TTS. It might be required, for example, that continuous and impulsive noise exposures be determined which would produce between 35-45 db shift rather than the 12-64 db shift permitted

in this experiment. It is possible that the relationship for susceptibility to continuous and to impulsive noise is not the same when TTS is high as when TTS is low. Experiments with restricted TTS ranges would settle this point.

Other experiments might be performed in which amount of TTS following a specified continuous noise exposure would be correlated with amount of TTS following a specified impulse noise exposure.

It becomes apparent here that "susceptibility" may have several different (perhaps related) meanings. The relationship between amounts of exposure required to produce specified TTS and amount of TTS following specified exposure is not currently known. Moreover, more animal experimentation will be necessary to determine which measure of susceptibility (if either) will predict susceptibility to permanent damage -- i.e., the probability that a given exposure or series of exposures will produce an irreversible loss. Such experimentation, of course, is in progress at a number of laboratories.

V. Summary and Conclusions

It was found that the helmet afforded significantly less attenuation of low frequency sound than the earplugs and roughly the same amount at higher frequencies. However, contrary to the findings of Cohen[3], the three devices were equally effective in eliminating the TTS following exposure to the continuous and impulsive noise. While the data did not lend themselves to definite conclusions regarding susceptibility to impulse and continuous noise, it appeared that susceptibility to one type of exposure was not necessarily significantly correlated with susceptibility to the other. The possible advantages of the TTSR method in the evaluation of earplugs are discussed.

References

1. American Standards Association, "Proposed Method for the Real Ear Evaluation of Ear Protectors at Threshold," 224.22/427 (1957).
2. J. Zwislocki, "New Types of Ear Protectors." J. Acoust. Soc, Am. 24, 762- (1952)
3. A. Cohen, J. Acoust. Soc. Am. 33, 858 (1961).
4. Bolt, Beranek, and Newman, Inc., Boston, Mass. "Characteristics of Noise Produced by Contemporary Army Weapons." Report No. 630, Surg. Genl. Contract DA 49-007-MD-985 (1959)
5. J. Zwislocki, Chapter 8 in Handbook of Noise Control, edited by C. M. Harris. (Mc Graw-Hill New York, 1957).
6. A. Glorig, W.D. Ward, and J. Nixon. Arch Otolaryng. 67, 71, (1961).
7. M. Loeb, and J.L. Fletcher. US Army Med. Res. Lab Report 533 (in press).
8. G. Flottorp and S. Quist-Hanssen. Acta. Otolaryng. Suppl 158, 286 (1960).

L28

FOURTH INTERNATIONAL CONGRESS ON ACOUSTICS
COPENHAGEN 21.-28. AUGUST 1962

PREDICTION OF NOISE FROM MOTOR VEHICLES IN FREELY FLOWING TRAFFIC

W. J. Galloway and W. E. Clark
Bolt Beranek and Newman Inc., Los Angeles, California, (U.S.A.)

I. INTRODUCTION

Vehicular traffic on large arterial highways is more and more becoming a major source of community noise. There is need, therefore, for a method to predict the noise to be expected from a new highway prior to its construction, or to predict the amount of noise control required in a building to be built adjacent to such a highway. We report herein a calculation procedure derived from a statistical model of freely flowing traffic. A series of noise level measurements on automobiles and trucks is used as input for the model. This procedure predicts the mean and variance in noise level expected adjacent to a highway if the mean speed and number of vehicles per second are specified.

II. SIMULATION OF TRAFFIC NOISE

It is possible to describe the noise produced by traffic by analyzing direct noise measurements on a wide range of traffic conditions. Such an approach is costly and time consuming if general conclusions are desired. An alternative method is to simulate traffic conditions with a simplified model which represents the important aspects of actual traffic flow.

A. Formulation of Model

Traffic traveling at a mean speed on a multi-lane highway is replaced by an equivalent number of vehicles clustered at the mid-points of a series of equal time intervals along a line. The contributions of all vehicles in the series of intervals to the instantaneous sound pressure level (SPL) at an observation point away from the highway are obtained from the expression:

$$SPL = 10 \log_{10} \left[(2\pi W_o)^{-1} \sum_i \sum_k \bar{W}_k n_{ik} d_i^{-2} e^{-\alpha_i d_i} \right]$$

Where: W_o is a reference power level; $\bar{W}_k$ is the mean acoustic power of a vehicle of the k-th class, as a function of speed; n_{ik} is the number of vehicles of the k-th class in the i-th interval; d_i is the distance from the mid-point of the i-th interval to the observation point; and α_i is the attenuation coefficient for propagation and shielding losses for the i-th interval as a function of d_i. Thus, if the speed and distribution of vehicles at any instant can be described, the corresponding value of SPL at the observation point can be determined. The simulation procedure consists of computing SPL from the model, using an adequate number of trials, and then analyzing the results by conventional statistical techniques.

B. Distribution of Vehicles

Investigators of traffic flow have found that in freely flowing traffic

the occurrence of vehicles per unit time is essentially random and can be approximated by a Poisson distribution. In the present simulation, we therefore assume that the probability P_n of having exactly n vehicles in an interval of time is:

$$P_n = \bar{n}^{-n} e^{-\bar{n}}/n!$$

where $\bar{n}$ is the mean number of vehicles per time interval.

The time interval to be used is determined by the distances involved. For speeds up to 60 mph (96.6 km/hr) and observation points 100 feet (30.5 m) or more from the highway, a time interval of one second is satisfactory. The maximum error introduced by assuming all vehicles at the mid-point of the interval is approximately ± 1 db, and less for slower speeds and greater distances from the highway.

We have verified the validity of the Poisson distribution assumption for occurrence of vehicles in one-second intervals with several sets of experimental data we have taken on representative multi-lane highways under free-flow conditions.

C. Acoustic Output of Individual Vehicles

A series of measurements were made of the noise produced by individual vehicles, taken at random, which were separated from other traffic. Speed was measured by timing the transit of the vehicle between two fixed points on the highway.

Sufficiently large samples were taken to insure a representative collection of vehicles of various ages, manufacturer, model, etc. Three sets of data were obtained; one on passenger cars on an almost level highway, a second for large trucks on an almost level highway, and a third for trucks climbing an approximately 5 percent grade. Sample checks on passenger cars indicate their noise output is relatively independent, at a given speed, of whether or not they are climbing a grade; thus, only one spectrum is presented.

All noise levels were obtained by recording the initial data on magnetic tape and subsequently analyzing the tape in octave frequency bands. To assist in evaluating the relative "noisiness" of different traffic conditions the data were then used to compute perceived noise level in PNdb at a distance of 100 feet (30.5 meters) from the highway. (A similar computation of loudness level could be easily performed.) The difference between overall SPL and perceived noise level at 100 feet is about 4 db. For noise control purposes, relating octave band data to PNdb is as adequate as relating to overall SPL. Fig 1 indicates the relative spectrum for passenger cars and Fig 2 the spectra for trucks. All observed speeds have been used in these curves, although for passenger cars there is greater variation between vehicles at lower than at higher speeds.

The data above have been least-squares fitted to obtain a prediction curve for each of the various vehicle classes to be used in the model simulation. These results are:

a) Passenger cars: PNdb at 100 ft = $35 + 30 \log_{10} V$
b) Trucks, level: PNdb at 100 ft = $44 + 30 \log_{10} V$
c) Trucks, 5% grade: PNdb at 100 ft = $66 + 20 \log_{10} V$

where V is speed in mph. The standard deviations for the three cases are 2.6, 2.8, and 2.0 db respectively.

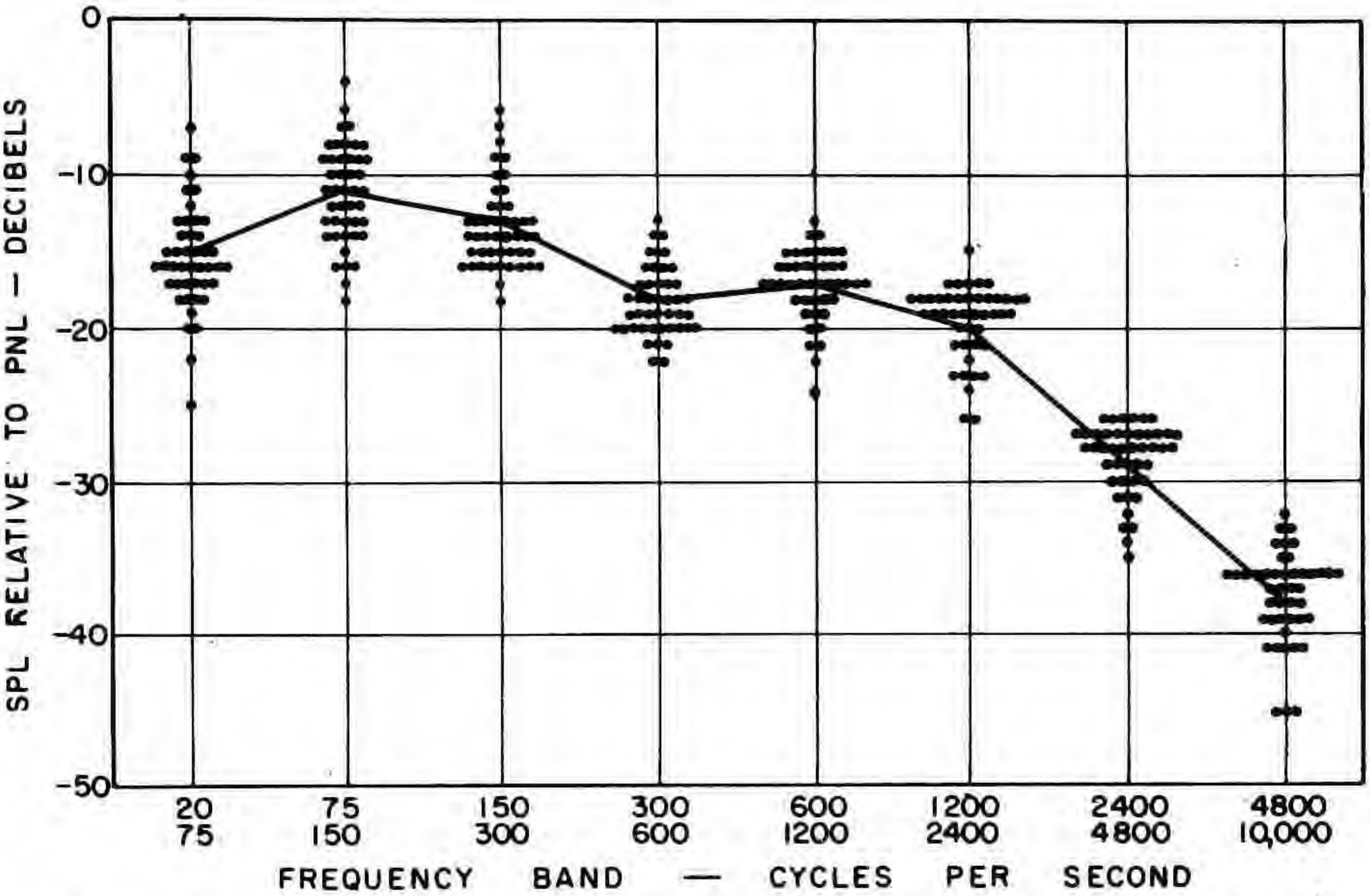

Fig 1. Octave Band Sound Pressure Level Relative to Perceived Noise Level for Passenger Vehicles

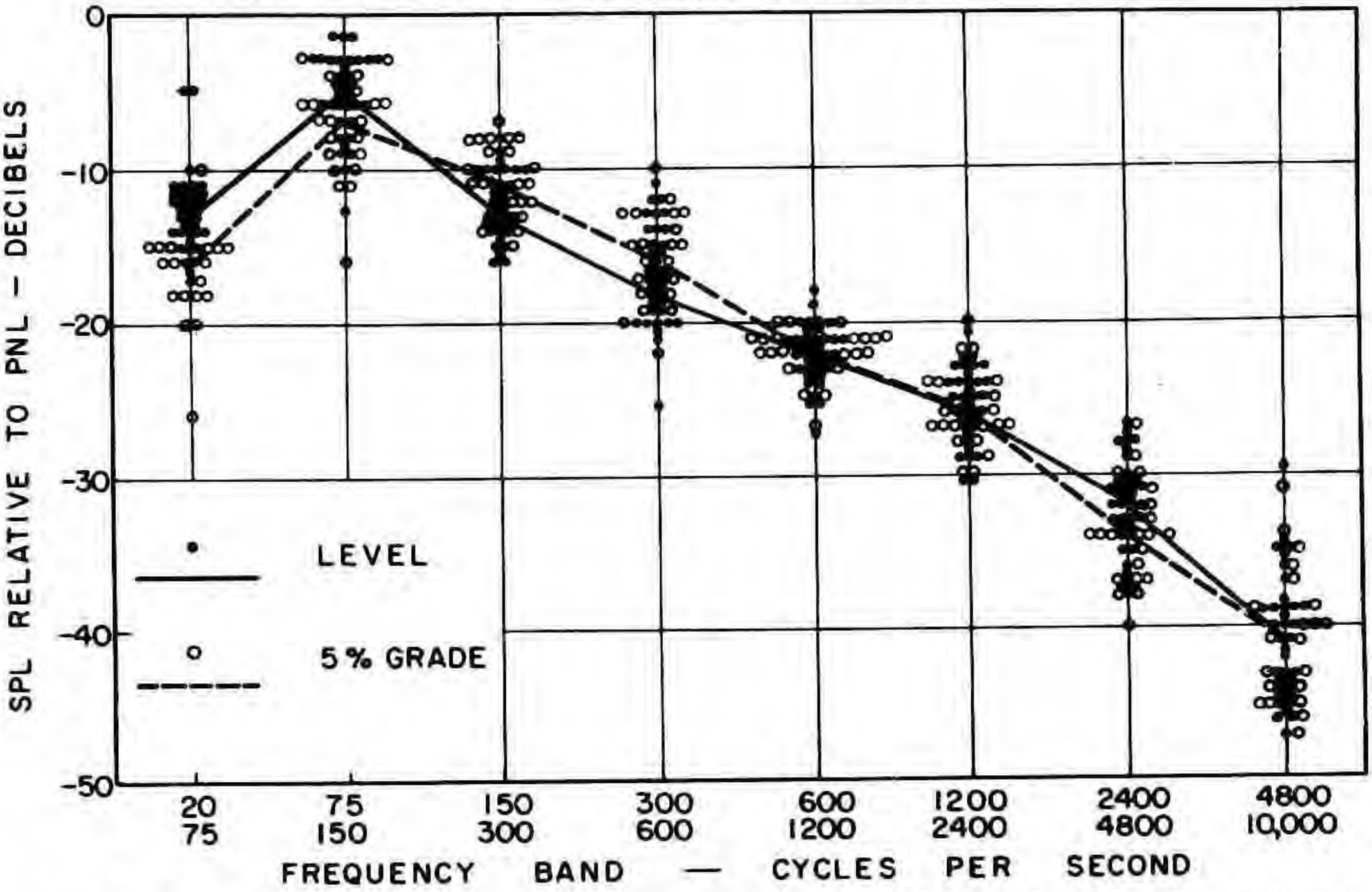

Fig 2. Octave Band Sound Pressure Level Relative to Perceived Noise Level for Heavy Trucks

D. Results of Model Simulation

The above data have been used to calculate simulations for flow rates of 0.1, 0.3, 1.0, and 3.0 vehicles per second, at mean speeds of 30, 45, and 60 mph (48.3, 72.5, and 96.6 km/hr). Sample sizes for the simulation were chosen to provide estimates within 1 db of the true mean. Typical results for level highways are plotted in Fig 3.

Experimental data, as well as the simulations, indicate that free traffic flow can be considered as a line source with sound level falling inversely as the distance away from the highway. If one assumes a normal distribution about the mean instantaneous level predicted by the model, fluctuations about the mean can be specified as shown in Fig 3. The assumption of normality in noise level distribution has been verified in checking the results of this simulation against actual observations at flow rates of 0.3 and greater vehicles per second.

It should be noted that, at low traffic flow rates, one should probably consider the noise from an individual vehicle rather than the statistical approach used herein. We consider a flow rate of about 0.1 vehicle per second as the lowest practical use for the model. At this flow rate, the distribution of noise levels departs substantially from normal, being skewed towards lower levels.

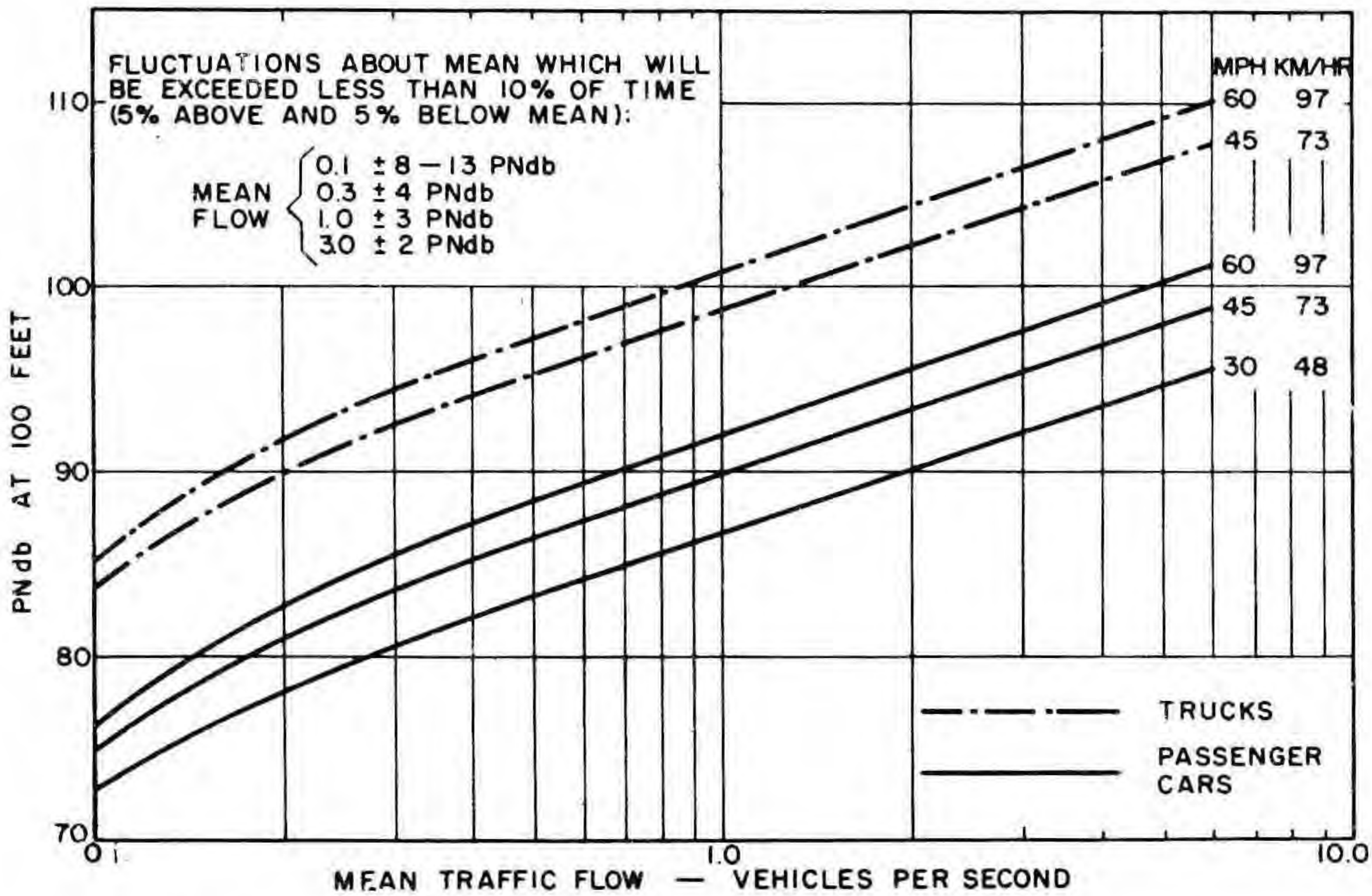

Fig 3. Mean Perceived Noise Level at 100 Feet from Edge of Multi-lane Highway with Freely Flowing Traffic on Level Highway (Grade Less than 2%)

M28

FOURTH INTERNATIONAL CONGRESS ON ACOUSTICS
COPENHAGEN 21.-28. AUGUST 1962

Die Kopplung von Doppelwänden am Fundament als Grenze ihrer Schalldämmung

W. Kuhl, Institut für Rundfunktechnik, Hamburg
W. Struve, Siemens und Halske, Karlsruhe

Vor einigen Jahren wurde von einem der Verfasser zusammen mit F.K.Schröder [1] über die Körperschalldämmung (Schnellepegeldifferenz) von Stoßstellen und von federnd gelagerten Wänden und Böden in Studiobauten berichtet. Durch Modellmessungen der Luftschalldämmung mehrschaliger Baukonstruktionen, durch fremde und eigene Untersuchungen der Körperschalldämmung verschiedener Stoßstellen sowie durch Körperschallmessungen in mehreren Studiobauten wurden die Kenntnisse inzwischen erweitert. Hier soll nur über eine spezielle Frage berichtet werden,nämlich über die notwendige Schnellepegeldifferenz der Doppelwände von Studios, die mögliche Pegeldifferenz bei einer Kopplung beider Wandschalen über das Luftpolster, sowie über die tatsächlich erreichbare Pegeldifferenz, welche durch die Körperschalldämmung des Fundamentes begrenzt ist.

Wenn ein Rundfunkstudio oder Fernsehstudio direkt unter einer Flugschneise liegt in etwa 4 km Abstand von der Startbahn eines Flughafens, muß die Differenz der Schalldruckpegel außerhalb und innerhalb des Studios gleich den Kurven D_R bzw. D_F in Bild 1 sein, wenn der Störschall von viermotorigen Maschinen und Düsen-Verkehrsflugzeugen in Rundfunkstudios bei tiefen Frequenzen unhörbar und bei hohen Frequenzen gleich dem Rauschpegel guter Kondensatormikrofone sein soll. Für die Dämmung eines Studios für großes Orchester zu einem benachbarten Studio gelten ungefähr die gleichen Werte. Die Forderung D_F entspricht bei tiefen Frequenzen der Kurve gleicher Lautstärke für 25 phon und bei hohen Frequenzen dem Störpegel während der Aufnahmen. Bei einer 25 cm dicken Ziegelmauer als äußerer Wand sind die zur Einhaltung der Pegeldifferenz erforderlichen Verbesserungen gleich ΔL_R bzw. ΔL_F. ΔL_O in Bild 2 ist die berechnete Differenz der Schnellepegel einer Außenwand und Hochlochziegelwand von 11,5 cm Dicke, die mit einseitigem Putz eine Masse von 150 kg/m^2 hat. Das 10 cm dicke Luftpolster ist zur Hälfte mit Fasermatten oder -platten gefüllt. Die Pegeldifferenz ist bei tiefen Frequenzen gleich der durch Wandmasse und Luftpolsterfederung bestimmten "Verbesserung" [2] , bei hohen Frequenzen gleich dem Luftschalldämmaß der Wand. Der Mittelwert im Frequenzbereich von 100 - 3200 Hz beträgt 39 dB. Die strenge Forderung für Rundfunkstudios wird auch mit einer solchen idealen Doppelwand bei tiefen Frequenzen nicht erreicht, wohl dagegen die für Fernsehstudios.

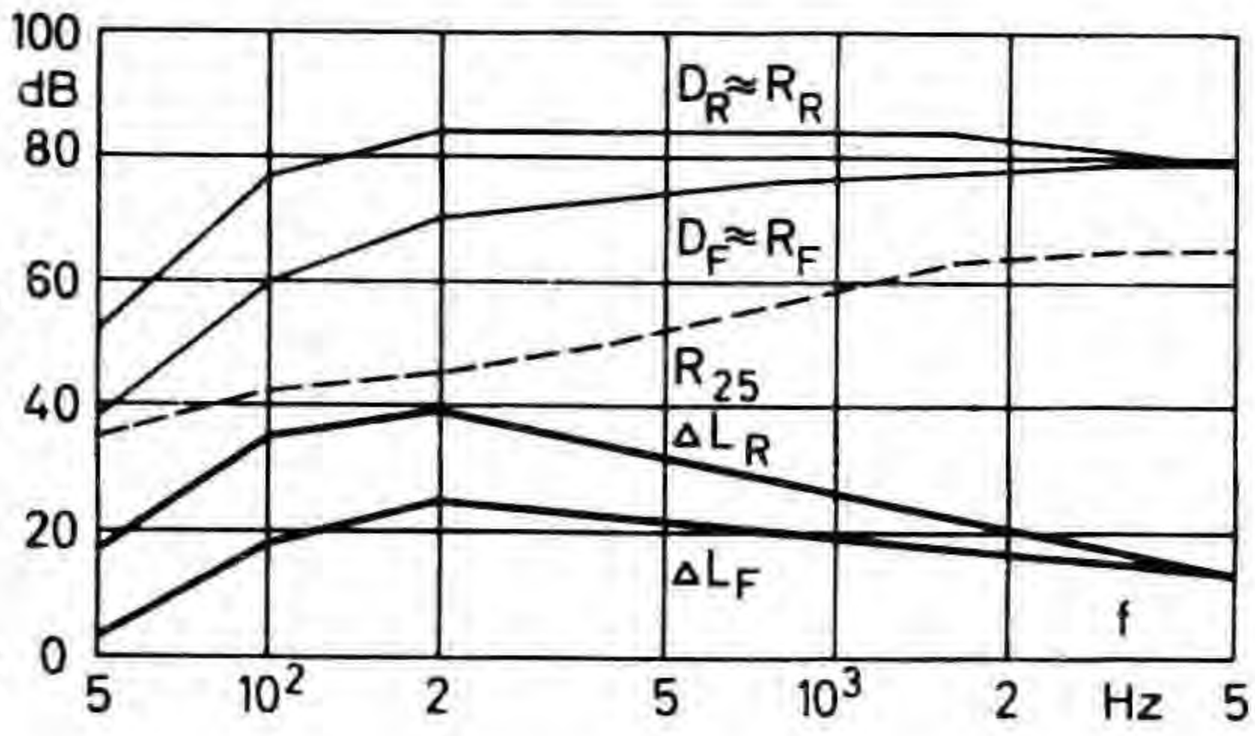

Bild 1 Erforderliche Luftschall-Pegeldifferenz für Studios in 4 km Entfernung vom Flughafen: D_R Rundfunkstudios, D_F Fernsehstudios. R_{25} Luftschalldämmäß einer verputzten Ziegelwand von 25 cm Dicke. Erforderliche Schnellepegeldifferenz der Doppelwand: L_R Rundfunkstudios, L_F Fernsehstudios

An einigen Beispielen wird nun gezeigt, wie die mögliche Pegeldifferenz beschränkt wird durch die Körperschallkopplung am Fundament, auf dem die Doppelwand steht. Es sei angenommen, daß die Vorsatzschale an den Seiten und oben keine Verbindung mit der tragenden Baukonstruktion habe.

Betonplatte als Fundament

Bild 3 zeigt Schnitte durch Doppelwände, bestehend aus je zwei 11,5 cm dicken Hochlochziegelwänden mit 10 cm dicken zur Hälfte mit Faserplatten gefulltem Luftraum. Bei a sind beide Wände starr mit der tragenden 17 cm dicken Betondecke verbunden, bei b nur die eine Wand, während die andere auf 1 m langen, bedämpften Stahlfederstreifen ruht, die in Wirklichkeit nicht quer zur Wand sondern in Längsrichtung angeordnet sind ("Längsdämmbügel"). Bei starrer Verbindung der Wände mit dem Boden beträgt die Pegeldifferenz nach Modellmessungen im Mittel 15 dB, also 24 dB weniger als der Mittelwert ohne Körperschallübertragung. Die Dämmung reicht weder aus für Rundfunkstudios noch für Fernsehstudios. Viel günstiger sind die Verhältnisse mit einer Wand auf Federn. Im Rohbau des neuen Münchener Funkhauses wurden viele Kontrollmessungen gemacht, an Hand deren einige schlecht gebaute Wände herausgefunden und verbessert werden konnten.

Bild 4 zeigt einige Resultate. Die Pegeldifferenz der zum Schwingen angeregten Wand 4 und der Wand 5 auf Federn ist fast gleich der berechneten Kurve ΔL_0. Bei der Lagerung beider Wände auf Federn liegt sie bei allen Frequenzen um 2,5 bis 3 dB höher und damit etwas über ΔL_0. Zwischen einigen Doppelwänden wurde eine Gipskartonplatte angebracht. Die Erhöhung der Pegeldifferenz um 5 dB oberhalb von 200 Hz ist ein Zeichen dafür, daß die reine Körperschalldämmung, einschließlich der Stoßstellendämmung L_4-L_6, bei Ausschaltung der Kopplung über das Luftpolster über ΔL_0 liegt. Die für Rundfunkstudios erforderliche Verbesserung ΔL_R wird mit Gipskartonplatten bei 260 Hz erreicht, ohne diese erst bei 350 Hz. Die ganze Sollkurve würde nur durch eine schwerere Konstruktion oder eine dritte Wandschale erreicht. Die kleinere Pegeldifferenz zwischen dem zum Schwingen angeregten Boden 6 und der auf Federn stehenden Wand 5, welche die Stoßstellendämmung von der Wand 4 zum Boden nicht enthält, beginnt bei 20 Hz, wie man durch Extrapolieren feststellt. Bei weichem

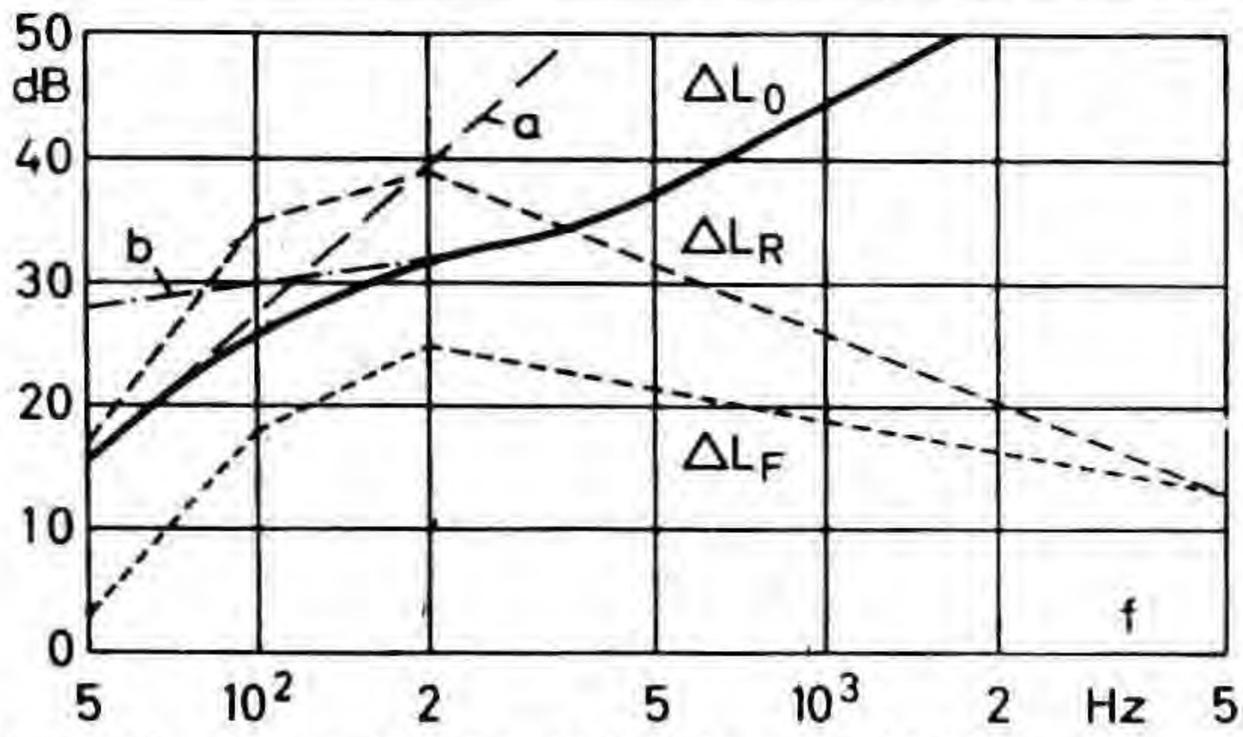

Bild 2 berechnete Schallpegeldifferenz bei einer verputzten 11,5 cm Hochlochziegelwand ohne Körperschallübertragung a) theoretische "Verbesserung", b) Luftschalldämmaß, ΔL_R, ΔL_F Sollwerte der Verbesserung für Studios

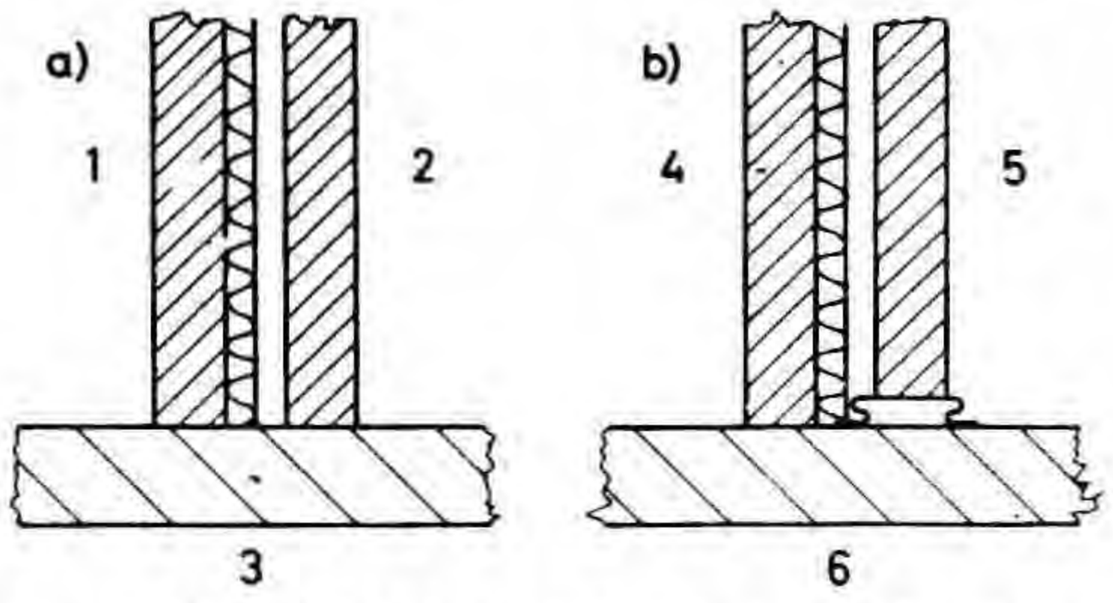

Bild 3 a) Schnitt durch 17 cm Betondecke und zwei 12 cm-Wände. b) wie a), eine Wand auf Stahlfederstreifen.

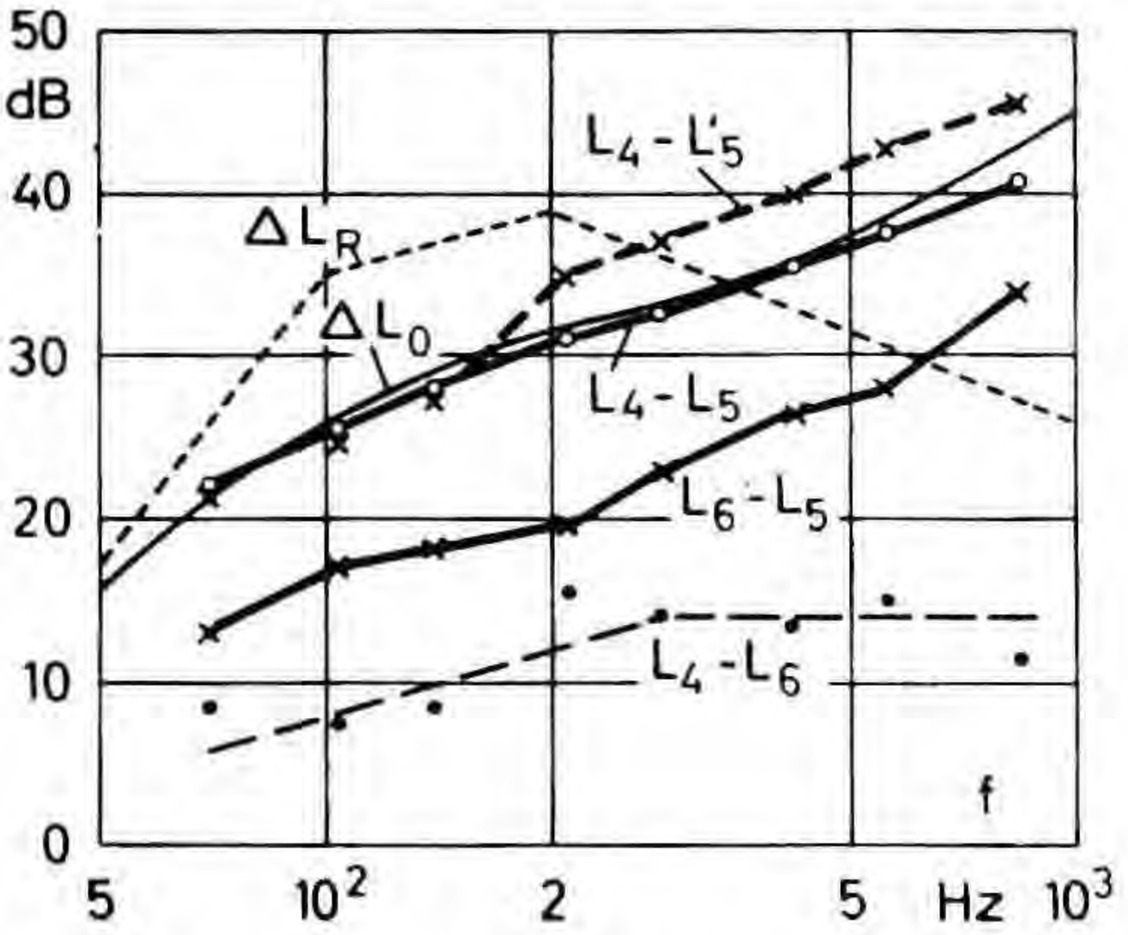

Bild 4 L_4-L_5; $L_4-L'_5$ (Gipskartonplatte im Luftraum); $(L_4-L'_5)-(L_6-L_5)$ Schnellepegeldifferenzen einer Doppelwand aus 11,5 cm Hochlochziegelsteinen im 10 cm Abstand nach Baumessungen (Mittelwerte von 54 - 86 Doppelwänden)

expandierten Kork von 4 cm Dicke beginnt sie erst bei 500 Hz [1]. Kork ist also für diesen Zweck ungeeignet, zumal er bei der zulässigen Belastung nach einigen Jahren nur noch die Hälfte der ursprünglichen Dicke hat.

Balken als Fundament

In Gebäude, die unterkellert sind, stehen die Doppelwände oft auf einem gemeinsamen, auf Pfeilern ruhenden Balken. Die äußere Wand möge eine Dicke von 25 cm, die innere von 12,5 cm und der Balken einen Querschnitt von 50 · 50 cm^2 haben. Nach Modellmessungen beträgt die Pegeldifferenz 12 dB von 50 bis 800 Hz. Unter 50 Hz geht sie gegen Null, bei hohen Frequenzen steigt sie an. Die mögliche Verbesserung ohne Kopplung am Fundament und die Sollwerte für Studios werden bei weitem nicht erreicht.

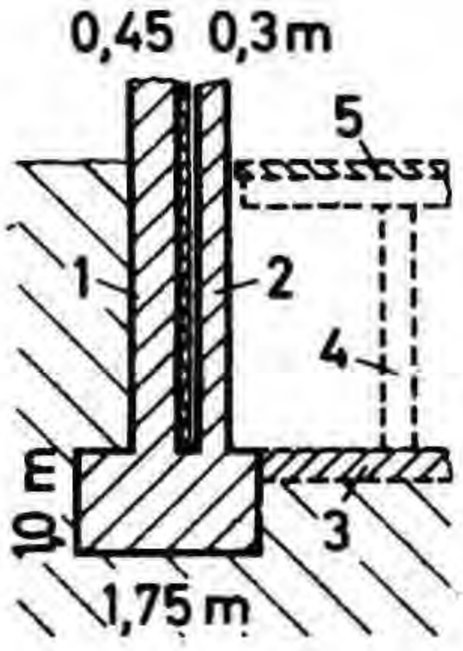

Bild 5a Schnitt durch das Fundament einer sehr schweren Doppelwand

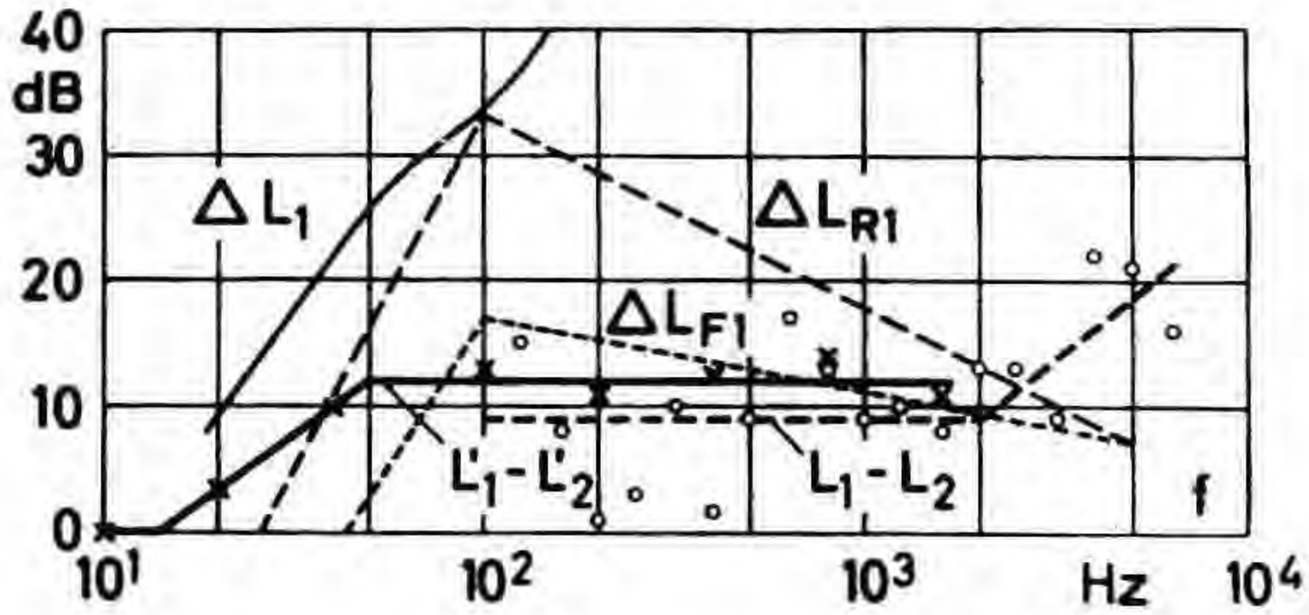

Bild 5b L_1-L_2 Schnellepegeldifferenz, Baumessung. $L'_1-L'_2$ Modellmessung. ΔL_1 berechnete Pegeldifferenz ohne Körperschallübertragung. Erforderliche Verbesserungen: L_{R1} Rundfunkstudios, L_{F1} Fernsehstudios

Bild 5a ist ein Schnitt durch eine sehr schwere Doppelwand aus 45 bzw. 30 cm dicken Betonmauern auf einem schweren Fundament. Die Luftraum ist zum Teil gefüllt. Die Pegeldifferenz wurde an einem Plexiglasmodell im Maßstab 1: 20 und am Bau gemessen (Bild 5b). Beim Modell fehlte die Kellerbodenplatte 3. Die Modellmessungen mit Rauschen in Oktavbreite (Mittel von je drei Meßwerten) zeigen, daß die Pegeldifferenz bei sehr tiefen Frequenzen Null ist und oberhalb von 50 Hz im Mittel 13 dB. Die Messungen am Bau mit Bodenplatte wurden mit Rauschen in Terzbreite ausgeführt (je ein Meßwert). Infolge der geringeren Bandbreite und geringeren Zahl der Meßwerte sind die Schwankungen hier größer. Der Mittelwert beträgt nur 9 dB. In Bild 5b sind außerdem die in diesem Fall anderen Werte für die mögliche Verbesserung ΔL_1 ohne Kopplung am Fundament und die Sollwerte der Verbesserung von Studios eingetragen. Sie werden alle nicht erreicht. Da das betreffende Studio "Villa Berg" in Stuttgart in einem ruhigen Park, weit entfernt von Flugschneisen liegt, reicht die Schalldämmung dort dennoch aus. Der Boden 5 des Erdgeschosses ist mit dem Kellerboden 3 über etliche dünne Pfeiler 4 verbunden. Am Bau wurde festgestellt, daß bei Frequenzen unter 100 Hz der Schnellepegel von 5 gleich dem von 3 ist. Die Pegeldifferenz steigt dann auf 12,5 dB oberhalb von 500 Hz. Pfeiler dieser Art bewirken also keine sehr wirksame Entkopplung.

Hintereinanderschaltung mehrerer Stoßstellen

Bild 6a zeigt einen schematischen Schnitt durch die mittleren Studiobauteile des neuen Funkhauses in München. Sie sind ringsum von technischen Räumen und Büros umgeben, die sich in insgesamt zehn Geschossen befinden. Die Pfeiler 3 und 4 haben den Querschnitt 1,2 m (in Zeichenebene) · 0,8 m und sind einmal durch das Fundament miteinander verbunden, zum anderen durch die Dachabdeckung, die aus Korkplatten und Kupferblech besteht.

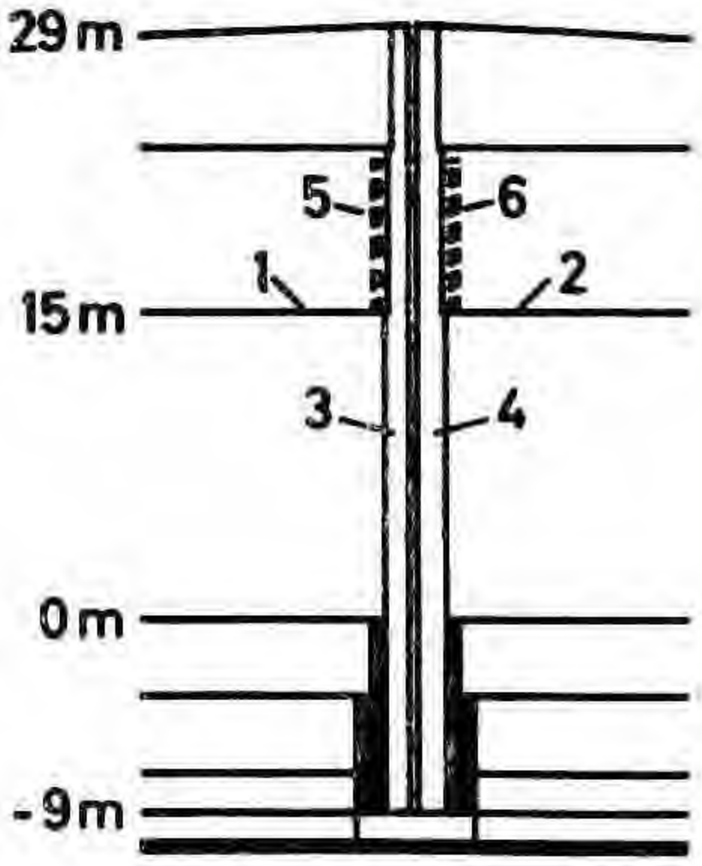

Bild 6a Schnitt durch Decken und Ansicht der Hauptpfeiler eines mehrteiligen zehngeschossigen Studiogebäudes

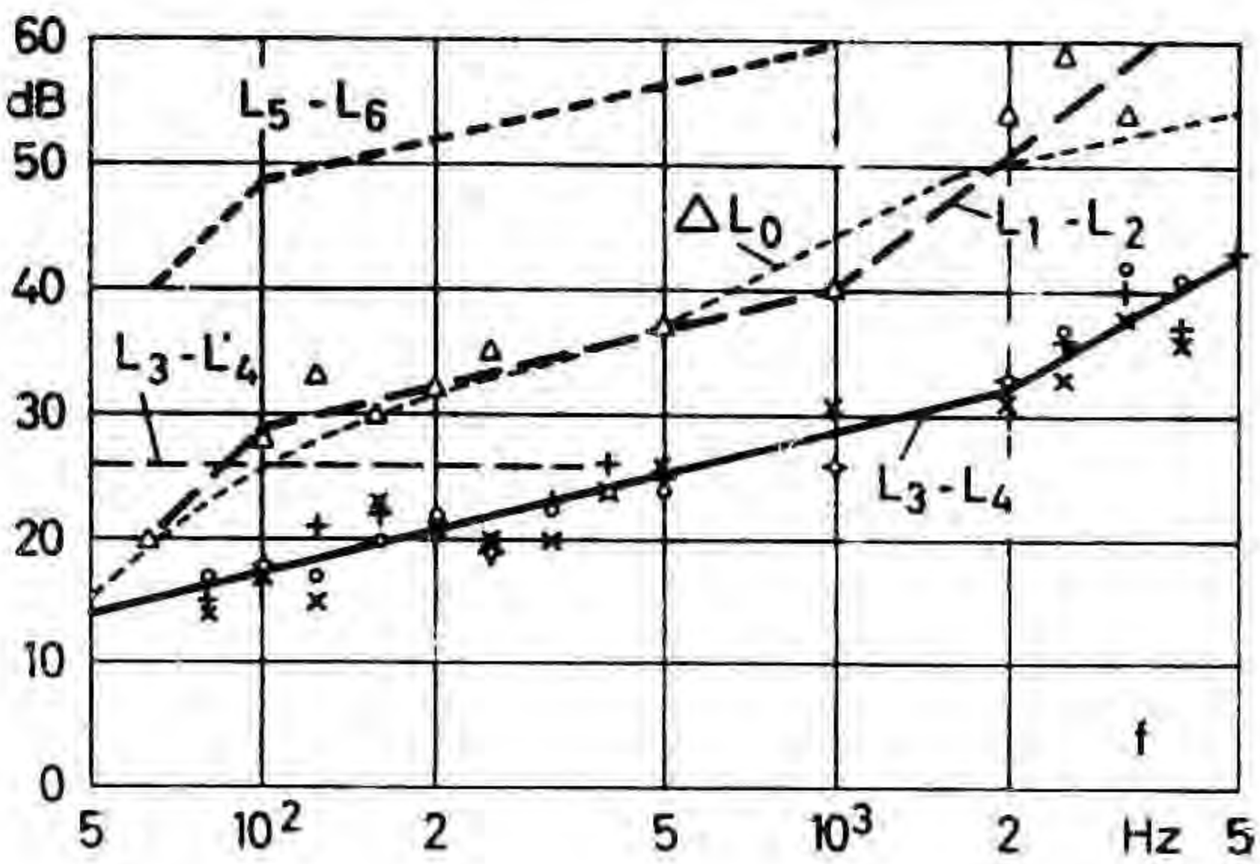

Bild 6b L_3-L_4 Pegeldifferenz eines Pfeilerpaares. $L_3-L'_4$, dasselbe bei Kopplung nur am Fundament. L_1-L_2 Pegeldifferenz der Deckenplatten. L_5-L_6 wahrscheinliche Pegeldifferenz zweier auf den Decken stehender Ziegelwände

Im Rohbau wurden umfangreiche Körperschallmessungen gemacht, von deren Ergebnissen zwei in Bild 6b enthalten sind. L_3-L_4 ist die Pegeldifferenz der Pfeiler, wenn die Deckenplatte 1 angeregt wird. Aus weiteren Messungen ergab sich, daß die Pegeldifferenz bei ausschließlicher Kopplung am Fundament bei tiefen Frequenzen der Geraden $L_3-L'_4$ entsprechen würde. Der tatsächliche Abfall bei tiefen Frequenzen ist auf die federnde Kopplung am Dach zurückzuführen. Der Körperschall gelangt von 1 über die nicht gezeichneten Deckenbalken auf den Pfeiler 3, mit der bekannten Dämmung auf Pfeiler 4, die Deckenbalken und die Deckenplatte 2. Die Pegeldifferenz der Platten ist ebenfalls in Bild 6b eingetragen. Zwei auf den Decken stehende 11,5 cm dicke Wände 5 und 6 hätten wahrscheinlich die Pegeldifferenz L_5-L_6, wenn sie mit den Pfeilern nicht direkt verbunden wären. Sie liegt weit über der Pegeldifferenz ΔL_0, bei reiner Luftschallübertragung. Man könnte also eine Doppelwand, deren Einzelwände zu beiden Seiten der Trennfuge stehen, ohne Federstreifen errichten, wenn man nicht die Übertragung des störenden Körperschalles von Türen, Tritten usw. vermeiden müßte. Aus dem letzten Grunde sollte man nie die innere Schale von Studios (Wände, Boden und Decke) ohne eine ringsum gleichwertige, federnde Lagerung bauen. Mit Stahlfedern lassen sich mittlere Luftschallpegeldifferenzen bis zu 90 dB erzielen.

Literatur

[1] W. Kuhl und F.K. Schröder Acustica 6 (1956), 73

[2] L. Cremer Acustica 2 (1952), 178

028

FOURTH INTERNATIONAL CONGRESS ON ACOUSTICS
COPENHAGEN 21.-28. AUGUST 1962

SOUND RADIATION FROM SLENDER BODIES IN AXISYMMETRIC VIBRATION

by

M. Strasberg

David Taylor Model Basin, Washington 7, D. C., U. S. A.

The caculation of the sound radiated by a vibrating body is a classical problem in acoustics and potential theory. Although calculation procedures are well known for certain shapes, e.g., for spheres, spheroids, and infinitely long cylinders, there is no general method for surfaces of arbitrary shape. This paper discusses a formula for the approximate calculation of the sound radiated by a slender body of revolution vibrating in an axisymmetric but otherwise arbitrary pattern of vibration.

The origin of the formula is seen most directly by examining the general solution for the sound from a vibrating body expressed in terms of Green's functions. For sinusoidal oscillations at a frequency f, with all oscillating quantities varying with time as $\exp(-2\pi i f t)$, the sound pressure $p(\underline{x})$ at a point given by position vector $\underline{x}$ in the fluid around the body can be expressed by an integral of the appropriate Green's function over the surface of the body, viz.,

$$p(\underline{x}) = \rho \int_S a_n(\underline{x}') \, G(\underline{x}|\underline{x}') \, dS \, , \qquad [1]$$

where ρ is the density of the fluid, $a_n(\underline{x})$ the normal acceleration at position $\underline{x}'$ on the surface S, and $G(\underline{x}|\underline{x})$ is the so-called Green's function which gives the increment dp of sound pressure at $\underline{x}$ due solely to unit acceleration over an element of area dS located at $\underline{x}'$, the remainder of the surface being immobile. The Green's function depends on the size and shape of the surface as well as on the frequency; the proper forms of the function are known only for special shapes. Accordingly, Eq.[1] can not be evaluated for arbitrary shapes.

The basis of the formula to be discussed here is the supposition, seemingly a naive one, that the Green's function for a point on a slender body of revolution in axisymmetric vibration is the same as the function for a point in free space, viz., $G(\underline{x}|\underline{x}') = (4\pi r)^{-1}\exp(ikr)$, where r is the distance between $\underline{x}$ and $\underline{x}'$ and k is the wave number $2\pi f/c$, with c the sound propagation velocity. Each element of the surface radiates like a free source pumping fluid at an acceleration volume rate $a_n dS$, and it is assumed that the surface does not scatter or "baffle" the radiation. With this supposition, the expression for the sound pressure at points $\underline{x}$ far from the vibrating body becomes simply

$$p(\underline{x}) = \rho(4\pi r)^{-1}\int_S a_n(\underline{x}')\, e^{ikr}\, dS\ , \qquad [2]$$

the term with r^{-1} being taken outside the integral because it can be considered to have a constant value r_c if r is very large compared with the dimensions of the body.

The order of error involved in the use of Eq.[2] is being investigated analytically, but no results are available. For the present, it is only possible to give a qualitative justification for the supposition. Such justification can be obtained by comparing Eq.[2] with the Helmholtz integral solution of the wave equation in terms of the boundary conditions. For a point in an infinite body of fluid far from the vibrating surface, the Helmholtz integral may be written as

$$p(\underline{x}) = (4\pi r)^{-1}\int_S [\rho a_n(\underline{x}') - ikp(\underline{x}')\cos\phi]\, e^{ikr}\, dS\ , \qquad [3]$$

where ϕ is the angle between the outward-pointing normal to the surface at $\underline{x}'$ and the line from $\underline{x}'$ to $\underline{x}$. This equation is exact, but it is an integral equation with the unknown pressure $p(\underline{x}')$ on the right side inside the integral, and it cannot be solved except in special cases. Comparison of Eq.[3] with Eq.[2] shows that the first term in the integrand of [3], involving $a_n(\underline{x}')$, is the same as the complete integrand of [2]. Accordingly, the assumption made in obtaining Eq. [2] is equivalent to neglecting the term in [3] involving the pressure $p(\underline{x}')$ on the surface of the body. The validity of the supposition made to obtain Eq.[2] is thus resolved into the question: Under what circumstances can the pressure term in the integrand of Eq.[3] be neglected?

It is immediately apparent that in the low-frequency limit, as $k \to 0$, the term containing $p(\underline{x}')$ in Eq.[3] will be negligible compared with the term containing $a_n(\underline{x}')$ provided only that the integral of the latter term remains non-zero. This is indeed the case whenever the body pulsates in volume; then the low-frequency value of the sound pressure is given simply by $p = \rho\ddot{V}/4\pi r$, where $\ddot{V}$ is the second time derivative of the volume. We are not concerned here with this simple case, however. A more interesting case is that of an oscillating rigid body. For this case, it can be shown[1] that the sound pressure at low frequencies is given by the formula $p = -ik(\rho V_o + M)(4\pi r)^{-1} a_o e^{ikr}\cos\theta$, where V_o is the volume of the body, a_o the acceleration of its centroid, and M the incompressible hydrodynamic added mass associated with the oscillating body when immersed in fluid. The ρV_o term is associated with the a_n term in the integrand of Eq.[3], and the M term with the p term in [3]. Now it can also be shown that the added mass of a body of revolution tends to zero as the body becomes very slender, for acceleration along its major axis.[2]

---

[1] M. Strasberg, J. Acoust. Soc. Am. 34, 520 (1962).

[2] H. Lamb, "Hydrodynamics" Cambridge Univ. Press, 1932; §114.

Accordingly, the integral in Eq.[3] involving the $p(\underline{x}')$ term must become small compared with the integral involving $a_n(\underline{x}')$, at low frequencies, even for an incompressible body. This leads to the conjecture that the same will be true at higher frequencies, if the body is slender enough.

Limiting attention to bodies of revolution, consider the contribution to the integral in Eq.[3] of a narrow ring around the body located at axial distance z from the center of the body. Let the ring have width dz and radius b. If the body is sufficiently slender, so that $b \ll r$ and $kb \ll 1$ for the maximum value of b, then all parts of the ring surface can be considered to be equidistant from the field point $\underline{x}$. If the vibration pattern is axisymmetric, the pressure $p(\underline{x}')$ will be uniform all around the ring and will result in a force entirely in the axial direction of magnitude $dF_z = 2\pi b\, p(z)(db/dz)\, dz$. For a cylindrical surface, $db/dz = 0$ everwhere, since b is constant; accordingly, the term in Eq.[3] involving $p(\underline{x}')$ is zero. Equation [3] then reduces to [2], and it is to be expected that the Green's function for a circular cylinder in axisymmetric vibration is just that used in Eq.[2]. The calculation by Nimura and Watanabe[3] confirms this supposition. Their results can be used to show that the magnitude of the Green's function for a narrow ring on an infinite cylinder is within 5 percent of $(4\pi r)^{-1}$ provided the cylinder radius b is small enough that $kb \lesssim 0.25$. For a non-cylindrical slender body of revolution, it is assumed that the cross-section changes its radius slowly, so that db/dz is always small enough over most of the surface to keep the contribution of the $p(\underline{x}')$ term negligible.

For a slender body of revolution in axisymmetric vibration, it is convenient to separate the normal surface acceleration into radial and axial components $a_r(z)$ and $a_z(z)$, respectively. Eq.[2] may then be written

$$p(\underline{x}) = (\rho/2r_o)e^{ik'r_o}\int [ba_r(z) + b(db/dz)a_z(z)]e^{-ik'z}dz\ , \qquad [4]$$

where r_o is the distance from $\underline{x}$ to the center of the body axis, $k' = k\cos\theta$, with θ the angle between the axis and a line to the point $\underline{x}$, and the integration extends over the entire axis of the body.

Values of the sound pressure for a slender spheroid in axial vibration have been calculated using Eq.[4] and compared with values obtained by Chertock[4] from spheroidal wave functions. The calculations have been caried out for two patterns of vibration: (a) rigid-body axial vibration, with $a_r = 0$ and $a_z(z) = a_o$, a constant, and (b) an axial "accordian mode" vibration, with $a_r = 0$ and $a_z(z) = a_o\sin(\pi z/2h)$, with h being half the length of the axis of revolution.

---

[3] Nimura and Watanabe, "Sound radiation from zonal radiators," Research Reports Inst. Elec. Communications, Tohoku Univ., Vol.5, No.3, p.155 (1953).

[4] G. Chertock, J. Acoust. Soc. Amer. 33, 871 (1961).

The integrals for both cases can be evaluated in closed form. For the rigid-body vibration,

$$p(\underline{x}) = i(\rho a_o R^2/r_o)e^{ik'r_o}\, j_1(k'h)\ , \qquad [5]$$

where R is the maximum radius (the minor axis) of the spheroid, and j_1 is a spherical Bessel function as tabulated by Morse.[5] Values given by this equation are compared with those deduced from Chertock's results in Fig. 1(a). For the "accordian mode" vibration,

$$p(\underline{x}) = (\rho a_o R^2/r_o)e^{ik'r_o}\,[(u^2+v^2)\cos.u + u(u^2-v^2)\sin.u][u^2-v^2]^{-2}, \qquad [6]$$

where $u = kh\cos\theta$ and $v = \frac{\pi}{2}$. These values are compared with Chertock's in Fig. 1(b). It is interesting that Chertock's values for this latter case all fall on one curve when plotted in this way for various angles θ, but the values are higher than those given by Eq.[6]. The cause of the disagreement is not yet understood.

---

[5] P.M. Morse, "Vibration and Sound," Mc-Graw Hill Book Co., 1948; Table VII.

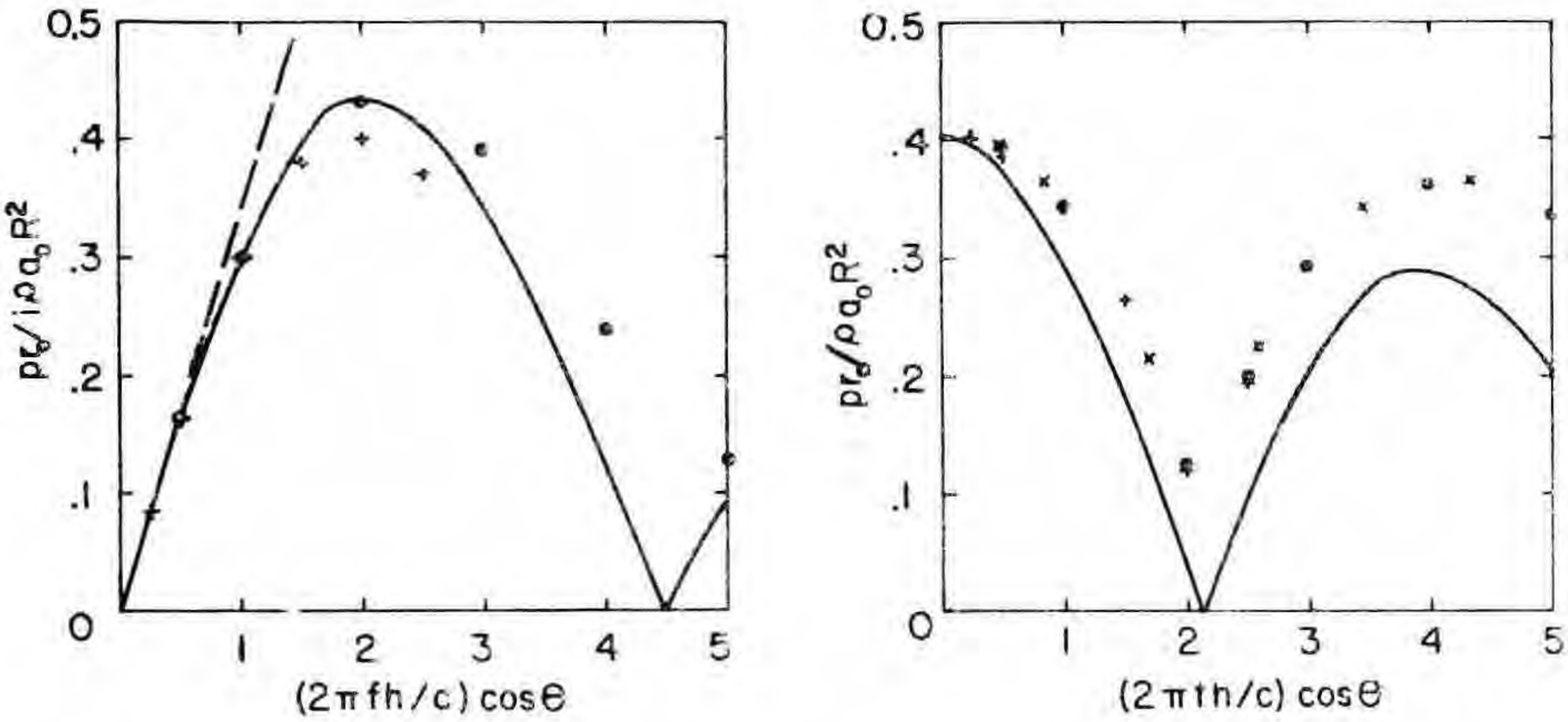

(a) (b)

Fig. 1– The sound pressure radiated by a slender spheroid in two modes of axial vibration: (a) rigid-body vibration, and (b) "accordian mode" vibration. The solid curves show the values given by Eqs. [5] and [6]. The dashed line is the low-frequency asymptotic value. For comparison, values deduced from Chertock's calculations[4] are shown as plotted points, with various angles θ indicated by the following symbols: o, x , + , for 0, 30, and 60 degrees, respectively; his values for 90 degrees are not shown, but they agree with the solid curve.

H29

FOURTH INTERNATIONAL CONGRESS ON ACOUSTICS
COPENHAGEN 21.-28. AUGUST 1962

La perception du son d'interruption dans la stimulation acoustique intermittente

Hélène GAVINI
Centre National de la Recherche Scientifique, MARSEILLE (France)

Les premières expériences sur la stimulation acoustique intermittente avaient pour but, à l'instar de celles sur le flicker visuel, de déterminer la fréquence critique de fusion, c'est à dire la fréquence de récurrence du stimulus à partir de laquelle la stimulation intermittente est perçue avec les mêmes caractéristiques que la stimulation continue. A la différence du flicker visuel, dont la fréquence n'est pas perçue par l'oeil comme excitation lumineuse, le flicker auditif n'est pas seulement une interruption périodique du stimulus sonore, il constitue lui-même une stimulation sonore, et il est perçu comme telle.

Nous cherchons depuis quelques années à préciser les caractéristiques de la perception de la stimulation acoustique intermittente et leurs rapports avec les caractéristiques physiques de cette stimulation.

DESCRIPTION DES STIMULUS ET DE L'APPAREILLAGE

La stimulation est constituée par un son pur (onde porteuse) interrompu à intervalles réguliers, avec une fréquence de récurrence qui peut être de 1 à 6 000 par seconde, et un rapport durée du son/durée totale qui peut varier très largement puisque, dans chaque segment du découpage, nous pouvons couper ou conserver seulement une demie période, avec tous les intermédiaires entre ces deux extrèmes (Fig. 1).

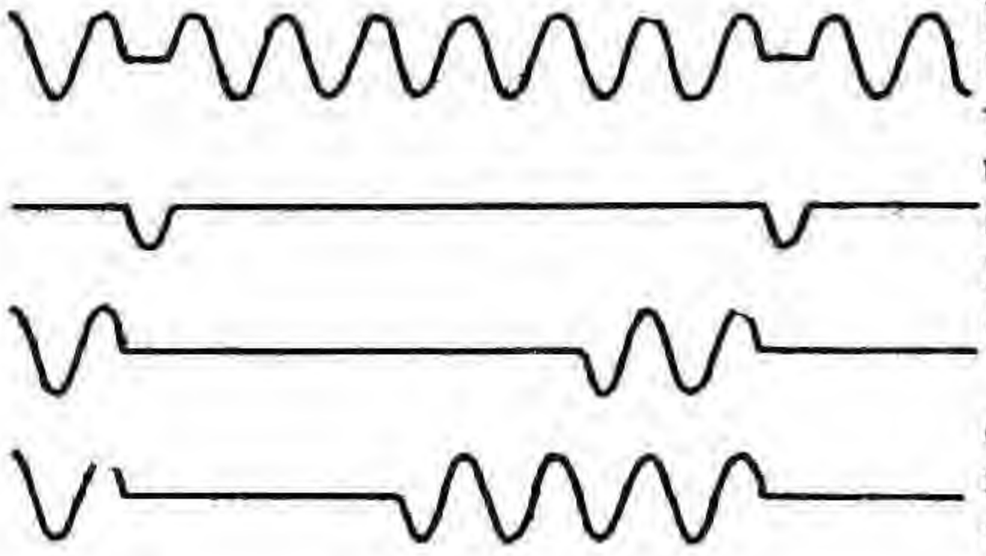

Figure : 1

Nous utilisons un dispositif original de découpage, établi par A. Clottes (brevet CNRS n° 1.176. 954). Une porte électronique à faibles parasites de commutation admet ou bloque la tension sinusoïdale d'un générateur B.F.; le circuit de commande de porte, à multivibrateurs et univibrateurs, reçoit des impulsions de truquage, afin que l'onde rectangulaire-pilote commence et finisse généralement aux moments où la tension instantanée est nulle.

Les ondes sonores sont émises dans une chambre anéchoïque par le haut-parleur ionique, donc sans traînage, de Klein; son corona H.F. est modulé en amplitude; aucune inductance ne se trouve dans la chaine de modulation, grâce à un dispositif particulier (A. Clottes, brevet CNRS n° 1.166.481).

L'émission du signal est contrôlée sur l'oscillographe à l'entrée du haut-parleur; à la sortie de ce dernier, le signal est recueilli par un microphone à faible inertie (Neumann), et on peut voir qu'il n'est guère déformé (projection).

MESURE DES CARACTERISTIQUES PHYSIQUES DE LA STIMULATION ACOUSTIQUE INTERMITTENTE

i) Analyse de fréquence

Elle est effectuée au moyen d'un analyseur Brüel et Kjaer. En général, la fréquence de l'onde porteuse est la seule qui ressorte dans les spectres sonores enregistrés, et la forme générale du spectre du son interrompu est peu différente de celle du son pur continu correspondant.

Cependant, dans quelques cas, nous avons enregistré des sons d'addition ou de soustraction, à une intensité voisine de celle de la porteuse; par exemple, un son pur de 3 000 Hz étant interrompu 300 fois par seconde, nous avons relevé dans le spectre des pointes à 2 700 et à 3 300 Hz, d'un niveau sonore peu différent de celui correspondant à la fréquence 3 000 Hz.

Dans d'autres cas, nous avons noté, dans le spectre, des fréquences qui n'ont de rapports simples, ni avec l'onde porteuse, ni avec la fréquence de récurrence, et qui sont toujours élevées.

Enfin, la fréquence de récurrence, correspondant au son de répétition ou d'interruption, n'est jamais présente dans le spectre à un niveau sonore différant significativement de celui du bruit de fond.

ii) Mesure de l'intensité

L'intensité de l'émission sonore, pour une fréquence déterminée, est exprimée en microvolts sur le cadran de l'analyseur.

L'intensité de la fréquence porteuse, la seule notable dans la plupart des cas, est approximativement proportionnelle au rapport durée du son/durée totale de la stimulation.

Si l'on mesure l'intensité globale de l'émission en système linéaire, c'est à dire sans passer par l'analyseur de fréquence, on obtient, à peu de chose près, les mêmes évaluations.

iii) Caractéristiques du pattern temporel de la stimulation

La fréquence de récurrence de la stimulation, ainsi que la durée des impulsions successives et des intervalles qui les séparent sont contrôlées sur l'oscillographe.

MESURE DES CARACTERISTIQUES DE LA PERCEPTION DE LA STIMULATION ACOUSTIQUE INTERMITTENTE

Les sons émis sont perçus par les sujets comme étant plus ou moins forts, aigus, harmonieux, "rugueux", désagréables.... Les deux premières caractéristiques, la sonie (loudness) et la tonie (pitch), peuvent être plus facilement évaluées objectivement. Pour cela, on demande aux sujets d'ajuster, au moyen de réglages d'intensité et de fréquence, le son émis par un autre haut-parleur à celui émis par l'ionophone. L'ajustement effectué, on peut déterminer la fréquence et l'intensité du son correspondant à la perception du sujet et les comparer à celles du stimulus.

i) Ajustement de la fréquence

Cet ajustement ne se fait pas sans difficulté: beaucoup de sujets n'y arrivent qu'après un apprentissage assez long, ou n'y parviennent jamais. Cela ne tient pas seulement au caractère complexe de la stimulation intermittente, ni au timbre un peu particulier de l'ionophone, qui ne font qu'augmenter la difficulté: cette dernière est inhérente à la tâche d'ajustement elle-même; en effet, de nombreux sujets ne parviennent même pas à ajuster deux sons purs, sur le même haut-parleur, sans faire des erreurs plus grandes que le 10 % généralement toléré. Aussi, les résultats expérimentaux que nous présentons ont été obtenus sur un petit nombre de sujets (de 1 à 5).

L'examen des données expérimentales fait ressortir la prédominance de la perception du son de répétition; en effet, quelle que soit la fréquence de l'onde porteuse, de 1 000 à 20 000 Hz, quelle que soit la fréquence de récurrence et quel que soit le rapport de la durée du son à la durée totale, le son d'interruption est toujours perçu et ajusté avec une précision suffisante, puisque la marge d'erreur tolérable de 10 % est rarement atteinte.

Les sujets ajustent parfois, mais rarement, l'octave inférieure ou supérieure du son d'interruption.

Influence de la fréquence de l'onde porteuse

Pour faire ressortir l'influence éventuelle de la fréquence de l'onde porteuse sur l'ajustement du son perçu, nous avons présenté aux sujets des sons purs de diverses fréquences (de 1 000 à 12 000 Hz), interrompus 250 et 500 fois par seconde, avec un rapport durée du son/durée totale égal à .50.

Fréquence de l'onde porteuse	Ajustements du sujet	
	Fréquence de récurrence	
	500	250
1 000	501,2	248,1
2 000	495,5	246,4
3 000	489,7	249,9
4 000	488,3	247,9
5 000	489,1	246,8
6 000	496,3	245,6
7 000	491,7	245,8
8 000	467,4	245,7
9 000	492,4	246,8
10 000	480,8	247,5
11 000	499,4	238,7
12 000	477,5	249.

Tableau I

On voit, tableau I, les résultats obtenus par un sujet; chaque valeur d'ajustement est la moyenne de 10 essais. On peut constater que, chaque fois, la fréquence du son de répétition a été ajustée de façon satisfaisante, bien qu'à une exception près, toujours un peu en dessous de 250 ou 500 Hz.

Des données moins complètes, recueillies sur d'autres sujets, recoupent ces résultats et les confirment.

Influence du rapport durée du son/ durée totale

Ce rapport, c'est à dire la durée de l'interruption, n'a pas, lui non plus, d'influence sur la perception du son de répétition. Nous donnons un exemple tableau II.

L'expérience a été faite par deux sujets, R. et H.; le stimulus est un son pur de 8 000 Hz coupé 800 fois par seconde. On peut constater que la tonie a toujours été ajustée aux environs de 800 Hz, que la coupure soit large d'1/4 de période (rapport durée du son/durée totale = .975) ou de 8 périodes (rapport durée du son/durée totale = .200).

Caractéristiques du stimulus		Rapports durée du son/ durée totale									
		1	.975	.950	.800	.700	.600	.500	.400	.300	.200
Intensité à 8000 Hz en microvolts		4500	4500	4400	3600	3200	2800	2150	1800	1350	900
en décibels		85	85	85	83	82	81	79	77	75	71
Ajustements des sujets											
Fréquence	R.	7897	752	793	801	792	778	790	775	786	807
	H.	7759	796	789	794	806	793	804	799	794	802
	moyenne	7828	774	791	797	799	785	797	787	790	804
Intensité en μv	R.	5300	220	235	210	190	160	400	200	300	290
	H.	3400	320	290	420	410	400	460	400	340	390
Intensité en dB	R.	86	60	61	61	59	57	65	61	63	62
	H.	82	63	63	65	65	65	66	65	64	65
	moyenne	84	61,5	62	63	62	61	65,5	63	63,5	63,5

Tableau II. Fréquence de l'onde porteuse: 8 000 Hz
Fréquence de récurrence: 800 par seconde

La fréquence de récurrence est aussi bien perçue et ajustée quand elle n'est pas un sous-multiple de la porteuse. Ainsi, un son de 2 000 Hz, interrompu toutes les 7 périodes est perçu avec une tonie correspondant à environ 285 Hz, quelle que soit la largeur de la coupure, de une demie période à six périodes et demie.

Evidemment, les sujets se rendent compte qu'ils n'entendent pas un son pur; ils sont gênés, dans leurs ajustements, par le timbre grinçant, rugueux de la stimulation intermittente. Ils signalent parfois qu'ils entendent, en même temps que le son d'interruption, plus grave, un son plus aigu qu'ils parviennent rarement à ajuster avec certitude. Ils arrivent généralement à ajuster correctement

la fréquence de l'onde porteuse dans les cas où la coupure est très étroite et où la fréquence de récurrence ne dépasse pas 150 ou 200 par seconde.

ii) Ajustement de l'intensité

L'ajustement de la sonie, qui donne l'impression d'être beaucoup plus facile que celui de la tonie, donne des mesures d'une plus grande variabilité inter et intra-individuelle. Cependant, si l'on fait la moyenne de plusieurs mesures, on arrive à des résultats cohérents.

Influence du rapport durée du son/durée totale

On peut voir, dans le tableau II, que, quel que soit le découpage, le son d'interruption est toujours perçu avec une sonie qui varie peu d'un essai à l'autre, alors que l'intensité du signal varie dans le rapport de 1 à 5. Tous nos résultats expérimentaux sont en accord avec cette constatation.

Ces observations nous amènent à penser que la sonie d'un stimulus intermittent n'est pas en rapport avec l'intensité globale du signal, mais plutôt avec son amplitude de pointe.

Influence de l'amplitude du stimulus

Toutes choses étant égales par ailleurs, la sonie varie en fonction de l'amplitude du signal: si nous atténuons ce dernier de 12 décibels par exemple, les sujets ajustent un son qui a une intensité (mesurée en microvolts) 4 fois moins grande que sans atténuation.

Il serait désirable de préciser le rapport de la sonie avec l'amplitude du signal. La sonie pourrait être en rapport, soit avec celle correspondant à l'intensité de l'onde porteuse continue, soit avec celle correspondant à un son de même amplitude que la porteuse et de même fréquence que le son d'interruption. Nous devons plus spécialement porter notre attention sur la seconde alternative puisque, dans certains cas, l'onde porteuse continue est inaudible (à 20 000 Hz, par exemple) et le son d'interruption est perçu.

Influence de la fréquence de l'onde porteuse

Ce qui précède ne veut pas dire que nous pensions que la fréquence de l'onde porteuse n'ait jamais de rapports avec la sonie du son d'interruption. Dans les cas où elle est perçue, distinctement ou non, elle pourrait, soit gêner la perception du son d'interruption et diminuer sa sonie, soit augmenter la sonie du signal et faire paraître plus fort le son d'interruption.

Influence de la fréquence de récurrence

Nous avons noté que la sonie de certains sons d'interruption était plus grande pour certaines fréquences de récurrence, mais nous n'avons pas encore pu déterminer les rapports entre ces deux caractéristiques.

CONCLUSION

Ainsi, l'émission d'un son pur, interrompue avec une fréquence de récurrence dans la marge des fréquences audibles, donne lieu à une perception dont les caractéristiques sont, dans une large mesure, indépendantes des caractéristiques physiques de fréquence et d'intensité mesurées à l'analyseur et au voltmètre.

Nous avons pu constater, en effet, quelles que soient la durée des impulsions successives, l'intensité et la fréquence de l'onde porteuse, que la tonie dominante correspond presque toujours au nombre d'impulsions par seconde. Comme cela a déjà été constaté par d'autres chercheurs, l'oreille est plus sensible à la structure temporelle de l'enveloppe de l'émission sonore qu'au spectre de fréquence qui lui correspond. C'est, en somme, l'image oscillographique de l'émission sonore qui nous donne le meilleur pronostic de la tonie de la perception.

En ce qui concerne la sonie, les pronostics sont plus difficiles à faire, car si, toutes choses étant égales d'ailleurs, elle varie proportionnellement à l'amplitude du signal et elle est indépendante de la durée des impulsions, elle dépend, dans une mesure que nous n'avons pas encore pu préciser, de la fréquence de récurrence et de la fréquence de l'onde porteuse.

M29

FOURTH INTERNATIONAL CONGRESS ON ACOUSTICS
COPENHAGEN 21.-28. AUGUST 1962

Schalldämmung von Fenstern und Türen mit Fugen verschiedener Luftdurchlässigkeit.

Dipl.Ing. Judith L a n g , Wissenschaftl. Assistent an der Staatlichen Versuchsanstalt für Wärme- und Schalltechnik in Wien.

1. Einleitung

Der Schallschutz der Fenster ist zur Sicherung der Ruhe in den Wohn- und Schlafräumen gegen den von außen eindringenden Verkehrslärm von entscheidender Bedeutung.

Die ÖNORM B 8115 "Hochbau, Schallschutz und Hörsamkeit" enthält deshalb auch Vorschriften über den Schallschutz von Fenstern und Türen. Diese müssen von den Bauteilen im eingebauten Zustand eingehalten werden, d.h. die vorgeschriebenen mittleren Schalldämmzahlen nach Tafel 1 müssen einschließlich des Schalldurchganges durch die Fugen gewährleistet sein. Es ist also keine Trennung in Schallschutz des Türblattes bzw. des Fensters allein und Fugendurchlässigkeit erfolgt, wie dies in der ÖNORM B 8110 "Hochbau, Wärmeschutz" der Fall ist, wo eine höchstzulässige Wärmedurchgangszahl k_o des Fensters bzw. der Türe ohne Einfluß der Fugen und eine höchstzulässige Luftdurchlässigkeit a in $m^3/m\ h\ (mmWS)^{2/3}$ nach Tafel 2 festgelegt ist.

T a f e l 1

Nach ÖNORM B 8115 für Fenster und Türen erforderliche mittlere Schalldämmzahlen (100-3200 Hz)

B a u t e i l	erforderliche mittlere Schalldämmzahl in dB bei Schallschutzgruppe	
	1 und 2	3 und 4 [1]
Fenster	30 [2]	35
Türen	25	30
Wohnungstüren	30	•

1) Für Nebenräume genügen die Anforderungen der Schallschutzgruppen 1 und 2.

2) Bei Lage an einer Verkehrsstraße oder in Nähe einer solchen sollen in den ihr zugewendeten Gebäudeseiten die Fenster der Haupträume möglichst die Schalldämmzahl 35 dB erhalten.

T a f e l 2

Höchstzulässige Luftdurchlässigkeit der Fugen von Fenstern und Türen nach ÖNORM B 8110

B a u a r t	Luftdurchlässigkeit a_{max} m^3/lm Fugenlänge h $(mmWS)^{2/3}$	
	Holz	Stahl, Aluminium
Einfach	2,25	0,75
Verbund	2,0	0,75
Doppelt	1,5	0,6
Gedichtet	0,5	•

Eine Trennung der Vorschriften auch für den Schallschutz in den des Türblattes bzw. des Fensters allein und die Luftdurchlässigkeit der Fugen erschiene wertvoll für die Hersteller dieser Bauteile; auch wäre es günstig zu wissen, ob die aus wärmeschutztechnischen Erkenntnissen vorgeschriebenen Werte der Luftdurchlässigkeit auch den schallschutztechnischen Anforderungen entsprechen.
In der Literatur[1] ist ein Zusammenhang zwischen Flächenausdehnung eines Spaltes und Schallschutzabnahme einer Wand (Türe) angegeben.
Es wurden daher Messungen des Schallschutzes und der Luftdurchlässigkeit von einigen Fenstern und Türen durchgeführt, um einen event. Zusammenhang zwischen diesen beiden Größen aufstellen bzw. höchstzulässige Werte für die Luftdurchlässigkeit ermitteln zu können.

2. Messungen an einem Verbundfenster üblicher Bauart

Die ersten Messungen wurden an einem üblichen Holz-Verbundfenster durchgeführt. Da schon beim Schließen des Fensters festgestellt werden konnte, daß die einzelnen Fugen verschieden dicht sind, wurde die Messung auch mit einer Trennung in einzelne Fugen (Luftdurchlässigkeit 0,23 bis 2,6) durchgeführt. Die übrigen Fugen waren jeweils verkittet.

Es ergab sich, daß der Schallschutz bei tiefen Frequenzen durch das Fenster selbst und bei den höheren Frequenzen durch die Fugen gegeben ist, u.zw. je größer die Luftdurchlässigkeit, desto geringer der Schallschutz. Auch die Frequenz, bei der die Verschlechterung einsetzt, ist abhängig von der Luftdurchlässigkeit. Die mittlere Schalldämmzahl lag zwischen 27 dB (alle Fugen offen) und 34 dB (Fugen verkittet).

3. Messungen an einem Verbundfenster mit verbessertem Schallschutz

Zur Ermittlung des event. Einflusses der Fugendurchlässigkeit bei tieferen Frequenzen wurde das Verbundfenster schalltechnisch verbessert durch Aufsetzen von "biegeweichen Vorsatzschalen" aus 4 mm Gummi auf den Fensterrahmen.
Zur Ermittlung des Einflusses der Fugenlänge wurden zusätzlich Versuche mit verschiedener Länge der Fugen gleicher Durchlässigkeit gemacht.
Die Ergebnisse sind im wesentlichen gleich wie beim Verbundfenster gewöhnlicher Bauart. Die Vergrößerung der Länge der Fuge ergibt etwa die zu erwartende Abnahme der Dämmung entsprechend dem Logarithmus des Verhältnisses der Längen. Die mittlere Schalldämmzahl lag zwischen 33 dB und 40 dB.

4. Ergänzende Messungen an einigen anderen Fenstern

Einige Messungen an anderen Fenstern wurden zur Ergänzung ausgeführt.
Die Messung des Schallschutzes mit verkitteten und offenen Fugen an einem Metallfenster mit Kunststoffüberzug (Luftdurchlässigkeit 0,14 $m^3/mh(mmWS)^{2/3}$) zeigte bei dem durch die Doppelscheiben gegebenen Schallschutz von im Mittel 28 dB keinen Einfluß der sehr dichten Fugen. Eine schallschutztechnische Verbesserung dieses Fensters wurde nicht durchgeführt.

Die Messung an einem Holz-Verbundfenster bei offenen und verkitteten Fugen (Luftdurchlässigkeit 2,8 $m^3/mh(mmWS)^{2/3}$) zeigte Übereinstimmung mit den Ergebnissen nach Pkt. 2 und 3.

5. Messungen an einer Holztüre üblicher Bauart

Ähnliche Messungen wurden an einer Holztüre üblicher Bauart durchgeführt.
Die Verschlechterung des Schallschutzes beginnt unter 100 Hz, entsprechend der großen Breite der Fuge, die bei einer Luftdurchlässigkeit von 11,6 $m^3/mh(mmWS)^{2/3}$ gegeben ist.

---

1) A. Schoch: Die physikalischen und technischen Grundlagen der Schalldämmung im Bauwesen. Verlag S. Hirzel, Leipzig 1937
F. Ingerslev und A.K. Nielsen: On the transmission of sound through small apertures and narrow slits. Ingeniorvidenskabelige Skrifter 1944, Nr.5, Kopenhagen

Eine Dichtung mit Schaumgummi verkleinerte die Luftdurchlässigkeit auf 2,3 $m^3/mh(mmWS)^{2/3}$ wesentlich, der Schallschutz wurde jedoch nur wenig verbessert; vor allem beginnt auch in diesem Fall die Verschlechterung bereits unter 100 Hz, gegeben offenbar durch die unveränderte Breite des Spaltes. Ob eine Dichtung mit Gummilippen im Falz oder andere Dichtungen diesbezüglich andere Ergebnisse bringen, wurde nicht geprüft.
Es wurde auch ein Versuch mit Erhöhung der Schallschluckung der Fuge durch 4 cm Filzleisten etwa gleicher Luftdurchlässigkeit durchgeführt[1]. Damit konnte die Schalldämmung erhöht werden, bei den höheren Frequenzen bis zu 5-7 dB.

6. Versuch der Berechnung der Schalldämmung der Fuge

Zum Vergleich und zur Auswertung der Ergebnisse wurde versucht die Schalldämmung der Fuge allein zu errechnen.
In Bild 1 sind die für 1600 Hz, 2500 und 3200 Hz erhaltenen Werte der Schalldämmung der Fuge in Abhängigkeit von der durch die Fugen durchgehenden Luftmenge l . a (Fugenlänge x Luftdurchlässigkeit) aufgetragen.

7. Zusammenfassung

Die Luftdurchlässigkeit der Fugen kann als angenähertes Maß für den zu erwartenden Schallschutz von Fenstern und Türen angesehen werden. Die Verschlechterung der Schalldämmung ist umso größer und setzt bei umso tieferen Frequenzen ein, je höher die Luftdurchlässigkeit ist. Eine Veränderung der Fugenlänge ergibt eine Änderung der Dämmung etwa entsprechend dem Logarithmus des Verhältnisses der Längen.
Als höchstzulässige Luftdurchlässigkeit der Fugen könnten nach den Meßergebnissen die Werte der Tafel 3 vorgeschlagen werden.
Die Werte sollen möglichst ohne zusätzliche Dichtung erreicht werden, da z.B. die gemessene Schaumgummidichtung zwar die Luftdurchlässigkeit wesentlich verringert, den Schallschutz jedoch nur vergleichsweise wenig verbessert.
Die mittlere Schalldämmzahl der Fenster- bzw. Türbauarten selbst, ohne Einfluß der Fugen, müßte um mindestens 3 dB, besser 5 dB, jeweils höher sein als der Sollwert für die Bauteile im eingebauten Zustand angibt.
Die angegebenen Sollwerte erscheinen durch die Herstellerfirma ohne weiteres erfüllbar und würden zum Schutz der Wohn-, Schlaf- und Arbeitsräume vor Lärm wesentlich beitragen.

Die vorgeschlagene Luftdurchlässigkeit sichert andererseits auch eine ausreichende natürliche Lüftung, sodaß eine Klimatisierung nicht erforderlich wird.

---

1) Auf die günstige Wirkung von schallschluckender Ausstattung der Schlitze bei Türen weist auch L. Cremer in seinem Buch "Die wissenschaftlichen Grundlagen der Raumakustik", Bd. 3, Verlag S. Hirzel, Leipzig 1950, hin.

Tafel 3

Vorschlag für höchstzulässige Luftdurchlässigkeit der Fugen

Bauteil	erforderliche mittlere Schalldämmzahl dB	höchstzulässige Luftdurchlässigkeit $m^3/m\,h\,(mm\,WS)^{2/3}$
Fenster	30	1,0
	35	0,5
Türen	25	1,5 [1]
	30	1,0 [1]

1) Bei Anordnung eines schallschluckenden Schlitzes von mindestens 4 cm Länge können die Werte auf 2,0 bzw. 1,5 erhöht werden.

Bild 1: Schalldämmung der Fuge in Abhängigkeit von der Luftdurchlässigkeit und der Länge

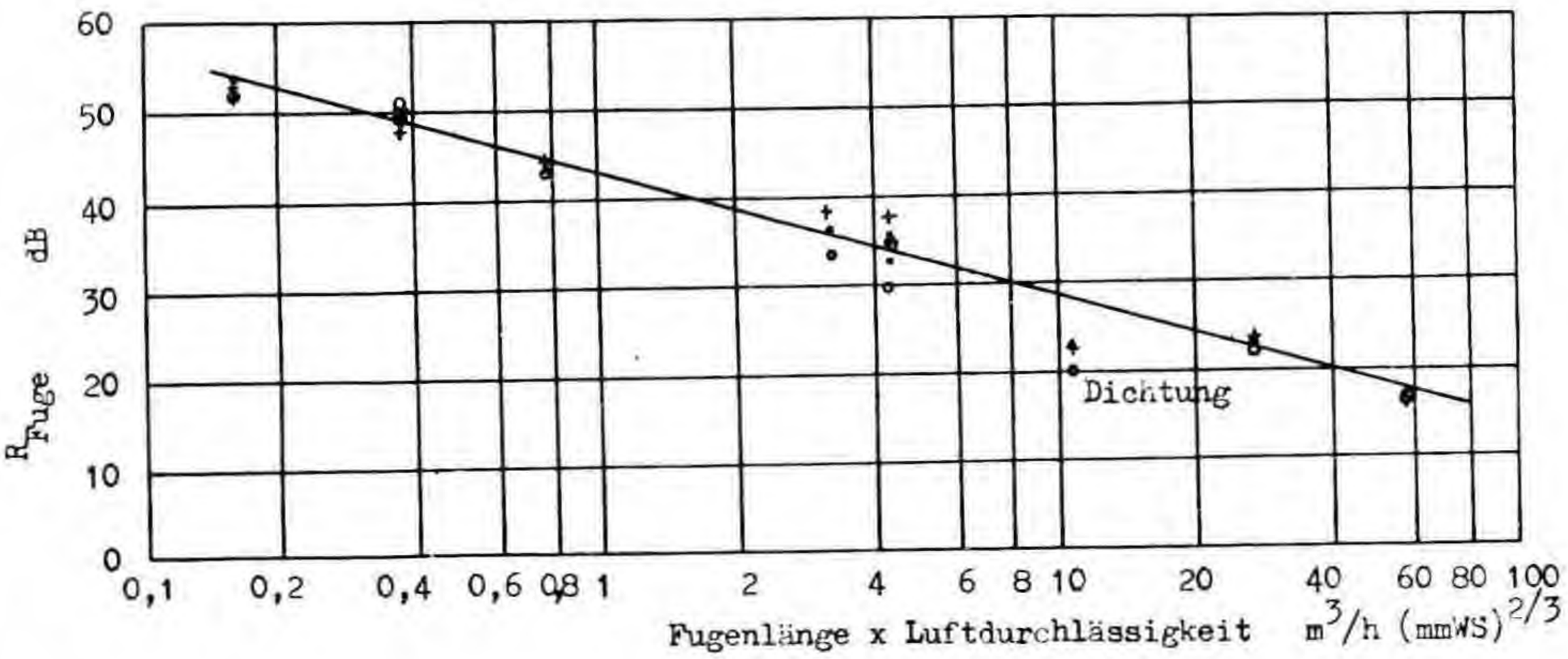

G31

FOURTH INTERNATIONAL CONGRESS ON ACOUSTICS
COPENHAGEN 21.-28. AUGUST 1962

L'ECOUTE STEREOPHONIQUE CHEZ L'AUDITEUR

J.F. ARNAUD

OBJET de l'Exposé.-

On se limitera strictement à l'influence de la partie électronique du récepteur de radiodiffusion sur l'écoute stéréophonique. Il s'agit d'un récepteur à modulation de fréquence auquel est ajouté un adaptateur idéal pour délivrer les deux signaux stéréophoniques gauche et droite, à partir d'un signal multiplex unique.

1.- Choix du récepteur.-

Quel que soit le système d'émission utilisé, la modulation contiendra toujours des fréquences supérieures à 15 000 Hz, afin de transmettre le signal supplémentaire (voie droite ou voie A - B). Le récepteur ne devra pas trop affaiblir ces fréquences et les restituera avec la phase convenable. En effet pour le système ZENITH-GENERAL ELECTRIC adopté aux U.S.A., l'affaiblissement ou le déphasage se traduisent par de la diaphonie, sélective ou non, pouvant facilement aller jusqu'à une interversion des signaux. Il faut donc que les circuits de détection du récepteur soient tout particulièrement soignés.

Accord du récepteur : si en radiodiffusion monophonique un accord à $\pm$ 60 kHz de la fréquence de l'émetteur désiré donne une écoute agréable, il en sera rarement de même en stéréophonie. Il faudra être plus exigeant, et rechercher une exactitude de $\pm$ 30 kHz. Bien souvent les indicateurs d'accord ne permettent pas d'apprécier de si faibles dérèglages. Des améliorations sont à apporter aussi de ce côté.

Influence du désaccord : il crée non seulement de la diaphonie et de la distorsion, mais aussi de la diaphonie non linéaire. Cette dernière se produit quand le quadripôle de diaphonie n'est pas linéaire . Son taux de Kf atteint facilement 10 % ce qui, même si son affaiblissement est de 20 dB ,

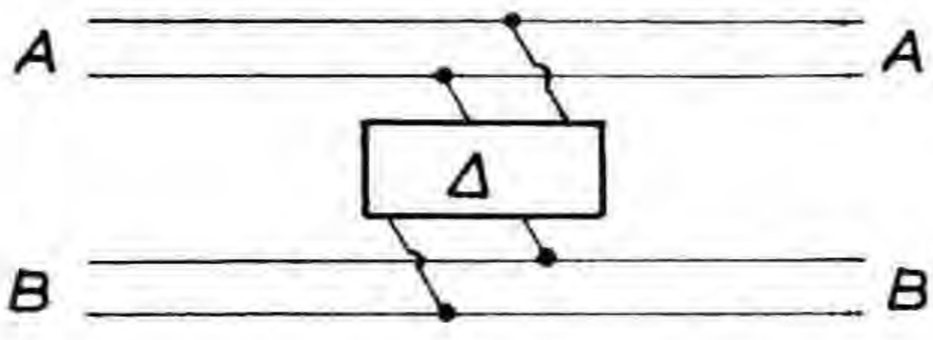

crée encore une distorsion appréciable. Ce défaut apparaît très rapidement avec le désaccord et est bien entendu ressenti comme de la distorsion harmonique habituelle.

Signalons enfin une difficulté spécifique à la stéréophonie. L'auditeur mélomane ne se fie pas toujours à l'indicateur d'accord mais plutôt à son oreille : il régle son appareil au minimum de distorsion. Or des mesures objectives ont montré que l'accord était souvent plus critique pour la diaphonie que pour la distorsion ; ainsi le réglage peut paraître correct bien que l'effet stéréophonique soit en partie détruit.

2.- Restitution des deux voies par la chaîne d'écoute correspondante.-

Bien souvent au cours d'une démonstration stéréophonique, les voies droite et gauche sont inversées par erreur à cause d'une commutation erronée. Il va de soi qu'il ne faudra pas que l'auditeur soit toujours exposé au doute : son écoute est-elle ou n'est-elle pas bien orientée ? A première vue il semble facile de réaliser des adaptateurs qui délivrent sur deux sorties marquées gauche et droite les signaux de gauche et de droite. Mais nous allons voir qu'avec un même adaptateur les signaux peuvent être intervertis par l'effet du récepteur. Nous considérons le cas du système américain ZENITH-GENERAL ELECTRIC.

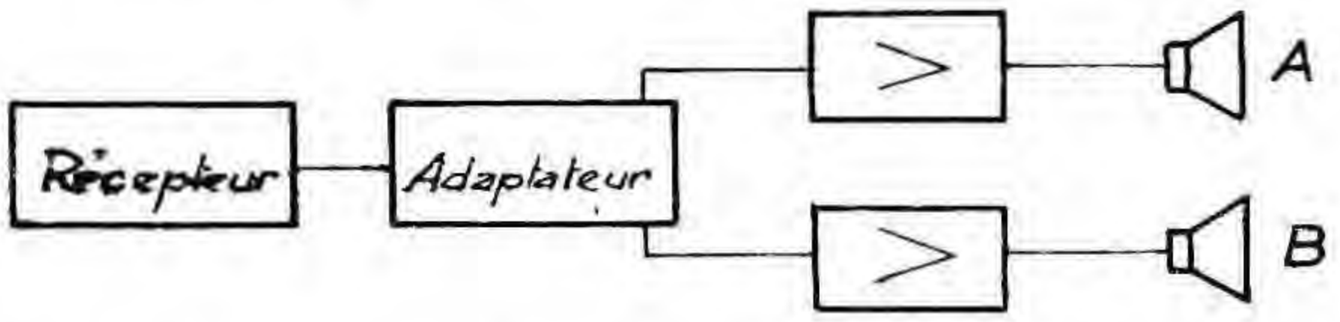

Rappelons que ce système transmet le signal A + B comme une modulation monophonique plus une sous-porteuse modulée en amplitude par A - B (1) . Quelle que soit la constitution du récepteur il délivrera la sous-porteuse de façon identique, car c'est un signal symétrique. Que la détectrice agisse sur l'enveloppe supérieure ou inférieure, la phase (ou le signe) de la tension sera la même, on aura toujours A - B. Il n'en va pas de même de A + B. En effet on peut symboliser le récepteur comme un élément qui traduit une variation de fréquence Δf en une variation de tension ΔU avec $\Delta U = k \Delta f$, k étant positif ou négatif.

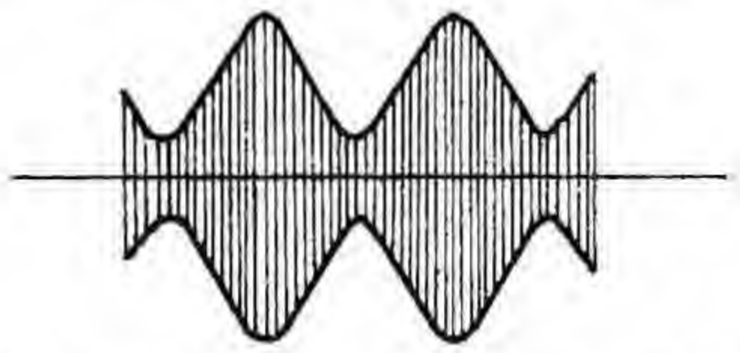

.../.

(1) On ne tient pas compte ici de la suppression de la porteuse et de la présence du pilote qui ne changent rien au phénomène.

Si k est positif, on restituera bien A + B , et l'organe chargé de restituer A et B effectuera : $\frac{1}{2}$ (A + B) + $\frac{1}{2}$ (A - B)= A et $\frac{1}{2}$ (A + B) - $\frac{1}{2}$ (A - B) = B , mais si k est négatif, on recueillera - A + B) et on trouvera B là où on attendait A et réciproquement. Une telle opposition de A + B peut être due à des amplificateurs à charge anodique, mais il est facile de la repérer. Elle peut aussi être due à d'autres organes du récepteur que l'auditeur n'a pas les moyens de tester lui-même: ce sont le changement de fréquence et le détecteur (discriminateur ou détecteur de rapport).

En effet ces deux organes ont une influence directe sur le signe de k et leur montage n'est pas le même dans tous les récepteurs. Il est clair que selon que l'oscillateur local sera inférieur ou supérieur à l'émetteur reçu, k sera positif ou négatif. De même le sens des enroulements du détecteur inversera la phase de A + B, et on ne peut diagnostiquer, à moins de disposer d'un véritable laboratoire, comment se comportera une récepteur donné. Comme d'autre part aucune normalisation n'existe sur ces 2 points-là, la phase de A + B sera correcte une fois sur deux, et une fois sur deux on "verra" l'orchestre dans un miroir. Qu'on ne nous dise pas que l'auditeur rectifiera de lui-même. A moins d'avoir une installation de toute 1ère qualité, il hésitera souvent sur la position des sources et c'est pourquoi il est utile de lui envoyer de temps en temps des signaux de réglage.

3.- Mise en phase - La phase des signaux A et B est aussi difficile à régler, mais en principe avec un système comme celui adopté auxUS et qui transmet A + B et A - B , l'erreur ne peut être due qu'à la partie proprement B.F. qu'il est plus facile de réaliser identique sur les 2 voies. Notons cependant qu'avec un système qui transmettrait A et B, les variantes des récepteurs que nous avons signalées plus haut se traduiraient non plus par une interversion de signaux gauche et droite, mais par l'opposition de phase des voies A et B.

4.- Emission de réglage.-

Afin de permettre à l'auditeur une écoute tranquille des émissions stéréophoniques, sans qu'il soit tenté de retoucher constamment ses réglages il peut être utile de diffuser une émission de réglage, dont on va montrer un exemple .

.../.

1°/ Signaux à 1 kHz, 10 kHz et 100 Hz sur la voie gauche, pour vérifier la fidélité et la position de cette voie.

2°/ Idem pour la voie droite.

3°/ Mêmes signaux sur les deux voies (parole et top de fréquences), en phase, pour contrôler la phase et les niveaux.

4°/ Signaux en opposition de phase pour mettre mieux en évidence l'opposition des chaînes.

5°/ Signaux en phase, pour les auditeurs qui, à la suite des 3° et 4°, auraient dû modifier leurs connexions.

5.- Ecoute : 4 mn 30 s

H31

FOURTH INTERNATIONAL CONGRESS ON ACOUSTICS
COPENHAGEN 21.-28. AUGUST 1962

PERCEPTION OF COLORATION IN FILTERED GAUSSIAN NOISE - SHORT-TIME SPECTRAL ANALYSIS BY THE EAR

B.S.Atal and M.R.Schroeder, Bell Telephone Laboratories, Incorporated, Murray Hill, New Jersey, U.S.A. and K. H. Kuttruff, University of Gottingen, Gottingen, Germany

Why have the large fluctuations of a room's frequency response no influence on sound quality? The hypothesis that the ear's limited frequency resolution is responsible was confirmed by paired comparison (AB) tests between filtered Gaussian noises and white noise. A spectral resolution function and a time weighting function (used in the short-time spectral analysis by the ear) are obtained in these experiments.

Introduction

It is well known that the steady-state frequency response between two points in a room is highly irregular. The response fluctuations are large, exceeding 30 db. It would seem therefore that rooms should be very poor media for transmission of speech and music. Actually, they are not. Why?

Many attempts[1,2,3] have been made to explain this anomaly. These are based on observations such as "speech and music do not excite rooms to a steady-state" or "our ears respond selectively to the first arrival" or "frequency response irregularities are averaged out because of head movements." However, none of them is satisfactory because the anomaly persists when the above mentioned factors are eliminated in controlled experiments.

Tests with Filtered Gaussian Noise

To investigate this problem systematically, we have conducted subjective tests based on listeners' ability to distinguish between white (flat spectrum) Gaussian noise and filtered noise having an irregular ("wavy") power spectrum. The noise stimuli were presented diotically (two-ear monophonically). The use of Gaussian noise as a signal enables us to observe any "coloration" due to the filters under reproduceable as well as under steady-state conditions. Since phase changes have no influence on the perception of Gaussian noise, the effect of irregularities in the frequency response can be studied independently of the phase response of the filter.

The filters used for these experiments were simulated on a digital computer (IBM 7090). We found it necessary to use a digital computer because the problem requires filters with exceptionally precise and stable frequency responses. The white Gaussian noise was also computer generated.

The impulse and frequency responses (in terms of power) of the filters used for these tests are shown in Fig. 1. All the filters have periodic frequency responses with maxima separated by $\Delta f = 1/\tau$. Although filters 1, 2 and 4 have different impulse responses, their frequency responses are identical. The frequency response of filter 3 is like that of filter 1 but maxima and minima are interchanged. The maxima of filters 5 and 6 have narrower bandwidths. Filter 7 has a nearly rectangular frequency response.

---

[1] A.F.Nickson and R.W.Muncey, "Frequency irregularity in rooms," Acustica 5, 44 (1955).

[2] J.P.A.Lochner and J.F.Burger, "The subjective masking of short-time delayed echoes by their primary sounds and their contribution to the intelligibility of speech," Acustica, 8, 1 (1958).

[3] F.V.Hunt, "Role of time integration in the discrimination of frequency responses," J. Acous. Soc. Am., 34, 125 (1962).

Eight subjects participated in paired comparison tests between white and filtered noise at a sensation level of 60 db. The threshold of perception of coloration (for which 50% of the judgments detected a difference between the white noise and filtered noise) was determined for the different filters. Figure 2 shows the threshold value of g as a function of delay τ for filters 1 to 4. The threshold curves for all filters are the same within the accuracy of the experiments. For delays τ exceeding 77 msec (Δf = 13 cps) no coloration is perceptible even for g = 1, which corresponds to maximum irregularity. Threshold curves for filters 5 and 6 are shown in Fig. 3. No coloration is heard in the case of filter 5 for delays τ exceeding 160 msec (Δf = 6.25 cps). In all cases the threshold value of g increases with increasing delays above 5 msec.

Interpretation of the Results

We assume the following model to explain these results: The ear performs a short-time power spectral analysis.* Whether a noise is perceived as colored does not depend on the irregularities of the actual power spectrum but the irregularities of the short-time power spectrum. Specifically, if the level differences between maxima and minima of the short-time power spectrum exceed a certain threshold A_o, coloration will be perceived.

The model is based on short-time Fourier analysis which implies a finite spectral resolution or a certain degree of smoothing of the power spectrum. Mathematically, the relationship between the actual power spectrum $G(\omega)$ and the short-time power spectrum $G_s(\omega)$ is as follows:

$$G_s(\omega) = \frac{1}{2\pi}\int_{-\infty}^{+\infty} G(x)E(\omega-x)dx \ , \qquad (1)$$

where $E(\omega)$ is the power spectrum of the weighting function r(t) employed in the short-time spectral analysis. Since $G_s(\omega)$, as Eq. (1) shows, is obtained by convolution of the actual power spectrum with $E(\omega)$, the closely spaced irregularities of $G(\omega)$ will be smoothed out. In terms of the short-time power spectrum, A_o is given by

$$A_o = 10 \log_{10} \frac{G_s(\omega)_{max}}{G_s(\omega)_{min}} \qquad (2)$$

Determination of the Weighting Function

Our model predicts a monotonically increasing threshold value of g as a function of τ. It can therefore not explain the decrease of g for values of τ up to 5 msec. To determine A_o and $E(\omega)$, we extrapolate the data for filter 1 above 10 msec for delays smaller than 10 msec (dashed line in Fig. 2). Because for τ = 0 no smoothing takes place, i.e., $G_s(\omega) = G(\omega)$, the value of A_o can be computed directly from the extrapolated data without knowing $E(\omega)$. The extrapolated data intersects the ordinate at g = - 24 db which corresponds to A_o = 1.1 db. This value for the just noticeable fluctuations of the power spectrum seems reasonable. (The intensity difference limen for white noise at a sensation level of 60 db is 0.5 db.)

With this value for A_o and Eqs. (1) and (2), we determine $E(\omega)$ which is shown in Fig. 4. The curve is very sharp at low frequencies and relatively flat for higher frequencies. To determine r(t), an assumption has to be made about its phase response, since our experiments give no information about phase. We assume a minimum-phase function for the phase response of r(t). The weighting function r(t) determined in this manner is shown in Fig. 5. r(t) has an initial slope corresponding to a time constant of 9 msec.

To test our model for the other filters, we calculate the short-time power spectrum $G_s(\omega)$ for filters 2 to 6, using Eq. (1), and determine A_o. A_o was found to be 1.1 ± 0.2 db which is in close agreement with the value of A_o for filter 1.

---

*The short-time power spectrum of a signal is obtained by multiplying the signal with a "weighting function" r(t) which vanishes for positive time (future) and has decreasing amplitude for negative time (past).

Short-time Autocorrelation Model

Although the above model is based on analysis in the frequency domain, an equivalent model based on analysis in the time domain can be given. The fact that $E(\omega)$ is very sharp (half-power bandwidth of 1 cps) suggests that the short-time analysis is not actually performed in the frequency domain. However, such high spectral resolution is easily obtained when the signal is analyzed in the time domain by correlation analyzers similar to those suggested by Licklider.[4] We define a short-time autocorrelation function $\varphi_s(\tau)$ as the Fourier transform of short-time power spectrum $G_s(\omega)$. $\varphi_s(\tau)$ is obtained, as in the case of $G_s(\omega)$, by multiplying the signal with a weighting function $r(t)$ which vanishes for positive time (future) and has decreasing amplitudes for negative time (past). The realization of short-time autocorrelation analysis in the auditory system can be visualized as follows: The multiplication of the binary-valued neural impulses is effected by neurons firing on coincidence of two inputs and the weighting function is represented by the distribution of "life-times" of the neural impulses.

From Eq. (1) follows:

$$\varphi_s(\tau) = \varphi(\tau) \cdot e(\tau) \ , \qquad (3)$$

where $\varphi(\tau)$ is the actual autocorrelation function and $e(\tau)$ is the autocorrelation function of $r(t)$. For white noise, $\varphi_s(\tau)$ has a single peak at $\tau = 0$. In the time domain model, coloration of a filtered noise is perceptible if the ratio of the maximum value of $\varphi_s(\tau)$ for any non-zero delay to its value at zero delay exceeds a certain threshold B_o. B_o is also a measure of the fluctuations in the short-time power spectrum at the threshold and is related to the previously defined A_o. However, in contrast to A_o, B_o is well defined even for non-periodic frequency responses which have irregularly spaced maxima and minima of different amplitudes. Results of recent tests with filters having non-periodic frequency responses are consistent with the short-time autocorrelation model but could not be predicted from the short-time power spectrum model thereby giving further credence to time-domain analysis.

We are indebted to Carol Bird of Bell Telephone Laboratories for preparing the test tapes on the digital computer and to G. M. Sessler, F. K. Harvey, D. J. McLean, J. G. Cisek, J. L. Perry and Barbara Meola who served as subjects.

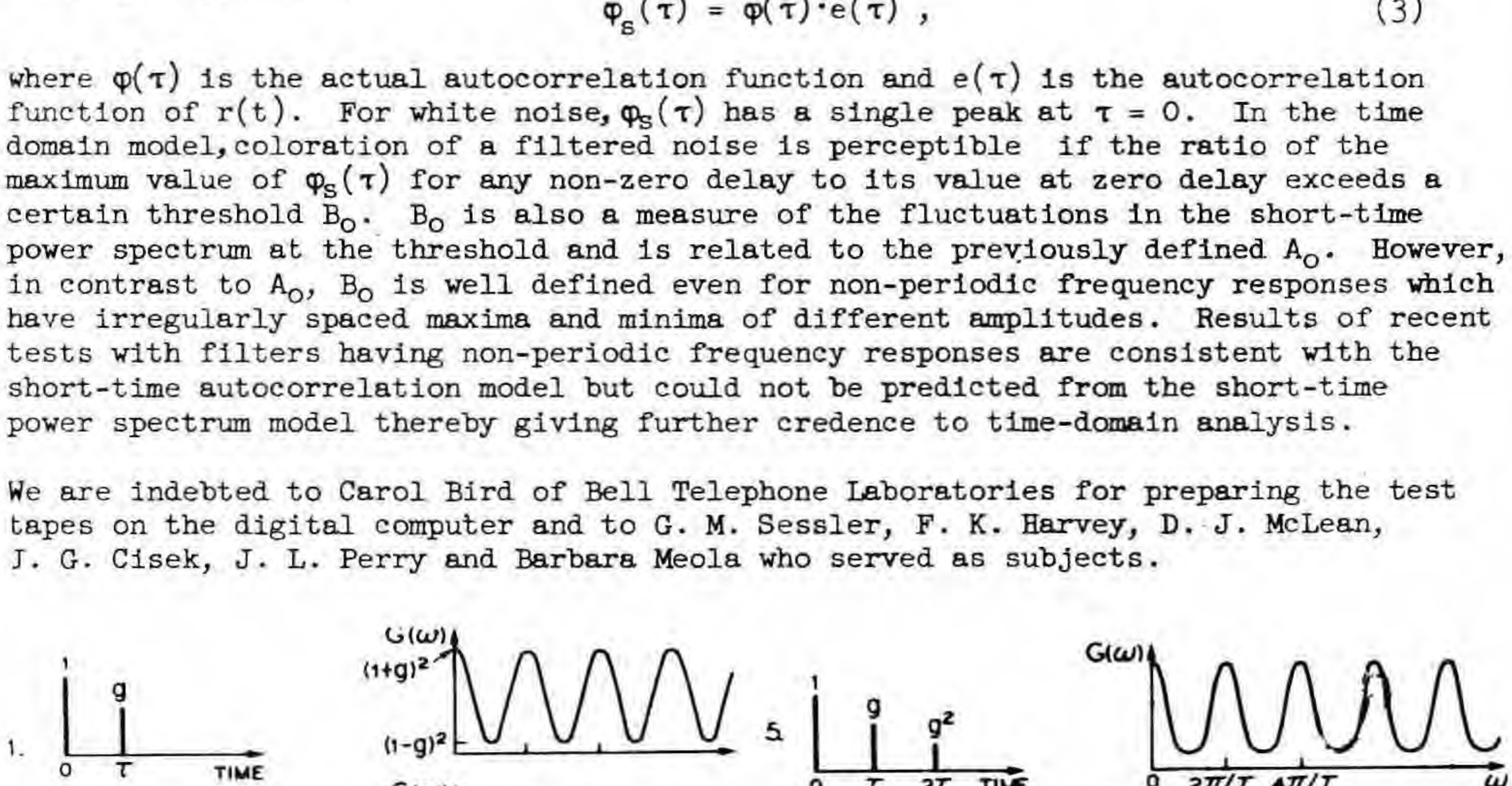

Figure 1

[4] J. C. R. Licklider, in Third Symposium on Information Theory, edited by Colin Cherry (Academic Press, Inc., New York, 1956).

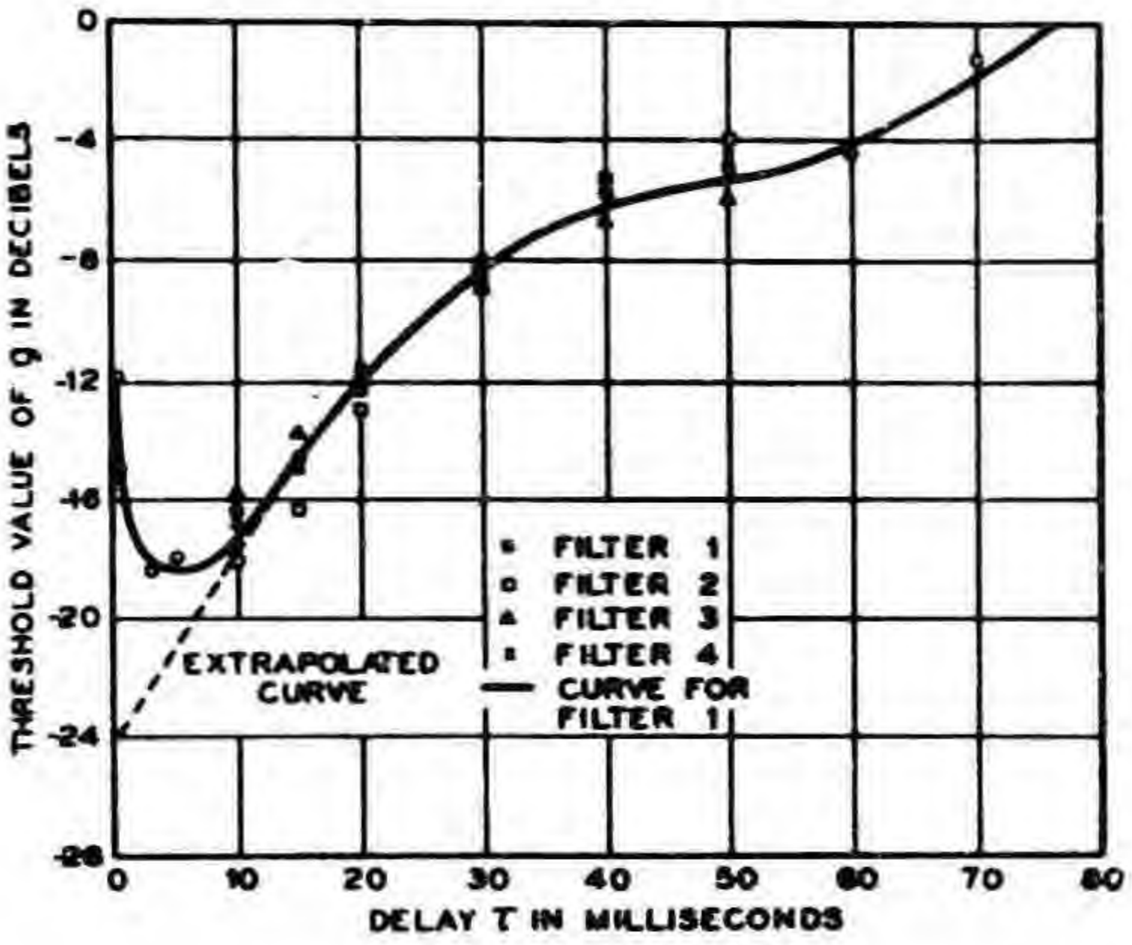

Figure 2

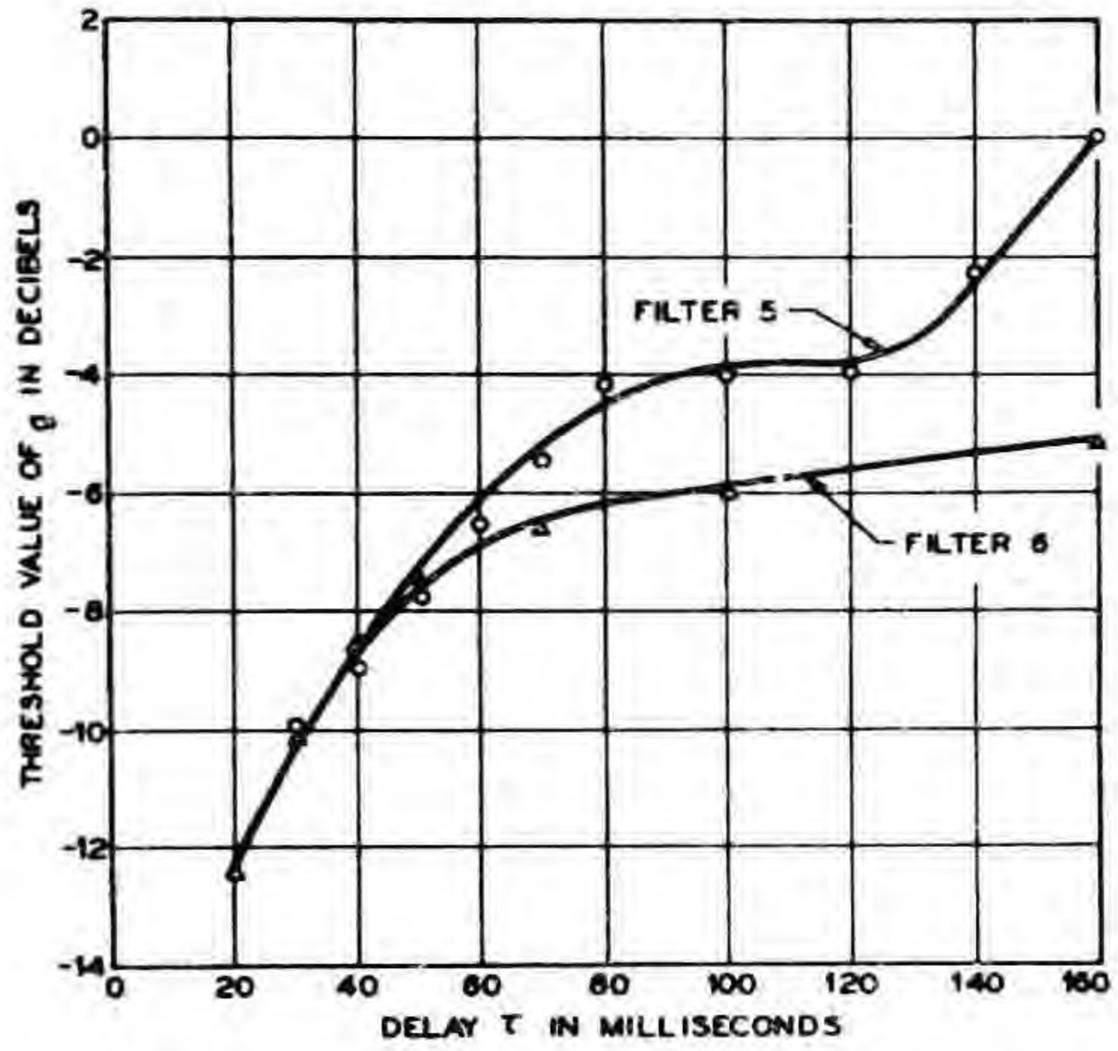

Figure 3

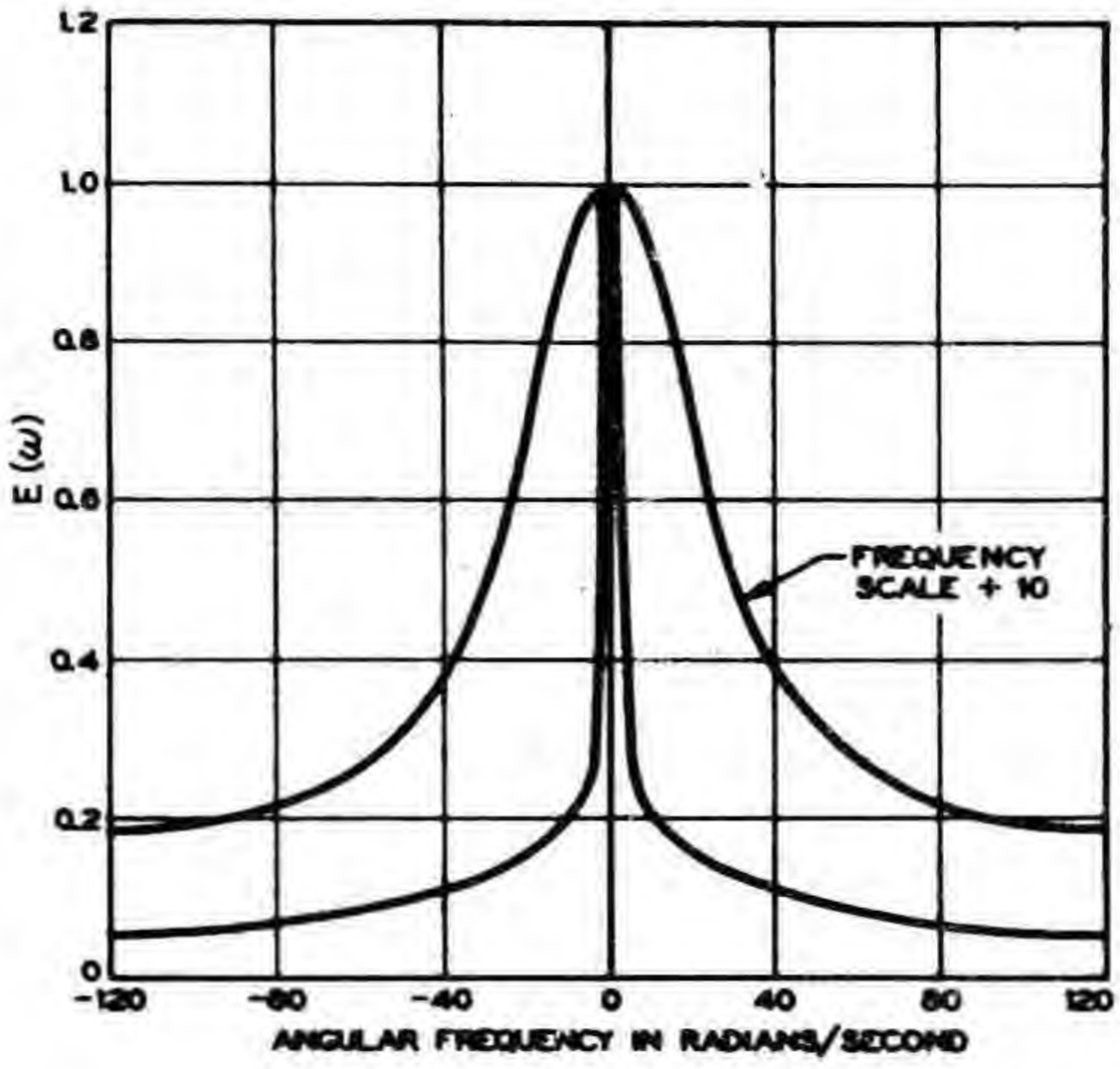

Figure 4

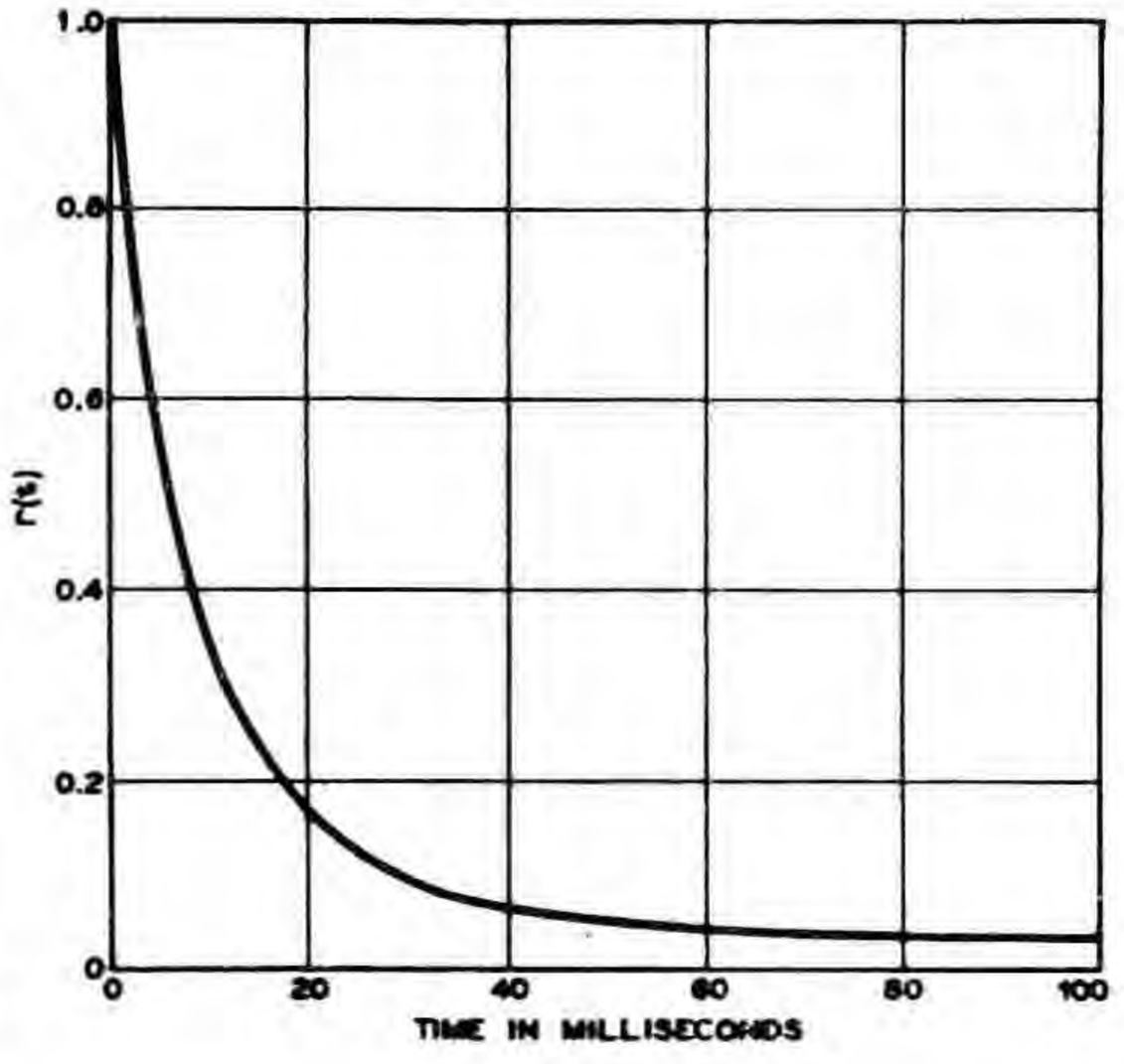

Figure 5

J31

FOURTH INTERNATIONAL CONGRESS ON ACOUSTICS
COPENHAGEN 21 - 28. AUGUST 1962

Vibrational Relaxation in Oxygen-Argon, Oxygen-Helium and Oxygen-Hydrogen Mixtures

R. Holmes, F. A. Smith and W. Tempest

Introduction A method has been developed for the measurement of sound velocity and absorption at frequency/pressure (f/p) ratios down to 15 c/s atm. The gas pressure is limited to 7 atm to keep corrections for non-ideality small. This has enabled a direct measurement of the vibrational relaxation time of oxygen to be made. The effect of several simple molecules on the deactivation of oxygen has been investigated.

Apparatus The method is an acoustic resonator technique, this being the most suitable at the frequencies involved. Several resonators have been used. The largest of these is a cylindrical steel tube with 1 cm thick walls, 388 cm. in length and 44 cm. in diameter. Flat brass plates 3 cm. thick are fitted into the ends and sealed with rubber "O" rings. The transducer, a moving coil pressure unit, is mounted behind a 1.6 mm hole in the centre of one end plate. The resonator can be evacuated through three similar sized holes in the other end plate. The resonators are immersed in a water tank of 1600 litres capacity, the water being continuously circulated at 140 litres per minute through a secondary tank containing an immersion heater. A thermistor bridge thermostat keeps the temperature constant within $\pm$ 0.03°C. In operation an audio frequency oscillator, with fine incremental tuning, is tuned to a resonant mode frequency (longitudinal) of the resonator. An automatic changeover switch connects the transducer alternately to the oscillator and the receiving system for periods of four seconds. In the first period the oscillations build up to a steady value and when the switch operates there is a delay of up to 0.5 seconds

before the transducer is connected to an amplifier which produces an output corresponding to the exponential decay of the sound field in the resonator. The frequency of the decaying signal is measured by a cycle counting unit and a Racal microsecond timer; a B. & K. level recorder measures the rate of decay. This method of measurement ensures that any non-plane wave modes excited in the resonator will have been damped out before measurements are made.

Accuracy Velocity measurements are estimated to be accurate to $\pm$ 0.07% and absorption measurements to $\pm$ 5%.

Treatment of results Velocities are corrected for the effects of the tube walls by the Kirchhoff-Helmholtz expression and for the effects of non-ideality. Absorption measurements are corrected empirically for the tube loss using a value for the absorption obtained from measurements above the absorption peak.

Results

Oxygen Measurements have been made in oxygen in the f/p range 15 c/s atm to 3 kc/s atm. The oxygen was of 99.5% purity. The impurities were argon (< 500 ppm), carbon dioxide (< 15 ppm), hydrogen (< 1 ppm), carbonaceous compounds (< 10 ppm), nitrogen (trace) and an unknown amount of water vapour. Initially measurements gave an absorption peak at about 50 c/s atm (Smith and Tempest[1]). However, with improved drying techniques the measurements now yield consistently a peak at 9 ± 1.5 c/s atm. The drying agents are phosphorous pentoxide, cold trap at - 126°C and molecular sieves. Hence the relaxation time is $\tau = 18 \pm 2.5$ ms. at 1 atm. The average number of collisions necessary for the deactivation of the first vibrational level of oxygen is $Z_{10} = N \tau \left\{ 1 - \exp (h\nu/kT) \right\} = (11 \pm 1.7)\ 10^7$ collisions.

Oxygen-Argon Measurements in oxygen-argon mixtures have been made at mole fractions of argon up to 0.5. It was found that the absorption peak

was shifted downwards in f/p indicating that argon is less efficient than oxygen in deactivating vibrationally excited oxygen. The relaxation time for argon-oxygen collisions was calculated from the equation

$$\frac{1}{\tau} = \frac{x}{\tau_{oo}} + \frac{1-x}{\tau_{oA}} \qquad \text{(all at 1 atm)}$$

where τ is the measured relaxation time in the mixture and x is the mole fraction of oxygen. The experiments yield a value $\tau_{oA} = 80 \pm 40$ ms and hence $Z_{10} = (47 \pm 23) 10^7$ collisions.

Oxygen-Helium Measurements have been made in oxygen-helium mixtures with mole fractions of helium up to 0.05. The absorption peak was shifted to higher f/p values showing that helium is more efficient than oxygen in deactivating oxygen. The measurements yield an average value of $\tau_{oHe} = (4.6 \pm .5) 10^{-2}$ ms which gives $Z_{10} = (3.9 \pm .4) 10^5$

Oxygen-Hydrogen These measurements are incomplete at the moment.

Discussion The theory of Schwartz and Herzfeld[2] has been used to calculate values of $(Z_{10})_{OO}$, $(Z_{10})_{OA}$ and $(Z_{10})_{OHe}$ at 30°C. The range of intermolecular forces, ℓ, was calculated by fitting the exponential repulsion potential to the Lennard-Jones potential with Lennard-Jones constants derived from viscosity measurements. For the mixtures the Lennard-Jones conetants for unlike collisions were calculated from the empirical combining rules

$\epsilon_{12} = \sqrt{\epsilon_1 \epsilon_2}$ and $r_{12} = (r_1 + r_2)/2$.

The calculated values of Z_{10} are as follows,

$(Z_{10})_{OO} = 3.1\ 10^7$, $(Z_{10})_{OA} = 7.2\ 10^7$, $(Z_{10})_{OHe} = 4.7\ 10^3$

It is probably better to compare the ratios $(Z_{10})_{OO} / (Z_{10})_{OA}$ and $(Z_{10})_{OO} / (Z_{10})_{OHe}$.

	Theory	Experiment
$(Z_{10})_{OO} / (Z_{10})_{OA}$	0.43	0.23 ± 0.16
$(Z_{10})_{OO} / (Z_{10})_{OHe}$	$6.6\ 10^3$	$(2.8 \pm .6)\ 10^2$

The agreement for oxygen-argon is good but the difference may be significant for oxygen-helium. The Lennard-Jones constants for oxygen and helium are very different; hence the combining rules may be invalid for calculating the force constants for oxygen-helium collisions. Chemical interaction between oxygen and helium can be discounted and if it is assumed that the mass effect is accurately represented in the Schwartz-Herzfeld expression for Z_{10} then the experiment suggests a softer interaction (i.e. larger ℓ) than the empirical combining rules imply.

References

1. Smith, F. A. and Tempest, W. J. Acoust. Soc. Amer. 33, 1626 (1961)

2. Schwartz, R. N. and Herzfeld, K. F. J. Chem. Phys. 22, 767, (1954).

K31

FOURTH INTERNATIONAL CONGRESS ON ACOUSTICS
COPENHAGEN 21.-28. AUGUST 1962

NEW TRENDS IN ULTRASONIC DEVICE TECHNOLOGY

John E. May, Jr., Bell Telephone Laboratories, Whippany, New Jersey

Introduction.

Recent advances in ultrasonics have resulted in a number of new and radically different solid state devices which have applications in performing a wide variety of functions. In the delay line field, application of guided elastic wave principles has resulted in several new types of delay lines[1-4] with capabilities which have greatly expanded the scope of applications[5]. New transducers using piezoelectric effects in semiconductors[6,7] or magnetostrictive effects in ferromagnetic oxides,[8] the ultrasonic traveling wave amplifier,[9] the experimental observation of non-reciprocal rotation of an acoustic wave,[10] the phonon maser,[11] and ultrasonic light modulators[12] are all developments based on the interaction of ultrasonics with other pheonomena of the solid state. These latter accomplishments represent progress toward extending the utilization of ultrasonic effects to microwave frequencies and indicate possibilities for complete ultrasonic transmission systems. This paper will review briefly the basic principles, general characteristics, and the applications of several of these acoustic solid state devices in order to emphasize the wide range of scientific disciplines already encompassed in this expanding field.

Guided Wave Delay Lines.

In the more conventional ultrasonic delay lines, e.g. a rod with a piezoelectric transducer on each end or one of the multiple reflection types, the wave propagation is essentially that of a plane wave in an infinite medium free of surface interactions. In the guided wave delay lines, however, the transducer dimensions are chosen comparable with a wavelength so that the wave interacts strongly with the bounding surfaces. Because in general many modes can exist at a given frequency, a useful delay line requires the preferential excitation of a selected mode and the suppression of all others by 20 to 60 db or more.

The thickness shear modes in a plate may be represented by two plane shear waves propagating with the shear wave velocity V_S and reflecting alternately from the two bounding surfaces. The variation of delay (plotted as V_S/U where U = group velocity) with thickness (h) frequency (f) product of the first two of the infinite set of dispersive modes is shown in Fig. 1 from the work of Meitzler.[1] Below the cut-off frequency, f_{c1}, the mode is evanescent and only the zeroth thickness mode can propagate. Being nondispersive, this mode is of great importance for distortionless transmission over long (millisecond) delay paths. Meitzler has developed the structure shown in Fig. 2a for the shear strip delay line. Thickness shear mode transducers are bonded to the ends of a rectangular strip 10 to 20 wavelengths in width and an absorbing material is applied to the edges in order to minimize interaction with the minor surfaces. Typical construction of a 4 millisecond line is of type 5052 aluminum strip 2.5 cm wide by 0.025 cm thick coiled within a 15 cm circle. PZT-5 transudcers resonant at 5 mc are bonded at the ends. Loss is about 30 db and bandwidth is sufficient for operation at a 2.5 mc bit rate when used for digital storage in computers, which is an important application of these lines.

Other delay characteristics are obtained by propagating the longitudinal or the flexural modes in a plate. These are characterized by particle displacement perpendicular to the plate and are described by the Rayleigh-Lamb frequency equations. The first two modes of each type are shown as delay versus frequency plots in Fig. 3 as calculated by Meeker.[2] The first longitudinal mode is of particular importance because

of the linear delay slope near the lower inflection point frequency. Using a structure similar to Fig. 2a with longitudinal mode transducers, Meeker has developed a linear line with unwanted mode suppression as high as 60db. Over a 20% bandwidth the delay characteristic is skewsymmetric with a maximum departure from linearity of 3.5%. Recently Fitch(3) has developed a tapered thickness strip line with which an arbitrary delay characteristic can be synthesized.

The linear delay lines possess a great advantage for pulse compression radar,(5) a system for increasing radar range without sacrificing range resolution. In a pulse compression system a short pulse is dispersed in a linear delay network and transmitted as a long frequency-modulated burst of high average power. In the receiver the overlapping signals from two adjacent targets are resolved after passing through another linear dispersive network of opposite slope which restores the pulses to their original short pulse length.

Preferential excitation at megacycle frequencies of the longitudinal and flexural modes in a circular wire described by the Pochhammer-Chree frequency equations was investigated by the author(4) using cylindrical longitudinal mode transducers mounted as shown in Fig. 2b. Mode shapes are similar to the plate modes but many more are possible. Unwanted mode suppression of 35db was attained in a delay line operating at the linear part of the first longitudinal mode which was sufficiently good to demonstrate the feasibility of using the acoustic line for pulse compression radar. The advantage of the wire line is compactness, particularly for low frequency operation, whereas the more recently developed strip line has superior unwanted mode suppression in the megacycle range and also has a lower electrical impedance because of larger transducer area.

Microwave Frequency Transducers.

In order to attain maximum efficiency the piezoelectric transducer at megacycle frequencies is designed as a half wavelength thickness resonator and bonded to the delay medium as shown in Fig. 4a. In studying acoustic wave propagation at microwave frequencies, Bommel and Dransfeld(13) and Jacobsen(14) excited the end of a quartz bar by the fringing field at the high field end of a reentrant cavity as in Fig. 4b. Mechanically nonresonant, this transducer requires the high field of a resonant electrical element which necessarily limits the bandwidth. An integral structure which has a half wavelength thickness is the depletion layer transducer of White(6) shown in Fig. 4c. A thin depletion layer (shaded) is formed within a piezoelectric semiconductor material at the interface with a metallic layer (dark) making a non-ohmic contact. In the high resistivity depletion layer a high electric field strength can be sustained and thus a piezoelectric strain is produced, whereas the low resistivity part of the bulk semiconductor serves only as a conducting electrode. Alternatively the depletion layer can be formed at a pn junction.

The thickness of the depletion layer depends on the square root of the ratio: applied voltage/concentration of impurity atoms. By applying a dc bias large compared to the ac signal, the layer thickness can be varied electrically by a factor of about three. Another consequence is that harmonics can be generated. Piezoelectric semiconductors are exemplified by the $A^{III}B^{V}$ sphalerite compound gallium arsenide and by the wurtzite compounds cadmium sulphide and zinc oxide. Unfortunately the concentration of impurity atoms in the samples of these materials currently available is relatively high with the result that the layer thicknesses attainable are in the 0.1 to 0.3μ range. These thicknesses would have resonant frequencies above 5Gc where acoustic losses in most materials are excessive at room temperature. Experiments conducted with gallium arsenide below 1Gc have demonstrated transducer action and an increase in layer thickness (exemplified by a decrease in loss and in capacitance) with increase in bias. It is expected that with improved materials the depletion layer transducer should prove to be an efficient wide band transducer at microwave frequencies.

An integral structure transducer like Fig. 4c can also be formed by epitaxial growth on the end of a bar of suitable material and by other means. In investigating this

general type of transducer, Foster[7] has succeeded in producing a structure exhibiting resonance at about 130 Mc. The delay line has a 30db loss and a 100 Mc acoustic bandwidth in good agreement with the bandwidth calculated by Strauss[15] for an integral transducer.

A magnetostrictive microwave transducer reported by Spencer, et.al.[8] operates under conditions of ferromagnetic resonance of the spins near the end of a YIG (yttrium iron garnet) rod. A dc magnetic field is applied along the axis of the rod, a (100) direction, and the ac field is applied in the (110) direction in the end face by a fine wire adjacent to the end face and forming a loop terminating a coaxial transmission line. An elastic strain is produced through a magnetostriction process accompanying ferromagnetic resonance. Spencer has operated this transducer at 500 Mc and 1000 Mc observing pulse propagation in a 1 cm length of YIG with as little as 25 μw of rf power. In addition to indicating that this effect is potentially a very high efficiency microwave transducer, the experiments show that at these frequencies YIG has a higher Q than quartz at room temperatures and is a very promising material for microwave delay line purposes.

Acoustic Wave Rotation.

Nonreciprocal rotation of the plane of polarization of a 500 Mc acoustic wave has been observed recently by Matthews and LeCraw.[10] An elastic wave is launched parallel to the magnetic field along the (100) direction in a YIG rod by a shear mode quartz transducer operating at a high overtone as shown in Fig. 5. Frequency and field conditions are chosen for strong magnetoelastic interaction. Maxima and minima in the return echoes are observed when the elastic wave has undergone a total rotation such as to align the polarization parallel to or perpendicular to that of the transducer respectively. In the YIG the linearly polarized wave from the shear wave transducer becomes two circularly polarized waves rotating in opposite directions. Interaction with the ferromagnetic spins causes a difference in the wave velocity of these two waves and thus at any point the difference in phase between the two oppositely rotating waves results in a rotation of the plane of polarization proportional to the distance traveled, and the direction of rotation is independent of the direction of wave propagation. This effect provides the basis for acoustic nonreciprocal devices.

Ultrasonic Traveling Wave Amplifier.

This discussion would not be complete without mention of the ultrasonic traveling wave amplifier which is described more completely in a paper by White in this volume. The amplifier is important not only as a new type of solid state amplifier but also as an amplifier of acoustic waves. As the losses in most materials are prohibitively high at kilomegacycle frequencies at room temperature, the amplifier will make possible much longer transmission paths.

Conclusions.

Several recent advances with important applications have been achieved by investigating the interaction of elastic waves with other solid state properties and with the bounding surfaces. Many possibilities for such interactions remain unexplored and it can be expected that the exploration and development of this field will become an increasingly important part of ultrasonics.

Acknowledgments.

The author wishes to thank J. H. Rowen, under whose guidance much of this work has been stimulated, for many helpful suggestions, and to thank the many colleagues referenced for many helpful discussions.

REFERENCES

1. A. H. Meitzler, IRE Trans. UE-7, 1(1960).
2. T. R. Meeker, IRE Trans. UE-7, 36(1960).
3. A. H. Fitch, J. Acoust. Soc. Am. 33, 1958(1961).
4. J. E. May, IRE Trans. UE-7, 44(1960).
5. J. R. Klauder, A. C. Price, S. J. Darlington and W. J. Albershein, BSTJ 39, 745(1960).
6. D. L. White, IRE Conv. Record 6, 304(1961).
7. N. F. Foster, (to be published).
8. E. G. Spencer, R. T. Denton and R. P. Chambers, Phys. Rev. 125, 1950(1960).
9. A. R. Hutson, J. H. McFee, D. L. White, Phys. Rev. Letters 7, 237(1961).
10. H. Matthews and R. C. LeCraw, Phys. Rev. Letters 8, 397(1960).
11. E. B. Tucker, Phys. Rev. Letters 6, 547(1961).
12. A. H. Rosenthal, IRE Trans. UE-8, 1(1961).
13. H. E. Bommel and K. Dransfeld, Phys. Rev. Letters 1, 234(1958)
14. E. H. Jacobsen, Phys. Rev. Letters 2, 249(1959).
15. W. Strauss, J. Acoust. Soc. Am. 34, Paper F4, June (1962).

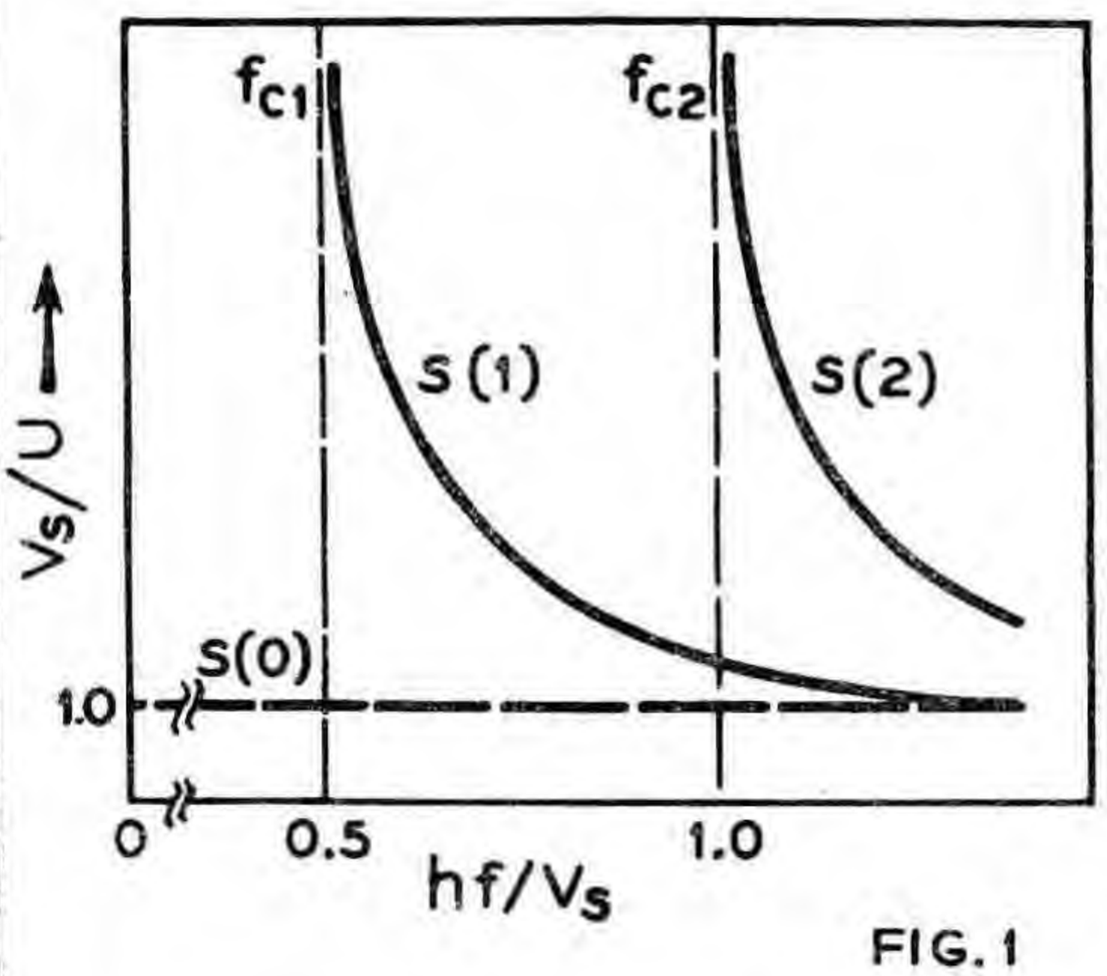

FIG. 1

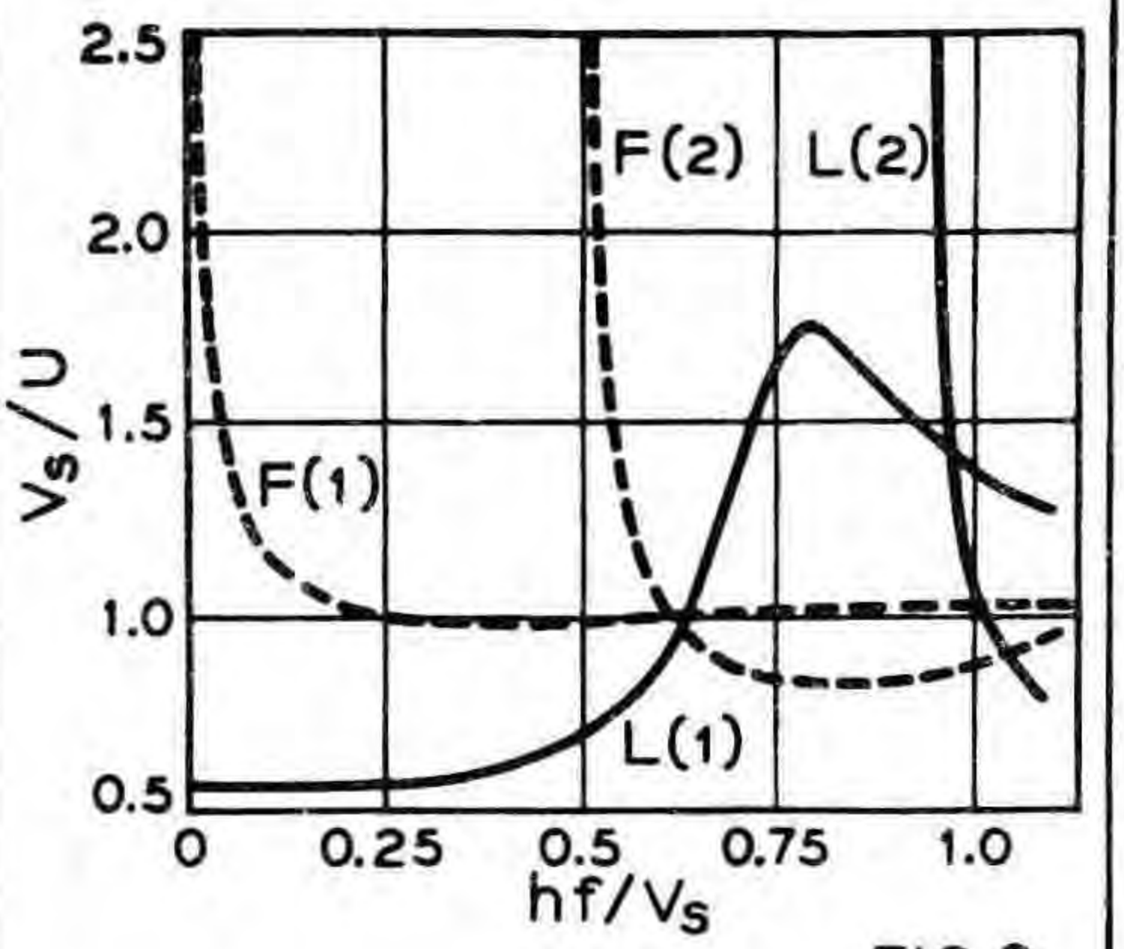

FIG. 2

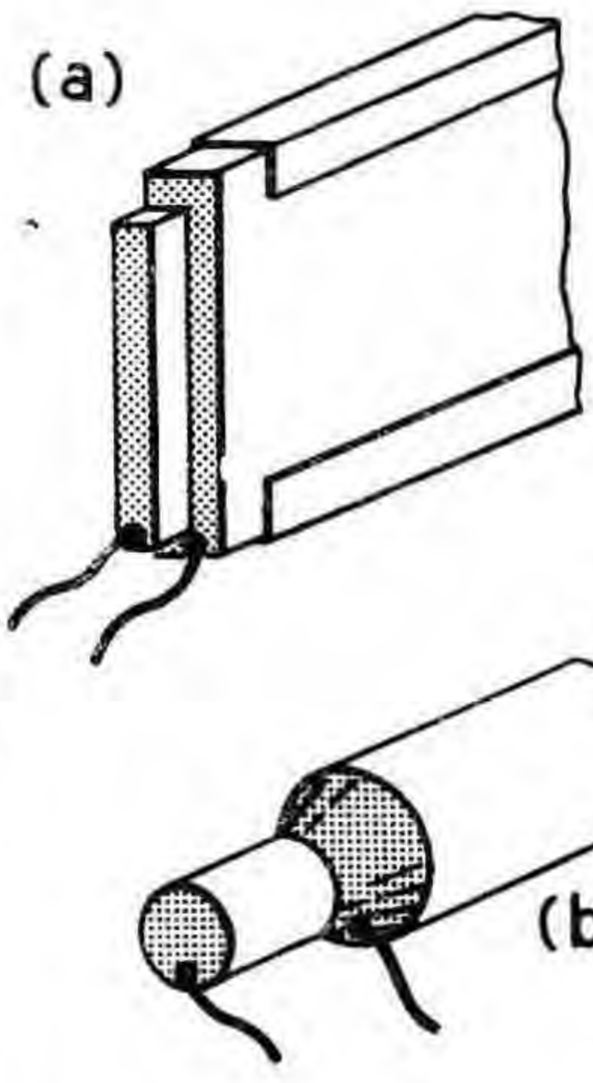

FIG. 3

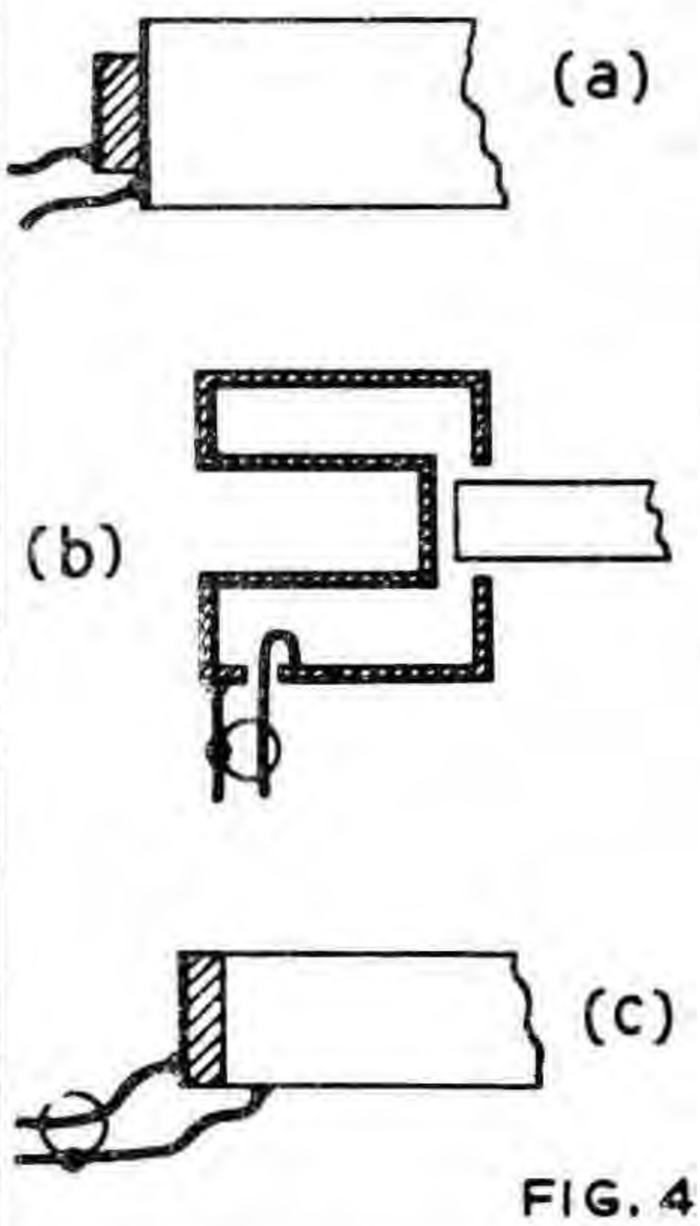

FIG. 4

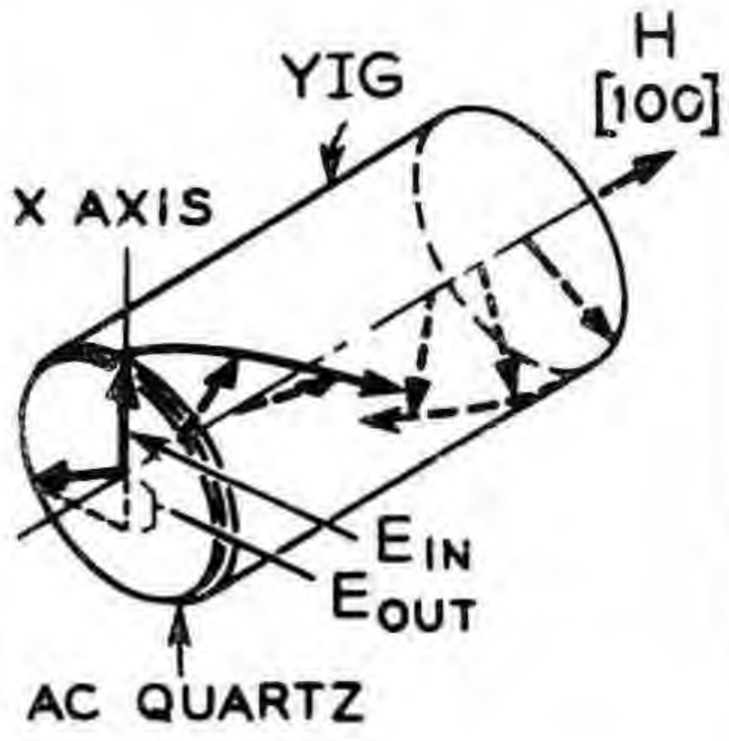

FIG. 5

L31

FOURTH INTERNATIONAL CONGRESS ON ACOUSTICS
COPENHAGEN 21.-28. AUGUST 1962

NOISE CHARACTERISTICS OF COAXIAL NOZZLES

P. Gregory and J. D. Voce

The ducted fan jet engine shows every sign of becoming the predominant aircraft powerplant in the immediate future. The use of this type of engine should go part way towards solving the aircraft noise problem since the required thrust is produced by using a higher engine mass flow with essentially a lower jet velocity. However, if the two exhaust streams of the ducted fan engine are not mixed prior to the final nozzle then it is not immediately obvious how an estimate of the jet noise would be made.

As a first step in their study of this problem Bristol Siddeley Engines have conducted a series of acoustic tests on a model of such an exhaust system. The model consisted of two coaxial nozzles, the central one 1.264 in. diameter and the outer one 1.806 in. diameter. Air was fed to the two nozzles at equal pressures and the central stream was preheated in the majority of the tests. The geometry of the nozzle gives approximately equal flow areas for each stream but the actual central stream flow for the heated tests was approximately half the outer stream flow. The model was tested at stream total pressures of 7.5, 15, 22.5 and 30 p.s.i.g. and with the central stream unheated and at temperatures of 400°, 600° and 800 °C. for each pressure condition.

In order to provide a datum to which the coaxial nozzle tests could be referred, a single 1.5 in. diameter nozzle was tested at stream total pressures of 7.5, 15, 22.5 and 30 p.s.i.g. and temperatures of 400°, 600° and 800 °C. For both sets of tests acoustic measuring positions were arranged on a circle about the nozzle exits 14.5 ft. diameter, at angles of 5°, 15°, 25°, 35°, 50°, 65°, 80°, 95° and 110°, to the downstream jet axis. At each microphone position and for each test condition the overall sound pressure level was measured and a third-octave frequency analysis carried out, using B & K equipment: a $\frac{1}{2}$ inch condenser microphone, type 2111 spectrometer and type 2304 level recorder, suitably calibrated.

SOUND PRESSURE LEVELS

In analysing the coaxial nozzle tests two approaches have been used. The exhaust has been considered on the one hand as a fully mixed jet, i.e. a single stream having the same mass flow momentum and total heat as the two separate streams. The characteristic dimension of this single stream was taken to be the diameter of the outer nozzle. On the other hand it was considered as a jet of which the only significant part is the inner, heated stream.

Comparisons have been made between the single nozzle tests and the coaxial nozzle tests on the basis of total acoustic power (power watt level), peak value of sound pressure level on a circle about the nozzle exit (polar peak) and peak value of sound pressure level on a line parallel to the jet (linear peak). This last quantity is the most significant one in considering the noise to the side of an aircraft or of an aircraft in flight. It was obtained by applying standard distance corrections to the measured polar results. For the purpose of comparison all noise levels were corrected for nozzle area and density squared.

Considered either as a fully mixed jet or as the central jet only, the various noise levels of the coaxial nozzle agree well with the single nozzle results. Scatter is about ± 3db for all but two or three of the tests. However the tests with a completely unheated stream show appreciably lower noise levels than would be expected.

FREQUENCY SPECTRA

In order to study the distribution of the noise energy over the range of frequencies measured, Strouhal number, frequency multiplied by diameter divided by velocity, has been used to take account of the different velocities and nozzle sizes. The limitations of this parameter are apparent from the single nozzle tests. High frequency noise is adequately correlated but at low frequencies there is a spread. This is not a random scatter but shows the influence of pressure and temperature. Some progress has been made in obtaining a better correlation of the results.

In comparing the coaxial nozzle tests with the single nozzle tests it seems sufficient to take a mean line through the latter as a datum. The low frequency spread on the coaxial nozzle tests is similar to that recorded on the single nozzles, so the comparison between the two tests will mainly refer to the high frequency component. This shows good internal agreement on either basis of considering the coaxial nozzle flow. The agreement with single nozzle tests is good when the central stream only is considered; when the jet is treated as a fully mixed stream, there is some displacement of the frequency spectrum relative to the single nozzle results.

CONCLUSIONS

It appears that the noise from the particular coaxial nozzle tested can be predicted satisfactorily from single nozzle data, both for noise level and spectral distribution, by considering only the central heated stream, the outer stream having no apparent effect. This confirms the results of what previous work has been done on the noise levels of coaxial nozzles; the fact that the central stream conditions also determine the frequency spectrum of the resultant noise suggests that the results can be extended to nozzles of other than 1:1 flow area ratio and to coaxial streams at different pressures.

However the results should not be extended too far as for outer stream flow areas much greater than the area of the central nozzle the relative velocity of the two streams must be the important parameter. The system in this case would be analogous to a single nozzle in a moving air stream or with due allowance for Doppler effect, a jet engine in flight.

The fact that the noise levels of this nozzle can also be predicted by considering the jet as a fully mixed stream is probably a peculiarity of this particular set of test conditions and the energy distribution between the two streams.

Co-Axial Nozzle Model Jet Tests.

Peak Linear OASPL - $10\log_{10}\rho^2 A\ V \log_{10} V_J$

Referred To Hot Jet And Mixed Jet Conditions.

Results Corrected To Equivalent Of 500ft. Alt.

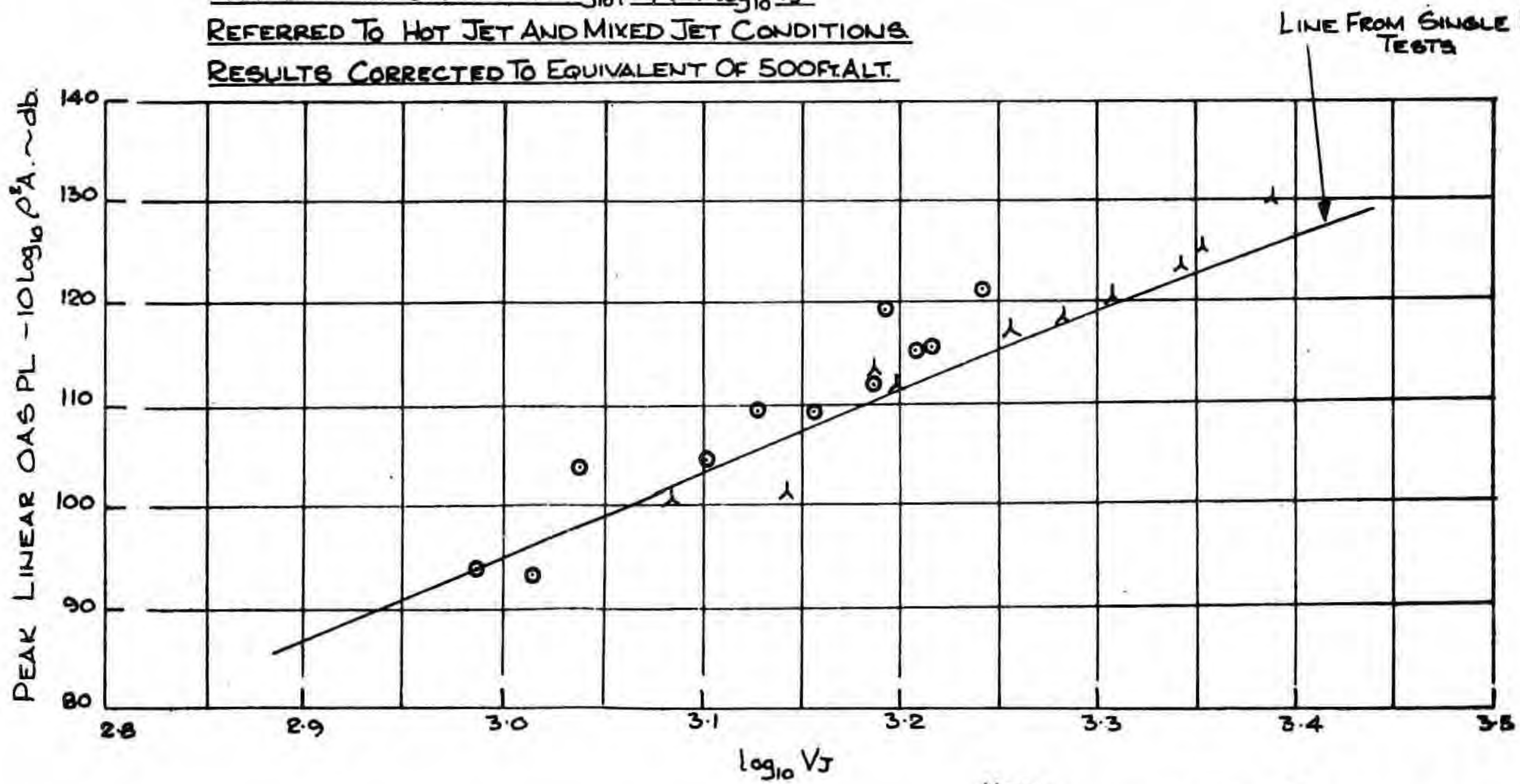

Key:- λ ~ Hot Jet Conditions.
⊙ ~ Mixed Jet Conditions.

M31

FOURTH INTERNATIONAL CONGRESS ON ACOUSTICS
COPENHAGEN 21.-28. AUGUST 1962

EIN BETONBUNKER WIRD KONGRESSHALLE

Max A d a m , Basel (Schweiz)

Die Regierung der Stadt Basel beschloss im Herbst 1959 eine Halle der Schweizerischen Mustermesse in eine Kongresshalle grossen Stils umzubauen. Diese Halle sollte der Universität Basel als Tagungsort der im Juli 1960 stattfindenden Feier des fünfhundertjährigen Bestehens dienen. Der Auftrag an den Akustiker erfolgte im Oktober 1959. Mit einem Kostenaufwand von drei Millionen Franken wurde die Beton-Halle in knapp 9 Monaten in eine Kongresshalle umgebaut.

Vor dem Umbau wies die 80 m lange und 40 m. breite Messehalle einen Asphaltboden von 3200 m^2 auf. Die Decke war über den 14 m hohen Wänden als Shed-Bedachung ausgebildet. Es stund im Vorneherein fest, dass die Shed-Dächer aus akustischen Gründen durch eine horizontale Decke unwirksam gemacht werden sollen. Vorgesehen wurde auch der Einbau einer Galerie, so dass das endgültige Volumen auf 42 000 m^3 vorberechnet wurde. Um eine möglichst flache Nachhallkurve zu erzielen, wurde eine Messung mit Heultönen und Oktavsieb vorgenommen. Die ausserordentlich ungünstige Kurve ist aus folgendem Bild zu ersehen:

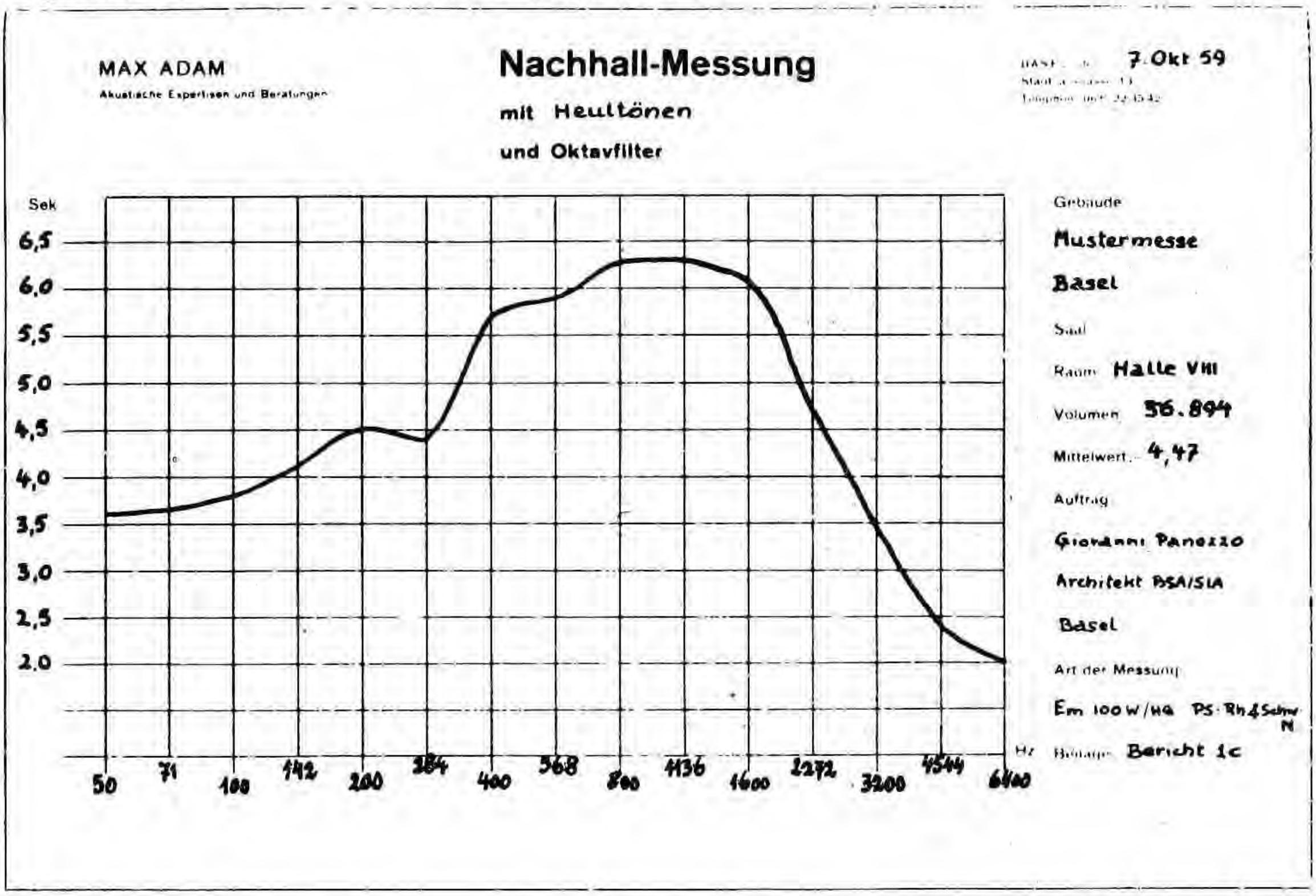

Zunächst galt es die Eigenresonanzen des Raumes zu eliminieren und gleichzeitig die Nachhallzeit von 4,47 Sek. Ø auf rund 3 Sek. in der

unbesetzten Halle zu reduzieren. Eine beschränkte Variabilität der Nachhallzeit war bei diesem Mehrzweck-Kongressgebäude erwünscht. Im Voraus wurde die Forderung aufgestellt, dass die Nachhallzeit auch bei 5000 Anwesenden nicht unter 2 Sek. sinken soll, damit die Schall=energien auch ohne elektrische Verstärkung genügend zur Entwicklung kommen.
Die weitaus schwierigste Aufgabe war das Erreichen einer guten diffu=sen Reflexion, da bei den gegebenen Dimensionen Laufzeitverschiebung=en bis zu einer halben Sekunde möglich waren. Da auch eine umfang=reiche Lautsprecheranlage geplant war, hätten sich bei schlechten Reflexionsverhältnissen die grossen Schallenergien besonders störend bemerkbar gemacht.
Als dritter Punkt war zu überlegen, dass Klangkörper jeder Grösse auch ohne elektrische Verstärkung den Raum so erfüllen sollen, dass der Eindruck eines "Forte" noch erhalten bleibt. Selbst ein einzel=ner Sprecher sollte noch, ohne Lautsprecherverstärkung, bis zu 2000 Hörern beschallen können.

Um die obgenannten Forderungen zu erfüllen, wurde wie folgt disponiert:

Die Wände wurden bis auf eine Höhe von 4 m mit sägezahnartigen Sperr=tafeln von je 2 m Breite verkleidet.Die Abstrahlungswinkel wurden nach einer gedachten Schallquelle in der Mitte der Längswand und ei=ner solchen in der Mitte der Querwand in die Pläne eingetragen und die Neigungsflächen derart verändert,bis die bestmögliche Verteilung der Reflexionen erzielt wurde. Darüber verblieben weitere 1600 m^2 Wandflächen für die akustische Behandlung. Die Hälfte davon wurden mit Spaltenresonatoren mit Hauptschluckvermögen von 200 - 2000 Hz, die andere Hälfte mit keilförmig geschliffenen Holzprofilen verklei=det. Diese Absorptions- und Reflexions-Elemente wurden in Tafeln von ca. 1.50 x 1.50 m abwechslungsweise montiert.

An der Decke wurden auf einer Fläche von 3000 m^2 drehbare Aluminium-Elemente von je 1 m^2 Grösse aufgehängt. Diese Aluminium-Elemente waren in asymmetrische Prismen geformt,deren eine Seite (Aluminium) reflektierend, die Kehrseite absorbierend wirken. Um einen Dröhn=effekt zu vermeiden, wurde die Rückseite des Aluminiums mit einer nach Gewicht und Absorption sorgfältig ausgesuchten Antidröhnmasse behandelt. Bei der Hälfte der Elemente, die gegen den Raum durch=hängen, wurde auf Anraten von Herrn Prof.W.Furrer eine gerade Glas=faser-Bauplatte eingehängt. Hierdurch entsteht ein unregelmässiger Hohlraum und somit ein guter Mitteltonabsorber. Bei den nach oben gekehrten Elementen wirkt die Antidröhnschicht absorbierend. Die 3000 Elemente sind hydraulisch gesteuert und können innert 30 Sek. von "reflektierend" auf "absorbierend" gedreht werden. Eine senkrech=te Stellung der Elemente gibt akustische Zwischenwerte und erlaubt das durch die Sheds fallende Tageslicht in den Hallenraum zu bringen.
Der ganze Boden wurde mit einem hartfaserigen Bouclé-Teppich belegt.

Mit besonderer Sorgfalt wählte der Akustiker die Stühle aus. Vor dem Entscheid wurden etwa 30 Arten Stühle akustisch und aesthetisch ge=prüft. Der endgültige Stuhl wurde nach genauen Angaben mit Schaum=gummi unterpolstert und mit Kunstleder überzogen. Die Absorption der Sitzflächen beträgt etwa die Hälfte der Kleider einer Person. Hier=bei werden wiederum die mittleren Frequenzgebiete im Schluckvermögen bevorzugt. Damit ist eine weitgehende Unabhängigkeit von der Besu=cherzahl erreicht.

Alle diese Massnahmen bewirkten eine zwischen 50 - 6400 Hz fast ge=radeverlaufende Nachhallkurve mit einem Maximum von 3,05 Sek. bei reflektierender Decke und einem Minimum von 2,42 Sek. bei absorbie=

render Decke. Die nachfolgenden Figuren zeigen verschiedene Möglich= keiten der Variabilität (Schussanalyse mit 4000 Anwesenden):

MAX ADAM
Akustische Expertisen und Berechungen

Nachhall-Messung

mit Pistolenknall

und Oktavfilter

BASEL, den 6. Juli 1960
Stadthausgasse 13
Telephon (061) 22 36 42

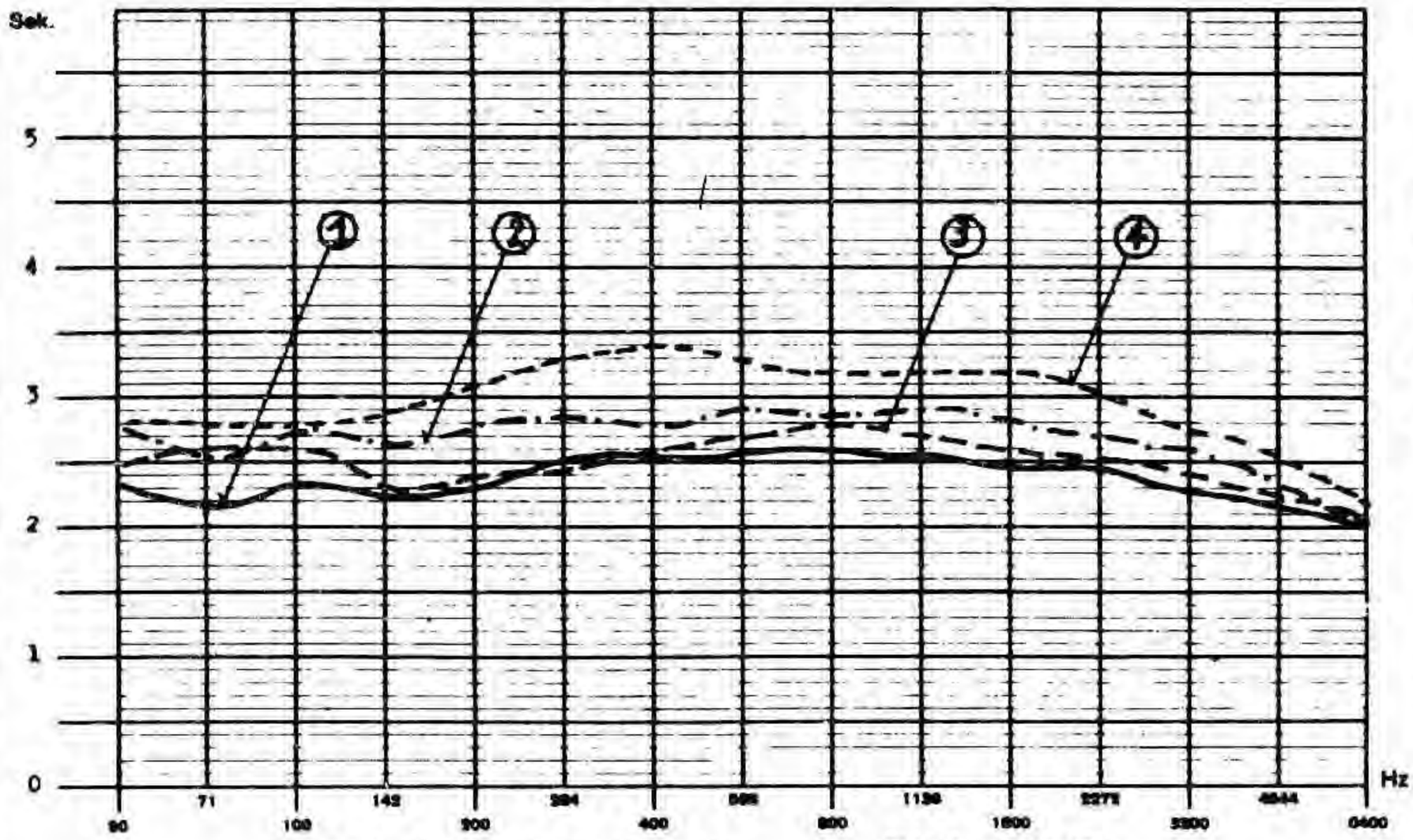

Gebäude: Mustermesse Basel

Saal: Kongresshalle, leere Halle, ohne Publikum

Raum:

Volumen: 42'000 m³

Mittelwert:

Auftrag:

Art der Messung:

Beilage:

Kurve 1: Mit absorbierender Decke, Mittelwert: 2,42 s
Kurve 2: Mit halbabsorbierender Decke, Mittelwert: 2,74 s
Kurve 3: Mit senkrecht gestellten Elementen, Mittelwert: 2,53 s
Kurve 4: Mit reflektierender Decke, Mittelwert: 3,05 s

MAX ADAM
Akustische Expertisen und Beratungen

Nachhall-Messung

mit Pistolenknall

und Oktavfilter

BASEL, den 6. Juli 1960
Stadthausgasse 13
Telephon (061) 22 36 42

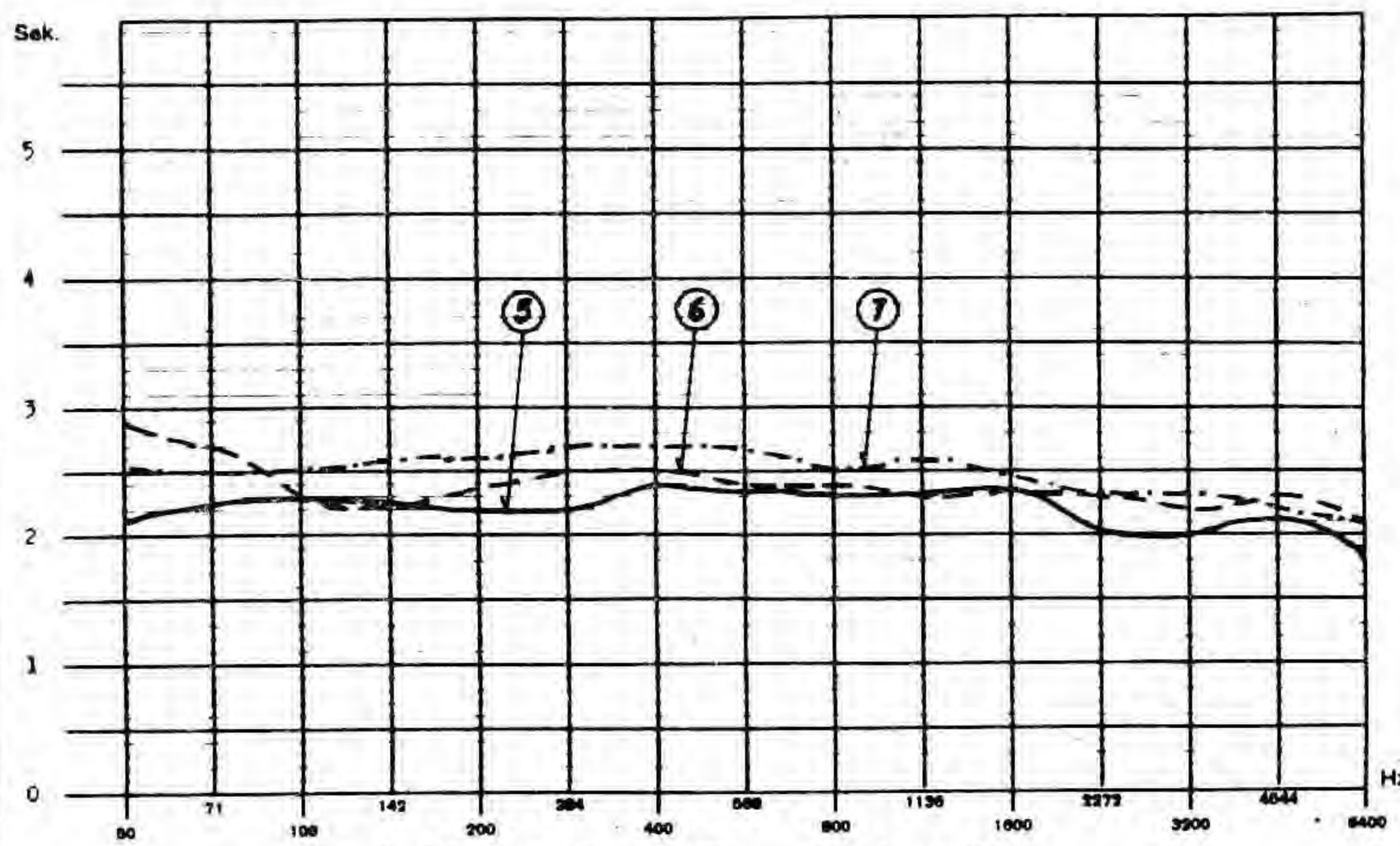

Gebäude: Mustermesse Basel

Saal: Kongresshalle, vollbesetzt mit Publikum

Raum:

Volumen: 42'000 m³

Mittelwert:

Auftrag:

Art der Messung:

Beilage:

Kurve 5: Mit absorbierender Decke, Mittelwert: 2,23 s
Kurve 6: Mit halbabsorbierender Decke, Mittelwert: 2,35 s
Kurve 7: Mit reflektierender Decke, Mittelwert: 2,51 s

Als Novum wurde 8 Tage vor der Universitätsfeier das Musik-Publikum der Stadt Basel zu einem Test-Konzert eingeladen. 4000 Personen folg= ten dem Ruf. Es wurden Klangkörper in verschiedenen Formationen auf= gestellt und ein Konzert mit kleinen und grossen Chören, mit Sinfonie= und Blasorchester geboten. Hierbei wurden 40 prominente Musiker ver= streut im Saale verteilt, die einen umfangreichen Fragebogen über alle Arten von Klangwirkungen und Verständlichkeit schriftlich zu beantworten hatten. Die Ergebnisse wurden hernach von einem Musik= wissenschafter, Herrn Dr. Franz Giegling ausgewertet und im Schluss= bericht des Akustikers veröffentlicht. Wir geben hier einen Auszug dieses Berichtes, da u.W. diese Testmethode durch Fachmusiker erst= mals angewendet wurde:

A) Dynamisches Verhältnis der verschiedenen Klangkörper zur Halle

Diese Frage,welche bei allen Nummern des Abends in einer Form auf= tauchte,gibt dem Akustiker vor allem Aufschluss über die Diffusität des Raumes,d.h.in welchen Grenzen ein grosser Klangkörper noch als angenehm klingend empfunden wird und bis zu welchem Wert ein kleiner Klangkörper noch ausreichend gehört werden kann;bei letzteren,zwei kleinen Chören,spielt vor allem die Verständlichkeit des Textes eine ausschlaggebende Rolle,beim Orchester und beim grossen Chor die Hör= barkeit der Stimmführungen.

Es sprechen sich aus:	positiv	befriedigend	negativ
beim Orchester	18	15	7
beim Männerchor (200 Sänger)	40 !	--	--
beim kleinsten Chor (40)	8	22	9
bei der Harmoniemusik	30	9	--

Dass verhältnismässig wenige die Dynamik des Orchesters völlig aus= reichend empfanden,liegt zu einem guten Teil an der besonderen Struk= tur des Orchesterwerkes (Richard Strauss:Don Juan),das für diesen Raum nicht sehr geeignet war. - Mehrere Experten der 22 bei den klei= nen Chören "befriedigenden" Voten drückten zudem ihr Erstaunen darü= ber aus, dass ein so kleiner Klangkörper in dieser grossen Halle überhaupt noch so gut gehört werden kann.

B) Eigenschaften des Orchesterklanges

Beim Orchestervortrag,der durchweg ohne Lautsprecherverstärkung er= folgte,hatten die Experten aus einer Reihe von vorgedruckten Eigen= schaften zu wählen. Es entschieden sich für:

glanzvoll	17	matt	9
hell	16	mager	2
weich	17	glanzlos	3
klangschön	24	kellerton	0
mächtig	4	spröd	1

Die beiden Experten,welche das Orchester zu mager im Klang fanden, sassen dicht am Podium und wurden durch die aussergewöhnliche Höhe desselben weitgehend vom Direktschall abgeschnitten.

C) Grad der Verschmelzung und klanglicher Ausgleich

Beim Orchester und bei der Harmoniemusik waren der Grad der Verschmel= zung zwischen den einzelnen Instrumentengruppen und deren Ausgleich zu beurteilen,eine Frage,die viel Hörerfahrung voraussetzt und daher auch einigemale unbeantwortet blieb. Für die gestellten zwei Fragen resultierten positive Stimmen 46 , befriedigende 27, negative 5 .

D) Die Verständlichkeit des Wortes wurde von 37 Experten mit sehr gut angegeben.

N31

FOURTH INTERNATIONAL CONGRESS ON ACOUSTICS
COPENHAGEN 21.-28. AUGUST 1962

Gerät zur Anzeige des "subjektiven Spektrums" und der Lautheit von Dauergeräuschen.

R. Fischer

Institut für Technische Akustik, Berlin.

1. Grundlagen

Vorliegende Aufgabe war, ein Meßgerät zu entwickeln, das die wichtigsten hörphysikalischen, -physiologischen und -psychologischen Gesetzmäßigkeiten der Lautstärkeempfindung bei Dauergeräuschen erfaßt. Nur so ist für alle möglichen Geräusche eine gute Übereinstimmung zwischen subjektivem Empfinden und dem objektiv gemessenen Lautstärkewert zu erwarten. In Anlehnung an die von ZWICKER und anderen gefundenen und heute allgemein gesicherten elementaren Zusammenhänge der Lautstärkeempfindung sollen folgende Eigenschaften des Gehörs nachgebildet werden:

a) Der Frequenzgang (Hörschwelle) des Ohres kann als Mithörschwelle einer durch körpereigene Geräusche stets vorhandenen, unhörbaren Grunderregung, die zu tiefen Frequenzen hin ansteigt, und einem frequenzabhängigen Übertragungsfaktor des Ohres bei den mittleren und hohen Frequenzen gedeutet werden.

b) Das Ohr faßt bei der Bewertung breitbandiger Geräusche spektrale Anteile innerhalb der sogenannten "Frequenzgruppen" zu einem gemeinsamen Effektivwert zusammen. Diese Frequenzgruppen sind unterhalb 500Hz etwa 100Hz breit und betragen oberhalb etwa 17% der jeweiligen Mittenfrequenz. Jeder dieser 24 aneinandergefügten Frequenzgruppe entspricht auf der Basilarmembrane eine konstante Kopplungsbreite von etwa 1,3 mm, in der die Haupterregung der Sinneszellen erfolgt.

c) Auch ein schmalbandiges Geräusch bzw. ein reiner Ton erregt die Basilarmembran außer am Ort der Haupterregung noch auf den benachbarten Abschnitten, besonders in Richtung Stapes, dh. zu hohen Frequenzen. Dieser Erregungsverlauf läßt sich durch die sogenannte "Mithörschwelle" ausdrücken. Er ist keine lineare Funktion des Maximalpegels. Bei hohen Pegeln erfolgt eine wesentlich stärkere Erregung der benachbarten Kopplungsbreiten; die Mithörschwelle verläuft flacher.

$$L_E(\zeta) \mathrel{\hat{=}} L_{MHS}(f)$$

(ζ = Ortskoordinate auf der Basilarmembrane, markiert durch die Gruppennummern n = 1 bis 24.)

Die Drosselung bzw. Verdeckung benachbarter spektraler Geräuschanteil kommt nun dadurch zustande, daß die Erregung z.B. eines zweiten Tones in einen Abschnitt der Basilarmembrane fällt, der bereits von einem anderen Ton bzw. Geräuschanteil erregt ist. Die zusätzliche Erregung wird nur dann als Lautstärkezuwachs hörbar, wenn in irgend einer Frequenzgruppe der Erregungspegel um mehr als 1 dB ansteigt.

d) Als addierbare Teillautheit erscheint jetzt eine Größe $N'(\zeta)$, die über ein Potenzgesetz mit der Erregung in den einzelnen Kopplungsbreiten zusammenhängt. $N'(\zeta) \sim E^{0,25}$. $N'(\zeta)$ nennen wir das "subjektive Spektrum".

Die Gesamtlautheit des Geräusches ist die Summe:

$$N = \sum_{z=1}^{24} N'(z)$$

Sie entspricht in unserer Darstellung der von der Kurve $N'(z)$ umschriebenen Fläche.

e) Die Gesamtlautheit N des Geräusches kann über die Lautheitsfunktion des 1 KHz-Tones wieder in einen Lautstärkewert umgewandelt werden.

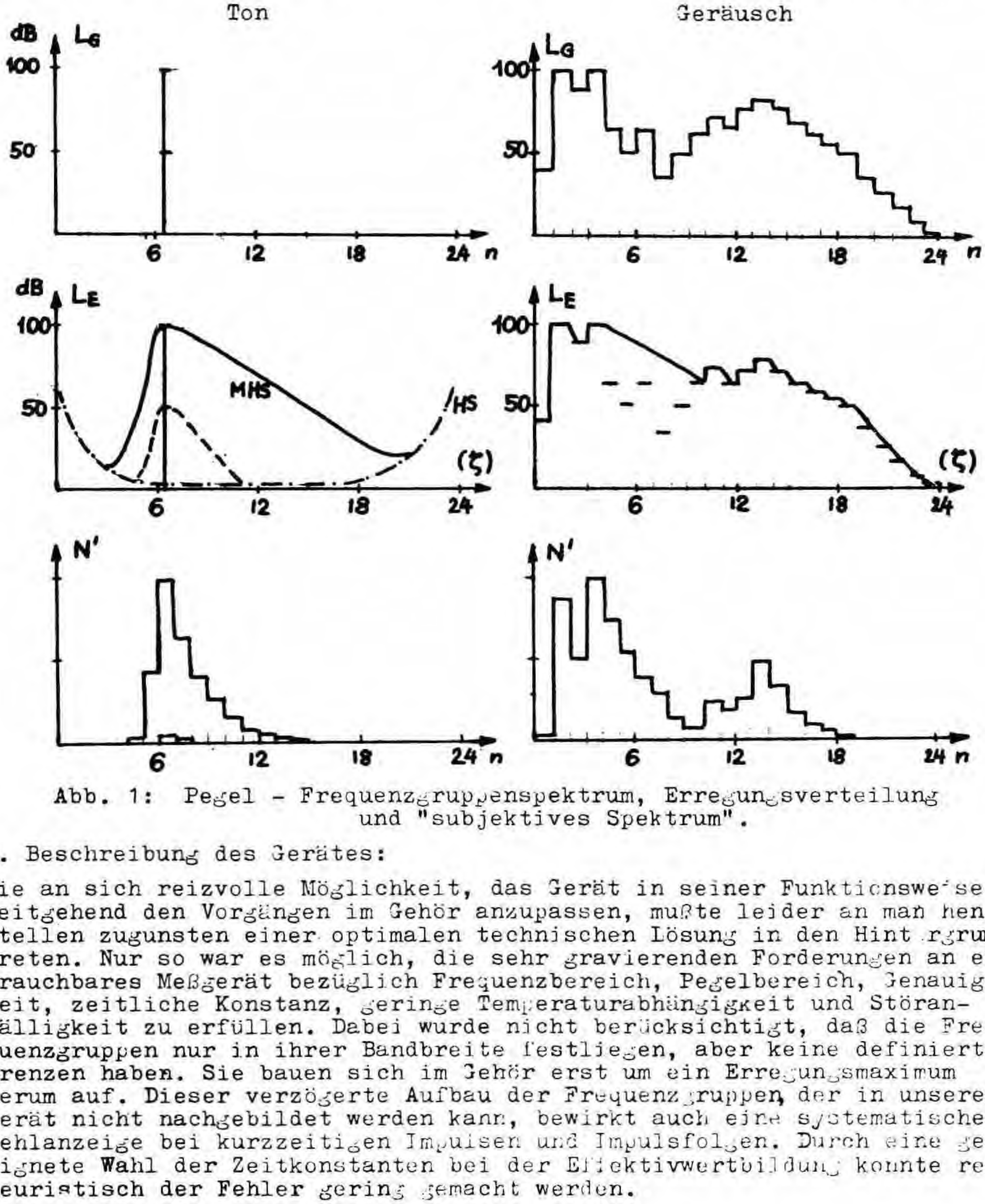

Abb. 1: Pegel - Frequenzgruppenspektrum, Erregungsverteilung und "subjektives Spektrum".

2. Beschreibung des Gerätes:

Die an sich reizvolle Möglichkeit, das Gerät in seiner Funktionsweise weitgehend den Vorgängen im Gehör anzupassen, mußte leider an manchen Stellen zugunsten einer optimalen technischen Lösung in den Hintergrund treten. Nur so war es möglich, die sehr gravierenden Forderungen an ein brauchbares Meßgerät bezüglich Frequenzbereich, Pegelbereich, Genauigkeit, zeitliche Konstanz, geringe Temperaturabhängigkeit und Störanfälligkeit zu erfüllen. Dabei wurde nicht berücksichtigt, daß die Frequenzgruppen nur in ihrer Bandbreite festliegen, aber keine definierten Grenzen haben. Sie bauen sich im Gehör erst um ein Erregungsmaximum herum auf. Dieser verzögerte Aufbau der Frequenzgruppen, der in unserem Gerät nicht nachgebildet werden kann, bewirkt auch eine systematische Fehlanzeige bei kurzzeitigen Impulsen und Impulsfolgen. Durch eine geeignete Wahl der Zeitkonstanten bei der Effektivwertbildung konnte rein heuristisch der Fehler gering gemacht werden.

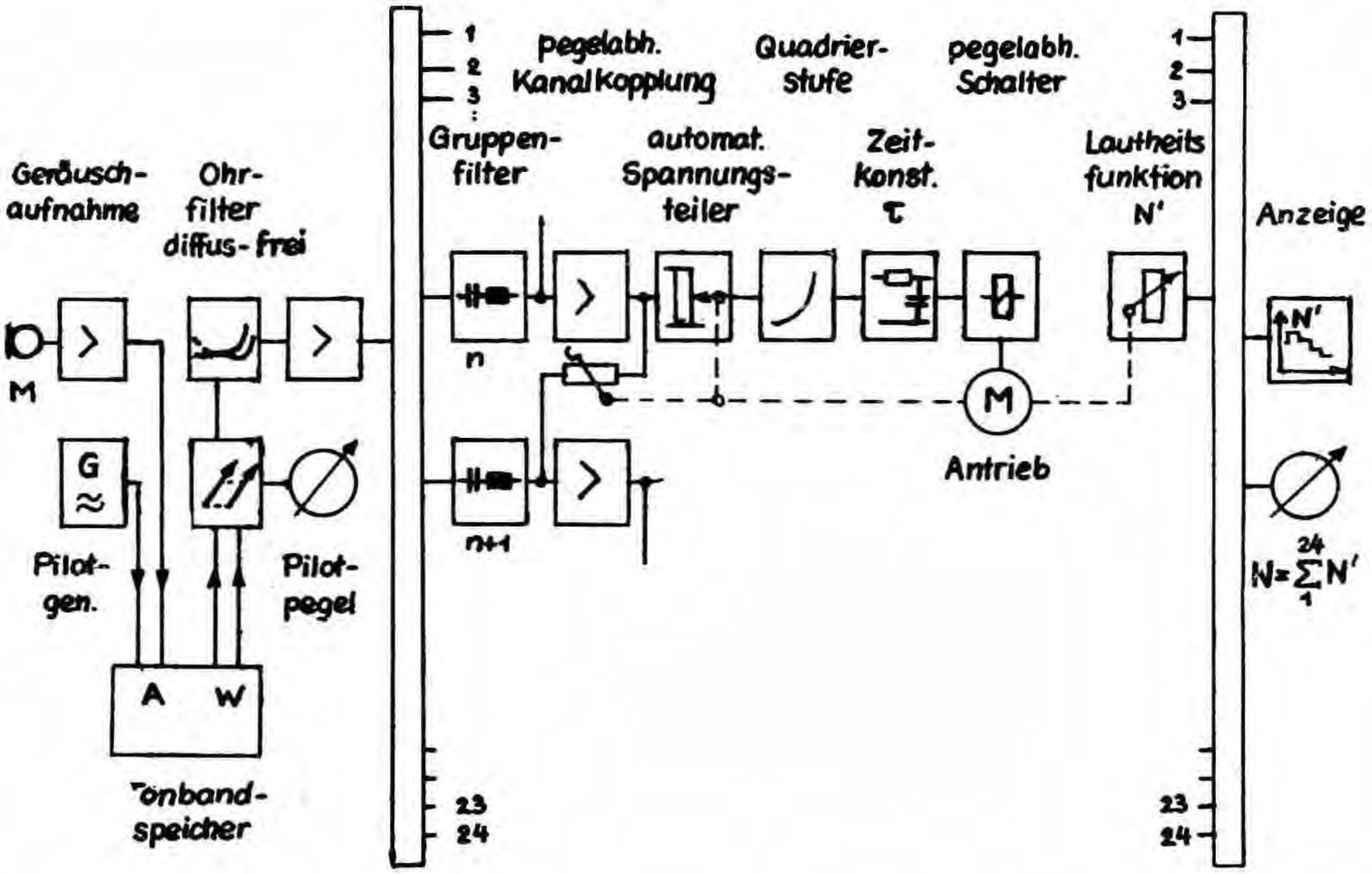

Abb. 2: Blockschaltbild

Der Meßbereich des Gerätes liegt zwischen 40 phon und 110 phon. Messungen außerhalb dieses Bereiches sind mit verminderter - spektrumsabhängiger - Genauigkeit möglich. Da die subjektive Lautstärkemessung erheblichen Streuungen unterliegt, ist eine Toleranzangabe des Gerätes nur gegenüber einem vorgeschriebenen Sollwert möglich. Als Toleranz wurde für den einzelnen Kanal ± 2,0 dB angestrebt, der Gesamtfehler wird wegen der teilweisen Kompensation der Fehler bei der Addition der Meßwerte sicherlich geringer.
Wegen der Richtcharakteristik des Gehörs ist die empfundene Lautstärke grundsätzlich auch von der Schallfeldform und der Kopfhaltung des Hörers abhängig. Die Schallfeldform wird im Gerät durch eine umschaltbare Frequenzgangentzerrung für zwei extreme Fälle, das freie und das diffuse Schallfeld berücksichtigt. Da eine Festlegung der Kopfhaltung des Hörers bei einem beliebigen Schallfeld nicht möglich ist, wurde der eindeutige Zusammenhang zwischen Lautstärke und Meßort durch eine hinreichende Kugelcharakteristik des Aufnahmemikrofons (12 mm$^{\varnothing}$) erzwungen. Das Geräusch wird an der Meßstelle auf Tonband mit 19,5 cm/sec aufgenommen, und dann zur Auswertung direkt, oder bei kurzzeitigen Geräuschen als endlose Schleife, im Gerät analysiert. Für die Spektrumsaufzeichnung ist der volle Dynamikbereich der Tonbandmaschine von 50 dB erforderlich, die Aussteuerung muß deshalb dem Geräuschpegel angepaßt werden. Ein auf den zweiten Kanal der Stereo-Tonbandmaschine gegebener Pilotton fester Frequenz und definierten Pegels, gestattet bei der Wiedergabe eine genaue Einregelung des originalen Geräuschpegels.

Das Geräusch wird nun durch 24 parallel-geschaltete Bandpässe in die Frequenzgruppen zerlegt. Die Bandpässe sind als 2-gliedrige Grundketten ausgelegt. Die Betriebsdämpfung beträgt in der Mitte der benachbarten Frequenzgruppe etwa 40 dB, eine Frequenzgruppe von der Grenzfrequenz entfernt mehr als 60 dB. Diese Filtersteilheit reicht aus, um die steile Flanke des Erregungsabfalls im Gehör zu tiefen Frequenzen nachzubilden.
Der ursprüngliche Plan, die Filter - ähnlich der Wirkungsweise des Innenohres - als Kettenleiter auszubauen und auch den flachen Abfall der Erregungsflanke zu hohen Frequenzen durch die sich überlappenden Filterflanken abzubilden, wurde aufgegeben. Ein pegelabhängiges Umschalten der Flankensteilheit der Filter wäre nur mit großen Aufwand möglich gewesen.
In unserem Gerät wird die Erregungsverteilung $L_E(\zeta)$ durch Koppelglieder zwischen den einzelnen Kanälen als ein $L_E(n)$ simuliert. Die Kopplung wird vom maximalen Gruppenpegel in 3 Stufen gesteuert, die je einer mittleren Steilheit des Erregungsabfalls für einen 30 dB umfassenden Bereich entsprechen.
Der Spannungspegel in den einzelnen Kanälen kann - auf absoluten Schalldruckpegel umgerechnet - 20 dB bis 110 dB betragen. Für diesen großen Pegelbereich ist eine Effektivwertbildung und anschließende Umwandlung in einen Lautheitswert durch nichtlineare Kennlinien vollelektronisch (d.h. ohne Bereichsumschaltung) mit der für ein Meßgerät benötigten Genauigkeit und Konstanz nicht durchführbar. Es wurde deshalb das Prinzip eines selbstabgleichenden Spannungskompensators verwendet. Der Abgleich erfolgt in 3 Stufen zu je 30 dB und einer Feinabstufung 30 x 1 dB durch eine Drehwähler, der als nichtlinearer Spannungsteiler beschaltet, automatisch bis zum Abgleich durchläuft.
Die Ausgangsspannung des Drehwählers wird zur Effektivwertbildung quadriert, über eine Zeitkonstante τ integriert und als Vergleichsnormal einem Schmitt-Trigger zugeführt. Erreicht nun die vom Drehwähler abgegriffene Spannung den vorgesehenen Effektivwert, dann spricht der Schmitt-Trigger an und schaltet den Wähler über ein Relais sofort ab. Die Stellung des Drehwählers nach der Abschaltung ist also eine eindeutige Funktion des Eingangspegels in dem betreffenden Kanal.
Aus der notwendigen Toleranz für ein sicheres Ansprechen des Triggers (10 V ± 0,3 V), einer durch das dynamische Verhalten bei Impulsfolgen vorgeschriebenen Zeitkonstanten von etwa 50 ms und einem geforderten Tastverhältnis 5:1 für die Effektivwertbildung ergibt sich die notwendige Ausgangsspitzenspannung der Quadrierstufe zu 100 V. Die Anforderungen an die Kennlinie brauchen nicht sehr streng sein, da der Effektivwert bei dieser Anordnung nur für einen bestimmten Spannungswert, bei dem die Abschaltung erfolgt, hinreichend genau sein muß. Eine befriedigende Lösung fand sich durch Verwenden einer E 90 CC in Gegentaktschaltung, deren Kennlinie bei geeigneten Betriebsdaten einen guten quadratischen Verlauf der Ausgangsspannung gewährleistet. Durch besondere Maßnahmen mußte noch ein Übersteuern der Quadrierstufe verhindert werden, da bei der Messung die Eingangsspannung von einem Maximalwert bis zum Abgleich heruntergeregelt werden muß.
Die Teillautheit N', die dem abgeglichenen Pegel in dem jeweiligen Kanal entspricht, wird von den mechanisch gekoppelten weiteren Dreharmen unseres Wählers als Widerstandswert abgegriffen. Die Pegelstufung erfolgt in 1 dB-Werten, das bedeutet für N' 0,5 dB-Stufen, also konstanten relativen Fehler von N' im gesamten Pegelbereich. Nach Beendung der Messung werden die N'-Werte der einzelnen Kanäle der Reihe nach einem Gleichspannungsschreiber zugeführt und von ihm automatisch als "subjektives Spektrum" aufgezeichnet. Die Gesamtlautheit N in sone als Summe der 24 N'-Werte wird unmittelbar angezeigt, der zugehörige Lautstärkewert kann grafisch abgelesen werden.

O31

FOURTH INTERNATIONAL CONGRESS ON ACOUSTICS
COPENHAGEN 21.-28. AUGUST 1962

EXPERIMENTS ON THE PROPAGATION OF SOUND IN FOAMS

G.A. Vignaux
Physics Department, Imperial College, London.

The propagation of sound in foams of very low density has been studied experimentally, (a) to check the applicability of a theoretical formula for the velocity, and (b) to investigate the variation of attenuation with frequency and to find the effect of bubble size and foam structure.

In order to obtain meaningful measurements it is desirable that the propagating medium should have uniform properties which do not change with time. In the present case mono-disperse foams (i.e. foams with bubbles of one size) will be uniform except for the effects of drainage and bubble collapse. These effects may be minimised by designing the foam-making apparatus to continuously produce a mono-disperse foam at a suitable fast rate.

The attenuation of sound waves in these foams was shown by preliminary measurements to be sufficiently high that within a working tube of moderate dimensions no standing-wave system could be set up. This allowed the use of a sealed probe tube connected to a condenser microphone which in turn fed into an amplitude and phase measuring system.

Fig. 1 shows in diagrammatic form the principle of the apparatus. Foam was produced by bubbling air from the jet, J, through the solution, S. This consisted of 5% of commercial detergent dissolved in distilled water. The bubble size was determined by the jet aperture and inlet air pressure, the latter being maintained at a constant value by a simple air bubbler. The foam passed to the measuring tube, T, closed at its upper end by a foam-tight gland Q which also acted as a low reflection termination. The lower end of T was closed by the sound source diaphragm, D, driven by a vibrator, V. To reduce the amplitude of the vibration transmitted from the base of the equipment to the tube, T, the latter was supported in a resilient mount, R. Since air bubbles of a constant volume can only be produced with a constant head of solution above J the foam leaving T was directed into the solution reservoir where it collapsed to liquid. Simultaneously a motor driven gear pump returned the solution to S to replace that lost in foam generation.

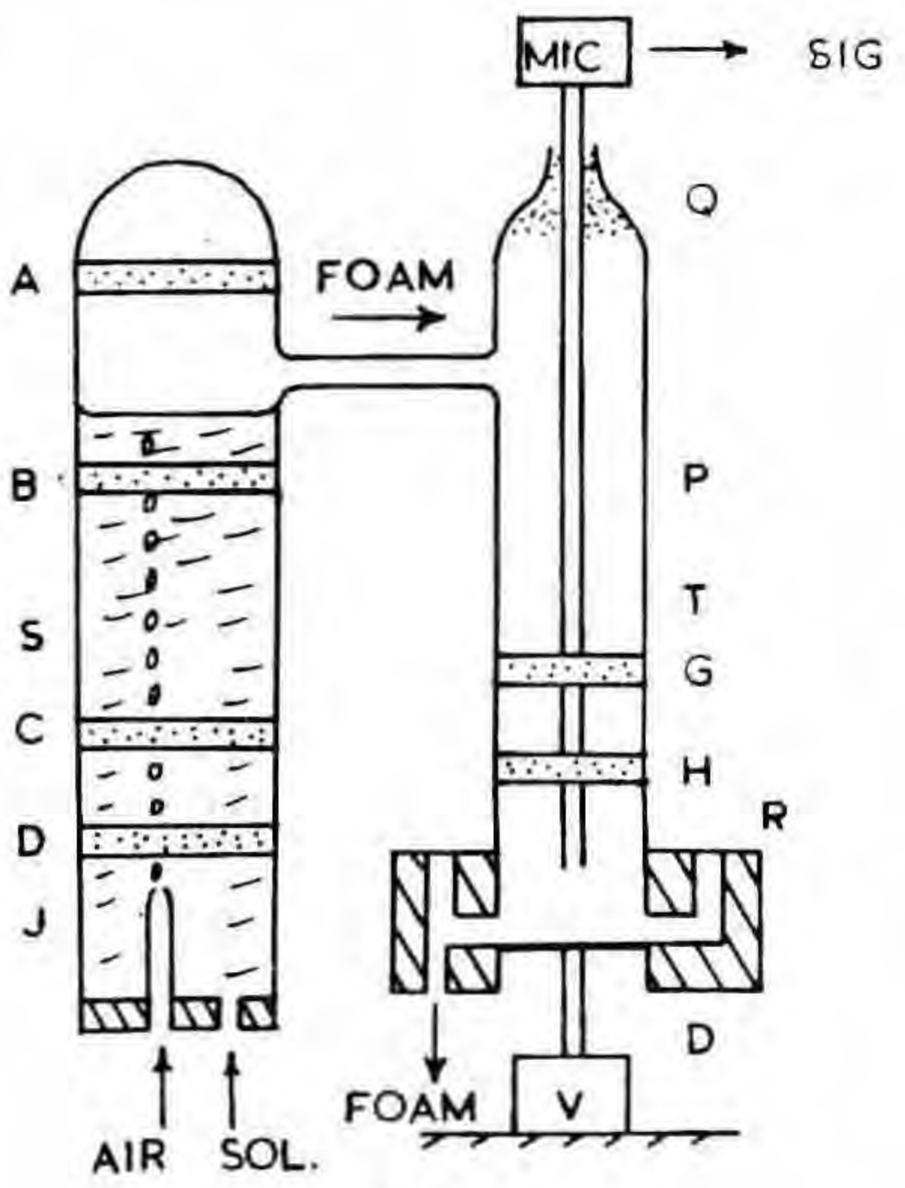

FIG 1

The motor was controlled by a servo system responding to the change in the electrical resistance between platinum electrodes A and B in contact with the liquid and foam. The foam density was calculated by finding the electrical conductivity ratio of foam to solution, from the ratio of the resistance between similar electrodes C and D in the solution to that between another pair, G and H, in the foam. A relation between foam density and foam conductivity was found to exist by Clark[1] and the appropriate relationship for the experimental system used by the author was found empirically in a calibration experiment.

The foam bubble volume was found from the rate of flow to J and the frequency of bubble formation. The rate was measured with a simple pressure-differential flow meter and the latter by allowing the bubble stream to interrupt a light beam passing through the solution above J to a phototransistor the output of which was fed to an electronic counter. The latter was also used to check the frequency of the vibrator.

Bubbles with volumes between 2 and 12 microlitre could be produced. For any given setting of the controlling devices, the bubble volume remained constant to within $\pm$ 10% over a period of several hours and within $\pm$ 1% over a number of minutes more than sufficient to explore the sound field in the measurement tube. Photographic observation showed that the variation in size between bubbles was negligible. The servo-control system was effective for the density range 0.5 to 0.003 gm. per millilitre and maintained the density constant to within $\pm$ 4% in the worst case.

The detecting system gave the amplitude and phase of the microphone signal relative to the input to the vibrator for any probe position. A plot of relative phase against distance moved by the probe gave the phase velocity and similarly a plot of amplitude against distance gave the attenuation per unit distance for the foam.

Theory predicts that for a mixture of air and water at s.t.p. the velocity of a compressional wave of very low frequency should vary with the expansion ratio E (= density of liquid/density of foam) as shown by the continuous line in Fig. 2. Using the values of the phase velocity found for low frequencies and them extrapolating to zero frequency yielded measured zero-frequency velocity values as shown by the plotted points. These are seen to be higher than the theoretical values but they fall substantially along a parallel curve.

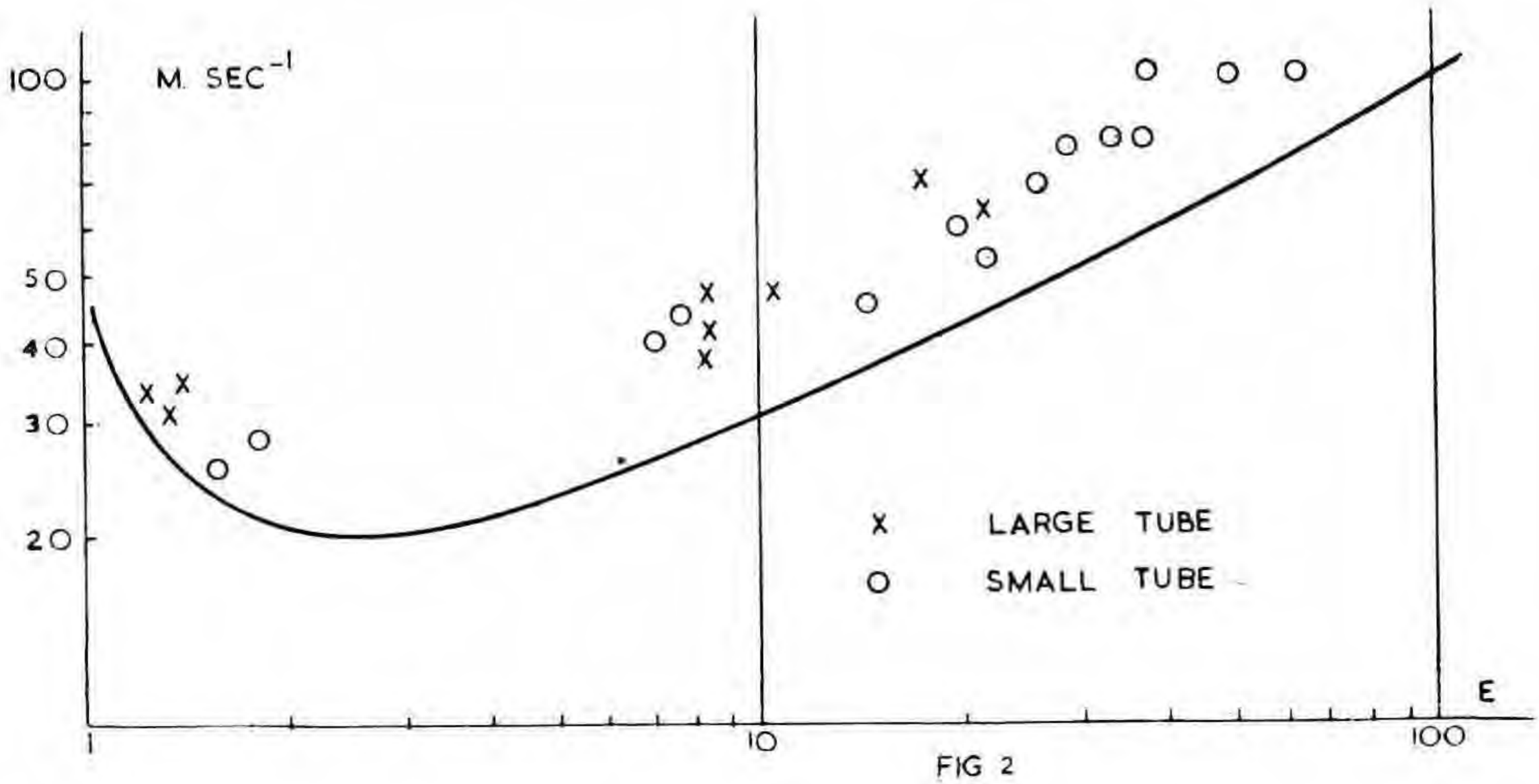

FIG 2

At higher frequency the phase velocity was found to vary in a discontinuous fashion at a succession of frequencies while the attenuation per unit length rose to quite high values at these frequencies. This is shown in Fig. 3. The frequencies for maximum attenuation varied with both measuring tube diameters and expansion ratio for the foam but were very much lower than the frequencies at which the normal cylindrical modes of vibration would be expected with a compressional wave.

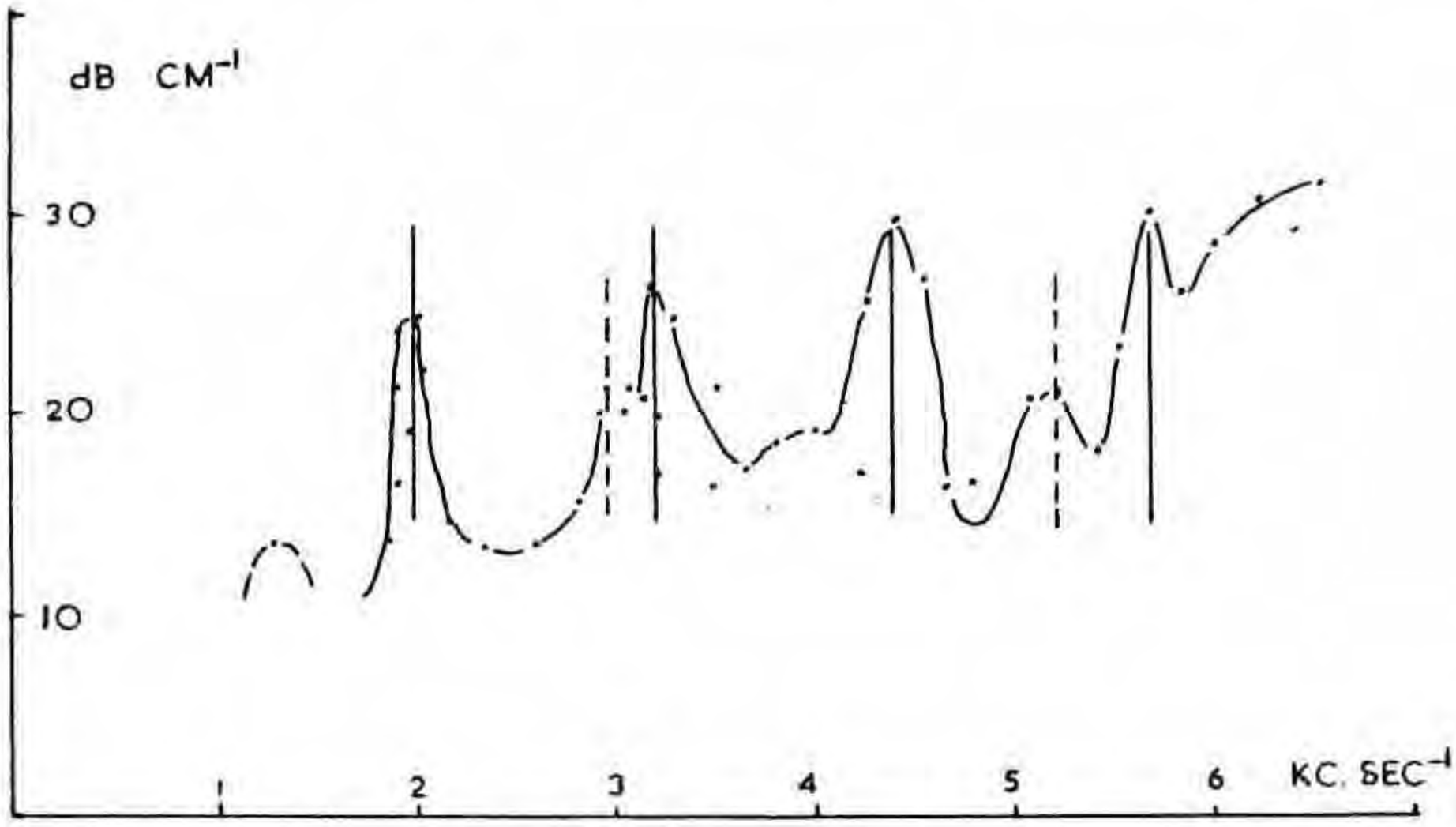

FIG 3

If a shear modulus is assumed for the foam then the behaviour and frequency of the modes can be predicted. From the experimental data an estimate of the shear modulus of the foams was made and from this a corrected "zero-frequency" compressional wave velocity could be calculated. When this was done the observed points plotted in Fig. 2, were found to be much closer to the values predicted by the theoretical relationship which is represented by the continuous line of that figure.

References

1. Clark, N.O. Trans. Farad. Soc., 44, 13 (1948)
2. Wood, A.B. A Textbook of Sound (1955) p.361.

P31

FOURTH INTERNATIONAL CONGRESS ON ACOUSTICS
COPENHAGEN 21.-28. AUGUST 1962

Mechanical Internal Energy Losses at Audio Frequencies in High Polymer Solids related to Cross Link Density.

P. Lord

E.R. Pithey

High polymer solids are often used in conjunction with piezo-electric transducers to control their mechanical and hence electrical behaviour, more specifically to damp out unwanted resonances. The authors have attempted to examine some of the physico-mechanical properties of certain high polymers with a view to devising a technique which would prove suitable as a routine quality control and which would act as a guide to the production of materials with tailor made properties.

Since damping seemed to be the parameter of greatest interest, it was presumed that a measure of the mechanical internal energy losses would be of value. This idea was encouraged by the fact that certain P.V.C. blends, which were known to give satisfactory performance in practice, were found to have a storage modulus and mechanical internal energy losses nearly independent of temperature in the range of interest, i.e. 15 °C to 35° C. (See Figure 1).

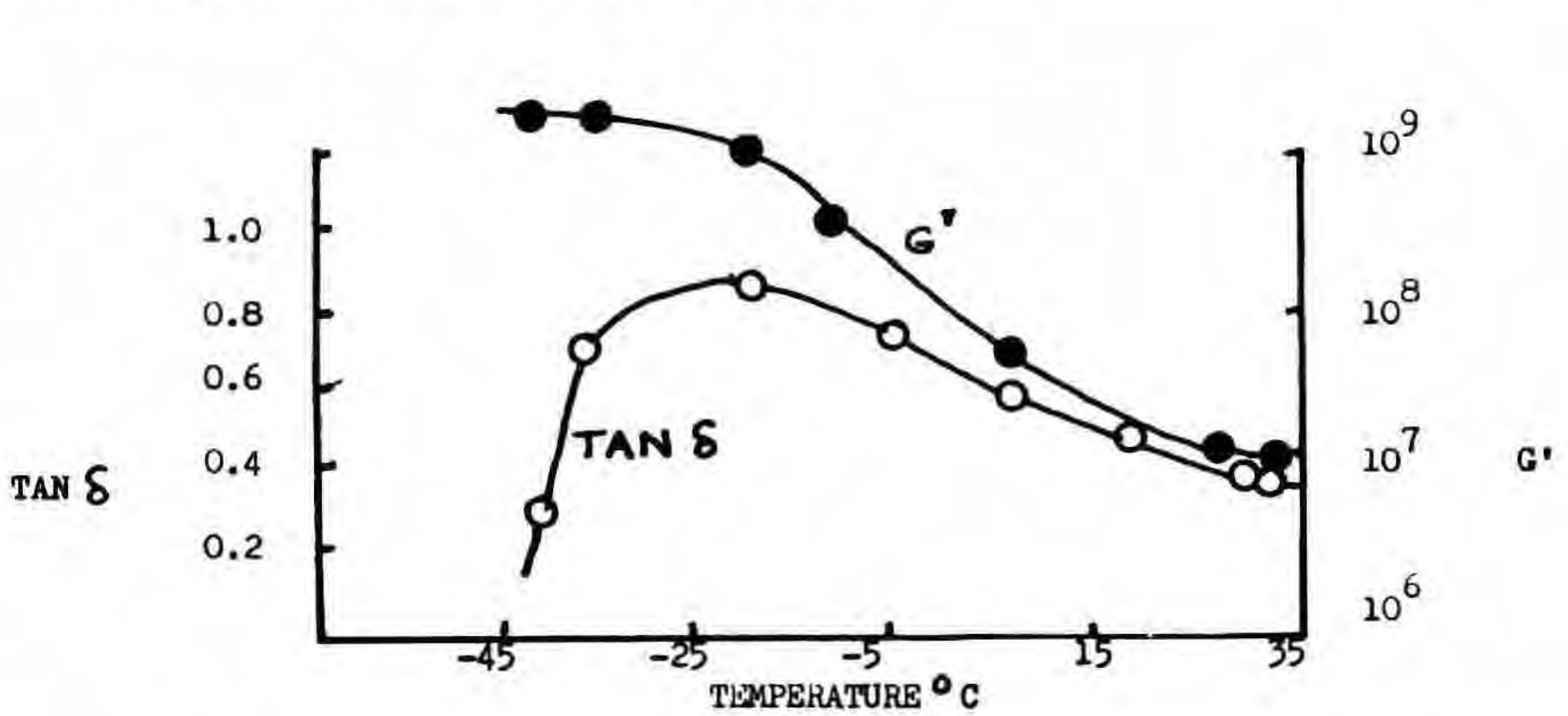

Figure 1.

An examination of certain other blends of polymers showed that unsatisfactory performance in certain climatic conditions were due to the fact that the polymer used suffered a sharp transition in mechanical properties in the temperature range covered.

It has been shown (1) that plasticizers and polymer blends can be used to displace the transition region on the temperature scale. The work reported here is an investigation into the effect of variations in cross link density on the mechanical properties of chlorobutyl.

Many piezo-electric transducers are vibrated in torsion so it was decided that the measurement would be more meaningful if the vibrations applied to the polymer were torsional.

The instrument developed to determine the mechanical internal energy losses over a wide range of frequency and temperature is described in detail elsewhere.[2] Nevertheless it will probably assist if the mode of operation is briefly outlined here.

The specimen, which is in the form of a cylinder, approximately 1 cm. long and 0.2 cm. diameter, is clamped at its lower end. The upper end is attached to a coil situated in an intense magnetic field and through which is passed an alternating current so that the specimen is sinusoidally stressed in torsion. The motion is detected by the capacitance changes which take place between three plates fixed in space and three radial plates attached to the coil former. The voltage output from a capacitance change meter and the voltage developed across a 10 ohm resistor in series with the coil are fed to a phase angle meter. The angle δ thus obtained represents the phase lag between applied stress and developed strain. Therefore $\tan\delta$ is a measure of the mechanical internal energy loss in the specimen. The whole of the mechanical assembly is surrounded by a vacuum system which enables the temperature to be accurately controlled.[3]

The polymer used for this investigation, although of no practical interest in the present context, was chosen because of the relatively simple systems involved in producing cross-linking. Since the chain back-bone is without large side-groups and the polymer possesses very little crystallinity, the effects of light cross-linking on the transition region should be more easily discernable.

Four specimens of different degrees of cross-linking were produced from a master-batch by vulcanization. The original polymer possesses approximately 2% unsaturation so that the specimen of highest cross-link density probably contains half this number of junction points.

The relationship between $\tan\delta$ and temperature for the four specimens is expressed graphically in Figure 3. These measurements were taken at 200 c/s which is representative of the audio-frequency range. The graph shows that the maximum value attained by $\tan\delta$ increases with decrease in cross-link density. This is to be expected since the production of cross-links restricts the mobility of the chains.

Figure 2 shows the variation in the in-phase rigidity modulus G' with temperature at 200 c/s. It appears that small changes in cross-link density have but little influence on G'.

These results lead one to suppose that cross-link density is worth considering as a device for controlling the damping of a polymer without adversely influencing the modulus.

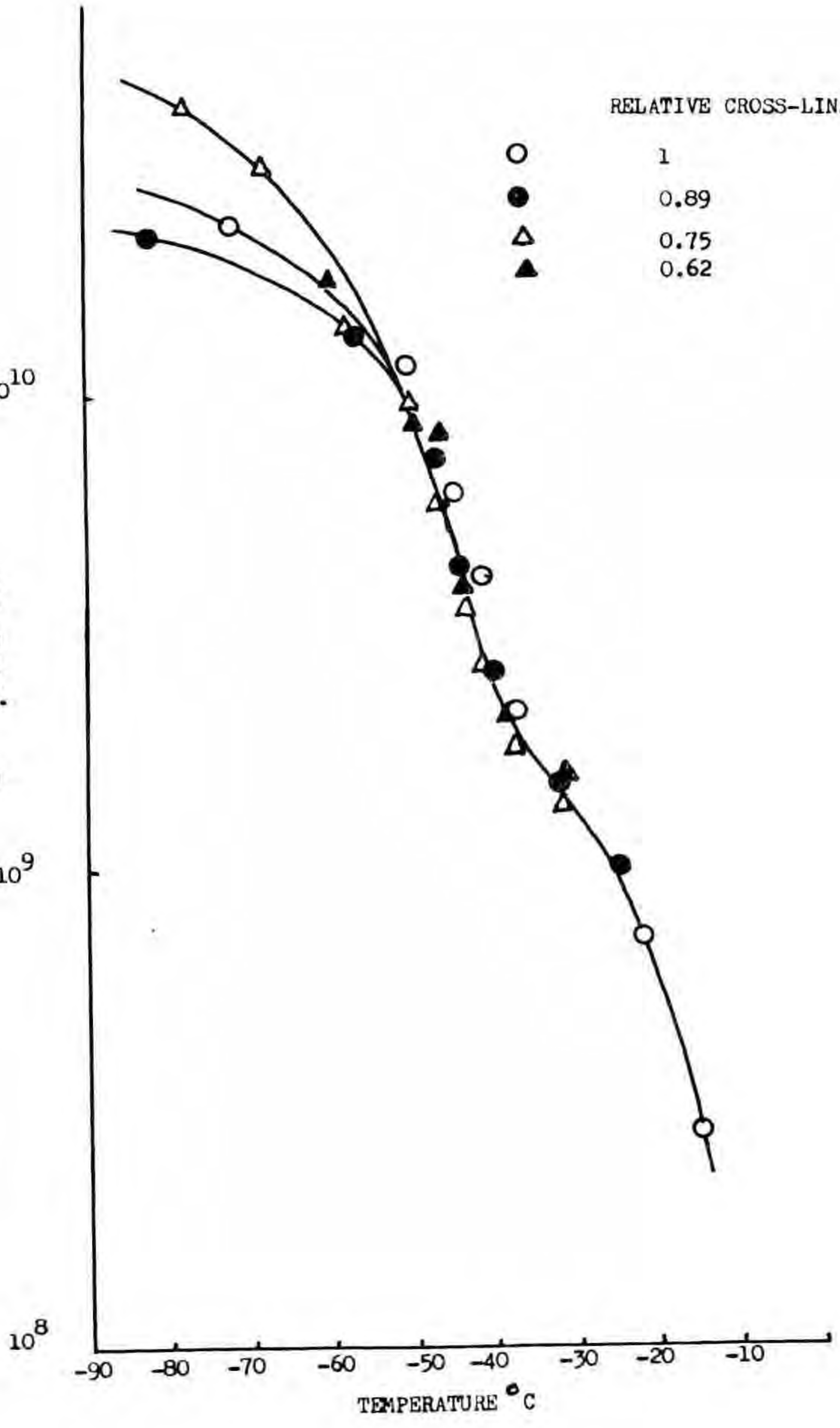
RELATIVE CROSS-LINK DENSITY
1
0.89
0.75
0.62
G' DYNE CM^{-2}
10^{10}
10^{9}
10^{8}
-90
-80
-70
-60
-50
-40
-30
-20
-10
TEMPERATURE °C

Figure 2

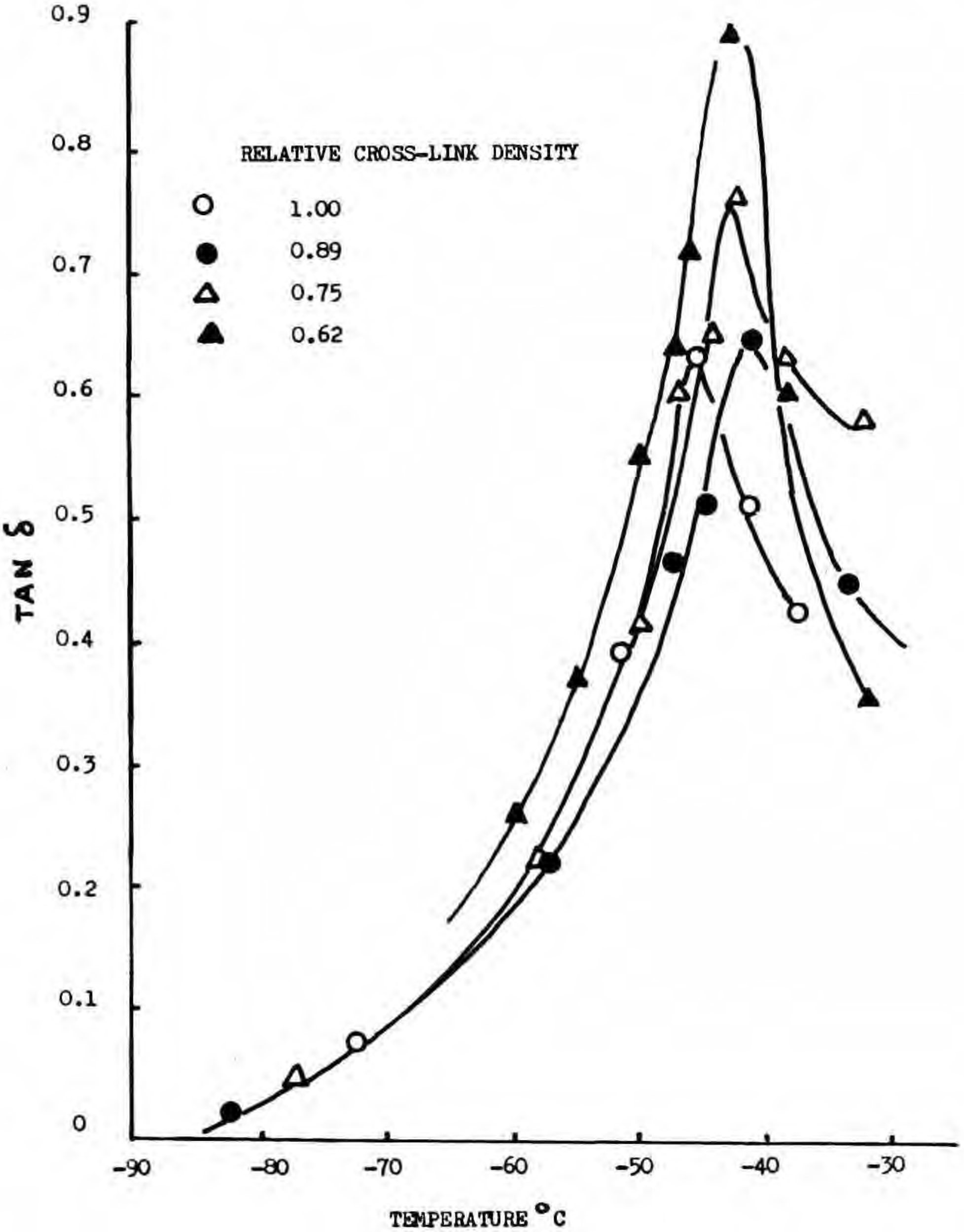

Figure 3

References

(1) Ferry, J.D., Viscoelastic properties of polymers. Wiley, 1961.

(2) Lord, P., Pithey, E.R., Wetton, R.E., Laboratory practice 10 884 (1961).

(3) Robinson, D.W., Oakes, W.J., J.Poly. Sci. 14 505 (1954).

G32

FOURTH INTERNATIONAL CONGRESS ON ACOUSTICS
COPENHAGEN 21.-28. AUGUST 1962

Speech Parameters extracted by processing of S.S.B.-clipping

Keiji Hiramatsu
Tokyo Electrical Engineering College
Kanda Nishikicho, Chiyoda-ku, Tokyo
Japan

Summary —— New speech parameters which was extracted from the processing of S.S.B.-clipping are discussed, one is for the recognition of vowels, consonants and spoken digit numbers.

The other contenuous signals extracted from each formant region are used for speech band compression system (Formac).

1. Introduction

If we take s (t) for the message function and σ (t) for the harmonic conjugate function, then the frequency shifted signal by $\omega_0/2\pi$ is

$$f_2(t) = \sqrt{s(t)^2 + \sigma(t)^2}\ \cos\left[\omega_0 t + \tan^{-1}\frac{\sigma(t)}{s(t)}\right]$$

$$= \alpha(t)\cos\left[\omega_0 t + \phi(t)\right] \qquad (1)$$

Consequently, both the envelope and the phase function involve the message information s(t)

As the time derivative of the phase function is angular frequency, we will get in general, instantaneous frequency: $\frac{1}{2\pi}\frac{d}{dt}\left[\omega_0 t + \phi(t)\right]$

Therefore the clipping wave of $f_d(t)$, if we take only primary spectrum (that which harmonics removed), we will find the frequency modulated wave with such frequency as:

$$f_s(t) = \frac{1}{2\pi}\frac{d}{dt}\phi(t) \qquad (2)$$

Consequently we will obtain such a signal almost equal to $f_s(t)$ by frequency discrimination.

We can imagine, according to eq(1), that there are some relation between $f_s(t)$, and the envelope function. We will show some actual wave-forms in slides. Consequently, if the envelopes of a signal have complicated variation, the frequency discriminated wave-form of the signal is also complicated, but if the envelopes of a sginal have simpler variation, the frequency discriminated wave-form of the signal is comparatively simple. Using for an example as the complex wave with a simple spectrum distribution like a certain formant region of a vowel, it has the envelope variation in its pitch period, therefore we will find that it is possible to obtain a pitch signal as the frequency discriminated signal of the instantaneous frequency of the complex wave.

Tihs principle is very useful in the pitch extraction.[1)]

2. Speech band compression

We have clearly explained in the other paper[2] how we can preserve the intelligibility and naturalness of S.S.B. clipping signal. One of that method is the restoration of the envelope information at the receiving end, and the other is the band division.

The band compression system presented in this paper is such a system that time variation of the instantaneous frequency in S.S.B.-clipping wave is extracted. The principal points for success are two procedures: the band division into formant region and the envelope restoration at the receiving end. As this is the system to compress the formant region, I shall name this system Formac (Formant compression).

We can say that the Formac have the information source having reduced the phase redundancy in speech signal, and is the system having compressed the band of the frequency discriminated signal of the formant region by filtering.

The speech signal is divided into three bands involving each formant region, then its partial band is shifted by frequency $\omega_o/2\pi$. The wave-forms of S.S.B. after clipping are discriminated by a wide-band discriminator (phantastron type).

It is obvious that the discriminated signals involve d. c. components and a. c. components, the former means the position of the formant frequency and the latter means the pitch frequency and its harmonics, and the levels of the a. c. components means the modulation index of the F. M. as delivered in the previous section.

At the receiving end, any carrier frequency is frequency modulated by the transmitted signals which involve d. c. and a. c. components. Thus we can obtain F. M. signal which is equivalent to the S. S. B.-clipping wave at the transmitter, and is added the envelope information at each channel. The demodulation of S. S. B. will carry at each channel, and is added the demodulated audio signal of each channel with the preset level, thus the speech signal with good quality will be obtained at the receiving terminal. Fig. 1 is the block-diagram of the system.

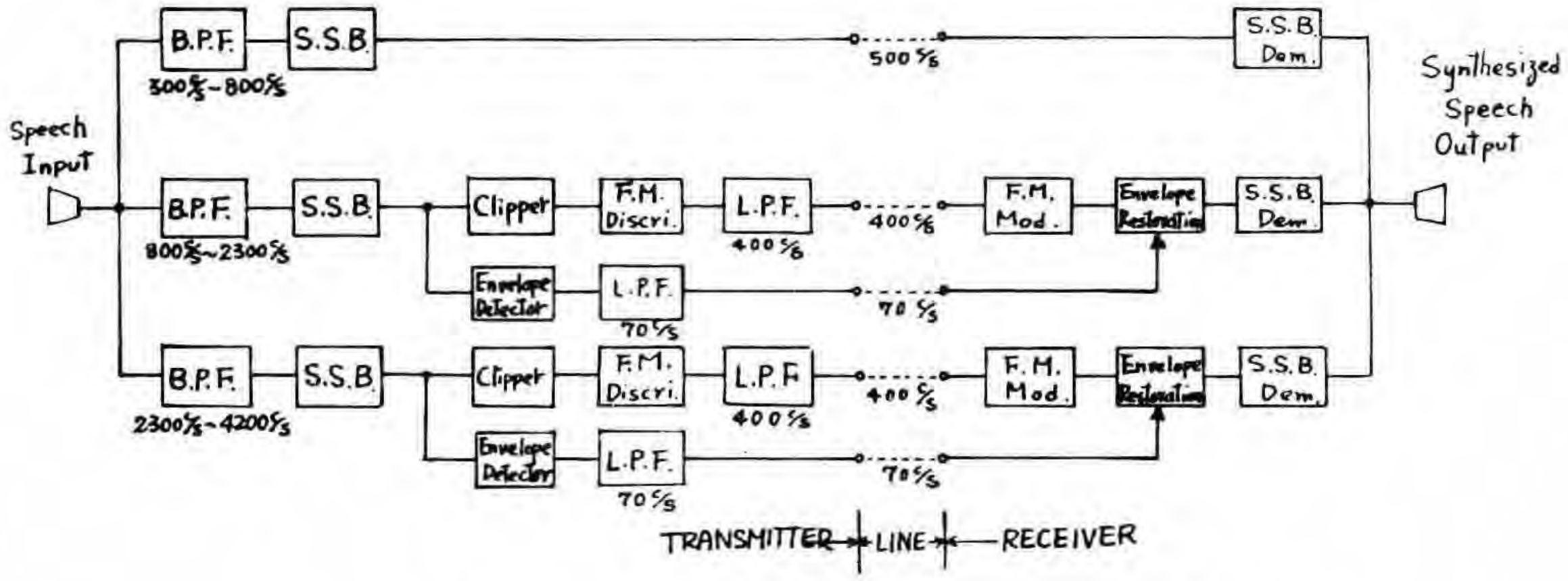

Fig. 1. Block diagram of the band-compression system

In the case of a single channel (300 c/s — 3400 c/s), we can't obtain any band compression system, because of the complicated spectrum pattern of vowels as stated in Cherry and Phillips's paper.[3] The syllable articulation score of this system which convey the imformation of 1200 c/s band width is about 54% and the sentence articulation is over 92%.
The system with band-division in two (300 c/s — 1500 c/s, 1500 c/s —3400 c/s) will not be expected.

In the case of three channels (300 c/s —800 c/s, 800 c/s — 2300 c/s, and 2300 c/s — 4200 c/s) with envelope restoration, rising or consonants parts is very similar with the original, and the preservation of information is very good.

Slides shows the wave-forms of vowels, the original wave-form, the transmitted wave-form, the regenerated wave-form in each channel, the synthesized vowels without envelope restoration and the synthesized signal patterns.

The articulation scores of the 3 channel Formac are shown in Table 1.

The articulation scores of the partial Formac which has the lst channel without processing are shown in Table II.

Table. 1. Articulation of 3 channel Formac

	without envelope restoration	with envelope restoration
Syllable articulation	60.7 %	69.6 %

Table. II. Articulation of Partial Formac

	without envelope restoration	with envelope restoration
Syllable articulation	70.3 %	78.6 %

The transmission band of the partial Formac is 500c/s (without processing 300c/s — 800c/s signal) in the lst channel, 400c/s in the 2nd channel and 400c/s in the 3rd channel, the envelope information being 70c/s in each channel. Then the total compression rate is

$$(500c/s+400c/s \times 2 + 70c/s \times 2)/(4200c/s - 300c/s)$$

$$= \frac{1440}{3900} \fallingdotseq \frac{1}{2.7}$$

We know in these tables that the envelope information is very important, and with envelope restoration about 9% in articulation is raised.

We stated mainly the Formac system which is limited in continuous signal transmission, and not stated the method of transmission and formant coding type Formac.

The channel capacity of the formant coding type Formac will be able to reduce the information rate to about 1200 bits/sec — 600 bits/sec,[4] but in the tranmission of continuous signal it will reduce the band-width as same as the Vocoder signal transmission.
In the Formac system, the receiver will need to have a pitch synchronous method to improve the regenerated voice quality.

Reference;
1) K. Hiramatsu; New Pitch Extractor, J.A.S.J., 16, No.4, p279, 1960.
2) K. Hiramatsu; Zero-crossing Information of I.F. speech wave, Comittee of Information Theory in Japan, 1960-June, or Reserch Report of Tokyo Electrical Engineering College, No.9, 1961-Dec.

3. Recognition of vowels

$F_1 - F_2$ diagram is used ordinary for recognition of vowels and another suitable parameters have not been obtained.

We propose to use the analogue signals which are extracted from the processing of S.S.B.-clipping.

$\phi'(t)$ containes both the d.c. component and the a.c. component, and the d.c. components preserve the information of the formant frequency and the spectrum distribution, a.c. components preserve the information of the relations between two or three formants.

We can easily show $F_1 - F_2$ diagram with analogue signals using the method as stated in the paper of C. Cherry[3] (which was already pointed out by our paper[2]).

Now, we can show d.c.-a.c. level diagram geting involve the further information of vowels; a.c. components as the signal preserving the information of the spectrum distribution in emphasized state or the information of the spectrum distribution of partial bands.

In case of proper emphasis, the feature of the vowels in Japanese are following.

i : d.c. levels are very high (uper 2kc), and a.c. levels are high.

e : d.c. level are high (under 2kc), and a.c. level are high.

a : d.c. level are holded in a region of 800c/s —1kc/s, and a.c. levels are very low.

o : a.c. levels are holded in a region of about 500c/s, and a.c. levels are very poor.

u : d.c. levels are very stable and low.

Fig. 2 shows a male's example of d.c.-a.c. diagram for recognition of Japanese vowels.

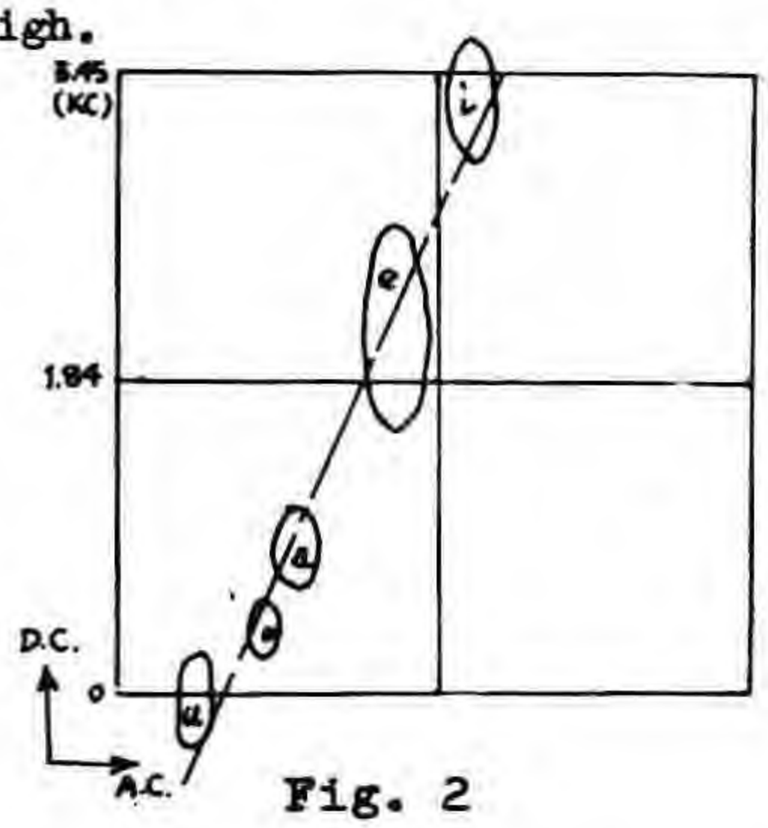

Fig. 2

4. Recognition of consonants

The d.c. components of $\phi'(t)$ in consonants are the signals preserving the informations of the 1st moment of the spectrum, and the a.c. components of $\phi'(t)$ are the signals preserving the informations of the spectrum distribution.

As the a.c. components are consist of the low frequency noise, the moments of the a.c. components of $\phi'(t)$ in consonants can use for the parameters for recognition of consonants.

5. Recognition of digit numbers

The d.c. signals of $\phi'(t)$ in consonants of 7kc bandwidth is useful for recognition as time sequential methods, as a example, [i-tʃ-i] in Japanese (means "one" in English) can be shown in d.c. levels in time sequence, consequently we can transform the digit words to the time sequential of the preset quantized level.

---

3) E.C.Cherry and V.J.Phillips, J.A.S.A, 33, p.1067, 1961-Aug.
4) K.Hiramatsu; The Speech Band Compression Systems, Symposium on the National Conference of E.E., 1960-July.

H32

FOURTH INTERNATIONAL CONGRESS ON ACOUSTICS
COPENHAGEN 21.-28. AUGUST 1962

PRELIMINARY REPORT ON COMPARISON OF BINAURAL AND MONAURAL GROUP HEARING AIDS.

John Boyd: Ontario School for the Deaf, Belleville, Ontario, Canada.

Anthony Jamroz: Northern Electric Co. Ltd., Ottawa, Ontario, Canada.

Recently, interest has grown in the advantages of binaural hearing aids for hearing impaired persons. Several advantages have been noted and reported in various texts and journals. Among these, the most frequently stated are:

1. The ability to gain lateral perception which permits localization of sound sources.
2. The ability to separate foreground from background sounds, which enable the listener to select the sound to which he wishes to attend.
3. The loudness factor which indicates that through the use of binaural hearing, there is a 3 db lower threshold than is found in either ear alone.

Purpose:

The purpose of the present project was to compare three systems of group hearing aids as used by hearing impaired children. The first system is a monaural, single attenuator system, meaning that there is one microphone, one amplifier, and one attenuator which controls the sound level to both ears. The second system is a monaural dual attenuator system, differing from the first in that now there is a separate attenuator for each ear. The third system is binaural in that there is one microphone, one amplifier and one attenuator controlling the input to one ear and a similar input system to the other ear.

Description of Apparatus:

The equipment used for this experiment consisted of the following:

Item	
1	2 - Ampex 601-2 Stereo tape recorders
2	2 - Northern Electric PA-35A amplifiers
3	2 - Northern Electric 633A microphones
4	2 prs. - Sharpe Instruments earphones
5	2 - Ballantyne Model 310A Electronic Voltmeters
6	1 - General Radio Model 1551-B Sound Level Meter
7	1 - Tektronix Model 502 dual beam oscilloscope
8	1 - Bruel & Kjaer Automatic Frequency Response and Spectrum Recorder Model 3320
9	1 - Bruel & Kjaer Model 4131 condenser microphone
10	1 - Bruel & Kjaer Model 4151 Artificial Ear.
11	- Attenuators, switches, and interconnecting cables.

Items 7 to 10 were required to calibrate the equipment used in the experiment.
Figure 1 shows the frequency response of the pair of earphones used by the subjects.

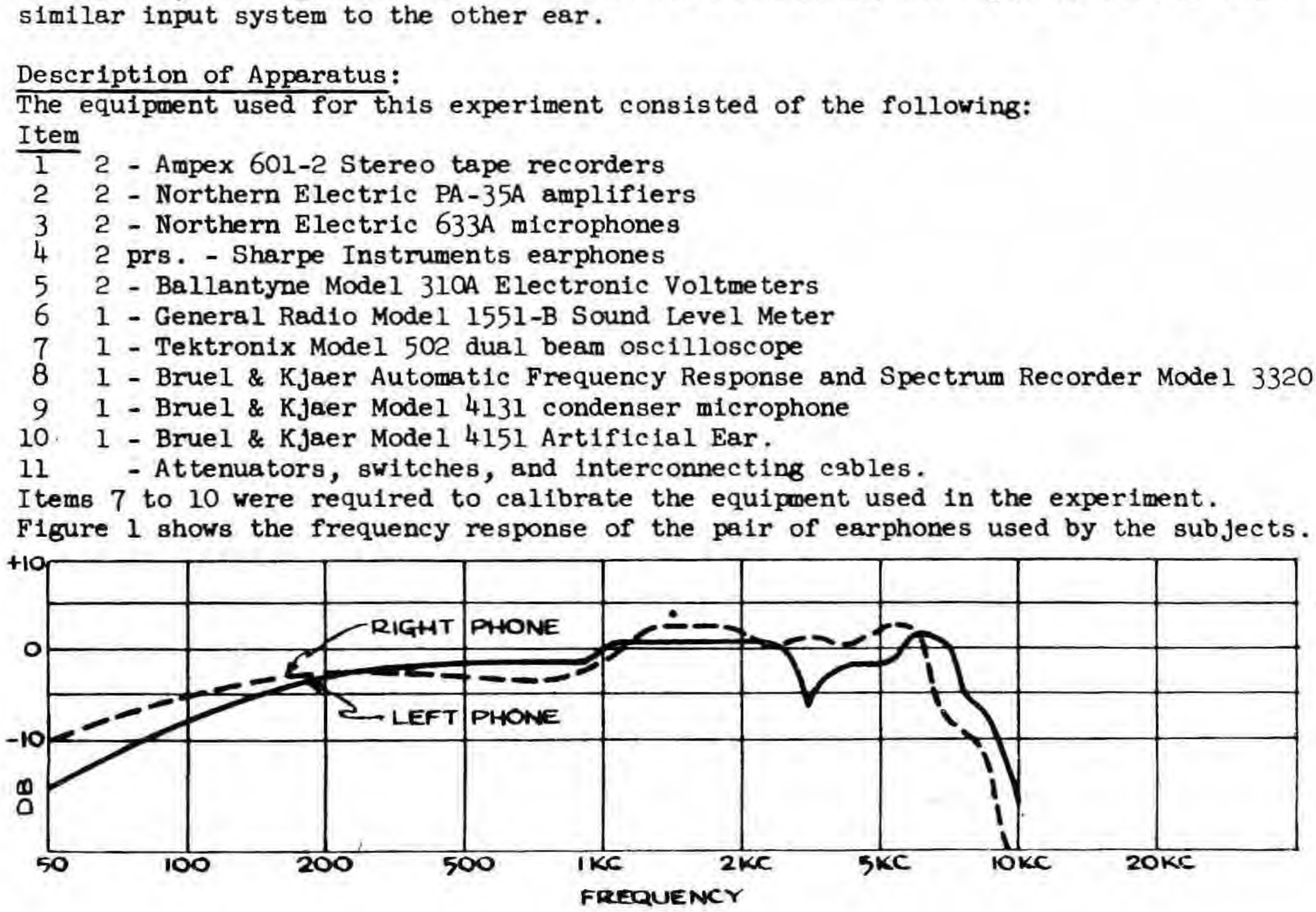

Figure 2 shows the frequency response of the two microphones.

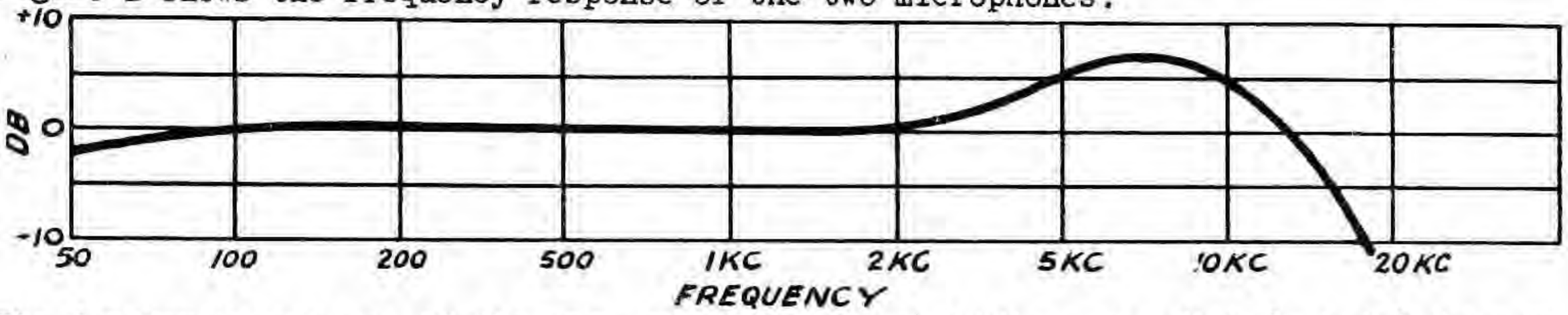

The frequency response of the tape recorders and amplifiers was flat (± 1 db) from 50 to 10,000 c.p.s.

The earphones were calibrated for sensitivity using 1000 cycle test tones. Figure 3 shows that a S.P.L. of 125 db could be obtained before the earphones began to overload.

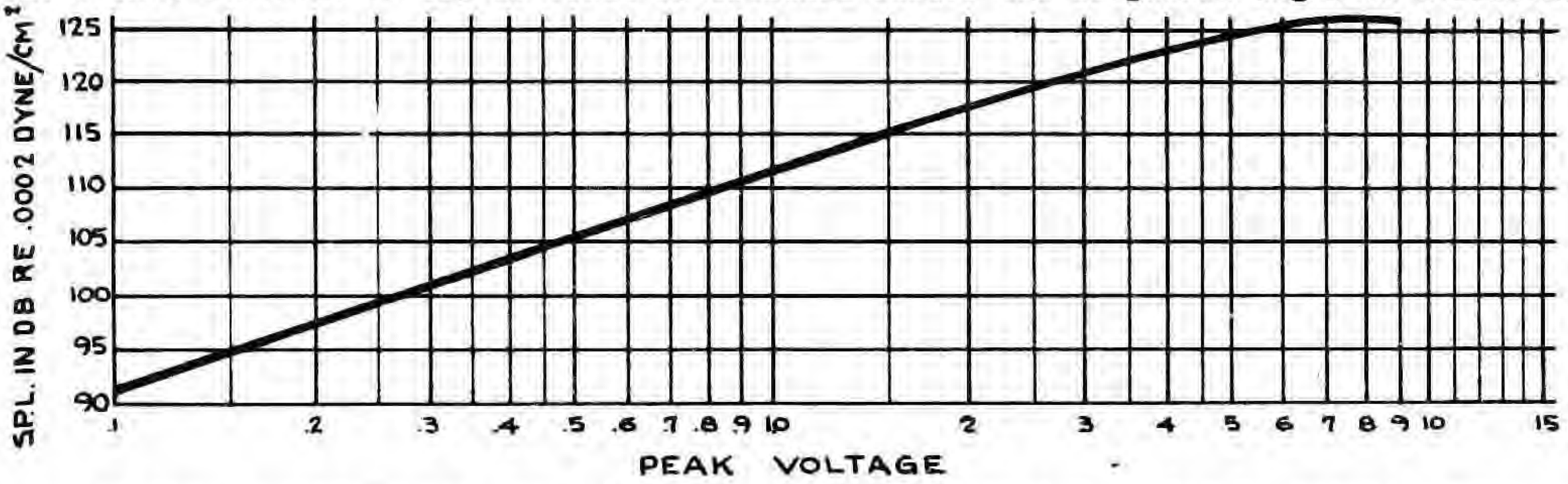

The two tape recorders were used to re-record the material in order to provide three test tapes differing from each other only in the order of presentation of the material.

Method:

Test Materials: A group of 50 words were selected and divided into five lists of ten. The criteria for the selection of these words were that they must be words known by the subject and they must be picturable. The total list must contain all the phonemes of English speech and in the approximate frequency of occurrence. Also, the words must have a companion word which differs only in the phoneme that one is trying to isolate, for example, coat and boat. To enlarge the list to 50 words, several blends were also included. It was decided to put fifteen pictures on a page. These fifteen pictures had the name of the object or action printed under them. Five of the pictures were alternatives for five of the actual test words. This was to reduce guessing and make the test more difficult. A multiple choice test of three words has also been prepared but has not been used as yet.

Each test list was recorded stereophonically on tape by one of the authors. Each word was monitored using the phrase, "Say the word," with a General Radio Company Sound Level Meter, Type 1551-B. The words were said ten seconds apart. A description of what the subject was to do and a practice list of ten words, repeated twice, was used at the beginning so that the subject could set the attenuators. One of the authors explained to the subjects what he was to do so they were not dependent on hearing the instructions. Figure 4 illustrates the three systems used.

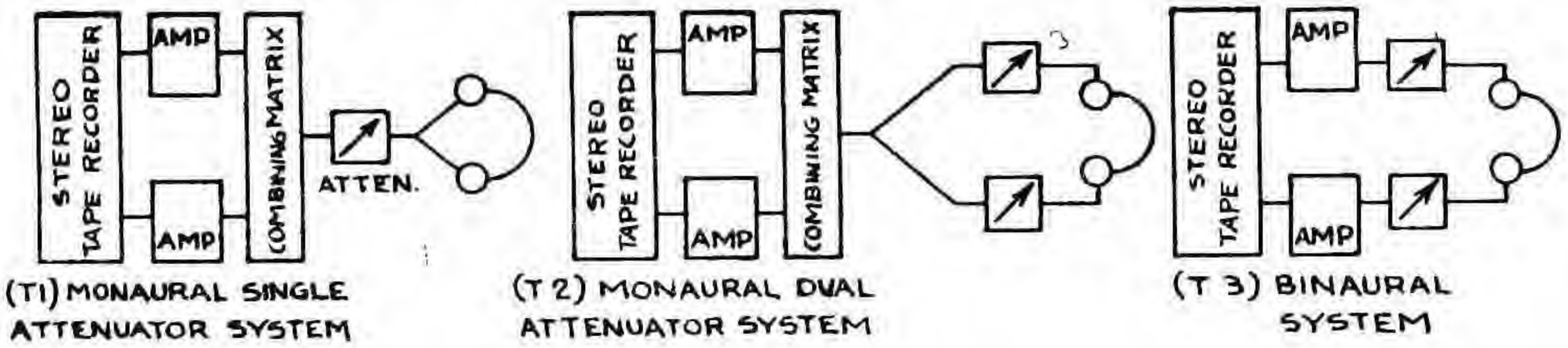

Subjects:
A total test group of 87 children ranging in age from 12 to 19 years were selected. This total group was divided into three sub groups based on the degree of hearing loss as measured by pure tone air conduction audiometry. Subjects were put in Group I if they had a best binaural average (BBA) of between 50 and 74 db, in Group II if the BBA was between 75 and 89 db and in Group III if the BBA loss was 90 db or more.
In some preliminary work using younger children it was decided to use Group II first as this group gave some scores but did not achieve perfect success.
Group II consisted of 24 subjects. These were divided into three sub groups, IIA, IIB, IIC, so that a comparison could be made between sub groups and the order of presentation of test situations could be randomized. The mean hearing loss of each group is shown as 79.6, 79.5 and 79.7 db. Each group also was arranged so that there was, as nearly as possible, an equal distribution of subjects representing academic and vocational pupils. All children had had considerable experience with a monaural, single attenuator system.
This paper is a report of the results obtained from Group II only.

Procedure:
Group IIA were given test 1, (T1) using the monaural one attenuator system first. The words were presented in groups of 10 in list order A,B,C,D,E. Later they were given test 2, (T2) using the monaural two attenuator system and lists in order B,D,C,A,E, and finally test 3, (T3) using the binaural system and the lists in order C,A,D,E,B.
Group IIB were given the tests in the order T2, T3, T1 and Group IIC were given the tests in the order T3, T1, T2.
The subjects were told whether to adjust one or two attenuators and to point to the picture of the word rather than say it. When doing the practice list they were encouraged to set the attenuators where they achieved greatest success as correct responses were acknowledged.

Findings:
It became apparent that there were great differences among individuals and among groups. It also appeared that there was improvement as the tests were repeated even though the lists were randomized and the subjects given no indication of whether they were correct or not during the actual tests.
Out of a possible 400 for each group, the total scores were as follows:

GROUP	T1	T2	T3
IIA	100	111	132
IIB	135	113	138
IIC	75	105	86
Three Group Total	310	329	356

A tendency is noted towards improved scores with the two attenuator and binaural systems; however, when subjected to statistical analysis, this tendency does not appear to be significant.
Some observations that may have a bearing on the results are of interest. It was noted frequently that subjects, even though they had the opportunity to use two attenuators, tended to set the one for their better ear and ignore to some degree any help that they might obtain from the poorer ear. It may well be that there was recruitment in the poorer ear or perhaps stimulation of the poorer ear was more disturbing because of high distortion and so the subject preferred to use only one ear. This was in spite of urging in some cases.
Of the 24 subjects, 7 had less than 5 db difference in hearing loss between the two ears while 17 had 5 db or more difference. Since two tests were presented to each subject in which the sound level for each ear could be controlled independently, there were, respectively, 1/4 and 3/4 opportunities offered for balancing the sound level against hearing loss. Of the 1/4 opportunities offered the equal loss group, equal level to each ear was selected 10 times. Of the 3/4 opportunities offered the unequal loss group, a higher level for the poorer ear was selected only 5 times; equal levels for both ears were selected 13 times; and a higher level for the better ear was

selected 16 times.
Perhaps prolonged training using two attenuator systems would produce significantly different results. At present these subjects have only used a single attenuator system.
Only two cases IIA5 and IIA7 indicated a marked improvement with the use of the binaural system.
Cases which had uniformly low scores of approximately 4 were guessing most of the time although there are indications of repeated recognition of a word such as "moon" with two or more of the systems.
Another observation was that many subjects could not distinguish between car and cow on the practice list. This would indicate that the frequently heard statement that pupils in a school for the deaf hear low frequencies and can perhaps discriminate vowels and dipthongs is questionable. There are other indications of contradiction to this statement and further investigation is necessary.
It was also noted that the pure tone average was not a good indicator of the ability of the subject to understand speech through the ears alone. It is, however, noted that subjects whose losses are less than 80 db on the average do much better than those with losses 80 db and over.
Further research is needed to determine whether:

1. Subjects whose BBA hearing losses are less than 75 db are able to utilize binaural hearing aids to a greater degree than the present group indicates.
2. The degree of difference between the two ears is a significant factor as suggested by Keyes.
3. These subjects can discriminate vowels and consonants and to what degree.
4. The type of hearing loss or audiometric configuration is a factor.
5. There are other contributing factors such as recruitment, central nervous system involvement etc.

		VOC. OR	AGE OF	HEARING LOSS			RESULTS		
SUBJECT	AGE	ACADEMIC	ONSET	RE	LE	BBA	T1	T2	T3
IIA1	18-5	V	birth	78	88	80	4	4	4
IIA2	15-10	A	18 mo.	93	77	77	31	32	33
IIA3	15-9	A	birth	82	93	82	6	9	8
IIA4	18-4	V	1½ yr.	77	95	77	14	14	11
IIA5	17-7	V	2 yr.	83	88	83	9	9	23
IIA6	18-3	A	birth	85	93	85	6	8	7
IIA7	14-3	V	6 mo.	78	78	78	12	13	22
IIA8	15-10	A	3½ yr.	75	98	75	18	22	24
						ΣA 637	100	111	132
						x̄A 79.6	12.5	13.8	16.5
IIB1	18-5	V	birth	80	97	80	7	2	7
IIB2	15-11	A	2 yr.	83	77	77	17	12	15
IIB3	15-4	V	birth	80	87	87	18	15	16
IIB4	18-3	V	2 yr.	75	73	73	17	21	25
IIB5	16-4	A	6 yr.	78	77	75	42	35	42
IIB6	14-11	A	9 mo.	85	92	85	4	7	3
IIB7	16-7	V	birth	82	87	82	8	6	7
IIB8	18-3	A	birth	80	78	77	22	15	23
						ΣB 636	135	113	138
						x̄B 79.5	16.8	14.1	17.3
IIC1	17-7	V	birth	80	95	80	5	7	6
IIC2	17-10	A	unk.	83	82	77	4	4	5
IIC3	15-8	A	birth	83	97	83	4	4	4
IIC4	14-8	V	3 yr.	82	82	78	29	39	32
IIC5	18-3	V	birth	80	77	77	20	21	19
IIC6	18-6	A	birth	95	83	83	2	5	2
IIC7	18-6	V	birth	77	83	77	6	11	5
IIC8	14-9	A	birth	83	93	83	5	14	13
						ΣC 638	75	105	86
						x̄C 79.7	9.3	13.1	10.7
							ΣII 310	329	356
							x̄II 12.9	13.7	14.8

J32

FOURTH INTERNATIONAL CONGRESS ON ACOUSTICS
COPENHAGEN 21.-28. AUGUST 1962

ULTRASONIC CAVITATION MEASUREMENTS BY CHEMICAL METHODS

Alfred Weissler, Air Force Office of Scientific Research
Washington 25, D.C.
(Work done in part at American University, Washington, D.C., with support from Office of Naval Research grant GD-55-62)

Conventional acoustic measurements, such as sound pressure, give erratic results and are not very useful with ultrasound waves in liquids which are intense enough to cause cavitation. However, cavitation is involved in many important uses of ultrasound, including for example the cleaning of small metal parts and the disruption of living cells; the magnitude of the useful effect obtained seems to depend on the amount of cavitation, rather than on the acoustic pressure as measured by a probe.

As a result, efforts are being made to find a convenient procedure for monitoring the cavitation intensity under different conditions, in a device such as an ultrasonic cleaner. Methods based on cavitation noise (1) and sonoluminescence (2) have been suggested, for example. Another principle, which utilizes the amount of sonochemical change produced by cavitation, is the subject of the present paper.

Sonochemical Reactions

It is well known that certain chemical reactions are brought about by ultrasonic cavitation (3, 4) . From among the many possibilities, two such reactions were chosen for study in the present work, on the basis of their simplicity and high sensitivity.

The first of these is the ultrasonic conversion of potassium acid phthalate in dilute solution into a fluorescent product, presumably the 3-hydroxyphthalate. This sonochemical reaction has already been utilized for the quantitative determination of phthalate (5) with a 400 kc focused-beam generator. Experiments have shown that it may also be used for dosimetry of cavitation, inasmuch as it gives a reasonably linear response of fluorescence intensity to successive increments of cavitation, under specified conditions. The fluorescence excitation wavelength was 3150 A, and the emission peak was at 4400 A, as measured in an Aminco-Bowman spectrophotofluorometer.

The second reaction studied was the ultrasonic liberation of chlorine from carbon tetrachloride dissolved in water (6, 7) ; the amount of chlorine liberated is determined by adding ortho-tolidine reagent and measuring the intensity of the resulting yellow color. With this reaction, studies were made of the effects of certain experimental conditions on the cavitation produced in commercial 25-30 kc ultrasonic cleaners from two different American manufacturers. A standardized method was used, as described below.

Details of Method

Two solutions are needed. One is a saturated solution of carbon tetrachloride in water, made by vigorously shaking distilled water with 2 ml. of carbon tetrachloride for each liter of water, and allowing to settle overnight or longer. The second solution, ortho-tolidine reagent, is prepared by dissolving 0.675 g. of ortho-tolidine dihydrochloride in a mixture of 75 ml. of hydrochloric acid and 425 ml. of distilled water. Both solutions should be stored in brown bottles, in order to minimize deterioration.

A simple procedure was evolved for measuring the relative amounts of cavitation. Twenty ml. of carbon tetrachloride solution and 1 ml. of ortho-tolidine reagent were pipetted into a convenient vessel. An ordinary glass test tube serves well, but most of the work to be described was done with a cell made by cementing a 0.002 inch Mylar sheet to the bottom of a length of 1 inch diameter glass tubing, for the sake of greater transparency to the ultrasound waves. The cell was clamped in place in the center of the tank, at such a height that the water level was the same inside as outside the tube. Then the generator was turned on for a specified time interval, usually 10.0 seconds. The intensity of the yellow color produced was measured in a 1 cm. cell in a Beckman spectrophotometer using blue light of 4360 A wavelength, and recorded as the optical density (D_{4360}) which is the negative logarithm of the fraction of light transmitted. Experiments showed that D_{4360} is a linear function of the concentration of dissolved chlorine, and that a D_{4360} value of 0.30 corresponded to one part per million of chlorine in the water, under the conditions used. Inasmuch as the color fades slowly, it should be measured within 15 minutes.

Some Results

One question was whether this method gives a linear response to linear increments of cavitation. A partial answer was obtained by an experiment in which the color of the solution was measured after each of several consecutive treatments in the tank, for 2.0 seconds each. These successive irradiations were taken as being uniform increments of cavitation. It was found that the method did respond linearly to such uniform increments of cavitation, when the line voltage supplied to the generator was either 120 volts or 100 volts. When the line voltage was as low as 80 volts, the initial treatment period of 2 seconds produced less color than the later periods, possibly because of the longer time needed to get optimum degassing of the test solution at a low level of cavitation. But even in this case the response is linear after the first 2 seconds of irradiation.

Another item of interest was the effect of a very wide range of line voltages (obtained with a Variac) on the cavitation in the tank. When the line supply for the generator was 30 volts or less, no cavitation streamers were visible in the tank, and no yellow color was produced in the test solution. At 40 volts, occasional cavitation streamers could be seen, and a small but perceptible amount of yellow color appeared. As the voltage was raised further, the amount of cavitation produced in 10 seconds increased gradually at first, up to 70 or 80 volts, and then more rapidly, up to the normal operating range of 110-120 volts. The initial slow increase is attributed in part at least to the long time

needed for weak cavitation to degas the solution down to the optimum value for either cleaning or chemical change.

The transition region where cavitation began, between 30 and 40 volts, was recognizable in various ways. Besides the appearance of bubble streamers and the onset of chlorine liberation, the output of a barium titanate probe immersed in the tank was observed on an oscilloscope. Below the threshold, the pattern was a smooth envelope of 120 cycles modulating the 26 kc carrier, but above the threshold the pattern showed clearly the superimposed irregular peaks of cavitation noise.

The distribution of cavitation intensity in the horizontal plane of an ultrasonic cleaning tank was also studied. A 32 x 200 mm. pyrex test tube containing the usual solution was clamped vertically in one of eleven positions about the tank (which was 10 inches long and 9 inches wide) and irradiated for 10 seconds. The tube was immersed to such a depth that the liquid level inside and outside the test tube were the same. It was found that there were striking variations in the amount of cavitation. At the geometric center of the horizontal plane, cavitation was more than 100 times greater than in the corners, and intermediate values were found at intermediate positions.

Other experimental conditions investigated included the height of water in the tank, and the temperature of the water.

Conclusion

A chemical method for measuring relative amounts of cavitation has been described, which is simple and rapid. Its response is reasonably linear, and its usefulness has been shown in studies of the effects of certain variables.

Literature Cited

1. L. D. Rosenberg and M.G. Sirotyuk, Soviet Physics--Acoustics 6, 477 (1961) .

2. M. G. Sirotyuk, Soviet Physics--Acoustics 7, 405 (1962) .

3. A. Weissler, J. Acoust. Soc. Am. 25, 651 (1953) .

4. A. Weissler, J. Am. Chem. Soc. 81, 1077 (1959) .

5. A. Weissler, Analyt. Chem. 33, 1963 (1961).

6. B.H. Jennings and S. N. Townsend, J. Phys. Chem. 65, 1574 (1961).

7. A. Weissler, H. W. Cooper, and S. Snyder, J. Am. Chem. Soc. 72, 1769 (1950) .

K32

FOURTH INTERNATIONAL CONGRESS ON ACOUSTICS
COPENHAGEN 21.-28. AUGUST 1962

Mise en évidence au moyen d'ondes ultrasonores transversales, des variations des constantes élastiques de solides soumis à des contraintes statiques. Application à la détection de faibles anisotropies initiales.

Suzanne PAUTHIER-CAMIER - Ecole Supérieure de Physique et Chimie

Industrielles, 10 rue Vauquelin PARIS.

I - CONSTANTES ELASTIQUES DU 2ème ORDRE - RELATION ENTRE LES VITESSES DE PROPAGATIONS DES ONDES ULTRASONORES ET LES CONSTANTES ELASTIQUES -

I.1- La théorie classique de l'élasticité suppose le solide parfaitement élastique et soumis à des contraintes telles que les déformations qui en résultent soient infinitésimales.

Les constantes élastiques $(C_{ij})^{(1)}$ sont les coefficients des relations linéaires qui relient les contraintes aux déformations. Dans le cas du solide isotrope, la matrice des constantes élastiques se ramène à 3 coefficients C_{11} C_{12} C_{44}, que l'on exprime généralement au moyen des coefficients de Lamé λ et μ . $C_{11} = \lambda + 2\mu$, $C_{12} = \lambda$, $C_{44} = \mu$ et d'où l'on tire immédiatement les constantes mécaniques usuelles E, G , η .

I.2- Nous nous sommes attachés à l'étude fine des relations contraintes déformations des solides élastiques isotropes soumis à des efforts de faibles intensités, tels que les déformations restent faibles et rigoureusement réversibles.

Nous avons choisi un mode de sollicitation simple - compression uniaxiale - afin de simplifier les relations générales.

On peut alors montrer, par des considérations de symétrie que le nouvel état du solide peut être représenté par 6 constantes élastiques (dont 5 indépendantes).

On peut définir 6 coefficients K_{ij} - constantes du 2ème ordre - qui représentent les termes correctifs à apporter aux expressions de Lamé.

I.3 - Vitesse de propagation d'uu ébranlement

Nous savons qu'une onde plane, de direction de propagation et d'orientation du vecteur déplacement des particules, convenablement choisi, se propage au sein d'un matériau avec une vitesse $K = \sqrt{\frac{C_{ij}}{\rho}}$

Si donc on excite, dans le solide soumis aux contraintes statiques, des vibrations convenables, on pourra par des mesures très précises des variations des vitesses de propagation $\triangle V_K$, déterminer les termes correctifs K_{ij}, qui représentent l'écart entre le comportement réel du matériau et l'approximation de Hooke.

Mais un échantillon soumis à des contraintes voit ses dimensions changer avec l'intensité des contraintes appliquées ; il est donc souhaitable de disposer d'une

...

méthode de mesure des variations de vitesse, indépendante des dimensions de l'échantillon, et de leurs variations.

Nous avons montré précédemment[2] en excitant la propagation d'ondes longitudinales dans des échantillons soumis à des contraintes σ_z, la variation des constantes C_{11} et C_{33} en fonction de σ_z. Cette mesure était basée sur une méthode de visualisation optique des ondes ultrasonores.

Pour déterminer les variations des constantes C_{44} et C_{66}, ou plutôt le facteur d'anisotropie transversale $C_{66}-C_{44}$ nous avons été amenés à utiliser une méthode qui s'est révélée d'une extrême sensibilité, et qui est applicable à tous les matériaux.

II - PRINCIPE DE LA MESURE DU FACTEUR D'ANISOTROPIE TRANSVERSALE -

II.1 - La méthode est basée sur l'emploi d'ondes ultrasonores transversales convenablement polarisées.

Les expériences sont effectuées sur des échantillons parallélépipèdiques de section carrée, environ 200 mm de longueur. La contrainte uniaxiale de compression est appliquée au moyen d'une machine Amsler de 10 tonnes, sur une section d'environ 30 cm2.

Les ondes transversales sont générées par un quartz coupe Y collé à l'échantillon et d'axe électrique soigneusement repéré. Le diamètre du quartz est de 20 mm et sa fréquence fondamentale de 2,4 Mhz.

Le quartz émetteur est excité par des impulsions de 2,4 Mhz de fréquence porteuse et d'une durée de 3 à 10 μsec.

A l'autre extrémité de l'échantillon, un détecteur transmet le signal reçu à un oscillographe cathodique par l'intermédiaire d'un amplificateur convenablement adapté.

Lorsque le quartz émetteur d'axe électrique dirigé suivant OZ, est excité, il engendre dans l'échantillon une contrainte dynamique de cisaillement σ_{XZ} (très faible devant la contrainte initiale σ_z) qui se propage suivant OX à la vitesse $V'_{TX} = \sqrt{\frac{C_{44}}{\rho}}$

Si par contre l'axe électrique est dirigé suivant oy, on provoque une contrainte dynamique σ_{xy} dont la vitesse de propagation est $V''_{TX} = \sqrt{\frac{C_{66}}{\rho}}$

Si l'on oriente la vibration rectiligne initiale à 45° des directions principales OZ, OY, on observera à la sortie de la pièce, une vibration elliptique ; le déphasage créé par l'anisotropie mécanique sera : $\Phi = 2\pi NX \left(\frac{1}{V'_T} - \frac{1}{V''_T}\right) = 2\pi NX \frac{\Delta V}{V_T^2}$

où N est la fréquence d'excitation du quartz émetteur, X la longueur parcourue dans le milieu rendu anisotrope, V'_T et V''_T , les vitesses de propagation des vibrations polarisées suivant Z et Y. V_T, vitesse de propagation des ondes de cisaillement dans le milieu non déformé $V_T = \sqrt{\frac{M}{\rho}}$, on se ramène ainsi à une mesure de phase qui peut être effectuée avec une très grande précision.

II.2 - Méthodes de détection

a) On peut utiliser un quartz de coupe Y collé à l'extrémité de l'échantillon de telle manière que son axe électrique soit croisé ou parallèle à la direction de vibration

...

du quartz émetteur. Le signal détecté est amplifié, puis relié aux plaques d'un oscillographe cathodique dont le balayage est déclenché par le générateur d'impulsions. La variation d'amplitude du top sera $V = V_o + V_1 \sin(\Phi/2)$ ou $V = V_o + V_1 \cos(\Phi/2)$ suivant que les axes électriques des quartz sont croisés ou parallèles. V_o, tension détectée, polariseur et analyseur croisés représente l'effet dû aux ondes dépolarisées au cours du trajet. V_1 défini par $V = V_o + V_1$ est la tension maximale obtenue lorsque les deux quartz ont leurs axes parallèles.

b) On peut interposer une lame $\lambda/4$, acoustique, entre l'échantillon et le quartz récepteur. La réalisation et l'utilisation d'une telle lame exigent de nombreuses précautions.

Pour des expériences dans le verre et le magnésium, nous avons obtenu de bonnes conditions avec une lame de fluorine taillée dans le plan (110).

III - RESULTATS EXPERIMENTAUX

III.1 - Echantillon de verre optiquement isotrope

Le verre présente une bonne transparence aux ondes U.S. et donne de nombreux échos. Cependant, à cause, a) des trajets dans les quartz

b) des réflexions parasites sur les parois, on s'est limité à l'examen du premier écho de réception.

Nous n'avons exercé que des contraintes statiques de faible intensité, 3 kg/mm2 au maximum.

Le déphasage Φ reste alors très faible et c'est en enregistrant la tension aux bornes du quartz récepteur, d'axe électrique soigneusement croisé avec celui de l'émetteur, que l'on obtient la précision maximale.

La tension lue sur l'oscillographe est alors : $V = V_o + V_1 \sin \frac{\Phi}{2}$

La fig. 1 présente les amplitudes successives du 1er écho lorsque l'on tourne de 5° en 5° le quartz analyseur par rapport à l'émetteur. Ceci donne un bon contrôle de l'isotropie initiale de l'échantillon et fournit les valeurs V_o et V_1.

La fig. 2 donne les variations d'amplitude du 1er écho en fonction de la charge appliquée.

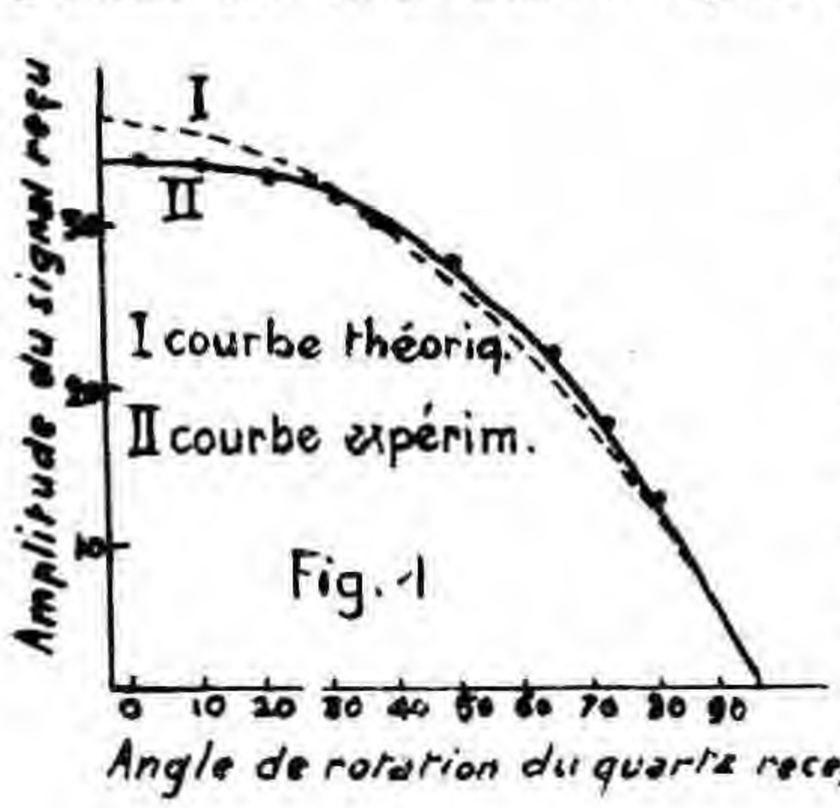

Fig. 1

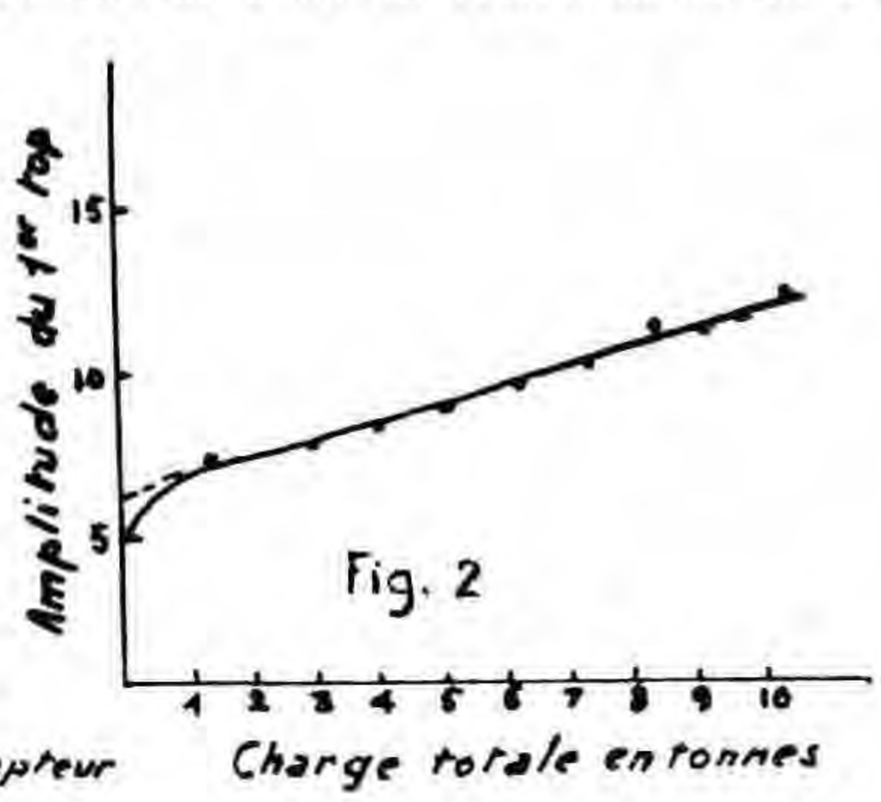

Fig. 2

...

Une série de mesures donnait l'expression $V = 1{,}3 \sin(\Phi/2) + 0{,}02$. La contrainte maximale appliquée était de $\sigma_z = 2{,}14$ kg/mm2. La tension lue sur l'oscillographe était de 0,06 V d'où $\Phi = 3°28'$. La variation de vitesse détectée ici est de $\Delta V/V = 1/7500$.

III.2 - Application à la détermination de l'anisotropie initiale d'un échantillon. Cas d'un barreau de magnésium.

La précision de la méthode peut permettre d'envisager son application pour la mise en évidence rapide de faible anisotropie élastique initiale, provoquée, par exemple, par des traitements susceptibles de créer une orientation privilégiée : laminage, tréfilage, etc... Nous avons pu, en particulier, mettre en évidence la très faible anisotropie initiale présentée par un barreau de magnésium de section carrée usiné dans une barre rectangulaire.

Les caractéristiques géométriques de la pièce avant usinage nous renseignaient sur les axes principaux probables de l'anisotropie initiale. Trois mesures effectuées en orientant convenablement les axes électriques des quartz émetteur et récepteur avant la mise en charge de l'échantillon donnent immédiatement V_o, V_1 et $\Phi_o = 2\pi N L \frac{\Delta V_{T\ initial}}{V_T^2}$

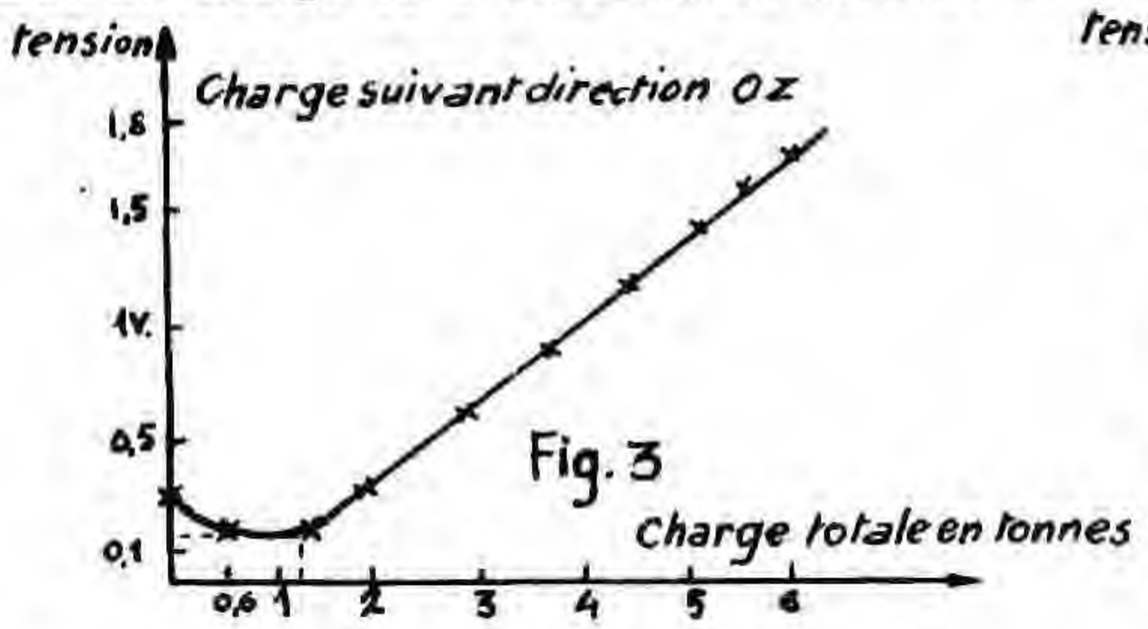

Fig. 3

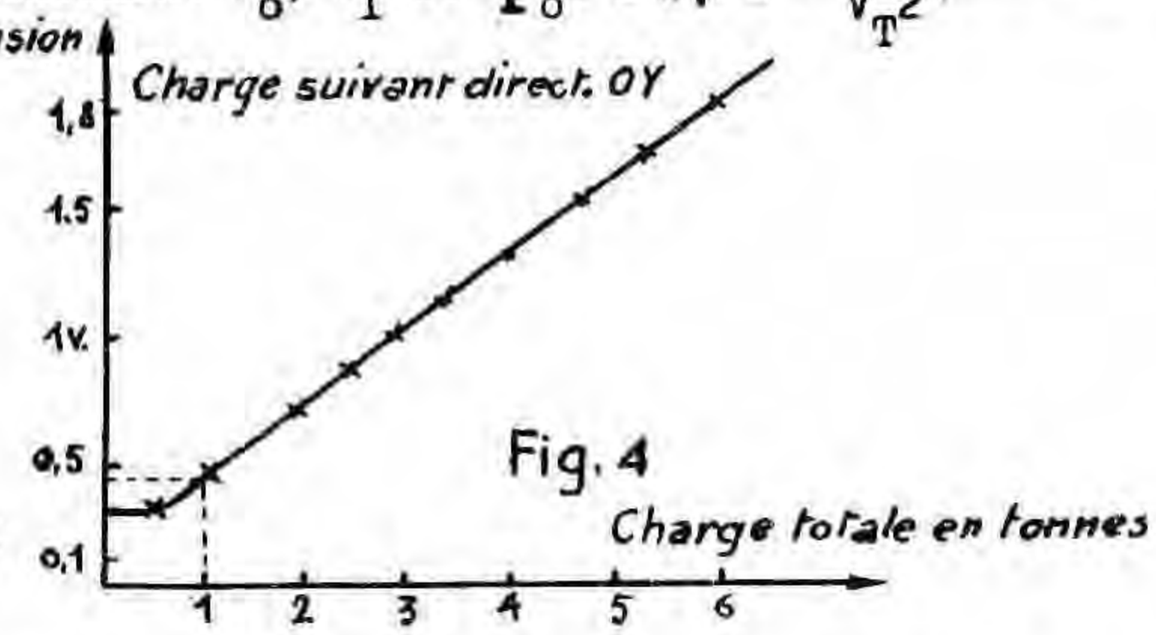

Fig. 4

Nous avons trouvé pour l'échantillon considéré de longueur L = 20 cm, une anisotropie initiale $\Phi_o = 45$ minutes, ce qui correspond à une variation de vitesse $\frac{\Delta V_T}{V_T} \gtrless 2.10^{-5}$

Si maintenant on exerce la charge et que l'on enregistre successivement la variation d'amplitude du premier écho de réception suivant que l'effort est exercé suivant OZ, ou suivant OY, on obtient les courbes suivantes (fig. 3 et 4)

La tension enregistrée $V = V_o + V_1 \sin \frac{\Phi + \Phi_o}{2}$ va augmenter ou diminuer avec la contrainte appliquée, suivant le signe de ϕ par rapport à ϕ_o.

Il est aisé à partir des courbes 3 et 4 de calculer Φ_o. La concordance avec la valeur déterminée plus haut est en moyenne de 3 %.

Paris, Mai 1962

(1) LOVE - Theory of Elasticity - Dover publications - New-York 1944

(2) S. PAUTHIER-CAMIER - Compte Rendu Acad. Sciences Séance du 9 mars 1959 pp.1473-1475.

L32

FOURTH INTERNATIONAL CONGRESS ON ACOUSTICS
COPENHAGEN 21.-28. AUGUST 1962

The Measurement of Flow Noise with the Aid of Buoyant Units

G. P. Haddle, Research Associate and E. J. Skudrzyk, B.S., Ph.D Professor of Engineering Research

WITHDRAWN.

M32

FOURTH INTERNATIONAL CONGRESS ON ACOUSTICS
COPENHAGEN 21.-28. AUGUST 1962

REVERBERATION CHAMBER POWER LEVEL MEASUREMENTS ON SOUND SOURCES

W. W. Lang and K. S. Nordby

International Business Machines Corporation, Poughkeepsie, N. Y., U.S.A.

INTRODUCTION

The diffusion of a sound field at a point has been defined[1] as the angular distribution of sound energy flux in the plane wave expansion of the sound field at that point. When the distribution over the solid angle is uniform, the sound field at the point is called "completely diffuse". Under such conditions, the acoustic power radiated by a source of sound could be calculated from the measured value of the mean squared pressure at any point in the sound field. The advantage of such a method would be that the sound pressure has to be measured at only one point. However, a "completely diffuse" sound field cannot be realized in practice. For this reason, sound pressure measurements are required at several points in a reverberant field.

A reverberation chamber was constructed as part of this study. While it was being designed, a careful investigation was made of the factors which influence the state of diffusion in the reverberant field. After completion, the power level spectra of two different sound sources were measured to check the performance of the chamber. These sources had dissimilar spectra. The octave-band spectrum of one of the sources[2] was within ± 1.5 decibels over the frequency range 100-6000 cycles per second (cps). The corresponding spectrum for the other source increased with a slope of 8 decibels per octave. These spectra were compared with similar spectra obtained in a free-field. While an absolute measure of the state of diffusion in the chamber is of interest and is currently being studied, it will not be considered here.

DESIGN OF REVERBERATION CHAMBER

Chambers for measuring power levels of sound sources and chambers for determining absorption coefficients of acoustical materials should both provide the best possible approximation of a "completely diffuse" sound field. The following factors were considered[3] in the design of the reverberation chamber (specifications are given in parentheses):

1. Volume of chamber (230 m^3) - The larger the volume of the chamber, the lower are the center frequencies of the lowest and highest frequency bands in which reliable measurements can be obtained. The degree of diffusion depends upon the number of normal modes of the room which are excited. An increase in volume increases the number of modes in a frequency band of constant width. However, it also increases the total absorption in the chamber due to the increased amount of air. Therefore, a compromise must be made. For the purposes of this study, reliable measurements were required in one-third octave bands between 100 and 8000 cps. The volume which was selected provides 25 normal modes of vibration in a one-third octave band centered at 100 cps and an adequate degree of diffusion for measurement purposes up to the one-third octave band centered at 8000 cps.

2. Shape (Rectangular: 4.77 x 6.31 x 7.66 m^3) - The frequency distribution of the normal modes depends upon the proportions of the chamber. A rectangular shape was selected with proportions 1 : 1.32 : 1.61 to provide a smooth distribution of the normal modes at low frequencies.

3. Diffusing elements (ISO diffusers) - To improve the degree of diffusion in a chamber, walls are frequently splayed, diffusing elements are built into one of the room surfaces or are placed in the room after completion. To provide a sound field which can be studied analytically and to minimize construction cost, it was decided to preserve rectangularity and to introduce removable diffusers if necessary according to the ISO recommendation[4]. This recommendation states that removable diffusers may be necessary for absorption measurements even in rooms with splayed walls and in rooms with three non-parallel polycylindrical boundaries.

4. Surface absorption (average absorption coefficient at 500 cps: 0.0085) - To maximize the number of reflections from the walls, floor and ceiling, surface absorption must be reduced to a minimum. Cement plaster was covered by a 50 micron layer of epoxy resin to provide a smooth, hard, reflective, interior finish for the chamber.

5. Other design factors - External noise and vibration should be isolated from the chamber. Temperature and humidity controls are necessary to insure repeatable atmospheric conditions.

RESULTS

It has been shown[5] that a chamber surface in close proximity can influence the power output, directivity pattern, extent of the near field, and radiation impedance of a noise source. Therefore, the measurements were obtained under two different conditions: (1) with the two sources just above the floor and (2) with the sources suspended from the ceiling in the reverberation and free-field chambers. The comparison measurements were made with the sources located at the same height above a reflecting plane in a free-field chamber (semi-anechoic) and in a completely free-field chamber (anechoic). To obtain the equivalent free-field output of the source in the reverberation chamber, it was important that the source be placed at sufficient distance from all reflecting surfaces so that interference effects would be negligible.

Figure 1 gives the free field power spectrum for the standard mechanical sound source compared with the power spectra obtained in the reverberation chamber with and without 22 diffusers. These data were obtained with the source resting on the floor in the reverberation and semi-anechoic chambers. Similar results were obtained for the source with spectrum sloping upward at 8 decibels per octave. All data lead to the same conclusions. The results for the standard mechanical source on the floor are presented here.

Figure 2 illustrates the reverberation times with and without the 22 diffusers. These data were used to obtain the reverberation chamber power spectrum from the relation given in the Appendix.

Figure 1 also shows that the deviations between the free-field data and the bare reverberation chamber data are within 0.4 decibel for the 400 through the 3150 cps octave bands and 2.6 decibels for the 100 through the 6300 cps octave bands. No reduction of these deviations was obtained with the 22 diffusers installed.

Table I shows the deviations of the power levels measured in the reverberation chamber with and without diffusers from the power levels measured in the semi-anechoic chamber.

Table II gives the variations in the power levels measured at 15 different microphone locations in the reverberation chamber. As expected, the variation decreases as the number of diffusers is increased. When averaged over all octave bands, this variation is + 0.5, -0.7 without diffusers and ± 0.4 with diffusers. Nevertheless, it is seen from Table I that the deviations in power level from the free-field values are greater with diffusers than without.

CONCLUSION

The results show that a rectangular reverberation chamber of sufficient volume and adequate surface hardness is entirely satisfactory for the measurement of the total acoustic power of wide-band sound sources. Within the accuracy of present-day measurements (± 0.5 decibel), the presence of diffusers in the chamber did not reduce the deviations between the power level data obtained under reverberant and free-field conditions. In fact, all diffusers could be removed from the chamber without sacrifice of accuracy. Therefore, no practical improvement can be anticipated with more costly chambers having splayed walls or polycylindrical surfaces.

In absorption measurements, it is the normal procedure to cover partially one surface of a chamber with absorbing material, thus decreasing the uniformity of the sound field. On the other hand, in power level measurements, the typical sound source introduces negligible absorption and the high degree of diffusion in the chamber is maintained.

The rectangular reverberation chamber has been shown to be an accurate tool for obtaining power spectra of sound sources at a considerable saving of labor and cost over the usual free-field technique.

REFERENCES

1. M. R. Schroeder, J. Acoust. Soc. Am., 31 (1959)1407.
2. H. C. Hardy, Noise Control, 5 (1959)158.
3. C. M. Harris (ed.), "Handbook of Noise Control", McGraw-Hill, New York, 1957, p. 17-35.
4. ISO TC/43 Recommendation (in preparation).
5. R. V. Waterhouse, J. Acoust. Soc. Am., 30 (1958)4.

APPENDIX

The source power levels in the reverberant field (PWL_R) and in the free field above a reflecting plane (PWL_S) were calculated from the following relationships (in decibels re 10^{-13} watt):

$$PWL_R = \overline{SPL}_R + 10 \log_{10} V - 10 \log_{10} T - 19.5 \quad (1)$$

$$PWL_S = \overline{SPL}_S + 20 \log_{10} r - 16.2 \quad (2)$$

In these equations, $\overline{SPL}_R$ is the average of the sound pressure levels measured at 15 microphone positions in the reverberant field, $\overline{SPL}_S$ is the sound pressure level averaged over a hemisphere using 12 measuring points, V and T are the volume and reverberation time of the chamber in cubic feet and seconds, and r is the radius of the test hemisphere in the free field in feet (6 feet).

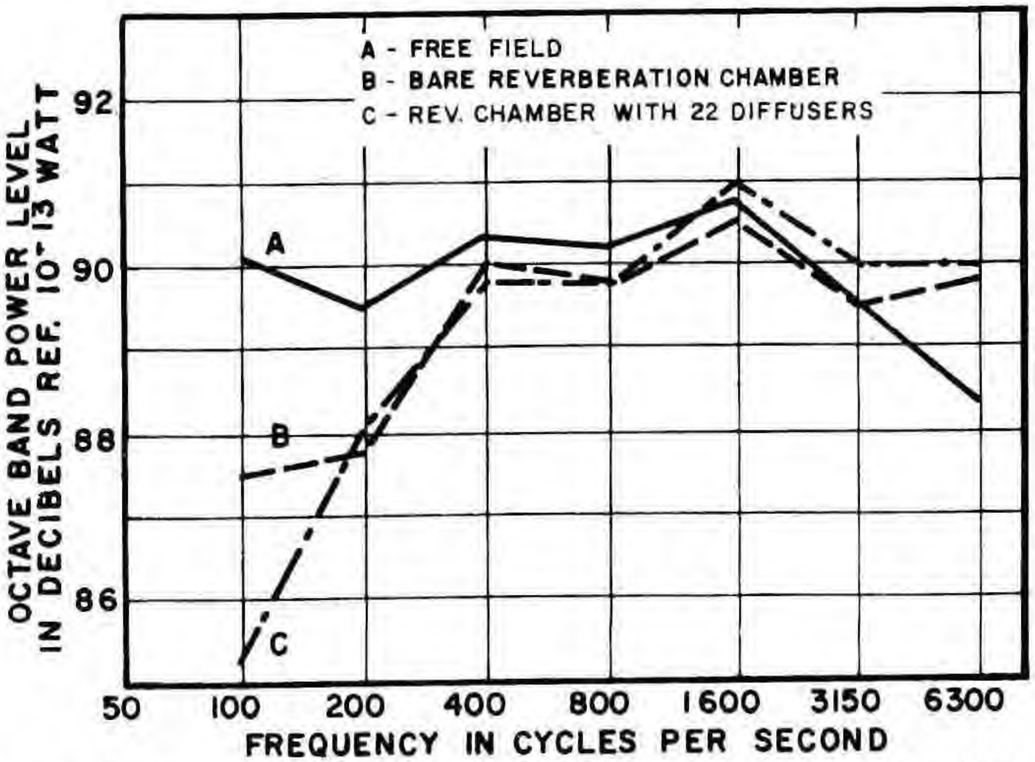

Fig. 1. Octave band power levels for standard mechanical noise source at 65% RH.

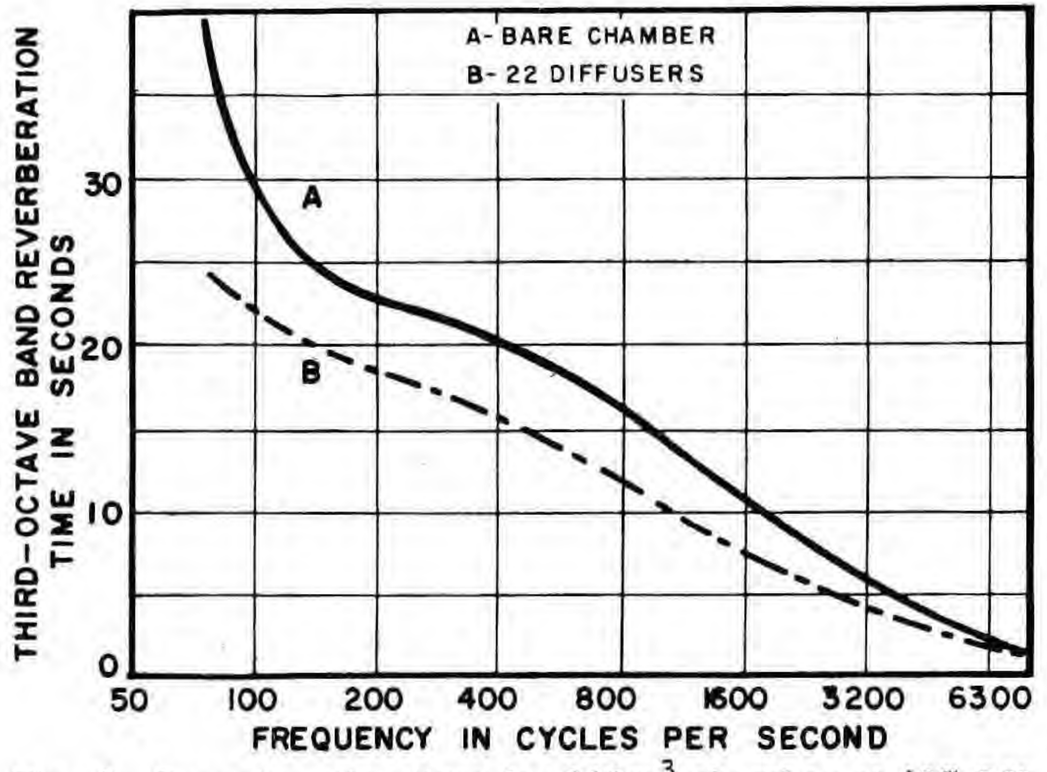

Fig. 2. Reverberation time for 230m^3 chamber at 65% RH excited by 1/2 octave noise measured in 1/3 octave bands.

TABLE I

Octave Band (cps)	Semi-Anechoic power level	Rev. Chamber Deviations	
		No diffusers	22 diffusers
100	90.1db	- 2.6db	- 4.8db
200	89.5	- 1.7	- 1.5
400	90.3	- 0.3	- 0.5
800	90.2	- 0.4	- 0.4
1600	90.8	- 0.3	+ 0.1
3150	89.6	- 0.1	+ 0.4
6300	88.4	+ 1.4	+ 1.6

TABLE II

Octave Band (cps)	Variation of Reverberation Chamber Power Level for 15 Different Microphone Positions (in decibels)		
	No diffusers	7 diffusers	22 diffusers
100	+ 0.7 ; - 1.8	+ 0.9 ; - 0.6	+ 1.1 ; - 1.7
200	+ 0.4 ; - 1.1	+ 1.0 ; - 1.0	+ 0.9 ; - 0.1
400	+ 0.8 ; - 0.7	+ 0.3 ; - 0.2	+ 0.1 ; - 0.4
800	+ 0.6 ; - 0.6	+ 1.0 ; - 1.5	+ 0.0 ; - 0.0
1600	+ 0.4 ; - 0.1	+ 0.0 ; - 0.0	+ 0.0 ; - 0.0
3150	+ 0.4 ; - 0.2	+ 0.0 ; - 0.5	+ 0.5 ; - 0.5
6300	+ 0.2 ; - 0.3	+ 0.0 ; - 0.0	+ 0.2 ; - 0.2
Average	+ 0.5 ; - 0.7	+ 0.5 ; - 0.7	+ 0.4 ; - 0.4

N32

FOURTH INTERNATIONAL CONGRESS ON ACOUSTICS
COPENHAGEN 21.-28. AUGUST 1962

Attenuation Measurements on a Mobile Audiometric Unit

Dr. Frank Fowweather

1. Introduction

Reliable field studies of industrial deafness are not easy on account of the problem of finding a sufficiently quiet environment in a factory to carry out the audiometry. To overcome this problem, the Nuffield Department of Occupational Health of Manchester University for their survey of deafness in the textile industry have constructed a vehicle in which the desired acoustic conditions would be obtained. A description of one such vehicle has been given by Pennington (1), and at least two vehicles (2,3) have been described for audiometry on airfields but there have been no serious measurements of the degree of attenuation achieved and of workable frequency range for audiometry.

2. Van Design and Construction

The mobile laboratory was built to the joint design of Dr. W.R. Lee, of the Nuffield Department, and Mr. J.N.J. Johns, the audiologist in the Manchester University Department of Deaf Education. It consists of a 3-ton van of internal dimensions 12 ft. long by 7 ft. wide and 8 ft. high; this is divided into two parts, a waiting-room, 7 ft. by 4 ft., and a clinical examination or consulting room 7 ft. by 8 ft., in one corner of which is placed a proprietary audiometric booth of size 3 ft. by 3 ft. and 7 ft.9ins. high.

The design requirements of attenuation were based on octave-band measurement of sound pressures in mill yards together with the minimum acceptable octave-band noise levels for audiometric rooms (4). The van has a glassfibre body built on a 1½" square timber framework; attached to the body is a 1" layer of fibre glass of 12 lb./cu.ft. density, then an air gap of ½", after which are 1" thick sheets of the man-made timber "Weyroc" of 42 lb./cu.ft. density with overlapping sealed joints, and finally the innermost layer is wood-fibre tiles which form the walls of the rooms. This construction gives an overall surface density for the walls and roof of 5 lbs./sq.ft. The floor consists of 1" tongue-and-grooved wood upon which are 1" Weyroc sheets; these are covered with hardboard and finally a rubber flooring material, giving an overall surface density of 6 lbs./sq.ft.

3. Attenuation Measurements

The initial problem was to find a high-intensity noise source that would produce a uniform field round a van of this size. The reverberant field in the generating hall of a power station was used for the first measurements; this had an overall level of 96.5 db varying by ±1.5 db. round the van. One-third octave band measurements were made of sound pressure using a Bruel and Kjaer condenser microphone and audiofrequency spectrometer. Measurements were made at six positions outside the van, two positions in the consulting-room and one in the audiometric booth. The attenuation was computed from average values, and the results are indicated by dots in Figure 1 for both the van-shell attenuation (i.e. outside to consulting-room) and the overall attenuation (i.e. outside to inside the booth). The range of measurement is restricted to 3150 c/s for the van shell attenuation and to 400 c/s for the overall attenuation, because of the fall-off in the power-station noise spectrum at the higher frequencies.

A second set of measurements was made using jet engines as noise source to extend the range of measurement. The van was placed about thirty yards from the nose of a four-engined aeroplane in line with the fuselage; the overall sound level was 116 db varying by ±2.5 db round the van, so giving a reasonably uniform noise

field. Measurements had to be made during the testing of the engines, which meant that the sound level was constant only for periods of the order of ten minutes; this necessitated the use of magnetic recording techniques. Two microphones and amplifiers were now used; a mechanical two-channel rotating selector was used to switch six seconds of each output to the tape-recorder. A pistonphone was used to calibrate the gain of each amplifying system and to record a calibration signal on the tape. Recordings were made with microphones in the same positions as at the power-station. The one-third octave band analysis was made using several tape loops cut from consecutive six-second recordings, the gain of the play-back system being adjusted by the tape loop of the standard source, and the attenuation was calculated from average values. These new results are indicated by crosses in Figure 1; the range of measurement was now extended to 12,500 c/s and the low frequency values are in good agreement with the earlier results.

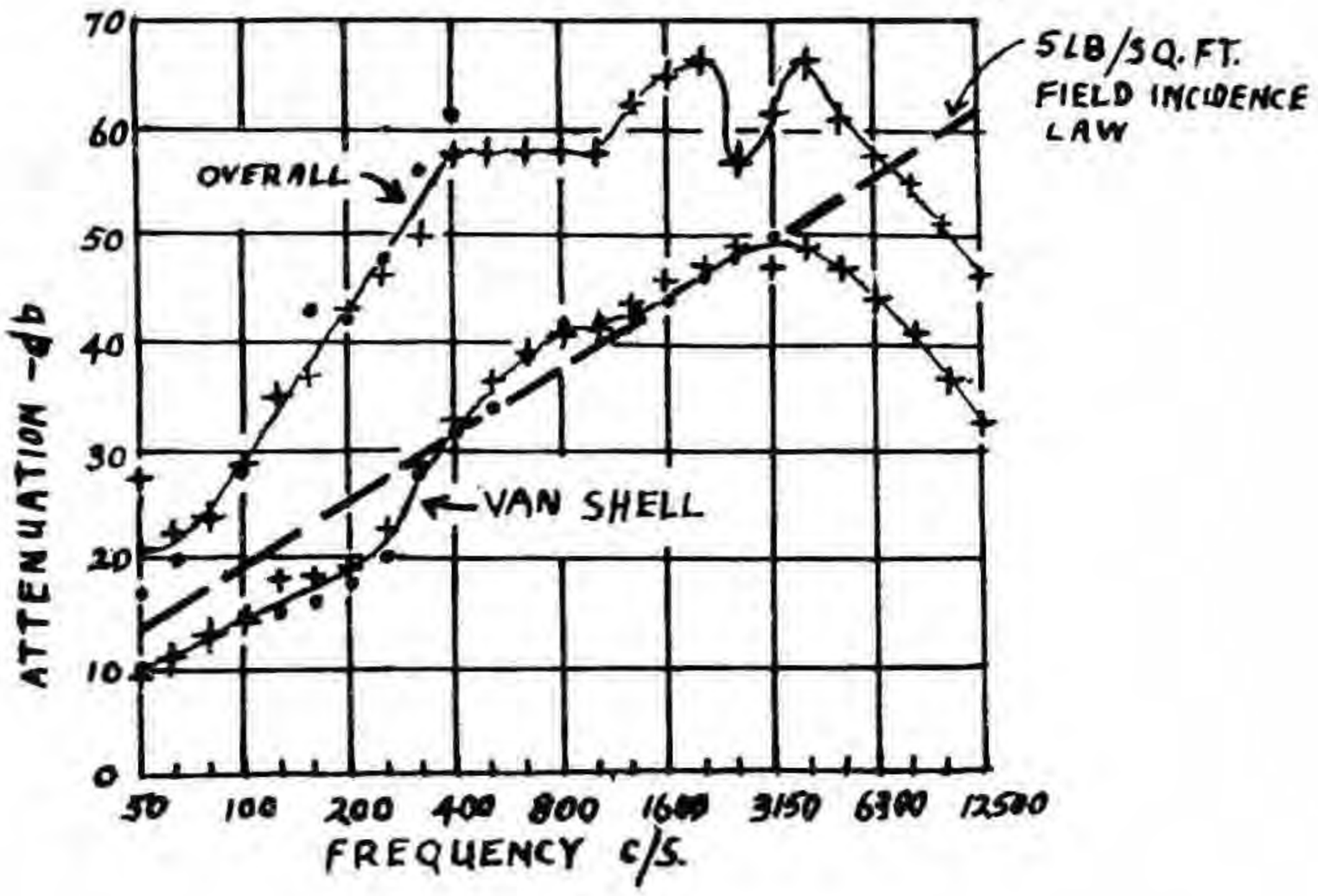

Fig.1. Van shell and overall attenuation

A 5 lb./sq.ft. field incidence law straight line is drawn on Figure 1; this is in reasonable agreement with the van-shell attenuation curve.

The audiometric booth is in one corner of the consulting-room and will not be in a uniform noise field; hence the measurements made with outside noise source will not give accurate values of attenuation. It was decided that the best measurement of booth attenuation would be obtained with an omnidirectional noise source inside the booth; this was a modified column loudspeaker fed from a tape loop of jet noise, giving a wide horizontal beam of sound. Measurements were made in the booth and at two positions in the consulting-room; the attenuation is shown in Figure 2 at one-third octave intervals.

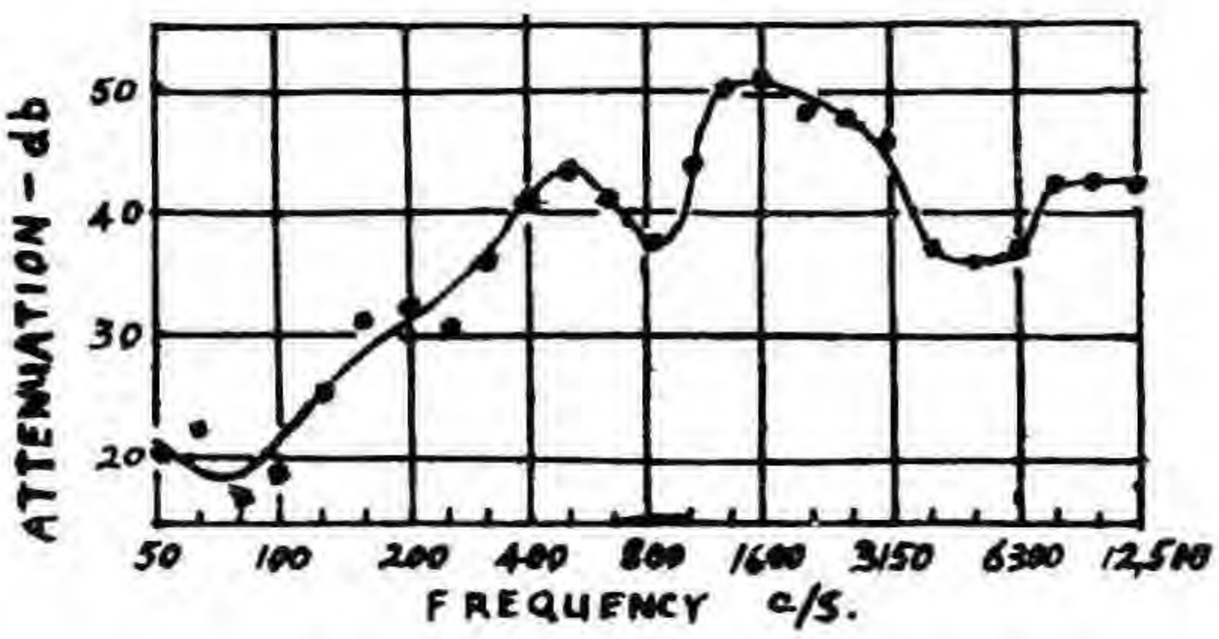

Fig.2. Booth attenuation

4. Conclusion

The workable frequency range for audiometric measurements can be obtained by computing the noise level in the booth from the octave band measurements in mill yards and the measured overall attenuation, and comparing the result with the Cox and Webster (4) data for the minimum acceptable octave-band noise levels for audiometric rooms. This comparison is made in Figure 3; the two curves cross at 100 c/s, and hence the van is satisfactory for audiometric measurements at frequencies above 100 c/s.

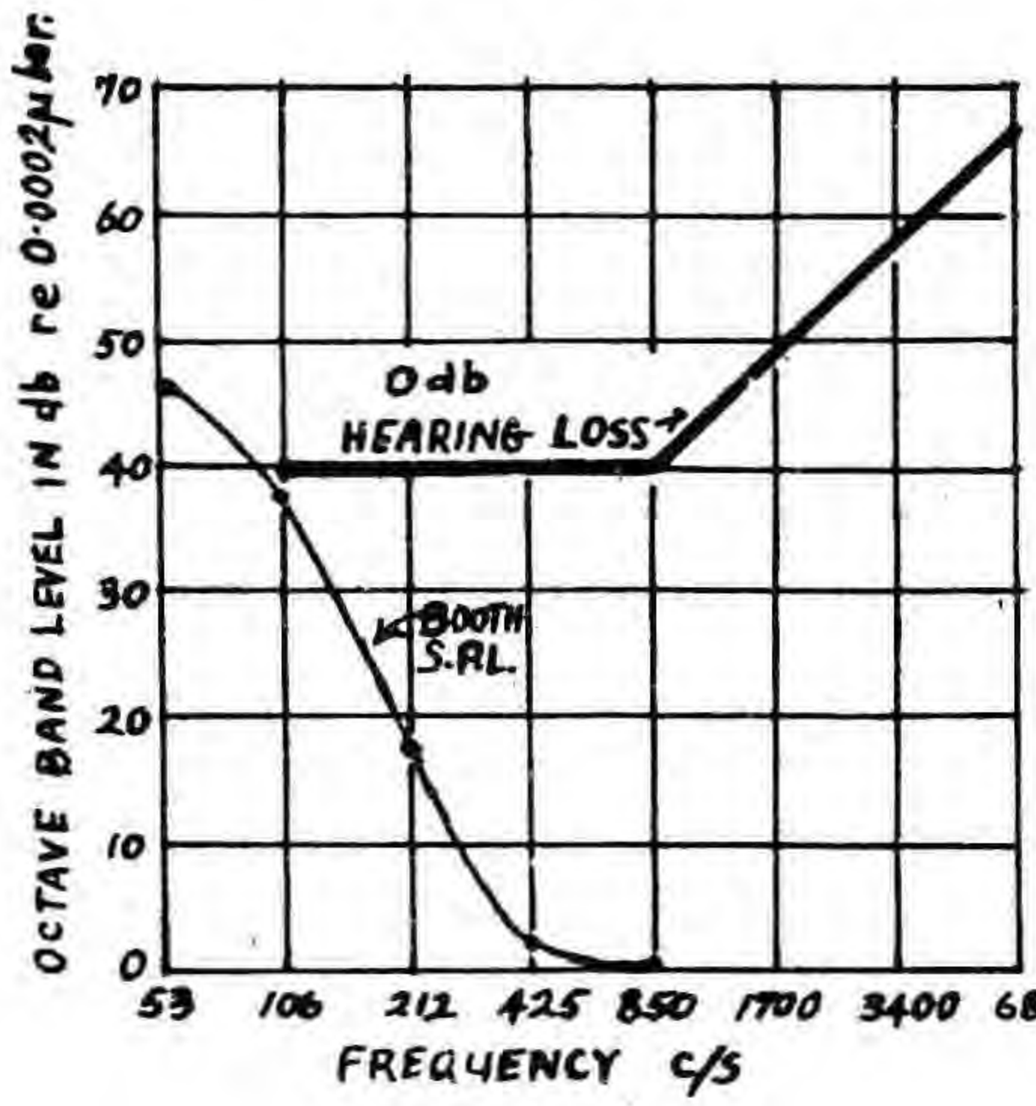

Fig.3. Comparison of "0 db hearing loss" contour with calculated average booth noise level in mill yards.

References

1. Pennington, G.F. Ann.occup.Hyg., Vol.1, 128 (1958).
2. Sullivan, J.A. and Hodges, W.E. Canad.J.Aviat.Med., Vol.23, 229 (1952).
3. Dickson, E.D.D. and Wheeler, L.J. Nature (London), Vol.172, 748 (1953).
4. Glorig, A. and Harris, J.D. in Chap.6 "Handbook of Noise Control" (Ed. C.M. Harris) - McGraw Hill Book Co., New York (1957).

O32

FOURTH INTERNATIONAL CONGRESS ON ACOUSTICS
COPENHAGEN 21.-28. AUGUST 1962

DIFFRACTION EFFECTS IN A RANDOM SOUND FIELD*

Richard V. Waterhouse

1. Introduction

In calibrating transducers in enclosures, and making measurements in random sound fields generally, it is desirable to know the diffraction pattern produced at the transducer, and to know what effect this pattern will have on the measurement. In the case of a sound field consisting of a travelling plane-wave train the diffraction effects have been fairly well studied and various analytical results are available. Some of these results are here extended to the case of a randomly incident sound field. The pressure field in the vicinity of a rigid reflecting sphere under these conditions is given as a function of the diameter of the sphere in wavelengths. The corresponding results for a pressure release boundary condition at the surface of the sphere, and for an infinite circular cylinder in a 2-dimensional random field are also given. It is shown that the reflected impedance for a point source in a randomly incident sound field is zero, and that this result holds for any transducer having constant volume-velocity. These results also have a possible application to measurements of hearing and loudness in random sound fields, the diffraction at a human head being approximated by that at a rigid reflecting sphere.

2. Pressure at Surface of Sphere for Random Incidence

We consider a reverberant enclosure in which a random sound field has been set up, with frequency f and wave number $k=2\pi f/c$. There is a fixed, rigid, reflecting sphere of radius a in the sound field sufficiently far from the walls and source for substantially plane sound waves to be incident on it with equal intensity from all directions and with random phase.

Fig. 1 shows the sphere. We take its centre as the coordinate origin and consider one wave train of the random sound field, incident on the sphere from the $\theta=0$ direction. It will cause an axisymmetric distribution of mean square pressure $\bar{p}^2(\theta)$ over the surface of the sphere. So will a wave train incident at any other angle. Since the phases of the wave trains incident at different angles are random, the total mean square pressure at any point on the sphere in the random sound field is

$$\bar{p}_a^2 = \oint \bar{p}^2(\theta)\, ds \qquad (2.1$$

i.e. the mean square pressure distribution for one incident wave train integrated over the sphere. The element of area on the sphere is ds.

We consider the ratio $\bar{p}_a^2 / \bar{p}_o^2$ as a function of ka, where $\bar{p}_o^2$ is the mean square pressure in the random sound field in the absence of the sphere, or at a point well away from it. Bounds on this ratio are obtainable by physical arguments. It is clear that as $ka \to 0$ the obstacle effect vanishes and $(\bar{p}_a^2 / \bar{p}_o^2) \to 1$; also, when the sphere is large and $ka \to \infty$, the spherical surface approaches planeness and $(\bar{p}_a^2 / \bar{p}_o^2) \to 2$, as in the case of a plane reflector.

The analysis, which will be given with fuller results in another paper, yields for the pressure on the surface of the reflecting sphere

$$\bar{p}_a^2 / \bar{p}_o^2 = (ka)^{-4} \sum_{m=0}^{\infty} (2m+1) [D_m'(ka)]^{-2} \qquad (2.2$$

---

* Research supported by the U. S. Office of Naval Research

The derivative of the spherical Hankel function of order m is

$$j'_m(ka) + i\,n'_m(ka) = -i\,D'_m(ka)\exp(i\,\delta'_{ms}) \qquad (2.3$$

These functions are fairly well tabulated.[1] A graph of 2.2 is given in Fig. 1. This curve bears some relation to that obtained experimentally for the pressure at the ear in a random sound field.[2]

3. Derivation by Reciprocity

The result 2.2 can also be obtained by applying reciprocity theory to the case of a radiating point source situated on the surface of the sphere. The argument is as follows.

With the reverberent enclosure as before (Fig. 1), A is an arbitrary point on the surface of the sphere. The origin of the random sound field is a point source at B. Then by reciprocity the mean square pressure at A with the source at B equals that at B when the source is moved to A. We express this in symbols as

$$\overline{p_A^2}\,,\,S_B = \overline{p_B^2}\,,\,S_A \qquad (3.1$$

Now

$$\overline{p_B^2}\,,\,S_A \propto W_A\,(\text{random field}) \qquad (3.2$$

where the latter term is the power output of a point source at A, on the sphere, in a random sound field. Since the radiation impedance of a point source in a random field is equal to that in a free-field (as shown in Section 6),

$$W_A\,(\text{random field}) = W_A\,(\text{free-field}) \qquad (3.3$$

Combining 3.1, 3.2 and 3.3 we have

$$\overline{p_A^2}\,,\,S_B \propto W_A\,(\text{free-field}) \qquad (3.4$$

But the latter quantity, the power output of a point source on a rigid reflecting sphere in a free-field, is already known. Rayleigh and others have treated this question, and Morse[3] gives results in a convenient form. We make 3.4 into an equation by normalizing as follows:

$$\left[\overline{p_A^2}(ka)\right] \Big/ \lim_{ka\to 0} \overline{p_A^2}(ka) = \left[W_A(ka)\right] \Big/ \lim_{ka\to 0} W_A(ka) \qquad (3.5$$

Now the left-hand sides of 3.5 and 2.2 are equal, and so are the right-hand sides. Thus we have shown that the reciprocal relations existing between a point source and a sphere in a free-field hold for an ideal random sound field also.

4. Pressure Pattern Outside the Sphere

In some cases it is desirable to know certain features of the diffraction pattern outside the sphere, for example to know the extent of the region around the sphere in which the pattern is appreciable.

The pattern is radially symmetric about the centre of the sphere, and to express the pressure field a convenient parameter is the ratio $\overline{p_r^2}/\overline{p_0^2}$. The radial distance from the centre of the sphere is r, and ka has any fixed value, a being the radius of the sphere. It is found that

$$\overline{p_r^2}/\overline{p_0^2} = \sum_{m=0}^{\infty} (2m+1)\left[j_m(kr).\cos\delta'_{ms} + n_m(kr).\sin\delta'_{ms}\right]^2 \qquad (4.1$$

The symbols are defined in 2.3. At the surface of the sphere r=a and 4.1 reverts to 2.2. A graph of 4.1 is given in Fig. 2 for the value ka=3, i.e. for a sphere whose diameter is approximately equal to the wavelength.

If there is a pressure release boundary condition at the surface of the sphere, the derivatives in 4.1 and 5.2 are replaced by the functions from which they are derived, while 2.2 and 5.1 become zero for all values of ka.

5. Diffraction at a Cylinder

Results analagous to those above can be derived for a rigid reflecting circular cylinder of infinite length in a two-dimensional random sound field. In this case unit length of the cylinder is considered, and sound waves are incident on it from all directions in the plane normal to the cylinder axis. The pressure on the surface of the cylinder is given by

$$\overline{p_a^2} / \overline{p_o^2} = 4(\pi ka)^{-2} \sum_0^\infty \epsilon_m \left[C_m'(ka)\right]^{-2} \qquad (5.1$$

and this is plotted in Fig. 1. $\epsilon_0 = 1$, $\epsilon_m = 2, m > 0$; $C_m'(ka)$ is defined below. As before, this result corresponds with a reciprocal case, the power output of a line source situated on the surface of the cylinder.

Fig. 1 shows that the cylinder gives an appreciably greater diffraction effect in the 2-dimensional field than does the sphere of the same diameter in the 3-dimensional case. This is not surprising, as the cylinder presents a rectangular cross-section to each approaching plane wave train, while the sphere presents a circular cross-section. An example is that for the cylinder a value of ka=1 corresponds to a 2 db pressure increase at the surface, whereas for the sphere this pressure increase occurs when the radius corresponds to ka=3.

The relative mean square pressure along a radius vector from the center of the cylinder is

$$\overline{p_r^2} / \overline{p_o^2} = \sum_0^\infty \epsilon_m \left[J_m(kr).\cos\delta_{mc}' + N_m(kr).\sin\delta_{mc}'\right]^2 \qquad (5.2$$

where the derivative of the Hankel function of order m is

$$J_m'(ka) + i\,N_m'(ka) = i\,C_m'(ka)\exp(i\delta_{mc}') \qquad (5.3$$

As before, when r=a, 5.2 reverts to 5.1.

6. Reflected Impedance for a Source in a Random Sound Field

It has been shown elsewhere[4] that a reflected impedance Z_r for a point source in a reflecting environment can be conveniently defined by analogy with its free-field acoustic impedance Z_o. Thus in a reflecting environment the point source sees the total impedance

$$Z_o + Z_r = (p_o + \textstyle\sum_n p_r) / v_o \cos\omega t \qquad (6.1$$

where p_o is the directly radiated pressure wave, $v_o \cos\omega t$ is the volume velocity of the source, and $\sum_n p_r$ is the sum of all the reflected wave trains at the point occupied by the source. We consider that the reflecting environment gives rise to a large number n of reflected wave trains at the source point, having the same frequency ω but different phase angles α_n. Thus

$$\textstyle\sum_n p_r = \sum_n A_n \cos(\omega t + \alpha_n) \qquad (6.2$$

$$Z_r = \left[\textstyle\sum_n A_n \cos(\omega t + \alpha_n)\right] / v_o \cos\omega t \qquad (6.3$$

For the purposes of this argument we can ignore the constants A_n and v_o which express amplitudes, and write

$$Z_r = \left[\textstyle\sum_n \cos(\omega t + \alpha_n)\right] / \cos\omega t \qquad (6.4$$

$$= \textstyle\sum_n \cos\alpha_n + i \sum_n \sin\alpha_n \qquad (6.5$$

in the usual complex-impedance notation.

Now the values α_n are assumed to be distributed at random over the range 0-2π. Then $y = \sum_n \cos\alpha_n$ has a distribution which for large values of n, as assumed here, approaches a normal distribution; this follows from the Central Limit Theorem. In the same way the distribution of $\sum_n \sin\alpha_n$ is also asymptotically normal.

It is assumed that to produce the ideal random sound field there is present some mechanism which continuously changes the phase angles α_n. (A rotating vane, such as Sabine used in his reverberation chamber, would have this type of action.) Under these conditions the time-averaged value of $\sum \cos\alpha_n$ equals the mean value of the distribution, which is zero. The same is true for $\sum \sin\alpha_n$. Thus under these conditions equation 6.5 shows that $Z_r=0$, i.e. that the reflected impedance on a point source is zero in an ideal random sound field.

This result can easily be extended to the case of a large transducer of constant volume velocity. For considering any small area or the vibrating surface of the transducer, the reflected impedance in a randomly-incident field must be zero, by the arguments above; therefore, it is zero for the vibrating surface taken as a whole. In cases where the assumption of ideally random incidence does not hold, a non-zero reflected impedance is to be expected.

References

1. "Scattering and Radiation from Circular Cylinders and Spheres" by A. Lowan et al. Mathematical Tables Project (N.B.S. for M.I.T.), U.S. Navy Department (ONR), Washington, D.C., July 1946.
2. D. W. Robinson and L. S. Whittle, Acφustica 10, 79, 1960. See Fig. 6.
3. "Vibration and Sound" by P. M. Morse, (McGraw-Hill, New York, 2nd Ed., 1948) p.322.
4. R. V. Waterhouse, J.A.S.A. 30, Jan. 1958, 4-13.

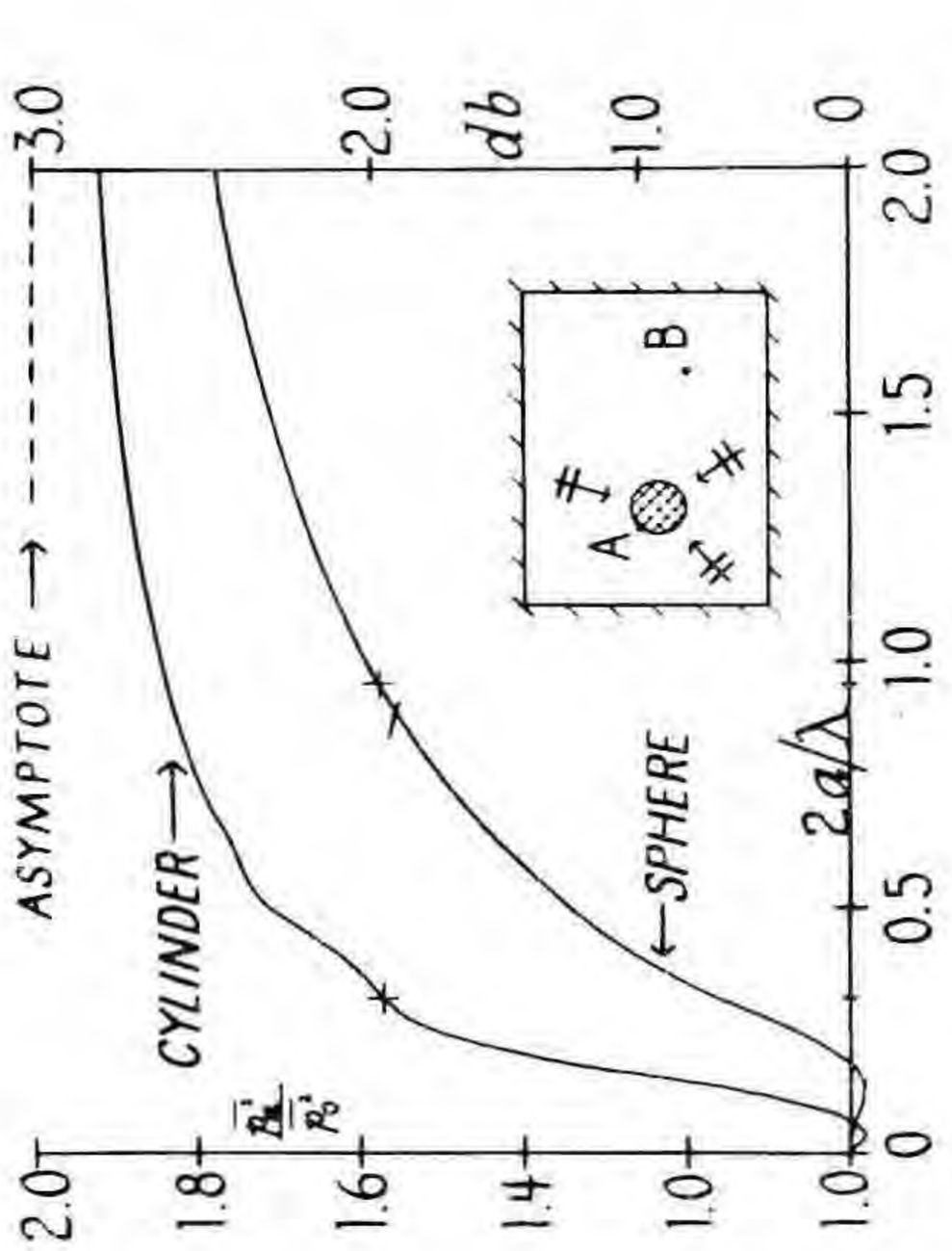

Fig. 1. Theoretical curves for the relative mean square pressure $\overline{p_a^2}/\overline{p_o^2}$ on the surface of a reflecting sphere and cylinder in a random sound field versus the diameter in wavelengths, $2a/\lambda$. On the right the ordinate shows the corresponding db scale. The curves are plots of 2.2 and 5.1.

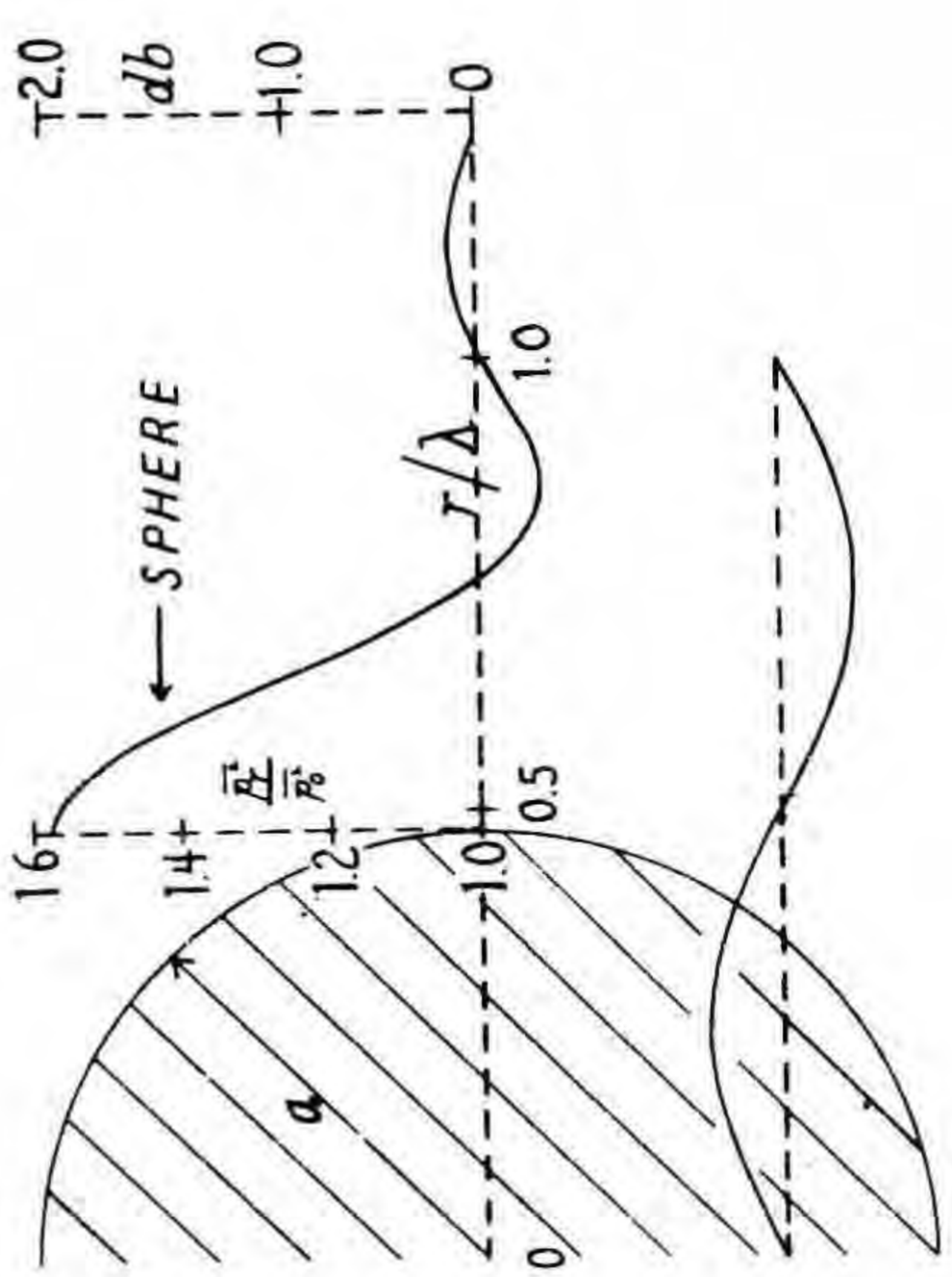

Fig. 2. Theoretical curve for relative mean square pressure $\overline{p_r^2}/\overline{p_o^2}$ versus radial distance in wavelengths r/λ from the centre of a reflecting sphere in a random sound field; ka=3. The other ordinate shows the corresponding db scale. The curve is a plot of 4.1.

P32

FOURTH INTERNATIONAL CONGRESS ON ACOUSTICS
COPENHAGEN 21.-28. AUGUST 1962

A SEISMIC DISPLACEMENT PICKUP+

R. A. WALKLING, Harvard University,
Cambridge, Massachusetts, U. S. A.

In the course of an investigation into a method for the dynamic measurement of the hardness of phonograph record materials, it became apparent that it would be necessary to measure peak dynamic displacements at least as small as 0.03 microns in the presence of low-frequency fluctuations considerably greater than 0.6 microns. The selection of a displacement pickup for performing these measurements was dependent upon the requirement that the size and weight of the pickup be quite small and that it be capable of operating at frequencies as low as 100 Hz. None of the vibration pickups commercially available appeared to meet these requirements. For example, the class of transducers which use an independent fixed mounting for one of the pickup elements could not be used on account of the presence of the low frequency fluctuations. On the other hand, the vibration pickups which do not require a fixed mounting are usually too large, too heavy, or too insensitive for this application.

The instrument to be described here makes use of a mass-spring system whose resonance frequency is adjusted to lie above the frequencies of the large-scale fluctuations but at least one octave below the lowest frequency to be measured. At the measurement frequencies, therefore, the mass is decoupled from the mounting base to which the mass support-spring is attached. In this situation, the mass remains stationary as the base vibrates, and the relative motion between the mass and the base is precisely the motion of the base itself. This principle of operation is most commonly used in the seismograph; hence the use of the term "seismic" pickup.

The seismic mass and its mounting base are electrically insulated from each other and form the two electrodes of a small capacitor. Since the value of this

---

+ This study was supported in part by funds made available under a contract with the

capacitor varies with the separation between the electrodes, the capacitance is directly related to the amplitude of vibration of the mounting base. The capacitor electrodes are used to vary the coupling between a fixed-amplitude rf generator and a double-diode detector circuit, whose rectified output voltage is proportional to the variation in capacitance, and hence to the displacement of the mounting base.

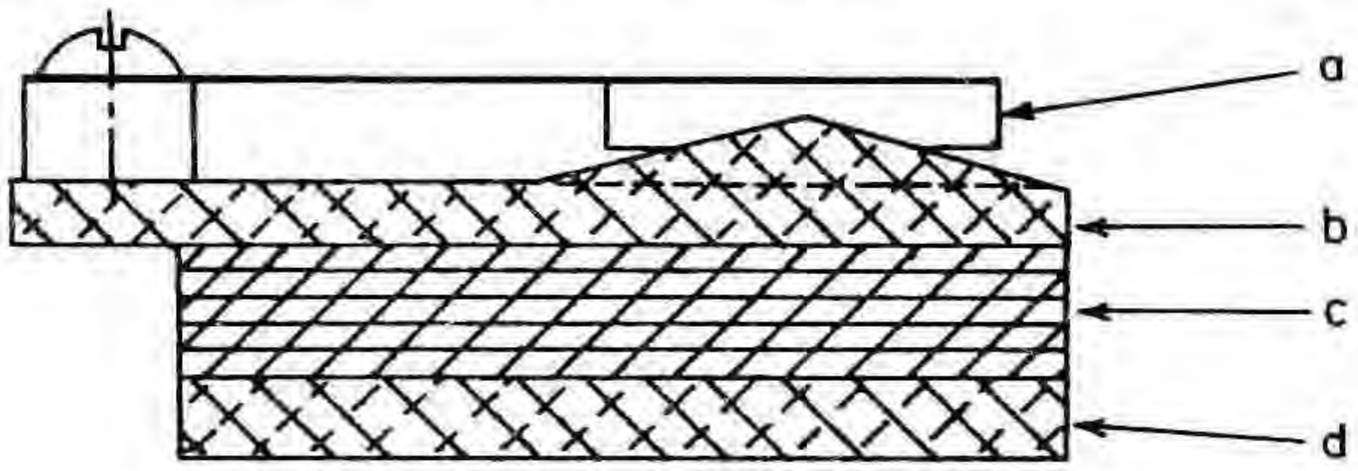

Fig. 1. Diagram of the seismic pickup.

The detector circuit employed requires that both electrodes of the capacitor be insulated from ground. For this reason the mounting base is composed of an aluminum top plate (b) which is the fixed electrode of the variable capacitor, a Teflon insulator (c), and an aluminum bottom plate (d), as indicated by the letters on the diagram in Fig. 1. The low dielectric constant of the Teflon minimizes the parasitic capacitance between the two plates. Two triangular shoulders are attached to the top plate (b), and rise on both sides of the seismic mass. These shoulders are designed to provide a large capacitance variation with displacement between the fixed electrode and the seismic mass and to make the variation approximately linear. The seismic mass itself (a) consists of a small brass block, which is attached to its phosphor-bronze, cantilever, leaf-spring support by means of a conductive epoxy cement. In order to convert the cantilever to a lumped system and provide more control over the system resonances, a transverse notch has been made in the support end of the leaf spring. The depth of the notch is adjusted by trial to provide the desired frequency of resonance. Since the parts of the pickup are held together by Nylon screws, the need for insulating bushings has been eliminated. The size of the present pickup is 2.0 cm long, 0.4 cm wide, and 0.8 cm high, and its total weight is less than 1.5 gm.

Figure 2 is a diagram of the detection circuit. An rf voltage from a 1-mc, crystal-controlled oscillator is applied to the seismic mass, which is one electrode

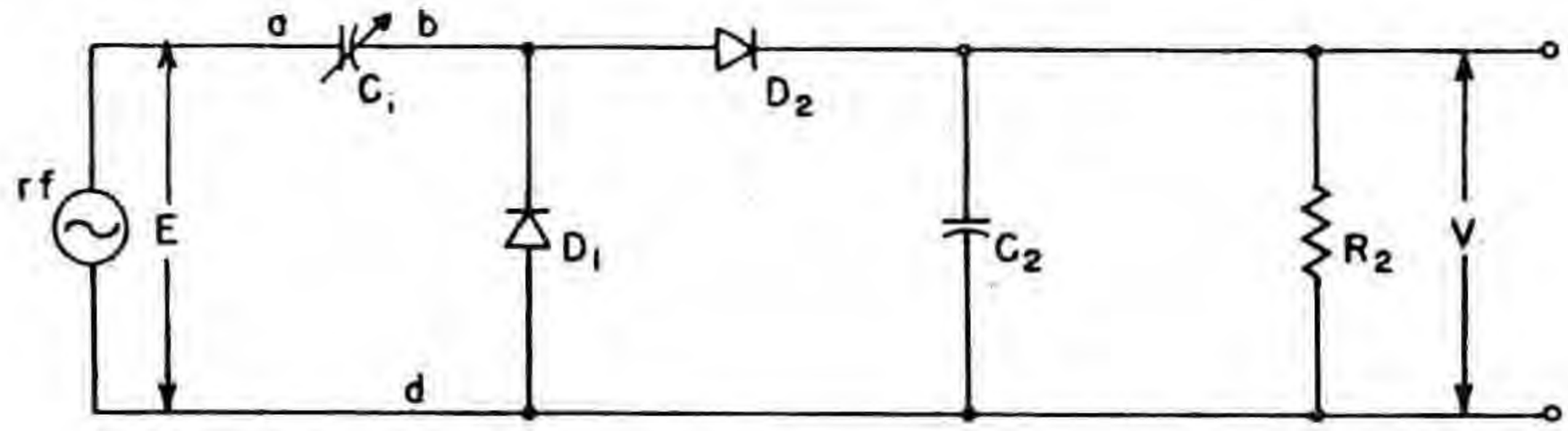

Fig. 2. Pickup detector circuit.

(a, Fig. 2) of the variable capacitor C_1. The output voltage from the pickup is taken from the top plate (b) of the pickup mounting base, which forms the other electrode (b) of C_1. The bottom plate of the pickup base (d) is held at ground potential, and is generally in contact with the system whose vibrations are being measured. The detection circuit is designed to satisfy the two conditions, $C_2 \gg C_1$ and $fR_2C_1 \approx 1$, where f represents the frequency of the applied rf voltage and R_2 includes the effect of the back resistance of diode D_2 on the rate of discharge of capacitor C_2. The total weight of the pickup has been kept to a minimum by using small, microminiature, semiconductor diodes. Diode D_2 is attached directly to the top plate of the pickup base in order to reduce the effects of stray capacitance. Diode D_1, which is connected between the top plate and the bottom plate of the pickup base, has been placed in a cavity hollowed out of the Teflon insulator. The mean value of the pickup capacitance for the present pickup is approximately 2 pF. Optimum operation for this pickup was found to occur when R_2 and C_2 were 0.3 MΩ and 1000 pF, respectively.

The application for which this pickup was designed entailed the measurement of vibration displacements at discrete frequencies. For this reason, no attempt has been made to ensure that the pickup response is not a function of frequency, and the pickup sensitivity must therefore be determined independently for each frequency at which measurements are to be performed. Representative values of the sensitivity for the present pickup at 200 and 500 Hz are, respectively, .495 and 1.06 volts/micron, are the units are given in terms of rms voltage and peak displacement. One extensive calibration was performed at 200 Hz in order to observe the variation in the pickup output voltage with displacement. This variation was found to be linear over a wide range of amplitude extending from 1.4 microns to about 0.002 microns (20 Angstroms). At the

latter level, the output signal from the detector was comparable to the noise voltage.

It should be pointed out that the percentage modulation of the pickup capacitor is extremely small for even the largest of the displacements mentioned above. At a peak displacement of 1.4 microns, when the rf generator output is 22 volts (rms), the signal output from the detector consists of a 15 volt dc carrier on which is superimposed a variational signal of only 6 millivolts. Hence, in order to suppress the noise to the level corresponding to peak displacements of the order of 20-50 Ångstroms, it is necessary to use a highly selective output indicator, such as a narrow-band wave analyzer, preceded by a low-noise amplifier, and to exercise great care in the selection of an rf oscillator and power supply. The oscillator and its power supply were the source of the noise that was most difficult to eliminate, and the results cited above were only obtained by the use of a crystal-controlled oscillator incorporating an AVC feedback network and supplied with a well regulated and filtered bias voltage and a dc filament current. Of course proper grounding of the system is also necessary.

The pickup described above was designed to measure vibrations at low audio frequencies which are superimposed on large-scale fluctuations at sub-audio frequencies. It is evident that its use is by no means limited to these conditions, however, and it is suggested that it may be useful in many situations where a sensitive pickup of small size and weight is required.

G33

FOURTH INTERNATIONAL CONGRESS ON ACOUSTICS
COPENHAGEN 21.-28. AUGUST 1962

Estimation of larynx-pulse timing during speech

J.S. Gill (Joint Speech Research Unit of the British Post Office, Eastcote)

High-speed cine-photography of the larynx during speech production reveals that the glottal area varies smoothly with time, usually in an approximately triangular and non-oscillatory manner[1]. The volume-velocity of the glottal airflow has been shown to vary similarly provided that the sub-glottic pressure remains constant[2]. Our measurements show that the relationship between the glottal area and the resulting sound pressure during phonation is typically of the form shown in fig. 1.

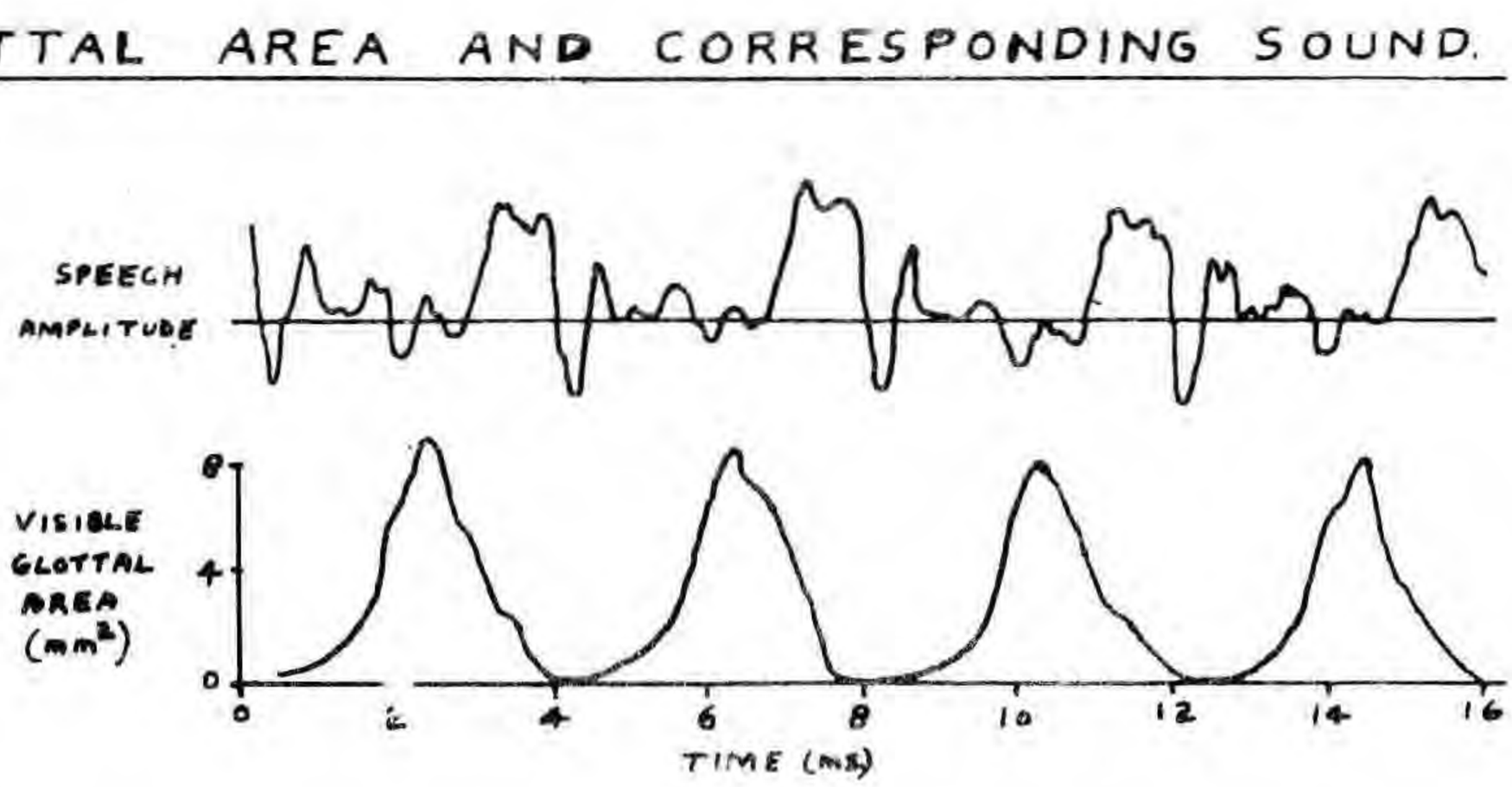

Fig. 1.

Data obtained from both high-speed cine-photography and inverse-filtration indicate that the difference in duration between successive glottal cycles usually varies smoothly with time although occasionally irregularities occur at the beginnings and endings of voicing. It can be seen from fig. 1 that although the larynx pulses are approximately equi-spaced in time they all differ slightly in shape.

During speech the main resonances of the vocal tract are excited two or three times during each larynx pulse, with the major excitation usually occuring at closure[3]. Quite small changes in the shape of the larynx pulse can vary the excitation pattern appreciably. Thus it is possible for the fundamental frequency of the glottal wave to vary smoothly whilst the excitation pattern of the majority of the speech spectrum is fluctuating.

The fine structure of the vocal excitation is not fully preserved in the existing systems of analysis-synthesis telephony. In many of these each larynx pulse is represented by a single narrow pulse which is situated, ideally, at the instant of maximum vocal excitation. Some of the properties of a pulse-by-pulse excited vocoder have been studied, using the "pitch-handwriting" technique[4].

The method of larynx-pulse estimation which is used when "handwriting" is described briefly in the following paragraphs.

First the recorded signal is examined to estimate, wherever possible, the approximate spacing of the larynx pulses and the locations of the major vocal tract excitations. These excitations are located by searching for those instants at which the speech waveform departs from the natural damped-oscillatory response of the vocal tract. The major point of excitation of each clearly-evident glottal cycle is recorded, in synchronism with the speech, on a second track of the recording.

When, occasionally, there appear to be two points of substantially equal excitation within a glottal cycle the handwriting pulse is placed in synchronism with whichever is the more compatible with the behaviour in the immediate vicinity. The effects of the glottal flow and of the vocal tract occasionally combine in a manner which conceals the excitational clues, leaving the speech waveform substantially sinusoidal at a fairly low harmonic of the estimated fundamental frequency of the adjacent regions. In this case a sequence of points is chosen to give the smoothest transition across the uncertain region and the second track of the tape is marked accordingly.

These twin-channel recordings of speech and "handwritten", one-pulse-per-larynx-pulse, excitation have been used with an 18-channel vocoder [5]. Speech synthesized from this material sounded slightly harsh. It seemed that this might be caused by the inherent positional uncertainties of the estimation process and so the effects of positionally-smoothing the excitation pulse stream were studied using the system shown in fig. 2.

PULSE-POSITIONAL SMOOTHING.

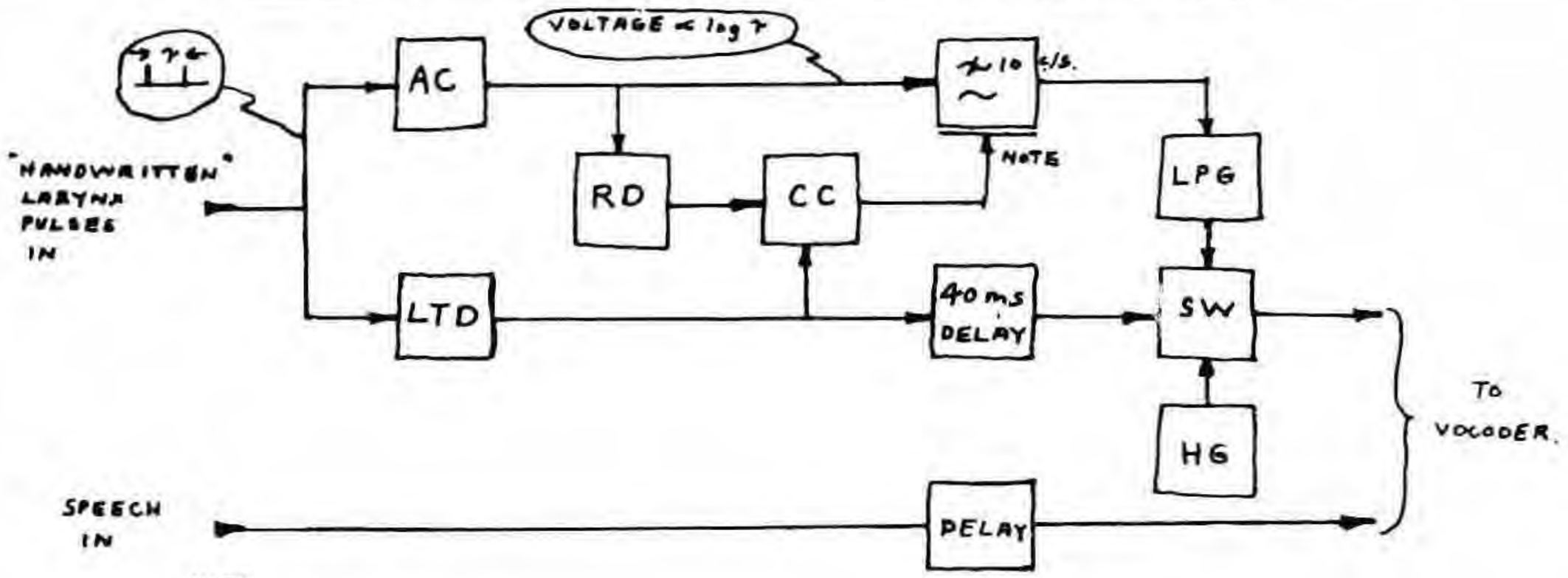

Fig. 2.

If, at the start of voicing, the "handwritten" pulses are regularly-spaced the excitation is switched to voiced, clamping is removed, the voltage analogue remains constant for about 40 ms at the initial value and then synthesis commences. When, however, the first few pulses are irregularly-spaced they are discarded by retaining the clamping until regularity is established. The corresponding speech is then synthesized from pulses which occur at the same spacing as that of the first regularly-excited part of the original sound.

A comparison of the two types of excitation showed that pulse-positional smoothing improved the naturalness of the synthetic speech. The result was obtained consistently from all of our "handwritten" recordings of spoken prose. A further experiment was therefore made, using "handwritten" recordings of conversational telephone-

quality speech. This further experiment used 40 different utterances each of about 2 seconds duration, from the speech of 3 male talkers, and none of the 12 judges had previously heard synthetic speech. This experiment also indicated that the naturalness was significantly improved by the smoothing.

These results indicate that if each larynx pulse is to be approximated by a single narrow pulse then the described method of positional smoothing, which incidentally simplifies the transmission requirements, also improves the naturalness of the synthesized speech. This tentative conclusion is not, however, supported by the results of Kersta, Bricker and David [6] and of Lieberman [7] which suggest that even small positional irregularities should be preserved to achieve naturalness. The reasons for this difference may lie partly in the choice of material and partly in the precise method of excitation estimation.

The effect of positionally-smoothing occasional gross glottal irregularities, such as occur in "creaky voice"[8] has not been studied. Further work on this subject is needed, based preferably on an inverse-filtration method of excitation estimation.

References

1. FARNSWORTH, D.W. "High-speed motion pictures of the human vocal cords". Bell Laboratories Record 18, 203-208 (1940).

2. FLANAGAN, J.L. "Some properties of the glottal sound source". J. Speech and Hearing Research, 1, 99-116 (1958).

3. HOLMES, J.N. "An investigation of the volume velocity waveform at the larynx during speech by means of an inverse filter". Paper submitted to IVth I.C.A., Copenhagen and to Speech Communication Seminar, Stockholm (1962).

4. GILL, J.S. "A study of the requirements for excitation control in synthetic speech". Proceedings of the IIIrd I.C.A., Stuttgart 1959, p. 221, Pub. Elsevier (1961).

5. SHEARME, J.N., HOLMES, J.N. "An experiment concerning the recognition of voices". Language and Speech, 2, 121-131 (1959).

6. KERSTA, L.G., BRICKER, P.D., DAVID, E.E. "Human or machine? - a study of voice naturalness". J. Acoust. Soc. Amer. 32, 1502(A), (1960).

7. LIEBERMAN, P. "Perturbations in vocal pitch". J. Acoust. Soc. Amer. 33, 597 (1961).

8. MOORE, P., LEDEN, H. VON, "Dynamic variations of the vibratory pattern of the human larynx". Folia Phoniatrica, 10, No. 4, 227-8 (1958).

H33

FOURTH INTERNATIONAL CONGRESS ON ACOUSTICS
COPENHAGEN 21.-28. AUGUST 1962

Die Bedeutung des vegetativen Nervensystems für die Entstehung des Reizfolgestroms

Wiktor Jankowski, Jerzy Giełdanowski, Władysław Birecki

Viele experimentelle Arbeiten befaßten sich bisher mit der Untersuchung des Einflusses des vegetativen Nervensystems auf die Funktionen des inneren Ohres. Die erzielten Ergebnisse weichen jedoch sehr voneinander ab. Um sich darüber ein eigenes Urteil bilden zu können, untersuchten die Verfasser die Wirkung gewisser, das sympatische und parasympatische System reizender und lähmender Mittel auf das Verhalten des Reizfolgestroms (MP) des Cortischen Organs.

Von den das sympatische System reizenden Mitteln wurden Corbasil (15oμg/kg) und Ephedrin (3mg/kg), von den lähmenden - Ismelin (3 mg/kg) und Hydergin (1 mg/kg) angewandt. Zugleich wurde der Arterienblutdruck registriert. Um die Zeit der Sekretionshemmung des Katecholamins in den Endungen der sympatischen Nerven nach der Ismelinverabreichung zu bestimmen, wurde die Kontraktion der Membrana nicticans beobachtet.

Als ein das parasympatische System reizendes Mittel wurde Physostygmin (2ooμg/kg) und als Lähmungsmittel - Atropin (2oμg/kg) gewählt.

Außerdem wurde auch Azapyrolidin verabreicht, welches beide Ganglienarten des Vegetationssystems lähmt.

Um nachzuprüfen, ob diese Mittel durch das vegetative Nervensystem auf das Cortische Organ einwirken können, oder ob es sich um eine spezifische Wirkung des chemischen Stoffes handelt, wurde ein typischer physiologischer Test angewandt: Man beobachtet die

Wirkung des das sympatische und parasympatische System reizenden Mittels vor und nach der Verabreichung der Präparate, welche die einzelnen Systeme blockieren. Während der Experimente wurde das MP bei der Reizung mit Reintönen mit 1o24, 2o48, 4o96, 8192 Hz beobachtet.

Nach der Verabreichung beider Sympatikotonika war kein eindeutiger Zusammenhang zwischen der hervorgerufenen Hypertension und der Depression des MP-Wertes festzustellen. Die beträchtliche Blutdruckerhöhung nach der Ephedringabe, ergab einen geringeren Potentialrückgang im Vergleich mit den nach der Corbasilgabe beobachteten Veränderungen. Jedoch entspricht die Zeitdauer der Blutdruckerhöhung ungefähr der Zeitdauer der Veränderungen im MP. Das kann dafür sprechen, daß die MP-Schwankungen vor allem von der Zeitdauer der Blutdruckveränderungen abhängen. Ein deutlicherer Zusammenhang zwischen dem Potential des sympatischen Systems und dem MP wurde nach der Ephedringabe festgestellt. Die Veränderungen waren in beiden Parametrien sehr ähnlich, d.h. ein plötzlicher Blutdruckanstieg wurde von einem eben so schnellen Sinken des MP-Wertes begleitet.

Die nach der Hyderginverabreichung erzielten Ergebnisse sprechen für eine gewisse Beziehung zwischen der Depression des sympatischen Nervensystems, welche die Senkung des Blutdrucks ausdrückt und den registrierten MP-Werten. Die nach der Ismelingabe erzielten Ergebnisse bestätigen jedoch diesen Zusammenhang nicht. Nach der Ismelingabe wird ein bedeutender Rückgang des MP noch vor der Blutdrucksenkung beobachtet. Außerdem besteht kein Parallelismus zwischen der Spannung des "microphonic response" und dem Hemmungsgrad der Adrenalinausscheidung im peripheren Nervensystem.

Die nach der Ephedrinverabreichung vor und nach der Blockade des sympatischen Nervensystems erhaltenen Ergebnisse sind deutlich

verschieden. Die Veränderungen des MP waren bei Tieren mit blockiertem sympatischen Nervensystem sichtlich geringer. Auch scheint es, daß das Entstehen und der Rückgang des MP-Wertes im letzten Falle langsamer vor sich ging, als nach Verabreichung des Ephedrins allein. Also muß das Ephedrin in gewissem Grade durch das vegetative Nervensystem auf das MP einwirken, wenngleich auch eine gewisse spezifische Wirkung der chemischen Bestandteile nicht ausgeschlossen werden kann.

Die Versuche mit der Blockade des parasympatischen Nervensystems mit Atropininjektionen zeugen dafür, daß dieses parasympatikolytische Mittel keinen Einfluß auf das MP hat.

Das Physostygmin, ein das parasympatische System reizendes Mittel, übt einen deutlichen depressiven Einfluß auf das MP des Cortischen Organs aus, welcher etwa eine Stunde andauert. Die Verabreichung derselben Physostygmindosis einem atropinbehandeltem Tier löste in dem MP Veränderungen mit ähnlichen Werten aus, wie vor der Atropinverabreichung. Im zweiten Fall verlief die Reaktion nur wenig langsamer, und die Veränderungen dauern etwas länger an. Die deutlichen MP-Senkungen wurden von unbedeutenden Blutdruckschwankungen begleitet. Diese Abweichung ist wohl nicht überraschend, wenn wir berücksichtigen, daß sich diese Verbindung schädlich auf das Zwischenepithel der Hirnkapilaren auswirkt. Das Physostygmin dringt leicht in den Liquor cerebro-spinalis ein und kann auch gleichzeitig in den Liquor labirynthi eindringen.

Die MP-Veränderungen nach Ausschaltung des Einflusses des vegetativen Nervensystems auf die Funktionen des inneren Ohres wurden nach Verabreichung zweier verschiedener Azapyrolidindosen beobachtet. Die kleine, 25 μg/kg-Dosis, welche das G. cervicale sup. lähmte, aber noch keinen Einfluß auf den Arterienblutdruck ausübte, verursachte keinerlei Störungen im MP. Dagegen rief die

große 2 mg/kg-Dosis, welche eine starke hypotensive Wirkung ausübte, eine deutliche MP-Spannungssenkung hervor. Das dürfte für einen verhältnismäßig geringen Einfluß des vegetativen Systems und für einen hohen Einfluß der Blutdruckveränderungen auf das MP in solchen Situationen sprechen, wo das innere Ohr mit einer gewissen Autonomie arbeitet.

Die Kontrolluntersuchungen wurden mit der Verabreichung von Mitteln durchgeführt, welche die Gefäßlumen (ausschließlich des vegetativen Nervensystems) zusammenziehen und erweitern (Vasopressin, Papaverin). Sie erwiesen, daß die MP-Werte jeweils bei größeren Arterienblutdruckschwankungen sinken.

Die dargestellten Untersuchungsergebnisse führten uns zu folgenden Schlüssen:

1. Das Fehlen eines Atropin- und Physostygmineinflusses auf das MP durch das parasympatische System zeugt für einen minimalen oder gar keinen Anteil des parasympatischen Systems an den bioelektrischen Funktionen der Haarzellen des Cortischen Organs.
2. Die Abschwächung der Ephedrinwirkung auf das MP nach Blockade des sympatischen Systems spricht für das Bestehen eines Zusammenhanges des "microphonic response" - Wertes und der Spannung im sympatischen System.

J33

FOURTH INTERNATIONAL CONGRESS ON ACOUSTICS
COPENHAGEN 21.-28. AUGUST 1962

BORDONI PEAK IN ALUMINUM

Fausta Fanti - Istituto Nazionale di Ultracustica "O.M.Corbino", Roma(Italy)
Mario Nuovo - Istituto Nazionale di Ultracustica "O. M.Corbino", Roma(Italy)

The dissipation peak due to dislocations in aluminum was originally noticed by Bordoni (1) and later confirmed by a large numebr of investigations on the same metal (2), (3), (4), (5), (6).

Notwithstanding this comparatively large amount of experimental evidence the characteristic parameters of the effect[1] (activation energy W, characteristic time τ_0, width of the relaxation spectrum) are not known as accurate enough for two main reasons. First, every set of self-consistent measurements (i.e. measurements made on specimens having the same purity and the same hystory) covers a rather narrow frequency range.

Secondly, the relaxation peak due to dislocations in aluminum anneals out at room temperature in a few days. Hence much of the experimental data concern very low peaks. Both difficulties have been overcome in the present work as the measurements have been carried out by an ultrasonic technique (10) on two specimens of 99.995% Aluminum machined from the same sheet (Table I).

TABLE I

Characteristic of the specimens

Specimen	Mechanical and heat treatments	Diameter mm	Final thickness
Circular plate 1	Machined from the casting and compressed to the final shape with a reduction in thickness of 1.6%	30.0	4.92
Circular plate 2	Machined from the casting and compressed to the final shape with a reduction in thickness of 2.7%	30.0	2.96

The frequency of the measurements covers the range from 28 kc.s^{-1} to 140 kc.s^{-1} and the peaks were kept high enough by maintaining the specimens cool enough during the whole set of experiments.

---

(1) For the meaning of the symbols see paper (7).

The experimental curves wich give the dissipation coefficient Q^{-1} as a function of the absolute temperature T show, (fig. 1), that two peaks of not very different amplitude are present, corresponding to two different relaxation effects both thermally activated but with different characteristic parameters (fig. 2). This result is consistent with those obtained for all, f.c.c. metals (9), (10)(11). It may by added that in b.c.c. metals the dissipation curves are also asymmetrical, the lower temperature branch being higher than the upper branch (12).

The frequencies f_m, f'_m and the temperatures T_m and T'_m of the peaks are listed in Table II with the maximum dissipation coefficients Q_m^{-1}, Q'^{-1}_m.

TABLE II

Experimental data of the two peaks

Specimen	f_m kc. s^{-1}	T_m °K	Q_m^{-1}	f'_m kc. s^{-1}	T'_m °K	Q'^{-1}_m
2	28.38	123.0	$71.5 \cdot 10^{-5}$	28.58	89.0	$64.0 \cdot 10^{-5}$
1	43.70	126.0	69.5	44.00	92.7	41.0
2	103.6	135.0	78.0	104.4	97.5	43.0
1	138.9	137.5	72.5	140.0	101.0	48.5

From this data the activation energies and the limiting times have been computed (7) obtaining the following values:

Peak at higher temperature: $\overline{W} = 0.16$ eV; $\overline{\tau}_o^{-1} = 6.9 \cdot 10^{11}\ s^{-1}$

Peak at lower temperature: $\overline{W}' = 0.107$ eV; $\overline{\tau}_o'^{-1} = 12.6 \cdot 10^{10}\ s^{-1}$

As it was shown by Verdini (13) a characteristic temperature may be defined for the relaxation effect according to the following equation

$$T_B = \frac{\overline{W}}{k} = \frac{\overline{W}}{8.617} \cdot 10^5 \quad °K$$

For all the investigated f.c.c. metals T_B appears to be related to the melting Temperature T_f by the empirical relation $T_B = (1.2 \pm 0.2)\ T_f$. From the above values of $\overline{W}$ and $\overline{W}'$ one finds,

$$T_B = 1,860\ °K \quad ; \quad T'_B = 1,240\ °K \quad .$$

The second of these values is very near to that computed according to the empirical relation ($1,2\ T_f = 1,117$ °K).

An approximate evaluation of the symmetrical part of the relaxation spectrum for the peak at higher temperature, was made by using the high temperature branch of the dissipation curves assuming that the spectrum of the relaxation times is of the bell-shaped type proposed by Fuoss and Kirkwood (7), (8).

The spectrum width (measured by the ratio between the times τ_1 , τ_2) for which the height of the spectrum is $1/\sqrt{2}$ of the maximum height, is:

$$\frac{\tau_1}{\tau_2} = 17.8$$

The analysis of the above results shows that the fundamental parameters of the relaxation effect in aluminum have values near to those found in the other f.c.c. metals (7), (10), (11). This gives additional support to the idea that the motion of dislocations has an intrinsic character (12) in agreement with the present theoretical treatments of the same problem.

References :

(1) P.G. BORDONI, J. Acoust. Soc. Am., 26 (1954) 495.

(2) T.S. HUTCHISON and G.J. HUTTON, Canad. J. Phys., 36 (1956) 1498.

(3) T.S. HUTCHISON and A.J. FILMER, Canad. J. Phys., 34 (1956) 159.

(4) T.S. HUTCHISON and G.J. HUTTON, Canad. J. Phys., 82 (1958) 36.

(5) N.G. EINSPRUCH and R. TRUELL, Phys. Rev., 109, (1958) 652.

(6) K. KAMISAKI and T. HIRONE, J. Phys. Soc. Japan, 16 (1961) 2077.

(7) P.G. BORDONI, Nuovo Cimento, suppl. al vol. 17 (1960) 43.

(8) R.M. FUOSS and J.G. KIRKWOOD, Journ. Chem. Phys., 63 (1941) 385.

(9) D.H. NIBLETT and J. WILKS, Phil. Mag., 1 (1956) 415; 2 (1957) 1427.

(10) P.G. BORDONI, M. NUOVO and L. VERDINI, Nuovo Cimento, 14 (1959) 273.

(11) P.G. BORDONI, M. NUOVO and L. VERDINI, Nuovo Cimento, suppl. 1 al vol. 18 (1960) 55.

(12) P.G. BORDONI: Internal friction in the body-centered cubic metals Niobium and Tantalum. Contract No DA91-591-EUC-1618 (01-7204-61), novembre 1961.

) L. VERDINI: Atti del Congresso Italiano di Fisica, 385 Como 1961 (in press).

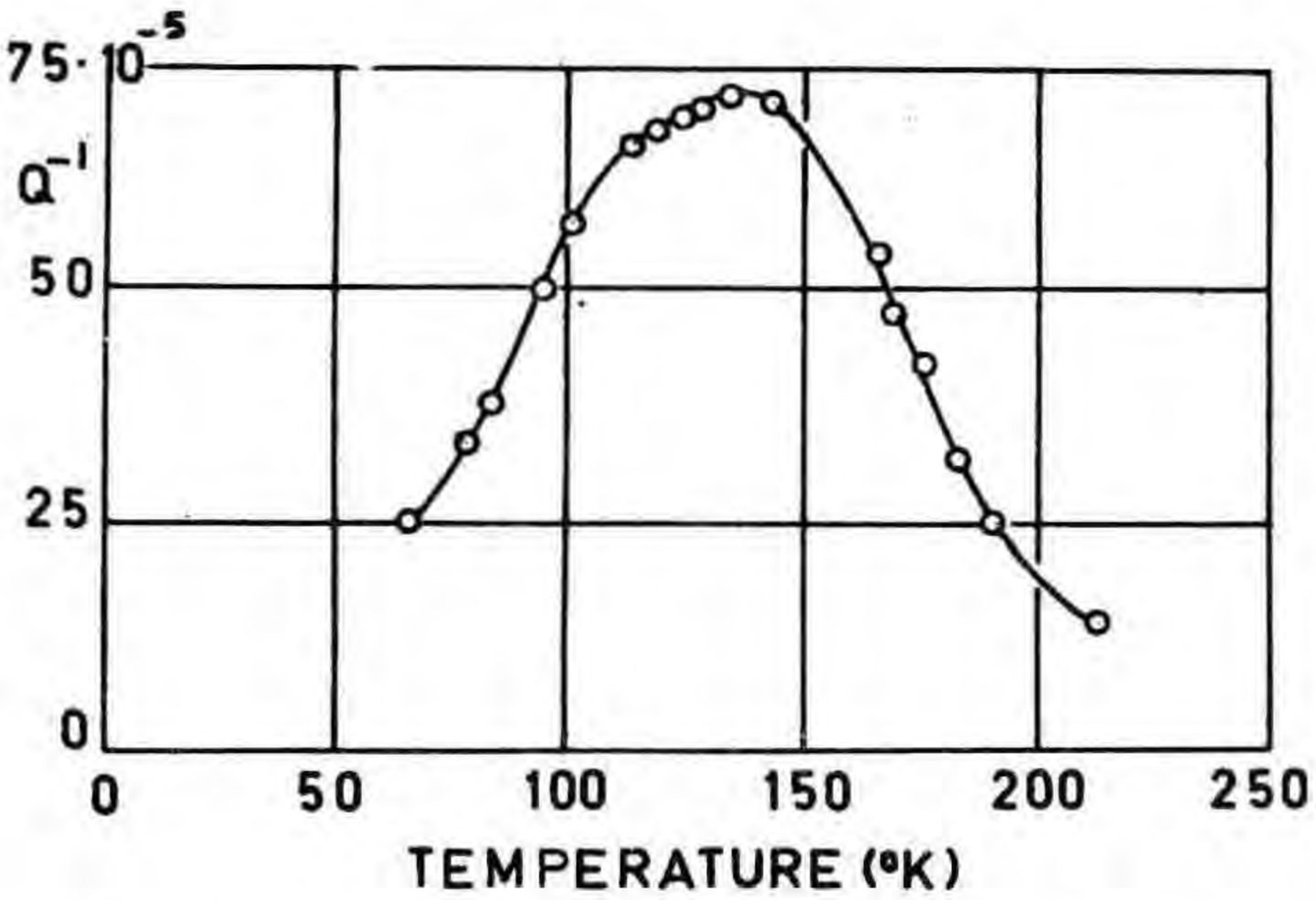

FIG. 1 - Dissipation peak at the frequency $f_m = 138.9$ kc. s^{-1}.

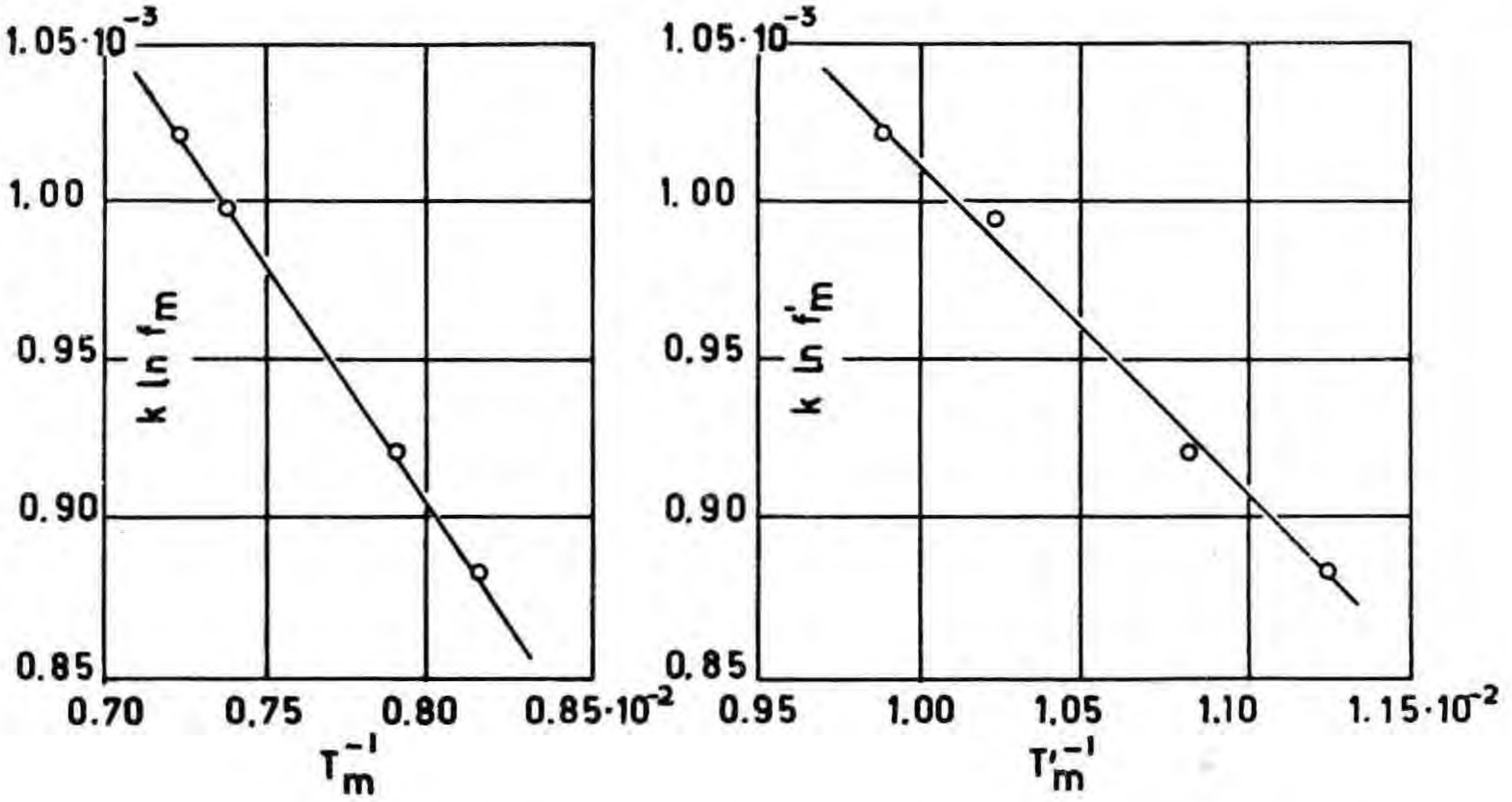

FIG. 2 - Frequency dependence of the temperatures T_m and T'_m for the two peaks.

K33

FOURTH INTERNATIONAL CONGRESS ON ACOUSTICS
COPENHAGEN 21.-28. AUGUST 1962

TRANSDUCER CALIBRATION FROM NEAR-FIELD DATA

W. James Trott and Robert J. Bobber
U. S. Navy Underwater Sound Reference Laboratory, Orlando, Florida, USA

If a transducer is effectively a point on a spherical wave, a line on a cylindrical wave (with the line parallel to the cylinder axis), or a plane on a plane wave, the ratio of output voltage to free-field sound pressure (the receiving sensitivity of the hydrophone) will be the same in each case. The transmitting current responses of a point, a line, and a plane are different, however, and depend on the mode and extent of the wave propagation. Normally, the transmitting current response S_s is defined in terms of the sound pressure in a spherical wave in the far field and the ratio of the receiving sensitivity to this transmitting current response is the reciprocity parameter calculated by MacLean[1] and Cook[2]. Simmons and Urick[3] have treated the plane-wave case where the transmitting response S_p is defined as the ratio of the average pressure in the plane-wave, nondivergent near field of a piston transmitter to the transducer current. Bobber and Sabin[4] have similarly treated the cylindrical-wave case where the transmitting current response S_c is the average pressure in the near field of a line or cylindrical transducer per unit input current.

The ratio of receiving to transmitting responses, or the reciprocity parameter, used in reciprocity calibrations in the three cases are

$$\text{Spherical} \qquad J_s = (2/\rho c)(d\lambda)$$

$$\text{Cylindrical} \qquad J_c = (2L/\rho c)(a\lambda)^{\frac{1}{2}}$$

$$\text{Plane} \qquad J_p = (2A/\rho c)$$

where ρ is the density of the medium, c is the speed of sound in the medium, d and a are the reference distances at which the transmitted sound pressures are measured, λ is the wavelength, L is the length of the line, and A is the area of the plane.

In a physical sense, all reciprocity parameters are the ratio of the volume velocity emanating from a transducer to the sound pressure at a specified reference point. Consequently, with a fixed volume velocity from one plane radiator transducer, the near-field average plane-wave pressure is related to the far-field spherical-wave pressure by the ratio J_s/J_p. It follows then that for a plane transmitter of finite area, the free-field voltage sensitivity M_p is given by

$$M_p = S_p J_p = S_s J_s. \tag{1}$$

This equation provides a simple and useful relation between near- and far-field calibrations.

The plane-wave transmitting response S_p can be found by scanning a plane of area A with a small probe transducer. The plane must, of course, be parallel to the source plane, and at a distance less than A/λ. The scanning area A must be equal to or greater than the real area of the transducer. Then

$$S_p = \int E_t dA / I_p M_t A \tag{2}$$

where E_t is the complex voltage output of the scanning transducer, I_p is the input current to the plane transducer, and M_t is the receiving sensitivity of the scanning transducer.

From equations (1) and (2)

$$S_s = S_p J_p / J_s = \frac{\int E_t dA}{I_p M_t A} \frac{2A}{\rho c} \cdot \frac{\rho c}{2d\lambda} = \frac{\int E_t dA}{I_p M_t} \frac{1}{d\lambda}. \tag{3}$$

If both the plane and scanning transducers are reciprocal, the system transfer impedance is the same in each direction, or $|E_t/I_p| = |E_p/I_t|$, where E_p is the voltage output of the plane and I_t is the current input of the probe. Then

$$\int E_t dA/I_p = \int E_p dA/I_t. \tag{4}$$

From equations (1), (3), and (4),

$$M_p = \frac{\int E_p dA}{I_t S_t} \frac{1}{d\lambda}, \tag{5}$$

where S_t is the transmitting current response of the probe transducer. Equations (3) and (5) thus provide formulas for finding far-field sensitivity of a plane transducer from near-field measurements.

Note that S_p is equation (2) depends on the arbitrary selection of A, but S_s is independent of A in equation (3). Using an A larger than the sound beam will lower the average sound pressure, but will not change the integral in equations (3) or (5). Simmons and Urick[3] have demonstrated experimentally and Williams[5] has shown theoretically that the average pressure in a plane in the near field of a piston radiator is 80–85 per cent of the pressure in a true uniform plane wave, or where A is infinitely large. This difference can be treated as an effective area smaller than the plane piston area. Since the area in this analysis is equal to or greater than the piston area, the integrals in equations (3) and (5) are not affected by the assumption that the average of complex pressures is equivalent to a true plane-wave pressure.

For a line or cylindrical transducer of finite length, the free-field voltage response M_L is given by

$$M_L = S_c J_c = S_s J_s. \tag{6}$$

By the same argument as before,

$$S_s = \frac{\int_0^L E_t dx}{I_L M_t} \frac{(a\lambda)^{\frac{1}{2}}}{(d\lambda)}, \tag{7}$$

where I_L is the current input into the line transducer and x is the scanning distance along a line, parallel to the source line, and at distance a such that $3 < ka < 2\pi(L/\lambda)^2$, where k is the wave number $2\pi/\lambda$.

Also

$$M_L = \frac{\int_0^L E_L dx}{I_t S_t} \frac{(a\lambda)^{\frac{1}{2}}}{(d\lambda)}. \tag{8}$$

Equations (7) and (8) are formulas for finding far-field sensitivity of line or cylindrical transducers from near-field measurements.

In practice, it is convenient to calibrate a line by scanning with a point and then scanning the plane with the line. The line will average the sound pressure in one dimension and the scan will average it in the second dimension.

With this technique, the line must be uniform. If the line is a series of elements electrically connected in parallel so that the E_L/M_L is the average pressure, then equations (3) and (5) become

$$S_s = \frac{\int_0^Y E_L L dy}{I_p M_L d\lambda} \tag{9}$$

$$M_p = \frac{\int_0^Y E_p L dy}{i_L S_c d\lambda}, \tag{10}$$

where y is the distance in the scanning direction and LY = A.

This theory and technique have been tested on three different types of transducers. The first was a relatively poor approximation to a line. It was 7.7 wavelengths long and consisted of 18 individual elements with broad but not omnidirectional radiation patterns. The second was a thick cylinder 5 wavelengths long and 6.5 wavelengths in diameter. The third was the same thick cylinder with phase delay circuitry fed to individual sectors of the cylinder so as to form an effective rectangular piston radiator 5 wavelengths long and 6 wavelengths wide. Although all configurations were severe tests of the theory, the near-field calibrations all agreed with conventional far-field calibrations within 1 db. Both types of calibrations were made at several distances. The near-field data were more consistent than the far-field data, and in the authors' opinions, tne near-field calibrations were probably the more reliable.

Since the submission of the abstract for this paper, equation (5) has been obtained by a theory that does not restrict the size and shape of the transducer.

Consider a point transmitting transducer scanning a plane area A. At each point in A the transducer is the source of spherical waves. If A is large compared to the wavelength λ, a plane wave is, according to Huygens' principle, simulated by integrating the pressure from the scanning transducer in a plane parallel to A and at a distance r_0.

Let the transmitting current response be S_T and the complex driving current I_T. Place an omnidirectional point hydrophone with free-field voltage sensitivity M_H and complex voltage output E_H in the simulated plane wave. For every point in the scan

$$E_H = M_H S_T I_T d/r, \tag{11}$$

where d is the reference distance used in defining S_T and r is the distance from the point transmitter to the hydrophone. Integrating over the area A produces

$$\int E_H dA = M_H S_T I_T d \int dA/r. \tag{12}$$

If $A \to \infty$, the pressure at the hydrophone becomes a free-field plane-wave pressure required for calibrating a hydrophone.

According to Fresnel zone theory[6] an infinite plane wave can be replaced by the first half-wave zone of area $\pi\lambda r_0$ and amplitude $1/\pi$ times the infinite plane wave

amplitude, insofar as the effect on the hydrophone is concerned. In the first Fresnel zone, $r \gg \lambda/2$, and r is approximately a constant equal to r_0. Equation (12) becomes

$$\int E_H dA = M_H S_T I_T d(1/\pi)(\pi\lambda r_0/r_0)$$

or

$$M_H = \int E_H dA / S_T I_T \lambda d. \tag{13}$$

Inasmuch as M_H is defined in terms of free-field pressure, equation (13) applies to any transducer sensitive at a point regardless of its directivity pattern. Also in a transducer consisting of many points, equation (13) applies point-by-point, and to the sum of the points. The integration in equation (13) is still required over $A \to \infty$. In practice, it is necessary only to scan a finite area where the integration is equivalent to that for an infinite area.

A small probe hydrophone was calibrated with both conventional far-field techniques and with the near-field method. The two calibrations agreed within 0.2 db.

References

1. W. R. MacLean, "Absolute measurement of sound without a primary standard," J. Acoust. Soc. Am. 12, 140 (1940).
2. R. K. Cook, "Absolute pressure calibration of microphones," J. Acoust. Soc. Am. 12, 415 (1941).
3. B. D. Simmons and R. J. Urick, "The plane wave reciprocity parameter and its application to the calibration of electroacoustic transducers at close distances," J. Acoust. Soc. Am. 21, 633 (1949).
4. R. J. Bobber and G. A. Sabin, "Cylindrical wave reciprocity parameter," J. Acoust. Soc. Am. 33, 446 (1961).
5. A. O. Williams, Jr., "Piston source at high frequencies," J. Acoust. Soc. Am. 23, 1 (1951).
6. A. B. Wood, A Textbook of Sound (The Macmillan Company, New York, 1955), Third (revised) edition, p. 333.

L33

FOURTH INTERNATIONAL CONGRESS ON ACOUSTICS
COPENHAGEN 21.-28. AUGUST 1962

Methods for Generation of High Intensity Sound

M. H. Hieken, Senior Engineer, Structures Laboratory
McDonnell Aircraft Corporation, St. Louis, Missouri

INTRODUCTION

The advent of high performance jet and rocket engines has brought with it, as an undesirable side effect, very high intensity noise fields. These noise fields are potentially damaging to the structures, the electronic equipment, and the human occupants of flight vehicles. Other problems, such as the ability to communicate in the presence of intense background noise and the psychological and physiological effects of prolonged exposure to high intensity noise, must also be resolved. In order to study these problems in the laboratory, it is necessary to simulate the noises whose effects are under investigation. This paper presents a survey of four basic types of noise generating devices which are suitable for laboratory use:

I. Conventional Loudspeakers
II. Air Stream Modulators
III. Sirens
IV. Air Jets

Some of the significant characteristics of each type will be discussed together with the advantages and disadvantages of each.

I. CONVENTIONAL LOUDSPEAKERS

The use of electrodynamic loudspeakers as a means of reproducing sound for ordinary communications and entertainment purposes is well established. The theory of operation, performance characteristics, and design principles of loudspeakers are documented in any number of references (1) (2)*.

In considering loudspeakers as a source of high intensity noise, however, one encounters the fact that the direct radiator loudspeaker is an inherently low efficiency device. The term "efficiency" as used here denotes the ratio of acoustic power produced by the loudspeaker to the total electrical power supplied to the loudspeaker. Typical values of efficiency are 3% to 5%. Thus, for a 25 cm. diameter loudspeaker rated at 20 watts, one would expect an acoustical power output of 0.6 to 1.0 watt. These acoustic powers correspond to sound intensities (relative to 10^{-16} watts/cm^2) of 131 db and 133 db, respectively, across the face of the loudspeaker. The loudspeaker thus becomes rather inefficient as a laboratory noise source for radiating large objects at sound pressure levels much in excess of 130 db. In the case considered above, for example, if it were required for the loudspeaker to produce a sound intensity of 150 db (0.1 watts/cm^2), the acoustic power output would be 49 watts. If the efficiency of the loudspeaker were 5%, then a power rating of almost 1000 watts would be required for this single 25 cm. loudspeaker.

* Numbers in parentheses refer to References listed at the end of this paper.

The efficiency of the loudspeaker as a high intensity source is somewhat increased by coupling the loudspeaker output to an appropriate matching horn. This technique may result in increasing the efficiency, and hence the acoustic power output, by a factor of 2 or 3, but the output of the speaker is now measured at the horn mouth, which may have an area greater than the speaker area by a factor of 10 or more. The increased acoustic power is therefore offset by a net reduction in the sound intensity at the mouth of the horn, which now serves as the sound source.

The main advantages of the loudspeaker are its simple control characteristics and low distortion. Since the loudspeaker will, within its linear operation range, closely reproduce any electrical signal, it can accurately simulate complex-wave sounds

II. Air Stream Modulators

The air stream modulator operates on a completely different principle than the electrodynamic and electrostatic loudspeakers. The air stream modulator consists of (a) a supply of compressed air, (b) a pneumatic flow system into which the compressed air is channeled, (c) an electromechanical modulating device which serves as a high frequency valve to modulate the air flow, and (d) a terminating horn which serves as acoustic matching of the modulator to free space, as well as to minimize turbulence in the air flow. Some of the energy contained in the flowing compressed air is converted into acoustic energy by the action of the modulator as the modulator causes pressure variations in the flowing air.

Burgess and Salmon (3) have investigated the theory of the air stream modulator. Assuming incompressible flow, these investigators estimate the sound pressure levels generated by the modulator from the following relation:

$$p = \gamma p_o \frac{u_o}{c} \frac{\Delta A}{A} \quad , \text{ where}$$

p = acoustic sound pressure
γ = ratio of specific heats
p_o = ambient pressure
u_o = average flow velocity
A = quiescent orifice area formed by the modulator element
ΔA = change of orifice area resulting from motion of the modulator
c = velocity of sound

The term, $\Delta A/A$, may be thought of as "per-cent modulation" taking place at the orifice, with 100% modulation being a desirable value. The optimum value of average flow velocity, u_o, must be based on a compromise between high values which produce large sound pressure levels and low values which result in less turbulent flow across the modulator orifice, and result in low ambient background noise levels. As a practical matter, most investigators have found an absolute pressure of 1.1 to 1.5 atmospheres just upstream of the modulator to be satisfactory.

The upper frequency limitation of air stream modulators is the resonance of the electromechanical modulating element. This resonance is in the 1000 cps to 2000 cps frequency range. Since the sound pressure level was shown to be proportional to the deflection (ΔA) of the modulator, the output will fall off rapidly above the modulator resonant frequency.

One of the most favorable aspects of the air stream modulator as a noise generator is its efficiency. The device actually requires two power sources: a pneumatic

power source to provide acoustic energy, and an electrical power supply to drive the modulating element. The electrical power supply may be an ordinary audio range power amplifier with a rating of 20 to 100 watts, depending on the electrical characteristics of the modulating element. The efficiency of the air stream modulator is generally stated as the percentage of pneumatic energy that is converted to acoustic energy. Under this definition, efficiencies of 25% have been measured.

The motion of the modulator element, and hence the acoustic output, is controlled directly by an electrical signal. This characteristic permits the modulator to reproduce complex wave signals with great accuracy. While the high frequency output of the air stream modulator falls off rapidly above the modulator resonant frequency, the air stream modulator is very useful for laboratory simulation of frequencies below 2000 cps, which is the band in which most jet and rocket engine noises have their maximum energy.

III. SIRENS

The use of a siren as a high-intensity noise generating device (sound pressure levels of 170 db or more) is attractive because of the relatively high efficiencies achieved with this type of acoustic transducer. R. Clark Jones (4) has shown that efficiencies (conversion of pneumatic energy to acoustic energy) up to 50% are possible for sine-wave output sirens. The large airflow requirements and the lack of complete control of sound waveshape are two siren characteristics which are somewhat undesirable. Since the acoustic output of a high intensity siren may be tens of thousands of watts, a correspondingly great airflow is required as an energy source. In addition, a muffled duct installation is necessary to attenuate the sound level of the exhausted air as it leaves the enclosure in which the siren is located. These problems have not detracted from the usefulness of the siren as a laboratory generator, particularly in the study of the effects of high intensity noise on structures.

The use of the siren as a source of complex-wave (random) sound has been given great impetus as a result of recent developments by von Gierke, Cole, and others, of the Aeronautical Systems Division of the US Air Force (5). Conventional sirens produce a periodic sound output as a result of a periodic port-opening and port-closing sequence. In the "wide-band" siren, a series of overlapping ports are irregularly spaced on several rotors, each of whose speed is separately controlled. This rotor and port arrangement produces a series of randomly spaced, variable width pressure pulses. A harmonic analysis of these pulses reveals a sound pressure spectral distribution very similar to the noise generated by jet and rocket engines. A degree of control of the spectral distribution is achieved by varying the speeds of the individual rotors of the siren. Thus it is possible to reproduce very high level complex wave sound fields at the high efficiencies found only in a siren.

IV. AIR JETS

The air jet is a simple device for generating high intensity noise, but the inefficiency and lack of frequency spectrum control of this device limit its usefulness as a laboratory sound source. In its most basic form, the air jet consists of a simple nozzle through which a volume of air is passed. The mechanism of sound generation is the shearing effect of the high velocity jet of air as it mixes with ambient air outside the nozzle. Sound pressure levels in excess of 160 db have been achieved with air jets. The acoustic output from a given air mass flow may be somewhat increased by heating the air, or by placing bends in the air pipe near the jet to increase the turbulence in the air flow.

Analysis and experimental data from jet engines and model air jets have shown that the air jet acoustic efficiencies (i.e., the fraction of mechanical power in the jet which is radiated as acoustic power) are typically less than 1% (6). Thus it is apparent that a large air supply is necessary for operation of air jets at any useful sound pressure levels.

The frequency spectrum of the air jet is not subject to accurate control, since the diameter of the nozzle and the velocity of the jet are the predominant factors influencing the frequency content of the generated noise. This situation is not without merit, however, since proper design of the air jet will permit adequate simulation of the noise generated by a particular jet engine (7). Some additional spectrum shaping of the output of an air jet could be obtained by employing acoustic filters to attenuate selected bands of noise.

An operational problem associated with the air jet is the large volume of air which must be discharged from the test chamber. Suitable mufflers must be provided to attenuate the noise, and yet permit the air to be exhausted at low velocities.

SUMMARY

It is evident that each of the four types of high intensity sound generators discussed - loudspeakers, air stream modulators, sirens, and air jets - has certain limitations. The loudspeaker, while producing a low-distortion sound, is inefficient as a high intensity noise source. At the other extreme is the siren, which generates high acoustic power levels but does not permit complete control of the acoustic waveshape. The air stream modulator combines some of the advantages of both the loudspeaker and the siren, in that it produces high sound levels at reasonable efficiencies and yet permits acoustic reproduction of an electrical signal within the limited bandwidth of the air stream modulator. The simple air jet is a convenient noise generator if a large supply of compressed air is available.

Further development work must be conducted on each of these types of acoustic generators to reduce their deficiencies, and thereby provide more useful instruments for generating high intensity sound.

REFERENCES

1. Philip M. Morse, "Vibration and Sound", McGraw-Hill Book Co. Inc., New York, N.Y. (1948).
2. Harry F. Olson, "Acoustical Engineering", D. Van Nostrand Co. Inc., Princeton, New Jersey (1957).
3. John C. Burgess and Vincent Salmon, "Development of a Modulated Air Stream Loudspeaker", Stanford Research Institute Final Report, SRI Project PU-886, Menlo Park, California (December, 1955).
4. R. Clark Jones, "A Fifty Horsepower Siren", Journal of the Acoustical Society of America, Volume 18, No. 2, page 371 (October 1946).
5. H. E. von Gierke, J. N. Cole, and H. L. Oestreicher, "Acoustic Siren for Generating Wide-Band Noise", Journal of the Acoustical Society of America, Volume 31, No. 1, page 116 (January, 1959).
6. C. M. Harris, Editor, "Handbook of Noise Control", Chapter 33, McGraw-Hill Book Co. Inc., New York, N. Y. (1957).
7. Philip M. Edge, Jr., "Random Noise Testing of Aircraft and Missile Components With the Aid of a Laboratory Air Jet", Bulletin of the 27th Symposium on Shock, Vibration, and Associated Environments, El Paso, Texas (February, 1959).

M33

FOURTH INTERNATIONAL CONGRESS ON ACOUSTICS
COPENHAGEN 21.-28. AUGUST 1962

Breitbandabsorber mit hohen Absorptionsgraden

E. HIRSCHWEHR
Technische Hochschule Wien, Österreich

Nach der Wirkungsweise kann man 3 Absorberarten unterscheiden: Poröse Absorber, Helmholtzresonatoren und schwingungsfähige Platten. Das Charakteristikum der beiden letzteren ist das Auftreten einer Eigenresonanz, bei der der Absorptionsgrad ein Maximum erreicht. Bei porösen Absorbern steigt der Absorptionsgrad mit der Frequenz an und erreicht ab einer bestimmten Frequenz einen etwa konstanten Wert, der in erster Linie nur mehr von der Schichtdicke, der Porosität und dem Formfaktor abhängig ist. Kombiniert man einen porösen Absorber mit einer Lochplatte, so sind 2 Fälle möglich: Beträgt die Lochfläche mehr als 20-30 % der gesamten Fläche, dann wirkt die Loch- oder Schlitzplatte nur als Abdeckung der porösen Schichte und ist im interessierenden Frequenzbereich akustisch nicht wirksam. Liegt der Prozentsatz tiefer, also etwa bei 5-15 %, oder ist die Dicke der Platte wesentlich größer als die Abmessung der Öffnungen, dann wirkt die Kombination als gedämpfter Helmholtzresonator und man kann eine breitbandige Absorption erreichen. Um auch tiefe Frequenzen in ausreichendem Maß absorbieren zu können, ist eine Abstimmung des ungefüllten Resonators auf 300-500 Hz erforderlich. Im folgenden werden 3 Kombinationsabsorber unterschiedlichen Aufbaues besprochen.

Für die Absorbertype 1 wurde neben einem genügenden Absorptionsgrad sehr hohe mechanische Festigkeit gefordert (Turnhallen). Aus einer Reihe von verschiedenen Möglichkeiten wurde eine Lochziegeltype ausgewählt, die 2.300 rhombische Löcher je m^2 besitzt, wobei die Diagonalen 1,2 und 2 cm betragen. Die Stärke der Lochziegel beträgt 10 cm. Zunächst wurde der Abstand von der festen Wand für eine Resonanzfrequenz von 300 Hz bestimmt (Bild 1, Kurve A). Bei dieser Frequenz liegt der Resonanzwiderstand unterhalb des Schallkennwiderstandes der Luft. Füllt man den Hohlraum zwischen den Lochziegeln und der festen Wand mit einem porösen Absorber, so erreicht man eine Erhöhung des Reibungswiderstandes. Dabei ist zu beachten, daß der zusätzliche Widerstand nur eine Erhöhung des Gesamtwiderstandes auf etwa das Zweifache des Wellenwiderstandes der Luft

bewirken darf, damit noch hohe Absorptionsgrade erzielt werden können. Im vorliegenden Fall war dies durch eine Schlackenwollefüllung von 4,5 kg/m^2 und einer 5 cm Holzwolleplatte möglich. Die im Kundtschen Rohr gemessenen Werte sind aus der Kurve B zu entnehmen. Die Entwicklung und Abstimmung von Absorbern ist mit einem Kundtschen Rohr leicht, übersichtlich und rasch durchführbar. Die Ergebnisse kann man jedoch nicht unmittelbar für Nachhallzeitberechnungen heranziehen. Zwei Räume wurden mit solchen Absorbern ausgestattet. Der Raum 1, mit einem Volumen von 900 m^3, besitzt - von den beiden, mit Lochziegelabsorbern verkleideten Stirnwänden abgesehen - nur Betonflächen. Der aus der Nachhallzeit nach SABINE berechnete Absorptionsgrad der Lochziegelwände (Kurve C) liegt etwas unterhalb der Meßrohrkurve, die Frequenzabhängigkeit bleibt jedoch erhalten. Die geringeren Werte im Vergleich zum Meßrohr sind auf die Raumdimensionen (langer, breiter, jedoch sehr niedriger Raum) zurückzuführen. Beim zweiten Raum mit großem Volumen (18.000 m^3) bleibt die Tendenz der Kurve ebenfalls erhalten, die Absorptionswerte sind jedoch 1,5 - 2mal so groß. Diese Kurven zeigen eindringlich, wie vorsichtig man bei der Beurteilung des Zusammenhanges zwischen Messungen mit dem Kundtschen Rohr und der Nachhallzeit sein muß.

Der Absorber 2, ein Schlitzplattenabsorber, zeigt folgenden Aufbau (Bild 2): Sperrholzschlitzplatte 0,5 cm mit 940 Schlitzen pro m^2 (0,2 x 5,5 cm), 5,5 cm Luftraum, 2 cm Weichfaserdämmplatte, Luftraumfüllung 5 kg Basaltwolle pro m^2. Die im Rohr gemessenen Werte (Kurve A) weichen bei tiefen Frequenzen stark von den im Raum gemessenen ab (Kurve B). Die Erklärung dafür ist die unterschiedliche Flächengröße im Zusammenhang mit der Einspannung (im Rohr 40x40 cm, im Raum 100x100 cm), die auch eine Änderung der Eigenschwingung der Platte bedingt. Bei der Rohrmessung fallen beide Resonanzen (schwingende Platte und Helmholtzresonator) zusammen, die Eigenresonanz der schwingenden Platte in der tatsächlichen Ausführung liegt jedoch wesentlich tiefer. Bei schwingungsfähigen Platten mit und ohne Helmholtzresonator darf man also, von der Rohrmessung ausgehend, nur unter Berücksichtigung der Resonanzverschiebung auf die Wirkung des Absorbers im Raum Schlüsse ziehen.

Für die akustische Auskleidung in Räumen mit hoher Luftfeuchtigkeit wurde eine spezielle Absorbertype entwickelt, die feuchtigkeitsunempfindlich ist und gleichzeitig ein sehr geringes Gewicht besitzt. Nach einer großen Zahl von Versuchen wurde ein blähfähiges Polystyrol, das unter dem Handelsnamen Frigolit bekannt ist, als Grundmaterial gewählt. Es besitzt

geschlossene Poren und weist an und für sich nur einen geringen Absorptionsgrad auf. In der ersten Ausführungsart wurde das Frigolit als Baustoff für einen ungefüllten Helmholtzresonator verwendet. Der erforderliche Reibungswiderstand mußte daher in den Resonatorhals verlegt werden. Es war aber nicht möglich, auch bei tiefen Frequenzen genügend hohe Absorptionswerte zu erzielen. Aus diesem Grund wurde die Deckplatte des Absorberelementes als luftleichte, schwingungsfähige Membran ausgebildet, deren Resonanzfrequenz stark gedämpft ist (Bild 3, Kurve A). Der Hohlraum des Elementes, dessen Ausmaße 50x50x10 cm betragen, wurde mit Sägespänen des gleichen Materials gefüllt. Zwischen den Sägespänen und der durchlochten Membran liegt noch eine speziell präparierte Plastikfolie, die den Reibungswiderstand auf einen optimalen Wert bringt. Die Kurve A zeigt die Frequenzabhängigkeit des Absorptionsgrades für senkrechten Schalleinfall. Zwischen 150 und 600 Hz pendelt der Absorptionsgrad um 90%. Dies ist möglich, da das Frequenzgebiet um 200 Hz durch das Mitschwingen der Deckplatte beherrscht wird, der Helmholtzresonator jedoch auf 450 Hz abgestimmt ist. Im Gebiet der höheren Frequenzen, in dem die Resonatorwirkung geringer ist, kommt die Eigenabsorption des Materials zur Wirkung. Um auch bei diesen Absorberelementen einen Vergleich mit den in Räumen zu erwartenden Absorptionsgraden zu haben, wurden Messungen in einem Hallraum durchgeführt. Das Volumen (145 m^3) und die Diffusität waren gegenüber den Normen jedoch zu gering, um einen für das gesamte Frequenzgebiet gültigen Vergleichswert zu erhalten. Aus der Kurve B ist der gemessene Absorptionsgrad für eine vollflächige Belegung einer Raumfläche (10,5 m^2) ersichtlich. Eine Übereinstimmung des Frequenzverhaltens ist nur im Bereich von 200-1000 Hz zu beobachten. Unter 200 Hz wirkt sich die etwas zu geringe Diffusität des Raumes schon zu stark aus. Dies war auch aus der außergewöhnlich starken Streuung der einzelnen Meßwerte untereinander bei den verschiedenen Mikrophonorten zu entnehmen. Über 1000 Hz liegt der Hallraumabsorptionsgrad unter dem im Rohr gemessenen. Diese Unstimmigkeit konnte bis jetzt noch nicht zufriedenstellend geklärt werden. In den meisten Fällen einer praktischen Anwendung würde jedoch bei einer vollflächigen Belegung einer Raumfläche (z.B. Decke) eine zu geringe Nachhallzeit erreicht werden. Aus diesem Grund wird meistens eine schachbrettartige Verlegung (Kurve C) verwendet, die eine Erhöhung des Absorptionsgrades im Vergleich zur tatsächlichen Belegung mit sich bringt, sodaß mit einem geringen Aufwand an Absorptionsmaterial eine weitgehende Beeinflussung der Nachhallzeit erreicht werden kann. Diese Absorbertype eignet sich speziell

auch für eine nachträgliche Behandlung von Räumen, bei denen eine zusätzliche Belastung der Decke nur gering sein darf. Das Gewicht eines Absorberelementes beträgt nur 0,45 kg. Neben der teilweisen oder vollständigen Belegung einer Fläche ist es auch möglich, die Absorberelemente frei im Raum einzeln oder zu Gruppen zusammengefaßt aufzuhängen.

Der Verfasser möchte der Österr. Frigolit AG. an dieser Stelle für die Überlassung des Materials und die Herstellung der Versuchsabsorber seinen besten Dank aussprechen.

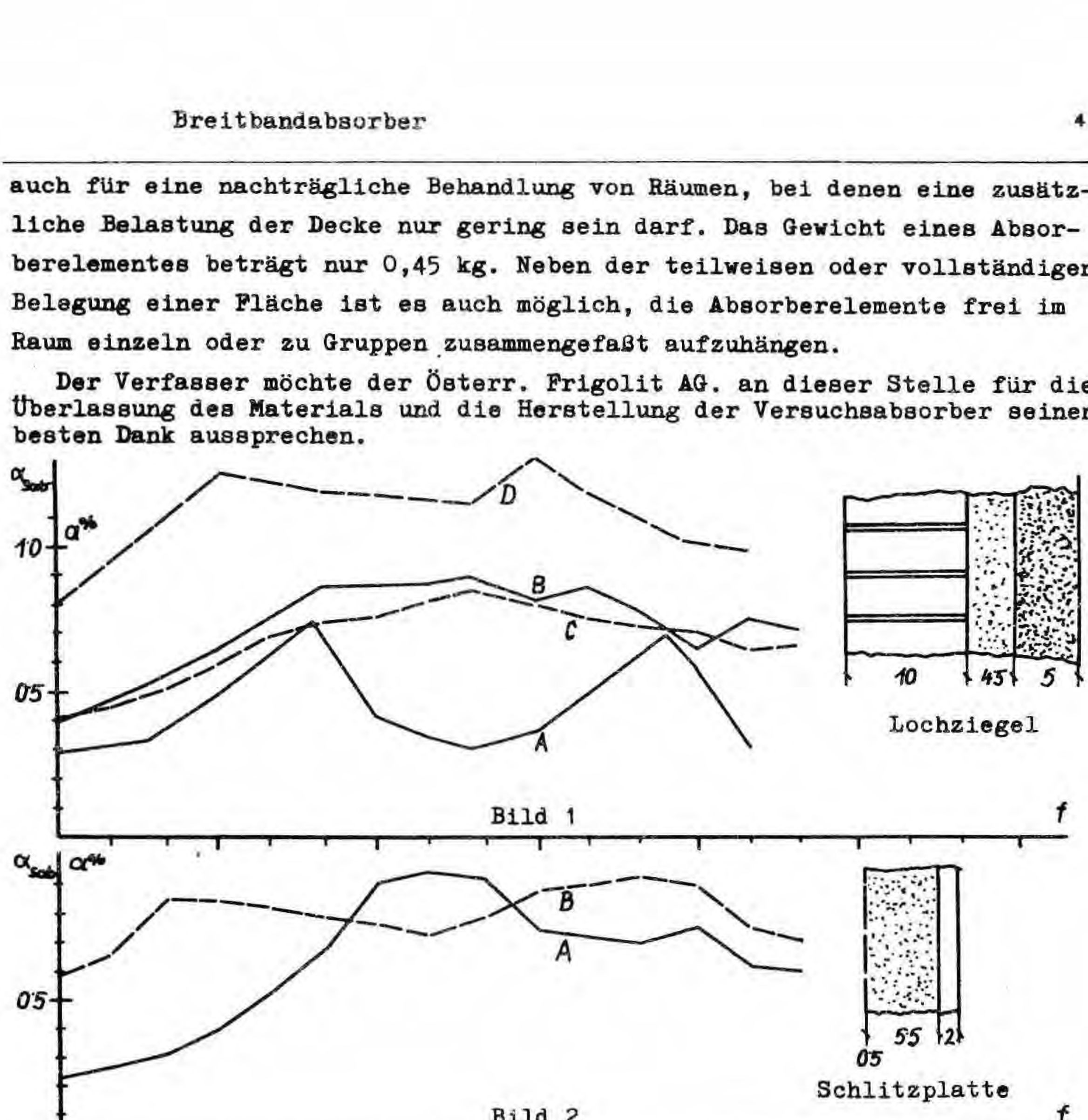

Bild 1

Bild 2

Bild 3

N33

FOURTH INTERNATIONAL CONGRESS ON ACOUSTICS
COPENHAGEN 21.-28. AUGUST 1962

DIE ERREGUNG VON SCHWINGUNGEN MIT EINER GROSSEN SCHALL-INTENSITÄT IN GASEN MITTELS EINES MAGNETOSTRIKTIVEN SCHALL-GEBERS.

Nowitzky B.G., Friedmann W.M.

Bekanntlich wird bei der Energieübertragung ins Gas wegen dessen geringer spezifischer Schallimpendanz eine große Volumgeschwindigkeit erfordert. Dementsprechend soll das Produkt der Verschiebungen und der abstrahlenden Fläche eines Schallgebers groß sein. Dadurch wird die Anwendung von bekannten Schwingertypen,verhindert. Bis jetzt wurden die Schwingungen mit einer grossen Schallintensität (etwa 150 bis 160 dB) in Gasen mittels aerodynamischer Schallschwinger (dynamische Sirene /1/, statische Strahlsirene /2,3/ u.s.) erzeugt.

Erst im Jahre 1961 veröffentlichte Kritz /4/ die von ihm erhaltenen Ergebnisse über die Erregung der US-Schwingungen in Gasen mittels Biegeschwingungen von piezokeramischen Platten aus Quarz und Bariumtitanat. Es gelang ihm, im Gasmedium Schallschwingungen zu erzeugen, die in der Nähe der Schwingerfläche eine Stärke von 150 bis 160 dB erreichten. Die Erregung der Schallschwingungen von einer so grossen Intensität ist in der Literatur noch nicht beschrieben worden. Bei den von uns durchgeführten Untersuchungen wurde ein magnetostriktiver Pakettschwinger 23,8 kHz verwendet, der steif mit einem hohlen Wellenleiter verbunden war /5/, siehe Abb.1.

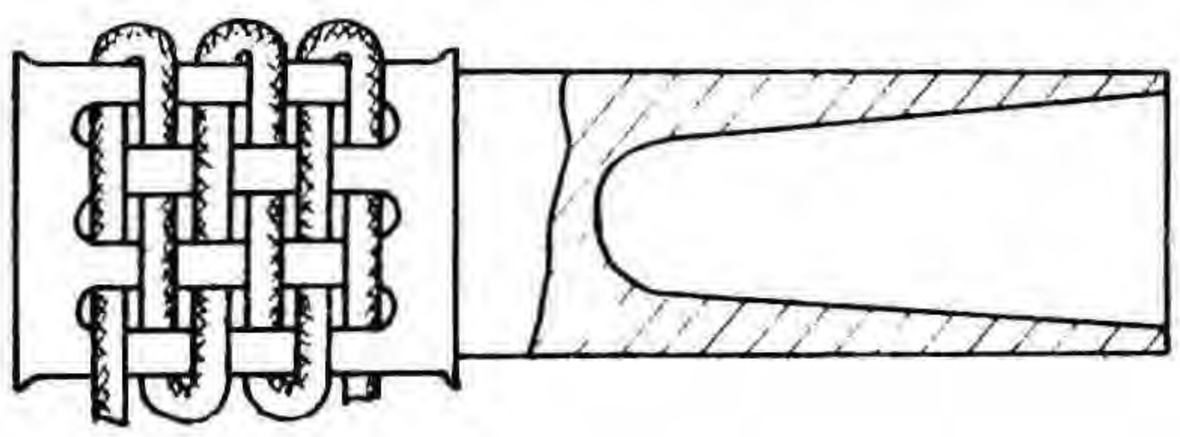

Abb.1. Eine magnetostriktive Anordnung für Erregung intensiver Schallschwingungen in Gasen.

Vermutlich werden die vom magnetostriktiven Schallgeber empfangenen Längsschwingungen im Wellenleiter in Radialschwingungen umgewandelt. Diese erregen Biegeschwingungen mit einer großen Amplitude (C,2 mm und über) am Ende des Wellenleiters, dessen Wände Schallschwingungen von grosser Intensität ins Gasmedium abstrahlen.

Es wurden folgende Grundcharakteristiken der von uns entwickelten Anordnung untersucht: das Frequenzspektrum (Abb.2) und die Richtkennlinien für beide Grundfrequenzen der US-Abstrahlung (Abb.3).

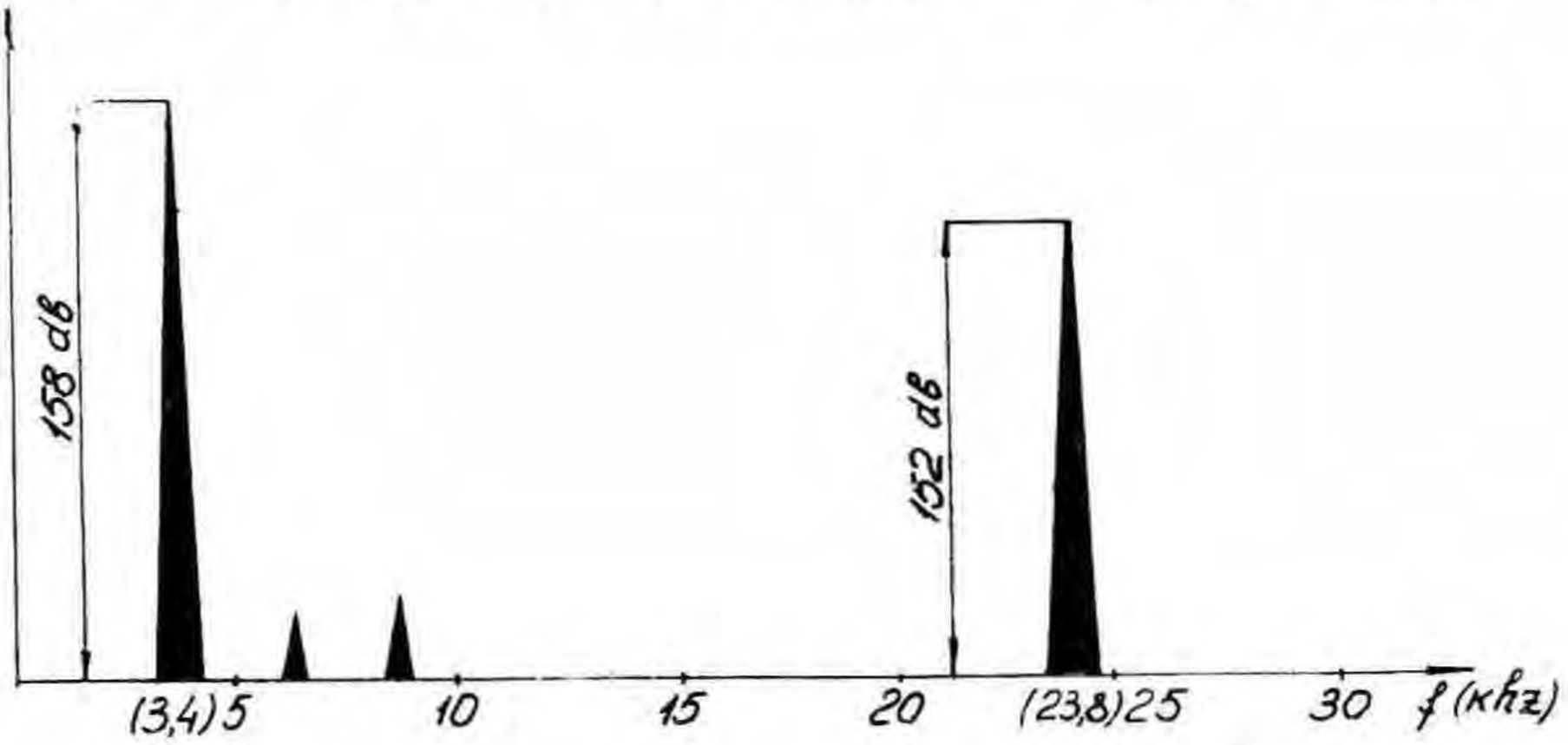

Abb.2. Frequenzspektrum, gemessen 350 mm weit von der magnetostriktiven Anordnung.

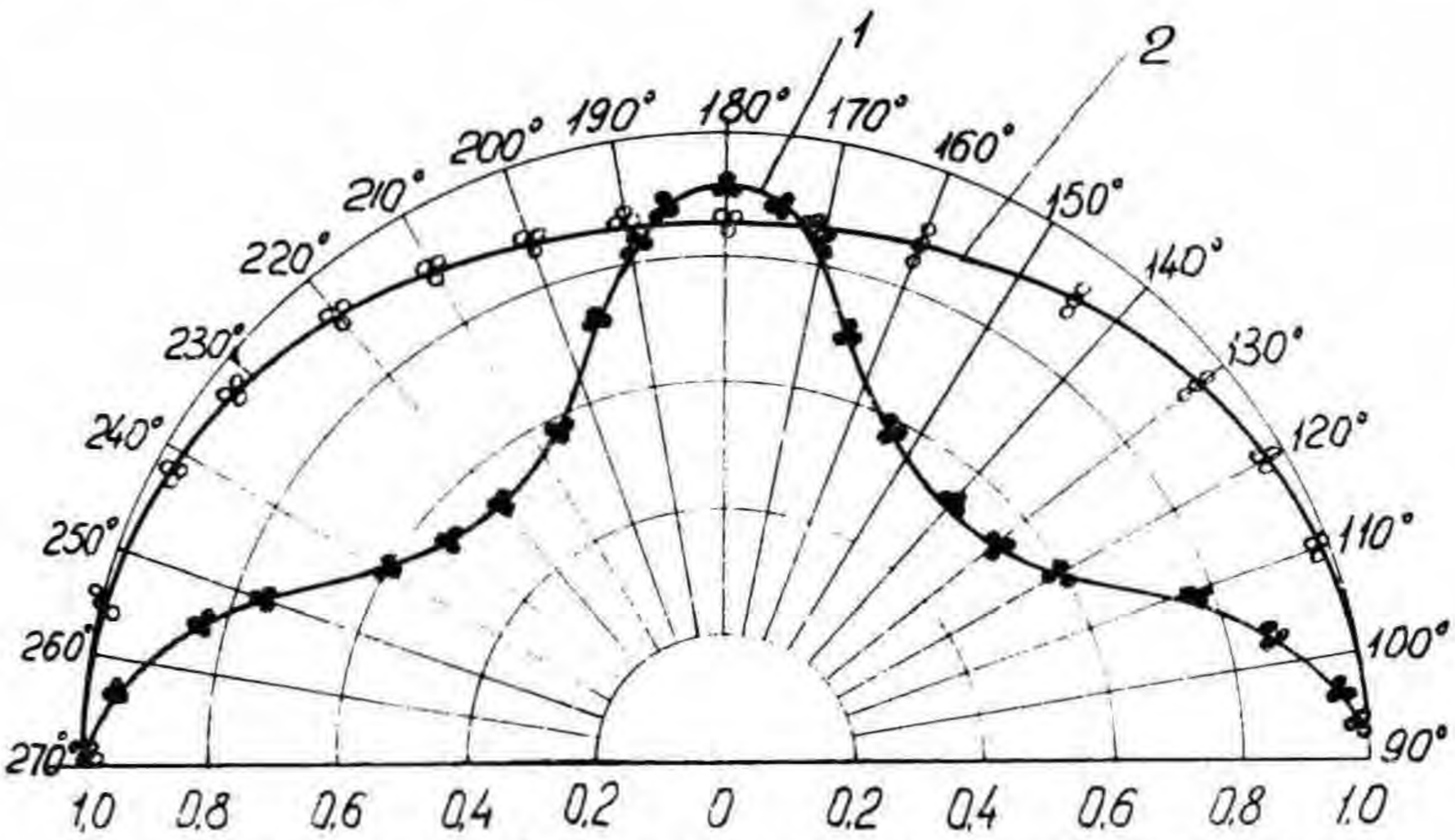

Abb.3. Richtkennlinien der magnetostriktiven Anordnung für zwei Grundfrequenzen 3,4 kHz (1) und 23,8 kHz (2), aufgenommen 350 mm weit von der Anordnung.

Durch Integrieren der Richtkennlinien für zwei senkrechtstehende Flächen wurde die US-Leistung der Anordnung zu 1,5KW ermittelt.

Das Verhältniss der elektrischen Leistung zur abgestrahlten akustischen Leistung der Anordnung ergab einen Wirkungsgrad, der bei 50% lag.

Dementsprechend läßt der obenbeschriebene Schallgeber, bei einer hohen US-Leistung und einem hohen Wirkungsgrad,der um 1,5-2 fache höher, als der der Strahlsirenen, intensive Schallschwingungen (bis 158 dB) im Gas erzeugen.

Dabei hat er eine Richtkennlinie, die inn besondere günstig für die Lösung einer Reihe von wirtschaftlichen und betrieblichen Problemen macht.

L i t e r a t u r :

1.Crawford A. "Ultrasonic engineering", London,1955.
2.Boucher R. Ultrasonic in Processing. "Chemical Engng", October,2, 1961.
3.Friedemann W.M. "Ultraschall", Verl."Znanie", 1960.
4.Kritz J. A heigh efficiency transducer for transmission to air, IRE Trans.Engng, 1961, 8, No1.
5.Friedemann W.M., Herschgall D.A. "Ultraschallapparatur", Gosenergoizdat, 1961.

O33

FOURTH INTERNATIONAL CONGRESS ON ACOUSTICS
COPENHAGEN 21.-28. AUGUST 1962

AMPLITUDE FLUCTUATIONS OF SOUND IN ATMOSPHERIC TURBULENCE*

Uno Ingard and George C. Maling, Jr., Department of Physics and Research Laboratory of Electronics, Massachusetts Institute of Technology, Cambridge, Massachusetts

The general aspects of sound propagation in a turbulent medium have been discussed in several basic papers by Obhukov, Krasilnikov, Chernov, Lighthill, Batchelor, Kraichnan, Mintzer, and others as well as in the recent books by Chernov[1] and Tatarski[2] in which extensive lists of references are given. There are, however, some aspects of the problem that have not as yet received a great deal of attention. One such problem is dealt with in this paper, the influence of turbulence on the propagation of sound in the presence of a boundary.

The fluctuation amplitude for a sound wave propagating in an unbounded inhomogeneous medium is of the order of $L = 20 \log(1+2\sqrt{\langle(a/A_o)^2\rangle})$, where $\langle(a/A_o)^2\rangle$ is the variance of the amplitude. According to Chernov, $\langle(a/A_o)^2\rangle \simeq \sqrt{\pi}(k_oL)(k_ox) \langle \mu^2\rangle/2$ for distances greater than $\sqrt{L\lambda}$. For values of λ, μ, L, and x that are often encountered in measurements of sound propagation over short distances above ground, the above relations predict fluctuation amplitudes of 2-3 db. However, measured values of the fluctuation amplitude frequently are as large as 10-15 db, and it is clear that the presence of a boundary must be accounted for in any calculation of the amplitude of the fluctuations.

In this paper we shall assume that the main influence of turbulence is to produce a fluctuation in phase between the wave that arrives directly from the source and the wave reflected from the boundary. The resulting "fading" of the sound pressure is assumed to have a characteristic period which is much longer than the period of the acoustic wave. Under these conditions, it is meaningful to speak of a time-dependent mean square sound pressure $(\overline{p^2})$. This mean square value is obtained by averaging over a time that is long compared to the period of the acoustic wave but short compared to the period of the turbulence. The essential problem in this paper concerns the statistics of the random function $(\overline{p^2})$.

In a homogeneous quiescent atmosphere the sound pressure in the direct wave at a horizontal distance x from the source may be expressed as $p_d = \exp(ikx - i\omega t)/x$, leaving out irrelevant constants. For the purposes of this paper, it is sufficient to use as an approximation for the reflected wave $p_r = R \exp(ikr - i\omega t)/r$, where R is the plane wave reflection coefficient $R = \cos\phi - \eta/\cos\phi + \eta$, r is the distance to the

---

*This work was supported in part by the U.S. Army Signal Corps, the Air Force Office of Scientific Research, and the Office of Naval Research.

image $r = \sqrt{x^2 + 4h^2}$, and ϕ is the angle of incidence, $\phi = \tan^{-1} x/2h$. For real values of η, the mean square pressure becomes

$$\overline{p^2} = x^{-2}\left[1 + R^2(x/r)^2 + 2R(x/r)\cos\beta\right] \tag{1}$$

$$\overline{p^2} = 2R(xr)^{-1}\left[r(2xR)^{-1}(1 - R\,x/r)^2 + (1 + \cos\beta)\right] \tag{2}$$

where $\beta = k(r - x)$ is the phase difference between p_d and p_r. As a result of the turbulence, the speed of sound c in the medium will be a function of time and position, but for small turbulent velocities the variations of c will be small. We therefore let $c = c_o(1 + \mu)$, where c_o is the unperturbed speed of sound and $\mu << 1$.

If the phase fluctuations in the wave are not identical over the direct and reflected path, the phase shift β will consist of a mean part $\beta_o = k_o(r - x)$ and a fluctuating component δ that may be expressed as

$$\delta \simeq k_o \int \mu_d dx - k_o \int \mu_r dr. \tag{3}$$

δ and $\overline{p^2}$ are therefore random variables whose statistical properties are of interest. The variance of δ, $\langle\delta^2\rangle$, may be estimated by assuming that the cross correlation between μ_d and μ_r may be neglected in comparison with the autocorrelation of μ_d and μ_r. We therefore obtain

$$\langle\delta^2\rangle = k_o^2 \iint\langle\mu_d(x_1)\mu_d(x_2)\rangle dx_1 dx_2 + k_o^2 \iint\langle\mu_r(s_1)\mu_r(s_2)\rangle ds_1 ds_2$$

which for a correlation function $\langle\mu(1)\mu(2)\rangle$ of the form $\mu_o^2 \exp(-\xi^2/L^2)$ becomes

$$\langle\delta^2\rangle = \sqrt{\pi}\,\mu_o^2(k_o x)(k_o L)\left[1 + \sqrt{x^2 + 4h^2}/x\right]$$

which for sufficiently large values of x becomes $\langle\delta^2\rangle = 2\sqrt{\pi}\,\mu_o^2(k_o x)(k_o L)$. L is a measure of the scale of the turbulence and $\xi = |x_1 - x_2|$.

It follows from Eq. (2) that the calculation of even the mean value of $\overline{p^2}$ requires a knowledge of the higher order moments of δ which in turn requires a knowledge of the higher order correlations of μ. We shall, for the purposes of this paper, assume that the variable δ is normally distributed with variance $\langle\delta^2\rangle$. Then, using this distribution function one can determine (numerically) the mean and variance of $\overline{p^2}$ from Eq. (2). These quantities can be compared with experimentally determined values described below. Two important results of the above analysis are that for a non-rigid boundary ($\eta \neq 0$) the quantity $(1 + \cos\beta)$ does not approach a value of two for large values of x.

Then, in a turbulent flow, according to Eq. (2), $\overline{p^2}$ will decrease with distance as $(1/r^2)$ rather than $(1/r^4)$ as in the case of a quiescent medium. For a rigid boundary and a homogeneous quiescent medium, $(1 + \cos \beta) = 0$ in the interference minima, and small values of $\overline{p^2}$ are obtained. In a turbulent medium, the mean value of $(1 + \cos \beta)$ is generally much larger than the first term in brackets in Eq. (2), and therefore the deep minima in $\overline{p^2}$ will be less pronounced.

In order to obtain some experimental values of the mean levels and fluctuation observed in the field, some studies of sound propagation over a large rigid plane surface were made. The sound pressure level was measured at various distances up to 232 ft from the source at frequencies of 500, 1000, and 2000 cps. The source and receiver heights were 4 ft.

The mean value of the measured levels is in good agreement with the calculated levels for frequencies of 500 and 1000 cps. The effect of the turbulence is relatively small except when the mean phase shift is an odd multiple of 180° which corresponds to the locations of distinct sound pressure minima in the quiescent atmosphere. In these minima the effect of the turbulence is to raise the mean level anywhere from 0 to 30 db depending on the frequency and location of the minimum.

The variance of $\overline{p^2}$ has also been calculated for a portion of the data. For example, the fractional standard deviation $\langle (\overline{p^2} - \langle \overline{p^2} \rangle)^2 \rangle / \langle \overline{p^2} \rangle$ for a 500 cps signal has peaks at the interference minima of 37 1/2 % and 7 1/2 % for $\beta_o = \pi$ and $\beta_o = 3\pi$ respectively. At the higher frequencies, much larger fluctuations, and hence much larger values of the fractional standard deviation, were observed.

References

1. L. A. Chernov, Wave Propagation in a Random Medium (McGraw-Hill Book Company, Inc., New York, 1961).

2. V. I. Tatarski, Wave Propagation in a Turbulent Medium (McGraw-Hill Book Company, Inc., New York, 1961).

P33

FOURTH INTERNATIONAL CONGRESS ON ACOUSTICS
COPENHAGEN 21.-28. AUGUST 1962

Flexural Waves of Finite Amplitude in a Plate.

I.A.Victorov.

A well known theory of linear flexural vibrations of a plane plate is only applied to the vibrations, the amplitude $\hat{U}$ of which is essentially less than the thickness of the plate h . By so called strong flexion, when $\hat{U} \sim h$ stress and deformation in the plate remain small and agree with the Gook's law (disagreement with Gook's law occurs by considerably more amplitudes, when $\hat{U} \sim \ell$ · where ℓ -is flexural region dimension), but together with pure flexion deformation it reveals deformation of all - round tension (see /1/). A linear equation of plate flexural vibrations in this case can not be applied. There is an exception for plane flexion in a cylindrical surface. At the plate propagation of flexural waves such flexion takes place in plane waves. In this case wholly analogical to rod strong flexion the flexural amplitude can be more than h , but all - round plate tension will not appear. In practice however (by strong vibrations of airplane bodies, ships and other thin-walled mechanical constructions) often can be met some cases, when strong flexion does not represent flexion in a cylindrical surface.

In the present lecture is given an attempt to consider the propagation of vibrations in plane infinite plate by this flexion. It is assumed, that vibrations are excited by harmonic displacements with the amplitude of α and the frequency of ω , distributed uniformly in the region of a circle radii R , besides $\alpha^2 \ll h^2$. A solution of the problem is given by subsequent approximation method with its exactness to second approximation includingly.

Using equilibrium equations by strong plate flexion given in /1/ we obtained the equation for free vibrations of strong plate flexion in cylindrical coordinates r, φ, z . For considered axial symmetrical motion the equation has the form:

$$\Delta^2 U(r,t) + \frac{12\rho(1-\nu^2)}{h^2 E} \cdot \frac{\partial^2 U(r,t)}{\partial t^2} = \frac{2(1-\nu^2)}{h^2} \cdot \frac{\partial}{\partial r}\left[\left(\frac{\partial U(r,t)}{\partial r}\right)^3\right] \quad /1/$$

It is given here: U -displacement in the z -axis, Δ -Laplace's operator, t -time, h -plate thickness, E -Young's module, ν -Poisson's ratio. Boundary conditions of the problem are:

$$\begin{cases} U(r,t) = \alpha \cdot \cos\omega t & \text{for } r \le R \\ \dfrac{\partial U(r,t)}{\partial r} = 0 & \text{for } r = R \end{cases} \qquad /2/$$

If $\hat{U}(r,t) \ll h$ than the right part /1/ is the value $\hat{u}^2/h^2$ of small order in comparison with terms of the left part, so that the first approximation of the problem solution is possible to take the desicion of the equation /1/ with a zero right part, which satisfies boundary conditions of /2/ and the extinction principle (see/2/). This solution can be written as follows:

$$U_1(r,t) = \alpha\, Re\, \frac{H_0^{(1)}(kr)H_1^{(1)}(ikR) + iH_0^{(1)}(ikr)H_1^{(1)}(kR)}{H_0^{(1)}(kR)H_1^{(1)}(ikR) + iH_0^{(1)}(ikR)H_1^{(1)}(kR)} \cdot e^{-i\omega t} \qquad /3/$$

$H_0^{(1)}(x)$, $H_1^{(1)}(x)$ -are Hankel's functions of the first kind order 1 and 0, Re -index of real part, k -wave number infinite small amplitude of flexural wave. Substituting the equation /3/ in the right part /1/ we shall obtain a linear inhomogeneous equation of the second approximation with the kind of right part $Re[F(r)e^{-i\omega t} + G(r)e^{-3i\omega t}]$ where $F(r)$, $G(r)$ - function r, α, h and elastic plate parameters. The solution of the equation satisfying together with /3/ boundary conditions /2/ and extinction principle can be found by the method of variable arbitrary constants.

Let us assume that the excitation region dimension is $kR \gg 1$. In the case of $k\Delta r > 1$ $(\Delta r = r - R)$ given solution has the following simple form:

$$U_2(r,t) = \alpha \cdot \frac{\alpha}{h^2}\sqrt{\frac{R}{r}}\, Re\Big[\Big(A_1 kr \ln\frac{r}{R} + A_2 \cdot \frac{R}{r} + A_3\Big)e^{i(k\Delta r - \omega t)} +$$

$$+ \Big(B_1 \cdot \frac{R}{r} e^{i(3-\sqrt{3})k\Delta r} + B_2\Big)e^{i(\sqrt{3}k\Delta r - 3\omega t)}\Big] \qquad /4/$$

Here A_1, A_2, A_3, B_1, B_2- complex constant of the order 0,1. Compared equations /4/ and /3/, which for first approximation can be written in the form:

$$U_1(r,t)=\alpha\sqrt{\frac{R}{2r}}\cdot\cos\left(k\Delta r-\omega t-\frac{\pi}{4}\right) \qquad (5)$$

it is easy to note, that rations of the terms of the second approximation to first are the values of the following order: $\frac{\alpha^2}{10h^2}kR\ln\frac{2}{R}$, $\frac{\alpha^2}{10h^2}\cdot\frac{R}{2}$, $\frac{\alpha^2}{10h^2}$. Second approximation of the solution describing nonlinear effect consist of the first and the third harmonics. The amplitude of the first harmonic of the second approximation grows with the distance according to law $\ln\frac{r}{R}$. The sum of the first harmonics of the first approximation and second can be considered as a flexural wave of the frequency ω with the amplitude and phase modulation. The third harmonic has pulsations, which attenuate with distance as $R/2$. The fact that higher harmonics have pulsations at sound propagation of finite amplitude in waveguides and in dispersive media (contrary to monotonous harmonic growth with the distance in a medium without dispersion of phase velocity) first was noticed by M.A.Issakovich in his work /3/

If the dimensions of region excitation are small in comparison with the length of flexural wave ($kR \ll 1$), in the vicinity of region excitation ($kr \ll 1$) the solution of nonlinear equation of the second approximation has the form:

$$U_2(r,t)=\alpha\cdot\frac{\alpha^2}{h^2}kr\ln kr\,\mathrm{Re}\left[C_1e^{-i\omega t}+C_2e^{-3i\omega t}\right] \qquad (6)$$

C_1, C_2 -complex constants of order 1. The solution of linear equation of the first approximation here is expressed by $U_1(r,t)=\alpha[1+O(k^2r^2)]$. Thus the amplitude term relation of the second approximation to the first for this case is rather small α^2/h^2. In the distance of region excitation ($kr \gg 1$) the solution of the second approximation and the first one can be written in the forms:

$$U_2(r,t)=\alpha\cdot\frac{\alpha^2}{h^2}\cdot\frac{1}{\sqrt{kr}}\mathrm{Re}\left[\left(A_1'\ln kr+A_2'\cdot\frac{1}{kr}+A_3'\right)e^{i(kr-\omega t)}+\right. \qquad (7)$$
$$\left.+\left(B_1'\cdot\frac{1}{\sqrt{kr}}e^{i(3-\sqrt{3})kr}+B_2'\right)e^{i(\sqrt{3}kr-3\omega t)}\right]$$

$$U_1(r,t)=\alpha\sqrt{\frac{2}{\pi}}\;\frac{\cos\left(kr-\omega t-\frac{\pi}{4}\right)}{\sqrt{kr}} \qquad (8)$$

Here A_1', A_2', A_3', B_1', B_2' -complex constants of the order 0,1 - 0,3.

In comparison of anologeous equations /4/,/5/ and /7/,/8/ is obvious

seen, that at large dimensions of region excitation the relation of nonlinear solution terms to linear terms is proportional to R , but in small dimensions of region excitation such proportionality does not excist.

We want also to note, that in case of $kR \gg 1$ and $kR \ll 1$ the amplitude finiteness changes of the flexural rigid plate. Due to its vibrations the first zero of the plate displacement moves towards the centre of excitation at a distance of the order $\frac{\alpha^2}{2h^2}\alpha$.

Literature Cited.

1. Landau L.D. and Lifshits E.M. Mechanics of Continuous Media, GITTL. M. 1954.

2. Malyuzhinets G.D. Generalizations of Reflection Methods in the Theory of Sinusoidal Wave Diffraction (doctoral dissertation), P.N. Lebedev Physics Institute, Acad.of Sciences, USSR, 1950.

3. Issakovich M.A. Nonlinear Effects in Some Acoustic Problems, Akust.Zh. 1960, v.6, N.3, p.321-325.

G34

FOURTH INTERNATIONAL CONGRESS ON ACOUSTICS
COPENHAGEN 21.-28. AUGUST 1962

DESCRIPTION OF A COMPUTER PROGRAM FOR PITCH DETECTION

Bernard Gold

A recent paper[1] described a computer program for extracting the pitch of a speech wave. The present paper, a sequel to the above, describes the rules of operation of a real-time pitch extractor which is presently being built as part of a vocoder.

This pitch extractor combines the tentative decisions made by six individual pitch extractors and computes a more accurate pitch period than could be obtained individually. Although the machine has not yet been constructed, its operation has already been simulated on a general purpose computer and sufficient data has been taken to indicate that we are building a practical machine.

The machine can conveniently be split into three parts, as shown in Figure 1.

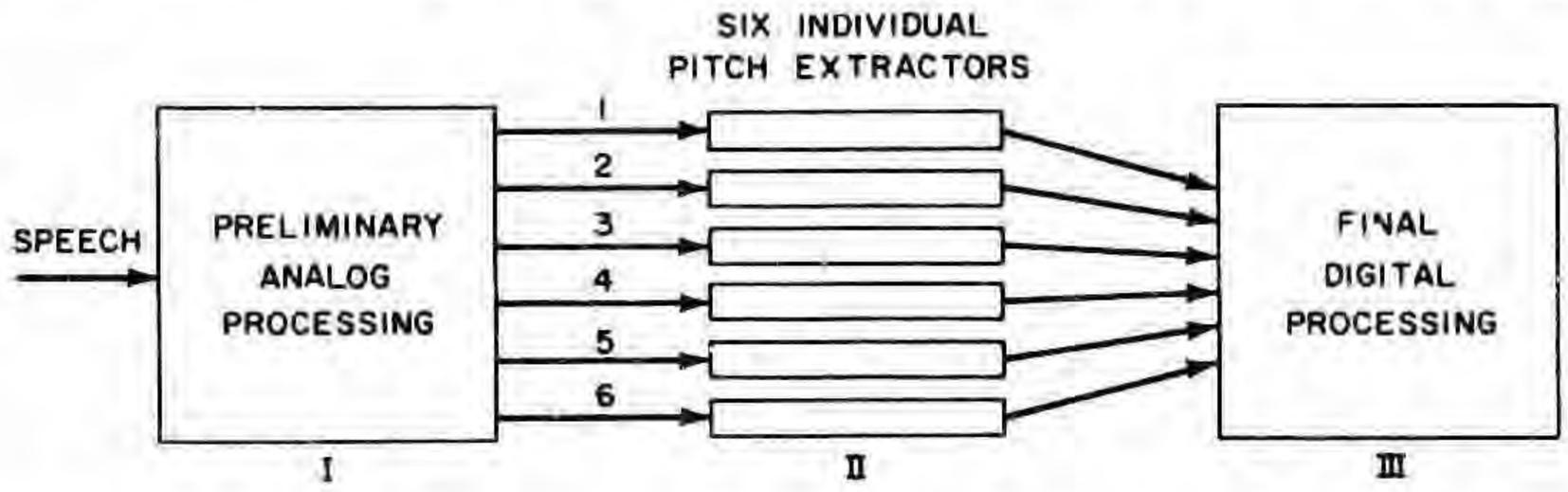

Fig. 1: The Pitch Extractor Divided into its Three Major Functions

The function of Box I, marked Preliminary Analog Processing, is described in Figure 2. The pulse trains appearing on the six output lines are shown in Figure 2 for a particular sample of speech. On Line 1 is a set of pulses with the amplitudes, f_i, of the positive peaks. The pulses on Line 2 are of amplitude $f_2 - g_1$, $f_3 - g_2$, $f_4 - g_3$, etc., that is, peak to peak swings of the waveform. The pulses on Line 3 have amplitudes $f_2 - f_1$, $f_3 - f_2$, $f_4 - f_3$, etc., the difference between a positive peak and the previous positive peak. If this difference is less than or equal to zero, no pulse is produced.

Lines 4, 5, 6 result from the same three operations on the negative peaks. All the lines are made to produce positive pulses so that each of the Six Individual Pitch Detectors can be identically constructed.

Although it is clear that the six sets of pulses are far from independent, it is still true that when it becomes difficult to find the pitch for one pulse train, it may be easy to find the pitch for another pulse train. For example, in Figure 2, it is exactly when Lines 3 and 6 are most useless (from a to b) that the other 4 lines are most accurate. This example illustrates the basic reason for operating on the speech in many (in our case 6) different ways; we want at all times to have a reasonable amount of correct pitch information.

A rundown voltage, consisting of a blanking gate followed by an exponential decay,

operating on each of the six lines from the Analog Processor, eliminates the pulses of amplitude less than the rundown voltage at any given time. Pulses whose amplitude exceeds the rundown voltage are passed tentatively as pitch pulses to a digital processor for final selection.

Figures 3a and 3b illustrate this process for Line 1 of Figure 2. The blanking gates are initiated by the tentative pitch pulses, the width of the gates being functions of the control voltage shown in Figure 3c. The control voltage is obtained by passing the exponential wave in Figure 3c through an R.C. filter with a 30 millisecond time constant. Since the exponential waves are reset by new pitch pulses, the control voltage (and blanking gate duration) are functions of a number of preceding pitch periods; hence the selective process in an individual pitch detector is influenced by preceding pitch period history.

Each line in Figure 2 is processed by the individual pitch detector we have just described. Therefore, six identical detectors are needed. The heavy dot below a pulse (on any of the lines in Figure 2) indicates that a pitch pulse has been produced by the operations pictured in Figure 3. Pitch periods are the time intervals between adjacent pitch pulses.

Given the outputs of six separate pitch period detectors, we must compute a final pitch period, which, on the average, is appreciably more accurate than that determined by any of the separate detectors. We now describe the algorithm for computing this final answer. Referring to Figure 2, at any given time c, we store the three most recent periods from each detector. For example, Pitch Detector 1 gives us p_{11}, p_{12} and p_{13}. From these, three other periods may be obtained; these are $p_{14} = p_{11} + p_{12}$, $p_{15} = p_{12} + p_{13}$ and $p_{16} = p_{11} + p_{12} + p_{13}$. (Note that the left subscripts correspond to the lines in Figure 2 and the right subscripts to the position of the periods relative to time c). From all the detectors a total of 36 periods are obtained, but only six of these periods will be eligible for selection. We are going to constrain our final choice of pitch period to one of the six numbers, p_{11}, p_{21}, p_{31}, p_{41}, p_{51} or p_{61}, that is, to the most recent period from one of the six detectors. Schedule 1 lists all 36 numbers in milliseconds. Each column corresponds to an individual detector. Thus, the only permissible solutions are the top entries in each column. We must now search for a sufficiently popular solution, i.e., one which agrees closely with the other periods in the schedule. To do this, we compile Schedule 2 which is obtained from Schedule 1 as follows:

Schedule 2 lists the "popularity" of each detector as a function of Window Size W. For example, Row 4, Column 3 of Schedule 2 tells us how many of the 36 numbers in Schedule 1 were within $\pm$300 microseconds of the entry in Row 1, Column 3 of Schedule 1.

The final step in the computation is illustrated in Figure 4. The step-like curve shows the maxima of each row in Schedule 2. Thus, for W = 0, the maximum is 4 (5th Column, 2nd Row of Schedule 2). The final decision as to the most probably correct period is achieved by a search process which is best described by referring to Figure 4. Imagine a point located at W = 0 and T = 8 (Point d). This point moves along the Line de. If it hits the corner of the step wave before it gets to e, the search is ended; otherwise it continues to search along Line fh. In the example illustrated in Figure 4, the search will end at Point g of Line fh. If the step wave had not been as high, the search would have continued along Line jk, etc. Now Point g corresponds to a window size of 600 or to Row 4 of Schedule 2. Since p_{21} is the most popular detector in that row, our final choice of period is 5.80 milliseconds.

REFERENCE

B. Gold, "A Computer Program for Pitch Extraction", J. Acoust. Soc. Am. (to be pub.).

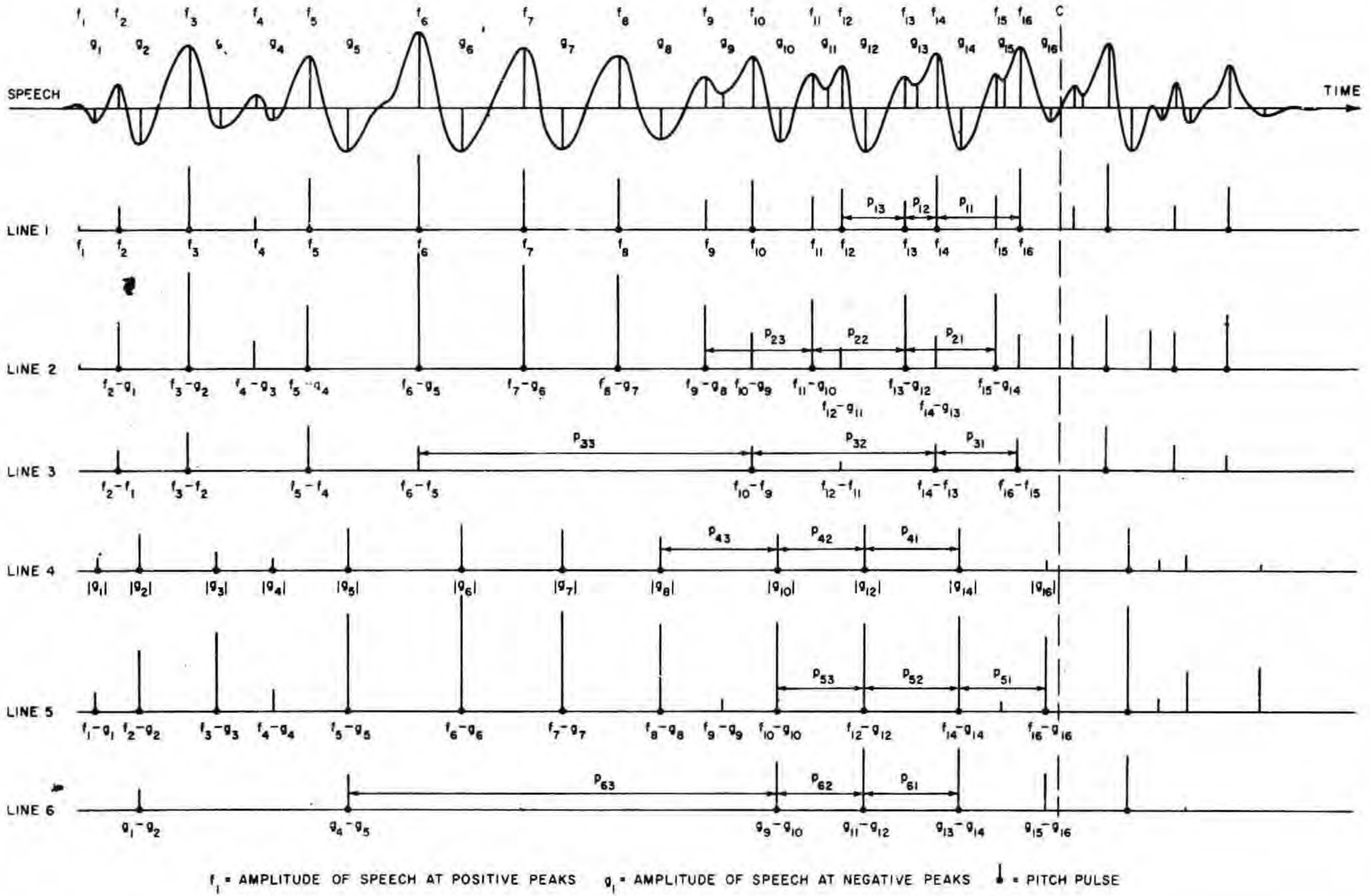

Fig. 2: Preliminary Analog Processing of Speech

SCHEDULE 1

P_{ji} (j → columns, i ↓ rows)

i \ j	1	2	3	4	5	6
1	5.25	5.80	5.25	6.10	5.54	6.10
2	1.50	5.95	11.73	5.54	6.10	5.54
3	4.00	6.80	21.30	7.50	5.54	27.20
4	6.75	11.75	16.98	11.64	11.08	11.64
5	5.50	12.75	33.03	13.04	11.64	32.74
6	10.75	18.55	38.78	19.14	16.62	38.84

SCHEDULE 2

N_{jW} (j →)

W	1	2	3	4	5	6
W = 0	2	1	2	2	4	3
W = 200	2	1	2	3	5	3
W = 400	2	1	2	4	5	4
W = 600	7	10	7	5	8	5
W = 800	7	10	7	5	8	5
W = 1000	7	10	7	5	8	5
W = 1200	8	12	8	10	12	10

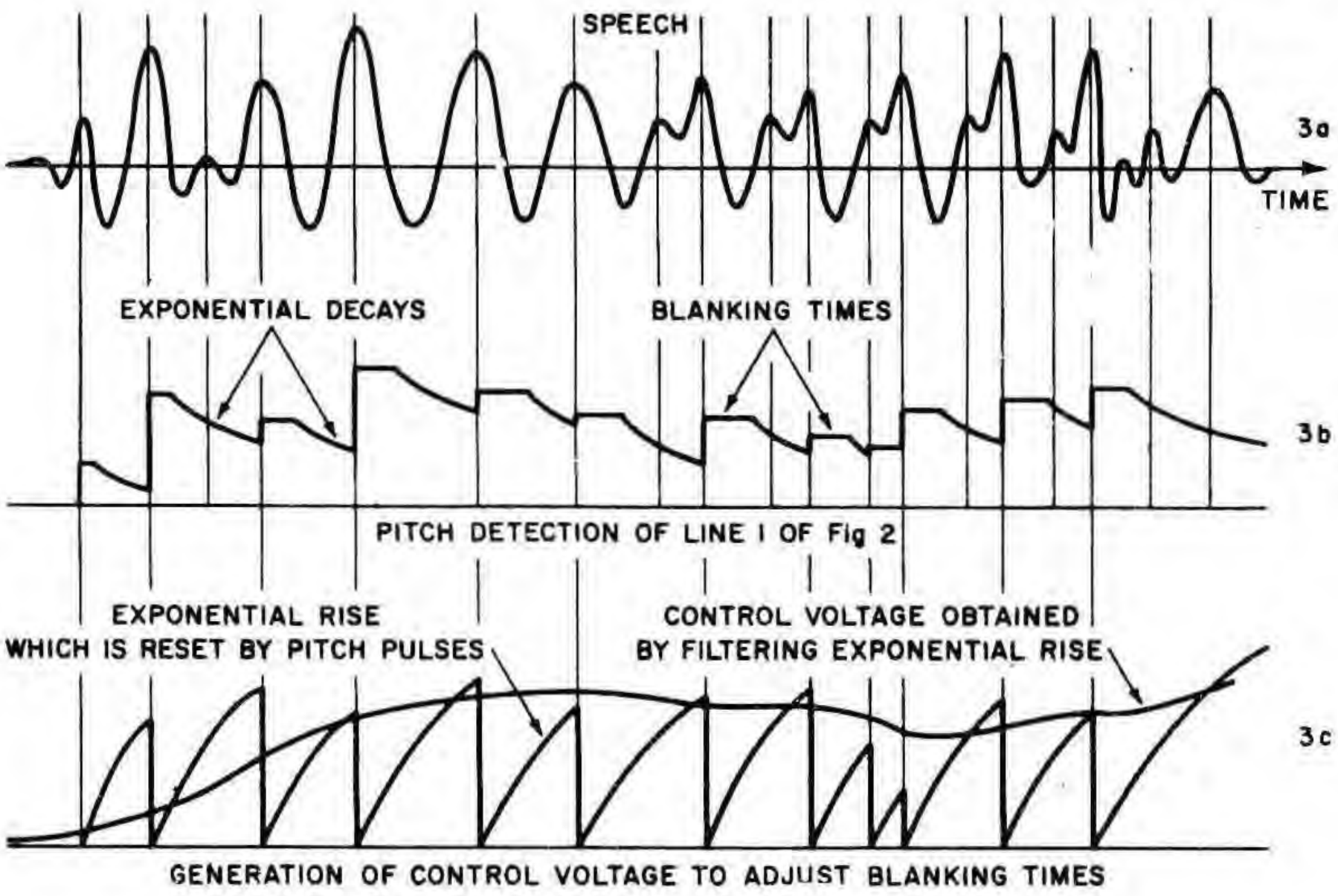

Fig. 3: Operation of Individual Pitch Detectors

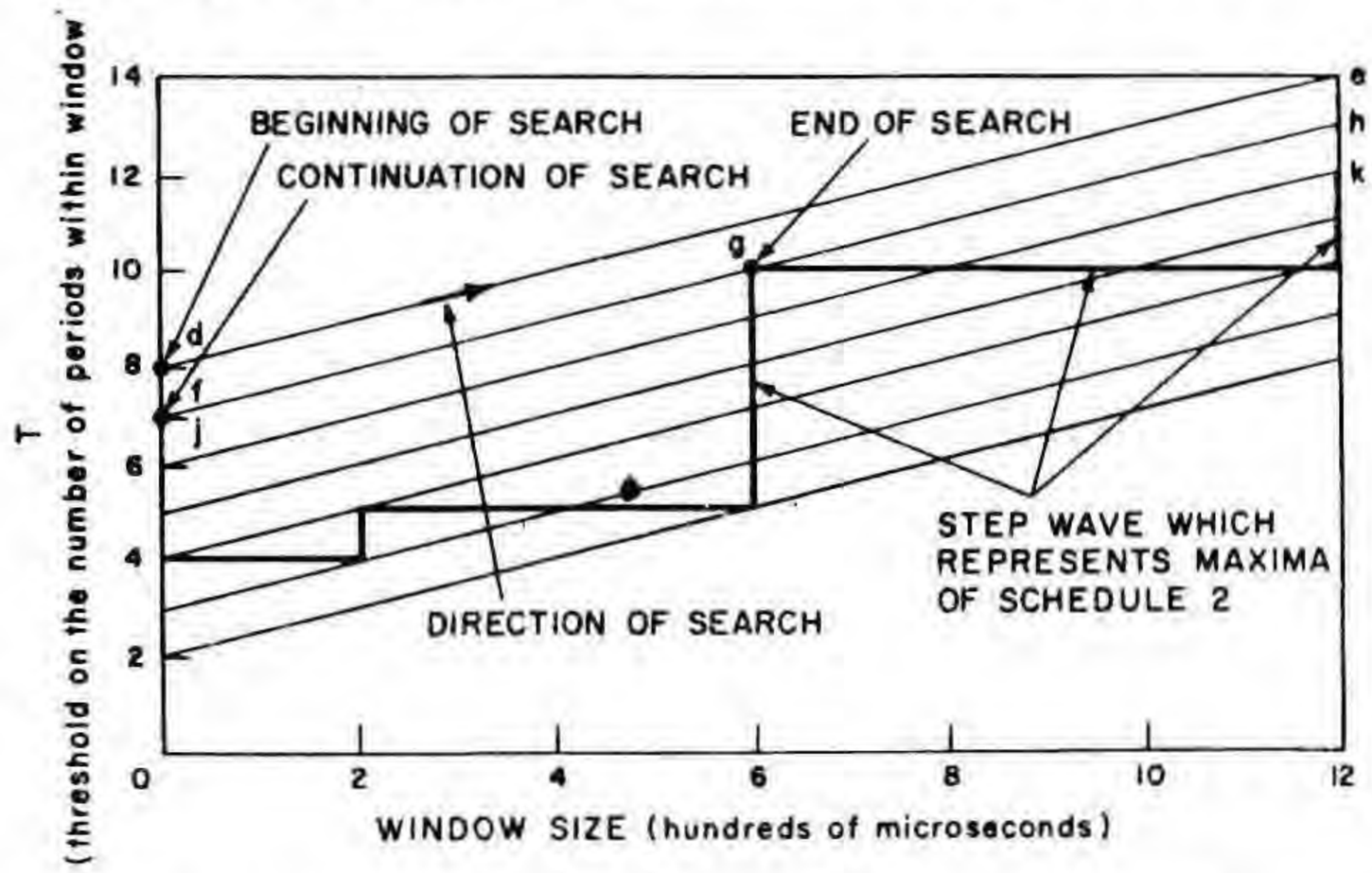

Fig. 4: Illustration of Search for Pitch Period

H34

FOURTH INTERNATIONAL CONGRESS ON ACOUSTICS
COPENHAGEN 21.-28. AUGUST 1962

Effect of Jet-Aircraft Noise on Hearing

J.J. Knight, Wernher Research Unit on Deafness,
British Medical Research Council.

Initially the danger to hearing from aircraft noise originated from piston engines and propellers, and it primarily concerned the flying crew but, with the advent of turbo-jet engines, the situation acquired a different emphasis. The greater thrust from jet engines is accompanied by greater noise but now the crew, protected in many ways from the noise, is positioned in front of the engines from which intense noise is directed towards the attendant ground staff. In a modern aircraft carrier, the aural hazard to the flight-deck party is particularly great on account of limitations in space and time for preparing aircraft for take-off. Also the steam catapults, from which the aircraft are launched, add to the noise at the time of release when the aircraft engines are run at full power.

Retrospective Survey

At the end of 1957 a retrospective audiometric survey of 224 men was undertaken to determine whether any damage to hearing had occurred among the flight-deck personnel of H.M. Ships ARK ROYAL and EAGLE when Sea Venom aircraft at squadron strength had been flying from both ships. With this new jet aircraft, overall noise levels of 131 dB had been measured between the catapults, and 121 dB on the Gunnery Direction Platform (where some of the ships' companies assembled to watch flying operations when off-duty). Ward (1957) had completed a similar investigation with the U.S. Navy and had reported that the evidence was "exceedingly flimsy" for a slightly depressed hearing level being due to aircraft noise. He found in his sample that a greater exposure to gunfire noise accompanied more aircraft-noise exposure, and he considered the gunfire exposure to be the more probable major cause of hearing loss.

A preliminary report was published (Coles and Knight, 1959) of the British investigation; the differences between the mean hearing losses of those most exposed to aircraft noise, and of those least exposed, was highly significant ($P < 0.01$) at 1 and 2 Kc/s. Ear protection in the form of flight-deck helmets was provided only after the men with the greatest noise exposure (about 2,500 take-offs in 18 months) had already experienced some 1,200 take-offs, and at first there were many who did not use the helmets to full advantage. Approximately 5 dB of average hearing loss at most test frequencies was found, even in those with least exposure. This was ascribed to long exposure to the general noise level of a ship at sea, and it has been found to be a temporary effect. Figure 1 shows the median hearing level of three groups with a minimum of gunfire exposure and different amounts of aircraft-noise exposure. Another group is included with considerable gunfire-noise exposure in addition, and this group shows the typical high-frequency notch associated with impulsive noise. Details of the experimental procedure and examination of the subjects were as described by Knight and Coles (1960).

Prospective Survey

During 1958 a prospective study was commenced into the hearing of men who were to work on the flight deck of the newly-commissioned H.M.S. VICTORIOUS. This ship was the first to carry a squadron of Scimitar aircraft and measurements in "ARK ROYAL" had shown that the overall noise level reached 149 dB during the free take-off of a single Scimitar.

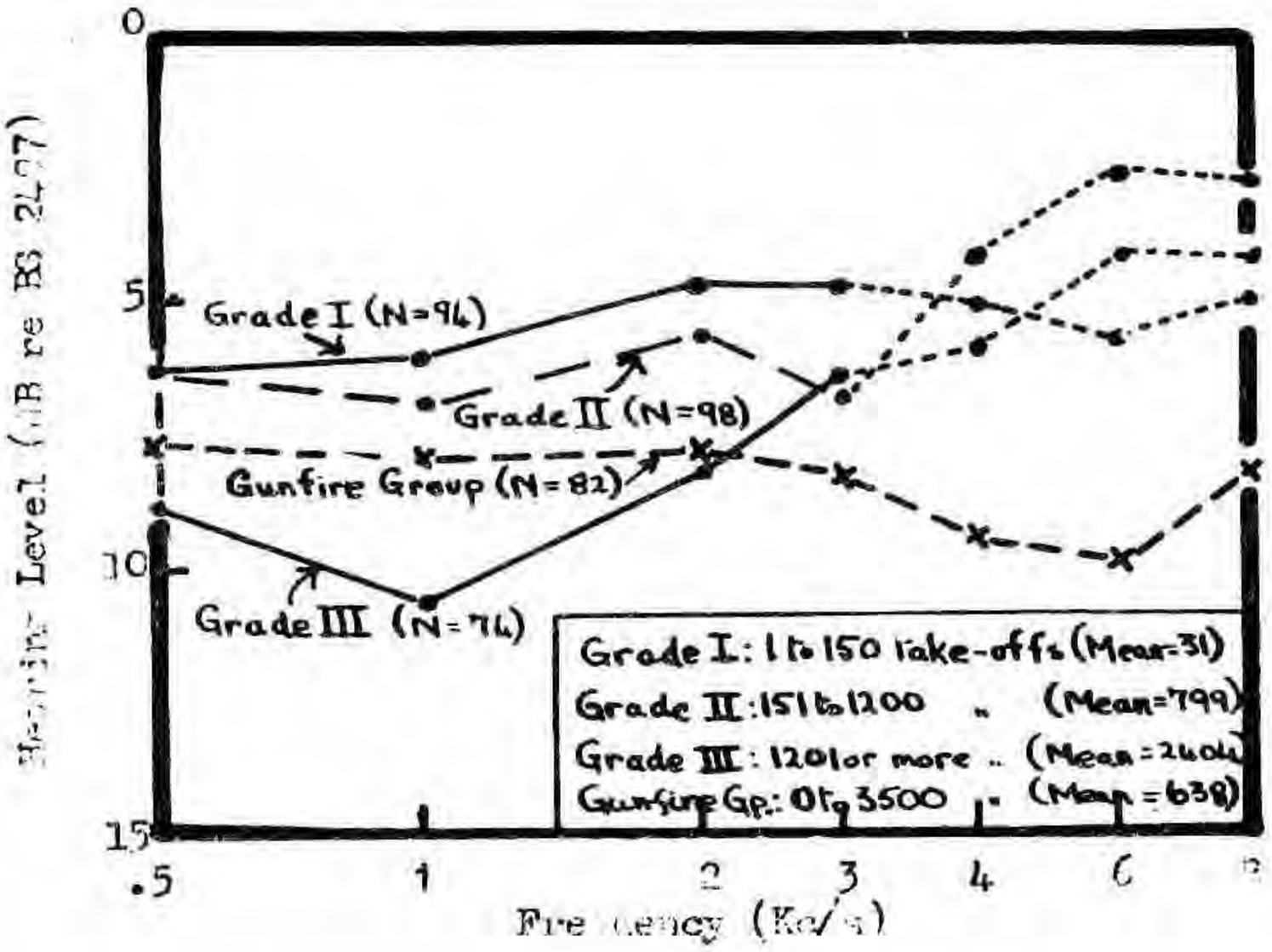

FIG.1 Retrospective Study. Median Hearing Level of Groups with Aircraft-Noise Exposure

The first hearing tests of a total of 120 men were completed before "VICTORIOUS" embarked her aircraft, and two main retests were made in 1959 and 1960 after successive periods of intensive operations. A ship-noise effect was detected at all these stages. After the retest in 1959 of 91 men, 15 were excluded for various reasons, and the remaining 76 men were graded according to their aircraft-noise exposure as:-

Grade A	0	to	50	take-offs	(Mean = 22)	17 men
Grade B	51	to	1300	" "	(Mean = 541)	59 men

A small average threshold shift in those most exposed (Grade B) had developed, which was significantly different ($P < 0.05$) at 0.5 and 1 Kc/s from the threshold shift of the men with the negligible exposure of Grade A. In fact the latter group showed an apparent improvement of hearing threshold averaging 1.2 dB throughout the test frequencies, when tested under identical conditions. This was taken to represent a measure of a practice effect obtained through an increased familiarity with the test procedure.

The final retest of 45 men was made at the beginning of 1960 after they had been away from aircraft noise for more than four weeks. The men were divided into three groups according to their exposure to aircraft noise, and their average threshold shifts since the initial test 19 months earlier are as shown in Figure 2 where the categories of exposure are as follows:-

Grade C	0	to	1500	take-offs	(Mean = 603)	16 men
Grade D	1501	to	2500	" "	(Mean = 2022)	5 men
Grade E	2501	to	4000	" "	(Mean = 3358)	24 men

Only five men were included in the intermediate group, but it was convenient to employ this group to segregate the least-exposed from the most-exposed.

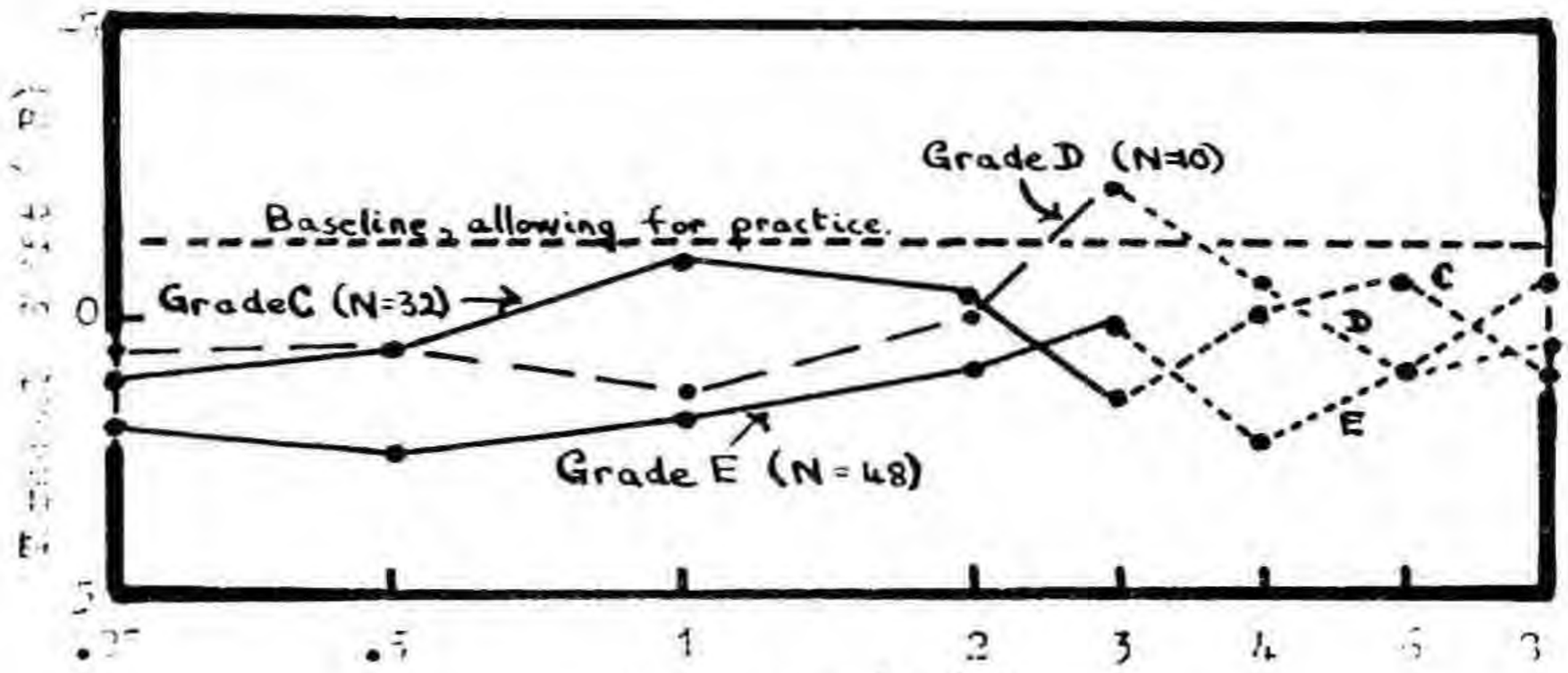

FIG.2 Prospective Study (H.M.S. VICTORIOUS)
Median Threshold Shift of Groups with
Reference to Initial Thresholds

The average threshold shift measured in the most exposed group was significant ($P < 0.05$) at 0.25, 0.5, 1 and 6 Kc/s, but addition of 1 dB for practice (as found in the 1959 retests) increased the degree of significance and extended its range, viz. 0.25, 0.5, 1 Kc/s ($P < 0.01$); 2 Kc/s ($P < 0.05$) and 4 and 6 Kc/s ($P < 0.01$).

Considerable interest attaches to the threshold shifts in the 24 men with an average of about 3,500 take-off exposures and attention was given to the distribution of these threshold shifts. Neglecting the small effect of practice it can be assumed that, to one 5 dB step of the audiometer attenuator, there was no reason for a greater threshold shift in the direction of a deterioration than in the direction of an improvement. Then there were at least 14 threshold changes of 15 dB or more for the worse, among the test frequencies; these were found to be associated with 9 ears of 8 men.

If further it can be considered that only the threshold shifts up to and including 4 Kc/s were the result of aircraft noise, the 14 threshold changes above reduce to 10, applying to 6 ears of 5 men. That is to say, about 20 per cent of the most-exposed group of men showed distinct signs of hearing damage after this single commission.

A flight-deck helmet, incorporating leather ear muffs to protect the ears, had been introduced in aircraft carriers during the retrospective survey, and its use became obligatory. Speech communication during quiet periods was possible by rotation of a speech valve on the side of the helmet. During the investigation with H.M.S. VICTORIOUS an improved form of flight-deck helmet was issued which employed ear muffs fitting the sides of the head by means of a fluid sealed into a thin plastic skin. The better seal of the ear muff to the head which was obtained, increased the attenuation at low frequencies to about 25 dB. Unfortunately, under the severe testing conditions of the flight deck, trouble was experienced through breakage of the fluid seal. When this happened much of the attenuation was lost, and hence the ear protection was not as complete as had been intended at this time.

Discussion and Conclusions

In both the retrospective and prospective phases of the study, the threshold shifts (measured sufficiently long after the last aircraft-noise exposure to ensure that any temporary effects had recovered) have been found principally at 2 Kc/s and below. At each stage, progressive increase in the average aircraft-noise exposure of the groups corresponded with an increase in their threshold shift. Additionally with the retrospective investigation, the difference in the threshold shifts of a group with moderate degree of exposure, divided on the basis of whether or not they had worn

ear protection, demonstrated that wearing the earlier form of flight-deck helmet gave a significant ($P < 0.05$) amount of hearing protection at 1 and 2 Kc/s.

The occurrence of noise-induced hearing loss in this middle range of audible frequencies is unusual. With the typical noisy industrial situation, the character of the noise is more often impulsive - either from a hammering process, or from some form of regular impact as with a circular saw or a train of gears. Here the resulting average hearing loss is found to be maximal at higher frequencies, usually at 4 or 6 Kc/s. This finding applies also to the effects of gunfire noise and, in Figure 1, where the hearing level of a group of men with aircraft-noise exposure and gunfire exposure is shown, a gunfire "notch" may be identified together with the lower frequency effect from aircraft noise.

As far as is known, the only other situation in which hearing loss for the lower tones has been reported is that of the borax-well workers in Tuscany studied by Bernabei (1953). Superheated steam and other gases gush at high pressure from the geysers producing a noise which closely resembles that of a jet engine in both spectral content and intensity. There is a peak in the noise spectrum in the region of 400 to 500 c/s and Bernabei found an average hearing loss at 500 c/s in a group of these workers.

Subjects with an occupational hearing loss about 4 Kc/s are generally unaware of any disability in the early stages, before the damage affects lower frequencies, but hearing loss which affects the lower and middle audible frequencies causes a greater social handicap. Men who have suffered 30 to 40 dB losses below 2 Kc/s, from exposure to jet noise on the flight deck, have sufficiently great hearing losses for speech to cause them difficulty. Further, the shape of the articulation curve is distorted, indicating that a hearing aid would be unlikely to restore full intelligibility at any output level. Two such cases have been examined recently after accidental exposure without adequate ear protection.

The uniform temporary threshold shift of approximately 5 dB, measured in men soon after leaving the aircraft carriers, has been noted in many other audiometric surveys of ship-borne personnel. It was not found, however, with naval recruits or with divers living in shore establishments. Similarly, a small group of men from the aircraft carriers, tested after spending more than a week in a hospital ashore, had substantially normal hearing. Hinchcliffe (1960) has lately found independent evidence of this effect in industrial workers tested soon after leaving a noisy working environment. It is possible that this temporary threshold shift might be due to the action of a protective mechanism in the middle ear (the acoustic reflex) rather than to auditory fatigue.

Acknowledgements

The investigations described above were performed as part of a joint research programme of the Wernher Research Unit on Deafness and of the Royal Naval Personnel Research Committee.

The author is indebted to Surgeon Lieutenant Commander R.R.A. Coles, R.N., for collaboration in examining the subjects and in many other ways. Grateful acknowledgement is given to Dr. T.S. Littler for his advice and encouragement throughout, and to the authorities concerned for permission to present this account.

References

Bernabei, L. (1953) Riv. Audiol. Practica (Milan) 3, 21.
Coles, R.R.A. and Knight, J.J. (1959) Nature (London) 184, 1803.
Hinchcliffe, R. (1960) Personal Communication.
Knight, J.J. and Coles, R.R.A. (1960) J. Acoust. Soc. Am. 32, 800.
Ward, W.D. (1957) J. Acoust. Soc. Am. 29, 1289.

J34

FOURTH INTERNATIONAL CONGRESS ON ACOUSTICS
COPENHAGEN 21.-28. AUGUST 1962

ON THE NUCLEATION PROCESS IN ULTRASONIC CAVITATION.

Diana MESSINO' - Istituto Nazionale di Ultracustica "O. M. Corbino" Roma
Daniele SETTE- Università di Roma - Istituto Nazionale di Ultracustica "O. M. Corbino" Roma
Francesco WANDERLINGH - Istituto Nazionale di Ultracustica "O. M. Corbino" Roma.

Previous research suggested that energetic neutrons may induce nucleation responsible for ultrasonic cavitation in water through the production of knocked-on Oxigen nuclei [1]. It was then pointed out that cavitatinn sets-in when a nucleus happens to be in a sound field of intensity sufficient for its growth from the original radius to visibility. The threshold therefore is to be considered as a suitable average of intensities as a consequence of the possible presence of nuclei of various radii. We have developed a technique [2] to get information on the size distribution of nuclei based on the determination of the probability of cavitation as a function of sound intensity in a large number of small specimens of the same liquid successively introduced in a plane wave sound field. One gets the number of nuclei present as a function of the sound intensity in which they may grow. This function may yeld a relation between number and size of nuclei if a growth mechanism is postulated.

We report here on the distribution functions obtained in this way in distilled water in the following conditions: a) normal; b) lead screened; c) lead screened and irradiated with a 10 mc Ra-Be neutron source. It is to be observed that the number of events in which cavitation is produced by nuclei of very small radii (very large sound intensities necessary for growth) is experimentally low because only in few specimens larger nuclei were absent. This fact puts limitation to the method used by us and allows one to get accurate

---

(1) D. SETTE, F. WANDERLINGH, Phys. Rev. 125, 409 (1962).

(2) To be reported elsewhere.

information only for nuclei present with concentrations between 10^{-4} and 10^{-2} nuclei/cm^3; they, however, determine the cavitation threshold. The distribution functions (i.e. concentration of nuclei vs sound pressure required for growth) found in the various cases have the general behavior of a regular raising curve with increasing pressure (i.e. decreasing radius) with added prominences around a few pressure (radius) values.

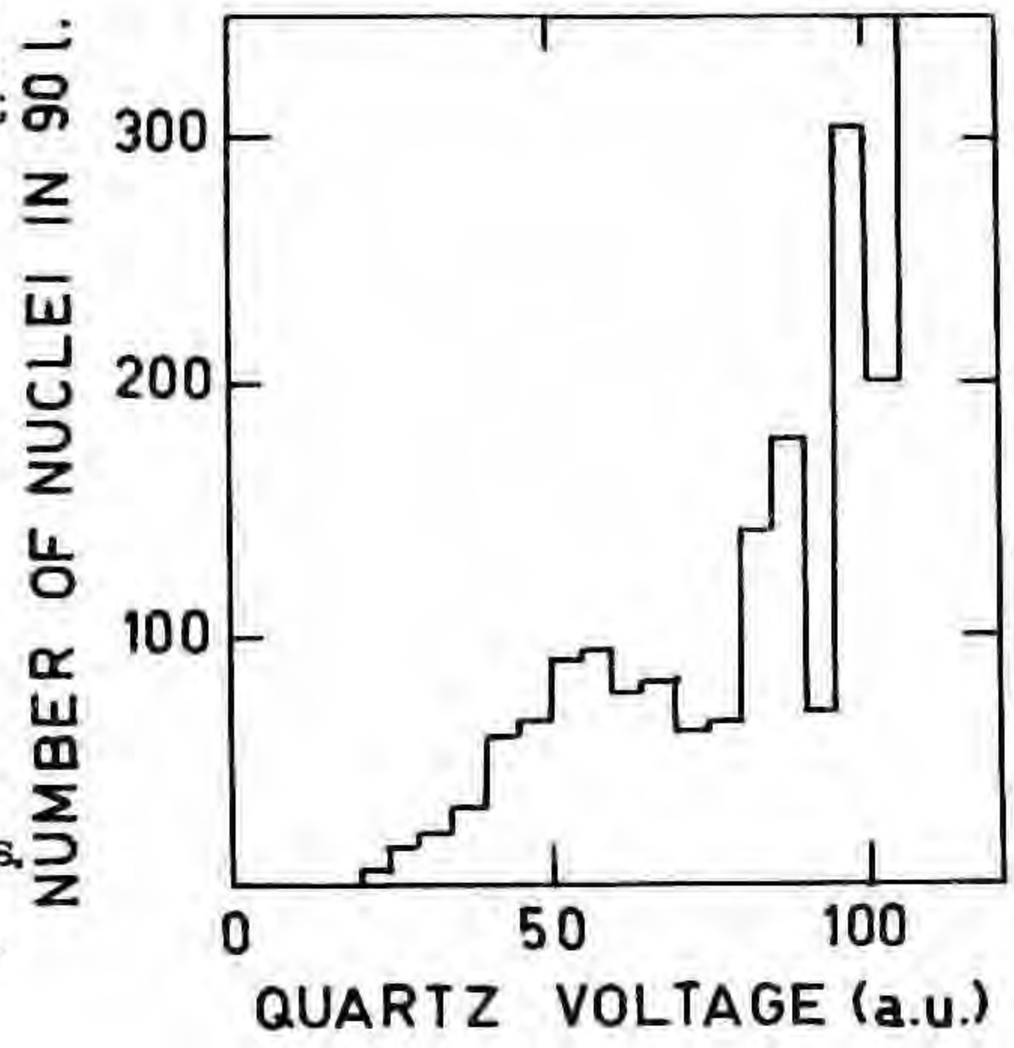

Fig. 1 - Distribution of nuclei in normal water

Figure 1 shows the results for normal distilled water: the number of nuclei found in 90 liters of water is put on the ordinates; the quartz voltage in arbitrary units is given on the x-axis it is possible to converte to sound pressure (bar) in the plane wave field by multiplying for 0.0204 the voltage data.

Figure 2 gives the variation of the distribution function due to the presence of a 15 mm lead screen: a general decrease of concentration of nuclei of all sizes has been found with a definite increase of nuclei which may growth in pressure fields of about 1.5 bar.

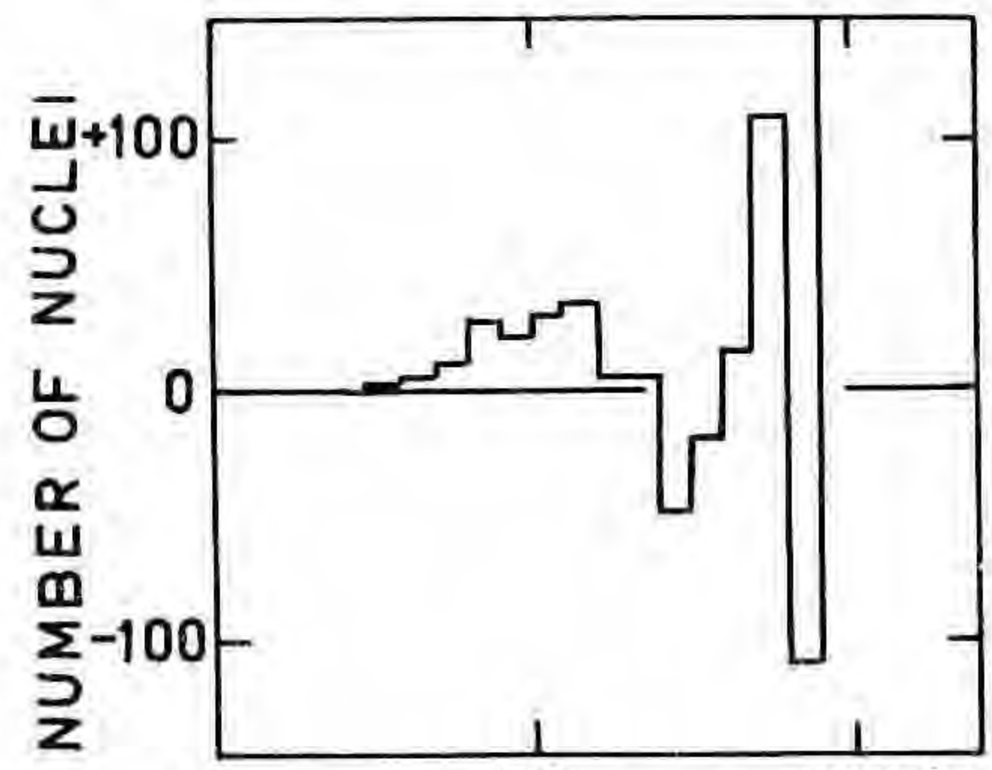

Fig. 2 - Excèss of nuclei in normal water compared with screened water.

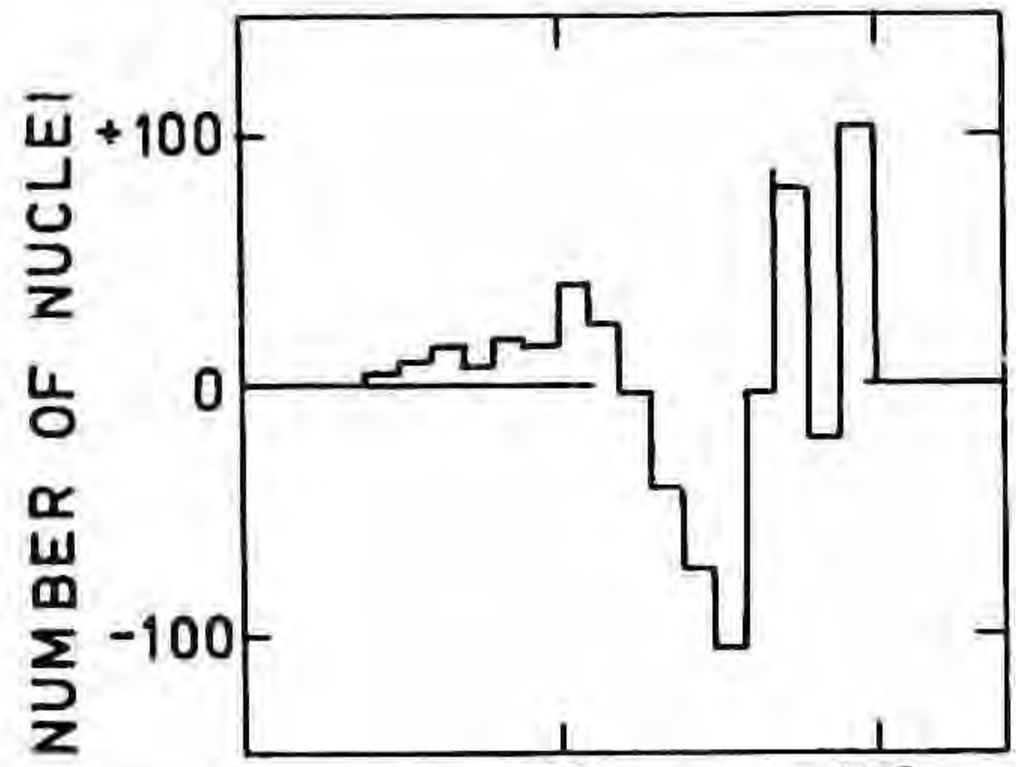

Fig. 3 - Excess of nuclei in normal water compared with screened irradiated water.

Figure 3 gives the similar variation between normal water and water enclosed by a 15 mm lead screen and irradiated by the neutron source: the increase of number of nuclei around the abscissa of 1.5 bar, already present in Fig. 2, is largely enhanced. This increase is more evident in fig. 4 where the differences between curves of Figg. 2 and 3 are plotted.

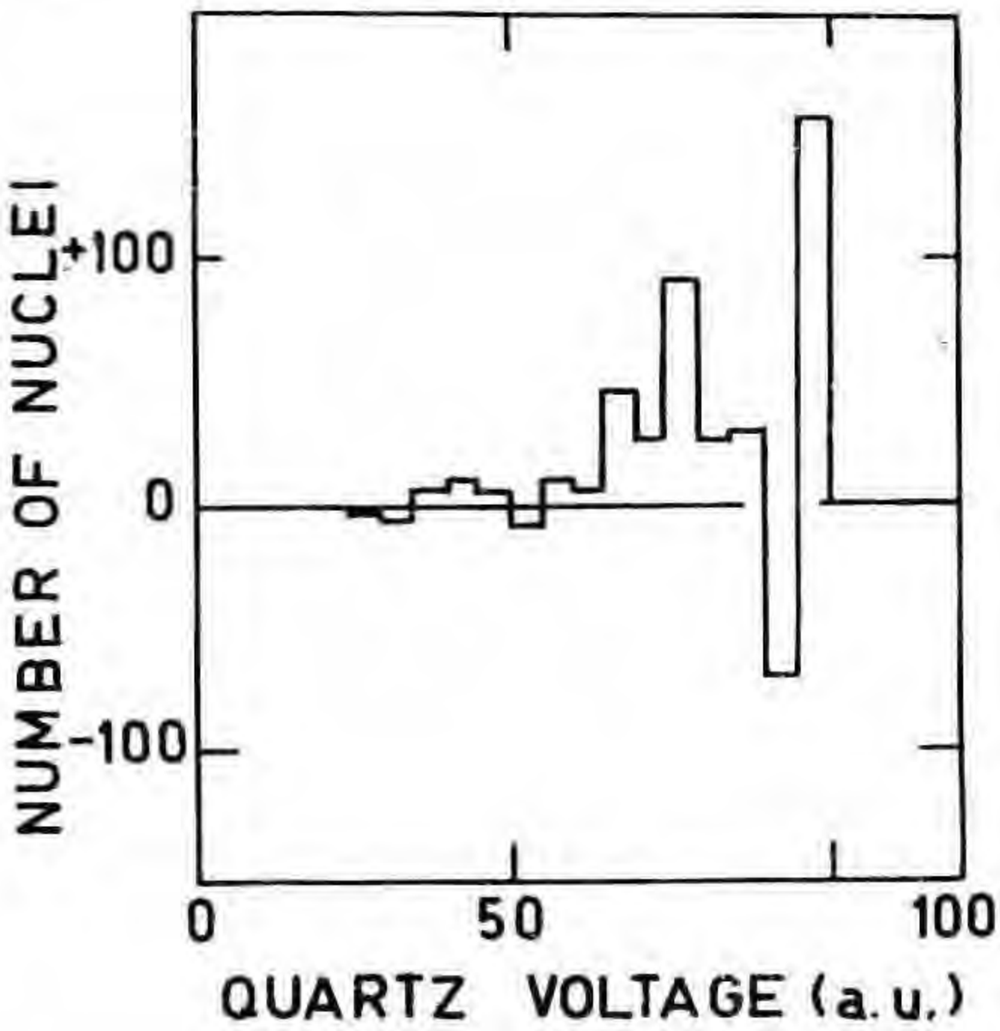

Fig. 4 - Excess of nuclei in screened irradiated water compared with screened water.

These results confirm first of all our conception of conventional cavitation threshold as a weighted average of sound intensities applied to the liquid, the weights depending on the distribution function and on a geometrical factor bound to the shape of the sound field. If we use the distribution functions obtained in the present research to calculate the weights for the experimental conditions used in paper (1), we get cavitation threshold values in agreement with those then found experimentally in the various situations. We get the calculated values 1.02, 1.26, 1.10 respectively for normal water, water with a 15 mm lead screen and water with screen and source, to be compared with experimental figures 1.00, 1.28, 1.02.

It is to be noted that in the case of water with lead screen the observed increase of concentration around the abscissa 1.5 bar is not sufficient to compensate the general decrease of the concentration values and we obtain a threshold increase. In the case of added neutron source the larger bump at 1.5 bar practically compensate the general decrease of the distribution curve for what the threshold value is concerned.

The Ra-Be neutron source produces nuclei and it is evident that those of larger size group around a radius to which corresponds 1.5 bar as sound pressure required for growth. Because it seems reasonable to assume that the size of nuclei increases with particle energy, these nuclei should be created by the more energetic neutrons emitted by the source, i.e. 10-12 MeV. This is in agreement with our previous calculations leading to the indication of cosmic neutrons as responsible for cavitation in normal water.

Lead enclosures have two effects: the first is a screening one which decreases the concentration of nuclei of all sizes. The second effect is a production of nuclei and it is interesting to note that the corresponding pressure necessary for growth is the same of that for nuclei created by 10 MeV neutrons from the source. It seem therefore possible to conclude that 10 MeV neutrons come into play also in the second effect in lead. This may happen for instance by means of the (μ^-, n) reaction in lead:

$$\mu^- + P \longrightarrow n + \nu$$

The presence of the two contrasting effects in lead screens gives support to the explanation already given of the presence of a maximum of the cavitation threshold as a function of the screen thickness: the probability of reactions, like that mentioned, produced by cosmic ray components, increases with thickness.

The present experiments therefore support previous indications on high energy neutrons as source of nucleation responsible for sound cavitation in water.

K34

FOURTH INTERNATIONAL CONGRESS ON ACOUSTICS
COPENHAGEN 21.-28. AUGUST 1962

QUANTUM ELECTRONICS OF OPTICAL PHONONS

Dr. C. H. Becker
Precision Instrument Company, San Carlos, California

Phonons are the elementary quanta of elastic radiation energy. Similarly, the elementary quanta of electromagnetic radiation energy are called the photons. Phonons occur in two principal kinds: (1) "Acoustical" phonons at, for example, kilomegacycle frequencies, in which the elastic medium vibrates as a whole; and (2) "Optical" phonons in the teracycle frequency range of 10^{12} cycles per second (MM c/sec.), where the molecular vibrational modes determine the elastic motion.

According to earlier theories by I. Tamm (TAM 30) and R. E. Peierls (PEI 56), optical phonons are spontaneously created and annihilated in alpha-quartz in connection with inelastic light scattering. Such processes became known as Raman scattering in the solid state. Discovery of alpha-quartz as the first known solid state material in which inelastic light scattering was produced is credited to the pioneer work of Landsberg and Mandelstam in 1928 (LAN 28).

On the basis of I. Tamm's hypothesis, optical phonon creation and annihilation occurs in two elementary propagating processes:

(1) A destruction of an incident light quantum $\omega_1, \bar{K}_1$ where, at the expense of this light quantum, a light quantum $\omega_s, \bar{K}_s$ and an optical phonon $\omega_\sigma, \bar{K}_\sigma$ are produced.

(2) A collision of an incident light quantum $\omega_1, \bar{K}_1$ with an optical

phonon ω_σ , $\bar{K}_\sigma$; thus, that at the expense of both, one light quantum ω_{AS} , $\bar{K}_{AS}$ is produced.

$\omega, \bar{k}$ are the angular frequencies and wave vectors of the respective quanta. The subscript I designates the incident light quanta (pump), the subscript σ indicates the optical phonon, and the subscripts S , AS characterize the scattered light quanta at the Stokes and Anti-Stokes frequencies, respectively.

Previously known inelastic light scattering processes represent strictly "spontaneous" and "incoherent" phenomena. However, it was recently postulated by the author (BEC 62) that under certain conditions "stimulated" (induced) optical phonon emission can be achieved in alpha-quartz by means of very high intensity ultraviolet optical pumping. Hence, in terms of quantum electronics, alpha-quartz can be operated as a traveling wave optical phonon-maser.

Applying I. Tamm's earlier theory to the second-order quantum mechanical interaction process in alpha-quartz, its operation is basically determined by the conservation laws of energy and momentum. After cancellation of Planck's constant, they obtain the form:

$$\omega_I = +\omega_\sigma + \omega_S \qquad \bar{k}_I = +\bar{K}_\sigma + \bar{K}_S$$

$$\omega_I = -\omega_\sigma + \omega_{AS} \qquad \bar{k}_I = -\bar{K}_\sigma + \bar{K}_{AS}$$

During the interaction, the wave vector $\bar{k}_\sigma$ of the optical phonons is related to the wave vector $\bar{k}_I$ of the incident light by means of $\bar{k}_\sigma = 2\bar{k}_p \sin \frac{\partial}{2}$ where ∂ is the scattering angle.

Parametrically speaking, an optical phonon-maser in alpha-quartz is equivalent to a four-frequency traveling wave parametric amplifier, with the dynamic (time-varying) polarizability of the alpha-quartz at the three dimensionally distributed "parameter" (LOU 60). According to S. Placzek (PLA 34), this polarizability is defined as $\sum_i \left(\frac{\partial \alpha}{\partial q_I}\right)_0 q_i$ where the q_I are certain

normalized vibrations of the alpha-quartz molecules. In a parametric presentation, the four optical frequencies are related as follows:

$\omega_1 \equiv$ angular pump frequency.

$\omega_{AS} \equiv$ signal frequency.

$\pm \omega_\sigma \equiv$ primary idler frequency.

$\omega_S \equiv$ second idler frequency.

Substituting these terms into the conservation laws above, one obtains the parametric equivalent to optical phonon-maser operation in alpha-quartz.

The transition probability W_{nk} per unit time for phonon creation in conjunction with the second-order photon-phonon-photon interaction is:

$$W_{nk} = \bar{\rho}(\omega_1)\,\Delta\omega_1\left[12\pi\hbar k_\sigma^3 + \rho(\omega_\sigma)\right].\Phi_{nk}$$

where $\rho(\omega_1)$ density of incident electromagnetic radiation.

$\rho(\omega_\sigma)$ density of present phonon radiation.

$\Delta\omega_1$ half width of incident electromagnetic pump.

with
$$\Phi_{nk} = \frac{\pi}{3}\left(\frac{1}{\hbar^2\epsilon_o^2}\right)\left(\frac{\omega_m}{\omega_\sigma}\right)\left|(\alpha_{xy})_{nk}\right|^2$$

$$\left|(\alpha_{xy})_{kn}\right|^2 = \frac{1}{\hbar^2}\sum_r\left[\frac{(M_y)_{kr}(M_x)_{rn}}{\omega_{rn}-\omega} + \frac{(M_x)_{kr}(M_y)_{rn}}{\omega_{rk}+\omega}\right]^2$$

Different writing discloses the relationship to A. Einstein's coefficients A, B for spontaneous and stimulated (induced) emission:

$$W_{nk} = \bar{\rho}(\omega_1)\,\Delta\omega_1\left[A_{nk} + B_{nk}\,\rho(\omega_\sigma)\right]$$

where $\frac{A_{nk}}{B_{nk}} = 12\pi\hbar k_\sigma^3$. In divergence from the usual factor 8π for photon-emission, the factor 12π appears for phonon-emission, because of the three polarization directions of the phonons compared to two polarization directions for the photons.

Hence, traveling-wave optical phonon-maser action at the molecular vibration frequencies ω_σ of the alpha-quartz theoretically occurs during

certain second-order quantum-mechanical interaction processes between very high intensity ultraviolet (pumping) radiation and the molecular vibrations.

Detection of optical phonon-maser action in alpha-quartz is conceived by means of measuring the ratio of the Anti-Stokes to the Stokes intensities of the scattered ultraviolet radiation for the various molecular modes. According to I. Tamm, S. Placzek and S. Mizushima, this ratio is proportional to the occupation ratio of the excited and non-excited quantum states $\frac{N_+}{N_o}$ of the molecular modes:

$$\frac{I_{AS}}{I_S} = \frac{N_+}{N_o} \left(\frac{\omega + \omega_\sigma}{\omega - \omega_\sigma}\right)^4$$

Successful operation of a traveling wave quartz phonon-maser was very recently achieved at Precision Instrument Company, San Carlos, California. Pertinent experimental data will be presented at this Conference.

* * * * *

Bibliography

BEC 62 C. H. Becker, "Quartz Phonon-Masers", Optical Maser Symposium, Electrochemical Society, Los Angeles, May 10, (1962)

LAN 28 G. Landsberg and L. Mandelstam "Eine neue Erscheinung bei der Lichtzerstreuung in Kristallen", Die Naturwissenschaften 16, 557 (1928)

LOU 60 W. H. Louisell "Coupled Mode and Parametric Electronics", New York, (1960)

MIZ 58 S. Mizushima, "Raman Effect", Handbuch d. Physik, Vol. 26 Berlin (1958)

PEI 55 R. W. Peierls, "Quantum Theory of Solids", Oxford (1955)

PLA 34 G. Placzek, "Rayleigh Streuung und Raman-Effekt", Handbuch der Radiologie, 6, II, pp. 209-374, Leipzig (1934)

TAM 30 I. Tamm, "Ueber die Quantentheorie der molekularen Lichtzerstreuung", Zeitschrift fuer Physik 60, 345 (1930)

L34

FOURTH INTERNATIONAL CONGRESS ON ACOUSTICS
COPENHAGEN 21.-28. AUGUST 1962

Vorausberechnung der aerodynamischen Geräusche elektrischer Maschinen

G. Hübner, Berlin, Siemens-Schuckert-Werke AG

Das Geräusch elektrischer Maschinen setzt sich aus mehreren Anteilen zusammen, die von unterschiedlichen physikalischen Vorgängen verursacht werden. Diese Anteile sind das magnetische und das aerodynamische Geräusch, ferner das Lager-und Bürstengeräusch. Mit einer Vorausberechnungsvorschrift der Pegelwerte dieser Geräusche kann die Erfüllung einer Geräuschgarantie schon im Stadium der Konstruktion geprüft werden. Ferner kann man von den Gesetzmäßigkeiten auch Hinweise für die Konstruktion leiserer Maschinen erhalten, sofern die Berechnungsvorschrift anhand eines physikalischen Modelles des Geräuschentstehungsmechanismus hergeleitet ist.

Die Untersuchungen über eine solche Berechnungsvorschrift bezogen sich bisher fast ausschließlich nur auf die magnetischen Geräusche [1] [2]. Dieser Anteil besitzt ein diskretes Spektrum und stellt die abgestrahlten Schwingungen der Maschinenständer dar, die von Radialkraftwellen des Luftspaltfeldes erzwungen werden. Der Gesamtgeräuschpegel wird meist nur bei Maschinen niedriger Umfangsgeschwindigkeit durch magnetische Geräusche merklich beeinflußt. Man ist heute im allgemeinen noch nicht in der Lage, mit Sicherheit die magnetischen Geräusche quantitativ vorauszubestimmen, was auf das komplizierte Schwingungsverhalten der Maschinenständer zurückgeführt werden konnte [3].

Der aerodynamische Geräuschanteil entsteht an den in Luft rotierenden Bauelementen der Maschinen. Er besitzt ein kontinuierliches Spektrum, dem außerdem auch noch Töne eingelagert sein können, die durch einen Sirenenmechanismus erzeugt werden. Es ist heute fast immer möglich, die Sirenentöne soweit zu mindern [4], daß sie neben dem rauschartigem Grundgeräusch nicht mehr wahrgenommen werden. Das Entstehen des breitbandigen Rauschens ist dagegen für die in einem Gas umlaufenden Maschinen grundsätzlich nicht zu vermeiden. Mit diesem aerodynamischen Rauschen wollen wir uns im folgendem ausschließlich beschäftigen, ihm kommt eine besondere Bedeutung zu, da das Gesamtgeräusch der schnellaufenden und damit der lautesten Maschinen fast immer allein durch

diesen Geräuschanteil bestimmt ist. Dies gilt für Maschinen mit Umfangsgeschwindigkeiten über 5o ms^{-1} in offener Bauform.
Zur Herleitung von physikalischen Gesetzen über das Entstehen des aerodynamischen Rauschens wird zuerst ein <u>frei</u> rotierender Maschinenläufer nach Bild 1 betrachtet. Entlang der Läuferoberfläche bildet sich bei der Rotation im Gas eine turbulente Schicht aus, deren zahlreiche Wirbel die Quellen für unser Geräusch darstellen. Die Gesamt-Schallleistung einer solchen flächenförmig verteilten Quelle ergibt sich aus der Summation der Wirkung aller Flächenelemente und ist der Läufer-Mantelobertläche $S=\pi DI$ proportional, da die Wirkung der Seitenflächen infolge ihrer geringeren Geschwindigkeiten vernachlässigt werden kann. Die Rauschleistung von Bauelementen, wie sie bei Läufern und Maschinenlüftern üblich sind, wachsen mit der 5.bis 6. Potenz der Umfangsgeschwindigkeit,sofern letztere 1oo ms^{-1} nicht wesentlich übersteigt, was durch Messungen an originalen Maschinenläufern bestätigt wurde (Exponent 5,5). Es zeigte sich dabei ferner, daß der Läuferdurchmesser im untersuchten Bereich nur in die Umfangsgeschwindigkeit und die Manteloberfläche eingeht[5]:

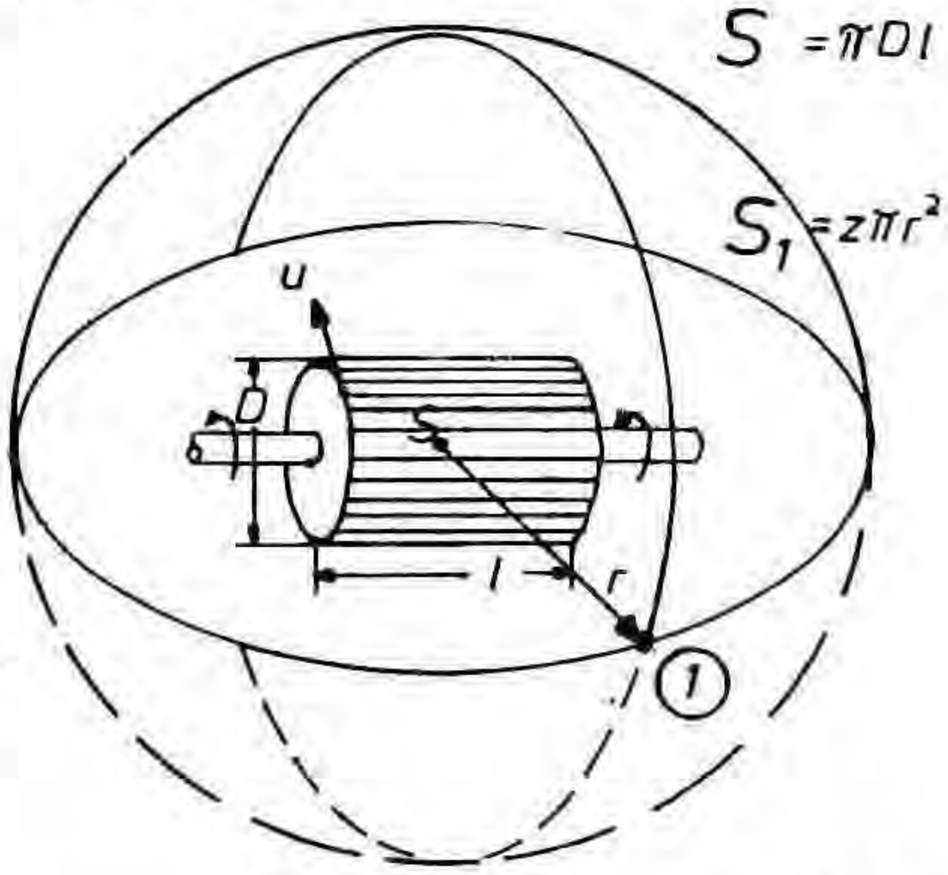

Bild 1

$$P = \gamma_0 S\left(\frac{u}{u_0}\right)^{5,5}$$

darin ist γ_0 die je Oberflächeneinheit bei der Bezugsgeschwindigkeit u_0 abgestrahlte, sogenannte "spezifische Schallleistung" , deren Zahlenwert experimentell bestimmt wurde. Hierbei zeigt sich, daß für die üblichen Maschinenkonstruktionen der Wert von γ_0 nur innerhalb einer Größenordnung schwankt, für u_0=5o ms^{-1} zwischen $1o^{-6}$ und $1o^{-5}$ $\frac{Watt}{cm^2}$ liegt. Die Auswertung von Geräuschmessungen von HOLLE an umlaufenden Profilstäben[6] und späterer Untersuchungen an Radialrädern[7] liegen ebenfalls in diesem Bereich (s.Bild 2). Der Effektivwert des Schalldruckes p_{eff} im Aufpunkt (1) ergibt sich dann zu:

$$p_{eff}=\sqrt{\varrho c \frac{P}{S_1}} \qquad \text{mit } S_1=z\pi r^2$$

falls der Aufpunkt hinreichend weit ab (Fernfeld) auf einer Voll-(z=4) bzw. Halb-(z=2)Kugel vom Radius r liegt.

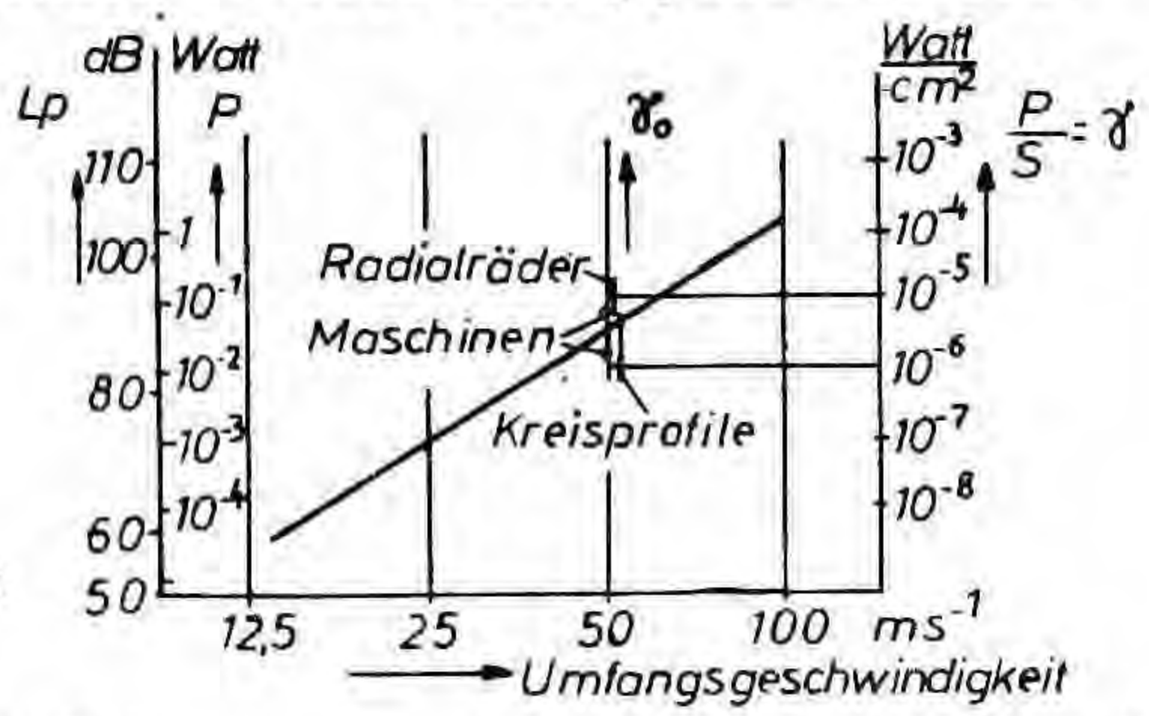

Bild 2

Der zugenörige Schalldruckpegel:

$$L_p = 10\,lg\frac{\gamma_o}{J_o} + 10\,lg\,\frac{S}{S_1} + 55\,lg\,\frac{u}{u_o} \quad \text{in dB} \quad \text{mit } J_o = 10^{-16}\ \frac{\text{Watt}}{\text{cm}^2}$$

Das Bild 3 stellt die letzte Gleichung in Abhängigkeit der Umfangsgeschwindigkeit dar, wobei als Parameter das Flächenverhältnis $\frac{S_1}{S}$ gewählt ist. Das normale Absorptionsvermögen im Inneren einer zusammengebauten elektrischen Maschine ist sehr klein ($\alpha < 0{,}1$), sodaß der im Bild 3 dargestellte Zusammenhang auch auf den in die Maschine eingebauten Läufer angewendet werden kann, sofern die Maschine eine offene Bauform besitzt. Im Falle einer geschlossenen Maschine vermindern sich diese Pegelwerte dagegen um die "wirksame" Dämmung der Kapsel. Zur Prüfung der angestellten Überlegungen wurden die so berechneten Schalldruckpegel mit zahlreichen gemessenen Werten verglichen. Bild 4 zeigt diesen Vergleich für eine Auswahl verschiedener Maschinentypen (■=2polige, ●=4polige Asynchronmaschinen, ▲=6polige, □=8polige Asynchron- und Synchronmaschinen). Die festgestellten Abweichungen sind danach kleiner ± 3 dB. Dabei ist von der 8poligen Synchronmaschine ($u = 125\ ms^{-1}$) abgesehen, die sich durch eine fast zylindrische Mantelobefläche, gebildet durch große abgerundete Pole, auszeichnet. Für derartige Sondermaschinen ist die Einführung einer geänderten, hier zahlenmäßig kleineren spezifischen Schalleistung γ_o zweckmäßig. Frühere Geräuschuntersuchungen an rotierenden glatten Scheiben [8] ergaben γ_o-Werte, die sogar um 40 dB unter denen der üblichen Maschinenläufer liegen.

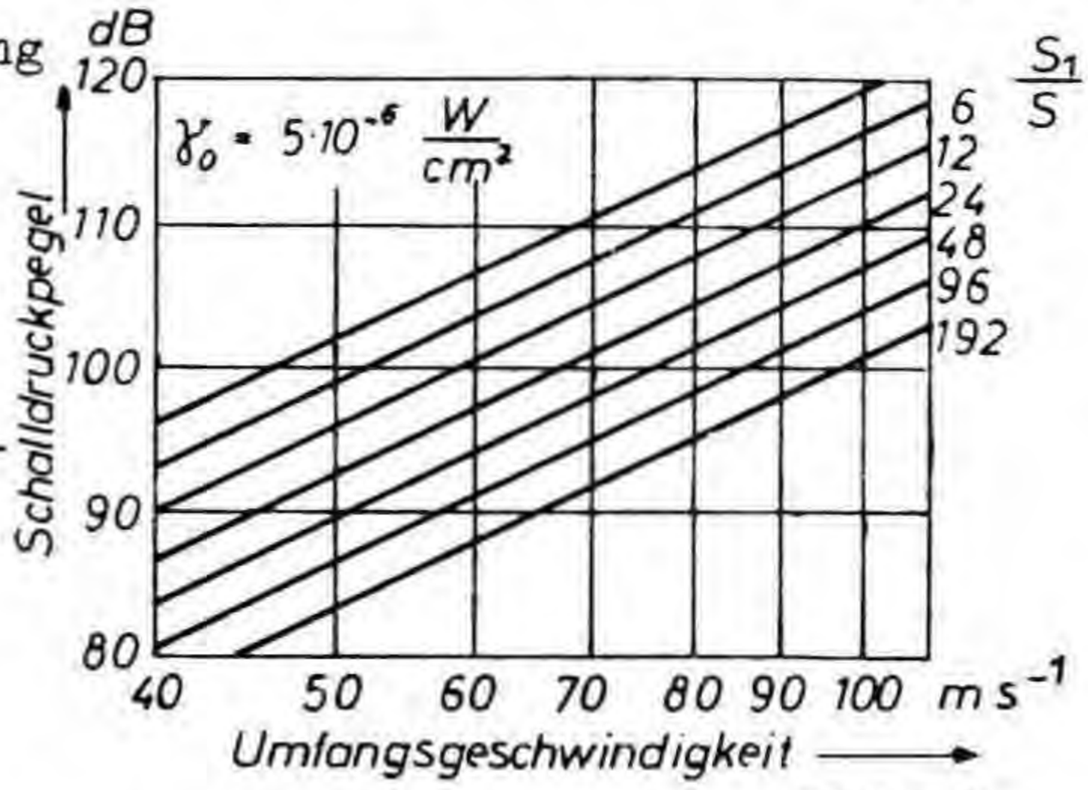

Bild 3

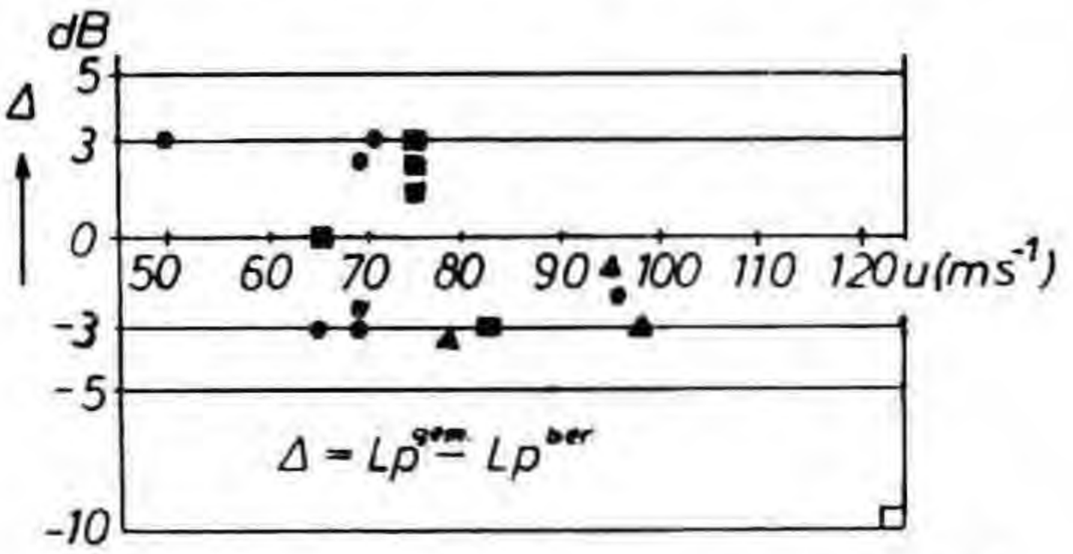

Bild 4

Eine verbesserte Beschreibung der aerodynamischen Geräuschentstehung kann erreicht werden durch Einführung weiterer Parameter wie z.B. der Drosselung des mitrotierenden Maschinenlüfters. Die erzeugte Schallleistung eines Radialrades ist nämlich gleich dem Produkt aus einem

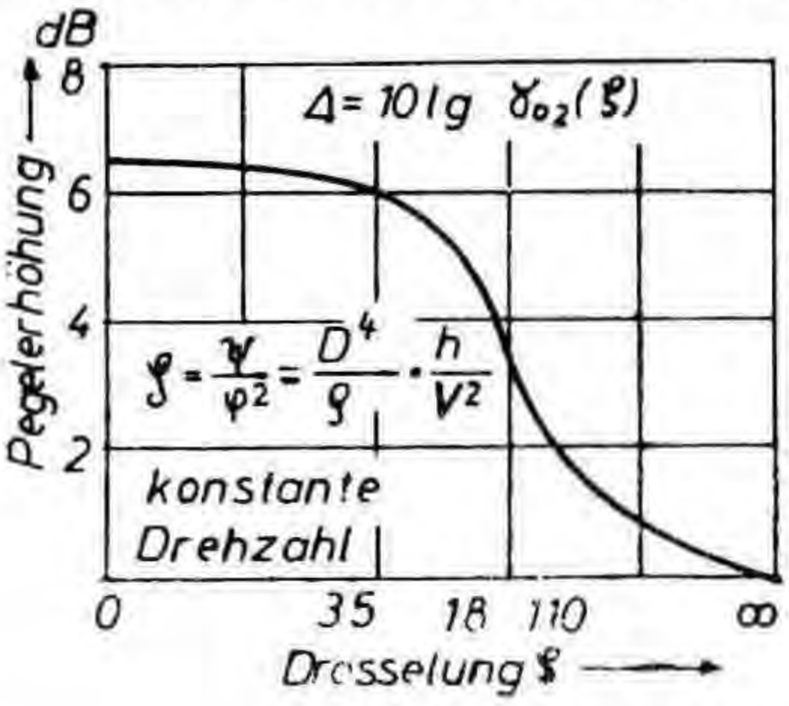

h=statischer Druck
V=geförderte Menge je Zeiteinheit
φ= Dichte

Bild 5

Rotationsanteil, welcher bei vollständiger Drosselung auftritt, und einem Förderanteil, entsprechend einer Aufteilung $\gamma_o=\gamma_{o1}\cdot\gamma_{o2}$ mit $10^{-6}<\gamma_{o1}<10^{-5}$ für $u_o=50$ ms^{-1} und $1\leq\gamma_{o2}(\xi)<10$ entspr. Bild 6.

In der deutschen Norm DIN 45 635 wird das Geräusch der elektrischen Maschine durch Messung des bewerteten Schalldruckpegels in einem Abstand von 1 m von der Maschinenoberfläche geprüft, wodurch bei großen Maschinen die oben getroffene Voraussetzung $r\gg\frac{D}{2}$ nicht zutreffen kann. Dann muß der kompliziertere Schalldruckabfall im "Nahfeld" berücksichtigt werden. Die Addition zweier (elektronischer) Rausch"leistungen" $P_1=\overline{p_1(t)^2}$ und $P_2=\overline{p_2(t)^2}$ erfolgt zur resultierenden Rausch"leistung" P nach der Beziehung [9]: $P=P_1+P_2+2\sqrt{P_1P_2}\,\phi_{12}$ mit $\phi_{12}=\overline{p_1(t)p_2(t)}:\sqrt{P_1P_2}$, dem Korrelationsfaktor. Im Falle einer Inkohärenz der beiden Quellen ($\phi_{12}=0$) ist $P=P_1+P_2$. Auf unser Nahfeld übertragen, erhält man für inkohärent strahlende Flächenelemente keine Interferenzerscheinungen, wohl aber einen schwächeren Abfall des Schalldruckes als mit $\frac{1}{r}$, der fast unabhängig von der Filtermittenfrequenz etwa dem eines elektrischen Potentials entspricht (exper. Bestätigung: Bild 6)

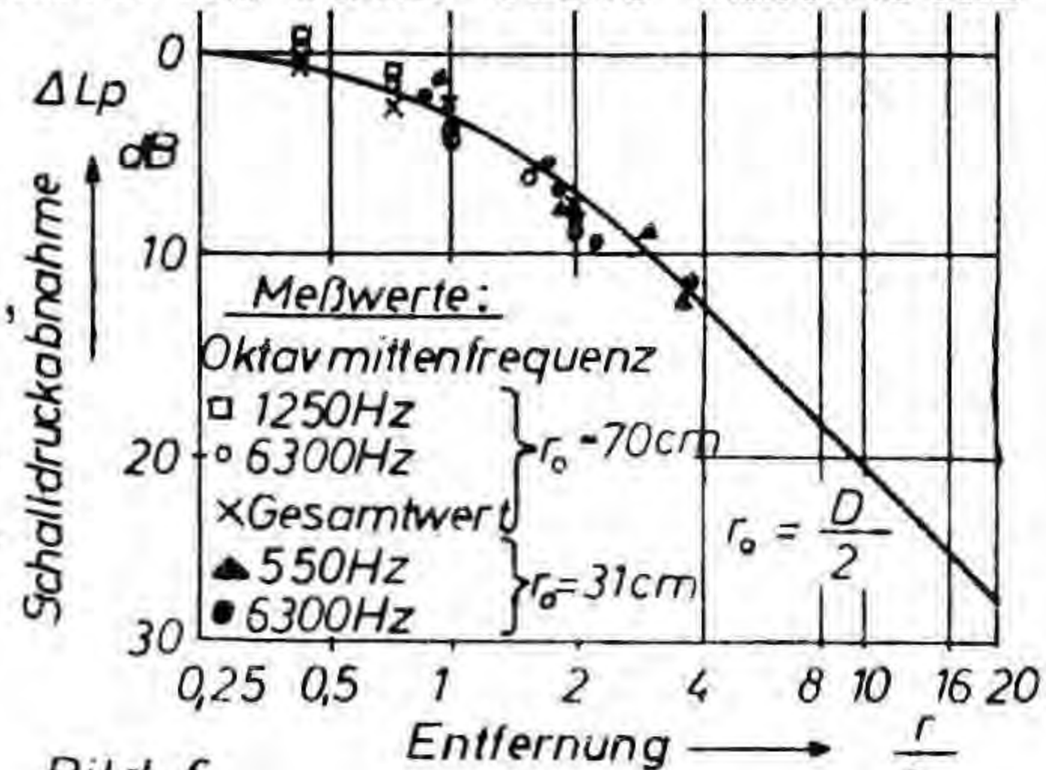

Bild 6

Literatur

1. Erdélyi, E.A.: Predetermination of the sound Pressure levels of magnetic noise in medium induction motors. Diss. University Ann. Arbor (Mich.) 1955
   siehe hierzu auch: Hübner, G.: Brief an die Schriftleitung. ETZ-A Bd. 81 (1960) S. 316
2. Jordan, H.: Der geräuscharme Elektromotor. Verlag W. Girardet Essen 1956
3. Hübner, G.: Untersuchungen über Schwingungen von Ständern elektrischer Maschinen. VDI-Ber. Bd. 24 (1957) S. 51-58
   Hübner, G.: Über das Schwingungsverhalten von Wechselstrommaschinenständern mit Rundschnittblechpaketen. ETZ-A Bd. 80 (1959) S. 33-39
4. Hübner, G.: Geräuschminderung bei großen elektrischen Maschinen. Siemens-Z. Bd. 35 (1961) S. 111-121
5. Hübner, G.: Aerodynamische Geräusche umlaufender Maschinenteile. VDI-Ber. Bd. 48 (1961) S. 113-117
   Hübner, G.: Entstehung und Bekämpfung der Geräusche elektrischer Maschinen. ETZ-A Bd. 82 (1961) S. 771-781
6. Holle, W.: Frequenz-und Schallstärkemessung an Hiebtönen. Akust. Z. Bd. 3 (1938) S. 321-331
7. Hübner, G.: Geräuschbildung von Radiallüftern. Siemens-Z. Bd. 33 (1959) S. 499-505
8. Hübner, G.: Geräuschbildung an rotierenden Zylindern und Radiallüftern. Kongreß-Ber. 3. ICA. Verlag Elsevier, Amsterdam 1961, Bd. II, S. 1171-1174
9. Montgomery, H.H.: Electrical noise in semiconductors. Bell Syst. techn. J. Bd. 31 (1952) S. 950-975

M34

FOURTH INTERNATIONAL CONGRESS ON ACOUSTICS
COPENHAGEN 21.-28. AUGUST 1962

Die Schallabsorption von gelochten und ungelochten Platten bei großen Wandabständen

Günter Venzke, Braunschweig

Physikalisch-Technische Bundesanstalt

Während über den Absorptionsgrad von gelochten und ungelochten Platten bei Wandabständen bis etwa 25 cm zahlreiche Meßergebnisse vorliegen (z.B. /1/), ist kaum etwas bekannt, wie sich diese Resonanzabsorber im diffusen Schallfeld bei größeren Wandabständen verhalten. Und doch treten häufig solche Schallschluckanordnungen in der Praxis auf, z.B. wenn unter einer weitgespannten Dachkonstruktion mit hohen Bindern frei aufgehängte Schallschluckdecken gezogen werden.

Messungen im Hallraum mit großen Wandabständen erfordern besondere Maßnahmen. Bei Verwendung der üblichen Prüfflächengrößen von 10 bis 12 m^2 müßten entweder entsprechend tiefe Nischen in den Hallraumbegrenzungen vorhanden sein, was kaum der Fall ist, oder man läuft Gefahr, durch die hohen Umfassungswände der im Hallraum aufgebauten Prüfflächen die Diffusität des Schallfeldes zu beeinträchtigen. Es wurde daher an ganzflächigen Wandverkleidungen gemessen, und zwar mit Luftraumtiefen von 10, 25, 60 und 150 cm.

Untersucht wurden 12,6 % und 19,6 % gelochte Gipskartonplatten von 9,5 mm Dicke (Rigips) sowie 8 mm dicke ungelochte Holzspanplatten. Die Lochplatten waren rückseitig mit einem textilen Vlies von etwa 8 Rayl Strömungswiderstand hinterklebt, hinter dieses Vlies waren zusätzlich noch Glasfasermatten von 20 mm Dicke und 1,3 kg/m^2 Flächengewicht (Masse je Flächeneinheit) gespannt. Das Tragegerüst für die Lochplatten bestand aus 48 mm breiten Holzlatten, die mit 39 cm Achsmaß in der Horizontalen parallelliefen. Bei den Spanplatten betrug der Lattenabstand 62,5 cm. Mit einer Ausnahme wurden die Spanplatten ohne Dämpfung des Hohlraumes gemessen.

Das Prüfmaterial bedeckte die 36,5 m^2 große ebene Längswand des Hallraumes der Physikalisch-Technischen Bundesanstalt (237 m^3), eine zweite Meßreihe wurde auf der 26,5 m^2 großen Querwand durchgeführt. Der Hallraum ist rechtwinklig und an zwei Wänden sowie der Decke mit zylindrischen Zerstreuungskörpern bedeckt, deren Achsen aufeinander senkrecht stehen. Wegen der großen Prüfflächen und der teilweise sehr breitbandig hochabsorbierenden Materialien wurden zusätzliche Diffusoren in Gestalt von Kugelkalotten und in den Raum gehängten gekrümmten Blechtafeln eingebracht. Über den jeweils notwendigen Aufwand an Diffusoren wurden Untersuchungen angestellt. Prüfschall (weißes Rauschen über Terzfilter) und Mikrophonstellungen entsprachen den deutschen und internationalen Normen.

Da der mittlere Absorptionsgrad im Hallraum mit Prüfmaterial im Gebiet der Resonanzmaxima den Wert 0,1 erheblich überschreitet, wurde nach der Eyringformel ausgewertet. Ferner mußte die bei großen Wandabständen beträchtliche Verkleinerung des Hallraumvolumens berücksichtigt werden. Die Auswerteformel hatte daher die Form

$$\alpha_{Eyr} = \frac{S_1}{S_p}\left[e^{-\frac{4V_1}{S_1}\left(0{,}67\cdot 10^{-3} d_1 - m_1\right)} - 1 \right]$$

$$- \frac{S_2}{S_p}\left[e^{-\frac{4V_2}{S_2}\left(0{,}67\cdot 10^{-3} d_2 - m_2\right)} - 1 \right]$$

Dabei sind:

$V_{1,2}$	die Hallraumvolumina	ohne und mit Prüfmaterial
$S_{1,2}$	die Hallrauminnenflächen	" " " "
$d_{1,2}$	die Abklingkonstanten	" " " "
$m_{1,2}$	die räumlichen Dämpfungskonstanten in Abhängigkeit von der Feuchtigkeit	" " " "
S_p	die Prüffläche.	

In der Formel ist das Glied, das die Absorption der vom Prüfmaterial bedeckten Hallraumfläche berücksichtigt, wie üblich fortgelassen. Die Druckerhöhung an den Prüfflächenkanten und in den Raumecken gegenüber der Wandmitte ist nicht korrigiert worden.

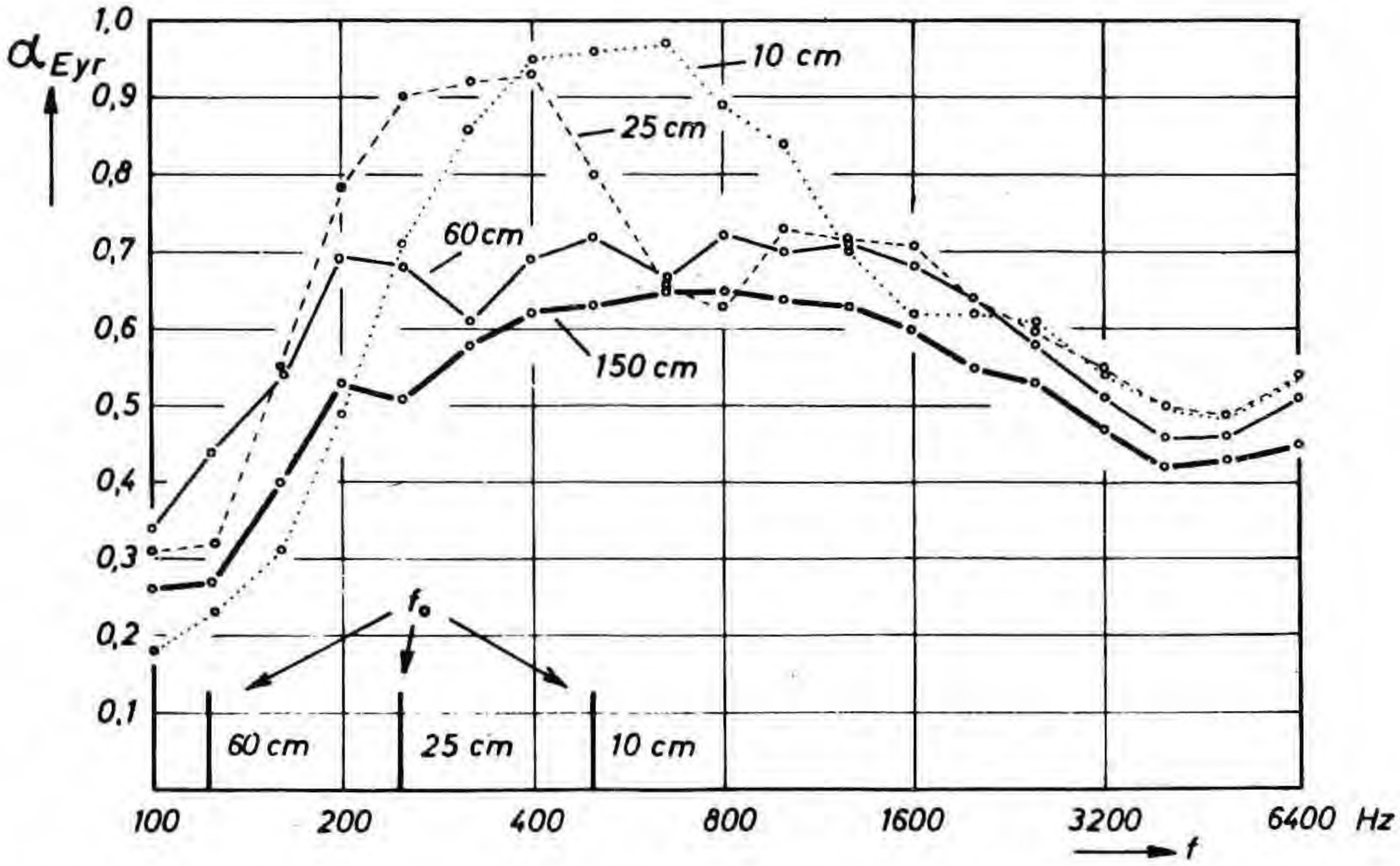

Bild 1 Absorptionsgrad von 19,6 % gelochten Platten bei verschiedenen Wandabständen (Realteil der Wandimpedanz: 1 bis 2 ϱc)

Die in Bild 1 aufgezeichneten Kurven des Absorptionsgradverlaufs, für Längs- und Querwand gemittelt, zeigen bei 10 cm Wandabstand die bekannte einfache Resonanzkurve. Bei 25 cm Abstand tritt noch ein zweites schwächeres Maximum in Erscheinung, während sich der Absorptionsverlauf mit größeren Abständen immer mehr verflacht. Bemerkenswert ist, daß bei 1,5 m Wandabstand die bei senkrechtem Schalleinfall und optimaler Anpassung zu beobachtenden Schwankungen zwischen 0 und 1,0 im Absorptionsgrad überhaupt nicht mehr in Erscheinung treten, jedenfalls nicht oberhalb 100 Hz.

Die Vergleiche mit dem theoretisch zu erwartenden Absorptionsgradverlauf müssen einer ausführlicheren Veröffentlichung vorbehalten bleiben. Die Übereinstimmung ist abgesehen von den Frequenzen $\leqq$ 200 Hz sogar in Einzelheiten recht gut. Die gemessenen Werte liegen durchweg etwas höher, da die Theorie (z.B. /1/) die Oberflächen-Absorption der Mattenhinterfüllung nicht berücksichtigt.

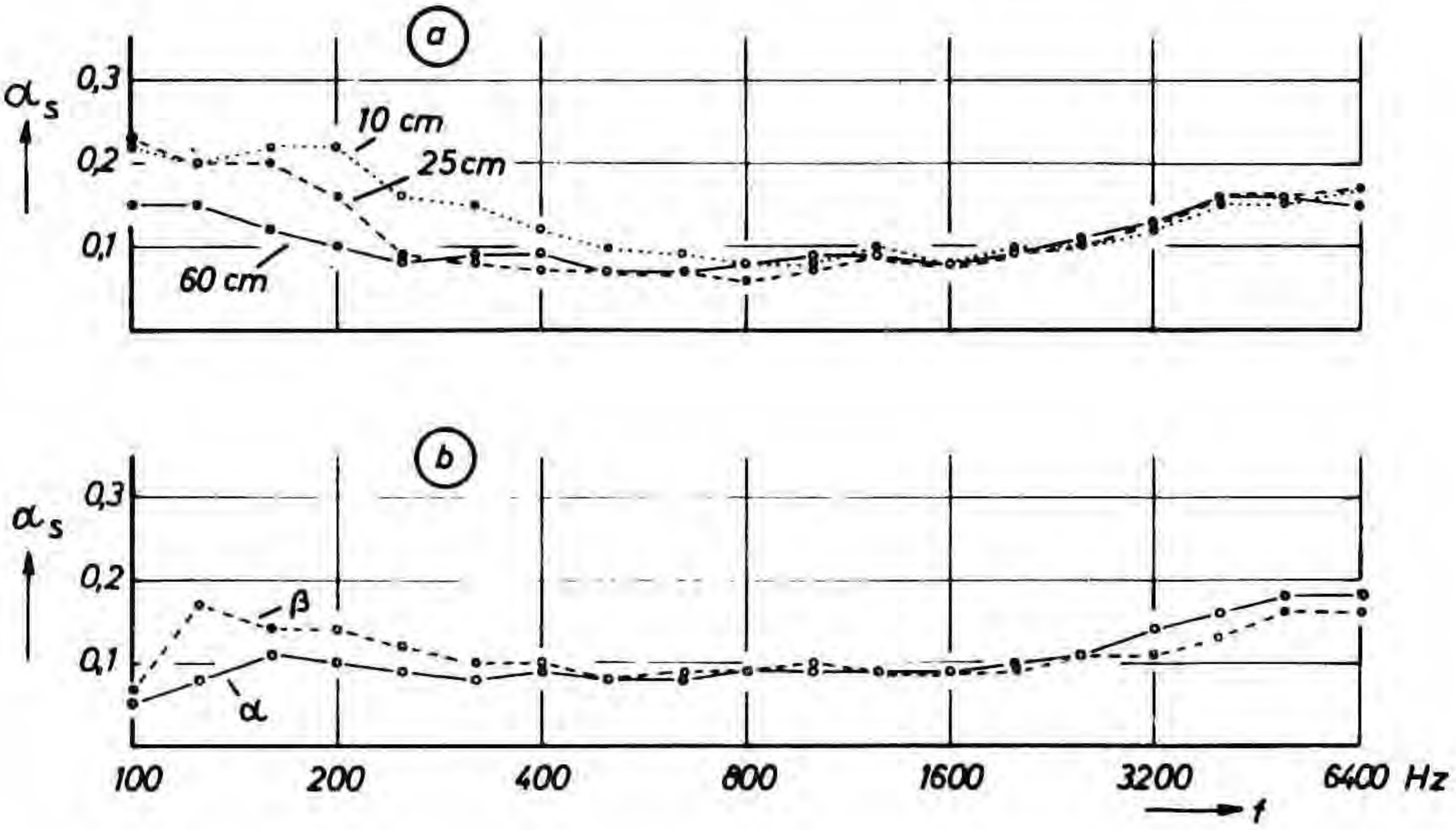

Bild 2 a) Absorptionsgradverlauf von 8 mm dicken Holzspanplatten bei verschiedenen Wandabständen

Bild 2 b) Absorptionsgrad bei 150 cm Wandabstand
α) ohne Hohlraumdämpfung
β) Hohlraum mit Mineralfaserplatten kassettiert

Die in Bild 2 wiedergegebenen Kurven für die Spanplatten von 8 mm Dicke und 5,6 kg/m^2 Masse je Flächeneinheit zeigen, daß der Absorptionsgrad bei großem Wandabstand sehr gering ist und auch bei 10 cm Wandabstand 0,2 nicht wesentlich überschreitet. Die Masse-Luftpolster-Resonanzen liegen bei sämtlichen Abständen unterhalb 100 Hz. In Bild 2 b ist noch ein zusätzliches Ergebnis für 1,5 m Abstand wiedergegeben, wobei der Hohlraum 1 m tief von der Plattenrückseite ausgehend mit Mineralfaserplatten (5 cm dick, 100 kg/m^3 Dichte) bei einer Maschenweite von 1 m x 1 m kassettiert war. Der Absorp-

tionsgrad steigt durch diese Maßnahme im unteren Frequenzbereich nur von 0,11 auf 0,17. Wegen der geringen Absorption wurde bei den Spanplatten nach Sabine ausgewertet.

Schrifttum:

/1/ U. Ingard, R.H. Bolt, Absorption Characteristics of Acoustic Material with Perforated Facings. Journ. Acoust. Soc.Amer. 23 (1951) S. 533

N34

FOURTH INTERNATIONAL CONGRESS ON ACOUSTICS
COPENHAGEN 21.-28. AUGUST 1962

ESSAIS DE MESURES OBJECTIVES DE LA FIDELITE DE TRANSMISSION D'UN QUADRIPOLE ACOUSTIQUE PAR CORRELATION.-

Jean GUILLERMIN

1.- CORRELATION.- Les travaux fondamentaux de N. WIENER ont montré l'intérêt des fonctions de corrélation dans l'étude des signaux de toutes natures : les ouvrages récents de D. MIDDLETON, de Y.W. LEE et d'autres développent le parallèle entre les notions d'analyses temporelles et spectrales des signaux et plus particulièrement des signaux aléatoires auxquels l'analyse temporelle est tout spécialement adaptée. L'optimalisation du filtrage et de la prédiction de signaux selon tel critère s'appuie sur la connaissance de leurs fonctions de corrélation. Rappelons que si $f_1(t)$ et $f_2(t)$ sont chacune fonctions membres d'un ensemble aléatoire stationnaire, la moyenne temporelle :

$$\psi_{12}(\tau) = \lim_{T \to \infty} \frac{1}{2T} \int_{-T}^{+T} f_1(t) \cdot f_2(t+\tau)\, dt$$

est identique à la moyenne d'ensemble des produits $\langle f_1(t) \cdot f_2(t+\tau) \rangle$ d'après le théorème "ergodique". On l'appelle corrélation mutuelle : si $f_2(t) \equiv f_1(t)$, c'est une autocorrélation. L'intérêt de ces fonctions réside dans l'extension analytique possible :

- aux fonctions périodiques sous la forme :

$$\psi_{12}(\tau) = \frac{1}{2T} \int_{-T}^{+T} f_1(t)\ f_2(t+\tau)\, dt$$ ou 2 T est la période

- aux fonctions apériodiques ou transitoires sous la forme :

$$\psi_{12}(\tau) = \int_{-\infty}^{+\infty} f_1(t)\ f_2(t+\tau)\, dt$$

Ces notions sont applicables à l'étude des signaux de modulation acoustique dont le caractère aléatoire n'est plus à souligner et à celle des quadripôles destinés à les transmettre à l'oreille.

2.- FIDELITE ACOUSTIQUE.- Un retard temporel, même important, ne modifie pas, sauf cas très particulier, la fidélité de la transmission d'un signal acoustique : ceci tient sans doute à l'absence de repères de temps originaux, mais aussi à la faible vitesse des ondes sonores dans l'air, et bien plus encore au développement de l'enregistrement sonore. Il semble utile pour tenir compte de ce retard éventuel, de développer un critère permettant de comparer une fonction $f_1(t)$ originale à sa transformée décalée dans le temps : $f_2(t+\tau)$. Le maximum de corrélation mutuelle s'obtiendra pour un retard représentant le décalage temporel moyen de la modulation : la valeur de ce maximum peut-elle "mesurer" la fidélité de la transmission ? C'est tout le problème du choix

.../.

du critère. Sans vouloir en faire une notion subjectivement valable, définissons a priori la "fidélité" par la valeur maximale de la fonction de corrélation mutuelle normée :

$$R_{12}(\tau) = \overline{f_1(t)\, f_2(t+\tau)}\ \left(\overline{f_1^2}\right)^{-\frac{1}{2}} \left(\overline{f_2^2}\right)^{-\frac{1}{2}}$$

Cette fonction dépend évidemment des propriétés statistiques du signal $f_1(t)$: il importe donc de définir un signal type qui soit le réflet des modulations diverses susceptibles de traverser la chaîne étudiée.

3.- ESSAIS DE MESURES OBJECTIVES.-

3.1 - Appareillage.- Nos mesures ont utilisé un appareillage analogique dont le schéma de principe est donne Fig. 1 : un enregistreur magnétique bipiste à têtes de lecture mobiles simule un décalage temporel positif ou négatif , de même qu'il permet la mise en mémoire sur boucle de la portion de signal analysée. La bande passante de l'ensemble est 60 Hz - 15 kHz, le temps d'intégration de 1,5 sec environ , la précision de calcul de 1 % . L'inscription automatique de $R_{12}(\tau)$ est réalisée à l'aide d'un servomécanisme avec variation continue de τ .

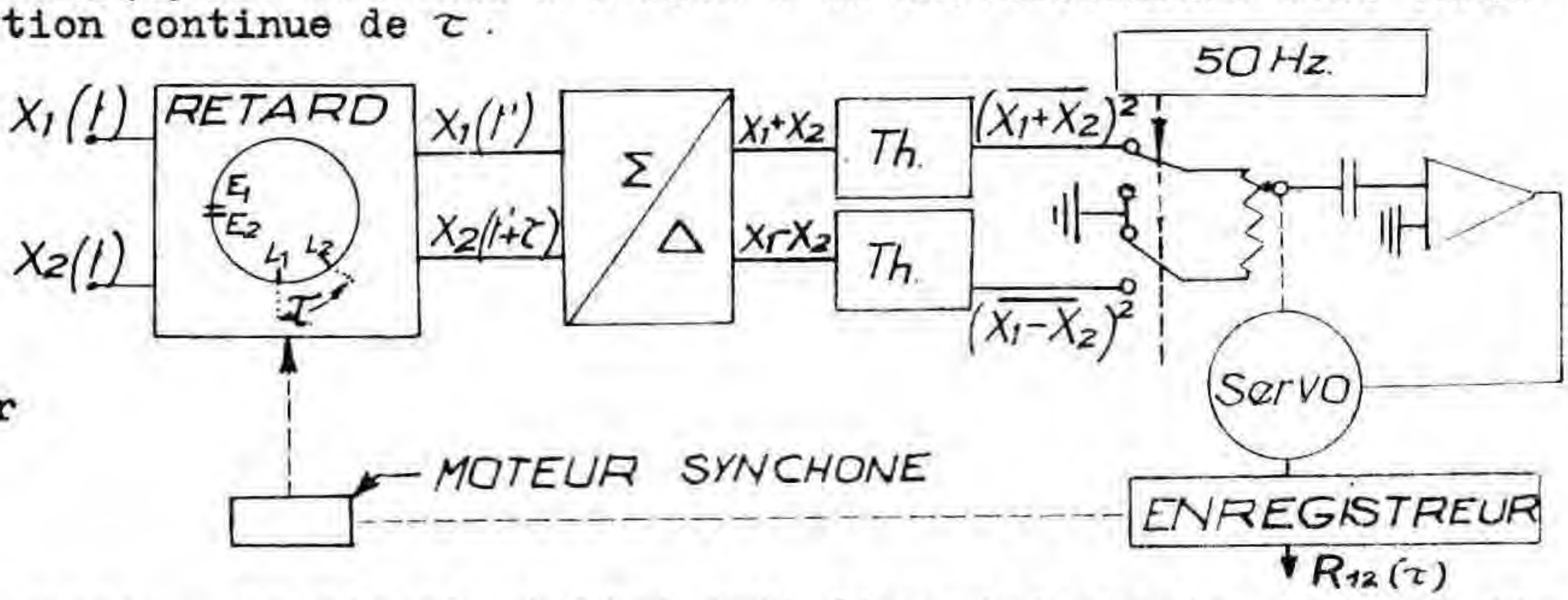

Fig. 1
Schéma du
Corrélateur

3.2 - Source.- Le signal utilisé doit être stationnaire à l'échelle de la constante de temps des thermocouples. Nous avons choisi un bruit blanc filtré. Un filtre à - 3 dB par octave nous a semblé fournir un équilibre des énergies graves-aigues plus comparable à celui des modulations réelles. L'échelle de hauteur en mels de l'oreille suggère aussi une densité d'énergie constante par bandes égales dans une échelle logarithmique plutôt que linéaire en fréquence. Les fréquences élevées et basses sont éliminées par un passe-bande donnant - 3 dB à 60 Hz et 10 kHz. La courbe d'autocorrélation de ce signal est donné sur la fig. 4 .

3.3 - Principe des mesures effectuées.- Nous nous limiterons aux éléments électroacoustiques (haut-parleurs et micros) et acoustiques (salles) de la chaîne. L'étude d'un élément est fait : - soit d'une manière absolue par l'observation des modifications des fonctions de corrélation entrée sortie de l'ensemble (Fig. 2).

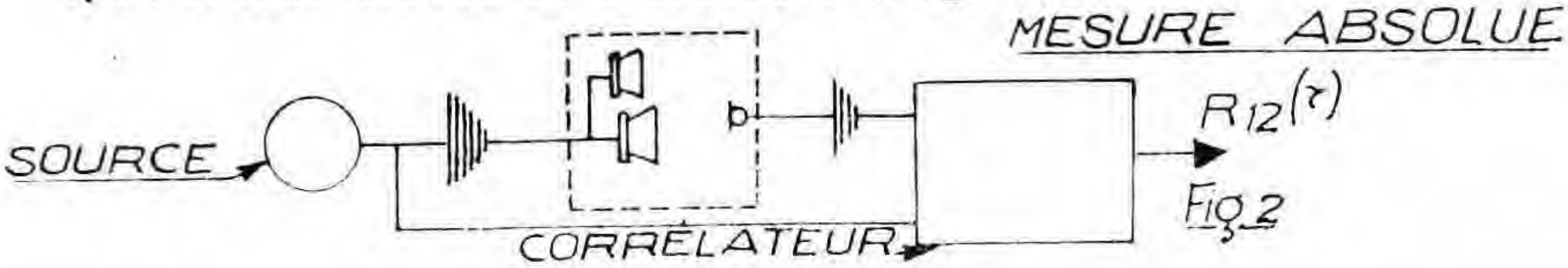

- soit d'une manière comparative par étude de la corrélation mutuelle sortie-sortie (fig. 3)

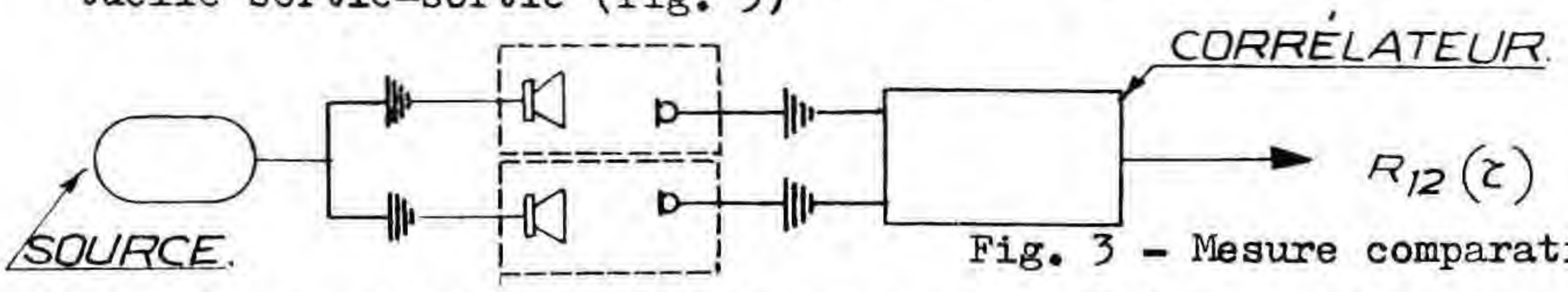

Fig. 3 - Mesure comparative

Notons l'importance particulière de ce procédé lors des tests de chaînes stéréophoniques. Nous avons étudié également d'après ce principe la transmission par émetteur à modulation de fréquence avec sous-porteuse des 2 canaux stéréophoniques.

4.- RESULTATS : Nous ne pouvons donner ici qu'un échantillon de chaque ensemble de résultats.

4.1.- Microphones : Etude comparative de micros par rapport à un micro de référence considéré a priori comme le meilleur.

RÉFÉRENCE								
B&K 4131	B&K 4131	R.C.A	MELODIUM 42B			WEST. ELEC. 630A	MEL. 55A	CARS. TELEPH.
CONDENS.	CONDENS.	RUBAN	DYNAMIQUE.			DYNAMIQUE	DYNAM.	CHARBON.
			MUS.	VOIX	PAROLE			
R_{12} max.	0,96	0,72	0,71	0,63	0,59	0,66	0,58	0,42

4.2.- Haut-parleurs : Mentionnons seulement une modification intéressante d'un ensemble haut-parleur à 3 canaux (aigu-médium-grave), faite à la suite d'une mesure de corrélation. On donne une coupe des dispositifs ainsi que les 2 séries de courbe de corrélation mutuelle obtenues avec un micro à 1 mètre en chambre sourde (Fig. 4).

Fig. 4

Recherche d'un haut-parleur de fidélité maximale.

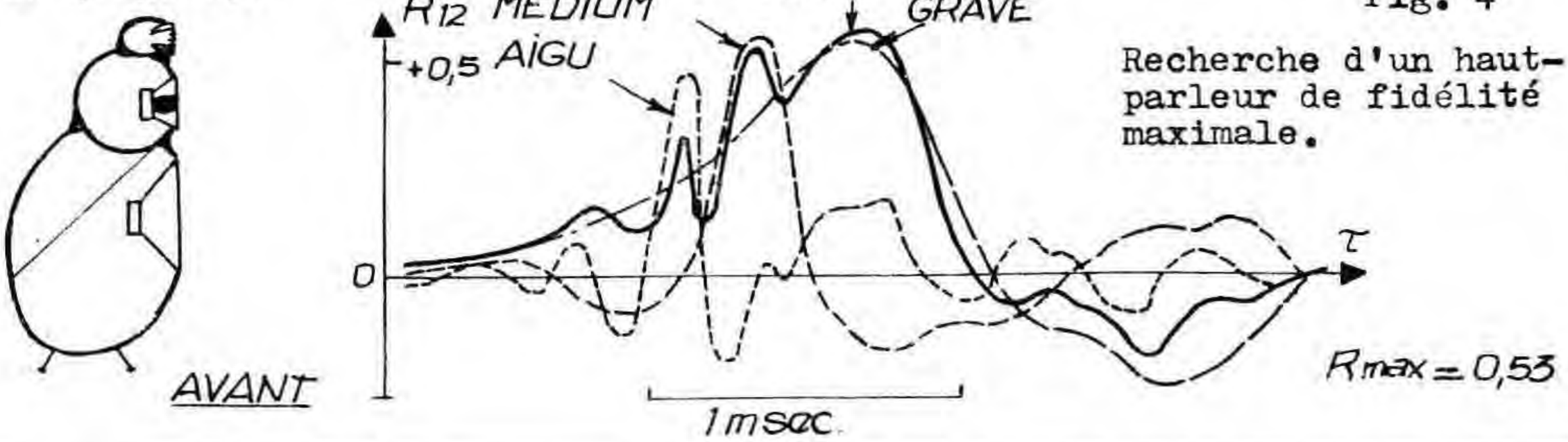

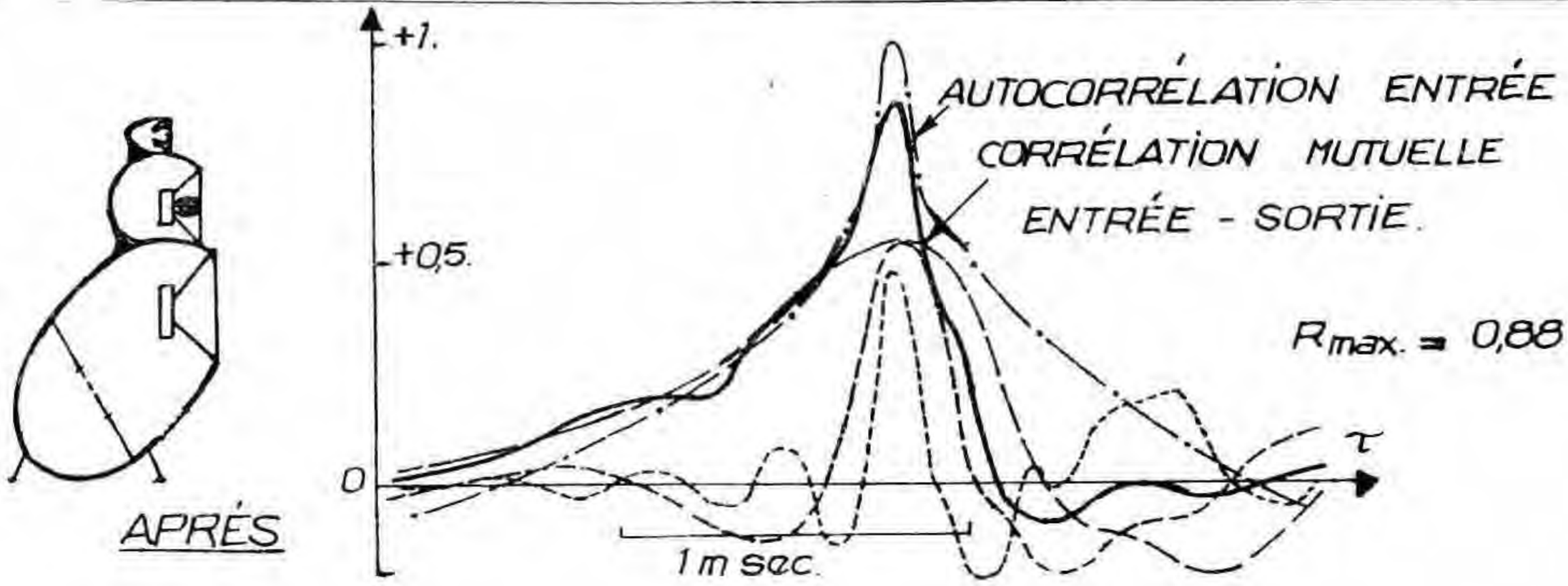

La recherche du maximum de corrélation a conduit à modifier les positions respectives dans l'espace des 3 sources émettrices de manière à faire arriver en phase les 3 signaux moyens au microphone. La comparaison des 2 systèmes à l'écoute est en faveur du 2ème système, bien qu'aucune modification sensible de la courbe amplitude-fréquence n'ait pu être constatée. Il donne une modulation à transitoires plus précis et une localisation bien plus nette du soliste si la modulation est prise à l'aide d'un micro unique alors qu'une prise de son à micros multiples ne fait ressortir aucune différence.

4.3.- Salles : Enfin le tableau ci-dessous donne un aperçu rapide de l'action du champ acoustique d'une salle sur la valeur maximale de $R_{12}(\tau)$ pour un ensemble haut-parleur-micro bien défini :

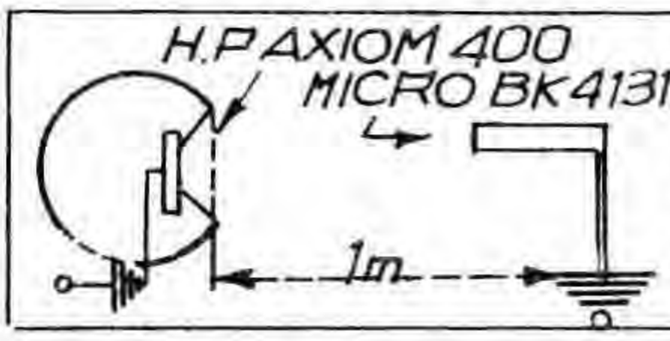

	R_{12} max.
CHAMBRE SOURDE.	0,70
LABORATOIRE	0,52
CHAMBRE REVERBER^te	0,31

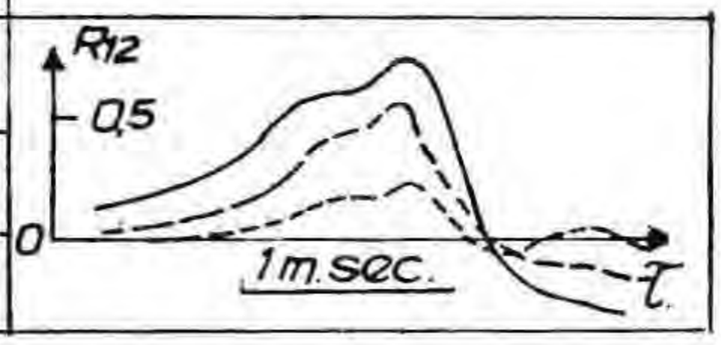

Les ondes réverbérées arrivant au micro avec un décalage supérieur au temps de cohérence propre du signal apportent une énergie incohérente qui fait diminuer le coefficient normé.

5.- CONCLUSION : Le critère choisi semble donner une importance prépondérante à la forme d'onde du signal. La mise en relief des phases relatives des éléments d'une modulation par cette mesure semble s'opposer aux conceptions classiques de la fidélité subjective en monophonie. La recherche de critères qui soient plus directement liés aux propriétés de détection de l'oreille est indispensable : mais l'étude de l'écoute monophonique avec deux oreilles pourrait bien faire comprendre notre sensibilité aux transitoires et donner au coefficient maximal de corrélation mutuelle une valeur qu'il est encore difficile de lui attribuer. La stéréophonie ne semble pas non plus devoir tirer grand avantage de la mesure dans son principe actuel. Le critère étudié fournit bien une condition suffisante de similitude, mais il n'est pas prouvé qu'elle soit nécessaire. Par contre, la notion de corrélation, liée à celle de redondance, du signal semble bien être la voix obligatoire aux problèmes de transmission codée.

B I B L I O G R A P H I E

(1) N. WIENER : The Extrapolation, interpolation & smoothing of stationary time series (Wiley - N.Y. 1949)
(2) D. MIDDLETON : Statistical Communication Theory (Mc GRAW HILL -1960)
(3) Y.W. LEE : Statistical Theory of Communication (Wiley-New-York 1960)
(4) F.H. LANGE : Nachrichtentechnik (Oct.55, p. 445 et suiv.)
(5) F. KRIEGER : Nachrichtentechnische Fachberichte 15 (1959),p. 17-20
(6) S.G. GUERSHMANN & E. ORLOV : Akust. Journ. 3 (1957),p. 285-288
(7) K.W. GOFF : J.A.S.A. 27, p. 236-246
(8) R.K. COOK & R.V. WATERHOUSE : J.A.S.A. 27, p. 1072
(9) J. GUILLERMIN : Rapport Corrélation R.T.F. (16-11-60)

O34

FOURTH INTERNATIONAL CONGRESS ON ACOUSTICS
COPENHAGEN 21.-28. AUGUST 1962

AN APPROACH IN NON-LINEAR ACOUSTICS

R.V.KHOKHLOV

Some recent progress in non-linear acoustics is due to the use of simplified reduced gasodynamic equations. This simplification is based on the fact of small values of Mach-number, absorbtion coeffi - cient and also on the time-space directivity of the progressive wave motion.

When Mach-number M is small enough and there is no energy losses, the gasodynamic variables of plane wave-density ρ, velocity V and pressure P are the functions of combination $\tau = t - \frac{x}{c}$ where c -the sound velocity. If one takes into account the presence of small energy losses and the finite value of Mach-number, the density and velocity are the functions of coordinate τ and, beside this, slowly varying functions of X. The gasodynamic equations for the plane waves reduce then to one equation:

$$\frac{\partial V}{\partial x} - \alpha V \frac{\partial V}{\partial \tau} = \delta \frac{\partial^2 V}{\partial \tau^2} \qquad (1)$$

where α the non-linearity coefficient $\alpha = \frac{\gamma+1}{2c^2}$, and δ - the absorbtion coefficient which is expressed through the viscosity coefficients and the heat-conductivity coefficient. There is relation between velocity and density:

$$\rho' = \frac{\rho_0}{c} V + a \frac{\rho_0}{c} V^2 - b \frac{\partial V}{\partial \tau}, \quad \text{where} \quad \rho' = \rho - \rho_0$$
$$a = \frac{3-\gamma}{4c}, \quad b = 2\rho_0 c^3 \delta$$

This relation can be considered as the generalization of the known Riemann's relation for simple waves for the case of slightly dissipative medium.

The analogous reduction can be made in more complicated cases than the plane waves in convectional gasodynamics. In these cases the initial equations reduce to the equation, similar to (I), but more complicated. Thus, the problem arises to find the effective solution of the equations of type (I).

Equation (I) with Hopf's substitution $V = \frac{2\delta}{\alpha} \frac{\partial u}{\partial \tau} \frac{1}{u}$ can be reduced to the linear equation of the heat-conductivity type and solved exactly. If the arbitrary sound disturbance is given at the cross - section $X=0$, the analysis of wave motion can be made on the basis of this exact solution. If, for example, at $X=0$, $V=V_0 \sin \omega t$, then, under the condition of large Reynolds-number $Re = \frac{\alpha}{2\delta} \gg 1$, initially sinusoidal wave propagates with a strong distortion. It is rational to distinguish three regions of distances X.

In the first region $0 < KX < KX_1 = \frac{1}{M}$, where $K = \frac{\omega}{c}$, the wave

is gradually distorted and becomes almost sawtooth one. In this region the energy losses do not play a noticeable role. At $X=X_1$ the discontinuities should have arisen if one neglects losses effects. The losses effects "keep up" arising of discontinuities and at $Re \gg 1$ the wave-shape becomes quasi-discontinuous, so, the phase-interval of wave front is equal, in order, $1/Re$.

In the next, second region $X_1<X<X_2$, where $KX_2=4\frac{Re}{M}$, the formed steep fronts diffuse under the action of dissipation and become more and more smooth. To the end of the second region the front in each wave becomes so wide that it takes the interval in a half wave length. This means asymmetry of wave shape disappears and the wave again becomes sinusoidal. At $X=X_2$ the amplitude is so damped that the influence of the non-linear forces becomes negligibly small.

In the third region $X>X_2$ the quasi-sinusoidal wave propagates according to the laws of the linear acoustics decreasing its amplitude because of losses.

Thus, in the first region one can neglect the dissipation effects and the wave distortion is described by the equations of first order. They can always be solved and the wave propagation can be analyzed on the basis of these solutions. In the third region one can neglect the non-linear effects and the propagation process, described by linear equations, can also be easily analyzed.

The most difficult for analysis and the most interesting is the second region, where the non-linear effects as well as the dissipative effects play essential roles. The solution in this region, obtained through the solution of the linear heat-conductivity equation is

$$V=\frac{V_0}{1+Z}\left[-\omega\tau+\pi\,\mathrm{th}\,\frac{\omega\tau}{\Delta}\right] \qquad -\pi\le\omega\tau\le\pi \qquad (2)$$

where $Z=\alpha\omega V_0 x$, and Δ -dimentionless front width is equal to

$$\Delta=\frac{1+Z}{\pi\,Re}$$

It follows from the solution(2), that in the second region the dissipative effects play noticeable role only on the stages of fast changes, wave-fronts. In fact, tangent-hyperbolic is equal to positive or negative unity almost everywhere, but when it is so, the solution(2) describes the sawtooth wave. The front structure describes "steady state" solution (tangent-hyperbolic) for which $\frac{\partial V}{\partial x}=0$. The equation for these steady-state waves are ordinary and can be solved much easier than (I).

In order to show directly the possibility of describing the front structure of non-stationary wave by the steady-state solution, write equation (I) in the form:

$$\frac{\partial V}{\partial x}=\frac{\partial S}{\partial\tau}\;; \qquad \delta\frac{\partial V}{\partial\tau}+\frac{\alpha}{2}V^2=S \qquad (3)$$

If the wave velocity C is chosen correctly, in the zero approximation $(\delta=0)$ is continuous function τ in the points, in which V changes abruptly. In the first approximation S changes a little on the wave fronts. This is illustrated on Fig.I, on which

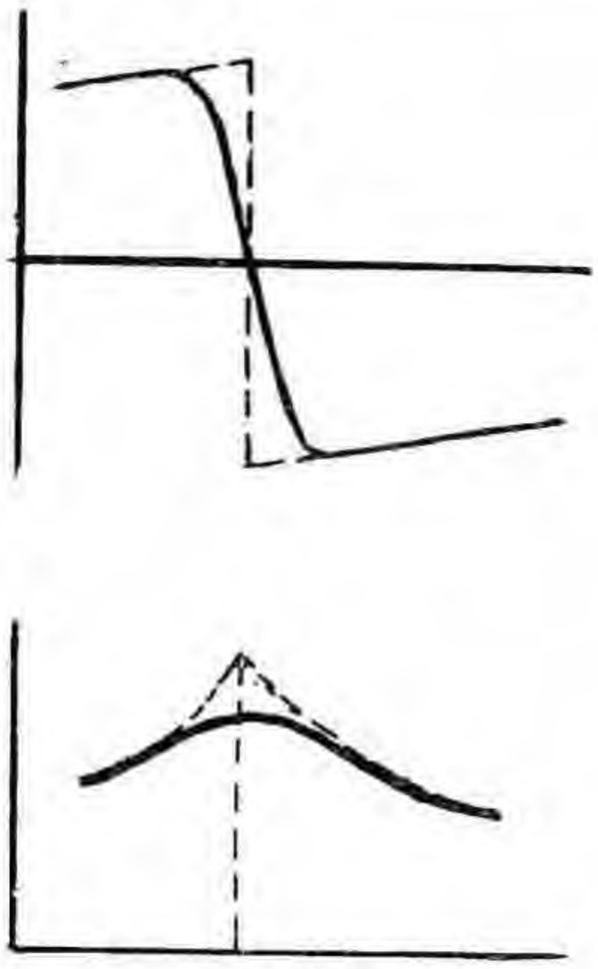

Fig.I

the behaviour of functions V and S are shown in the "region of discontinuity". The solid curves show V and S when $\delta \neq 0$, and dashed curves show V and S for the limit case $\delta = 0$. According to the first relation (3) the value $\frac{\partial V}{\partial x}$ on the wave fronts is equal approximately to zero. The exceptions are the front edges, in which one can neglect term $\delta \frac{\partial V}{\partial \tau}$.

So, the solution describing the wave motion in the second region can be "sewed up" from the solution, in which one neglects dissipative effects and which describes "slow" changes in the wave, and from "steady-state" situation, describing the structure of discontinuity. It is necessary to note that as in the case $\delta = 0$ the amplitude of discontinuity decreases and as the width of the steady-state shock wave increases with the decrease of its amplitude, the front structure is not constant when the wave propagates.

If one applies the idea of simplification of the gasodynamic equations to more complicated non-linear problems, then contrary to the above considered case, the simplified equations cannot be solved exactly and the direct analysis becomes impossible. The propagation of spherical and cylindrical, divergent and convergent waves, the propagation of waves in the chemically active mediums and so on belong to these problems. If one is interested in the wave motions for large Reynolds-number, then it is possible to pick the small parameter up in the simplified equation. Mathematically the problem is to find solution of the non-linear partial equation with the small parameter as multiplier by the highest derivative.

The general form of the simplified equations, which describe the wave motions for large Reynolds-number can be reduced to the form:

$$\frac{\partial V}{\partial x} = \frac{\partial S}{\partial \tau}; \qquad \delta f\left(V, \frac{\partial V}{\partial \tau}, \xi, \frac{\partial \xi}{\partial \tau}, \tau, x\right) + \varphi(V) = S \qquad (4)$$

where ξ are the other variables, which describe the wave motion and the equation for which is

$$\Phi\left(\frac{\partial \xi}{\partial \tau}, \xi, V, \frac{\partial V}{\partial \tau}\right) = 0 \qquad (5)$$

The above consideration points out the approach to the analysis of these problems. The distances divide up in several regions in which one can neglect either dissipative effects or non-linear effects. In the regions in which these effects play essential roles in equal degree the wave-motion can be divided in the slow stages and the fast ones and can be analyzed separately. On the slow stages one can neglect dissipative effects, and the fast stages-"fronts" can be described by the steady-state solutions.

In fact, if the wave velocity C is equal to the front velocity, $\varphi(V)$ in (4) is the even function in the neighbourhood of the "discontinuity". It means that in the first approximation S changes a little on the wave fronts and term $\frac{\partial V}{\partial x}$ in the first equation (4) is appro-

ximately equal to zero.

The actual limitation of the above approach to the problems is the necessity to have the steady state (or quasi steady state) solution which asymptotically tends to the constant, when $\tau \to +\infty$ and to the same constant with the opposite sign when $\tau \to -\infty$.

The concrete analysis of one of such problems, made on the basis of this approach is presented at this Congress in Soluyan's report.

P34

FOURTH INTERNATIONAL CONGRESS ON ACOUSTICS
COPENHAGEN 21.-28. AUGUST 1962

Die Messung der absoluten Schwingungsauslenkung bei tiefen Frequenzen ohne festen Bezugspunkt

Dr.Ing. Ulrich Arns, München

Aufgabe:

Wenn irgendwo ein störendes Geräusch auftritt, dann ist im allgemeinen eine unerwünschte mechanische Vibration die Ursache. Wenn in der Werkzeugmaschinenfertigung die geforderte Bearbeitungsgenauigkeit nicht erreicht wird, dann ist ebenfalls eine unerwünschte mechanische Vibration die Ursache. Während für die Schallerzeugung nur Schwingungen oberhalb von 30 Hz von Bedeutung sind, interessiert den Ingenieur des Werkzeugbaues ein wesentlich tieferer Frequenzbereich, der sich bis annähernd Null Hertz hinunter ausdehnt. Aber auch für den Akustiker ist dieser tiefe Frequenzbereich nicht ganz uninteressant, weil Nichtlinearitäten der langsamen mechanischen Schwingungen mit ihren Oberwellenanteilen an einer akustisch günstigen Stelle, nämlich dort, wo der Strahlungswiderstand groß genug ist, Hörschall abstrahlen können.

Es wird also ein Meßverfahren gefordert, mit dem man ohne zeitraubenden Aufwand an vielen verschiedenen Stellen des zu untersuchenden Gegenstandes die mechanischen Schwingungen fehlerfrei in elektrisch analoge Schwingungen umwandeln kann, um sie dann durch die anpassungsfähige elektronische Meßtechnik einer näheren Untersuchung unterziehen zu können. Um die leichte Ortsveränderlichkeit des Meßwertaufnehmers zu gewährleisten, muß man sich aus physikalischen Gründen auf schwingungsmäßig abgeschlossene Systeme beschränken, die einen festen Ruhebezugspunkt nicht benötigen.

Methode:

Welche Verfahren bieten sich für diese Aufgabe an? (Bild 1). Grundsätzlich kann man zwischen selbständigen mechanisch-elektrischen Wandlern mit einer direkten Spannungsabgabe und solchen unterscheiden, die als steuernde Wandler eine Speiseenergie benötigen, welche entsprechend moduliert wird. Der tabellarischen Übersicht (Bild 2) kann man

entnehmen, daß der Parameter für die Umwandlung der mechanischen Bewegung in eine analoge elektrische Funktion entweder die Auslenkung oder die Kraft ist.

Da die Auslenkung die mechanische Beanspruchung des Wandlerelementes bedeutet, kann man die Kraft bzw. die mechanische Verformung als die einzige Größe bezeichnen, die für den Umwandlungsvorgang der mechanischen in die elektrische Energie verantwortlich ist. Weder die Geschwindigkeit noch die Beschleunigung hat eine direkte Bedeutung für die Umwandlungsvorgänge.

	selbständ.Wandler	steuernde Wandler
induktiv	u Geschwindigkeit ($\frac{\text{Auslenkung}}{\text{Zeit}}$) f f_{res}	Induktivität Auslenkung f f_{res} Induktivität Kraft f. Modulation einer Wechselspg. f f_{res}
magnetisch	u Durchflutungsänd. ($\frac{\text{Auslenkung}}{\text{Zeit}}$) f f_{res}	magn.Widerst. Auslenkung f f_{res} magn.Widerst. Kraft f. Modulation einer Wechselspg. f f_{res}
magneto-striktiv	u mechan. Verformung (Kraft) f f_{res}	
kapazitiv		Kapazität Auslenkung f f_{res} Modulation einer Gleich- oder Wechselspg.
piezo-elektr.	u mechan. Verformung (Kraft) f f_{res}	
ohmisch		Widerstand Auslenkung f f_{res} Modulation einer Gleich- oder Wechselspg.

Damit diese Schwingkraft bei einem seismisch abgeschlossenen Schwingungssystem auch unabhängig von der Schwingungsfrequenz ist, dürfen die aufgezählten Wandler nur in dem angegebenen Arbeitsfrequenzbereich betrieben werden. Zusammengefaßt bedeutet das: Will man den Anwendungsbereich nach tiefen Frequenzen hin nicht durch die Resonanzfrequenz des Aufnehmersystems beschränken, so stehen für die bezeichnete Aufgabe nur hochabgestimmte seismische Systeme zur Verfügung. Alle anderen Systeme, deren Resonanzfrequenz im oder unterhalb des

Arbeitsfrequenzbereiches liegt, haben Amplituden- und Phasenfehler, besonders dann, wenn die Schwingsysteme gedämpft sind.

Allein die hochabgestimmten ungedämpften Systeme arbeiten immer proportional der Kraft, die im seismisch abgeschlossenen System der D'Alambert'schen Hilfskraft entspricht. Die an der seismischen Masse angreifende Hilfskraft erzeugt am Wandlerelement eine Größe, die der Beschleunigung der Schwingungsbewegung direkt proportional ist. Diese Schwingbeschleunigung am Meßort des Prüflings wird also exakt in einem Frequenzbereich von 0 Hz bis etwa zu einem Drittel der Resonanzfrequenz über dem Wege der Kraft auf das empfindliche Wandlerelement übertragen. Durch zweimalige Division dieser Beschleunigungsgröße mit der Frequenz bzw. durch zweimalige Integration eines Frequenzgemisches läßt sich also theoretisch bis zu null Hertz hinab die absolute Schwingweggröße erhalten.

Schwierigkeiten:

Diesem Vorhaben liegen aber folgende Schwierigkeiten im Wege. Wenn Die Schwingungsfunktion der Beschleunigungsgröße eine sehr langsame Periode hat, beispielsweise eine solche von nur einer Stunde, dann darf der elektrische Rechenverstärker sich während dieser Zeit nicht verändert haben. Würde nämlich der erste elektrische Integrator, der die Beschleunigungsfunktion in eine Geschwindigkeitsfunktion verwandelt, nur eine ganz kleine Instabilität aufweisen, dann würde diese Änderung des elektrischen Nullpunktes einer analogen, tatsächlich aber nicht vorhandenen Beschleunigung entsprechen. Die anschließend durchzuführende zweite Integration, die die Geschwindigkeitsfunktion zur Wegfunktion verwandelt, würde diese elektrische Nullpunktschwankung zu einer ständig steigenden Ausgangsspannung wachsen lassen. Je höher die elektronische Verstärkung getrieben wird, um eine möglichst große Empfindlichkeit dieses Aufnahmeverfahrens zu erhalten, desto störender sind die Wirkungen der Instabilitäten der 1. Integrationsstufe bzw. des Schwingungsaufnehmers selber.

Entweder muß man die elektrische Verstärkung durch bessere Gegenkopplung verringern oder die ganz langsamen Frequenzen, die in der Größenordnung der Instabilitätsschwankungen liegen, durch ein Hochpaßfilter

aussperrer. Beides läuft darauf hinaus, daß die Meßanlage unempfindlicher wird und die Frequenz Null Hertz nicht ganz erreicht werden kann, obwohl das physikalische Prinzip des beschleunigungsproportionalen Aufnehmers bis zur Frequenz Null richtig arbeitet. Aus diesem Dilemma gibt es keinen Ausweg. Mit besonders guten Verstärkern kann man heute bis zur Frequenz von etwa 0,1 Hz hinunter Schwingwege ab 1/um messen. Der scheinbar nur geringe Abstand von 0,1 Hz bis zum theoretischen Ziel - nämlich 0 Hz - ist durch eine unüberbrückbare Kluft technischer Schwierigkeiten nicht zu beseitigen.

Vereinfachung:

Durch Ausnutzen einer physikalischen Eigenart kann aber die hohe Forderung an die Gleichspannungsverstärkerstark gemildert werden.
Man wird fast immer voraussetzen können, daß der Meßort vor und nach der Messung wieder den Ausgangspunkt einnimmt, bzw. immer nur um diesen Punkt herum schwingt. Unter dieser Voraussetzung ist die Schwingungsfunktion der Schwinggeschwindigkeit immer symmetrisch zum Nullwert, d.h. sie besitzt keinen Gleichspannungsanteil. Man darf daher einen aufgrund von Instabilitäten der 1. Integrationsstufe entstandenen Gleichspannungswert abtrennen, ohne daß der Verlauf der Wegfunktion dadurch verändert wird. Der Gleichspannungsanteil einer nur einseitigen Auslenkung des Meßortes vom Ausgangsruhepunkt bleibt im Meßergebnis trotzdem erhalten. Nur eine Bedingung ist dabei zu berücksichtigen: Das Abtrennen des Gleichspannungsanteiles des ersten Integrators darf frequenzmäßig noch nicht die symmetrische also gleichspannungsfreie Funktion der Beschleunigung verändern.

Unter Berücksichtigung dieser Tatsache lassen sich heute bereits mit kleinen handlichen elektrischen Meßgeräten, die das Prinzip der Beschleunigungsmessung ausnutzen, absolute Schwingwege von 1/1000 mm an bei Frequenzen knapp unterhalb 1 Hz messen. Da die Resonanzfrequenz des Aufnahmesystems weit außerhalb des schwingungstechnisch interessierenden Bereiches liegt, sind Änderungen des Funktionsverlaufes durch Phasenfehler des Schwingungsaufnehmers ausgeschlossen, die dann besonders unangenehm sind, wenn die Eigenresonanz des Schwingsystems stark gedämpft ist. Da die Wegauslenkung nicht direkt, sondern erst über die Beschleunigungsfunktion erhalten wird, bietet sich dieses Verfahren für schnelle Schwingungsuntersuchungen an, wobei kein äußerlich fester Ruhebezugspunkt benötigt wird, dessen Aufbau immer mit großem Zeit- und Kostenaufwand verbunden ist.

G35

FOURTH INTERNATIONAL CONGRESS ON ACOUSTICS
COPENHAGEN 21.-28. AUGUST 1962

MOBILE PALATOGRAPHY AS A TOOL FOR ACOUSTIC STUDY OF SPEECH SOUNDS

Y.I.KUZMIN
Pavlov Institute of Physiology, Leningrad, USSR.

Rather primitive and imperfect techniques used in experimental phonetics are in contrast with the powerful and elaborated devices which are at the disposal of students of acoustic speech characteristics. At the same time it is obvious that the decoding of acoustic speech flow can be attained by correlating articulatory and acoustic parameters of speech. Thus there is an urgent need in such a method of articulatory movement registration that provided simultaneous recording of articulatory and acoustic parameters.

According to phonetics the location of contact areas between the tongue and the hard palate is a useful parameter for the description of the vast majority of consonants. The method of mobile palatography to be described here makes it possible to register such contact points unceasingly during speech production.

A special device called "artificial palate" is used in the procedure. The palate consists of a plastic plate similar to those used in experimental phonetics. On the surface of the plate pairs of electrodes are mounted as schematically shown in Fig.1. Wires from the electrodes are embedded in the plate and leave the palate at its posterior corners. The left-hand electrodes are connected to the sound frequency generator (frequency 2000 cps, voltage 250-500 mv). The potencial on the right-hand electrodes is available only at those moments when when the tongue covers a corresponding area of the plate. The signals from the palate are fed into the set of amplifiers and then are registered at the multi-

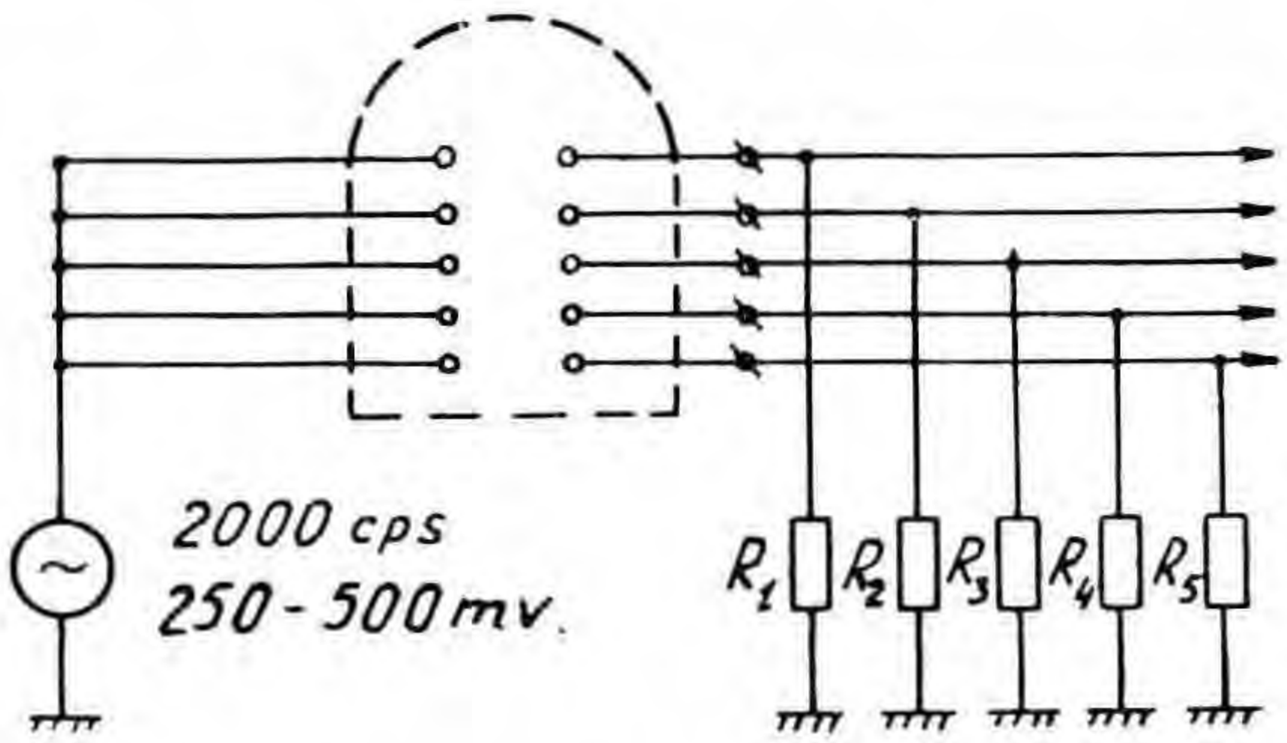

FIG. 1.

channel ink-recorder.

The palate being well adjusted to the roof of the mouth no additional fixation is needed. The use of the palate doesn't interfere with the intelligibility of speech provided the training of the speaker is sufficient.

The procedure described was realized in the laboratory of Dr. L.A. Chistovich. All electronic equipment necessary for its realization was elaborated by Dr. Kozhevnikov and V.S.Shupl akov.

"Artificial palates" for six speakers have been made and tested in experiments. The number of electrodes on these palates varied from 15 to 22 pairs. The set of amplifiers available permitted the experimenter to register eleven parameters simultaneously.

In the course of the experiments it became clear that symmetrical disposition of electrodes is not absolutely necessary. Secondly, the registration of a large number of contact points appeared to be unnecessary due to their intercorrelation. Seven points given in Fig. 2 are likely to be sufficient to differentiate all tongue positions characteristic of Russian consonant articulation.

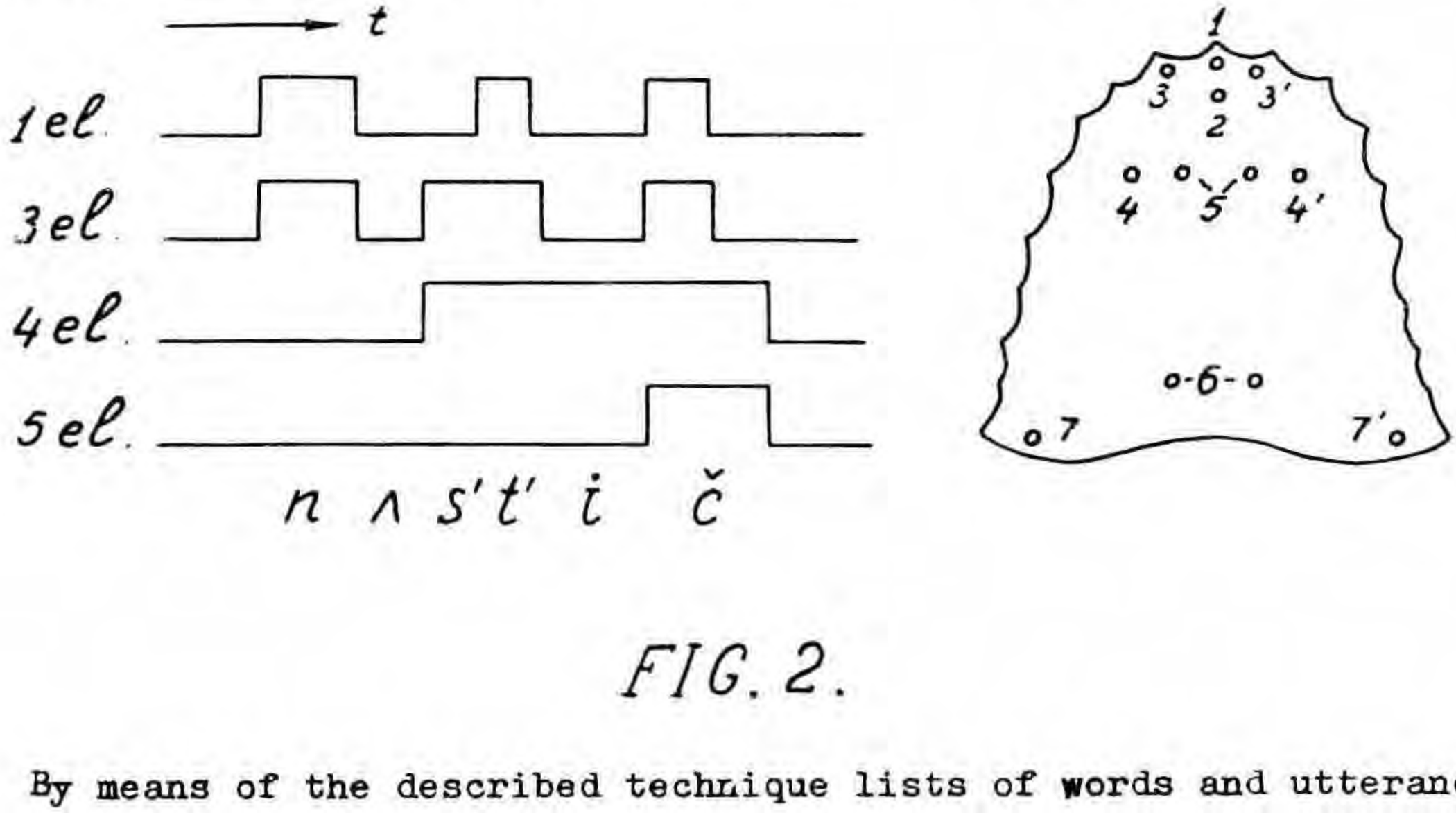

FIG. 2.

By means of the described technique lists of words and utterances were recorded. The obtained mobile palatograms are like the one schematically drawn in Fig. 2. The parameters on the left part of the figure correspond to the points on the scheme on its right part. In accordance with phonetics the signal at point 3 is registered during articulation of alveolar consonants. The absence of the signal at point 1 when the signal at the third parameter is present is

characteristic of the fricatives s , z and the affricate portions of t' and c . It can be seen that tongue positions during close vowel articulacion can also be recorded (see i).

The method described enables us to register tongue positions continuously in the process of speech production. The materi$_a$l can be obtained in any amount necessary for statistical analysis. Obtained electrical signals can be registered simultaneously with acoustic parameters of speech or used for speech flow segmentation. In the latter case the segments that strictly correspond to particular articulatory positions can be separated. Vowels can be "cut out" by means of articulatory parameters of adjacent consonants.

The method proved to be extremly useful for the measurement of temporal characteristics of speech. Automatisation of the measurements is possible.

H35

FOURTH INTERNATIONAL CONGRESS ON ACOUSTICS
COPENHAGEN 21.-28. AUGUST 1962

Der Einfluss des Geräusches auf die Lokalisierung und Verständlichkeit bei der dreikanaligen Stereophonie

Felix Kolmer, Forschungsinstitut für Ton, Bild-und Reproduktionstechnik, Prag, Tschechoslowakei

1. Einleitung

Dieser Artikel bestrebt sich die angeführten Abhängigkeiten vom psychophysikalischen Gesichtspunkt klarzulegen und eine Erläuterung der erzielten Ergebnisse von dem Standpunkt der Physiologie darzubieten.

Das Signal für die durchgeführten Prüfungen war das gesprochene Wort. Für die Nachbildung des Geräusches wurde ein Rauschen benützt, das von drei selbstständigen Rauschgeneratoren erzeugt wurde, deren Frequenzcharakteristik übereinstimmend war und von denen ein jeder eine Geräuschquelle für einen Wiedergabekanl war. Die selbstständige Speisung der einzelnen Kanäle mit Rausch wird deshalb durchgeführt, damit nicht eine Lokalisierung des Geräusches eintrete. Die Rauschgeneratoren wurden durch Bandfilter mit den Bereichen von 40 Hz - 200 Hz, von 200 Hz - 4 kHz und von 4 kHz - 16 kHz ergänzt. Die Teilungsfrequenzen des mittleren Bereiches wurden mit Rücksicht auf die Frequenzen gewählt, welche bei den Formanten der Sprache auftreten. Bei allen Prüfungen war der durchschnittliche Schallpegel des Signals konstant, 75 dB (B). Der Schallpegel änderte sich in den Grenzen von 42 - 88 dB (B).

2. Die Versuchsergebnisse

Insgesamt wurden 54.600 Hörproben ausgewertet. Bei dem ersten Versuch wurde die Lokalisierung und die Verständlichkeit des wiedergegebenen Wortes in Abhängigkeit von drei Frequenzbereichen und bei ansteigendem Geräuschpegel verfolgt. Die Versuchsergebnisse der Lokalisierung für eine Männerstimme sehen wir auf Abb. 1. Aus dem Bild ist ersichtlich, dass alle Messungen in dem Fehlerbereich der Auswertungsmethode liegen. Aus der Verteilung der gemessenen Punkte kann mit Bestimmtheit konstatiert werden, ob höhere Geräuschfrequenzen auf die Lokalisierung störender als die übrigen Frequenzen wirken. Bei Auswertung der Versuchsergebnisse bei einer Frauenstimme erhielten wir die gleichen Ergebnisse. Die Prüfungen zeigten, dass kein Unterschied in der Lokalisierung der Männer-und der Frauenstimme existiert. Das Geräusch aller Frequenzbereiche verschlechtert nicht die Lokalisierung bis zu dem Geräuschpegel, welcher gleich dem Schallpegel des Testsignals ist. Diese Erscheinung kann durch die Erhöhung der Aufmerksamkeit der Hörer bei der Unterscheidung des Nutz- und Störschalles und des Geräusches bei den sich nähernden Pegeln erklärt werden. Erst eine weitere Geräuscherhöhung hat eine Verschlechterung der Lokalisierung zur Folge.

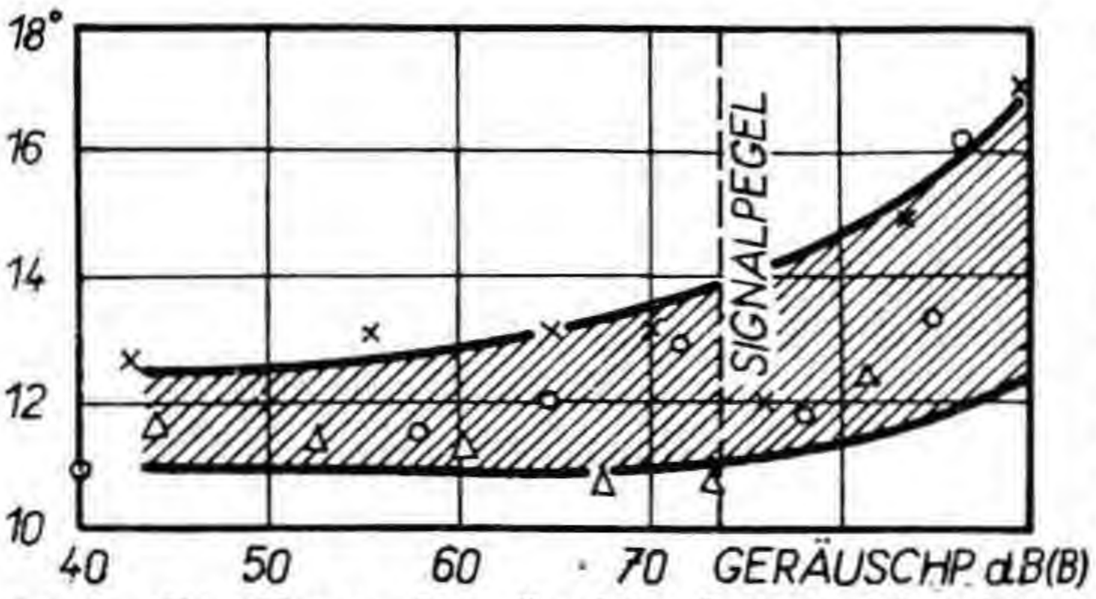

Bild 1. Einfluss der Spektralcharakteristik des Geräusches auf die Lokalisierung. Männerstimme - Geräusch des Frequenzbereiches: △ 40Hz ÷ 200Hz, ○ 200Hz ÷ 4kHz, × 4kHz ÷ 18kHz, • Grundgeräuschpegel im Saal.

Die Versuchsreihe wurde zwecks einer Feststellung des Einflusses der Spektralcharakteristik des Geräusches auf die Verständlichkeit des wiedergegebenen Wortes bei der dreikanaligen Wiedergabe wiederholt. Die Versuchsergebnisse der Verständlichkeit sehen wir

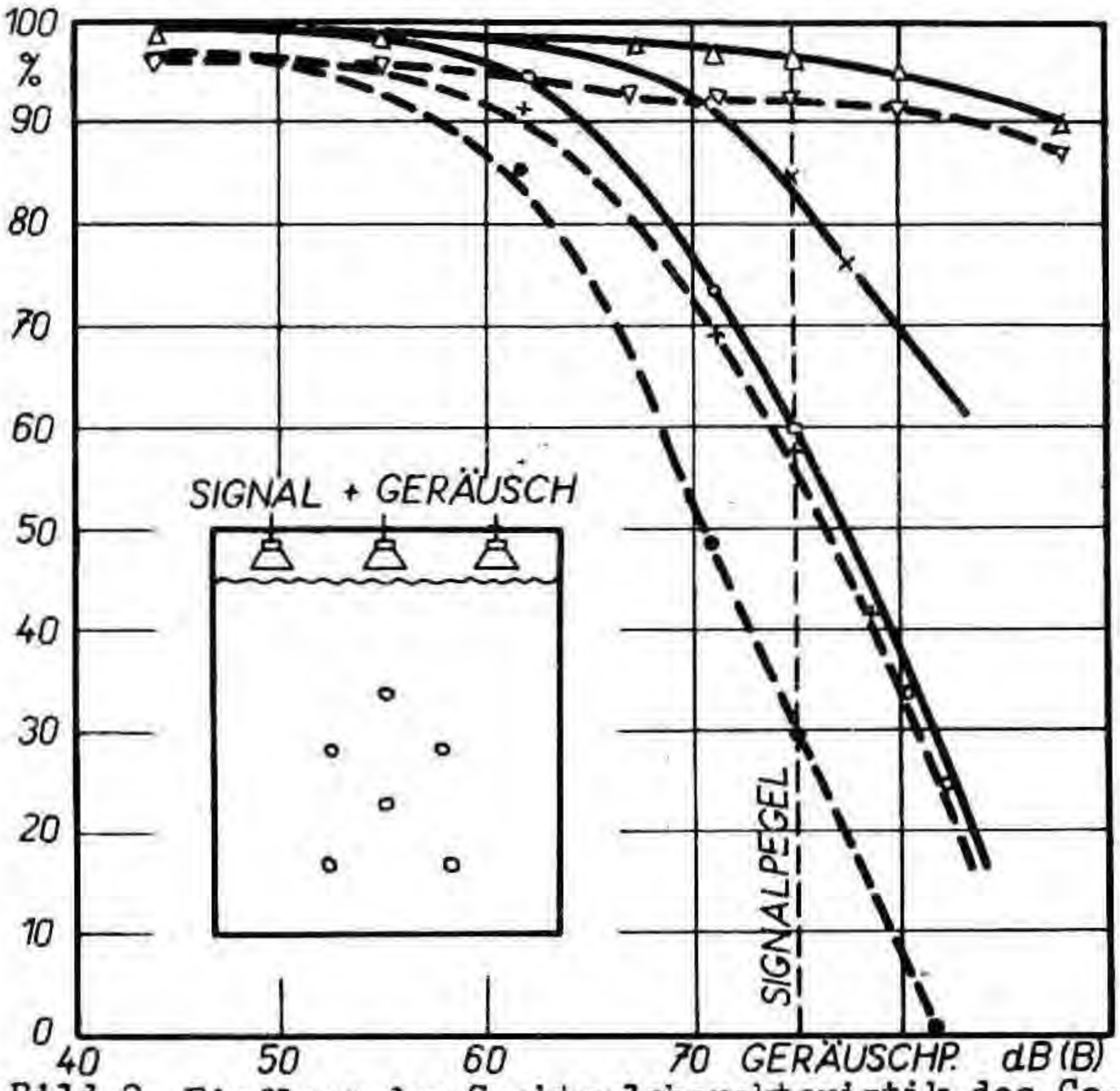

Bild 2. Einfluss der Spektralcharakteristik des Geräusches auf die Verständlichkeit des wiedergegebenen Wortes bei der dreikanaligen stereophonischen Wiedergabe. a) Männerstimme - Geräusch des Frequenzbereiches: △ 40Hz ÷ 200Hz, ○ 200Hz ÷ 4kHz, × 4kHz÷18kHz. b) Frauenstimme - Geräusch des Frequenzbereiches : ▽ 40Hz ÷ 200Hz, • 200Hz ÷ 4kHz, + 4kHz ÷ 18 kHz.

quenzgebietes erklärt, anderseits dadurch, dass dieses Frequenzgebiet des Geräusches mit dem Formantengebiet übereinstimmt, welches der Träger der Verständlichkeit der Sprache ist. Die schlechtere Verständlichkeit der Frauenstimme ist dadurch erklärlich, dass das Frequenzgebiet der Formanten näher dem Grundgebiete liegt als es bei der Männerstimme der Fall ist. Die Verständlichkeit nimmt schon bei Geräuschpegeln ab, bei denen die Lokalisierung noch gut ist. Die Verständlichkeitsabnahme ist wesentlicher als der Fehleranstieg in der Lokalisierung.

Einen qualitativen Vergleich der dreikanaligen stereophonischen Wiedergabe mit der einkanaligen hatte der zweite Versuch zum Ziel, der mit dem ersten Versuch in der Art und Weise übereinstimmte, nur die Geräuschwiedergabe wurde durch die gleiche Lautsprecherkombination, mit welcher das Testsignal wiedergegeben wurde übermittelt. Als Quelle des Prüftestes und des Störschalles diente der mittlere Kanal des dreikanaligen Wiedergabesystems. Die Versuchsergebnisse sind auf den Kurven der Abb. 3 zusammengefasst, wo sich auch eine Skizze der Anordnung der Hörer bei dem Versuche befindet. Die Kurven weisen eine annähernde Übereinstimmung im Verlauf der Verständlichkeit bei niedrigen Geräuschpegeln mit den dreikanaligen Prüfungen auf Abb. 2.

Der Störschall des niedrigen Frequenzbereiches hat fast keine Wirkung auf die Verständlichkeit des wiedergegebenen Wortes auch bei Schallpegeln, die höher als die Schallpegel des wiedergegebenen Testes sind. Das Geräusch des mittleren und hohen Frequenzbereiches verschlechtert wesentlich die Verständlichkeit. Das gilt für die Männer,-sowie für die Frauenstimme. Bei der Frauenstimme ist die Verständlichkeitsabnahme höher und äussert sich schon bei niedrigeren Schallpegeln als bei der Männerstimme. Der verschiedene Einfluss frequenzunterschiedlicher Bereiche des Geräusches auf die Verständlichkeit wird einerseits durch die erhöhte Empfindlichkeit des Ohres für Frequenzen des mittleren Fre-

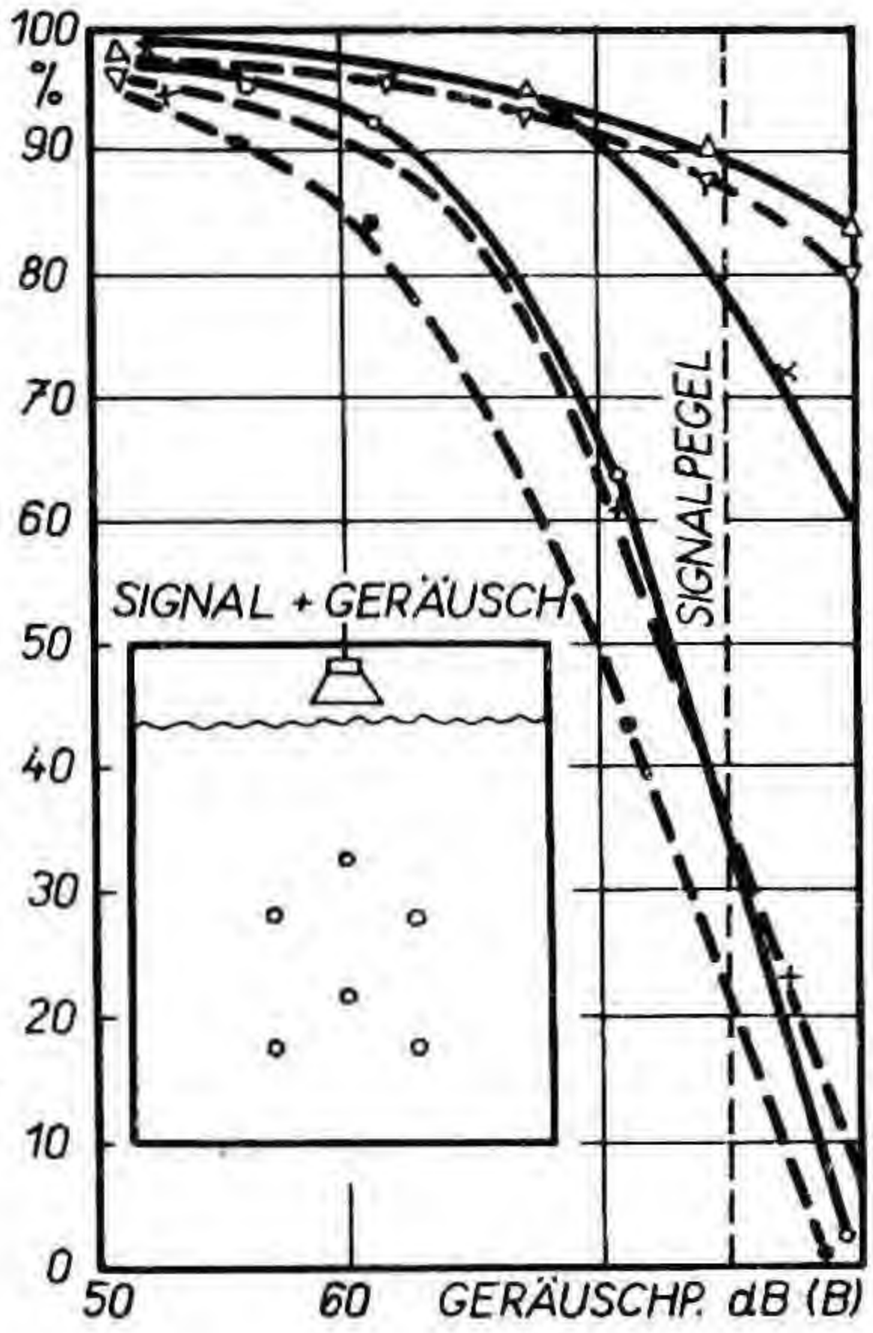

Bild 3. Einfluss der Spektralcharakteristik des Geräusches auf die Verständlichkeit des gesprochenen Wortes bei der einkanaligen Wiedergabe. a) Männerstimme-Geräusch d. Frequenzbereiches: △ 40Hz ÷ 200Hz, ○ 200Hz ÷ 4kHz, × 4kHz ÷ 18kHz. b) Frauenstimme-Geräusch d. Frequenzbereiches: ▽ 40Hz ÷ 200Hz, • 200Hz ÷ 4kHz, + 4kHz ÷ 18kHz.

auf, jedoch bei einem ansteigenden Geräuschpegel tritt eine schnellere Verständlichkeitsabnahme ein als im vorhergehenden Falle. Der Einfluss der Frequenzcharakteristik des Geräusches ist der gleiche wie bei der dreikanaligen Prüfung, ebenso auch die schlechtere Verständlichkeit der Frauenstimme als die der Männerstimme. Die schnellere Verständlichkeitsabnahme bei der einkanaligen Wiedergabe im Vergleich mit der einkanaligen kann nach I. Pollak dadurch erklärt werden, dass im Fall einer einkanaligen Wiedergabe bei einem gleichzeitig wiedergegebenen Signal und Geräusch eine für die Wahrnehmung bestimmte Stelle auf dem Gebiete der Hirnrinde von dem Signal, sowie von dem Geräusch gemeinsam erregt wird, währenddem im Fall einer dreikanaligen Wiedergabe durch den Einfluss der Lokalisierung eine Stelle der Hirnrinde und durch das unlokalisierbare Geräusch das ganze zugehörige Gebiet der Hirnrinde erregt wird. Deshalb muss die Verschlechterung besonders bei den niedrigen Abständen des Signals vom Geräusch bei der einkanaligen Wiedergabe eintreten, wo eine erheblichere Vermischung des Nutzschalles und Störschalles infolge der in der Intensität wenig unterschiedlichen Erregungen der gleichen Stelle der Hirnhaut stattfindet. Auf dem Gebiet der in der Praxis vorkommenden Abstände der Geräuschpegel von dem Signal ist die dreikanalige stereophonische Wiedergabe bei dem gegebenen System und der Platzverteilung der Mikrofone bei der heute im Film angewandten stereophonischen Aufnahme (eine kleiner Pegelunterschied des akustischen Druckes in den einzelnen Kanälen, maximal 6 dB) ein unwesentlicher Beitrag für die Verständlichkeit. Bei diesem System der Platzverteilung der Mikrofone (eine 2 m lange Basis zwischen den beiden äusseren Mikrofonen) bei der Tonaufnahme wird die Stereophonie nur wenig ausgenützt.

Zwecks Beglaubigung der physiologischen Erklärung des vorhergehenden Falles wurde eine dritte Versuchsreihe veranstaltet, in welcher das Test einkanalig mit einer am rechten Saalende angebrachten Lautsprecherkombination, und der Störschall mit einer zweiten in der gegenüberliegenden Saalecke angebrachten Kombination wiedergegeben wurde. Dadurch wurde erzielt, dass die Erregungsstellen des zugehörigen Gebietes der Hirnrinde, voneinander entfernt waren, und demnach sollte der Einfluss des Geräusches auf die Verständlichkeit kleiner sein als im Falle der ersten und sogar im Falle der zweiten Versuchsserie wo das Geräusch im Raum mittels dreier Lautsprecher räumlicher verteilt war. Die Prüfungsergebnisse auf Abb. 4 zeigen, dass die angenommene Voraussetzung richtig war, der Verlauf der Verständlichkeit, in diesem Fall bei höheren Pegeln, sinkt im Vergleich mit den zwei ersten Versuchen am wenigsten. Bei der vierten Versuchsreihe bestrebte man sich die Verhältnisse im stereophonischen Kino bei der Benützung von Effektkanälen nachzuahmen. Die Versuche wurden dermassen angeordnet, dass der Text dreikanalig und der Störschall getrennt aus drei Lautsprechern, die bei dem Hinterteil der Seitenwände angebracht waren, wiedergegeben wurde.

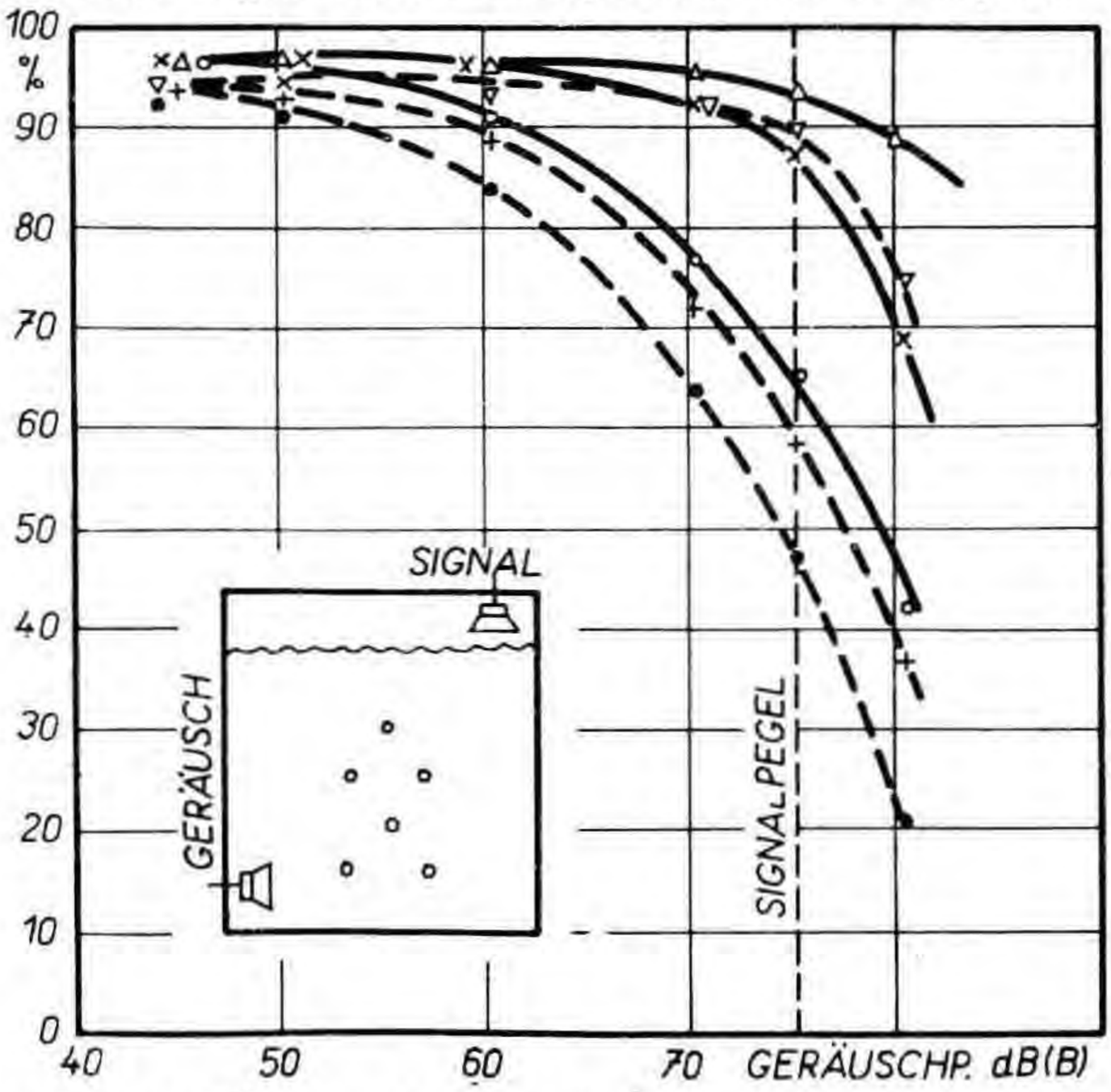

Bild 4. Einfluss der Spektralcharakteristik d. Geräusches auf die Verständlichkeit des wiedergegebenen Wortes bei der getrennten einkanaligen Wiedergabe. a) Männerstimme-Geräusch d. Frequenzbereiches: △ 40Hz ÷ 200Hz, ○ 200Hz ÷ 4kHz, × 4kHz ÷ 18kHz.
b) Frauenstimme-Geräusch d. Frequenzbereiches: ▽ 40Hz ÷ 200Hz, • 200Hz ÷ 4kHz, + 4kHz ÷ 18kHz.

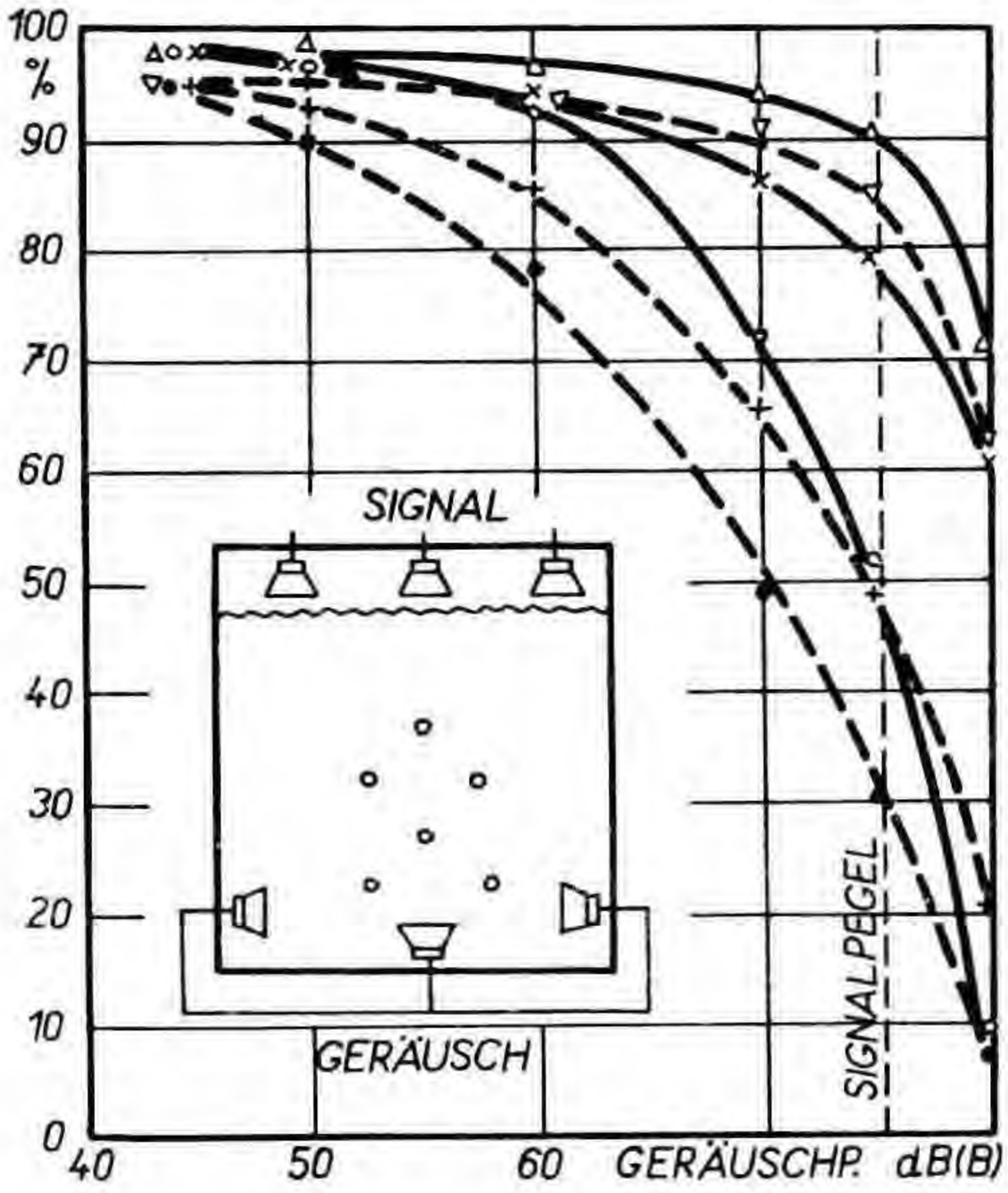

Bild 5. Einfluss der Spektralcharakteristik d. Geräusches auf die Verständlichkeit d. wiedergegebenen Wortes bei gegenüber d. Signalquellen des Testes angebrachten Geräuschquellen. a)Männerstimme Geräusch d. Frequenzbereiches:Δ40Hz÷200Hz ○ 200Hz ÷ 4kHz, × 4kHz ÷ 18kHz. b) Frauenstimme-Geräusch d. Frequenzbereiches : ▽ 40Hz ÷ 200Hz, • 200Hz ÷ 4kHz, + 4kHz ÷ ÷ 18kHz.

Die Versuchsergebnisse der Abb. 5 zeigen, dass die Verständlichkeitsabnahme auch bei niedrigeren Schallpegeln etwas grösser ist, als wenn das Geräusch von vorne kam; dieses könnte durch eine erhöhte Wahrnehmung des von hinten kommenden Geräusches (oder der Richtungscharakteristik der Maskierung) bewirkt werden, denn ein ähnlicher Verlauf kann auch bei dem vorhergehenden Test beobachtet werden. Im Vergleich mit der einkanaligen Prüfung, wo die Quelle des Geräusches und des Signals getrennt war, (siehe Abb. 4) weist diese Prüfung eine schlechtere Verständlichkeit auf. Diese Erscheinung ist dadurch erklärlich, dass das Geräusch zwar getrennt wirkt, aber schon so zerstreut ist, dass die Trennung beider Quellen und dadurch auch die Erregungsstellen der zugehörigen Gebiete der Hirnrinde nicht im vollen Masse eintritt.

3. Schlussfolgerung

Nach [1] und [2] ist die Satzverständlichkeit gut, wenn die Silbenverständlichkeit wenigstens 85% ist und annehmbar, wenn sie wenigstens 75% beträgt. Diesem Wert entspricht eine Wortverständlichkeit [3] von cca 92% für den ersten und von 87% für den zweiten Fall. Aus Angaben für eine gute Verständlichkeit und aus Schallpegeln, die man bei Dialogen bei der Dialogenwiedergabe in Kinos erzielt (60 - 85 dB), kann mittels Abb. 2 abgeleitet werden, dass zwecks einer guten Verständlichkeit der wiedergegebenen Sprache bei einer dreikanaligen Wiedergabe der Pegel des Grundgeräusches in Kinos nicht cca 35 dB (A) und das Grundgeräusch im Studio in den Tonaufnahmestellen cca 25 dB (A) nicht überragen darf.

Für eine richtige Einstellung der Pegel der Effektkanäle erfolgt aus Abb. 5 und aus dem Erfordernis einer annehmbaren Verständlichkeit, dass der Schallpegel minimal 22 dB unter dem Schallpegel des stereophonischen Signals liegen muss.

Zum Abschluss halte ich es für meine angenehme Pflicht, H. Prof.Ing.RNDr J.B. Slavík DrSc aus dem Physikalischen Institut der Technischen Universität in Prag und dem verstorbenen Ing. J. Ledrer aus dem Forschungsinstitut für Ton, Bild-und Reproduktionstechnik in Prag für zahlreiche anregende Hinweise zu danken, mit denen sie mir bei meiner Arbeit behilflich waren gleichzeitig gehört auch mein Dank dem Arbeitskollektiv der akustischen Abteilung des genannten Institutes für die unter der Leitung des H. J. Tomáš sorgfältig ausgeführten Messungen.

4. Literatur

[1] Slavík J.B. : Akustika kinematografie, Ústř. Čs. filmu, Praha 1947.
[2] Skudrzyk E. : Die Grundlagen der Akustik, Springer-Verlag, Wien 1954.
[3] Januška I. : Statist. převodní vztah mezi slabikovou a slovní srozumitelností české řeči. Sborník Čs. VTS - Současné problémy v prostorové a stavební akustice, Praha 1962.

K35

FOURTH INTERNATIONAL CONGRESS ON ACOUSTICS
COPENHAGEN 21.-28. AUGUST 1962

Hysteresis and Residual Stress in Solids

Robert W. Benson, Professor of Electrical Engineering,
Vanderbilt University, Box 1540, Nashville 5, Tennessee, USA

The design of mechanical vibrating systems such as transducers, matching stubs, etc., requires sufficient information to predict frequencies of components and information for the prediction of bandwidth, "Q", or damping for each component. Sufficient information is available in the literature to design simple vibrators of various sizes and shapes to produce a given natural frequency. However, the design of optimum configuration versus "Q" can only be accomplished with a thorough knowledge of losses within the material chosen. Simple ultrasonic measurements are available for the determination of the various elastic moduli of a material and are well supplemented by quasi-static methods. The most common method for measurement of losses is by the determination of the decay rate of a shock excited bar or by the determination of the bandwidth of amplitude of vibration of the bar when driven with a constant force with respect to frequency. Small amplitude behavior of the material is readily determined by these techniques, but the greatest interest in transducing systems is for large amplitude excitation. Due to the non-linear behavior of most materials, it is advantageous to measure the losses at actual operating amplitudes.

A bar, when shock excited, will vibrate at its natural frequency and decay exponentially with time. If the same bar is driven at its natural frequency, it is necessary to supply the loss per cycle in order to maintain constant amplitude of vibration. A system with this behavior is said to exhibit "hysteresis." If it is possible to dynamically excite a material which exhibits hysteresis, and measure the resultant effect, it is found that a plot of the dependent versus independent variables produces a loop known as a hysteresis loop. The area of the loop is the loss per cycle for the level of excitation chosen.

Experimental techniques are now available to directly obtain hysteresis loops for mechanically excited materials. The independent variable, stress, displayed against the dependent variable, strain, produces a typical hysteresis loop such as that commonly found for magnetic materials. The basic technique employs ultrasonic shear waves to perform measurements similar to those obtained with polarized light in the photoelastic method of stress analysis. The change in angle of polarization is a measure of stress, and strain is measured by more conventional means, such as strain gages. Samples are prepared which are a half-wavelength long at the exciting frequency so that peak stress levels above the elastic limit are obtainable. The stress-strain hysteresis loop is presented on a cathode ray oscilloscope and may be obtained as a function of stress for any given material. The behavior of the same material at other frequencies requires additional samples of the material.

Since the techniques of obtaining mechanical hysteresis loops are available, it is of interest to compare mechanical behavior with magnetic behavior of materials with the hopes of utilizing the vast knowledge available concerning the use of magnetic materials to aid in the design of mechanical vibrating systems. First of all, the static or quasi-static characteristics show a marked similarity. A typical stress strain curve is shown in Figure 1 and is compared to a typical magnetization curve. The general shape of the curves is similar having a linear region for low values of excitation and saturating at higher values of excitation. The curves are plotted in the usual orientation, where magnetic intensity H, the horizontal axis, and stress, s, the vertical axis are the independent variables and the magnetic flux density B and strain e, are the dependent variables.

When a material is dynamically excited either magnetically or mechanically typical hysteresis loops are obtained for magnetic materials and mechanical hysteresis loops are obtained by the experimental method described briefly above. If the path of the loop for a megnetic material is traced, it is found that the loop follows a counter-clockwise direction as illustrated by the arrows in Figure 2. In the case of mechanical excitation, a similar loop is traced, however, the loop follows a clockwise direction. Static measurements of stress versus strain beyond the elastic limit, easily show this pattern of behavior.

On the hysteresis curves two points are marked where the curve crosses the axis of the dependent variable or where the independent variable has "zero" value. At this point, there is no external excitation and the amount of the dependent variable remaining is referred to as "residual-magnetism" or "residual-strain." One will note that in the two cases the "residual" is in terms of the dependent variable because there is no external excitation. Although many text books refer to "residual-stress" the diagrams illustrate the phenomena of residual-strain. This does not say that there cannot be residual stresses, but the diagrammatic explanation of the phenomena results in an explanation of residual strains rather than stresses. Since the independent variable is an "applied" excitation it, of course, cannot exist after it is removed.

Nevertheless, there is reason to believe that there are residual stresses that exist in materials. For instance, if a flat plate as is ground, it is found that there are stress concentrations near the ground surface extending 0.010 to 0.020 inch below the surface. Although according to the previous discussions, one would tend to call these residual strains, they are indeed residual stresses since when the top surface is removed by etching, the formerly flat plate will bend. The tensile forces near the surface were opposed by compressive forces which were distributed throughout the rest of the sample. When the material which was under tension is removed, the sample bends illustrating the presence of stresses or forces capable of doing work. These are not the same stresses as referred to previously as being an applied force, but stress trapped within the material. The integrated stresses over the sample must necessarily be zero. However, there may be many combinations of tensile and compressive stresses which oppose each other and keep the sample in equilibrium.

Now let us examine another phenomena similar in magnetic and mechanical excitation of materials. If there exists a residual flux density in a material, a method of reducing this to zero is to excite it dynamically until the peak magnitization exceeds that which is

necessary to produce the residual magnetism, and then slowly reduce the peak excitation to zero. The corresponding hysteresis loops traced out will follow a path illustrated in Figure 4. In the case of the plate with stresses near the surface, one finds that it is common practice to subject the sample to a ball mill in order to relieve the surface stresses. A large number of small steel balls hit the sample randomly with relatively high velocities thus producing high peak stresses at the point of impact. If one now thinks of the sample as being made up of a number of parallel masses setting on damped springs (5A), that is, an elastic sample with damping, a pulse input of force or stress will result in a damped oscillation as shown in (5B). The corresponding plot for a given impact of a single ball is illustrated in Figure 4. The hysteresis loop is traced in a clockwise direction with ever decreasing magnitude and thus for a single point the stress would theoretically be reduced to zero. The adjacent parts of the sample are, however, still stressed and the stresses are redistributed accordingly. With sufficient impacts, however, it should be possible to entirely stress relieve the sample.

Although the foregoing discussion is based partly upon experimental evidence and partly on hypothesis, the similarity in behavior of magnetic and mechanical materials appears to be sufficient to warrant a study of the relationships between like phenomena. The explanation for residual strain and for residual magnetism appears to be straight-forward, if one assumes hysteresis within the material. However, a more interesting problem lies in the explanation of the possibility of residual stresses since they must add directly to external applied forces and thus influence any design. Actually all materials thus far examined appear to have significant amounts of residual stress even after considerable care in heat treatment to allow for the reduction of these stresses. One must be careful in discussing residual stresses by defining what is meant by stress since it usually is the independent variable and is determined from "applied" loads rather than from an equivalent applied load. For the purposes of this discussion, a residual stress may be defined as the equivalent applied force per unit area necessary to produce a stress of a given indicated magnitude. This implies that a technique is available which will indicate the state of stress in a given material.

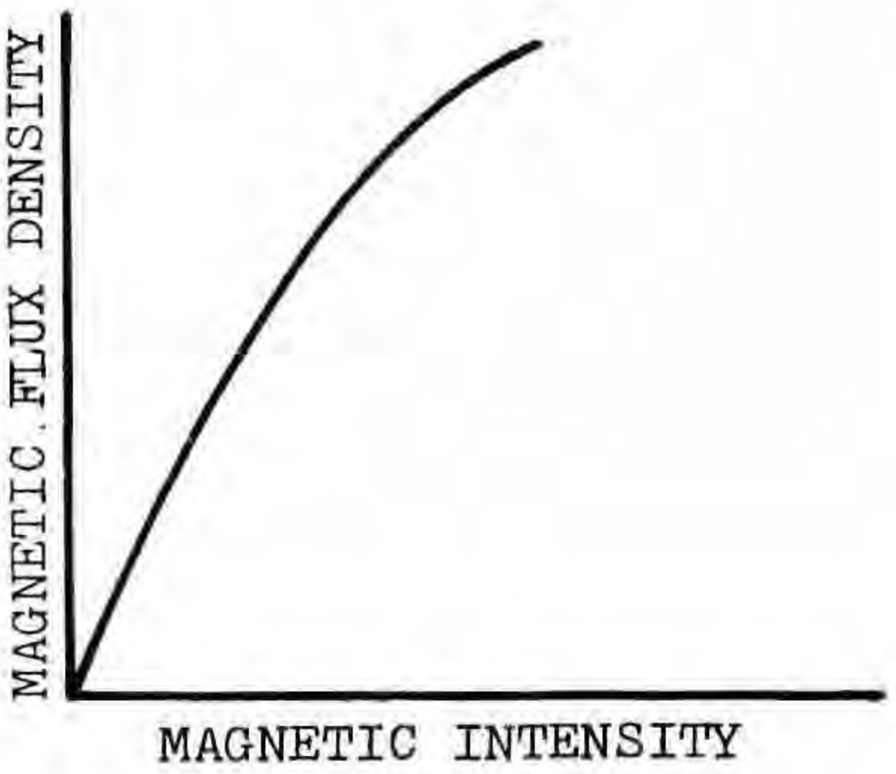

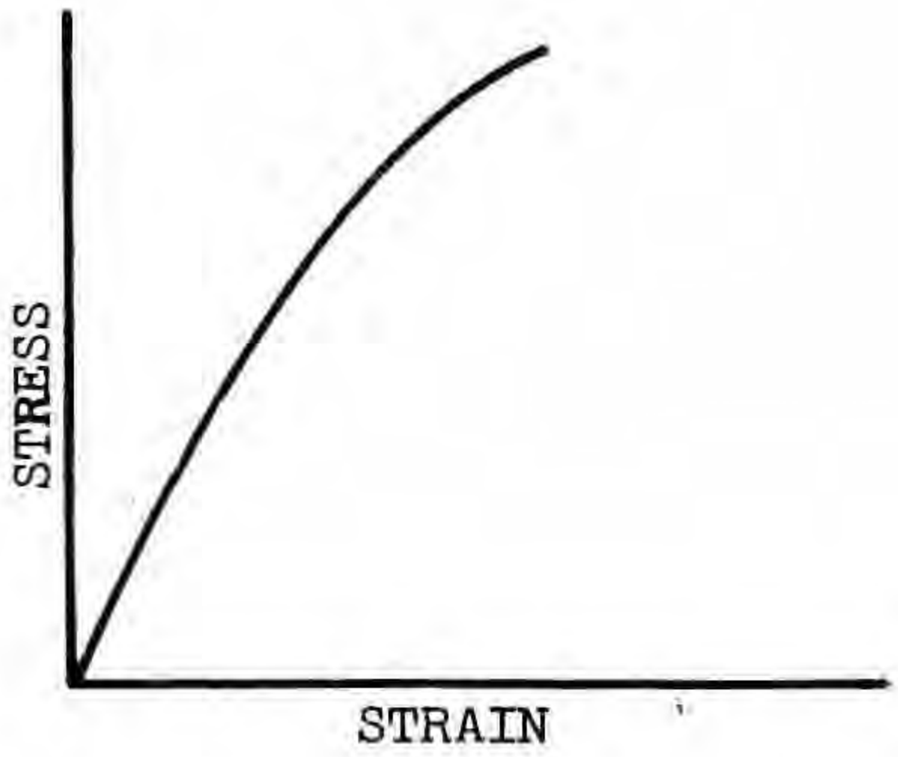

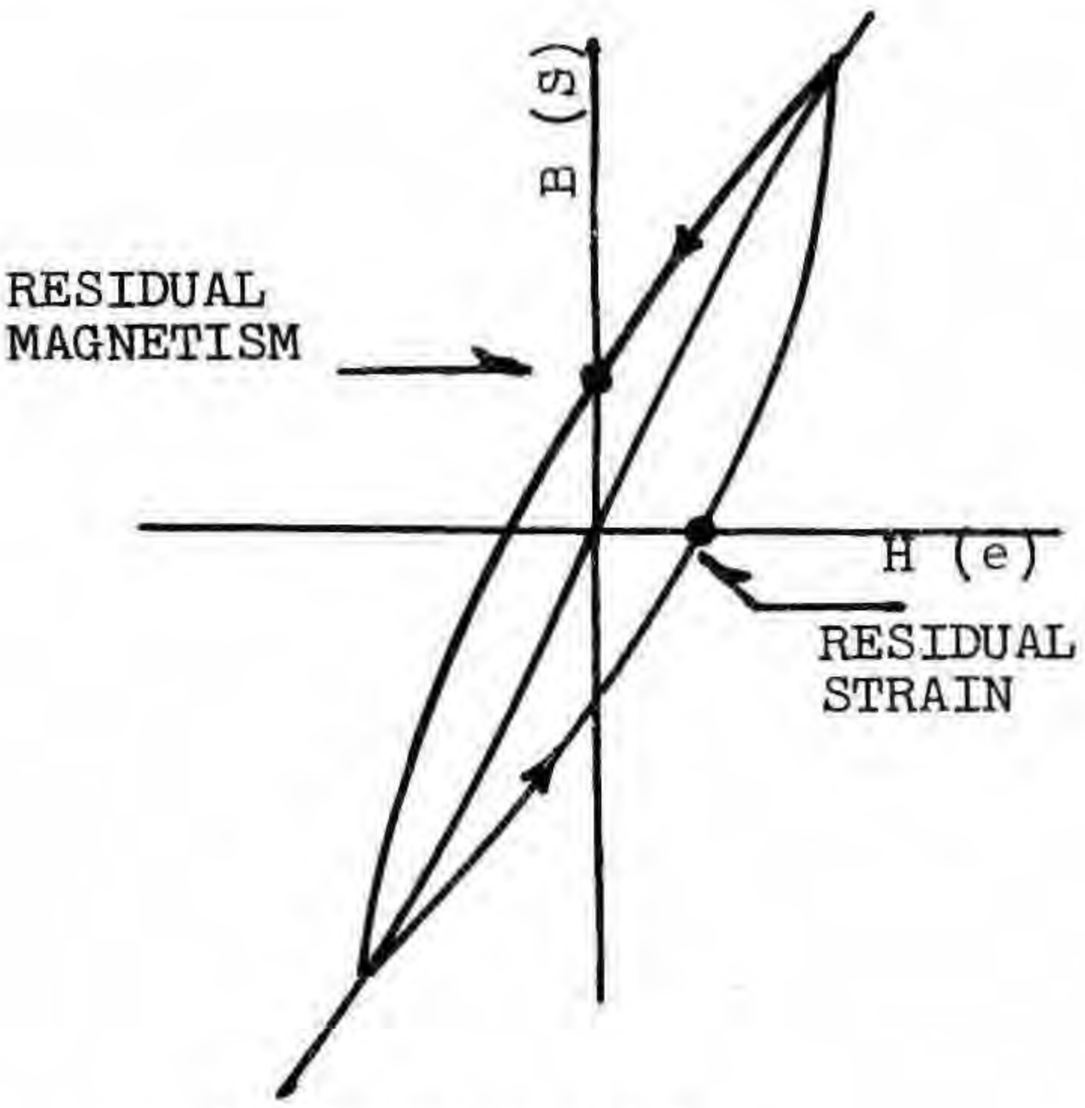

2. HYSTERESIS LOOP

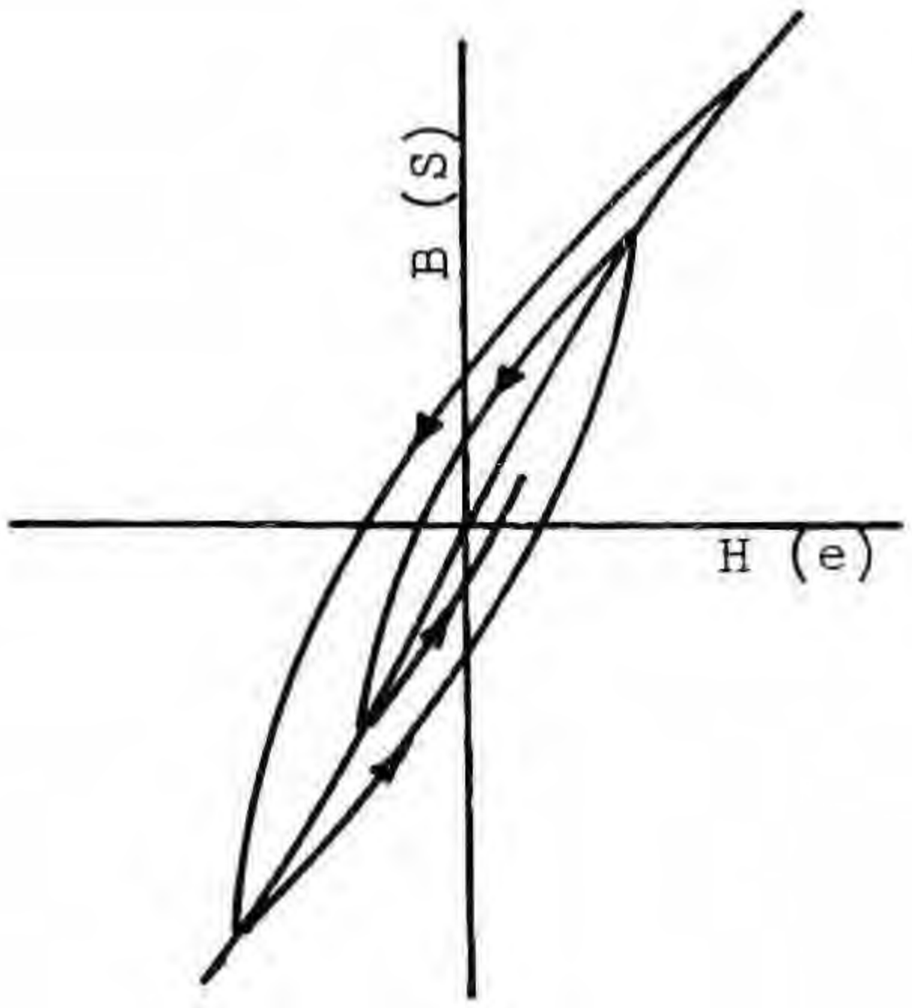

4. DEMAGNETIZATION OR STRESS RELIEF

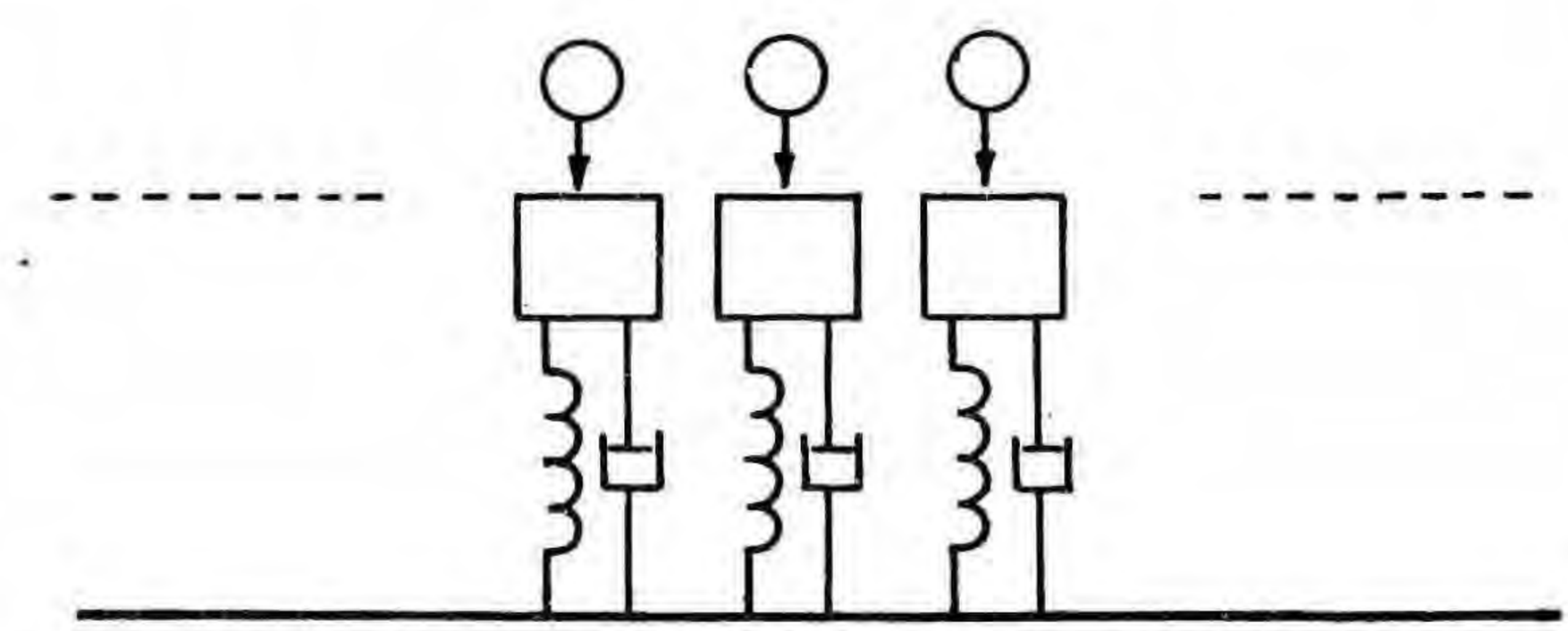

5A. CIRCUIT REPRESENTATION OF SURFACE STRESS RELIEF

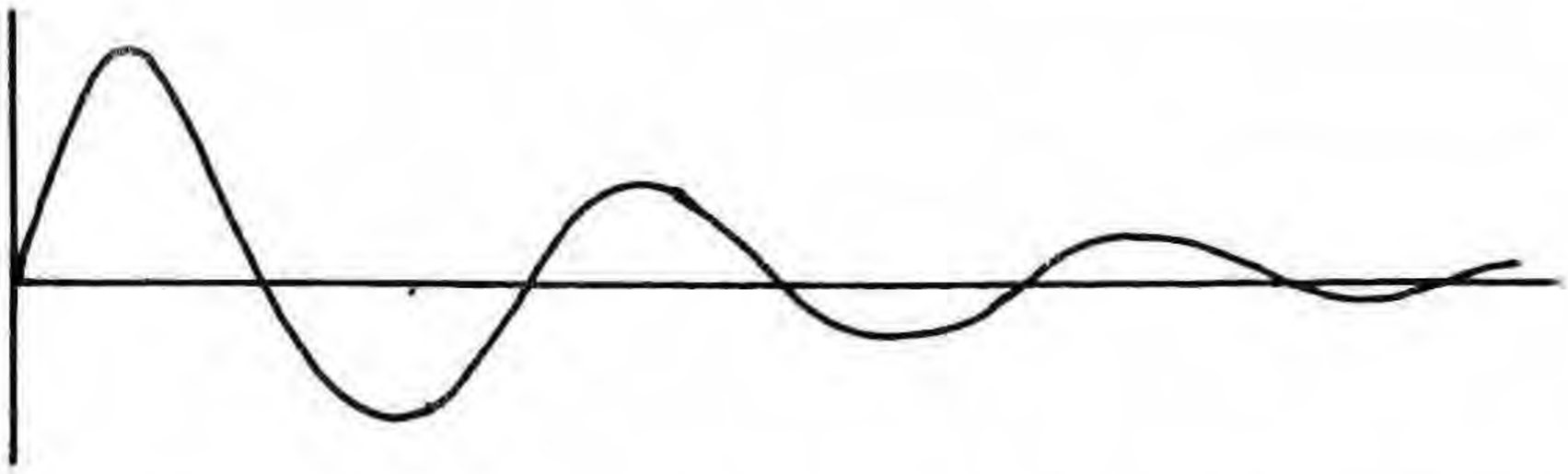

5B. STRESS VERSUS TIME, ILLUSTRATING DAMPED WAVE TRAIN

L35

FOURTH INTERNATIONAL CONGRESS ON ACOUSTICS
COPENHAGEN 21.-28. AUGUST 1962

"QUALITY CONTROL by NOISE ANALYSIS".

J.August Jensen, electr.eng. and Holger Larsen electr.eng.

A/S Brüel & Kjær.

Recent years have developed a new need in the field of quality testing, a need for instrumentation to test products with rotating or moveable parts for noise and vibration. This requirement has arised mainly because it has become necessary to reduce the noise level produced by equipment used in daily life (office machinery, household machinery, workshop equipment etc.) in order to provide more comfortable conditions for the operators of such equipment. However, analysis of the noise and vibration produced, has proved to be an aid in the manufacture of such equipment. By analysing the noise or vibration produced by a certain apparatus, it is often possible to locate faults on this apparatus which would otherwise have remained hidden until the apparatus had been in use for some time. By investigating the noise and/or vibration components produced by a certain piece of machinery, it is not only possible to locate mechanical faults, but it is most often so, that a certain mechanical defects, in for instance rotating machinery, always produces a noise of a certain frequency and loudness, thus making it possible to check the machinery for mechanical defects by means of a noise check. The advantage of a noise check is obvious as far as the noise check can be carried out in seconds when the right equipment is used, while mechanical measurements of similar phenomena consume much more time. This again means that this kind of checks are suitable for mass-produced units.

Typical areas where such noise or vibration tests are required, are all kind of machinery containing motors or gear boxes. On gear boxes a noise test will indicate if it contains any inaccurately cut gear wheel, faulty ball bearings etc. In, for instance, small electric motors a vibration test will indicate unbalance of the rotating parts, oil-agitation in bearings etc. This kind of quality tests is suitable for a very wide range of equipment covering anything from oil burners, vacuum cleaners, kitchen aids, ventilators, office machinery to all kinds of gears and motors, also such ones used in automobiles, etc., etc.

Quality tests by means of noise analysis should preferably take place at the time where the product leaves the assembly line to be carried in stock. The test should be carried out on fully completed units and under simulated working conditions i.e. with power applied, motor running at full speed etc. In some cases though, it will be advantageous to place the test at an earlier stage, such as in the automobile industri where motors, gearboxes, differential gears etc.may be tested on their own, before mounting in the chassis.

A problem arises in most cases because of the background noise that is normally present in a factory near the assembly lines. Of course it is a condition that the background noise level does not exceed or even come near the noise level generated by the test object. (In a few cases the background noise may though be eliminated by the use of filters in the measuring systems; this applies to conditions where the background noise mainly consists of noise of one predominant frequency). In most cases, however, it will be necessary to employ some kind of screening to damp the background noise at the place where the noise test is carried out. Quite often the noise level generated by the test object is of the order of 30-40 db or even less. This level is comparable to the level in a silent living room, but far below, what is normal in a factory (depending on the kind of manufacturing this level varies from 60-100 db SL). IT is

therefore necessary to isolate the test object from factory noise. In most cases the object can be tested in a hard walled chamber, the walls of which are made heavy enough to provide sufficient damping.

Besides the practical problems of opening and closing the heavy doors or gates of such a chamber, this solution is also a rather expensive one, as regards the construction of the chamber. Especially when it is desired to measure at frequencies below 100-200 c/s, such a chamber becomes less practical and more expensive. It has therefore become more common in noisy areas to carry out the noise test as a vibration test i.e. by means of vibration pick-ups instead of microphones as the sensitive elements. It has proved to be much easier to isolate the test object from unwanted vibration than from background noise, in that the object can be placed on a test stand mounted on foam rubber pads or other kinds of shock- and vibration absorbers. Also this does not involve as many practical problems for the test stand operators. Another advantage in using a vibration pick-up is that it can be placed at a position on the test object where the vibration is most pronounced for certain critical operation modes, which makes the measurement more selective. Disadvantages of this method are that the pick-up must be fastened in some way to every test item, and which is more serious, at higher frequencies the number of vibration nodes and antinodes in the test object increases considerably, thus making the measurement inaccurate due to incertainty in pick-up fastening, and retroaction of the pick-up.

A suitable solution to the problem of measuring noise in areas with conspicuous background noise will thus be to employ vibration measurements at lower frequencies and noise measurements in a fairly light and inexpensive chamber at higher frequencies. The dividing point is somewhat dependent upon the special arrangements, but is normally chosen to be between 400 and 800 c/s. (A measuring chamber with a volume of approximately 10 m^3 will be suitable for noise measurements in the frequency range between 500 c/s and 5000 c/s).

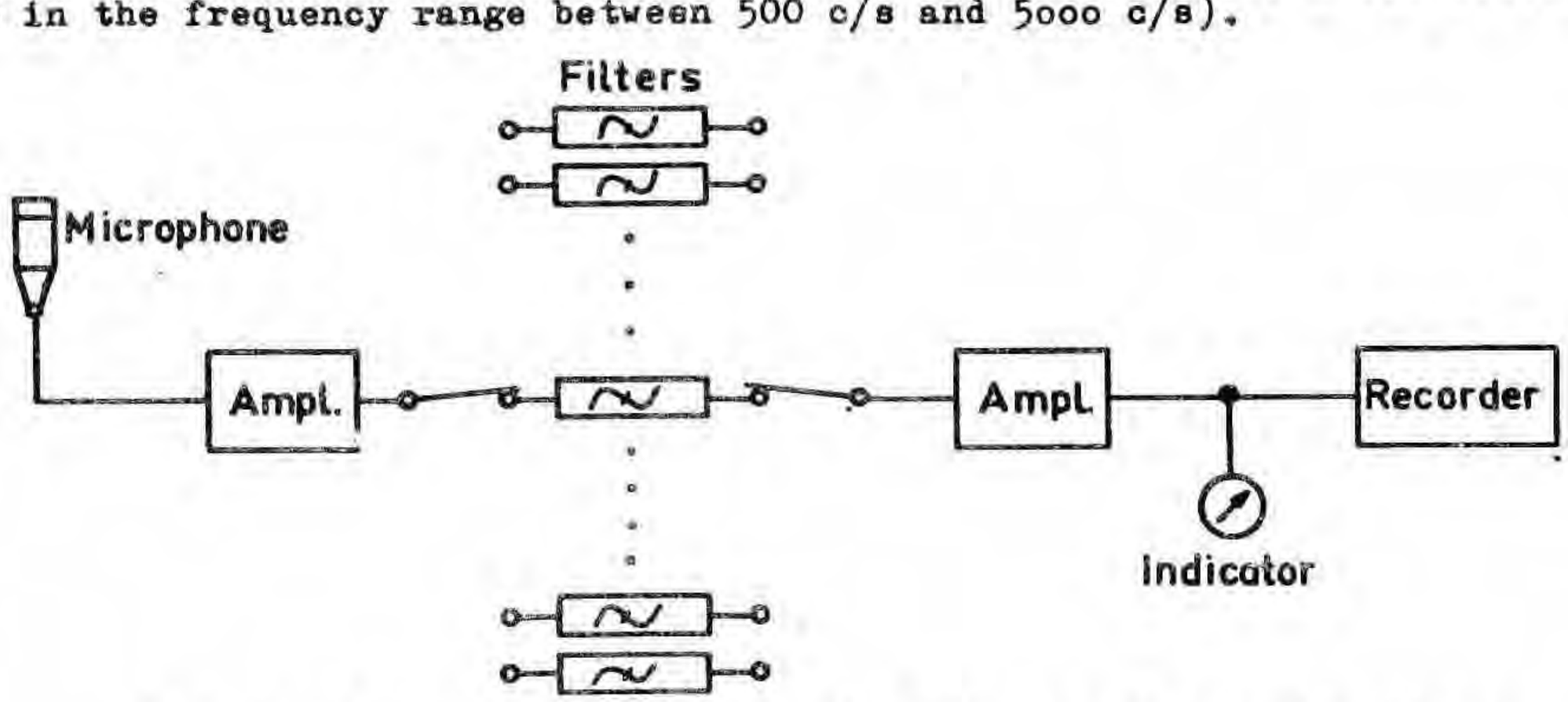

Fig. 1. Analysing arrangement for laboratory investigations.

For laboratory investigation of noise an arrangement as shown above is normally employed. It consists of a microphone, an amplifier, a number of band-pass filters that can be switched in successively, a second amplifier and a meter or recording device. The signal from the microphone is analyzed by means of the band-pass filters and recorded. Analysis is carried out by inserting the filters, one by one, and recording the noise level for each filter. A similar arrangement is used for the analysis of vibration, but in this case the microphone is interchanged with a vibration pick-up. f.ex. an accelerometer.

This arrangement is excellently suited for laboratory investigations and may also be used for production control in cases where the time factor does not play a too important role and where qualified personel is available. However, such conditions are very seldomly fulfilled in manufacturing, thus another set

of instruments is required. The main requirements to such an instrumentation system can briefly be stated as follows:

1. It should be an analysing instrument.
2. It should provide for both noise and vibration measurement.
3. It should give fast and accurate measurements to facilitate high-speed production.
4. It should be easy to operate, also for untrained personel.
5. It should be easy to readjust for different types of production.

To fulfil these requirements an instrument has been developed at the laboratories of Brüel & Kjær, Nærum, Denmark. The principle of this instrument is outlined in fig.2, and in the following shall shortly be described its main advantages and disadvantages.

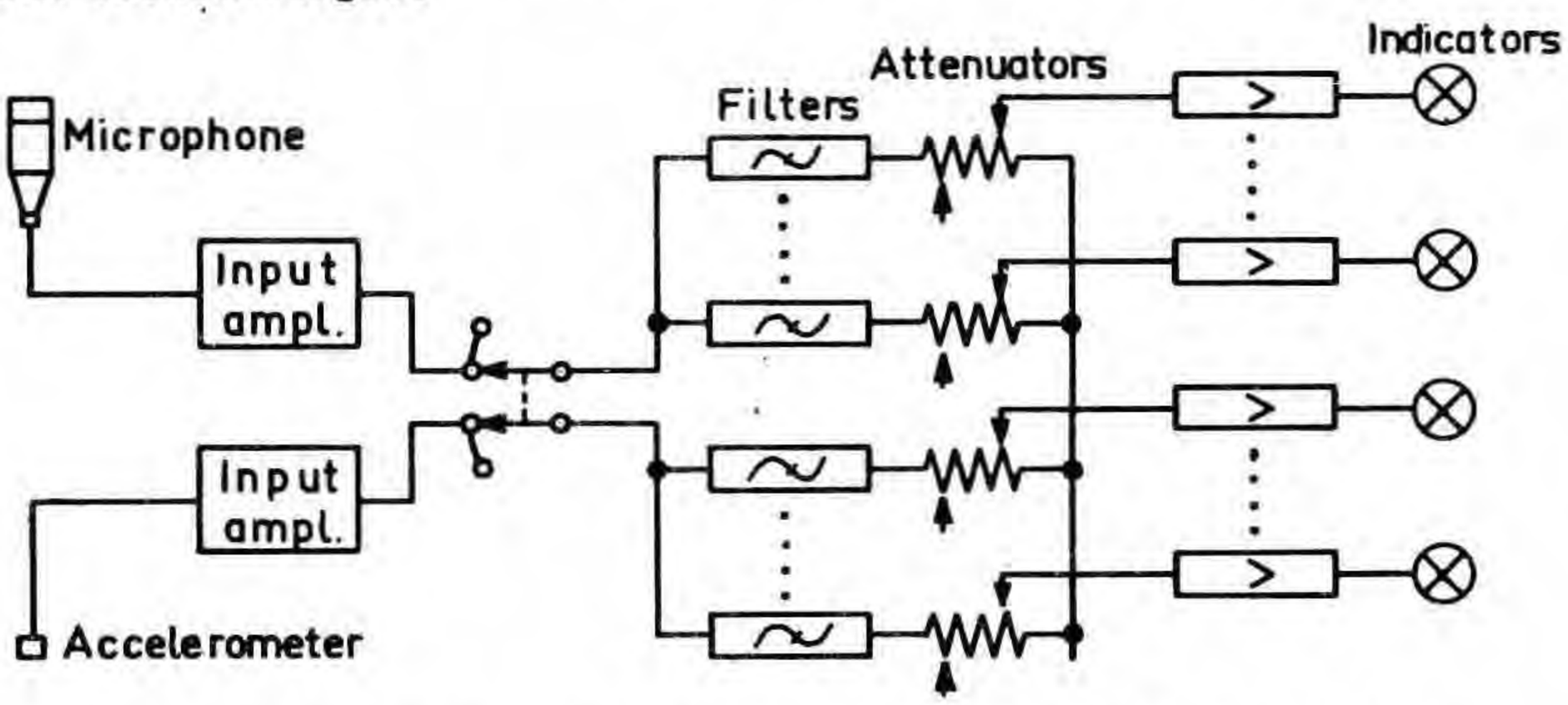

Fig. 2. Basic principle of the Noise Limit Indicator.

The instrument is called a Noise Limit Indicator. As the sensitive element it employs a condenser microphone and/or an accelerometer. As shown in fig.2, it is possible to connect either a microphone and a vibration pick-up, two microphones or two accelerometers. When employing condenser microphones or piezoelectric accelerometers it is necessary to obtain a high input impedance. In this instrument two cathode follower stages are used for this purpose. Next are two input amplifiers followed by a set of filters. The filter inputs are permanently connected in parallel with each other, and the whole set of filters can be switched to one or the other of the two inputs. Also it is possible to switch one input to the first half part of the filters and the other input to the remaining half part. In this way the instrument can be used for noise testing and vibration testing, one after the other, with the full set of filters, or for simultaneous noise and vibration testing with half the number of filters. The filters are plug-in units, and may be chosen as 1/1 octave or 1/3 octave band-pass filters. To obtain a reading of the overall sound level, one of the internationally standardized weighting networks can also be inserted. Each filter is followed by a double attenuator and an output amplifier, the latter feeding the indicator circuit. The indicator circuit contains a rectifier, a threshold circuit, a relay with two passive positions and an indicator lamp.

The attenuator serves to adjust the amplification for each individual filter channel. The attenuator has two tappings, one for each of the input channels, so that pre-adjustments can be carried out for both noise and vibration measurements.

Prior to measurements it is necessary to determine the frequency bands in which it is desired to measure and also the allowable noise level for each of these bands. This must be based on laboratory investigations carried out by normal analysing equipment (see fig.1), so that at the production stage the Noise Limit Indicator, properly adjusted, only functions to indicate that the pre-determined limits at the different frequencies are not exceeded.

For normal "go-no go" tests, the amplification of each of the filter channels are adjusted in such a way that the threshold and indicator circuit makes the indicating lamp light-up when the pre-determined noise limit is exceeded. The lamp remains lit until it is manually switched off. The instrument is put into operation by depressing a push-button which activates a relay, switching in the chosen input amplifier. After the measurement is carried out a "release" button is depressed,switching off the instrument until the next object is ready for measurement. A control panel, which can be placed remote from the main unit, contains the control push-buttons and indicator lamps necessary for the operator. Pre-adjustments for the particular type of measurement desired are carried out on the main unit, which can be locked after adjustment.

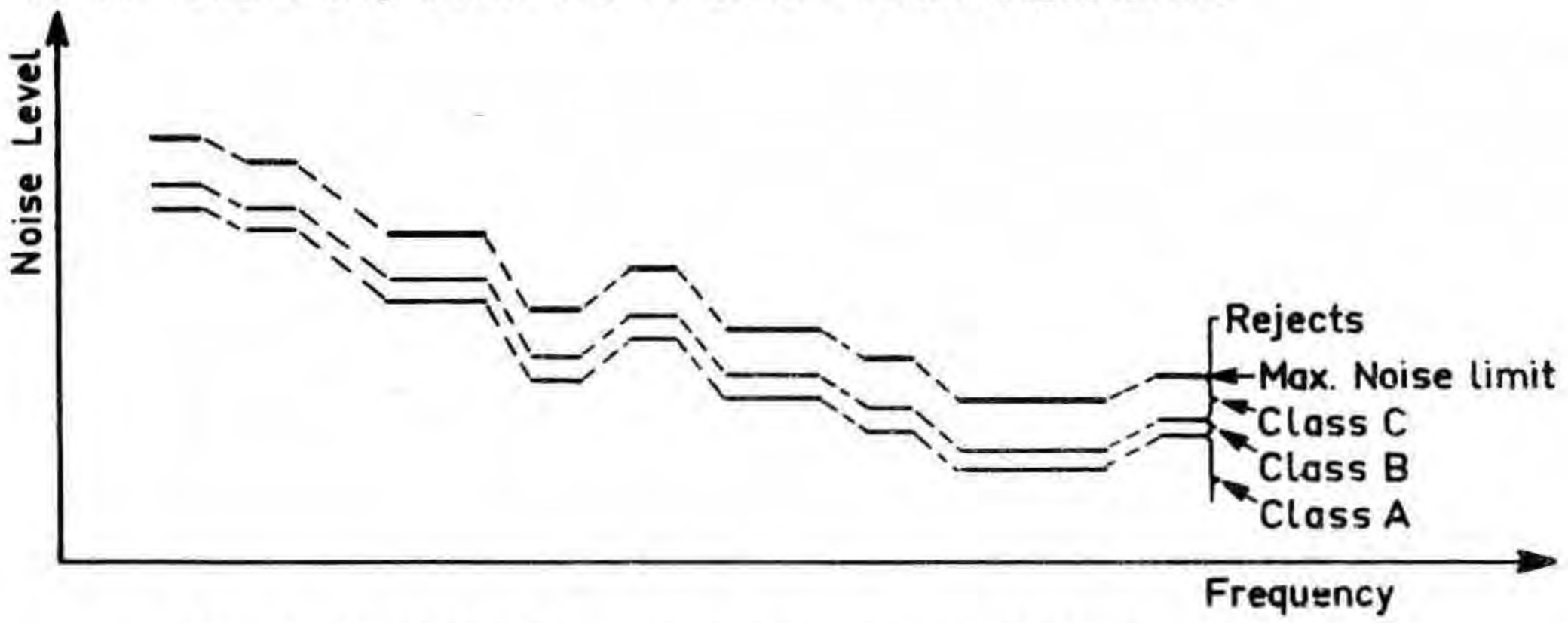

Fig. 3. Besides the normal "go-no go" test an actual noise or vibration classification may be carried out.

A special circuit provides an overall increase in amplification at the input stage. This lowers the pre-set noise limit for all filter channels with an amount of o-5 db (pre-adjusted). The normal "go-no go" classification is in this way extended with a third class, which may be named "extra". Combining the two input stages makes it possible to divide a series of test items into five noise or vibration classes. This will not only be an aid to better analysis of production quality, but also it may in many cases determine what kind of installation the produced units are suited for.

The instrument outlined above is thus capable of checking that the noise limit produced by a test object does not exceed the pre-determined limits for a number of frequency bands (up to 12) simultaneously. The limit for each frequency band can be set anywhere between 32 db and 140 db re 2 x 10^{-4} µbar. The time needed for a normal "go-no go" test amounts to only a few seconds (3-10 seconds) besides the time it takes to install the object in the test stand. It measures both noise and vibration, and the control panel, containing only five push-buttons, is easily interpreted even by untrained personel. In addition to the primary requirements stated above the instrument is also capable of dividing the test items into several noise or vibration classes.

M35

FOURTH INTERNATIONAL CONGRESS ON ACOUSTICS
COPENHAGEN 21.-28. AUGUST 1962

Studies on flanking transmission in an experimental building

O. Brandt
G. Westerberg

The Swedish sound insulation requirements for dwellings are based on the normalized level difference between neighbouring rooms as well as on the reduction faktor for the partitions and floors. It is therefore necessary to consider all transmission paths of importance.

In modern prefab building techniques the trend is towards light outer walls with good heat insulation, for instance sandwich constructions. Such outer walls may very often allow flanking transmission equal to or bigger than the direct transmission through floors and partitions.

Flanking transmission through outer walls has been studied in an experimental building by means of special techniques. The experimental building, where these studies were made, has been described elsewhere[1]. The concrete walls and floors in the four rooms are of the minimum thickness at present allowed in Sweden: 14 cm for partitions and 16 cm for floors. In earlier studies we have found that it is possible to fullfil the requirements with these concrete constructions if the insulation is not reduced by flanking transmission through the outer wall or through flanking partitions.

For a given outer wall covering two adjoining rooms the technique was to measure the different components of the flanking transmission through the outer wall as well as the direct transmission through the separating partition. In order to do this we covered the various surfaces in both the room of origin and the receiving room with a screening construction having properties, which have been described elsewhere [1]. However, the floors and ceilings were not covered during the investigations, as we supposed these surfaces would add little to the transmission. This supposition has been proved correct for the cases so far studied.

The following symbols for level differences are used:
(Reference absorption 10 m^2)

Fig. 1.

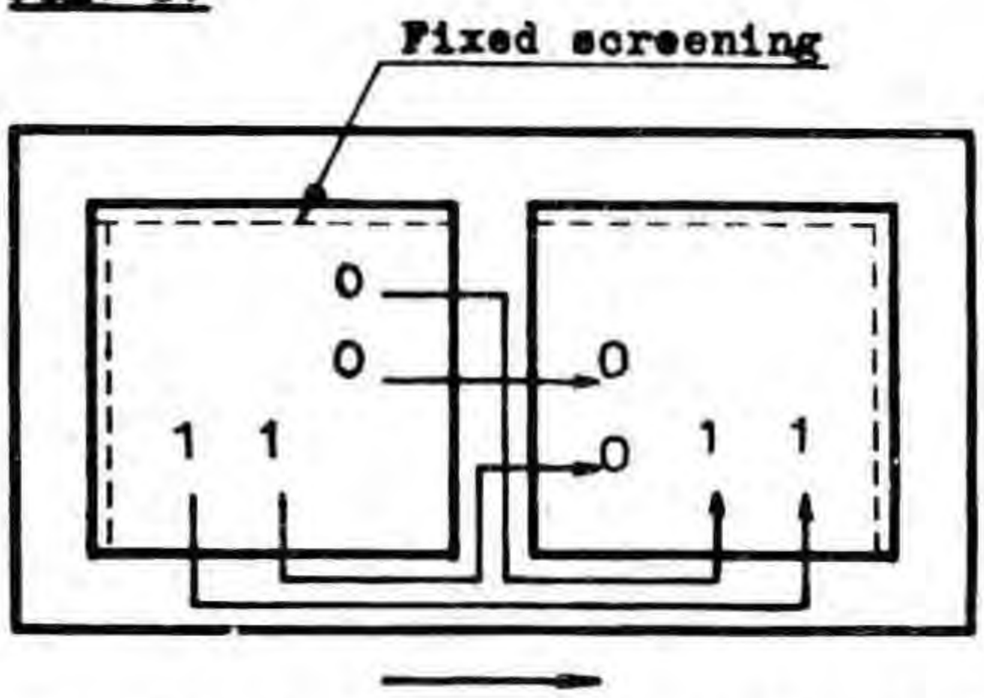

D_{10} Measured total normalized level difference

D_{0-0} Normalized level difference caused by direct transmission through the separating partition.

D_{1-1} Normalized level difference caused by flanking transmission through the outer wall.

D_{0-1}, D_{1-0} Similar components involving the partition and the outer wall.

The sizes of the transmission surfaces were:

Surface 0	9 m^2
Surface 1	6 m^2
Ceiling, floor	9 m^2

When measuring the components D_{0-0}, D_{1-1}, D_{0-1}, D_{1-0} the ceiling and floor components are included. If the total transmission is controlled only by the four components mentioned the following equation must be valid.

$$D_{10} = 10 \cdot {}^{10}\log \frac{1}{\sum_{j=0}^{1} \sum_{i=0}^{1} 10^{-0.1 \cdot D_{i-j}}}$$

It was shown by vibration measurements that the amplitudes of the floor and ceiling in the receiving room were about 10 dB below the amplitudes of the partition, Fig. 2. At this measurement the outer wall was of 25 cm lightweight concrete built from 50 cm wide, floor height elements.

Fig. 3 and 4 show that the measured total level difference D_{10} is nearly the same as the level difference computed from the four components mentioned. Consequently it is possible, at least for lighter outer walls, to carry out the measurements neglecting the transmission paths

through floors and ceilings. Obviously it is not possible to neglect these paths for outer walls with very high sound insulation, for instance thick concrete walls.

The following is an example of the problems studied in the experimental building. An outer wall with details as in Fig. 5 and 6 was erected. It was desirable to determine if such a wall contributes more or less to the sound transmission than a 14 cm concrete partition wall. It was also desirable to find out if the flanking transmission could be reduced by making vertical breaks through the outer wall on each side of the partition. From a practical point of view it was possible to do this if the breaks could be covered afterwards with a thin layer of plaster. The results of these studies are shown in Fig. 3 and 7-10. The effects of the breaks and the plastering are most evident for the paths 1-1 and 1-0, (Fig. 7, 9) which together give results in total effect according to Fig. 10. Obviously the plaster reduces the insulation improvement due to the breaks considerably.

Fig. 2. Vibration amplitudes of floor and ceiling below the amplitude of the concrete partition.

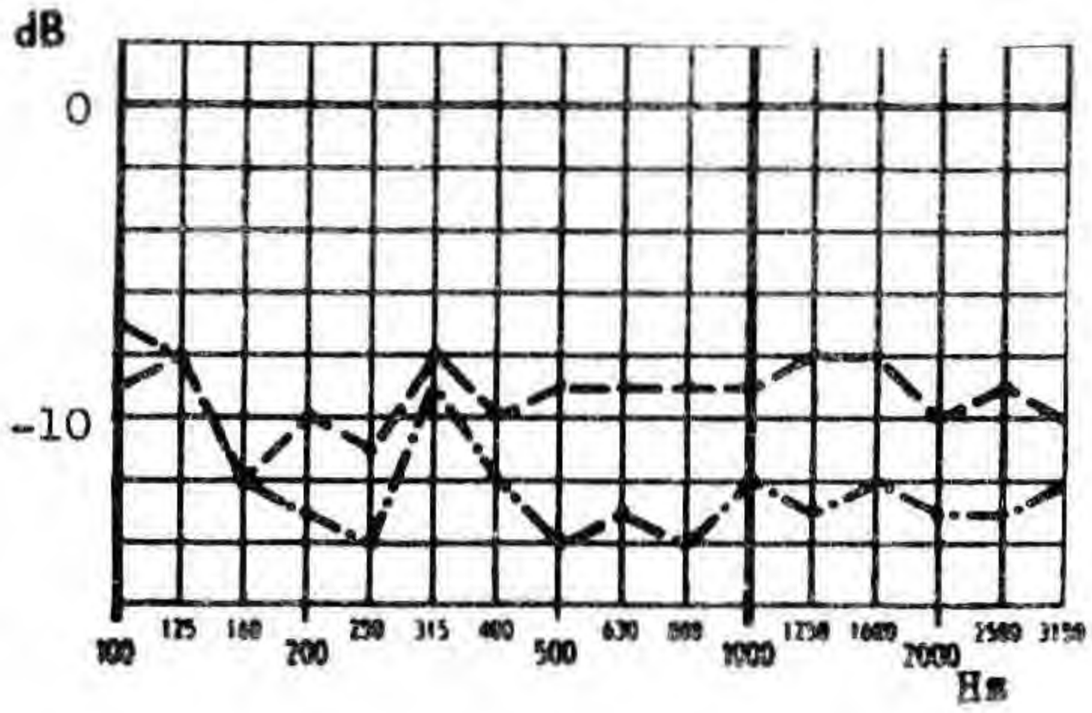

Fig. 3. D_{0-0} ····· D_{0-1} —·— D_{1-1} ——— D_{1-0} — — —

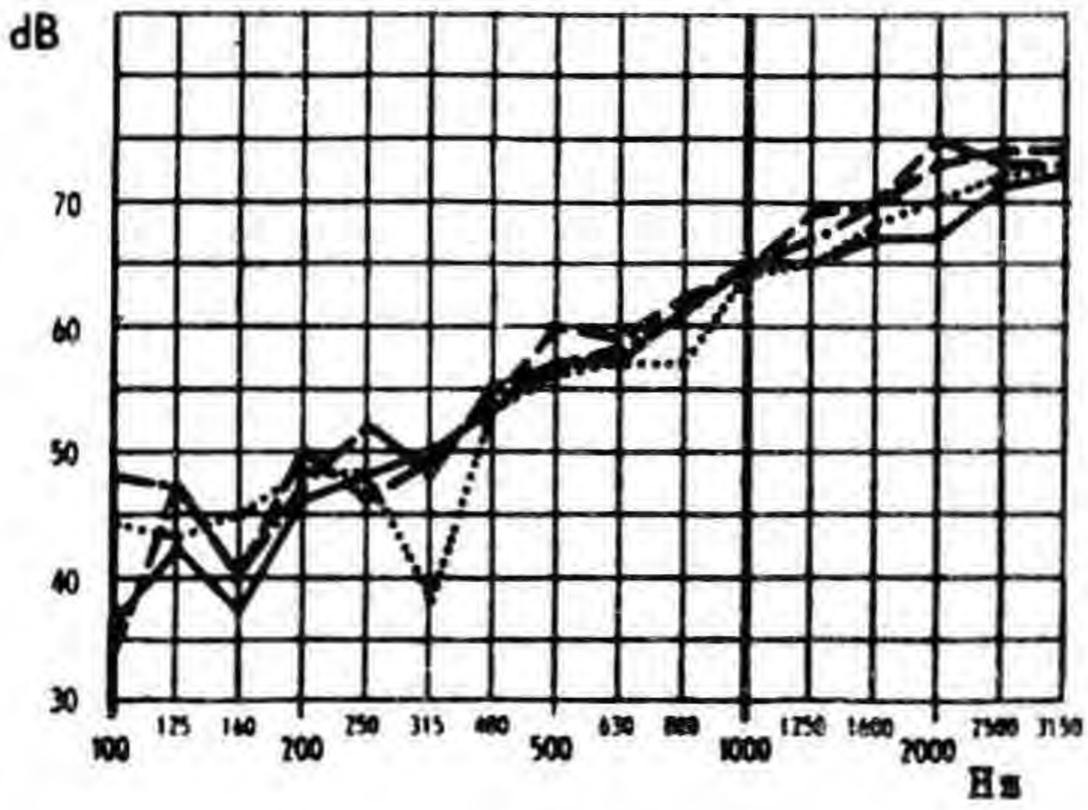

Fig. 4. D_{10} Computed ····· Measured ———

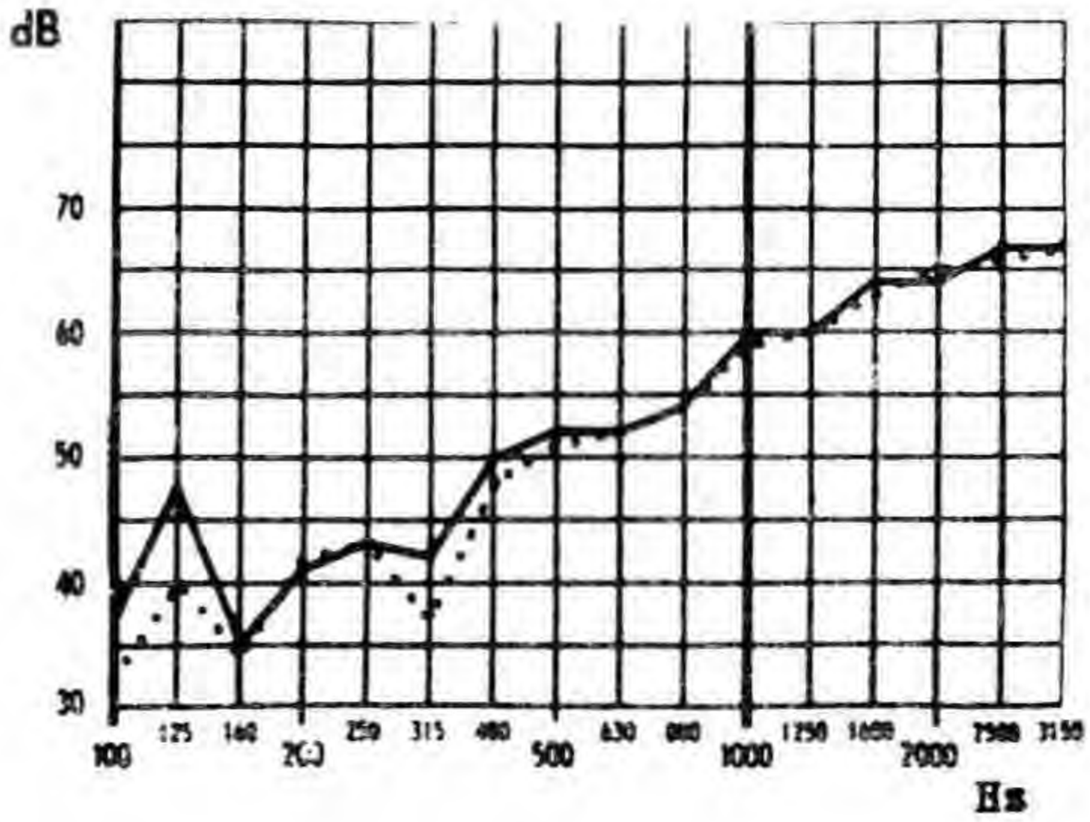

Reference

1. Brandt, O. and Wahlström, S.: Experimental buildings for sound insulation studies.

Fig. 5.

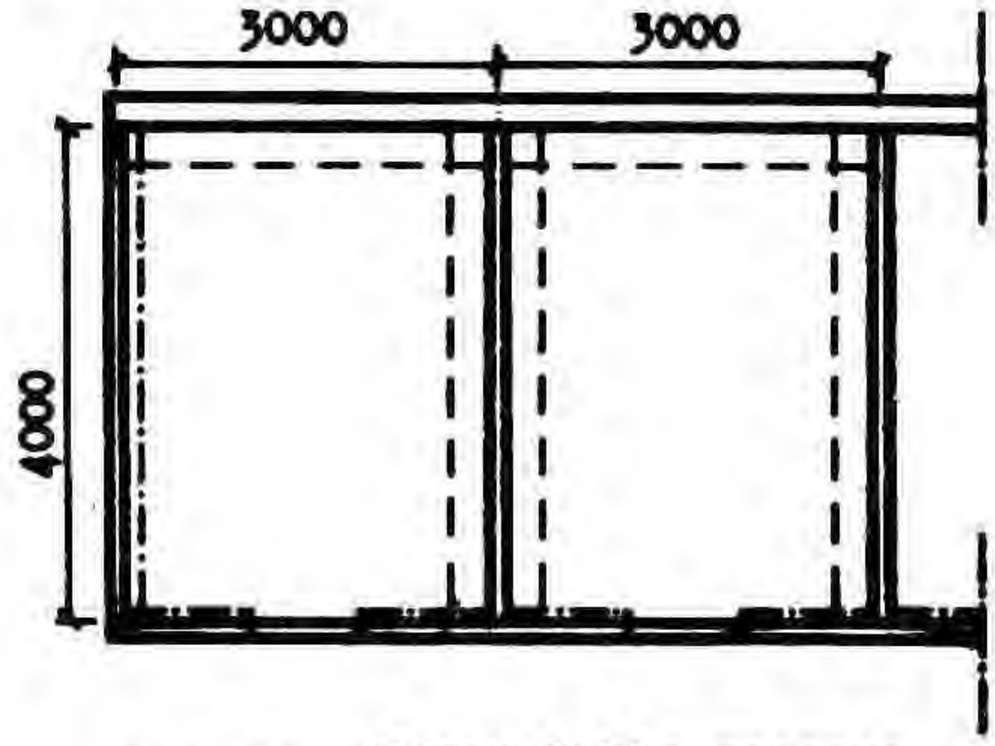

Fig. 6.

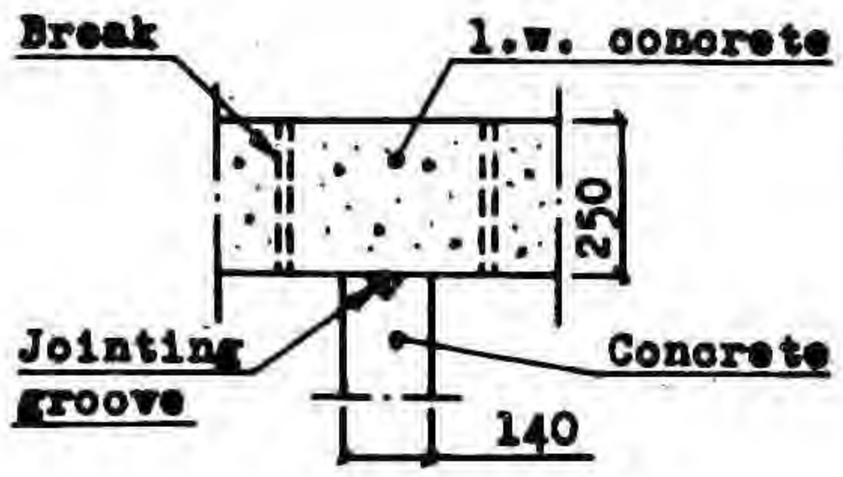

Fig. 7. D_{1-1}

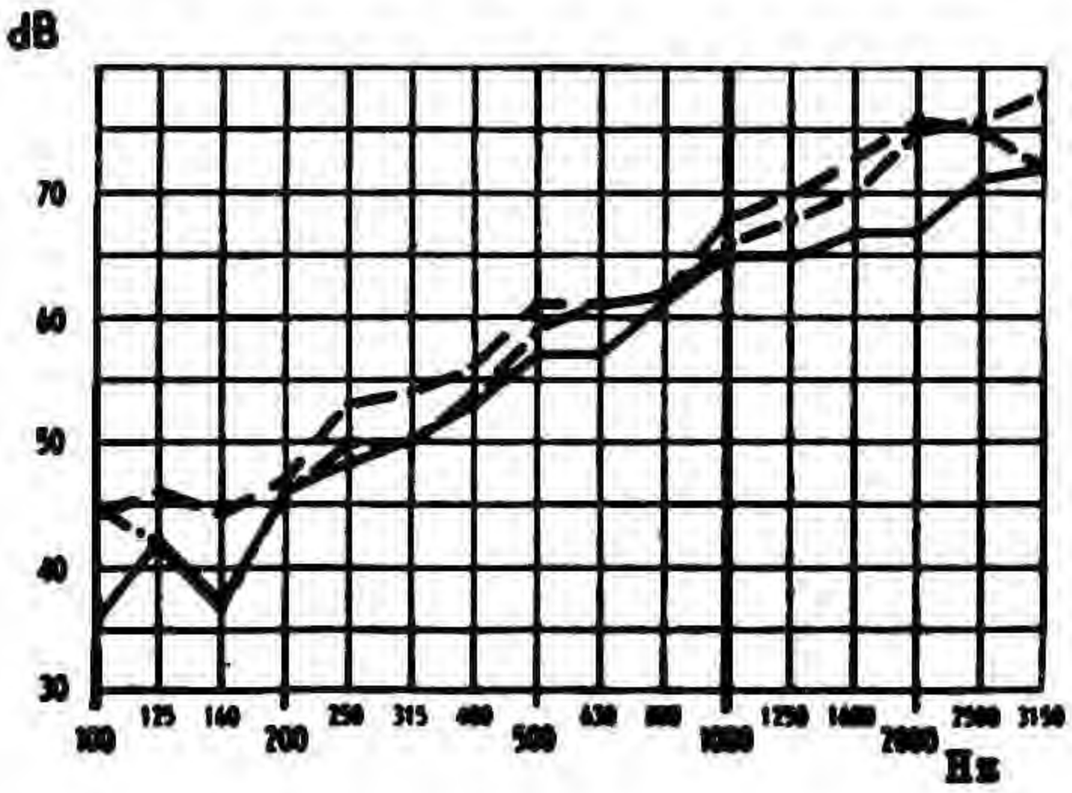

Fig. 8. D_{0-1}

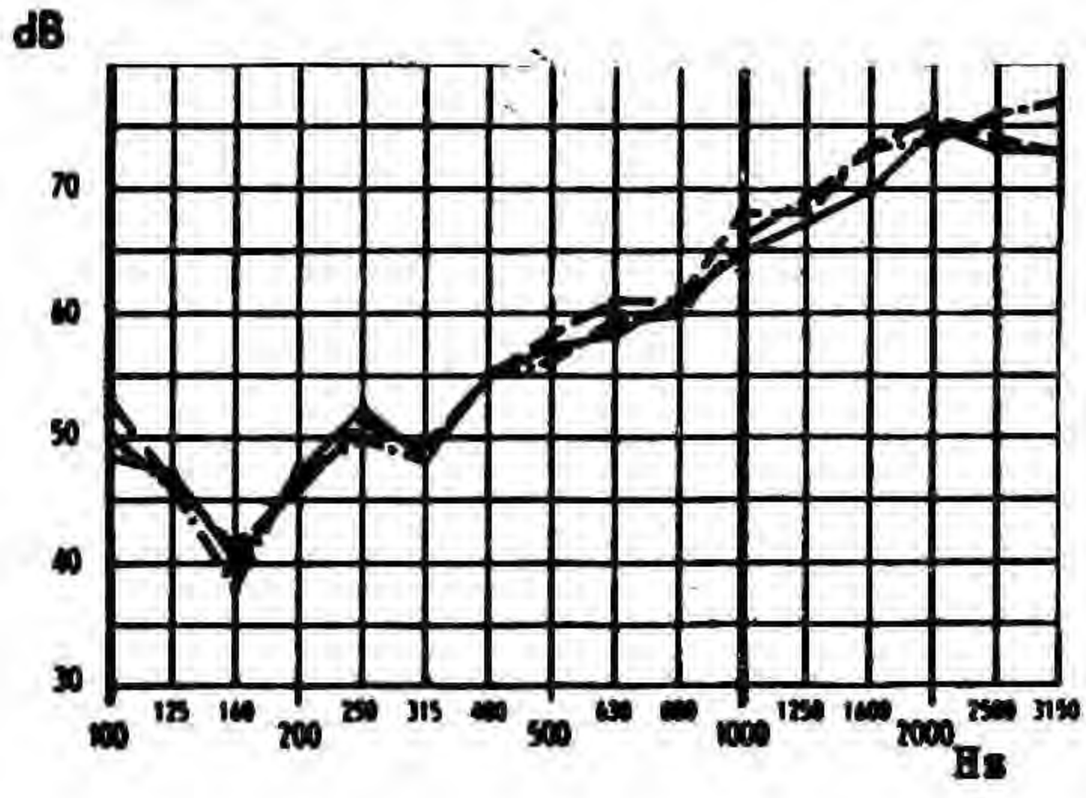

Fig. 9. D_{1-0}

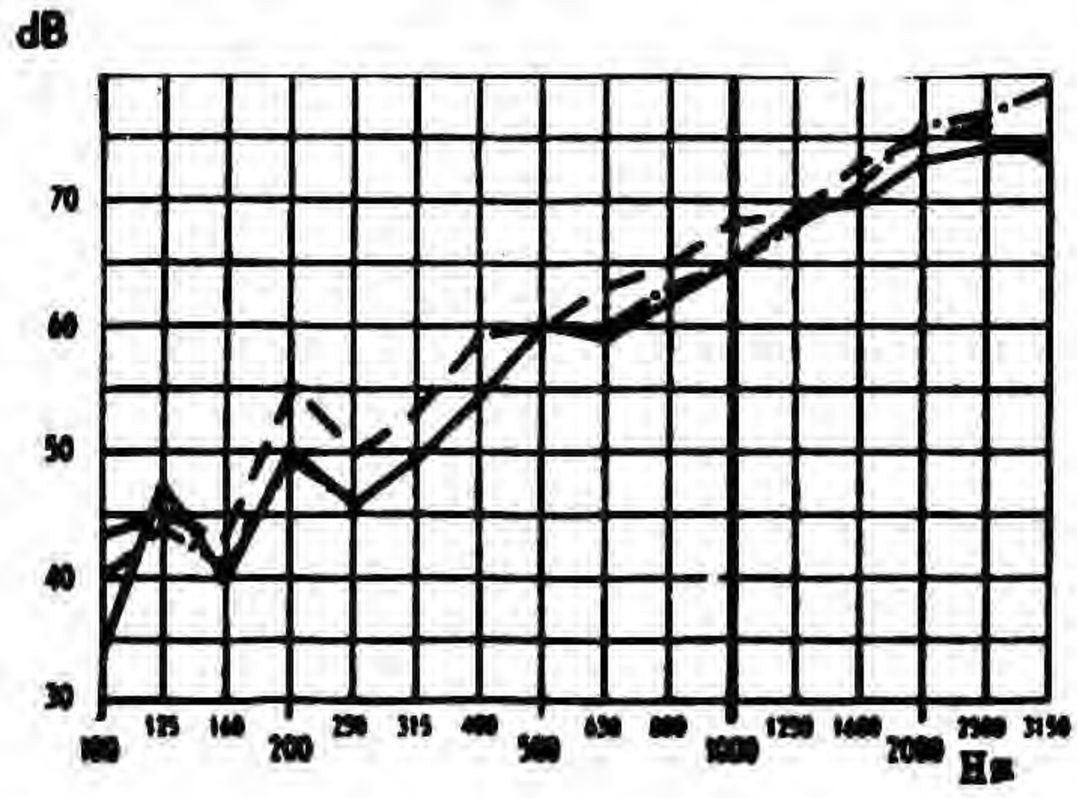

Fig. 10. D_{10}

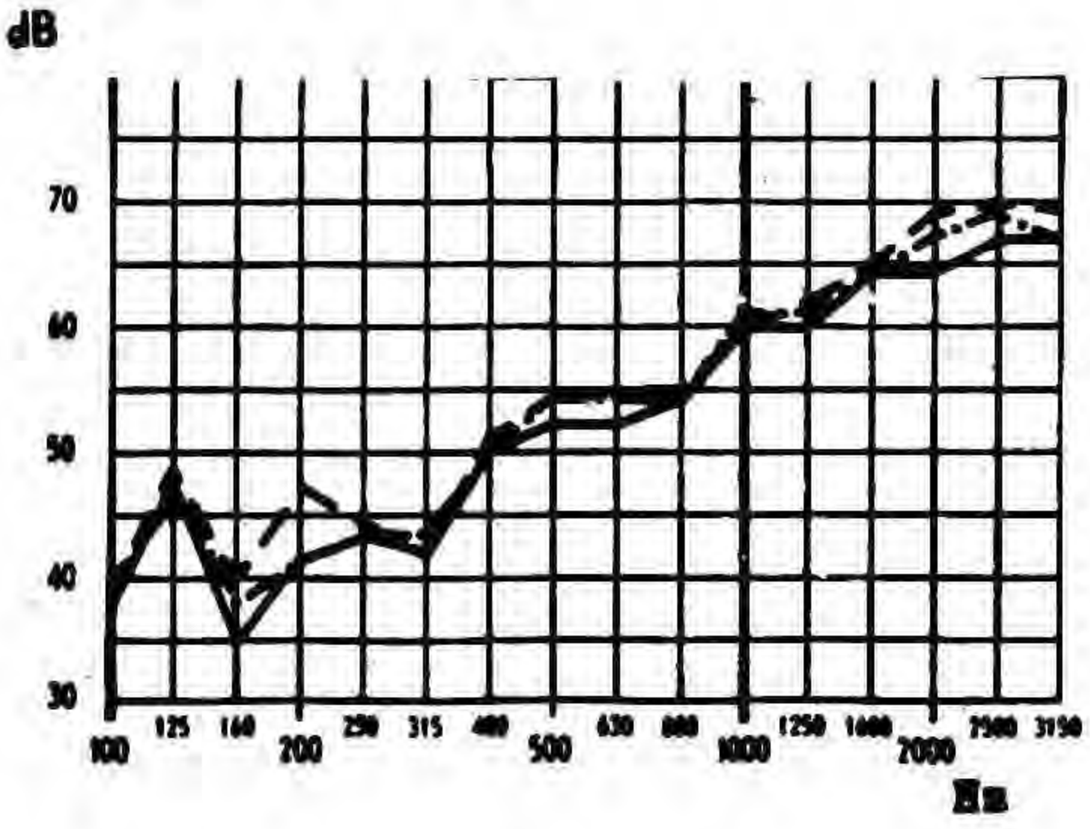

N35

FOURTH INTERNATIONAL CONGRESS ON ACOUSTICS
COPENHAGEN 21.-28. AUGUST 1962

THE EFFECT ON STEREOPHONIC REPRODUCTION OF FREQUENCY-DEPENDENT CROSSTALK BETWEEN LEFT AND RIGHT CHANNELS

H.D. Harwood, B.Sc., A.Inst.P., A.M.I.E.E.

Research Department, British Broadcasting Corporation.

SUMMARY: Crosstalk between the left and right channels of a stereophonic system may cause displacement or blurring of the sound images. The relationship between the degree of crosstalk and the amount by which the image is displaced or dispersed has been determined subjectively, and the effects of variables such as sound level, observer's position, acoustic environment and bandwidth of the programme have been investigated.

1. GENERAL: A serious difficulty in stereophonic sound systems is the unintentional transference of a portion of the signal from one of the channels to the other producing a displacement of the acoustic images. We borrow from the vocabulary of the telephone engineer and call this phenomenon "crosstalk". When the inter-channel crosstalk is dependent on frequency the different components of a complex sound are affected in varying degrees so that blurring and anomalous movement of the images may be observed. If the crosstalk is inversely proportional to frequency it will be most evident at low frequencies; the converse applies at high frequencies. In this connection it may be noted that time delay between the sum and difference channels (M and S) of a transmission system is equivalent to crosstalk, proportional to frequency, between left and right channels which is therefore most noticeable at high frequencies.

Experiments have been carried out to determine the subjective effects of various amounts of crosstalk. These effects depend on the position of the images and the frequency range of the programme, but are also influenced by the masking at the ends of the sound spectrum by the remainder of the signal. It is not permissible therefore to employ artificial signals such as bands of noise, and experiments were therefore carried out with recorded programme material covering various bandwidths. To investigate the most extreme variations in acoustic environment likely to be encountered, tests were made in a listening room designed for quality monitoring and also in a "dead" room employed for microphone calibration.

2. EXPERIMENTAL DETAILS: The experiment was intended to render the effects of crosstalk readily observable, thus simulating the most critical conditions likely to be encountered in practice. Other things being equal, the effect of crosstalk is greatest when the signal in one stereophonic channel is zero, and the experiments were therefore confined to this condition; the programme was applied to one channel only, producing an image which, in the absence of crosstalk, appeared at one side of the stage. The observers were eleven engineers experienced in judging the quality of stereophonic programmes.

For the first series of experiments, which were concerned with crosstalk occurring predominantly at high frequencies, the programme material consisted of a typical piece of Latin-American music, the bandwidth being restricted when required by low-pass filters. In a second series of tests, in which crosstalk was greatest at low frequencies, separate recordings of organ, bass drum and plucked double-bass were employed high-pass filters being used when it was desired to limit the frequency band in the bass. For the sake of completeness and as a check on earlier estimates a third set of tests was carried out, in which the crosstalk was independent of frequency and here the programme material consisted of male speech unrestricted in frequency range.

The listening room has a volume of 85 m^3 and a reverberation time of 0·3 sec. Fig. 1 shows the plan of the room and the experimental layout; a similar arrangement was adopted in the dead room. The observer faced the centre of the stage, a chair with a neck rest being used to provide accurate location of his head without interfering with those small movements which are thought to play an essential part in directional hearing. Most of the experiments were carried out with the observer in

the middle position, but the most critical tests were repeated with the observer to one side, and further to the rear, to investigate conditions in the usual triangular seating layout.

For the experiments concerned with crosstalk varying with frequency, the rate of change was maintained at 6 dB/octave over the whole audio-frequency range, which, in the absence of phase correction, involves a lag or lead of 90° in the phase of the crosstalk relative to that of the direct signal. The resulting 90° phase difference between the crosstalk and the direct signal was accepted as being generally associated with this form of crosstalk.

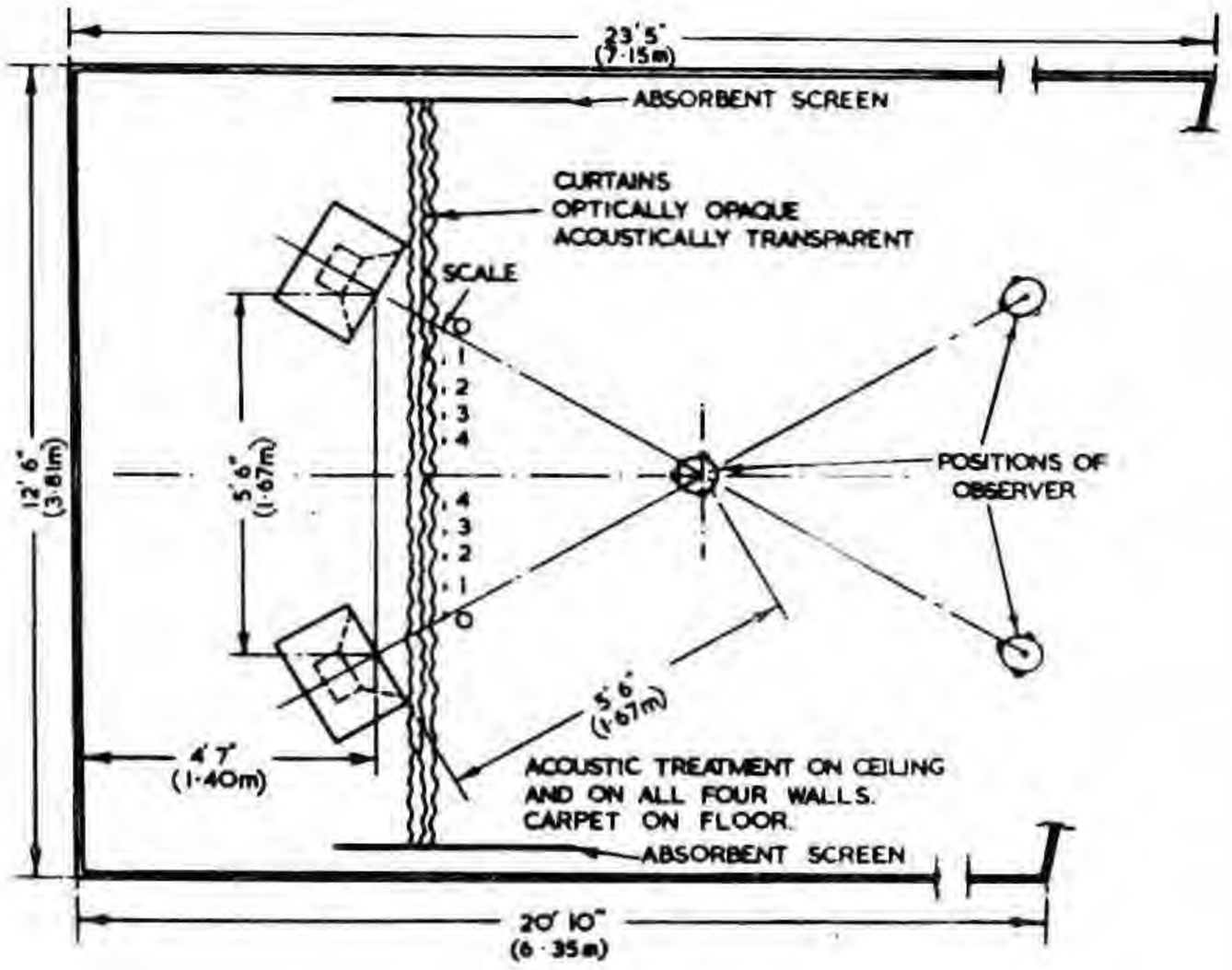

Fig. 1 - Plan of listening room

The filters employed to limit the programme frequency range were inserted in the common input channel and so did not introduce any further phase difference between left and right channels. The rate of cut-off of the filters was restricted to 12 dB/octave; the nominal cut-off frequency was that at which the attenuation was 3 dB. The axial frequency characteristic of the loudspeakers was within ± 2 dB of a smooth curve from 80 c/s to 13 kc/s and ± 3 dB to 40 c/s; the response curve at ± 45° in the horizontal plane was within 4 dB of the axial curve up to 10 kc/s. The greater part of the crosstalk energy is contained in the two octaves at either end of the spectrum, and over this range, the axial responses of the two loudspeakers were equal within ± ½ dB.

3. PRESENTATION OF TEST MATERIAL: Programme was presented on the loudspeaker on the left, artificial crosstalk being applied to the other, thus displacing some components of the image inwards, i.e. towards the centre of the stage. An attenuator which controlled the level of crosstalk was adjusted by the observer until the position of the inner edge of the image coincided with one of the divisions of the numbered scale shown in Fig. 1. The observer was also asked to determine the degree of crosstalk necessary to give the minimum perceptible displacement from position 0. This procedure was carried out twice and the whole experiment was then repeated with programme on the right-hand loudspeaker and crosstalk on the left. To avoid learning or adaptation by the observers during the tests, all were allowed to accustom themselves to the signals before the tests commenced. When the observer was in either of the side positions, the crosstalk was applied to the loudspeaker nearer to him, this being the more critical condition.

4. LOUDNESS LEVEL OF PROGRAMME: In a preliminary test, observers were asked to adjust the programme to their own preferred loudness and the mean level for the team was determined. The first set of tests was carried out at this level (corresponding to a maximum reading of 74 dB on a sound level meter when no weighting was used) which agrees with previously published data on the loudness preference of the general population.

It has been estimated that in the United Kingdom 75% of the population listen at sound levels between 68 dB and 84 dB, and further measurements were therefore carried out at these levels.

5. RESULTS: For each of the experimental conditions the position of the estimated inner edge of the image was plotted against the level of crosstalk, taken at a convenient reference frequency. Fig. 2, for a central observer in the listening room shows two such curves for crosstalk at high frequencies at sound levels of 68 dB and 80 dB. The curve for the preferred sound level of 74 dB lies exactly midway between them. It will be seen that the effect of the 12 dB difference in level is

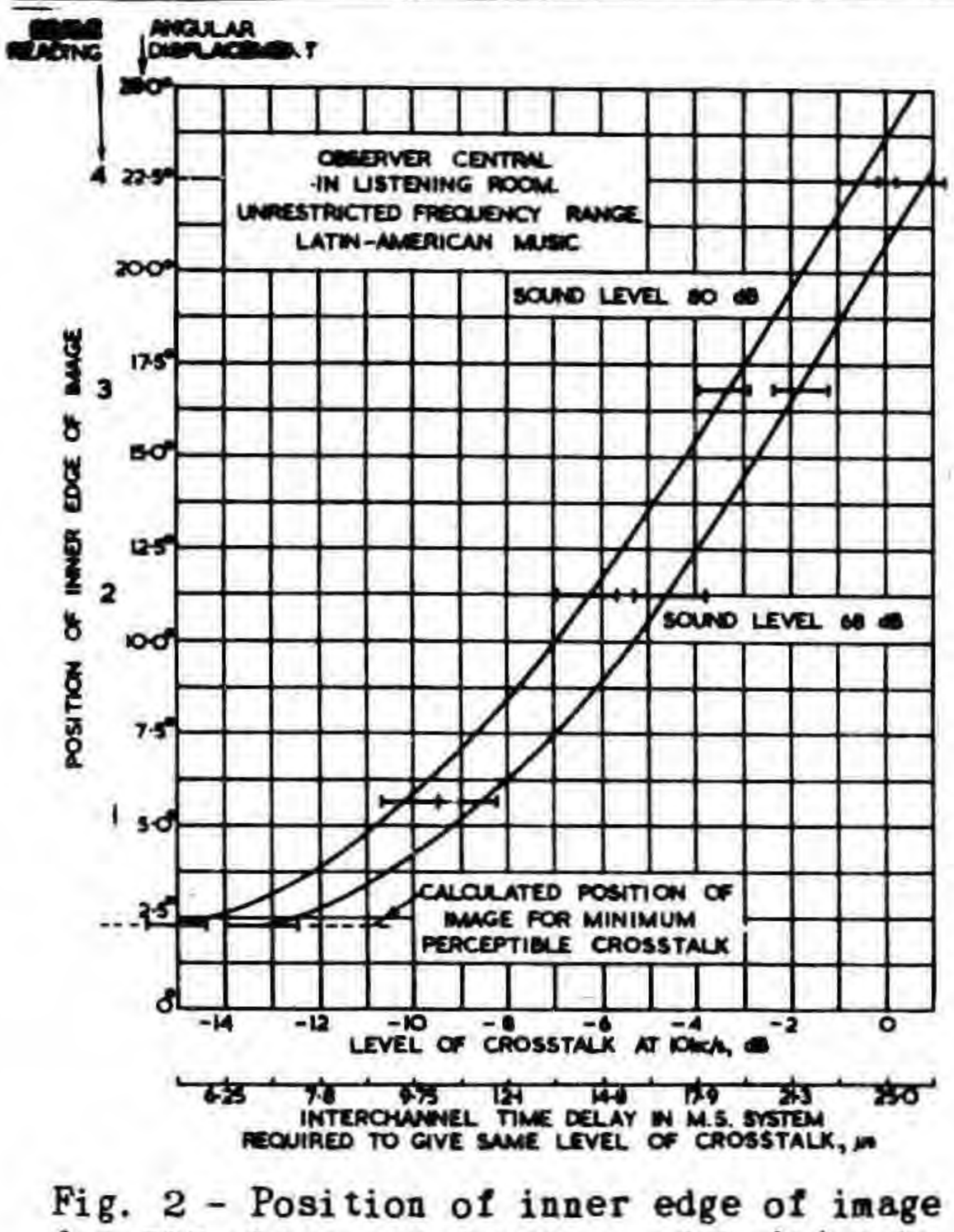

Fig. 2 - Position of inner edge of image for 50% of team as function of left/right crosstalk

⟷ Standard error

significant but small; a similar difference was found for crosstalk at low frequencies.

It is of interest to estimate a value of displacement corresponding to the minimum perceptible level of crosstalk. This displacement is the smallest image shift which can be detected in the particular experiment, and for this purpose it seems reasonable to assign a value corresponding to the probable error in the crosstalk levels obtained by individual observers. The mean of the probable error has been calculated for position 1 in Fig. 2 and is equivalent to ± 1/3 of a scale division or about ± 2°; this position is indicated in the figure and is in good agreement with the values of displacement obtained by extrapolation. The effect of a greater degree of crosstalk, and of the equivalent time delay in an M-S system can be read directly from the curves.

The levels of minimum perceptible crosstalk for a central observer are plotted as points in Fig. 3 for the different test conditions. Full lines have also been drawn to represent the 6 dB/octave variation in crosstalk with frequency and it was found possible to adjust the level of each line so that it lies very close to all the points relating to a particular test condition. It follows that, for the form of crosstalk under consideration, the amount by which the image is displaced or dispersed is almost unaffected by quite drastic limitation in programme bandwidth. A similar relation exists for the points corresponding to an image extending to scale divisions 1, 2, 3 and 4; this conclusion was confirmed directly by observing the position of the image while the cut-off frequency of the filter was being varied.

From the above it will be seen that the amount of crosstalk corresponding to a prescribed degree of impairment of the stereophonic image can be specified by a single figure giving the attenuation between left and right channels at some convenient frequency. The results which follow are given as attenuation in decibels at 50 c/s and 10 kc/s for low frequency and high frequency crosstalk respectively.

It will be seen from Fig. 3 that for 50% of central observers in the listening room, the minimum perceptible level of crosstalk at low frequencies, referred to 50 c/s, is equal to that of the programme; the corresponding figure at high frequencies, referred to 10 kc/s, is -13 dB. The minimum perceptible level for crosstalk independent of frequency is -19 dB. The statistical distribution of the results for the team was closely Gaussian and the figures for the most sensitive 10% of the observers are respectively -6 dB for the low-frequency crosstalk, -21 dB for the high-frequency crosstalk and -23 dB for the crosstalk independent of frequency. The difference between the two listening environments has a negligible effect on the results at high frequencies, possibly because the level of reflected sounds in front of the observer in the listening room is reduced by the directional properties of the loudspeaker. On the other hand, at low frequencies, for which the loudspeakers are omnidirectional, the effect of room acoustics is appreciable.

The levels required to displace the inner edge of the image to scale divisions 1, 2, 3 and 4 in the listening room are also shown in Fig. 3 for Latin-American music and for organ music. It will be seen that some of the points plotted involve a

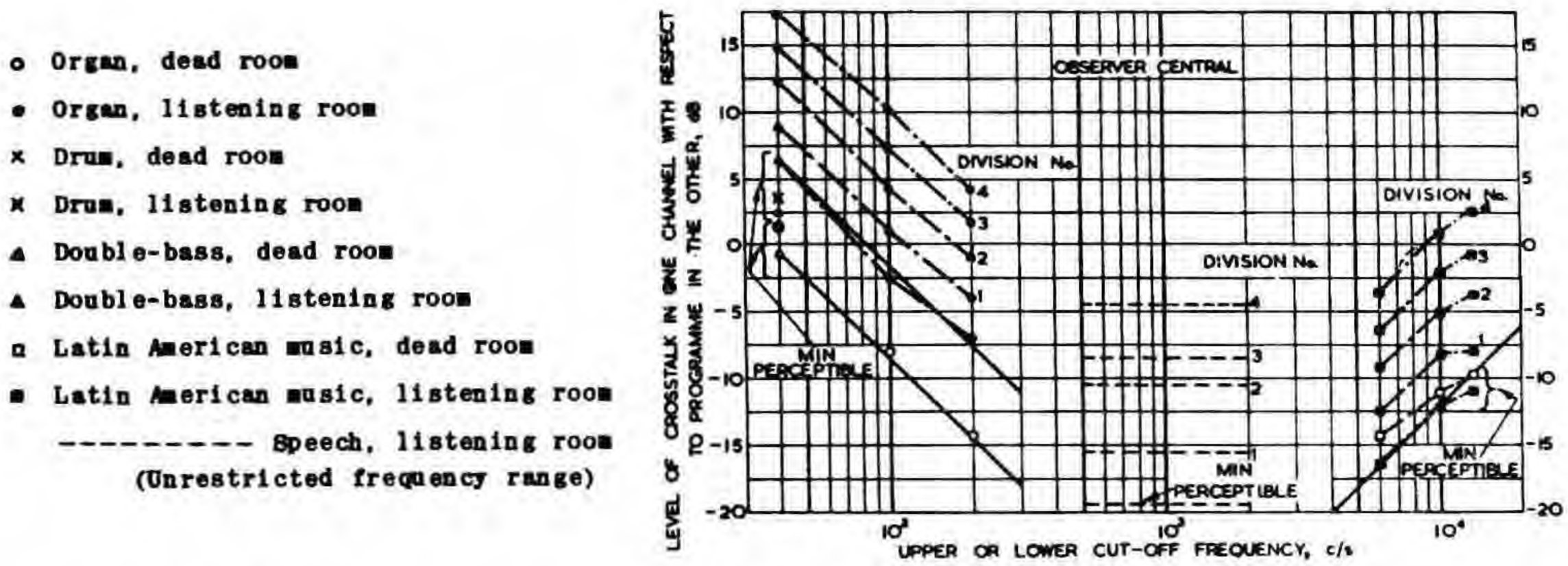

Fig. 3 - Level of crosstalk for 50% of team for different scale divisions, listening conditions and cut-off frequencies (-3 dB point)

greater level of crosstalk than of programme. This condition may easily occur at high frequencies if the crosstalk is the result of a difference in time delay between M and S signals; at low frequencies it is unlikely to arise but the points have been shown to complete the series. It should be noted that at low frequencies, at which the crosstalk lags 90° behind the programme signal, a greater amount of crosstalk is required to produce a given image displacement than if the two were in phase. The change of level needed for a particular image displacement in the dead room follows a law similar to that obtained in the listening room. With organ music however the effect of the difference in acoustics on the displacement becomes slightly less as the level of crosstalk is increased.

When the observer is seated to one side in the dead room, the level of minimum perceptible crosstalk is reduced at low frequencies by 3 dB and at high frequencies by 2 dB and the change is therefore in the direction expected. For the tests in the listening room the level was reduced by 4 dB at low frequencies but increased by 2 dB for high frequencies. The standard error in these measurements was 2 dB so the results at high frequencies are hardly significant statistically. It is, however, evident that there is no major difference in the minimum perceptible crosstalk for a central observer and one in the side position chosen.

Examination of the displacements calculated for the edge of the image at the minimum perceptible levels of crosstalk for a central observer shows that the distributions, which are again closely Gaussian, show no significant difference between displacements at high and at low frequencies for tests in either the listening room or the dead room. On the other hand, the mean displacement in the listening room, 1·9° in from the side of the stage, is significantly different from that of 2·7° obtained in the dead room, the standard errors being 0·17° and 0·25° respectively. Both image displacement and variation are therefore greater in dead than in normal listening conditions.

6. ACKNOWLEDGEMENTS: This paper is published by permission of the Director of Engineering of the British Broadcasting Corporation. The author wishes to thank his colleagues, J.R. Chew and A.A. Harris, for their help in the experimental work and calculations.

O35

FOURTH INTERNATIONAL CONGRESS ON ACOUSTICS
COPENHAGEN 21.-28. AUGUST 1962

Anisotropic Elastic Wave Propagation

Dr. Edgar A. Kraut , Institute of Geophysics and
Planetary Physics, University of California
Los Angeles 24, California, U.S.A.

A function theoretic method has been developed by the author for the solution of mixed initial and boundary value problems in anisotropic elastic wave propagation. The method has been sucessfully applied to compute the transient response of beryl and zinc crystals to pulsed excitation.
Consider the displacement field generated by a pulsed line source of normal stress lying on the surface of a transversely isotropic, homogeneous elastic half space. The line source lies in the boundary plane and is normal to the symmetry axis of the medium. The displacement field is of the form

$$\hat{U} = (u(x,z,t), 0, w(x,z,t)) \tag{1}$$

The components of the displacement field are subject to the equations of motion

$$A \frac{\partial^2 u}{\partial x^2} + (F + L) \frac{\partial^2 w}{\partial x \partial z} + L \frac{\partial^2 u}{\partial z^2} = e \frac{\partial^2 u}{\partial t^2} \tag{2}$$

$$L \frac{\partial^2 w}{\partial x^2} + (F + L) \frac{\partial^2 u}{\partial x \partial z} + C \frac{\partial^2 w}{\partial z^2} = e \frac{\partial^2 w}{\partial t^2} \tag{3}$$

In the isotropic limit
$A = \lambda + 2\mu \qquad F + L = \lambda + \mu \qquad L = \mu \qquad C = \lambda + 2\mu$
where λ and μ are the familiar Lame' parameters and e is the density.
On the boundary of the half-space

$$T_{zz} = F \frac{\partial u}{\partial x} + C \frac{\partial w}{\partial z} = -\delta(x) F(t) \qquad \text{at} \quad z = 0 \tag{4}$$

$$T_{xz} = L\left(\frac{\partial w}{\partial x} + \frac{\partial u}{\partial z} \right) = 0 \qquad \text{at} \quad z = 0 \tag{5}$$

where $F(t) = 0$ for t less than 0 .
The displacement field satisfies the initial conditions

$$(u, 0, w) = 0 \qquad \text{for} \quad t = 0 \tag{6}$$

$$\frac{\partial}{\partial t} (u, 0, w) = 0 \qquad \text{for} \quad t = 0 \tag{7}$$

In addition, the solution is to converge in the half-space defined by positive values of z. By taking the Laplace transform in time of the above equations and introducing

$$\hat{U} = \int_0^\infty \exp(- st)\hat{U} \, dt \tag{8}$$

the time transformed displacement field, we can construct integral representations for the displacement field of the form

$$\hat{U} = 1/2\pi i \int_{c-i\infty}^{c+i\infty} \hat{A} \exp(px - nz) \, dp \tag{9}$$

The condition that (9) satisfies the equations of motion (2) and (3) after they have been transformed with respect to time leads to a homogeneous set of linear equations of the form

$$M \hat{A} = 0 \tag{10}$$

The condition that the system have a non-trivial solution is that the determinant of the system must vanish

$$\Omega(p, n) = 0 \quad \text{where} \quad \Omega = \det | M | \tag{11}$$

This equation is called the slowness surface of the medium and it provides the relation between p and n .
In explicit form

$$n(p) = \pm \left(\frac{\Gamma \pm (\Gamma^2 - 4L C R S)^{\frac{1}{2}}}{2 LC} \right)^{\frac{1}{2}} \tag{12}$$

where

$R = (e - p^2 A)$
$S = (e - p^2 L)$
$\Gamma = (RC + LS + p^2 J^2)$
$J = (F + L)$

It is necessary to represent n(p) as a single valued function of p on a Riemann surface of four sheets over the complex p plane. The sheets are so chosen that

$$0 \leq \text{Re } n_1(p) \leq \text{Re } n_2 (p)$$

$$0 \geq \text{Re } n_3(p) \geq \text{Re } n_4 (p)$$

The restriction that the solution is to converge for $z \geq 0$ requires that the integration be confined to sheets 1 and 2 of the Riemann surface.
Corresponding to the two branches n_1 and n_2 there are two amplitude vectors, $\hat{A}_1$ and $\hat{A}_2$, which satisfy (10). This equation determines the ratio of the components of each of these vectors. Thus of the four scalar functions associated with the two vectors only two are independent and these two are determined by applying the two boundary conditions (4) and (5). Application of the boundary conditions to

$$U = 1/2\pi i \sum_{k=1}^{2} \int_{c-i\infty}^{c+i\infty} \hat{A}_k \exp s(px - n_k (p) z) \, dp$$

using the integral representation

$$\delta(x) = s/2\pi i \int_{c-i\infty}^{c+i\infty} \exp (spx) \, dp$$

yields the time transformed displacement field components,

$$\bar{u}(x,z,s) = \bar{F}(s)/2\pi i \int_{c-i\infty}^{c+i\infty} A(p, n_1,n_2)/D(p,n_1,n_2) \exp s(px - n_1 z) \, dp + \bar{F}(s)/2\pi i \int_{c-i\infty}^{c+i\infty} A(p,n_2,n_1)/D(p,n_2,n_1) \exp s(px - n_2 z) \, dp \tag{13}$$

$$\bar{w}(x,z,s) = \bar{F}(s)/2\pi i \int_{c-i\infty}^{c+i\infty} (A(p,n_1,n_2)/D(p,n_1,n_2)) L(n_1) \exp s(px - n_1 z) \, dp + \bar{F}(s)/2\pi i \int_{c-i\infty}^{c+i\infty} (A(p,n_2,n_1)/D(p,n_2,n_1)) L(n_2) \exp s(px - n_2 z) \, dp \tag{14}$$

where,

$A(p,n_1,n_2) = (Jpn_1)((L - J)n_2^2 - R)$
$D(p,n_1,n_2) = J(n_2 - n_1)((RC + p^2F^2)(RS/LC)^{\frac{1}{2}} + R(S + p^2L))$
$L(n_1) = (Ln_1^2 - R)/ Jpn_1$
$n_1(p) = +\left(\frac{\Gamma - (\Gamma^2 - 4LCRS)^{\frac{1}{2}}}{2LC} \right)^{\frac{1}{2}}$
$n_2(p) = -\left(\frac{\Gamma + (\Gamma^2 - 4LCRS)^{\frac{1}{2}}}{2LC} \right)^{\frac{1}{2}}$

The inversion of (13) and (14) into the time domain is accomplished by applying the Cagniard - De Hoop technique. This involves making a pair of conformal transformations

$$\mathrm{Re}\,(px - n_1 z) = -t\,, \quad \mathrm{Im}\,(px - n_1 z) = 0, \quad \mathrm{Re}\,(px - n_2 z) = -t \quad \mathrm{Im}\,(px - n_2 z) = 0$$

Inserting the functions $n_1(p)$ and $n_2(p)$ into these transformations and then squaring twice to remove the radicals yields the quartic parametric equation for the new paths of integration

$$p^4 + A(t/R,\theta)p^3 + B(t/R,\theta)p^2 + C(t/R,\theta)p + D(t/R,\theta) = 0 \qquad (15)$$

In this equation $\theta = \arctan x/z$. The coefficients are rational functions of $\sin\theta$, $\cos\theta$, and t/R. $R = (x^2 + z^2)^{\frac{1}{2}}$. Equation (15) can be solved exactly. The coefficients are real and therefore the roots, $p(t/R,\theta)$ occur in complex conjugate pairs. As the parameters t/R and θ vary the roots $p(t/R, \theta)$ trace the contours of integration upon the four sheeted Riemann surface over the complex p-plane. The shape and behavior of these paths as the parameters t/R and θ vary were determined using a digital computer. Paths were computed as a function of t/R for a representativeset of angles θ, using the numerical values of the elastic constants of beryl. The integrals in (13) and (14) can be rewritten in the form

$$\bar{u}(s,R,\theta) = 1/\pi \sum_{l,k} \int_{t_{a,b}}^{t_{c,d}} \mathrm{Im}\left(\frac{((A(p_{1,k}(t/R,\theta);n_1(p_{1,k}) ,n_2(p_{1,k})))}{((\ D(p_{1,k}(t/R,\theta);n_1(p_{1,k}),\ n_2(p_{1,k})))} \frac{dp}{dt}_{1,k}\right) e^{-st}\,dt$$

$$\bar{w}(s,R,\theta) = 1/\pi \sum_{l,k} \int_{t_{a,b}}^{t_{c,d}} \mathrm{Im}\left(\frac{A(p_{1,k}(t/R,\theta);\ n_1(p_{1,k}),n_2(p_{1,k}))\ L(n_1(p_{1,k})}{D(p_{1,k}(t/R,\theta);\ n_1(p_{1,k}),n_2(p_{1,k}))} \frac{dp}{dt}_{1,k}\right) e^{-st}\,dt$$

where the sum is understood to range over piecewise continuous portions of arc. It is assumed that the source strength $F(t)$ is a delta function so that $\bar{F}(s) = 1$. The inversion into the time domain can be accomplished by inspection. It gives

$$u(t/R,\theta) = \sum_{l,k} (H(t - t_{a,b}) - H(t - t_{c,d})) \times \frac{1}{\pi}\ \mathrm{Im}\left(\frac{A(p_{1,k}(t/R,\theta),\ n_1(p_{1,k}),n_2(p_{1,k}))}{D(p_{1,k}(t/R,\theta),\ n_1(p_{1,k}),n_2(p_{1,k}))} \frac{dp}{dt}_{1,k} \right)$$

$$w(t/R,\theta) = \sum_{l,k} (H(t - t_{a,b}) - H(t - t_{c,d})) \times \frac{1}{\pi}\ \mathrm{Im}\left(\frac{A(p_{1,k}(t/R,\theta),n_1(p_{1,k}),n_2(p_{1,k}))}{D(p_{1,k}(t/R,\theta),n_1(p_{1,k}),n_2(p_{1,k})} L(n_1(p_{1,k})) \frac{dp}{dt}_{1,k} \right) \qquad (16)$$

The summation is again understood to be over arcs of the path obtained by solving (15). The pieces of arc are numbered with the index l, while the index k refers to the sheet of the Riemann surface on which the arc lies. The indices a,b and c,d refer to the beginning and ending points of the lth .arc lying on the kth. sheet. (k = 1,2). H is the Heaviside unit step function. When θ = 90 degrees so that the source and receiver are on the surface of the half space there is a pole on the path of integration which gives rise to a delta function singularity propagating parallel to the surface direction and traveling with the appropriate Rayleigh speed for the medium. This is the so called Rayleigh pulse and its presence in an anisotropic solid with an axis of rotational symmetry normal to the boundary surface should be expected.

The displacement field response to a pulsed surface line source of normal stress exhibits the same pulse fronts as would be observed in the case of an un--bounded medium. There are in addition certain new pulse fronts arising from the presence of the boundary of the half-space. These new pulse fronts are plane and and correspond to the conical pulse fronts that are observed in the solution of the corresponding isotropic problem. The natural critical angle associated with the conical pulse front is the angle that the conical pulse front makes with the horizontal. In the isotropic case the angle of a position vector to the point of tangency of the conical pulse front is the critical angle and this is equal to the angle that the conical pulse front makes with the horizontal, since for isotropy the wave surfaces are of circular cross-section. The disturbance at the receiver will consist of a suite of pulses, each followed by a decay whose time constants depend on the degree of anisotropy. The number of pulses in the suite depends on the receiver angle θ. It can vary between two and five in beryl. In addition there is also a Rayleigh pulse which has been previously mentioned. The quantitative time dependence of the solution in the vicinity of a pulse front with onset time $t_{a,b}$ can be determined by expanding the exact solution (16) in powers of $(t - t_{a,b})$. The singularity in the time dependence is determined by the order of the saddle point associated with the pulse arrival. In the case of the conical pulse, the singularity in time near the onset is determined by the order of the branch point associated with the onset. The results for beryl give displacement field components behaving as $O(t - t_{a,b})^{-\frac{1}{2}}$ for pulses associated with the passage of a sheet of the wave surface passed the receiver. However, there are certain singular angles at which there are tips of cusps on the wave surface. This is connected with the confluence of saddle points and results in a time dependence for the displacement field components behaving like $O(t - t_{a,b})^{-2/3}$. Near the onset of the conical pulse the field components behave like $O(t - t_{a,b})^{+\frac{1}{2}}$. Numerical calculations were made for the displacement field experienced by a receiver on the surface and by a receiver on the epicenter of the half-space. An examination of the computational results in these two special cases does not reveal any marked differences in the general shape of the transient response as compared to the isotropic case. This result is not unexpected, because the cuspidal edges on the wave surface of beryl are not intercepted at zero or ninety degrees. It can be expected that even at receiver angles which do intercept the cusps the general transient response exhibited by the components of displacement will strongly resemble the isotropic results at the same receiver angle. There will be, however, additional deflections superposed at the times corresponding to the arrivals of edges of the cusps at the receiver. The time constants of the pulse tails are also somewhat altered by the introduction of anisotropy.

In summary, the introduction of anisotropy of the type considered here has the following effects on the theoretical displacement field:

1). The number of arrivals can vary between two and six depending on receiver angle.
2). The times of the arrivals are shifted by an amount depending on the magnitudes of the elastic constants of medium.
3). The time constants of the pulse tails depend on the degree of anisotropy.
4). The overall shape of the transient response in displacement retains a strong resemblance to the corresponding isotropic result.

P35

FOURTH INTERNATIONAL CONGRESS ON ACOUSTICS
COPENHAGEN 21.-28. AUGUST 1962

Propagation des ondes de torsion dans le plexiglas

M. W.Bismuth, Mlle D.Bonsignour (Centre de Recherches Scientifiques, Marseille) & M. J. Wehr (Inst.Probl.fond.Tech.Varsovi

Nous avons étudié le comportement dynamique d'un barreau de plexiglas de sections différentes et soumis à des températures variable

La méthode utilisée consistait à mesurer la vitesse de propagation et l'amortissement d'une onde de torsion par une méthode de phase; elle a été employée antérieurement pour étudier la propagation des ondes élastiques dans le caoutchouc type "pure gomme". /1/

PRINCIPE DE LA METHODE

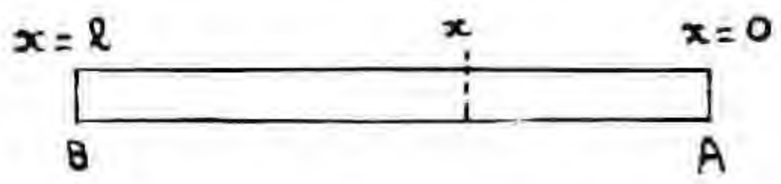

On entretient dans un barreau visco-élastique AB de longueur ℓ des vibrations transversales à l'extrémité B .

Une onde amortie peut s'écrire d'une façon générale sous la forme

$$y = y_o \; e^{-\alpha x + i\omega(t - \frac{x}{c})}$$

Le mouvement vibratoire au point x dans le cas de ce barreau est donné par la somme de toutes les vibrations dues aux différentes ondes qui se réfléchissent sur les faces A et B et qui arrivent en x des deux côtés.

Si cette réflexion se fait sans absorption, on a au point x

$$y(x,t) = e^{i\omega t}\left[e^{\alpha x + i\omega\frac{x}{c}} + e^{-(\alpha x + i\omega\frac{x}{c})}\right].$$

Soit $y(0,t) = 2\, e^{i\omega t}$, et $y(x_1,t) = Z_1\, e^{i\omega t}$

Le déphasage de $y(x_1,t)$ sur $y(0,t)$ sera θ , tel que

$$tg\ \theta_1 = -\, tg\ \frac{\omega}{c}\, x_1 \;\; th\ \alpha\, x_1$$

En fait, on peut mesurer le déphasage entre les amplitudes et x_1 et 0 au moyen d'un appareillage électronique qui introduit un

déphasage supplémentaire constant θ_o de sorte que la formule précédente devient :

$$tg\ (\theta_o - \theta_1) = tg\ \frac{\omega}{c}\ x_1\ th\ \alpha x_1 \qquad (1)$$

On pourra donc tracer la courbe théorique reliant θ et x (Fig.1). La relation (1) montre que les zéros successifs $\frac{n\pi}{K} = \frac{n\pi c}{\omega}$ peuvent nous donner c. En appliquant cette relation où le premier membre est l'ordonnée lue sur la courbe pour une abscisse donnée et en donnant à c la valeur précédemment trouvée, on pourra déterminer α.

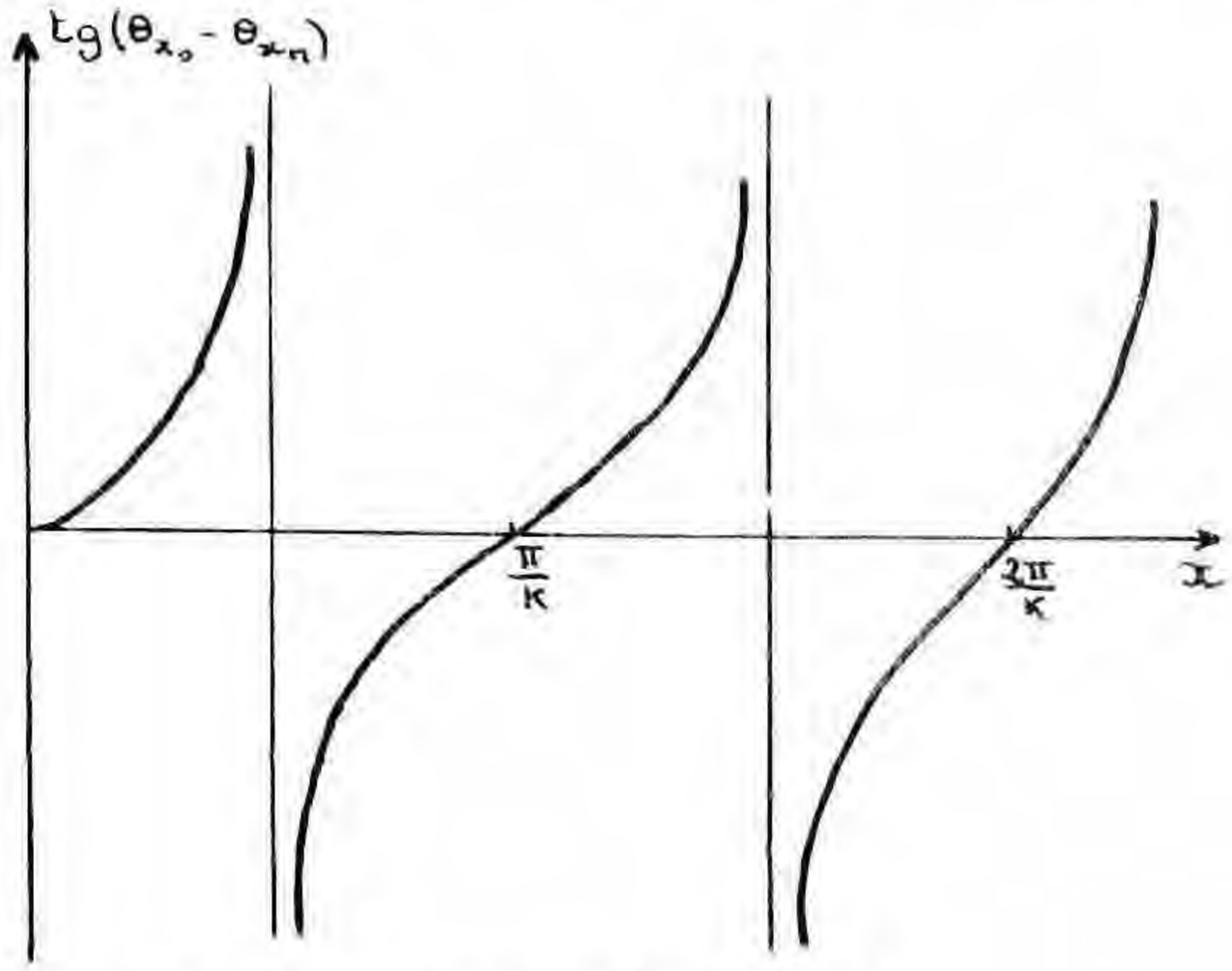

Fig.1 - Courbe théorique

METHODE EXPERIMENTALE

Les vibrations étaient excitées dans le barreau par un générateur et recueillies en un point variable par un récepteur. Nous avons choisi, comme générateur, un graveur de disque légèrement modifié et dont le burin avait été remplacé par une aiguille se terminant par une demi sphère. Les vibrations mécaniques du plexiglas recueillies au point x étaient transformées en tension électrique par un récepteur constitué par une barre au titanate de baryum monté de façon à avoir une courbe de réponse aussi linéaire que possible en fonction de la fréquence.

Dans une première série d'expériences, on avait disposé le graveur de façon que l'aiguille vibre parallèlement à l'axe du barreau. On s'est aperçu que les ondes produites contenaient une composante longitudinale et une composante de flexion, ce qui apparemment déformait les courbes. On a donc cherché à exciter des ondes de torsion pures.

Après maints essais, on a adopté le dispositif suivant.

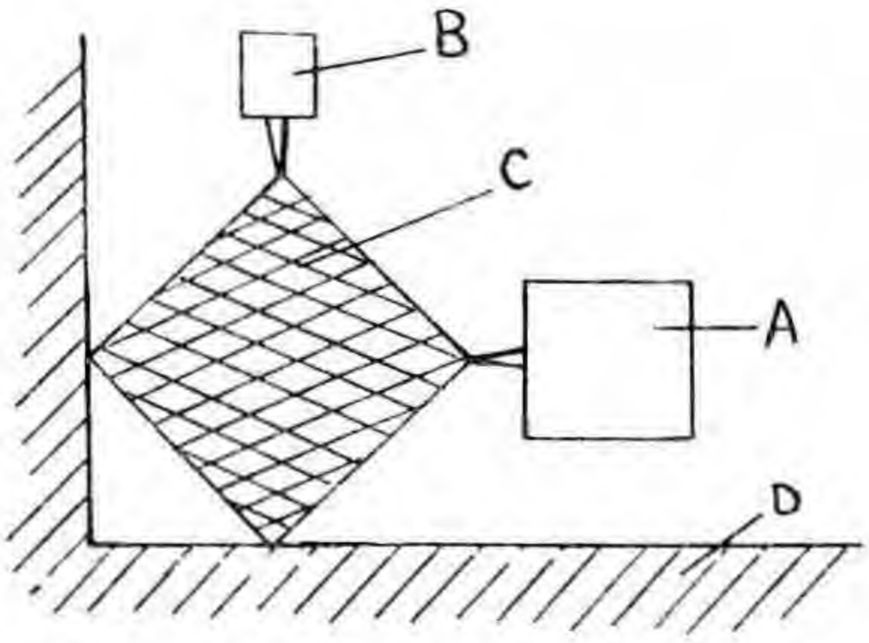

A - graveur C - barreau
B - récepteur D - support

On place le barreau sur une arête et on l'y maintient à l'aide d'un étau dont les faces intérieures sont recouvertes de caoutchouc. L'aiguille du graveur est placée sur une arête et vibre perpendiculairement à la direction de propagation de l'onde dans le barreau. On pose le pick-up sur l'arête adjacente et on mesure ainsi la phase existante entre le point $x = 0$ (graveur) et les points successifs x_1, x_2, ... x_n.

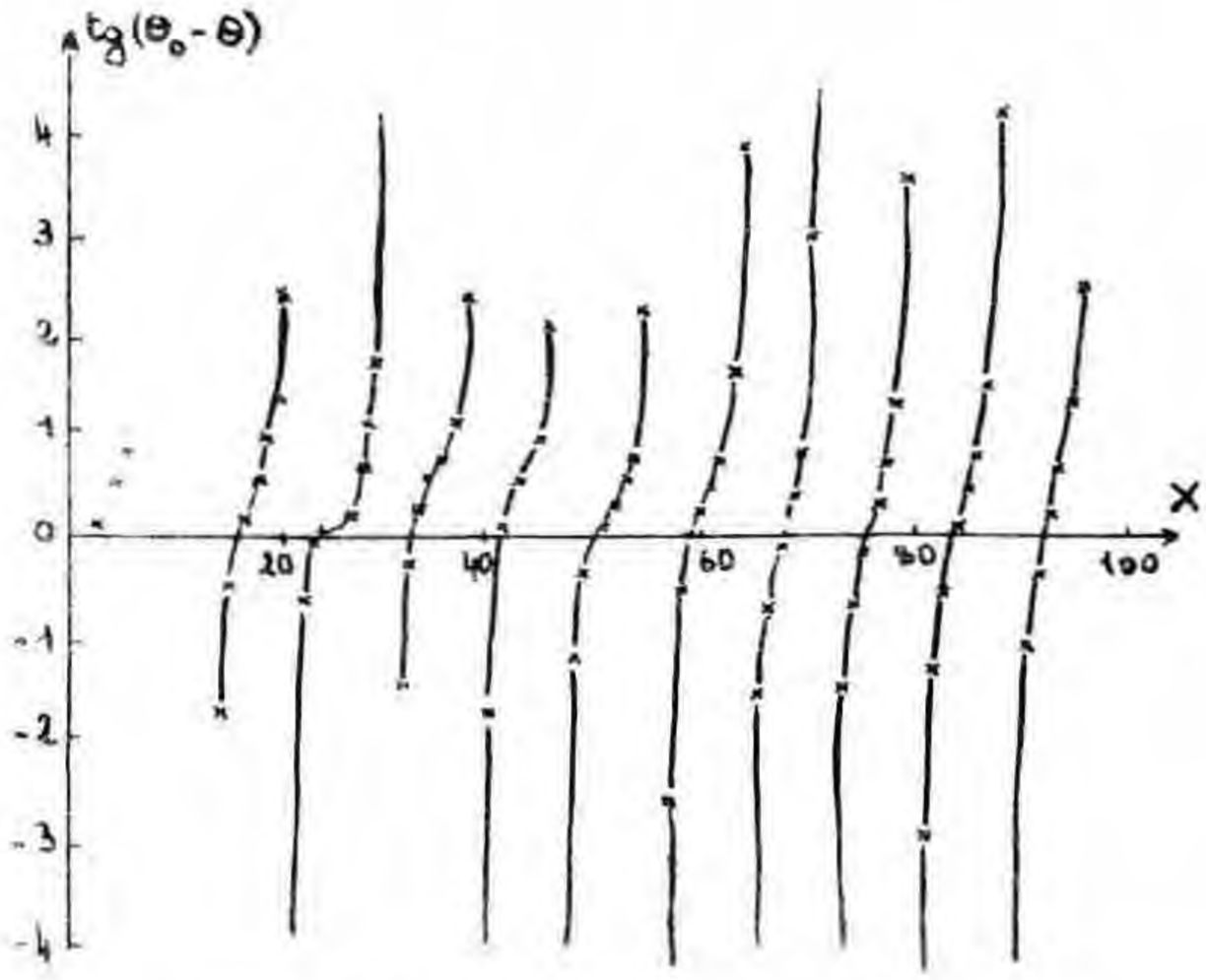

Fig.2 - Ondes de torsion dans la barre n°1

L'expérience a confirmé que l'on obtenait ainsi des ondes de torsion car les courbes expérimentales se sont révélées semblables à la courbe théorique (Fig.2).

L'ensemble du montage était enfermé dans une enceinte thermostatique qui, grâce à un jeu de thermocouple, nous donnait une température constante (a ± 0,25 % près).

Tout le montage expérimental reposait sur une fondation flottante constituée par un bloc lourd en pierre placé en sandwich entre deux semelles de liège de 10 cm d'épaisseur.

La tension du graveur était fournie par un générateur type Férisol. La tension électrique recueillie par le récepteur, amplifiée par un amplificateur de mesure était filtrée par l'intermédiaire d'un filtre demi octave. On mesurait la différence de phase entre la tension du graveur et la tension de sortie du filtre par l'intermédiaire d'un phasemètre électronique.

RESULTATS EXPERIMENTAUX

Nous avons étudié la propagation des ondes de torsion dans des barreaux de plexiglas de 1 m de long et de sections carrées de 1 cm et 1,5 cm de côté. Nous avons mesuré ainsi $c(\omega)$ et $\alpha(\omega)$ à différentes températures. Nous avons ensuite exprimé ces résultats, en parties réelle et imaginaire E_1 et E_2 du module complexe E^*.

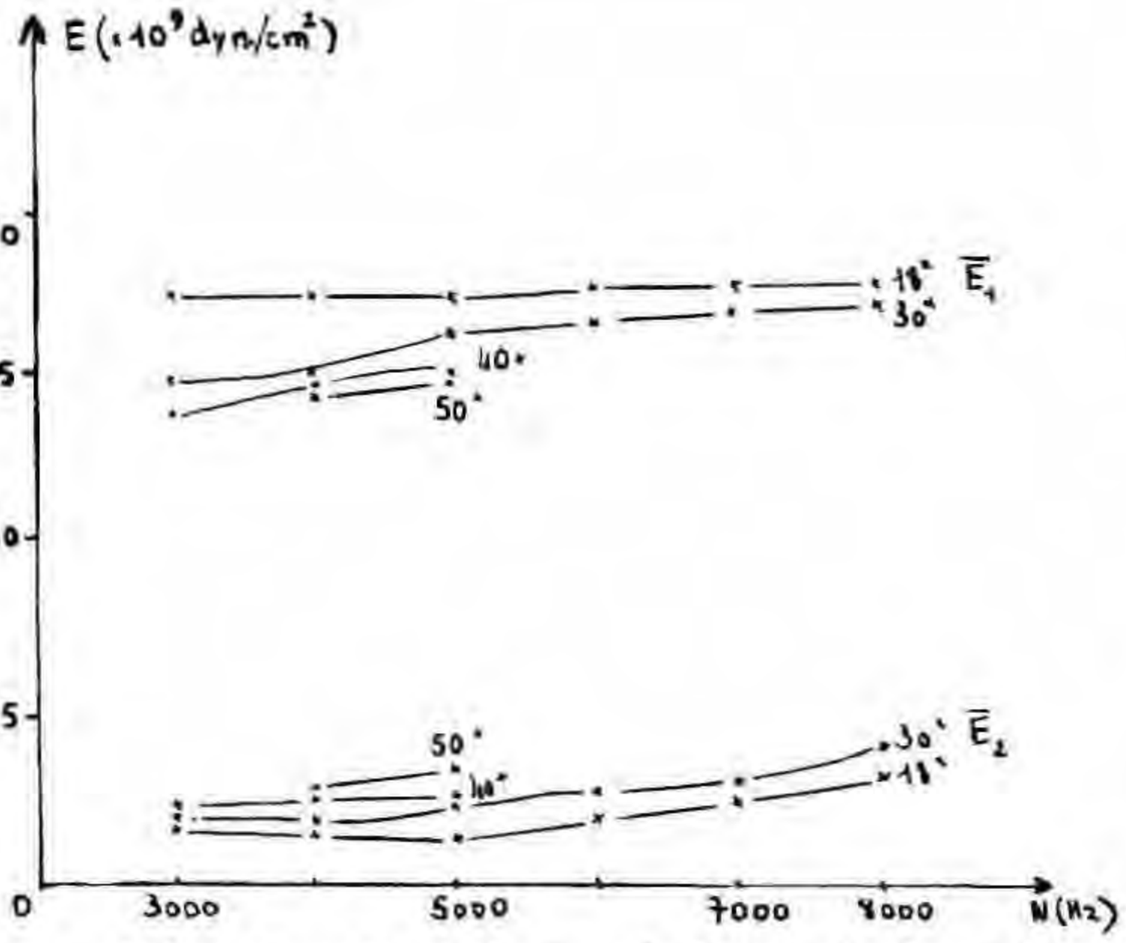

Fig.3 - Parties réelle et imaginaire du module complexe dans la barre n°1

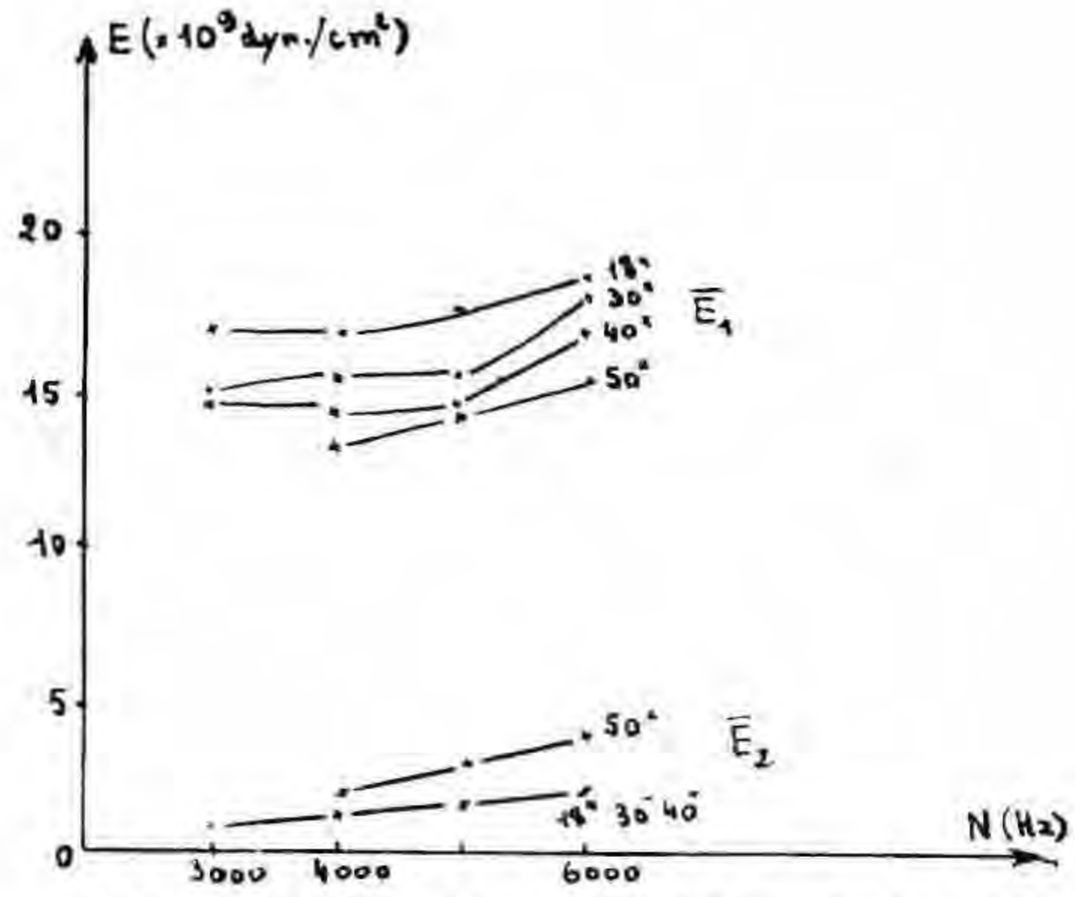

Fig.4 - Parties réelle et imaginaire du module complexe dans la barre n°2

On a appliqué ensuite la méthode des variables réduites et nous avons obtenu ainsi pour les deux barreaux les courbes des figures 5 et 6, ce qui vérifie la théorie de Ferry.

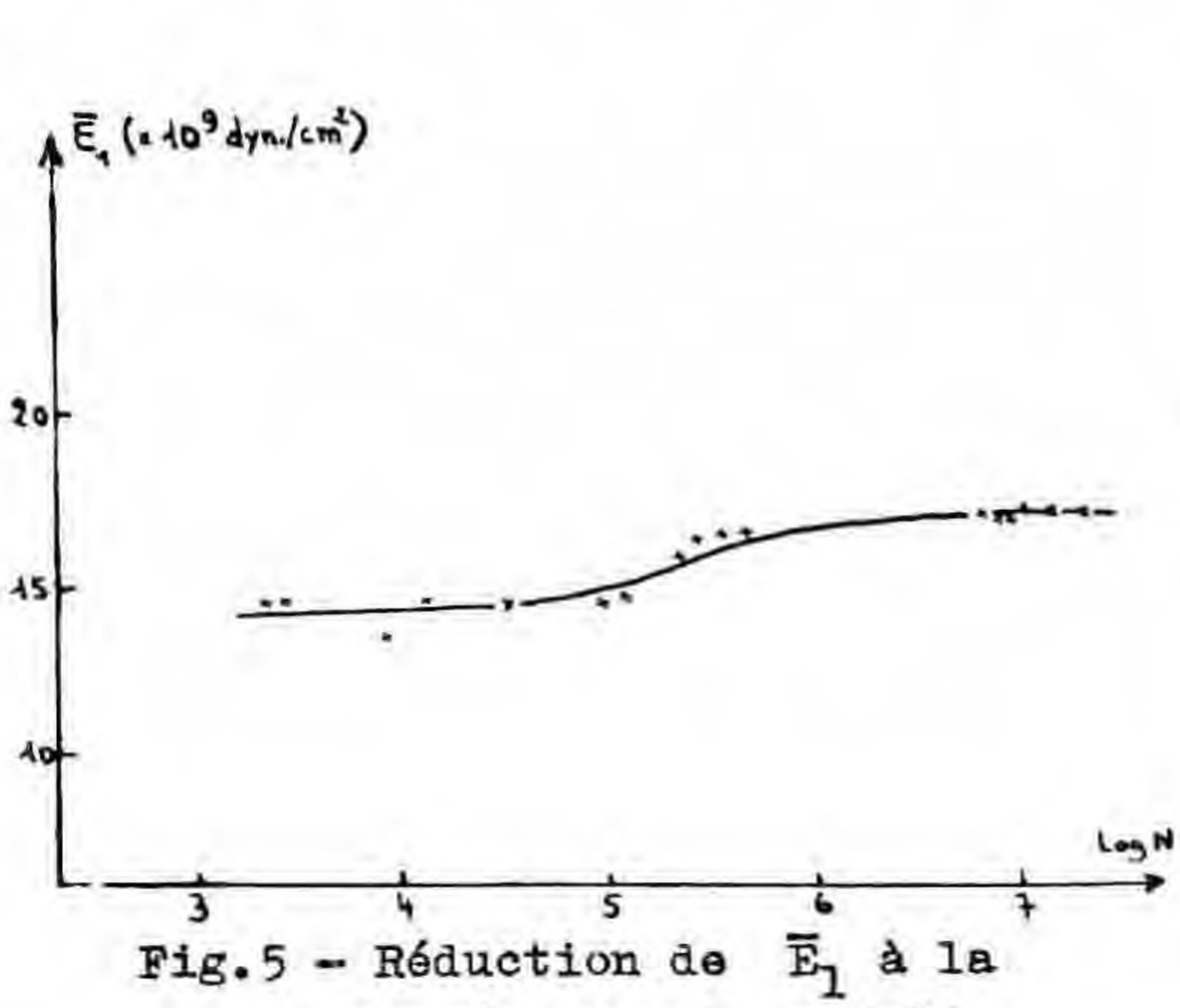

Fig.5 - Réduction de $\bar{E}_1$ à la température T_s = 45°C Barre n°1.

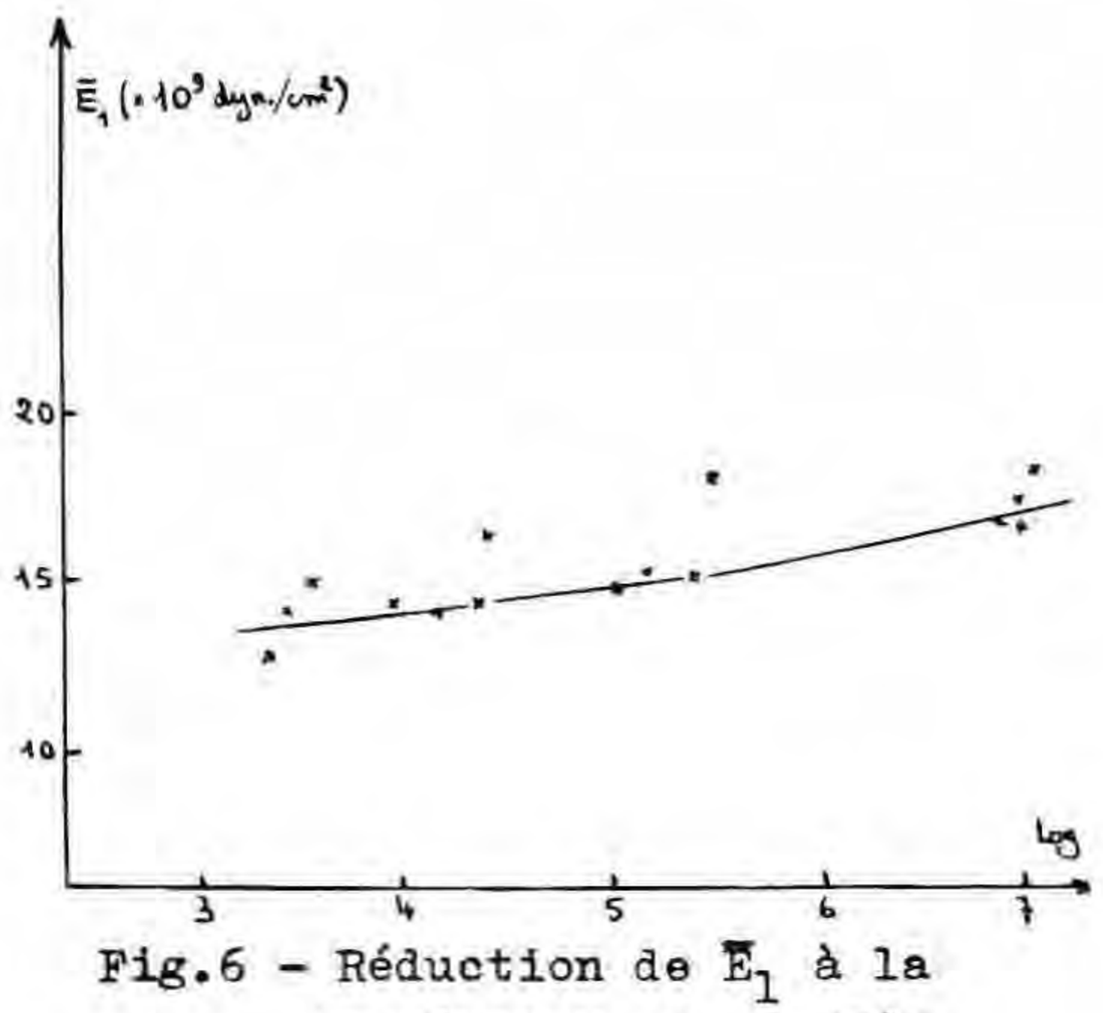

Fig.6 - Réduction de $\bar{E}_1$ à la température T_s = 45°C Barre n°2.

/1/ 3° Congrès international d'Acoustique, Stuttgart, 1959.

G36

FOURTH INTERNATIONAL CONGRESS ON ACOUSTICS
COPENHAGEN 21.-28. AUGUST 1962

Shape of Human Mouth based on Speech Pressure Distribution close to the Mouth.

H. S. LEMAN

Standard Telecommunication Laboratories Limited, Harlow (England).

Summary

These measurements were made to provide information on the shape of the human mouth, for use in the development of an artificial mouth.

The average size and shape of the human mouth can be obtained from speech pressure distributions in horizontal and vertical planes close to the mouth.

The apparent width of the mouth whilst talking is greater than the height. The opening is large at low frequencies, and both width and height decrease for the higher speech frequencies.

Introduction and Method

In order to determine the size and shape of the human mouth, it is necessary to make measurements closer than 4 cms. to the lips so that the effect of small changes in size can be observed.

Papers have been published [1, 2, 3] for measurements from 5 to 100 cms. from the lips, but very few at less than 4 cms.

The basic method is similar to that used by other observers, in which a selected test sentence is repeated a number of times and the average speech pressure determined at different positions by a small exploring microphone. A fixed monitor microphone is used to measure the speech level, the position of the head of the talker being controlled by a lip gauge and a pad on the forehead.

The "puffs" of air from the mouth, whilst speaking, give spurious readings from a microphone placed close to the mouth. A graded wire mesh "puff" screen was placed round the tip of the exploring probe microphone. This gave adequate protection for all sounds except the plosive /p/. In the test sentence "The speech sounds in english ..", used by Dunn and Farnsworth[1], the /p/ has been replaced by /v/. The sentence can still be spoken easily with this modification and the excessive air blast is avoided.

The complete sentence was used for each talk and the output from both microphones measured on an r.m.s. speech energy meter. It was found by experiment that greater consistency was obtained by using the complete sentence, instead of a fixed time portion.

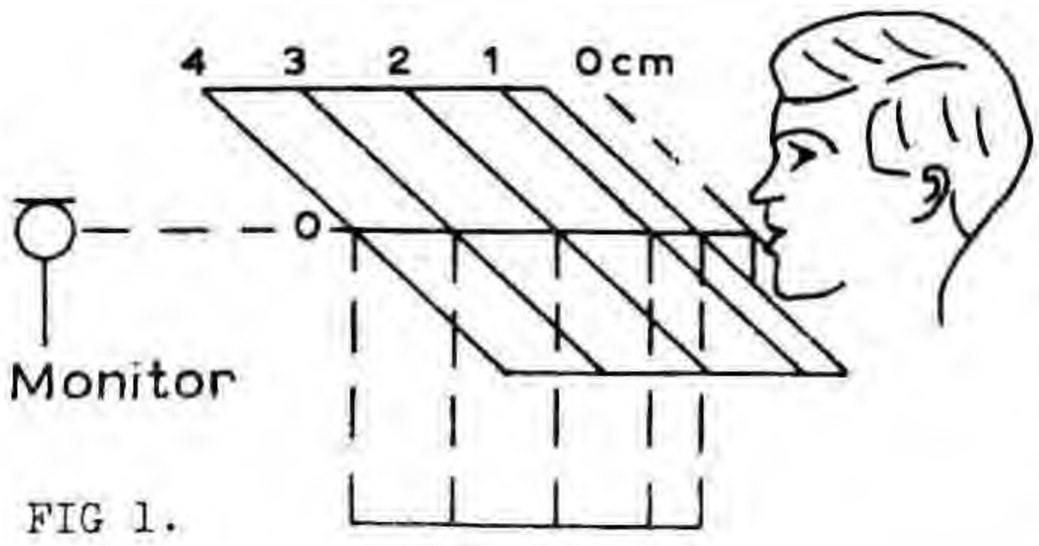

FIG 1.

Fig.1 shows the horizontal and vertical planes in which speech pressure measurements were made. The exploring microphone was moved along the lines shown, at distances from 0.5 cm. in front of the lip plane, up to 4 cms. in an axial direction. In the horizontal and vertical directions, measurements extended to 4 cms. from the axis. Rectangular coordinates were used to define the position of the microphone, because this gave a convenient method of graphical display.

The outputs from the two microphones were recorded on a twin-track tape recorder through a "white speech" network and the outputs examined in three frequency bands, 200 - 400, 1000 - 1600 and 2800 - 3400 c/s. Instrumental errors on repetitions were less than 0.2 db.

Results

The speech pressure measurement for each position was adjusted by the corresponding reading from the fixed microphone to compensate for changes in talking level.

The pressure along a transverse horizontal line, parallel to the plane of the lips, was plotted from 4 cms. to the right, across the mouth axis to 4 cms. to the left, as shown in Fig. 2a. This gave a pressure which was low at either side and increased to a maximum in front of the mouth orifice. At 0.5 cm. from the lips the

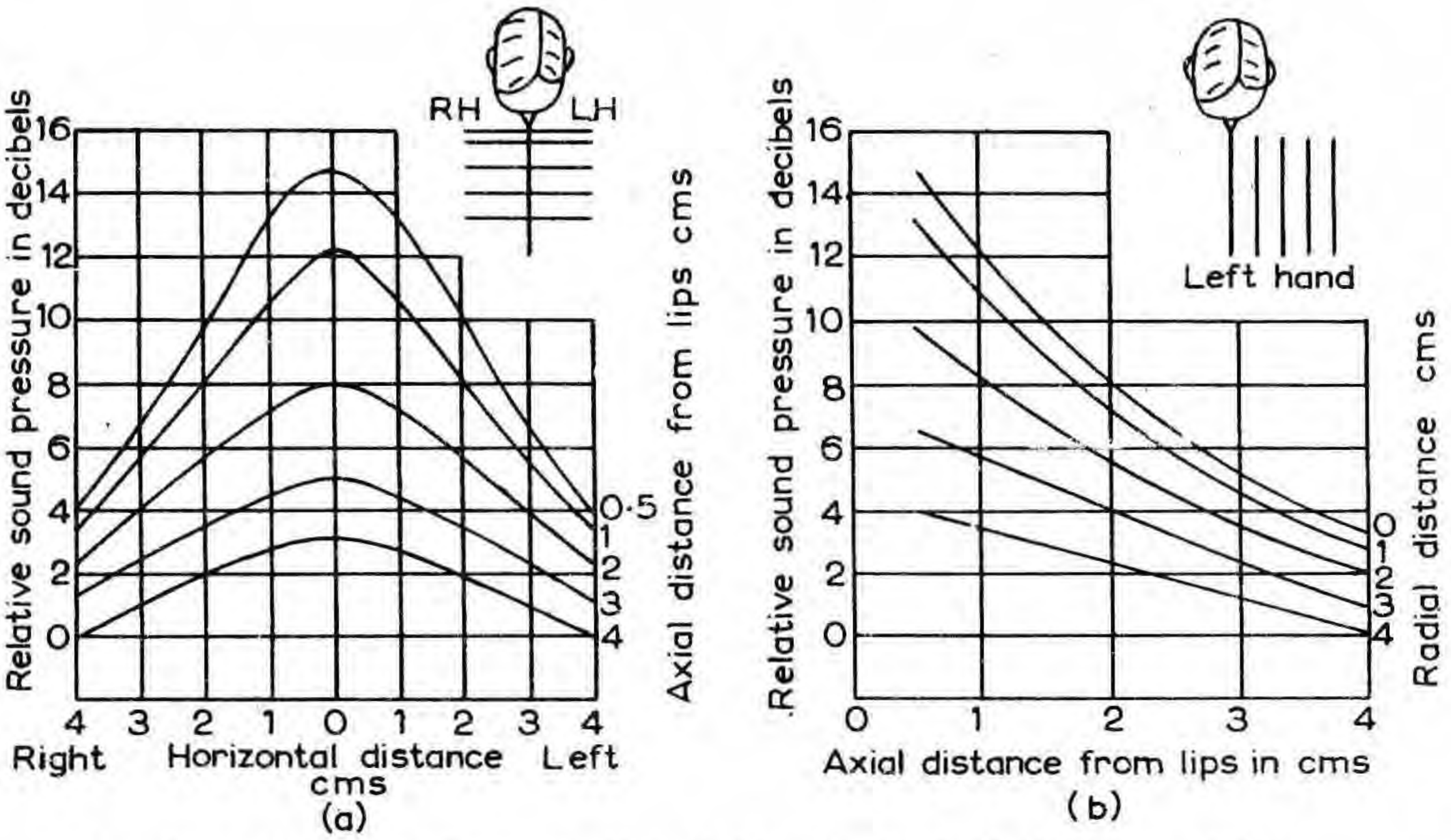

Fig. 2. Speech sound pressure distribution in front of the human mouth. Horizontal plane. Midfrequency 1300 c/s.

pressure changes rapidly with distance on either side of the axis, whilst at 4 cms. from the lips the change is more gradual. This change of pressure with transverse distance can be used to determine the size of the orifice. For a small orifice the change of transverse pressure is more rapid than for a large orifice.

The information in Fig. 2a has been replotted in Fig. 2b. The curve marked Radial Distance 0 shows the axial pressure at different distances from the lips. The other curves show the pressure along lines parallel to the axis, but displaced at distances 1, 2, 3 and 4 cms. to one side, as indicated in the diagram at the top of the figure. The shape and spacing of these extra curves gives additional information about the pressure distribution on either side of the axis, which cannot be obtained from the axial curve alone. The steady air stream from the mouth and "puff" from plosives does not affect the readings obtained at the side of the mouth as much as those directly on the axis.

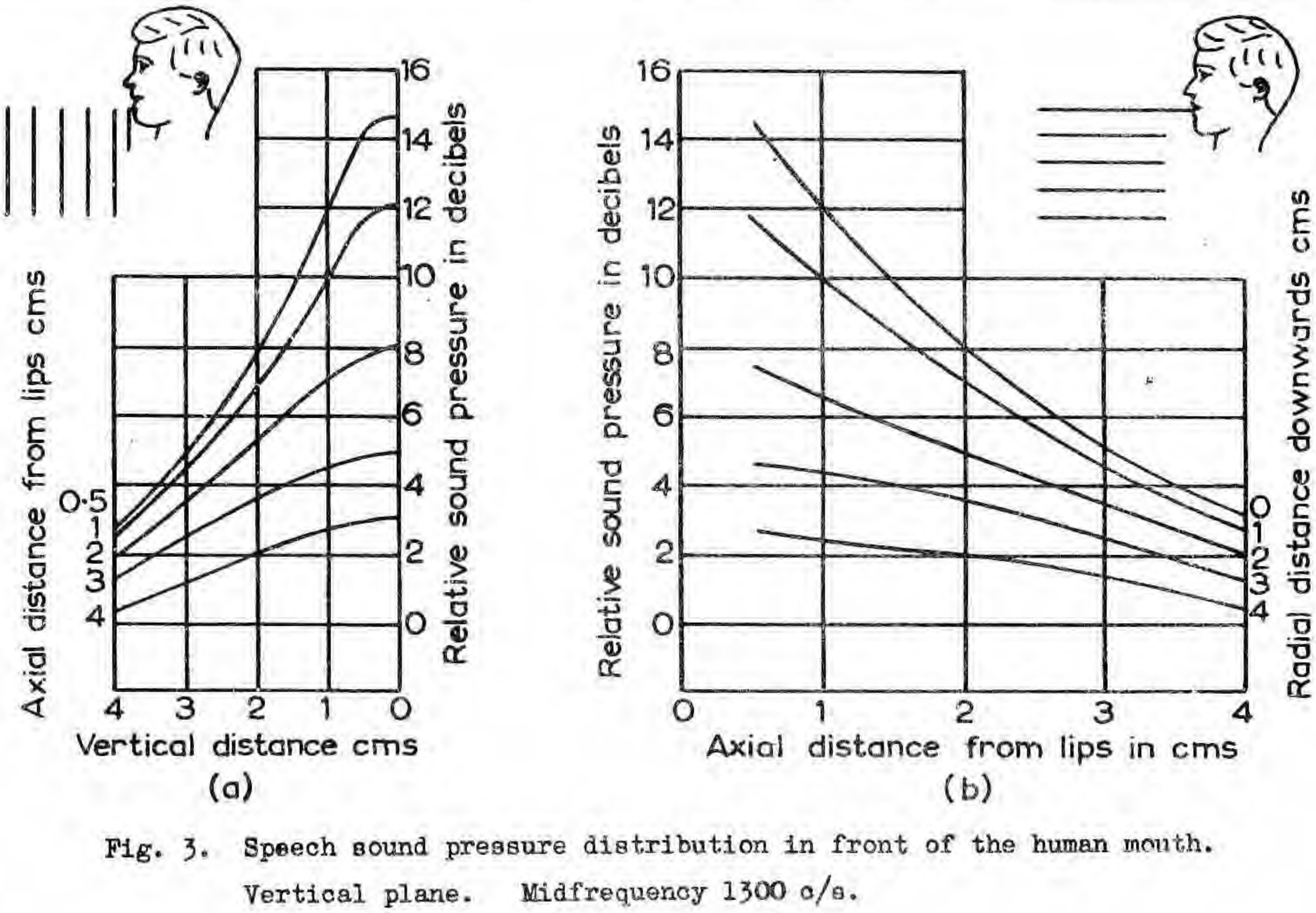

Fig. 3. Speech sound pressure distribution in front of the human mouth.
Vertical plane. Midfrequency 1300 c/s.

By using the type of plot shown in Fig. 2b, it is possible to compare these with similar plots from artificial mouths, and slide one trace over the other to obtain a best fit for the curves. Thus the size and shape of an orifice which is equivalent to a human mouth whilst talking, can be obtained. When the best fit is obtained, it is found that the plane of the orifice of an artificial mouth does not normally coincide with the lip position obtained in the human distribution. For a small orifice of 18 mm. diameter, the "equivalent lip position" of the artificial mouth is 1 cm. in front of the orifice. As the orifice gets larger, the "equivalent lip position" moves nearer to the orifice.

The curves in Fig. 2 are for the mid-frequency region of 1300 c/s. The sharpness of the curves for the horizontal distribution at 0.5 and 1.0 cm. from the lips, shown in Fig. 2a, changes with the frequency band measured. At the lower frequency band around 400 c/s. they are broader than in Fig. 2a, and become more narrow at 3100 c/s, thus indicating a decrease in the apparent size of the mouth opening as the frequency increases.

Corresponding plots in the vertical plane through the mouth axis enabled a comparison to be made between the horizontal and vertical opening of the mouth during speech. These are shown in Figs. 3a and 3b.

The sound pressure in the vertical plane at 0.5 cm. from the lips, shown in Fig. 3a, changes more rapidly with distance from the axis than the corresponding curve for the horizontal plane in Fig. 2a. This indicates that the vertical height of the mouth opening is smaller than the horizontal width, and shows that the mouth opening is not circular.

There are difficulties in interpreting these results, because the mouth is continually changing whilst talking. These measurements were the average of a test sentence which contained 80% of the speech sounds in english, and might be different for another language. The analysis in different frequency bands contained the components of speech in those bands, and were not sounds chosen to have important components in those frequency bands.

Measurements were made on three subjects, and individual differences were observed.

Attempts have been made to simulate the spatial speech sound pressure distributions obtained on human mouths, by models of artificial mouths with different shapes and sizes of orifice. It was found that, in the middle-frequency range of 1300 c/s, a rectangular orifice 16 mm. by 42 mm. on the surface of a sphere 16 cm. in diameter gave a better approximation to the human mouth measurements than a 35 mm. diameter circular orifice. This could not take account of the change in apparent size of the human mouth with frequency.

In the horizontal direction, the equivalent size of a human mouth was 45 mm. at low frequencies, decreasing to about 18 mm. at the higher speech frequencies.

Conclusions

During continuous speech the apparent width of the human mouth opening is greater than the height.

The equivalent size of opening is larger for the low-frequency components than for the high-frequency components, in both horizontal and vertical directions.

This work was carried out in the laboratories of Standard Telecommunication Laboratories Limited.

1. H.K.DUNN and D.W.FARNSWORTH. J.Acoust.Soc.Am., 10 (1939) 184
2. M.E.HAWLEY and A.H.KETTLER, J.Acoust.Soc.Am., 22 (1950) 365
3. J.L.FLANAGAN. J.Acoust.Soc.Am., 32 (1960) 1613

H36

FOURTH INTERNATIONAL CONGRESS ON ACOUSTICS
COPENHAGEN 21.-28. AUGUST 1962

Ein Zusammenhang zwischen Schwerpunktsfrequenz, Tiergröße und akustischer Reichweite.

Dr. Th. Lange
Westfäl. Metall Industrie KG Hueck & Co, Lippstadt

Zusammenfassung: Die Schwerpunktsfrequenz wird als Mittenfrequenz der Hörfläche (Lautstärke über Tonhöhe) eines Tieres oder auch aus anatomischen Daten ermittelt. Sie wird in Abhängigkeit von der Körpergröße dargestellt. Es ergibt sich bei Säugetieren und Vögeln, für die genügend zahlreiche Daten vorliegen, ein Abfall mit wachsender Körpergröße. Diese Regel gibt Hinweise auf die günstigste Signalfrequenz als Funktion der Reichweite.

Einleitung: Schallwellen werden von unserer Technik wie von vielen Tieren zur Information über die Umgebung benutzt. Die Frage nach der optimalen Signalfrequenz ist technisch ungelöst für die Schallausbreitung im Freien bei Wind und Wetter. Der meßtechnisch erfaßte Frequenzbereich für Luftschall reicht von jährlichen Luftdruckschwankungen, das ist Infraschall von $3 \cdot 10^{-8}$ Hz bis zu Ultraschallfrequenzen von mehreren 10^8 Hz, also über 16 Zehnerpotenzen. Nur ein geringer Teil dieser Skala wird von den Sinnesorganen erfaßt. Welche Frequenzbereiche hat die Tierwelt im Laufe ihrer Entwicklung ausgewählt, und warum bevorzugte sie gerade diese Frequenzen?

Definition der Schwerpunktsfrequenz: Zunächst soll der von jeder Tierart benutzte Frequenzbereich durch eine einzige Zahl einfach gekennzeichnet werden. Bei den Stimmfrequenzen ist die Grundfrequenz am einfachsten zu ermitteln. Richtiger betrachtet man die stärksten Obertöne, also die Formantbereiche, über die leider viel weniger Messungen bekannt sind. Bei den Gehörfrequenzen ist die Charakterisierung durch eine einzige Zahl noch wichtiger und schwieriger, weil obere und untere Grundfrequenz weiter auseinanderliegen. Die von uns benutzte Schwerpunktsfrequenz soll definitionsgemäß die Hörfläche in zwei gleiche Teile halbieren.

Die Hörfläche wird bekanntlich von Hörschwelle und Schmerzschwelle begrenzt, wenn man die Lautstärke als Funktion der Frequenz (beide logarithmisch) aufträgt. Abb.1. Beim Menschen gibt die Planimetrierung eine Schwerpunktsfrequenz von 0,9 kHz. Noch besser teilt man die Koordinaten in gleiche Empfindungsstufen ein, für die Tonhöhe z.B. in Mel. Dadurch wird die Hörfläche annähernd symmetrisch, und hieraus ergibt sich ein neues Verfahren zur Bestimmung der Schwerpunktsfrequenz: Die Mel-Skala kann ja bekanntlich hergeleitet werden aus der Verteilung der Orte maximaler Erregung auf der Basilarmembran in Abhängigkeit

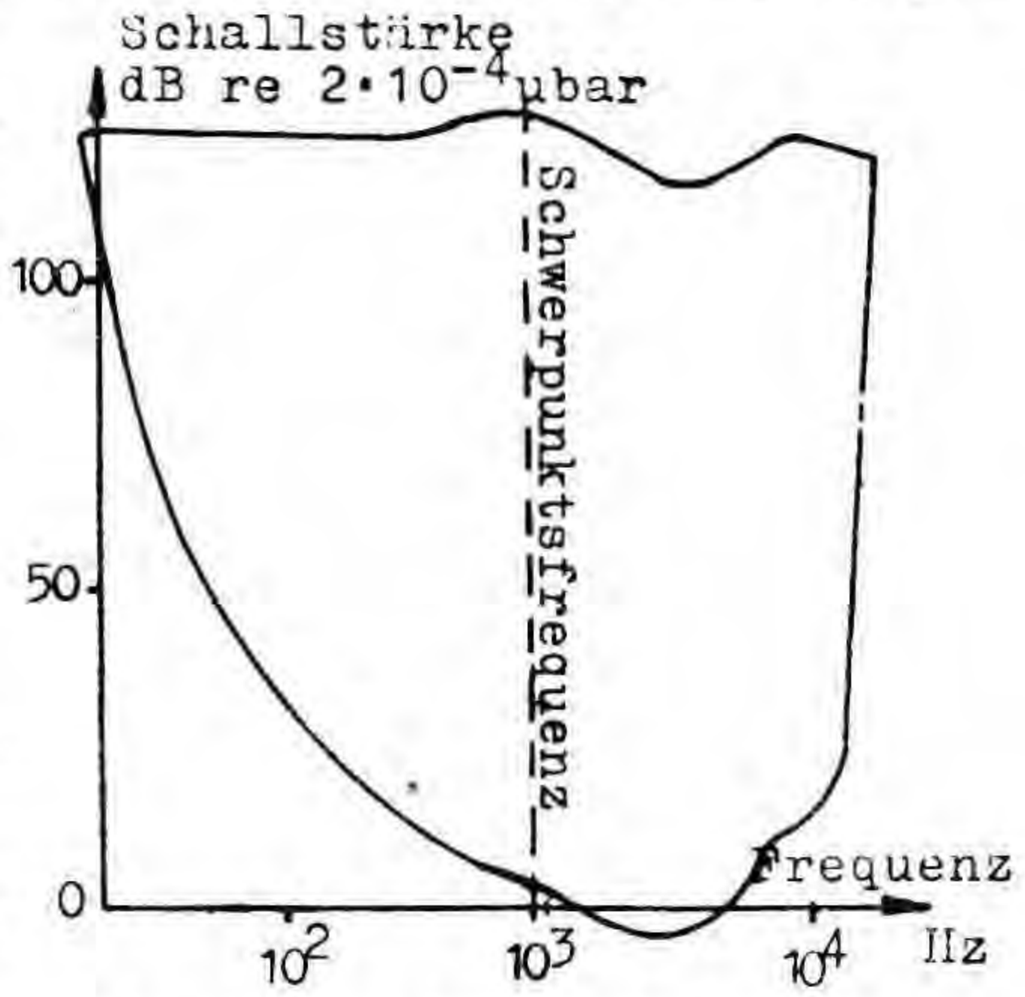

Abb.1 Hörfläche d.Menschen

von der Frequenz. Als Schwerpunktsfrequenz setzt man die Frequenz ein, welche die Basilarmembran gerade auf halber Länge erregt, also in der Mitte zwischen ovalem Fenster und Helicotrema. Abb.2: Für das menschliche Ohr erhält man so eine Schwerpunktsfrequenz von 1,2 kHz. Das Verfahren wurde ferner geprüft am Katzengehör, für das sich aus der Planimetrierung der Hörfläche 2,5 kHz ergibt und aus anatomischen Messungen 3 kHz, also ebenfalls gute Übereinstimmung. Messungen der ganzen Hörschwelle sind nur an wenigen Tieren bekannt. Nach dem geschilderten Verfahren wurde die Schwerpunktsfrequenz in einigen Fällen berechnet, in denen nur die anatomischen Angaben vorliegen. Es wäre interessant, wenn diese Art der Berechnung nachträglich durch direkte Hörflächenmessungen nachgeprüft würden, z.B. am Elephanten.

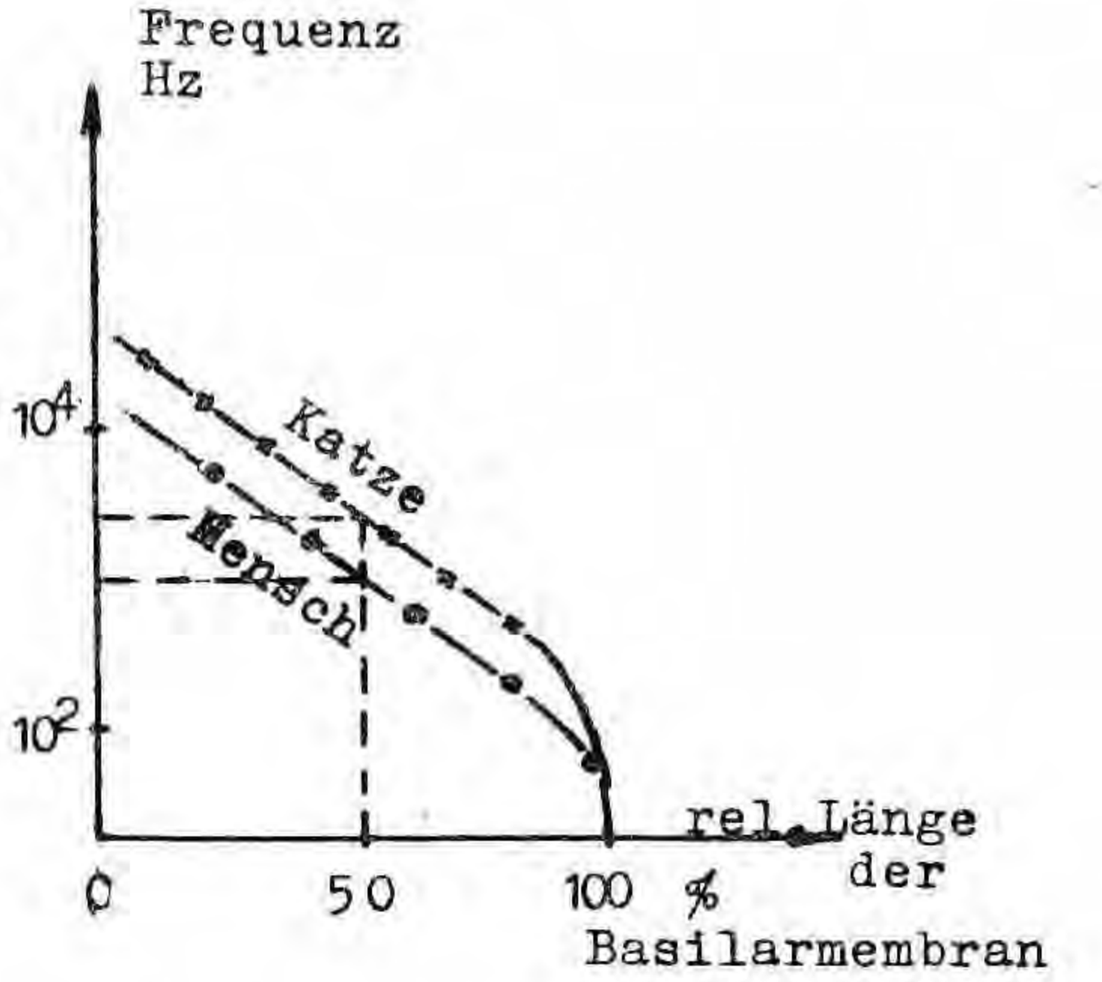

Abb.2 Schwerpunktsfrequenz aus anatomischen Daten

Tiergröße und Schwerpunktsfrequenz: In 60 Lit. Stellen wurden über 100 verschiedene Tiere Frequenzangaben über Stimme und Gehör gefunden und in einer Tabelle zusammengefaßt, (aus Platzmangel nicht veröffentlicht). Die Schwerpunktsfrequenzen liegen im Bereich von wenigen 100 Hz bis fast 100 kHz, überdecken also 3 Zehnerpotenzen; der Gesamtbereich überdeckt 4,5 Zehnerpotenzen. Um diese Meßwerte zu ordnen, kann man eine zweite Variable suchen, die mit den akustischen Frequenzbereichen im Zusammenhang steht. Sehen wir uns darauf einmal die Größe des Innenohres an. Abb,3 zeigt die Schneckenlänge im Innenohr von Vögeln in Abhängigkeit von der Körpergröße, Abb.4 das Gleiche von Säugern. Man erkennt ohne Zweifel einen Zusammenhang, und zwar wächst die Schneckenlänge und damit das Organ der mechanischen Frequenzauflösung, die Basilarmembran, etwa mit der 6-ten Wurzel des Körpergewichtes.

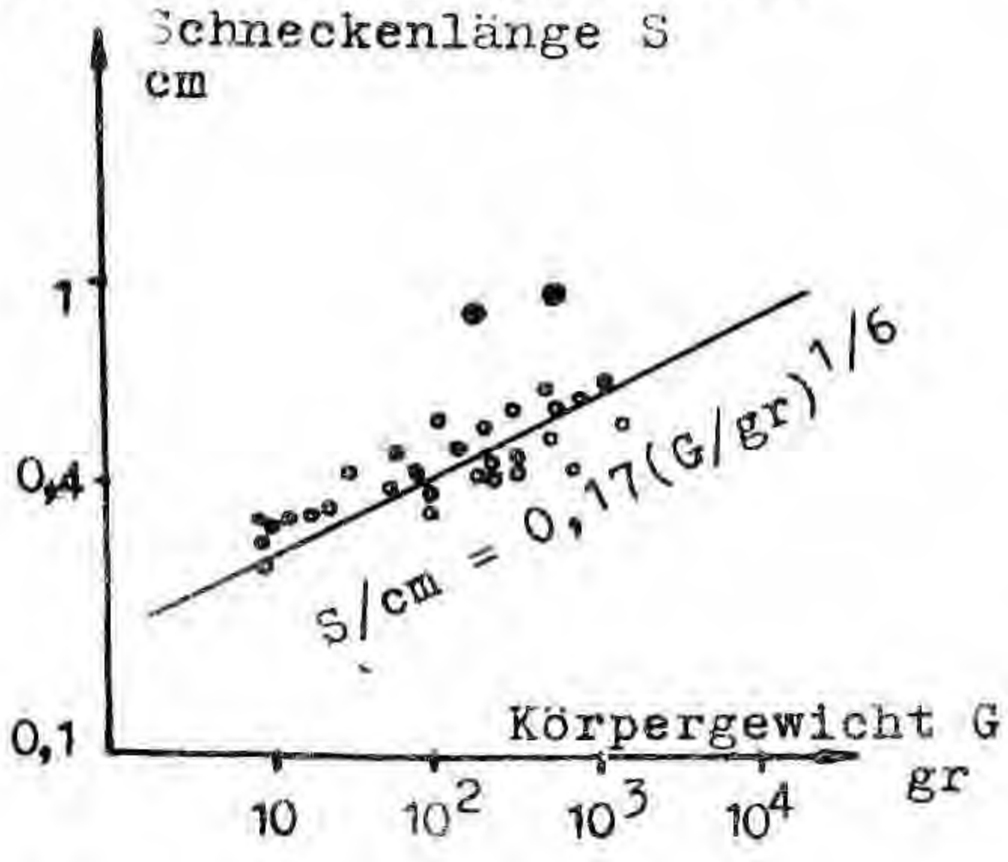

Abb.3 Innenohrgröße, Vögel

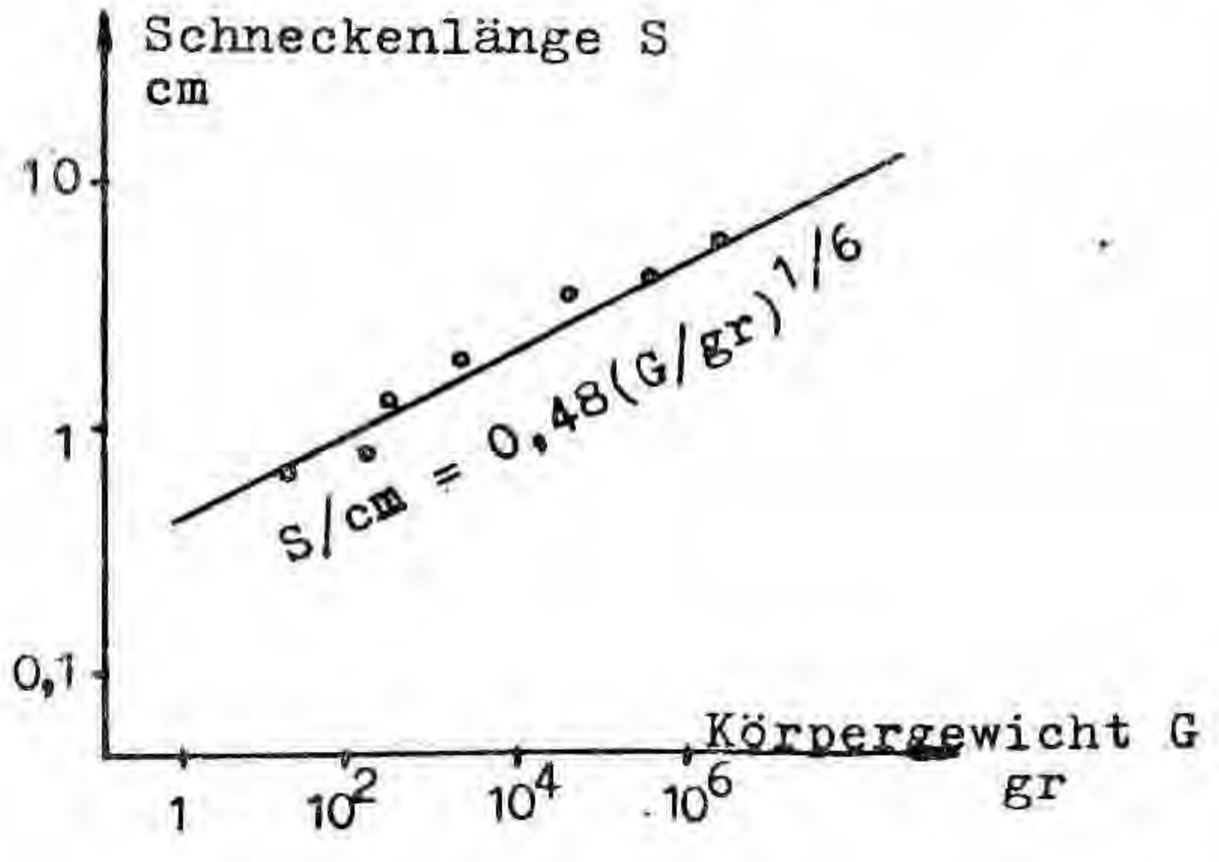

Abb.4 Innenohrgröße, Säuger

Nachdem diese Beziehung zwischen Körpergröße und Länge der Innenohrschnecke klar ist, liegt es nahe, einen weiteren Zusammemhang zwischen Schneckenlänge und Frequenzschwerpunkt zu vermuten. Existiert solch ein Zusammenhang, muß der Schwerpunkt auch von der Körpergröße abhängen. Die Stimmfrequenzen sind auf Abb.5. für Säuger dargestellt. Jeder Punkt stellt einen Mittelwert dar, nämlich für den Frequenzbereich und für die Streuung innerhalb der Art. Die Kreise gelten für die Grundtöne, die Kreuze für die stärksten Obertöne, die um den Faktor 5 höher liegen. Man kann sehen, daß die Punkte rechts tiefer liegen, m.a.W. große Tiere besitzen tiefere Stimmen als kleine. Der Zusammenhang ist sicherer auf Abb.6. der Darstellung der Schwerpunktsfrequenz des Gehörs zu erkennen. Das Gehör ist i.a. also für die wichtigsten Stimmfrequenzen der eigenen Art am empfindlichsten.

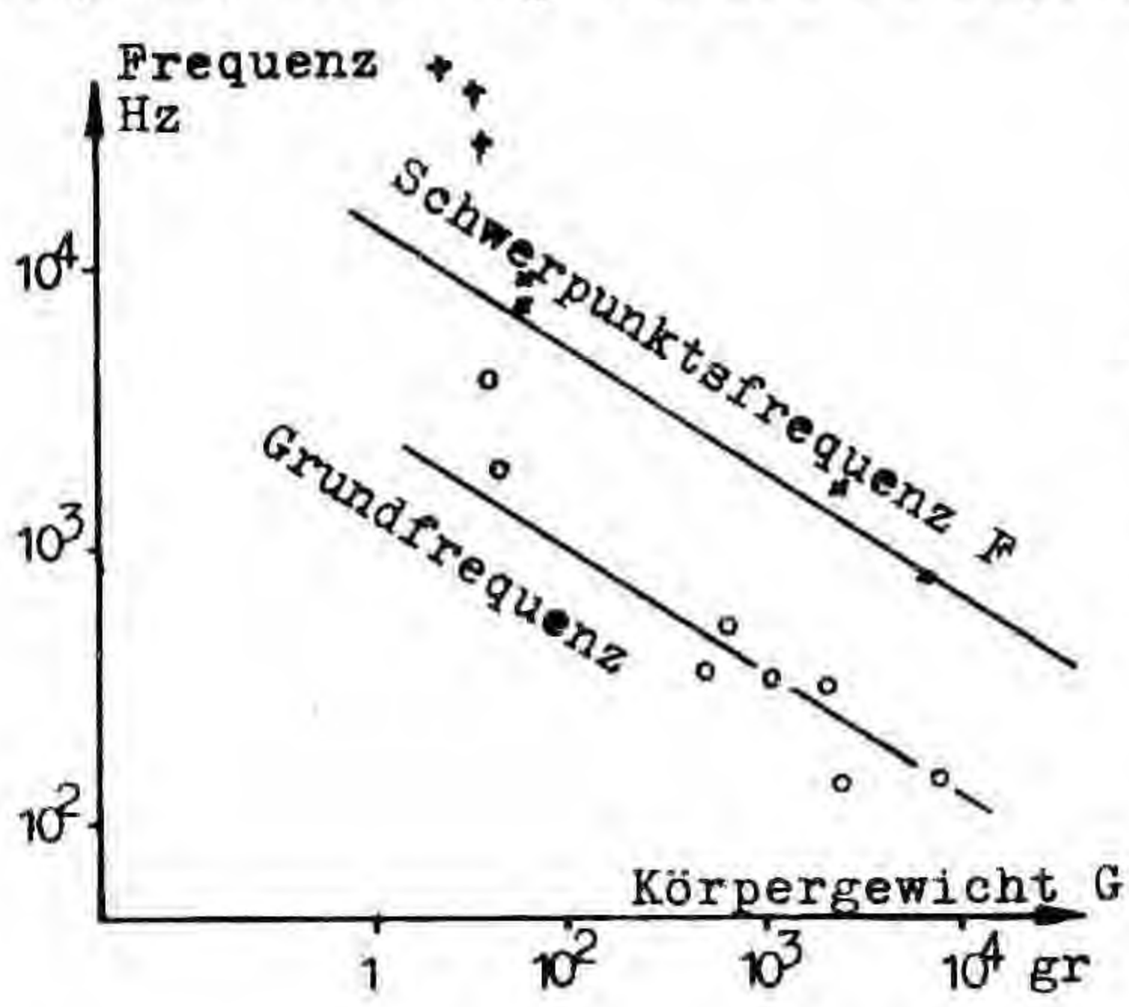

Abb.5 Stimmfrequenzen, Säuger

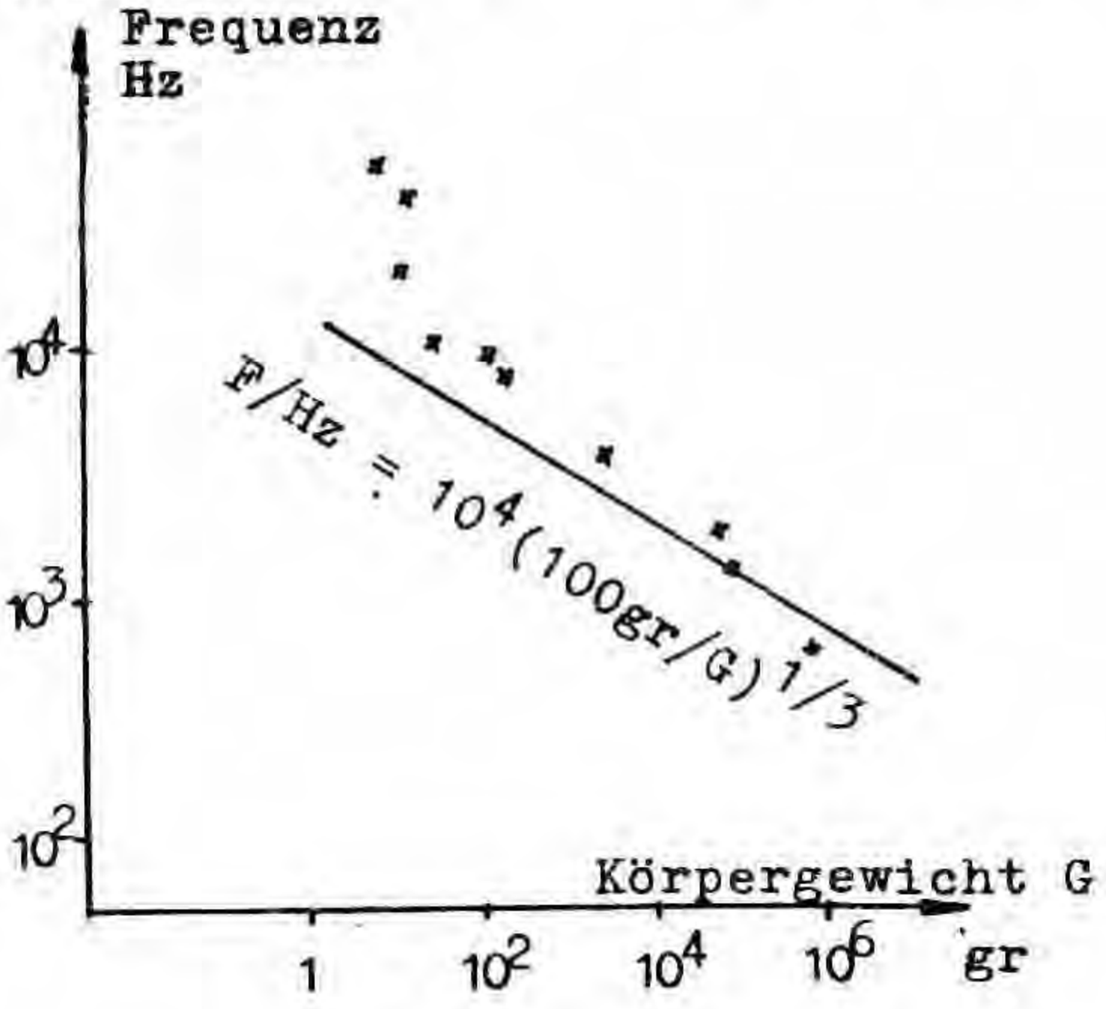

Abb.6 Gehörfrequenz, Säuger

Die geschilderte Abhängigkeit der Frequenz von der Körpergröße wird nur bei Betrachtung genügend großer Bereiche, also über mehrere Zehnerpotenzen, erkennbar. Aus der alltäglichen Erfahrung ist der Zusammenhang schon lange bekannt. Eine ähnliche Frequenzabhängigkeit von der Körpergröße besteht auch für tote Gegenstände wie Pfeifen, Saiten, Membranen, Balken und Platten. Man ordnet als psychologische Folge erfahrungsgemäß einer unsichtbaren Schallquelle einen großen Gegenstand oder ein großes Tier zu, wenn sie einen tiefen Grundton besitzen, und umgekehrt.

Da mit dem Gewicht der Tiere auch ihr Volumen wächst, besteht der gleiche Zusammenhang also auch mit dem Körpervolumen. Musiker sprechen auch vom Volumen eines Klanges, ohne daß ein quantitativer Zusammenhang mit der Frequenz bekannt ist. Weitere Parameter für dieses Tonvolumen sind Intensität, Obertongehalt, räumliche Ausdehnung der Schallquelle, Vibrato, Nachhall, Echos. Die Grundtonhöhe ist aber die entscheidende Größe.

Reichweite und Schwerpunktsfrequenz: Dennoch ist nicht die Körpergröße der Tiere die primäre Ursache für die Frequenzlage des Gehörs, die außer von der Schneckenlänge sehr wesentlich von der Elastizität der Schneckentrennwand beeinflußt wird. Man erkennt gerade an Abweichungen von der diskutierten Regel (wie z.B. Fledermäuse und Raubvögel) deutlich, daß das Gehör auch bei abweichenden Frequenzen besondere Empfindlichkeiten erreichen kann. Ich glaube, die primäre Ursache ist nicht die Körpergröße, sondern die Anpassung der hochentwickelten Gehörorgane an die Umgebung, Anpassung der Frequenz ebenso, wie es von der Lautstärke schon bekannt ist. Diese Anpassung während der Entwicklung des Gehörs ist in langer Zeit erfolgt, und so sind auch die Einflüsse der Umgebung als Mittelwert über ähnlich große Zeiträume berücksichtigt. Daher gestattet die Auswahl der von den hochentwickelten Tieren benutzten Frequenzen Rückschlüsse auf die Schallausbreitung im Freien und zwar unter Bedingungen, die über sehr große Zeiträume gemittelt sind.

Die wesentlichen physikalischen Einflüsse sind der Störpegel, meist durch Wind hervorgerufen, die Schallextinktion durch Wind- und Temperaturschwankungen. Sie sind als allgemein gültige Mittelwerte noch unbekannt, und nur die Absorption in ruhender Luft ist wohlbekannt. Diese Größen, die die Schallausbreitung im Freien beeinflussen, sind frequenzabhängig, so daß auch die Reichweite, die sich mit einem Signal bestimmter Intensität erreichen läßt, frequenzabhängig wird. Die Frage lautet: Welches ist die optimale Frequenz, mit der man im Freien mit dem geringsten Aufwand eine Information übermitteln kann? Die untere Frequenzgrenze ist gegeben durch zu lange Einschwingzeiten und den stärkeren Störpegel bei Wind. Die obere Frequenzgrenze ist gegeben durch Beugung und Streuung an Wind- und Temperaturungleichheiten, welche die Richtcharakteristik ungünstig beeinflussen, und durch die Absorption in der Luft und am bewachsenen Boden. Zwischen diesen beiden Grenzen liegt die günstigste Signalfrequenz. Sie hängt von der Reichweite ab, die akustisch überbrückt werden soll. Aus den biologischen Daten wurde eine Abschätzung versucht mit folgendem Resultat: Die optimale Frequenz mit der sich bei kleinstem Aufwand unter den meisten Wetterbedingungen ein akustisches Signal übermitteln läßt, fällt mit der Wurzel aus der Reichweite, oder als Formel:

$$\nu_{kHz} = \frac{16}{\sqrt{R/m}}$$

Danach ist 500 Hz die optimale Signalfrequenz für eine Reichweite von 1 km und entspricht den Nebelsendern an der Küste. Die menschlichen Rufe reichen fast bei jedem Wetter bis 100 m, das Mäusefiepen mit 5 kHz ist optimal für Entfernungen um 10 m und das Zirpen von Heuschrekken bei 16 kHz für 1 m. Auch das Pfeifen des Verlassenseins und die Ultraschall-Laute junger Mäusenestlinge passen gut zu diesen Anschauungen: sie besitzen zweckmäßig nur eine begrenzte Reichweite, um keine Raubtiere aufmerksam zu machen. Das als Gleichung formulierte Resultat ist auch insofern plausibel, als es die gleiche quadratische Frequenzabhängigkeit besitzt wie die klassische Formel für die Absorption in ruhender Luft. Die Zahlenwerte stellen nur eine erste Abschätzung dar.

K36

FOURTH INTERNATIONAL CONGRESS ON ACOUSTICS
COPENHAGEN 21.-28. AUGUST 1962

Hypersonic Attenuation in Fused Quartz at Low Temperatures.

H. E. Bömmel and C. K. Jones
University of California, Los Angeles.

It is well known that the attenuation of ultrasonic waves in fused quartz is very small at room temperature. This is one of the reasons why fused quartz is so widely used for ultrasonic delay lines. McSkimin[1] first discovered that the attenuation increased enormously as the temperature was lowered to tha of liquid air. Fine (2) and Bömmel (3), extending the measurements to 4.2°K, found that this increase was part of a broad absorption band which for a frequency of 20 Mc/sec peaks around 45°K. The position of this peak shifts to higher temperatures as the frequency is raised and its amplitude increases. Anderson and Bömmel (3) were able to explain the observations by assuming that this absorption band is caused by a structural relaxation mechanism due to the small deviations of the Si-O-Si bonds from a straight line in fused quartz. The broadness of the absorption curve suggested the presence of a distribution of relaxation times rather than a single relaxation process, with an average activation energy of 1030 cal/mole. Anderson and Bömmel calculated the distribution of activation energies by fitting the experimental data. Their distribution curve shows a concentration at very low energies. This in agreement with the interesting fact that the absorption at 4.2°K is still appreciably larger than at room temperature.

We have performed a series of new experiments, extending the frequency range up to 1000 Mc/sec and the temperature down to 1.4°K, using techniques for the generation and detection of hypersonic waves recently developed by Bömmel and Dransfeld (4). The specimen was a cylindrical rod of optical quality, 20 mm long and 3 mm in diameter. X-cut quartz transducers were attached to its ends by the Indium bonding technique. At 1000 Mc/sec the absorption band was found to be so broad and the absorption increasing so rapidly below room temperature that no sound pulses were observable between about 250°K and 1.5°K. At this temperature sound could just be observed again. At a frequency of 525 Mc/sec the attenuation increased about 24 db between room temperature and 180°K and became again so large that no sound could be observed until the temperature was lowered to 3.3°K. Between 3.3°K and 1.4°K the attenuation dropped about 30 db with no apparent change in the slope of the curve at the latter temperature.

The estimated width, magnitude of the absorption band and position of the peak at 525 Mc/sec seems to be in agreement

with the model for the relaxation mechanism proposed by Anderson and Bömmel. The abnormally large specific heat of fused quartz at low temperatures (5) should also be related to this phenomenon. It is intended to extend the measurements to temperatures below $1^{o}K$.

References.

(1) H. J. McSkimin, J. Appl. Phys., 24, 988, (1953).
(2) M. E. Fine, H. Van Duyne and N. T. Kenney, J. Appl. Phys., 25, 402, (1954).
(3) O. L. Anderson and H. E. Bömmel, J. Am. Ceram. Soc. 38, 125, (1955).
(4) H. E. Bömmel and K. Dransfeld, Phys. Rev. 117, 1245, (1960).
(5) See for example: P. Flubacher, A. J. Leadbetter, J. A. Morrison and B. P. Stoicheff, J. Phys. Chem. Solids, 12, 53, (1959).

L36

FOURTH INTERNATIONAL CONGRESS ON ACOUSTICS
COPENHAGEN 21.-28. AUGUST 1962

ON THE RELATION BETWEEN THE EXHAUST NOISE AND THE MECHANICAL OUTPUT POWER OF SOME COMBUSTION ENGINES

Ken'iti Kido, Noriyoshi Chubachi and Tadamoto Nimura
Tohoku University, Japan

§1 Introduction

There have been many troubles in Japan caused by the noise of combustion engines. Many of the troubles were brought into our labolatory to solve them. Whenever a trouble is brought in, we used to measure the power level of the noise radiated from the engine in the first place, to make the most effective measure to solve it. But their measurement is frequently very difficult, mereover, it is not always possible. Then we tried to make a table or chart to read directly the radiated noise power and the spectrum of engines from their nominal data. The radiated noise power and their spectra were measured with some kinds of the engines at their nominal horse power. Consequently we got the very interesting results, that is to say, the linear correlatin between the exhaust noiselevel and the mechanical out-put power level. On that point, we were interested to know, why the results came out and whether we can get the same results about all engines every time.

§2 Experiments on the relation between the exhaust noise and the mechanical power output of some combustion engines.

§ Experiments on the engines made by an engine maker.

To get a designing aim of the silencers which are installed to the diesel engines made by a diesel engine maker Niigata Tekkosho, a series of the noise measurements were carried on. The results are shown in Figs. 1 and 2. In Fig. 1, the measured exhaust noise levels at the nominal horsepower of the engines, listed in the table are shown. We can find the linear correlation between the exhaust noise level and the mechanical output power in three groups. The mean noise spectra analysed with 1/3 octave filter set are shown in Fig. 2 for each group. The band power level can be found by reducing the value of the ordinate from the power level shown in Fig. 1 At the low frequency region, some higher harmonics of the fundamental combustion frequency are observed. Some additional results are shown in Fig.3, in which the mechanical output power is varied keeping the revolution numbers of each engine constant.

These results are very useful to make the designing aim of the silencers which are installed to the diesel engine made by the maker.

§ Further experiments.

The above mentioned results

No.	Diameter of Cylinder	Stroke	Number of Cylinder	rpm	Power	
	mm	mm		rpm	ps	
1	160	220	5	750	100	conventional
2	250	320	6	600	300	
3	250	290	6	600	300	
4	200	240	6	900	220	4 cycle
5	430	500	6	360	1,500	
6	310	360	6	600	750	with super
7	250	320	8	600	600	charger
8	250	320	6	600	450	4 cycle
9	180	200	6	1,200	340	
10	430	500	8	360	1,900	
11	250	290	V.12	750	1,500	
12	250	320	8	600	750	with super
13	250	320	6	600	600	charger and air
14	200	240	6	900	375	cooler 4 cycle
15	540	900	6	170	2,900	super charged 2 cycle

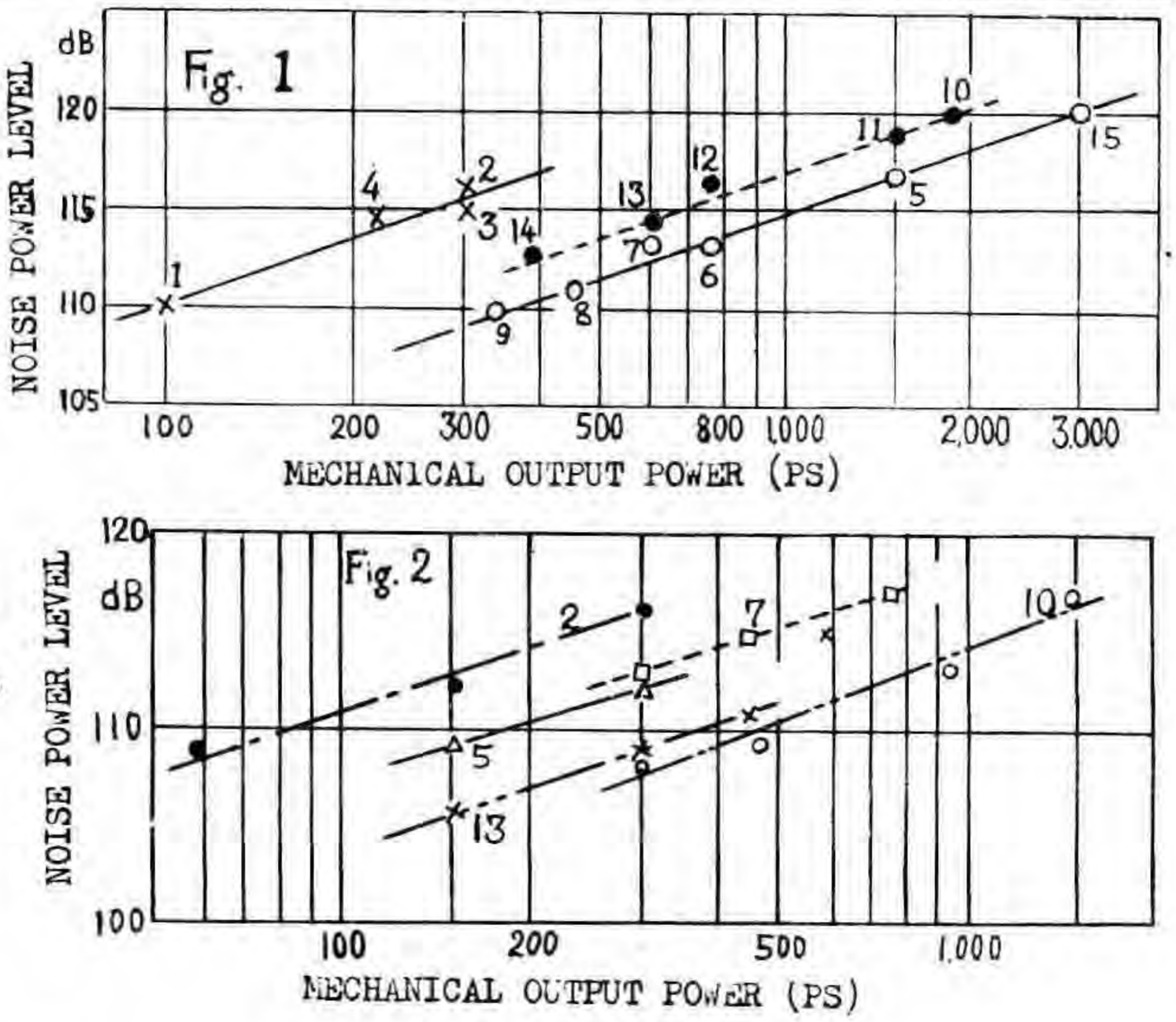

were very interesting but they cannot predict the value of the other engines unless the experimental or theoretical verifications are made. To clear how and why the linear correlations come out, we have carried on further experiments on the other engines. Some of the experimental rosults by the other engines are shown in Fig. 4. The linear correlations observed in Fig. 1 holds good in some limit, but the slopes of the straight lines connecting measured points differ a lettle from the former results. If the revolution frequencies are increased, the output noise level grows up largely as shown in Fig. 6.

§3 Considerations on the experimental results.

From the above experiments, we can estimate what is prominent factor to produce the exhaust noiso of engines, though no certain explanation can be made why the lenear correlation between the exhaust noise level and the mechanical output power levelis. The estimation is based on the above mentioned experiments and the relation that the mechanical output power is approximately proportional to the product of the revolution numbers, the number of the cylinders, the volume of each cylinder and the effective mean pressure inside the cylinders.

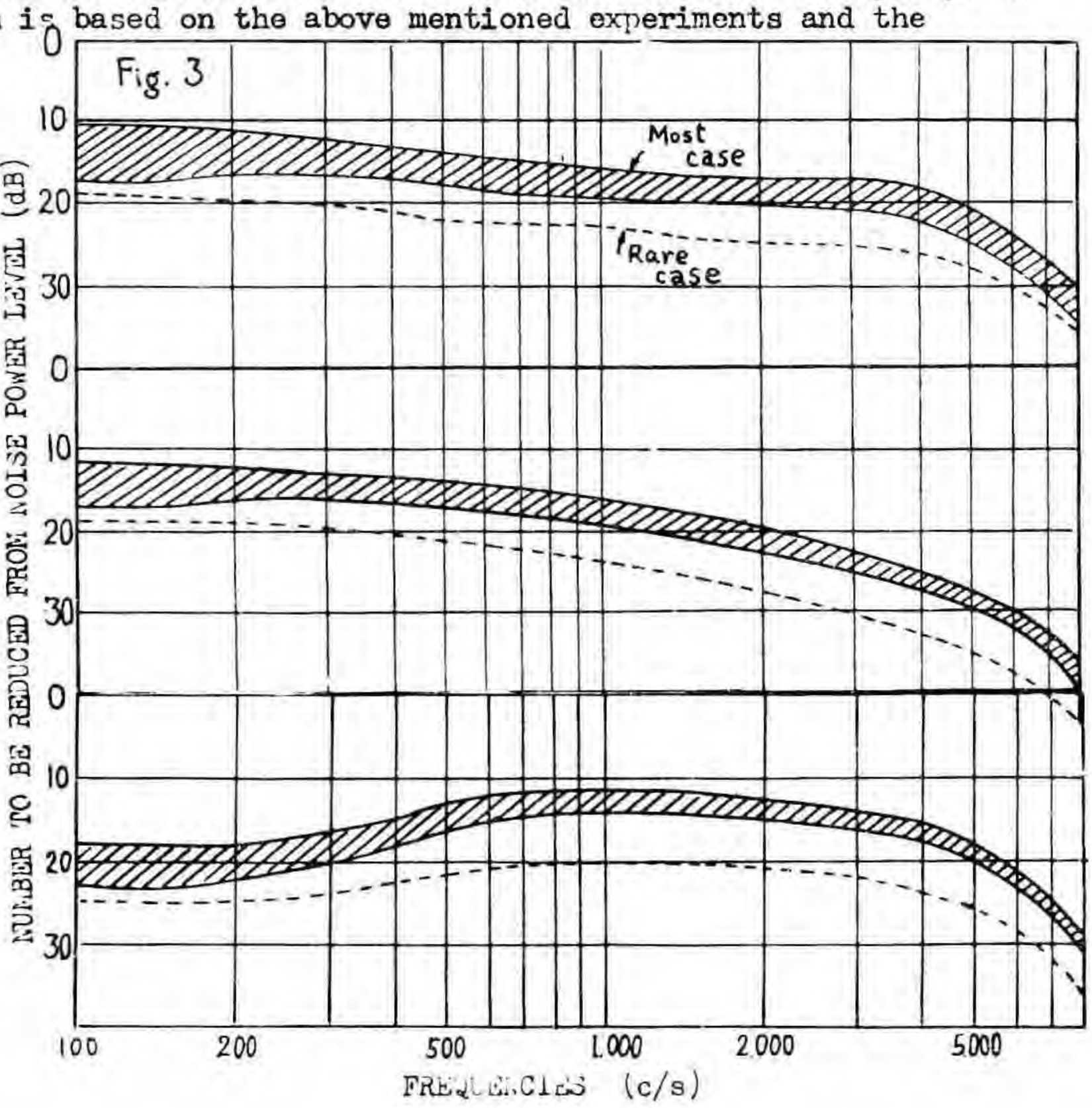

From the results of the considerations , it is derermined that we must investigate how effective the di dimension of the pressure at the opening of the exhaust valve on the exhaust noise levelis.

§4 Researches on a simple model

Some theoretical considerations can be made with the Euler's equation on

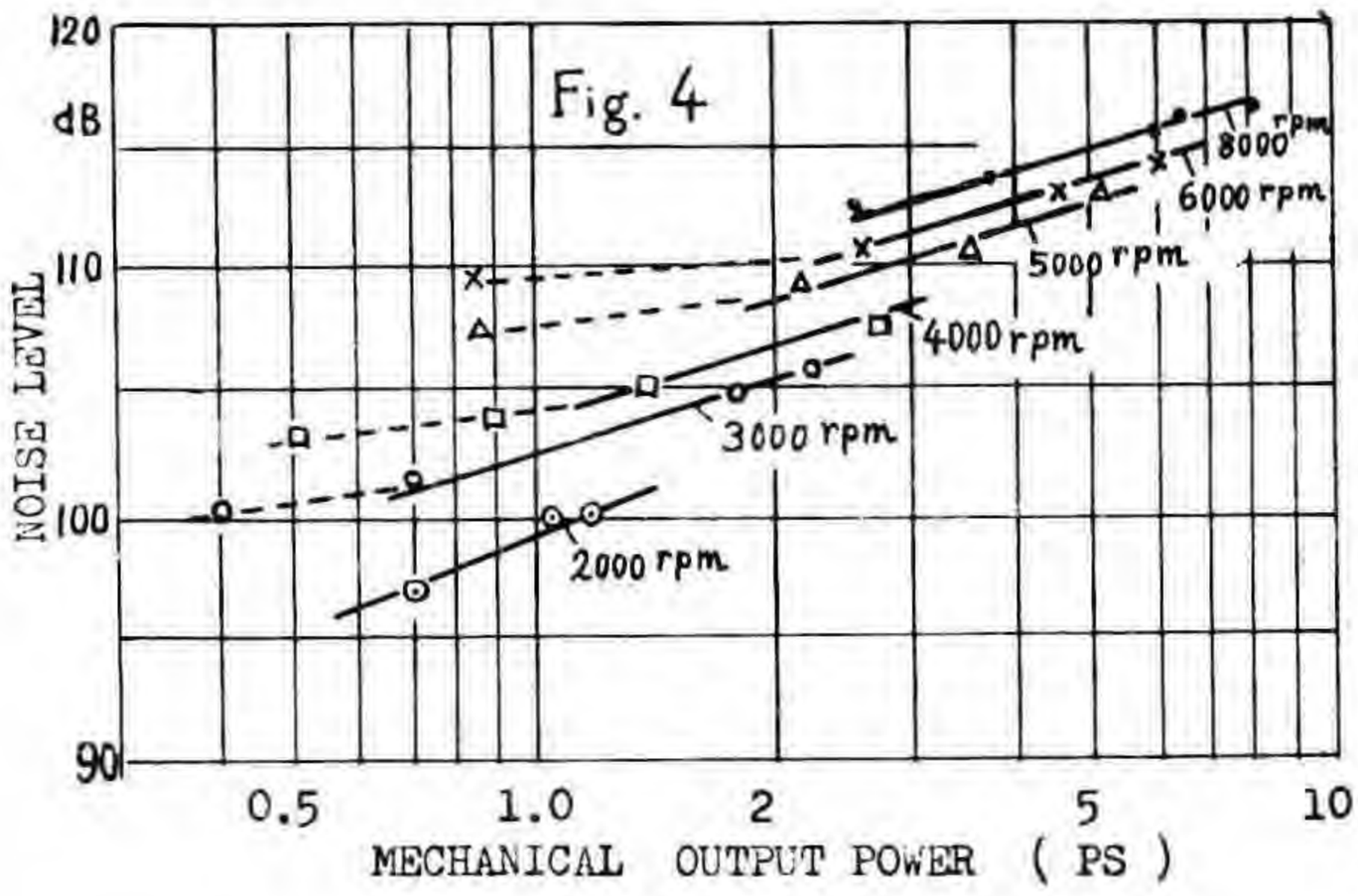

the one dimensional flow of the compressible gas:

$$\frac{\partial u}{\partial t} + u\frac{\partial u}{\partial x} = -\frac{1}{\rho}\frac{\partial P}{\partial x}$$

where u is the flow velocity of the gas, P is the pressure, and ρ is the density.

The transient phenomena can be divided into four periods.
(1) Short interval after the exhaust port is opened. Shock wave will be generated.
(2) The period when $\partial u/\partial t$ can be neglected compared with the other terms. In this period, the air flow with large velocity may be superposed by the shock wave and the viscosity of the gas.
(3) The period, when the all terms of the Euler's equation can not be neglected, as the pressure difference of the inside and the outside of the cylinder decreases. This period may be very short and the noise generated in this period may be already less than in the former period.
(4) The period, when $u\partial u/\partial x$ can be neglected, and linear equation holds good.

The exhaust noise may be mainly generated in the first and the second period.

Some experiments were carried on respecting these points. To simplify the conditions, cylindrical cavities having a circuler hole in one plate were used, the hole was closely sealed by a number of cellophane paper. Initially, the air closed was compressed into the cavity, then the cellophane seal was pricked by a needle to initiate sudden expansionof gas.

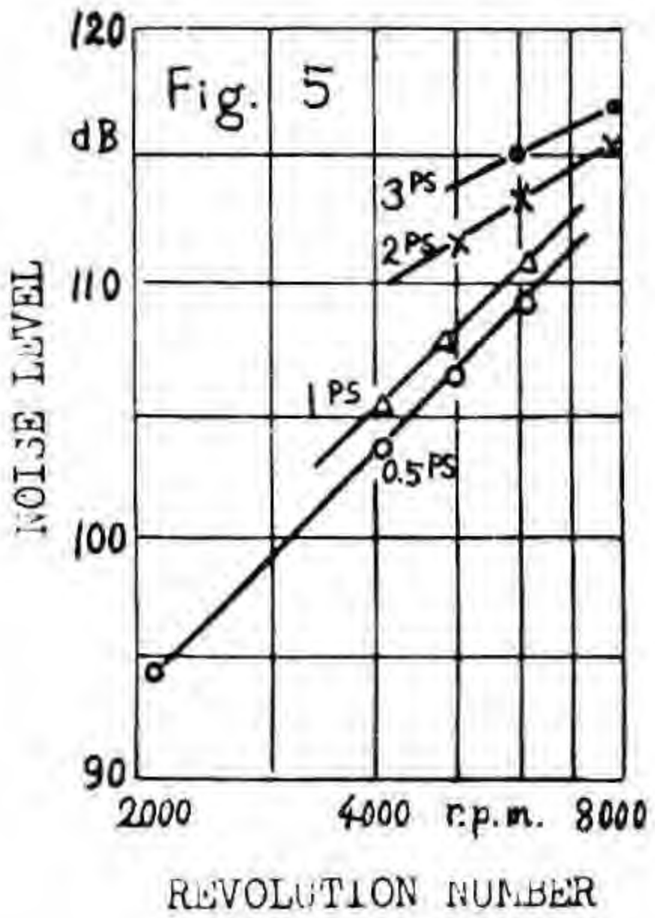

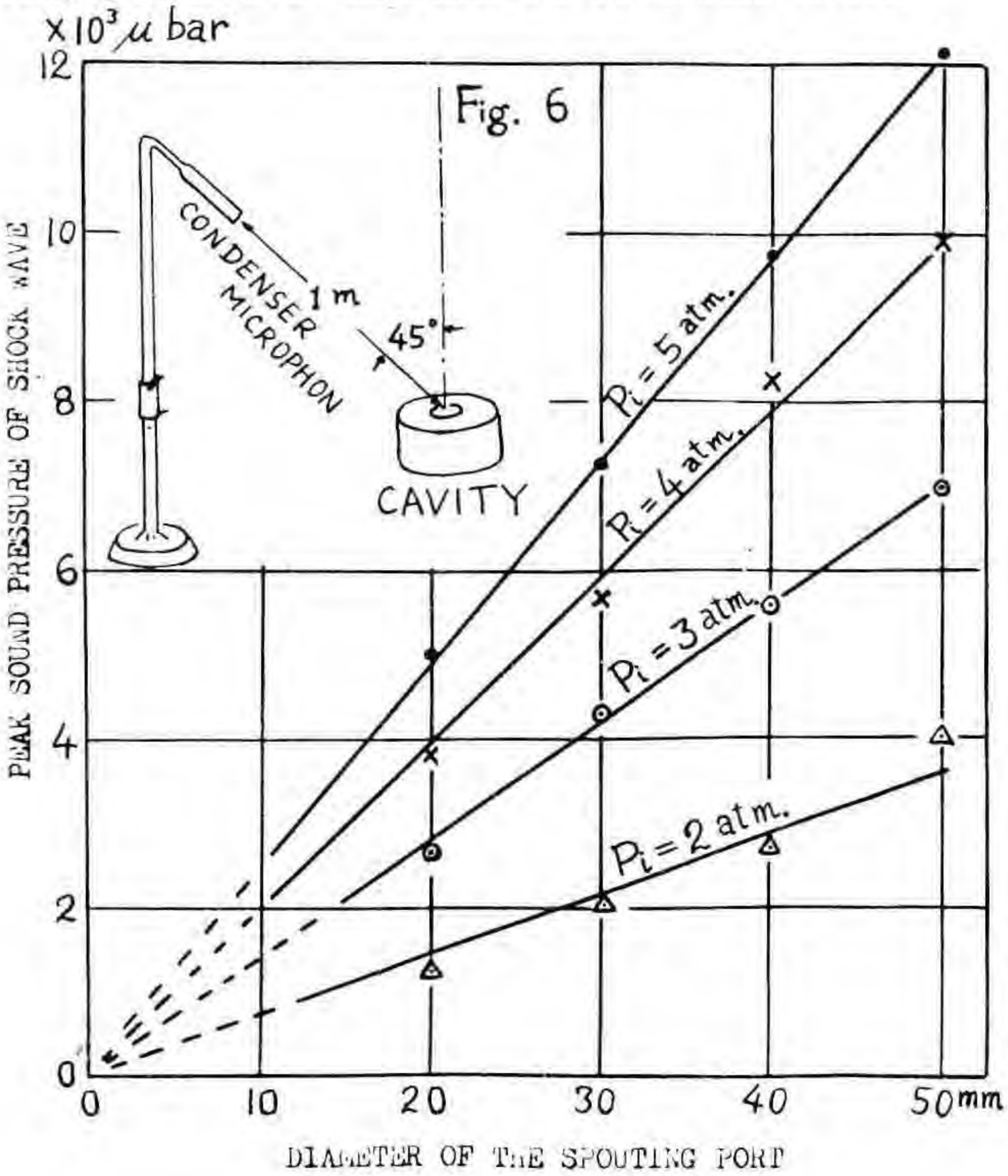

The sound pressure one or two meter apart from the opening was picked out by condenser microphone (Brüel Kjaer, Type 4133), the wave form was photographed with a cathode ray tube oscilloscope. From these experiments, the following results were obtained:

(1) The peak values of the shock wave are the same as theoretically expected, (Fig 6 and 7) and the wave contains the high frequency components. But the power of the shock wave is not so large.

(2) Higher noise is produced when the areas of the spouting hole is made large. (Fig. 8) By the spectrum analysis, the frequency components calculated as the resonances in the cylinder are prominent.in this case.

(3) When the area of the spouting hole is small, the high frequency noise is predominant. But the whole noise power is less than that at larger hole. (Fig. 8)

(4) The sound power caused by the Helmholtz' resonator is small than the others.

§5 Summary

We found a systematic relations between the exhaust noise level and the mechanical output power level of some kinds of combustion engines. We investigated how the exhaust noise is generated and it is found that the transient phenomena caused by spouting the exhaust gas from the cylinder are significant. The transient phenomena were investigated theoretically and experimentally. According to those researches, the exhaust noise may be increased when the pressure inside cylinder is increased a little before the openning of the exhaust port, and also when the area of the exhaust port is enlarged. In the latter case, the frequency component below 2,000 c/s rapidly grows up with the area of the spouting port. From these results, it is estimated in the actual engines that the exhaust noise can be diminished by changing the construction of the exhaust valve. More investigations are now carried on. But in the case of the actucal engines, we can conclude neither how to make low noise engines nor why the above mentioned correlation exists, because there are more complicated factors concerning with the exhaust noise.

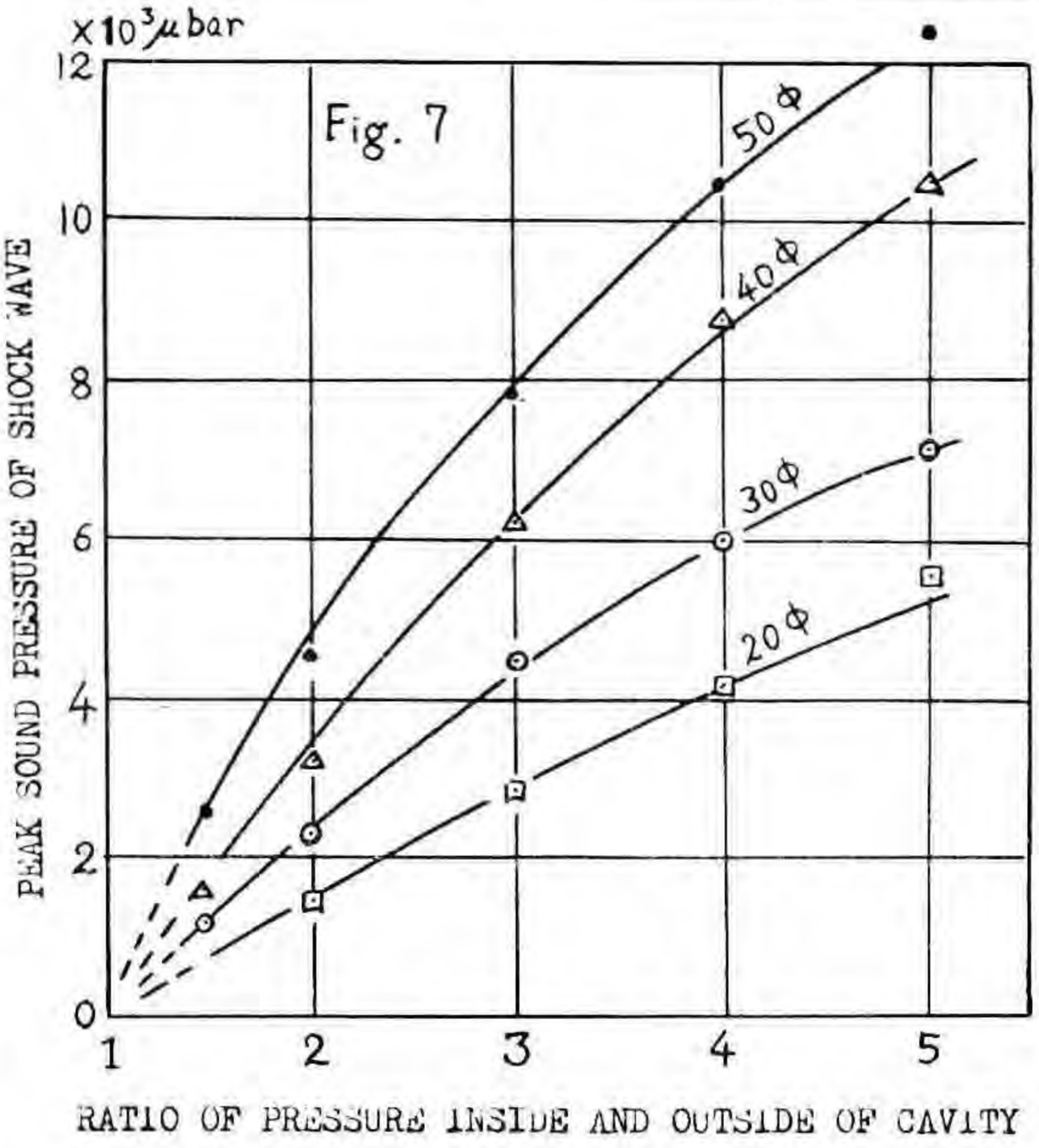

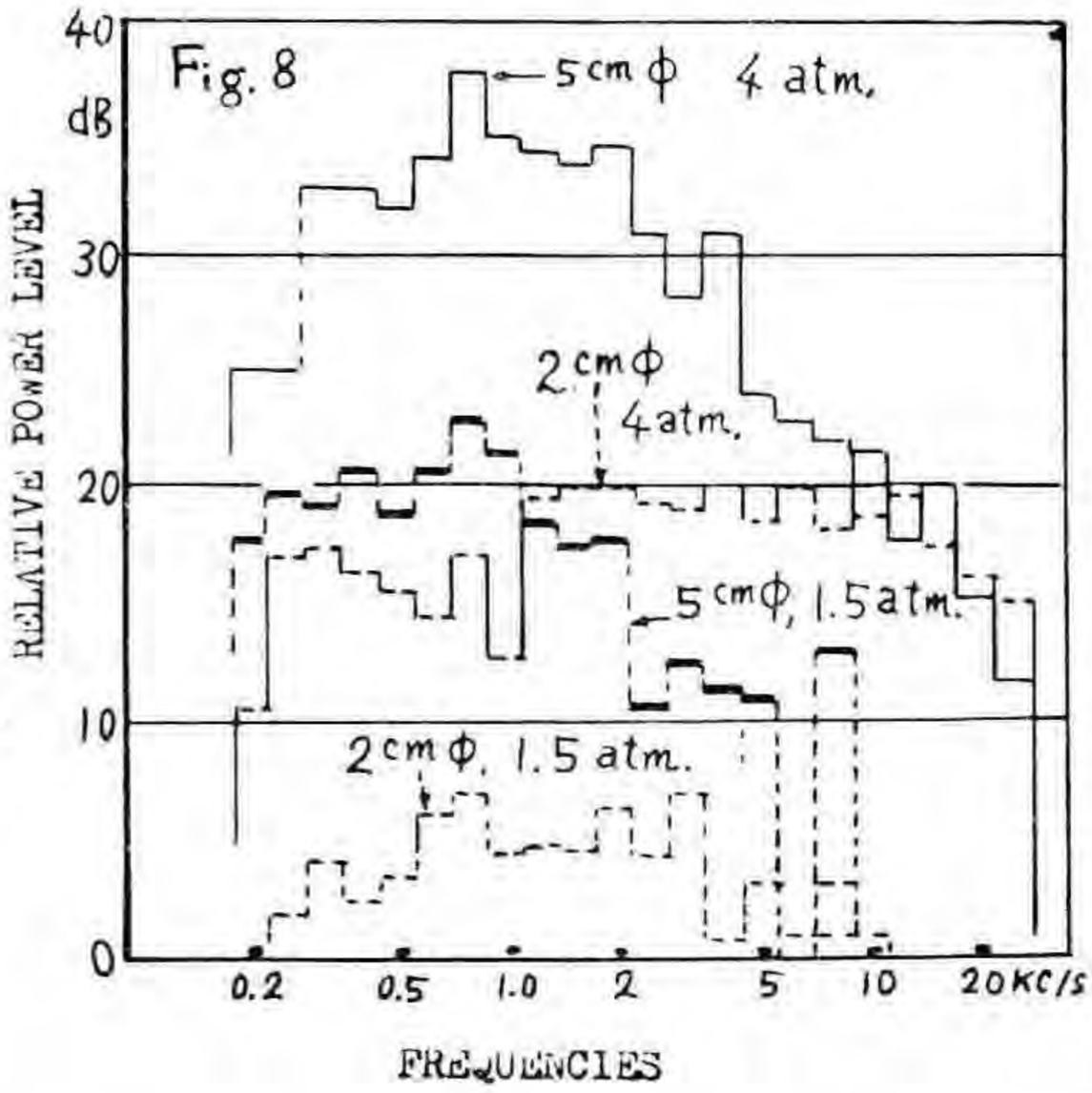

M36

FOURTH INTERNATIONAL CONGRESS ON ACOUSTICS
COPENHAGEN 21.-28. AUGUST 1962

Beeinflussung der Schalldämmung von Wänden durch Resonatoren

Wolfgang Westphal

Bei einer Einfachwand hängt die Schalldämmung in erster Linie von der Masse des Elementes ab. Wenn wir uns auf senkrechten Schalleinfall beschränken und idealisierend die Randeinspannung vernachlässigen, ist die Wandmasse die allein ausschlaggebende Größe. Für diesen Fall kann man - wie bekannt - ein sehr einfaches elektrisches Ersatzschaltbild angeben (Abb.1), wobei die Masse der Wand pro Flächeneinheit M als Induktivität und der Wellenwiderstand der Luft $Z = \varrho c$ als reeller Widerstand auftreten. Bei der gewählten Analogie ist der Strom in dem Kreis mit der Schnelle v der Wand zu identifizieren. Hat man eine auf die Wand auftreffende Welle mit dem Druck p, so errechnet sich das die Schalldämmung charakterisierende Verhältnis von auftreffender Schalleistung N_1 zu rückwärts abgestrahlter Schallleistung N_2 zu

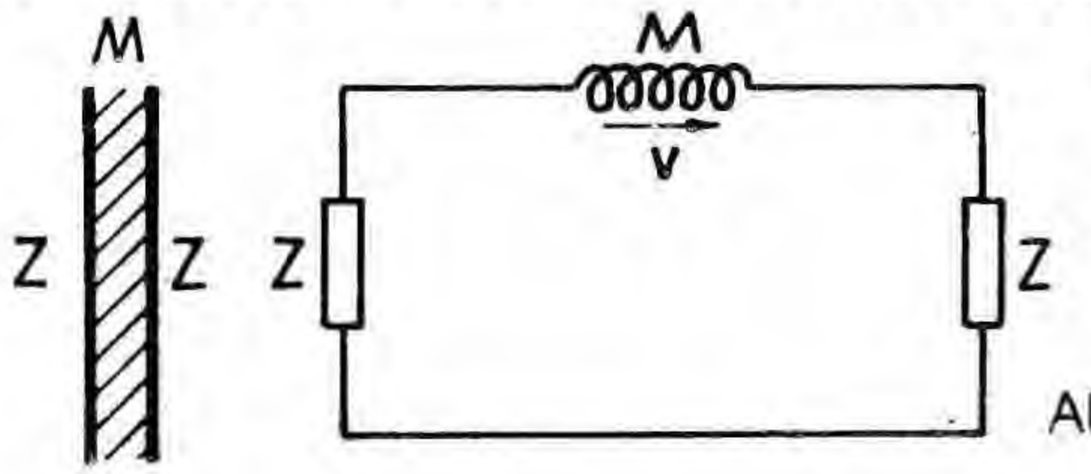

Abb.1

$$\frac{N_1}{N_2} = \frac{\frac{1}{Z}|p|^2}{Z|v|^2} \cdot \quad (1)$$

Den Quotienten p/v erhält man aus den Impedanzen, wenn man im Ersatzschaltbild auf der Seite der einfallenden Welle einen Generator mit der Urspannung 2p einfügt. Dann ist

$$\frac{2p}{v} = Z + j\omega M + Z \quad (2) \text{ und} \qquad \frac{N_1}{N_2} = \frac{1}{(2Z)^2}\left|j\omega M + 2Z\right|^2. \quad (3)$$

In dem meist interessierenden Frequenzbereich ist $Z \ll \omega M$, so daß sich aus (3) das bekannte "Massegesetz" der Schalldämmung für senkrecht einfallende Wellen ergibt (4).

$$\frac{N_1}{N_2} \approx \left(\frac{\omega M}{2Z}\right)^2 \quad (4)$$

Das durch Gl.(4) gekennzeichnete ideale Verhalten, bei dem die Dämmung mit 6 dB pro Frequenzverdopplung ansteigt, ist bei realen Wänden leider nicht zu finden. Vor allem bei leichten Wänden ist der Anstieg oftmals viel geringer. Man kann deshalb die Frage stellen, ob sich z.B. durch Anbringen von Resonatoren eine wesentliche Verbesserung der Schalldämmung erzielen läßt. Im Folgenden soll dies untersucht werden, wobei wir uns zur Vereinfachung wieder auf senkrechten Schalleinfall beschränken.

Eine Möglichkeit ist, daß die Masse m des Resonators über seine Federung F an die vorgegebene Wand der Masse M angekoppelt ist. Dies ist bei einer vorgesetzten zweiten Wandschale der Fall, wobei die Federung durch ein Luftpolster gegeben ist. Berücksichtigt man die Dämpfung durch einen Reibungswiderstand R, dann ergibt sich als Ersatzschaltbild Abb.2.

Wichtig ist bei der realen Ausführung einer solchen Anordnung, daß keine Wellenausbreitung im Federungshohlraum stattfindet, was durch Kassettierung oder Füllung mit Absorptionsmaterial erreicht werden kann. In unserer Betrachtung spielt das keine Rolle, da wir uns auf senkrechten Schalleinfall beschränkt haben.

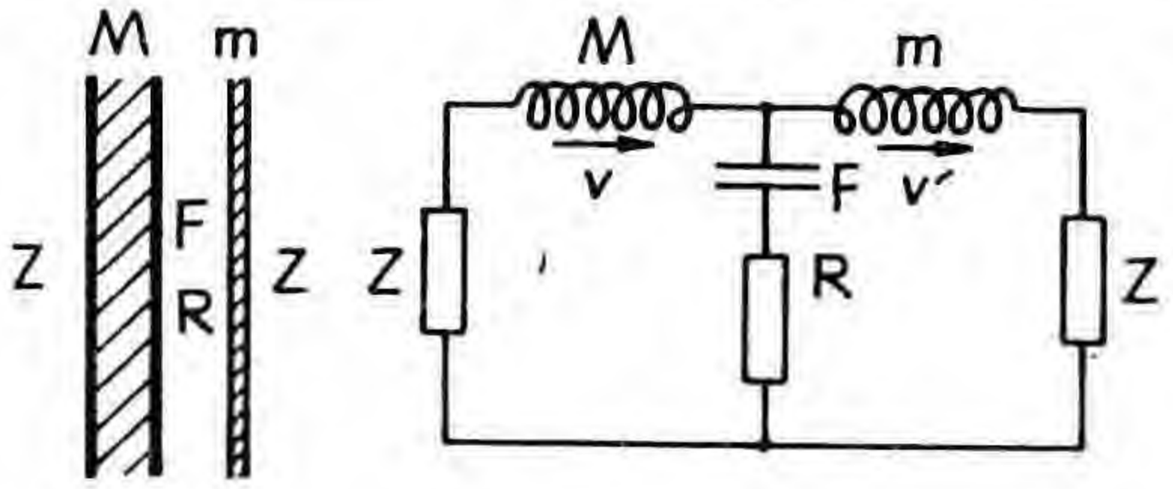

Abb. 2

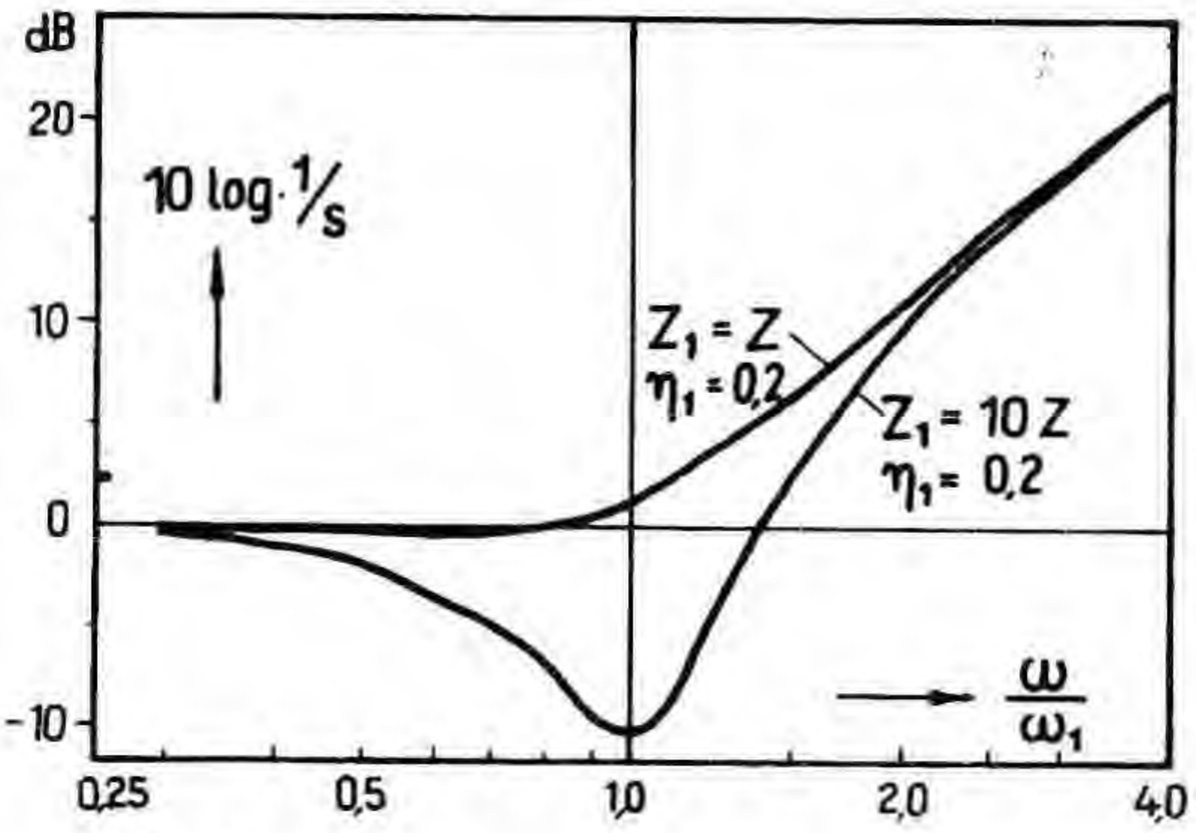

Abb. 3

Für die Schalldämmung, die wir wieder durch das Verhältnis von auftreffender zu durchgelassener Leistung kennzeichnen wollen, erhält man

$$\frac{N_1}{N_2} = \frac{1/Z\,|p|^2}{Z\,|v'|^2} = \frac{1}{Z^2}\left|\frac{p}{v}\right|^2 \cdot \left|\frac{v}{v'}\right|^2 . \quad (5)$$

In einem weiten Bereich ist nun die Impedanz des aus m, F, R und Z gebildeten Resonanzkreises klein gegen ωM. Dann ist nach (1) und (2) wie bei der Einfachwand

$$\frac{1}{Z^2}\left|\frac{p}{v}\right|^2 \approx \left(\frac{\omega M}{2Z}\right)^2$$

Somit ergibt sich aus (5)

$$\frac{N_1}{N_2} \approx \left(\frac{\omega M}{2Z}\right)^2 \cdot \left|\frac{v}{v'}\right|^2 . \quad (6)$$

Der Faktor $|v/v'|^2$ gibt also die "Verbesserung" der Schalldämmung an, die der Resonator bei der Einfachwand der Masse M bewirkt.

Üblicherweise wird die Größe $s = |v'|^2/|v|^2$ als Abstrahlgrad bezeichnet, somit ist die Verbesserung gleich dem reziproken Abstrahlgrad. Zu bemerken ist hierbei noch, daß auch bei den Wänden, deren Schalldämmung stärker von dem Massegesetz abweicht, die Verbesserung sehr gut durch den Faktor $1/s$ wiedergegeben wird.

s läßt sich an Hand des Ersatzschaltbildes leicht errechnen. Mit den Kenngrößen (7) ergibt sich $1/s$ nach Gl.(8).

$$\omega_1 = \frac{1}{\sqrt{mF}} \; ; \; Z_1 = \sqrt{\frac{m}{F}} \; ; \; \eta_1 = \frac{R}{Z_1} \quad (7) \qquad \frac{1}{s} = \left|\frac{v}{v'}\right|^2 = \frac{\left(\frac{\omega}{\omega_1} - \frac{\omega_1}{\omega}\right)^2 + \left(\eta_1 + \frac{Z}{Z_1}\right)^2}{\left(\frac{\omega_1}{\omega}\right)^2 + \eta_1^2} \quad (8)$$

Die Frequenzabhängigkeit von $1/s$ ist für zwei Fälle in Abb.3 aufgetragen. Man sieht den für eine vorgesetzte Wandschale typischen Verlauf, daß nur oberhalb der Resonanzfrequenz eine Verbesserung zu erzielen ist, während im Gebiet $\omega \approx \omega_1$ meist eine Verschlechterung auftritt. Weiter ist aber zu erkennen, daß der Resonanzeinbruch zum Verschwinden zu bringen ist, wenn man den charakteristischen Widerstand Z_1 des Resonators klein macht. Das bedeutet, daß Resonatoren mit geringer Masse günstiger sind, als solche mit großer Masse. Bei einem Helmholtz-Resonator, bei dem die Masse durch Luftpfropfen in Öffnungen gebildet wird, kann man einen Wert $Z_1 \approx Z$ erreichen, wohingegen massive Wandschalen meist einen charakteristischen Widerstand Z_1 von mehr als 10 Z aufweisen.

Diese Überlegungen zeigen also, daß bei der Resonanzfrequenz nicht unbedingt eine Verschlechterung der Schalldämmung eintreten muß, nämlich dann nicht, wenn der Resonator einen hinreichend kleinen charakteristischen Widerstand Z_1 hat.

Es ist aber auch der Fall denkbar, daß gerade im Bereich der Eigenfrequenz eines mit einer Wand gekoppelten Resonators eine wesentliche Verbesserung der Schalldämmung eintritt. Dieser ergibt sich, wenn man den Resonator über den Strahlungswiderstand Z an die vorgegebene Wand der

Masse M ankoppelt. In Abb.4 ist eine derartige Konstruktion und ihr Ersatzschaltbild angegeben.*

Bei der dargestellten Konstruktion handelt es sich um starr an der Wand befestigte Helmholtz-Resonatoren, im Ersatzschaltbild ergibt sich ein Serienkreis parallel zum Wellenwiderstand Z. Aus der Schaltung ersieht man unmittelbar, daß bei kleinen Werten von R der Serienkreis in Resonanz den Widerstand Z kurzschließt, so daß es dann zu verminderter Abstrahlung kommt.

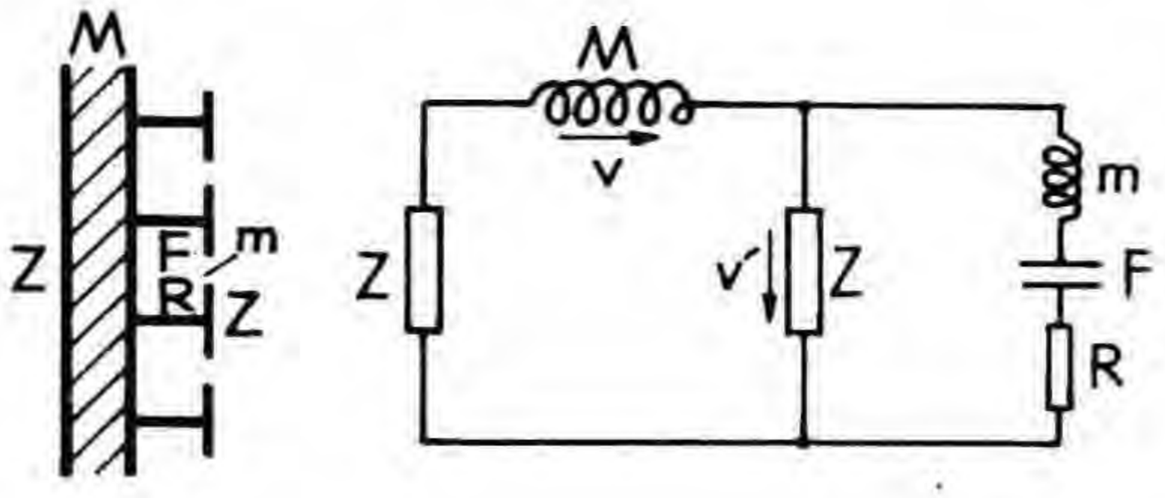

Abb.4

Bei hinreichend kleinem charakteristischem Widerstand Z_1 des Serien-Resonanzkreises können alle Widerstände gegen ωM vernachlässigt werden. Dann ergibt sich für die Schalldämmung, wenn man wieder eine einfallende Welle mit dem Druck p und eine rückwärts abgestrahlte Welle mit der Schnelle v' hat, Gl.(9). Diese Beziehung (9), die der im vorhergehenden Fall gefundenen Beziehung (6) analog ist, besagt wieder, daß die Verbesserung der Schalldämmung durch den reziproken Abstrahlgrad gegeben ist.

$$\frac{N_1}{N_2} = \frac{\frac{1}{Z}|p|^2}{Z|v'|^2} = \frac{1}{Z^2}\left|\frac{p}{v}\right|^2 \cdot \left|\frac{v}{v'}\right|^2 \approx \left(\frac{\omega M}{2Z}\right)^2 \cdot \frac{1}{s} \qquad (9)$$

$$\frac{1}{s} = \left|\frac{v}{v'}\right|^2 = \frac{\left(\frac{\omega}{\omega_1} - \frac{\omega_1}{\omega}\right)^2 + \left(\eta_1 + \frac{Z}{Z_1}\right)^2}{\left(\frac{\omega}{\omega_1} - \frac{\omega_1}{\omega}\right)^2 + \eta_1^2} \qquad (10)$$

Unter Benutzung der Kenngrößen nach (7) errechnet man Gl.(10). Diese Funktion ist in Abb.5 dargestellt.

Wie erwartet, ergibt sich eine Verbesserung nur in der Nähe der Resonanzfrequenz. Diese Verbesserung ist um so größer, je kleiner η_1 ist und um so breitbandiger, je kleiner Z_1 ist.

Bei einem Helmholtz-Resonator sind Resonanzfrequenz ω_1 und Widerstand Z_1 nicht unabhängig voneinander, vielmehr ist ihr Produkt durch die Hohlraumtiefe d bestimmt.

$$(11) \quad \omega_1 \cdot Z_1 = \frac{\rho \cdot c^2}{d}$$

Da man zur Erzielung einer Verbesserung in einem größeren Frequenzbereich einen kleinen Wert von Z_1 wünscht, andererseits aus praktischen Gründen d nicht zu groß machen kann, muß man bei der Dimensionierung für unsere Zwecke geeigneter Resonatoren einen Kompromiß schließen.

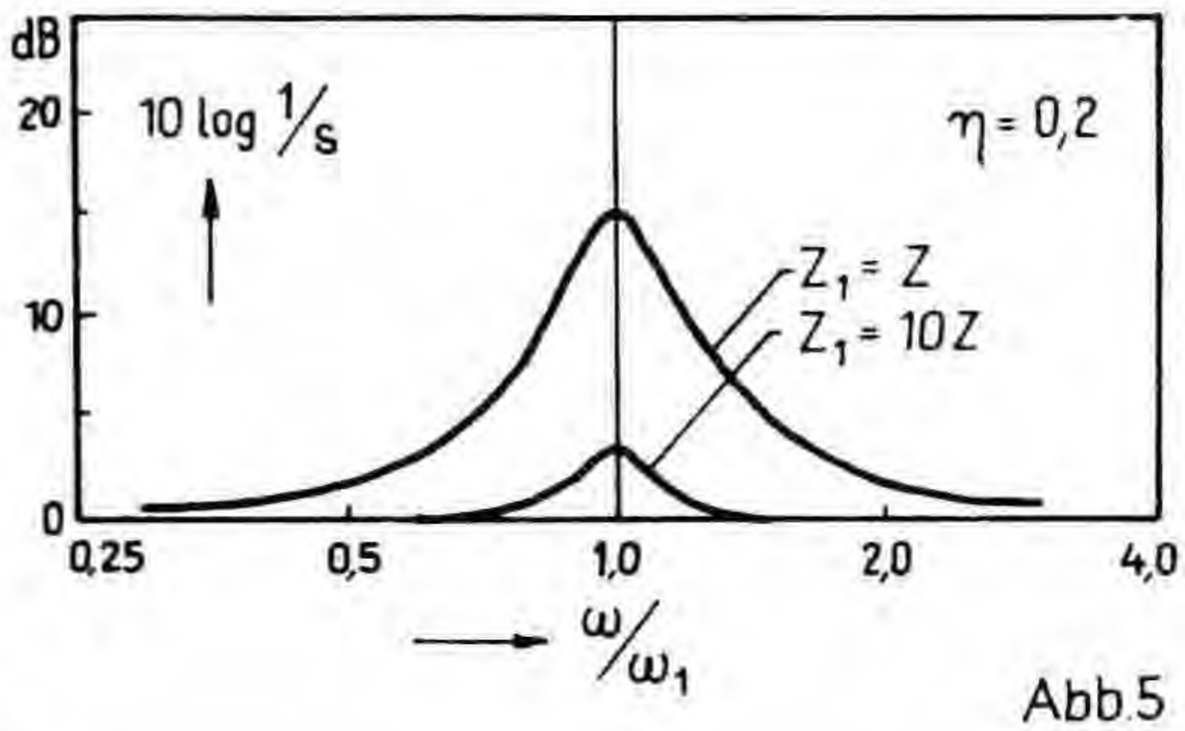

Abb.5

Die praktische Ausführung einer Wand mit Helmholtz-Resonatoren, von der nachfolgend Meßergebnisse mitgeteilt sind, bestand aus einem Wabenkern von 5 cm Stärke und beiderseits aufgeklebten 3,5 mm dicken Deckschichten (Abb.7), wobei die eine Deckschicht mit Bohrungen von 5 mm Durchmesser versehen war. Diese Wand wurde zunächst im Urzustand, dann mit den Bohrungen gemessen.

Die Resonatoren hatten folgende Kenngrößen, die sich aus der Geometrie bzw. aus der im Kundt'schen Rohr gemessenen Absorptionskurve (Abb.6)

* Dieses Ersatzschaltbild wurde zuerst von G. Kurtze angegeben.

errechnen: $\frac{\omega_1}{2\pi} = 700\,Hz$; $Z_1 = 1{,}5 \cdot Z$; $\eta_1 = 0{,}19$

Abb.7 zeigt die an der Wand mit und ohne Bohrungen gemessene Schalldämmung. Ferner sind die gemessene Verbesserung durch die Resonatoren sowie die theoretisch sich ergebende Verbesserung dargestellt. - Der berechnete Maximalwert von $^1/_s$ bei 700 Hz beträgt 13 dB, die Messung ergab im Terzbereich um 640 Hz 11,5 dB. Die mittlere Verbesserung über drei Frequenzoktaven wurde mit 3,8 dB errechnet, während 4,4 dB gemessen wurden.

Der gemessene Verlauf der Verbesserung $^1/_s$ steht in guter Übereinstimmung mit den berechneten Werten, hingegen weicht die Dämmungskurve der Wand <u>ohne</u> Resonator vom Massegesetz stark ab, was aber hier ohne Belang ist.

Es liegt hier also ein Fall vor, in dem im Resonanzbereich keine Verschlechterung der Schalldämmung eintritt, sondern im Gegenteil eine wesentliche Verbesserung. Gleichzeitig zeigt eine solche Wand mit Resonatoren eine erhöhte Schallabsorption, was in manchen Fällen von Vorteil ist.

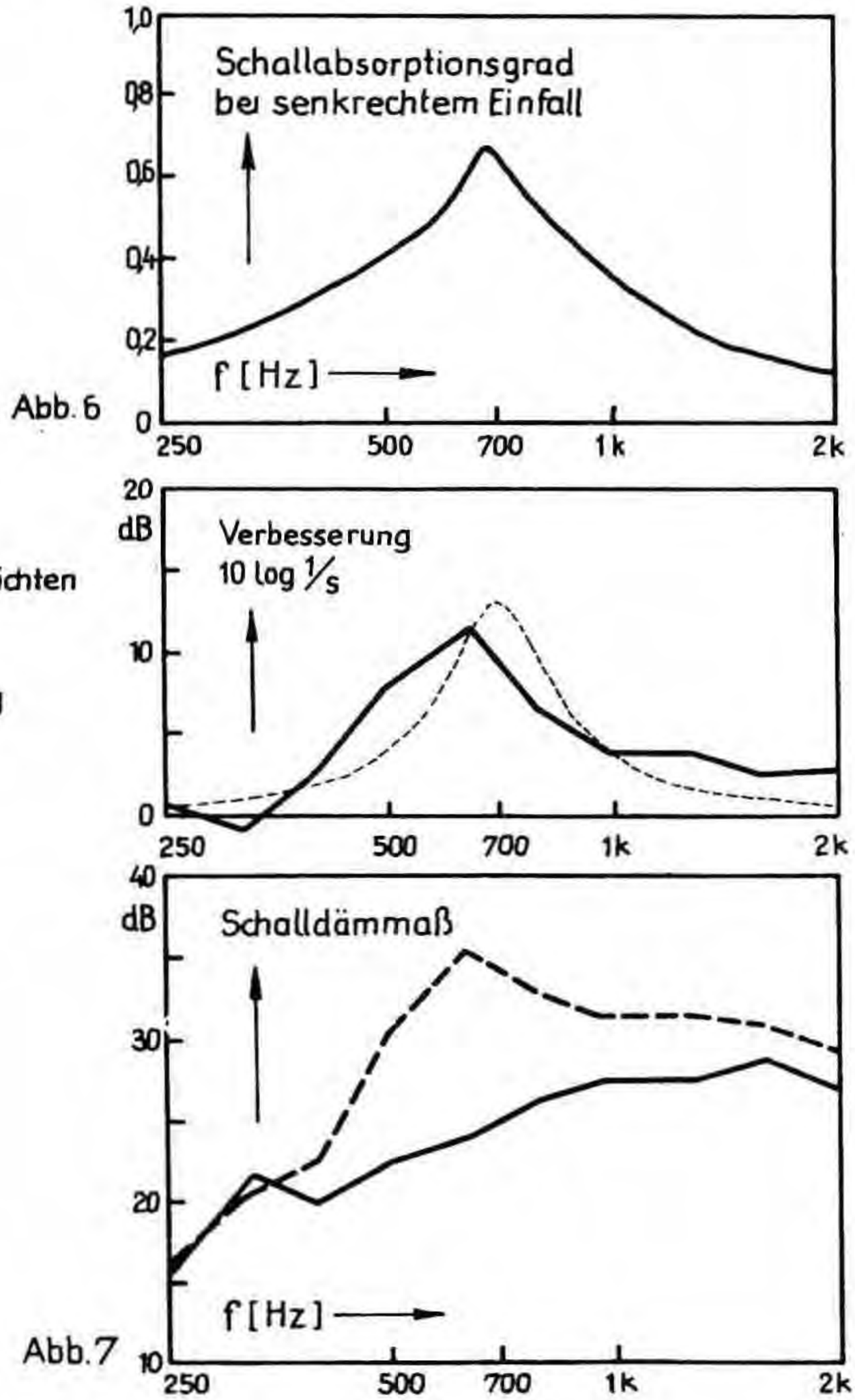

Abb.6

Abb.7

N36

FOURTH INTERNATIONAL CONGRESS ON ACOUSTICS
COPENHAGEN 21.-28. AUGUST 1962

THE AIR MODULATED LOUDSPEAKER AND ITS APPLICATION TO ACOUSTIC ENVIRONMENTAL TESTING

John K. Hilliard, Walter T. Fiala, and John J. Van Houten

Three principle types of transducers are now available for generating the large amounts of acoustic power required for high intensity sonic environmental testing. These are:

1. Conventional dynamic loudspeakers
2. Sirens
3. Air modulated devices.

The conventional dynamic transducers include large area cone speakers for frequencies up to 1,000 cps and compression type drivers above this frequency. These provide a source of random or periodic acoustic noise capable of delivering a maximum of 145 db SPL or 200-300 acoustic watts with efficiencies from 5% to 20%. Above this level, absorption of the units themselves and the surrounding enclosure limit their use.

Sirens may be designed for either random or limited sinusoidal output. They average 4% conversion of pneumatic to acoustic energy. Acoustical power levels of 25 Kw per unit have been achieved. The limitation of this device is the fixed spectrum output for either sine or random operation, inherent in the design of the rotor configuration. However, the random output can be essentially uniform up to 10 KC.

Air modulated transducers are now available which produce power in excess of 2,000 acoustic watts. The device to be described is capable of sine wave and random spectra programmed electrically with suitable wave generators or tape recordings. This device has a pneumatic efficiency of 14%

The principle of operation of an electro-pneumatic transducer extends back at least twenty-five years. However, the earlier devices had severe limitation in frequency response, distortion, and total generated acoustical power (100 watts).

Figure 1 shows a cross section of the unit now in use. It has a diameter of seven inches and a length of twelve inches.

The air valve consists of a stationary, inner modulator ring; a movable, outer modulator ring; and a supporting ring. The inner ring contains two rows of eight slots equally spaced around its circumference, each slot having a height of 0.060 inch. The outer ring, which is fitted closely over the inner ring, contains eight slots. These slots are of the same width and spacing as those of the inner ring, and have a height of 0.060 inch.

The outer modulator ring is supported by eight ¼" x ¼" x ¼" butyl rubber blocks bonded on one end to this ring in the spaces between the slots.

On the other end, each block is bonded to the fixed supporting ring.

In the quiescent state, that is with no modulation but with air flowing radially inward, the slots of the inner ring are half closed by the outer ring, presenting an effective slot height of 0.030 inch to the air flow. With electrical signal input, the outer ring moves up and down, changing the area of the air passage and thereby modulating the air flow in accordance with the electrical signal.

For maximum acoustical output, 300 scfm of air at 40 psi is required. The electrical power to obtain 100% modulation is 100 watts. Figure 2 is a typical random noise distribution generated by the unit. Figure 3 illustrates the sinusoidal frequency response. The random noise response is uniform to 2,400 cps and falls at the rate of 6 db per octave above this frequency.

Test Chamber Configurations

The reverberant chamber and progressive wave tube are the most widely used configurations for acoustical testing. Progressive wave testing offers the advantage of compact test equipment size with the capability of generating wideband acoustical energy over the entire audio spectrum. The reverberant chamber is used when a highly diffused sound field is desired. The physical dimensions of the reverberation room determine the lowest operating frequency.

The remainder of this paper will be devoted to examples of the application of the previously described electro-pneumatic transducer to progressive wave and reverberation chamber testing.

Two types of progressive wave tubes are required for sonic environmental testing. One is a narrow channel used to generate high intensity noise for panel fatigue studies. Another tube having a square cross section is required for electronic and/or mechanical component testing.

An Overall Sound Pressure Level of 167 db has been obtained in a 6" x 30" cross section of a progressive wave channel. The fatigue of panels having maximum dimensions of 30" x 40" are studied by use of this channel. The electro-pneumatic transducer is ideal for this application since a sinusoidal sweep is performed and the response of the panel established. Having this information, a random noise test is then performed simulating the operational environment anticipated. In view of the versatility inherent with the noise generator, no arguments of sine-random equivalents become necessary.

A progressive wave channel with a cross section of 6" x 5' has been fabricated and is in operation at the Douglas Aircraft Company plant in Santa Monica. An Overall Sound Pressure Level of 170 db is achieved by use of ten electro-pneumatic transducers. Both random and periodic signals are programmed in order to subject a panel having maximum dimensions of 5' x 10' to simulated operational environments.

For testing electronic or mechanical equipment items to high intensities, particularly at low frequencies, progressive wave tubes having cross sectional dimensions in the order of 2' x 2' have been designed and are in operation. Figure 4 indicates the SPL available for various test chamber configurations. High frequency transducers complement the electro-pneumatic device for programmed spectrums in the seventh and eighth octave bands.

A reverberation chamber size which appears to meet the bulk of test requirements has interior dimensions in the order of ten feet. A typical laboratory arrangement outlined in Figure 5 shows the previously mentioned progressive wave channel and square cross section tube. A reverberation chamber is also included. The three environmental chambers each will accommodate the same transducer array. The array is fabricated on casters and is readily portable to be positioned at either of the test chamber locations, depending on the specific requirements of the test to be performed.

A modular concept in both transducer and exponential connector design permits considerable future growth of the progressive wave units and reverberation chamber in both size and sound level. Figure 6 exemplifies this concept. You will note that as the requirements change, additional transducers are added to the exponential connector with little sacrifice in previously fabricated hardware. A single modular consisting of transducer and exponential horn is fabricated for this purpose.

CONCLUSION

The electro-pneumatic transducer has proven to be a versatile tool for a wide variety of applications requiring large amounts of acoustic power. We have described various applications of this device in the area of sonic environmental testing. Equipment also has been designed in which the transducer plays an important roll as a signalling device for speech and warning installations.

Research is in progress which will result in an improved air modulated transducer with response to 5,000 cps to accommodate the evergrowing demands of qualification and evaluation testing of flight vehicle elements. Also, it will accommodate the need of acoustic warning systems with ranges of several miles.

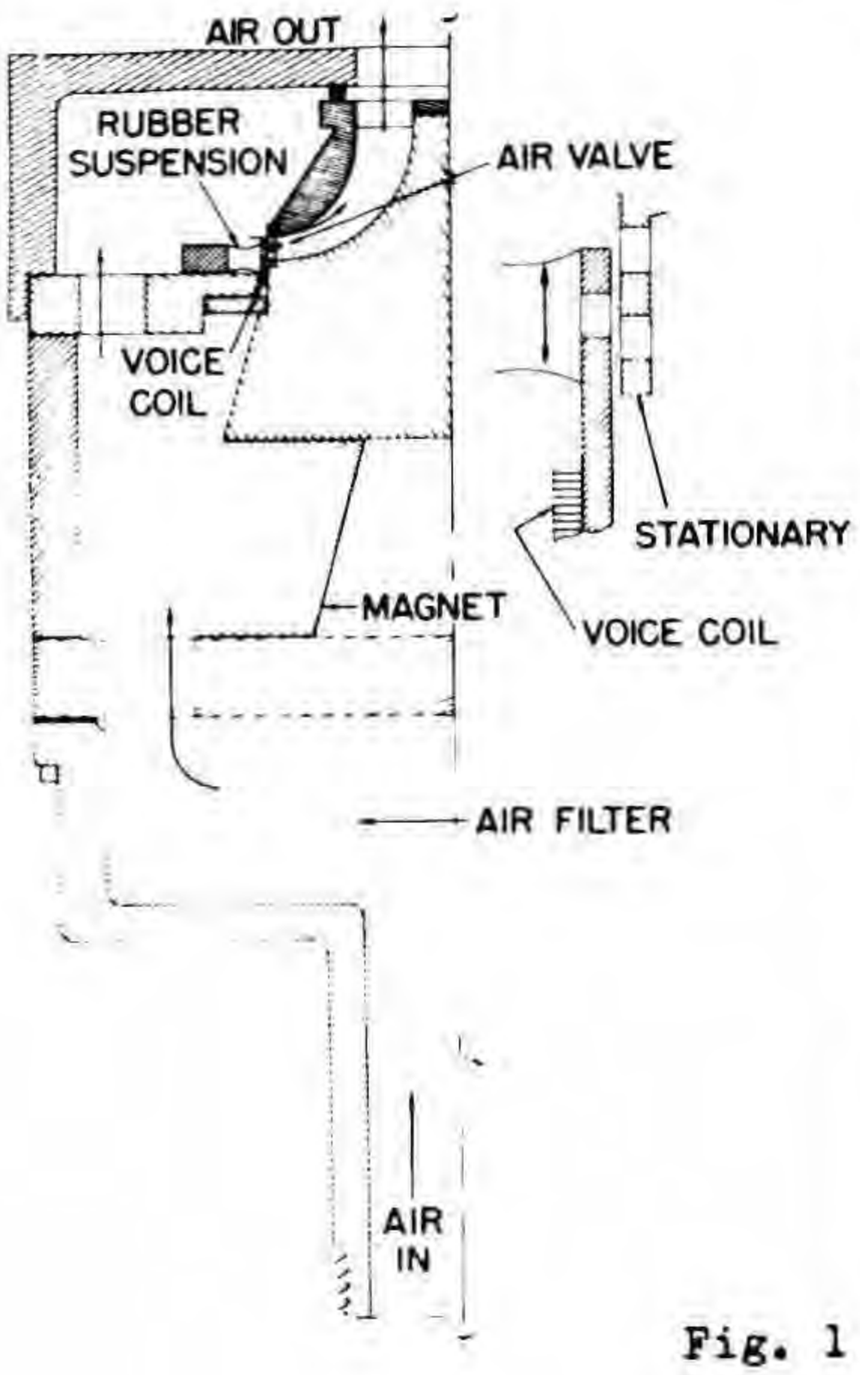

Fig. 1

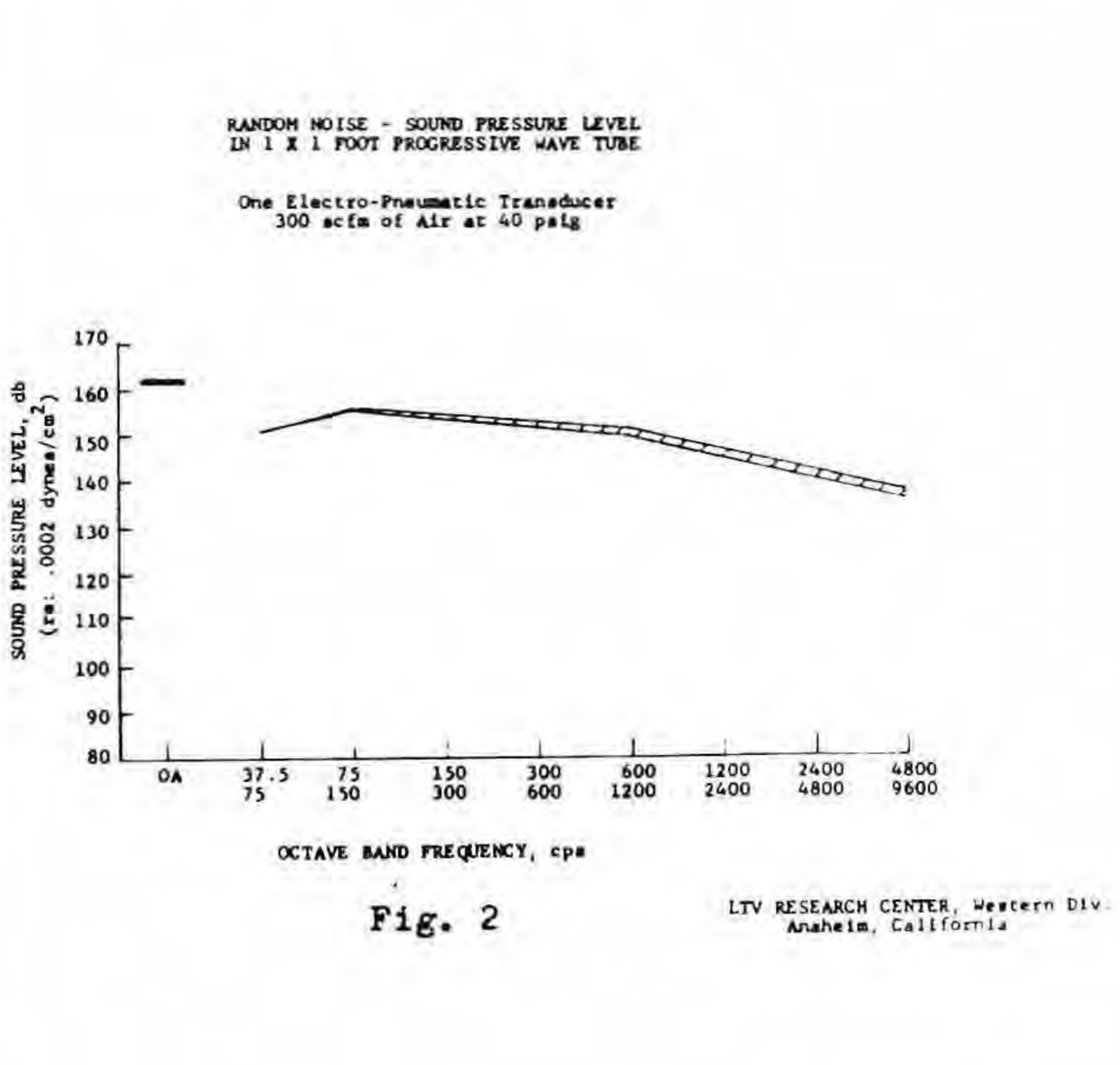

Fig. 2

LTV RESEARCH CENTER, Western Div.
Anaheim, California

RESPONSE OF 1 x 1 FOOT PROGRESSIVE WAVE TUBE

One Electro-Pneumatic Transducer

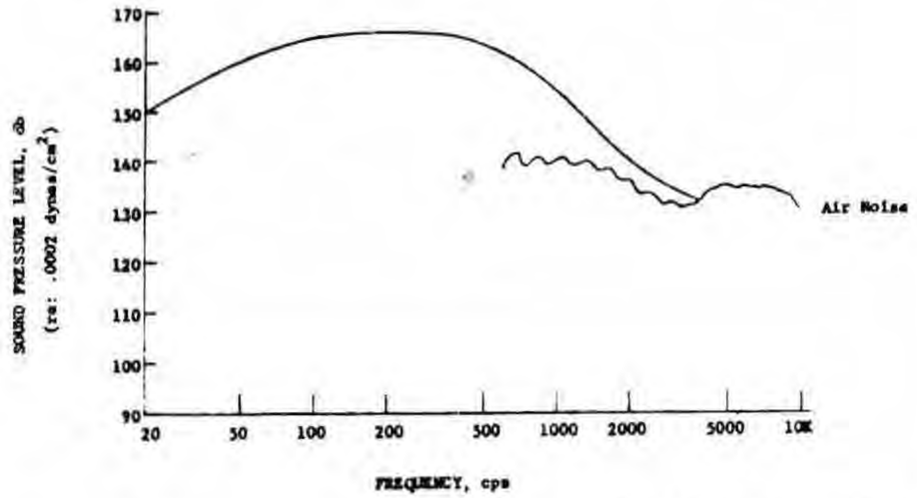

Fig 3

LTV RESEARCH CENTER, Western Division
Anaheim, California

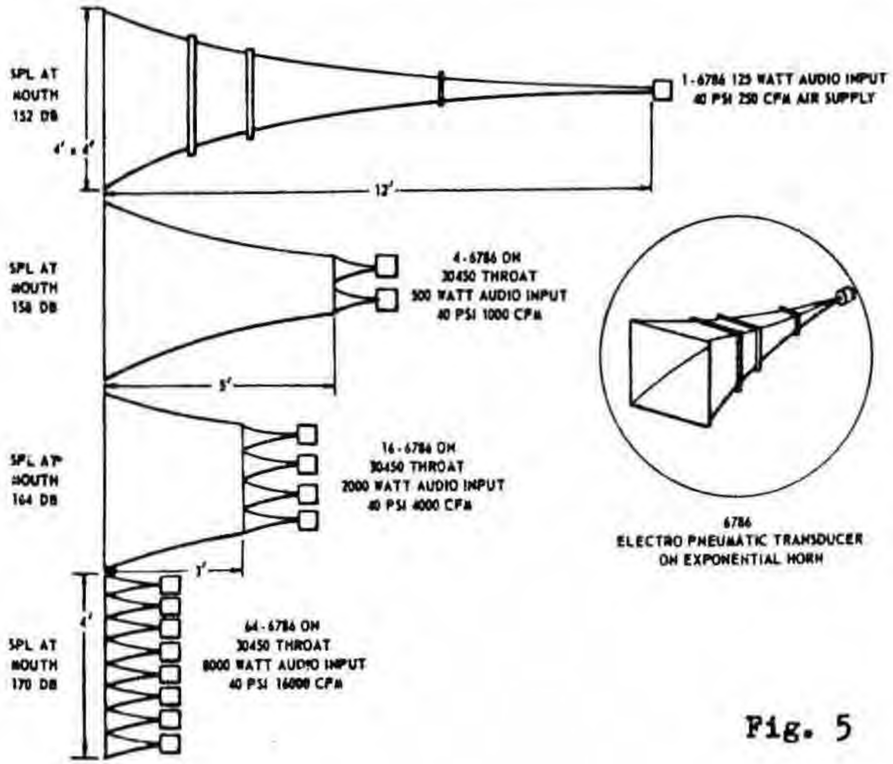

Fig. 5

Fig. 4

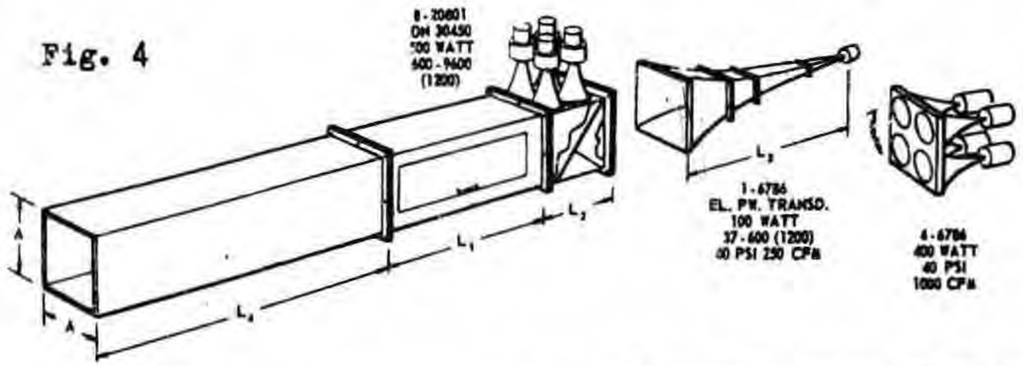

TEST SECTION		MIXING UNIT	EXPON. CONNECTOR	ABSORPTION UNIT	164 DB SPL		170 DB SPL	
					NO. OF 20801 EL. POWER	NO. OF 6786 EL. POWER AIR SUPPLY	NO. OF 20801 EL. POWER	NO. OF 6786 EL. POWER AIR SUPPLY
A'	L_1'	L_2'	L_3'	L_4'				
1	3	1½	6	8	8 500 WATT	1 125 WATT 40 PSI 250 CFM	8 500 WATT	4 500 WATT 40 PSI 1000 CFM
2	5	2½	9	8	16 1000 WATT	4 500 WATT 40 PSI 1000 CFM	16 1000 WATT	16 2000 WATT 40 PSI 4000 CFM
4	6	4½	12	8	64 4000 WATT	16 2000 WATT 40 PSI 4000 CFM	16 4000 WATT	64 8000 WATT 40 PSI 16000 CFM

HIGH INTENSITY SONIC ENVIRONMENTAL TESTING LABORATORY

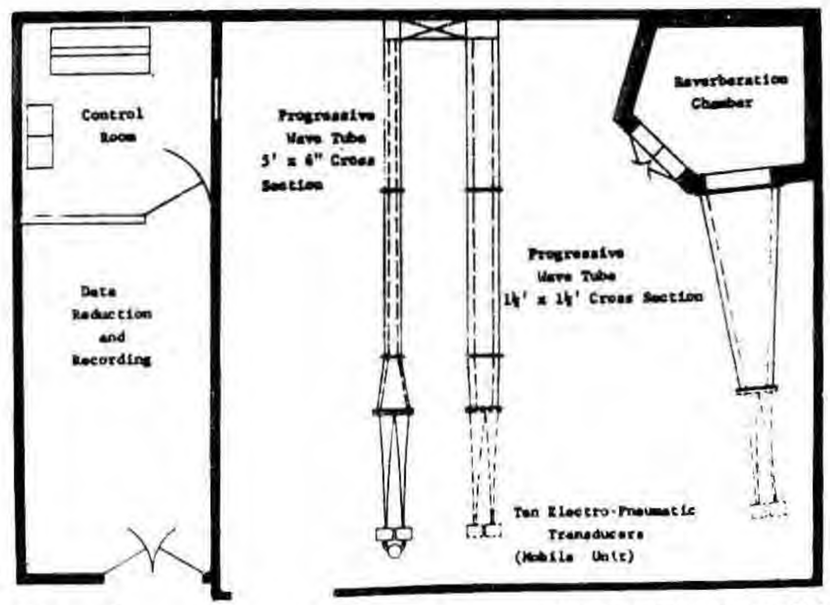

Fig. 6

LTV RESEARCH CENTER, Western Division
Anaheim, California

O36

FOURTH INTERNATIONAL CONGRESS ON ACOUSTICS
COPENHAGEN 21.-28. AUGUST 1962

Diffraction Theory of Noise Generated by Turbulent Flows and Boundary Layers.

L.M.Lyamshev

We consider sound radiation by turbulent infrasonic aerodynamic flows with thin elastic bodies placed in the flow. The statistical processes are assumed to be stationary in time. However, this consideration may be generalised for nonstationary processes. Let us write the equation for the propagation and generation of sound in the turbulent moving medium /1-3/.

$$\frac{1}{c^2}\frac{D^2}{Dt^2}p^{(1)}(\bar{x}_0) - \Delta p^{(1)}(\bar{x}_0) = \frac{\partial^2}{\partial x_{0i}\partial x_{0j}} P_{ij}(\bar{x}_0) \qquad /1/$$

here $\frac{D}{Dt} = -i\omega + \bar{v}_j\frac{\partial}{\partial x_j}$; $\bar{v}_1 = V$, $\bar{v}_2 = v_3 = 0$; $P_{ij}(\bar{x}_0) = S_{ij}(\bar{x}_0) - p^0(\bar{x}_0)\delta_{ij}$

$S_{ij}(\bar{x}_0)$ the viscous stress tensor, $p^0(\bar{x}_0)$ pressure fluctuations in the turbulent flow of an incompressible gas. Fluctuations $p^0(\bar{x}_0)$ are connected with velocity fluctuations $v_j^0(\bar{x}_0)$ due to the equation

$$\Delta p^0(\bar{x}_0) = -\rho_0\frac{\partial^2}{\partial x_{0i}\partial x_{0j}} v_i^0 v_j^0 \qquad /2/$$

We require that the solution of the equation /1/ satisfies with the radiation condition in infinity and the following boundary conditions hold on the surface of elastic bodies.

$$L w^{(1)}(\bar{x}_0) = p^{(1)}(\bar{x}_0)|_S \qquad /3/$$

$$-\frac{\partial p^{(1)}(\bar{x}_0)}{\partial n} = \rho_0\left(-i\omega + V\frac{\partial}{\partial x_2}\right)^2 w^{(1)}(\bar{x}_0) \qquad /4/$$

Here L is the linear differential self-adjoint operator; eq./3/ represents the equation of motion of the streamlined elastic body - the shell or plate; $W(\bar{x}_0)$ are the displacements of the shell or plate surface S in the direction of the outward normal to S, namely $\bar{n}$.

Eq./4/ follows from the condition of the surface impenetrebility for the gas flow: $\frac{D}{Dt}F(\bar{x},t)=0$, $F(\bar{x},t)=0$ is equation of the surface S. We introduce the auxibiliary solution $\tilde{p}^{(2)}(\bar{x}/\bar{x}_0)$ of the adjoint boundary problem. Eq. $\tilde{p}^{(2)}(\bar{x}/\bar{x}_0)$ discribes a regular (nonstatistical) acoustical field. That satisfies the equation

$$\frac{1}{c^2}\frac{\tilde{D}}{Dt^2}\tilde{p}^{(2)}(\bar{x}/\bar{x}_0)-\Delta\tilde{p}^{(2)}(\bar{x}/\bar{x}_0)=-4\pi\delta(\bar{x}-\bar{x}_0) \qquad /5/$$

the radiation condition and the adjoint boundary conditions on S. It follows from the adjointment of the basic and auxiliary problems, the radiation condition and Green's theorem that the solution of the eq./1/ may be written in the form:

$$p^{(1)}(\bar{x})=\int_{\Omega}P_{ij}(\bar{x}_0)\frac{\partial^2}{\partial x_{0i}\partial x_{0j}}\tilde{p}^{(2)}(\bar{x}/\bar{x}_0)d\Omega(x_0)+i\omega\rho_0\int_S \ell_i v_i^0(\bar{x}_0)\tilde{p}^{(2)}(\bar{x}/\bar{x}_0)ds(\bar{x}_0)-$$
$$-\int_S \ell_j\frac{\partial}{\partial x_{0i}}\tilde{p}^{(2)}(\bar{x}/\bar{x}_0)P_{ij}(x_0)\,ds(x_0) \qquad /6/$$

From the eq./6/ it is evident that the acoustic field of a turbulent flow with elastic bodies placed in the flow is a superposition of the fields of radiation from volume sources - pressure and viscous stress fluctuations in the flow and the fields of surface sources. Pressure and viscous stress fluctuations and velocity fluctuations acting from the f'ow on the elastic surface are surface sources. Dimensional analysis can be used to establish the fact that the radiation power of the volume sources is proportional to the ration of the flow velocity to the velocity of sound in the medium, raised to the eight power /M^8/; the radiation power of the surface sources, pressure and viscous stress fluctuations are proportional to M^6 and the velocity fluctuations to M^4. Consequently, in the case of infrasonic turbulent flows /$M < 1$/ and elastic, but "soft" surfaces, when the velocity fluctuations in the flow around the surface are large compared with the pressure and viscous stress fluctuations, the acoustic radiation is caused mainly by velocity fluctuations. On the other hand, when the

surface is relatively "rigid", the role of the velocity fluctuations is insignificant. In this case the radiation field is caused mainly by the action of the pressure of viscous stress fluctuations on the elastic surface. S . A significant sound radiation by vibrating bodies takes place in a given above cases. The so called "pseudosound" transforms into true sound.

In the radiation field of the flow the cross-correlation function and average meaning of the square pressure fluctuation can be obtained from the eq./6/. Under the conditions that the flow velocity is relatively small and in some other cases, when $|\rho^0(\bar{x}_0)| >> |S_{ij}(\bar{x}_0)|$ the average meaning of square pressure fluctuation should be calculated as follows:

$$\overline{\rho^{(1)}(\bar{x}_1)\rho^{(1)*}(\bar{x}_2)} \approx \iint_{SS} \frac{\partial \tilde{p}^{(2)}(\bar{x}_1/\bar{x}_0')}{dn} \frac{\partial \tilde{p}^{(2)*}(\bar{x}_2/\bar{x}_0'')}{dn} \overline{p^0(\bar{x}_0')p^0(\bar{x}_0'')} ds(\bar{x}_0) ds(\bar{x}_0'') \quad /7/$$

The average meaning of square pressure fluctuations is obtained from eq./7/ when $\bar{x}_1 = \bar{x}_2$

Consequantly, for the calculation of the cross-correlation function of the sound pressure fluctuations and the average of the meaning square of these fluctuations it is necessary to solve the corresponding auxiliary adjoint diffraction problem and to determine the correlation function of the pressure fluctuations at the elastic surface in a turbulent flow. If the auxiliary solution and correlation function are given the solution of the problem of sound radiation by a turbulent flow and by elastic bodies placed in the flow reduces to the calculation of the quadratures.

The correlation function of the pressure fluctuation can be determined both experimentally and from eq./2/. This equation can be considered as Poisson's equation for $\rho^0(\bar{x}_0)$ and be solved with the appropriate boundary conditions. Thus, if the velocity fluctuations in the flow at the surface of elastic bodies are insignificant, we can assume

that $\frac{\partial p^0(\bar{I}_0)}{\partial n|_S} = 0$ as was given, e.g. in /4/.

Eq./6/ can be used for the calculation of the cross-correlation function and avarage meaning of the square pressure fluctuations in a sound field of the free turbulent flow. In this case surface integrals in eq./6/ are vanished and it can be shown that Lighthill's solution /(2)/ follows from eq./6/. Eq./7/ can be applied for a calculation of statistical characteristics of a sound field of turbulent boundary layers.

We should like to note, in conclusion, that the results published by N.Curle /5/, R.Kraichnan /4/, P.Doak /6/ and A.Powell /7/ are particular cases of the more general solution given here.

Literature Cited

/1/ D.I.Blokhintsev, Acoustics of a Inhomogeneous Moving Medium, M.-L. 1946. p.43 /In Russian/. /2/ M.Lighthill, Proc.Roy.Soc. 1952. A211, 564; 1954, A222, 1. /3/ L.Lyamshev, Doklady A.N.SSSR. 1961. 137. 1343 /Eng.trans.in:Sov.Phys. - Doklady, v.6, N.4, p.341-43/, Akust.Zh. 1960, 6, 471; 1961, 7, 59; 1962, 8, 91 /Sov.Phys. - Acoust.(USA). /4/ R.Kraichnan, JASA, 1956, 28, 378; 1957, 29, 65. /5/ N.Curle, Proc.Roy.Soc. 1955, A231, 505. /6/ P.Doak, Proc.Roy.Soc. 1960, A254, 129; /7/ A.Powell, JASA, 1960, 32, 382.

L.M.Lyamshev

P36

FOURTH INTERNATIONAL CONGRESS ON ACOUSTICS
COPENHAGEN 21.-28. AUGUST 1962

On Anomalous Resonances in Stressed Crystalline Solids

Sol R. Bodner

Brown University, Providence, Rhode Island, U.S.A.

Introduction

This paper is concerned with the anomalous resonance dispersions that have been observed by E. R. Fitzgerald in his measurements of the audio frequency complex compliance of prestressed crystalline solids, e.g. Refs. 1-5. Some corroborating experiments and attempts at an explanation of the unusual results have been previously reported by the author, Refs. 6 and 7. Recent experiments have led to more definite indications on the nature and source of the resonances and associated effects. In particular, the resonances are presently viewed as being due to coupling of an elastic system such as a testing machine with a material property similar to a negative damping characteristic that occurs in stressed crystalline solids.

Previous Experiments

Fitzgerald's basic experimental procedure is to compress the specimen to about the yield stress of the material and to subject it to an oscillatory shear by means of a light weight driving tube, Fig. 1. The complex compliance components are obtained by measuring the in and out of phase strain to stress ratios. The specimen dimensions are small, about 0.25 in. and are appreciably smaller than the wave lengths of the oscillatory stresses so that the cyclic loading can be considered as quasi-static. Normal results were obtained in tests on amorphous polymers but unusual and unexpected results were obtained for crystalline solids such as lead, aluminum, crystalline quartz and NaCl. These were very high compliance values at the lower frequencies (about 100~500 c./s.) and the occurrence of sharp resonance dispersions that were independent of the specimen geometry. The compliance for aluminum, for example, was 20 times the usual value. A strong resonance at about 2800 c./s. was common for the various metals tested.

The author's initial tests involved forced lateral oscillations of preloaded aluminum bars and of aluminum bars containing residual stresses. Unexpected double resonance peaks were observed in the vicinity of 2800 c./s. when a natural frequency had this value. The double resonance peaks vanished upon unloading of annealing. In other respects the specimens subjected to forced lateral oscillations behaved in the normal manner and no change in the dynamic elastic modulus was noted even when the specimens were stressed into the inelastic range. Although these experiments demonstrated the importance of an applied or residual stress to obtain the effects, they were not conclusive as to their origin.

Recent Experimental Results

In Ref. 7 an attempt was made to devise a linear viscoelastic stress strain relation that would correspond to both Fitzgerald's and the author's results for the different test conditions. However, Fitzgerald's very low dynamic elastic modulus values and the author's observations of the usual values were not reconcilable. The possibility existed, however, that for Fitzgerald's test conditions of initial preloading to the inelastic range the material would exhibit a lower modulus for superimposed quasi-static cyclic stresses. The author's tests and other similar tests differ in that they involve the inertia of the test specimens. Further experiments were devised in which the specimens were a pair of thin walled tubes about 1 ft. long, 1 in. in diameter and having a wall thickness of 0.05 in. They were connected through a large mass (about 13 lb.) so that natural frequencies in the range of 100-300 c./s. could be achieved for longitudinal, torsional and bending oscillations of the combined spring mass system, Fig. 2. These frequencies were much less than the natural frequencies of the specimens by themselves.

The oscillations for the various modes were forced and measured by coil and magnet arrangements on extension arms to the central inertial mass. The natural frequencies for the different modes were observed as the specimens, which were of pure aluminum and various aluminum alloys, were subjected to a variety of loading conditions including plastic flow under applied strains and applied loads. In all instances the dynamic modulus remained the same to within the experimental accuracy (about 1%) after the slight corrections due to geometry changes and continuum mechanical effects were made to the observed frequencies. These experiments duplicated Fitzgerald's conditions except for overall size and the flexibility of the testing apparatus. They strongly indicated that Fitzgerald's very low moduli values are a consequence of the flexibility of his apparatus and are not dynamic moduli in the usual sense.

Discussion

The evidence that the resonances are of the self-excited oscillation type was previously discussed by the author in Ref. 7. These included the negative damping values observed by Fitzgerald, the sharpness of the resonances, and the apparent conversion of the energy of initial compression into oscillatory energy. Stressed crystalline solids appear to contain the required negative damping property required for self excited oscillations. On the microscopic level, the fine slip mechanism of dislocation motion has properties similar to those of dry friction including the initial negative slope of the force velocity relation. This negative slope property has been observed macroscopically in various stress-strain rate measurements, e.g. Ref. 8, and is generally recognized to be responsible for the acoustic emission observed in tension tests with flexible machines. The acoustic emission effect is well represented by the dry friction chatter model, Fig. 3, in which the friction characteristic is the material stress-strain rate relation, the spring and mass represent the testing machine, and the moving belt velocity is the testing speed.

The experiments of Fitzgerald and of the author can be viewed as a variation of the acoustic emission test. The relevant model appears to be that shown in Fig. 3 but in which the belt undergoes small harmonic oscillations. It is therefore a system having inherent capabilities for self-excited oscillations that is subjected to parametric excitation. The harmonic variation in this case occurs in the damping term rather than as a simple forcing function. Fitzgerald's results, the high compliance values and the apparent resonances, would then be due to the output of such a complicated system. As in the related acoustic emission case, an elastic system is required for self-excited oscillations to be present. This would be the flexibility of the apparatus in Fitzgerald's tests and, seemingly, the specimen itself vibrating in one of its natural modes in the author's tests. The need for flexibility in the testing system to obtain results similar to Fitzgerald's has also been shown recently by Le Grand, Ref.9.

Although the basic cause of the resonances and associated effects is considered to be better understood, a number of important questions remain. These include the determination of the physical properties responsible for the negative damping characteristic and, particularly, the nature of the common property that results in the frequently observed resonance at 2800 c./s. In addition, a proper mathematical description of the different experiments is highly desirable. The possibility of the utilization of these results as a simple low frequency amplifier also appears worthy of exploration.

References

1. Fitzgerald, E. R., Phys. Rev., 108, 690 (1957).
2. Fitzgerald, E. R., J. Chem. Phys., 27, 1180 (1957).
3. Fitzgerald, E. R., Phys. Rev., 112, 1063 (1958).
4. Fitzgerald, E. R., J. Acoust. Soc. Amer., 32, 1270 (1960).
5. Fitzgerald, E. R., Devel. in Mechanics, vol. 1, Plenum Press, N. Y., 10 (1961).
6. Bodner, S. R., Trans. Soc. Rheology, 4, 141 (1960).
7. Bodner, S. R., Trans. Soc. Rheology, 5, 297 (1961).
8. Manjoine, M. J., Trans. ASME, 66, A211 (1944).
9. Le Grand, D. G., "Dynamic Mechanical Properties of Polymers," General Electric Research Lab Report No. 61-RL-2714C, Schenectady, N. Y., (1961).

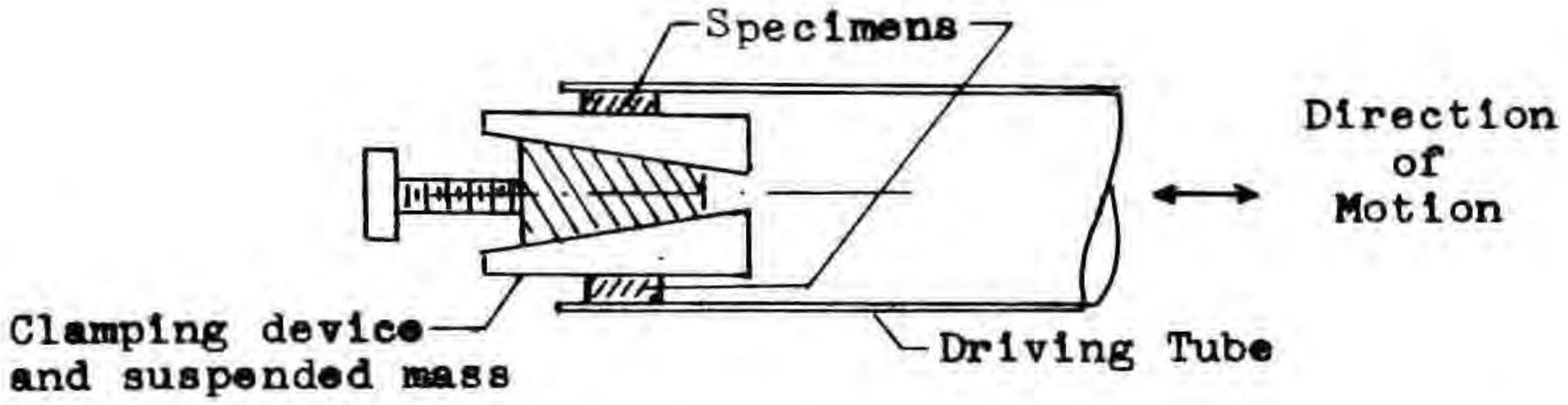

FIG. 1 SCHEMATIC OF FITZGERALD'S TEST ARRANGEMENT

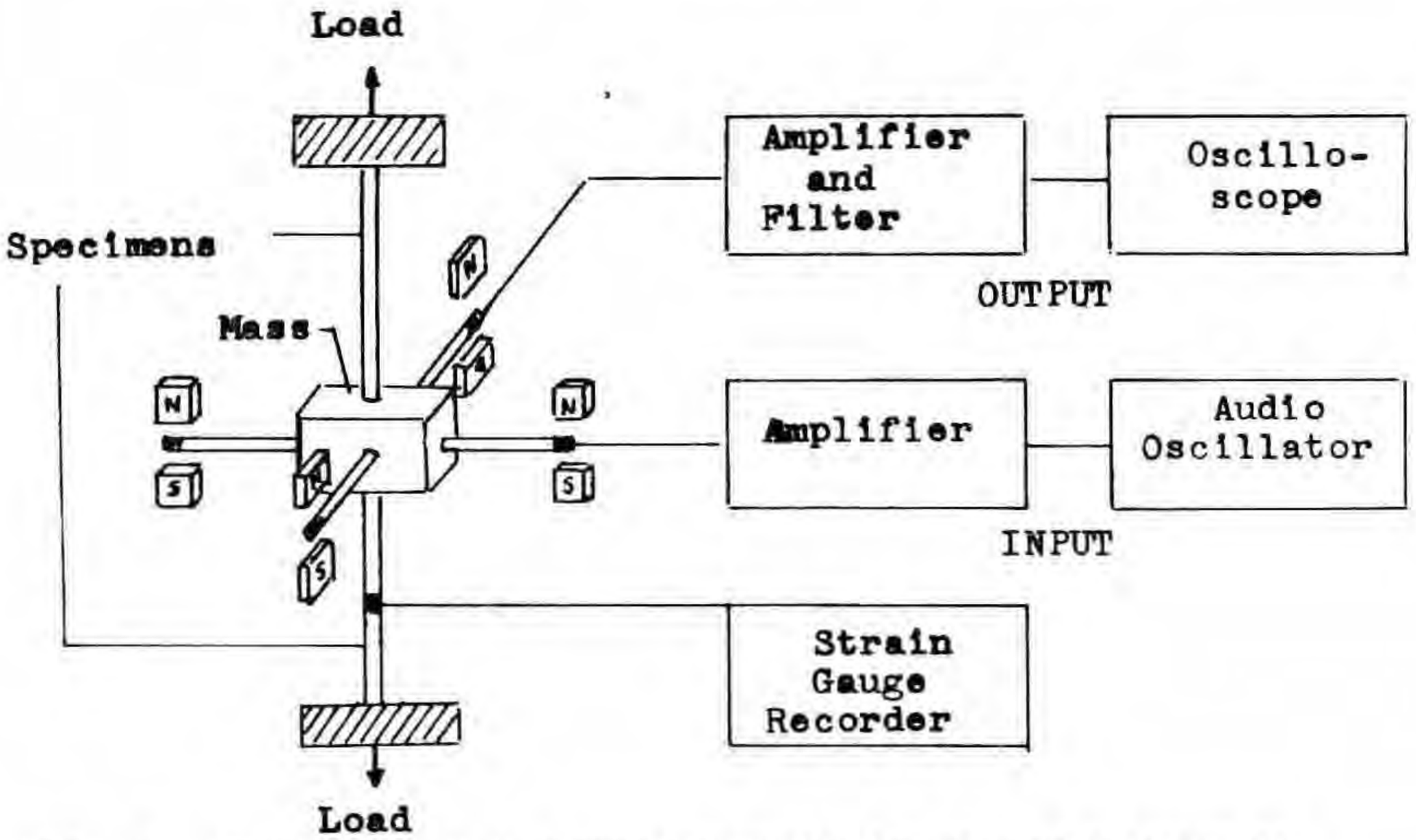

FIG. 2 APPARATUS FOR DETERMINATION OF DYNAMIC MODULUS OF LOADED SPECIMENS

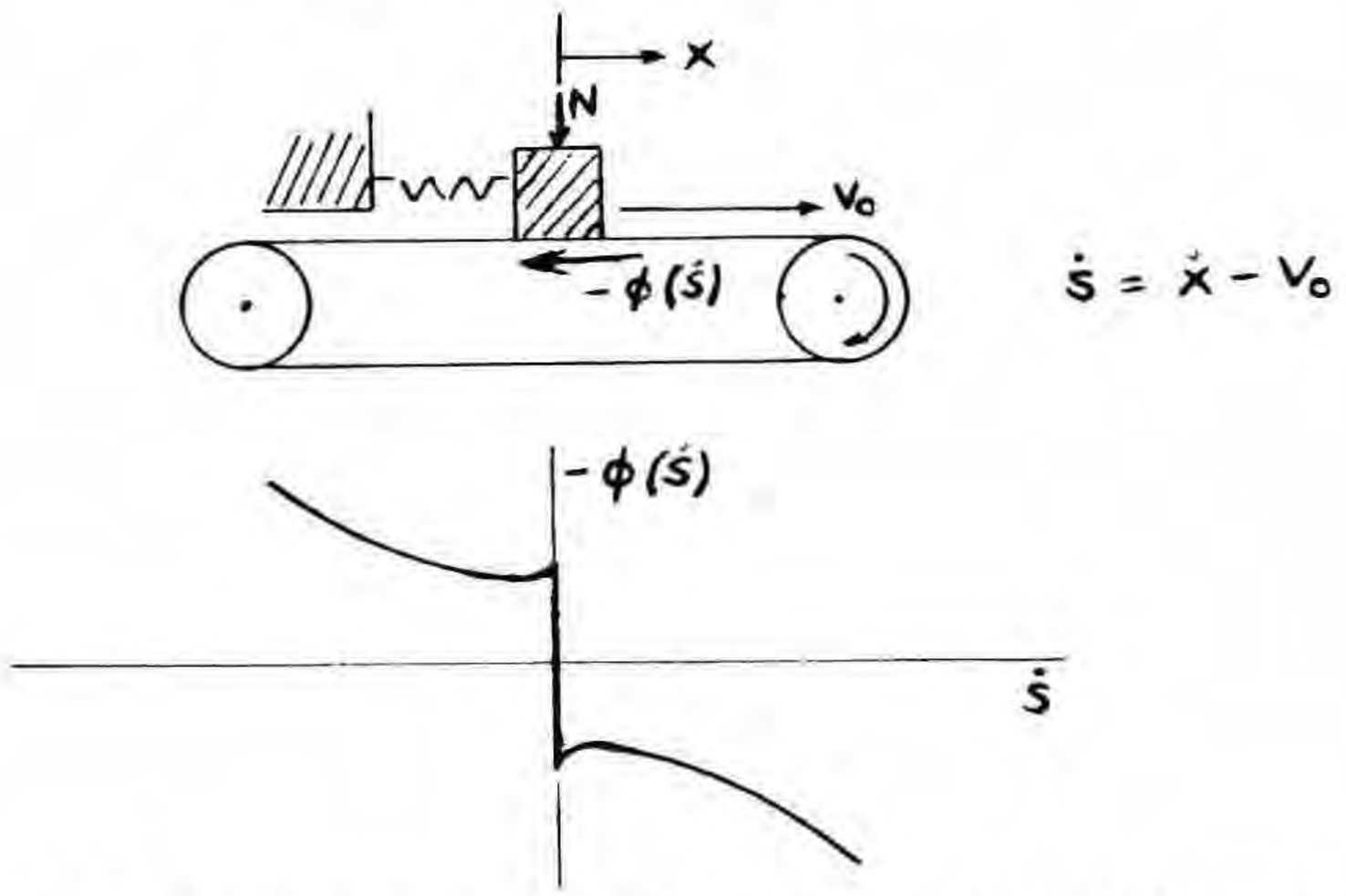

FIG. 3 MECHANICAL SYSTEM CAPABLE OF SELF-SUSTAINED OSCILLATIONS

G37

FOURTH INTERNATIONAL CONGRESS ON ACOUSTICS
COPENHAGEN 21.-28. AUGUST 1962

PITCH PERTURBATIONS OF NORMAL AND PATHOLOGIC LARYNXES

Philip Lieberman

AF Cambridge Research Laboratories
Bedford, Massachusetts, U. S. A.

I. Object

This experiment deals with pitch perturbations, that is, the small but rapid variations that occur in the glottal periodicity of normal connected speech. The object of the experiment was to see whether the pitch perturbations of speakers with pathologic larynxes were different from those of normal speakers. In a sense this is a pilot study to determine the feasibility of detecting pathologic larynxes through acoustically derived pitch perturbation measurements.[1]

II. Procedure

The voices of thirty-two speakers of American English whose ages ranged from 24 to 71 years were recorded for this experiment. Twenty-three of these speakers had pathologic larynxes, i.e., tumors, polyps, etc. These samples were collected with the cooperation of Dr. Ralph M. Caulk of the Washington Hospital Center, Washington, D.C., who provided a medical diagnosis of each case. The speakers were recorded in an acoustically treated audiometric room using an Altec 633A microphone and an Ampex 601 tape recorder. Each speaker read a three-minute selection. The sentences, "Joe took father's shoe bench out," read as a statement and, "They have bought a new car," read as a statement, a question, and a confidential communication were selected for analysis.

The waveforms of the set of four sentences selected from each speaker's recording were displayed on an oscilloscope and photographed with a Dumont oscillographic record camera at 1,200 inches per minute. Two sinusoids, one of 500 cps and one of 5 kc were also recorded and photographed with the utterances of each speaker. The processed 35 mm film was then read on a Gerber Digital Data Reduction System, type GDDRS-3B, on which the duration of each pitch period was measured and automatically punched on IBM cards. The overall time resolution of the entire system was 0.05 msec. Wideband sonagrams were made of two of the sentences of each speaker. In addition, recordings were processed of normal speakers uttering sustained vowels.

An IBM type 7090 computer was programmed to process the pitch periods punched on cards by the Gerber apparatus. The computer first calculated the pitch perturbations by subtracting the duration of each period, Tn, from that of the period immediately proceeding it, T_{n-1}. The computer listed and graphed the sequences of perturbations, $D = T_n - T_{n-1}$, for each speaker.

III. Findings: Air Pressure Transients as a Cause of Perturbations

When the sonagrams were compared with the sequence of pitch perturbations it was noted that perturbations exceeding 0.5 msec generally occurred at formant transitions for connected speech (many perturbations exceeded 1.0 msec). Perturbations exceeding 0.5 msec almost never occurred within the steady state portions of sustained vowels in which no formant transitions occurred. This raised the question of whether perturbations were due to the changes in phase associated with the change in the vocal tract's transfer function. If this were so the vocal cords might have little to do with the pitch perturbations of the acoustic waveform. A Western Electric type 5 artificial larynx was therefore used to excite a normal vocal tract. The output of the artificial larynx was used to synchronize an oscilloscope sweep, and the output of a Western Electric type 640AA microphone was displayed on the

oscilloscope. The largest perturbations that could be induced in the waveform by changing vocal tract configurations was less than 0.5 msec. The perturbations $\geq$ 0.5 msec were apparently attributable to variations in the glottal cycle. Since a recent study by Ladefoged has shown that the fundamental frequency is a function of the pressure drop across the glottis[2] it was hypothesized that large perturbations are instead induced by transients in the pressure drop across the glottis. These pressure transients are in turn caused by changes in vocal tract configuration.

To test this hypothesis sustained /a/'s were uttered while a variable external acoustic load impinged on the mouth of the speaker. Large perturbations exceeding 0.5 msec (some exceeded 2.0 msec) occurred when the external acoustic load rapidly reduced the air path at the mouth. When the vocal tract was excited by the artificial larynx the external load did not induce large perturbations.

IV. Findings: The Detection of Pathologic

The normalized integral of all perturbations having an absolute value $\geq$ 0.5 msec, which shall be termed the Perturbation Factor, was computed for each speaker. In Fig. 1 the Perturbation Factor is plotted on the abcissa for a control group of normal speakers, each of whom is marked by a solid dot, and for speakers 4, 18 and 21, who all had comparatively large masses on their vocal cords. The median pitch of each speaker is plotted on the ordinate. Speaker 21 in this group had squamous carcinoma of his right vocal cord with a mass measuring approximately 15 x 5 x 5 mm, while speaker 4 had a polypoid tumor on his right vocal cord. Speaker 18 had a fairly large keratotic polyp-like area on the anterior half of his left vocal cord.

In Fig. 2 the same normal group is repeated and compared with a group of speakers who had smaller growths on their vocal cords. Speaker 23, for example, had recurrent 5 mm polyps on his right vocal cord while Speaker 5 and 11 had singer's nodes. Note that these pathologic cases fall into a lower region than those plotted in Fig. 1.

In Fig. 3 the normal control group is repeated and compared with a group of speakers who had either very small growths or inflammations on their vocal cords. Speakers 7 and 16 had very small nodules while Speakers 6 and 9 had inflammatory conditions. No anomalies could be detected for Speaker 15. These cases almost merge with the normal controls.

In Fig. 4 the normal control group is again repeated and compared with speakers who had large growths or carcinoma near their vocal cords. Speaker 2 in this group had a large subglottic mass which filled the area below his left vocal cord anteriorly while Speaker 22 had a recurrent cancer to her posterior pharyngeal wall with extension to the posterior cricoid area. Speaker 12 had squamous carcinoma of his epiglottis. Note that these cases also fall into a lower region than those on Fig. 2.

The speakers with advanced cases of cancer who were recorded shortly before total laryngectomys were performed are not plotted since it was impossible to visually measure pitch periods. Their vocal cords apparently never completely closed and their waveforms were completely filled in. Fill in also occurred in two cases where large multiple polyps apparently caused the same effect.

V. On Accuracy and Stability of Measurements

The 500 cps sinusoids as recorded through the tape recorder and oscilloscope trace camera were measured on the Gerber Digital Data System to check the total system error. . Perturbations $\geq$ 0.25 msec occurred less than 5 percent of the time while perturbations $\geq$ 0.4 msec were never found. The Perturbation Factors plotted in Figs. 1 - 4 are therefore not artifacts of the measuring system.

The waveforms of Speakers 4, 18, 21, 5, 22, and several of the normal controls were measured two or more times on the Gerber apparatus by different operators.

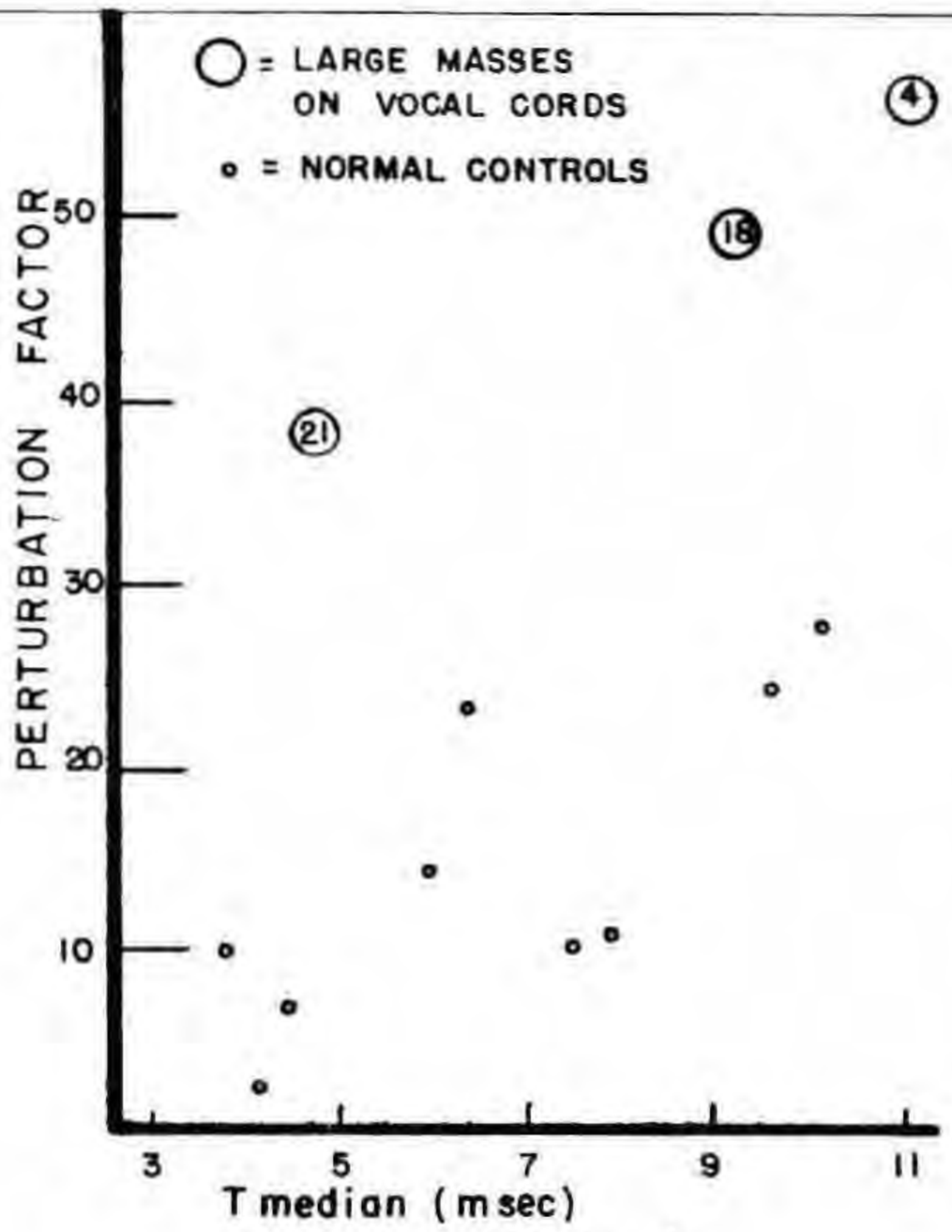

FIG. 1

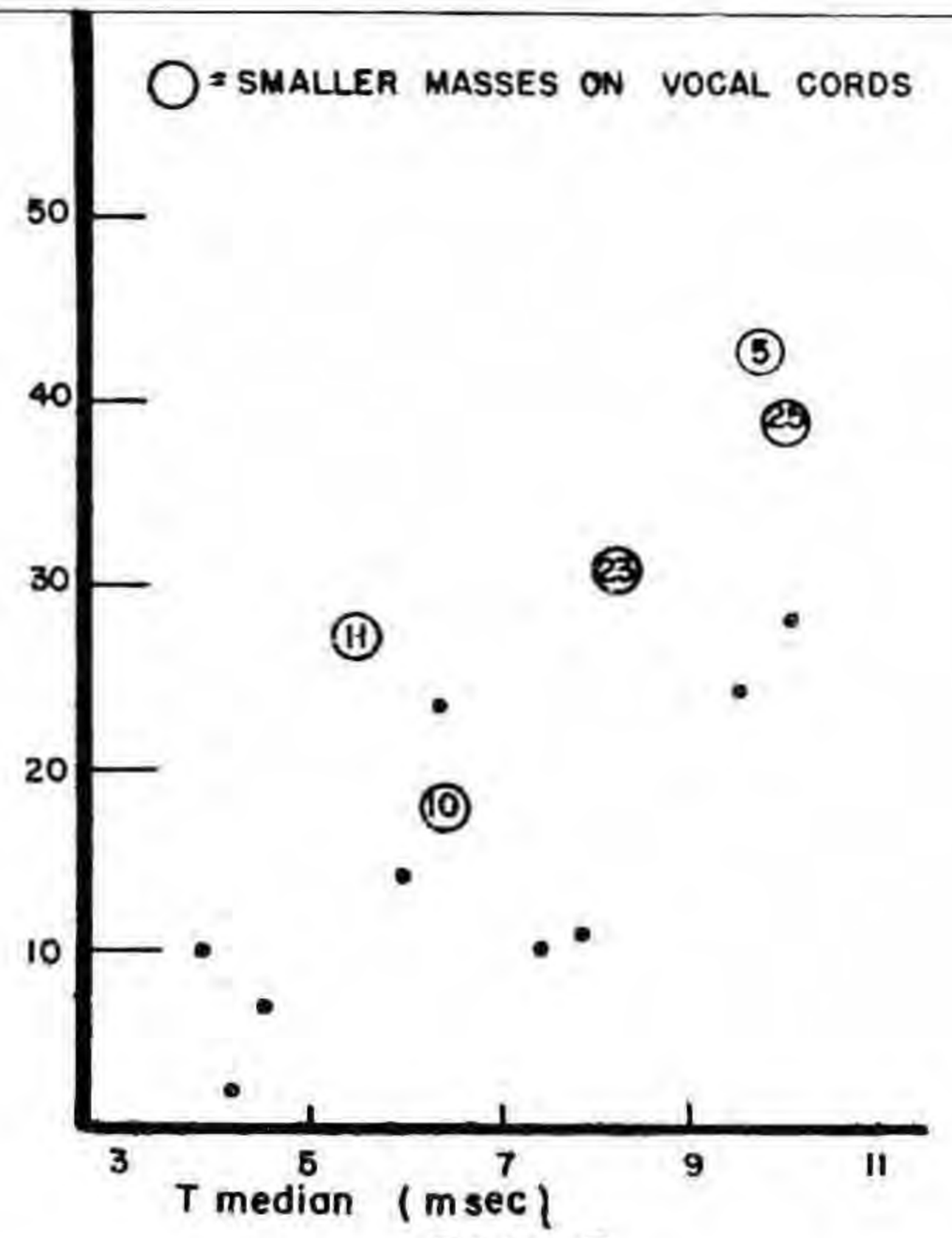

FIG. 2

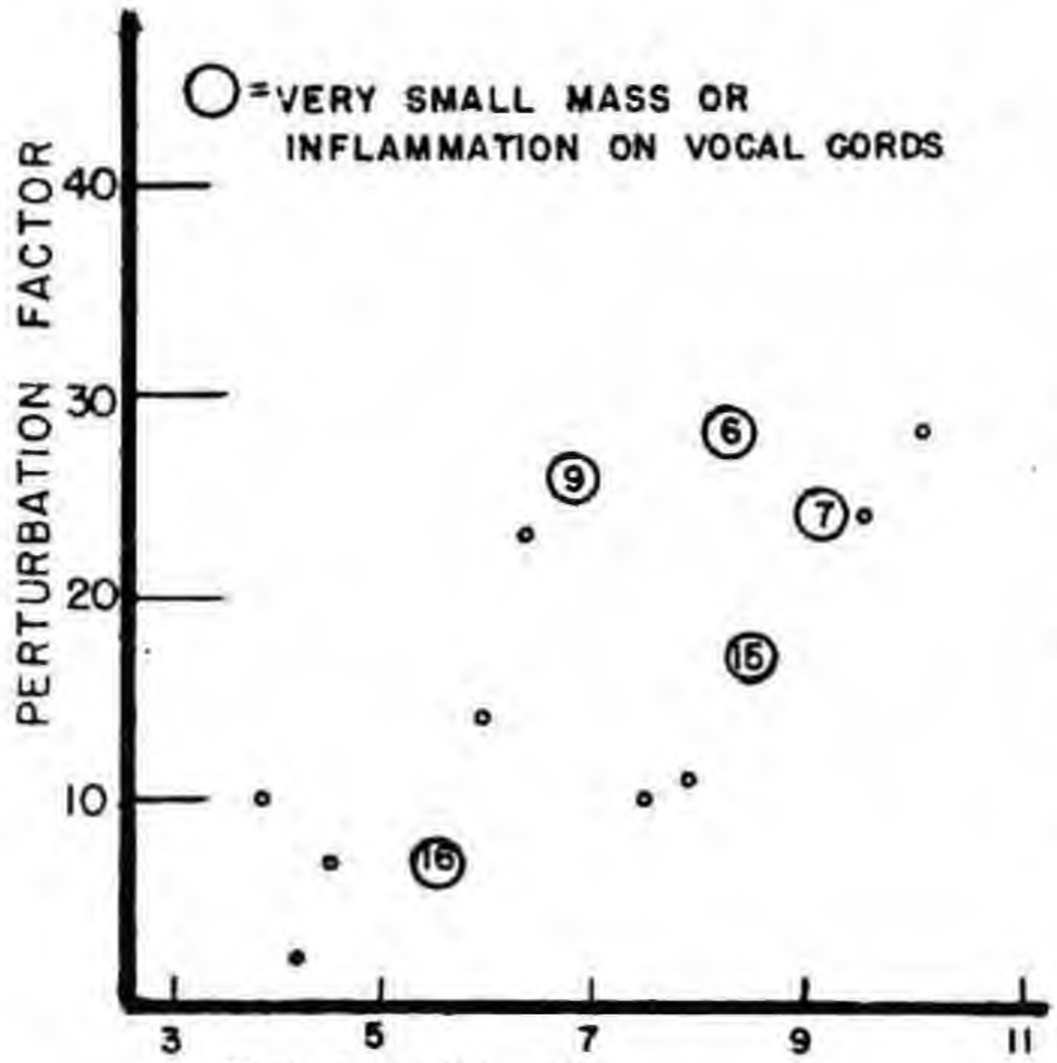

FIG. 3

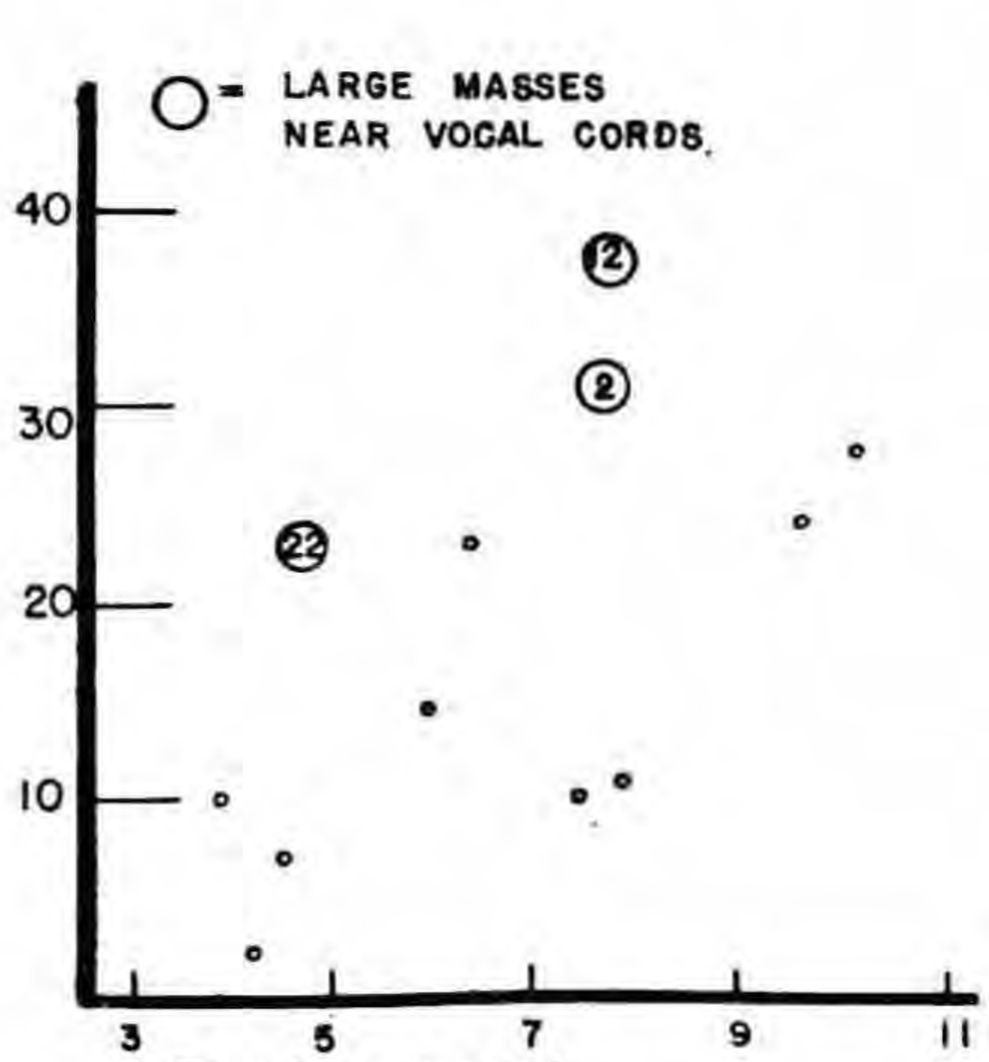

FIG. 4

In Figs. 1-4 the Perturbation Factor and median pitch period are plotted for a control group of normal speakers, each of whom is marked by a solid dot, and for speakers with pathologic larynxes, each of whom is numbered. In Fig. 1 the normal group is compared with speakers who all had comparatively large masses on their vocal cords. In Fig. 2 the normal group is compared with speakers who had smaller masses on their vocal cords. In Fig. 3 the normal group is compared with speakers who had either very small growths or inflammations on their vocal cords. In Fig. 4 the normal group is compared with speakers who had large growths or carcinoma near their vocal cords. Note how the difference between the Perturbation Factors of the normal and pathologic larynxes is proportional to the size of the pathologic growths when these growths are on the vocal cords.

The measurements were consistent.

The Perturbation Factor was also rather stable with respect to the total sample size. The computer in one run was programmed so that it read only one third of the pitch periods of each speaker. The Perturbation Factors were generally within 2 percent of those computed from all the pitch periods.

VI. Discussion and Summary

1. Speakers with longer pitch periods tend to have larger pitch perturbations.

2. Speakers with pathologic larynxes have larger pitch perturbations than do normal speakers with the same median pitch period.[3] The Perturbation Factor is mass sensitive. The differences between the Perturbation Factors of the normal and pathologic larynxes is proportional to the size of the pathologic growths when these growths are on the vocal cords. Inflammatory conditions, though extensive generally have comparatively little effect.

3. Large pitch perturbations apparently may be induced by transients in the pressure drop across the glottis, which are in turn caused by movements of the vocal tract.[4] The activity of the larynx is regulated by the pressure against the glottis and the tension of the vocal cords. Imbalanced pathologic masses on the vocal cords reduce the system's mechanical damping factor and pressure transients therefore induce larger and more prolonged transients.

VII. Practical Applications

The Perturbation Factor detected masses on the vocal cords far smaller than those associated with advanced cases of cancer of the larynx. Although this procedure would not replace direct examination of the vocal cords, it may be possible to develop this measure into a screening test for the early detection of pathologic conditions in which the patient would merely have his voice recorded while reading some standard phrases. The recording could then be processed at a central facility or with a specialized apparatus that would obviate the necessity for a general purpose computer.

---

1. The author would like to acknowledge the role of Dr. William R. Smith of Northeastern University, Boston, Massachusetts, in pointing out this problem.

2. P. Ladefoged, Report 3/61, Speech Transmission Laboratory, Royal Institute of Technology, Stockholm, Sweden, pp 16-21.

3. Age may influence the Perturbation Factor. The sample size of this study was however too small to resolve its effects.

4. The relation between pitch perturbations and emotional information noted in Lieberman, "Perturbations in Vocal Pitch," J. Acoust. Soc. Am., 33, 597 and Lieberman and Michaels, "Some Aspects of Fundamental Frequency, and Envelope Amplitude as Related to the Emotional Content of Speech," scheduled J. Acoust. Soc. Am., July 1962, may therefore be a concommitant effect of slower movements of the vocal tract in certain very deliberate emotional modes.

H37

FOURTH INTERNATIONAL CONGRESS ON ACOUSTICS
COPENHAGEN 21.-28. AUGUST 1962

ETUDE DU POTENTIEL MICROPHONIQUE COCHLEAIRE DANS DIVERSES CONDITIONS MODIFIANT LES PROPRIETES MECANIQUES DE L'OREILLE INTERNE

J.-P. Legouix
Collège de France, Paris

Ainsi que l'a montré Békésy (1) le potentiel microphonique cochléaire est produit par les déplacements des cellules ciliées de l'organe de Corti. Il est donc possible par l'observation de ce potentiel d'obtenir des indications précises sur les mouvements qui animent les structures qui sous-tendent ces cellules et en particulier la membrane basilaire. Dans le présent travail nous nous sommes attachés à observer les modifications d'amplitude et de phase du potentiel microphonique, produites par diverses conditions mécaniques à l'intérieur de l'oreille interne. Les résultats obtenus permettent de tirer des conclusions sur les propriétés de la membrane basilaire et sur le transfert de l'énergie acoustique du liquide aux structures solides du canal cochléaire.

TECHNIQUE

L'animal utilisé était le Cobaye. La technique d'enregistrement du potentiel microphonique était celle décrite par Davis et Coll. (2, 3). Elle consiste à introduire des paires d'électrodes dites "differentielles" constituées de fil d'acier inoxydable, dans des trous de fin diamètre percés dans les rampes tympanique et vestibulaire, de part et d'autre de l'organe de Corti.

Dans la plupart des expériences deux paires de semblables électrodes étaient placées, l'une dans la spire basale l'autre daus la troisième spire. Les potentiels produits en ces deux endroits étaient observés et photographiés simultanément sur un oscillographe à deux voies.

I.- MODIFICATIONS DU POTENTIEL MICROPHONIQUE PRODUITES PAR LES CHANGEMENTS DE PRESSION INTRALABYRINTHIQUE

Dans ces expériences la pression des liquides intracochléaires était augmentée ou diminuée au moyen d'un dispositif comprenant une pipette reliée à une seringue par un tube de plastique. Cette pipette était introduite dans un trou percé dans la rampe vestibulaire ou tympanique de la première spire

cochléaire. En poussant le piston de la seringue une petite quantité du liquide qui remplissait la partie inférieure de la pipette était introduite dans la cochlée et contribuait à augmenter la pression. Au fur et à mesure que la pression hydrostatique était accrue, une réduction sélective du potentiel microphonique enregistrée dans la troisième spire était observée. - Dans un premier temps, pour des pressions modérées, seul le potentiel microphonique de la troisième spire était réduit. La phase et la forme de l'onde microphonique n'étaient pas alors modifiées. - Dans un deuxième temps, pour des pressions plus élevées, le potentiel microphonique de la spire basale était également réduit, mais toujours moins que celui du troisième tour. A ce moment le rapport de phase des potentiels de la première et de la troisième spire était nettement changé, et une distorsion importante de l'onde microphonique était notée.

Dans d'autres expériences la pression intracochléaire était augmentée en poussant l'étrier dans la fenêtre ovale. Dans ce cas le son était introduit non pas par voie aérienne, mais directement à l'intérieur de la cochlée au moyen d'une pipette reliée par un tube de plastique à un haut-parleur. Dans ces conditions une réduction sélective du potentiel microphonique de la troisième spire était observée, mais ceci seulement d'une manière transitoire au moment où l'étrier était déplacé. Un phénomène analogue a pu être mis en évidence au cours des contractions des muscles ossiculaires qui surviennent spontanément chez les animaux légèrement anesthésiés.

II.- MODIFICATIONS DU POTENTIEL MICROPHONIQUE PRODUITES PAR UNE PRESSION LOCALE APPLIQUEE SUR LA MEMBRANE BASILAIRE

Dans une autre série d'expériences un blocage local était réalisé en appuyant sur la membrane basilaire par l'intermédiaire d'un poil de Cobaye, selon une technique déjà utilisée par Békésy (4) et Tasaki (3).

En appliquant la pression au niveau de la spire basale, à une faible distance des électrodes réceptrices, on obtenait une diminution du potentiel microphonique enregistré à cet endroit. Une variation de la phase était notée mais seulement lorsque la pression était assez forte. Le potentiel microphonique de la troisième spire n'était pas modifié par cette action. Lorsque la pression était appliquée au niveau du troisième tour de spire, on obtenait des changements analogues dans cette spire. Le potentiel microphonique des régions basales n'était pas modifié.

Un résultat différent était observé lorsque la pression était appliquée sur la membrane basilaire au niveau du deuxième tour de spire. Dans ce cas

la réduction du potentiel microphonique ne se limitait pas à cette spire mais affectait également les régions distales, c'est-à-dire la troisième et la quatrième spire, alors que les potentiels restaient inchangés dans la spire basale. Une variation de phase accompagnait cette réduction lorsque la pression était exercée avec une force suffisante et en certaines positions.

III.- MODIFICATIONS DU POTENTIEL MICROPHONIQUE PRODUITES PAR DES LESIONS LOCALES DE LA MEMBRANE BASILAIRE

Des lésions étendues de la membrane basilaire provoquent une disparition complète des potentiels dans toute la cochlée. Il a été possible cependant de réaliser des lésions locales introduisant une discontinuité de la membrane basilaire sans faire disparaître tous les potentiels. Ainsi une perforation complète du canal cochléaire dans la spire basale supprime les potentiels dans cette spire mais ne modifie pas les potentiels des régions apicales. D'autre part des destructions très étendues des régions apicales laissent subsister les potentiels de la première spire et ne modifient pas leur phase.

DISCUSSION ET CONCLUSIONS

L'effet sélectif de la pression hydrostatique sur la partie apicale de la cochlée peut s'expliquer par le fait démontré par Békésy (4) que l'élasticité de la membrane basilaire est plus grande dans ces régions. Tonndorf (5) a pu mettre en évidence sur des modèles de cochlée qu'une augmentation de pression liquidienne pouvait affecter sélectivement les régions où la membrane est plus élastique. Cependant à la différence de ces modèles, la phase n'est pas modifiée dans la cochlée, tout au moins pour des pressions modérées. En fait, comme l'a montré Békésy (4), la membrane basilaire ne présente aucune tension et ceci peut expliquer que pour des pressions modérées aucun changement de rigidité ne survient. La réduction du potentiel microphonique qui s'observe alors peut être interprété comme étant dû à un accroissement de l'amortissement. C'est seulement pour des pressions élevées que la rigidité peut être modifiée et que les déphasages peuvent survenir. Lorsque la pression est exercée localement et modérément sur la membrane basilaire au moyen d'un poil de Cobaye l'amortissement est vraisemblablement modifié de la même manière. Cependant il semble que dans certains cas l'action de blocage se limite à produire en écrêtage aux fortes amplitudes.

Les résultats décrits ci-dessus semblent apporter également des indications sur le mécanisme du transfert de l'énergie des liquides cochléaires

aux structures solides. Selon Wever, Lawrence et Békésy (6), deux mécanismes pourraient coexister: une transmission directe de l'énergie du liquide aux différents points de la membrane basilaire (comme dans la Théorie de la résonance de Helmholtz), qui serait prépondérante à la base; une transmission de la base au sommet, de chaque point de la membrane basilaire au point voisin, à la manière d'une onde propagée. Ce double mécanisme semble trouver une confirmation dans nos résultats qui montrent que le blocage local de la membrane basilaire dans les régions basales n'affecte pas les parties distales, mais que le même blocage pratiqué au niveau de la deuxième spire supprime l'activité des parties plus apicales. Toutefois aux fréquences très basses où seulement de faibles déphasages surviennent entre les différents points de la membrane basilaire, la transmission de l'énergie semble se faire par l'intermédiaire du liquide. Aux fréquences plus élevées pour lesquelles on observe des retards de phase progressifs vers l'apex, la transmission se fait vraisemblablement, dans les régions où se font ces déphasages, comme dans le cas d'une onde propagée. Ces régions correspondraient à la "secundary zone" envisagée par Wever, Lawrence et Békésy.

REFERENCES

1) G. v. BEKESY, J. Acoust. Soc. Amer., 1951, 23, 29-35.
2) H. DAVIS, B.E. GERNANDT and J.S. RIESCO-MacCLURE, J. Neurophysiol., 1950, 13, 73-87.
3) I. TASAKI, H. DAVIS and J.-P. LEGOUIX, J. Acoust. Soc. Amer., 1952, 24, 502-519.
4) G. v. BEKESY, J. Acoust. Soc. Amer., 1948, 20, 227-241.
5) J. TONNDORF, Ann. of Otol. Rhinol. Laryngol., 1957, 66, 766-784.
6) E.G. WEVER, M. LAWRENCE and G. v. BEKESY, Proc. Nat. Acad. Sc., 1954, 40, 508-512.

L37

FOURTH INTERNATIONAL CONGRESS ON ACOUSTICS
COPENHAGEN 21.-28. AUGUST 1962

VIBRATION AND NOISE CONTROL BY HIGH EFFICIENCY VISCOELASTIC DAMPING MATERIALS.

Francis Kirschner, Chief Engineer
Korfund Dynamics Corporation, Westbury, L.I., N.Y.

1. INTRODUCTION

The damping of steel plates is important in many technological areas. Automobile undercoating is standard practice and many modern airplanes, electrical home appliances, business machines are constructed of sheet metal which require damping. We wish to present here a report on the damping obtained for noise control, and our concern is with the damping introduced by viscoelastic damping materials applied to the metal and the resultant noise reduction. In comparison to the empirical methods of the past where only the viscous constants were exploited in felts and bituminous mastics, our aim is to use the viscoelastic damping materials on sheet metal structures, metal and homogenous damping layers, and we are able to obtain a loss factor larger than $\eta = 0.2$ (10% of the critical damping) over a broad frequency and temperature range. Fig. 1 illustrates the vibration amplitude of a reed 12" long, 3/8" wide and .040" thick, with and without the damping material, over a broad frequency range. The homogenous viscoelastic damping layer effectively reduces vibration amplitudes over the broad frequency range. The method and apparatus developed by Dr. Oberst was used for these measurements. (Ref. 1)

2. ELECTRICAL INDUSTRY

As a first example, we have chosen the electrical industry and a pròblem common to all buildings where fluorescent lighting fixtures are used. Recent trends in fluorescent lighting fixtures have been towards longer illuminating tubes with higher illuminating power, so more driving force is present in the form of magnetic excitation which is picked up by the sheet metal and radiated as noise into the surrounding atmosphere. The fluorescent lamp, because of its non-linear impedance characteristics, draws current of many harmonic frequencies through the ballast. Although the exciting force driving the sheet metal structure is predominantly the 120 cycle magnetic force from the ballast transformer, the sheet metal has its own resonances, which are closer to higher harmonics, and peaks are present in the noise spectrum at 240 cycles, 480 cycles, and up to 720 cycles. A viscoelastic damping material has been selected which was most effective at 120°F, approximately the temperature to which the sheet metal structure is heated during the use of the fluorescent fixture when powered.

The amplitude of vibration acceleration has been measured by means of PZT Accelerometers feeding into a Sound Level Meter and a Frequency Analyzer, and the result of amplitude vs. frequency have been plotted on the attached Fig. 2. The graphs illustrating the acceleration amplitudes, with and without damping, show a reduction in acceleration level of 22 db at 240 cps, and 20 db at higher frequencies. At 120 cps, the fundamental driving force, the acceleration level reduction was only 3 db. This illustrates that the damping material is very effective at frequencies where the sheet metal's resonant frequency appears, and only a small reduction is obtained at the forcing frequencies.

3. AIRCRAFT SKIN DAMPING

In the transportation industry, particularly with respect to the aircraft section, the use of vibration damping materials has been valuable. Transmission loss of typical airplane fuselages with/without damping materials was measured. The transmitting room was a reverberation chamber in which both high and low frequency loud-

speakers were located, with microphones measuring the overall sound pressure level, at both the reverberation chamber end of the fuselage wall, and at the anechoic termination at the receiving end of the other side of the fuselage wall to measure the transmitted sound. The fuselage wall was made of 0.100" thick aluminum with a radius of 20 ft. The cross section area measured 6' x 6'. A broad band sound field generated in the reverberation room excited the fuselage.

Fig. 3 illustrates third octave band noise reduction obtained both with and without the damping material under laboratory conditions. The damping material used in this experiment was Korfund Type 80A with loss factor 0.2 in the measured range of 100 to 1800 cps with the Oberst Reed method.

Note in the transmission loss curves, Fig. 3, that the noise reduction of the fuselage increased by 7 db at 160 cps, and by 8 db at 400 cps, when coated with the damping material. The transmission loss also increased 8 db at 500 and at 600 cps, about 3 db at 1000 cps, about 6 db at 1600 cps. The elimination of an anti-resonance at 315 cps causes a drop of 5 db in the transmission loss with the application of a damping material.

Besides noise reduction, the advantages of viscoelastic damping materials are particularly outstanding near the jet exhaust where a considerable increase of metal fatigue life has been obtained by the panels which had to be replaced frequently in the past because of sonic fatigue problems.

4. INCREASE IN WORKING LIFE OF METALS

One interesting example of application of damping materials to increase metal fatigue life is on a high intensity random noise generating siren. These sirens are designed to produce sound pressure levels of 160 to 170 db of broad band noise to test components and structures which go into vehicles, propelled by rocket engines.

Obviously, the first requirement for this siren is to survive its own noise environment. A steel exponential horn is connected to the siren to increase radiation efficiency into a reverberation chamber. The first designs used heavy steel casings made out of steel plates, 3/8" thick, with stiffeners placed every 5". These stiffeners were made of 3" x 3" x 1/2" thick angle beams as illustrated on Fig. 4.

The measured Q (resonant amplification) of these stiffened panels was approximately $Q \simeq 30$ to 60, with resonant frequencies between 100 and 300 cps. These steel horns would show visible fatigue cracks after a maximum of ten hours and some in less than five hours. If any bolts were used to connect the exponential horn to a progressive wave tube, the bolt would shear off in a short period of time. With the application of the viscoelastic damping material, the Q was reduced to approximately 5 to 6, and the life of the sirens increased to a point where no fatigue could be detected after six months of use. Not only would the use of the damping material extend the life of the first construction, but present models use 1/8" steel plates for the exponential horn with stiffeners placed at a distance of 8" to 12", and the size of the stiffeners is 1" x 1" x 1/8" angle. The savings in construction costs are appreciable. The same considerations as far as damping is concerned apply to the reverberation chamber which is coupled to the horn. Within its walls are contained the samples to be tested for sonic fatigue. The chamber walls have to survive the 170 db sound pressure level as well. This has been successfully achieved, plus the transmitted noise through the exponential horn wall has been substantially reduced because, (a) the amplitude of steel panel vibration has been reduced; (b) at the steel panels resonant frequencies the walls were transparent to sound, causing total transmission through the walls. With damping, the resonant peaks were eliminated and transmission loss of the walls was increased by 20 db.

5. GAS TRANSMISSION PIPE LINE NOISE CONTROL

The increased popularity in the use of natural gas in the U.S.A. requires pumping natural gas over long distances. This is done at high pressures, approaching 600 p.s.i. The compressor stations pumping gas are usually located in remote areas, but near the cities where the gas is actually consumed, so-called "reducing" stations are required to drop the pressure in these lines from 600 p.s.i. to 15 p.s.i. and less for the users. The reduction is made by the control valve automatically operated to maintain the set downstream pressure. These valves raise or lower plugs with "V" notches cut in them. The vast volumes of gas rushing through the constrictions produce a hissing roar much like that of a waterfall, thus generating noise levels in excess of 110 db. This is particularly annoying because highest noise peaks occur in the bands between 1200 and 2400 cps and this noise level is radiated over large areas by the pipes themselves. This high intensity noise and vibration has been greatly reduced by the use of viscoelastic damping materials, as illustrated on Fig. 5. Overall noise reduction of 16 db has been achieved within the station itself. The noise reduction outside is even more substantial.

6. DAMPING OF BALL MILLS

Another interesting example of noise control is the application of the damping material on a ball mill. Ball mills are extensively used in process industries around the United States by ink, paint, chemical, mining, and concrete manufacturers. These ball mills consist of a steel drum with a wall thickness from 3/8" to 1" (from 1 cm. to 2.54 cm.) steel plates. Steel balls or rods from 1/4" to 2" diameter are rotating inside of this drum to break up the solid particle compositions with the refinement required for the particular industry. These ball mills vary from sizes of a mill of 2 ft. in diameter, 1 ft. long for laboratories, to mills of 20 ft. in diameter and 100 ft. long for the concrete industry. A high efficiency viscoelastic damping material was applied over the steel casing of such a mill. The drum of this mill had a steel wall thickness of 5/16". The damping material was applied in increments of .050" thickness. The attached graph, Fig. 6, illustrates the noise reduction obtained with successive damping layers. The decibel reduction in high frequencies is almost a direct function of the thickness of the damping layer, up to the point where the steel and damping layer thicknesses are about the same. After this, very little noise reduction was achieved.

7. INSTRUMENT NEEDLE DAMPING

A common problem in planes, automobiles, in general where background vibration is present and instruments are used, is the vibration of an instrument indicator needle. An indicator needle vibration was causing a problem for an auto pilot. The application of the damping material in the form of a droplet of a fraction of an ounce at the root of the mode of vibration eliminated this resonant condition and the attached graph, Fig. 7, shows the reduction in vibration levels in the temperature range of -35°F to +70°F. These tests were run on a vibration shaker table and the first and second mode of vibration were recorded as a function of displacement amplitudes in inches vs. temperature in centigrades for a 1G input.

The vibration amplitude at the tip of the needle has been reduced by a factor of 6 - 10. Displacement of the tip reduced from .4" to .04".

8. CONCLUSION

Applications of high efficiency viscoelastic damping materials have been described in industry and architecture. These damping compounds provide tools for the control of vibration and sound, not hitherto available. Instead of the rough, massive, unsightly, sometimes toxic coatings of the past, light-weight materials with good appearance provide smooth, paint-like finishes.

The broad band - in frequency and temperature - high polymer, viscoelastic plastics, developed for these applications are the best tools available for the control of steady state and shock-excited structure-borne sound. They provide the most economical solution as well by cutting down sound and vibration problems at the source.

REFERENCES

1. Oberst, H.: Werkstoffe mit extrem hoher innerer Dampfung, Acustica, vol. 6, pp. 144-153, 1956 (Akustische Beihefte, no. 1).

2. Fig. 4 - Courtesy John Joiner, Joiner-Meade-Capers, Inc. Dallas, Texas.

3. Fig. 5 - Courtesy Tenney Engineering, Union, New Jersey

4. Hamme, Richard N. - Geiger and Hamme -: Vibration Control by Applied Damping Treatments, Shock and Vibration Handbook, Edited by Cyril M. Harris and Charles E. Crede, vol. 2, p. 37-1, 1961

M37

FOURTH INTERNATIONAL CONGRESS ON ACOUSTICS
COPENHAGEN 21.-28. AUGUST 1962

Über den Einfluß der Deckenhöhe auf die Klangqualität in Konzertsälen

Fritz Winckel, Technische Universität Berlin

Zur Feststellung der raumakustischen Kriterien hervorragender Musikaufführungsstätten hat der Verfasser 1946 bis 1955 eine Umfrage bei Dirigenten veranstaltet und als Ergebnis nachfolgender Untersuchungen gefunden, daß die höchste musikalische Wirksamkeit in Bauten des vorigen Jahrhunderts gegeben war. Hierzu werden jetzt noch zwei Säle ergänzt.

Saal	Baujahr	Höhe m	Nachhall-zeit bes.	Vol.	Platz-zahl	m^3/ Platz	Höhe: Länge
Alte Philharmonie Berlin	1888	15,00	1,9	18000	1960	9	?
Gewandhaus Leipzig	1886	14,50	1,5(?)*)	10310	1560	6,6	4 : 9
Musikvereinssaal Wien	1870	18,00	2,0	15000	1950	7,5	2 : 3
Concertgebouw Amsterdam	1887	17,50	2,1	20000	2200	8	2 : 5
Symphony Hall Boston	1900	19,50	1,8	19000	2631	7,3	5 : 9
St. Andrew Glasgow	1877	20,00	1,9	17000	2500	7	3 : 7
Massey Hall Toronto	1893	30,00	1,9	17000	2760	6,2	1 : 1

Diese Säle sind vom gleichen Typ einer Architekturperiode, des Neoklassizismus (der letztere ist von maurischem Stil): Rechteckgrundriß mit Balkon, Mauerwerk mit Gips- oder Holzverkleidung, Gliederung der Wandungen und reichlich Verzierungen. Damit wird gute Schalldiffusität erzielt und die für symphonische Musik im Mittel optimale Nachhallzeit von nahezu 2 sec. Die Nachhallzeiten von acht bedeutenden, nach dem Kriege gebauten Konzertsälen haben den mittleren Wert von 1,6 sec, während die in der Tabelle aufgeführten Säle einen Mittelwert von 1,88 sec ergeben.

Es ist nun versucht worden, weitere Kriterien zu finden, um die Konzertsäle für großes Orchester einer neuen Stilepoche (Nachkriegszeit) mit den älteren, vor dem Krieg gebauten zu vergleichen. Wenn man die Gesamtsitzfläche von Zuschauern, Orchester und Chor als eine nur wenig schwankende Größe annimmt, die sich in Zukunft wohl noch mehr standardisieren wird, und die Ausstattung von Decke und Wänden aus Holz oder Gips annimmt bei Vermeidung zusätzlicher Schluckflächen, die als

*) Messungen um 1930 waren noch nicht zuverlässig.

fehlerhaft angenommen werden können,so bleibt als noch mögliche variable Größe die Deckenhöhe. Sie kann daher bei der Betrachtung von Platzzahlen für das Symphoniekonzert von häufig 2000 in Europa und 2700 durchschnittlich in Amerika als direkter Gütefaktor angesehen werden. Die Nachkriegsbauten haben erheblich geringere Deckenhöhen (Durchschnitt 14m bei Annahme von Maximalhöhen der heute meist gekrümmten Deckenflächen) im Gegensatz zu 19,2m Durchschnitt bei Vorkriegsbauten. War früher das Verhältnis Höhe zu größter Saallänge höchstens 1:3,vor 1900 im Mittel 1:2,so ist nach dem Krieg vereinzelt das Verhältnis 1:4 überschritten worden. Schon im Handbuch der Architektur (IV.Teil,I S.349-1906) wird auf die Höhe von Konzertsälen hingewiesen,"die so entscheidend für eine gute Akustik besonders der entfernteren Plätze ist".

Beranek hat, um gesetzmäßige Zusammenhänge zu finden, eine Höhendimension ersatzweise durch die reziproke Größe S_T/V eingeführt, worin S_T die Gesamtfläche von Publikumsbesetzung, Orchester und Chor einschließlich der Zwischengänge bis etwa 1m Breite bedeutet, und diese Größe als Funktion der Nachhallzeit in der Form 1/T durch eine gerade Linie dargestellt erhalten.Diese Gesamtfläche nimmt bei Sälen der Tab. Werte von 0,56-0,7m^2/Person an,bei Nachkriegssälen 0,65-0,80. Bei Einführung der Gesamt-Begrenzungsflächen des Raums S ergibt das Verhältnis V/S den ziemlich konstanten Wert 10 feet. Natürlich geht eine Zunahme der Höhe mit einer Erhöhung der Nachhallzeit ein, allerdings weniger als in linearem Anstieg. Wenn S_T konstant bleibt und die Gesamtfläche aller Wandungen S mit h ansteigt,so wird auch ein günstiger Einfluß auf den Frequenzgang der Nachhallzeit ausgeübt, dergestalt,daß die Absorption des mittleren Frequenzgebietes relativ einen kleineren Anteil beiträgt.
Über diese funktionell gebundenen Zusammenhänge hinaus kann gezeigt werden,wie mit zunehmender Höhe bei dem hier betrachteten Konzertsaaltyp die Schalldiffusität besser wird. Auf die Beleutung der Deckenhöhe, absolut genommen,soll im folgenden eingegangen werden.

H.J.Sabine hat in einer Arbeit über Maschinengeräusch darauf hingewiesen,daß die Beziehungen des Gesamtschallpegels zur Raumabsorption nur gültig sind,wenn der Schalldruckpegel des reflektierten Schalls gleichmäßig über den Raum vorherrscht.Das ist erfüllt, wenn das Signal statistischen Charakter hat und keine der Grundriß-Dimensionen mehr als 5mal die Deckenhöhe beträgt. Bei größeremVerhältnis als 1:5 fällt der reflektierte Pegel gleichmäßig mit der Entfernung. Messungen ergeben dann Werte, als seien die Wände nicht existent und die Reflektion nur zwischen Boden und Decke vorhanden.

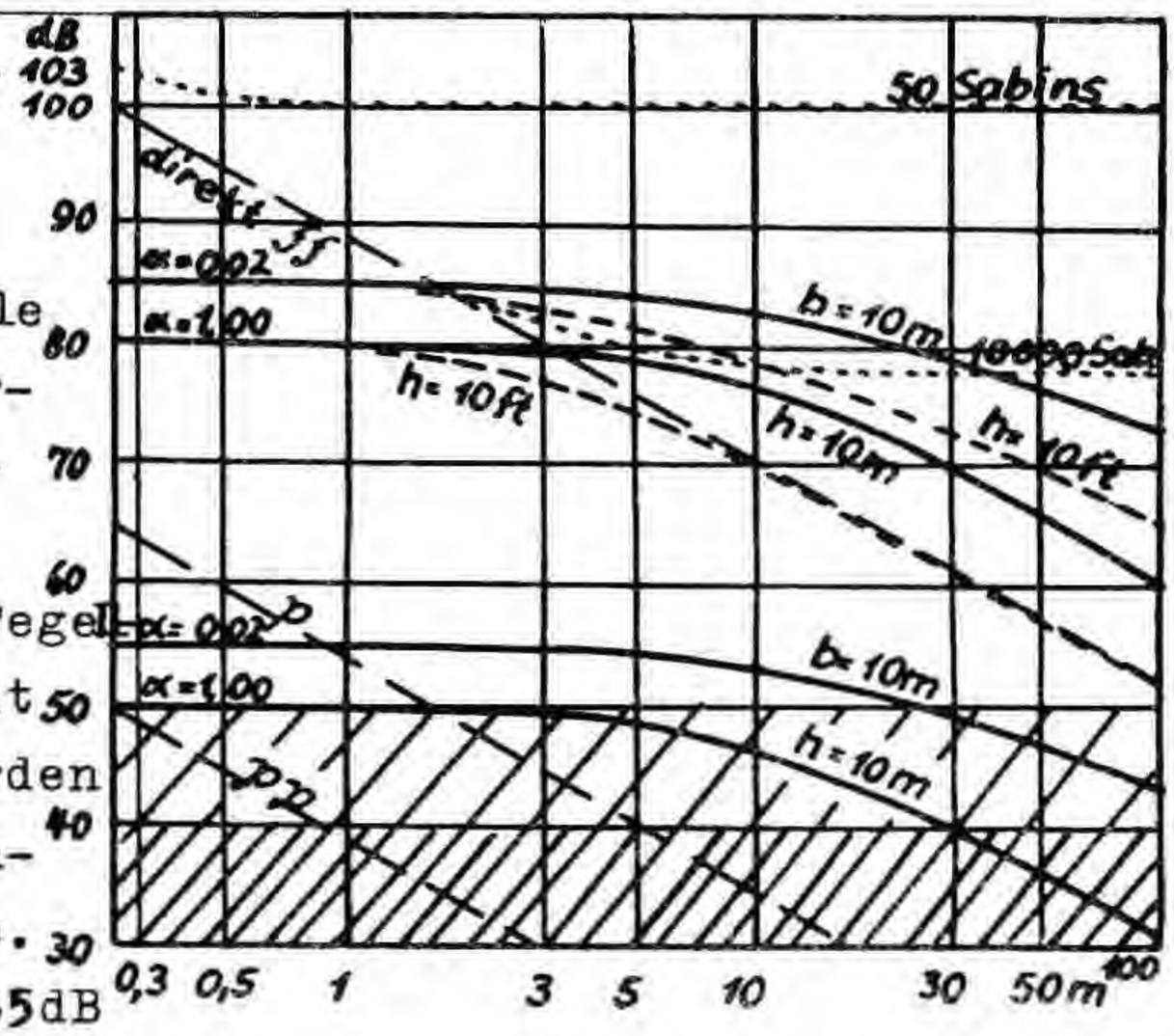

Fig.1 zeigt dieses Verhalten in der Kurve $\alpha \approx 1$ (Bodenabsorption durch Publikum) für eine Deckenhöhe von 3m (10 ft)für eine Kugel-Schallquelle von 100 dB (0,0115 W),also etwa Fortissimo-Orchestereinsatz.Mit zunehmender Deckenhöhe verschieben sich die Kurven nach rechts,woraus der Pegelgewinn des reflektierten Anteils mit wachsender Entfernung abgelesen werden kann,z.B.auf 30m Entfernung 9 dB zugunsten des reflektierenden Anteils. Ein Piano-Instrumenteneinsatz von 65dB bei 10m Deckenhöhe zeigt, wie der direkte Schall bereits in 10m Entfernung im 40 dB-Rauschpegel des Konzertsaals untergeht und ein reflektierter Anteil von nur 7 dB übrig bleibt. Im Pianissimo-Einsatz verschwindet der reflektierte Anteil vollkommen im Rauschpegel und auch der direkte Anteil bei einer Entfernung von mehr als 1m. Somit kann mit zunehmender Deckenhöhe ein Pegelgewinn des reflektierten Anteils erzielt werden,falls der Pegel der Schallquelle größer als 60 dB ist.

Bei höheren Pegeln (*f* bis *ff*) erhält man mit zunehmender Entfernung von der Schallquelle und mit größer werdender Deckenhöhe ein Überwiegen des reflektierten Schallanteils, bis bei ausgeglichenen Raumdimensionen (Grenzfall Kubus) die bekannten Kurven des resultierenden Schalldrucks mit dem Parameter der Total-Absorption in Sabins zustandekommen (10 000 Sabins für einen Konzertsaal von ca. 10000m^3).Damit ist die Klangqualität für das diffuse Schallfeld an verschiedenen Stellen des Raums quantitativ bestimmt, wogegen die Lautstärke sich gegenüber dem stärkeren Schallanteil höchstens um 3 dB verändern kann. Als Korrektur sind noch die Richtcharakteristiken der Musikinstrumente gegenüber der angenommenen Kugelschallquelle zu berücksichtigen.

Mit abnehmender Deckenhöhe tritt eine Verarmung an indirektenSchallanteilen ein, damit ein Verlust an Plastizität des Klangs, selbst bei Optimalbedingungen von Nachhallzeit und Diffusität. Außerdem wird die untere Grenze des Nutzpegels heraufgesetzt und damit die Dynamik des Orchesters eingeengt. Das Pianissimo muß bei 60dB angesetzt werden.

Quantitative Angaben erhält man nach J.C.Allred und A.Newhouse, die für verschiedene Raumproportionen die mittlere freie Weglänge und weiter die Zahl der relativen Zusammenstöße mit den begrenzenden Wänden berechnet haben.

Raumverhältnis	mittl.freie Weglänge	4 V/S	Frequ. yz/n_x	Wand -Kollisionen xz/n_y	xy/n_z
10 : 10 : 10	6,350	6,667	1,005	1,013	0,983
10 : 10 : 2	3,035	2,857	0,830	0,857	1,081

Die Wand mit den kleineren Dimensionen wird öfter getroffen, sie hat also eine größere absorptive Wirksamkeit. Die optimalen Raumdimensionen ergeben sich demnach in der Annäherung an den kubischen Raum,also einem Höhenmaß $h=\sqrt[3]{V}$. Würde man aus dem Verhältnis 1:5 zu 5:5 darüber hinaus entwickeln in Richtung 5:1, so bekäme man den "Steilraum"wie er in gotischen Kathedralen,besonders den englischen, entwickelt ist. Die Tendenz der erhöhten Absorption an den beiden Schmalseiten, Boden und Decke, wird noch gefördert dadurch,daß der Boden, mit Publikum besetzt, den Absorptionsfaktor α nahezu eins hat und die Spitzbogenstruktur der Decke Keilflächen mit streifendem Einfall darstellt. Mit Bezug auf die Breite b ist im Diagramm $\alpha \approx 0{,}02$ angegeben, wo dann auch der erhöhte Rauschpegel mit 50 dB eingetragen ist.

Im Vergleich des Klangverhaltens der alten und neuen Säle ist ferner zu beachten, daß man heute einem Ansteigen des Parketts aus optischen und akustischen Gründen den Vorzuggibt, während früher die Säle einen horizontalen Boden hatten. Durch die Überhöhung zur Rückwand zu geht diese zum Teil als Reflektionsfläche verloren, während die zusammenhängende Publikums-Absorptionsfläche vergrößert wird. In der Festival Hall z.B. ergeben sich dreigeteilt Anstiege von 12° bis 15° bzw. ein Ausschalten von Rückwandhöhe von 13m, bezogen auf 18m Gesamthöhe, entsprechend auch die Seitenwände. Die Publikumsfläche ist durch das Ansteigen um 5% vergrößert, zugleich die durchschnittliche Deckenhöhe im Vergleich zu einem Saal von gleichem Außenvolumen mit horizontalem Boden verringert, abgesehen von dem beträchtlichen Innenraum-Volumenverlust durch den ansteigenden Fußboden. Entsprechend wird die Schalldiffusität vergleichsweise verringert.

Die Praxis bestätigt die Überlegungen. Zu den besten Konzertsälen(Klangqualität) gehört die Massey Hall in Toronto mit h= 31m über dem Parkett und 30m über dem Orchester.Die musikalischen Darbietungen sind echofrei, innerhalb des Orchesters besteht Verständigung,und der Dirigent fühlt große Sicherheit in der Gestaltung. Die Publikumsfläche ist in drei Absorptionseinheiten günstig aufgeteilt (Parkett und zwei Ränge). Gleiche Erfahrungen teilt Somerville über St.Andrews Hall in Glasgow mit 20m Deckenhöhe mit.

N37

FOURTH INTERNATIONAL CONGRESS ON ACOUSTICS
COPENHAGEN 21.-28. AUGUST 1962

THE RATIONAL DESIGN OF PHONOGRAPH PICKUPS*+

F. V. HUNT, Harvard University
Cambridge, Massachusetts, U.S.A.

In the systematic design of a stereo phonograph pickup, it is useful to deal separately with the mechanism of signal transduction and the mechanical parameters which control proper groove tracking. This paper is concerned with the latter, and its primary objective is the specification of the important mechanical parameters of a pickup in terms of its bearing weight, the requirements for perfect tracking, and the limiting characteristics of typical recorded material.

The total bearing force is balanced in static and dynamic equilibrium by the groove-wall reaction forces. These forces can never reverse sign because there is no adhesion between stylus and groove, and they cannot disappear because the stylus must remain in continuous contact with both groove walls. As a consequence, the maximum dynamic force which is available to drive both the stylus and the tone arm is just the static groove-wall reaction force which balances the bearing weight. The primary design variables can be separated by arbitrarily allocating this available driving force in some proportion, perhaps equally, among the three independent and uncorrelated driving-force demands imposed by tone-arm acceleration, stylus acceleration, and the low-frequency tracking requirements. These separate demands can be assessed quantitatively by relating them to typical recording practice and the standardized dimensions of records, and these assessments then allow the basic mechanical parameters of the pickup and tone arm to be specified in terms of the bearing weight.

The symmetry of stereo groove modulation dictates that the stylus compliance C_{LV} should be the same for either vertical or lateral deflection. The elastic stylus-groove contact is initially pre-loaded by the static bearing weight M_B, but part of this

---

* This study was supported in part by funds made available under a contract with the (U. S.) Office of Naval Research.

+ A more extended discussion of these design principles has been submitted for publication in a forthcoming issue of the Journal of the Audio Engineering Society.

pre-loading is relieved periodically as the stylus executes large excursions in tracing low-frequency groove modulation. The standard groove dimensions and the typical variations of recording pitch combine to limit the maximum vertical amplitude of such stylus excursions to about 0.05 mm. According to the postulated principle of design, the part of the pre-loading removed in this way must not exceed one-third of the total pre-loading which represents the available driving force. It follows then, that the lateral and vertical stylus compliances will each be governed by the design inequality $M_B C_{LV} \geqq 15 \times 10^{-6}$, gm x cm/dyne. This specification may also be interpreted as a requirement that the static deflection produced by the total bearing weight should be about 0.150 mm.

The allowable values of equivalent tone-arm mass M_{ta} are based on estimates of the radial accelerations and velocities evoked by transitions in the recording pitch, bumps due to warpage, and the tracking of eccentric grooves. For example, a radial acceleration of about 0.026 g is demanded for a short interval if the transition from normal recording pitch to the pitch of the lead-out spiral is completed within 35 to 50 milliseconds (i. e., within 10--15° of record rotation). A comparable radial acceleration is required in order to track the eccentric finishing groove of a 78-rpm record, and a similar acceleration in the vertical plane would arise in tracking a bump which rises 1.6 mm and then subsides within 1/5 of a period of record rotation at $33\frac{1}{3}$ rpm. Steady radial velocities as high as 0.95 cm/sec can also occur in the lead-out spiral of a 45-rpm record and these can impose demands on the driving force which will be comparable with the acceleration demands if the tone arm has enough viscous damping to suppress the tone-arm resonances. These considerations lead to the general design inequality $M_{ta}/M_B \leqq 13$, but this limit on tone-arm mass should be lowered further to $M_{ta}/M_B \leqq 6$ if the steady-state damping is comparable with the damping at tone-arm resonance.

The allowable value of the stylus mass M_s is established by the acceleration demand aroused by tracking the second-harmonic components of tracing distortion. All second-order components of tracing distortion are additive in the vertical plane, whether the fundamental groove modulation is lateral or vertical, and they include a steady component which causes the stylus to ride at a mean elevation slightly above its position in an unmodulated groove. The second harmonics must all be tracked faithfully, therefore, in order to avoid intermittent loss of stylus-groove contact. The required accelerations can readily be estimated in terms of the same curvature ratio (kakr) which appears in the description of tracing distortion; they are given explicitly

by $a_s = (V^2/r)(kakr)^2$, where a_s is the peak acceleration, V is the groove velocity, r is the stylus radius, λ is the recorded wavelength, $k = 2\pi/\lambda$, and a is the amplitude of lateral or vertical groove modulation. Values of (kakr) in the range 0.5 to 1 can and do occur occasionally so it is necessary to provide for accelerations as high as 1000 g. It follows, therefore, that the stylus mass should be governed by the design inequality $M_s/M_B \leqq 0.33$ milligrams/gram.

When C_{LV}, M_s, and M_{ta} are selected in accordance with the foregoing specifications, the frequency of tone-arm resonance f_{ta} will be about 11 Hz and the frequency of free resonance of the stylus system $f_{1,cf}$ will be about 2300 Hz. Neither of these frequencies is a function of the bearing weight and, since the designer's latitude in choosing C_{LV} is relatively limited, either frequency can be lowered only slightly but can be raised by a factor of 2 or 3 if substantial reductions of tone-arm mass or of stylus mass can be achieved. The frequency of free resonance turns out not to be located at the geometric mean of the upper and lower cutoff frequencies; on the contrary, these design considerations indicate that M_s and C_{LV} are controlled by independent and unrelated factors which lead to the proper placement of $f_{1,cf}$ well above the geometric mid-point of the frequency range of interest.

The driving-point impedance of the stylus system is characterized in general by an alternating sequence of maxima and minima which correspond to the clamped-supported modes of a distributed vibrating system. In practice, however, the "support" of the stylus tip at the groove walls is not rigid but has the finite compliance of the stylus-groove contact. As a result, the frequencies of the clamped/rigidly-supported modes are each lowered slightly to the new values $f_{n,cr}$ (n = 1, 2...) which designate the "stylus-groove resonances" or the compliantly restrained modes of the stylus-groove system. These resonances produce spurious responses in the system output and degrade the channel separation so they must be placed well above f_u, the upper limit of the frequency range of interest. Unfortunately, these resonances cannot be adequately suppressed by damping except at the heavy cost of overdamping the stylus system at frequencies below f_u and of increasing the stylus-groove frictional work with consequent increase of stylus and record wear.

Translation loss originates in the differential change of groove-wall stiffness brought about by the wall curvature due to modulation. Scanning loss, on the other hand, is an aperture effect stemming from the finite size of the circle of contact between the stylus and the groove wall. Both loss components vary with M_B, V, r, and

the elastic modulus of the record material, and each is independent of the dynamics of the stylus system. The translation loss can be held to less than 2 dB if the translation-loss cutoff frequency for the slowest (inside) groove velocity f_{gi} is placed at or above $2 f_u$, but this in turn requires M_B to be less than 1 gram if $f_u \geqq 15$ kc/s. Scanning loss does reduce the playback level of the higher harmonics but it cannot suppress tracing distortion adequately except when the translation loss at fundamental frequency is already intolerable. Attempts to compensate for translation loss by pre-equalization are to be strongly deprecated since this practice leads inevitably to a substantial increase of the net tracing distortion.

The stylus-groove contact is inherently nonlinear and a stylus-groove resonance at any frequency can make a contribution to the in-band noise through intermodulation. This intermodulation noise component can be eliminated if the scanning loss is used beneficially to suppress the stylus-groove resonance. Such suppression will occur if the first compliantly restrained mode of the stylus system is located at or above the translation-loss cutoff frequency for the maximum (outside) groove velocity, i. e., if $f_{1,cr} \geqq f_{go}$. For the calculable case of a stylus suspension which behaves as a lumped-constant system, this condition requires that the stylus mass satisfy a low-noise design inequality $M_s/M_B \leqq 0.14$ mg/g. This restriction on stylus mass is more than twice as severe as the one stated above and currently available pickups fail to meet it by almost an order of magnitude.

Most of the pickups and tone arms now offered commercially do meet the suggested specifications for C_{LV} but almost none meets the stated requirements for M_s and M_{ta}. Each of the postulated demands on the available driving force will have an independent statistical distribution in time and their peak demands will coincide only occasionally. It follows, therefore, that the typical overweight pickup and tone arm will perform satisfactorily during a large fraction of its playing time; but it follows with equal certainty that tracking difficulties will arise during a small and non-vanishing fraction of the playing time unless these pickups are operated with bearing weights lying in the range embraced by the design inequalities given above.

O37

FOURTH INTERNATIONAL CONGRESS ON ACOUSTICS
COPENHAGEN 21.-28. AUGUST 1962

The transmission of a spherical transient wave through a liquid layer

Gunnar Lindh
Kungl. fortifikationsförvaltningen, Stockholm

Let us consider two liquid halfspaces separated by a liquid layer of finite thickness but otherwise of infinite extension, cf. Fig.1. At the distance h from the upper surface of the liquid layer a pressure pulse is emitted from a source. The pressure-time process of this disturbance can be characterized with the aid of Dirac´s delta function, cf. Broberg/1/. To describe the wave propagation we use cylindrical coordinates both for the two halfspaces and for the liquid layer, see further the indications in Fig.1. The wave propagation in the upper halfspace is characterized with the aid of the velocity potential φ_1. For this velocity potential the following differential equation is valid:

$$\nabla^2\varphi_1 - \frac{1}{c_1^2}\frac{\partial^2\varphi_1}{\partial t^2} = -k\,\delta(r)\,U(t)/r^2 \qquad (1)$$

where $\delta(r)$ = Dirac´s delta function
$U(t)$ = Heaviside´s unit step function
k = a constant that will be determined further on.

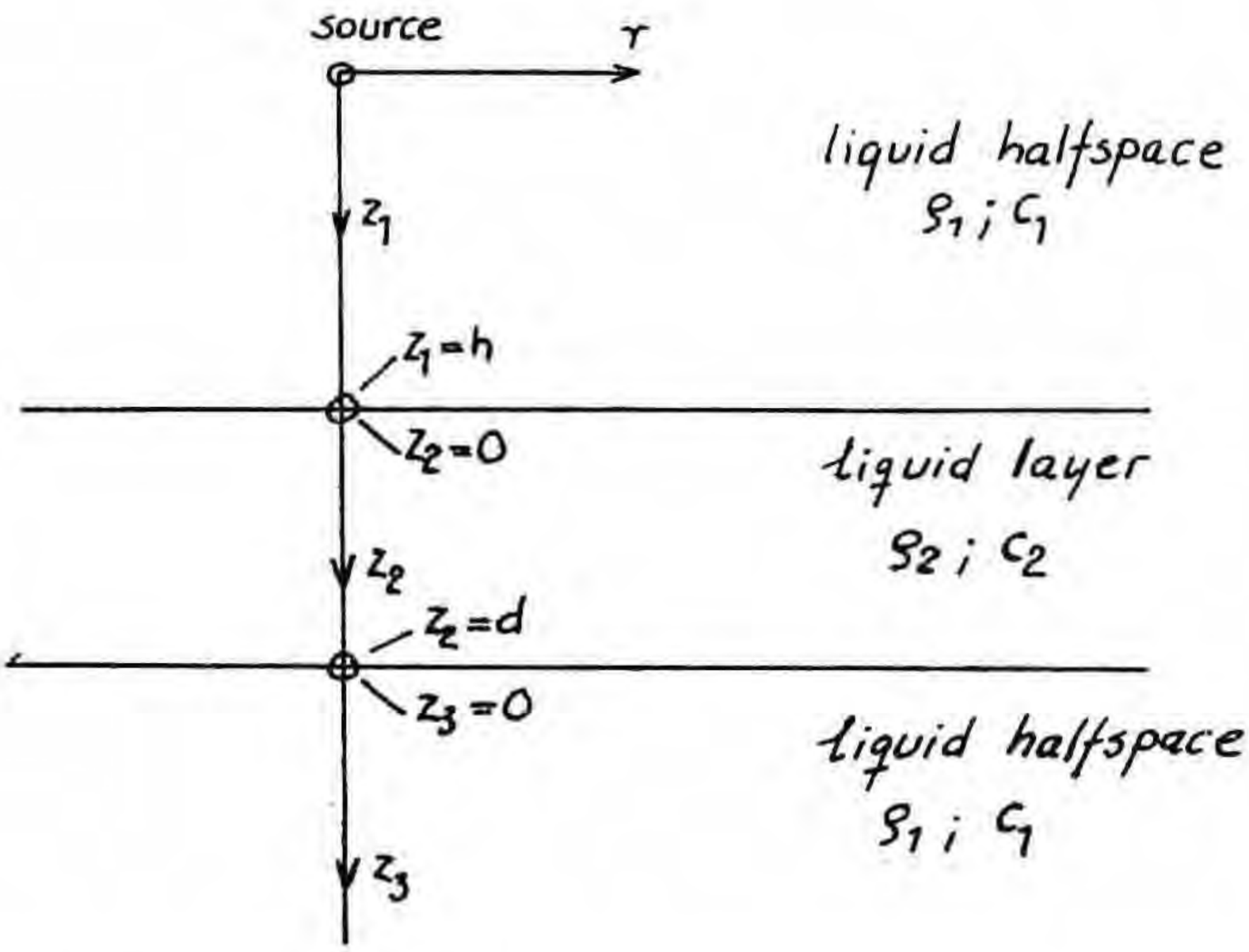

Fig.1. Coordinate systems chosen when studying the transmission problem.

Using the Laplace transform

$$\tilde{\varphi}_1 = s \int_0^\infty exp(-st)\, \varphi_1\, dt \tag{2}$$

we transform the equation (1) into

$$\nabla^2\tilde{\varphi}_1 - \frac{s^2}{c_1^2}\tilde{\varphi}_1 = -k\,\delta(r)/r^2 \tag{3}$$

the particular solution of which is

$$\tilde{\varphi}_p = k\, exp(-sr/c_1)/r \tag{4a}$$

In our case, the solution of the differential equation (3) will be

$$\tilde{\varphi}_1 = \int_0^\infty A_1(\alpha,s)\, exp\left(z_1\sqrt{\frac{s^2}{c_1^2}+\alpha^2}\right) J_0(\alpha r)\, d\alpha + k\int_0^\infty \frac{\alpha}{\sqrt{\frac{s^2}{c_1^2}+\alpha^2}}\, exp\left(-z_1\sqrt{\frac{s^2}{c_1^2}+\alpha^2}\right) J_0(\alpha r)\, d\alpha \tag{4b}$$

Here we have used Sommerfeld's integral representation and $A_1(\alpha,s)$ is a function not yet determined. The following differential equations and solutions, obtained by Laplace transformations, are valid for the wave propagation in the liquid layer and the lower halfspace.
In the liquid layer:

$$\nabla^2\tilde{\varphi}_2 - \frac{s^2}{c_2^2}\tilde{\varphi}_2 = 0 \tag{5a}$$

$$\tilde{\varphi}_2 = \int_0^\infty A_2(\alpha,s)\, exp\left(-z_2\sqrt{\frac{s^2}{c_2^2}+\alpha^2}\right) J_0(\alpha r)\, d\alpha + \int_0^\infty B_2(\alpha,s)\, exp\left(z_2\sqrt{\frac{s^2}{c_2^2}+\alpha^2}\right) J_0(\alpha r)\, d\alpha \tag{5b}$$

In the lower halfspace:

$$\nabla^2\tilde{\varphi}_3 - \frac{s^2}{c_1^2}\tilde{\varphi}_3 = 0 \tag{6a}$$

$$\tilde{\varphi}_3 = \int_0^\infty A_3(\alpha,s)\, exp\left(-z_3\sqrt{\frac{s^2}{c_1^2}+\alpha^2}\right) J_0(\alpha r)\, d\alpha \tag{6b}$$

where A_2, B_2 and A_3 are arbitrary functions, which - together with A_1 - can be determined by help of the following boundary conditions (continuity of pressure and particle velocity at the two boundary surfaces):

$$(\rho_1 s\tilde{\varphi}_1)_{z_1=h} = (\rho_2 s\tilde{\varphi}_2)_{z_2=0} \tag{7a}$$

$$\left(\frac{\partial\tilde{\varphi}_1}{\partial z_1}\right)_{z_1=h} = \left(\frac{\partial\tilde{\varphi}_2}{\partial z_2}\right)_{z_2=0} \tag{7b}$$

$$(\rho_2 s\tilde{\varphi}_2)_{z_2=d} = (\rho_1 s\tilde{\varphi}_3)_{z_3=0} \tag{7c}$$

$$\left(\frac{\partial\tilde{\varphi}_2}{\partial z_2}\right)_{z_2=d} = \left(\frac{\partial\tilde{\varphi}_3}{\partial z_3}\right)_{z_3=0} \tag{7d}$$

Now let us investigate the wave transmitted to the lower halfspace with our attention confined to the case for which $r=0$ and $z_2=0$. The potential $\tilde{\varphi}_3$ can now be written

$$\tilde{\varphi}_3 = 4\varrho_1\varrho_2 k \int_0^\infty \frac{\alpha\sqrt{\frac{s^2}{c_2^2}+\alpha^2}\exp\left(-h\sqrt{\frac{s^2}{c_1^2}+\alpha^2}\right)}{s\left[\varrho_1\sqrt{\frac{s^2}{c_2^2}+\alpha^2}+\varrho_2\sqrt{\frac{s^2}{c_1^2}+\alpha^2}\right]^2}\sum_{n=0}^{\infty}\left[\frac{\varrho_1\sqrt{\frac{s^2}{c_2^2}+\alpha^2}-\varrho_2\sqrt{\frac{s^2}{c_1^2}+\alpha^2}}{\varrho_1\sqrt{\frac{s^2}{c_2^2}+\alpha^2}+\varrho_2\sqrt{\frac{s^2}{c_1^2}+\alpha^2}}\right]^{2n}$$

$$\cdot \exp\left[-(2n+1)d\sqrt{\frac{s^2}{c_2^2}+\alpha^2}\right]d\alpha \qquad (8)$$

Using Cagniard's method /2/ we make the following substitutions

$$\alpha = s\,\varepsilon \qquad (9a)$$

and

$$h\sqrt{\frac{1}{c_1^2}+\varepsilon^2} + (2n+1)d\sqrt{\frac{1}{c_2^2}+\varepsilon^2} = \upsilon \qquad (9b)$$

We will also observe that the particular solution /eq.(4a)/ is equivalent to a pressure pulse which in Laplace transformed quantities can be expressed as follows:

$$\tilde{\rho}_p = -\varrho_1 s\,\tilde{\varphi}_p = -\varrho_1 s\,k\exp(-sr/c_1)/r \qquad (10a)$$

i.e.

$$p_p = -\varrho_1 k\,\delta\left(t-\frac{r}{c_1}\right)/r \qquad (10b)$$

With this pressure-time process we can associate an impulse density i(r), thus being able to determine the constant k in the following way:

$$i(r) = \int_{-\infty}^{\infty} p_p\,dt = -\int_{-\infty}^{\infty}\varrho_1\frac{k}{r}\delta\left(t-\frac{r}{c_1}\right) = -\varrho_1\frac{k}{r} \qquad (11a)$$

For r=h we obtain

$$k = -h\,i(h)/\varrho_1 \qquad (11b)$$

Using the substitutions in eq.(9) and the expression determined above for the constant k we obtain

$$p_3 = 4\varrho\,i(h)\frac{c_1}{h}\,\frac{L}{V^3(1-\sigma^2)(L+M)^3}\,U(\tau-1-\sigma c)\cdot$$

$$\cdot\left\{V(\varrho L+M)\left\{4\varrho LM\frac{M^2-L^2}{(\varrho L+M)^2}\sum_{n=0}^{\infty}n\left(\frac{\varrho L-M}{\varrho L+M}\right)^{2n-1} + \right.\right.$$

$$\left.\left. + (L^2+2M^2)\sum_{n=0}^{\infty}\left(\frac{\varrho L-M}{\varrho L+M}\right)^{2n}\right\} - LM\left\{2V(\varrho M+L)+\tau(\varrho L+M)\right\}\sum_{n=0}^{\infty}\left(\frac{\varrho L-M}{\varrho L+M}\right)^{2n}\right\} +$$

$$+ 4\varrho i(h)\frac{c^2}{(\varrho c+1)^2(c+\sigma)}\sum_{n=0}^{\infty}\left(\frac{\varrho c-1}{\varrho c+1}\right)^{2n}\delta(\tau-1-\sigma c) \qquad (12)$$

where

$$\varrho = \varrho_1/\varrho_2\,, \quad c = c_1/c_2\,, \quad \tau = c_1 t/h\,, \quad \sigma = (2n+1)d/h$$

$$V = \sqrt{\tau^2+(1-c^2)(\sigma^2-1)}\,, \quad L = V-\sigma\tau\,, \quad M = \tau-\sigma V$$

The above analysis is made on the basis of the assumption of an incident wave of delta function character. Should the incident wave have an arbitrary pressure - time process, say $p_i(t)$, the pressure-time process of the transmitted wave (P_3) could in this case be obtained by a method of superposition. We find that

$$P_3 = \int_{-\infty}^{\infty}\frac{P_i(\tau_1)}{i(h)}\cdot p_3(\tau-\tau_1)\,d\tau_1 \qquad (13)$$

The foregoing study refers to the case when a wave is transmitted through a liquid layer. If this layer is replaced by a plate of infinite extension a considerably more complicated transmission problem arises, as in this case we must take into account the capability of the plate to support shear stresses. However, this problem has been thoroughly studied by the author, and the results obtained will be published later on.

Literature: /1/ Broberg,B: Trans. Roy. Inst. Techn., Stockholm 139 (1959)
/2/ Cagniard,L: Réflexion et réfraction des ondes séismiques progressives. Gauthier-Villars, Paris 1939

H38

FOURTH INTERNATIONAL CONGRESS ON ACOUSTICS
COPENHAGEN 21.-28. AUGUST 1962

CONTRIBUTION A L'ETUDE DU MASQUAGE DE LA PAROLE

R. LEHMANN (Centre National d'Etudes des Télécommunications - Paris - France)

I°) - INTRODUCTION

L'étude des phénomènes de masquage de la parole présente actuellement un intérêt indéniable, l'expérience journalière montrant qu'il est possible de percevoir et même de comprendre le langage dans des conditions de bruit ambiant souvent pénibles ; on peut d'ailleurs être surpris de cette faculté que présentent tout à la fois l'oreille et l'intelligence de l'individu de distinguer certains sons utiles parmi divers autres sons dont il peut alors faire, en partie tout au moins, abstraction.

Cependant, il est bien connu que lorsque le bruit ambiant a un niveau trop élevé ou lorsque le rapport signal sur bruit est trop faible, le langage n'est plus intelligible et l'effet de masque devient alors prépondérant. Cet effet dépend de divers facteurs dont les plus importants sont évidemment les spectres et les niveaux relatifs des sons masqués et masquants.

Dans ce travail, nous avons tout principalement cherché à mettre en évidence l'influence des modes de présentation respectifs de la parole et du bruit de masque, car on ne peut admettre, a priori, d'une part que la sonie soit la même pour des conditions de champ libre et de champ diffus, d'autre part que les phénomènes de localisation et de latéralisation puissent être négligés et, enfin, que l'audition binaurale supraliminaire en présence d'un bruit de masque soit la même pour l'écoute par écouteurs et par haut-parleurs.

Nous avons étudié successivement les conditions expérimentales suivantes :

1°) Parole et bruit dans des haut-parleurs,
2°) Parole et bruit dans des écouteurs,
3°) Parole dans des écouteurs et bruit dans des haut-parleurs,

et nqus verrons que certains écarts systématiques existent dans les résultats, écarts pouvant être expliqués, en partie, par des phénomènes de nature psychophysiologique.

Afin de ne pas faire intervenir les effets bien connus de fatigue auditive, nous avons utilisé des niveaux acoustiques inférieurs à 100 dB, tant en ce qui concerne le bruit de masque qu'en ce qui concerne la parole. D'autre part, toutes les mesures ont été exécutées en utilisant des listes de 25 mots français dissyllabiques et, après chaque liste, était observé un arrêt de plusieurs minutes. Toutes les mesures ont été effectuées avec cinq opérateurs qui recevaient, chacun, 100 mots (soit 500 mots au total) et l'intelligibilité calculée correspondait à la moyenne obtenue sur ces cinq opérateurs. Quant au bruit de masque utilisé, il

consistait en un bruit blanc présentant une énergie pratiquement constante par Hz, entre 100 et 8000 Hz.

II°) - ETUDE DU MASQUAGE DANS LE CAS DE L'EMISSION DES STIMULI DANS DES HAUT-PARLEURS

Trois séries d'essais successifs ont été exécutées en émettant la parole à des niveaux croissant de 10 en 10 dB, entre 50 et 100 dB, et le bruit de masque à des niveaux tels que les rapports signal sur bruit soient égaux à + 10, 0, -5 et - 10 dB. Dans une première expérimentation, la parole était émise en champ pratiquement libre par un haut-parleur faisant face à l'auditeur (à 2 m environ) et le bruit de masque par quatre haut-parleurs disposés autour de lui. L'auditeur était assis au point d'intersection des axes acoustiques de ces quatre haut-parleurs, à une même distance de leur centre acoustique (les 5 haut-parleurs étaient pratiquement disposés sur une sphère, les angles de leur axe acoustique étant de 72° environ). Dans une seconde expérimentation, les conditions de présentation des stimuli ont été inversées : la parole était émise simultanément par les quatre haut-parleurs et il était alors impossible de lui donner une direction préférentielle (conditions appelées de champ quasi-diffus). Quant au bruit de masque, il était produit par le haut-parleur qui faisait face à l'auditeur. Enfin, dans une troisième expérimentation, la parole et le bruit de masque ont été émis dans un seul et même haut-parleur faisant face à l'auditeur : les deux stimuli ont alors la même origine et parviennent en phase aux deux oreilles.

La figure 1 groupe les résultats comparatifs de ces trois séries d'essais desquels il est permis de tirer les conclusions suivantes :

1°) l'intelligibilité décroît toujours lorsque le rapport signal sur bruit (S/B) diminue ; elle varie pratiquement entre 0 et 100 % lorsque le rapport S/B passe de - 20 à + 10 dB,

2°) l'intelligibilité décroît toujours, pour un rapport S/B donné, lorsque les niveaux du signal et du bruit augmentent (la baisse est de l'ordre de 5 % lorsque les niveaux de S et de B passent de 40 à 100 dB, pour un rapport S/B nul),

3°) pour des rapports S/B 0, l'intelligibilité est pratiquement la même que le bruit soit émis en champ libre (et la parole en champ quasi-diffus) ou en champ diffus (et la parole en champ libre). Pour des rapports S/B 0, l'intelligibilité est nettement meilleure lorsque la parole est émise en champ quasi-diffus (et le bruit en champ libre) qu'en inversant les modes de présentation des stimuli,

4°) dans le cas de l'émission de la parole en champ libre, l'intelligibilité est davantage dégradée lorsque le bruit de masque provient de la même origine que lorsqu'il provient de plusieurs directionsdifférentes de celle du son utile (la différence est de l'ordre de 10 %),

5°) il semble que l'homme présente ce que l'on peut appeler un certain facteur de directivité dû au fait que dans le cas de sources séparées dans l'espace, le signal et le bruit siègent apparamment en deux endroits différents de la tête (phénomènes de localisation spatiale).

III°) - ETUDE DU MASQUAGE DANS LE CAS DE L'EMISSION DES STIMULI DANS DES ECOUTEURS

Deux séries d'essais ont été exécutées en émettant la parole à

des niveaux compris entre 40 et 90 dB et le bruit de masque à des niveaux tels que les rapports S/B soient compris entre + 10 et - 40 dB. Dans la première expérimentation, la parole et le bruit de masque étaient envoyés simultanément et ensemble dans les deux écouteurs, tandis que dans la seconde, les deux stimuli étaient envoyés simultanément, mais séparément, dans des écouteurs différents. La figure 2 donne les résultats de ces essais qui conduisent aux conclusions suivantes :

1°) dans le cas de l'écoute binaurale simultanée des deux stimuli (parole et bruit de masque), l'effet est le même que lors de l'écoute des mêmes stimuli en champ libre. Aux niveaux supérieurs à 90 dB, cependant commencent à apparaître certains effets interauraux dus aux phénomènes d'audition croisée (1 et 2),

2°) dans le cas de l'écoute monoaurale simultanée des deux stimuli (parole dans une oreille et bruit de masque dans l'autre), l'intelligibilité est évidemment beaucoup moins détériorée que dans le cas précédent (pour un rapport S/B de - 15 dB, elle est de l'ordre de 70 % dans ce cas et pratiquement négligeable dans le cas précédent) : il n'y a alors pas localisation au centre du crâne, mais lorsque le rapport S/B diminue, la latéralisation tend toujours inconsciemment à se faire du côté où le niveau est le plus élevé,

3°) enfin, encore dans ce cas de l'écoute monoaurale simultanée des deux stimuli et pour un rapport S/B nul, les niveaux du signal et du bruit étant peu élevés (30 à 45 dB), nous avons pu observer une légère mais très nette augmentation de l'intelligibilité (5 à 8 % environ) par rapport au cas où aucun bruit de masque ne parvenait à l'oreille opposée à celle recevant le signal.

Dans le cas de l'utilisation de fréquences pures comme sons masquants, une légère augmentation de l'intelligibilité a pu être notée pour les fréquences 125 et 250 Hz, mais aucune augmentation pour des fréquences supérieures. Il faut donc admettre, soit une activation corticale, soit une action stimulatrice sur la musculature de l'oreille moyenne contralatérale, soit l'excitation d'un nombre suffisant de fibres sous l'effet d'un bruit blanc ou d'un son de basse fréquence, effets se traduisant par une augmentation de la sonie de la parole (3).

IV°) - ETUDE DU MASQUAGE DANS LE CAS DE L'EMISSION DE LA PAROLE DANS DES ECOUTEURS ET DU BRUIT DE MASQUE DANS DES HAUT-PARLEURS

Dans ces conditions, trois séries d'essais successifs ont également été exécutées, pour des niveaux de la parole compris entre 40 et 100 dB et pour des rapports signal sur bruit compris entre 0 et - 30 dB. Dans une première série d'essais, la parole a été émise dans les deux écouteurs simultanément et le bruit blanc de masque en champ libre, tandis que dans une seconde expérimentation, le bruit masquant parvenait aux auditeurs de plusieurs directions simultanément. Enfin, dans la troisième série d'essais, la parole n'était envoyée que dans un seul écouteur, le bruit masquant parvenant toujours aux auditeurs de plusieurs directions. La figure 3 groupe les résultats comparatifs de ces essais dont on peut tirer les conclusions suivantes :

1°) même en tenant compte de l'indice d'isolement acoustique des écouteurs utilisés, l'intelligibilité est moins dégradée que lorsque l'écoute de la parole se fait à l'aide de haut-parleurs,

2°) la baisse d'intelligibilité, pour un rapport S/B donné, est plus marquée lorsque le bruit de masque est produit en champ diffus que lorsqu'il est produit en champ libre,

3°) il semble que la sonie d'un bruit soit plus élevée lorsqu'il

parvient aux oreilles de plusieurs directions que lorsqu'il parvient en champ libre, la différence se situant entre 2 et 3 dB pour un bruit blanc,

4°) dans un bruit blanc émis par des haut-parleurs en champ quasi-diffus le phénomène de sonie est prépondérant dans le cas de l'écoute de la parole à l'aide d'écouteurs, tandis que le phénomène de directivité de l'auditeur est prépondérant dans le cas de l'écoute de la parole en champ libre,

5°) dans le cas de l'écoute de la parole dans le bruit à l'aide d'un seul écouteur, la protection de l'oreille contralatérale est utile, quoique non indispensable pour un rapport S/B 0. Elle devient d'autant plus utile que le rapport S/B est plus faible. D'autre part, il y a intérêt à ce que l'indice d'isolement acoustique de l'écouteur utilisé soit toujours aussi élevé que possible. Enfin, il y a évidemment toujours intérêt à écouter la parole dans le bruit à l'aide de deux écouteurs (phénomènes de sommation et de protection de l'oreille opposée), tout principalement dans le cas où le rapport S/B 0.

B I B L I O G R A P H I E

(1) - I. POLLACK et J.M. PICKETT : masking of speech by noise at high sound levels (J.A.S.A. - 1958 - p. 127).
(2) - I. POLLACK et J.M. PICKETT : interaural effects upon speech intelligibility at high noise levels (J.A.S.A. - 1958 - p. 293).
(3) - J. P. EGAN : the effect of noise in one ear upon the loudness of speech in the other ear (J.A.S.A. - 1948 - p. 58).

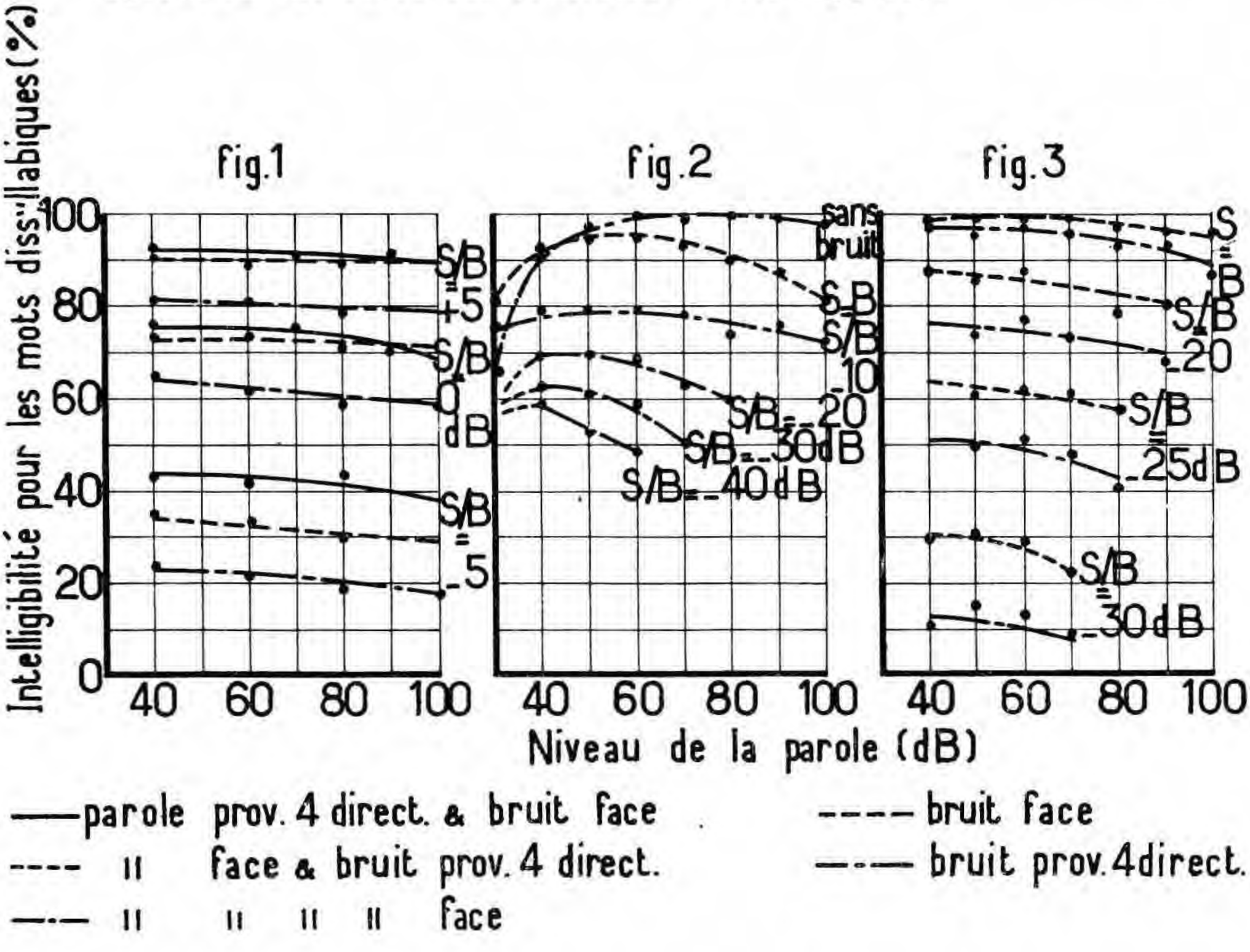

N38

FOURTH INTERNATIONAL CONGRESS ON ACOUSTICS
COPENHAGEN 21.-28. AUGUST 1962

Analyse des stereofonen Schallfeldes.

Andrá: Illényi,
Akustische Forschungsgruppe, Budapest, Ungarn.

Die Notwendigkeit der weiteren Untersuchungen des stereofonen Schallfeldes haben wir in einer früheren Arbeit aufgeworfen (1). Wir haben damals als ersten Schritt unserer Arbeit die klassische Anordnung mit zwei Lautsprecher als idealisiertes akustisches Dipol betrachtet, und haben dessen Schallfeld mit einem anderen Dipol (mit den zwei Ohren) abgetastet. Die Zahl der Anfangsbedingungen herabsetzend, wird jetzt die Analyse eines sowohl praktisch, als auch mathematisch durchführbaren stereofonen Schallfeldes angegeben. Die Strahler mit endlicher Ausdehnung werden in freiem Schallfeld aufgestellt und in dem auf den einzelnen Strahler bezüglichen Fernfeld wird das entstehende Nahefeld des akustischen Dipols untersucht. Das Feld wird der Wahrheit gemäss mit dem menschlichen Körper gestört. Die untersuchungen werden mit Sinustöne durchgeführt, da die Richtcharakteristik, als eine charakteristische Angabe der Strahler, für statistisches musikalisches Signal und für Transienten einstweilen noch nicht gedeutet ist.

Der sich in den Ohren abspielende Wirkungsmechanismus wird nicht eingehend behandelt. Unser Ziel ist, die Charakteristiken des Schallfeldes (Schalldruck, Teilchengeschwindigkeit) bei Öffnung des äusseren Gehörganges anzugeben. Bei eigenen Untersuchungen gehen wir von den aus der Literatur (Tröger, Sivian-White, Jahn-Vogelsang, Robinson-Whittle, Schirmer) (2) bekannten einohrigen Richtcharakteristiken aus. Bisher waren nämlich die Modellversuche (Kugel, verschiedene Kunstköpfe, usw.) und die mathematische Näherungen auf die Diffraktionswirkung des Kopfes ungenügend. Die neueren Messergebnisse von Robinson und Whittle und von Schirmer stimmen mit guter Näherung überein. Sie haben kein Modell, sondern während der Messung eine passive Rolle spielende Versuchsperson angewandt, bei welcher mit einem im Gehörgang angebrachten Sondenmikrophon der Schalldruck untersucht wurde. Aus ihren Messungen berechnete ich die Richtcharakteristik mit Hilfe der Bessel'schen Formeln der angenäherten harmonischen Analyse, mit trigonometrischer Interpolation.

Sei die so ausgerechnete Funktion bei Frequenz ω, in Richtung

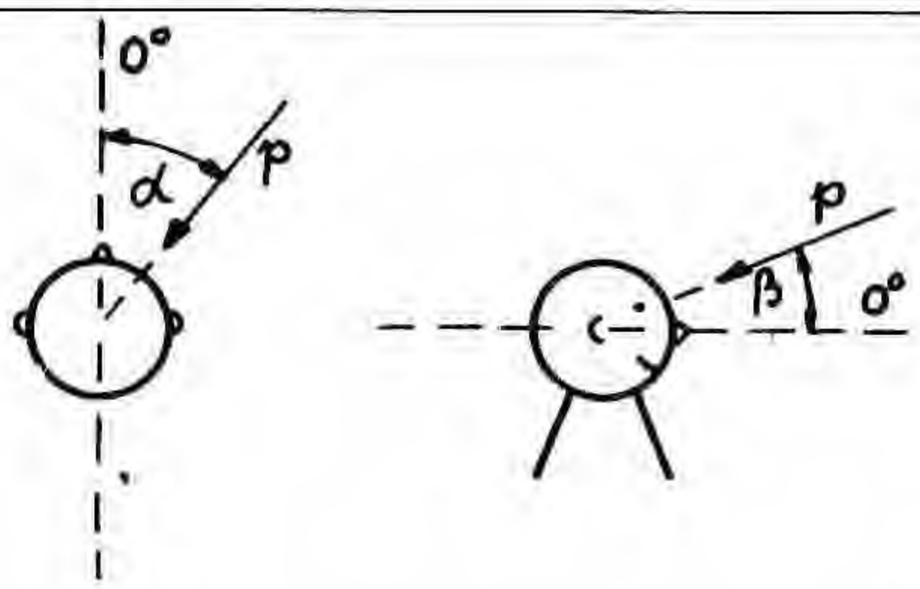

Abb.1. Bezeichnungen für in Text behandelten Formeln.

(α,β) für das rechte Ohr $d_r[\alpha,\beta,\omega]$ für das linke Ohr $d_l[(2\pi-\alpha),\beta,\omega]$ wobei α in der Asimutal-Ebene, β in der Symmetrie-Ebene gemessener Einfallswinkel (Abb.1.) ist. Der einfallende Schalldruck p wird auf Grund des Helmholtz-Prinzipes für $p\ d[\alpha,\beta,\omega]$ wahrgenommen, wo nach unserer Erklärung das zweiohrige Hören folgende Richtcharakteristik hat:

$$d[\alpha,\beta,\omega] = d_r[\alpha,\beta,\omega] + d_l[(2\pi-\alpha),\beta,\omega]$$

Da das Ohr hauptsächlich ein Organ für Druckempfindung ist, und unsere Messmikrophone grösstenteils auch druckempfindlich sind, richtete sich die Analyse zuerst auf die Untersuchung des Schalldruckes im äusseren Gehörgang.

Aus dem mit Gleichung $(\nabla^2+k)\phi = 0$ abschreibbaren Schallfeld - wo ϕ das Geschwindigkeitspotenzial des Schallfeldes bildet - kann die für die Entfernung und räumliche Empfindung wesentliche Teilchengeschwindigkeit ausgerechnet werden.

Die Differenz des in den zwei Ohren entstehenden Schalldruckes, welche mit dem Richthören proportionell ist, wird als $\Delta p = p\,\delta[\alpha,\beta,\omega]$ betrachtet, wobei $\delta[\alpha,\beta,\omega] = d_r[\alpha,\beta,\omega] - d_l[(2\pi-\alpha),\beta,\omega]$ ist. Es ist ersichtlich, dass im Falle der aus Richtung der Symmetrieachse ($\alpha=\beta=0^\circ$) eingelaufener "Schallstrahlen" $\delta[0,0,\omega]=0$ ist, d.h. es gibt garkeine Schalldruckdifferenz. Man kann aber solche, sich von der Achse abweichenden (α,β) Werte finden, wo ebenfalls $\Delta p = 0$ ist, z.B. bei Richtcharakteristik von 700 Hz, wenn $\beta = 0^\circ$ und $\alpha = 180^\circ$ ist (Abb. 2.) Da der vorwärts-rückwärts-Eindruck gut zu unterscheiden ist (3), müssen bei Bestimmung des Richtungshörens auch die Harmonischen in Betracht gezogen werden. Bei dem obigen Beispiel ist nämlich für die fünfte Harmonische $\delta[\alpha,\beta,\omega_5] \neq 0$, was aus der Richtcharakteristik von 3,5 kHz ersichtlich ist. Danach wird die Analyse anstatt einer einzigen Frequenz, auf das Frequenzspektrum des untersuchten Tones ausgebreitet, welches einen F(t) zeitlichen Verlauf hat.

$$F(t) = \sum_i A_i \exp(j\omega_i t) \quad \text{und} \quad \delta[\alpha,\beta,t] = \sum_i \delta_i[\alpha,\beta,\omega_i]$$

Nun ist $\Delta p = \sum_i p_i \delta_i[\alpha,\beta,\omega_i]$, wo i = 0, 1, 2, ... die Ordnungszahl der Harmonischen ist.

Die Versuchsperson soll in einem Feld gestellt werden, wo aus

einer (α_1, β_1) Richtung p_1 und aus einer anderen (α_2, β_2) Richtung p_2 Schalldrücke einfallen. In dem rechten und linken Ohr bilden sich die Schalldrücke von

$$p_r = p_1 d_r [\alpha_1, \beta_1, \omega_1] + p_2 d_r [\alpha_2, \beta_2, \omega_2]$$

$$p_l = p_1 d_l [(2\pi - \alpha_1), \beta_1, \omega_1] + p_2 d_l [(2\pi - \alpha_2), \beta_2, \omega_2]$$

Die Schalldruckdifferenz ist also

$$\Delta p = p_1 \delta_1 [\alpha_1, \beta_1, \omega_1] + p_2 \delta_2 [\alpha_2, \beta_2, \omega_2]$$

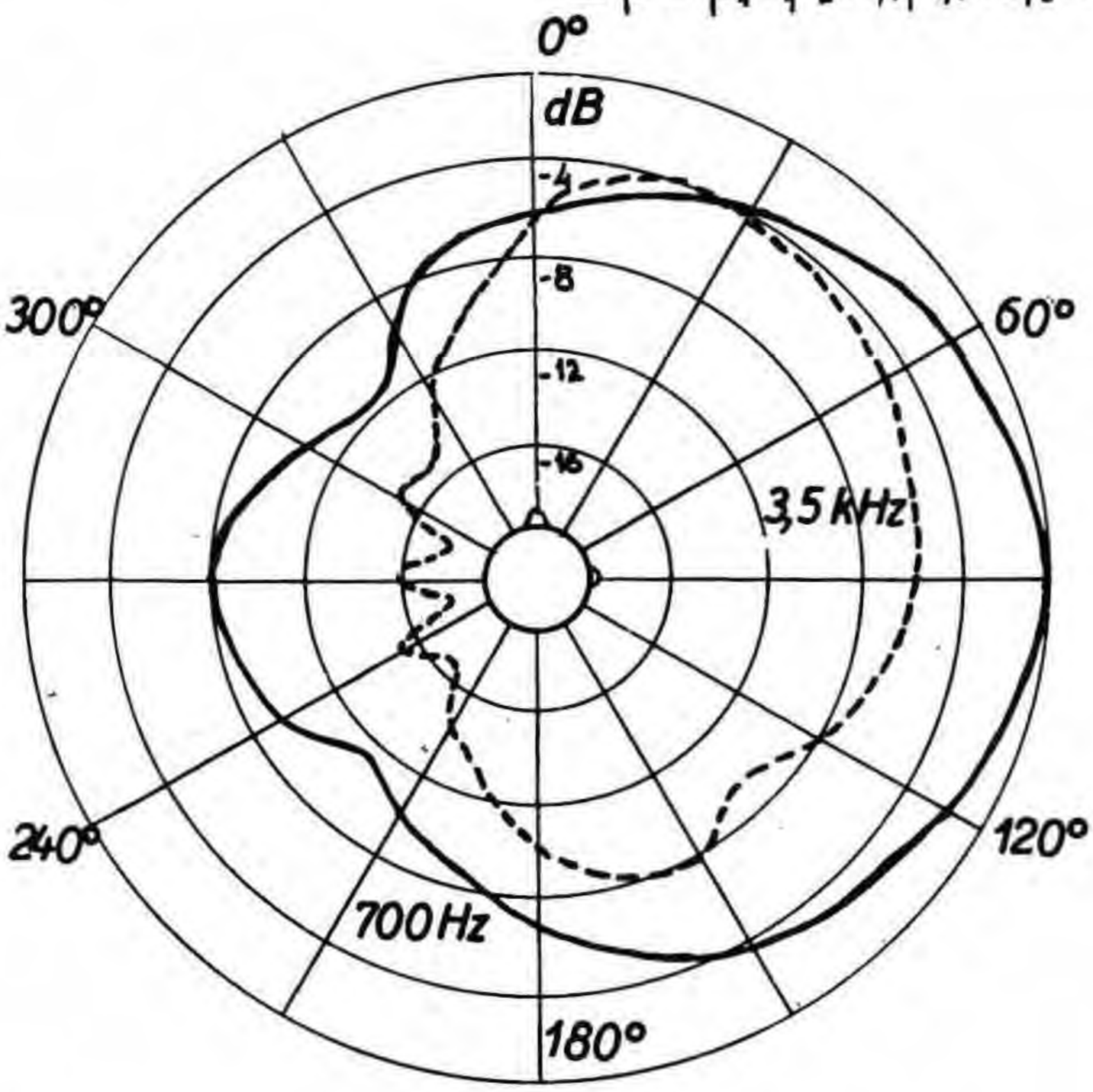

Abb. 2. Die einohrigen Richtcharakteristiken (700, 3,5 kHz) nach Schirmer.

d.h. die auf die zwei verschiedenen Einfallsrichtungen bezogenen Schall- druck- (bzw. Teilchengeschwindigkeits-) Differenzen summieren sich. Auf "n" Schallquellen ausgebreitet:

$$\Delta p = \sum_{l=1}^{m} \Delta p_l$$

Die Zusammenhänge geben eine Erklärung auf die Beobachtungen von Kösters, Kuhl, Schodder, Knowels, (4), wonach die Wiedergabsysteme mit mehreren Lautsprechern (z.B. der Köster'sche Lautsprecher, weiters die Spiegelschallquellen) den räumlichen Eindruck des Klangbildes verbreiten.

Letztens untersuchte man die Rolle der Strahler. Der Schalldruck eines Strahlers mit Oberfläche A, Richtcharakteristik D, ist in einer Entfernung R von dem Mittelpunkt (5)

$$p = p_0 \exp(j\omega t - kR)\ D(\psi, \vartheta)$$

Hier ist p_0 der Schalldruck der Punktquelle, (ψ, ϑ) sind die Richtungswinkel des Strahlers.

Auf Grund der obigen ergibt sich auf die übliche Anordnung mit zwei Lautsprechern:

$$\Delta p = p_{01} \exp(j\omega_1 t - k_1 R_1)\ D_1(\psi_1, \vartheta_1, \omega_1) \delta_1 [\alpha_1, \beta_1, \omega_1] + p_{02} \exp(j\omega_2 t - k_2 R_2)\ D_2(\psi_2, \vartheta_2, \omega_2) \delta_2 [\alpha_2, \beta_2, \omega_2]$$

Auf die Symmetrieachse ist auch dieser Ausdruck gleich Null. Das Interessante ist, dass hier auf die Bedeutung der Richtcharakteristik in Ausbildung des stereofonen Schallfeldes hingewiesen wird. Man kann leicht einsehen, dass die sich aus der Anordnung des Strahlungssystems ergebende Verzerrung des originalen Schallfeldes abnimmt, falls die Strahler innerhalb eines breiten Frequenzbandes frequenzunabhängige Richtcharakteristik haben. Als experimenteller Beweis kann die bei Einführung der Kugellautsprecher hinfällig gewordene Behauptung erwähnt werden, wonach eine richtige Mittellokalisation nur in einer sehr schmalen Zone möglich ist (4). Der letzterwähnte Ausdruck beweist weiters, dass die Vorbedingung der Symmetrie des stereofonen Schallfeldes die Identität der zwei Strahler ($D_1 = D_2$) ist, was in der Praxis durch Zusammenwählen von Lautsprechern gleichen Typs gesichert werden kann.

Die geeignete Anwendung der Richtcharakteristik ermöglicht auch zahlreiche Tricke. Solche Lösungen werden bei pseudostereofon Systemen ausgenützt, die zwei verschiedene Lautsprecher ($D_1 \neq D_2$) verwenden. Bei mehreren Lautsprechern mit speziell ausgebildeten Richtcharakteristiken kann der "Schwerpunkt" des Schallfeldes in Abhängigkeit von der Frequenz verschoben werden. So kann auch schon mit einkanäliger Übertragung ein gewisser scheinbarer Raumeffekt gesichert werden, was von uns mit drei Lautsprechern erfolgreich geprüft geworden ist. Im allgemeinen sind die Zusammenhänge, auf "n" Strahler und auf das Frequenzspektrum der untersuchten Töne ausgebreitet:

$$\Delta p = \sum_n \sum_i p_{o,n,i} \exp(j\omega_{n,i} t - k_{n,i} R_n) D_{n,i}(\varphi_n, \vartheta_n, \omega_{n,i}) \delta_i[\alpha_n, \beta_n, \omega_{n,i}]$$

Die Rechnungen einiger konkreten Fällen sind mit elektronischer Rechenmaschine im Gange.

Literatur:

1. A. Illényi: II. Akust. Konf. Budapest (1961).
2. W.Schirmer: II. Akust. Konf. Budapest (1961).
3. Th.Tarnóczy: Acustica 8. 343. (1958).
4. W. Kuhl, J.M. Zosel: Acustica 6. 474. (1956).
5. H. Stenzel, O. Brosze: Leitfaden zur Berechnung von Schallvorgängen. Springer Berlin, 1958.

O38

FOURTH INTERNATIONAL CONGRESS ON ACOUSTICS
COPENHAGEN 21.-28. AUGUST 1962

A new method for determining the end correction of pipes by means of pulses.

Mohy Louden

Radiohouse Cairo (U.A.R.), at the time a guest in Physikalisch-Technische Bundesanstalt, Braunschweig, (Germany)

The resonance frequencies f_r of the air column inside a circular pipe with both ends closed can be determined exactly. The boundary conditions necessitate that the particle velocity at the closed ends is zero. Hence multiples of half the wave length fit into the length of the pipe l·

$$l = n \frac{\lambda_r}{2} \quad \text{or} \quad f_r = \frac{nc}{2l} \tag{1}$$

where n = 1, 2, 3, ..., and c is the sound velocity. Whereas in the case of a pipe with one or both ends open it is only approximate to assume that the pressure node occurs at the plane of the open end. Therefore a simple formula such as (1) can only give approximate values for the resonance frequencies. The sound pressure node cannot be at the open end since that means no communication of sound energy to the outside, or the outside air inertia is zero. The pressure node occurs at a certain distance a from the open end which is a function of the pipe diameter. To get correct values when calculating the resonance frequencies, this distance a called "end correction" must be added to the real length of the pipe. Lord Rayleigh[1] estimated the end correction for a circular pipe fitted at its open end with a rigid flange to be 0.82 the radius of the pipe. Experimentally he found the end correction of an unflanged open pipe to be 0.6 its radius.

The complicated exact calculation of the end correction for an unflanged circular pipe was first carried out by Levine and Schwinger[2], and independently, by Weinstein[3]. The solution is valid assuming axially symmetric excitation of the air column, and up to the cutoff frequency where only the first mode of cylindrical waves can propagate in the pipe[4].

From the theoretical calculations it is evident that the end correction is not only a function of the pipe diameter, but also of the frequency. This fact was early found experimentally by Bosanquet[5],

Blaikley[6], and Anderson and Ostensen[7]. Meyer[8] carried out recently expiriments on the same subject. By using modern electronic apparates he obtained results which agree partially with the theoretical calculations. His method consisted in measuring the resonance frequencies of the air column inside the pipe which are actuated with sinusoidal tones. Having the actual length of the pipe he calculated the end correction in phase angle units, i.e., the end correction in length units multiplied by the wave number.

The method mentioned here consists in generating a single acoustic pulse, at one end of the pipe, which travels to the other open end. Due to the mismatching of the acoustical impedances at the open end a negative pulse is generated there. This one, which can be considered as an echo or a reflection of the incident pulse, travels in the opposite direction inside the pipe. Both of these two pulses can be analysed into a series of sinusoidal tones. Each component of the reflected pulse should be retarded by a phase angle, from its respective one of the incident pulse, which is equal to $\pi + \theta$. The π phase shift is due to the fact that the resultant sound pressure, that is the excess pressure, at an open end must be zero, owing to the free expansion occuring there. Thus a compression is reflected at an open end as a rarefaction, and vice versa. Whereas θ is due to the fact that the reflection does not occur exactly at the plane of the open end, but at a certain distance from it.

By means of a condenser microphone the acoustic pulse, and its echo coming from the open end are picked up, amplified and displayed on an oscillograph screen. Photographs are then taken for the pulse and its echo, Fig. 1 and Fig. 2.

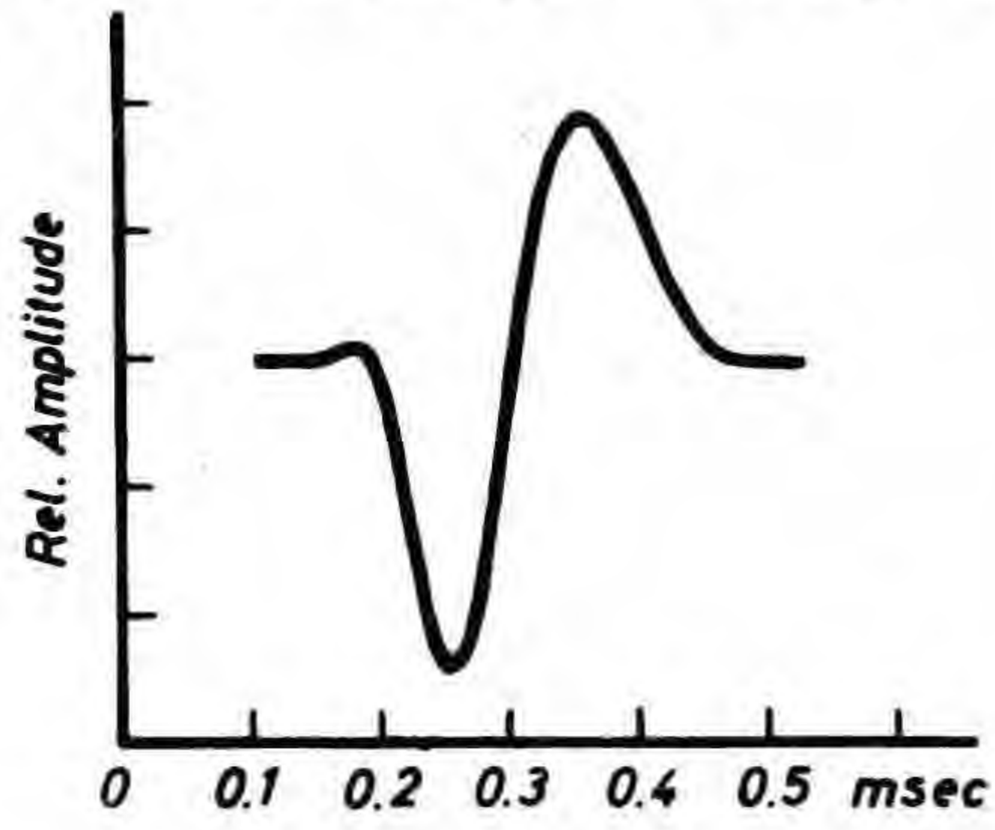

Fig. 1 The acoustic pulse

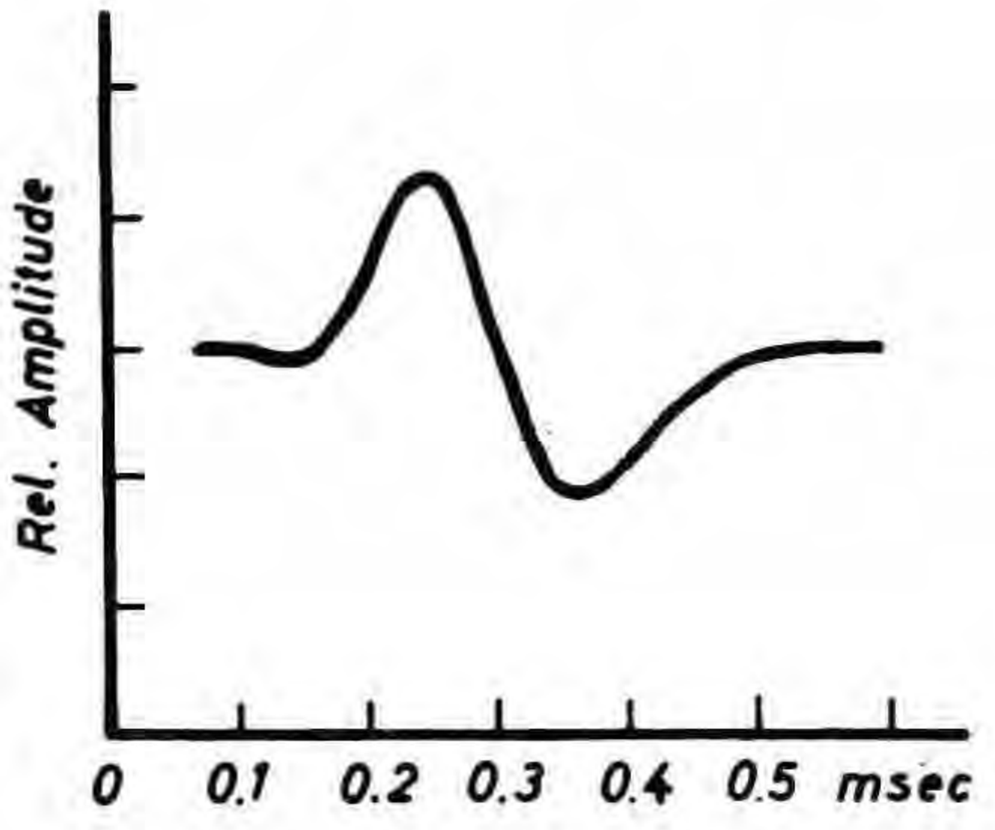

Fig. 2 The reflected acoustic pulse (echo)

The easiest and quickest method to analyse the photographs of the pulses is to use the mechanical curve analyser of Grützmacher[9]. The analyser gives the phase angle for each component directly without any calculation. The phase difference between each two respective components of the pulse and its echo is $\pi + \theta$, and hence θ can be determined. It is easy to see that the relation between θ and the end correction a is such that

$$\theta = 2 k a$$

where $k = \frac{2\pi}{\lambda}$ is the wave number.

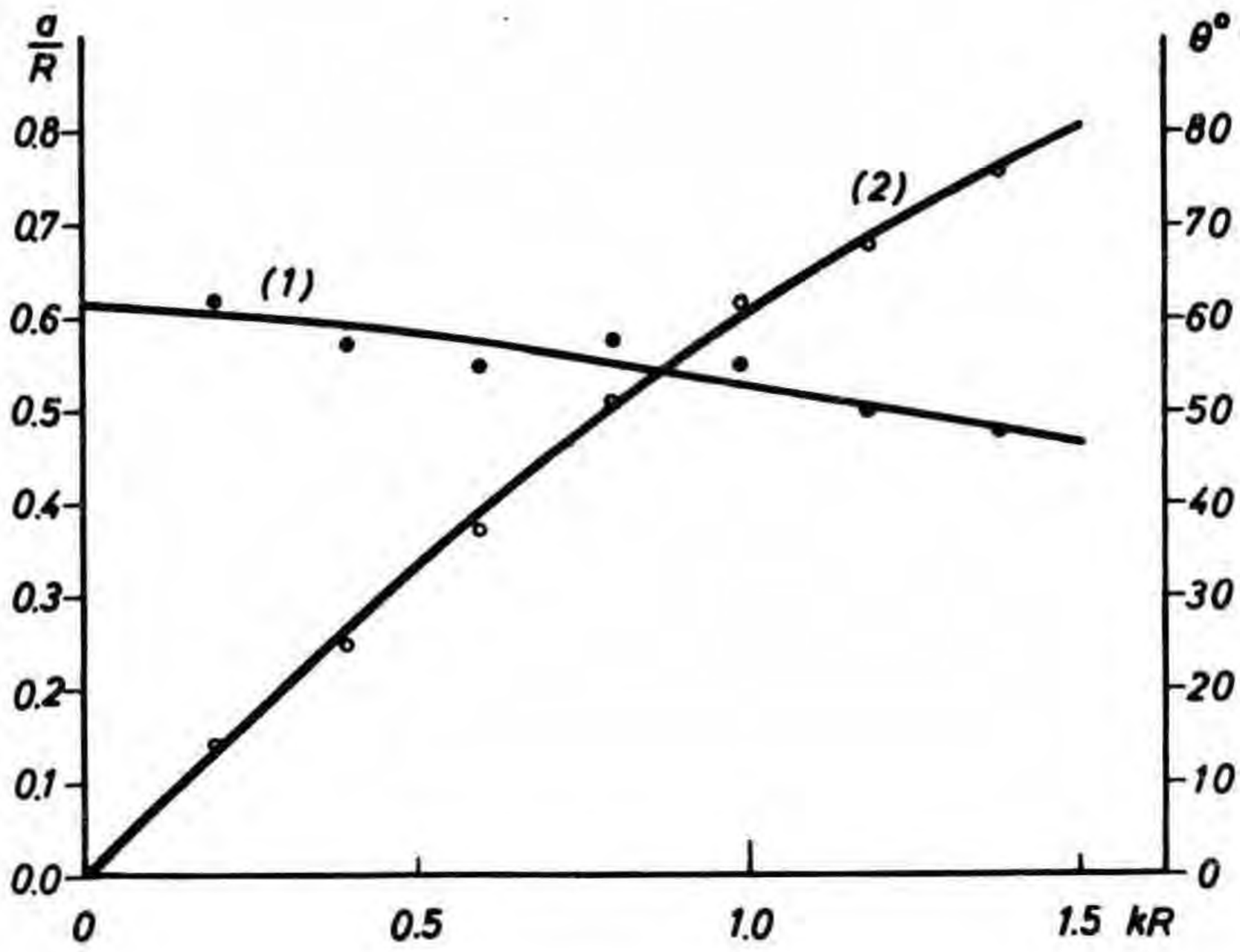

Fig. 3 Curve (1) gives the dependence of $\frac{a}{R}$, curve (2) of θ, on kR. The circles show the measured values.

Fig. 3 shows the results of the measurements carried out on a pipe with a radius R = 1.4 cm compared with the theoretical curves[2,3]. Curve 1 gives the relation between $\frac{a}{R}$, the ratio of the end correction to the radius of the pipe, and kR. Curve 2 shows the dependence of θ on kR. At low frequencies the end correction is 0.613 the radius of the pipe, and it decreases gradually with the increase of frequency for a constant pipe radius. It must be kept in mind that the above results are true so far only the first mode of cylindrical sound waves

(plane wave) exists in the pipe.

I would like to thank Professor Grützmacher and Dr. Lottermoser from the Physikalisch-Technische Bundesanstalt for the useful discussions and provision of apparates.

References

1. Lord Rayleigh, Theory of Sound, Vol. 2, Chap. 16 and Appendix A. (Macmillan and Co., London, 1940).
2. H. Levine and J. Schwinger, Phys. Rev. 73, 383 (1948).
3. L.A. Weinstein, Doklady Akad. Nauk SSSR II, S. 58, 1957 (1947).; J. Tech. Phys. (U.S.S.R.) XIX, 911 (1949).
4. E. Skudrzyk, Die Grundlagen der Akustik, Chap. VII. (Springer Verlag, Wien, 1954).
5. R.H.M. Bosanquet, Phil. Mag. 4, 216 (1877).
6. D.J. Blaikley, Phil. Mag. 7, 339 (1879).
7. S.H. Anderson and F.C. Ostensen, Phys. Rev. 31 267 (1928).
8. J. Meyer, Acustica 11, 385 (1961).
9. M. Grützmacher, Akust. Z. 8, 49 (1943).; Proceedings 3rd International Congress on Acoustics, 723. (Elsevier Pub. Co., Amsterdam, 1961).

H39

FOURTH INTERNATIONAL CONGRESS ON ACOUSTICS
COPENHAGEN 21.-28. AUGUST 1962

SOME EXPERIMENTS ON THE ASSESSMENT OF SUBJECT JUDGEMENT TO THE QUALITY AND SIGNAL TO NOISE RATIO OF PROGRAMME.

D.M.J.P. Manley, Ph. D., B. Sc., A. Inst. P., Grad. I.E.E.
(Farnborough Technical College, Farnborough, England.)

1. Introduction.

With the introduction of high quality audio reproducing equipment, many listeners to speech and music programmes have become increasingly aware of unwanted noise. Unwanted noise can, inter alia, be due to motor vehicles, aircraft, ventilation systems, and structure borne sounds. Decisions have to be made by Broadcasting Corporations as to the critical signal to noise ratio that can be tolerated. Surveys (1) have often been made in broadcasting studios and consequent decisions made on the maximum permissible noise level before a transmission becomes unsatisfactory. Very little work has been done analysing results of questions put to people listening to samples of programmes with various levels of background noise. This paper gives a short account of some experiments carried out in the last two years.

2. The Experiments.

A sample of speech or music free from any appreciable unwanted noise is reproduced using high quality loudspeakers. Wide band random noise is produced at different intensity levels, either by mixing the noise electronically in the programme channel, or by the use of a separate loudspeaker. Many samples of programme each lasting between a half and one minute are arranged with different noise levels in each case. For a given type of noise, about eight samples are necessary with signal to noise ratios varying from 12 db. to 40-50 db. In order to obtain an unbiased judgement from the listener, care is taken to set the signal to noise ratios of the samples in random order.

The listener is asked to place the unwanted noise into one of the following five categories:

Np ... Not perceptible;

P ... Perceptible;

PD ... Disturbing at times;

D ... Disturbing all the time;

DD ... Very distracting and the unwanted noise constitutes a serious deterioration of the programme.

A careful verbal definition of these grades is given to the listener before the test.

Three different series of tests using the method above have been conducted by the Author:

(1) On about forty individuals using the listening rooms of the British

Broadcasting Corporation (2).

(2) A referendum broadcast on the Overseas Network of the British Broadcasting Corporation (3) (September 1961.). Replies were received from nearly 300 people.

(3) A demonstration in the Main Hall of Farnborough Technical College, Farnborough, Hampshire, England. (4). About 90 persons were present.

For the first two series of tests, the samples with unwanted noise were prerecorded on tape.

3. The Results.

The first series of tests were mainly designed to compare listeners' judgements to different types of noises mixed with both music and speech. Wide band random noise of different octave bands was used. The results provided by about 40 listeners were tabulated and the critical signal to noise ratio corresponding to the difference between NP and P and also between P and PD was found in each case. These two conditions were known as the just perceptible and just disturbing conditions respectively. The complete results were plotted on Gaussian distribution paper as shown in fig. 1. For music with unwanted random noise of an octave band centred at 1000 cycles, the disturbing and perceptible signal to noise ratios are 39 and 49 db. respectively corresponding to 50% of the listeners.

Fig. 2 shows the perceptible and disturbing critical conditions as a function of the mid-frequency of the octave band of unwanted noise. Fig. 3 shows these results plotted in terms of loudness units (sones). This graph shows that a slightly higher level of unwanted noise can be tolerated if the noise is at the same frequency as the programme material.

Considering the tests broadcast on the General Overseas Programme of the B.B.C., some three hundred results were sent by post from all parts of the world to the B.B.C. In this case, only wide band unfiltered random noise was used as the unwanted signal, in addition to the normal atmospheric noise. heard on the short wave bands. Fig. 4 shows the distribution of the critical perceptible and disturbing conditions, showing the 50% disturbing and perceptible judgement to be 8 and 25 db. respectively. These results show a much higher tolerable noise level; but it must be appreciated that noise due to reception conditions on short waves is generally very high.

Some ninety people took part in a test in the Main Hall at Farnborough Technical College. This test used 14 samples of music fed through two electrostatic loudspeakers. A third loudspeaker reproduced the unwanted random noise.

Fig. 5 shows the results obtained and although there seems to be a wider range of opinion on the disturbing condition compared with the B.B.C. results, it is seen that the results for the condition of disturbance and perception to 50% of the listeners, namely 39 and 49 db. respectively, does agree well with the first set of experiments.

4. Conclusions.

This technique of plotting the statistical analysis of the judgement of

listeners has led to qualitative results that appear to agree well with the criteria set from the experience of acoustic engineers and broadcast studio designers. The Overseas Service referendum has shown that short wave conditions on the whole considerably raise the limits of perception and disturbance of unwanted noise occurring at the broadcasting end.

Most modern disc and tape reproducing equipment should be capable of better than 49 db. signal to noise ratio - the perceptible critical condition found in two of the series of tests - but investigations into certain broadcasts, especially on television, suggest that due to ventilation noise the signal to noise ratio is worse than the disturbing limit of 39 db.

Plans have already been made to extend this research technique with modifications to investigate the effect of aircraft and other common noises on mental and physical performance of individuals.

5. Acknowledgements.

The author wishes to acknowledge the help of the research department and General Overseas Service of the B.B.C. and to thank the Principal of Farnborough Technical College for permission and facilities to carry out part of this work. The author is also grateful to Mr. C.L.S. Gilford for his help and advice.

6. References.

(1) Beranek: 'Criteria for Noise in Buildings'. Noise Control, Jan. 1957, p. 19.

C.W. Koslen and G.J. Van Os: 'Community Reaction Criteria for External Noises'. Conference proceedings 'The Control of Noise.' National Physical Laboratory, Teddington, England (in publication).

(2) Research Department, B.B.C. Report in publication.

(3) General Overseas Service of the B.B.C. Broadcast as part of a programme 'Short Wave Listeners' Corner', September 1961.

(4) Part of a demonstration of high quality audio equipment on Friday April 6th. 1962 in the Main Hall of Farnborough Technical College.

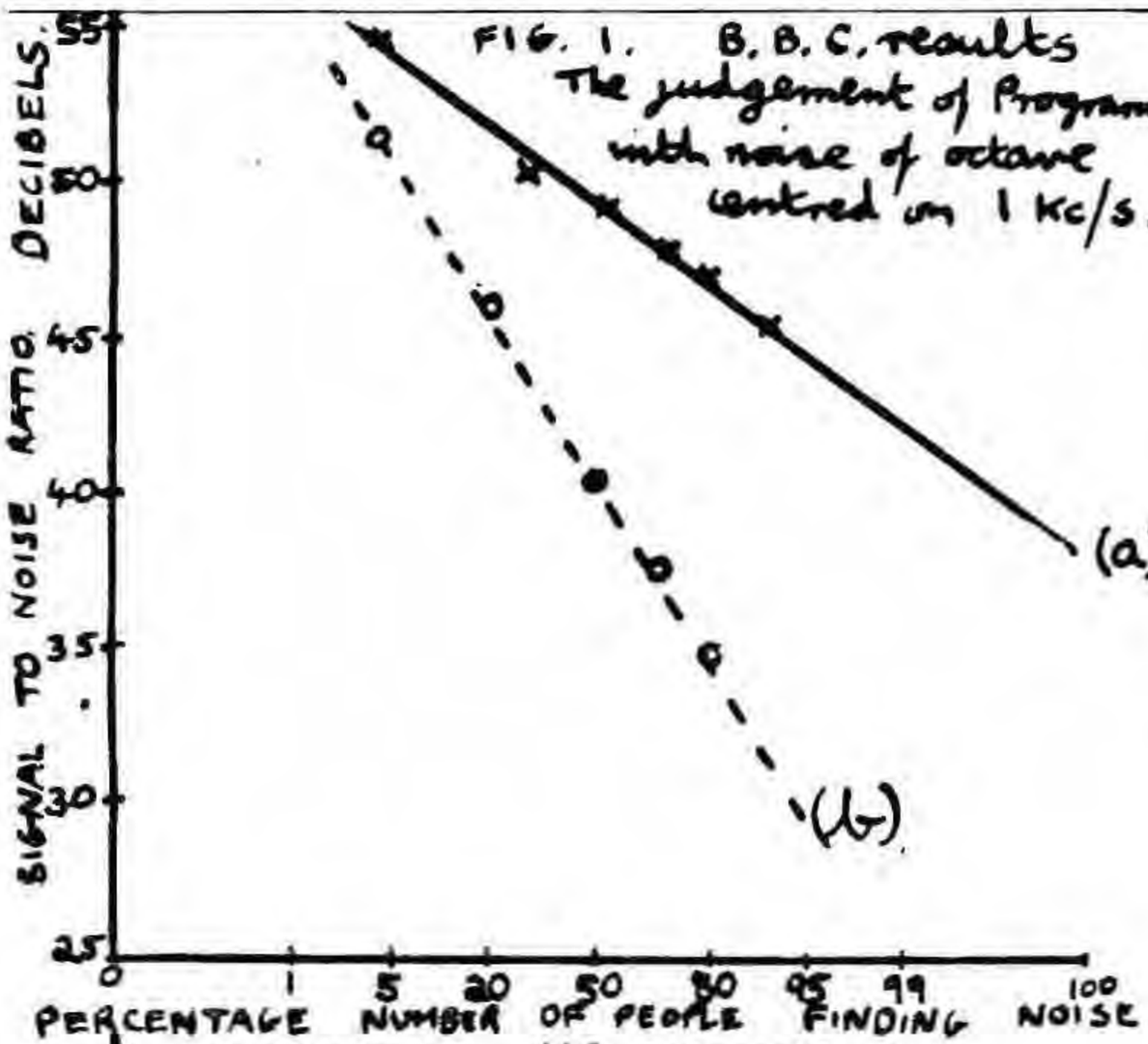

FIG. 1. B.B.C. results
The judgement of Programme with noise of octave centred on 1 kc/s.

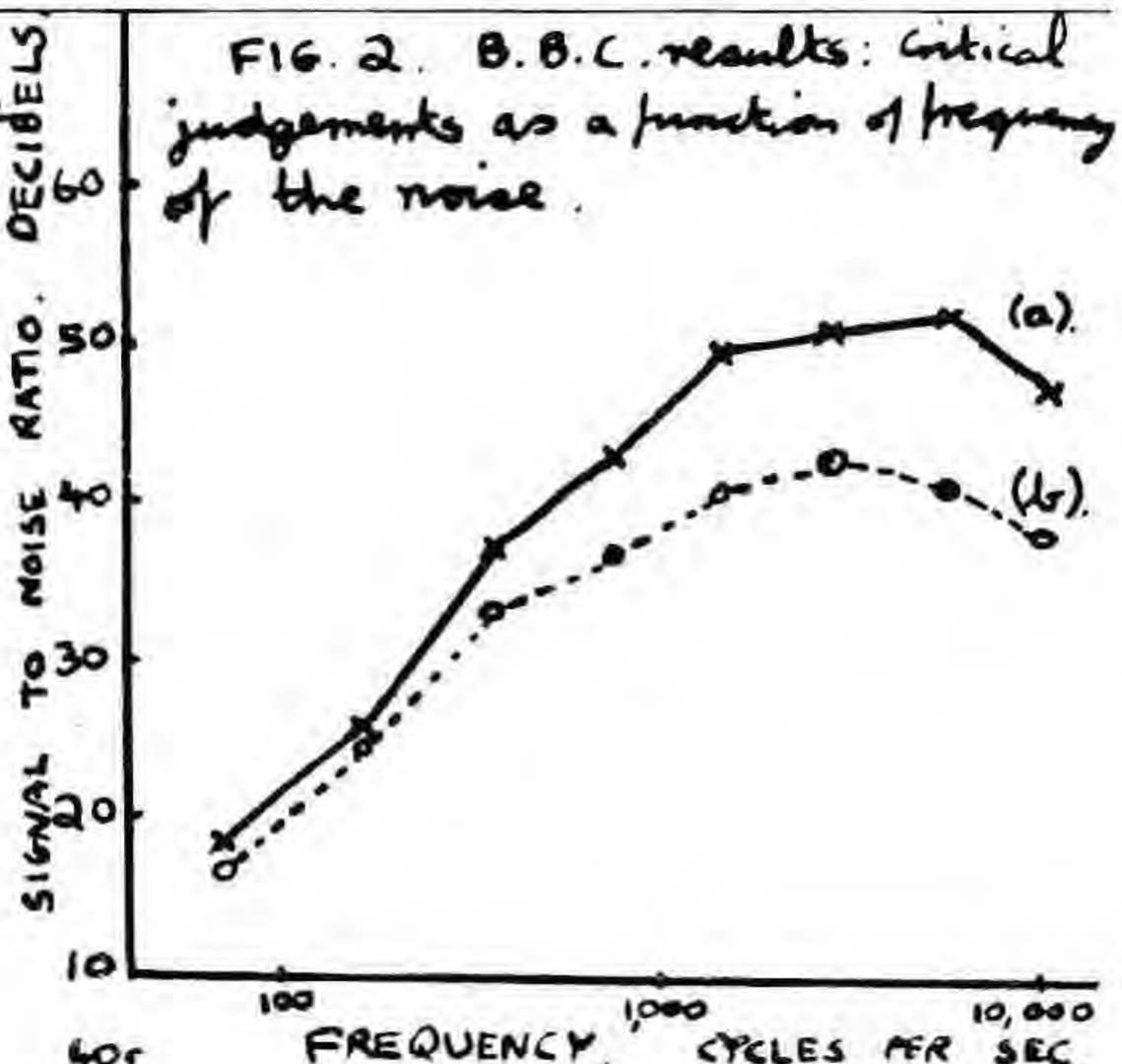

FIG. 2. B.B.C. results: Critical judgements as a function of frequency of the noise.

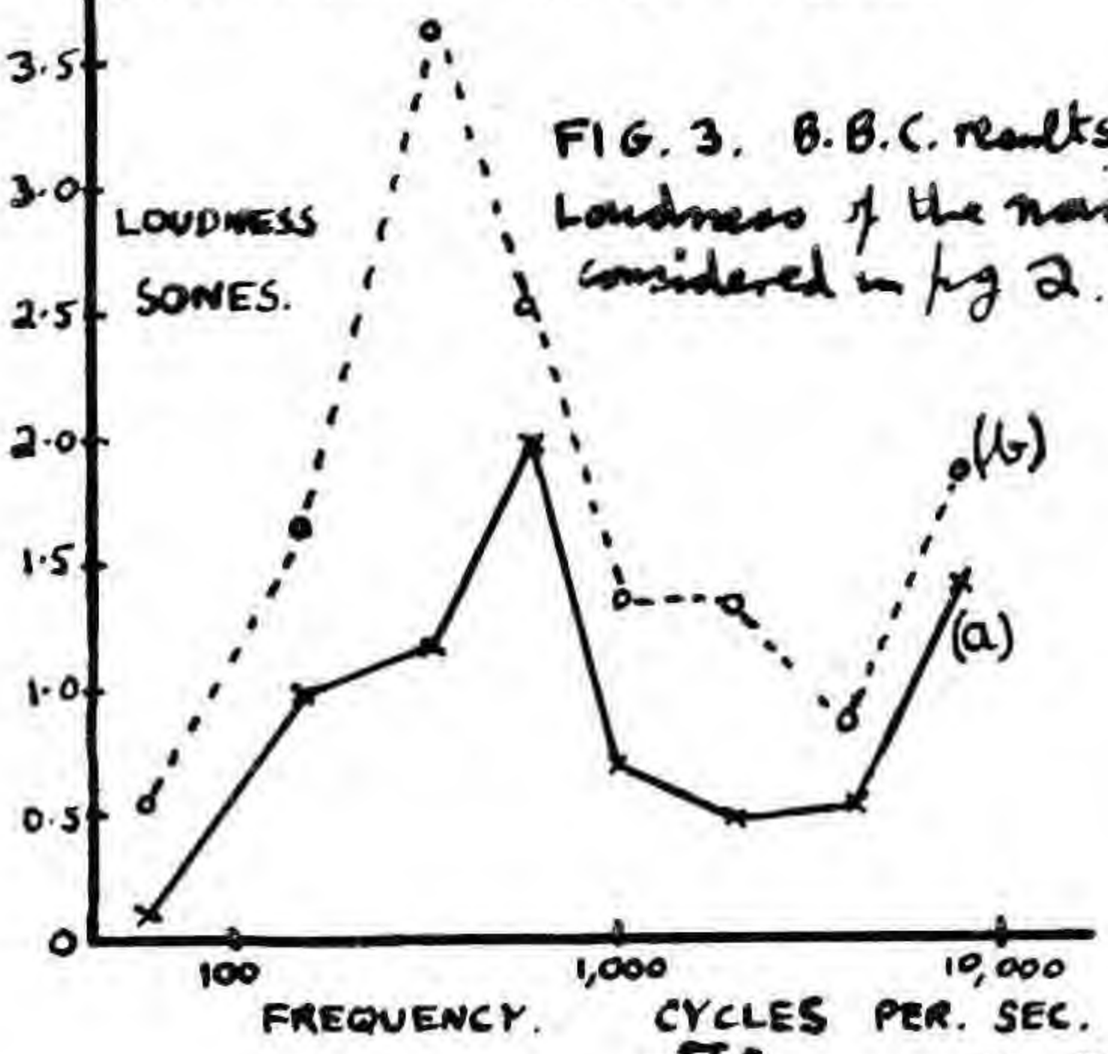

FIG. 3. B.B.C. results.
Loudness of the noise considered in fig 2.

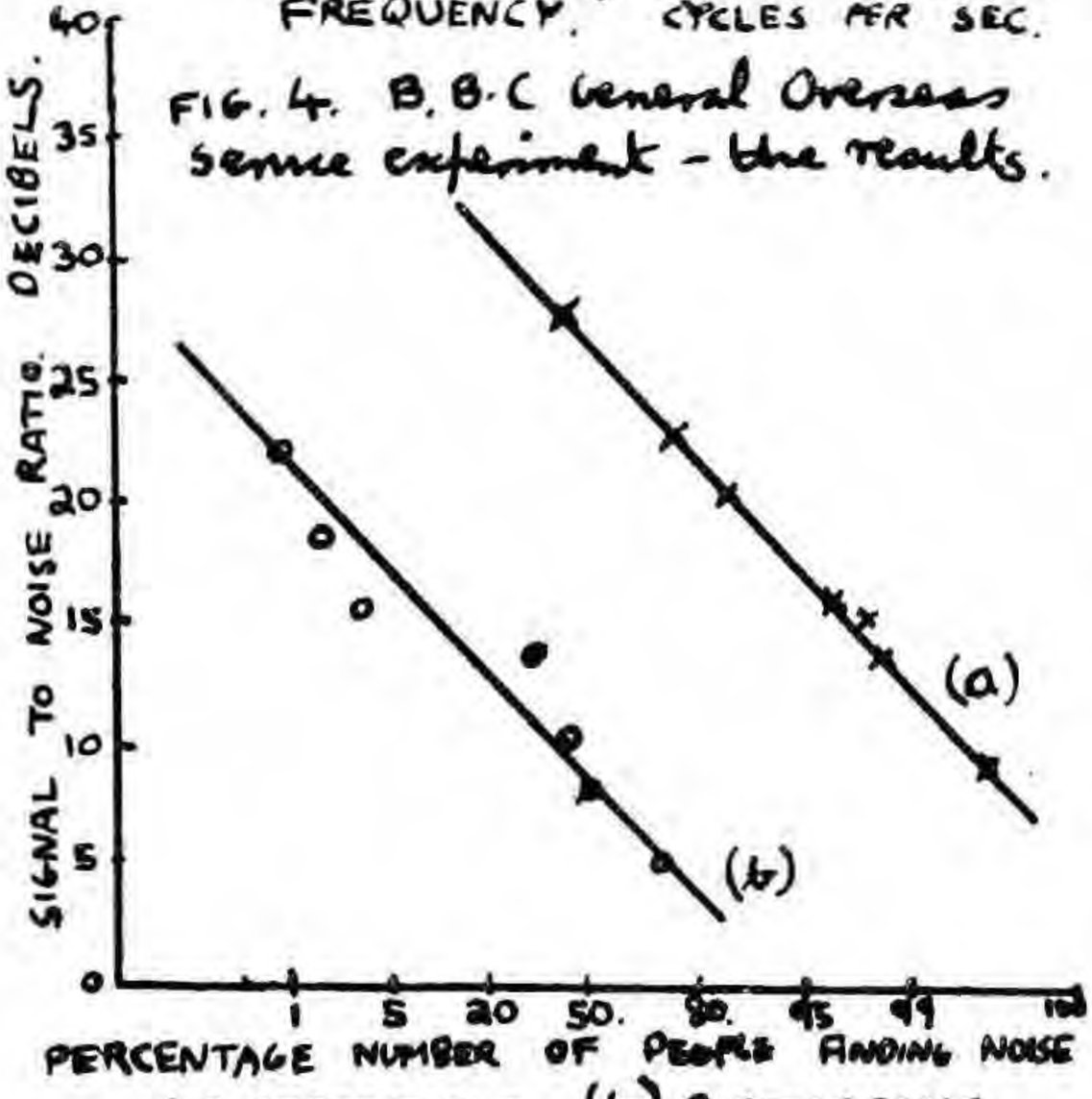

FIG. 4. B.B.C General Overseas service experiment - the results.

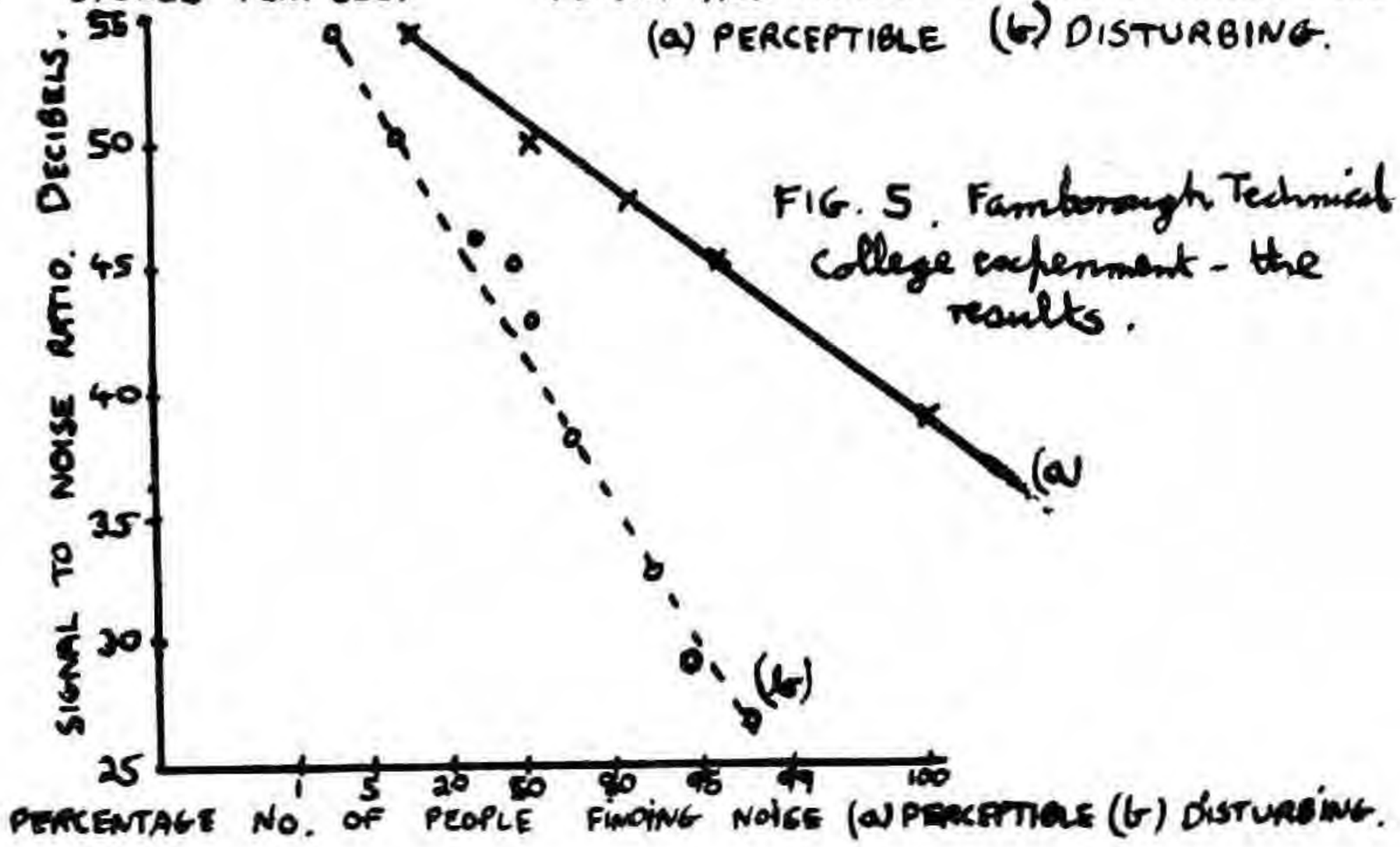

FIG. 5. Farnborough Technical College experiment - the results.

N39

FOURTH INTERNATIONAL CONGRESS ON ACOUSTICS
COPENHAGEN 21.-28. AUGUST 1962

Die obere Frequenzgrenze bei der Kalibrierung piezoelektrischer Beschleunigungsaufnehmer mit elektrodynamischen Schwingtischen.

Dipl.-Ing. Jan-Peter HIRSCHFELD, Dresden, DDR

Für die Kalibrierung von piezoelektrischen Beschleunigungsaufnehmern sind tief abgestimmte dynamische Schwingtische besonders geeignet. (Bild 1) Durch mechanische Bauteil- oder Verbindungsresonanzen des Schwingtisches ist der für die Kalibrierung ausnutzbare Frequenzbereich zu hohen Frequenzen hin begrenzt. An einer großen Zahl von Schwingtischen wurden das Auftreten und die Ursachen solcher Resonanzen bis 100 kHz systematisch untersucht, um Hinweise für eine Konstruktion mit möglichst hoher Grenzfrequenz zu erhalten.

Schwierig war zunächst die Vermeidung von Verbindungsresonanzen durch die Ankopplung der Wicklung und des Messobjektes an den Schwingspulenkörper. Durch eine gute Klebeverbindung oder ein Einklemmen der Wicklung in eine Nut des Schwingspulenkörpers mit einem beim Aushärten treibendem Füllharz im ersteren Fall und durch feste Schraubverbindung mit zwischenliegendem Silikonfettpolster im zweiten Fall können diese Resonanzen im Gebiet bis 100 kHz sicher vermieden werden.

Ebenfalls in diesem Frequenzbereich vermeidbar waren Bauteilresonanzen bei sehr dünnem und langem Trägerteil für die Wicklung. Das entstehende ringförmige Schwingungsgebilde läßt sich durch entsprechende konstruktive Gestaltung ebenso vermeiden, wie eventuelle Resonanzen an stabförmigen Verbindungen.

Die Forderungen zur Erhöhung der Biegegrundresonanz und der Längsgrundresonanz des Schwingspulenkörpers stehen einander entgegen, es muß deshalb eine Optimierung vorgenommen werden.

Bei Spulenkörpern, deren Durchmesser D sehr viel größer als seine Dicke l ist, kann man unter der vereinfachenden Annahme, daß sich über dem Durchmesser eine halbe Biegewellenlänge erstreckt, die auftretende Biegegrundresonanz der Scheibe näherungsweise berechnen.

$$\text{Für } \lambda_B > 6l \text{ bzw. } D > 3l \quad \text{ist} \quad f_{0B} \approx \frac{1.8 \cdot c \cdot l}{4 D^2} \qquad (1)$$

Durch Verkleinerung des Durchmessers D, Wahl eines Materials mit großer Schallgeschwindigkeit c und durch Vergrößerung der Scheibendicke l läßt sich prinzipiell die Biegegrundresonanz erhöhen.

Bei Vergrößerung der Dicke l nähert man sich schließlich einer Stabform des Schwingspulenkörpers, an dessen einem Ende die Kraftanregung durch die Schwingspule, am anderen Ende die Ankopplung des zu messenden Schwingungsaufnehmers erfolgt. Die Längsgrundresonanz eines solchen homogenen unbelasteten Stabes ergibt sich bei $l = \frac{\lambda}{2}$, d.h.

$$f_{0L} = \frac{c}{2l} \qquad (2)$$

Auch hier erreicht man durch Material mit großer Schallgeschwindigkeit eine hohe Resonanz, jedoch wird im Gegensatz zur Biegeresonanz die Längsresonanzfrequenz erhöht, wenn ich den Spulenkörper verkürze. Unsere Forderung war, für beide Fälle eine möglichst hohe Resonanz zu erreichen. Aus Bild 2 erkennt man, daß das bei konstantem Durchmesser für eine Länge l_{opt} eintritt, wenn also beide Resonanzen zusammenfallen. Durch Messung der jeweils tiefsten Resonanzfrequenz an einem extrem langen Rütteltischkörper, der stufenweise verkürzt wurde, konnte dieser Verlauf bestätigt werden.
Im Bereich der Biegeresonanzen ergab sich selbst bei Spulenkörperabmessungen bis zu D = l noch eine recht gute Übereinstimmung von berechneten Werten und Messergebnissen. Ein Einfluß des aufgesetzten Beschleunigungsaufnehmers konnte dabei nicht festgestellt werden.
Im Bereich der Längsresonanzen ist dieser Einfluß jedoch besonders bei kurzen Stäben sehr groß, da Gleichung (2) nur für unbelastete Stäbe gilt. Eine Belastung des Stabes berücksichtigt man bei der üblichen Darstellung als Vierpols allgemein durch eine Kettenschaltung des Stabvierpols mit einer punktförmigen Masse. Die so berechneten Frequenzen der Längsresonanz nähern sich zwar den gemessenen, weichen aber noch immer z.T. recht erheblich von diesen ab. Das ist verständlich, wenn man bedenkt, daß die Längsabmessungen des Schwingtisches und des an diesen angekoppelten Schwingungsaufnehmers in der gleichen Größenordnung liegen. Für eine exakte Berechnung muß man also die Kettenschaltung zweier Stabvierpole zugrunde legen (Bild 3). Aus der Matrix dieser Kettenschaltung erhält man für die am leerlaufenden Vierpolausgang ($F_2 = 0$) vorhandene Schnelle

$$v_2 = \left| \frac{F_1'}{A_{21}'} \right| = \frac{F_1}{w_{z1}\left[\left(1+\frac{w_{z2}}{w_{z1}}\right)\cdot\sin\left(\frac{l_1}{c_1}+\frac{l_2}{c_2}\right)+\left(1-\frac{w_{z2}}{w_{z1}}\right)\cdot\sin\left(\frac{l_1}{c_1}-\frac{l_2}{c_2}\right)\right]} \qquad (3)$$

Die gesuchte Längsgrundresonanz der Beschleunigung am Aufnehmer läßt sich aus der ersten Nullstelle des Zählers in Gleichung (3) berechnen. Dabei erweist sich die Anwendung eines grafischen Verfahrens als vorteilhaft. Berücksichtigt man noch die Änderung der Ausbreitungsgeschwindigkeit c für kurze Stäbe infolge der größeren Querkontraktion, so konnte in den zahlreichen aufgebauten Anordnungen eine völlige

Übereinstimmung von Rechnung und Messung nachgewiesen werden. Diese Übereinstimmung rechtfertigt die bei der Berechnung gemachte Annahme, daß wir den Schwingungsaufnehmer als homogenes Stabgebilde mit den äußeren Abmessungen des Aufnehmers ansehen dürfen.
Im Bild 4 sind die Ergebnisse von Messung und Rechnung für eine der untersuchten Anordnungen dargestellt. Man erkennt, daß die optimale Schwingtischlänge recht kritisch ist, aber nach dem angegebenen Verfahren mit ausreichender Genauigkeit berechnet werden kann. Sie gilt aber nur für den zugrunde gelegten Belastungsfall und ändert sich bei Verwendung eines Schwingungsaufnehmers mit anderen mechanischen Daten.

Bei der praktischen Dimensionierung geht man deshalb zweckmäßig vom Aufnehmer aus.
Aus Gleichung (3) kann man folgende Bedingungen zur Erzielung einer hohen Längsresonanz ableiten:

1) $\frac{l_1}{c_1} > \frac{l_2}{c_2}$ i $w_{z_1} = S_1 \cdot \rho_1 \cdot c_1 > w_{z_2} = S_2 \cdot \rho_2 \cdot c_2$

2) $\frac{l_1}{c_1} < \frac{l_2}{c_2}$ i $w_{z_1} = S_1 \cdot \rho_1 \cdot c_1 < w_{z_2} = S_2 \cdot \rho_2 \cdot c_2$

Welche der beiden Möglichkeiten infrage kommt, entscheidet wesentlich der Schwingungsaufnehmer mit seinen Kenngrößen (l_2, c_2, S_2, ρ_2).
Da die Schallgeschwindigkeit c und die Dichte ρ durch Wahl verschiedener Materialien nur sehr geringfügig variiert werden können, sind Länge l und Fläche S bei der Optimierung meist ausschlaggebend.
Die Wirkung der Flächentransformation ist an einem Beispiel in Bild 5 anschaulich dargestellt. An einem trapezförmigen Schwingspulenkörper wurden die Längsresonanzen mit Belastung gemessen, wobei Anregungs- und Belastungsseite am Trapezkörper jeweils vertauscht wurden. Für die verwendeten Materialien von Aufnehmer und Spulenkörper ergab sich $\rho_1 c_1 \approx \rho_2 c_2$, so daß gemäß der obigen Bedingung infolge $\frac{l_1}{c_1} > \frac{l_2}{c_2}$ der Fall mit $S_1 > S_2$ eine höhere Resonanzfrequenz ergibt. Die berechneten und gemessenen Werte stimmen überein und sind im Bild 5 angegeben. Das Flächenverhältnis darf aber nicht beliebig vergrößert werden, da sonst wieder eine Verringerung der Biegeresonanz des Grundkörpers eintreten kann.
Bei sehr hohen Frequenzen wird die Kalibrierung von Schwingungsaufnehmern meist durch Vergleich mit einem zweiten Aufnehmer durchgeführt, der am Schwingtisch angebracht oder eingebaut ist. Besitzen beide Aufnehmerzentren einen endlichen Abstand voneinander, so sind bei Längsschwingungen besonders in Resonanznähe die Beschleunigungen in beiden Zentren nicht gleich. Die Beschleunigung kann für jeden Punkt längs

des Leitungsweges ($l_1 + l_2$) annähernd berechnet werden. In der Nähe von Resonanzen ist jedoch eine solche Korrektur nicht sehr genau. Besser ist es, wenn man die Meßzentren beider Aufnehmer in die gleiche Ebene legt oder zumindest so weit wie möglich aneinanderrückt.

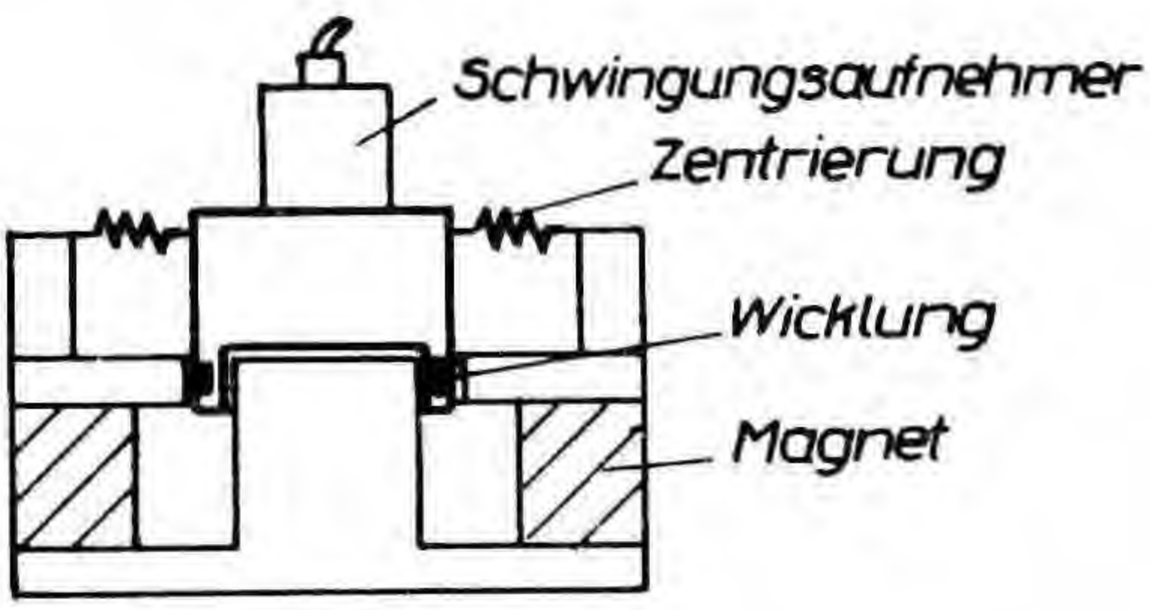

Bild 1

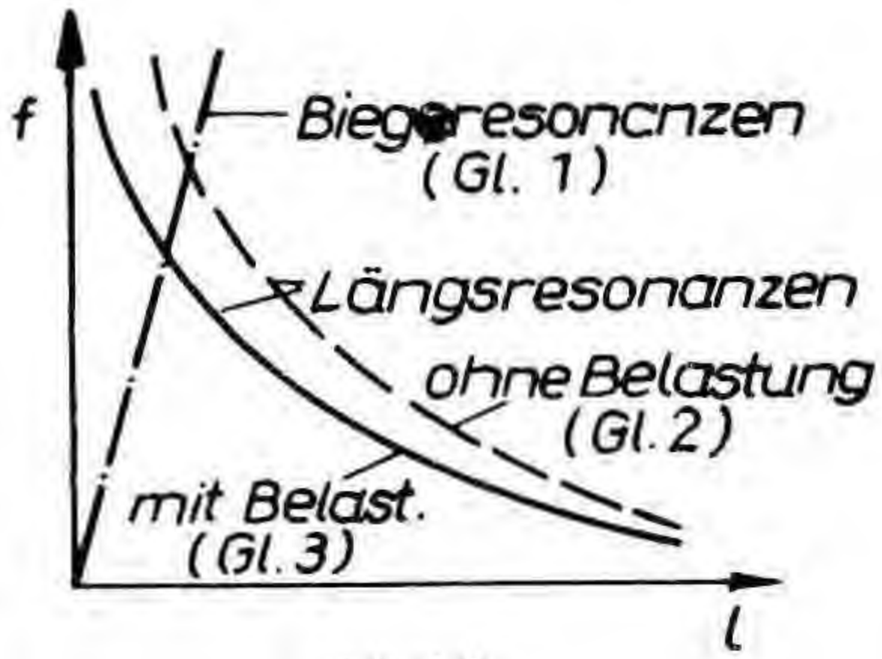

Bild 2

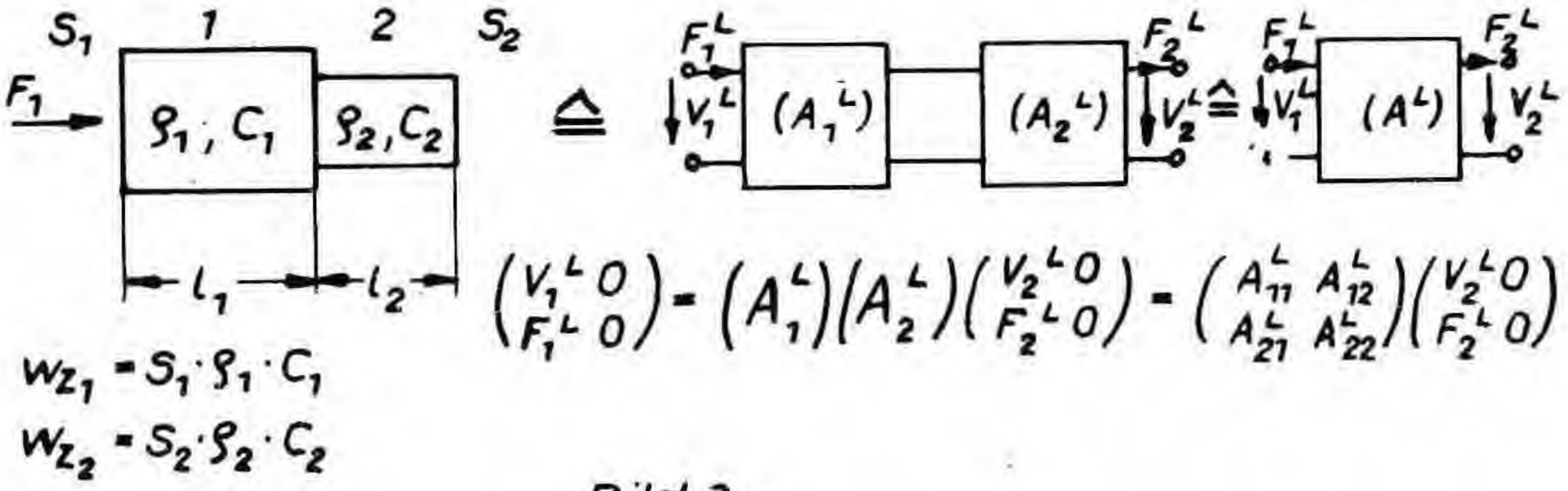

Bild 3

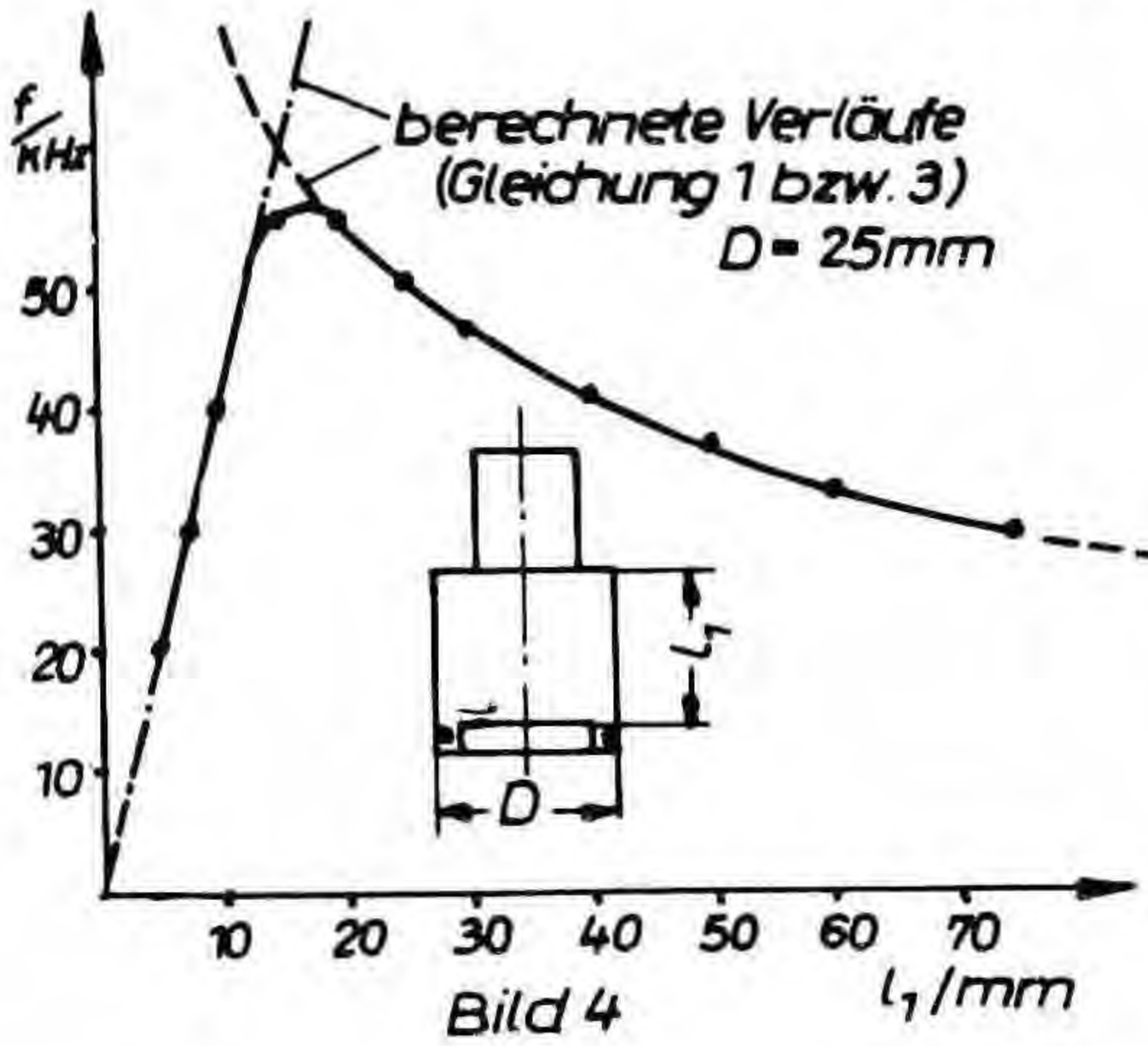

Bild 4

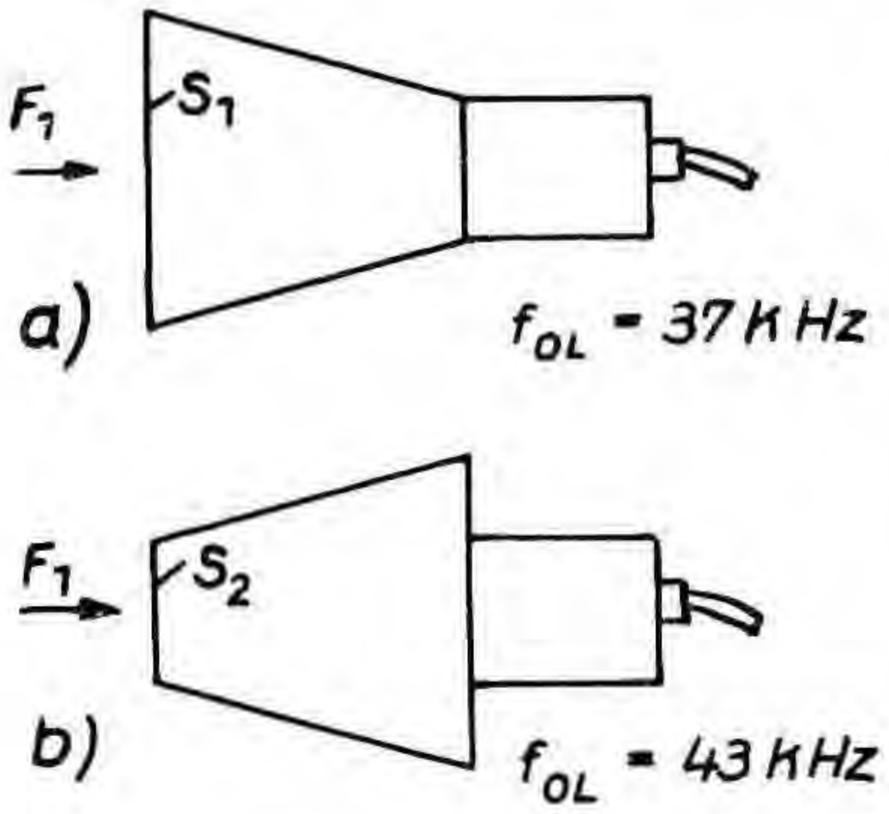

Bild 5

G41

FOURTH INTERNATIONAL CONGRESS ON ACOUSTICS
COPENHAGEN 21.-28. AUGUST 1962

NEW METHODS FOR SPEECH ANALYSIS-SYNTHESIS AND BANDWIDTH COMPRESSION

M. R. Schroeder, B. F. Logan and A. J. Prestigiacomo, Bell Telephone Laboratories, Incorporated, Murray Hill, New Jersey

A "harmonic compressor" is described which halves the frequencies of individual harmonic frequency components, transmits the compressed signal, and resynthesizes an approximate replica of the input speech signal by frequency doubling. The analyzer or synthesizer alone can be used to speed up or slow down the syllabic rate of speech. Harmonic compression can also be applied to the baseband of voice-excited vocoders, thereby considerably reducing the required transmission bandwidth while maintaining the advantages of voice excitation.

An autocorrelation vocoder with a bandwidth (or time) compression of about 10:1 before multiplexing is also described. A time-varying equalizer compensates for the spectrum squaring inherent in the autocorrelation analysis. In resynthesizing speech from the autocorrelation signals, special "taper" functions are used to minimize the distortion due to the fact that the maximum delay in the autocorrelation analysis is fixed and does not vary with the fundamental period of the input speech signal. Excitation of the synthesizer can be either conventional or voice excited.

Description of Harmonic Compressor

Figure 1 shows the block diagram of a harmonic compressor. The speech signal is applied to a bank of 50 bandpass filters A, each 60 cps wide and spaced 60 cps apart. The purpose of filter bank A is to separate a voiced speech input into its individual harmonic frequency components. The outputs of filters A are applied to frequency dividers which divide the instantaneous frequencies of the narrow band signals by 2. The resulting waveform at one divider output for a sinewave input is shown in Fig. 1. It consists of a sinewave with every other period inverted. This signal contains a frequency component whose instantaneous frequency is one half of that of the input signal with an amplitude proportional to the input. The filters of filter bank B remove the distortion components from the half-frequency signal. The outputs of filters B are added together to form the compressed signal ready for transmission over a channel of one half bandwidth.

In the synthesizer (right half of Fig. 1) the compressed signal is applied to filter bank C covering the compressed frequency scale (120-1620 cps). The individual filter bandwidths must be small enough to separate the compressed signal into individual

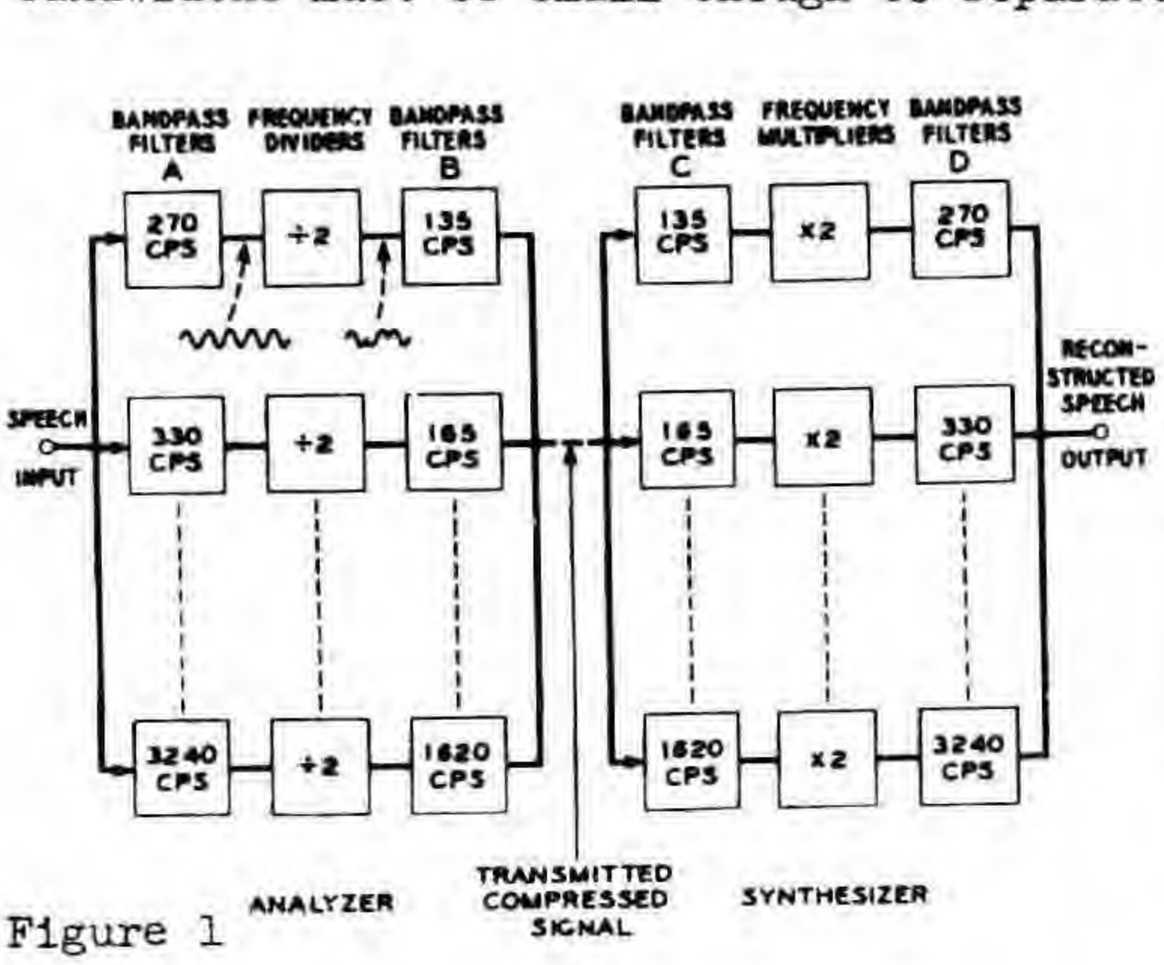

Figure 1

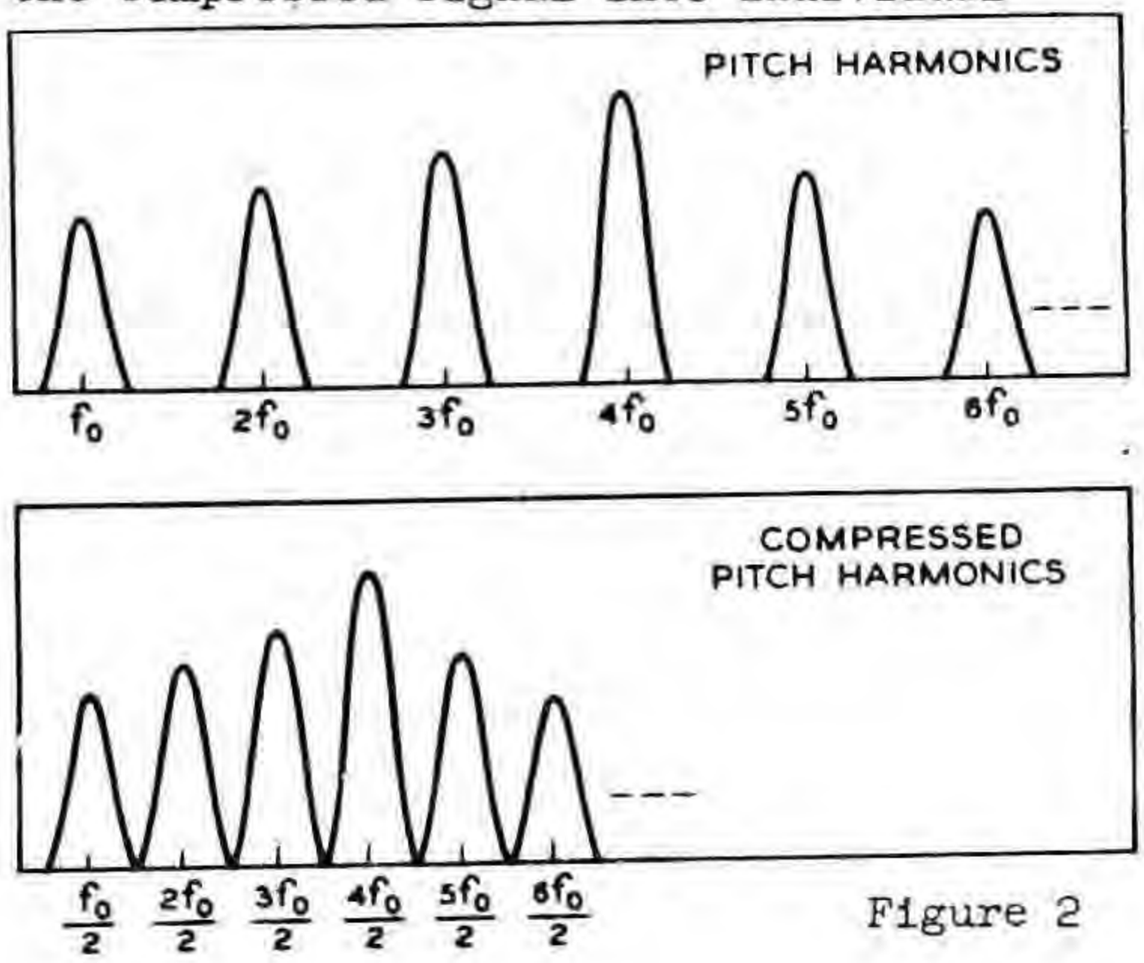

Figure 2

harmonics of half the fundamental frequency. The filter outputs are connected to fullwave rectifiers which double the instantaneous frequencies, thereby regenerating the original harmonic frequencies. Filter bank D removes the distortion products resulting from the fullwave rectification.

If any of the filters in filter bank C passes two or more adjacent halved harmonics, the fullwave rectifier will generate frequencies which are multiples of half the fundamental frequency of the input speech signal. These "subharmonics" will appear in the output and, if sufficiently intense, constitute an audible distortion reminiscent of diplophonia.

The harmonic compressor capitalizes on the quasi-periodic nature of speech sounds. Figure 2 shows (schematically) harmonics of the short-time amplitude spectrum of a monotone speech sound of fundamental frequency f_o. Each harmonic has a certain bandwidth which reflects the quasi-periodic nature of speech and is proportional to the syllabic rate. From experiments with spectrum vocoders, it is known that spectrum channel signals can be low-passed to about 20 cps for average syllabic rates. Therefore, the width of each harmonic component can be limited to about 40 cps. The spectrum of the analyzer output is also illustrated in Fig. 2. The frequency gaps between the harmonics are reduced or eliminated; but adjacent lines do not significantly overlap.

Quasi-periodicity, the property of speech signals on which the harmonic compressor is based, is absent in unvoiced sounds. Therefore, we must expect some sort of degradation for this class of speech sounds. The main distortion results from the frequency doubling in the synthesizer. The fullwave rectifiers double the phase modulation without changing the amplitude modulation of the narrow-band signals from filter bank C. After frequency doubling, these signals no longer exhibit the relationship between amplitude and phase modulation appropriate for Gaussian noise. The resulting sound is known (from Vobanc[1] experience) to resemble that of burbling water. "Burbles" have also been observed in the harmonic compressor output for a steady Gaussian noise input. Fortunately, for short aperiodic speech sounds, the distortion is hardly noticeable.

Computer Simulation of Harmonic Compressor

The harmonic compressor described above was simulated on a large digital computer (IBM 7090) programmed by means of a "block diagram compiler" (BLØDI).[2] The basic building block of the bandpass filters, is a recursive filter with a cosine impulse response. It requires only one multiplication per sample. To construct one bandpass filter, the outputs of two blocks with frequencies corresponding to the desired cut-off frequencies are subtracted from each other and their impulse responses are truncated after one beat cycle of the two chosen frequencies. The total number of multiplications in the computer is only slightly more than two per bandpass filter per sample time. The computation time for the combined analyzer and synthesizer with a total of 200 narrow bandpass filters is 530 times real time.

Compared to vocoders, the harmonic compressor possesses the following advantages: There are no pitch or voiced-unvoiced decision problems. No multiplexing of channel signals is required. The compressed signal has speech-like characteristics on the reduced frequency scale and is therefore well suited for transmission over speech circuits. The relative phases of the individual harmonic frequency components are preserved.

In informal listening, members of our Laboratories have ranked the remade speech quality of the harmonic compressor between that of an unmultiplexed voice-excited vocoder (with a 700 cps baseband) and unprocessed speech of the same bandwidth. We are presently studying the application of harmonic compression to the baseband of a voice-excited vocoder.

---

[1] B. P. Bogert, "The Vobanc--a two-to-one speech bandwidth reduction system," J. Acoust. Soc. Am. 28, 399 (1956).

[2] John L. Kelly, Jr., Carol Lochbaum and V. A. Vyssotsky, "A block diagram compiler," Bell Syst. Tec. J., 40, (May 1961), p. 669.

Description of Autocorrelation Vocoder

Figure 3 shows the block diagram of a complete autocorrelation vocoder. In the analyzer, the short-time autocorrelation function is derived for a number of discrete delays $\tau_0, \tau_1, \ldots, \tau_N$. Because the autocorrelation function is bandlimited to the same frequency band as the input speech signal, the former is completely specified by its values for discrete delays with a spacing $\Delta\tau = 1/2f_c$, where f_c is the cut-off frequency of the speech. For $f_c < 5$ kc, a $\Delta\tau$ of 0.1 msec suffices. The maximum delay τ_N influences the speech quality. For $\tau_N = 2.5$ msec, there are 26 "delay channel" signals, each representing a time-varying sample of the short-time autocorrelation function for a fixed delay. If each delay channel signal is bandlimited to about 20 cps, the total transmission bandwidth (without multiplexing and excitation) is 520 cps corresponding to a compression of approximately 10:1.

At the synthesizer, a symmetrical replica of the autocorrelation function is generated for every pitch period. This is achieved by a forward-backward scanning operation. A convenient method of realizing the symmetrical scanning is illustrated on the right of Fig. 3. Each pitch pulse samples all delay channel signals. These samples are fed to taps of a delay line corresponding to the one in the analyzer. However, this delay line has one end terminated to give complete reflection. This causes every sample pulse to appear in the output twice. When all the pulses are combined, they form a sampled and symmetrical replica of the short-time autocorrelation function at the time of the sampling pitch pulse. For aperiodic excitation, the synthesizer can be viewed as a time-varying transversal filter multiplying the excitation spectrum by the power spectrum of the input signal.

To compensate for the spectrum squaring in the output waveform, a time-varying equalizer, performing an approximate square rooting, precedes the autocorrelation analyzer. The equalizer (Fig. 4) separates the input speech signal into three frequency bands and takes the square root of the average amplitude of each before recombining. The time-varying equalizer performing the required (approximate) spectrum square rooting operation is shown in Fig. 4. The effect of this equalizer on two speech spectra is illustrated in Fig. 5. If the spectral intensity is plotted in decibels, all level differences with respect to some reference level should be halved--as should be the average slope of the spectrum. Figure 5 shows that the equalized spectrum (solid curve) approaches this condition closely.

The most serious distortion in time-domain vocoders using a fixed (not pitch tracking) maximum delay is the abrupt truncating of the output signal at the beginnings and ends of individual pitch periods which gives a rough and nasal character to the remade

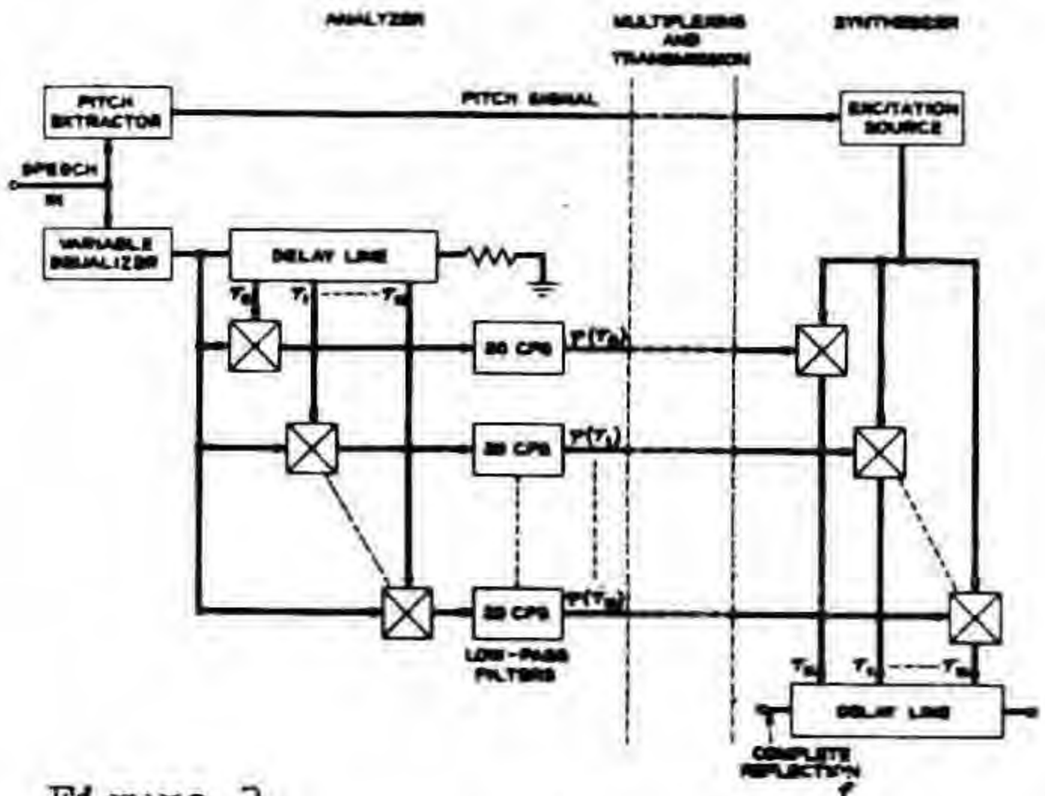

Figure 3

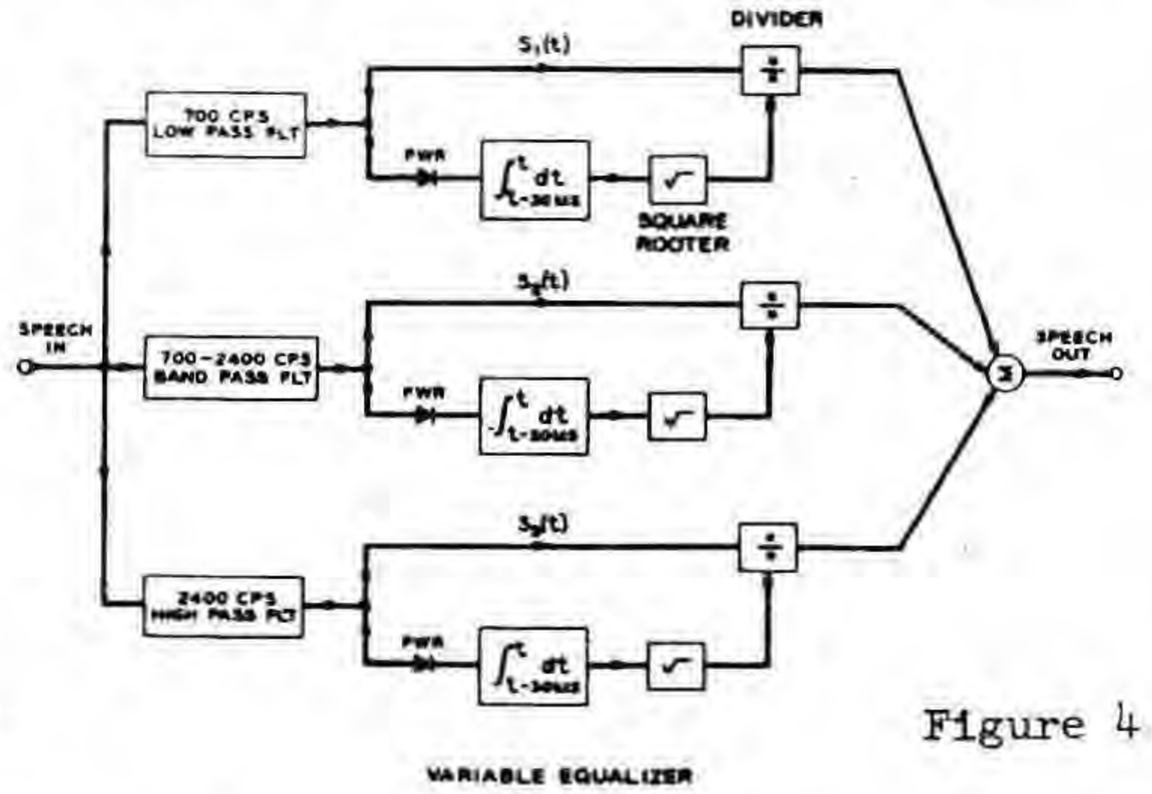

Figure 4

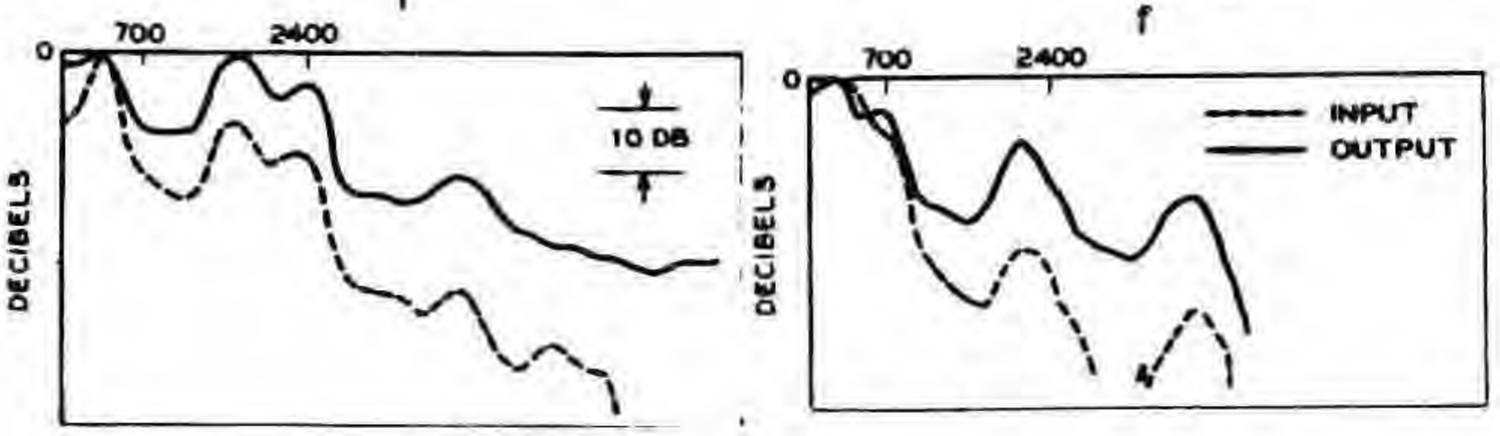

Figure 5

speech. To minimize this distortion, the autocorrelation function has been gradually tapered. As a tapering function the so-called "Hamming window"[3] function has been used.

However, with tapering and a maximum delay of 2.5 msec, the spectral resolution is insufficient, especially at the low-frequency end of the speech spectrum. The obvious remedy, a substantial increase in the maximum delay, would result in an intolerable increase in the number of delay channels and the required transmission bandwidth. Yet, because of the large sampling interval $\Delta\tau$ possible for low-frequency components, there is a possibility of improving the resolution at low frequency without substantially increasing the number of channels. Simultaneously, the resolution for the highest frequency components may be slightly degraded, resulting in a significant reduction of the number of channels because of the small delay interval $\Delta\tau$ required at those frequencies. To incorporate these ideas into the autocorrelation vocoder, the following modifications have been made. After the 16th tap (at 1.5 msec) a phase-linear 2.5 kc lowpass filter has been inserted into the delay line of the analyzer and the delay intervals have been lengthened to 0.2 msec. After 5 more taps (at 2.5 msec) another lowpass filter with a cut-off frequency of 1.25 kc is inserted into the delay line and the delay intervals are lengthened to 0.4 msec. The maximum delay is 4.9 msec, requiring 6 more taps for a total of 27 delay channels. Thus, with a negligible increase in the number of delay channels and a slight degradation of the spectral resolution for frequency components above 2.5 kc, the resolution below 1.25 kc has been doubled. The result is a considerable improvement of the remade speech quality. In the synthesizer, bandpassed pulses and noise are used to excite the three different frequency bands. Except for the bandpass filters, no additional equipment is required for the improved autocorrelation vocoder.

Conclusions

Time-domain vocoders are not susceptible to the problems resulting from the arbitrary division of the spectrum by a fixed filter bank whose frequency bands do not coincide with the harmonic structure of voiced speech sounds. However, time-domain vocoders encounter a corresponding problem if the analysis is performed for a fixed maximum delay regardless of the fundamental frequency. Yet, if pitch-tracking analysis is desired, it can probably be instrumented more easily by time-domain vocoders: only one parameter, the maximum delay has to be variable. When time-multiplexing the channels of a time-domain vocoder by forward-backward scanning, speech-like signals (on a reduced frequency scale) result which are particularly well suited for transmission over speech circuits. Another advantage of autocorrelation vocoders is that they produce symmetrical (zero-phase) pitch periods without special effort. Thus, degradation due to time-varying phase distortion is avoided. Further, minimum phase (derived from the amplitude spectrum) can be added for vowel sounds if this refinement should prove important for high quality.

There are two basic disadvantages in autocorrelation analysis compared to spectrum analysis, both related to the fact that operations are performed on time signals: linear multipliers with a wide dynamic range are required and quantizing of the "delay channel" signals for digital transmission requires 6 to 7 bits per sample as opposed to 3 to 4 bits required for the quantization of spectrum channel signals.

The autocorrelation vocoder described here has been simulated on an IBM 7090 digital computer. The programming technique and effort are similar to that used for the harmonic compressor. Computation time is 260 times real time for variable equalizer, analyzer and synthesizer combined. The quality of the reconstructed speech using a three-channel equalizer and three different maximum delays and window functions for low, middle and high frequency components is comparable to spectrum vocoders using similar excitation.

We are grateful to J. F. Kaiser for the design of the digital lowpass filters used in the autocorrelation vocoder, to Carol Bird for writing the complex simulation programs, and to E. E. David, Jr., for stimulating discussions.

---

[3] R. B. Blackman and J. W. Tukey, "The measurement of power spectra from the point of view of communications engineering--Part I," Bell Syst. Tech. J. 37 (Jan. 1958), p. 185.

H41

FOURTH INTERNATIONAL CONGRESS ON ACOUSTICS
COPENHAGEN 21.-28. AUGUST 1962

ON THE TRANSMISSION CHARACTERISTIC OF THE MIDDLE EAR

. Aage R. Møller, Speech Transmission Laboratory
Royal Institute of Technology, Stockholm 70, Sweden

The purpose of most investigations on the middle ear is to get more knowledge about the sound transmission through the middle ear which would make it possible to predict what the stapes displacement would be for a given sound at the eardrum. This is of importance in the study of the auditory system in general as well as in the study of middle ear diseases. Measurements which directly lead to such information cannot be gained from normal human subjects. It is necessary to perform animal experiments and experiments on human cadavers.

If only a gross approximation of the transfer function is wanted the mean value of measurements on several ears can be used. The results which are based on the mean value, however, do not necessarily give exact information about the vibration of the middle ear mechanism. If there are resonance peaks in the transfer function and the frequency of these peaks varies from ear to ear, then the mean value will be a curve where the peaks are broadened and the magnitude of the corresponding friction components in the analog system will be much too high and may be higher than in any of the investigated ears. That would influence the pulse response very much while the absolute value of the transfer function will look almost correct. A more correct damping could be achieved from a sufficient number of measurements performed on one single ear to reveal the analog network of that particular ear. A representative analog can then be achieved by taking the mean value of the components in a number of such models. This would give an analog network which represents also the damping.

The vibration amplitude of the different parts of the middle ear in experimental animals can be measured fairly easily by means of a capacity probe which measures the change in capacity between two electrodes. A block scheme of the apparatus used in this investigation is seen in Fig. 1. The signal to noise ratio of the apparatus must be high in order to be able to measure the amplitude with a moderate sound pressure level at the eardrum. The signal to noise ratio can be improved by measuring through a narrow filter. That, however, makes direct phase angle measurements almost impossible. This is avoided by the arrangement shown in Fig. 1. A signal with the same frequency as the sound is added to the output of the capacity probe and the amplitude and phase of this signal is adjusted until it cancels the

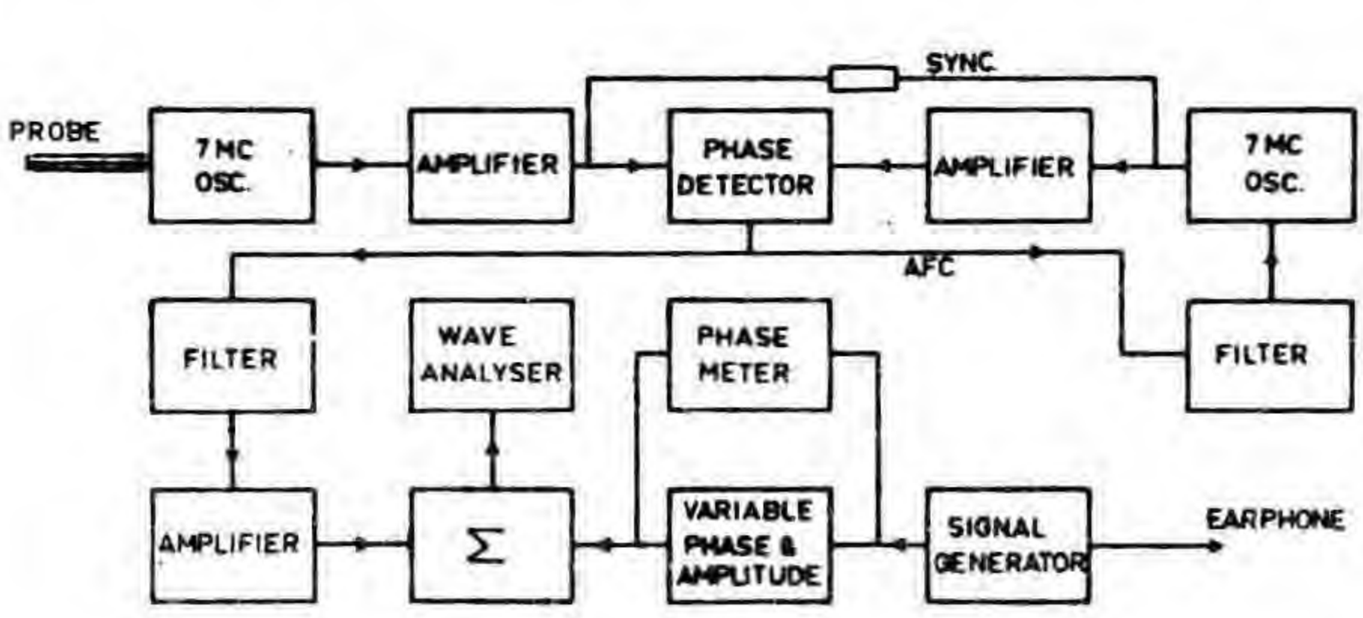

Fig. 1

signal coming from the capacity probe. The signal to noise ratio of this apparatus is approximately 150 db re 1 pf. At 500 cps the manubrium of the malleus in a cat produces a capacity change equal to the noise level for a sound level at the eardrum of 75 db re 0.0002 μb when the electrode distance is about 0.5 mm and the area of the electrode approximately 1 sq mm.

Measurements of the vibration of the different parts of the middle ear mechanism can be most easily performed with the bulla open. The effect of this operation can be seen from the acoustic impedance measured before and after opening the bulla (Fig. 2). It is seen that the impedance at low frequencies is lower with the bulla open. This is because the air in the middle ear cavity adds stiffness to the middle ear mechanism. It is also seen that the change is not very great. With the bulla intact there is a great peak in the impedance at about 4 kcps. This peak disappears totally when the bulla is opened and is probably responsible for the dip in sensitivity of the cat ear around 4 kcps which is seen in most reports.

The first question on the transfer function of the middle ear concerns the ability of the eardrum to convert sound into vibration of the manubrium of the malleus. Fig. 3 shows the inverse velocity of the malleus for constant sound pressure at the eardrum compared with the acoustic impedance at the eardrum. The acoustic impedance at the eardrum is proportional to the inverse velocity of the eardrum. The reference for the velocity is arbitrary. It is seen that the ability of the eardrum convert sound into mechanical vibrations is somewhat frequency dependent.

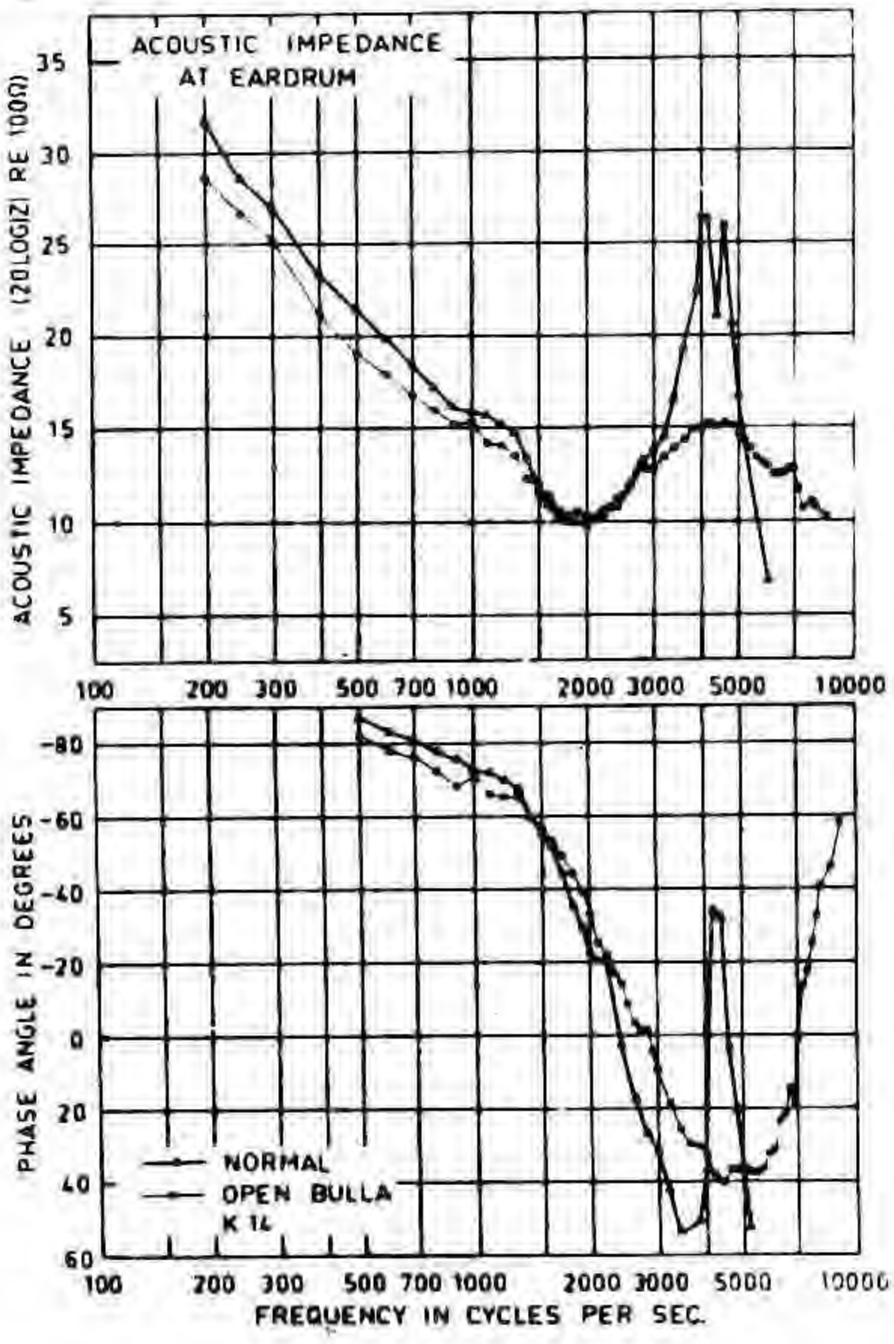

Fig. 2

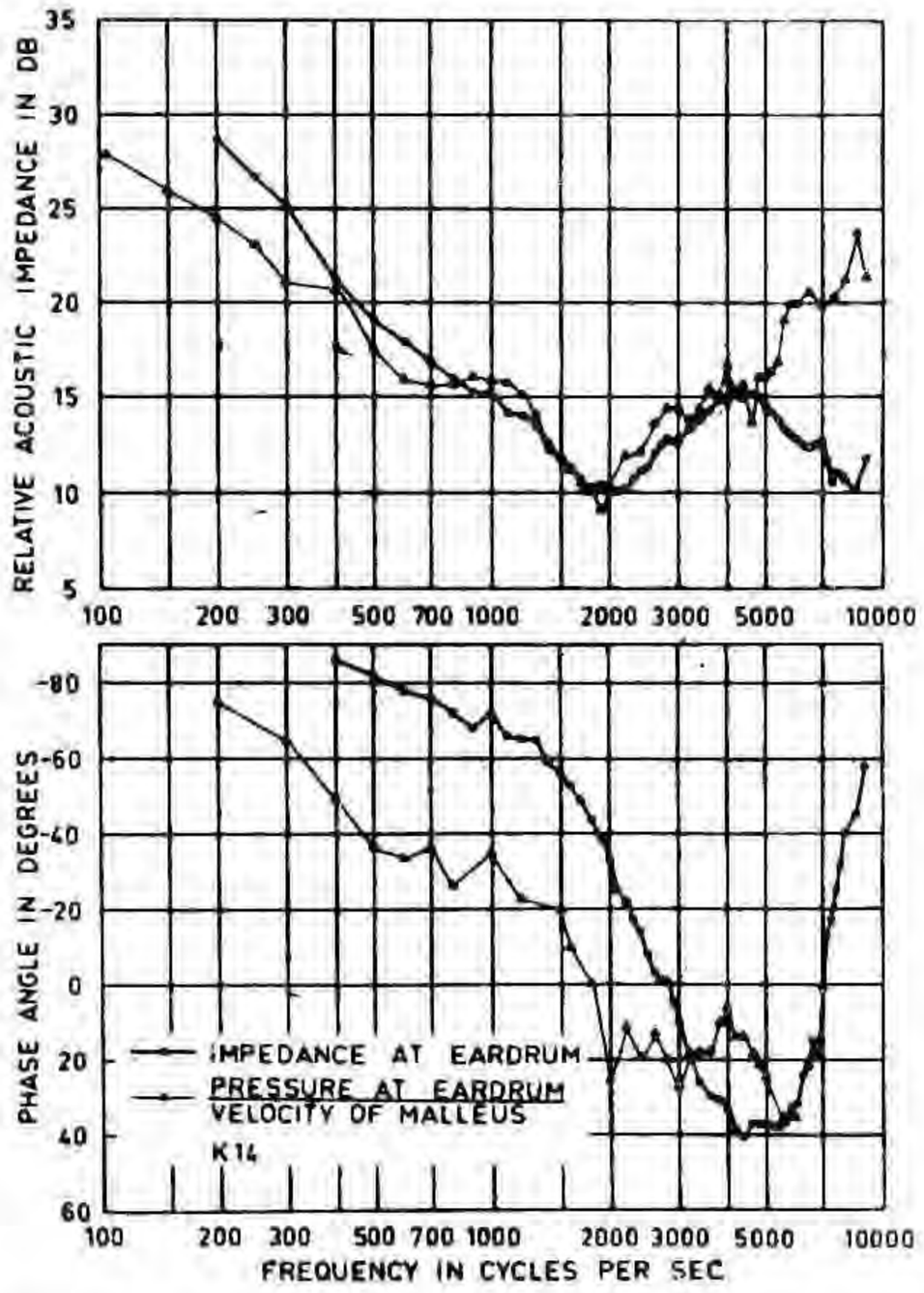

Fig. 3

The displacements of the stapes is very well represented in the amplitude of the round window which can also be measured by the capacitive probe. A comparison of the amplitude of the malleus and the round window shows how rigid the ossicular chain is (Fig. 4).

Fig. 5 shows how the velocity of the different parts of the middle ear corresponds to electrical current in an electrical analog [1] of the middle ear mechanism. It is seen that the difference in the inverse acoustic impedance at the eardrum and the velocity of the malleus depends on the shunt impedance which represents the impedance of the eardrum when the malleus is blocked. The difference between the velocity of the malleus and that of the round window is caused by the shunt impedance which represents the lack of rigidity in the rotational axis of the malleus and incus, and, at least at higher frequencies, the elasticity in the incudostapedial joint.

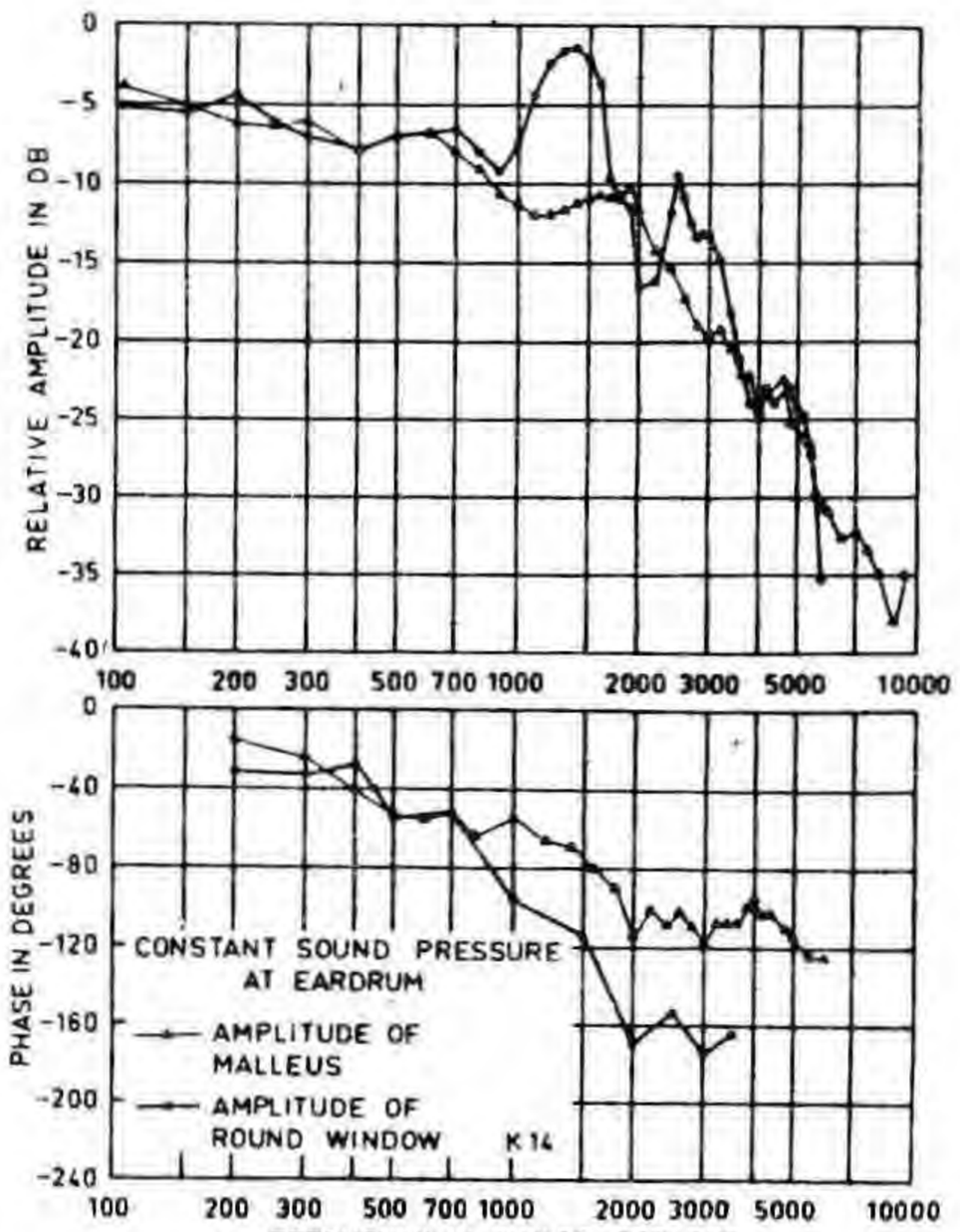

Fig. 4

These data make it possible to investigate the function of the middle ear of a cat. It is well known, however, that the middle ear of cats and men exhibit differences. The acoustic impedance at the eardrum can be measured in normal human subjects as well as in experimental animals. Fig. 6 shows the acoustic impedance of a cat compared with that of a typical human subject. The frequency scale for the impedance of the human subject was multiplied by 1.65. This factor makes the impedance of the ear of the cat more comparable with that of the human ear and maybe also to other properties of the ear. Fig. 7 shows the amplitude of the round window of a typical cat compared with the results on a human subject reported by von Békésy [2]. Fig. 8 shows a comparison between the experimental data on a

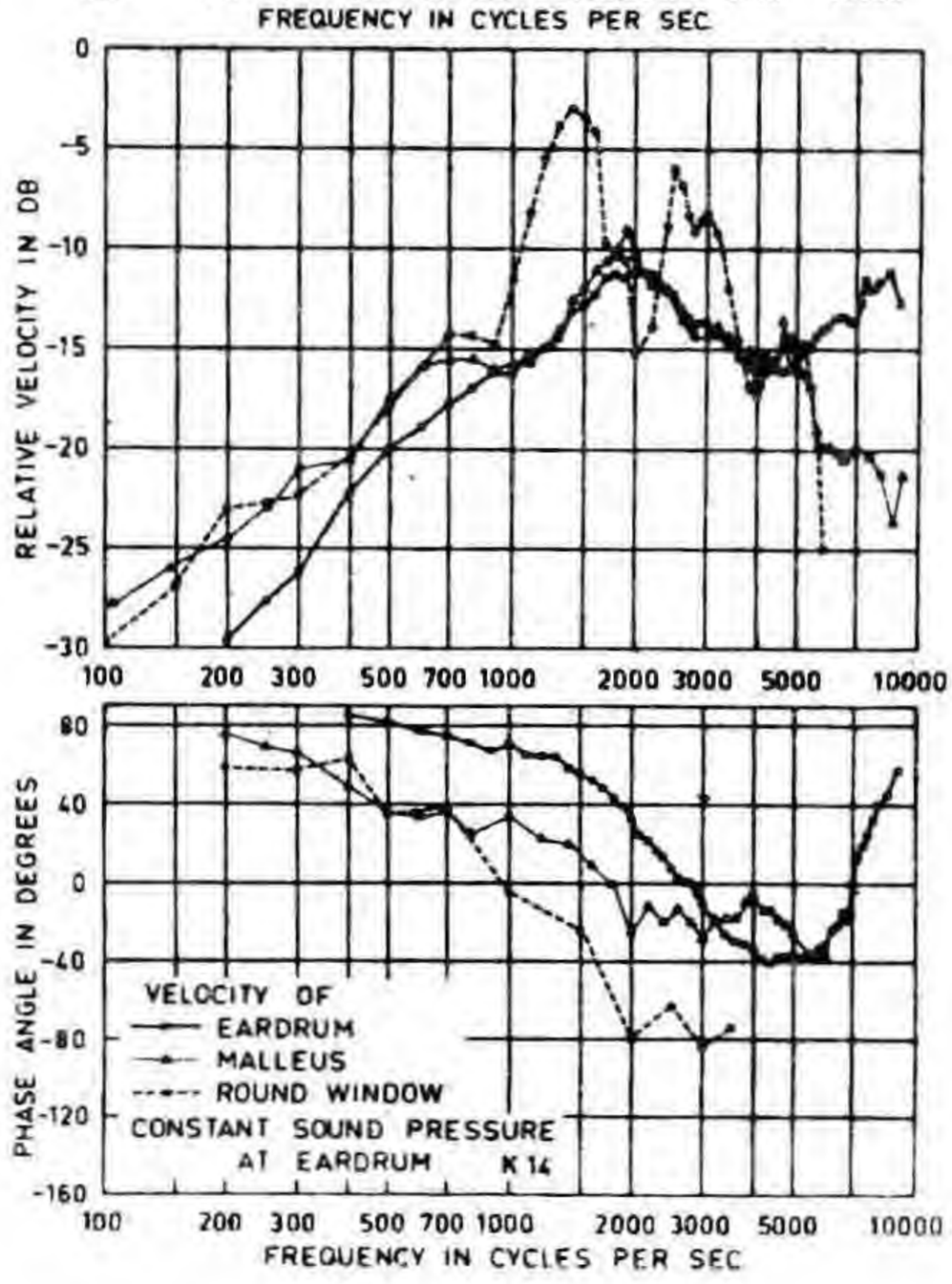

Fig. 5

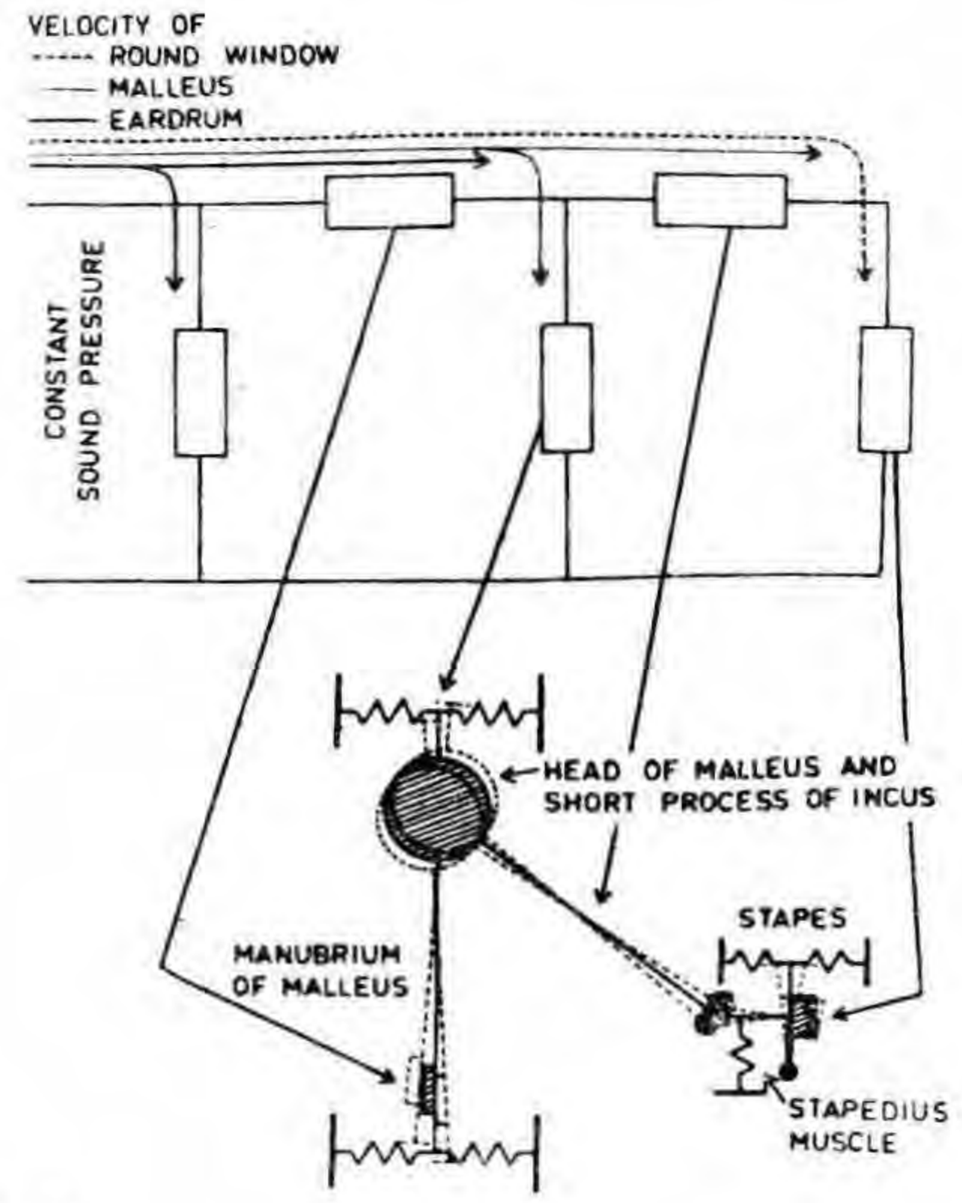

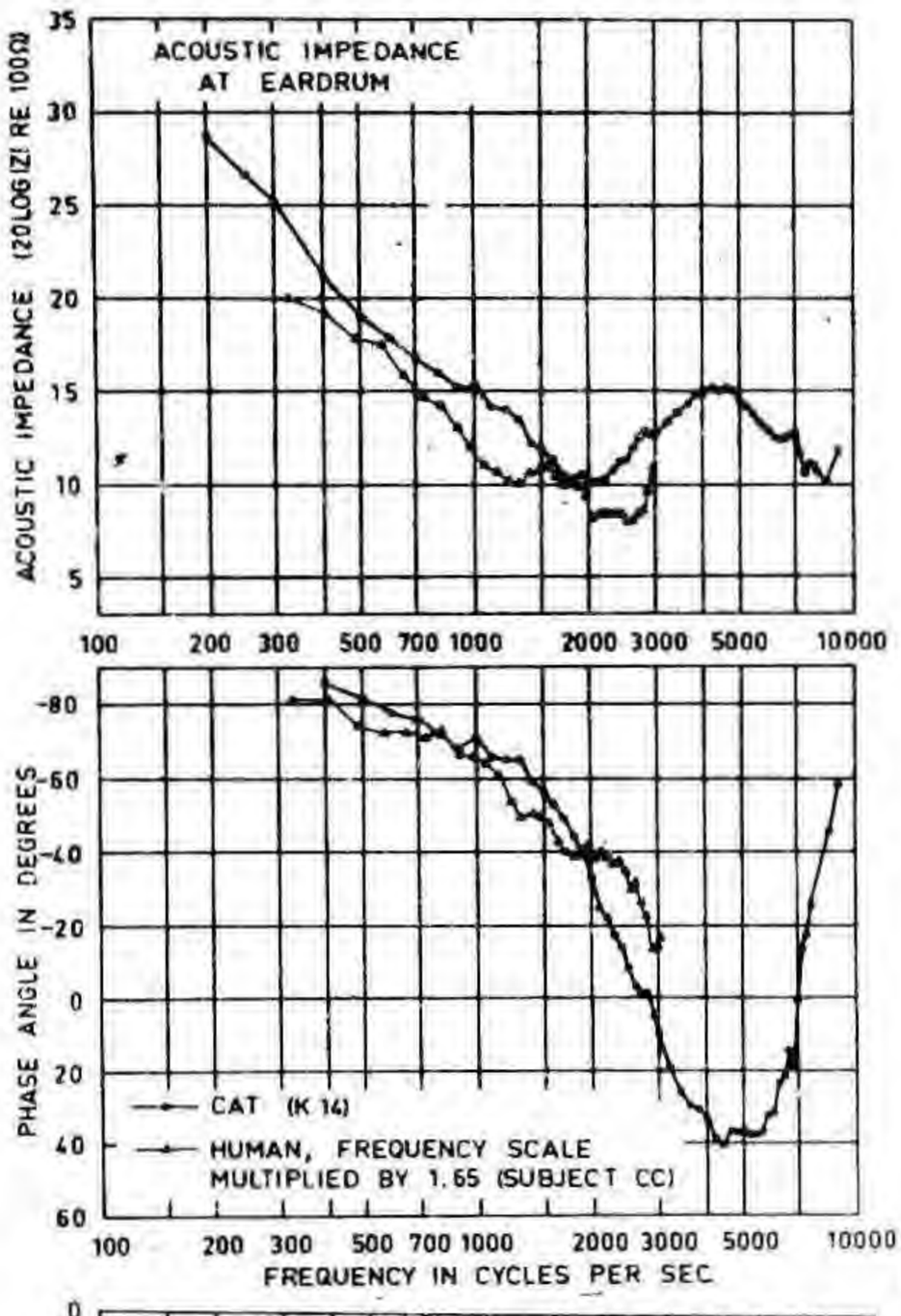

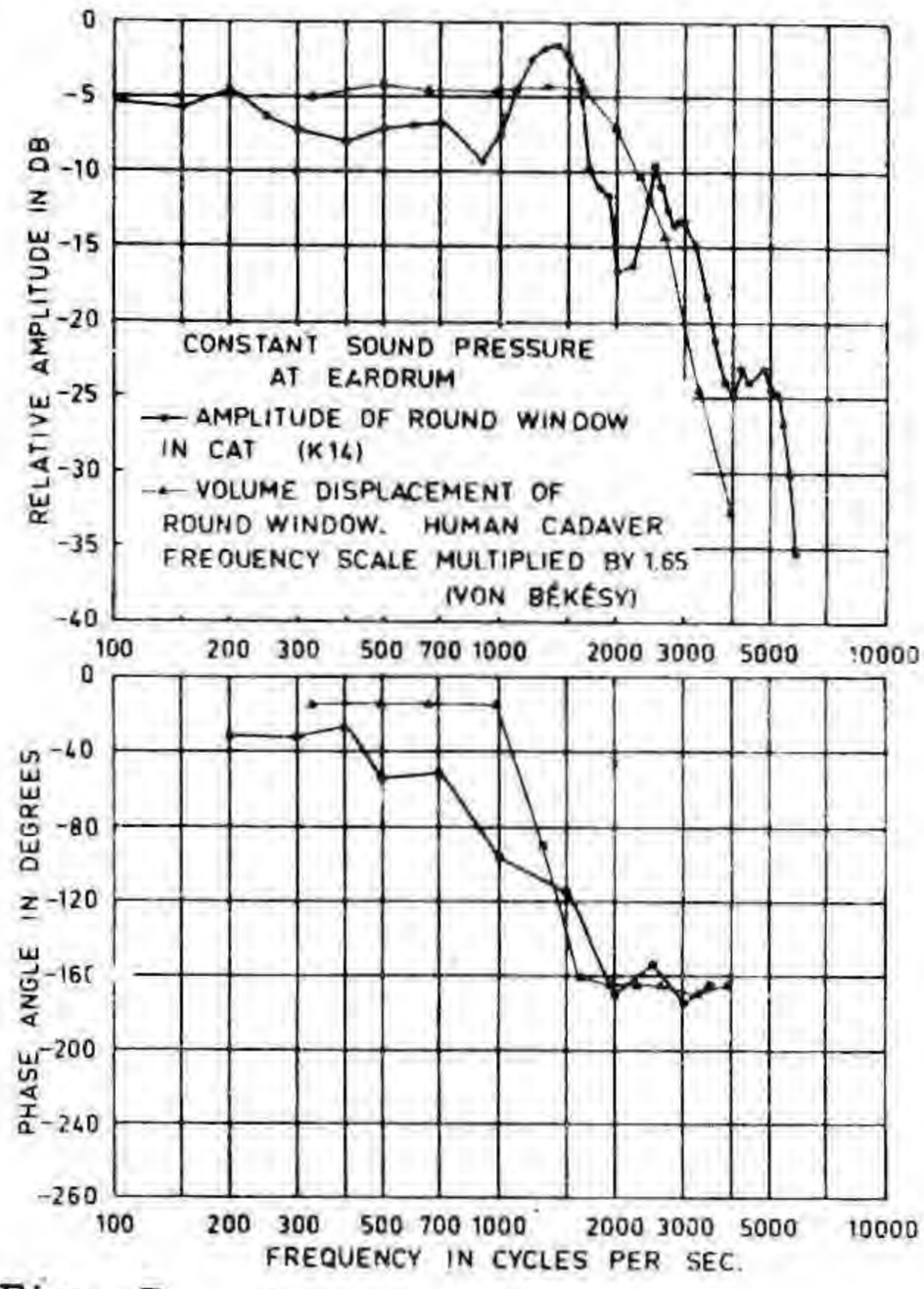

Fig. 6 Fig. 7

cat with the response of two models.[1)3)] The frequency scale for the models of the human ear have been multiplied by the same factor as that for the acoustic impedance in Fig. 6. It is seen that the results on human ears can be made to agree more closely with the experimental data on the cat by means of this scale factor.

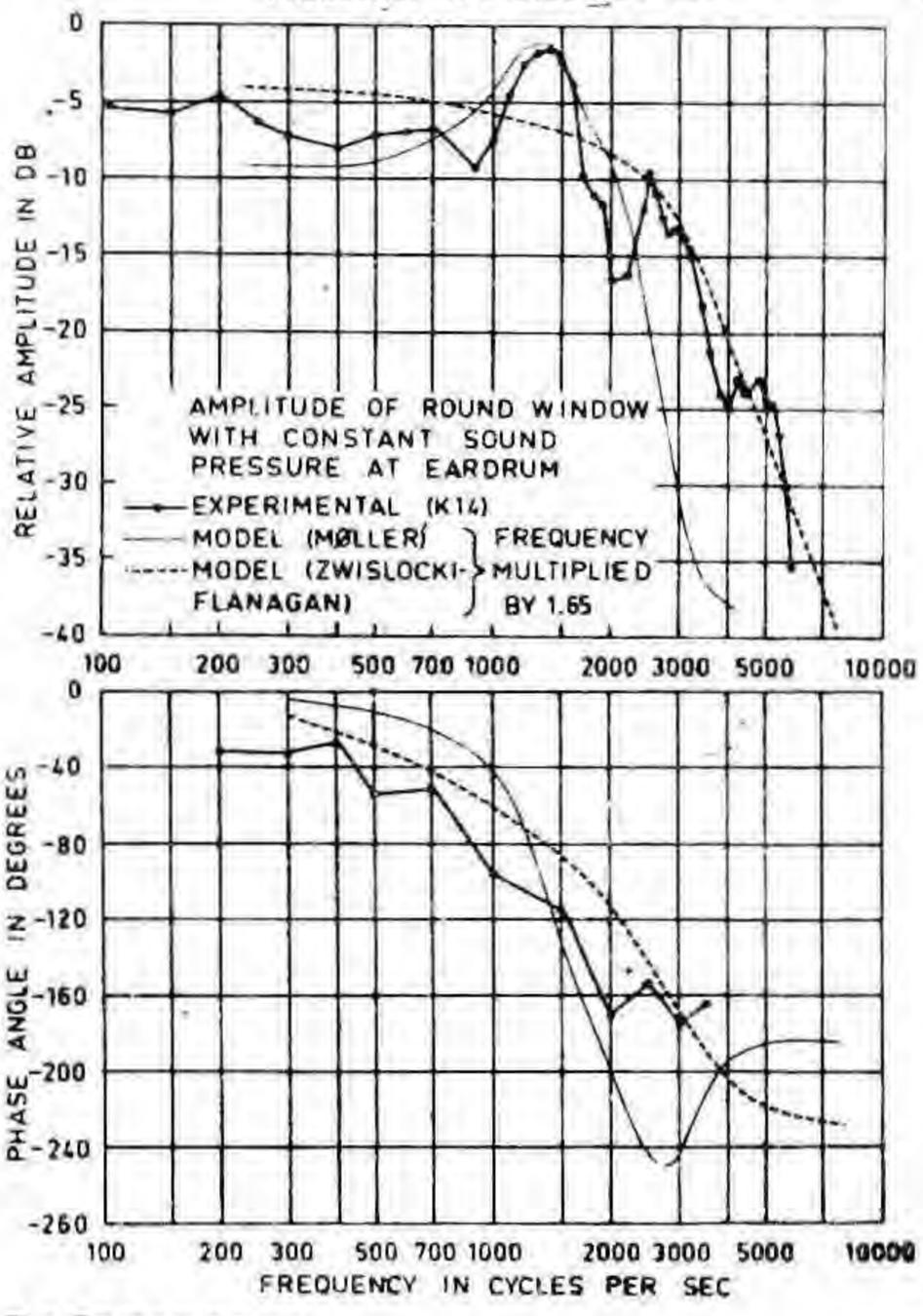

Fig. 8

References:

1) A.R.Møller: "Network model of the middle ear", J.Acoust.Soc.Am. 33 (1961) pp. 168–176.

2) G. von Békésy: Experiments in Hearing, McGraw-Hill Book Co. 1960, p. 436

3) J.L.Flanagan: "Models for approximating basilar membrane displacement; Part II", Bell Systems Tech. J., May 1962.

J41

FOURTH INTERNATIONAL CONGRESS ON ACOUSTICS
COPENHAGEN 21.-28. AUGUST 1962

A Characteristic Number for the Interaction Between a Sound Field and a Colloid.

Egon A. Hiedemann, Department of Physics, Michigan State University, East Lansing, Michigan, U.S.A.

Abstract: The interaction between a sound field and a colloid depends on the degree of participation by the suspended particles in the vibration of the medium. A characteristic number is given which determines this degree of participation in aerosols as well as in liquidosols.

Sewell[1] was the first to show theoretically that additional absorption of sound in a fog can occur if the suspended water particles do not participate completely in the vibration of the air. The discovery of the orthokinetic aggregation of aerosols in a sound field by Brandt and Freund[2] showed the importance of the difference in response to the sound field by the different-sized particles of a polydisperse system.

The ensuing detailed theoretical study of the interaction between an aerosol and a sound field made by Brandt, Freund and Hiedemann[3] showed that many significant physical quantities can be represented by simple functions of the phase angle ϕ between the motion of the suspended particle and that of the gas. The phase angle ϕ is given by

$$\tan \phi = m\, b\, \omega = S \qquad (1)$$

where m is the mass of the particle, b its mobility and ω the circular frequency of the sound wave. For spherical particles the mobility in a medium of viscosity η is given by the Stokes formula

$$1/b = 6\pi\eta r, \qquad (1a)$$

where r is the radius of the particle. The ratio of the amplitude of the particle motion X_p to that of the gas X_g is given by

$$X_p/X_g = \cos \phi = [1 + S^2]^{-1/2} \quad . \qquad (2)$$

The ratio of the amplitude δ of the difference in velocity of the particle and the gas is given by

$$\delta/V_g = \sin \phi = S\,[1 + S^2]^{-1/2} \quad . \qquad (3)$$

Furthermore the additional absorption coefficient α^* caused by the viscous forces between gas and particles can be expressed by

$$\alpha^* = \frac{c_m}{\rho\,\lambda} \cdot \pi \sin 2\phi = \frac{2c_m}{\rho\,\lambda} \cdot \pi\, S\,[1 + S^2]^{-1} \qquad (4)$$

where λ is the wavelength of sound, $c_m = n \cdot m$ is the mass concentration and ρ the density of the gas.

It is obvious that these important relations are simple functions of the dimensionless number $mb\omega$. As Sewell first found this number for the special case of spherical particles in the form

$$\frac{2\,d\,r^2\,\omega}{9\eta}$$

where d is the density of the particle, it is suggested to call this dimensionless number S after his name.

Figure 1 illustrates the simplicity of the representation of the quantities given by equations (2), (3) and (4) in a single diagram if one plots them as functions of Sewell's number S.

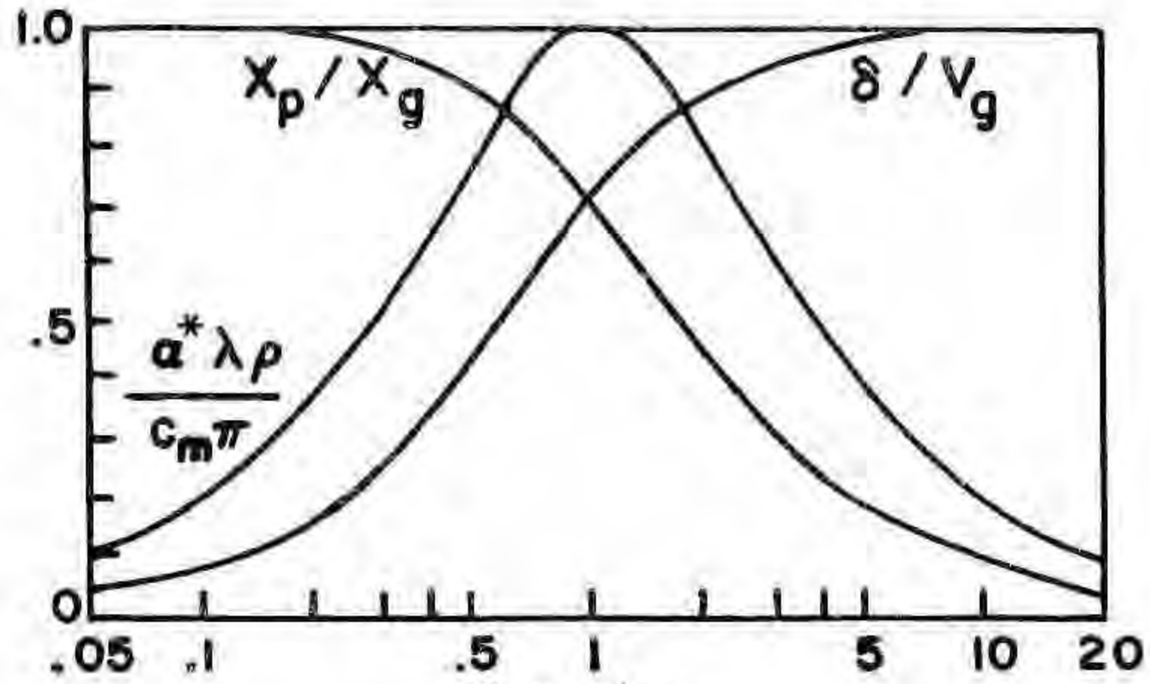

Figure 1.

The case of the aerosol is so simple because only viscous forces are involved. In case of liquidosols mass forces have to be considered and then the relations become much more involved. However, it can be shown that a dimensionless number given by

$$S^* = \omega\, b(m_p - m_L) \qquad (6)$$

is characteristic for the participation of the particle in the vibration of the medium. m_L is defined as the mass of a liquid particle of the same size as the suspended particle. It is obvious that for an aerosol the more general form of Sewell's number (6) reduces to the form given by eqs. (1) or (5).

Bibliography.

1. C. J. T. Sewell, Proc. Roy. Soc. (A) 83, 547 (1910); Phil. Trans. (A) 210, 239 (1910).
2. O. Brandt and H. Freund, Z. f. Physik, 92, 385 (1934); 94, 348 (1935).
3. O. Brandt, H. Freund and E. Hiedemann, Kolloid-Zs. 77, 103 (1936); Z. Physik, 104, 511 (1937).

K41

FOURTH INTERNATIONAL CONGRESS ON ACOUSTICS
COPENHAGEN 21.-28. AUGUST 1962

INFLUENCE OF LARGE AMPLITUDE SOUND WAVES UPON AEROSOL SCRUBBING

R.M.G. Boucher, Ph.D. Macrosonics Corp., Carteret, N.J.

I - EXPERIMENTAL SET-UP - ANALYTICAL TECHNIQUES

The purpose of our experiments was to evaluate the effect of high amplitude airborne sound waves produced by air-jet whistles upon the collection efficiency of a wet precipitator when dealing with the difficult problem of low concentration micronic liquid aerosols.

The Schmieg wet collector (500 CFM Swirl-type) is essentially a device which creates a turbulent sprayed water area by means of a pressure difference exerted upon water levels. The collector is divided into two compartments by a vertical baffle as shown in fig. 1. The dirty gases or aerosol first impinge on the water surface in compartment I, before being forced into a S-shaped device by means of the suction created by a fan at the top of compartment III. When the mixture of aerosol and water flows in the intermediate passage II, the water is broken into long liquid filaments and droplets. The latter are violently shaken in the turbulent channel and therefore collide with the aerosol microdroplets to form larger drops. These large drops are entrained by the gas stream and deflected (inertia effect) against the liquid surface at the bottom of compartment III.

FIGURE 1

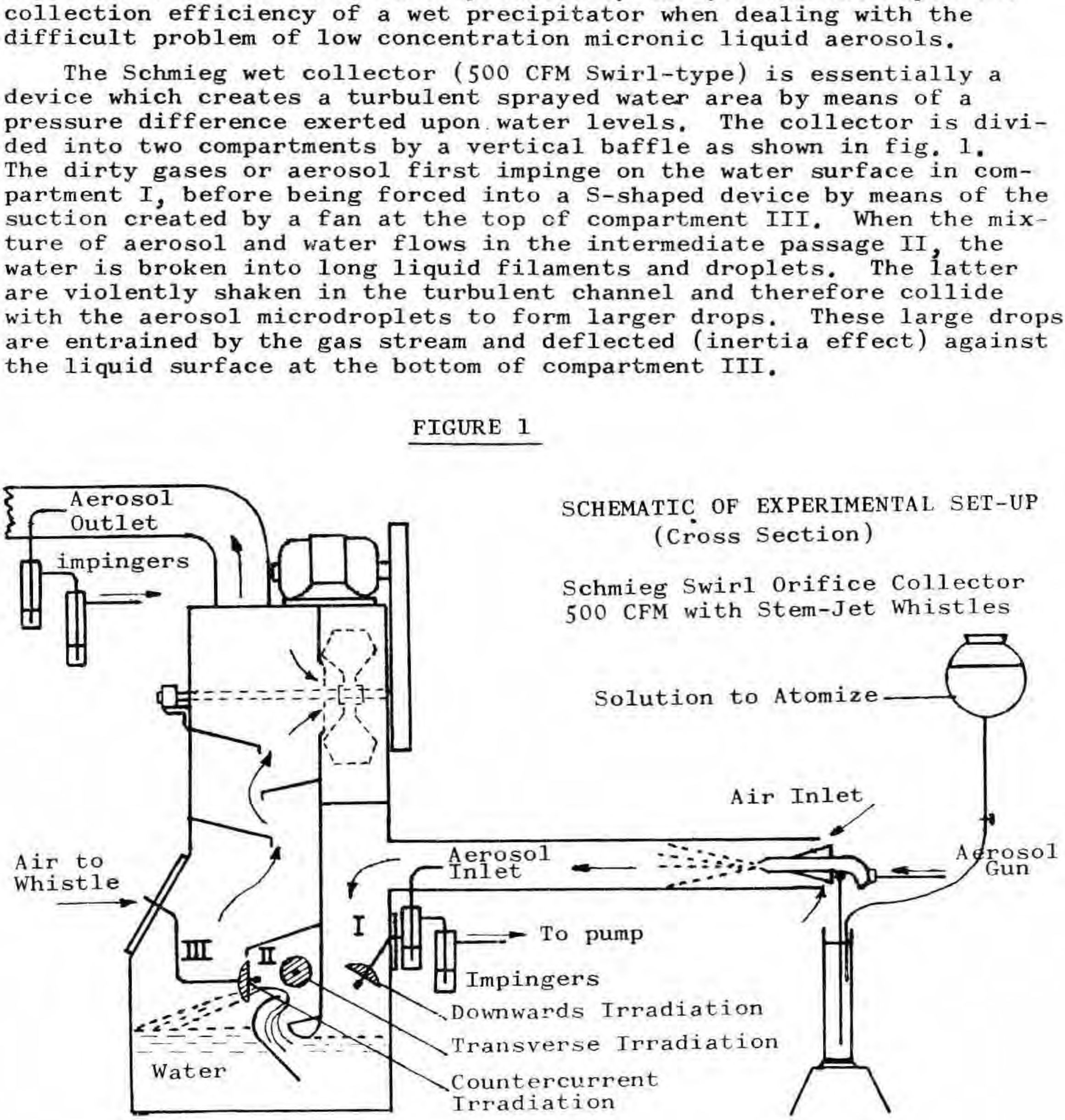

It is easy to understand that the higher the pressure drop through passage, the stronger the turbulence and the greater the overall collection efficiency. For practical reasons, our first series of tests was limited to the processing of 444 CFM of aerosol with a 2-1/2 inch pressure drop which was the value recommended to us by the manufacturer. A four inch pressure drop would of course enhance the performance of this wet collector.

The processed aerosol was a solution of triethylene glycol and water. Dissolved in this solvent was a known quantity (10 mg. Li per cc of mixture) of reagent grade lithium chloride. The lithium chloride which is quite soluble in the glycol-water solution acted as a "tracer" in the aerosol. The soluble glycol-water aerosol was sampled isokinetically and collected into two sets of impingers in series. The contents of these midget impingers placed upstream and downstream from the collector (see fig. 1) were analyzed by means of a Beckman Flame Photometer. Concentration versus percentage of transmittance curves for the expected concentration ranges were drawn and the instrument was calibrated before each sample was analyzed. The instrument was capable of detecting the presence of Lithium* up to .002 parts per million. The aerosol (average diameter 2.5 microns) produced by pneumatic atomization was injected in a straight 7 foot length duct** and its mass concentration at the scrubber inlet ranged from 79 to 136 mg./cu. meter.

II - SONIC IRRADIATION - RESULTS OF EXPERIMENTS

Table 1 shows the results of a series of tests which correspond to four different types of sonic irradiation by means of one or two Stem-Jet Whistles. As known, this airborne sound source consists of a cylindrical rod or stem fastened on the axis of a classical air jet nozzle-resonator system. The whistle used in our experiments was of Swedish make (Demister AB, Model 50 S) and its output varied between 60 and 100 watts according to the air nozzle pressure. In most of the tests, the whistle was operated at 44 psi and the intensity at 10 inches on the axis averaged 144-1/2 db. The free air consumption of the whistle is then 17 CFM and the frequency is close to 11 KC***. For each run, duplicates were performed to establish the reproducibility of the experimental procedure.

---

* It should be noted that lithium was chosen in these experiments since its occurrence in water as a contaminant is very small and will not interfere with the analysis.

** Inlet duct diameter 0.5 ft. (average inlet duct aerosol velocity $\bar{U}$ = 2260 ft/min.)

***Acoustic intensities checked with a General Radio Condenser Microphone (type 1551 PIH) and frequencies distribution studies with a Probescope Spectrum Analyzer (Model SS500). 11 KC is the frequency which corresponds to the best coagulation for 2.5 microns droplets when using the orthokinetic theory of E. Hiedemann and O. Brandt.

TABLE I

Run No.	Aerosol Inlet Concentration (mg/m^3)	Aerosol Outlet Concentration (mg/m^3)	Aerosol Collection Efficiency	Type of Experiment
1	95.7	46.9	50.9%	150 db 11 KC
2	79.8	52.8	33.7%	No sound Air inject.
3	94.3	41.1	56.4%	No sound No air inject.
4	94.3	44	53.3%	150 db 11 KC
5	101.2	40.3	60.1%	151 - 152 db 11 KC
6	102.7	50.6	50.7%	No sound Air inject.
7	136	42.5	68.6%	150 db 11 KC
8	128.7	49.9	61.1%	No sound Air inject.
9	131.4	39.6	69.8%	150 db 11 KC
10	112.1	39.4	64.8%	No sound Air inject.

The runs No.1 and 4 (See table I) consisted of a downwards sonic irradiation in compartment I. The idea behind these experiments was that a powerful acoustic field would cavitate the upper surface of the liquid and thus would improve the collection efficiency in this highly turbulent zone. To the contrary, the collection yield sharply decreased because the superimposed acoustic field produced some channeling effect underneath the separation baffle. The collection efficiency oscillated between 51 and 53% while the scrubber alone (no sound, no air from the whistles) had a 56.4% efficiency, as in run No. 3. As expected, the channeling effect was still more important when the whistles were detuned (air jets, but no sound*) since the collection yield averaged only 33.7% in run No. 2.

The runs No.5 and 6 consisted of a transverse sonic irradiation through the lateral ports. The whistle in run No.5 was tuned in resonance and the acoustic emission was so powerful that the whole liquid at the bottom of compartment III was surface cavitated. The aerosol inlet concentration was fairly constant (around 101 mg/m^3) and a marked difference was observed in the outlet concentration when the sound was on (40 mg/m^3) or off (50 mg/m^3). When the sound was off, we always maintained the same flow of compressed air through the Stem-Jet whistle with a view to evaluate the influence of the air jet alone. However, through visual observation, it was difficult to see any difference between the state of turbulence in the water curtain when the air jet was applied and when sound was applied.

*This detuning is achieved by sliding the resonator away from the nozzle in a region where it cannot produce any oscillations of relaxation.

The runs No. 7 and 8 consisted of a transverse sonic irradiation by means of two identical whistles fastened in opposition through the lateral ports. During these experiments we were not able to synchronize the sound sources and we observed wave cancellation effects. Therefore the average intensity level (150 db) was lower than in the preceding tests. The difference in collection efficiency between the runs, with sound off and on, was approximately 7.7%. However, the absolute value of the precipitation yield was higher than in the first six experiments, because the inlet concentration was also higher (around 130 mg/m^3).

The runs 9 and 10 represent the best set up when the radiation pressure field was directed countercurrent against the water curtain. By visual observation, one can see the difference when the whistles operate with sound or with air alone. In the first case (run No. 9) the liquid filaments are instantaneously blasted and broken into small water droplets,while with air alone (run No. 10) one can still distinguish large water drops in the turbulent zone. An overall efficiency of nearly 70% on the fine aerosol droplets was reached for an inlet concentration around 131 mg/m^3. This result was obtained with two Stem-Jet whistles located at 7-1/2 inches from the baffle, but we believe that identical results could also be achieved with one whistle equipped with a proper diffuser.

III - CONCLUSION

From the preceding series of tests, one can draw the following conclusions:

(a) A Stem-Jet whistle used in the configuration of run No. 9 and with a proper diffuser seems to be able to handle up to 500 CFM of micronic aerosol even at low concentration (80 to 130 mg/m^3). A minimum increase in mass collection efficiency of 10 to 15% can be expected if the energy level in the turbulent zone is equal to or higher than 0.07 watts/cm^2 ($\cong$ 148 db). Any intensity increase will correspond to an improvement in collection efficiency.

(b) A suitable frequency seems to be the frequency computed from the "orthokinetic coagulation" theory which promotes not only efficient impingements between aerosol droplets, but also a good coagulation rate between large water drops and fine aerosol droplets.

(c) From the energy point of view, our first series of experiments corresponded to a supplementary electrical energy consumption of approximately 3 KWH per whistle. This figure can be decreased in the future when using steam driven or low pressure whistles.

(d) The pressure drop of the scrubber (2.1 to 2.8 inches of water) was not affected by the sonic emission and the intensity level at one foot from the collector varied between 100 and 103 db. With a proper insulation, the noise level around the precipitator can certainly be brought under permissible limits from the industrial point of view.

This study was performed at the Research Division of the New York University under the sponsorship of Schmieg Industries, Inc., Centerline, Michigan.

L41

FOURTH INTERNATIONAL CONGRESS ON ACOUSTICS
COPENHAGEN 21.-28. AUGUST 1962

Anwendung von Sandwichblechen zur Lärmbekämpfung

Günther Kurtze
Grünzweig u. Hartmann A.G., Ludwigshafen/Rhein

Zur Dämpfung von Biegeschwingungen dünner Bleche existieren heute eine Reihe von Verfahren, die eines gemeinsam haben, nämlich die Ausnutzung von Relaxationsverlusten in Kunststoffen, mit denen die Bleche beschichtet werden. Die Art der Beschichtung ist aber sehr unterschiedlich und daraus ergeben sich anwendungstechnische und schalltechnische Unterschiede, die die Entscheidung, welches Verfahren im Einzelfall vorzuziehen ist, wesentlich beeinflussen.



Abb. 1 Prinzipieller Aufbau der zur Biegewellendämpfung benutzten Schichtstrukturen.

Eine Übersicht über den bei den verschiedenen Verfahren gewählten Schichtenaufbau gibt die Abb. 1.
Fall a) [1, 2] ist das bekannteste Verfahren, bei dem die Dämpfungsschicht als homogene Masse einseitig aufgebracht wird. Diese Methode ist besonders geeignet zur nachträglichen Anwendung. Die Frequenzabhängigkeit der erzielten Dämpfung ist allein vom Kunstostoff abhängig. Der maximal erzielbare Verlustfaktor beträgt etwa $\eta = 0,3$. Ein Nachteil ist die durch den Belag bedingte Erhöhung der Steife des Bleches, die dessen Schalldämmung beeinträchtigt.

Fall b) ist das vor allem im Flugzeugbau gern verwendete "damping tape" [3], bestehend aus einer Metallfolie, die mit einer Klebschicht, die zugleich Dämpfungsschicht ist, auf das zu dämpfende Blech aufgeklebt wird. Das Verfahren ist also ebenfalls nachträglich anwendbar, wobei das zusätzliche Gewicht wesentlich kleiner ist als im Fall a). Die erzielte Dämpfung ist hier bereits von der Anordnung her frequenzabhängig, also zusätzlich zu den Eigenschaften der Kunststoff-Klebschicht. Die größtmögliche Bandbreite beträgt etwa 4 Oktaven bei einem maximalen Verlustfaktor von etwa $\eta = 0,1$, wenn die Folienstärke 1/10 der Blechstärke beträgt. Die Erhöhung der Steife durch die Dämpfungs-

schicht ist nur bei tiefen Frequenzen wirksam, so daß die Schalldämmung nicht beeinträchtigt wird.

Die Wirksamkeit, aber nicht die Bandbreite des "tapes" kann bei geringem zusätzlichem Gewichtsaufwand durch Abstandshalter erhöht werden. Mit diesem sog. "spaced tape" [4] (Fall c) in Abb. 1) kann ein Verlustfaktor von maximal etwa $\eta = 0,3$ unter sonst gleichen Bedingungen erreicht werden.

Die symmetrischen Sandwich-Anordnungen d) und e) in Abb. 1 stellen vom Aufbau her die zur Erzielung hoher Verlustfaktoren günstigste Lösung dar [5]. Nachteilig ist jedoch, daß eine nachträgliche Anwendung wegen der erforderlichen Gewichtsverdopplung in der Regel nicht möglich ist. Allerdings wird auch durch die Schicht a) das Gewicht der zu dämpfenden Platte nahezu verdoppelt. Die Dämpfung ist auch hier von der Anordnung her bereits frequenzabhängig, ihr Maximalwert hängt von der Dicke der Kernschicht ab. Beim Sandwich mit dünner Kernschicht (Kernschichtdicke $d \ll$ Blechstärke h einer Deckschicht) gilt $\eta > 0,3\ \eta_o$ für $\omega_1 < \omega < \omega_2$. Dabei ist η_o der Verlustfaktor der Kernschicht und ω_1, ω_2 zwei Frequenzen, die durch die Steife der Deckschichten und den Schubmodul der Kernschicht bestimmt sind und die sich bei der dünnen Kernschicht um den Faktor 2 unterscheiden. Beim Sandwich mit dicker Kernschicht ($d \gg h$) gilt $\eta > 0,5\eta_o$ im Bereich $\omega_1 < \omega < \omega_2$ und $\eta = \eta_o$ für $\omega_1 \ll \omega \ll \omega_2$. Das Verhältnis ω_2/ω_1 wächst mit der Kernschichtdicke und beträgt bereits für $d = 5h$ mehr als eine Zehnerpotenz. Die Verlustfaktoren verfügbarer, als Kernschicht geeigneter Kunststoffe liegen in der Größenordnung $\eta_o = 1$. Es können also für die Kombination bei Verwendung dicker Kernschichten sehr viel höhere Verlustfaktoren erzielt werden als mit den übrigen Anordnungen. Da die Materialbedingte Frequenzabhängigkeit bei weitem nicht so breitbandig ist wie die vorstehend erwähnte Anordnung, ist die durch die Anordnung bedingte Frequenzabhängigkeit hier ohne Belang.

Ein weiterer Vorteil der symmetrischen Anordnungen d) und e) in Abb. 1 liegt in der geringen dynamischen Biegesteife, die diese Platte bei hohen Frequenzen aufweist. Bei tiefen Frequenzen kann die Kernschicht als starr angesehen werden. Damit ist die Biegesteife wesentlich höher als die einer homogenen Metallplatte gleichen Gewichtes. Bei hohen Frequenzen dagegen, in dem Bereich also, in dem die Biegewellengeschwindigkeit der Platte normalerweise die Luftschallgeschwindigkeit überschreiten würde, wirkt die Kernschicht weich. Die Biegesteife nimmt mit steigender Frequenz ab, bis sie im Grenzfall der Steife der einzelnen Deckschichten gleich wird. Ein Koinzidenzeinbruch

in der Schalldämmkurve wird auf diese Weise vermieden.

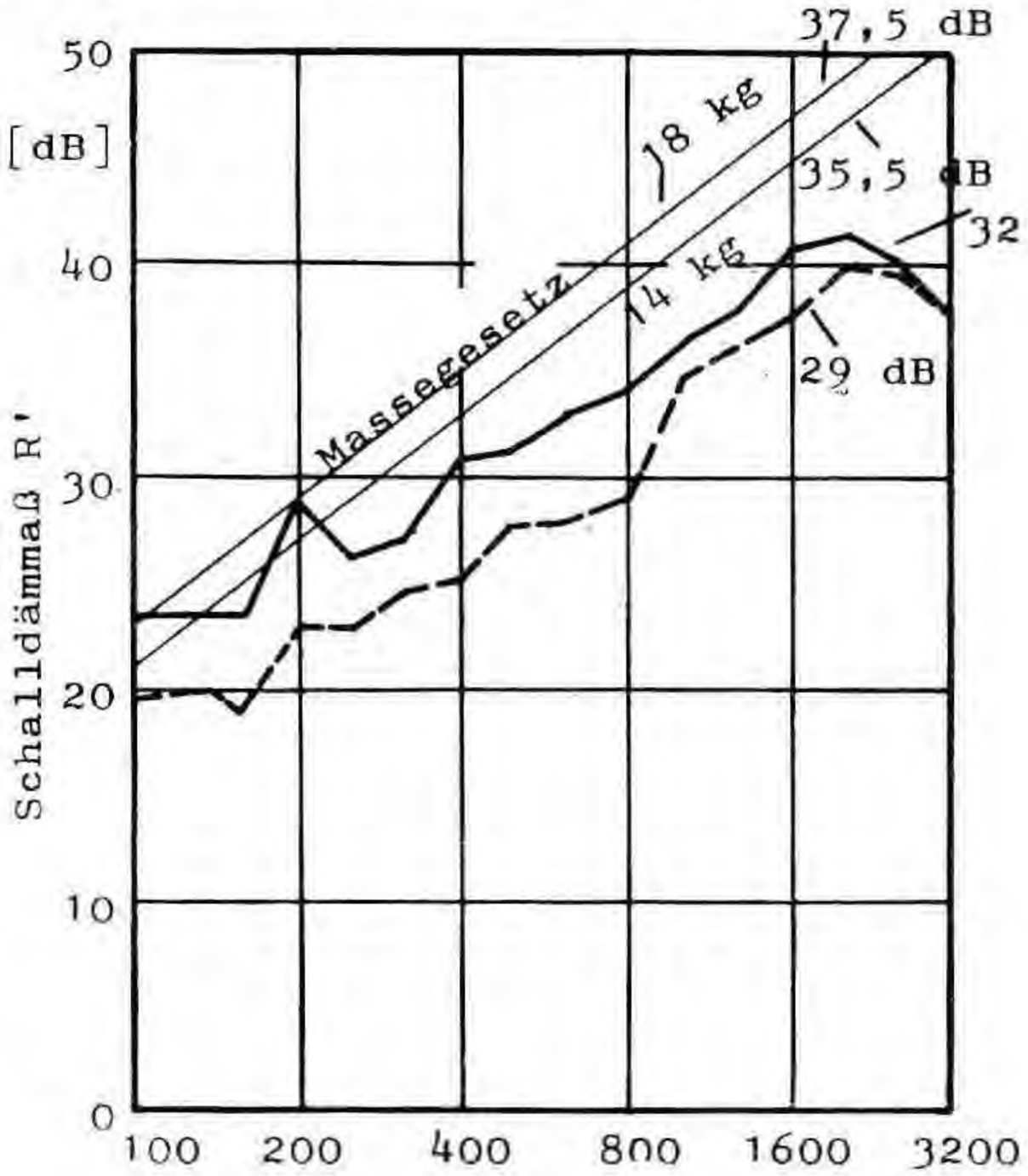

Abb. 2 Schalldämmung von symmetrischen Sandwichplatten
—— 2 x 1 mm Blech, 1 mm Kunststoffkern
--- 2 x 0,76 " , 1 mm "

Abb. 2 zeigt die Schalldämmung von zwei symmetrischen Sandwichblechen mit 1 mm Kern und 1 bzw. 0,76 mm Deckschichten (Eisenblech). Die ebenfalls eingetragenen, dem Massegesetz entsprechenden Geraden gelten für senkrechten Schalleinfall, sind also zur Berücksichtigung der statistischen Winkelverteilung um etwa 3 dB zu vermindern. Der Verlustfaktor einer Sandwichplatte aus 1 mm starken Blechen mit 1 mm Kunststoff-Kernschicht ist in Abhängigkeit von Frequenz und Temperatur in Abb. 3 wiedergegeben. Bei diesem Aufbau der Platte handelt es sich um ein Mittelding zwischen den Fällen d) und e) aus Abb. 1. Die gestrichelte Kurve gilt für eine 5 mm starke Kernschicht bei sonst gleichem Aufbau. Der geringe Unterschied im Frequenzgang zeigt, daß dieser im wesentlichen durch die Eigenschaften des Kunststoffes bestimmt wird.

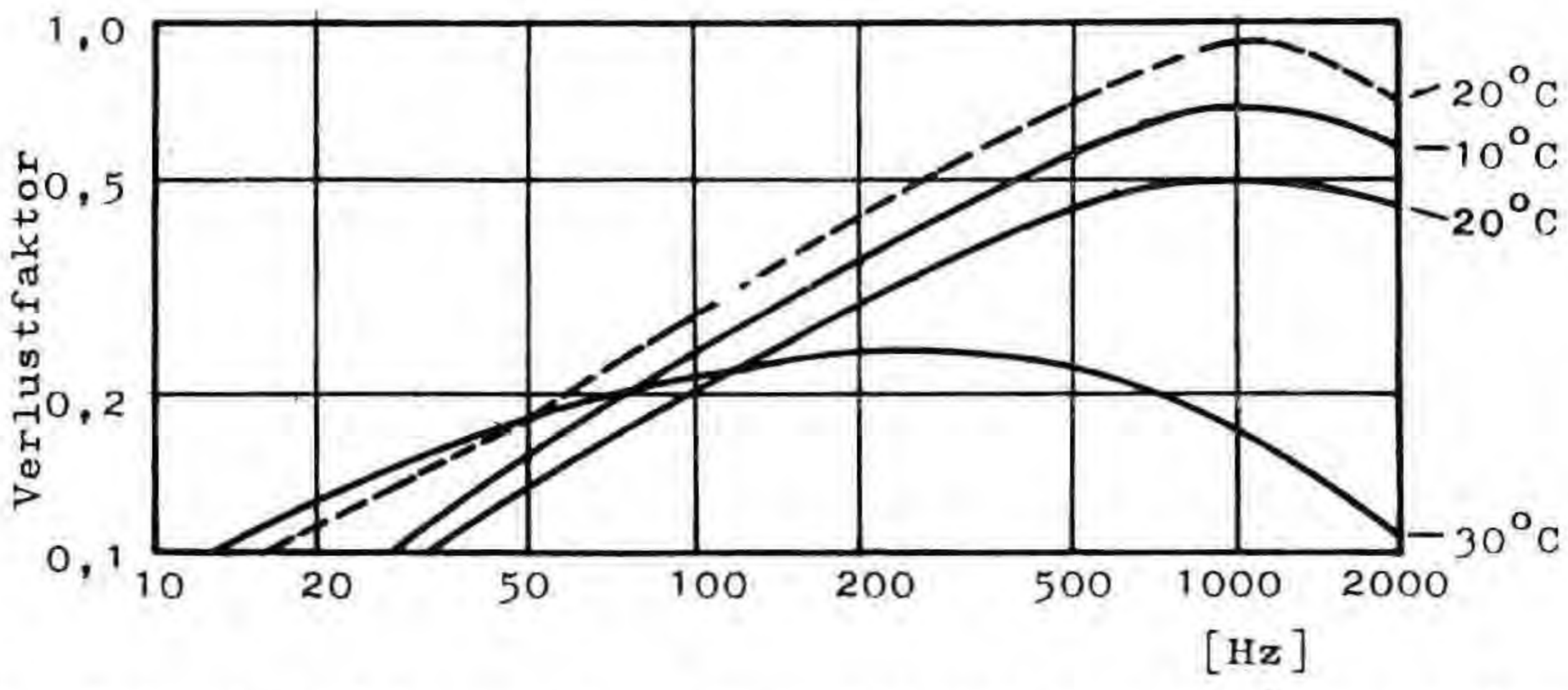

Abb. 3 Verlustfaktor einer Sandwichplatte mit 1 mm starken Eisenblech-Deckschichten in Abhängigkeit von Frequenz und Temperatur —— Kernschicht 1 mm stark, ---- Kernschicht 5 mm stark.

Hohe Schalldämmung bei zugleich hohem Verlustfaktor machen symmetrische Sandwichplatten besonders geeignet für Trennwände und Vorsatzschalen in Land-, Luft- und Seefahrzeugen, sowie für schalldämmende Hauben. Abb. 4 zeigt die Wirkung einer Sandwich-Vorsatzschale vor einer körperschallerregten Schiffs-Außenwand. Gegenüber einer gleich schweren Schale aus homogenem Blech ergibt sich eine Verbesserung, die anderenfalls nur mit dem doppelten Gewichtsaufwand zu erzielen wäre. Beide Schalen waren punktweise starr befestigt.

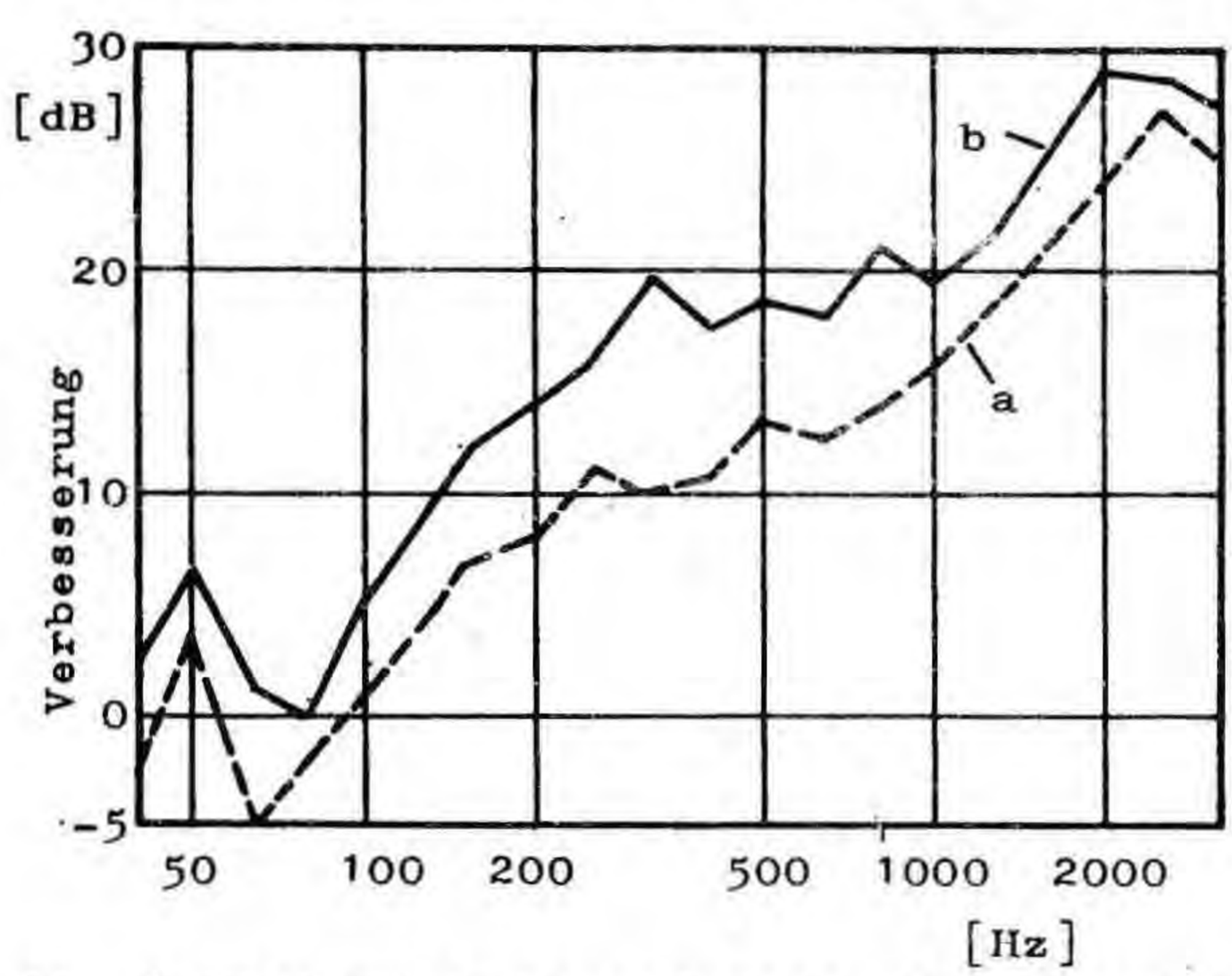

Abb. 4 Minderung des Schallpegels in einem von einer körperschallerregten Schiffswand begrenzten Raum:
a) durch Vorsatzschale aus homogenem Blech
b) durch gleich schwere symmetrische Sandwichplatte.

Insbesondere bei der Verwendung von Sandwichplatten für Wände und Vorsatzschalen macht sich deren hohe Steife bei tiefen Frequenzen vorteilhaft bemerkbar. Die übliche biegeweiche Schale, die hinsichtlich Schalldämmung das gleiche leistet, hat in der Regel keine ausreichende Standfestigkeit. Leider ist aber hohe Steife bei tiefen Frequenzen nicht gleichbedeutend mit hoher statischer Steife. Da alle Kunststoffe Fließerscheinungen zeigen, gilt für alle hier erwähnten Platten, daß die zusätzliche, durch den Kunststoff bedingte Steife für Dauer-Biegebeanspruchung statisch nicht in Rechnung gestellt werden darf. Bei der symmetrischen Sandwichplatte ist dieser Nachteil allerdings dadurch etwas gemildert, daß die Deckschichten dieser Platten punktweise durch Nieten oder Schrauben starr miteinander verbunden werden können, ohne daß eine wesentliche Beeinträchtigung der akustischen Eigenschaften erfolgt.

Literatur:

[1] Oberst, H., Acustica 2 (1952) 181
[2] Lienard, P., La Recherche Aeronautique 20 (1951) 11
[3] Kerwin, E.M., Ross. D., Proc. IIIrd ICA Congr. S. 410
[4] Kerwin, E.M., Proc. IIIrd ICA Congr. S. 412
[5] Kurtze, G., Watters, B.G.. Journ. Acoust. Soc. Am. 31 (1959) 739

M41

FOURTH INTERNATIONAL CONGRESS ON ACOUSTICS
COPENHAGEN 21.-28. AUGUST 1962

Modellversuche zur Ermittlung des Einflusses von Schallspiegeln auf die Hörsamkeit

Ekkehart Krauth und Roland Bücklein

Das Modellverfahren nach F. Spandöck (1), welches durch maßstabsgerechte Frequenztransponierung klanggetreue raumakustische Untersuchungen in akustisch ähnlichen Modellräumen ermöglicht, hat mit Unterstützung der Deutschen Forschungsgemeinschaft nun einen Stand erreicht, der das Verfahren zur Klärung raumakustischer Fragen als geeignet erscheinen läßt.

Die subjektiven Auswirkungen von Nachhallzeitänderungen oder die Unterschiede in der subjektiven Wahrnehmung, die durch verschiedene Wahl des Zuhörerplatzes bedingt sind, konnten schon seit längerer Zeit durch solche Modellversuche ermittelt werden. Dies zeigten Aufnahmen, die bereits vor drei Jahren anläßlich des 3. Internationalen Kongresses für Akustik in Stuttgart vorgeführt wurden (2).

Es wurden nun neben der Nachhallzeit auch die Diffusität und die Deutlichkeit im Modell gemessen und ihre subjektiven Auswirkungen durch Hörvergleich bestimmt.

Im folgenden wird über die Möglichkeit berichtet, durch Aufhängung reflektierender Flächen die Deutlichkeit am Ort des Zuhörers zu beeinflussen. Unter Deutlichkeit versteht man das Verhältnis der innerhalb der ersten 50 ms am Ort des Beobachters eintreffenden zur gesamten dort ankommenden Schallenergie eines Knallimpulses (3). Um zu großen Deutlichkeiten zu gelangen muß also dafür gesorgt werden, daß innerhalb von 50 ms, entsprechend einem Schallaufweg von 17 m, ein möglichst großer Anteil der abgestrahlten Schallenergie beim Zuhörer eintrifft. Bei großen hohen Sälen erreichen Reflexionen, die z.B. über die Decke kommen, leicht einen größeren Laufweg als 17 m und machen sich störend bemerkbar. Man versucht daher vielfach durch Aufhängen von niedrigeren Reflektoren bestimmter Größe den Schall auf kürzerem Wege ins Publikum zu leiten.

Durch Modelle kann geklärt werden, wie groß ein wirksamer Spiegel sein muß und wie man ihn zweckmäßig anordnet. Für die Untersuchungen wurden 7 Glasspiegel benutzt, die sich optisch leicht einrichten ließen. Alle Spiegel hatten Rechteckform mit einem Seitenverhältnis von 2:3. Die Messung der Deutlichkeit erfolgte mittels eines Fluxmeters der AEG, das über ein Thermokreuz an einer Relaisschaltung angeschlossen war, die nach 50 ms nach Eintreffen des ersten Knallimpulses abschaltete (3). Da alle Knallaufnahmen gemäß dem Prinzip des Modellverfahrens bei schneller Geschwindigkeit aufgesprochen und entsprechend dem Modellmaßstab bei langsamer Geschwindigkeit des Tonbandes wiedergegeben wurden, konnte jeder Knall beliebig oft wiederholt und somit der Gesamtanteil sowie der innerhalb der ersten 50 ms eintreffende Anteil der Schallenergie mit demselben Fluxmeter gemessen werden.

Das Ergebnis der Deutlichkeitsmessungen mit 7 Spiegeln verschiedener Größe als Reflektoren, die nacheinander am selben Ort angebracht waren, zeigt Bild 1.

Bei allen Messungen standen der Funkenknallgeber auf der Bühne und das Mikrofon in 18 m Entfernung (bezogen auf die Hauptausführung) in der Mitte des Saales. Die drei Kurven, die bei verschiedenen Anordnungen der Reflektoren im leeren und "besetzten" Modell gewonnen wurden, zeigen ähnlichen Verlauf. Wenn eine bestimmte Reflektorgröße erreicht ist, läßt sich kein wesentlicher Deutlichkeitsgewinn mehr erzielen. Von einer Spiegelgröße von 100 mal 150 cm^2 (bezogen auf die Hauptausführung) an, bleibt die Deutlichkeit auch bei Verwendung noch größerer Spiegel an einem Hörerplatz nahezu konstant.

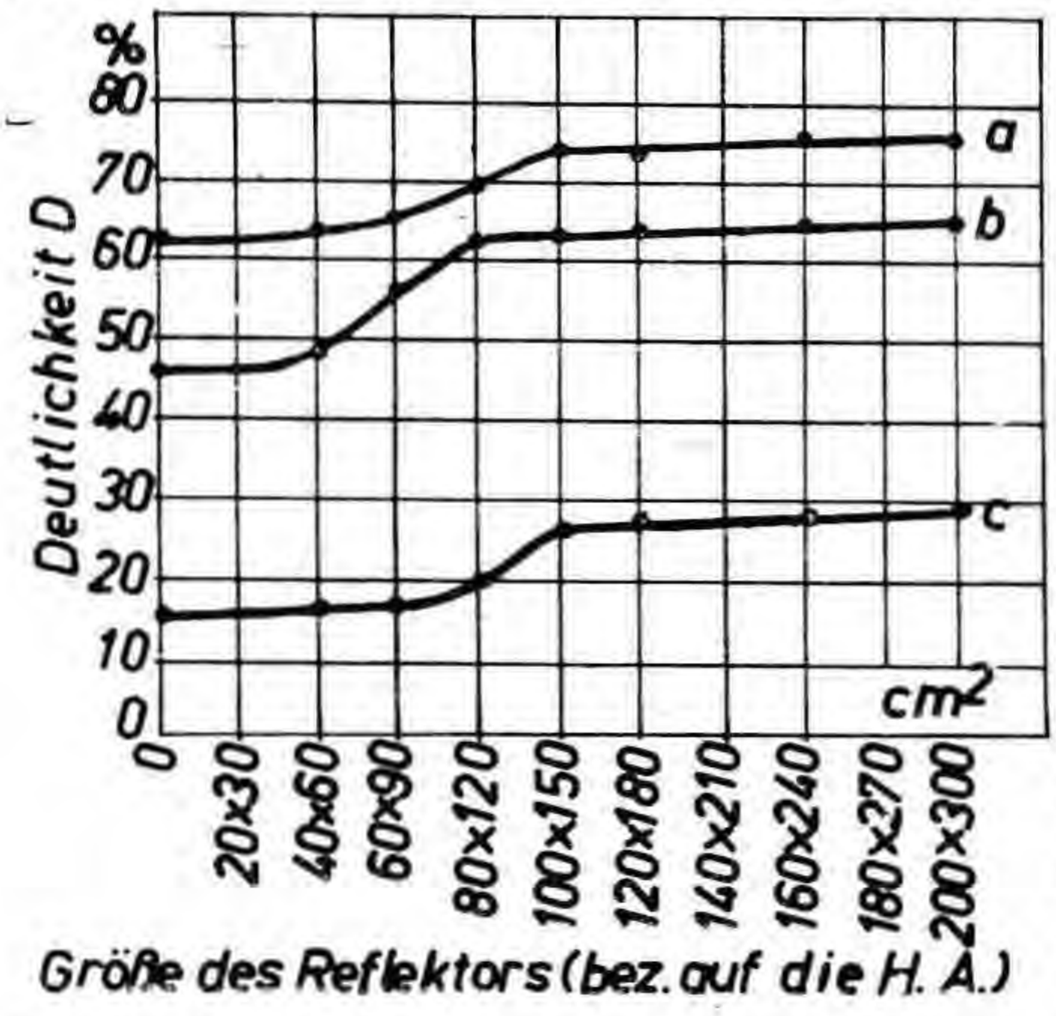

Bild 1 Einfluß eines Schallreflektors variabler Größe auf die Deutlichkeit D
Kurve a: Reflektor über dem Sender, $T_H \cong 3$ s
Kurve b: Reflektor über dem Mikrofon, $T_H \cong 3$ s
Kurve c: Reflektor über dem Mikrofon, $T_H \cong 10$ s

Zur Beantwortung der Frage, von welcher Reflektorgröße an Unterschiede in der subjektiven Wahrnehmung bemerkbar sind, wurden Hörvergleiche kurzer Testsätze, jeweils mit und ohne Spiegel, vorgenommen.

Die Ergebnisse dieser Abhörversuche sind in Bild 2 dargestellt. Über der Größe der Spiegelfläche ist der Anteil der Beobachter aufgetragen, die einen Unterschied hören, d.h. von 10 in beliebiger Reihenfolge gemachten Aufnahmen mit und ohne Reflektor wurden pro Beobachter mindestens 8 richtig beurteilt.

Die Kurven der Wahrnehmbarkeit zeigen einen Verlauf, der nach den in Bild 1 dargestellten Ergebnissen über die Wirksamkeit von Reflektoren verschiedener Größe zu erwarten war. Unterhalb der Mindestgröße der Reflektorfläche sinkt die Wahrnehmbarkeit stark ab, größere Reflektoren bringen keinen Gewinn mehr. Für diese Hörversuche wurde der Reflektor stets am selben Ort über dem Mikrofon aufgehängt.

Wie aus den Kurven nach Bild 2 hervorgeht, ergibt sich in der Wahrnehmbarkeit von Reflektoren ein wesentlicher Unterschied je nach dem Standort des Mikrofons. Wenn das Mikrofon frei im Mittelgang des Modells steht, ist der Einfluß eines Schallspiegels sehr viel weniger zu erkennen, als wenn das Mikrofon direkt ins Publikum gestellt wird. Bei der Aufstellung des Mikrofons im Mittelgang hören erst bei einer Reflektorgröße von 100 mal 150 cm^2 (bezogen auf die Hauptausführung) 60 % der Beobachter einen Unterschied im Vergleich zu Aufnahmen ohne Reflektor. Auch bei zunehmender Größe der Spiegelfläche ändert sich der Anteil der Beobachter, die einen Unterschied hören, nicht mehr. Das Ergebnis dieser Hörversuche stimmt somit überein mit dem Verlauf der mittleren Kurve nach Bild 1, die ebenfalls bei Reflektoranordnung

über dem Mikrofon im Mittelgang des mit Publikum besetzten Modells erhalten wurde. Wenn das Mikrofon zwischen dem Publikum steht, hören schon bei einer Größe der Reflektorenfläche von 80 mal 120 cm^2 (bezogen auf die Hauptausführung) alle Beobachter einen Unterschied.

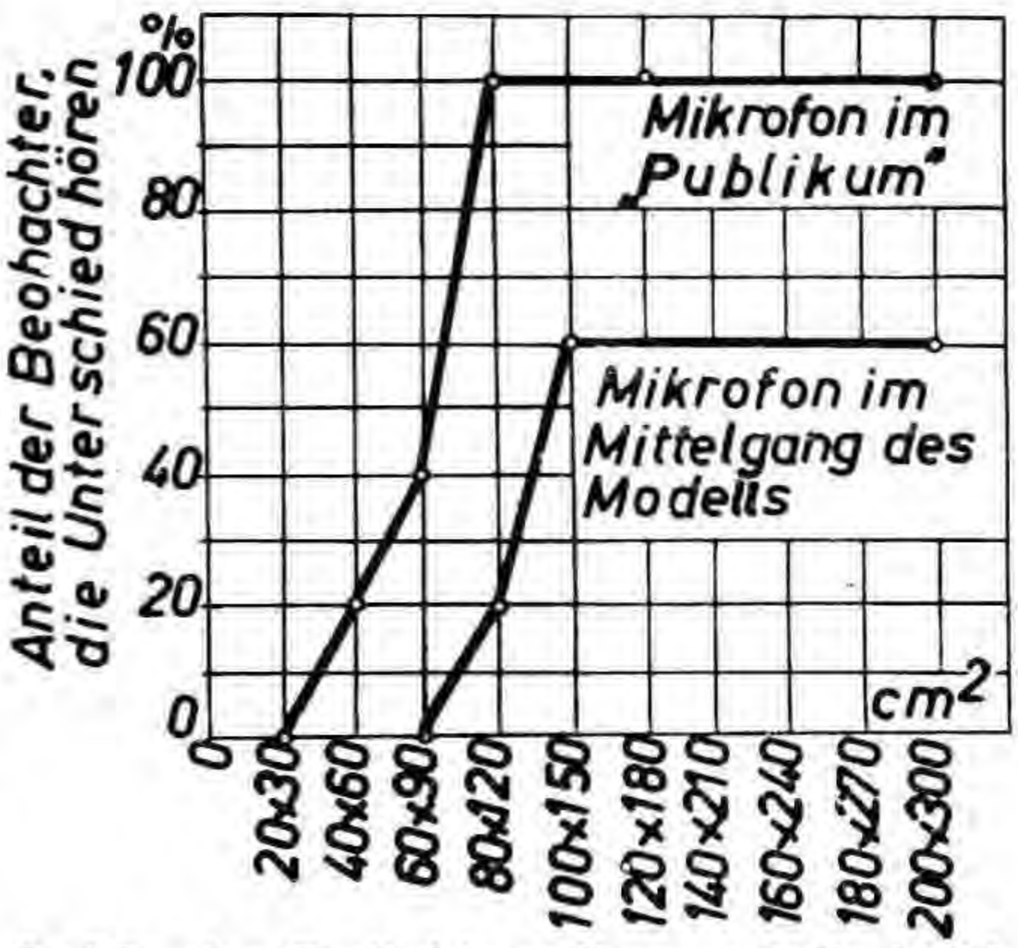

Bild 2 Hörbarkeit eines Schallreflektors variabler Größe bei Sprache im "besetzten" Modell, $T_H \cong 3$ s

Wie Messungen von G.v.Békésy sowie W. Janowsky und F.Spandöck (4) ergaben, wird eine Schallwelle, die sich über einer schallschluckenden Fläche (Publikum) ausbreitet, gleichsam in das Absorptionsmaterial hineingesogen und kommt somit am Ort des Beobachters mit kleinerer Intensität an als Schallwellen, welche in größerer Höhe sich über das Schluckmaterial hinweg ausbreiten. Ein Reflektor über dem absorbierenden Publikum erweist sich also in diesem Fall von größerer Wirksamkeit als im leeren Modell, was durch die obere Kurve in Bild 2 bestätigt wird.

Bei der Aufhängung eines Reflektors ist natürlich auch die Größe des Bereiches von Interesse, innerhalb dessen ein solcher Reflektor eine Anhebung der Deutlichkeit bewirkt. Im Modellversuch wurden für drei verschiedene Aufhängungen der Wirkungsbereich eines Schallspiegels gemessen. Der Modell-Spiegel hatte eine Fläche von 10 mal 15 cm^2, die nach den vorangegangenen Versuchen als ausreichend anzusehen ist. Als Schallempfänger dienten 6 Mikrofone, die in das "Publikum" hineingestellt wurden. Die Anordnung der Reflektoren und der Mikrofone sowie die gewonnenen Meßergebnisse sind aus Bild 3 ersichtlich.

Der Reflektor, der einmal über dem Mikrofon (Anordnung a), dann in der Mitte zwischen Sender und Empfänger (b) und schließlich über dem Sender (c) angebracht wurde, war immer auf das in der Mitte der 6 Empfänger stehende Mikrofon 1 ausgerichtet. Die am Ort der einzelnen Mikrofone gemessenen Deutlichkeitswerte wurden in der Richtung der Mikrofone 4,3,1,2 in Bild 3 links und in Richtung der Mikrofone 5,1,6 rechts jeweils im Vergleich zu den ohne Reflektor gemessenen Deutlichkeitswerten (ausgezogene Kurven) eingetragen.

Aus den Kurven erkennt man, daß die Anordnung a des Reflektors über dem Empfänger zwar einen großen Deutlichkeitsgewinn bringt, jedoch nur für das Mikrofon 1, auf das der Reflektor besonders ausgerichtet war. Eine Anordnung des Reflektors zwischen Sender und Empfänger bringt dagegen keinerlei Vorteile, wie die Kurven b zeigen. Günstig ist dagegen die Aufhängung eines Spiegels über dem Sender (Kurven c). In diesem Fall ergibt sich der größte Bereich, innerhalb dessen eine merkliche Verbesserung der Deutlichkeit erzielt wird. Gegenüber der Reflektoranordnung über dem Empfänger ist die am Ort des Mikrofons 1 gemessene Deutlichkeit nicht mehr so groß, dafür wird aber die Deutlichkeit für mehr Zuhörerplätze verbessert. Diese Art der Reflektoraufhängung ist also mit Recht die in der Praxis gebräuchlichste. Es kann aber auch, wie die Messungen zeigen, ein über dem Empfänger angebrachter Reflektor besonders dann von Vorteil sein, wenn einzelne, ungünstig gelegene Zuhörerplätze besser beschallt werden sollen.

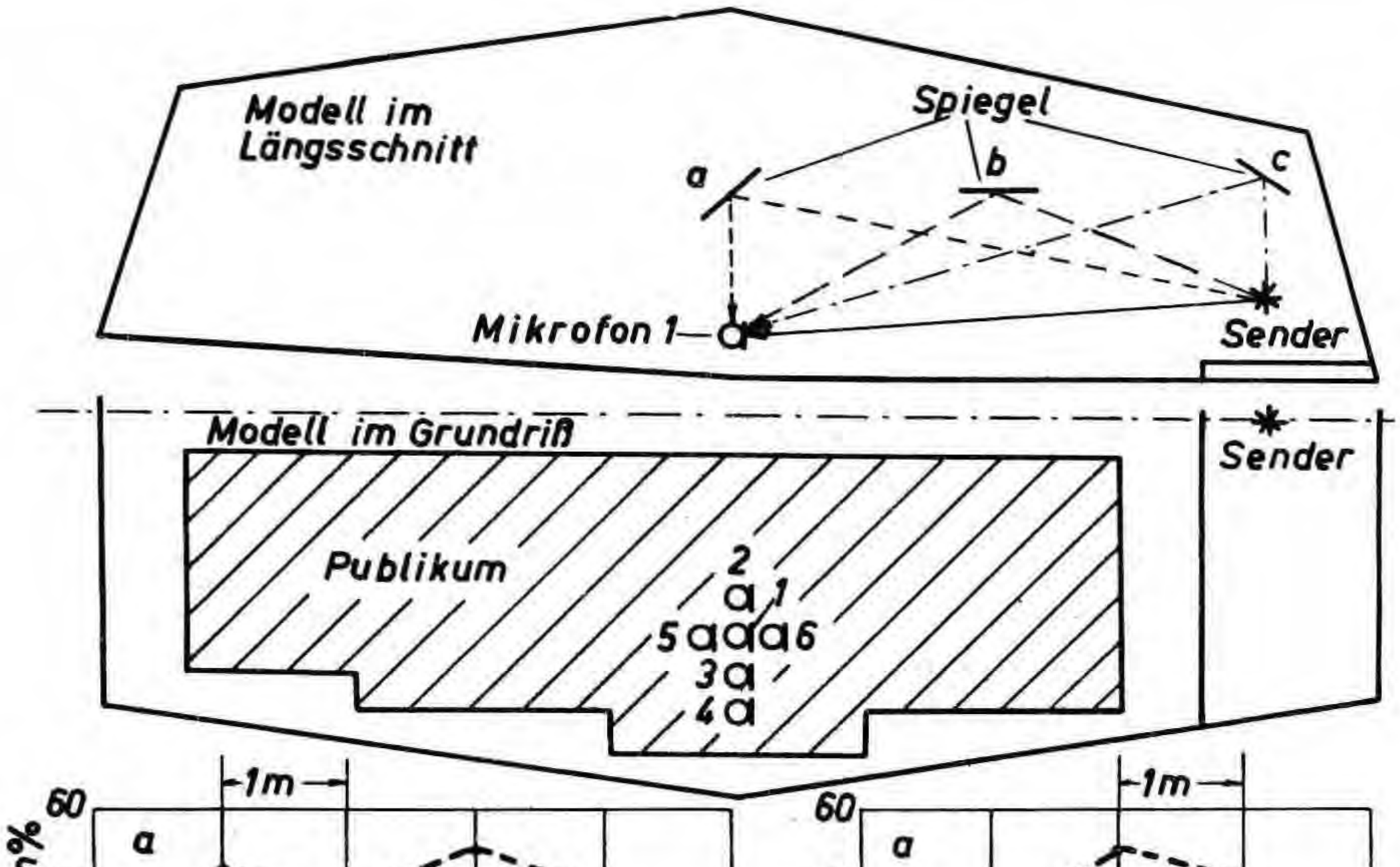

Bild 3 Im Modell gemessene Deutlichkeitswerte D für die verschiedene Anordnung eines Spiegels der Größe 10 cm mal 15 cm

Einige diesbezügliche Beispiele werden während des Vortrages mit Hilfe von Tonbandaufnahmen vorgeführt werden.

Literatur

(1) F.Spandöck, Akustische Modellversuche, Annalen der Physik, 20(1934)338.
(2) F.Spandöck, R.Boutros-Attia, E.Krauth, Proceedings of the third ICA Congress in Stuttgart 1959, Vol.II, Elsevier, Amsterdam, 1961, S.925, 929, 932.
(3) R.Thiele, Richtungsverteilung und Zeitfolge der Schallrückwürfe in Räumen, Acustica, 3(1953)291.
(4) G.v.Békésy, Zeitschrift für technische Physik, 14(1933)6.
W.Janowsky und F.Spandöck, Akustische Zeitschrift, 2(1937)322.

N41

FOURTH INTERNATIONAL CONGRESS ON ACOUSTICS
COPENHAGEN 21.-28. AUGUST 1962

PROBLEMS in FEEDBACK CONTROL of NARROW BAND RANDOM NOISE

P.E.Møller Petersen, electr.eng.
A/S Brüel & Kjær

Introduction.
Random Noise has been used for acoustical test purposes for several years and a large number of noise generators with various frequency characteristics are available. Most commonly the output of the generators can be characterized as white noise which means that the energy per unit frequency is constant through the frequency range of interest. Generators intended for applications where filters with constant percentage bandwidth are involved can in addition often supply a noise spectrum where the output voltage per unit frequency decreases 3 db per octave. This type of noise is sometimes described as pink noise. There are also noise generators capable of generating noise in selectable frequency bands, for example one octave or one third of an octave.

The purpose of the generator described in the following is to produce narrow band random noise with constant absolute bandwidth and continuously variable center frequency in the audio frequency range.

The generator utilizes the heterodyne principle which has made it possible to incorporate automatic feedback control of the output voltage. The feedback circuit has been so designed that Rayleigh distribution of the output peaks can be maintained over a compression range of 45 db. Some of the problems which arose during the development work will be discussed in this paper and an instrumentation set-up for recording peak response probability density curves will be described.

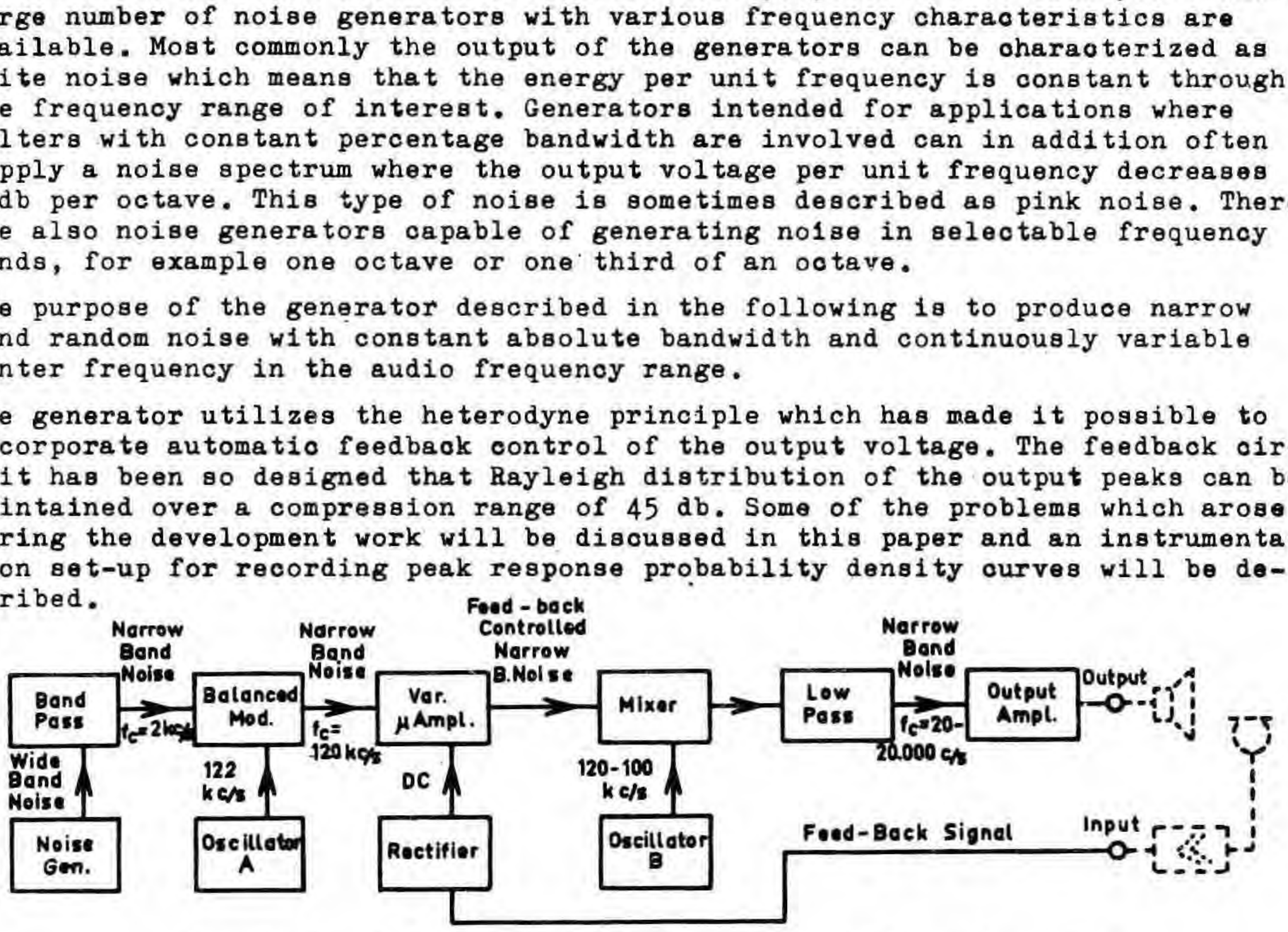

Fig. 1. Block Diagram of the Narrow Band Noise Generator

A Narrow Band Noise Generator.
The block diagram in fig.1. shows the different sections of the Generator. The basic noise signal is produced in the Noise Generator section where the noise from 2 silicone diodes is added and amplified. The silicone diode is an excellent noise source as far as frequency spectrum is concerned, but the magnitude distribution is unsymmetrical and not gaussian. This draw-back can be overcome by adding the signals from two diodes.
The noise generator is followed by a band pass filter which determines the bandwidth of the final output noise band. The center frequency of the pass band is 2ooo c/s.
In the Balanced Modulator following the band pass filter, the center frequency of the noise band is converted to 120 kc/s by beating with a 122 kc/s sine wave signal.

The unwanted frequencies, which include among others the 122 kc/s from the sine wave oscillator, the 2 kc/s noise signal and the 124 kc/s sum frequency, are rejected partly in the balanced modulator and partly in the following selective variable μ amplifier which also forms an important part of the feedback control circuit.
As a net result a narrow band noise signal with a center frequency of 120 kc/s is present at the output of the variable μ amplifier the bandwidth being adjustable to 10, 30, 100 or 300 c/s.
The final output center frequency is produced by a second frequency conversion where the 120 kc/s noise signal is beated with the signal from Oscillator B the frequency of which is continuously variable in the range 120 to 100 kc/s by means of a tuning condenser. This condenser is specially designed to give a logarithmic variation of the output frequency and intended for outside motor drive. The narrow band noise signal the center frequency of which is now variable between 20 and 20ooo c/s is passed through a low pass filter to the output amplifier and is finally available at the output terminals.

The output signal level is practically independent of the center frequency and will remain constant during a frequency sweep. For many applications, however, other quantities such as current, sound pressure or vibration level should be kept constant. For this purpose a voltage proportional to the quantity to be regulated can be applied to the input of a "compressor" circuit.

The feedback signal which may be the amplified voltage from a condenser microphone as indicated in fig.1 is rectified and used to regulate the gain in the variable μ amplifier thereby automatically controlling the output voltage and keeping the quantity in question constant.

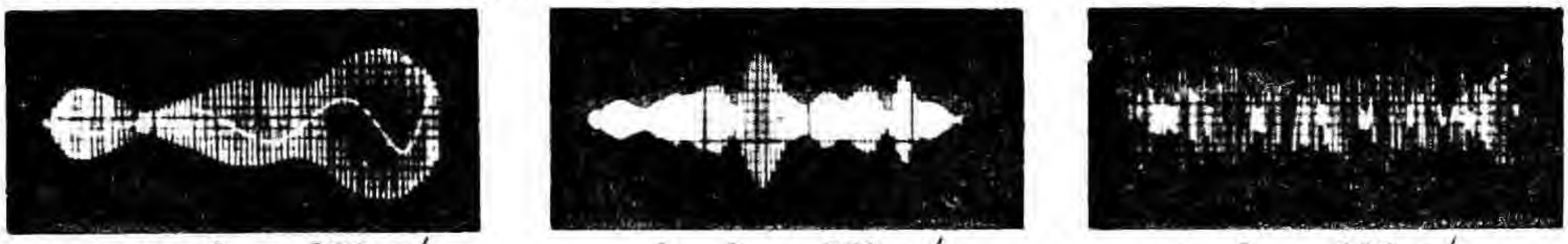

a. f_c = 200 c/s
Δf = 10 c/s

b. f_c = 200 c/s
Δf = 30 c/s

c. f_c = 200 c/s
Δf = 100 c/s

Fig. 2. Narrow Band Gaussian Random Noise

Magnitude Distribution. Oscillograms of narrow band Gaussian random noise of different bandwidths are shown in fig.2. It may be seen that the appearance is similar to that of an amplitude modulated sine wave signal. The instantaneous response is distributed according to the Gaussian distribution and the peak response or envelope according to the Rayleigh distribution. The narrow band noise output from the generator described must be in accordance with these distribution laws when working with as well as without feedback control.

The magnitude distribution of the output from the basic wide band noise generator is not critical as only a very small frequency band is passed through the following filter but all the amplifier sections including the Band Pass Filter and the variable μ amplifier must have a linear voltage characteristic.

In the variable μ amplifier, the gain is controlled by the rectified feedback signal which is used as bias voltage for two amplifier tubes working near cut-off. To obtain a sufficiently linear voltage characteristic here, it has been necessary to operate at very low signal levels.

Compressor Speed. To maintain Rayleigh distribution during automatic frequency scanning when the output voltage is feedback controlled, a sufficiently low compressor speed is just as important as a linear voltage characteristic. Too high a compressor speed will cause unwanted regulation of the noise signal envelope, the compressor trying to keep the amplitude constant. See fig.3.

The speed of the compressor is determined by the time constant of the rectifier for the feedback signal and can be adjusted in steps of 3 to 1. The time constant required for a particular test is a function of the bandwidth of the output signal and the compressor speed should be selected according to table 1:

Bandwidth c/s	10	30	100	300
Compr.Speed db/sec	3	10	30	100

Scanning Speed. The maximum permissible scanning speed depends on the selected compressor speed as the change in frequency must take place at such a rate that the compressor has time to correct the output level.
Considering the test time the compressor speed should thus be as high as possible without affecting the magnitude distribution of the output voltage.
This demand has been the decisive factor in the choice of type of rectifier for the feedback signal.

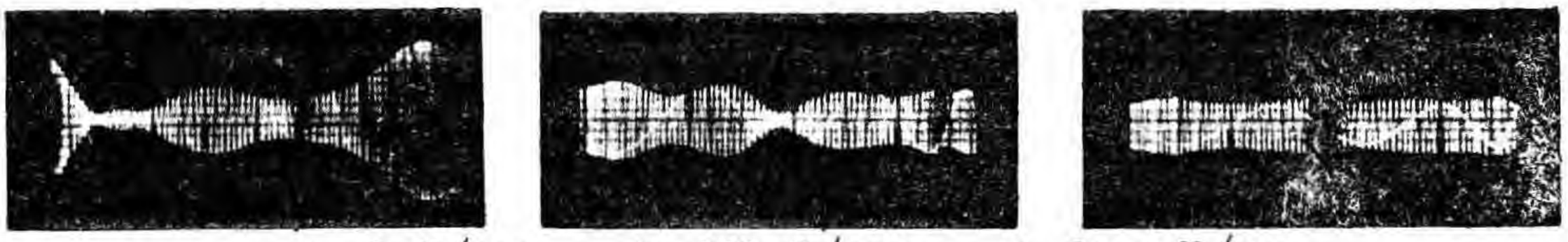

a. 3 db/sec b. 100 db/sec c. 3000 db/sec
f_c = 200 c/s; Δf = 10 c/s

Fig. 3. The Effect of too high Compressor Speed

Rectifier Considerations. The first aim was to incorporate a square law detector as the rms value of the reference signal should be kept constant during the frequency sweep, but with this design of rectifier, the compressor speed for increasing and decreasing reference voltages are different. For increasing levels the regulation is faster and thus determined by the bandwidth of the output voltage. The maximum possible scanning speed, however, will depend on the slower compressor speed at decreasing levels and an unneccessarily long test time will result. In order to obtain equal compressor speeds for increasing and decreasing levels, thereby reducing the test time, an arithmetic average rectifier has been chosen for the compressor circuit. The average value of the reference signal is thus kept constant during the frequency sweep instead of the rms value, but in practice this is of no significance as the ratio between the rms value and the average value of the feedback signal is constant (approx.2 db) for normal applications where the magnitude distribution of the reference signal is gaussian.

Recording of Probability Density Curves.
The figures in table 1 have been found by measuring the magnitude distribution of the positive as well as the negative envelope of the output signal at different bandwidths and different compressor speeds. At correct compressor speed the probability density curve of the envelope shall obey the Rayleigh distribution law. The instrumentation developed for recording the distribution curves includes a rectifier section which can be switched to apply either the positive or the negative envelope to the Y-deflection input of a DC oscilloscope having a short persistence cathode ray tube. The front of the tube is masked by a plate of ebonite with a one millimetre high slit in it and the light passing through the slit reaches a photo multiplier tube mounted in front of the oscilloscope.

The voltage balance in the Y-amplifier output stage can be varied by an external motor drive so that the picture of the envelope is moved slowly from the top to the bottom of the screen. During the movement the current in the photo multiplier will change, being proportional to the time for which the voltage of the envelope has a value causing the electron beam to be opposite the slit in the mask.

After several experiments with different cathode ray tubes, different shapes of slit and different amplitudes of picture on the screen a linear working range of 50 db has been obtained.
By moving the picture of the envelope relative to the slit and applying a voltage proportional to the photo multiplier current to a level recorder the probability density curves can be recorded.

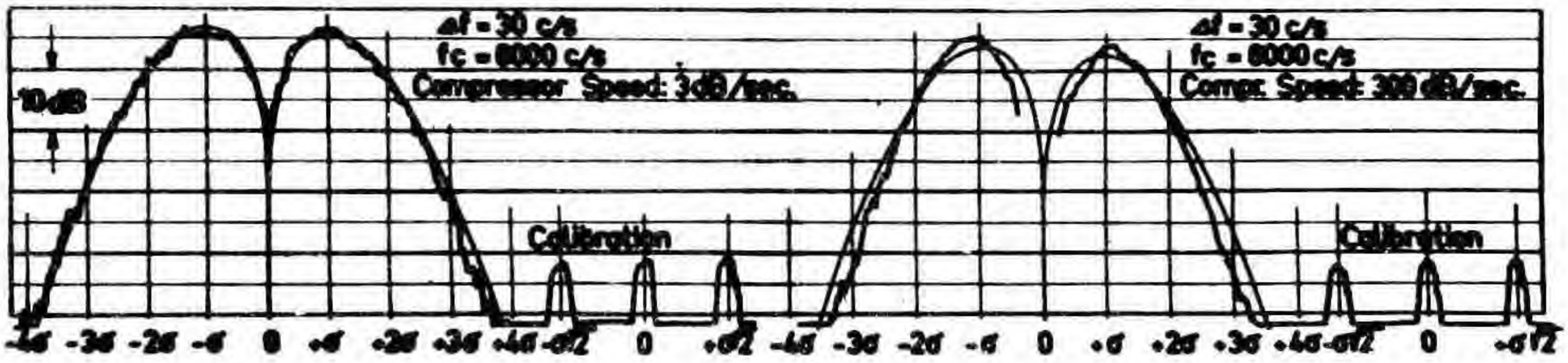

Fig. 4. Peak Distribution Curves.

Fig.4 shows as an example the distribution curves for a noise signal with 30 c/s bandwidth at compressor speeds of 3 and 300 db/sec. At 300 db/sec. the depression of the higher amplitudes is easily detected. The integrating network, which is averaging the voltage applied to the level recorder, must have a time constant, at least in the order of 100 seconds when the bandwidth of the noise is 30 c/s. The recording time is consequently fairly long: for each of the distribution curves shown in fig.4 the time used was 6 hours.

As may be seen from the curves, first the magnitude distribution of the negative envelope and then that of the positive is recorded.
The calibration is carried out by applying a sine wave signal having the same rms value as the investigated signal to the input of the rectifier, and then recording first the negative peak value, then the zero line, and finally the positive peak value. For comparison the Rayleigh distribution curve has been plotted on each recording to the correct scale.

The probability density curves are recorded in logarithmic form to obtain a better accuracy at the high amplitudes than is possible with a linear scale.

If the band noise signal to be analyzed is applied direct to the oscilloscope by-passing the rectifier, the probability density of the instantaneous voltage response can be recorded. For a signal with gaussian distribution the probability density curve will be a parabola when recorded with logarithmic ordinate.

The feedback problems outlined here are mainly related to the design of the Narrow Band Noise Generator. In addition other problems will have to be considered by the user of the instrument. Besides choosing the correct compressor speed it must for instance be checked that amplifiers and transducers incorporated in the feedback loop are capable of handling signals with a crestfactor of at least 3,5.

It is expected that the Narrow Band Noise Generator will be a valuable supplement to existing Noise Generators and will find its applications where advantage can be taken of the constant absolute bandwidth, the exact defined magnitude distribution and the automatic output voltage regulation.

041

FOURTH INTERNATIONAL CONGRESS ON ACOUSTICS
COPENHAGEN 21.-28. AUGUST 1962

SYNTHESIS OF DIRECTIVE ARRAYS - II *

C. D. Lowenstein

Acoustics Research Laboratory, Harvard University
Cambridge, Massachusetts (USA)

Just as electric networks can be built up from standard combinations of circuit elements to obtain a specified transmission characteristic, acoustic arrays can be built up from standard simple arrays to obtain a specified directional characteristic. Although a single lattice network of sufficient complexity will achieve any realizable transmission characteristic, the difficulty of calculating the requisite element values has brought about the development of simple circuits which can be used in combination. Networks have been devised which can be connected in tandem so that the over-all transmission is the product of the transmission characteristics of the individual network sections while the characteristic of one section is not affected by the presence of the other sections. Particular examples are filters designed on an image-parameter basis, and constant-resistance equalizer networks. In either of these cases, networks with the same image impedance can be connected in tandem and each section will make its individual, easily calculable, contribution to the over-all transmission characteristic.

In a similar fashion, we can now form a multi-element array having a directional characteristic which is the product of the characteristics of individual simple two- and three-element arrays. Although the physical procedure for combining the simple arrays is not as easy as merely connecting networks in tandem, the source strengths of the resultant array are easily calculated, as we will see. We will also see that the arrays which are to be combined should have the same inter-element spacing, just as networks to be combined should have the same image impedance. The filter designer has at hand a tabulation of the transmission characteristics of various types of network sections. We must likewise have a tabulation or catalog of the directional responses of various types of simple arrays. From this catalog we can select a combination of arrays having the kind of directivity which we desire for any particular application. Before considering this further, let us discuss the mathematical principles involved.

---

* This work was supported in part by funds made available under a contract with the Office of Naval Research.

The far-field directional response of a linear array of point sources depends only on the relative strengths of the sources and the phase-shift differences in the transmission paths from the sources to the observer. The phase shift between signals arriving at the observer from adjacent sources is $\phi = (2\pi d/\lambda) \sin\theta$, where d is the distance between the sources, λ is the wavelength, and θ is the angle of observation, measured from the normal to the line of the array. The directional characteristic of an array of several equally spaced elements can now be expressed as

$$K(\phi) = \sum C_n e^{-jn\phi},$$

in terms of the phase-shift variable ϕ and the relative strength C_n of the nth source. If the source excitation is uniformly in-phase, then all the C_n's will be positive numbers. If any source is excited 180° out of phase, its C will be negative. Other phases of excitation would correspond to complex C's. We will exclude this possibility, however, so that we can take advantage in this work of the algebraic properties of polynomials with real coefficients.

Following a method of analysis first used extensively by Schelkunoff,* we will represent an array and its directional response as a polynomial in a complex variable $z = e^{-j\phi}$. As the angle of observation θ is varied from 0 to $\pi/2$, the phase shift ϕ varies from 0 to $2\pi d/\lambda$ and the point z travels clockwise around the unit circle from +1 to $e^{-j2\pi d/\lambda}$. For the common half-wave spaced array, $d = \lambda/2$, and z travels around the unit circle from +1 to -1 as θ varies from 0 to $\pi/2$.

By substituting $z = e^{-j\phi}$ in the above representation of the directional response as a complex function of the real variable ϕ, we obtain a representation of the response as a real polynomial in the complex variable z:

$$K(z) = \sum C_n z^n.$$

Each term of this polynomial represents the response of one element of the array; the response of the whole array is the sum of the contributions from all of its elements. We may say that each term of the polynomial corresponds to an element of the array; thus the kth element has strength C_k and is represented by $C_k z^k$.

It follows that every array with in-phase excitation can be represented by a polynomial with real coefficients and, conversely, every real polynomial can be interpreted as corresponding to an in-phase array. The product of two polynomials is also, of course, a polynomial, and it too may be considered to represent an array.

---

* Schelkunoff, S. A., "A mathematical theory of linear arrays," Bell System Tech. J. 22, 80 (1943).

This product array has as its directional characteristic the product of the directional characteristics of the arrays represented by the two original polynomials.

The multiplication of array responses in this way corresponds physically to the substitution of an entire array of one type for each element of an array of a second type. When the inter-element spacing of the two arrays to be compounded is the same, nearly all of the elements of the product array are located so that they can be merged into one another, thus reducing the total number of elements in the product to less than the sum of the numbers of elements in the original arrays. It is in this case that the multiplication of array responses can be most easily represented by the multiplication of the corresponding polynomials, since the variable z in the two polynomials is the same.

The polynomial K(z) which represents an array has all of the usual algebraic properties of polynomials with real coefficients. In particular, any arbitrary K(z) can always be factored into real linear and quadratic factors (Gauss, 1799). By our identification of real polynomials and arrays, each linear factor of an array polynomial corresponds to a two-element array and each quadratic factor to a three-element array. Since the whole array is the product of its factors, its directivity is the product of the directional responses of the corresponding simple two- and three-element arrays.

This method of finding the directivity of an array in terms of its simple factors is not a suitable means for the calculation of the response of an arbitrary array. The work expended in finding the factors of an arbitrary polynomial far outweighs the work saved by the simplicity of the calculation of the responses of the simple arrays.

On the other hand, since the response of a simple array can be calculated easily, we can select a representative sample from among all possible simple arrays and then synthesize a more complicated directivity function from combinations of these elementary functions. Because every polynomial can be factored in this simple way, we are sure that no possibilities will have been overlooked when we restrict ourselves to combinations of two- and three-element arrays as the basis for our synthesis.

Two problems remain to be solved before this synthesis method can be applied. What is needed is a systematic method for compiling the catalog of representative array responses, and a simplified method for multiplying selected responses to form the directional characteristic of the resultant array. The second of these problems can readily be solved by plotting the responses of the simple arrays on a logarithmic or decibel scale. In this way the multiplication is reduced to a graphical addition.

In the compilation of the catalog of array responses, there are several parameters of the array which can be varied. The power supplied to each source can have any value, and each of the end sources can have either of two phases relative to the center source. The representation of "all possible" arrays can be systematized by first normalizing the total power input to unity. To do this, we need to select three excitation coefficients such that the sum of their squares is 1. This suggests that we make the coefficients a set of direction cosines. The variation of one "angle" will vary the proportion of the total power delivered to the center element through the entire range of possibilities. The variation of the other "angle" over half of its range will cover all possible distributions of the remaining power between the end elements. The second half of its range will again cover the same power distributions, but will produce arrays with the opposite phasing. Two-element arrays can be treated as the special case in which the power supplied to one end element of a three-element array is zero. In this way, the variation of these "angles" through their ranges will generate all possible two- and three-element arrays. As we have previously seen, it is possible to construct every linear array as a combination of these elementary arrays; thus our method is all-inclusive.

P41

FOURTH INTERNATIONAL CONGRESS ON ACOUSTICS
COPENHAGEN 21.-28. AUGUST 1962

The Propagation of Acoustic Pulses in Linear Viscoelastic Solids

H. Kolsky , Division of Applied Mathematics, Brown University, Providence, Rhode Island, USA

The mechanical behavior of a linear viscoelastic solid may be represented in a number of mathematically equivalent ways. For studying wave propagation in such materials, probably the most convenient description is in terms of complex elastic moduli. If for simplicity we consider a uniaxial stress σ, acting on a section of a linear viscoelastic rod and this stress varies simusoidally with time at angular frequency p, so that $\sigma = \sigma_o \exp(ipt)$ then the longitudinal strain ε will be given by

$$\varepsilon = \varepsilon_o \exp(ipt - \delta)$$

so that

$$\sigma/\varepsilon = (\sigma_o/\varepsilon_o)\exp(i\delta) = E_1 + iE_2 \qquad (1)$$

where E_1 and E_2 are termed the real and imaginary parts of the complex modulus E. For the limiting case of an elastic solid E_2 is zero and E_1 has a constant value, namely Young's modulus. For viscoelastic solids both E_1 and E_2 are found to depend on the angular frequency p. Often $E^* = \sigma_o/\varepsilon_o = \sqrt{(E_1^2 + E_2^2)}$ and $\tan\delta = E_2/E_1$ are used to describe the behavior instead of E_2 and E_1 since E^* and $\tan\delta$ are quantities which can be determined directly from vibration experiments.

If we now consider the propagation of a longitudinal wave along a thin viscoelastic rod, the equation of motion is

$$\partial\sigma/\partial x = \rho(\partial^2 u/\partial t^2) \qquad (2)$$

where u is the longitudinal displacement a distance x along the rod at time t, and $\varepsilon = \partial u/\partial x$. From (1) and (2) we then find

$$(E_1 + iE_2)\partial^2 u/\partial x^2 = \rho(\partial^2 u/\partial t^2) \qquad (3)$$

and the solution of (3) for a sinusoidal displacement $u = u_o \exp(ipt)$ at the origin $x = 0$ is

$$u = u_o \exp[-\alpha x + ip(t - x/c)] \qquad (4)$$

where

$$c = (E^*/\rho)^{\frac{1}{2}} \sec(\delta/2) \quad \text{and} \quad \alpha = (p/c)\tan(\delta/2) \qquad (5)$$

Since for most viscoelastic solids $\tan\delta < 0.1$ equations (5) may be approximated to by

$$c = \sqrt{(E^*/\rho)} \quad \text{and} \quad \alpha = (p/2c)\tan\delta \qquad (6)$$

Thus if we know the values of E^* and $\tan\delta$ (or E_1 and E_2) for the rod at an angular frequency p, equations (6) give us the phase velocity and attenuation of a train of simusoidal waves of that frequency along the rod. Since the medium is linear, the shape of any disturbance can be represented as a Fourier integral and if the values of E^* and $\tan\delta$ are known over a sufficiently wide range of frequencies, the spatial distribution of the disturbance at any time or the temporal distribution at any point in the rod can be calculated. Thus we may describe the displacement at the origin $x = 0$ by $u \int_0^\infty A_p \exp(ipt)dp$, where A_p is in general complex. Then at a distance x along the rod we have

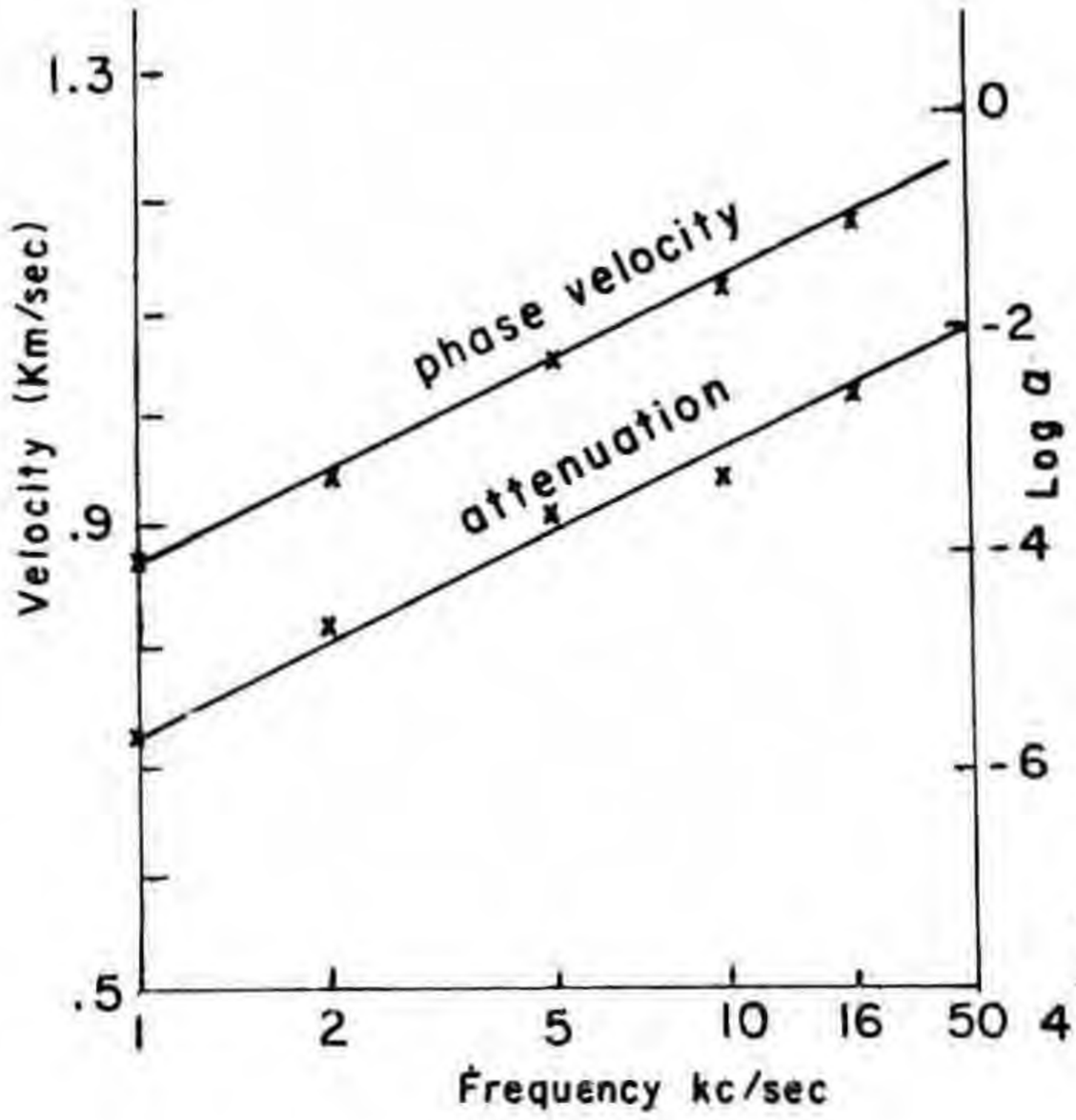

FIG. 1

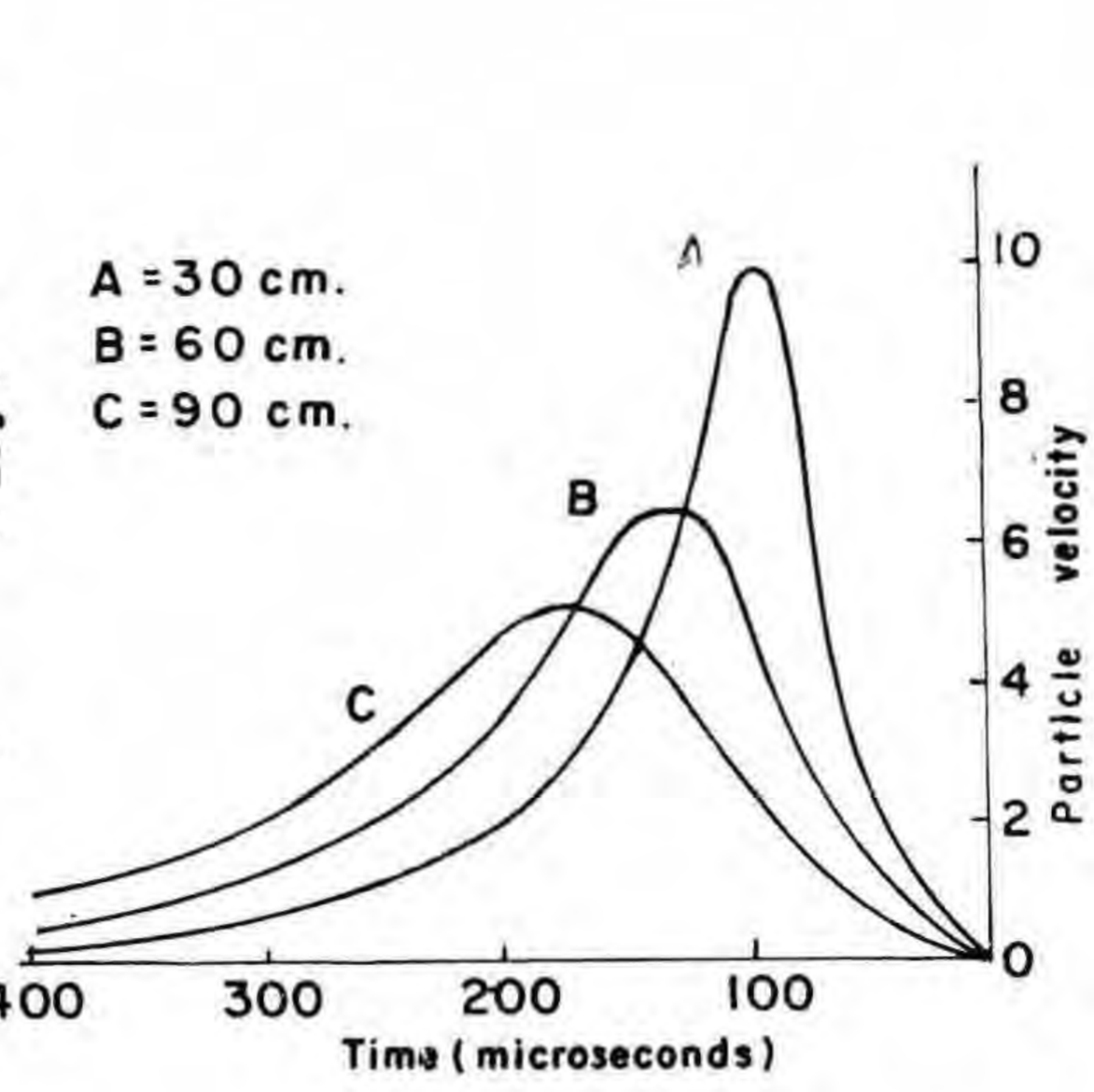

FIG. 2

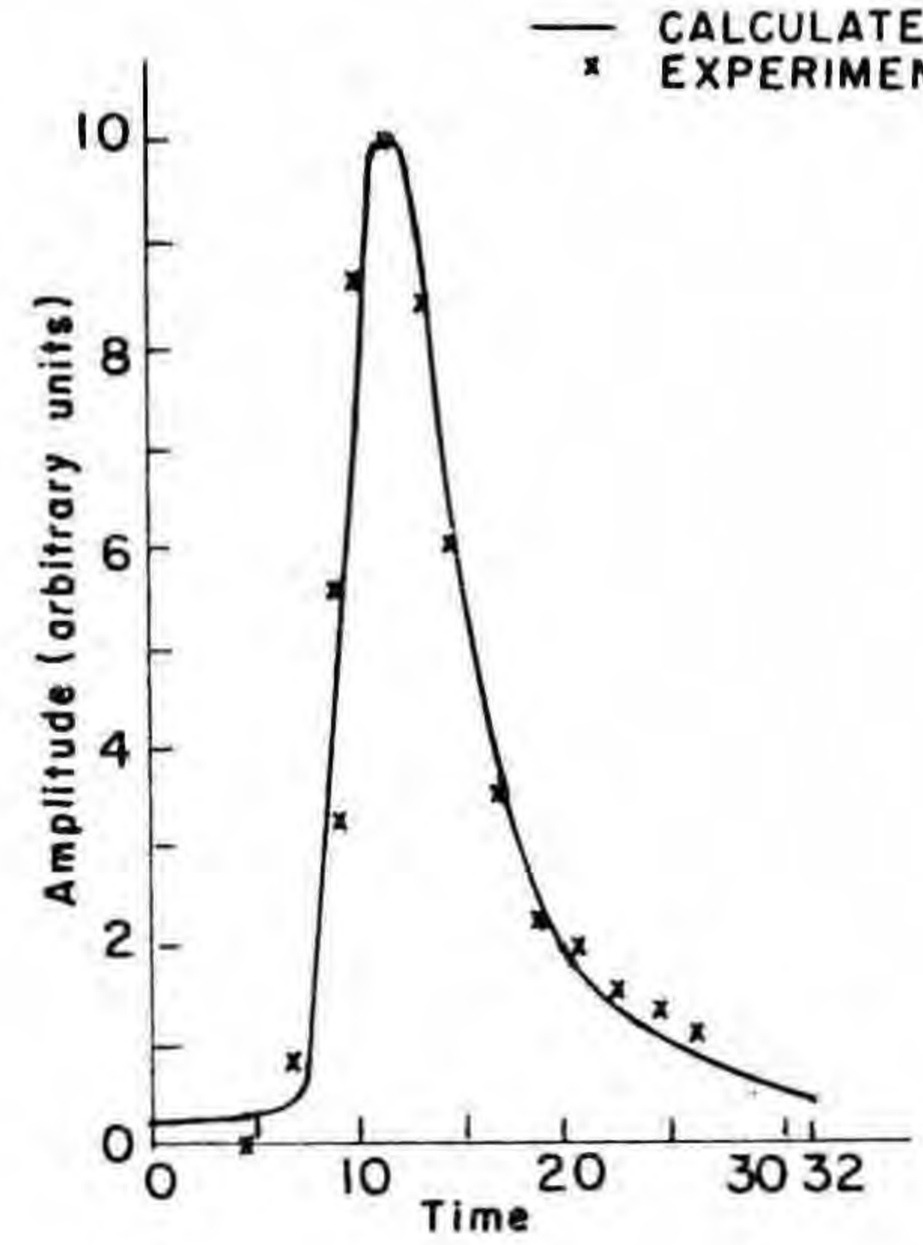

FIG. 3

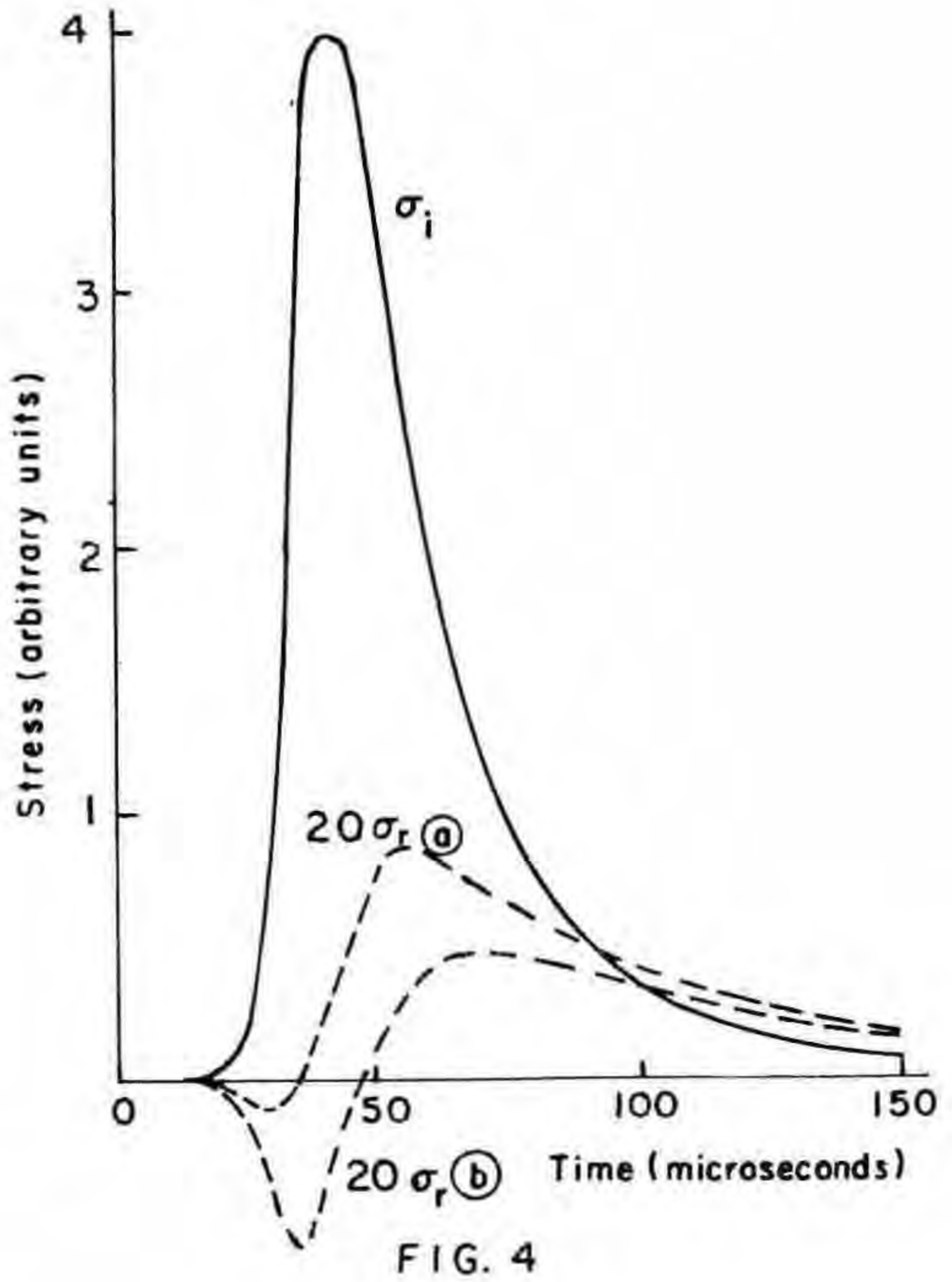

FIG. 4

$$u = \int_o^\infty A_p \exp[-\alpha x + ip(t - x/c)]\,dp \qquad (7)$$

where α and c are functions of frequency given by equations (5).

Now for many real viscoelastic solids such as polystyrene, polymethylmethacrylate (Plexiglas, Perspex), polyethylene, ebonite, $\tan\delta$ is reasonably constant over wide ranges of frequency. For such materials it may be shown from the theory of linear viscoelasticity that an approximate relation exists for expressing the modulus E^* as a function of p. (See references 1, 2, 3). This relation is

$$E_p^* = E_o^* [1 + (2 \tan\delta/\pi)\log (p/p_o)] \qquad (8)$$

where E_o^* is the value of E^* at some reference frequency p_o. From equation (6) we see that if $\tan\delta$ is sufficiently small for $\tan^2\delta$ to be neglected, we may write

$$c = c_o[1 + (\tan\delta/\pi)\log p/p_o] \qquad (9)$$

For such materials α should be proportional to p and the velocity of propagation should increase linearly with the logarithm of the frequency. Figure 1 shows experimental results for the propagation of longitudinal sinusoidal waves along filaments of polyethylene at a number of different frequencies [4]. It may be seen that a linear relation between c and log p exists over this frequency range. On the same figure, log α is plotted against log p and since the graph is here a straight line of unit gradient, α is proportional to p.

We will now consider some of the consequences of equation (6) for a material for which $\tan\delta$ is substantially constant over a reasonably wide range of frequency so that equation (9) represents the dependence of velocity on frequency. As a mechanical pulse is propagated through such a material the high frequency components travel with higher phase velocities than those of lower frequency and are at the same time attenuated more rapidly. As a result a symmetrical pulse becomes asymmetrical in shape and at the same time decreases in amplitude as it travels along a viscoelastic rod. Figure 2 shows the experimental results of the change in the shape of a pulse travelling along a rod of polyethylene; the initial pulse was here a sharp impulse produced by the detonation of a very small explosive charge. In Figure 2 the pulse shape is expressed in terms of particle velocity, and it should be emphasized that whereas in an elastic rod the pulse shape is the same whether particle velocity, stress or strain are considered, this is no longer true for viscoelastic solids. Thus for an elastic pulse the displacement u is given by $u = f(x-ct)$ so that the particle velocity is $\partial u/\partial t = -cf'(x-ct)$, and the strain ε is $\partial u/\partial x = f'(x-ct)$ and the stress $\sigma = E\varepsilon = Ef'(x-ct)$. For a viscoelastic solid the expression for u is given by equation (7) so that the particle velocity v is given by

$$\frac{\partial u}{\partial t} = \int_o^\infty ip\, A_p \exp[-\alpha x + ip(t - x/c)]\,dp \qquad (10)$$

the strain ε is

$$\frac{\partial u}{\partial x} = \int_o^\infty (-\alpha + ip/c)A_p \exp[-\alpha x + ip(t - x/c)]\,dp \qquad (11)$$

and the stress σ is given by

$$\sigma = [E_1 + iE_2]\partial u/\partial x = \int_o^\infty (E_1 + iE_2)(-\alpha + ip/c)A_p \exp[-\alpha x + ip(t - x/c)]\,dp \qquad (12)$$

since α, c, E_1 and E_2 all depend on p it is clear that (10), (11) and (12) will all be different in shape. Some computations on real viscoelastic solids [5] have shown, however, that for smooth pulses so long as $\tan\delta$ is small the difference in pulse shape, though appreciable, is not large except very near the beginning and the end of the pulse. Equations (7), (10), (11) and (12) enable us to predict changes in pulse shape if we know how c and α vary with frequency for a given solid. Where experimental data for these qualities are available over a considerable frequency range numerical Fourier syntheses yield pulse shapes which are found to be close to those observed experimentally [3]. For a large class of solids however equation

(9) can be used for predicting pulse shapes to a high degree of accuracy. Under these conditions, if the pulse is assumed to be a sharp blow which can be represented by a Dirac δ-function at the origin ($x = 0$); the pulse shape at any distance x along the rod can then be represented by an approximate expression derived from Equation (10). In order to do this, a frame of reference travelling with the pulse with velocity c' must be used, and the pulse shape is given with time abscissae in units of $(x \tan\delta)/c'$. Figure 3 shows this 'universal pulse shape' calculated by numerical Fourier synthesis, the particle velocity is in arbitrary units, whereas on the time axis each unit corresponds $(\pi x \tan\delta)/16c'$. The experimental results obtained for the distribution of particle velocity in a pulse which was initially one or two microseconds in duration, and which travelled six metres along a rod of polymethylmethacrylate, are shown on the same figure, and the agreement between theory and experiment may be seen to be very good.

Another interesting problem is the reflection of stress waves at the boundary between two viscoelastic solids, or between an elastic and a viscoelastic solid. The amplitude and phase of the reflected and transmitted waves will depend on frequency, so that when a pulse is reflected at such a boundary, the Fourier spectra of the transmitted and reflected pulses may be quite different from those of the incident pulse. An extreme example of this is shown in Figure 4. Calculations have here been carried out for a pulse produced by a δ-function input in stress at one end of a polymethylmethacrylate rod 120 cms. in length. The other end of the rod is assumed to be in contact with the end of an elastic rod for which the value of ρc is such that the low frequency Fourier components of the pulse are reflected in one phase, and the Fourier components above a certain frequency are reflected in the opposite phase. (This situation occurs in certain frequency ranges, if the second rod is a polystyrene one.) The shapes of the reflected stress pulses for two different values of ρc for the elastic rod are shown in the figure, and it may be seen that the reflected pulses are s-shaped, although the initial pulse was unidirectional. The reflected pulses σ_r in the figure are shown at twenty times their true scale compared with the incident pulse σ_i.

References

(1) Gross, B., Mathematical Structure of Theories of Viscoelasticity, Paris, Hermann, (1953).

(2) Hunter, S. C., Progress in Solid Mechanics, Vol. I, p. 1, North Holland, Amsterdam, (1959).

(3) Kolsky, H., Int. Symposium on Stress Wave Propagation, p. 59, Interscience, New York, (1960).

(4) Hillier, K. W., Proc. Phys. Soc., B 63, p. 70, (1949).

(5) Kolsky, H. and Lee, S. S., Brown University Technical Report No. 5, Contract Nonr 562(30), (1962).

The work described in this paper was supported by the Office of Naval Research, under Contract Nonr 562(30), with Brown University.

G42

FOURTH INTERNATIONAL CONGRESS ON ACOUSTICS
COPENHAGEN 21.-28. AUGUST 1962

SPEECH SYNTHESIS

John L. Kelly, Jr., and Carol C. Lochbaum, Bell Telephone Laboratories, Incorporated, Murray Hill, New Jersey

Introduction

The goal of the investigations reported in this paper is the production of synthetic speech from an input consisting only of the names of phonemes and a minimum of pitch and timing information. The work was all done on a digital computer, the IBM 7090. Two general approaches were attempted, based respectively on a terminal analogue and an artificial vocal tract. The first approach uses for an intermediate language formant frequencies, bandwidths, and excitation parameters; while the second uses cross-sectional areas of the vocal tract, nasal coupling and excitation parameters. The two programs work on the same general principle: stored tables give values of the parameters (acoustic or articulatory, respectively) corresponding to each phoneme, and various ad-hoc rules cause smooth transitions to occur between phonemes. The ultimate output of each program is a digital tape representing the sound pressure waveform, which can be translated to analog. The terminal analog has been described elsewhere, and therefore we will concentrate mainly on the vocal tract analog.

The Artificial Vocal Tract

Several practical considerations served to determine the method of integrating the wave equation in the computer. The most important of these was running time. For reasons of economy, it was necessary that the program run in about forty times real time on an IBM 7090. Another requirement was that the output sampling rate be no greater than 20 kc. It was found that these requirements could be met be approximating the tract with 21 delay lines with one fortieth of a millisecond delay and characteristic impedance proportional to the area of the tract at a given place. Figure 1 shows a typical junction between sections and a signal flow diagram which is equivalent. The flow diagram shown in Fig. 2 is equivalent except that the ultimate output is delayed. Since the delays of Fig. 2 are the same as the sampling times, it can be simulated with difference equations in the computer.

The figures are included merely to give a rough idea of the principle involved. Many features are not shown and will be explained below:

Damping - Since there is no way to obtain frequency dependent damping with the model, a constant damping was inserted by attenuating the backward-going pressure wave at each junction. The amount (one part in 128) was chosen to give the formants the right average widths (and to avoid a multiplication).

Terminal Impedances - The reflection coefficient at the glottis is computed to correspond to source impedance of 0.2 cm^2 (a nice thing about computer simulation is that all proportionality constants may be taken to be one). This is the value used by Fant.[1] Strictly speaking the

---

[1] Gunnar Fant, "Acoustic Theory of Speech Production," published by Mouton and Co., 'S-Gravenhage, 1960.

radiation impedance is zero to the same order of accuracy that holds for the entire model. Nevertheless, some extra damping was included at the mouth end of the tract.

Nasal Tract - The nose was approximated by four sections three times as long as those of the oral tract and with more damping.

Voice Excitation - The excitation is obtained by operating on a pair of pulses (one for opening and one for closing of the glottis) with difference equations for spectral shaping. These correspond to several poles and zeros in the complex plane and tend to control voice quality.

Aspiration and Affrication - These are inserted at the glottis and place of greatest constriction respectively.

Control Methods

Before discussing the signal generator program, which controls the motions of the tract in response to a phonemic input, I will discuss in some detail the timing of the control system. This is not due to a desire to delve into programming techniques, but because some of the compromises made in the interest of speed might affect performance. To begin with, the tract configuration is held constant for intervals of ten samples (0.5 msec). It is changed over eight of these intervals (4 msec) by linearly interpolating the excitation parameters and reflection coefficients to new values determined by the signal generator program. Thus, it is only at the end of each 4 msec interval that new area information can be supplied.

The Signal Generator

To drive the tract, it is necessary to supply 26 parameters as functions of time. These consist of 21 cross-sectional areas, nasal coupling, pitch, buzz, aspiration, and affrication. The signal generator program accomplishes this by reading the names of phonemes off of input cards and following certain rules.

An imput card consists of 6 columns. The first contains the name of the phoneme, in a machine readable code equivalent to the IPA, and the next indicates the stress of vowels. The other 4 may be left blank or may be used to control loudness, pitch, transition time, and duration. If any of these columns are left blank, the program computes the corresponding parameters by rule.

The general principle of operation of the program consists of one simple rule and endless exceptions. The rule is that all parameters change linearly with time from their old values to a set obtained from stored tables, one for each phoneme. The transition time is a function of the old and the new phoneme. All parameters are then held constant for a duration determined by more tables. Some of the more interesting exceptions are the following:

Nasalized Vowels - Vowels adjacent to nasal consonants are partly nasalized.

Labials - B,M,P, and W have no fixed configuration. The stops are formed by closing the lips, leaving the remainder of the tract as it was. While the lips are closed the remaining sections change over to their values for the next sound. W is made similarly but with the lips only partly closed.

Neutral Tract - This is a tract configuration corresponding to a sound between æ and ʌ . The tract returns to this position during silence. This serves to give a release on stops.

Unstressed Vowels - These are formed by averaging the configuration corresponding to the stressed vowel with that of the neutral tract. The duration is zero, i.e., these sounds are all transition.

Context - Some sounds (other than the labials mentioned above) are made by contextual rules. K,G, and NG use different configurations according as the adjacent vowels are front, back or middle. If they are different, the tract is changed during closure.

Conclusions and Results

At the time of writing of this paper the speech quality is far from satisfactory. The authors believe, however, that the trouble is mainly in the stored configurations and not in the principles involved. Accurate area information for all the sounds involved is difficult to acquire. The X-ray data in Fant's excellent book[1] served as a starting point, but experimentation is laborious with a digital computer. Also there is no simple way to correct configurations by the examination of spectrograms. The terminal analog is much better off in this respect. In fact the authors are convinced that a superior talking program could be written using a terminal analog driven by a program with the contextual features of the one described here.

Nevertheless, the vocal tract analog has many clear advantages. The complex sequence of spectral events occurring in the production of a consonant comes about quite naturally. For example, if excitation containing a DC component is left on during the closure time of a stop consonant, a burst will occur automatically upon release. It is quite possible that experimentation with this model will prove valuable in the design of a more satisfactory terminal analog.

TITEL SPEECH SYNTHESIS

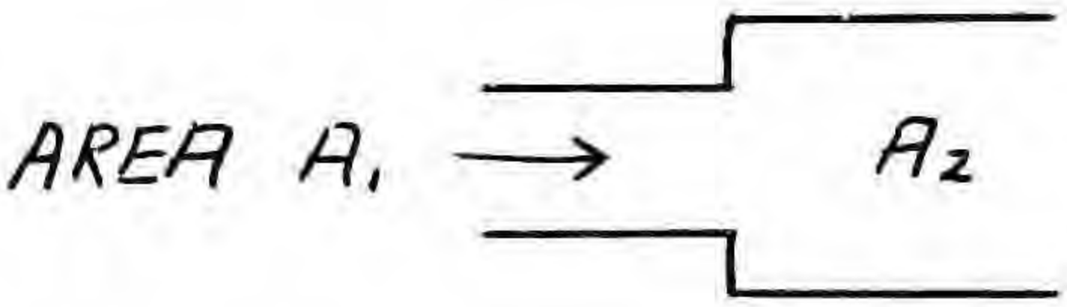

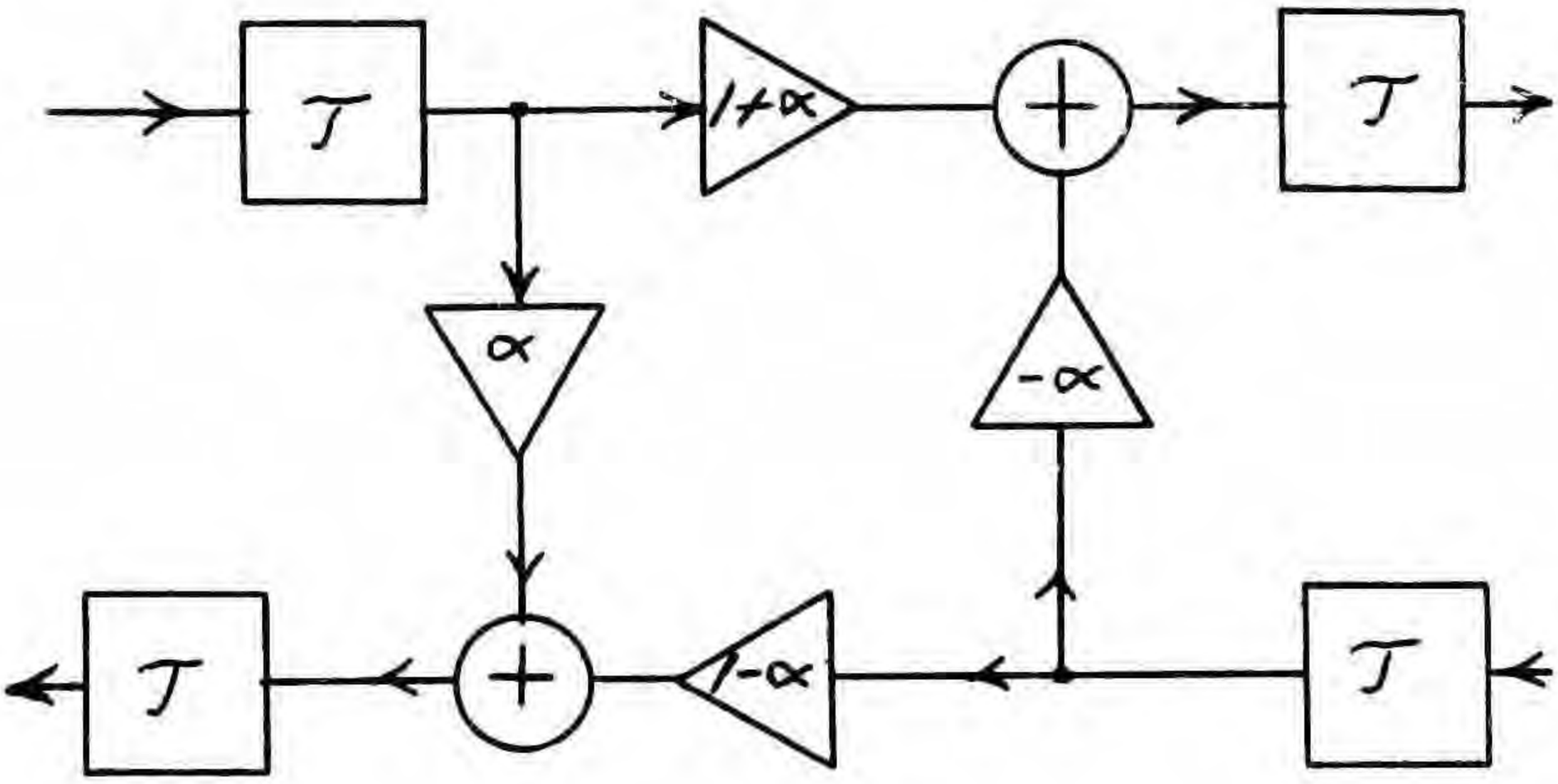

$$\alpha = \frac{A_1 - A_2}{A_1 + A_2}$$

Figure 1 - Junction of two sections and equivalent flow diagram.

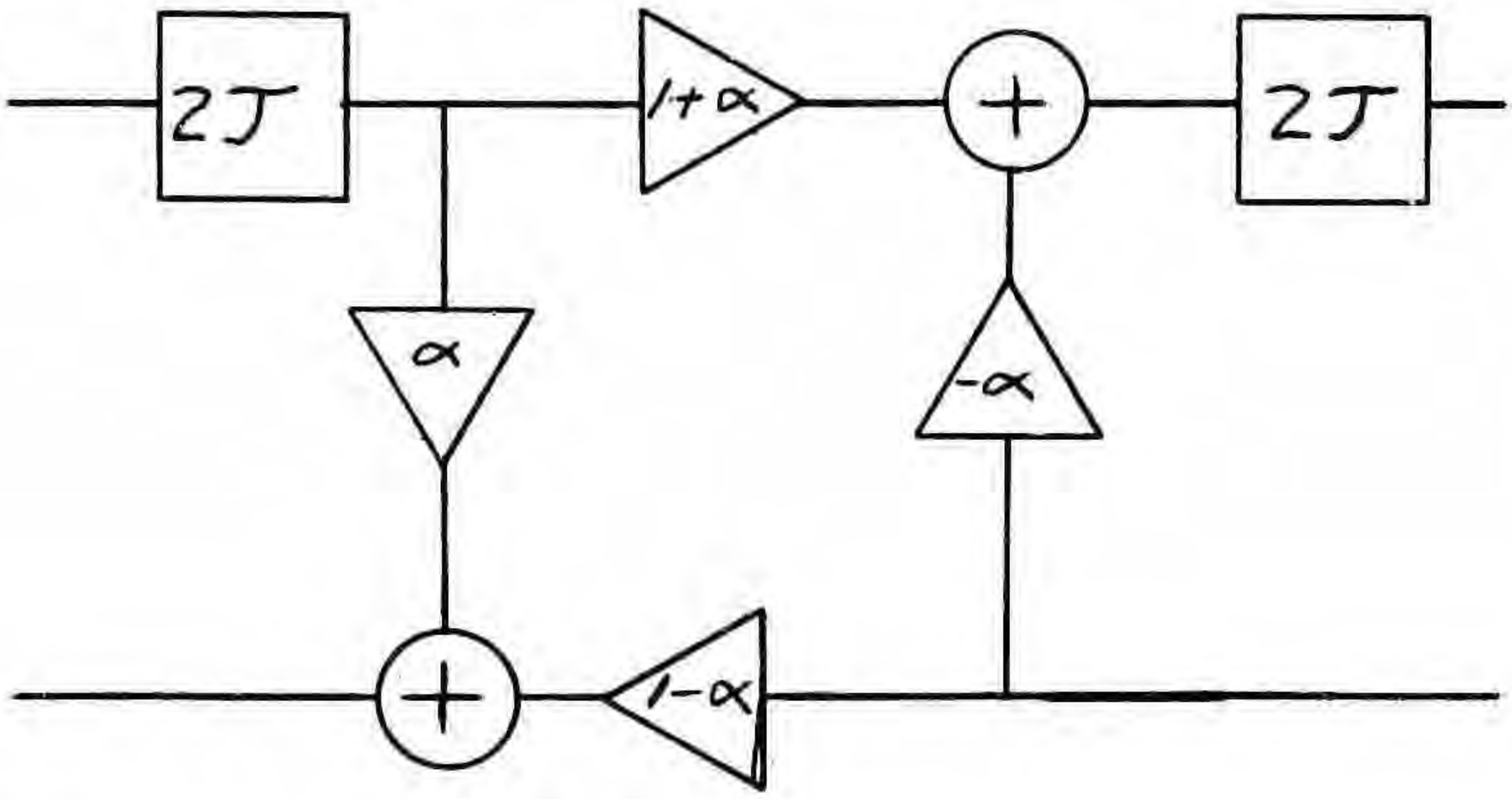

Figure 2 - Simplified flow diagram.

H42

FOURTH INTERNATIONAL CONGRESS ON ACOUSTICS
COPENHAGEN 21.-28. AUGUST 1962

THE IMPLEMENTATION OF A HEARING CONSERVATION PROGRAM*

Dr. Keith K. Neely,
Defence Research Medical Laboratories, Toronto, Ontario, Canada.

Adequate Hearing Conservation Programs will prevent most individuals from suffering losses in hearing due to exposure to high-intensity sound, i.e., continuous or interrupted sound that exceeds 85 decibels (db re: 0.0002 microbar).

The possible results of exposure to high-intensity sound include, in addition to temporary or permanent losses of hearing, non-auditory effects such as disruption of voice communication, changes in behaviour and in the performance of skilled and unskilled tasks, and mechanical or pathological damage to the body[3]. Directly or indirectly these effects may compel changes in operational procedures or may even preclude the successful completion of an assignment.

The degree and type of hearing loss suffered by any individual will be determined by his susceptibility to noise, the overall level and spectrum of the noise, and the number of hazardous exposures and length of time between such exposures.

Several years ago the Defence Research Medical Laboratories of the Defence Research Board of Canada were asked to assist in developing a Hearing Conservation Program for the Canadian Armed Forces. A program was developed which includes the designation of hazardous exposure areas, hearing conservation criteria, sound abatement procedures, hearing testing (enlistment, monitoring and discharge), use of efficient ear protection devices, an education program and periodic review of results[4].

Designation of Hazardous Exposure Areas

Measurements of noise in potentially hazardous areas should be made by trained personnel and should include overall level and spectral analyses[2]. Measurements should be made at the head level of the individual(s) working at these positions. Equipment is available that permits such analyses to be made efficiently, quickly and economically. Information should also be obtained as to the number and length of the hazardous exposures. Such information should permit prediction of maximum permissible exposure times. Wherever the overall sound pressure levels of the noise exceed 85 db exposure should be considered as potentially hazardous.

Hearing Conservation Criteria

Criteria for the conservation of hearing should ensure protection for most individuals and permit effective conservation measures in a majority of situations, with no need for the continual collection of large amounts of data and complex calculations. Once the environment of a particular noise generator has been designated as

*Defence Research Board of Canada, DRML Report 242-3.

hazardous, periodic surveys will indicate any change in this status or the requirement for changes in hearing conservation or sound abatement procedures. Modification of the noise generator or changes in operating procedures should always be accompanied by a survey of the noise levels and spectra.

The Defence Research Medical Laboratories have prepared criteria for protection of hearing during exposure to high-intensity sound (see Table I).

Table I

CRITERIA FOR PROTECTION OF HEARING DURING EXPOSURE TO HIGH-INTENSITY SOUND

Sound Pressure Level (db re: 0.0002 microbar)	Exposure Time	Type of Protection Required
85 - 100	4 hours per day	Ear Plugs or Earmuffs
100 - 130	any	Ear Plugs or Earmuffs
130 - 150	any	Ear Plugs and Earmuffs
150 -	any	Whole Body Protection

If these criteria are properly applied adequate hearing protection should be achieved for most individuals. In noise environments of 90 to 120 db the efficiency of communication by voice or other sounds may be increased by the use of ear plugs or earmuffs.

Sound Abatement Procedures

The sound abatement procedures, depending upon the sources and nature of the noise environment, may include modification of the noise sources, operation of the noise-generators at reduced power, isolation of such generators with sound-attenuating structures, and reduction of the number and duration of generator operations.

Hearing Testing

Hearing tests should be conducted by qualified personnel with calibrated instruments in proper sound environments. Patients being tested must be free from head colds and temporary deafness; the ear canals must be clean and free of wax. Both automatic and manual types of audiometers are suitable for routine and screening tests; manually operated audiometers only are satisfactory for clinical evaluations.

Accurate audiograms may be obtained only when at least 48 hours has elapsed since the individual's last exposure to high-intensity sound. A complete air conduction hearing test should be administered as part of the medical examination at the time of enlistment and discharge. A test with frequencies of at least 2000 and 4000 cps should be given at intervals of not more than six months to all personnel routinely exposed to high-intensity sound. For individuals exposed to continuous noise, hearing losses at these frequencies are indicative of losses at the other speech frequencies also[1].

Any changes of 15 decibels or more in hearing acuity requires the administration of a complete air conduction hearing test three times during a period of several days in which the individual is not exposed to high-intensity sound.

The insertion of the audiometer earphones into adequate sound-attenuating earmuffs may provide a proper sound environment for many testing situations. Prefabricated hearing-test booths are usually more efficient and more economical than testing areas built into existing structures. Mobile hearing-test vehicles are useful when tests must be conducted on personnel in scattered locations.

Use of Efficient Ear Protector Devices

Ear protectors are effective only when worn[5]. Strict insistence upon their use is mandatory when exposure to noise is hazardous although it may not result in discomfort or pain. Training and patience will overcome initial difficulties in the perception of auditory stimuli in noise conditions, while in quiet environments the loosening or removal of the ear protecting device may be desirable.

Maximum hearing protection can be obtained only by properly fitted ear plugs, earmuffs or helmets. The sound attenuation characteristics of some devices used by the Canadian Armed Forces are shown in Table II.

Table II

SOUND ATTENUATION (DECIBELS) OF VARIOUS EAR PROTECTOR DEVICES

Device	Frequencies (cps)								
	125	250	500	1000	2000	3000	4000	6000	8000
NRC Type Earmuff	25	27	39	40	41	44	45	36	32
NRC Type Earmuff in Nylon Helmet	23	26	31	39	36	44	46	35	33
V-51R Type Ear Plug	15	14	16	19	28	28	23	25	31

The V-51R type ear plug was developed at the Psycho-Acoustic Laboratory, Harvard, by Veneklasen[7]. The NRC earmuff was developed at the Canadian National Research Council by Shaw and Thiessen[6]. Both of these types may be worn for many hours without discomfort and both should be made personal issue items.

Education Program

The success of any Hearing Conservation Program will depend on the practicability of the procedures, the enthusiasm of the supervisors, the information given to the personnel involved and the degree of cooperation between the various members of the hearing conservation team (engineers, physicians, audiologists, and administrators). Individuals who are exposed to high-intensity sound should be aware of the risks accompanying such exposure and of the simple procedures and proper protective equipment by which these risks can be eliminated.

Review of Results

The results of the hearing conservation program should be reviewed periodically to ascertain its effectiveness. Such reviews will permit amendments to be made quickly and effectively.

Summary

Exposure to high-intensity sound need not result in hearing losses provided that suitable but simple precautions are taken. Information is available from which an adequate program for hearing conservation can be developed and successfully completed.

What is needed, in many instances, is recognition of the problem.

References

1. Glorig, A., Noise and Your Ear, (New York: Greene and Stratton, 1958), 152 pp.
2. Neely, Keith K., "The Measurement of Noise", Bulletin, Academy of Medicine (Toronto), December, 1956, pp. 60-63.
3. Neely, Keith K., "Noise - Some Implications for Aviation", Can. Aeronautical Journal III, November, 1957, pp. 312-317.
4. Neely, Keith K., "Hearing Conservation for the Armed Forces", Med. Ser. Jour. (Canada), April, 1959, pp. 235-247.
5. Neely, Keith K., "Protection from Noise", Flight Comment, RCAF, July-August, 1961, pp. 10-11.
6. Shaw, E.A.G., and G.J. Thiessen, "Improved Cushion for Ear Defenders", Jour. Acoust. Soc. Am. XXXI, January, 1958, pp. 24-36.
7. Shaw, W.A., "The Development of Ear Wardens Type V-51R", OSRD Report No. 5122, 1 July, 1945, 31 pp.

J42

FOURTH INTERNATIONAL CONGRESS ON ACOUSTICS
COPENHAGEN 21.-28. AUGUST 1962

Effect of Interstitials Due to Water on the Attenuation and Velocity of Ultrasonic Waves, and on the Thermal Resistance of Sodium Chloride Crystals

Warren P. Mason and Konrad Brugger

Bell Telephone Laboratories, Incorporated, Murray Hill, New Jersey

Recently measurements[1] of the attenuation and velocity of shear and longitudinal sound waves in sodium chloride crystals, have shown effects connected with a spectrum of relaxation frequencies at temperatures below 10°K. These effects occur for crystals grown in the atmosphere (Harshaw) but are absent for vacuum grown crystals (Isomet). By annealing the Isomet crystals in a water vapor atmosphere at 750°C for 11 hours, the same set of relaxations can be made to occur. Measurements were made for a variety of waves and directions and it was found that if a wave produced shear stress in the {110} planes and along <110> directions, the effect occurred. This is the same stress sensitivity as found for dislocations in NaCl. Figure 1, solid line, shows the measured attenuation for a 57MC shear wave propagated along a [110] direction with the polarization along [1$\bar{1}$0]. The relaxation effect is the difference between the solid line and the short dashed line, which is caused mostly by dislocation damping. This is confirmed by shear wave measurements with the polarization along [100] - an orientation which produces no active shear stress in the {110} planes - which shows no relaxation effect and practically no rise in the back ground dislocation loss out to 60°K.

Measurements were made from 18MC to 200MC, and if one plots the natural logarithm of the measuring frequency against the inverse temperature of the attenuation peak, as shown by Fig. 2, a straight line results. Hence, the relaxation satisfies an Arrenhius type equation

$$f_i = f_o \exp(-E_i/RT) \quad \text{where} \quad f_o = 5\times10^{9\pm0.2} \; ; \; E_i = 21\pm2.3 \text{ cal./mole} \qquad (1)$$

A distribution of relaxations of this type satisfies attenuation equations of the form

$$A = Q^{-1}\omega/2V = (\pi f/v)\sum_{i=1}^{n} B_i (f/f_i)/\left(1+(f/f_i)^2\right) \qquad (2)$$

where Q^{-1} is the internal friction, ω is 2π times the frequency, v is the velocity and B_i is a constant determining the height of the ith peak. The peak satisfying equation (1) is shown by the highest temperature dashed line. This agrees with the measured difference above 2.5°K, but it requires a distribution of relaxation frequencies below 2.5°K. Taking a ratio of 1.23 between activation energies, the top three relaxations are shown by the dashed lines. Below 1.4°K, which is the lowest temperature attained, a curve between the two limiting lines is most probable.

The values of B_i determined by the 57MC measurements were tested for the higher frequency measurements and were able to reproduce the results. Since an acoustic wave can be considered as being composed of a number of phonons which are scattered as the wave is propagated, a distance λ for which the attenuation has reached one neper, (a factor e^{-1}) can be considered as a mean free path. By extrapolating the calculations to the dominant frequencies for thermal phonons, given by

$$hf = kT \quad \text{or} \quad f \doteq (k/h)T = 2\times10^{10}T\ , \qquad (3)$$

it was shown[1] that the extrapolated results gave the same mean free path as that determined by the drop in thermal conductivity as measured by Klein[2] for a similar set of Harshaw NaCl crystals.

Figure 3 shows the velocity change with temperature for 57MC shear waves, for both Harshaw and Isomet crystals. The Harshaw velocity <u>decreases</u> as the temperature approaches 0°K while the Isomet values are constant. For crystals grown in a water vapor atmosphere, the best evidence[3]--obtained from cleaving the crystal--is that water itself enters the crystal. Hence, the model that we consider most likely is shown by Fig. 4. Oxygen substitutes for the chlorine and to agree with the stress sensitivity observed, the hydrogens have to make bonds to the sodiums. For a (110) shear stress, directed as shown, the bond distance of one set of sodiums is increased while that of another set is decreased. Two other possibilities, i.e., bonding to chlorines, or positions in [111] directions, do not react to this stress. The bond between sodium and hydrogen in sodium hydride has a strength of 52.3 kilocalories per mole. Hence, the small activation energy of 21

calories per mole requires a quantum mechanical tunneling process. Although the model with two tunneling atoms and six equivalent positions is too complicated to calculate in detail, a comparison with the familiar tunneling process in ammonia (NH_3) shows that the energy values are in the right order of magnitude. In ammonia the nitrogen atom tunnels between the triangle of hydrogens. The two energy levels are represented by the antisymmetric and symmetric combinations of the wave functions of the two positions and their difference is determined by the equation

$$E_2 - E_1 = hf(\text{ergs}) \tag{4}$$

where f is the tunneling frequency 23,870MC. This corresponds to an energy difference of 2.3 cal./mole or (1/9)th that of equation (1). Since there are two atoms and six equivalent positions for the hydrogen atoms, there will be many energy levels. The occupation numbers of the energy levels follow Boltzmann's statistics, and the relaxation time $\tau_i = 1/(2\pi f_i)$, to go from one equilibrium condition to another, will follow the form of (1).

This model explains the <u>decrease</u> in stiffness as the temperature decreases. The effect of a shearing strain S_{12} in the {110} planes is to cause a separation in the energy levels proportional to S_{12}^2. The total elastic energy plus the energy of the impurity levels is of the form

$$U = \left(\frac{\mu}{2}\right)S_{12}^2 + \frac{CN_A}{V}\left[\frac{\Sigma(E_i - E_{i-1})}{N_A} + KS_{12}^2\right] = \frac{\mu}{2}S_{12}^2 + \left[1630 + 2.24\times10^{17}KS_{12}^2\right]\frac{\text{ergs}}{\text{c.c.}} \tag{5}$$

where C the impurity concentration[2] is 10^{-5}, V the molal volume is 26.8cc, N_A is Avogadro's number, $E_i - E_{i-1}$ are the separations of successive energy levels in ergs per mole, and K a constant which measures the total energy addition caused by the separation of the energy levels. The sum total of the energy differences used in calculating the relaxations causing the attenuation is given on the right-hand side of (5). At $0^\circ K$ all the impurity atoms will be in the lowest energy state and do not add to the elastic modulus. At a high temperature all the states will be equally populated and an impurity energy $(CN_AK/2V)S_{12}^2$ is associated with the square of the strain. This adds to the elastic energy $\mu S_{12}^2/2$ and hence the elastic constant increases with temperature. From Fig. 3 this increase adds about 0.6 percent to the

$0^{o}K$ shear modulus of $2.37x10^{11}$ d./cm^2. Hence $CN_AK/V = 1.4x10^9$ d./cm^2 and $K = 6.25x10^{-9}$. To double the separation of the energy levels requires a strain of about 10^{-3}.

(1) K. Brugger and W. P. Mason, Phys. Rev. Letters, 7, 270-273, October (1961).
(2) M. V. Klein, Phys. Rev. 122, 1393-1402(1961). Klein's suggestion of a carbonate impurity does not seemr to be as probable as the water molecule.
(3) N. R. Whetten and T. A. Vanderslice, Bull. Am. Phys. Soc. 6, 360(1961) and General Electric Research Laboratory Report No. 62-RL-2967 (private communication).

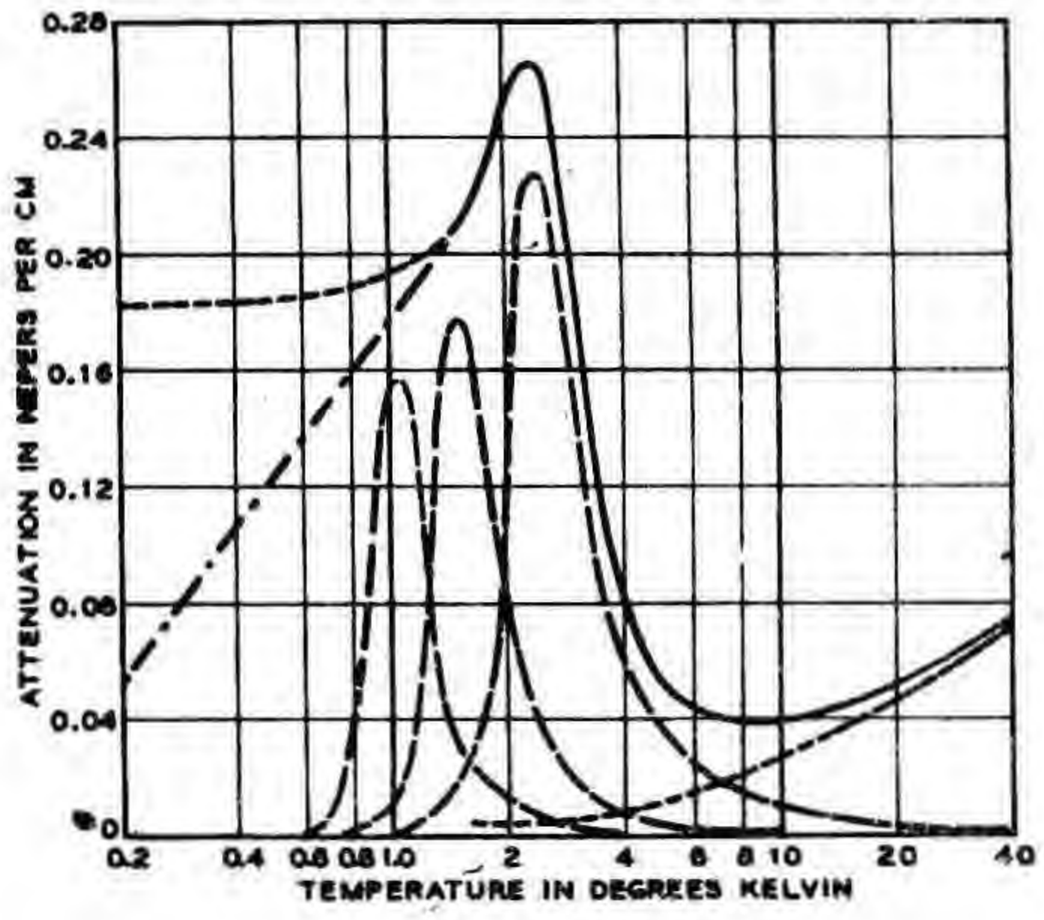

FIG. 1

Measured attenuation of 57MC shear wave along [110], Polarization along [1$\bar{1}$0]

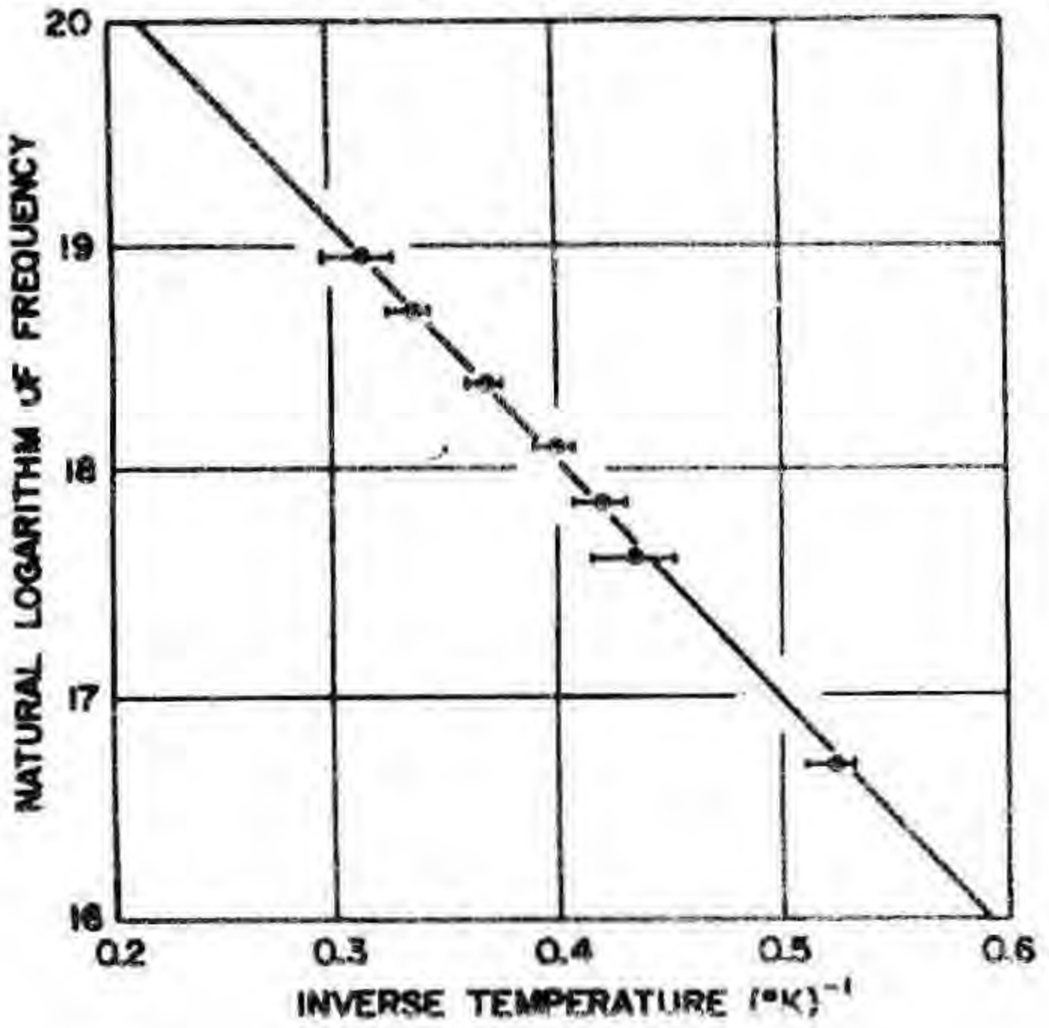

FIG. 2

Temperature shift of attenuation peak with frequency

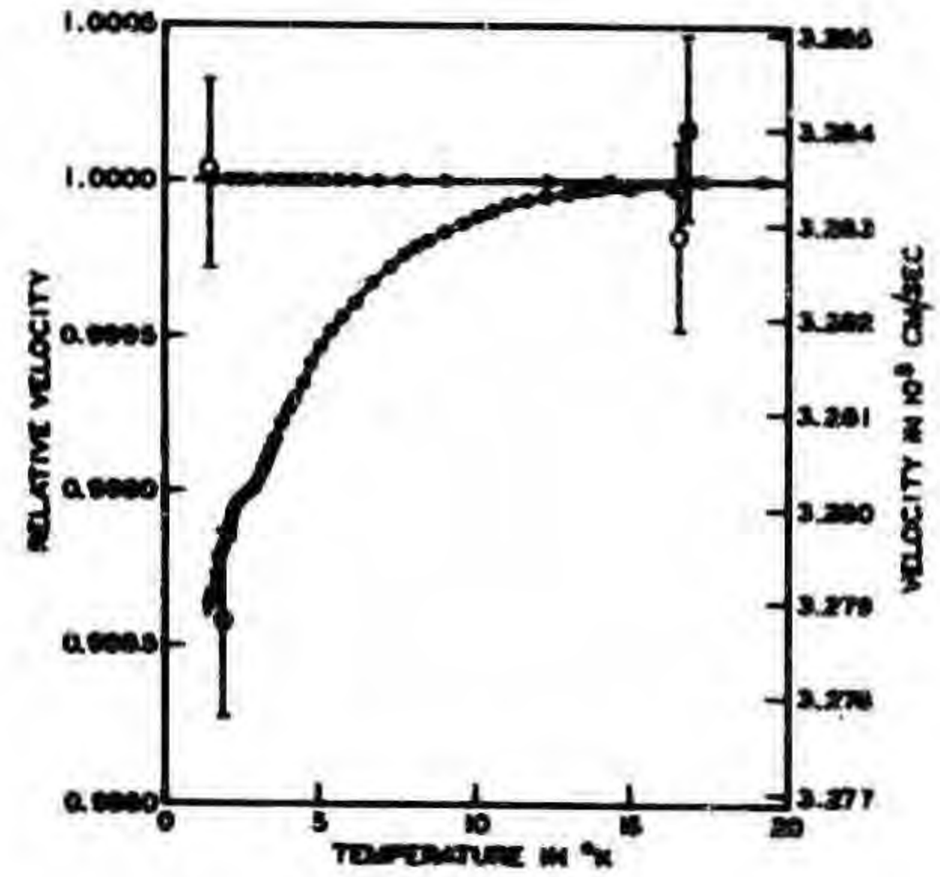

FIG. 3

Relative velocity of 57MC shear waves as a function of temperature • Harshaw; o Isomet

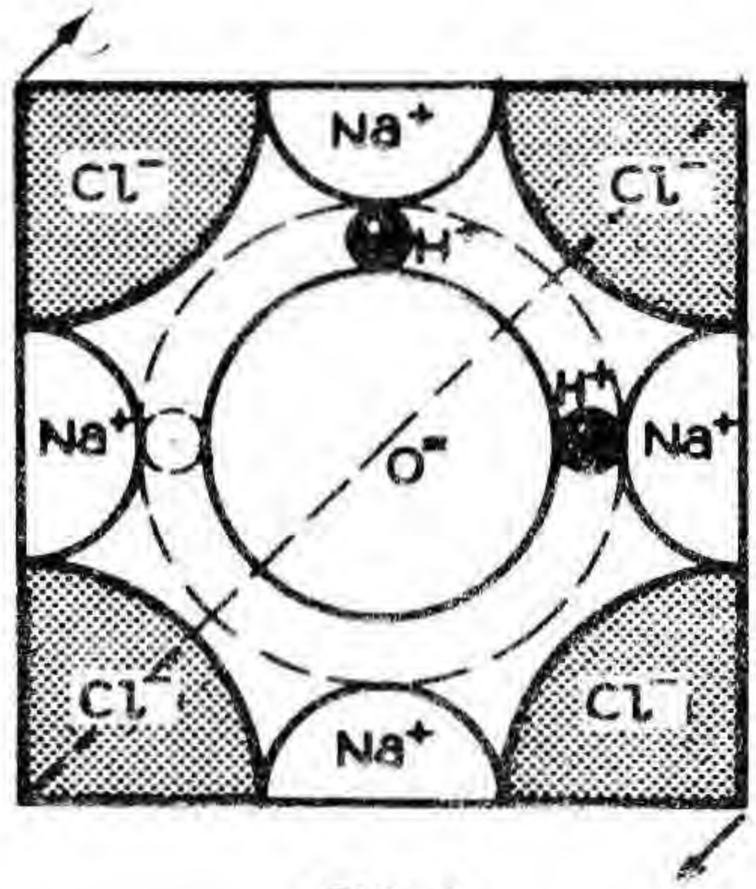

FIG. 4

Proposed model for relaxation effect

K42

FOURTH INTERNATIONAL CONGRESS ON ACOUSTICS
COPENHAGEN 21.-28. AUGUST 1962

Mechanisches Verhalten von Polymeren bei sinusförmigen Deformationen großer Amplitude

G.W. BECKER und H.-J. RADEMACHER
Physikalisch-Technische Bundesanstalt, Braunschweig, Deutschland

1. Einführung

Der lineare Zusammenhang zwischen den Deformationen und Spannungen im Festkörper (HOOKEsches Gesetz) ist auf den Fall hinreichend kleiner Deformationen bzw. Spannungen beschränkt. Beim Übergang zu größeren Beanspruchungen wird dieser Zusammenhang wesentlich komplizierter, und man spricht ganz allgemein vom nichtlinearen Deformationsverhalten eines Materials.

Kautschuk-Vulkanisate und Hochpolymere im gummielastischen Zustand zeichnen sich durch einen besonders breiten nichtlinearen Deformationsbereich aus. Daher ist gerade das nichtlineare Verhalten dieser Stoffe vielfach untersucht worden. Meistens wurden dabei zeitlich konstante (statische) Beanspruchungsformen benutzt (vgl. z.B. [1]). Messungen bei zeitlich sinusförmigen (dynamischen) Deformationen wurden im allgemeinen nur in Verbindung mit einer gleichzeitigen statischen Deformation vorgenommen, so daß die Gesamtbeanspruchung entweder auf den Druck- oder den Zugbereich beschränkt blieb (vgl. z.B. [2]).

Die theoretische Behandlung des bei dieser Beanspruchungsform gemessenen Deformationsverhaltens ist jedoch außerordentlich schwierig, zumal eine einwandfreie theoretische Beschreibung des Verhaltens selbst bei der einfachen statischen Beanspruchung bisher noch nicht gelungen ist (vgl. z.B. [3]). Aus diesem Grunde wurde ein Meßverfahren entwickelt, das eine vorspannungsfreie sinusförmige Deformation der Meßproben bei Frequenzen oberhalb 5 Hz gestattet (Abschnitt 2). Hiermit wurden erste Messungen an einer Reihe gefüllter Kautschuk-Vulkanisate und an einem weichgemachten Polyvinylchlorid durchgeführt. Sie wurden teilweise ergänzt durch Messungen bei niedrigeren Frequenzen, die mit Hilfe eines bereits vorhandenen Gerätes ausgeführt wurden (Abschnitt 3).

2. Meßverfahren

Den prinzipiellen Aufbau der Meßapparatur zeigt Bild 1. Die vertikal angeordnete stabförmige Probe PR ist an beiden Enden in Klemmen gehaltert. Die untere Klemme ist über eine Stahlwelle mit der Schwingspule eines elektrodynamischen Schwingungserzeugers (Fa. Goodmans, Modell 8/600 A) starr gekoppelt. Die obere Klemme ist mit der Achse des Vertikalsupports VS unter Zwischenschaltung eines Kraftmeßgliedes KM verbunden. Der Support, der zur Anpassung an verschiedene Probenlängen, zum Ausgleich der thermischen Ausdehnungen und der durch das Einklemmen der Probe entstehenden Längsdehnungen dient, ist auf das Querjoch eines aus starkem Profileisen aufgebauten Gestelles montiert, mit dessen

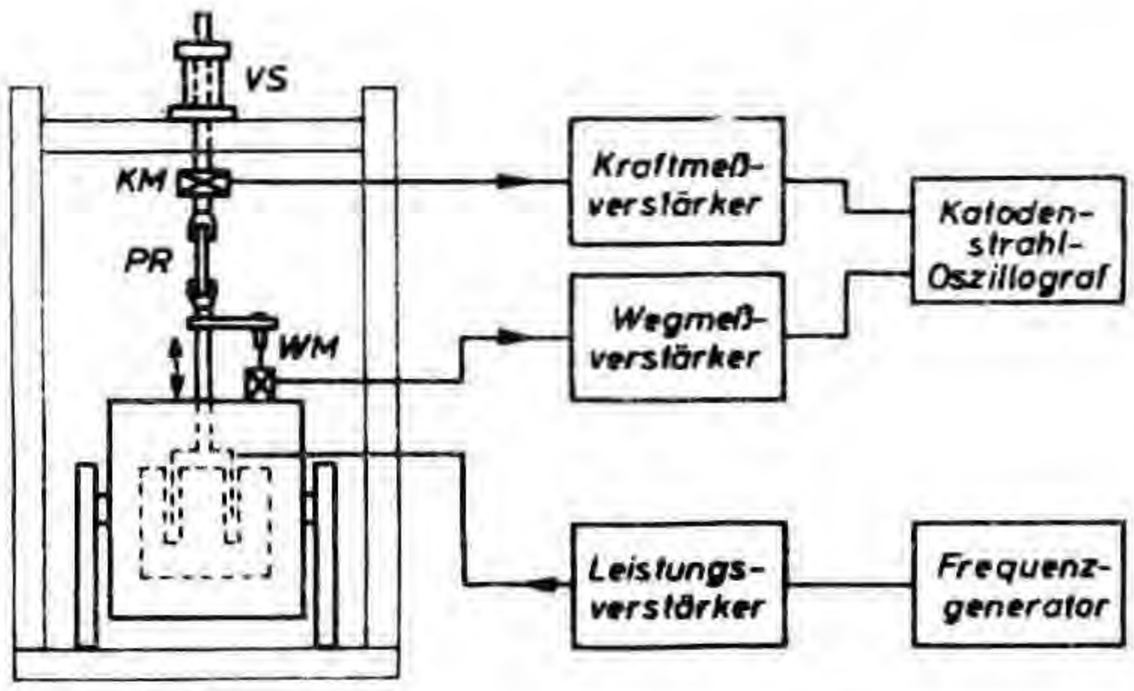

Bild 1. Prinzipieller Aufbau der Meßapparatur.

Grundplatte der Schwingungserzeuger fest verschraubt ist.

Der Vertikalsupport und der Schwingungserzeuger sind in der horizontalen Ebene verschiebbar, und das Querjoch kann geschwenkt werden. Dadurch ist es möglich, das Kraftmeßglied, die Probe und die Schwingspule genau axial auszurichten, was für eine einwandfreie Ausführung der Messungen unerläßlich ist.

Der Schwingungserzeuger wird von einem Frequenzgenerator über einen Leistungsverstärker gespeist. Die Verstärkerleistung von 1 kW ermöglicht über den gesamten Frequenzbereich von etwa 5 bis 1000 Hz eine maximale Kraftamplitude des Schwingungserzeugers von etwa 90 kp bei festgeblocktem System. Die Wegamplitude bei unbelastetem System beträgt unterhalb der Eigenfrequenz (etwa 25 Hz) maximal 1,25 cm; oberhalb ergibt sich der übliche Abfall mit dem Quadrat der Frequenz.

Als Kraftmeßglieder dienen elektromechanische Wandler verschiedener Empfindlichkeit, die mit induktiv arbeitenden Gebersystemen oder auch mit Dehnungsmeßstreifen ausgerüstet sind. Zur Wegmessung werden induktive Systeme (WM) verwendet. Die der Kraft bzw. dem Weg proportionalen Widerstandsänderungen führen in nachgeschalteten Trägerfrequenzbrückenverstärkern zu Diagonalspannungen, die nach Aussiebung der Trägerfrequenz an die Vertikal- bzw. Horizontalplatten eines Katodenstrahloszillografen gelegt werden. Hierdurch entsteht auf dem Bildschirm eine Hysteresisschleife (vgl. das Beispiel in Bild 2), aus deren Amplitudenwerten die Kraft- und die Wegamplitude $\hat{K}$ bzw. $\hat{\Delta l}$ ermittelt werden. Bei Kenntnis der Querschnittsfläche F_o und der Länge l_o der nichtdeformierten Probe ergeben sich hieraus die Spannungs- und die Deformationsamplitude $\hat{\sigma} = \hat{K}/F_o$ bzw. $\hat{\varepsilon} = \hat{\Delta l}/l_o$. Der Verlustfaktor $d = \operatorname{tg}\delta$ (δ = Phasenwinkel zwischen Spannung und Deformation) wird aus der relativen Breite $2 \cdot \sin\delta$ der Hysteresisschleife bei $\sigma = 0$ bestimmt.

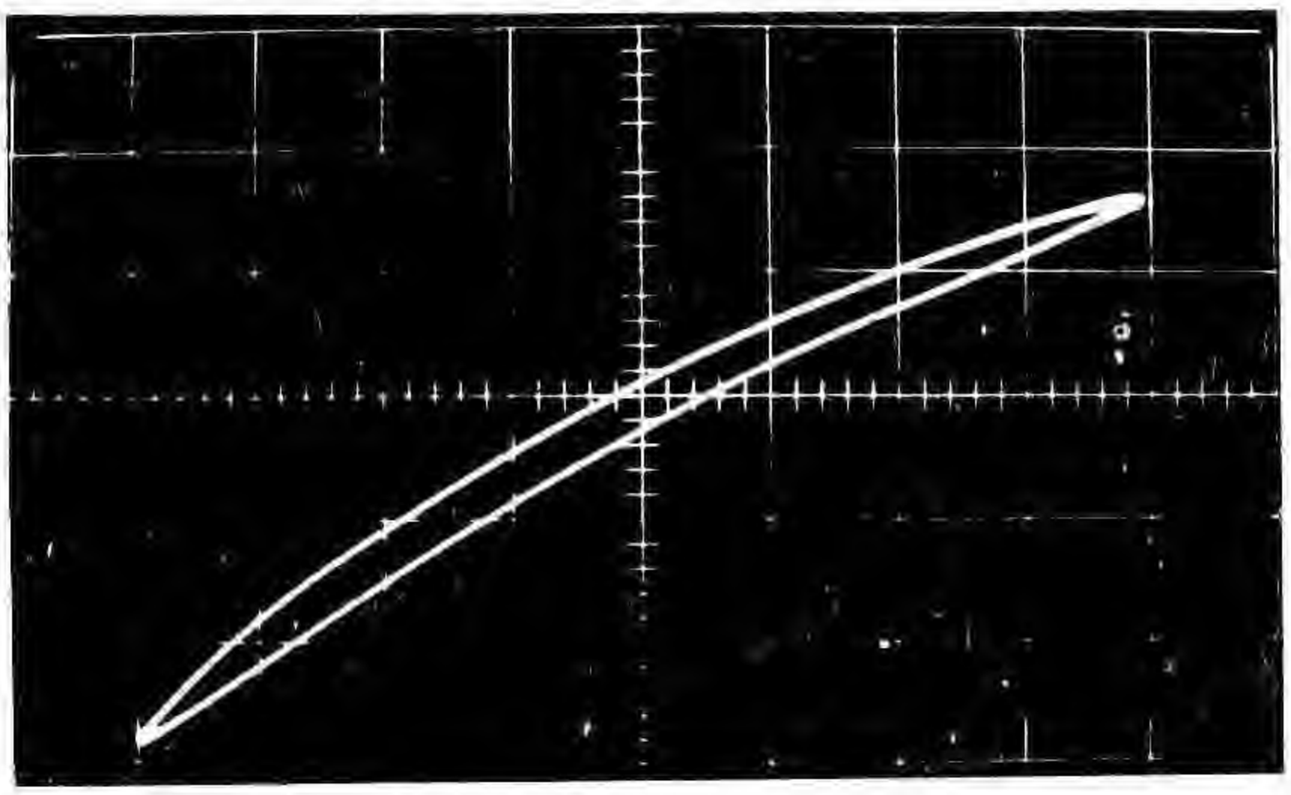

Bild 2. Oszillogramm einer Hysteresisschleife; Horizontalablenkung: Weg, Vertikalablenkung: Spannung (nach oben Zug). Kautschuk-Füllstoff-Mischung mit $V_2/V_1 = 0{,}4$. Frequenz = 40 Hz, $\hat{\varepsilon} \approx 0{,}2$.

Ein besonderes Problem stellt die gleitfreie Halterung der Meßproben in den Klemmen dar. Hierzu wurden die verhältnismäßig weichen Proben aus den Kautschuk-Füllstoff-Mischungen mit ihren Endflächen auf Metallklötzchen geklebt, die in die Klemmen der Apparatur eingespannt wurden. Die Proben aus weichgemachtem Polyvinylchlorid wurden unmittelbar eingeklemmt, wobei in die Klemmen zusätzlich mit Schmirgelleinen beklebte Metallbacken eingelegt waren.

Zur Vermeidung eines "Ausknickens" der Proben bei Druckbeanspruchung mußte das Verhältnis der Probenlänge zu den Querabmessungen genügend klein gewählt werden; bei Längen von etwa 8 bis 20 mm betrug die Querschnittsfläche etwa 32 bis 40 mm^2. Wegen der Querkontraktionsbehinderung an den Probenenden ist bei den benutzten Probenformen bereits mit einem merklichen Fehler des Absolutwertes der als Verhältnis $\hat{K}/F_o$ bestimmten Spannung zu rechnen; die so ermittelten Spannungswerte liegen um etwa 10 bis 20 % zu hoch, wie Vergleichsmessungen an hinreichend langen Proben im Zugbereich in Übereinstimmung mit theoretischen Abschätzungen (vgl. [4]) ergaben. Die im folgenden mitgeteilten Ergebnisse wurden jedoch nicht korrigiert, da dieser Einfluß bei allen Meßbedingungen annähernd gleich groß ist.

Zusätzlich zu den Messungen der Spannung und des Verlustfaktors wurde in parallelen Meßreihen die Temperaturerhöhung in der Mitte der Proben mit Thermoelementen gemessen.

3. Meßergebnisse

3.1. Gefüllte Kautschuk-Vulkanisate

Zur Verfügung stand eine Reihe von Vulkanisaten aus reinem Naturkautschuk mit Titandioxyd als Füllstoff. Die Mischungsverhältnisse waren V_2/V_1 = 0; 0,1; 0,2; 0,3; 0,4 (V_2: Füllstoffvolumen, V_1: Kautschukvolumen) (Einzelheiten über die Proben sind in anderem Zusammenhang mitgeteilt worden [5]). In Bild 3 sind die für die verschiedenen Vulkanisate gemessenen Werte $\hat{\sigma}$ und d in Abhängigkeit von $\hat{\varepsilon}$ für die Frequenz f = 40 Hz dargestellt. Es zeigt sich, daß das HOOKEsche Gesetz selbst bei kleinen Füllstoffgehalten und $\hat{\varepsilon}$-Werten von 0,003 nicht mehr erfüllt ist; denn die $\hat{\sigma}$-Kurven verlaufen keineswegs unter 45° gegen die Achsen. Ein merklicher Unterschied zwischen den $\hat{\sigma}$-Werten für Zug und Druck ist jedoch erst oberhalb $\hat{\varepsilon} \approx 0{,}02$ zu beobachten. Der Verlustfaktor d durchläuft mit wachsendem $\hat{\varepsilon}$ ein Maximum; bei verschwindender Deformation ergibt sich für alle Vulkanisate bei 40 Hz der Wert $d \approx 0{,}1$ [6]. Ähnliche Kurvenverläufe wie in Bild 3 ergaben sich bei den Frequenzen f = 5 Hz sowie f = 0,13 und 0,00814 Hz; die Messungen bei den beiden letztgenannten Frequenzen wurden mit einem früher entwickelten Gerät [7] ausgeführt.

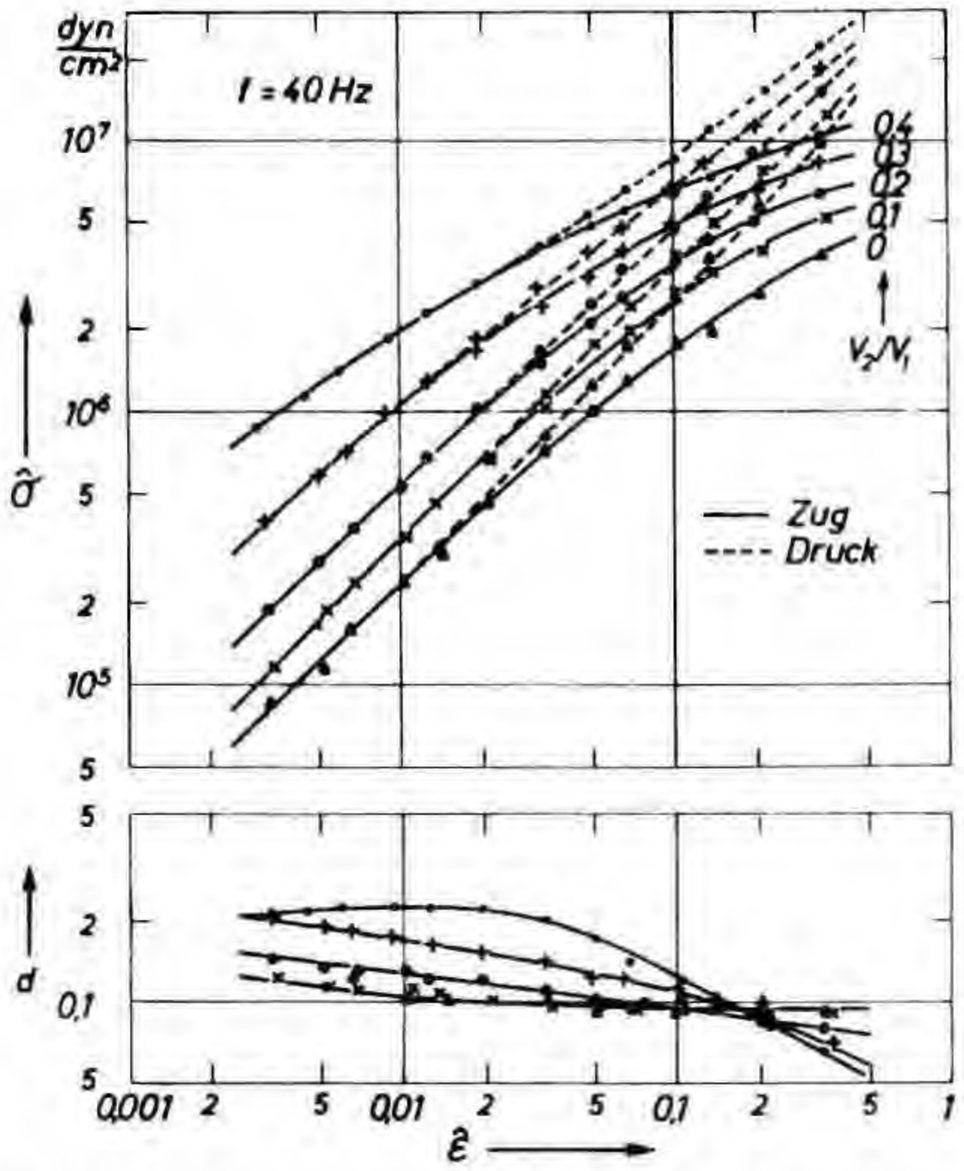

Bild 3. Spannung $\hat{\sigma}$ und Verlustfaktor d in Abhängigkeit von der Deformation $\hat{\varepsilon}$ für mit Titandioxyd gefüllte Kautschuk-Vulkanisate bei f= 40 Hz. Punktbezeichnung : V_2/V_1 = 0 (▲), 0,1 (x), 0,2 (o), 0,3 (+), 0,4 (●).

Die Frequenzabhängigkeit von $\hat{\sigma}$ und d zeigt Bild 4 für die beiden Deformationen $\hat{\varepsilon}$ = 0,03 und 0,3. Der Verlauf der Frequenzkurven zeigt, daß sich die Werte $\hat{\sigma}$ und d nur wenig mit der Frequenz ändern. Der schwache Anstieg der $\hat{\sigma}$-Kurven bei $\hat{\varepsilon}$=0,03 (bei dieser Deformation besteht noch kein nennenswerter Unterschied zwischen den $\hat{\sigma}$-Werten für Zug und Druck; vgl. Bild 3)steht in Übereinstimmung mit dem Frequenzverlauf des Elastizitätsmoduls bei verschwindender Deformation [6]. Bei $\hat{\varepsilon}$=0,3 deutet das Abknicken der $\hat{\sigma}$-Kurven für Zug bei höheren Frequenzen und höheren Füllstoffgehalten auf den zunehmenden Einfluß der Temperaturerhöhung bei diesen Meßbedingungen hin.

Die Temperaturerhöhung im Probeninneren ist in Bild 5 in Ab-

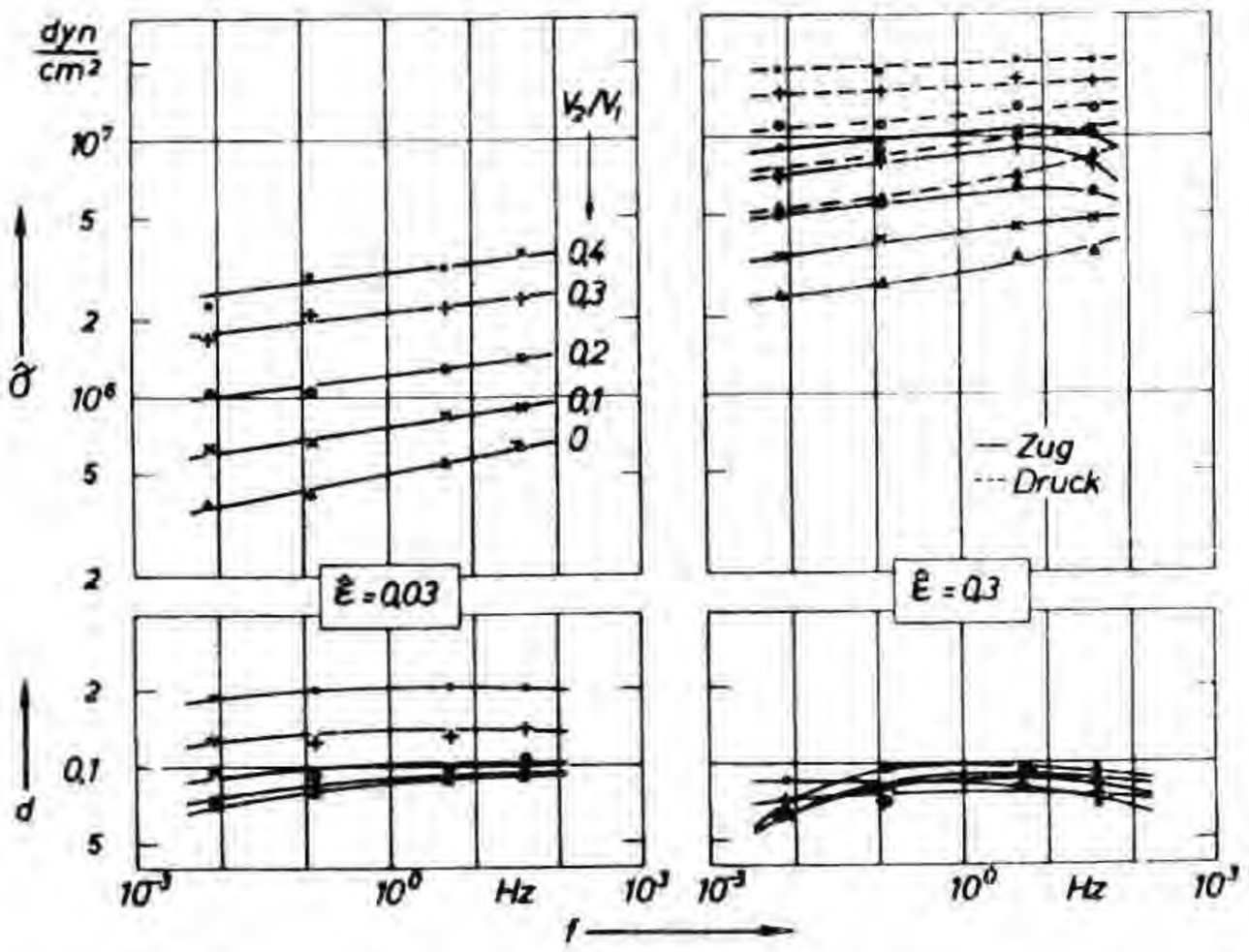

Bild 4. Spannung $\hat{\sigma}$ und Verlustfaktor d in Abhängigkeit von der Frequenz f für mit titandioxyd gefüllte Kautschuk-Vulkanisate bei $\hat{\varepsilon}$=0,03 und 0,3.Zch.s.Bild 3.

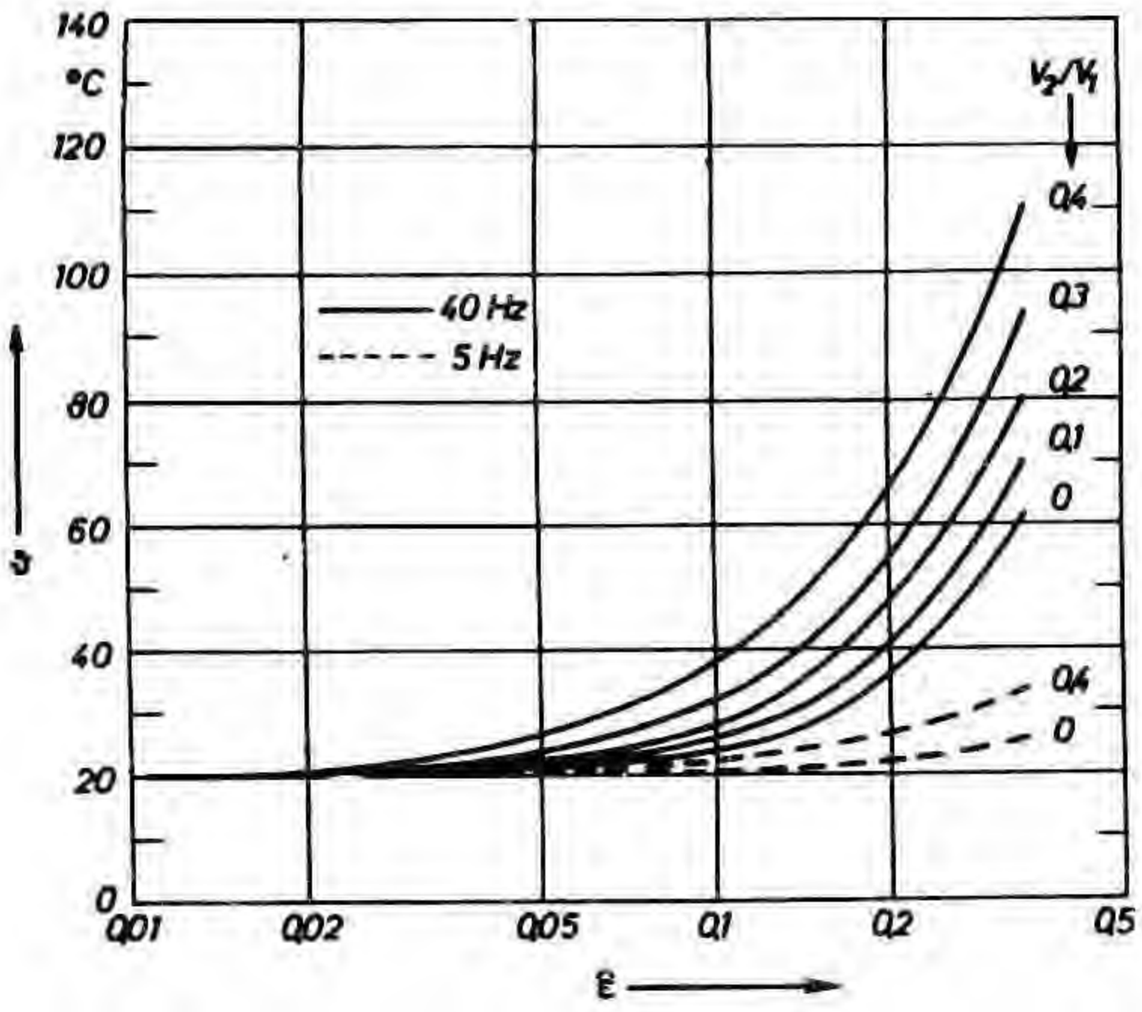

Bild 5. Temperatur ϑ im Probeninnern als Funktion der Deformation $\hat{\varepsilon}$ für mit Titandioxyd gefüllte Kautschuk-Vulkanisate bei f = 5 und 40 Hz.

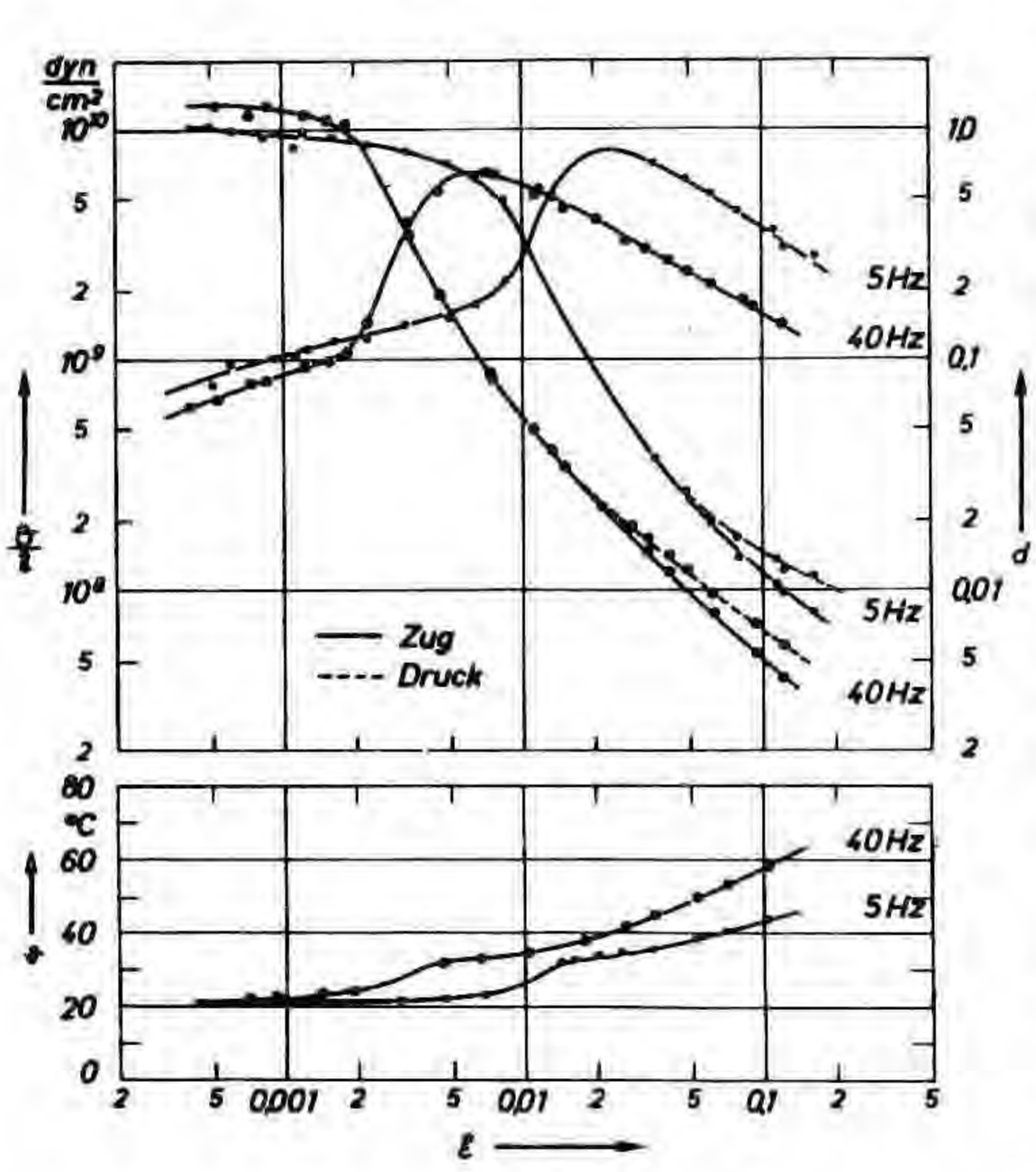

Bild 6. Verhältnis $\hat{\sigma}/\hat{\varepsilon}$, Verlustfaktor d und Temperatur ϑ in Abhängigkeit von der Deformation $\hat{\varepsilon}$ für weichgemachtes Polyvinylchlorid (80 Gew.-% PVC+ 20 Gew.-% Dioctylphthalat) bei f = 5 und 40 Hz.

hängigkeit von der Deformation für die beiden Frequenzen 5 und 40 Hz dargestellt; die eingetragenen Kurven sind durch Mittelung über mehrere Messungen gewonnen. Bei den niedrigeren Frequenzen war keine Temperaturerhöhung feststellbar. Die gemessenen Temperaturerhöhungen lassen sich durch die Beziehung $\Delta\vartheta \sim \hat{\sigma}\cdot\hat{\varepsilon}\cdot d\cdot f$, die von verschiedenen Autoren angegeben wurde (vgl.z.B. [2]), befriedigend beschreiben.

3.2. Weichgemachtes Polyvinylchlorid

Die für das weichgemachte Polyvinylchlorid (80 Gew.-% PVC+20 Gew.-% Dioctylphthalat) gemessenen Werte $\hat{\sigma}/\hat{\varepsilon}$, d und ϑ sind in Abhängigkeit von $\hat{\varepsilon}$ für die Frequenzen 5 und 40 Hz in Bild 6 dargestellt. Das Verhältnis $\hat{\sigma}/\hat{\varepsilon}$ wurde als Kenngröße gewählt, da es ein übersichtlicheres Verhalten zeigt als $\hat{\sigma}$ allein. Aus den Kurven folgt, daß das Material mit wachsendem $\hat{\varepsilon}$ ein "Dispersionsgebiet" durchläuft, das dem der Temperaturdispersion [8] ähnelt: $\hat{\sigma}/\hat{\varepsilon}$ fällt in einer steilen Stufe ab, während d maximale Werte annimmt. Die Probentemperatur nimmt zu und durchläuft dabei ebenfalls eine kleine Stufe bei einer Temperatur von etwa 30°C, die näherungsweise mit der Erweichungstemperatur des Materials zusammenfällt. Dabei werden alle Kurven mit steigender Frequenz im wesentlichen nur nach kleineren $\hat{\varepsilon}$-Werten verschoben. Dieses Verhalten ist durch die Temperaturerhöhung allein nicht zu erklären (vgl. [9]): die gemessenen Temperaturerhöhungen sind danach offenbar viel zu gering. Im "gummielastischen" Bereich, d.h. bei großen Werten $\hat{\varepsilon}$, beobachtet man, wie bei den Kautschuk-Vulkanisaten, eine Aufspaltung der Spannungswerte für Zug und Druck.

Schrifttum: [1] STUART, H.A., Die Physik d.Hochpolymeren IV, Springer-Verl.Bln-Göttg.-Heidelbg 1956, Kap.5. - [2] KAINRADL, P. u. HÄNDLER, F., Kautsch.u.Gummi 11 (1958) WT 222. - [3] BECKER, G.W. u. RADEMACHER, H.-J., J.Polymer.Sci., im Druck. - [4] BECKER, G.W., Acustica 9 (1959) 135. - [5] BECKER, G.W., Acustica 11 (1961) 264. - [6] BECKER, G.W., unveröff.Mess.- [7] SOMMER, W., Koll.-Z. 167 (1959) 97. - [8] SCHMIEDER, K.u.WOLF, K., Koll.-Z. 127 (1952) 65. - [9] KOPPELMANN, J., Koll.-Z. 144 (1955) 12.

L42

FOURTH INTERNATIONAL CONGRESS ON ACOUSTICS
COPENHAGEN 21.-28. AUGUST 1962

Zur Deutung einiger typischer Frequenzanalysen von Fahrzeuginnengeräuschen

Karl Kurz

Einige typisch fahrzeugakustische Erscheinungen sind in den relativ kleinen Abmessungen der Fahrzeuginnenräume begründet. So hat häufig die Lautstärke bei bestimmten Geschwindigkeiten ausgeprägte Maxima. Als Beispiel zeigt Bild 1 die Lautstärke eines Personenwagens in Abhängigkeit von der Geschwindigkeit mit solchen Maxima bei 55 km/h und 72 km/h. Ihre Entstehung lässt sich erklären, wenn man den Fahrzeuginnenraum durch einen Rechteckraum idealisiert. Bobbert (1) hat bereits vor längerer Zeit darauf hingewiesen, dass man auch im Spektrum von Fahrzeuggeräuschen drehzahlabhängige und drehzahlunabhängige Spektralkomponenten voneinander unterscheiden muss. Drehzahlunabhängige Frequenzanteile sind die Eigentöne des Rechteckraumes:

$$f_R = \frac{c}{2}\sqrt{\left(\frac{o}{\ell}\right)^2+\left(\frac{p}{b}\right)^2+\left(\frac{q}{h}\right)^2} \qquad (1)$$

Die drehzahlabhängigen Komponenten ergeben sich aus der Drehzahl und ihren Vielfachen:

$$f_D = \frac{n \cdot \mu}{60} \qquad (2)$$

Stimmen nun bei einer bestimmten Drehzahl die Frequenzen f_R und f_D der Gleichung 1 und 2 überein, so kann bei dieser Resonanz besonders grosse Schallintensität erwartet werden:

$$U = \frac{30c}{n}\sqrt{\left(\frac{o}{\ell}\right)^2+\left(\frac{p}{b}\right)^2+\left(\frac{q}{h}\right)^2} \qquad (3)$$

In einem Koordinatensystem, auf dessen Abszisse die Frequenz und auf dessen Ordinate die Drehzahl als Mass-Stäbe gewählt sind, ergeben die Gleichungen 1 und 2 zwei Scharen von Geraden, deren Schnittpunkte den Lösungen der Gleichung 3 entsprechen und jeweils eine Resonanz zwischen Drehzahl und Eigenton des Fahrzeuginnenraumes darstellen (Bild 2).

Die stehenden Wellen quer oder in Richtung der Fahrzeuglängsachse sind erfahrungsgemäss besonders resonanzanfällig. Für den bereits in Bild 1 erwähnten PKW sind die Resonanzen eingezeichnet. Wie man sieht, ist bei diesem Wagen bei 55 km/h die Zündfrequenz in Resonanz mit der Grundschwingung in Längsrichtung und bei 70 km/h mit der Grundschwingung quer zur Fahrzeuglängsachse, so dass sich die experimentellen Befunde mit dieser Darstellung befriedigend erklären lassen.

Mit stehenden Wellen haben bereits Becker und Oberst (2) sowohl ausgeprägte Intensitätsmaxima in Fahrzeuggeräuschspektren als auch örtliche Schallstärkeunterschiede im Fahrzeuginnenraum erklärt. Solche örtlichen Intensitätsunterschiede lassen sich in fast jedem Fahrzeug im Bereich tiefer Frequenzen nachweisen. Bild 3 zeigt die Spektren an zwei Mess-Stellen in einem LKW-Fahrerhaus. Die an Mess-Stelle 2 festgestellte Resonanz bei 180 Hz ist an Mess-Stelle 1 nur schwach bemerkbar, dagegen tritt die Resonanz bei 450 Hz nur an Mess-Stelle 1 in Erscheinung, jedoch nicht an Mess-Stelle 2.

Oberhalb 1.000 Hz stimmen die örtlichen Pegel innerhalb der Messgenauigkeit überein. Der Bereich der durch die Raumresonanzen bedingten örtlichen Pegelunterschiede erstreckt sich, wie man erkennt, bis etwa 300 - 400 Hz, und bei hohen Frequenzen sind die örtlichen Pegelunterschiede wieder gering. Dieses Verhalten kann übereinstimmend an verschiedenartigen Fahrzeugen, wie PKW's, LKW's, Omnibussen, Diesellokomotiven u.a., festgestellt werden.

Diese deutlich voneinander getrennten Frequenzbereiche lassen sich aus der zunehmenden Dichte der Eigentöne des Innenraumes bei höheren Frequenzen mit Hilfe des Eigentonnetzes erklären. Für sie ergibt sich bekanntlich:

$$\frac{\Delta N}{\Delta f} = \frac{4\pi f^2 V}{c^3} + \frac{2\pi f V}{c^2}\left(\frac{1}{l}+\frac{1}{b}+\frac{1}{h}\right)+\frac{2}{c}(l+b+h) \qquad (4)$$

Setzt man hierin $\Delta N/\Delta f = 1$ d.h. alsol Resonanz in einem Frequenzbereich von 1 Hz Breite, erhält man für den bereits erwähnten PKW eine Frequenz von 780 Hz. Die angenommene Resonanzdichte bedeutet praktisch die Grenze zum statistischen Schallfeld, so dass entsprechend den Beobachtungsergebnissen oberhalb dieser Frequenzgrenze kaum mehr örtliche Pegelunterschiede zu erwarten sind. Die untere Frequenzgrenze ist durch das spektrale Auflösungsvermögen der Messapparatur und durch die unvermeidlichen Drehzahlschwankungen gegeben. Zu diesem Zweck sei die Formel 4 für die Drehzahl und ihre Vielfachen entwickelt.

$$\Delta N = \left[U\Delta n + n\Delta U\right]\left[\frac{\pi^2 U^2 V}{1{,}72\cdot 10^4 c^3}+\frac{\pi U\cdot V}{5{,}7\cdot 10^2 c^2}\left(\frac{1}{l}+\frac{1}{b}+\frac{1}{h}\right)+\frac{1}{30c}(l+b+h)\right] \qquad (5)$$

Im Durchlassbereich des Oktavsiebes um 300 Hz werden Raumresonanzen nur von der 5. - 8. Vielfachen der Drehzahl angeregt, so dass also $\Delta n = 3$ zu setzen ist. Bei einer Drehzahlschwankung von $\pm$ 50 U/min. werden dann nach Gleichung 5 etwa 30 Eigentöne in der bei 300 Hz liegenden Oktave erregt. Infolge dieser unvermeidlichen Drehzahlschwankungen ist daher eine Trennung der einzelnen Resonanzen auch bei bestem Auflösungsvermögen der Messgeräte oberhalb 400 Hz nicht mehr möglich.

Es lässt sich ebenso zeigen, dass diese unvermeidbaren Drehzahlschwankungen die Messgenauigkeit der Lautstärke und der Schallpegel im Bereich tiefer Frequenzen bestimmen, und dass ebenfalls in Übereinstimmung mit der Erfahrung die Messgenauigkeit der Schallpegel im Fahrzeug oberhalb 1000 Hz praktisch durch die Güte der Schallpegelmesser gegeben ist.

Literatur:

(1) G. Bobbert: " Verkehrsgeräusche, ihre Messung und ihre Beurteilung"
Dt. Kraftfahrtforschung Heft 91, VDI-Verlag 1956

(2) G.W.Becker "Grenzen der Geräuschminderung durch Körperschalldämpfung
u.H. Oberst im Kraftfahrzeug"
Acustica 8. (1958) S. 11

Zur Deutung einiger typischer Frequenzanalysen v. Fahrzeuginnengeräuschen

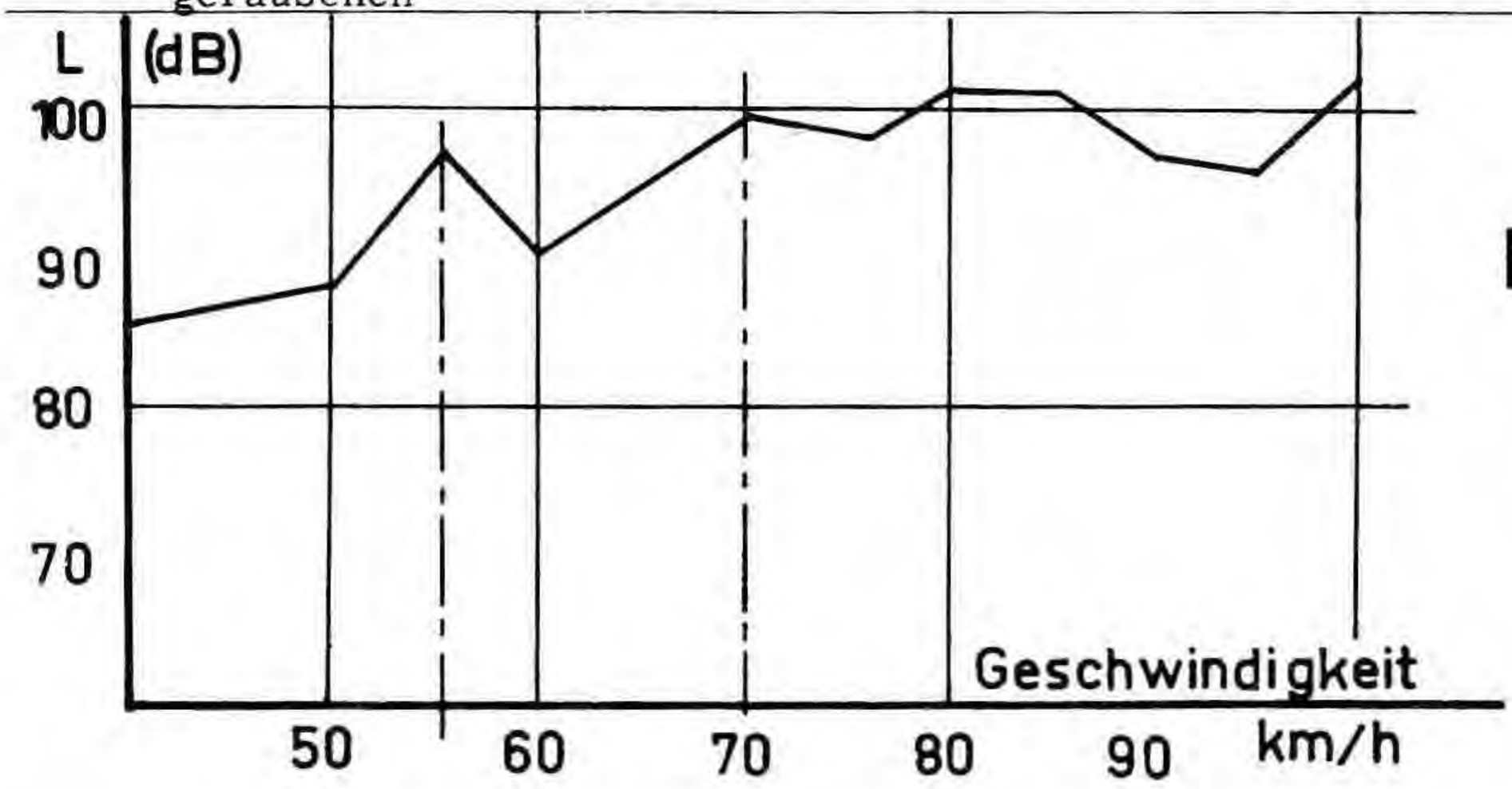

Bild 1

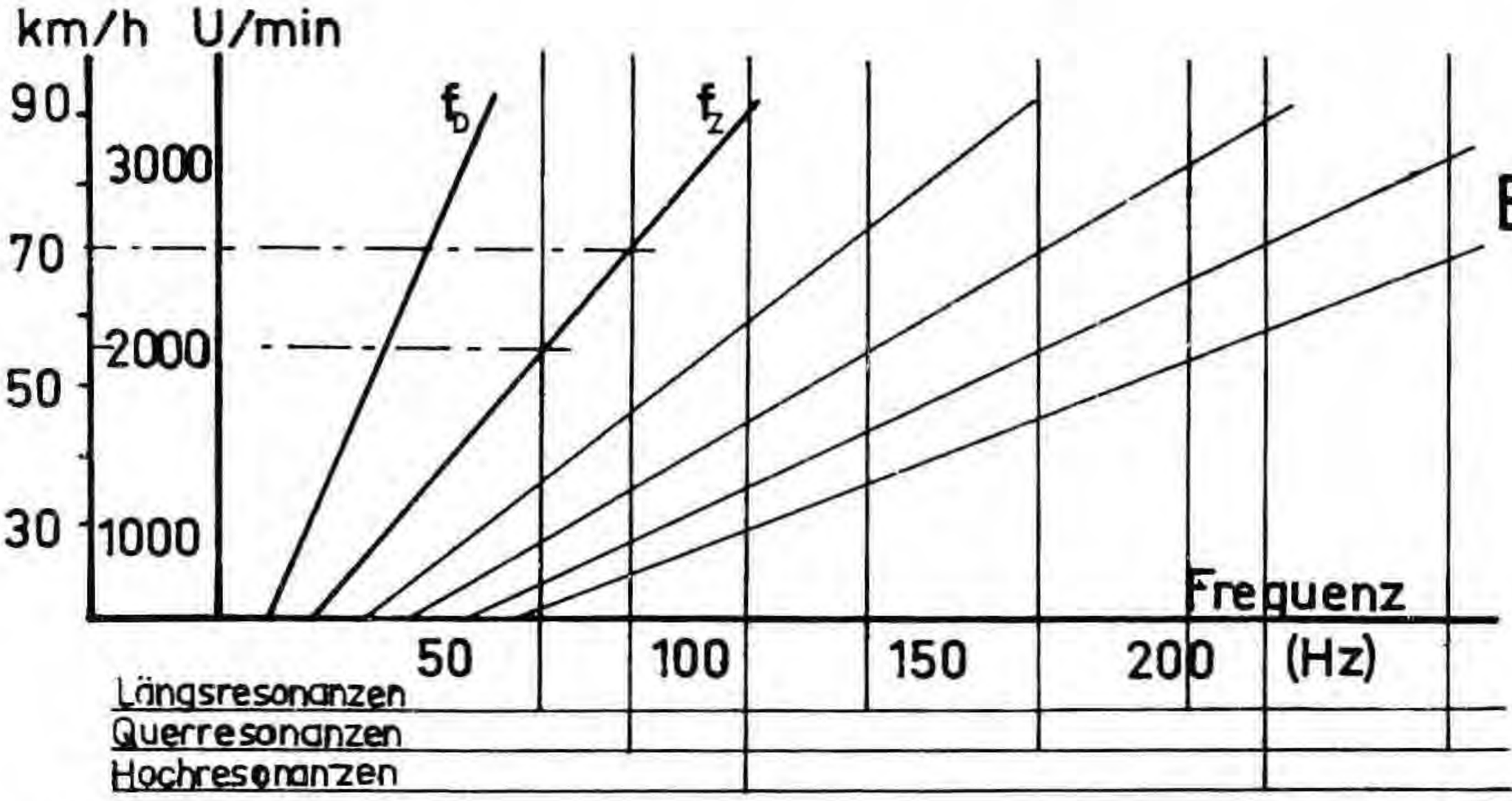

Bild 2

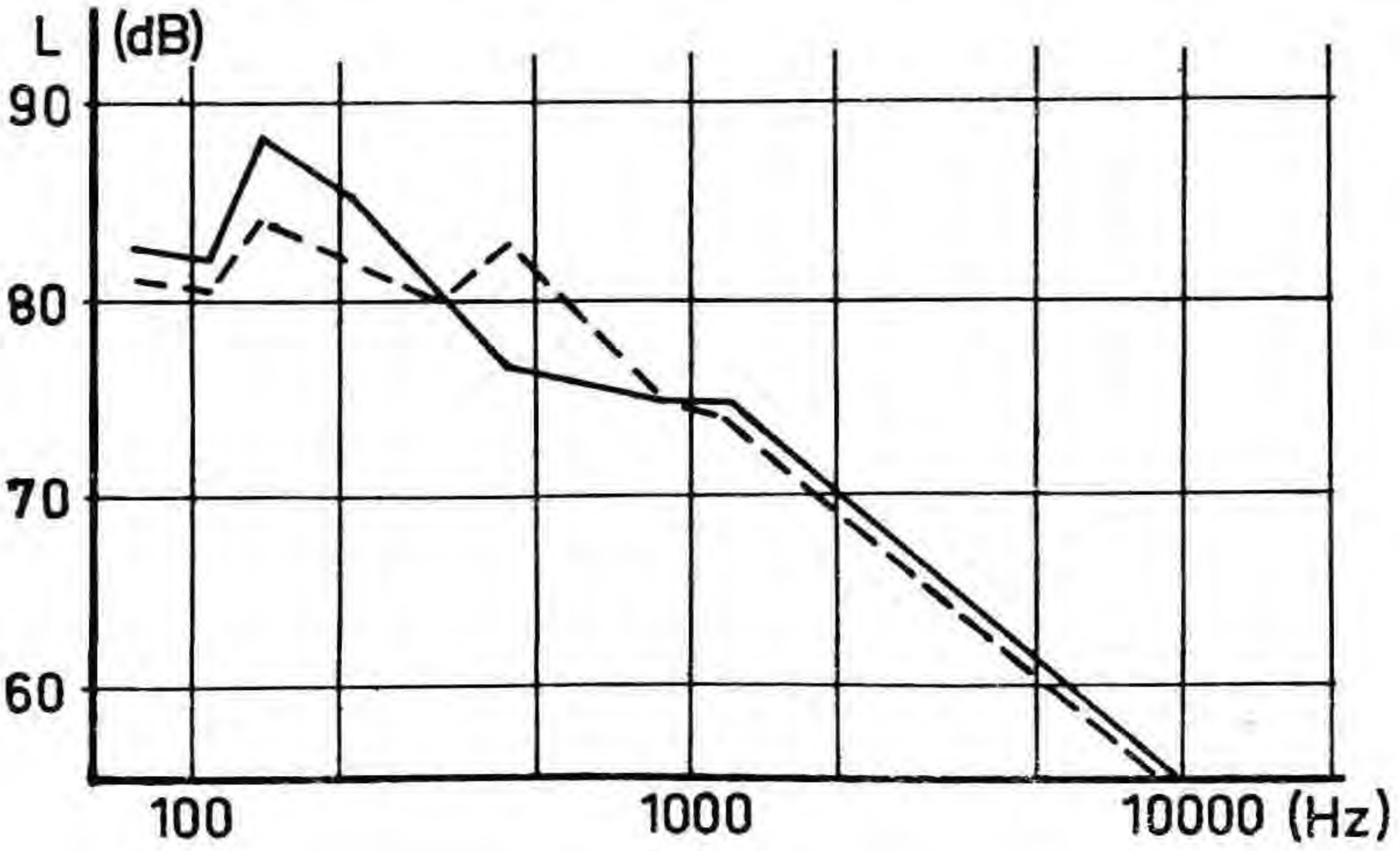

Bild 3

M42

FOURTH INTERNATIONAL CONGRESS ON ACOUSTICS
COPENHAGEN 21.-28. AUGUST 1962

INSTANTANEOUS SUBJECTIVE PRE-DETERMINATION OF ROOM ACOUSTICS.

Dr.-Ing. Radamis BOUTROS-ATTIA,
Faculty of Engineering, Alexandria University, Egypt (U.A.R.)

Subjective investigation of room acoustics by means of magnetic tape recordings in models was first reported to the German Physisists' Congress in Munich (Sept. 1956). In the original method (see fig. 1) a two-channel two-speed magnetic tape recorder was used in which the higher speed was n-times the lower one; 1:n being the room model scale. In this way normal audio frequencies recorded at low speed on cannel 1 could be transferred into an n-times higher frequency range (up to 100 kc/sec.) when played back at the high speed. The played-back high frequencies were then fed into an ultrasonic sound transmitter placed in the model. The ratio of sound wavelengths to room dimensions was thus kept the same in both the model and the original room to be investigated. Another essential condition had been also fulfilled; namely that the model should be made of materials having the same sound absorption coefficients at the high frequencies as those of the original room materials at the corresponding normal audio frequencies.

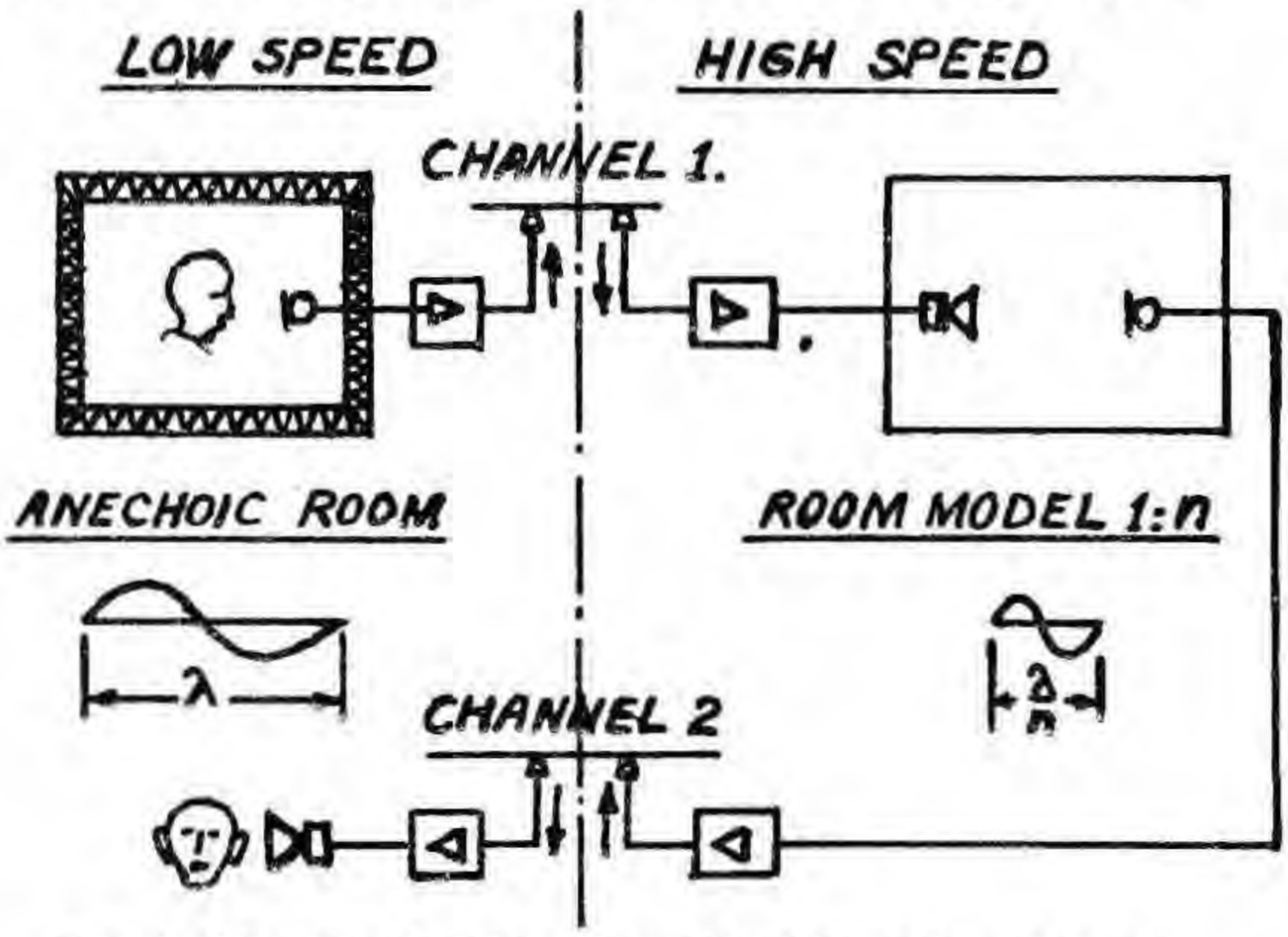

FIG.1 - MONOPHONIC APPARATUS FOR MODEL INVESTIGATION OF ROOM ACOUSTICS.

Sound at any specified position in the model was then picked-up by an ultrasonic microphone and recorded at the high speed on channel 2. This last model recording, when played-back at low speed, gave an idea about the acoustical conditions to be expected in the room, even before it existed at all. There is no need to emphasize the economical importance of this method of subjective pre-determination of room acoustics to acousticians and architects.

In the above-mentioned stage of development the method was still suffering from two main drawbacks:

1) excessive absorption of ultrasonic waves in air inside the model, rendering the model boundary surfaces ineffective at the high frequencies, and
2) monophonic model recordings always sounded more reverberant than the original recordings directly and binaurally heard in the original room.

Modifications to overcome these difficulties were reported to the 3rd ICA Congress (papers 7F6, 7F7 and 7F8). A drying apparatus (see fig. 2) has been applied to reduce the relative humidity of air inside the mo-

del to the low value of about 5%. The attenuation of sound in air inside the model was thus reduced to the extent that the ratio of sound absorption in air to that at the boundary surfaces was nearly the same in both the model and original room.

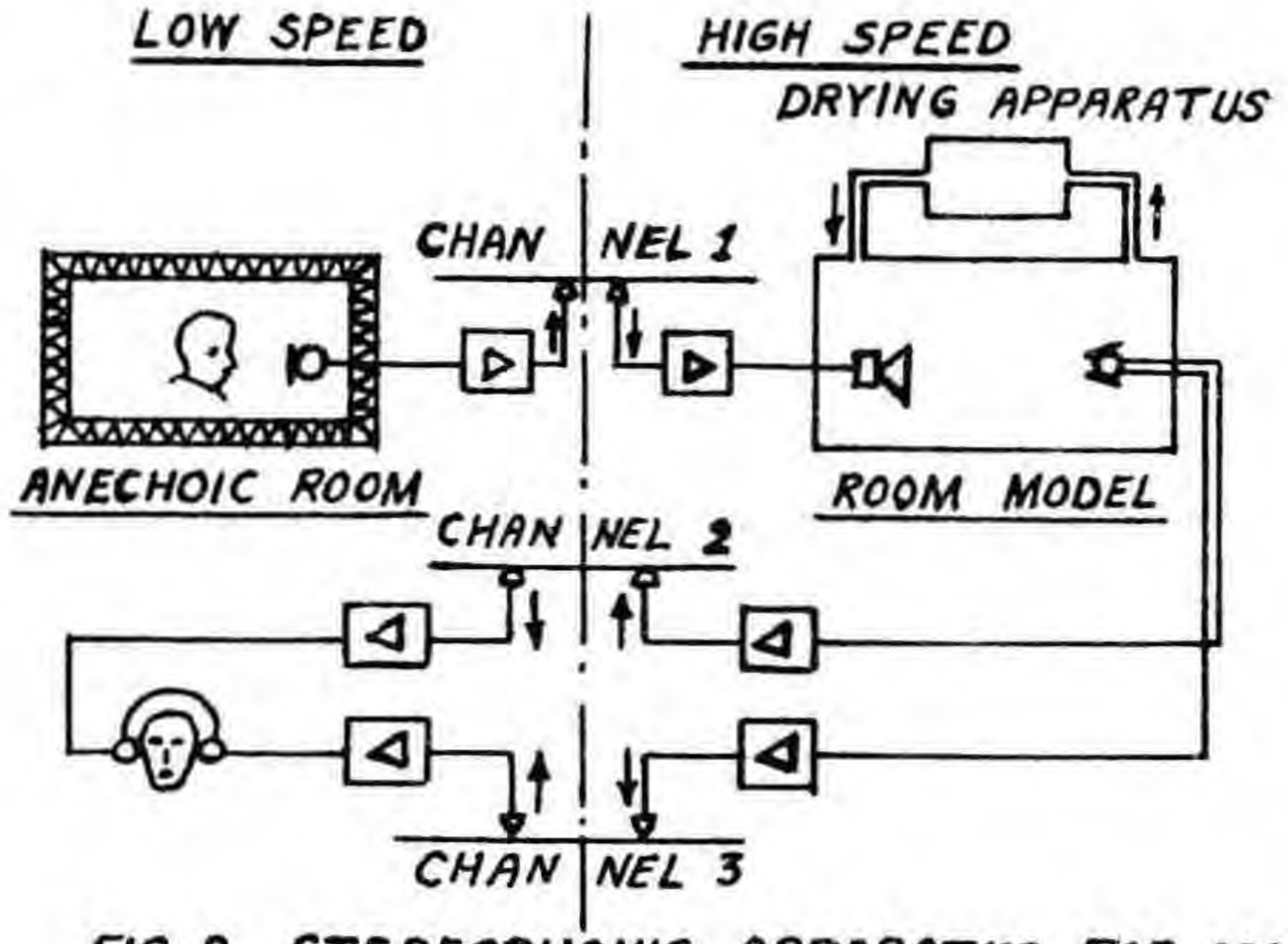

FIG. 2. STEREOPHONIC APPARATUS FOR MODEL INVESTIGATION OF ROOM ACOUSTICS

The ultrasonic condenser microphone in the model has been also replaced by an artificial head in which two separate electrostatic capsules were mounted at a certain angle to imitate the binaural directional characteristics of the human head. The two outputs from the artificial head were recorded on two separate channels of the tape recorder (now 3-channel) and then played-back at low speed and heard by separate headphones.

Stereophonic recordings obtained after these modifications gave much better results. However, both the original and the modified apparatus presented a serious disadvantage resulting from the use of longitudinal recording with stationary magnetic heads. In the original apparatus, the mechanical part of the tape recorder (Fig. 3) consisted of an endless piece of tape (3 meters long) driven at both speeds (20 and 200 cms per sec.) by a single motor through two separate couplings applied alternatively. In this way supply and take-up reels and motors were dispensed with for simplicity on the expense of the total time of recording which was limited to 15 seconds, i.e. just enough for one sentence or a short piece of music. Although rewinding was not necessary in this apparatus before a model recording could be played-back at low speed, yet the process of changing the motor couplings resulted in an appreciable loss of time when carrying out investigations.

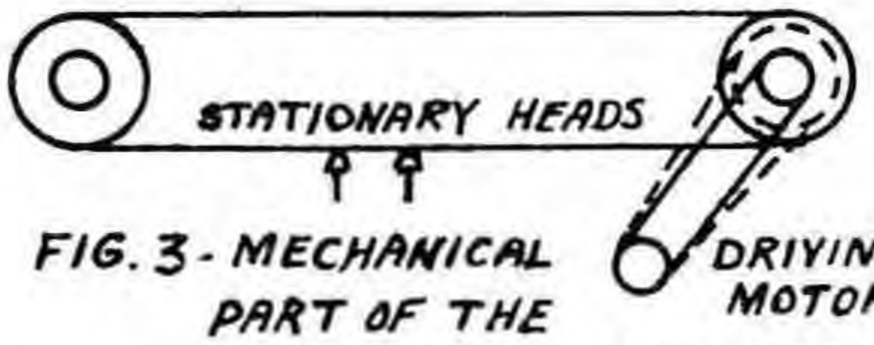

FIG. 3 - MECHANICAL PART OF THE ORIGINAL TAPE RECORDER

In the modified apparatus of Fig.2, the difficulty of limited recording time has been overcome by using a 30 meter long endless tape wound on an external auxiliary loop. Magnetic tape was driven by a toothed wheel and a single motor. A special mechanism was developed to allow immediate change-over from one speed to the other.

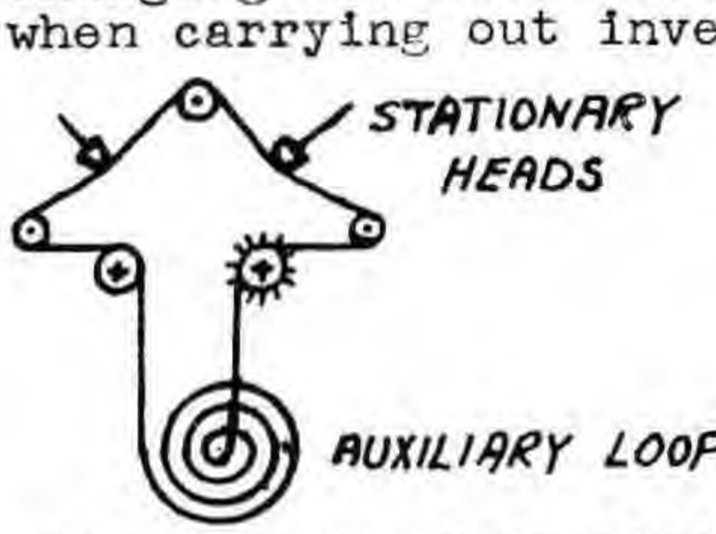

FIG. 4. MECHANICAL PART OF THE MODIFIED APPARATUS

In this improved apparatus, however, speed change-over was necessary before a

model recording could be heard. In other words, an original problem still remained unsolved, namely that a model recording could not be heard at normal audio frequencies while being made in the model at ultrasonic frequencies. If this could be realised, then, for instance, the effect of a certain absorbing surface on the sound level at different locations in the model could be immediately determined by moving the artificial head to these locations successively and hearing the recordings simultaneously. Also, the effect of the inclination of a certain reflecting surface on the sound level at a certain region in an auditorium could be instantaneously investigated in the model by listening to the model recording while rotating that surface slowly. It is obvious that many other investigations could be carried out applying this method.

The present paper deals with a suggestion to solve this problem by transverse recording on magnetic tape using rotating heads. Fig. 5

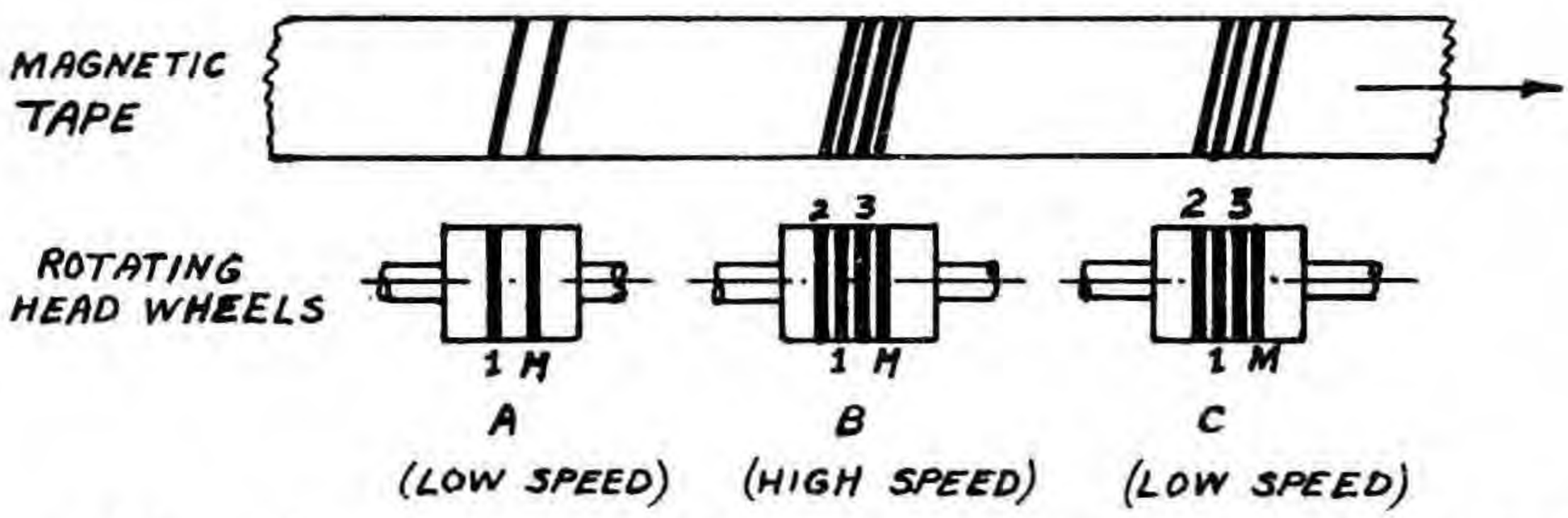

FIG. 5. ROTATING HEAD SYSTEM FOR ROOM ACOUSTICS' INVESTIGATION

illustrates the principle of the suggested apparatus which is actually a modification of a television tape recorder. With normal TV magnetic tape (breadth 50 mms) three head wheels should be used, A and C rotating at low speed (for recording or play-back of audible frequencies) and B at high speed(for ultrasonic frequencies). The ratio of low to high speed is again the same as that of the model to original room linear dimensions. The heads of wheel A work on two tracks only (designated 1 and M), the first for making the original "dry" recording and the second M for monitoring purposes of synchronisation. Wheel B comprises heads for two extra tracks 2 and 3 for recording model sound while wheel C comprises similar heads for playing it back at low speed.

Compared to a normal TV tape recorder, the suggested apparatus has the following design characteristics:

1) Peripheral speed of rotating heads is much less due to the fact that the upper frequency limit in a TV recorder is about 4 Mc/sec whereas in the suggested apparatus it is 100 kc/sec only (highest investigation frequency in a 1:10 acoustical model corresponding to f = 10 kc/sec in the original room). As a result peripheral speed of high speed heads may be limited down to about 2 meters/sec correspoding to a head wheel speed of about 10 revs/sec (in a TV tape recorder about 240 revs/sec).
2) As a consequence rotating head life as well as tape life will be appreciably longer than in a TV recorder.
3) With a reasonable angle of inclination α of recording tracks on tape where:

$$\tan \alpha = \frac{\text{total width of tracks}}{\text{tape width}} \simeq \frac{10 \text{ mm}}{50 \text{ mm}} = \frac{1}{5}$$

$$= \frac{\text{tape speed}}{\text{peripheral speed of high speed heads}}$$

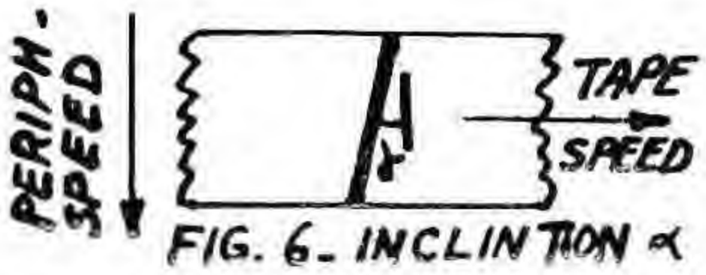

FIG. 6 - INCLINATION α

The tape speed here will be nearly the same as in a TV tape recorder (about 38 cms/sec) in spite of the much larger width required for the four tracks. Thus, similar to a TV recorder, a total recording time of 96 minutes will be available, using 35.5 cm reels (15").

4) Due to the fact that the head wheels A and C will rotate at 1/10 the speed of headwwheel B, they will be unable to follow the recording tracks on the tape unless given a longitudinal speed = 0.9 the tape speed and in the same direction (about 34 cms/sec). However, provision should be made that these head wheels return immediately to their original longitudinal position each time they lose contact with one side of the tape and start contact at the other side.

Beside mechanical considerations there is a series of other problems associated with this suggested apparatus and which should be solved, e.g. synchronisation (servomechanisms), distortion limits, signal-to-noise ratio, etc... As a result the cost of the apparatus will be naturally higher than that of the apparatus of Fig. 2, but in the long run the increased number of consultations which could be made in the same span of time will be more than paying for the extra charges.

Another important application of the suggested apparatus will be the systematic and quick testing of model materials in model reverberation rooms. The absorption coefficients of two samples of materials at high model frequencies could be measured simultaneously (Fig.7). Square wave pulses modulated with different test frequencies successively and having sufficient intervals in-between are recorded on track 1. They are then played back, supplied to the speakers in the model reverberation rooms, picked-up together with reverberation by the microphones and recorded at high speed on tracks 2 & 3. When played back at low speed, reverberation time will be elongated in the ratio of the high to the low speed and could therefore be immediately recorded on normal sound level recorders. Absorption coefficients of model materials could thus be easily and quickly determined. This allows for much quicker development of new types of such materials to cope with the enormously increasing rate of production of new building materials.

MODEL REVERBERATION ROOMS

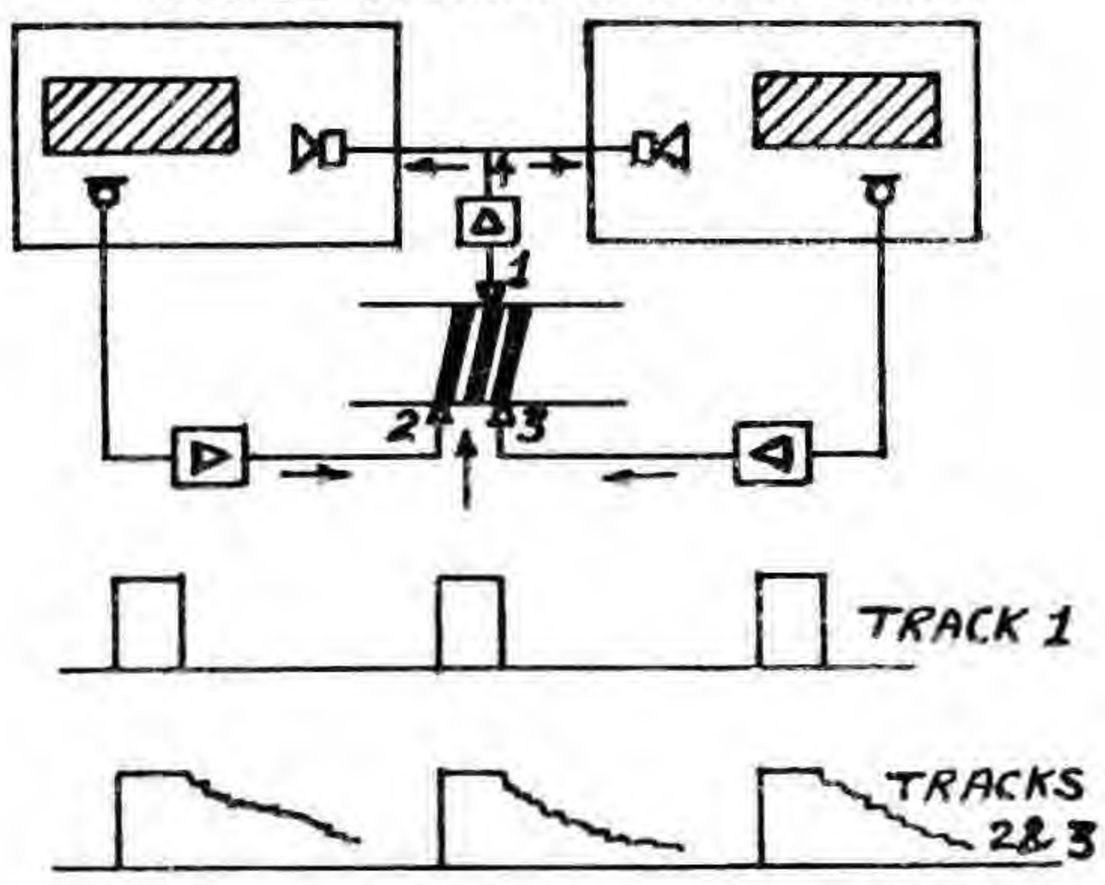

FIG. 7. TESTING OF MODEL MATERIALS IN MODEL REVERBERATION ROOMS

N42

FOURTH INTERNATIONAL CONGRESS ON ACCUSTICS
COPENHAGEN 21.-28. AUGUST 1962

DEVELOPMENT OF A SPHERIC ARTIFICIAL HEAD FOR ACOUSTICAL MEASUREMENTS OF TELEPHONE INSTRUMENTS

Eero Lampio, Finland Institute of Technology

Introduction

The objective acoustic measurements on the telephone systems are divided into two groups, one of which is the sending attenuation measurement and the other the receiving attenuation measurement. These measurements have been made already three decades in various countries. Both CCITT and IEC are interested in these measurements and they have set the special study groups, whose duty is to study an international recommendation of objective acoustic measurements on telephone systems. For this purpose an artificial head which is spherical has been designated in the acoustic laboratory of Finland Institute of Technology for an acoustic standard source on the sending telephone systems.

Requirements

A criterion of the quality of the telephone instrument in the sending systems is expressed in dB as a reference equivalent attenuation against the SFERT of the CCITT. But as a basis of this criterion can be also the measurements made as the function of a pure sound at constant sound level 1 N/m^2 at the distance of 5 cm from the lips of mouth opening in various frequencies. The variation of sound pressure with distance along the axis of mouth must be hyperbola. The radiating area at the mouth must be representative of a medium small mouth opening so that the distribution of sound pressure is reasonably uniform in the front hemisphere.

The requirements of the international co-operation for tests on telephone instruments with same measuring methods constrain the simple shape to the outside of the sound source. The speed, the accuracy and the economy in measurements of the sending telephone systems are notable characteristic, because every to telephone network joining telephone instruments should receive and take care with a simple, but technically complete system, which should be cheap to supply and easy to use.

Construction

The sound source construction for measurements of the sending systems is called the artificial head analogically after the artificial ear of the receiving systems. Life-size head is geometrically next an ellipsoid so that the spheric form is not far. Influences of the spheric surface on the free sound field have been treated much so that it is mathematically much easier to handle as a in life-size head shape artificial head.

The recommendation of the CCITT determine the distance and fixing position of the handmicrotelephone in front of talker's mouth in the comparative articulation tests. Now a artificial head is set on the place of the talker's head. According to recommendations of the CCITT the diameter of the artificial head can be taken 140 mm, so that "ears" for fixing of the handmicrotelephone are

---

CCITT = Comité Consultatif International Téléphonique et Télégraphique
IEC = International Electrotechnical Commission

still on the outer side of the surface of the sphere. Into this spheric artificial head can be set 5" loudspeaker. Because inside the crust of the artificial head is very high sound level versus the outer side of the crust, so the crust has to be made very rigid so that it does not vibrate with any measurement frequency.

The measurements of sound radiation from mouth which have earlier been made are showing that the opening of the artificial mouth must be elliptic and the area of mouth opening has to be about 2 cm^2, which is a medium-to-small mouth area. When it is taken a spheric mouth opening, its diameter is about 15 mm, which is less than the smallest futher known artificial mouth opening. In the construction of the sound source of the artificial head a requirement of 1 N/m^2 without a notable distortion at the distance of 5 cm from mouth opening is determining. Then the volume velocity by 100 Hz at the 15 mm mouth opening is $1,6 \cdot 10\text{-}3$ m^3/s. If the radiation area of the sound source should be of the same size as that of the mouth opening, the displacement of the radiation membrane of the sound source should be 1,4 mm r.m.s. By using the 5" radiation membrane the displacement is only 0,04 mm r.m.s.

The recommendations of the CCITT for international calls require a frequency range from 300 Hz to 3400 Hz, so that in this frequency range the frequency response of the artificial head must be flat. The laboratoryworking requires from 160 Hz to 6400 Hz, because it is basis research work. The flatness of frequency response of the artificial head has to be in basis laboratory measurements ± 0,5 dB, but in speed serie measurements the requirements are not tight, so that ± 2 dB should be satisfactory.

Characters

The construction of the spheric artificial head is shown in fig. 1. The diameter of this head is 140 mm and its crust is a castbrass with a thickness 5 mm. The surface of the artificial head is turned. On the end of the spheric artificial head there is the mouth opening and on the other side there is the fastening point of the head. One fitting ear for handmicrotelephone is in accordance with the AEN-system of the CCITT and the other ear in accordance with the SFERT-system of the CCITT. Crust of the spheric head is in two parts.

Both a commercial 5" loudspeaker and the self made loudspeaker with a 0,05 mm aluminium membrane have been used as the sound source. The flatness of frequency response of the commercial loudspeaker, when it is in the spheric artificial head, is about ± 5 dB a constant voltage at the distance of 5 cm from mouth opening, but by the self made loudspeaker frequency response is ± 2 dB from 160 Hz to 4900 Hz, see fig. 2. Every harmonics are less than 2 % from his fundamental by both loudspeaker types.

If the input voltage to the sound source of the artificial head is taken as a function of the frequency from a magnetic tape, so frequency response of the spheric artificial head is flat in ± 0,6 dB limit from 100 Hz to 8000 Hz, see fig. 2. A principle of this method is to regulate by a control microphone, which is at a point in the front of mouth opening, the output voltage of the oscillator to the sound source of the artificial head so that the sound level is constant at the reference point. The output voltage of the oscillator is taken as a function of the frequency on the magnetic tape. At the later time the magnetic tape can be recorded and the output fed through an amplifier to the artificial head. Implicit is the fact that the tape recorder employed must be of high quality and dependable. The distortion of the sound by the tape recorder method is 3 % or less from 160 Hz to 5000 Hz.

The directivity pattern of the artificial head is very spheric, see fig. 3., and the greatest differencies between sound levels at the axis of the mouth and at any spatial angle are by 1 kHz 5 dB, by 3,15 kHz 15 dB and by 5 kHz 17 dB. The sound pressure as a function of the distance along the axis of the

mouth in the near field falls at the rate of 7 dB per doubling of distance below 1,5 kHz, but after this frequency the rate is less than 7 dB and by 10 kHz the pressure falls at the rate of 5,7 dB per doubling of distance.

Comparative measurements

In the Green Book of the CCITT it is showing a mathematical method of Braun by which from frequency response curve of a telephone instrument the reference equivalent against the SFERT-system of the CCITT can be determined. By this new spheric artificial head the frequency response curves of some telephone instrument were taken on the level recorder paper. Thereafter the reference equivalent against the SFERT-system of the CCITT could be determined according to the Braun-method. The same telephone instruments were measured also by the germanish objective telephone measurement system which is used by the Federal German Administration. These comparative measurements are showing that this new spheric artificial head gives the reference equivalent about 0,15 N = 1,3 dB less than the germanish objective telephone measurement system. The differencies may be caused by the size of the control microphone in front of the mouth opening, by the pressure gradient and by measurement errors.

Using as an acoustic standard source

As an acoustic standard source for free-field calibration of acoustic transducers this new spheric artificial head can be used without the fixing "ears". Only at the low frequencies, below 160 Hz you have to use another sound source which has very large radiation membrane, because the distortion of the spheric artificial head is at these low frequencies to high. By the tape recorder method a sound level of 70 dB relative to $2 \cdot 10^{-5}$ N/m^2 can be got at a distance of 1 m from the mouth opening on its axis.

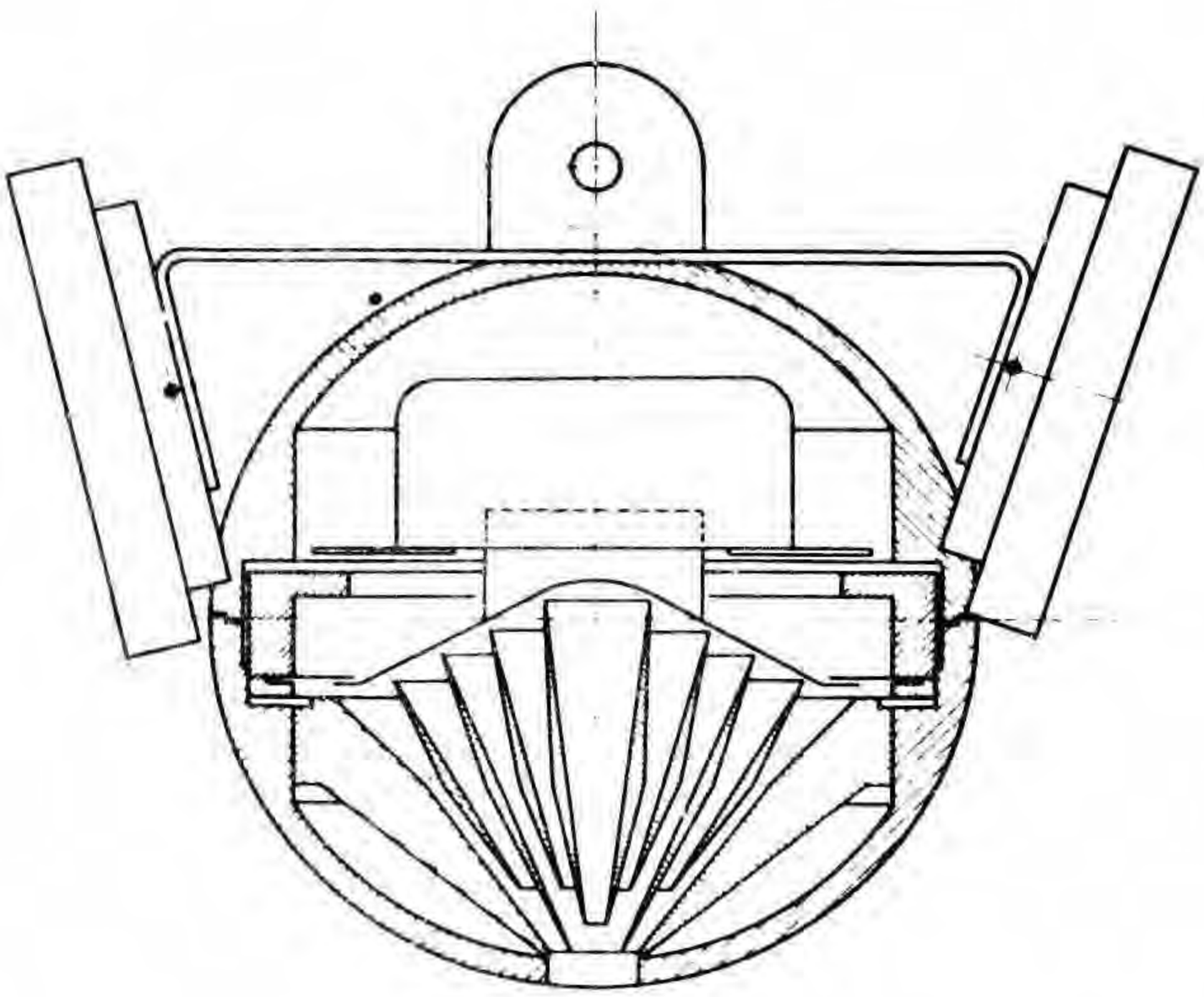

Fig. 1. Cutaway drawing of the spheric artificial head. The left "ear" has been made in accordance with the AEN-system of the CCITT and the right "ear" in accordance with the SFERT-system of the CCITT.

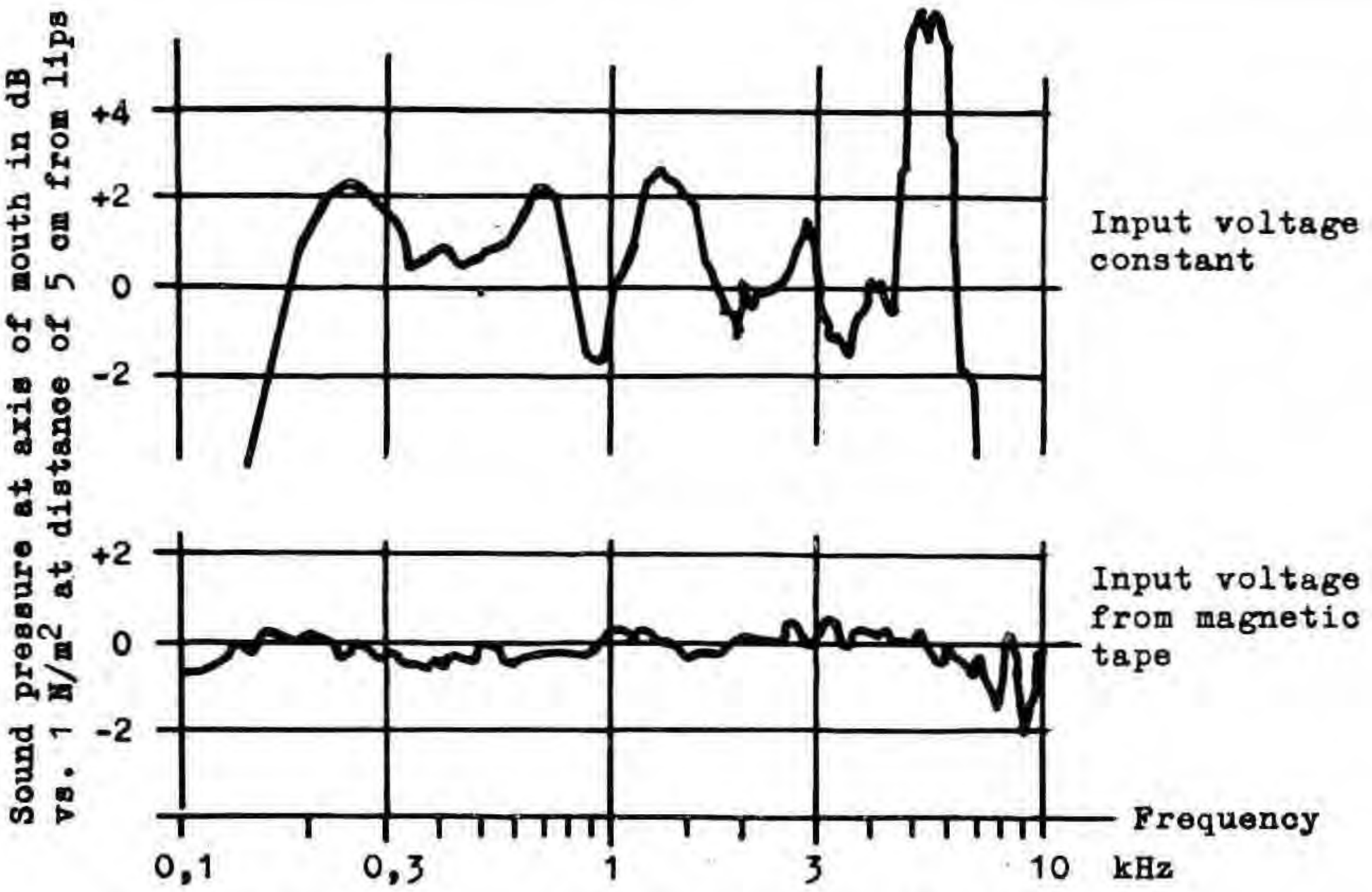

Fig. 2. Frequency response of the spheric artificial head.

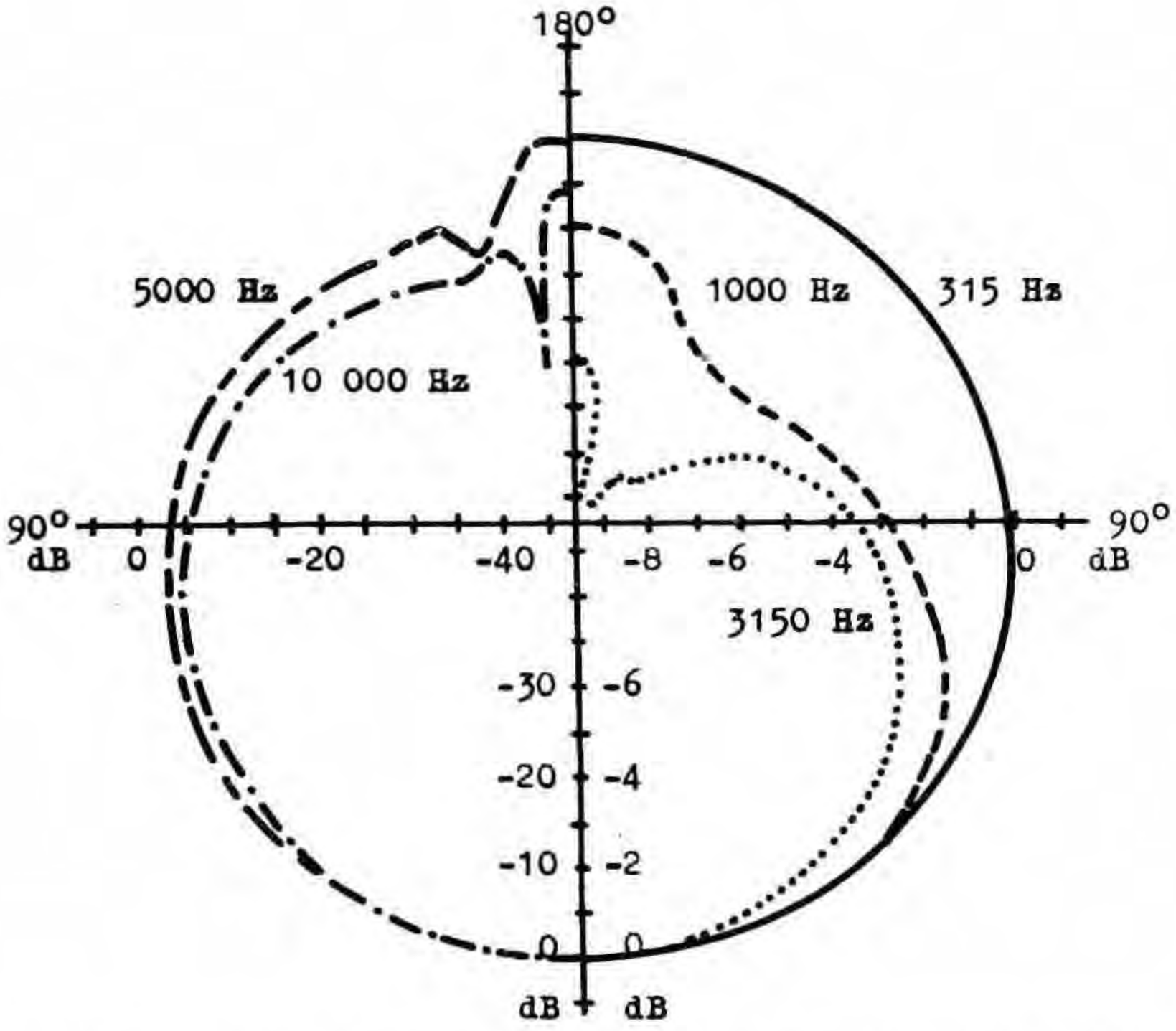

Fig. 3. Directivity pattern of the spheric artificial head. On the figure has been drew only the directivity pattern of the right side or of the left side. The scale on the left side is not same than on the right side.

042

FOURTH INTERNATIONAL CONGRESS ON ACOUSTICS
COPENHAGEN 21.-28. AUGUST 1962

Radiation Impedance of Systems with Arbitrary Shape

Ignacy Maleoki - Wincenty Pajewski

The object of research was a theoretical and experimentäl investigation concerning the influence of the shape of a radiating system on its mechanical impedance. The accustic potential Φ produced in the point P by a vibrating surface of any shape is determined by means of the Kirchhoff integral formula. For a far field this potential is

$$\Phi(p) = \frac{jk}{4\pi} \cdot \frac{e^{jkr_0}}{r_0} \left[\cos(\bar{n},\bar{r}) + \cos(\bar{n},\bar{r}_0)\right] \iint_S \Phi(s) e^{-jk(r-r_0)} \cdot dS \qquad /1/$$

Hence we can calculate in an approximate manner the specific impedance Z of the radiating surface:

$$Z = \frac{Z_0}{(1+q^2)}(1+q) \qquad /2/$$

where $q = \frac{1}{kF}\frac{\delta F}{\delta r}$

The function F is calculated for a given shape of the vibrating surface from /1/ . It appears that if the surface is convex $\frac{\delta F}{\delta r} > 0$ and the influence of the medium is characterized by an increase of the mass of the system .If however, the system has a concave radiating surface. $\frac{\delta F}{\delta r}$ is, over a certain region, negative, and the medium acts as an elastic load. In such a case the imaginary power of the source is also negative and can be written as:

$$N_x = \frac{1}{k}\iiint_V p\frac{\delta p}{\delta t} dV - \frac{1}{2}\iiint_V \rho v^2 dV \qquad /3/$$

The load of the source by the medium is not then a co-vibrating mass but a spring with the stiffness:

$$K = \frac{N_x}{j\omega p^2} \qquad /4/$$

Theoretical calculations were carried out for different shapes

of the vibrating system, however, they proved to be valuable only for balls with a small depth /the ratio of the depth to the radius of the aperture being not greater than 0,3/. If the ball is deeper /olosed system /, there occur then resonance vibrations of the whole internal oavity.

Depending on the ratio of the wavelength to the dimensions of the olosed system, we alternately deal with frequency bands for which the load of the system is either inert or oompliant. The behavior of a radially vibrating and hollow oylinder was investigated as an example. The acoustic field inside the oylinder with the radius R is determined by $p=AJ_0(kr)+BN_0(kr)$

The resonance frequencies are determined by oondition : /5/

$$J_1(kr)=0$$

The bands of the compliance load are below these frequencies.

Experimental investigations have confirmed theoretical calculations. Barium titanate transducers were used as vibrating systems. The changes in the mechanic impedance of the transducer were measured by means of the changes in its electric impedance. When the transducer works in the air, its radiation is minimal, and therefore the difference in the impedance of a transducer vibrating in a liquid /e.g.in water/ and in the air is equal to the radiation impedance Z_s .From the circular diagrams of the electric admittance, measured by means of an R L C bridge,we can then determine the radiation impedance

$$Z_s=R_s+jX_s \qquad /6/$$

The ratio of the components X_s and R_s can be found from the changes in the resonance frequency with the transducer working in the air and water.

$$\frac{X_s}{R_s}=2\frac{\Delta fe}{\Delta fm}\frac{R_0}{Z} \qquad /7/$$

R_0 - series resistance of the transducer in the air,

Δfe - the difference of frequency for the maximum electric reactance and the maximum electric inductance of the transducer in the air /from the circular diagram/,

Δfm - the change in the resonance frequency of the transducer due to the influence of the medium,

ζ - radiation resistance measured on the electrical side:

In the case of vibrations of a spherical ball, it follows from the theoretical calculus that

$$\frac{X_s}{R_s} = \pm \frac{\lambda}{2\pi R} \qquad /8/$$

where: R - radius of the transducer curvature,

λ - wavelength in the medium,

- the sign + corresponds to a convex transducer , the sign - corresponds to a concave transducer.

If $R \gg \lambda$ we can assume that $R_s = \rho c S$

where the radiating surface S

It turns out that for shallow balls vibrating in thickness and having the angle $\alpha < \frac{\pi}{2}$ the values $\frac{X_s}{R_s}$ and $\frac{X_s}{\rho c S}$ are equal to each other within the limits of the measurement error, and X_s has the nature of elastic load.

With an increase of α , or growth of the depth of the ball, the ratio $\frac{X_s}{\rho c S}$ increase and in the neighborhood of $\alpha \cong \pi$ it shows a several times greater value than that which has been calculated as: $\frac{X_s}{R_s}$

A comparison between the values of the quality factor Q of the transducer in a liquid and in the air shows that for the case $\alpha < \pi$, not only X_s increase but also the radiation impedance R_s decrease.

This signifies that the concentration of acoustic energy by means of radiating systems with the shape of a hollow sphere , or a deep spherical ball, is limited by the capability of the transducer surface to radiate energy.

The fact that of decisive importance is here the shape of the transducer rather than its dimensions, was confirmed by measurements carried out on a radially vibrating and hollow cylinder which was filled up with fluids with different ρc .The quality factor Q of the transducer remained in such a case unchanged, and the imaginary component of the impedance changed its sign in accord with Eq./5/.

Further details of the experiments carried out will be presented during the Congress.

P42

FOURTH INTERNATIONAL CONGRESS ON ACOUSTICS
COPENHAGEN 21.-28. AUGUST 1962

UMWANDLUNG MECHANISCHER ROTATIONSENERGIE IN MECHANISCHE SCHWINGUNGSENERGIE.

von R. Pohlman und E.G.Lierke, Aachen
Laboratorium für Ultraschall der Technischen Hochschule Aachen.

Die Forschung hat in den letzten Jahren eine Reihe neuer Anwendungsmöglichkeiten für den Ultraschall erschlossen, deren technische Verwirklichung in vielen Fällen nur am hohen Preis der akustischen Energie scheitert. Die allgemein übliche Gewinnung der akustischen Energie mit magnetostriktiven oder piezoelektrischen Gebern auf dem Umweg über elektrische Hochfrequenzenergie ist trotz aller Vorzüge für manche Verwendungszwecke zu kostspielig, während die bekannten mechanischen Generatoren in der Regel zu "schallweich" gegenüber Flüssigkeiten sind und deshalb für technische Zwecke kaum eingesetzt werden. Als Ausnahmen mit speziellem technischen Anwendungsbereich seien die Flüssigkeitspfeife von Pohlman und Janovski, sowie ein in der "Ultrasonic News" (1958) beschriebener "Hydrodynamischer Ventiloszillator" von Boujoukos genannt.

In der vorliegenden Arbeit wird die Möglichkeit untersucht, hochfrequente mechanische Schwingungen auf direktem Wege aus mechanischer Rotationsenergie zu gewinnen und mit gutem Wirkungsgrad als akustische Energie in Flüssigkeiten abzustrahlen.

I. Zwei Möglichkeiten der Rotationserregung.

Als Schallgeber wird ein auf Resonanz abgestimmter, im Bewegungsknoten starr gehalterter Zylinderstab verwendet, der am Eingang durch eine periodische Kraft erregt und am Ausgang durch eine Flüssigkeit belastet wird. Zwei Anregungsarten wurden untersucht :

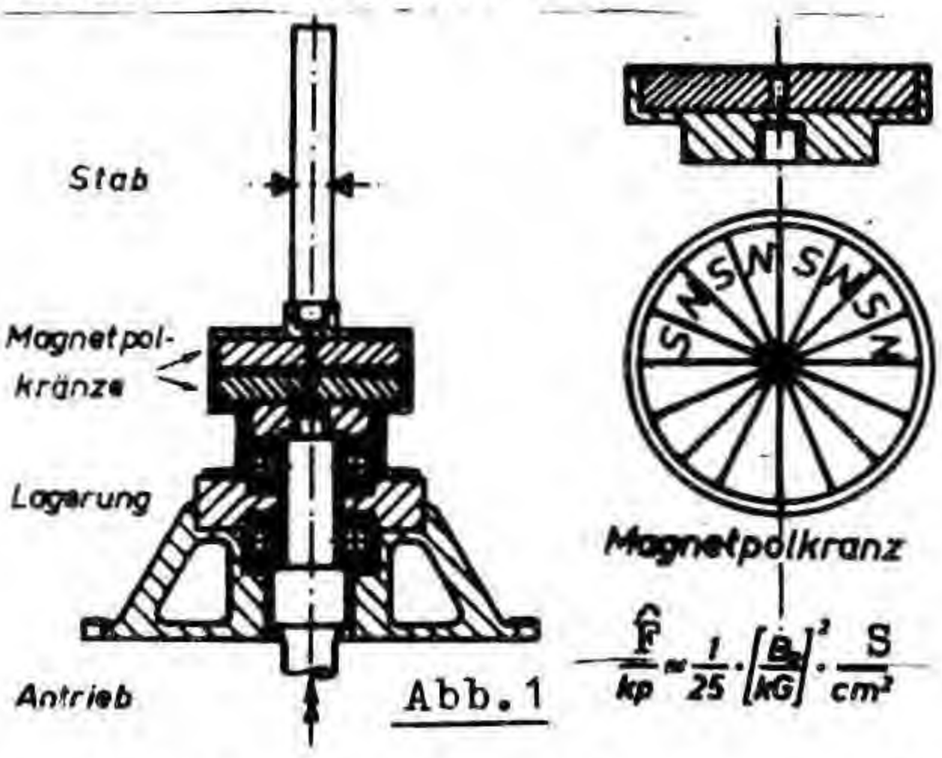

Abb.1

1. die extrem "schallharte" Massenkrafterregung durch rotierende Axial-Rillenkugellager mit aufgeprägter Sinuscharakteristik (nach Art der "Berg-u.Talbahn")
2. die praktisch verschleißfreie aber weniger "schallharte" Erregung durch hochkoerzitive Permanentmagnete (schematisch dargestellt in Abb. 1). Der Stab ist am Eingang mit einem Kranz von Magnetpolen (vgl.Abb.1 rechte Seite) gekoppelt. Ein gleicher Magnetpolkranz rotiert, durch einen dünnen Luftspalt vom Stabanhang getrennt und durch Axial-Lager an der Vertikalbewegung gehindert, hochtourig und erzeugt eine periodische Wechselkraft $F \approx \hat{F} \cdot \frac{4}{\pi}(\sin\omega t - \frac{\sin 3\omega t}{9} + \frac{\sin 5\omega t}{25})$

Da die Untersuchungen am magnetisch erregten Schwinger bei Redaktionsschluß noch nicht abgeschlossen waren, kann hier nur über die Kugellagererregung ausführlicher berichtet werden.

II. Massenkrafterregung durch Spezial-Kugellager.

Verwendet wurden Axial-Rillenkugellager vom Typ 51110 der Firma Kugelfischer, Schweinfurt, bei denen durch automatisches Schleifen in je eine Lagerschale in axialer Richtung eine in sich geschlossene Sinuskurve von 10 μm Amplitude eingesenkt wurde (Laufrillendurchm.2 R = 60 mm, Wellenzahl n = 95, Wellenlänge λ = 2 mm und Kugelradius r = 3 mm).
Die Lager wurden so kombiniert, wie das aus den schematischen Abbildungen 2a u. 2 b ersichtlich ist. Zwei komplette Lagersätze sind notwendig, weil die Kugeln nur Drucke zwischen den Lagerschalen übertragen können, also jeweils nur in der positiven Halbperiode der Belastung wirksam werden. Die Kombination zweier Lager

mit einer Wellringversetzung um $\lambda/2$ gestattet dann die Übertragung der vollen Belastungsperiode. Normallagerschalen (N) und Wellringe (W) sind unter sich starr gekoppelt, so daß die Rotation der äußeren Lagerschalen (N) eine periodische Massenkraft am Stabeingang bewirkt.
Die Erregerfunktion ergibt sich unmittelbar aus der Bewegungsgleichung der Kugelmittelpunkte auf der Sinuskurve. Man wählt zweckmäßig Zylinderkoordinaten R, φ ξ und bezieht zunächst auf die Koordinaten R=const.φ_0 und $\xi_0=\hat{\xi}_0\cos n\varphi_0$ des Berührungspunktes P (vgl.Abb.2c). Für $\hat{\xi}_0 \ll \lambda$ erhält man als gute Näherung

(1) $\varphi=\varphi_0 \pm \frac{2\chi}{n}\sin n\varphi_0$ und $\xi=\hat{\xi}_0(\cos n\varphi_0 \pm \frac{\chi}{2}\cos 2n\varphi_0) \pm \text{const.}$

wobei χ der Quotient aus Kugelradius r und doppeltem Krümmungsradius $2\rho_0$ der Sinuskurve in den Umkehrpunkten ist. Die doppelten Vorzeichen sind zur Unterscheidung des oberen Lagers (oberes Vorzeichen) vom unteren (unteres Vorzeichen) angegeben. Die Koordinate φ_0 ist bei einem mit konstanter Tourenzahl rotierenden Normallager eine lineare Funktion der Zeit t, der sich beim "gewellten" Lager eine periodische, für kleine x annähernd harmonische Zeitfunktion überlagert. Man erhält für $x<1/2$ als gute Näherung $\varphi_0=\bar{\omega}t \mp x\sin\omega t$

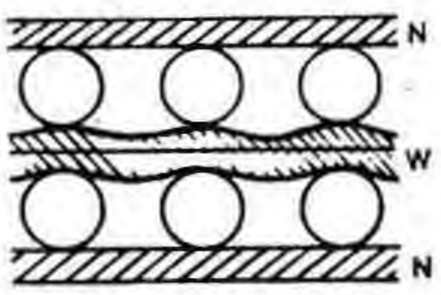

Abb.2a

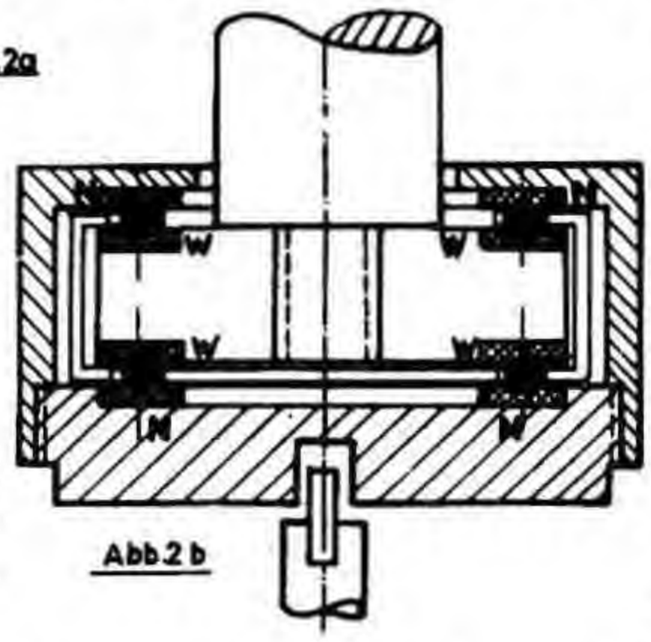

Abb.2b

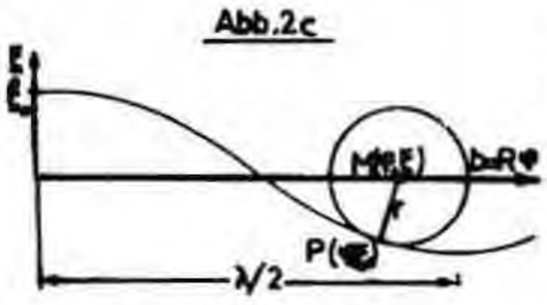

Abb.2c

wenn $\bar{\omega}$ und ω die mittlere Kreisfrequenz der Kugeln auf der Kreisbahn bzw. auf der Sinuskurve bedeuten. Die Gleichungen (1) lassen sich dann als Fourrierreihen

(2) $\varphi(t)=\bar{\omega}t+\Sigma a_k \sin k\omega t$ und $\xi(t)=\hat{\xi}_0\Sigma b_k\cos k\omega t$

darstellen, wobei die Berechnung der Fourrier-Koeffizienten a_k und b_k auf Besselfunktionen $J_k(x)$ führt. Man findet

(3) $a_k(n,x) = \pm\frac{2\chi}{n}[J_{\frac{1}{2}(1-k)}(x)-J_{\frac{1}{2}(1+k)}(x)]$ $(k>1)$ $a_1(n,x) = \pm\frac{2\chi}{n}[J_{\frac{1}{2}(0)}(x)-J_{\frac{1}{2}(2)}(x)-\frac{1}{2}]$

$b_k(x) = [J_{\frac{1}{2}(1-k)}(x)+J_{\frac{1}{2}(1+k)}(x)] \pm \frac{\chi}{2}[J_{\frac{1}{2}(3-k)}(2x)-J_{\frac{1}{2}(3+k)}(2x)]$ $\quad k = 1,2,3\cdots$

In Abb. 3 sind die Fourrierkoeffizienten b_k als Funktion von x angegeben. Man erkennt, daß für die verwendeten Läger mit x=0,15 die Erregerfunktion praktisch rein harmonisch ist, d.h. $\xi=\hat{\xi}\cos\omega t$ Die periodischen Abweichungen zweier (in Abb.2a) übereinanderstehender Kugeln von ihren Normalabständen zum Zeitpunkt t=0 sind so gering, daß sie innerhalb der Lagerpräzision liegen. Für größere x muß man sie dagegen berücksichtigen. Man erhält :

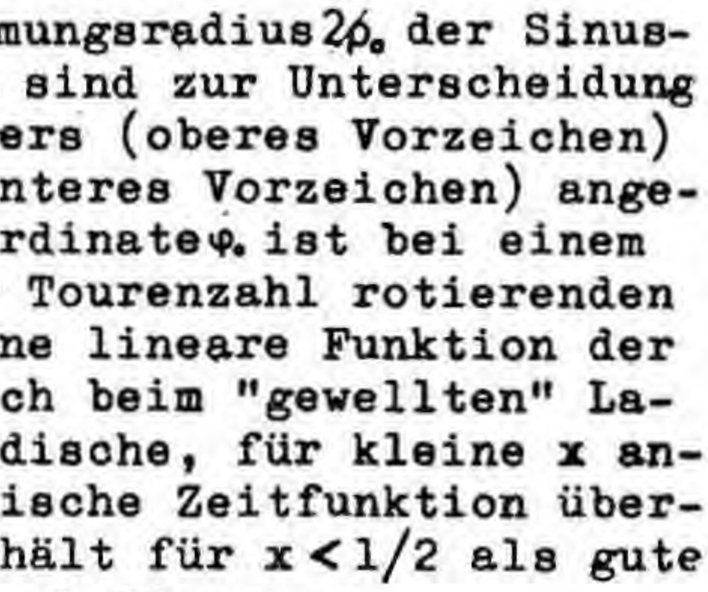

Abb.3

$\Delta\xi \ll -\frac{x^3}{4}\hat{\xi}_0$ $\quad \Delta b = R\Delta\varphi \ll (x-x^3)\frac{\lambda}{\pi}$

III. Stabschwinger mit Massenkrafterregung.

Das Schwingerprinzip ist aus Abb. 4 ersichtlich. Der Stab von der Länge l, mit dem Wellenwiderstand $w_0=\rho vS$, der Querschnittsfläche S, der Anhangsmasse m_1 und dem Abschlußwiderstand R_α wird durch die Fliehkräfte zweier gegenläufig rotierender Massen $m_2/2$ harmonisch erregt. Gesucht ist die Amplitude $\hat{F}$ der an den beiden Drehpunkten angreifenden harmonischen Kraft F, die identisch ist mit der (axialen) Belastungsamplitude des Kugellagers. Es interessieren weiterhin die Amplituden $\hat{u}_{1e}$ und $\hat{u}_{1a}$ der Schallschnelle am Eingang und Ausgang des Stabes, sowie die vom System aufgenommene und die an R_α abgegebene Leistung, aus der sich der Wirkungsgrad des Schwingers berechnen läßt. Gegeben ist die Erregerfunktion $\xi=\hat{\xi}\cos\omega t=\frac{u}{\omega}$ Unter Berücksichtigung der "dualen"mechanisch-elektrischen Analogien (vgl.Abb.4) kann man das mechanische

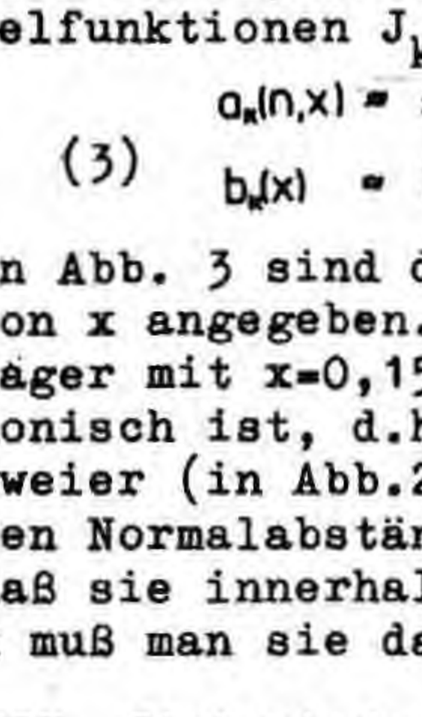

Abb. 4a

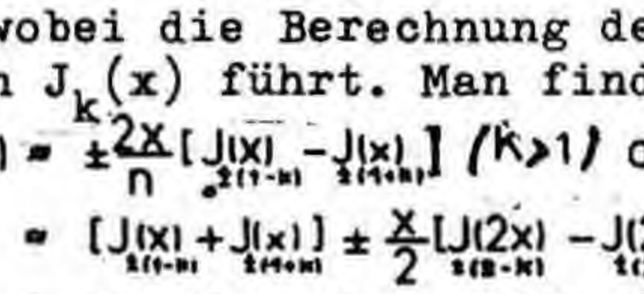

Abb.4b

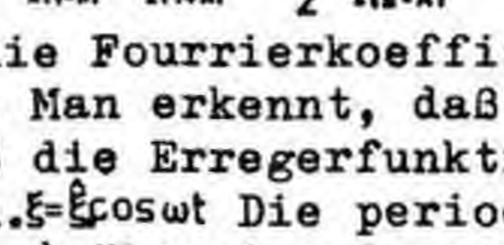

Abb.4c

Kraft ⟷ Spannung
Schnelle ⟷ Strom
Masse ⟷ Induktivität
Stab ⟷ Doppelleitung

System in ein mathematisch analoges elektrisches System transformieren.Man findet das Ersatzschaltbild Abb.4b, in dem die elektrischen Größen bereits wieder durch ihre mechanischen Äquivalente ersetzt sind. Zur Berechnung der Belastungsamplitude $\hat{F}$ und der Schnelleamplitude $\hat{u}_{1e}$ am Stabeingang kann man den Stab durch seine komplexe Eingangsimpedanz $Z_e = R_e + jX_e$ ersetzen. Das Ersatzbild vereinfacht sich dann (vgl.Abb.4c) und man findet:

$$(4) \qquad \hat{F} = \omega m_2 \hat{u} \sqrt{\frac{R_e^2 + [\omega m_1 + X_e]^2}{R_e^2 + [\omega(m_1+m_2) + X_e]^2}} \qquad \hat{u}_{1e} = \frac{\hat{u}\,\omega m_2}{\sqrt{R_e^2 + [\omega(m_1+m_2)+X_e]^2}}$$

Da die Verluste am Abschlußwiderstand R_a bei hoher Stabgüte ($Q_M \approx 10^4$) die inneren Verluste des Stabes um Größenordnungen übersteigen, kann der Stab bei den folgenden Betrachtungen praktisch als verlustfrei angesehen werden. Dann wird aber

$$(5) \qquad R_e = \frac{R_a/\cos^2\frac{\omega}{v}l}{1+(R_a/w_e)^2\tan^2\frac{\omega}{v}l} \qquad X_e = w_e \tan\frac{\omega}{v}l\,\frac{1-(R_a/w_e)^2}{1+(R_a/w_e)^2\tan^2\frac{\omega}{v}l} \qquad \frac{\hat{u}_{1e}}{\hat{u}_{2e}} = \sqrt{\frac{R_e}{R_a}}$$

Aus (4) und Abb.4c erkennt man, daß zwei Resonanzfrequenzen auftreten.

$$(6) \qquad \omega_1 = -\frac{X_e(\omega_1)}{m_1+m_2} \quad \text{mit} \quad \hat{F}_1 = m_2\hat{\xi}_e\omega_1^2\left[1+(a_1\sin 2\tfrac{\omega_1}{v}l)^2\right]^{1/2} \qquad \text{wobei} \quad 2a_1 = \frac{m_2}{m_1+m_2}\left(\frac{R_a}{w_e} - \frac{w_e}{R_a}\right) = \frac{2m_e}{m_1+m_2}a_1$$

$$(7) \qquad \omega_2 = -\frac{X_e(\omega_2)}{m_1} \quad \text{mit} \quad \hat{F}_2 = m_2\hat{\xi}_e\omega_2^2\left[1+(a_2\sin 2\tfrac{\omega_2}{v}l)^2\right]^{1/2} \qquad \omega_1 < \omega_2$$

Während bei der "Parallelresonanz" (ω_1) ein schmales Belastungsmaximum auftritt, liegt bei der "Reihenresonanz" (ω_2) ein relativ breites Belastungsminimum. Die Frequenz ω_2 ist also (Belastungsmaximum-instabiler Zustand) als Arbeitsfrequenz ungeeignet. Der mechanisch-akustische Wirkungsgrad ist etwas kleiner als bei ω_1. Die Frequenz ω_{1a} ist als Arbeitsfrequenz (Belastungsminimum-stabiler Zustand) gut geeignet. Man findet mit $R_e = R_a/\cos^2\frac{\omega_1}{v}l$ und $R_a = (\rho v)_{fl}S$

$$(8) \qquad \hat{F} = \frac{R_a\omega_1\hat{\xi}_e}{\sqrt{1+(R_e/\omega m_2)^2}} = \hat{u}_{1a}R_a = \hat{u}_{2a}\sqrt{R_eR_a}$$

Für den Mittelwert der abgestrahlten Wirkleistung ergibt sich $P_a = \frac{R_a\hat{u}_{1a}^2}{2}$

Mit $m_2 = 600g$, $m_1 = 350g$ und $f_2 = \omega_2/2\pi = 6kHz$ erhält man theoretisch für einen in Wasser abstrahlenden Aluminiumstab ($S = 16\ cm^2$) eine Lager-Belastungsamplitude $\hat{F} \approx 128$ kp, eine Schwingeramplitude $\hat{\xi}_{1a} \approx 12\,\mu m$ und eine abgestrahlte akustische Leistung von 240 Watt (das entspricht einer Schallintensität von etwa 15 Watt/cm^2

Die Belastung im Arbeitspunkt wächst bei konstanter Lageramplitude annähernd linear, die akustische Leistung dagegen annähernd quadratisch mit ω_2.Auf die Lebensdauer der Lager wird die relativ niedrige Axiallast im Arbeitspunkt keinen bestimmenden Einfluß haben. Jedenfalls ergibt sich bei der konventionellen Lebensdauerberechnung unter alleiniger Berücksichtigung der Axiallast ein viel höherer Wert als man erwarten darf. Die Lebensdauer wird in erster Linie von der Lagerreibung und den Belastungsspitzen im Anlaufbereich (vgl.Abschn.IV) abhängen, wobei die Tangentialbeschleunigung der Kugeln $b_t = -\omega^2\Sigma k^2 a_k \sin k\omega t$ (vgl.(2)) einen starken Einfluß auf die Lagerreibung haben dürfte. Der Einfluß der genannten Parameter ist theoretisch schwer zu erfassen, so daß man auf umfangreiche Verschleißmessungen angewiesen ist. Der Verschleiß wurde nach wiederholten Laufversuchen durch Abtasten des Rillengrundes nach dem Talyrond-Verfahren ermittelt (bei Redaktionsschluß waren diese Messungen noch nicht abgeschlossen).Da mit wachsendem Verschleiß auch das Krümmungsverhältnis x und die Belastungsamplitude $\hat{K}$ kleiner werden, ist zu erwarten, daß die Lageramplitude nach einer Exponentialfunktion abnimmt.

IV. Der Anlaufvorgang

Um auf die zur Arbeitsfrequenz gehörige Tourenzahl zu kommen, muß der Antriebsmotor einen Anlaufbereich $0 \leq \omega \leq \omega_1$ durchlaufen, in dem der Stab wegen seiner nicht im Bewegungsknoten liegenden, starren Einspannung eine andere Eingangsimpedanz als (4) besitzt. Auch hier ergibt sich, wie im vorigen Abschnitt, eine "kritische" Frequenz mit einem Belastungsmaximum (Parallelresonanz) und ein Belastungsminimum (Reihenresonanz). Da aber der Abschlußwiderstand R_a wegen der starren Einspannung am Eingang nicht wirksam werden kann, ergibt sich für die beiden

Komponenten der Eingangsimpedanz:

(9) $$R_e = w_0 \frac{a l' (1 - \sin\varphi/\varphi)}{\sin^2\varphi} \qquad X_e = -w_0 \cot\varphi$$

wobei a die Dämpfungskonstante und l' der Abstand zwischen Stabeingang und Einspannung bedeuten ($\varphi = \frac{\omega}{v} l'$). Infolge der außerordentlich niedrigen Dämpfungskonstanten ($\alpha_{Al} \approx 10^{-3} \omega^2$ cm^{-1}) erhält man im kritischen Punkt eine sehr hohe Belastungsspitze, die das Lager zerstören oder den Motor zum Stillstand bringen kann. Um dies zu vermeiden, wurde der Stab direkt über der Anhangsmasse durch ein Dreibackenfutter starr eingespannt. In diesem Falle liegt der kritische Bereich oberhalb der Arbeitsfrequenz . Außerhalb des kritischen Bereichs kann der Stab wieder als praktisch verlustfrei betrachtet werden, so daß man für den Belastungsverlauf im Anlaufbereich findet :

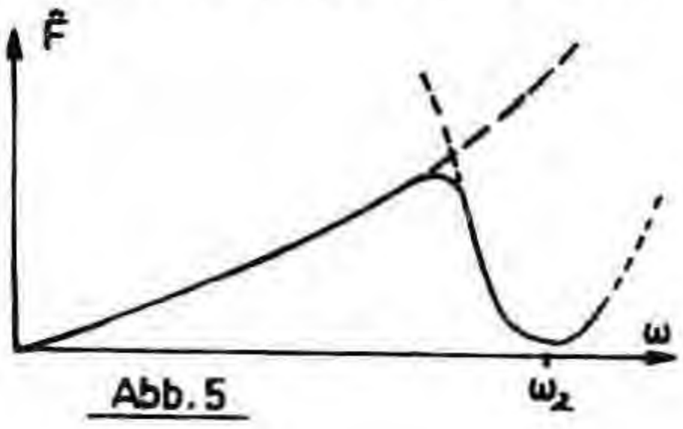

Abb.5

$$\hat{F} = \omega m_2 \hat{u} \frac{m_1/M' - \cot\varphi/\varphi}{(m_1+m_2)/M' - \cot\varphi/\varphi}$$

mit $M' = \rho S l'$ als mitschwingender Stabmasse

Ist die Arbeitsfrequenz ω_2 erreicht, so wird das Dreibackenfutter gelöst, und der Stab kann (nunmehr im Bewegungsknoten gehaltert) "frei" schwingen. Die vollständige Belastungskurve hat den in Abb. 5 skizzierten Verlauf.

Zur Erhöhung der Frequenz muß man entweder die Tourenzahl des Antriebsaggregats oder die Wellenzahl auf den Wellringen erhöhen. Letzteres hat eine Vergrößerung der Massen m_1 und m_2 zur Folge, da man zu größeren Lagern übergehen muß. Die Massenvergrößerung kann allerdings dadurch kompensiert werden, daß man m_1 federnd am Stab befestigt und die Federung so berechnet, daß sich im Anlaufbereich ein weiteres Belastungsminimum ergibt.

Anstelle des zylindrischen Stabes können selbstverständlich auch konische Stäbe sowie Exponential-, Kathenoid- oder Stufenrüssel verwendet werden.

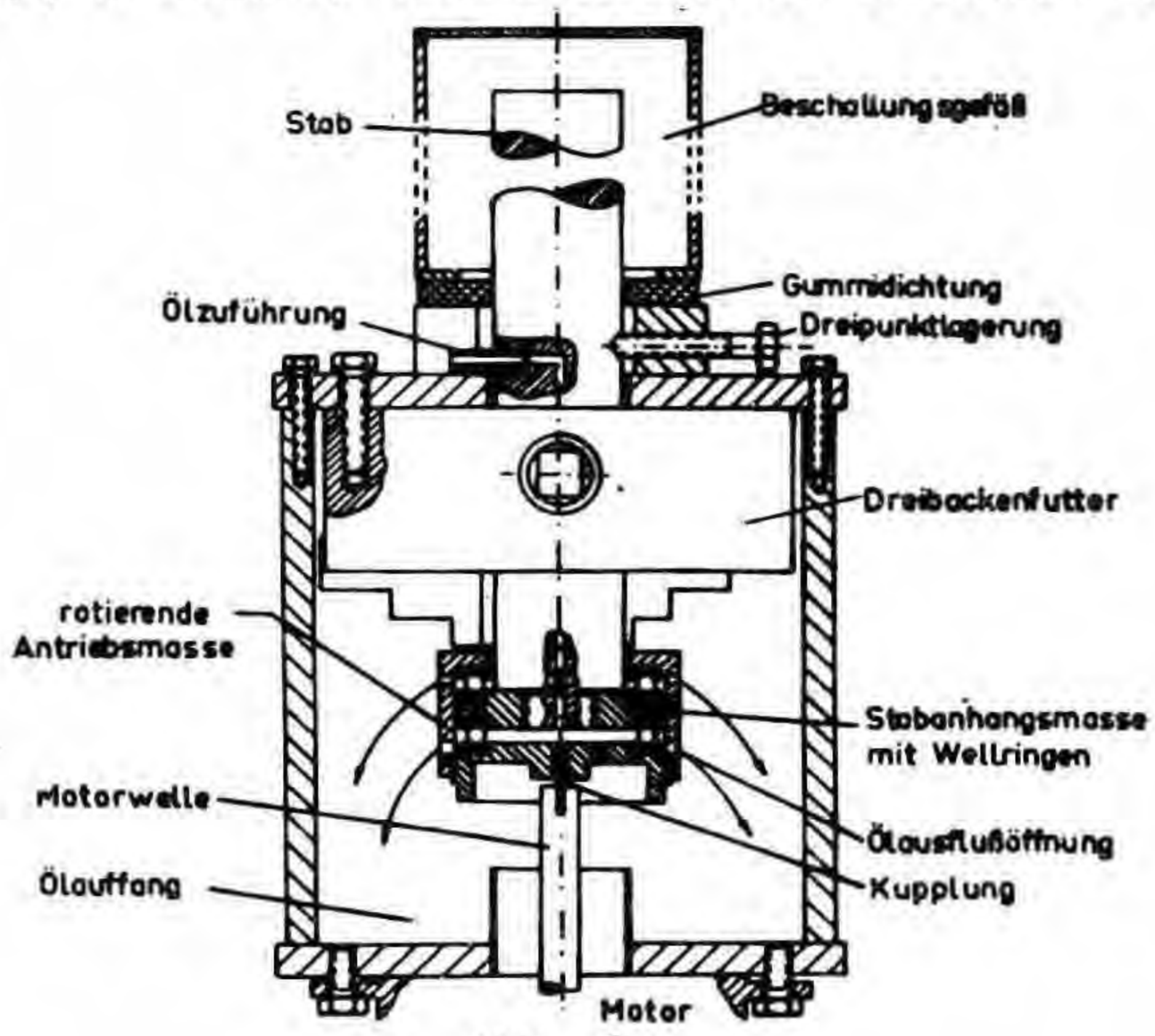

Abb. 6

Literatur:

1. L. Bergmann: "Der Ultraschall", S.Hirzel-Verlag, Stuttgart 1954

2. I.I.Teumin: "Ultraschall-Schwingungssysteme", Maschgis-Verlag,Moskau 1959 deutsche Übersetzung bei S.Hirzel-Verlag, Stuttgart in Vorber.

G43

FOURTH INTERNATIONAL CONGRESS ON ACOUSTICS
COPENHAGEN 21.-28. AUGUST 1962

A RESONANCE ANALOGUE SPEECH SYNTHESISER.

J. Anthony, A.M.I.E.E.,
Phonetics Department, Edinburgh University.

W. Lawrence, A.M.I.E.E.,
Signals Research & Development Establishment, Ministry of Aviation.

This Synthesiser is an electrical analogue of the human vocal mechanism. With suitable control of parameters related to various features found in the complex speech wave, steady-state speech sounds or continuous speech can be simulated. The present instrument has been developed from the Parametric Artificial Talking Device designed by Lawrence[1] to demonstrate that intelligible speech could be generated from a small number of signals which had a low information rate. Development has been made in several directions, notably in closer conformity to the mathematical model dictated by acoustic theory, in improved precision of control, in an increase in the number of parameters, and in increased skill in the interpretation and use of the data obtained from analysis. The intention is to improve the quality of the speech by progressive modification of the machine while retaining flexibility and ease of control for research purposes.

[At this point a demonstration on tape was given of two items of synthesised speech. The first was the phrase "How do you do?" as demonstrated in 1952 using only four parameters and the second a short fable lasting 45 secs. using eight parameters.]

In the production of human speech various types of excitation are applied to the resonant cavities of the throat, mouth and nose. For voiced sounds the source is of a pulse-like nature, produced by the action of the vocal cords periodically interrupting the air stream from the lungs. For fricative sounds the source consists of turbulent noise or hiss formed when air is forced through a narrow orifice.

FIG. 1

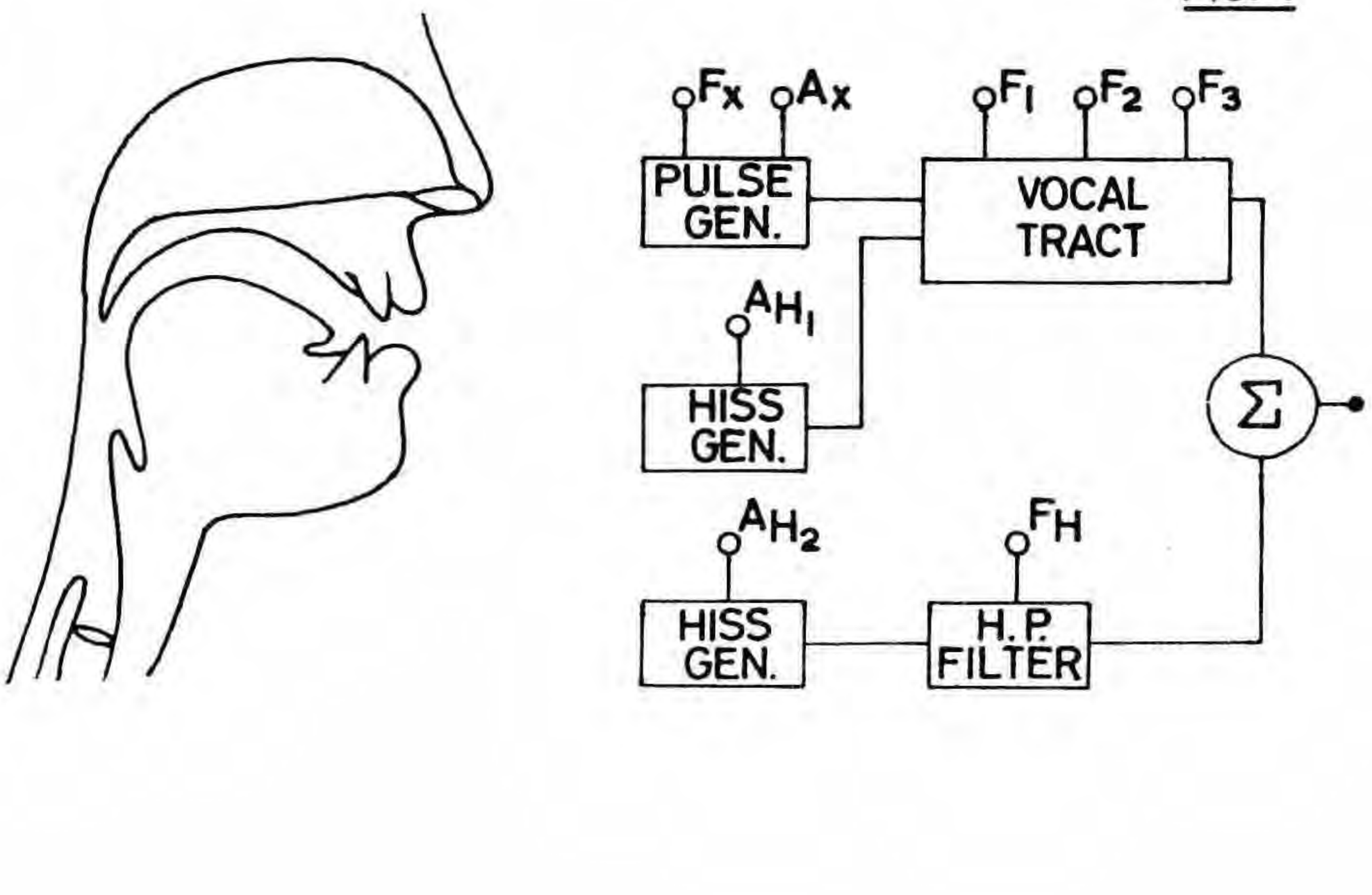

FIG. 5

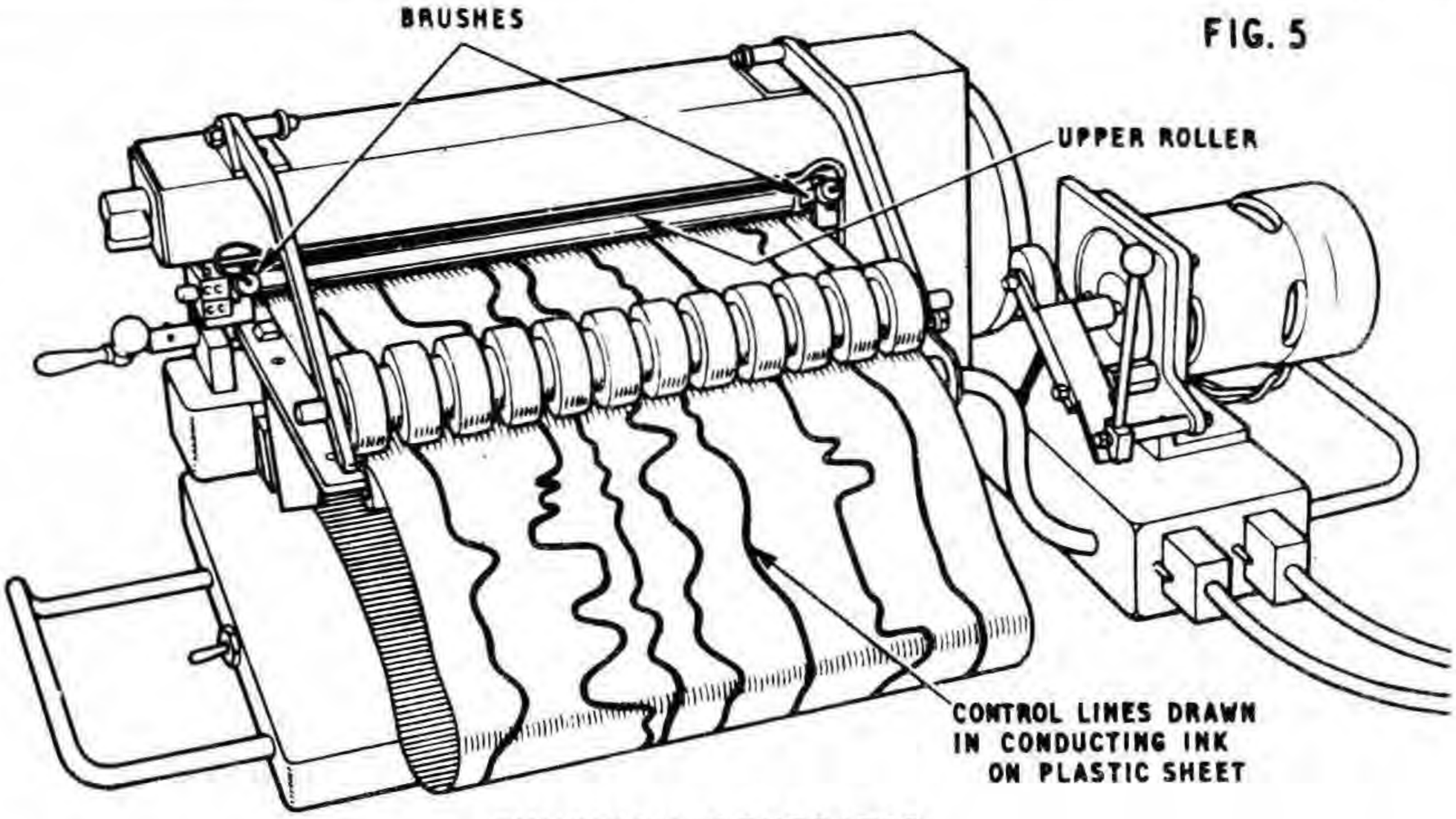

FUNCTION GENERATOR

The Function Generator used at present to provide the time varying voltages for dynamic control of the synthesiser was described by FOURCIN[3]. It is of the Potential Divider type as also used in the Speech Transmission Laboratory at R.I.T., Stockholm. The basic arrangement is shown in Fig. 5. The upper roller is uniformly coated with an electrically conducting material and a constant potential gradient is maintained along its length. Control lines about 1 mm. wide are drawn in conducting ink on a plastic sheet. The point at which the line makes contact with the roller determines the potential of that whole line. As the sheet is moved under the roller, variation of line position gives a corresponding change of potential. In principle any number of lines may be drawn providing that they do not interact. Normally the speed of the sheet is the same as that of the Kay Electric Spectrograph to allow formant and pitch values to be traced directly.

The transmission of speech in terms of a small number of slowly varying parameters allows great reductions in bandwidth to be achieved: the synthesiser as here described, constitutes essentially the receiving terminal of an analysis synthesis transmission system. Research using speech synthesis at the Phonetics Department of Edinburgh University has been undertaken not only for the general illumination it throws on the whole speech process but also with the direct purpose of contributing to the development of bandwidth compression systems to meet the ever-increasing demand for speech communication.

[1]Lawrence, W.
"The synthesis of speech from signals which have a low information rate", Proc. of the 1952 Symposium on the Applications of Communication Theory, ed. W. Jackson, 460-469 (London, 1953).

[2]Fant, G.
"Acoustic Theory of Speech Production". Mouton & Co. 1960.

[3]Fourcin, A.
"A Potential Dividing Function Generator for the Control of Speech Synthesis". J.A.S.A. p. 1501, 32, 11, Nov. 1960 (Abstract).

This work was undertaken under a contract between the Ministry of Aviation and the University of Edinburgh for research into the specification of speech by means of acoustic parameters.

H43

FOURTH INTERNATIONAL CONGRESS ON ACOUSTICS
COPENHAGEN 21.-28. AUGUST 1962

RÉPONSE DE L'OREILLE AUX PHENOMENES TRANSITOIRES

PIMONOW Léonid, Dr. de l'Université de Paris. Ing. au Centre National d'Etudes des Télécommunications - Paris.

Pour établir la bande passante d'une chaîne de haute fidélité, on a entrepris les essais suivants dans le Laboratoire du Département Acoustique du C.N.E.T.:

Deux séries A et B d'impulsions d'une durée de 5 microsecondes environ et d'intervalles de 1 s. ont été transmises à travers deux préamplificateurs à un amplificateur "commun" suivi d'un ionophone.

La série (A) précédait la série (B) de 0,5 s. De cette manière l'oreille était attaqué chaque 0,5 s par un signal parvenant d'une série différente et entendait les signaux dans l'ordre qui suit : A - pause 0,5 s, B - pause 0,5 s, A - .....

La bande passante de la chaîne était de 100 kHz. En réglant convenablement le gain de chaque préamplificateur ont entendait une succession d'impulsions parfaitement identiques.

Ensuite, on a introduit dans le préamplificateur qui transmettait la série B un filtre passe-bas avec $R_{lim.}$ = 10 kHz. En essayant de compenser la différence d'énergie des impulsions des deux séries par une préamplification plus grande (de B), on a tenté d'obtenir une sensation identique pour toutes les impulsions. Or, l'oreille percevait toujours une différence entre les impulsions des deux séries.

Ensuite, on a progressivement élargi le filtre passe-bas de 5 kHz chaque fois et on a répété l'opération.

Selon les sujets (l'expérience a été faite avec 6 sujets) la différence de perception entre les deux séries d'impulsions disparaisait quand la bande du passe-bas dépassait 20 à 45 kHz. Un jeune garçon de 15 ans percevait une différence jusqu'à 45 kHz. Pour les personnes plus agées, la fréquence limite était plus basse mais elle était toujours et au moins deux fois supérieure à celle de la bande passante de l'oreille.

Une seconde expérience analogue a été faite par application des deux séries d'impulsions à travers des chaînes semblables d'une largeur identique (ΔF = 100 kHz avec gain réglable dans les préamplificateurs

séparément) mais avec des impulsions qui se distinguaient par la durée. Les impulsions plus courtes étaient toujours de l'ordre de 2 microseconde et la durée des impulsions plus longues pouvait être progressivement diminuée de 0,5 ms jusqu'à 2 micros.

Lors de cette expérience aussi, on a constaté qu'on ne pouvait pas obtenir une sensation identique malgré la compensation d'énergie (par une amplification plus grande) si la différence de la durée était inférieure, selon les sujets, de 0,02 à 0,2 ms.

En conclusion, l'oreille perçoit des différences d'intervalle de temps qui sont très inférieures à la période réfractaire des influx nerveux qui est de l'ordre de 2 ms et, de même que dans le cas de phénomènes transitoires, l'oreille est sensible aux bandes passantes des chaînes acoustiques qui sont deux à trois fois supérieures à celles de la bande passante (statique) de l'oreille, qui est de l'ordre de 16 kHz.

Pour expliquer ce phénomène, il nous semble que l'on doit faire appel à l'analyse spectrale.

En effet, entre la largeur du spectre et la durée du signal, il existe la relation

$$S_k = k \int_{-\infty}^{\infty} f(kt) e^{-j\omega t}\, dt = S\ (\omega/k)$$

Si on augmente k fois la durée de la fonction f(t), le spectre se rétrécit dans la même proportion.

Plus particulièrement, l'étendue du spectre instantané est fonction de la durée du signal. On peut donc, d'après la décroissance progressive de la densité spectrale qu'on observe dans une fraction de la bande du spectre instantané, déduire ce qui se passe en dehors de la gamme de mesure. La figure 1 donne ces relations pour l'organe de l'ouïe.

Les signaux (fig. 1a) supposés appliqués à un analyseur physique ayant un très grand nombre de filtres fortement amortis, branchés en parallèle et couvrant la gamme de 0 à 55 kHz, auront des spectres évolutifs tels qu'ils sont représentés en trois dimensions sur la figure 1b.

Le signal le plus bref (en haut de la figure) aura évidemment un spectre plus large (sur l'axe des fréquences) que le signal arrondi (en bas de la figure). Si, au lieu d'être appliqués à un analyseur physique, les signaux sont appliqués à l'analyseur auditif qui ne couvre qu'une gamme de 16 Hz à 16 kHz, seules les fractions de spectre comprises entre les points A et B (fig. 1b) seront mesurées par cet analyseur.

Comme on peut facilement l'observer d'après la pente de la fraction du spectre AB, on peut en déduire la durée des signaux.

Or, pour transmettre le spectre d'un signal très bref, la chaîne acoustique doit avoir une bande passante très large et, en tout cas, beaucoup plus large que celle de l'oreille. En effet, une bande étroite arrondit le signal, et l'oreille qui peut, par la mesure d'une fraction de la gamme, en déduire l'étendue du spectre, le percevra.

Certes, dans le cas d'une chaîne de transmission à bande étroite on peut recourir à une amplification supplémentaire des hautes fréquences. Toutefois, cela ne fera que corriger la pente AB, et n'aura pas d'infuence sur la durée du spectre sur l'axe des temps, qui exerce également une influence sur la sensation si les signaux deviennent plus longs.

D'autre part, il faut tenir compte de ce que les mélanges acoustiques comportent outre des signaux brefs, ou, plus généralement des variations d'amplitudes rapides, également des phénomènes périodiques. Or, une amplification des composantes de fréquence élevée déforme le spectre périodique. En conséquence, l'amélioration de la sensation relative au transitoire bref produite par une amplification supplémentaire des hautes fréquences est pratiquement annihilée par la déformation des phénomènes périodiques. Cette compensation ne peut donc avoir de raison d'être que si on ne transmet que des informations, comme c'est le cas pour la parole.

Par contre, dans le cas de la musique, où la transmission des informations est d'une importance secondaire et où le rôle prépondérant est joué par les états "périodiques" agréables que présentent des notes soutenues, une telle correction est plutôt gênante. Mais dans tous les cas, si on veut obtenir une transmission dite de "haute fidélité", la bande passante du système doit être environ deux fois plus large que celle de l'oreille.

On construit d'ailleurs actuellement des amplificateurs et des haut-parleurs de haute fidélité qui couvrent une bande passante de 20 à 25 kHz.

Il en résulte aussi que si la fraction du spectre est trop réduite par les troubles, l'estimation de l'étendue des spectres instantanés devient peu précise et l'oreille n'arrive plus à suivre convenablement les phénomènes transitoires rapides formés par l'articulation de la voix, ce qui diminue l'intelligibilité.

Or, c'est précisément la transformation en signaux perceptibles de ces parties des spectres instantanés inaccessibles à l'oreille déficiente, c'est-à-dire la mise à sa disposition d'un moyen de suivre convenablement l'articulation de la parole, que représente l'essentiel du problème de la compensation qui doit être exigée d'une prothèse moderne.

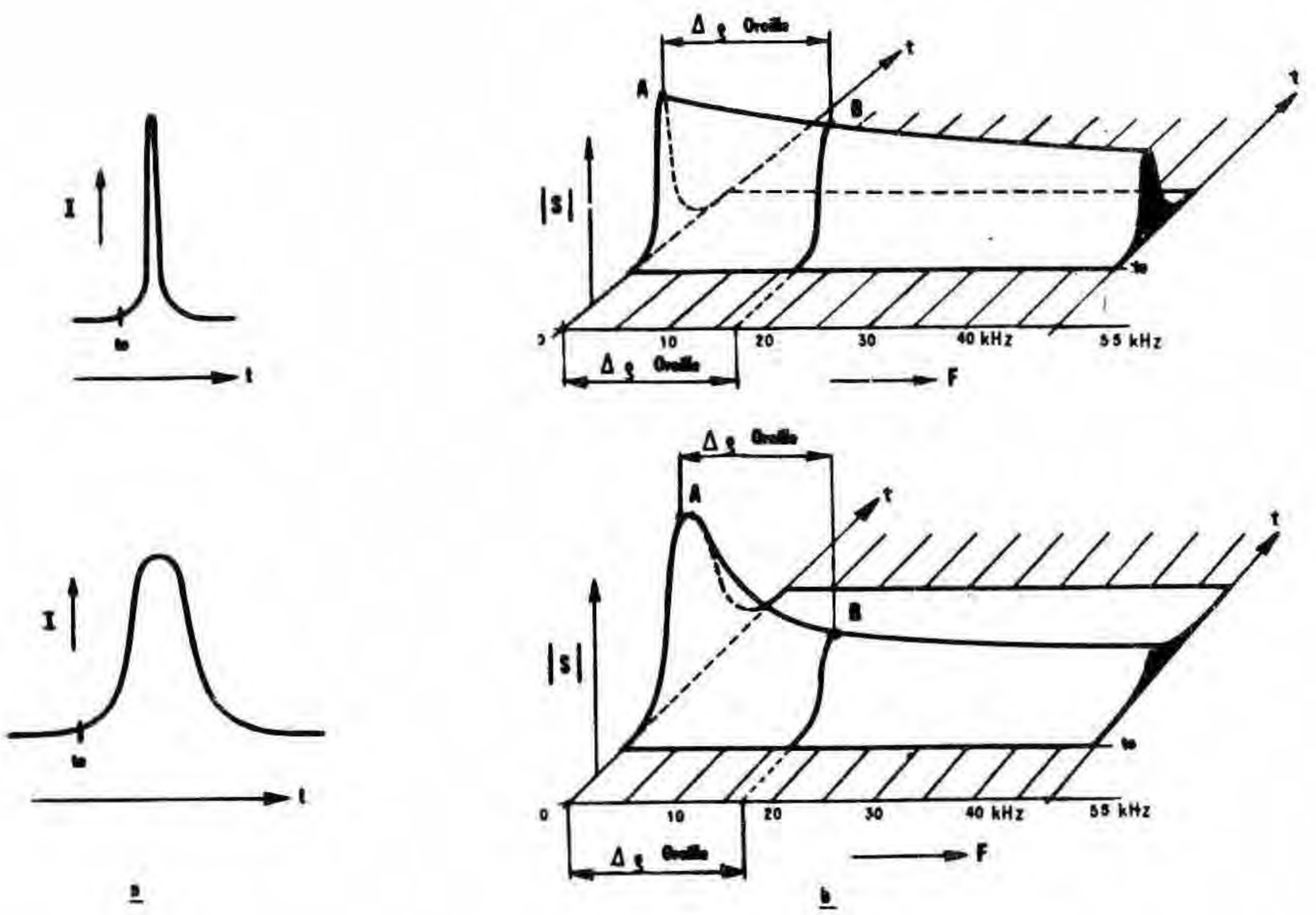

a b

Fig. 1

J43

FOURTH INTERNATIONAL CONGRESS ON ACOUSTICS
COPENHAGEN 21.-28. AUGUST 1962

New data on sound velocity in aquaeous solutions

I.G. Mikhailov

The measurements of sound velocity in aquaeous solutions of electrolytes and non-electrolytes have been carried on at the ultrasonic laboratory of Leningrad University for the last few years.[1-7] These measurements were carried in the extensive temperature and concentration range.Some very interesting results have been achieved in the process of work.Here we are going to dwell only on the question of the behaviour of temperature maximum of sound velocity or solution compressibility minimum.

It is a well-known fact that in pure water in distinction from all other liquids, sound velocity has its temperature maximum at $\sim 74^{\circ}$ and its compressibility has a minimum respectively. Such an anomalous dependence of sound velocity on the temperature is connected with some pecularities of water structure. At present water is considered to be a mixture of two structures: the first one-a friable ice-type structure and the second one - a closely-packed structure. As the temperature is raised the concentration of the closely-packed structure increases which corresponds to the negative value of the temperature coefficient of compressibility.In the other hand as the temperature is raised the mean distance between the molecules increases as well,that is the loosening of water structure takes place and the temperature coefficient of compressibility has a positive value.The presence of these opposite tendencies brings to existence the compressibility minimum. Any change in water structure caused, for example, by the increase of outer pressure or by the presence of ions must result in some displacement of the minimum position and change its value.

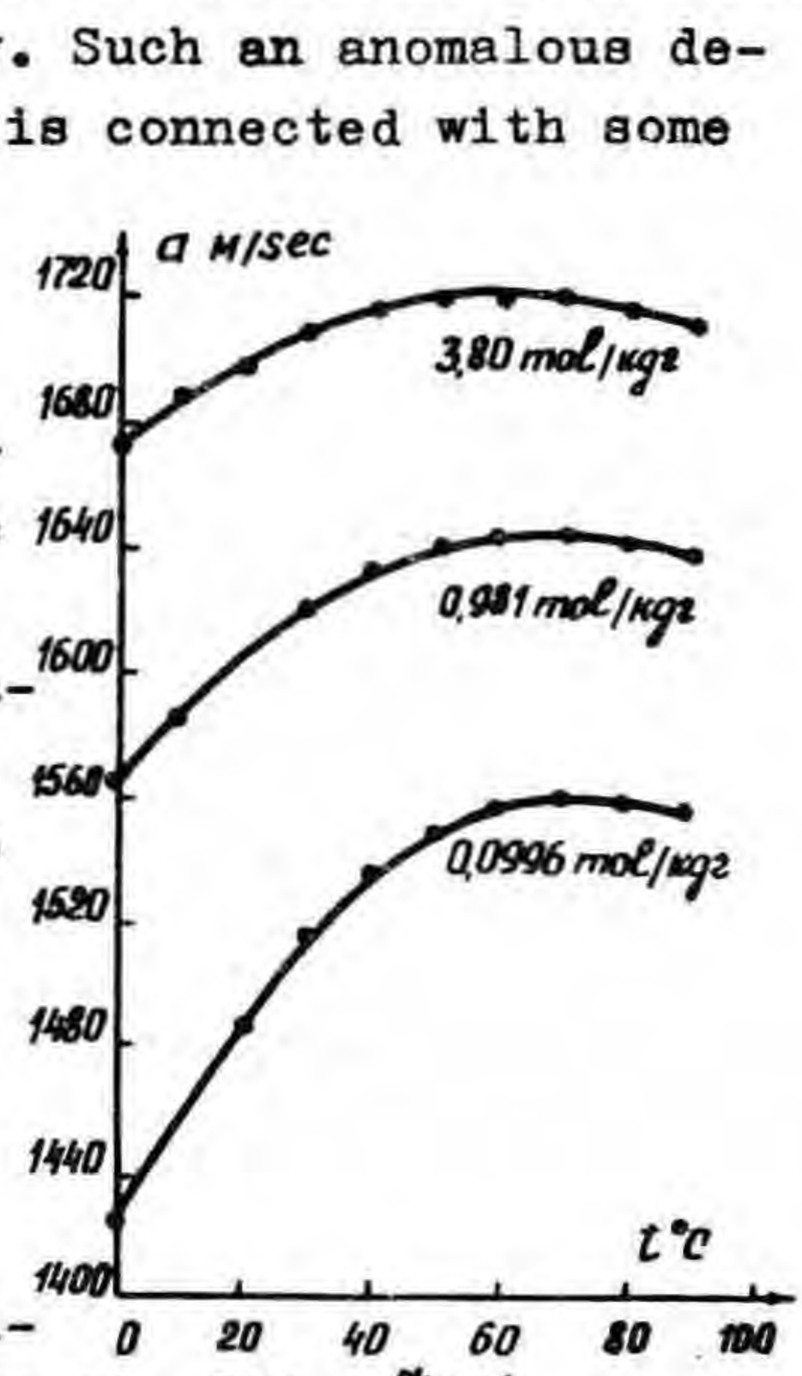

Fig. 1.

Thus we can regard the maximum of sound velocity or compressibility

minimum as a value responsive to structural changes. It was found by our investigations that in all solutions of average and strong concentrations sound velocity maximum is displaced towards lower temperatures. The size of this displacement is different in the solutions of various kind. Fig.1 shows an example of the dependence of sound velocity on the temperature in NaCl solutions of different concentrations.(2) There exists a rule found from the analysis of the experimental data according to which "Any given quantity of water in solution bahaves in the same way as the same quantity of water which is under the outer pressure".(10) The displacement of density maximum in solutions as well as their other properties obey this rule. So it was quite natural to expect agreement between the experiments with the electrolyte solutions and those studying the change of properties of water with the increase of pressure. But as the experimental data show with the increase of outer pressure the compressibility minimum is displaced towards higher temperatures.(9) In the course of a through measurements of water compressibility and some aquaeous solutions of electrolytes it was found quite unexpectedly that the displacement of compressibility minimum is of a rather complicated nature.(3) While in small concentrations, compressibility minimum is displaced towards higher temperatures but then beginning from a certain concentration it tends to lower temperatures. Fig.2 shows the dependence of the temperature of compressibility minimum on H_2SO_4 solution concentration.(1) The first three points on the curve correspond to the weight concentrations of the acid: 4,2%; 8,0% and 12,3%. This is the phenomenon which requires some special theoretical considerations. No exact calculations of this kind are theoretically possible, and it is difficult even to give any approximate ones. We preferred to make a model which allows us to carry out some calculations.(3) We have used a two-structural model of water quite analogous to that used by Hall for the calculation of ultra-sonic absorption.(9) We consider also that there co-exist two structures in water; structure "1" and structure "2" having different values of their thermodynamic potentials and molar volumes. The equilibrium constant for $1 \rightleftarrows 2$ reaction may be written as: $n_2/n_1 = \exp \frac{\Delta\Phi}{RT}$ where $\Delta\Phi$ is the difference of thermodynamic potentials of the two structures, n and n_2 - the number of molecules in the first

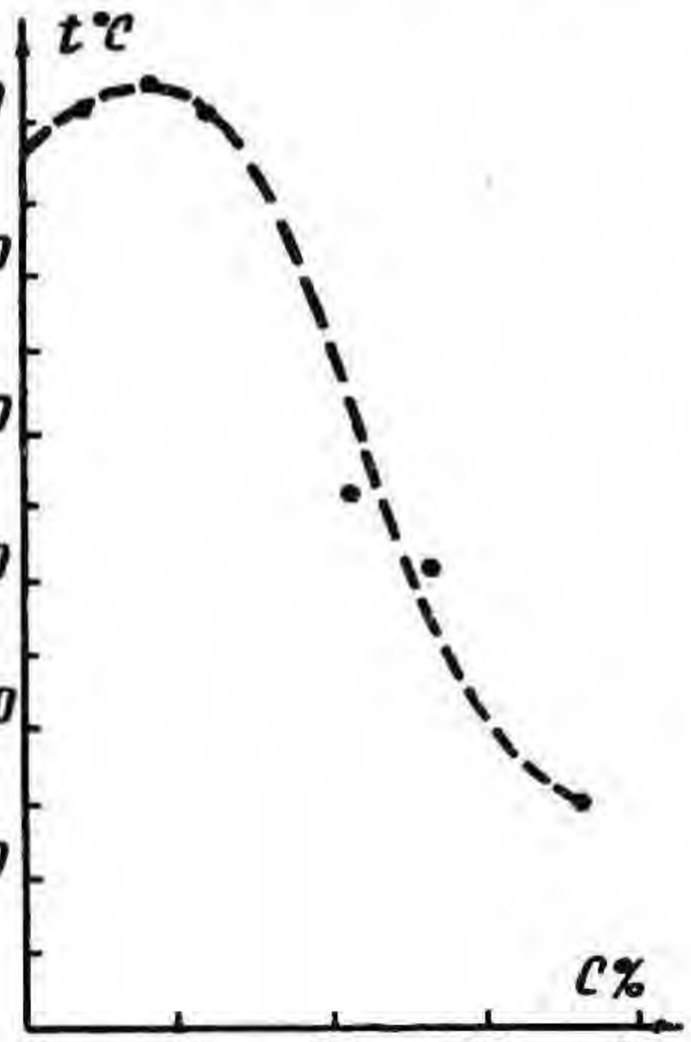

Fig. 2.

and in the second structure.As thermodynamic potentials of these structures are different,their compressibility must be different too.Such a model gives possibility to derive an expression for the temperature minimum of water compressibility.This temperature mainly depends on $\Delta\Psi$ Further we assumed that ions present in water not only caused hydratation but also greatly influenced the water structure which is not included into hydratic shells.Some calculations showed that any increase of concentration result in the decrease of $\Delta\Psi$ and there appeared some displacement of the reaction equilibrium towards the second denser structure.An account of this the compressibility minimum must be displaced towards the higher temperatures which is the case at small concentrations.

The value of compressibility minimum displacement towards higher temperatures varies in the solutions of different kind.In some cases this displacement is quite unnoticeable,and only some delay in displacement towards lower temperatures is observed.At strong and average concentrations to be necessary to take into account the interaction of ions.Generally the electrolyte solution may be thought of as two structures,where one of them is inserted into another; these are solvent and ionic lattice,both structures occupying the whole volume.The energy of such a system can be written in the following form: $U=U_1+U_2$,where U_1 is solvent energy + the energy of the interaction of ions with the solvent which is taken into account through hydratation and the influence of ions on the free water structure; U_2- is the energy of ionic lattice. For the ionic lattice compressibility we have taken its expression from the ionic crystal theory,while Madelung constant was taken as a mean value for all possible types of lattices for the salt of a given valency.Further we derived an expression for the temperature minimum of water compressibility which has taken into account both effects:the influence of ions on water structure and the presence of ionic lattice in the solution.From the analysis of the obtained expression it follows that the temperature of compressibility minimum must develop in the way shown at Fig.2.From the theory described here it is possible to calculate a number of other properties of solutions,such as maximum density displacement with the increase of concentration.[7] In the case of aquaeous solutions of non-electrolytes it was found that none of these solutions displayed any displacement of compressibility minimum towards higher temperatures.[5] The absence of such a displacement shows that the influence of the dissolved substance on the free water structure is quite negligible.It is to be supposed that in the case of non-

dissociated molecules their effect on the water structure is limited to the nearest layer,constituting the socalled hydratic shell.(6) Indeed, the forces of interaction of non-electrolyte molecules with those of water are active only at a short distance so it is not to be expected any noticeable influence of this molecules on water structure at a distance exceeding several radii of its molecules.This interaction may essentially depend on the type and structure of the molecules of dissolved substance,and the hydratatic shell structure may sharöly differ from the structures characteristic of the pure water.It is quite natural that thermodynamic equilibrium conditions for the three structure are much more complicated than for the two.When there are present three structures: two of them inherent to pure water and the third one-some new structure, there may be the following "monomolecular" reactions:1⇄2, 1⇄3 and 2⇄3 and at the same time the principle of reaction independence is sure to be preserved for them.Further calculations are carried on in the way anologous to that in the case of electrolyte solutions,but this time the expression for compressibility is more complicated.(6) We suceeeded in analysis the obtained expression and got convinced that the available experimental data could be satisfactorily explained.These data are very diverse.There are solutions both with positive and with negative concentration compressibility coefficient and in some solutions and at definite temperatures this coefficient changes its sign.

This theory will give us fuller idea of the character of water molecules interaction with the molecules of the dissolved substance.

Literature.

1. Mikhailov I.G. Shutilov V.A. Vestnik Leningr.Univers.16,3(1956)16-23.
2. Mikhailov I.G. Savina L.I. Feofanov G.N.,Vestnik L.U.22,4(1957)25-42.
3. Mikhailov I.G. Syrnikov U.P. Vestnik L.U. 10,2 (1958), 5-14.
4. Mikhailov I.G. Phen-Zhau, Vestnik L.U., 16,3 (1960) 22-35.
5. Mikhailov I.G. Phen-Zhau. Vestnik L.U. 4,1, (1961) 51-56.
6. Syrnikov U.P. Phen-Zhau. Vestnik L.U. 16,3 (1961) 59-65.
7. Mikhailov I.G. Syrnikov U.P. Jurn.Struc.Chim. 1, 1 (1960) 12-27.
8. Hall L. Phys Rev 73 (1948) 475.
9. Smith H.H. Lawson A.W. J.Chem. Ph. 22 (1954) 351.
10. Tamman K. Zs.f. Phys. Chem. 11. (1893) 676.

K43

FOURTH INTERNATIONAL CONGRESS ON ACOUSTICS
COPENHAGEN 21.-28. AUGUST 1962

ON THE DIRECTIVITY CONTROL OF THE UNDERWATER SOUND RECEIVING SYSTEM

Isao Saito, Yasumasa Urabe and Takahiko Otani

Doshisha University, Kyoto, Japan

(1) INTRODUCTION

We must, in the scanning sonar, swing the receiving beam with high speed without rotating the receiving transducer (or the group of transducers) itself. Various methods have been reported on this line. Recently D.G.Tucker and others have developed a new method in which they used a linear array of receiving transducers and a tapped delay line. Then by introducing suitable phase-shifts varying with time by swept-frequency carrier modulation, they scanned the receiving beam across a sector.[1,2]

We are going to report two methods on the directivity control of the scanning sonar. In both cases, we use two receiving transducers. In the first case, we use the sum and the difference of the two transducer outputs to control the sharpness of the directional pattern. For beam bearing control, we introduce a phase-shift to one of the transducer outputs. In the second case, we use the time difference of the two transducer outputs which are transformed into two groups of pulse trains to get a suitable directional pattern. For beam bearing control, we introduce a time-delay to one of the pulse trains. The former method is named here the SD system and the latter TD system.

These methods have some merrits as compared with other methods. For instance it is very easy in these methods to control the bearing of the receiving beam and the sharpness or width of the beam. Moreover, the directional patterns have the special shapes which seem to be preferable to the scanning sonar.

(2) SD SYSTEM

In Fig.1, H_1 and H_2 are the two receiving transducers and the sound wave incidents from θ-direction. The directional pattern of the sum of the outputs H_1 and H_2 will become something like the S-curve in Fig.2, and that of the difference

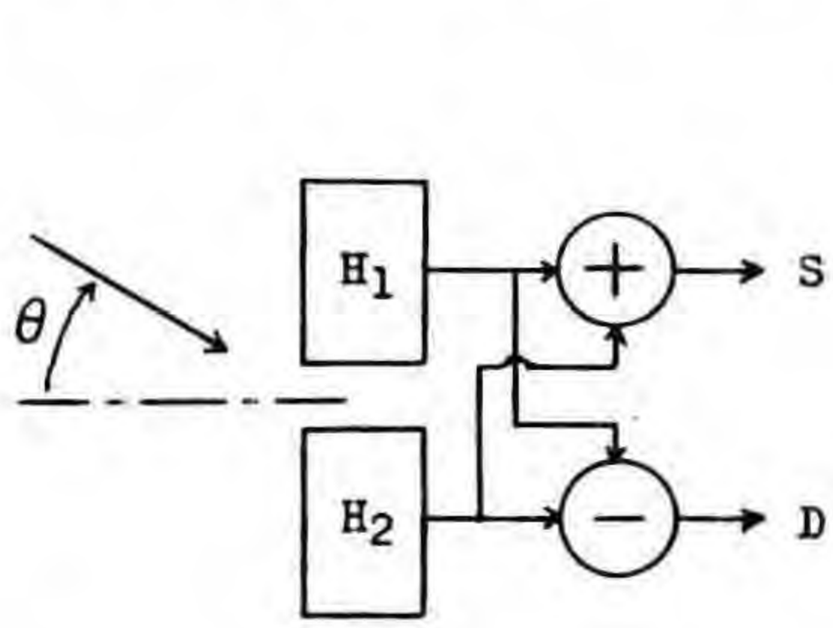

Fig. 1

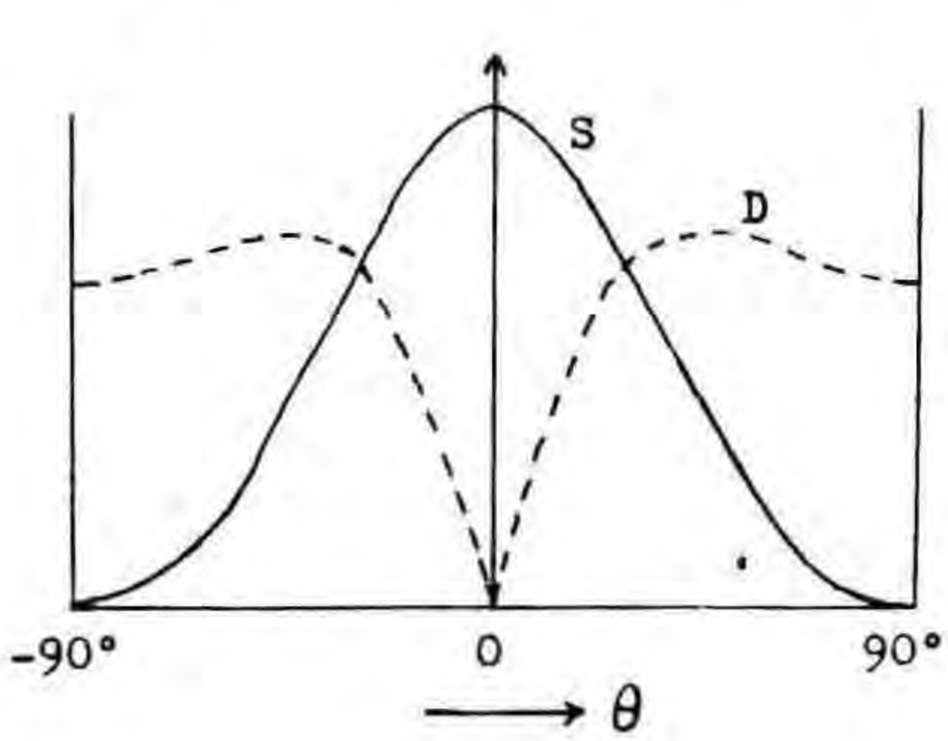

Fig. 2

like the D-curve. These directional patterns vary, of course, as the directivity of each transducer varies. As shown in these figures, there is very little change of the S-pattern near the direction of $\theta = 0$, while the D-pattern changes very rapidly. In ordinary sonars, the directional patterns of the same quality as the S-pattern are used, and hence the bearing accuracy is very low. We make use of this characteristic of the D-pattern to increase the bearing accuracy. One method is shown schematically in Fig.3, where A_1 and A_2 are the amplifiers of the sum and the difference of outputs of the transducers respectively and P.S. is a phase-shifter. Let the amplifications of A_1 and A_2 be μ and $c\mu$ respectively, then we get as the output of the system,

$$K \propto |S| - c|D| .$$

The directional pattern of K becomes as shown in Fig.4. This shows a special triangular form which seems to be very useful in the scanning sonar. The sharpness can be easily controlled by varying the parameter c as shown in the figure.

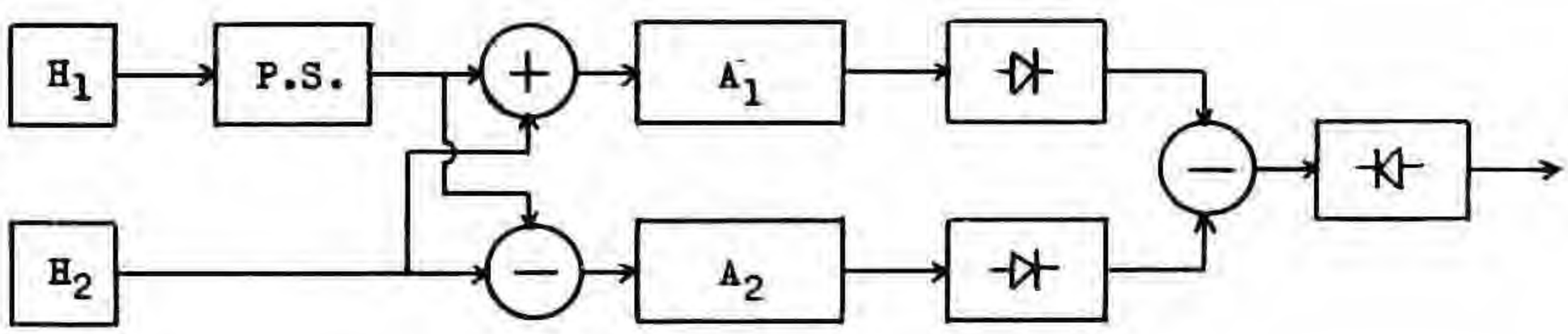

Fig. 3 Block diagram of SD system.

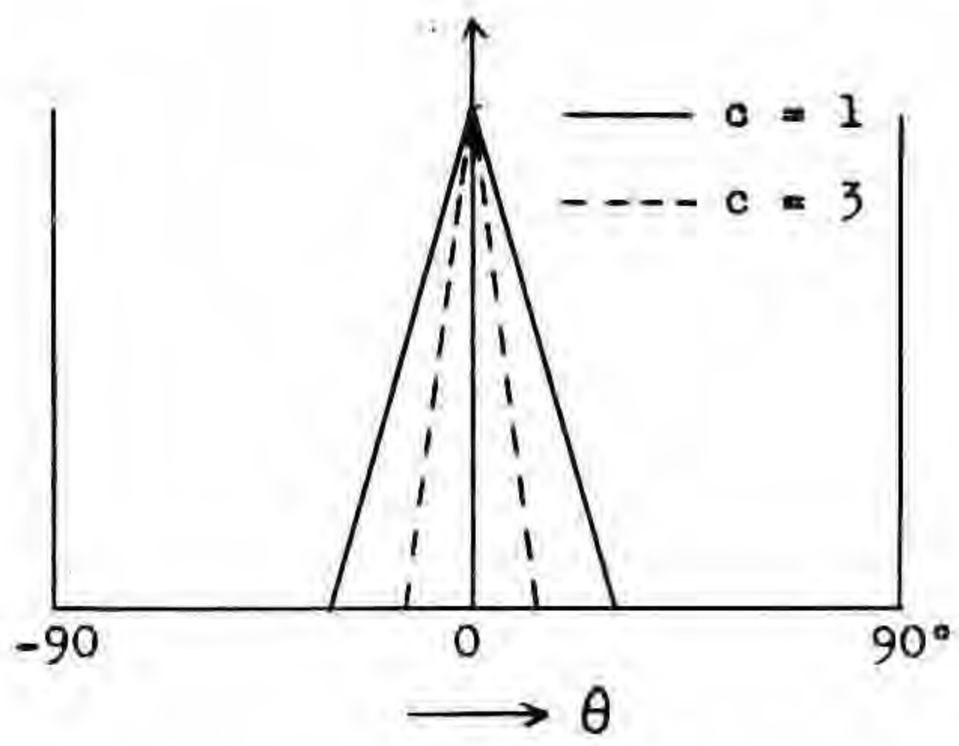

Fig. 4 Directional patterns by SD system.

Another method is shown in Fig.5 where the output of the difference amplifier A_2 is used to suppress the gain of the sum amplifier A_1. In this case, we also get the same kind of directional pattern as shown in Fig.4, but the sharpness is influenced by the intensity of the incoming wave. It becomes sharper as the intensity increases.

We may swing easily the receiving beam by giving some phase-shift, varying with time, to one of the outputs of the transducers by a phase-shifter as shown in Fig.3 and Fig.5. In Fig.6, A-curve shows an experimental result of the directivity when no phase-shift is given, and B, C and D are those when phase-shifts are

given.

The preliminary tests of scanning sonar by this system were carried out successfully.

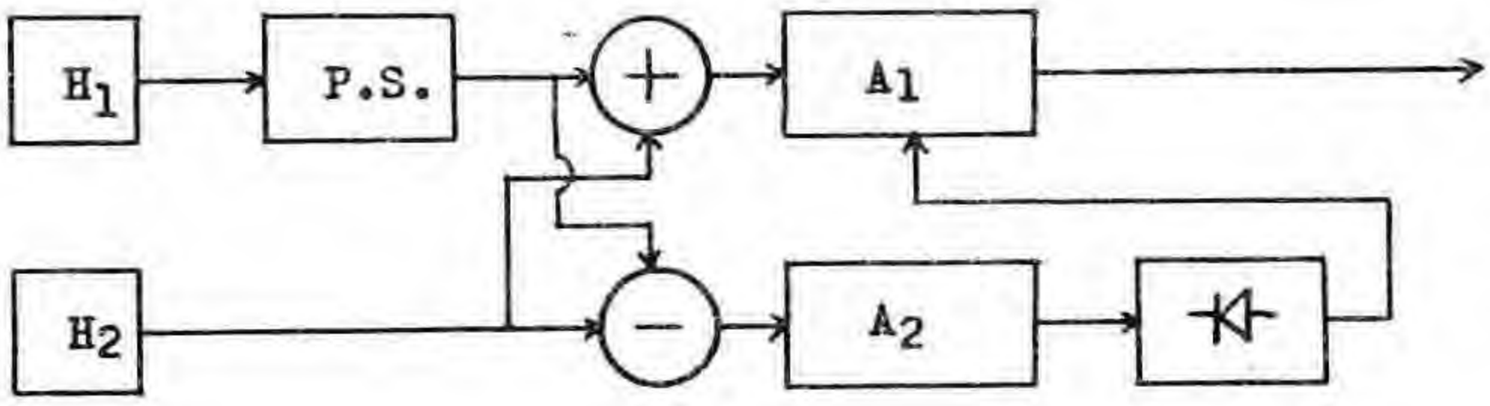

Fig. 5 Block diagram of SD system by amplification control method.

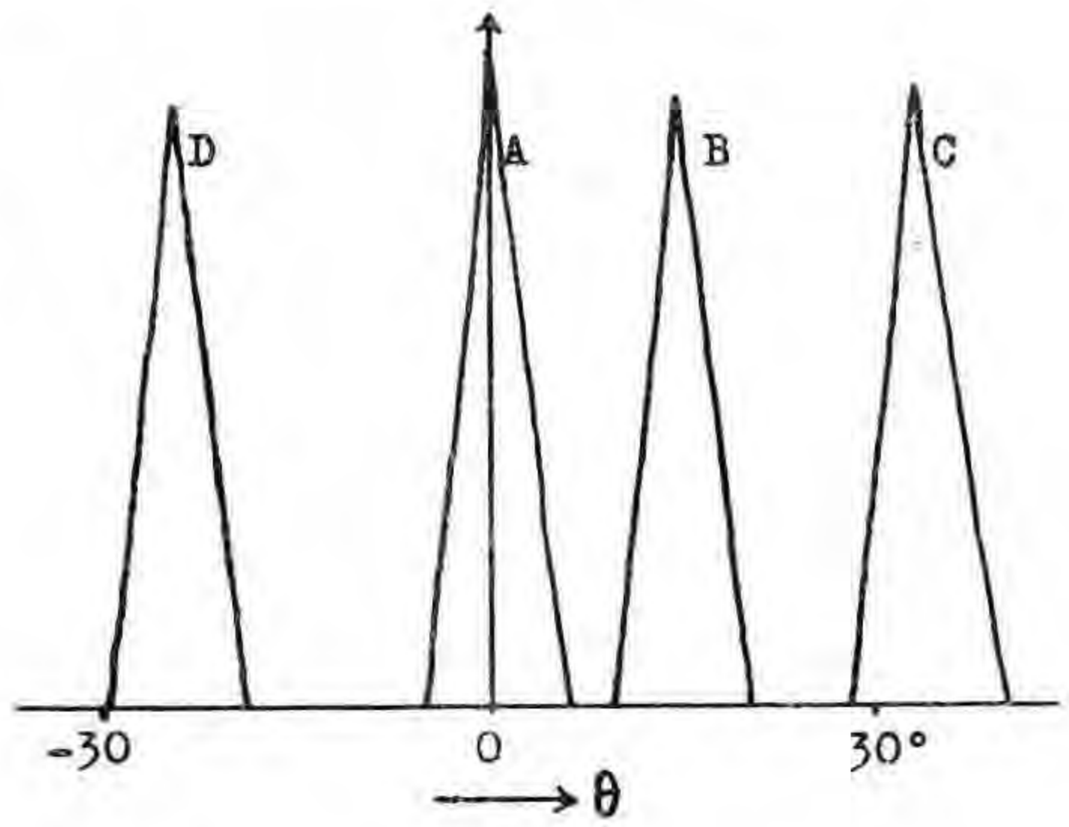

Fig. 6 Experimental results of beam bearing control by SD system. Transducer spacing is 5/6 of wavelength; angles of phase-shift are (A) 0°, (B) -90°, (C) -180° and (D) 135°.

(3) TD SYSTEM

Between the outputs of H_1 and H_2 in Fig.1, there is a time difference which is determined by the direction of the incoming wave. Let this time-difference be denoted by t_{12}. Now the two outputs are transformed into two pulse trains, and these pulse trains are made to have suitable pulse width τ_1 and τ_2 respectively. Between the two pulse trains, there also exists the same time-difference t_{12}. If we make the summation or the product of these two pulse trains, we get quite different results as these two pulse trains become superposed or not. For example if we use a device which can deliver the output only when two pulse trains become superposed, we can get such rectangular shaped directional patterns as shown in Fig.7. This is an example of our experimental results, in which A, B, C, and D represent the patterns when the pulse width τ_1 of one of the pulse trains is changed while the other width τ_2 remains unchanged.

If we want to swing the receiving beam, we need only give a time delay, varying with time, to one of the pulse trains. The experimental result shown in Fig.8 represents this relationship.

This TD system for controlling the directivity is quite new, and has many interesting points.

The preliminary tests of the scanning sonar by this system were carried out successfully.

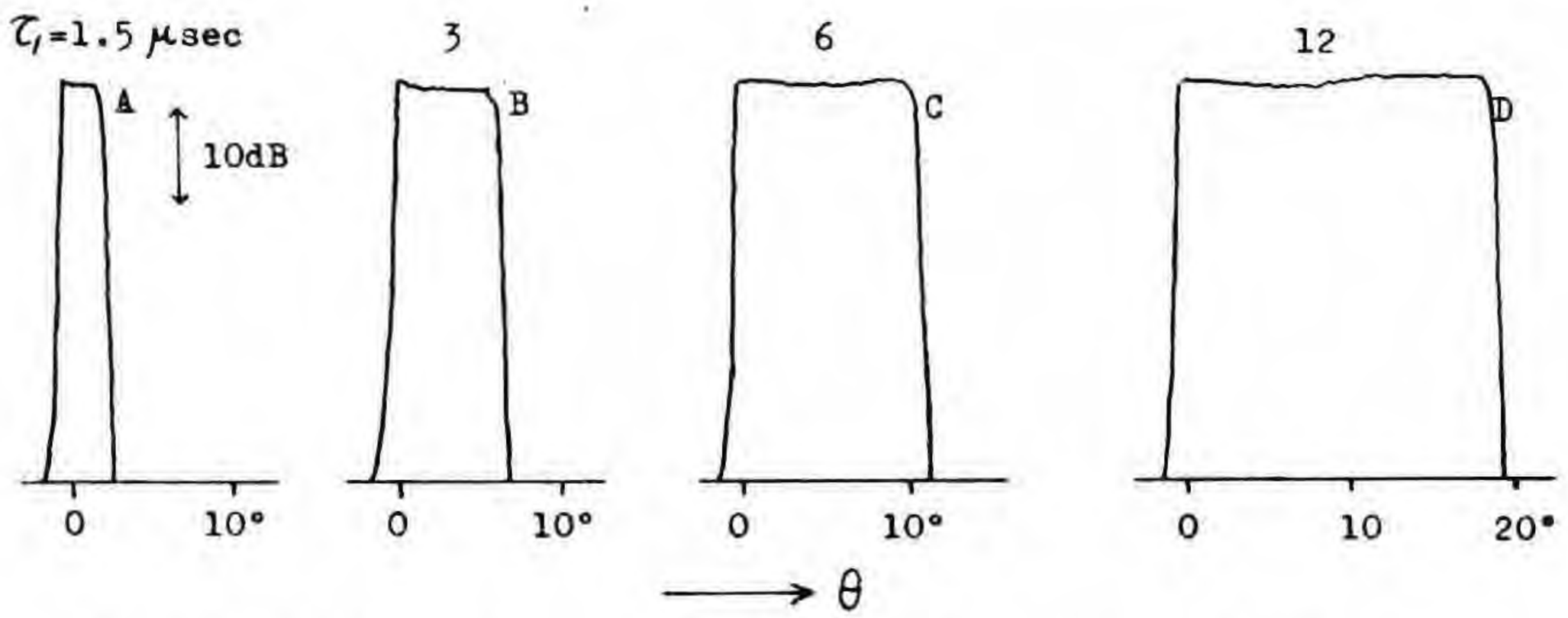

Fig. 7 Experimental results of beam-width control by TD system. (τ_2=1 μsec)

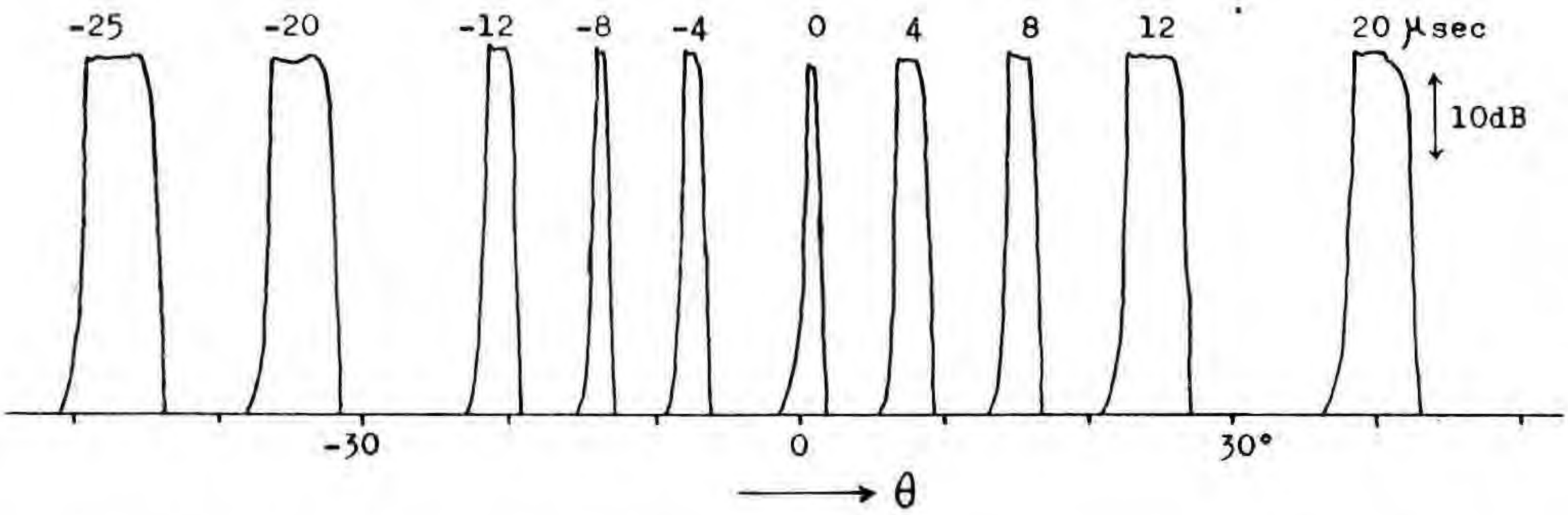

Fig. 8 Experimental results of beam-bearing control by TD system, recorded for various values of relative delay of two pulse trains. Transducer spacing is 5/9 of wavelength and frequency is 16kc.

REFERENCES

1. Tucker, D. G., Welsby, V. G. and Kendell, R.: "Electronic sector scanning" J. Brit. I.R.E., 18, p.465 (1958).

2. Welsby, V. G.: "Multiplicative receiving arrays", J. Brit. I.R.E., 22, p.5 (1961).

L43

FOURTH INTERNATIONAL CONGRESS ON ACOUSTICS
COPENHAGEN 21.-28. AUGUST 1962

Die Anwendung elektronischer Rechenmaschinen bei Lärmbekämpfungsarbeiten

Anselm Lauber

Die Arbeiten auf dem Gebiet der Lärmbekämpfung haben in den vergangenen Jahren an Umfang bedeutend zugenommen.

Das mag damit zusammenhängen, dass unser Leben tatsächlich geräuscherfüllter geworden ist, indem immer stärkere Maschinen eingesetzt werden; andererseits scheint aber auch das Publikum lärmbewusster geworden zu sein, sodass es heute kritischer und schärfer auf Lärmbelästigungen reagiert.

Es ist üblich bei Lärmklagen die akustische Situation nebst der subjektiven Beurteilung auch durch objektive Schallmessungen zu beschreiben.

Bei grösseren Schallgutachten, zum Beispiel bei der Abkärung der Schallstörungen in der Umgebung eines grossen Flugplatzes oder Aehnlichem - können die akustischen Messungen und ihre Auswertung sehr viel Arbeit verursachen und man wird daher möglichst wirkungsvolle und rationelle Arbeitsmethoden einsetzen.

Bei eingehenderen Schallmessungen wird fast immer neben dem Schallpegel auch das Schallfrequenzspektrum gemessen, letzteres meistens in Form einer 1/1- oder 1/3-Oktavbandanalyse.

Aus solchen Frequenzanalysen können zum Beispiel folgende Daten berechnet werden:

1. Bewertete Schallpegel
   durch Bewertung der Frequenzbandpegel mit den international genormten Gewichtskurven A, B und C (CEI publication 123)
2. Lautheit und Lautstärke
   nach der Methode von Professor S.S. Stevens
   (JASA, Vol. 33, No.11, Nov. 1961, p.1577 oder
   ISO TC 43 (secrtariat-135) 230).
3. "Noisiness" und "Perceived Noise Level"
   nach der Methode von K.D. Kryter (Noise Control Vol. 6,No.5)

4. Lautheit und Lautstärke
   nach der Methode von Professor E. Zwicker
   (Acustica 1960, Vol.10 oder ISO TC 43 (secretariat-145) 241)
5. "Noise Rating Number" (Grenzkurven- Kriterium)
   (ISO TC 43 (secretariat-139) 235).

Alle diese Berechnungen lassen sich von Hand ausführen; bei den ersten Hundert Schallspektren mag das amusant und lehrreich sein - bei den nächsten Hundert Schallspektren wird diese Berechnungsarbeit bestimmt zur Plage.

Unser Institut hat sich daher entschlossen diese Berechnungen auf der elektronischen Rechenmaschine der Eidg. Techn. Hochschule in Zürich ausführen zu lassen und die entsprechende Programmierung vorzunehmen. (Diapositiv)

Mit Ausnahme der Lautheitsberechnung nach der Methode von Professor E. Zwicker sind heute alle anderen genannten Rechnungen programmiert.

Die Eingabe der Daten erfolgt mit dem Lochstreifen eines Fernschreibers (Diapositiv).

Auch die Resultate können mit dem Fernschreiber übermittelt werden (Diapositiv).

Mit diesem Vorgehen kann erstaunlich viel Zeit bei den Auswertungsarbeiten gewonnen werden was sich natürlich auch auf die Kosten vorteilhaft auswirkt.

Besonders gross ist der Vorteil einer elektronischen Datenverarbeitung bei den Lautheitsberechnungen nach der Methode von Prof. E. Zwicker. Unsere Freunde vom National Physical Laboratory in Teddington haben auch für diese Rechnung ein Computer- Programm entwickelt und sie verwenden es seit mehr als einem Jahr mit viel Erfolg.

Nach unseren Erfahrungen sind die Vorteile bei der verwendung einer elektronischen Rechenmaschine bei Lärmbekämpfungsarbeiten bedeutend und überzeugend, und wir möchten daher folgende Anregung zur Diskussion stellen:

Wäre es vielleicht nicht zweckmässig
- im Rahmen der sich ganz langsam abzeichnenden europäischen Zusammenarbeit-

ein europäisches elektronisches Rechenzentrum zu schaffen,

das solche akustische Berechnungen, speditiv und zuverlässig, für ganz Europa ausführen könnte?

Es ist ja ohne weiteres möglich von jedem Postamt aus telegraphisch oder mit Fernschreiber die nötigen Daten zu übermitteln und die Resultate wieder zu empfangen.

M43

FOURTH INTERNATIONAL CONGRESS ON ACOUSTICS
COPENHAGEN 21.-28. AUGUST 1962

TRANSIENT SOUND TRANSMISSION LOSSES

AUGUSTE C.RAES
BRUSSELS ,BELGIUM.

1. INTRODUCTION

The common standard practice for measuring sound transmission losses is to apply constant amplitude sounds such as warbled tones or bands of white noise, and diffuse sound fields.

Let us compare this with other techniques,e.g.building construction and the practice of designing beams.Beams are not invariably designed for evenly distributed loads,but either for evenly distributed or for concentrated loads, according to their particular case.These loads are not necessarily supposed to be static,due consideration is given to their dynamic properties.

Beam testing machines in the laboratories always apply concentrated loads. This is because concentrated loads are more easily made variable than evenly distributed loads.Field tests,on the contrary,are not submitted to any rule imposing the imitation of laboratory tests.They apply uniformly distributed loads,which are more easily obtained and adjusted in situ.

Applying this practical experience to architectural acoustics leads to the following conclusions.

a - The use of sounds which's amplitudes do not vary with time and space is not the consequence of the requirements of any problem,especially not of the reproduction of frequently appearing practical conditions.It is the consequence of the fact that the most easily found sound sources such as warble tone or white noise generators only produce steady sounds.

b - In practice,except in cases of machine noises,steady sounds are not the majority.We encounter much more often transient sounds,from human speech to office machinery,music to pneumatic hammers a.s.o.

c - Diffuse sounds are excepfionally met.In practice,no partition is submitted to sound pressures which are evenly distributed over it's surface.

d - Laboratory testing conditions,as defined by usual standards,do not

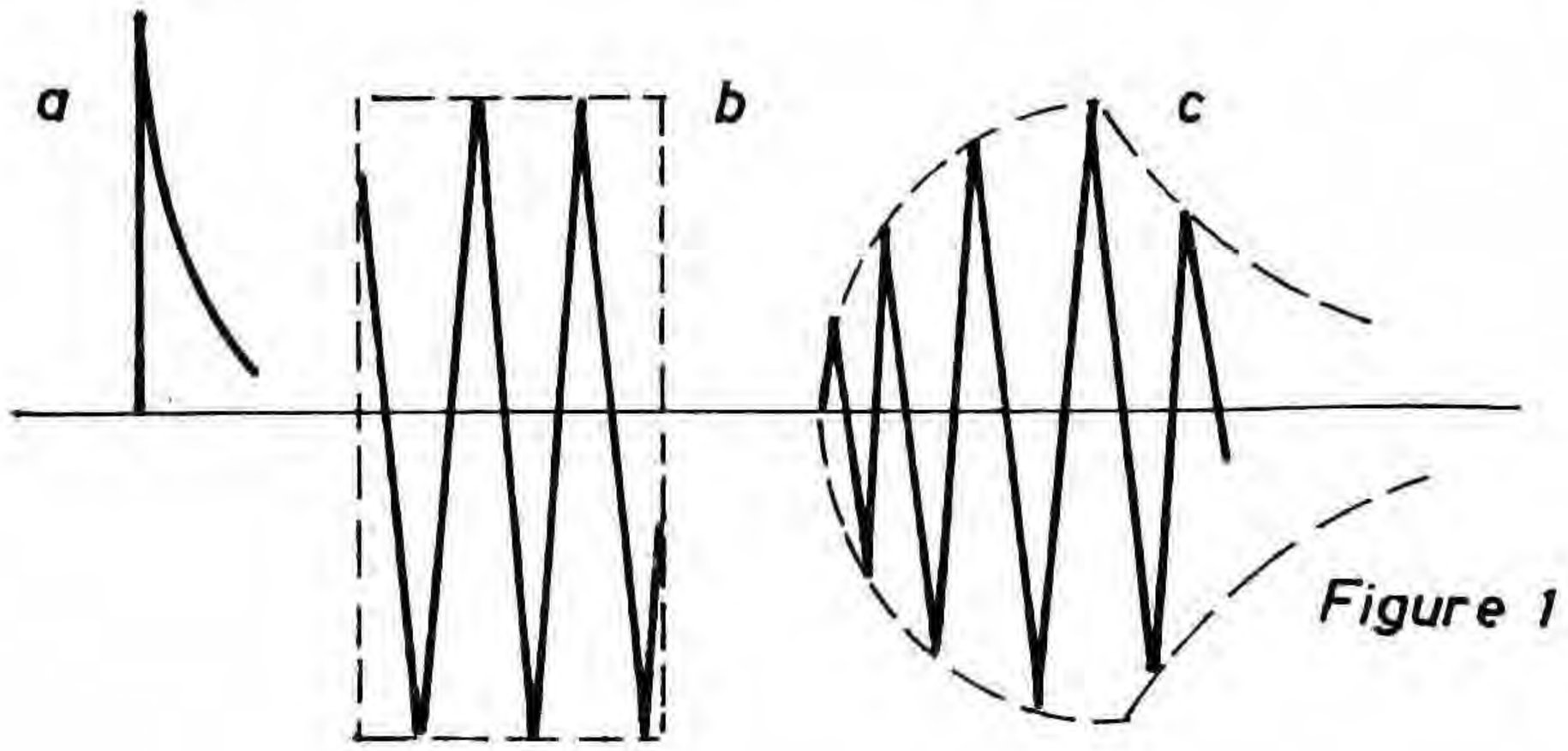

Figure 1

reproduce practical conditions.

e - We should know the relations between transmission losses obtained with steady and transient sounds,with diffuse and concentrated sound fields.

f - According to the experience of other sciences,there is no reason why field tests should reproduce laboratory tests.On the contrary,laboratories should try to reproduce practical conditions as closely as possible.

g - Data on transient and concentrated sound transmission losses are of greater practical value than steady and diffused sound data in most designing problems

It is the purpose of this paper to present a tentative standard transient,apparatus to use it,and some results obtained with it.

2.SELECTION OF THE TYPE OF TRANSIENT

Single pulses such as shown by fig.1 (a) are easiest to produce,but their spectra are hard to draw and they give exagerated values .
Rectangular pulses,fig.1b,cannot be produced by convenient 15 to 25 W loudspeakers.They have complicated spectra.Their envelope distortions are hard to analyse.
Exponential pulses,fig.1c,are convenient when the sound waves are synchronised with the envelopes.
Their rising part only is used,each wave being separately measured.
In the present state of our research work,we find that the most convenient transient is a pure sine wave which's amplitude increases linearly with time.It can be expressed by

$$p = K\ t\ f \sin 2H\ t\ f$$

K being a constant,t the time in sec. and f the frequency in cps of the sine wave.Such a transient is shown in fig.3

3.METHOD OF MEASUREMENT

We apply a method for the measurement of transmission losses in situ which we presented at the G.A.L.F. in June 1954 and which was published in the J.A.S.A.,vol.27,Jan.1955.

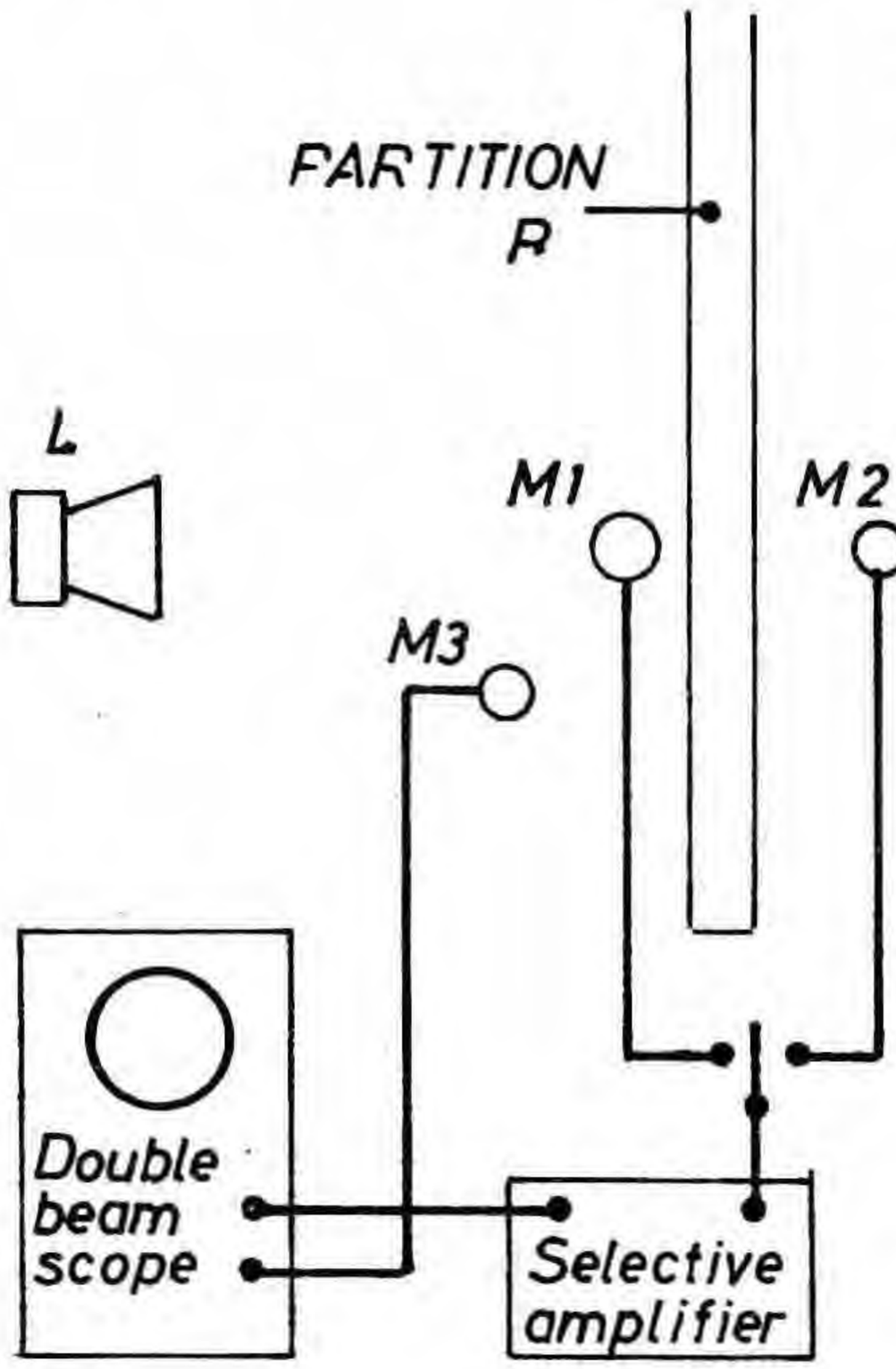

Figure 2

Sounds emitted by the loudspeaker L take abour 2mS to pass from microphone M1 to microphone M2 through the partition under test P.They take at least 10 mS to reach M2 around the partition.If L emits a sound starting from zero in pressure and in time,we have thus about 9 mS to measure the sound waves coming through the partition.This is easily done with M2,the selective amplifier A, and the double-beam oscilloscope O. M1 and the switch S are used to measure the incident sound pressure.M3 is used to locate the zero of the time scale and thus measure the time lag between the incident and outcoming sound waves.
This method has been applied in 1955 by the Radiodiffusion Française,adding an electronic switching to limit the signals measured by M2with a single beam scope,no filter and no special pulse shape.This scheme reduces the accuracy of

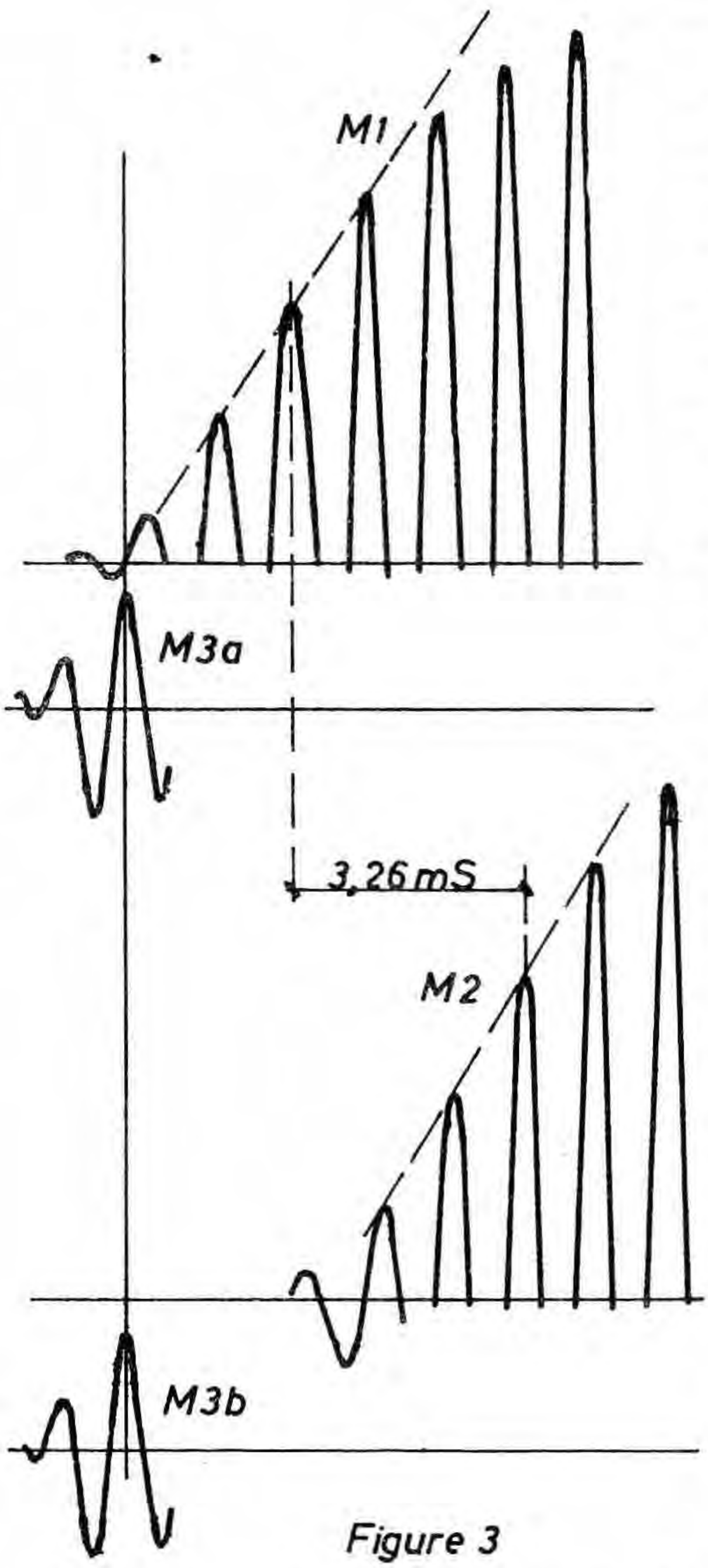

Figure 3

the measurements, since it does not allow a close control of wave shapes and positions.

4. TYPICAL SET OF OSCILLOGRAMS

Figure 3 shows pictures obtained at 1000 cps. They are part of a series of tests made on a set of 3 glass panes, resp. 4 , 5 & 6,5 mm thick, separated by two 1/2 in air spaces. They are drawn in ink from photographs of the screen. M2 and M3b have been taken about 2 minutes after M1 and M3a. The amplification for M2 was 30 dB higher than for M1.

For current field tests we only read from the screen. For more important tests it is safer to take photographs. All the data for a given partition are thus stored on a 36 exposures Leica film.

5. DATA

Space limitations allow to show only a few cases which can easily be compared with those obtained with steady and evenly distributed sounds.

5.1. Glass.

All the figure are obtained by making at least 2 measurements for 3 angles of incidence for every standard $\frac{1}{3}$ octave central frequency, and averaging the results for every octave. The panes tested measured 2 x 1 meter and were framed in a 3 x 3 m heavy Linex and Fiberglass partition.

5.1.1. Single panes.

Transmission loss in dB

Frequency, cps	250	500	1000	2000	4000
Thickness, mm					
3,4	18	27	33	39	42
5,3	28	34	40	46	51
10,0	29	37	47	50	55

5.1.2. Two 5 mm panes. Var. air spaces.

Transmission loss in dB

Frequency, cps	250	500	1000	2000	4000
Air space, mm					
5,5	25	34	40	42	50
12,5	28	35	42	45	53
15,0	29	38	40	45	53

5.1.3. One 12,5 mm air space between different panes.

Transmission loss in dB

Frequency, cps	250	500	1000	2000	4000	
Panes, mm						
2,5 + 5	29	30	34	38	46	
3 + 3	28	34	35	34	46	
3 + 6	25	36	37	38	49	
4 + 6	28	40	46	51	56	Incidence on the 4 mm pane
6 + 4	29	38	44	52	57	Incidence on the 6 mm pane

5.2.Asbestos-cement board,12 mm thick,bonded between one 2 mm and one 1 mm sheet steel.

Frequency,cps	250	500	1000	2000	4000	
Transmission loss	19	20	22	48	35	dB

5.3.Expanded polystyrene sheet,34 mm,bonded between 5 mm asbestos-cement sheets.

Frequency,cps	250	500	1000	2000	4000
Transmission loss,dB	24	24	33	30	35

5.4.Accordion doors.
Sound projected at half-distance between two joints.Average from 4 specimens.

Frequency,cps	250	500	1000	2000	4000
Transmission loss,dB	7	26	38	46	35

5.5.Porous concrete,10 x 3 ft slabs,4 in.thick.

Frequency,cps	250	500	1000	2000	4000
Transmission loss,dB					
Unplastered	37	48	50	56	51
Light plastering, both faces	37	48	50	59	64

6.TIME-LAG MEASUREMENTS

Considering the oscillograms of M1 and M2 in figure 3,we can locate any particular wave top on the time scale by measuring the horizontal distance between that top and a characteristic point of M3,(a or b),curve,which we select as the zero time marker.

When the microphones M1 and M2 are placed at a suitable distance from each other,normally 30 cm,and are separated by air only ,these locations differ by about 0,9 mS,the differences being determined by the microphones's characteristics and the frequencies.

When a partition is placed between the microphones,which otherwise keep the same relative positions,we find that this difference of time locations can increase considerably.This time-lag depends upon the frequencies and the structure of the partition under test.

We have drawn some characteristic curves,which cannot be shown here for lack of space.The following table sums up some typical results.

Time-lag in mS Frequency,cps	250	500	1000	2000	4000
Partitions					
17 mm plate glass	5,9	3,9	2,2	1,6	2,4
2 x 6,5 mm glass,air space 12,5 mm	7,5	2,9	2,4	2,2	2,3
4 + 5 + 6,5 mm glass,air spaces 2 x 12,5mm	5,2	2,0	2,1	2,1	2,0
Light steel partition,double faced,fiber-glass blanket,60 mm total thickness	4,0	5,1	5,2	7,3	8,5
Double plasterboard partition,50 mm wood studs,70 mm total thickness	1,5	2,1	1,6	1,8	1,8

We are not yet able to suggest an accurate relation between that time-lag and the insulating properties of a partition.A long time lag seems to be favorable.

N43

FOURTH INTERNATIONAL CONGRESS ON ACOUSTICS
COPENHAGEN 21.-28. AUGUST 1962

"Akustisches Goniometer" *)

G.A. Liaghati (Teheran)

Anlässlich der Tonmeistertagung in Detmold (Deutschland) im Oktober 1957 berichtete H. Lauridson (Kopenhagen) von einem neuartigen Tonortungsgerät, von ihm "akustisches Goniometer" genannt.

Lauridson hatte ursprünglich dieses Verfahren zum Orten von nacheinander einfallenden Schallreflexen in Studioräumen verwendet. Er wollte damit hauptsächlich die richtige Aufstellung von Reflexionsflächen in Konzertsälen demonstrieren. Die Apparatur bestand aus zwei unter einem Winkel von 90° gekreuzten Mikrophonen mit Achtercharakteristik. Die abgegebenen Spannungen wurden den beiden Plattenpaaren eines Kathodenstrahloszillographen zugeführt. Wurde nun der Raum mittels eines von einem Lautsprecher erzeugten Tons angeregt, so entstand auf dem Oszillographenschirm ein Strich, dessen Länge proportional dem Schalldruck wächst und der die Einfallsrichtung des Schalls anzeigt.

Lauridson hatte seinerzeit mit dieser Apparatur einige Versuche durchgeführt, die seiner Meinung nach ein gutes Kriterium für raumakustische Eigenschaften bilden könnten, wobei er aber selbst nicht mehr dazu kam, seine Ideen zu verwirklichen.

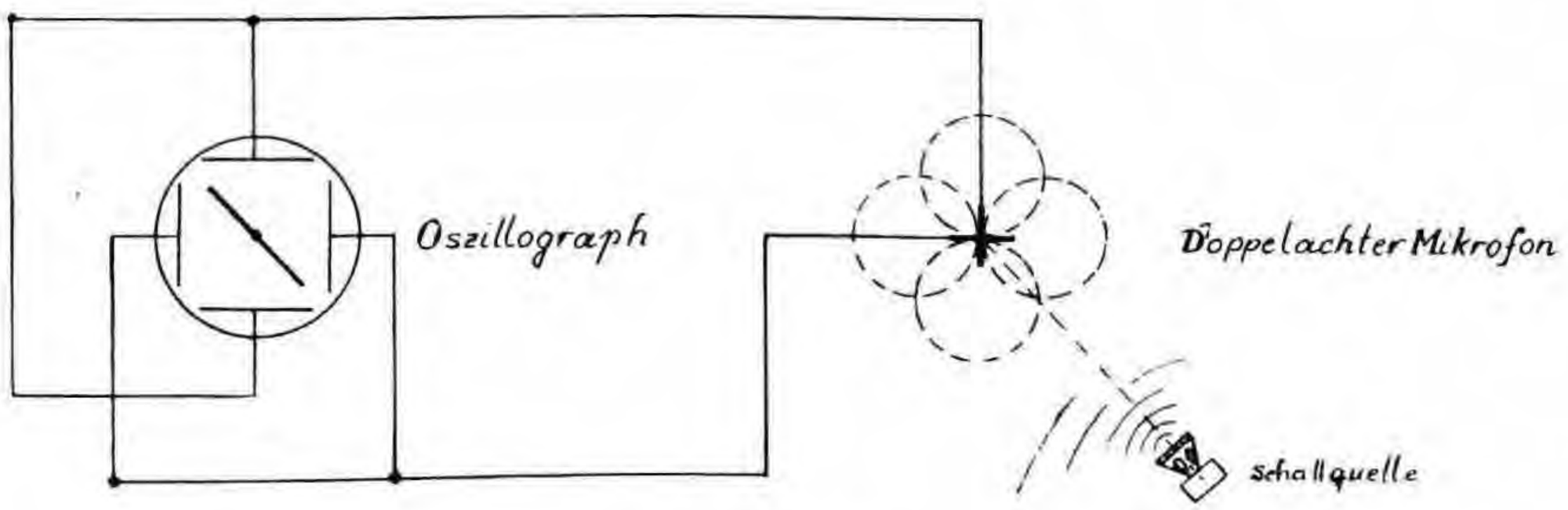

Lauridson'sches Goniometer

---

*) Auszug aus der gleichnamigen Dissertationsarbeit, eingereicht bei der Technischen Hochschule München. - Kurzvortrag mit Sondergenehmigung.

Um die Brauchbarkeit des Lauridson'schen Goniometers für allgemeine raumakustische Untersuchungen zu überprüfen, wurde zunächst eine der ursprünglichen ähnliche Apparatur aufgebaut. Nach diesem Prinzip wurden Versuche in einem freien Gartengelände mit einigen definierten Reflexionsflächen sowie im Konzertsaal der Staatlichen Hochschule für Musik in München durchgeführt. Von den Meßergebnissen, die auf einem Stereoband gespeichert waren, wurden mit Hilfe eines Kathodenstrahloszillographen Goniometer-Bilder von dem Schallfeld erzeugt und davon eine Zeitlupenaufnahme mit einer 16mm-Filmkamera gemacht. Diese Aufnahmen hatten kein zufriedenstellendes Ergebnis gezeigt. Da eine sehr kurze Belichtungszeit erforderlich war, um eine Bildanalyse machen zu können, wurde eine elektronische Belichtungsapparatur zum Oszillographen gebaut, die Aufnahmen mit einer Belichtungszeit von 0,1 msec bis einige msec ermöglichte.

Die Bildanalyse vom Schallfeld zeigte, daß das vorhandene akustische Goniometer für allgemeine raumakustische Untersuchungen nicht geeignet ist, so daß eine weitere Entwicklung notwendig ist. *) Die abgewandelte Apparatur besteht aus 4 getrennten Kanälen, von welchen jeder mit einer Platte des Oszillographen verbunden wurde. Als Schallempfänger wird ein umgebautes Neumann-Stereomikrophon, bestehend aus 4 Mikrophonkapseln mit Nierencharakteristik, welche nach allen 4 Raumquadranten gerichtet sind, benutzt. Die gewonnenen Reflexionen werden verstärkt und von störender Tonfrequenz mit einem geeigneten Gleichrichter und Tiefpaßschaltung befreit (Hüllkurvenspannungsbildung).

Das nach diesem Verfahren gebaute 4-Kanal-Goniometer besteht aus allen Einrichtungen, die zur Aufnahme und Auswertung von 4 getrennten Signalen notwendig sind. Die Spannungen, die durch vier Nierenmikrophone aufgenommen werden, können entweder auf Band gespeichert und nachher vom Band ausgewertet werden (2- oder 4-Spurgerät) oder man kann sie direkt an den Auswerter schalten. Untenstehendes Blockschaltbild zeigt einen Kanal des Aufnahme- und Auswertegerätes.

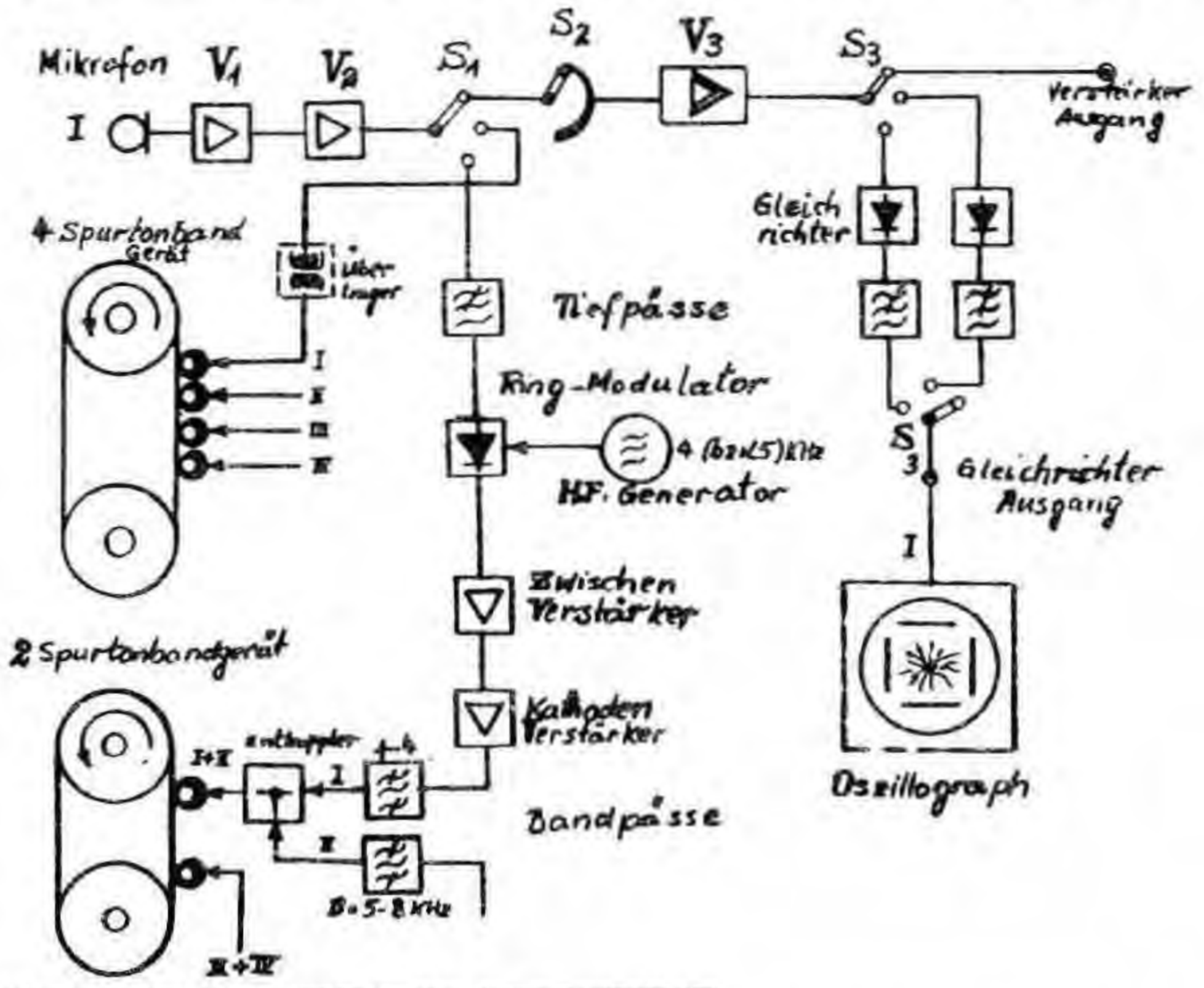

*) Diese Entwicklung wurde im Zentral-Laboratorium der Firma Siemens & Halske AG, München, durchgeführt.

"Akustisches Goniometer"

Diese Apparatur hat gegenüber der Lauridson'schen den großen Vorteil, daß anstatt eines undefinierten Striches auf dem Bildschirm nur ein einziger Punkt ausgelenkt wird, der jeweils die Schalleinfallsrichtung anzeigt.

Man kann mit vorhandener Apparatur folgende Messungen durchführen:

1. Nachhallmessung: Mit den auf das Band aufgenommenen Knallvorgängen kann man in Verbindung mit einem Pegelschreiber die Nachhallzeit messen (Dias).
2. Stoßprüfung: Aus den einkanaligen Ablaufbildern der gleichgerichteten Reflexionen kann man die wichtigen Reflexionen einzeln für jeden Raumquadranten getrennt betrachten (Dias).
3. Die Deutlichkeit: Man kann aus Echogrammen, die man in der vorgenannten Weise gewonnen hat, theoretisch die Deutlichkeitsintegrale :

$$D = \int_0^{80} p^2(t)\,dt \Big/ \int_0^{\infty} p^2(t)\,dt$$

   aus dem Flächenverhältnis bestimmen.
4. Goniometrie: Das Hauptanwendungsgebiet der entwickelten Apparatur ist die Meßmöglichkeit für raumakustische "Güte" durch Reflexionsbildbewertung auf dem Goniometer-Schirmbild (Dias).

O43

FOURTH INTERNATIONAL CONGRESS ON ACOUSTICS
COPENHAGEN 21.-28. AUGUST 1962

Radiation of Sound by Ocean Waves

Richard K. Cook
National Bureau of Standards, Washington, D. C.

I. Microbaroms

Amongst the many natural sounds at infrasonic frequencies (less than 1 c/s) occurring in the atmosphere, those having dominant periods of oscillation between about 4 and 7 secs. seem to be particularly widespread. They are characterized by their persistence at a given geographic location for many hours, by a rather constant period of oscillation, and by an amplitude which seldom exceeds 3 or 4 dynes/cm^2 in the area of Washington, D.C. Microbaroms of 4 sec. periods were observed by Gutenberg and Benioff[1] at Pasadena in southern California. They found the microbaroms to be sound waves traveling approximately parallel to the earth's surface, and coming from a direction southwest of Pasadena. Saxer[2,3] and Dessauer et al.[4] observed microbaroms at Fribourg in Switzerland. They found the waves traveling parallel to the earth's surface to come from a direction northwest of Fribourg, periods $\approx$ 5 secs., and sound pressures $\approx$ 0.5 -1 dynes/cm^2. Furthermore, the sound pressures seemed to be correlated with the heights of water waves in the north Atlantic Ocean due to storms, and with the strength of microseisms in the earth observed at Strasbourg (about 200 km north of Fribourg). Observations on microbaroms in the Washington area will be discussed later.

What causes microbaroms? Similarities between them and microseisms on the earth's surface suggest that one causes the other. But it can be easily shown[5] that, on the one hand, the sound waves radiated into the atmosphere by microseisms are much weaker than microbaroms; on the other hand, sound pressure of the latter on the earth's surface is not strong enough to produce observable microseisms.

Daniels[6] has supposed that the water waves created by storms radiate sound into the atmosphere. In the analysis which follows we shall show (a) that long trains of such waves cannot radiate sound power, and (b) that sound power radiation can occur when the waves come to an abrupt stop as, for example, on a beach.

II. Radiation by an infinite train of surface waves on water

We consider first a sinusoidal gravity wave on water, of amplitude A and period T, the wave-fronts being straight lines parallel to the z-axis, see Fig. 1. We suppose the depth to be substantially greater than $\frac{1}{k_o} = \lambda_o/2\pi$ (λ_o = wave-length), and so the

---

[1] B. Gutenberg and H. Benioff, Trans. Am. Geophysical Union 22, 424 (1941).

[2] L. Saxer, Helvetica Physica Acta 18, 527 (1945).

[3] L. Saxer, Archiv f. Meteorologie, Geophysik, u. Bioklimatologie 6, 451 (1953-54).

[4] F. Dessauer, W. Graffunder, and J. Schaffhauser, Archiv f. Meteorologie etc. 3, 453 (1951).

[5] R. K. Cook and J. M. Young, "II Strange Sounds in the Atmosphere", Sound-Its Uses and Control 1, No. 3 (May - June 1962).

[6] F.B. Daniels, J. Acoust. Soc. Am. 24, 83 (1952).

deep-water wave speed is $c_o = gT/2\pi = g/\omega$, where g = acceleration of gravity. Therefore the surface displacement can be represented by

$$h_o = A \exp i(\omega t - k_o x) \qquad (1)$$

for all x.

In the atmosphere above the water a distribution of sound pressure and particle motions is caused by the surface wave. The velocity potential for this distribution must satisfy the sound wave equation and the boundary condition at the water surface. The final result is that the sound pressure in the atmosphere above the water is

$$p = \frac{\rho c\, \omega A}{\sqrt{\beta^2 - 1}} \exp\left[-\sqrt{k_o^2 - k^2}\, y + i(\omega t - k_o x)\right] \qquad (2)$$

where ρ = density of the atmosphere, c = speed of sound, $\beta = c/c_o$, and $k = \omega/c$.

We note the sound pressure at the water surface is in phase with the displacement. Hence no net work is done and no sound power is radiated into the atmosphere.

For water waves of period $T = 2\pi = 6.28$ secs., $\omega = 1$/sec., $c_o = 9.8$ m/sec., and $\lambda_o = 61$ meters. Suppose the displacement amplitude A = 100 cm. Then the sound pressure at the water surface is $|p| \approx 120$ dynes/cm^2. But at a height of 100 m. above the surface the sound pressure is reduced by a factor of $e^{-10} \approx 1/22000$ down to less than 10^{-2} dynes/cm^2.

III. Radiation by a semi-infinite wave train

We consider next a sinusoidal gravity wave on water coming from $-\infty$ and stopping abruptly at x = 0, the wave-fronts again being straight lines parallel to the z-axis, see Fig. 2. The surface displacement h_o is the same as in eq (1) for $-\infty < x < 0$, and $h_o = 0$ for $x > 0$. We imagine the z-axis in the xz-plane to be the beach, and the region $x > 0$ to be the landward side.

The velocity potential ψ for the total wave field at y = 0 is readily found by superposition of the hemi-cylindrical waves generated by each line element, parallel to the z-axis and of width du, of surface waves.

$$\psi = -\frac{\omega A \exp(i\omega t)}{2} \int_{-\infty}^{o} [J_o(kx - ku) - i\, Y_o(kx - ku)] \exp(-ik_o u)\, du \qquad (3)$$

for $x > 0$.

A good approximation to this integral is found as follows. We first replace the Bessel functions J_o and Y_o by the first terms of their asymptotic expansions. This leads to a Fresnel integral expression for ψ, whose asymptotic form for large x yields

$$\psi \sim \frac{cA}{\sqrt{2\pi}\,(\beta - 1)} \cdot \frac{-i \exp[\pi i/4 + i(\omega t - kx)]}{\sqrt{kx}} \qquad (4)$$

From this we find the sound pressure on the landward side ($x \gg 0$) to be

$$|p| = \frac{\rho c A}{(\beta - 1)T} \sqrt{\frac{\lambda}{x}} \qquad (5)$$

where λ = wavelength of the atmospheric sound. As before we suppose the water waves to have a period $T = 2\pi$ secs. and A = 100 cm. Then $\beta = 35$ and $\lambda = 2130$ m. At a distance x = 185 km from the beach, the sound pressure will be 2.1 dynes/cm^2.

Suppose the wave starts abruptly at the beach x = 0 and travels towards $x = -\infty$. We find the sound pressure on the landward side to be almost the same as before; for such a wave the factor $\beta - 1$ in eq (5) above is replaced by $\beta + 1$. Therefore a standing wave caused by reflection of an incoming wave by a beach will also give rise to a radiated sound field.

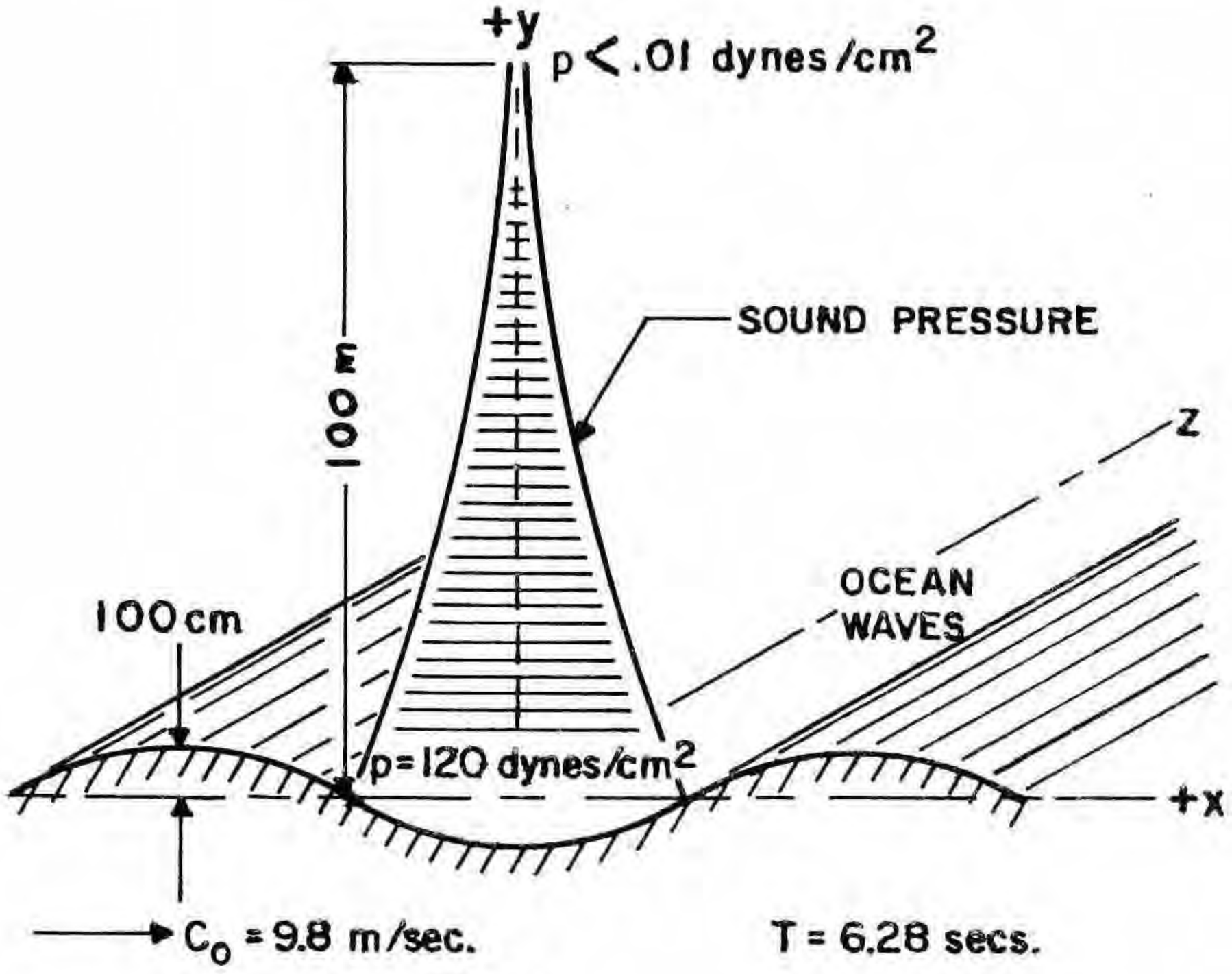

Figure 1

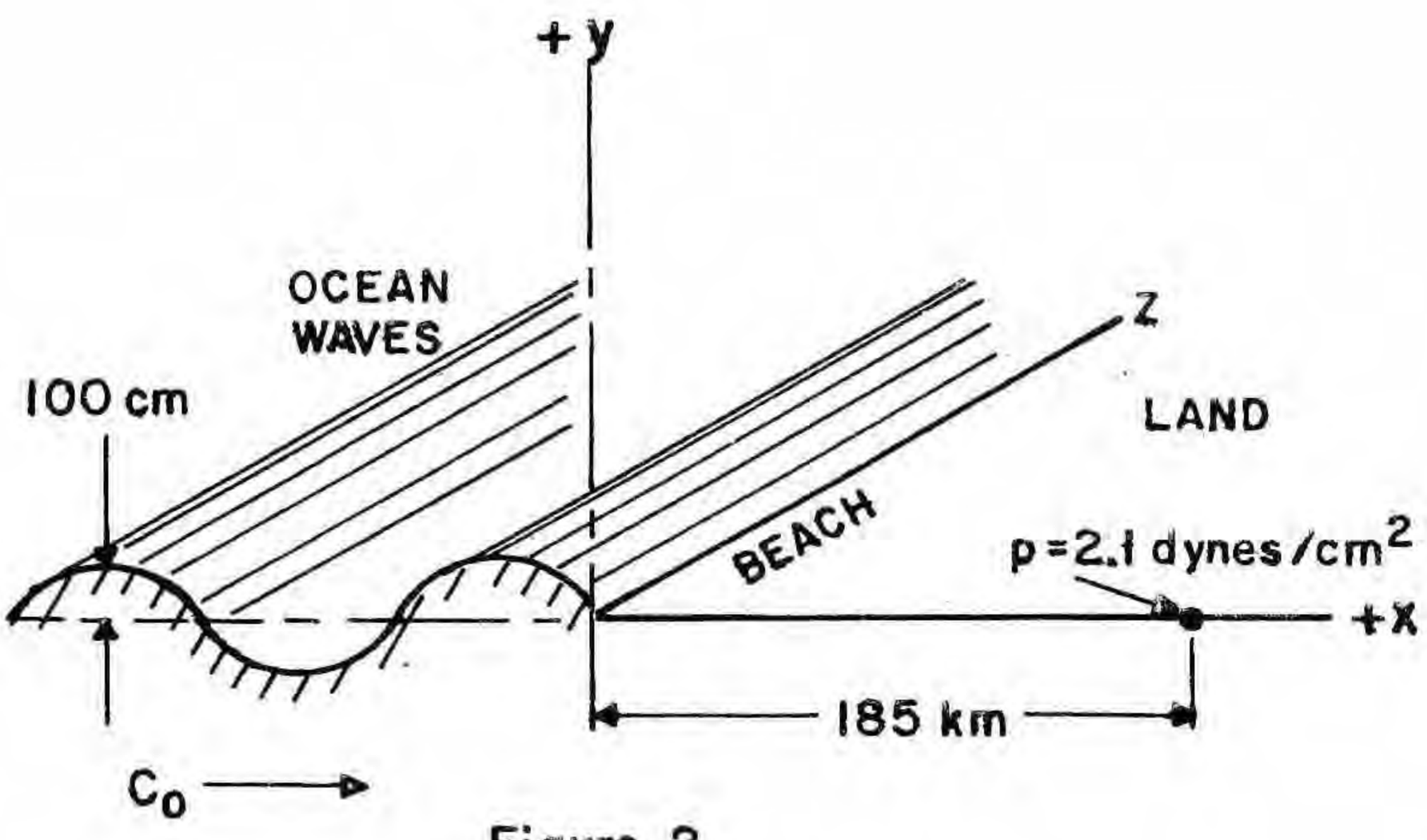

Figure 2

Since an infinite wave train radiates no sound power, whereas there is radiation by a semi-infinite train stopping abruptly at x = 0, we can imagine that the radiated power is due to a line source on the beach. The assumption is not strictly correct, but we can use it to estimate the power by means of eqs (4) and (5). For the water waves of the period T and amplitude A considered above, we find the radiated sound power to be about 30 kw per kilometer of beach.

IV. Comparison with observed microbaroms

The foregoing analysis is for the idealized case of straight-line wavefronts of infinite length, the waves being perpendicularly incident on a straight-line beach. But natural beaches are not very straight; the waves arriving at one point might not be coherent with those arriving at a point on the beach a few kilometers away; the strength of the wave can be affected by reflection from the upper atmosphere; etc. The mathematically derived sound fields of eqs (4) and (5) can therefore be expected to yield only order-of-magnitude estimates for sound pressures at a large distance from a beach.

Microbaroms have been observed in the Washington area with an infrasonic system of microphones, filter-amplifiers, and recorders which has been described before[7]. The Atlantic Ocean beach is 185 km east-southeast of the infrasonic station. Generally speaking, the microbarom sound waves come from the east and travel parallel to the earth's surface. They appear at almost all times of the year, and occasionally have sound pressures as great as 6 dynes/cm^2. A typical recording made on March 11, 1961, has T $\approx$ 5.5 secs. and p $\approx$ 1 dynes/cm^2. Fuller details will be published elsewhere. On the basis of the analysis given above, microbaroms at Washington could be caused by waves on the Atlantic Ocean beaches ranging in amplitude from about 20 cm to 100 cm.

Fribourg is about 650 km from the Atlantic Ocean beach on the west coast of France. Microbaroms observed at Fribourg often had daily average sound pressures $\approx$ 0.4 dynes/cm^2. From the above analysis the expected pressure at Fribourg due to ocean waves of A = 100 cm would be 1.0 dynes/cm^2. A more puzzling observation is that the sound waves were reported as arriving from a northwest direction. The Atlantic Ocean is about 1500 km away in this direction, beyond north Ireland and Scotland.

Available data are not quite complete enough to verify the proposed theory. Sound pressure measurements made at several distances from a long straight beach, combined with concurrent wave-height measurements, should serve as a test of the theory.

---

[7] R.K. Cook, "I Strange Sounds in the Atmosphere", Sound 1, No. 2, p. 12 (1962).

P43

FOURTH INTERNATIONAL CONGRESS ON ACOUSTICS
COPENHAGEN 21.-28. AUGUST 1962

On Vibration of Layered Plate with Losses.

B.D.Tartakowskii, S.A.Rybak.

In connection with the problem of vibroabsorption it is necessary to study wave propagation in plates when the thickness (h) is comparable with a bending wave length ($\kappa h \sim 1$). In published papers the investigation of some properties of vibrodissipative construction /1,2/ is based on the thin plate theories ($\kappa h \ll 1$).
On the base of general methods of elasticity we considered thin plate vibrations for the general case ($\kappa h \gtrsim 1$) and the transition to a thin plate was followed.
In the case of a homogeneous plate with the accuracy in term $(\kappa h)^8$ the equation of bending vibrations has the form:

$$m\frac{\partial^2 u}{\partial t^2}+\frac{E}{1-\sigma^2}\frac{h^3}{12}\Delta^2 u-m\frac{h^2}{12}a_1\Delta\frac{\partial^2 u}{\partial t^2}+m\frac{h^2}{12}\frac{E}{1-\sigma^2}\frac{h^2}{4\mu}a_2\Delta^2\frac{\partial^2 u}{\partial t^2}=0$$

$$a_1=3\left(\frac{9}{5}-\frac{4}{3}\frac{\mu}{\lambda+2\mu}\right);\quad a_2=\frac{2}{5}+\frac{1}{15}\frac{\mu}{\lambda+2\mu}-\frac{11}{700}\frac{\lambda+2\mu}{\lambda+\mu};\quad \frac{E}{1-\sigma^2}\equiv\frac{4\mu(\lambda+\mu)}{\lambda+2\mu}.$$

The corresponding Timoshenko's equation /3/ with its corrections due to rotatory inertion and shear differs slightly from ours. The differencies are in some other meanings of the coefficients (by $\sigma=0{,}3$ these differencies, however , don't exceed 2%) and in the last term of the equation /1/ $\sim\Delta^2\frac{\partial^2 u}{\partial t^2}$ when Timoshenko's corresponding term is $\sim\frac{\partial^4 u}{\partial t^4}$. With the accuracy in term $(\kappa h)^8$ these differencies are not principal. However, formal solution of Timoshenko's equation gives two meanings for the velocity of wave propagation, that proves misunderstanding in some papers. The equation

/1/ contrary to /3/ does not yeald wrong roots $\omega(\kappa)$, because there is not time derivatives higher than second.

In the case of plates, consisting of arbitrary thick layers ($\kappa_i h_i \sim 1$) each layer vibration is convenient to split both on symmetrical and antisymmetrical vibration, characterizing each vibrational type by three impedances Z_{is} and Z_{ia}. Six impedances, characterizing vibrations of the total plate, are expressed through separate layer impedances. Their physical meaning comes from the equation:

$$\begin{vmatrix} P_s \\ \tau_s \end{vmatrix} = \begin{vmatrix} Z_{1s} & Z_{2s} \\ -Z_{2s} & Z_{3s} \end{vmatrix} \cdot \begin{vmatrix} u_s \\ V_s \end{vmatrix} \qquad \begin{vmatrix} P_a \\ \tau_a \end{vmatrix} = \begin{vmatrix} Z_{1a} & Z_{2a} \\ -Z_{2a} & Z_{3a} \end{vmatrix} \cdot \begin{vmatrix} u_a \\ V_a \end{vmatrix} \qquad /2/$$

Where P_s, P_a, τ_s, τ_a symmetrical and antisymmetrical forces (normal and tangent) applied to the layer (the plate); u_s, u_a, V_s, V_a corresponding components of boundary point velocities. The impedances depend upon the frequency, elastic parameters of a layer, the thickness and incident wave angle. In that case when the plate is emerged in liquid ($\tau = 0$) it is characterized by normal impedances:

$$\zeta_s = \frac{P_s}{u_s} = Z_{1s} + \frac{Z_{2s}^2}{Z_{3s}} ; \quad \zeta_a = \frac{P_a}{u_a} = Z_{1a} + \frac{Z_{2a}^2}{Z_{3a}}$$

Let's consider, for example, three layered symmetrical plate with external thin layers. Then

$$\zeta_a = 2\zeta_a^{(1)} + \zeta_a^{(2)} - \frac{\xi_s^{(1)} \left(\frac{Z_{2a}^{(2)}}{Z_{3a}^{(2)}} + \frac{Z_{2a}^{(1)}}{Z_{3a}^{(1)}} \right)}{1 + \frac{\xi_s^{(1)}}{Z_{3a}^{(2)}}},$$

where $\xi_s = 2\left(Z_{3s} + \frac{Z_{2s}^2}{Z_{1s}} \right)$

If the internal layer is also thin, the result will be similar to Kerwin's, who studied bending vibrations of the three layered thin

plate [1]

The difference lies in the fact that the inertion corresponding to longitudinal vibrations in external layers, was not taken into consideration in [1]. In the problem of bending wave propagation it doesn't bring to considerable failuress, though it can be essential in some other cases. There is the same lack of the well known Oberst formula, used for the determination of soft coating Joung's modul, put on metal rod [2]. Here, however, it is rather great and by modul determination will bring to absurd result, if the vibration frequency is increased. The formula obtained with the aid of the method, given above,

$$\frac{E_2}{E_1} = \frac{\left(\frac{B^*}{B}-1\right)(1-q_1-\beta q_2)+q_2(1-q_1)3\beta(1+\beta)^2}{\beta\left[4+6\beta+4\beta^2-\frac{B^*}{B}-\beta^2(q_1+\beta q_2)-3q_1(1+\beta)^2\right]}. \qquad (4)$$

differs from Oberst formula by the presence of inertion terms:

$$q_{1,2} = \frac{\rho_{1,2}}{E_1}\omega\sqrt{\frac{B^*}{m^*}}$$

where

$$\beta = \frac{h_2}{h_1}\ ;\ B^* = \frac{m^*\omega^2}{K^4};\quad B = \frac{E_1 h_1^3}{12};\quad m^* = \rho_1 h_1 + \rho_2 h_2.$$

Calculation to this formula give correct modul in wide frequency range.

Let's consider losses in layered plates. The wave number in plate will be

$$K = K_0(1+i\varkappa);\quad E = E_0(1+i\eta).$$

In the case of small losses we obtained , given through normal impedance $\zeta_{a,s}$:

$$\varkappa = \frac{\sum_p \frac{\partial\zeta}{\partial E_p}(E_0\eta)_p}{\frac{\partial\zeta}{\partial K}K_0} \qquad (5)$$

Particularly the absorption in threelayered plate discribed by impedance $\zeta_a(3)$ was considered. It was found an essential difference between frequency characteristic of losses in the threelayered plate and that in the thinlayered construction, described by Kerwin [1]. For determination of different mechanismus of the losses in vibrations of

multilayered structures an energetic method should be applied. The advantage of it lies in the fact that the terms corresponding to different mechanismus of the losses are additive in the formula of summarized energy.

It can be shown that

$$\chi = \frac{C_{ph,x} \int \bar{\varphi} dz}{C_{g,x}\, \omega \int \bar{E} dz} . \qquad /6/$$

$C_{ph,x}, C_{gx}$ phase and group velocities along the X -axis, φ -loss function, E -density of energy.

For example, in condition of the resonanc. in internal layer, determined by the equality for proections of wave numbers of longitudinal and transverse waves on Z -axis

$$K_z, q_z = \frac{2n_{t,e}+1}{2}\pi , \quad n_t > n_e .$$

and in condition of relative softness of the internal layer $\frac{E_2}{E_1} \ll 1$ we obtain, from /6/ that $\chi = \frac{\eta}{4}$.

So the losses in a layered plate in this case are equal to that in internal layer, vibrating separately. It twice exceeds the maximum losses when intermediate layer is thin. The theory agrees with the experiment.

Literary Citied

1. D.Ross. E.Ungar. E.Kerwin, Structural Damping. 1959. p.49-57.

2. H.Oberst. Akust.Beih. 1952. 4. 181-188.

3. S.Timosherko. Phil.Mag. Ser.6. v.41. 744. 1922.

G44

FOURTH INTERNATIONAL CONGRESS ON ACOUSTICS
COPENHAGEN 21.-28. AUGUST 1962

ON PEAK FACTORS AND ASYMMETRIES OF ACOUSTICAL SPEECH SIGNALS

Weiant Wathen-Dunn — AF Cambridge Research Laboratories
Bedford, Massachusetts, U. S. A.

In single-channel voice communications the peak factor of the signal is of particular importance, but no meter has yet been devised to measure it -- or even the peak and rms values from which it may be calculated -- and no mathematical model exists whereby these quantities can be determined analytically. Recourse must be had, therefore, to statistical description, which yields the desired measures, but only at the expense of much labor.

Whenever a speech signal is "processed" -- even by so simple a technique as band limiting -- the peak and rms values are altered, and so is the peak factor. Furthermore, the new values cannot be predicted but must be measured, which is most readily done from the density function and distribution of the instantaneous signal amplitude.

In order to appreciate the effects of various processing techniques, it is desirable to have a standard of comparison. The pressure wave produced by an "average" speaker in a free field might well be taken as a standard, and accordingly this paper reports a measurement of the average density function and cumulative distribution for the instantaneous amplitudes of the acoustical pressure waves generated by 16 male speakers in an anechoic chamber.

The actual measurements were made on electrical waveforms, and the results are valid only to the extent that these waveforms are replicas of the original pressure waveforms. The transducer used is therefore crucial, and only a small condenser microphone is really suited to the purpose. At the lower frequencies, where the effects of diffraction and diaphragm resonance are negligible, the output voltage is directly proportional to the pressure. At higher frequencies this is no longer true, for the reasons indicated, but components of the speech signal in this part of the spectrum are more Gaussian in nature and consequently more invariant under transformation. This rationale serves to justify the validity of the measurement in lieu of a knowledge of the exact effects of resonance and diffraction.

Measurements of the density and distribution functions for the instantaneous amplitudes of electrical speech waveforms have been reported previously, notably by Dunn and White[1] and Davenport[2]. The former used a condenser microphone in a free field, but the experiment did not have the advantage of modern measurement techniques, and a comparison of their data with one of Davenport's curves showed some discrepancy[3]. The latter used a pressure-gradient microphone and direct magnetic recording, and there was a question as to how well these represented the acoustical signal.

In the present experiment the speakers talked "across", i.e., at right angles to the axis of, a 640-AA condenser microphone placed 30 cm from the speakers' lips in an anechoic chamber. The electrical signal was recorded at 60 ips on an FM (frequency modulation) magnetic tape recorder to preserve waveform, even though the playback speed might be changed, and a high-quality transmission line carried the signal to the location of the recorder as shown in Fig. 1. The over-all system response-frequency characteristic was flat within ±0.5 db from 50 cps to 10 kcps, but above this the response of the playback amplifier fell repidly so as to eliminate frequencies actually recorded on the tape. A 1 kcps square wave, inserted across a resistor in series with the microphone, came out of the tape reproducer in very respectable shape.

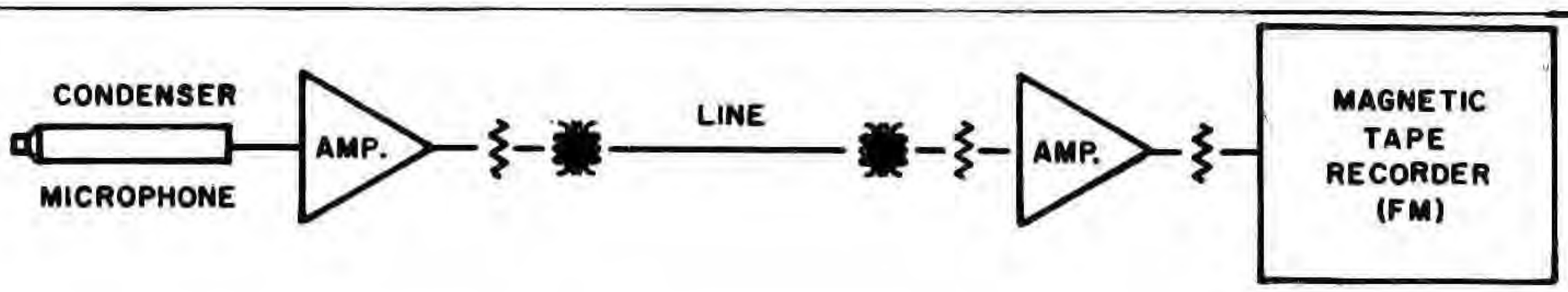

FIG. 1 BLOCK DIAGRAM OF EQUIPMENT

Each speaker read from text for more than 2-1/2 minutes and then remained silent for over half a minute while the tape continued to record the actual noise condition that prevailed. The text material was chosen so that it could be read in a manner approximating normal conversational speech. The speakers were chosen mostly as a matter of convenience, and there is no assurance that they are a representative population.

The tapes containing the recorded speech samples were reproduced at half speed at MIT's Lincoln Laboratory. The output of the playback system was confined to a range of ±1.0 volt to satisfy the input requirements of an analog-to-digital converter, which provided 7-bit digitizations at approximately the Nyquist rate on computer command. The computer calculated the probability of being in each of the 128 voltage quantization intervals (Δe) and then the mean and the standard deviation of the function. The latter is identical to the rms value of the signal, e_{rms}. Later versions of the program normalized the voltage amplitude against the rms value.

The computer also provided a plot of the histogram, and a typical result is shown in Fig. 2. Certain irregularities will be noted, but these always occured at the same voltage step and are ascribable to irregularities in the reference network against which comparisons were made for the digitization process. One high value was always balanced by a correspondingly low value next to it.

It turned out that the noise of the electrical system was below the acoustical noise in the anechoic chamber, which consisted primarily of frequencies below 5 cps due to building vibration. This, together with the system noise, showed up as a single,

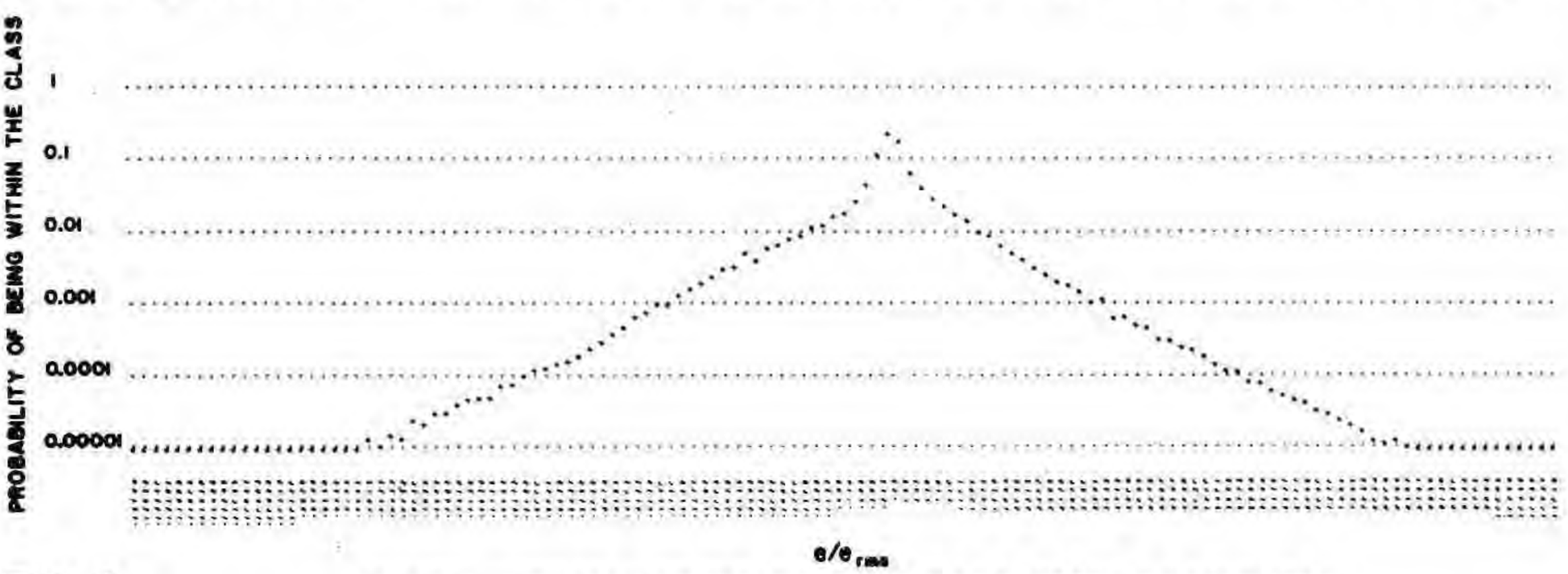

FIG. 2 TYPICAL HISTOGRAM OF SPEECH AMPLITUDES PLOTTED BY COMPUTER

smooth, sharp hump when plotted by the computer in the manner shown in Fig. 2. The noise histogram dropped below $p = 10^{-5}$ at roughly 4.5 times its rms value. The ratio of the rms values of speech and noise ranged from 12 to 20 db, increasing toward the latter value as the recording technique improved with experience.

The data were averaged on the basis of equal rms values (normalized amplitudes). A density curve was prepared for each speaker by drawing a smooth curve through representative points determined by examining the histogram. Each point value was taken equal to the probability read from the histogram multiplied by $e_{rms}/\Delta e$. This resulted in a density curve with a scale change that made the area under the curve integrate to one. All curves were then comparable. They were divided into small increments of normalized amplitude, and the probabilities of all 16 speakers being within each increment were averaged. The average density function was obtained by dividing the average probability by the width of the increment, while the average distribution was obtained by summing the average probabilities, beginning at the two ends of the curve and working toward the middle.

The average density function is plotted in Fig. 3 on a logarithmic probability scale against the absolute value of normalized amplitude. There are two curves, one for positive and one for negative pressure values. The points fall on a remarkably smooth curve, which exhibits an asymmetry at small amplitudes which is typical of all speakers. At larger amplitudes the variations among the speakers are greater. Sometimes the two curves cross, while at other times they spread apart slightly. The average is well represented by two straight, parallel lines and bears out Davenport's contention that, except at the center, the function is exponential[2].

Fig. 4 presents the two halves of the average cumulative distribution. The dotted curves bend because only probabilities derived directly from the data in Fig. 3 were included in the summation. The curves in Fig. 3 can be extrapolated and additional probabilities included in the summation to give the points next to the solid lines in Fig. 4. Mathematical integration of the proper exponential functions from $\pm \infty$ would yield the solid lines.

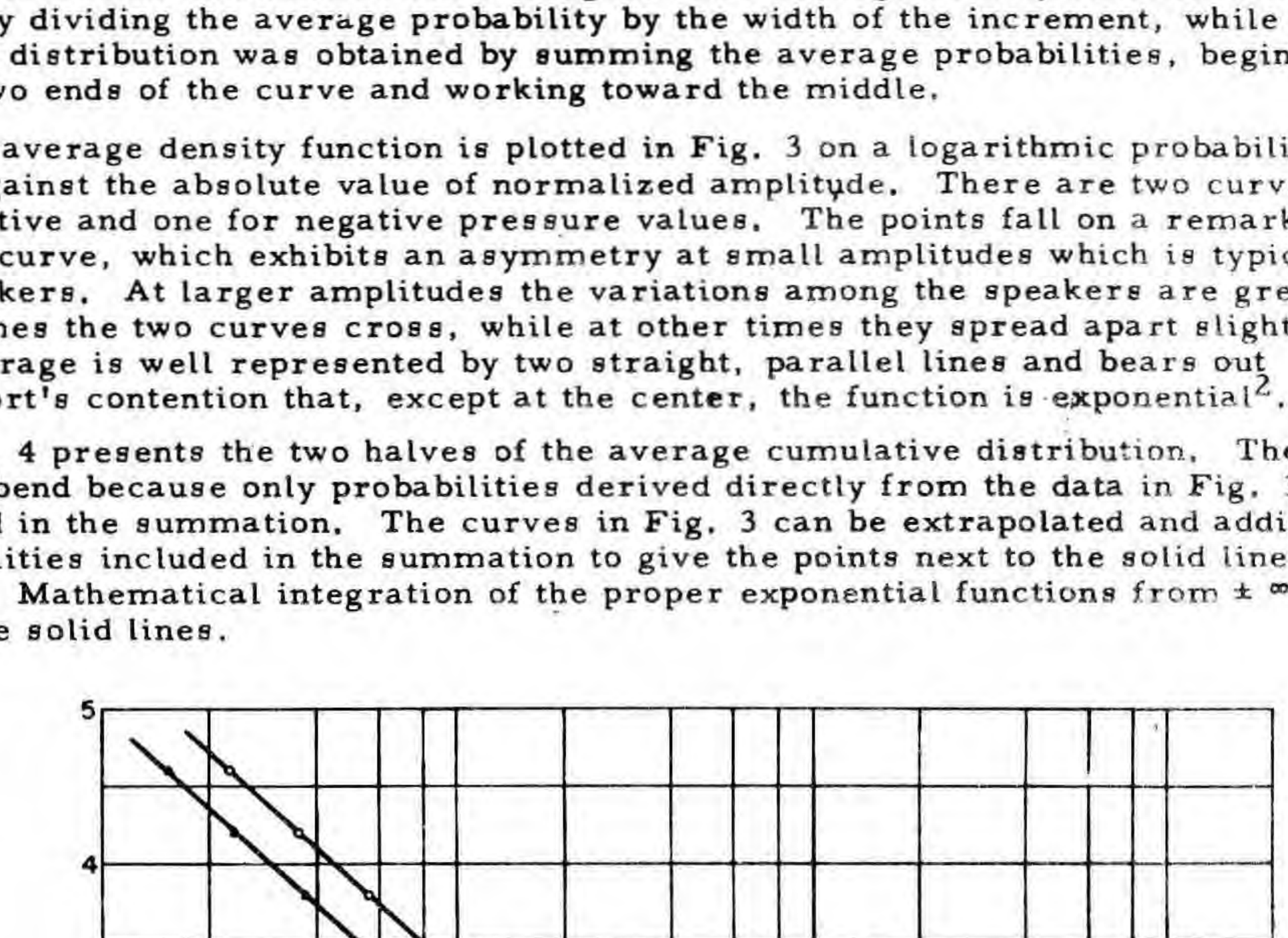

FIG. 3 AVERAGE PROBABILITY DENSITY FUNCTION FOR ACOUSTICAL PRESSURE AMPLITUDES OF MALE SPEECH

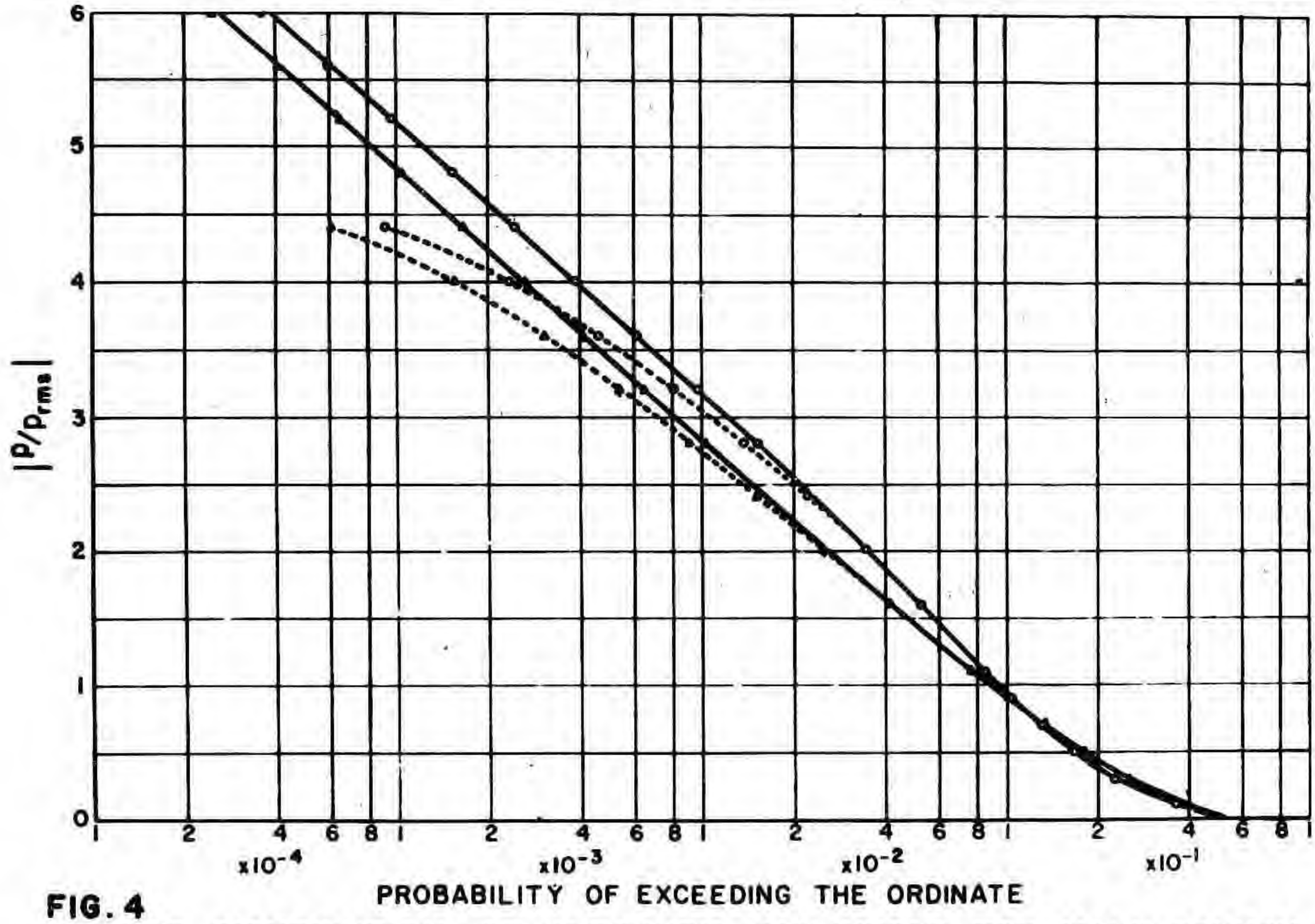

FIG. 4
AVERAGE DISTRIBUTION OF PRESSURE AMPLITUDES FOR MALE SPEECH

This cumulative curve turns out to be in close agreement with the curve previously integrated from one of Davenport's density functions by Wathen-Dunn and Lipke[3], which must be considered in part fortuitous, since the curve integrated was chosen at random and was not an average of all his data. This comparison leads one to the conclusion, however, that these distributions do not seem to be as greatly affected by the type of microphone and recording system as the author had at first supposed, provided, however that both are high-quality, wide-range systems. The author has other data which definitely indicate that a communications type microphone has a large effect on these distributions.

Acknowledgements

The author is indebted to the Lincoln Laboratory for the use of the TX-2 computer and to Mssrs. James Forgie and Mason Groves, at Lincoln, for the program and assistance in running it.

---

[1] Dunn, H. K. and S. D. White; "Statistical Measurements on Conversational Speech." J. Acoust. Soc. Am., Vol. 11, No. 3, pp. 278-288 (Jan 1940).

[2] Davenport, W. B., Jr.; "A Study of Speech Probability Distributions." J. Acoust. Soc. Am., Vol. 24, No. 4, pp 390-399 (July 1952).

[3] Wathen-Dunn, Weiant and David W. Lipke; "On the Power Gained by Clipping Speech in the Audio Band." J. Acoust. Soc. Am., Vol. 30, No. 1, pp 36-40 (Jan 1958).

H44

FOURTH INTERNATIONAL CONGRESS ON ACOUSTICS
COPENHAGEN 21.-28. AUGUST 1962

METHODS FOR OBTAINING UNBIASED RATING SCALES

Irwin Pollack
Operational Applications Laboratory, ESD, Bedford, Mass., U.S.A.

Abstract: Sound rating, or category, scales are usually sensitive to the arbitrary selection of sounds being rated. Six methods for obtaining unbiased scales, which are independent of the initial distribution of sounds, are presented. All were experimentally effective in obtaining unbiased scales (end of abstract).

Despite the recent substantial advances in magnitude scaling, primarily by Stevens, Ekman, and their collaborators, there remains an important role for category or rating scales. In particular, when sounds are not precisely defined, e.g. truck vs motorcycle vs scooter noises, magnitude scaling may be clearly less appropriate than category or rating scaling.

Rating scales, however, have one serious drawback. As compared with magnitude scales, rating scales are sensitive to the particular distribution of stimulus objects arbitrarily selected for rating. That is, rating scales are sensitive to stimulus bias.

The aim of the present paper is to consider six methods for minimizing stimulus bias in rating scales, and to outline briefly the results of experiments which test the methods. The general approach employed will be to start with stimulus distributions which are markedly different from each other; to obtain rating scales for these distributions; to derive new stimulus distributions from the resulting rating scales, and, finally, to continue the entire process until the "descendents" of the initially markedly different distributions are alike. This process, when successful, will be referred to as the convergence upon stimulus bias.

EXPERIMENTAL METHODS

A. Method of Iterative Scaling.

This method is primarily due to S.S. Stevens and associates. It derives new stimuli based upon previous ratings. The process is called iterative because it is repeated over and over until a stable rating scale is achieved. The method derives new stimuli in the regions where the slope of the category function is steep and deletes stimuli in the region where the slope of the category function is shallow.

This is done from a plotting representing the mean category rating (ordinate) vs stimulus magnitude (abscissa). The range of ratings assigned to the extreme stimuli is divided into (n-1) equal intervals, where n is the number of stimuli to-be-derived for rating. The corresponding stimuli are determined from the plot.

The assumptions underlying this procedure are: the stimuli objects can be ordered so that a monotonic category scale is obtained; intermediate stimuli may be derived from the stimulus scale; and the appropriate basis of selection of new stimulus objects corresponds to equal linear extents along the rating scale.

B. Method of Category Production.

This method is primarily due to Miss G. Stone. The procedure provides a "reasonable" distribution of stimulus objects by preliminary selection before more intensive category scaling takes place. In preliminary tests for scaling sound levels, for example, each listener is presented with the extreme sound levels of the range of levels to-be-examined. He is then instructed to adjust attenuators to find good examples of the intermediate categories. The average levels produced by several listeners then serve as the sound distribution in further tests.

When the required number of sound levels is equal to the number of produced categories, no assumptions are required by the method of category production. When the required number of sound levels is different from the number of produced categories, it is necessary to assume that the sound levels can be ordered and that intermediate stimuli can be derived.

C. Method of Single Presentation.

This method has long been used in consumer sampling of large populations and has been used extensively in the loudness scaling of naive listeners. Only a single sound is presented to each listener for rating. In this way, the distribution of sounds arbitrarily chosen cannot affect the listener's ratings. The method, in effect, solves the problem of stimulus bias by avoiding it.

While the method avoids the problem of stimulus bias, it is an empirical question whether rating scales generated by this method will be identical to scales generated by the other methods.

D. Method of Unequal Stimulus Frequencies.

The method of unequal stimulus frequencies is specifically designed for situations in which additional sounds are not available to the method of iterative

scaling. For example, you may wish to rate the noisiness of five specific fans. The method presents sounds more often in the region where the initial category function is steep and less often where the category function is shallow. The method produces sounds with a frequency-of-presentation proportional to the slope of the category function at that sound.

The method attempts to provide an unbiased category scale with a given set of sounds with a minimum number of assumptions. No assumption is made other than the sounds can be rank-ordered to yield a monotonic category scale. This rank-ordering need not be done before the initial scaling, it may be done after the initial scaling. This permits one to scale qualitative objects as well as well-defined scales such as sound level or audio frequency.

E. Method of Equal Response Frequencies.

When a listener is presented with a heavily weighted distribution of sounds, he will often apologize for not using the various rating categories equally often. That is, listeners expect to employ their rating categories equally often. The method of equal response frequencies attempts to capitalize upon this expectation to yield an unbiased set of sounds.

The method spreads out sounds in the region where a given response category is used often and concentrates sounds in the region where a given response category is seldom used. The method of equal response frequencies requires the first two assumptions of the method of iterative scaling since additional new sounds must be derived by the method. However, the assumption that sounds must be chosen to correspond with equal spacing along the rating scale is not required. Instead, it is assumed that the listener attempts to employ the various rating categories equally often.

F. Method of Average Ratings.

Stimulus bias effects are demonstrated to the extent to which the sound distributions depart from a relatively balanced distribution of sounds. This finding suggests that we can minimize the departure from a relatively balanced distribution of sounds simply by averaging the ratings assigned to two or more distributions. In turn, from this average distribution of ratings, a new distribution of sounds can be obtained by the method of iterative scaling.

RESULTS

The results of an extensive testing program demonstrate: (a) weighted stimulus distributions produce biased rating scales which reflect the direction of weighting; and, (b) all six of the procedures are effective in eliminating the introduced bias.

The summary conclusion is based upon a testing program which included tests:

1. in Great Britain and the United States.

2. with a wide range of subjects including British Naval Ratings, university students, and laboratory personnel.

3. rating variables ranging from the poorly defined judgment of facial beauty to the well defined judgment of auditory frequency.

4. extending over a narrow stimulus range to a wide stimulus range, e.g. ranges in auditory frequency subtending a small fraction of an octave to one subtending several octaves or ranges in sound level subtending 10db to 60db.

5. with a wide range of rating procedures, including the judgment of "twice" brightness, selection of "ideal gray," category naming of audio frequencies, category sorting of weights, category production of sound levels, and the category marking of gray papers.

CONCLUSION

The effect of a weighted distribution of sounds may be easily and quickly eliminated by a wide range of methods in preliminary experimentation. Their use may be recommended unequivocally before more extensive scaling.

REFERENCES

The implication of bias effects for the validity of psychophysical scaling was pointed up by: W. R. Garner, Context effects and the validity of loudness scales. J. exp. Psychol., 1954, 48, 218-224.

The problem of stimulus bias is examined in several papers by S.S. Stevens and collaborators. Of special note : S.S. Stevens and E.H. Galanter, Ratio scales and category scales for a dozen perceptual continua. J. exp. Psychol., 1957, 54, 377-411.

FOURTH INTERNATIONAL CONGRESS ON ACOUSTICS
COPENHAGEN 21.-28. AUGUST 1962

Schwingungsrelaxation von CO_2 in Mischungen mit Helium.

H.-J. Bauer und E. Liska
I.Physikalisches Institut der Technischen Hochschule Stuttgart

Den Anlaß für die vorliegende Arbeit bildeten frühere Untersuchungen der Schallabsorption in CO_2-Edelgas-Mischungen, die am I.Physikalischen Institut der Technischen Hochschule Stuttgart durchgeführt wurden[1]. Aus der Verschiebung der Relaxationsfrequenz mit der Zumischung des Edelgases B sollte die Stoßausbeute $1/Z_{AB}$ für die Schwingungsanregung des CO_2-Moleküls (A) in AB-Stößen

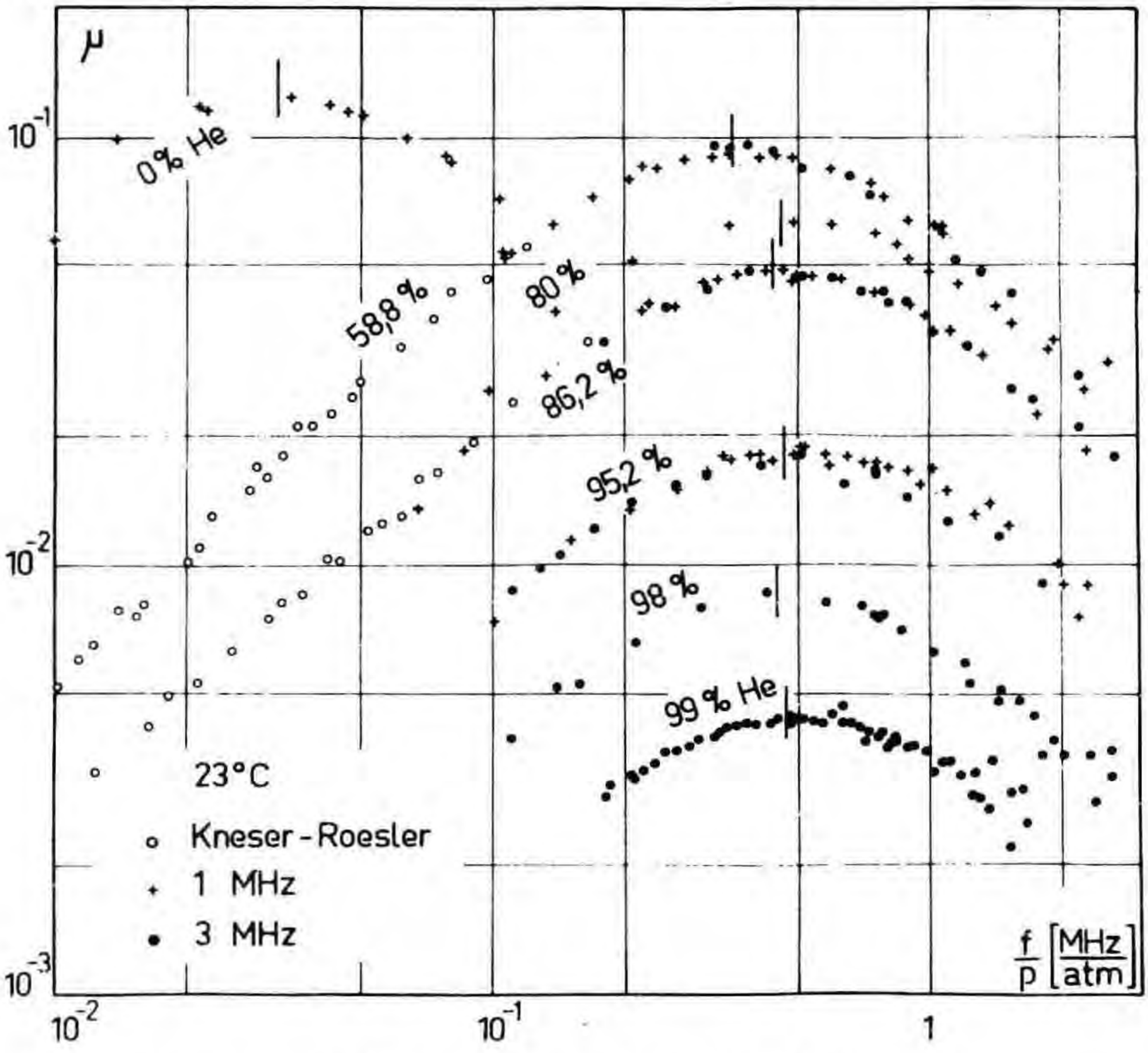

Fig.1 Überklassische Absorption in CO_2-He-Mischungen

bestimmt werden. Das Absorptionsmaximum für CO_2-He-Mischungen lag oberhalb des Meßbereichs der damals verwendeten Apparatur; diese Mischungen wurden daher einer neuerlichen Untersuchung mit einer Impulsapparatur unterzogen (Meßbereich von 0,02 bis 30 MHz/atm).

In Fig.1 ist die erhaltene überklassische Absorption für reines CO_2 und 6 Mischungen dargestellt. Dabei wurde von der gemessenen Gesamtabsorption der klassische Anteil - Absorption infolge innerer Reibung, Wärmeleitung und Diffusion - abgezogen. Fig.2 zeigt die nach Kohler[2] berechnete klassische Absorption bei 1 MHz/atm. Ein weiterer zu f/p proportionaler Anteil an der Gesamtabsorption - von der Rotationsrelaxation herrührend - ist stets kleiner als 1 % und wurde daher nicht berücksichtigt. Wegen der vergleichsweise hohen klassischen Absorption im Relaxationsgebiet wurde auch die Nichtadditivität zwischen klassischer und überklassischer Absorption nach Meixner[3] abgeschätzt. Es ergab sich nur ein geringer Einfluß (< 1 %). Korrekturen wegen der Nichtidealität des CO_2 waren nur oberhalb von 1 atm Partialdruck von wesentlichem Einfluß und wurden dort berücksichtigt.

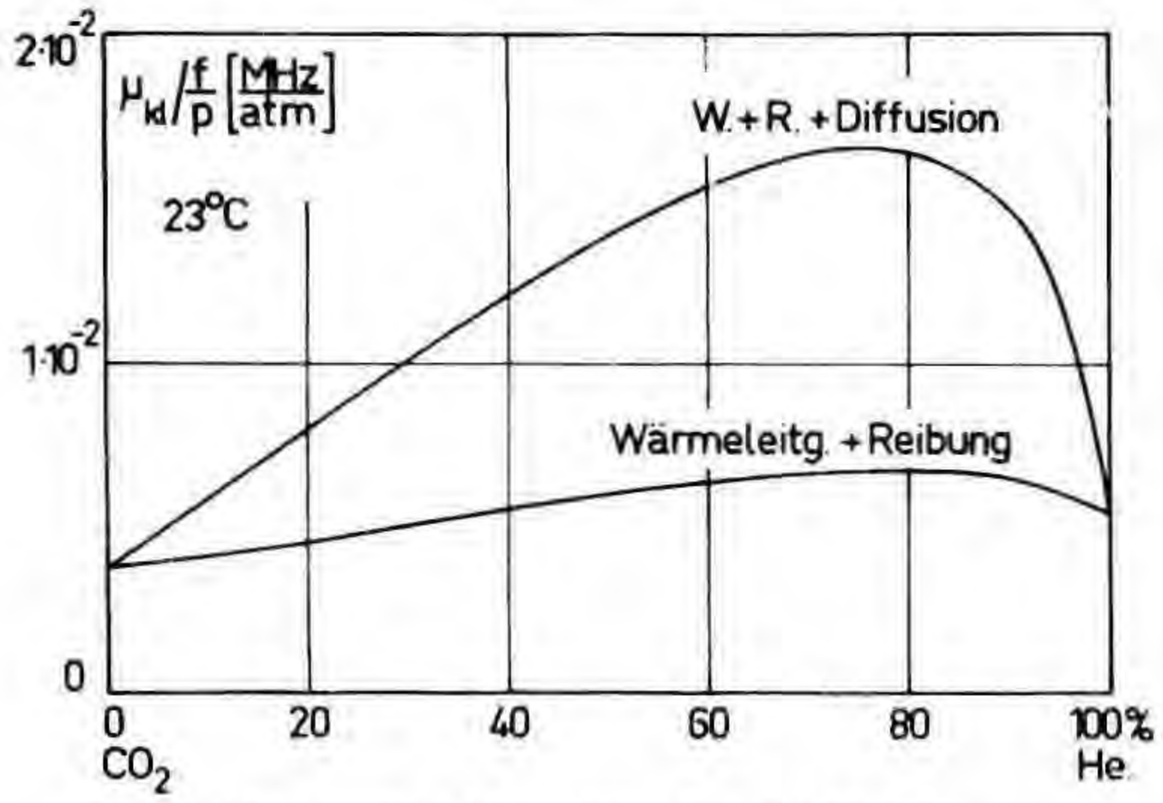

Fig. 2 Klassische Absorption bei 1 MHz/atm

Aus der Lage der Absorptionsmaxima in Fig.1 wurden die auf 1 atm bezogenen isotherm-isochoren Relaxationszeiten $\bar{\tau}_{VT}$ bestimmt. Dabei wurde ein einfacher Relaxationsprozeß vorausgesetzt:

$$\bar{\tau}_{VT} = \frac{c_p^0}{2\pi c_p^\infty \sqrt{1-\varepsilon}} \left(\frac{f}{p}\right)_{max}$$

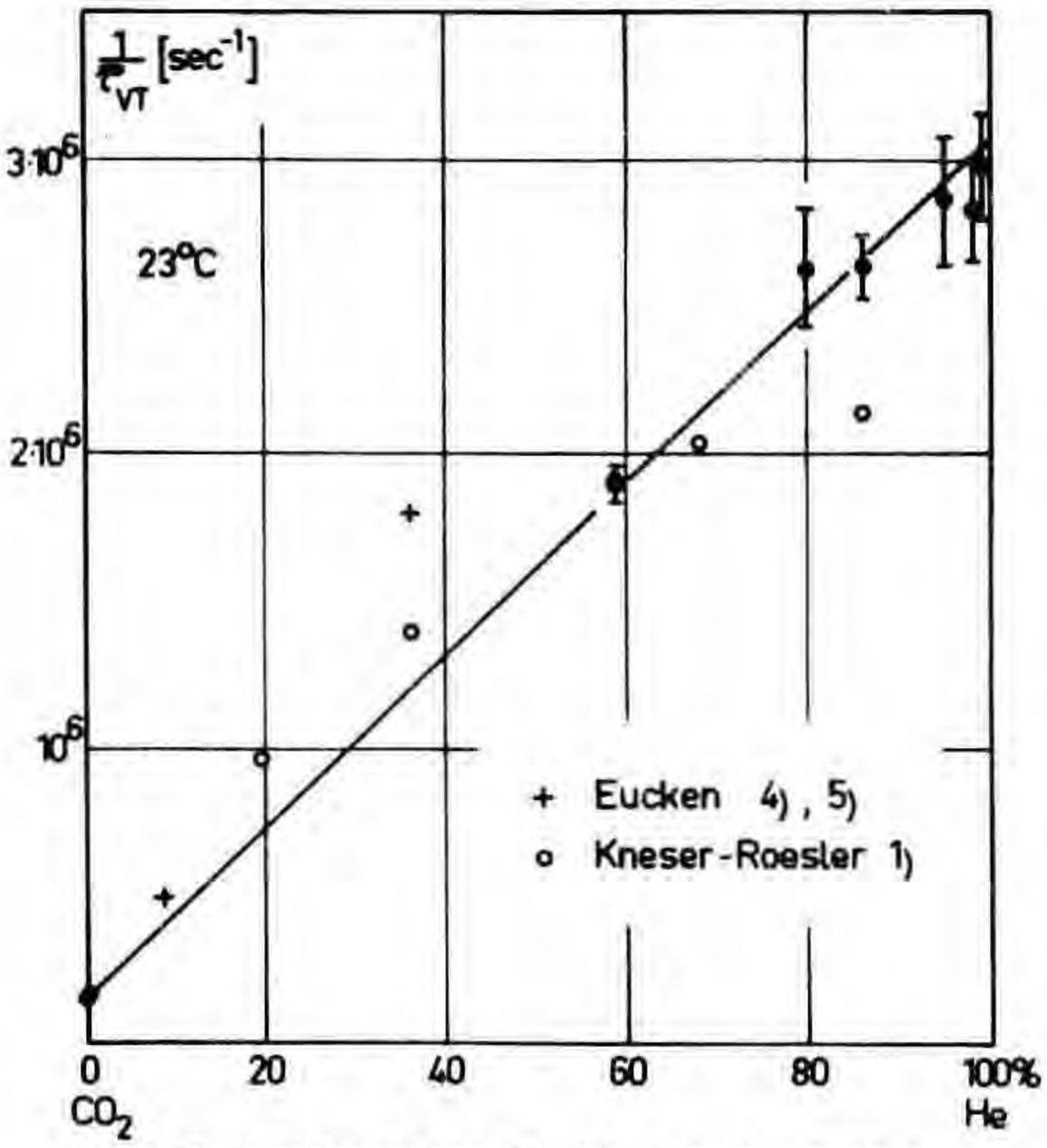

Fig. 3 Relaxationszeiten für CO_2-He-Mischungen.

Fig.3 zeigt $1/\bar{\tau}_{VT}$ als Funktion der Zusammensetzung. Obwohl der Anschluß der Meßpunkte von Kneser und Roesler[1] an unsere Ergebnisse (s.Fig.1) ausgezeichnet ist, zeigen sich erhebliche Abweichungen der $1/\bar{\tau}_{VT}$. Kneser und Roesler mußten $\bar{\tau}_{VT}$ durch eine Extrapolation auf das Absorptionsmaximum gewinnen. Unsere Messungen ergeben nun eine systematische Abweichung der Maximalabsorption von der für einen einfachen Relaxationsprozeß der gesamten Schwingungswärme berechneten. In Fig.4 ist diese Abweichung als Verhältnis von gemessener zu berechneter Maximalabsorption dargestellt.

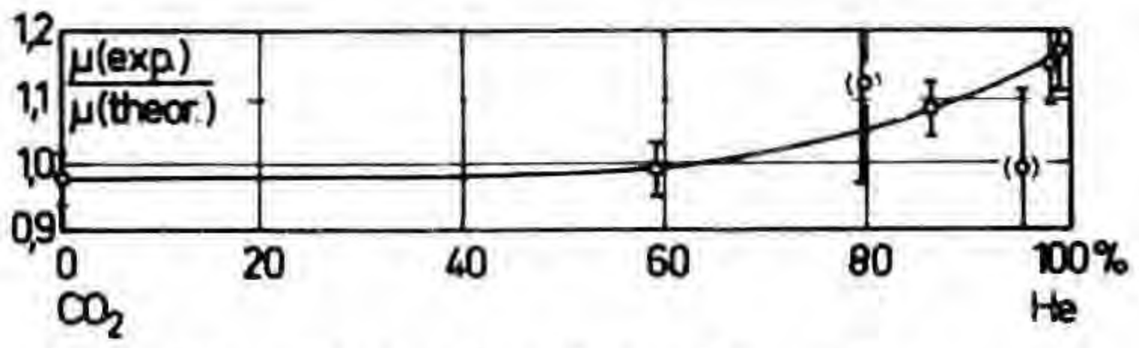

Fig. 4 Abweichungen der Maximalabsorption.

Die Deutsche Forschungsgemeinschaft unterstützte die Arbeit wesentlich durch Bereitstellung von Sachmitteln.

1) H.O. Kneser und H. Roesler, III.ICA-Kongress 1959 Stuttgart
2) M. Kohler, Phys. Z. 127, 40 (1949)
3) J. Meixner, Acustica 2, 101 (1952)
4) A. Eucken und S. Nümann, Z. Phys. Chem. B 36, 163 (1937)
5) L. Küchler, Z. Phys. Chem. B 41, 199 (1938)

K44

FOURTH INTERNATIONAL CONGRES ON ACOUSTICS
COPENHAGEN 21.-28. AUGUST 1962

RELATION DANS CERTAINS LIQUIDES ULTRASONNES ENTRE LA LUMINESCENCE ET LA RELAXATION DES CAVITATIONS DE GAZ ET DE VAPEUR

MM. DEGROIS et B. BADILIAN - Lab. Physiologie Acoustique - I.N.R.A.
JOUY-en-JOSAS (S.&.O.)

RESUME .

Des disparitions soudaines, suivies de réapparitions de la luminescence, sont constatées à une température définie dans des liquides ultrasonnés, les conditions de traitement étant constantes.

Cette température particulière est étudiée pour des solutions de KI, et on montre que celle-ci est liée à l'apparition spontanée et relaxée des cavitations de gaz et de vapeur.

INTRODUCTION .

Dans une solution aqueuse ultrasonnée, toutes conditions expérimentales restant constantes, nous avons constaté que certaines des manifestations des effets physico-chimiques de la cavitation se représentaient périodiquement (1-2-3-4). Si la luminescence, entre autre, subit une disparition soudaine ainsi que l'ont relaté sommairement LEWSIN et RSCHEVKIN (5), elle réapparaît également spontanément. Ces phases d'extinction et d'apparition se succèdent cycliquement.

Les caractéristiques et les origines du phénomène font l'objet de cette étude.

CONDITIONS EXPERIMENTALES .

La luminescence ultrasonore a été étudiée sur l'eau et des solutions de KI, de diverses concentrations : 20 - 30 - 50 %; Volume traité : 90 cm3; Fréquence : 1 MHz; Puissance ultrasonore : environ 30 w pour 12 cm2 de surface active du transducteur. L'intensité de la luminescence est mesurée dans le spectre visible par un photomultiplicateur d'électrons dont la tension de sortie est appliquée à un galvanomètre enregistreur.

Dans la cuve de traitement, de forme parallélipipédique, on dispose :

a) - d'un thermocouple étalonné pour la mesure de la température et éventuellement,

b) - d'un 2ème thermocouple (à 2 soudures dans le liquide) pour la mesure simultanée de l'intensité U.S. ou,

c) - d'un hydrophone pour la mesure du bruit de cavitation.

RESULTATS .

I. - Intensité de la luminescence (δ) en fonction du temps -

Si on enregistre l'intensité de la luminescence en f(temps), pour une puissance US (30 w) et une température (25° C) données, on constate, et ce indépendamment de la concentration de la solution, (fig. I) que la luminescence croît à partir d'une valeur δo, passe par un maximum δ_{MAX}, décroît plus ou moins rapidement suivant les conditions de traitement et atteint un palier δp, au bout d'un temps plus ou moins long selon les conditions expérimentales.

Pour étudier l'influence de la température sur l'intensité de la luminescence, nous partirons des valeurs paliers de la luminescence.

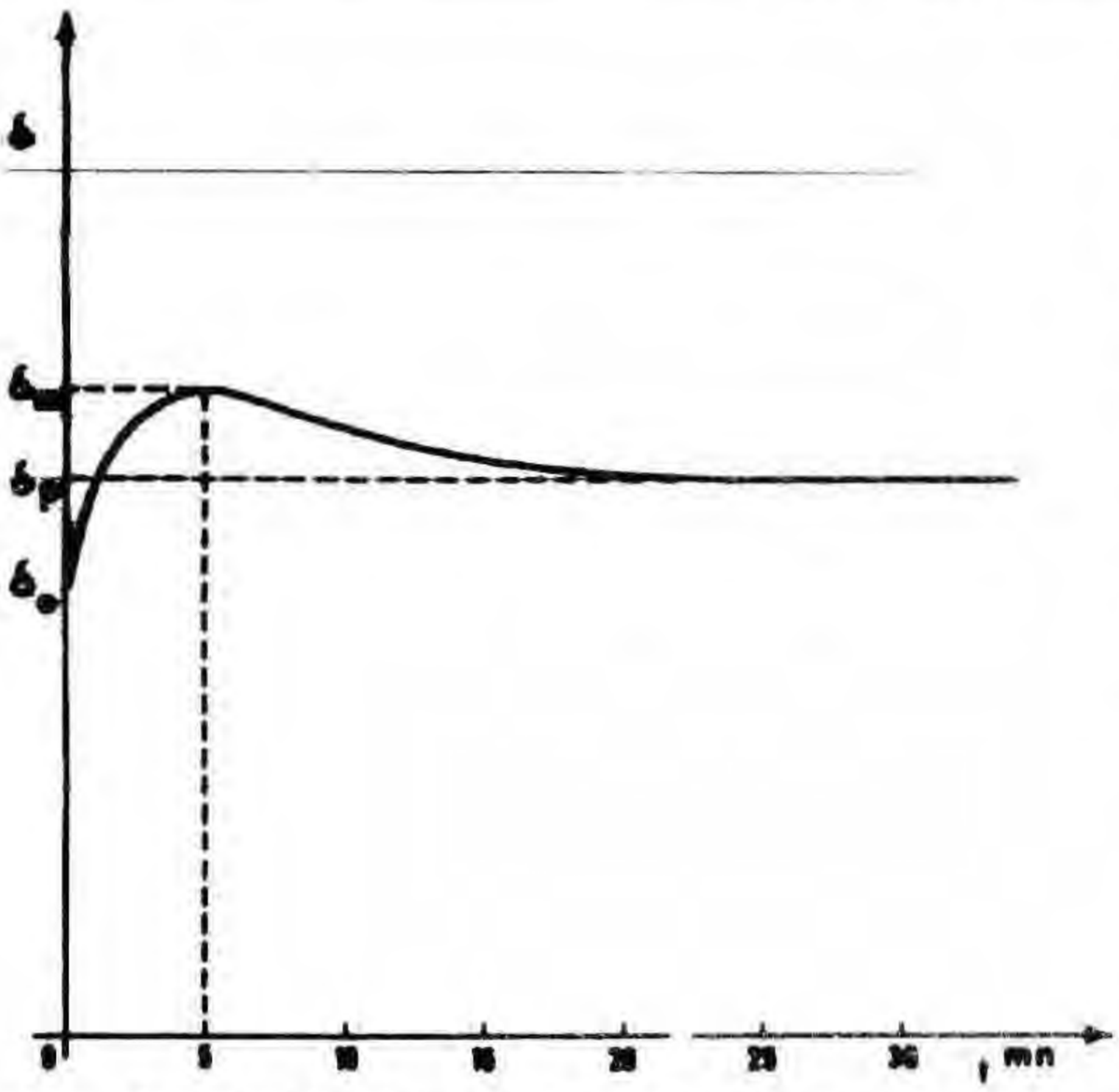

Fig. I - Variation de la luminescence en f(t) - (KI 50 %)

II. - <u>Variation de la luminescence en fonction de la température</u> -

La <u>fig. II</u> montre que :

a) - la luminescence décroît linéairement avec la température,

b) - la luminescence disparaît à des températures différentes qui dépendent de la concentration en sels.

Soit Tp, cette température de disparition de la luminescence.

III. - <u>Variation de la température de passage (Tp) avec la concentration de la solution</u> -

La courbe de la <u>fig. III</u>, extraite de la fig. II, montre que Tp décroît en fonction inverse de la concentration.

Cette variation semble linéaire aux fortes concentrations, mais la linéarité dépend de la nature de la solution et des conditions expérimentales.

IV. - <u>Apparition de la relaxation</u> -

Si à la température de la disparition de la luminescence, (Tp), les conditions expérimentales sont maintenues constantes, après quelques minutes la luminescence réapparaît et subit des disparitions et réapparitions successives selon un rythme périodique.

Pour suivre le phénomène, divers paramètres énumérés précédemment sont enregistrés (<u>fig. IV</u>) pendant que se déroulent les phases d'apparition et d'extinction successives de la luminescence. Le tracé montre que l'intensité US et la température mesurées au sein de la solution subissent une augmentation soudaine et non négligeable, au moment de la disparition de la luminescence.

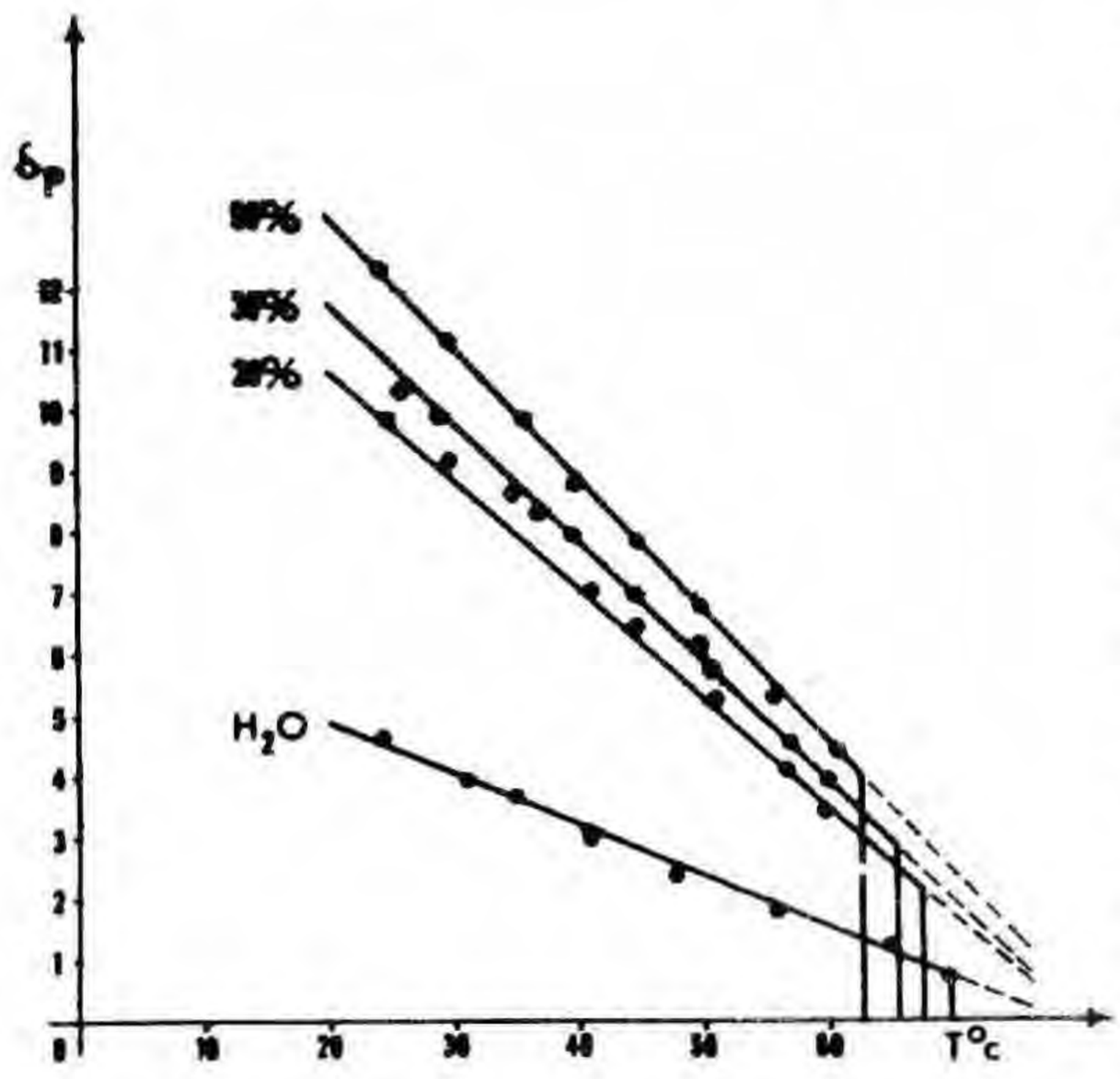

Fig. II - Variation de la luminescence en fonction de la température.

Les oscillations périodiques et particulières de ces paramètres autour d'une valeur moyenne, mise en évidence par les enregistrements, peuvent être assimilées à des courbes de relaxation classique.

On peut émettre une hypothèse sur l'origine de ce phénomène. Depuis longtemps il est admis que les liquides à forte tension de vapeur : éther, chloroforme, etc... annihilent complètement la luminescence formée dans les liquides, en donnant naissance à la cavitation de vapeur. On peut alors penser que la luminescence est produite par la cavitation de gaz et que son extinction a lieu lors de la cavitation de vapeur, la relaxation précédente se ramène donc à la relaxation des cavitations de gaz et de vapeur.

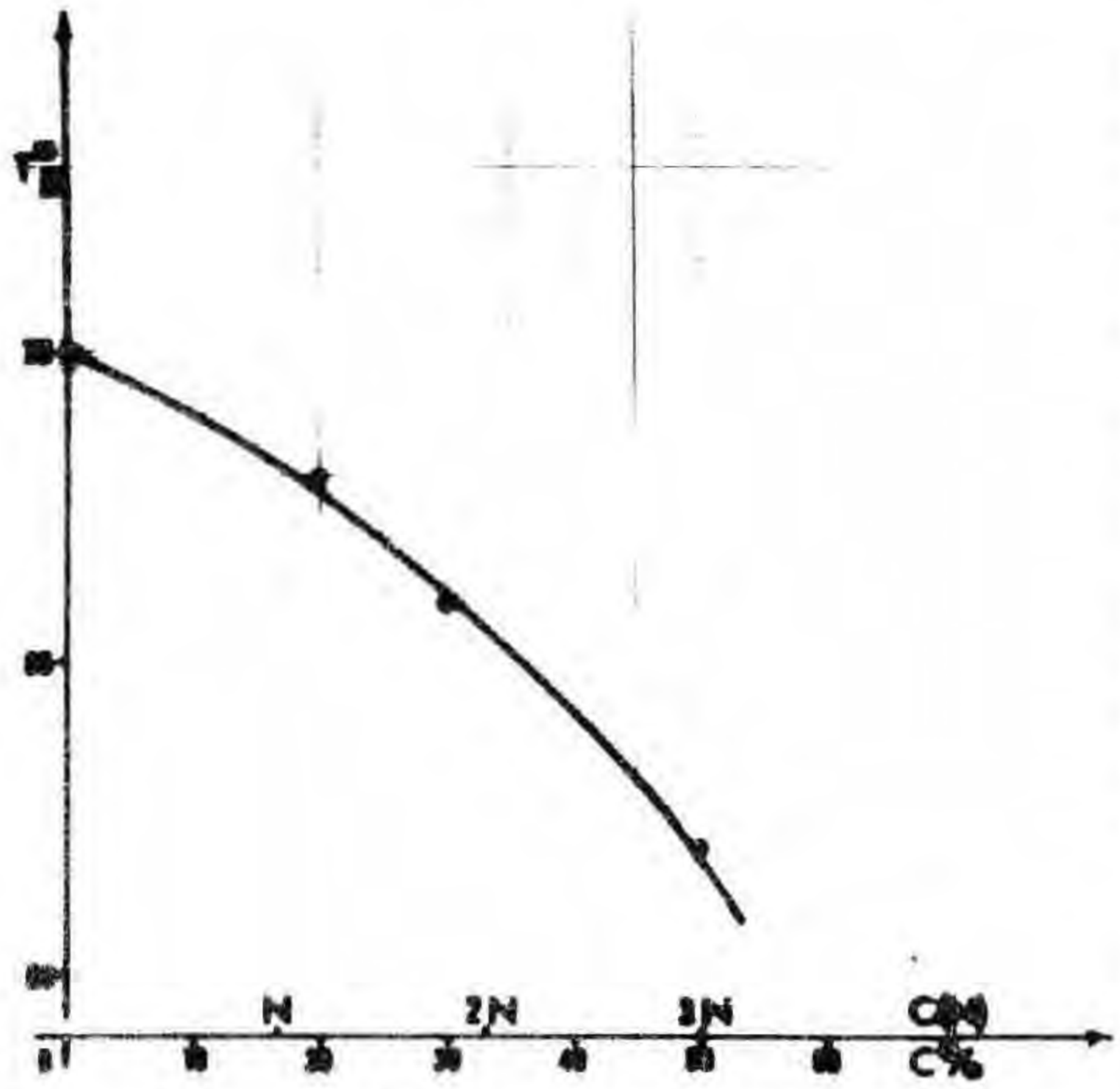

Fig. III - Variation de la température de passage avec la concentration.

Pour vérifier cette supposition on considèrera la courbe de tension de vapeur de la solution étudiée en fonction de la température T, (fig. V). Soit To la température initiale de la solution, p_o la pression au-dessus de la solution, p la pression acoustique liée à l'intensité US, I, par la relation $I = \Delta p^2 / 2 \rho V$ - ρ la densité - V la vitesse du son dans la solution - p_v la pression de vapeur.

Un point M (T_o, $p_o - \Delta p$) peut être défini dans le système de coordonnées p, T.
En ce point, $(p_o - \Delta p) > p_v$, la cavitation observée dans ce cas est donc la cavitation gazeuse.

Si à partir de To la température est augmentée; l'intensité US subit un accroissement par suite de la diminution de la viscosité de la solution et de l'absorption qu'elle entraîne. Le point figuratif M se déplace selon le chemin MA. En même temps la luminescence diminue selon une des droites de la fig. II. Lorsque la température atteint Tp, le point M devient le point A sur la courbe de tension de vapeur. La cavitation change alors soudainement de nature et se transforme en cavitation de vapeur qui entraîne, d'une manière concomitante, l'extinction de la luminescence.

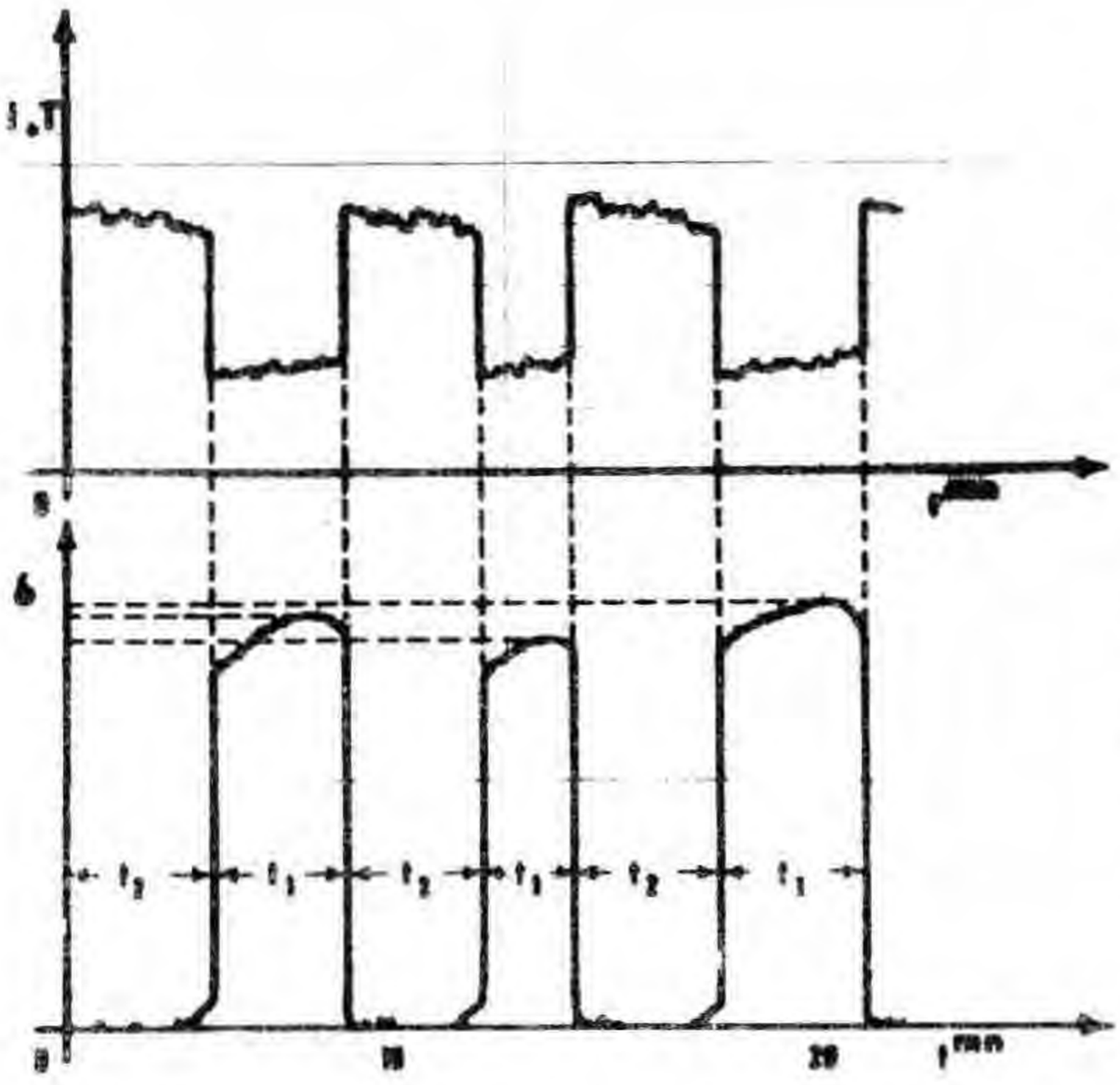

Fig. IV - Variation de l'intensité ultrasonore et de la luminescence en f(t).

MECANISME DE LA RELAXATION

Si on fixe à Tp la valeur de la température, au point A de la courbe de la figure V, l'intensité US et la température subissent une augmentation soudaine, car les bulles de gaz viennent de disparaître. On atteint rapidement le point B. La température diminue alors par absorption de l'énergie calorifique mise en jeu par la vaporisation, et entraîne en même temps une diminution de l'intensité ultrasonore provoquée par l'augmentation de la viscosité. Le point C est lentement atteint. A cet instant, la traversée en sens inverse de la courbe de tension de vapeur provoque le retour à la cavitation de gaz. L'intensité US et la température subissent une brusque diminution avec la réapparition des bulles et l'on atteint le point D, à partir duquel le cycle recommence. Les bulles gazeuses absorbent de l'énergie US et échauffent la solution, on atteint le point A, etc...

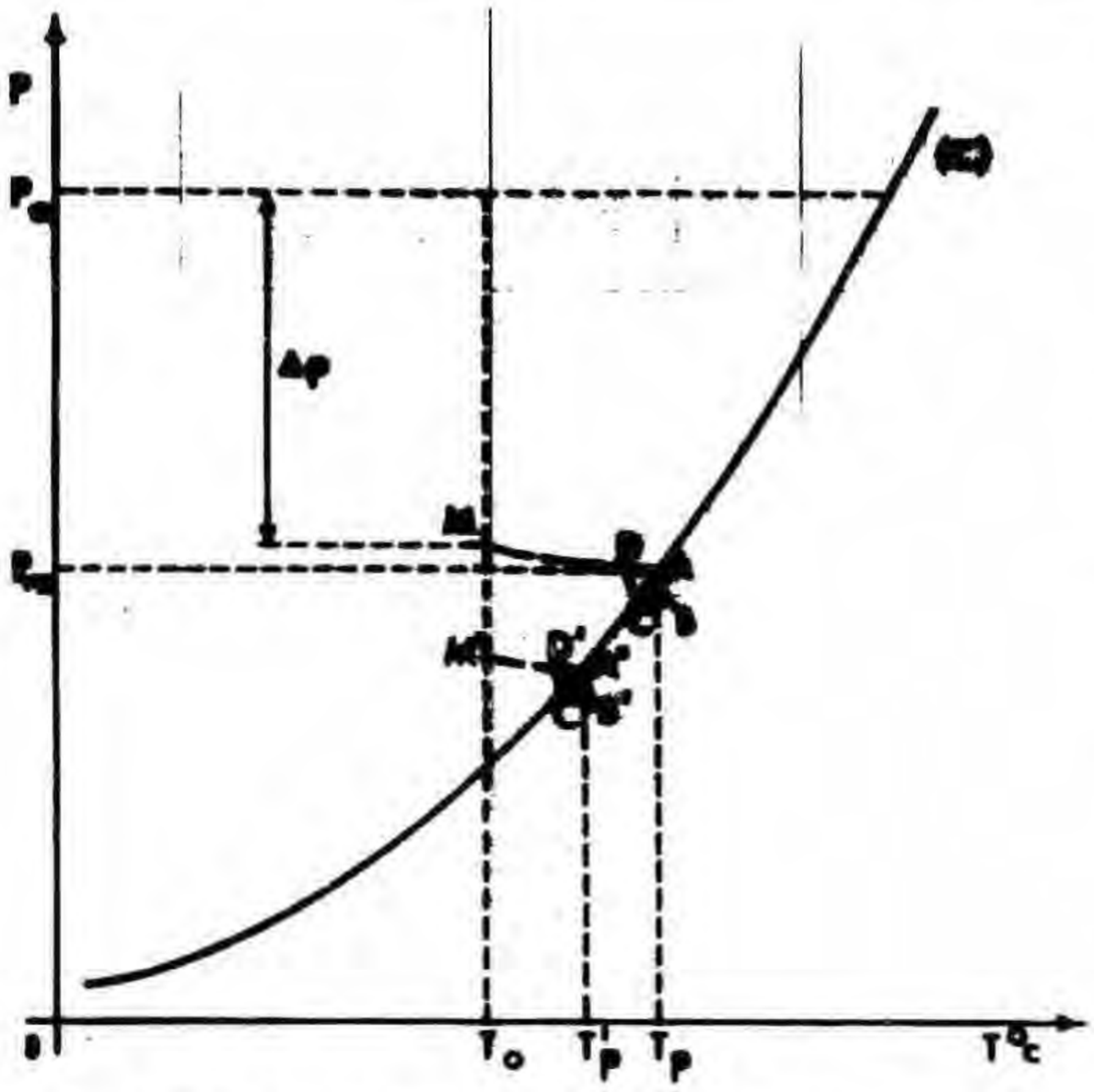

Fig. V - Relaxation des cavitations.

D'après la fig. V l'effet d'une augmentation de la concentration, donc de la masse spécifique ρ de la solution, augmente p puisque $\Delta p = \pm \sqrt{2 \rho IV}$ ce qui déplace le point figuratif M en M' et détermine une nouvelle température de passage $T'p < Tp$. Il y a donc accord avec la relation de $Tp = f(C)$, fig. III.

CONCLUSION .

Les phases d'extinction et d'apparition périodiques de la luminescence sont donc identifiables à celles des relaxations des cavitations de gaz et de vapeur.

BIBLIOGRAPHIE .

1. M. DEGROIS et B. BADILIAN - C.R. Acad. des Sci. 1962, t. 254 p. 231-233.
2. M. DEGROIS et B. BADILIAN - C.R. Acad. des Sci. 1962, t. 254 p. 837-839.
3. M. DEGROIS et B. BADILIAN - C.R. Acad. des Sci. 1962, t. 254 p. 1213-1215.
4. M. DEGROIS et B. BADILIAN - C.R. Acad. des Sci. 1962, t. 254 p. 1943-1945.
5. V.L. LEWSIN et S.N. RSCHEVKIN - Acad. des Sci. de l'URSS - 1937 - Vol. XVI n° 8.

L44

FOURTH INTERNATIONAL CONGRESS ON ACOUSTICS
COPENHAGEN 21.-28. AUGUST 1962

Die zulässigen Störpegel in den Studios.

Dezső Lázár

Bei der Untersuchung dieses Problems hielten wir es vor allem für notwendig festzustellen, mit welcher Methode wir die Störpegel messen, zweitens aus welchem Gesichtspunkt wir die Störpegel beurteilen und endlich wie gross der Wert jener sein darf.

1. Messungsmethode.

Die in den Rundfunk- und Fernsehstudios durchgefürten Geräuschmessungen und die daraus gewonnenen Erfahrungen führten uns zur Überzeugung, dass die aus der "A", "B" und "C" Kennkurve erhaltenen Werte mit der Lautempfindlichkeit nicht eindeutig übereinstimmen. Übereinstimmende dB_A Geräuschwerte hat unser Ohr nämlich als verschieden starke Lautheit wahrgenommen, gemäss der Zusammensetzung des gemessenen Geräuschspektrums. Dies war hauptsächlich dann warnehmbar, wenn die Klimaanlage in Betrieb war. Desswegen haben wir unsere Messungen nicht mit der Kennkurve "A", "B" und "C" durchgeführt, sondern haben das Geräuschpektrum der Studios registriert. Zur Registrierung verwendeten wir das Brüel-Kjaersche Messmikrophon Typ 4131, den Mikrophonverstärker Typ 2603, und den Terzanalysator Typ 2109 gekoppelt mit dem Pegelschreiber Typ 2304. Zur Feststellung des kleinsten messbaren Geräuschpegels registrierten wir das eigene Geräuschspektrum der obigen Messeinrichtung /Abb.1. Kurve a./. Dann zeichneten wir das Grundgeräuschspektrum in verschiedenen Rundfunkstudios ohne Personen und ohne dem Betrieb der Klimaanlage auf. Daraus geht hervor dass der Geräuschpegel eines Studios im tiefen Frequenzbereich mit 6 dB/oktav-Steilheit sinkt bis dieser nicht den Geräuschpegel der Messeinrichtung erreicht /Abb.1. Kurve b./.

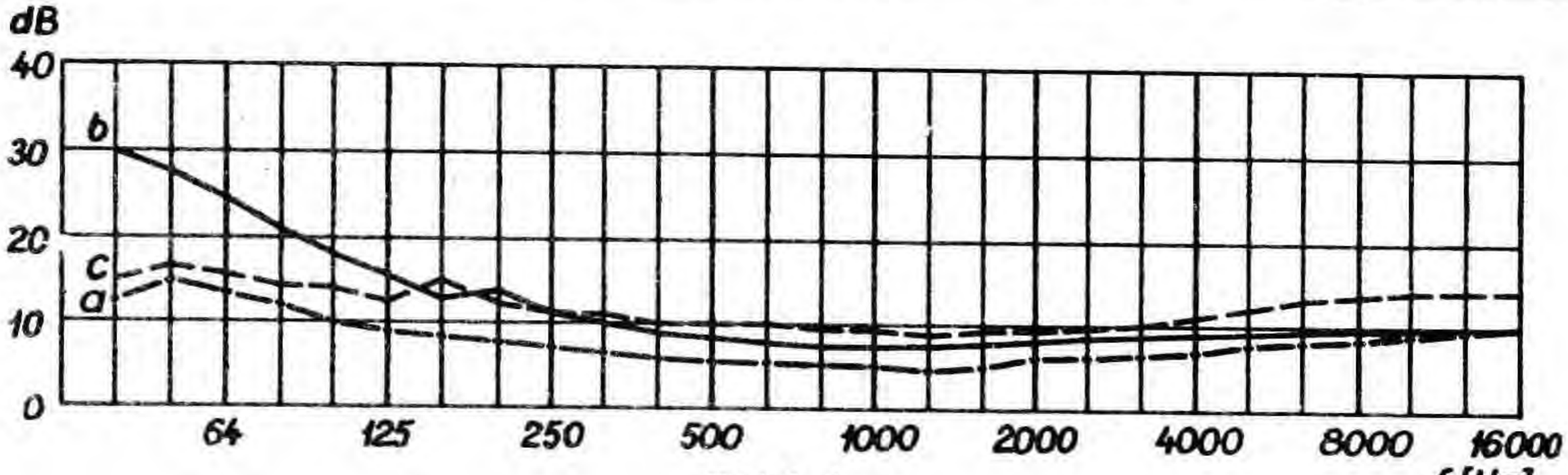

Bild 1.

2. Die Beurteilung des zulässigen Geräuschpegels.

Nach der Feststellung des Messverfahrens und nach der Registrierung des Spektrums der Studios ergibt sich die Frage auf Grund welcher Erfordernisse in den Studios der zugelassene Störpegel in Frequenzabhängigkeit zu beurteilen ist.

Die Konstruktion der bei industriellen Geräuschen verwendeten zugelassenen Kurvenschar, beruht auf der Wahrnehmung der Schäden die die Geräusche auf den menschlichen Organismus und auf die Gehörschwächung ausüben. Wegen der daraus folgenden Charakteristik und wegen seines hohen Pegels sind diese Kurven bei Studios nicht anwendbar. Die auf Grund der Sprachverständlichkeit errechneten Kurven sind im Vergleich zu den in den Studios zulässigen Störpegel von derart grossem Werte, dass diese auch nicht in Betracht gezogen werden können.

Unserer Meinung nach müssen wir danach trachten, dass in den Rundfunkstudios der zugelassene Störpegel in keinem einzigen 1/3 Oktavband grösser sein soll, als Geräuschpegel der elektroakustischen Übertragungskette, welcher den Grundstörpegel und den Dynamikbereich der Programmübertragung determiniert.

Um das Geräusch der Studios mit dem der Übertragungskette vergleichen zu können, registrierten wir das Geräuschspektrum der Übertragungskette /Kondensator-Mikrophon U 47 + Mischpult + Magnetophongerät M 10/ /Abb.1. Kurve c./.

3. Determinierung zugelassener Störpegel.

Vergleichen wir das Grundstörspektrum des Studios /Abb.1. Kurve b./ mit dem Störspektrum der elektroakustischen Kette /Abb.1. Kurve c./ dann sehen wir, dass in den tiefen Frequenzen der Störpegel des Studios höher liegt wie der Störpegel der Übertragungskette, sinkt aber in der nähe von 125 Hz unter diesen und bei hohen Frequenzen bleibt er tief darunter. Damit der Wert des Dynamikbereiches der Programmübertragung breit sein soll, ist es nicht nötig, dass der Störpegel des Studios im ganzen Hörbereich kleiner sein soll, als der Störpegel der Übertragungskette. Grund der Messung der in den Studios zugelassenen Störpegel können wir folgende Werte feststellen: In den mittleren Frequenzen soll der zugelassene Störpegel nicht höher liegen wie der Geräuschpegel der elektroakustischen Übertragungskette, d.h. nicht über 10 dB bei einem Grundpegel von 2.10^{-5} N/m^2. Bei höheren Frequenzen steigt der Geräuschpegel der Übertragungskette ein wenig da aber bei diesen Frequenzen das Studiogeräusch viel kleiner ist als bei der Übertragungskette, so ist die Erhöhung der Sollkurve bei hohen Frequenzen nicht notwendig. Bei tiefen Frequenzen bleibt der Geräuschpegel der Übertragungskette weit unter der Hörschwelle wegen deren steilen Erhöhung. Wenn daher die Sollkurve in dem tiefen Frequenzbereich mit dem Geräuschspektrum der Übertragungskette zusammenfiele, würde dies in Bezug auf die zugelassene Störung im Studio eine zustrenge Forderung bedeuten. Es genügt wenn die Sollkurve unter der Hörschwelle bleibt. Ab 200 Hz/dort wo der Geräuschpegel der elektroakustischen Einrichtung die Kurve der Hörschwelle schneidet/ steigt die Sollkurve mit der Steilheit der Hörschwelle in der Richtung der tiefen Frequenzen, so wie es die Kurve a. auf Abb. 2. zeigt.



Bild 2.

Wollen wir den Umstand beachten, dass bei der Übertragung von Programmen bzw. Tonaufnahmen zu einem bestimmten Grade eine dynamische Kompression vor sich geht und die Lautstärke der Wiedergabe grösser ist wie die der Aufnahme, dann nehmen wir um die tiefen, hörbar werdenden Komponenten vermeiden zu können den zugelassenen Wert mit 10 dB kleiner so wie dies auf der Abbildung mit gestrichelter Linie angedeutet is.

In Studios für grosse Orchester kommt zum Grundgeräusch noch das Geräusch der Musiker hinzu. Da dies zur Produktion immer dazu gehört, wäre es überflüssig das Grundgeräusch des leeren Studios wesentlich herabzuzetzen. Berücksichtigen wir das messbare Spektrum des Geräusches in Anwesenheit der Musiker, so ändert sich die Sollkurve gemäss der punktierten Linie.

Der zugelassene Störpegel für Rundfunkstudios wäre auch ein strenges Erfordernis für Fernsehstudios. Der Grundgeräuschpegel der Fernsehstudios ist wegen des Geräusches der Kameraventilatoren und wegen der Bewegung der Kameras und der Kabel grösser als der Grundgeräuschpegel der Rundfunkstudios, so müssen auch diese zusätzlichen Geräusche bei der Determinierung des zulässigen Störpegels in Anbetracht gezogen werden. Wir haben durch Messungen den Durchschnittswert des Grundgeräuschpegels in Fernsehstudios festgestellt und auf Grund dieser Ermittlung haben wir die zugelassene Kurve des Störpegels konstruiert /Abb.2. Kurve b./.

4. Zusammenfassung.

Vom Standpunkt subjektiver Empfindung aus gesehen geben die Messungen mit den Kennkurven "A", "B" und "C" keine eindeutige Aufklärung. Zur Determinierung der zugelassenen Störpegel ist der Terz- oder Oktavanalysator viel geeigneter. Zur Beurteilung der in den Studios zugelassenen Störpegel sind die bei industriellen Geräuschen gebrauchten Kurvenscharen nicht geeignet. Bei Rundfunkstudios wird die Sollkurve durch das Geräuschspektrum der Elektroakustischen Übertragungskette festgestellt, während bei Fernsehstudios auch die zusätzlichen Geräusche bei Übertragungen und Szenen eine Rolle spielen.

Ich möche an dieser Stelle meinen Kollegen den Herren I.Antal und S.Steinbach meinen besten Dank für Ihre wertvolle Mittarbeit bei den Messungen abstatten.

M44

FOURTH INTERNATIONAL CONGRESS ON ACOUSTICS
COPENHAGEN 21.-28. AUGUST 1962

Prinzip und Anwendung einer neuartigen Wandverkleidung für reflexionsarme Räume

Peter Rother, Joachim Nutsch
Institut für technische Akustik der Technischen Universität Berlin

Im Rahmen der Erweiterungsbauten der Technischen Universität Berlin entstand im Jahre 1961 in der Prüfhalle des Instituts für technische Akustik ein neuer großer reflexionsarmer Raum. Beim Bau dieses Raumes wurde ein neues Verfahren zur schallschluckenden Verkleidung der Wände entwickelt und erprobt, bei der das zur Schallabsorption verwendete poröse Material in einzelne Schluckstoffkörper aufgelöst ist, die an Drähten vor den Raumbegrenzungsflächen hängen.

Die Packung soll für möglichst alle Schalleinfallsrichtungen und einen möglichst weiten Frequenzbereich eine gute Anpassung an den Wellenwiderstand der Luft gewährleisten und in Material- und Montagekosten möglichst niedrig liegen. Die Schluckstoffkörper sollen in Größe, Form und Material variabel sein und in unregelmäßiger Anordnung aufgehängt werden, um die noch vorhandene schwache Reflexion diffus zu machen.

Schon die ersten Messungen ergaben, daß mit einer derartigen Anordnung niemals eine Anpassung des Strömungswiderstandes der Packung an den hohen Wandwiderstand der Raumbegrenzung erreicht werden kann. Die Ursache lag in dem Zwischenraum zwischen den einzelnen Schluckstoff — körpern, die direkt vor der Wand angeordnet waren. Daher wurde die Pakkung in zwei Teile aufgegliedert: eine "lockere Verkleidung" bestehend aus einzelnen an Drähten aufgehängten Schluckstoffkörpern und eine "dichte Verkleidung", die als Schicht die ganze Raumoberfläche abdeckt.

Wirtschaftliche Gesichtspunkte führten dazu, nur handelsübliches Material zu verwenden und dieses möglichst ohne Abfall zu verarbeiten. Das billigste auf dem Markt erhältliche Material ist lose Mineralwolle. Diese bedingt jedoch einen hohen Arbeitsaufwand bei der Montage. Günstiger erschien die Verwendung von kunstharzgebundenen Mineralwolleplatten, wie sie aus Glas-, Stein- oder Schlackenwolle gefertigt werden. Bei der hier beschriebenen Anordnung wurden Glaswolleplatten in einer Stärke von 5cm verarbeitet.

Auf Grund der Größe des auszukleidenden Raumes (H. 10 m, B. 11 m, L. 16 m) wurde die untere Grenzfrequenz, oberhalb derer der Reflexionsfaktor nicht größer als 0,1 sein soll, auf 70 Hz festgelegt. Zur Erreichung dieser unteren Grenzfrequenz wurde eine Packungstiefe von 1 m vorgesehen. Die Rohrmessungen für die Decken- und Bodenpackung und für die Wandpackung wurden getrennt durchgeführt, da sie sich in der Ausführung der "dichten Verkleidung" unterscheiden. Der optimale Aufbau der Schluckstoffanordnung wurde durch systematische Rohrmessungen ermittelt.

Für die Auskleidung an Decke und Boden erwies sich die Anordnung nach Bild 1 als die günstigste. Es wurden hierbei drei Materialien unterschiedlicher Dichte und unterschiedlichen Strömungswiderstandes verwendet:

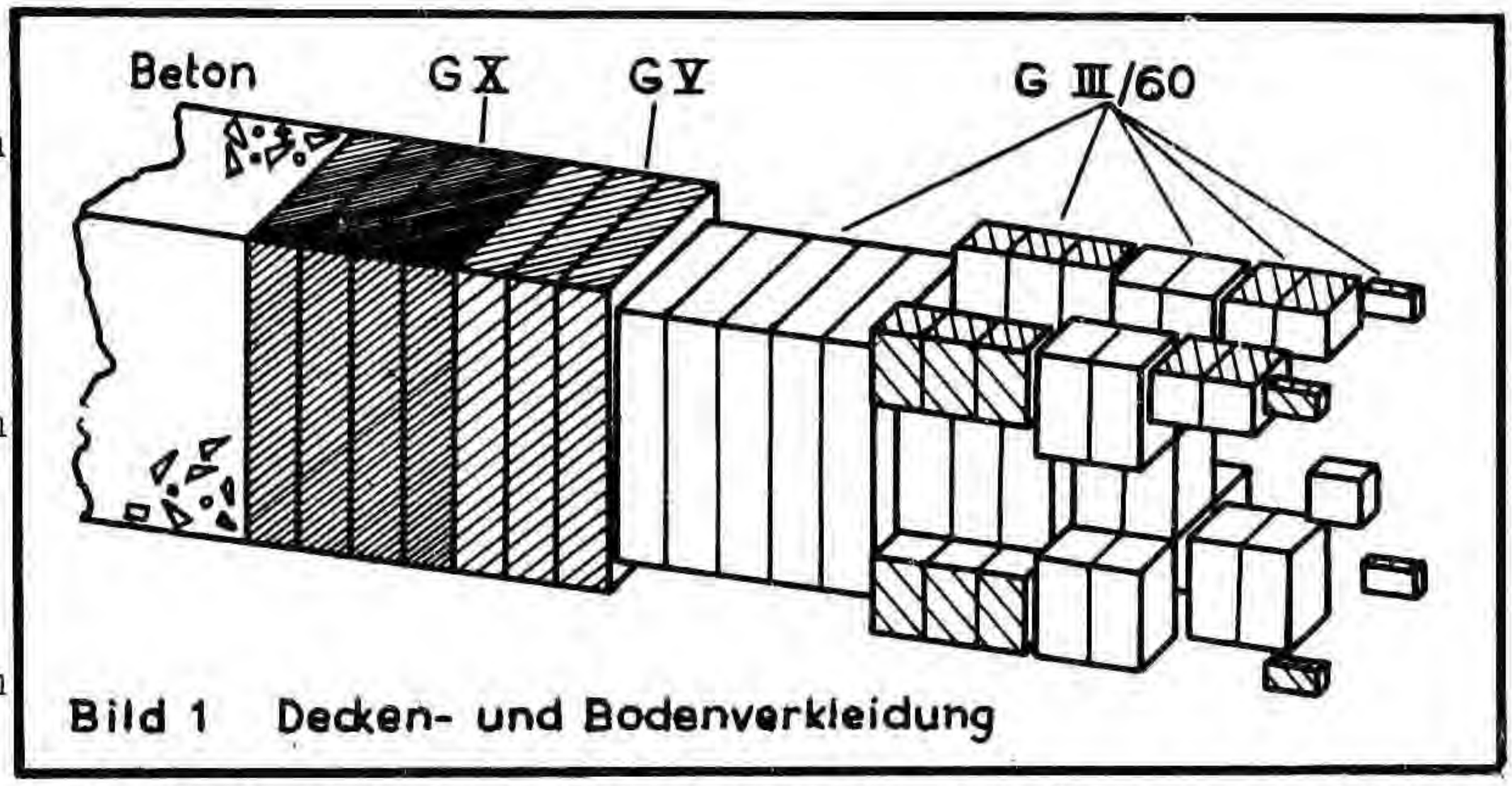

Bild 1 Decken- und Bodenverkleidung

Die Anordnung gliedert sich in 7 Schichten.Die dem Raum zugewandten ersten fünf Schichten bestehen aus würfelförmigen Körpern,während die beiden vor der Wand liegenden Schichten 6 und 7 aus ganzen Schluckstoffplatten aufgebaut sind.Die einzelnen Schichten decken unterschiedliche prozentuale Anteile der Wandoberfläche ab:

Schicht	1	2	3	4	5	6	7
Flächenanteil	11 %	22 %	33 %	50 %	70 %	100 %	100 %
Kantenlänge	5 cm	10 cm	10 cm	15 cm	25 cm	-	-
Material	----------G III/60----------					G V	G X

Für die Wandverkleidung wurde der Aufbau der Packung abgeändert und nur die beiden Materialien GX und GIII/60 verwendet.Die Anordnung der "lockeren Verkleidung", bestehend aus dem leichten Material, G III/60 wurde ohne Änderung übernommen; dagegen erfolgte der Aufbau der dichten Packung aus dem schweren Material GX entsprechend Bild 2 aus zwei unterschiedlich breiten Platten.

In Bild 3 sind die aus den Rohrmessungen gewonnenen Frequenzgänge des Reflexionsfaktors für die beiden Anordnungen dargestellt.Die eingetragenen Meßpunkte sind Mittelwerte aus jeweils acht unabhängig voneinander durchgeführten Messungen.Auch die ungünstigsten Meßwerte überschreiten oberhalb 70 Hz nicht die 0,1 Grenze des Reflexionsfaktors. Es wurden auch Rohrmessungen mit Steinwollematerial durchgeführt.Dabei zeigte sich,daß auch dieses Material bei geeignetem Strömungswiderstand und geeigneter Dichte verwendet werden kann.

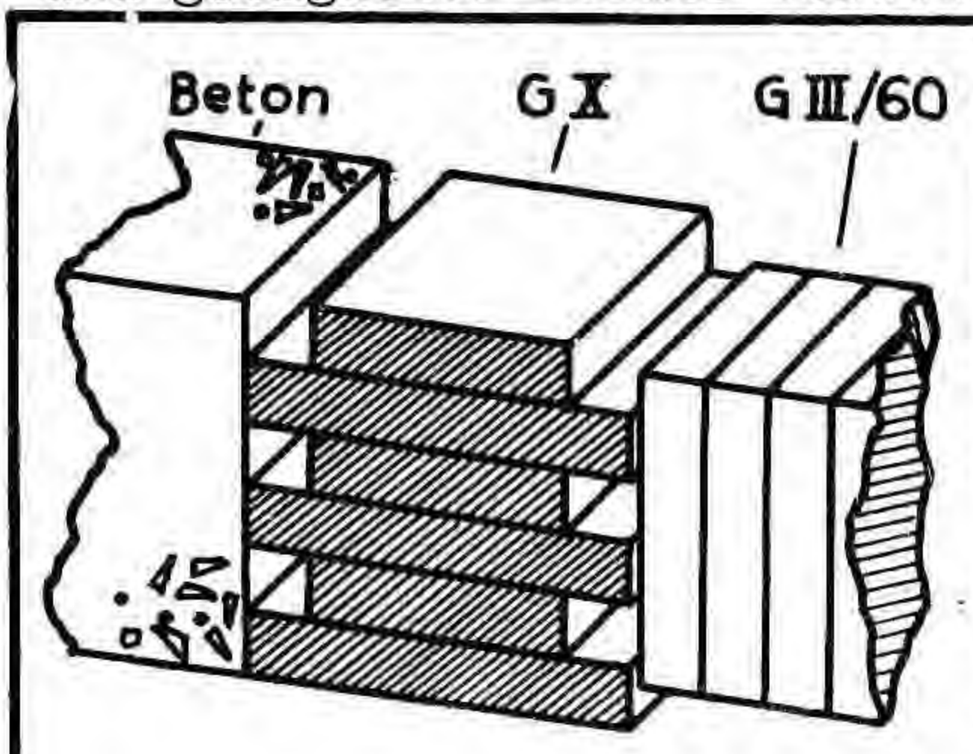

Bild 2 Dichte Wandverkleidung

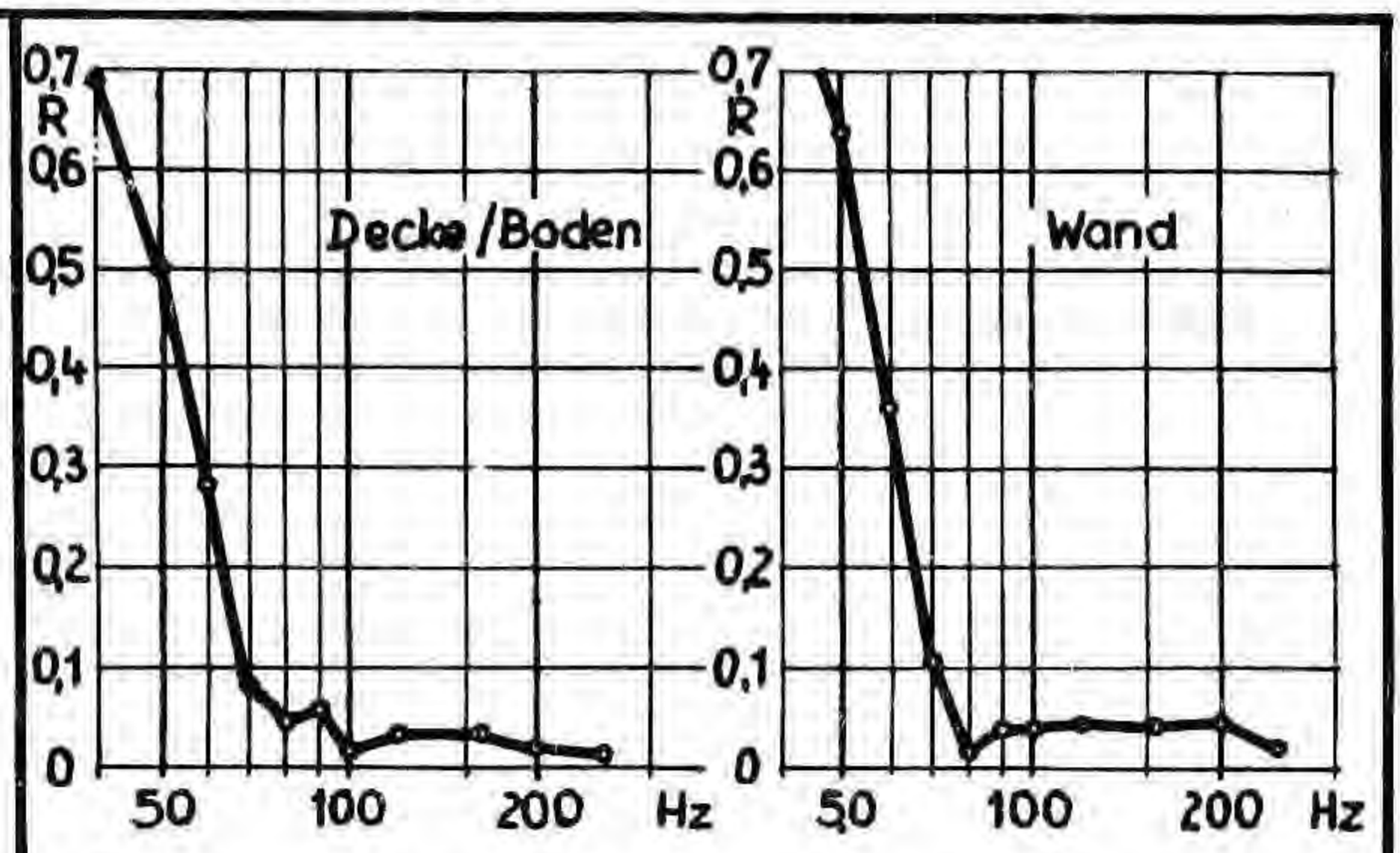

Bild 3 Frequenzgang des Reflexionsfaktors

Das Anbringen der durch die Rohrmessungen ermittelten Schluckstoffanordnung ist an Decke, Wandflächen und Boden jeweils verschieden. Auch innerhalb der Packung werden jeweils das schwere Material (GX) und das leichte Material (GIII/60) gesondert montiert.

An Decke und Boden erfolgt der Einbau des schweren Materials (GX) in den angelieferten Plattengrößen (50 cm x 100 cm), während für die Wände die Platten durch einen Schnitt in Streifen von 20 cm und 30 cm Breite geteilt wurden. An der Decke wurden die Schluckstoffplatten auf Roste aus Baustahlgewebe gelegt, die durch Stahlrohrrahmen (1m x 2m) versteift sind. Diese Rahmen sind an Deckenunterzügen befestigt, die durch ihre Höhe von 35 cm die Stärke der dichten Packung bestimmen. Am Boden wurden die Platten direkt in die Wanne geschichtet. An den Wänden ist das schwere Material vom Boden aus durch Übereinanderlegen der unterschiedlich breiten Streifen bis zur vollen Höhe der Wand aufgestapelt worden. Davorgespannte und in der Wand verankerte Drähte verhindern ein Umkippen der Schicht.

Die Würfel der "lockeren Verkleidung" aus dem leichten Material (GIII/60) werden an der Decke auf senkrecht nach unten hängenden Drähten (73 cm lg) aufgefädelt, die an den Kreuzungspunkten in das Baustahlgewebe eingehängt sind. Auf den Drähten sind jeweils die verschieden großen, voreinander angeordneten Würfel aufgereiht. Für den Aufbau der Deckenverkleidung wurden 4 verschiedene Elemente benötigt (Bild 4), die in einem bestimmten Raster über die gesamte Decke verteilt sind. Ähnlich wurde die Bodenverkleidung ausgeführt. Hier hängen die Drähte, die die Schluckstoffwürfel tragen, an den Knotenpunkten eines etwa 1,2m über dem Betonboden angeordneten Netzes mit einer Maschenweite von 15cm. Dieses Netz verhütet zudem durch seine schalltransparente Nesselauflage die Verunreinigung der Schluckanordnung des Bodens und fängt herunterfallende Gegenstände über der Schluckanordnung ab. Das Fangnetz ist nur durch die ersten vier Schichten der "lockeren Verkleidung" belastet. Die Würfel mit 25 cm Kantenlänge aus dem lockeren Material (GIII/60) liegen direkt auf den Platten aus dem schweren Material (G V, G X), die auf den Boden geschichtet sind.

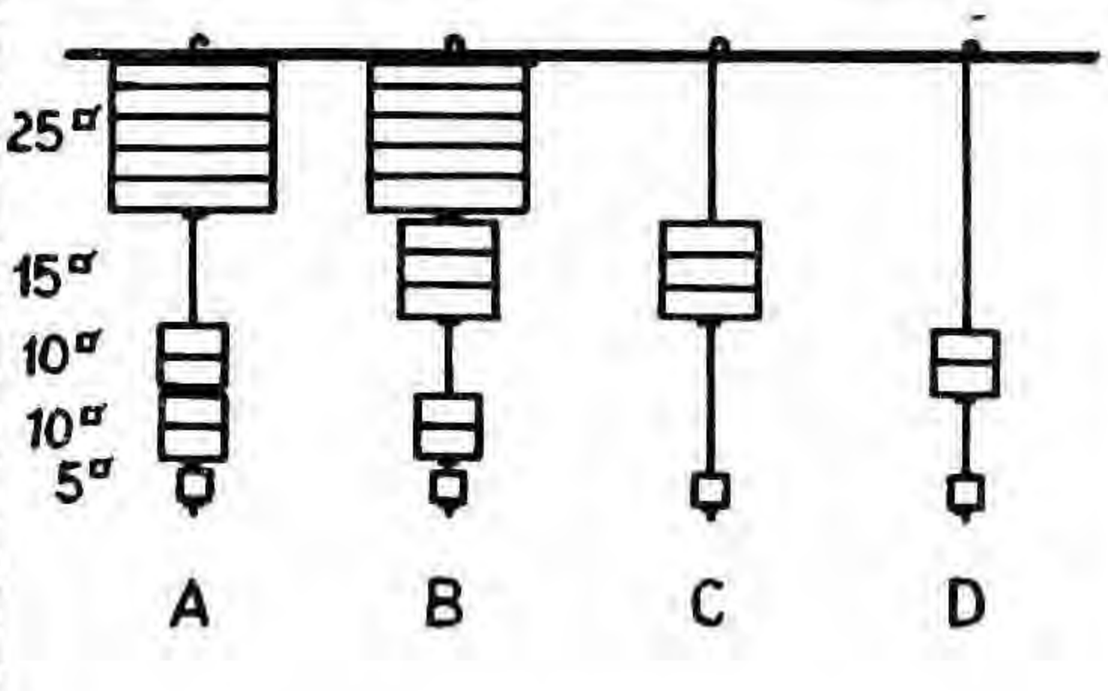

Bild 4 Deckenelemente

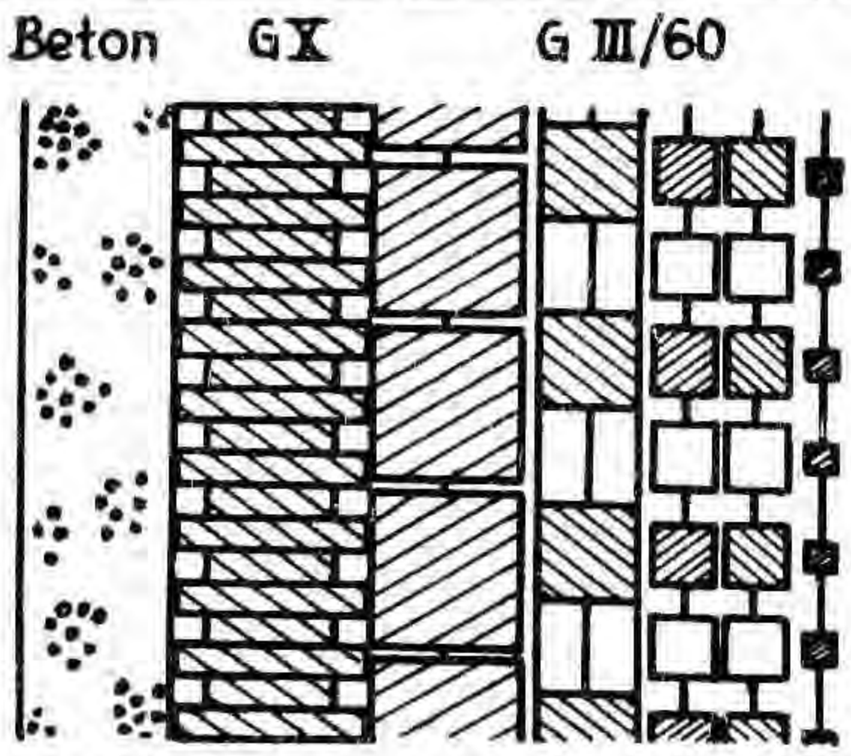

Bild 5 Wandverkleidung (Schnitt)

Bei der Wandverkleidung werden die Würfel auf von der Decke herabhängenden Drähten aufgereiht. An der Wand befinden sich auf einem Draht jeweils die gleichen Würfel in gleichem Abstand. Hier wird die Verkleidung schichtweise ausgeführt (Bild 5). Es werden, von der Wand beginnend, die Würfel mit 25 cm Kantenlänge vor der dichten Packung (GX) von der Decke aus aufgehängt. Danach folgen die davorliegenden Schichten.

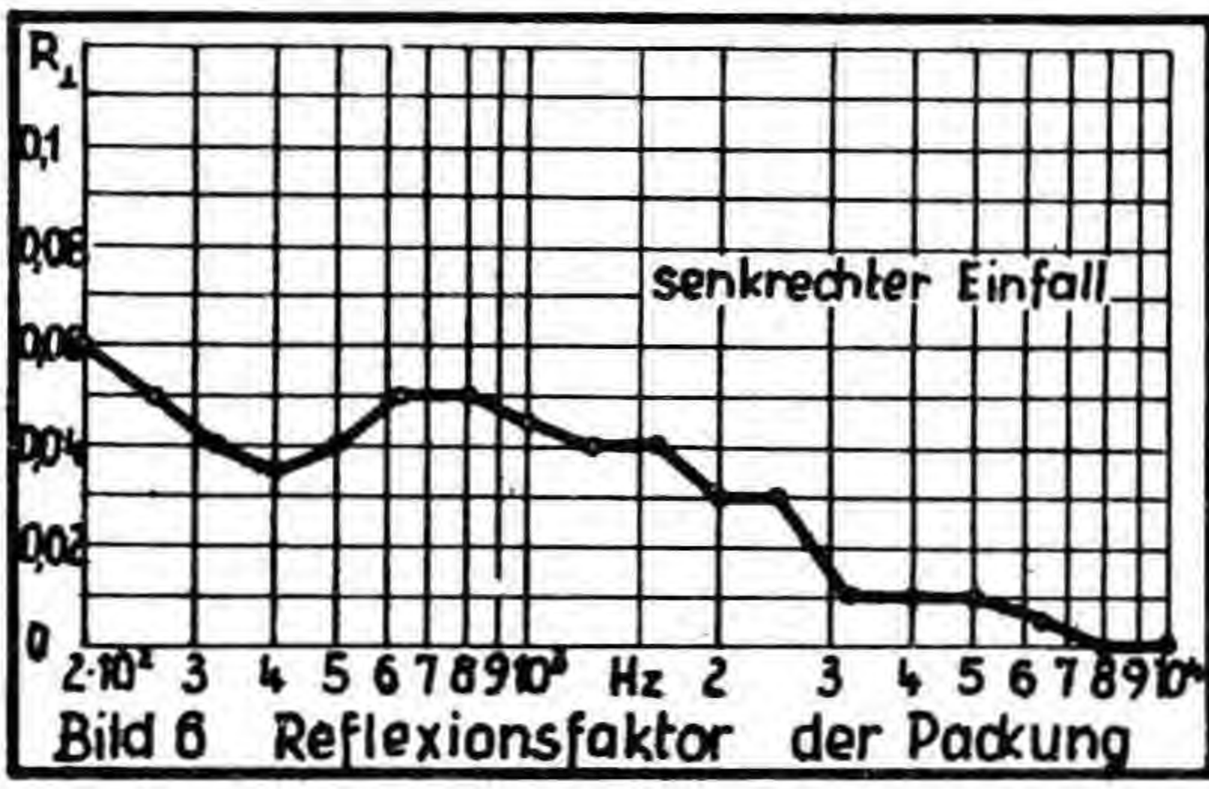

Bild 6 Reflexionsfaktor der Packung

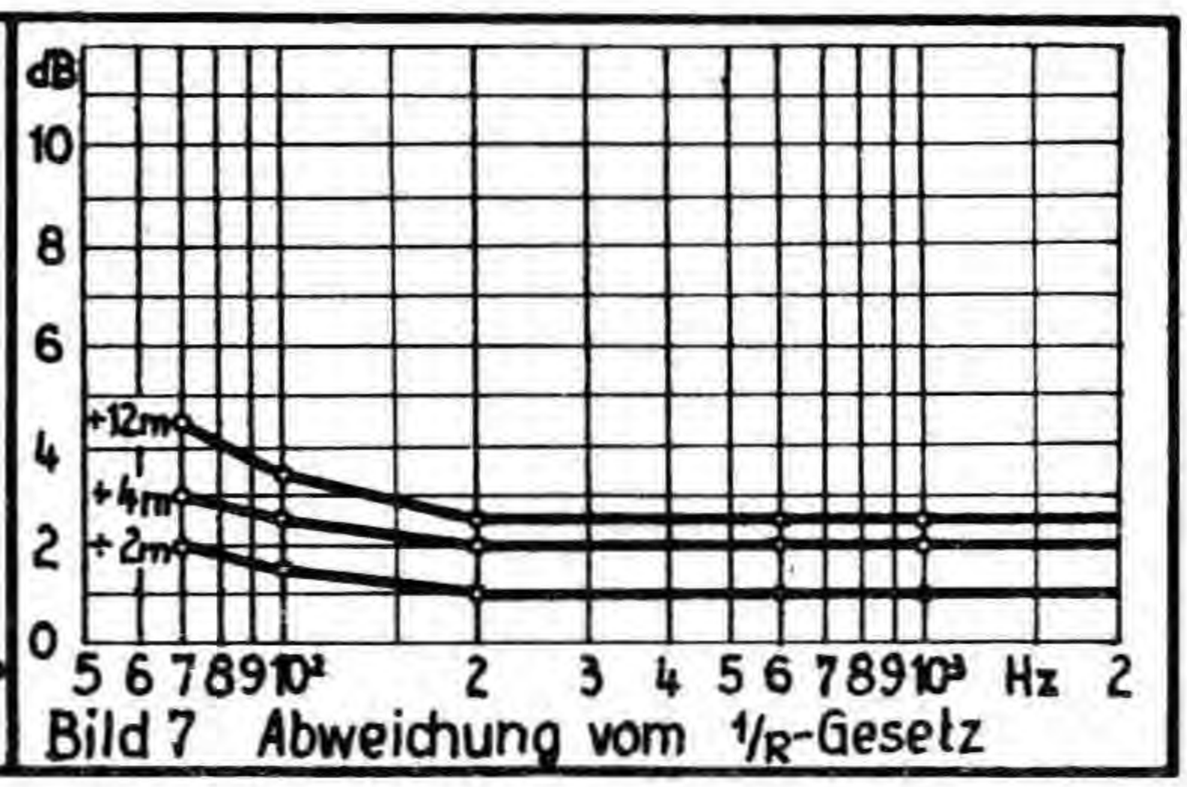

Bild 7 Abweichung vom 1/R-Gesetz

Die Ergebnisse der Messungen im fertigen Raum sind in den Bildern 6 bis 9 dargestellt.

Bild 6 zeigt den Reflexionsfaktor der Packung bei senkrechtem Schalleinfall. Als Sender wurde dabei für die Frequenzen 200 Hz bis 1 kHz ein in ein Gehäuse eingebauter Konuslautsprecher verwendet, für die Frequenzen 500 Hz bis 10 kHz ein Druckkammersystem, das mit seiner Schallaustrittsöffnung im Brennpunkt eines Parabolspiegels angeordnet war. Als Empfänger diente ein Mikrofon mit besonders großer Richtwirkung. Die Messungen wurden mit Tonimpulsen durchgeführt, die nach einer Gaußschen Fehlerkurve amplitudenmoduliert waren.

Bild 7 stellt die Ergebnisse der Ausbreitungsmessungen dar. Als Sender dienten Kugelschallquellen und als Empfänger ein Meßmikrofon, das bis 10 kHz eine kugelförmige Richtcharakteristik hat. Der Einfluß der Dissipation der Luft bei hohen Frequenzen wurde berücksichtigt und eliminiert. Die Meßkurven stellen die maximalen Abweichungen der gemessenen Schalldruckpegel vom 1/R-Gesetz dar, wobei als Parameter die Entfernung Lautsprecher - Mikrofon angegeben ist.

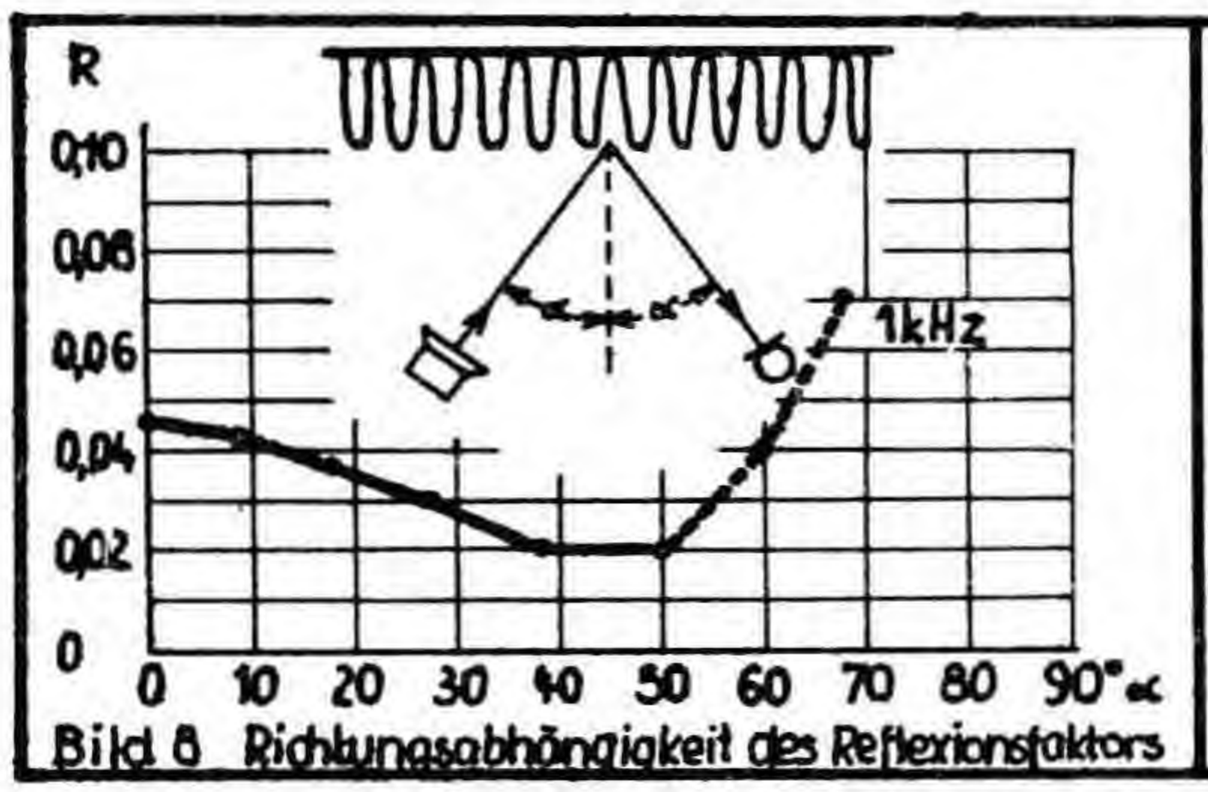

Bild 8 Richtungsabhängigkeit des Reflexionsfaktors

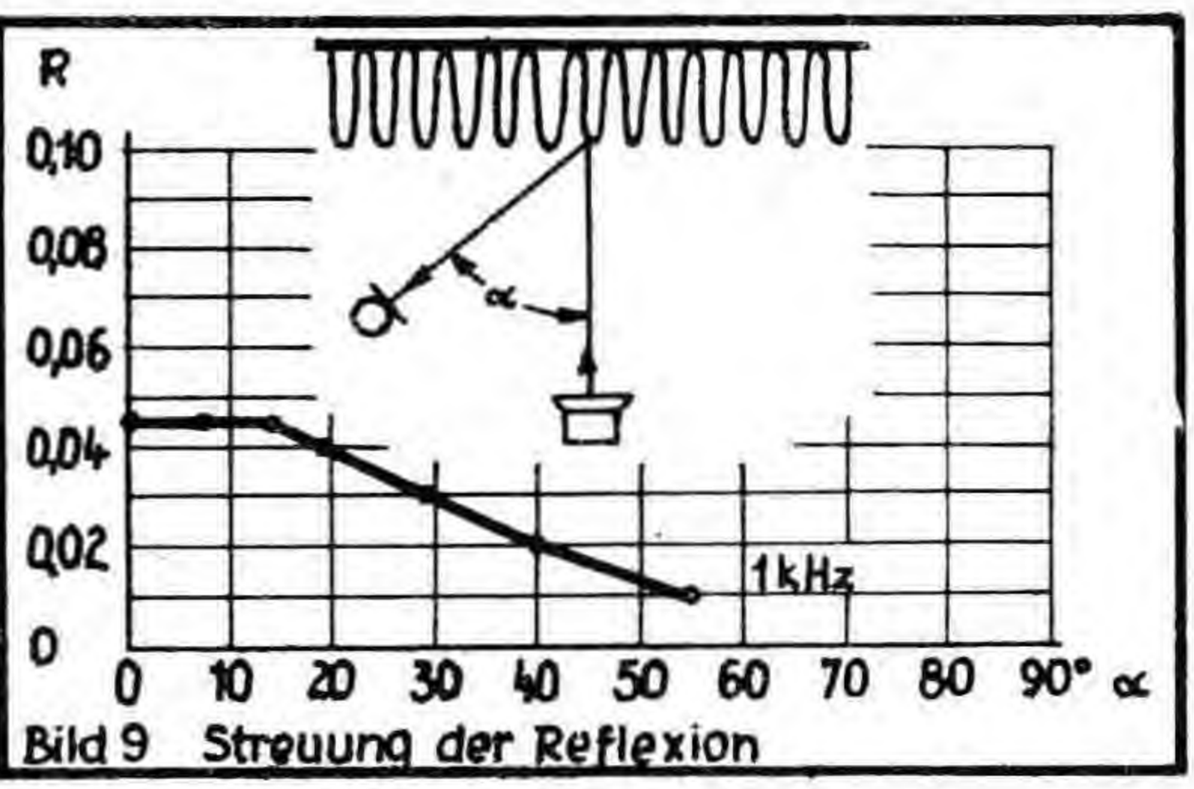

Bild 9 Streuung der Reflexion

Bild 8 zeigt die Richtungsabhängigkeit des Reflexionsfaktors bei 1kHz. Die Messung wurde ebenfalls mit Impulsen und unter Verwendung eines Richtlautsprechers und eines Richtmikrofons durchgeführt.

Bild 9 läßt die Streuung der reflektierten Schallenergie erkennen. Bei dieser Messung war die Halbwertsbreite von Mikrofon und Lautsprecher ca. 20°. Der hier für 1 kHz gezeigte Verlauf ergab sich prinzipiell auch für tiefe Frequenzen (160 Hz) und für hohe Frequenzen (8 kHz).

-o-o-o-o-o-o-o-o-o-

N44

FOURTH INTERNATIONAL CONGRESS ON ACOUSTICS
COPENHAGEN 21.-28. AUGUST 1962

Effects of High Electromechanical Coupling on Characteristics of Piezoelectric Ceramic Transducers

Morio Onoe* and Allen H. Meitzler
Bell Telephone Laboratories, Inc.
Whippany, New Jersey

1. Introduction. Over the past few years, piezoelectric ceramic transducer materials have become available with electromechanical coupling factors, k, in the range of 0.40 to 0.70. These materials are finding increasing use in applications such as ultrasonic delay lines because the high k makes it possible to obtain wide bandpass transmission characteristics without incurring the losses associated with the techniques of mechanical and electrical loading often used to broaden passbands. In the course of developing delay lines using high coupling transducers made of PZT-5(1) ceramic bonded to metals having mechanical impedances greater than that of the transducer material, certain unusual admittance and transmission characteristics were observed which were not interpretable by means of analyses heretofore carried out by Fagen(2), May(3), McSkimin(4), Konig, Lambert, and Schilling(5). This paper presents an analysis which is consistent with the observed experimental results. It is based on the equivalent circuit for thickness-mode transducers, first derived by Mason(6), which includes a negative capacitance element. This element has been neglected in the previous analyses, except the one by May, because it produces little effect on the overall characteristics if k is small. For materials like PZT-5, this element has indeed a significant effect on the characteristics of transducers. In addition, the effects of finite thickness bonding layers have been included into the analysis because it was found that certain observed characteristics could not be fully interpreted until this was done.

2. Equivalent Circuit. Figure 1(a) shows a piezoelectric transducer, C, attached by means of a bonding layer, B, to a medium, A. The behavior of the composite electromechanical system is well represented by cascading the equivalent circuits for each element. Included in the complete circuit is a source with internal resistance, R_0, and a shunt inductor, L_0, which usually antiresonates the clamped capacitance, C_0, at the resonant frequency of the transducer. Since the transducer is used for pulse transmission, the mechanical impedance of the medium can be represented as a pure resistance, Z_A. The behavior of the bonding layer is expressed by a transmission line of length, L_B, with a characteristic mechanical impedance, Z_B. Usually the length is less than one-tenth of a wavelength at the operating frequency. The equivalent circuit of the transducer(6) has two pairs of mechanical terminals, a-a and b-b', one pair of which is short circuited because only one major surface of the transducer is loaded. This is usually the case for ceramic transducers because a high k makes it possible to obtain wide bandwidths without additional losses due to mechanical loading. Hence the present analysis is limited to this case, although the effect of backing is easily included by connecting the appropriate mechanical impedance to the terminals a-a'. A special feature of the circuit is the presence of the negative capacitance, represented by the shaded element in the series arm. This equivalent circuit is valid for all thickness-shear mode, thickness-dilatational mode, and length-longitudinal mode transducers. Thickness-shear mode transducers are widely used for delay lines, both polygon(7) and strip-type(8). Thickness-dilatational mode transducers are frequently used in non-destructive testing as well as in several types of delay lines(3)(9). Length-longitudinal mode transducers find applications in certain low-frequency devices.

A computer program was set up to calculate the input admittance, transmission loss, and reflection coefficient for any combination of material constants

*On leave of absence from Institute of Industrial Science, Univeristy of Toyko, Azabu, Tokyo, Japan

and electrical termination conditions. Before presenting the results, a brief qualitative discussion of the effects of high k and bonding-layer thickness will be given. It is well known that the circuit of the transducer in Fig. 1(b) can be transformed to the circuit in Fig. 1(c). In Fig. 1(c) the impedance element, Z_2, in the series arm has a resonant frequency which coincides with the antiresonant frequency of the element, Z_3, in the shunt arm. In the case when Z_A is low compared to Z_C, both the bonding layer and the shunt element have little effect. The overall behavior is chiefly determined by the series arm, the resonant frequency of which is shifted lower than f_C because of the presence of the negative capacitance. As a result, the input conductance can have a single peak occurring appreciably lower than f_C for high k transducers. The similar shift in the resonant frequency of an unbonded transducer (Z_A=0) has been reported in a previous paper.(10) In the case when Z_A is high compared to Z_C, the effect of the shunt arm is significant, producing a second peak in the input conductance around f_C. The height and position of this peak are affected by the bonding layer.

3. Results of Analysis and Experiment. Figs. 2 and 3 present the input conductance, susceptance, and the insertion loss calculated for the impedance ratio Z_C/Z_A = 1.65, which fits approximately the case of a PZT-5 transducer bonded to either aluminum or fused silica. The first two quantities are actually the input admittance seen at the terminals c-c'. The calculated insertion loss is based on that termination which gives a perfect match at the frequency of the conductance peak. Fig. 2 shows the family of curves with k as the parameter and with the bonding-layer thickness taken as zero, while Fig. 3 shows the same quantities plotted with bonding-layer thickness as the parameter and k taken as 0.50. The parameter D is defined as the ratio L_B/Λ_B, in which L_B is the bonding-layer thickness and Λ_B is the wave-length of the motion in the bonding layer when $f=f_C$. The impedance ratio Z_B/Z_A is taken to be 1.20, corresponding a low-melting-point solder as the bonding material. The downward shift in the frequency of the conductance peak and the small effect of the bonding-layer are readily apparent, as previously mentioned.

Figs. 4 and 5 present similar results for the impedance ratio Z_C/Z_A = 0.80, which fits approximately the case of a PZT-5 transducer bonded to a brass medium. The impedance ratio Z_B/Z_A becomes 0.57 for the same solder bonding layer. The second conductance peak due to the effect of the shunt arm is apparent and the thickness of the bonding layer has a considerable influence, as explained before.

Figs. 6, 7, and 8 show comparisons between calculated (solid lines) and observed (dots) values of input admittance for thickness-shear mode transducers bonded to aluminum, brass and nickel-iron alloys, respectively. The structure is the same as used in strip delay lines and has the advantage that the mode of motion has nearly the one-dimensional dependence assumed in the theory. The values of parameters assumed in calculation are shown in Table 1. Although slight discrepancies are observed in the susceptance curves, the overall agreement in the three individual cases is good considering the various assumptions made in the calculations. The bonding layer-wavelength ratio shown in the table corresponds to a layer thickness of 2×10^{-3} cm, which is verified by microscopic observation.

REFERENCES. (1) This is a commercial lead zirconate-titanate composition manufactured by Clevite Corporation, Cleveland, Ohio, U.S.A. (2) M. D. Fagen, Proc. National Electronics Conf., 7, 380 (1951). (3) J. E. May, Jr., J. Acous. Soc. Am., 26, 347 (1954). (4) H. J. McSkimin, J. Acous. Soc. Am. 27, 302 (1955). (5) W. F. Konig, L. B. Lambert, and D. L. Schilling, 1961 IRE International Convention Record, 9, Part 6, 285. (6) W. P. Mason, "Electromechanical Transducers and Wave Filters," (D. Van Nostrand Co., Inc., New York, Second Edition 1948) pp. 399-404. (7) J. E. May, Jr., IRE Trans. on Ultrasonics Eng., UE-7, 7(1960). (8) A. H. Meitzler, IRE Trans. on Ultrasonics Eng., UE-7, 35 (1960). (9) J. E. May, Jr., IRE Trans. on Ultrasonics Eng., UE-4, 3 (1956). (10) M. Onoe, H. F. Tiersten, and A. H. Meitzler, (Submitted for publication in J. Acous. Soc. Am.)

	Z_C/Z_A	Z_B/Z_A	D	k	f_C(MC)	C_0(PF)
ALUMINIUM	1.4	1.2	0.05	0.55	2.40	59.5
BRASS	0.72	0.57	0.05	0.55	2.40	60
NICKEL-IRON	0.59	0.43	0.06	0.55	2.35	54

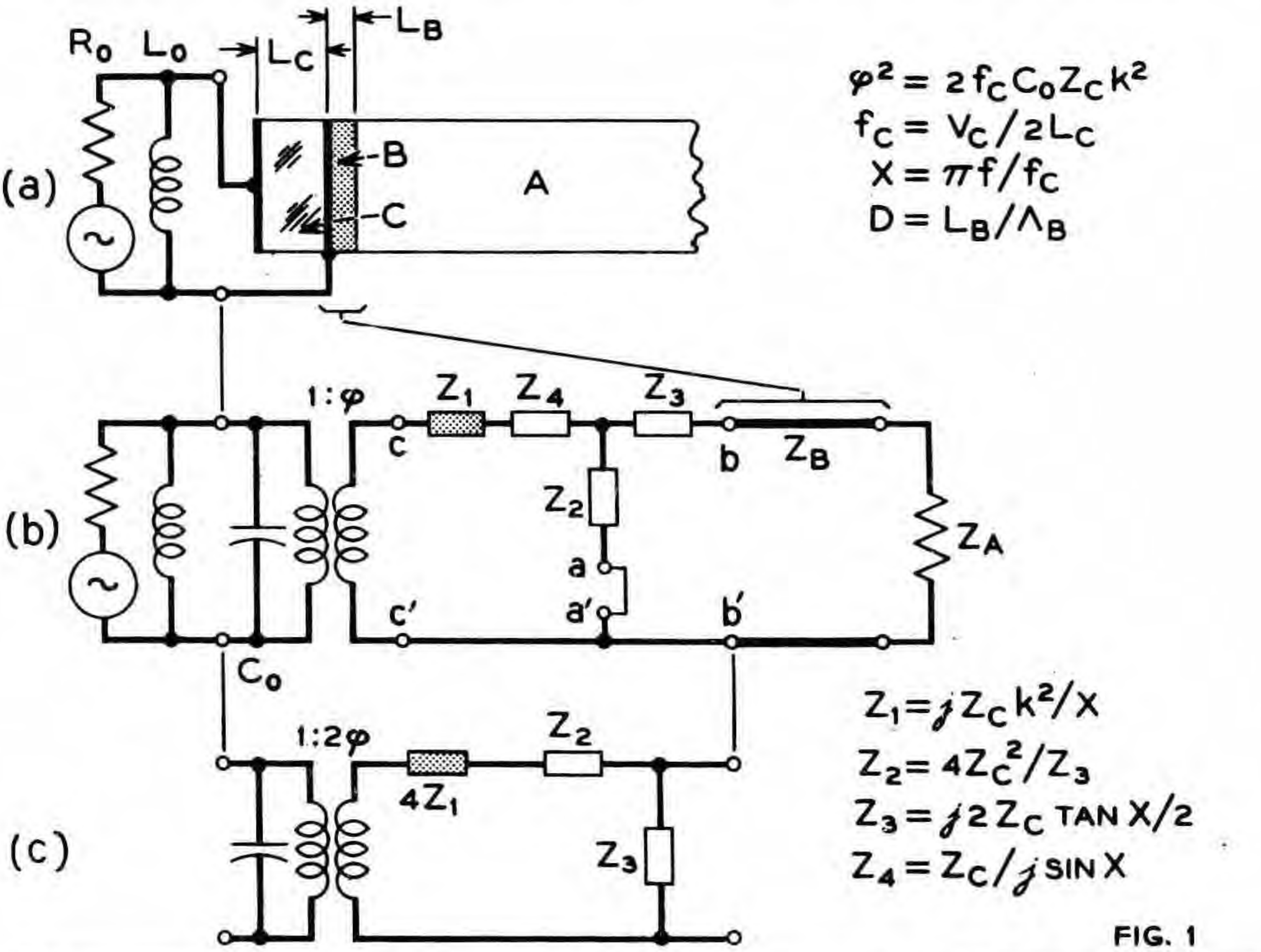

FIG. 1

FIG. 6

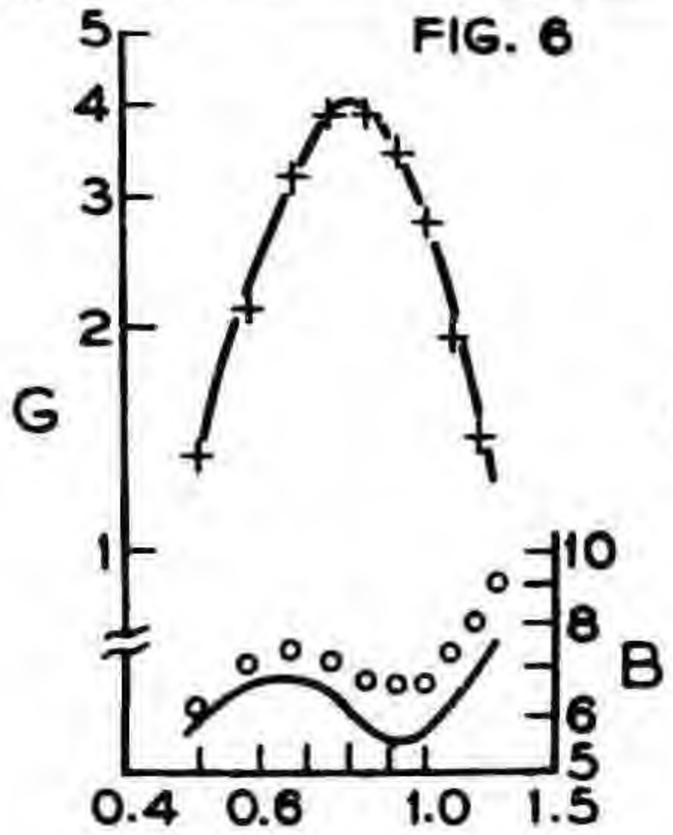

FIG. 7

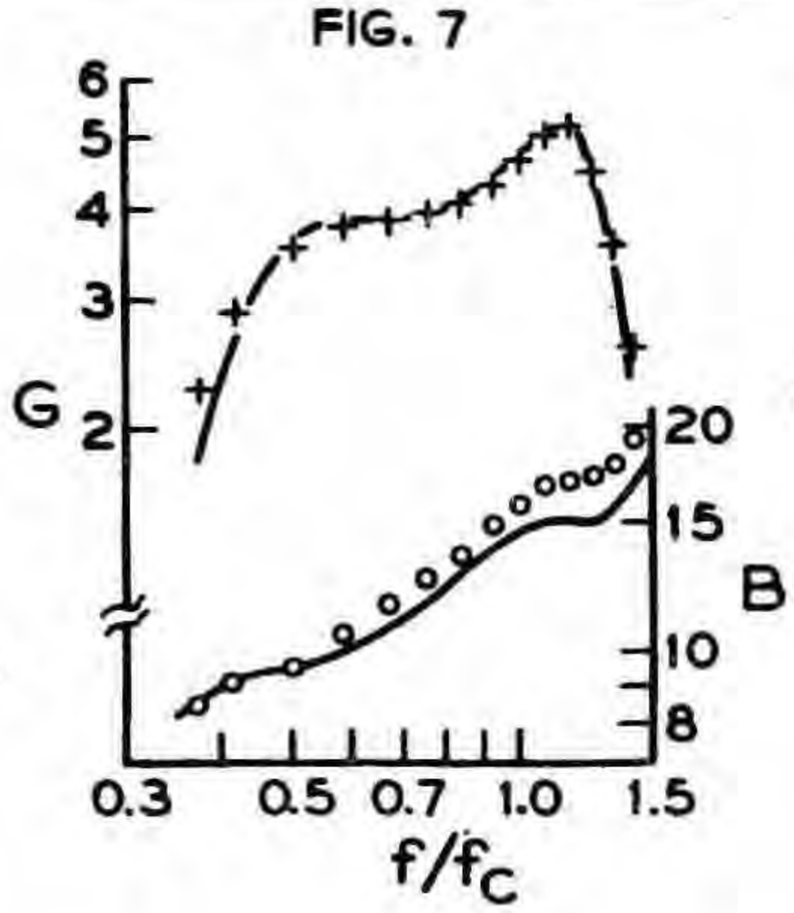

FIG. 8

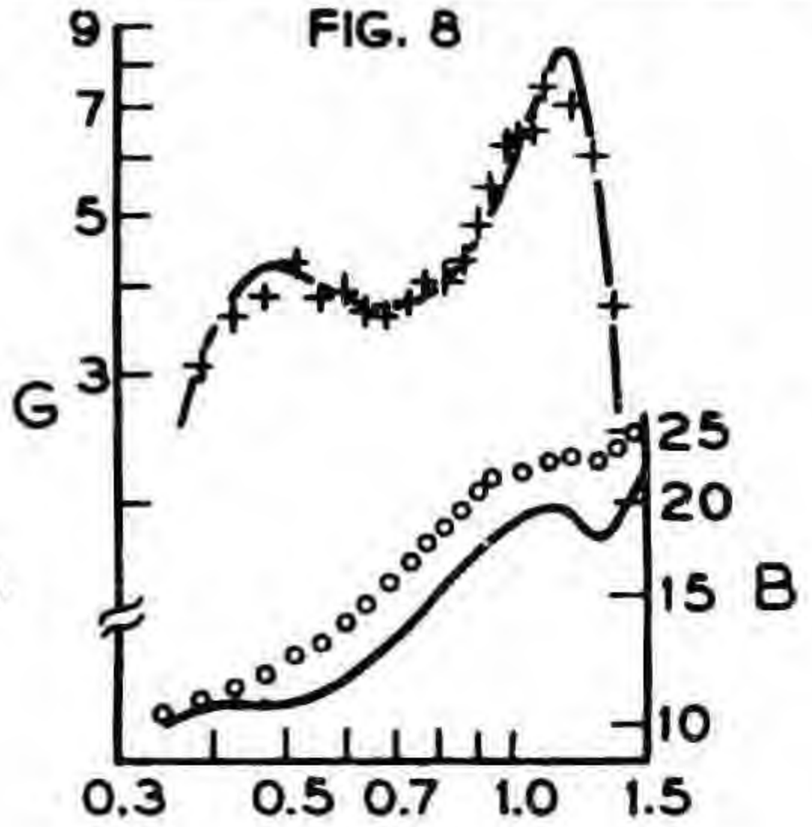

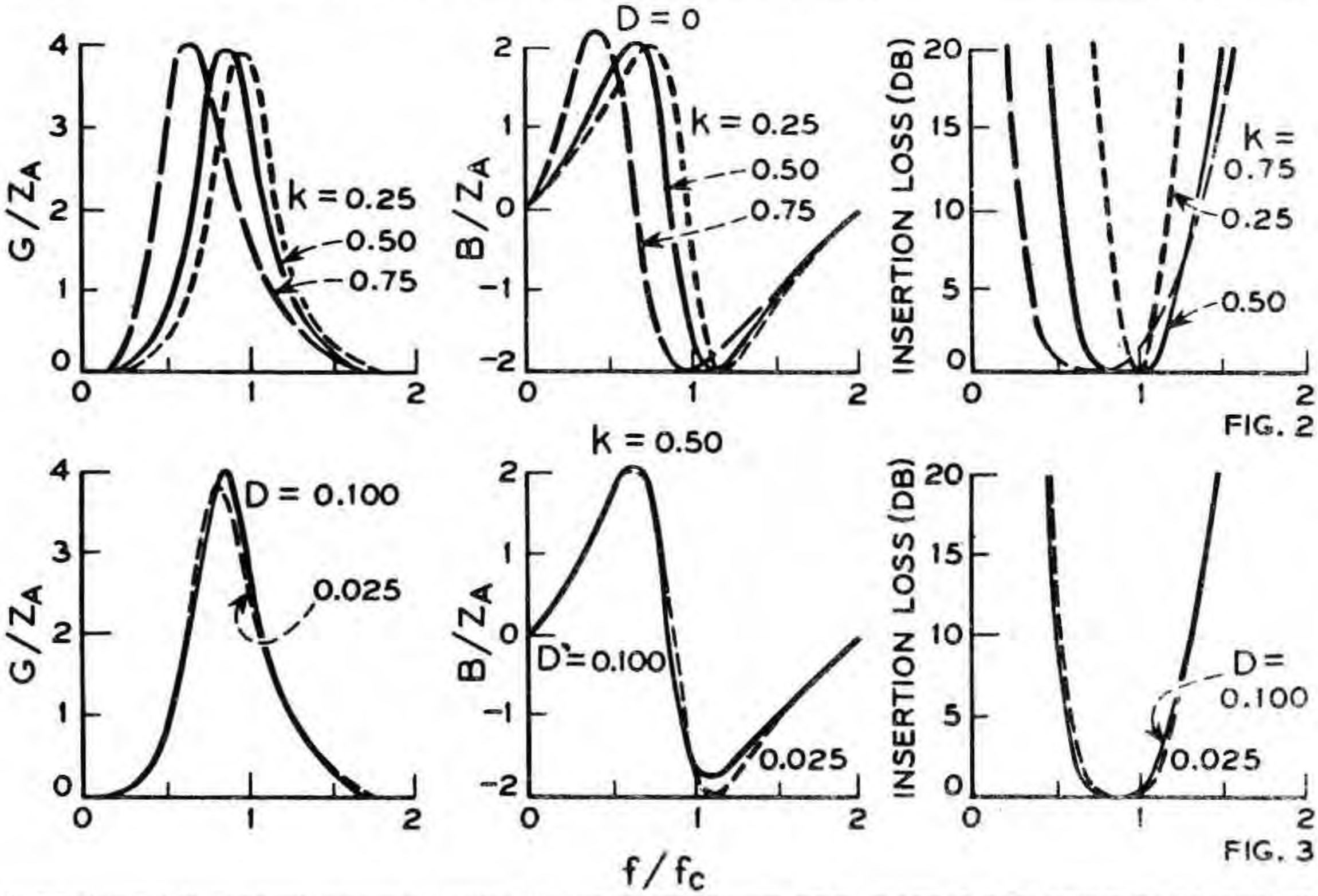

FIG. 2

FIG. 3

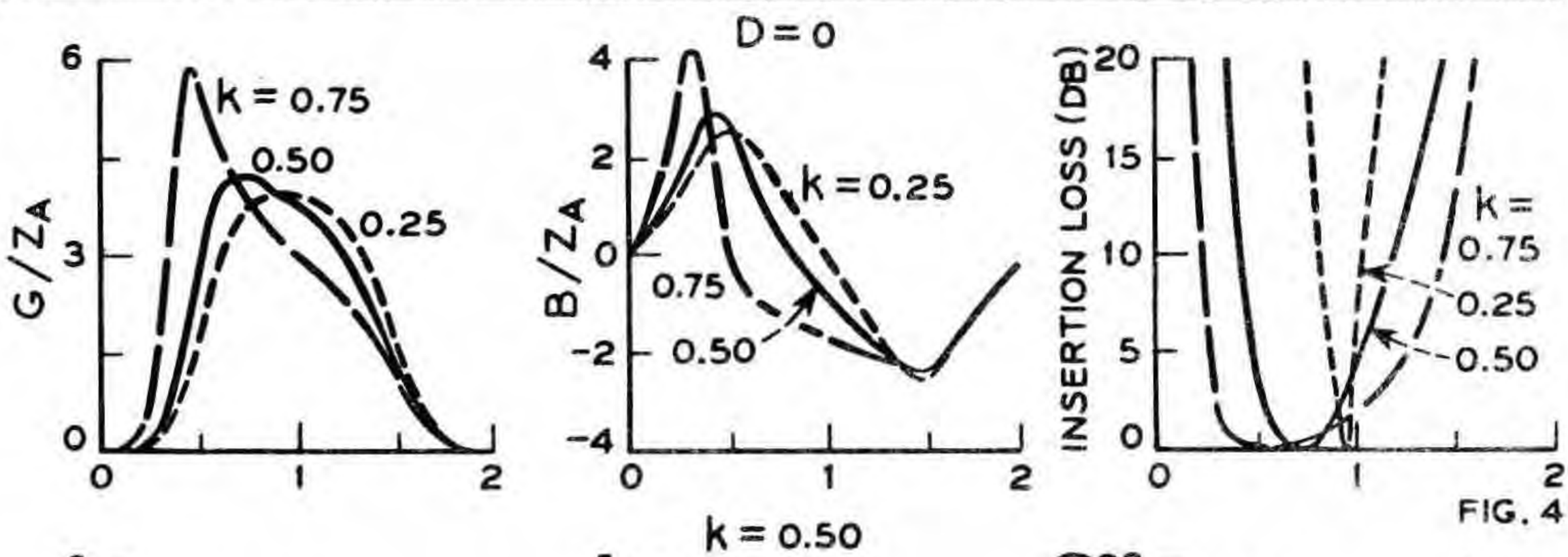

FIG. 4

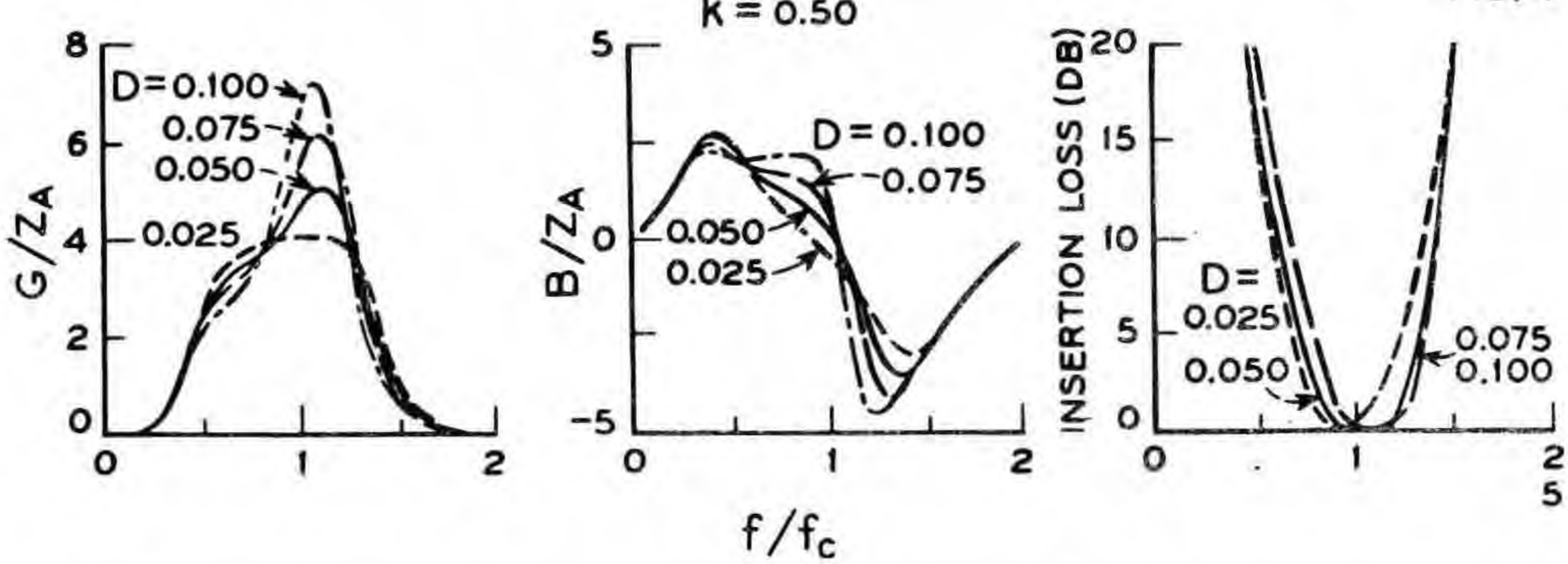

O44

FOURTH INTERNATIONAL CONGRESS ON ACOUSTICS
COPENHAGEN 21.-28. AUGUST 1962

Acoustic Instability of Burning Gases

Dr. Ira Dyer
Bolt Beranek and Newman Inc., Cambridge, Massachusetts, USA

The burning rate of gases evolved during the combustion of solid propellants is a function of the pressure of the gas. The burning gas may therefore act as a sound source if the burning rate oscillation (i.e., mass flow oscillation) m_1 is of proper magnitude and phase compared to the pressure oscillation p_1. Recently, McClure and his coworkers (Refs. 1,2,3) have derived a criterion, in terms of the complex ratio m_1/p_1, for the source-like or unstable behavior of burning gases evolved from solid propellants. We show that McClure's criterion may be inadequate, and that burning gases may have greater instability ranges than he predicted.

We consider a one-dimensional geometry in which gas combustion takes place at x=0. The burnt gases flow in the positive x direction which, in the absence of perturbations, would have a velocity v_o, a pressure p_o, and a density ρ_o. We assume the perturbations to be plane, and to propagate in the positive x direction only. We wish to examine the conditions under which the combustion at x=0 tends to produce sound.

The combustion region is very thin compared to wavelength, so that its oscillations may be represented by an acoustic admittance $Y = -v_1/p_1$ evaluated at x=0, where v_1 is the oscillatory velocity (Ref. 2). McClure concludes that if the real part of Y is negative [$Re(Y) < 0$] the combustion region acts as a sound source. While the source condition $Re(Y) < 0$ is valid for gases without mean flow, we show that the presence of flow alters the situation significantly. To do this we shall calculate the acoustic intensity emanating from a thin layer at x=0.

Like McClure, we assume the burnt gases to be ideal, inviscid, and non-radiative (Ref. 4), for which the vector intensity N is (Ref. 5)

$$N = \left[\frac{1}{2}\rho v^2 + \frac{\gamma p}{\gamma - 1}\right] v \quad , \tag{1}$$

where ρ, v, and p are the total gas variables, and where γ is the ratio of specific heats. We expand the gas variables to second order ($\rho = \rho_o+\rho_1+\rho_2$, etc.) and compute the time-average of the difference between the intensity N and zero-order intensity N_o. This difference is the acoustic intensity I, which turns out to be

$$I = \overline{N-N_o} = \frac{\gamma}{\gamma-1}\left[\overline{p_1 v_1} + p_o\overline{v_2}\right] + v_o\left[\frac{3}{2}\rho_o\overline{v_1^2} + \frac{1}{2}\overline{\rho_2}\,v_o^2 + \frac{3}{2}\rho_o v_o\overline{v_2} + \frac{3}{2}\overline{\rho_1 v_1}\,v_o + \frac{\gamma}{\gamma-1}\overline{p_2}\right] , \quad (2)$$

where the bar signifies the time-average operation. This expression for the acoustic intensity, correct to second order, is in agreement with the calculations of Pridmore-Brown (Ref. 6). With the use of the time-averaged Navier-Stokes equations, the second order quantities in Eq. (2) may be related to first order quantities, resulting in

$$I = \overline{p_1 v_1} + v_o\left[\frac{1}{2}\rho_o\overline{v_1^2} + \frac{1}{2}\frac{\overline{p_1^2}}{\rho_o c^2}\right] , \quad (3)$$

where c is the sound speed. The acoustic intensity is thus composed of the usual $\overline{p_1 v_1}$ term plus a term representing the convection of kinetic and potential energy densities. If v_1 and p_1 are related by the admittance of a freely propagating plane wave, then the convection term can be shown to be v_o/c times the $\overline{p_1 v_1}$ term; this simplification is not possible in general.

It is usual to express the behavior of burning gases in terms of mass flow rather than velocity. Mass conservation in the present case may be expressed as:

$$\frac{m_1}{m_o} = \frac{v_1}{v_o} + \frac{1}{\gamma}\frac{p_1}{p_o} \quad (4)$$

Thus the admittance of the combustion layer may be expressed as

$$Y = -\left(\frac{v_1}{p_1}\right)_{x=0} = \frac{v_o}{p_o}(\theta + i\chi) ,$$

$$\theta = -\left[\frac{\overline{m_1 p_1}}{m_o p_o}\frac{p_o^2}{\overline{p_1^2}} - \frac{1}{\gamma}\right]_{x=0} = -\mathrm{Re}\left[\frac{m_1/m_o}{p_1/p_o} - \frac{1}{\gamma}\right]_{x=0} , \quad (5)$$

$$\chi = -\mathrm{Im}\left[\frac{m_1/m_o}{p_1/p_o} - \frac{1}{\gamma}\right]_{x=0} \qquad (5)$$
(continued)

The quantities θ and χ are expressed in terms of the complex ratio m_1/p_1; this ratio is ordinarily used to characterize burning processes. Then the acoustic intensity at x=0 becomes

$$I_{x=0} = p_o v_o \frac{\overline{p_1^2}}{p_o^2}\left[-\theta + \frac{1}{2\gamma} + \frac{\gamma M_o^2}{2}(\theta^2 + \chi^2)\right] \quad , \qquad (6)$$

where $M_o = v_o/c$. The intensity must be positive for the combustion layer to act as a sound source. That is, it is assumed that the seat of potential acoustic instability is the combustion layer, and that energy must flow from the combustion layer to overcome losses in the acoustic system. Further, it is assumed that acoustic intensity represents the totality of energy flux available to overcome acoustic losses.

Equation (6) for the intensity at x=0 is zero for a particular value of $\theta = \theta_o$ given by

$$\theta_o = \frac{1 - \left[1 - M_o^2 - \gamma^2 M_o^4 \chi^2\right]^{1/2}}{\gamma M_o^2} \quad , \qquad (7)$$

and the source condition is therefore

$$\theta < \theta_o \quad . \qquad (8)$$

In comparison, McClure's criterion is $\theta < 0$. Thus, Eq. (8) predicts a wider range of the real part of the acoustic admittance for which the combustion tends to act as a sound source. Further, Eq. (8) shows that the combustion has an increasingly wider range of potential instability as the mean flow is increased. Both these effects are significant, even for small M_o, and are a direct consequence of the energy convection term in the acoustic intensity.

REFERENCES

1. McClure, Hart, and Bird, "Solid Propellant Motors as Acoustic Oscillators", Solid Propellant Rocket Research, M. Summerfield, Editor, Academic Press, N. Y., 1960.

2. McClure, Hart, and Bird, J. Appl. Phys., 31, 884-896, 1960.

3. McClure, Hart, and Bird, A.R.S.J., 31, 367-368, 1961

4. The thermoviscous nature of the combusting gas should be taken into account in a more complete discussion of instability. For example, it is likely that the oscillations near the combustion layer are more nearly isothermal than adiabatic. However, we proceed with these simplifying assumptions to parallel the work of McClure.

5. D. I. Blokhintsev, Acoustics of an Inhomogeneous Moving Medium, (translated from the Russian), Brown University, 1952.

6. D. C. Pridmore-Brown, J. Fluid Mech., 4, 393-406, 1958.

P44

FOURTH INTERNATIONAL CONGRESS ON ACOUSTICS
COPENHAGEN 21.-28. AUGUST 1962

PROPAGATION OF ULTRASONIC WAVES IN SPIRALS

Leszek Filipczyński, Warsaw, Poland

THEORETICAL PART

Let us consider a spiral of infinite length, in the form of a screw line, and made of a rod the transverse dimensions of which are very small as compared with its diameter 2r and with the wave length λ. It is assumed that the material of which the spiral is made is homogenous, isotropic and perfectly elastic and that the processes occurring are variable in accordance with the dependence $e^{j\omega t}$. The phenomena taking place in the spiral will be considered in the system of cylindrical coordinates /Fig.1/.

The equation of dynamic equilibrium in this system takes the form[2]

$$\begin{aligned}
\rho\frac{\partial^2 u_r}{\partial t^2} &= \frac{\partial \sigma_{rr}}{\partial r} + \frac{1}{r}\frac{\partial \tau_{r\theta}}{\partial \theta} + \frac{\partial \tau_{rz}}{\partial z} + \frac{\sigma_{rr}-\sigma_{\theta\theta}}{r} \\
\rho\frac{\partial^2 u_\theta}{\partial t^2} &= \frac{\partial \tau_{r\theta}}{\partial r} + \frac{1}{r}\frac{\partial \sigma_{\theta\theta}}{\partial \theta} + \frac{\partial \tau_{\theta z}}{\partial z} + \frac{2\tau_{r\theta}}{r} \\
\rho\frac{\partial^2 u_z}{\partial t^2} &= \frac{\partial \tau_{rz}}{\partial r} + \frac{1}{r}\frac{\partial \tau_{\theta z}}{\partial \theta} + \frac{\partial \sigma_{zz}}{\partial z} + \frac{\tau_{rz}}{r}
\end{aligned} \qquad /1/$$

where u_r, u_θ, u_z - components of the displacement vector
$\sigma_{rr}, \sigma_{\theta\theta}, \sigma_{zz}, \tau_{r\theta}, \tau_{rz}, \tau_{\theta z}$ - normal and tangential components of stress
ρ, t - density and time

For the free surface of the rod the following equality holds

$$\sigma_{rr} = \sigma_{zz} = \tau_{r\theta} = \tau_{rz} = \tau_{z\theta} = 0 \qquad /2/$$

Since the transverse dimensions of the rod are very small as compared with the length of the wave under consideration the equality /2/ being satisfied on the surface of the rod, is also satisfied approximatly inside the rod. Taking into account the equality /2/ in the relations /1/, we obtain

$$\frac{\partial u_r}{\partial \theta} = -u_\theta \qquad /3/$$

Taking into consideration the Hooke's law we have from /1/,/2/ and /3/ the equation

$$u_\theta\left[\omega^2 r^2\frac{\rho}{E} - 1\right] + \frac{\partial^2 u_\theta}{\partial \theta^2} = 0 \qquad /4/$$

where ω denotes the frequency and E the Young's modulus.

The general solution of the equation /4/ takes the form

$$u_\theta = \left[C_1 e^{-jk\theta} + C_2 e^{jk\theta}\right] e^{j\omega t} \qquad C_1, C_2 = const. \qquad /5/$$

where

$$k = \sqrt{\omega^2 r^2\frac{\rho}{E} - 1} \qquad /6/$$

We determine the circumferential phase velocity of the wave as

$$c_p = r\frac{\omega}{K} = c_0\sqrt{\frac{1}{1-\left(\frac{c_0}{\omega r}\right)^2}} \quad , \quad c_0 = \sqrt{\frac{E}{\rho}} \qquad /7/$$

Hence it follows that the phase velocity is a function of frequency, and consequently there occurs the phenomenon of dispersion.

We can thus determine the circumferential group velocity

$$c_g = r\frac{d\omega}{dK} = c_0\sqrt{1-\left(\frac{c_0}{\omega r}\right)^2} \qquad /8/$$

If the radius of the spiral tends to infinity, then the wave velocity as follows from the relation /7/, becomes equal to the velocity c_o of the waves propagating in the straight rod.

A similar phenomenon occurs if the frequency increases. However, with decrease in the frequency we observe a decrease in the group velocity which for the value $\omega = c_o/r$ becomes equal to zero. At the same time the phase velocity increasing constantly, becomes equal to infinity. This frequency is the cutoff frequency below which the type of wave described above cannot propagate in the spiral.

EXPERIMENTAL PART

Two methods were applied for measuring the wave velocity in the spiral. The first was the resonance method with the application of the continous wave; the second was the pulse method.

The principle of the resonance method is shown at Fig. 2. Between the transmitting and the receiving coils a spiral made of ferromagnetic rod was placed, which - for simplicity - is represented in the form of a straight rod. The element to convert electromagnetic energy into mechanical and vice versa is in this case the examined ferromagnetic rod itself because of its magnetostrictive properties[1].

A sinusoidal signal was applied to the transmitting coil and the receiving coil was connected with an indicator through an amplifier. If n hakves of the wavelength are distributed in the spiral, we write the relation

$$l = n\frac{\lambda}{2} = n\frac{c_p}{2f} \qquad /9/$$

If we increase the frequency by the value Δf, so that the next maximum can be observed on the indicator, than we can write the following

$$l = (n+1)\frac{\lambda'}{2} = (n+1)\frac{c_p + \frac{dc_p}{df}\Delta f}{2(f+\Delta f)} \qquad /10/$$

From the formulae /9/,/10/ we obtain; when $n \gg 1$

$$\frac{1}{\frac{1}{c_p} - \frac{f}{c_p^2}\frac{dc_p}{df}} = 2l\Delta f \qquad /11/$$

However

$$\frac{1}{c_g} = \frac{dK}{d\omega} = \frac{1}{c_p} - \frac{f}{c_p^2}\frac{dc_p}{df} \qquad /12/$$

By comparing /11/ and /12/ we finally have

$$c_g = 2l\Delta f \qquad /13/$$

Thus, by means of the resonance method described, we can determine the group velocity occuring in a disoersive system on the basis of the formula /13/. The measured group velocities calculated by means of this forma-

la are presented in the function of frequency at Fig.3. The black points concern the spiral, while the white ones refer to the straight rod. The continous line denotes the theoretical curve calculated from the formula/8/.

The experiment thus confirmed the anticipated relationships of the wave velocity in the range above the cutoff frequency. In the direct neighborhood, and below this frequency it was hard to draw any conclusions from the complex system of maxima obtainde by this method. The block diagram of the measurement system used in this case is shown at Fig. 4.

Using the pulse method a pulse with a frequency of about 80 kc with a high value of the second harmonic was transmitted through the spiral. It could be shown that the velocity of the pulses of the second harmonic is approximately twice as high as that of the pulses of the basic frequency of 80 kc. This fact confirms the dependece between the group velocity and the frequency in the spiral according to the Fig.3.

More details of this work will be given during the Congress.

REFERENCES

1. L.Filipczyński - Ultradźwiękowa impulsowa metoda badania drutów ferromagnetycznych przy wykorzystaniu ich właściwości magnetostrykcyjnych./Ultrasonic pulse method of testing of ferromagnetic wires using their magnetostrictive properties/. Conference on Nondestructive Methods of Testing Materials.PAN.,Warsaw, 15-20.V.1961, Zeszyty Problemowe Nauka Polska, in print.
2. A.E.Love. - The Mathematical Theory of Elasticity. Cambridge 1944

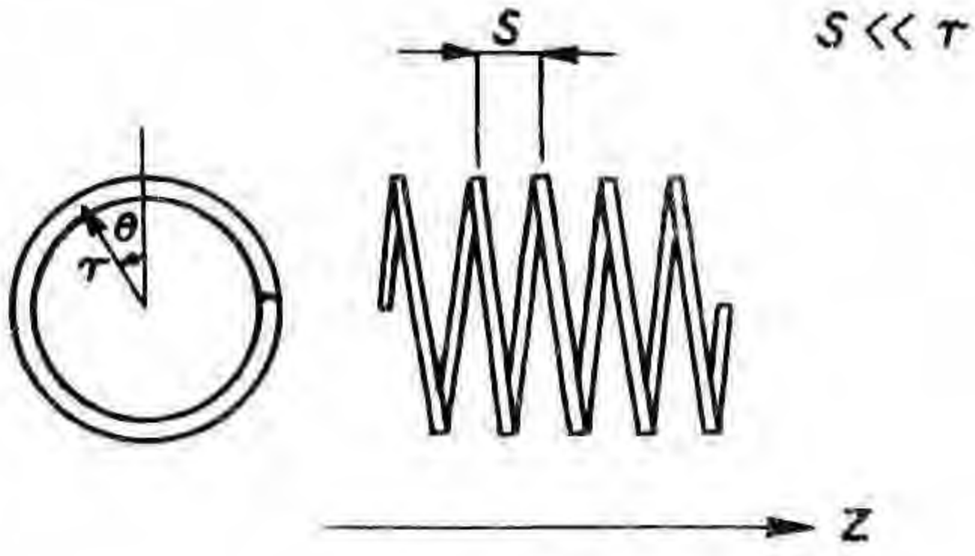

Fig.1. Spiral rod in the system of cylindrical coordinates

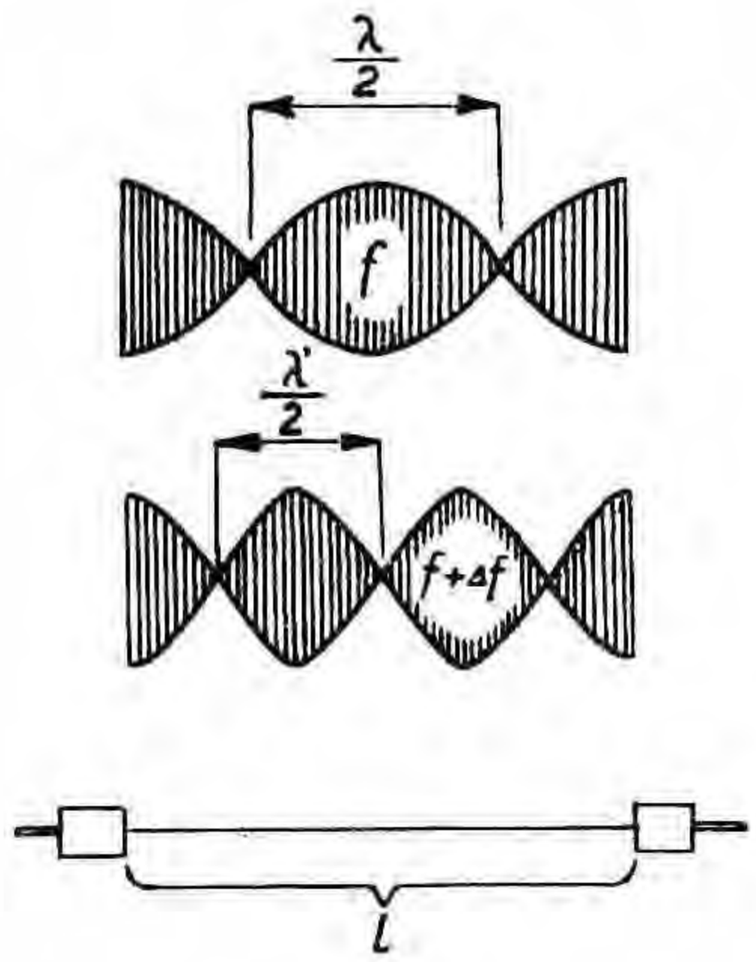

Fig.2. The resonance method used for measuring the group velocity of waves in a dispersive system

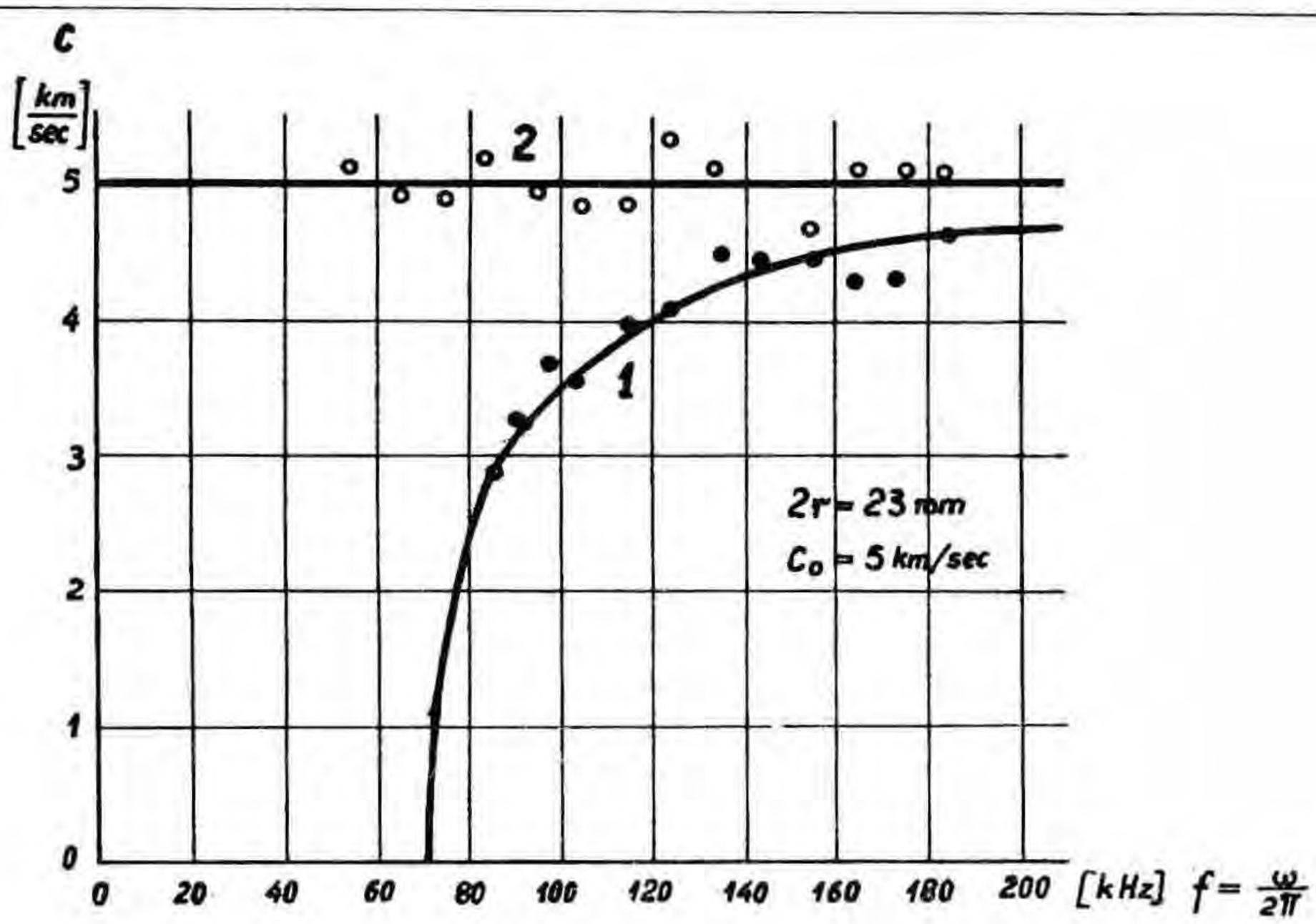

Fig.3. Results of measurements performed with reference to the velocities of wave propagation in a spiral /1/, and in a straight rod /2/. The continuos line denotes the theoretical curves

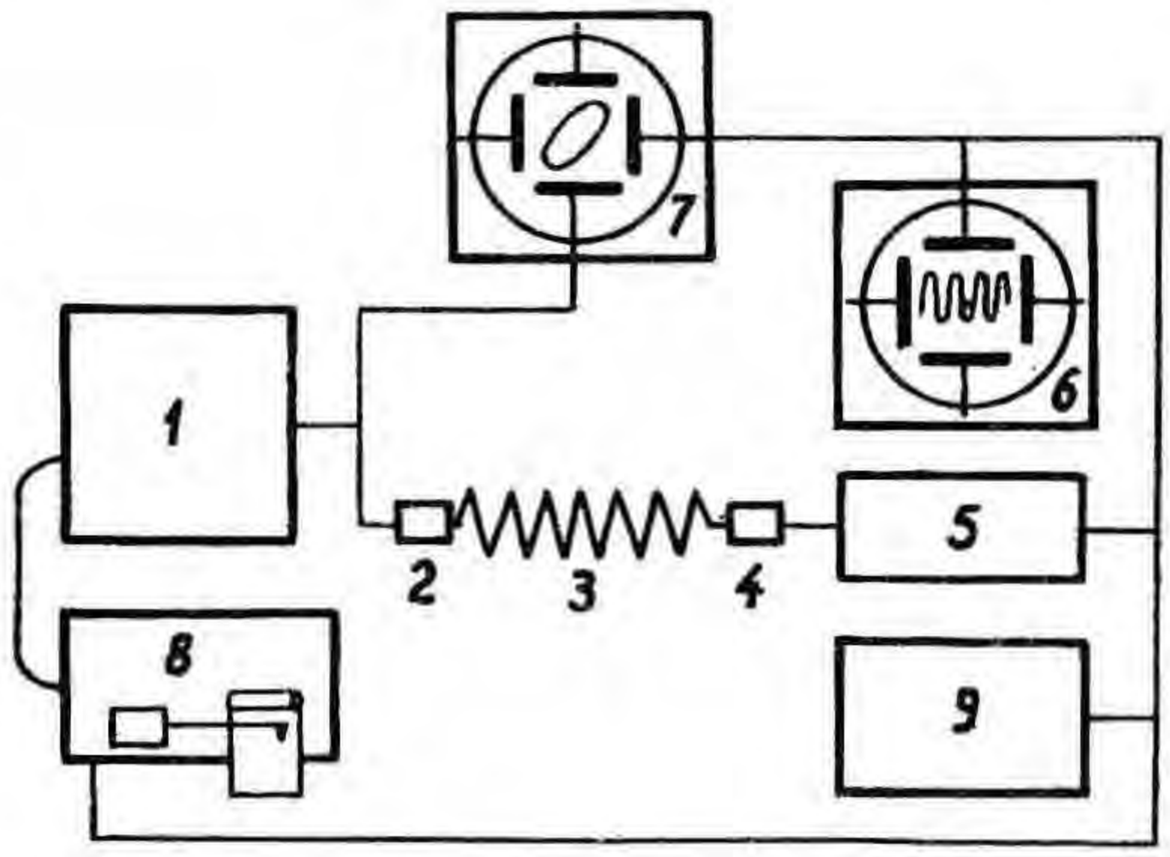

Fig.4. Measurement system for determination of velocities of the waves propagating in spirals by means of the resonance method

1 - signal generator, 2 - transmitting probe-head, 3 - spiral, 4 - receiving probe-head, 5 - amplifier, 6 - indicator of the amplitude, 7 - indicator of the phase, 8 - recorder Bruel Kjaer, 9 - wavemeter

G45

FOURTH INTERNATIONAL CONGRESS ON ACOUSTICS
COPENHAGEN 21.-28. AUGUST 1962

ON PERCEPTUAL CUES FOR SWEDISH FRICATIVES

János Mártony, Dipl.ing. (E.T.H.), Speech Transmission Laboratory
Royal Institute of Technology, Stockholm 70 Sweden

The purpose of the experiments reported here is to gain better insight into the perception of Swedish voiceless fricatives and the importance of various cues for the identification of these sounds. The cues that have been investigated in the present study are the transitional pattern of the vowel adjacent to the fricative, spectral properties of the fricative, and the relative intensity of the friction.

The material was limited to fricatives in initial and intervocalic positions. In the first study it consisted of four Swedish words which were pronounced by a Stockholm speaker so as to differ only with respect to the fricative. The words are /ˈfena/ /ˈsena/ /ˈr̰sena/ /ˈç̰ena/. The /r̰s/ phoneme has two important variants, the prepalatal and usually retroflex [ʂ] and the velar strongly labialized [ʃ]x). Both sounds were included in the present experiment. Natural stimuli and synthetic speech produced with OVE II were used. The variation of parameters in the human speech was effected by means of a tape-splicing technique which made it possible to select any desired combination of transitional pattern, spectrum, and intensity of the fricative.

The 5 transitional patterns associated with /f, s, ʂ, ʃ and ç̰/ were combined with the 5 fricative segments. Each fricative segment had been copied at four different levels (-5, -10, -15 and -25 dB rel to the most intense part of the rest of the word xx). Thus 5x5x4 = 100 stimuli were obtained. The fricative and the transitional segments were separated by a cut just before the initial larynx pulse. The formant frequencies of /e/ at the cutting point and at the subsequent "steady-state" interval are:

---

x) An alternative sign for the phoneme /r̰s/ is /s̰j/, and /t̰j/ is sometimes used instead of /ç̰/. A third variant of the /r̰s/ phoneme of quality between [ʂ] and [ʃ] is [ʃ] (cf. the report by W. Jassem for IVth ICA).

xx) The intensity differences between the fricative and the following reference point in the original material were for [f] -22 dB, [s] -11, [ʂ] -7, [ʃ] -16, and for [ç̰] -9 dB.

	cutting point			"steady state"		
	F_1	F_2	F_3	F_1	F_2	F_3
/ˇfena/	375 c/s	1900 c/s	2400 c/s	375 c/s	2150 c/s	2600 c/s
/ˇsena/	375	1750	2400	375	2100	2500
/ˇʂena/	420	1700	2250	375	2000	2400
/ˇʃena/	400	1250	2050	375	2000	2500
/ˇʂena/	250	1900	2600	375	2000	2400

The voiced segment is preceded by an aspirative segment with marked traces of F2 and F3. To evaluate the importance of this segment a series of stimuli were prepared in which this aspirative segment has been removed. Only transitions and fricative parts were varied giving a total of 5x5 = 25 combinations. There were thus two different sets of stimuli based on human speech to be identified by groups of listeners. A third series of stimuli was then made of the same material as above synthesized on OVE II. The synthesis enabled greater freedom in the variation of transitions and frictional segments. One part of the test was a synthetic copy of the first experiment on the natural material. Another part involved a systematic variation of the selected cues i.e. transitions and spectrum.

The simulation of fricatives started with a very accurate reproduction of spectra specified by a large number of poles and zeros. An approximate reproduction involving only 2 poles and 1 zero in the transfer function was then attempted. In addition to the "fricative" noise as specified by the K-pattern there was added noise excited sound from the vocalic part of the synthesizer. This "aspirative" noise specified by the F-pattern was superimposed on the entire noise segment of the sound [ʃ]. In other fricatives it was added as a transitional segment next to the vowel only.

When listening to the synthesized sounds through a hi-fi system no difference could generally be detected with the possible exception of /ʂ/ and /ʐ/ between the detailed and the approximated simulations where the difference in the reproduction of the high-frequency region was perceptible. The two poles and one zero were selected as follows.

	K_0	K_1	K_2
[f]	1900 c/s	2100 c/s	9000 c/s
[s]	3000	4100	6300
[ʂ]	1500	2200	2800
[ʃ]	3200	3400	6100 x)
[ʐ]	2800	2800	3800

x) This K-pattern represents the high frequenoy formant of [ʃ] only. The main formant of [ʃ] was derived from the F-pattern through the added aspirative noise.

Test I and II were presented to a group of naive listeners whose task was to identify the stimuli as one of /f/ /s/ /ʂ/ or /ɕ/ (/ʂ/ being the only response for [ʂ] and [ʃ]) and to rate their quality as bad, fairly good, good. The synthetic stimuli were listened to informally in a test involving expert judgments.

The results obtained for natural and synthetic stimuli are similar. These tests and the experiment in which friction and transitions were varied can be summarized as follows.

Friction is the primary cue for identification. Exceptions are found for /ʂ/-friction combined with /ɕ/-transitions or /ɕ/-friction and /ʂ/-transitions. As can be seen from the frequencies of the 2 poles and the zero the approximated spectra of /ʂ/ and /ɕ/ are rather similar. The entire pole-zero configuration is for [ɕ] shifted upwards in frequency by approximately 1/4 octave compared with [ʂ] and is less than 3/4 octave below the pole-zero configuration for [s] x). The fact that the /ʂ/ and /ɕ/ spectra resemble each other so closely enhances the importance of the transitions. An exception is also afforded by the [ʃ]-transitions. The stimuli made up of this transitional pattern and a fricative segment which is not [ʃ] sounds very unnatural. Subjects get the impression of a kind of [v] or [w] inserted between the friction and the voiced interval. Subject's responses appear to be based by their own pronunciations of /ʂ/ and we get /ʂ/-responses to these stimuli from people who use [ʃ] and responses corresponding to the friction from subjects who do not use [ʃ].

A faithful reproduction of the relative intensity did not prove to be very important except for the identification of /f/ which tended to be confused with /s/ at high intensities. Too high noise intensity was judged to be more objectionable for synthetic speech than natural speech.

Transitions are of minor importance except in connection with [ʂ] [ɕ] and [ʃ] as discussed above.

To study in greater detail the /ʂ/ : /ɕ/ distinction in other combinations than /ʂena/ /ɕena/ transitions and fricative spectra were varied also in the words /ʂɔk/ /ɕɔk/ and the syllables /ʂi:/ /ɕi:/. The variations were always made with respect to the synthetic copies of the original natural material.

The basic K-pattern adopted for the synthesis was

K_0 = 2.2 kc/s
K_1 = 2.8 kc/s
K_2 = 3.5 kc/s

These values were shifted in steps of ± 1/4 octave ranging from K_1 = 1.75 kc/s to K_1 = 4.5 kc/s. For the K-patterns of lowest frequency the responses were

---

x) We have observed large individual variations in the K-pattern approximation of [ɕ]. The values K_0 = 4500, K_1 = 4000, and K_2 = 5600 c/s were obtained for a speaker different than the one used in the present study.

consistently /ʂ/ and for the highest configuration /s/. For transitions at low F_2 and F_3 loci a shift in the K-pattern from low to high frequencies resulted in a change of responses from /ʂ/ to /s/. In case of higher F_2 and F_3 loci, typical for [ç], the noise frequency variation gave a shift in response from /ʂ/ to /s/, with /ç/ responses for intermediate values of the noise frequency. K_1 was 2.8 kc/s for a maximum of /ç/ responses.

Fricatives in intervocalic position

The test stimuli were of VCV-type, V standing for short /a/ and C for /f/ /s/ /ʂ/ /ç/. The /ʂ/ phoneme was represented by the [ʂ] alone. The results are similar to those obtained, for initial fricatives. The identification of intervocalic /f/ and /ç/ seemed to rely more on transitions.

Conclusions: The friction is the most important cue for all fricative sounds. Transitional segments may also contribute somewhat especially for the identification of the velar labialized [ʃ] and in the /ʂ/ : /ç/ distinction. Low intensity is an important cue for /f/ but not a primary one.

H45

FOURTH INTERNATIONAL CONGRESS ON ACOUSTICS
COPENHAGEN 21.-28. AUGUST 1962

Zur Lautstärke einzelner Rauschimpulse.

E.Port
Inst.f.Nachrichtentechnik, Technische Hochschule Stuttgart

Übersicht.

Die Abhängigkeit der Lautstärke von der Darbietungsdauer eines Schalles wurde schon von einigen Autoren bei Tönen [1 - 5] und auch bei Ausschnitten aus weißem Rauschen gemessen. Als Ergänzung hierzu wird in dieser Arbeit dieselbe Fragestellung bei Verwendung eines schmalbandigen Rauschens untersucht. In einem zweiten Experiment soll geklärt werden, ob auch bei sehr kurzen Ausschnitten aus Rauschen die Bandbreite des Rauschens einen wesentlichen Einfluß auf die Lautstärke hat.

Meßmethode.

Verkürzt man die Darbietungsdauer eines beliebigen Schalles, dann unterscheidet sich das Spektrum des entstehenden Schallimpulses von dem des ursprünglichen Dauerschalles. Nur bei Verwendung eines breitbandigen Rauschens verändert sich dessen spektrale Verteilung nicht, auch wenn man die Darbietungsdauer bis zu sehr kurzen Zeiten verringert. Aus diesem Grund wurde ein weißes Rauschen verwendet, aus dem mit Hilfe eines elektronischen Schalters Impulse beliebiger Dauer ausgeschnitten werden konnten. Nach dem Schalten wurde das Spektrum der Impulse durch ein Terzbandfilter mit einer Mittenfrequenz von 2,5 kHz begrenzt. Infolge der Einschwingzeit des Terzfilters konnten die Impulse nicht beliebig weit verkürzt werden.

Die Beobachter hatten während der Messung die Aufgabe, die Lautstärke des schmalbandigen Rauschimpulses mit der des spektral gleichen schmalbandigen Dauerrauschens zu vergleichen. Ein solcher Vergleich ist relativ schwierig. Erleichtert wird er, wenn der Beobachter nicht nur einen Impuls, sondern einige Impulse hintereinander hört, deren zeitlicher Abstand aber so groß sein muß, daß sie sich nicht gegenseitig in ihrer Lautstärke beeinflussen. Hier wurde eine Pulsfolge mit einer Pulsfrequenz von $f_p = 3$ Hz gewählt. Der Beobachter hörte jeweils abwechselnd 6 Rauschimpulse hintereinander und dann ein 1,25s langes Dauerrauschen.

Es wurde bei jedem Meßpunkt sowohl die Methode des pendelnden Angleichens (method of tracking) wie auch die Methode des Angleichens (method of adjusting) verwendet. Ein systematischer Unterschied zwischen den Ergebnissen beider Methoden war nicht erkennbar. Jeweils 8 Beobachter nahmen an den Messungen teil. In den Bildern 1 und 3 wurden als Meßergebnis die Zentralwerte (median), samt den zugehörigen wahrscheinlichen Schwankungen (interquartile range) eingezeichnet.

Die Abhängigkeit der Lautstärke von der Impulsdauer.

Nach dem oben beschriebenen Verfahren wurde die Lautstärke von schmalbandigen Rauschimpulsen verschiedener Dauer t_i gemessen. Das Ergebnis zeigt Bild 1. Aufgetragen sind die Pegeldifferenzen, um die die kurzen Impulse beim Lautstärkevergleich höher eingestellt wurden als das Vergleichsdauerrauschen. L_i ist der Pegel des Dauerrauschens aus dem die Impulse ausgeschnitten wurden. Die links von den Abszissenwerten ein-

gezeichneten Werte zeigen das Ergebnis der Messung, bei der von den Beobachtern der Pegel der Impulse eingestellt werden konnte; bei den rechten Werten konnte das Vergleichsdauerrauschen verändert werden.

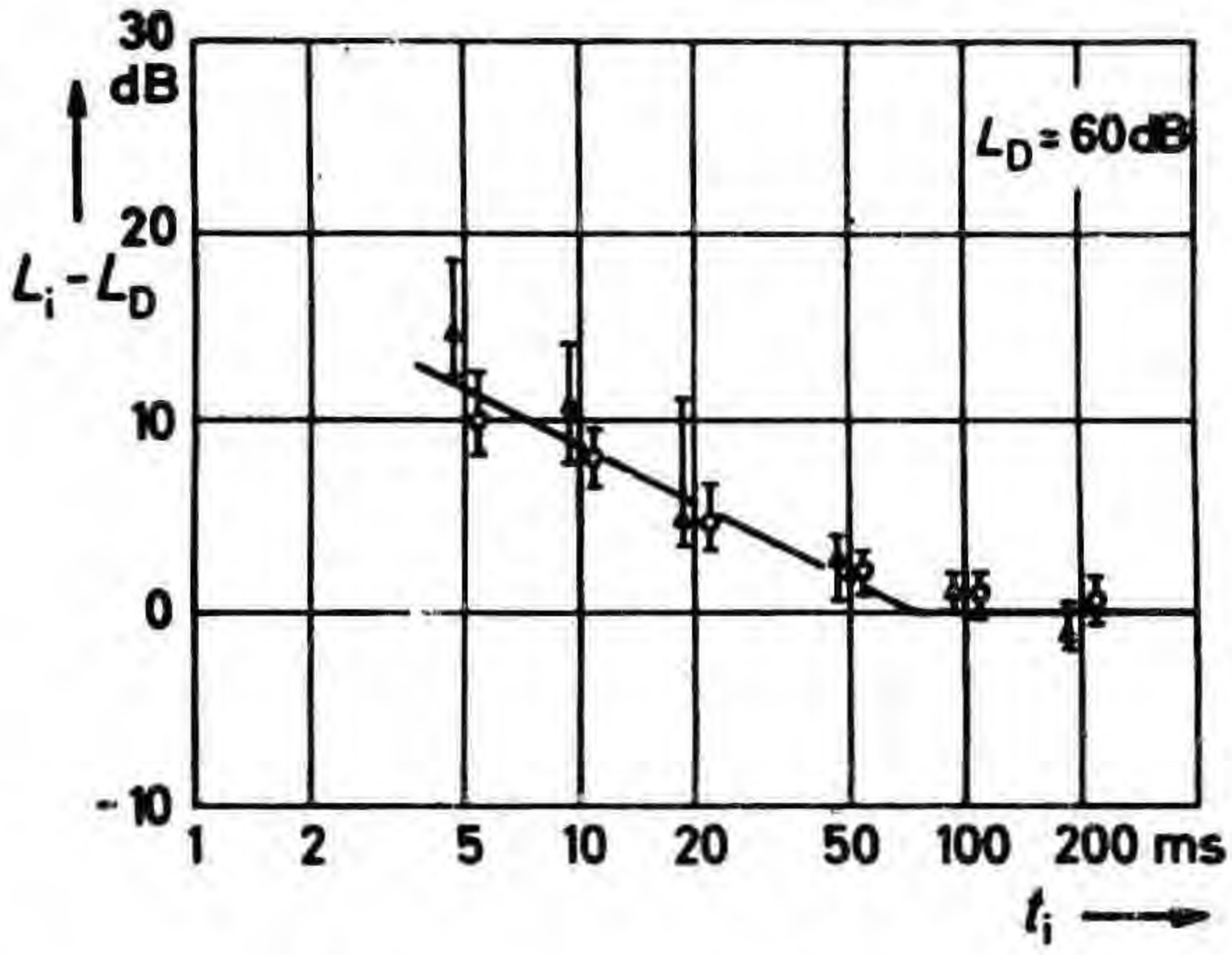

Bild 1.

Lautstärkevergleich von schmalbandigen Rauschimpulsen mit einem schmalbandigen Dauerrauschen in Abhängigkeit von der Dauer der Impulse.

Dreiecke: Impulse verändert.
Kreise: Dauerrauschen verändert.

Man sieht, daß bis herab zu einer Impulsdauer von etwa t_i = 70ms die Impulse noch genauso laut sind wie das Dauerrauschen. Verringert man aber die Impulsdauer zu noch kleineren Werten, dann muß der Pegel L_i der Impulse gegenüber dem Pegel L_D des Dauerrauschens erhöht werden, um gleiche Lautstärkeempfindung zu erzeugen. Der Anstieg des Pegels kann durch die im Bild 1 eingezeichnete Gerade, deren Neigung 10 dB pro Dekade der Impulsdauer beträgt, angenähert werden. Längs einer solchen Geraden ist die Schallenergie der Impulse konstant. Das Gehör scheint demnach bei Rauschimpulsen, die kürzer als etwa 70 ms sind, nicht die Schallintensität, sondern die gesamte Schallenergie zu bewerten. Wie schon erwähnt, haben eine Reihe von Autoren ähnliche Versuche mit Tönen verschiedener Dauer durchgeführt. Zum Vergleich wurden alle bisher bekannten Ergebnisse in Bild 2 aufgetragen.

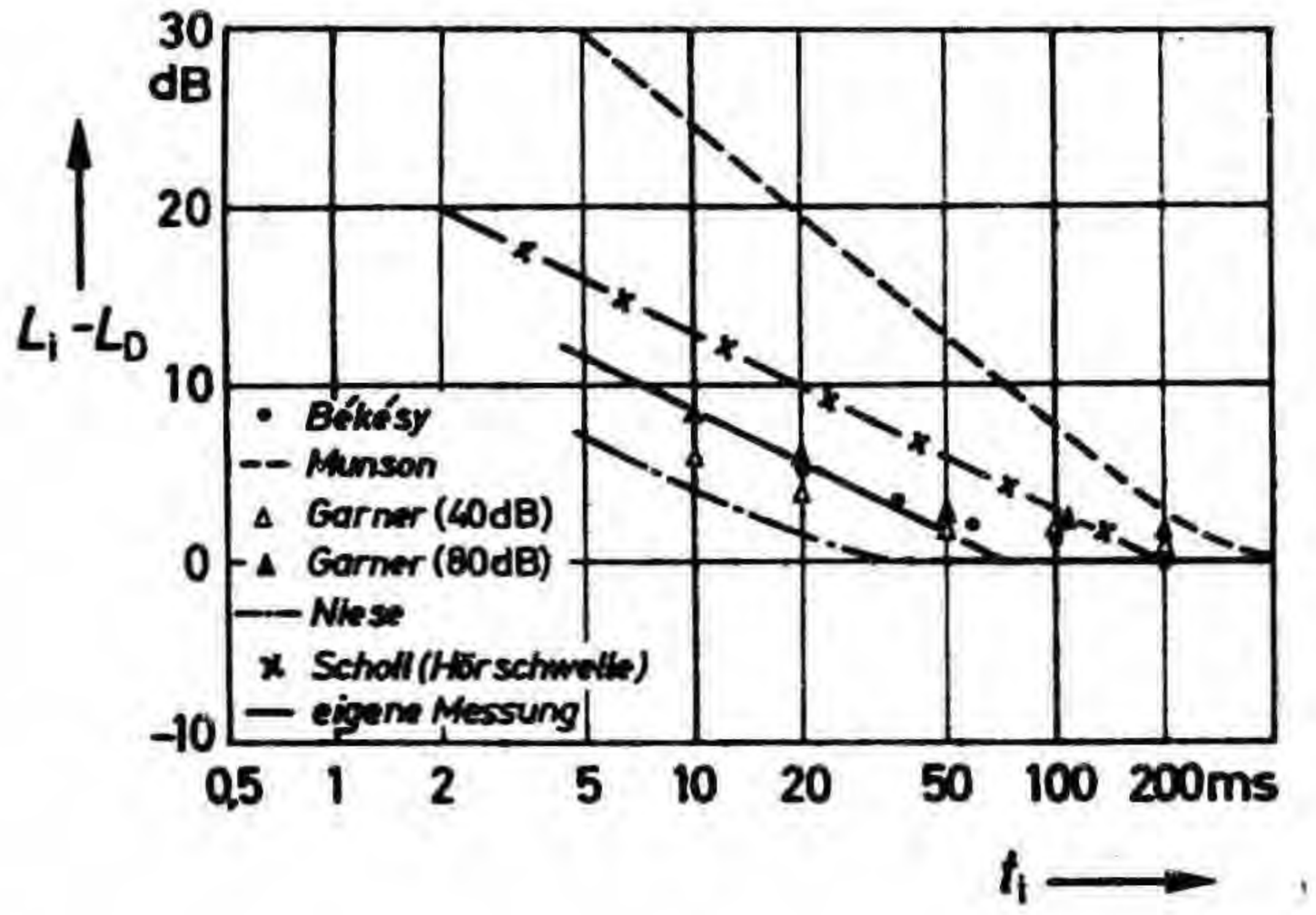

Bild 2.

Vergleiche der Messungen verschiedener Autoren, Kurven gleicher Lautstärke schmalbandiger Schallimpulse in Abhängigkeit von der Dauer der Impulse.

Die von Garner und von von Békésy gemachten Messungen stimmen recht gut mit der in dieser Arbeit gemessenen Kurve überein, während die Messung von Niese und besonders die von Munson abweichende Werte liefert. Zum Vergleich wurde außerdem noch die von Scholl [6] angegebene Hörschwelle von Ton- und schmalbandigen Rauschimpulsen verschiedener Dauer eingezeichnet. Die Hörschwelle ist mit wesentlich größerer subjektiver Genauigkeit meßbar. Man erkennt, daß die an der Hörschwelle gemessene Grenzdauer mit 200 ms etwa 3 mal so groß ist wie die bei der Lautstärke gemessene. Der Anstieg der an der Hörschwelle gemessenen Kurve beträgt aber auch 10 dB pro Dekade der Impulsdauer.

Die Abhängigkeit von der Bandbreite bei kurzen Impulsen.

Mißt man die Lautstärke von Dauerrauschen in Abhängigkeit von der Bandbreite des Rauschens und hält den Schalldruckpegel des Rauschens während der Messung konstant, dann zeigt es sich, daß oberhalb einer kritischen Bandbreite - der Frequenzgruppe - die Lautstärke mit wachsender Bandbreite ansteigt [7]. Breitbandige Dauerschalle sind bei gleichem Pegel lauter als schmalbandige. Ob dies auch bei kurzen Impulsen zutrifft, wurde in der im Folgenden beschriebenen Messung nachgeprüft.
Den Beobachtern wurde abwechselnd eine Serie von 6 Tonimpulsen verschiedener Bandbreite mit jeweils einer Pulsdauer von t_i = 5 ms und einer Pulsfrequenz von f_p = 3 Hz dargeboten. Der Pegel der Tonimpulse konnte von den Beobachtern verändert werden; der Pegel der Rauschimpulse blieb dagegen konstant L_{iR}=50 dB. Das Ergebnis der Messung wurde als Pegeldifferenz $L = L_{iT} - L_{iR}$ in Bild 3 links von den zugehörigen Abszissenwerten eingezeichnet.

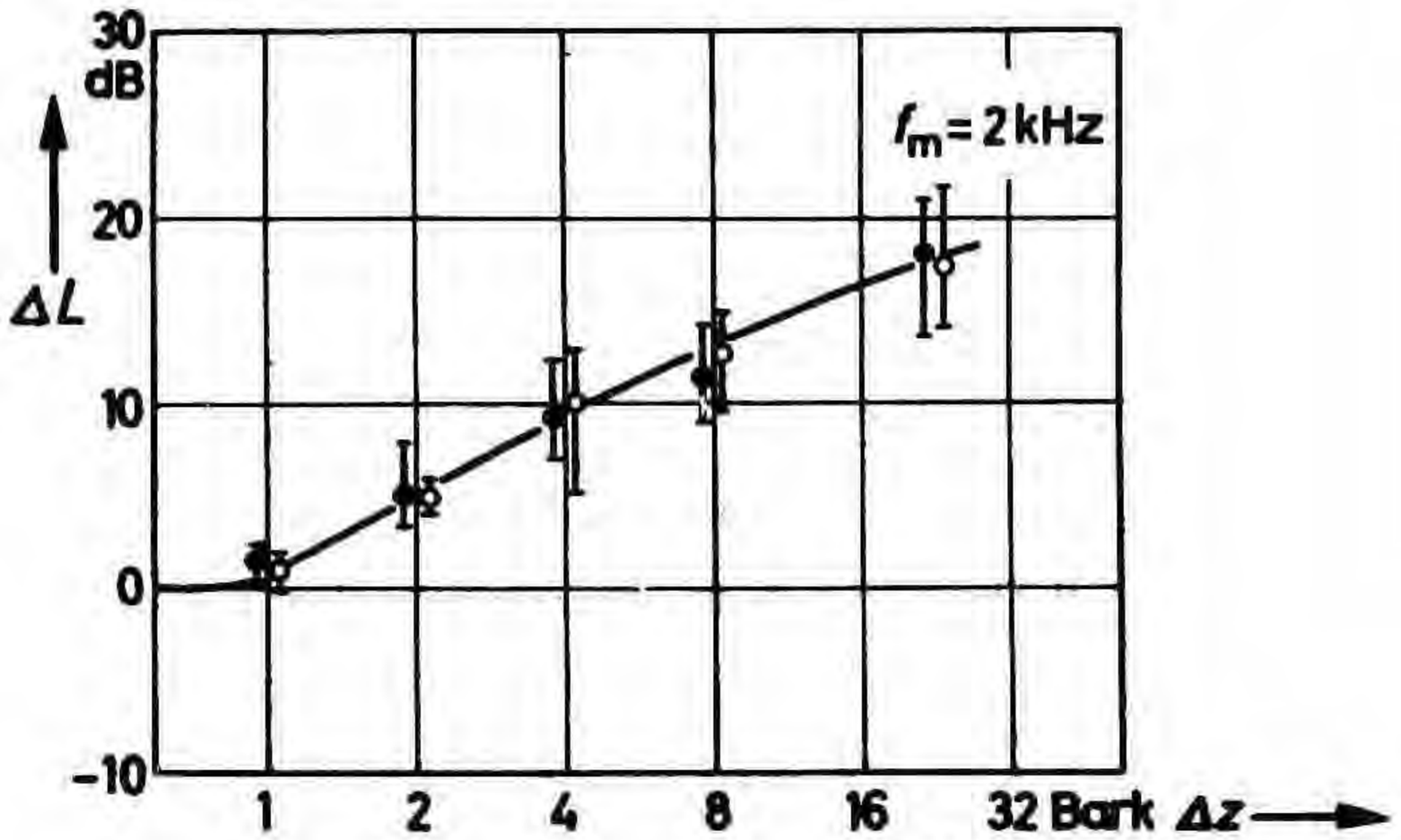

Bild 3. Die Abhängigkeit der Lautstärke von der Bandbreite bei Schallimpulsen und bei Dauergeräuschen.
Punkte: Meßwerte bei Rauschimpulsen mit einer Dauer von 5 ms.
Kreise: Meßwerte bei Dauerrauschen.

Um einen guten Vergleich mit den Verhältnissen bei Dauergeräusche zu bekommen, wurde der entsprechende Versuch auch mit Dauerrauschen von denselben Beobachtern durchgeführt. Die Beobachter hatten ein schmalbandiges Rauschen mit der Breite einer Frequenzgruppe so einzustellen, daß es ihnen gleichlaut wie ein Rauschen verschiedener Bandbreite und konstantem Pegel L_{DR} = 40 dB erschien. Das Meßergebnis ist in Bild 3 rechts von den Abszissenwerten eingetragen. Man sieht aus diesem Bild daß die Lautstärke kurzer Rauschimpulse mit wachsender Bandbreite in völlig gleicher Weise zunimmt wie die Lautstärke von Dauerrauschen. Bei kurzen Einzelimpulsen scheint das Spektrum des Schalles für die Lautstärkeempfindung praktisch ebenso wie bei Dauergeräuschen bewertet zu werden. Dieses Verhalten des Gehörs weicht von dem Verhalten bei der Hör- bzw. Mithörschwelle ab. Bei der Messung der Mithörschwelle von Dauerrauschen verschiedener Bandbreite bei Verdeckung durch ein breitbandiges Dauerrauschen zeigt sich eine starke Abhängigkeit der Mithörschwelle von der Bandbreite des verdeckten Rauschens. Die Mithörschwelle liegt umso höher je breitbandiger das verdeckte Rauschen ist. Mißt man dagegen die Mithörschwelle von einzelnen Rauschimpulsen mit einer Impulsdauer $t_i < 5$ ms, dann bleibt die Mithörschwelle völlig unabhängig von der Bandbreite der Impulse [6][8].

Schrifttum:

1) v.Békésy, G.Phys.Ztschr. 30 (1929), 118.
2) Munson, W.A., J.acoust.Soc.Amer. 9 (1947), 584.
3) Garner, W.R., J.acoust.Soc.Amer.21 (1949), 398.
4) Niese, H. Hochfrequ. u. Elektroak. 65 (1956), 4.
5) Niese, H. Hochfrequ. u.Elektroak. 68 (1959), 143.
6) Scholl, H. Acustica 12 (1962) im Druck.
7) Zwicker, E. et al. J.acoust.Soc.Amer. 29 (1957), 548.
8) Scholl, H., Acustica 12 (1962) im Druck.

J45

FOURTH INTERNATIONAL CONGRESS ON ACOUSTICS
COPENHAGEN 21.-28. AUGUST 1962

ULTRASONIC VIBRATION POTENTIALS IN POLYELECTROLYTES

JONATHAN BOOKER, ERNEST YEAGER, and FRANK HOVORKA
Western Reserve University, Cleveland, Ohio (U.S.A.)

Introduction

The propagation of ultrasonic waves through an ionic solution produces alternating potential differences within the solution between points separated by a phase distance other than an even multiple of the wave length. This effect was first predicted by Debye[1] in 1933 and results because differences in the dynamic reactions of the cations and the anions to the material wave produce periodic excesses of either type of ions. The mathematical treatments of the effect by Debye[1] and others[2] as well as experimental studies[3-8] indicate that the effect is of the order of 1 to 10 μV per unit velocity amplitude (cm/sec) at frequencies of 10^5 to 10^6 cycles/sec.

A similar effect has been found in colloidal systems[4,7,9-13] consisting of charged colloidal particles surrounded by a diffuse ionic atmosphere of predominantly opposite charge. In the sound field the ions of the ionic atmosphere are displaced with an amplitude and phase which differ from those of the central colloidal particle. As a result, the ionic atmosphere is periodically distorted and a dipole of varying moment is produced. The associated alternating potentials are known as colloidal vibration potentials and are much larger than the ionic vibration potentials. This effect in colloidal systems has been examined theoretically by Hermans[9], Enderby[14], and Booth[15] and experimentally by various workers[7-13]. Theory and experiment are in reasonable agreement (as close as 25% in some instances). A value of 10^{-3} volts per cm/sec is typical for a suspension of low specific conductance.

The purpose of the present study has been to establish if a comparable effect exists in solutions of polyelectrolytes and, presuming that it does, to establish how the effect depends on the charge characteristics and configuration of the polyelectrolyte. The solutes in such solutions consist of polymer molecules which acquire charge through the ionization of certain functional groups associated with the monomeric units of the polymer. Thus, polyelectrolytes incorporate features of simple electrolytes and colloidal systems yet possess additional unique features associated with the linkage of like-charged groups together in an appended structure.

The present measurements have involved polyacrylic acid

$$\left(\begin{array}{cc} H & H \\ -C- & -C- \\ H & | \\ & COOH \end{array} \right)_n$$

with a molecular weight of $1.4 \cdot 10^5$ corresponding to n = 2000. In the absence of other electrolytes, this polyelectrolyte is only slightly ionized, and hence, the total charge on a given polymer molecule is small. Under such circumstances the structure is probably described satisfactorily by the random coil model proposed by Kuhn[16] and may approach that of a non-charged polymer molecule. If alkali is added to the polyacrylic acid suspension, the acid groups in the polymer chain will ionize and the negative charge on the polymer molecule will increase by a large factor. Intramolecular repulsion between these negatively charged groups will cause the polymer coil to expand and, in the limiting case, the polymer might extend to a rod-like configuration. This is unlikely, however, since cations will be attracted into the polymer coil as the concentration of negatively charged groups within the coil increases. The screening effects of these cations will greatly reduce the intramolecular repulsion, and hence, far less dilation of the coil will occur.

Ultrasonic vibration potentials may offer promise as a means for obtaining information concerning the configuration of such polyions at various stages of neutralizatior provided an adequate mathematical treatment of the effect for such systems is

forthcoming. The mathematical description of the effect for polyelectrolytes is much more difficult than for either the simple electrolytes or colloidal systems. Just as in the case of a simple colloid, the polyion is surrounded by a time-average symmetrical ionic atmosphere. Periodic distortion of the ionic atmosphere occurs in the sound field but in contrast to the rigid colloidal particle with its localized charge, the shape of the central polyion is dynamic and the charge distribution within the polyion can shift. Information concerning charge mobility within the polyion is not readily available. Thus the image-charge problem and the complex hydrodynamics anticipated for a non-rigid particle contribute to the present inability to calculate reliably the magnitude of the effect to be expected at various stages of neutralization.

Experimental Procedure

In the present work the effect has been measured with pulse-modulated ultrasonic waves at frequencies from 200 to 1000 kc with equipment similar to that used in earlier studies in the authors' laboratory[17]. Pulse techniques permitted the true acoustically-produced effects to be differentiated from false, electromagnetically induced signals and minimized problems associated with multiple reflections. The sound waves were generated by means of either barium titanate or quartz transducers mounted at one end of a 250-gal tank. The sound waves were propagated through a 6-ft path in the tank into a plastic cell which contained the polyelectrolyte and the electrode assembly for the detection of the effect. A ρ-c rubber window separated the polyelectrolyte in the plastic cell from the water in the large tank.

The vibration potentials were measured on a single platinum probe relative to ground. This is equivalent to measuring the alternating potential at any one position relative to the position-average potential of the solution and has been shown experimentally to yield an observed effect equivalent to one-half of that measured between points separated by a phase distance of one-half wave length. The probe consisted of a 0.02-cm diameter Pt wire with 1.0 cm exposed to the solution and was sealed in the end of a glass tube with its axis parallel to the wave front.

A hydrophone utilizing a barrium titanate cylinder with an outside diameter of 0.32 cm was used to measure the pressure amplitude of the ultrasonic waves in the polyelectrolyte solutions. The hydrophone was calibrated at each frequency involved in the measurements by direct comparison with a radiation pressure gauge.

The signals from the Pt probe were amplified with a tuned amplifier and displayed on an oscilloscope. Loading effects associated with the finite input impedance of the detection equipment were shown to be negligible for the solutions involved in this research. The signals were measured with a precision of $\pm 10\% \pm 1\mu V$ by direct comparison with the signal from a standard signal generator (General Radio Model 605). The absolute accuracy of the measured values for the effect per unit velocity amplitude is estimated to have been $\pm$ 20% with the non-homogeneity of the ultrasonic field the major factor limiting the accuracy.

The polyacrylic acid was obtained from the Rohm and Haas Co. of Philadelphia in the form of a 25% (by weight) stock solution. This solution was diluted to the desired concentrations for the ultrasonic measurements with distilled water. The charge characteristics and rheological properties of the diluted solutions were determined by pH, conductance, and viscosity measurements. The measurements have been made in solutions of sufficient conductance that the false microphonic effects encountered in previous work[18] should not be expected to cause any significant error in the present work.

Experimental Results

In Figures 1 and 2 are graphed typical results for 0.1% and 0.5% by weight solutions at 200 and 1000 kc as a function of the percent of the acid groups which have been neutralized through the addition of sodium hydroxide. From these figures, it is evident that the effect in polyacrylic acid suspensions is intermediate in value between the ionic and the colloidal vibration potentials. The change of the effect with neutralization is surprisingly small and qualitatively indicates that the cations rather completely screen the negative charges of the anions within the polymer chain and/or the polyion dilates to such an extent that it moves with substantially the same phase and amplitude as the solvent. It is interesting to note that the

amplitude of the observed effect correlates rather well with the dependence of the viscosity on percent neutralization.

In the limiting case of a reasonably tightly coiled polyion, the effect may approach the value expected for a simple colloidal system. Since the polyion should be in the most compact configuration in the unneutralized state, an attempt has been made to calculate the order of magnitude of the effect for this case with the equations developed by Enderby[14] for a simple colloidal system. The following are the numerical values used for the 0.1% polyacrylic acid suspension in this calculation:

pH = 3.3
polyion radius = $5 \cdot 10^{-7}$ cm
specific conductance = $1.5 \cdot 10^{-3}$ ohm^{-1} cm^{-1}
density of polyion = 1.12 g/cm
net charge per polyion = 70e
effective thickness of ionic atmosphere = $7 \cdot 10^{-7}$ cm
zeta potential = 200 mV

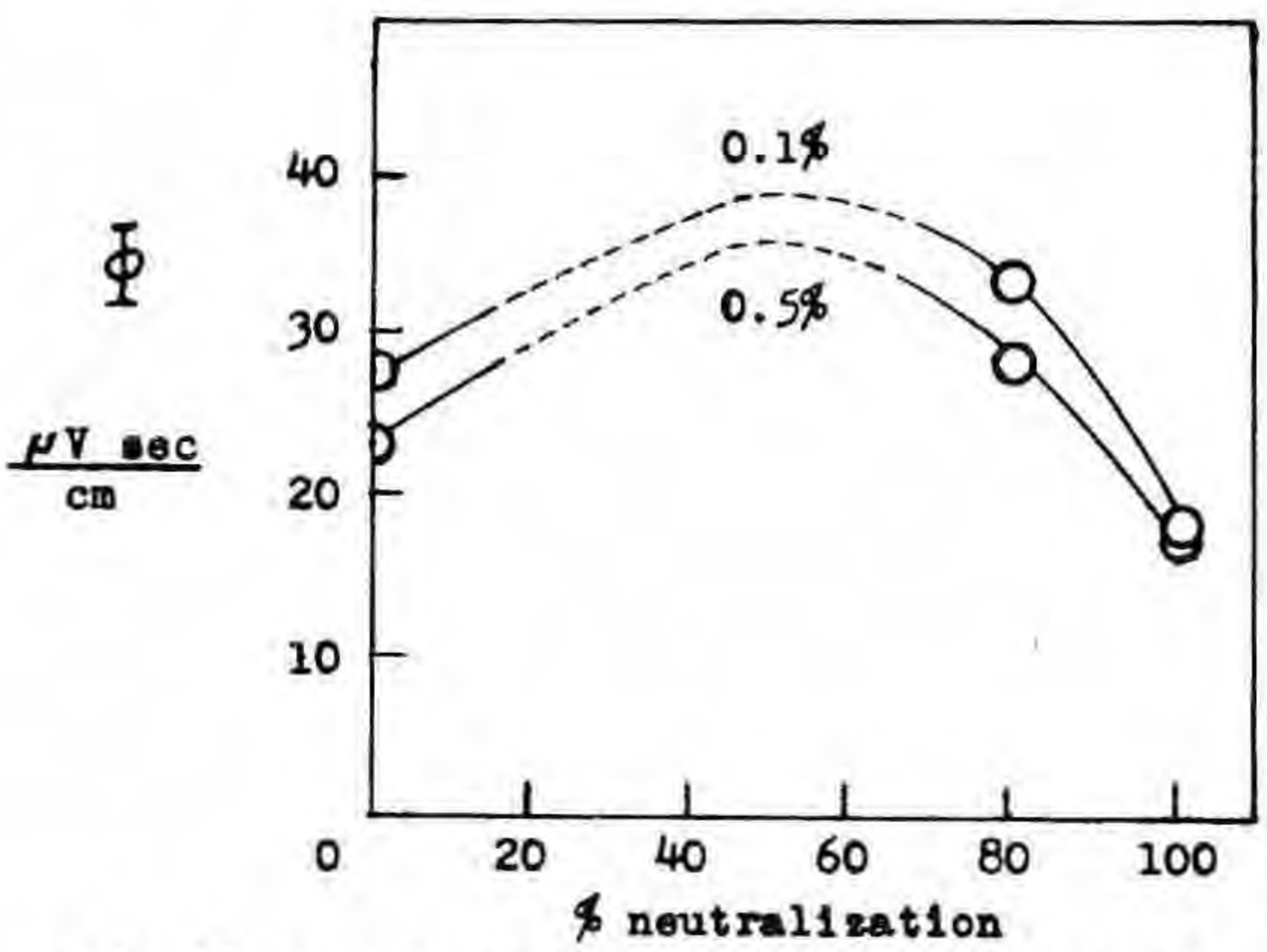

Figure 1. Ultrasonic vibration potentials in polyacrylic acid at 200 kc.

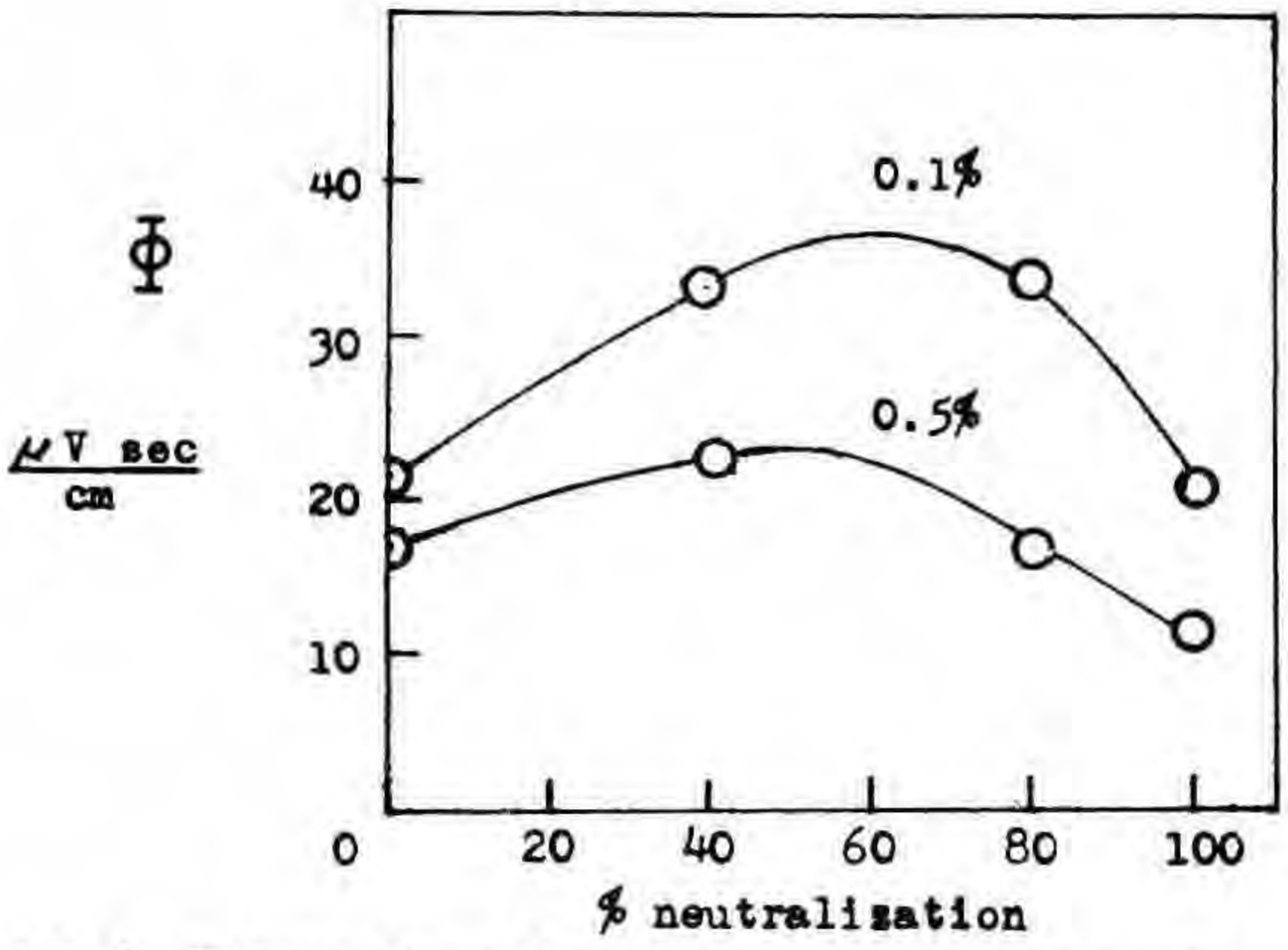

Figure 2. Ultrasonic vibration potentials in polyacrylic acid at 1000 kc.

The calculated amplitude of the effect is $3 \cdot 10^{-5}$ volt-sec/cm as compared with an experimental value of $3.2 \cdot 10^{-5}$ volt-sec/cm. The close agreement is probably fortuitous since the calculated value is not expected to indicate much more than the order of magnitude of the effect.

Acknowledgement

The authors acknowledge the support of this research by the U.S. Office of Naval Research.

References

1. P. Debye, J. Chem. Phys. 1, 13 (1933).
2. Bugosh, Yeager, and Hovorka, ibid. 15, 592 (1947).
3. Yeager, Bugosh, Hovorka, and McCarthy, ibid. 17, 411 (1949).
4. Yeager, Dietrick, and Hovorka, J. Acoust. Soc. Am. 25, 456 (1953).
5. Yeager, Booker, and Hovorka, "Quantitative Measurements of Ionic Vibration Potentials," Chapter 6 in Structure of Electrolytic Solutions, W. Hamer, editor, John Wiley and Sons, Inc., New York, 1959.
6. A. Hunter, Proc. Phys. Soc. 71, 847 (1958).
7. Rutgers and Rigole, Trans. Faraday Soc. 54, 139 (1958).
8. R. Millner, Z. Elektrochem. 65, 639 (1961).
9. J. Hermans, Phil. Mag. 25, 426 (1938); 26, 674 (1938).
10. A. Rutgers, Physica 5, 46 (1938).
11. Rutgers and Vidts, Nature 165, 109 (1950).
12. J. Causse, ibid. 230, 826 (1950).
13. Dereout and Denizot, Compt. rend. 233, 368 (1951).
14. J. Enderby, Proc. Roy. Soc. (London) 207A, 329 (1951).
15. Booth and Enderby, ibid. 208A, 321 (1952).
16. W. Kuhn, Kolloid, Z. 68, 2 (1934); 76, 258 (1936).
17. Saunders, Yeager, and Hovorka, J. Acoust. Soc. Am. 27, 556 (1955).
18. Yeager, Booker, and Hovorka, Proc. Phys. Soc. 73, 690 (1959).

K45

FOURTH INTERNATIONAL CONGRESS ON ACOUSTICS
COPENHAGEN 21.-28. AUGUST 1962

THE RELATIONSHIP BETWEEN WIND SPEED AND SHALLOW WATER AMBIENT NOISE

Frank T. Dietz, J. Steven Kahn and William B. Birch
University of Rhode Island, Kingston, R. I.

During the period from October 1958 through September 1959, the University of Rhode Island, supported by the Office of Naval Research, made a systematic series of ambient noise spectrum determinations in the lower West Passage of Narragansett Bay, Rhode Island. This body of water extends in a north-south direction and, in the vicinity of the hydrophone installation, is approximately one mile in width. It is bounded on the west by the mainland and on the east by an island. The mid-channel depth is 40 - 50 feet.

The purposes of the measurement program were to study the characteristics of the ambient noise and to determine possible correlations between the noise and certain environmental factors, such as: wind speed, wind direction, wave height, rainfall, and tidal currents.

In order to accomplish this, a sampling schedule was devised which called for a total of 864 spectrum determinations over the course of a year. Readings were made each month during two weeks chosen at random within the month. During each of the two weeks, two days of the five weekdays and one of the two weekend days were selected at random. Further, each of the three sampling days was divided into six equally spaced hour groups, and two spectrum determinations were made within each of the hour groups at times chosen at random. Thus, the acoustic spectrum was measured twelve times per day, three days per week, two weeks per month. This resulted in seventy-two spectra per month.

The receiving system consisted of a Brush Type AX-58C hydrophone, with preamplifier, supported one foot above a silty-sand bottom in forty feet of water approximately 900 feet from the west shore of the bay. The signals from the hydrophone were amplified and frequency analysed by a Bruel and Kjaer Spectrum Analyser on a one-third octave basis and recorded by a B & K Graphic Level Recorder. The recorder was operated at a paper speed of 1 mm/sec and approximately 1.9 min. were required to scan the spectrum between 40 cps and 10 000 cps.

Calibration was accomplished by injecting a random noise signal into the hydrophone preamplifier and recording it, after it passed through the complete system, on the same paper tape as the sound spectrum. This procedure allowed the determination of the average spectrum levels associated with nineteen selected frequencies, distributed over the frequency band, to be made in under ten minutes.

Acoustic and environmental information were entered in IBM punch cards and processed with the aid of the Computation Centers at Brown University and the University of Rhode Island. Significant correlations between ambient noise and the environmental variables were found for wind speed, rainfall, and tidal currents.

The effect of wind on the sea surface in our locality is a complex one and no attempt has been made to present any correlations between ambient noise and sea state. Tidal currents influence the noise spectrum below 100 cps and are likewise omitted from this presentation.

This paper is concerned with some of the relationships between wind speed and ambient noise. Wind speed and direction measurements were obtained from a Bendix-Friez recording anemometer mounted fifteen feet above the water surface and approximately 900 feet from the hydrophone. The results to be presented are based on a total of 651 spectrum determinations. Of the original 864 spectra, 213 were excluded from the analyses because of the presence of rainfall or the presence of ship and biological noise.

Included in the data sample are wind speeds ranging from 0 mph to 29 mph. The distribution of wind speed observations is given in Table 1.

Table 1

Distribution of Observations at Various Wind Speeds

Wind Speed	No. of Obsvs.	Wind Speed	No. of Obsvs.	Wind Speed	No. of Obsvs.
0	56	10	60	20	7
1	27	11	24	21	9
2	35	12	26	22	5
3	39	13	10	24	5
4	58	14	12	25	5
5	31	15	14	27	1
6	59	16	20	29	2
7	32	17	8	Total	651
8	49	18	16		
9	33	19	8		

Unpublished studies conducted in deeper water by the Admiralty Research Laboratory, the U.S. Navy Electronics Laboratory, and the Canadian Naval Research Establishment indicate that the ambient sound pressure level may be linearly associated with the logarithm of the wind speed, for wind speeds exceeding certain threshold values. Our data show similar results.

The average spectrum level, corresponding to particular wind speed, was computed for each of the nineteen frequencies and plotted versus the logarithm of the wind speed. A typical plot for a given frequency shows that the levels associated with small wind speeds are essentially the same. At higher wind speeds, above a threshold value, the sound level increases in a linear fashion. The threshold value was determined from the graphs by eye, and a linear regression line was computed for the pressure points corresponding to the higher wind speeds. Table 2 summarizes the results.

Table 2

Summary of Regression and Correlation Statistics, including the Number of Observations, (n), beyond the Threshold Velocity (v_t); Correlation Coefficient (r); Slope of Line of Best Fit (b); y Intercept (a); Wind Speed (x) in Miles Per Hour

Frequency cps	n	v_t mph	r	b	a	Regression
40	-	-	.14NS	1.0	-25.5	log y = -25.5 + 1.0 log x
50	6	21	.77NS	25.9	-60.8	-60.8 + 25.9
60	6	21	.75NS	30.5	-68.7	-68.7 + 30.5
80	4	24	.48NS	21.7	-59.3	-59.3 + 21.7
100	17	20	.78NS	32.3	-74.5	-74.5 + 32.3
150	15	12	.86*	21.4	-57.8	-57.8 + 21.4
200	17	10	.93*	29.7	-66.9	66.9 + 29.7
300	19	8	.97*	28.3	-65.0	-65.0 + 28.3
400	20	7	.98*	30.2	-66.5	-66.5 + 30.2
500	21	6	.99*	30.2	-67.6	-67.6 + 30.2
600	21	6	.99*	31.1	-69.0	-69.0 + 31.1
800	21	6	.99*	31.2	-69.5	-69.5 + 31.2
1 000	2	6	*	30.0	-69.9	-69.9 + 30.0
1 500	20	7	.99*	28.4	-70.9	-70.9 + 28.4
2 000	20	7	*	29.5	-73.3	-73.3 + 29.5
3 000	19	8	.98*	30.6	-77.0	-77.0 + 30.6
5 000	19	8	.98*	28.6	-78.1	-78.1 + 28.6
7 000	18	9	.98*	27.3	-81.2	-81.2 + 27.3
10 000	18	9	.89*	20.8	-76.0	log y = -76.0 + 20.8 log x

NS = correlation not significantly different from 0.
* = correlation significantly different from 0.
y = average pressure (dynes/cm^2/cycle).

It will be noted that statistically non-significant correlations between sound pressure and wind speed were obtained for frequencies less than 150 cps. These results for shallow water are in conformity with the results of oceanic ambient studies reported by various laboratories [For example, see G.M. Wenz, J. Acoust. Soc. Am. 33, 64 - 74 (1961)].

It is also seen from Table 2 that noise levels are most sensitive to wind in the frequency range 500 cps - 1 000 cps, and that the maximum regression line slope occurs at 800 cps. The minimum threshold wind speed is 6 mph.

The influence of wind speed on the acoustic spectrum can also be shown by graphing average ambient noise spectrum levels associated with a given frequency for various wind speed groupings. Table 3 displays these results.

Table 3

Average Ambient Noise Spectrum Levels for Various Frequencies and Wind Speed Groups
(Db re 1 dyne/cm^2/cycle)

Frequency	Wind Speed Groups (mph)				
cps	0 - 5	6 - 10	11 - 15	16 - 20	21 - 29
40	-25.4	-25.4	-25.5	-22.5	-19.5
50	-27.2	-26.3	-27.0	-24.3	-26.2
60	-29.5	-28.4	-29.0	-26.4	-27.7
80	-32.5	-31.5	-32.1	-31.0	-31.1
100	-33.8	-33.0	-33.3	-32.0	-31.4
150	-35.2	-35.0	-33.8	-32.5	-29.6
200	-36.6	-35.6	-34.1	-32.2	-27.6
300	-39.0	-37.8	-34.2	-32.2	-26.8
400	-40.6	-38.8	-33.7	-30.8	-27.0
500	-44.0	-40.2	-34.6	-32.1	-26.5
600	-45.1	-41.0	-34.9	-32.9	-26.8
800	-46.5	-41.8	-35.0	-32.9	-27.9
1 000	-47.9	-43.0	-36.5	-34.3	-29.4
1 500	-48.5	-44.4	-38.8	-36.8	-31.7
2 000	-49.1	-45.5	-40.3	-38.2	-33.3
3 000	-50.2	-47.1	-42.9	-41.8	-
5 000	-52.4	-49.7	-44.3	-44.3	-38.0
7 000	-53.9	-51.7	-48.9	-47.0	-41.5
10 000	-55.8	-54.9	-52.4	-51.0	-46.8

Spectrum level versus frequency graphs of these data are, in general, characterized by two or three regions. Between 40 cps and 100 cps, the data points lie within 3 db of one another for all wind speeds measured. The slope of this portion of the spectrum is approximately -7 db per octave. Above 100 cps, the curves diverge. For the 0 - 5 mph and the 6 - 10 mph groups, the trend from 100 cps to 10 000 cps is of the order of -3 to -4 db per octave. Characteristic of the 11 - 15 mph and the 16 - 20 mph curves is the plateau region which occurs between 100 cps and 800 cps. Beyond 800 cps, the slopes of these two curves are approximately -4.5 db per octave. The highest winds measured produced a convex-shaped curve in the 100 cps - 800 cps region, and a slope, beyond 800 cps, of between -4 to -5 db per octave.

These results do not differ appreciably from the Knudsen curves, [V.O. Knudsen. R.S. Alford, and J.W. Emling, J. Marine Research 7, 410 - 429 (1948)], except that the slopes of the lines for small wind speeds are 1 - 2 db less than those reported by Knudsen, et al.

In summary, data accululated over a year's time have been presented which show the effect of wind speed on the average acoustic ambient noise spectrum for a shallow water location free of shipping, biological noise, and rainfall. The results which have been presented include winds without regard to their directions. Investigations of the effects of winds blowing with, against, or across the tidal currents show that the average spectra are only slightly influenced by the wind direction.

L45

FOURTH INTERNATIONAL CONGRESS ON ACOUSTICS
COPENHAGEN 21.-28. AUGUST 1962

THE CORRELATION OF JET NOISE FREQUENCY SPECTRA

W. J. LEWIS

When considering the spectral distribution of the noise of jets of differing diameters, pressures and temperatures, some method is required for reducing the data to a form in which comparisons can be made with other results. The normal method of presentation involves the use as a correlating parameter of Strouhal number, fd/V, where f is the frequency of the noise measured, d a characteristic dimension of the jet (normally nozzle diameter) and V the fully expanded jet velocity. Following an extensive series of tests carried out by Bristol Siddeley Engines in the course of their noise research it was apparent that the accepted form of Strouhal number was not very satisfactory, as indeed had been reported by other workers, and an attempt was made to find a better parameter.

Over the fairly wide range of temperatures and pressures covered by Bristol Siddeley model tests and for nozzles ranging from a 1.5 inch diameter model to the Olympus engine at 22 inches diameter, the use of Strouhal number with nozzle exit velocity substituted for fully expanded jet velocity leads to a satisfactory correlation, though the small number of subsonic tests included in the programme show rather more spread than the supersonic ones.

Investigation

The first part of the investigation dealt with the influence of diameter. Results were taken from various Bristol Siddeley tests and including as a check, a test point on an Avon engine obtained from data published by Rolls Royce. Tests were chosen for which the conditions in the jet were as near identical as possible so as to isolate the effect of diameter and it was found that the product of frequency and diameter successfully correlated the spectra.

For the investigation of the effect of pressure and temperature, results were used from a programme in which a 1.5 inch diameter nozzle was tested at pressures of from 7.5 to 30 p.s.i.g. and at temperatures of 400, 600, and 800°C. Using the normal Strouhal number to correlate the frequency spectra resulted in a considerable spread in the results, apparently the consistent effect of changes of the pressure and temperature of the jet. The use of nozzle exit velocity in place of fully expanded jet velocity when deriving Strouhal number lead to a much improved correlation. The tests involving a subsonic jet, on which the correlation is not completely satisfactory, are probably too few in number entirely to eliminate experimental scatter.

The method proved successful when extended to other model tests, including unheated jets, and to full scale engine results though in this case the range of temperatures and pressures covered by normal operating conditions is too small for any dramatic improvement in correlation to be apparent.

In view of certain difficulties experienced in obtaining agreement between the overall noise levels of heated and unheated jets using fully expanded jet velocity as a correlating parameter, the possibility of substituting nozzle exit velocity in this case also was considered. Assuming the noise level to be dependent on nozzle diameter, nozzle density and nozzle velocity it is possible to fit all the supersonic points on to a single line using the normal diameter squared correction and a factor of density to the fifth power. However the subsonic points do not follow this empirical relationship and the data at present available is insufficient to carry the investigation any further.

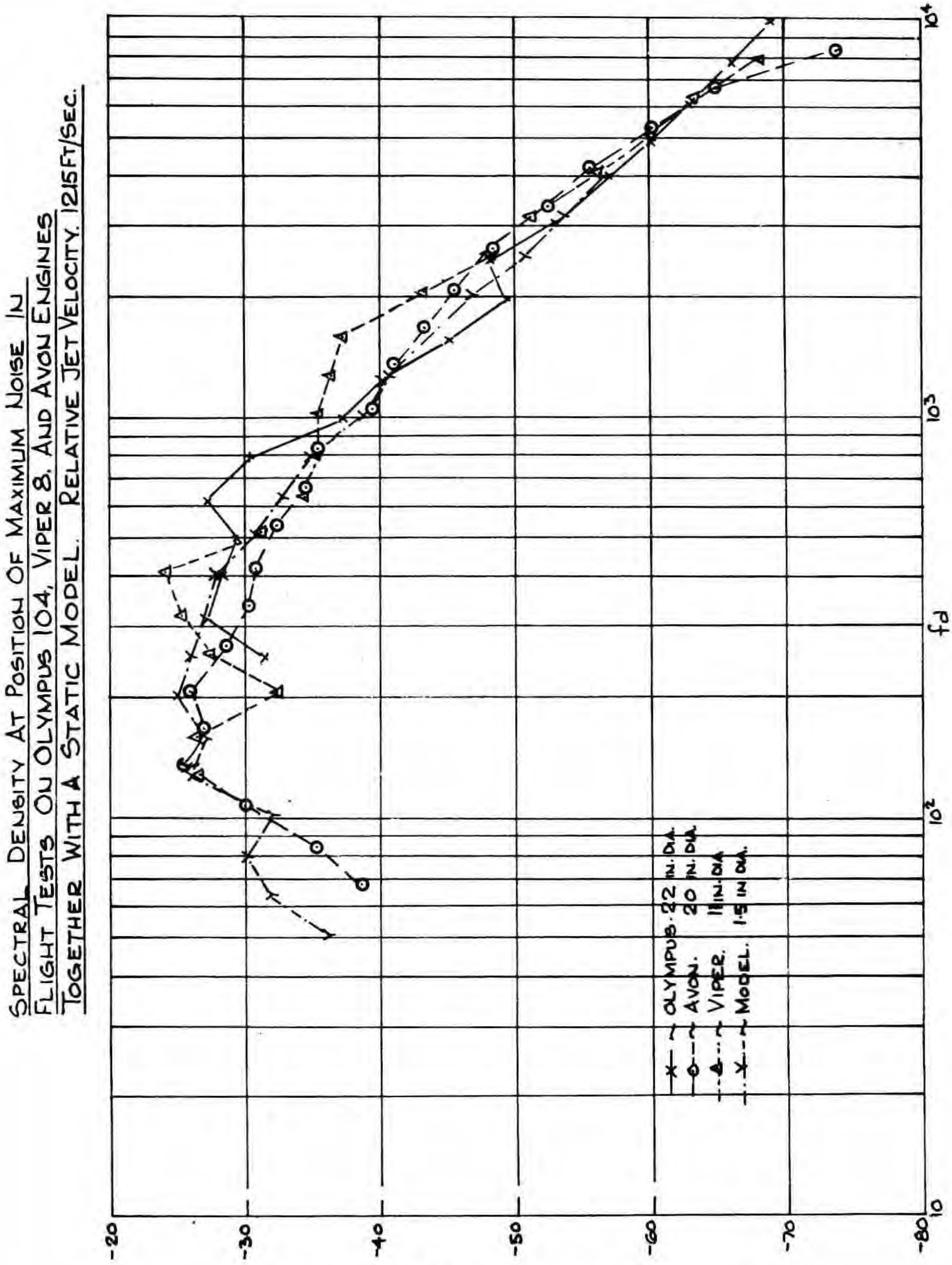
SPECTRAL DENSITY AT POSITION OF MAXIMUM NOISE IN
FLIGHT TESTS ON OLYMPUS 104, VIPER 8, AND AVON ENGINES
TOGETHER WITH A STATIC MODEL. RELATIVE JET VELOCITY. 1215FT/SEC.
SPL/CYCLE -(SPL o/A - 10log10 1/d)~db
-20
-30
-40
-50
-60
-70
-80
10
10²
fd
10³
10⁴
OLYMPUS 22 IN. DIA.
AVON. 20 IN. DIA.
VIPER. 18 IN. DIA.
MODEL. 1.5 IN DIA.

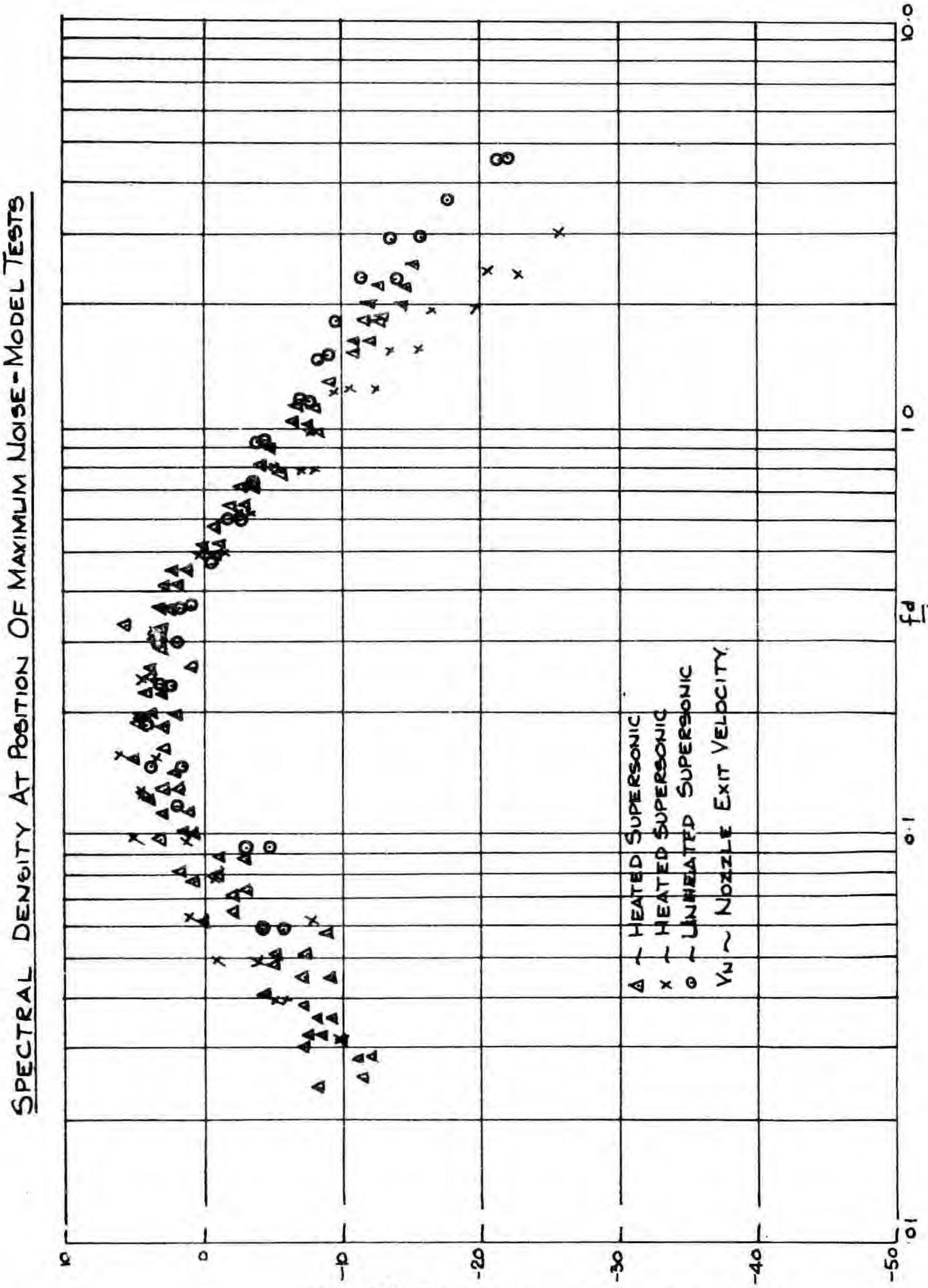
SPECTRAL DENSITY AT POSITION OF MAXIMUM NOISE - MODEL TESTS
SPL/CYCLE - (SPL o/A - 10 log10 Vd/d) ~ db
Δ - HEATED SUPERSONIC
x - HEATED SUPERSONIC
o - UNHEATED SUPERSONIC
VJ ~ NOZZLE EXIT VELOCITY
fd/Vj
0.1
1.0
10
0
-10
-20
-30
-40
-50

M45

FOURTH INTERNATIONAL CONGRESS ON ACOUSTICS
COPENHAGEN 21.-28. AUGUST 1962

THE NEW ACOUSTIC FACILITIES AT UCLA

R. W. LEONARD, I. RUDNICK, L. P. DELSASSO

Introduction

We are pleased to be able to report to the Congress on the development of the new facilities for acoustics at the University of California on the Los Angeles campus. This development is a part of the general expansion of the Department of Physics and will be located in the new Physics Building, Unit II, which is in the process of construction on a site just south of Unit I where all of the Physics Department is located at the present time. The 90,000 square feet of net usable floor space in Unit II plus the space in Unit I will more than double the space occupied by the Department of Physics at the present time. Even in a climate as mild as that in Southern California, it is pleasant to look forward to Unit II as a building completely air-conditioned with humidity control.

The net usable square feet of floor space in Unit II set aside for acoustics is 12,500. Of this total 1600 is marked for teaching laboratories; 8000 is to be used as research space; 2300 is occupied by the special facilities which include an anechoic room, a transmission room, a reverberation room, and an under-water sound laboratory; and 600 for storage space.

The special facilities for acoustics are located in a wing separated from the main building by a vibration break. This wing, which has two floors above ground and one below, provides the height necessary for the anechoic room. The research and teaching laboratories are located both in the wing and in the main building on the first and second floors. As a matter of interest, the main building has six floors above ground level and two below.

Teaching Laboratories

This space will have facilities quite similar to the research laboratories. A greater number of circuits on individual breakers will be supplied to reduce the interference between student groups working on different experiments. To provide a maximal flexibility in their use, these rooms will have no built-in furniture except the sink enclosures.

Under-Water Sound Laboratory

This facility contains a pool $12\frac{1}{2}$' x 16' with a depth of 10'. A closed control area with a clear view of the pool will be provided so that the electronic equipment used in experiments will have an environment of moderate humidity. The water will be filtered and treated with chemicals to prevent the growth of biological materials. The water temperature will be that of the surrounding earth which should be quite stable. The pool is located in the basement of the wing.

This space is to be regarded largely as a teaching facility although small scale research problems may be undertaken in this laboratory.

Research Laboratories

The research rooms vary in size from 375 to 600 square feet. The space allocated to an individual researcher will not be less than 275 square feet and probably not more than 500 square feet although this will depend on individual needs.

These laboratory rooms will be equipped with the usual utilities such as: compressed air, vacuum, gas, hot and cold water. Electricity will be supplied in single phase 115 volt outlets and three phase 208 volt outlets.

The acoustics group has adopted a policy of no built-in cabinets except the sink enclosures. It is believed that the use of movable furniture will result in much more flexibility and in a maximal use of floor area.

The airconditioning will provide a temperature control of about $\pm 2^{o}F$ for mean room temperatures lying between 70° and $75^{o}F$. The relative humidity control will hold the relative humidity to $50\% \pm 10\%$.

Anechoic Room

This space is designed to provide essentially free field conditions from 80 c.p.s. up to frequencies where the absorption of the air in the room becomes a dominant factor. The upper useful frequency limit will depend on temperature and humidity as well as the scale of the experiment. The lower limit is pretty well defined by the cut-off frequency of the wedges which for the four foot treatment used is about 80 c.p.s.

The available floor space in the room is 31' x 23 2/3' giving a floor area of 734 square feet. The vertical dimension of the anechoic room is 21' with the wire floor set about 5' above the wedges at the bottom of the room. This places the eyelevel of the experimenter at about the median height of the room. The wire floor consists of steel cables woven into a 2'x2' mesh with 200 lbs tension applied to each cable.

A light monorail is provided for the suspension of transducers which require the maintenance of accurate orientation while the experimenter moves about on the wire floor. This monorail runs parallel to the length of the room at a height of about 7' from the wire floor.

A heavy monorail enters through the large doors at the side of the anechoic room and turns to become parallel to the light monorail. The purpose of the heavy monorail is to facilitate the handling of large sources which may be brought into the anechoic room for test.

Reverberation Room

The reverberation room has the dimensions 30' x 19' x 24' giving it a volume of 13,700 cubic feet or 390 cubic meters. This is a little over twice the volume of our present reverberation room. The ratios of the dimensions of the new room are very close to the 2 which should reduce the number of degenerate modes at the lower frequencies. The room is rectangular with plane parallel walls. The walls are of 8 inch reinforced concrete as are the floor and the ceiling.

No additional diffusion over that supplied by the room itself is planned at the present time. It may prove necessary to add fixed diffusers after the room has been tested. The low-frequency sound source will be placed in one corner of the room where it will excite a maximal number of normal modes per half octave bandwidth. A number of high-frequency sources may be required to produce a diffuse

sound field in the presence of the molecular sound absorption in air. The microphone used to pick up the sound will probably be placed in a corner of the room where the sound pressure is a maximum for all normal modes excited by the sources.

Transmission Room

The transmission room is identical in size and construction to the reverberation room. The only difference between the two rooms is in the number of doors opening into each. The transmission room has 5 doors while the reverberation room has only the two connecting it to the transmission room. These two sets of doors when open provide test openings for transmission tests on 8' x 8' and 7' x 3'6" panels. The larger opening is for testing partition sections; the smaller opening for testing doors.

During transmission tests, the transmission room will act as the source room, and the reverberation room as the receiving room. The use of two large rooms will provide a more nearly diffuse sound field in the source and receiving room during the test. The fact that the two rooms are essentially identical in their acoustics may permit the use of equivalent points in the two rooms for microphone pickup and thus eliminate the space averaging procedures which are necessary at the present time.

A heavy monorail serving both the transmission room and the anechoic room comes in at the top of the doors leading to the loading area. This will make it possible to handle heavy sound sources and test panels.

Vibration Isolation of the Special Purpose Rooms

The anechoic room, the reverberation room, and the transmission room are separate structures within the external shell of the building. Each one of them is isolated by a set of air springs located around the perimeter of the floor just below the supporting beams. The anechoic room, because of its lighter structure, requires only 48 of these springs. The other two rooms require 60 springs each. The total number of springs for each room is divided into four groups supplied from a separate manifold. This grouping is necessary for stability against rolling or pitching displacements. Each individual spring is supplied with a shut-off valve so that it may be removed for repair or replacement without deflating the other springs in the same group. The operating pressure for the springs in our application is about 90 pounds per square inch.

An air spring consists of a light-weight tubeless casing which seals to a flat plate at the top where it is held in place by a shaped washer. The casing passes downward through a constraining cylinder, takes on a reentrant form and seals to a pedestal smaller in diameter than the constraining cylinder. The constraining cylinder is attached to the top plate by four straps. This markedly increases the shear rigidity of the whole assembly by preventing the constraining cylinder from rocking relative to the top plate which is attached to the load above in such a way as to prevent the top plate from rocking. The pedestal of the air spring fastens to the supporting surface below.

The loading vs. height of spring is essentially a hyperbolic curve with small irregularities due to the variation of the effective area with spring height. Calculations based on data received from the General Tire and Rubber Company of Wabash, Indiana, indicate that the natural frequencies of the rooms will be less than 2 cycles per second for vertical motion.

The air springs appear to have enough damping so that no additional damping is necessary.

Slides will be shown.

N45

FOURTH INTERNATIONAL CONGRESS ON ACOUSTICS
COPENHAGEN 21.-28. AUGUST 1962

SOME RESULTS ON USING A SIGNAL WITH A CONTINUOUS SPECTRUM FOR DISTORTION MEASUREMENTS.

S.BOEL PEDERSEN,
ACOUSTICAL LABORATORY, ROYAL TECHNICAL UNIVERSITY, COPENHAGEN, DENMARK

Introduction.

For the determination of the nonlinear distortion of a quadripole it is common practice to use a test signal consisting of one or several pure tones. The harmonics and intermodulation frequencies arising from the nonlinearity are in well known ways related to the linear transfered signal.

However, in many cases of practical interest the mentioned test signals cannot be said to be adequate signal models. This is true when speaking about loudspeakers, headphones, amplifiers, and similar devices which are determined to reproduce signals with a statistical character.

Testing such items a more natural test signal is e.g. bandlimited white noise which can be treated mathematicaly in a rather simple way. However, working with a signal with a continuous power spectrum it is nessesary to get a powerfree domain in the input spectrum so that the distortion products can be measured in that frequency band in the output signal. A test procedure along this line has been in use since the late 193o's in long line telephony. A similar test method for use in the AF-range has been proposed by V.M.Volf (A) in 1954 and apparently independent hereof by A.Darré (B) in 1955.

In the following sections a short summary of the theoretical basis of the test method shall be given.

Theory.

If a test signal $x(t)$ is applied to the input of a nonlinear device, the output signal $y(t)$ can be written

$$y(t) = g(x(t)).$$

In certain cases the function $g(x(t))$ can be approximated by

$$g(x(t)) = \sum_{n=o}^{m} a_n \, x^n(t). \qquad (1)$$

For a nonlinear network of very simple kind - i.e. where all distortion takes place in one frequency independent nonlinear device - the constants a_n can be determined by a measurement using one pure tone only.

Using the test method suggested above (with a gaussian test signal) it is not convenient to use the approximation (1) for the transfer function of the nonlinear device. As shown by several authors (e.g. Rice (C)), the evaluation of $g(x(t))$ in Hermite polynomials simplifies the mathematical treatment of the problem. If $R_x(0)$ is the autocorrelation function of the input signal $x(t)$ for $\tau = 0$,

$$g(x(t)) = \sqrt{\frac{R_x(0)}{2}} \sum_{i=o}^{k} b_i \, H_i\left(\frac{x(t)}{\sqrt{2R_x(0)}}\right) \qquad (2)$$

where the b_i's are constants and $H_i(z)$ is the Hermite polynomial of i'th order of argument z.

(Using the quantity $\sqrt{R_x(0)/2}$ in front of the summation the special case $y(t) = x(t)$ takes place for $b_1 = 1$, all other $b_i = 0$).

It can now be shown that the autocorrelation function $R_y(\tau)$ of y(t) can be calculated from

$$\frac{R_y(\tau)}{R_x(0)} = \sum_{i=o}^{k} 2^{i-1}\ i!\ b_i^2 \left(\frac{R_x(\tau)}{R_x(0)}\right)^i \qquad (3)$$

In most cases the two limits of summation (m in (1) and k in (2) & (3)) will be equal for convergence reasons. Therefore, a relation between the a_n's and the b_i's can be established.

To compute the power spectral density of the output signal from eq. (3) it is nessesary to handle integrals of the form

$$\int_{-\infty}^{\infty} R_x^{\,n}(\tau)\ e^{-j2\pi f\tau} d\tau\ ,\ n = 0,\ 1,\ 2,\ \ldots.$$

It can be shown that

$$\int_{-\infty}^{\infty} R_x^{\,n}(\tau)\ e^{-j2\pi f\tau} d\tau = \int_{-\infty}^{\infty} S(f-f')\ S^{(n-1)}(f')\ df'$$

where the integral to the right of the sign of equation is the convolution integral of the input spectrum with the (n-1)'th convolution integral of the input spectrum. In table 1 the mathematical expressions for the first four convolution integrals are given for the case that $S_x(f)$ is bandlimited white noise from zero to B (c/s).

The power spectral density $S_y(f)$ of the output function y(t) can thus be expressed as a sum of convolution integrals i.e.

$$S_y(f) = \sum_{i=o}^{k} c_i\ S_x^{(i)}(f) \qquad (4)$$

where the c_i's are constants depending on the actual nonlinear network.

Considering eq. (4) the following quantity

$$D(f) = \frac{\sum_{i=2}^{k} c_i\ S_x^{(i)}(f)}{\sum_{i=1}^{k} c_i\ S_x^{(i)}(f)} \qquad (5)$$

can be used as a distortion measure. (It shall be noted that the DC-term (i = o) has been left out here as being of little practical interest). D(f) is of course a function of frequency.

When using this measure of distortion, knowledge of the nominator of eq. (5) can be obtained by introducing a notch in the input signal power spectral density i.e., a frequency interval in which the power is reduced to a great extent. The power spectral density at the location of this notch in the output spectrum will then be made up from distortion products.

The bandwidth of the notch and its position in the input spectrum affects the magnitude of the various distortion products in the output spectrum. Fig. 1 shows the reduction of the second and third order distortion products resulting from the introduction of a notch of bandwidth ΔB in a bandlimited white noise spectrum extending from zero to B (c/s). The relative width of the notch is used as parameter. A correction for the loss of input power as a consequence of the presence of the notch is applied to the curves so that the nonlinear device is fed with the same amount of power in the two cases.

Example.

A simple example will illustrate some of the results that can be obtained. Consider a very simple frequency independent nonlinear device whose output signal y(t) is given as follows in terms of the input signal x(t)

$$y(t) = a_1 x(t) + a_2 x^2(t) + a_3 x^3(t) \ .$$

In this case

$$D(f) = \frac{2a_2^2 S_x^{(2)}(f) + 6a_3^2 S_x^{(3)}(f)}{(a_1 + 3a_3 R_x(0))^2 + 2a_2^2 S_x^{(2)}(f) + 6a_3^2 S_x^{(3)}(f)} \ .$$

Using bandlimited white noise as test signal and f = B/5 the figures 2, 3, and 4 show D(f) as a function of $\beta = a_3/a_1$ with $\alpha = a_2/a_1$ as parameter for 3 different values of $R_x(0)$.

References.

A: V.M.Volf, Journal der techn. Physik (UdSSR), 24(1954)2054.

B: A.Darré, Frequenz, 9(1955)84 & 127.

C: S.O.Rice, B.S.T.J., 23(1944)282, B.S.T.J., 24(1945)46.

Table 1.

Freq. f	0<f<B	B<f<2B	2B<f<3B	3B<f<4B	4B<f<5B	f>5B
$S(f)$	A	0				
$S^{(2)}(f)$	$A^2(2B-f)$		0			
$S^{(3)}(f)$	$A^3(3B^2-f^2)$	$A^3(f^2/2-3Bf+9B^2/2)$		0		
$S^{(4)}(f)$	$A^4(f^3/2-2Bf^2+16B^3/3)$		$A^4(-f^3/6+2Bf^2-8B^2f+32B^3/3)$		0	
$S^{(5)}(f)$	$A^5(f^4/4-5B^2f^2+115B^4/12)$	$A^5(-f^4/6+5Bf^3/3-5B^2f^2+5B^3f/3+55B^4/6)$		$A^5(f^4/24-5Bf^3/6+25B^2f^2/4-125B^3f/6+625B^4/24)$		0

Figure 1.

Reduction in level of distortion products caused by an ideal notch of bandwidth ΔB as a function of the center frequency of the notch.

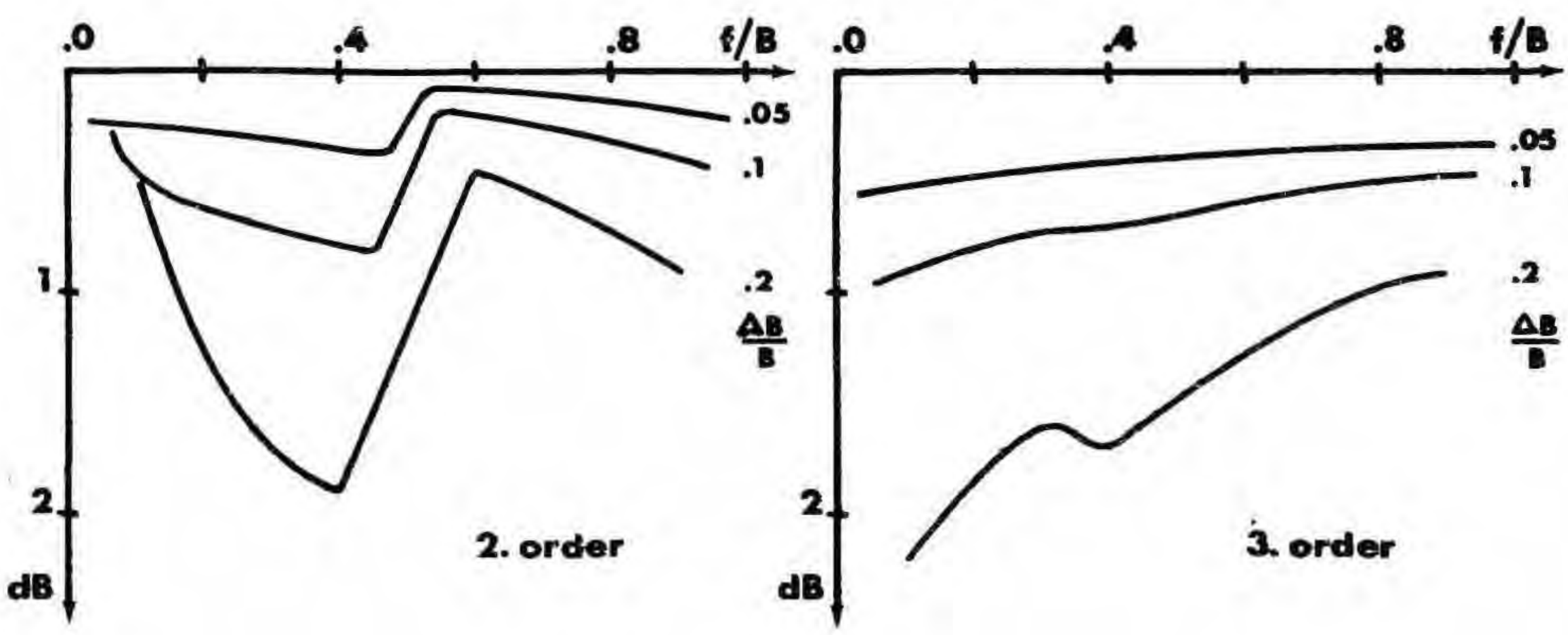

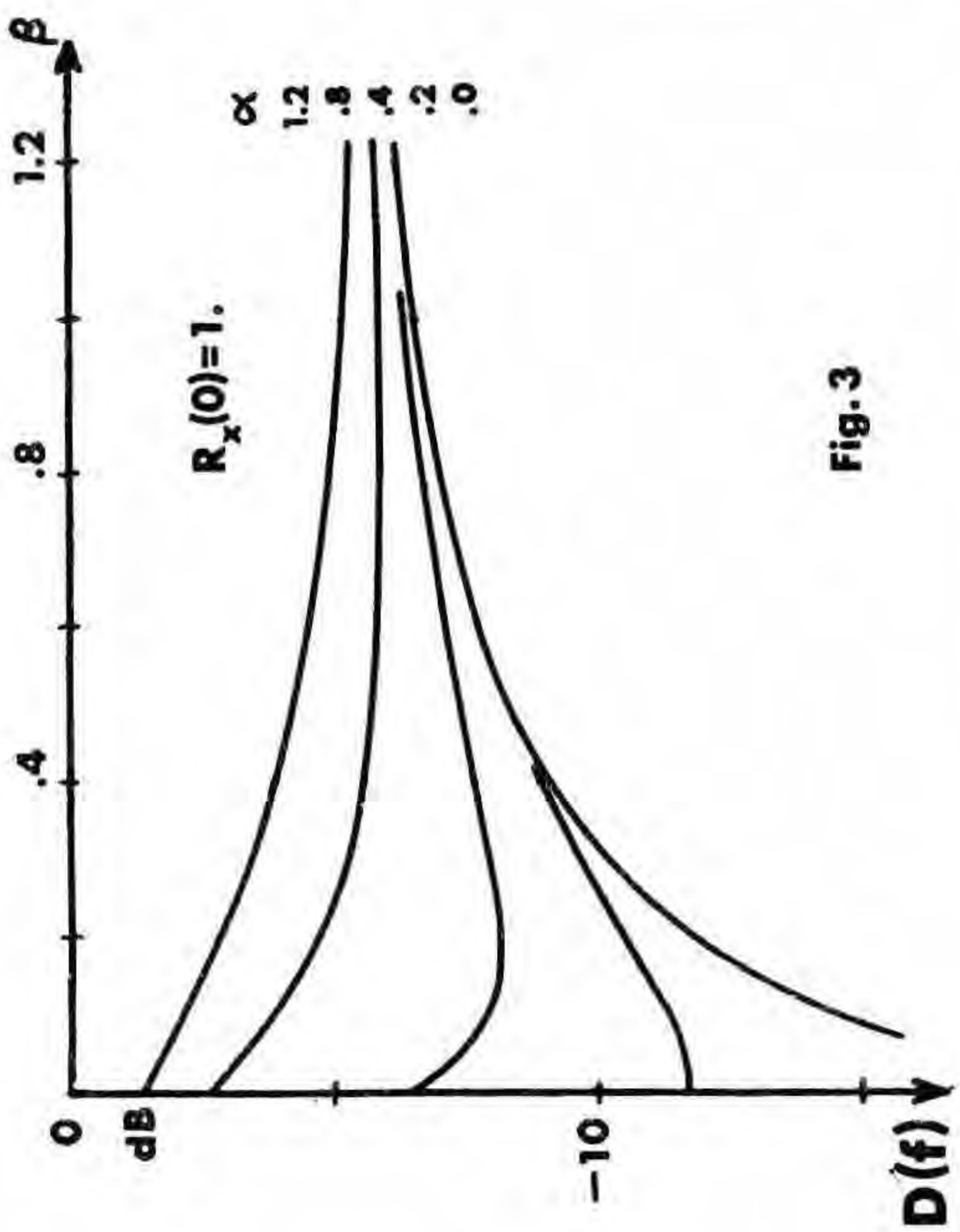

Fig. 3

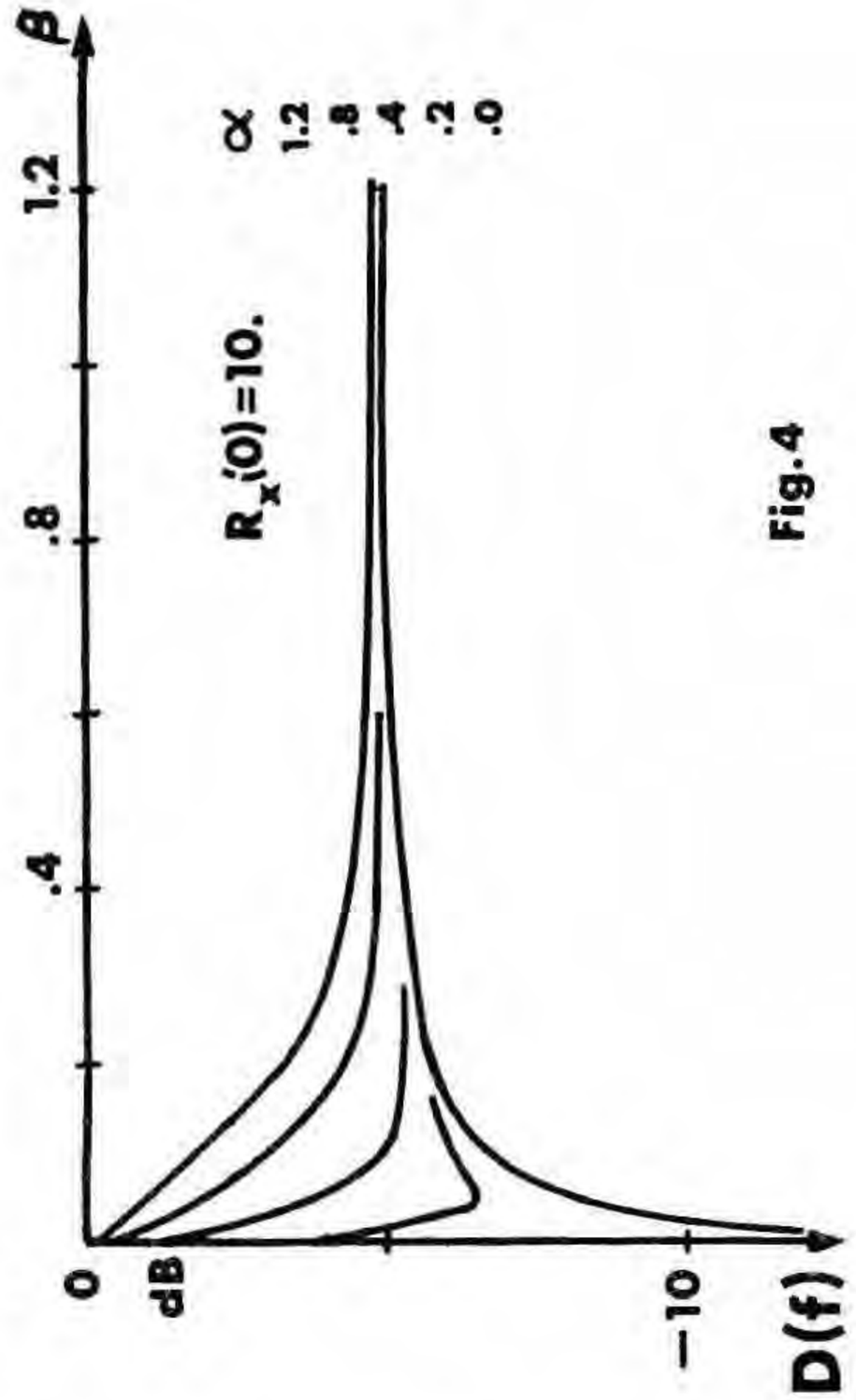

Fig. 4

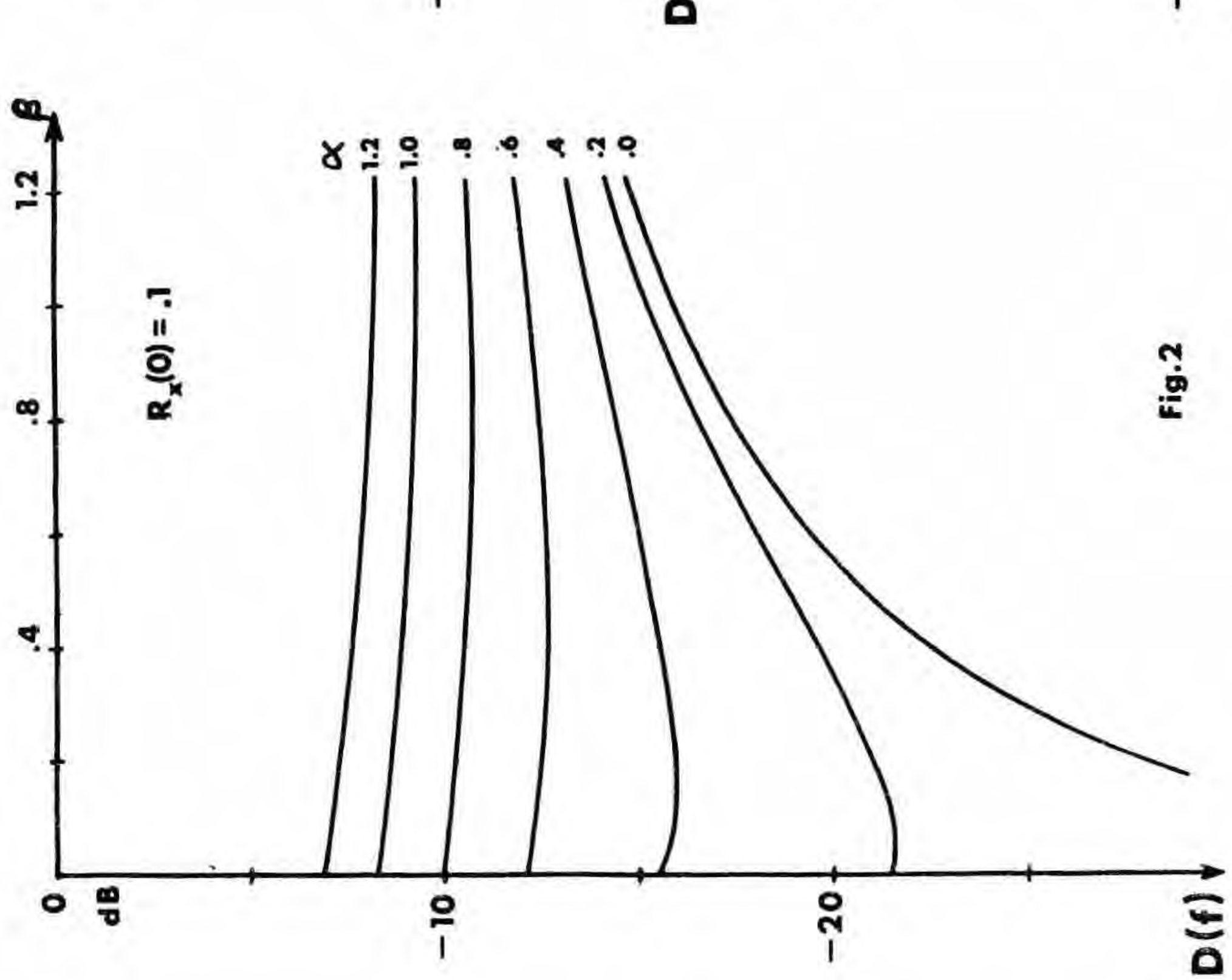

Fig. 2

045

FOURTH INTERNATIONAL CONGRESS ON ACOUSTICS
COPENHAGEN 21.-28. AUGUST 1962

On the Radiation Pressure of Standing Waves.

Z.A.Goldberg, K.A.Naugolnich

A sound wave impinging on an obstacle exets a constant pressure on it (radiation pressure). The amount of this pressure in certain conditions is measured by a volume density of the sound energy. A similar relation exists also for light pressure.

For example, the sound beam impinging normally on the boundary between two liquid media produces on it the radiation pressure $\overline{p'}$,which can be expressed by the formula [1] :

$$\overline{P'} = \overline{E}(1+k) ,$$

where E -volume density of sound energy, k - reflection coefficient, a bar above a letter indicates that time average is taken.

However in acoustics the nonlinear characteristics of the medium are sometimes to be taken into account.

In fact, according to Rayleigh 2 the radiation pressure produced by a plane standing wave on a rigid surface is expressed as follows:

$$\overline{p'} = (\gamma+1)\rho_0 v_0^2 = \frac{\gamma+1}{2}\overline{E'} , \qquad /2/$$

where ρ_0 -equilibrium density, v_0 -velocity amplitude, $\overline{E'}$ -time averaged energy density, $\gamma = \frac{\partial c^2}{\partial \rho_0}\frac{\rho_0}{c_0^2} + 1$ - nonlinear parameter, C_0- sound velocity. In the present paper 1)Rayleigh's data [2] , obtained for the case of free vibrations between two plane rigid boundaries, are generalized for a case of forced vibrations caused by a harmonic motion of one of the boundaries; 2) radiation pressure of standing spherical waves both for free and for forced vibrations are considered.

Jet's consider first a plane standing wave between two plane boundaries,

one of which is fixed and the other vibrates harmonically.

If Lagrange's coordinate of the vibrating boundary is $a_0 = 0$, coordinate of the fixed boundary is $a_1 = \ell$, than the sound fild between these boundaries can be described in such a way:

$$\xi = -\frac{A}{2}\,\frac{\sin k(\ell - a)}{\sin k\ell}\cos\omega t\,, \qquad /3/$$

where ξ -particle displacement, A -wave amplitude, k -wave number, ω -frequency. To obtain the radiation pressure on a fixed boundary we have to time average the equation of motion $\frac{\partial v}{\partial t} = -\frac{1}{\rho_0}\frac{\partial p}{\partial a}$ in respect to time. Taking into account the condition $\overline{\frac{\partial v}{\partial t}} = 0$ we get:

$$\overline{p'} = const\,. \qquad /4/$$

Now we use the equation of state $p' = c_0^2\rho' + \frac{\gamma-1}{2}\,\frac{c_0^2}{\rho_0}\,\rho'^2$ for determining this constant.

Averaging this equation in respect to time, applying /4/ and integrating according to a between the limits 0 and ℓ, we obtain:

$$const = \frac{c_0^2}{\ell}\int_0^\ell \overline{\rho' da} + \frac{\gamma-1}{2}\,\frac{c_0^2}{\rho_0}\,\frac{1}{\ell}\int_0^\ell \rho'^2 da\,. \qquad /5/$$

Taking into account the equation of continuity $\rho dx = \rho_0 da$, where $x = a + \xi(a,t)$ -Euler's coordinate, and the relation $\rho dx = (\rho_0 + \rho')(da + d\xi)$ and averaging in the respect of time we can transform the first integral in the right side /5/ to the form:

$$\int_0^\ell \overline{\rho' da} = -\int_0^\ell \rho'\frac{\partial\xi}{\partial a}\,da \qquad /6/$$

Using the relation $\rho' = -\xi_a$, we obtain from /4/ and /5/:

$$\overline{p'} = \frac{\gamma+1}{2\ell}\,\rho_0 c_0^2\int_0^\ell \overline{\left(\frac{\partial\xi}{\partial a}\right)^2} da \qquad /7/$$

Substituting /3/ in /7/ we find sound pressure on a fixed wall:

$$\overline{p'} = \frac{\gamma+1}{2}\,\rho_0 v_0^2\left(1 + \frac{\sin 2k\ell}{2k\ell}\right) \qquad /8/$$

Note, that if $k\ell$ approaches $2n\pi$, where n -an integer while v_0 is held constant, than /3/ gives:

$$\xi = \frac{V_0}{\omega} \sin ka \cos \omega t \qquad /9/$$

while /8/ assume the forme /2/.

Now let's consider a standing spherical wave between two concentric spheres with the internal one pulsating harmonically and the external one fixed.

If R is Lagrange's spherical coordinate this standing wave in a linear appoximation can be described by the equation:

$$\xi = \frac{A}{\omega}\left(\frac{k \cos kR}{R} - \frac{\sin kR}{R^2} \right) \sin \omega t \,. \qquad /10/$$

For determination of radiation pressure on fixed external sphere we use the equation of motion:

$$\frac{\partial V}{\partial t} = - \frac{r^2}{R^2} \frac{1}{\rho_0} \frac{\partial P}{\partial R} \qquad /11/$$

where $r = R + \xi(R,t)$ -Eulear's spherical coordinate.

Integrating /11/ with respect to R we obtain

$$\rho' = - \rho_0 \int_{R_1}^{R_2} \frac{R^2}{r^2} \frac{\partial V}{\partial t} dR + C_1 \,. \qquad /12/$$

Here R_1, R_2-radii of internal and external spheres respectively, C_1 -constant.

Now we use the equation of state in order to determite this constant. Substituting in it the equation /12/, multiplied by r^2 ,integrated with respect to r ,averaged with respect to time and using the equation of continuity we would obtain the relation for C_1 .

In view of the complicity of this equation we will restrict ourselves with the consideration of some particular cases.

For example, if $kR_1 = 2n\pi$ we find the following equation for radiation pressure on a fixed sphere

$$\overline{\rho'}_{R_1} = \rho_0 \frac{A^2 k^2}{8} (3\gamma - 1) \frac{\sin^2 kR_2}{R_1^2} + \rho_0 k^2 A^2 \frac{3}{8} (\gamma - 1) \left[\frac{R_2 \sin^2 kR_2 - R_1}{R_2^3 - R_1^3} - \frac{\sin^2 kR_2}{R_2^2} \right] \qquad /13/$$

If $R_1 = 0$ $\overline{P'_{R_2}} = \rho_0 \frac{A^2 k^2}{8} (3\gamma - 1) \frac{\sin^2 kR_2}{R_2^2}$

which agrees exactly with the result of [3] .

If $R_1 \approx R_2 \gg \lambda$ where λ -wave length the expression /10/ assumes the form

$$\xi = \frac{A}{\omega R_1} k(l-x) \sin kR_2 \sin \omega t . \qquad /14/$$

The same approximation gives /8/ for $\overline{P'}$.

We remark in conclusion that the radiation pressure is exerted the internal sphere too.

This circumstance gives a theoretical possibility of creating original "acoustic bearings", a central part of which would be supported by sound pressure. However, there are some difficultes in putting these ideas into practice [4] .

Literature Cited

1. L.D.Landau, E.M.Lifchiz. Mechanics of Continuous Media,CITTL, Moscow, 1954.

2. Reilegh. On the momentum and pressure of gaseous vibrations and on the connexion with the virial theorem. Phil.Mag. 1905. X. 364-374.

3. R.Lucas. On the radiation pressure of spherical waves. Compte. Rend. 1950. 230. 2004-2006.

4. M.I.Segal. The acoustical bearing. J.Acoust.Soc.Amer. 1961. 33, 5, 566-574.

P45

FOURTH INTERNATIONAL CONGRESS ON ACOUSTICS
COPENHAGEN 21.-28. AUGUST 1962

Method of Measurements of Acoustic Material Visco-Elastic Parameters.

E.A.Vovk, R.N.Viktorova, V.V.Tiutekin.

Measurements of complex Young's modulus $\bar{E} = E(1-i\eta)$ of acoustic materials in continuous frequency range from 200 to 3000sps can be conveniently made using samples in the form of cylindrical rods, only simple equipment is needed for these measurements.

The block diagram of the experimental set-up is shown in the fig.1. The coil of electrodynamic transducer (II) is fed by the voltage of a sound generator (I). Duraluminium pintle /1/ is fastened to the coil of electrodynamic transducer on the upper end of which a piston /2/ is screwed. A small pick-up /4/ is fastened to the bottom of this piston. The whole represents the moving unit of the set up. A sample to be measured /3/ is placed on the piston and acoustic contact between these two is achieved either with water or with oil. The voltage from pick-up is proportional to velocity of moving unit and measured by the vacuum tube voltmeter (IV) via amplifier (III). The phase shift between this voltage and driving voltage is measured by phasometer (V). (VI)-control oscilloscope.

The velocity $\bar{\xi}$ (bar upper indicates that the value is complex) of the coil is related to mechanical and electrical parameters of the system by the relation.

$$\bar{\xi} = \frac{\bar{E}\,K}{K^2 + \bar{Z}_{el}\,\bar{Z}_m} \qquad /1/$$

where $\bar{E}$ -driving voltage, K -electromechanical coupling coefficient. $\bar{Z}_{el}$ -electrical impedance of the coil. $\bar{Z}_m = \bar{Z}_o + \bar{Z}_e$ -total mechanical impedance of the system, $\bar{Z}_o$ -impedance of the moving system, $\bar{Z}_e$ -load

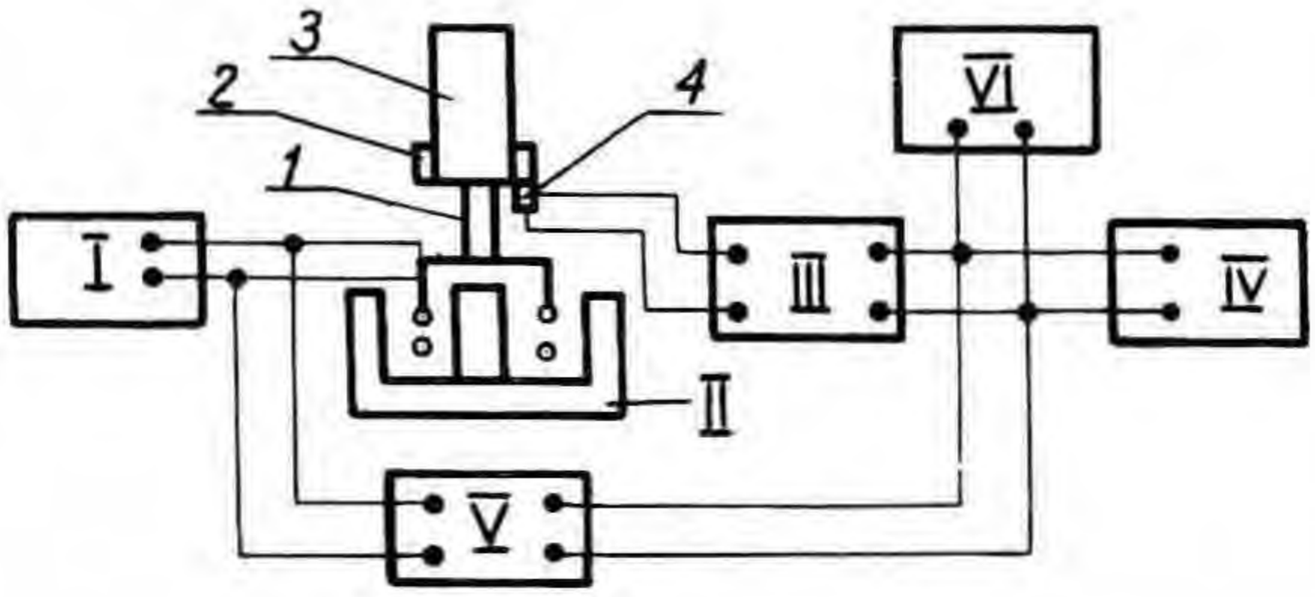

Fig.1

impedance.

The value E during the experiment is held constant; values of $K, \bar{Z}_{el}, \bar{Z}_0$ can be eliminated by means of special measurements with loads of known impedance. For this purpose $\bar{\xi}$ is measured without load ($\bar{Z}_l = 0$ $\bar{\xi}_0 = \bar{\xi} e^{i\varphi_0}$) with a load in form of a known mass m ($\bar{Z}_l = -i\omega m$ $\bar{\xi} = \xi_m e^{i\varphi_m}$) After that, measuring the velocity of the system with the sample ($\bar{\xi} = \xi_x e^{i\varphi_x}$) we can determine its impedance $\bar{Z}_{lx}$ according to formula:

$$\bar{Z}_{lx} = \frac{\bar{\alpha}_x - 1}{\bar{\alpha}_m - 1}(-i\omega m) \qquad /2/$$

where $\bar{\alpha}_x = \frac{\xi_0}{\xi_x} e^{i(\varphi_0 - \varphi_x)}$, $\alpha_m = \frac{\xi_0}{\xi_m} e^{i(\varphi_0 - \varphi_m)}$.

The experiment proved that due to small losses in a free system α_m is real and $\varphi_0 = \varphi_m$. The value $M = \frac{m}{\alpha_m - 1}$ represents the effective mass of the moving system. The length of the experimental sample is l, its cross section is S, its impedance is equal to

$$\bar{Z}_{lx} = -i\rho\bar{c}\, tg\, \bar{\kappa} l \qquad /3/$$

where $\bar{c}$ -velocity in the rod.

The values of E and η are obtained from equation /3/ with the aid of special nomogram.

Frequency characteristics for measured values of α_x and φ_0 (see equation /2/) for an experimental sample from plastic in the form rod with l = 8cm and S = 12,5 cm^2 are shown in the fig.2.

The fig.3 represents the frequency dependence of the sample impedance $\bar{Z} = R - iX$ from wich elastic complex modulus is calculated.

Results obtained by this method are in good agreement with that of another methods.

The experimental samples and the electrodynamical transducer could be placed together in a thermostat and in this case E and η could be measured at different temperatures.

Using a recorder it is possible to automatize measurements.

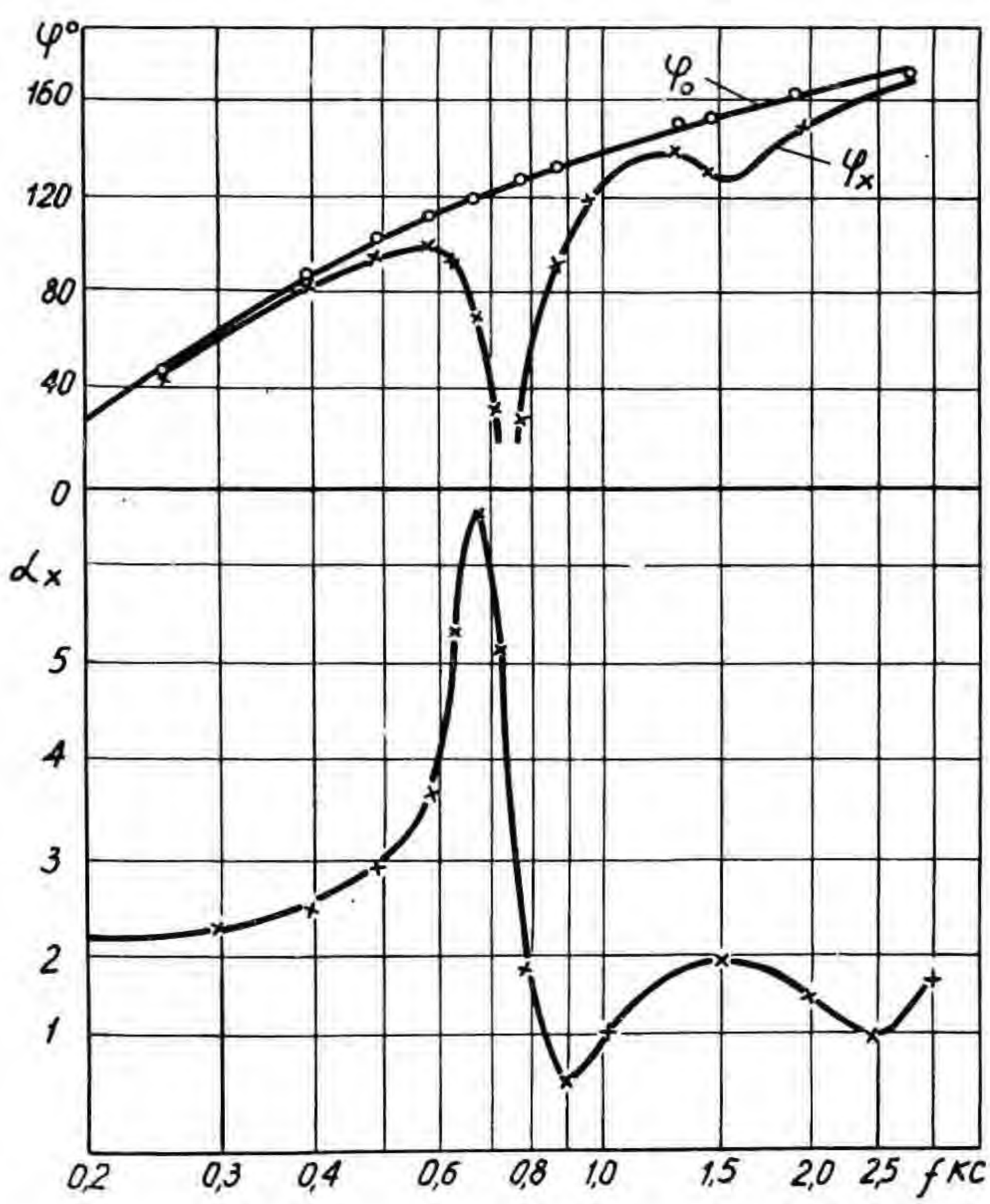

Fig.2

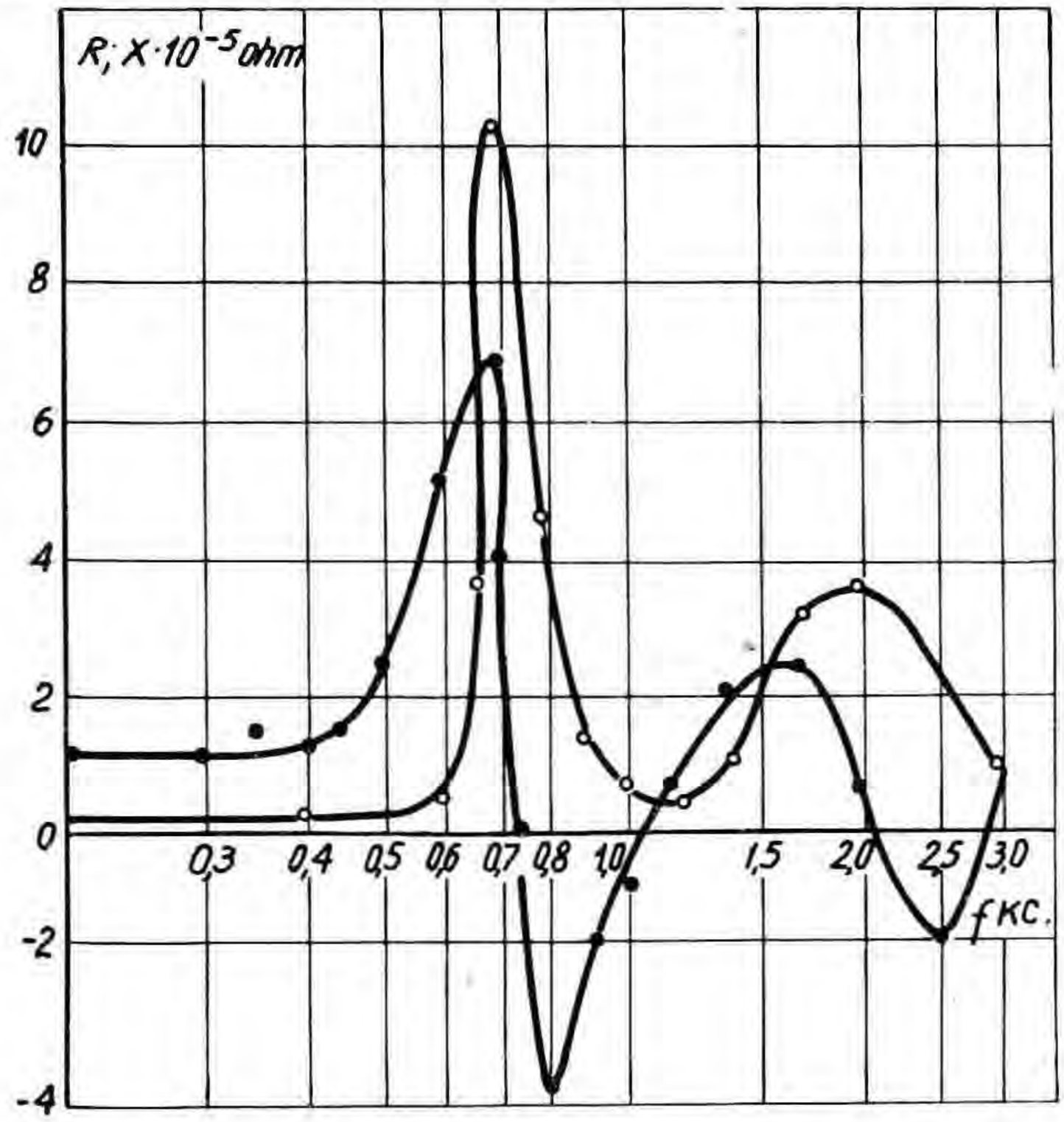

Fig.3

G46

FOURTH INTERNATIONAL CONGRESS ON ACOUSTICS
COPENHAGEN 21.-28. AUGUST 1962

AN ANALYSIS OF SPEECH SPECTRA IN TERMS OF A MODEL OF ARTICULATION*

J. M. Heinz, Research Laboratory of Electronics, Massachusetts Institute of Technology, Cambridge, Mass.. U. S. A.

I. Introduction

The analysis-by-synthesis technique as applied to the analysis of speech spectra requires a model capable of generating speech spectra when given the values of certain parameters which are descriptive of the speech production.[1] The analysis procedure consists of varying the input parameters in the model until an output spectrum is obtained which optimally matches the spectrum to be analyzed. The values of the parameters needed to give this best match constitute the results of the analysis. This procedure is schematized in the block diagram of Fig. 1.

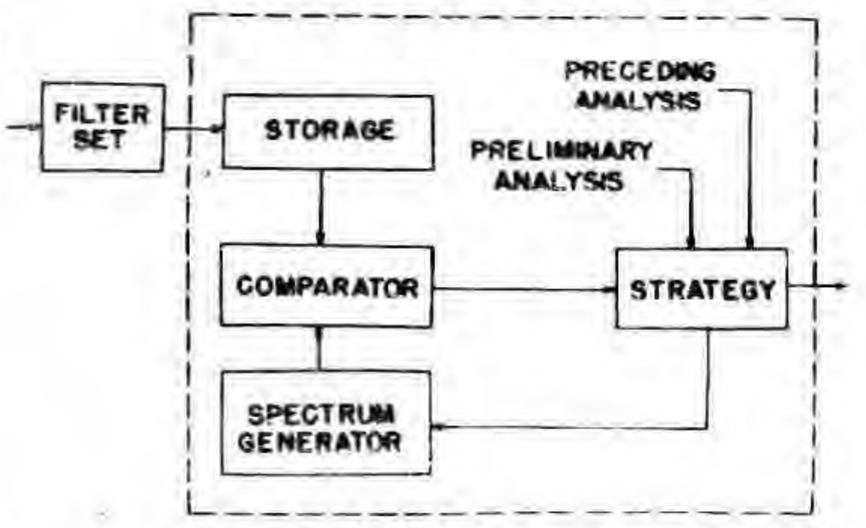

Fig. 1. Block diagram of an analysis-by-synthesis process for the reduction of speech spectra.

Models which have been utilized previously in such systems have as their input parameters the locations in the complex-frequency plane of the poles and zeros of the vocal-tract transfer function. The poles of the transfer function are independent of the source location and depend only on the vocal-tract configuration.[2] Thus, the poles move in a continuous manner during the production of connected speech even though the source may change in type and location. One difficulty with models of this type arises from the fact that the zeros do depend on source location as well as on the vocal-tract shape and so may appear and disappear and in general change in a discontinuous fashion as different types of sources are introduced at different locations within the tract. This discontinuous behavior of the zeros and the resulting drastic changes in the general characteristics of the speech spectrum make the tracking through connected speech of the parameters involved in this type of model very difficult. Furthermore, the number of parameters that need to be specified varies as zeros are introduced in the transfer function, leading to additional complications.

In order to investigate the possibility of analyses in which the parameters employed are more closely related to the physical processes involved in speech production, a different model is under study. In this model the input parameters are the cross-sectional areas of the vocal tract at a specified number of positions along the tract. Changes in these area parameters are closely related to changes in the physical dimensions of the vocal tract and therefore vary in a continuous way. Thus, it is hoped that these area parameters or other physical parameters simply related to these may prove useful in an analysis-by-synthesis scheme for speech analysis and may in addition

produce an even more efficient description of speech signals than the pole-zero description of the previous system.

II. The Spectrum Generator

The spectrum generator to be described is based on a model for generating speech spectra when vocal-tract area functions and source locations are known. The calculation of a spectrum takes place in two steps, though ultimately these steps will be combined into one. First, the locations of the poles and zeros of the transfer function are determined from the area parameters and, second, using the previous model,[1] the spectrum itself is determined. Since the distribution of acoustic losses within the vocal tract is not known in detail (and is of secondary importance here), an initial version of this model provides only the imaginary-axis coordinates (center frequencies) of the poles and zeros. Thus, the real-axis coordinates (half-bandwidths) also constitute input parameters for this version of the model.

An acoustic description of the vocal tract is provided by Webster's horn equation, expressing the approximate behavior of acoustic volume velocity $U(x,t)$ in a non-uniform tube in terms of the area of the tube $A(x)$.[3,4,5,6] For exponential time dependence of complex frequency $s = \sigma + j\omega$, the wave equation reduces to a frequency dependent equation involving the complex volume velocity $U(x,s)$:

$$A \frac{d}{dx} \left(\frac{1}{A} \frac{dU}{dx}\right) - \left(\frac{s}{c}\right)^2 U = 0 \qquad (1)$$

The appropriate homogeneous (source-free) boundary conditions represent an assumption of infinite glottal impedance ($U = 0$) and a constraint on the ratio of complex sound pressure $p(x,s)$ to complex volume velocity $U(x,s)$ imposed by the radiation mass loading at the mouth. As losses are not included in these equations, all such characteristic values of s must be imaginary so that the poles obtained all lie on the $j\omega$-axis.

With a modification of the boundary conditions, equation (1) can also be used to locate the zeros of the transfer function for a pressure-difference source (a pressure source "in series" with the vocal tract) located at a distance ℓ_1 from the glottis. Zeros in the output spectrum for such a source occur at frequencies which are "open-circuit" natural frequencies of that portion of the vocal tract lying between the glottis and the source. These are the frequencies at which the impedance looking back from the source toward the glottis has poles.[7,8] Since the source is in series with this impedance, the output at these frequencies is zero. The boundary conditions corresponding to open-circuit conditions are infinite glottal impedance and zero volume velocity at the source location. Thus equation (1) can be used along with the appropriate boundary conditions to find either the poles or zeros of the vocal-tract transfer function.

III. The Computer Program

A digital computer has been programmed to obtain solutions to equation (1) subject to the appropriate boundary conditions in order to determine the pole locations (and possibly zero locations) for a

given vocal-tract configuration. The tract is divided into a number of intervals of equal length and the differential equation is reduced to a difference equation for numerical solution.

In the present program the cross-sectional area can be specified at as many as 40 locations spaced as close as 1/2 cm apart. One version of the program provides a type-out of the pole and zero locations when an area function and source location are specified. In addition, an oscilloscope is available to display cross-sectional area and volume velocity as functions of distance along the tract while the program progresses through its calculations. A photograph of such a display is shown in Fig. 2 depicting an area function and a volume velocity distribution appropriate to the second formant frequency for the vowel /i/.

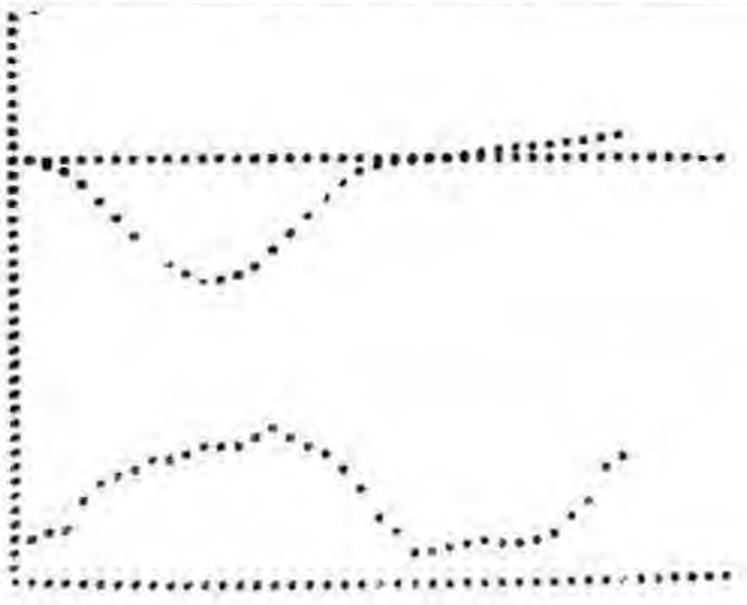

Fig. 2. Photograph of a cathode-ray tube display. The upper curve shows the volume velocity along the vocal tract at the second formant frequency. The lower curve shows the effective vocal-tract diameter versus distance along the tract. The configuration was derived from data for the vowel /i/ (Wendahl, R. W., Ph.D. Thesis, University of Iowa, 1957).

In order to reduce the number of input parameters for some applications, a slight modification of the Stevens-House three parameter model of articulation has also been programmed.[9,10] For this modification four parameters must be specified: (1) d_o, the location of the tongue constriction in the tract, (2) r_o, the radius at d_o, (3) A_o, the area of the mouth opening and (4) ℓ_o, the length of the mouth section. Thus, it is possible to generate an area function by specifying the four parameters and then to calculate the corresponding pole and zero locations.

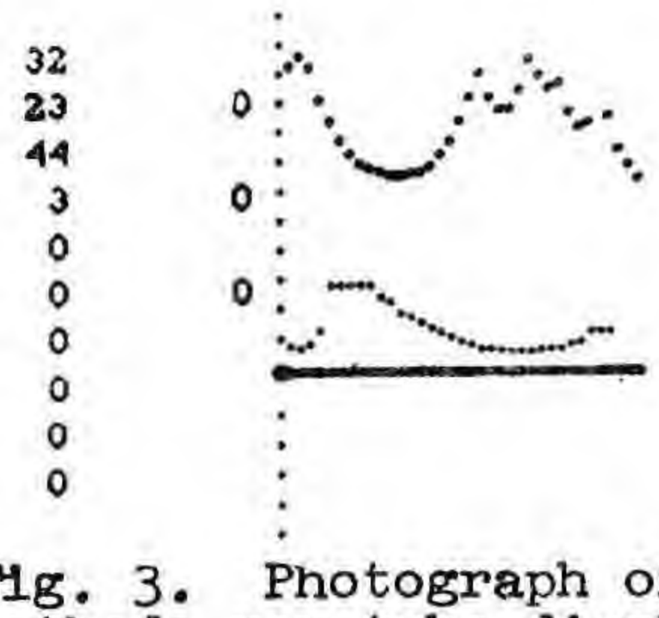

Fig. 3. Photograph of a cathode-ray tube display The lower curve depicts a vocal-tract diameter function generated by the four-parameter model for values appropriate to the vowel /i/. The upper curve shows the spectrum resulting from excitation of the tract with a volume velocity source at the glottis.

A second version of the program incorporates the first version, but goes further to calculate a spectrum from the lossless pole-zero locations plus pre-stored average bandwidth data. This spectrum is then available for comparison with actual measured speech in the manner described previously.[1] Fig. 3 shows a photograph of a cathode-ray tube display depicting an area function generated according to the four-parameter model with values of the parameters appropriate to the vowel /i/ as well as the resulting spectrum for a volume velocity source at the glottis.

IV. Conclusion

It is possible with these programs to compare an internally generated spectrum with an actual speech spectrum and to vary manually the input parameters until an optimum match is obtained. The results of the match are

parameters which relate to the physical dimensions of the vocal tract and thus make it possible to study the dynamics of the articulatory system through analyses of the acoustic signal. Currently, data are being collected by this procedure, particularly in the vicinity of vowel-consonant boundaries. It is hoped that the programs will prove useful also for investigating other possible models for generating vocal-tract area functions from the specification of a small number of parameters.

References

1. C. G. Bell, H. Fujisaki, J. M. Heinz, K. N. Stevens and A. S. House, Reduction of speech spectra by analysis-by-synthesis techniques, J. Acoust. Soc. Am. 33, 1725 (1961).

2. C. G. M. Fant, "Transmission properties of the vocal tract with application to the acoustic specification of phonemes," Technical Report No. 12, Acoustics Laboratory, Mass. Inst. of Tech., January 1952.

3. A. G. Webster, Acoustical impedance and the theory of horns and the photograph, Proc. Natl. Acad. Sci. 5, 272 (1919).

4. T. Chiba and M. Kajiyama, The Vowel: Its Nature and Structure, Tokyo-Kaiseikan Publishing Co., Ltd. Tokyo, 1941.

5. E. S. Weibel, Vowel synthesis by means of resonant circuits, J. Acoust. Soc. Am. 27, 858 (1955).

6. S. Meyer-Eppler and G. Ungeheurer, Die Vokalartikulation als Eigenwertproblem, Zeit. f. Phonetik 10, 245 (1957).

7. G. Fant, Acoustic Theory of Speech Production, Mouton and Company, The Hague, 1960.

8. J. M. Heinz and K. N. Stevens, On the properties of voiceless fricative consonants, J. Acoust Soc. Am. 33, 589 (1961).

9. K. N. Stevens and A. S. House, Development of a quantitative description of vowel articulation, J. Acoust. Soc. Am. 27, 484 (1955).

10. K. N. Stevens and A. S. House, Studies of formant transitions using a vocal tract analog, J. Acoust. Soc. Am. 28, 578 (1956).

---

* This work was supported in part by the U. S. Army Signal Corps, the Air Force Office of Scientific Research, and the Office of Naval Research; in part by the National Science Foundation under Grant G-10800; and in part by the U. S. Air Force Cambridge Research Laboratories under Contract No. AF 19(604)-6102.

H46

FOURTH INTERNATIONAL CONGRESS ON ACOUSTICS
COPENHAGEN 21.-28. AUGUST 196[illegible]

AUDIOMETRY AND PHYSIOLOGICAL NOISE

E.A.G. Shaw and J.E. Piercy
Division of Applied Physics, National Research Council, Ottawa, Canada.

When an earphone encloses the ear, physiological noise may be present in the cavity at levels sufficient to affect hearing threshold determinations. This possibility, recognized by Sivian and White in 1933,[1] has since received the attention of a number of others including Brogden and Miller,[2] Rudmose,[3] Munson and Wiener[4] and Lochner and Burger.[5] However, the subject has clearly suffered from a lack of physical measurements of the noise. Such measurements are included in recent work by Rudmose[6]. A primary purpose of this paper is to provide physiological noise data for a number of earphones used in audiometry and standard threshold determinations.

A diagram of the apparatus used in these experiments is shown in Fig. 1. An enclosure, simulating a given supra-aural earphone, is formed by a plastic housing sealed to the auricle either by the rubber cushion of the earphone or in the case of the STC Type 4026A, by a machined replica of the plastic earphone surface engaging with the auricle. The enclosure simulating a circumaural type earphone[7] (not shown) was sealed to the head by the liquid filled cushion of the Sharpe earphone.

A Bruel and Kjaer type 4132 condenser microphone is coupled to the enclosure by a short probe tube which is sealed to the housing by means of a soft rubber washer which also provides resilient support. The remote end of the microphone cathode follower is supported by a rubber band attached to a head frame (not shown). The frame is suspended from the ceiling to take most of the weight off the head and is provided with means of adjusting the force applied to the enclosure and its position with respect to the ear.

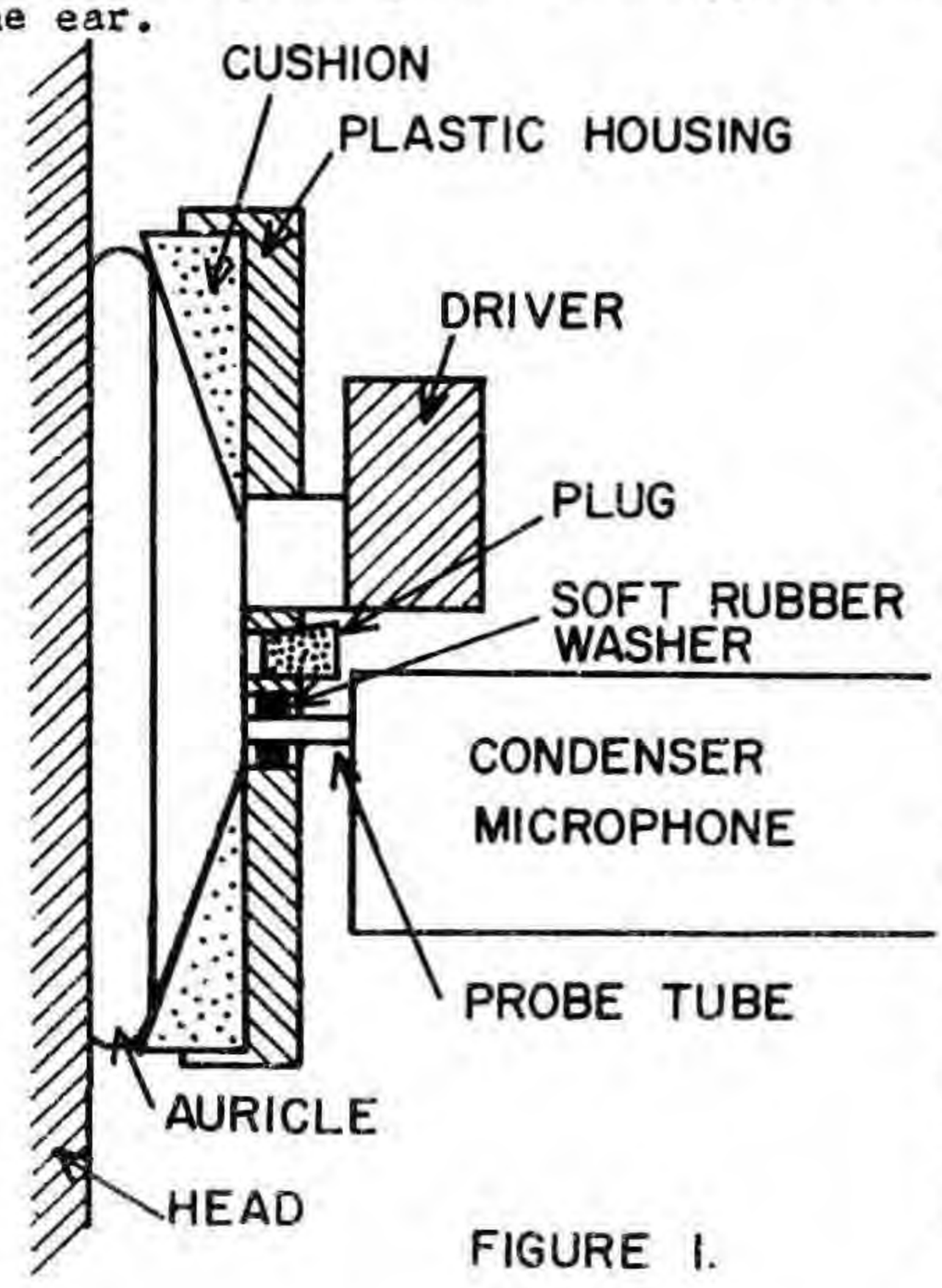

FIGURE 1.

To increase microphone sensitivity and hence minimize instrumental noise level the microphone is operated at a polarizing voltage just below the instability point (around 280 volts). A further increase in sensitivity is provided by probe tube resonance giving a maximum response of about -37 db re 1 volt/dyne cm^{-2}. To avoid overloading the 1/3 octave spectrometer used for frequency analysis, the spectrum was preshaped by a filter between cathode follower and preamplifier which reduced the dynamic range to 40 db.

The plug to be seen above the probe tube may be replaced by an aperture of appropriate size. The low frequency signal is then greatly reduced demonstrating that the recorded signal is indeed acoustic. Furthermore, the enclosure with aperture becomes a Helmholtz resonator enhancing the signal by 5 - 10 db at the resonance frequency. Measurements at 500, 800 and 1000 c/s are made in this manner.

The magnitude of the enclosure acoustic impedance (expressed here as an equivalent volume) is determined from the pressure generated when a known acoustic signal is injected by the dyanmic driver.

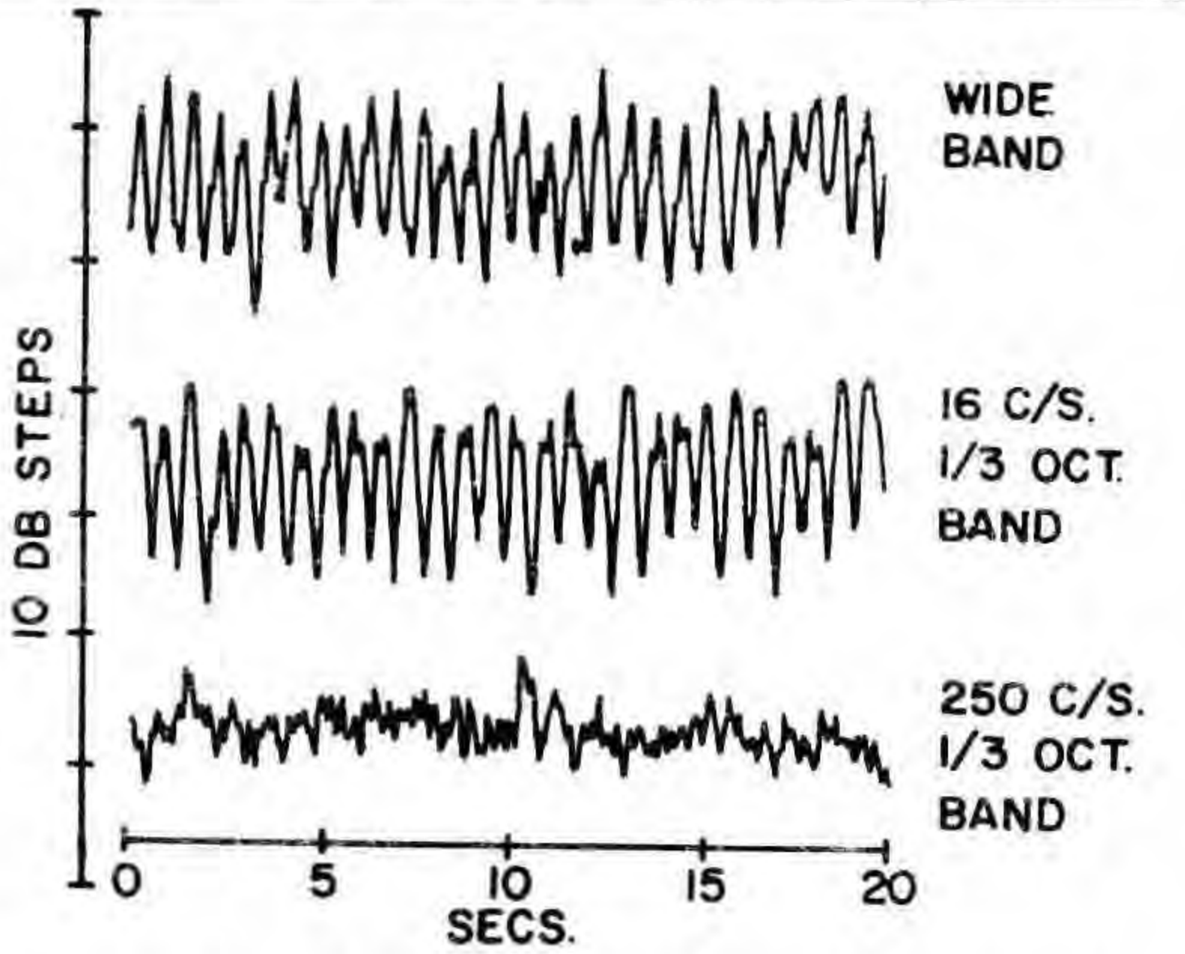

Typical recordings of physiological noise made with a level recorder operating at 63 db/sec writing speed are shown in Fig. 2. The wide band and 16 c/s 1/3-octave noise clearly rise and fall at the heart beat frequency. Above 100 c/s the noise is quite smooth except for the enclosures simulating the Beyer DT48 and Western Electric 705A earphones, the records for which frequently show a definite heart pulse up to 500 c/s. During these measurements, and others described below, the subject sat in a chair and was required to hold his breath while the bands above 160 cps were being recorded. Without such controlled breathing, noise spikes 10-20 db above the level of smooth noise were recorded. The pulsed noise is clearly caused by the circulatory system. It is conceivable that the smooth component of noise is muscular in origin[2] similar to the arm muscle tremor observed by Brogden and Miller.

Fig. 3 shows the estimated average 1/3 octave band physiological noise levels for one circumaural and four supra-aural earphones. In each case the noise levels were determined for six subjects using an enclosure which closely simulated the corresponding earphone as regards engagement with the head or auricle, and, with one exception, total mass. The contact force was adjusted to a fixed value for each enclosure and the position of the enclosure with respect to the ear was adjusted to give the minimum equivalent enclosure volume at 20 c/s. The equivalent volume as a function of frequency was measured for each subject, and an estimated "true" volume for earphone and subject was determined, making use of measured equivalent volumes for the various driver units. (Paragraph is completed in footnote on page 4.)

Perhaps the most significant feature of Fig. 3 is the low level of physiological noise in the circumaural earphone compared with the levels in the supra-aural earphones. This is caused by the very large volume of the circumaural earphone. With equal enclosed volumes the levels for the circumaural enclosure are about 8 db higher than the corresponding levels for a typical supra-aural enclosure. It may be noted that this is the approximate ratio of exposed skin area for the two cases. It is also worth noting that much of the indicated spread between supra-aural earphones is also due to differences in equivalent enclosed volume. For example, the estimated difference of 9 db at 250 c/s between the STC4026A and Beyer DT48 would be reduced to 3.6 db with equal volumes.

Earphone		Enclosure		Average Equivalent Volume of Earphone and Subject (cm^3)		Equivalent Volume of Driver alone (cm^3)	
Type	Mass (gm)	Mass (gm)	Applied Force (Kg-wt)	25 c/s	250 c/s	25 c/s	250 c/s
WE705A	190	210	1.5	35	25	11	11
TDH39/MX41AR	130	310	1.5	37	19	13	12
Beyer DT48	180	210	1.5	44	29	21	16
STC 4026A	190	210	1	31	16	9	4.5
Sharpe (circumaural)	230	240	1	Approx 180	Approx 150	-	-

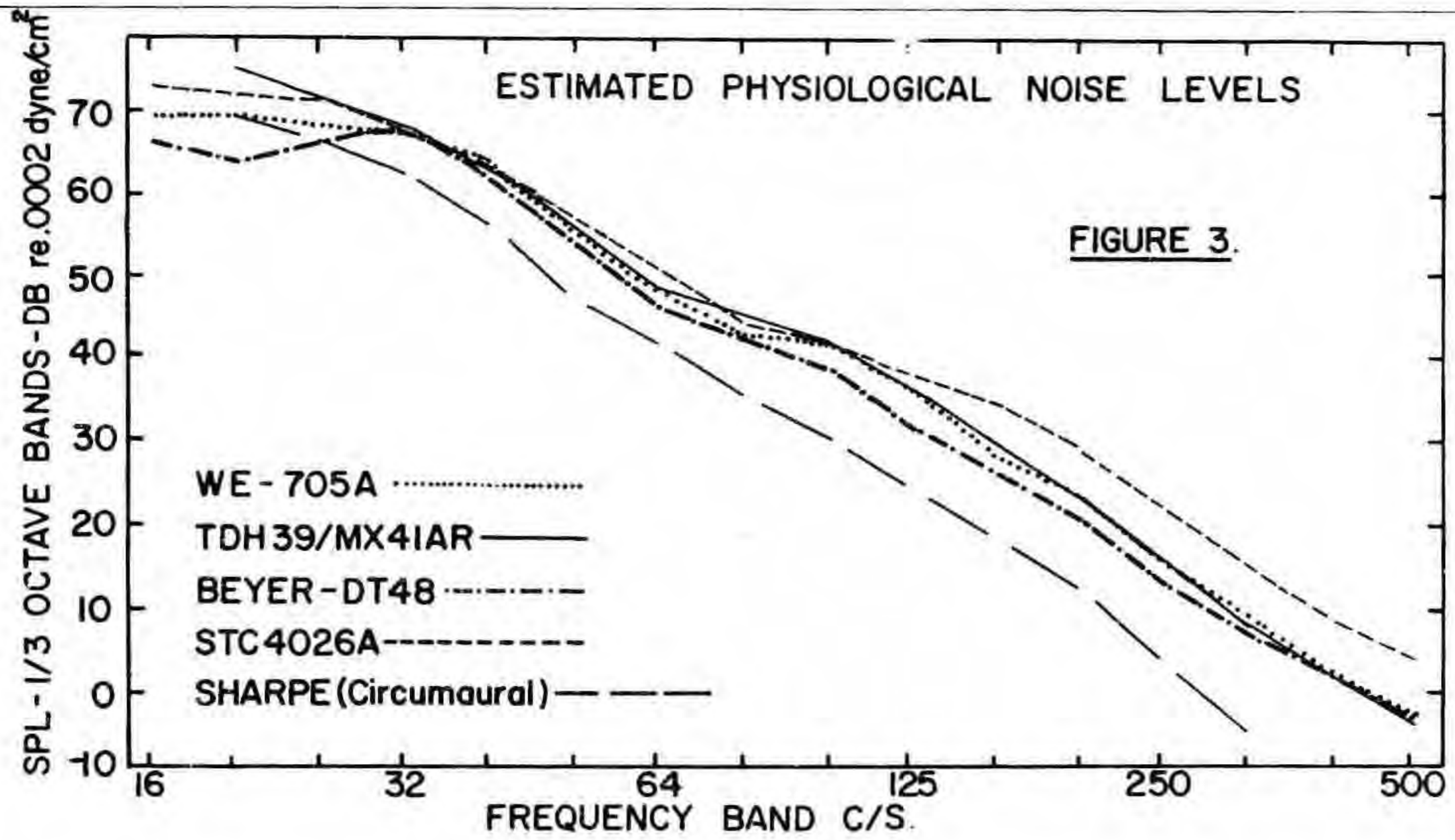

FIGURE 3.

The intersubject variations of noise level for the Western Electric 705A are shown in Fig. 4. Similar variations are found with other earphones. The small range found with six subjects suggests that the average levels in Fig. 3 may reflect accurately the levels for other populations.

The average 1/3 octave band levels of physiological noise for the four supra-aural earphones are compared with various earphone threshold determinations in Fig. 5. Curve B is part of the Sivian and White MAP curve.[1] Curve C was given by von Békésy.[8] The squares show recent UK (NPL) data[9] and the circles show values given by U.S. Bureau of Standards and U.S. Army.[10] The tentative ISO levels are also shown. It is recognized that it might be more meaningful to plot physiological noise levels for critical bands but this presents difficulties at very low frequencies. Around 250 cps the critical band is about 1/3 octave. In any event, it is doubtful whether the published masking data would allow one to make an accurate prediction of the masking effect of the observed physiological noise on pure tones. Masking experiments with steeply sloping wide band noise spectra would appear desirable.

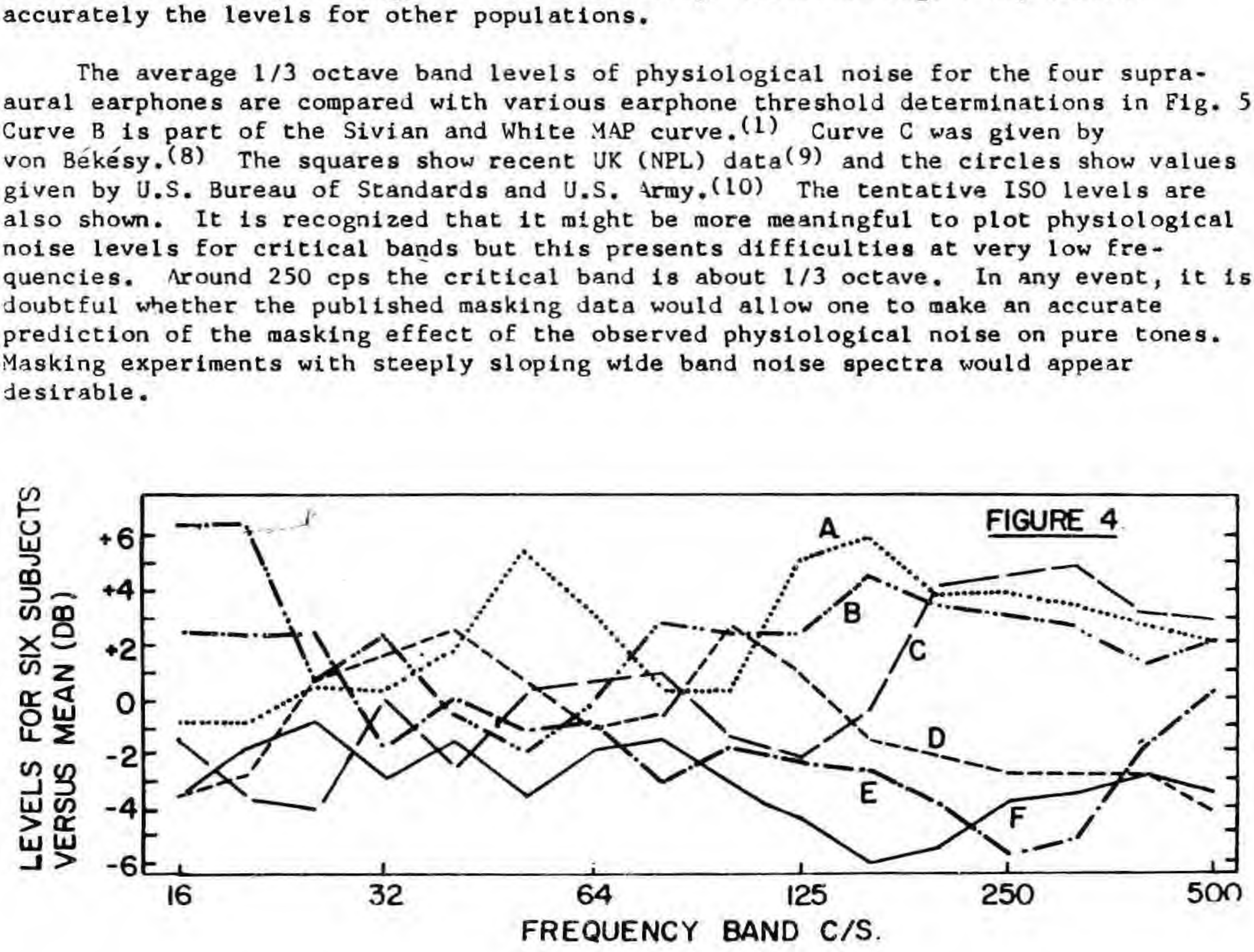

FIGURE 4

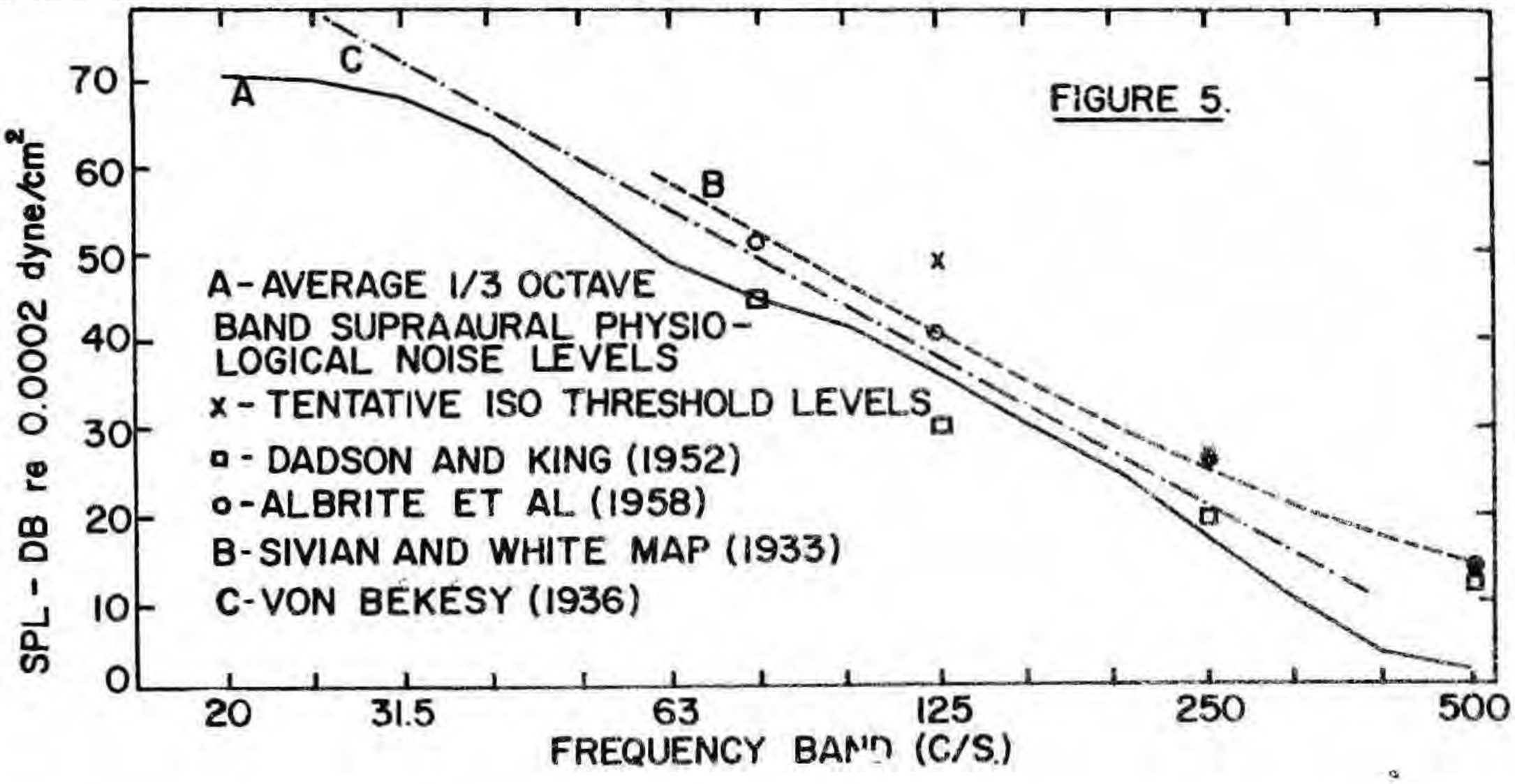

In the meantime it will be noted that the 1/3 octave physiological noise band levels and the normal minimum audible pressure thresholds for pure tones almost coincide over 3 octaves covering a 50 db range of level. The obvious inference is that the low frequency minimum audible pressure is a masked threshold, and the equality of slope of noise and threshold curves suggests local masking. Similar conclusions have also been reached from recent studies of binaural masking phenomena,(11) interaural phase and threshold level,(11) and the shape of the loudness function.(5)

If this inference is accepted then one must observe that the minimum audible field is only a few db lower than MAP. One must therefore ask whether the low frequency minimum audible field is also masked by or at least adapted to physiological noise transmitted directly to the hearing mechanism. It would not be difficult to construct a model which would give low frequency physiological noise pressures at the hearing mechanism of about the same level as those found in a cavity enclosing a free surface of the body.

REFERENCES

1. L.J. Sivian and S.D. White, Jour. Acoust. Soc. Am. 4, 288-321 (1933).
2. W.J. Brogden and G.A. Miller, Jour. Acoust. Soc. Am. 19, 620-623 (1947).
3. W. Rudmose, Jour. Acoust. Soc. Am. 22, 674A (1950).
4. W.A. Munson and F.M. Wiener, Jour. Acoust. Soc. Am. 24, 498-501 (1952).
5. J.P.A. Lochner and J.F. Burger, Jour. Acoust. Soc. Am. 33, 1705-1707 (1961).
6. W. Rudmose, Proceedings of 4th International Congress in Acoustics, Copenhagen, (1962).
7. E.A.G. Shaw and J.E. Piercy, Jour. Acoust. Soc. Am. 34, 745A (1962).
8. G. von Békésy, Experiments in Hearing, p. 258, McGraw Hill Book Company Inc., New York (1960).
9. R.S. Dadson and J.H. King, Jour. of Laryngology and Otology, 66, 366-378 (1952).
10. J.P. Albrite et al, AMA Archives of Otolaryngology, 68, 194-198 (1958).
11. K.J. Diercks and L.A. Jeffress, Jour. Acoust. Soc. Am. 34, (1962) (In press).

Footnote: The enclosure physiological noise levels were then corrected assuming the inverse relationship between physiological noise pressure and enclosure equivalent volume demonstrated by a separate experiment. These corrections were usually less than 3 db. The masses of the various earphones and enclosures, the values of applied force, the average equivalent enclosed volumes at 25 and 250 cps and the equivalent driver volumes are shown in the table.

K46

FOURTH INTERNATIONAL CONGRESS ON ACOUSTICS
COPENHAGEN 21.-28. AUGUST 1962

Bestimmung der Stoßfrontdicke in Flüssigkeiten aus dem akustischen Spektrum

W. Eisenmenger
III. Physikalisches Institut der Universität Göttingen

Einleitung: Untersuchungen an Stoßwellen gestatten insbesondere im Hinblick auf Dicke und Verlauf der Stoßfront Aussagen über die akustischen Dämpfungseigenschaften des Übertragungsmediums. Bei Flüssigkeiten ist einmal die Frage nach der Konstanz von Schub und Volumenviskosität bei hohen Schnellegradienten hervorzuheben, zum anderen ergibt sich prinzipiell die Möglichkeit, Relaxationserscheinungen bei Frequenzen im Bereich von 10^9 Hz zu untersuchen, da diese Frequenzen schon bei mäßigen Stoßwellendrucken (20 und mehr atm) auftreten. (Anstiegszeit der Stoßfront im Bereich 10^{-9} sec).

Eine Messung derart kurzer Anstiegszeiten (Stoßfrontdicke ca. 10^{-4} cm) ist mit gewissen experimentellen Schwierigkeiten verbunden. Optische Methoden unter Ausnutzung der Lichtreflexion an der Stoßfront haben bei Flüssigkeiten im Gegensatz zu Gasen nicht zu befriedigenden -Resultaten geführt. Eine elektroakustische Anordnung soll im folgenden beschrieben werden.

Stoßwellenerzeugung Stoßwellen können in einem flüssigkeitsgefüllten, dickwandigen Stahlrohr mittels einer elektromagnetischen Impulsschallquelle erzeugt werden [1]. Die Schallquelle besteht aus einer Flachspule mit eng anliegender, an die Flüssigkeit grenzender Kupfermembran. Über die Flachspule erfolgt die Entladung eines Kondensators, so daß zwischen Flachspule und Membran starke Abstoßung auftritt und damit verbunden die Abstrahlung eines ebenen Überdruckimpulses in die Flüssigkeit. Der Druckbereich beträgt 20 bis 700 atm bei einer Impulsdauer von 3 - 10 µsec. Im Laufe der Ausbreitung des Kosinusquadrat-förmigen Druckimpulses bildet sich dessen Vorderseite infolge der nichtlinearen Eigenschaften der Wellenausbreitung zu einer Stoßfront aus. Für möglichst gute Annäherung an die Verhältnisse bei einem idealen Stoß gilt die Bedingung, daß die Anstiegszeit an der Stoßfront sehr klein gegenüber der Zeitkonstante des Druckabfalls hinter dem Stoß ist. Um diese Bedingung auch bei niedrigen Drucken unter 20 atm. erfüllen zu können, ist es erforderlich, daß der von der Schallquelle abgestrahlte Druckimpuls bereits eine kurze Anstiegszeit bei vergrößerter Impulsdauer be-

sitzt. Dies konnte durch Verwendung einer Laufzeitkette anstelle des Kondensators erreicht werden.

Stoßwellenmikrofone Die bekannten Methoden der Erzeugung und Messung höchstfrequenter Schallwellen (Hyperschall) an Quarzeinkristallen legen nahe, die dabei wesentliche kapazitive Abtastung der Oberfläche auch auf breitbandige Signale wie z.B. Stoßwellen anzuwenden. Eine Beschreibung des Empfangsvorganges wird für Stoßwellen (Einschwingverhalten bei Drucksprung) besonders übersichtlich, s.Bild 1. Trifft auf eine ebene x-Quarzplatte z.B. aus der auf einer Seite angrenzenden Flüssigkeit, ein Drucksprung, so breitet sich ein entsprechender Drucksprung in die Platte hinein aus. Betrachtet man einen Zeitpunkt vor der Reflexion des Drucksprunges an der schallweich begrenzten Rückseite der Quarzplatte, so tritt an der Vorderseite des Drucksprunges eine Ladung auf und ebenso eine entgegengesetzte Ladung an der an die Flüssigkeit grenzenden Quarzseite. (Der unter mechanischer Spannung stehende Teil der Quarzplatte entspricht dem Fall einer gleichförmig belasteten Quarzplatte, deren Endflächen Ladungen tragen). Die mit dem Drucksprung verknüpfte Ladung bewegt sich nun mit Schallgeschwindigkeit auf die freie Endfläche zu, nach der Reflexion erfolgt lediglich Richtungsumkehr. Sind die Endflächen der Quarzplatte nun mit Elektroden versehen, die über einem niederohmigen Widerstand verbunden sind, so folgt der zeitliche Verlauf des durch den Widerstand fließenden Stromes gemäß Bild 1 unten. Man beobachtet sowohl einen Stromsprung beim Auftreffen des Drucksprunges als auch einen Stromsprung doppelter Amplitude bei seiner Reflexion an der schallweichen Rückseite des Quarzes. Somit liefert eine Strommessung ein verzerrungsfreies Bild des Drucksprunges. Lediglich bei hohen Frequenzen muß die akustische Dämpfung im Quarz berücksichtigt werden, wenn der der Reflexion an der Rückseite entsprechende Stromsprung zur Messung herangezogen werden soll. Demgegenüber ist für den ersten Stromsprung kein Dämpfungseinfluß zu erwarten. Da Messungen an Flüssigkeiten nicht bei sehr tiefen Temperaturen ausgeführt werden können, bei denen die Dämpfung im Quarz extrem klein wird, muß man zur

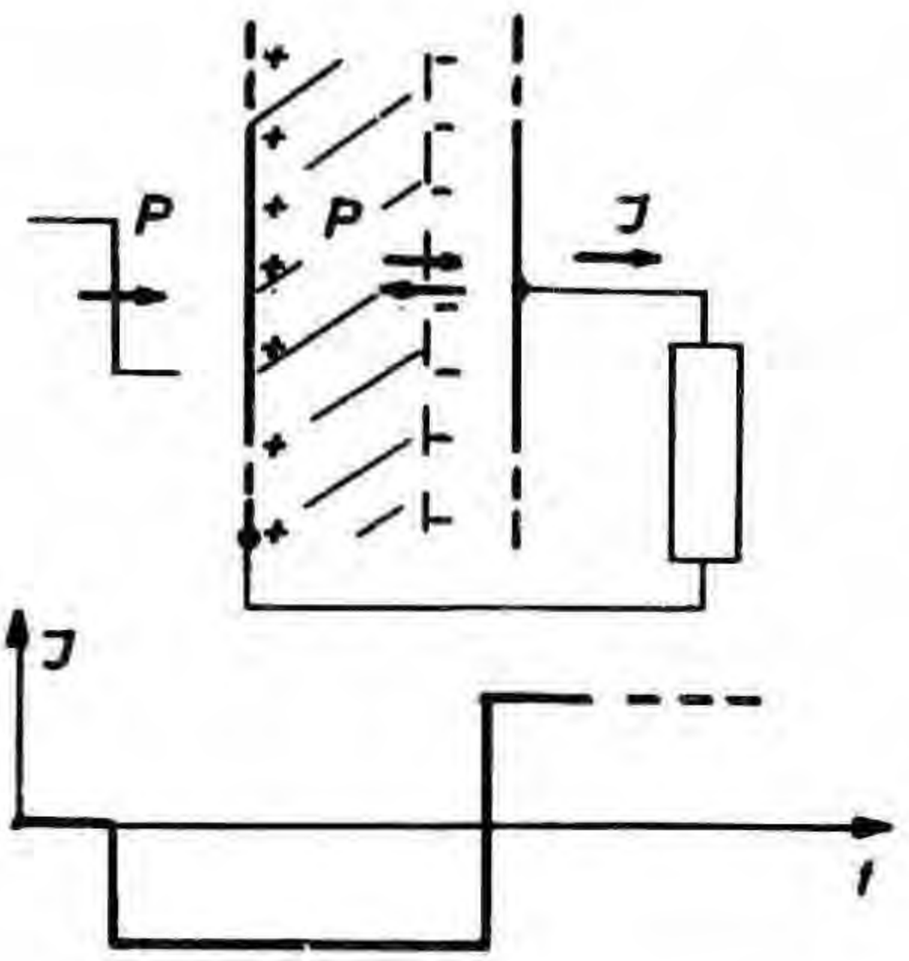

Bild 1

Messung im Frequenzbereich oberhalb 10^9 Hz den ersten Stromsprung ausnutzen, (Vorderflächenabtastung), dagegen ist für Frequenzen bis 10^9 Hz die Rückseitenabtastung wegen der doppelt so hohen Empfindlichkeit vorzuziehen. Bei der praktischen Ausführung von Stoßwellenmikrofonen mit Vorderseiten- bzw. Rückseitenabtastung muß man von den ebenen Feldbedingungen abweichen. Bild 2 und 3 zeigen schematisch ein Stoßwellenmikrofon für Rückseiten und Vorderseitenabtastung. In Bild 2 ist die Rückseitenelektrode als kapazitive Sonde ausgebildet (Innenleiter einer Koaxialleitung). Die Vorderseite ist elektrodenlos, es genügt die Streukapazität des Außenleiters als Erdung. Bei relativ großem Durchmesser des Quarzzylinders Ø 20 mm beträgt der Durchmesser der Sonde nur 2,5 mm. Dies ist erforderlich, um die Parallel-Justierung zur Wellenfront zu erleichtern. Die Endflächen des Quarzzylinders sind optisch plan und parallel. Bei der Vorderseitenabtastung ist der Durchmesser des Quarzzylinders nur 3 mm, um eine entsprechend kleine Abtastfläche zu gewährleisten. Beide Anordnungen geben den Druckverlauf in der Nähe des Sprunges gut wieder. Abweichungen treten nur bei Frequenzen unter 3 MHz auf. Sie sind durch den endlichen Laufweg im Quarz und Abweichungen von der ebenen Feldverteilung bedingt.

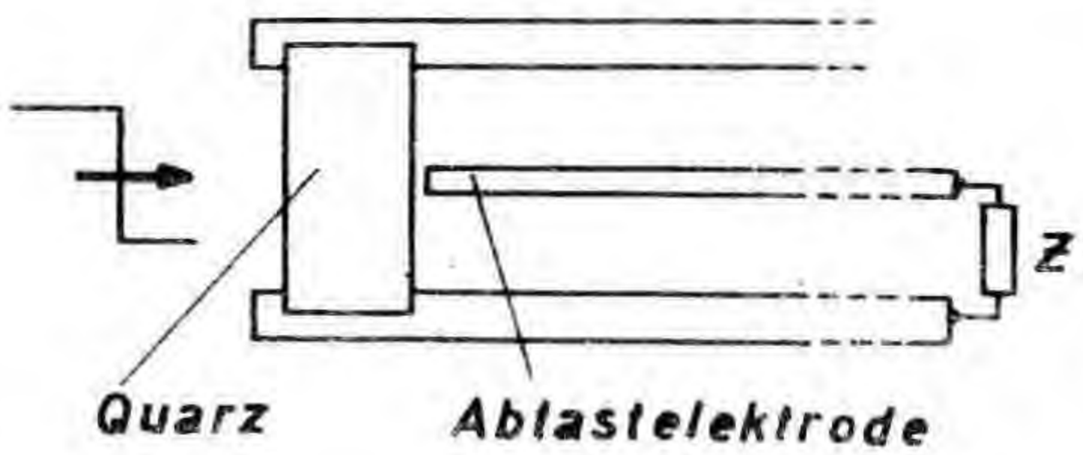

Bild 2

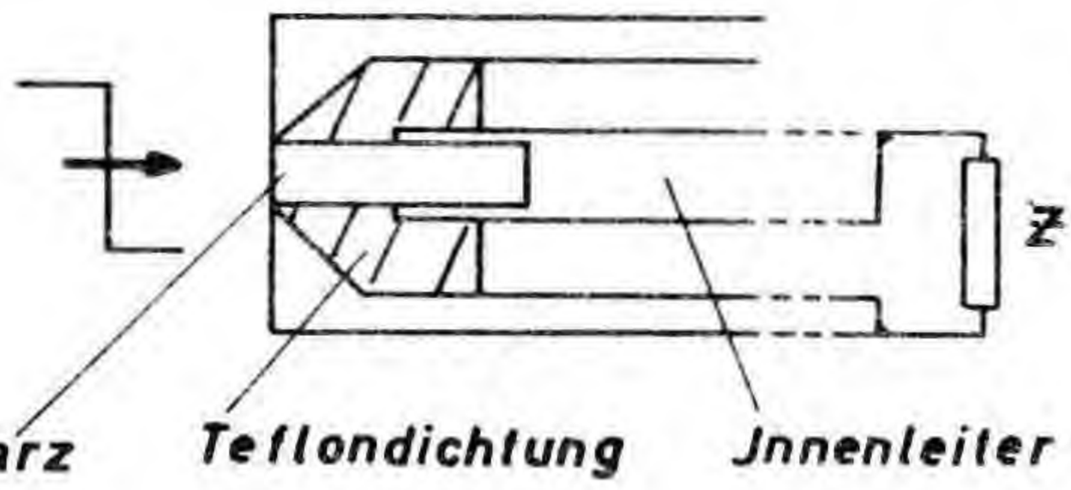

Bild 3

<u>Frequenzanalyse zur Bestimmung der Stoßfrontdicke</u> Wegen der geringen Empfindlichkeit der Anordnungen (ca. 0,1 Volt bei 50 atm) stößt die direkte oszillografische Wiedergabe des Stoßfrontsignals (oberhalb der Frequenz von 10^8 Hz) zur Zeit noch auf Schwierigkeiten. Aus diesem Grunde wurde mit der Anordnung nach Abb. 2 eine Frequenzanalyse des Stoßfrontspektrums ausgeführt. Hierzu wurde die an den Quarz anschließende Koaxialleitung als Koaxialresonator ausgebildet. Der Resonator wird durch den Stromsprung zu gedämpften Schwingungen angeregt, deren Amplitude nach induktiver Auskopplung mittels eines Überlagerungsempfängers zu bestimmen sind. (Oszillografische Anzeige). Nach Berücksichtigung der Quarzdämpfung sowie der Eigenschaften des elektrischen Über-

tragungsweges erhält man das Frequenzspektrum der ersten zeitlichen Ableitung des Druckverlaufes in der Stoßfront. Hieraus kann die Anstiegszeit, sowie die Stoßfrontdicke bestimmt werden. Meßresultate an Wasser zeigen eine charakteristische Druck- und Temperaturabhängigkeit. Lediglich bei 16°C und einem Druck von 44 atm ergibt sich eine mit der Theorie [2] übereinstimmende Stoßfrontdicke von $1{,}7 \cdot 10^{-4}$ cm.

Mögliche Fehlerquellen Naturgemäß erhebt sich bei dem beschriebenen Verfahren die Frage nach möglichen Fehlerquellen. Hierzu sind zu nennen: Beeinflussung der Stoßfrontform durch die Reflexion an der Vorderseite des Quarzmikrofons; Abweichungen von der Ebenheit der Wellenfront im Bereich der Abtastfläche sowie Abweichungen von der Planparallelität zwischen Wellenfront und Abtastfläche. Zum ersten Punkt gehören: Weitere Aufsteilung der Stoßfront infolge der Druckverdopplung während der Reflexion, Dämpfungsabweichungen vor der schallharten Wand bei senkrechter Inzidens (Zähigkeitsgrenzschicht), Strukturänderung der Flüssigkeit in der Nähe der Kristalloberfläche. Durch einfache Abschätzungen kann man zeigen, daß diese Einflüsse bei schwacher Nichtlinearität (d.h. Stoßgeschwindigkeit nur wenig höher als Schallgeschwindigkeit, hier 1 %) vernächlässigbar sind, zumindest bis zur Frequenz von 10^9 Hz. Abweichungen zum zweiten Punkt können durch Kontrolle der Richtcharakteristik der Mikrofone experimentell ausgeschlossen werden. Als weitere Fehlerquelle kommt eine grundsätzlich mögliche Frequenz- und Druckabhängigkeit der piezoelektrischen Eigenschaften von Quarz in Betracht, für die aber bis jetzt im interessierenden Bereich keine experimentellen Hinweise bestehen.

Literatur:

[1] W. Eisenmenger
Proc. 3rd Internat.Congr.Acoustics 1959
Part C; P 326-329 Elsevier Publish.Comp. 1961
Acustica Jahrg. 1962 in Vorbereitung

[2] L.D.Landau; E.M. Lifshitz
Fluid Mechanics
Transl.Pergamon Press 1959 P 337-340

L46

FOURTH INTERNATIONAL CONGRESS ON ACOUSTICS
COPENHAGEN 21.-28. AUGUST 1962

Etude sur Maquette de la Réduction du Bruit par l'interposition d'une Barrière

P. E. Magyar
Institute Tecnologique d'Aeronautique
São José dos Campos, S. Paulo (Brésil)

Lorsqu'on place un obstacle, acoustiquement opaque et de certaines dimensions, entre une source sonore et un point de réception, on obtient une réduction du niveau sonore. Cette réduction est définie comme la différence en décibels entre le niveau sonore mesuré à la réception, avant la mise en place de l'obstacle, et le niveau sonore aprés la mise en place de l'obstacle.

Si la longueur d'onde était trés faible par rapport aux dimensions géométriques de l'obstacle, le niveau sonore reçu aprés l'interposition serait nul, puisque la région de réception serait couverte par une ombre sonore analogue à l'ombre qu'on obtient dans le cas de l'éclairage lumineux. En fait, la longueur d'onde pour les fréquences audibles n'est pas assez petite par rapport aux dimensions des obstacles pratiques et ceux-ci ne produisent qu'une "pénombre sonore" au lieu d'une ombre bien définie. Dans ce cas on dit que l'existence d'un certain niveau sonore au lieu de réception est dû à la diffraction du son par les bords de l'obstacle.

La réduction du niveau sonore est fortement influencée par la géométrie de la barrière et par les conditions atmosphériques: le vent, les gradients de température, etc.. La longueur L de la barrière joue aussi un rôle important parce que, dans les cas pratiques, cette dimension ne peut atteindre des valeurs trés élévées soit pour des raisons économiques soit à cause des limitations de terrain. Dû au nombre limité des applications pratiques de la méthode, et aux differentes géometries utilisées, il parait difficile d'arriver à une conclusion sur la longueur qu'une barrière doit avoir pour accomplir effectivement la réduction sonore pour laquelle elle a été projetée. D'autre part les auteurs se plaignent du manque de données expérimentales pour différentes géometries. Pour cette raison nous avons étudié le problème sur maquette. La Fig. 1 représente le montage que nous avons utilisé pour ces mesures. Le Tableau I donne les relations entre les paramètres.

Nous avons fait construire plusieurs murs en briques à échelle réduite et nous les avons placés en salle sans écho pour éviter toute perturbation externe. Le sol était en céramique lisse, fortement réfléchissant de manière à garder une absorption à peu prés convenable avec l'échelle utilisée.

Cette étude a été réalisée pendant un stage de l'auteur au Centre de Recherches Scientifiques, Industrielles et Maritimes, Marseille (France)

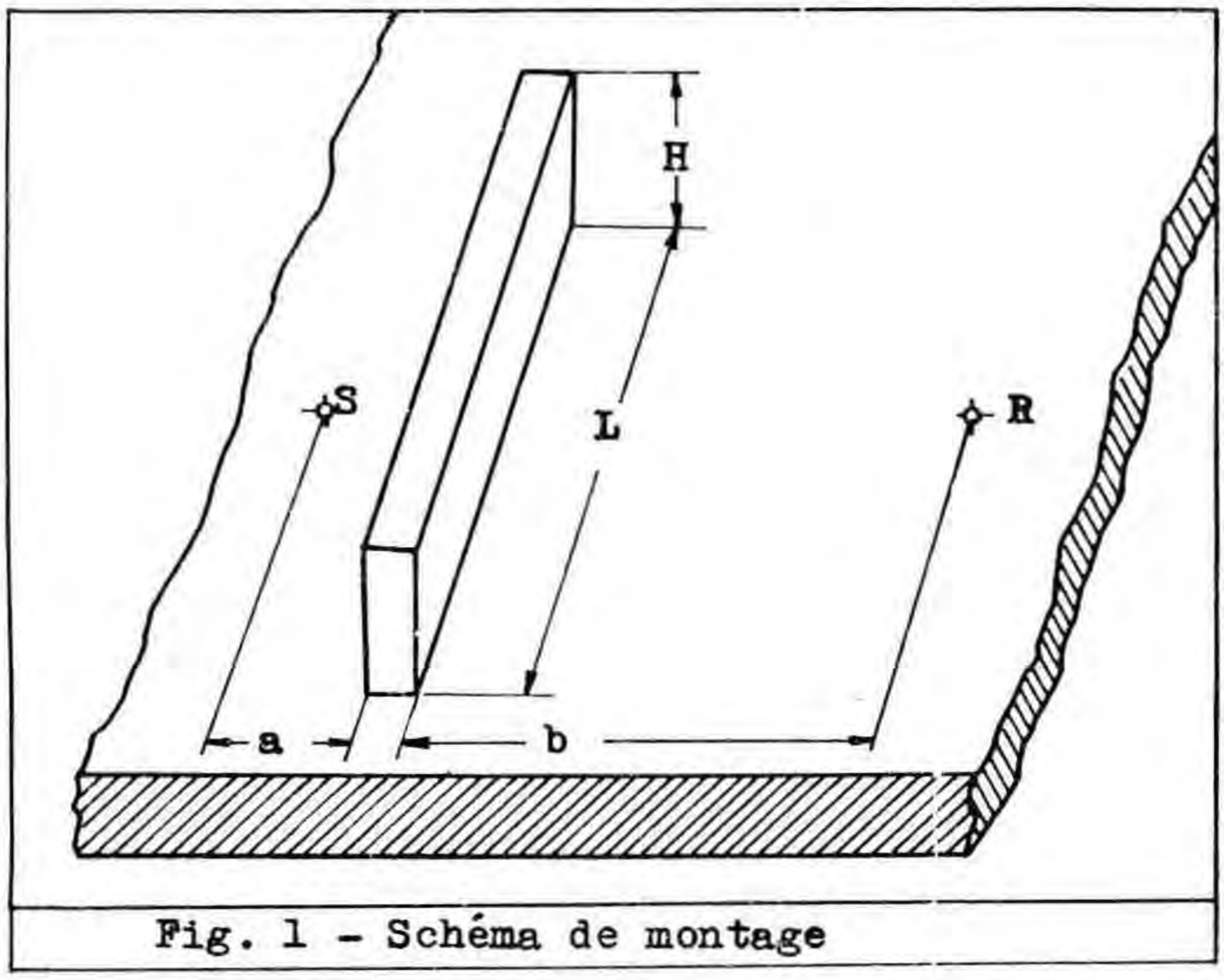

Fig. 1 - Schéma de montage

b=3,50m=constant
0,10m ≤ a ≤ 0,70m
0,10m ≤ H ≤ 0,50m
0 m ≤ L ≤ 4,00m
1,25KHz ≤ f ≤ 16KHz
5a ≤ b ≤ 35a
$0,2 \leq \frac{a}{H} \leq 7$
$0,37 \leq \frac{a}{\lambda} \leq 32$

Tableau I

La source sonore (S) était une sonde de faible section posée sur le sol et reproduisant un bruit blanc provenant d'une chambre de compression. Pour les fréquences d'essais la source était sphérique. Le récépteur (R) était un petit microphone éléctrostatique, placé au niveau du sol et suivi d'un système de filtres tiers d'octave.

Le procédé de mesure était le suivant: pour chaque hauteur H on a fait construire deux murettes de 4,00 mètres de long. Pour chaque valeur de a (b étant toujours égal à 3,50 mètres) on relevait les niveaux sonores reçus par le microphone et cela pour plusieurs valeurs de la fréquence. Après cette opération le mur était raccourci (des deux cotés) d'une certaine longueur et on reprenait les mesures ci-dessus. Par ce procédé, le mur a été raccourci successivement jusqu'à atteindre une longueur égale à zéro, c'est-à-dire H = 0. Les mesures ont été répétées avec le deuxième mur à titre de confirmation.

Nous avons ainsi construi 8 murettes et pour chaque ensemble de valeurs (a, H, L) nous avons mesuré la réduction sonore par bands de 1/3 d'octave centrées en 1,25KHz, 2,5KHz, 5KHz, 10KHz et 16KHz. Pour des raisons de simplicité, nous avons calculé le pourcentage de la réduction maximun en fonction de L/H pour les 160 courbes obtenues. La Fig. 2 donne les points experimentaux obtenus avec une certaine valeur de H et la courbe moyenne pour les géometries etudiées.

Nous avons constaté que les courbes sont systematiquement les mêmes pour toutes les géometries examinées.

D'après ces résultats, il apparait qu'on obtient une réduction sonore maximun à partir de L/H $\cong$6. Ceci revient à dire que pour des valeurs de L/H plus grandes que 6 nous sommes déjà dans la région de

Fig. 2

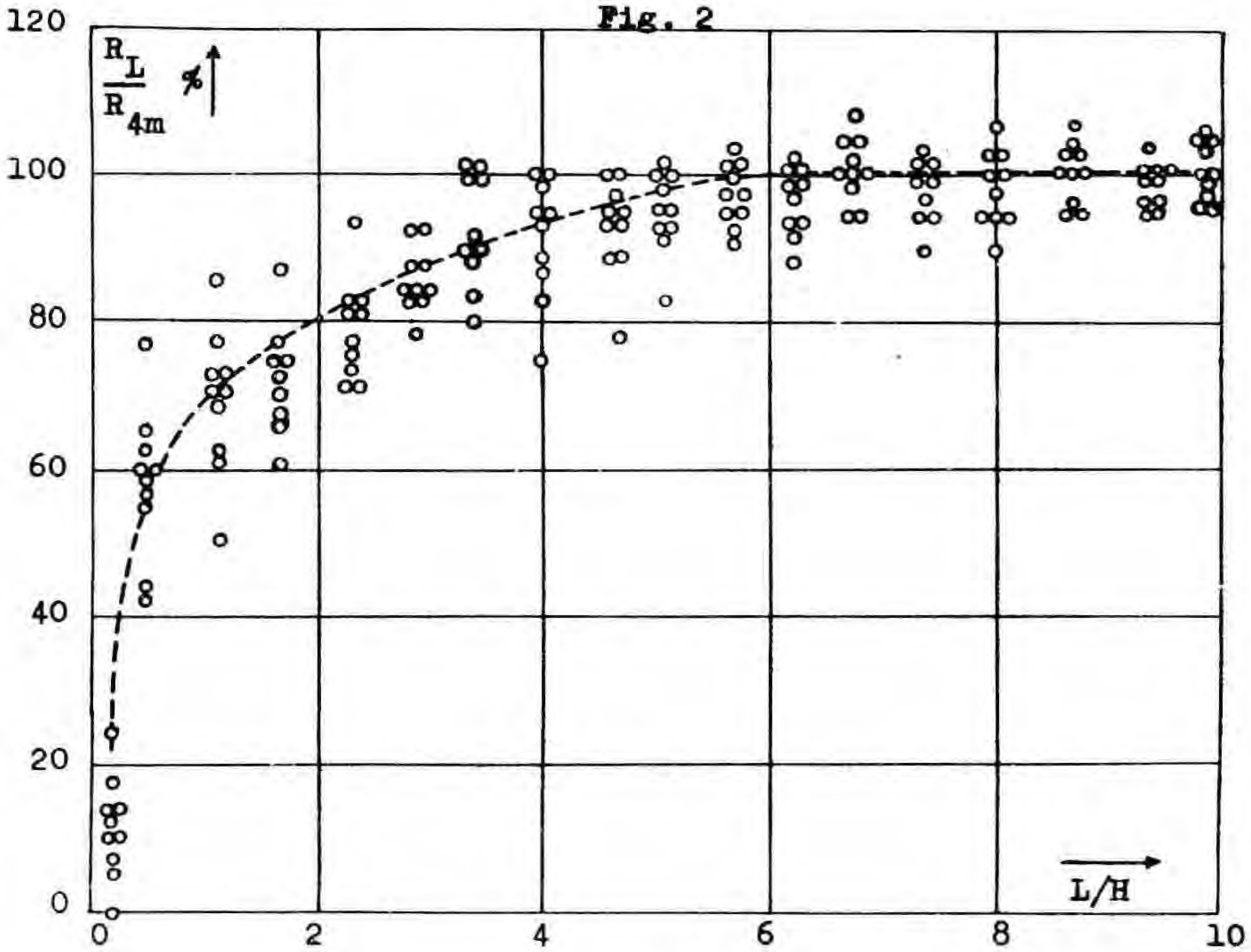

saturation de la courbe, et la barrière pourrait être considerée comme ayant une longueur infinie ne présentant pas de fuites sonores apréciables par les bords lateraux.

On pense que les résultats obtenus dans cette étude pourront être utilisés comme référence dans les projets des barrières de manière à corriger les reductions sonores calculées d'aprés les formules théoriques valables pour des obstacles de longueur infinie.

Une étude théorique est en cours pour essayer d'expliquer les résultats des mesures qui nous avons fait a ce sujet.

REMERCIEMENTS:

Nous sommes heureux à cette occasion d'adresser nos sincères remerciements à M. Th. Vogel, Directeur du CRSIM qui nous a accuilli si gentiment et aussi à MM Fabre et Cerillo pour leur aide dans la réalisation des essais et des montages.

M46

FOURTH INTERNATIONAL CONGRESS ON ACOUSTICS
COPENHAGEN 21.-28. AUGUST 1962.

DEMONSTRATION BOX FOR SOUND INSULATION

by W.K.R. Lippert and P. Dubout
Division of Building Research, C.S.I.R.O., Melbourne, Australia

Summary: A simple apparatus has been designed for demonstrating the sound insulation properties of various materials and acoustical systems. It has proved an excellent tool for general education and for instruction of laymen interested in acoustics.

APPARATUS

A sketch based on a photograph of the apparatus during a demonstration is shown in Figure 1. A loudspeaker on the bottom of the box (not visible in the Figure) produces loud sound (music, speech, white noise, octave bands of white noise, or single tones, and this

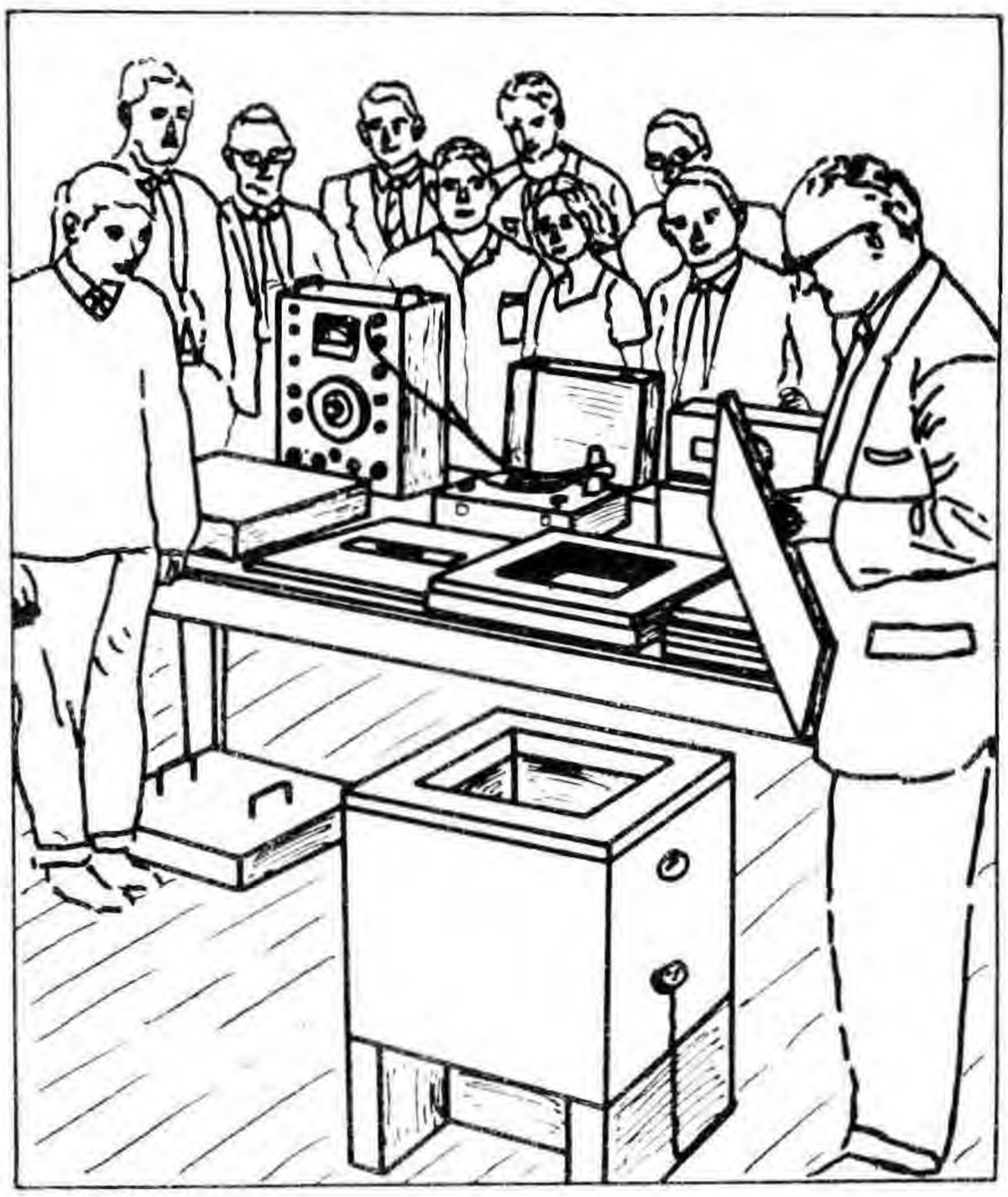

Fig. 1 Sketch of apparatus during demonstration

sound leaves the box through the opening at the top. The demonstrator can close the opening of the box (30 cm by 30 cm) with a sample of material (50 cm by 50 cm). The sound insulating effect of a particular sample is determined subjectively by listening to the loudness in the room before and after the sample has been placed tightly on the box. Quick changes of samples and repetitions are possible whence effects obtained with different kinds of samples and sounds can be compared quite easily.

A set of samples and sound generators used during demonstrations can be seen on the table behind the box.

The demonstration box has been designed in such a way (Fig. 2) that leakage of sound through the bottom and side walls has been kept as small as possible, but the overall weight does not exceed 75 kg. With this aim the design includes a double box construction with walls made of 24-mm plywood reinforced by 2-mm lead sheet in the centre, resilient suspensions and mountings of the inner box and of the loudspeaker, felt linings and gaskets, rubber edgings, and sound absorbent treatment on the bottom of the boxes. A description in greater detail will be published elsewhere.

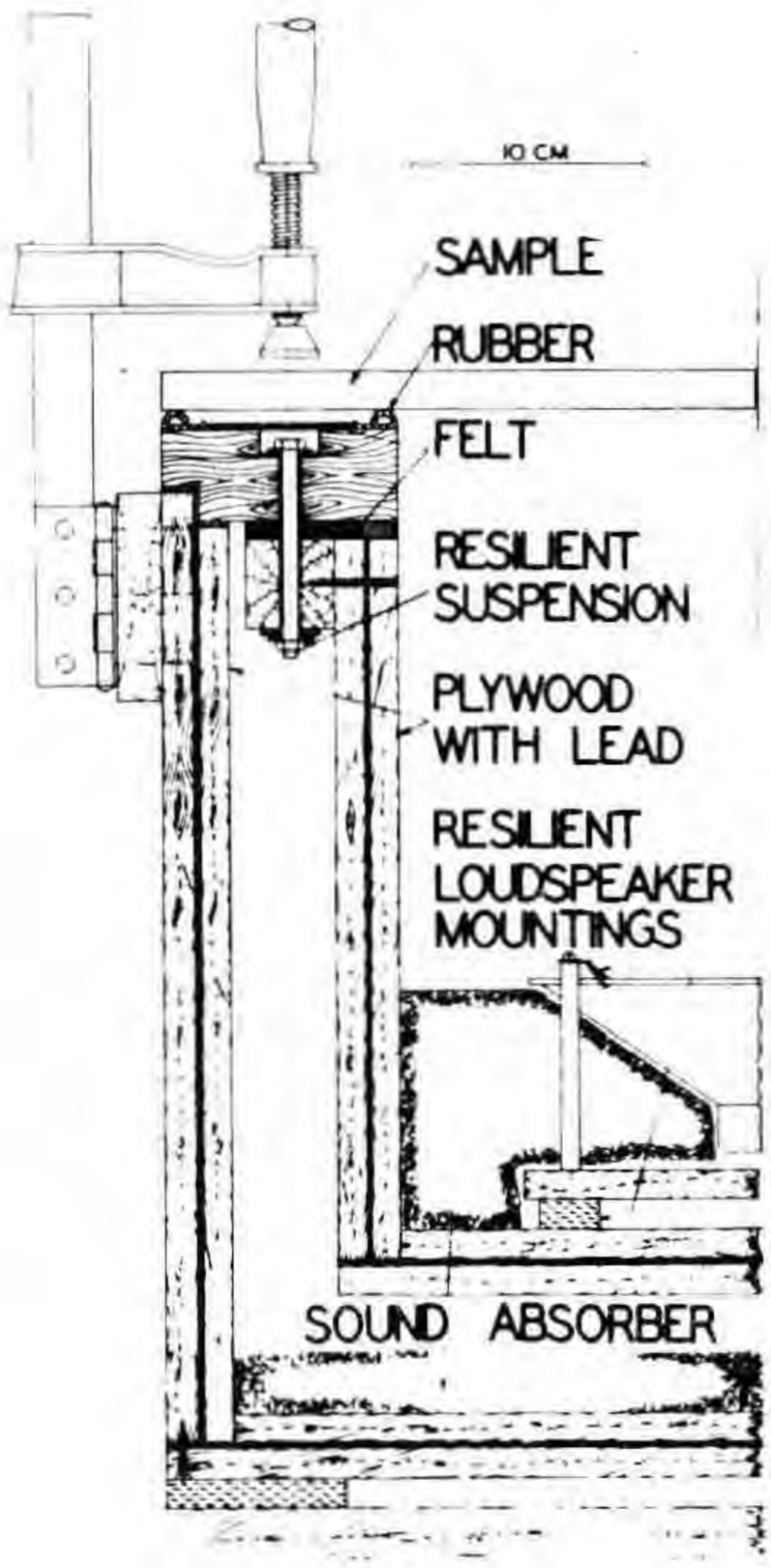

Fig. 2 Half cross-section of demonstration box

TEST OF PERFORMANCE

A simple subjective test can be made to show whether leakage of sound has been reduced sufficiently. Loud music or white noise is played, a 5-cm plywood sample is placed on top of the box and the loudness heard outside the box is assessed. Another heavy sample (for example a 10-cm concrete slab) is placed on top of the plywood sample, and if a noticeable reduction in loudness is observed the performance of the box is likely to be satisfactory.

Sound pressure levels were also measured with the box in a reverberation chamber, using white noise of various octave bands and a microphone 120 cm above the top. The measured level differences (in dB) with the box open and when blocked by a 10-cm slab of solid concrete are shown in Table I.

TABLE I

Octave bands (c/s)	75 150	150 300	300 600	600 1200	1200 2400	2400 4800	4800 9600
Level difference (dB)	41	45	39	49	47	55	57

DEMONSTRATIONS

Some typical results with various materials are as follows:

Plywood panels - Average noise reductions achieved with panels of various thicknesses are: 3 mm, 15 dB; 12 mm, 25 dB; 48 mm, 35 dB. Noise reductions of up to 35 dB are not affected by imperfections in the insulation of the box.

Lead sheet with plywood - A 2-mm lead sheet with 12-mm plywood bonded to each side has about the same weight as a plywood panel 48 mm thick and produces the same average noise reduction. This indicates that surface density is more important than thickness for sound insulation.

Porous materials - A 27-mm slab of compressed glass fibre board (specific density 0.15 $g.cm^{-3}$, specific flow resistance 28.5 $rayl.cm^{-1}$, average absorption coefficient between 200 and 2000 c/s on rigid backing 0.47) produces an average noise reduction of 5 dB. A 100-mm batt of soft mineral wool (specific density 0.073 $g.cm^{-3}$, specific flow resistance 7.7 $rayl.cm^{-1}$, average absorption coefficient 0.81) produces an average noise reduction of 10 dB. Porous materials are poor sound insulators. Octave bands of white noise disclose that the noise reduction has a flat frequency characteristic.

Sheets of foil - Polythene film 0.2 mm thick either alone or in combination with porous slabs shows an average noise reduction comparable with that of thick porous slabs.

Metal plates with slots - A rectangular opening 5 cm by 25 cm in the centre of a 20-mm plywood panel is covered by a 3-mm brass plate (7.5 cm by 30 cm) with a slot 12.5 cm long in the centre. Two brass plates were used, one having a slot 1 mm wide and the other a slot 0.25 mm wide (Both plates were machined so that a V-shaped groove was formed underneath the slot to make the slot depth equal to the slot width). Leakage of sound through these slots is quite substantial, and the reduction in loudness when the slots are blocked is very striking.

Glass panels in wooden frames - A 35-mm wooden frame with outer and inner dimensions of 50 cm by 50 cm and 30 cm by 30 cm respectively holds a 2.5-mm glass plate in the centre. This glass plate is fitted in the wooden frame in a groove 9 mm deep. Two similar frames are placed on top of each other on the box, forming a kind of double window. The frequency of sinusoidal sound is slowly changed until resonance occurs at about 200 c/s. Removal of the upper panel reduces the loudness of the tone heard outside, which means that the sound insulation of a single panel at that resonance frequency is greater than that of the double panel.

Another version of this resonance demonstration is equally impressive. By switching to a higher frequency than the double panel resonance mentioned above, (e.g. 1000 c/s) and lifting the upper frame slowly, keeping it horizontal, a sharp resonance occurs at the first standing wave between the panels at a height of about 17 cm, and a weaker resonance occurs at the next standing wave at about 34 cm height.

The resonance effect of the double glass panel can be shown to be reduced by various means of damping, for instance, by touching the upper panel with the finger tips. This effect is not noticeable with music or white noise.

CONCLUSION

The method proposed permits sound insulation effects of various materials and systems to be demonstrated in quick succession to give readily comparable subjective impressions. An advantage of the method is its simple technique, which is easily understood by the layman. It is true that the results derived from these demonstrations are more qualitative than quantitative, but some of the most common misconceptions regarding sound insulation properties, especially of porous materials, can be clarified by comparing relative sound insulation properties as suggested here.

It is not known to the authors if similar equipment is in use elsewhere. However, there seems to be a need to demonstrate the acoustical properties of various materials, particularly in the building industry, and the equipment and method described here might well be helpful to other workers.

N46

FOURTH INTERNATIONAL CONGRESS ON ACOUSTICS
COPENHAGEN 21.-28. AUGUST 1962

Eine Methode zur Bestimmung ~~des~~ Querkontraktionskoeffizienten piezoelektrischer Keramiken

Ludwig W a l t h e r

Einleitung und Problemstellung

In den letzten 2o Jahren ist zur Gruppe der bis dahin praktisch verwendeten piezoelektrischen Kristalle eine weitere Gruppe piezoelektrischer Materialien dazugekommen. Während erstere fast ausschließlich Einkristalle waren, die entweder in der Natur gefunden wurden oder in langdauernden Ziehprozessen aus Lösungen erhalten wurden, läßt sich die zweite Gruppe verhältnismäßig schnell nach herkömmlichen Methoden der keramischen Sintertechnik herstellen und ist in ihrem Aufbau polykristallin. Zur ersten Gruppe gehören Quarz, Seignettesalz, ADP, KDP usw. Zur zweiten Gruppe gehört als klassischer Vertreter das Bariumtitanat und in neuerer Zeit das Bleizirkonat-Bleititanat, Bleimethaniobat und ähnliche. In der Gruppe der polykristallinen Piezoelektrika gelingt es, durch Änderung der Zusammensetzung bestimmte Eigenschaften mechanischer, piezoelektrischer oder dielektrischer Art zu erzielen und damit Materialien zu erhalten, die für bestimmte Anwendungsbereiche besonders gut geeignet sind. Bei der Entwicklung solcher Piezoelektrika und auch bei ihrer späteren Produktion spielt die Messung ihrer Materialkoeffizienten eine wesentliche Rolle.
Da der piezoelektrische Effekt die Verkopplung zwischen mechanischen und elektrischen Größen darstellt, interessiert sich von Seiten der Anwender verständlicherweise der Elektroakustiker sehr für derartige Stoffe, weil er damit bequem einen mechanischen Vorgang in einen elektrischen und umgekehrt einen elektrischen Vorgang in einen mechanischen umwandeln kann. Außer den Erkenntnissen auf dem Gebiete der Theorie der Wandler müssen dem Berechnungsingenieur aber auch hier die reinen Materialeigenschaften des von ihm verwendeten piezoelektrischen Materials bekannt sein. Zur Bestimmung dieser Materialkoeffizienten sind eine ganze Reihe von Methoden angegeben worden. Überwiegend wird eine Methode verwendet, bei der der elektrische Eingangswiderstand eines geeignet vorbereiteten Stückes des zu untersuchenden Materials in einer bestimmten Resonanz gemessen wird und

aus den Meßwerten einzelne Koeffizienten bestimmt werden. "Geeignet vorbereitet" heißt dabei, daß man Form, Polarisation, Anregung und Art der Schwingung des Materialstückes so wählt, daß in 1. Näherung nur ein mechanischer, ein piezoelektrischer und ein dielektrischer Koeffizient das Verhalten des Stückes bestimmt. Aus den Meßwerten kann man dann eben diese Koeffizienten berechnen.
Die Anzahl der für ein bestimmtes Material vorhandenen Koeffizienten richtet sich nach der Kristallklasse, in der das Material kristallisiert. Für Bariumtitanat z.B. beträgt die Anzahl der vorhandenen Koeffizienten 2o, wobei die Zahl der in ihren Werten verschiedenen Koeffizienten durch die Gleichheit einiger Koeffizienten auf 11 herabgesetzt wird. Bei diesen 11 Koeffizienten handelt es sich um 6 elastische, 3 piezoelektrische und 2 dielektrische Koeffizienten. Um diese Koeffizienten alle bestimmen zu können, muß man meist eine ganze Anzahl verschiedener Materialproben herstellen, messen und die Koeffizienten berechnen. Erfahrungsgemäß macht dabei die genaue Bestimmung der beiden elastischen Koeffizienten $s_{12} = \partial S_1/\partial T_2$ und $s_{13} = \partial S_1/\partial T_3$ bzw. $c_{12} = \partial T_1/\partial S_2$ und $c_{13} = \partial T_1/\partial S_3$ mit T_1 = Elastische Spannung in Richtung 1 und S_1 = Elastische Dehnung in Richtung 1 oft einige Schwierigkeiten.
Es soll deshalb hier über eine Methode berichtet werden, mit der sehr schnell, auch an kleinen Proben von wenigen Zentimeter Länge, diese Koeffizienten zuverlässig bestimmt werden können, wenn man außerdem die Koeffizienten s_{11} und s_{33} bzw. c_{11} und c_{33} schon bestimmt hat.

Das Prinzip

Wie bekannt, ändert sich die Wellengeschwindigkeit einer Dehnwelle in einem langen Stab eines Festkörpers, sobald die Wellenlänge in die Größe der Querabmessungen des Stabes kommt. Die Größe dieser Änderung ist in erster Linie abhängig von dem Querkontraktionskoeffizienten des Stabmaterials und zweitens von der Querschnittsform des Stabes. Für isotropes Material und einen langgestreckten Zylinder gilt die von Pochhammer [1] angegebene Lösung. Ihre graphische Darstellung zeigt Bild 1. Man ersieht daraus, daß man durch Messen der Dehnwellengeschwindigkeit in einem langen Stab und in einem Stab von Längsabmessungen etwas größer als Querabmessungen den Querkontraktionskoeffizienten bestimmen kann, vorausgesetzt, daß die Messung mit der genügenden Genauigkeit geschieht. Da die Messung aber auf die Aufnahme der Resonanzfrequenz dieser Zylinder hinausläuft, läßt sich z.B. bei Me-

tallen bequem eine Meßgenauigkeit von 1 ‰ erreichen. Da nun der Querkontraktionskoeffizient μ_{12} definitionsgemäß $-s_{12}/s_{11}$ ist, läßt sich auf diese Art bei bekanntem s_{11} der Koeffizient s_{12} bestimmen.
Da die piezoelektrischen Keramiken unter dem Einfluß der Vorpolarisation aber anisotrop werden, und damit mehrere Querkontraktionskoeffizienten auftreten, ist der zylindrische Stab nicht geeignet, um an solchen Materialien die Querkontraktionskoeffizienten zu bestimmen. Dazu müßte man zu Stäben übergehen, deren Breitenabmessungen groß gegenüber ihrer Dicke sind. Genügend genaue mathematische Lösungen sind dem Autor für dieses Problem nicht bekannt geworden. Es wurde deshalb folgender Weg eingeschlagen: An zylindrischen Stäben von isotropen Materialien, deren Querkontraktionskoeffizienten zunächst mit völlig anderen Methoden bestimmt worden waren, wurde die Lösung von Pochhammer experimentell nachgeprüft. Das Ergebnis zeigt Bild 2.

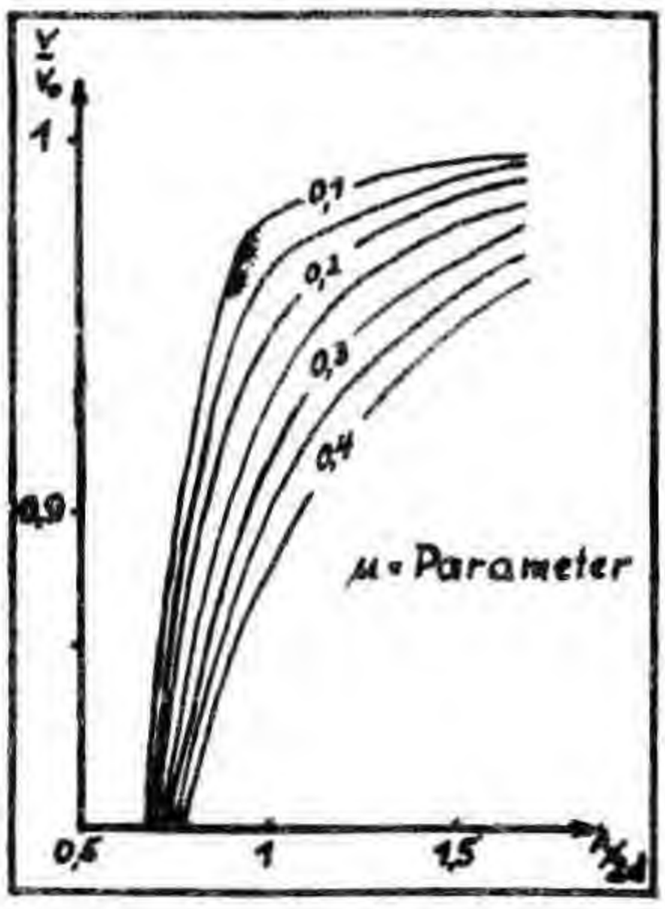

Bild 1

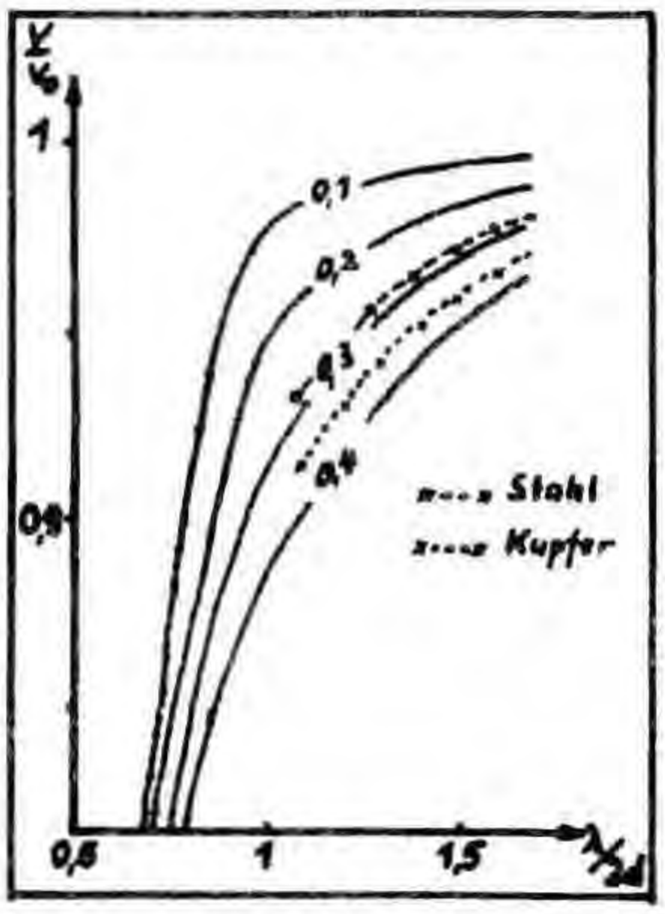

Bild 2

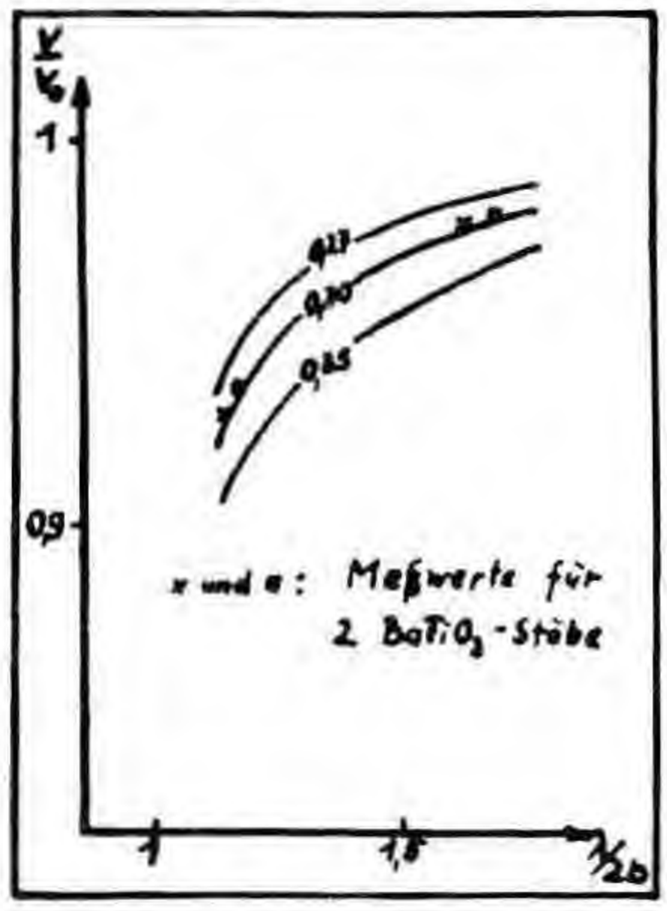

Bild 4

Nachdem so die Genauigkeit der Meßmethode zu besser 1 ‰ gefunden worden war, wurde versucht, mit rechteckigen Stäben, deren Breitenabmessungen >> die Dicke waren, ein neues Diagramm für rechteckige Stäbe aufzustellen, das die Abhängigkeit der Dehnwellengeschwindigkeit für verschiedene Querkontraktionskoeffizienten liefert. Dieses einmal aufgestellte Diagramm kann dann dazu dienen, an flachen Stäben aus piezoelektrischer Keramik, deren Dehnwellengeschwindigkeit bei einem langen Stab und einem verkürzten Stab, dessen Länge nur etwas größer als seine Breite ist, gemessen wurde, den Querkontraktionskoeffizienten zu bestimmen. Man muß den Stab auch nicht verkürzen, sondern kann mit einer Oberschwingung messen, bei der die halbe Wellenlänge nur wenig

größer als die Stabbreite ist. Mit den leicht zu bestimmenden Koeffizienten s_{11} und s_{33} kann man daraus dann die Koeffizienten s_{12} und s_{13} leicht erhalten.

Die Meßmethode

Die Erzeugung der Longitudinalschwingungen in den Proben und die Messung der Resonanzfrequenzen geschah nach folgendem Blockschaltbild:

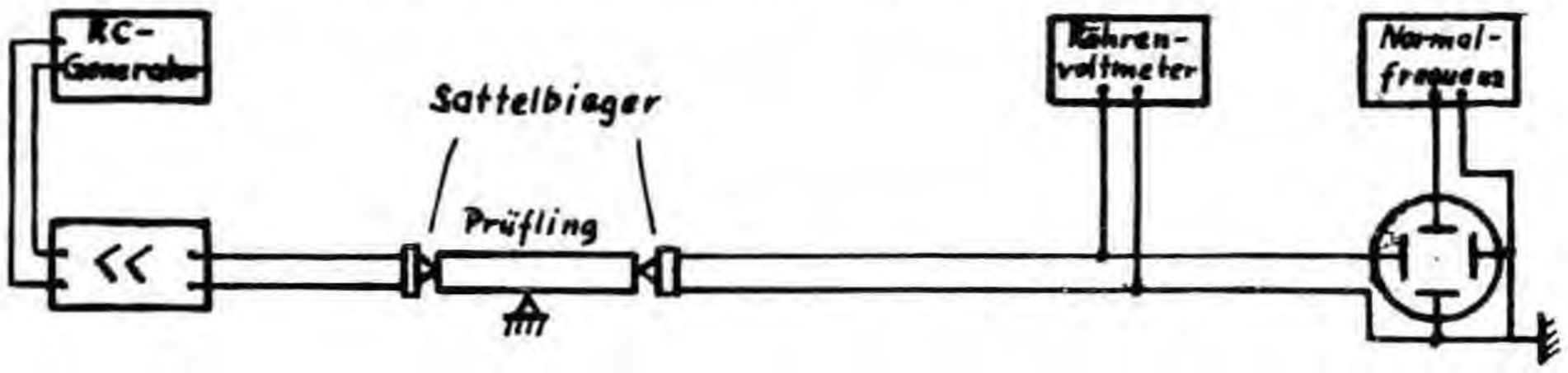

B i l d 3

Als Anregungssystem diente ein Seignettesalz-Sattelbieger, der je nach Frequenz von verschiedenen Generatoren über einen Verstärker gespeist wurde. Die Prüflinge wurden in der Mitte unterstützt und schwangen frei. Als Empfangssystem diente ein gleichartiger Sattelbieger, dessen Spannung einem Röhrenvoltmeter zugeführt wurde und außerdem auf einem Oszillografen mit einer aus einer Frequenzdekade entnommenen Normalfrequenz verglichen und gemessen wurde. Die Meßgenauigkeit war stets besser als $\pm$ 2 Hz und ist damit in jedem Falle besser als 1 ‰.

Meßergebnisse

Die Ergebnisse der Nachprüfung der Pochhammer schen Theorie zeigte schon Bild 2. Das für Stäbe mit rechteckigem Querschnitt für Werte von μ = 0,27 ... 0,35 erhaltene Diagramm zeigt Bild 4. Das Verhältnis von Breite zu Dicke der gemessenen Stäbe betrug 5:1. Für 4 aus der gleichen Art von Bariumtitanat hergestellte Schwinger sind die Meßwerte mit eingetragen. Die Abweichungen der einzelnen Meßwerte an 4 gleichartigen Schwingern untereinander waren in jedem Falle $\leq \pm 3\%$. Die Reproduzierbarkeit der Meßwerte an einem Schwinger war stets besser als $\pm 2\%$. Die Meßmethode hat sich bei der Entwicklung von piezoelektrischen Keramiken gut bewährt und dazu geführt, daß die Materialkoeffizienten schnell und mit genügender Genauigkeit bestimmt werden konnten.

[1] Pochhammer, L. Crelles J. Math. 81, 324 (1876)

O46

FOURTH INTERNATIONAL CONGRESS ON ACOUSTICS
COPENHAGEN 21-28 AUGUST 1962

On Sound Propagation in a Randomly Inhomogeneous Medium*

Professor William C. Meecham, Department of Aeronautics and Engineering Mechanics, University of Minnesota, Minneapolis, Minnesota, USA

I. INTRODUCTION

This work is concerned with the problem of the propagation of sound in a medium having random inhomogeneities. The inhomogeneities may be caused by temperature fluctuations or turbulence. It will be seen that in order to make progress, we shall have to assume that the fluctuations are small compared with the average properties of the medium. Problems of this type are of importance for sound propagation in water and in the atmosphere.

There has been a considerable amount of theoretical effort expended on problems of the type described above. Usually a single scattering approximation is made, and attention is centered on the first order scattered field. The average field can be found by calculating the total amount of energy removed from the beam by the scattering process. Extensive reviews of this kind of treatment are given in two recent books by Chernov[1] and Tatarski[2].

II. THE GREENS FUNCTION FOR RANDOMLY INHOMOGENEOUS MEDIA

We shall examine here only the case of the propagation of a scalar field in the randomly inhomogeneous medium. We also confine attention to single frequency effects, i.e., we replace the wave equation with the Helmholtz equation for an inhomogeneous medium. We find the Greens function, i.e., the field obtained from a point source of a single frequency located in the medium.

It is necessary to describe the statistical nature of the problem, in particular the type of averaging to be considered. The simplest theoretical situation is one in which we are given an ensemble of randomly inhomogeneous media, each member of which has similar statistical characteristics; ensemble averaging is used. Unfortunately, this situation is not of much practical interest. There are two other types of averaging which can be considered. For space averaging, we imagine transporting the source and field point, maintaining their relative positions, and average the observed field. Alternatively, if the characteristics of the medium change with time, a simple time average may be used. In this case, it is important that the medium should change little in one period of the source, for otherwise frequency spreading (Doppler effects) become important. According to the ergodic hypothesis either of the latter two types of averaging may be assumed to be equivalent to ensemble averaging.

With this preparation we proceed to consider the field generated by a point source. The equation to be satisfied is,

$$[\nabla^2 + k_0^2 + k_0^2 U_{st}(\underline{r})][G_0(\underline{r}, \underline{r}_0) + G_{st}(\underline{r}, \underline{r}_0)] = \delta(\underline{r} - \underline{r}_0) \qquad (1)$$

where k_0 is the propagation constant for the average medium, $\underline{r}_0$ is the source position, $U_{st}(r)$ is the fluctuation in $1/c^2$, with C the velocity of sound, if the inhomogeneity is produced by temperature. For turbulence effects U_{st} is a random dif-

1. L. A. Chernov, Wave Propagation in a Random Medium, Translated by R. A. Silverman (McGraw-Hill Book Co., New York, 1960).
2. V. I. Tatarski, Wave Propagation in a Turbulent Medium, Translated by R. A. Silverman (McGraw-Hill Book Co., New York, 1961).

* This work was partially supported by ONR.

ferential operator involving the turbulence velocity components, as will be seen. We have written the Greens function as the sum of two contributions. The quantity G_o is the average field at $\underline{r}$ due to the source at $\underline{r}_o$ and G_{st} is the fluctuation in the field under the same conditions. It follows from these definitions that[3]

$$\langle U_{st} \rangle = \langle G_{st} \rangle = 0, \tag{2}$$

where the brackets $\langle\rangle$ indicate averages, as defined above. We now rearrange terms of (1), define two integral operators P and Q,

$$\left\{ \begin{matrix} P \\ Q \end{matrix} \right\} F = \frac{1}{4\pi} \int \frac{e^{ik_o|\underline{r}-\underline{r}'|}}{|\underline{r}-\underline{r}'|} \left\{ \begin{matrix} k_o^2 U_{st}' \\ \nabla'^2 + k_o^2 \end{matrix} \right\} F(\underline{r}')\, d\underline{r}' \tag{3}$$

the prime on U_{st} indicating $U_{st}(r')$, (similarly later for G'), and solve (1) for G_{st} to obtain formally,

$$G_{st} = (1 + P + P^2 + \cdots) \left\{ (P+Q) G_o - \frac{1}{4\pi} \frac{e^{ik_o|\underline{r}-\underline{r}_o|}}{|\underline{r}-\underline{r}_o|} \right\}. \tag{4}$$

As the next step we take the average of (4), use (2) to find

$$0 = (Q + \langle P^2 \rangle + \langle P^2 \rangle Q + \cdots) G_o - \frac{1}{4\pi} (1 + \langle P^2 \rangle + \cdots) \frac{e^{ik_o|\underline{r}-\underline{r}_o|}}{|\underline{r}-\underline{r}_o|}. \tag{5}$$

The higher order terms involve averages over higher powers of P which in turn will be seen to involve higher order correlation functions of the fluctuation.

We see Eq. (5) is an integral equation for the determination of G_o. In order to obtain an approximate solution, we now assume that the fluctuations in the medium are small compared with the average properties of the medium. In this case, we can neglect higher powers of U_{st}, equivalently of P; furthermore, we shall see that G_o is of order U_{st}^2, except for a term which cancels the source term, and consequently, we neglect products of P and Q. If desired, the solution of (5) could be continued by iteration beginning with the lowest order solution obtained here. We proceed by retaining the first two terms of the first series of (5) and the first term of the second series. After substituting definitions and operating with $\nabla^2 + k_o^2$ the equation for G_o which we obtain is,

$$(\nabla^2 + k_o^2) G_o(\underline{r}, \underline{r}_o) + \frac{k_o^4}{4\pi} \int \mathcal{H}(\underline{r}, \underline{r}') G_o(\underline{r}', \underline{r}_o)\, d\underline{r}' = \delta(\underline{r} - \underline{r}_o), \tag{6}$$

where

$$\mathcal{H}(\underline{r}, \underline{r}') = \langle U_{st}(\underline{r}) \frac{e^{ik_o|\underline{r}-\underline{r}'|}}{|\underline{r}-\underline{r}'|} U_{st}(\underline{r}') \rangle. \tag{7}$$

Of course if U_{st} is a function, not an operator, the spherical wave can be taken out of the average. We suppose now, as is often the case physically, that the medium fluctuation is homogeneous so that $\mathcal{H}$ is a function of the difference of its arguments. Further, we restrict U_{st} to be a function; the more general case is discussed later. Then the integral in (6) is of convolution form and that equation can be solved for G_o by taking the Fourier transform (F.T.).

Although the assumption is not essential, the development is simplified if we assume that the fluctuations in the medium are statistically isotropic. Then $\mathcal{H}$ is a function of $|r - r'|$ alone. Using F. T., setting $r_o = 0$, and integrating over angles, we find to lowest order in $\mathcal{H}$ from (6)

---

[3] As will be seen, formulating the problem in this way leads to the result that the average of first order scattering is zero.

$$G_0(\underline{r},0) = (4\pi^2 r)^{-1} \int_{-\infty}^{\infty} \frac{s \sin sr \, ds}{k_0^2 - s^2 + \frac{k_0^4}{4\pi} \int e^{i\underline{s}\cdot\underline{R}} \mathcal{H}(R) d\underline{R}} \tag{8}$$

By treating (8) as a contour integral we obtain

$$G_0(\underline{r},0) = -\frac{1}{4\pi} \frac{e^{is_0 r}}{r} \tag{9}$$

where

$$s_0 = k_0 \left\{ 1 + \frac{k_0^2}{8\pi} \int e^{i\underline{k}_0\cdot\underline{R}} \mathcal{H}(R) d\underline{R} \right\}. \tag{10}$$

The result is that the coherent spherical wave is slightly damped, at a rate dependent on the transform of $\mathcal{H}$. It can be shown that

$$s_0 = k_0 + \frac{k_0^2}{2} \left\{ \frac{1}{8\pi^2} \int_0^{\infty} k\, h(k) \ln \frac{k+2k_0}{|k-2k_0|} dk + \frac{i}{8\pi} \int_0^{2k_0} k\, h(k) dk \right\} \tag{11}$$

where h is F. T. of $\langle U_{st}(\underline{r}) U_{st}(\underline{r}') \rangle$. We see the rate of loss of energy from the coherent beam is determinedby the long wave length components of the medium fluctuation. Further the phase velocity of thecoherent beam is lowered, since $h > 0$, being the transform of a correlation.

For propagation in a turbulent medium U_{st} is an operator. We find by a straightforward application of Lighthill's theory[4]

$$U_{st}(\underline{r}) = \frac{2}{i\omega k_0^2} \frac{\partial^2}{\partial r_i \partial r_j} u_i(\underline{r}) \frac{\partial}{\partial r_j}$$

where u_i are the components of the (presumed given) turbulent fluid velocity, r_i are the components of $\underline{r}$, and ω is the angular frequency of the source. The summation convention is used. Substituting in (7) and (6) and following a procedure like that above yields a result similar to that of (9) and (10), though considerably more complicated, involving the correlation of the turbulent velocity.

4. See for instance G. W. Ford and W. C. Meecham, J. Acoust. Soc. of Am. 32, 1668 (1960).

G47

FOURTH INTERNATIONAL CONGRESS ON ACOUSTICS
COPENHAGEN 21.-28. AUGUST 1962

CONCERNING THE EFFECT OF WORD LENGTH ON RATES OF CHANGE OF FORMANT FREQUENCIES

Mark R. Weiss, Federal Scientific Corp., New York 27, N. Y.
Cyril M. Harris, Columbia University, New York 27, N. Y.

This paper is concerned with an application of computer techniques to the high-resolution analysis of speech. Details of the analysis equipment and of the programming logic for the extraction of formant frequencies and pitch are being presented shortly at the Speech Communication Seminar in Stockholm. Here, only a brief mention is made of these aspects of our research program. Instead, attention is focused on one interesting facet currently being studied---the effect of word length on rates of change of formant frequencies of voice sounds. For example, if the same word is spoken a number of times but said slowly first, more rapidly a second time, and still more rapidly a third time, what is the relation between the rates of change of formant frequencies in the three cases?

ANALYSIS SYSTEM

The spectrum analyzer used in this research effectively synthesizes a continuum of filters, each having a uniform frequency resolution of 50 cps. Analysis is performed simultaneously over a 7500-cps frequency band. This SIMORAMIC Spectrum Analyzer (produced by the Federal Scientific Corporation) contains a closely-regulated memory loop of unity gain. The device is, essentially, a correlation-type analyzer. The signal to be analyzed is heterodyned to the megacycle region, applied to the input of an ultrasonic delay line and fed back to the input of the loop so that it is recirculated around the loop many times. The memory loop includes a time-variable phase shifter. By special phase-modulation of the stored signals, a wave interference phenomenon takes place which leads to a presentation of the Fourier spectrum. Immediately after presentation of the spectrum, the contents of the memory loop are discharged rapidly and a new processing cycle is initiated. Details of the operation of this system as a spectrum analyzer and coherent signal integrator are available in the literature.[1]

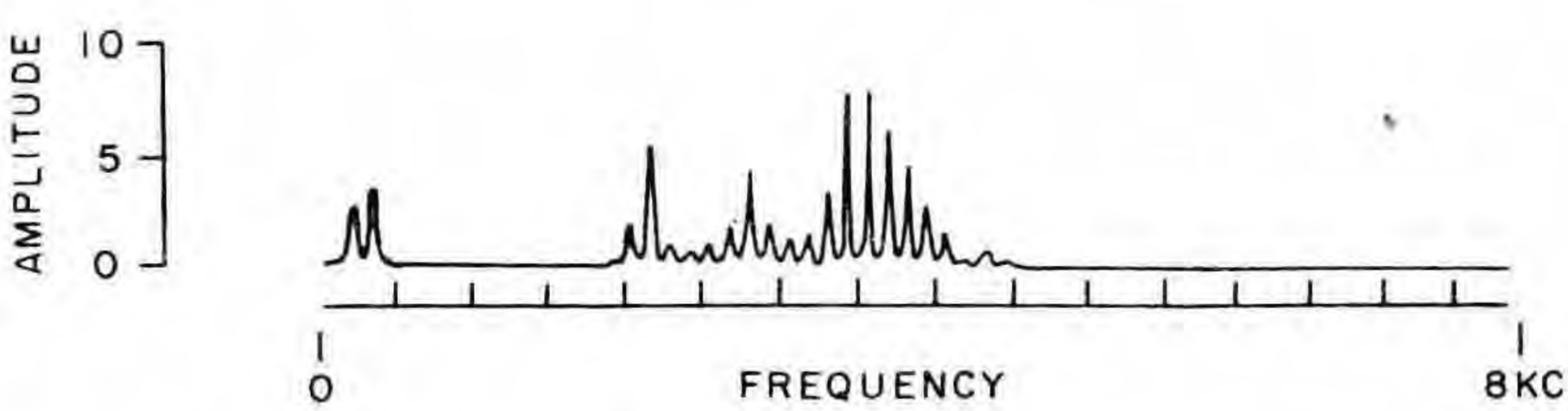

FIG. 1 SPECTRUM ANALYSIS OF THE VOWEL, / i /

[1] Technical Report FSC-T-1/100, Federal Scientific Corporation, New York, N. Y., 1958.

Figure 1 is a reproduction of an oscillographic display of the analyzer which illustrates some of the characteristics of the data that are provided. The analysis is of a segment of the vowel sound, /i/, from the spoken word "the." Below the main trace is a line of frequency calibration markers, spaced 500 cps apart. Note that the envelope of the harmonics of the fundamental voice frequency has peaks at 400 cps, 2200 cps, 2800 cps, and 3500 cps. (Frequency equalization of the speech signal is employed for visual presentation to enhance the higher frequencies.) Such an analysis appears on the face of an oscilloscope of the analyzer each 30 msec. It represents the Fourier analysis of the signal fed into the analyzer for the preceding 30 msec. (A shorter time interval for processing can be selected if desired.) Simultaneously the analog signal which feeds the oscilloscope is converted to a digital output so that it can be employed as data input to a high-speed computer. Thus the analyzer provides spectral data essentially in real time, either in the form of a series of oscillograms or in the form of bursts of information. For operation in conjunction with a computer that has the capacity for handling information at a high-bit rate, a compatible analog-to-digital read-out system has been constructed. Because of the high resolution of the data which are supplied by the analyzer, the sample rate must be sufficiently high (as high as 330 kc with seven-bit accuracy) and the scanning aperture must be sufficiently narrow, to avoid a loss of useful spectral information. The output of the read-out system is applied to an IBM 729-II digital recorder, operated in the high-density mode. Tape from this unit then feeds into an IBM 7090 computer.

SPEECH RECORDINGS FOR ANALYSIS

All of the speech sounds that have been analyzed in this program first were recorded on a high-quality magnetic tape unit. Then the analyses were performed using these recordings as a source. The words were selected arbitrarily from a table[2] listing the frequency of occurrence of words in written English. The first 27 words, representing 38% of the words in written English, were selected. In addition, three of the words were included in variant form.

The recordings were prepared at the University of Michigan under the supervision of Professor Gordon E. Peterson, assisted by Miss J. Shoup. For our study of rates of change of formant frequencies, twenty-five male speakers having general American speech were employed. The speakers were instructed to use what can be described as normal pronunciation, natural intonation, medium emphasis, and natural duration. The list was repeated three times with the words spoken at a normal rate. Then the entire word list was repeated two more times---for rapid speech (short duration) and for slow speech (long duration); an attempt was made to keep the other attributes relatively constant. Thus there are a total of 2,250 recorded words. In addition, there are 5,250 other recordings in which other parameters are varied.

---

[2] Fletcher, H.,"Speech and Hearing," Table 8, p. 90, D. Van Nostrand, New York, N. Y., 1953.

EXTRACTION OF FORMANT FREQUENCIES AND PITCH

In establishing a computer program to provide data on rates of change of formant frequencies, it was necessary to develop a program that extracts formant frequencies; pitch also is extracted. As a first step, a sequence of photographs (such as the one reproduced in Fig. 1) was obtained which provided a Fourier analysis as a function of time. Next, a program was established to reduce these data by mechanical techniques. Once the manual computer program was checked, it was converted to a digital computer routine employing Fortran language, with FAP language employed in sub-routine programs. The digital computer program was then checked and rechecked many times through study of processed data obtained from the computer until a computer program was developed that was more precise in obtaining both formant frequencies and pitch than the mechanical procedure. Several routine system calibrations are used throughout the process of data reduction with the computer. At periodic intervals between words to be analyzed, a known spectrum of sine waves is presented for analysis; also a word previously analyzed is repeated at periodic intervals as a running check on the overall system. The ability of the present program to extract both pitch and formant frequencies has been checked by independent analysis techniques.

RATES OF CHANGE OF FORMANT FREQUENCIES

In a large-scale program of spectrum analysis, whether it be that of analyzing acoustic background noise in the ocean or radio frequency noise from outer space, the problem of recording and analyzing the signals often is not as complex as the problem of reducing the data from thousands of analysis records to some common denominator. High-speed and relatively inexpensive operation, as we have here, only compounds the problem since much more data are extracted. Thus, it is necessary that the computer be employed in an effective program to reduce the large volume of analysis data that it provides.

At the present time, our formant and pitch extraction programs can obtain these quantities accurately for conditions tested to the present date. For example, Fig. 2 shows data obtained from a typical IBM 7090 computer output from the analysis of the word I, /aɪ/. These data are for a single speaker, talking at three different rates: fast, normal, slowly. Even for one individual, it can be seen that some form of time normalization is required to reduce the data to a common denominator. This is essential in obtaining statistical data on a number of speakers. Thus the problem of data reduction here is essentially the same as that faced in automatic speech recognition.

In attacking the time normalization problem, the power of high-speed computer techniques becomes evident. Since all information is available on tape in digital form at the computer input, various hypotheses can be checked extensively in hours instead of months by hand-reduction methods. Nevertheless, a hand-reduction program still is required to check the logic of the computer program.

At the present time we are taking two methods of approach. The first method is to characterize a word by a series of parameters (not necessarily restricted to the formant frequencies, but including such parameters as rates of change of formant frequencies and rate of change of power) which are sampled at critical times during the phonation of the word. Thus the analog form of the presentation of these parameters as a function of time is represented by a pattern of discrete events. This approach has two advantages. It presents a convenient method of normalizing data so that they may be tabulated statistically---allowing one to obtain mean values, variances, etc.---and it presents the data in a natural form for utilization in automatic speech recognition. Conditions which we have tried for determining critical events vs. time include: (1) maximum rates of change of F_1, F_2, and F_3, (2) inflection points of these parameters and of pitch, (3) maximum rates of change of power, and (4) change from voiced to unvoiced (or vice versa).

The second method, which has been employed by other investigators, is a simple expansion or compression of the time scale to a value that has been arbitrarily selected as "normal." Examples of both of these methods for use in developing a computer program for time normalizing the various parameters will be presented as slides at the Congress, together with other aspects of the computer program.

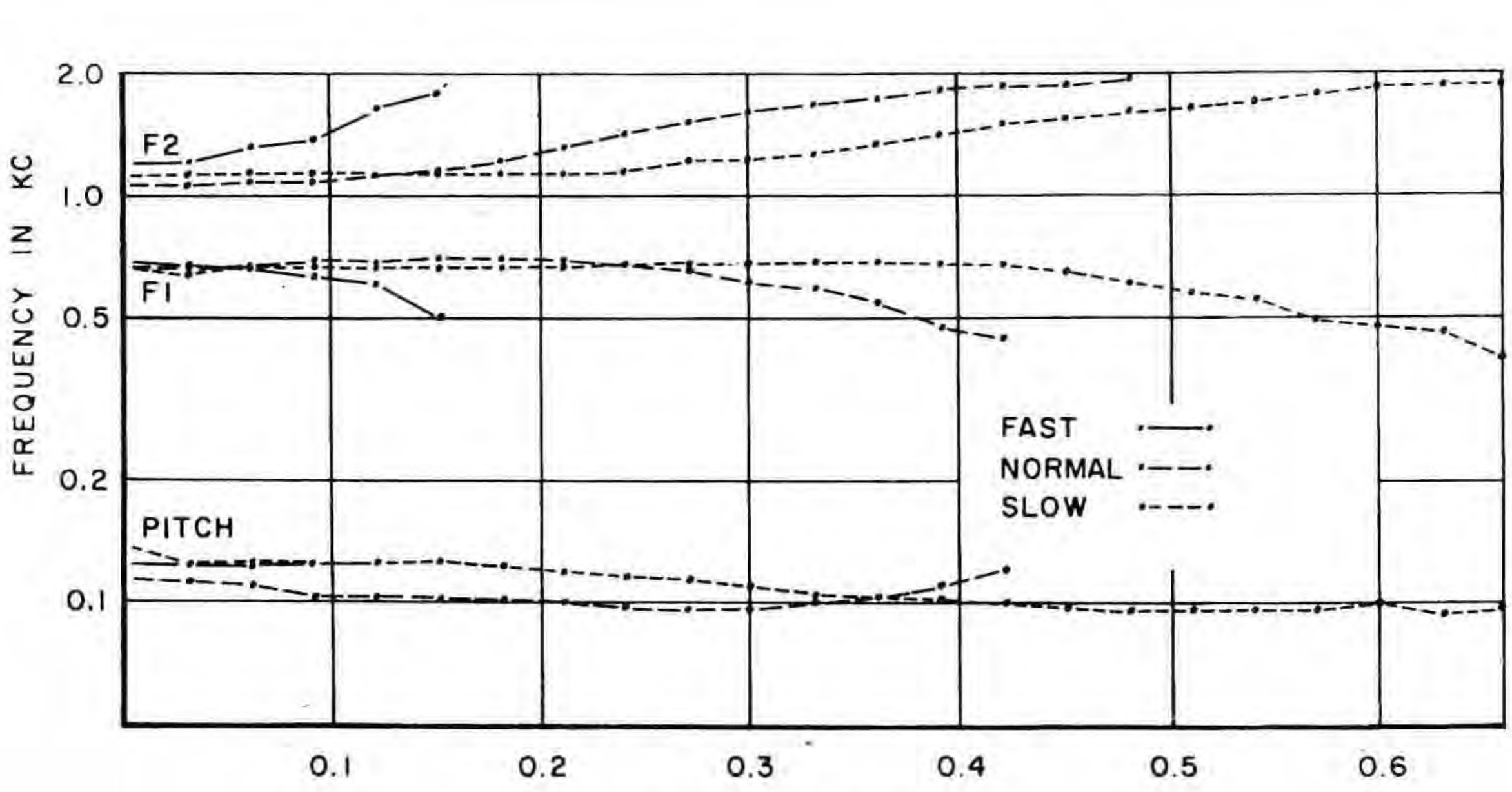

FIG. 2 PITCH AND FORMANT FREQUENCIES VS. WORD LENGTH FOR THE WORD I, /a ɪ/

H47

FOURTH INTERNATIONAL CONGRESS ON ACOUSTICS
COPENHAGEN 21.-28. AUGUST 1962

Über die Kurven gleicher Sprachverständlichkeit

Věra Chalupová - Josef B. Slavík, Physikalisches Institut
der Technischen Universität, Prag, Tschechoslowakei

1. Einleitung

S. J. L i f š i c /1/ hat schon früher die Kurven gleicher Sprachverständlichkeit bestimmt. Dazu verwendete er das Silbenmaterial. Die Untersuchungen wurden im freien sowie im geschlossenem Raume durchgeführt. Solche Kurven hat auch V. O. K n u d s e n /2/ bestimmt, welcher für die Untersuchungen auch das Silbenmaterial benützte. Die Kurven von Lifšic und Knudsen unterscheiden sich. Um diesen Unterschied zu erklären, haben wir uns ebenfalls mit der Bestimmung der Kurven gleicher Sprachverständlichkeit für die tschechische Sprache befasst.

2. Bestimmung der Kurven gleicher Sprachverständlichkeit

Die Bestimmung der Kurven gleicher Sprachverständlichkeit haben wir in Zusammenarbeit mit dem Forschungsinstitut für Ton-, Bild- und Reproduktionstechnik in Prag durchgeführt. Wir untersuchen die Sprachverständlichkeit der männlichen und weiblichen Stimme bei Benützung des Wörter- und Silbenmaterials. (Die Silbenprüfungen ergeben nur ein Bild der deutlichen Erkennung der Mitlaute und Selbstlaute der Sprache.) Die Kurven wurden für den freien und auch für den geschlossenen Raum festgestellt.

Als freies Gelände wurde das Stadion für die Spartakiadenfeste benützt, dessen Ausmass 200 x 300 Quadratmeter beträgt. (Siehe Abb. 1 für männliche und Abb. 2 für weibliche Stimme.)

Für die Untersuchungen im geschlossenen Raume wurde ein Saal benutzt, dessen Rauminhalt 51 900 m^3 betrug. Die Nachhallzeit im leeren

Saal war 3,5 s bei 1000 Hz. (Siehe Abb. 3 für männliche und Abb. 4 für weibliche Stimme.)

Die erzielten Ergebnisse für das Wörter- und auch für das Silbenmaterial zeigen, dass die Kurven gleicher Sprachverständlichkeit in freiem und geschlossenem Raume in der Achse vor dem Sprechenden in grösserer Entfernung vor diesem ein Absinken der Sprachverständlichkeit aufweisen.

Im geschlossenen Raume ist das Absinken in der Achse vor dem Sprechenden durch den Einfluss der Reflexion von den Wänden geringer als im freien. Infolgedessen ist das Absinken in der Achse für weibliche Stimme beim Wörtermaterial fast nicht bemerkbar.

Das erwähnte Absinken der Sprachverständlichkeit in der Achse des Sprechenden ist nach J. C. W e b s t e r wahrscheinlich eine Angelegenheit des Gehörorgans, dessen Richtungsempfindlichkeit nicht die gleiche ist. Eine weitere mögliche Erklärung beruht nach T. T a r n o c z i , dessen Behauptung auch wir uns anschliessen, in der räumlichen Verteilung der Energie des Formantengebietes der einzelnen Sprachenlaute, d.h. diese Erscheinung ist eine Angelegenheit der Mundschallausbreitung.

Zur näheren Erklärung des Absinkens der Sprachverständlichkeit in der Achse des Sprechenden werden wir weitere Untersuchungen anstellen.

3. Schlussfolgerungen

Die festgestellten Kurven der gleichen Sprachverständlichkeit zeigen für männliche und weibliche Stimme und für das Wörter- und Silbenmaterial im freien und geschlossenen Raume in der grösseren Entfernung vom Sprechenden ein Absinken der Sprachverständlichkeit oder deutlichen Erkennung der Sprachlaute in der Achse vor diesem.

Ob diese Erscheinung eine Angelegenheit des Gehörorgans oder der Mundschallausbreitung ist, darüber werden weitere Untersuchungen durchgeführt werden.

Literatur:

/1/ S. J. Lifšic, Kurs architekturnoj akustiki, 1937, S. 88 - 89.

/2/ V. O. Knudsen, Architectural Acoustics, 1949, S. 498 - 499.

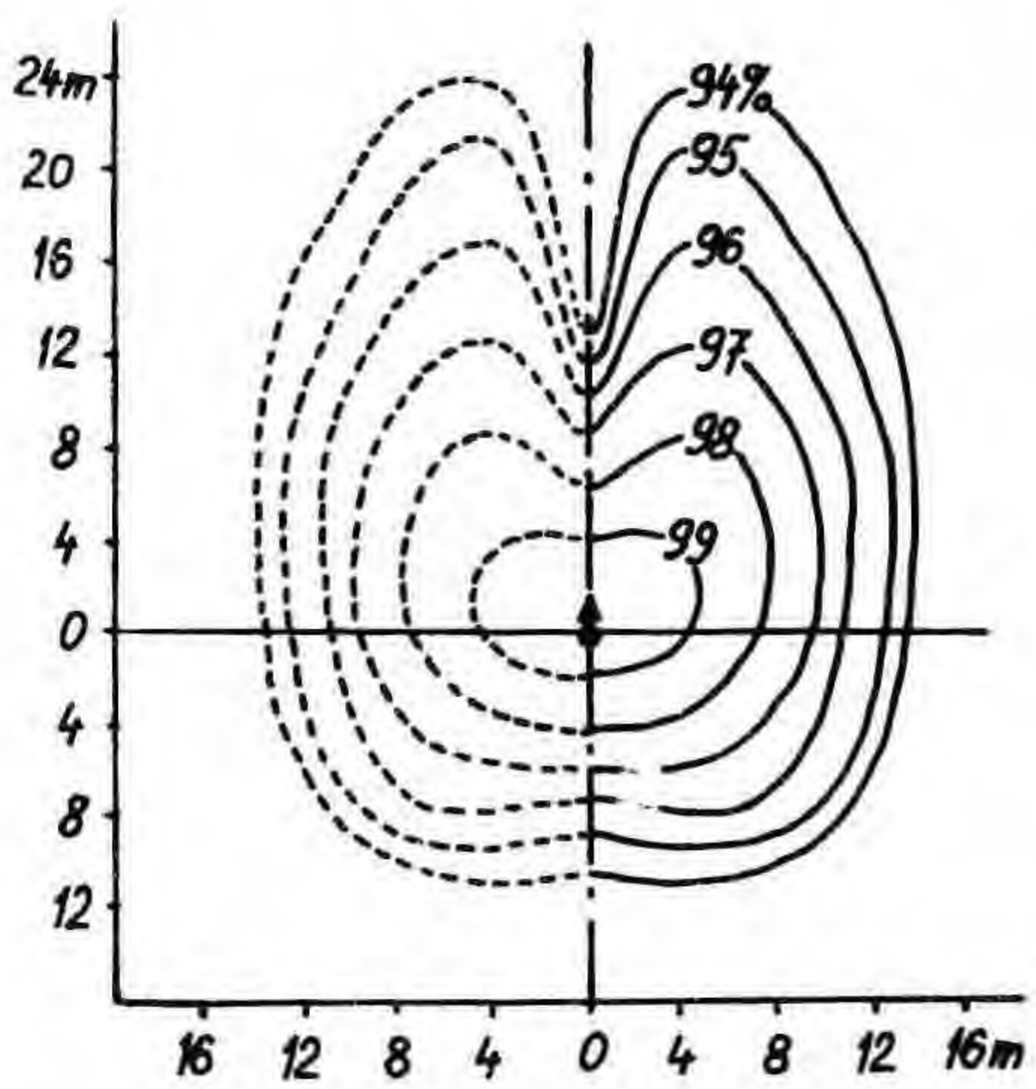

Abb. 1.
Kurven gleicher Verständlichkeit im freien Raume für Wörter und männliche Stimme. Die Sprachverständlichkeit ist in % angegeben.

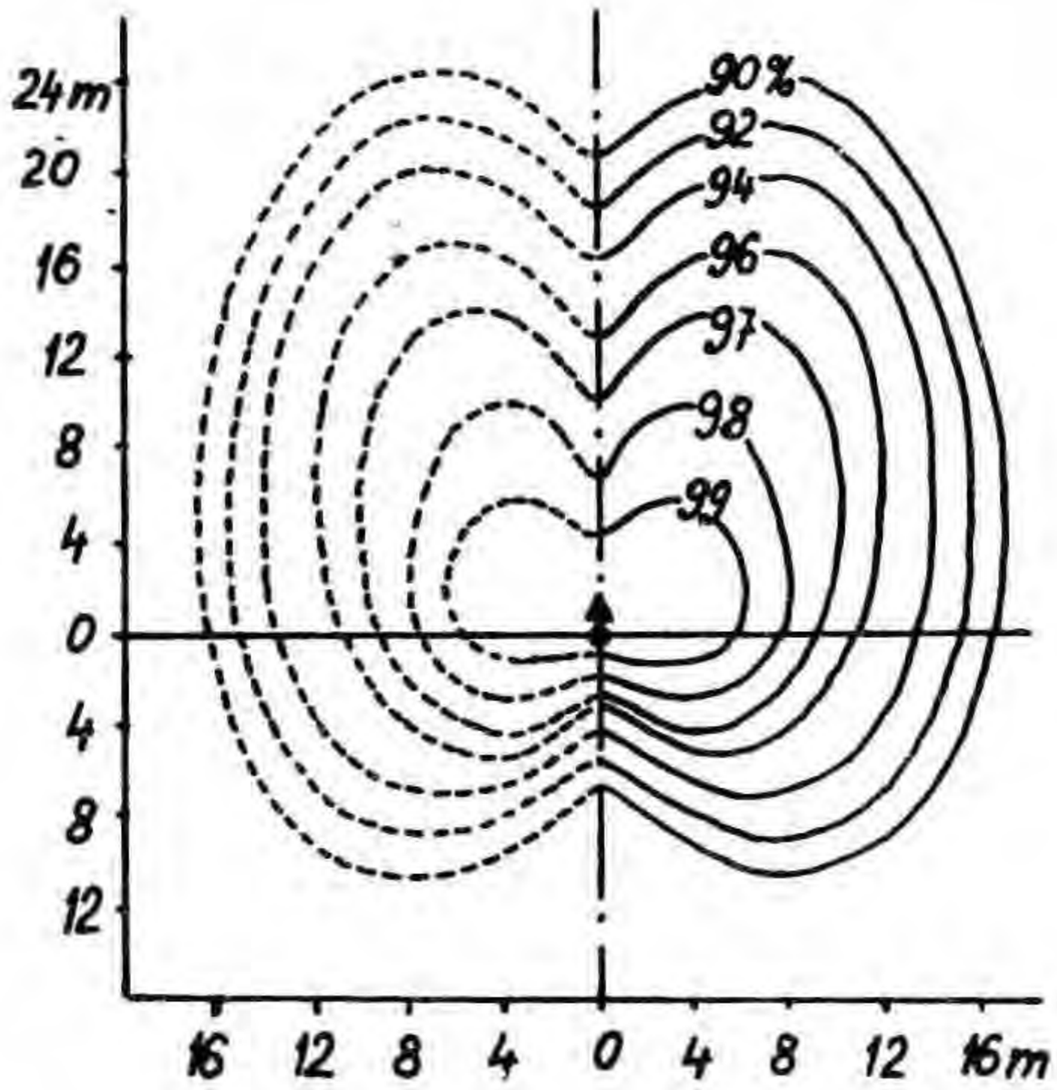

Abb. 2.
Kurven gleicher Verständlichkeit im freien Raume für Wörter und weibliche Stimme. Die Sprachverständlichkeit ist in % angegeben.

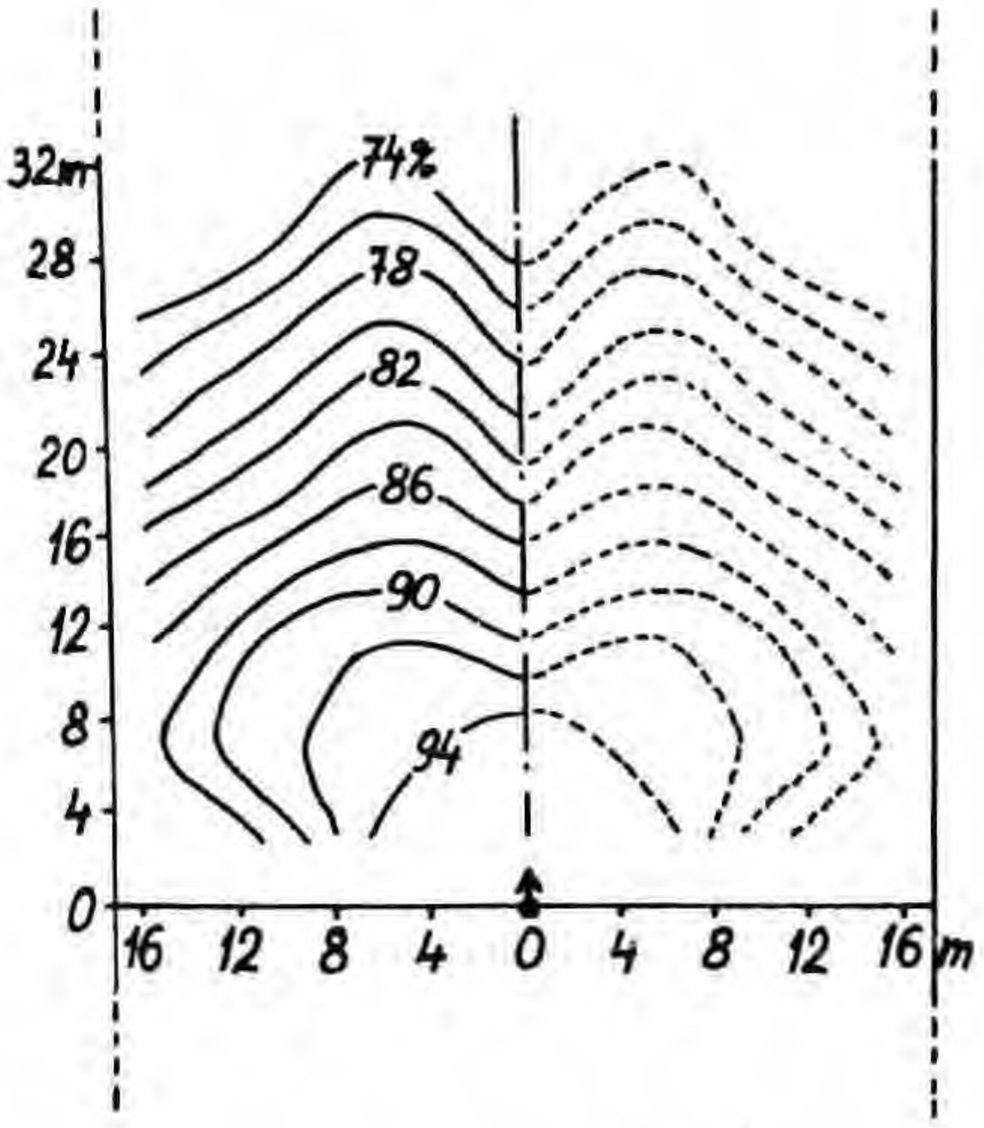

Abb. 3.
Kurven gleicher Verständlichkeit im geschlossenen Raume für Wörter und männliche Stimme.Die Sprachverständlichkeit ist in % angegeben.

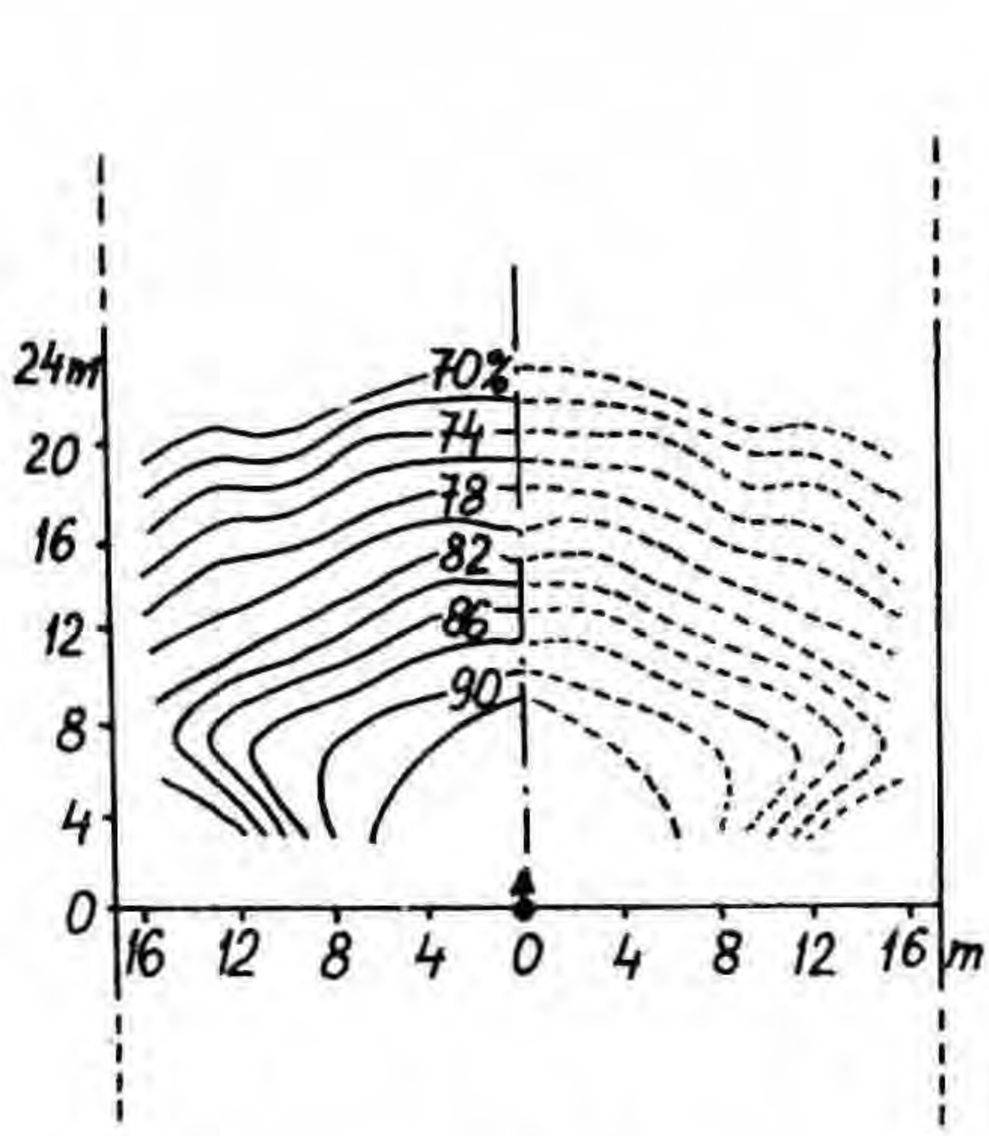

Abb. 4.
Kurven gleicher Verständlichkeit im geschlossenen Raume für Wörter und weibliche Stimme.Die Sprachverständlichkeit ist in % angegeben.

L47

FOURTH INTERNATIONAL CONGRESS ON ACOUSTICS
COPENHAGEN 21.-28. AUGUST 1962

A PROPOSED SOUND-ABSORBING DEVICE IN THE HIGH VELOCITY DUCT SYSTEMS

Masayuki Matsui: Ass. Prof. of Training Institute for Engineering Teachers, Tokyo Institute of Technology

Kinya Nakamura : Marunouchi Manufacturing Co., Ltd.

PREFACE

High velocity duct systems(v=15-30m/sec) for air conditioning are gaining wide acceptance in the field of modern buildings. The use of these systems permits substantial reduction in the space requirement as compared with conventional low velocity duct systems. With sound absorbing methods which have hitherto been used in the low velocity duct systems(v=5m/sec), it is difficult to obtain a sufficient air conditioning effect. Objectionable noise is inherent in these systems which results from the friction of air flow of high velocity. It is also to be noted that horse power required for blowers leads to increase, if used in a high velocity system, because the large attenuation by muffling devices is often in proportion to the resistance to air flow.

In this study, we designed the device for mufflers with a screen duct of the same size as the supply duct with a sound-absorbing layer around it and with the mitigation zone between the screen and the layer. To solve the vibration problem inherent in the high velocity air flow and other objectionable properties, and to provide for the durability of the screen duct, we built a screen duct consisting of a rigid perforated plate lined with a sheet of glass fabric. From the test, with this muffling device, a large amount of attenuation was obtained. The static pressure of the air flow in the muffling device is 3 to 4 times that in a vinyl tube of the same size and 1/10 time that in a sound attenuator connected with a diffuser.

APPARATUS AND MEASURING METHOD

Measuring equipment(Fig.1) We used the white noise and the blower noise as the sound-sources. To prevent the vibration of the duct due to air flow and white noise, the ducts in front of and behind the test

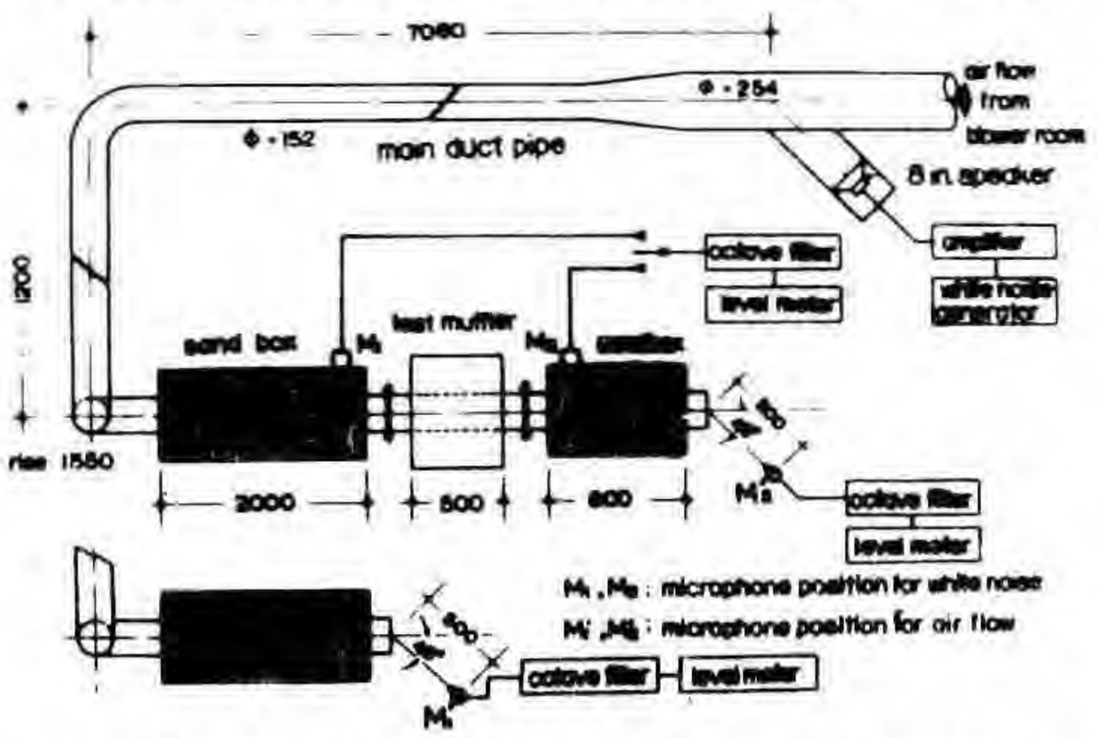

Fig.1 A schematic equipment lay-out for measuring attenuation by muffler.

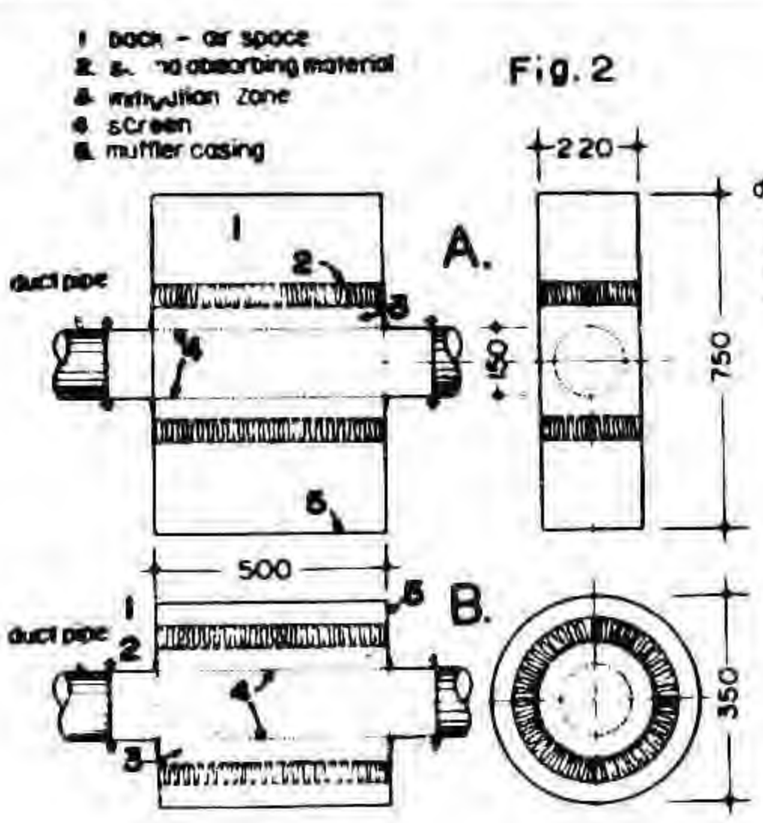

Fig.2

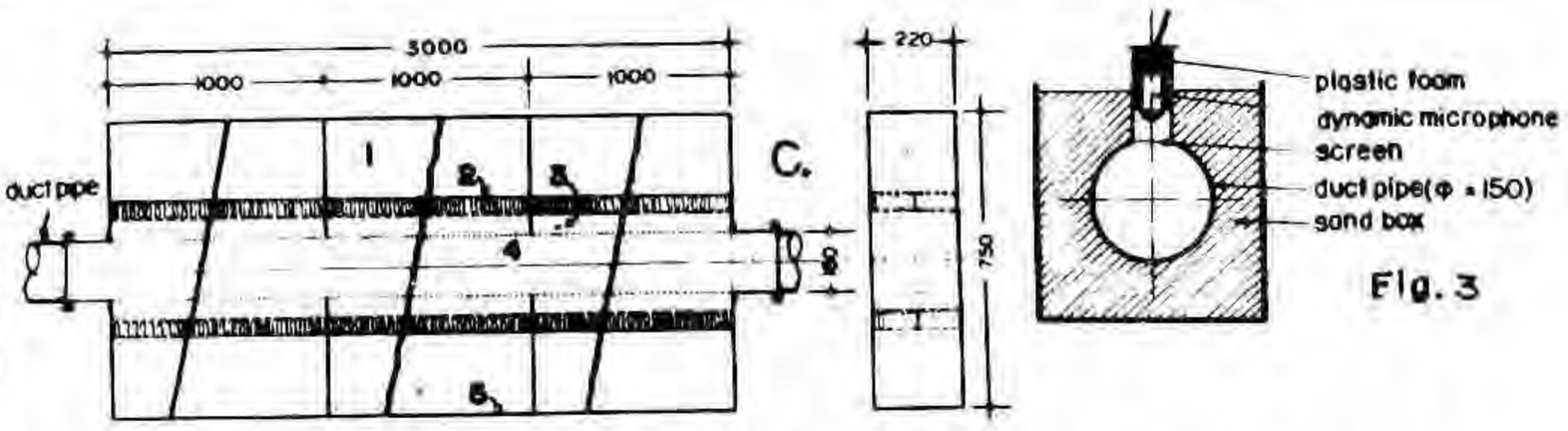

Fig.2 Various forms of cross-section for mufflers.

Fig.3

Fig.3 Detail of sand box and microphone position for white noise.

muffler are surrounded by sand boxes. The blower, placed in another room, generates maximum air velocity of 30m/sec for a duct size of 150mm in diameter with a variable volume damper.

Test mufflers The test mufflers(Fig.2) are of the following types: (A)rectangular, (B)cylindrical, and (C)continuous. The screen duct was made of a rigid cylindrical perforated plate(p=60%,p:perforation degree) with a glass fabric inside. An air space, 50mm wide, was prepared around the screen duct as a mitigation zone. The air flow in the duct passes through the screen duct of the same size as the supply duct, and the noise from the sound source is absorbed in the layer through the screen duct and the mitigation zone. The muffler has the feature of separating the high velocity air flow which is mingled with the noise into two components, noise and air flow, and then absorbing the noise. The layer consists of a sound-absorbing material, glass wool or plastic foam, etc.

A. The rectangular mufflers(Fig.2-A) This type is placed most suitably in the space between the slab and the ceiling of a building. With this, a large space of air is secured behind the sound-absorbing material to increase the absorption of the low frequency band noise.

B. The cylindrical mufflers(Fig.2-B) This type of muffler, when placed in such a shallow space as between the slab and the ceiling of a building, has the drawback of lessening the air space necessary for the absorption of the low frequency band noise.

C. The continuous muffler(Fig.2-C) For this type, not less than two rectangular mufflers are lined up, end to end.

Methods for measuring attenuation Experiments were carried out on the white noise and the blower noise. The attenuation was indicated by the level difference from the sound level meter, through the octave filter between M_1 and M_2, which were set in two tubes in the sand boxes(Fig.3), in front of and behind the test muffler used for the white noise. The amount of attenuation for the blower noise was expressed as a

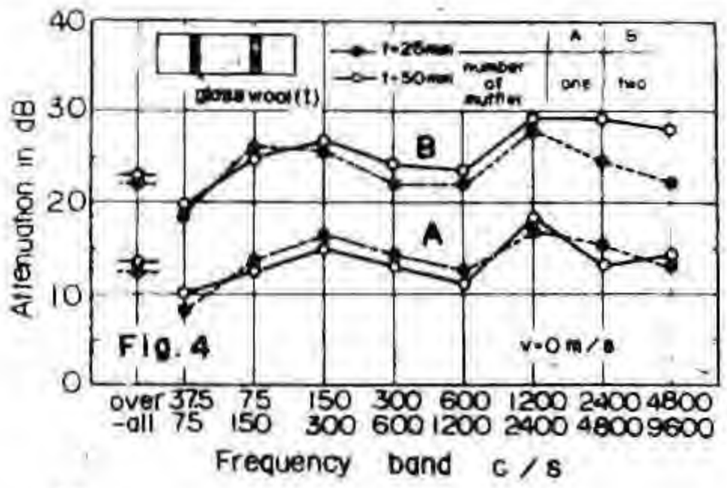

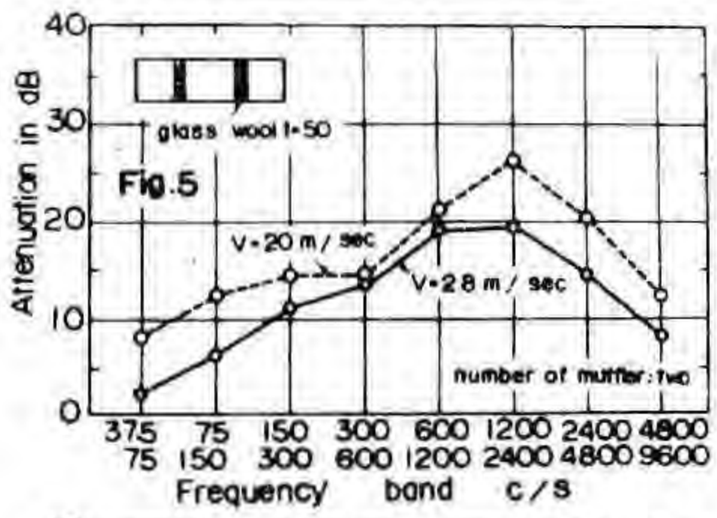

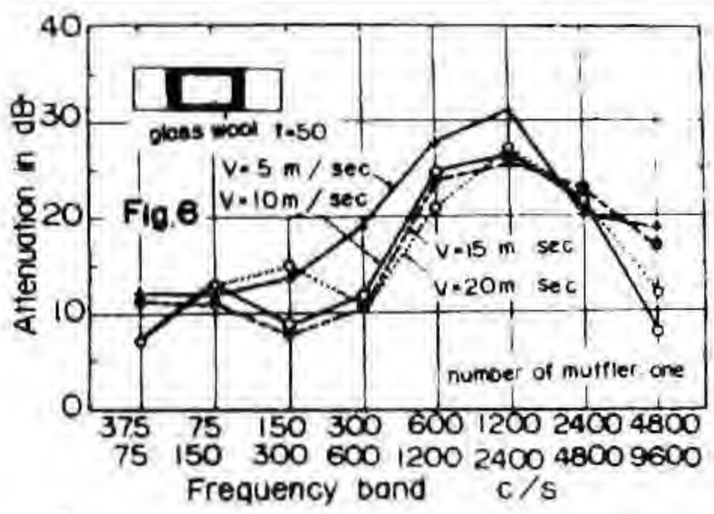

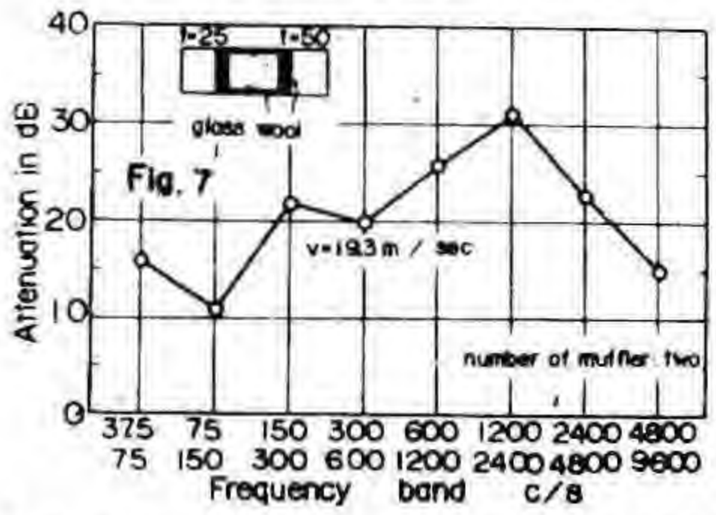

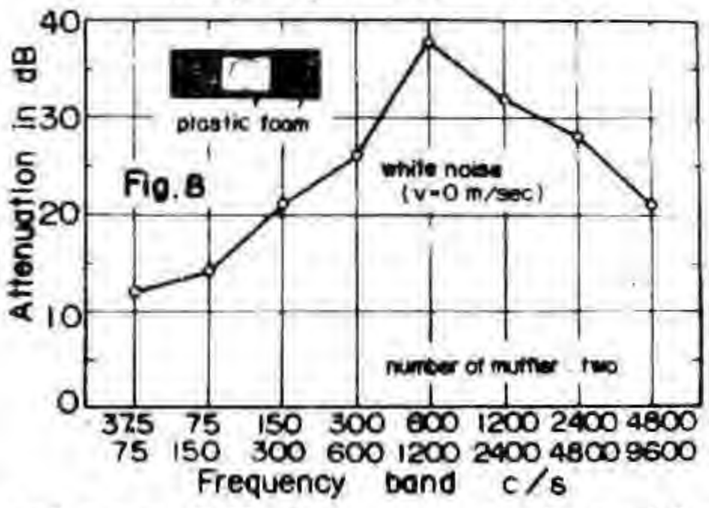

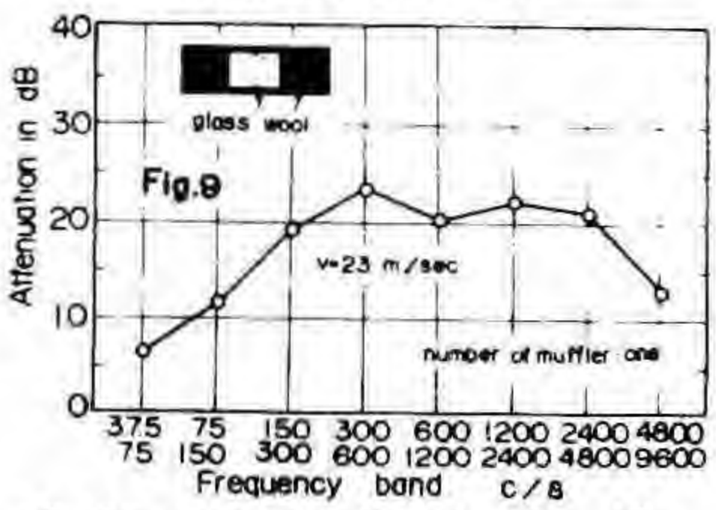

Fig.4-9 Attenuation of rectangularmufflers, as a function of frequency band, in dB.

difference in level between M_1' and M_2', which represented conditions with and without the muffler respectively, and were placed at points 500mm distant from the outlet center, and at an angle of 45° with it.

RESULTS OF MEASUREMENTS

1. Attenuation by rectangular muffler(Fig.4-9) For the white noise measurements, an average attenuation of about 12 dB was obtained on a single muffler. The thickness of the glass wool did not have much influence on the attenuation(Fig.4). In the measurements of the blower noise combined with the air flow, a considerable amount of attenuation was obtained, despite the co-existence of the air flow, and the amount of attenuation is larger with a smaller velocity of the air flow. Generally speaking, the muffler has a peak of attenuation in a three frequency band of 600-4800 c/s. This is more effective in bringing the Speach Interference Level down(Fig.5-7).

The attenuation leads to an increase over the middle frequency bands if the sound-absorbing material fills the whole air space in the rear.

2. Attenuation by cylindrical mufflers The results of the measurements for the white noise(Fig.10) show almost the same inclination as those for the rectangular mufflers(Fig.4). The attenuation is smaller in the low frequency bands in measuring the blower noise. With the lower velocity in air flow, the amount of sound attenuation increases (Fig.11, 12).

3. Attenuation by continuous mufflers(Fig.13, 14) In the case of the white noise, Fig.13 shows an average attenuation of about 30 dB as the absorption inside is smaller, and Fig.14 shows an average attenuation of 42 dB. The attenuation increases in high

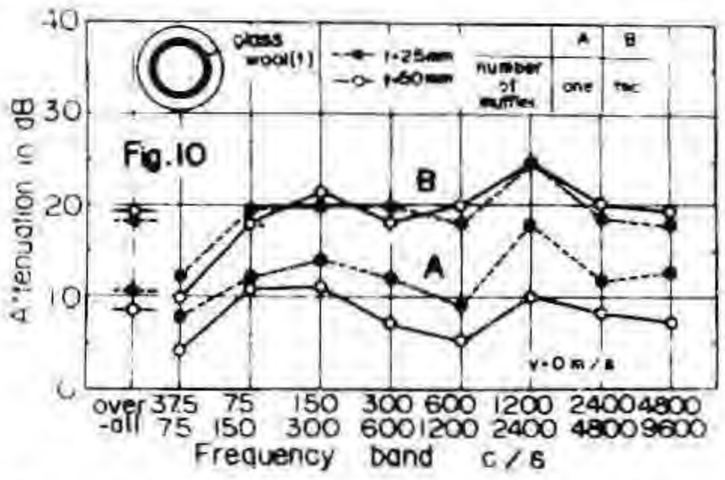

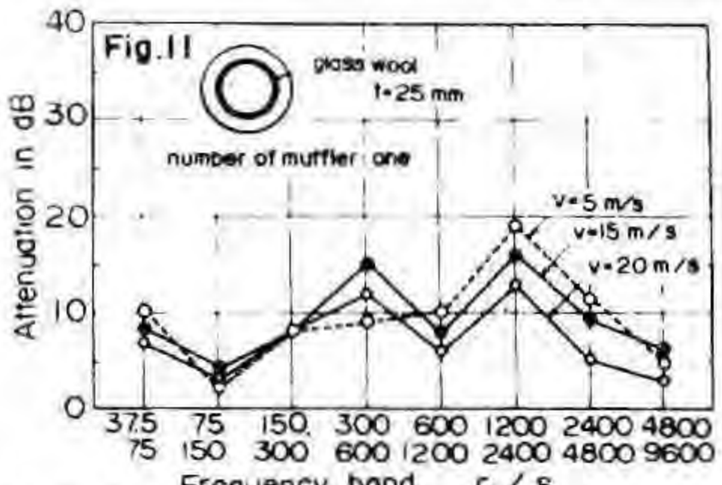

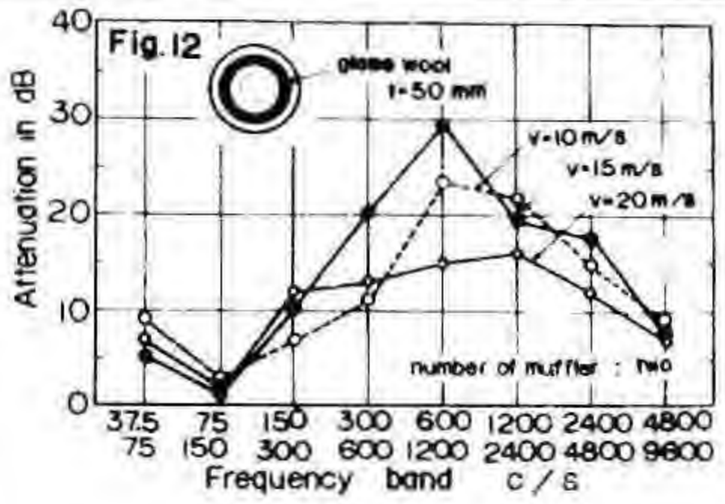

Fig.10-12 Attenuation of cylindrical mufflers, as a function of the frequency band, in dB.

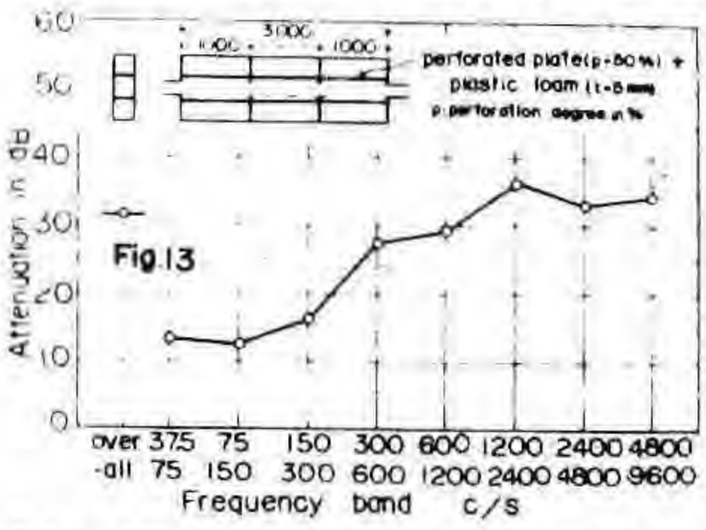

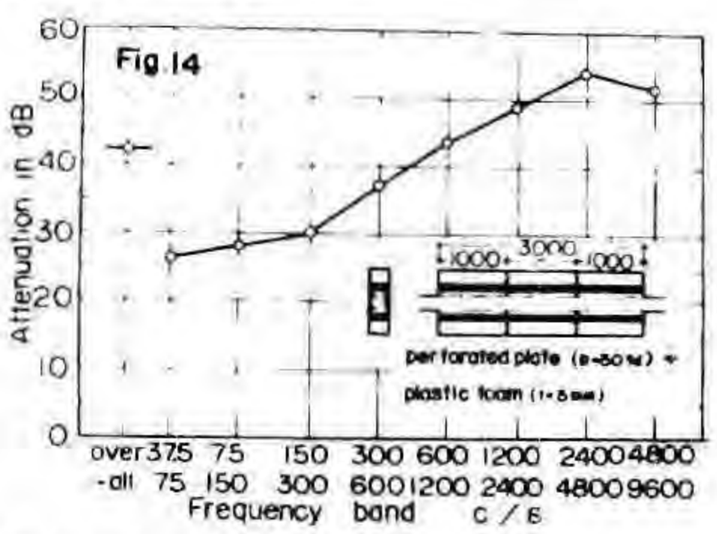

Fig.13,14 Attenuation of continuous mufflers

frequency bands. For the blower noise, an average attenuation, subtracted by 10 dB from that for the white noise, can be estimated from the above-mentioned results.

CONCLUSION

The results of the above measurements, using the method by which the separation of the high velocity air flow into two components, noise and air flow, was performed, met our expectations. A conclusion was derived, from an experiment which had proved that the difference in attenuation made by varying the thickness of the absorbing material was small, that the effect of the attenuation through the screen duct was not negligible, although at the beginning of the experiment the effect was ignored. It is considered that because of the influence of the noise leakage from the main duct the low frequency band attenuation was smaller as compared with that for the white noise. Much attention was paid in the study, to the problem of the noise level measurements accompanied by air flow, and to the elimination of the friction-noise generated in the screen duct because of the high velocity air flow. Of the former, the measurements were made by placing cloth-covered microphones at the points, M_1', M_2'. With this device, we are confident of having obtained an air velocity up to 30m/sec.

ACKNOWLEDGMENT

Grateful acknowledgment is made of the assistance granted by Mr. Fukuo Saeki, president of Marunouchi Manufacturing Co., Ltd. and Mr. Masaki Makihara, factory manager for that company. Our thanks are also due to Mr. Yoshio Namba, Mr. Fumiaki Shinjo, and others, for their co-operation in and contribution to the test.

M47

FOURTH INTERNATIONAL CONGRESS ON ACOUSTICS
COPENHAGEN 21.-28. AUGUST 1962

INFLUENCE OF ACOUSTICS ON DESIGN AND CONSTRUCTION OF BUILDINGS IN AMERICA TODAY

Robert B. Newman

Bolt Beranek & Newman Inc., Cambridge, Mass., U.S.A.

More than sixty years have passed since Professor Wallace C. Sabine did his historic work on room acoustics at Harvard University. We are all familiar with his equation for reverberation time that we use today. In the ensuing years there has been a growing number of workers in this field all over the world. Although architects occasionally turned to these experts for help in the design or remodeling of an important concert room or church, until the recent post-war period, architectural acoustics has never been considered very important in the process of building design. The past fifteen years, however, has seen tremendous progress in applied acoustics, and a great many buildings being designed today are influenced by the vast fund of available knowledge in this field.

Perhaps the most important task of the acoustics consultant is to educate architects and engineers to realize that the acoustical environment is important and basic in every building project, not only in churches and concert halls! They can be taught that there is no need for surprises in buildings and that results can be predicted in advance. Today with the use of lighter weight building materials and demands for movability of partitions, many hotels, office buildings, and apartment houses are put up with too little attention to acoustics. This almost always results in unsatisfactory buildings. Through the efforts of workers in the field, the architectural profession and the public at large are becoming increasingly aware of the fact that good acoustics conditions can be the result of careful initial planning of buildings, and that the occupants can be assured of a satisfactory acoustic environment.

Until recently, very few architectural students in America had anything more than one or two casual lectures on architectural acoustics and usually by some one from the physics department who is more interested in atomic fission. Today in many of our important architectural schools, courses in acoustics are being taught regularly, often by people who are in active practice in the field. The effect of this training of the younger architects is making itself evident. We are often delighted to find ourselves being asked to collaborate in the design of a project that has been done by a well-informed architect who has already set the stage for an excellent result by sensible basic planning and disposition of elements. He has made a good selection of a structural scheme that can be made to work acoustically, and he is usually not asking us to perform any miracles with a domed auditorium!

In spite of this increased understanding of the basic principles of architectural acoustics, many new buildings are put up in America (and in other parts of the world!) in which auditoria have ceilings covered entirely with sound absorbing materials, in which a sound reinforcement system consists of those ubiquitous brown boxes placed along each side of the room facing the opposite side, and in which the air-conditioning system massages the feet of the lecturer and makes a noise like a waterfall. Too many designers still think that, if they want good acoustics, they must use "acoustical" materials, and they fail to understand the basic influence of acoustics on design. In fact, the well-informed architect realizes that acoustics can be a resource for design and can influence strongly the kind of building he does.

We in acoustics play an important role in the design of many new buildings, both commercial and public. In the modern office building in America there is an almost universal demand for some degree of flexibility. Bearing partitions are almost never used, and it is expected that partitions will at least be removable without affecting the structure of the building, and in many cases there is a demand for "over the weekend" re-arrangement of office spaces. This demand for flexibility, coupled with the fact that floor slabs are thinner, that windows are fixed, and air conditioning is almost always used, have imposed a whole series of problems that must be solved if the occupants of these new buildings are to enjoy "old-fashioned" privacy. This has led to some very careful study on just what it is that gives speech privacy, and the quantitative criteria have now been rather well established.

It is now commonplace that both minimum and maximum background noise levels are specified for occupied spaces in new office buildings (usually a minimum around NC-30 and maximum NC-35). Almost any desired background noise spectrum is obtainable in a building that is totally air-conditioned because we have available the air-distributing devices which can be operated and controlled to produce the desired noise levels. In an urban environment we may have to count on traffic or other sources as well if they influence the background noise condition. Only with such an assured background sound level can we have privacy with the types of readily movable partitions that are in use today. Even with this much background level, care must be taken in detailing and installing partitions. The problem of adequate sealants between movable partition components and the basic structure has not been completely solved, but most manufacturers are now aware of the needs. In fact, several test laboratories in the U.S. for measuring the sound isolation of prefabricated building components have irregularities built into the test opening to assure that the results will be indicative of the performance of the complete assembly rather than just that of a part of the construction. The gaskets are very much a part of any movable partition assembly.

With the advent of the totally air-conditioned office building comes the problem of excessive noise from the mechanical equipment. Large fans and compressors are almost always located on the roof, directly above the president's office! In very tall buildings there are often a number of floors of air-conditioning equipment located at intermediate levels so that sound and vibration is of concern both upwards and downwards. In any case, it is almost always desirable to have reasonably quiet conditions in the spaces located very near the major mechanical equipment rooms. This means great

care in mounting such mechanical equipment. Good practice requires heavier-than-normal floor slabs for mechanical equipment spaces and often that pieces of equipment themselves be mounted on massive slabs of concrete weighing three or four times as much as the equipment itself. These "inertia" slabs may be carried on glass fiber or cork with the machine, in turn, supported with highly compliant spring and rubber mounting assemblies. We find that, with careful initial installation, the owner can be assured of quiet in the occupied space directly below such equipment.

Another problem not present a few years ago is that associated with the high velocity distribution of air. Air is frequently distributed at 4000 ft per minute (1300 meters per minute) or more. While air is seldom delivered to occupied spaces at these velocities, it can create serious turbulence noise problems in the ductwork en route. Turns and transitions must be designed and constructed very carefully to avoid serious noise problems. We have seen cases where whole floors of new buildings were quite unusable because of noise from duct turbulence. The problems are well understood, however, and design in advance can assure good conditions.

The mania for flexibility is even greater in the field of school design. Many educators demand not only that the partitions between classes be movable almost at will, but that a large space with uniform ceiling height be subdividable for groups ranging from ten to two hundred people. This philosophy unfortunately is sometimes incorporated in schools, although we can usually persuade architects that a 200-seat lecture room should have more ceiling height than a ten-man seminar room! Educators and architects must understand that true flexibility in a school comes with the provision of a variety of spaces, each ideally adapted to its particular use, and all usable at the same time. It is easy in the initial planning (but so hard later) to arrange things so that the band rehearsal will not be audible in the study hall or in the auditorium. We saw a new classroom building in a college recently in which alternate classrooms had to be left vacant because the sound isolation was inadequate (sound transmission through a lightweight, porous, suspended ceiling into the plenum and down again on the other side!). Manufacturers in the U.S. have given a good deal of attention in recent years to developing high sound isolating acoustical tile units to solve this particular problem and many products are available which allow uninterrupted plenums above the partition systems. We also looked at a high school where a lecture in one classroom gave the students in the adjoining room all the answers to an examination in the same subject. This was a case of a poorly-installed partition. Good components -- bad installation.

It has become almost commonplace now to expect that a school or community auditorium will be an excellent room in which speech and music can be heard and enjoyed by everyone. While the techniques for electronic sound amplification have been continually improved, we feel that we must do everything we can with natural sound reinforcement in the space, and then use the sound amplification system to supplement the "natural acoustics". This often requires an integrated architectural-electroacoustics approach, especially in large auditoria. With small capacity auditoria, simple forms with hard, sound reflecting ceilings almost always give good results if proper attention is paid to the control of extraneous noise. When amplification is needed, it must be designed for the particular room in question and usually

involves as much engineering effort as all other aspects of the design together. Worth noting too is the recent work of Beranek and others of my colleagues in the field of concert hall design. There is considerable construction and planning activity on new performing arts centers throughout America and the owners and public alike are no longer satisfied with symphonic concerts in the large "dead" motion picture houses so many of which were built in the past.

A rather minor, but still important, aspect of our professional work in acoustics in America is helping the designer sift truth from fiction in the advertising of "acoustical" products. A glass manufacturer advertises that his laminated glass "cuts out 50% more noise" when he has achieved a three decibel improvement in transmission loss! The uninformed architect may think that something really great has been accomplished, and we have to temper his enthusiasm. Recently, there have been at least two companies that have advertised an "acoustic" paint. This material is reported to reduce noise in some way. Some meaningless data have been taken which prove absolutely nothing, and the test results are written into an advertisement to convey the impression that the paint has almost magical properties. It sells for almost twice the price of ordinary paint, and in both cases is ordinary paint with some grit in it!

Thin felt is advertised as a remarkable "acoustical" material, and we even saw one case in which the architect applied this material to a concrete block wall to increase its sound isolating properties! Incredible though it may seem, there are always people who will buy almost any product if the advertising is skillfully done.

Recently an article appeared in one of our best newspapers telling of a restaurant being planned for the 1964 New York Fair (to be near La Guardia Airport) that would be open on three sides and would be "quiet and restful" inside because air curtains would be used to keep out weather, insects, and noise!

In America, today, the acoustician is indeed becoming influential in building design. He finds his most successful and creative collaboration with designers who have somehow been educated in the fundamentals of good acoustics practice. Within the next decade we expect to see acoustics thinking brought to bear on almost all building design.

047

FOURTH INTERNATIONAL CONGRESS ON ACOUSTICS
COPENHAGEN 21.-28. AUGUST 1962

Blast Waves in a Heterogeneous Atmosphere

J. Menkes
E. H. Plesset Associates, Los Angeles, California

The blast wave produced by an intense explosion can be idealized to possess spherical symmetry; the medium is in most cases stratified and therefore adequately described by a one-dimensional model. Two coordinate systems are therefore required for the simplest description of the boundary conditions; polar coordinates are imperative for the blast wave, Cartesian coordinates for the ambient medium. The incompatibility of the two systems is probably the most serious obstacle to a simple description of the problem under study.

It will be assumed that the density is a function only of the radial distance from the source of the explosion. This assumption permits one to describe both the ambient medium and the blast wave by spherical polar coordinates. It is a consequence of the spherical symmetry and the stipulation that the energy content of the wave must be fixed that in general the shock will decay eventually into a sound wave. Initially the shock is very strong as well as nondecaying, and finally the shock is infinitely weak. Of interest in this paper is the initial stage of the shock propagation.

By the introduction of appropriate similarity variables it is possible to reduce the governing partial differential equations to ordinary differential equations, as long as the density can be represented by a power law. The present discussion is concerned primarily with the energy density and the temperature immediately behind the shock front as functions of the shock radius. The latter distance, R, is assumed to be given by $\eta_1 R^{\lambda} = t$. The constant η_1 can be obtained from dimensional analysis and is found to be given by

$$\left(\frac{E_0}{\alpha A}\right)^{1/5-a}$$

where E_0 is the total energy released by the explosive; α is a function of γ; and $A = \overline{\rho} L^{1/3}$, where $L = (\mu/\overline{\rho})^{1/3}$, which is an "energy length."

The fundamental assumptions are (1) the system possesses spherical symmetry, (2) the medium is a perfect and ideal gas, (3) there are no external forces. Under these circumstances, the following equations govern.

The momentum equation:

$$\frac{\partial u}{\partial t} + u\frac{\partial u}{\partial r} = -\frac{1}{\rho}\frac{\partial p}{\partial r} \tag{1.1}$$

The continuity equation:

$$\frac{\partial \rho}{\partial t} + \frac{1}{r^2}\frac{\partial}{\partial r}(r^2 \rho u) = 0 \tag{1.2}$$

The energy equation:

$$\frac{\partial E}{\partial t} + \frac{1}{r^2}\frac{\partial}{\partial r}(r^2 uI) = 0 \tag{1.3}$$

where

$$E = \frac{1}{2}\rho u^2 + \frac{p}{\gamma - 1} \text{ and } I = E + p \tag{1.4}$$

Solutions of the following form are sought:

$$u = V(R)\, f(x) \tag{1.50}$$

$$\rho = \rho_0(R)\, h(x) \tag{1.51}$$

$$p = \frac{1}{\gamma}\rho_0(R)\, V^2(R)\, g(x) \tag{1.52}$$

where $x = r/R$ and $\rho_0(R) = \bar{\rho} R^{-a}$ with the boundary conditions simplified for the case of an infinitely strong shock:

$$f(1) = \frac{2}{\gamma + 1} \tag{1.60}$$

$$g(1) = \frac{2\gamma}{\gamma + 1} \tag{1.61}$$

$$h(1) = \frac{\gamma + 1}{\gamma - 1} \tag{1.62}$$

Substituting Eqs. (1.50) to (1.52) into Eqs. (1.1) to (1.3) yields

$$(x - f)\, f' = \frac{1}{\gamma}\frac{g'}{h} + \frac{a - 3}{3} f \tag{1.70}$$

$$(x - f)\frac{g'}{g} = \gamma\left(f' + \frac{2f}{x}\right) - 3 \tag{1.71}$$

$$(x - f)\frac{h'}{h} = f' + \frac{2f}{x} - a \tag{1.72}$$

where a prime denotes differentiation with respect to x.

Two independent integrals of the system of differential equations can be obtained by quadrature. Introduction of these integrals into the system yields a differential equation of the homogeneous type that can be integrated. The important results are summarized in Fig. 1. The dependence of the energy density and the temperature behind the shock (which is proportional to the energy density) is clearly apparent.

This work was performed under sponsorship of the United States Air Force under contract to AFSWC.

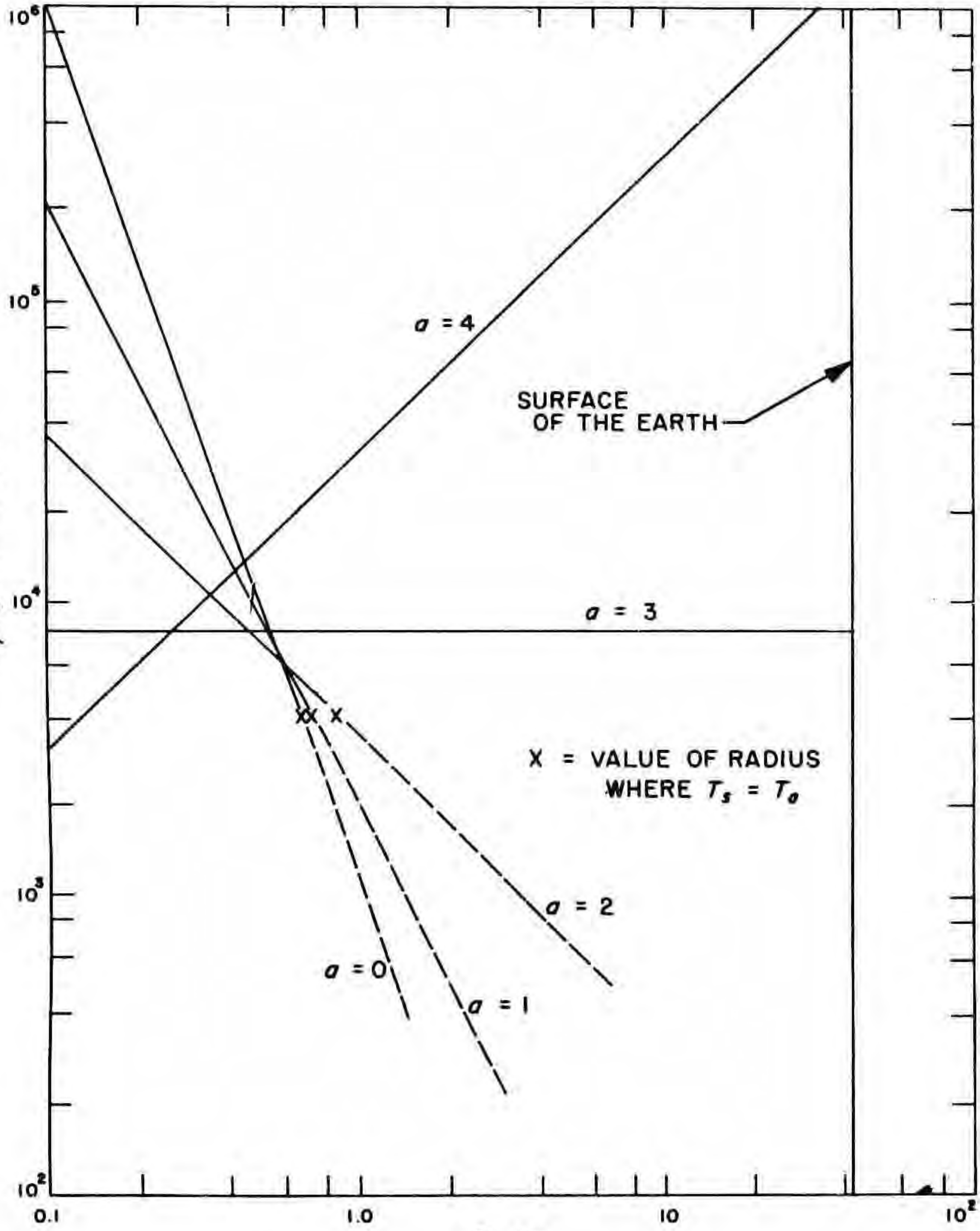

Fig. 1. Energy density vs shock radius (assumed energy input is 20 metric kilotons of TNT at an altitude of 30 km)

H48

FOURTH INTERNATIONAL CONGRESS ON ACOUSTICS
COPENHAGEN 21.-28. AUGUST 1962

Relative Power Transmission Characteristics of the Ear and the Skull from Hearing Threshold Data

Ernest L. Smith
National Bureau of Standards, Washington, D. C.

Sound transmitted to the cochlea by bone conduction can be completely cancelled by proper adjustment of the phase and amplitude of sound introduced into the ears[1]. Under these conditions the vibration pattern of the basilar membrane is the same for acoustic stimulation by air and bone conduction. At the hearing threshold, then, the motion of the basilar membrane must be the same whether the stimulus is supplied through the ear or through the bones of the skull.

This fact has been used to derive a motion transmission characteristic for the skull from threshold data for air and bone conduction for a group of young people with normal hearing. Bone thresholds were determined in terms of the least rms amplitude of vibration of the driver tip[2], while air thresholds were determined in terms of the least rms pressure introduced at the entrance to the auditory meatus.

To arrive at a bone conduction transmission characteristic, data from air conduction experiments were used to calculate the maximal displacement at the basilar membrane. The threshold pressures measured at the entrance to the ear canal were first converted to pressures at the eardrum[3]. Bekesy[4] has given two curves which when combined relate the sound pressure at the eardrum, p_t, to the difference in pressure, p_o, between the fluid behind the oval window and that behind the round window. The values of p_o/p_t thus obtained give the pressure amplification of the middle ear and are shown in Figure 1.

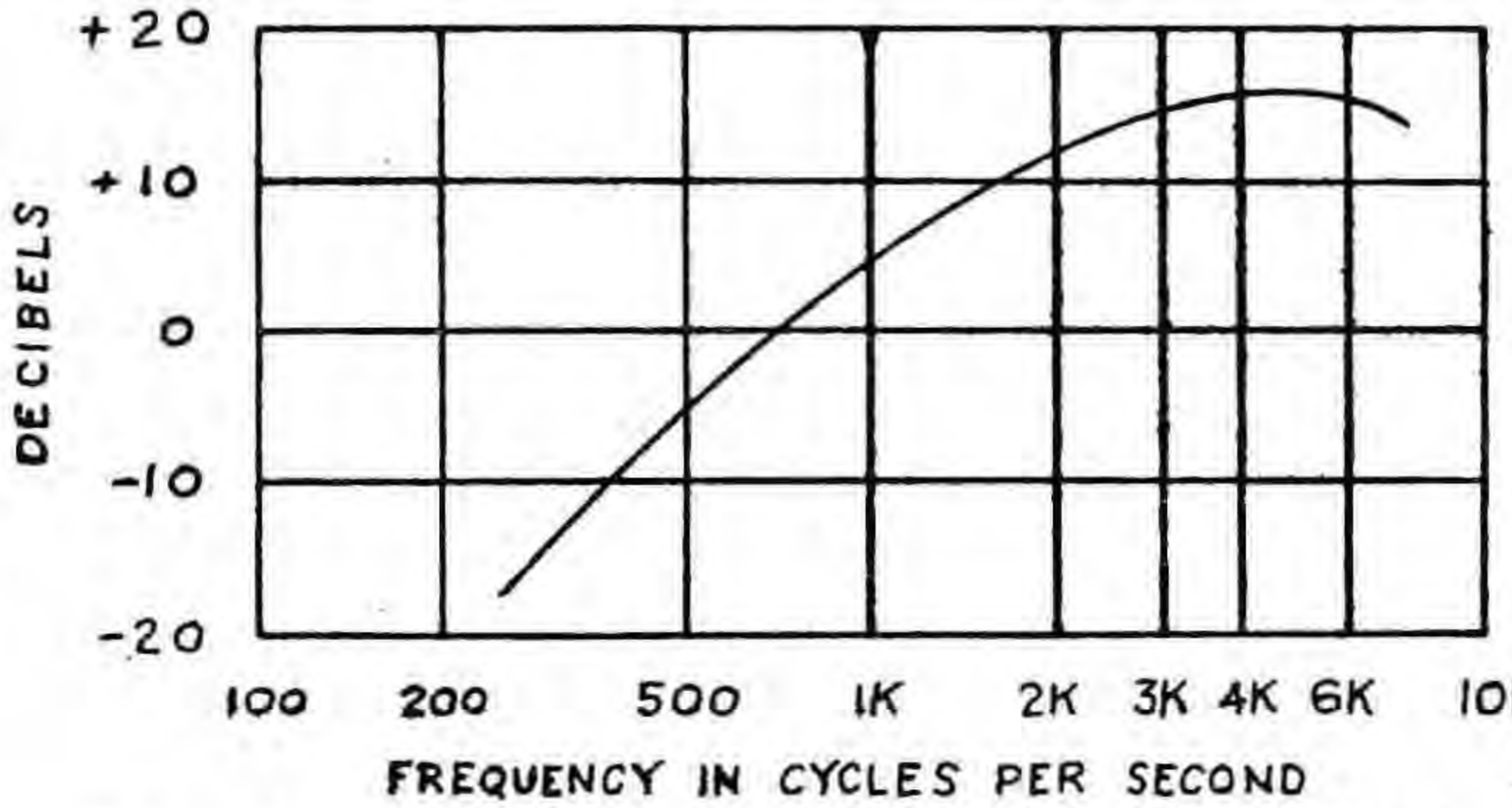

Figure 1. p_o/p_t, Pressure amplification of the middle ear.

---

[1] G.V. Bekesy, Ann. Physik, Vol. 13, 111-136 (1932).

[2] E.L.R. Corliss, E.L. Smith, & J.O. Magruder, Proc. 3rd ICA Congress, Vol. 1, 53-55 (1959)

[3] J. Pollack, Amer. J. Psychol., Vol. 59, 193-219 (1949).

[4] G.V. Bekesy, J. Acoust. Soc. Am., Vol. 21, 233-245 (1949).

Fletcher[5] has derived the dynamical equations for the cochlea from basic hydrodynamical equations and the experimental constants obtained by Bekesy. Solution of the equation of motion by numerical integration, yields the pressure differences on the two sides of the basilar membrane and displacement amplitudes at distances from the stapes corresponding to the resonance positions for the test frequencies. The maximal displacement amplitudes of the basilar membrane for threshold pressures at the eardrum are shown in Figure 2. Also shown are displacement amplitudes for the forehead and mastoid.

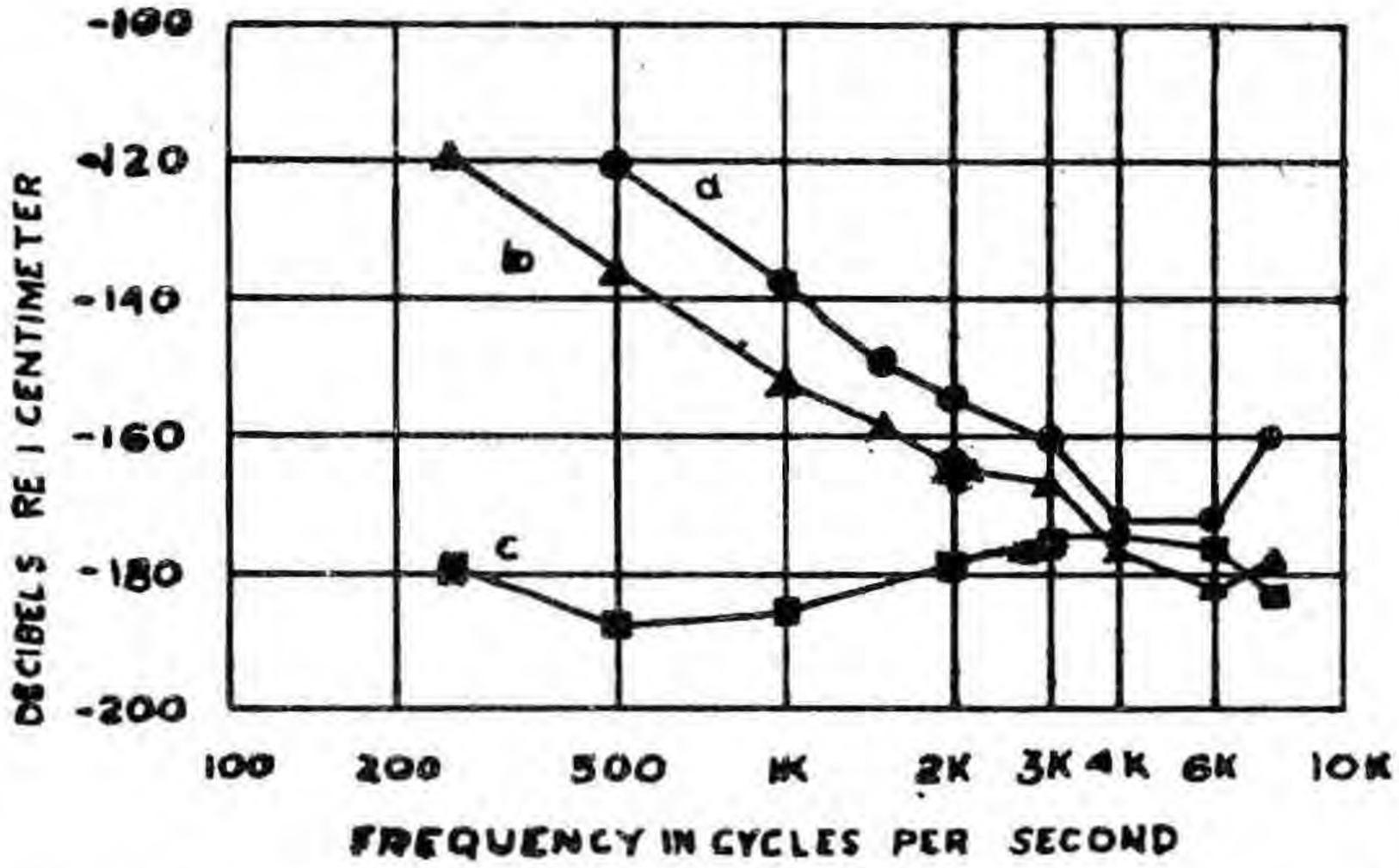

Figure 2. Displacement amplitudes of the forehead, mastoid and the basilar membrane at threshold.
a. Forehead
b. Mastoid
c. Basilar membrane

Since the motion of the basilar membrane is the same for bone conduction, the ratio of the bone conduction threshold displacements to the maximal displacements of the basilar membrane gives the overall motion transmission characteristic of the skull. This ratio d/y_m is shown for the forehead in decibels in Figure 3.

If the impedance of the ear is known it is possible to determine the rate energy is dissipated in the ear, using the threshold pressures at the eardrum and the resistive component of the ear impedance. Similarly, knowledge of the impedance of the head and the displacement for threshold stimulation give values of the energy dissipated by the skull for bone conduction.

$$P_A = \omega^2 d^2 R$$

where R is the resistive component of the mechanical impedance the head presents to the driver, d is the threshold displacement and $\omega = 2\pi f$. The power consumed by each subject at threshold was determined. The median value of these determinations is shown in Figure 4 expressed in decibels relative to 1 erg/sec.

[5] H. Fletcher, J. Acoust. Soc. Am., Vol. 23, 637-645 (1951).

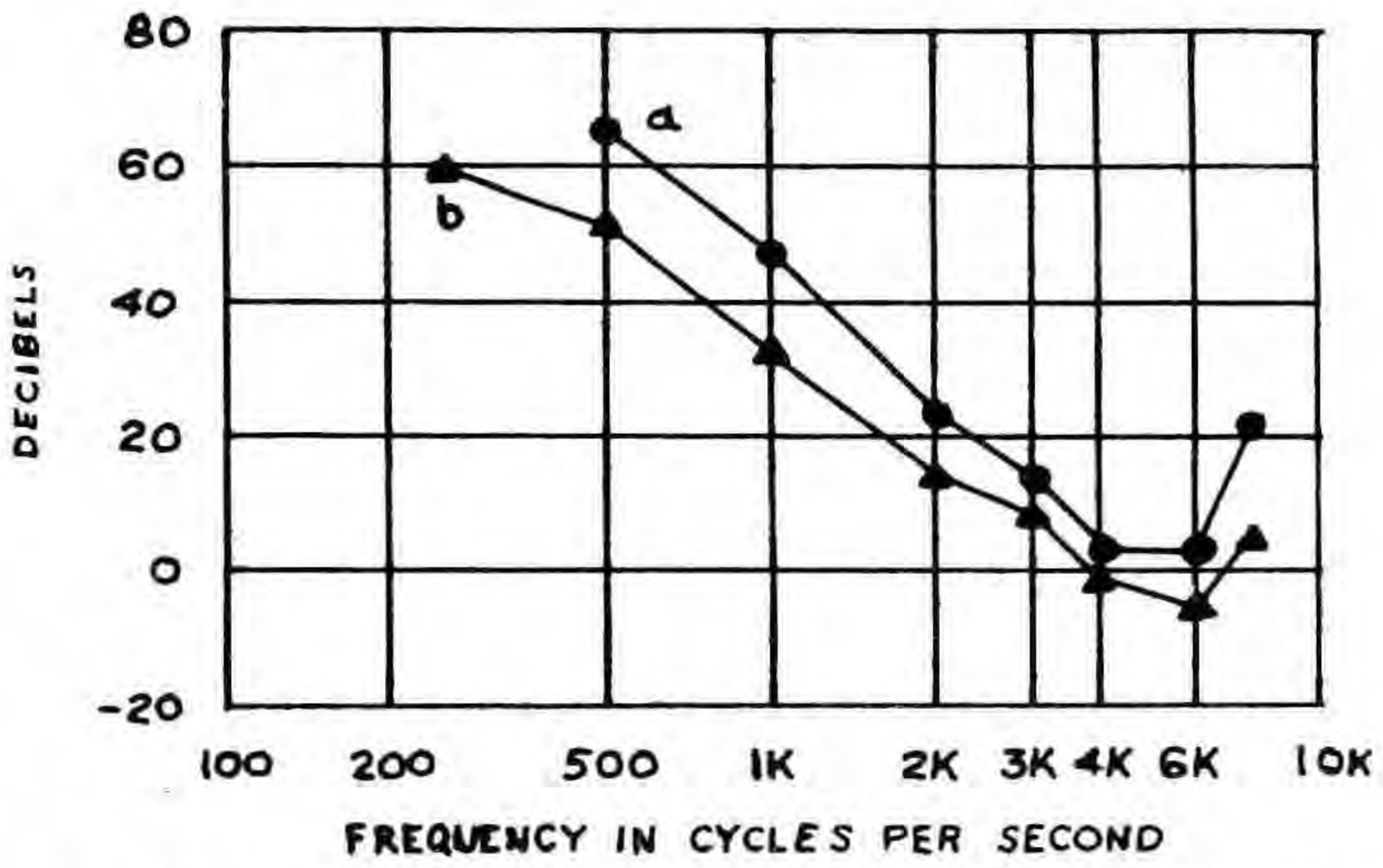

Figure 3. Motion transmission characteristic of the skull.
a. Forehead
b. Mastoid

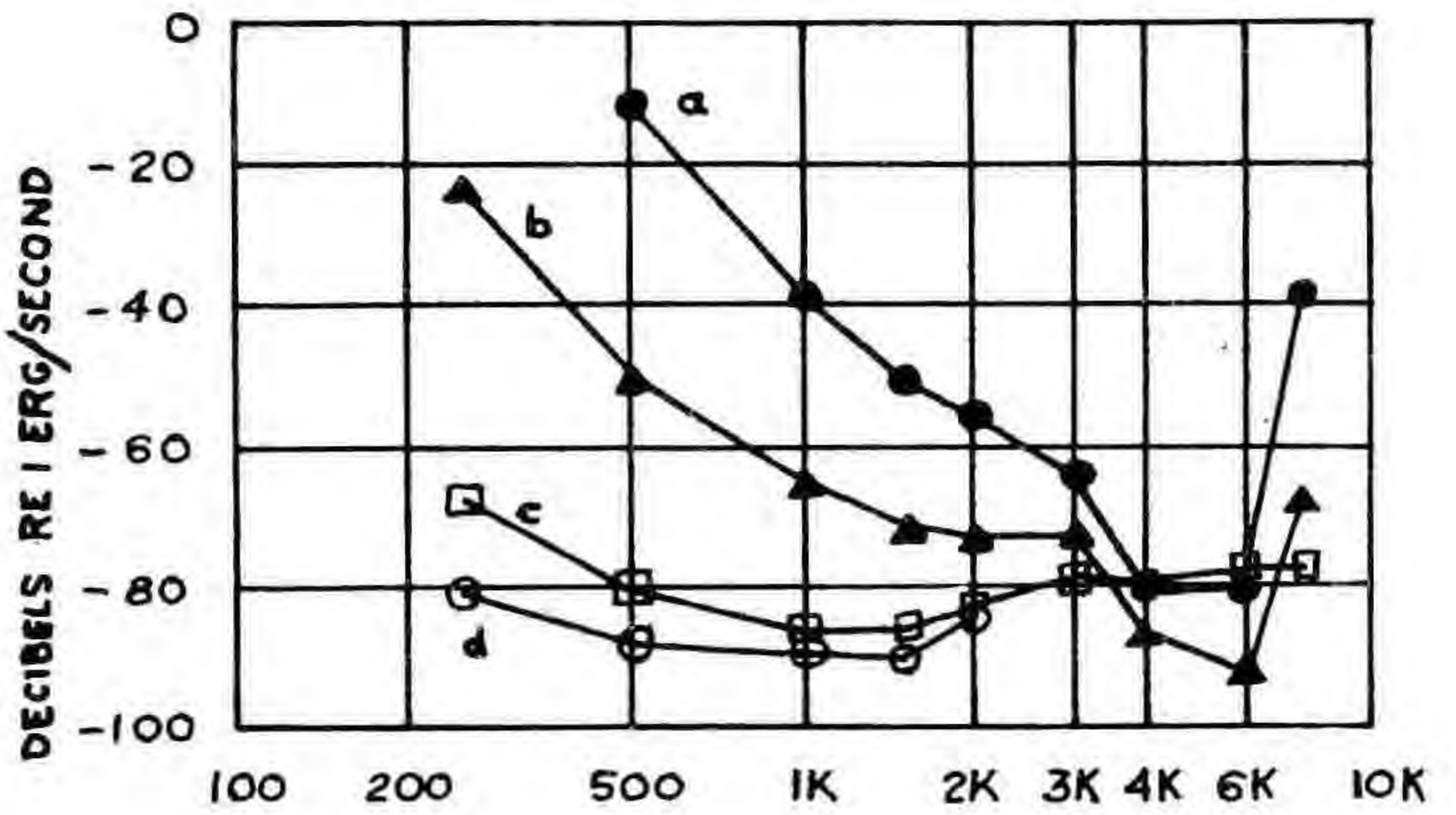

Figure 4. Threshold power consumption.
a. Forehead
b. Mastoid
c. Meatus
d. Tympanum

Ear impedances were not measured for the subjects of this study, however estimates of the threshold power for air-borne sound have been made using data from recent literature. Nabelek[6] gives values of the impedance of ears measured at the entrance to the auditory meatus and Zwislocki[7] has made measurements of the impedance at the eardrum. Median values of the threshold pressure have been used in calculating the power consumed by ears at threshold and are also shown in Figure 4 for comparison.

[6] I. Nabelek, Proc. 3rd ICA Congress, Vol. 1, 25-28 (1959).

[7] J. Zwislocki, J. Acoust. Soc. Am., Vol. 29, 349-356 (1957).

FOURTH INTERNATIONAL CONGRESS ON ACOUSTICS
COPENHAGEN 21.-28. AUGUST 1962

FAA- Richtlinien der Flughafenrand-bebauung und akustische Belastung.

F.J. Meister, Akustisches Laboratorium in der Medizinischen Akademie Düsseldorf (Deutschland).

a) Allgemeine Bewertungsmaßstäbe.

Bei der Beurteilung einer Geräuschbelastung hinsichtlich ihrer Zumutbarkeit ist neben der Größe der spektralen Schallpegel, die Art des zeitlichen Einsatzes und die Dauer der Belastung von entscheidender Bedeutung. Bei Fluglärm durch Über- und Vorbeiflug schwerer Strahlflugzeuge entsteht so eine Belastungsgrenze für die Anwohner eines Flughafens, die sowohl durch die Größe der spektralen Schallpegel, als auch durch die Häufigkeit des Auftretens und damit der je Stunde wirksamen gesamten Belastungsdauer gegeben ist. Die Grenze wird kritischer für Häfen mit hohem Verkehrsaufkommen, auf denen mit schwereren Maschinen als 100 to Startgewicht geflogen werden soll. Es sind deshalb von der Federal Aviation Agency Richtlinien für die Randbebauung von Flughäfen und ein Schema für die Schutzbereichgrenze festgelegt worden, das z.Z. in seiner Brauchbarkeit vielerorts diskutiert wird. Neben Flugsachverständigen werden Akustiker, Landesplaner und Ärzte angesprochen. Auch in Deutschland ist die Frage der zulässigen Bebauungsgrenze an Flughäfen, vor allem für die Errichtung öffentlicher Bauten, wie Krankenhäuser und Schulen, sehr aktuell. Bei Beratungen des Landesausschusses für Fluglärm und Planungsfragen in Nordrhein-Westfalen wurde gefunden, daß die obige Empfehlung der FAA für Krankenhäuser und Schulen mit Rücksicht auf die psycho-physiologischen Wirkungen starker Geräusche im Bereich dieser beiden öffentlichen Institutionen nicht ausreicht bezw. einer Ergänzung bedarf. Es wurde eine Außenbeschallung durch Fluglärm für Krankenhäuser und Schulen festgelegt, die 80 dB_A vor den Fenstern nicht überschreiten soll, solange die Häufigkeit des Auftretens solcher Schallpegel einen Grenzwert einhält, der durch die Form des Schallanstieges und durch die Gesamtbeschallungsdauer je Tagesstunde gegeben ist. Für ähnliche Belastungsspektren könnte diese Häufigkeit aus den auf ruhigen Stadtstraßen gemessenen Verkehrsgeräuschstatistiken entnommen werden, wodurch für den Luftverkehr

eine der heutigen allgemeinen Geräuschbelastung angepaßte Bewertung benutzt würde[x], was auch von B.Lundberg empfohlen wird.
Es ergibt sich für statistische Schallimpulse mit gleichgroßem langsamem Druckanstieg und -abfall eine einfache Beziehung für den Zeitvergleich:

$$H_V \cdot t_V = H_F \cdot t_F \cdot \delta$$

worin H_V die Häufigkeit des Auftretens eines größeren Impulses bei Straßenverkehrslärm und H_F die Häufigkeit des Auftretens von Fluglärm im gleichen Siedlungsraum bedeutet. t_V und t_F sind mittlere Belastungsdauern für diese Schallarten. δ ist ein spektraler Faktor, der für nicht zu niedrig fliegende Maschinen den Wert 1 bis 2 hat. H_F wird für Strahllärm immer wesentlich kleiner als H_V bleiben und in die Größenordnung von 2 bis 6% kommen. Das besagt im Zusammenhang mit der vorher mitgeteilten Empfehlung für die Grenzlautstärke, daß während der Tagesstunde 2 bis 6 % der Lärmbelastung einen Schallpegel von 80 dB_A erreichen darf; für höhere Schallpegel als 80 dB_A würden sich Häufigkeiten unter 1 % ergeben.

b) Handhaben aus der Änderung des Spektrums.
Betrachtet man das von einem Strahlflugzeug mit mehr als 100 to Startgewicht erzeugte Spektrum für verschiedene vertikal unter dem Flugpfad gemessene Entfernungen, so erkennt man die grundsätzliche Regel, daß bis zu einer Entfernung von 1600 m das breite Frequenzband oberhalb 1000 Hz den psychologisch wirksamen Schallpegel bestimmt und die tiefen Frequenzen bis zu Entfernungen von 1600 m von untergeordneter Bedeutung bleiben, was auch aus der Geräuschbewertung nach Kryter, Miller und Beranek erhellt. Es sollte die Frequenzbewertung des Meßgerätes bis zu dieser Entfernung auf jeden Fall darauf Rücksicht nehmen. Sicherlich genügt zunächst für die Bestimmung des wirksamen Schallfeldes der kritischen Belastung im Frequenzbereich oberhalb 1000 Hz bei den hier auftretenden Entfernungen der Bebauungsgrenzen von 800 bis 1600 m die Bewertung nach dB_A zu benutzen. Man erhält so ein bereits nach einer Iso-Norm für Lautstärkenmessung bewertetes Schallfeld, das man nun mit der FAA-Bebauungsgrenze vergleichen kann.

---

x) Diese Frage kann auch in anderer Form behandelt werden. Vergl. hier F.J.Meister, Unterschiede der Schallbewertung, V.Kongreßbericht der internat. Gesellschaft für Audiologie, Bonn 1960. S. 379-382, Verlag Audin, Lyon.

c) Vergleiche der Belastungsflächen.

Die Felddarstellung soll auf die starttechnischen Gegebenheiten Rücksicht nehmen[xx]. Climb up-Kurven der Flugzeuge und die Schallabstrahlung für sog. Normalpunkte müssen bekannt sein. Unter diesen Voraussetzungen sind für 3 Steigwinkel des Flugzeuges (4°, 6° und 9°) die Verteilung der drei für das vorliegende Kriterium wichtigen Normpegel: 80 dB_A, 85 dB_A und 90 dB_A bei einem häufig geflogenen Maschinentyp (DC8) dargestellt (s. Abb.). Im Falle des steileren Steigwinkels von 9° ist nur ein Startgewicht von 98 to, also eine kontinentale Flugroute angenommen, während für die Winkel 4° und 6° ein Startgewicht von 140 to bezw. 130 to zugrundegelegt wurde. Gleichzeitig wurde die FAA-Grenzlinie gestrichelt eingezeichnet.

Es läßt sich leicht übersehen, daß nur für den kontinentalen Start die FAA-Bebauungsgrenzen bis zu etwa 9 km Entfernung in Startrichtung den eingangs aufgestellten Forderungen für Krankenhäuser und Schulen entspricht. Für schwerere Maschinen als 100 to kann bis etwa 130 to Startgewicht bei den derzeitigen Abstrahlverhältnissen 90 dB_A an der FAA-Bebauungsgrenze erreicht werden. Der Wert erscheint für Krankenhäuser auch bei nur bis zweimaliger Belastung je Tag zu hoch. Für Startgewicht von 130 bis 145 to ergeben sich in Startrichtung sehr große über 12 km Länge reichende Beschallungsgebiete. Krankenhäuser und Schulen sollten in diesem Fernbereich daher mehr als 600 m seitwärts der Flugspur gelegt werden, d.h. einen größeren Abstand haben als die FAA-Bebauungsgrenze angibt. Es wäre daher zu empfehlen, eine Ergänzung zu den FAA - Richtlinien zu bringen, die ausdrücklich darauf hinweist, daß die FAA-Grenze für Krankenhauser und Schulen nur dann gewählt werden sollte, wenn die Sicherheit einer zulässigen Grenzbelastung gegeben ist.

---

xx) Über die Darstellung vergl. Beitrag F.J.Meister, Geräuschmessungen an Verkehrsflugzeugen usw. Sitzungsbericht der Arbeitsgemeinschaft für Forschung des Landes Nordrhein-Westfalen, Heft 94, Westdeutscher Verlag Köln-Opladen.

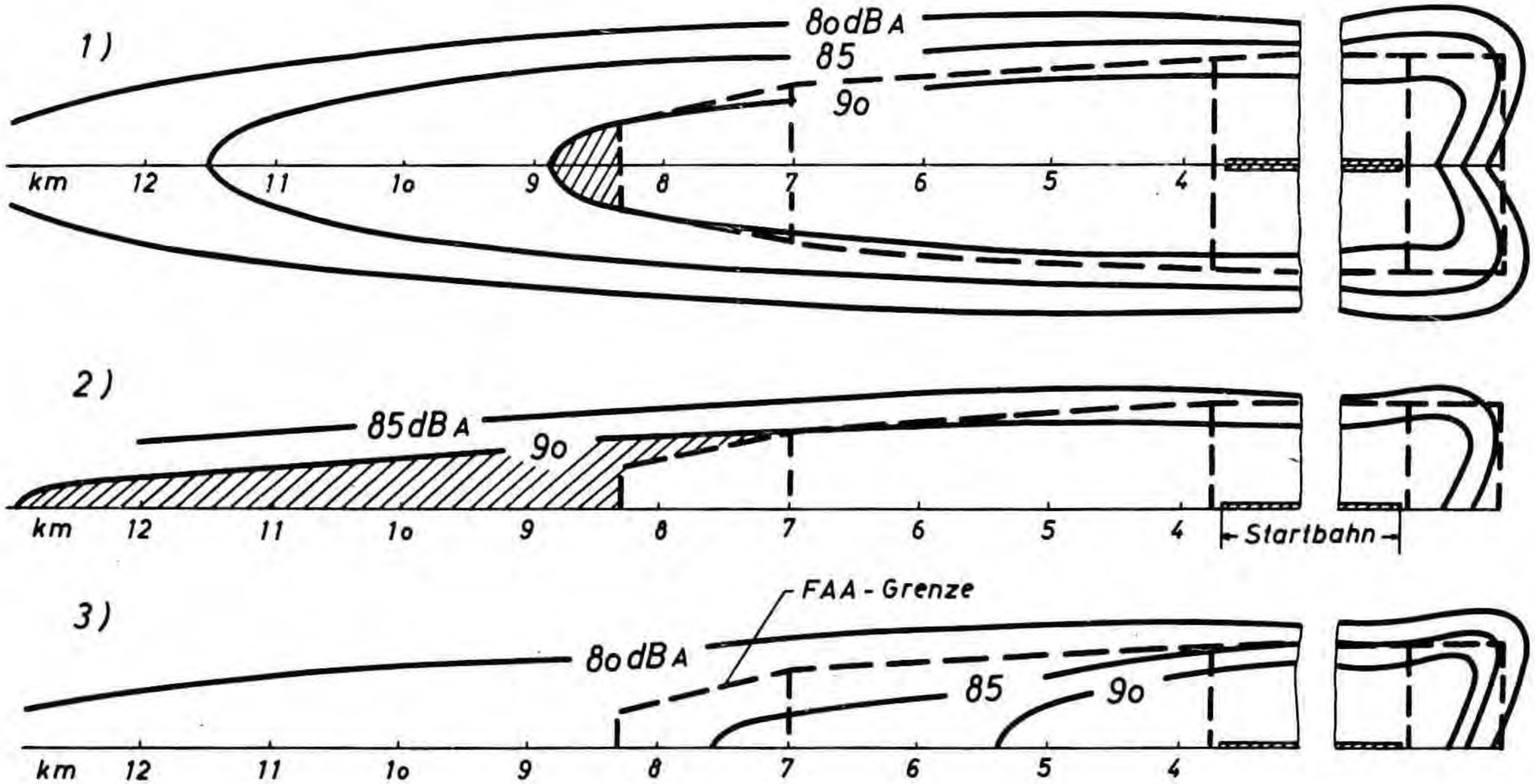

Unterschiede zwischen FAA-Grenzlinie des Schallschutzes und der tatsächlichen Schallbelastung für die gleiche Maschine (DC8 mit PW JT4-A5 Triebwerken) aber bei verschiedenem Steigwinkel α. (für den steilen Anstieg mit $tg\alpha = 0{,}17$ ist das Startgewicht auf 98 to herabgesetzt)

1) $tg\alpha = 0{,}1$ 2) $tg\alpha = 0{,}07$ 3) $tg\alpha = 0{,}17$

FOURTH INTERNATIONAL CONGRESS ON ACOUSTICS
COPENHAGEN 21.-28. AUGUST 1962

Rôle d'un baffle sur l'émission sonore d'un jet d'air sonique

Marie MERLE, Maître de Recherches au C.N.R.S., Marseille

Un jet d'air sonique, à structure périodique, issu d'une buse convergente rectangulaire, émet des ondes acoustiques dont la fréquence et l'intensité sont en relation étroite avec la pression génératrice. Nous avons montré précédemment (1) que toutes choses égales d'ailleurs, la longueur d'onde du son émis croît avec la pression génératrice jusqu'à devenir égale au double de la largeur de la buse. Ce travail a été fait en utilisant des buses de forme et de dimensions différentes mais comportant toutes le même baffle. Les expériences antérieures faites avec des baffles de différentes formes et dimensions nous ayant montré l'influence de ceux-ci sur l'intensité et la répartition du champ sonore, nous nous sommes proposée d'étudier systématiquement une série de 12 baffles de différentes dimensions, équipant une même buse.

Nous avons utilisé pour cela trois méthodes d'observation qui se contrôlent et se complètent :

1°) Observation à l'oeil nu des ondes par la méthode strioscopique, en cherchant la fréquence de modulation de la lumière qui les fait apparaître. Ce procédé stroboscopique permet, d'une part de déterminer avec une très grande précision les fréquences émises en fonction de la pression génératrice et, d'autre part de noter les fréquences extrêmes d'apparition ou de disparition.

2°) Remplacement de l'oeil par un appareil photographique. Les fréquences limites se déterminent par disparition des ondes sur les clichés. On peut, de plus, noter la répartition spatiale des ondes et leurs centres d'émission.

3°) Repérage du son par un ensemble microphone-analyseur électronique (à bande passante très étroite), en passant ou non par l'intermédiaire d'un enregistrement sur bande de magnétophone. Cette méthode permet, d'une part, d'avoir les intensités relatives des sons en fonction de la pression génératrice et de la fréquence et, d'autre part, de se faire une idée de la répartition spatiale en utilisant plusieurs microphones.

La buse utilisée, de dimensions constantes (3,5 x 21 mm) a été équipée successivement avec 12 baffles différents répartis en 3 séries de 4 (Fig.1).

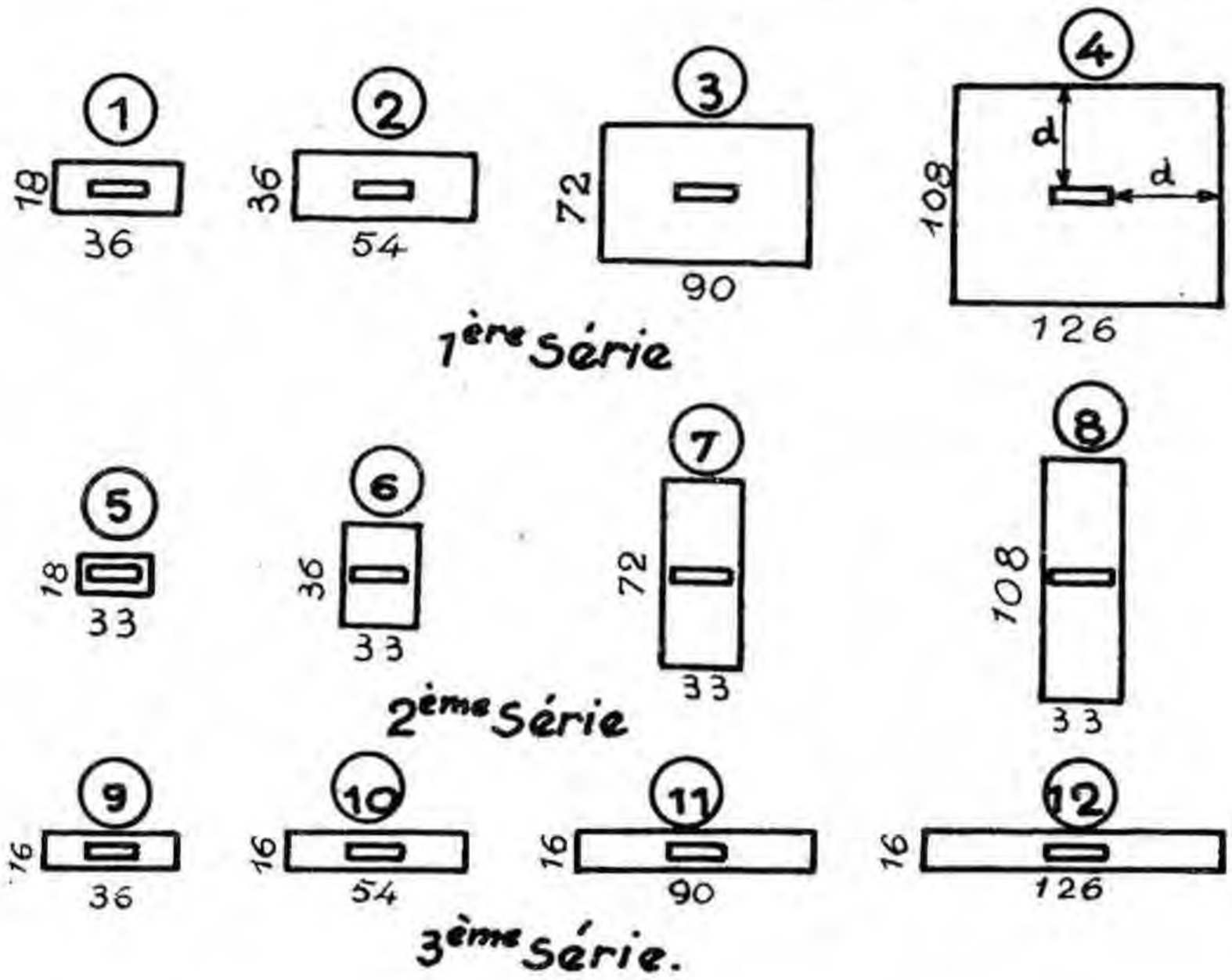

fig.1

On remarquera :

a) sur la 1ère série de ces baffles (1 à 4) que la partie utile (d) verticale et horizontale est sensiblement égale dans chacun d'eux.

b) sur la 2ème série (5 à 8) que les hauteurs sont égales deux à deux à celles des baffles de la 1ère série et que la largeur, identique pour tous (33 mm), est juste suffisante pour encadrer la buse aux épaisseurs de métal près.

c) enfin, sur la 3ème série (9 à 12) que les largeurs sont égales deux à deux à celles des baffles de la 1ère série et que la hauteur, identique pour tous (16 mm) est juste suffisante pour encadrer la buse aux épaisseurs de métal près.

Les trois méthodes d'observation ont été utilisées conjointement. Nous avons ainsi pu établir les courbes de fréquence et d'intensité en fonction de la pression génératrice desquelles nous avons extrait les remarques suivantes :

Baffles	Niveaux maximum d'intensité		Remarques
0 (pas de baffle)	dans le plan perpendiculaire à la fente	aval - 5dB amont + 5dB	Les intensités sont en général très faibles. L'émission amont est supérieure à l'émission aval.
	dans le plan parallèle à la fente	aval -18dB amont -10dB	Les niveaux sur le plan horizontal (parallèle à la fente) sont nettement plus faibles que sur le plan vertical (perpendiculaire à la fente).

Baffles	Niveaux maximum d'intensité		Remarques
1	dans le plan perpendiculaire à la fente	aval + 2dB amont +15dB	Les intensités sont nettement plus fortes que dans le cas précédent. L'émission amont est encore supérieure à celle aval.
	dans le plan parallèle à la fente	aval -12dB amont - 9dB	Les niveaux sur le plan horizontal sont encore nettement plus faibles que sur le plan vertical.
2	dans le plan perpendiculaire à la fente	aval +12dB amont +16dB	Les intensités sont supérieures à celles du baffle précédent. L'émission amont est encore supérieure à celle aval.
3	dans le plan perpendiculaire à la fente	aval +16dB amont +10dB	Les intensités semblent se stabiliser. L'émission amont devient inférieure à celle aval.
	dans le plan parallèle à la fente	aval 0dB amont - 7dB	Les niveaux sur le plan horizontal sont toujours nettement inférieures à ceux du plan vertical.
4	dans le plan perpendiculaire à la fente	aval +16dB amont + 3dB	Les intensités en aval sont sensiblement les mêmes que celles du baffle 3. Celles de l'émission amont diminuent nettement.
5 6 7 8	Les courbes d'intensité aval sont sensiblement les mêmes que celles des baffles correspondants de la 1ère série 1, 2, 3, 4.		
9 10 11 12	Les courbes d'intensité aval sont sensiblement égales pour ces 4 baffles.		

De ces remarques jointes aux observations faites à l'oeil nu et sur les striogrammes, nous avons tirer les conclusions suivantes :

1°) La relation "fréquence-pression" se traduit par une courbe unique quel que soit le baffle; seules les limites extrêmes varient avec les dimensions de celui-ci (Fig.2).

2°) Le champ acoustique comprend deux sources principales de même fréquence : l'une se propageant vers l'aval, centrée sur l'orifice de sortie du jet; l'autre se propageant vers l'amont, centrée approximativement sur le dernier "chaînon" organisé du jet, là où la structure périodique se perd dans la turbulence.

Ces deux émissions n'ont pas la même intensité pour les différents baffles et diffèrent également entre elles pour un même baffle (Fig.2).

La présence du baffle défavorise l'émission vers l'amont et favorise celle vers l'aval. Cette action est d'autant plus marquée que la hauteur vertical du baffle est plus grande.

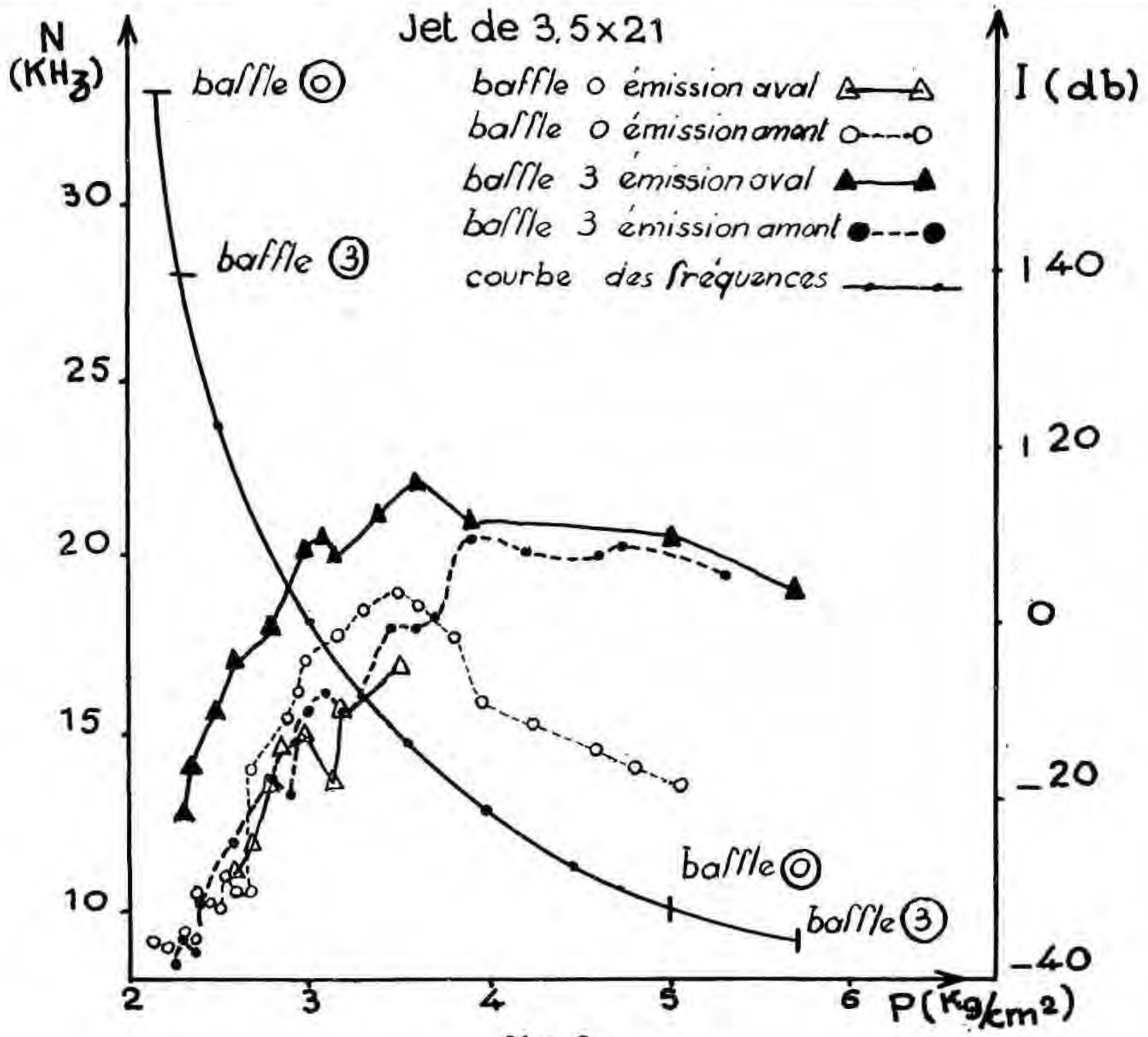

fig.2

3°) Le niveau moyen de l'intensité du son croît avec la hauteur verticale du baffle (perpendiculaire à la fente) tout au moins tant que celle-ci ne dépasse pas la longueur d'onde supérieure limite du son émis (baffles 0, 1, 2, 5, 6). Au-delà de cette dimension, le baffle ne semble que défavoriser l'émission amont (baffles 3, 4, 7, 8).

4°) Latéralement au jet, dans le plan parallèle à la fente, les émissions sont toujours très faibles et la largeur du baffle (parallèle à la fente) ne paraît pas intervenir (baffles 9, 10, 11, 12).

---

(1) C.R.Acad.Sci., 248, 1/4/1959, 1953-4.

H49

FOURTH INTERNATIONAL CONGRESS ON ACOUSTICS
COPENHAGEN 21.-28. AUGUST 1962

Middle Ear Muscle Effects on Round Window Responses During Prolonged Sound

Carmel, Peter W. and Starr, Arnold

We are attempting to analyze electrical responses recorded from electrodes chronically implanted along the auditory pathway of waking cats before, during and after some hours' exposure to steady loud sounds. During unchanging sound stimulation changes in recorded responses can be observed all along the auditory pathway. Some of these dynamic changes are introduced initially at the cochlea as a result of action of the middle ear muscles, stapedius and tensor tympani. Contraction of these muscles results in a decrease of electrical response recorded from round window. These muscles contract to both acoustic and non-acoustic influences. This paper presents an analysis of some of the mechanisms underlying muscle induced changes occurring at round window.

METHODS: Cats are prepared with an electrode implanted at round window some days prior to sound exposure. The stimulating sound is a white noise 85 db re. .0002 dynes/cm^2 projected from a loud speaker 1 meter above the animal's head. Electrical responses recorded from round window are photographed on an oscilloscope and also averaged continously on an electronic summator. Experiments are carried out with cats awake and free to move about a wire cage within a sound attenuating room. The same animals are tested while under Nembutal anesthesia or following intercollicular decerebration. Effects of surgical division of the tendons of the middle ear muscles or of paralyzing their contraction by Flaxedil are studied. The functions of these muscles in animals having unilateral or bilateral interruption of the VIII nerve are analyzed. Middle ear muscle action is also monitored by electromyography. Ontogeny of middle ear muscle action is observed in kittens ranging from birth to 10 weeks of age.

RESULTS: 1) Round window responses in waking cats. Between 40 and 70 milliseconds after onset of loud white noise initial round window responses decrease in amplitude. This decrease ranges from 6 to 18 db,

averaging 10 db. With continuing steady sound stimulation responses gradually increase again in amplitude; taking 30 to 90 minutes to reach a maximum, which is usually within 2 db of the initial onset response. During continuing sound exposure the gradually rising response is interrupted by transient decreases, averaging 4 db, which are regularly associated with bodily movements of the cat.

2) The role of middle ear muscles. The initial attenuation of round window response at onset of loud white noise, the gradually rising response thereafter, and the intervening decreases associated with movement all result from effects of middle ear muscle action. Surgical section of the tendons of m. stapedius and m. tensor tympani, or administration of Flaxedil, results in a round window response that is maximal at onset and does not change in amplitude with prolonged sound exposure. Of the two middle ear muscles, the stapedius exerts the predominant effect. However, the two muscles act synergistically since there combined effects are greater than the sum of their independent effects.

3) Acoustic reflex contraction of middle ear muscles. Middle ear muscle action is, in part, dependent upon hearing. Behaviorally deafened animals, with both VIII nerves crushed and with the internal auditory artery left intact, show no decrease in round window potentials following onset of loud noise, nor do they show any gradually rising response during prolonged exposure. Animals with only one VIII nerve crushed have essentially normal action of middle ear muscles on both sides. Thus, middle ear muscles are capable of reflex action which depends upon at least one intact acoustic input.

4) Non-acoustic influences affecting contraction of middle ear muscles. The middle ear muscles of deafened animals contract during bodily movements, even though they show no acoustic reflex contractions. Deafened animals' round window responses decrease in amplitude during bodily movements just as do those in normal animals. Even in spinal animals, attenuation of round window responses is seen in association with movements of just face and eye musculature. Thus, middle ear muscles are capable of contracting in the absence of hearing and in association with movements.

5) Central Nervous System influences on acoustic reflex contractions. Nembutal anesthesia abolishes acoustic reflex middle ear muscle contractions. Inter-collicular decerebration is also associated with profound

alterations in middle ear muscle action. Here, the initial decrease in round window responses develops within 20-30 milliseconds following onset of sound, in contrast to the minimum of 40 milliseconds required in normal animals. However, the decerebrate animal does not sustain middle ear muscle contractions, apparently relaxing completely within ten minutes following onset of sound. Finally, in the intact animal repetitive exposure to loud noise is correlated with a shortening of the time till onset of acoustic refelx contractions.

6) Electromyographic studies. Middle ear muscles discharge with an abrupt burst of activity within 20 milliseconds after onset of loud white noise. Thereafter, the averaged electromyogram decreases during continuing sound exposure. Bodily movements are associated with an increase in electromyogram, independent of the presence of an acoustic stimulus.

7) Ontogenetic studies. Middle ear muscle contractions do not appear during the first week of life. Non-acoustic contractions associated with bodily movements develop during the second week. At this age no acoustic reflex contraction is present. During the third week of life middle ear muscle acoustic reflex responses first appear, and this is correlated with a behavioral response to the sound.

G51

FOURTH INTERNATIONAL CONGRESS ON ACOUSTICS
COPENHAGEN 21.-28. AUGUST 1962

SEGMENTATION OF THE SPEECH CONTINUUM

A.COHEN and J.'t HART

INSTITUUT VOOR PERCEPTIE ONDERZOEK
- EINDHOVEN - NETHERLANDS -

1. Anyone wishing to study speech sounds more closely is confronted with the notorious problem of deciding how he can retrace the phonetic segmentation in the speech samples he is investigating, on any one level, articulatory, acoustic, and auditory.

   Thanks to the tape-recording machine and the spectrograph the traditional predominantly articulatory approach has been supplemented, if not partly eclipsed, by studies of the acoustic parameters of speech.

   The most refined technique of analyzing spliced portions of tape recorded speech was devised by Truby 1), who correlated listening tests with spectrographic evidence.

   A method closely resembling the one to be described in this paper is that of Menzerath 2), who used the sound track of a closed loop of film, together with the sprocket holes of a blank strip of slightly different length, to get a stroboscopic effect. This technique enabled him to listen closely to the gradual building-up of the original word on the sound track.

   We deliberately refrain from mentioning other experimenters who have tried, by means of the substitution method, to check in a concrete way the commutation test, used in linguistic analysis, to establish the distinctive function of the speech sounds. This involves replacing portions cut from one word on tape by those obtained from another word. It turned out, that in a number of cases, notably with regard to stop consonants, the variants of one phoneme were no longer recognizable as such.

   Much of the evidence obtained by the various methods brings out the large interdependence of neighbouring sounds in the normal speech, thus warranting the use of the term speech continuum. All this goes to show, that it is hard to maintain that speech can be regarded as a series of independent units ordered in time, which is the normal procedure in linguistic analysis.

2. In the experiments to be described an electronic gating circuit is used. A word is recorded on a closed loop of tape and reproduced at the same fixed speed (30 in/sec). An electronic gate is set to open at a frequency slightly lower than that of the loop; in other words the tape will gradually gain on the gating system, and an ever increasing portion of the word on the tape can be made audible, gradually building up from beginning to end. Once the complete word has been heard, an ever decreasing amount remains audible at successive steps, until the word has vanished completely.

   The value chosen for the difference between the periodicity of the loop and that of the gate is 10 msec. This value is large enough to secure an acceptable reproduceability and small enough to warrant that no interesting details will be neglected. To obviate any harmful effects, such as spectral widening caused by switching clicks, the rise and decay times in the gates used are at least 10 msec.

   The operation of the gate is made possible by having the grid of a triod controlled by a square pulse generated by a monostable multivibrator. The slopes of this pulse can be modified by means of RC circuits so as to bring about variable onset and decay times of the acoustic signals to be passed by the gate.

The interval between successive presentations is about 1.2 sec., a convenient value for listening experiments. This interval was arrived at as a compromise between an upper limit, set by the desirability at each presentation of remembering the previous one, and a lower limit required for adequate concentration on each individual presentation.

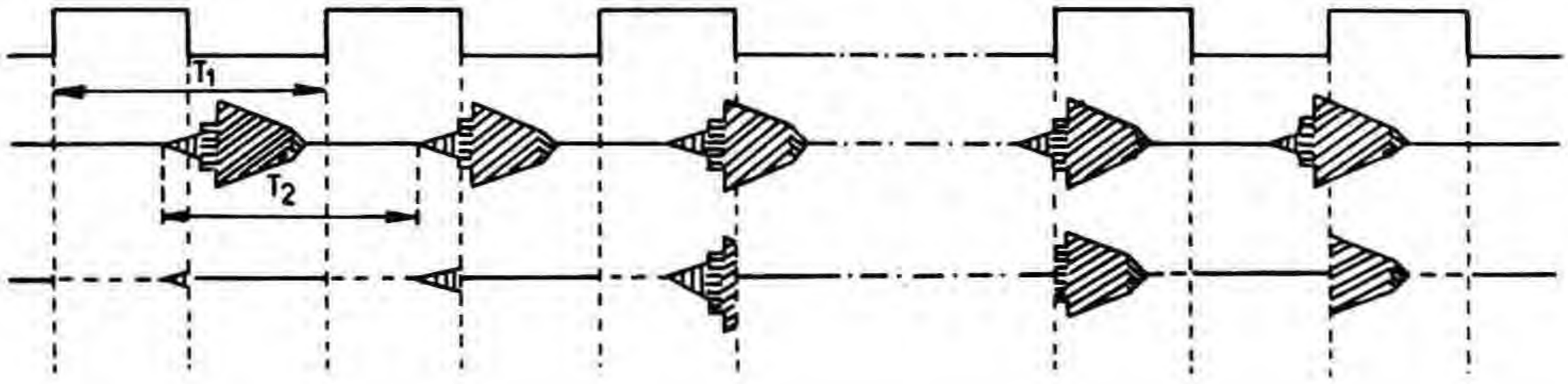

Fig.1. The gating process used in perceptual analysis of speech. T1 - T2 = 10msec.

In fig. 1 the width of the gate was made to encompass the length of the word. In principle the range of values of the gate width is between 20 and 800 msec. due, respectively to instrumental limitations and the length of the words normally investigated.

3. The impetus to this approach was given by the consideration, that an interference with the normal time pattern has been shown to play havoc with the perception of acoustic signals in general. A noteworthy example is afforded by reversing the normal time order of the tape recorded sounds of a piano. Speech processed in the same way will be completely unintelligible. One may expect, therefore, to gather relevant data about the contribution of the time parameter to speech perception through carrying out experiments in which arbitrary portions of a spoken utterance can be submitted to a listener's judgment.

Invoking responses of a subject, whose main qualification will be that he should be a native speaker of the language investigated, implies that his answers will be guaranteed to reflect the common structure of the linguistic pattern underlying both his own speech and the recorded utterances.

Previous tape splicing experiments carried out by Jones 3) had shown that shortened versions of fricative sounds gave rise to the perception of affricates and stops. Similar results might be expected to be obtained with respect to vowels, viz. that quantitative variations in time would lead to qualitative differences in perception. In all these experiments a necessary prerequisite for such qualitative differences to be possible is, that they should closely match phonemic differences in the language investigated.

The main object in carrying out perceptual experiments of this nature is to find out which speech units can be identified under varying conditions of time.

4. It turned out that it was possible, while listening to the recorded word being slowly built up, to determine with a high degree of accuracy whether new presentations formed a homogeneous part with the previous ones, or else constituted a break. This outcome leads to the feasibility of indicating border marks between seperate fragments.

The subject, whose task it is, while listening for instance to the word fly, to write down any identification of speech sounds he is able to make, will only arrive at his first identification after about the first five presentations, viz. /f/. Initially he is only aware of a noiselike signal. After the /f/ has been perceived, a new voicelike element comes in , which is

only identifiable as /l/ , once the very first fragment of the diphthong is passed by the gate. For a long time the vowel /a/ is heard until a turning point is reached, where a new vowel sound is heard which is hard to identify. After a few more steps the perception of /ai/ comes about.

It is only after the beginning of the word has been eliminated, that the additional vowel sound turns out to be /ɛ/. During this process of elimination the original /f/ part passes through the stage /pf/ to /p/.

The process described above was based on having the width of the gate encompass the length of the word to be analyzed. When applying much shorter gate widths, e.g. of 20 msec., no clear /f/ can be heard, while the /l/ recognition presents no difficulties and the vowel parts are equally well identifiable, though no diphthongal identification takes place at any one moment. It therefore turns out that the /l/, as opposed to /f/, has a characteristic stop-like nature, although in itself it may have a length exceeding that of a real stop consonant (it can easily be proven that elimination of this stop-like character, by presenting a closed loop of the tape with sustained /l/, changes it out of recognition).

Generalizing the experimental findings, established in analyzing Dutch speech sounds, the following results may be generally valid:

a. Fricatives both voiced and unvoiced can be reduced to homorganic affricates and stops.
b. Sonorants like /l,m,n,w,j/ are only recognizable when the first fragment of a following vowel is presented.

   In postvocalic positions identification of these consonants is dependent on the presence of some part of the previous vowel.
c. Diphthongs can generally be heard to consist of only two components. Some so-called long vowels, that are normally considered to be homogeneous, also turn out to be analyzable into two components.

In principle, the method described above can also be applied to carry out experiments on intonation features, notably by means of the smallest value of the gate width, viz. 20 msec. This guarantees the subject's concentration being directed to the pitch variations thanks to the exclusion of the disturbing influence of the more complete phonetic pattern. This method seems preferable to others, using filter techniques, since a) pitch sensation need not coincide with the fundamental, which b) is in a frequency area where pitch sensation is relatively poor, and c) when presented as a continuous stimulus is even harder to trace.

In determining the perceptual fragments obtained through analysis, the procedure is as follows: in a running analysis of a tape recorded word first of all the number of perceptually clear turning points are established. In fact, every new presentation is compared with the previous one and if either at the beginning, or at the end of the audible stretch a heterogeneous part disappears or appears respectively, this is made the criterion for the occurrence of a turning point. The stretches between such turning points are provisionally called perceptual fragments.

In order to be able to decide whether these fragments can indeed be regarded as so many perceptual segments into which the speech continuum can be divided the technique of synthesizing speech from steady-state segments will be employed.

5. For this purpose the facility of variable onset and decay times, as well as the duration, of the electronic gating circuit mentioned above (section 2). plays a predominant part. The components needed are continuous signals derived from two sources (periodic and noise-like) by means of filtering.

   Next these components each require a specific time envelope, brought about by experimentally established gate values necessary for evoking acceptable speech.

   Thus, in synthesizing a word, the rough-sounding filtered components are each led through a gate with tentative settings, then ranged in the required

serial order, after which adjustments can be made for the appropriate gate settings. It was found possible to make acceptable speech utterances in this way.

A special facility, inherent in the gating system, makes it possible to introduce pitch inflection, resulting in a much more natural sounding output.

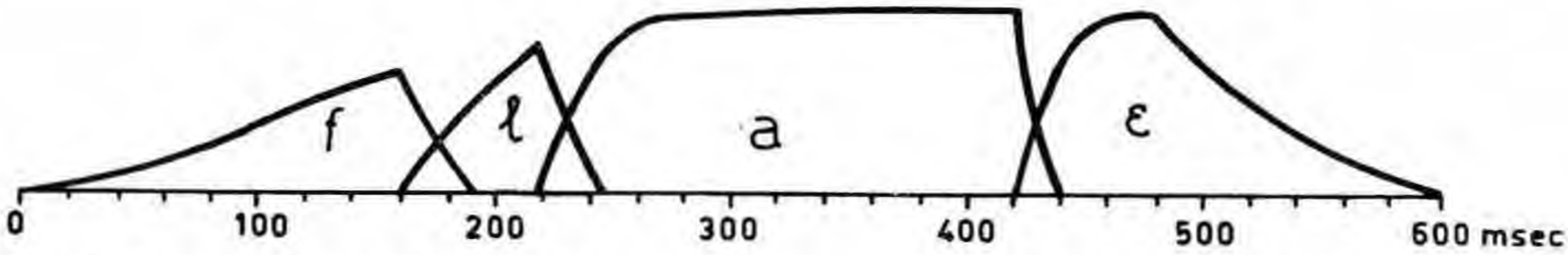

Fig.2. Time pattern of individual segments used in synthesizing fly.

The way is now cleared for investigating the relative contribution of the perceptual fragments obtained in analysis.

It turns out, that the expected relationship between homorganic fricatives, affricates and stops can be corroborated in synthesis. Starting from one specific spectral composition per series, each of its members can be generated by applying the proper gate settings (e.g. /f,pf,p/ and /z,dz,d/).

The crucial point in the recognition of the sonorants mentioned above, is the short decay time in prevocalic position and the equally short rise time postvocalically.

Perfectly natural sounding diphthongs can be generated from two steady-state segments without any intermediate formant bending, although in analysis sometimes more than two perceptual fragments can be heard. The long vowels that were heard to consist of two fragments could satisfactorily be synthesized by using a single segment.

In other words, one is forced to the conclusion that the speech continuum can indeed be segmented if perceptual cues are used as a criterion, both in analysis and synthesis. In a way this segmental approach closely resembles the linguistic practice of analyzing speech into a series of phonemes, in so far as the number of perceptual segments obtained generally coincides with that of a phonemic description. However, it differs in attaching more importance to the identificatory aspect of the units as moments in a total pattern to be recognized, rather than to the distinctive function, which is the sole criterion in a phonemic analysis.

Far from being abstract like phonemes, the perceptual segments presuppose, in order to be perceptible, to have an extension in time. The specific time values at issue, both with respect to each individual segment and to their collective functioning as a whole, in combination with frequency information, may well be responsible for their eventual identification as speech.

References:

1. H.M.Truby — A Note on Visible and Indivisible Speech, Proc.8th Int.Congr. of Linguists, Oslo, 1958, 393-400.
2. P.Menzerath — Der Diphthong, Bonn-Berlin, 1941.
3. R.Jakobson, C.G.Fant, M.Halle — Preliminaries to Speech Analysis, Cambridge, Mass. 1952, p.22.

H51

FOURTH INTERNATIONAL CONGRESS ON ACOUSTICS
COPENHAGEN 21.-28. AUGUST 1962

THE DOMAIN OF EXISTENCE OF THE TONAL RESIDUE

R.J.RITSMA, INSTITUUT VOOR PERCEPTIE ONDERZOEK
EINDHOVEN - NETHERLANDS

INTRODUCTION

The residue phenomenon is defined by Schouten 1)2) as the joint perception of a number of neighbouring higher harmonics of a periodic signal. Schouten has found that the characteristic low pitch of such a percept (a tonal residue) is equal to that of the fundamental. This phenomenon makes it necessary to assume that each area of the basilar membrane may give rise to sensations of widely different pitch, depending upon the pattern of stimulation. A closer study of the residue phenomena is of interest as the residue implies situations where average frequency and periodicity are separate parameters and may be varied independently to a certain extent. No such possibility of seperately dealing with frequency and periodicity exists when working with pure tones or limited bands of noise.

The literature shows that the tonal residue does not occur at all frequency values though it can be perceived at specific frequency combinations 3)4)5)6)7) . Measurements have been carried out to determine the frequency region in which a tonal residue can be established.

A stimulus was generated by modulating a sinusoid of centre frequency f with a second sinusoid with frequency g. The modulation depth m could be varied from 0 up to 100%. If the centre frequency f is an integral multiple of the spacing frequency g , the complex sound is an harmonic one. At all values of the frequencies f and g where a tonal residue could be observed using a modulation depth m=100% , it is possible to turn down the value of m in such a way that the tonal residue is just noticeable. This value m for a just noticeable tonal residue could be reproduced very accurately. This method was chosen to find out experimentally the frequency boundaries within which the tonal residue for a three component complex can be obtained.

INSTRUCTIONS TO THE SUBJECT

For a subject it is hard to decide without matching whether there is tonality with the right pitch in a complex sound or not. Therefore the subject was instructed to ask himself whether the stimulus had the same pitch as that of a reference tone of pitch g. The reference tone was provided by an harmonic residue since more accurate pitch matchings of residues can be obtained rather than using a sinusoid as a reference 8). In case of a positive answer it was assumed that the tonal residue had been established. In the case of a negative answer by the subject it was assumed that no residue could be established.

APPARATUS

Fig. 1 illustrates the apparatus used.
The centre frequency was presented continuously at a loudness level of about 35 db above threshold. By using button A, the subject could switch the modulating signal on and off. In this way the subject's attention could be concentrated on the addition of the modulation to the original signal. The modulation depth could

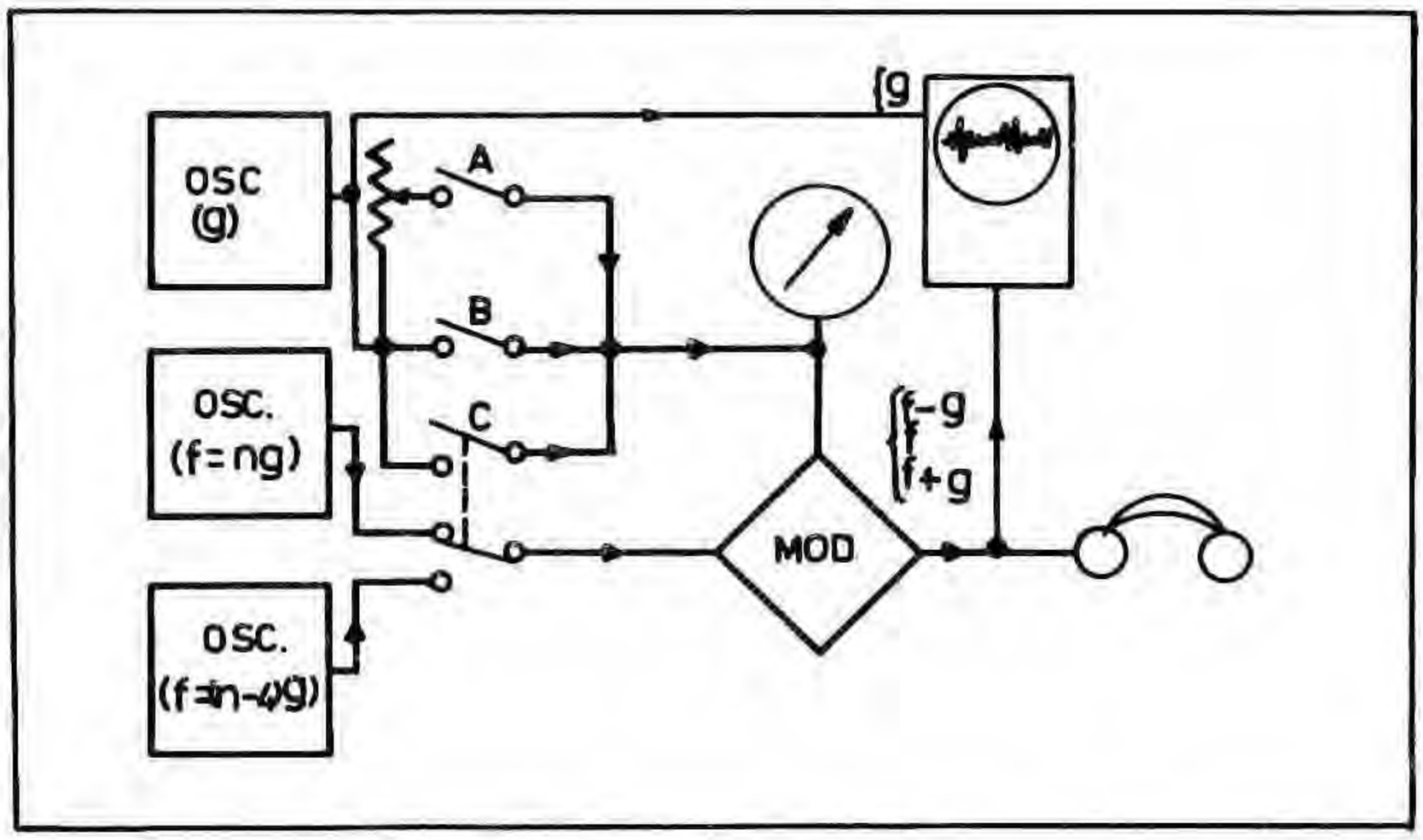

Fig.1 Block diagram of apparatus

be controlled by the subject himself. In choosing the reference tone the following empirical data were taken into account:
a. The tonal residue is observed more clearly as the modulation depth increases.
b. For a constant modulation depth the tonal residue is observed more clearly as the centre frequency decreases.

By pressing button B the subject could hear the reference tone: the same frequencies with a modulation depth m =100%. If this reference tone became too weak the subject could press button C: a reference tone was heard consisting of an harmonic complex (m =100%) of which the centre frequency is 4 g below that of the stimulus, the pitch being equal to that of the reference tone 'B'.

PROCEDURE

In principle any combination of centre and spacing frequency ought to be tested as to the minimal modulation depth at which the tonal residue would be just noticeable. Since the relation f/g =n =integer is maintained it is possible to carry out measurements keeping f,g or n constant. Keeping the spacing frequency g constant during a test series results in keeping the pitch constant in such a series. This helps the subject in better recognizing the proper pitch of the stimulus presented to him. Therefore, this type of test series has been mainly applied while control series have been carried out keeping the centre frequency f constant.

Minimal modulation depths m were determined for a number of selected values of g for n =4,5,6,7 etc.

Measurements where n =2 are meaningless owing to the fact that the residue pitch has a value corresponding to t pitch of the lowest component.

Measurements where n =3 have also been excluded since the lowest component of the complex has a pitch which is an octave apart from the pitch of the residue. Each test series was run at least three times at various days.

RESULTS

Three subjects participated in the experiment. They had participated in auditory experiments before and they had been exposed to residue tones rather extensively. For each spacing frequency g the experimentally found minimal modulation depths m have been plotted as a function of n. The averaged values of the individual plottings of the series for each subject have been collected in one diagram. Fig. 2 shows such a diagram for one subject.

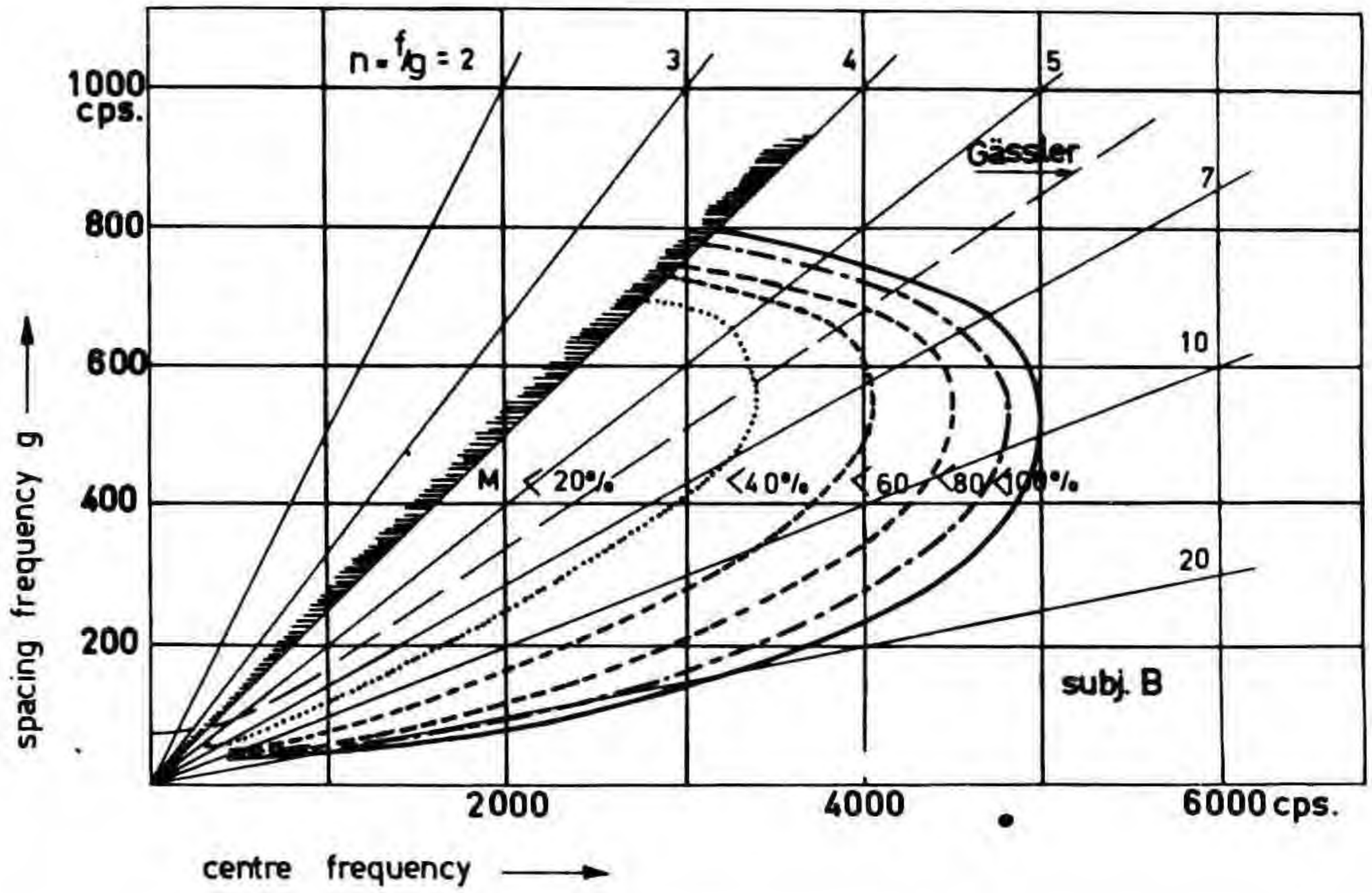

Fig.2 The frequency region of the tonal residue (harmonic complex of three components) for various modulation depths m (subj.B).

On the **abscissa** the centre frequency f is indicated while the **ordinate** represents the spacing frequency g.

Inside the area marked by the solid line m = 100% a tonal residue could be observed. Outside this area no tonal residue was found. Only a kind of high buzz is observed of an indefinable pitch. As one chooses a stimulus further removed from the marked off frequency region the buzz assumes a more noise like character where the centre frequency obtrudes more clearly as a pure tone. At low values of the spacing frequency g the tonal residue gradually changes its character into that of a rattle.

For a modulation depth m = 80% the area in which a tonal residue was observed is slightly reduced as enclosed by the dash-dotted line. For modulation depths m = 60%, 40% and 20% the size of the area in which the tonal residue can be established, is getting increasingly smaller.

There are certain experimental indications to the effect that for values of n below n = 4 the frequency region of the tonal residue is also limited. In addition a series of measurements was made involving modulation depths above 100% at one specific spacing frequency g = 200 cps.

Fig.3 shows the minimal and maximal modulation depths in perceiving a tonal residue as a function of n. For values of m > 100% the value of n first increases by one unit (m = 115%) before a decrease at higher m-values sets in. It appears that the tonal residue of the stimulus is optimal at a modulation depth m of 115% .

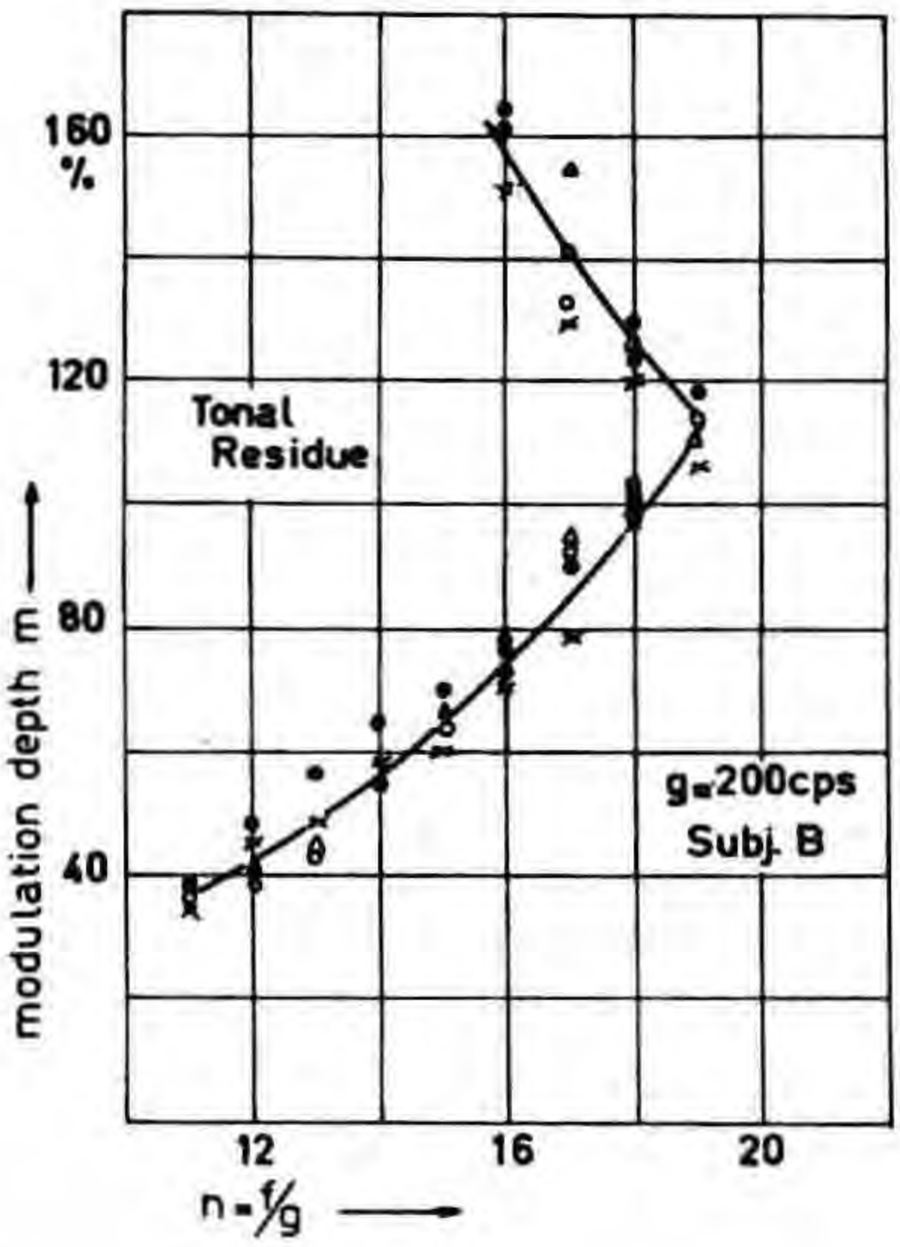

Fig.3 Individual plottings of the minimal and maximal modulation depths in perceiving a tonal residue as a function of n = f/g (subj.B).

REFERENCES:

1. J.F.Schouten — Proc.Koninklijke Nederlandse Akad.van Wetenschappen XLI, 1086-1093 (1938)
2. J.F.Schouten — Proc.Koninklijke Nederlandse Akad.van Wetenschappen XLIII, 356-365 (1940)
3. G.A.Hoogland — The Missing Fundamental, Ac. thesis, Utrecht 1953
4. W.A.Rosenblith — Progress Report II of the Psycho-Acoustic Laboratory, Harvard University 1947
5. E.de Boer — On the ''residue'' in hearing, Ac.thesis, Amsterdam, 1956
6. W.R.Thurlow and A.M.Small Jr. — J. Acoust. Soc. Am. 27, 132 (1955)
7. A.M.Small Jr. — J. Acoust. Soc. Am. 27, 751 (1955)
8. J.F.Schouten , R.J.Ritsma B.Lopes Cardozo — On the pitch of the residue. Submitted for publication in J. Acoust. Soc. Am.

J51

FOURTH INTERNATIONAL CONGRESS ON ACOUSTICS
COPENHAGEN 21.-28. AUGUST 1962

MEASUREMENTS OF VELOCITY AND ATTENUATION OF SOUND IN IRON UP TO THE MELTING POINT

D.R. HUB
ROYAL NAVAL COLLEGE, GREENWICH, LONDON

1. Summary.

The velocity of sound in iron has been measured by a pulse method from room temperature to just below the melting point. Phase change, attenuation and crystal growth effects are described; these effects are demonstrated with a cine film of echo patterns over parts of the temperature range.

2. Introduction.

Pure iron exists in three phases. The body centred form is stable below 900°C (α) and above 1400°C (δ). Between these two temperatures the γ phase (face centred form) is stable. (A β phase was once thought to exist between the Curie point, 770°C, and 900°C). As is seen from phase diagrams (iron-carbon for example) the temperatures at which phase changes occur are sensitive to contamination.

Recent surveys of methods of measuring sound velocities and elastic moduli (1,2) show that of the many methods available few have been used successfully at high temperatures. Measurements up to 1000°C have been reported (1,3,4). The one reported at higher temperature (5) does not claim great accuracy. Observations on iron are reported in the temperature range 0-200°C (6). With the present equipment measurements have been taken above 1500°C and use at still higher temperature appears quite feasible. The method allows continuous monitoring of velocity.

3. Experimental Method.

To examine strain pulses over a wide temperature range, rod specimens, 2 mm. diameter and about 17 cm. long were cemented into an alumina tube, which acts as a low attenuation lead into a furnace. These pulses were longitudinal, about 9μsec. long (4 cm. in iron at room temperature) and were produced by magneto-striction in a nuckel tube. An atmosphere of purified argon was used to protect the specimen from contamination. Some details of the apparatus have been reported previously (7,8). Full details will be published later.

A pulse passing into the alumina produces two readily identifiable echoes, one from the alumina-iron junction and the other from the end of the iron. Three distinct features appear from the echo pattern. The separation of the echoes gives the velocity, the relative heights are a measure of the attenuation and the small echoes between the main ones show crystal boundaries within the iron. Figure 1 shows typical echo patterns over the full range of measurements up to 1450°C.

4. Velocity.

Figure 2 shows the echo delay time (approximately the reciprocal of velocity for longitudinal pulses as a function of temperature. The extent to which the displacement between heating and cooling curves could be attributed to temperature gradients was tested in the second cooling run. The temperature, having fallen to 100°C, was raised to 1300°C and allowed to fall again. The three sets of data over this range were spread over about 15°C. The displacements observed between the various cycles are therefore attributed to the iron.

The two marked changes in velocity correspond to phase changes. The extra sharpness of the first phase change on the second heating is thought to be due to the almost complete removal of strain energy brought about by the annealing

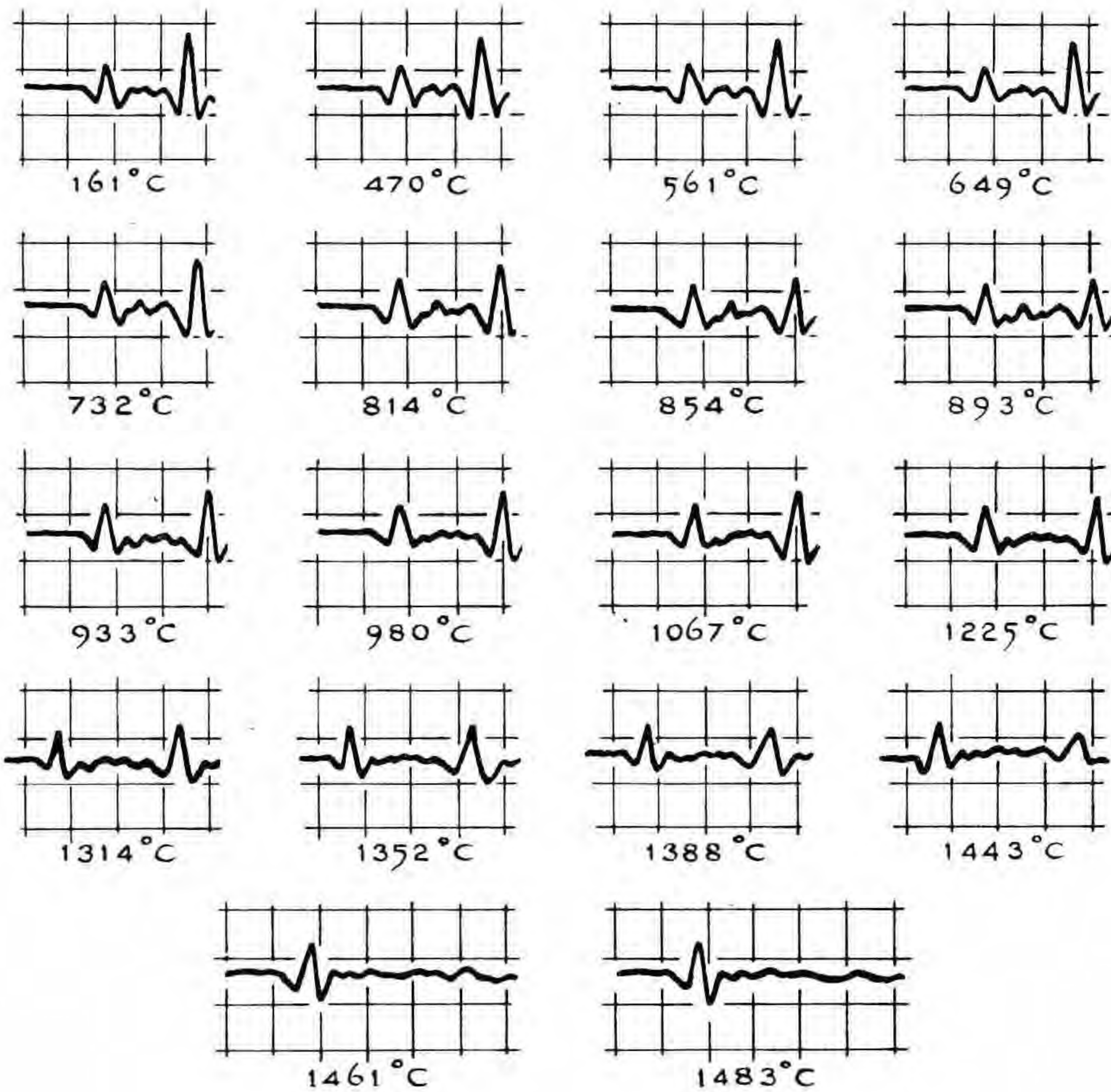

FIG. 1

Fig. 1: Typical echo patterns for iron from room temperature to just below the melting point.

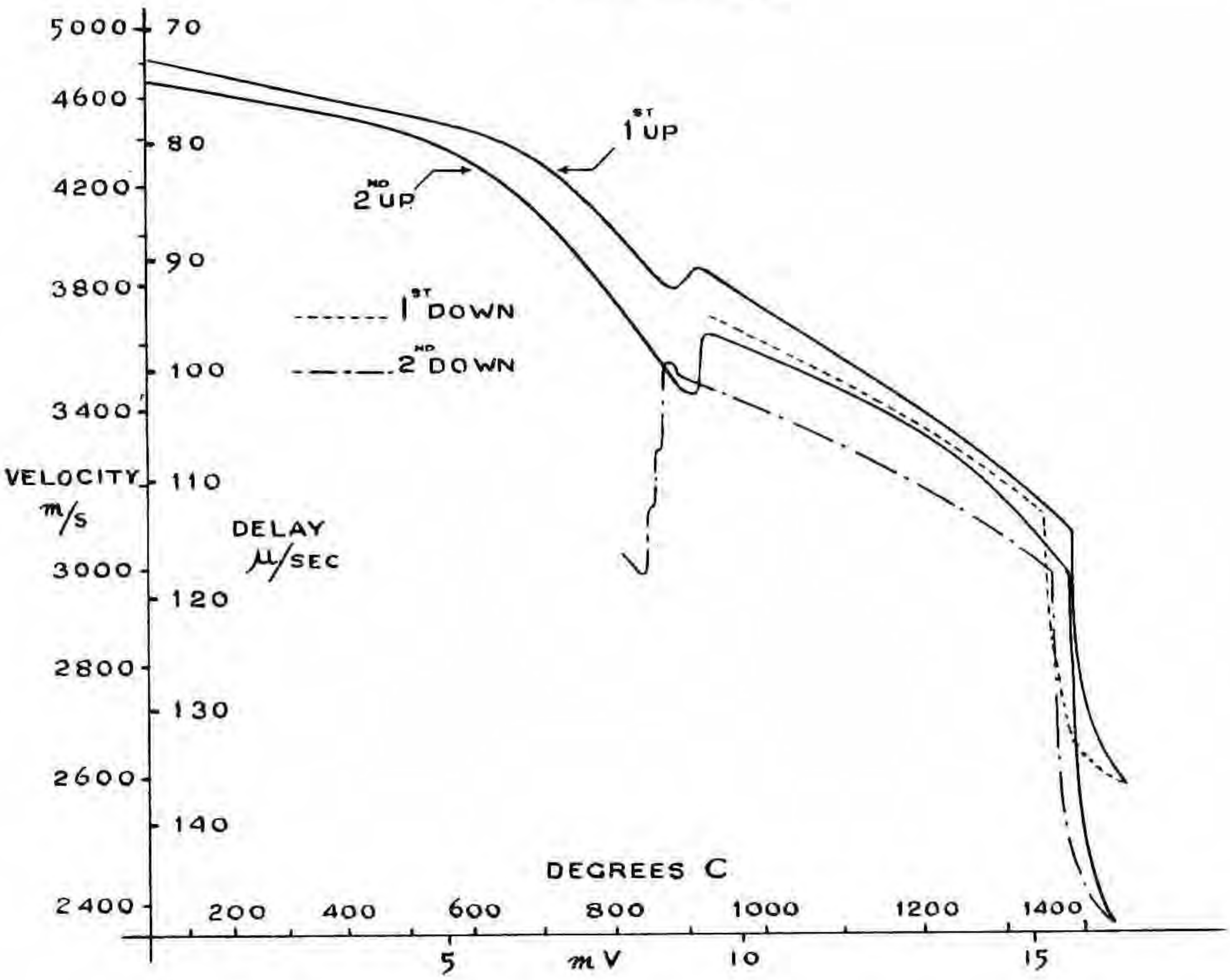

Fig. 2: Variation of velocity with temperature.

effect of the first heating cycle. Examining the second phase change the features are: the temperature hysteresis between heating and cooling runs; the well defined temperature at which the change starts on the heating cycles; the displacement between the various curves arises mainly from the recrystallisation at the phase change. Due to the anisotropy of iron the new set of crystals having a different orientation will result in a different velocity. Some contamination (nitriding) took place, mainly during the second cooling run when the specimen was above 1100°C for about 24 hours. The change in character of the lower phase change is a fairly definite confirmation of this.

5. Attenuation.

The attenuation, shown in Figure 3 by the change in echo heights is a combination of the energy dissipated in the material and the energy lost by echoing from the crystal boundaries.

The qualitative picture is fairly obvious. The attenuation is very low up to 500 or 600 degrees. It increases rapidly (and echo height falls) to the $\alpha - \gamma$ phase change and decreases spectacularly as the phase changes. It then increases slowly until the δ phase is reached when it rises suddenly to a very high value indeed, the end echo being only just measurable.

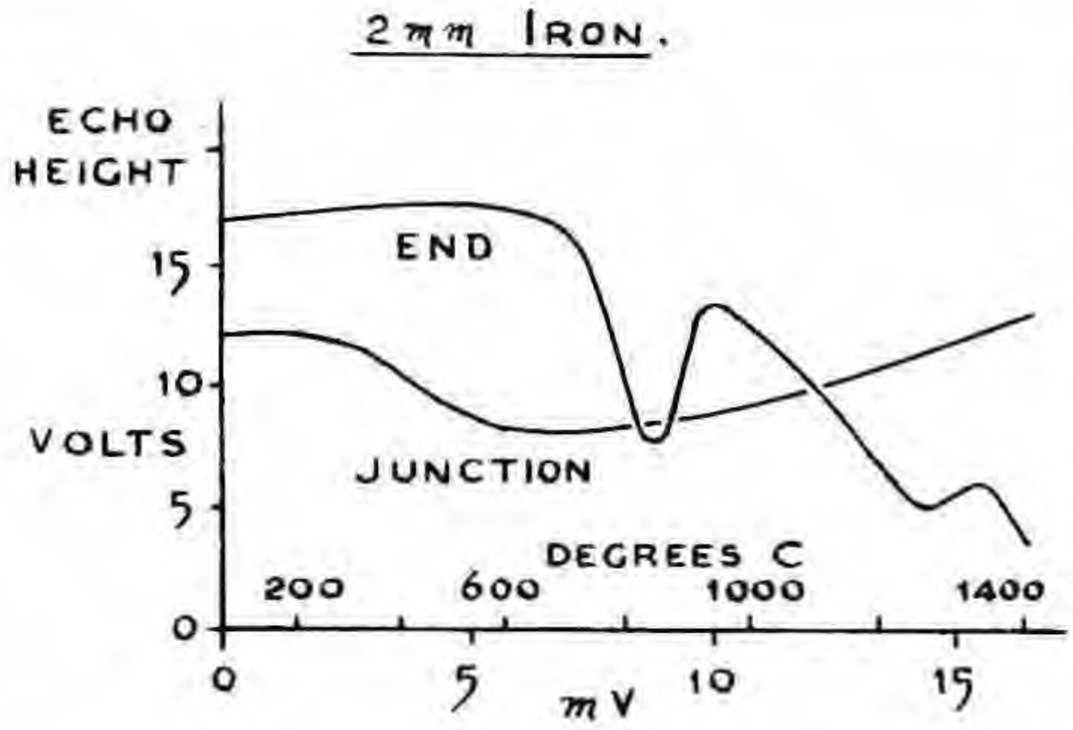

Fig. 3: Changes in attenuation shown by changes in echo heights.

6. Crystal boundaries.

The small echoes between the two main echoes arise from the velocity discontinuities at the crystal boundaries. As the pulse used is 3 or 4 cms. long the crystals must be at least an appreciable fraction of this length (say 1 cm.) to give an echo. Metallurgical examination of the specimens after cycling shows various crystals of this size. In the α phase the echoes are much stronger above 700°C than below (Figure 3), indicating that the material is more anisotropic at the higher temperature. The phenomenon was quite unexpected but was confirmed by cycling the specimen between 400°C and 850°C. As the temperature fell the echoes almost disappeared. As the temperature increased the echoes reappeared to give exactly the same pattern as before. The change in slope of the velocity temperature curve near 700°C could be another manifestation of the anisotropy.

The recrystallisation which occurs at the phase change is well in evidence in Figure 1. A cine film with frames taken at one minute intervals showed the phase change and crystal growth effects very strikingly and clearly. There is some indication that a crystal in one phase changes into a complete crystal in the next phase but with the pulse length used the apparatus lacks the resolving power to do other than suggest this.

Improvement in resolution could be attained, with increase in attenuation, by using a shorter exploring pulse. The change would involve using a smaller, thinner-walled launching tube and redesign of the acoustic matching to the lead-in alumina. The use of 1 mm. diameter specimens would increase the probability of crystals occupying the complete diameter of the specimen and so give better echoes.

This is being pursued. Measurements have also been made of torsional velocity.

Acknowledgments.

This work was carried out in the Physics and Electrical Engineering Department of the Royal Naval College, Greenwich, England as part of a research contract for the O.E.C.D. High Temperature Reactor Project Dragon.

The author's grateful thanks are due to Mr. S.G. Smith and Mr. B.P. Doyle whose valued assistance considerably facilitated this work.

References.

(1) H.J. McSkimmin, "Notes and References for the Measurement of Elastic Moduli by Means of Ultrasonic Waves" J.Acoust.Soc.Am. 33, 606, (1961). (2) H.J. McSkimmin, J.Acoust.Soc.Am. 31, 287, (1959). (3) J.W. Marx and J.M. Siversen, J.App.Phys. 24, 81, (1953). (4)(a) W.H. Hill, K.D. Shimmin and B.A. Wilcox, "Elevated-Temperature Dynamic Moduli of Metallic Materials" A.S.T.M. Preprint No.74 (1961). (4)(b) G.G. Conradi and E.P. Zamilatskii, Zavod.Lab, 10, 1286-9, (1961). (5) F.E. Faris, L. Green and C.A. Smith, J.App.Phys. 23, 89, (1952). (6) G. Wertheim, Ann.de Chimie, 12, 385, (1844). (7) J.F.W. Bell, "The Velocity of Sound in Metals at High Temperatures", Phil.Mag. (8), 2, 1113, (1957). (8) J.F.W. Bell, D.R. Hub and S.G. Smith, "Elastic Properties of Graphite", D.P. Report 5, O.E.E.C. High Temperature Reactor Project, Dragon.

K51

FOURTH INTERNATIONAL CONGRESS ON ACOUSTICS
COPENHAGEN 21.-28. AUGUST 1962

The Measurement of Liquid Borne Ultrasonic Power.

F.E. Freeman and E.A. Lloyd,
Northampton College, London, E.C.1.

INTRODUCTION. Because of other work proceeding in our laboratories on water borne ultrasonics in the frequency range 2-4 Mcs and power levels between 1 and 4 watts it was found desirable to have a ready means of measuring the ultrasonic power present in water within these ranges. It is to be noted that the quantity we sought to measure was the Gross Acoustic Power Transfer (G.A.P.T.) (1) that is the actual power present in the liquid medium. Although the calorimetric method of measurement is the most direct some quicker means was sought and one also capable of probing the field.

It was decided to utilise the results of Fox (2) for the sound pressure on spheres, by experimentally measuring the force exerted on a sphere in a progressive wave and to compare this result with calcrimetric measurements. The insertion loss of the transducer was also measured (3) and the value of the water borne power deduced from this method was compared with the calorimetric and radiometer methods.

RADIOMETER METHOD. The fundamental requirements when using the radiometer method are similar in principle to the requirements dictated by the electro-magnetic microwave power measurements using directional couplers (4). From a practical point of view this resulted in the use of a perspex water tank with a matched terminating impedance consisting essentially of a volume of transformer oil separated from the water by a polythene membrane the characteristic impedances of these materials being close to that of water, the oil also being a good absorber. To increase the efficiency of the termination, the portion of the tank containing the oil was set at right angles to the water container and the end of the water container angled at 30°. With this arrangement the ultrasound entering the oil suffered multiple reflections from the sides of the tank thus increasing the total absorption obtained (see figure 4.).

Considering the transducer as a piston source there will be an effective Fresnel field for distances from the source up to about $\frac{a^2}{\lambda}$ where a is the radius of the transducer and λ is the wavelength of ultrasound in water. For the frequency range 2-4 Mcs conveniently short distances from the transducer bring measurements well within the Fresnel field. The method of tackling this problem may best be seen by reference to Figure 2 where Lommels curve (5) for the intensity distribution from a circular aperture has been replotted with an abcissae $p = \frac{\pi r^2}{\lambda}$ instead of r, where r is the radius measured from the centre of the circularly symmetrical diffraction pattern, this means that the area under the graph gives the power transmitted. Thus knowing the radius of the radiometer ball one can find the fraction of the total power intercepted by the ball and thus calculate the total power from measurements made on the radiometer. The graph drawn is for a distance (x) from the transducer such that three half period zones are subtended this allows several combinations of values for a, x, λ, still other combinations may be catered for by obtaining similar curves for other numbers of subtended half period zones. The force on the radiometer

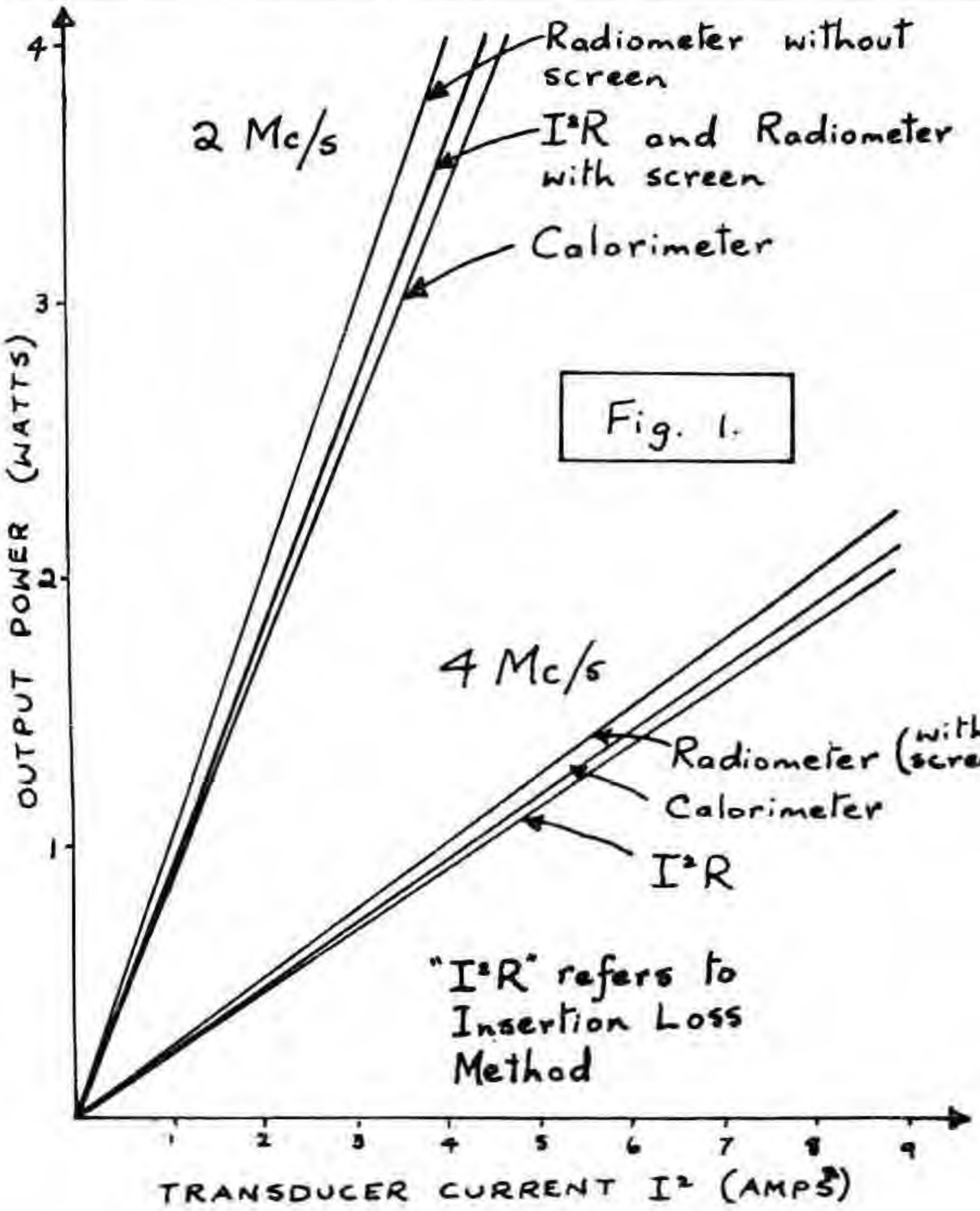

Fig. 1.

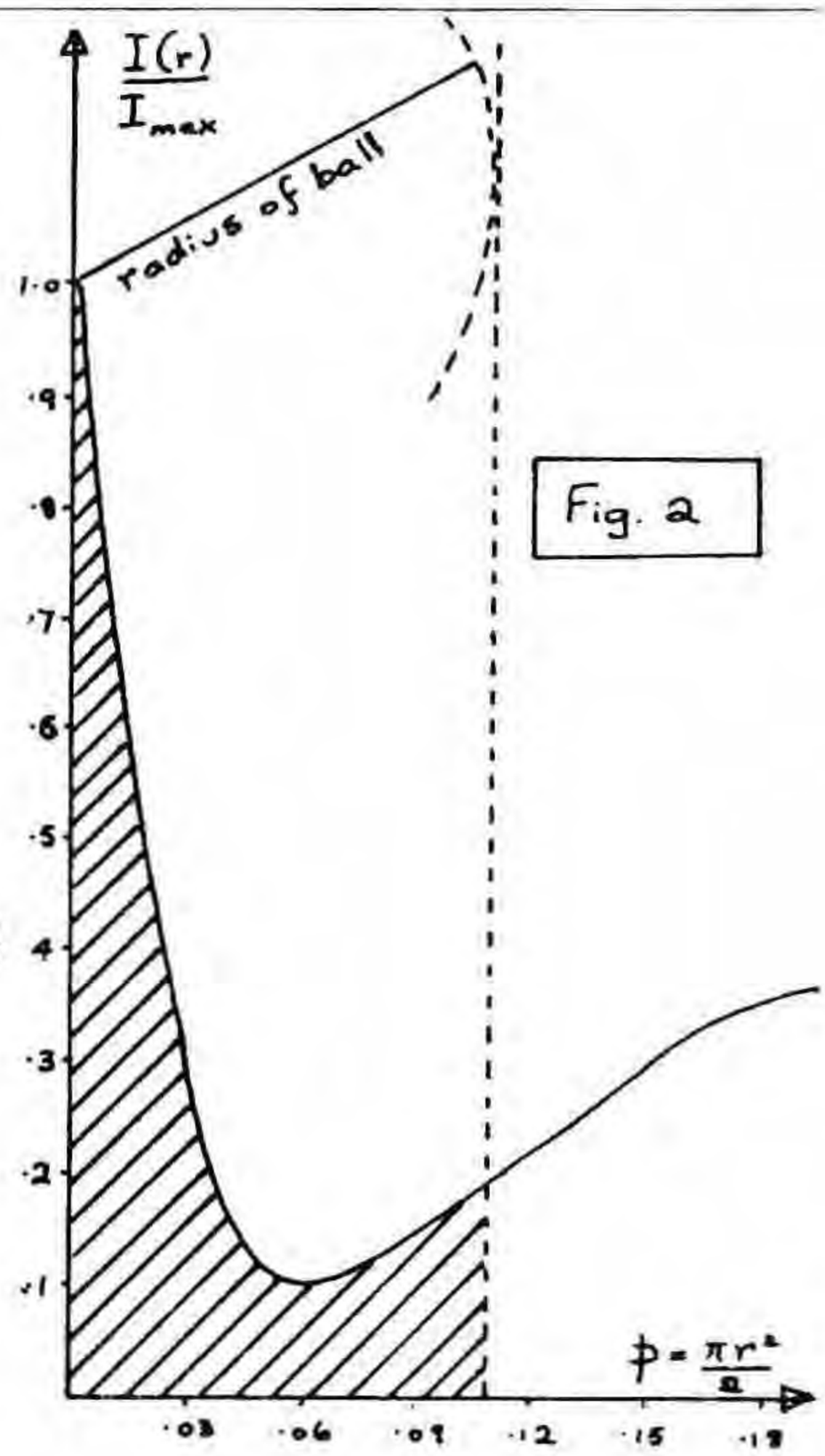

Fig. 2

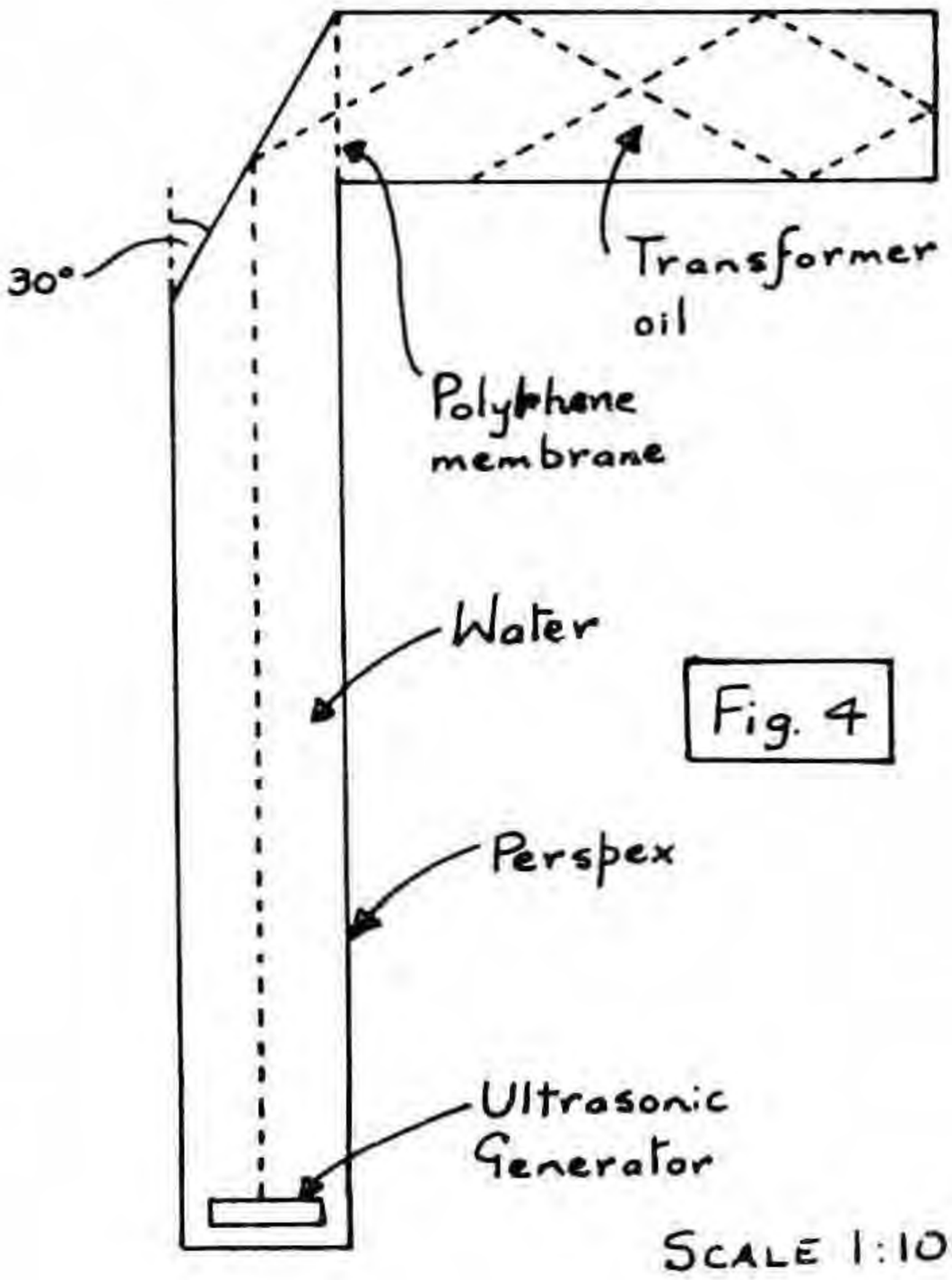

Fig. 4

SCALE 1:10

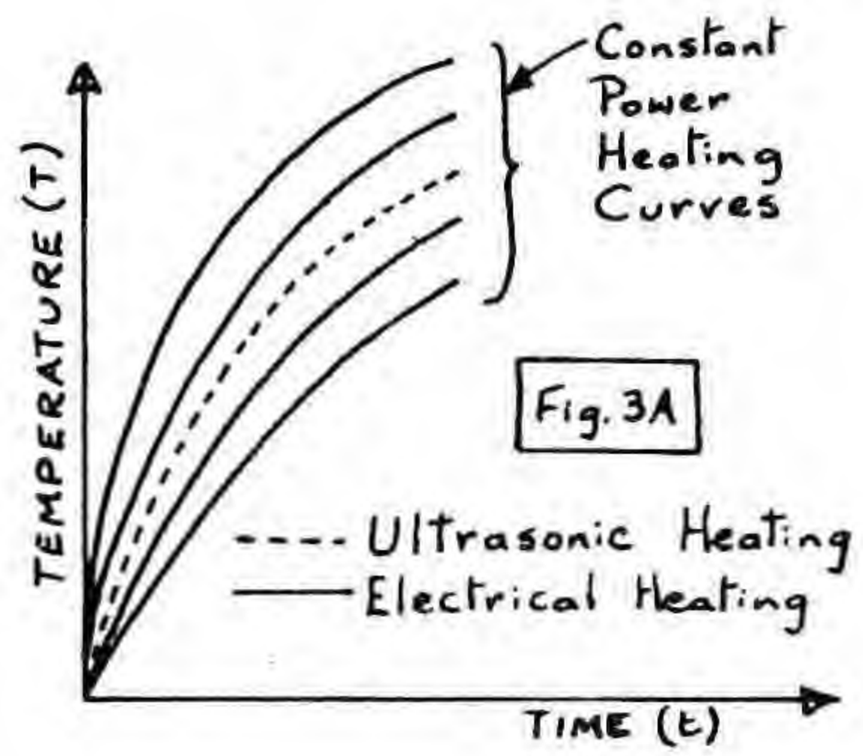

Fig. 3A

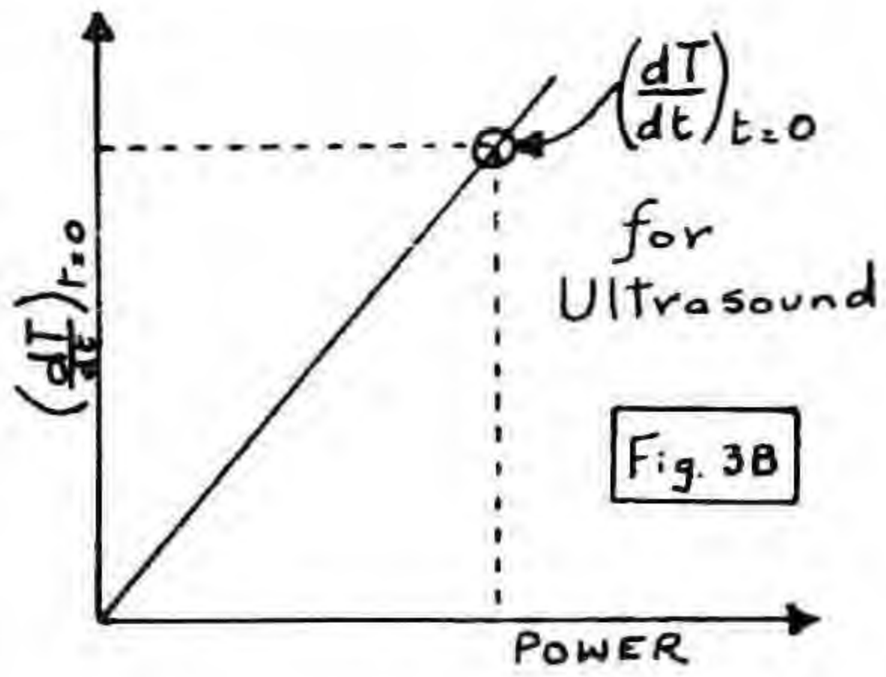

Fig. 3B

ball was obtained by suspending it by means of a thin brass strip from a pivoted support, the deflection of the ball due to the incidence of ultrasound was reduced to zero by adding small weights to a scale pan thus the force on the ball could be measured whilst keeping the ball on the axis through the centre of the transducer. To avoid the effect of streaming or mass flow of water a polythene membrane was interposed between the transducer and the radiometer. The effect of this "quartz wind" is shown in Figure 1 which at 2 Mcs gives results both with and without the use of the membrane.

CALORIMETRIC METHOD. A simple calorimeter was constructed consisting of a perspex vessel containing castor oil as an absorber with a polythene window to admit the ultrasound. The calorimeter was supplied with an electric heater coil and a mercury in glass thermometer. Heating curves were drawn for the input energy due to both ultrasonic and electrical heating. These are shown in Figure 3a which together with Figure 3b illustrates the method of evaluating the ultrasonic input power. It must be emphasised that this method depends upon the electrical heating curves being of the same family as those due to ultrasonic heating; for this reason the internal structure of the calorimeter was adjusted until satisfactory matching was obtained. This adjustment was effected by altering the geometry of the heater coil and the provision of a deflector plate for the ultrasound. Additional stirring was found to be unnecessary.

INSERTION LOSS. The following quantities are defined.

P_i = power fed to the transducer.

P'_o = " " " " water under perfect coupling conditions.

P_o = " " " " " for the actual case in hand.

IL = insertion loss = $10 \log \frac{P'_o}{P_o}$

Since for perfect coupling $P_i = P'_o$ then IL = $10 \log \frac{P_i}{P_o}$

Thus to calculate P_o, IL and P_i must be found. P_i may be measured directly for the case of the transducer operated at minimum impedance.

To find IL a pulse reflection technique was employed. The pulsed output from the transducer was reflected from a polythene sided air cell. On the arrival back of the pulse the transducer now acted as a receiver. The voltage amplitude (V_1) of the transmitted pulse (transducer open circuit) and the received pulse across the transducer (V_2) were displayed on an oscilloscope. The IL was calculated by considering the system to be equivalent to two identical transducers one transmitting the other receiving. For such a system it may be shown that the total insertion loss is given by $20 \log \frac{V_1}{V_2}$ -6db (3)

thus the insertion loss per transducer is $10 \log \frac{V_1}{V_2}$ - 3db and therefore knowing P_i we may calculate P_o.

CONCLUSIONS. In spite of the fact that we extended the use of Fox's results beyond that for a strictly plane wave, reference to the experimental results (Fig.1) shows that a very satisfactory agreement was obtained between the radiometer measurements,& the calorimeter and insertion loss measurements. For the 2 Mcs case the curves for the insertion loss and radiometer measurements lie so close to one another as to be indistinguishable on the scale drawn. From the original graph of the results it is estimated that the radiometer measurements differ from the calorimeter measurements by not more than 10%.

The radiometer used thus provided a very convenient and rapid method of measuring the ultrasonic power present in the liquid when working in the Fresnel field and could also, of course, be used for the Frauenhofer region. The apparatus in its present form would not be sensitive enough to deal with intensity levels much below 10^{-1} Watts cm^{-2} but this could probably be improved together with the general accuracy of the method by a refinement of the balance mechanism from which the radiometer ball was suspended.

REFERENCES.

1. Trans. I.R.E. P.G.U.E.5. (1957).

2. J.A. Fox. J.A.S.A. 12. 147 1940.

3. R.N. Thurston I.R.E.Convention Record 1959. p.260.

4. Handbook of Microwave Measurements Vol.1. Section 4.
Measurement of Power by E.Torgow.
Polytechnic Institute of Brooklyn.

5. Bayerisch. Akad.d.Wiss., 15, 233, 1886.

L51

FOURTH INTERNATIONAL CONGRESS ON ACOUSTICS
COPENHAGEN 21.-28. AUGUST 1962

TRANSMISSION OF SOUND IN DUCTS

C.L. Morfey

Introduction

Throughout the last six decades of development of Civil Aircraft one common factor has linked their propulsion units: rotating blades. These have taken a variety of forms, from the tractor propeller to the helicopter rotor on one hand and the axial compressor rotor on the other: but until recently the ground noise from rotating blades has not set an urgent problem to aircraft designers. This situation is now changing with the use in airliners of increasingly powerful turbojet engines. The question arises, what effect has the air intake duct on the sound radiated from an axial compressor.

This paper considers only pure-tone radiation. The source of such radiation in a compressor is the pressure fluctuations felt near the rotor owing to the repeated passing of blades. The amplitude observed will depend on position relative to nearby objects, such as stator blades, which affect the flow round the rotor. In this way, a complicated distribution of pressure is set up over the intake annulus in a turbojet compressor. The problem is, how effectively are these fluctuating pressures propagated. The fact that the far end of the duct is open clearly affects the problem; this will be mentioned in conclusion. The following theory assumes for simplicity an infinitely long duct, of uniform section.

Simplified Mechanism of Propagation

The shape of the duct, bounded by concentric circular cylinders, strictly requires a solution of the acoustic wave equation in cylindrical polar co-ordinates. This has been done by Tyler and Sofrin (Ref. 1). The mathematics is difficult, however, and it is the purpose of this paper to present a simpler approach. This should make it practicable to insert the characteristics of a given source, and to extend the study of duct transmission to short ducts of varying section.

The simplifying assumption on which the following theory is based is that the duct walls are close enough for their curvature to be negligible. The boundaries become parallel planes, and sound can propagate as plane waves reflecting between the walls. It will be shown (Equations 1, 2) that once the wave number is specified (as it can be for pure tones), these plane wave fronts are confined to certain directions by the boundary conditions. Waves travelling in any one of these directions set up a characteristic distribution of pressure over the annulus: examples are shown in Fig. 1, where the lines are nodes of pressure. These are the normal-mode pressure distributions; from these, any complicated distribution can be built up, including that due to an axial compressor.

FIG.1.

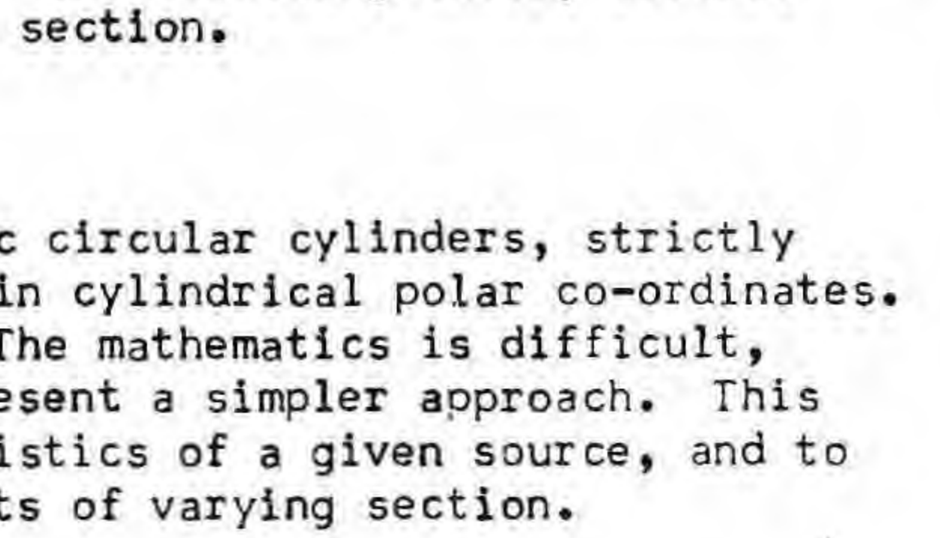

However, the number of modes, or directions, in which waves can propagate along the duct is not unlimited. It will be

shown (Equation 4) that for a specified wave number, only certain modes can propagate. This means that a given distribution of pressure over one section of the duct cannot propagate unchanged if it contains the excluded modes. The same fact can be seen another way by fixing attention on a single mode, one component of the given distribution: there is a range of wave numbers which will propagate this mode, but in fact below a certain minimum wave number, the mode cannot propagate along the duct.

Conditions for Propagation

FIG.2.

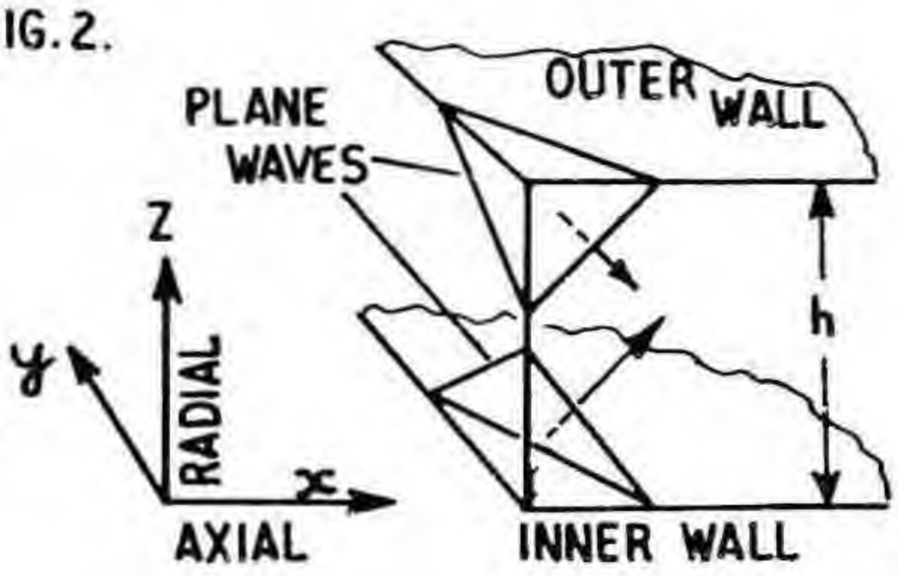

Fig. 2 shows part of the duct in section, with the walls taken as plane. The distance between the walls is h, and the mean perimeter ℓ. A succession of plane waves, wave number k, is travelling between the walls: the normal to the wave-fronts has direction cosines α, β, γ, referred to the axes x,y,z. Waves are reflected from the wall with direction cosines $\alpha, \beta, -\gamma$; the combination of these wave systems produces standing waves between the walls.

The boundary conditions are:

(1) The pressure gradient is zero at the walls. There must therefore be a whole number of half-waves standing between the walls: and since the wave number in the z-direction is γk, $\gamma kh = n\pi$ (n integer) ...(1)

(2) Pressure and pressure gradient are continuous around the annulus. There must therefore be a whole number of waves around the duct: i.e. $\beta k\ell = 2m\pi$ (m integer) ...(2)

Since $\alpha^2 + \beta^2 + \gamma^2 = 1$, ...(3)

It follows that $\beta^2 + \gamma^2 \leqslant 1$

i.e. from (1) and (2) $\left(\frac{2m\pi}{k\ell}\right)^2 + \left(\frac{n\pi}{kh}\right)^2 \leqslant 1$

If k is to be real, i.e. propagation is to be possible, it follows that

$$k \geqslant \frac{2\pi}{\ell}\left(m^2 + \frac{n^2\ell^2}{4h^2}\right)^{\frac{1}{2}} = k^* \text{ say} \quad ...(4)$$

FIG.3.

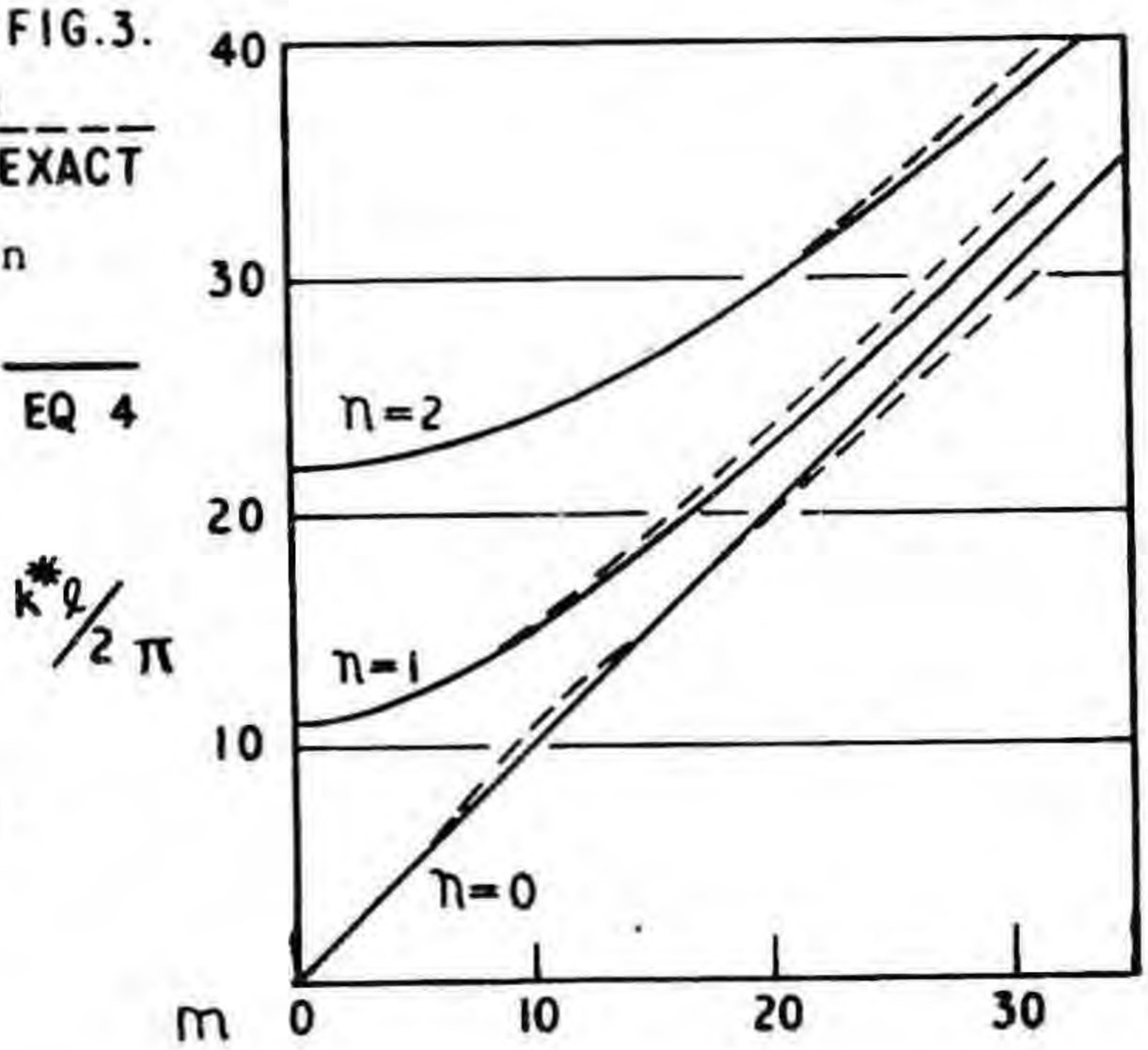

A comparison is shown in Fig. 3 between Equation (4) and Tyler and Sofrin's exact solution, taking the case of a duct with hub-tip ratio $\frac{3}{4}$.

Finally, from (1),(2) and (3),

$$k = (k^2 - k^{*2})^{\frac{1}{2}}$$

i.e. if the wave number k is greater than the critical value k^*, the wave number component in the x-direction is

$$(k^2 - k^{*2})^{\frac{1}{2}} ;$$

but if k is less than k^*, the pressure decays exponentially along the duct, with a decay constant

$$(k^{*2} - k^2)^{\frac{1}{2}} \qquad \ldots(5)$$

(as may be verified from a formal solution).

Experimental Results

Tests at Southampton University have confirmed the operation of this "cut-off" effect, as it is called. A $2\frac{1}{2}$" I.D. steel pipe was used as a duct, for which the lowest propagation frequency in the (m = 1, n = 0) mode (Fig. 1A) was calculated at 3.15 Kc/s. As the approximation described above is inaccurate for a plain cylinder, the exact solution was used. One end of the duct was fitted with an

FIG. 4.

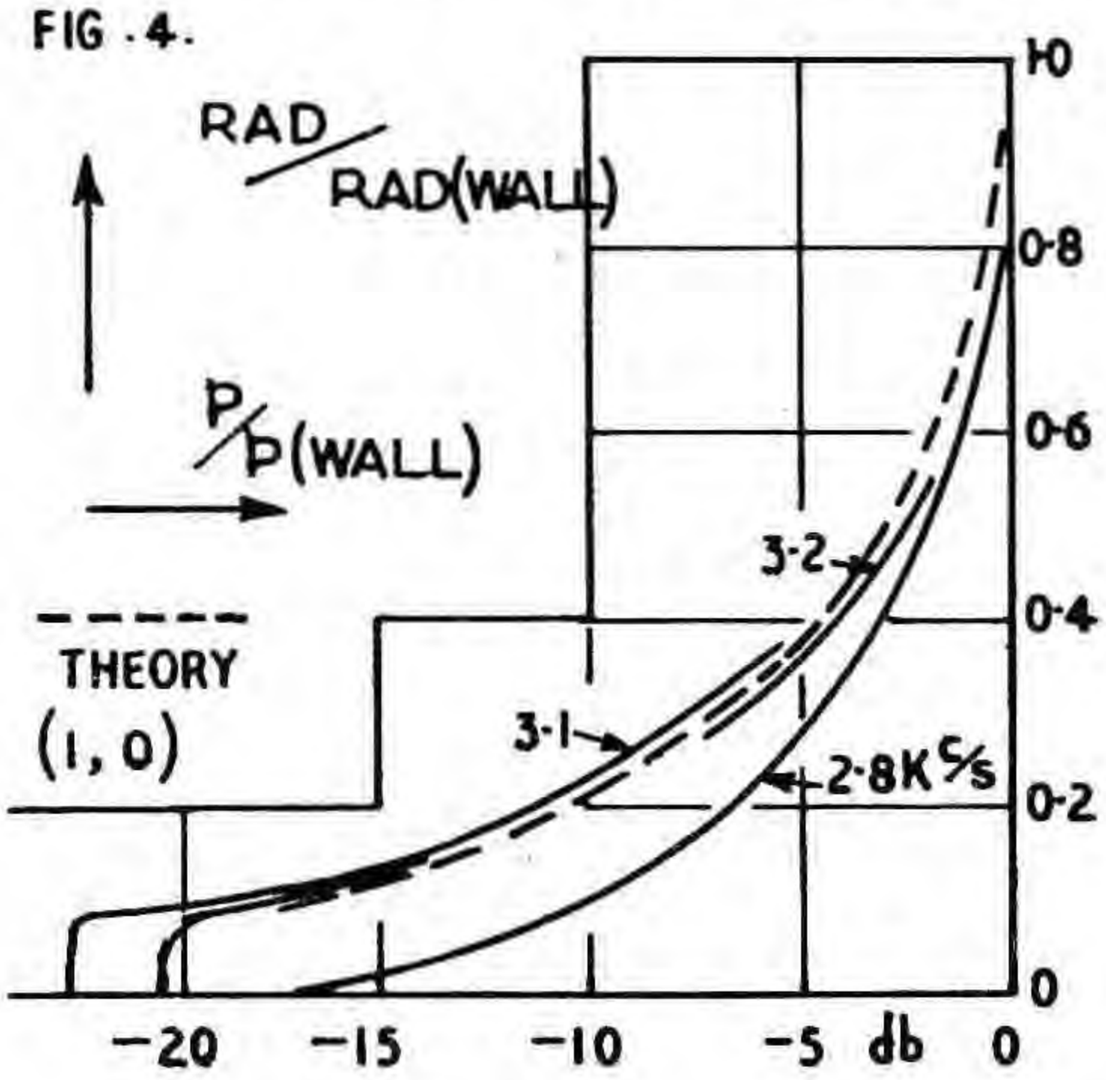

FIG. 5.

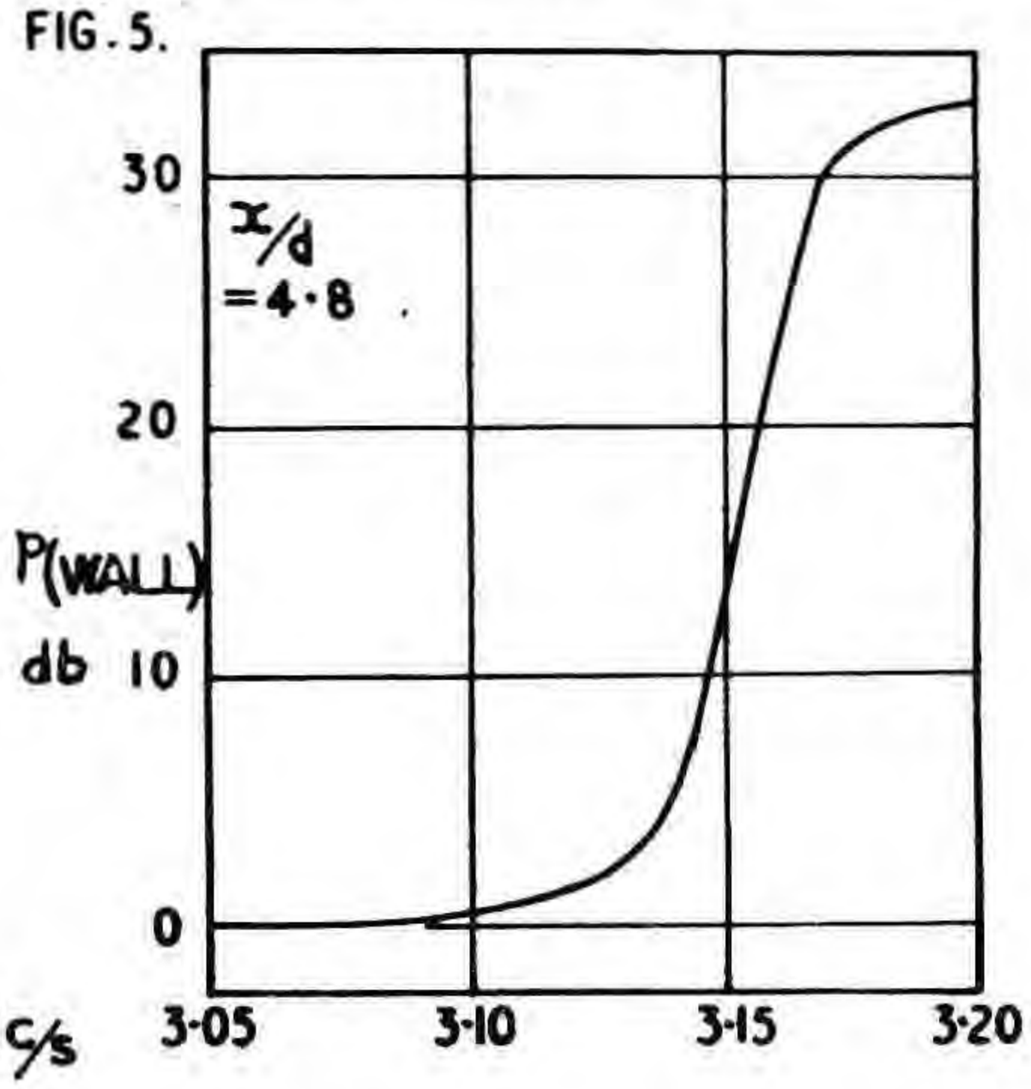

(1, 0) MODE PRESSURE WAVES IN CYLINDRICAL DUCT

FIG. 4 PRESSURE VARIATION ACROSS DUCT

FIG. 5 VARIATION WITH FREQUENCY

FIG. 6 VARIATION ALONG DUCT

FIG. 6.

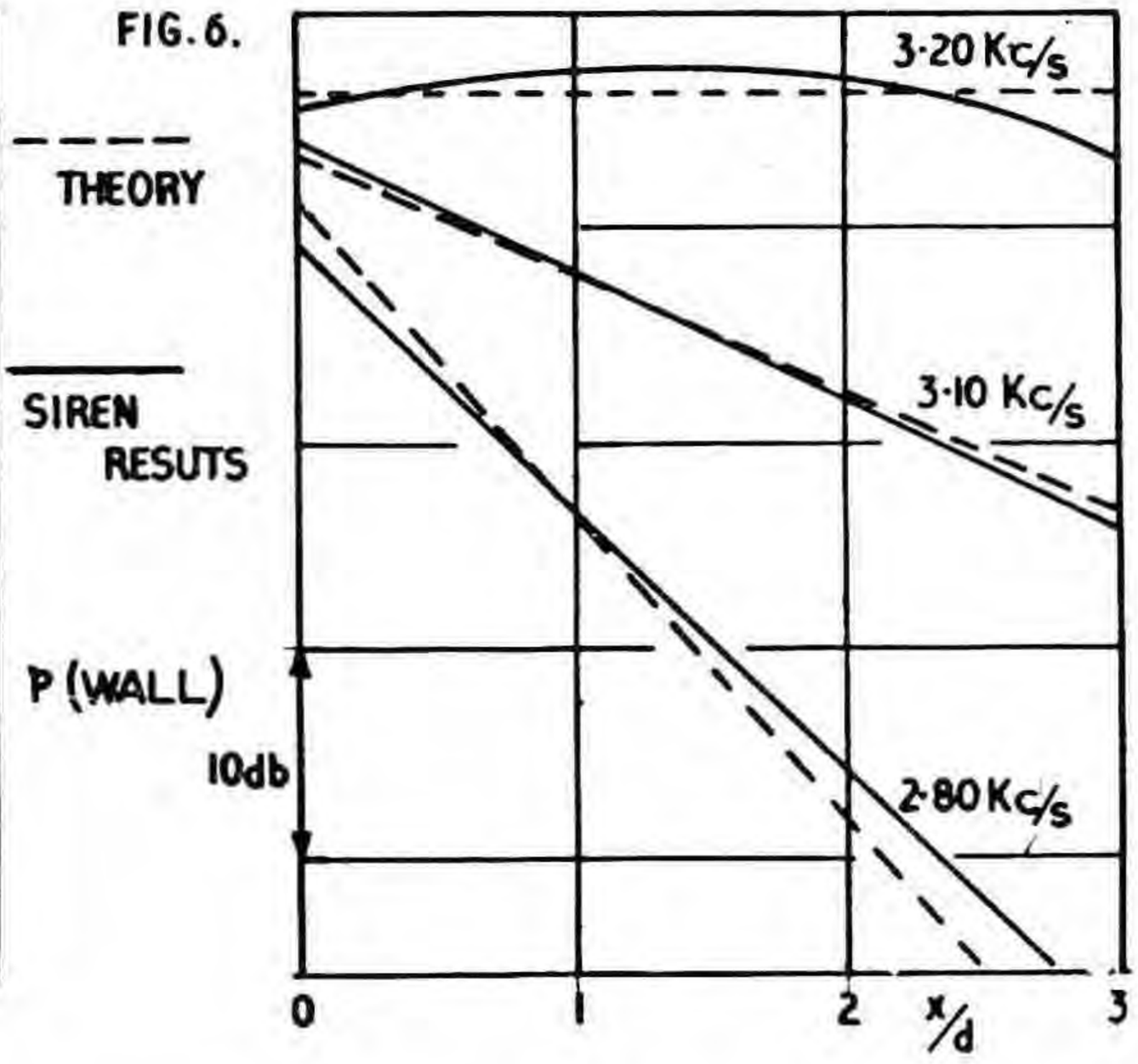

anechoic termination, making the length effectively infinite. A small siren inside the other end excited the (1,O) mode with frequencies around 3.15 Kc/s.

Fig. 4 shows radial traverses of the pressure level in the duct, taken with a 4 mm microphone probe. The theoretical (1,O) distribution is drawn for comparison.

Fig. 5 shows how the pressure level varies with frequency through cut-off, at a fixed point in the duct. The sharp rise around 3.15 Kc/s is consistent with theory.

Fig. 6 shows how the (m = 1, n = O) mode, generated strongly by the siren, varies in amplitude along the duct. The amplitude is measured by the sound pressure at the wall (p_w), and plotted against the ratio of axial distance (x) to duct diameter (d). The mode propagates undiminished at 3.2 Kc/s, i.e. $k/k^* = 1.016$. At 3.1 and 2.8 Kc/s, i.e. $k/k^* = 0.984, 0.889$, the amplitude of the mode decays along the duct. The decay rates are consistent with the general result (5). Similar results have been obtained for the (m = O, n = 1) mode using a loudspeaker as source

Conclusions

A complicated distribution of pressures, fluctuating at discrete frequencies, and generated within a duct as by an axial compressor, will not propagate unchanged even if the duct is infinitely long. The simplified theory gives a criterion (4) for propagation of normal mode components which is quite accurate for annular ducts of hub-tip ratio down to $\frac{1}{2}$; it is hoped that it will allow further work on propagation in short ducts of varying section. Experiments have shown that in a long duct, sound can propagate in higher order modes in accordance with theory. Current experiments with an open-ended duct show similar trends, but there is no conclusive evidence yet of a cut-off in the radiated sound.

Acknowledgment

I am indebted to Professor E.J. Richards for guidance in the experimental work at Southampton University.

Reference

(1) Tyler, J.M. Sofrin, T.G. "Axial Flow Compressor Noise Studies" Society of Automotive Engineers, 1961 Aeronautic Meeting Preprint 345 D.

M51

FOURTH INTERNATIONAL CONGRESS ON ACOUSTICS
COPENHAGEN 21.-28. AUGUST 1962

Acoustical Effects of Movable Sound Reflectors in Auditoriums

FUNAKOSHI, Yoshifusa

Recently, many cities in Japan have built their own community centers in order to provide their citizens with the multi-purpose building for the public gatherings of various kinds. I and my associates have designed more than twelve such community centers for the past several years.

Due to the financial reasons for its construction and maintenance, the general trend has been that to have a community center with one main auditorium, which can be used for diverse civic activities including public lectures, the displays of motion pictures, the performances of dramas, dances, orchestras, and others.

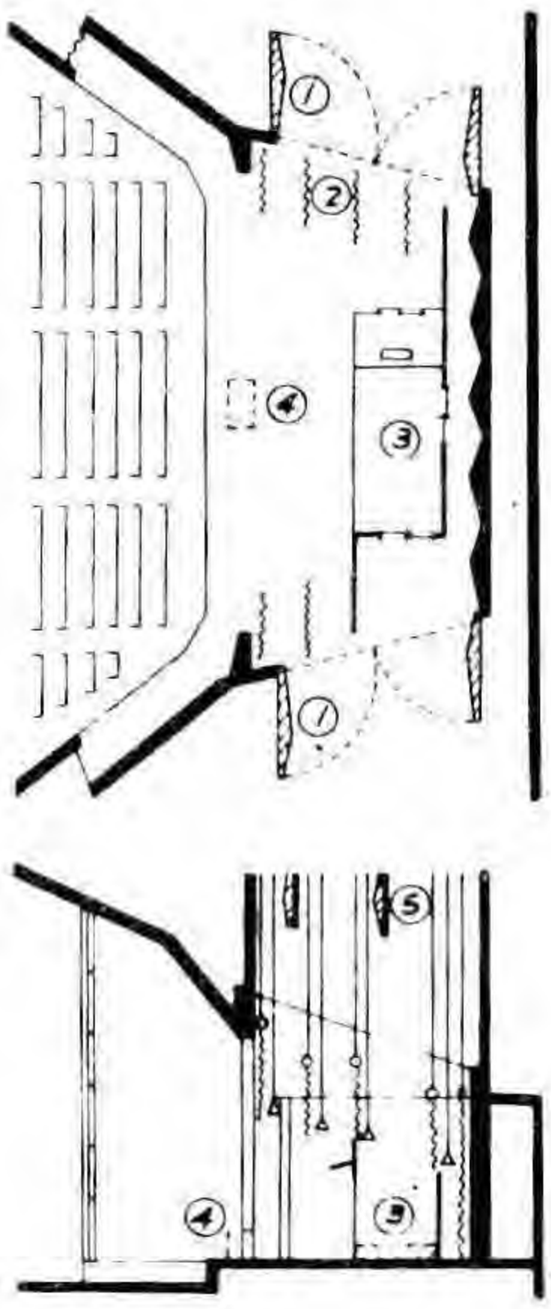

Fig.1: Stage for speech, ballet & drama (Kabuki and modern plays)

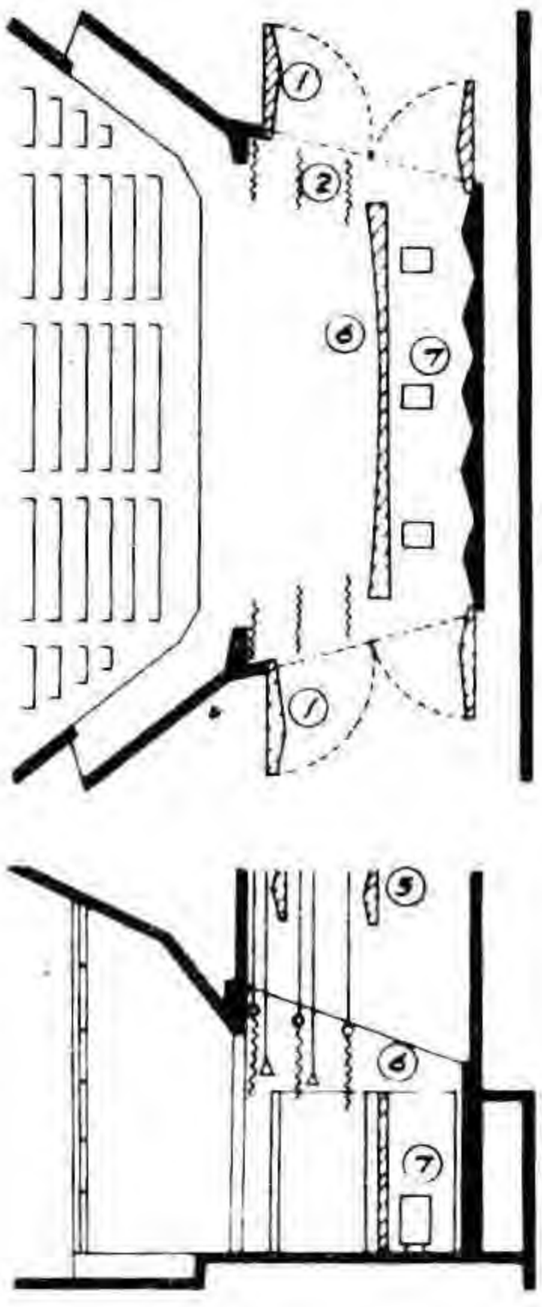

Fig.2: Stage for motion picture

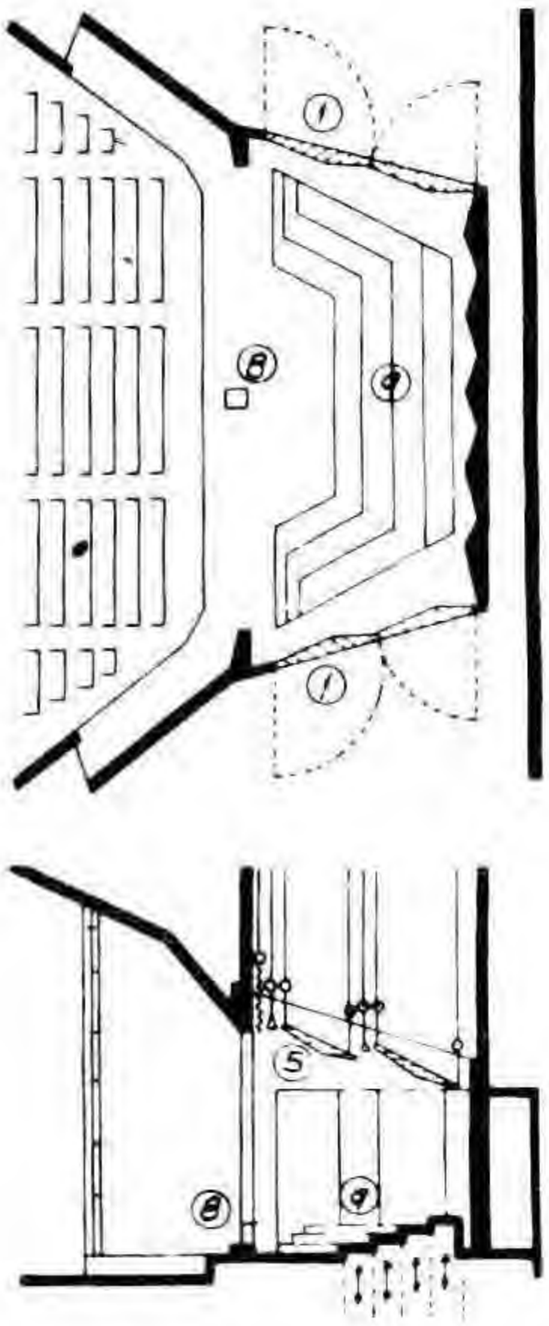

Fig.3: Stage for music & orchestra

① & ⑤ movable sound reflectors ② side curtains ③ scernery ④ speaker's desk
⑥ motion picture screen ⑦ loud speaker for motion picture ⑧ conductor's desk
⑨ stepped floor for orchestra

In designing the auditorium, which can meet such diverse demands satisfactorily, it is essential to take the reverberation time into full consideration, besides making proper provisions for the conversion and control of stage equipments and lightings.

The numbers of relevant problems have been solved by:

1) Installing the movable sound reflectors overhead the stage, at the both sides and sometimes also at the back of the stage (see Fig. 1-3).

2) Using movable screen and loud speakers for motion pictures (see Fig. 2).

3) Utilizing table elevators in a part of the stage to provide desired stepped levels for musicians playing orchestral or other musics (see Fig. 3).

4) In some special cases, using revolving panels in the side walls of auditorium to permit a wide control range of reverberation time (see Fig. 4).

In the acoustical design of any multi-purpose auditorium, the proper control of reverberation time always presents the most important as well as the most difficult problem. For most of auditoriums designed by us, which have the volume of 10,000-15,000 cu. meters, the optimum reverberation time is, at the sound of 500 cps, about 1.0 sec. for speeches, 1.3 - 1.7 sec. for musics. The optimum reverberation times for other performances range between these two limits. It, therefore, is preferable that this kind of auditoriums should permit the reverberation control range of 0.7 sec. at the maximum.

To secure such a wide control range of reverberation time, the large parts of interior surfaces on ceilings or side walls of the auditoriums, besides around the stage, must be capable of providing the variable degrees of sound absorption.
"Sapporo Civic Center" in Hokkaido is an example of this type. Figure 4 shows the constructional features of the side walls of that auditorium. The revolving panels have front faces made of artificial wooden sheets (20 mm) hardly pressed, with back faces of thin plywoods (6 mm), and the spaces behind those panels are finished with

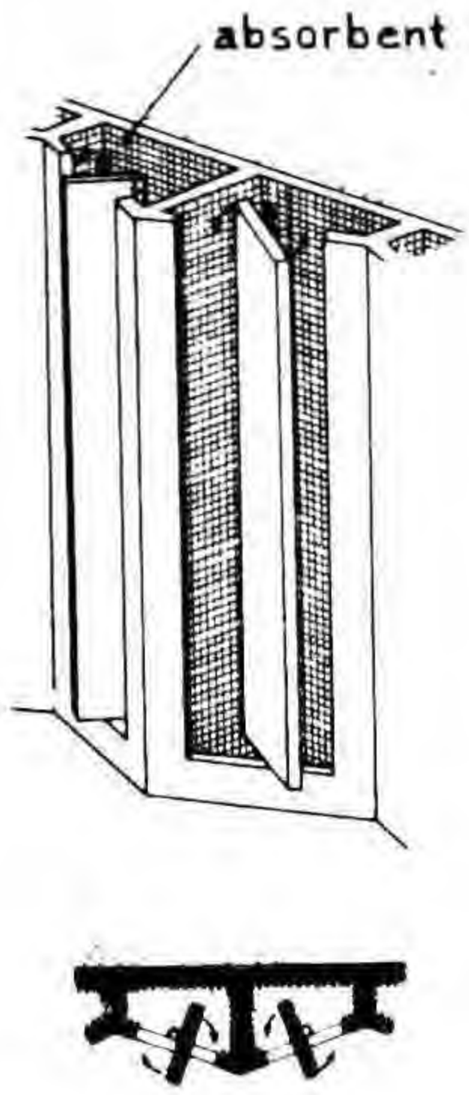

Fig.4: Revolving panels in side walls for controlling the reverberation time

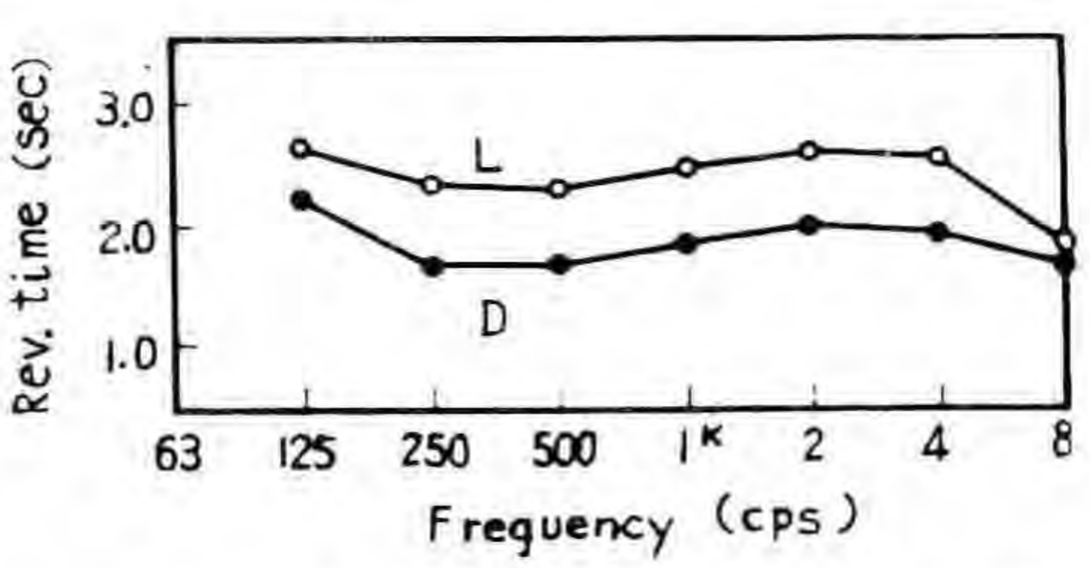

Fig. 5: Reverberation time of "Sapporo Civic Center", as all movable panels operated.
(L: closed, D: opened)

absorbents. The total of movable reflectors, in the side walls and around the stage, in that Center is about 340 M^2, while the area of the interior surfaces of that auditorium is 4,400 M^2 when all reflectors closed. Figure 5 shows the reverberation times with all movable panels closed(L), and opened (D). In the latter case, the revolving panels in the side walls are opened to an angle of 60°.

Controlling of the reverberation time to such a wide range assures the flexibility of the multipurpose auditorium. However, because of the high installation cost, such a controlling system has a limited use.

For the control of reverberation time in narrower ranges, satisfactory results (see Fig. 6) have been obtained by opening or closing the movable reflectors placed only around the stage. The total area of movable reflectors in such an auditorium is about 180-200 M^2, while the total of interior surfaces of that auditorium is about 3,500 - 4800 M^2, when all reflectors are closed.
(Only "Meitetsu Hall" has the surface area of 2,800 M^2). The data shown in Figure 6 have been obtained by measuring the reverberation time with the reflectors,

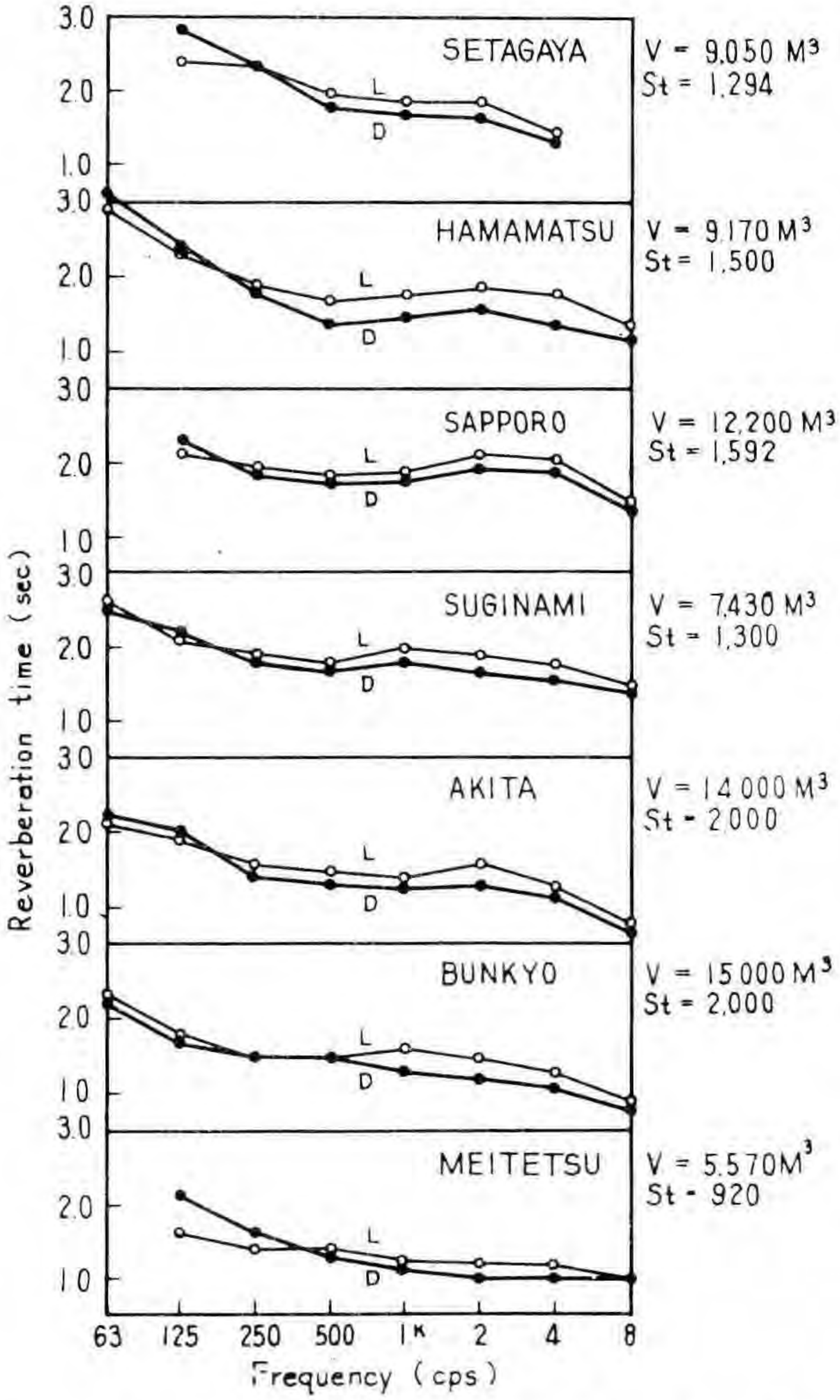

Fig. 6: Variation of reverberation time according to the operation of movable reflectors around the stage.

installed overhead and at both sides of the stage, opened and closed in empty auditorium. Figure 7 is plotted based on the difference of reverberation times as obtained from Figure 6.

It has been found to be common in almost all auditoriums investigated that when these movable reflectors are open, the reverberation time is reduced by 0.2 - 0.3 sec. for the sound of 250 cps or higher. On the contrary, when the frequency is lower than 250 cps, the opened reflectors result in slightly prolonged the reverberation time. These phenomena seem to be attributed to the fact that when the reflectors are open, the higher frequency sound is largely absorbed by the curtains behind the reflectors, and low frequency sound remains unabsorbed in large space behind the proscenium. And in this case, it is assumed that this large space behind the proscenium and the space over the audience seats form a coupled room. The opened reflectors result in giving a prolonged reverberation time for low frequency sound, thus disadvantageous in case of lectures and the like. However, since the speech is always amplified electrically, the necessary adjustment can be made in the loud speaker system. Besides, further measurements have indicated that the reverberation is reduced by about 0.2 - 0.3 sec., if the auditorium is seated to its full capacity.

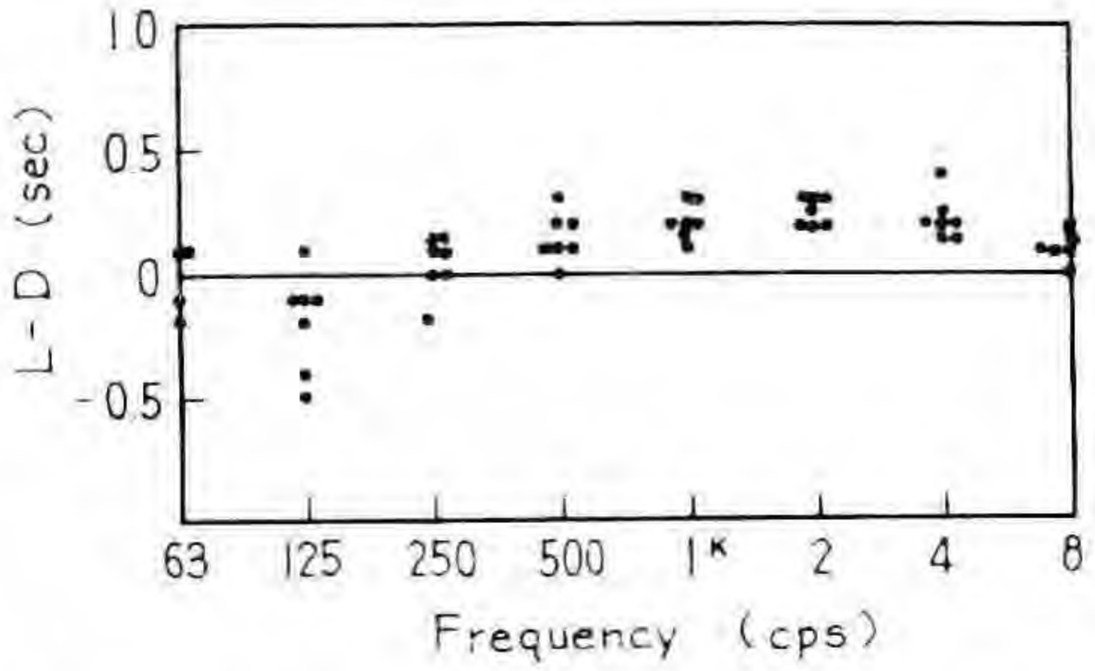

Fig. 7: Difference of reverberation times as obtained from Fig. 6

Previous example indicate that it is possible to increase or decrease the reverberation time to a certain extent by closing or opening the movable sound reflectors.

This leads to a conclusion that by the use of these reflectors, we can successfully design a multi-purpose auditorium, which permits a reasonable performance acoustically.

N51

FOURTH INTERNATIONAL CONGRESS ON ACOUSTICS
COPENHAGEN 21.-28. AUGUST 1962

MINIATURE PRESSURE MICROPHONES

Gunnar Rasmussen , Electrical Engineer , Brüel & Kjær A/S

In his textbook"Electroacoustics, the analysis of transduction and its historical background" F. V. Hunt writes about Wente' s "uniformly sensitive instrument" of 1917: It ushered in a new and thrilling era for the quantitative measurement of acoustical phenomena. The principal changes introduced in the condenser microphone itself during the next three decades consisted of the virtual elimination of the cavity in front of the diaphragm and a drastic reduction in the size of the instrument.

The removal of any cavity in front of the diaphragm ,and also an increase in the effective sensitive area of a condenser microphone will make the transducer appear smaller in an acoustic sound field. This effect is best illustrated in fig.1 where the free field correction for 0° incidence are shown for two microphones. The front cavity is only 2 mm deep with an internal diameter of 18.6 mm, but it will make the microphone look more than 10% larger in diameter and increase the free field correction by more than 1.5 db between 7 and 12 kc/s. It is possible , however, to utilize the effect of cavities and obstacles in front of a microphone diaphragm to increase the linear frequency range and the omnidirectional properties far beyond the frequency range given by the conventional considerations regarding dia - phragm resonance, wavelength and diameters. In fig. 2 are shown the frequency response curves obtained by optimizing the properties of a front cover in order to obtain the best possible uniform ity of sensitivity for a 1" microphone at any angle of incidence . In fact this 1" type 4131 microphone with random incidence corrector UA 0055 is more omnidirectional up to 15 kc/s than a conventional microphone, only

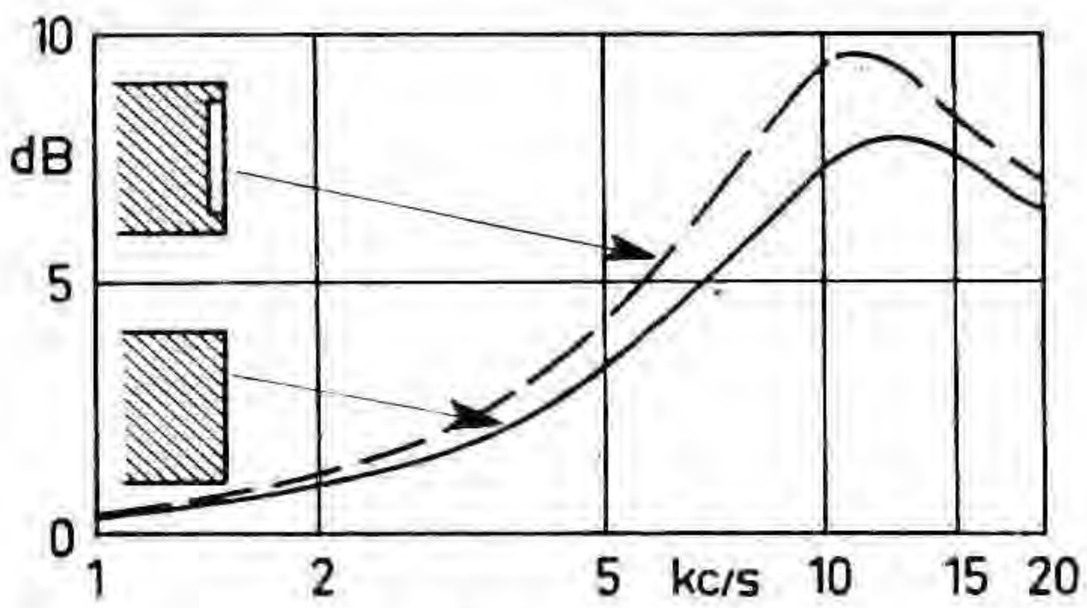

Fig. 1

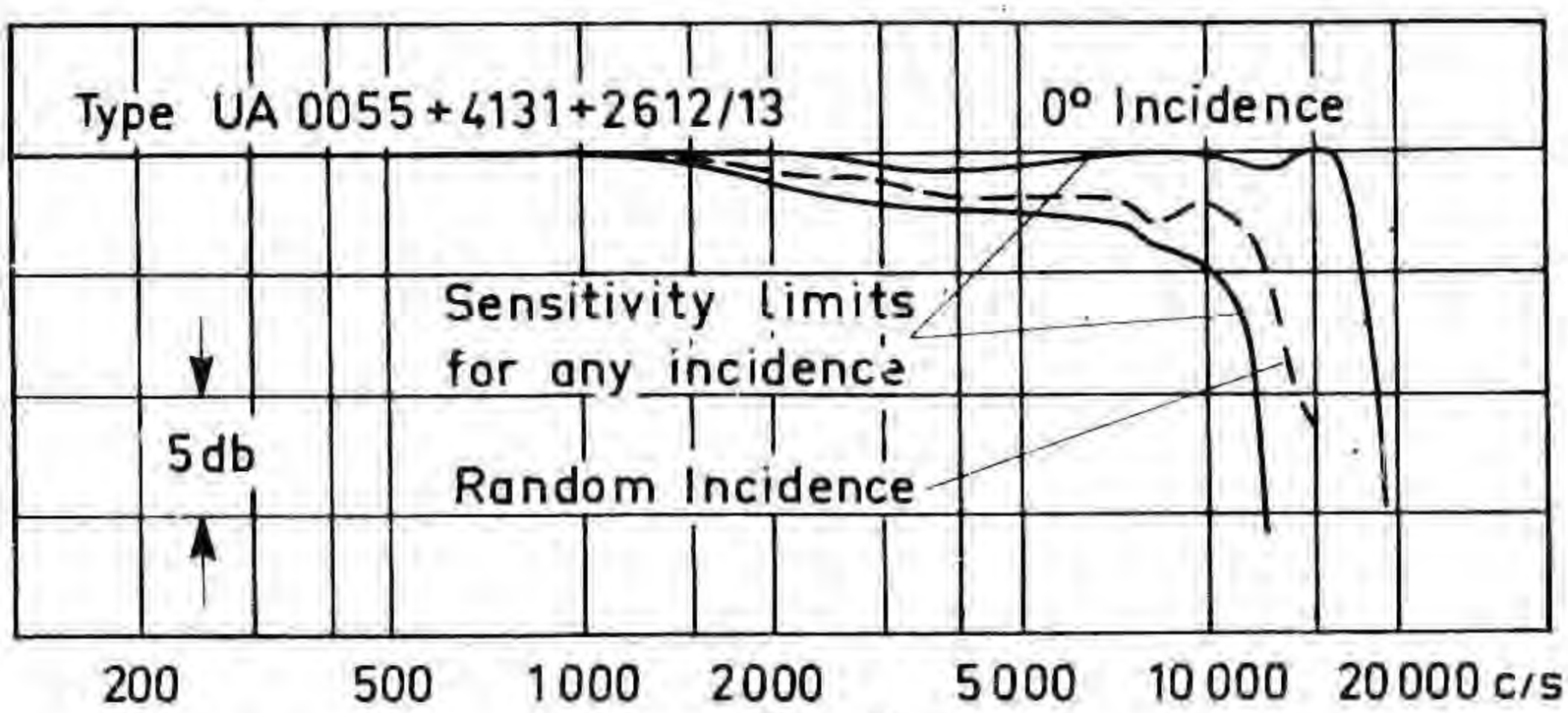

Fig. 2

1/2" in diameter. Some of the experimental steps leading to this design are shown in fig. 3. - It is thus possible to optimize some of the properties of a given cartridge size, one could say make it look acoustically smaller in some respects than it really is.



Fig. 3

Now for acoustical-and for fluctuating air pressure measurements in general -properties other than omnidirectivity may be called for, and we have investigated the possibilities of miniaturization of both the microphone cartridge itself and the succeeding preamplifier.

It should be kept in mind that the miniature microphones must still be stable with time temperature and ambient pressure. They must have reasonable dynamic range, a high resonant frequency, and a flat frequency response. They should be unaffected by severe environments, including high vibration levels. The condenser microphone seems at the moment to be the only one which is able to fulfil all these requirements. In particular it must be a stretched metal diaphragm type in order to ensure the stability.

The resonant frequency is given by the root of the compliance and the mass of the diaphragm. The sensitivity is controlled by the compliance below and by the mass above resonance. The effective mass is determined by the mass of the diaphragm material itself plus the mass of the moving air loading the diaphragm. The mass of the diaphragm itself should thus be less than the mass of the moving air in order to obtain the maximum sensitivity and highest resonant frequency. The mass of moving air near a diaphragm 4.5 mm in diameter is given by: $0,\frac{8}{3}\frac{\cdot q \cdot \varrho}{\pi}\pi a^2 = 0,43\,\frac{8}{3}\cdot 1.29\cdot 10^{-3}\cdot 0.45^3 \cdot 1.7\cdot 10^{-4}$ gr.

q is a reduction factor for the diaphragm movement below the first resonance, $\frac{8}{3}\frac{a}{\pi}$ is the air columne as given by Lord Rayleigh[x], and ϱ the density of air and "a" the diaphragm radius[xx]. This mass will equal that of a 5μ nickel diaphragm if we calculate the effective moving diaphragm mass using a reduction factor of 0.27 (see [xx]).

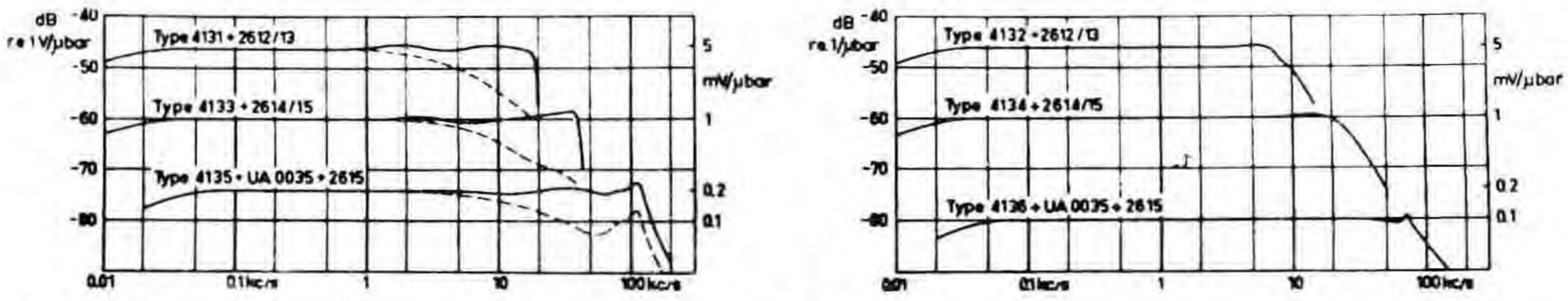

Fig 4

Fig. 4 shows the relationship between the frequency responses and sensitivities for

1", 1/2" and 1/4" microphones. It is possible by the technique used to make microphones of similar design of still smaller diameters. A 1/8" type has been made for laboratory use.

In fig. 5 is shown a 1/4" type. This microphone has only recently come on the market and I should like to mention some of the design problems faced during its development. The diaphragm is made up in a way which will give a maximum free moving area. The diaphragm tension is adjusted by tighting up the diaphragm on the housing from the front. The diaphragm thickness is 6μ for one type and 2μ for another. The material is nickel. The diaphragm thickness is choosen in order to give a flat and uniform pressure response for the one type and a flat free field response at 0° incidence for the other type. The frequency response for the pressure type is linear up to 70 kc/s within ± 2 db. It is interesting that the natural frequency of the diaphragm with no air loading and no air cushion between the diaphragm and the back plate is 50 kc/s.

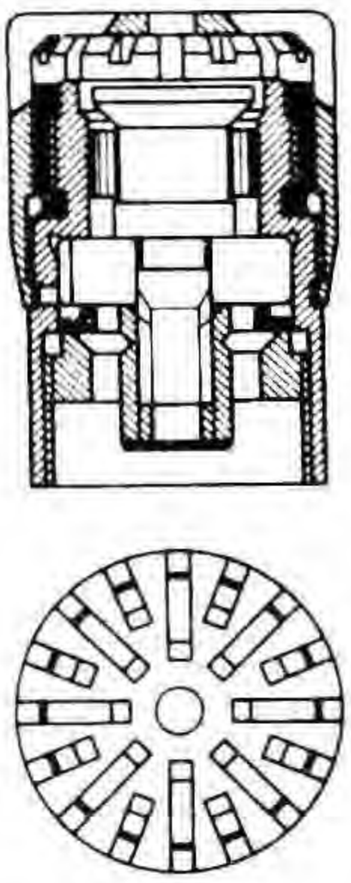

Fig. 5

It is possible to increase the frequency range to 70 kc/s by choosing the correct size of back plate and using maximum damping of the diaphragm center around resonance, thereby virtually blocking the diaphragm center and increasing the resonance. In this way the maximum sensitivity will be located at the edge of the back plate. This will make the microphone more sensitive to wave motions in the space between the diaphragm and the insulator. A special shaped Teflon damping ring is introduced inorder to overcome this. How this works is shown in fig. 6. This standing wave effect is incidentally also present in 1/2" and 1" microphones but normally does not manifest itself within the working frequency range. In 1949 Isadore Rudnick proposed the effect as a reason for resonances in the W. E. 640 A. A. at 36 kc/s. xxx) The sensitivity and thus the compliance of the type with 2μ diaphragm is around 2-3 times that of the type with 6μ. The resonance of the free moving diaphragms are the same. However, it is possible to damp the 2μ diaphragm in order to compensate for the pressure increase in front of the diaphragm for 0° incidence and obtain a flat response above 120 kc/s still with good sensitivity.

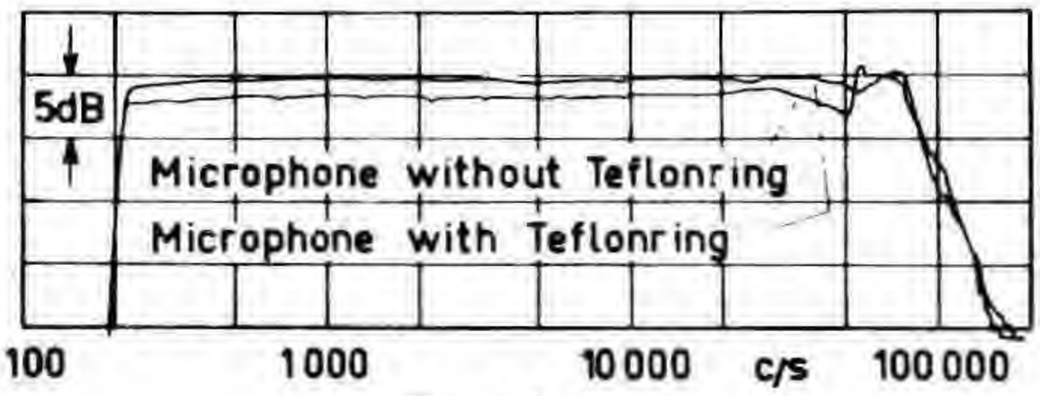

Fig. 6

The stiffness of the back space is kept very low in order to maintain the sensitivity stable at low ambient pressure as encountered at high altitudes. The stiffness is less than 8% of the diaphragm stiffness as seen from the curves in fig 7. This again gives the equivalent volume of the microphone as less than 0.0005 cm^3. The back space volume is 0.005 cm^3. The resonance damping will of course decrease at low ambient pressure and it is interesting to see that Q values of the order of 500 are obtained for the diaphragm resonance at 14 mm of mercury. The equalisation of the pressure from the back space takes place through a small slot to the front of the cartridge and

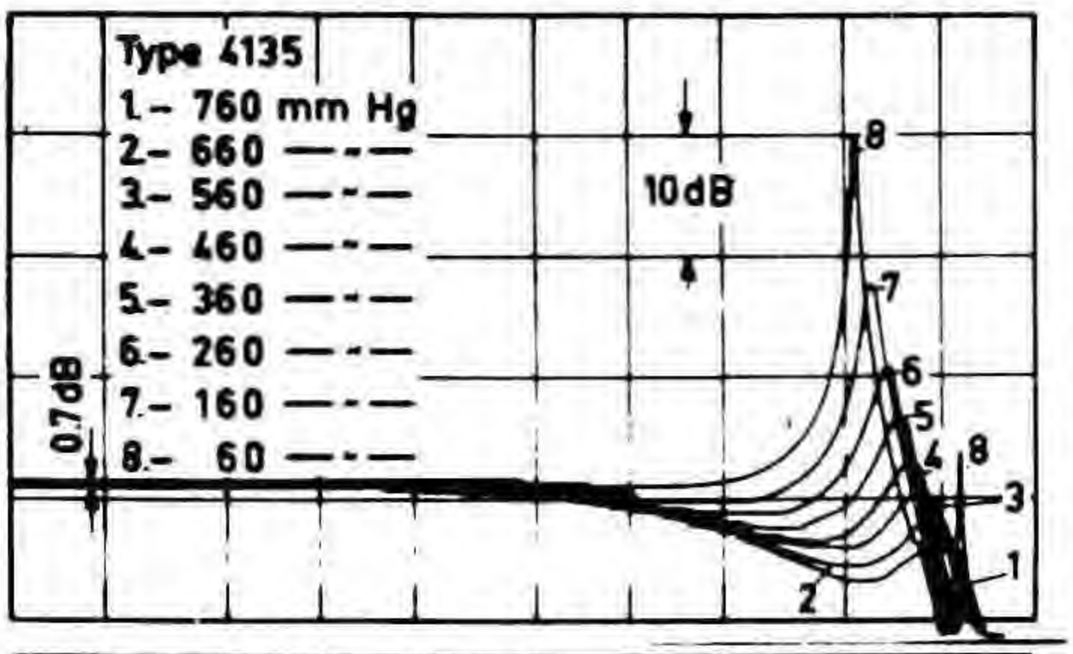

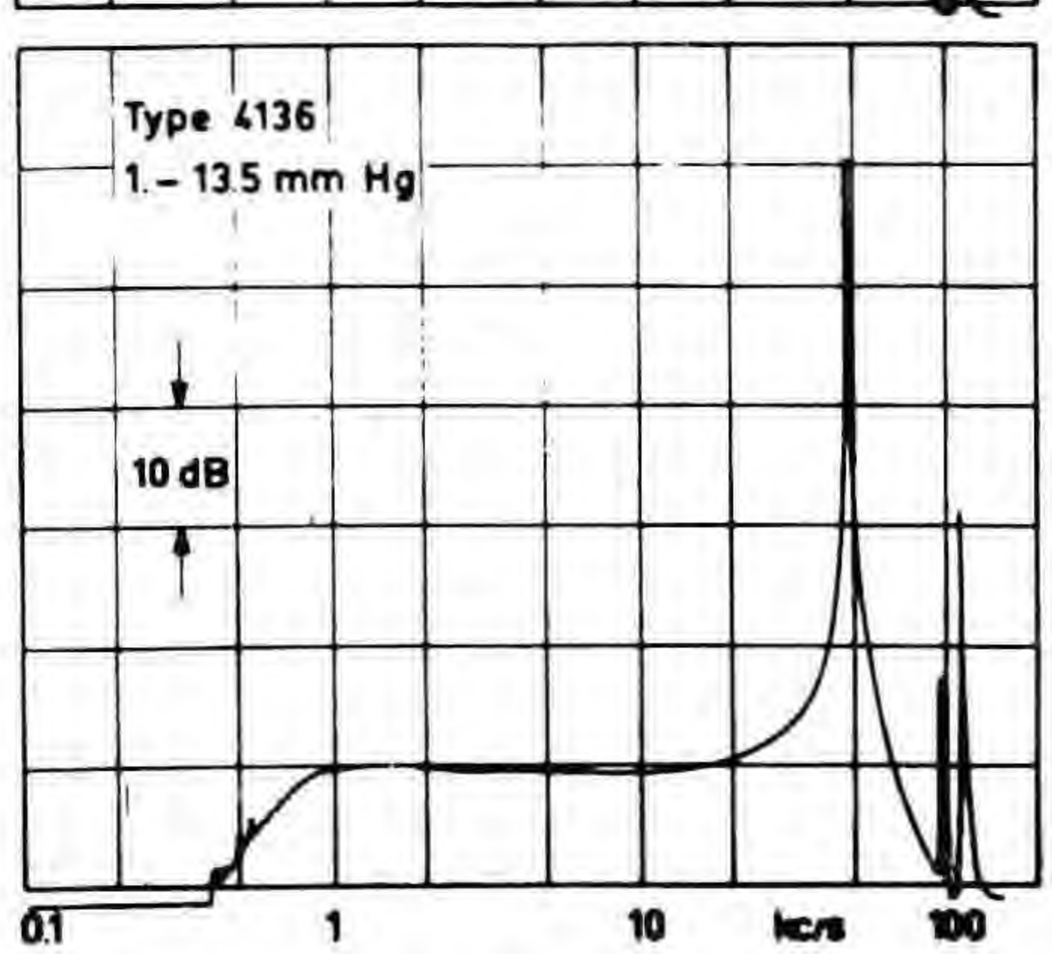

Fig. 7

and it is adjusted to a lower limiting frequency of 1-5 c/s. The rate of climb allowed for less than 1 db change in sensitivity is greater than 20 000 m/sec.

The microphones are aged at 150°C for several days and exposed to controlled temperature variations for at least two weeks and checked for stability during that period. They are tested in a humidity chamber overnight and must work properly under normal conditions within 15 min after they have been withdrawn from the humidity chamber.

Having produced condenser microphone cartridges for several years we have found it possible to avoid most of the troubles with moisture sensitivity normally believed to be an inherent failure in microphones of that type. This requires trained personnel and good working conditions, but once established it seems possible to prove that condenser microphones can be made to withstand even one of the most severe environments-the dessicator. People sometimes still store their condenser microphones in dessicators-an old practice maybe. But if there are any disturbing particles in the microphone they will dry out, maybe become loose and drop in between the diaphragm and back plate, or be attracted by the polarizing voltage when taken into use again. After 7-15 min the microphone will sometimes get noisy when the dried-out particles absorb moisture again. Therefore we do not recommend the use of dessicators, although we try to make microphones which can stand this treatment.

By further miniaturization, employing the technique from which I have mentioned a few examples and peculiarities, i should be possible to extend acoustical measurements into fields hitherto not well investigated. Careful design may offer stability and accuracy comparable to that of the associated electronic instrumentation.

x)Theory of Sound, Vol. II, Chapter XVI, 2nd Ed.
xx)Die Grundlagen der Akustik von E. Skudrzyk, page 430
xxx)IASA Vol. 20, No. 6, 1948 , I. Rudnick et M. N. Stein

O51

FOURTH INTERNATIONAL CONGRESS ON ACOUSTICS
COPENHAGEN 21.-28. AUGUST 1962

Neuere Beiträge zur Theorie der Schallstrahlung.

Dénes Huszty,
Akustische Forschungsgruppe, Budapest, Ungarn.

Es ist leicht zu beweisen, dass die Richtfunktion eines in unendlicher Wand strahlenden Linienstrahlers mit einer Länge von 2ℓ durch

$$D_\ell(x_\ell) = \frac{1}{2}\int_{-1}^{1} \exp(jx_\ell u)\ \varphi_\ell(u)du, \qquad (1)$$

d.h. durch die FOURIER'schen Transformierten der Geschwindigkeitsfunktion $\varphi_\ell(u)$ gegeben ist, wobei $x_\ell = k\ell\sin\gamma$ ist.

In der Fachliteratur benennt man nach STENZEL [1] die Funktion D - missverständlich - als Richtfaktor. Mit Rücksicht darauf, dass der Ausdruck offenbar eine Funktion ist, scheint die Benennung "Richtfunktion" zweckmässiger zu sein. Es wäre richtiger den Begriff "Richtfaktor" für die Bezeichnung des Wertes D , im Falle irgendwelchen festgesetzten x-Wertes anzuwenden.

Die Richtfunktion eines Strahlers mit radialsymmetrischer Erregung und Halbmesser r wird daher mit der HANKEL'schen Transformierten der Geschwindigkeitsfunktion $\varphi_r(u)$ beschrieben [2]:

$$D_r(x_r) = 2\int_0^1 J_0(x_r u)\ \varphi_r(u)udu, \qquad (2)$$

wobei $J_0(z)$ die BESSEL'sche Funktion von Ordnung Null ist, während $x_r = kr\sin\gamma$ ist. Hier ist γ der Winkel zwischen der Normalen des Strahlers und des zu dem im Fernfeld befindlichen Beobachtungsort führenden Vektors $\bar{a}$, welcher im Uhrzeigersinne als positiv betrachtet wird, während $k=2\pi/\lambda = \omega/c$ die reelle Wellenzahl, ω die Kreisfrequenz und c die reelle Fortpflanzungsgeschwindigkeit ist.

Im Folgenden wollen wir voraussetzen, dass $x_\ell = x_r = x$, d.h. $\ell = r$ ist, ausserdem nehmen wir an, dass die als komplexwertig angenommenen Funktionen φ_ℓ , φ_r gerade sind und zur Klasse L^2 gehören. Wir wollen solche Funktionen mathematisch realisierbare Geschwindigkeitsfunktionen nennen. Die zu solchen Funktionen φ gehörenden Richtfunktionen D bezeichnen wir dementsprechend als mathematisch realisierbare Richtfunktionen.

1. Einige Eigenschaften des Linienstrahlers.

Es sei f(z) irgendwelche Funktion der komplexen Veränderlichen $z=x+jy$. Definieren wir jetzt die Funktionenmenge W_σ wie folgt: $f(z) \in W_\sigma$,

wenn $f(x) \in L^2(-\infty,\infty)$ und wenn $f(z) \in E_\mu$, $\mu \in [0, \sigma]$, wobei E die Menge der ganzen transzendenten Funktionen von Ordnung Null ist, während μ den Typ der Funktionen bezeichnet. Betreffend der Funktionen $f(z) \in W_\sigma$ besteht der Satz von PALEY--WIENER (P.W.), [3] wonach jede solche Funktion als FOURIER'sche Transformierte irgendeiner Funktion $\varphi(u) \in L^2(-\sigma, \sigma)$ darstellbar ist wie folgt:

$$f(z) = \frac{1}{\sqrt{2\pi}} \int_{-\sigma}^{\sigma} \exp(jzu)\ \varphi(u)du. \qquad (3)$$

Nehmen wir jetzt irgendeinen Linienstrahler mit modifizierter Richtwirkung [2], wobei die Richtfunktion ${}_mD_\ell(mx)$, $m \in (0,\infty)$ ist, dann erhalten wir nach (1):

$${}_mD_\ell(mx) = \frac{1}{2} \int_{-1}^{1} \exp(jxu)\ {}_m\varphi_\ell(u)du \qquad (4)$$

Aus diesem, sowie aus dem P.W. Satz, weiters aus dem PARSEVALschen Satz der FOURIER'schen Transformation folgt unmittelbar, dass

1) Wenn ${}_mD_\ell(mx) \in W_1$, jede mit $m \in (0,\infty)$ modifizierte Richtfunktion ${}_mD_\ell(mx)$ mathematisch realisierbar ist, und ${}_m\varphi_\ell(u) \in L^2(-1, 1)$, so dass

$$\int_{-1}^{1} |{}_m\varphi_\ell(u)|^2\, du = \frac{2}{\pi} \int_{-\infty}^{\infty} |{}_mD_\ell(mx)|^2 dx$$

ist. Die modifizierte Geschwindigkeitsfunktion ${}_m\varphi_\ell(u)$ ist wie folgt:

$${}_m\varphi_\ell(u) = \frac{1}{\pi}\ \underset{n\to\infty}{\text{l.i.m.}} \int_{-n}^{n} \exp(-jxu)\ {}_mD_\ell(mx)dx$$

Die Umkehrung ist auf Grund des P.W. Satzes wie folgt:

2) Der FOURIER'sche Transformierte einer Geschwindigkeitsfunktion ${}_m\varphi_\ell(u) \in L^2(-1, 1)$ stellt eine Richtfunktion der Klasse W_1 dar.

Die Fernfeldrichtcharakteristik des Strahlers ist durch den Abschnitt $x \in [0, x_0]$ der Funktion $|D(x)|$ gegeben, wobei $x_0 = kl = kr$ bei Linienstrahler, resp. bei einem radialsymmetrischen Strahler ist.

Da ${}_mD_\ell(mx) = 1 \notin W_1$, ist es offenbar, dass

3) es keinen Linienstrahler gibt, welcher von der Frequenz unabhängige, halbkreisförmige Fernfeldrichtcharakteristik zeigen könnte.

Wir bemerken hierzu, dass die Menge der physikalisch realisierbaren Funktionen D offenbar enger ist, als die der mathematisch realisierbaren Funktionen, weil in der Wirklichkeit ja nur beschränkte Funktionen realisierbar sind, die in L^2 gehörenden Funktionen können dagegen an Nullmengen beliebig grosse Werte annehmen.

Wir wollen uns in der folgenden Terminologie vereinbaren. Nennen wir physikalisch realisierbare Geschwindigkeitsfunktionen jene Funktionen φ, welche in ihrem Bereiche beschränkt sind. So liegt es an der Hand, dass eine solche Richtfunktion D als physikalisch realisierbar

bezeichnet wird, zu welcher eine beschränkte Geschwindigkeitsfunktion φ gehört. Es ist klar, dass in der Praxis zuerst diese Richtfunktionen interessant sind, da sich keine unbeschränkte Geschwindigkeitsfunktionen realisieren lassen.

Auf Grund der PLANCHEREL--PÓLYA'schen Ergänzung (P.P.) des P.W. Satzes [4] kann aber erklärt werden, dass

4) falls mit $m \in (0,\infty)$, ${}_mD_\ell(mx) \in W_1$ und ${}_mD_\ell(x) \in L(-\infty,\infty)$, dann ist der Linienstrahler physikalisch realisierbar und die modifizierte Geschwindigkeitsfunktion ist durch den Ausdruck

$$ {}_m\varphi_\ell(u) = \frac{1}{\pi} \int_{-\infty}^{\infty} \exp(-jxu)\, {}_mD_\ell(mx)\,dx $$

gegeben, wobei das Integral fast überall konvergiert.

Dies folgt einfach daraus, dass wenn ${}_mD_\ell(x) \in L(-\infty,\infty)$, dann ist mit jedem $m \in (0,\infty)$ ${}_mD_\ell(mx) \in L(-\infty,\infty)$. In diesem Falle ist aber der P.P. Satz erfüllt, falls ${}_mD_\ell(mx) \in W_1$. Gleichzeitig ist auch Satz 1) und 2) erfüllt, also auch ${}_m\varphi_\ell(u) \in L^2(-1, 1)$.

Wir haben hier jedenfalls zu bemerken, dass Satz 4) nur eine genügende, aber keine notwendige und genügende Voraussetzung der physikalischen Realisierbarkeit einer Richtfunktion ist. So wissen wir z. B. im Falle der Funktion

$$ D_\ell(z) = z^{-1} \sin z \in W_1, $$

dass - obwohl $x^{-1} \sin x \notin L(-\infty,\infty)$, - doch dazu eine beschränkte Geschwindigkeitsfunktion gehört, undzwar auf Grund von 1) leicht nachweisbar gerade die Funktion $\varphi_\ell(u) = 1$.

2. Einige Eigenschaften des radialsymmetrischen Strahlers.

Setzen wir in (2) ${}_mD_r(mx)$ statt $D_r(x)$ ein, dann ist die modifizierte Richtfunktion des radialsymmetrischen Strahlers wie folgt:

$$ {}_mD_r(mx) = 2 \int_0^1 J_0(xu)\, {}_m\varphi_r(u)\,u\,du. \qquad (5) $$

Dabei ist ${}_m\varphi_r(u) \in L^2(0, 1)$ die modifizierte Geschwindigkeitsfunktion.

Nun soll folgende Definition eingeführt werden. Benennen wir die Menge derjenigen Funktionen $f(z) \in E_0$, für welche besteht, dass $x^{1/2} f(x) \in L^2(0,\infty)$, als $H_0^{(\omega)}$. Dann ergibt sich, dass

5) die modifizierte Richtfunktion ${}_mD_r(mx)$ jedes mathematisch realisierbaren radialsymmetrischen Strahlers zur Menge $H_0^{(\omega)}$ gehört.

Wenn der Strahler mathematisch realisierbar ist, so ist definitionsmässig ${}_m\varphi_r(u) \in L^2(0, 1)$. Dann folgt aber auf Grund des PARSEVALschen Satzes der HANKEL'schen Transformation, dass $x^{1/2}\, {}_mD_r(mx) \in L^2(0,\infty)$, es ist nämlich

$$ \int_0^\infty x\,|{}_mD_r(mx)|^2\,dx = 4 \int_0^1 u\,|{}_m\varphi_r(u)|^2\,du < 4 \int_0^1 |{}_m\varphi_r(u)|^2\,du < \infty. $$

Jetzt müssen wir noch einsehen, dass in diesem Falle ${}_mD_r(mz) \in E_0$. Berücksichtigen wir, dass $|J_0(z)| < K_1 e^{\varepsilon|z|}$, $K_1 < \infty$, $\varepsilon > 0$, dann bekommen wir auf Grund der BUNJAKOVSKY-SCHWARTZ'schen Ungleichung Folgendes:

$$|{}_mD_r(mz)|^2 < 4 \int_0^1 |J_0(zu)|^2 u^2 du \cdot \int_0^1 |{}_m\varphi_r(u)|^2 du < 4 K_1^2 K_2^2 \exp(2\varepsilon|z|),$$

wobei $K_2 < \infty$ eine von ${}_m\varphi_r$ abhängige Konstante ist. So ist ${}_mD_r(mz)$ tatsächlich eine ganze transzendente Funktion von minimalem Typ.

Aus der Definition der Menge $H_0^{(\omega)}$ und W_1 folgt, dass

6) $H_0^{(\omega)} \subset W_1$, d.h. die Richtfunktion ${}_mD_r(mx)$ jedes mathematisch realisierbaren radialsymmetrischen Strahlers fast überall mit der Richtfunktion ${}_mD_\ell(mx)$ irgendeines mathematisch realisierbaren Linienstrahlers zusammenfällt.

Wenn nämlich ${}_mD_r(mz) \in H_0^{(\omega)}$, dann ist ${}_mD_r(mx) \in L^2(-\infty,\infty)$, weil in $x \in [0,$ $|{}_mD_r(x)| < \infty$ ist. Da aber $E_0 \subset E_\mu$, $\mu \in [0, \sigma]$, dann ist $H_0^{(\omega)} \subset W_1$. Da nun auf Grund des P.W. Satzes die Funktion ${}_mD_r(mz)$ auch als FOURIER'scher Transformierte einer Funktion ${}_m\varphi_\ell(u) \in L^2(-1, 1)$ darstellbar ist, gibt es eine Funktion ${}_mD_\ell(mz)$, welche mit der Funktion ${}_mD_r(mz)$ längs der reellen Achse äquivalent ist. Dass die Menge $M_1 = W_1 - H_0^{(\omega)}$ nicht leer ist, folgt daraus, dass nicht jede Funktion $f(z) \in W_1$ zur Menge $H_0^{(\omega)}$ gehört. Das gilt z.B. für die schon erwähnte Funktion

$$D_\ell(z) = z^{-1} \sin z \in W_1 .$$

Dass offensichtlich $z^{-1} \sin z \notin H_0^{(\omega)}$, ist durch folgenden Ausdruck erklärt:

$$\int_0^\infty x |D_\ell(x)|^2 dx = \int_0^\infty x^{-1} \sin^2 x \, dx = \infty .$$

Auf Grund der Sätze 3), 5) und 6) folgt die Behauptung:

7) Ein Strahler mit radialsymmetrischer Erregung, dessen Richtcharakteristik von der Frequenz unabhängig halbkreisförmig ist, lässt sich mathematisch nicht realisieren.

Literatur.

1. H. Stenzel: Leitfaden zur Berechnung von Schallvorgängen. Springer, Berlin, 1939.
2. D. Huszty: Proc.III. ICA Congress, Stuttgart, 1959. Elsevier, Amsterdam 1961. 696.
3. R.E.A.C. Paley, N. Wiener: Fourier Transforms in the Complex Domain. Am.Math.Soc.Coll.Publ.No.19. New-York, 1934.
4. M. Plancherel, G. Pólya: Comm.Math. Helvetici, Vol. 9. 224-248, 1937.

P51

FOURTH INTERNATIONAL CONGRESS ON ACOUSTICS
COPENHAGEN 21.-28. AUGUST 1962

LA CAVITÉ BUCCALE , PARAMÈTRE SENSIBLE DES SPECTRES RAYONNÉS PAR LES INSTRUMENTS A VENT .

E . L E I P P Paris

Iº POSITION DU PROBLÈME

L'expérience montre qu'un musicien habile peut modifier systématiquement et dans une large mesure le timbre des sons d'un instrument à vent,en agissant sur les conditions de l'excitation par ce qu'il est convenu d'appeler les "effets de bouche".
On sait,d'autre part,que la sensation de timbre est liée à la forme de la courbe enveloppe des spectres. (I)
D'où l'idée d'étudier la relation entre les effets de bouche et les enveloppes des spectres (*).

Exemple: Nous avons demandé à un clarinettiste de répéter la même note (RE 2 , 147 Hz) en modifiant le timbre le plus possible par des effets de bouche.Les sons obtenus ainsi furent analysés à l'aide d'un spectrographe à bande étroite.On porte en abcisse les numéros des harmoniques,en ordonnée,le % d'énergie par rapport à l'harmonique prédominant.

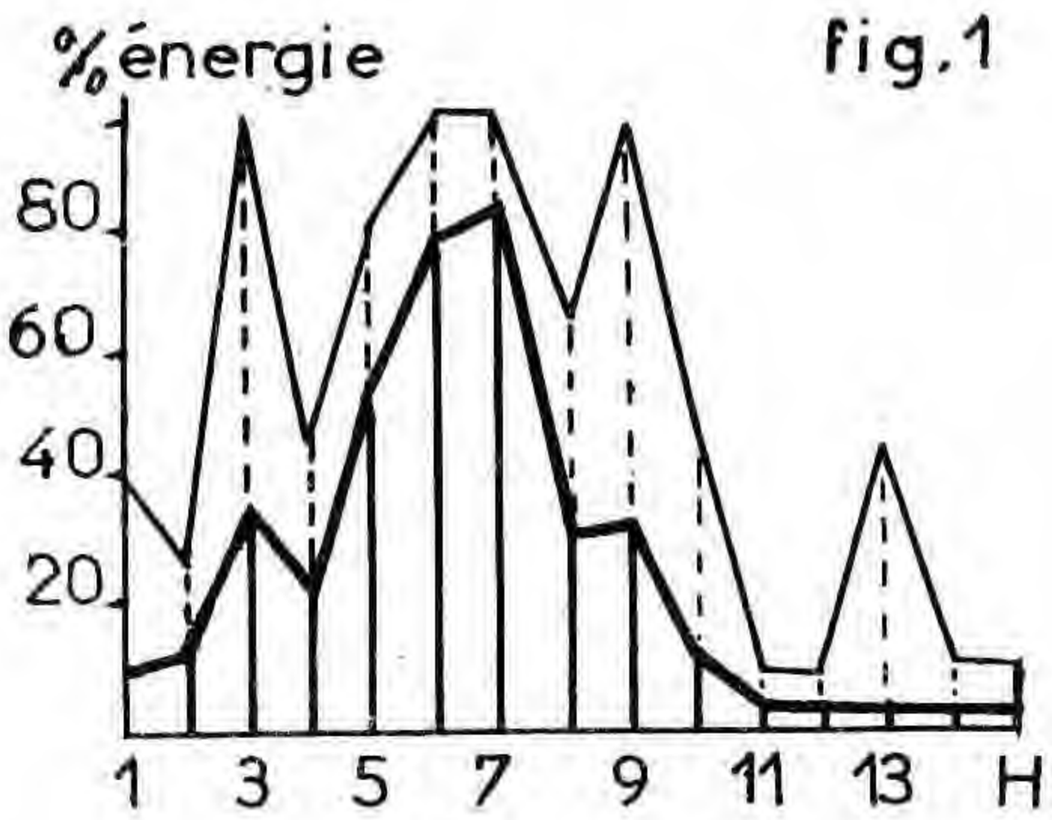

fig.1

On a représenté (fig I) les spectres extrêmes,entre lesquels le musicien peut faire fluctuer les courbes enveloppe.Des relevés identiques faits sur l'ensemble des notes de l'instrument,montrent que la part du musicien, dans la répartition de l'énergie à l'intérieur des spectres est importante et oscille de 30 à 70%.Le rôle des effets de bouche est donc déterminant.
Nous avons observé,cependant,que le musicien englobe dans le terme "effets de bouche" toute une série de paramètres distincts,d'importance variable,mais dont aucun n'est indifférent.
Ces paramètres sont:

- le volume de la cavité buccale
- la situation du point d'appui sur l'anche
- la force d'appui de la lèvre inférieure
- la surface de contact lèvre-anche
- la pression à l'intérieur de la bouche.

---

* Travaux réalisés au Laboratoire de Mécanique Physique de l'Université de Paris,dirigé par M. le Professeur SIESTRUNCK.

Notre propos étant l'étude de la seule cavité buccale,il fallait d'abord isoler ce paramètre.Dans ce but :

-nous avons choisi un instrument à anches libres,le plus simple possible,l'harmonica à bouche,où les lèvres ne sont pas en contact avec l'anche et ne peuvent par conséquent agir sur elle et en modifier le fonctionnement.

-Nous avons opéré à pression constante.

- Nous avons mis en évidence au préalable le rôle des résonances propres de l'instrument en relevant sa courbe de réponse par la méthode des impulsions (2). Un dispositif électromagnétique excite l'instrument par chocs (8 Hz);le signal obtenu,enregistré sur boucle magnétique et analysé au spectrographe fournit la courbe de réponse(fig 2a) qui met en évidence les résonances principales de l'instrument.Les pointes de résonance sont situées sur 250, 400, II00 et 2000-3500 Hz environ.

On sait (3) que les instruments de musique sont très généralement la somme d'un excitateur pulsatoire et d'une série de résonateurs couplés qui déforment le signal de l'excitation par résonance et filtrage aboutissant au spectre rayonné.Si une pointe du signal de l'excitation coincide avec une des bosses de la courbe de réponse de l'instrument,le spectre rayonné présentera un maximum à ce point.Ainsi,si nous considérons la note UT 3,260 Hz,nous pouvons prévoir des surrésonances sur les harmoniques dont la fréquence est voisine des pointes de résonance de la courbe de réponse de l'instrument,soit les harmoniques 4 (I040 Hz) et le groupe d'harmoniques de 8 à I4 (2080 à 3640 Hz). Les invariants des spectres étant précisés,on peut maintenant étudier le rôle de la cavité buccale.

2ª) METHODE

La cavité buccale peut être considérée comme un résonateur à caractéristiques variables,la fréquence de résonance principale étant fonction de l'ouverture lippale et du volume de la cavité.Lors du jeu de la note,la surface de l'ouverture lippale reste constante (9mm^2). Par contre,le volume de la cavité peut diminuer continuement par modifications de la position de la mâchoire inférieure,de la langue et des joues.La fréquence de résonance de la cavité varie alors corrélativement de 500 à 2000 Hz environ,bande de fréquence que nous appelons:

"zone formantique de la cavité buccale"

Nous avons d'abord observé,à l'audition directe,qu'en diminuant graduellement le volume de la bouche lors du jeu d'une note,on entendait distinctement émerger,les uns après les autres,tous les harmoniques placés à l'intérieur de la zone formantique de la cavité buccale.
Nous appelons cette série d'harmoniques :

"harmoniques sensibles de la cavité buccale"

Nous avons vérifié que leur émergence correspond effectivement avec la coincidence entre la fréquence de la cavité actuelle et la fréquence de l'harmonique sensible considéré.
Un entrainement suffisant permet "d'accorder" systématiquement la bouche sur tel ou tel harmonique sensible.Nous avons alors enregistré sur 7 boucles les 7 notes obtenues en faisant émerger chaque fois un harmonique sensible différent.Les boucles furent analysées au spectrographe (analyseur à bande étroite + enregistreur de niveau).
Les resultats,pour la note UT 3 , 260 Hz, sont représentés par les figures 2b à 2h : en abcisse les numéros des harmoniques,en ordonnée leurs niveaux relatifs.

FIG. 2 a) Courbe de réponse de l'instrument
b à h): Emergence des harmoniques sensibles

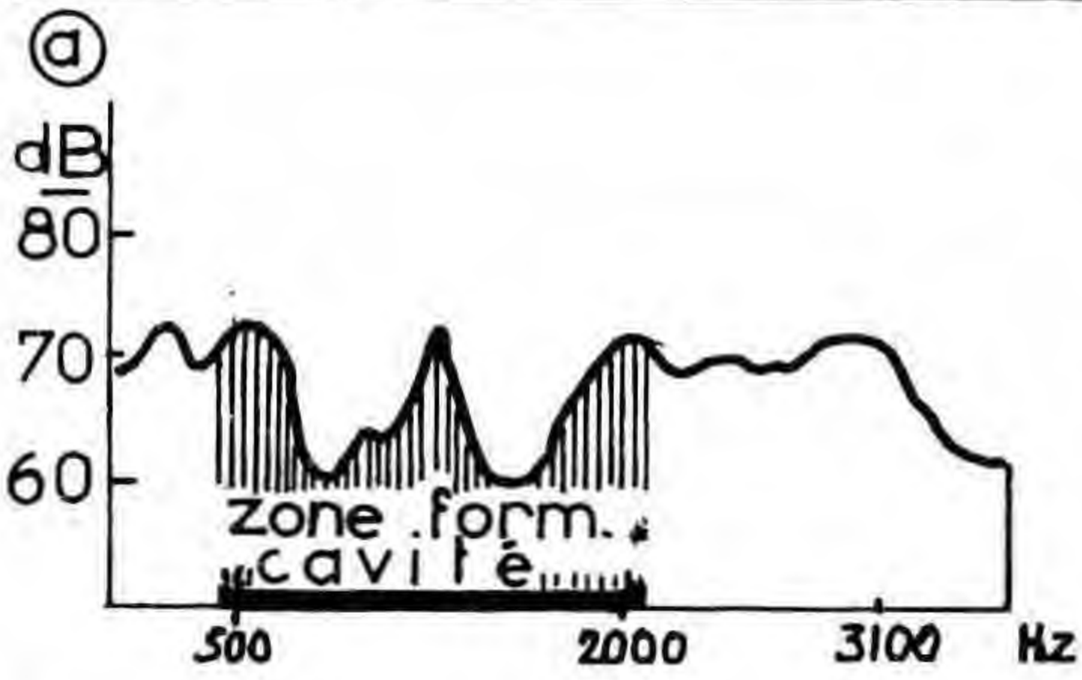

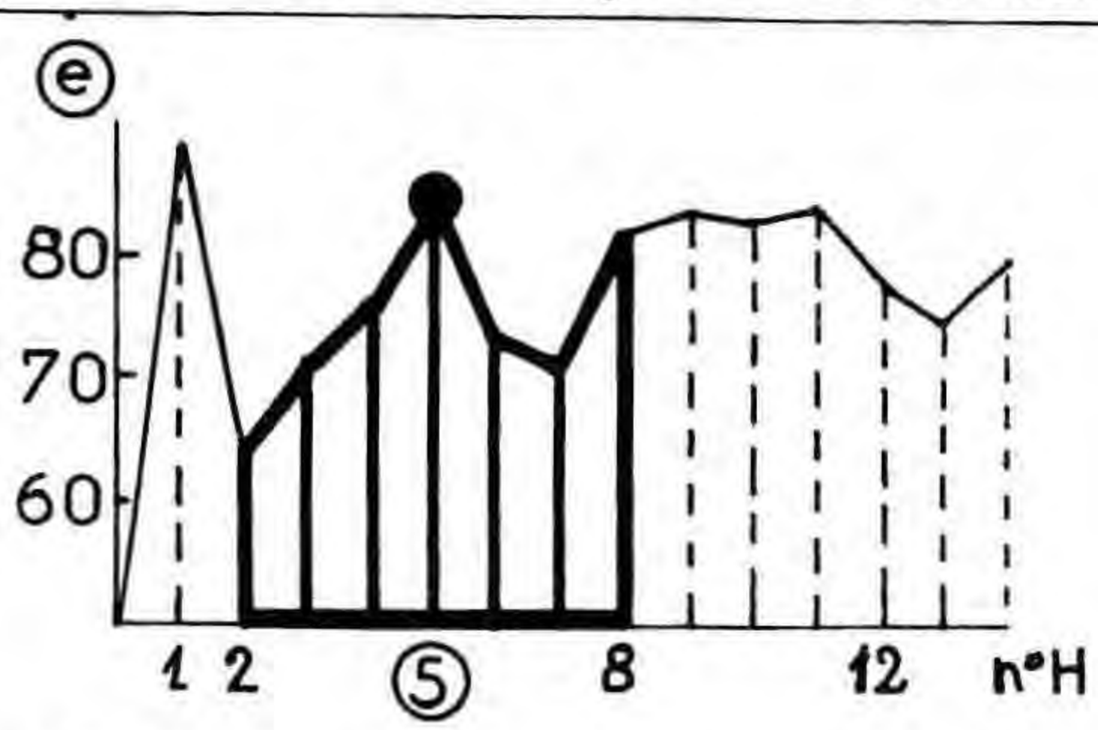

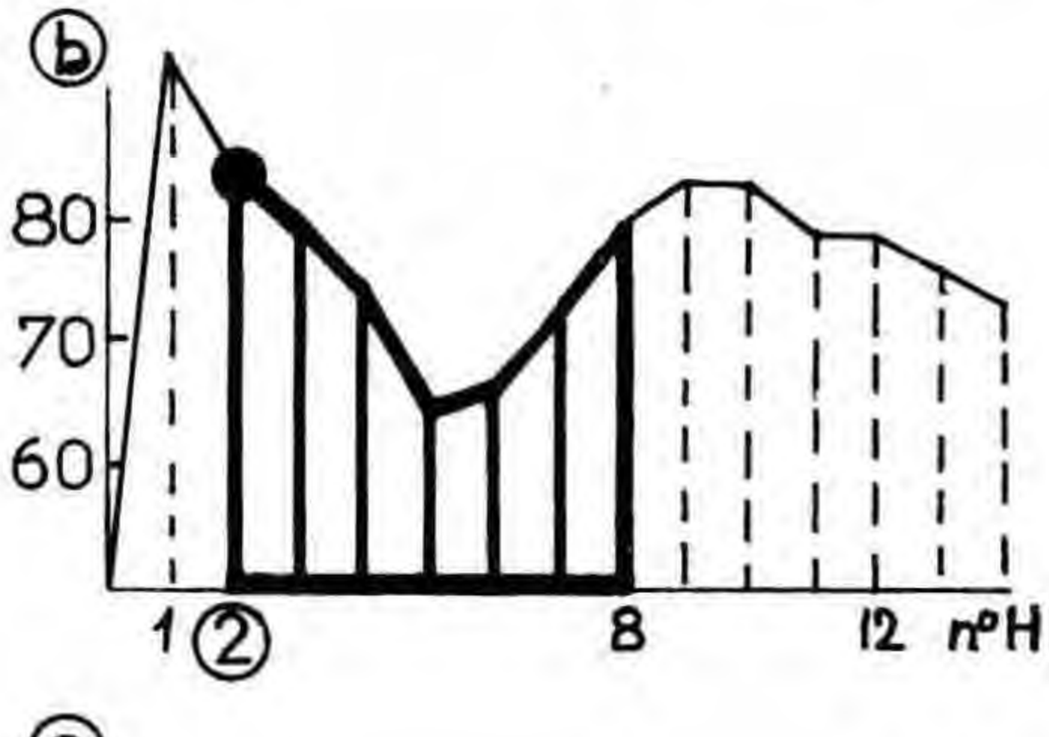

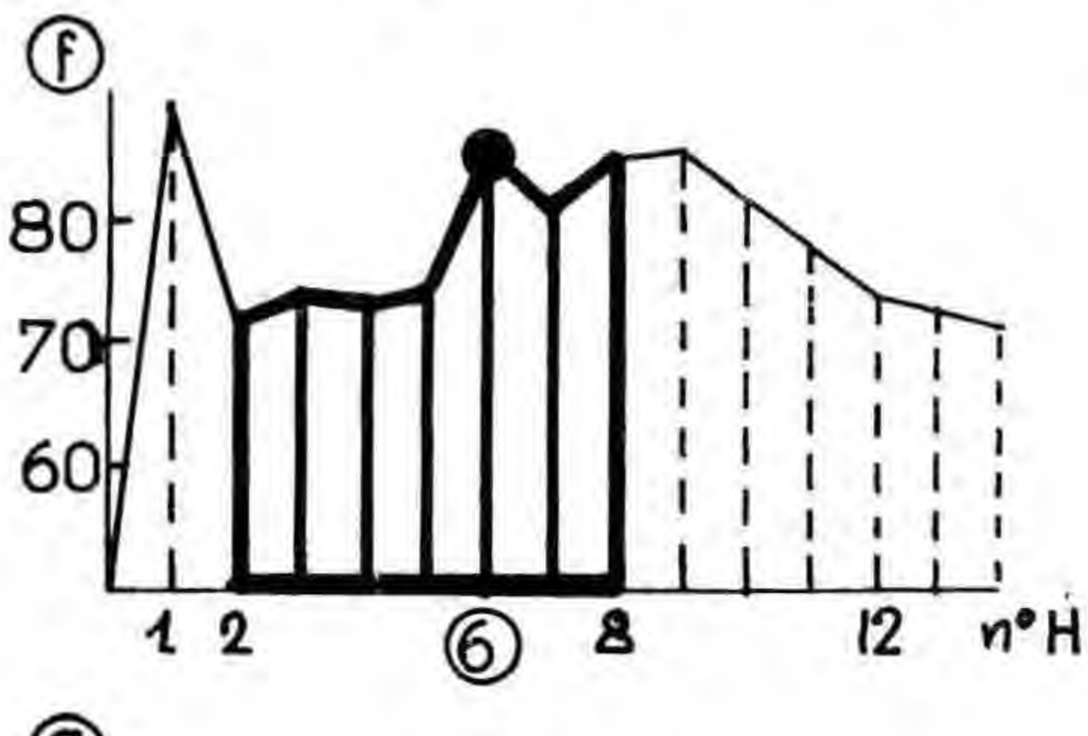

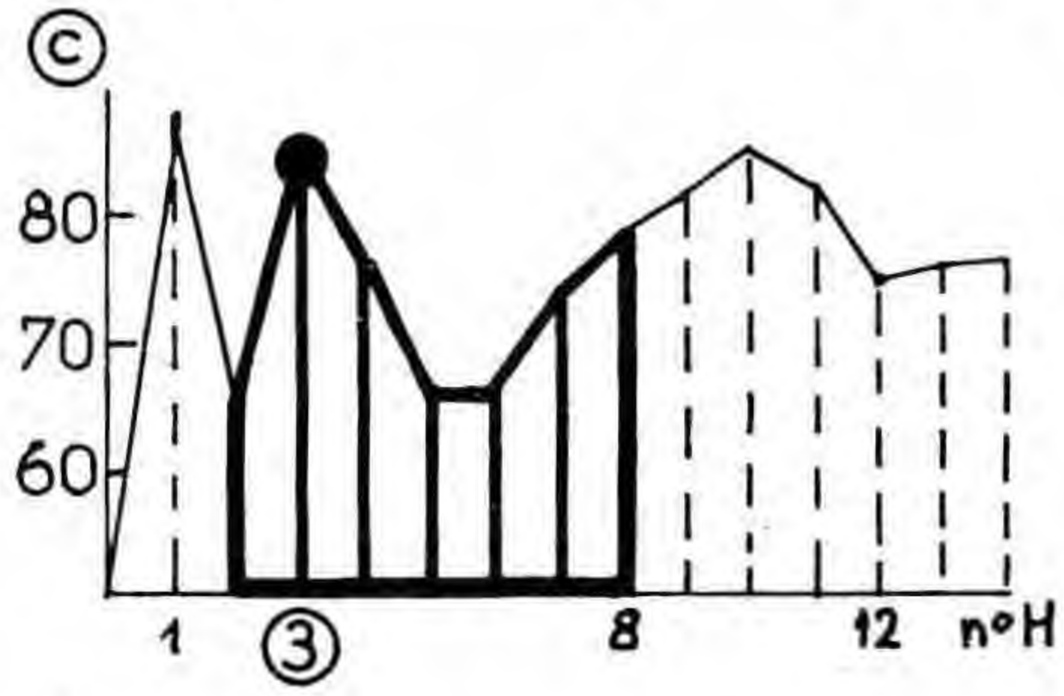

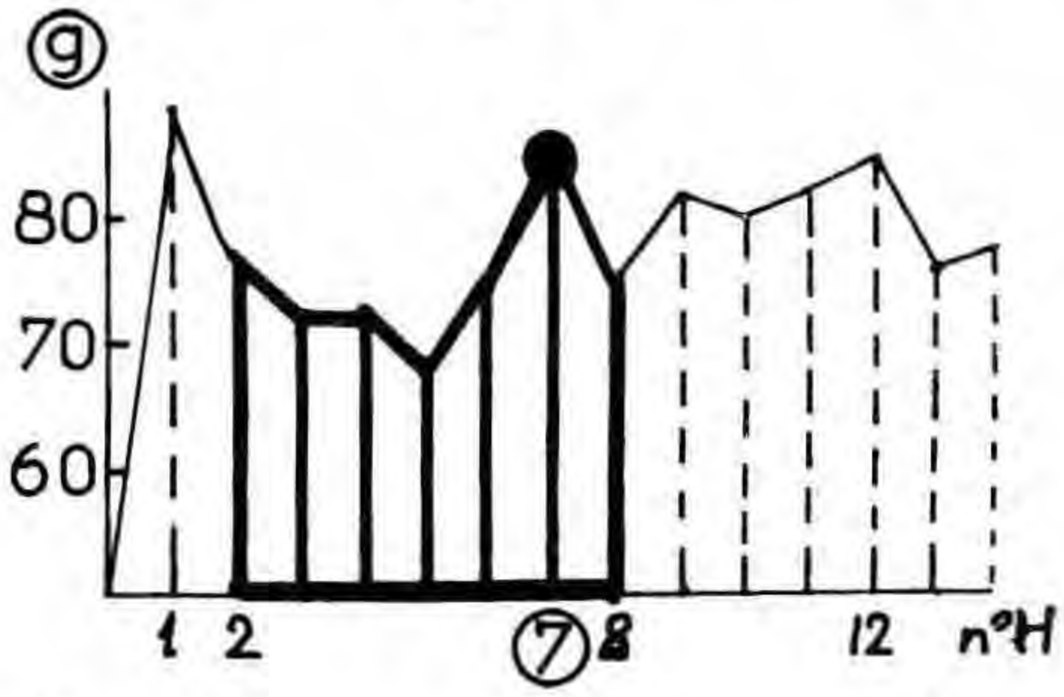

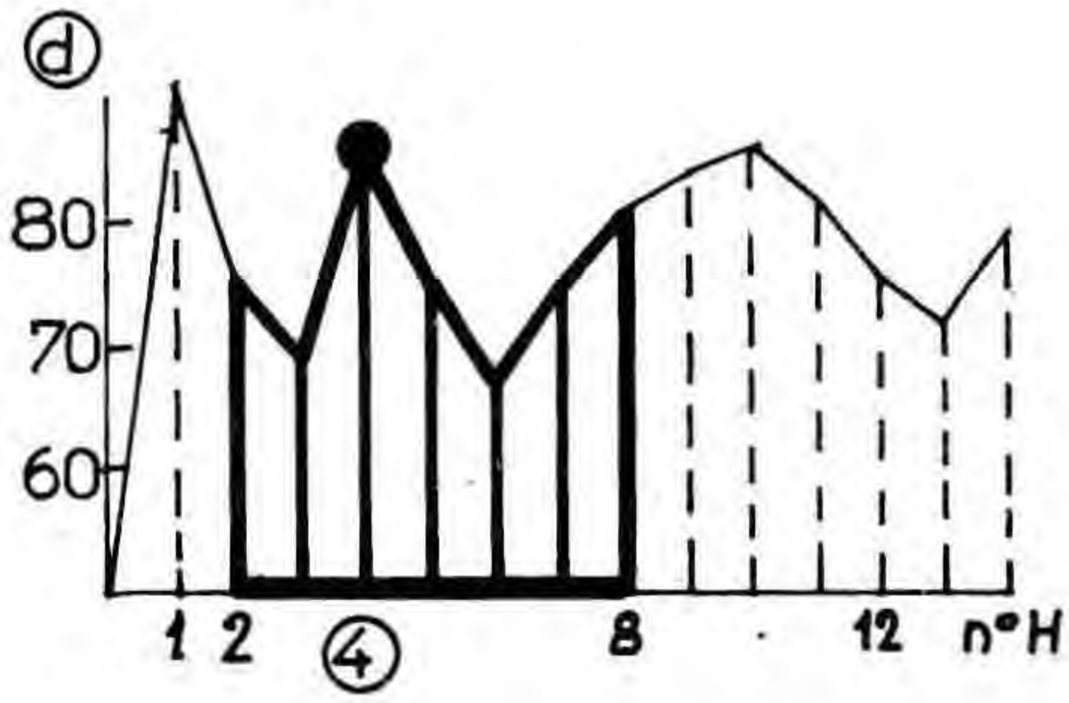

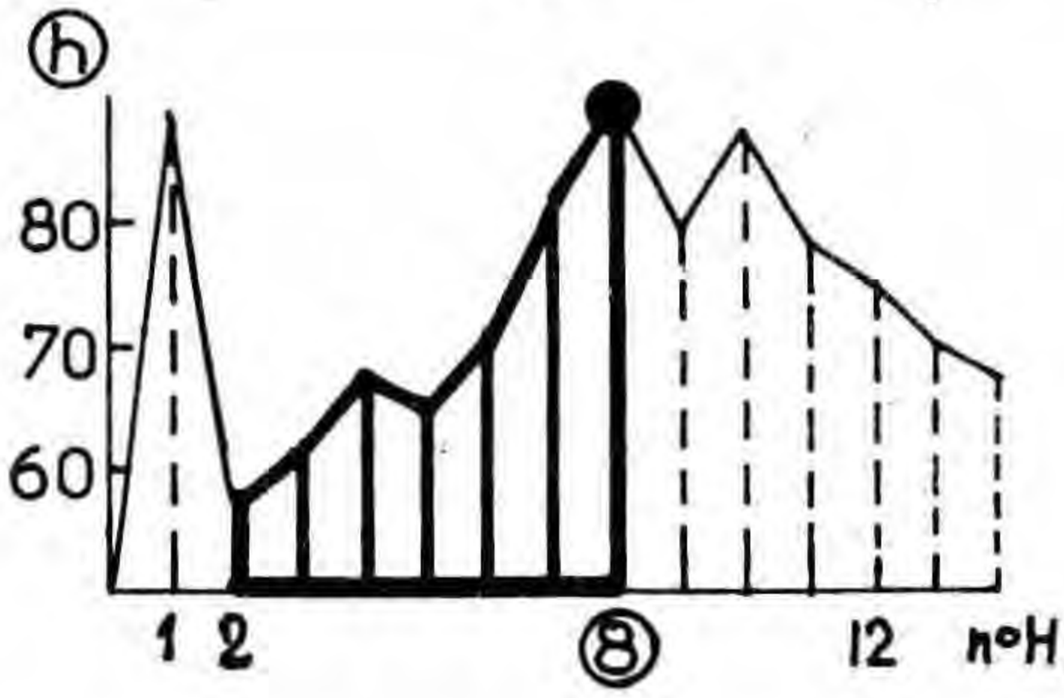

3º) RÉSULTATS

Les spectres sont schématisés,mais les niveaux sont respectés.L'enveloppe est en trait gras à l'intérieur de la zone formantique de la cavité buccale.
L'harmonique sensible prédomine constamment et détermine sur l'enveloppe du spectre une bosse qui glisse graduellement vers la droite au fur et à mesure du rétrécissement de la cavité buccale.Auditivement, on vérifie que le timbre "sonne l'octave" avec l'harmonique sensible 2 la quinte avec l'harmonique sensible 3 etc.En bref,le musicien peut régler systématiquement le timbre à l'intérieur de la zone formantique de la cavité buccale.
Si on considère maintenant l'enveloppe de part et d'autre de cette zone,on observe des fluctuations notables de forme;ces fluctuations secondaires proviennent du fait que,pour certaines positions de la langue,la bouche devient une cavité multirésonante (4).La bouche agit donc sur l'ensemble du spectre,avec une zone préférentielle située entre 500 et 2000 Hz environ.

4º) CONCLUSION

Nous avons montré que les fluctuations spectrales dues à la cavité buccale sont considérables.Par conséquent l'étude spectrographique d'un instrument à vent n'a de sens que dans la mesure ou les conditions de bouche sont strictement précisées,éventuellement normalisées. En fait,ces fluctuations,réalisées plus ou moins consciemment par les musiciens,sont la condition,la définition même du "son musical". Un son de composition spectrale fixe devient inintéressant en une fraction de seconde (5),ce qui justifie la pratique des effets de bouche. On s'explique également pourquoi tel musicien a une "jolie" ou une "vilaine sonorité": apprendre à jouer d'un instrument à vent,c'est d'abord apprendre à accorder la cavité buccale sur tel ou tel harmonique sensible en fonction de l'effet esthétique recherché.

BIBLIOGRAPHIE

I) MOLES (A) Structure physique du signal musical.Thèse Sciences Paris I952.Bibl.Sorbonne Y Phys.I952 (I2) 4º

2) MEYER (J) Impulsmethode zur Messung von Geigenresonanzen Gravesaner Blätter I9-20 (I960) p.I06-II9

3) LEIPP (E) - Les paramètres sensibles des instruments à cordes Thèse Sciences Paris I960 (Bibl.Sorbonne)

- Acoustics and musical instruments Gravesaner Blätter 22 (I96I) p. II8-I29

4) FANT (G) The acoustics of speech Proc.3rd Intern.Congress of Ac. Elsevier Amsterdam (I96I) pI88-200

5º) WINCKEL(F) Phänomene des Musikalischen Hörens Max Hesse Berlin (I960)

G52

FOURTH INTERNATIONAL CONGRESS ON ACOUSTICS
COPENHAGEN 21.-28. AUGUST 1962

Manipulation of The Acoustical Component of Language By A Specially Structured Orthographic System

Herbert J. Oyer

I. Introduction

In many parts of the world the English language is the international language of the air. Frequently it is not a simple task to achieve maximum efficiency when, for example, a Japanese pilot is attempting to land his plane on a French airfield with the help of a French tower operator, as both pilot and operator are communicating in English.

II. Problem

The problem involved in this study was to arrive at the best method whereby foreign pilots could be taught the General American pronunciation of English words that are important in air traffic communication.

Specifically three questions were asked:

1. Can foreign nationals pronounce English words acceptably after reading the printed word?
2. Can foreign nationals pronounce English still more acceptably when they see the printed word and also see the words represented phonically with orthographic symbols peculiar to their language?
3. Can foreign nationals pronounce English most acceptably when (a) seeing the printed words, (b) seeing the words represented phonically with orthographic symbols peculiar to their language, and (c) in addition receiving auditory stimulation by a general American speaker who is saying the words they are viewing?

III. Procedure

In order to answer these questions a number of tasks had to be accomplished.

1. The first was to select words most frequently used in air traffic control. These words selected were from the frequency listing of M. Y. McCormick and from recordings made at several airports handling transoceanic traffic. In addition to single words, phrases were also utilized. A total of 500 words were chosen (250 monosyllables and 250 polysyllables). There were 25 phrases.
2. The second task was to construct "tailored orthographies," for several languages that represented the 500 words and 25 phrases. To accomplish this, services of nine persons were retained, representing the following languages: Chinese, Dutch, French, German, Italian, Japanese, Korean, Spanish and Thai. Five were language scholars, the other four were persons who had extensive training and experience in both English and their native tongues.
3. The third task was then to try out the use of (a) printed words as stimuli, (b) the printed words plus the tailored orthography, and (c) the printed words, tailored orthography and auditory stimulation on a group of foreign pilots. The pilots employed in the study were found at the Air Force Language School at Lackland Air Force Base, Texas.

IV. Evaluation of Orthographies

Although it would have been desirable to have tested all of the prepared orthographies, it was decided to limit the study to three groups of foreign nationals who had just arrived at the Air Force Language School, Lackland Air Force Base, Texas. This decision was made in order to restrict the population of subjects to those whose training in the English language had been received chiefly in their native countries.

A. Recording

All of the foreign pilots met in a group on three consecutive days to record the English words and phrases. Each man occupied a relatively isolated booth, thus permitting simultaneous recording. Condition one on the first day consisted of the reading of the materials from a printed page into microphones connected to separate tape recorders. On the second day the pilots read under condition two. This consisted of their reading from a printed list which also included the special modified spelling alongside each printed word. On the third day the pilots recorded under condition three. This condition was the same as condition two but in addition, each man listened to recorded pronunciations of the materials by a native American speaker of General American dialect. Each word was pronounced three times by the American speaker and fed through a master unit to individual sets of headphones for each foreign pilot. Five seconds were allowed after each set of auditory stimulations for the pilot to record his own pronunciation into his individual recording system.

B. Preparation of Tapes for Evaluation

The tapes of 15 foreign pilots were selected for evaluation. This group was composed of three subgroups of German, Japanese, and Spanish pilots, five in each group. These subsamples permitted the study of the various conditions of speech stimulation for different language groups.

The tapes of each speaker were transcribed and edited. The editing was done to eliminate any clues that would allow raters to identify which of the three conditions was employed to stimulate the speaker.

C. Evaluation of the Recorded Speech of Pilots

The intelligibility of the pronunciations of selected English words and phrases was evaluated. Various methods of determining intelligibility were considered. A decision was made to have the intelligibility rated by trained listeners.

Several conditions were established to provide a desirable rating procedure. Four trained raters were employed. These persons had background and experience in speech intelligibility testing, phonetics, and clinical speech. Each rater worked independently while evaluating word intelligibilities. The raters were not informed of the specific purpose of the study, nor were they told which condition of stimulation they were rating at a given time. It is possible, because of differences in pausing and pronunciation, that the raters became aware that speakers were reading aloud under different conditions. During each rating session, the rater had a typed list of materials available to him. This was done so that the rater would know the speaker's goal in each speech attempt, and thus rate his intelligibility against a standard of correctness. The rater used headsets, adjusting volume to the most comfortable loudness.

The raters evaluated the words and phrases spoken by each speaker. For all speakers, standard English spelling (Condition 1) was rated first; words spoken with the additional aid of orthographic spelling (Condition 2) were rated next; words spoken with still further aid of auditory stimulation (Condition 3) were rated last. Raters were instructed to cover up prior ratings; the tapes provided a fairly rapid presentation of words to the raters, which made referrals to prior ratings difficult.

The raters were instructed in the use of a four-point rating scale. They were to rate a word:

1. If judged highly intelligible - no distortion.
2. If judged intelligible with some distortion.
3. If judged distorted, but intelligible.
4. If judged not intelligible.

V. Outcomes

The ratings of intelligibility of individual speakers under three conditions of stimulation were analyzed. Comparisons between conditions of recording were made.

It was found that on a sample of 240 ratings of the four raters there was a standard deviation of 0.596. This suggests a low inter-rater variability which further suggests that the raters were probably using similar criteria in making judgments.

Further analysis disclosed none of the 15 speakers experienced detrimental effects in intelligibility during Conditions 2 and 3. Of 27 tests comparing Conditions 2 and 3, seven did not show Condition 2 as significantly better than 3. However, all tests showed Condition 3 to be significantly better than 1.

A Friedman two-way analysis of variance or ranks revealed that Condition 2 was significantly better than Condition 1 for polysyllabic but not for monosyllabic words, but that Condition 3 is significantly better than either 1 or 2.

In terms of the greatest improvement per language group, it was shown that the largest improvement occurred under Condition 3 with the Germans. Japanese speakers did least well.

With these considerations in mind, the following conclusions may be stated and tentatively generalized.

Conclusion 1: All speakers improved their word intelligibilities with the aid of either a manipulated orthography or auditory stimulation for both monosyllabic and polysyllabic words.

Conclusion 2: For this sample of speakers the average improvement with aid of a manipulated orthography or with orthography supplemented by auditory stimulation, probably would make a distinguishable difference in word intelligibility to air traffic controllers.

Conclusion 3: For individuals, the addition of auditory stimulation is more likely to result in significantly greater word intelligibility improvement than a manipulated orthography alone.

Conclusion 4: The utilization of a tailored orthography with auditory stimulation is distinctly more effective than orthography alone for polysyllabic words as compared with monosyllabic words.

Conclusion 5: The advantage that auditory stimulation has over a tailored orthography alone does not increase as the need for intelligibility increases.

Conclusion 6: The comparative value of the special orthography alone, vs. the special orthography plus auditory stimulation varies considerably among language groups.

(This research was supported by United States Air Force Contract Number 19-(604-4575) -- Dr. Henry M. Moser, Project Director.)

H52

FOURTH INTERNATIONAL CONGRESS ON ACOUSTICS
COPENHAGEN 21.-28. AUGUST 1962

PRESSURE VS FREE FIELD THRESHOLDS AT LOW FREQUENCIES[1]

WAYNE RUDMOSE

ACOUSTICS LABORATORY, SOUTHERN METHODIST UNIVERSITY, DALLAS, TEXAS

INTRODUCTION. THE "MISSING 6 DB" WAS DESCRIBED FIRST BY SIVIAN AND WHITE[2] AND HAS SINCE BEEN REPORTED MANY TIMES. THE AUTHOR PRESENTED AN ORAL PAPER IN 1950[3] SHOWING THAT MINIMUM AUDIBLE PRESSURES (MAP) AND MINIMUM AUDIBLE FIELDS (MAF) FOR 100 Hz COULD BE MADE TO AGREE, OR DISAGREE, DEPENDING UPON THE METHOD USED TO PRESENT THE PRESSURE SIGNAL. THIS WORK WAS NOT PUBLISHED DUE TO OTHER ACTIVITIES. THREE YEARS AGO THE RESEARCH WAS REVIVED AND NEW DATA ON MORE SUBJECTS HAVE VERIFIED THE ORIGINAL FINDINGS.

WHEN THE EAR IS SEALED BY AN EARPHONE MOUNTED IN A CONVENTIONAL CUSHION, PHYSIOLOGICAL NOISE IS GENERATED IN THE SMALL VOLUME UNDER THE EARPHONE. THE AMOUNT OF NOISE GENERATED IN THE EAR CANAL DEPENDS UPON THE ENCLOSED VOLUME, THE HEADBAND PRESSURE, PHYSICAL CONTACT OF THE HEADBAND WITH THE HEAD, ETC. BROGDEN AND MILLER[4] MEASURED PHYSIOLOGICAL NOISE UNDER EARPHONE CUSHIONS MOUNTED ON CLAMPS BY SUBJECTIVELY COMPARING THE CUSHION NOISE WITH NOISE GENERATED BY LOUDSPEAKERS. THEY DID NOT, HOWEVER, REPORT EITHER ATTEMPTS TO MINIMIZE THE NOISE WHILE MAINTAINING A SMALL VOLUME OVER THE EAR NOR ATTEMPTS TO MEASURE PRESSURE THRESHOLDS AT LOW FREQUENCIES.

THE PHYSIOLOGICAL NOISE APPEARS TO EXCITE THE EAR CANAL CAVITY BY TRANSMISSION FROM THE EAR TO THE CUSHION (ASSUMING HEADBAND ISOLATION). THE SIZE OF THE CONVENTIONAL CUSHION IS SUCH THAT WHEN IT IS IN CONTACT WITH THE PINNA, EVEN THOUGH THE CUSHION IS SUPPORTED BY EXTERNAL MEANS, SUFFICIENT LOW FREQUENCY NOISE IS GENERATED IN THE EAR CANAL TO PRODUCE MASKING OF A 100 Hz SIGNAL AT LEVELS CORRESPONDING TO FREE FIELD THRESHOLD. HOWEVER, IF THE EARPHONE (HEARING AID TYPE) IS REMOVED FROM THE EAR BUT CONNECTED TO IT BY A SMALL FLEXIBLE TUBE WHICH ATTACHES TO AN EARPLUG SEALED IN THE CANAL (THE TOTAL ENCLOSED VOLUME MAINTAINED AT 6 cm^3), THE PHYSIOLOGICAL NOISE GENERATED IN THE EAR CANAL IS GREATLY REDUCED.

EXPERIMENTAL METHOD. SIX EXPERIENCED SUBJECTS WERE FITTED WITH SPECIAL EARMOLDS MADE OF SOFT PLASTIC. THE USUAL "CANAL" WAS BORED IN THE EARMOLD TO PERMIT SOUND TO REACH THE EAR CANAL. A SNAP RING, AS USED FOR HEARING AID EARPHONES, WAS EMBEDDED IN THE OUTER END OF THE EARMOLD TO PERMIT CONNECTION TO AN EXTERNAL DRIVER UNIT. A FITTING, DESIGNED TO MATE WITH THE RING, HAD A SHORT METAL TUBE ATTACHED, AND A PIECE OF RUBBER TUBING (4 MM ID, 8 MM OD) WAS FITTED OVER THE METAL TUBE. THE OTHER END OF THE RUBBER TUBE WAS ATTACHED TO A CONVENTIONAL HEARING AID EARPHONE BY MEANS OF A METAL ADAPTOR. THE EARPHONE WAS SUSPENDED FROM THE WEDGES OF THE ANECHOIC CHAMBER AND NOT FROM THE SUBJECT'S CHAIR. THE LENGTH OF THE RUBBER TUBE (19 CM) WAS SUCH THAT THE VOLUME ENCLOSED BETWEEN THE EARPHONE DRIVER UNIT AND THE EARDRUM WAS 6 cm^3. THE SOUND PRESSURE IN THE EAR CANAL PRODUCED BY THE DRIVER UNIT WAS MEASURED BY MEANS OF A CAPILLARY PROBE WHICH WAS EMBEDDED IN THE EARMOLD AND TERMINATED IN THE "EARMOLD CANAL". THE OTHER END OF THE CAPILLARY WAS ATTACHED TO A BRUEL AND KJAER CONDENSER MICROPHONE BY A SMALL PLASTIC TUBE (1 MM ID, 2 MM OD) ATTACHED TO A METAL CAP WHICH SCREWED ONTO THE MICROPHONE. THUS THE MICROPHONE MEASURES THE SOUND PRESSURE AT APPROXIMATELY THE ENTRANCE TO THE EAR CANAL. THE SEAL OF THE ENTIRE

[1] THIS RESEARCH WAS SUPPORTED IN PART BY THE CALLIER TRUST.

[2] ON MINIMUM AUDIBLE SOUND FIELDS, SIVIAN AND WHITE, J. ACOUS. SOC. AM. 4, 288, 1933.

[3] FREE-FIELD THRESHOLDS VS PRESSURE THRESHOLDS AT LOW FREQUENCIES (A), RUDMOSE, J. ACOUS. SOC. AM. 22, 674, 1950.

[4] PHYSIOLOGICAL NOISE GENERATED UNDER EARPHONE CUSHIONS, BROGDEN AND MILLER, J. ACOUS. SOC. AM. 19, 620, 1947.

SYSTEM WAS CHECKED BY COMPARING THE PRESSURE IN THE EAR CANAL WITH THE PRESSURE IN A 6 cm^3 METAL CAVITY. THE EARPHONE DRIVER UNIT WAS MOVED FROM THE RUBBER TUBE AND ATTACHED TO THE METAL CAVITY WHILE CONSTANT VOLTAGE WAS MAINTAINED ON THE DRIVER UNIT. THE PRESSURES WERE FOUND TO BE EQUAL FOR A 100 Hz SIGNAL. FOR PURPOSES OF ABBREVIATION, THRESHOLDS OBTAINED USING THE ABOVE SYSTEM ARE REFERRED TO AS MAP(EARMOLD).

WHEN A CONVENTIONAL EARPHONE WAS USED AS THE PRESSURE DRIVING SYSTEM, THE SMALL PLASTIC TUBE (ONE END ATTACHED TO THE MICROPHONE) WAS ATTACHED TO THE EAR WITH ADHESIVE TAPE AND THE OPEN END OF THE TUBE TERMINATED AT THE ENTRANCE OF THE EAR CANAL. THE EARPHONE CUSHION SEAL WAS NOT AFFECTED BY THE PLASTIC TUBE COMING OUT FROM UNDER THE CUSHION VIA THE SMALL NOTCH IN THE FRONT PART OF THE PINNA. A PERMOFLUX EARPHONE, MOUNTED IN AN MX41AR CUSHION (FLAT TYPE), WAS USED AND THRESHOLDS OBTAINED WITH THIS SYSTEM ARE REFERRED TO AS MAP(PDR).

FREE FIELD THRESHOLDS WERE OBTAINED USING A LOUDSPEAKER ACROSS THE ANECHOIC CHAMBER FROM THE SUBJECT. THE CHAIR USED BY THE SUBJECT WAS MECHANICALLY ISOLATED FROM THE WOVEN WIRE FLOOR BY PLACING AUTOMOBILE INNER TUBES, PROPERLY INFLATED, BETWEEN THE WIRE FLOOR AND THE WOODEN BOARD ON WHICH THE CHAIR RESTED. THE PURPOSE OF THIS ISOLATION WAS TO MINIMIZE THE TRANSMISSION OF THE 100 Hz SIGNAL THROUGH THE WIRE FLOOR TO THE SUBJECT'S CHAIR. (THIS MECHANICAL ISOLATION WAS ALSO MAINTAINED WHEN PRESSURE THRESHOLDS WERE MEASURED.) THE MICROPHONE PROBE WAS ATTACHED TO THE EAR IN THE MANNER USED FOR THE EARPHONE. THUS FREE FIELD AND PRESSURE THRESHOLDS WERE MEASURED USING THE SAME PROBE SYSTEM ATTACHED AT THE EFFECTIVE ENTRANCE TO THE EAR CANAL. SINCE THE PRESSURE THRESHOLDS WERE MONAURAL, THE NON-LISTENING EAR WAS OCCLUDED. THE SUBJECT WAS ASKED TO CHECK THE EFFECTIVENESS OF THE EAR PLUG USED IN THE OCCLUDED EAR BY LISTENING TO THE 100 Hz SIGNAL AT A LEVEL ABOVE THRESHOLD AND THEN CLOSING THE "LISTENING EAR" WITH HIS FINGER TO ASCERTAIN THAT THE 100 Hz SIGNAL COULD NOT BE HEARD BY THE OCCLUDED EAR.

ALL THRESHOLDS WERE OBTAINED USING THE BEKESY TECHNIQUE WHERE THE SUBJECT OPERATES A MOTOR DRIVEN ATTENUATOR BY MEANS OF A HANDSWITCH. HE PRESSES THE SWITCH WHEN HE HEARS THE TONE AND RELEASES THE SWITCH JUST AS SOON AS THE TONE IS NO LONGER HEARD. THE MICROPHONE AMPLIFIER AND GRAPHIC RECORDER WERE STANDARD BRUEL AND KJAER EQUIPMENT; HOWEVER, A GENERAL RADIO MODEL 736-A WAVE ANALYZER (4 Hz BANDWIDTH) WAS INSERTED BETWEEN THE OUTPUT OF THE AMPLIFIER AND THE INPUT TO THE RECORDER. THE WAVE ANALYZER WAS MODIFIED TO PERMIT ITS 50 kHz SIGNAL TO DRIVE THE RECORDER. THE ACTUAL SOUND PRESSURE AT THRESHOLD WAS RECORDED IN ALL MEASUREMENTS - NOT THE ATTENUATOR SETTING. SOME DRIVER UNITS WERE FOUND TO BE NON-LINEAR NEAR THRESHOLD LEVELS; HENCE THE ABOVE TECHNIQUE WAS ADOPTED.

PHYSIOLOGICAL NOISE WAS ANALYZED USING THE SAME PROBE MICROPHONE SYSTEM THAT WAS USED FOR THRESHOLD MEASUREMENTS. THE TUNING DIAL OF THE WAVE ANALYZER WAS MOTOR DRIVEN FROM 20 TO 100 Hz, AND THE SPECTRUM, IN A 4 Hz BANDWIDTH, WAS GRAPHICALLY RECORDED. THE FREQUENCY RESPONSE OF THE PROBE WAS UNIFORM WITHIN PLUS OR MINUS ONE DECIBEL OVER THE 20 - 100 Hz RANGE. IN MANY CASES THE NOISE WAS ANALYZED DURING THE SAME SESSION WHEN THRESHOLD DETERMINATIONS WERE MADE, BUT THIS WAS NOT ALWAYS TRUE.

SUBJECTS REPEATED MEASUREMENTS ON DIFFERENT DAYS TO DEMONSTRATE ANY EFFECT OF LAPSE OF TIME. THERE WERE NO EFFECTS OF TIME EXCEPT THE USUAL VARIATIONS IN ABSOLUTE VALUES OF THRESHOLDS. ALTERNATE FREE FIELD AND PRESSURE THRESHOLDS WERE OBTAINED, I.E., A PRESSURE THRESHOLD WAS MEASURED, THEN THE EARPHONE OR TUBE WAS REMOVED AND THE FREE FIELD THRESHOLD MEASURED. THE PROCEDURE WAS REVERSED PERIODICALLY FOR BALANCE. SINCE THE AIM OF THIS RESEARCH WAS TO MEASURE THE DIFFERENCES BETWEEN PRESSURE AND FREE FIELD THRESHOLDS, ANY DIFFERENCES COULD BE SEEN CLEARLY BY COMPARING THE "SIDE-BY-SIDE" GRAPHIC RECORDINGS. BY THIS TECHNIQUE THE DIFFERENCES BETWEEN MAP AND MAF HAD A SMALL STANDARD DEVIATION EVEN THOUGH THE ABSOLUTE VALUES OF THE THRESHOLDS HAD A LARGER STANDARD DEVIATION. IN RECORDING THE DATA, THE SOUND PRESSURE LEVEL OF THE FREE FIELD THRESHOLD WAS SUBTRACTED FROM THE SOUND PRESSURE LEVEL OF THE PRESSURE THRESHOLD OBTAINED EITHER JUST BEFORE OR JUST AFTER THE FREE FIELD THRESHOLD.

RESULTS. THE RESULTS OF THE THRESHOLD MEASUREMENTS ARE SHOWN IN TABLE 1. THE VALUES

GIVEN ARE AVERAGE VALUES. IN ALL CASES THE MAP(PDR) THRESHOLDS ARE SIGNIFICANTLY DIFFERENT, AT THE 5% LEVEL, FROM MAF THRESHOLDS; WHEREAS MAP(EARMOLD) THRESHOLDS ARE NOT SIGNIFICANTLY DIFFERENT FROM THE MAF THRESHOLDS. THE STANDARD DEVIATIONS FOR THE THRESHOLD DIFFERENCES ARE GIVEN AS WELL AS THE NUMBER OF PAIRS OF THRESHOLD DETERMINATIONS. THE TEST OF SIGNIFICANCE WAS BASED ON THE PRESSURE DIFFERENCES, I.E., THRESHOLDS WERE DIFFERENT IF THEIR DIFFERENCES VARIED FROM ZERO BY A SIGNIFICANT AMOUNT.

TABLE 1. MONAURAL THRESHOLDS IN DECIBELS RE .0002 MICROBAR. 100 HZ. STANDARD DEVIATIONS (S) OF PRESSURE DIFFERENCES ARE IN DB. N IS THE NUMBER OF PAIRS OF JUDGMENTS.

SUBJECT	MAF	MAP(PDR)	MAP(EARMOLD)	MAP(PDR) − MAF		MAP(EARMOLD) − MAF	
				S	N	S	N
DB	35.1	37.8	34.3	1.1	15	1.4	14
RS	37.7	44.1	37.9	2.3	15	1.3	12
RW	37.4	43.6	37.2	1.2	15	1.1	14
WC	34.7	40.1	34.9	1.4	10	1.6	10
WR	37.2	45.8	37.4	1.8	17	1.6	16
LS	39.4	43.6	39.2	1.1	12	1.2	12

THE DATA IN TABLE 1 SHOW THAT MAP(EARMOLD) IS THE SAME AS MAF, AND THE NOISE SPECTRA, IN TABLE 3, SHOW THAT THERE IS A SIGNIFICANT REDUCTION IN PHYSIOLOGICAL NOISE WHEN THE EARMOLD SYSTEM IS USED COMPARED WITH THE NOISE WHEN THE EARPHONE SYSTEM IS USED. THUS IT SEEMS CLEAR THAT THE 100 HZ THRESHOLDS REPORTED IN THE LITERATURE ARE ELEVATED RE MAF DUE TO MASKING RESULTING FROM PHYSIOLOGICAL NOISE. TO SHOW THE CHANGE IN MASKING OF MAP AS FREQUENCY INCREASES, THE DATA IN TABLE 2 WERE OBTAINED. FOR THESE MEASUREMENTS ONLY THE PERMOFLUX EARPHONE IN THE CONVENTIONAL HEADSET WAS USED. THE PRESSURE PROBE WAS ATTACHED AT THE EAR CANAL OPENING AS BEFORE, AND THE TECHNIQUE WAS THE SAME; HOWEVER, ONLY THE DIFFERENCES BETWEEN MAP(PDR) AND MAF ARE REPORTED; NOT THE THRESHOLD PRESSURES. FOR ALL SUBJECTS EXCEPT DB THE 200 HZ DIFFERENCES ARE SIGNIFICANT AT THE 5% LEVEL; HOWEVER, FOR 400 HZ, NONE OF THE DIFFERENCES ARE SIGNIFICANT. THERE IS NO QUESTION THAT PHYSIOLOGICAL NOISE IS PRODUCING MASKING AT 200 HZ FOR THESE THREE SUBJECTS. IN THE CASE OF 400 HZ, THE PROBE ON THE EAR DOES NOT MEASURE TRUE FREE FIELD VALUES DUE TO HEAD DIFFRACTION, BUT THE PURPOSE OF THIS RESEARCH IS TO SHOW THAT PRESSURE THRESHOLDS AND FREE FIELD THRESHOLDS AGREE EXCEPT FOR DIFFRACTION AND RESONANT EFFECTS.

TABLE 2. MAP(PDR) MINUS MAF IN DB. MAF MEASURED AT ENTRANCE OF EAR CANAL.

SUBJECT	200 HZ	400 HZ
DB	0.4	0.1
RS	1.1	0.3
WR	1.8	−0.6
LS	2.1	0.0

THE NOISE SPECTRA ARE SHOWN IN TABLE 3. THE AMBIENT NOISE SPECTRUM IS GIVEN IN THE FIRST COLUMN OF SPECTRA. IN THE CASE OF SUBJECT DB, THE HEADBAND USED FOR HIS THRESHOLD

TABLE 3. PHYSIOLOGICAL NOISE SPECTRA. VALUES ARE AVERAGE SOUND PRESSURE LEVELS IN A 4 HZ BANDWIDTH IN DECIBELS RE .0002 MICROBAR.

FREQ.		DB		RS		RW		WC		WR		LS	
HZ	AMB	PDR	MOLD	PDR	MOLD	PDR	MOLD	PDR	MOLD	PDR	MOLD	PDR	MOLD
20	25	37	41	52	43	55	50	49	32	58	49	53	52
30	19	35	36	54	40	49	52	43	32	53	45	55	45
40	16	32	28	46	30	43	39	40	22	49	39	47	37
50	15	29	25	45	25	41	31	38	17	46	36	42	34
60	13	26	23	38	21	36	28	34	15	41	30	36	28
70	12	26	20	34	19	34	26	31	14	39	23	3[illegible]	26
80	10	25	16	32	16	31	22	28	13	36	22	33	18
90	7	24	14	30	15	30	18	28	13	34	19	28	16
100	4	23	12	28	13	28	14	26	12	27	16	26	14

THE INITIALS AT THE TOP INDICATE THE SUBJECT. THE COLUMN LABELED AMB IS THE AMBIENT SPECTRUM. COLUMNS LABELED PDR ARE THE SPECTRA FOR THE NOISE UNDER THE PDR EARPHONE IN A FLAT CUSHION (MX41AR). COLUMNS LABELED MOLD ARE THE SPECTRA OF THE NOISE IN THE EAR CANAL WITH THE EARMOLD SYSTEM IN THE EAR.

AND NOISE MEASUREMENTS WAS DIFFERENT FROM THAT USED BY THE OTHER SUBJECTS. LESS PRESSURE EXERTED BY THIS HEADBAND (FOR DB) ACCOUNTS FOR THE LOWER LEVEL OF PDR NOISE. NOTE ALSO THAT SUBJECT DB OBTAINED THE SMALLEST DIFFERENCE BETWEEN MAF AND MAP(PDR) OF ALL SUBJECTS. THE CHANGE IN NOISE WITH CHANGE IN HEADBAND WAS MEASURED ON SUBJECTS RS AND LS, AND THE RESULTS CONFIRM THE STATEMENT JUST MADE ABOUT THE HEADBAND USED BY DB. NOISE WAS NOT MEASURED AT EVERY THRESHOLD SESSION; HENCE IT WOULD BE EXPECTED THAT THE ACTUAL NOISE PRESENT DURING A PARTICULAR THRESHOLD DETERMINATION MIGHT DIFFER FROM THE VALUES OF TABLE 3.

TO CHECK THE MASKING EFFECT ON 100 Hz OF A SLOPING SPECTRUM, A WHITE NOISE GENERATOR WAS EQUALIZED TO PRODUCE A NOISE IN THE PDR EARPHONE OF APPROXIMATELY THE SAME SHAPE AS THE MEASURED PHYSIOLOGICAL NOISE SPECTRA OF TABLE 3. ONLY THREE SUBJECTS WERE USED IN THIS EXPERIMENT. THE NOISE WAS ADJUSTED WELL ABOVE THRESHOLD AND THE 100 Hz SIGNAL WAS ADJUSTED TO ITS THRESHOLD LEVEL IN THE PRESENCE OF THE NOISE. A 4 Hz BANDWIDTH ANALYSIS SHOWED THE NOISE AND THE PURE TONE. THE DATA ARE GIVEN IN TABLE 4. IF ONE CALCULATES THE NOISE LEVEL IN A CRITICAL BAND (TAKEN AS 80 Hz) CENTERED AT 100 Hz, THE VALUES SHOWN AS "CBW LEVEL" IN TABLE 4 ARE OBTAINED. RETURNING TO TABLE 3 AND CALCULATING THE SOUND PRESSURE LEVEL OF THE PDR NOISE SPECTRA IN AN 80 Hz BAND CENTERED AT 100 Hz, THE VALUES OBTAINED ARE: 35, 44, 42.7, 40.4, 47.4 AND 43 DB FOR THE SUBJECTS DB THROUGH LS RESPECTIVELY. COMPARISON OF THESE VALUES WITH THE MAP(PDR) VALUES SHOW SATISFACTORY AGREEMENT IN VIEW OF THE VARIABILITY OF THE NOISE SPECTRA EACH TIME A THRESHOLD MEASUREMENT IS MADE THIS LENDS ADDITIONAL EVIDENCE TO THE FACT THAT THE MAP(PDR) VALUE OF TABLE 1 ARE "MASKED" THRESHOLDS.

TABLE 4. MASKING OF 100 Hz TONE IN PRESENCE OF SIMULATED PHYSIOLOGICAL NOISE. NOISE SPECTRA IN 4 Hz BAND (DB), MASKED TONE LEVEL AND CALCULATED CRITICAL BAND LEVEL.

FREQ	RS	WR	LS
20	83	80	75
30	80	78	75
40	76	75	74
50	74	72	72
60	70	70	70
70	68	68	69
80	65	65	65
90	63	64	63
100	60	62	61
TONE	75	75	74
CBW LEVEL	76	76	76.4

CONCLUSIONS. THE DATA INDICATE THAT IF CARE IS TAKEN TO REDUCE THE MASKING EFFECTS OF PHYSIOLOGICAL NOISE AT LOW FREQUENCIES, THEN THERE IS NO DIFFERENCE BETWEEN MAP AND MAF UNTIL DIFFRACTION AND RESONANT EFFECTS BECOME SIGNIFICANT. EXPERIENCE HAS CONVINCED THE AUTHOR THAT THE USE OF A PROBE MEASUREMENT TECHNIQUE TO MONITOR CONTINUOUSLY THE EAR CANAL PRESSURE IS A NECESSITY IN THIS TYPE OF WORK. FURTHERMORE, THE SUBJECT'S CHAIR SHOULD BE MECHANICALLY ISOLATED; CORDS LEADING TO THE EARPHONE DRIVER UNIT SHOULD NOT CONTACT THE SUBJECT'S BODY; THE PRESSURE PROBE SHOULD BE FLEXIBLE AND NOT CONTACT THE SUBJECT'S HEAD AFTER IT LEAVES THE CUSHION; AND THE CATHODE FOLLOWER TO WHICH THE MICROPHONE IS ATTACHED SHOULD BE SUSPENDED FROM SOME SUPPORT FREE OF THE SUBJECT'S CHAIR. IT IS HOPED THAT THIS PART OF THE MISSING 6 DB PROBLEM WHICH HAS BEEN IN THE LITERATURE FOR ALMOST 30 YEARS HAS FINALLY BEEN RESOLVED.

AUDIOMETRIC THRESHOLDS OBTAINED WITH CONVENTIONAL HEADSETS WILL, IN GENERAL, MEASURE "MASKED" THRESHOLDS AT FREQUENCIES BELOW 200 Hz. CARE MUST BE EXERTED IN MEASURING ATTENUATION OF EARPLUGS AND SMALL VOLUME EAR COVERS AT LOW FREQUENCIES USING THE THRESHOLD SHIFT TECHNIQUE.

FURTHER COMMENTS. IT IS RECOGNIZED THAT THE MISSING 6 DB ALSO EXISTS AT LEVELS WELL ABOVE THRESHOLD WHERE PHYSIOLOGICAL NOISE CANNOT POSSIBLY PRODUCE MASKING. MOST OF THE AUTHOR'S RESEARCH HAS BEEN DIRECTED TOWARD EXPLAINING THE "LOUDNESS MATCH" DIFFERENCE. THERE IS NO SINGLE ANSWER WHICH EXPLAINS THIS DIFFERENCE FOR ALL OF THE EXPERIMENTS THAT HAVE BEEN REPORTED. RESULTS DEPEND UPON THE ACTUAL SUBJECT AND THE TECHNIQUES. DIFFERENT EXPLANATIONS ARE REQUIRED IN MANY OF THE CASES. A FORTHCOMING PAPER BY THE AUTHOR WILL DEAL WITH THIS PART OF THE MISSING 6 DB PROBLEM.

ACKNOWLEDGMENTS. THE AUTHOR IS INDEBTED TO THE CALLIER TRUST FOR SUPPORT WHICH MADE POSSIBLE THE RESUMPTION OF THIS RESEARCH. SINCERE THANKS ARE DUE THE SUBJECTS WHO SPENT MANY HOURS MAKING JUDGMENTS WITH PROBES, PLUGS, EARMOLDS, ETC., ATTACHED TO OR INSERTED INTO THEIR EAR CANALS.

J52

FOURTH INTERNATIONAL CONGRESS ON ACOUSTICS
COPENHAGEN 21.-28. AUGUST 1962

SOME ACOUSTIC EFFECTS AT PHASE CHANGES.

J. F. W. BELL

ROYAL NAVAL COLLEGE, GREENWICH, LONDON

The elasticities of a solid and hence the velocities, longitudinal and torsional, are governed by the forces between the atoms and their lattice arrangement. When the lattice changes with rising temperature (a phase change) there is an almost discontinuous change in physical quantities, either an increase or a decrease. In terms of energy, atomic separation corresponds to minimum potential energy, the elasticity gives the second coefficient of energy. Other quantities such as the various temperature coefficients have similar dependencies. By carrying out observations through a phase change it should be possible to separate the features which are common to the material and the structure. Changes in density have been widely investigated. The work described adds changes in elasticities of uranium, zirconium, titanium, thallium, cobalt and iron.

All measurements were carried out on polycrystalline specimens. Each excursion through a phase change changes the number and orientation of the crystals. For this reason elasticity temperature curves differ slightly from one cycle to another. The differences are small enough to be ignored when qualitative effects are being examined.

The technique, previously described, uses video pulses 10 μ sec long similar to those used in magnetostriction delay lines. Figure 1 shows the nickel transducer, the matching unit to the "lead in" rod and the specimen. There are sufficient variables in the design to enable a single arrangement suitable for both torsional and longitudinal pulses to be made. This makes it possible to measure both velocities without remounting the specimen. Figure 2 shows the echo patterns for such a system. The specimen is uranium.

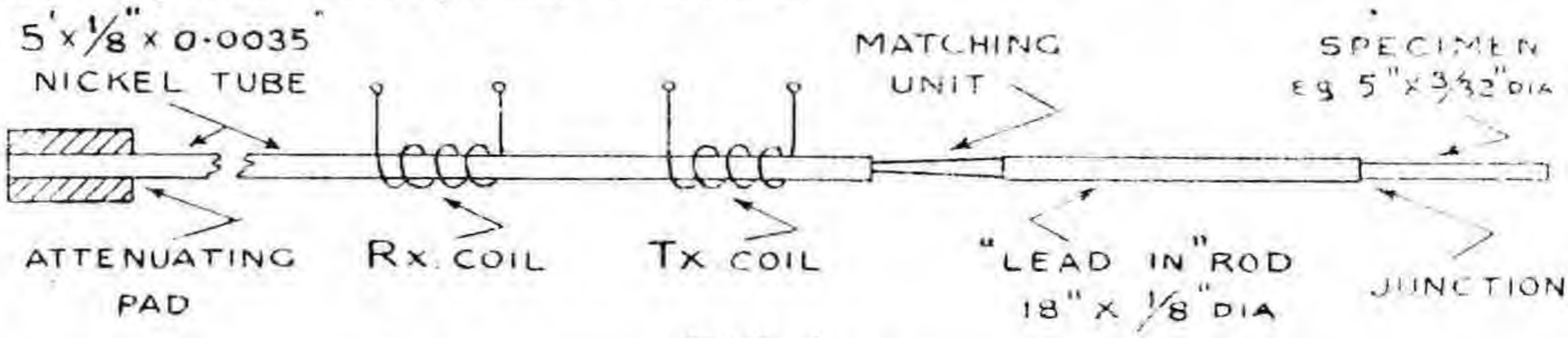

FIG 1.

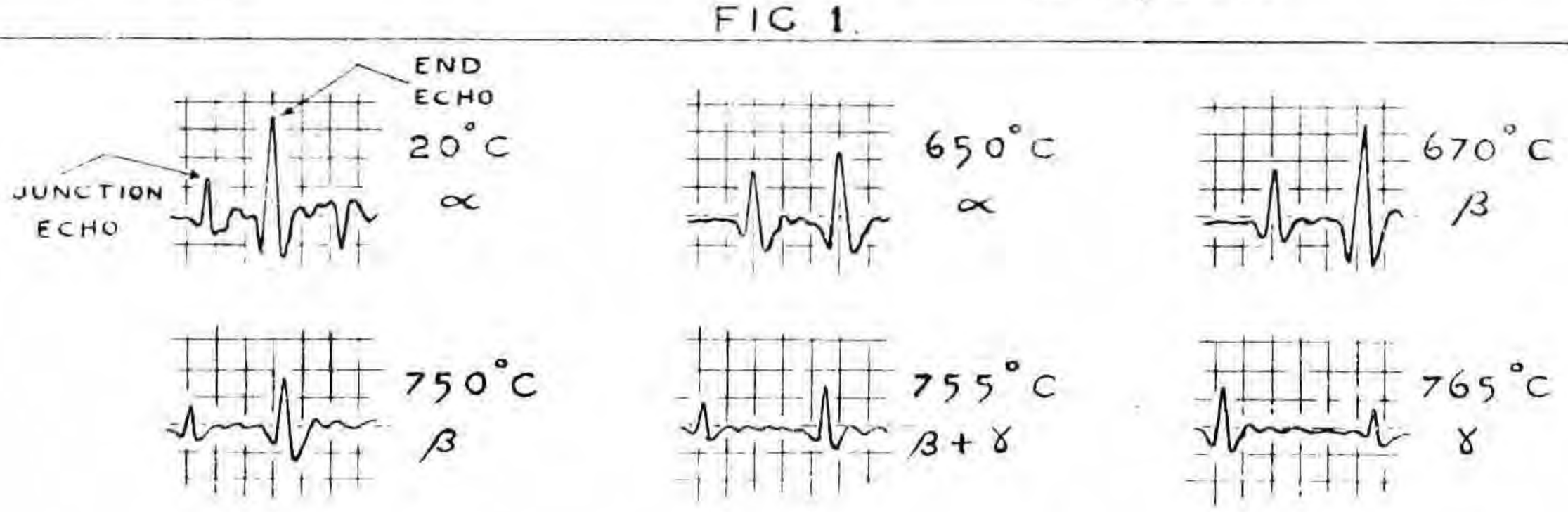

FIG 2.

A typical phase change is shown in figure 3. The specimen consists of a 1/8" diameter rod of polycrystalline uranium, an easy metal to investigate as the phase change is uninfluenced by small amounts of contamination. The curves show a large fall in velocity as the uranium changes from α (orthorhombic) to β (tetragonal). The temperature difference between rising and falling curves is due to temperature hysteresis, common to all phase changes. The velocity temperature curve on return to the phase has suffered a slight displacement due to crystal growth and reorientation. The coefficients of velocity are less negative in the phase than the α. In the δ phase (body centred cubic) the coefficient is positive. The attenuation, deduced from the relative heights of junction and end echoes follows the velocity change.

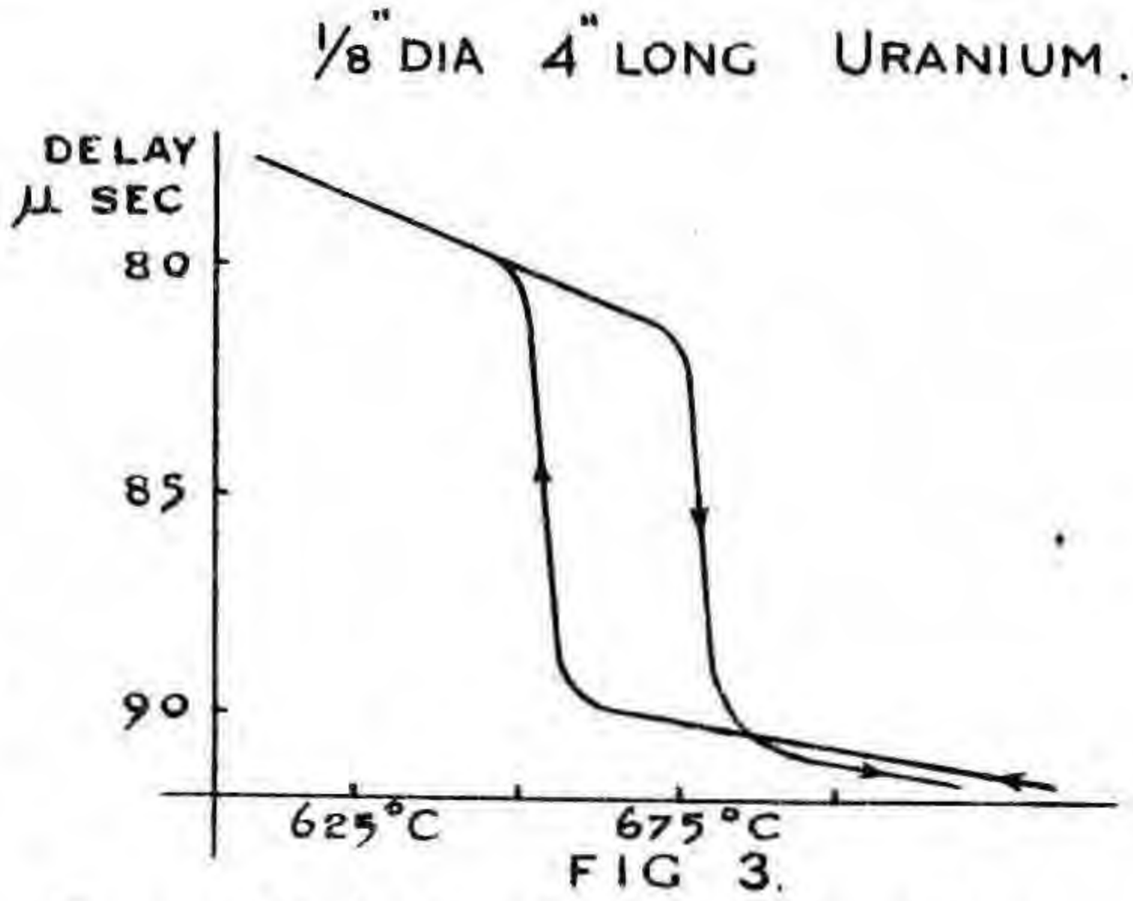

FIG 3.

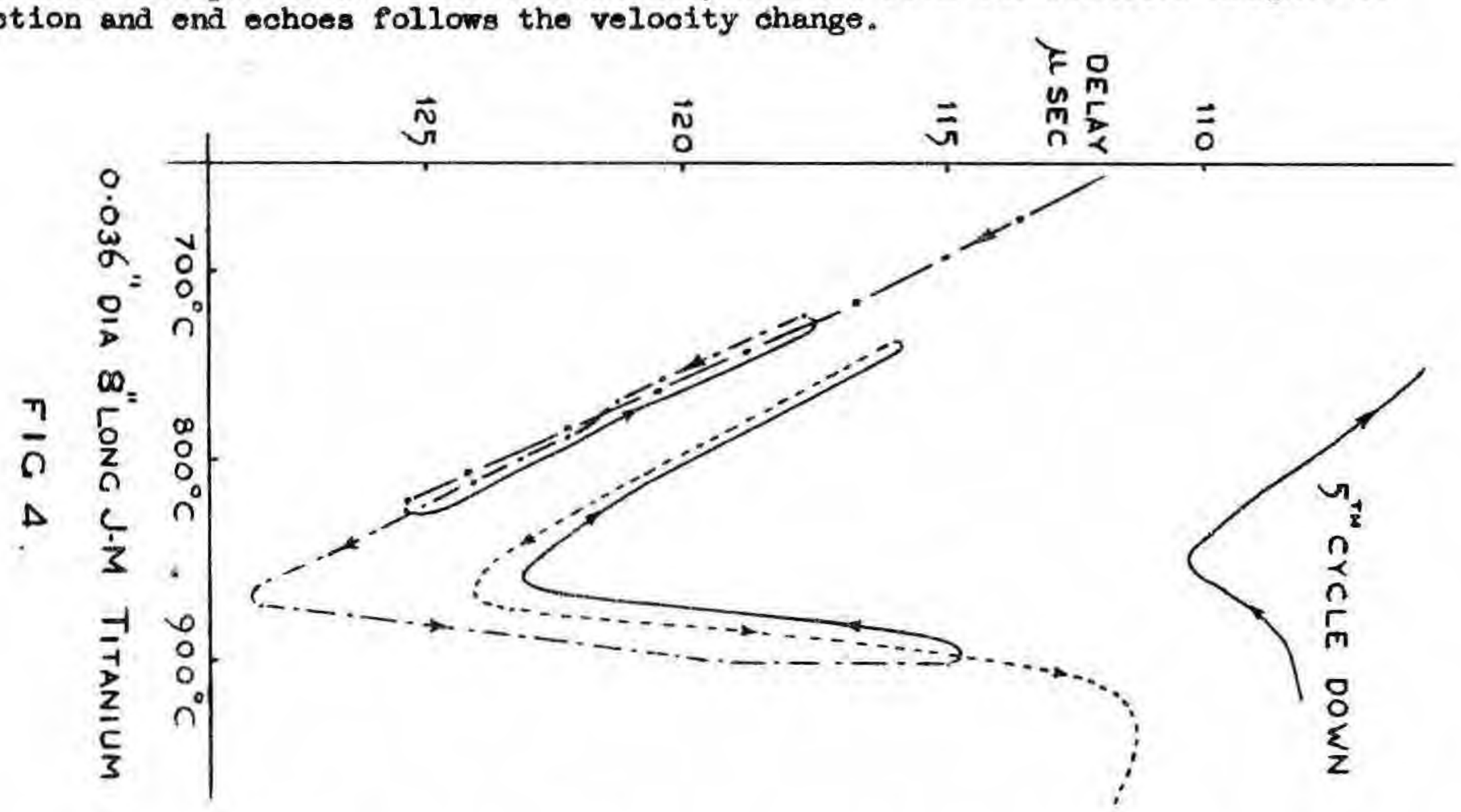

FIG 4.

Figure 4 shows similar measurements on titanium as it goes from α hexagonal close packed to β body centred cubic. The metal has a strong affinity for nitrogen and oxygen, particularly in the β phase. The coincident cycles in the α phase shows that there is no contamination. A few minutes in the β phase produces enough contamination to cause a large shift in velocity.

The ~~table~~ below summarises qualitatively changes which occur when the metallic elements of column one are heated through the phase changes shown in column two. Velocity coefficients $\frac{1}{v}\frac{dv}{d\theta}$ are normally negative. In cases where they become less negative they are classified in the table as "up". With the exception of attenuation the properties shown are dependant on structure and the energy distance law of the atoms. Density gives the atomic separation for which the potential energy of the structure is a minimum. The second coefficient of potential energy gives the elasticity. The magnitude of the velocity change is often of the order of 10% or more, that of the density $\frac{1}{2}$%. The information in column five (velocity) is thus also applicable to elasticity.

Material	Phase change rising temp.	Approx. temp.	Density	Velocity	Velocity coeff.	Attenuation
Titanium	HCP to BCC	880	Up	Up	Up	Down
Zirconium	HCP to BCC	860	Up	Up	Up	Down
Iron	BCC to FCC	900	Up	Up	Up	Down
Iron	FCC to BCC	1400	Down	Down	Down	Up
Uranium	Ortho- to Tetra-rhombic gonal	670	Down	Down	Up	Down
Uranium	Tetra- to BCC gonal	750	Down	Down	Up	Up
Cobalt	HCP to FCC	450	Down	Up	Up	Down

An objective of this work is to separate the factors which are structure dependant from those which arise from the velocity distance law in the determination of the physical properties of a metallic crystal. Theoretical support for this work is needed and would be most welcome.

Acknowledgments.

The work described was carried out in the department of Physics and Electrical Engineering at the Royal Naval College, Greenwich, England as part of an O.E.E.C. "Project Dragon" contract.

The author expresses his thanks to Mr. S.G. Smith and Mr. B.P. Doyle, who have played a major part in this work.

K52

FOURTH INTERNATIONAL CONGRESS ON ACOUSTICS
COPENHAGEN 21.-28. AUGUST 1962

TIME DEPENDENT OPTICAL METHODS FOR THE STUDY OF ULTRASONIC WAVES.

K. L. Zankel and H. M. Colbert

Many studies have been made on the effects of ultrasonic waves on light. Those studies were made in order to either determine the characteristics of the ultrasonic waves or to obtain modulated light. Most previous measurements were time averages of the light intensities. The measurements of light fluctuation were made indirectly, with the stroboscope effect and were very approximate.[1]

We have theoretically and experimentally investigated the time dependant behavior of light passing through progressive ultrasonic waves.[2] Light fluctuations during one ultrasonic period are measured. This investigation suggests several possible uses: 1) As a method of accurately measuring relative ultrasonic pressures; 2) As a method of determining ultrasonic waveform. This method includes the determination of phase relationships between various harmonic components of a periodic wave. This is not possible using time average measurements; 3) As a method of accurately measuring ultrasonic wavelength of progressive waves; and 4) As a method of predicting the light fluctuation in various regions of the light beam for use in light modulation or stroboscopes.

Only a brief description of the method and results can be given here. In these experiments collimated light is passed through and normal to the ultrasonic wave, as is shown schematically in Fig 1. For moderate pressures and frequencies (to which this discussion is limited), a phase modulated wavefront emerges from the ultrasonic wave. This wavefront is represented by the line P. The light can then be focussed by the lens L' to form diffraction orders at D. Previously, measurements of the time average light intensity have been made for stationary ultrasonic waves in the region between P and L' (the near light field region which is sometimes called the visibility region), at D (the position of the diffraction orders) or at P' (which is the image of P and is referred to as the "schlieren"). In addition such measurements have been made at D (the position of the diffracted orders) for progressive waves. Time average measurements in the near light field region give no information for progressive waves. A pattern is formed here for progressive waves, but it moves with the speed of sound. Time average measurements give only the total light intensity. Other information is lost. A similar statement can be made for most of the information at the schlieren P', when progressive waves are used.

The discussion here will concern light measurements as a function of time in the two regions (in the near light field and at the schlieren). These measurements were made by placing a slit followed by a photomultiplier in the region to be studied. The photomultiplier output was put through a wide band amplifier and then displayed on an oscilloscope. Measurements were made using 2Mc ultrasonic waves in water which in some cases were allowed to become finite amplitude distorted.

The near field region will be discussed first. The relative light amplitude in this region can be obtained from the integral

$$A = A_o \int \exp \{i\omega t - 2\pi i[r + \phi(x,t)]/\lambda\}\, dx$$

where

$$r \cong y(1 + x^2/2y^2)$$

x being the distance along the sound wave and y the distance from it, t is the time. Also,

$$\phi(x,t) = \sum_{p=o}^{\infty} v_p \sin p(\omega_1 t - 2\pi x/\lambda_1) + w_p \cos p(\omega_1 t - 2\pi x/\lambda_1)$$

here $v_p = 2\pi u_p L/\lambda$ and $w_p = 2\pi \gamma_p L/\lambda$.

The angular frequency and wavelength of light are given by ω and λ; those of the sound wave fundamental have the subscript 1. u_p and γ_p are the maximum changes of the index of refraction of the pth fourier sine and cosine components respectively of the sound wave. Therefore $\phi(x,t)$ is proportional to the sound pressure. Note that any completely arbitrary periodic ultrasonic wave is being considered. L is the geometrical path length of light through the ultrasonic wave. One obtains from this that

$$A' = A_o \lambda y \sum_{\rho,\sigma=o}^{M-1} \exp[2\pi i(\rho^2 a + \rho\sigma)/M - ik\phi(\lambda_1 \sigma/M, t)]/M$$

where A' times its complex conjugate is the light intensity as a function of time. Here $a/M = \lambda y/2\lambda_1^2$ where a and M are integers. This expression becomes particularly simple for certain values of $\lambda y/\lambda_1^2$.

When comparing the predicted and experimental results, close correspondence was obtained; The experimental information will be presented during the talk but due to reproduction difficulties cannot be shown here. The results shown in Fig 2 are for an almost sinusoidal wave and for $v=\pi/2$ which corresponds to about 0.35 atm for the one inch square transducer used in the experiments. v is the peak value of $\phi(x,t)$, and is therefore proportional to peak pressure. The curves are those predicted for various distances of photomultiplier slit from the sound wave. In the left curve the slit was placed in the near light field region at $\lambda y/\lambda_1^2 = 1/8$; the curve next to it at $\lambda y/\lambda_1^2 = 2/8$; the other two at $\lambda y/\lambda_1^2 = 3/8$ and $4/8$. The ordinates of these curves are light intensity and the abscissa are time. One wave length is plotted for each curve. Therefore for 2Mc the curve would be one-half u sec. wide. For $\lambda y/\lambda_1^2$ greater than $4/8$, the curves repeat in reverse order.

If the ultrasonic waves are allowed to travel a distance they become finite amplitude distorted. The theoretical curves in Fig 3 are for a wave which has traveled 0.3 of the discontinuity distance (distance of shock formation). Here from left to right $\lambda y/\lambda_1^2 = 1/2$, $1/3$ and $1/4$. The experimental curves for ultrasonic waves which have traveled about 0.3 of the discontinuity distance agree within experimental error to these.

We can look at what results when the photomultiplier slit is kept at one position and the amount of ultrasonic distortion is increased. Fig 4 is for $\lambda y/\lambda_1^2 = 1/3$. Here the left curve is for an ultrasonic wave which has traveled 0.1 of the discontinuity distance. The middle curve is for 0.3 of the discontinuity distance and the right 0.5.

In all of the curves shown the maximum value of v was about $\pi/2$. The next figure (Fig 5) is for different pressures or values of v. For these $\lambda y/\lambda_1^2 = 1/4$. The values of v from left to right are π, $5\pi/4$ and $6\pi/4$ for sinusoidal waves. The shapes of these curves are very sensitive to pressure. Very accurate relative pressure measurements may be made in this way.

The experimental curves show that the light fluctuations as a function of time can be, within experimental error, predicted and measured. Uses for light modulation, pressure measurements and waveform determination can be inferred. We will mention one further use, that is for wavelength or velocity measurement. This is accomplished by synchronizing the scope trace to the signal applied to the transducer and then moving the transducer or photomultiplier slit an accurately measured distance in the direction of sound travel. One can then determine the number of wavelengths corresponding to this distance by counting the number and fraction of wavelengths which have swept across the oscilloscope face during the motion. In this way one can get quite accurate measurements of velocities of progressive waves.[3]

We have discussed some of the experiments concerning light fluctuations in the near field region. We will now turn to such measurements at the "schlieren".[4] The experimental procedure is the same. Two Mc. progressive ultrasonic waves traveling in water were again used. Clearly, if the light were allowed to reach the schlieren unhampered, an image of the phase modulated light wave front would result and no fluctuations would be observed. However, if one or more of the diffracted orders

were blocked out, interference would occur and the light would fluctuate. Although other cases were investigated, we will discuss only what happens when the zero order is blocked out. The light intensity predicted for this case is

$$I = E_o^2 + E_1^2 - 2E_oE_1 \cos \phi(x,t)$$

where E_o is the intensity of light without sound, E_1 the intensity of light in the zero diffracted order and $\phi(x,t)$ was given previously. $\phi(x,t)$ is proportional to the ultrasonic pressure and therefore describes the waveform completely. We see that the light fluctuates simply as the cosine of the waveform. Examples of predicted results are seen in Fig 6. The theoretical curves shown are for sinusoidal waves. These are for values of v, reading from left to right, of about .85, 3.75, 7.0 and 10.2. Corresponding experimental curves agree within experimental error. Again we have plotted light intensity vs time. The next figure (Fig 7) shows the effects of finite amplitude distortion. The predicted results are, reading from left to right, for waves which have traveled 0, .275 and 0.5 of the discontinuity distance. Corresponding experimental curves again agree. From experimental curves similar to these we obtained the parameters which determine the discontinuity distance and obtained results within experimental agreement with previously measured values.

To summarize then, it appears that for progressive ultrasonic waves light fluctuations in the near light field region and in the schlieren can be predicted and measured. Sound pressure, waveform and sound velocity can be obtained at least in theory from these measurements. The use of a better light source such as a maser should extend the usefullness of these experiments. We are now in the process of developing a stroboscope and of studying phase relationships between harmonic components of finite amplitude distorted waves which have traveled in a relaxing medium.

This work was supported by ONR, U. S. Navy.

- - - - - - -

1 See for example Ch. Bachem, Phys. 87 (1934), p. 788.

2 For previous theoretical discussion of similar problems concerning sinusoidal ultrasonic waves, see D. Nomoto, Proc. Phys. Math. Soc. Jap. 3 (1937) p. 337: and J. Phys. Soc. Jap. 9 (1954) p. 267.

3 This method essentially extends that of Bachem and Hiedemann [Z. Phys. 94 (1935) p. 68] to include progressive waves.

4 These measurements were reported on briefly at the Sixty-Second Meeting of the Acoustical Society of America.

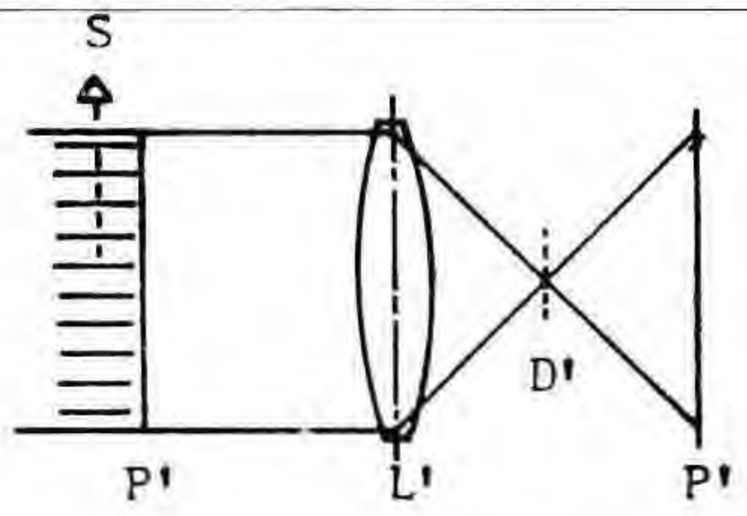

Fig 1

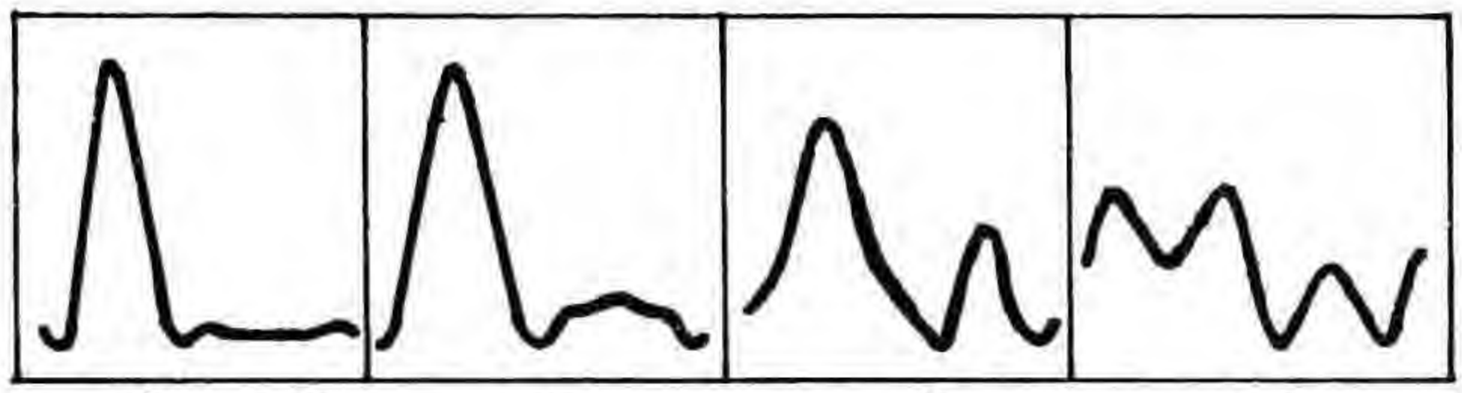

$\lambda y/\lambda_1^2$ = 1/8 2/8 3/8 4/8

K = 0 $\nu = \pi/2$

Fig 2

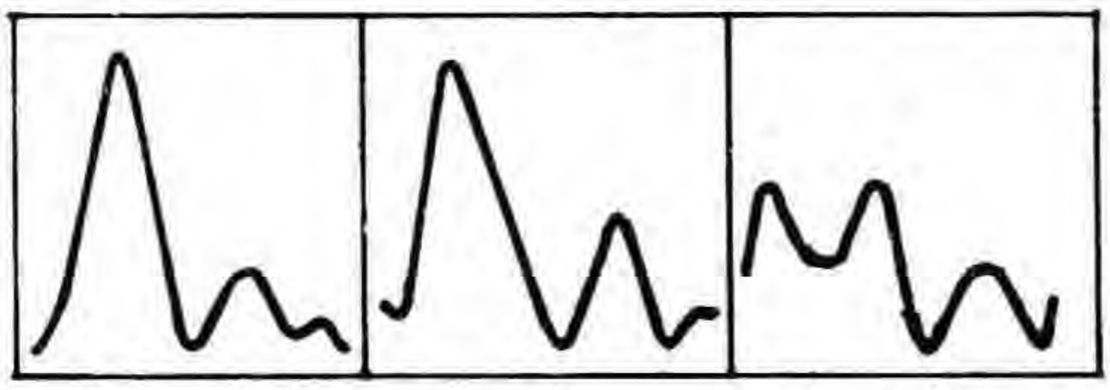

$\lambda y/\lambda_1^2$ = 1/4 1/3 1/2

K = 0.3 $\nu = \pi/2$

Fig 3

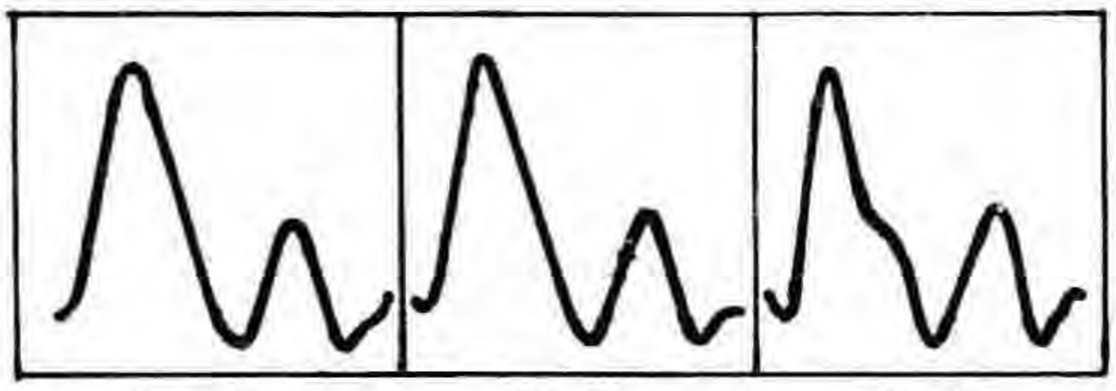

K = 0 0.3 0.5

$\lambda y/\lambda_1^2$ = 1/3 $\nu = \pi/2$

Fig 4

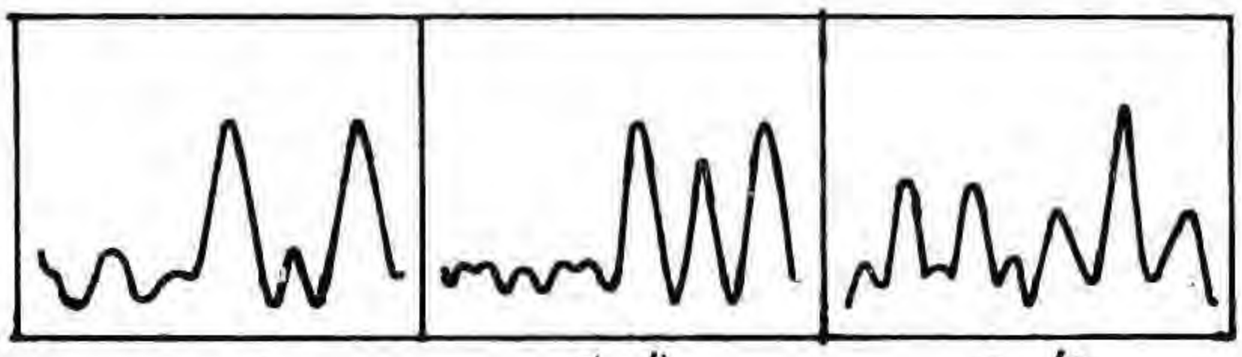

$\nu = \pi$ 5π/4 3π/2

$\lambda y/\lambda_1^2$ = 1/4 K = 0

Fig 5

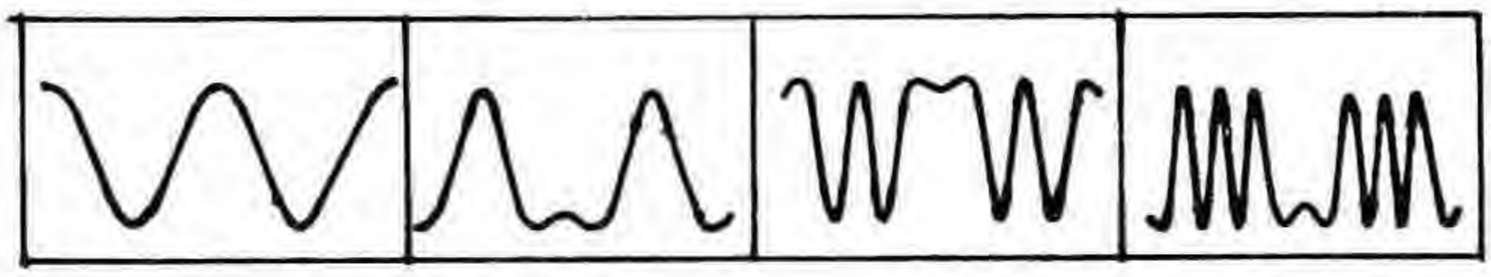

ν = 0.85 3.75 7.00 10.2

K = 0

Fig 6

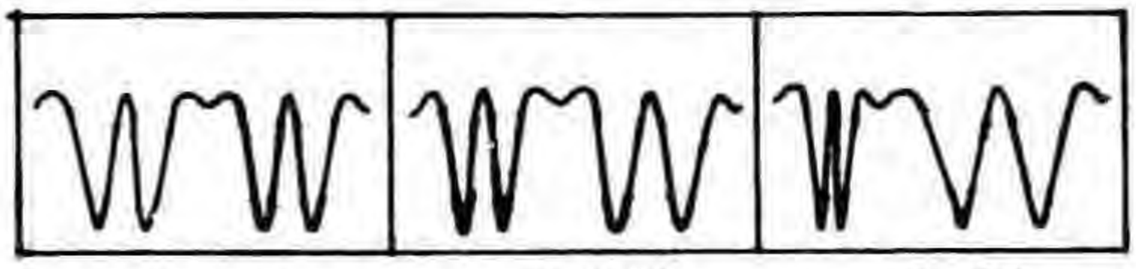

K = 0 0.275 0.55

V = 7

Fig 7

L52

FOURTH INTERNATIONAL CONGRESS ON ACOUSTICS
COPENHAGEN 21.-28. AUGUST 1962

THE BLADING OF FANS IN ITS INFLUENCE ON NOISE

Ing.Dr Jaroslav Němec C Sc, SVUTT, Prague, ČSSR

In axial-flow fans and compressors, a very large component of the noise produced is due to irregularities of flow in the flowing medium. We may call it the siren noise.

It has been found that some fan designs prove more silent than other ones. Suggestions have been made to choose the number of fixed and moving blades in such a way as not to have a common measure.

Siren noises in fans are caused by flow irregularities created, for instance, behind the individual blades. Pulsation forces thus initiated are the cause of noise emission (Yudin [1]). Fig. 1 indicates details of flow conditions occuring in an axial fan. It can be shown that the rotating fan blade 2 passes through a field of variable velocity w_1 with the result that it is acted upon by alternating forces ΔF .

Let us consider one pitch of the entry blades 1 comprising one blade and its wake. One rotating blade after the other passes through this place, the number of pressure pulsations per second occuring in the irregular field of velocity c_1 being f_1 .
The variable portion of the velocity profile is represented by a curve of rather complicated a shape which repeats itself in each pitch of the entry blades, Fig. 2.
A harmonic analysis of the variable portion c_1 of the velocity profile enables us to separate it into a basic component of the order k = 1 and components of a higher order (k = 2, 3, 4 etc.).

Let us contemplate now the relation between the emitted acoustic output and the alternating forces resulting from the fluctuating flow. Yudin [1] bases his deductions on the fact that the periodical force acting upon the medium is equivalent to an acoustic dipole. Some years ago already, it was Lamb [2] who busied himself with contemplating the acoustic effect of a concentrated periodical force upon a medium. From his work it

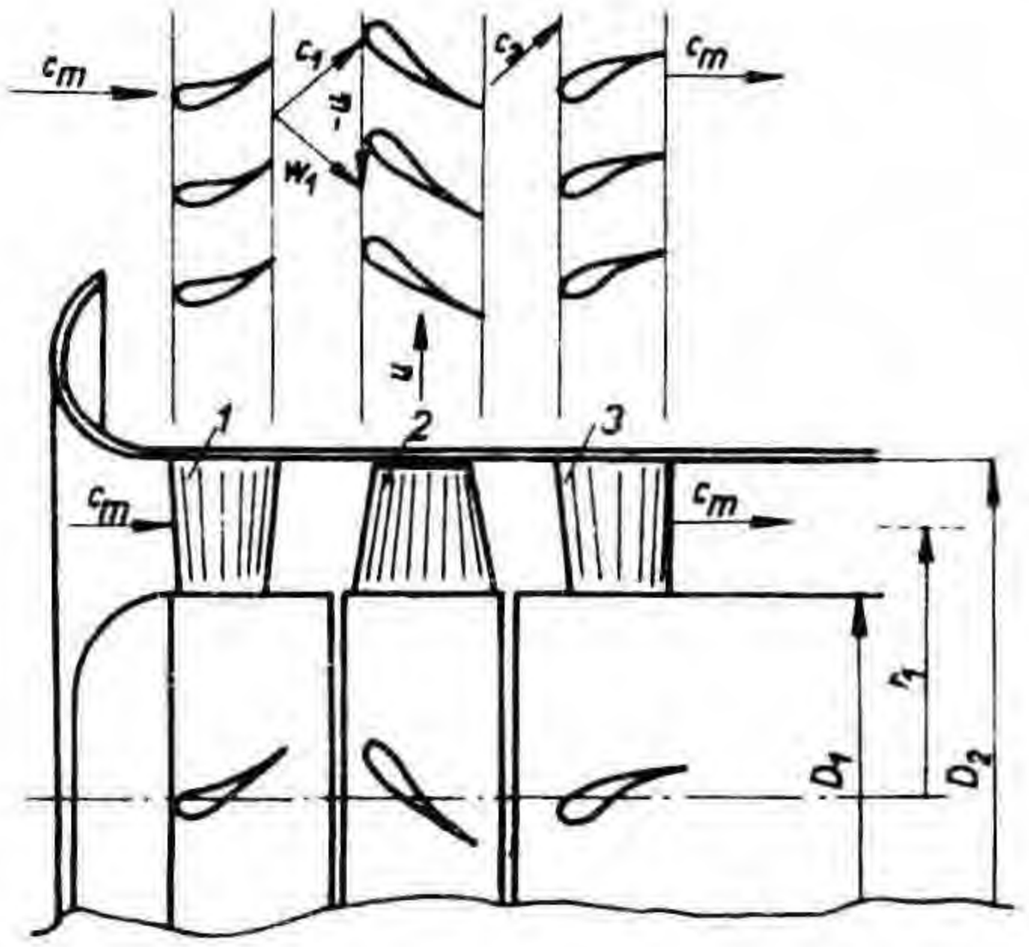

Fig. 1.

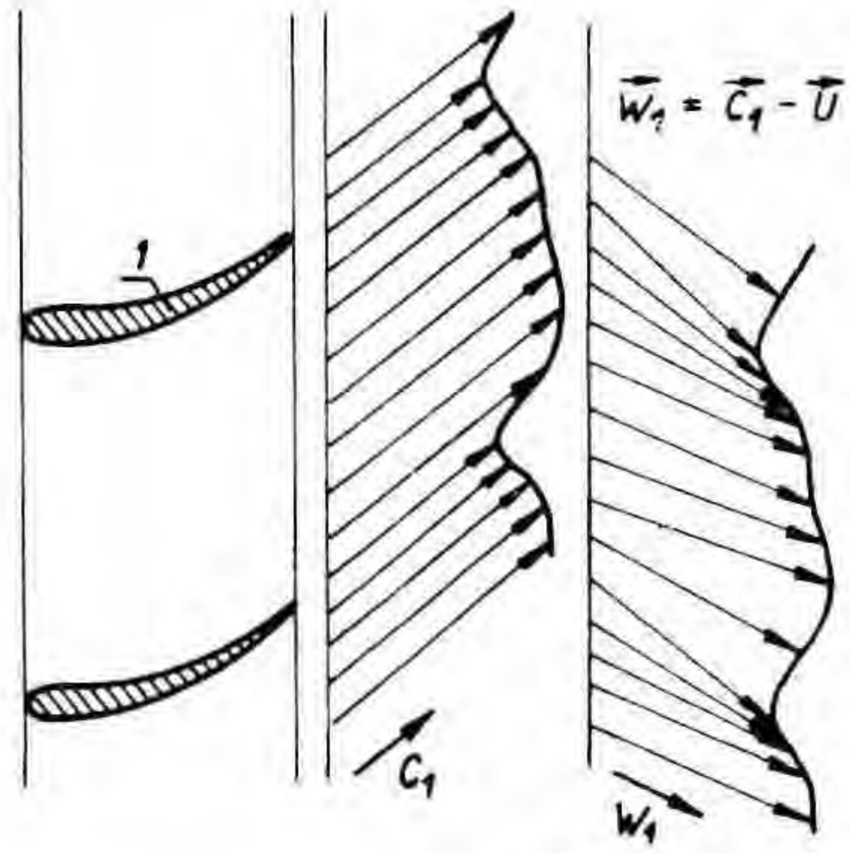

Fig. 2.

results that the effect of an alternating force with an amplitude ΔF_k is equal to the effect of an acoustic dipole.

With respect to other developments we can write

$$A = \frac{\Delta F_k \cdot \omega_k}{4\pi \cdot c} \tag{1}$$

As to the sound pressure created, at point M, by an individual dipole, the following relation applies

$$p = \frac{A}{r} \cdot e^{-j\frac{\omega_k}{c} r \cdot \cos\theta} \cdot e^{j\omega_k t} \tag{2}$$

The value of A is to substituted from relation (1).
Thus we find that the acoustic pressure is proportional to the force ΔF_k

From the above it follows that pressure pulses occur at the place of each wake behind the entry vane and that they act as individual acoustic sources i.e. as acoustic dipoles. The number of these sources is given either by the number of entry vanes z_1 of the axial fan or by the number z_2 of the outlet vanes.

In regard of the above interpretation, the fan can be looked upon as a regular group of axial acoustic sources (dipoles) distributed along a circle. We may imagine them to be distributed upon a medium radius r_1 (Fig.2), their number being z_1 and z_2 respectively. Here, the individual sources have the same frequency, a mutually fixed phase and the same amplitude p .

The axis of the individual dipoles may be parallel to the axis of the fan or form a certain angle with it. In practice, this angle does probably not exceed 45°.

The sound pressure created in a distant point M on the fan axis by the i-th source (dipole) is given by the general expression

$$p_i = \frac{A}{r} e^{-j\frac{\omega_k}{c} r} e^{j[\omega_k(t-t_i)+\varphi_k]\cos\theta} \tag{3}$$

t_i representing the phase of the process taking place in the i-th source in relation to the first source.

$$t_i = (i-1)\frac{60}{n \cdot z_1} \tag{4}$$

The resulting sound pressure in M as a sum of p_i is given by

$$p = \sum_{i=1}^{z_1} p_i = \frac{A}{r} e^{-j\frac{\omega_k}{c} r} \cdot e^{j(\omega_k t + \varphi_k)\cos\theta} \sum_{i=1}^{z_1} e^{-j(i-1)2\pi \frac{z_0}{z_1} k} \tag{5}$$

Therefore the magnitude of the sound pressure p depends on the magnitude of the term

$$\sum_{i=1}^{z_1} e^{-j(i-1)2\pi \frac{z_0}{z_1} k} \tag{6}$$

This term represents the sum of the vectors of unit length rotated, against the first one, through an angle of $(i-1)2\pi k\, z_0/z_1$. Its magnitude depends on the ratio z_0/z_1 and on k .

Due to the circumstance that a wake originates also behind the rotating vanes, velocity changes take place on the outlet blades (located behind the rotor) and take effect in noise making. If z_2 is the number of the outlet blades, the number of the partial sources of dipole character is also z_2 . We can proceed in the same way as in the case of the entry vanes.

The results can be represented on a synoptic table (Fig. 3) showing the ratios z_0/z_1 of rotating to entry vanes or those z_0/z_2 of the rotating to the outlet vanes.as indicated by the above analysis. The ratios in question are distinguished by the order of the harmonic k and by their suitability. Unsuitable ratios are marked by a full framing, they correspond to the highest value of the above expression (6). The

order of harmonic k										
k = 1				k = 2				k = 3		
not suitable	degree of suitability			not suitable	degree of suitability			not suitable	degree of suit.	
	1	2	3		1	2	3		1	2
							1:8			1:9
						1:6			1:6	
										2:9
			1:4		1:4					
		1:3				1:3		1:3		
							3:8			4:9
	1:2			1:2					1:2	
							5:8			5:9
		2:3				2:3		2:3		
			3:4		3:4					
										7:9
						5:6			5:6	
							7:8			8:9
1:1				1:1				1:1		
							9:8			10:9

Fig. 3.

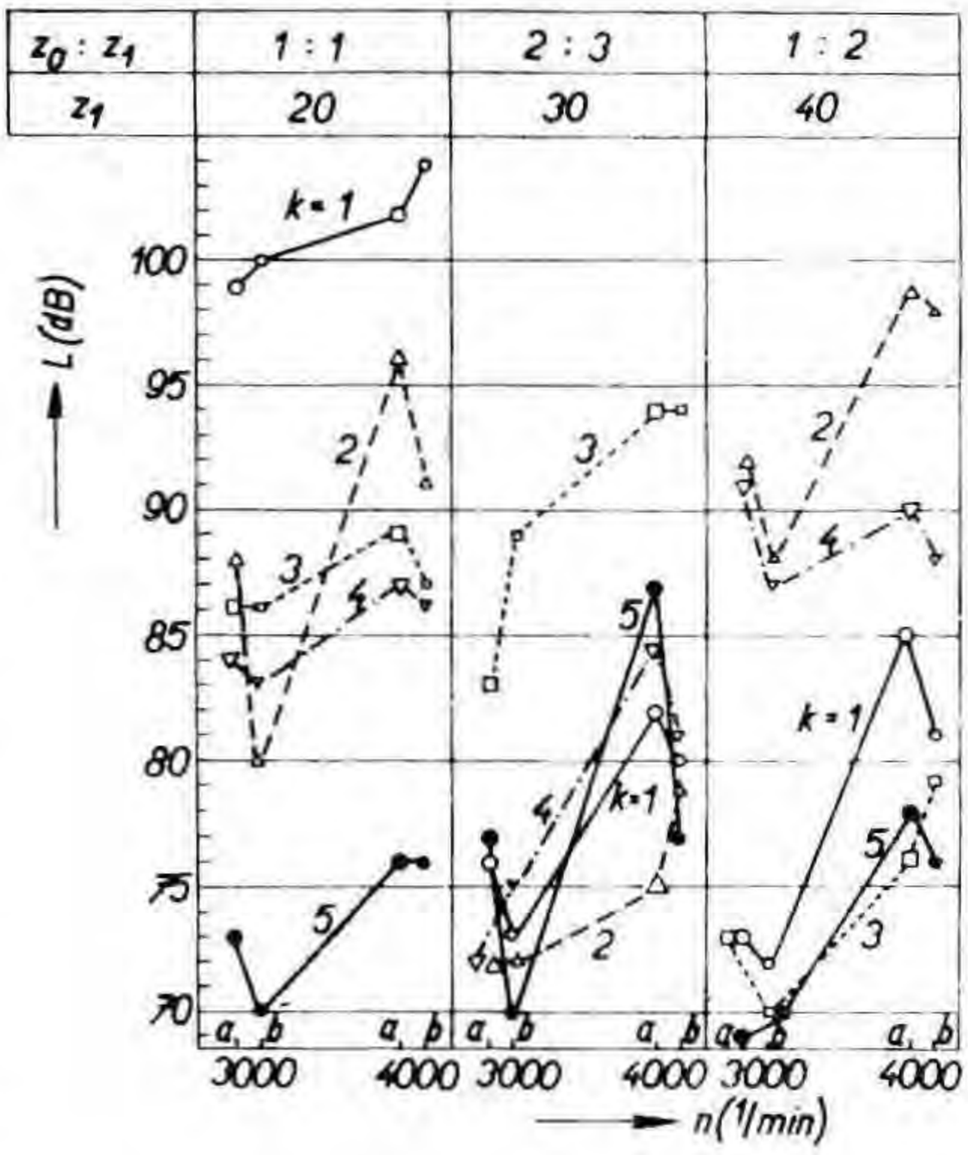

Fig. 4.

suitable values are graded (1 to 3 grades) whereby the first grade is considered the most suitable.

The table is filled up to ratios 1 : 1 considering that higher ratios seldom occur in practice. Similarly, the table is made only up to the order of k = 3. It can be completed in accordance with the indicated part, if required.

Should the point M not be situated in the axis of the fan but at a distance r_0 from the centre of the fan, the radius r_0 forming an angle θ with the axis of the fan, the distance r of the individual sources will be different. For practical purposes, it will be interesting to know the criterium when phase variations will reach large values at the point M between two adjacent vanes at a large angle θ, i.e. approximately π. This will occur when the pitch T_1 between the entry vanes (or between the outlet vanes) is smaller than the half wave length $\frac{\lambda_k}{2}$, i.e.

$$2\frac{T_1}{\lambda_k} \ll 1 \qquad T_1 = \frac{\pi D_2}{z_1} \qquad \lambda_k = \frac{c \cdot 60}{n\, z_0 \cdot k} \tag{7}$$

Then we write

$$2\frac{T_1}{\lambda_k} = 2\pi \frac{D_2}{c} \frac{n}{60} \cdot k \cdot \frac{z_0}{z_1} \ll 1 \tag{8}$$

As can be seen, the ratio T_1 / λ_k depends on the speed n of the machine and the ratio z_0 / z_1. With respect to this it is advantageous to choose a low number z_0 and a high number z_1.

Experimental verifications were carried out on an axial fan having a diameter of 320 mm, 20 rotating vanes (z_0), 15 outlet vanes (z_2). The number of the entry vanes was gradually increased; z_1 = 20, 30, 40.

The sound pressure levels of siren noise components measured next to the axis of the fan at a distance of 1 m from the suction point are represented on diagram of Fig. 4. They are in a very good agreement with the table values. For a component having the order k = 1, for instance, a difference of 20 - 28 dB was attained and for k = 2 a difference of 8 - 21 dB. This shows that the influence of blade numbers is very

substantial.

Considering the indications of Fig. 3, it can be recommended to use ratios z_0/z_1 = = 1 : 4, 1 : 3, 2 : 3, 3 : 4, 5 : 4, 4 : 3. These ratios shloud be exactly adhered to.

[1] Yudin J.J.: Issledovaniye shuma ventilyatorovych ustanovok i metodov borby s nim. Moskva, Oborongiz, 1958.

[2] Lamb H.: The dynamical Theory of Sound, London 1931.

M52

FOURTH INTERNATIONAL CONGRESS ON ACOUSTICS
COPENHAGEN 21.-28. AUGUST 1962

Measuring methods for Distinctness in time and Distinctness in frequency in Studio Acoustics.

J.J. Geluk - Netherlands.

For some years the idea has been generally accepted, that the reverberation time of a studio is only one factor determining its acoustic quality. Besides this oldest criterium some other quantities have been introduced like: definition and directional diffusivity. [1] Both factors were introduced in the field of room-acoustics, although the measurements were all done with the aid of single microphones. One may doubt whether the results so obtained could ever be representative for a judgment by a binaural listener. For broadcasting and disc-recording, microphones have to be used and the signals transmitted should have such characteristics that an optimal reproduction may be obtained. In stereophony two signals are responsible for an adequate sound picture, and only these signals should be treated corresponding to the earlier mentioned quantities of "definition" and "directional diffusivity". To avoid confusion the analogon of the term: definition will be named distinctness in time whereas the directional diffusivity finds its counterpart in the apparent diffusivity in the case of stereophonic sound reproduction.

Distinctness in time could be measured in the same way as given for the determination of the "definition" i.e. the energy in 50 msec divided by the total energy, resulting from a short acoustic pulse and measured at the microphone output. Although reasonable in concept, the measurement needs special equipment, apart from the normal studio technique. With the introduction of stereophony coincident microphones and double level-meters are becoming generally available. From a coincident microphone-pair one may be directed towards the sound source, while the other to a large extend cancels the direct sound; by taking pressure-difference type of microphones this condition can easily be met. Level-meters in studio equipment transform the line voltage u into a logarithmic current $i = \log u$; in addition these meters have a peak reading with a small time-constant ($\approx$ 20 msec) whereas the discharge time amounts to 3 sec. [2] Two level-meters, connected to the coincident microphone, deliver currents $i_1 = \log u_1$ and $i_2 = \log u_2$. By taking the difference $i_1 - i_2 = \log u_1/u_2$, one immediately gets the level-difference between u_1 and u_2 being independent from the acoustic power-level of the source. [3]. In stereo sound reproduction the voltage u_1 will belong to the so-called M channel and be fed to both loudspeakers in phase; the other voltage u_2 (S-channel) will represent the indirect sound field only and be fed to the loudspeakers in phase-opposition. Because of the random phase-correlation between u_1 and u_2 , a listener localizes the mainly direct sound (u_1) in the middle between the loudspeakers, while the other voltage gives rise to a completely undirected sound-impression. The level-difference therefore is to some extend a measure for the distinctness of localization, although other factors may also become important. In monophonic listening however only the M channel is available; in the voltage u_1 the same

amount of indirect sound is incorporated as present in the non-connected S channel. In a stationary state the level-difference between u_1 and u_2 directly gives the relative importance in the M-channel alone of the total sound level to the indirect sound level.

For transient sounds the division between these two can either be obtained by taking the signal u_1 only and introducing some sort of gating process or taking both signals u_1 and u_2 as time-functions and comparing both after appropriate transformation. If peak-reading programme-meters are used and properly matched, two time-constants play an important role, namely that of the musical instrument and the reverberation of the studio; the meter integration time is so short that this is of minor importance. The level-difference between u_1 and u_2 , both instruments working in the logarithmic range, shows irregularities if a sound source is suddenly switched on.

In general the transient of u_1 is steeper than that of signal u_2 , resulting in a maximum level-difference between both signals occurring shortly after the switching on of the source and reducing afterwards to the steady-state value determined by the ratio of distance to the source and the reverberation-radius. If a source in itself has a slow transient behaviour this maximum value vanishes corresponding to a poor "definition". Because of the great fall-back time of the programme-meters the mentioned maximum can easily be read-off and it is proposed to call this value (in dB) the distinctness in time (d_t).

In stereophony one would aim at a wide continuous spreading of the reproduced sound originating from the indirect sound field in the studio. To measure this spreading a coincident microphone can be placed at a location free of direct sound. Either a distance large in respect to the reverberation radius may be chosen or as sound source a dipole can be taken. Placing two pressure-difference cartridges under resp. + and - 45° with respect to the "line of sight" one expects the same voltage level for both signals under ideal diffuse conditions. For sine waves however the pressure-gradiënt changes both magnitude and direction in a random way, hence the signal-level difference is a random function of the frequency. Each difference in dB means an apparent angle α of the sound image, according to De Boer. [4], leading to a random function of $\alpha(f)$. In a certain frequency range Δf one may find $n.\Delta f$ times the occurrence of the angle α , n being a function of α and f. For a given frequency the irregularity in spreading Δn is $2/\pi . \int_{-\pi/4}^{+\pi/4} \left| n_{average} - n \right| d\alpha$, while the apparent diffusivity D_S is given by $D_S = 1 - \frac{\Delta n}{n_{average}}$.

Distinctness in frequency.

If a frequency modulated tone is produced in a room, reflections arriving later than the foregoing sound will have a different momentaneous frequency. Vectorial this means that the later reflection vector of the sound-pressure rotates around the primary vector; if the amplitudes of both are comparable the resulting vector shows momentaneous frequencies far beyond the deviation of the frequency modulation. Especially strong separated reflections turn out to be most harmful; for diffuse reflections a cancellation occurs leading to frequencies within the deviation range while moreover the resulting average pressure-amplitude tends to be more smoothly distributed throughout the room. This latter effect is frequently taken as the reason why musicians use "vibrato" but "liveliness" may be another good reason; even in anechoic rooms

"vibrato" improves the fullness of tone.

If however the acoustics superimpose extra frequency-deviation this may result in objectionable phenomena; if e.g. a reverberation device with a poor reflection-rate but otherwise linear frequency-characteristic is taken the sound becomes highly "coloured"[5][6] If we assume a microphone-signal consisting out of a frequency-modulated signal: $\underline{a} = \hat{a} \cos \alpha_a$ and a rather strong reflection with a delay-time τ : $\underline{b} = \hat{b} \cos \alpha_b$ in which $\alpha_a = \omega_o t - \frac{\Delta\omega}{\Omega} \cos \Omega t$, then

$$\alpha_b = \omega_o(t - \tau) - \frac{\Delta\omega}{\Omega} \cos \Omega (t - \tau).$$

The momentaneous frequencies resp. are $\omega_a = \omega_o + \Delta\omega \sin \Omega t$ and $\omega_b = \omega_o + \Delta\omega \sin \Omega(t - \tau)$, thus the vector $\underline{b}$ rotates around the $\underline{a}$ vector-end with an angle-velocity $\omega_b - \omega_a = \frac{d\psi}{dt}$, ψ being the angle between $\underline{a}$ and $\underline{b} = \alpha_b - \alpha_a$. The resultant vector $\underline{m} = \underline{a} + \underline{b}$ forming an angle φ with $\underline{a}$ will have an angle-velocity $\omega_m = \omega_a + \frac{d\varphi}{dt}$. After some calculation one finds $\omega_m = \omega_a + H(d,\psi).(\omega_b - \omega_a)$, in which $H(d,\psi)$ is an angle function of ψ and the reflection factor $d(\tau) = \hat{b}/\hat{a}$:

$$H(d,\psi) = \frac{d + \cos\psi}{d + \frac{1}{d} + 2.\cos\psi} .$$

If ψ varies over a wide range, $\cos\psi$ will reach values of - 1 or $|\hat{H}| = \left|\frac{d}{1-d}\right|$

The momentaneous frequency ω_m will then deviate from ω_o by an amount $\Delta\omega_m = \Delta\omega + 2\,|\hat{H}.\Delta\omega \sin \frac{1}{2}\Omega\tau|$ or $\Delta\omega_m/\Delta\omega = [1 + d(2.|\sin \frac{1}{2}\Omega\tau| - 1)]/(1-d)$. By changing Ω one scans roughly the reflection factor d for $\frac{1}{2}\Omega\tau = \frac{\pi}{2}$ or $\tau_m = \frac{\pi}{\Omega}$, giving rise to $F_d = \Delta\omega/\Delta\omega_m = \frac{1-d(\tau_m)}{1+d(\tau_m)}$. In order ψ to vary over a large angle, $2\frac{\Delta\omega}{\Omega}$ should be kept larger than π or $\frac{\Delta\omega}{\Omega} > \frac{\pi}{2}$.

The number of extreme deviations per period depends on the largest variation in ψ in respect to 2π ; because this variation alternates 4 times per period one finds an average "sequency" of extremities given by $\bar{\omega}_p \approx \frac{4}{\pi} .\Delta\omega \sin \frac{1}{2}\Omega\tau$ or if $\tau = \tau_m$, $\bar{\omega}_p \approx \frac{4}{\pi}.\Delta\omega$.

A criterium for frequency distinctness may be found in the function $F_d = \Delta\omega/\Delta\omega_m$ while varying the rhythm Ω and keeping $\Delta\omega > \frac{\pi}{2}\Omega$.

When this function does not diverge too much from 1 in the region where Ω can be carried out manuelly, on a musical instrument, one may say that the intention of the musician is maintained and kept distinct; if on the other hand the function F_d takes values of 1/2 or less there is evidence that some reflections are preponderant, occurring at $\tau_m \approx \frac{\pi}{\Omega}$, leading to phenomena outside the musician's intention. Normally the deviation $\Delta\omega$ is only a few percent of the

carrier-frequency (e.g. $\Delta\omega \approx 5\%$ of ω_o), while the rhythm Ω lies between 1 and 10. This means that tones above a few hundred cycles per second may give rise to these extreme deviations having a sequency $\bar{f}_p \approx \frac{4}{\pi} \cdot \frac{1}{20} f_o = \frac{1}{5.\pi} f_o$.

The measurement can be performed with rather freely chosen parameters thereby increasing Ω beyond the manuel limits. In this way the continuity and randomness of the reflection-rate may be checked at intervals $\tau_m = \frac{\pi}{\Omega}$ as short as a few milliseconds or for path differences of appr. 1 m. Because accidental phase-relations do not influence the measurement, the method disregards statistical fluctuations but clearly shows non-random irregularities in the soundpressure composition.

The analysing apparatus consists out of a very effective limiter and pulse former. These pulses trigger a constant saw-tooth generator, thus giving a voltage-rise during each period of the microphone-voltage. A display is formed on an oscilloscope having a time base governed by Ω and the triggered saw-tooth voltage as vertical deflection. The lengths of the vertical lines thus are a measure for the momentaneous frequency.

Some typical results will be given during the reading of the paper.

References.

1) Acustica 1956/2. E. Meyer u. R. Thiele: Raumakustische Untersuchungen in zahlreichen Konzertsälen und Rundfunkstudios unter Anwendung neuerer Mess-Verfahren.

2) O.T.M. 1962/1. H.J.v.d.Heide: Een programma-uitsturingsmeter met halfgeleiders.

3) E.B.U.-Review 72-A; April 1962. J.J.Geluk: A direction-meter for stereophony.

4) Thesis Delft 1940. K. de Boer: Stereofonische Geluidsweergave.

5) EBU conference on magnetic recording - Hamburg 1952. J.J.Geluk: Artificial reverberation.

6) Tonmeistertagung - Detmold 1960. M.R.Schroeder and B.F.Logan: "Colorless" artificial reverberation.

N52

FOURTH INTERNATIONAL CONGRESS ON ACOUSTICS
COPENHAGEN 21.-28. AUGUST 1962

Qualitive Study of Transmission Frequency Response

Shuzo Saito And Ryoichi Matsuda

Electrical Communication Laboratory, NTTPC, Tokyo, Japan

Introduction

In telephone transmission system, fidelity of received telephone speech is not necessarily needed, but satisfactory intelligibility of conversation is essential in a reduced frequency band. So it is an important problem to determine the optimum frequency response of the telephone system in the some restricted frequency band. With regard to such a problem, the subjective assessment of transmission quality of the peak response which is usually seen in various transmission apparatus, is studied in this paper.

Model System (I)

The model system studied here is a two-terminal circuit of L, C and R in series. The transmission characteristic related to the input voltage and the flowing charge is simple and the amplitude characteristics are shown in Fig. 1. This is proportional to the terminal voltage of C and could be simulated easily. Resonance frequencies of the simulating circuits are 1000, 2000 and 4000 cps, and in each resonance frequency, the peak heights are set to 0, 10, 20 and 30 dB.

Fig. 1

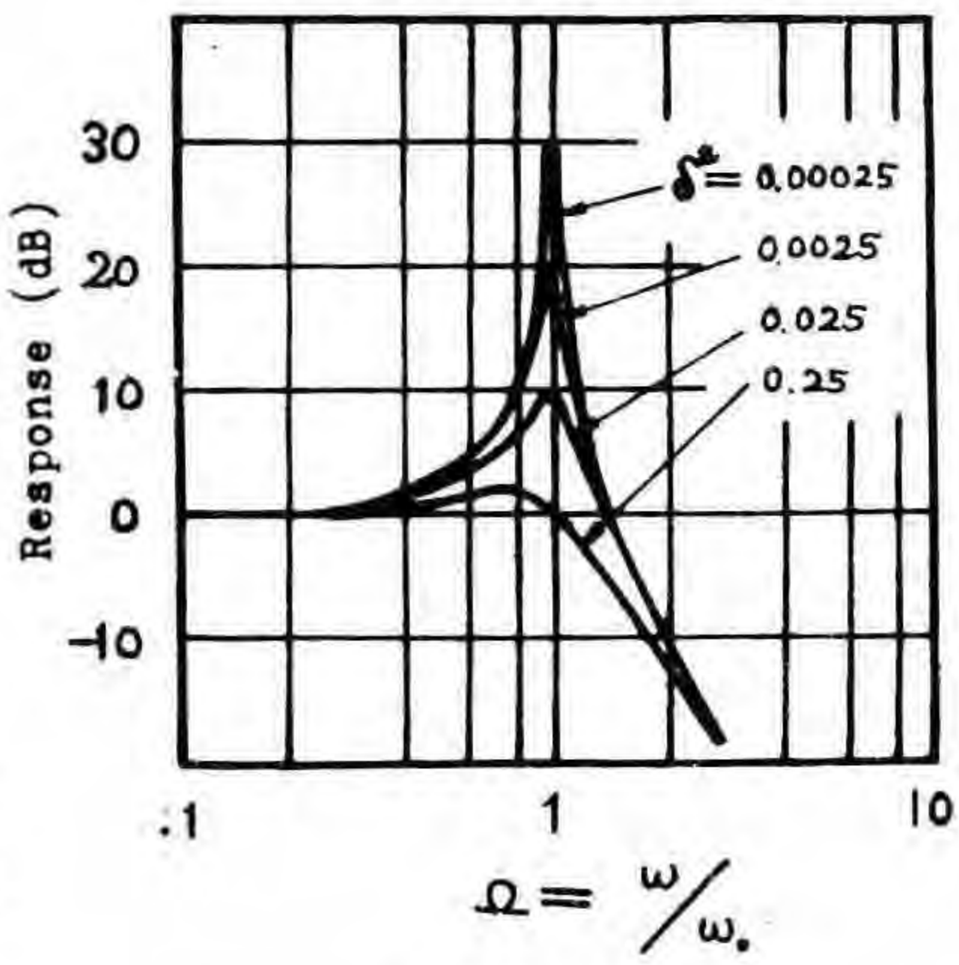

Articulation Test of Model System (I)

Articulation tests were practiced by the use of the Japanese Master Reference System for Telephone Transmission, whose transmitter wasMR-103 condenser microphone and earphones were DR-305 electrodynamic receivers. The response deviation of the reference system in orthotelephonic gain is less than 4 dB within 200~7000 cps frequency region. Twelve kinds of peak response systems were tested in several orthotelephonic gain of 0~-50 dB. Five female adults were engaged in articulation test who were well experienced in such tests. A test syllable list contains 100 kinds of Japanese monosyllables of C-V type.

Results of articulation tests are shown in Fig. 2. It appears that the effect of peak height on the articulation score is most prominent in the case of 1000 cps resonance frequency and in the lower system gain a few peak height is rather preferable, although the flat response is better in the higher system gain. So it seems that the optimum peak height may exist in the region tested here. In the case of higher resonance frequency the effect of the peak height becomes

Fig. 2

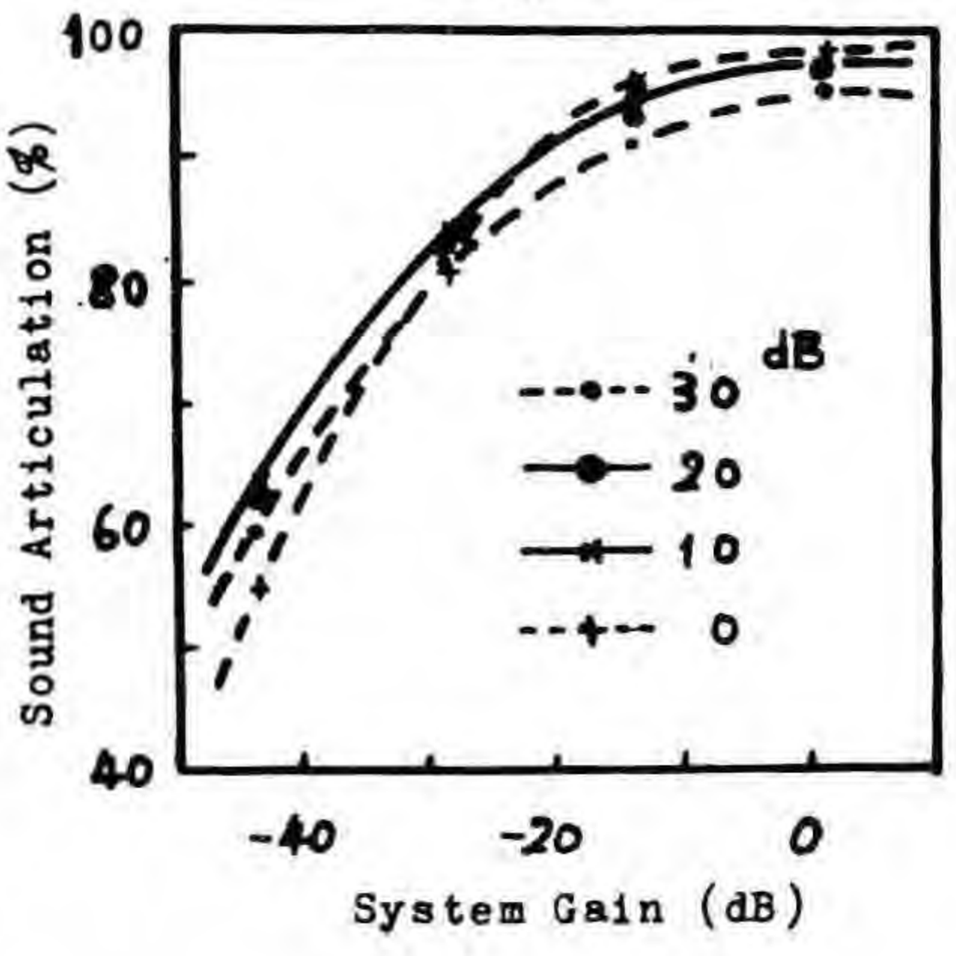

faint, but a few peak height is still preferable.

As a matter of course, higher the resonance frequency becomes, higher the articulation score does in the same system gain. These relation may be well confirmed in Fig. 3, which is represented in equal articulation contours. It shows that the relation between the resonance frequency and the system gain in the equal articulation score is the concave form in general and suggests the existence of the saturation resonance frequency.

By the use of Fig. 3, the optimum resonance frequency of the peak system in the point of view of interpretation aspect can be estimated in various situations. If it is assumed that the sensitivity of earphone is in inverse proportion to the three second power of the upper limit frequency [1], the optimum resonance frequency will lie in the 1500 1700 cps region. It is also shown that the peak height of 10 dB is excellent and is succeeded by that of 20 dB for the 95 % sound articulation, but for the 90 or 80 % sound articulation the peak height of 20 dB is a little better than that of 10 dB. In general, the peak height of 10 or 20 dB is preferable for the articulation score. These results are attributed in quantitative to the effect of enlargement of effective frequency band and the generation of the transient sound. So hereafter the characteristic of the peak system is analyzed more precisely and tested in the tonal aspect.

Fig. 3

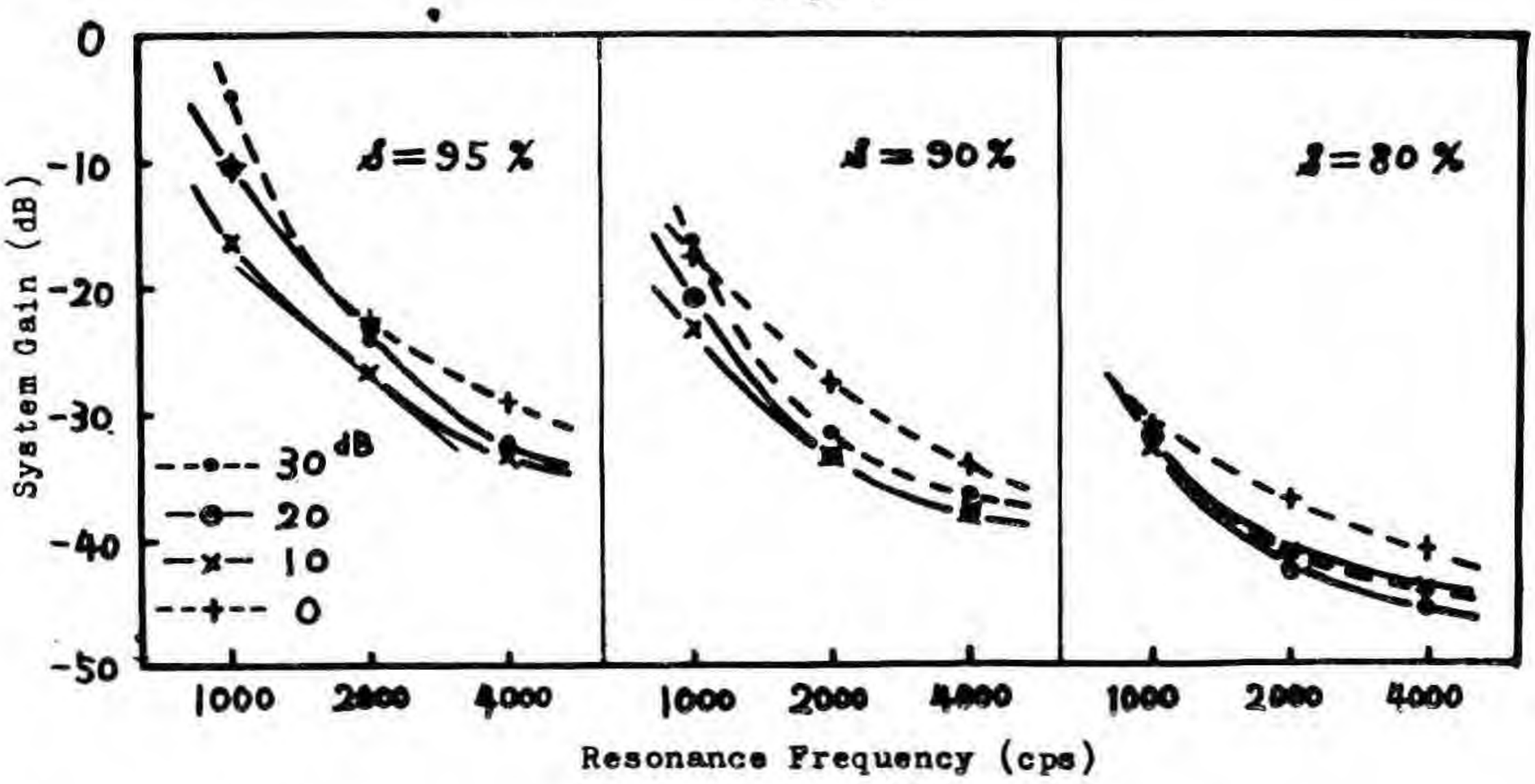

Model System (II)

For the assessment of peak transmission system the tonal differential limen is chosen for scaling which is thought to be more fundamental than the articulation score. Then the model system is replaced with an another one, which is shown in Fig. 4. The peak height of this system is $p = 1 + \Delta\Omega \cdot Q$, where $\Delta\Omega = R/\omega_0 L$, $Q = \omega_0 L/r$. Resonance frequencies tested here are 500, 1000, 2000 and 3000 cps.

Fig. 4

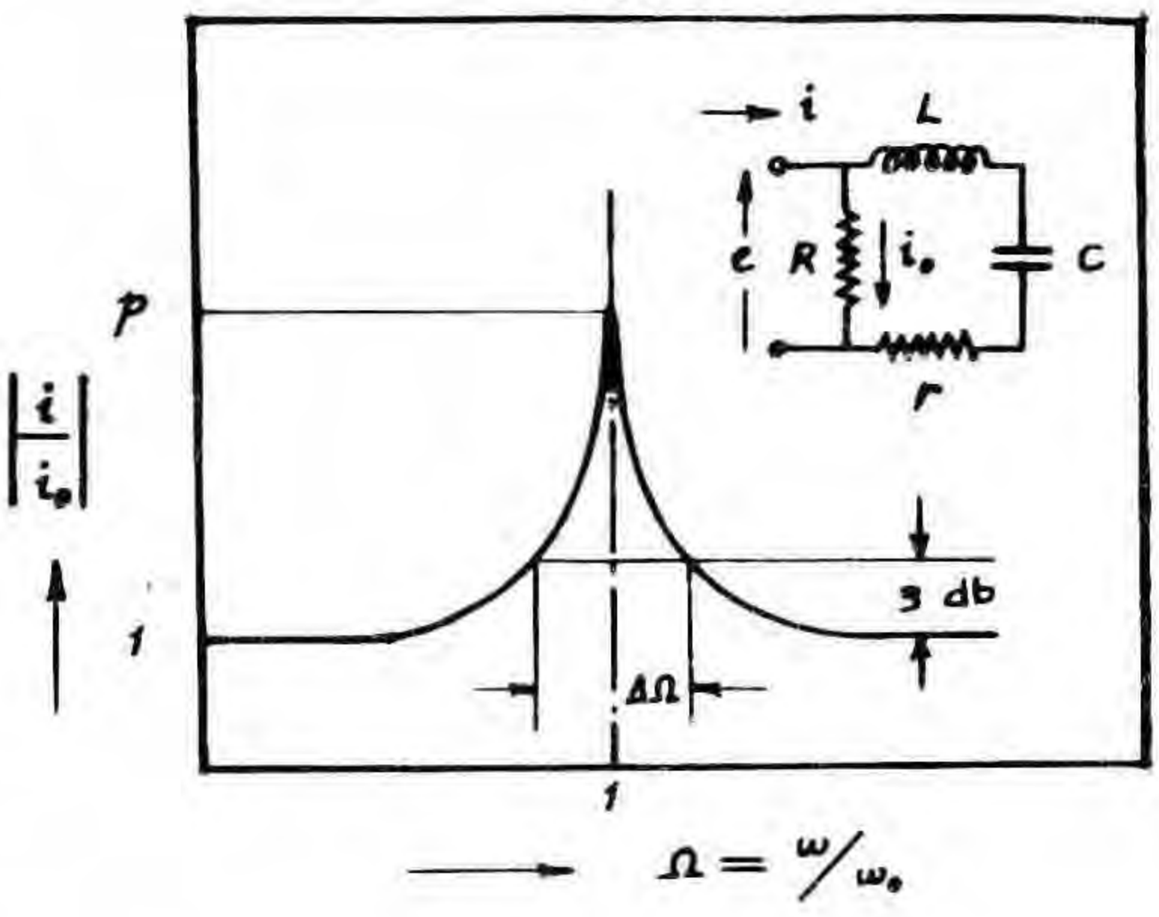

Response of Model System (II) for Speech Signal

Speech or music signal transmitted through the system which contains a lot of peaks is perceived as suffi-

ciently high quality as that of the flat system in many situations. It may be one of the reasons that the dynamic response of the peak system differs from the static one for such signals as speech or music, whose parameters vary in every moment. Fluctuation in speech signal may be divided into the four components and at the first approximation the fluctuating speech signal may be represented by the model tone whose components are in a harmonic relation and those frequencies fluctuate in a constant rate and their intensities exceed the proper threshold levels with some probabilities.

Response of the model system states above for the signal whose frequency varies in a constant rate has reported by several authors in the case of $R=\infty$.[2] Analytical result states that the dynamic response differs from the static one in the peak system of a high Q or in the signal of a high fluctuating rate. The ratio of the flowing current at the resonance frequency in the static response (p_s) to the maximum flowing current in the dynamic response for the signal of the fluctuating rate of h cps^2 (p_h) is shown in Fig. 5. For finite values of R, ratios are measured and illustrated in this figure. In this analysis it is assumed that the transient vibration caused by interruption of the signal has vanished.

As the time constant of the transient vibration is proportional to the logarithmic decrement in peak system, the transient sound which affects the tonal differential limen occurs in the peak system of a high Q and it may be related to the auditory threshold of pused sinusoidal.

Fig. 5

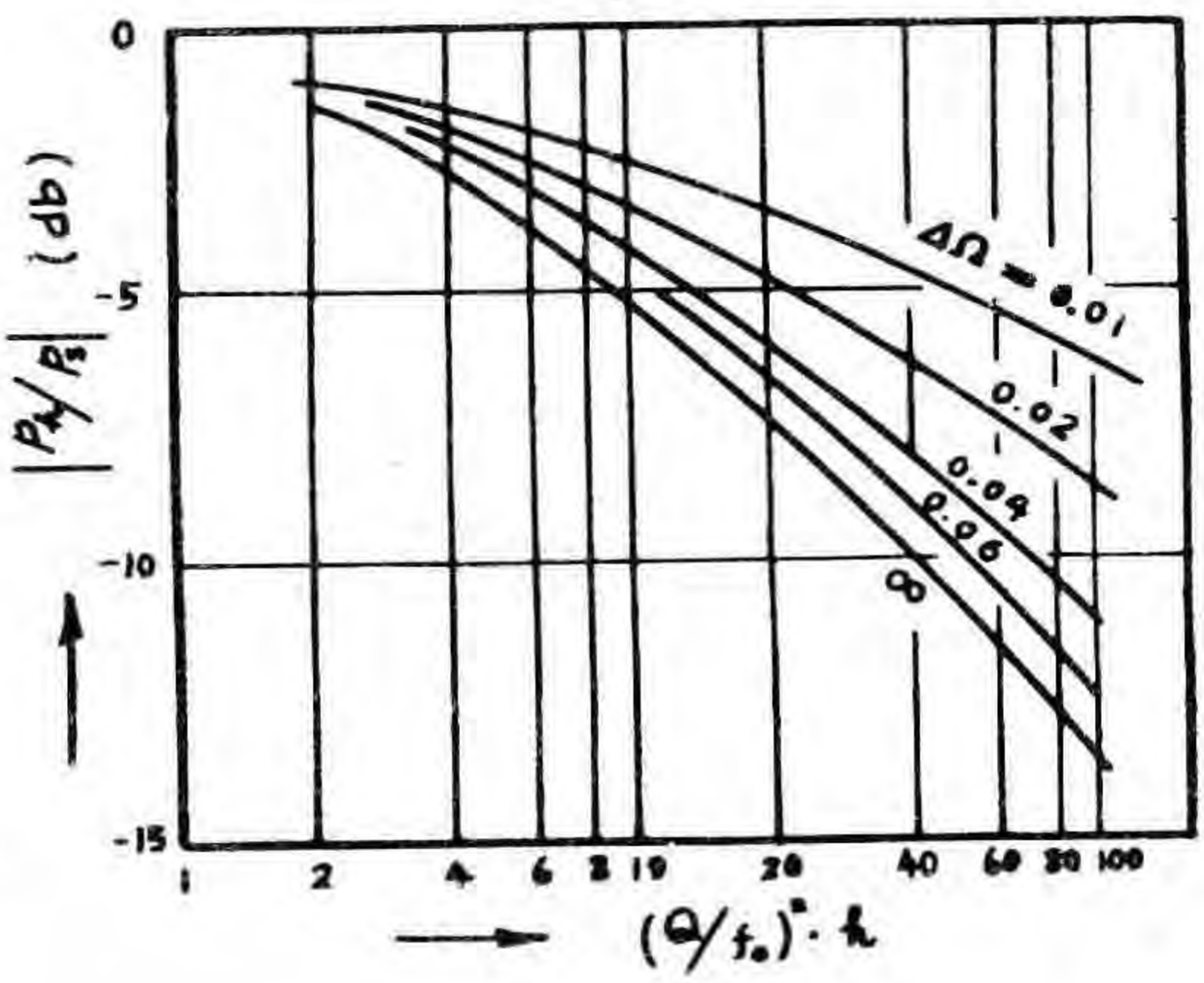

Tonal Differential Limen of Synthesized Sound

The synthesized test sound is composed of 14 sinusoidal waves of equal amplitude in a harmonic relation and its fundamental frequency is 250 cps. The measurement of the tonal differential limen of the peak system was practiced by the use of the reference system described above. Tonal differential limen was determined by the method of constant stimuli, comparing the output of the flat respose system with that of the peak system. Variables of the peak system are the resonance frequency, Q and $\Delta\Omega$. The system gain was fixed to 0 dB in orthotelephonic gain.

Fig. 6

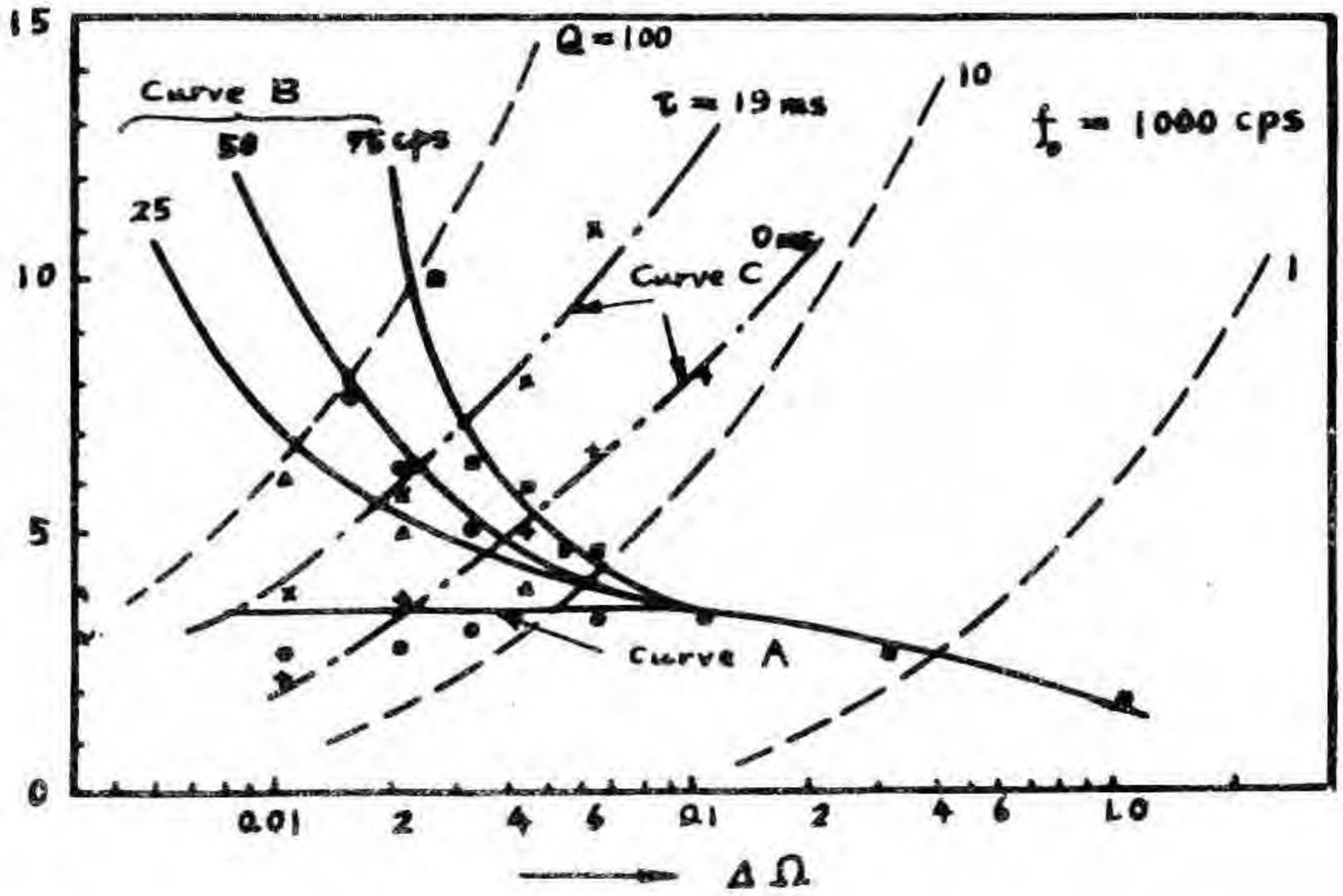

Four femal and four male adults were engaged in this test.

Results of tests are shown in the curve A of Fig. 6. In the case of larger $\Delta\Omega$ the just noticeable peak height approaches to the intensity differential limen of the test tone, but in the lesser $\Delta\Omega$, as the intensity rise in the test tone is restricted to few components near the resonance frequency, the just noticeable peak height increases.

Assuming that the tonal differential limen corresponds to the peak height, the differential limen for the sinusoidal fluctuating tone may be estimated by Fig. 5 and 6. The calculated differential limen is shown in the curve B of Fig. 6.

The steady test tone is fluctuated in frequency by the use of the magnetic tape recorder with a eccentric capstan. The fluctuating tones thus produced are those of a sinusoidal fluctuating rate of 5 cps and of fluctuating widths of 25, 50 and 75 cps in their fundamental frequencies. Results of the tonal differential limen measurements of the fluctuating tones are shown in Fig. 6 for the 1000 cps peak system. Data agree fairly well with the calculated values.

The effect of the interruption was tested in such a case that the interruption rate was 3.3 cps and the time fraction was 0.5. Auditory threshold of the transient sound was measured and is shown in the curve C of Fig. 6. It is found that it accords well with that of the pulsed sinusoidal [3].

The effect of the occurrence probability (α) of the resonance frequency component of the fluctuating test tone was also measured. It is found that as the occurrance probability decreases, the just noticeable peak height becomes larger.

Tonal Differential Limen of Speech

The tonal differential limen of speech was measured and shown in Fig. 7 for the 500 cps peak system. It is seen that the just noticeable peak height for speech signal is composed with the several factors analyzed in the previous section. The occurrance probabilities of the 500, 1000, 2000 and 3000 cps components in speech estimated by the experimental data are 0.83, 0.77, 0.56 and 0.40 respectively.

Conclusion

It is concluded that in the qualitive study of the peak system, the dynamic response should be considered for the signal of speech or music. The reflection of the analyzed factors of fluctuating speech signal to the articulation score is the problem under considerations.

Fig. 7

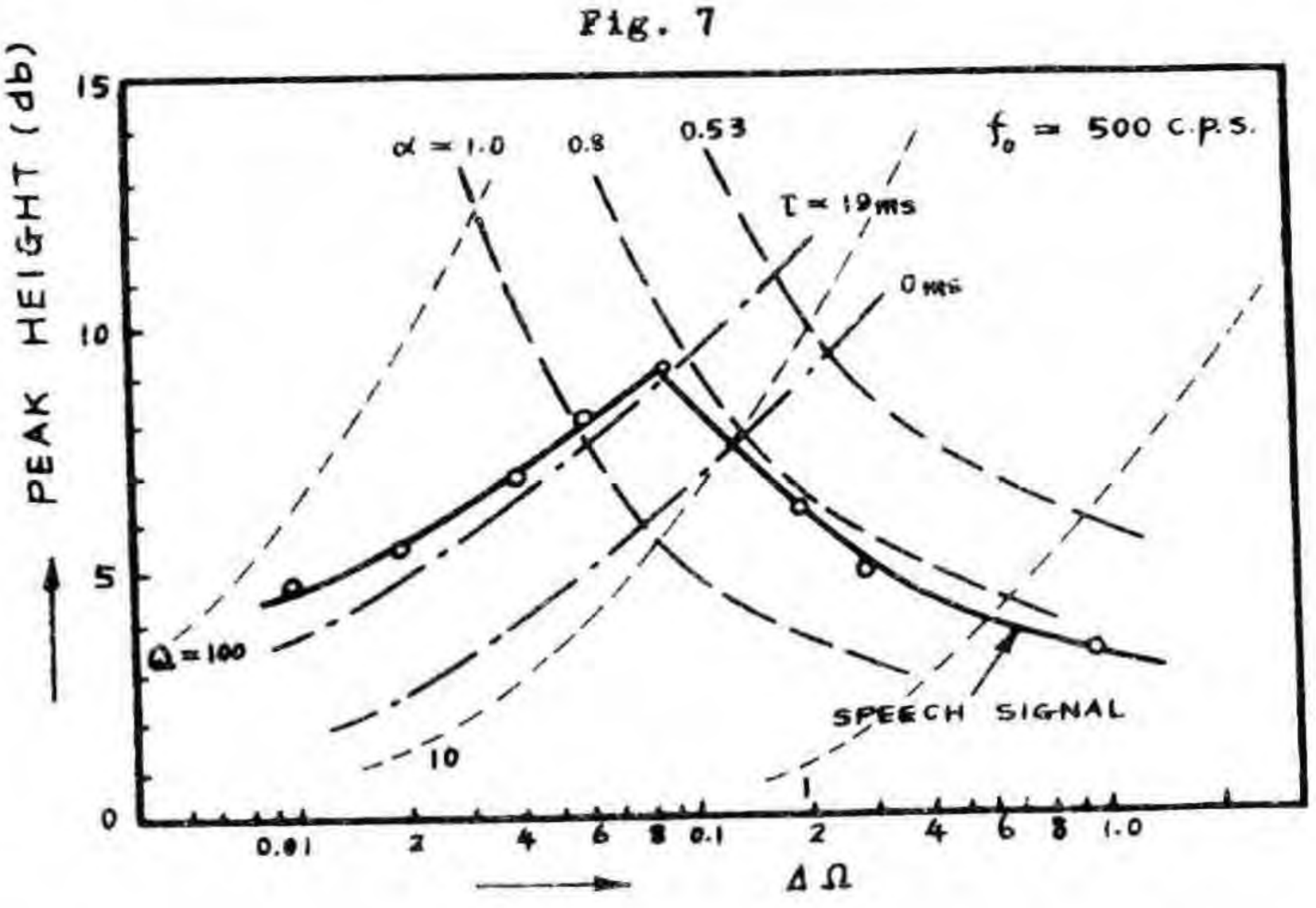

Literatures

(1) K. Masuzawa, E. C. L. T. J., 1, p.129, 1952
(2) N. Yamada & K. Kuriyama, Trans. J. I. E. E. J., 4, p.109, 1943
(3) R. Matsuda, J. I. E. C. J., 45, p.542, 1962

O52

FOURTH INTERNATIONAL CONGRESS ON ACOUSTICS
COPENHAGEN 21.-28. AUGUST 1962

ON ACOUSTIC WAVE PROPAGATION IN HORNS

HANS L. OESTREICHER
Aerospace Medical Research Laboratories
Wright-Patterson Air Force Base, Ohio

The rigorous determination of the sound propagation in horns requires the solution of a boundary value problem of the wave equation. Only for very few shapes of a horn (e.g. conical, hyperbolic, parabolic) can this boundary value problem be solved by the separation of variables, while for other types of horns approximation methods must be used. One widely used approximation method is Webster's horn equation which is derived (Ref. [1],[2]) from the continuity equation of Hydrodynamics under several simplifying assumptions, the effect of which on the degree of approximation is, however, difficult to estimate. Although families of horns have been determined (Ref. [1]), for which Webster's equation may be expected to give a good approximation, no systematic effort has been made to determine the error of the approximation or to improve the Webster solution.

This paper is concerned with an attempt to improve the Webster approximation by considering it as the first step of an iterative procedure for the solution of the exact boundary value problem which, if repeated, leads in further steps to more accurate approximations.

In order to obtain such a procedure, we formulate the problem as a rigorous boundary value problem in the appropriate coordinate system, compare it to Webster's equation and consider the difference between the two as perturbation term.

We begin with the formulation of the rigorous boundary value problem as the first step. If the shape of the horn (Figure 1), which is assumed to be infinitely long and axially symmetric, is described by the equation $y = \pm h(x)$ for $x \geq o$, then the problem is to find a solution of the wave equation

(1) $$\Delta \psi + k^2 \psi = 0$$

with the boundary conditions

$$\partial \psi / \partial n = 0 \qquad \text{for} \qquad y = \pm h(x)$$

$\partial \psi / \partial n$ = normal velocity for $-a \leq y \leq a$, or another surface $x = m(y)$ which represents the membrane M over this circular area (Figure 1), and the radiation condition at infinity.

In order to treat such a problem it is convenient to transform the wave equation (1) to an orthonormal coordinate system containing the horn surface as coordinate surface. Transformation to the coordinates of Figure 1, axially symmetric about the x-axis, is accomplished by

(2) $x = g(\mu, \vartheta)$, $y = f(\mu,\vartheta)\sin\varphi$, $z = f(\mu,\vartheta)\cos\varphi$

Equation (1) transformed to this coordinate system becomes (Ref. [3])

$$\Delta\psi + k^2\psi =$$

(3) $$= \frac{1}{f\cdot f_\vartheta\cdot\sqrt{1+f_\mu^2}}\left[\frac{\partial}{\partial\mu}\left(\frac{f\cdot f_\vartheta}{\sqrt{1+f_\mu^2}}\psi_\mu\right) + \frac{\partial}{\partial\vartheta}\left(\frac{f\sqrt{1+f_\mu^2}}{f_\vartheta}\psi_\vartheta\right)\right] + k^2\psi = 0$$

if we also assume an axially symmetric boundary condition, so that ψ does not depend on φ . The boundary conditions become

(4) $$\begin{cases} \partial\psi/\partial\mu = \text{prescribed on M} \\ \partial\psi/\partial\vartheta = 0 \quad \text{on S} \end{cases}$$

if M and S are orthogonal surfaces, and indices denote partial differentiation with respect to the index. Equations (3) and (4) represent the exact formulation for the problem of sound propagation in an axially symmetric horn.

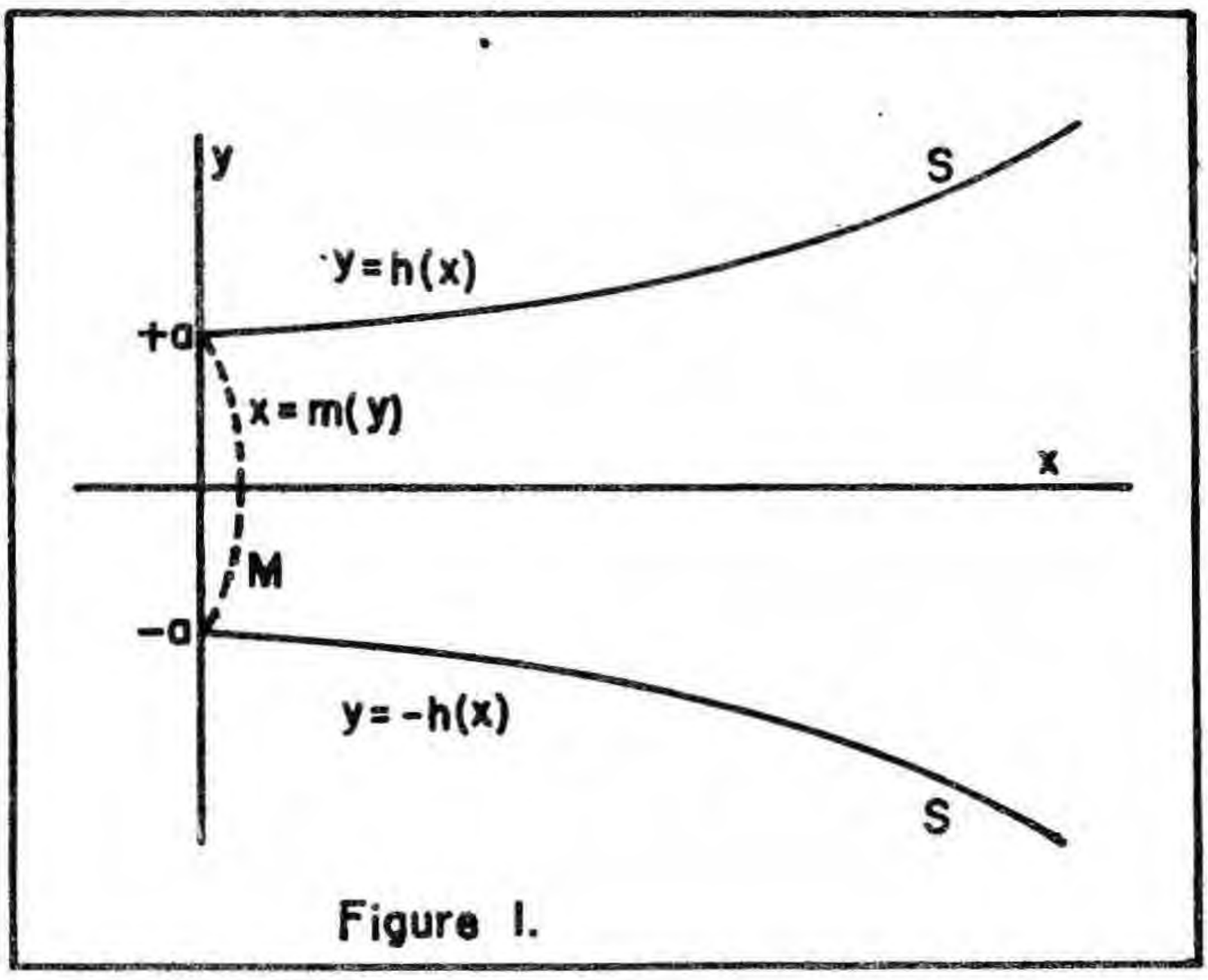

Figure 1.

Compared to this complicated problem the Webster equation is very simple. It is derived (Ref. [1] [2]) under the assumption that the wave motion in the horn is a one-parameter motion, i.e. depends only on the coordinate μ and that the horn does not flare too much over one wavelength. For narrow horns and low frequencies, these assumptions are in general valid. One obtains then, on physical arguments, for the horn of Figure 1

(5) $$W(\psi) + k^2\psi = \frac{1}{h^2(\mu)}\frac{\partial}{\partial\mu}\left(h^2(\mu)\psi_\mu\right) + k^2\psi$$

with the boundary condition

(6) $$\partial\psi/\partial\mu = \text{prescribed for } \mu = 0$$

and an outgoing wave condition for $\mu \to \infty$

Combination of (3) and (5) permits now the formulation of the rigorous problem as an inhomogeneous Webster equation

$$(7) \qquad W(\Psi) + k^2 \Psi = -\left(\Delta \Psi - W(\Psi)\right)$$

with the boundary conditions (6).

Equation (7) already is in a form permitting an iterative procedure by introducing the usual Webster solution on the right-hand side and obtaining improved values by solving the inhomogeneous Equation (7) although it turns out that this form is useful for improving the μ dependence in μ only, with little effect on the ϑ-dependence. For many purposes it is convenient to transform Equation (7) into an integral relation by means of Green's identity and a fundamental solution (Ref. [4]) $g(\mu, \mu_0)$ of the left-hand side of Equation (7).

$$(8) \qquad \Psi = \Psi_W - \int_0^\infty \left[\Delta \Psi - W(\Psi)\right] g(\mu, \mu_0)\, d\mu_0$$

This relation is equivalent to (7) and therefore still a rigorous formulation of the horn problem, obtained without approximation. Equation (8) is, of course, not a solution of the problem because the unknown function appears also on the right hand side, but it can be considered as an integral equation and is suitable for an iterative procedure.

Equation (8) is also useful for a discussion of the influence of various factors on the accuracy of the Webster approximation:

The first term in Equation (8) is an expression involving the boundary values of Ψ .If we have a strictly one-parameter motion, then $g(\mu, \mu_0)$ can be chosen so that this term reduces precisely to the usual Webster solution. The contributions of the second integral can be divided into two parts. The first is

$$(9) \qquad V_1 = \int_0^\infty \frac{1}{f \cdot f_\vartheta \cdot \sqrt{1+f_\mu^2}} \frac{\partial}{\partial \vartheta}\left(\frac{f\sqrt{1+f_\mu^2}}{f_\vartheta}\, \Psi_\vartheta\right) g(\mu, \mu_0)\, d\mu_0$$

which is caused by the fact that the wave motion is not a one-parameter motion in μ and therefore $\Psi_\vartheta \neq 0$. The second part

$$(10) \qquad V_2 = \int_0^\infty \left[\frac{1}{f \cdot f_\vartheta \cdot \sqrt{1+f_\mu^2}} \frac{\partial}{\partial \mu}\left(\frac{f \cdot f_\vartheta}{\sqrt{1+f_\mu^2}}\, \Psi_\mu\right) - W(\Psi)\right] g(\mu, \mu_0)\, d\mu_0$$

originates because the coefficients of the derivatives with respect to μ in the Webster Equation (5) are different from the correct expressions of Equation (3).

If iteration is applied to solve Equation (7) or (8), an error estimate, confirmed by numerical experience, shows that convergence is good if the term V_1 is negligible. This is understandable from a physical point of view because $g(\mu, \mu_0)$ as fundamental solution, or Green's function in one coordinate can improve the solution only in the μ-direction.

In order to design a procedure which improves also the ϑ-dependence, the terms in Equation (7) must be rearranged. Taking

the terms containing the ν-derivatives in $\Delta\psi$ to the left-hand side, gives

$$(11)\quad W(\psi)+\frac{1}{f\cdot f_\nu\sqrt{1+f_\mu^2}}\frac{\partial}{\partial\vartheta}\left(\frac{f\sqrt{1+f_\nu^2}}{f_\nu}\psi_\nu\right)+k^2\psi=-\left[\frac{1}{f\cdot f_\nu\cdot\sqrt{1+f_\mu^2}}\frac{\partial}{\partial\mu}\left(\frac{f\cdot f_\nu}{\sqrt{1+f_\mu^2}}\psi_\mu\right)-W(\psi)\right]$$

If $g(\mu,\nu,\mu_0,\nu_0)$ is a fundamental solution of the left-hand side of Equation (11) this can be transformed again into an integral equation

$$(12)\quad \psi(\mu,\nu)=\int_{H+M}\left(\frac{\partial\psi}{\partial n}g+\psi\frac{\partial g}{\partial n}\right)dS-\iint\left[\frac{1}{f\cdot f_\nu\sqrt{1+f_\mu^2}}\frac{\partial}{\partial\mu}\left(\frac{f\cdot f_\nu}{\sqrt{1+f_\mu^2}}\psi_\mu\right)-W(\psi)\right]g\,dV$$

which looks similar to (8) but is more powerful, however also more complicated than (8) because $g(\mu,\vartheta,\mu_0,\nu_0)$ is more difficult to construct than is $g(\mu,\mu_0)$ and leads to another iterative procedure for its determination.

Again convergence of iteration in Equation (12) is good as soon as we have a fairly good approximation to $g(\mu,\vartheta,\mu_0,\nu_0)$. The convergence for $g(\mu,\vartheta,\mu_0,\vartheta_0)$ depends strongly on the resonance frequencies of the horn, and is much more sensitive than the convergence of Equation (12).

Preliminary numerical calculations have been performed for two types of horns, exponential horns with an angle of opening too large for the Webster approximation and the conical horn with a non-radial motion, as e.g. excited by an axially moving spherical segment. Results of the numerical calculations and comparisons with known solutions (Ref. [5]) will be reported later in detail.

REFERENCES

[1] Morse, P. M., Vibration and Sound. New York, 1948.

[2] Crandall, I. B., Theory of Vibrating Systems and Sound. New York, 1927.

[3] Magnus, W., Oberhettinger, F., Formeln und Sätze für die Speziellen Funktionen der Mathematischen Physik, Berlin, 1943.

[4] Morse, P. M., Feshbach, H., Methods of Theoretical Physics, New York, 1953.

[5] Buchholz, H., Das Schallfeld in einem Kegelhorn unter verschiedenen Anregungsbedingungen, Akustische Zeitschrift, Vol. 5, (1940), p. 13.

P52

FOURTH INTERNATIONAL CONGRESS ON ACOUSTICS
COPENHAGEN 21.-28. AUGUST 1962

MUSICAL IMPLICATIONS OF STANDARDIZED TUNING FREQUENCY

D. W. Martin
The Baldwin Piano Co., Cincinnati, Ohio, U.S.A.

It is more than a century since a frequency of 435 cps was decreed in 1859 for tuning the la (A_4) tone of musical instruments in France. The International Conference in Vienna (1885) set a Continental tuning standard of the same frequency. In 1896 in England the Philharmonic Pitch was lowered to 439 cps at 68° F, with the intent to agree with 435 cps at 15° C, and to compensate for the 4 cps rise in organ flue pipe frequency between these temperatures. (However temperature effects were perhaps irrelevant to an absolute standard, because instruments differ greatly in the magnitude (and even direction) of their temperature coefficients of frequency.)

These agreements were made by men whose experience in music had demonstrated the necessity for a standard tuning reference; and whose knowledge of acoustics implemented the necessity. The physicist Blaserna, who with Boito represented Italy at Vienna in 1885, noted that ". . . the scale of pitch is plainly a musical question, but its introduction should be effected with all the means at the disposal of science." Boito had previously consulted with Giuseppe Verdi, the acknowledged master of Italian opera, who emphasized the necessity for a unified pitch standard (and urged the adoption of 432 cps).

Clearly this was not an attempt by scientists to put the art of music into a straitjacket. Rather it was a joint attempt to provide through science the means by which music could discipline itself in the matter of average reference frequency in musical performance, while allowing those variations around the average value which are needed for artistic, melodic and harmonic purposes.

The result in the fifty years after the Vienna conference was that musicians and musical organizations succeeded in holding their progressive tendency toward higher average pitch to a rise of approximately 5 cps. In comparison to England's Philharmonic Pitch rise of 30 cps between 1813 and 1874, this was real restraint!

In 1939 the International Standards Association meeting in London agreed upon a new standard of 440 cps conforming to modern practice. In 1954 the international standard ISO/TC43 reaffirmed 440 cps. National surveys in many countries reveal that a majority of musical organizations and almost all musical instrument manufacturers intend to conform to the standard. Yet some of the most outstanding concert orchestras in the world deviate intentionally (usually upward) for musical reasons. Some use tuning standards of 444 cps or even higher. The intent of this paper is not to question the practice of raising the average reference frequency, or to argue for conformity. Music is an art. The performance of an artist or of a musical organization is to be judged by musical listeners and critics, not by scientists and engineers as such.

Art is unbounded. Like science, its evolution comes from venturing beyond frontiers. However freedom carries with it some responsibility. For example, in the rendition of classical works musical conductors have a responsibility to the composers of the works they interpret, in all of the musical factors including pitch. And just as the physicists of the last century had a responsibility to provide music with better scientific instruments for tuning musical instruments, the psychophysicists of today have a responsibility to provide modern musical pioneers with the beginnings of experimental knowledge about musical tone and hearing. Eventually this should enable progressive composers, conductors and performers to determine their musical course even more creatively than at present. It is in this spirit that the following questions of possible significance to both music and science are asked. In some cases tentative answers are postulated to help introduce other questions.

1. If the <u>average</u> reference frequency of an orchestral rendition were shifted upward or downward as much as one semitone, would it make an <u>audibly detectable</u> difference to the (a) audience, (b) critics, (c) orchestra, (d) cooperating singers, (e) composer?

To many musicians the answer will seem obviously affirmative, and this is probably a safe assumption for all classes of listeners but the musically naive portion of the audience. However a carefully designed and controlled experiment with rigorous statistical analysis would be enlightening. Preferably the successive orchestral renditions would be identical, with pitch the only tonal parameter. Transposition between successive renditions will not necessarily be sufficient, because of timbre changes in the tones of the individual instruments.

2. Assuming an affirmative answer to question 1, what percentage of a semitone shift in average reference frequency will be <u>just</u> noticeable to each of groups (a) - (c) above? Also what percentage would be considered musically <u>significant</u>?

Detectability and significance are not necessarily the same. From Verdi's 432 to a recent 444 cps is nearly a quarter tone. Continuation of the trend would permit eventual return to 432, along with transposition of keys upward by a semitone.

3. What frequency corresponds to the A4 of musicians with "absolute" pitch? What is the just noticeable difference in their reference tones? If the ability is inherent (not learned) would it be the same in 1962 as in 1862? Are such endowed musicians bothered by having to perform in "fractionally" different keys as a result of variations in standard tuning frequency?

4. When a just noticeable difference is produced by shifting the reference frequency in orchestral rendition, will the listeners identify the difference as one of pitch? Or, if they have been asked whether there is a "difference" (rather than whether there is a change in pitch), will they identify the change with some other tonal attribute such as timbre?

When the reference frequency is increased the purpose may be to obtain a "brighter" timbre, or a more "electrifying" overall performance. Increased pitch as such may not be the audible result but rather the means for achieving it. Perhaps alternative means could be used without shifting the reference frequency.

5. Is there a musically optimum reference frequency, based upon tradition, learning, or absolute origin, or a combination of these? If so, are there good musical reasons why the optimum should change gradually, or in small increments from time to time? If there is no critical optimum, is there an optimum range? If the latter, doesn't an invariant value midway in the optimum range have musical, as well as practical, merit?

All of these questions have been concerned with real orchestral renditions of musical text, not with the single tones or isolated simple musical phrases used by musicologists, physicists, or psychologists, in previous experiments of wide variety. This is not to decry the analytical approach using the basic elements of musical sound. Nor is it intended to cast doubt upon the findings of scientific investigators within the context of their experimental frame of reference. It simply recognizes that (a) the control of trends in reference tuning frequency for orchestras lies with the conductors; (b) the conductors have both the freedom to deviate from standards (even those they have helped to create) and the responsibility for the effects; (c) the most realistic, effective, and influential answers to questions about reference tuning frequency could well come from experiments conceived and executed by orchestra conductors, in consultation and cooperation with the related scientific specialists in knowledge about matter, human beings, and music; (d) the best subject material for the experiments is music itself.

What are the practical impediments to this research approach? What ways and means can be conceived to overcome them?

There may be few conductors who have the interest, the understanding, the patience, or the resources to follow through. However only one is needed, if he has these prerequisites and the ear and the confidence of other conductors.

If real orchestral renditions of musical texts are to be used, how can the experiments afford the manpower for both the rendition and the audition of major musical works? If successive renditions are to be identical except for reference frequency, how can the musicians and instruments perform reproducibly? And if transposition on the musical instruments is to be avoided, in the interests of identical timbre rendition, how can the reference frequency be changed? All three of these questions suggest the substitution of the best possible recording and playback system for live performance. If the time has come when science and technology can reproduce orchestral sounds with sufficient integrity for the experiments, repetitions can substitute for successive identical renditions, saving manpower and eliminating transposition or difficult retuning.

How can the reference frequency be changed without simultaneous change of tempo and timbre (e.g. formant frequency)? Springer's pitch regulator, a magnetic tape playback system which skips (or inserts) very minute portions of tone waves and retards (or advances) the tape transport speed to retain the musical tempo, is capable of changing the reference frequency without altering other musical parameters, at least in principle. Certainly gross changes in pitch by this means would be expected to result in audible degradation of the tone wave. However in the proposed experiments

the frequencies would never be changed more than six percent, and generally the changes would be much smaller. This system appears to overcome a major obstacle to the experiments.

There are no doubt many psychological problems to be solved in the experimental design and the statistical analysis. An example is how to obtain successive answers on question 4 from the same listener without giving inadvertent clues. It may also be necessary to develop techniques for temporary "erasure" of short-term reference pitch memory, for example, by interposing bursts of broad-spectrum noise or combinations of tones purposely tuned to grossly inharmonic or non-scalar frequencies. Listeners with absolute or good relative pitch may be quite resistant to such techniques. These or similar problems may already be solved by the experimental psychologists.

However for the knowledge and techniques of the sciences related to acoustics to make substantial contributions to music, the active involvement of people guiding the artistic destiny of music will be required. This is only one of the areas where such cooperative effort should be fruitful.

G53

FOURTH INTERNATIONAL CONGRESS ON ACOUSTICS
COPENHAGEN 21.-28. AUGUST 1962

Perception of gated Swedish consonants in VC and CV syllables

S.E.G. Öhman, fil.lic. , Speech Transmission Laboratory,
Royal Institute of Technology, Stockholm 70/Sweden

The perceptual role of those acoustical features of the speech sound wave which determine the phonetic identities of linguistic message elements, is a matter of general interest and is furthermore of immediate relevance to many speech communication engineering problems. This paper describes some results of an experiment which was made last year at the Speech Transmission Laboratory of the Royal Institute of Technology in Stockholm[x], and which was designed to examine an aspect of the question just mentioned. The basic reasoning was briefly as follows.

An utterance such as the Swedish nonsense word /aba/ (Fig.I-1a.) may be cut twice into two parts by means of a suitable electronic gating equipment in such a way that the second cut occurs e.g. 20 msec later than the first cut. The part of the utterance which comes before the first cut is here called VC stimulus No.1, and the part after the first cut, CV stimulus No.2. Similarly, the second cut gives rise to VC stimulus No.2 and CV stimulus No.1. That is, the VC stimuli are numbered in the direction <u>with</u>, and the CV stimuli <u>against</u> time. The two stimuli in both the VC and CV pairs obviously differ by what is contained in the 20 msec interval between the two cut points. Now, let a native listener compare the two stimuli in each pair separately. Whatever difference he hears, it must be due to the 20 msec long "difference segment". It is also clear that the <u>difference</u> in perceived quality gives an indication of the role of this difference segment in the original utterance. (The procedure is illustrated in Fig.I-1. Observe that the numbering of segments in the Figure differs from that in the example above.)

If the pair of cut points is allowed to move about within the utterance, then any segment may be studied in this way. Specifically, one may, as was done in the experiment to be described, divide the whole word into adjacent 20 msec intervals and study the perceptual effect of a successive extension of the VC and CV stimuli to include more and more of the intervocalic consonant. Twenty-two words were treated in this way, i.e., all Swedish consonants in position between two short a-vowels, pronounced with the so-called grave accent by one male Swedish talker. The recording was made in an anechoic room. A condenser microphone and an Ampex tape-recorder were used. The experiment was divided into two parts; in the first of these 18 subjects listened to the stimuli of VC character, and in the second, 17 subjects listened to the stimuli of CV character. In both sessions the stimuli occurred in random order, and the subjects were instructed to <u>identify</u> the (respectively, final and initial) consonant. Their choice of response symbols was restricted.

Before the results are discussed it should be pointed out that the role of an arbitrary segment of an utterance is not independent of its surroundings. For instance, the technique outlined above permits the study of the perceptual effect of the first part of the noise interval of an intervocalic voiceless fricative by including and excluding this part in both VC and CV stimuli. This effect turns

---

[x]I wish to express my sincere thanks to Dr. Fant of the Speech Transmission Laboratory, RIT, Stockholm, for the benevolence, interest, and generosity which he has shown me during my work with the thesis summarized here. See further ref.1.

out to be quite different in the two cases; in a VC stimulus the noise segment signals "fricativeness", whereas it adds nothing new to the subjective impression in a CV stimulus.

Every point of truncation in each test word defines two stimuli - a VC stimulus and a CV stimulus - and the experiment associates with each of them a certain response distributuon. The percentage of "correct" responses is one of the many interesting parameters of these distributions, and, for each test word, this percentage changes (usually monotonically) with the time location of the truncation point. Regarding the correct percentage as a continuous "time" function (in the following called the identification function), one may obviously plot two identification curves for each test word, viz. a VC curve and a CV curve. (Fig. I-1b.) The independent variable of the CV identification function is considered to increase with negative time, the VC function with positive time.

On the basis of these functions it is possible to define a measure of "importance" which works as a numerical estimate of the weight of the various segments tested, in their role as determinants of the subjective quality of the consonant. This measure is simply taken to be the derivative of the identification function. Usually, of course, the VC importance of a segment is different from its CV importance.

The motive for this definition is, in brief, that an extension of a stimulus in one or the other time direction by a certain segment causes a change in identification, the magnitude of which depends on how important the added segment is. The derivative is then postulated as the (hypothetical) limiting case when the intervals between the truncation points are made indefinitely short.

Of course, the importance of any given segment, measured in the above manner, does not necessarily have to be the same as its importance <u>inside</u> an untruncated utterance, granted that the latter kind of importance can be given a reasonable interpretation. The proposed measure does give, however, a picture of what parts of the tested words are more important than others.

The importance function is interesting also because there is a close relationship between its maxima and the time location of the acoustical vowel-consonant and consonant-vowel boundaries of the words in the investigated material. The latter boundaries are determined in accordance with the practice common in, for instance, modern studies of duration, and the data show that whenever the importance maxima exist (which is the rule) their time coordinates deviate from the corresponding acoustical boundaries by less than 20 msec on the average. Hence, taking the maxima of the derivative of the identification functions as a sort of perceptual phoneme boundaries we have, by definition, that the perceptual boundaries coincide with the maximally important segments, in the above sense, and, by observation, that the segments of maximum importance generally are located about the acoustical time boundaries.

In some cases the identification functions are not monotone. In the successive addition of segments a point is sometimes reached where the percent correct responses momentarily <u>decrease</u>. Such a dip is usually followed by a strong increase of identification. These dips correspond to cut points at which the truncation effectively changes the identity of the consonant, rather than merely blurs it. The consonants suddenly appearing in this way are all very "similar" to the "correct" ones, and hence, what appears in the correct response curves as an impairment of identification, looks like an improvement in the confusion matrices.

For this reason a systematic analysis of the response errors was also undertaken. This was based on a grouping of the consonants into five larger classes: Voiced, Closed, Sonorant, Anterior, and Peripheral. (For definitions see ref.1.) The percentages of the responses falling in these classes were calculated for each stimulus and then weighted with respect to the number of phonemes occurring in each group. Finally, two matrices were obtained for each test word, one called the VC matrix and the other, the CV matrix. In these the rows represent the above mentioned consonant classes and the columns correspond to the points of truncation in the words. The VC and CV matrices condense the raw data to a form which should serve as a complement to the identification curves, more handy than the unprocessed responses would be.

Space considerations forbid a complete summary of the conclusions drawn by using the two analysis methods outlined in this paper. It must suffice to quote a few reflexions concerning the stops. A more detailed account is to be found in ref.1.

Excepting the VC parts of the words containing labial, dental, and supradental stops, where no perceptual boundaries could be found, the deviation between the perceptual and accoustical boundaries is always within 20 msec. The parts of the formant transitions which terminate in the occlusion interval effect more drastic changes in the identification than the other parts of the transitions.

When the final vowel (together with the burst, if this is present) is separated from a test word containing a voiceless stop, the stimulus obtained sounds like an homorganic voiced stop. Hence, the cues for voicelessness cannot be located in the final vowel. But in all voiceless stop stimuli, except those cut out of /aka/, the information contained in the initial vowel alone caused a correct identification of the non-voicing component only. (The initial vowel of /aka/ caused correct identification of the voicelessness as well as of the place of articulation.) This suggests that in voiceless intervocalic the initial vowel together with the occlusion interval, provides cues for the non-voicing, and the burst and the final vowel contain place and manner cues.

During the inclusion of larger and larger parts of the initial vowel in the VC test, the responses to all voiced stops first fall predominantly into the Voiceless class, but then switch over to the correct, Voiced, class. This Switch-over point occurs near the acoustical boundary. A corresponding (converse) phenomenon does not occur in the words containing voiceless stops. It is inferred that a postvocalic stop (without voice bar) is heard as voiceless if the vowel is sufficiently short, and otherwise as voiced.

References: S.Öhman: On the perception of Swedish consonants in intervocalic position, The Royal Institute of Technology, Stockholm Sweden. Report Np.25, March 1st, 1962. The Speech Transmission Laboratory, Div. Telegraphy-Telephony.

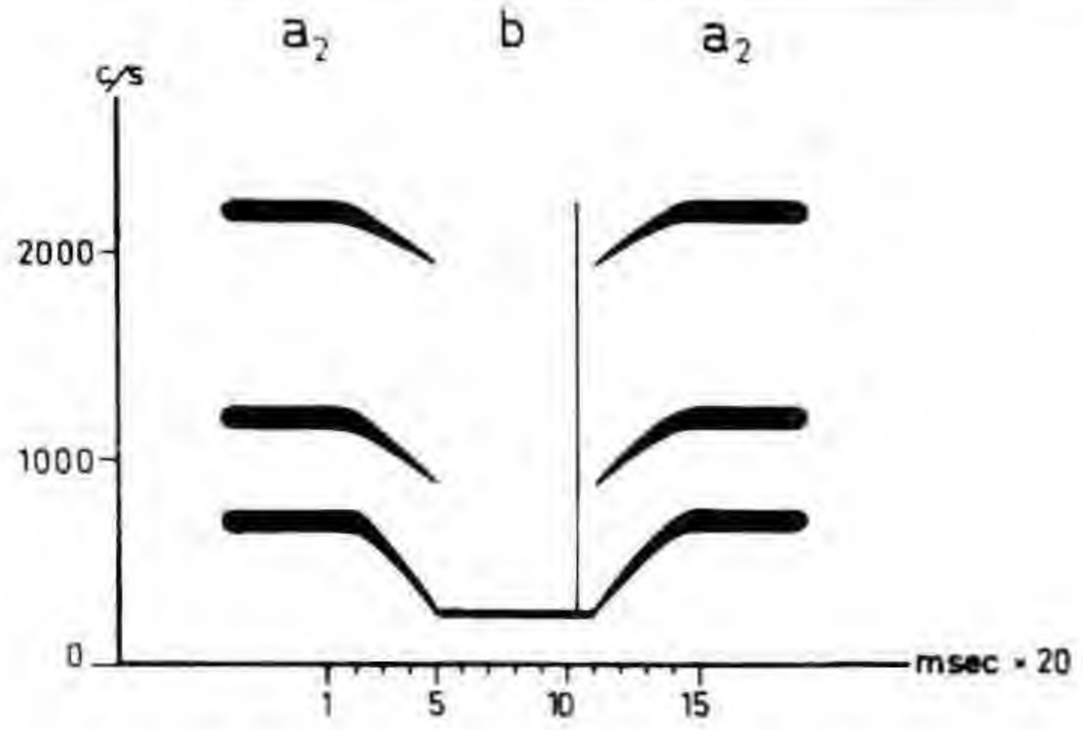

Fig. I-1a. Schematic of stimulus word /aba/.

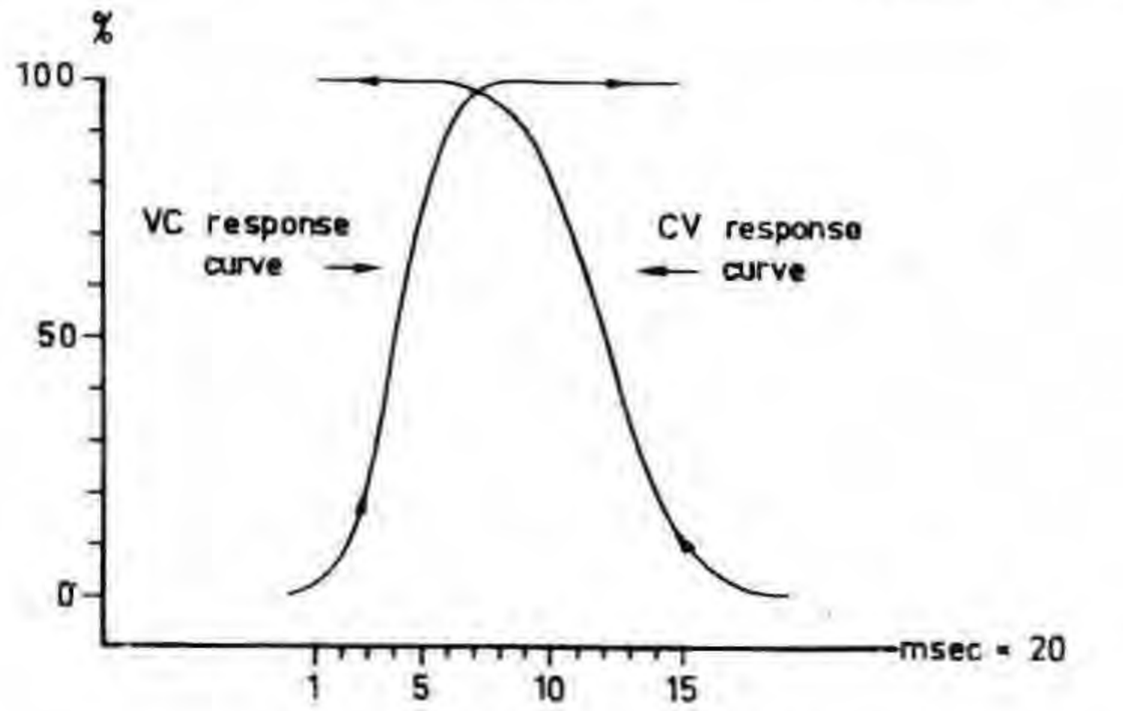

Fig. I-1b. Fictitious correct response curves (VC and CV curves) for /aba/.

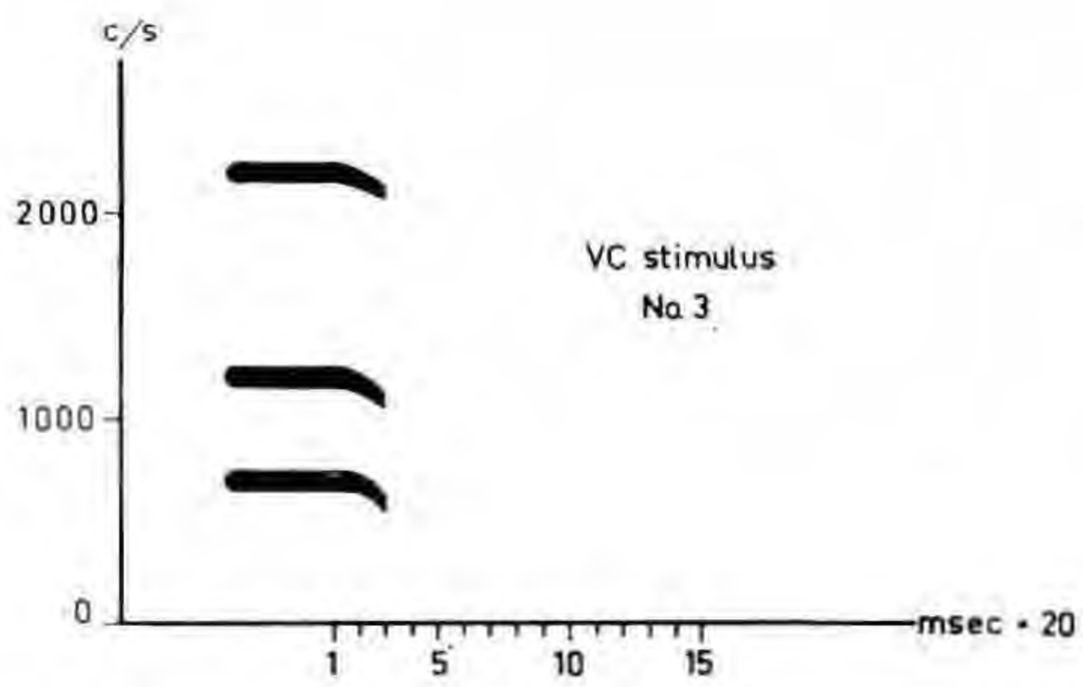

Fig. I-1c.

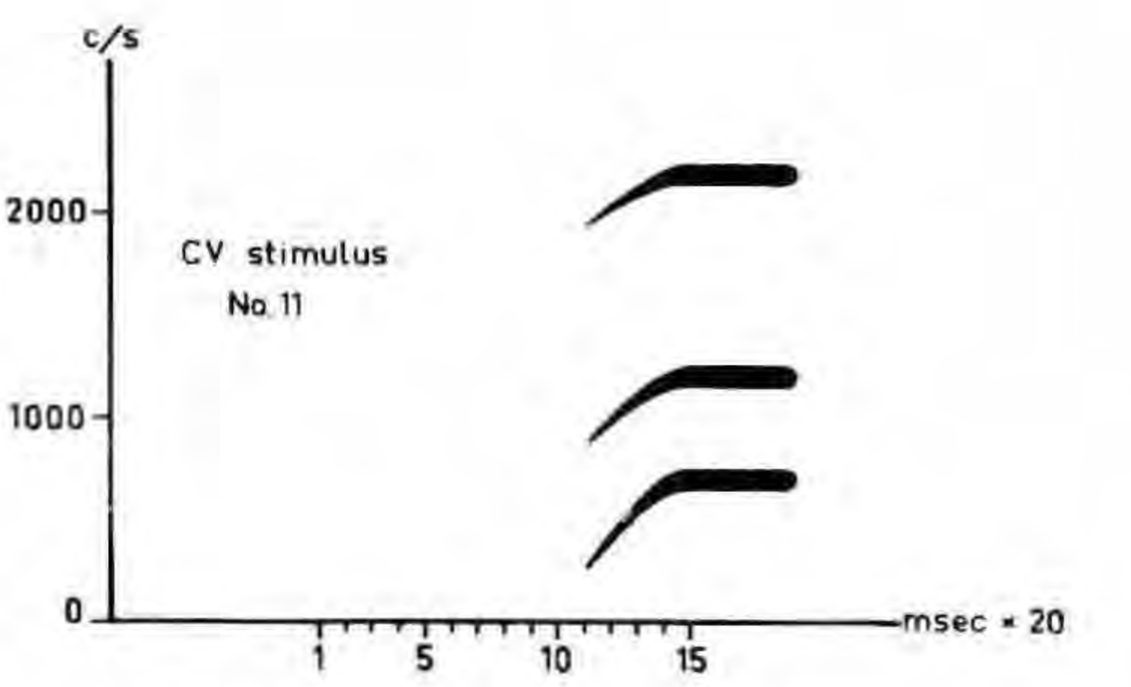

Fig. I-1d.

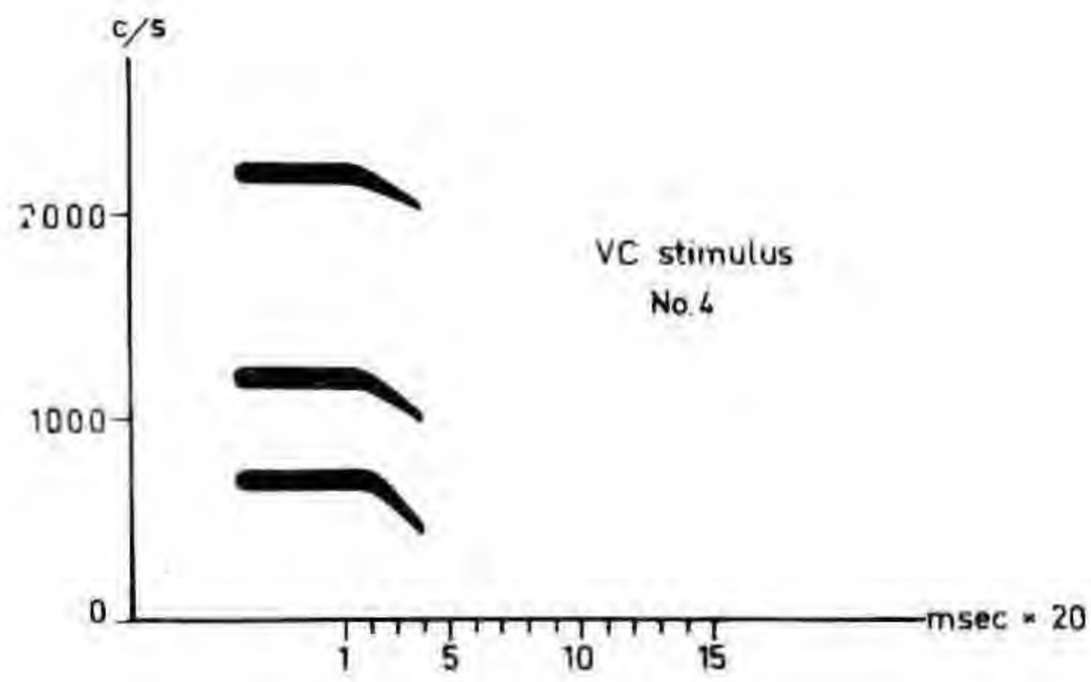

Fig. I-1e.

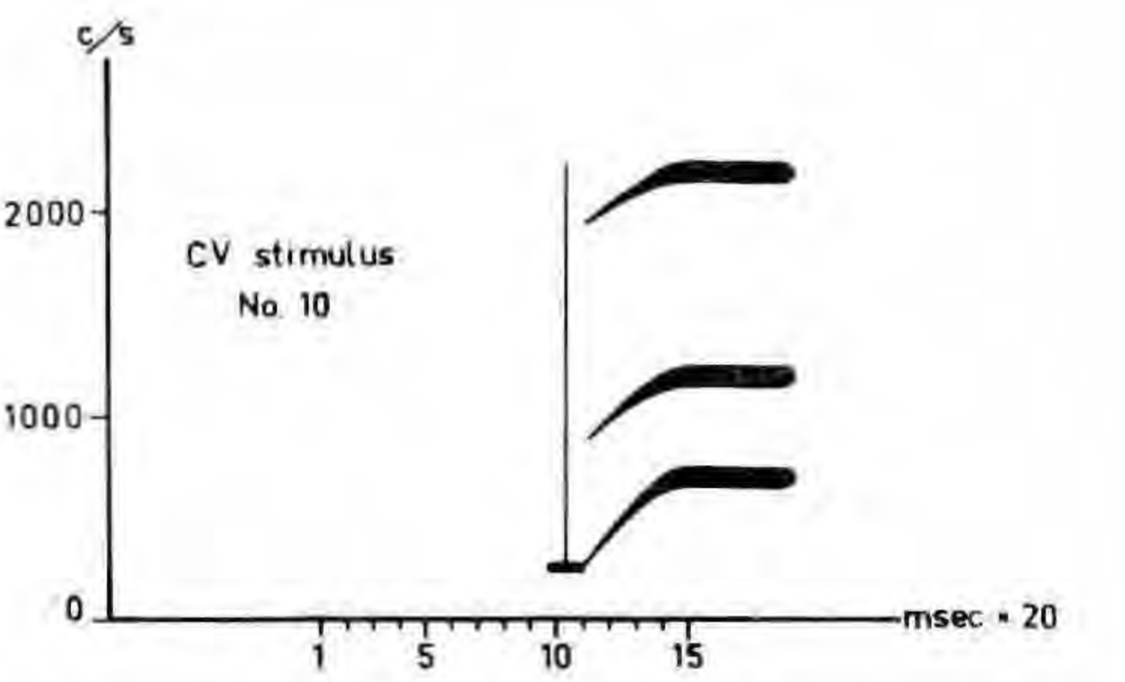

Fig. I-1f.

Fig. I-1. Schematic illustration of experimental procedure. For details, see text.

H53

FOURTH INTERNATIONAL CONGRESS ON ACOUSTICS
COPENHAGEN 21.-28. AUGUST 1962

Loudness Summation in Conductive Deafness*

Bertram Scharf
Northeastern University, Boston, Mass.

Our understanding of the mechanisms underlying loudness summation may be aided by a comparison of loudness summation in normal and abnormal ears. Such a comparison could tell us how loudness summation proceeds as a function of level in ears with high thresholds, with and without loudness recruitment. It may then become clearer why in the normal ear the summation of loudness is greater at moderate sound pressure levels than at lower and higher levels (1). We could also find out whether the critical band (Frequenzgruppe) plays the same role in the abnormal ear that it does in the normal ear where the loudness of a complex sound begins to increase with bandwidth only when the width exceeds the critical band (1,2). This paper provides some answers to these questions for ears showing little or no recruitment but suffering impairment of the conductive mechanism.

Loudness summation was measured for complex sounds composed of four sinusoids, generated by four Hewlett-Packard oscillators (200A/B) and combined in a mixing amplifier. The four tones of the complex were equally spaced around a center frequency of 2000 cps and were usually set equally loud. The over-all spacing, ΔF, between the lowest and highest component frequencies was set at two values, 150 and 280 cps, which are smaller than the critical band and at two values, 1100 and 2200 cps, which are larger than the critical band. (At a center frequency of 2000 cps, the value of the critical band is 300 cps (3).) For each of these values of ΔF, the complex was matched to the tone at levels between 5 and 55 db above threshold. The relative loudness of the complex was measured by having the subject use a sone potentiometer to adjust the intensity of the complex until it sounded equal in loudness to a 2000-cycle tone. Sound stimuli were presented through a single PDR-8 earphone mounted in a Permoflux rubber and chamois ear cushion (No. 1505).

Of the six subjects, three were tested on both ears separately and three on only one ear. Table 1 gives the thresholds of the nine ears tested, as well

Table 1. The Six Experimental Subjects.

Subject	Sex	Age (yrs)	Diagnosis	Threshold in db at 2000 cps (S.L.)
M.B.	F	46	Conductive loss[m]	AD 71.5, AS 73
[illegible]	[illegible]	36	Congenital[s]	AD 73
G.G.	F	31	Otosclerosis[m]	AD 66.5, AS 61
S.H.	F	39	Otosclerosis[s]	AS 44
F.W.	F	42	Middle ear infection[s]	AD 48
E.S.	F	37	Chronic adhesive otitis[m]	AD 41.5, AS 69

m: diagnosis by Mass. Eye and Ear Hospital; s: report by subject; AD: right ear; AS: left ear.

*Research supported by the U.S. Public Health Service (grant B-2223).

as each subject's sex, age, and diagnosis. For each subject, pure-tone thresholds for frequencies from 100 to 8000 cps were measured on a self-recording Békésy audiometer. Measurements of recruitment by binaural and monaural loudness balances were possible in five of the nine ears. Each subject was tested in three or four two-hour sessions. Although hospital records were available for only three of the subjects (for six of the nine ears), the other three subjects gave self-consistent reports of previous medical diagnoses. Most important, none of the subjects showed appreciable loudness recruitment or other signs that would contra-indicate the reported diagnosis. All but one subject have some form of middle-ear impairment. The one exception, P.E., suffers an apparently congenital central loss, but he showed no recruitment, and his results were similar to those of the other subjects.

Figure 1 gives the median results for all nine ears. The difference between the level of the 2000-cycle comparison tone and that of the equally loud

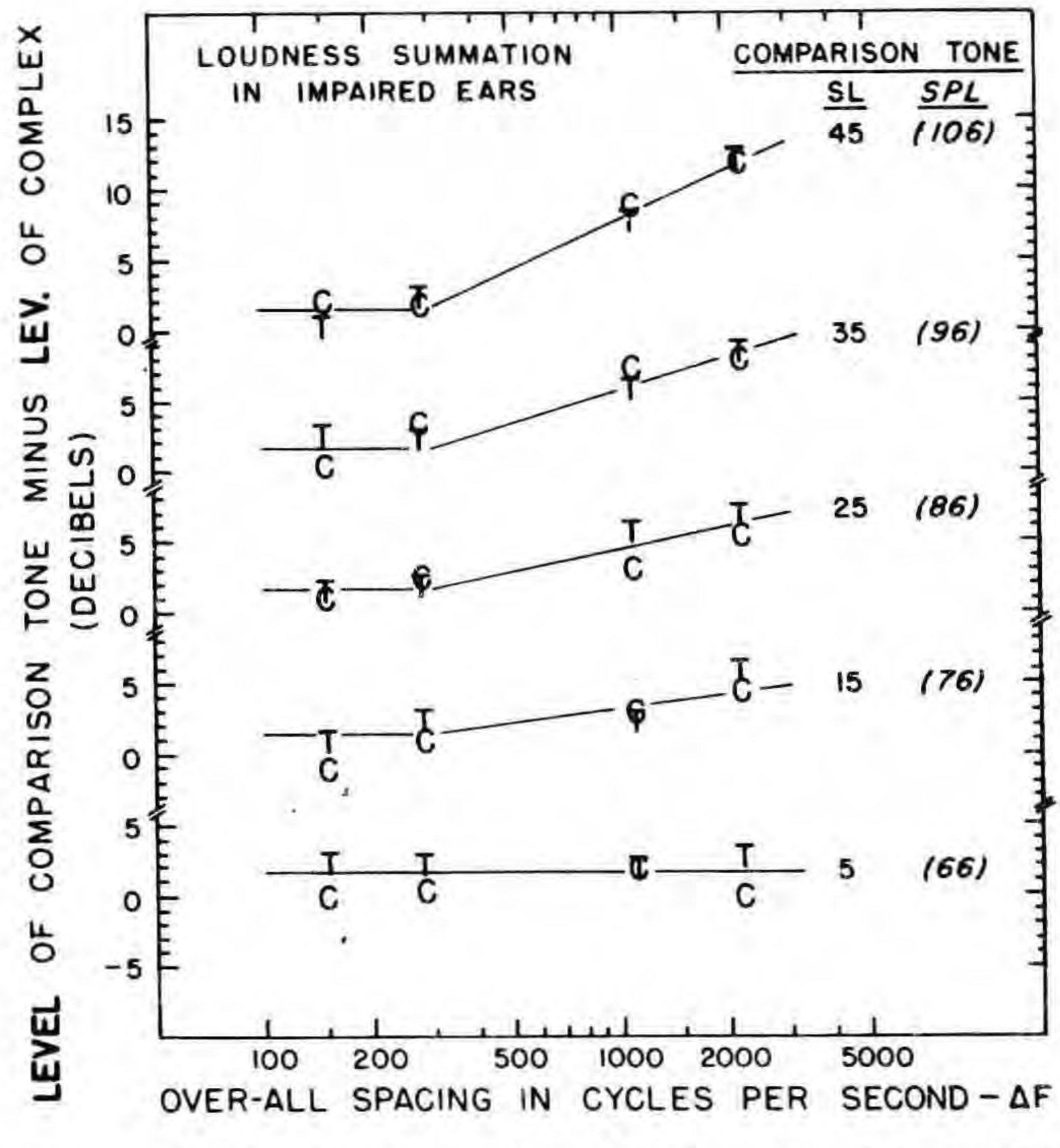

Fig. 1. The change in the loudness of a four-tone complex centered at 2000 cps as a function of the over-all spacing, ΔF. The ordinate shows the difference in "effective" intensity between a 2000-cycle comparison tone and the equally loud complex. The parameter on the curves is the sensation level (SL) and the corresponding median SPL of the comparison tone. Each symbol, T and C, is the median of nine judgments by six subjects with an average hearing loss of almost 50 db. The solid lines are fitted to the data with a break at 300 cps, the value of the critical band.

complex is shown as a function of the over-all spacing, ΔF, of the complex.* Both the sensation level (SL) and the corresponding median SPL of the comparison tone are shown, in decibels, as the parameter on the curves. The symbol C means that the subject adjusted the complex until it sounded as loud as the tone; T means he adjusted the tone. The results are quite clear. The loudness of the complex remains constant as the over-all spacing is increased up to the value of the critical band. At values greater than the critical band the loudness begins to increase with ΔF. As in the normal ear, however, the increase in loudness with ΔF is greater at a moderate sensation level than at lower levels. Near threshold the loudness does not increase at all with ΔF.

The points from Fig. 1 are replotted in Fig. 2 with some additional data at high levels. Figure 2 shows more directly that the course of loudness summation, measured as a function of over-all spacing and sensation level, is quite similar in normal ears and in ears suffering a conductive hearing loss. The present results, given by the symbols T and C, lie very close to the solid lines, which are representative of the results obtained in previous studies with normal ears (4,5). Figure 2 also shows more clearly how the efficiency of loudness summation for a given value of ΔF changes with level.

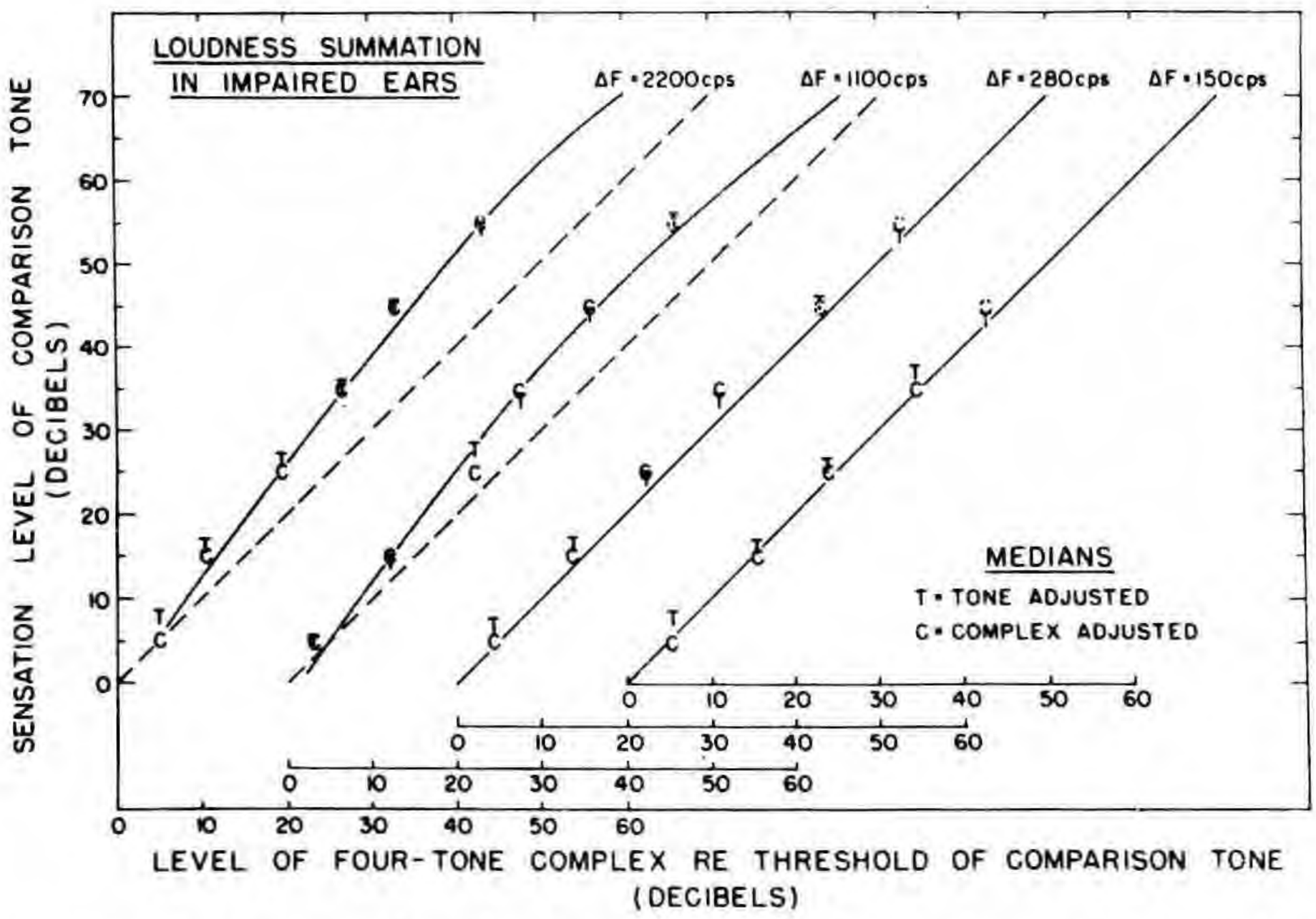

Fig. 2. Loudness summation in impaired ears (experimental points) compared to that in normal ears (solid lines). The ordinate shows the sensation level at which the comparison tone sounded as loud as the complex, whose effective level is given on the abscissa. The parameter on the curves is the over-all spacing, ΔF, of the complex. Solid symbols are the medians of nine judgments; broken symbols of three judgments.

*The values on the ordinate are the differences between the loudness level of the comparison tone and the computed sum of the loudness levels of the four components in any given complex. This measure was necessary because of the highly uneven loudness contours of these impaired ears, which meant that the stimulation values of the components, being highly dependent on frequency, would change with changes in ΔF. As a consequence of this measure, references to intensity often have a somewhat special meaning in this paper.

The efficiency of loudness summation is indicated by the degree to which the experimental points depart from the straight 45° lines. For ΔF less than the critical band, the points lie close to the diagonal lines, indicating that the tone and subcritical complexes (ΔF less than the critical band) were judged equally loud when approximately equally intense. (The diagonal lines for the subcritical complexes are drawn solid since in normal ears a subcritical complex is generally judged equal in loudness to an equally intense pure tone having the same frequency as the center of the complex (2,4).) For ΔF greater than a critical band, the points fall to the left of the diagonals, indicating that the tone and supercritical complexes were judged equally loud when the tone was more intense than the complex. Moreover, the intensity difference between the tone and complex increased as the SL increased up to 45 or 55 db. Accordingly loudness summation may be said to be most efficient at moderate sensation levels for impaired ears, just as it is for normal ears (2).

Several interesting conclusions may be drawn from these data. In both the non-recruiting abnormal ear and the normal ear, the loudness of a complex sound does not begin to increase with ΔF until the critical band is exceeded. Furthermore, the changes in loudness summation with sensation level are the same in the normal and abnormal ears, despite an almost 50-decibel difference in their average thresholds. This finding was expected since in the ears studied here, the middle-ear impairment acted as a simple attenuator that reduced the amount of sound energy reaching the inner ear. That the degree of loudness summation is more directly related to the energy reaching the cochlear than to the sound pressure at the ear drum (or in a 6-cc coupler) is hardly surprising. The next question, however, has a less obvious answer. What happens to loudness summation when no abnormal attenuation reduces the energy reaching the inner ear, but when neural impairment within the inner ear produces a high threshold with recruitment? Loudness summation in such an ear might be expected to look like that in a normal ear exposed to a masking noise (4), since under these two conditions the loudness functions for single tones are very similar. It is thought, however, that the degree of loudness summation depends not only on the loudness functions for the individual components of a complex, but also on the amount of masking or mutual inhibition among these components (1). Not much seems to be known about the masking patterns in impaired ears, so we may be in for some surprises.

Perhaps even more interesting is the question of how loudness summation proceeds in subjects suffering a central hearing loss, without recruitment. If the summation of loudness is completed within the inner ear, then it may be possible in some cases of central deafness to show that loudness summation is similar to normal summation, measured as a function of SPL, i.e., the loudness summation in central deafness would be greatest near threshold.

Now that we have gathered consistent and meaningful data from naive, partially deaf subjects who gave even less variable results (mean interquartile range was 3.4 db) than normal subjects, we may proceed with some confidence to the study of loudness summation in ears that show recruitment and perhaps also in ears where the loss is central in origin. With the data from these ears, we may hope to move closer to an understanding of the psychophysical and perhaps also of the physiological processes underlying the summation of loudness.

REFERENCES

1. E. Zwicker and R. Feldtkeller, Acustica, 5 (1955) 303.
2. E. Zwicker, G. Flottorp, and S. S. Stevens, J. Acoust. Soc. Am., 29 (1957) 548.
3. E. Zwicker, J. Acoust. Soc. Am., 33 (1961) 248.
4. B. Scharf, J. Acoust. Soc. Am., 33 (1961) 503.
5. B. Scharf, J. Acoust. Soc. Am., 34 (1962) 228.

J53

FOURTH INTERNATIONAL CONGRESS ON ACOUSTICS
COPENHAGEN 21.-28. AUGUST 1962

DISLOCATION RELAXATION IN SOME B.C.C. METALS

BORDONI prof. Piero Giorgio - Università di Roma
NUOVO prof. Mario - Istituto Nazionale di Ultracustica - Roma
VERDINI prof. Livio - Istituto Nazionale di Ultracustica - Roma

The resonant frequency and the coefficient of energy dissipation Q^{-1} have been measured for several specimens of niobium, tantalum and molibdenum as a function of temperature between 60 °K and 300 °K. The measurements have been made in the frequency range 18 - 180 kc. s^{-1} for niobium, 19 - 440 kc. s^{-1} for tantalum and 25 - 97 kc. s^{-1} for molibdenum. The specimens are thin circular plates vibrating on their lowest symmetrical modes with one or two nodal circles. The experimental technique is the same which has been used in previous investigations on f.c.c. metals (1). The strainswere generally smaller than 10^{-6}, and non-linear effects have not been detected (2).

EXPERIMENTS

a) Niobium.

When the material is permanently strained by means of an axial compression with a thickness reduction to about 1/2 of the original value a pronounced peak is observed in the dissipation-temperature curve, with a maximum value Q_m^{-1} of the dissipation coefficient of about $400 \cdot 10^{-5}$. The peak shifts toward the high temperatures when the vibration frequency increases as it is shown by the following Table, where T_m is the temperature of the peak, and f_m is the resonant frequency at the temperature T_m.

f_m (kc . s^{-1})	T_m (° K)	Q_m^{-1}
18.62	173.0	$438 \cdot 10^{-5}$
63.73	184.5	404
118.11	193.0	384
174.38	197.6	400

For this shift an activation energy $\bar{W} = 0.26$ eV is computed for the relaxation process. The limiting value $\tilde{\tau}_o^{-1}$ of the inverse relaxation time for very high temperatures is $61 \cdot 10^{11}\ s^{-1}$. The peak is about twice as broad as the peak for a Zener's relaxation effect characterized by a single relaxation time, and there is some evidence of a subsidiary peak at lower temperatures.
An anneal at about 365 °K reduces the peak to less than 1/10 of its value, and at the same time gives rise to a considerable shift toward the low temperatures.

When the material is treated for some hours at about 900 °C in high vacuum the interstitial hydrogen is almost entirely eliminated, and the dislocations are cancelled or made inactive. After this treatment a low temperature run shows very small values of the dissipation coefficient ($Q^{-1} \simeq 1 \cdot 10^{-5}$). Adding hydrogen by an electrolytic treatment introduces only a small peak ($Q_m^{-1} \simeq 10 \cdot 10^{-5}$). It has also

been checked that grinding the specimen with some abrasive material after annealing does not give rise to any appreciable relaxation process. As it happens with f.c.c. metals a pronounced peak can be reintroduced in the annealed and degassed material by a permanent pre-strain. An axial compression with a permanent thickness reduction of about 3% gives rise to a peak as high as that found when the material is strained without previous degassing.

b) Tantalum.

The behaviour of the very pure specimens of this material supplied by the Hynes Stellite Co. is very similar to that of niobium. Pre-straining the material in the as-received condition introduces a relaxation peak in the dissipation-temperature curves. This peak shifts toward the high temperatures when the vibration frequency increases, as it is shown by the following Table. The values of the activation energy ($\bar{W}$ = 0.25 eV) and of the limiting value $\bar{\tau}_o^{-1}$ of the inverse of the relaxation time ($\bar{\tau}_o^{-1} = 18 \cdot 10^{11}$) are near to those found in niobium. As in the last material there is also evidence of a relaxation spectrum and of a subsidiary peak at lower temperatures. A rather different behaviour has been observed in other tantalum specimens having a different origin. In these specimens a permanent pre-strain, however large, rises the dissipation-temperature curve by an amount which is almost independent of temperature in the interval 100 - 300 °K, but does not introduce even the faintest trace of a relaxation peak. The dissipation introduced in this way is not completely stable at room temperature, but it anneals out in several days, the final value of the dissipation coefficient being somewhat higher than the coefficient of the undeformed material. To introduce the dissipation peak already observed in the Hynes specimens in this second kind of tantalum specimens, the material must be first permanently strained and then ground with some abrasive material. However if this type of tantalum is treated for some hours at about 900 °C in high vacuum, its behaviour becomes identical to that of the Hynes material. In this condition only a permanent pre-strain is required to introduce a relaxation peak. Adding hydrogen by an electrolitic treatment or grinding without a permanent strain give rise, as in niobium, to a very low peak. The influence of anneal upon the height of the peak is the same as in niobium.

f_m (kc . s^{-1})	T_m (°K)	Q_m^{-1}
19.14	176.8	$255 \cdot 10^{-5}$
27.18	182.5	276
87.67	196.8	287
440.7	220.8	227

c) Molibdenum.

A permanent pre-strain at room temperature gives rise to a relaxation peak which is less pronounced than those found in niobium and tantalum, owing to a large "background" dissipation which changes in a gradual way with temperature and is due to some other process. The experimental curves obtained show that the activation energy must be very near to that found in niobium (0.26 eV) whilst the value of $\bar{\tau}_o^{-1}$ for molibdenum is possibly somewhat higher that the value computed for the other material ($60 \cdot 10^{11}$ s^{-1}).

CONCLUSIONS

The above experimental results show that the relaxation effect observed in niobium, tantalum and molibdenum is similar in several respects (activation energy, value of $\bar{\tau}_0$, evidence of a subsidiary peak) to the relaxation effect due to the dislocations in f.c.c. metals. Some differences seem however worth of notice:

I) the annealing temperature for the effect in niobium and tantalum is lower than in f.c.c. metals; the difference is still more evident when the reduced temperature are considered (ratio of the annealing temperature to the temperature of melting);

II) the relaxation spectrum is narrower in niobium and tantalum than in f.c.c. metals;

III) the values of the activation energies for the three b.c.c. metals are very near to each other and somewhat higher than those found for f.c.c. metals; moreover the latter values are spread over a wider range.

The experiments on the degassed specimens of niobium and tantalum show that the effect cannot be due to an interaction of dislocations and hydrogen atoms, as it has been suggested (2). The effect seems to be due to the dislocations alone, and the theory which fits best the experimental evidence presently available is that due to Seeger and collaborators (4). However it may not be excluded that other imperfections (divacancies or interstitial atoms different from hydrogen) play a role in determining the width of the relaxation spectrum and the annealing temperature.

The anomalous behaviour which has been observed in some tantalum specimens; may also be explained by an interaction of this type.

REFERENCES

(1) P.G. BORDONI, Nuovo Cimento, 4, 177 (1947); P.G. BORDONI, M. NUOVO and L. VERDINI, Nuovo Cimento, 14, 273 (1959). For a review of the experimental methods see: M. NUOVO, Ricerca Scientifica, 31, (II-A), 212 (1961).

(2) Low-temperature relaxation peaks have been observed by several A.A. without any attempt to measure the fundamental parameters of the effect or to investigate its structural causes; see for instance J.W. MARX, G.S. BAKER and J.M. SIVERTSEN, Acta Met., 1, 193 (1953); L.J. BRUNER, Phys. Rev. Letters, 3, 411 (1959); R.H. CHAMBERS and J. SCHULTZ, Acta Met., 8, 585 (1960); L.J. BRUNER, Phys. Rev., 118, 399 (1960); R.H. CHAMBERS and J. SCHULTZ, Phys. Rev. Letters, 6, 273 (1961).

(3) See also P.G. BORDONI, M. NUOVO and L. VERDINI, Phys. Rev. 123, 1204 (1961).

(4) A. SEEGER, Phil. Mag., 1, 651 (1956); H. DONTH, Zeits f. Phys., 149, III (1957); A. SEEGER, H. DONTH and P. PFAFF Discussions Faraday Soc. 23, 19 (1957). For a review of these theories see also: W. P. MASON, Physical Acoustics and the Properties of Solids (New York, 1958) p. 266- 271; P. G. BORDONI: Resonance and Relaxation in Metals (American Society for Metals, Chicago 1962) VI, Dislocation Relaxation at High Frequencies or by the same A. Nuovo Cimento, Suppl. 17, 43 (1960). More recent theories of dislocation motion and of their influence upon relaxation effects have been given by J. LOTHE and J. P. HIRTH, Phys. Rev., 115, 543 (1959); A. D. BRAILSFORD, Phys. Rev. 122, 778 (1961); J. LOTHE, Phys. Rev. 117, 704 (1960).

K53

FOURTH INTERNATIONAL CONGRESS ON ACOUSTICS
COPENHAGEN 21.-28 AUGUST 196[illegible]

A New Variational Method for Ray Path Calculations

Ralph R. Goodman

SACLANT ASW Research Center, La Spezia, Italy.

In the various fields of physics the development of variational techniques for approximate solutions is considerable[1]. No effort seems to have been made to develop similar methods in ray acoustics although its basis is a variational principle. In this paper a small effort is made in this direction with the derivation and application to ray tracing of a variational method developed by Luttinger[2] for classical mechanical one dimensional vibrating systems. The method is useful for approximating quickly certain points along ray paths. The derivation is given in the section below, followed by a section containing a few simple applications. A discussion of the use of the method along with some general comments on the analogous mechanical problems are given in the last section. The entire discussion is limited to the two dimensional case of a sound channel in which the velocity C is only a function of one coordinate (depth in the sea water case, height in the atmospheric case).

I. Derivation of the Variational Method

From Fermat's principle, that the function

$$T = \int_{(x_0,y_0)}^{(x_1,y_1)} \sqrt{1+y'^2}\, C^{-1}(y)\, dx \qquad (1)$$

be an extremum between (x_0, y_0) and (x_1, y_1), Snell's law

$$C(y)\sqrt{1+y'^2} = \text{constant} \qquad (2)$$

is easily obtained[3]. Horizontal and vertical coordinates are given by x and y respectively. The symbol $y' = dy/dx$. The basic problem in ray tracing is to find $y(x)$ for a given $C(y)$ and initial conditions x_0, y_0, y_0'. The exact $y(x)$ is known only for a few simple functions $C(y)$. Due to the generally complicated nature of $C(y)$ found for realistic cases approximation methods are used[4]. All

/ of .....

of these methods approximate the velocity profile by segments of curves for which the solution $y(x)$ is known. There is, with an extremum principle, another possibility. A trial function $y(x, A_0, A_1, \cdots A_n)$ with a set of parameters $A_0, \ldots A_n$ may be used and the extremum condition used to find the best set of values of $A_0, \cdots A_n$. This is essentially the method used here. Using Fermat's principle, however, (x_0, y_0) and (x_1, y_1) must be given. Normally in ray tracing x_0, y_0 and y_0' are known. Thus Eq.(1) is not the proper form for this approach since it is easily shown that it is not an extremum in (x, y_1). Another function is easily found which is an extremum in the final position as well. For the purpose of simplicity the source of rays will be taken at $x_0 = y_0 = 0$ and the point (x, y_1) will be taken to be $x_2 = L, y_2 = 0$, the distance at which the ray again crosses the axis. By subtracting a term from (1) a new extremum is found

$$U = \int_0^L dx \left\{ \frac{\sqrt{1+y'^2}}{c(y)} - \frac{1}{c(0)\sqrt{1+y_0'^2}} \right\} \tag{3}$$

which is very useful for finding the approximate value of L. This may be seen as follows: call the exact solution of the ray y_e, the distance at which it crosses the axis L_e, and the trial solution $y(x, L, A_1, \cdots A_n)$. For the trial solution U may be written as

$$U = \int_0^L dx\, \tau(y, y') - \frac{L}{c(0)\sqrt{1+y_0'^2}} \tag{4}$$

where τ abbreviates the integrand in Eq.(1). Expanding τ in a Taylor series about y_e and y_e', partially integrating and using the general techniques of variational calculus it is possible to show that U given above differs from the exact expression by terms of order $(L - L_e)^2$, thus it is an extremum for variations in L. The procedure for finding an approximate solution is then

(1) Choose some function $y(x, L, A_1, \cdots A_n)$ as a "guess".
(2) Solve for U
(3) To find the best choice for $L, A_1, \cdots A_n$ use the conditions that

$$\frac{\partial U}{\partial L} = 0$$
$$\frac{\partial U}{\partial A_i} = 0 \qquad i = (1, 2, \cdots n)$$

must be satisfied. Some sample calculations of L will be given in the next

/section .....

section.

II. Application of the Variational Method for Predicting L.

As a first example a linear velocity gradient is considered. The distance L may be found by simple trial functions. Using $C = C_0(1+\alpha y)$, U may be written, by symmetry considerations as

$$U = \frac{2}{C_0}\int_0^{L/2} \frac{\sqrt{1+y'^2}}{C(y)}\,dx - \frac{L}{2C_0\sqrt{1+y_0'^2}} \tag{5}$$

using the trial function $y = y_0'x$ and taking $\frac{\partial U}{\partial L} = 0$ leads to the necessary condition that $L = \frac{2}{\alpha}y_0'$ which is the exact result[5]. Obtaining exact results is unusual. For example the choice $y = \frac{L}{\pi}y_0' \sin\frac{\pi x}{L}$ for small angles $\theta_0 = \tan^{-1}y_0'$ (with respect to the horizontal gives the approximate result $L = \frac{3\pi^2}{16}\frac{y_0'}{\alpha} = 1.851\frac{y_0'}{\alpha}$ Additional terms with more parameters may be taken to obtain more accuracy.

For the simplest trial function $y = y_0'x$ an expression is easily obtained for arbitrary $C(y)$. Suppose

$$C(y) = C_0(1+f(y)) \tag{6}$$

The condition for L derived from $\frac{\partial U}{\partial L} = 0$ is

$$f\left(y_0'\frac{L}{2}\right) = y_0'^2 \tag{7}$$

For the case $f = \beta^2 y^2$ the value of L is approximated by $L = \frac{2}{\beta}$ in satisfactory agreement with the exact result[6] in the small angle $L = 2.222/\beta$. More complicated profiles may be calculated in the same manner. Space does not allow the presentation here. These results will be discussed at the Congress.

III. Discussion

The method presented above allows the calculation of only certain points with any accuracy. It is especially useful in finding crossover points L and maxima (or minima) along ray paths. These are clearly at $x = \frac{L}{2}$, y being fixed from Snell's Law for the condition $y' = 0$. It does not therefore replace present ray tracing methods but supplements them with a rapid approximation of a few points along the ray path. Just like all of the methods used in ray tracing, more accuracy may be obtained at the expense of more work. A thorough

/ discussion ...

discussion of the accuracy of the method is given by Luttinger for mechanical systems. It may be shown in the limit of small angles θ_o and under the condition $f(y) \ll 1$ in Eq.(6) that the equations above reduce to the form of the mechanical case. This is not surprising since it has been shown elsewhere[6] that Snell's Law under these approximations reduces to

$$\tfrac{1}{2} y'^2 + f(y) = \text{constant} \qquad (8)$$

ignoring higher order terms. In this limit, then, any of the techniques used in analysis in classical mechanics should hold. The extension of the method to additional parameters and to more complicated forms of $f(y)$ will be presented at the Congress.

List of References

1. c.f. Morse, P.M. and Feshbach H. Methods of Theoretical Physics. McGraw-Hill Book Company (1953) Chapter 9 and reference list at the end of that chapter.

2. Luttinger, J.M. and Thomas, R.B. Jr. J. Math. Phys. 1. (2) (1960).

3. Officer, C.B. Introduction to the Theory of Sound Transmission McGraw-Hill Book Company (1958) Chapter 2.

4. Pedersen, M.A. J. Acoust. Soc. Am. 33 465 (1961).

5. Reference 3 page 60.

6. Goodman, R.R. and Duykers, L.R.B. J. Acoust. Soc. Am. 34, No.6. (1962) (To Be Published).

L53

FOURTH INTERNATIONAL CONGRESS ON ACOUSTICS
COPENHAGEN 21.-28. AUGUST 1962

QUIETENING A CYCLONE EXTRACTOR TO REDUCE COMMUNITY ANNOYANCE

by A.F.B. Nickson

Division of Building Research, C.S.I.R.O., Melbourne, Australia

Summary: Noise from a cyclone extractor annoyed a residential neighbourhood but no information was available on how such systems could be quietened. The system was broken into sections and the effect on the noise measured as each part was removed. Noise-reducing techniques were applied to the offending components, and the annoyance to the community was reduced.

A mill exhaust system consists of a main suction pipe and necessary branch pipes from each machine, leading to the inlet of a fan. A discharge pipe leads from the outlet of the fan to a cyclone collector which separates the solid material from the conveying air. Such systems are used for collection of wood shavings and often require fan units of considerable power. These units create a large amount of noise at frequencies related to the speed and number of blades of the impeller, thereby producing a characteristic whine. Neighbours usually complain of this noise, and this paper describes one manner in which such a system was treated to make it acceptable to the surrounding neighbourhood. The sound level measurements have been compared with the suggestions of section 4 of the report[1] produced by Technical Committee 43 of the International Organization for Standardization, and were found to agree satisfactorily with the proposal that noise ratings with respect to annoyance may be made with readings taken with the "A" scale weighting of sound level meters.

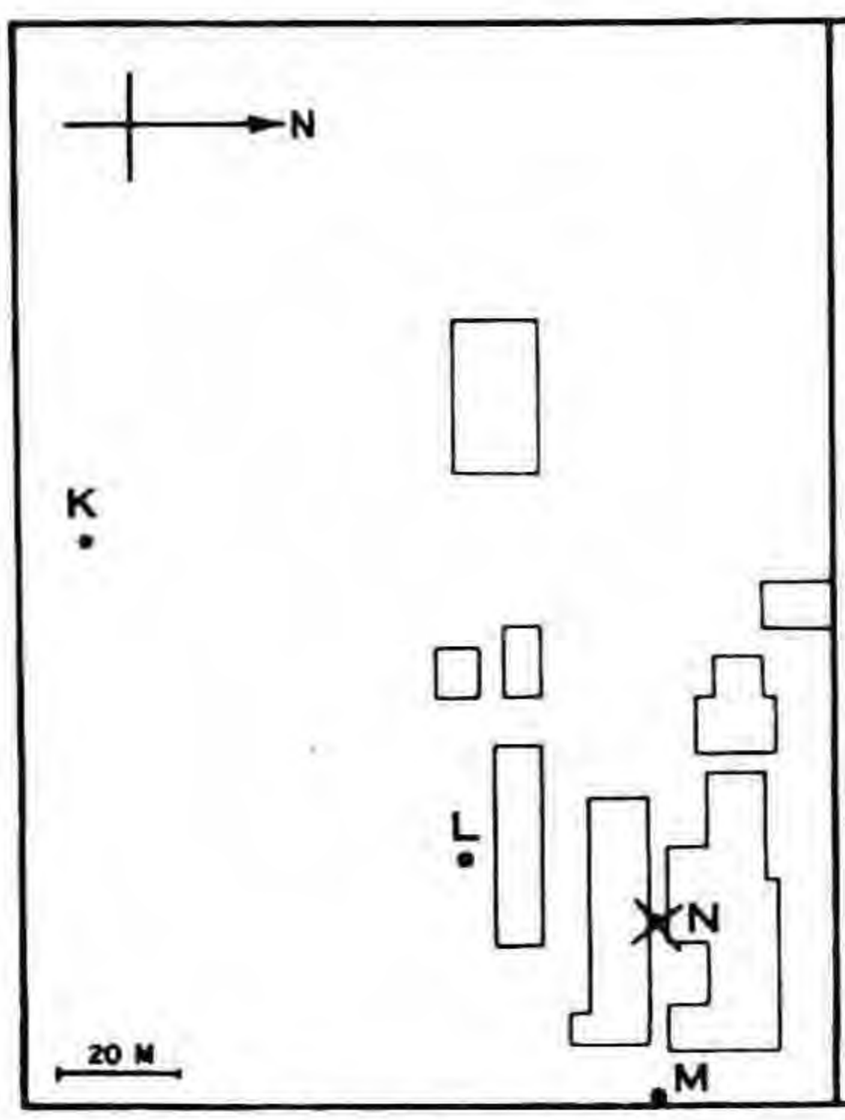

Site plan

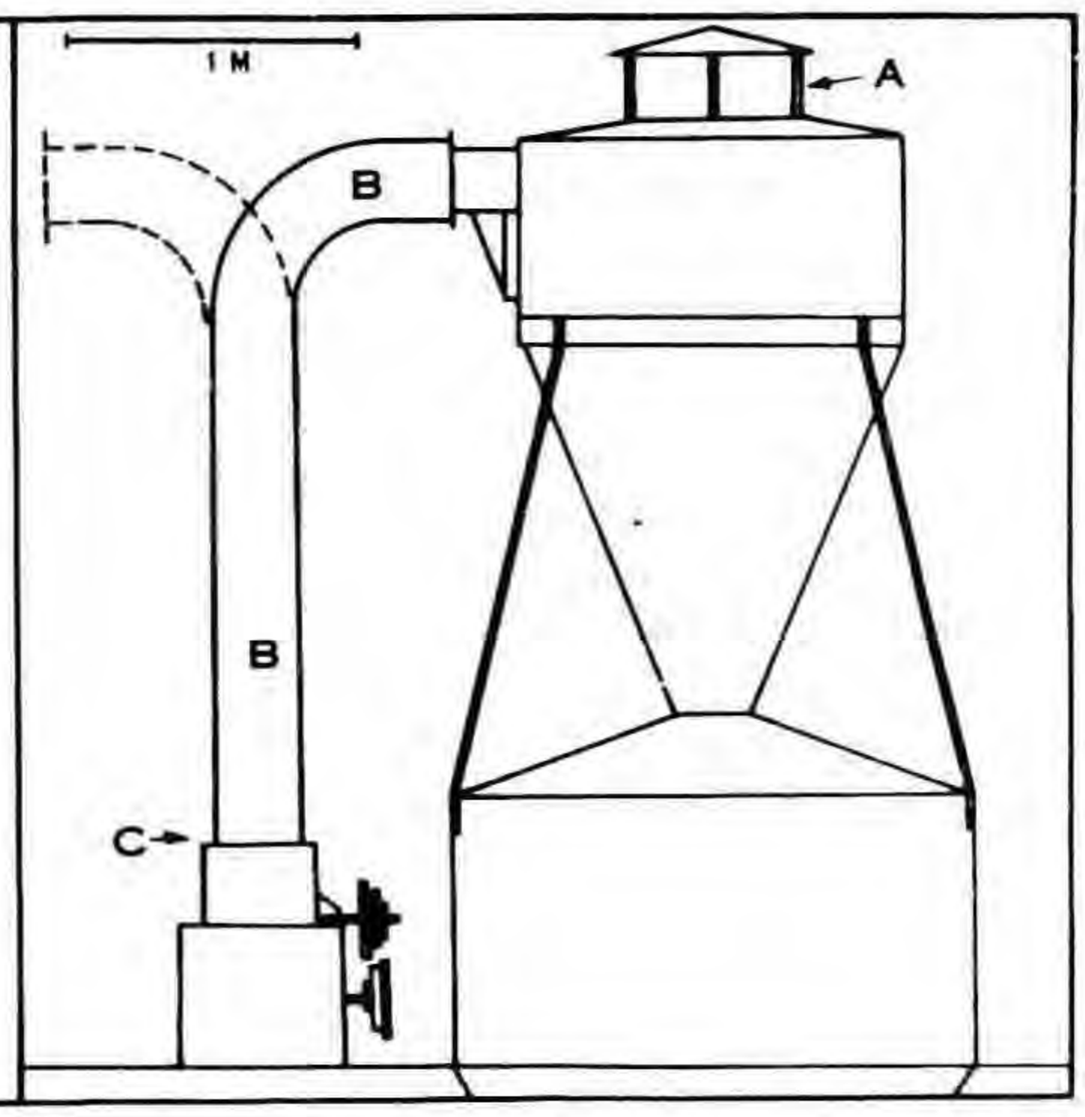

Elevation of extractor

The accompanying figure shows an outline of the main parts of the exhaust system. Sound level measurements were made at four points in the field, using wave analysers at the two points nearest the extractor and portable sound level meters at the other two points. These points are also shown in the figure; K is in the open about 100 m from the plant, L is in the shadow of a nearby building from which complaints had been made, M is at the nearest street boundary, and N is close to the exhaust fan. Sound level measurements were made at each point under the following conditions:

(1) With the system intact.
(2) With the cyclone outlet at A closed.
(3) With the duct section B removed.
(4) With the fan outlet C closed.
(5) With the duct section B reversed (dotted position) and end open.
(6) As in (5) but with end closed.
(7) With the system reassembled.

Table I shows the "A" scale measurements (in dB) at positions K, L, M, and N as the various tests were made.

TABLE I

	Test							
Position	1 (dB)	2 (dB)	3 (dB)	4 (dB)	5 (dB)	6 (dB)	7 (dB)	Background level
K	-	59	53	48	55	54	56	50
L	55	58	51	48	58	54	56	
M	69	74	71	69	73	67	71	
N	84	84	92	87	88	86	88	

It is apparent from these figures that the fan unit was contributing the most noise. The noise spectrum showed peaks at 220, 440 and 660 c/s, as would be expected from a 6-blade fan rotating at 220 rev/min producing a fundamental frequency with harmonics.

The fan unit was therefore enclosed in a lead-lined wooden box having the inner surfaces faced with a mineral wool absorbent. Rubber seals were fitted to those parts of the fan unit which must protrude. The exhaust system was then reassembled and the same seven tests were repeated. The results are shown in Table II.

TABLE II

	Test							
Position	1 (dB)	2 (dB)	3 (dB)	4 (dB)	5 (dB)	6 (dB)	7 (dB)	Background level
K	55	54	50	Undetected	52	Undetected	52	42
L	56	51	52	Undetected	55	44	49	42
M	71	71	74	58	73	67	71	51
N	84	83	91	83	91	86	83	

Two features are apparent from these results: the sound level close to the fan unit did not change greatly (about 4 dB reduction), and (b) that, while the sound level at a distance was almost the same as before for the complete system, there was a considerable reduction (about 10 dB) when the cyclone and connecting duct was disconnected from the fan unit (test 4), or when the connecting duct was re-connected with its opening blocked (test 6). It was therefore obvious that duct section B should be made as an acoustic filter. Accordingly the duct was lined with 0.05 m thickness of mineral wool (density 0.25 g cm^{-3}) for its entire length of 3 m, the wool being protected with a perforated facing of metal with 50 per cent open area.

It was the intention that the same seven tests would be made with this filter in position, but measurements at the four field points showed that this was unnecessary as the sound level had been reduced sufficiently and was comparable with the background level measured when the exhaust system was inoperative. Table III shows the improvement obtained.

TABLE III

Position	Test 1 (dB)	Background level (dB)
K	46	44
L	48	42
M	51	42
N	78	-

The residual noise is that of a rushing air stream with undertone frequency of 220 c/s. The generally random nature of this noise was favourably commented upon by all concerned with the experiment.

It is instructive to compare these results with the suggestion that in residential districts the public reaction to noise can be estimated from readings made with "A" scale weighting of a sound level meter. It is suggested that the meter reading minus 8 dB may be taken as a rough indication of the noise rating number, provided that this number is corrected for such factors as the noise spectrum, whether it is day or night, and the type of the neighbourhood, e.g. industrial, residential, or rural. For the particular noise of the cyclone these corrections are +5 dB because of the pure tone components of the noise, -5 dB for the noise being only in the day, and 0 dB for all other factors, giving a total correction of 0 dB. Thus with these corrections the estimated public reaction in this case should be "no observed reaction" if the noise rating number is less than 40, "sporadic complaints" if between 40 and 50, and "widespread complaints" if between 45 and 55.

Table IV compares the predicted reaction with the observed reaction.

TABLE IV

Position	"A" Scale (dB)	Noise Rating Number	Expected Reaction	Observed Reaction
Initially				
K	56	48	Sporadic complaint	Complaints from 3 residences
L	56	48	Sporadic/widespread complaint	Determined complaints
Finally				
K	46	38	No reaction	No further complaints
L	48	40	No reaction/ sporadic complaint	No further complaints

It may therefore be concluded that the cyclone extractor has been quietened satisfactorily as judged by the community reaction, and that this reaction to the noise produced by the system was correctly assessed by the recommendations suggested in the report prepared by the Technical Committee 43 of the International Organization for Standardization.(1)

Reference

(1) International Organization for Standardization (1961) - Technical Committee 43 (Acoustics). Report 235. Draft proposal for noise rating numbers with respect to conservation of Hearing, Speech Communication, and Annoyance.

M53

FOURTH INTERNATIONAL CONGRESS ON ACOUSTICS
COPENHAGEN 21.-28. AUGUST 1962

A Method for the Investigation of Sound Diffusiveness in Rooms

G.A.Goldberg

Sound diffusiveness (in the sense of the angular distribution of reflexions, "Richtungsdiffusität") attracts the attention of acousticians in connection with two problems. One is the influence of diffusiveness upon the effectiveness of an absorber in a room (e.g.in a reverberation chamber) and upon the rate of decay of sound energy. The other is the influence of diffusiveness upon the quality of a concert hall. We are principally interested in this latter problem.

It is allready known [1] that different degrees of the diffusiveness in different halls or in different places in a hall are observed chiefly in the initial part of the reverberation. In the "tail" of the reverberation diffusiveness is usually everywhere good.

For the investigation of this phenomenon a convenient method of observation and measurement is needed. A well known method worked out by prof. E.Meyer and his collaborators [2] is irreprochable in all respect but one: it is too complicated. It should be reminded that at the end of a long procedure we get a photograph (i.e.a projection on a plane) of a three dimentional metallic model, a so called "hedgehog". The length of each needle of a "hedgehog" is proportional to the energy flux coming from a corresponding direction.

A much simpler method many be proposed allowing to get oscillographic pictures similar to the photographs of a "hedgehog". We call these pictures briefly "reflexion roses". The length of a petal of a "rose" is proportional to the sound pressure instead of sound intensity in a "hedgehog". The method is specially destined for the investigations of the earliest reflexions where the exact coincidence of two or more reflexions has a low probability.

A simple device makes the light beam flash only for a given part of the reverberation thus allowing (when comparing a serie of pictures) to observe the change in the angular distribution of reflexions during the reverberation.

The method is based on two ideas.

First is the use of two joint pressure gradient microphones with their

axes shifted by 90°. When the sound wave is travelling parallel to the plane of both axes (we shall call it "the main plane"),then the outputs of the microphones are proportional to the sound pressure times $\sin\varphi$ for one microphone and $\cos\varphi$ for the other, φ being the angle of incidence of the sound wave with respect to the axis of one of the microphones. The microphones with their amplifiers are connected to a pair of plates of an CR -oscillograph. When a sound wave strikes the microphones, there appear a line on the screen of the oscillograph, it's length being proportional to the sound pressure and it's inclination depending on the direction of the sound wave.
Pictures obtained in this way are very instructive but have a serious defect. Due to the bilateral deflection of the light point on the screen, it is impossible to distringuish between the two opposite directions.
It is the same as an uncoloured compass needle shows the position of the meridian but not separately the north or the south direction. We need an one-side image like a needle of a clock.
To get a unilateral deflection of the electron beam a following system is proposed. An electric spark giving a shock wave is used as a source of sound. The oscillogram of such a wave taken by means of a high quality microphone consists of one nearly sinusoidal vibration of a large amplitude, followed by several much smaller vibrations. From this curve an one-side curve is easily obtained by means of integration, the integral of $\sin x$ being $(1-\cos x)$. The sign of the integral shows the direction of the arrival of the sound wave.
Fig.1 represents a serie of oscillograms taken when the sound wave came to a pressure gradient microphone from the front(a), from one side (b) and from behind (c). The left hand curves were taken without integration, the right hand curves - with an integrating circuit inserted between the output of the microphone amplifier and the input of the CR-oscillograph. In our tests the width of the curve was about 0,25 msec and therefore the difference of about 8cm in the path length was sufficient for an independent reception of consecutive reflexions.

Fig.1

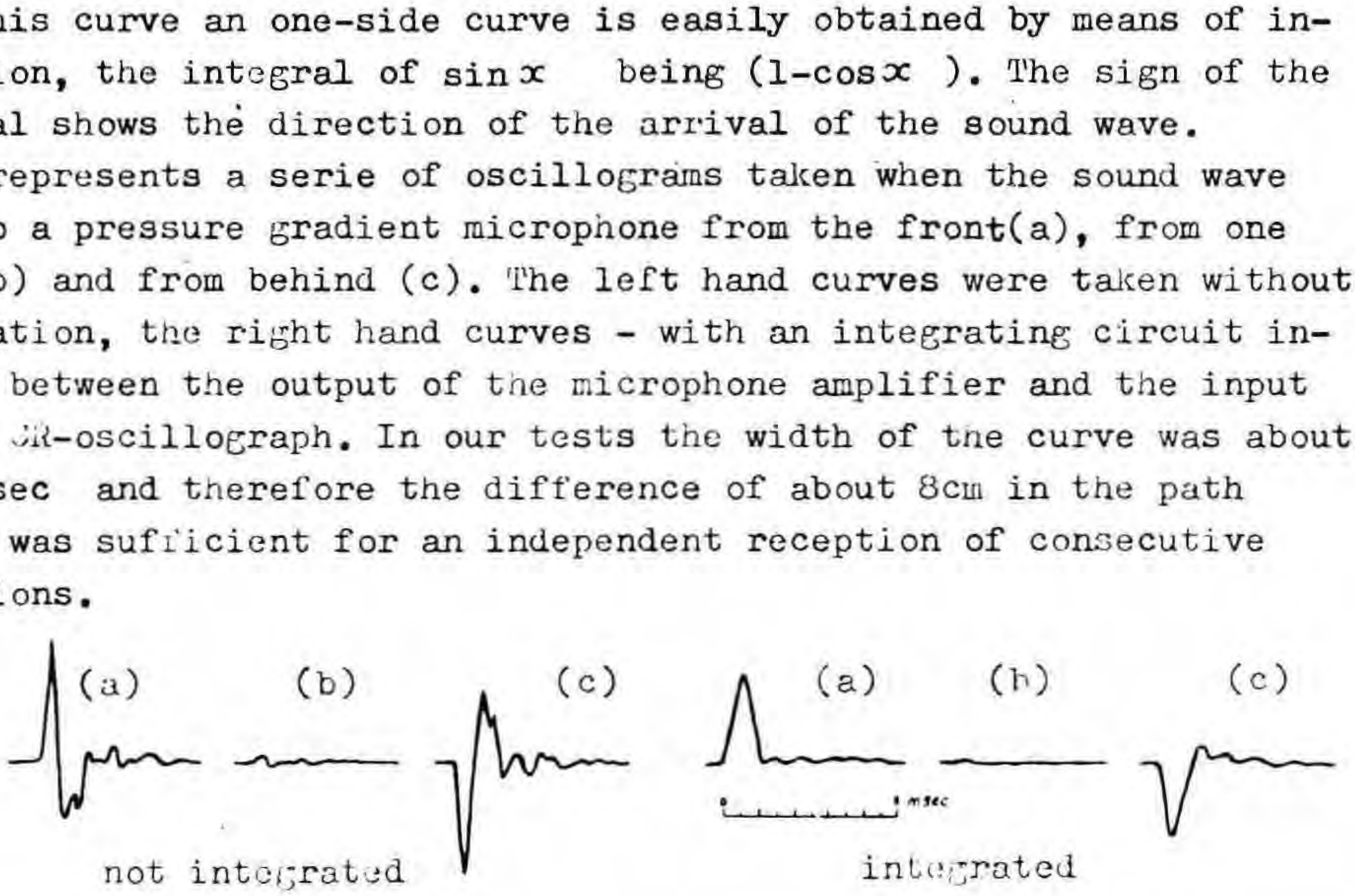

The block diagram of the device is shown on fig.2. It was tested in the following way. Pulse waves were sent to the microphones and the images of the direct waves (without any reflected) were obtained on the screen. Between the sound pulses the microphone pair was turned each time by about 45°.

Fig.2

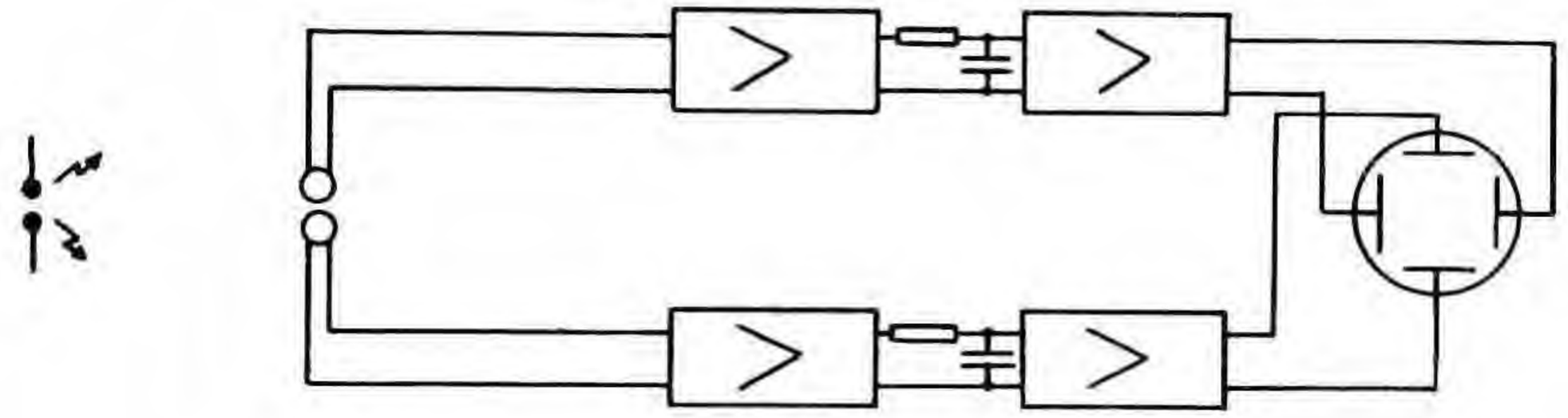

To show clearly the unilateral deflection caused by each wave, two pictures were taken for the complete turne of the microphones. They are shown on fig.3.

Fig.3

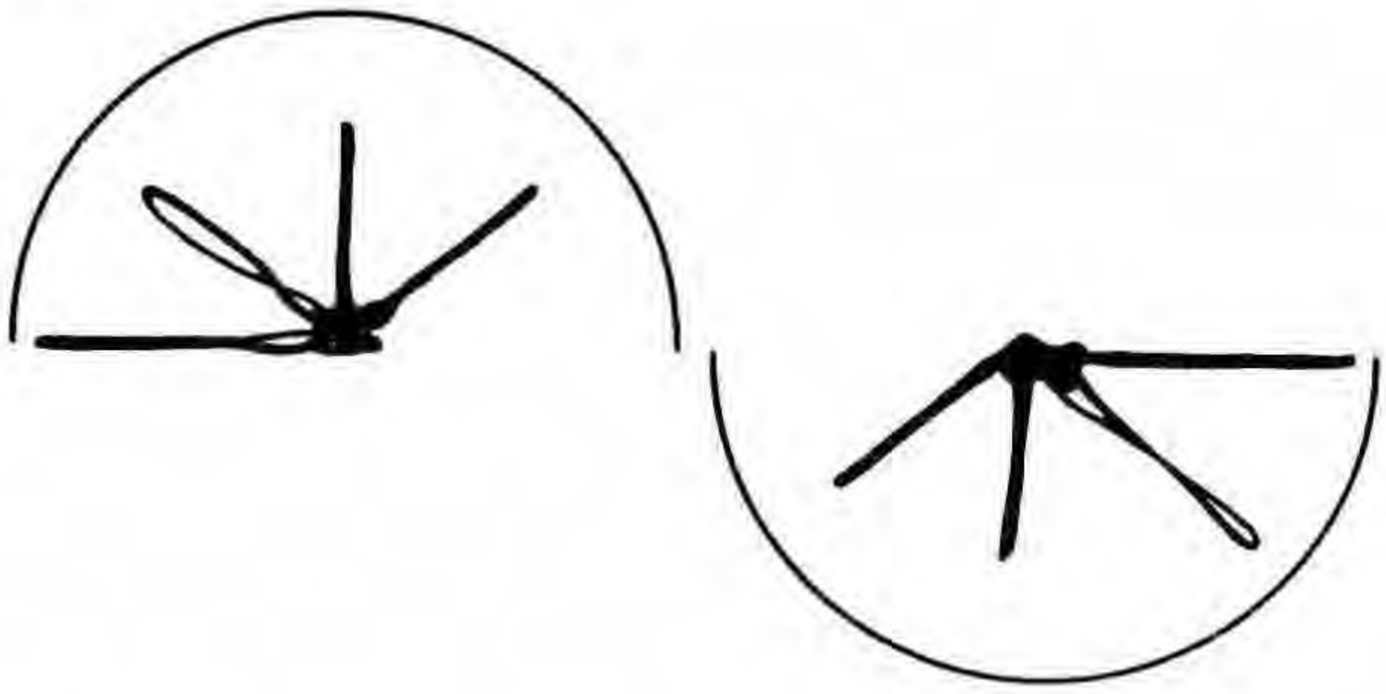

If the direction of the sound wave forms an angle ϑ with the main plane two cases should be considered. When the wave travels approximately in the zero plane of one of the microphones (so that only the other is answering) then the deflection is proportional to the sound pressure times $\cos\vartheta$, i.e. it represents the projection of a three dimentional vector on the main plane just in the same way as on the picture of a "hedgehog". When both microphones are acting, then a phase shift arises due to the distance between the two microphones. In this case a loop appears on the screen instead of a strait line (see fig.4). This effect is favorable as it helps to distringuish on the picture reflexions occuring in the main plane and out of it.

Fig.4

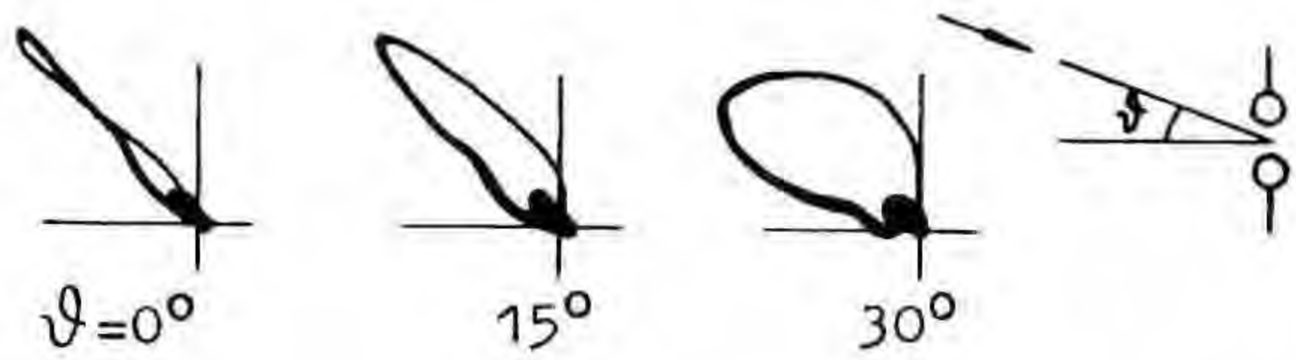

Fig.5. shows a "reflexion rose" taken in a room. In order to get strong reflexions from different sides, the microphone pair was placed near a wall and reflecting screens were used. Picture (a) represents the first 10 msec of the reverberation, picture (b)-about half a second.

Fig.5



(a) (b)

It should be mentioned that the method described above is also convenient for the development of an automatic measuring device. The vector components having different signs may be used for the angular selection of signals. The total energy passing during a given time interval within a certain angle may be obtained as a sum of the time integrals of the squares of the corresponding components.

The author thanks Mr. V.D.Sher, chief engineer of the Moscow House for Broadcasting and Soundrecording, for the permission for experimenting in studios with a number of microphones and Mr. K.R.Krastyn of the Institute for Soundrecording for his help in performing tests.

Literature

[1]. W.Junius. Acoustica. 1959. 9. 289.
[2]. E.Meyer, D.Thiele. Acustica, 1956, 6, 425.

N53

FOURTH INTERNATIONAL CONGRESS ON ACOUSTICS
COPENHAGEN 21.-28. AUGUST 1962

Eine Apparatur zur ohrgemäßen Tonhöhenanzeige

Ludwig S c h r e i b e r , Institut für Technische Akustik der Technischen Universität Berlin-Charlottenburg *)

Es wird ein Gerät beschrieben, das die Tonhöhe von Tönen und Klängen zweidimensional anzeigt. Eine Dimension ist die Oktavlage oder ungefähre Tonhöhe, bestimmt durch eine Spektralanalyse, die andere die Tonhöhe innerhalb der Oktave ("Chroma"), für alle Oktaven gemeinsam durch eine Periodizitätsanalyse bestimmt. Das Gerät bildet einige charakteristische Eigenschaften des Gehörs (Hüllkurvenhören, Oktavverwandtschaft, zweifache Tonhöhenperzeption) qualitativ ab. Es enthält unseres Wissens die erste Modellvorstellung für das Phänomen der Oktavverwandtschaft.

Die bekannte "Duplex Theory of Pitch Perception" von J.C.R. LICKLIDER /1/ ist die erste Theorie, die das Hüllkurvenhören physiologisch zu deuten versucht. Sie hat den Vorteil großer Anschaulichkeit, ist aber keine Einortstheorie, sondern eine Art "Klangbildertheorie" (EWALD, siehe /2/). Sie gibt ebensowenig wie die HELMHOLTZsche Theorie /3/ eine befriedigende Erklärung für die Oktavverwandtschaft. Für eine apparative Abbildung ist sie zu unökonomisch.

Der Verfasser hat sich nun auf Anregung von Herrn Prof.Dr.-Ing. CREMER die Aufgabe gestellt, von der LICKLIDERschen Theorie ausgehend und unter Verzicht auf die Dimension der Lautstärke und auf physiologische Ähnlichkeit eine möglichst einfache Modellvorstellung zu finden, die einer Einortstheorie entspricht, das Oktavphänomen abbildet und sich leicht in einem Gerät zur Tonhöhenanzeige technisch realisieren läßt.

Die gefundene Lösung wird im folgenden anhand eines vereinfachten Schemas (Abb. 1) in ihren Grundzügen beschrieben:

Wird auf den Frequenzanalysator, der der einfacheren Darstellung halber die Eigenschaften eines Oktavsiebanalysators mit vier aneinandergrenzenden Durchlaßbereichen haben möge, ein Ton gegeben, dessen Tonhöhe in der Oktave N (1,2,3,4) liegt, so wird er zu dem entsprechen-

---

*) Jetz: M Ü L L E R - B B N G m b H , Schalltechnisches Beratungsbüro, M ü n c h en 2, Herzogspitalstr. 10

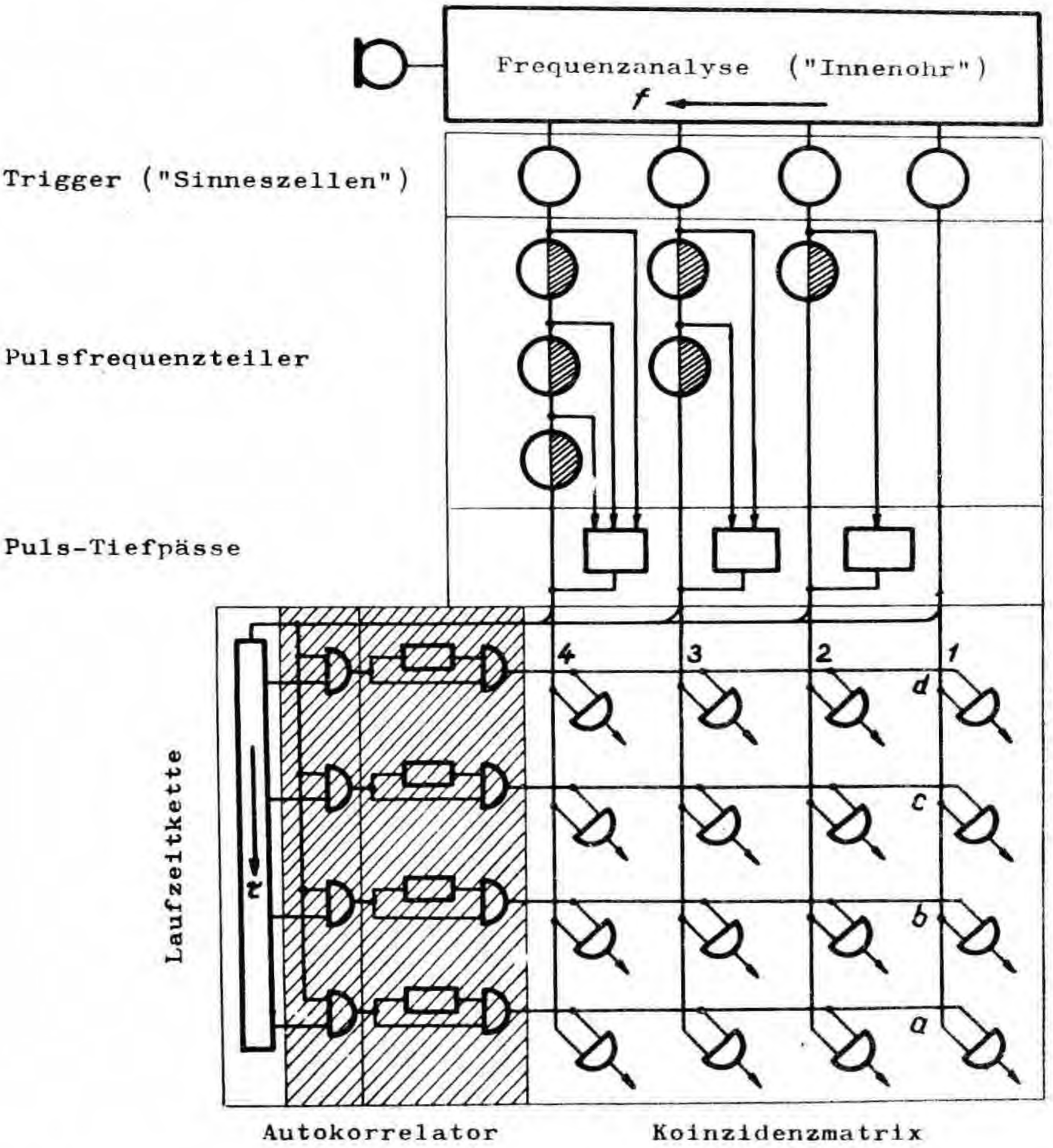

A b b . 1 Prinzipschema der apparatur zur Tonhöhenanzeige

den Ausgang durchgelassen und löst in dem angeschlossenen Trigger eine synchrone periodische Impulsfolge der gleichen Frequenz aus. Jeder der folgenden Puls-Frequenzteiler (Flip-Flops) läßt nur jeden zweiten auf seinen Eingang gelangenden Impuls passieren, sodaß die Pulsfrequenz nach (N - 1)maliger Frequenzhalbierung in der Oktave 1 liegt. Vom Ausgang des letzten Frequenzteilers gelangt der Puls auf die senkrechte Leitung N der Koinzidenzmatrix und auf den Eingang einer Laufzeitkette. Die Laufzeit zwischen deren Eingang und einem Aus-

gang n (a,b,c,d) betrage τ_n . Auf den horizontalen Leitungen, die man sich zunächst von den Ausgängen der Laufzeitkette durch den schraffierten Bereich durchgehend denke, erscheint also der gleiche Puls, aber um die Laufzeiten $\tau_{a,b,c,d}$ verzögert. Hat der Puls nach der Frequenzteilung die Periode τ_n , so koinzidiert an der Stelle (N,n) der Matrix der verzögerte Puls auf der horizontalen Leitung n zeitlich mit dem unverzögerten auf der senkrechten Leitung N und am Ausgang der Koinzidenzstufe, die beide Leitungen verbindet, entsteht ein Puls der gleichen Frequenz $\frac{1}{\tau} = f \cdot 2^{(1-N)}$.

Die Tonhöhe eines Tones der Frequenz $\frac{1}{\tau_n} \cdot 2^{(N-1)}$ wird demnach durch einen Puls der Periode τ_n am Ausgang (N,n) der Matrix gekennzeichnet.

Das Tonhöhenunterscheidungsvermögen des Modells für nacheinander dargebotene Töne ist durch die Schärfe der Periodizitätsanalyse (im wesentlichen durch die Impulsbreite) und die Zahl der Ausgänge der Laufzeitkette gegeben. Soll das Modell z.B. innerhalb einer Oktave zwölf Halbtonschritte unterscheiden, so muß die Laufzeitkette zwölf Ausgänge mit den entsprechenden Laufzeiten haben und die Matrix zwölf horizontale Leitungen.

Zwei gleichzeitig erklingende Töne können in dem gezeigten Beispiel nur dann getrennt angezeigt werden, wenn sie nicht in der gleichen Oktave liegen. Soll das Modell innerhalb einer Oktave ebenso wie das Gehör mehrere gleichzeitig erklingende Töne unterscheiden, so muß man eine entsprechende feinere Frequenzselektion und entsprechend mehr Trigger, Frequenzteiler und senkrechte Leitungen der Matrix vorsehen.

Beim gleichzeitigen Einwirken mehrerer Töne in verschiedenen Oktaven treten auch an anderen als den diesen Tönen zugeordneten Ausgängen der Matrix Impulsfolgen auf, die aber nicht die Frequenzen $\frac{1}{\tau_n}$ haben. Diese "falschen Anzeigen" können durch eine nachfolgende Integration oder Nachselektion unterdrückt werden. In dem Schema Abb. 1 ist (schraffierter Bereich) bereits vor der Matrix jedem Ausgang der Laufzeitkette eine Koinzidenzstufe und ein Selektor - bestehend aus einem Laufzeitglied und einer weiteren Koinzidenzstufe - zugeordnet.

Bei Klängen und Residualklängen (Klängen ohne Grundton) werden zu den Ausgängen des Frequenzananlysators, die höheren Oktaven über dem Grundton entsprechen, mehrere Teiltöne durchgelassen, so daß dort Spannungsverläufe entstehen, in deren Hüllkurven unter bestimmten Phasenbedingungen die Periodizität des Klanges ausgeprägt ist. Schreibt man den

Triggern die Eigenschaft zu, bei spitzenhaltigen Hüllkurven nur einen Impuls je Periode abzugeben, so treten in diesem Fall auf den senkrechten Leitungen vor den Frequenzteilern Pulse auf, die die Periode der Hüllkurve haben. Dieser Periode entspricht die Residualtonhöhe. Durch die den Frequenzteilern parallel liegenden Puls-Tiefpässe (Trigger, die besonders dimensioniert sind), deren Grundfrequenz gleich der zwischen erster und zweiter Oktave ist, werden diese Pulse direkt oder erst nach noch notwendiger Frequenzteilung zur Matrix und zum Autokorrelator durchgelassen.

Das Modell zeigt das Chroma eines Tones, Klanges oder Residualklanges immer richtig an. Bei einem Ton wird das Chroma nur in dessen Oktave angezeigt, bei einem Klang mit Grundton in dessen Oktave und in höheren Oktaven, bei einem Residualklang hingegen nur in höherenOktaven (Formantbereich, Formanttonhöhe). Ein Beobachter, der nach der Anzeige des Gerätes die Tonhöhe eines Tones auf gleiche Tonhöhe mit einem anderen Ton, Klang oder Residualklang einstellen soll, wird in allen Fällen das Chroma des Tones richtig einstellen, sich aber beim Klang und besonders beim Residualklang über die Oktave unsicher sein. Das entspricht genau den Beobachtungen, die der Autor bei solchen Tonhöhenvergleichen gemacht hat. Small /4/ und Davis et al./5/ berichten ebenfalls von Oktavverwechslungen, und Bachem /6/ hat bei Versuchen mit Personen mit absolutem Gehör festgestellt, daß diese sich selten im Chroma, aber häufig in der Oktave irren.

Das Modell bildet also trotz seines einfachen Prizips wesentliche Eigenschaften der Tonhöhenperzeption qualitativ erstaunlich gut ab. Eine quantitative Übereinstimmung anzustreben erscheint dagegen nicht sinnvoll.

In Berlin wurde von den Herren GRUBER und SMAGO ein solches Gerät mit wenigen Oktaven und Chromen provisorisch aufgebaut und zeigte die erwarteten Eigenschaften. Für die Koinzidenzstufe der Matrix werden darin Kaltkatodenröhren verwendet, deren Glimmentladung gleichzeitig zur Anzeige dient. Das Gerät soll mit Mitteln der Deutschen Forschungsgemeinschaft zu einem umfangreicheren Demonstrationsmodell ausgebaut und sein Verhalten bei verschiedenen Schallereignissen untersucht werden

Literatur: /1/ Experientia 7 (1951), 128
/2/ Wever, Theory of Hearing, New York, 1949
/3/ Die Lehre von den Tonempfindungen, 6.Ausg., Braunschweig 1913
/4/ JASA 27 (1955), 751
/5/ JASA 23 (1951), 40
/6/ JASA 9 (1932), 146

O53

FOURTH INTERNATIONAL CONGRESS ON ACOUSTICS
COPENHAGEN 21.-28. AUGUST 1962

Finite Perturbations in Relaxing Media.

A.L.Polyakova

Thermodynamically irreversible process - the relaxation of internal degrees of freedom leads to additional sound absorption and to dispersion of sound velocity. On the other hand nonlinear effects in propagation of finite amplitude waves lead to the steepening of the wave form. The conflicting influence of these processes is worth while to consider. Let us study relaxing media in which deviations from equilibrium are small and the parameter $m = \frac{C_\infty^2 - C_0^2}{C_0^2}$ is much less than unity ($m \ll 1$). This parameter characterizes the sound dispersion in the medium: C_0 is the sound velocity for very slow processes when the medium is always in equilibrium ($\omega\tau \ll 1$,where ω -sound frequency, τ -relaxation time); C_∞ is the sound velocity for rapid processes that is when the medium has no time to reestablish the equilibrium state during the external perturbation ($\omega\tau \gg 1$). Let us consider the propagation of a hydrodynamical perturbation amplitude of which is so large that it is necessary to consider nonlinear equations, but the ratio of particular velocity v to sound velocity C is less than unity. We shall assume that $\frac{v}{C}$ and m are values of the same order, that is $\frac{v}{C} \sim m \sim \mu$, where μ is some small quantity. We will restrict our study to first and second order terms in respect to μ . In this approximation it is possible to obtain the equation giving the relation between pressure p and density ρ in the relaxing medium

$$p - p_0 + \tau \frac{dp}{dt} = C_0^2(\rho - \rho_0) + \left(\frac{\partial p}{\partial \rho^2}\right)_{eq} (\rho - \rho_0)^2 + \tau\left[C_\infty^2 + \left(\frac{\partial^2 p}{\partial \rho^2}\right)_{eq}(\rho - \rho_0)\right]\frac{d\rho}{dt} \qquad /1/$$

This equation replaces the equation of state for finite amplitude perturbations in the relaxing media.

In order to simplify the problem let us consider the equation /1/ and hydrodynamical equations in new independent variables $y = t - x/c_0$ and $z = \mu x$. This substitution permits us to distinguish two different types of processes: the rapid processes expressed by the variable y for instance, periodical oscillation of pressure in the sound wave, and the slow processes expressed by z such as the slow change of the sound amplitude due to absorption. This small value μ represents that the derivatives of all hydrodynamical values in respect to x are small. Taking into account the terms of order μ^2 it is possible to obtain the nonlinear equation describing the propagation of finite-amplitude waves in the relaxing media:

$$\mu \frac{\partial v}{\partial z} - \frac{\gamma+1}{2c_0^2} v \frac{\partial v}{\partial y} - \frac{m\tau}{2c_0} \frac{\partial^2 v}{\partial y^2} + \tau \frac{\partial}{\partial y}\left(\mu \frac{\partial v}{\partial z} - \frac{\gamma+1}{2c_0^2} v \frac{\partial v}{\partial y} \right) = 0 \qquad /2/$$

We will consider this equation for some particular case.

At first we shall consider the shock wave form in the relaxing media. This question has been studied with the aid of conservation laws at the shock (Hugonio-relations). In this report the problem is solved with the aid of continuous equation /2/. Indeed in the case of a steady wave form (i.e. when the wave form is not changed during the propagation) the solution of the equation /2/ is

$$y = \tau \ln \frac{v_0^2 (v + v_0)^{\kappa-1}}{(v_0 - v)^{\kappa+1}} \qquad /3/$$

where $2v_0$ -total velocity change in shock wave and $\kappa = \frac{m c_0}{v_0(\gamma+1)}$.

For $\kappa > 1$ the function $v(y)$, given by /3/ represents the wave form; it is continuous and nonsymmetrical (fully-dispersed shock). For $\kappa < 1$ $v(y)$ is a multivalued function and therefore cannot represent the wave form. This ambiguity signifies the appearence of a discontinuity in the wave front (partly-dispersed shock). Taking into

account shear viscosity it is possible to obtain the value of the velocity jump.

$$\Delta v = v_0 - \frac{2 m c}{\gamma + 1} \qquad /4/$$

In the case $\kappa > 1$ the velocity $\mathcal{D}$ of wave propagation through the medium satisfies the inequality $c_0 < \mathcal{D} < c_\infty$ it means that $\mathcal{D}$ can vary within a very small range. For higher amplitudes ($\kappa < 1$) the velocity of shock propagation is supersonic: $\mathcal{D} > c_\infty$.

It is interesting to consider the propagation of finite amplitude periodic waves in the case when the sound frequency is of the same order as the reláxation frequency ($\omega\tau \sim 1$). The equation /2/, with the boundary condition $v = v_0 \sin \omega t$ by $x = 0$, was solved by a numerical method with the aid of an electronic computer.

The velocity $v(z, y)$ was expanded in a Fourier series, the Fourier amplitudes being functions of distance z . Differential equations for Fourier amplitudes were solved numerically. It was shown that the wave form becomes steeper and unsymmetrical during the propagation. The slope of the front of rarefied parts of the wave is steeper than the slope of compessed parts. In this case as usually the nonlinear effects lead to higher harmonic appearence. But there is some difference in the behaviour of harmonics in relaxing medium. At first the amplitudes of higher harmonics increase with the distance from the radiator and reach their maxima at some distance. Further these amplitudes don't decrease monotonously as is the case for medium with the shear viscosity, but they begin to oscillate. The period of this oscillation is inversely proportional to the number of harmonic; it decreases slowly as $\omega\tau$ increases. These pulsations may be explained by the phase lag of harmonics due to sound dispersion.

P53

FOURTH INTERNATIONAL CONGRES ON ACOUSTICS
COPENHAGEN 21.-28. AUGUST 1962

Unharmonische Komponenten im "Klang der Orgelpfeifen"

Jürgen Meyer
Physikalisch-Technische Bundesanstalt, Braunschweig, Deutschland

Analysiert man den von einer Orgelpfeife abgestrahlten Schall in einem großen Dynamik-Bereich (z.B. 75 dB), so zeigt sich zwischen den einzelnen Teiltönen ein Rauschspektrum, aus dem eine größere Anzahl mehr oder weniger hoher Spitzen herausragt. In der Zeile a der beigefügten Abbildung ist das Ergebnis einer Suchtonanalyse bei einer Prinzipal-Pfeife wiedergegeben. Der Grundton liegt bei etwa 250 Hz, die einzelnen Teiltöne liegen streng harmonisch dazu. Zwischen den ersten beiden Partialtönen bildet das Untergrundgeräusch eine annähernd symmetrische Senke, aber bereits zwischen dem 2. und 3. Teilton rückt das Minimum aus der Mitte heraus zu einer etwas höheren Frequenz. Die folgenden Obertöne zeigen auf ihrer rechten Flanke eine Anhebung der Geräuschanteile, und vom 5. Teilton an trennt sich eine Spitze des Rauschpegels von dem eigentlichen Partialton ab, bis schließlich die 11. Harmonische wieder mit einer solchen Spitze zusammenfällt.

Diese Charakteristik des Rauschuntergrundes läßt sich aus der unharmonischen Lage der einzelnen Pfeifenresonanzen erklären. Regt man nämlich eine Orgelpfeife statt durch den Luftstrom mit einem kleinen Lautsprecher vor der Labienöffnung an, so zeigt sich, daß die einzelnen Resonanzen stets höher liegen als die ganzzahligen Vielfachen der Grundresonanz. Dieser Efekt tritt um so stärker in Erscheinung, je weiter die Mensur der Pfeife ist und je kleiner die Labienöffnung ist [1] . In der Zeile c der Abbildung sind die gemessenen Resonanzfrequenzen eingetragen. Man erkennt, daß sie ziemlich gut mit der Lage der unharmonischen Spitzen übereinstimmen. Im Bereich um 2000 Hz liegen demnach die Teiltöne dieses Prinzipalklanges (s. auch Zeile b) genau zwischen den Resonanzen, während der 11. Teilton wieder mit der 10. Resonanz zusammenfällt.

Bei Pfeifen anderer Mensur ändern sich die Verhältnisse naturgemäß in ziemlich starkem Maße. So wurde festgestellt, daß bei einem sehr weiten "Nachthorn" bereits der 5. Teilton auf die 4. Resonanz traf, während bei einer engen Pfeife des Registers "Zartgeige" erst wieder die 15. Harmonische mit der 14. Resonanz zusammenfiel.

Gegenüber diesen durch die Rohrresonanzen hervorgerufenen Komponenten treten die Metalleigentöne stark zurück. In der Zeile d der Abbildung ist eine Resonanzkurve des Pfeifenkörpers wiedergegeben. Dazu wurde die Pfeife am Oberlabium mit einem elektrodynamischen System, das mit weißem Rauschen gespeist wurde, erregt und der von der Wandung abgestrahlte Schall analysiert. Auf dem Registrierstreifen erkennt man eine große Anzahl von mehr oder weniger hohen Resonanzspitzen; doch nur die stärkste, die bei etwa 2200 Hz liegt,

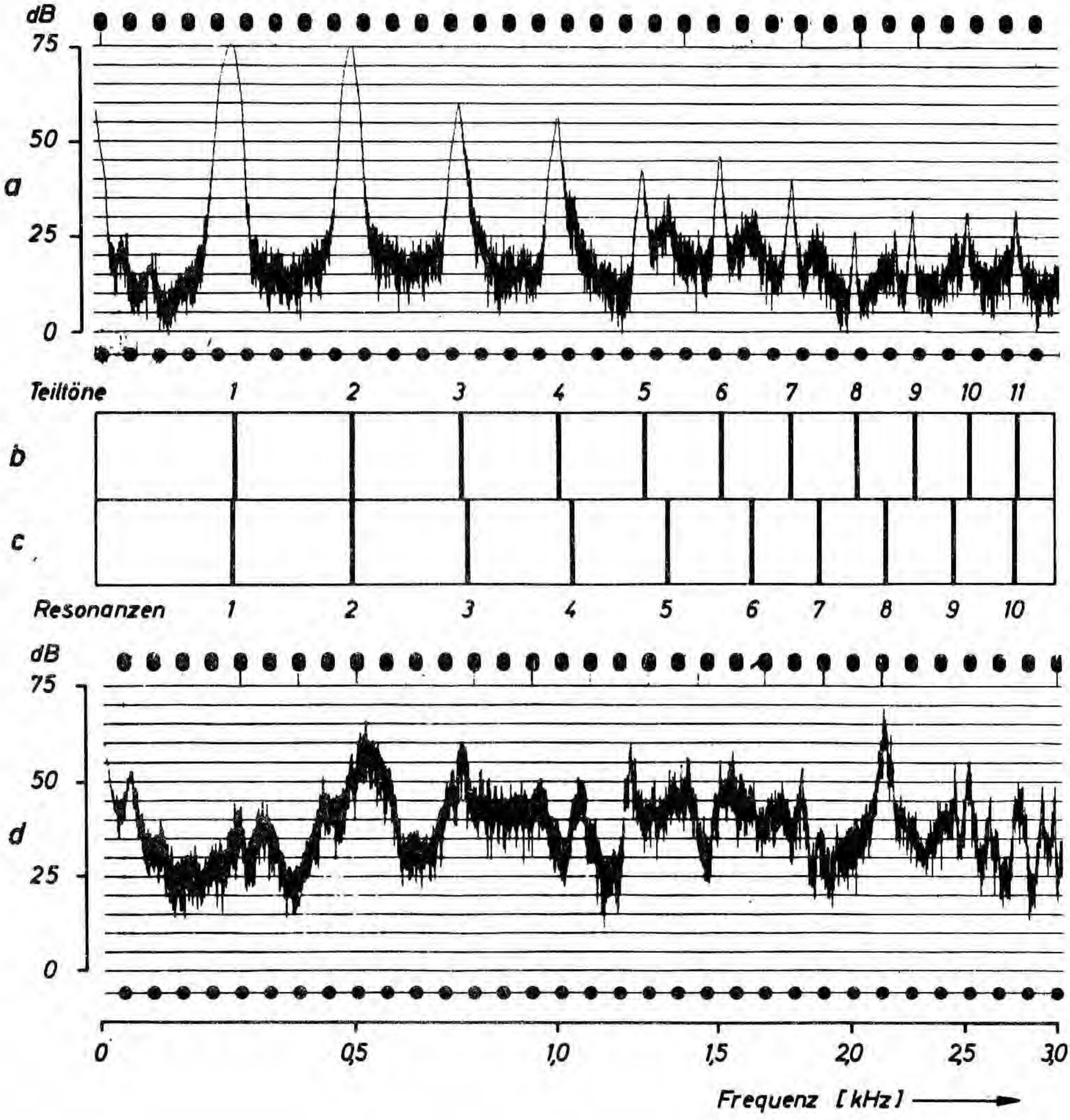

Klanganalyse einer Prinzipalpfeife 8' c'

a Suchtonanalyse bei normalem Anblasen
b Frequenzlage der Teiltöne
c Frequenzlage der Luftraumresonanzen
d Resonanzkurve des Pfeifenkörpers

prägt sich in der Analyse des Pfeifenklanges deutlich aus, während vor allem in tieferen Frequenzlagen die Einflüsse der Luftsäulen-Resonanzen überwiegen. Wie frühere Untersuchungen gezeigt haben, spielen die Eigenschaften des Wandungsmaterials besonders in höheren Frequenzlagen eine bedeutende Rolle. In diesen Bereichen liegt der Rauschpegel bei Zink- und auch Kupferpfeifen erheblich höher als bei Zinn- und Blei- oder gar Holzpfeifen, wodurch die ersteren einen schärferen Klangcharakter erhalten [2].

Die Anregung aller dieser unharmonischen Komponenten erfolgt durch das vom Anblasen herrührende Rauschspektrum. Eine Untersuchung der Schneidengeräusche, zu deren Analyse die Pfeifenrohre mit einer lockeren Wattefüllung gedämpft wurden, ergab, daß die Anregefunktion aus einem Rauschpegel besteht, aus dem einige Gebiete stärkerer Amplituden wie Resonanzüberhöhungen herausragen. Es handelt sich dabei um die sog. Schneidentöne, welche durch die Spalt-Schneiden-Kombination am Pfeifenlabium hervorgerufen werden. Ihre Frequenzlage und Bandbreite hängt von den Abmessungen der Anordnung sowie vom Winddruck ab. Der tiefste Schneidenton entspricht der Folgefrequenz der Luftwirbel, die am Kernspalt abgelöst werden, wenn keine Rückwirkung zum Pfeifenresonator besteht. Im stationären Schwingungszustand geht die Wirbelfolge allerdings auf die Frequenz des Grundtones der Pfeife über, wie sich auf Grund der Phasenlage der Obertöne in Oktavsieb-Oszillogrammen nachweisen läßt.

Dieser Übergang der Wirbel-Folgefrequenz von dem durch die Pfeifenabmessungen gegebenen Wert auf den Grundton des Klanges ist von entscheidender Bedeutung für den Verlauf des Einschwingvorganges, der naturgemäß noch stärkere unharmonische Anteile aufweist als der stationäre Zustand. Meßtechnische Untersuchungen bei einer größeren Anzahl von Pfeifen der verschiedensten offenen Labialregister ergaben, daß sich diese je nach der Lage des untersten Schneidentones in drei Gruppen einteilen lassen. Während bei einigen Pfeifen der Schneidenton in der Nähe der Grundresonanz liegt (z.B. Nachthorn), fällt er bei der Hauptgruppe der Pfeifen (Prinzipale, Flöten) zwischen die 2. und 3. Resonanz. Bei einer weiteren kleineren Gruppe befindet er sich sogar oberhalb der 3. Resonanz (Streicher) [3].

Liegt der erste Schneidenton in der Nähe der Grundresonanz, so wird diese auch zuerst angeregt, und die Folge der Luftwirbel wird sehr schnell durch diese Frequenz gesteuert. Da bei jenen Pfeifen meist auch der zweite Schneidenton verhältnismäßig tief liegt, wird auch die 2. Resonanz sofort erregt. Wenn sie von dem Grundton weiter als eine Oktave entfernt ist - im Falle des Nachthornes war es eine None -, so schwingt der 2. Teilton mit dieser unharmonischen Frequenz ein und wird erst langsam von dem Grundton in die reine Oktave mitgezogen. Für das Ohr ist dieser Vorläufer deutlich als None wahrnehmbar.

In dem am häufigsten vorkommenden Fall, daß der unterste Schneidenton zwischen der 2. und der 3. Resonanz liegt, schwingt zunächst der Oktav-Teilton ein. Die Impulsfolge in den höherfrequenten Bereichen eines Oktavsieb-Oszillogrammes zeigt dabei ebenfalls die Frequenz der 2. Resonanz, erst später geht sie auf den Grundton über. Da die Dämpfung der Grundresonanz stets größer ist als die der zweiten, wird der Grundton von seiner

Resonanzfrequenz auf den halben Wert der 2. Resonanz hinaufgezogen; jedoch ist dieser Effekt sehr schwach, da bei den Prinzipalen und Flöten die ersten Resonanzen noch ziemlich genau harmonisch liegen. Infolgedessen treten bei dieser Gruppe der Pfeifen keine hörbaren unharmonischen Anteile im Bereich der unteren Teiltöne auf.

Liegt dagegen der Schneidenton zwischen der 3. und 4. Resonanz, so wird zunächst der 3. Teilton angeregt, die bei-den tieferen folgen erst später. Auch die Luftwirbel zeigen eine entsprechende schnelle Folge und gehen nur langsam über die Frequenz der Oktave auf den Grundton über. Die Pfeifen dieser Gruppe neigen stark zum Überblasen, was auf die hohe Schneidentonlage zurückzuführen ist.

Besonders charakteristisch für den Klangeinsatz von Labialpfeifen sind unharmonische Vorläufertöne in höheren Frequenzlagen. Es handelt sich dabei um Schwingungen von meist nur einer Frequenz, die vor dem Erreichen des stationären Zustandes wieder verschwinden. Bei Prinzipalen liegen sie im allgemeinen im Bereich der 6. oder 7. Harmonischen [4] , bei Gedackten etwas tiefer, bei Streichern höher. Der Grund dafür, daß hierbei stets nur eine Resonanz - oder höchstens zwei benachbarte - angeregt werden und nicht etwa die gesamte Folge der höheren Eigentöne, liegt darin, daß die Schwingungserregung nicht durch ein gleichmäßiges Rauschspektrum erfolgt, sondern durch die Schneidentöne höherer Ordnung, welche nur auf die angrenzenden Resonanzen einwirken. Sobald die Wirbelfolge vom Grundton synchronisiert wird, gehen diese Schwingungen daher in ihrer Amplitude wieder zurück. Da bei vielen Pfeifen die Teiltöne im Bereich des zweiten Schneidentones zwischen die einzelnen Resonanzen fallen, macht sich die unharmonische Lage dieser Vorläufer im Höreindruck besonders deutlich bemerkbar.

Literatur:

[1] J. Meyer, Acustica 11 (1961), 385

[2] W. Lottermoser und J. Meyer, Metall 16 (1962), 108

[3] s.auch die Berechnungen von
F. Ingerslev und W. Frobenius, Trans. Dan. Acad.Techn. Sci.Nr.1(1947), 7

[4] s.a. F. Trendelenburg, E. Thienhaus und E. Franz,
Akust. Zeitschr. 1 (1936), 59

G54

FOURTH INTERNATIONAL CONGRESS ON ACOUSTICS
COPENHAGEN 21.-28. AUGUST 1962

The Perception of Real and Synthetic Vowels After Very Sharp Filtering

by

EDWARD C. CARTERETTE
University of California,
Los Angeles, U.S.A.

and

A. MØLLER
Speech Transmission Laboratory
Royal Institute of Technology, Stockholm

Introduction

The concept of format frequency has proved powerful in speech research and theory. The role of the formant has been studied both analytically and synthetically. Among the major results, workers at the Haskins Laboratories showed that the formants are sufficient cues for vowel identification and that changes in formant position are vital to perception in certain consonant types (1). The formant's role in speech perception grows even more important given Fant's (4) proof that the four lowest formant frequencies completely specify the spectrum of a vowel.

This intimate connection of formant frequencies with the spectrum calls for a very close look at the perception of vowels from which various formants have been removed. Modern studies using electrical methods have dealt with relatively large linguistic units. For example, the extensive work of French and Steinberg and others (2) on the intelligibility of filtered vowels used consonant-vowel-consonant sounds. The consonant context was, however, a random variable. Miller (7) found interconfusions for 16 English vowels in a uniform context, using a very sharp low-pass (M-derived) filter – but only for 670 c/s. Lehiste and Peterson (6) describe the confusions that arise from filtered steady-state vowel segments. Although a wide range of filters were used, they were not very sharp, nor was there enough data to give stable estimates of confusions.

Our work, briefly reported here, had two major aims. One was to obtain enough data to get stable estimates of confusions among vowels after "ideal" filtering. The other was to obtain data on the same listeners using synthetic vowels as stimuli having, in a sense to be defined, nearly the same properties as the human vowels. Beyond this, such data would be useful in evaluating the analog vocal tract developed in the Speech Transmission Laboratory. One hardly needs to say how valuable an artificial voice that spoke with the tongue of man would be as a research tool and as a speech standard.

The basic problem of this paper is to assess the contribution of the formant frequencies to vowel recognition in both real and synthesized speech, as distorted by very sharp high- and low-pass filtering, and to test a quantitative model of the process.

Procedure

Real vowels

Fourteen Swedish vowels were chosen. IPA symbols, key words, mean formant frequencies, etc., are given in Table I. Five male Swedish talkers (Stockholm dialect) spoke briefly sustained vowels with constant vocal effort. Each talker recorded 14 lists each of which had 42 randomly arranged vowels (3 samples of each of the 14 vowels). This material was transferred to an identical recorder through a gate to give steady-state vowel segments 500 msec in duration with rise-fall times of 50 msec.

Synthetic vowels

Using the values of the formant frequencies shown in Table I, gated, shaped vowel segments 500 msec in duration were prepared with the electrical analog vocal tract OVE II, designed by Dr. Gunnar Fant (5). After gating, vowels were recorded through the filter system exactly as described for real vowels.

IPA Symbol	Key Word	F_1 R	F_1 S	F_2 R	F_2 S	F_3 R	F_3 S	F_4 R	F_4 S
u:	mos	270	280	630	600	2350	2250	3040	3250
o:	kål	365	410	660	750	2490	2450	3075	
ɔ	olja	470	500	780	850	2490	2550	3025	
ɑ	mat	580	650	910	1000	2450	2500	3240	
a	matt	725	750	1180	1200	2470	2600	3390	
ɛ	ära	675	650	1525	1600	2460	2450	3310	3500
ɛ:	även	425	475	1890	1950	2500	2550	3350	
e:	ek	310	340	2140	2100	2715	2700	3420	
i:	is	270	240	2100	2050	3015	3000	3510	
y:	fy	260	240	1980	2000	2540	2350	3120	
ʉ:	ute	300	240	1750	1600	2130	2150	3130	3250
ɵ	ull	440	450	1115	1050	2370	2300	3090	3250
ø:	ösa	360	375	1700	1700	2200	2300	3190	3500
ø	för	505	550	1145	1150	2405	2450	3125	3250

Table I. A comparison of the first four formant frequencies for real (R) and synthetic (S) speech. Each R value is the median of the means of samples of size 3 for each of five male talkers, as measured from broad band Kay sonagrams. Each synthetic speech value (S) is that used to program the RIT Speech Transmission Laboratory's OVE II formant generator. The S values are based on extensive measurements of the speech of male Swedes.

The filters

If formant frequencies are important determiners of perception, it is apparent that the sharpness of the filter cutoff must be a crucial factor. The heterodyne filter designed by Dr. Gunnar Fant (3) and used in our study attenuated energy beyond the cutoff frequency, f_c, at a rate of about *one db per c/s* independently of f_c. Nine LP and 8 HP filter cutoff frequencies, f_c, were used.

LOW PASS f_c: 410, 690, 980, 1175, 1391, 1576, 1765, 2550, and 3300 c/s.
HIGH PASS f_c: 335, 418, 582, 732, 1048, 1358, 1881, and 3130 c/s.

The experiments

Nine Swedish subjects (six women and three men) with normal hearing and ages ranging from 19 to 28 years listened over binaural telephones. The average total system response was flat within ± 2.5 db over the range of filtering.

After a single practice tape, listening test began. Presentation was in random sequence. Subjects were required to respond with one of the 14 vowels after each stimulus by writing down the key word (Table I). The vowels were spoken at a rate of 10 per minute.

Results

Real vowels

A gross analysis of the data (Fig. 1) gives mean per cent correct responses *vs* f_c in c/s. Both LP and HP functions are shown by solid points. Data from two related studies are included, French and Steinberg (2) and Lehiste & Peterson (6). The most obvious similarity is that the cross-over point of the HP and LP curves is near 1050 c/s in our study compared to 1100 c/s in the other two. This holds in spite of differences in context, duration of vowels, filter sharpness, and language and training of talkers and listeners (e.g., Lehiste & Peterson's subjects were phonetics students). This result strongly implies that vowel perception depends very little on the peculiarities of a subject, but on basic properties of the hearing mechanism. The fact that per cent correct responding at cross-over ranges from 85 (French & Steinberg) to 45 (our study) is due most probably to differences in context and filter sharpness, and the number of different vowels to be discriminated. In our study the context was minimal, vowel duration least, and the

number of different vowels the largest. We believe, however, that the results are due largely to filter sharpness, for in spite of the other factors, asymptotic responding for our untrained subjects was nearly equal to that of the trained and selected subjects in, e.g., Lehiste & Peterson's study.

Synthetic vowels. A comparison of per cent correct identification as a function of f_c is summarized in Fig. 2. Synthetic vowels behave very much like real vowels under HP filtering, but the first formant, F_1, has more importance for discrimination of synthetic vowels under LP filtering. This is borne out by a regression analysis which showed the (simple) correlation coefficients between the probability of a correct response ($p_f(C)$) and $F_1(r_{p,1})$ and $F_2(r_{p,2})$ to be 0.753 and 0.988, respectively, for real vowels. For synthetic vowels, $r_{p,1} = 0.871$ and $r_{p,2} = 0.885$. This also accounts for the cross-over of the synthetic functions at about 900 c/s, rather than at 1050 c/s as for real vowels. The comparative anatomy of an individual vowel in its real and synthetic form naturally reflects these differences, as we shall show in a paper to be published elsewhere. It should be said, however, that a given synthetic vowel behaves under LP or HP filtering in general much like its Platonic ideal, the real vowel.

The linear model. It was assumed that the expected probability of a correct response, $p_f(C)$, was a linear function of the weighted number of formants that remained after the filtering process. More precisely,

$$p_{f_c}(C) = W_o + \sum_i^m \sum_j^n W_i \mathfrak{F}_{ij} + \epsilon \qquad \text{Equation (1)}$$

where f_c is a given HP or LP filter condition, m is the number of formants (3 in our case), j refers to the number of samples of each formant in the whole ensemble (in our case n = 70 for real vowels, and n = 14 for synthetic vowels). The number $\mathfrak{F}_{ij}$ is a random variable function of F_{ij} such that, for HP filtering,

$$\mathfrak{F}_{ij} = \begin{cases} 1 \text{ (HP) or } 0 \text{ (LP), if freq. in c/s of } F_{ij} > f_c, \\ 0 \text{ (HP) or } 1 \text{ (LP), if freq. in c/s of } F_{ij} \leq f_c. \end{cases}$$

The quantity ϵ is a normally distributed random variable, $N(0, \sigma^2)$. The value of $\mathfrak{F}_{ij}$ was found from the distribution of formant frequencies as measured from Kay sonagrams of 210 samples of real and 42 samples of synthetic vowels.

Computations to test this sample, quantitative model were done on the IBM 7090 Computer (the senior author (ECC) is indebted to one of his students, Mrs. Bernyce Byars, for assistance with the program). Here we can give only the major results of the test of the linear model comprised by Equation (1). Table II gives the multiple correlation coefficients (MCC), and maximum likelihood estimates of the constant W_o and the weights W_i to be associated with the *number* of formants of frequency F_i passed by the filter (maximum number of each $F_i = 70$). That the model gives an excellent account of the data is clear from Fig. 2. Solid lines connect theoretical values. Circles and triangles are experimental values. A useful interpretation of the MCC is to associate its square with that part of the total variation which has been accounted for by the independent variables using the *a priori* chosen Equation (1). On this view, the model accounts for 99.6 per cent of the variation in the best case and 98.6 per cent in the worst. A wrong model would prohibit high correlations even if the right variables and good data were used with it.

Condition	MCC	W_o	W_1	W_2	W_3
LP (R)	0.997	0	.00301	.00930	0
LP (S)	.994	−.1805	.00982	.00592	0
HP (R)	.995	0	.00358	.00985	−.00274
HP (S)	.993	.1500	.00520	.00612	0

Table II. Multiple correlation coefficients and weights. See text.

In summary, we found that (1) contrary to the smooth functions obtained by earlier workers of per cent correct identification of vowels *vs* filter cut-off frequency, discontinuities existed reflecting the non-uniform distribution of formant frequencies; (2) confusions ensuing when certain formants are eliminated may be explained by the relationship among those remaining – in either HP or LP filtering; (3) real and synthetic vowels behaved much alike; and (4) a simple, linear regression model describes the data adequately, on the assumption that correct responding will be proportional to the weighted sums of the number of formants available in a given filter pass-band. The model appears to hold equally well for real or synthetic vowels. Solution of the regression equations gives coefficients that may be used to adjust parameters of the analog vocal tract making possible even closer matches to real vowels.

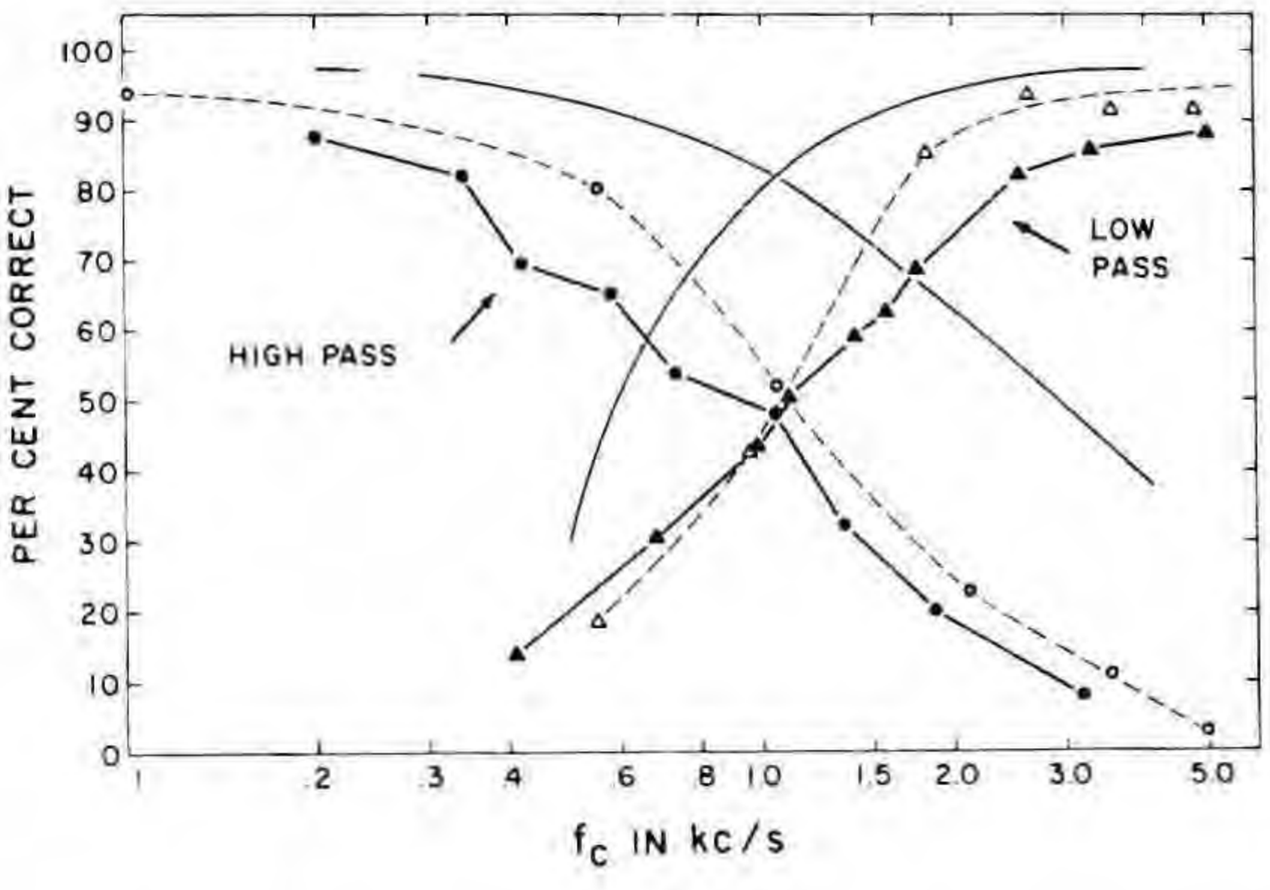

Figure 1. A comparison of the results using real vowels with those of two earlier studies. The Steinberg data (1929; topmost solid lines) were obtained with long vowels in consonant context, and ideal filters. Lehiste & Peterson (1959; broken lines) used 1500 msec vowel segments, and 40 db/octave filters. In our study the 500 msec vowel segments were passed through ideal filters.

Figure 2. Theoretical curves for probability of correct identification *vs* f_c in c/s, computed from Eq. (1) (solid = real; broken = synthetic). See text. The solid circles and triangles are real vowel data points, each based on 1638 observations. Open circles and triangles are synthetic vowel data points, each based on 378 observations.

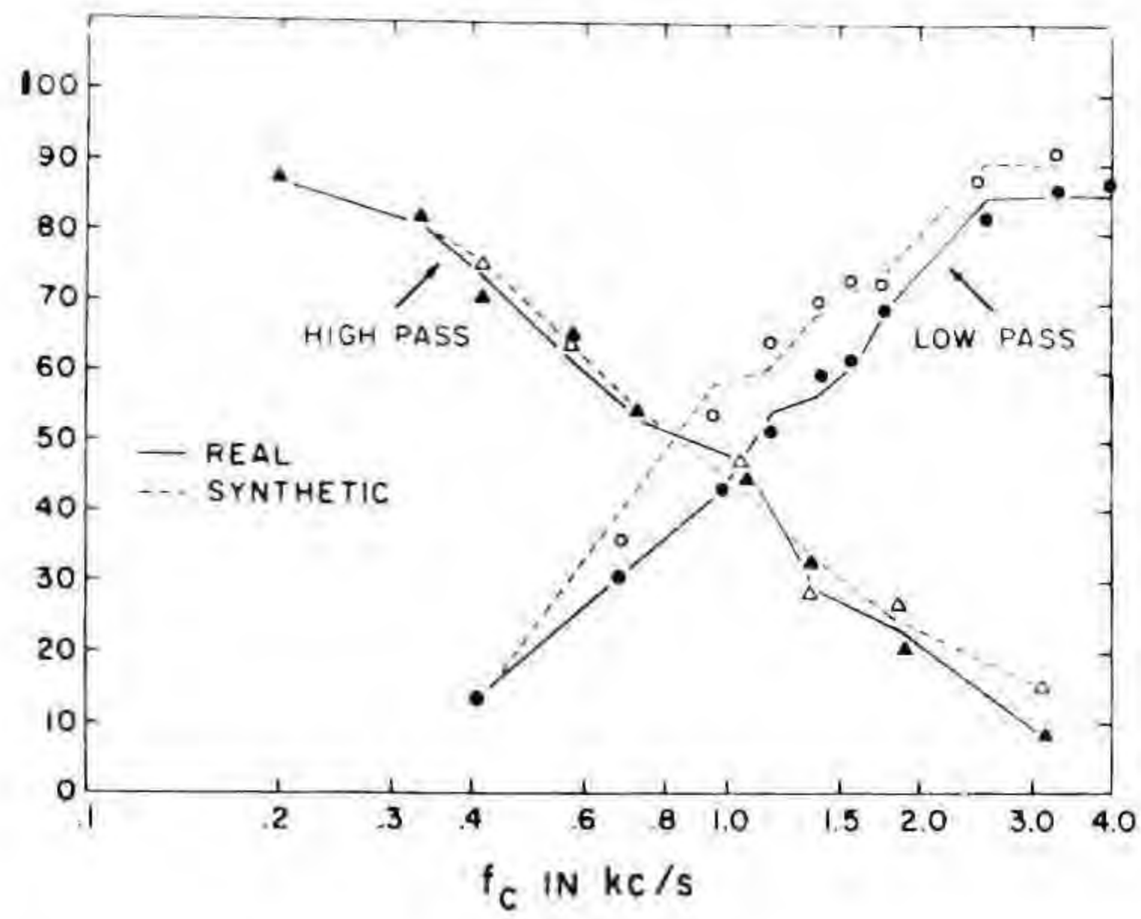

References

1. Cooper, F. S., *et al, J. Acoust. Soc. Amer.*, 24, 297-606 (1952).
2. Fletcher, H. *Speech and Hearing in Communication* (New York, 1953).
3. Fant, G. *Transactions of the Royal Inst. of Tech.*, 55 (Stockholm, 1952).
4. Fant, G. In *For Roman Jakobson* (The Hague, 1956) pp. 109-121.
5. Fant, G. *Acoustic Theory of Speech Production* (The Hague, 1960).
6. Lehiste, I., and Peterson, G., *Phonetica*, 4, 161-177 (1959).
7. Miller, G. A. In *For Roman Jakobson* (The Hague, 1956) pp. 353-360.

FOURTH INTERNATIONAL CONGRES ON ACOUSTICS
COPENHAGEN 21.-28. AUGUST 1962

Clinical determinations of the acoustic impedance of the eardrum.

K. Terkildsen, M.D.

Within clinical otology measurements of the impedance of the eardrum were met with hopes, that it would be possible to obtain a diagnosis in middle ear disease by entirely objective methods. As it happens in biological investigations the road has been tortuous and the findings often controversial. Attempts have been made to construct electrical analogue networks of the middle ear. Knowledge about many of the elements involved, however, is still uncertain, and it is fair to say, that such work is still at the level of basic science. The clinical value of such determinations is mainly attached to indirect evidence.

Metz (1946) found the impedance method suited to measure the intra-aural muscle reflexes, that are elicited acoustically via the cochlea as a bilateral reflex. In normal ears reflexes are present at an intensity of 70 -90 db. It is however not absolute intensities, that determine the onset of reflexes, but the subjective loudness sensation evoked by sound. In this manner the reflex threshold becomes objective evidence for the suprathreshold response of the ear, which is of diagnostic importance in the differentiation between hearing-losses of cochlear and retrocochlear origin. In cochlear disease the subjective loudness level will increase at an abnormally fast rate over the threshold of hearing. The existence of this phenomenon of loudness recruitment can be established by several methods. Clinical experience has shown that among these the reflex method is one of the most reliable, with the further advantage of being essentially a monaural procedure, so that it can be used also in patients with bilateral symmetrical hearinglosses.

In otosclerosis the intra-aural reflexes are absent due to fixation of the stapes. This fact is of diagnostic value in early stages of this disease, and where the perceptive element of the hearingloss is so pronounced, that ordinary audiometric results are inconclusive. In patients with paralysis of the stapedius muscle reflexes will also be missing. This muscle derives its innervation from the facial nerve, and evaluation of the intra-aural muscle response is an important part of our diagnostic means to locate the site of pathological conditions in this nerve. Psychogenic hearing disorders are often difficult to evaluate; also here the presence of acoustically elicited reflexes at a normal threshold may help to disclose the true nature of this condition.

The impedance of the ear is to a large extent determined by the pressure gradient across the eardrum. Pressure differences cause an increase of stiffness, and the impedance will be at a minimum under circumstances where the pressure in the middle ear and in the ear canal are exactly equal. Through measurements of the impedance at the same time as the pressure in the ear canal is changed, it is possible to determine this level of minimal impedance, which comes to indicate the pressure in the middle ear cavity. The middle ear pressure is controlled by the Eustachian tube, and normally it is very close to

the atmospheric level. Deviations from this level constitute a rather exact measure for the degree of pathological conditions in and around the Eustachian tube.

This short review shows the diagnostic range of the impedance method. All relevant informations are derived from measurement of the small changes of the eardrum impedance, which are caused by contractions of the intra-aural muscles, and those somewhat larger variations, that are produced in an artificial way through manipulations with external ear canal pressure. In consequence of this the requirements to an apparatus designed for clinical use should be a high degree of sensitivity, and the possibility of introducing artificial pressures towards the eardrum. On the other hand it is sufficient to use a single measuring frequency.

A block scheme of such an apparatus is seen in the figure

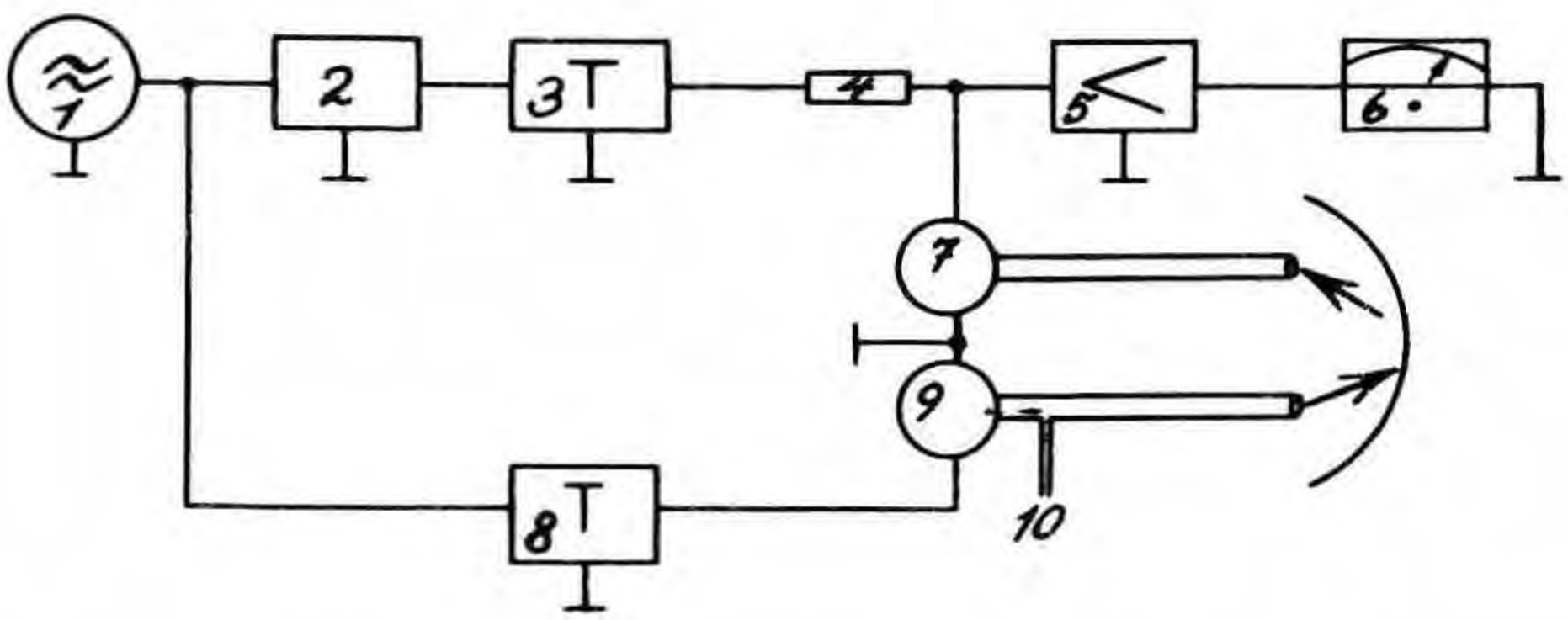

1. oscillator, 220 cps; 2. var. phase shift; 3. attenuator (amplitude); 4. resistor; 5. selective amplifier; 6. vacuum tube voltmeter; 7. microphone; 8. attenuator (sound pressure); 9. telephone; 10. pressure control inlet.

The main part of the apparatus is an earpiece with two hearing aid type earphones. One of these generates a test sound of 220 cps. Its opposite number acts as a sound probe microphone, which is activated according to the sound level in the measuring area. Both are connected to the ear canal by means of long narrow tubes, that are contained in a common insert tubing. Because of the deep test frequency it is essential to obtain an absolutely airtight closure of the ear canal so that the deep part of this canal is converted to a closed space in which the measuring takes place. For this purpose there is an inflatable rubber cuff around the distal part of the common insert tubing. From an acoustical standpoint all variations in the physically constant ear canal space are referable to the eardrum. The test frequency is so low in relation to the resonance of the ear, that stiffness is the main limitation to transmission of sound through the eardrum, and a change in stiffness will be reflected as a change of sound level in the measuring area. The increase of impedance that occurs during intra-aural muscle contractions is so small, that it was found necessary to introduce a balancing principle in order to obtain a satisfactory degree of sensitivity. The balancing is performed by means of a voltage from the original sound generator, passed to the sound probe microphone via an attenuator and a phase control stage. Through adjustments in these two stages the microphone is gradually brought to a zero state. The degree of balancing obtained at any spe-

cific time is read on a vacuum tube voltmeter, which is preceded by a selective amplifier.

Examination for the middle ear pressure level is carried out in the following way: A preliminary artificial plus 30 cm waterpressure is established in the ear canal space, and the sound probe microphone balanced to zero at this stage. When the pressure is made to pass via zero to negative levels, the middle ear pressure will be indicated on the voltmeter as a deflection of the pointer, which reaches a maximum and then returns towards zero. The magnitude of impedance variations during this procedure are so large that the selective amplifier preceding the voltmeter should be set somewhat below its maximum.

Measurements with this apparatus were calibrated against closed cavities of a hard plastic material. In 39 normal ears the average impedance was 1,69 ml. The impedance of the eardrum itself was estimated as the difference between values found with and without a pressure applied to it. In the same 39 ears the average result was 0,79 ml. This is very close to the figures given by Zwislocki (0,81 ml in his own investigations and 0,86 ml as calculated from the results of Metz). These values appear to indicate that the international 2 ml coupler is too large, but on the other hand individual variations are so large, that the acceptance of a fixed standard has no real meaning.

Because of the high degree of sensitivity obtained with this apparatus it was easy to record the period of latency for the muscle reflexes. With an intensity of 110 db at 1000 cps it averaged 44 msec. The same result was found in a series of persons, that for many years had been exposed to intense industrial noise. Nothing was found to indicate, that there is any relation between susceptibility to industrial noise trauma and the function of the middle ear muscles.

The intensity of the muscle reflexes as ascertained by the present method was found to depend upon the pressure gradient across the eardrum. For unknown reasons reflexes are strongest with slightly negative pressures in the ear canal. This is especially conspicuous in patients with cicatricial eardrums; thus a quantitative comparison of reflexes from one person to another is unreliable without having access to artificial control of the external ear canal pressure. To some extent there is a relation between the threshold of the reflexes and the reflex intensity, so that this demand for pressure control also applies to comparative threshold determinations.

At the present stage measurement of the eardrum impedance is a valuable method in clinical otology, but with further technical progress we expect even more information from such methods.

References.

Metz, O.: Acta oto-laryng. 1946, suppl. 63.

Zwislocki, J.: J. Acous. Soc. Amer. 1957, 29: 349.

J54

FOURTH INTERNATIONAL CONGRESS ON ACOUSTICS
COPENHAGEN 21.-28. AUGUST 1962

The Influence of Texture and Plastic Deformation on the Elasticity of Polycrystalline Metals

G. Bradfield

National Physical Laboratory, Teddington, Middlesex, England

(1) Introduction

Texture in metals is important industrially for the reasons that firstly the strength of, for example, wires[1] may be much greater when there is pronounced preferred orientation compared with wires which have random texture. This may also be true of rolled plates[2] in certain directions. Secondly, metals which have pronounced texture of certain types may "draw"[3,4] unevenly during fabrication and perhaps crack. Finally, and most basically, any attempt to investigate the elasticity of polycrystalline metals in the form of alloys will be almost worthless unless account is taken of the texture of the specimens. For example, two specimens of copper of identical composition but of different textures[5] may have Young's modulus values differing by 25% and the apparent Poisson's ratio of one may be as much as $\times 2\frac{1}{2}$ that of the other.

A great deal of information has been collected on the texture of deformed metals, especially with the help of X-rays. We have found, however, that simple X-ray examination is considerably less sensitive than certain measurements of elasticity for revealing non-random texture; these measurements are also able to reveal heterogeneous texture.

The problems involved in this subject are not simple. To avoid undue complication, attention will first be confined to texture which is circularly symmetrical, but even then not only do face-centred and body-centred cubic metals behave very differently but body-centred metals differ markedly between themselves. Hexagonal metals, though again different, vary their elasticity under deformation similarly among themselves, but to differing degrees. The elasticity of rolled plates rarely possesses circular symmetry and more complex treatment is needed.

(2) Polycrystalline Specimens with Random Texture. Krönner and Kneer Corrections

Hill[6] and others[7,8,9] considered the discrepancy between the elastic constants G_V (modulus of rigidity) and K_V (bulk modulus) deduced for the isotropic (i.e. random textured) metal by Voigt[10] integration of elastic constants and alternatively G_R and K_R deduced by Reuss[11] integration of the modulii of compliance over all possible orientations of the crystallites and Hill recommended taking averages of these: G_{VR}, K_{VR}. Assuming, for cubic metals, invariance of bulk modulus K, Krönner[12] and Hershey[13] independently evaluated a much more rigorous solution, G_{KH}, and the writer[14] has found that this fitted experimental data excellently. Kneer[15] applied the technique to hexagonal metals and Krönner[16] has further applied it to systems of still lower symmetry.

The Krönner[12] corrections[13] are functions of two variables which can conveniently be the anisotropy $A = 2c_{44}/(c_{11}-c_{12})$ and a Poisson's ratio, $\sigma_{VR}=(3K-2G_{VR})/(6K+2G_{VR})$ The writer[14] found Krönner's[12] solution, G_{KH}, of a cubic equation could be expressed in terms of a normalised difference, Δ_G, such that $\Delta_G = G_{KH}/G_{VR}-1$ which, for a limited range of variables, ($A = 2$ to $3\frac{1}{2}$, $\sigma_{VR} = 0.25$ to 0.35), is found to be $0.083\left(A+\frac{1}{A}-1.8\right)\sigma_{VR}^2$; rather similar simplifications in the case of the hexagonal single crystal may be possible and are being studied.

(3) Elastic Constant Matrices of Polycrystalline Aggregates of Non-Random Texture

The common deformations which affect texture are drawing, extrusion, axial

compression and rolling. The former, in general, result in textures possessing circular symmetry about the specimen axis and an elastic system also of circular symmetry. This requires five elastic constants to describe its behaviour not all of which are, however, necessarily independent [5,17]. Rolled plates, to be considered later, are less simple elastically and cross-rolled plates still less so. The five elastic constants derived by Voigt [10] averaging for the circularly symmetric textured specimens are $\overset{V}{c}_{11}$, $\overset{V}{c}_{12}$, $\overset{V}{c}_{13}$, $\overset{V}{c}_{33}$ and $\overset{V}{c}_{44}$, ($\overset{V}{c}_{66} = \frac{1}{2}(\overset{V}{c}_{11} - \overset{V}{c}_{12})$ accompanied by a corresponding compliance matrix, $\overset{R}{s}_{ij}$ derived by Reuss [11] averaging.

For single crystal constants of c_{11}, c_{12}, c_{44} for cubic metals and c_{11}, c_{12}, c_{44} c_{13}, c_{33} for hexagonal metals, the expressions in Table I [17,18] hold when the degree of departure from random texture and the extent of the anisotropy of the single crystals are both small.

Table I. Elastic Constants of Cubic and Hexagonal Metals with Circularly Symmetric Texture

	Cubic Metals		Hexagonal Metals
$\overset{V}{c}_{11}$ =	$\overset{OV}{c}_{11} + a_4 c_0/60$	=	$\overset{OV}{c}_{11} + 2a_2 c_1/105 + 3a_4 c_3/315$
$\overset{V}{c}_{12}$ =	$\overset{OV}{c}_{12} + a_4 c_0/180$	=	$\overset{OV}{c}_{12} - 2a_2 c_2/105 + a_4 c_3/315$
$\overset{V}{c}_{13}$ =	$\overset{OV}{c}_{12} - a_4 c_0/45$	=	$\overset{OV}{c}_{12} + a_2 c_2/105 - 4a_4 c_3/315$
$\overset{V}{c}_{33}$ =	$\overset{OV}{c}_{11} + 2a_4 c_0/45$	=	$\overset{OV}{c}_{11} - 4a_2 c_1/105 + 8a_4 c_3/315$
$\overset{V}{c}_{44}$ =	$\frac{1}{2}(\overset{OV}{c}_{11} - \overset{OV}{c}_{12}) - a_4 c_0/45$	=	$\frac{1}{2}(\overset{OV}{c}_{11} - \overset{OV}{c}_{12}) - a_2(c_1+c_2)/105 - 4a_4 c_3/315$

where $c_0 = c_{11} - c_{12} - 2c_{44}$; $c_1 = 4c_{11} - 3c_{33} - c_{13} - 2c_{44}$;

$c_2 = c_{11} + c_{33} + 5c_{13} - 7c_{12} - 4c_{44}$; $c_3 = c_{11} + c_{33} - 2c_{13} + 4c_{44}$;

and where $\overset{OV}{c}_{11}$, $\overset{OV}{c}_{12}$ are the two elastic constants (Voigt [10] averaging) of the random textured metal and where a_2 and a_4 are the second and fourth zonal harmonic coefficients of the texture [17,18] and higher order coefficients are disregarded. Similar expressions exist for the terms of the compliance matrix $\overset{R}{s}_{ij}$ based on Reuss [11] averaging.

When the elastic anisotropy of the single crystal is considerable, the compliance matrix no longer inverts to the elastic constant matrix. We can, however, from the $\overset{R}{s}_{ij}$ etc. matrix, deduce a $\overset{R}{c}_{ij}$ matrix and similarly deduce a $\overset{V}{s}_{ij}$ matrix from the $\overset{V}{c}_{ij}$ matrix, and use these as below; the reasons for this duality are the same as for the case of random texture.

(4) Application of Corrections to Cases of non-random Textures with Circular Symmetry

The nearer the approach to random texture the more precisely can the corrections of Kröner [12] and Kneer [15] be applied even in the cases of single crystal constituents of pronounced anisotropy.

For more pronounced textures, useful approximations result from Hill [6] averaging for the e.g. $\overset{V}{c}_{ij}$ and $\overset{R}{c}_{ij}$ derivatives. Although the hexagonal case still presents difficulties, for the cubic case, the Kröner [12] analysis [13] can be extended to yield a closer approximation thus. Compute a normalised difference $\overset{VR}{\Delta}_{ii} = (\overset{V}{c}_{ii} - \overset{R}{c}_{ii})/\frac{1}{2}(\overset{V}{c}_{ii} + \overset{R}{c}_{ii})$ Let Δ_{GVR} be the corresponding expression for the random texture case. Then the required corrections for i = 4 or 6 are approximately $\Delta_G \cdot \Delta_{ii}/\Delta_{GVR}$. For the corrections to the constants with i = 1 or 3, apply a reducing factor $G_{VR}/(\frac{3}{4}K + G_{VR})$. Using the values for i = 1 and 6, the corrections for i = i, j = 2 are obtainable and thence, by invariance of K, the corrections for i = 1, j = 3.

(5) Deformation Texture [19] and Elasticity of Copper, Iron and Niobium

The operation of drawing or extruding an f.c.c. metal results in a texture

approximating to [111] , but similar working of a b.c.c. metal, because quite different slip systems come into play, produces a texture more nearly approximating to [110] , though displaced in the stereographic triangle somewhat towards the [100] corner. In general, however, the textures which result from deforming f.c.c. metals in this way are similar, the main fluctation being a minor but variable amount of [100] texture. Textures in deformed b.c.c. metals, though different from the f.c.c. metals, are also similar among themselves. The changes in strength due to texture which occur in f.c.c. metals due to drawing and extruding are similar and so are the changes in elasticity, though the resulting degree of the anisotropy of the polycrystalline metals differ. But, as Table II shows, b.c.c. metals seem to possess more widely varied types of elastic anisotropy than f.c.c. metals. Thus, in practice the Young's modulus of drawn copper is perhaps 20% greater than for random texture while that for drawn niobium is perhaps only 7% greater while for drawn iron it is perhaps about 2½% less than for random texture, the percentages depending on drawing severity.

Table II. Comparison of f.c.c. and b.c.c. Elastic Anisotropy

	Ref		A	c_{11}	c_{12}	c_{44}	Young's Modulus(10^{11}dyn/cm^2) in Directions:- [100]	[110]	[111]	Random	σ_{VR}
				x 10^{11}dyn/cm^2							
Copper	(20)	f.c.c.	3.2	16.9	12.2	7.6	6.69	13.1	19.1	13.0	0.34
Silver	(21)	f.c.c.	3.0	12.4	9.3	4.6	4.38	8.4	12.1	8.3	0.37
Iron	(20)	b.c.c.	2.4	23.7	14.1	11.6	13.2	22.0	28.4	21.1	0.27
Tantalum	(22)	b.c.c.	1.6	26.7	16.2	8.2	14.6	19.4	21.8	18.6	0.34
Molybdenum	(23)	b.c.c.	0.8	46	17.6	11.0	35.6	30.4	29.0	31.6	0.31
Niobium	(22)	b.c.c.	0.5	24.6	13.5	2.9	15.2	9.2	8.2	10.5	0.37

(6) Deformation Texture[19] and Elasticity of Titanium and Zinc

When hexagonal metals are drawn or extruded their basal planes tend to align themselves with the drawing or extrusion direction; when such metals are uniaxially compressed the basal planes turn off orthogonally. It is curious to observe that the basal planes tend to align themselves with respect to the plastic vector very much the same as a Rayleigh disc in acoustics with respect to the displacement vector. It will thus be found that the Young's Modulus of a bar cut normal to the plastic vector in the case of strong uniaxial compression, is closely similar to $1/s_{11}$ for the single crystal e.g. about 1.2×10^{12} dyn/cm^2 for a zinc specimen.

The effects on the various elastic constants of a uniaxial compression on extruded titanium are very different, values for increments being:-
Δc_{11}, -2.72%; Δc_{33}, 3.43%; Δc_{12}, 7.8%; Δc_{13}, -10.4%; Δc_{44}, 6.38%; Δc_{66}, -11.9%.
These data enable the texture coefficients a_2 and a_4 to be calculated with the help of the single crystal constants, which are approximately:- c_{11}, 16.3; c_{12}, 9.3; c_{13}, 6.2; c_{33}, 18.0; c_{44}, 4.6 all$\times 10^{11}$ dyn/cm^2 units.

(7) Texture in Rolled Plates

The texture in rolled plates in general results in an elastic system of the orthorhombic system with 9 elastic constants. Nevertheless, an approximate procedure enabling the general trend of the changes of elasticity for weak deformations to be evaluated is to consider the superposition of the effects of a uniaxial extension in the rolling direction, together with a uniaxial compression in the plate thickness direction; in the simplest case these deformations can be numerically nearly equal.

(8) The use of the Ultrasonic Goniometer for the Examination of Elasticity in textured Metals

The ultrasonic goniometer described by the writer in the 1959 I.C.A. Congress is a most valuable instrument for the investigation of texture in metals. The fundamental reason is that texture must be described by reference to a plane in the anisotropic specimen and to a direction lying in that plane e.g. a (110) [1$\bar{1}$2] texture. This is exactly the type of examination into elasticity provided by the ultrasonic goniometer, for the surface wave used is allowed to propagate in the desired surface

and its behaviour when travelling in a particular direction in that surface in the specimen can then be studied. This device is also very useful for measuring the constant c_{13}. These matters are discussed in more detail by the writer in National Physical Laboratory Note on Applied Science No. 30.

Using this device there are three principle waves in testing a specimen with circular symmetry of texture. The results of such tests for extruded brass and in titanium and zinc of various textures are given in Table III expressed as the elastic constant associated with the surface wave; the units are 10^{11} dyn/cm^2.

Table III. Effective Surface Wave Elastic Constants for Three Metals

Sagittal Plane Direction	Surface	Brass	← Titanium →			← Zinc →		
		Texture						
		Extruded	Extruded	Random	Uniaxially Compressed	Extruded	Random	Uniaxially Compressed
Basal	Basal	2.94	3.67	3.81	3.95	3.76	3.54	3.33
// to Axis	Axial	3.32	3.65	3.81	3.96	3.60	3.54	3.12
⊥ to Axis	Axial	3.22	4.01	3.81	3.61	2.75	3.54	3.94

(9) References

1. Phillips, A.S. and Smith, A.A., ASTM Proc., 1936, 36, p.62, p.263. Schmid, E. and Wassermann, G., Zeits. f. Phys., 1927, 42, p.779.
2. Baldwin, W.M., Trans. AIME, 1946, 166, p.591.
3. Kaiser, K., Z. Metallkunde, 1927, 19, p.435.
4. Cook, M. and Richards, T.L., J. Inst. Metals, 1943, 69, p.201.
5. Bradfield, G., Pursey, H., Phil. Mag., 1953, 44, p.437.
6. Hill, R., Proc. Phys. Soc. Lond., A65, 1952, p.351.
7. Goens, E. and Schmid, E., Naturwissenschaften, 19, 1931, p.520.
8. Bruggeman, D.A.G., Z.Physik, 92, 1934, p.561.
9. Weerts, J., Z. Metallkunde, 25, 1933, p.101.
10. Voigt, W., Lehrbuch d. Kristallphysik, 1910, Leipzig and Berlin, (Teubner).
11. Reuss, A., Z. angew. Math. Mech., 9, 1929, p.49.
12. Kröner, E., Z.P.Phys., 1958, 151, p.504.
13. Hershey, A.V., J. Appl. Mech., 21, 1954, p.236.
14. Bradfield, G., (in course of publication).
15. Kneer, G., (Private communication). 16. Kröner, E., (Private communication).
17. Pursey, H. and Cox, H.L., Phil. Mag., 1954, 45, p.295.
18. Bradfield, G., Hearn, C.J. and Pursey, H., Unpublished work.
19. Barratt, C.S., "Structure of Metals" 1953: London, New York (McGraw-Hill).
20. National Physical Laboratory. Unpublished work.
21. Bacon, R. and Smith, C.S., Acta Metallurgica, 1956, 4, p.337.
22. Bolef, D.I., J. Appl. Phys. (U.S.A.), 1961, 32, p.100.
23. Druyvesteyn, M.J., Physica, 1941, 8, p.439.

Acknowledgment

The work forms part of the research programme of the National Physical Laboratory and is published by permission of the Director.

K54

FOURTH INTERNATIONAL CONGRESS ON ACOUSTICS
COPENHAGEN 21.-28. AUGUST 1962

ACOUSTIC WAVEGUIDE MODE INTERFERENCE AND DAMPING IN VISCOUS FLUIDS

RICHARD A. ELCO and WILLIAM F. HUGHES
Carnegie Institute of Technology, Pittsburgh, Pa., U.S.A.

I. INTRODUCTION

The mode interference and waveguide effects observed in the measurement of ultrasonic absorption in liquids have stimulated interest in the acoustic waveguide modes. The early work by Rayleigh[1] for an inviscid fluid gives the propagation constants for each mode and relates the mode amplitude to the boundary conditions at the sound source. Recent works[2,3] have for the most part also assumed the fluid to be inviscid. Some attempts have been made to include viscous effects but, because of the inhomogeneous boundary conditions on pressure, only solutions for the lowest mode have been obtained.[1,4] To describe properly the experimental observations it is necessary that the effects of viscosity on the modes of propagation be determined. However, there appears to be some question as to the proper form which the viscosity coefficients should take. From the literature[5,6,7] it can be concluded that the second coefficient of viscosity, μ', can be complex and frequency dependent (thus accounting for relaxation effects) and that the Stokes relationship is not generally true. Therefore if a generalized μ' is used a realistic description of the waveguide modes is possible.

In the following analysis the modes of propagation and propagation factors are determined for a cylindrical pipe of radius a, filled with a liquid of viscosity μ and a second coefficient of viscosity μ'. Experimental measurements of pressure profiles are described and discussed.

II. BASIC EQUATIONS

The equation of motion for small amplitude waves is

$$\rho_o \frac{\partial \vec{u}}{\partial t} = -\nabla P + \frac{4}{3}(\mu + \mu')\nabla(\nabla \cdot \vec{u}) - \mu \nabla \times \nabla \times \vec{u} \tag{1}$$

where ρ_o is the unperturbed mass density, $\vec{u}$ the velocity vector, and P the perturbed pressure. The equation of continuity is

$$\rho_o \nabla \cdot \vec{u} = -\frac{\partial \rho}{\partial t} \tag{2}$$

where ρ is the perturbed mass density. The equation of state can be written

$$\rho = \frac{P}{c^2} \tag{3}$$

where c is the isentropic sound velocity in the fluid. By introducing the fluid vorticity as $\vec{\Omega} = \nabla \times \vec{u}$ (where $\nabla \cdot \vec{\Omega} = 0$) and combining equations (1) through (3) the following wave equation in P and diffusion equation in $\vec{\Omega}$ result:

$$\nabla^2 P + \frac{4}{3}\frac{(\mu + \mu')}{\rho_o c^2}\nabla^2 \frac{\partial P}{\partial t} = \frac{1}{c^2}\frac{\partial^2 P}{\partial t^2} \tag{4}$$

$$\nabla^2 \vec{\Omega} = \frac{\rho_o}{\mu}\frac{\partial \vec{\Omega}}{\partial t} \tag{5}$$

Then assuming a steady state solution for P and $\vec{\Omega}$ of the form $\exp(j\omega t + k_n z)$ equations (4) and (5) become

$$\nabla_t^2 P + P\left[\frac{K_n^2\left(1 + j\frac{\omega}{\omega_o}\right) + \frac{\omega^2}{c^2}}{1 + j\frac{\omega}{\omega_o}}\right] = 0 \tag{6}$$

$$\nabla_t^2 \vec{\Omega} + \vec{\Omega}\left(K_n^2 - j\frac{\omega \rho_o}{\mu}\right) = 0 \tag{7}$$

where ∇_t^2 is the transverse scalar and vector operator for equations (6) and (7) respectively, and $\omega_o = \rho_o c^2/(4\mu/3 + \mu')$. The velocity $\vec{u}$ in terms of P and $\vec{\Omega}$ is from equation (1):

$$\vec{u} = -\frac{1}{j\omega\rho_o}\left[\left(1 + j\frac{\omega}{\omega_o}\right)\nabla P + \mu\nabla\times\vec{\Omega}\right] \tag{8}$$

Assuming cylindrical symmetry and using the identity $\nabla\cdot\vec{\Omega} = 0$ it can be shown that only the ϕ component of (7) is needed to determine the velocity $\vec{u}$. Then the solutions to (6) and (7), requiring that P and Ω_ϕ remain finite at r = 0, are:

$$P = A J_o(\gamma_n r) \quad ; \quad \Omega_\phi = B I_1(\tau_n r) \tag{9}$$

where A and B are arbitrary constants. The eigenvalues γ_n and τ_n are given by

$$\gamma_n^2 = K_n^2 + \frac{\omega^2}{c^2}\left[\frac{1 - j\frac{\omega}{\omega_o}}{1 + \frac{\omega^2}{\omega_o^2}}\right] \tag{10}$$

$$\tau_n^2 = -\left(K_n^2 - j\frac{\omega\rho_o}{\mu}\right) \tag{11}$$

Evaluation of (8) using the boundary condition that $\vec{u} = 0$ at r = a leads to the following relationship for γ_n and τ_n.

$$K_n^2\,\frac{I_1(\tau_n a)}{I_o(\tau_n a)} = \gamma_n\tau_n\,\frac{J_1(\gamma_n a)}{J_o(\gamma_n a)} \tag{12}$$

which together with (10) and (11) specify completely the values of k_n, γ_n, and τ_n.

At this point the assumption will be introduced that $\omega \ll \rho_o c^2/\mu$ which for most fluids (including water) implies that $\omega \ll 10^{12}$ rad./sec. This condition is easily met in ultrasonic measurements. Then the value of τ_n^2 in equation (11) can be approximted by

$$\tau^2 \cong j\frac{\omega\rho_o}{\mu} >> 1 \tag{13}$$

where the subscript is dropped since τ^2 has only one value. Equation (12) can then be approximated by

$$K_n^2 = \gamma_n\tau_n\,\frac{J_1(\gamma_n a)}{J_o(\gamma_n a)} \tag{14}$$

The value of ω_o for most fluids will be of order $\rho_o c^2/\mu$ even if μ' is three or four orders of magnitude greater than μ. Therefore the condition $\omega/\omega_o < 1$ is valid over the range of most ultrasonic investigations.

III. SOLUTIONS FOR γ_n AND K_n.

An exact solution of equation (14) for the values of γ_n cannot be readily obtained since the γ_n are generally complex. However, at low frequencies or for situations where the viscous effects are very small, the solution of (14) should differ only slightly from the solution for zero viscosity. The solution for the inviscid modes (which correspond to the boundary condition $\partial P/\partial r = 0$ at the wall) is

$$\gamma_n = \frac{\lambda_{n1}}{a} \qquad n = 0, 1, 2, \ldots \tag{15}$$

where λ_{n1} are the zeroes of $J_1'(x)$. Then using a Taylor series expansion of $J_1'(x)$ about its zeroes and retaining only the first two terms of the series, equation (14) becomes

$$K_n^2 = \gamma_n\tau a\left(\gamma_n - \lambda_{n1}/a\right) \tag{16}$$

Substituting (10) for k_n^2 and solving for γ_n there results

$$\gamma_n = \frac{1}{2}\left[\frac{\lambda_{n1}}{a} + \left(\frac{\lambda_{n1}^2}{a^2} - 4\,\omega^2/\tau a c^2\right)^{\frac{1}{2}}\right] \tag{17}$$

where terms of order ω/ω_o are neglected. For (17) to be valid $\left|\frac{4\omega^2}{\tau a c^2}\right| \ll 1$ and using this condition the eigenvalues are

$$\gamma_o = j\frac{\omega}{c\sqrt{\tau a}} \quad ; \quad \gamma_n = \frac{\lambda_{n1}}{a}\left(1 - \frac{\omega^2 a}{\lambda_{n1}^2 c^2\tau}\right) \qquad n = 1, 2, 3, \ldots \tag{18}$$

When $\left|\frac{\omega^2 a}{\lambda_{n1}^2 c^2 \tau}\right|$ approaches unity, it is apparent that the eigenvalues no longer correspond to values of λ_{n1}/a. This fact indicates that at frequencies of the order $\nu = (\rho_0 c^4/\mu a^2)^{\frac{1}{3}}$ the modes are significantly different from the inviscid modes. This change in the modes is due to the viscous damping of the radial waves which upon reflection from the walls establish the mode patterns. There appears to be some experimental evidence for water at frequencies near 5 mc. that the pressure at the wall is zero and the mode interference pattern seems to fit the modes corresponding to pressure relieved boundary conditions at the wall.[8] Physically, however, the boundary condition $\vec{u} = 0$ applies at the wall and it is probable that solutions of (14) for high frequencies correspond to the pressure relieved modes. For high frequencies then the solution is approximated by expanding about the pressure relieved eigenvalues which are (using P = 0 at r = a):

$$\gamma_n^* = \lambda_{no}/a \quad ; \quad n = 1, 2, 3, \cdots \tag{19}$$

where λ_{no} are the zeroes of $J_0(x)$. Then expanding $J_0(\gamma_n a)$ about its zeroes and retaining the first order terms, (14) becomes

$$K_n^2 = \gamma_n \tau/(\gamma_n^* - \gamma_n)a \tag{20}$$

Now assuming that $\gamma_n = \alpha \gamma_n^*$ (for α close to unity) the solution for α is

$$\alpha = (1 - \tau c^2/\omega^2 a)^{-1} \tag{21}$$

and γ_n is

$$\gamma_n = \frac{\lambda_{no}}{a}\left(1 - \tau c^2/\omega^2 a\right)^{-1} \cong \frac{\lambda_{no}}{a}\left(1 + \tau c^2/\omega^2 a\right) \; ; \quad n = 1, 2, 3, \cdots \tag{22}$$

The condition for the validity of (22) is that $\left|\frac{\omega^2 a}{\tau c^2}\right| \gg 1$ which is indeed the case at high frequencies.

These results show that as frequency increases the n = 0 and n = 1 low frequency modes degenerate into the n = 1 pressure relieved mode and that the n = m modes go into the corresponding pressure relieved modes. This transition occurs in the region of $\omega \approx \nu$ which for water in a 10. cm. diameter pipe is approximately 1 mc.

The propagation factor k_n from equation (10) is

$$K_n = \pm j \frac{\omega}{c\left(1 + \frac{\omega^2}{\omega_0^2}\right)^{\frac{1}{2}}} \left[\left(1 - \frac{\gamma_n^2 c^2}{\omega^2}\left(1 + \frac{\omega^2}{\omega_0^2}\right)\right) - j\frac{\omega}{\omega_0}\right]^{1/2} \tag{23}$$

and the value of γ_n is given by (18) if $\omega \ll \nu$ or by (22) if $\omega \gg \nu$. Because of the complicated nature of the general expression for the real and imaginary parts of (23) only two special cases will be considered here. The first case is for $\lambda_{n1}c/a < \omega < \omega_0$ which corresponds to the range of frequencies used in ultrasonic measurements. The second case is for $\mu/\rho_0 a^2 < \omega < \lambda_{n1}c/a$ which is the audio and sub- audio range in such phenomena as water hammer. The approximate solutions of (23) for the ultrasonic case are:

$$K_0 \cong \pm j\frac{\omega}{c} \pm \left[\omega^2/c\omega_0 + \frac{1}{c}\sqrt{2\omega\omega_L}\right] \tag{24}$$

$$K_n \cong \pm j\frac{\omega}{c}\left(1 - \frac{\lambda_{n1}^2 c^2}{2a^2\omega^2}\right) \pm \frac{\omega^2/c\omega_0 + \frac{1}{c}\sqrt{2\omega\omega_L}}{2\left(1 - \frac{\lambda_{n1}^2 c^2}{2a^2\omega^2}\right)} \; ; \quad n = 1, 2, 3, \cdots \tag{25}$$

where $\omega \ll \nu$ and $\omega_L = \frac{\mu}{\rho_0 a^2}$. For $\omega \gg \nu$, k_n is:

$$K_n \cong \pm j\frac{\omega}{c}\left(1 - \frac{\lambda_{no}^2 c^2}{2a^2\omega^2}\right) \pm \frac{\omega^2/c\omega_0 + \frac{\lambda_{no}^2 c}{a^2\omega}\left(\frac{2\nu}{\omega^3}\right)^{\frac{1}{2}}}{2\left(1 - \lambda_{no}^2 c^2/2a^2\omega^2\right)} \; ; \quad n = 1, 2, \cdots \tag{26}$$

It is apparent that in the vicinity of $\omega \approx \nu$ the imaginary part of γ_n increases the attenuation of each mode. The approximate solution of (23) for the audio range is:

$$K_n \cong \pm j\frac{\omega^2 a}{2c^2}\left[\frac{\omega/\omega_0 + \sqrt{2\omega_L/\omega}}{\lambda_{n1}}\right] \pm \frac{\lambda_{n1}}{a} \; ; \quad n = 1, 2, 3, \cdots \tag{27}$$

and k_o is identical to (24). Hence only the n = 0 mode predominates because of the large damping of the $n \geq 1$ modes.

IV. EXPERIMENTAL PRESSURE PROFILE MEASUREMENTS

Pressure profile measurements for a water filled vertical waveguide were made using a magnetostriction probe [9] which was inserted radially into the waveguide of radius 2.4 cm. The probe diameter was 1 mm. and the upper cutoff frequency of the probe was 350 kc. The ultrasonic waves were excited by a circular quartz transducer of radius 1.27 cm. Standard pulse techniques were used.[8] The frequency range investigated was from 100 kc. to 300 kc. The output of the probe consisted of a series of pulses the first of which was the incident transmitted pulse, and the later pulses were alternately relections from the free surface and reflections from the transducer plate. Knowing the geometry, the time interval between pulses was accurately determined. Future measurements are planned over the entire transition region. Typical pressure profiles are shown in Fig. 1 for various distances from the sending transducer. The decay of the higher order modes is very apparent.

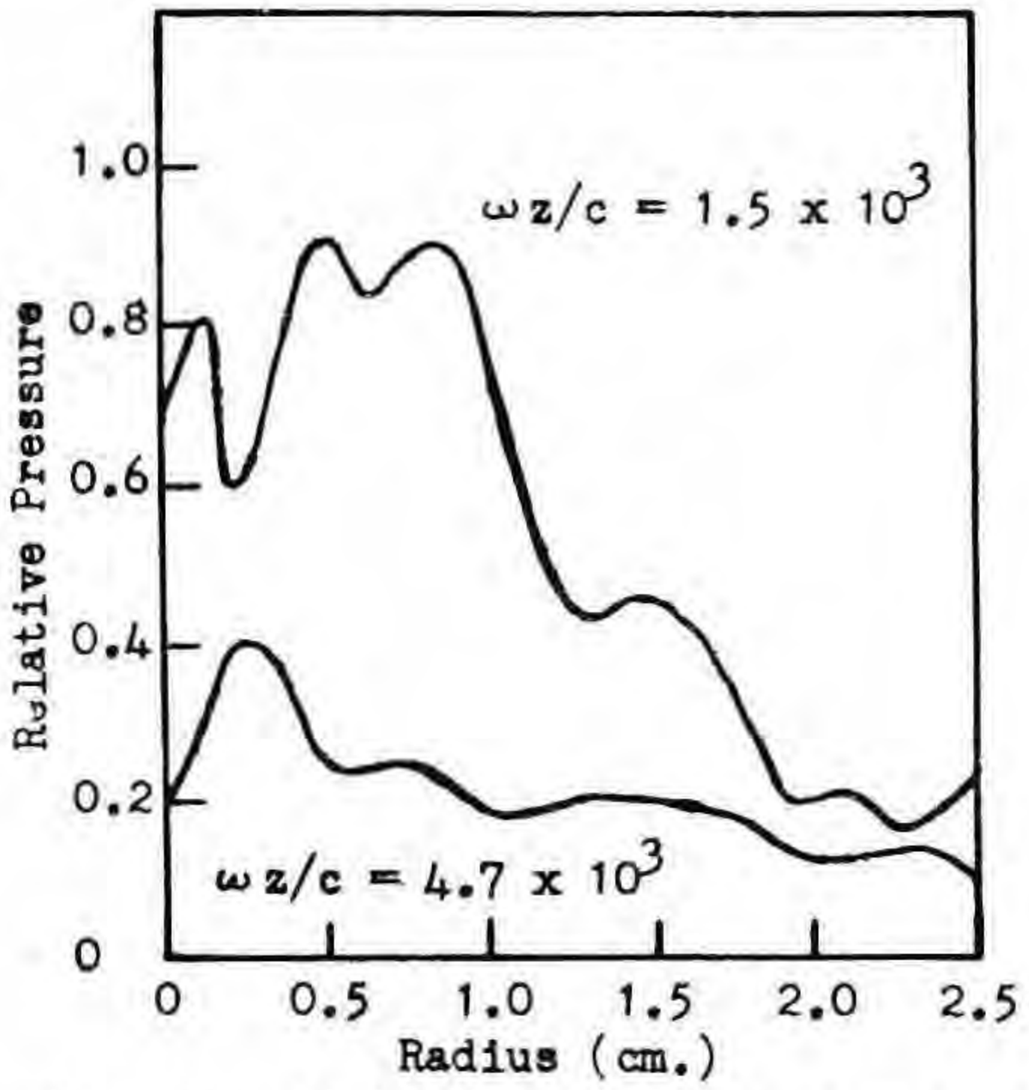

Fig. 1. Plot of relative pressure vs. radius for various axial distances from the sending transducer. ($\omega/2\pi$ = 200 kc.)

V. CONCLUSIONS

It has been shown that approximate solutions can be obtained for a wide range of frequencies by expanding about asymptotic eigenvalues. For $\omega \ll \nu$ the wall boundary condition of $\partial P/\partial r = 0$ is a good approximation, and for $\omega \gg \nu$ the condition $P = 0$ at the wall is a good approximation. It follows that solutions can be constructed by an ortho-normal expansion since the eigenfunctions will still be orthogonal to the order of the eigenfunction approximation. This type of expansion is classical and is not repeated here.[2,3] It may be concluded that water hammer solutions can be approximated as in ref. 10.

REFERENCES

1. Lord Rayleigh, The Theory of Sound, Vol. II, Chapters 13 and 19, Dover, N. Y.
2. M. Redwood, Proc. Phys. Soc. (London), Vol. 70, 1957, p. 721.
3. E. F. Carrome and J. M. Witting, J. Acoustical Soc. Amer., Vol. 33, 1961, p. 187.
4. H. Cohen and Yih-O Tu, A. S. M. E. paper No. 61 - WA - 48, 1961.
5. L. Tisza, Phys. Rev., Vol. 61, 1942, p. 531.
6. L. Rosenhead, Proc. Royal Soc. London, Vol. 226A, 1954, p 1.
7. K. F. Herzfeld and T. A. Litavitz, Absorption and Dispersion of Ultrasonic Waves, Academic Press, New York, 1959.
8. E. F. Carrome and J. M. Witting and P. A. Fleury, J. Acoustical Soc. Amer., Vol. 33, 1961, p. 1417.
9. L. Bohn, Acustica, Vol. 7, 1957, p. 201.
10. W. F. Hughes, Some Aspects of Wave Propagation in Viscous Liquids in Conduits, submitted to Applied Scientific Research, (Holland).

Acknowledgement. The work underlying this paper was supported by a grant from the National Science Foundation.

L54

FOURTH INTERNATIONAL CONGRESS ON ACOUSTICS
COPENHAGEN 21.-28. AUGUST 1962

MULTI-MOUNT ISOLATION SYSTEMS

Alan O. Sykes
David Taylor Model Basin
Washington 7, D. C.

INTRODUCTION

A commonly used method for estimating the effectiveness of an isolation mount system in reducing machine-excited foundation vibration is to find the transmissibility of the machine-mounts system treating the machine as a rigid mass, the system of mounts as a massless paralleled spring-dashpot combination, the foundation as being infinitely stiff and massive.

In recent years this approach has been modified by use of impedance and mobility concepts to take account of inertia, elasticity, and dissipation in the machine, mounts and foundation[1,2].

This paper attempts a generalization of the latter approach employing somewhat expanded concepts of point and transfer impedance. Coupling between mounts by machine and foundation is accounted for, and provision is made for estimating the effectiveness of the system of mounts in reducing vibration at each mounting point on the foundation.

It is assumed that the machine, mounts, and foundation are linear mechanical elements which obey the reciprocity principle, and that the forces generated by the machine, which are responsible for the foundation vibration, are independent of what structure the machine is attached to.

POINT AND TRANSFER MOBILITY AND IMPEDANCE MATRICES

Consider a set of rectangular cartesian coordinate axes, each coordinate axis designated by a subscript 1, 2, or 3, located at an arbitrary point p on a mechanical system S. A sinusoidal vibratory force exerted at p, parallel to any one of the coordinate axes, will, in general, generate a vibratory velocity having components parallel to each of the three coordinate axes. The relations between the phasors F_k^P and $\dot{x}_k^P$ of the components of the force and the velocity at p are given by the matrix equations

$$\dot{x}^P = Y_S^{PP} F^P \quad (1) \qquad F^P = Z_S^{PP} \dot{x}^P \quad (2)$$

where $\dot{x}^P$ and F^P are column matrices of the type y^P, and Y_S^{PP} and Z_S^{PP} are square matrices (3 x 3) of the type R_S^{PP}.

---

1. C. Molloy, Use of Four Pole Parameters in Vibration Calculations, JASA 29, 842, 1957.
2. A.O. Sykes, Vibration Isolation When Machine and Foundation are Resilient and Wave Effects Occur in the Mounts, David Taylor Model Basin Report 1404, September 1960; see also Noise Control, May - June 1960.

$$y^P = \begin{bmatrix} y_1^P \\ y_2^P \\ y_3^P \end{bmatrix} \quad (3) \qquad R_S^{PP} = \begin{bmatrix} R_{S11}^{PP} & R_{S12}^{PP} & R_{S13}^{PP} \\ R_{S21}^{PP} & R_{S22}^{PP} & R_{S23}^{PP} \\ R_{S31}^{PP} & R_{S32}^{PP} & R_{S33}^{PP} \end{bmatrix} \quad (4)$$

Y_S^{PP} is the matrix of point mobility coefficients of S at p; Z_S^{PP} the matrix of point impedance coefficients; Y_{Sij}^{PP} and Z_{Sij}^{PP} are the mobility and impedance coefficients respectively. Since by hypothesis, the systems under discussion are reciprocal, $R_{Sij}^{PP} = R_{Sji}^{PP}$, it follows from Equation (4) that six mobility or impedance coefficients are required to characterize a single point on a mechanical system.

Consider now two arbitrarily selected points p and q on S, each with its own set of coordinate axes. A sinusoidal vibratory force exerted at p parallel to one of the coordinate axes at p will, in general, generate a vibratory velocity at q having components parallel to each of the three coordinate axes at that point; similarly a vibratory velocity applied at p parallel to one coordinate axis will generate a vibratory force at q with components parallel to each of the three axes at q.

The relations between the phasors F_k^P and $\dot{x}_k^q$ of the components of the force applied at p and the components of the resulting velocity at q, and between the phasors $\dot{x}_k^P$ and F_k^q of the components of the velocity applied at p and of the resulting force at q are given by the equations

$$\dot{x}^q = Y_S^{qP} F^P \quad (5) \qquad F^q = Z_S^{qP} \dot{x}^P \quad (6)$$

where $\dot{x}^q$, $\dot{x}^P$, F^q, F^P are defined by Equation (3), Y_S^{qP} and Z_S^{qP} by Equation (4) with the first superscript p replaced by q.

Y_S^{qP} is the matrix of transfer mobility coefficients; Z_S^{qP} the matrix of transfer impedance coefficients; the Y_{Sij}^{qP} and Z_{Sij}^{qP} being the transfer mobility and impedance coefficients respectively. The matrices Y_S^{qP}, Z_S^{qP} are not, in general, symetrical, but have 9 different coefficients. Since as a consequence of reciprocity Y_S^{qP} and Z_S^{qI} are equal to the transposes of the matrices Y_S^{Pq} and Z_S^{Pq} respectively, it follows that any two-terminal mechanical system whose terminals may be represented as points which move in three dimensions requires 21 independent mobility or impedance coefficients to characterize it: 6 independent coefficients being required for each drive point matrix; 9 for the transfer matrix.

MOUNT EFFECTIVENESS

The effectiveness of a mounting system in isolating a vibrating machine from a foundation can be defined at each mounting point on the foundation in terms of two conceptual experiments indicated respectively in Figures 1 and 2:

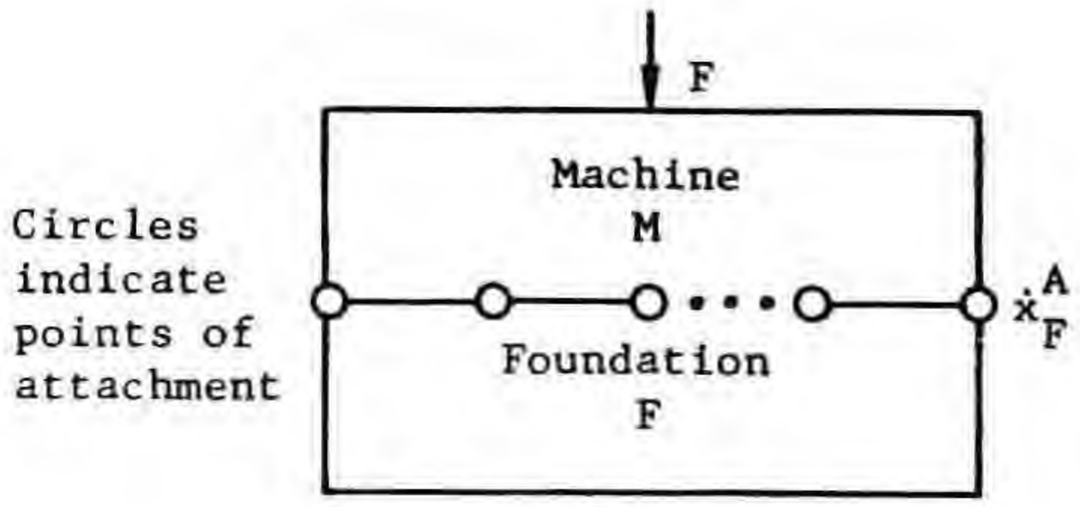

Fig. 1
Machine-Foundation System

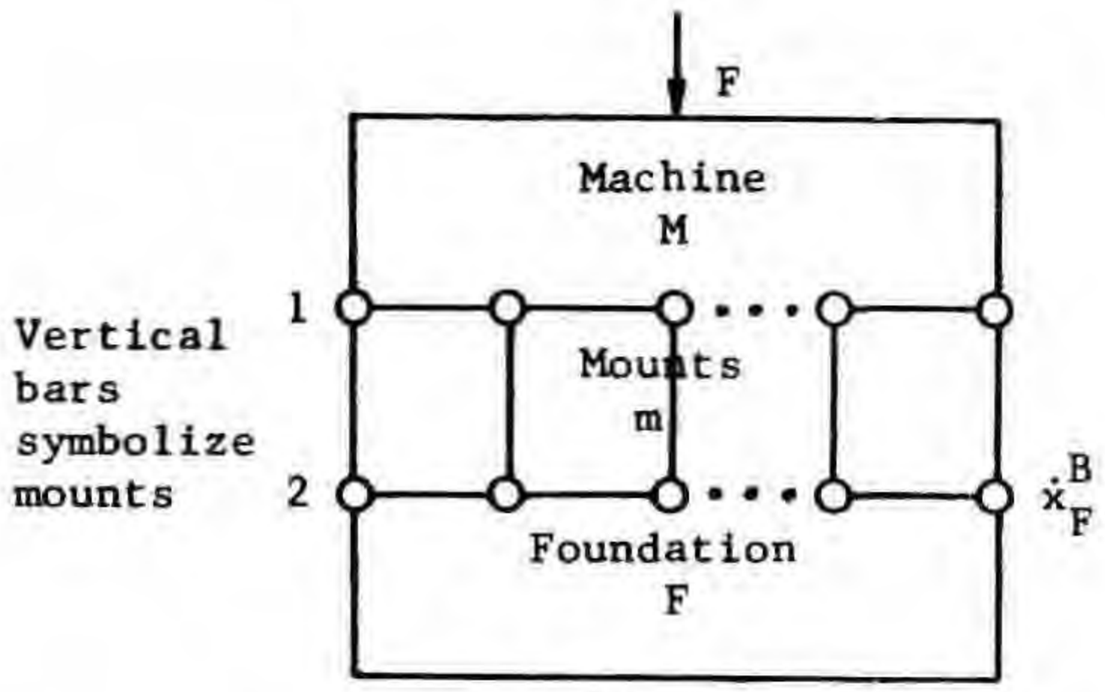

Fig. 2
Machine-Mounts-Foundation System

In the first experiment, the machine is fastened directly to the foundation, and the phasor $\dot{x}_{Fk}^{Ai}$ of each component of the vibratory velocity at each mounting point on the foundation is determined.

In the second experiment the machine is fastened to the foundation by the system of mounts m, and the phasor $\dot{x}_{Fk}^{Bi}$ of each component of the vibratory velocity at each foundation mounting point is again determined.

The ratio of the phasor of the kth component of the vibratory velocity at the ith foundation mounting point in the first experiment to the phasor of the kth component of the vibratory velocity at the ith foundation mounting point in the second experiment, $\dot{x}_{Fk}^{Ai}/\dot{x}_{Fk}^{Bi}$, can be taken as a measure of the effectiveness of the system of mounts at that attachment point for that component of velocity.

The problem to be solved is the calculation of the ratios $\dot{x}_{Fk}^{Ai}/\dot{x}_{Fk}^{Bi}$ in terms of the separate characteristics of the machine, mounts and foundation. The calculation can be performed most easily by application of multiterminal network theory.

It can be shown that for the first experiment

$$\dot{x}_F^A = \left[Y_M^{-1} + Y_F^{-1}\right]^{-1} F_{Mb} \qquad (7)$$

and that for the second experiment

$$\dot{x}_F^B = \left[Z_m^{22} - Z_m^{21}\left(Y_M^{-1} + Z_m^{11}\right)^{-1} Z_m^{12} + Y_F^{-1}\right]^{-1} Z_m^{21}\left[Y_M^{-1} + Z_m^{11}\right]^{-1} F_{Mb} \qquad (8)$$

where

$\dot{x}_F^A$, $\dot{x}_F^B$, F_{Mb} are column matrices (3n x 1), the first two of the phasors $\dot{x}_{Fk}^{Ai}$ and $\dot{x}_{Fk}^{Bi}$ of the three components k of the vibratory velocities at each of the n foundation mounting points i, the third of the phasors F_{Mbk}^{i} of the three components of the vibratory forces that would be experienced at each of the n mounting points of the machine if they were constrained so as to allow no motion (blocked); Y_M and Y_F are square supermatrices (n x n) of matrices of mobility coefficients for the machine and foundation respectively, measured at the terminals of machine and foundation to be attached to the mounts, of the form $Y_E = \left[Y_E^{pq}\right]$, (p, q = 1, ..., n), the diagonal submatrices Y_E^{pp} being

matrices of driving point mobility coefficients, the off-diagonal submatrices Y_E^{pq} being matrices of transfer mobility coefficients relating force phasors at mounting point q with velocity phasors at point p, Y_E^{pq} being of the form $Y_E^{pq} = \left[Y_{Ek\ell}^{pq}\right]$, (k, ℓ = 1, 2, 3).

Z_m^{pq}, (p, q = 1, 2), are square diagonal supermatrices (n x n), each element of which Z_m^{ipq}, is associated with a particular mount, Z_m^{ipq} being of the form $Z_m^{ipq} = \left[Z_{mk\ell}^{ipq}\right]$, (k, ℓ = 1, 2, 3). Z_m^{11} and Z_m^{22} are supermatrices of the matrices of the drive point impedance coefficients of the mounts, Z_m^{12} and Z_m^{21} are supermatrices of the matrices of the transfer impedance coefficients of the mounts, where, for example, Z_m^{12} relates velocity phasors at the terminals of the mounts to be attached to the foundation to force phasors at the terminals of the mounts to be attached to the machine.

It follows that the effectiveness of the mounting system at any mounting point, $\dot{x}_{Fk}^{Ai}/\dot{x}_{Fk}^{Bi}$, can be calculated from Equations (7) and (8) if the characteristics of the machine, Y_M and F_{Mb}, of the mounts, Z_m^{11}, Z_m^{22}, Z_m^{21}, Z_m^{12}, and of the foundation, Y_F, are known.

The calculations can also be carried out in terms of the free velocities that would exist at the terminals of the machine were it operated free in space with no connections to its mounting points.

$$\dot{x}_F^A = \left[I + Y_M\, Y_F^{-1}\right]^{-1} \dot{x}_{Mf} \quad (9)$$

$$\dot{x}_F^B = \left[I + \left[Z_m^{22} - Z_m^{21}\left(Y_M^{-1} + Z_m^{11}\right)^{-1} Z_m^{12}\right]^{-1} Y_F^{-1}\right]^{-1} \left[Z_m^{22}\right]^{-1} Z_m^{21} \left[I + Y_M \left(Y_m^{11}\right)^{-1}\right]^{-1} \dot{x}_{Mf} \quad (10)$$

where $\dot{x}_{Mf}$ is a (3n x 1) column matrix of the phasors $\dot{x}_{Mfk}^i$ of the components of the free velocities at the n mounting points on the machine and I is the unit matrix (3n x 3n), and $Y_m^{11} = \left[Z_m^{11} - Z_m^{12}\left(Z_m^{22}\right)^{-1} Z_m^{21}\right]^{-1}$

$\dot{x}_{Fk}^{Ai}/\dot{x}_{Fk}^{Bi}$ can be easily evaluated if the off-diagonal elements of the matrices Y_M, Y_F, Y_M^{PP}, Y_F^{PP}, Z_m^{i11}, Z_m^{i22}, Z_m^{i12}, Z_m^{i21} are zero, these elements representing coupling between mounting points on machine or foundation, or between different directions at each mounting point on machine or foundation, or between different directions at each mount terminal, or between different directions at the two mount terminals. For this special case

$$\frac{\dot{x}_{Fk}^{Ai}}{\dot{x}_{Fk}^{Bi}} = \frac{1}{T_{12bk}^i}\left[\frac{Z_{Mk}^i\left(\dfrac{Z_{21bk}^i}{Z_{12bk}^i}\right) + Z_{Fk}^i\left(1 + \dfrac{Z_{Mk}^i}{Z_{12bk}^i}\right) + Z_{21fk}^i}{Z_{Mk}^i + Z_{Fk}^i}\right] \quad (11)$$

where $T_{12bk}^i = \dfrac{Z_{mkk}^{i21}}{Z_{mkk}^{i11}}$, $Z_{Mk}^i = \left[Y_{Mkk}^{ii}\right]^{-1}$, $Z_{12bk}^i = Z_{mkk}^{i11}$, $Z_{21bk}^i = Z_{mkk}^{i22}$,

$$Z_{Fk}^i = \left[Y_{Fkk}^{ii}\right]^{-1}, \quad Z_{21fk}^i = Z_{mkk}^{i11} - Z_{mkk}^{i12}\left[Z_{mkk}^{i22}\right]^{-1} Z_{mkk}^{i21}$$

Equation (11) has been discussed in Reference 2 in some detail for the case of a mount which is a massless paralled spring-dashpot combination.

M54

FOURTH INTERNATIONAL CONGRESS ON ACOUSTICS
COPENHAGEN 21.-28. AUGUST 1962

The "Sound Insulation" of Circular and Slit-shaped Apertures

M.C. Gomperts
Institute for Public Health Engineering T.N.O., Delft

Reference to different books on sound insulation soon reveals the fact that there is little agreement regarding the degree in which sound insulation diminishes as a result of an aperture in a party wall.

In the present paper simple formulae are deduced for the sound transmission factor of circular and slit-shaped apertures. For circular apertures it is found that the formulae agree very well with the more accurate but very complicated formulae of Y. Nomura and S. Inawashiro [1]. For slit-shaped apertures there only exist formulae for a few special cases (a very thin wall, resonance); these formulae, too, agree fully with the more general formulae that will be deduced below.

We define the sound transmission factor q as being the quotient of the power radiated by the aperture on the receiving side and the power supplied originally (i.e. before the aperture was made) on the transmitting side at the position of the aperture.

According to Helmholtz and Rayleigh the velocity potential of the plane wave (angular frequency ω) inside a cylindrical aperture of circular cross-section (radius ε) is:

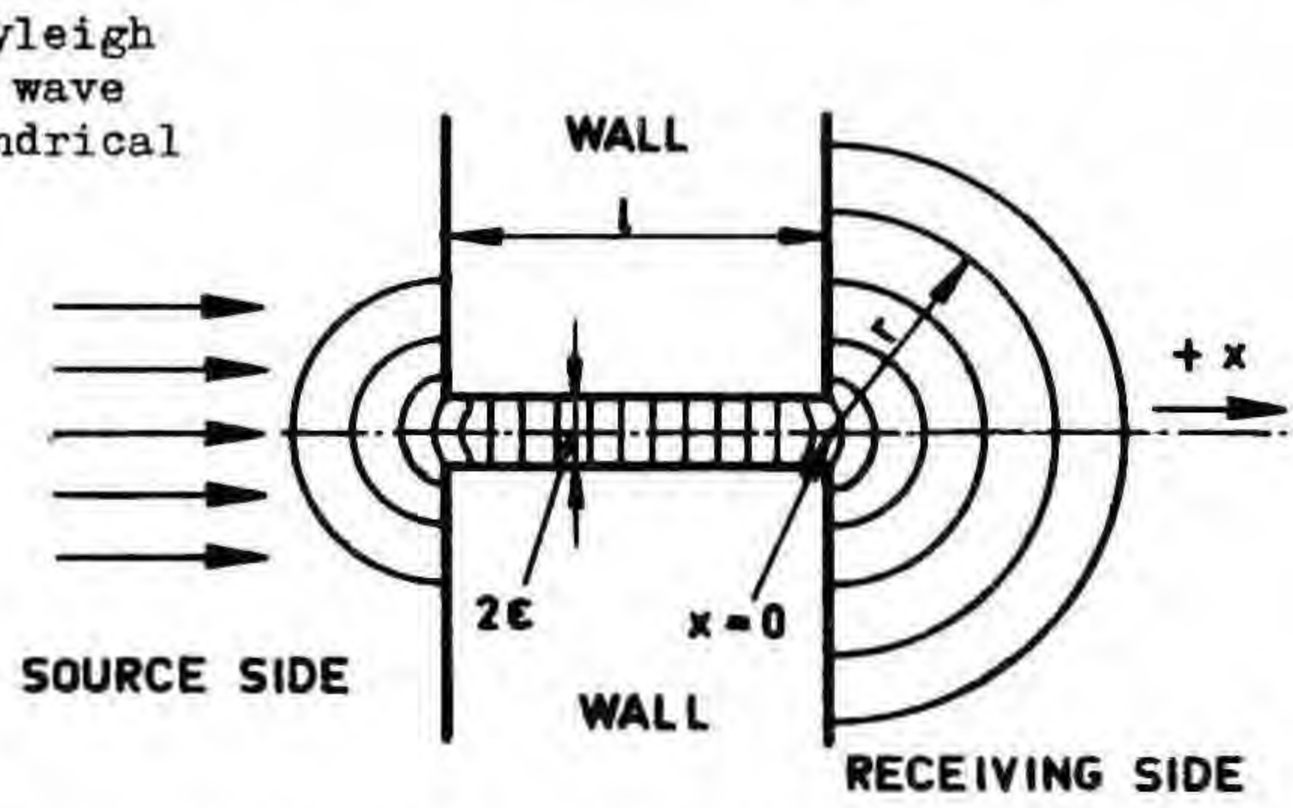

Schematic representation of the wavefronts of sound passing through a cylindrical aperture in a wall.

$$\phi(x,t) = b\left[\frac{\sin k(x-\alpha)}{\cos k\alpha} \cdot \cos \omega t - \frac{k^2\varepsilon^2}{2} \cdot \cos kx \cdot \sin \omega t\right] \qquad (1)$$

where the real coefficient b determines the amplitude of the wave; $k = \frac{2\pi}{\lambda}$ is the wave number and α the end correction ($\alpha \leq 0{,}82\varepsilon$, smaller according as k is greater).

The velocity potential of the spherical wave outside the aperture on the receiving side is:

$$\phi(r,t) = \frac{N}{r} \cdot e^{i(\omega t - kr)} \qquad (2)$$

where N is again a real constant which determines the amplitude of this wave.

- According -

According to Helmholtz and Rayleigh, there exists between the plane wave in the aperture and the spherical wave on the receiving side the relation:

$$\pi \varepsilon^2 k b = -2\pi N \qquad (3)$$

Now we still need the relation between the plane wave in the aperture and the incident acoustical field on the transmitting side. We begin by assuming that there is a plane harmonic wave impinging perpendicularly upon the transmitting side of the still undamaged wall. The velocity potential at the site of the wall may in that case be represented by:

$$\phi = M \cos(\omega t + \theta) \qquad (4)$$

If the acoustical field on the transmitting side would not vary as a result of making the aperture, the "imposed" acoustical field (4) in the aperture would result solely in a velocity potential:

$$\phi(x,t) = M \cos k(1+x) \cdot \cos(\omega t+\theta) \qquad (5)$$

But the acoustical field before the aperture on the transmitting side does vary as a result of making the aperture. Sound radiates from the aperture back to the transmitting side in the form of a spherical wave. Between this spherical wave on the transmitting side and the corresponding plane wave in the aperture there again exists a relationship identical with the one we found above for the receiving side, provided we shift the origin of the X axis to the transmitting side, since we have to consider now the whole phenomenon from the transmitting side.

The total potential field in the aperture, considered from the transmitting side, will be a superposition of the velocity potential (5) and a velocity potential of the form (1), but differing from (1) in amplitude and phase.

As the wave in the aperture as considered from the receiving side, is of course identical with the wave in the aperture as considered from the transmitting side, the applicable equation must be:

$$M \cos k(1+x)\cos(\omega t+\theta) + b'\left[\frac{\sin k(x'-\alpha)}{\cos k\alpha}\cdot\cos(\omega t+\theta') - \frac{k^2\varepsilon^2}{2}\cdot\cos kx'.\sin(\omega t+\theta')\right] =$$

$$= b\left[\frac{\sin k(x-\alpha)}{\cos k\alpha}\cdot\cos\omega t - \frac{k^2\varepsilon^2}{2}\cdot\cos kx.\sin\omega t\right] \qquad (6)$$

where $x' = -(x+1)$.

This gives us the desired relationship between b and M:

$$b = \frac{M \sin kl}{\sqrt{\left[\frac{\cos^2 k(1+\alpha)}{\cos^2 k\alpha} + \frac{k^4\varepsilon^4}{4}\sin^2 kl\right]^2 - 2\left[\frac{\cos^2 k(1+\alpha)}{\cos^2 k\alpha} - \frac{k^4\varepsilon^4}{4}\cdot\sin^2 kl\right] + 1}} \qquad (7)$$

From the equations (3) and (7) the relationship is now known between the acoustical field on the transmitting side (established by M) and the acoustical field on the receiving side (established by N).

For the sound transmission factor q_a for the circular aperture we finally obtain (in dimensionless form) the expression:

$$q_a = \frac{2K^2\cos^2 Ke}{\frac{\sin^2 K(L+2e)}{\cos^2 Ke} + \frac{K^4}{2}\left[1 + \cos K(L+2e).\cos KL\right]} \qquad (8)$$

where: $K = k\varepsilon$, $L = \frac{l}{\varepsilon}$ and $e = \frac{\alpha}{\varepsilon}$

Formula (8) is not directly applicable to sound insulation problems, because the incident acoustical field upon the wall, originating from a sound source of constant radiation situated in the confined transmitting room, is not a plane acoustical wave. However, with the aid of the theorem of reciprocity it can readily be seen that the sound pressure level at the walls is in this case 3 dB higher than at a sufficiently remote distance from the walls (hereinafter

termed "in the middle of the room"), where the acoustical field may be considered to be diffuse. As is well known [2,3], a point-like source situated in the immediate vicinity of a wall radiates twice as great a power as in unconfined space, that is, at a remote position from the confining walls, i.e. in the middle of the (not too small) room. With this positioning of the sound source, the sound pressure level in the middle of the room is therefore 10 log 2 = 3 dB higher than if the sound source were positioned in the middle of the room. According to the theorem of reciprocity, if the point-like source is positioned in the middle of the room, the sound pressure level near the wall will be equal to the sound pressure level that existed in the middle of the room when the point-like source was situated near the wall. But, now that the point-like source is in the middle of the room, the sound pressure level in the middle of the room, where the reverberant field predominates the direct field of the point source, is 3 dB lower than when this source was near the wall. Hence it follows that the sound pressure level near the wall is now 3 dB higher than in the middle of the room (not, of course, measured in the direct field of the sound source).

Similarly, it can be proved that the sound pressure level in the middle of an edge of the room is 6 dB higher, and in a corner of the room 9 dB higher than in the middle of the room.

By allowing for this higher sound pressure level near walls, edges and corners and also allowing for the fact that an aperture in an edge only radiates into a quarter of the space and that an aperture in a corner only radiates into an eighth part, we ultimately obtain the following expression for the sound transmission factor q_a of a circular aperture:

$$q_a = \frac{m.K^2.\cos^2 Ke}{n^2.\left\{\frac{\sin^2 K(L+2e)}{\cos^2 Ke} + \frac{2K^4}{n^2}\left[1 + \cos K(L+2e).\cos KL\right]\right\}} \qquad (9)$$

where: m=8 and n=2 for an aperture in an infinitely extended wall upon which a plane wave impinges perpendicularly (formula 8).

m=16 and n=2, 1 or 1/2 in the "diffuse" acoustical field in a room, according to whether the aperture is situated in the middle of a wall, in the middle of an edge or in a corner.

It has been found by experiment that formula (9) not only applies to cylindrical apertures of circular cross-section but also to cylindrical apertures of rectangular, triangular, crescent-shaped or otherwise shaped cross-section.

In an analogous manner, we find the following expression for slit-shaped apertures:

$$q_{sl} = \frac{m.K.\cos^2 Ke}{2n^2.\left\{\frac{\sin^2 K(L+2e)}{\cos^2 Ke} + \frac{K^2}{2n^2}.\left[1 + \cos K(L+2e).\cos KL\right]\right\}} \qquad (10)$$

where: $K = k\beta$, $L = \frac{l}{\beta}$, $e = \frac{\alpha}{\beta}$, β = breadth of the slit,

l = depth of the slit = thickness of the wall.

m=4 and n=1 for a slit in an infinitely extended wall upon which a plane wave impinges perpendicularly.

m=8, n=1 or 1/2 in a "diffuse" acoustical field in a room, according to whether the slit is situated in the middle of a wall or in an edge.

Bearing in mind that for the limiting case L=0, m=4, n=1, formula (10) must be identical with Bouwkamp's formula:

$$q_{sl} = \frac{\pi}{2K} \cdot \frac{1}{(\ln\frac{K}{8} + \gamma)^2 + (\frac{\pi}{2})^2} \qquad (11) \qquad (\gamma = 0{,}57722)$$

which is the formula for a slit-shaped aperture in an infinitely extended screen upon which a plane wave impinges perpendicularly, we find the following expression for the end correction factor e of a slit-shaped aperture:

$$e = \sqrt{\frac{(\ln\frac{K}{8} + \gamma)^2 + (\frac{\pi}{2})^2}{\pi^2}} \qquad (12)$$

The above theory has been applied to certain practical cases (see figs. 2 and 3).

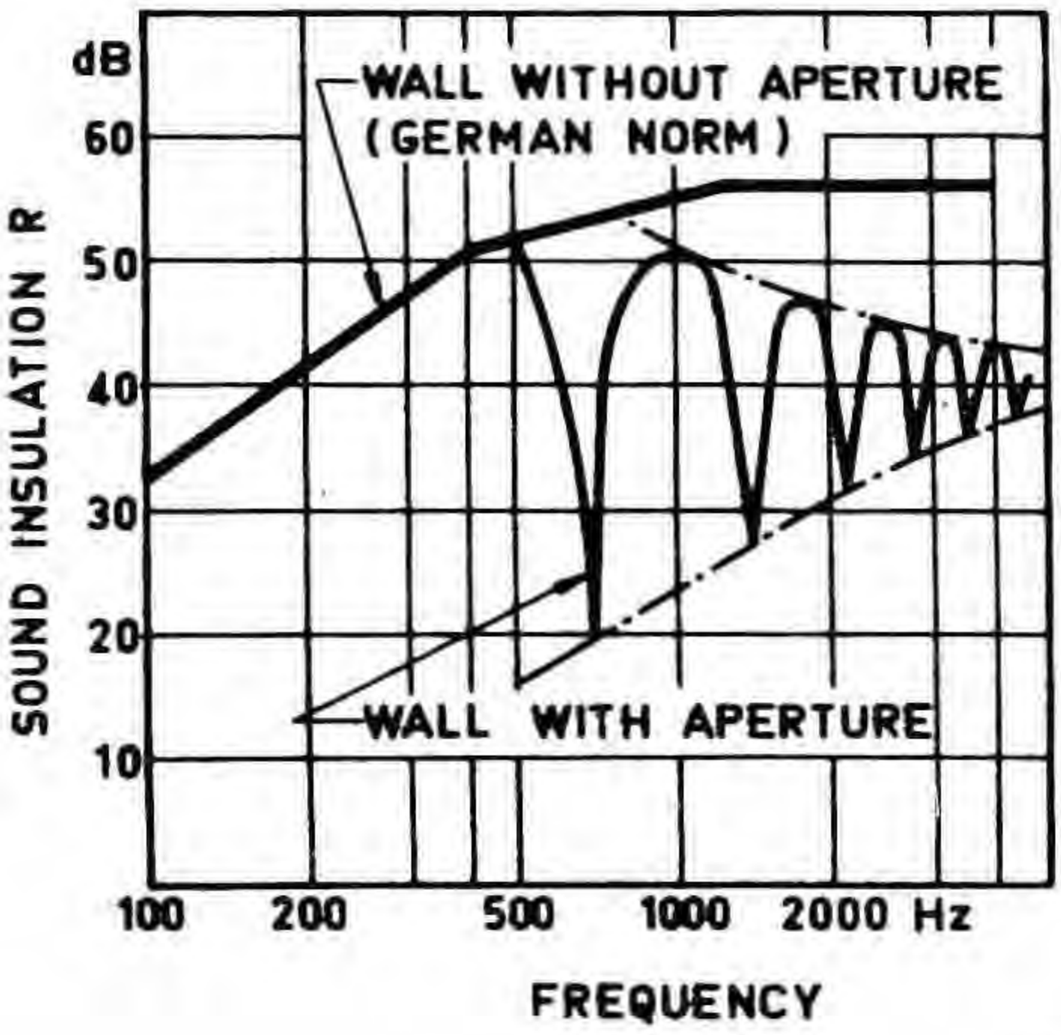

The sound insulation R of a fictitious wall 22 cm thick and 11 m^2 in area without and with a cylindrical aperture 2.2 cm in diameter.

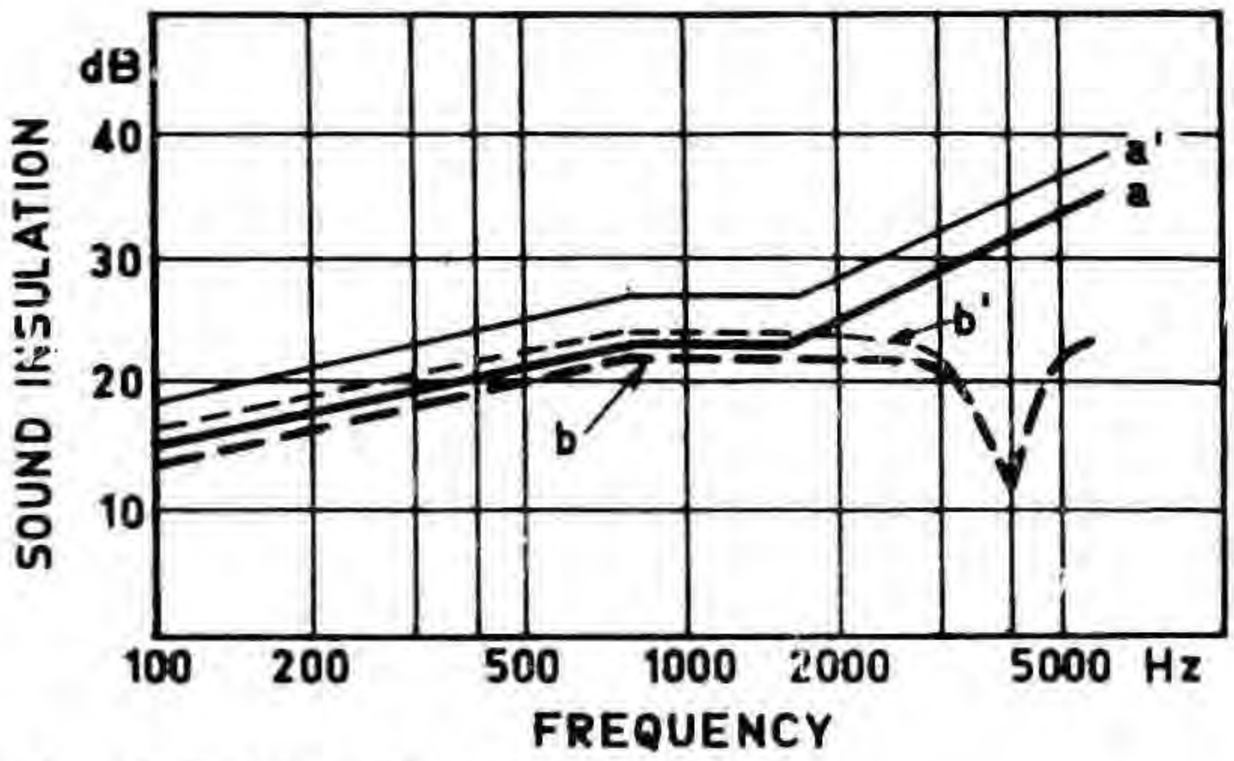

Curve a : Sound insulation of an ordinary inside door with chinks sealed home.

Curve b : Sound insulation of the same door with chinks open (only chinks at the top and at the bottom; width 0.35 cm).

Curve a' : Sound insulation of a fictitious door with a 3 dB higher sound insulation than the door corresponding to curve a.

Curve b' : This door with chinks open.

References

(1) Y. Nomura and S. Inawashiro: Sci. Rep. Tohoku Univ. (1), 123, 57 (1960)
On the Transmission of Acoustic Waves through a Circular Channel of a Thick Wall.

(2) Rayleigh. Dover (1955)
The Theory of Sound.

(3) R.V. Waterhouse. J. Acoust. Soc. Am. 30,4 (1958)
Output of a Sound Source in a Reverberation Chamber and other Reflecting Environments.

N54

FOURTH INTERNATIONAL CONGRESS ON ACOUSTICS
COPENHAGEN 21.-28. AUGUST 1962

Non-Linear Effects in Quartz Resonators

A. Seed, Physics Department, Imperial College, London, S.W.7, England.

Experiments have been conducted on the excitation of quartz resonators at large amplitudes and the effects observed are explainable in terms of non-linear theory, see Stoker, Andronow and Chaikin. A brief resume is given below.

A typical non-linear equation of a body undergoing periodic forced vibration, using standard notation, is

$$m\ddot{x} + c\dot{x} + \alpha x + \beta x^3 = F\cos(\omega t + \psi) \qquad \ldots\ldots\ldots(1)$$

Provided the condition $m\omega^2 = \alpha + {}^3/_4\beta A^2 - F\cos\psi/A$ .....(2) is satisfied, then the periodic solution of equation (1) is given approximately by

$$x \sim A\cos\omega t + \frac{\beta A^3}{32m\omega^2}\cos 3\omega t \qquad \ldots\ldots\ldots(3)$$

where the second term is negligible for the small perturbation considered. The corresponding equation giving the response function (i.e. the amplitude variation with frequency for a given excitation force) is

$$F^2 = c^2A^2\omega^2 + \left[(\alpha - m\omega^2)A + {}^3/_4\beta A^3\right]^2 \qquad \ldots\ldots\ldots(4)$$

this may be exhibited graphically as in figs. (1) and (2)

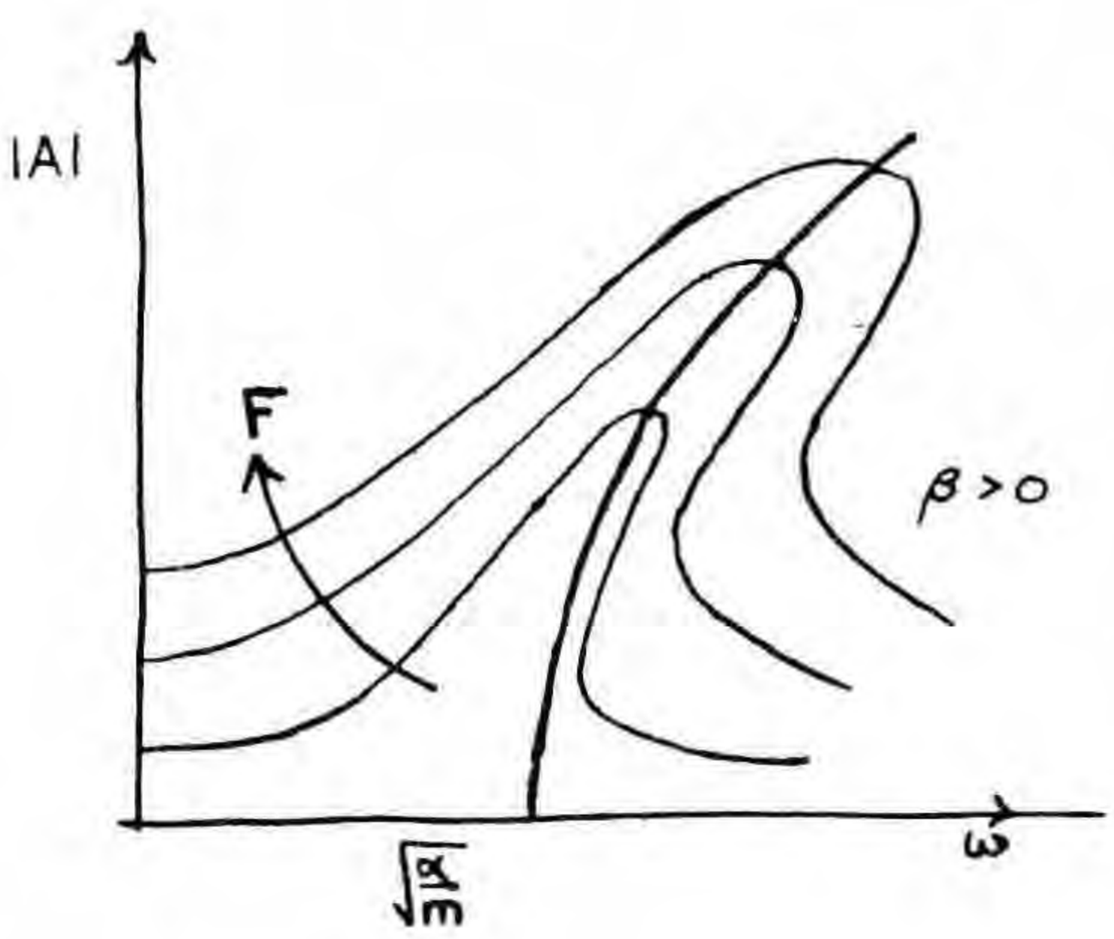

fig 1

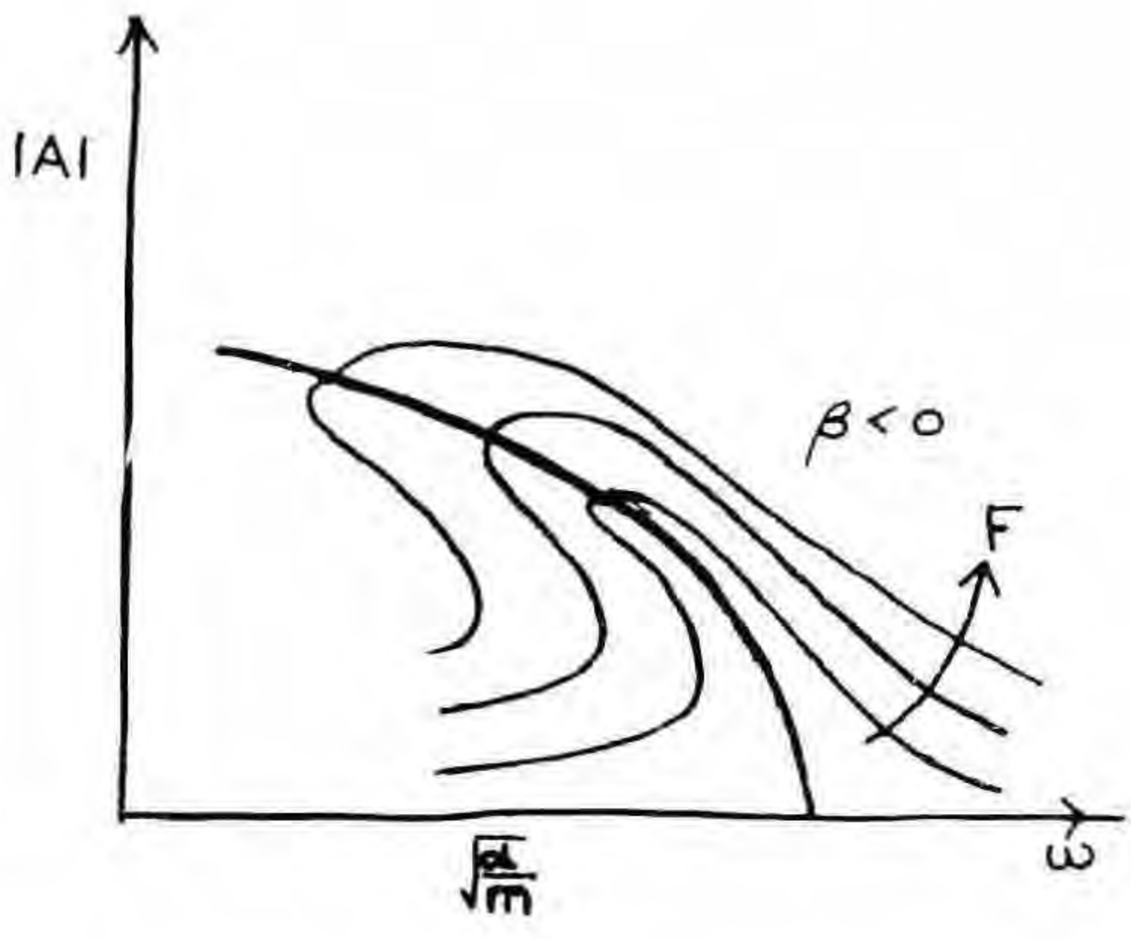

fig 2

Experimental response curves, figs (3) and (4), similar to the theoretical curves of figs (1) and (2) have been obtained, using the technique of King and Jones, for 5 Mc/s thickness shear vibrating quartz resonators. The results were obtained using fifth overtone AT-cut crystals and a fundamental BT specimen.

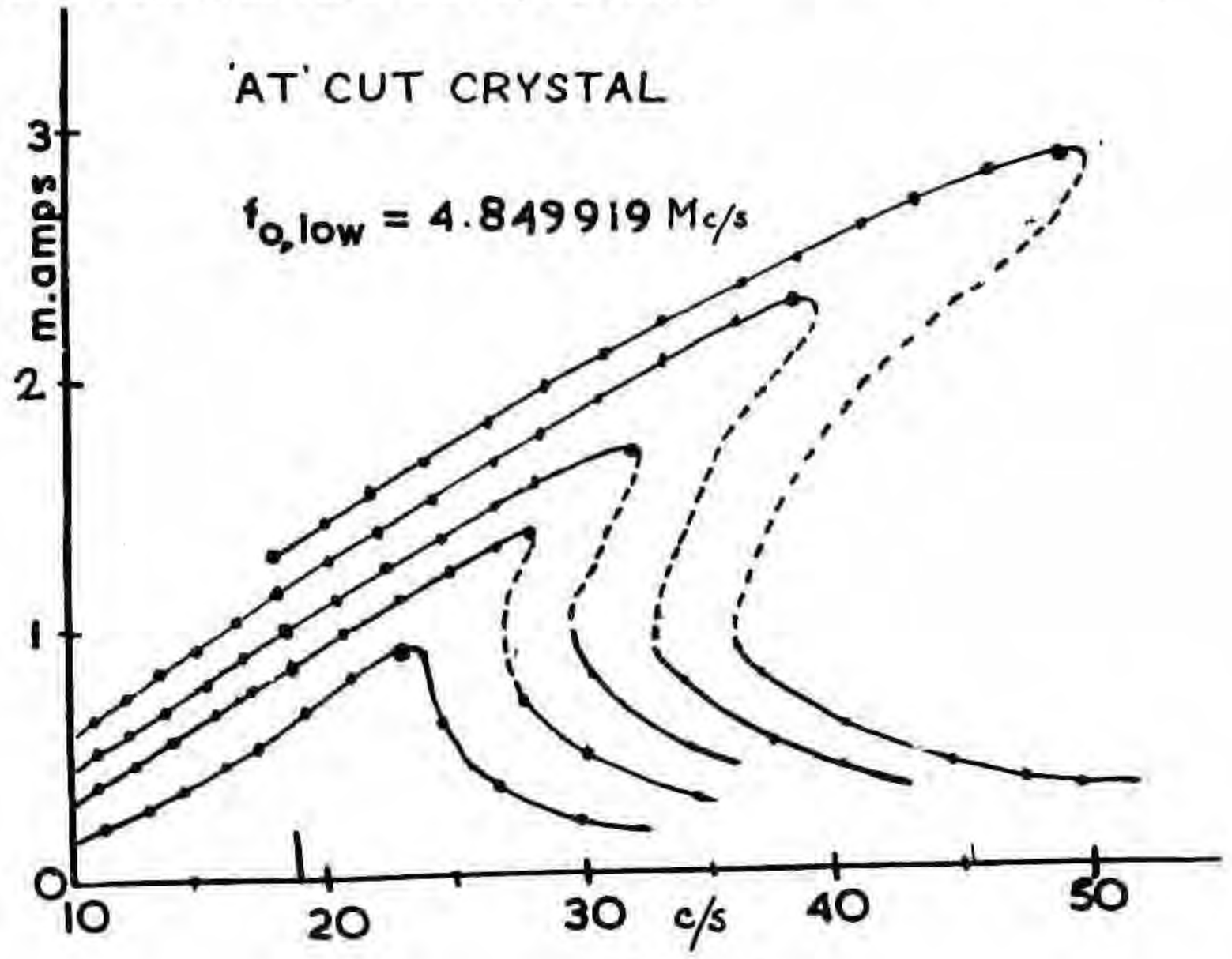

fig 3

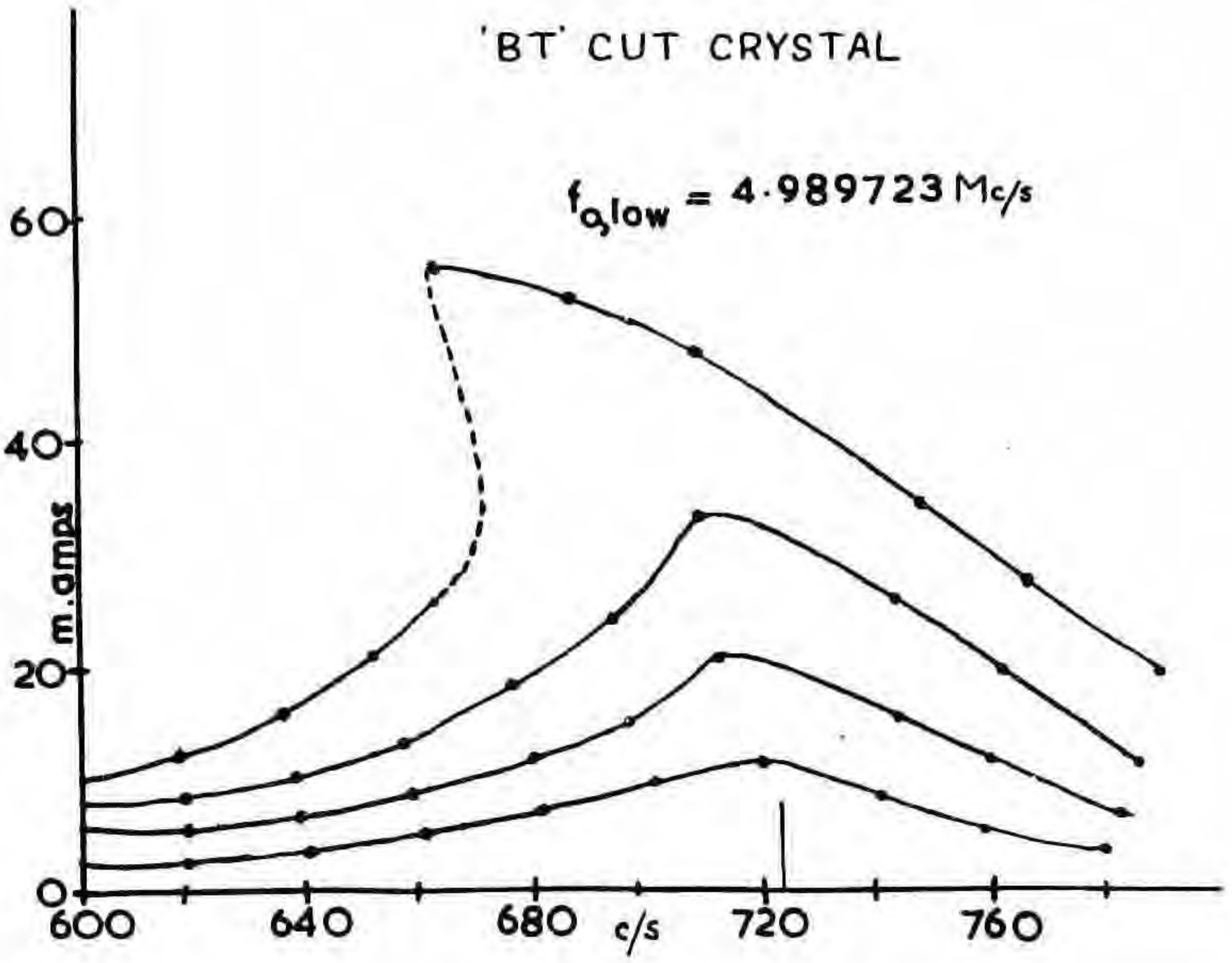

fig 4

It was found that the degree of non-linearity for the AT specimens was unaffected by the mounting and electrode assemblies, and it was not a critical function of the thickness to diameter ratio of the specimen. Crystals fabricated from synthetic quartz gave a slightly different non-linear coefficient β, although the difference was comparable with experimental error, and the non-linearity was found to be unaffected by irradiation with γ -rays.

The cause of the phenomena would therefore appear to be found in the quartz material itself and not in the geometry or the mounting of the element. A further step in the elucidation of the problem was to formulate the equation of motion involving the higher order elastic constants. Two assumptions are made:-

(1) The effect of damping can be neglected, as it only yields information close to resonance.

(2) The piezoelectric relationships are linear.

Following the finite deformation theory of Murnaghan in which strain is defined as

$$\lambda = 1/2\ (JJ^* - E_3)$$

where E_3 is a 3 x 3 unit matrix and

$$J = \begin{pmatrix} 1+u_x & u_y & u_z \\ v_x & 1+v_y & v_z \\ w_x & w_y & 1+w_z \end{pmatrix}$$

$u_x = \delta u/\delta x$ etc. and u, v, w, are displacements in the coordinate system x, y, z. The stress matrix

$$T = \frac{1}{\text{Det } J} J.\frac{\delta V}{\delta \lambda} J^*$$, where V is the deformation energy. The general equation of motion for a deformable medium is

$$\text{div}_x\ T = \rho\ \ddot{u} \quad \text{etc.} \qquad \ldots\ldots\ldots(6)$$

Gross simplification can be achieved when one considers the special case of the 'rotated Y-cut' crystals used in the experiment. When the appropriate reductions are made the equation of motion assumes the form

$$\rho\ \ddot{u} = A\frac{\delta^2 u}{\ell_J^2} + B\left(\frac{\delta u}{\delta s}\right)^2 \frac{\delta^2 u}{\delta s^2} \qquad \ldots\ldots\ldots(7)$$

where s defines the normal to the wave front, A is the second order elastic constant, and B is a linear combination of third and fourth order elastic constants. As the case considered is one of forced vibration the solution must be of the form

$$u = X\ (t)\ Y\ (s), \qquad \ldots\ldots\ldots(8)$$

where X(t), Y(s) are periodic functions. The condition for a periodic solution is similar in form to equation (3), more specifically the non-linear parameter β occurring in that equation can be related to the coefficient B in equation (7).

From the results, therefore, one is able to determine B quantitatively and thus give an estimate of the magnitude of some high order elastic constants in quartz. In particular the fourth order elastic constant C'_{6666} can be estimated from knowledge of B and certain constants of the crystal unit.

For natural AT crystals

$$C'_{6666} = (2.3 \pm 0.4)10^{14} \text{ dynes/sq.cm.}$$

For the natural BT crystal

$$C'_{6666} = -(5.4 \pm 1.6)10^{13} \text{ dynes/sq.cm.}$$

References:

(1) Stoker, J.J., Non-linear Vibrations. Interscience Publishers Inc. New York, 1950.

(2) Andronow, A.A., and C.E. Chaikin, Theory of Oscillations. English. translation by S. Lefschetz. Princeton Univ. Press, 1949.

(3) Murnaghan, F.D., Finite Deformation of an Elastic Solid. Wiley, New York, 1951.

(4) King, J.C., Phys. Rev. 109, 1552, 1958.

(5) Jones, C.K. and C.S. Brown, Proc. Phys. Soc. Vol. 79, 930, 1962.

O54

FOURTH INTERNATIONAL CONGRESS ON ACOUSTICS
COPENHAGEN 21.-28. AUGUST 1962

ABSORPTION OF SOUND IN AIR

IN THE AUDIO FREQUENCY RANGE

CYRIL M. HARRIS

COLUMBIA UNIVERSITY, NEW YORK 27, N.Y.

This paper is a progress report on a program of the determination of the absorption of sound in air as a function of humidity in the frequency range between 2,000 cps and 12,500 cps. Measurements have been carried out during the past two years. Although the data analysis is not yet complete and some additional measurements are to be made, preliminary results at 20°C are described here and are compared with other published data in the same frequency range.

Introduction. The classic work of Knudsen[1] provided data on sound absorption in air that has been widely used for the past several decades. The method he employed was to measure the rate of decay of sound in two chambers having different volumes 6.11 m^3 and 0.23 m^3 . Both chambers had steel walls 4.8 mm thick, reinforced with angle irons spot-welded to the walls. In this "two-chamber technique" it is assumed that the absorptive effects of the walls of both chambers are identical. If this is the case, one may calculate both the absorption due to walls and to the air within the chambers from decay measurements in both chambers.

Another approach to the evaluation of air absorption was taken by Evans and Bazley[2] who made a series of decay rate measurements in a single reverberation room with air under various conditions of humidity. From a comparison of their experimental data and calculations of the contribution to absorption in the chamber by molecular absorption, classical absorption and ideal surface absorption, the angular relaxation frequency $\underline{k}$ was determined as a function of the percent molar concentration of water. Using this value of $\underline{k}$, a set of curves then was computed for the absorption of sound in air vs. humidity. Over portions of the frequency range, these curves differ considerably from the measurements of Knudsen, and those of Knotzel[3] (who employed a resonance tube technique). Such data on air absorption are of considerable importance in the field of architectural acoustics in computing the reverberation time in large rooms. Because of these discrepancies, a program was undertaken to re-evaluate the absorption of sound in air in the frequency range indicated above, employing some equipment and control techniques not available in the earlier studies. Measurements were made of the decay rate of diffuse sound in a spherical chamber. The effects of the boundary were evaluated from measurements of the decay rate when the chamber was filled with nitrogen as described below.

Spherical Chamber. The spherical chamber, which has an inner diameter of 1.68 meters, was specially fabricated in two halves from hot-rolled steel having a thickness of 16 mm. That the boundary losses are low is illustrated by the fact that at 1000 cps the reverberation time, when the chamber (volume = 2.48 m^3) is filled with dry air, is 43 seconds. Measurements both with nitrogen and with dry air show that, over the frequency range employed, there are no isolated mechanical resonances of the spherical chamber housing that have any significant effect on the decay

rate of sound in the enclosure. The entire chamber is packed in glass fiber blankets to provide heat insulation. Its temperature is controlled by pumping a methanol coolant through copper tubing fastened to the exterior surface of the sphere. The temperatures at various points of the air circulation system, and temperature differences between points in the system, are measured by means of calibrated thermocouples.

Humidity Control. The problem of accurately controlling and measuring the humidity in a chamber in which air absorption measurements are made has always presented difficulties. The accuracy of usual humidity measurement techniques is low at low values of humidity, a range of considerable interest. Furthermore there is the problem of insuring that the humidity measured is representative of conditions within the chamber. One approach is to insert a known amount of water into a dry chamber, but problems arise in this technique because of the absorption of water vapor by the wall surfaces. Humidity control and measurement probably account for one of the greatest sources of discrepancy among published data on air absorption.

The method used here is illustrated in the diagram below. Air is circulated through a closed system by means of a small highspeed turbo-fan. The exhaust of the spherical chamber passes through a "saturator" which is a small cylinder whose temperature can be controlled accurately from approximately -60°C to room temperature. Water is contained in the bottom of the saturator. Moisture is either added to or taken from the air that passes through the saturator, depending upon the relative temperatures of the spherical chamber and the saturator. Two electric hygrometers (manufactured by Hygrodynamics, Inc.) are employed. The operation of these devices is based upon the change in the resistance, with humidity, of a lithium chloride sensing element (Class A, type H) which is in a bridge circuit. Eight such sensing elements are required in a single set to cover the range from 1.6% to 88% relative humidity. Two such sets were closely matched against each other and calibrated to an accuracy of about 1% R.H. One set is placed at the entrance of the spherical chamber and the other at the exhaust. When both indicate the same steady reading of relative humidity, equilibrium conditions have been established. Then the value of the relative humidity can be deter-

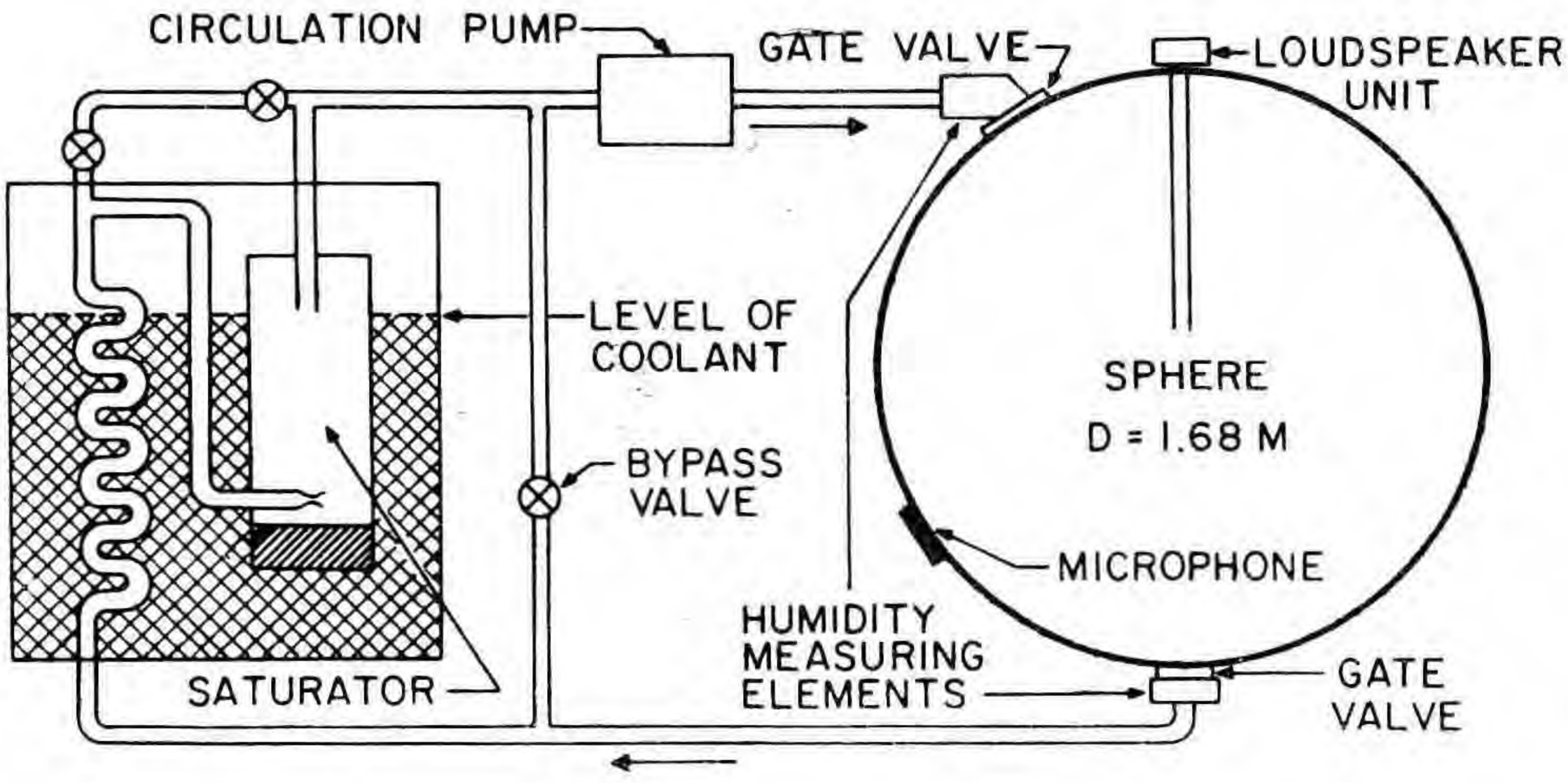

mined independently by a calibration procedure developed by Wexler and Daniels[4] at the National Bureau of Standards, which they call the "two pressure principle." This requires a measurement of the temperatures of the spherical chamber and the saturator to obtain pressure in the two volumes.

Electro-Acoustic Measurement System. Sound is produced in the spherical chamber by a random noise generator that feeds a 25 watt electrodynamic loudspeaker unit. The unit is attached to a stainless steel tube ($\frac{1}{4}$ inch in diameter) that is inserted in the sphere. This arrangement provides an effective point source at the open end of the tube. Because of the very poor impedance match between the loudspeaker unit and probe tube, little acoustic energy is absorbed by this transducer while it is inactive during decay measurements. A small dynamic microphone is located in one of the insert plugs in the walls of the spherical chamber. The output of the microphone is amplified, fed through a Bruel & Kjaer third-octave filter, Type 2109, and thence to a high-speed level recorder. When the random noise source is turned off, a curve of the rate of decay of sound in the spherical chamber is obtained. The slope of this curve determines the decay rate in db/sec at the center frequency for which the third-octave band analyzer is set.

Calibration Procedure. As a routine procedure before any measurements were made on air (or on nitrogen, for calibration purposes), the entire air handling and measurement system was evacuated to a few microns for a day -- or longer, if required -- to eliminate all traces of moisture or other forms of contamination. Thus the entire system, including the spherical chamber, loudspeaker unit, microphone, turbo-fan used in air circulation, humidity-measuring elements, etc., is vacuum-tight. Other precautions were then taken to avoid contamination, such as the use of silicone vacuum grease in the fan, in place of the usual lubricant.

The decay rate of sound in the spherical chamber is given in decibels per second by

$$R_{total} = R_{medium} + R_{wall} \qquad (1)$$

where R_{medium} is the decay rate due to absorption in the gas, and R_{wall} is the decay rate due to absorption at the walls. The total decay rate R_{total} is the value that one measures. Thus, when the chamber is filled with pre-purified dry nitrogen,

$$R_{measured(N)} = R_N + R_{wall} \qquad (2)$$

where R_N is the classical value of absorption for nitrogen, in db/sec. When filled with air,

$$R_{measured(air)} = R_{air} + R_{wall} \qquad (3)$$

If it is assumed that the wall losses for N_2 and air are approximately the same because these gases are closely similar in molecular weight and characteristic impedance, then subtracting Eq. (2) from Eq. (3):

$$R_{air} = R_{measured(air)} - R_{measured(N)} + R_N \qquad (4)$$

The first two terms on the right are obtained from decay measurements while the third term is computed from values of the constants for nitrogen[6]. To convert the value of R_{air} in db/sec to absorption m per meter as expressed in the equation $I = I_o e^{-mx}$, merely divide R by 4.34 c where c = the velocity of sound in meters/second; i.e.:

$$m = \frac{R_{air}}{4.34c} \text{ meters}^{-1}$$

Results. Measurements have been made at 20°C on air having a CO_2 content of 300 parts per million. The data were taken at atmospheric pressure at the following frequencies: 2000, 2500, 3200, 4000, 5000, 6400, 8000, 10,000 and 12,500 cps. The maximum values in the curves of absorption vs. humidity for constant frequency show close agreement with the values predicted by Kneser[5]. The measured values of absorption are considerably above the theoretical values, which has been observed by previous investigators. In some frequency regions, the values are quite close to those measured by Knudsen, while at other frequencies the measured values are closer to those given by Evans and Bazley. These results will be illustrated by slides at the ICA meeting.

Acknowledgement. The author appreciates the support given this project for the past several years by the Acoustics Programs Branch, Office of Naval Research. He is grateful for the assistance of Prof. J. Igarashi on many of the measurements.

References.

1. Knudsen, V. O., J. Acous. Soc. Am., 5, 112 (1933) and 6, 119 (1935).
2. Evans, E. J. and E. N. Bazley, Acustica, 6, 238 (1956).
3. Knotzel, H., Akus. Zeits., 5, 245 (1940).
4. Wexler, A., and R. D. Danielis, Jr., J. of Research of the N.B.S., 48, 269 (1952).
5. Kneser, H. O., J. Acous. Soc. Am., 5, 122 (1933).
6. Tables of Thermal Properties of Gases, National Bureau of Standards, Circular 564, Washington, D. C. (1955).

P54

FOURTH INTERNATIONAL CONGRESS ON ACOUSTICS
COPENHAGEN 21.-28. AUGUST 1962

MUSICAL TRANSFER FUNCTIONS
Fonctions de transfert musicales
Musikalische Übertragungsfunktionen

ANEDREW G. PIKLER

Increasing complexity in the connections of music and electronics necessitates a general model of the musical transfer function.

SLIDE I.
(Illustrates the 7 blocks in the diagram of the conventional transfer function and the expanded audiences).

In the conventional transfer process, the composer selects musical messages from some Universe of musical signals, i.e. a finite set of acoustical waveforms ordered in some musical scale system. The composer generally uses a music instrument for his reference and produces a permanent record, i.e. a musical score. With this score before him, the performer generates a physical output from a mechanical or an electronic musical instrument, or from the mechanism of his vocal organ. This audible musical sound reaches the live audience.

The channels of the conventional transfer function may be expanded (I), contracted (II) or modified in six cases which will be discussed under "Processed Music". (III).

SLIDE II. Illustrates guidance and control between soloist and accompanist.

SLIDE III. Illustrates guidance and control in larger ensembles.

I. Expansions of the conventional transfer function.

1. Ensemble music. The single performer may be re-

placed by an ensemble of performers, i.e. a man-to-man system. To secure precision in a live ensemble, control and guidance has to be organized. Ensemble performances can be rationalized as a complex form of auditory pursuit tracking simultaneously in the three dimensions of pitch, loudness and musical time scale. As shown on Slides II. and III., many different tracking patterns and tracking aids are used in the various forms of musical ensembles.

SLIDE I. again.

(2) To the live audience may be added broadcast and phonograph channels and different combinations of remote and delayed audiences.

II. Contractions of the conventional transfer function.

A composer relying on his "mental pitch" may dispense with a reference instrument.(1) He may perform his compositions before preparing the written score.(2). Composition and performance are simultaneous in the case of improvisation.(3). Mental pitch may serve reading or memorizing of unfamiliar musical contexts as well as rehearsal of familiar contexts in the absence of a music instrument.(4). In the limiting case a composer may compose and rehearse his music mentally.(5).

III. Processed Music. Various combinations of man and machine components lead to six principal modifications of the transfer function.

SLIDE IV.
(Synchronization by Juxtaposition).

(1). Combinations of live and mechanical music. Live performances may alternate with prerecorded portions or be synchronized with them. The esthetic and technological requirements of such combinations will be discussed and demonstrated.

SLIDE V.

(Tabulation for types of automated performances in the preelectronic and electronic age) .

(2) Automation of the performance. In the preelectronic age the performer's manual actions could be replaced by spikes on revolving drums, or holes on revolving discs or punched paper tapes. These elicited music from a music box, from a barrel organ or from a pianola instead of some conventional music instrument. In the electronic music synthesizer, the performer is replaced by digital coding on punched tapes and the musical instruments are substituted for signal generaters. Electronic synthesis of music has three principal objectives:

(a). Reproduction of existing music pieces in the synthesized form;

(b) Composing original music pieces for the tape recorder to exploit tonal and temporal patterns which could be generated only by means of electronic synthesis;

(c) Producing sound effects, "musique concrete", from a white noise.

(3) Processing music for the stage. For better theatrical effects, especially in the opera, music actually produced by an orchestra, vocal soloists and choruses, is processed to simulate different localizations and to emphasize dynamics.

SLIDE V.
(Composing music by a computer)

(4) Composing music by a computer. Computer music is created in two ways. In one, musical notes are generated in random sequences in the form of binary coding. Hereafter, the actual selections are made by the computer programmed in terms of the rules of composition. In the second application of the computer, musical notes are sequenced in terms of transition probabilities calculated from note-to-note combinations from actual music samples. The music emerges in binary language. From computer models are expected to come the understanding of

the composition process itself and statistical analyses of particular composers and styles.

(5) Time-processed music. The technique of time expanded recording and time-compressed playback may be used for preparing mastercopies of difficult music compositions. (Demonstration).

SLIDE VII.
(Scheme of the Polyphonic Separator).

(6) Polyphonic separation. The design of a polyphonic separator is suggested for reducing polyphonic contexts to component parts with the intervention of the human operator.

Finally, the channels of performance may be displayed and evaluated. Seashore used phono-photography and stroboscopic analysis, tone by tone. My personal interest centers on the possibility of running, automated forms of performance scoring.

SLIDE VIII.
(The analog process of performance scoring).

I synchronized my piano accompaniment to Caruso's voice on a separate track and computed the statistical time-lag of this ensemble. This experiment covered the time-intensity domain only. Digital techniques are required for analysis of the time-frequency dimension and of the musical time scale.

SLIDE IX.
(The digital process of performance scoring).

I propose an automatic scoring system assigning one punched card to each tone performed in a sole part or in an ensemble. Appropriate numerical manipulations permit, among other things, statistical analyses of the intonational standards (Diatonic, Pythagorean) in various musical contexts.

Audible playback from the punched cards through the channels of the electronic synthesizer is interpreted as reversible cycle.

G55

FOURTH INTERNATIONAL CONGRESS ON ACOUSTICS
COPENHAGEN 21.-28. AUGUST 1962

PRELIMINARY SYNTHESIS OF POLISH VOWELS BY MEANS OF THE "TERMINAL-ANALOG" SPEECH SYNTHESIZER

JANUSZ KACPROWSKI - Institute of Basic Technical Problems
Polish Academy of Sciences, Warsaw, Poland

Introduction

Vowel synthesis in formant-circuit analog synthesizers consists in exciting the chain of n independent formant filters, each being described by the transfer function of the type

$$H_i(s) = \frac{s_i \cdot s_i^*}{(s - s_i)(s - s_i^*)} \qquad [i = 1; 2; 3...n] \qquad (1)$$

by a source function $u(t) \triangleq U(s)$ simulating the recurrent larynx-source pulses of the human organ of speech. The output of the synthesizer is given by the formula

$$r(t) = \mathcal{L}^{-1}\left\{U(s) \cdot H(s) \cdot Z_r(s)\right\} \qquad (2)$$

where $Z_r(s)$ is a function simulating the radiation characteristics of the human mouth [1][7].

It is well known, that the phonetic features of the vowel to be synthesized depend mainly on the transfer function $H(s) = \prod_n H_i(s)$ of the resonance analog and that the dislocation of each pair of conjugated poles $s_i, s_i^* = \alpha_i \pm j\,\omega_i$ in the complex frequency plane describes sufficiently the formant frequencies as well as the formant band-widths of the synthetic sound. Additional information is given by the relative formant levels [2][3]. The source function U(s) and the radiation function $Z_r(s)$ are of minor importance as they do not change significantly during vowel production and may thus be treated as constant factors in the formula (2), at least when synthesis of sustained vowels is considered. In consequence of this fact many different approximations concerning the glottal wave, the nature of which is still somewhat obscure, may be found in the literature.

It has been of interest to our further work to know how important is the influence of the shape of the source function on the acoustic features of Polish vowels and how precisely should the glottal pulse wave be simulated in an equivalent circuit so that the naturalness of the synthetic sound be sufficient. In this connection another problem has arisen, namely that of dynamical synthesis of Polish vowels. For the time being we have had rather poor experimental data concerning the variations of the voice fundamental frequency and amplitude as well as those of formant frequencies during vowel production. It seemed that the only possible way was to get the necessary information by preliminary dynamical synthesis of Polish voiced sounds. Many different sounds had to be synthesized before one was found that may be appreciated as being compatible with the original sound. This method has been proved very useful for our purposes, as it let us know what are the limits of approximation of parametric functions to be used to control the amplitude and frequency parameters of the sound being synthesized.

Theoretical considerations

The response of one or more formant filters to different driving functions has been investigated by means of conventional mathematical methods. The response of a chain of n decoupled resonators to the driving function having the form of

recurrent rectangular or exponentially decaying pulses has been discussed in details by G.E.Peterson and others [4]. Our first attempt at Polish vowel synthesis was to simulate the glottal wave with a saw-tooth shaped source function, which resembles the laryngeal wave more closely than do pulses mentioned above.

The complete response $r(t)$ of n decoupled resonators to a train of recurrent saw-tooth pulses of unit amplitude and width T may be written as

$$r(t) = r_1(t) + \sum_{g=1}^{\infty} r_g(t) \qquad (3)$$

and represents the superposition of the response $r_1(t)$ to a linear increasing function $f_1(t) = t/T$ and of the response $\sum r_g(t)$ to the infinite train of negative unit step functions, successively transfated by a whole number of periods. The formula (3) has a quite simple physical interpretation provided the decay time constants of all formant filters are so large, that the damped sinusoids excited once during each fundamental period die out within each cycle. In this case the response $r_1(t)$ to the first saw-tooth pulse represents the increase of the oscillations when voicing is suddenly applied at the moment $t = 0$, whereas the quasi-stationary conditions within every next period are given by the expression

$$r_o(t) = -k/T + t/T - \sum_{i=1}^{n} \frac{A \cdot e^{\alpha_i t}}{\omega_{oi} \cdot \omega_i \cdot M_i} \cdot \sin\left(\omega_i t - \psi_i\right) \qquad (4)$$

where: k - is a constant factor depending on RLCG parameters of all filters,

$$A = \prod_{i=1}^{n} \omega_{oi}^2 = \prod_{i=1}^{n} \left(\omega_i^2 + \alpha_i^2\right)$$

$$M_i = \prod_{\substack{j=1 \\ j \neq i}}^{n} \left\{\left[\left(\alpha_i - \alpha_j\right)^2 - \left(\omega_i^2 - \omega_j^2\right)\right]^2 + 4\,\omega_i^2 \left(\alpha_i - \alpha_j\right)^2\right\}^{1/2}$$

The curves corresponding to the increase of the oscillations, to the sustained part of the response and to the decay period, concerning for the sake of simplicity one formant filter only, that is the case when $n = 1$, will be given in Fig.1 during the lecture at the Congress. Some illustrations will be shown in Fig.2.

The frequency components of the output $r(t)$ of the synthesizer are given by the following general expression

$$r(t) = A_o + \sum_{i=1}^{n} A_i \cdot e^{\alpha_i t} \cdot \sin\left(\omega_i t - \theta_i\right) + \sum_{k=1}^{\infty} A_k \cdot \sin\left(k\Omega t + \Delta_k\right) \qquad (5)$$

which includes a d.c. term, a series of n exponentially decreasing sinusoids for each of n resonance circuits, having initial amplitudes A_i, frequencies ω_i and logarithmic decrements α_i, and an infinite series of harmonics of the fundamental frequency $F_o = \Omega/2\pi$. Of interest here are the amplitudes A_k of the harmonics given by the formula

$$A_k = - \frac{A}{k\,\pi\,N_k} \qquad (6)$$

where: $N_k = \prod_{i=1}^{n} \left[\left(\omega_{oi}^2 - k^2\Omega^2\right)^2 + 4\,\alpha_i^2\,k^2\Omega^2\right]^{1/2}$

as they are closely related to the original amplitude spectrum of the source

function U(s) which in this case decreases 6 dB/octave. This is not compatible with the amplitude spectrum of the natural glottal wave decreasing about 12 dB per octave, but includes the correction for the radiation function $Z_r(s)$ increasing 6 dB/octave. The preliminary results of Polish vowels synthesis when using this type of source function have been unsatisfactory from the viewpoint of the naturalness of those vowels, which like Polish "e" and "i" have rather high second and third formants [5][6]. The correction of the source spectrum proved to be necessary. To this end the response to other driving functions have been investigated, and particularly to those obtained by differentiation or integration of the saw-tooth wave. The process of differetiation, achieved with a simple RC network, leads to a function which may be approximated as a series of recurrent exponentially decaying pulses; its amplitude spectrum, related to the frequency components of the steady-state response given by the expression

$$A_k = \frac{A \cdot \Omega}{\left[(RC)^{-2} + k^2\Omega^2\right] \cdot N_k} \quad , \tag{7}$$

is flat up to the pole frequency $s = -(RC)^{-1}$ and then decreases 6 dB/octave. The process of integration, on the other hand, results in a function the amplitude spectrum of which decreases 6 dB/octave up to $s = -(RC)^{-1}$ and 12 dB/octave at higher frequencies, as in this case

$$A_k = \frac{A}{\pi \cdot k \cdot RC \cdot \left[(RC)^{-2} + k^2\Omega^2\right] \cdot N_k} \quad . \tag{8}$$

The best results from the viewpoint of naturalness and recognition of Polish vowels have been obtained in the latter case with $s = 2\pi \cdot 1600$ sec^{-1}. This form of driving function, which includes the correction for radiation function $Z_r(s)$ and corresponds to the primary source spectrum decreasing approximately 12 dB/octave beneath 1600 c/s and 18 dB/octave at higher frequencies, has been adopted for further experiments.

Description of the synthesizer

To prove the results of the analysis experimentally a simple cascaded formant-circuit analog for synthesis of Polish vowels has been built. Its simplified block and circuit diagram is given in Fig.3.

The voice source is simulated by a saw-tooth pulse generator with necessary controls for varying the pulse amplitude A_o and fundamental frequency F_o either manually or electrically, in the latter case by controling the grid potentials of two separate tubes with d.c. voltages delivered from special function generators to be described later. The generator itself is based on the conventional principle of a saw-tooth thyratron oscillator as used in oscilloscopes and similar devices; its simplified schematic diagram is shown in Fig.4. Two separate RC networks are provided to change the amplitude frequency spectrum of the primary pulse wave according to the rules given above. Some examples of the spectrum are given in Fig.5.

Four formant filters of the variable capacitance type are all based on the well-known Miller-effect principle. The resonance frequency of of the circuit formed by a variable capacitance and a fixed inductance may be changed either manually or electrically by means of a d.c. control voltage varying the gain of a variable-mu pentode. The frequency control is used only in filters F1, F2 and F3, the frequency F4 being constant and fixed to a given value between 3200-4300 c/s. The simplified circuit diagram of one filter is given in Fig.6. The quality factors of each formant circuit are so chosen, that the resulting formant band-width follows dr.Fant's empirical formula $\Delta F = 50 \cdot (1 + F/2000)$, see Fig.7. The best order of cascading the formant circuits has been proved to be F3, F2, F1, F4, the corrective networks for higher formants being connected between F2 -F1 and F1-F4 respectively.

Five separate function generators have been designed and used to control the fundamental frequency F_o and the pulse amplitude A_o as well as the frequencies of

the lower formants F1, F2 and F3. The basic form of the d.c. control voltage is chosen in such a way that it remains constant and equal to U_o for a given time period τ_1, then increases linearily from U_o to U_{max} during the time period τ_2, remains constant and equal to U_{max} for τ_3 and decreases to the initial value during the time τ_4. The basic shape of the control voltage is shown in Fig.8. All the time periods τ are independently adjustable in rather broad limits, from 100 msec or even less to a few seconds. The circuit diagram of the function generator is given in Fig.9. Its action consists in successive process of charging and discharging a capacitor, controled by a trigger circuit cooperating with an electromagnetic high-speed relay and a silicon diode.

The absolute values of the d.c. control voltages U_o and U_{max}, which correspond to the initial conditions and to the sustained parts of the vowels, respectively, are so chosen that the whole range of the amplitude and frequency parameters of the synthetic sound may be covered without any difficulty. An additional switching circuit lets the polarity of the output control voltage be changed from +U to -U and vice versa. Fig.11 may be used as an example of a set of five control voltages corresponding to different Polish vowels and groups of vowels.

Conclusions

It has been proved that the synthesis of Polish vowels by means of a simple "terminal-analog" formant synthesizer may give satisfactory results from the view point of their identification as well as naturalness. The radiation characteristic of the mouth may easily be included into the source function U(s) having in the case discussed a fairly simple amplitude spectrum. The formant parameters of six sustained Polish vowels have been determined experimentally and compared with the data obtained by analysis [5][6]. The results are shown in Fig.10.

It has been proved, too, that the dynamical synthesis of separate Polish vowels and some combinations of vowels may be easily done when using only five d.c. control signals changing the amplitude A_o and fundamental frequency F_o as well as the formant frequencies F1, F2 and F3, respectively. It is worth while to mention here, that the shape of the control signals may be significantly simplified without affecting the quality of synthetic sounds. In our case this simlification consisted in approximating the original smooth time function with straight lines corresponding to the increase, sustained part and decay of the sound. Some examples are given in Fig.11. It seems, that these approximations may be useful for future speech compression systems based on formant coding methods.

Literature

1 . Fant G.: Acoustic Theory of Speech Production. - Mouton and Co., 's-Gravenhage, 1960.
2.. Fant G.: On the Predictability of Formant Levels and Spectrum Envelopes from Formant Frequencies. - For Roman Jakobson, 's-Gravenhage 1956, pp.109-120.
3.. Flanagan J.L.: Note on the Design of "Terminal-Analog" Speech Synthesizer. - J.Acoust.Soc.Amer., vol.29, 1957, No 2, pp.306-310.
4 . Gandhi O.P., Peterson G.E. and Yu F.: Recurrently Impulsed Resonators in Speech and Psychophysical Studies. - Language and Speech, vol.3, part 3, July September 1960, pp.140-154.
5 . Jassem W.: A Spectrographic Study of Polish Speech Sounds. - Phonetic Department, Edinburgh University, March 1961.
6 . Jassem W.: The Formants of Sustained Polish Vowels; A Preliminary Study. - Tokyo 1957.
7 . Kacprowski J.: Theoretical Fundamentals of Polish Vowels Synthesis by Means of Resonance Formant Synthesizers. - Rozprawy Elektrotechniczne, vol.VIII, No 1, Warsaw 1962, pp.28-103 /in Polish/.

H55

FOURTH INTERNATIONAL CONGRESS ON ACOUSTICS
COPENHAGEN 21.-28. AUGUST 1962

ON THE SHORT ACOUSTICAL SIGNAL INTENSITY MEASUREMENT AT THE FIRST NEURON LEVEL OF THE AUDITORY SYSTEM

E.A.Radionowa
Pavlov Institute of Physiology, USSR, Leningrad.

The short acoustical signal intensity measurement within the auditory system can be performed by two ways: 1) by the number or by the frequency of the nerve impulses in the individual neurons and 2) by the number of neurones which respond to the sygnal synchroniously. On the basis of some data in literature, it can be supposed that in the case of short acoustical signals their intensity measurement is performed mainly with the help of the second mechanism, e.g. by the number of neurones synchroniously responding to the signal. We investigated this mechanism using as the method of registration of the cochlea neural response to the click, as the psychoacoustical experiment.

When presenting the short acoustical signal we can register near the round window of the cochlea the electrical reaction which consists of the microphonic response (M) of the cochlea receptors and of the summated response of the auditory nerve fibres (fig.1). The summated neural response (N_1) is the result of the synchronious discharge of a group of neural units. The duration of the N_1 response is about 0.5 msec. In this time interval each nerve fibre can give only one spike. Therefore the amplitude of the N_1 response represents the number of nerve units synchroniously responding to the click. Thus when measuring the amplitude of the N_1 response we can get an information of the number of the nerve units sinchroniously responding to the signal.

It is known that with the increasing of the click intensity the amplitude of the N_1 response increases too; however in the middle part of the amplitude characterstic curve (at the level of about 60 db over the threshold) the curve has a bend, that proves the complicated character of the function (fig.1). This bend is not an occasional one, we find it not only by the construction of the amplitude characteristic curve on the points corresponding to the amplitude values of the negative phase of the N_1 response (as it was done in this work), but also by the construction of the amplitude characteristic curve on the points corresponding to the area of the N_1 response or its amplitude from peak to peak (Frishkopf, 1956). Considering the amplitude characteristic curve as an integral curve of the distribution of the nerve units according to their thresholds we can conclude (on the basis of the complicated character of the amplitude characteristic curve) that the whole population of the nerve units responding to the click is distributed according to their thresholds in two groups - with lower and higher thresholds. Frishkopf & Rosenblith (1958), Davis (1961) and other authers came also to this conclusion.

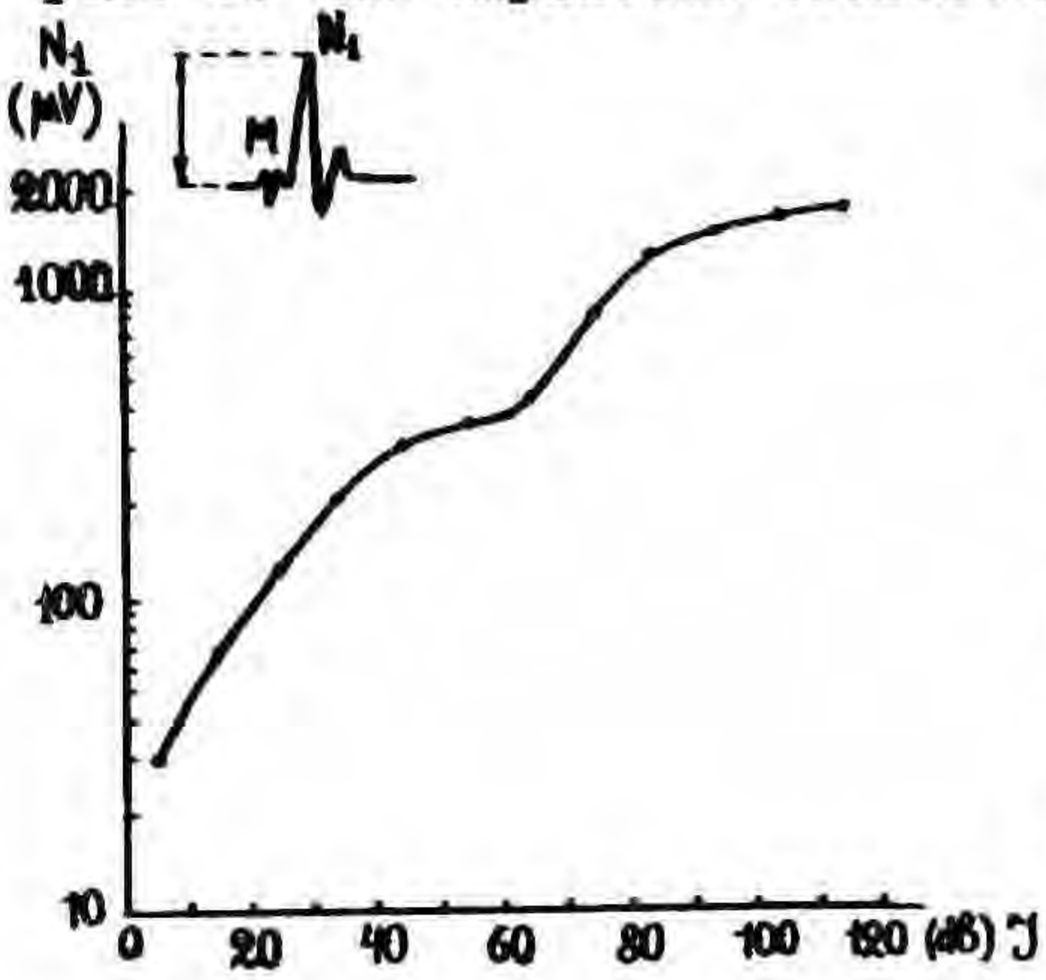

Fig.1

The investigation of the variance of the amplitude of the N_1 response confirms the presence of the two groups of units. The measurement of the amplitude of the N_1 response by the repeated presenting of the constant intensity click results in some distribution of the amplitude values characterized by the mean value $\bar{N}_1$ and by the variance σ^2. The dependence of the σ^2 on the click intensity, experi-

mentally, results in a curve with two humps (fig.2, the average data for 10 animals; below them - the data of one of the experiments). It may be shown that this function is the expression of the distribution of the auditory nerve units according to their thresholds, it is the approximate expression of the probability density of this distribution. Then the two-hump character of the curve

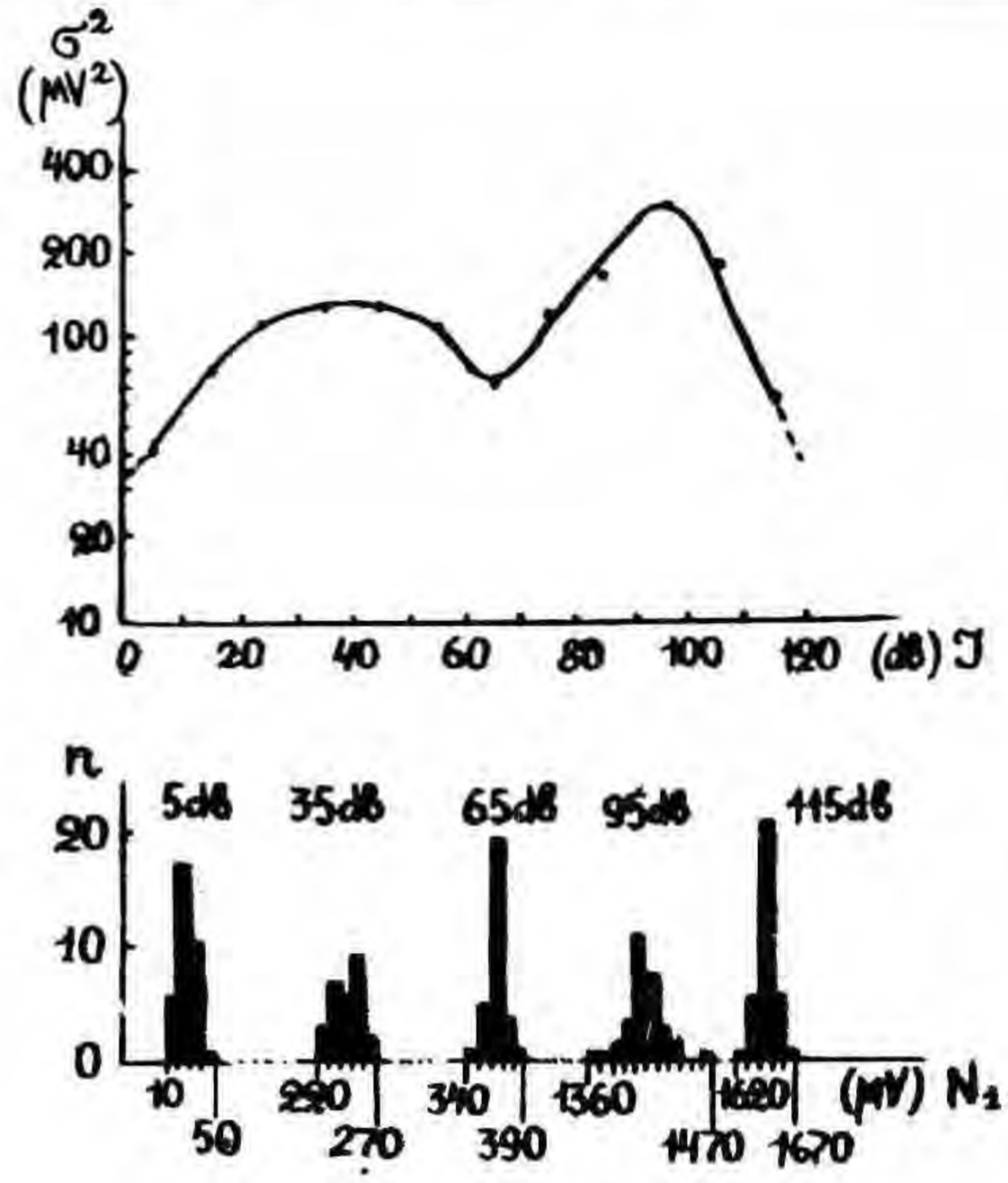

Fig.2

shows that all the auditory nerve units really distribute in two groups according to their thresholds.

The presence of two groups of units seems to produce some decrease of the precision of the signal intensity measurement in the middle intensity range, corresponding to the bend of the amplitude characteristic curve. In order to examine this assumption the difference limen (DL) for intensity were calculated in the whole click intensity range. If the mean value $\bar{N}_1$ and the variance σ^2 of the amplitude of the N_1 response are known, the mean value of the amplitude ($\bar{N}_1'$) different from $\bar{N}_1$ with the probability $p=0.5$ can be calculated. Then

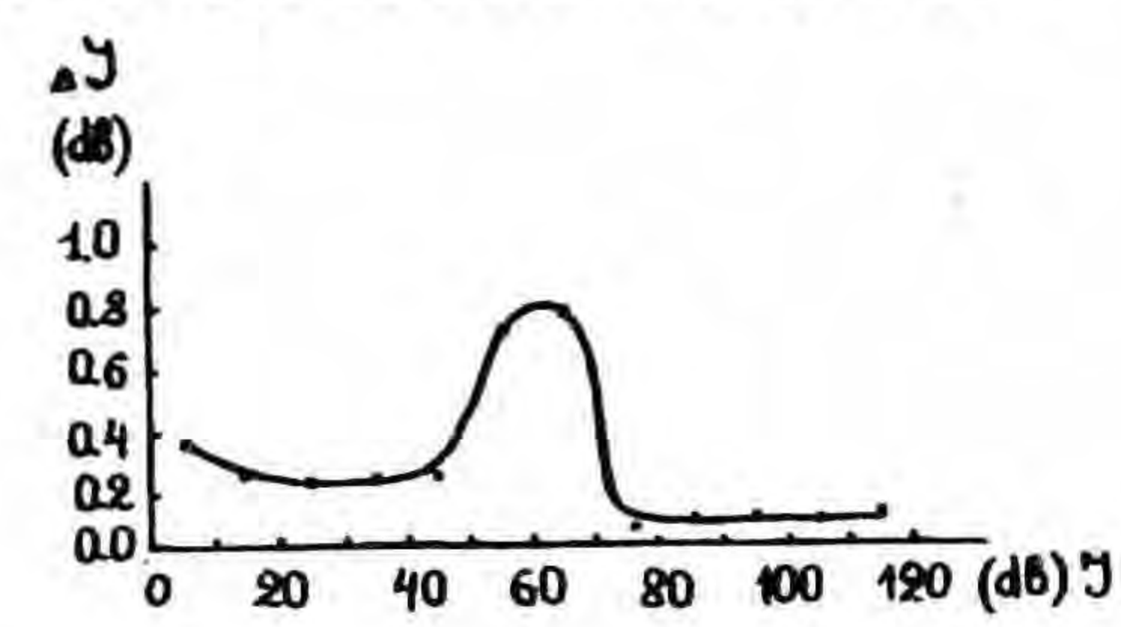

Fig.3

on the amplitude caracteristic curve (fig.1) we can find the inten-

sity change (ΔJ) corresponding to the change of the amplitude from $\bar{N}_1$ to $\bar{N}_1'$. The calculated values of the DL (ΔJ) really show some increase in the middle intensity range (fig.3).

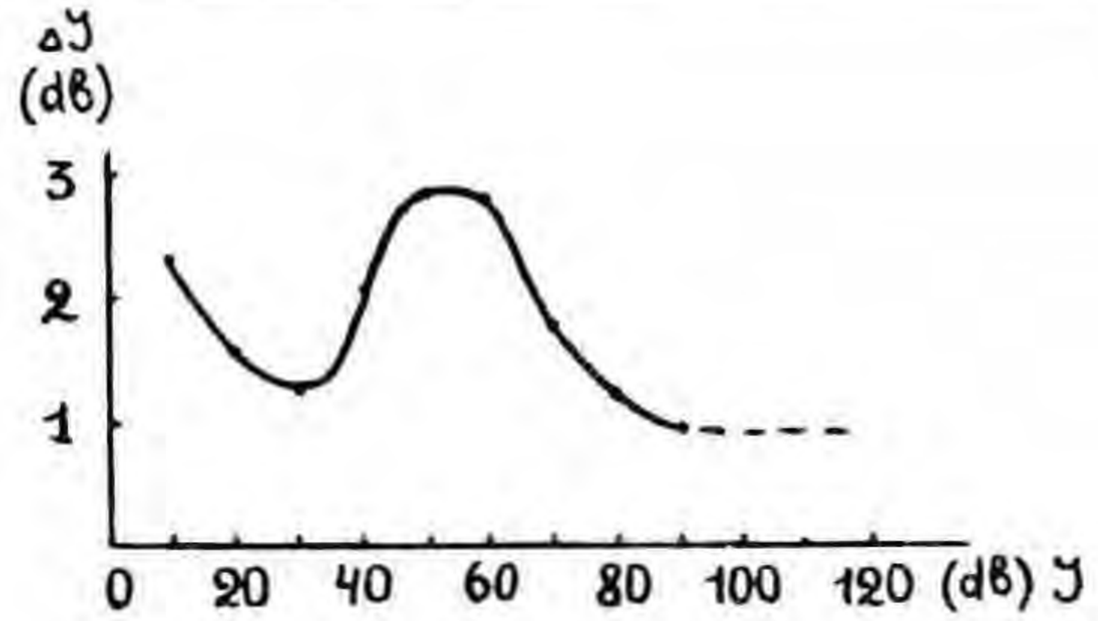

Fig.4

In order to be sure that the particular character of our DL-curve is not connected with the object specifity (the peripheral part of the auditory analyser of the cat) we measured, together with R.V.Avakjan, the DL for clicks on men. As a result we got a DL- curve (fig.4) in its form very much like the curve in the fig.3.

Thus supposing the measurement of the short acoustical signal intensity to be performed by the number of the nerve units synchroniously responding to the signal (resp. by the amplitude of the N_1 response) we can conclude that there are two groups of units in the peripheral part of the auditory analyser, which give some DL increase in the middle intensity range, however together they provide for the possibility of the short acoustical signal intensity measurement in a wide range.

J55

FOURTH INTERNATIONAL CONGRESS ON ACOUSTICS
COPENHAGEN 21.-28. AUGUST 1962

Schwingungsrelaxation in flüssigem und festem Brom.

H.G.Danielmeyer und H.O.Kneser
I.Physikalisches Institut der Technischen Hochschule Stuttgart.

1) Einleitung

Viele Arbeiten beschäftigen sich mit der Abhängigkeit der Schwingungsrelaxationszeit von der Dichte der Substanz im Bereich gasförmig-flüssig. Da sie leichter meßbar sind, wurden drei- und mehratomige Substanzen untersucht, obwohl dann die Zuordnung einer Reaktion wegen der vielen möglichen Schwingungszustände unter Mehrdeutigkeit leidet.
Von zweiatomigen Substanzen sind nur die Halogene mit Meßbarkeitsbedingungen verträglich. 1960 hat Shields (L1) die Schwingungsrelaxation in gasförmigem Cl_2, Br_2 und J_2 gefunden und die Übergangswahrscheinlichkeiten für die Schwingungsquanten bestimmt. Bittig (L2) gelang dies für gasförmiges und flüssiges Chlor. Die vorliegende Arbeit beschäftigte sich daher zunächst mit flüssigem Brom. Da Brom einen Molekülkristall bildet, lag es nahe, die Relaxation auch im festen Zustand zu suchen; seine thermodynamischen Eigenschaften sind hierfür sogar besonders günstig. Für Benzol und Zyklohexan wurde das Problem von Liebermann (L3) und Rasmussen behandelt. Das Relaxationsmaximum liegt dort weit oberhalb der Meßfrequenzen.

2) Die Apparatur

Für obiges Meßprogramm wurde eine Zwei-Quarz-Impulsapparatur mit parallel geschaltetem Vergleichzweig entwickelt. Ihre Stabilität reichte aus, um die Absorption auch in festem Brom im einfachen Durchgangs-Verfahren und die Schallgeschwindigkeit mit der Laufzeit des Impulses zu messen. Die Reinigungsanlage (vor allem Trocknung) und der Meßraum bildeten ein vakuumdichtes System.

3) Ergebnisse in flüssigem Brom

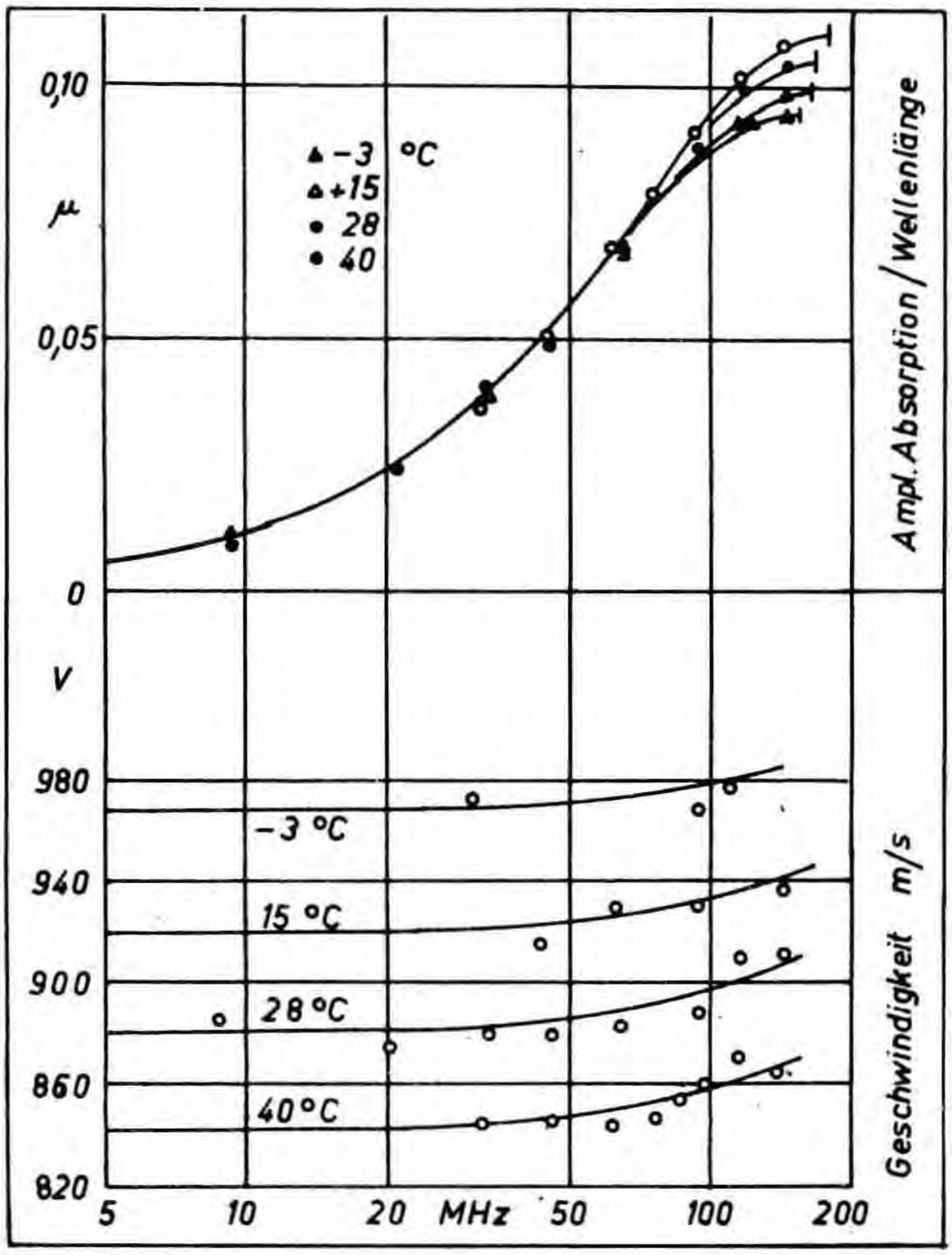

Bild 1: Schallabsorption und -Dispersion in flüssigem Brom.

Die Meßpunkte liegen innerhalb des Meßfehlers auf den theoretischen Kurven für Einfachrelaxationen. Die klassische Absorption erreicht bei der höchsten Meßfrequenz nur etwa 1 % des Meßwerts.
Mit Literaturwerten des Ausdehnungskoeffizienten ß, der spezifischen Wärme c_{po}, der relaxierenden spezifischen Wärme c_i und der Schallgeschwindigkeit v_o (aus Bild 1) ergibt sich Tabelle 1. Durch die Übereinstimmung der Maximalabsorptionen ist die Schwingungsrelaxation sichergestellt.

T	c_i	c_{po}	$10^3 ß$	c_o	c_∞	μ_{max}	μ_{max}
^oK	$\frac{cal}{Mol\,^oC}$	$\frac{cal}{Mol\,^oC}$	$^oC^{-1}$	$\frac{m}{sec}$	$\frac{m}{sec}$	theor	exp
270	1,556	16,73	1,028	968	1000	0,101	0,096
288	1,607	17,30	1,089	920	951	0,105	0,100
301	1,635	17,72	1,146	880	910	0,108	0,105
313	1,658	18,10	1,201	842	872	0,111	0,111

Shields erhielt im Gaszustand bei 28°C als Relaxationszeit

$$\tau_{VT} = 0{,}854 \cdot 10^{-6} \text{ sec}$$

Aus Bild 1 folgt für flüssiges Brom bei 28°C

$$\tau_{VT} = 1{,}06 \cdot 10^{-9} \text{ sec.}$$

Nimmt man an, daß sich die Übergangswahrscheinlichkeit pro Stoß nicht geändert hat, dann liefert das kubische Zellenmodell die beste Übereinstimmung.

3) Meßergebnisse in festem Brom.

Es wurden insgesamt 6 Kristalle mit Wachstumsgeschwindigkeiten von 0,3 bis 2 mm pro Stunde und 1 bis 12 mm Länge eingefroren. Da eine Orientierungskontrolle des Wachstums nicht möglich war, ist die Streuung entsprechend groß, jedoch zeigten alle Kristalle den wichtigen Dämpfungsabfall bei 3 MHz.

Ein anomales Verhalten der Absorption in der weiteren Umgebung des Schmelzpunkts, wie sie von Nozdrev und Mitarbeitern (L4) an verschiedenen Substanzen beobachtet wurde, trat nicht auf.

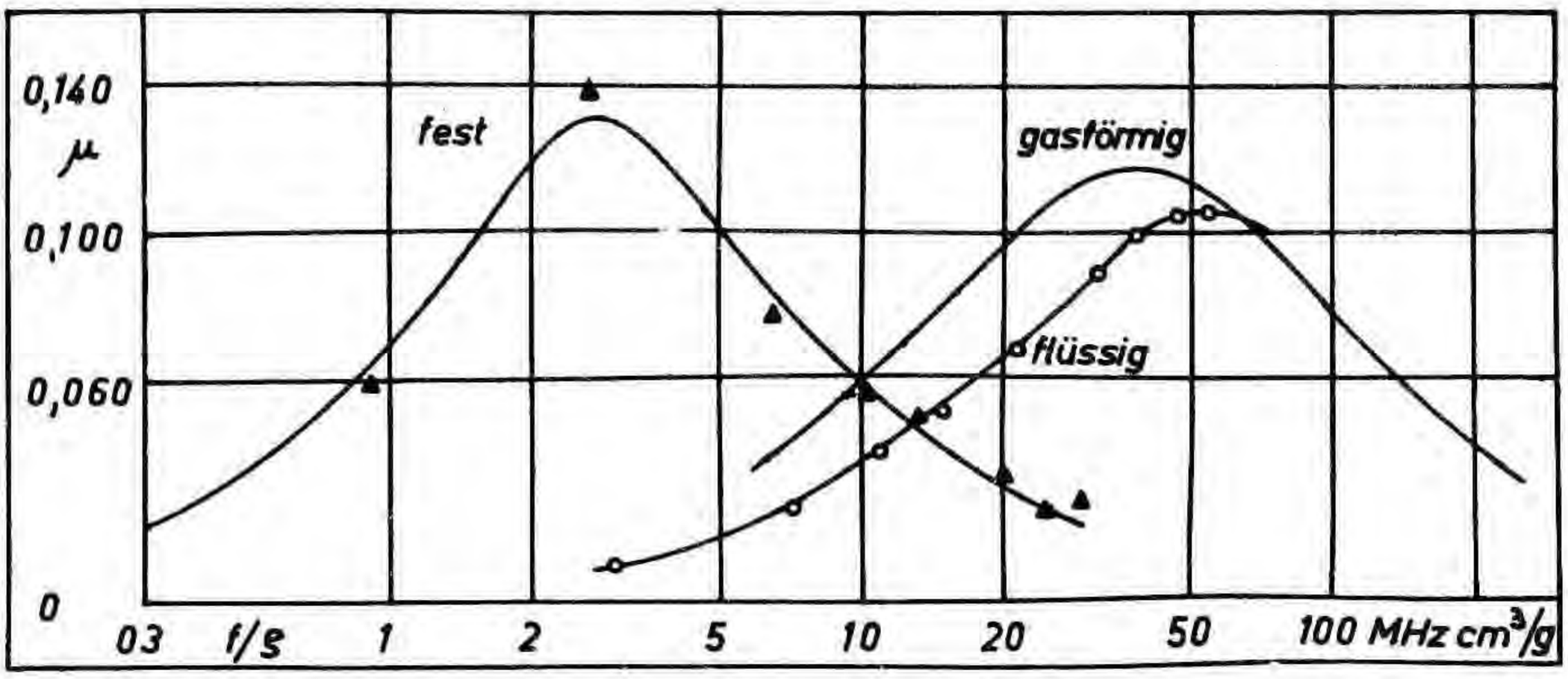

Bild 2: Schallabsorption in den drei Aggregatzuständen.

In Bild 2 sind die Mittelwerte der Meßpunkte aufgetragen. Zum Vergleich sind die Messungen von Shields im Gaszustand und unsere Messungen im flüssigen Zustand bei 28°C aufgenommen. Zur Erklärung des Absorptionsverlaufs im festen Brom kommt vor allem die Schwingungsrelaxation in Frage. Eine Berechnung der Relaxationszeit nach Liebermanns Theorie ist aber immer noch wenig erfolgversprechend, zumal dort nicht genau bekannte Größen bis zur 7. Potenz eingehen. Besser steht es um den Relaxationsbetrag. Berücksichtigt man dabei noch die Querkonstraktion im Festkörper mit der Poisson-Konstante 0,3 (Korrektur der Schallgeschwindigkeit), erhält man ensprechend

Tabelle 1

T	c_i	c_{po}	$\beta \cdot 10^3$	v_{exp}	$\mu_{maxtheor}$	μ_{maxexp}
265	1,55	14,80	0,70	1890	$0,142 \pm 0,02$	$0,132 \pm 0,02$

Diese Übereinstimmung kann als hinreichend für die Annahme der Schwingungsrelaxation betrachtet werden. Aus der Relaxationszeit bei -8°C nach Bild 2

$$\tau_{VT} = 1,9 \cdot 10^{-8} \text{sec}$$

folgt, daß sich das Gleichgewicht in der festen Phase rund 20 mal langsamer einstellt, als in der flüssigen.

Literatur:

L1 F.D.Shields, J.Acoust.Soc.Am. 32, 1960, 180
L2 E.Sittig, Acustica 10, 1960, 81
L3 L.Liebermann, Phys.Rev. 113, 4, 1959, 1052
L4 V.F.Nozdrev, N.I.Koshkin, M.A.Gorbunov, III.ICA-Congr. 1959, 549

Folgenden Firmen sei für ihre Arbeit und Großzügigkeit bei Sonderanfertigungen gedankt:

Carl Huth u. Söhne, Bietigheim (Teflonbälge)
Vereinigte Deutsche Metallwerke AG. Zweigniederlassung
Basse u. Selve, Altena (Nickelmaterial)
Heraeus Quarzschmelze GmbH., Hanau (Delay-lines)
Eberhard Hoeckle GmbH., Stuttgart (Hon- und Schleifarbeiten)

K55

FOURTH INTERNATIONAL CONGRESS ON ACOUSTICS
COPENHAGEN 21.-28. AUGUST 1962

A Solid Resonant Device for Ultrasound Focusing

M.A.Issakovich, M.G.Sirotyuk.

Ultrasound focusing in a liquid is limited by cavitation: when the cavitation threshold in a converging ultrasonic beam is surpassed further energy concentration will be hindered or stopped altogether. It is expedient therefore to use as a material for focusing devices a noncavitating medium-solid body - obtaining in it a converging sound beam and transmitting the ultrasonic energy into the liquid only when vibration amplitude has reached the desired value. The use of solid body for transmitting medium practically remouves also nonlinear absorption - another obstacle for ultrasonic concentration in a liquid medium.

The focusing device could be made of a material with low mechanical losses in the form of a sphere with a concentric cavity and channels for filling the cavity with liquid, for introducing probes and so on.

The excitation of vibrations could be achieved with the aid of piezoelectrical mozaic on the outer surface of the device. On resonant frequencies of the solid sphere and the cavity working chamber a considerable concentration could be obtained with a device of comperatively moderate dimensions. The frequency equation for the solid sphere is of the form

$$tg\,k(B-a) = \frac{4ka\left[(\varkappa B)^2-4\right]-4kB\left[(\varkappa a)^2-4\right]}{4ka\,4kB+\left[(\varkappa B)^2-4\right]\left[(\varkappa a)^2-4\right]}$$

Where a and B -internal and external radii of the device and k and $\varkappa$ -wave numbers for longitudinal and transversal waves.

A model of such concentrator was made in the form of a part of a

sphere shown in the fig.1.

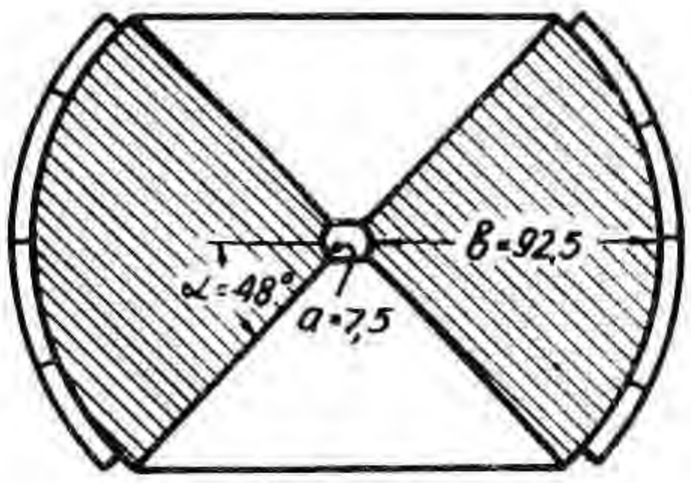

fig.1.

Resonance frequency of the barium-titanate mozaic was about 580 kc. The cavity was filled with water and was placed a miniature barium-titanate hydrophone (diameter 0,2mm) was placed in its center.

Fig.2 gives frequency dependence of the pressure amplitude in the center of the cavity with the electrical tension on the mozaic held constant. Two series of maximums were obtained; one corresponding to sphere resonances and the other to the cavity resonances.

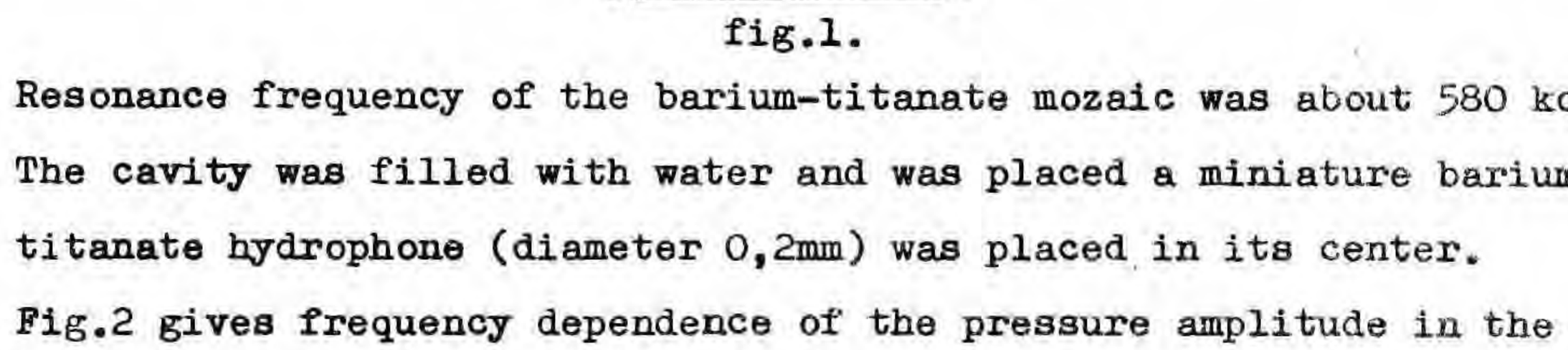

fig.2

Fig.3 gives a part of the frequency characteristic of the concentrator obtained on the electrical side, with the cavity either filled with water (solid line) or emptied (broken line).

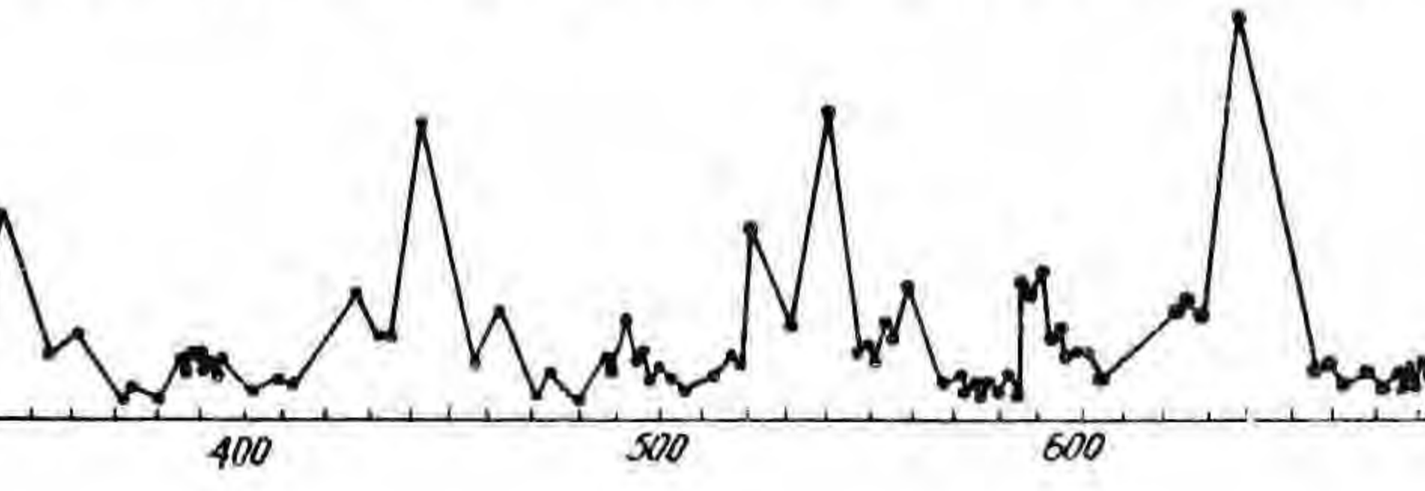

fig.3

According to these curves the efficiency of the concentration was calculated. In this model 30% of energy supplied to piezoelectric mozaic could be transfered to water. Cavitation was obtained on several resonant frequencies with electrical tension reaching only 15-25 volts.

Nonlinear Effects Accompanying the Dipole Radiation.

M.A.Issakovich

Radiation from a harmonic vibrator is always accompanied by a wave of doubled frequency corresponding to the nonlinear (second order) correction to the solution of linearized acoustic equations.

In this report this effect is considered for a small sphere oscillating harmonically. According to linear approximation it radiates a dipole wave; in the far-zone the pressure in this wave is

$$\frac{e^{i\kappa r}}{r}\cos\theta$$

The generation of double frequency wave results from the action of several different mechanisms. First of all such a wave is generated directly by the oscillating boundary of the sphere. The explanation lies in the fact that to the second order of approximation harmonic oscillations of a sphere correspond to the nonharmonical normal velocities on fixed surface. This mechanism gives rise to a quadrupole wave. For a dipole consisting of two simple sources of opposite signs this mechanism would be lacking; a dipole source and an oscillating sphere cannot therefore be considered as equivalent when nonlinear effects are studied.

Secondly, a spherically-symmetrical wave of double frequency is radiated by the near-zone of the oscillating sphere because particle velocities are relativēly high in this zone.

And lastly, the nonlinear correction in the far-zone results in a diverging wave of double frequency propagating as the sum of a spherically-symmetrical and a quadrupole wave. Their amplitudes increase proportionally to the logarithm of the distance.

It appears that nonlinear correction to the dipole radiation is represented by sperically-symmetrical and quadrupole waves. Thus the nonlinearity besides doubling the frequency causes also transformation of radiation modes. Directivity patterns of the primary wave and its nonlinear correction for a given radiator are therefore different (the case of pulsating spheres is the exception).

The total second-order correction calculated for the far-zone is

$$\frac{e^{i2\kappa r}}{r}\left[2M\cos\theta + iM\frac{\gamma+1}{8}(\kappa a)^3 \ln(2\kappa r)\cos^2\theta\right]$$

where a -radius of the sphere, M -Mach number: ratio of sphere oscillating velocity to the sound velocity; γ -ratio of specific heats. Except for very great distances the logarithmic member is vanishingly small in comparison with the first member. For instance for $\kappa a = \frac{1}{2}$ logarithmic member will be sensible only at distances greater then about 10^{20} wavelengths.

The validity of calculations for the first member requires that $M \ll \kappa a$ rather than $M \ll 1$ as is the case for plane waves. It means that oscillation amplitude of the sphere is to be small compared with its radius.

FOURTH INTERNATIONAL CONGRESS ON ACOUSTICS
COPENHAGEN 21.-28. AUGUST 1962

Geräuschmessungen an den normalen und geschweissten Schienen

dipl. ing. Széchey, Béla
Akustische Entwiklungsabteil der MÁV. Ungarn.

Die Geräuschmessungen, die wir in unserem Iande bisher vorgenommen hatten, haben gezeigt, dass die Riffelbildung für uns keine Aufgaben gibt und zur Zeit keine grosse Rolle spielt. So haben wir uns eine andere Aufgabe gestellt. Wir sollen Erläuterungen geben über die Geräuschverhältnisse der geschweissten Schienen. Alle Fachleute, die in diesem Gebiete interessiert waren, haben einen möglichst grossen Erfolg erwartet, der subjektiven Empfindung entsprechend. Bei dem Zusammengleich der Messergebnisse der normalen und geschweissten Schienen, kam es vor, dass der Unterschied nur 1-2 db war, was zu beschreiben der richtigen Iage zu wenig war. Die Untersuchungen hatten es schnell gezeigt, dass die Dinamik grösser als 6 db ist, und so eine Durchschnittliche Ablesung keinen Zweck hat, und was wichtiger ist: die Untersuchungen, was die Dinamik anbelangt, nicht nur eine interessante wissentschaftliche Aufgabe ist, sondern eine sehr wesentliche praktische Rolle spielt. So muss man also das Frequenz- und Dinamikspektrum des Geräusches in Betracht nehmen. Unsere Aufgabe war, wegen den biologischen Bezihungen, nicht nur bessere Festlegung der Erscheinungen, sondern auch eine Beschreibung, consultieren, die der menschlichen Empfindung richtig entspricht. In Folge, da kein Heulen, und so auch keine echte tonale Komponente stattfanden, haben wir nur Oktaveband- Analyse für notwendige gefunden und als solches beurteilt. Entsprechende, oder gut brauchbare dinamische Daten zu bekommen, das ist etwa schwerer. Es ist klar, dass die Messangaben den dinamischen Eigenschaften für das Ohr gemäss sein sollen. Die Messgeräte, die mit einem ähnlichen Zeitkonstanten arbeiten,können,nur die subjektive Wirklichkeit feststellen oder registrieren. Mehrere haben es schon festgestellt, dass die früher gebrauchte Zeitkonstanten für das Ohr, T=0,2 sec, nicht mehr gültig sind. Die von uns bekannten Messdaten /E. Port/ stellen die Werte über die Zeitkonstanten von 15 msec bis 5o msec fest. Auch das kann man beobachten, dass das Ohr in dinamischer Hinsicht, sich sättigt, d. h. der Anlaufabteil des Empfindens etwa steiler ist. Die Geräuschzeichen, die aus der Durchschnittnivo herauszuheben sind, haben meistens einen Impul-

sekarakter /Schienenfügen, Überlauf an den Weichen, Wagenstossen/, deswegen haben wir die kleinste Zeitkonstante gewählt, mit einem Wert von 10-15 msec. Mit einem bekannten Brüel-Kjaer Apparat arbeitend, die eine Registrierbreite mit 5o mm und allgemein mit einem dementsprechenden Umfassung von 5o db ausgestattet ist, haben wir die Registriergeschwindigkeit mit 7oo mm/sec gewählt. Die Registraten, die wir so angenommen haben, zeigten,es, dass unsere Wahl übereins stimmt mit der subjektiven Empfindung, und der Impulskarakter gut beobachtbar ist. Was mit einem Schreibgeschwindigkeit von loo mm/sec unmöglich war, das hat diese Schreibgeschwindigkeit für möglich gemacht:die Schienstosen und die Weichen ebenso einen bestimmten Charakter haben, laut Registrierpapieren was auch von den reisenden Publikum festgestellt wurde. Durch diese Metode wurden unsere Messergebnisse als Vorbereitung zur dinamischer Analise. Mit einem Bruel-Kjaer Apparat kann man einen sehr bequeme Methode anwenden, und die dinamische Eigenscaften des Frequenzspektrums beobachten. Mit einer relativ kleiner Vorschiebung sind auch statistische Geräusche sofort analisierbar, wenn man einen endlosen Magnettonband dazu lauffen lässt. Dadurch wird die Dokumentation einfacher, und die Möglichkeit ist geschaffen, auch in konventioneller Einteilung die Dinamik abzeichnen. /Abbildung 1. und 2./.

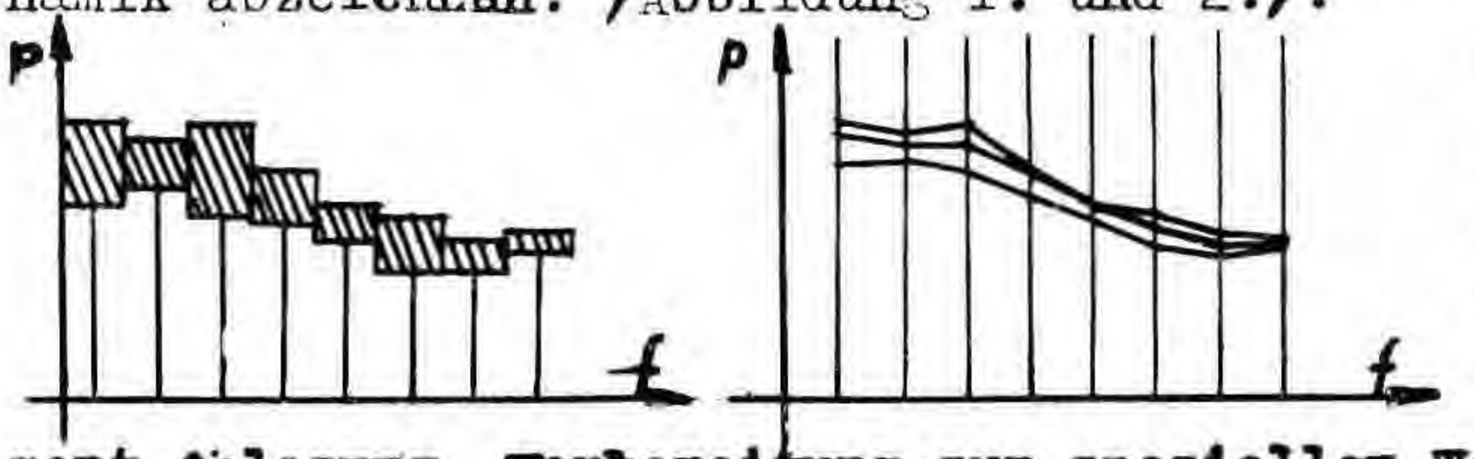

Wenn man die Messwerte mit Ziffern feststellen will, haben wir als unbrauchbar beurteilt, einen einzigen Wert anzugeben. /Instrument Ablesung, Vorbereitung zur speziellen Wertausrechnungen/. Wir fordern den Durchschnittwert, das Maximum desselben, und den Spitzenwert anzugeben. /Abb. 3./

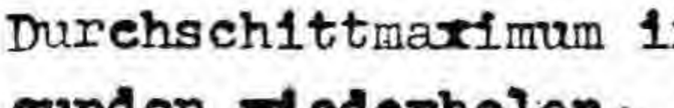

Als Maximalwert nehmen wir grundsätzlich die Werte an, die eine Folgerungszeit = lo min. haben. /Durchschnittlicher Stationabstand bei einer Geschwindigkeit 8o km/St/ als Durchschittmaximum inBBetracht genommen, die sich mindestens in 2 secunden wiederholen, /höchste Gleislänge/, als durchschnittliches dessen Frequenz grösser ist, als lo/sec. Spitzenwert, als überflüssigen Parameter verhindern will, muss man daran denken, dass ZB. in einem Schlafwagen der Spitzenwrt der entscheidenste Wert - eben man bei Überlauf andden Weichen und bei dem Beginn des Bremsens - ist. Die weitere Analise der Dinamik kann durch Realisierung und Zusammengleich der Häufigkeitskurven stattfinden. Selbstverständlich, eine Normalisierung an dem Nullpunkt, schafft die Möglichkeit zu einem allgemeinen Zusammen-

gleich, was auch wertvoll ist; in speziellen Falle aber eine Häufigkeitskurve, – die wir an Ihrer originelle Stelle gelassen – mehrere praktische Informationen geben kann. /Abb. 4. Entsprechend der Natur der Aufgabe, muss man an der Gleichheit der Beobachtungsperiode aufmerksam sein.
Die Funktion: $h/y, y+ y/= \frac{\sum_{1}^{n} \Delta t_i}{T}$ (—· . Es ist noch eine Frage: was man analisieren soll? Unserer Meinung nach, ist etwa erfolgreicher, die gleichgerichtete und logaritmizierte Funktion analisieren. Diese Kurven sind sofort Gebrauchfähig. Die Auswertung eines Oscillogrammes ist zweifellos einfacher.

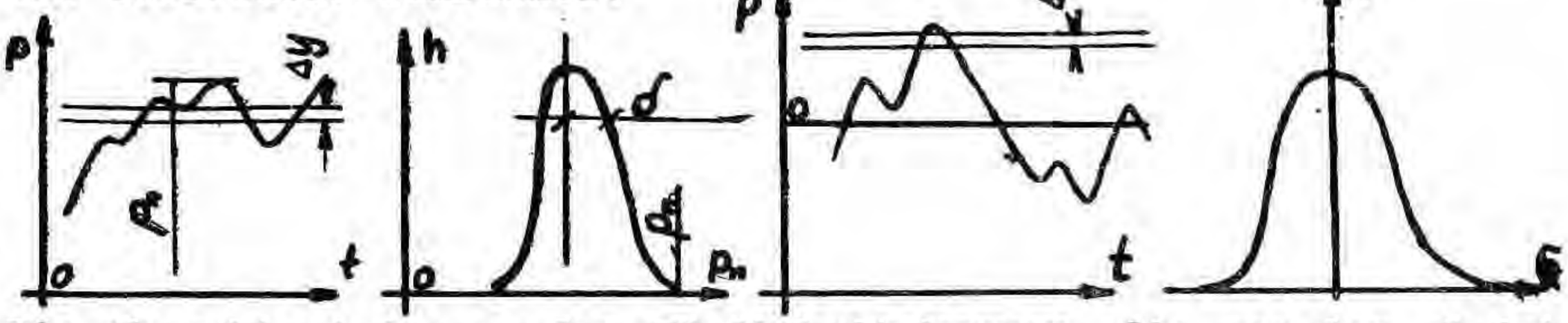

Die Charakterisierung der Häufigkeitskurven, die vom der gleichgerichtetem Funktionen geschaffen wurden, kann nicht durch bestättigt werden, sondern es ware nötig die Brandbreite in dem gewöhnlichen Form – definieren. In der Folge, dass die eben besprochene Kurve – beziehend dem häufigsten Wert – allgemein keinen Simmetrie hat, die Bandangabe nur an dem breiteren Halb-band stimmen kann. In diesem Falle, neben der Frequenzspektrum-Kurve auch die sogewonnene Dinamikkurve antragbar wäre.

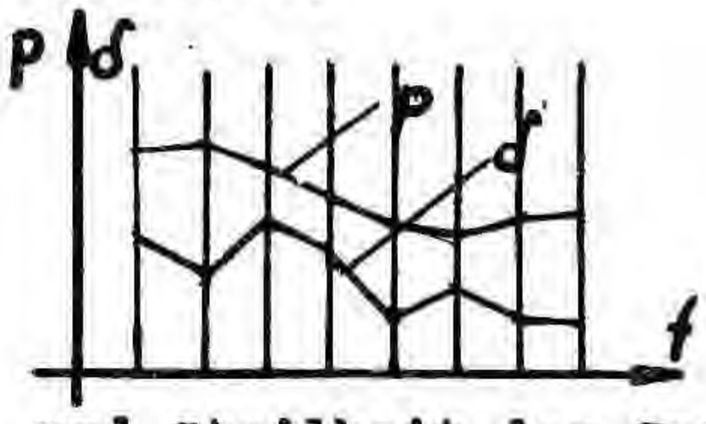

Bei den Auswertungen der Messungen, haben wir mit Hilfe einer Analogie, zwei neue Parameter eingeführt, die bei der Besprechung der Dinamik viel geholfen haben. Die neue Parametern sind: Lautstärke Irregularität und Steilheit der Lautstärke Irregularität.

$$LLi = \frac{\sum p_y - p_m}{T} \text{ db/sec} \qquad LLis = \frac{LLi}{n} \text{ db/sec/Stk}$$

Bei dem Vergleich T muss gleich sein.
Mit der Hilfe der neuen Parametern ist es möglich geworden, pregnante Unterschiede zwischen den zwei Schienesorten anzuweisen. Es ist klar, wenn diese Parametern auch in anderen Fällen gut funktbnieren, muss man Zusammenhänge feststellen, wie diese aus Mittelwert festgestellten Gleichbelastung-kurven, bei uns die FCx- Kurven modifizieren.

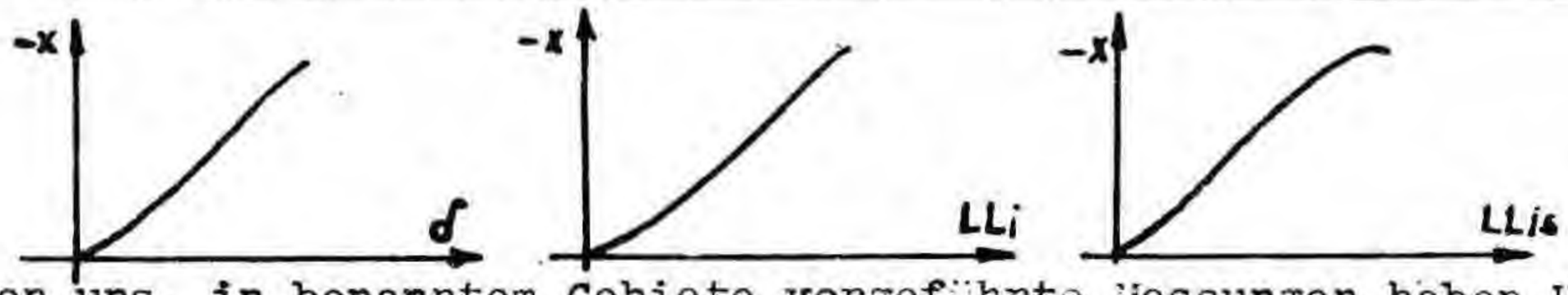

Die von uns, in benanntem Gebiete vorgeführte Messungen haben Unsere Theorie gerechtfertigt. Die Werte Zeigen dass:

1/ Mittelwert Angaben nicht ausreichend sind.

2/ Mit der Hilfe der Dinamik kann man schon einen Unterschied feststellen.

3/ Die eingeführte IIi und IIis Werte sind als brauchbar festgestellt.

MESSERGEBNISSE

	Normale Schiene			Geschweisste Schiene		
Bandmitte	p_D	p_{DI}	p_v	p_D	p_{DII}	p_v
50	84	90	97	83	89	94
100	78	84	92	78	84	92
200	80	86	101	78	82	93
400	79	84	96	80	83	96
800	74	77	96	72	75	82
1000	89	70	80	86	88	71
3200	86	70	77	83	84	84
6400	83	87	74	81	81	81
lin	90	96	107	91	95	102
ACA B	84	90	99	83	89	94
SII	89	72	82	86	86	72
S_{tph}	93	98	110	92	90	100
S_{tp}-SII	24	20	29	20	28	34
IIi, lin	82 db . sec			32 db . sec		
IIis lin	0,99			0,30		
PII	95	98	111	92,5	90	105

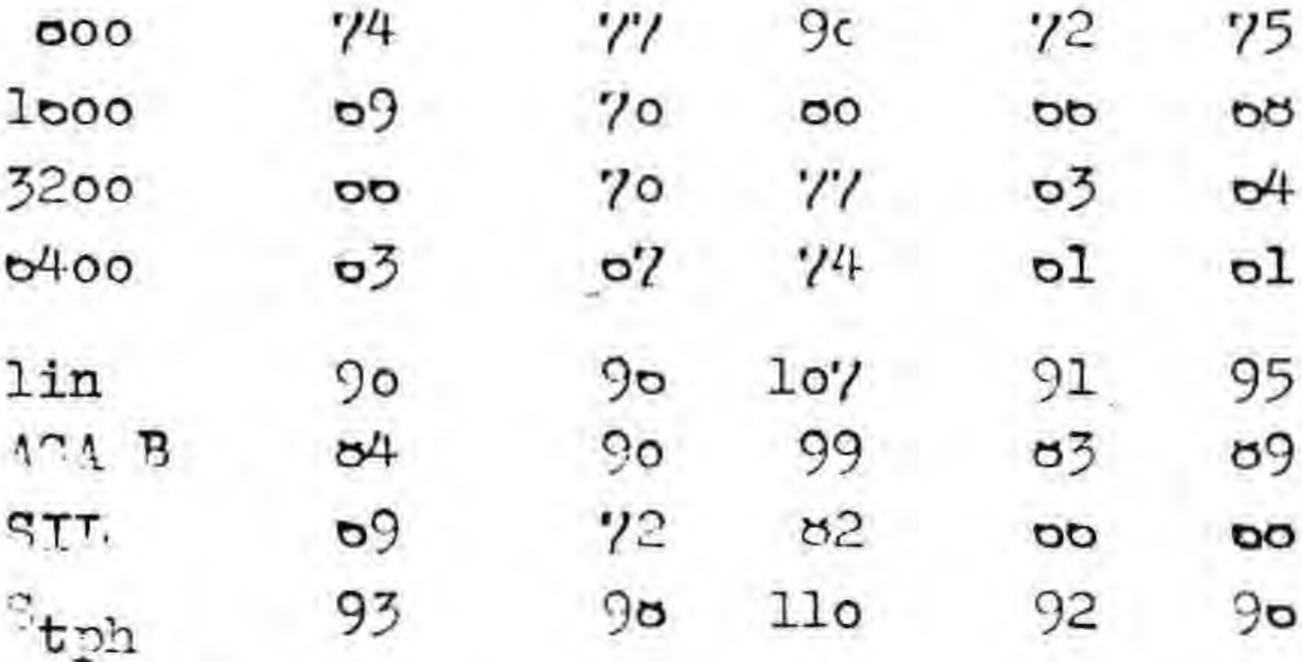

M55

FOURTH INTERNATIONAL CONGRESS ON ACOUSTICS
COPENHAGEN 21.-28. AUGUST 1962

CONSIDERATIONS SUR L'EFFICACITE DU TRAITEMENT ACOUSTIQUE POUR L'INSONORISATION DES SALLES BRUYANTES

Ing. M. Grumăzescu

Le traîtement acoustique d'un espace clos a pour effet une réduction du niveau de pression acoustique, en même temps qu'une diminuation du temps de réverbération. Nous tâcherons d'examiner de plus près ces effets afin de pouvoir établir les conditions optima pour l'insonorisation des salles bruyantes , tout en indiquant un moyen expéditif pour le calcul de l'opération.
Considérons une source sonore ponctuelle, placée au centre d'un espace clos. Dans la situation initiale - de la salle non traîtée - la pression acoustique dans un point situé à la distance r de la source sonore est

$$p_o^2 = W\rho c\left(\frac{1}{4\pi r^2} + \frac{4}{R_o}\right) \qquad (1)$$

Après avoir appliqué le traîtement acoustique, la pression acoustique en ce même point devient

$$p^2 = W\rho c\left(\frac{1}{4\pi r^2} + \frac{4}{R}\right) \qquad (2)$$

où $R = \frac{\bar{\alpha} S}{1-\bar{\alpha}}$ désigne la constante de la salle , S - l'aire totale et $\bar{\alpha}$ le coefficient moyen d'absorption acoustique.
L'application du traîtement acoustique produit à l'endroit considéré une réduction du niveau de la pression acoustique, qui s'exprime par

$$\Delta L = 10 \lg \frac{p_o^2}{p^2} = 10 \lg \frac{1 + \frac{16\pi r^2}{R_o}}{1 + \frac{16\pi r^2}{R}} \qquad (3)$$

Si l'on tient compte de l'expression de R, respectivemeht R_o, la relation (3) revêtira la forme

$$\Delta L = 10 \lg \frac{1 + k\frac{1-\bar{\alpha}_o}{\bar{\alpha}_o}}{1 + k\frac{1-\bar{\alpha}}{\bar{\alpha}}} \qquad (4)$$

où $k = 16\pi r^2/S$.
En mettant en évidence les absorptions acoustiques correspondant à la salle non traîtée (A_o) et à la salle traîtée (A) et en tenant compte que $A = A_o + A_a$ où A_a désigne l'absorption aditionnelle due au traîtement acoustique appliqué, il s'ensuit que

$$\Delta L = 10 \lg \frac{(A_o + A_a)\left[A_o(1-k) + kS\right]}{A_o\left[(A_o + A_a)(1-k) + kS\right]} \qquad (5)$$

On constate que la réduction du niveau de la pression acoustique dépend du paramètre k, donc de la distance par rapport à la source. Par conséquent, lorsque l'on indique la valeur de ΔL, il faut préciser en même temps l'endroit où la réduction est réalisée. Pour $k = 0$, $\Delta L = 0$, c'est à dire qu'au centre de la source on ne perçoit aucune réduction du niveau de la pression acoustique.

En admettant que la différence minimum du niveau sonore perceptible à l'oreille de l'homme est de 1 dB, la relation (5) permet de déduire la valeur de r, c'est à dire de la distance minimum à la source sonore, à laquelle l'auditeur peut recevoir l'effet du traîtement acoustique.

$$r_{min} = \left(\frac{0,02}{\frac{1}{S} + \frac{4}{A_o} - \frac{5}{A}} \right)^{1/2} \qquad (6)$$

Pour des valeurs de S suffisamment grandes, le premier terme du dénominateur de la fraction peut être négligé. On a alors

$$r_{mm} = \left(\frac{0,02}{\frac{4}{A_o} - \frac{5}{A}} \right)^{1/2} \qquad (7)$$

Au moyen de ces relations, on peut aussi déterminer la distance minimum admissible entre deux sources de bruit voisines, afin que par le traîtement acoustique appliqué, le niveau de la pression acoustique soit réduit avec le minimum perceptible. On constate que cette distance dépend des absorptions initiales et finales et qu'elle est d'autant moindre que l'absorption finale est plus grande. Dans ce qui précède il n'a pas été tenu compte de la caractéristique de directivité de la source sonore, ni de la caractéristique de directivité de l'organe auditif.
La relation (5) permet en outre de déduire l'absorption acoustique qu'il faut introduire dans une salle bruyante, afin de réaliser dans un point déterminé la réduction du niveau nécessaire

$$A_a = A_o \frac{S + A_o\left(\frac{1}{k} - 1\right)}{\frac{S}{10^{\frac{\Delta L}{10}} - 1} - A_o\left(\frac{1}{k} - 1\right)} \qquad (8)$$

Si k = 1, la relation (8) se simplifie et devient

$$A_a = A_o\left(10^{\frac{\Delta L}{10}} - 1\right) \qquad (9)$$

Il s'ensuit qu'à une distance appréciable de la source sonore, l'absorption aditionnelle ne dépend plus des dimensions de la salle.
D'autre part, puisque l'introduction d'un absorption aditionnelle apporte une modification du temps de réverbération (T) de la salle, on aura par l'application de la formule de Sabine

$$A_a = \frac{0,161\,V}{T} - A_o \qquad (10)$$

Nos recherches nous on conduit à la conclusion que, pour réaliser une ambiance favorable au travail, le temps de réverbération devra être de 1,5 s.
Pour une salle donnée et un endroit donné dans cette salle, on peut, en tenant compte de cette condition et en utilisant les formules (8) et (10), tracer deux courbes $A_a = f(A_o)$ qui se coupent en un point M (fig. 1) et partagent le plan en quatre zones:
La zone I comprend les points auquels correspondent des valeurs de l'absorption acoustique aditionnelle (A_a) satisfaisant aussi bien à la condition de reverbération optimum, qu'à la condition d'un niveau de bruit admissible.
La zone II comprend les points auxquels correspondent des valeurs de l'absorption aditionnelle satisfaisant à la condition du bruit limite, mais avec un temps de reverbération de la salle supérieur à la valeur limite. La salle est

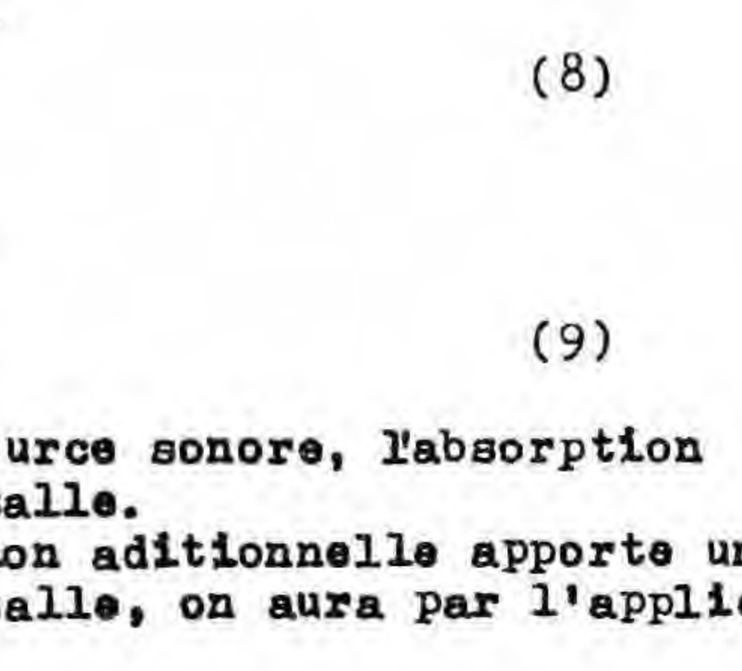

Fig 1

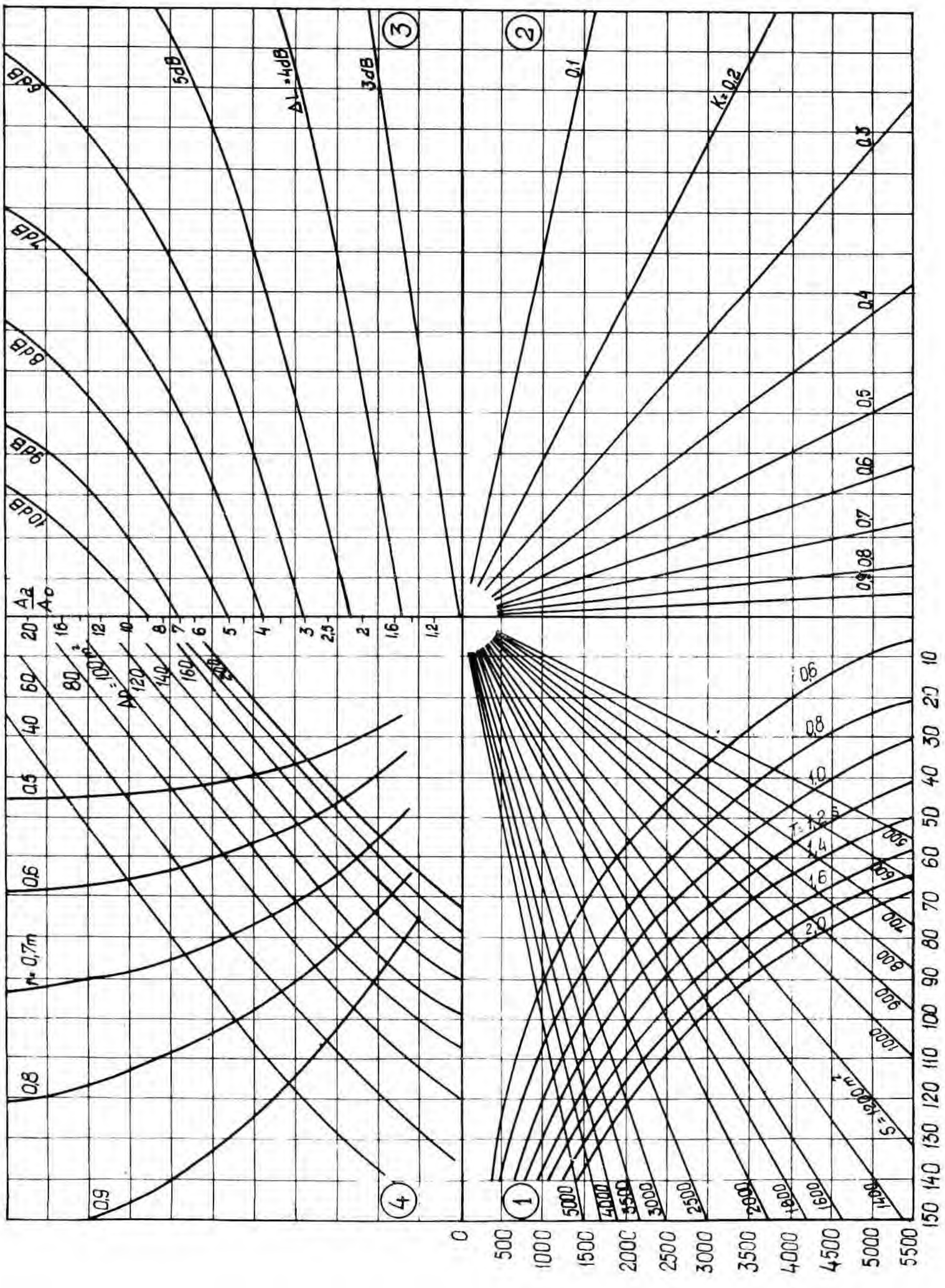
1
2
3
4
9dB
8dB
7dB
6dB
5dB
4dB
3dB
ΔL
K=0.2
0.1
0.4
0.5
0.6
0.7
0.8
0.9
1.0
1.2
1.4
1.6
2.0
r=0.7m
S=1200m²
A=100m²
A=120
A=140
A=160
A=200
Aa/Ao
0
500
1000
1500
2000
2500
3000
3500
4000
4500
5000
5500

résonante et contribue à diminuer l'intelligibilité de la parole et à créer une ambiance désagréable.
La zone III contient les points auxquels correspondent les valeurs de l'absorption additionnelle pour lesquels le temps de réverbération a des valeurs inférieures à la limite nécessaire, tandis que le niveau de bruit est supérieur à la valeur admissible.
La zone IV contient les points auxquels correspondent des valeurs de l'absorption additionnelle ne satisfaisant ni à la condition de réverbération optimum, ni à celle du niveau de bruit admissible. C'est une zone défavorable du point de vue acoustique.
Dans les salles à forte réverbération, l'introduction d'une absorption acoustique additionnelle permet plus facilement la réduction nécessaire du niveau de la pression acoustique que d'assurer un temps de réverbéartion favorable. Par contre dans les salles possédant une acoustique moins réverbérante, c'est la réduction du niveau de la pression acoustique qui constitue une opération malaisée.
La détermination de l'absorption additionnelle à introduire dans une salle afin d'obtenir la réduction du niveau sonore voulu, dans une zone déterminée et la vérification des conditions de réverbération de la salle après son traîtement acoustique peuvent être faites au moyen de l'abaque de la figure 2, qui permet aussi de déterminer la distance minimum donnée par la relation (7). Dans la partie (1) de l'abaque, on calcule graphiquement le rapport A_o/S; les valeurs de A_o, en mètres quarrés, sont données en abscisse, tandis que celles de S sont représentées par un faisceau de droites. Dans la partie (2) de l'abaque on effectue le produit $A_o\ (1/k - 1)/S$; les valeurs de k sont représentées par la famille de droites passant par l'origine. Dans le quadrant (3) on détermine en fonction de la valeur de L le rapport A_a/A_o dont les valeurs sont marquées en ordonnée. Lorsque ce rapport est connu, l'abaque permet ensuite de déterminer le temps de réverbéartion en fonction de l'absorption acoustique initiale, représentée par les courbes tracées dans le quadrant (4) et du volume de la salle en mètres cubes indiqués en ordonnée dans le quadrant (1). Les courbes des temps de réverbération égaux, en secondes, sont tracées dans le quadrant (1). En outre, si l'on connaît le rapport A_a/A_o, l'abaque permet de déterminer la distance minimum. Les courbes d'égales distances minima, en mètres, sont tracées en fonction du rapport A_a/A_o et de l'absorption acoustique initiale (A_o) dans la partie de l'abaque marquée par (4)

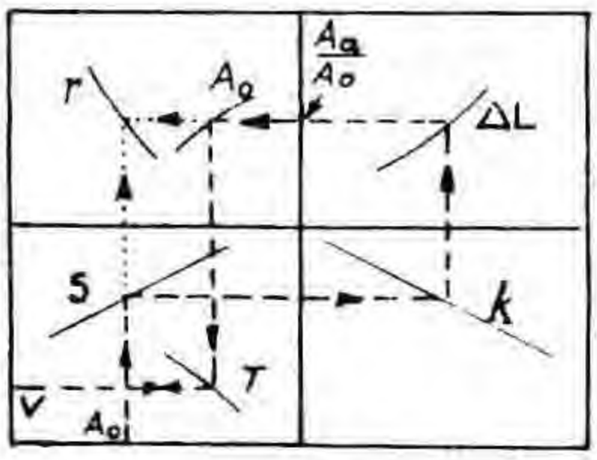

Fig.2

La succession des opérations pour résoudre graphiquement les formules (8) et (10) est indiquée sur la figure 3 par un traît interrompu et la résolution graphique de la formule (7) est indiquée sur la même figure en traîts pointillé.
L'abaque permet de plus de déterminer graphiquement la réduction du niveau de la pression acoustique que l'on obtient dans une salle et à un endroit donné de la salle par l'introduction d'une certaine quantité de matériel, caractérisé par l'absorption acoustique additionnelle.

N55

FOURTH INTERNATIONAL CONGRESS ON ACOUSTICS
COPENHAGEN 21.-28. AUGUST 1962

HIGH-QUALITY PUSH-PULL CONDENSER TRANSMITTERS

G. M. Sessler and J. E. West, Bell Telephone Laboratories Incorporated,
Murray Hill, New Jersey

ABSTRACT

A special type of push-pull condenser transmitter which operates without dc-bias is described in this paper. This transmitter consists of two metallized solid dielectric foils which are prepolarized. With the metal layers facing each other, these foils are sandwiched between two perforated metal plates. The force equation for this three electrode system shows that if ac-signals of opposite polarity are applied to the plates, the electrical force on the foils is free of nonlinear distortion.

Used as earphones, such systems have frequency responses which are flat within ±3 db from 30 to 11,000 cps. The harmonic distortion is less than 0.9% at 100 db SPL in this frequency range. The earphones show impulse responses which are almost exact replicas of the applied signal voltage.

Introduction

The qualities of condenser transmitters with solid dielectric are well known.[1] Until now the disadvantage of these systems has been the relatively high dc-polarizing voltage required for high efficiency and low distortion. This disadvantage can be eliminated by (1) using prepolarized foil, (2) driving the foil in push-pull, and (3) using multiple layers of foil. If these three methods are combined, condenser transmitters can be built which operate without dc-bias. These systems have a flat frequency response as well as high efficiency and low distortion.

Physical principles

The system which we consider here consists of two metallized and two nonmetallized mylar foils sandwiched symmetrically between two equal metal plates, as shown in Fig.1.

Figure 1
Enlarged Section of Push-Pull System

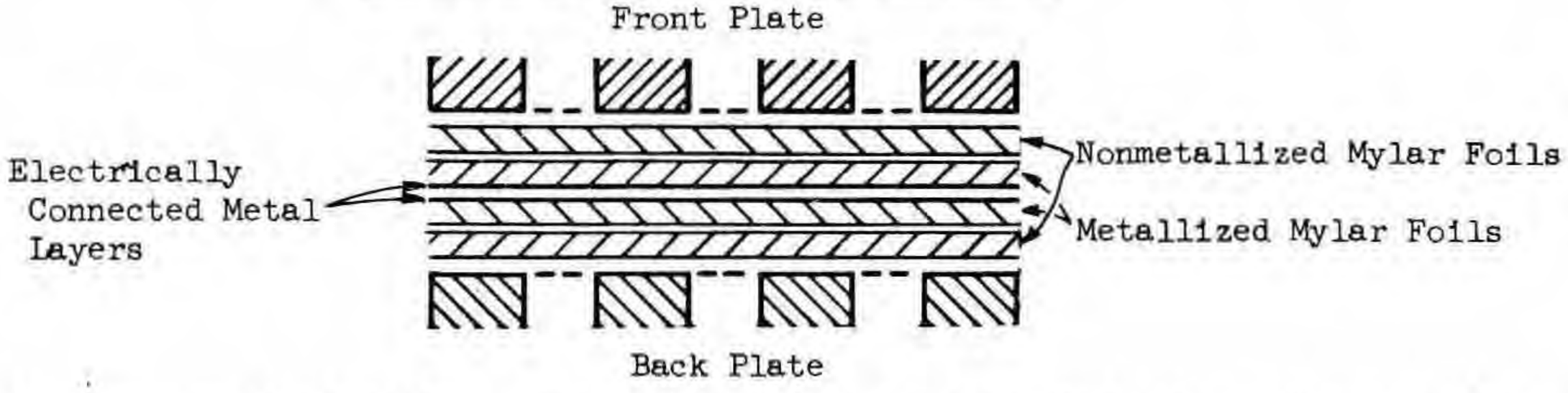

The foils are prepolarized in a process which will be described later. The two plates are insulated from each other and are also insulated from the foil. The electrical signal is applied to the two plates and the foil as shown in Fig. 2. It is apparent that the signal is of opposite polarity at the two plates. According to Coulomb's law, the force on the metallized foils is:

$$F \approx (E_{dc} + E_{ac})^2 - (E_{dc} - E_{ac})^2 = 4E_{dc}E_{ac} \qquad \text{Eq. (1)}$$

---

[1] G. M. Sessler and J. E. West, "A Condenser Earphone with Solid Dielectric," (to be published).

where E_{dc} is the dc-potential produced by the prepolarized foils and E_{ac} is the applied signal voltage. This equation shows that the electrical force on the foils is free of nonlinear distortion.

Only the combination of the two features, namely (1) the use of a three-electrode push-pull principle and (2) the use of prepolarized foils makes a system possible that operates without external dc-bias, and which, according to Eq. (1), shows an electrical force on the foils free of nonlinear distortion. This can be seen by considering systems which use only one of these features: (1) A push-pull system with unpolarized

Figure 2, Electrical Circuit

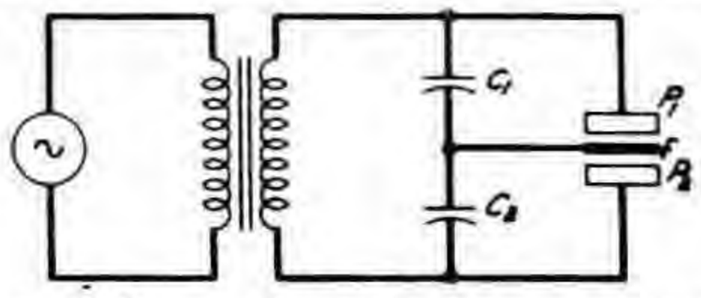

C_1 and C_2 - Equalizing condensers
P_1 - Perforated front plate
P_2 - Perforated back plate
f - Prepolarized foils

foil requires an external dc-bias for operation (otherwise the force on the foil would be zero). Moreover, for good efficiency, this bias has to be relatively high. (2) A two-electrode system with prepolarized foil still shows a distortion term in the electrical force.[1]

The pressure amplitude (for constant signal voltages) which can be generated in a small closed coupler is independent of the signal-frequency for frequencies lower than the resonant frequency. Therefore, a flat frequency response for pressure is expected. Mechanical distortion can result if the foils strike the plates when a high ac-signal is applied. This distortion is not included in Eq. (1). However, by use of the multilayer system, part of this distortion is removed.[1]

The impulse response is an almost true image of the input signal. The displacement of the foil follows the input signal because the pulse voltage adds to the polarizing dc-potential. Because of the very flat frequency response, no overshoots are expected.

Description of the Systems

The back and front plate of the earphone used for the experiments are completely equal. Each plate consists of a perforated brass disc 36 mm in diameter and about 1 mm thick. Each plate has about 200 holes which are 0.6 mm in diameter. The plates are arranged in such a manner that the holes are aligned. The plates are placed in a retainer ring which prevents them from turning when adjustments are made. Thus sliding contact between the foils and plates is avoided. The separation of the plates can be changed by two adjustment rings. Two rubber rings give a restoring force when greater separation is desired.

The foils are supported and stretched by two circular clamps. Therefore, the tension on the foils is independent of the position of the front and back plates. The foils are 0.25 mil nonmetallized and metallized mylar and are arranged as shown in Fig. 1 with the metal layers facing each other. Front plate, back plate and foils are electrically insulated from each other. The whole system is placed into a standard size telephone case. The volumes of the front and back cavity are relatively unimportant.

Prepolarized Foils (Inorganic Electrets)

Electrets[2] have been known for a long time but most research has been confined to relatively thick materials. Little work has been done in polarizing thin foils.[3]

---

[2] F.Gutman, Reviews of Modern Physics, 20 (1948), p.457.

[3] D.E.Richardson, et al., "A System of Electrostatic Recording," 1962 IRE International Convention.

In our case electrets have been formed by exposing the foil to a high electric field in a gap between two parallel metal plates. This method has been used previously for the forming of thick electrets.[4] The plates are separated by about 3 mm and the applied voltage is about 3500 volts dc. With this voltage applied the temperature of the foil is raised to roughly 120 ° C (forming temperature) and held constant for about 15 minutes. While the voltage is still applied, the temperature is decreased to room temperature. After this treatment a polarization exists on the foil.

This polarization corresponds to about 200 volts outer bias if the foil is used in a condenser transmitter. This can be shown by applying a dc-voltage of opposite polarity with respect to the polarization to the transmitter. If this dc-voltage is increased until only second harmonic of the applied signal results, the outer dc-voltage is equal to the polarization of the electret.

According to Gross[5] the mechanism of polarization is the formation of an ionic space charge within the dielectric material at the forming temperature. This polarization is frozen when room temperature is restored. The relaxation time of this poarlization is very long. For 1/4 mil mylar foil life-times in the order of several hundred years have been extrapolated.[3]

Method of Measurements

The earphone measurements reported in this paper were made with the earphone loaded with a standard 6 cm^3 artificial ear coupler in conjunction with the Western Electric 640 AA condenser microphone. The frequency response was automatically recorded with a Mosely X-Y plotter driven by a logarithmic amplifier. The distortion was measured in approximately third octave steps with a General Radio distortion meter.

Results

The measurements reported here were taken with the earphone shunted by two capacitors C_1 and C_2 (see Fig. 2) which balanced the (unavoidable) mechanical asymmetry of the system. The signal voltage required for a sound pressure of 100 db SPL is 36.5 volts from a symmetrical output. Because of the very high resistance, the power consumption of the unit is relatively low.

The frequency response, which is within ±3 db from 30 to 11,000 cps is shown in Fig. 3

Figure 3
Frequency Response of the Earphone
Balancing Capacitors $C_1 = 0.0018\mu F, C_2 = 0.0029\mu F$
$E_{ac} = 36.5$ volts

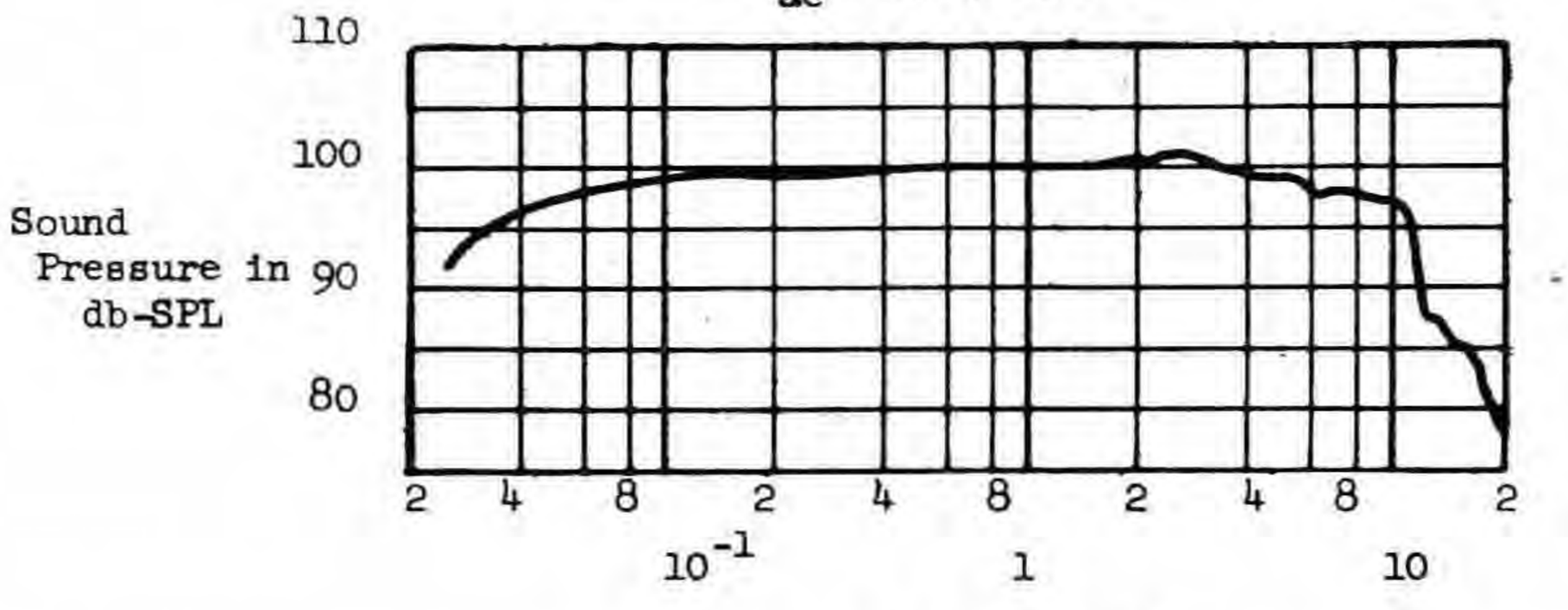

[4] A.N.Gubkin and G.I.Skanavi, English translation of The Bulletin of the Academy of Science of the USSR, 22 (1958), p.327.

[5] B.Gross, Phys. Rev. 66 (1944), 26.

The harmonic distortion at 100 db SPL is plotted in Fig. 4.

Figure 4
Harmonic Distortion of the Earphone at 100 db SPL
Balancing Capacitors $C_1 = 0.0018\mu F$, $C_2 = 0.0029\mu F$

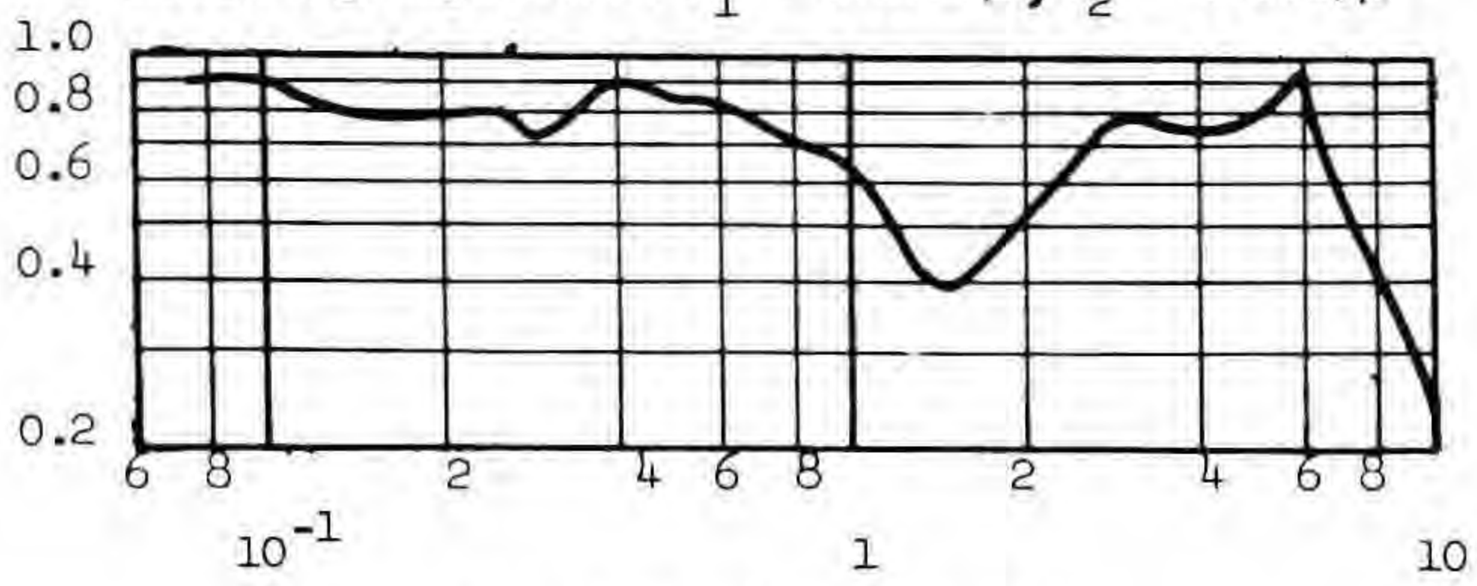

Figure 5 shows an impulse response. The input signal with a pulse duration of 120 μ sec is shown in the upper part and the response of the earphone in the lower part of the figure.

Figure 5
Impulse Response of the Earphone

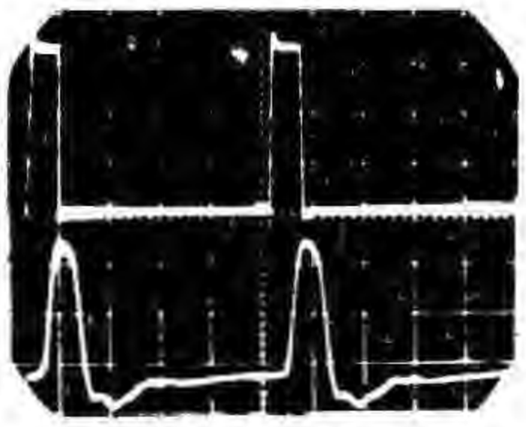

Pulse Duration 120μ sec, 1000 pulses per second

Conclusions

The main advantage of this push-pull system, compared to prior condenser transmitters, is it does not require an external dc-bias. This makes it completely safe for the user. The good frequency response, the low distortion and the excellent impulse response makes this transmitter useful for many purposes.

The stability of the system is relatively good after the surface charge of the foil has disappeared, which takes several days. One of the systems has been operating more than a month without noticeable change in efficiency or frequency response. The above mentioned investigation[3] into the relaxation time of polarization on mylar foils points to very high lifetimes of the described transmitters.

While the described push-pull earphone is superior to conventional earphones, improvements are possible with respect to frequency response, efficiency and distortion. For example, efficiency and distortion can be improved by increasing the area of the back and front plates and by increasing the perforation of these plates.

Acknowledgments

We are pleased to acknowledge the suggestions of E. E. David, Jr., and M. R. Schroeder and the aid in mechanical design of C. F. Mattke, and J. H. Kronmeyer.

O55

FOURTH INTERNATIONAL CONGRESS ON ACOUSTICS
COPENHAGEN 21.-28. AUGUST 1962

Einfluß der Randbedingungen auf die Schallabstrahlung von Platten

Manfred H e c k l , Müller-BBN GmbH, München

Die Schallabstrahlung von Platten, die Biegeschwingungen ausführen, deren Wellenlänge kleiner ist als die Wellenlänge im umgebenden Medium, wurde bereits von mehreren Autoren [1-7] untersucht. Dabei wurde festgestellt, daß die abgestrahlte Leistung im allgemeinen nicht proportional der Fläche der abstrahlenden Platte, sondern proportional der Länge irgendwelcher Linien unstetiger Schwingungsverteilung ist. Diese Tatsache läßt vermuten, daß die Schallabstrahlung hauptsächlich von der Plattenbegrenzung oder von anderen Gebieten unstetiger Schwingungsverteilung ausgeht. Demzufolge ist es auch denkbar, daß eine Änderung der Schwingungsverteilung an diesen Gebieten die Schallabstrahlung der Platte stark beeinflußt, obwohl dadurch die Schwingungen der übrigen Teile der Platte nur wenig geändert werden.

Einfluß des Reflexionsfaktors auf die Abstrahlung von einem einfachen Plattenmodell

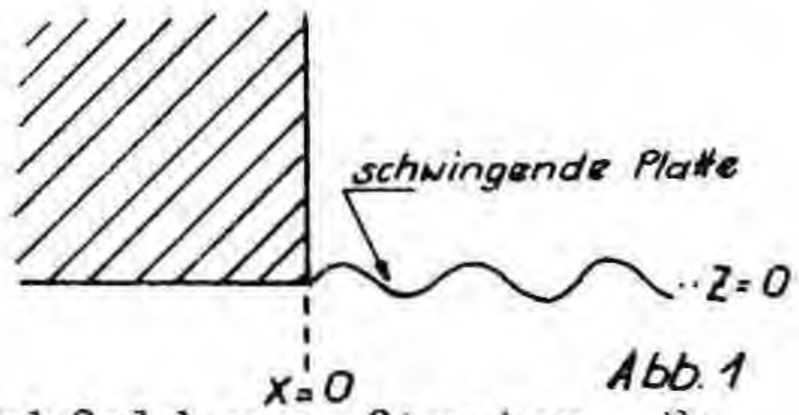

Abb. 1

Wir betrachten eine halbunendliche Platte, die an der Stelle x=o an einen starren Körper anschließt. Über die Art der Verbindung an der Stelle x=o nehmen wir nur - der Einfachheit halber - an, daß keine Biegewellen-Nahfelder auftreten. Es sollen also Biegewellen, die sich von rechts zur Verbindungsstelle ausbreiten, nur als fortlaufende Biegewellen mit einem Reflexionsfaktor r reflektiert werden.

---

1) Cremer, L., Die wissenschaftlichen Grundlagen der Raumakustik, Bd. III, § 62. S. Hirzel Verlag, Leipzig 1950.
2) Gösele, K., Acustica 3 (1954), 243.
3) Westphal, W., Acustica 4 (1954), 603
4) Skudrzyk, E., Acoust. Soc. Amer. 30 (1958), 1150.
5) Heckl, M., Acustica 9 (1959), 371.
6) Maidanik, G., J. Acoust. Soc. Amer. 34 (1962), Juni Ausg.
7) Lyon, R. H., Radiation from Plates supported by Beams, to be published in JASA.

Die Schnelle v in der Ebene z=o ist also gegeben durch

$$v(x) = 0 \quad \text{für } x < 0$$
$$v(x) = v_0 \left(e^{-ikx} + re^{ikx}\right) \text{ für } x \geq 0 \qquad 1)$$

Hierbei ist k die Wellenzahl für Biegeschwingungen.

Führt man eine Fouriertransformation von Gl.(1) durch, so kann man sofort [5] nach der Gleichung

$$P = \tfrac{1}{2} \rho_0 c_0 \int_{-k_0}^{+k_0} |\tilde{v}(k')|^2 \frac{k_0}{\sqrt{k_0^2 - k'^2}}\, dk' \qquad 2)$$

die von der schwingenden Platte abgestrahlte Leistung P bestimmen. In Gl.(2) bedeuten ρ_0, c_0, k_0 die Dichte, Schallgeschwindigkeit, Wellenzahl im umgebenden Medium. $\tilde{v}(k')$ ist die Fouriertransformation von Gl.(1). Führt man die Integration in Gl.(2) durch, so erhält man für den hier allein interessierenden Fall $k \gg k_o$ näherungsweise

$$P \approx \frac{\rho_0 c_0 k_0}{4k^2} v_0^2 |r-1|^2 = \frac{\rho_0 c_0 k_0}{4k^2} v_0^2 \left(|r|^2 - 2|r|\cos\varphi + 1\right). \qquad 3)$$

(φ = Phasenwinkel bei der Reflexion.)

Gl.(3) zeigt deutlich, daß der Phasenwinkel bei der Reflexion, d.h. die Art der Verbindung an der Stelle x=o das Ergebnis stark beeinflußt. Die abgestrahlte Leistung wird umso geringer, je kleiner der Phasenwinkel, d.h. je größer die Amplitude der Schwingung an der Stelle x=o ist.

Die Tatsache, daß die Details der Schwingung an der Verbindungsstelle für die gesamte abgestrahlte Leistung von großer Bedeutung sind, läßt sich noch etwas veranschaulichen, wenn man die Schalldruckverteilung

---

8) Morse, P.M. und Ingard, U., Handbuch der Physik, Vol. XI, Bd. Akustik Verlag Springer, Berlin, 1961.

p(x,z) berechnet. Zu diesem Zweck kann man die Formel

$$p(x,z) = \frac{\rho_0 c_0}{\sqrt{2\pi}} \int_{-\infty}^{+\infty} \tilde{v}(k') \frac{k_0}{\sqrt{k_0^2 - k'^2}} e^{ik'x} e^{i\sqrt{k_0^2 - k'^2}\, z} \, dk' \qquad 4)$$

benutzen. Eine näherungsweise Durchführung der Integration [8] gibt für $k \gg k_0$

$$p(x,z) \approx \rho_0 c_0 \frac{k_0}{\sqrt{k_0^2 - k'^2}} \left[v(x)\, e^{i\sqrt{k_0^2 - k'^2}\, z} - i v_0 (r-1) \frac{k_0}{2k} J_0\left(k_0 \sqrt{x^2 + z^2}\right) \right] \qquad 5)$$

($J_0(k_0)$ = Besselfunktion nullter Ordnung)

Wie man sieht, klingt der erste Term, der genau die Schwingungsverteilung der Platte hat, mit wachsender Entfernung von der Platte exponentiell ab. Der zweite Term stellt eine normale Zylinderwelle dar, die ihren Ausgangsort an der Linie x=o, z=o hat. Da nur diese Zylinderwelle akustische Leistung überträgt, ist es nicht verwunderlich, daß Änderungen an ihrem Ausgangsort die abgestrahlte Leistung sehr beeinflussen.

Einfluß eines schallschluckenden Materials in der Nähe der Plattenbegrenzung

Da für das in Abb. 1 skizzierte Modell die Schallabstrahlung als Zylinderwelle von der Plattenbegrenzung ausgeht, ist auch zu erwarten, daß ein schallschluckendes Material in der Nähe dieser "Schallquelle" einen starken Einfluß auf die Schallabstrahlung von der Platte ausübt. Für eine erste Näherungsrechnung wurde für das Gebiet $x < o$, $z < o$ ein Material mit dem - vom Einfallswinkel unabhängigen - akustischen Widerstand Z angenommen. Das bedeutet, daß die Schnelle in der Ebene z=o durch

$$v(x) = p(x,0)/Z \quad \text{für} \quad x < 0$$

$$v(x) = v_0 \left(e^{-ikx} - e^{ikx}\right) \quad \text{für} \quad x \geq 0 \qquad 6)$$

gegeben ist. (Es wurde hier r=-1 gesetzt, d.h. die Platte wurde bei x=o als unterstützt angenommen.)

Führt man die Fourierungstransformation von Gl.(6) durch und setzt das Ergebnis in Gl.(4) ein, so erhält man eine Integralgleichung in p(x,o) die man durch ein Integrationsverfahren annähern kann.

Die Durchführung der Rechnung in der ersten Näherung, d.h. für hohe Werte von Z, zeigt, daß durch einen imaginären, ziemlich hohen Wandwiderstand die Abstrahlung nicht verringert wird. Dagegen bewirkt ein reeller Wandwiderstand, wie zu erwarten, stets eine Verminderung der abgestrahlten Leistung.

Dieses Ergebnis wurde auch durch einen einfachen Versuch bestätigt. Es wurde hierzu eine 1,5 mm dicke Blechplatte in die etwa 2 m^2 große Öffnung zwischen zwei Räumen montiert. Die Platte wurde punktförmig von einem Körperschallsender angeregt. Beim ersten Versuch wurde die Platte von schallhartem Material (Zimmertrennwand) begrenzt. Beim zweiten Versuch wurde die Zimmertrennwand in der Umgebung der Platte mit Mineralwolleplatten von mehreren Zentimetern Dicke abgedeckt. Durch diese Maßnahme wurde die Nachhallzeit des Meßraumes nicht beeinflußt, da die Mineralwolleplatten bereits beim ersten Versuch an einer Stelle im Raum waren. Abb. 2 zeigt die in beiden Fällen gemessenen Schallpegel. Die Messungen wurden mit weißem Rauschen, das empfangsseitig in Oktaven gefiltert wurde, vorgenommen. Wie man sieht, sind bei der zweiten Messund die Luftschallpegel um mehrere dB geringer obwohl in beiden Fällen die Schwingungsamplituden der Blechplatte gleich waren.

Schallabstrahlung von einer Platte mit und ohne schallschluckende Umrandung.

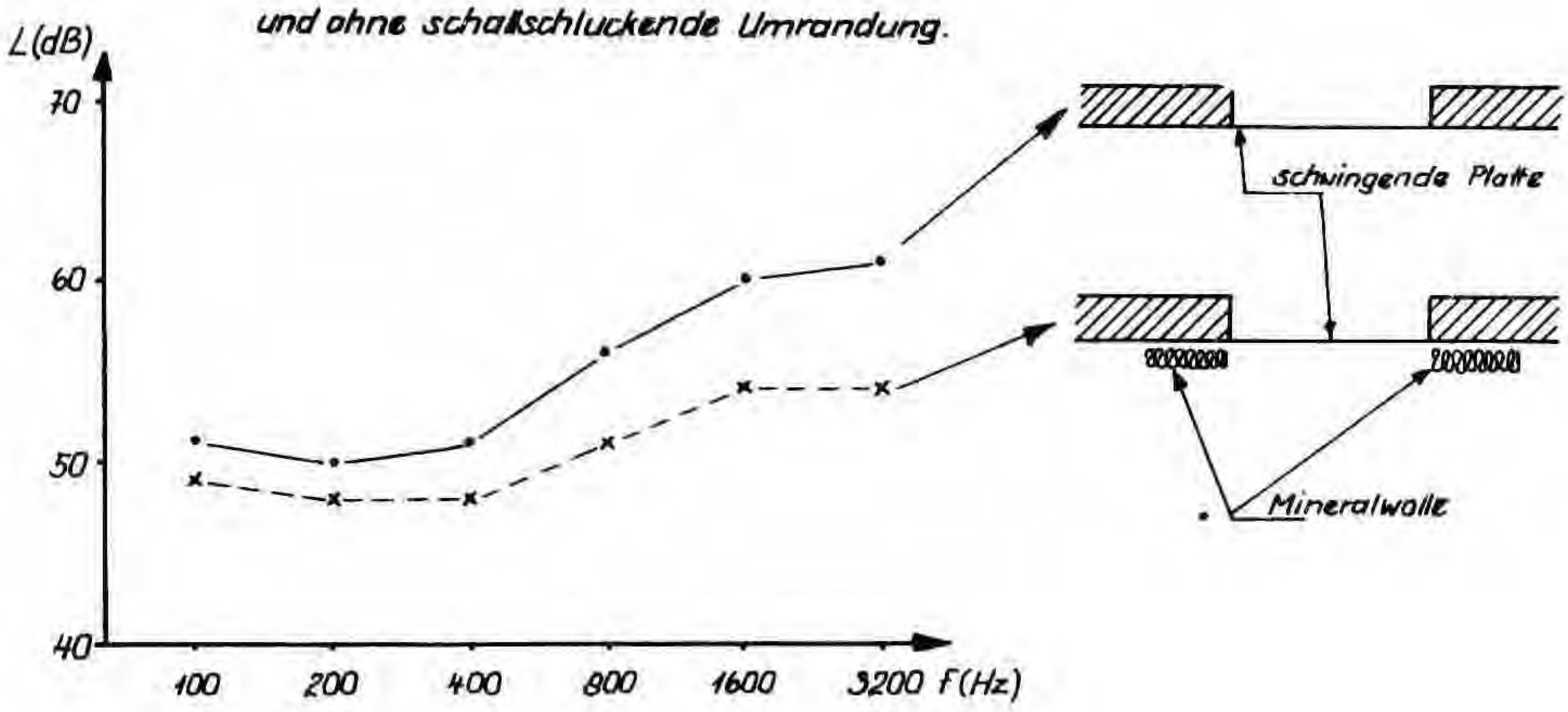

P55

FOURTH INTERNATIONAL CONGRESS ON ACOUSTICS
COPENHAGEN 21.-28. AUGUST 1962

MUSICAL CONSONANCE AND CRITICAL BANDWIDTH

R.Plomp and W.J.M.Levelt
Institute for Perception RVO-TNO, Soesterberg, The Netherlands

1. Introduction

This year just a century ago H. von Helmholtz (1821-1894) published his book "Die Lehre von den Tonempfindungen als physiologische Grundlage für die Theorie der Musik". His treatment of musical consonance, the central problem of the book, has proved to be the most acceptable explanation of the well-known fact that the consonant chords correspond with simple frequency ratios of the tones (octave 1:2, fifth 2:3, fourth 3:4, major third 4:5, major sixth 3:5, minor third 5:6, minor sixth 5:8).

Von Helmholtz's explanation was based on the hypothesis of Ohm (1787-1854) that the hearing organ performs a Fourier analysis of sound, so each periodical vibration is dispersed in its partials (fundamental tone plus overtones). After Von Helmholtz dissonance occurs when two or more partials differ so little in frequency that they cannot exist independently but interfere with each other (minimum consonance at 30-40 beats/sec). The more partials of a tone coincide with partials of another one, the less the chance on interferences is. This can explain the fact that simple frequency ratios give the most consonant chords.

Especially by Stumpf (1848-1936) many objections against these considerations were raised, for instance that after Von Helmholtz consonance alters by transposing a chord. Stumpf[1] introduced "fusion" ("Verschmelzung") as the origin of consonance: a chord is more consonant as it is easier perceived as one tone. Though undoubtedly a relation between consonance and fusion exists, at least for complex tones, this notion does not explain the consonance phenomenon at all as Révész[2] rightly stated.

During the last decennia the physiological knowledge of the hearing process, the physical equipment and the psychological methods of experiment are improved so much that a reconsideration of Von Helmholtz's explanation might be of value. This paper gives only a brief survey of research in this field carried out by the authors during the last years.

2. The connotation of musical consonance

As a preliminary to further research an exploratory investigation was made on the different modes of judgments of musical intervals. In this way it was tried to determine what subjects mean by their qualification of chords as consonant or dissonant. 23 combinations of two pure tones were used, all within the octave. The frequency ratios of the intervals could be described by the numbers 1....12, so the intervals were 1:2, 2:3, 3:4, 3:5, 4:5,.....,7:12, 11:12. Only multiples of 85 cps were available as pure tones, so it was not possible to have all intervals of the same height. Ten intelligent subjects (non-musicians) judged these chords against ten 7-points rating scales: high-low, sharp-round, beautiful-ugly, active-passive, consonant-dissonant, euphonious-diseuphonious, wide-narrow, sounds like one tone-sounds like more tones, tense-quiet, rough-smooth. The correlations between the scales were computed and the correlation matrix factor-analysed.

It appeared that all data could be summarized by assuming 3 basic dimensions, which we called height, evaluation and fusion. Evaluation was closely related to consonance, beautiful and euphonious; with other words: consonance had a definite meaning coinciding with the two other notions, not with fusion. This result was used in further experiments by circumscribing consonance as beautiful and euphonious.

3. Consonance as a function of the distance between two pure tones

From the foregoing and other experiments it appeared that the degree of consonance is a function of the distance (frequency difference) between the two tones of a chord, as far as pure tones are concerned. To investigate this relation more closely, a series of experiments were carried out in which test subjects had to judge chords of two pure tones on consonance against a 7-points rating scale as in the experiments described above. To eliminate the factor height as good as possible, each subject judged only chords with a constant geometric mean. Different groups of 10-12 subjects were used to judge chords with a geometric mean of 125, 250, 500, 1000 and 2000 cps. The subjects were exposed to each interval 5 times and only the data of the subjects with a reasonably consistent judgment (a correlation above about 0.5 between the first and the last judgment of the intervals) were maintained. The average scores at 125, 500 and 2000 cps are plotted in fig. 1.

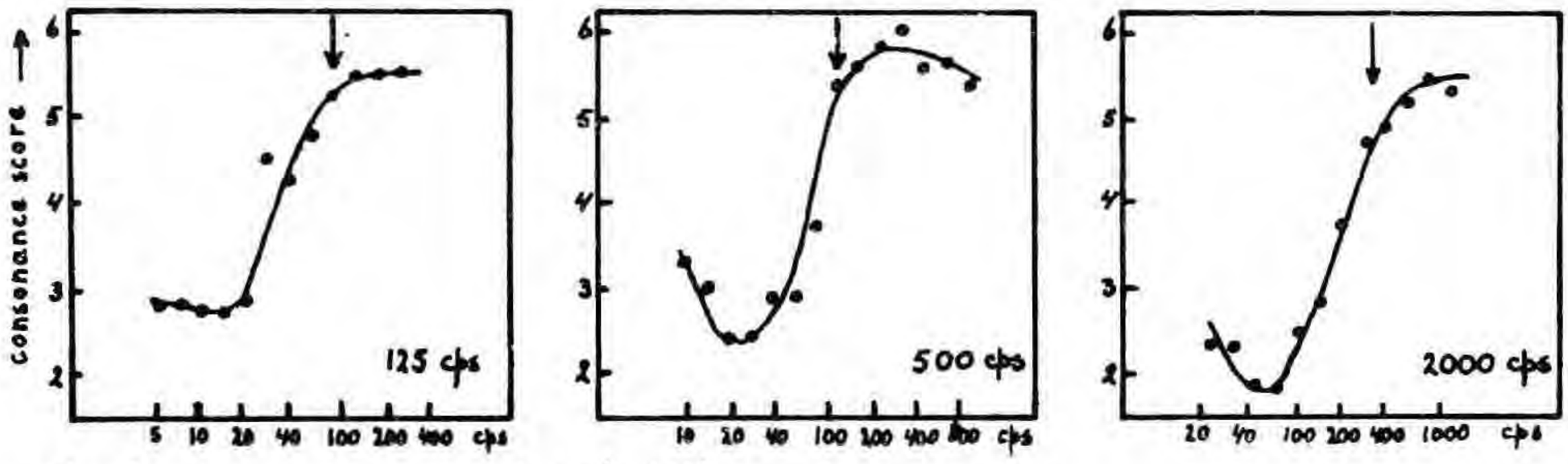

Fig. 1

The arrows indicate the critical bandwidth after Zwicker[3], derived from psychophysical hearing experiments. Fig.1 shows that the upper bend of the curves agrees very well with the critical band; the lower bend corresponds with about 0.2 x this bandwidth. In fig.2 this is demonstrated more explicitly.

This means that intervals with a frequency difference exceeding the critical bandwidth are judged as consonant; below this value the consonance appreciation falls rather sharp, reaching a minimum at about 0.2 x the critical bandwidth. For still smaller frequency differences we get slow beats which are appreciated more and more positively as the frequency difference decreases. This is shown in detail by a comparable experiment of Guthrie and Morrill[4] at one frequency.

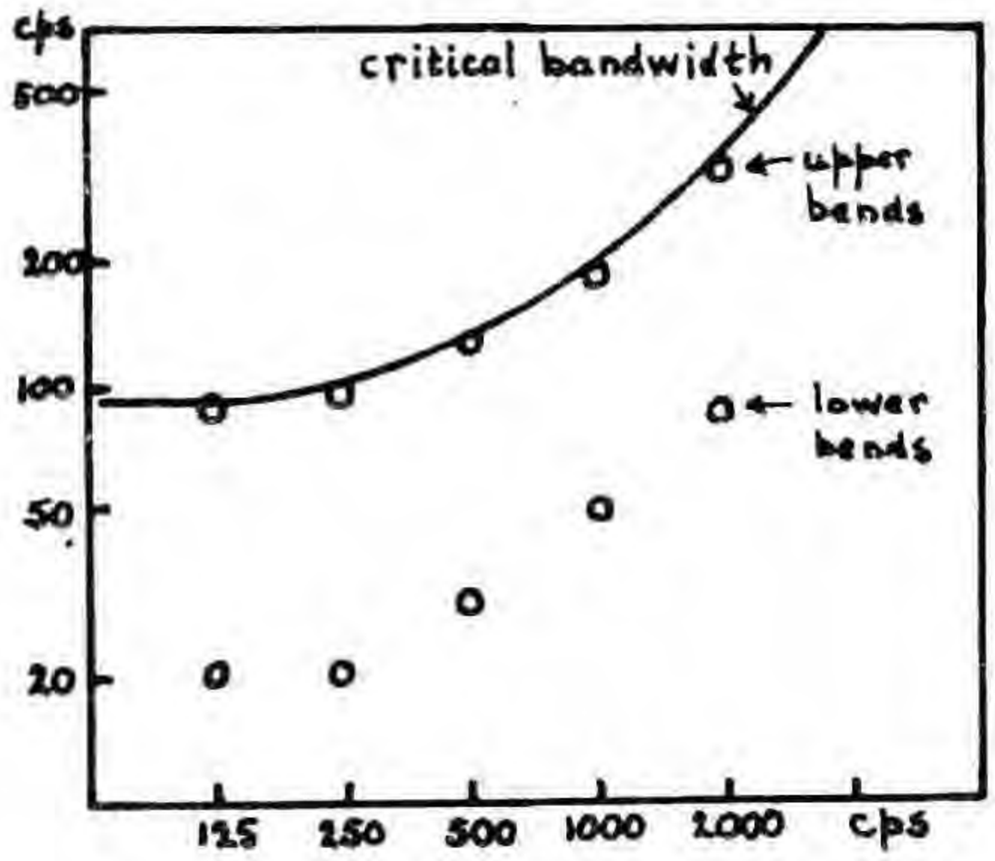

Fig. 2

These results show that the critical band is an important factor in relation to consonance. We may state that this conclusion represents a valuable modification of Von Helmholtz's conception that dissonance is caused by interference of pure tones. Moreover it demonstrates that for pure tones consonance is not related to simple frequency ratios though for musicians the recognition of well-known intervals may affect their consonance appreciation of chords consisting of pure tones.

4. Consonance as a function of the distance between two complex tones

Using the results of the foregoing paragraph we can show that for complex tones (fundamental tone plus overtones) consonance is indeed related to simple frequency ratios. Plotting the consonance scores of fig.1 together with the corresponding data at 250 and 1000 cps as a function of the critical bandwidth and averaging these

curves we get a standard curve which is reproduced in fig.3. By a linear transformation the evaluation scale is replaced by a "consonance scale", 1 corresponding with maximum and 0.1 with minimum appreciation. For small frequency differences the curve is extended in accordance with the data of Guthrie and Morrill[4].

We can use this diagram to get some impression how consonance varies as a function of the distance (frequency difference of the fundamental tones) between two complex tones. As an illustration we take the case of a constant tone of 250 cps and a variable tone between 250 and 500 cps, each tone composed of the first 6 partials. We define as the consonance of the chord the sum of the dissonances (right scale of fig.3) of the intervals between each two adjacent partials, subtracted from 1. This consonance value is calculated as a function of the frequency of the variable tone and plotted in fig.4.

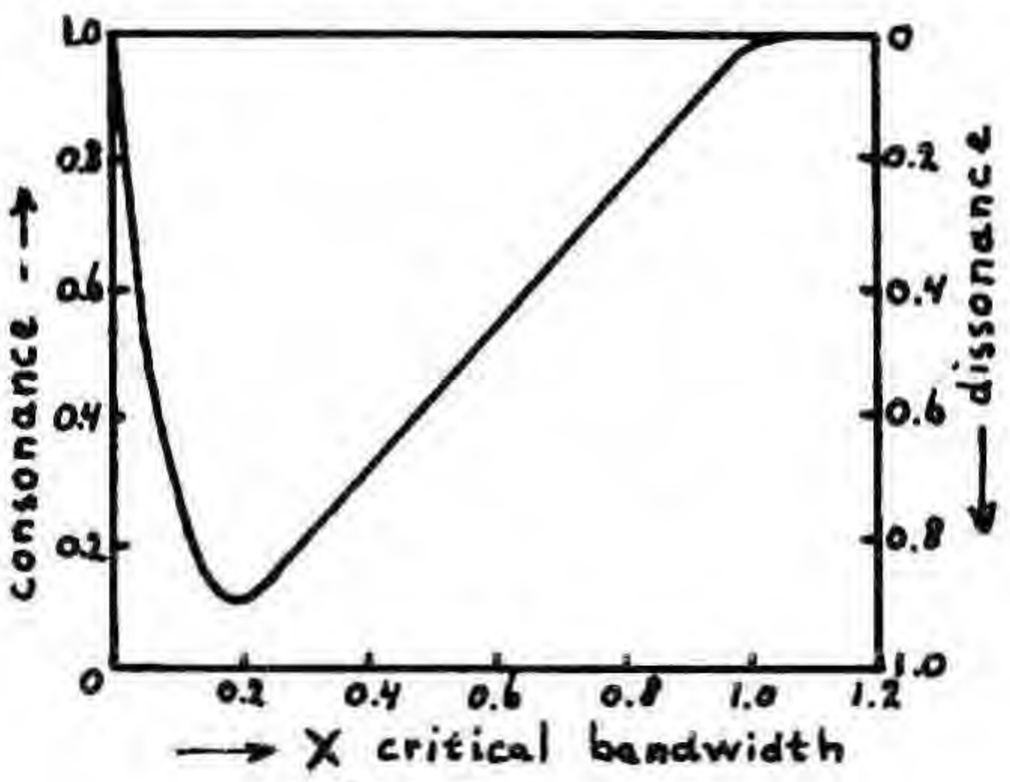

Fig. 3

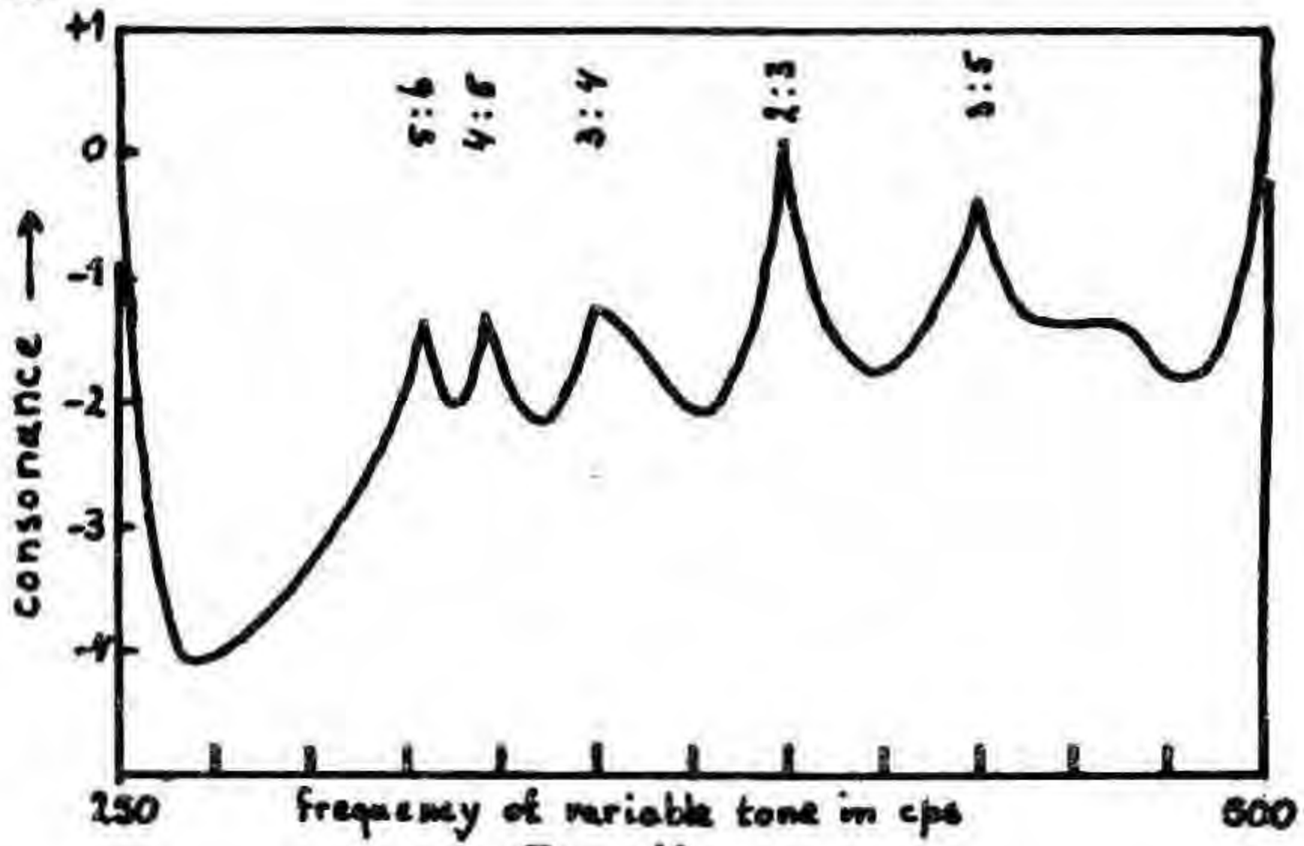

Fig. 4

Though the definition of this consonance is arbitrary, we believe that some interesting conclusions are justified:

a. The simple frequency ratios (1:1, 1:2, 2:3, 3:4, 3:5, 4:5, 5:6) are singular points of the curve, each being surrounded by a region of lower consonance. This explains that for complex tones consonance is related to simple frequency ratios.

b. The consonance of 1:1 and 1:2 is 1, which means that the distances between the adjacent partials exceed the critical bandwidth. It appears that this only applies for 6 and fewer partials; this is in agreement with the fact, also underlined by Von Helmholtz, that tones with strong higher partials sound sharp and dissonant.

c. A small deviation from a simple frequency ratio has much more influence on the unison (1:1), octave and fifth than on the other consonant intervals. This corresponds with the practice of tuning musical instruments by octave and fifth relations. In connection with this the fact is important that the impure thirds of the equi-tempered intonation are much better tolerated than impure octaves and fifths would have been (compare the position of the maxima of the curve with the vertical dashes in fig.4, giving the intervals of the equi-tempered intonation).

d. The octave and fifth are the most consonant intervals, which is in agreement with practice.

Fig.5 illustrates how the consonance of simple frequency ratios varies with frequency. The curves show that the mutual relations of consonance of the different intervals are nearly independent of frequency. The fall at low frequencies is caused by the fact that below 500 cps the critical bandwidth is nearly constant and the fall at high frequencies by the fact that in this range the critical bandwidth increases more rapid than frequency. The curves of fig.5 are important in relation to the controversy

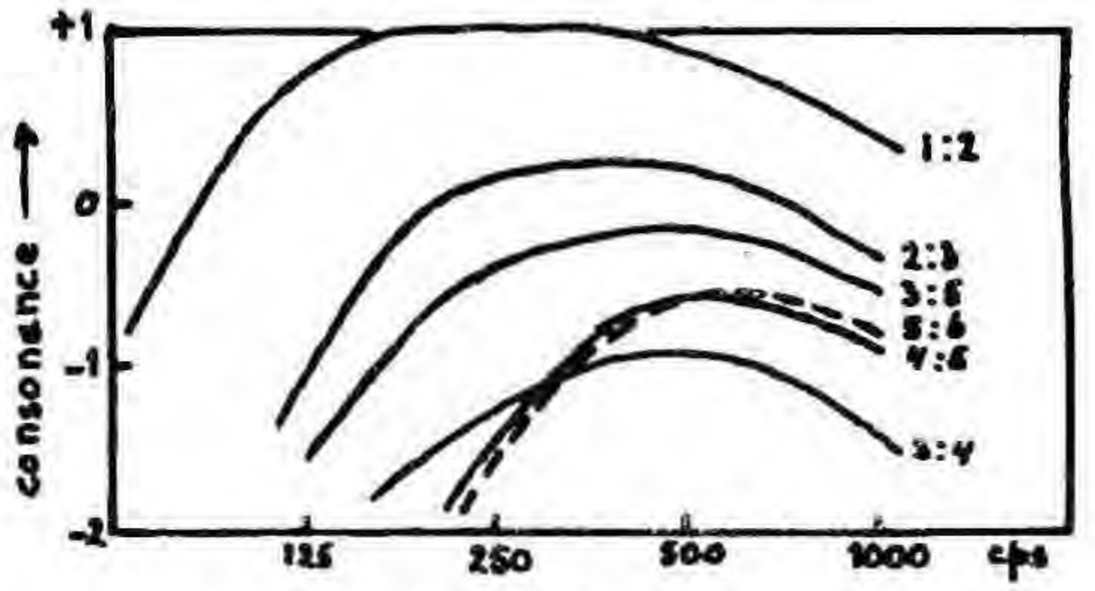

Fig. 5

Von Helmholtz-Stumpf about the dependence of consonance on frequency. After Von Helmholtz the consonance of an interval increases with frequency, after Stumpf consonance is independent of frequency. Von Helmholtz seems to be right below about 250 cps and Stumpf in a range of 1-2 octaves above this frequency.

5. The distance between partials in music

It is of interest to examine to which extent the relation of consonance to critical bandwidth can be found back in musical compositions. Only some preliminary investigations are made and one of the most interesting results will be shown.

We analysed the chords of compositions in the following way. After choosing a note, for instance b^1 (494 cps), we determined which fraction of its total time of presentation this note sounds together with a tone at a distance of 1/2 tone (b^1-flat or a^1sharp and c^2), which fraction together with a tone at a distance of 2/2 tone, etc. The result of such an analysis we called the interval distribution of b^1. Such interval distributions can be calculated for different tones and also taking into account the presence of overtones.

In figure 6 the mean value of interval distributions of tones around 125, 250, 500, 1000 and 2000 cps is plotted as a function of the number of partials taken into account. The interval distributions were calculated from all chords of 4 chorals of J.S.Bach (St. Matthew Passion, nos. 3, 16, 23 and 31). The ordinate is given in cps, so the graph shows the "density" of partials (mean frequency difference between adjacent partials) at a number of frequencies. As we may expect, introducing more partials affects more the "density" at high frequencies than at low frequencies. In fig.7 the asymptotic values of the curves of fig.6 are plotted as a function of frequency together with the critical bandwidth. It is very interesting that the curves are almost parallel, demonstrating that the composer selected his chords in such a way that on the average over the whole frequency range the critical band is "penetrated" to the same degree.

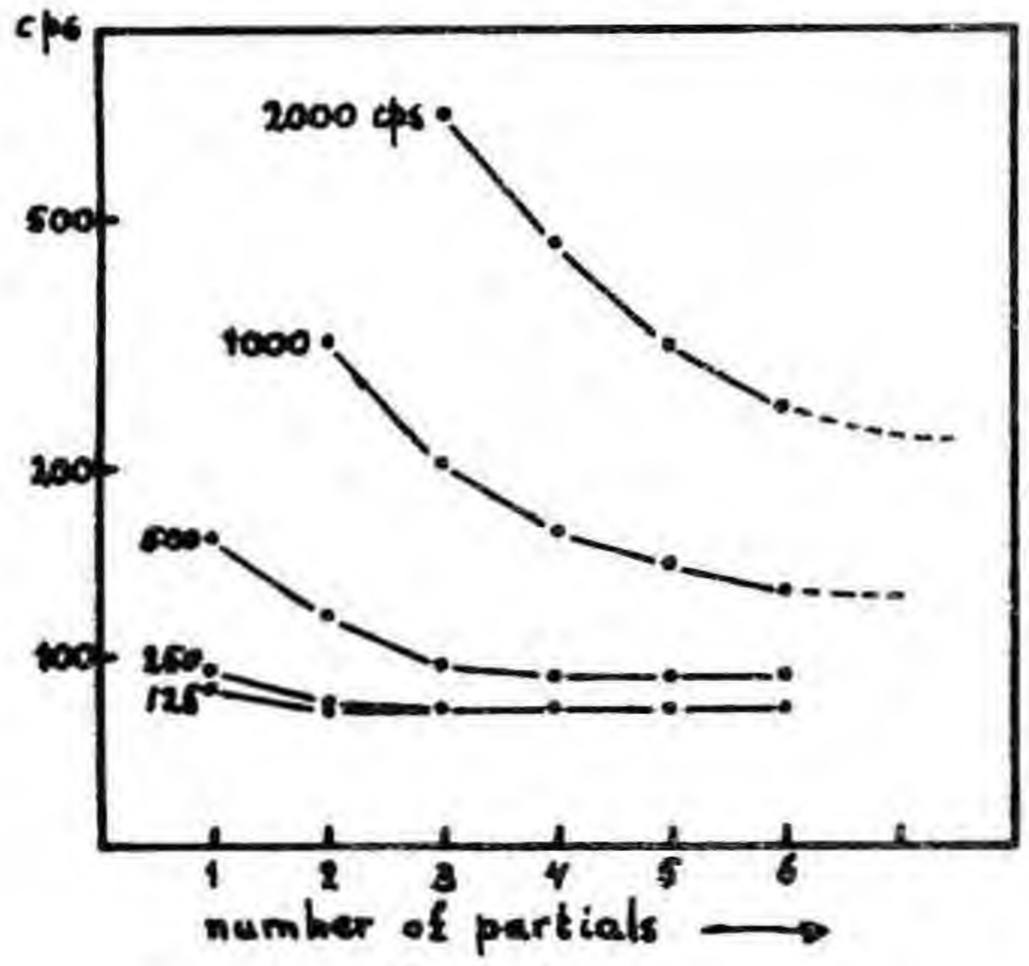

Fig. 6

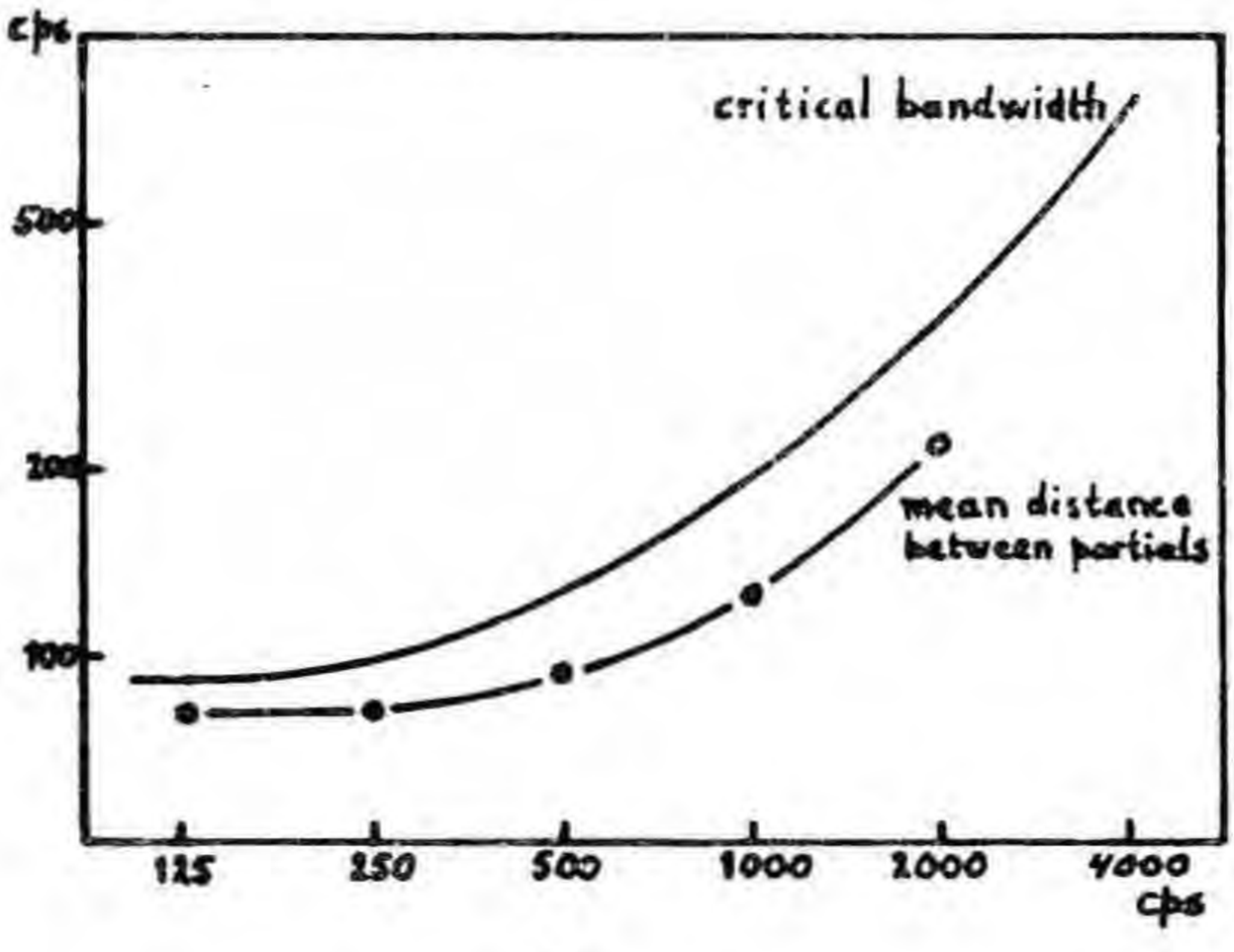

Fig. 7

References
1 C.Stumpf, Beiträge zur Akustik und Musikwissenschaft 1, 1-108 (1898).
2 G.Révész, Inleiding tot de muziekpsychologie, 2nd impression, Amsterdam (1946).
3 E.Zwicker, Acustica 10, 185 (1960).
4 E.R.Guthrie and H.Morrill, Amer.J.Psychol. 40, 624-625 (1928).

H56

FOURTH INTERNATIONAL CONGRESS ON ACOUSTICS
COPENHAGEN 21.-28. AUGUST 1962

Verdeckung von Tönen durch pulsierende Geräusche.

H. S c h o l l
Inst.f.Nachrichtentechnik d. Technischen Hochschule Stuttgart

Einleitung.

In den letzten Jahren wurde in einer Reihe von Arbeiten der Einfluß der Zeitfunktion bei der Verdeckung untersucht. Dabei stand im Vordergrund die Frage nach der Abhängigkeit der Mithörschwelle von den zeitlichen Eigenschaften des Testschalles. Als verdeckender Schall wurde ein Dauerschall, im allgemeinen Rauschen verwandt. Der umgekehrte Fall, die Verdeckung eines Dauerschalles durch eine Folge von Impulsen wurde bisher nur durch Miller und Garner (1) und durch Pollack (2) untersucht. Es soll hier auf der Grundlage ähnlicher Messungen versucht werden, Aufschlüsse über die zeitliche Integration des Gehörs zu gewinnen.

Meßverfahren.

Es wurden die Mithörschwellen von Sinustönen bei Verdeckung durch Rauschimpulse gemessen. Die Rauschimpulse wurden mittels eines elektronischen Schalters aus gleichmäßig verdeckendem Rauschen ausgeschnitten. Gleichmäßig verdeckendes Rauschen wird durch einen speziellen Tiefpaß aus weißem Rauschen gewonnen und besitzt die Eigenschaft, eine von der Frequenz des Testtones unabhängige Mithörschwelle zu erzeugen. Die Messungen wurden mit zwei Beobachtern nach dem Verfahren des pendelnden Angleichens (method of tracking) mit einem Békésy-Audiometer durchgeführt. Gemessen wurde mit Kopfhörern (beidohrig)

Ergebnisse.

Bild 1 zeigt die Mithörschwellen von Tönen bei Verdeckung durch pulsierendes Rauschen. Die Zeitfunktion des Rauschens ist rechts im Bild dargestellt, es sind Impulse mit dem Tastverhältnis 1:2, ihr Pegel beträgt 80 dB. Den Impulsen überlagert ist ein Dauerrauschen von 40 dB, das dazu dient, eine wohldefinierte künstliche Ruhehörschwelle zu erzeugen, die von der Frequenz des Testtones und weitgehend auch vom Beobachter unabhängig ist.
Im Bild ist die Mithörschwelle L_T des Testtones über der Pulsfrequenz f_p der Rauschimpulse aufgetragen. Parameter ist die Frequenz des Testtones. Die Kurven haben alle den gleichen Charakter. Bei hoher Pulsfrequenz verläuft die Schwelle horizontal. Man kann sich diesen Verlauf folgendermaßen erklären: Der Effektivwert der Rauschimpulse ist unabhängig von der Pulsfrequenz f_p, da das Tastverhältnis konstant ist. In dem horizontalen Bereich der Mithörschwellen integriert offenbar das Gehör über die Impulse, d.h. es merkt gar nichts von der Lücke dazwischen. Bei einem Dauerrauschen von 80 dB würde die Mithörschwelle bei 60 dB liegen. Bei den Impulsen liegt sie im Mittel bei 57 dB, also 3 dB tiefer, weil die Impulsfolge eine um Faktor 2 geringere Intensität besitzt. Man muß daraus schließen, daß das Gehör über die Schallintensität, also eine Leistungsgröße integriert.
Ab einer bestimmten Pulsfrequenz f_p, die von der Frequenz des Testtones abhängt, fällt die Mithörschwelle plötzlich steil ab und mündet asymptotisch in die Ruhehörschwelle, die hier durch das Grundrauschen von 40 dB bestimmt wird. Ein derartiges Verhalten kann wie folgt erklärt werden: Bis zu einer bestimmten Pulsfrequenz scheint das Gehör den verdeckenden Schall zu integrieren; die Pause zwischen zwei Im-

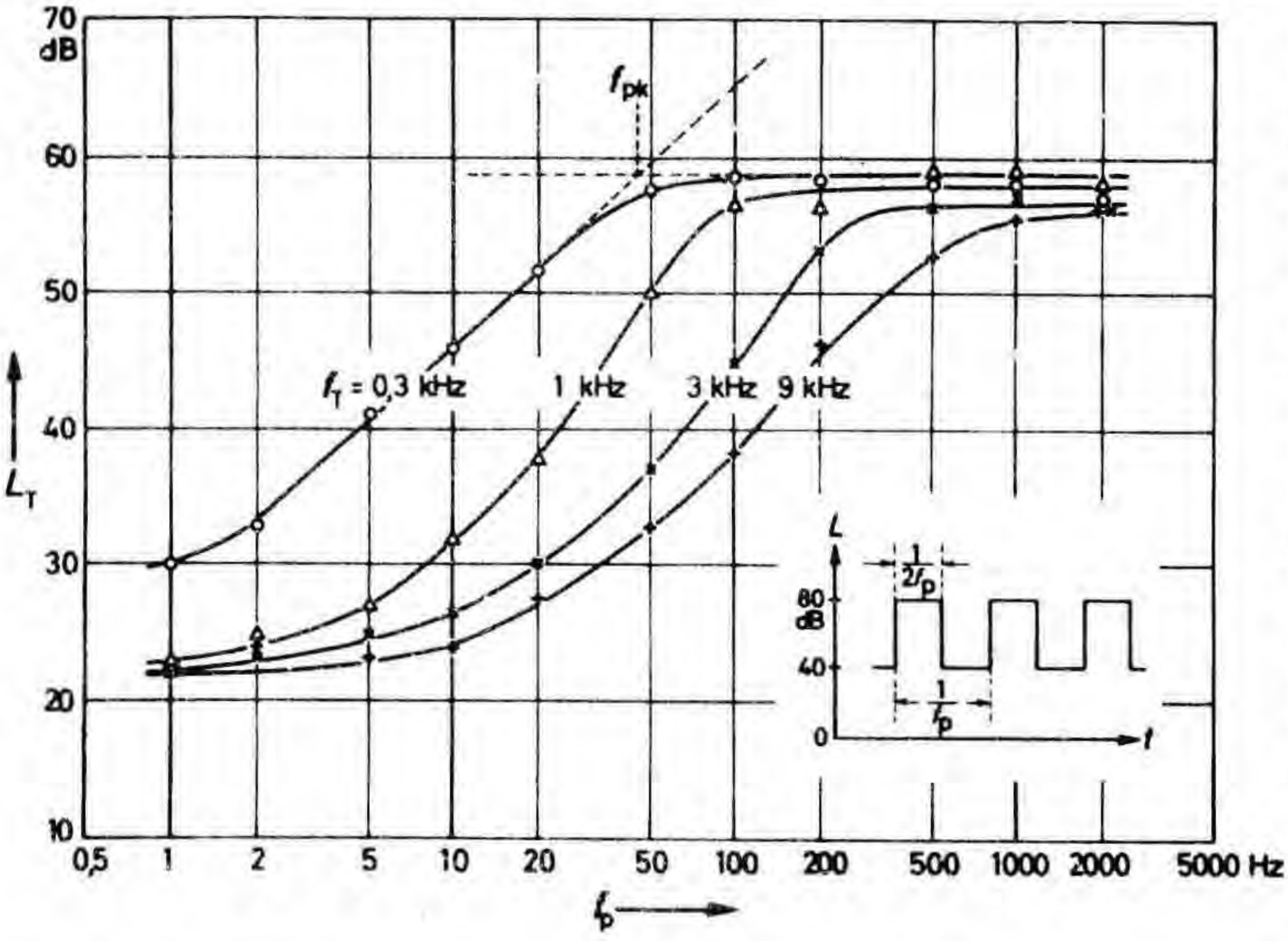

Bild 1. Mithörschwelle L_T von Tönen bei Verdeckung durch Rauschimpulse in Abhängigkeit von der Pulsfrequenz f_p. Die Dauer der Impulse ist $t_i = \frac{1}{2f_p}$; Parameter ist die Frequenz f_T der Töne.

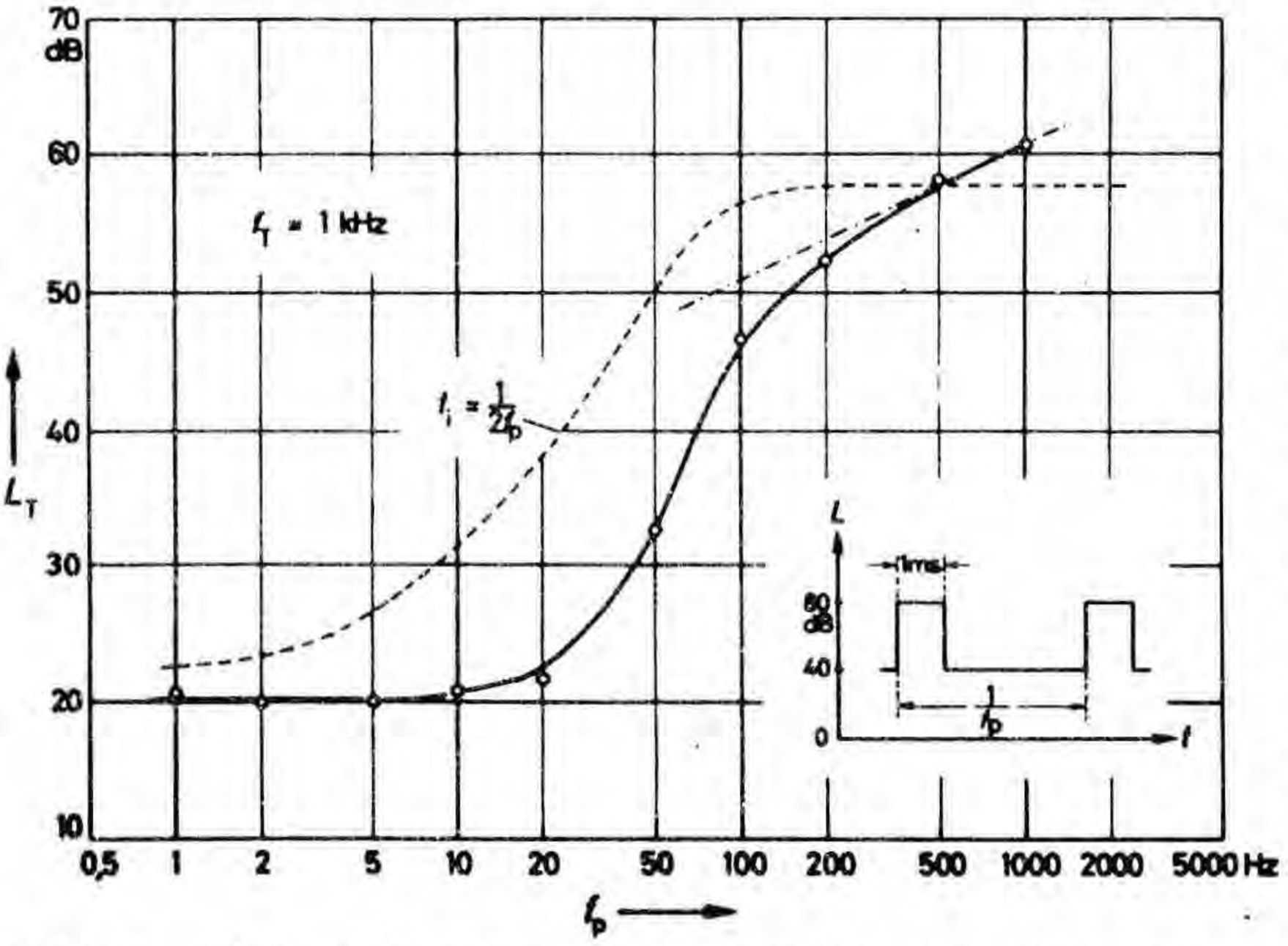

Bild 2. Mithörschwelle L_T eines Tones der Frequenz f_T= 1kHz bei Verdeckung durch Rauschimpulse der Dauer t_i= 1ms in Abhängigkeit von der Pulsfrequenz f_p.
Gestrichelt: Mithörschwelle aus Bild 1 für f_T = 1kHz.

pulsen tritt nicht in Erscheinung. Mit abnehmender Pulsfrequenz wird die Pause schließlich größer als die Integrationszeit des Gehörs, die Erregung des Gehörs klingt daher in der Pause ab, und der Testton wird bei einem tieferen Pegel schon hörbar. Im Extremfall sehr niederer Pulsfrequenz klingt die Erregung des Gehörs zwischen zwei Impulsen praktisch völlig ab, es wird dann die Ruhehörschwelle erreicht.

Die Mithörschwellen für die verschiedenen Testtonfrequenzen fallen nicht zusammen. Daraus folgt, daß die Integrationsdauer von der Frequenzlage abhängt und bei hohen Frequenzen sehr viel geringer ist als bei tiefen Frequenzen.

In Bild 2 ist das Ergebnis einer ähnlichen Messung dargestellt. Der einzige Unterschied besteht darin, daß jetzt bei den Rauschimpulsen nicht das Tastverhältnis, sondern die Impulsdauer konstant ist. Im letzteren Fall ist die mittlere Intensität des

verdeckenden Schalles proportional zur Pulsfrequenz.
Man kann auch hier aus dem Verlauf der Mithörschwelle entnehmen, daß das Gehör bei hoher Pulsfrequenz über die Intensität des Störschalles integriert. Der Meßpunkt bei f_p= 1 kHz bedeutet Dauerrauschen, weil hier die Lücke zwischen zwei aufeinanderfolgenden Impulsen verschwindet. Mit abnehmender Pulsfrequenz folgt die Mithörschwelle zunächst der strichpunktierten Geraden, die mit 10 dB pro Dekade abfällt und der abnehmenden Intensität der Impulsfolge entspricht. Ab einer bestimmten Pulsfrequenz biegt die Mithörschwelle wie im vorigen Bild nach unten ab und nähert sich asymptotisch der Ruhehörschwelle. Der Abfall erfolgt bei etwas höheren Pulsfolgefrequenzen und steiler als bei der zum Vergleich gestrichelt eingezeichneten Mithörschwelle von Bild 1, weil die Dauer der Pause mit abnehmender Pulsfrequenz immer mehr überwiegt (Dauer der Rauschimpulse ist konstant und 1 ms).

Deutung der Ergebnisse.
Es soll zum Schluß versucht werden, die Ergebnisse der Messungen mit anderen Eigenschaften des Gehörs in Verbindung zu bringen. Aus beiden Messungen kann entnommen werden, daß im Gehör eine zeitliche Integration der Schallintensität innerhalb eines bestimmten Zeitintervalles stattfindet. Das Gehör scheint die Eigenschaft eines trägen Systems mit der Zeitkonstanten τ zu besitzen. Diese Zeitkonstante hängt von der Frequenzlage ab und ist gekennzeichnet durch die Pulsfrequenz f_{pk}, bei welcher in Bild 1 die Mithörschwelle abknickt (Schnittpunkt der in Bild 1 gestrichelt eingezeichneten Geraden). Wir können näherungsweise annehmen, daß der Knick dann erfolgt, wenn die Impulsdauer bzw. die Pause zwischen zwei Impulsen gleich der Zeitkonstanten τ ist. Es gilt dann

$$\tau = \frac{1}{2f_{pk}} \qquad (1)$$

Wie eine große Anzahl subjektiver Messungen gezeigt hat, findet im Gehör eine spektrale Zerlegung des Schalles in einzelne Frequenzbänder statt, die als Frequenzgruppen (3) bezeichnet werden. Diese Eigenschaft des Gehörs ist vergleichbar mit der Funktion von Bandfiltern. Schon die Übertragungsfunktion zwischen Schalldruck am Trommelfell und Auslenkung der Basilarmembran hat Bandfiltercharakter. Ein Bandfilter besitzt eine von der Bandbreite Δf abhängende Einschwingzeit

$$\tau = 1/\Delta f. \qquad (2)$$

Diese Eigenschaft bewirkt, daß Impulsfolgen am Eingang (z.B. breitbandige Rauschimpulse) mit einer Folgefrequenz größer als die reziproke Einschwingzeit am Ausgang des Bandfilters ihren Impulscharakter verlieren. Während am Eingang die Energie als Funktion der Zeit impulsförmig schwankt, zeigt sich am Ausgang ein praktisch gleichmäßiger Energiefluß. Dieser Effekt kann als eine Art Integration der Energie über der Zeit beschrieben werden.
Die Bandbreite Δf_G der Frequenzgruppe hängt nach der im Bild 3 dargestellten Funktion von der Bandmittenfrequenz f_m ab. Aus den Gleichungen (1) und (2) ergibt sich die zur Knickfrequenz f_{pk} gehörende Bandbreite

$$\Delta f = 2 f_{pk} . \qquad (3)$$

Nach dieser Beziehung wurden zu den 4 Knickfrequenzen aus Bild 1 die zugehörigen Bandbreiten bestimmt. Sie sind im Bild 3 als Kreuze eingezeichnet, wobei die Frequenz f_T des Testtones gleich der Bandmittenfrequenz f_m gesetzt wurde. Die Übereinstimmung mit der Bandbreite der Frequenzgruppe ist erstaunlich gut. Dies deutet darauf hin, daß auch beim Gehör möglicherweise ein fester Zusammenhang zwischen Bandbreite und Einschwingzeit besteht.

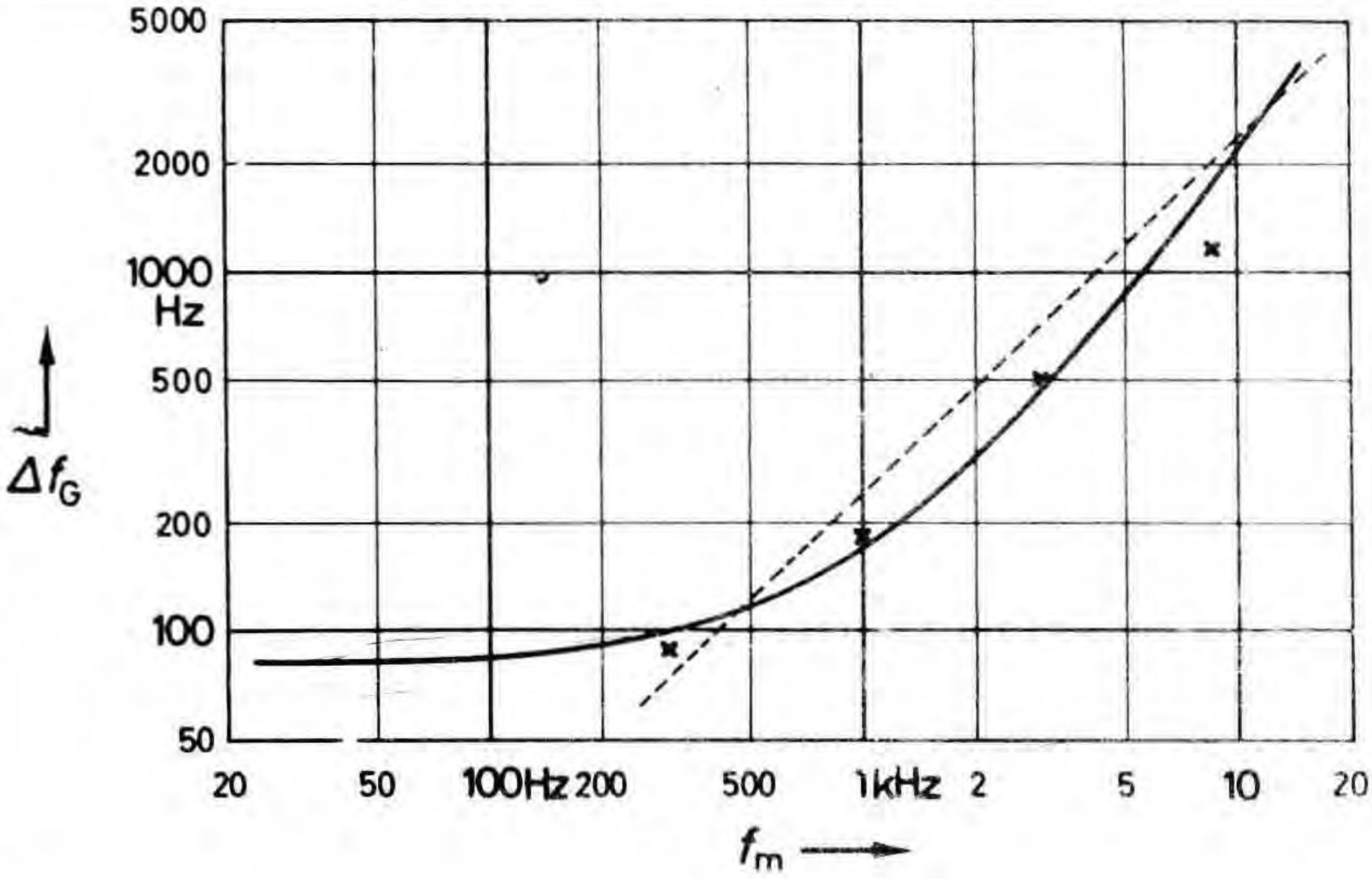

Bild 3. Bandbreite Δf_G der Frequenzgruppen (3) in Abhängigkeit von der Bandmittenfrequenz f_m.
Gestrichelt: Bandbreite der Terz. ✖ aus den Knickfrequenzen f_{pk} berechnete Bandbreiten.

Literatur:

(1) G.A. Miller and W.R. Garner, J.Acoust.Soc.Am. 20, S.691 (1948)
(2) I. Pollack, J.Acoust.Soc.Am. 27, S.353 (1955)
(3) R.Feldtkeller u. E.Zwicker, Das Ohr als Nachrichtenempfänger
Verlag Hirzel Stuttgart 1956

J56

FOURTH INTERNATIONAL CONGRESS ON ACOUSTICS
COPENHAGEN 21.-28. AUGUST 1962

THE ORIGIN OF SOUND ABSORPTION IN WATER

C. M. DAVIS, JR.*
U. S. NAVAL ORDNANCE LAB.
SILVER SPRING, MD., U.S.A.

T. A. LITOVITZ
CATHOLIC UNIV. OF AMERICA
WASHINGTON, D. C., U.S.A.

In 1946, Fox and Rock[1] showed that excess sound absorption in water near 4°C does not result from an exchange of energy between internal and external degrees of freedom. Hall[2] extends these results by assuming structural relaxation, emphasizing a relaxing isothermal contribution, and using a 2-state approach with no specific model. Hall's assumption of isothermal loss appears inconsistent to the authors in view of Eucken's[3] estimate of the large relaxational contribution to the specific heat of water (nearly 1/2 of the total).

The excess sound absorption in water, is reconsidered in this investigation to determine whether thermal effects contribute. This requires a knowledge of the relaxational portions of: specific heat, $C_{p,r}$, thermal expansion coefficient, β_r, and isothermal compressibility, $k_{T,r}$. Estimates of these parameters were obtained from a new model of the structure of water proposed by the authors, and Eucken's[3] estimate of $C_{p,r}$ at 0°C (Table I). The proposed model consists of puckered hexagonal rings like those in ice. The presence of such rings in water is explained by the fact that the hydrogen bond is partially covalent leading to highly directional cooperative effects which favor the formation of hexagonal rings. In water these rings occur in an equilibrium distribution of an open packed ice-like structure (Fig. 1) and a close packed structure (Fig. 2). This model accounts for:

a. The difference in the number of nearest neighbors estimated by means of x-ray scattering and Raman spectra

Hydrogen bonding occurs between nearest neighbors in the open packed structure and within rings in the close packed structure. Since bonds between close packed rings do not occur along tetrahedral angles, they do not exhibit covalent properties. Such non-covalently bonded neighbors have little effect on the strength of the O-H bonds within molecules, and for this reason, are not indicated by the Raman line corresponding to the O-H extensional mode. This Raman line shift therefore indicates only hydrogen bonded nearest neighbors; however, the x-ray radial distribution curve indicates the presence of all neighbors. The obvious difference in the number of nearest neighbors estimated by these two methods is therefore accounted for by the proposed model.

b. X-ray radial distribution function

The rings in the close packed structure are located in a manner which allows the water molecules to occupy a nearly complete body

---

*This paper is abstracted from a portion of a thesis presented in partial fulfillment of the requirements for the Degree of Doctor of Philosophy in the Graduate School of the Catholic University of America.

---

[1] F. Fox and G. Rock, Phys. Rev. 70, 68 (1946).
[2] L. Hall, Phys. Rev. 73, 775 (1948).
[3] A. Eucken, Z. Elecktrochem. 52, 255 (1948); 53, 102 (1949).

centered cubic structure. While in ice, alternate cube corners are vacant, in the close packed structure of water many previously vacant corners are occupied. In water, therefore, one expects the appearance of intermolecular spacing equal to the cube edge. This distance corresponds to the position of the "extra" peak at 3.6Å in the radial distribution curve of water. Using the number and position of neighbors, calculated from the model, one can account for the portion of the radial distribution curve below 4Å, including the "extra" peak.

c. Anomalous thermal expansion of water

The anomalous thermal expansion of water results from the shift in the equilibrium distribution towards closer packing with increasing temperature. This leads to a thermal expansion coefficient consisting of a negative relaxational term and a positive instantaneous term. Below 4°C the relaxational term is largest resulting in the negative value of β while above 4°C the instantaneous term is largest resulting in the positive value of β.

d. Anomalous sound absorption in water

The expression for excess sound absorption[4], α', given in terms of density, ρ, structural relaxation time, τ_p, frequency, f, velocity, θ, and relaxational adiabatic compressibility, $k_{s,r}$, or the adiabatic volume viscosity, $\eta_{v,s}$ is:

$$\alpha' = 2\pi^2 f^2 \theta \tau_p k_{s,r} = 2\pi^2 f^2 \eta_v / \rho \theta^3 \qquad (1)$$

The volume viscosity, η_v, compressibility, k, and structural relaxation time, τ_p, may be measured adiabatically or isothermally. The adiabatic volume viscosity is given by the expression[4]

$$\eta_{v,s} = \frac{k_{s,r}}{k_{s,0}^2} \tau_{P,s} \qquad (2)$$

For isothermal η_v the subscript s is replaced by T. $\tau_{p,s}$ is equal to $C_{P,\infty}\tau_{P,T}/C_{P,0}$.

The quasi-static adiabatic and isothermal compressibilities (k_s and k_T) are related by means of the well known thermodynamic expression

$$k_s = k_T - TV\beta_0^2/C_{P,0} \qquad (3)$$

containing the temperature, T, volume/mol, V, thermal expansion coefficient, β, the specific heat at constant pressure, Cp. A similar relation exists between the corresponding instantaneous parameters (designated with the additional subscript ∞) at frequencies well above the relaxation frequency. A relation between the relaxational compressibilities, obtained from the difference between the instantaneous and quasi-static values ($k_{s,r} = k_s - k_{s,\infty}$ and $k_{T,r} = k_T - k_{T,\infty}$) is

$$k_{s,r} = k_{T,r} + TV\left[\beta_\infty^2/C_{P,\infty} - \beta_0^2/C_{T,0}\right]. \qquad (4)$$

---

[4] K. Herzfeld and T. Litovitz, Absorption and Dispersion of Ultrasonic Waves (Academic Press, New York and London, 1959).

Taking the ratio $\eta_{v,T}/\eta_{v,s}$ one obtains

$$\frac{\eta_{v,T}}{\eta_{v,s}} = \frac{k_{T,r}\, C_{P,0}\, k_{s,0}^2}{k_{s,r}\, C_{P,\infty}\, k_{T,0}^2} \tag{5}$$

In water at 4°C, where $\beta_0 = 0$ and $k_{s,0} = k_{T,0}$, the right hand side of Eq. 5 reduces to unity if the Prigogine[5] relation [$k_{T,r}\, C_{P,r} = TV\, \beta_r^2$] is applied.

Values of relaxational parameters obtained from the proposed model and Eucken's[3] estimates are given in Table I. Values of the ratio calculated from Eq. 5 are given in Table II. At 4°C the value of $\eta_{v,T}/\eta_{v,s}$ obtained using the proposed model is one as expected. The corresponding ratio, obtained from Eucken's estimates is 1.2. Eucken's estimates[3] of $k_{T,r}$ and β_r were obtained by assuming that water behaves normally at 10,000 atms. (Eucken's estimate of $C_{p,r}$ is independent of this assumption.) Smith and Lawson[6] show from their investigation of the velocity of sound, that the anomalous behavior is still present at 10,000 atm. It therefore appears that Eucken's assumption leads to an underestimate of the relaxational contribution; nevertheless, calculations based on Eucken's estimates are given as a lower limit on $k_{T,r}$ and β_r.

At 100°C, $\eta_{v,T}/\eta_{v,s}$ has decreased to less than 0.5. This can be understood if one considers the effect on structure caused by applying pressure. An isothermal increase in pressure shifts the equilibrium towards closer packing. The resulting structural rearrangement gives rise to an excess loss. When T>4°C and the pressure is increased adiabatically, a temperature increase which also favors closer packing occurs; therefore, a larger amount of structural rearrangement results. This leads to $k_{s,r} > k_{s,T}$ and thus $\eta_{v,s} > \eta_{v,T}$ as shown in Table II.

In most liquids the increased temperature accompanying adiabatic compression favors structural rearrangements which lead to a more open structure. Since this opposes the effect of pressure, the amount of structural rearrangement resulting from adiabatic compression should be less than that resulting from isothermal compression. This would lead to $\eta_{v,T}/\eta_{v,s} > 1.0$. Using data given by Davies and Jones[7], this ratio was calculated for glycerol, glucose, selenium and rubber and found to lie between 1.6 and 1.95 in accord with the argument above.

Conclusion

Using the proposed model and available estimates of $C_{p,r}$ for water values of the relaxational parameters $k_{T,r}$ and $\beta_{T,r}$ were estimated. Hall's assumption of isothermal losses in water is shown to be true only at 4°C. At higher temperatures the ratio $\eta_{v,T}/\eta_{v,s}$ decreases from one at 4°C to less than 1/2 at 100°C. For liquids which exhibit a normal expansion coefficient $\eta_{v,T}/\eta_{v,s}$ was found to lie between 1.6 and 1.95. It therefore appears the thermal contribution to the excess sound absorption can not be neglected when structural relaxation occurs. The volume viscosity of water is anomalous in that $\eta_{v,s} > \eta_{v,T}$ for most temperatures.

---

[5] I. Prigogine and R. Defay, Chemical Thermodynamics (Longman, Green, New York, 1954).
[6] A. Smith and A. Lawson, J. Chem. Phys. 22, 351 (1954).
[7] R. Davies and G. Jones, Advances in Phys. 2, 370 (1953).

TABLE I. RELAXATIONAL PARAMETERS

T°C	Proposed Model				Eucken[3]			
	$k_{T,r}$ [a]	β_r [b]	$C_{P,r}$ [c]	$k_{s,r}$ [a]	$k_{T,r}$ [a]	β_r [b]	$C_{P,r}$ [c]	$k_{s,r}$ [a]
0	22.96	-1.296	8.6	42.66	11.6	-0.738	8.6	17.75
20	22.14	-1.163	7.73	44.76	7.2	-0.515	8.4	13.68
40	20.60	-1.013	6.76	43.02	4.2	-0.320	8.2	9.95
60	18.57	-0.859	5.73	39.16	2.0	-0.186	7.8	7.02
80	16.43	-0.720	4.93	35.46	1.2	-0.101	7.4	5.94
100	14.62	-0.604	4.17	32.09	0.6	-0.053	7.0	5.48

[a] $cm^2/dyne \times 10^{-12}$ [b] $(°C)^{-1} \times 10^{-3}$ [c] cal/°C-mol

TABLE II. RATIO $\eta_{v,T}/\eta_{v,s}$ IN WATER

T°C	Present	Eucken[a]	$\eta_{v,s}$ [b] (millipoise)
0	1.03	1.25	80
4	1.00	1.20	70
20	0.86	0.98	47
40	0.73	0.74	29
60	0.63	0.46	21
80	0.55	0.30	14
100	0.49	0.15	--

[a] Calculated from the relaxational parameters given by Eucken[3].
[b] L. Hall, Phys. Rev. 73, 775 (1948).

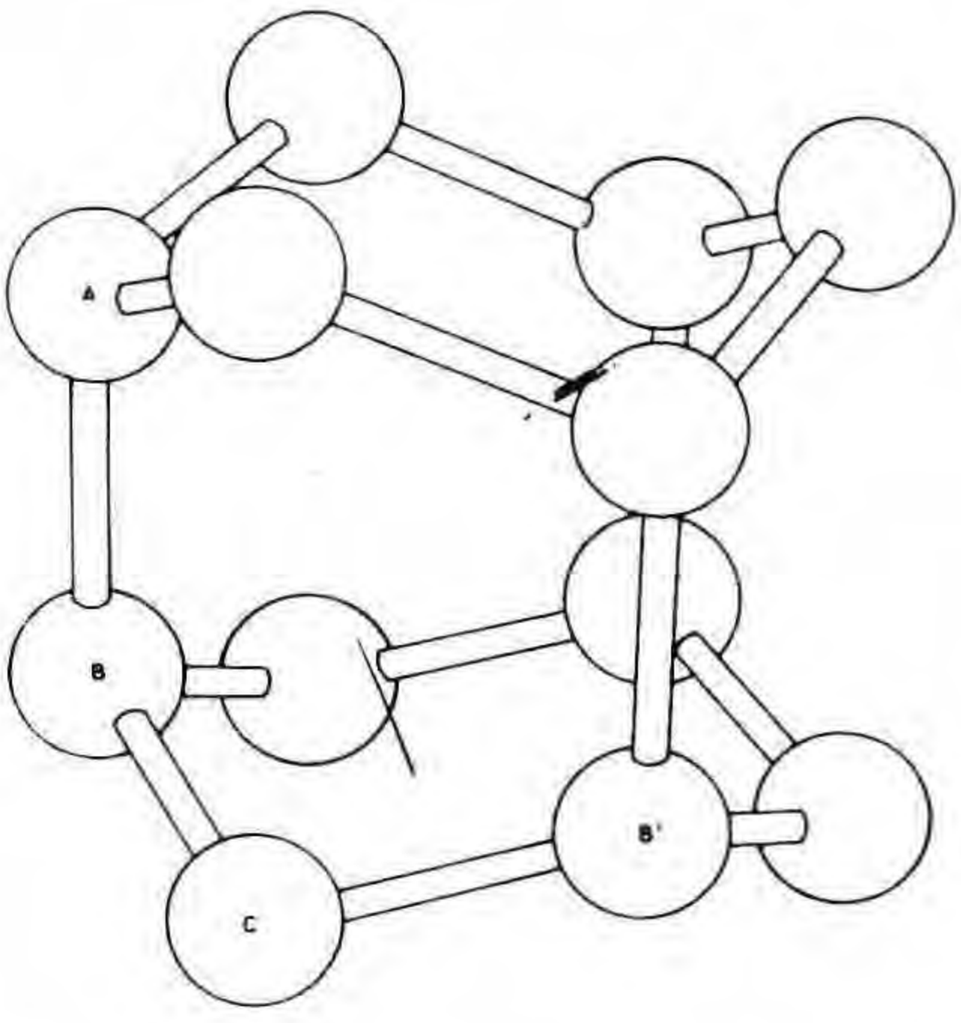

FIG. 1. OPEN PACKED STRUCTURE

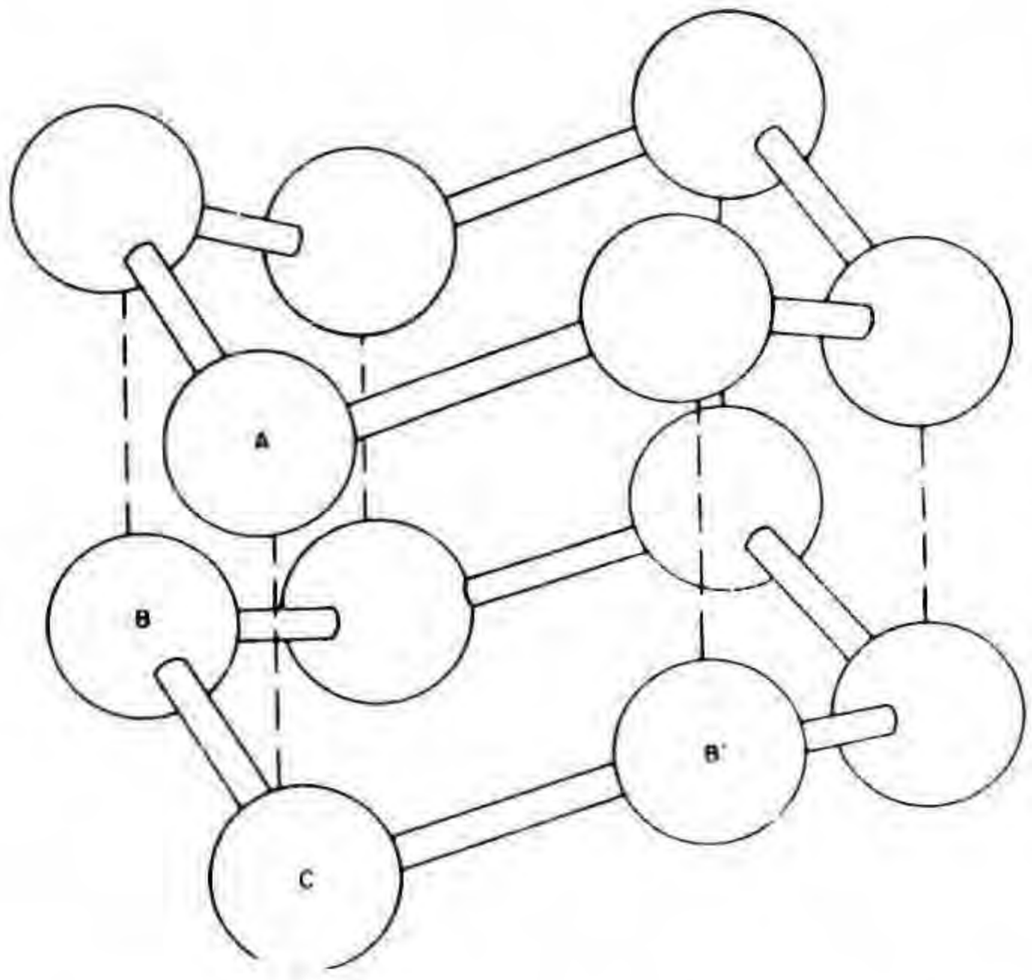

FIG. 2. CLOSE PACKED STRUCTURE

K56

FOURTH INTERNATIONAL CONGRESS ON ACOUSTICS
COPENHAGEN 21.-28. AUGUST 1962

Mechanische und dielektrische Relaxationserscheinungen in Hochpolymeren bei Ultraschallfrequenzen

Jan Koppelmann
Physikalisch-Technische Bundesanstalt, Braunschweig

Einleitung

Bereits vor einigen Jahren haben Thurn und Wolf [1] und Thurn und Würstlin [2] vergleichende dielektrische und mechanische Messungen bei 2 MHz an verschiedenen hochpolymeren Stoffen in einem größeren Temperaturbereich durchgeführt. Hiernach liegt das Maximum des dielektrischen Verlustfaktors durchweg bei höheren Temperaturen als das Maximum des Verlustfaktors des Longitudinalwellenmoduls. Thurn und Wolf versuchen dies damit zu erklären, daß im elektrischen Fall die Molekülbewegung oberhalb der Einfriertemperatur aus Drehbewegungen und im mechanischen Fall zu erheblichem Teil aus Translationsbewegungen besteht.

Nach dieser Deutung liegt die Vermutung nahe, daß die Platzwechselprozesse sich bei mechanischer und dielektrischer Beanspruchung eines hochpolymeren Stoffes unterscheiden und z.B. verschiedene Aktivierungsenergien haben, wie man sie aus der Temperatur-Frequenz-Lage der Verlustfaktormaxima ermitteln kann. Es erschien daher eine interessante Frage, diese Folgerung durch eigene Messungen und anhand der Ergebnisse anderer Autoren am Beispiel des Polyvinylchlorid (PVC) ohne Weichmacherzusatz nachzuprüfen.

Meßapparatur

Messungen des Elastizitätsmoduls von PVC in einem größeren Frequenzbereich sind den Arbeiten von Becker [3] und Sommer [4] und dielektrische Messungen einer Arbeit des Verfassers [5] zu entnehmen. Es blieb daher die Aufgabe, möglichst zuverlässige Ultraschallmessungen in einem größeren Frequenz- und Temperaturbereich durchzuführen. Hierzu wurde eine bereits früher beschriebene Apparatur [6] benutzt, bei der eine Kunststoffplatte in einem Flüssigkeitsbad von einem Schallimpuls durchstrahlt wird, und die in folgenden Punkten verbessert wurde:

1) Um höhere Temperaturen zu erreichen und das Quellen der Proben zu vermeiden, wurde das Wasserbad durch ein Bad aus Silicon-Öl ersetzt.

2) Durch eine Dunkeltastung des Oszillographen wurden die Null-Linie, störende Mehrfachechos im Meßtrog und der Ein- und Ausschwingvorgang des Schallimpulses unterdrückt, um eine bessere Auswertung des Leuchtschirmbildes zu ermöglichen.

3) Die Berücksichtigung der stehenden Wellen in der Platte und der Reflexionsverluste an deren Vorder- und Rückseite ist bei der Auswertung der Messungen in einfacher Weise nur dann möglich, wenn die Plattendicke ein Vielfaches der halben Schallwellenlänge beträgt (siehe [6]). Um diese Bedingung zu

erfüllen, wurden die Eigenresonanzen der verwendeten Zirkontitanat-Schwinger durch auf der Rückseite angebrachte Bleikörper so stark gedämpft [7] , daß eine Frequenzvariation jeweils im Verhältnis 1 : 2 bei ausreichender Schallintensität möglich war.

Meßergebnisse an PVC

Nach Thurn und Würstlin [2] liegen bei einer Frequenz von 2 MHz das dielektrische Verlustfaktormaximum (137°C) und das Verlustfaktormaximum des Longitudinalwellenmoduls (110°C) um etwa 27°C auseinander. Nach eigenen Messungen bei einer Frequenz von 0,4 MHz beträgt die Temperaturdifferenz zwischen dem dielektrischen (120°C) und dem mechanischen (107°C) etwa 13°C. Bei einer Frequenz von 1 kHz erhält man zwischen dem dielektrischen Verlustfaktormaximum (96°C) und dem Verlustfaktormaximum des Elastizitätsmoduls (104°C) eine Temperaturdifferenz von etwa 8°C in umgekehrter Richtung.

Diese Betrachtungsweise scheint zu der Folgerung zu führen, daß mechanische und dielektrische Beanspruchungen eines hochpolymeren Stoffes unterschiedliche Molekülbewegungen mit unterschiedlichen Aktivierungsenergien hervorrufen. Eine eingehende Auswertung aller bisher bekannten Messungen an PVC führt jedoch zu völlig anderen Vorstellungen.

Diskussion

1) Trägt man die Temperaturlage der Verlustfaktormaxima der Dielektrizitätskonstanten und des dynamischen Elastizitätsmoduls über dem Logarithmus der Frequenz anhand der Ergebnisse der Arbeiten [3] , [4] und [5] vollständig auf, so erhält man eine Kurve für das Verlustfaktormaximum des Elastizitätsmoduls und eine für das der Dielektrizitätskonstanten. Beide Kurven sind gekrümmt, das heißt: die in der üblichen Weise ermittelte scheinbare Aktivierungsenergie (siehe [6]) ist temperaturabhängig. Beide Kurven lassen sich jedoch durch eine Verschiebung um 1 1/2 Zehnerpotenzen entlang der logarithmischen Frequenzachse zur Deckung bringen. Das bedeutet: innerhalb der Meßfehlergrenzen sind die Aktivierungsenergien der molekularen Umlagerungsprozesse bei mechanischer und dielektrischer Beanspruchung gleich. Hieraus ergibt sich der erste Hinweis dafür, daß die Relaxationserscheinungen bei beiden Beanspruchungsarten durch denselben Elementarprozeß verursacht werden.

2) Wie sich aus den Frequenzkurven des Verlustfaktors der Dielektrizitätskonstanten von PVC [5] ablesen läßt, tritt im Temperaturbereich zwischen 90°C und 120°C oberhalb einer Frequenz von etwa 0,1 MHz eine Überlagerung zwischen dem Nebendispersionsgebiet (zugeordnet der Bewegung der Chloratom-Dipolgruppen) und dem Hauptdispersionsgebiet (zugeordnet der Kettensegmentbewegung) ein. Die gleiche Erscheinung tritt bei dem Verlustfaktor des Longitudinalwellenmoduls auf. Jedoch ist der Beitrag des Nebendispersionsgebietes zum Verlustfaktor bei mechanischer und dielektrischer Beanspruchung verschieden. Um bei vorgegebener Temperatur einen Vergleich der Frequenzlage des mechanischen und des dielektrischen Hauptdispersionsgebietes anstellen zu können, müssen daher jeweils Haupt- und Nebendispersionsgebiet bei der Auswertung der Messungen von einander separiert werden. Dies ist in einfacher Weise nur möglich, wenn sich beide Anteile linear superponieren. Nach der Theorie der Relaxationsprozesse gilt für den Verlustfaktor nicht das Gesetz der linearen Superposition. Dieses Gesetz ist

nur für die Imaginärteile des dynamischen Longitudinalwellenmoduls und der reziproken Dielektrizitätskonstanten gültig. Nimmt man eine Umrechnung in die Imaginärteile und anschließend eine Trennung der Anteile von Haupt- und Nebendispersionsgebiet vor, so rücken die Hauptmaxima für mechanische und dielektrische Beanspruchung zusammen.

3) Ferner zeigen die Ergebnisse, daß das Verlustfaktormaximum des Elastizitätismoduls und das des Longitudinalwellenmoduls bei gleicher Temperatur um mehrere Zehnerpotenzen der Frequenz auseinander liegen. Demnach muß man auch bei mechanischer Beanspruchung je nach der Deformation eines Volumenelementes zwischen verschiedenen Beanspruchungsarten unterscheiden. Auch hier läßt sich jedoch anhand der Theorie der Relaxationserscheinungen nachweisen, daß es sinnvoll ist, nicht die Verlustfaktoren, sondern die Imaginärteile der elastischen Moduln miteinander zu vergleichen. Diese Art der Auswertung führt wiederum zu dem Ergebnis, daß die Hauptdispersionsgebiete von Elastizitätsmodul und Longitudinalwellenmodul hinsichtlich der Frequenz- und Temperaturlage zusammenrücken. Das Gleiche läßt sich für den Vergleich zwischen Elastizitätsmodul und Kompressionsmodul bei sehr tiefen Frequenzen zeigen.

Schlußfolgerungen

Nach den bisher vorliegenden Ergebnissen an PVC liegen die Hauptdispersionsgebiete, wie sie bei verschiedenen Beanspruchungsarten auftreten, annähernd jeweils bei gleicher Frequenz und Temperatur, wenn man die Maxima der Imaginärteile der verschiedenen elastischen Moduln und der reziproken Dielektrizitätskonstanten miteinander vergleicht und, sofern notwendig, den Beitrag des Nebendispersionsgebietes vorher separiert.

Daher liegt die Vermutung nahe, daß die Relaxationserscheinungen bei verschiedenen Beanspruchungsarten auf ein- und denselben elementaren Platzwechselprozeß zurückgeführt werden können. Es wäre interessant, diese Vorstellung durch Messungen an anderen hochpolymeren Stoffen nachzuprüfen.

Literaturverzeichnis

[1] Thurn, H. und K. Wolf, Koll.-Z. 148, 16 (1956)
[2] Thurn, H. und F. Würstlin, Koll.-Z. 156, 21 (1958)
[3] Becker, G.W., Koll.-Z. 140, 1 (1955)
[4] Sommer, W. Koll.-Z. 167, 97 (1959)
[5] Koppelmann, J. und J. Gieleßen, Z. f. Elektrochemie 65, 689 (1961)
[6] Koppelmann, J., Koll.-Z. 144, 12 (1955)
[7] Koppelmann, J., F. Frielinghaus, Fr. J. Meyer, Acustica 8, 151 (1958)

L56

FOURTH INTERNATIONAL CONGRESS ON ACOUSTICS
COPENHAGEN 21.-28. AUGUST 1962

EFFECT OF REVERBERATION ON REACTION TO IMPACT NOISE

G.J. Thiessen and K. Subbarao[A]

National Research Council : Ottawa : Canada.

I. Introduction

In 1959 Embleton[1] and others reported on a survey of office noise in the Canadian Civil Service and they found that equal noise levels elicited different subjective responses depending on the amount of absorbing material in the offices. Experiments by Jahn[2], Wiener and Ross[3,4] and Robinson et al[5] have shown that the sound pressure level produced at the eardrum is dependent on the angle of incidence. The magnitude of this directional effect is of the same order as that of the subjective change caused by introducing absorbing material in an office. It is tempting, therefore, to conclude that in a non-reverberant room a listener will automatically orient himself so as to face the noise source and thus experience a reduced physical stimulus and that this is the explanation of the results of Embleton et al. A psycho-acoustical or physiological contribution cannot be ruled out, however, and these experiments were performed to test such effects. Directional effects were eliminated by simply presenting the signal by means of earphones.

II. Procedure

Since impact sounds are an important basic component of most office noises simple pulses in the shape of the letter lambda and a width of 0.5 msec. were produced electronically. These were recorded on a tape at 4 pulses per second and then fed into two channels, one of which contained an electronic reverberation unit. The subject listened to the signals through earphones and could control the level of the reverberant signal. By pushing a button he could listen to the reference tone at will but its level could be controlled only by the operator. The subjects were asked to match the two channels in "noisiness". The instructions were given in printed form to assure uniformity.

The reverberation time was measured by using white noise as the input into the reverberation unit and recording its decay when the input was cut off.

The reference and test signals were compared in level by reading the peak levels. The contribution due to the reverberation was measured by introducing white noise into the reverberation unit and then reading the output with an RMS voltmeter with the tape running and stopped. The contribution was less than half a decibel and hence no correction has been applied to the results.

A Present address: Andhra University, Waltair, India.

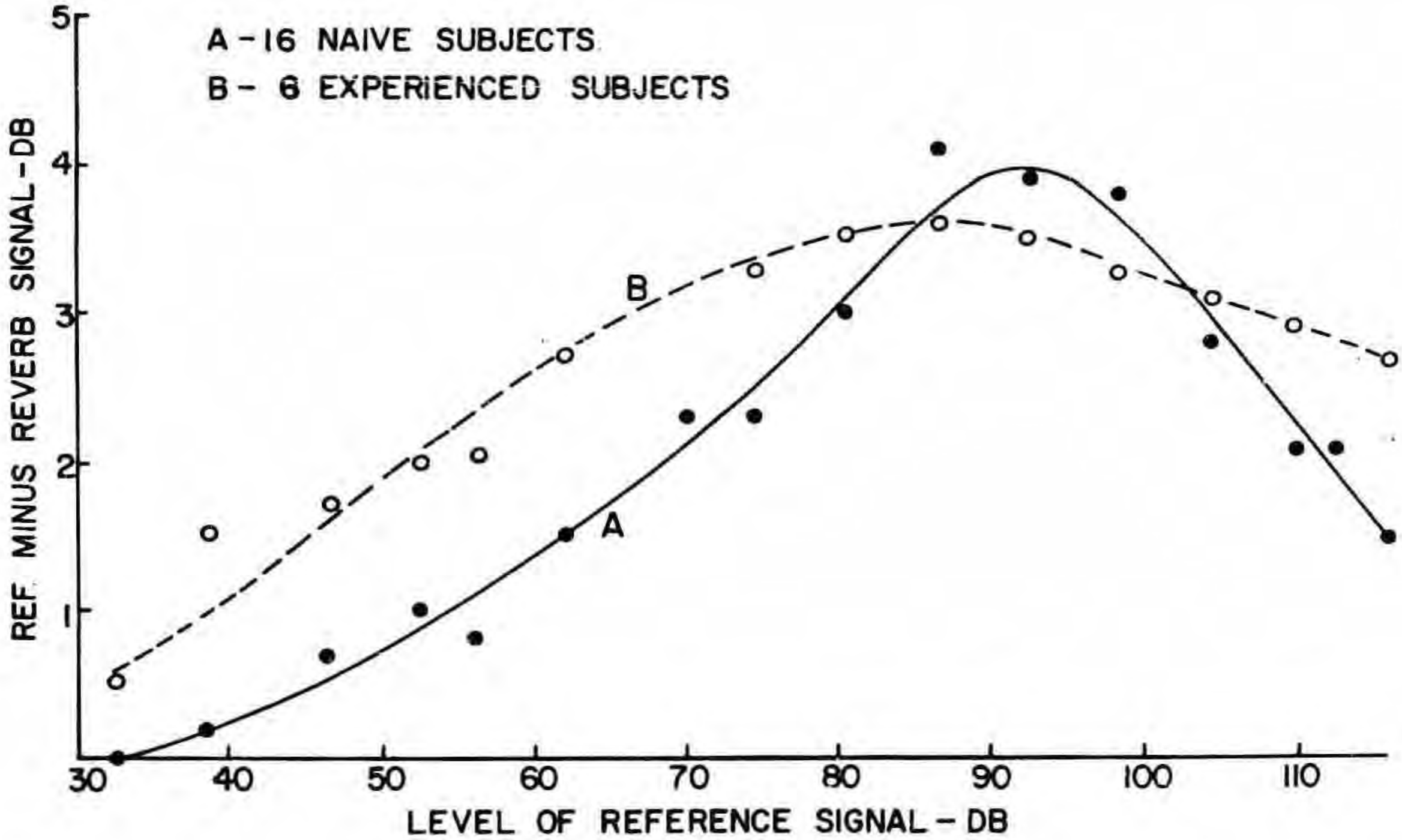

III. Results

Figure 1 shows some of the results for two groups of subjects. The ordinate gives the amount, in decibels, by which the reference signal exceeds the reverberant or test signal when the subjects matched them to be equal in "noisiness". The abscissa is the reference signal level. From curve A we see that for pulse levels around 90 db 16 naive subjects judge a reverberant pulse with a reverberation time of $\lambda = 1.1$ sec. to be equal in noiseness to one without reverberation provided its level is lower by 4 db. At low levels no difference exists. At higher levels this difference again drops off rapidly.

Curve B was obtained for 6 experienced subjects. A definite change in shape seems to have occurred and by an amount which is beyond statistical error. Experienced subjects appear to be more discriminating than naive ones. Qualitatively, however, the results are similar, viz. at low signal level reverberation seems to have a negligible effect on "noisiness". Its maximum influence is in the 85 to 90 db region and beyond this it drops off again.

IV. Interpretation and Comments

The question will no doubt be asked: What does a person, working in an office, have in mind when he says that his environment is too noisy? These experiments do not answer this question. It is possible that concepts like annoyance, noiseness, loudness and speech interference are mixed in appropriate proportion to determine his response. But there seems little

doubt that reverberation makes impact noise less acceptable.

It is too early to interpret the meaning of the details of the curves but some suggestions can perhaps be offered. It is reasonable to expect that at low levels of signals the reverberation part of the noise may drop below the threshold of hearing or may be masked by other noise. For example, Burgtorf(6) has shown that a primary signal is a better mask of an echo at low levels than at high levels. Thus very little or no difference in character is perceived by the ear between the two signals. Hence the curves drop down to the abscissa.

As for the drop at higher levels it is possible that the middle ear muscle is brought into play here and suppresses the reverberation part of the signal after being stimulated by the main pulse.

In conclusion we may say, therefore, that by the treatment of an office (or other environment in which the noise is in the nuisance area) by means of absorbing material perhaps three separate effects are achieved.

1. The sound pressure level is actually reduced by a small amount by reducing reflections.

2. The number of directions from which the noise arrives at the ear is reduced thus enabling the listener to find a preferred orientation and thus reduce the physical stimulus at the ear drum due to head diffraction.

3. The character of the impact noise is rendered more acceptable and it is this last item which represents the subject of this report.

Experiments with different rates of presentation of pulses, different reverberation times, and different criteria for matching are in progress.

References

1. T.F.W. Embleton, I.R. Dagg and G.J. Thiessen. Noise Control, 5, p.37 (Nov. 1959).

2. G. Jahn, Wissensch, Z. Tech. Hochsch. Dresden, 8, 530, 1958.

3. Francis M. Wiener and D.A. Ross, J. Acoust. Soc. Am. 18, 401 (1946).

4. Francis M. Wiener, J. Acoust. Soc. Am. 19, 143, (1947).

5. D.W. Robinson, L.S. Whittle and J.M. Bowsher, Acustica, 11, 397, 1961.

6. W. Burgtorf, Acustica, 11, 97 (1961).

M56

FOURTH INTERNATIONAL CONGRESS ON ACOUSTICS
COPENHAGEN 21.-28. AUGUST 1962

Graphic Solution for Acoustical Designing in Auditorium.

Naoto Hida, Takenaka Komuten Building Research Institute,
3-3, Fukagawa Hiraicho, Koto-ku, Tokyo, Japan.

I. Foundation and Development of the Graphic Solution for the Acoustical Design.

The graphic calculation in the applied mathematics is very important in the engineering. According to author's system, a graphic calculation based upon the primary polynominals of many variables can apply to the architectural acoustics. This graphic calculation system is called the Massau's solution, which is structurally so simple and reasonable as to observe the whole aspect in a moment. In the architectural acoustics, this system can be especially applied to the reverberation design.

If this method is utilized, a large number of weighted values can be obtained.

If the following expression is given;

$$m = \frac{a_1X_1 + a_2X_2 + a_3X_3 + \cdots\cdots + a_nX_n}{a_1 + a_2 + a_3 + \cdots\cdots\cdots + a_n} \qquad \text{- - - - - - - - - - (1)}$$

,such a construction as shown in the Fig. 1 can be made, if the above values are plotted therein.

Fig. 1

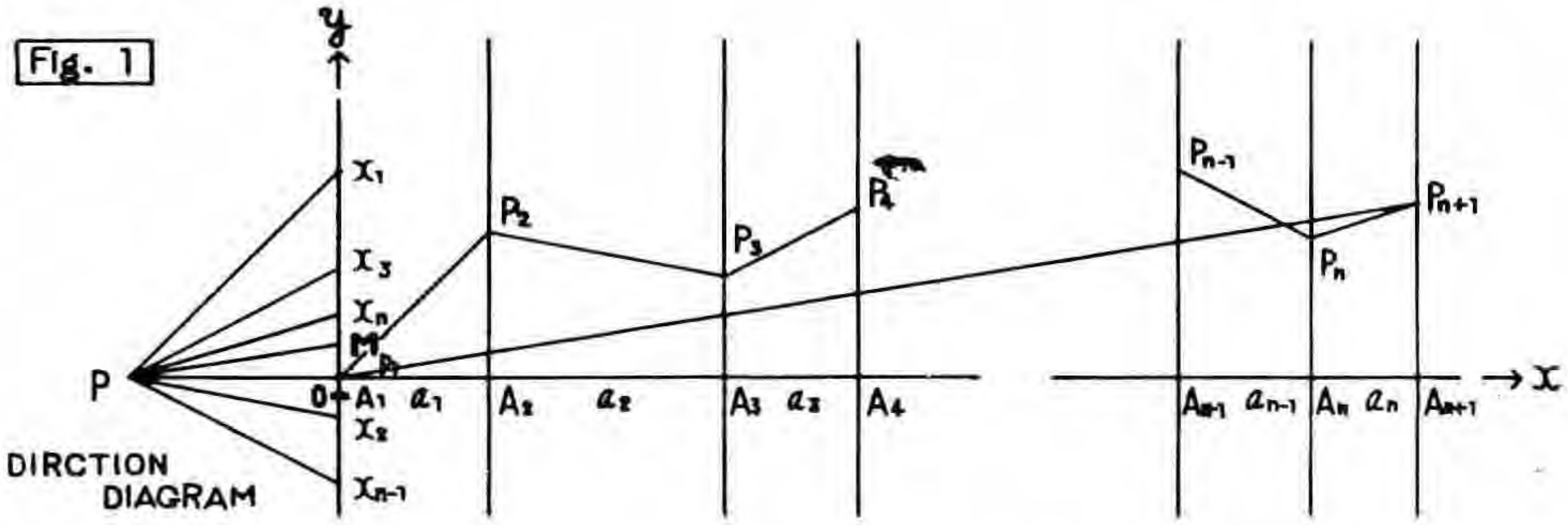

Wherefore, the average sound absorption coefficient ($\bar{\alpha}$), which plays an important role in the acoustical calculation, is expressed in the following formula, which can be regarded as the same as the formula (1). Therefore, its graphic calculation is

Possible.

$$\bar{\alpha} = \frac{\alpha_1 S_1 + \alpha_2 S_2 + \alpha_3 S_3 + \cdots\cdots + \alpha_n S_n}{S_1 + S_2 + S_3 + \cdots\cdots + S_n} = \frac{\sum \alpha_i S_i}{\sum S_i} \qquad \cdots\cdots\cdots (2)$$

If the weighted S_1, S_2, S_3 ... S_n are plotted on the $\mathcal{X}$ axis, while the coefficients α_1, α_2, α_3, ... are plotted on the $\mathcal{Y}$ axis (α is constantly on the positive side), the $\bar{\alpha}$ can be obtained on the $\mathcal{Y}$ axis of the direction diagram. In this case, the S_1, S_2, S_3... S_n can be expressed in terms of m^2, ft^2 or % areas.

According to this system, for instance, if the values of the $\bar{\alpha}$ is given, the point P_n becomes an altimate arrival point, when the $\bar{\alpha}$ is plotted on the $\mathcal{Y}$ axis of the direction diagram and the $\overline{A_1 P_n}$ is drawn in parallel with the $P\bar{\alpha}$. Meanwhile, the area weight on the $\mathcal{X}$ axis can be the area % per finishing, or the roughly classified area % of the ceiling, wall and the floor. In these case, the α_i on the $\mathcal{Y}$ axis of the direction diagram corresponding to the interim P_i can be controlled. On the other hand, the condition before and after the reconstruction can be viewed at a glance on the same graph. In the meantime, as the absorption coefficient never becomes negative, the route from the P_i (P on the way) to the next P, i.e. the P_{i+1} never becomes downgrade. In addition, as for the interim route (P_2, P_3 ..., P_{n-1}) from the origin A_1 to the final point P_n, the same P_n(final point) is reached through any route so long as the condition is the same. The Fig. 2 is a general solution of the system applied to the architectural acoustics.

The author has called it the "acoustical designing nomogram".

Fig. 2

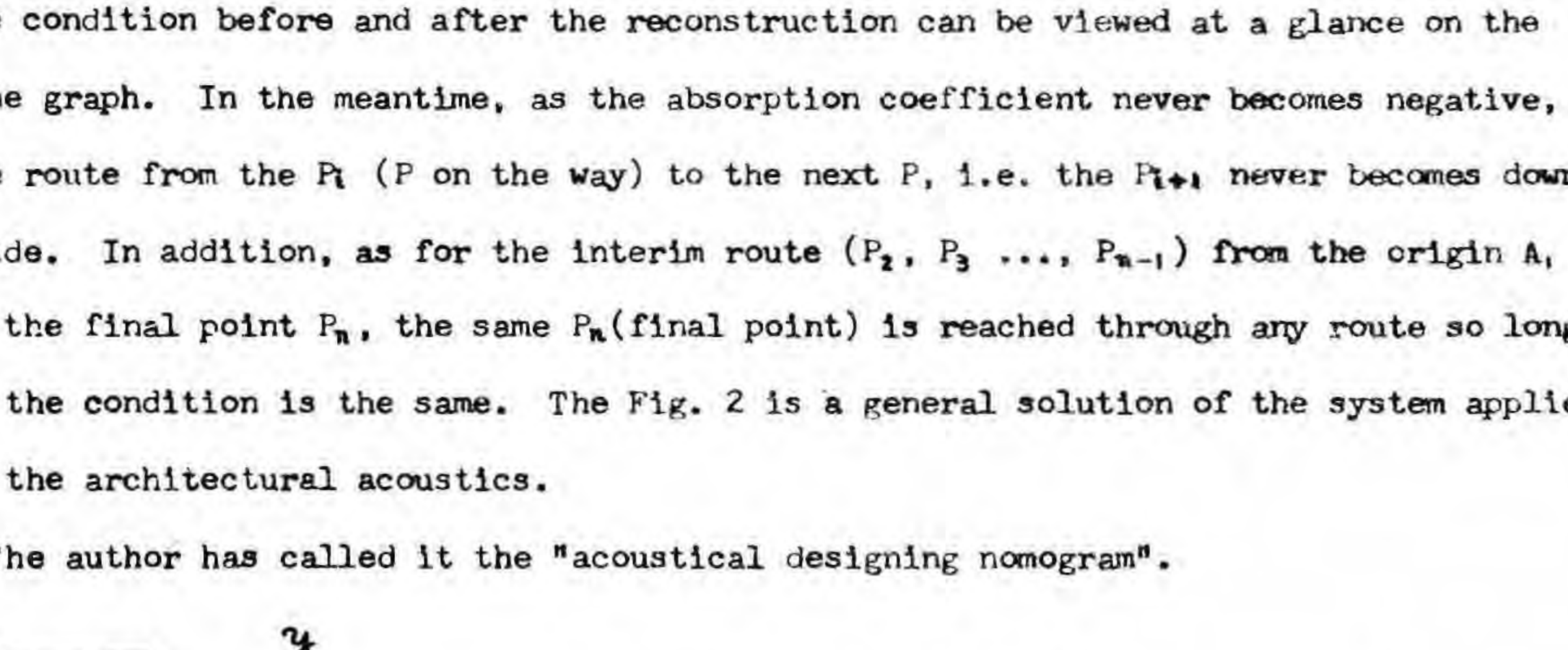

If the form of the sound absorption ($\alpha \cdot S$) in this nomogram is examined, a rectangle each area in which the α (height) of the y axis is given to each area S_i, is formed, when a horizontal line to the x axis is drawn on the points P_2, P_3, P_4, P_5 and P_n in the previously shown Fig. 3.
This rectangular area expresses the ($\alpha \cdot S$) of each section.

Fig. 3

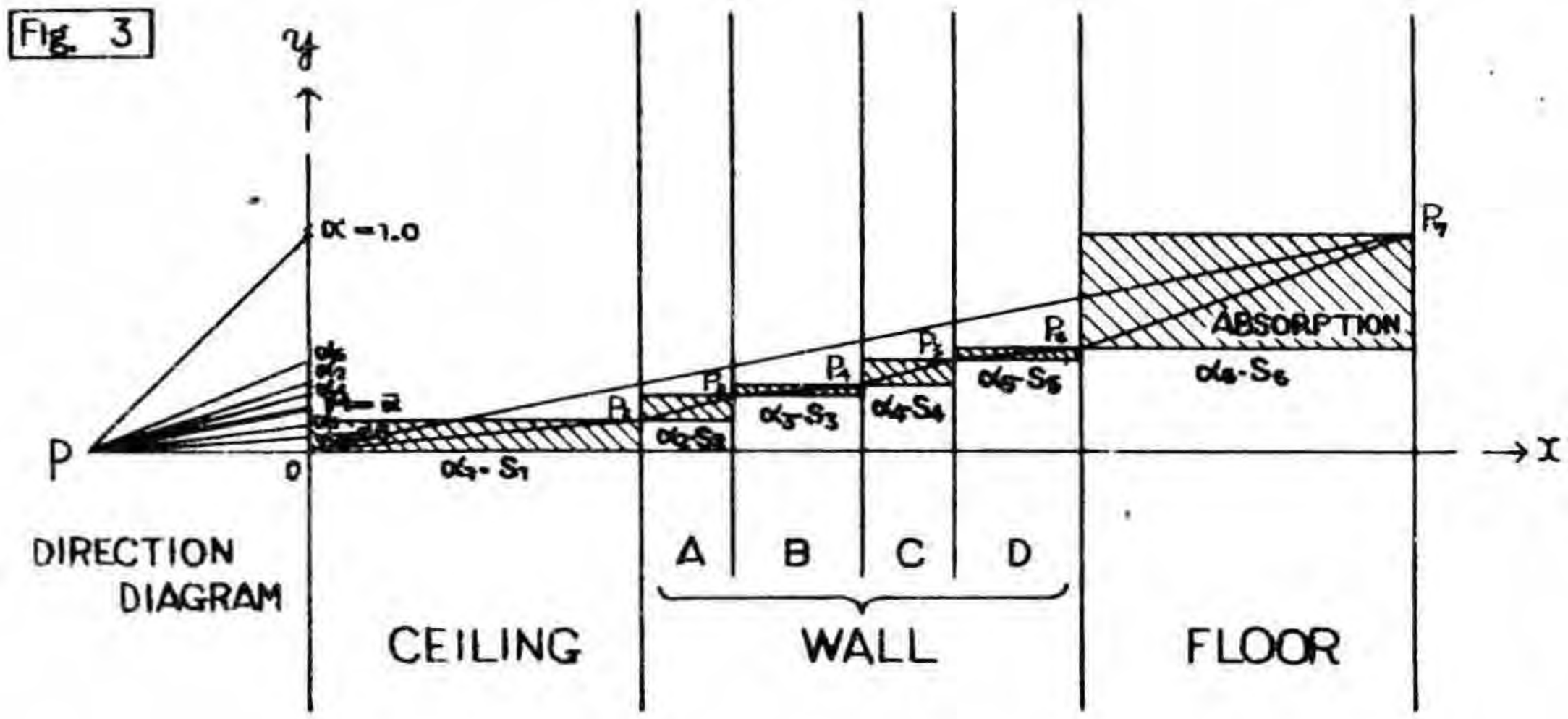

II. Establishment of the Direction Diagrams.

The graduation on the y axis is defined in making the direction diagram. The graduation is given to the absorption coefficient, which is generally regarded as the variable. As the absorption coefficient never becomes smaller than 0, it shall be an origin of the coordinates of the $x-y$ system. So the height of the y in the direction diagram is unit 1. This scale is called the "standard scale".

As a result of the solution, the average value appearing on the standard scale becomes the $\bar{\alpha}$. On the other hand, if the average absorption coefficient is previously given, the absorption coefficient for each section can be obtained.

III. Executed example (Asahi Hall, in Tokyo.).

Hall capacity (V); 2740 m^3 = 96.722 ft^3, Number of the seat; 616

Total surface area (S); 1641 m^2

As for the optimum reverberation time, the Knudsen's recommended value for the volume was evaluated from the application and use required by the customer. Then the reverberation time of the empty room was estimated at 1.1 sec. (500 c/s).

When the graphic method at the final stage of the design for the Asahi Hall case was completed, the whole calculation as shown in the Fig. 4 can be obtained. It may be called the new statement of the calculation, in which the $\bar{\alpha}$ obtained on the y axis of the direction diagram is 0.219 (as the empty room).

Fig. 4 Graphic Solution (ex. ASAHI·HALL)

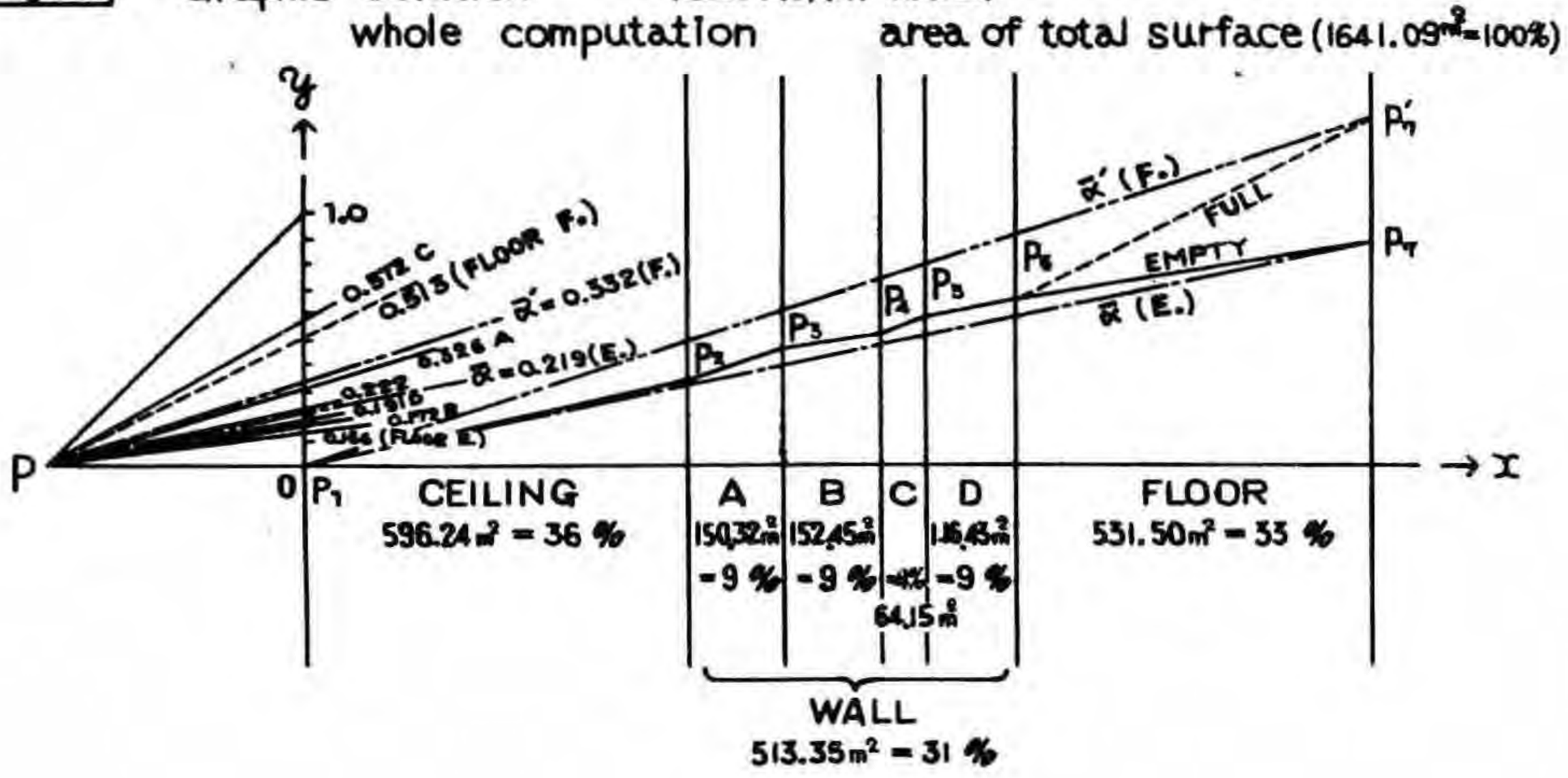

This graphic solution which had been developed as a new acoustic designing method, is characterized by the architectural acoustic engineering method that the design can be put forward, the overall acoustic design being observed, sometimes the following design being induced, and still that the design can rapidly meet any interim change.

Not only that, two design operations can be placed on the same calculation process.

For example, it is significant that the design before and after the reconstruction can be expressed on the same nomogram.

N56

FOURTH INTERNATIONAL CONGRESS ON ACOUSTICS
COPENHAGEN 21.-28. AUGUST 1962

ELECTROMECHANICAL CONSTANTS OF THICK BARIUM TITANATE DISKS

KIMIO SHIBAYAMA and YOSHIMITSU KIKUCHI
Research Institute of Electrical Communication,
Tohoku University, Sendai, Japan

Introduction

Recently,the vibration of thick disks has received much attention, with particular reference to the distribution of resonance frequencies.[1] We have also studied the vibration of the barium titanate transducers to obtain a broad view of their characteristics over the whole range of shape from the circular plates to long circular columns.[2] In this paper,design charts which give the equivalent mass,force factor and electromechanical coupling coefficient of the longitudinal symmetrical fundamental mode are presented. This mode is often used in practical applications.

The theory is based on two alternative approximations. Approximation I is accurate for thin disks and Approximation II holds for long thin bars. These approximations are overlapped to cover the intermediate region.[3]

Amplitude ratio

An example of the fundamental symmetrical mode is illustrated in Fig.1,where the dimension ratio l/a (thickness to diameter) of the disk is 0.42. The maximum amplitude of W-component ,W_{max},occurs at the center of the end surface of the vibrator, while the maximum U-component,U_{max},is found on the circumferential surface. Fig.2 shows the ratio of W_{max} to U_{max} versus l/a . It is apparent that the W_{max}/U_{max} is approximately $2(l/a)$ for all values of l/a , provided Poisson's ratio is in the neighbourhood of 1/3.

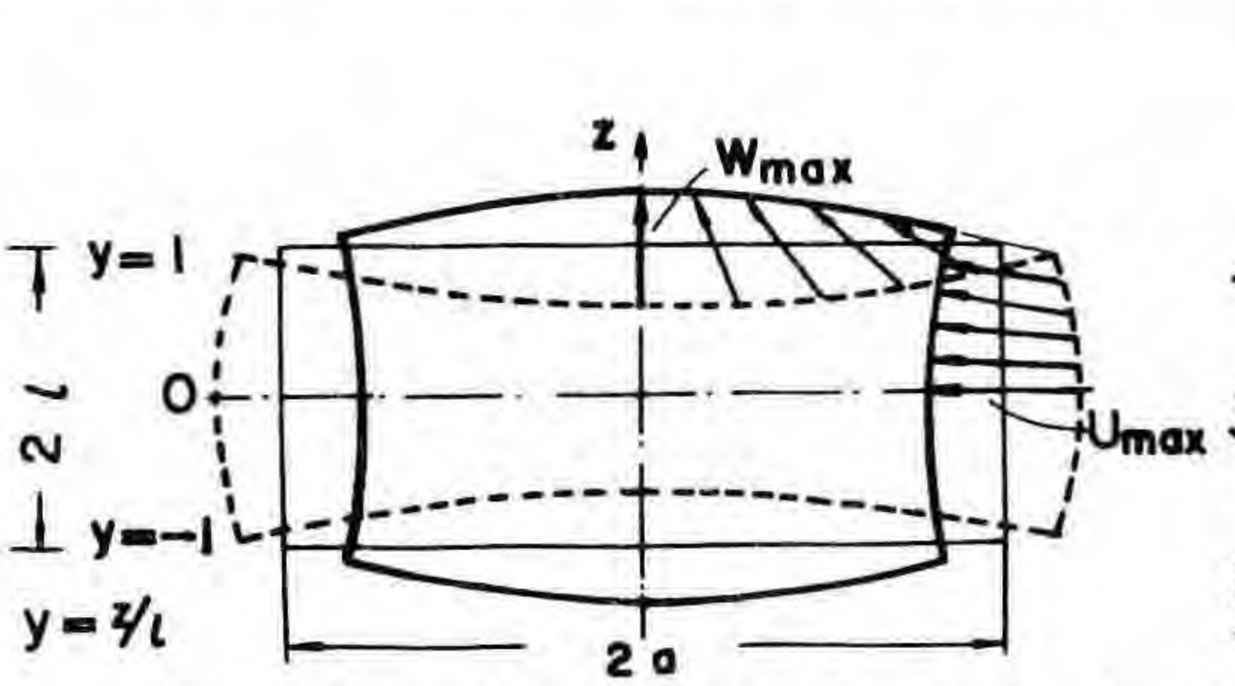

Fig.1. Velocity Distribution ($l/a = 0.42$).

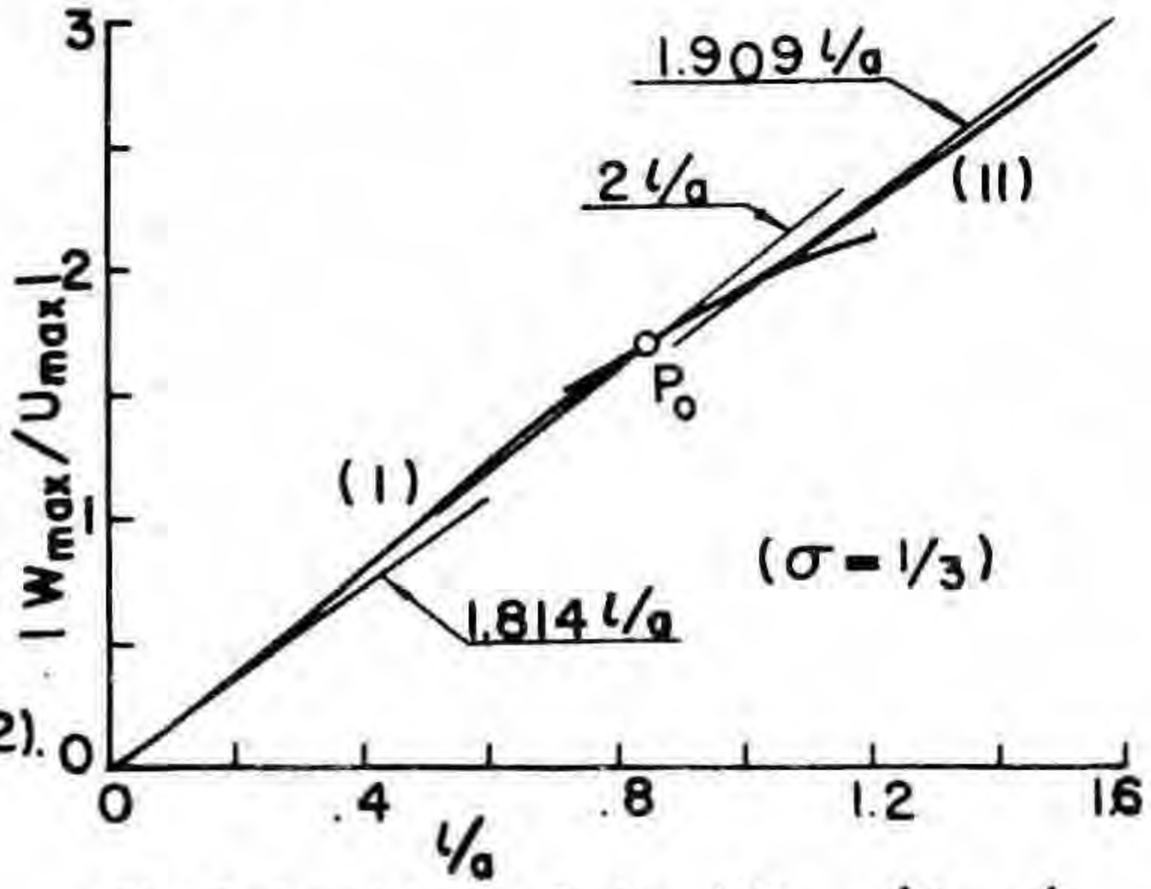

Fig.2. Amplitude Ratio, $|W_{max}/U_{max}|$.

Equivalent mass

Fig.3 shows the equivalent masses at particular mechanical terminals for the fundamental mode. Curve(a) refers to the pair of center points

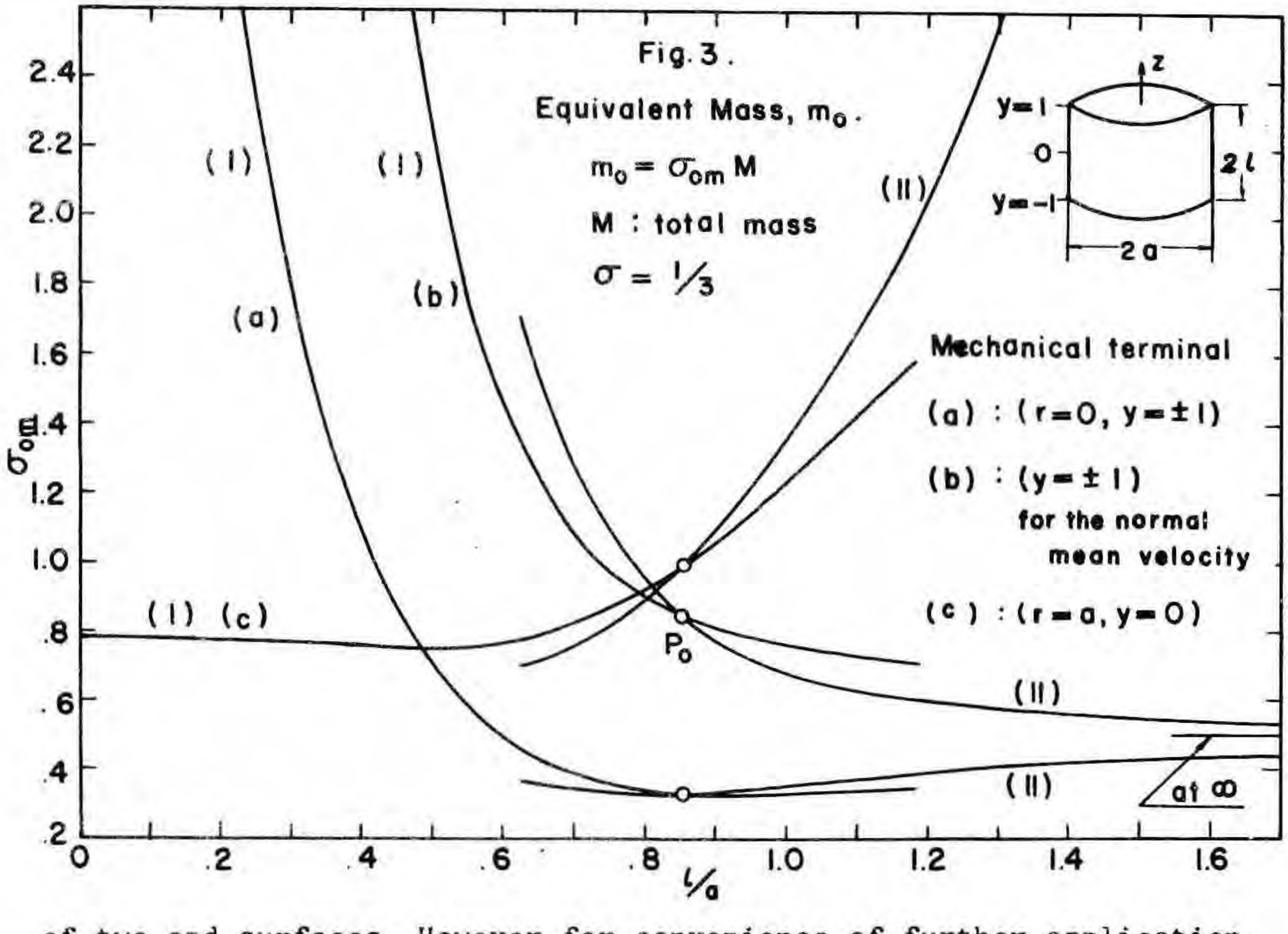

of two end surfaces. However, for convenience of further application, we often employ a vibration having a uniform distribution over the end surface with the mean normal velocity of original disk. The equivalent mass with reference to this uniform velocity is given by Curve(b). On the other hand, if we choose as the mechanical terminal the medial circular line on the cylindrical surface ($r=a, z=0$ in Fig.1), the equivalent mass has the value shown by Curve(c). For $l/a \to 0$, it tends to the equivalent mass of thin disks refered to the circular boundary. In this figure, if Approximation I is linked to Approximation II by smooth curves through the points P_0's whose common abscissa is $l/a \simeq 0.853$, we may expect better approximations to the equivalent masses of thick disks.

<u>A tentative assumption for electrostrictive characteristics of barium titanate disks</u>

Barium titanate should, of course, be treated as an anisotropic transducer material. But if one assumes the elastic constants to be isotropic, analysis becomes considerably easier. Accordingly, we make the tentative assumption that a disk polarized in its thickness direction is an isotropic body as far as the elastic constants are concerned. However, the absolute values of the elastic constants are affected by the electrical working conditions of the vibrator. Here, we consider only the effect on Young's modulus:-

$$1/E^G = (1/E^P)\left\{1 + \epsilon\sigma\Gamma_{11}^2/E^P\right\}, \qquad (1)$$

where E^P is Young's modulus for the state of constant electric polarization and E^G for the state of constant electric field intensity.

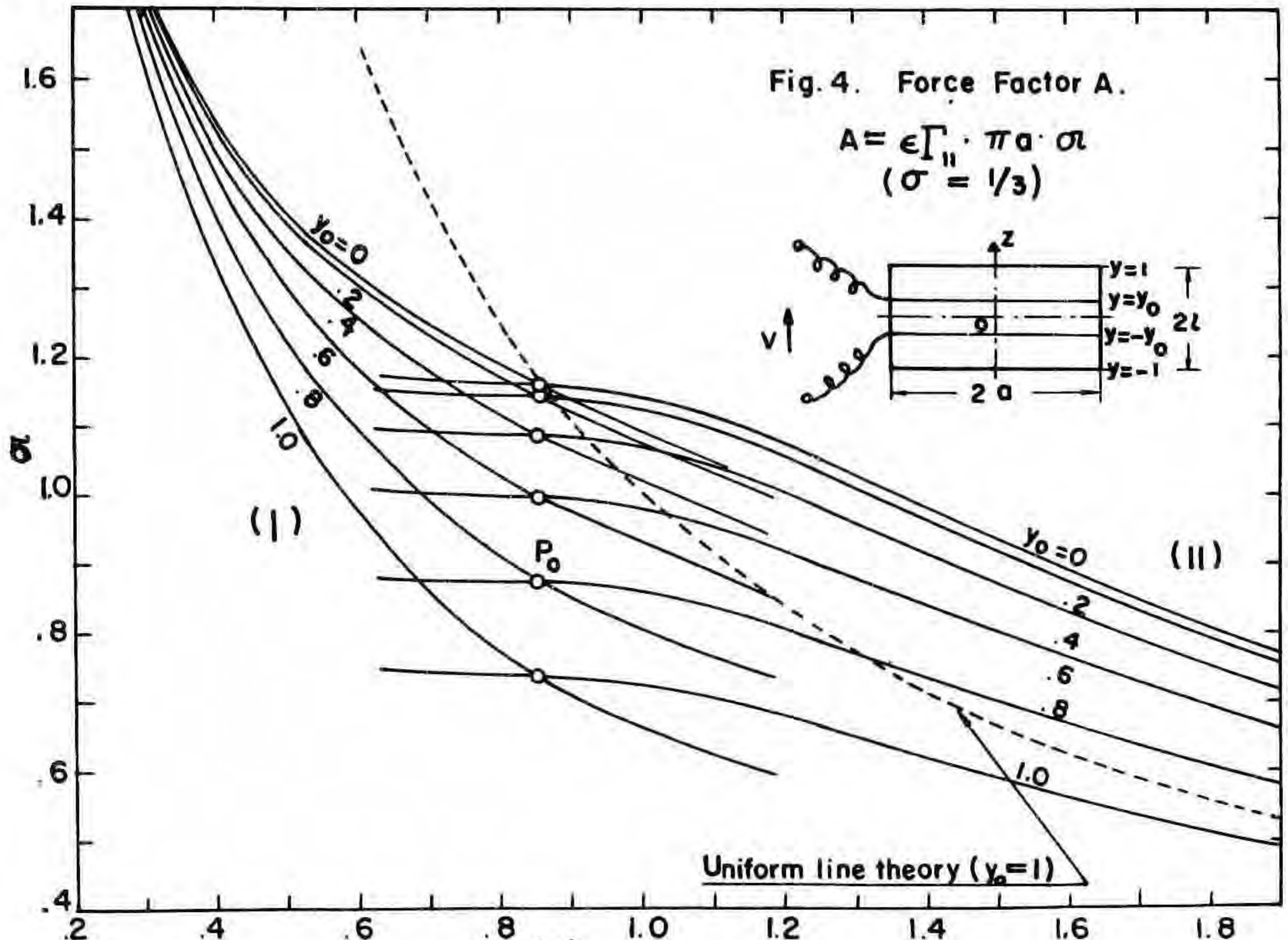

Poisson's ratio σ and the electric susceptibility ϵ are constant. The following assumption concerning to "electrostrictivity Γ " has already been used *:-

$$\Gamma_{12} = \sigma \Gamma_{11} , \qquad (2)$$

where Γ_{11} is the longitudinal electrostrictive constant and Γ_{12} the lateral constant. These assumptions are based on the general equation of the electrostrictive vibrator and several experimental results.

Force factor

Numerical values of the force factor, A, have been calculated for a transducer polarized in the thickness direction. Fig.4 shows the results obtained when the mechanical terminals are the pair of centers of the flat surfaces. The broken line of the figure shows the force factor of a composite bar which is analyzed by an electrical transmission line analogy.

Electromechanical coupling coefficient

It is well known that the electromechanical coupling coefficient is defined as the square root of ratio of available mechanical energy to input electrical energy. Usually, the coefficient is calculated assuming vibration in the region of stiffness controlled region. When the transducer vibrates at resonance, the energy ratio k_v^2 is dependent

---

* $\epsilon\Gamma$ corresponds to the piezoelectric strain constant e .

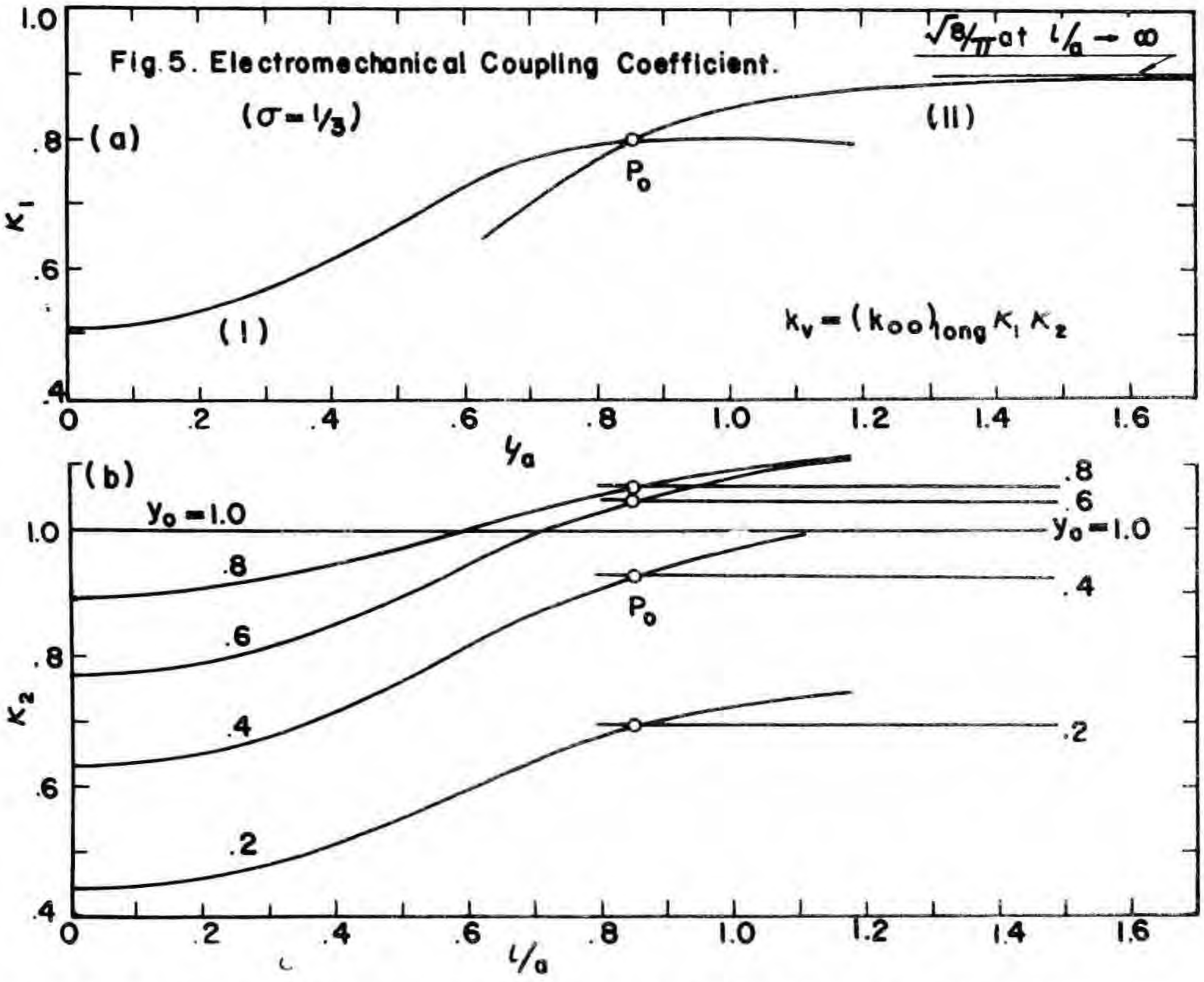

on the mode of vibration. For symmetrical fundamental mode, k_v may be written

$$k_v = (k_{oo})_{long} K_1 K_2 , \qquad (3)$$

where $(k_{oo})_{long} = \sqrt{\epsilon \Gamma_{11}^2 / E^P}$ corresponds to the electromechanical coupling coefficient for a long thin bar in the stiffness controlled region. Fig.5(a) and 5(b) give the values of K_1 and K_2 when $\sigma = 1/3$. As the figure shows, k_v for the thick disk is always lower than that of the long thin bar for which $(k_v)_{y_0 \to \infty} = \sqrt{8}/\pi (k_{oo})_{long}$ For example, if $y_0 = 1$ and $(k_{oo})_{long} = 50\%$, $(k_v)_{y_0 \to \infty}$ is 45% and as one proceeds to smaller l/a, it falls, reaching a value of 25% for thin disks.

The above results have been derived from simple assumption in order to obtain general view of the situation. Some errors are to be expected in the results. Neverthless, the agreement between experiment and theory is good.

References
(1) For example: in experiment; E.A.G.Shaw, Jour. Acoust. Soc.Amer. Vol.28,(1956)p.38, and in theory; D.C.Gazis & R.D.Mindlin, Jour.Applied Mechanics Vol.27,(1960)p.541.
(2) K.Shibayama & Y.Kikuchi, SCI.REP.RITU,B-(Elect.Comm.)Vol.8,No.3 (1956)p.133,Vol.9,No.2(1957)p.113 and Vol.11,No.3-4(1959)p.203.
(3) Y.Kikuchi, Proc. 3. ICA,1959

H57

FOURTH INTERNATIONAL CONGRES ON ACOUSTICS
COPENHAGEN 21.-28. AUGUST 1962

CORRELATION OF BINAURAL NOISE SIGNALS AND SOUND IMAGE LOCALIZATION

A. V. Rimski-Korsakov
Acoustic Institute, Academy of Sciences, Moscow (U.S.S.R.)

Studies of binaural effect, done by meanes of sinusoidal tones lead to the conclusion, that in the high frequency range finding the direction to the sound source is possible due to a certain difference of sound intensities between ears, caused by diffraction of sound waves near the head [1,2] . However, the effect of phase difference on the direction finding can be detected, and the experiments with short impulses show that sounds of high frequencies are localised due to the time difference of arrival between the ears [3,4,5] .

In practice a man meets the necessity to determine the direction to the sources of complex sounds (speech, music), so it appears interesting to study the possibility of localization of continuous non-periodical sounds. Sui Huan Chang and the autor [6] in Acoustic Institute and in Moscow Communications Institute made some experiments on localisation of band noises. Binaural noise signals were produced in a dead room by a loudspeaker and a dummy head with microphones in place of ears. Signals from microphones were fed in another room to a two-channel amplifier with the standard headphones. A semicircular azimuth-scale was joint to the headphones. Listeners with the hedphones on could see the scale in front of them and indicate the azimuth of the imagined sound source. Phase and amplitude characteristics of the channels were adjusted from the acoustical input to the acoustical output. At the amplifier autput the sound pressures at the dummy head and their correlation factor were measured. In another series of tests binaural signals were produced by the same microphones, placed 21 cm one from another on a turntable.

Tests, made on the groups of 15-20 persons have shown, that the determination of azimuth for continuous noises of 1/2 octave bands is practicaly equally successful in both series of tests. The subjective mean square error of direction finding for a group of listeners was, depending on the noise frequency and the azimuth determi-

ned,from 5° to 15° .Localisation becomes more precize,especially for low frequency noise,if the noise is intermittend (manipulated in telegraph-code breaks).The binaural noises correlation factors,calculated by their energy vs. frequency spectrum,time delay vs. azimuth dependance $\tau = a(\theta + \sin\theta)/c_o$,derived from simple geometric considerations,and by the data for the dummy head sound diffraction are in good agreement with the measured values,if the equivalent head radius (a) is taken to be 9.5 cm, and c_o = 340 m/sec.

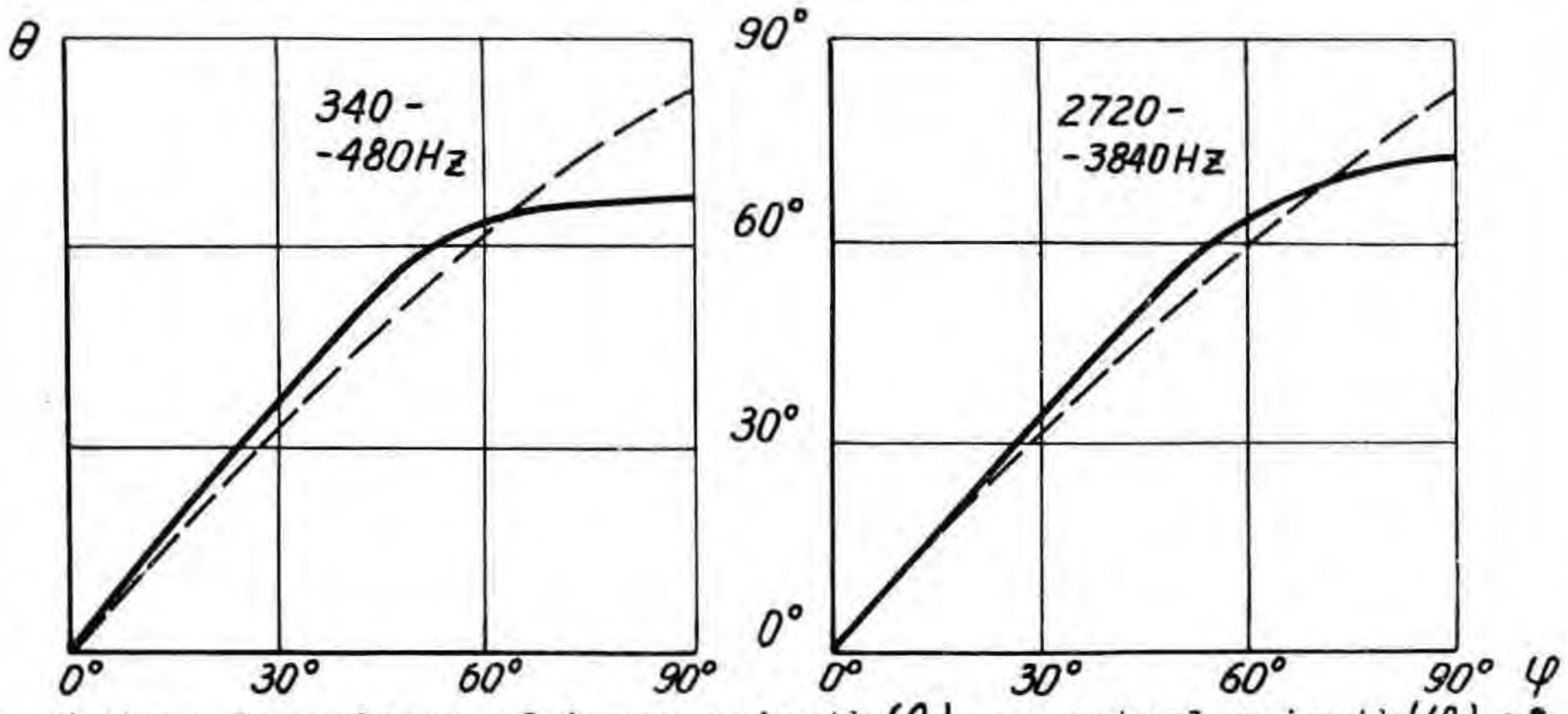

Fig.1.Mean dependence of image azimuth(θ) on actual azimuth(φ) of noise at the dummy head. ——— continuous noise measurements,– – – – intermittend noise measurements.

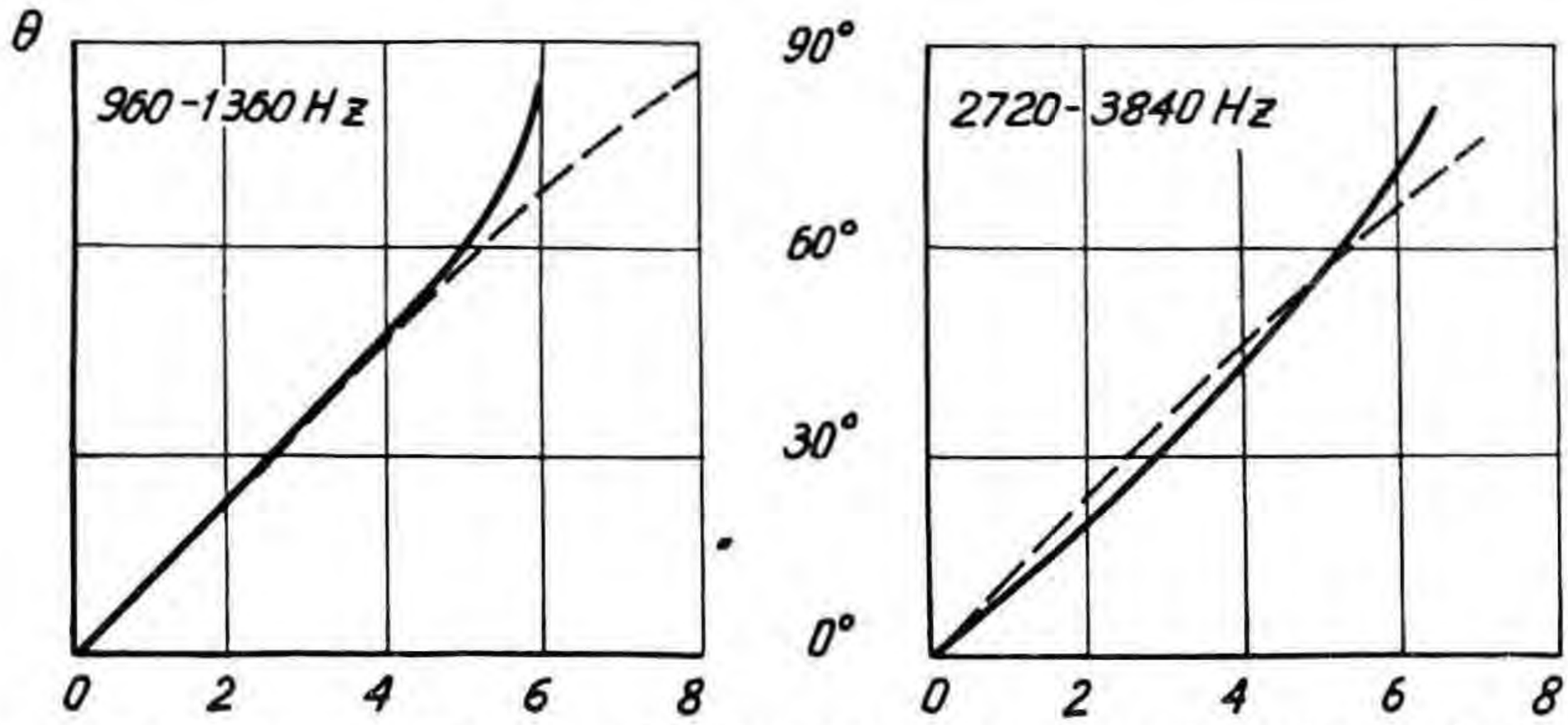

Fig.2.Mean image azimuth (θ) dependence on time delay between ears.Time delay (τ) in 10^{-4} sec. ——— microphones in ears of dummy head,– – – – microphones on a turntable.

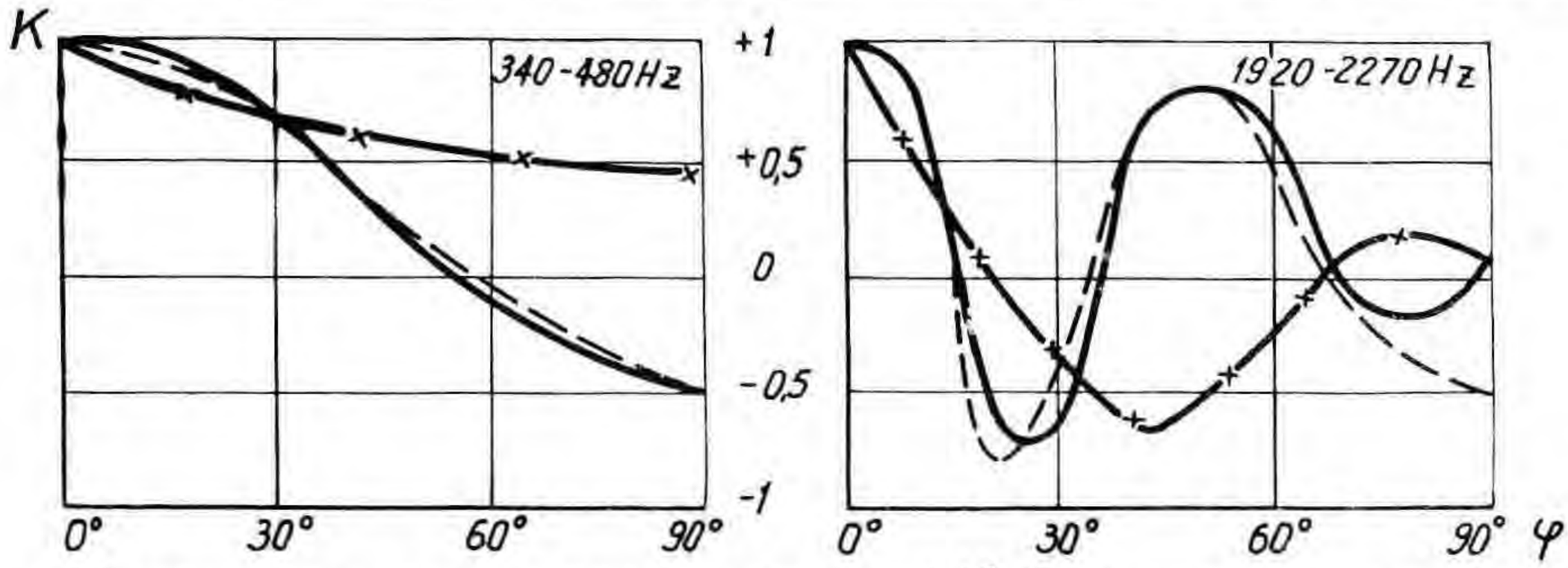

Fig.3. Dependence of correlation factor (K) of sound pressures at the ears of dummy head on the azimuth (φ) of loud speaker. Continuous noise: ——— measured, — — — calculated. Intermittend noise, measured —×——× .

It can be supposed, that the human azimuth determination mechanism is a correlational one, i.e. that the nervous system can have a circuit with a delay line and coincidence detector. The effect of sinaptic time summing can be an analogue of such a sheme [7] . Nerve impulces from ears afferent centers are delayed for different times, before coming to efferent centers, connected to neurones, running from both ears. The efferent neurones are activated, depending on the number of coincidencies from both ears. The neurones, for which the resulting difference of time delay in coming through the nervous lines (τ_θ) and the time delay of sound between ears is zero, are maximally activated: $\tau_\theta - a(\theta + \sin\theta)/c_0 = 0$. It corresponds to the maximum maximorum of pressures correlation function. The place of maximum neuron activation is the measure of asimuth. For sinusoidal sound the correlation function degenerates into a periodical one, all its maximums are alike and the azimuth finding by means of one maximum activation at high frequencies becomes impossible. The better localization of intermittend noise also becomes understandable. If the intermittend noise is represented as a product of stationary noise (u) and a modulating process of manipulation ($\frac{1}{2} + v$), where v recieves at random values $\pm 1/2$ with a mean frequency $\mu/2$, then:

$$\overline{u\left(\tfrac{1}{2}+v\right) \times u_\tau\left(\tfrac{1}{2}+v_\tau\right)} = \overline{uu_\tau}\left(\tfrac{1}{4} + \overline{vv_\tau}\right) = R_{uv} .$$

For a noise of mean frequency ν and band width $\Delta\nu$ the correlation function $R_u=\overline{uu_\tau}=[\sin(\pi\Delta\nu\tau)\cos\nu\tau]/\pi\Delta\nu\tau$,but $R_v=\overline{vv_\tau}=\frac{1}{4}\exp\{-2\mu|\tau|\}$ so that in absence of manipulation $R'_u(0)=0$,and in its presence $R'_{uv}(0)=\pm\mu/2$. A sharp maximum simplifies the localisation of intermittend noises. Another experiment confirms the correlation mechanism: 1/2 oct. noise signal is fed to two telephones with a magnetic delay line in the circuit of one of them, to create a seeming azimuth of source. In one of the telephones is olso fed an undistinguishable by timbre, but not correlated with the first, noise signal of the same spectrum from another generator. The resulting mixed noise loudness is kept constant, as the parts of mixture are varied. The azimuth determination remains unvaried (though it is difficult for the listener) until the mixed noise voltage remains lower, then of the principal one, i.e. maximum maximorum is higher than 0.7 . From this value down the direction finding becomes impossible. Persons listening to two completely uncorrelated noises imagine, that they hear the noise of the rain, falling on a big level roof over their heads. It seems, that the maximum value of correlation factor of 0.7 can be taken as a criterium of possibility of creating the stereophonic effect.

REFERENCIES

1. E.R.Whiteman and F.A.Firestone, J.A.S.A. No 2, 1930
2. Л.Д.Розенберг и А.Б.Славинский, ДАН СССР № 6, 1940.
3. E.M.Hornbostel und M.Wertheimer "Über die Wahrnehmung der Schallrichtung". Verlag d. Academie d. Wissenschaften, Berlin, 1920.
4. G.Bekesi, J.A.S.A. No 5, 1948; Phys.ZS. No 31, 1930.
5. J.R.C.L.cklider, J.A.S.A. No 1, 1950.
6. Сюй Хуан Чжан, Диссертация, Институт Связи, Москва 1959.
7. М.Брайзе "Электрическая активность мозговой системы", Издание ИЛ, Москва, 1955.

L57

FOURTH INTERNATIONAL CONGRESS ON ACOUSTICS
COPENHAGEN 21.-28. AUGUST 1962

Experimental buildings for sound insulation studies

O. Brandt

S. Wahlström

General

Measurement of the reduction index for airborne sound in traditional laboratories gives certain information about what is to be expected for constructions under field conditions. However, in some cases great deviations occur between the laboratory and the field. This is true when using light constructions, i.e. lightweight concrete single and double walls. Usually, lower sound insulation is then obtained in the field than in the laboratory. One reason for this is flanking transmission. Another reason is the different edge conditions in laboratory and in the field.

The use of models and vibration studies gives valuable information about the way the sound energy is divided by junctions between walls and floors but the picture has only two dimensions and to completely clarify the circumstances it is necessary to work in full scale and three dimensions.

The time at disposal between the completion of a building and the appearance of the first occupiers is usually very short and gives few possibilities for complicated acoustical measurements or experiments.

For these reasons we have in Sweden in the past few years built experimental buildings for sound insulation studies in connection with the planning of bigger building projects. In these houses several room units are built together in the same way as in the planned building but with possibilities for changing elements such as outer walls, floors, partitions etc.

By sound insulation measurements in these experimental houses it has been possible to predict the conditions in the final construction with considerable accuracy. Certain unexpected faults have also been revealed and put right in this earlier period of the planning.

So far four such houses have been built in Stockholm and used for the study of flanking transmission in light outer and inner walls, the use of non-radiating panels in lightweight buildings and similar problems.

One of our latest buildings (Storängsbotten), erected in order to study flanking transmission in normal Swedish outer walls for dwellings, is described in the following.

The experimental building at Storängsbotten

Plan and section of the experimental building are found in Fig. 1. The partitions and the floors are made of 14 and 16 cm concrete respectively, the minimum thickness according to the Swedish Building Code. To get the same conditions as in a big house with several floors the concrete slabs are mounted on 14 cm broad beams of concrete under the partitions. One of the long side walls and both end walls of the house are made of concrete and these three walls are screened on the inside with gypsum board on studs to prevent sound radiation from these part of the rooms.

The outer walls which are to be studied are erected along the other long side of the house and the measurements of airborne level difference are made between the rooms.

Measuring methods

The method used for the measurement of sound insulation is as described in ISO Recommendation R 140. The standard deviation for the normalized level difference D_{10} has been calculated to be 3.2, 1.2 and 1.2 dB at the frequencies 160, 630 and 2500 Hz, respectively.

One method for estimating the flanking transmission is to measure the vibration amplitudes. Such measurements are done with a ceramic pick-up fastened in ten different positions on each surface to be investigated. The contacts between pick-up and walls are made by screws plugged into holes with selfhardening plastic. The contact resonance between pick-up and concrete lies high enough over the highest measuring frequency to be neglected, while for lightweight concrete it lies at about 2000 Hz which is quite independant of the fastening method used; in this case it is possible to simplify the fastening by using conical pins attached to the pick-up and forcing

them by hand into the lightweight concrete. The vibrations to be measured in the vibration investigations are initiated in the wall surfaces in the same way as for the measurement of the airborne sound transmitted, i.e. with loudspeaker and filtered white noise in the range of 100-3150 Hz.

Screening walls

In connection with investigations of the flanking transmission it is necessary to reduce the sound transmission via one or more walls in a simple way, to such a size that its contribution to the total sound transmission can be neglected. For practical reasons the desired construction must be flexible in use and be easy to put up and take down quickly. A suitable compromise between the different claims we have found to be a framed wall, erected at a distance of 30 cm from the basic construction and with a sound absorbing mat in between. The studs in the frame work are fastened permanently in place, while the wall cladding consisting of 13 mm gypsum board, covered on both sides with 6 mm hard masonite board, is screwed to the studs with wing nuts.

To get high insulation with this type of wall it is important that it be absolutely tight, which is achieved by placing the fastening arrangements close to each other and by using a foam plastic strip as a seal between the framing system and the cladding.

The cladding is made in pieces 54 by 228 cm^2, each with a weight of about 30 kg. The entire wall cladding is easily put up or taken down in a few minutes.

The above mentioned construction has been tested in the laboratory using a 70 mm thick lightweight concrete wall as the basic construction, Fig. 2. The airspace was 200 mm. The average improvement of the sound reduction index was $\overline{\Delta R}$ = 31.6 dB, Fig. 3.

Conclusion

The use of experimental buildings has proved to be a valuable complement to laboratory measurements of sound insulation.

Some results of the method are shown in a separate paper [1].

Reference

1) Brandt, O. and Westerberg, G.: Studies on flanking transmission in an experimental building.

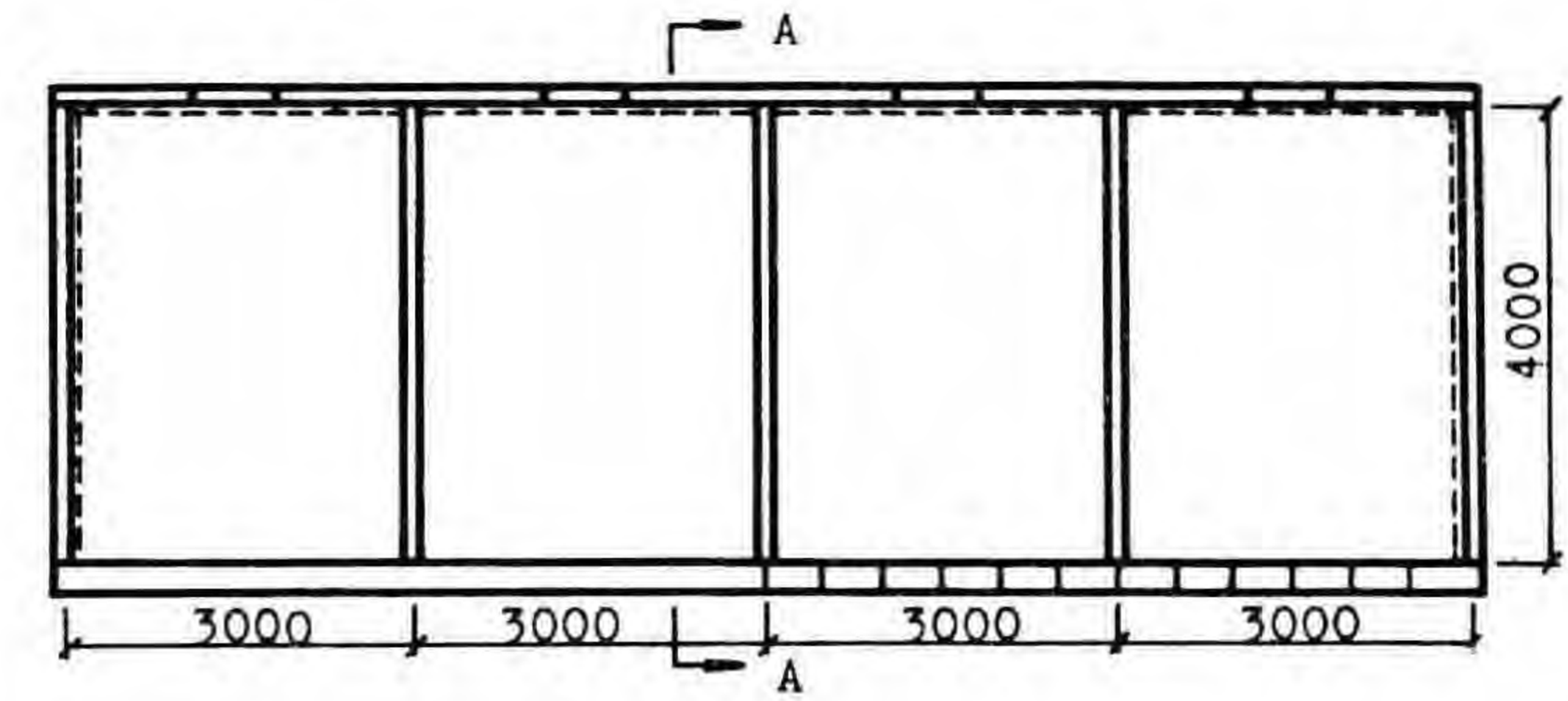

Fig. 1. Plan and section of experimental building at Storängsbotten, Stockholm.

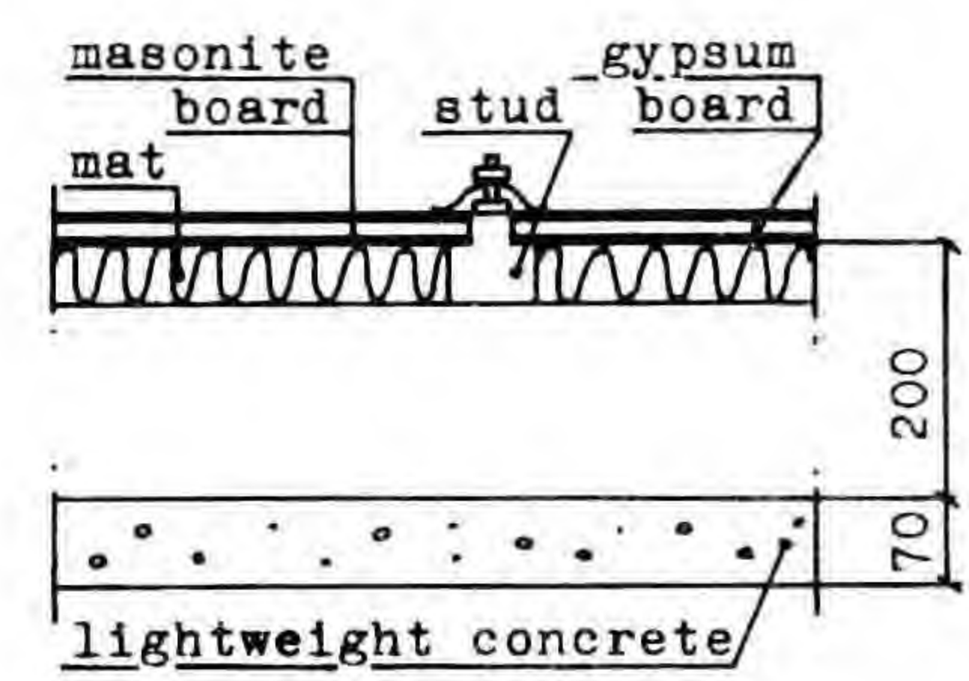

Fig. 2. Construction of screening wall in front of lightweight concrete.

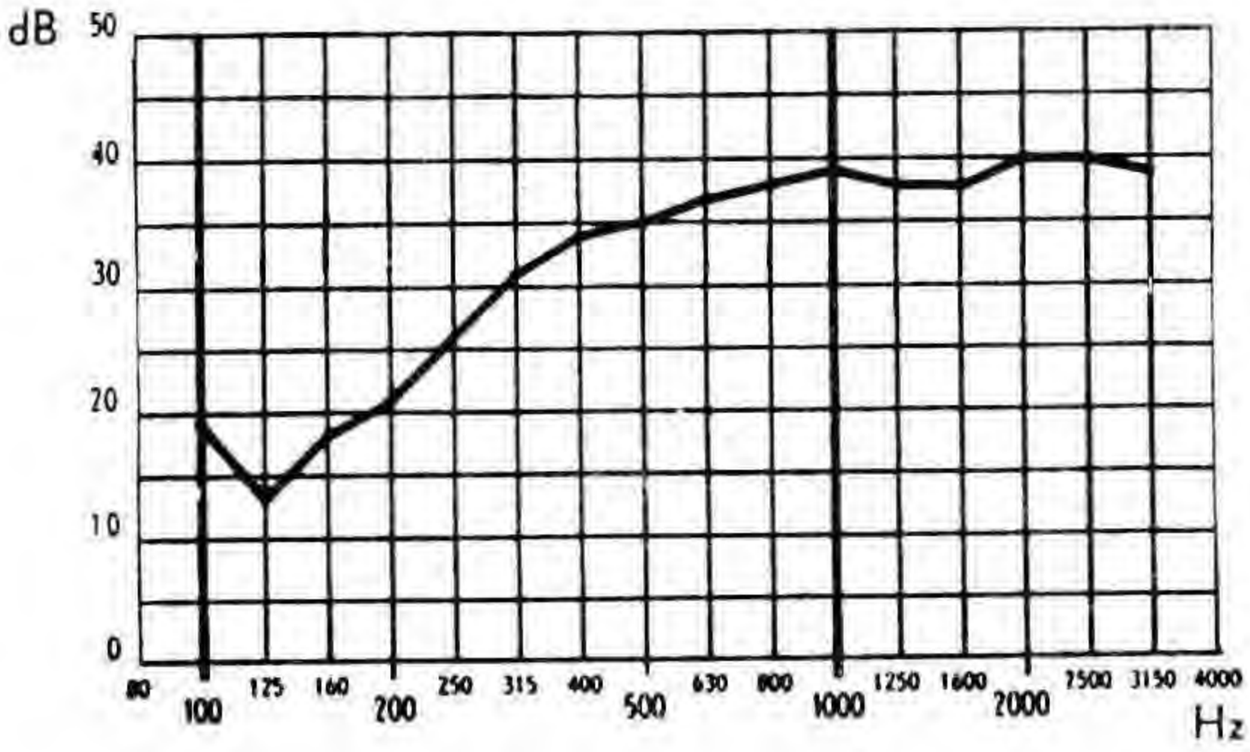

Fig. 3. Improvement of sound reduction index, Δ R, when using screening walls.

M57

FOURTH INTERNATIONAL CONGRESS ON ACOUSTICS
COPENHAGEN 21.-28. AUGUST 1962

Geschlossenzelliger Weich-PVC-Schaumstoff als Luftschallabsorptionsmittel

Hermann Oberst
Farbwerke Hoechst AG., vormals Meister Lucius & Brüning
Frankfurt (Main)-Höchst

Einleitung

Neben den geschäumten hochpolymeren Stoffen, wie Latex- oder Polyurethan-Schaumstoff, die bereits als Luftschallabsorptionsmittel angewandt werden[1-3], ist auch geschäumtes Weich-Polyvinylchlorid (-PVC) ein für diesen Anwendungszweck geeignetes Material. Dieser Schluckstoff ist dadurch ausgezeichnet, daß seine Zellen geschlossen sind. Er ist abwaschbar und weist die bekannte Chemikalienbeständigkeit von Weich-PVC auf. Der Vorteil dieser Eigenschaften bei Anwendungen in chemischen Betrieben, in feuchten oder staubigen Räumen usw. liegt auf der Hand. Durch Auswahl geeigneter Weichmacher kann der Schaumstoff schwer entflammbar gemacht werden.
Unter diesen Umständen ist die Frage, ob aus geschäumtem Weich-PVC hochwertige Luftschallabsorptionsmittel hergestellt werden können, von größerem Interesse[4]. Bei früheren Untersuchungen[5] wurden bereits die Bedingungen diskutiert, die der Schaumstoff erfüllen muß, wenn eine befriedigende Luftschallabsorption erreicht werden soll. In der vorliegenden Arbeit wird über den gegenwärtigen Stand der Entwicklung berichtet.

Dynamisch-elastische und akustische Eigenschaften des Weich-PVC-Schaumstoffs

Beim gegebenen Anwendungszweck kann der Schaumstoff mit geschlossenen Zellen als homogener, isotroper Stoff angesehen werden, dessen akustische Eigenschaften durch seine dynamisch-elastischen Kenngrößen und seine Rohdichte ϱ ausreichend charakterisiert sind. Der dynamische Elastizitätsmodul E' ist im wesentlichen durch das Kunststoffgerüst bestimmt und hängt nur wenig von dem in diesem eingeschlossenen Gaspolster ab[6]. Bei der Schallschluckmatte aus dem Schaumstoff, die unmittelbar auf die harte Wand geklebt sein soll - nur dieser Fall wird im folgenden behandelt -, ist für die Wandimpedanz die Gesamtsteifheit der Matte maßgebend, die sich aus der Steifheit des Gerüstes und der des Gaspolsters zusammensetzt. Wenn der Wert des Moduls E' unter den Wert des Kompressionsmoduls K_G des in den Zellen eingeschlossenen Gases absinkt, der von der Größenordnung 1^G. $1o^6$ dyn/cm^2 ist, wird das Gaspolster mehr und mehr allein bestimmend für die Steifheit der Schaumstoffmatte bei der Schalldruckbeanspruchung. In diesem Falle ist der Longitudinalwellenmodul L' die dynamisch-elastische Kenngröße, durch die die Schallgeschwindigkeit c in der Matte bestimmt ist: $c \approx \sqrt{L'/\varrho}$.
Vereinfachend soll im folgenden angenommen werden, daß sich L' aus E' und K_G additiv zusammensetzt; die Versuchsergebnisse in der Entwicklung des Weich-PVC-Schaumstoffs haben die Brauchbarkeit dieser Annahme für die Abschätzung von c bestätigt. Die Energieverluste in der Schluckmatte sind überwiegend durch diejenigen im Kunststoff bestimmt, die durch den zum Modul E' gehörigen Verlustfaktor d charakterisiert sind.
Um eine hohe Schallabsorption in der Schaumstoffmatte zu erreichen, muß man die Schallkennimpedanz ϱc, die vereinfachend als rein reell angenommen sei, nach Möglichkeit an diejenige der Luft anpassen, d. h. praktisch, man muß ϱc so klein wie möglich machen. Die vorliegende Schallschluckanordnung gehört zur Gruppe der Resonanzabsorber. Maximale Schallabsorption tritt ein, wenn die Mattendicke $l = (2n - 1)\lambda/4$ ist, $\lambda = c/f$ die Wellenlänge im Schaumstoff, n eine ganze Zahl, f die Frequenz. Um bei gegebener Mattendicke l hohe Absorption bei möglichst tiefen Frequenzen zu erzielen, muß c und damit λ möglichst klein gemacht werden. Es folgt also, daß ϱ und c einzeln so klein wie möglich gemacht werden müssen.

Das Weich-PVC wird in der geschlossenen Form geschäumt. Man kommt dabei bisher günstigstenfalls auf Rohdichten von etwa o,o5 g/cm^3. Im vorliegenden Falle wurden Rohdichten$\varrho \approx$o,o6 g/cm^3 erzielt. Um eine kleine Schallgeschwindigkeit c zu erhalten, muß man E' möglichst klein machen. Tatsächlich ist es möglich, Werte $E' < K_G$ zu erreichen. Das PVC muß dazu so stark weichgemacht werden, daß der Kunststoff im interessierenden Frequenzbereich bei Raumtemperatur im quasigummielastischen Zustand ist; E' hat dann kleine Werte und ist von der Frequenz nur verhältnismäßig wenig abhängig. Daß dieses Ziel erreicht werden kann, veranschaulicht Abb. 1, in der gemessene Temperaturkurven von E' und d für die Frequenzen 1oo und 1ooo Hz wiedergegeben sind. In diesem Falle ist der Kunststoff unterhalb etwa -5o° C im glasartig harten Zustand. Oberhalb seiner Einfriertemperatur erweicht er mit zunehmender Temperatur allmählich, E' sinkt ab, und d durchläuft ein hohes Maximum mit Werten d ≈1. Werte E' ≈1 . 1o^6 dyn/cm^2 werden bei 2o° C erreicht und bei höheren Temperaturen noch unterschritten.
Um bei der tiefsten Resonanzfrequenz (n = 1) ein hohes Absorptionsmaximum zu erzielen, muß d optimal eingestellt werden. Es sei hier schon vorweggenommen, daß im Falle der Abb. 1 die d-Werte bei 2o° C noch etwas zu hoch sind. Durch noch stärkere Weichmachung könnte man sie auf das gewünschte Maß senken; die E'- und d-Kurven verschieben sich mit zunehmender Weichmachung des PVC in Richtung tieferer Temperaturen.

Meßtechnik und Meßergebnisse

Zur Messung von E' und d wurde die Biegeschwingungsmethode benutzt[7,8] (Apparatur Brüel & Kjaer, elektromechanisches Gerät Typ 393o, elektronische Apparatur Typ 3324). Die Meßproben sind aus der Matte* geschnittene Streifen (Dicke o,8 cm, Breite 1,4 cm, Länge 2o cm), zum Teil auf Hart-PVC-Streifen gleicher Breite von 1 oder 2 mm Dicke geklebt. Die Temperaturkurven von E' und d in Abb. 1 sind Schnitte durch gemessene Frequenzkurvenscharen.
Bei Temperaturen oberhalb 0° C konnten die Kennwerte nicht mehr genügend sicher mit der Biegeschwingungsmethode ermittelt werden. Die in Abb. 1 eingetragenen Meßwerte von E' und d für 2o° C wurden mit dem Schaumstoff-Vibrometer gewonnen[9]. Als Probekörper wurden dabei aus den Matten geschnittene zylindrische Proben von 3 cm Durchmesser und 2 oder 3 cm Höhe verwendet. Die in Abb. 1 eingetragenen Meßwerte E' und d für 1oo Hz sind aus den Frequenzkurven im Meßbereich zwischen 1o und 1oo Hz extrapoliert.
Der Schallabsorptionsgrad α_o der Schallschluckmatten mit hartem Abschluß bei senkrechtem Schalleinfall kann im Impedanzrohr gemessen werden[3,5]. Zahlreiche Messungen dieser Art** haben ergeben, daß man im Rahmen der Meßgenauigkeit befriedigende Übereinstimmung zwischen den gemessenen Werten α_o und den an Hand der dynamisch-elastischen Kenngrößen des Schaumstoffs berechneten Werten α_o erhält. Deshalb wurde hier auf Impedanzrohrmessungen verzichtet.
In bekannter Weise wird α_o aus der spezifischen Schallimpedanz $\underline{W}$ an der Oberfläche der Schaumstoffmatte berechnet[3,6]. $\underline{W}$ kann an Hand der Größen ϱ, c, d und 1 berechnet werden. Das Ergebnis der Rechnung ist aus Abb. 2 zu ersehen. Die Größen c und d sind streng genommen frequenzabhängig; hier wurden vereinfachend konstante mittlere Werte aus dem hauptsächlich interessierenden Bereich um 1ooo Hz der Rechnung zugrunde gelegt. Der Wert c wurde in der oben angegebenen Weise abgeschätzt. Bei der Schätzung des nicht gemessenen Wertes E' für 2o° C und 1ooo Hz aus dem Wert E' für 1oo Hz (Abb. 1) wurde ein schwacher Anstieg von E' mit der Frequenz berücksichtigt. Danach wird c etwa im Bereich 6,3 bis 6,8 . 1o^3 cm/s erwartet. Auch der Verlustfaktor d, der hier auf den Modul L' zu beziehen ist, kann nur grob nach Abb. 1 geschätzt werden; d wird etwa im Bereich o,4 bis o,8 erwartet.
Die Kurven I und II in Abb. 2 a geben die mit den in der Abbildung vermerkten Grenzwerten von c und d berechneten Frequenzkurven von α_o für die Mattendicken 1 = 2 und 3 cm wieder. Hohe Absorptionsmaxima werden in der $\lambda/4$-Resonanz (n = 1)

* Die Weich-PVC-Schaumstoffmatten von ca. 1 x 1 m^2 Fläche wurden hergestellt von der Firma Indewerk, Eschweiler (Rhld.).
**Messungen im Laboratorium für Raumakustik der Physikalisch-Technischen Bundesanstalt (PTB), Leiter Regierungsrat Dr. G. Venzke.

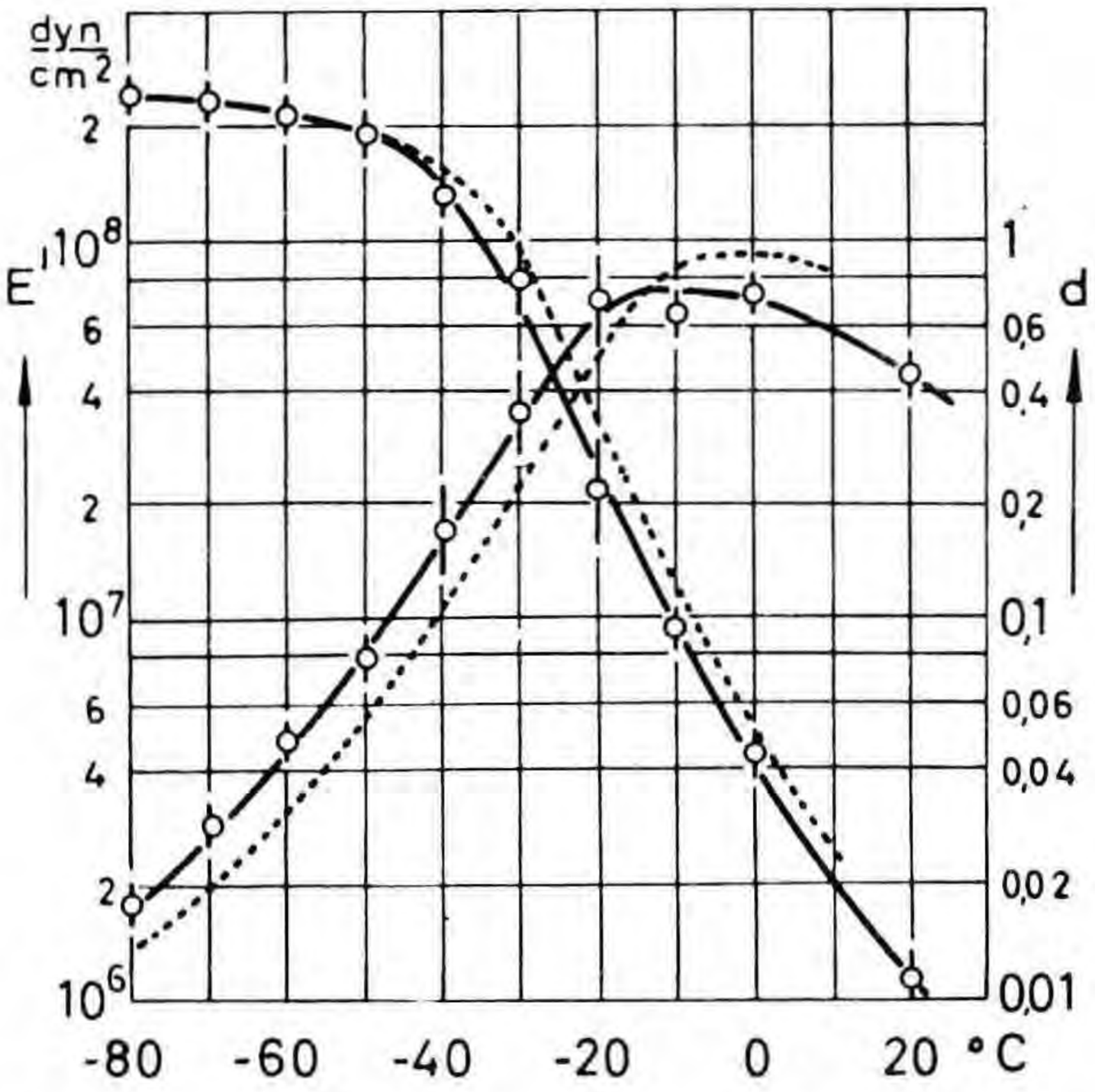

Abb. 1

Dynamischer Elastizitätsmodul E' und Verlustfaktor d von Weich-PVC-Schaumstoff der Rohdichte $\varrho = 0{,}063\ g/cm^3$ in Abhängigkeit von der Temperatur

——— 1oo Hz

---------1ooo Hz

ϕ Mittelwerte der Meßpunkte mit Streubereich

bei den Resonanzfrequenzen $f_r = c/4\,l$ erreicht. Durch Verteilung der Mattendicken l zu gleichen Anteilen über die schallabsorbierende Wandbekleidung, was in verschiedenen Weisen realisierbar ist, erreicht man eine Verbreiterung des Hauptabsorptionsbereichs. Durch Mittelung aus den Kurven I und II ergibt sich für eine solche Schluckanordnung die α_o-Kurve III. Aus der Wandimpedanz $\underline{W}$ kann man außerdem in bekannter Weise den Schallabsorptionsgrad α_s für den Fall des diffusen Schallfeldes (Schalleinfall statistisch über alle Richtungen verteilt) berechnen[10]. Kurve IV in Abb. 2 a ist die zur Kurve III gehörige α_s-Kurve. In Abb. 2 b ist als Kurve II die α_s-Kurve IV nach Abb. 2 a wiedergegeben, dazu als Kurve III die in gleicher Weise für die oberen Grenzwerte von c und d berechnete α_s-Kurve. Beide Kurven grenzen etwa den Bereich ein, in dem α_s bei der Messung des Schallabsorptionsgrades im Hallraum erwartet wird. Bei dieser Prüfung wurde eine Schachbrettanordnung mit Abmessungen der Felder von etwa 52 x 52 cm^2 benutzt***. Als Prüfschall diente Rauschen von Terzbandbreite. Bei drei Meßreihen ergaben sich mit Hilfe der Sabineschen Formel die in Abb. 2 b eingetragenen Meßpunkte; sie bestimmen die α_s-Kurve I in Abb. 2 b.

Diskussion

Die im Hallraum gemessene Frequenzkurve des Schallabsorptionsgrades α_s paßt sich befriedigend dem durch Kurven II und III in Abb. 2 b abgegrenzten Erwartungsbereich an, wenn man die vereinfachenden Annahmen bei der Abschätzung dieser Kurven berücksichtigt. Man ersieht aus dieser Abbildung, daß der mittlere Verlustfaktor bei 2o° C noch verhältnismäßig hohe Werte ($d \approx o{,}8$) aufweisen muß. Durch stärkere Weichmachung und damit Verschiebung der E'- und d-Kurven in Abb.1 in Richtung tieferer Temperaturen ließe sich eine Senkung des Verlustfaktors und damit eine Erhöhung von α_s im Sinne der Kurve II in Abb. 2 b erreichen. Dem Weichmachergehalt ist eine obere Grenze gesetzt. Bei den hier untersuchten Schaumstoffmatten wurde mit Rücksicht auf die Schwerentflammbarkeit ein Weichmachergemisch verwendet. Mit der stärker weichmachenden Komponente allein wurden bei einheitlicher Mattendicke im Maximum Werte $\alpha_o \approx 1$ erreicht (vgl. Kurven I und II in Abb. 2 a). Man würde also in diesem Falle wesentlich höhere Absorptionsgrade α_s erreichen; die Brennbarkeit der Schluckstoffmatten mußte dabei

*** Messung im Hallraum der PTB nach der deutschen Norm DIN 52212.

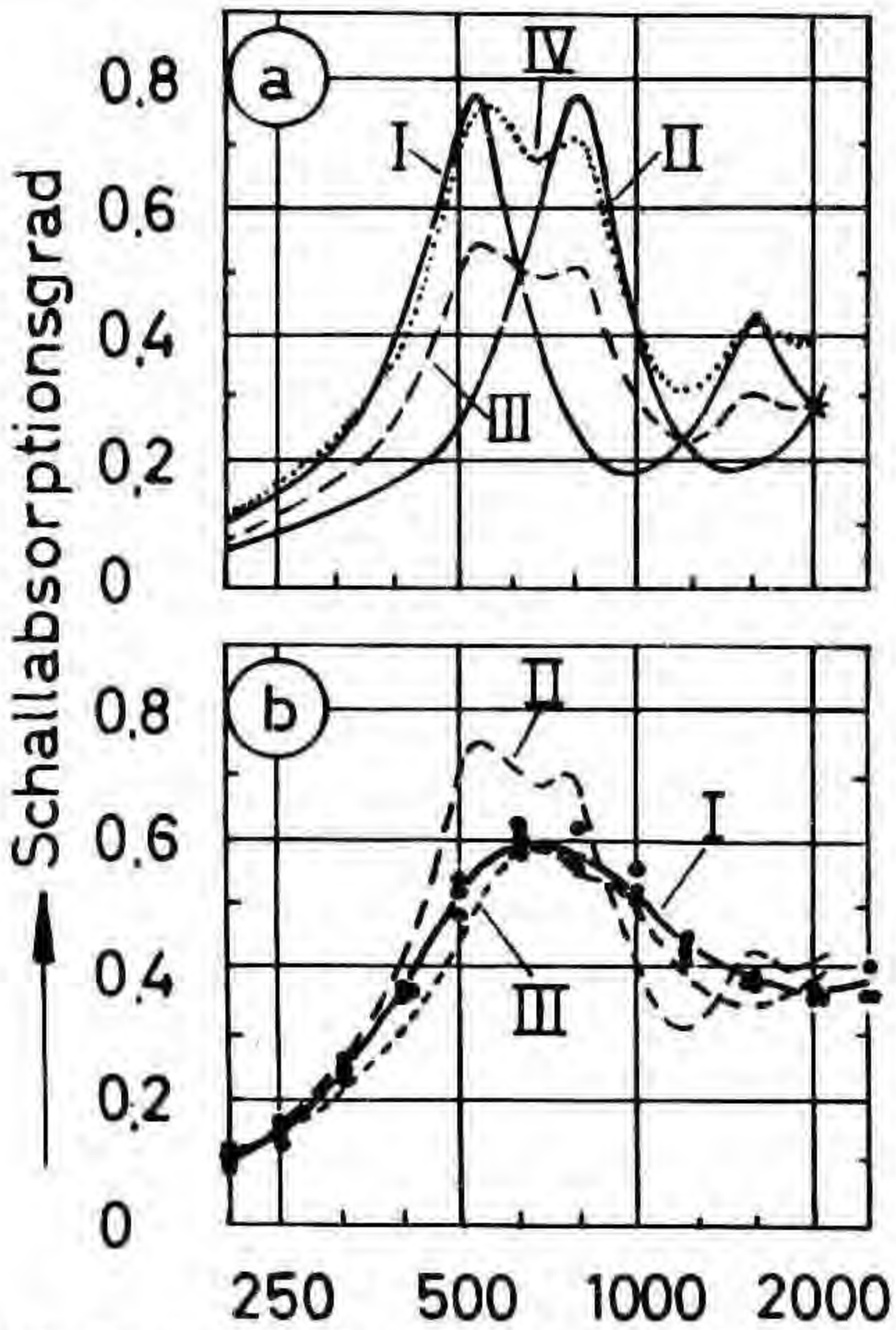

Abb. 2 Schallabsorptionsgrad (Sch.-A.) von Weich-PVC-Schaumstoffmatten

a: Sch.-A. berechnet mit den Kennwerten $\varrho = 0{,}063\ g/cm^3$, $c = 6{,}3 \cdot 10^3\ cm/s$, $d = 0{,}4$ und der Mattendicke l
Sch.-A. α_o bei senkrechtem Schalleinfall
Kurve I : l = 3 cm
Kurve II : l = 2 cm
Kurve III: l = 2 und 3 cm, zu gleichen Anteilen im Schachbrettmuster wechselnd.
Sch.-A. α_s bei statistischem Schalleinfall
Kurve IV (Mattenanordnung wie unter III)

b: Sch.-A. α_s im diffusen Schallfeld
Kurve I: gemessen im Hallraum, Matten im Schachbrettmuster, l = 2 und 3 cm
Zum Vergleich α_s näherungsweise berechnet in
Kurve II mit $\varrho = 0{,}063\ g/cm^3$, $c = 6{,}3 \cdot 10^3\ cm/s$, $d = 0{,}4$ (gleich Kurve IV unter a),
Kurve III mit $\varrho = 0{,}063\ g/cm^3$, $c = 6{,}8 \cdot 10^3\ cm/s$, $d = 0{,}8$.

jedoch in Kauf genommen werden. Die vorliegende Weich-PVC-Rezeptur stellt also eine Kompromißlösung dar; zugunsten der Schwerentflammbarkeit wurde eine gewisse Minderung der erreichbaren Schallschluckgüte hingenommen.
Bei weiterer Senkung von ϱc könnte der Grenzwert, dem sich die α_s-Kurven bei hohen Frequenzen nähern, angehoben werden. Es bleibt schließlich zu bemerken, daß Alterungserscheinungen bei den Weich-PVC-Absorbern nach den bisherigen Erfahrungen keine wesentliche Rolle spielen.
Der Verfasser ist den Herren Dr.H.Becker und Ing. W.Sommer für die Beratung in den chemischen Fragen dieser Arbeit zu Dank verpflichtet. Herrn Dr.G.Venzke (PTB) schuldet er Dank für seine Mitarbeit in den experimentellen Untersuchungen und für eingehende Diskussionen der akustischen Probleme.

Literatur

1. C. Zwikker und C. W. Kosten, Sound Absorbing Materials, New-York - Amsterdam - London - Brüssel (1949); siehe auch E. G. Richardson, Technical Aspects of Sound, Bd. I, New York-Amsterdam-London-Brüssel (1953), Kap. 4, C. W. Kosten.
2. H. W. Paffrath, Kunststoffe, 47 (1957) 638.
3. G. Venzke, Acustica, 8 (1958) 295.
4. G. Kurtze, Kunststoffe, 51 (1961) 595.
5. H. Oberst, Kunststoffe, 46 (1956) 190.
6. Nitsche/Wolf,Kunststoffe, Bd. 1, Struktur und physikalisches Verhalten der Kunststoffe, hrsg. von K. A. Wolf, Berlin-Göttingen-Heidelberg (1962), Kap. 4.4, H. Oberst.
7. Nitsche/Wolf, Kunststoffe, Bd. 2, Praktische Kunststoffprüfung, hrsg. von R. Nitsche, zu Ende geführt von P. Nowak, Berlin-Göttingen-Heidelberg (1961), Kap. 3.4.2, H.Oberst.
8. H. Oberst, L. Bohn und F.Linhardt, Kunststoffe 51 (1961) 495.
9. G. W. Becker, Acustica, 9 (1959) 135.
10. P. M. Morse und R. H. Bolt, Rev.Mod.Phys., 16 (1944) 69; siehe auch L. L. Beranek, Acoustic Measurements, New York-London (1949), Kap. 19.

N57

FOURTH INTERNATIONAL CONGRESS ON ACOUSTICS
COPENHAGEN 21.-28. AUGUST 1962

METHODS OF CHECKING THE RMS PROPERTIES OF RMS INSTRUMENTS

Carl Gustav Wahrman, M.Sc.,
A/S Brüel & Kjær

For a long time the Root Mean Square has been accepted as the most practical measure determining the magnitude of an alternating variable. This is also the case within the field of acoustic although it is not evident whether the primary standard for noise measurement: the human ear, makes any root mean squaring at all.

Unfortunately, it has also for a long time been common practice to calibrate electrical instruments so as to show the RMS value of a sinusoidal input even though the instrument actually measures either the arithmetic average value or the peak value. This has been because it is simpler to make average or (approximate) peak measuring instruments, than a true RMS instrument. (Another point is that it is also difficult to make a good peak measuring instrument).

The user of such an instrument may risk great errors when measuring acoustical signals as they are very often far from sinusoidal.

However, it is now possible to make instruments measuring an approximate RMS value. It is therefore of interest to have a good method of checking whether an instrument claimed to show the RMS value really is an RMS instrument, and how good a possible approximation is.

To this end some national and international standards for sound level meters have included a check where the reading for the combination of two non harmonically related sinusoidal voltages of the same amplitude is compared to the reading for each of the sinusoidal components. The RMS value of the combination is exactly $\sqrt{2}$ times the RMS value of the single sinusoidals. If the combination is attenuated 3 db, the three readings should be the same within suitable tolerance.

This is a necessary but unfortunately not a sufficient condition for an RMS instrument. This condition excludes the simple average or peak measuring instruments, but the circuits shown in the following can be made to satisfy the above check as accurately as desired, and some of these are very bad approximations to an RMS instrument.

The signals measured with a sound level meter are often non-sinusoidal and very seldom similar to the above two tone signals. Very often the signals have a more or less Gaussian probability distribution. Therefore it would be natural to use a Gaussian random noise signal as another signal for checking RMS instruments at least in sound level meters. The Gaussian noise check has the drawback of not being absolute as the RMS value of the signal has to be measured by another RMS instrument. A Gaussian noise check has been included in some standards for sound level meters.

Let us consider first the simple average and peak measuring circuits and their current voltage characteristics shown in Fig. 1 A and B. Their characteristics are very bad approximation to a parabola which is the curve wanted for an RMS instrument. The RMS value of a signal is always between the average and the peak values, and therefore a compromise between the average and the peak measuring circuits as shown in Fig. 1 C seems to be an obvious solution to a better approximation. The horizontal arrows on the characteristic Fig. 1 C indicate that the characteristic moves with the reading on the instrument. This property takes care of the "root extraction" in this RMS circuit.

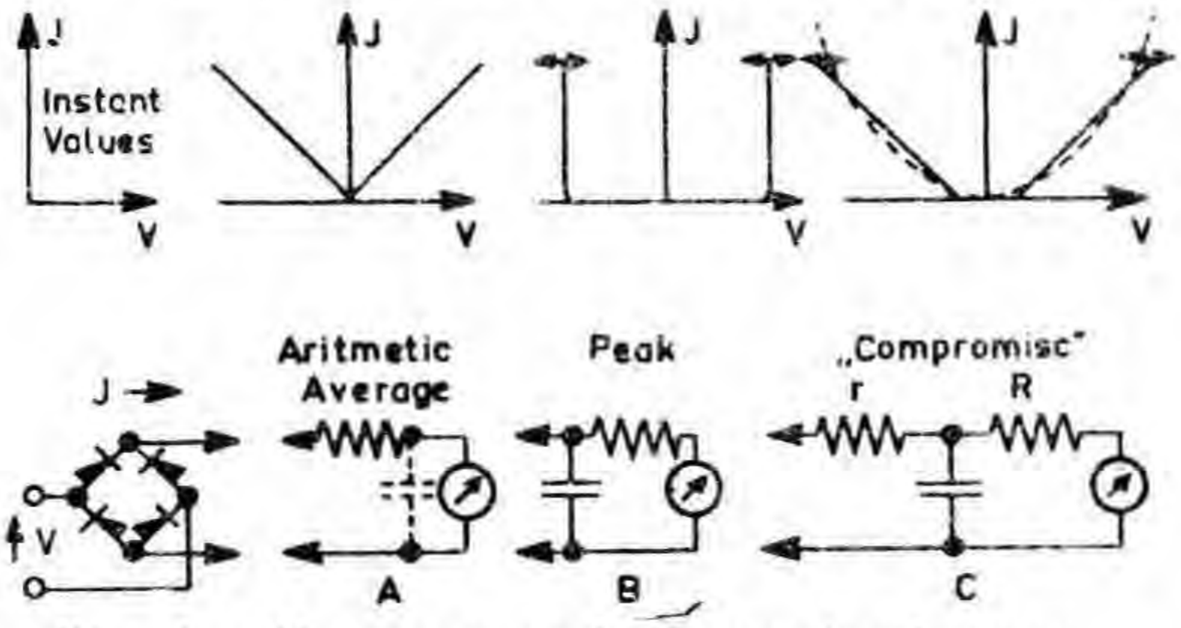

Fig.1. Diagrams and characteristics of some simple meter circuits.

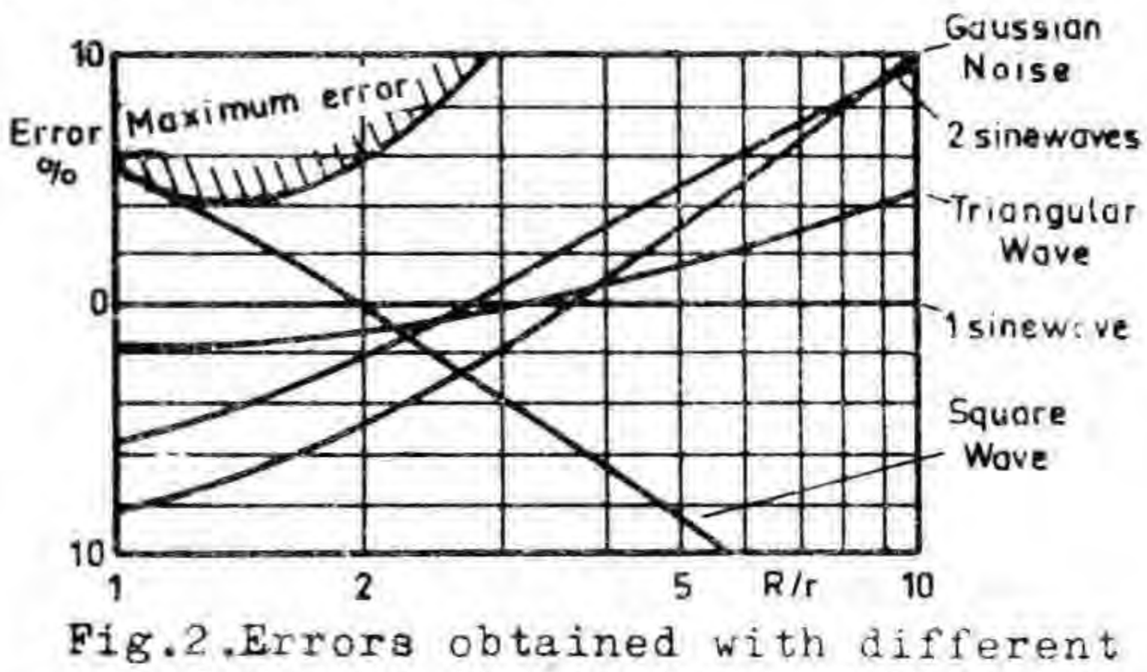

Fig.2.Errors obtained with different waveforms on the "compromise"circuit fig. 1 C.

In Fig. 2 is shown the error obtained with this circuit for different input signals as a function of the ratio between the two resistors R and r. These curves are also valid for similar circuits using either single rectification or voltage doubling, if the R/r scale is simply multiplied by 2 or 4 respectively. It is seen that an R/r of about 2.7 gives zero error with the two tone test, whereas the error with a Gaussian signal is about -3%. A value of R/r = 3.6 gives zero error for Gaussian signals and about +2% for the two tone signal. An error of 3% is negligible compared to all the other errors normally appearing in sound level measurements, and therefore this circuit seems usable for such measurements.

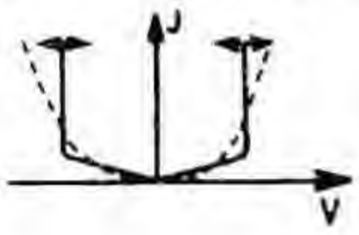

signal	Ave.	Peak	RMS
1 tone	o.90	1.41	1
2 tones	o.81	2	1

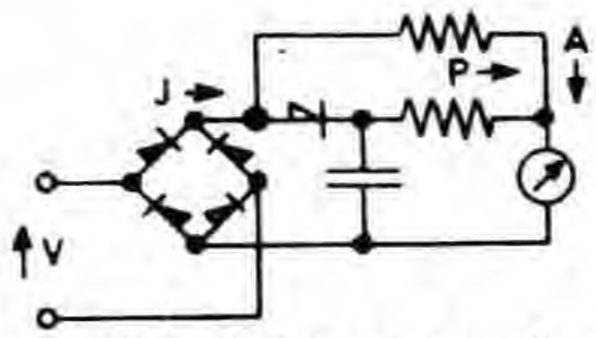

1 tone o.90A+1.41P=1
2 tones o.81A+2P =1
A = o.90 P = o.137
A/P = 6.57

Fig.3.Diagram,characteristic and calculation for a combined average-peak circuit satisfying the two tone test.

Instead of making a compromise between the average and the peak measuring circuit, a combination of the two can be made as shown in Fig.3 A. The current in the meter consists of A parts proportional to the average value and P parts proportional to the peak value of the input signal. Two equations can now be set up and a ratio A/P can be found so that this circuit satisfies the two tone test. This is shown in Fig. 3 B.

How does this circuit behave when measuring Gaussian noise . Theoretically, the peak value of Gaussian noise is infinite, and the meter should thus show infinity. However, in practice it is hard to make a simple peak measuring circuit, which shows more than 3 to 4 times the RMS value of the Gaussian noise. This causes the combined circuit to measure 1 to 2 db too much. This circuit may thus be worse than the simple average measuring circuit which shows only -1 db error on Gaussian noise.

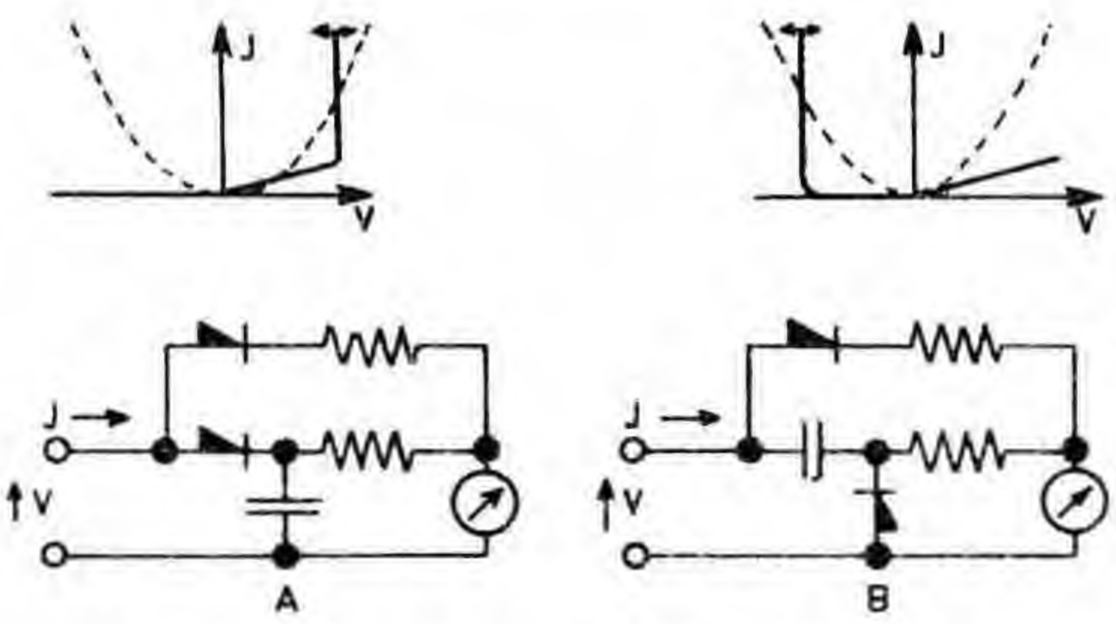

Fig.4. Two simple combined average - peak circuits and their characteristics.

The combined circuit in Fig. 3 can be simplified as shown in Fig. 4. The characteristics of these circuits are very unsymmetrical, but the above-mentioned standards do not require a symmetrical characteristic, and neither the two tone test nor a Gaussian noise test checks this property. If less "effort" is put into the peak measuring part of the "combined" circuits, that is if a resistance is put in before the condenser just as in the "compromise" circuit Fig. 1C, these circuits may even be made so that they satisfy both the two tone test and a Gaussian noise test.

It is obvious that such "unsymmetrical" circuits are not recommendable as approximate RMS circuits. Although most acoustical signals have more or less symmetrical distributions, the signal may sometimes happen to be rather unsymmetrical, and the reading on this meter will then depend on the polarity of the signal and possible 180° phase inversion in the amplifier.

Thus the two tone and the Gaussian noise tests are not very satisfying for testing approximate RMS instruments, at least not when the construction is unknown. An unknown characteristic cannot be determined by only two or three measurements. The most obvious way of checking such a characteristic is to check a great number of points on the curve. Sometimes this can be done by DC measurements, if access can be made to the interior of the instrument.

However, in most cases a complete instrument containing AC amplifiers has to be checked, and therefore an AC test has to be used. A square wave of varying amplitude might seem usable at first sight, but it only checks that an error in the squaring is compensated by an error in the root extraction. Instead a waveform consisting of rectangular pulses can be used as the peak value here can be varied in proportion to the RMS value by varying the pulse width in proportion to the time between the pulses.

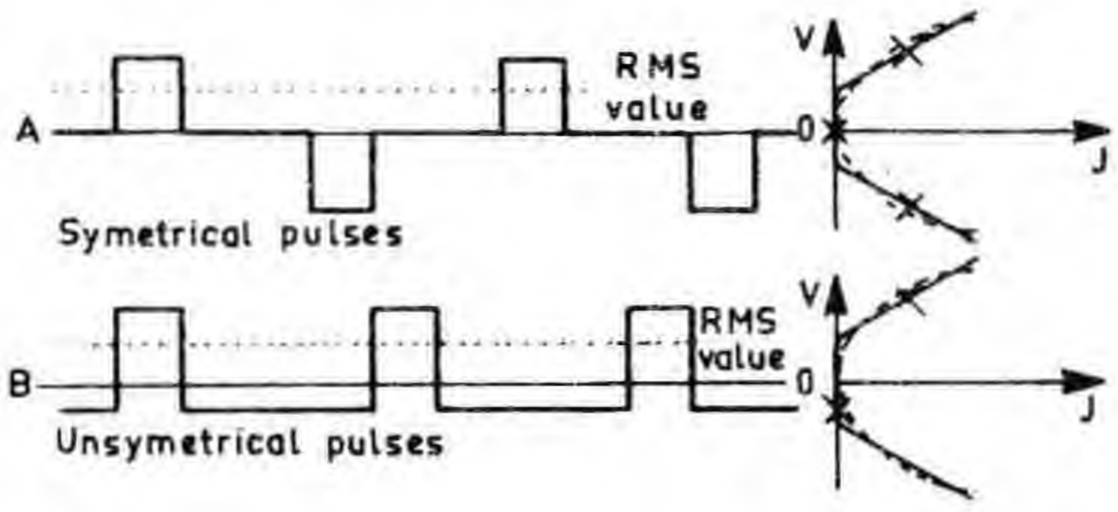

Fig.5.Rectangular pulse signals for checking the characteristic of RMS instruments.

Symmetrical pulses as shown in Fig. 5 A check two or rather three points on the characteristic as the zero point is checked also. By varying the crest factor (that is the ratio peak value to RMS value), the two outer points can be moved outwards from the RMS value up to as high a crest factor as desired. Like the two tone test and the Gaussian noise test, symmetrical pulses alone do not check whether the characteristic is symmetrical. Errors on the positive side may be compensated by errors on the negative side. Besides the part within the RMS value are not checked.

To this purpose the unsymmetrical pulses as shown in Fig. 5 B can be used. Here a point outside the RMS value on one side is checked together with a point inside the RMS value on the other side. By changing the polarity of the pulses and by varying the crest factor all parts of the characteristic are checked.

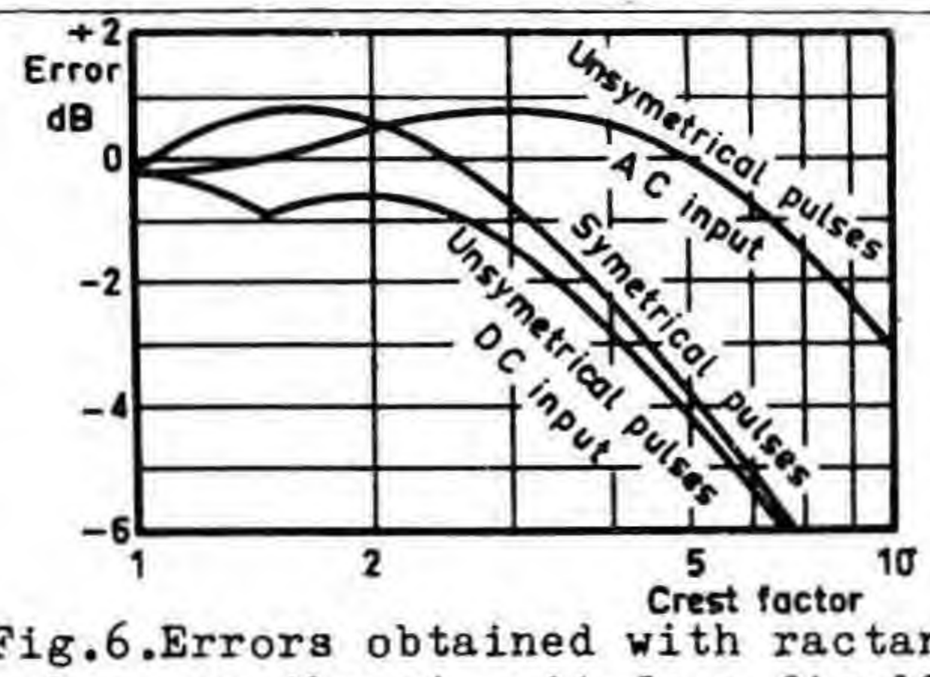

Fig.6.Errors obtained with ractangular pulses on the circuit from fig.1C (R/r = 2.7)

However, unsymmetrical pulses alone are not sufficient, because errors on the two points being checked together may counteract each other. An example of this is shown in Fig.6 which shows the error obtained with the "compromise" circuit from Fig. 1 C. With a condenser in series with the input of the circuit a much smaller error is obtained for unsymmetrical pulses of high crest factors than for symmetrical pulses.

In most cases a combined test using symmetrical and unsymmetrical pulses of both signs will be sufficient. The unsymmetrical pulses check whether the characteristic is symmetrical. They also check the inner part of the characteristic together with the outer part, whereas the symmetrical pulses check the outer part of the characteristic alone.

These tests always check two or three points on the characteristic at a time. Although it is not very probable, it might therefore happen that errors on the positive and the negative side were compensating each other, so that the test would erroneously show a correct RMS instrument. To avoid this, the waveforms shown in Fig. 7 can be used.

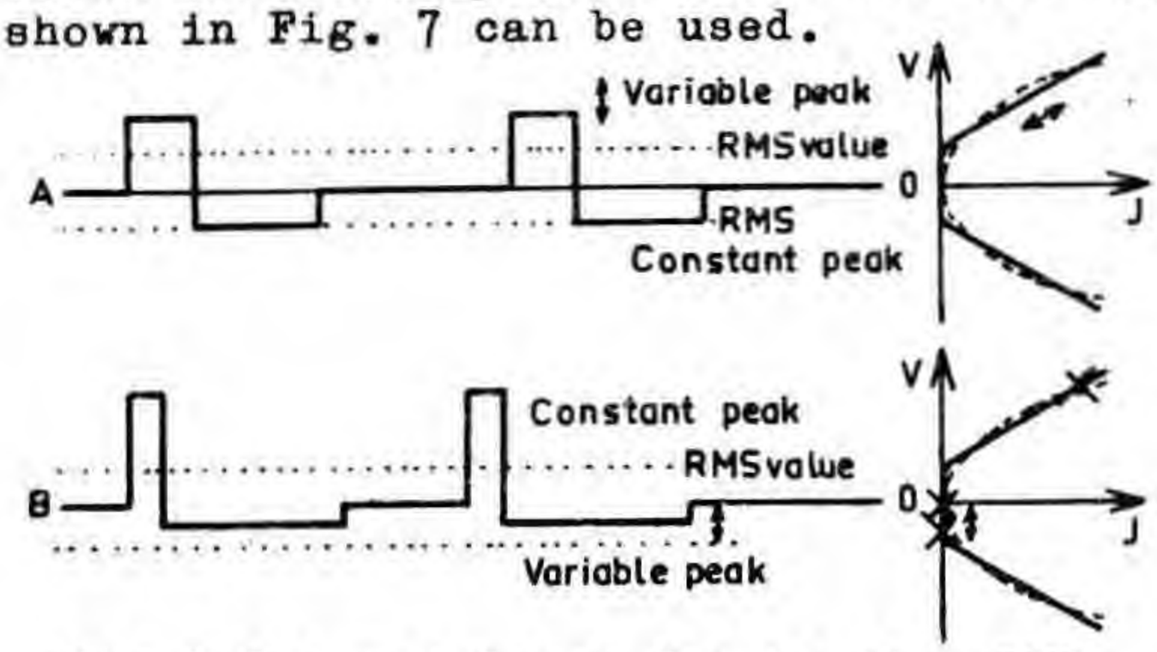

Fig.7.Two waveforms for testing RMS characteristics where only one check point is varied at a time.

The first waveform has a variable maximum peak (here positive) whereas the other two check points, the zero and the RMS points are fixed. In this way the two parts of the characteristic from the RMS value outward, can be checked. After this the inner part of the characteristic can be checked by the second waveform. This time the maximum peak value is constant at a suitable large value within the range, which was found correct by the first curve, whilst the minor peak value is varied.

In those cases where the characteristic varies with the waveform as in Fig. 3 and 4, these pulse tests do not give the true characteristics. The true characteristic can only be measured by breaking into the circuit. However, it is a problem whether the true characteristic is of greater interest than the apparent characteristic as measured by the pulses.

It should be noted that the pulse tests do not necessarily give the maximum possible error with a given crest factor. A more complicated waveform, which seeks out the points on the characteristic having the greatest deviation from the ideal curve may show greater error.

Finally a practical hint when making the pulse tests: The RMS value or rather the meter reading should be held constant whilst the crest factor is varied. If for example the peak value is held constant instead, the meter reading will vary, and possible scale errors may falsify the test. The nonlinearity of the diodes may also cause the circuit to look better than it is.

H58

FOURTH INTERNATIONAL CONGRESS ON ACOUSTICS
COPENHAGEN 21.-28. AUGUST 1962

A MODEL OF HUMAN PITCH - EXTRACTION BASED ON ADDITIVE CORRELATION

R.J.RITSMA, INSTITUUT VOOR PERCEPTIE ONDERZOEK
EINDHOVEN - NETHERLANDS

This paper is not supposed tc introduce a new theory of hearing but rather a further development of a trend of thinking which has found some currency during the last twenty years in both perceptual and anatomical investigations 1) 2) 3) 4).

This line of thinking starts from the one to one relation that exists between the frequency of an acoustic signal and the area of maximal stimulation on the basilar membrane. This relation causes the human ear to perform a kind of Fourier analysis with a limited resolving power. A trained observer is capable of hearing the lower harmonics of a periodic pulse as separate entities. Apart from this analysing faculty the human ear can perceive a complex sound as a single percept, the residue. This phenomenon occurs whenever a number of successive higher harmonics of a periodic signal are perceived as a single whole.

This residue can have a decidedly low pitch provided the constituent frequencies fulfil certain conditions. If so the phenomenon observed will be called a tonal residue as distinguished from an atonal residue which does not have a well defined low pitch. A residue consisting of the frequencies 1800, 2000 and 2200 cps has a well defined low pitch of 200 cps which means that a pitch of 200 cps is generated at the location of the constituent frequencies of the complex on the basilar membrane.

Consequenly one may conclude that each area of the basilar membrane may give rise to sensations of widely different pitch, depending upon the pattern of stimulation.

The pitch extractor, operating upon the selected spectral region of such a particular area, must derive its information on pitch from certain physical parameters of the spectral region involved. In order to get this information the excitation curves of the various components have to overlap to a certain extent. Due to the limited resolving power of the basilar membrane such an overlap is likely to occur. This implies that the residue phenomenon can only occur if at a given centre frequency f the spacing frequency g does not exceed a certain maximum value.

The location of the pitch extractor must be postulated to be posterior to the basilar membrane where a frequency analysis takes place and must therefore be looked for in the neural system.

The pitch extractor might, in principle, operate in two entirely different ways. Either it operates in the frequency domain or in the time domain. When operating in the frequency domain a residue pitch equal to that of the fundamental tone could be derived by some process measuring the spacing of the spectral components.

When operating in the time domain, however, the pitch of the residue is determined by the spacing of certain marking points in the time function. Though the spacing remains 200 cps, an anharmonic residue consisting of the frequencies 1850, 2050 and 2250 cps has a pronounced pitch of about 205 cps. Therefore, the pitch extractor must be interpreted as a time measuring instrument. Moreover, the envelope of the time function cannot be a relevant parameter in determining pitch, since the frequency of the envelope remains 200 cps, irrespective of the frequency shift.

A clue to the input signal of the pitch extractor may be obtained from the experimental fact that no residue with a decidedly low pitch is observed when the constituent frequencies exceed about 5000 cps. From the literature on neurophysiology it is known that volleys occur for pure tones also at frequencies up to about 5000 cps 5) 6).

The maximum rate of firing of a nerve fiber amounts to 800-1000 spikes per second. Normally a fiber emits only 100-300 spikes per second. At higher frequencies the fiber will emit spikes only intermittently. From the literature it appears that this intermittent firing occurs at a specific phase of the signal 7).

In the case of a modulated signal the odds are greater for a spike being emitted near the maximum of the envelope than near a minimum. This applies to all fibers constituting a single integrating bundle. The integral output of such a bundle will therefore consist of a number of impulses occuring in groups.

Fig. 1 shows a schematic representation of this mode of operation. The resulting integral output of a bundle must contain all the data necessary for a pitch determination.

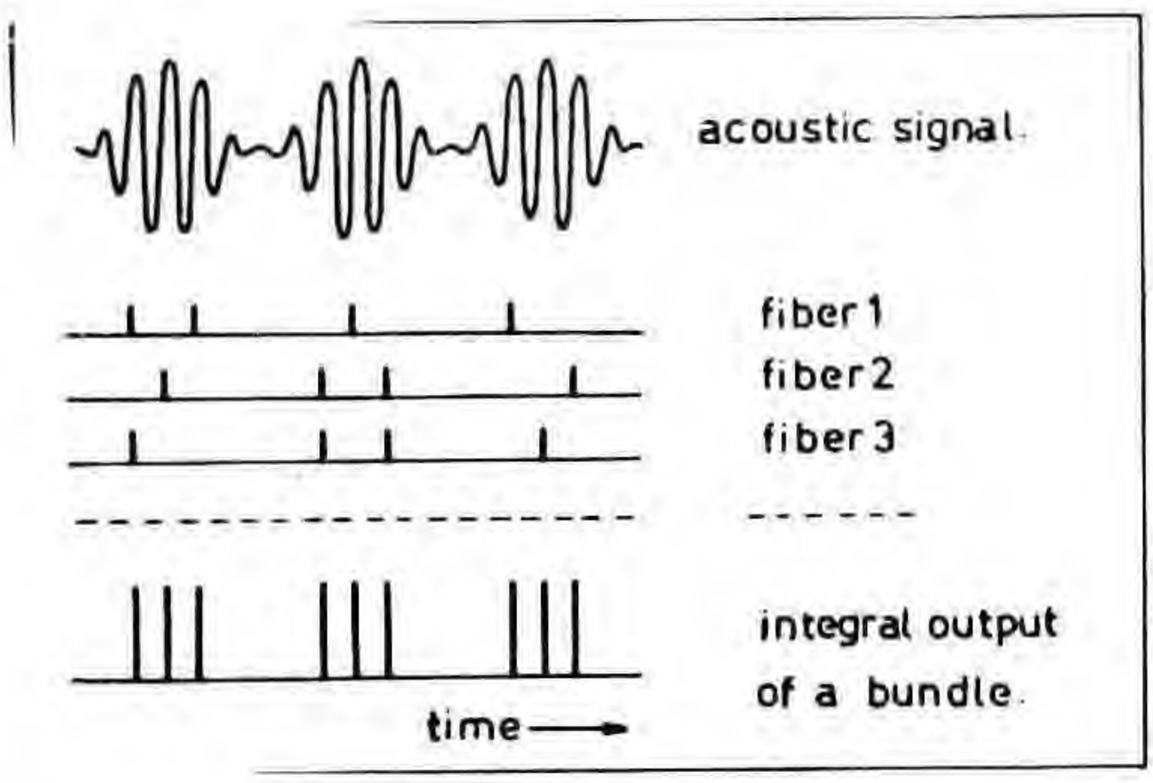

Fig.1 A schematic representation of the volley-principle with respect to a modulated signal.

As the pitch extractor is assumed to operate in the time domain, it seems legitimate to hypothesize that this is due to the presence of a number of delay lines. In the trapezoid body time delays up to 30 msec can be found 2). Consequently it might be not too far-fetched to assume that the pitch extractor is made up of a great number of coïncidence elements corresponding to specific delay-times. Once a signal as schematized in fig. 1 and derived from an acoustic signal with centre frequency f and spacing frequency g, has been made to coïncide with itself after a certain delay, the resulting output as a function of the delay may be represented as shown in fig. 2.

A number of maxima occur at delay times corresponding with 1/g, 2/g, 3/g,....sec. If the first maximum is taken to be a measure of pitch whereas the successive maxima at 2/g, 3/g,.....sec. all contribute to a more pronounced character of that pitch, then a pitch determination would be possible whose characteristics agree with the experimental findings. In the case of fig. 2 one may conclude that there will be a well pronounced pitch of 1000/5 = 200 cps.

In addition to the first maximum with a delay time of 1/g sec, there also exist sub maxima corresponding with delay times of 1/g ± 1/f; 1/g ± 2/f sec. The signals having double and triple delay times which thus form a series with each of the sub maxima, rapidly decrease in intensity. As these signals are assumed to contribute only to a more pronounced pitch, the sub maxima should have to correspond with ambiguous pitches of low intensity. In the case of fig. 2 the residue should also contain pitches of 1000/4,5 = 222 cps and 1000/5,5 = 181 cps. These predicted values of secondary pitch in an harmonic residue have recently been confirmed experimentally 8). Part of the experimental results is given in fig. 3.

Starting from an harmonic residue consisting of three components with frequencies f-g= 1800; f= 2000 cps and f+g= 2200 cps, a change of pitch is clearly heard when shifting all frequencies an equal amount. In continuing this shift up to the adjoining harmonic situation, the sensation of pitch fades away gradually rather than jumping abrubtly towards a lower pitch of increasing intensity.

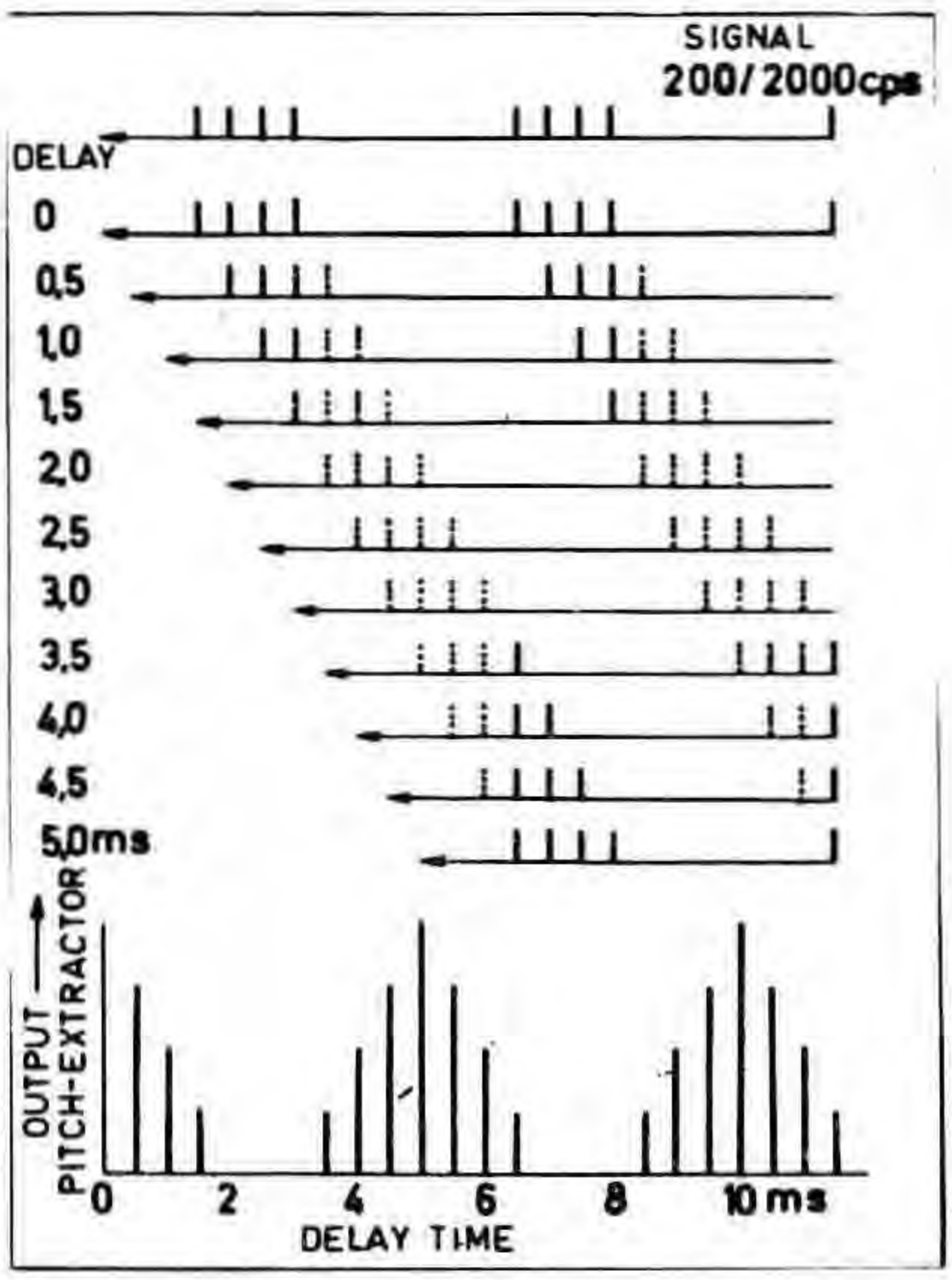

Fig.2 A schematic representation of operation of the hypothetical pitch extractor, based on the principle of coïncidence of the input signal with itself after a well defined delay time.

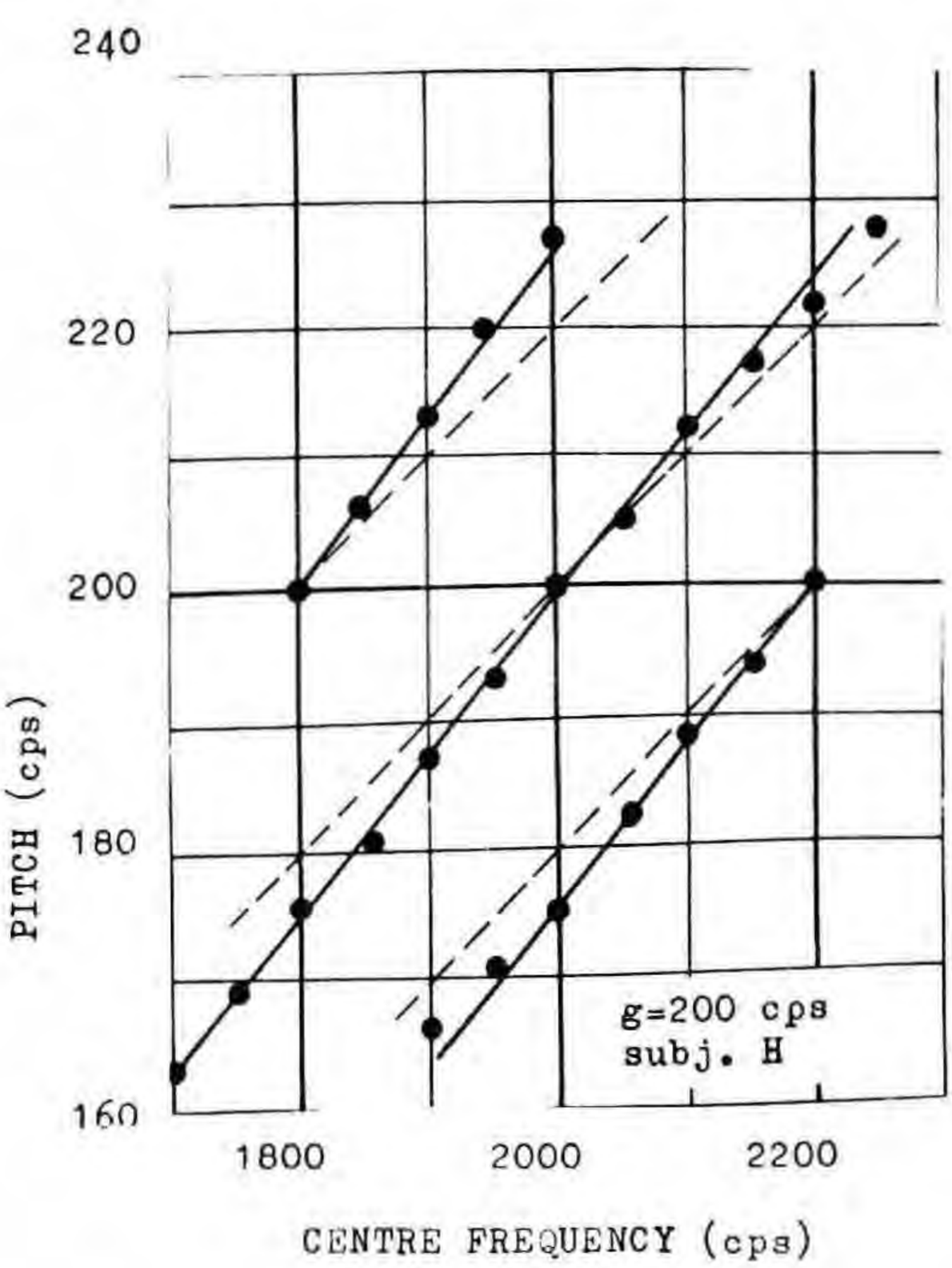

Fig.3 The pitch as a function of the centre frequency for a three component complex. The spacing frequency g is 200 cps.

In the description of the hypothetical pitch extractor no account has yet been given of the finite duration of the spikes. This would tend to slur the schematized representation as a function of the delay time. The influence of this slur increases with the centre frequency f. In general it may be concluded that the detectability of the (sub) maxima decreases with increasing number of impulses per group and/or with decreasing length of the 'silent' interval between the groups in the input signal of the pitch extractor. Both phenomena, an increase of the number of impulses per group and a reduction of the 'silent' interval between the groups in the input signal occur with higher values of f/g and with decreasing modulation depth. This would account for the experimental finding that either an increasing value of f/g or a decreasing modulation depth results in a decrease of the tonal character of the residue.

References

1. J.F.Schouten — Proc. Koninklijke Nederl_ndse Akad. van Wetenschappen, XLIII, 991 (1940)

2. J.C.R.Licklider — Experientia VII/4, 128 (1951)

3. I.C.Whitfield — Progress in Biophysics 8, 43 (1947)

4. M.H.Goldstein — Techn.Rep. 323, Res.Lab.Electronic. M.I.T. 1957

5. E.G.Wever — Theory of hearing, New York and London (1949)

6. J.Schwartzkopff — N.T.G.-Fachtagung, Karlsruhe (1961)

7. I.Tasaki — J.Neurophysiology 17, 97-122 (1954)

8. J.F.Schouten, R.J.Ritsma, B. Lopes Cardozo — 'On the pitch of the residue'. submitted for publication in J.Acoust. Soc.Am.

L58

FOURTH INTERNATIONAL CONGRESS ON ACOUSTICS
COPENHAGEN 21.-28. AUGUST 1962

Geräuschkontrolle und Lärmbekämpfungsmassnahmen an Heizkesseln

Prof.Herbert Werner, Zentralschweiz. Technikum Luzern
Prof.Dr.Ulrich Winkler, Universität Fribourg und ZTL, Luzern

Schon immer erzeugten die Heizeinrichtungen unserer Wohnungen Geräusche, ohne dass dadurch eine Belästigung entstand. Im Gegenteil, das Knistern und Knacken eines Zimmerofens gehörte sozusagen zum Behaglichkeitsgefühl der Wärmeentwicklung im Raum. Der Uebergang vom festen Brennstoff zum Oel brachte durch die geräuschreichere Oelflamme schon eine Aenderung. An Stelle der gusseisernen Heizkessel,die wahrscheinlich für die Flammengeräusche gute Absorptionseigenschaften hatten, wurden zur Steigerung der Wirtschaftlichkeit bald geschweisste Stahlkessel mit sehr gutem Wirkungsgrad, aber auch höherem inneren Widerstand entwickelt. Hochtourige Oelbrenner zur Erzeugung des höheren Druckes und andere akustische Eigenschaften des Stahlkessels gaben bald an vielen Stellen Anlass zu Klagen über Lärmbelästigung. Wie in den meisten europäischen Ländern, so entwickelte sich auch in der Schweiz eine intensive Neubautätigkeit mit neuen Ideen. Bei grossen Wohnblocks gewann die sogenannte Attikabauweise an Bedeutung, wo auf das flache Dach des Gebäudes noch mehrere Wohnungen aufgesetzt sind, die ringsum von Balkons, Terrassen und Dachgärten umgeben werden. Der auf dem Dach dieses Attikastockwerkes austretende Heizungskamin ergab mit seinen Geräuschen für die Bewohner dieser Wohnungen und auch die der Nachbarhäuser eine teilweise unerträgliche Belästigung. An verschiedenen Stellen waren Beschwerden und Kündigungen der Mieter die leider nicht ausbleibenden Folgen.

Das Zentralschweizerische Technikum in Luzern erhielt den Auftrag, diese Probleme zu untersuchen und geeignete Massnahmen vorzuschlagen. Die Versuche wurden von der Abteilung für Physik und der Abteilung für Heizungs- und Lüftungstechnik in Gemeinschaftsarbeit durchgeführt. Als Messgeräte standen Instrumente der General Radio, nämlich der Sound Level Meter (Type 1551-A) und der Sound Analyzer (Type 760-B), zur Verfügung. Die Untersuchungen wurden an einem fünfstöckigen Wohnblock durchgeführt, an dem die Belästigungen besonders akut waren. Die Messergebnisse sind in Figur 1 wiedergegeben. Auf dem Dach (obere Darstellung) ergab sich eine Gesamtschallstärke von 100 db, die für die Bewohner des Attikastockwerkes als unzumutbar bezeichnet werden mussten. Geräuschspitzen traten bei Frequenzen von 50 und 100 Hz auf. Im Heizkeller selbst (untere Darstellung) liegen diese beiden Spitzen bei 53 und 117 Hz und eine dritte Spitze bei ca. 560 Hz. Vom Keller bis auf das Dach tritt also eine geringe Verschiebung der Frequenzen und eine vollständige Absorption der Schallstärke bei 560 Hz auf. Diese Frequenz entspricht der Schaufelfrequenz des Brennergebläses, das bei 12 Schaufeln mit 2800 min^{-1} umläuft.

Nun wurde durch Messung anderer Oelbrennerkessel mit Variation der Brennereinstellung, des Brennerfabrikates, der Kesselgrösse, der Rauchrohr- und Kaminlänge versucht, die Ursachen für diese Geräusche zu finden.

Aber alle dabei ermittelten Schallstärken lagen in ähnlicher Grössenordnung und die störenden Frequenzen ebenfalls zwischen 35 und 130 Hz, sodass keine eindeutige Ursache festgestellt werden konnte.

Anschliessend wurde ein Oelbrenner im Freien durchgemessen. Es ergab sich (Fig. 2), dass an den auftretenden Geräuschen die Frequenzen von 35 bis 250 Hz fast gleichmässig beteiligt sind. Betreibt man den Oelbrenner mit geringerer Leistung (46 l/h- Düse gegen eine von 30 l/h ausgetauscht), so nimmt die Schallstärke etwas ab (von 83 db auf 80,5 db) und die Frequenzen unter 50 Hz gehen in ihrer Wirkung zurück.

Offensichtlich sind im Geräusch der Brennerflamme Frequenzen von 30 Hz bis 400 Hz vorhanden und insbesondere treten die Frequenzen von 50 bis 250 Hz mit etwa gleicher Energie auf, werden aber von Kessel. Rauchrohr und Kamin zum grössten Teil absorbiert, sodass auf dem Dach meist nur zwischen 50 und 100 Hz noch 2 bis 3 störende Frequenzen vorhanden sind.

Da eine nachträgliche Umkonstruktion einer grossen Zahl bereits eingebauter Kessel nicht in Frage kam, entschlossen wir uns, den auftretenden Lärm durch den Einbau eines Schalldämpfers zu verringern. Bei einer vorgegebenen Mindestdämpfung von 10 db der Gesamtschallstärke wurden theoretisch verschiedene Arten von Schalldämpfern durchgerechnet. Auf Grund der niedrigen Frequenzen werden alle Schalldämpfer zu voluminös, um nachträglich in einem Heizkeller untergebracht zu werden. Nur beim Interferenzschalldämpfer ergaben sich günstigere Verhältnisse. Für die Wahl der Schalldämpferart war auch ausschlaggebend, dass die Vielfachen einer Frequenz (50 Hz, 100 Hz) in ihrer Schallstärke zu dämpfen waren. Der Interferenzschalldämpfer beruht bekanntlich darauf (s.Fig.3, Abb. oben links), dass man zwei Wellen gleicher Frequenz und Amplitude mit der Phasenverschiebung einer halben Wellenlänge überlagert, sodass sie sich auslöschen. Praktisch erreicht man die Phasenverschiebung dadurch, dass man den Gasstrom verzweigt, durch zwei Kanäle mit einer Weglänge von λ und $\lambda/2$ strömen lässt und anschliessend wieder zusammenführt.

Bei der Vorausberechnung machte die Bestimmung der Schallgeschwindigkeit in den Rauchgasen Schwierigkeiten, da Temperatur und Zusammensetzung der Gase schwankt. Auch die Auslegungsfrequenz war nicht ganz eindeutig. Um diesen Gesichtspunkten Rechnung zu tragen, sollte ein Versuchsschalldämpfer gebaut werden, bei dem die Längen der Rauchgaswege in gewissen Grenzen verstellbar waren. Die Forderung nach raumsparender Bauweise führte zu einer Anordnung, wie sie in Fig. 3 (Abb. oben rechts) zu sehen ist. Die Abzweigrohre sind kreisringförmig, konzentrisch um das Rauchgasrohr angeordnet. Die obere halbe Ringfläche (λ-Segment) wird als Strömungsquerschnitt für den Gasweg $l_1 = \lambda$ und die untere halbe Ringfläche ($\lambda/2$ - Segment) für den Gasweg $l_2 = \lambda/2$ benutzt. Die Gase werden in jedem Segment hin- und hergeführt, sodass die Baulänge kurz bleibt, sie benutzten also etwa die Viertelkreisringfläche als Strömungsquerschnitt. Die Segmente sind in ihrer Segmentführung verschiebbar, das λ-Segment um 0,5 m, das $\lambda/2$- Segment um 0,25 m. Die Gase aus dem Rauchgasrohr werden in der Mitte zugeführt, dann nach vorne (entgegen der Strömung im Rauchgasrohr) in das λ- und $\lambda/2$-Segment umgelenkt.. Dann strömen sie bis zur vorderen Kante, wo sie um 180° umgelenkt werden, legen die gleichen Wege wieder nach hinten zurück, vereinigen sich im Rauchgasrohr und treten in den Kamin aus. Der

Schalldämpfer hat nur eine Länge von 2,8 m und einen Durchmesser von 0,8 m und lässt sich auch bei engen Raumverhältnissen gut unterbringen.

Vor und nach Montage des Schalldämpfers wurden die Geräuschverhältnisse messtechnisch überprüft. Dabei wurden die Segmentstellungen systematisch verändert. Die optimalen Verhältnisse traten ein, wenn die Gase im λ-Segment einen mittleren Weg von 4,6 m und im $\lambda/2$- Segment einen solchen von 2,3 m zurücklegen mussten. Die hauptsächlich gedämpfte Wellenlänge musste also bei 4,6 m liegen, um die beste Dämpfung der Gesamtschallstärke zu erreichen. Die Dämpfung erfasst ein relativ breites Frequenzband (Fig. 3 unten), was auf die vom mittleren Weg abweichenden Wege der Gasteilchen auf der Innen- und Aussenbahn zurückzuführen ist. Die erreichte Dämpfung ist besonders stark bei 50 und rund 100 Hz. Die Gesamtschallstärke wurde auf dem Dach von 100 db auf 85,5 db und auf dem Attikabalkon, wo die Mieter sich aufhalten, von 80 db auf 67 db gesenkt. Die Herabsetzung der Geräusche auf dem Balkon entspricht in dem Frequenzbereich mehr als 20 phon und kann als Erfolg betrachtet werden. Der Druckverlust im Schalldämpfer beträgt 1,7 mm WS bei einer Gasgeschwindigkeit von ca. 5 m/s im Rauchrohr und einer mittleren Rauchgastemperatur von 200° C.

Von den Bewohnern der Häuser und der Umgebung wurde das Resultat der Geräuschdämpfung dankbar begrüsst und als grosse Erleichterung empfunden.

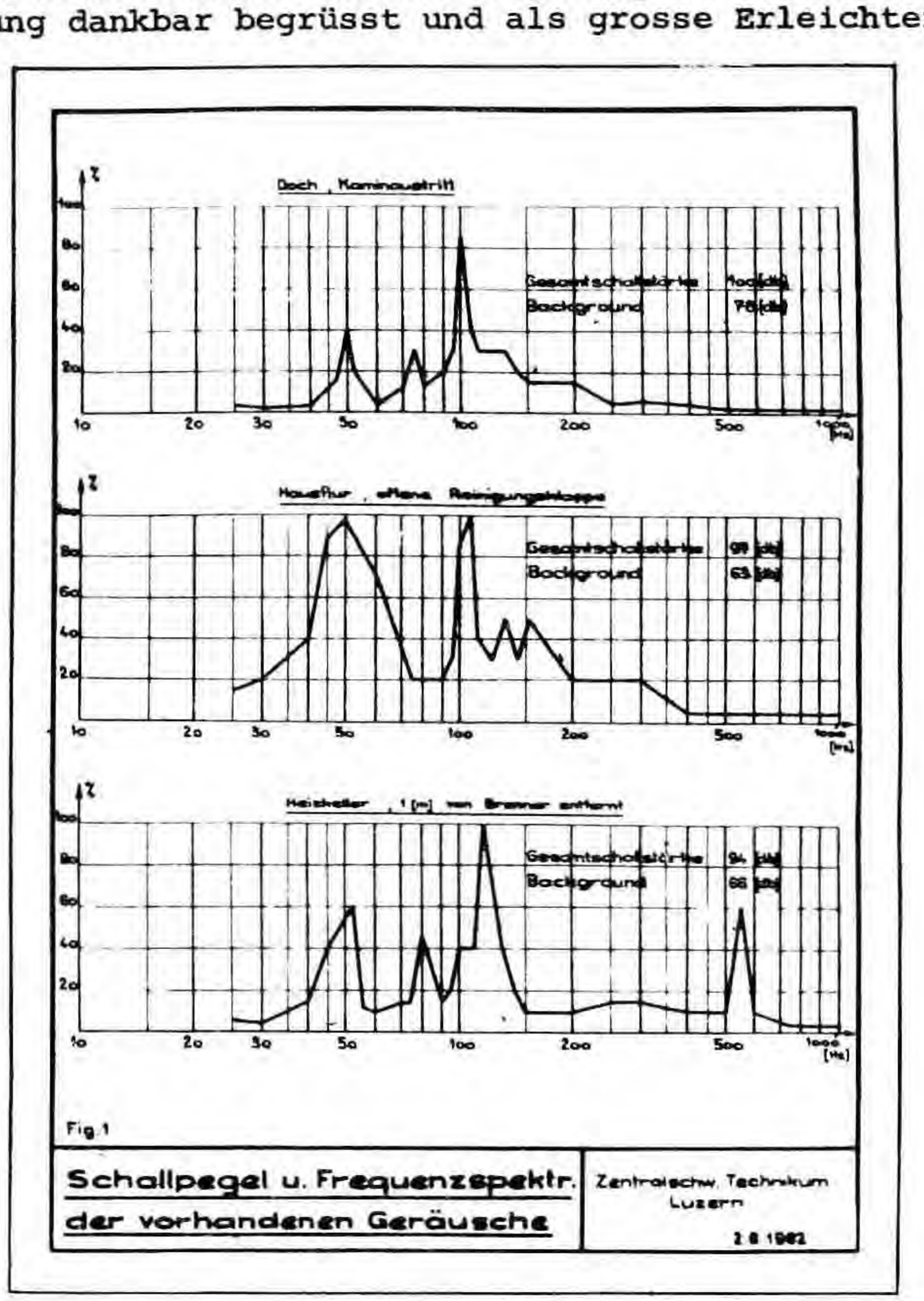

Fig. 1

Schallpegel u. Frequenzspektr. der vorhandenen Geräusche

Zentralschw. Technikum Luzern

2.8.1982

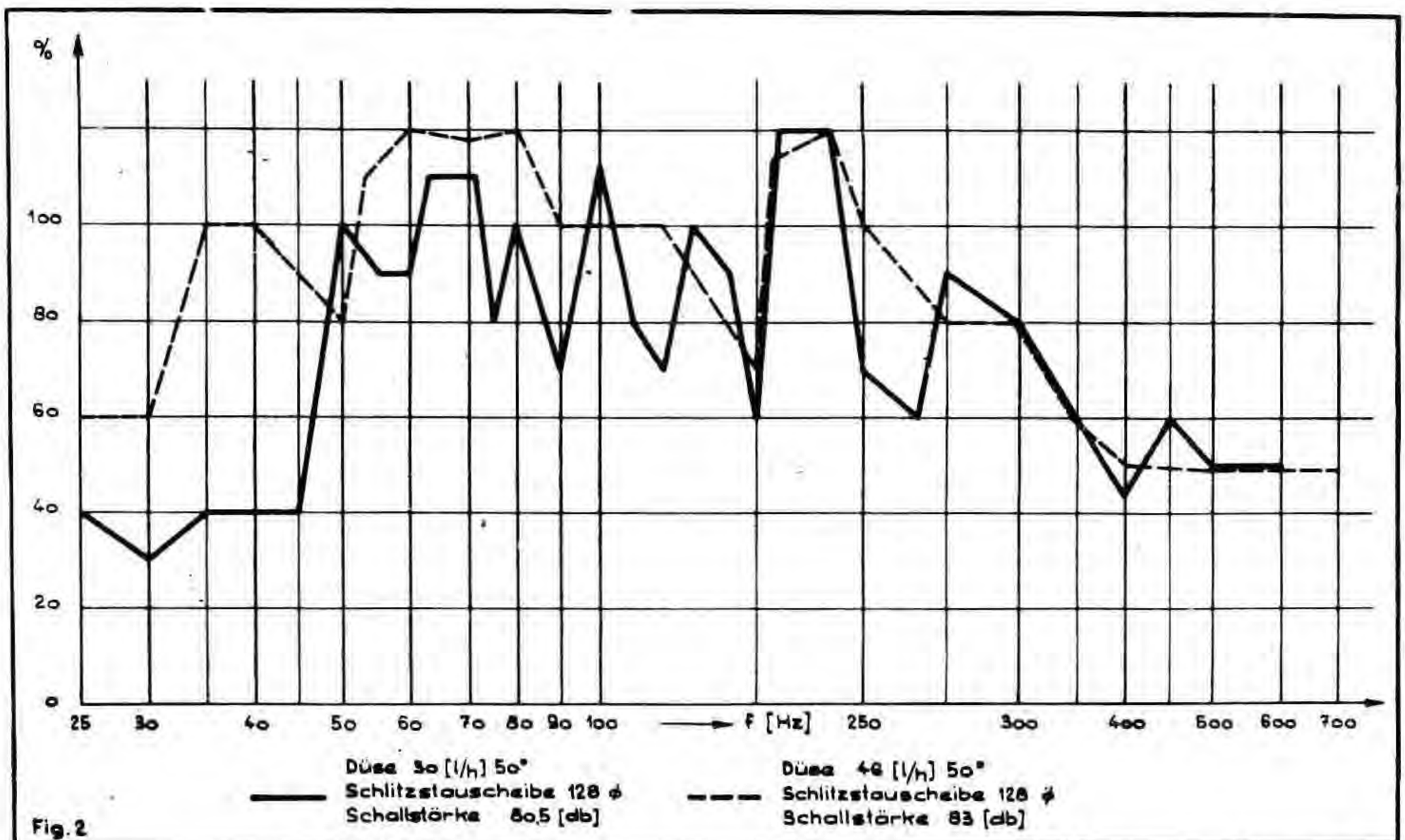

Fig. 2

Brennerspektren

Zentralschw. Technikum Luzern

2.6.1962

Prinzip des Interferenzschalldämpfers

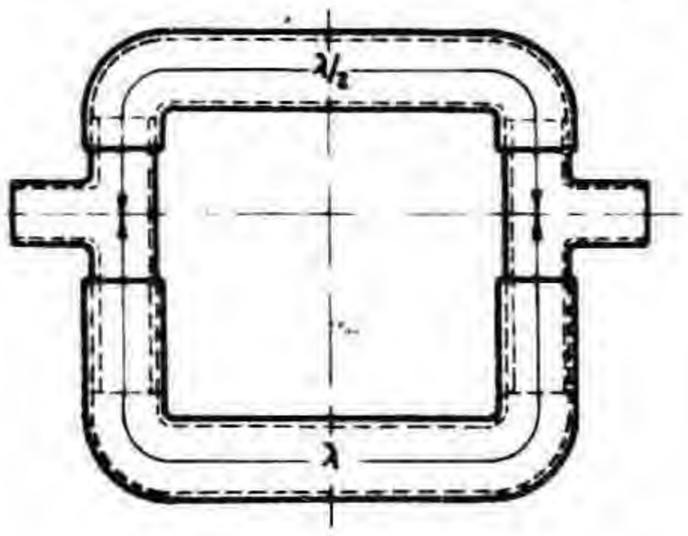

Ausführung für Heizkesselanlage (Versuchsschalldämpfer mit variablen λ-Segmenten)

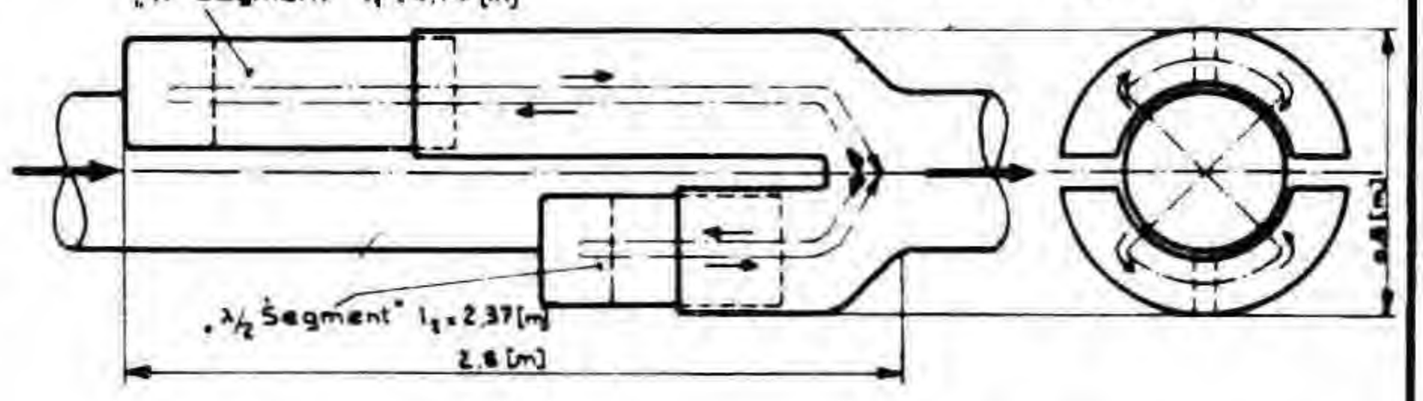

	Gesamtschallstärken [db]		
	Hausflur	Dach	Attikabalkon
ohne Schalldämpfer	97	100	80
mit Schalldämpfer	85,5	85,5	67

Frequenzspektren

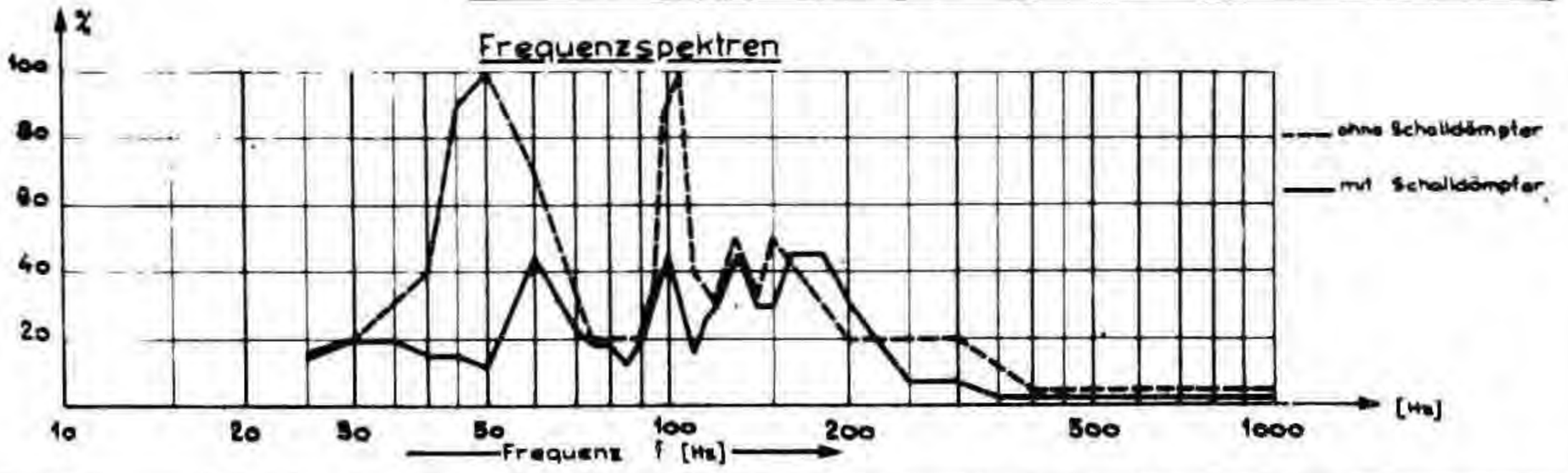

Fig. 3

Interferenzschalldämpfer

Zentralschw. Technikum Luzern

2.6.1962

M58

FOURTH INTERNATIONAL CONGRESS ON ACOUSTICS
COPENHAGEN 21.-28. AUGUST 1962

The Use of Lead in Improving Sound Transmission Loss

Paul B. Ostergaard
Lewis S. Goodfriend & Associates Little Falls, New Jersey

The trend toward lighter-weight architectural materials in the United States and Canada has been spurred since 1946 by the increasing costs of materials and labor to install them. With this trend have come the thin, lightweight, low-cost partitions for offices, multiple dwellings, and private homes. Lowest first cost is an important factor in the economics of these buildings. Because the acoustical properties, or the lack of such properties, of low-cost building materials are not fully appreciated by many architects, contractors, and owners, too many buildings have been constructed with low-cost floors and partitions between offices or dwelling units which are acoustically inadequate. In most of western Europe, where cost of masonry construction still is not prohibitive, the use of lightweight partitions is not yet common except in new or remodelled office buildings. However, the information currently at hand including personal inspection of recently built offices in Paris by a member of our firm indicates that sound transmission problems are occurring in new office construction throughout western Europe.

In separate efforts to improve the sound isolation offered by lightweight partitions and floor-ceiling constructions, groups working independently in Australia, England, France, and the United States have been studying the application of both rolled and cast sheet lead as a means of improving the sound isolation of lightweight partitions without returning to the high floor, column, and footing loadings required by masonry construction. This work has led to one very encouraging conclusion: thin, relatively inexpensive lead sheets can increase the sound transmission loss of a wide variety of common architectural materials used for wall panels in office and residential construction. This paper will outline the basic acoustical properties of lead when applied in combination with conventional building panels.

The conventional approach to the study of lead in combination with building materials is to consider the lead-building-board assembly as a rigid combination of two materials and compute the combined stiffness, mass and damping factor of the new board. From these parameters it is possible to calculate the transmission loss as approximated by straight lines after the method of Watters.[1] When this is done no consideration is given to the added damping provided by the use of elastomeric adhesives. The elastomeric adhesives are much more common in the building industry today in the United States and Canada than are the rigid adhesives. Among the rigid adhesives are casein adhesives, epoxy cements, and conventional furniture glue. The elastomeric adhesives include the synthetic resins in the class referred to as contact adhesives. One caution must be observed in the use of contact adhesives. When applied to lead, any rubber base adhesive which would permit the formation of lead sulphide at the lead-adhesive interface must be avoided since this will cause the eventual delamination of the lead.

Tests on samples of steel bars indicated that the complex modulus of elasticity for soldered bars follow theory rather well. However, with an elastomeric adhesive between the steel and the lead the damping is markedly increased. The result of this difference is that the actual sound transmission loss as measured in both the laboratory and the field turns out to be considerably higher than anticipated. When due allowance is made for the damping provided by the adhesive, the results are somewhat closer to that predicted by theory. The effect of damping can be accounted for in both the bending stiffness plateau and the damping of the coincidence dip by application of the shear damping theory of Kerwin.[2] A comparison of the transmission loss predicted from theory with and without taking the added damping into account is shown in Figure 1 along with the TL measured in the laboratory.

Our firm has had a large series of panels tested with and without lead. For some panels of a simple nature it was possible to estimate the transmission loss. By accounting for the effects of the adhesive the measured and calculated transmission loss agreed well at middle and high frequencies. To eliminate any arguments that the effects were achieved by the adhesive alone or by any shear damping, 1/8" sheet lead was used.

The mechanical properties of lead which contribute to its acoustical performance are: low stiffness, high density, and high internal damping. Lead has a density of 710 lbs/ft^3, its modulus of elasticity is 2×10^6 lbs/in^2 and its internal damping is approximately 0.015 at 1000 cps.

In addition, lead is malleable and thus readily formed to unusual contours. It may be sawed, planed, and fastened in the field with the usual carpenters tools. It is all of these mechanical properties which make it a good acoustical isolation material for use in building construction.

Watters has stated that the sound transmission loss ($10 \log_{10} \frac{1}{\tau}$) in the plateau region caused by trace matching may be approximated by the equation:

$$TL = 60 + 30 \log_{10} W - 10 \log_{10} B + 2 \log_{10} \eta \text{ db}$$

where W is the surface weight of the panel in pounds per square foot
B is the bending stiffness per unit width in lb-in^2, and
η is the damping factor.

Writing this more directly:

$$\frac{1}{\tau} = C_1 \frac{\rho^3 h^3}{E h^3} \eta^{0.2}$$

$$\frac{1}{\tau} \approx C_2 \frac{\rho^3}{E}$$

Thus to achieve the highest degree of sound isolation a material with high ρ^3/E becomes extremely desirable. Table I shows the values of W^3/E for a variety of materials.

TABLE I

	W	E	W^3/E
Lead	710 lbs/ft^3	20 x 10^5 psi	178
Steel	490	300 x 10^5	3.92
Gypsum board	48	2 x 10^5	0.539
Hardboard	67	8.1x 10^5	0.371
Plywood	45	7 x 10^5	0.130

Note the outstanding position of lead. To achieve a given sound transmission loss in the plateau region we need less thickness or weight of lead than of any other material.

To produce satisfactory architectural units the lead must be combined with suitable architectural materials. When this is done the transmission loss is degraded somewhat by the stiffness of the architectural material. This is shown in Figure 2. Thus it is most desirable to use a minimum thickness of gypsum building board, plywood or hardboard to achieve a given sound transmission loss.

In laminating the materials with lead, an energy absorbing elastomeric adhesive has been used most effectively to obtain maximum η. Many contact-type adhesives are suitable for this service. In our own laboratory adhesive lamination of lead to building materials has been carried out using simple techniques. A trisodium phosphate solution is used to clean the lead and deposit a stable phosphate surface layer. Adhesive is applied to both lead and building material, the surfaces are joined and rolled with a water-filled lawn roller. More sophisticated production methods may be used but none are as inexpensive for a small quantity of material as the method described.

Nailing the lead to studs and nailing the building board over it does not produce the same results since advantage is not taken of the shear damping of the adhesive. Also lead may readily be applied to existing surfaces using thin double-coated adhesive tapes. The technique is expensive, but for small areas such as doors, closet interiors or bathroom cabinets, it is most convenient. The lead is readily painted to match existing finishes.

Certain applications can make use of leaded boards as single sheets to develop a maximum transmission loss. The use of single panels set into the framing between stops, as shown in Figure 3 offers considerable sound isolation in a minimum of thickness. Note the requirements for perimeter seals. Here again the lead face may be painted readily, and intriguing architectural designs may be achieved by use of random horizontal framing and patterns of coloring for the panels.

Materials costs are quite modest compared to conventional sound isolation constructions. There are appreciable price differentials around the world for rolled lead sheet in the 2-6-pound-per-square-foot surface-weight range. The price in sizeable quantities in the U.S. and Canada is $.15/lb. In Europe the price is $.08 to $.10/lb. In Australia the price is $.10/lb. This results in varying economic situations. In the U.S., high quality sound retardent office partitions cost over $4.00 per square foot in large quantity. Light-weight leaded partitions using not more than 6 lb. of lead with steel or hardboard capable of much higher TL are available at prices from $2.50 to $3.50 per square foot including posts and removable base. The use of trowelable plastic compounds loaded with lead granules applied only 1/8" thick can provide a 3 to 4 lb. increase in surface density. These plastics have high damping and are easy to apply. This material is also excellent for application to new construction of gypsum board on studs, when applied to one side during erection. The cost of this method is between $.36 and $.45 per square foot of finished partition above the cost of the plain gypsum board wall.

In Australia the cost of competitive materials set a maximum limit of four pounds of lead which can be used in a premium wall. In Europe, where sheet metal partitions are replacing masonry construction in new high-rise buildings, the cost of lead is negligible compared to any other means of achieving the TL of the masonry formerly used. Actually, with the rising labor costs in Europe, the use of 4 pound lead, at its present low rolled price, will be economically sound. Six pound lead should easily fit within the cost limits of premium partitions.

Leaded vinyl plastic sheeting in the range of .5 to 1.5 lb/ft^2 is also available for a wide variety of uses. Its cost is about $\$1.50/ft^2$ and is now in use in some new educational facilities in the U.S. in weights of 3 lb/ft^2 as remedial sound closures and barriers. It is hoped that the cost can be greatly reduced by new production methods.

The use of lead has been shown to provide maximum sound isolation per pound. Its ease of lamination, fabrication and paintability make it an ideal architectural material for high TL at modest cost.

References:
1. B.G. Watters, J. Acoust. Soc. Am. 31 , P. 898-911 (1959)
2. E.M. Kerwin, Jr., J. Acoust. Soc. Am. 31 P. 952-962 (1959)

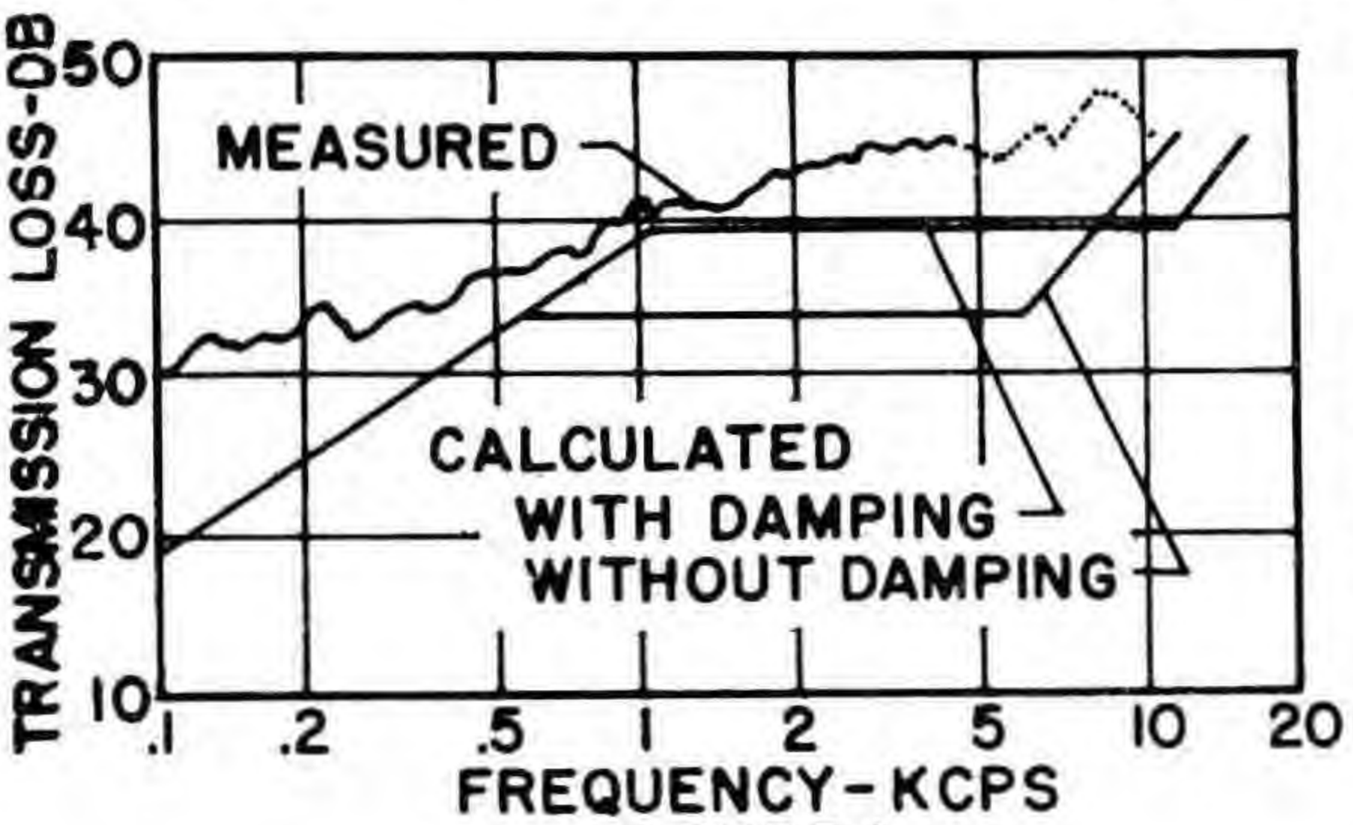

FIGURE 1

Calculated and measured transmission loss of 3/8" plywood with 3/32" lead adhered to one face. The increase in transmission loss above 500 cps results from the inclusion of damping in the calculations.

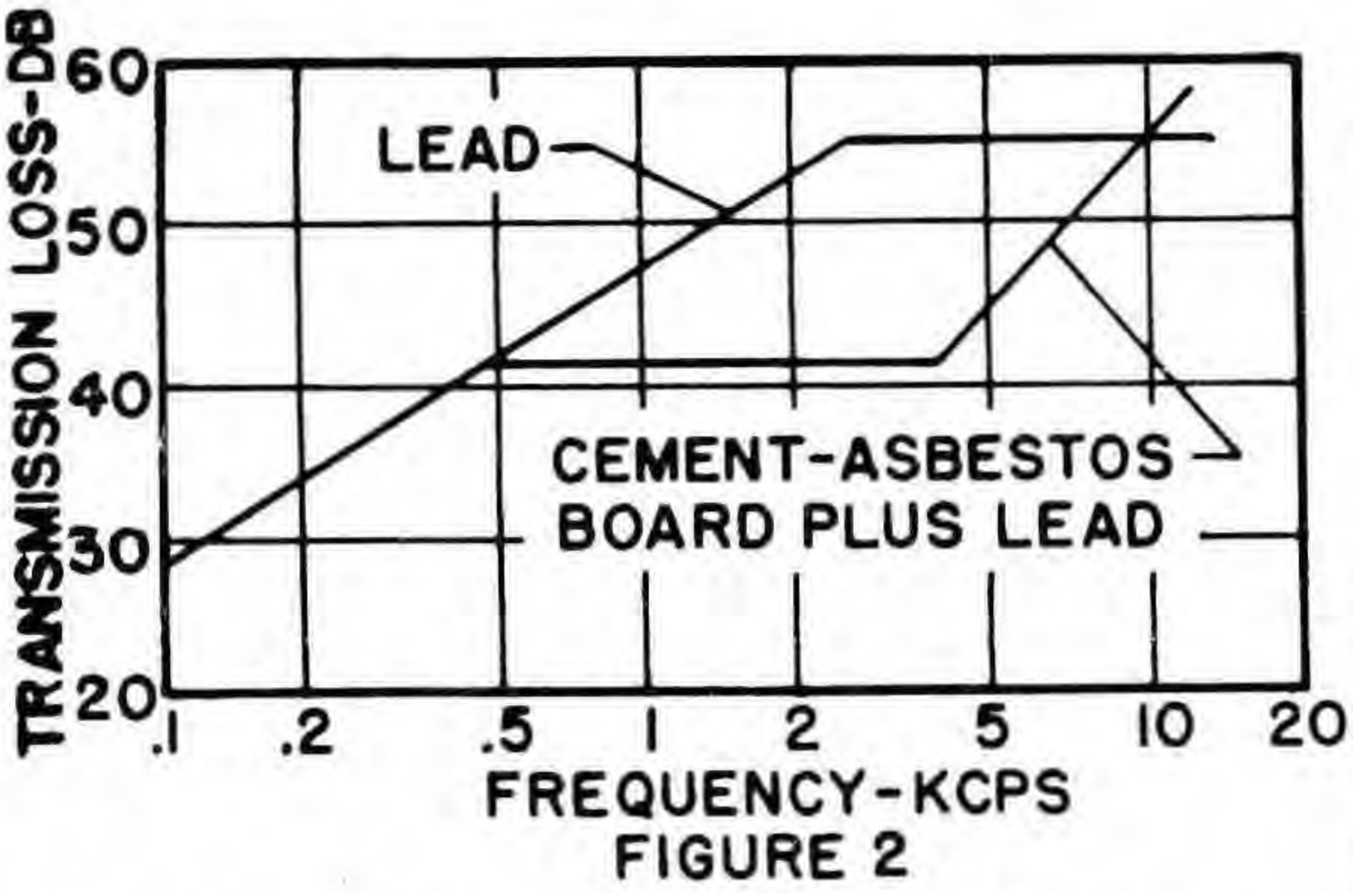

FIGURE 2

Calculated transmission loss of 3/8" cement-asbestos board and lead, and a sheet of lead of equal weight. The reduction in transmission loss above 500 cps is due to the stiffening effect of the cement-asbestos board.

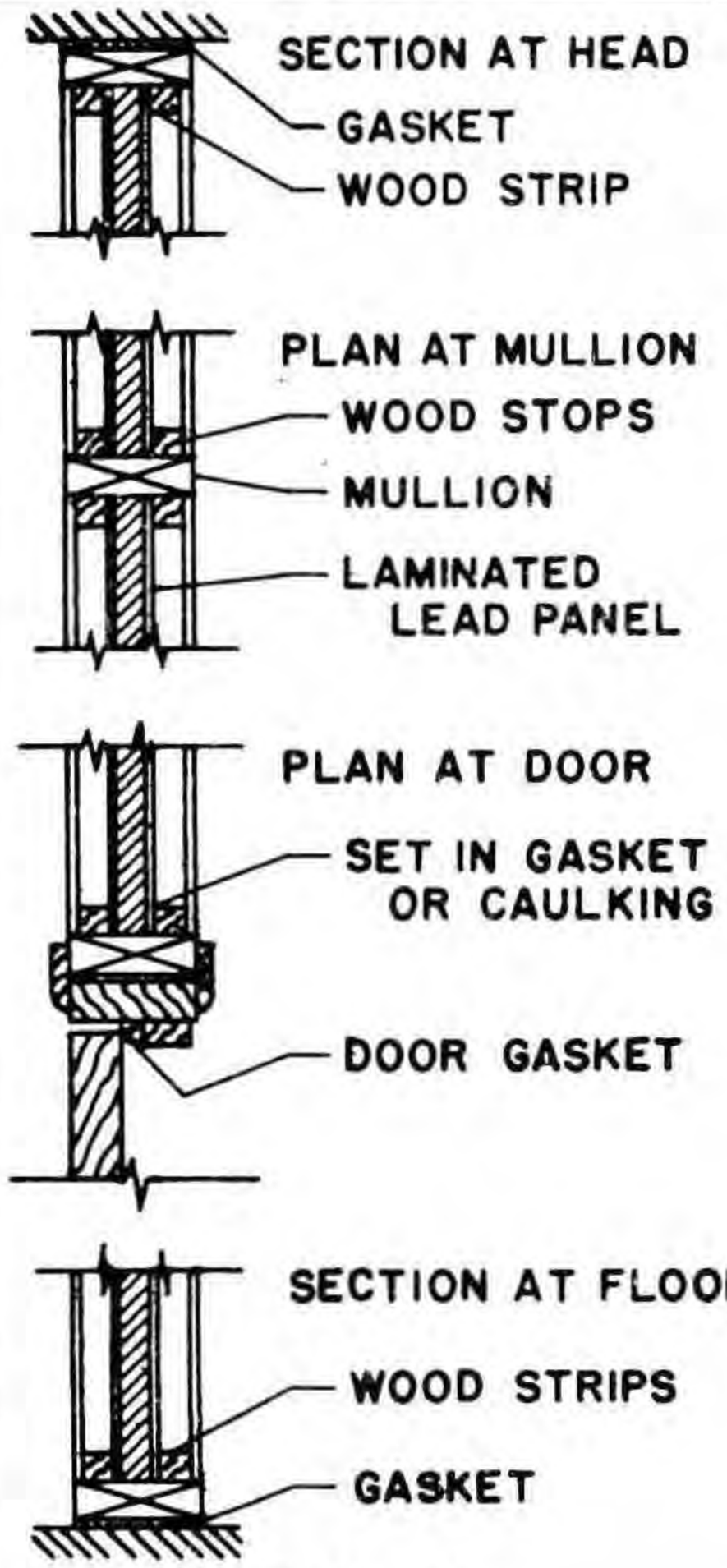

FIGURE 3

Architectural details for a lead laminated panel wall. The perimeter seals are a very important part of the assembly.

N58

FOURTH INTERNATIONAL CONGRESS ON ACOUSTICS
COPENHAGEN 21-28 AUGUST 1962

PRODUCTION OF HIGH-INTENSITY ACOUSTIC VIBRATIONS BY MEANS OF HYDRODYNAMIC TRANSDUCERS

FRIDMAN V.M., NOVITSKY B.G.

As early as in 1948 Polmann and Janovski W.[1] suggested to use liquid whistle (Hydrodynamic transducer) to produce acoustic vibrations. The authors propose the following mechanism of production of acoustic vibrations: a liquid flow, leaving a narrow slit at high velocity, strikes a nonstreamlined obstacle (a plate) forming vortexes near the surface of the obstacle. The vortex has an excessive pressure at the centre. The continuous liquid flowforms a series of vortexes and a sequence of pressure drops resembling a sound wave. These waves excite the plate into acoustic vibrations of the frequency given by

$$f = \frac{0,5 \cdot V.n}{h} \qquad /1/$$

where

V = velocity of the liquid outflow from the nozzle,

h = distance between nozzle and plate,

n = number of harmonics.

The possibility to use hydrodynamic transducer to generate acoustic vibrations was studied in the Soviet Union too /2,3/. The tests carried out by Shi-Go-Bao, directed by prof. Rosenberg L.D., allowed to work out a new mechanism of excitation of acoustic vibrations.

High-speed filming showed an important role of the jet's vibrations in the transducer operation. The frequency of these vibrations is given by the relationship proposed by Rosenberg L.D.

$$f = \frac{V.n}{h} \psi\left(\frac{h}{bn}\right) \qquad /2/$$

where

b - nozzle width

ψ - universal ratio, depending on $\frac{h}{bn}$

The above mentioned tests were carried out on the hydrodynamic transducers giving acoustic vibrations of relatively low intensity. Therefore Rosenberg's mechanism seems more suitable in this case. We faced the problem of producing acoustic vibrations of much higher

intensity compared to those received by Polmann R. and Janovski.The results of our investigations allowed to design (4) high intensity hydrodynamic transducer for low liquid pressure (~5 ata).

This transducer has the following technical features:

a) small distance between nozzle and plate (~ 0,4 mm),
b) a nozzle with a jet-forming device,
c) the plate has a relatively low flexural rigidity and variable section of equal resistance,
d) the plate material has low density (ρ) and high Young's modulus (E) (titan and its alloys).

Here are the results of the tests carried out on the above mentioned hydrodynamic transducers. The intensity of the transducer is 4-5 times higher than the intensity of Polmann-Janovski transducer. (Fig.1).

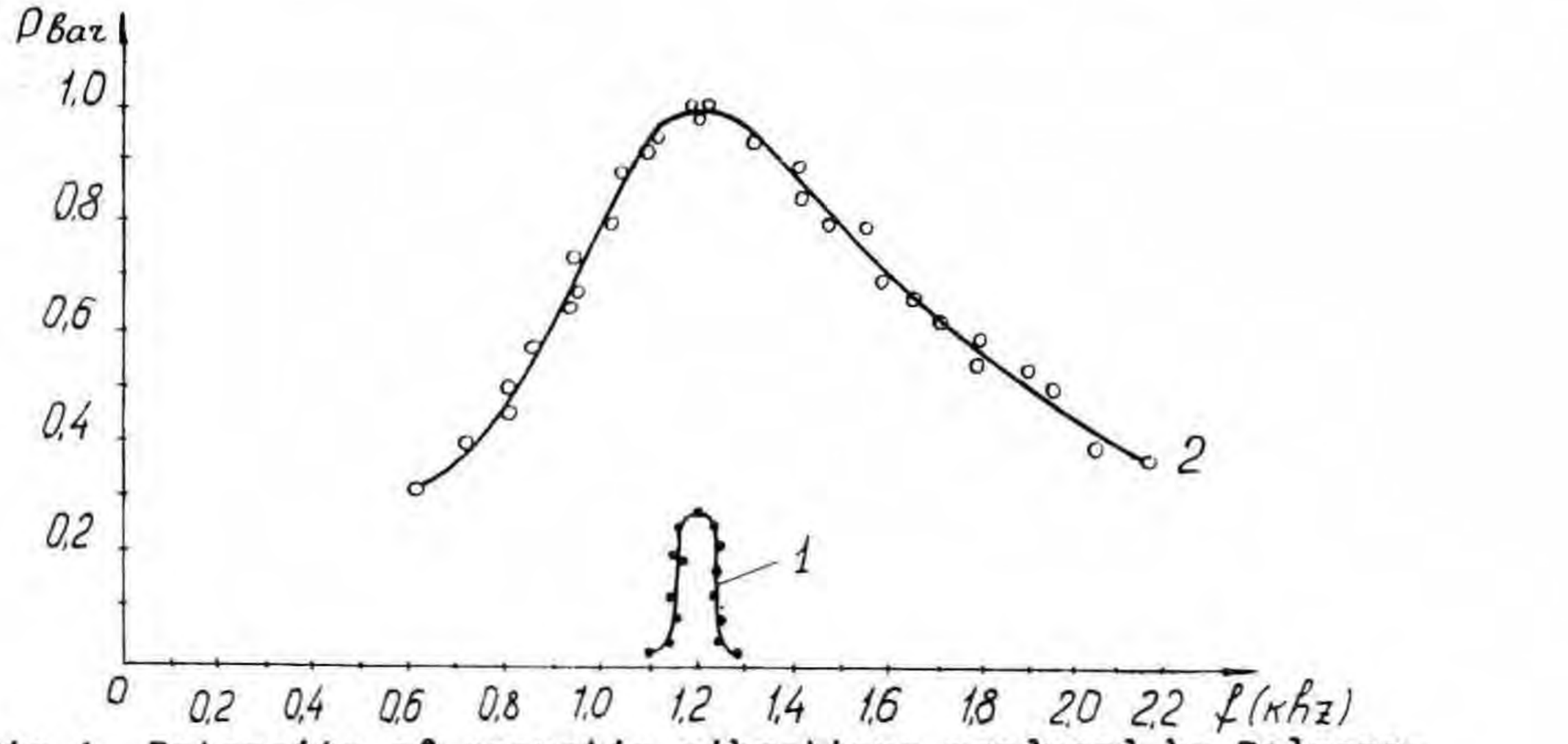

Fig.1. Intensity of acoustic vibrations,produced by Polmann-Janovski hydrodynamic transducer (1) and high intensity transducer (2) (in comparable units).

The pressure and flow rate were maintained constant. Frequency of vibrations was changed by varying the plate length while the other parameters remained constant. The liquid pressure, necessary for the radiation of the same intensity (vibration frequency is the same) is 2-3 times less than in Polmann-Janovski transducer.(Fig.2).

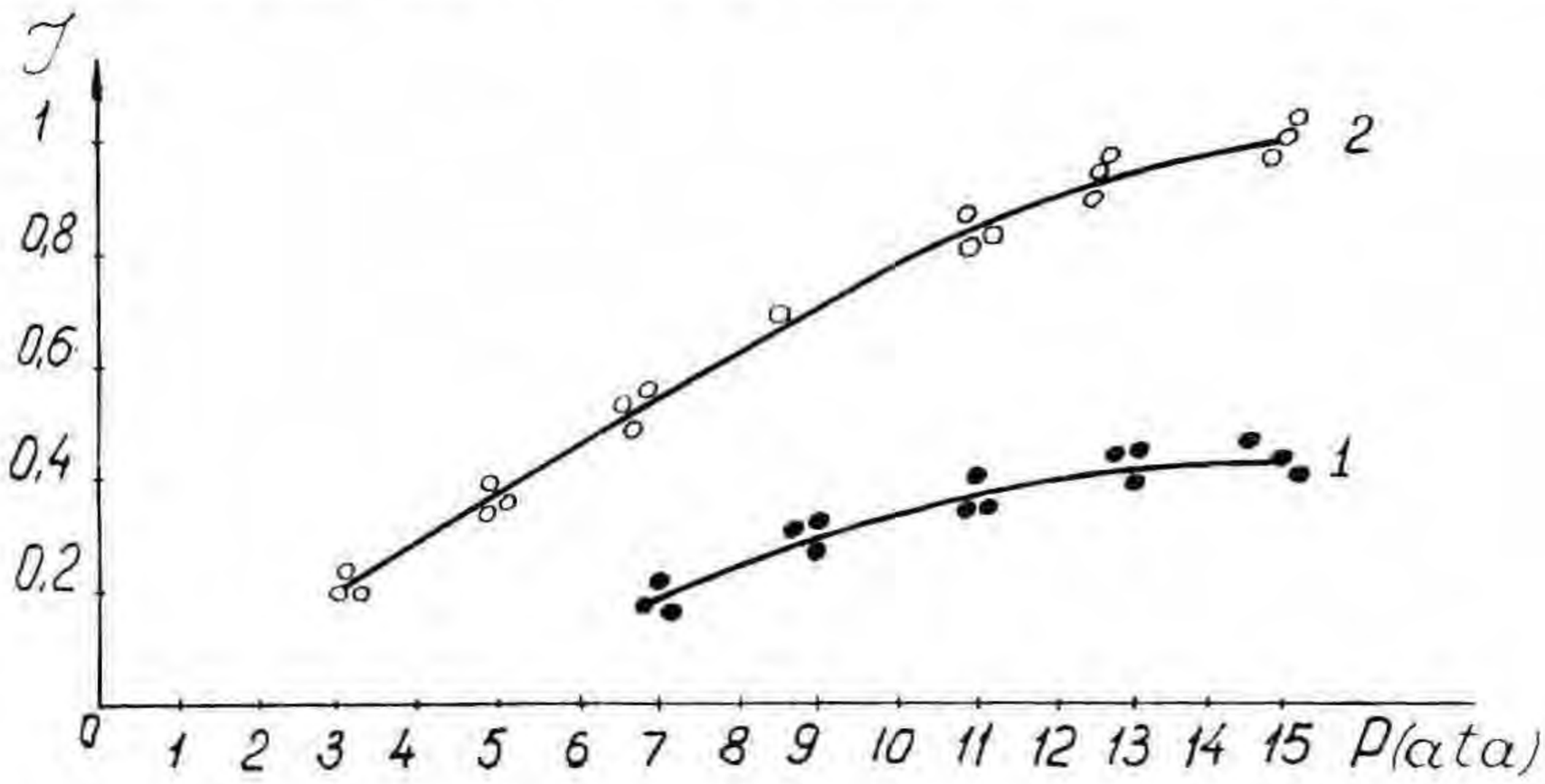

Fig.2. Relationship between liquid pressure and intensity of accoustic vibrations (in comparable units) in Polmann-Janovki hydrodynamic transducer (1) and high-intensity transducer (fluid pressure and flow rate are the same).

Titanium plate of equal resistance variable section works much longer in the same operation conditions, and gives much intensive vibrations.

The above mentioned mechanisms do not explain all the results of the investigations on hydrodynamic transducer. So experimental frequences of acoustic vibrations differ from those given by the formulas (1,2). The pressure change from 3 to 15 ata at the nozzle inlet has no effect upon the resonant tuning of the transducer (Fig.3).

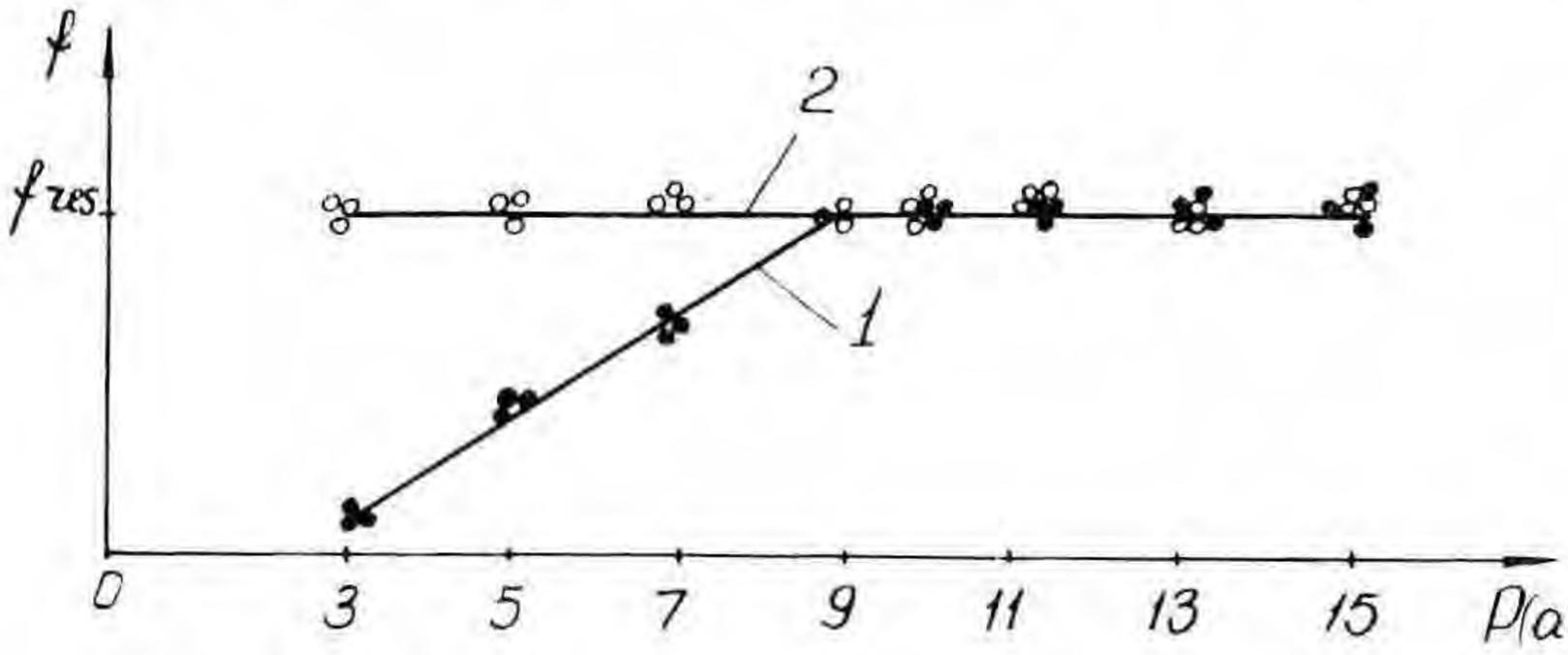

Fig.3. Effect of the liquid pressure on the excitations of the plate into resonant frequwncy in Polmann-Janovski hydrodynamic transducer (1) and in high intensity transducer (all the other conditions are equal).

This fact is also difficult to explain from the point of view of the above mentioned mechanisms. All this means that the mechanism of acoustic vibrations' excitation by means of high-intensity hydrodynamic transducer differs from all the known mechanisms of the kind.

The jets from the nozzle with a jet preforming device, is supposed to act directly upon the transducer plate, if the distance between nozzle and plate does not exceed 0,4 mm. At present this process undergoes a thorough study.

Soviet scientists designed industrial ultrasonic apparatus based on the above mentioned high-intensity hydrodynamic transducers.

L I T E R A T U R E

1. Janovski W., Polmann R., Schall und Ultraschall Erzeugung in Flüssigkeiten für industrielle Zwecke.- Zeitschrift angew. Physik, 1948, 1, 222.

2. Fridman V.M. Sonic and ultrasonic vibrations and their applications, Gislegprom, 1956.

3. Rosenberg L.D. Ultrasonics applications. Izdatelstvo Akademii Nauk SSSR, 1955.

4. Fridman V.M., Gershgal D.A. Ultrasonic apparatus. Gosenergoisdat, 1961.

---o---

H59

FOURTH INTERNATIONAL CONGRESS ON ACOUSTICS
COPENHAGEN 21.-28. AUGUST 1962

Auditory Adaptation in Pitch Shift Detection *

Andrew Sekey

Department of Electrical Engineering, Imperial College, London, S.W.7.

Introduction

The pitch of short bursts of tone has been the subject of several investigations, and it is found that as the duration of the burst is reduced to a few milliseconds its pitch quality becomes almost completely lost. This process appears to be continuous, although some authors (1) prefer to describe it in terms of marked 'thresholds'. The subjective indeterminacy of pitch, characterized by listeners' inability to associate the pitch of a burst with that of a pure tone, is analogous to the frequency indeterminacy Δf in the Uncertainty Principle $\Delta f.\Delta t \geq 1$ of signal analysis (2). Due to the essentially introspective nature of the pitch uncertainty, however, a similar inequality in subjective acoustics has so far eluded an experimentally verifiable quantitative formulation (9).

A related phenomenon is the reduction in the differential sensitivity to frequency for tonal pulses of gradually shortening durations (4,5,6,8,10). This effect is observed at the presentation of two, slightly different stimuli, and therefore cannot be directly related to the Uncertainty Principle, which applies to a single waveform. A more appropriate analogy can be found with the statistical problem of signal reception in a noisy environment. The relevance of a statistical approach is borne out by the nature of perceptual experiments: as the ultimate sensitivity is approached, judgements become contaminated by random errors, reflecting the presence of some fluctuating, unpredictable attribute inherent in the human decision process. This interference is conveniently regarded, in the terms of communication engineering, as some 'noise' process superimposed on the received stimulus.

In this paper the function relating differential pitch uncertainty to stimulus duration is studied, on the basis of new experimental evidence. Human performance is compared to that theoretically attainable, and a satisfactory measure of agreement is found. It is subsequently argued that this provides preliminary evidence supporting the view that the auditory system is capable of short-term adaptation to stimuli of varying duration.

Experimental Technique and Results

Subjects, all male College students aged 20-30, were seated in an acoustically treated testing booth, whose attenuation was supplemented by that of the padded circumaural Sharpe Type A. earphones, model HF-15. Binaural stimuli were generated by means of an apparatus containing an oscillator, counting circuits, a pedestal- and transient-free linear gate and a band-pass filter. A typical waveform is drawn schematically below, and is seen to consist of two sinewave pulses.

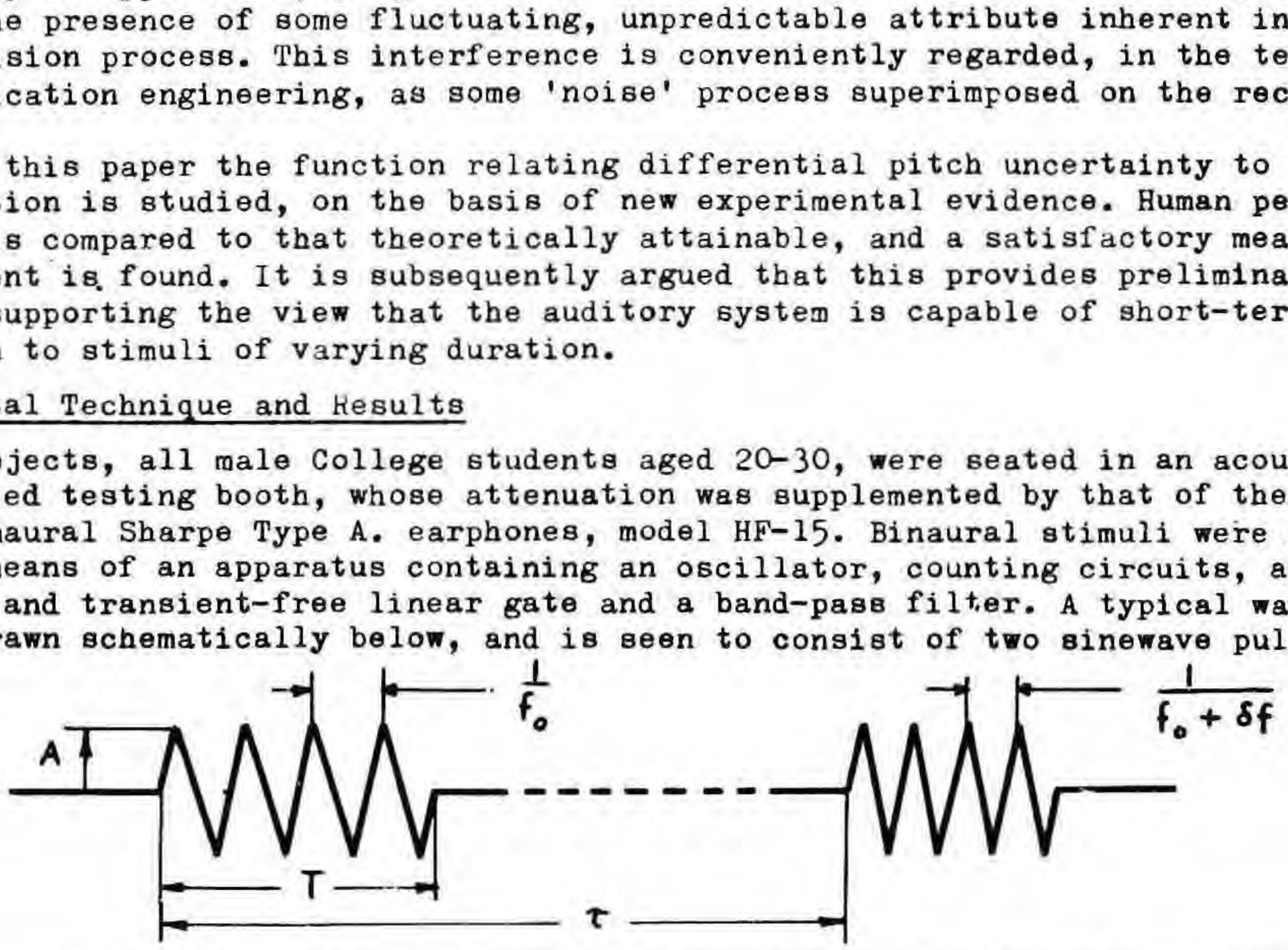

* This paper is based on a Ph.D.Thesis to the University of London.(See ref.7.)

The carrier frequency f_o, duration T, frequency deviation δf and amplitude A were all adjustable; the delay τ was a constant 0.5 seconds.

Subjects were told that the stimuli consisted of short 'pips' or 'clicks' separated by an interval, and that the pitch of the second click was either higher or lower than that of the first click, the two possibilities occuring at random with equal probabilities. Further, they were asked to indicate after each presentation of a paired stimulus whether the pitch moved up or down, by pressing one of two switches. In doubtful cases they were told to guess; withholding a judgement or pressing both switches simultaneously was not permitted.

The object of the experiments was to obtain a functional relationship between the stimulus parameters δf and T and the probability of a decision error $P_e = P_e(\delta f, T, \text{other parameters})$. In practice only a limited number of δf_i-T_j combinations could be investigated, and the observed relative frequency of errors, F_{ij}, was regarded as a binomially distributed estimator of the 'true' value, P_{ij}. Data were obtained in listening tests of about 30 minutes duration, during which only δf and T were varied. The effect of other parameters was examined separately.

The table shows the range of T and δf in the main experimental series. Each dot denotes 15 judgements for positive and 15 for negative values of δf. Stimuli were presented 'row by row': one of the values T_j was chosen at rando. and held constant, whilst δf varied over its range in a quasi-random manner, then another value of T was picked, etc. Subjects were thus able to 'anticipate' pulses of a given duration.

T ms \ $\lvert\delta f\rvert$ - c/s	5	10	20	40
4	•	•	•	•
8	•	•	•	
16	•	•		
32	•			

It was found from preliminary experiments that the error probability function (EPF) has the general form:

$$P_e = \text{Erf}\,(e^{-k}\,|\delta f|^a\,T^b) \qquad \text{where} \qquad \text{Erf } Y = \frac{1}{\sqrt{2\pi}} \int_{-\infty}^{-Y} e^{-\frac{1}{2}x^2}\,dx\ ,$$

and δf is to be substituted in c/s and T in ms. The constants k, a and b must be estimated separately for each test from the observations. To determine the influence of certain factors on these constants, the main experiment was designed in the form of a 4 x 4 Greco-Latin square containing the following factors: Subjects (4 'levels'), Order of Test (4 levels), Carrier frequency f_o (4 levels, 0.5 - 2.0 kc/s), Intensity (2 levels with 6 db variation) and Bandwidth (2 levels). The constants and their standard deviations were estimated by a maximum likelihood iterative technique, developed on the lines of the probit method. The values obtained by averaging over the 16 tests were:

$$a = 0.7 \quad (\sigma_a = 0.4) \qquad b = 0.95 \quad (\sigma_b = 0.47) \qquad k = 4.34 \quad (\sigma_k = 2.0)$$

(These figures are based on 30 x 10 x 16 = 4,800 binary judgements. Very similar results were obtained by graphical estimation from the preliminary experiments, in which 8 subjects were tested on three occasions each, yielding a total of 8,150 judgements.)

Analysis of variance calculations failed to show up significant effects (on the 10% level) due to any of the factors listed above. (It must be remembered, however, that the Latin square design is based on the assumption that interactions are absent which, if unwarranted, renders the results less significant.)

The average EPF is thus of the form:

$$P_e = \text{Erf}\,(e^{-4.34}\,|\delta f|^{0.7}\,T^{0.95})$$

The goodness of fit, as determined by the χ^2-test, was found acceptable.
The condition for the error probability to remain constant is set by the equations:

$$|\delta f|^{0.7}\,T^{0.95} = C' \qquad \text{or} \qquad |\delta f|\,T^{1.35} = C$$

This is a kind of "trading relationship", showing how the hearing mechanism can 'barter' frequency shift for duration and vice versa.

A Decision Theory Model of Spectral Shift Detection

Consider now that the listener is replaced by an 'abstract mechanism' or 'model', to which is attributed a consistent strategy for coping with the given task. The model is purely behavioural - it is designed to simulate the function, but not the structure, of the auditory process. One hopes, however, that its

calculated performance will correspond to the average behaviour of human listeners.

In transforming the problem from the psychological into the physical domain a certain amount of arbitrariness is inevitable; the following are only the most important assumptions:

(i) The perceptual uncertainty inherent in human observers can be adequately represented by an additive Gaussian noise process in the model.

(ii) For the test signal employed, pitch (a subjective sensation) is positively correlated with frequency (a physical parameter).

(iii) Changing f_o to $f_o \pm \delta f$ in the stimuli is psychologically equivalent to shifting its spectrum by $\pm \delta f$.

With these conditions the problem can be formulated as one of estimating the relative frequency shift between two spectra, and the solution can be obtained by the application of statistical decision theory. This type of approach has been successfully applied to other problems in psycho-acoustics, and its main attractions are that (a) it enables the language of statistical signal theory to be applicable to both human and instrumental members in a communication system and (b) decision theoretic solutions are usually optimal in terms of some rational criterion, thus providing useful, though somewhat arbitrary, standards of comparison (11).

The structural details of the model have been presented elsewhere (7), and here only a broad outline is given. The complex Fourier spectra $\sigma_1(f)$ and $\sigma_2(f)$ of the received signals $s_1(t)$ and $s_2(t)$ are related to some 'reference' spectrum $\gamma(f)$ (only known to the external observer) in the following way:

$$\sigma_1(f) = \gamma(f) + \lambda_1(f) \quad ; \quad \sigma_2(f) = \gamma(f - \phi_o) + \lambda_2(f) \ ,$$

where λ_1 and λ_2 are independent white Gaussian noise processes having N_o (Wattsec) mean energy associated with each degree of freedom. For the estimation of the relative spectral shift ϕ_o, $\gamma(f)$ may be eliminated by combining the two noise terms:

$$\sigma_2(f) = \sigma_1(f - \phi_o) + \lambda(f) \ ,$$

where $\lambda(f)$ has $2N_o$ mean energy per degree of freedom.

This equation is formally identical to:

$$y(t) = u(t - \tau_o) + n(t) \ ,$$

representing the relationship between transmitted and reflected signals in radar range measurements, where the quantity τ_o is the unknown echo delay (12). The problem of spectral shift estimation can thus be regarded as the 'dual' in the frequency domain of delay estimation. The solution, when carried out along similar lines as in (12), leads to the posterior probability distribution:

$$p_o(\phi) \cong k\, p_o(\phi) \exp\left[- \frac{(\phi - \phi_{max})^2}{2/R\alpha^2} \right] , \quad \text{where} \quad R = \frac{\int |\gamma|^2 \, df}{N_o} = \frac{E_g}{N_o} \gg 1 \ ,$$

$$\alpha^2 = \frac{2\pi^2}{E_g} \int g^2(t)\, t^2 \, dt \quad ; \quad g(t) = \int \gamma(f) \exp(2\pi j\, t\, f)\, df \ .$$

α is a measure of the 'effective duration' of $g(t)$, (2). The prior distribution $p_o(\phi)$ of ϕ is assumed to be uniform and bounded.

It is now recalled that the model is not required to yield an estimate of ϕ_o but only to state its polarity. In the absence of external 'costs', or if the payoff matrix is symmetrical, the 'best' strategy involves computing the generalized Bayes Preference, which is the ratio of average posterior probabilities on the hypotheses that ϕ_o is positive and that it is negative. If this is greater than unity then $\phi_o > 0^o$ is accepted, otherwise $\phi_o < 0$. From the known (Gaussian) distribution of ϕ_{max} the distribution of the Bayes Preference, and thence the probability of a decision error can be determined:

$$p_e = \mathrm{Erf}\ (\sqrt{R}\,\alpha|\phi_o|)$$

For the signal $g(t) = A \sin 2\pi f_o t \quad (0 \leq t \leq T = 2\pi n/f_o)$ used in the experiments, we get:

$$R = A^2 T / 2N_o \ , \qquad \alpha = \frac{2\pi}{\sqrt{3}} T \ ,$$

and thus

$$p_e = \mathrm{Erf}\ (k\, |\phi_o| T^{1.5}) \ , \quad \text{where} \quad k = \frac{\sqrt{2/3}\ \pi\ A}{\sqrt{N_o}}$$

The Case for Aural Adaptation

Let us now compare p_e and P_e, the theoretical and experimental EPF's. The general form of both functions is the same, but in relation to p_e the exponents of δf and T in P_e are too low. Amongst the possible causes for this are some mathematical approximations in the model, and the fact that for pure tones pitch is a non-linear function of frequency. Of particular interest in each formula is the 'trading' condition for constant error probability:

$$|\delta f| T^{1.35} = C \qquad \text{and} \qquad |\phi_o| T^{1.5} = c$$

By noting that the difference in the exponents of T is insignificant, one may speculate as follows: the model uses an optimum detection technique which, for white Gaussian noise, is cross-correlation or the equivalent matched filtering. Since T is a variable, the filters must also be capable of adjusting their impulse responses in order to maintain the condition of matching. For the aural mechanism, however, it has been frequently suggested ever since Helmholtz, that an appropriat description can be given in terms of fixed filters (or resonators) with specified time constants (3). Consider therefore an alternative model which follows the same decision strategy as the one discussed, but contains fixed filters with time constants equal to T_o milliseconds. Calculations show (7) that a constant error rate is characterized by the conditions:

$$|\phi_o| T^{3.0} = c\, T_o^{1.5} \quad \text{for} \quad T < T_o \; ; \quad |\phi_o| T_o^{1.5} = c \quad \text{for} \quad T > T_o$$

Thus once the signal duration has attained the value of the filter time constant and matching occured, further increase in T is not rewarded by any improvement in the observational accuracy. This is manifest in a plot of ϕ_o against T: the curve descends monotonically up to the value T_o where a break occurs, beyond which ϕ_o remains constant. Observations show that T_o cannot be less than 50 ms; but even if it were greater, the discrepancy between the exponents 1.35 and 3.0 is so much greater than between 1.35 and 1.5 that, in the face of the observations, an 'adaptive filter' model still represents the 'preferred hypothesis'. It is to be noted, however, that the situation examined represents only a special case. More specific investigations are now being carried out into the flexibility of the aural system in pitch shift detection as well as other modes of operation.

The writer wishes to express sincere thanks to his Supervisor, Professor E.C.Cherry, for encouragement and continued interest during the course of this work. Thanks are also due to the Admiralty for financial support.

References

1. DOUGHTY,J.M. and W.R.GARNER, J.Exp.Psychol. 37, Aug.1947.
2. GABOR,D., Journ.I.E.E., 93, Part III. 429, 1946.
3. GOLD,T. and R.J.PUMPHREY, Proc.Roy.Soc. B. 135, 462, 1948.
4. KÖNIG,E., J.A.S.A. 29, 606, 1957.
5. LIANG CHIC-AN and L.A.CHISTOVICH, Soviet Physics, Acoustics, July,1960.p.75.
6. OETINGER,R., Acustica, 9, 431, 1959.
7. SEKEY,A. " A study of auditory perception in the time-frequency domain", Ph.D.Thesis, University of London, March, 1962.
8. STEVENS,K.N., J.A.S.A. 24, 76, 1952.
9. STEWART,G.W., J.A.S.A. 2, 325, 1931.
10. TURNBULL,W., Journ.Exp.Psychol., 34, 302, 1944.
11. VOELCKER,H.B. in Information Theory, Ed.E.C.Cherry, Butterworth, 1961.
12. WOODWARD,P.M., Probability and information theory, with applications to radar, Pergamon Press, 1953.